Diagnostic Gynecologic and Obstetric Pathology

An Atlas and Text


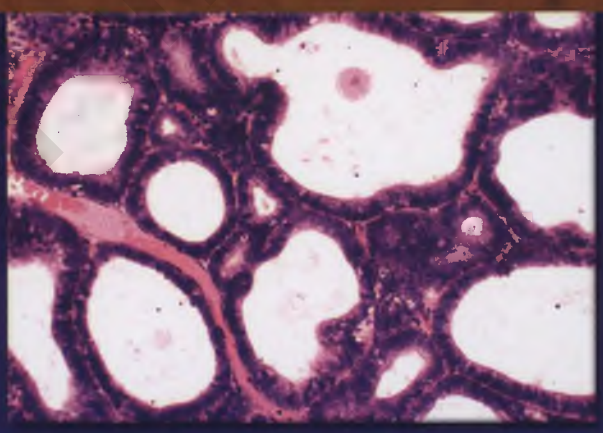
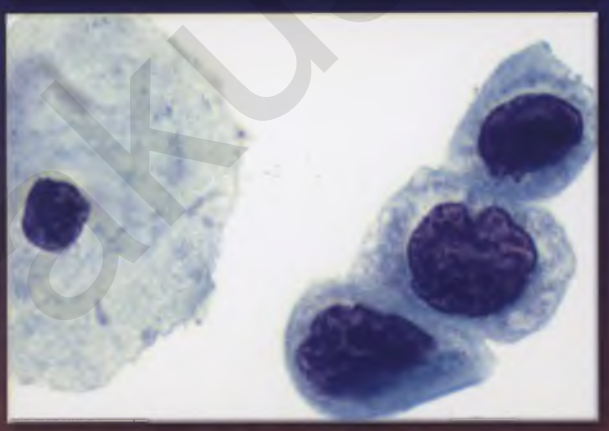


Roger A. Reichert

Includes online access to fully searchable text & image bank

Wolters Kluwer | Lippincott Williams & Wilkins

Diagnostic Gynecologic and Obstetric Pathology

An Atlas and Text

Roger A. Reichert, M.D., Ph.D.

Consultant in Gynecologic Pathology
http://www.reichertpathology.com

Emeritus Chief of Pathology
St. Luke's Hospital
St. Louis, Missouri

Wolters Kluwer Health | Lippincott Williams & Wilkins

Philadelphia • Baltimore • New York • London
Buenos Aires • Hong Kong • Sydney • Tokyo

Senior Executive Editor: Jonathan W. Pine, Jr.
Product Manager: Marian Bellus
Vendor Manager: Bridgett Dougherty
Senior Marketing Manager: Angela Panetta
Senior Manufacturing Manager: Benjamin Rivera
Graphic Designer: Stephen Druding
Production Service: SPi Global

Two Commerce Square
2001 Market Street
Philadelphia, PA 19103 USA
LWW.com

Printed in the People's Republic of China

Library of Congress Cataloging-in-Publication Data
Reichert, Roger Alan.
Diagnostic gynecologic and obstetric pathology : an atlas and text / Roger A. Reichert. — 1st ed.
p. ; cm.
Includes bibliographical references.
ISBN 978-1-60831-077-7
I. Title.
[DNLM: 1. Genital Diseases, Female—diagnosis. 2. Genital Diseases, Female—pathology. 3. Genital Diseases, Female—diagnosis—Atlases. 4. Genital Diseases, Female—pathology—Atlases. WP 141]
618.1'075—dc23

2011028222

To purchase additional copies of this book, call our customer service department at (800) 638-3030 or fax orders to (301) 223-2320. International customers should call (301) 223-2300.

Visit Lippincott Williams & Wilkins on the Internet: at LWW.com. Lippincott Williams & Wilkins customer service representatives are available from 8:30 am to 6 pm, EST.

10 9 8 7 6 5 4 3 2 1

Legends for Cover Figures: **Top Left:** Endophytic ovarian serous borderline tumor (see Fig. 7.8). **Top Right:** Simple hyperplasia without atypia of the endometrium (see Fig. 4.130). **Bottom Left:** Pap smear with high-grade squamous intraepithelial lesion, metaplastic type (see Fig. 3.128). **Bottom Right:** Vesicles from a complete hydatidiform mole (see Fig. 10.1).

CCS1111

To Valerie, Elaine, and Elizabeth

PREFACE

In covering the topic of gynecologic and obstetric pathology, this book attempts to carve out its own niche midway between an atlas and a traditional textbook. It takes an image-intensive and practical approach that provides the reader with the information necessary to evaluate the vast majority of the wide range of diseases encountered within this subspecialty. Much can be learned from the gross examination of pathology specimens, and this often neglected and undervalued aspect of pathology practice is herein given its proper respect. The gross and microscopic images in this work are presented exclusively in color, and are supplemented by pertinent clinical information and discussions of differential diagnostic considerations. When deemed appropriate, images of immunohistochemical and "special" stains are included. This book also includes numerous Pap smear images and cytologic–histologic correlations. In addition to coverage of pathology of the organs of the female genital tract, brief overviews of the normal histology of these sites are provided as necessary background information. Separate chapters are also devoted to placental and peritoneal pathology.

The material presented places an emphasis on diagnostic-related issues pertaining to common lesions and their variants, although attention is also given to classic forms of many rare lesions. In selected instances, recommendations on the processing of gross pathology specimens, discussions regarding the optimal approach for intraoperative consultations, and recommendations on the phrasing of key portions of pathology reports are provided. The 10 chapters are organized by site, and the beginning of each chapter lists the entities discussed and their corresponding page numbers. The bibliography sections include both recommendations for general reading and selective lists of references.

This book is intended to be used by pathologists in community and academic practices, as well as pathologists-in-training, as a source of high-quality images and condensed diagnosis-related information in this complex field of pathology. My target audience also includes gynecologists and obstetricians with an interest in clinicopathologic correlation, and I hope that cytopathologists and cytotechnologists will appreciate the numerous Pap smear images and the sections on peritoneal cytology. Pathologists-in-training and those responsible for the billing of gynecologic surgical pathology specimens may also find the material in the appendices to be of use.

This work represents the culmination of 25 years of effort. Taking a page from my childhood hobby of collecting baseball cards, I painstakingly collected and organized slides and images of gynecologic and obstetric pathology specimens as I encountered them during my training at Stanford and throughout my career as a pathologist at St. Luke's Hospital. Years of hands-on experience at the surgical pathology bench have allowed me to personally photograph most of the surgical specimens that are presented. After a 25-year gestation period, it is with great satisfaction that I deliver this book to you, and I hope that it exceeds your expectations.

Roger A. Reichert, M.D, Ph.D

For information on how to send consultations in gynecologic pathology to Dr. Roger Reichert, please visit http://www.reichertpathology.com. This website also contains information on how to contribute images to Dr. Reichert to enhance possible future editions of this book.

All images were optimized using Adobe Photoshop. In some instances, this included changing the color of the background, balancing the color, correcting minor imperfections in the stained tissue sections, and/or removing extraneous tissue and objects. In rare situations in which I could best demonstrate a particular disease process by using images from another organ, this approach was utilized. My intent is not to deceive the reader with these maneuvers, but rather to provide the highest quality images possible.

Please note that images that span the full width of both columns in Chapters 6 and 8 were selected for enlargement by the compositor.

ACKNOWLEDGMENTS

I am forever indebted to four professors from Stanford University: Drs. Richard L. Kempson and Michael R. Hendrickson for sparking and encouraging my interest in the field of gynecologic pathology, and Drs. Irving L. Weissman and Eugene C. Butcher for nurturing my development as a physician scientist and author. Special thanks to histotechnologist extraordinaire Mark Richardson of St. Luke's Hospital, whose dedication, attention to detail, and technical skills are second to none. Several colleagues, most notably Drs. Colin J.R. Stewart, Deborah J. Gersell, Julio A. Lagos, Enrique Higa, and Richard L. Payne, enhanced the quality of this book by generously providing selected images or glass slides as cited in the figure legends. I am also grateful to Dr. Cheryl M. Reichert (AKA Big Sis) for helpful suggestions made during her review of Chapters 4 and 10, Dr. Julio A. Lagos for sharing with me his expertise in placental pathology, Dr. Sherman Silber for the donation of his 35-mm slide scanner, Dr. Richard L. Payne for allowing me to use his photomicroscope to fill in the gaps in my image collection, St. Luke's Hospital for providing an atmosphere that attracts a high volume of interesting gynecologic cases and promotes physician education through the use of pathology images, and St. Luke's librarians Marlene Pelton, Jean Henderson and Jane Isaak for their friendly and helpful assistance.

Roger A. Reichert, M.D, Ph.D

FOREWORD

Image-intensive textbooks are one of the most important resources available to surgical pathologists. The photomicrographs serve as a reminder of histologic patterns that characterize rare or unfamiliar lesions, and are also a valuable learning tool for both experienced and neophyte pathologists. To be most useful, the photomicrographs should be of the highest quality, in color, and accompanied by legends that fully describe the salient features of each photograph. Equally as important is a text that focuses on diagnostic criteria and differential diagnosis. Dr. Reichert has produced a book that far exceeds these requirements. The photomicrographs, all in color, are superb, and the legends fully describe what the observer should see. The text is practical and not only emphasizes definitions and differential diagnoses but also provides clues about avoiding diagnostic errors. Information about relevant immunohistochemical stains is a prominent feature, and the references are timely and pertinent. Readers faced with a diagnostic problem within the area of gynecologic and obstetric pathology will often find the solution in this book without having to consult other texts.

The chapter on the uterine cervix amply demonstrates the outstanding nature of this book. Following an overview of normal histology and cytology, the various lesions encountered in the cervix are illustrated and described in a thorough and organized fashion. The beautiful histologic photomicrographs and the comprehensive text are complemented by descriptions and illustrations of abnormal cytologic preparations. In the chapter on the uterine corpus, Dr. Reichert provides a balanced discussion of the merits and demerits of the atypical hyperplasia and endometrial intraepithelial neoplasia systems of nomenclature, and also presents his own point of view. The section on uterine smooth muscle tumors thoroughly reviews the morphologic predictors of outcome and their utilization. The chapter on ovarian tumors is detailed and fully illustrated. The sections on noninvasive versus invasive implants, micropapillary serous tumors, and the new system for grading ovarian serous carcinomas are both timely and useful. These are but a few examples of the many highlights contained in this superb book, which is a unique work that will have great appeal to diagnostic pathologists at every level of experience.

Although primarily intended for pathologists, this book also will serve as a useful resource for gynecologists and obstetricians as they prepare for board examinations, interpret pathology reports, and strive to better understand the nature of the diseases that they treat. Beyond its value as a diagnostic aid, this book is written in a style that makes it a pleasure to read. There is no doubt in my mind that Dr. Reichert has produced a work that will become a classic and one most pathologists will find to be an essential and integral part of their practice of gynecologic and obstetric pathology.

Richard L. Kempson, M.D.
Emeritus Professor of Pathology
Stanford University School of Medicine
Stanford, California

CONTENTS

CHAPTER 1

Pathology of the Vulva

OVERVIEW OF VULVAR ANATOMY AND HISTOLOGY

The major externally visible components of the vulva are the mons pubis, labia majora, labia minora, clitoris, and vestibule. These structures are all lined by stratified squamous epithelium, which is nonkeratinized in the vestibule and keratinized elsewhere. Within the vestibule, which is the space between the labia minora, are the entrance to the vagina, the urethral orifice, the openings of the ducts of the major (Bartholin) and minor vestibular glands, and the duct openings of the paraurethral (Skene's) glands. The acini of the paired Bartholin's glands are lined by mucinous columnar cells (Fig. 1.1). Each Bartholin's duct is lined by mucinous epithelium proximally, transitional epithelium distally, and squamous epithelium at its point of exit into the vestibule, which has implications for the histology of the Bartholin's cyst. Further details on vulvar anatomy and histology are available in *Histology for Pathologists* and other standard texts of gynecologic pathology (see suggested readings list in bibliography).

NONINFECTIOUS VULVAR DERMATOSES

Terminology and Classification

As modified skin, the vulva is subject to the same dizzying array of noninfectious dermatological disorders as skin elsewhere in the body. Since the focus of this book is on gynecologic pathology rather than dermatopathology, only the few major lesions of this type that are likely to be commonly encountered by general surgical pathologists are presented in this chapter. The 2006 classification scheme of these lesions that was developed by the International Society for the Study of Vulvovaginal Disease (ISSVD) represents its third iteration.[1] Dating back to the ISSVD's first classification system in 1975, the terminology used for hyperkeratotic, acanthotic, nondysplastic lesions

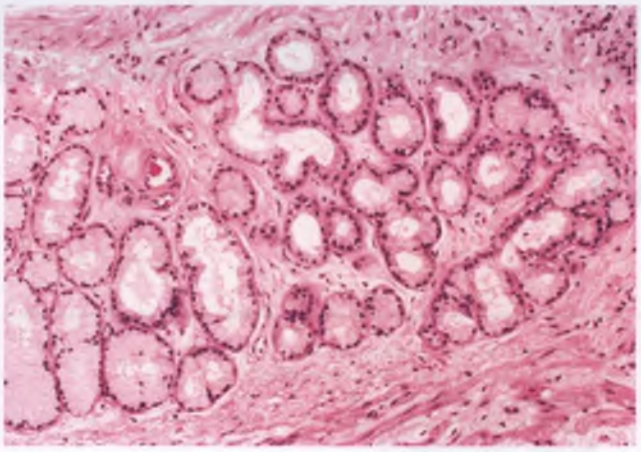

FIGURE 1.1. Acini of normal Bartholin's gland lined by mucinous columnar epithelium.

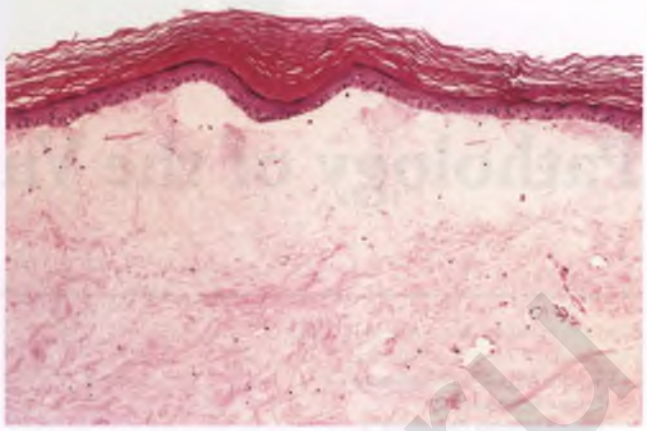

FIGURE 1.2. Lichen sclerosus. The dermis is hyalinized and edematous, and is separated from the epidermis centrally, which will lead to formation of a blister. The epidermis is thin with loss of rete pegs, and there is an overlying layer of hyperkeratosis. A bandlike lymphocytic infiltrate is beyond the field of view within the deeper aspect of the dermis.

of vulvar skin has been controversial. Terminology for these lesions has evolved from hyperplastic dystrophy in 1975 to squamous cell hyperplasia in 1987 to "acanthotic pattern" in 2006. The vast majority of these acanthotic skin lesions represent a primary or secondary form of lichen simplex chronicus (see below).

As advocated by most dermatopathologists for many years, the 2006 classification system utilizes standard dermatologic terminology for the vulvar dermatoses, and avoids use of the older, nonspecific terms squamous cell hyperplasia and vulvar dystrophy.[1,2] By basing the classification system on histologic patterns and including a list of the most likely diagnoses for each pattern, the 2006 version has its greatest utility precisely when it is needed the most, which is when neither the pathologist nor the clinician can render a specific diagnosis. In addition to the acanthotic pattern, the other histologic categories in this system are spongiotic, lichenoid, dermal homogenization/sclerosis, vesicobullous, acantholytic, granulomatous, and vasculopathic patterns.[1] If the pathologist can place the lesion within the proper histologic category, clinicopathologic correlation focused on the list of the most likely disease possibilities for that pattern will often allow the clinician to make the correct diagnosis. In difficult cases, consultation with a dermatologist and/or dermatopathologist is suggested.

Lichen Sclerosus

Lichen sclerosus, formerly known as lichen sclerosus et atrophicus, is a skin disorder of unknown etiology that commonly involves the vulva and perineum.[2,3] Most patients are postmenopausal, but children and young adults can also be affected. The lesions are typically intensely pruritic, and may also result in dyspareunia or a burning sensation, although some patients are asymptomatic. Chronic cases of lichen sclerosus are at an increased risk for the development of vulvar squamous cell carcinoma, and lichen sclerosus is an associated finding in roughly one-third of patients with this type of cancer.[4,5]

Grossly, lichen sclerosus appears as shiny white patches with interspersed erythematous/telangiectatic areas that may exhibit a symmetrical distribution. The lesions may form blisters or ulcerate, and can produce vulvar scarring with resorption of the labia minora or fusion of tissue overlying the clitoris. Histologically, typical cases of lichen sclerosus exhibit hyalinization and edema ("homogenization") of the upper dermis, some degree of vacuolar degeneration of basal keratinocytes, and a bandlike lymphocytic infiltrate beneath the layer of homogenized dermis (Figs. 1.2–1.4).[2,3] The epidermis is usually thin and exhibits loss of rete pegs, although chronic scratching can produce hyperkeratosis, excoriations, or superimposed lichen simplex chronicus.[2]

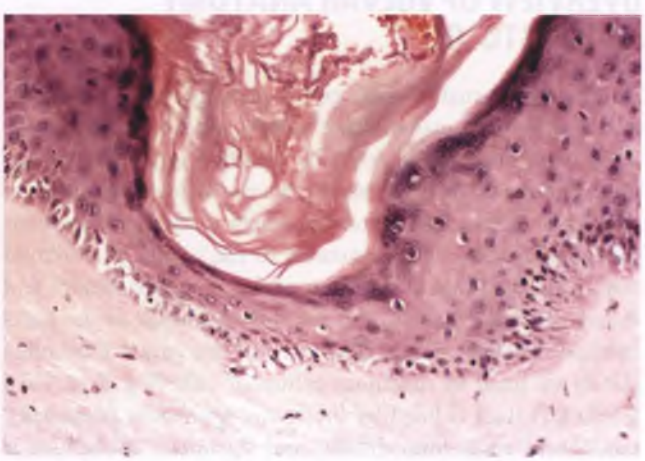

FIGURE 1.3. Lichen sclerosus. This example features prominent vacuolar degeneration of the basal keratinocytes.

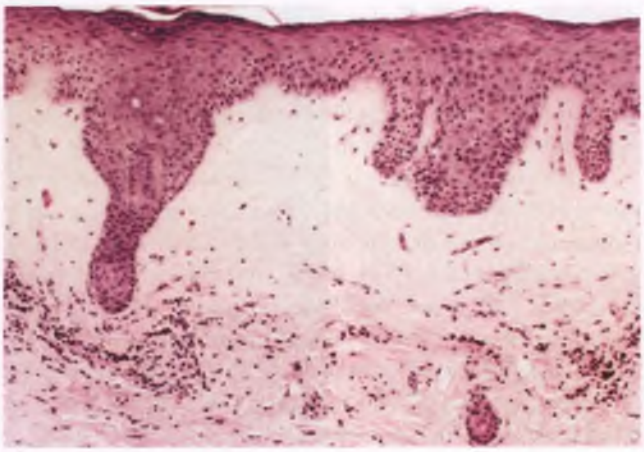

FIGURE 1.4. Lichen sclerosus. The diagnosis of lichen sclerosus is secured by the characteristic dermal homogenization and the bandlike lymphocytic infiltrate. As this case illustrates, epidermal atrophy may not be present.

Atypical lichen sclerosus features nuclear atypia of cells in the lower portion of the epidermis, and may represent a precursor or variant of differentiated vulvar intraepithelial neoplasia (VIN).[4] A pattern of strong, continuous p53 staining in the basal layer has been reported by some to be supportive of a diagnosis of atypical lichen sclerosus,[4] but others have found both discontinuous and continuous patterns of p53 immunoreactivity in the basal cells of ordinary lichen sclerosus to be commonplace.[6] Since there is no evidence that lichen sclerosus is a human papillomavirus (HPV)-related lesion, its lack of immunoreactivity for p16 is not surprising.[7]

Differential Diagnosis

Whether or not an early phase of lichen sclerosus can be reliably recognized in the absence of homogenization of the upper dermis is controversial.[8,9] The ability to distinguish early lichen sclerosus from lichen planus is made more difficult by the fact that vulvar lichen planus often lacks the saw-toothed rete ridges, wedged-shaped hypergranulosis, and cytoid bodies that characterize lichen planus in other sites.[9] In this regard, a limitation of the Fung and Leboit study that specifies criteria to help distinguish early lichen sclerosus from lichen planus is that vulvar lichen sclerosus was compared to *penile* rather than to vulvar lichen planus.[8] The dermal sclerosis of postradiation dermatitis can also simulate lichen sclerosus, but is recognized by the clinical history of radiation, the extension of the sclerosis deep into the reticular dermis, and the presence of damaged, thick-walled vessels and atypical stromal cells (radiation fibroblasts).

Treatment

Management of lichen sclerosus includes topical application of potent corticosteroids, with patients monitored over the long term due to their increased risk for the development of squamous cell carcinoma.[3]

Lichen Simplex Chronicus

Lichen simplex chronicus is the dermatologic term given to a nonspecific pattern that is produced as a reaction to chronic rubbing and/or scratching. There is often an underlying noninfectious or infectious pruritic process such as chronic contact dermatitis, an infection with *Candida* organisms or lichen sclerosus. However, this lesion can also be seen in patients with a localized area of skin that is chronically rubbed or scratched for no apparent reason or as a consequence of ill-fitting clothing.[2] Although a search for an underlying etiology should be undertaken in all cases of lichen simplex chronicus, this search is often thwarted by the fact that any residual causative lesion may be partially or completely obscured by the secondary reactive changes of lichen simplex chronicus.

In the region of the vulva, the most common sites of involvement are the mons pubis and labia majora, and these lesions appear as thick, leathery, scaly skin with exaggeration of the normal skin markings (lichenification).[2] Histologically, lichen simplex chronicus exhibits marked hyperkeratosis (usually orthokeratotic, but sometimes focally parakeratotic), hypergranulosis, and irregular epidermal hyperplasia (Fig. 1.5). In addition, the papillary dermis is thickened, vertical streaks of dense collagen may be found between rete ridges, and scattered lymphocytes may be present within the dermis.[2] By definition, the epithelium exhibits no significant nuclear atypia.

Differential Diagnosis

The differential diagnosis of lichen simplex chronicus includes fungal infection (the presence of neutrophils within the epidermis should prompt fungal stains; see Figs. 1.16 and 1.17), chronic contact dermatitis (look for foci of epidermal spongiosis as in Fig. 1.6), and psoriasis (rete ridges are regularly elongated to uniform lengths, suprapapillary plates are thinned, surface is parakeratotic, and intraepidermal pustules are often present, as illustrated in Fig. 1.7).[2,10]

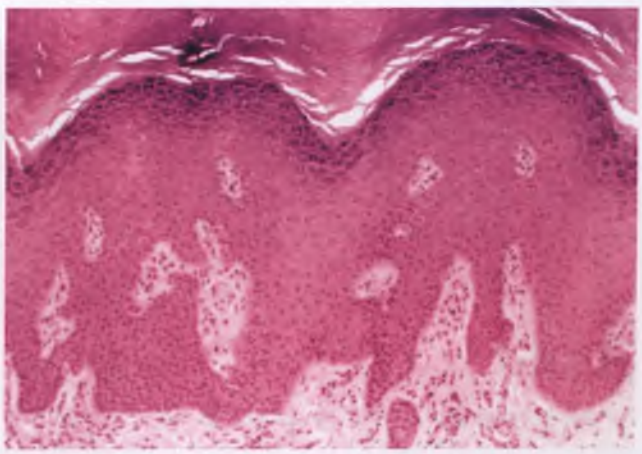

FIGURE 1.5. Lichen simplex chronicus. Note the orthokeratotic (anucleate) hyperkeratosis, hypergranulosis, and acanthosis with irregular elongation and thickening of the rete ridges.

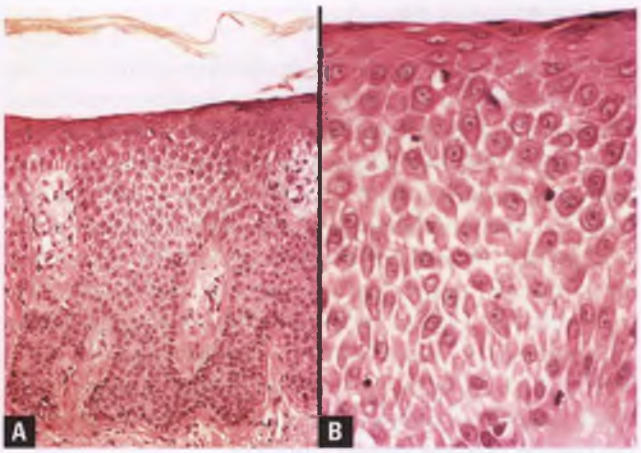

FIGURE 1.6. Spongiotic dermatitis. **A**: The hyperkeratosis, acanthosis with elongated rete ridges, and collagenization of the papillary dermis are indicative of a component of lichen simplex chronicus that has been superimposed on this subacute (active chronic) dermatitis. **B**: The presence of intercellular edema within the epidermis partially separates the keratinocytes from one another and accentuates their intercellular bridges.

CONDYLOMA ACUMINATUM[11]

Vulvar condyloma acuminata ("genital warts") are a common form of sexually transmitted disease caused by HPV. In the vast majority of cases, these condylomata represent a manifestation of infection with low-risk HPV type 6 or 11. Condyloma acuminata are frequently multiple and range from barely perceptible micropapillary lesions to lesions with grossly recognizable papillations to large, cauliflower-like masses (Fig. 1.8A). In their most recognizable and typical form, condyloma acuminata feature modest amounts of hyperkeratosis and parakeratosis, prominent papillomatosis with fibrovascular cores lined by acanthotic squamous epithelium, and foci of koilocytosis in the superficial to middle regions of the epidermis (Figs. 1.8B and 1.9). Koilocytes are keratinocytes with HPV-induced cytopathic changes that include perinuclear vacuolization and nuclear abnormalities, and are described in more detail and more extensively illustrated in the section on squamous intraepithelial lesions in Chapter 3.

Although koilocytosis is the most specific histologic feature of HPV-related lesions, this feature may be absent in squamous proliferations that are otherwise histologically consistent with condyloma (Fig. 1.10). In this situation, opinions vary as to whether such lesions should still be diagnosed as out-and-out condyloma or whether hedge phrases such as "consistent with," "suggestive of," or "equivocal for" should be utilized. Although not practical and rarely necessary, these lesions can be subjected to molecular methods to detect HPV nucleic acids that can help to establish a diagnosis of condyloma when a positive result is obtained. In a recent study, 30% of histologically equivocal cases were positive for HPV by in situ hybridization, with all of the positive results due to HPV types 6 or 11.[12]

Condylomas that have been recently treated with podophyllin may exhibit spongiosis, intracellular edema, keratinocyte necrosis, and arrest of mitotic activity with resultant presence of mitotic figures in the same phase of development in the lower portion of the epidermis.[13] To avoid these potentially confusing histologic features, podophyllin-treated condylomas should not be excised within 1 week of the last treatment.[13]

Differential Diagnosis

A small percentage (<5%) of warts occurring in the genital region of adults are actually of the verruca vulgaris (common cutaneous wart) type and are associated with HPV type 2 infection.[12] Histologic clues to the presence of a verruca are more marked hyperkeratosis than typical condylomata,[12] vertical tiers of parakeratosis, and elongated rete ridges at the margins of the wart that are bent inward (Fig. 1.11). In contrast to the situation for adults, approximately 40% of genital warts in girls <5 years of age are of the verruca vulgaris type with a

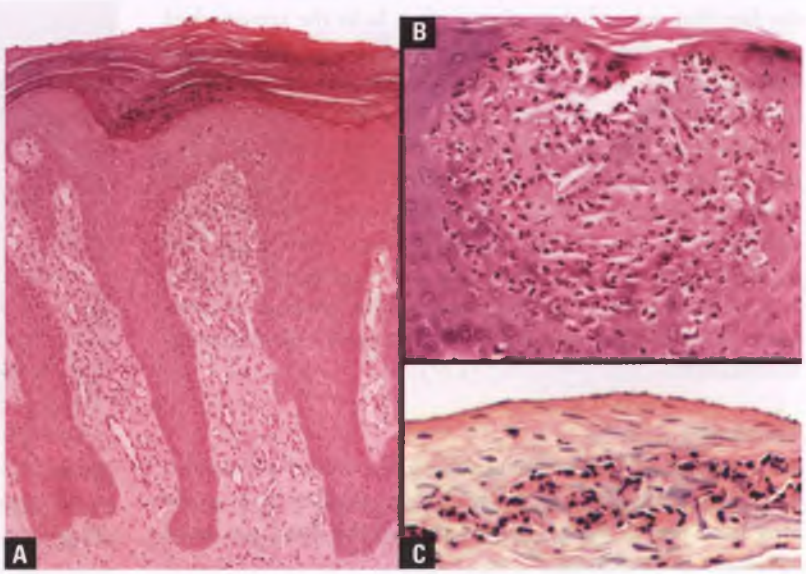

FIGURE 1.7. Psoriasis. **A**: Note parakeratosis, the uniform length of the elongated rete ridges, and the thinning of the suprapapillary plates. **B**: A spongiform pustule is present within the spinous layer of the epidermis. **C**: Small collections of intracorneal neutrophils with pyknotic nuclei are present within the parakeratotic layer (Munro microabscesses).

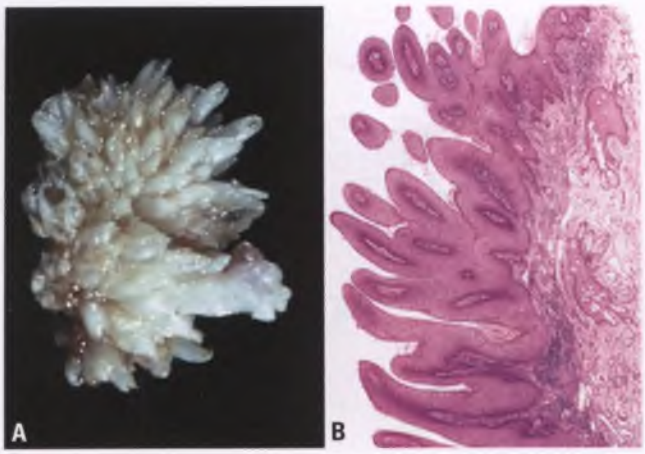

FIGURE 1.8. Condyloma acuminatum. **A**: Excised condyloma (1 cm) with an exophytic, papillary growth pattern. **B**: Low-magnification view of a condyloma with prominent papillomatosis.

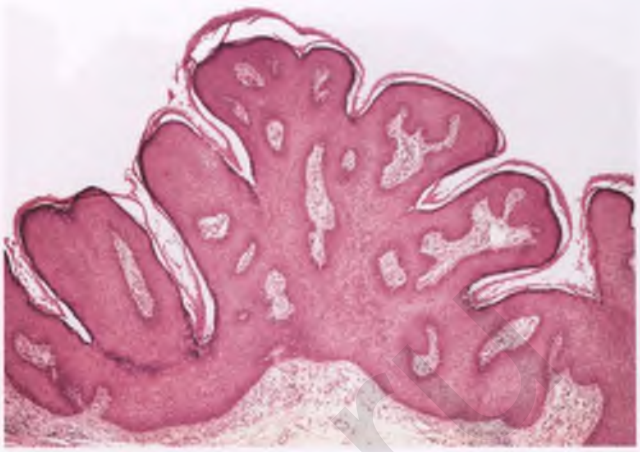

FIGURE 1.10. This acanthotic, papillomatous, cauliflower-like lesion lacks koilocytosis, and is considered equivocal for or consistent with condyloma acuminatum.

mode of transmission that is presumably not related to sexual contact.[12] Since the distinction between a condyloma acuminatum and a verruca vulgaris is important in cases of possible child abuse, the utility of HPV subtyping in helping to make this distinction should be kept in mind.

In addition to verruca vulgaris, the differential diagnosis of condyloma acuminata includes fibroepithelial polyp, vestibular papillomatosis, seborrheic keratosis, warty VIN, verrucous carcinoma, and condyloma lata.

- Fibroepithelial polyps share the features of hyperkeratosis and papillomatosis with condylomas, but lack viral cytopathic effect, exhibit a less impressive degree of acanthosis and may even have an attenuated epithelial lining, and usually have a loose connective tissue stalk that may contain atypical stromal cells.
- The squamous papillomas of vestibular papillomatosis are small, usually multiple, confined to the structures within the vulvar vestibule, and are lined by nonkeratinized, well-glycogenated, stratified squamous epithelium (Fig. 1.12). If papillomatous lesions of the vestibule that exhibit koilocytosis are considered condylomas and excluded from the category of vestibular papillomatosis, as they should be, there is no compelling evidence that HPV plays a role in the etiology of these squamous papillomas.[14]
- Some vulvar condylomas can resemble seborrheic keratoses, and HPV in situ hybridization or polymerase chain reaction may be indicated if their distinction is deemed necessary.[15]
- The presence of a papillomatous architecture and koilocytes in warty VIN can cause it to be mistaken for condyloma, but the increased mitotic activity at various levels of the epithelium, often including atypical division figures, and the presence of significant nuclear atypia that spares only the

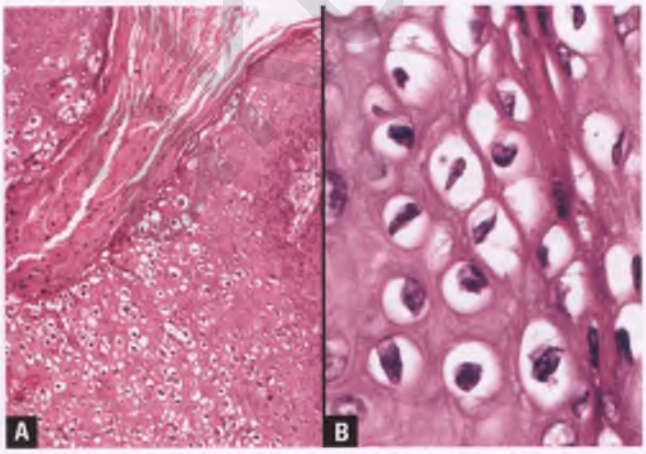

FIGURE 1.9. Condyloma acuminatum. **A**: Prominent koilocytosis is evident in the upper epidermis in this portion of the lesion. **B**: High-magnification view of a cluster of koilocytes within a condyloma.

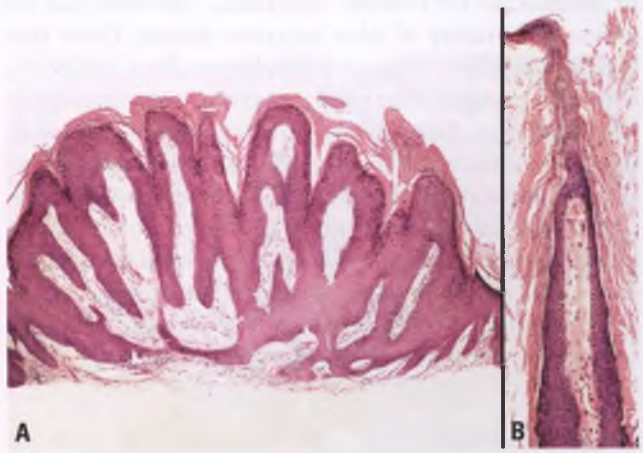

FIGURE 1.11. Verruca vulgaris. **A**: Note the prominent hyperkeratosis, papillomatosis, acanthosis, and the inward bending of the elongated rete ridges at the periphery of the lesion. **B**: A mound (vertical tier) of parakeratosis is perched atop one of the spikes of papillomatous epithelium in this image from a different cutaneous wart.

FIGURE 1.12. Vestibular papillomatosis. The small squamous papillomas are lined by glycogen-rich, nonkeratinized squamous epithelium, and have fibrovascular cores.

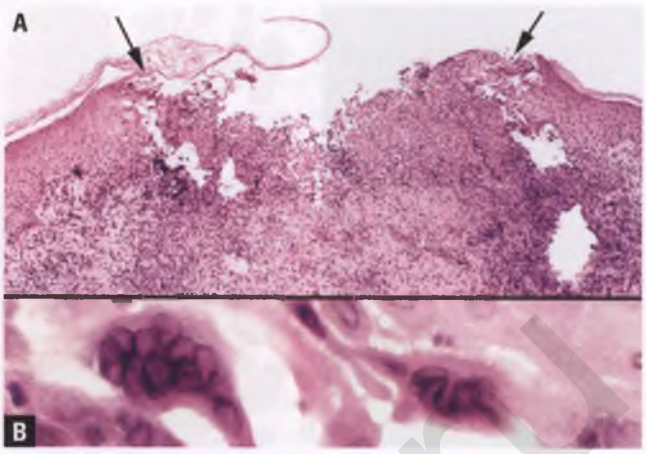

FIGURE 1.13. Vulvar skin with herpes-induced ulcer. **A**: Diagnostic herpetic inclusions are most likely to be found at the margins of the ulcer (*arrows*). **B**: Multinucleated cells with "ground glass" intranuclear inclusions characteristic of herpes virus infection.

superficial aspects of the epithelium should allow for its proper identification.

- The distinction between verrucous carcinoma and condyloma acuminatum is discussed in the section on the former entity.
- Condyloma lata of secondary syphilis are papular or plaque-like lesions with acanthosis, papillomatosis, and a chronic inflammatory infiltrate in the dermis that is rich in plasma cells. The plasma cell infiltrate should prompt ordering of a Warthin–Starry or equivalent stain in an attempt to identify spirochetes, and serologic tests for syphilis should also be obtained.

SELECTED INFECTIOUS DISEASES OF THE VULVA OTHER THAN CONDYLOMA ACUMINATUM

In addition to HPV-related condyloma, the vulva can be affected by a variety of other infectious diseases. Given that syphilis, granuloma inguinale, lymphogranuloma venereum, chancroid, parasitic infestations, infections with cytomegalovirus or Epstein–Barr virus, and tuberculosis produce vulvar lesions that are rare and/or only rarely seen by surgical pathologists, the reader is referred to more in-depth textbooks of gynecologic pathology for a discussion of these entities. The only non–HPV-related infectious diseases of the vulva that surgical pathologists encounter with appreciable frequency are those related to infection with herpes virus, molluscum contagiosum, and fungus, which are discussed below.

Herpes Genitalis

Infection of the vulva by herpes virus produces vesicles that are rapidly converted into painful ulcers.[16] Biopsy is usually not necessary to make the diagnosis, since a clinical suspicion of herpes genitalis can be confirmed by culture or by cytologic examination of material scraped from the edges of an ulcer or an opened vesicle. When tissue samples are obtained, the characteristic intranuclear inclusions will typically be found within altered squamous cells from the margins of ulcerated skin (Fig. 1.13). The nature of the herpes-induced intranuclear inclusions is discussed and illustrated in more detail in the section on selected microorganisms of the lower female genital tract in Chapter 3 (see Figs. 3.36 and 3.37).

Molluscum Contagiosum[17]

Molluscum contagiosum is a DNA poxvirus that most commonly presents as self-limited papules on the face, trunk, or extremities of young children. In the setting of vulvar involvement in an adult woman, the mode of transmission is typically via sexual contact. Immunodeficient patients are more likely to develop lesions related to molluscum contagiosum, which characteristically take the form of asymptomatic, small (usually 3–6 mm), multiple, flesh-colored, smooth, firm papules with umbilicated centers.

Although the diagnosis of molluscum contagiosum is often made clinically, biopsies are occasionally obtained. In optimally oriented histologic sections, the cup-shaped nature of the lesion is readily apparent (Fig. 1.14). Hyperplasia and downward expansion of the infected squamous epithelium (thought to be derived from a hair follicle in most instances) produce a lobulated, squamous-lined nodule within the dermis that contains diagnostic molluscum bodies. These bodies are large, homogeneous, eosinophilic intracytoplasmic inclusions that become more numerous and more deeply stained as they approach the surface (Fig. 1.15A). In the region of the granular layer, aggregates of large, basophilic keratohyalin granules are associated with the altered keratinocytes (Fig. 1.15B). Although molluscum bodies bear some resemblance to the large intracytoplasmic inclusions of HPV type 1–induced palmoplantar warts, this type of wart does not occur in the vulvar region.

Chronic Fungal Infections

Chronic fungal infections of the vulva such as those produced by *Candida* organisms and dermatophytes are pruritic lesions

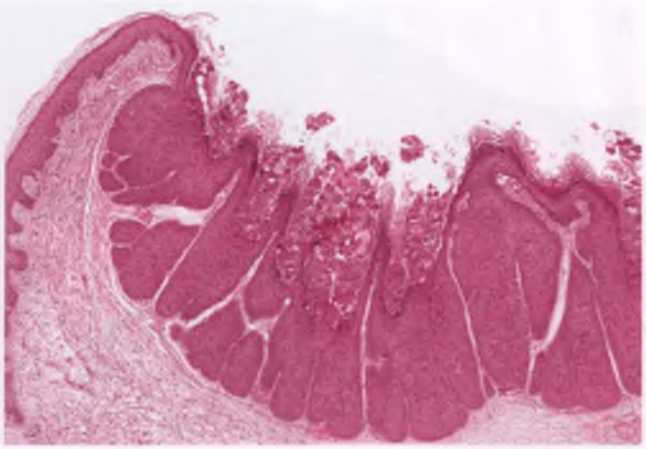

FIGURE 1.14. Molluscum contagiosum. Portion of a cup-shaped lesion showing prominent epidermal hyperplasia with lobulated margins. The molluscum bodies are most numerous within the aggregates of dead keratinocytes that are enmeshed within keratinous debris near the surface.

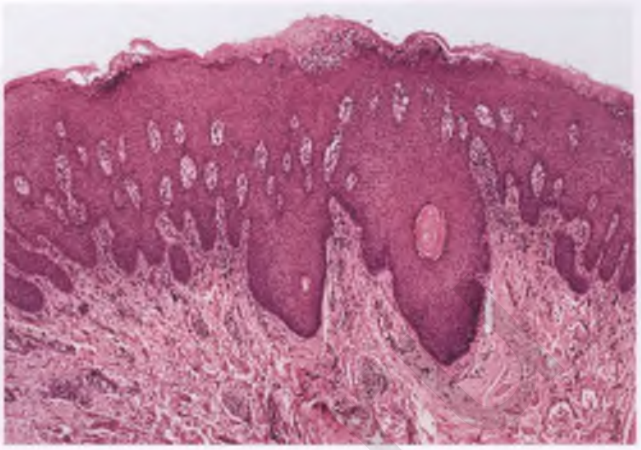

FIGURE 1.16. Chronic fungal infection. The hyperkeratosis and irregular acanthosis produce a pattern that is similar to lichen simplex chronicus. The key to making the correct diagnosis is noting the presence of neutrophils within the cornified layer and/or epithelium (top center), which should prompt ordering of a fungal stain.

that are usually diagnosed by identification of fungus within skin scrapings or culture. If biopsied, these lesions are often found to be keratotic and acanthotic, and can be misinterpreted as lichen simplex chronicus (Fig. 1.16). The presence of neutrophils within the cornified layer ("neuts in the horn") and/or epithelium is an indication to order a fungal stain, as are patches of parakeratosis or epidermal spongiosis. If present, the fungal organisms will usually be found within the cornified layer and/or superficial epithelium (Fig. 1.17). Candida organisms are the most frequent causative agent and are usually recognized by the combination of yeast forms, pseudohyphae, and true hyphae, but may be difficult to differentiate from some other fungal species in the absence of a culture result.

CYSTS

Bartholin's Cyst

The Bartholin's cyst is a common type of vulvar cyst that is due to duct outlet obstruction with subsequent retention of mucinous secretions and conversion of the duct into a cyst wall. The cysts are located on either side of the posterior portion of the vestibule, which is where the Bartholin's gland ducts normally exit.

Bartholin's cysts are unilocular, have a smooth inner lining, and contain mucoid, partially translucent fluid when there is not a superimposed infection (Fig. 1.18). The cyst may be lined by nonkeratinizing stratified squamous, transitional, or mucinous epithelium (Figs. 1.19 and 1.20A), which reflects the normal lining of the duct as one proceeds from the orifice

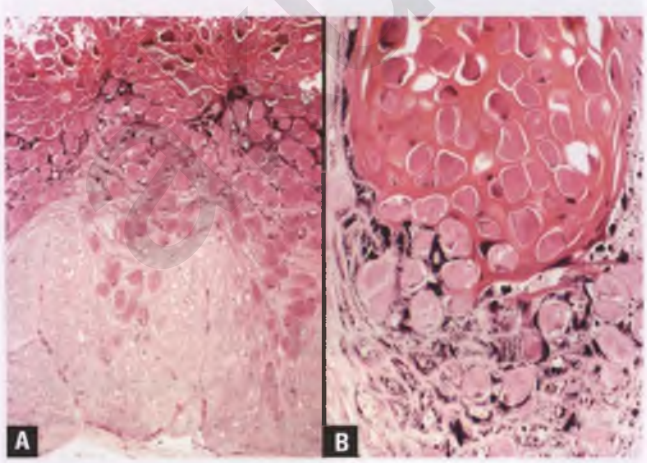

FIGURE 1.15. Molluscum contagiosum. **A**: Note how the molluscum bodies become more numerous and more deeply stained as they approach the surface at top. **B**: Large, darkly stained keratohyalin granules are prominent in the region of the granular layer in close association with molluscum bodies.

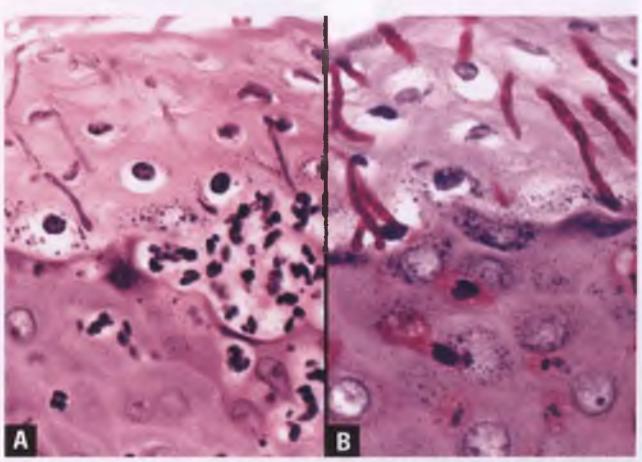

FIGURE 1.17. Chronic fungal infection. **A**: As in this example, fungal elements are often recognizable near the skin surface when examined at high magnification. Note the presence of associated neutrophils. **B**: Fungal elements are highlighted with a periodic acid-Schiff stain (with diastase pretreatment to remove "noise" from intraepithelial glycogen).

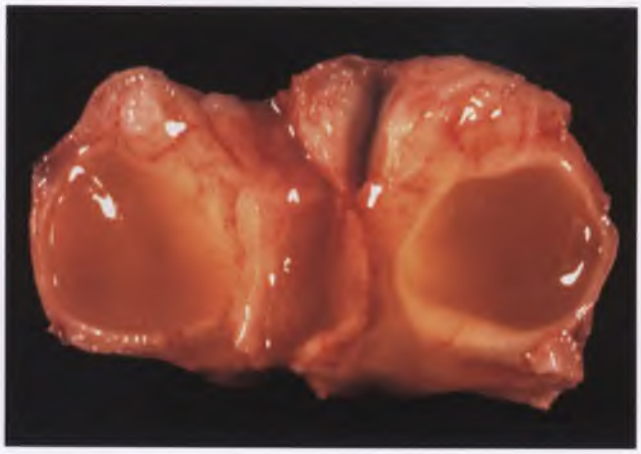

FIGURE 1.18. Bartholin's cyst. This 1.5-cm unilocular cyst has been bisected, revealing its mucoid contents.

to the acini of the gland. Patches of ciliated cells may also be present (Fig. 1.20B), and pressure atrophy may result in the lining epithelium assuming a nondescript, flattened appearance. Superimposed bacterial infection can result in formation of a Bartholin's abscess, in which case the cyst contents consist of purulent material, portions of the epithelial lining are destroyed, and there is marked inflammation in the stroma adjacent to the obliterated epithelium. The varying appearance of the lining epithelium and the presence of lobules of residual Bartholin's gland acini within the cyst wall help to differentiate Bartholin's cysts from cysts originating from minor vestibular glands.

Keratinous Cyst

Keratinous cysts (sometimes incorrectly referred to as sebaceous cysts) can be of either the epidermoid or pilar type. The latter

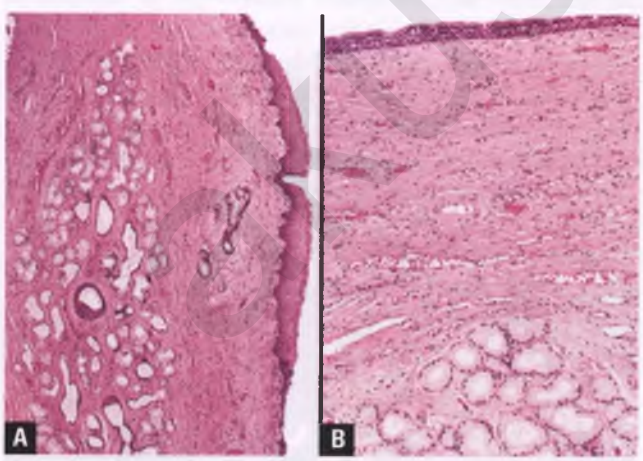

FIGURE 1.19. Bartholin's cyst. **A**: In this example, the cyst lining at right consists largely of nonkeratinizing stratified squamous epithelium. **B**: This portion of a different Bartholin's cyst is lined by transitional epithelium (top). Note: The presence of lobules of Bartholin's gland acini within the cyst wall, as shown in both these images, is a helpful diagnostic feature.

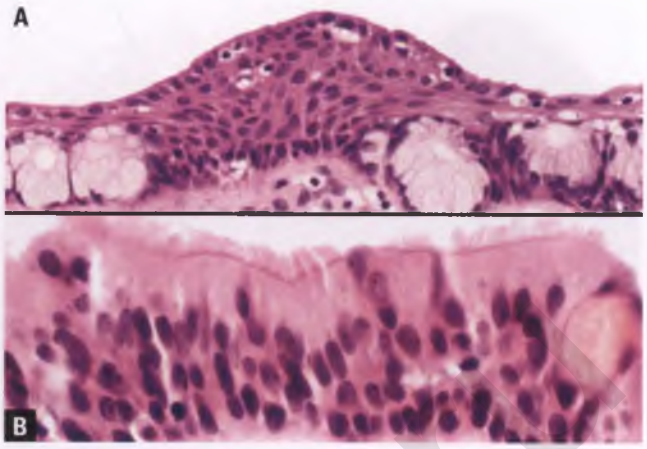

FIGURE 1.20. Bartholin's cyst. **A**: This portion of the epithelial lining consists of an admixture of squamotransitional and mucinous epithelial cells. **B**: Ciliated cells may also be a component of the lining of a Bartholin's cyst.

are also known as pilar cysts or trichilemmal cysts, occur predominantly on the scalp, and are differentiated from keratinous cysts of epidermoid type (the so-called epidermal inclusion cysts) mainly by the absence of a granular layer. Keratinous cysts encountered in the vulvar region are almost always of the epidermoid type. These unilocular, spherical cysts are filled with keratinous debris that is malodorous and white to pale yellow, and are lined by a peripheral rim of stratified squamous epithelium that contains a granular layer (Fig. 1.21). If the cyst ruptures, there is an ensuing multinucleated foreign body giant cell reaction to the released cyst contents within the dermis and there may also be partial to complete destruction of the epithelial lining.

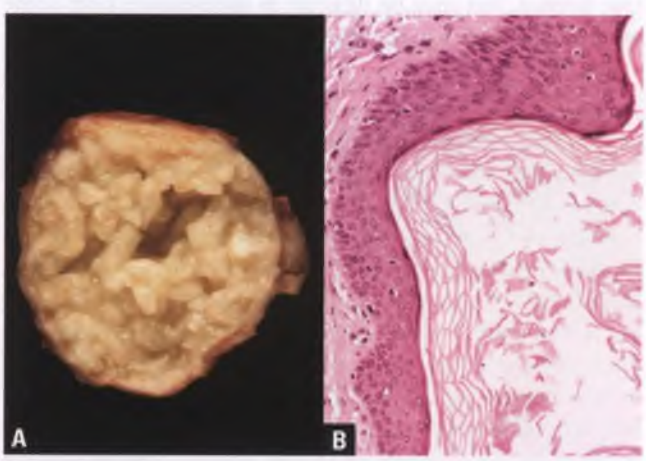

FIGURE 1.21. Keratinous cyst, epidermoid type. **A**: Cross section through a cyst that is filled with keratinous debris. A small amount of skin that was excised with the cyst is present at the 3 o'clock position. **B**: Histologic section through a portion of a keratinous cyst that includes its epithelial lining, which consists of stratified squamous epithelium with a granular layer. Flakes of keratinous material from the cyst contents are at right.

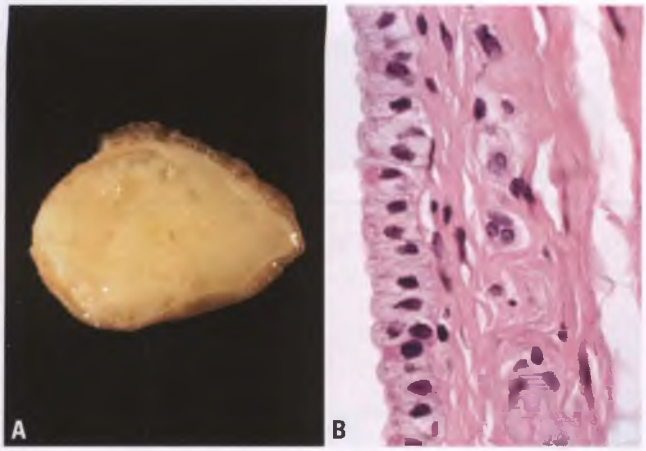

FIGURE 1.22. Mucinous vestibular cyst. **A**: Cross section through a 2-cm cyst beneath vulvar skin. Note the creamy, mucinous cyst contents. **B**: High-magnification view of the cyst lining reveals a simple layer of columnar mucinous epithelium similar to that found lining the endocervical canal.

Vestibular Cysts (Mucinous and/or Ciliated)[18]

Obstruction of the outflow tract of one of the minor vestibular glands is the presumed mechanism for the formation of a vestibular cyst, whose lining typically consists predominantly of a single layer of columnar mucinous epithelial cells similar to that found lining the endocervical canal (Fig. 1.22). In addition to these mucinous vestibular cysts, some vestibular cysts are lined by an admixture of mucinous and ciliated epithelium, and ciliated epithelium dominates the lining of occasional cysts (Fig. 1.23). The ciliated cells in these cysts are thought to be of metaplastic origin, as are occasional foci of squamous epithelium.

Distinction of vestibular cysts from Bartholin's cysts is discussed in the section on Bartholin's cysts. Ciliated cysts with a tuboendometrioid-type lining are distinguished from endometriotic cysts by their absence of associated endometrial stroma and lack of hemosiderin-laden macrophages.

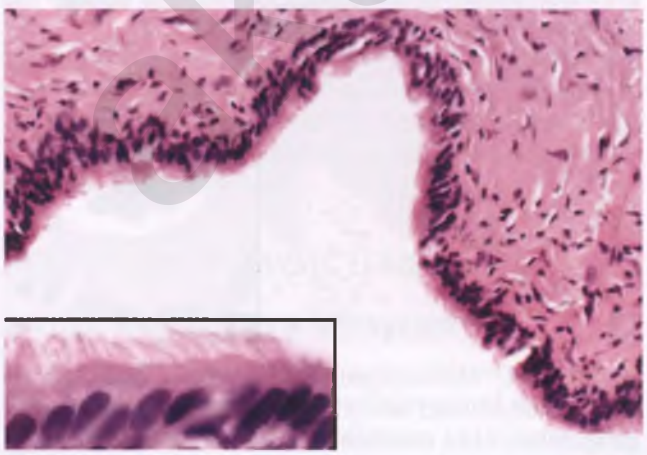

FIGURE 1.23. Ciliated vestibular cyst. The inset highlights the ciliated epithelial cells that are the dominant cell type lining this cyst.

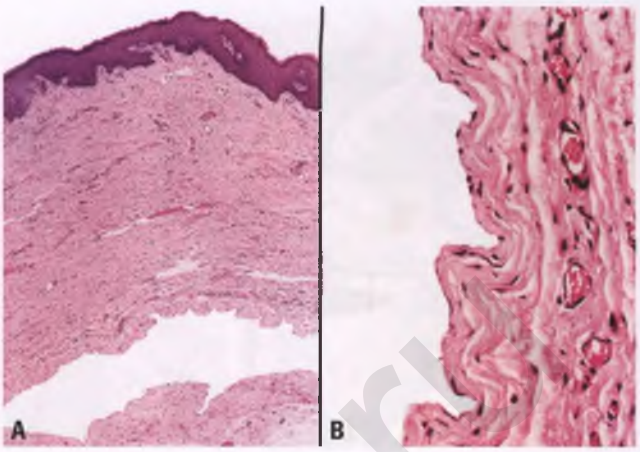

FIGURE 1.24. Cyst of the canal of Nuck. **A**: The cyst is located within the stroma, 2 mm beneath the squamous-lined skin surface. **B**: The cyst is lined by a flattened layer of inconspicuous cells that are consistent with atrophic mesothelial cells.

Cyst of the Canal of Nuck (Mesothelial Cyst)

A cyst of the canal of Nuck represents an encysted remnant of mesothelial-lined peritoneum related to incomplete obliteration of the processus vaginalis. These cysts are typically found in the superior portion of the labia majora or the inguinal canal and are lined by a single layer of flattened mesothelium (Fig. 1.24).

Miscellaneous Cysts

Other cysts that occur on occasion in the vulvar region include mesonephric-like cysts, mammary-like cysts, Skene's duct cysts, steatocystomas, and apocrine hidrocystomas.

FIBROEPITHELIAL POLYP

Vulvar fibroepithelial polyps that also qualify as mundane acrochordons/skin tags usually occur on the hair-bearing skin, and typically present as one or more small, flesh-colored papillomas. These lesions are lined by squamous epithelium that usually exhibits hyperkeratosis, papillomatosis, and acanthosis, although fibroepithelial polyps can also have an attenuated epithelial lining (Fig. 1.25). When the papillomatosis is pronounced and repetitive, some pathologists prefer the diagnosis of squamous papilloma (Fig. 1.26), but this distinction is arbitrary and has no clinical impact other than to potentially cause confusion with the generally nonkeratinizing squamous papillomas of vestibular papillomatosis as depicted in Figure 1.12.

The diagnostic terms fibroepithelial polyp and fibroepithelial stromal polyp are also used for the more interesting, larger lesions with prominent stroma that may contain atypical stromal cells (Fig. 1.27). Polyps of this type are more commonly seen in the vagina, and are discussed in greater detail in Chapter 2. The distinction between fibroepithelial polyp and condyloma is addressed in the section on condyloma

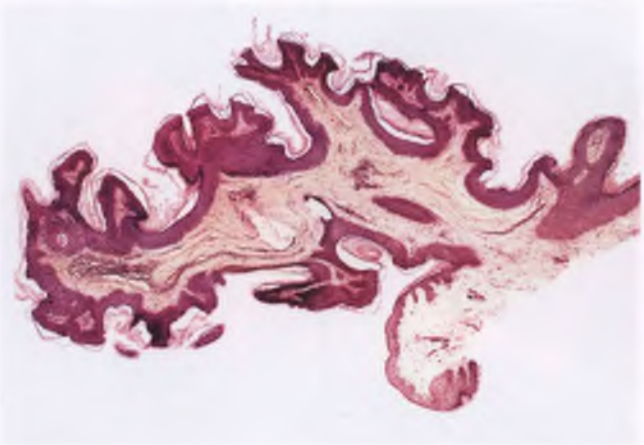

FIGURE 1.25. Common type of fibroepithelial polyp, also known as an acrochordon or skin tag. In this low-magnification view, the lesion protrudes from the skin surface at right and exhibits hyperkeratosis, papillomatosis, and a squamous lining of variable thickness.

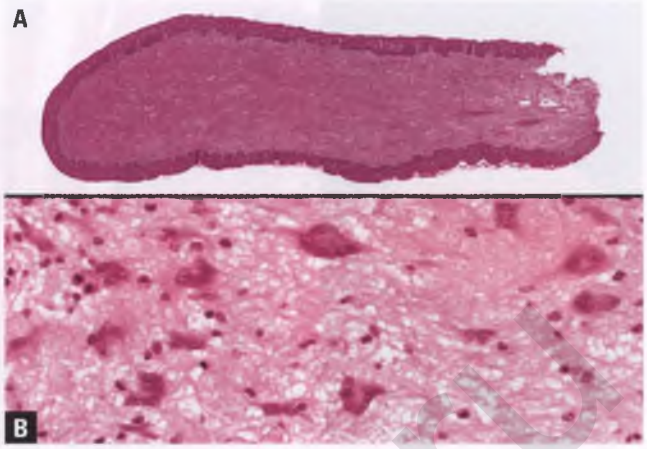

FIGURE 1.27. Fibroepithelial polyp with atypical stromal cells (fibroepithelial stromal polyp). **A**: Low-magnification view shows a squamous-lined polyp with a dense stromal core. **B**: Several multinucleated cells are present within the stroma, which are of no clinical significance.

acuminatum. Fibroepithelial polyps of the vulva with stromal edema can resemble aggressive angiomyxoma and massive vulval edema, as discussed in the sections on these other entities.

MISCELLANEOUS NONINFECTIOUS/ NONNEOPLASTIC PROCESSES

Multinucleated Epithelial Atypia[19]

Multinucleated epithelial atypia of the vulva refers to the uncommon finding of multinucleated keratinocytes within the lower to midportion of the epithelium that are unrelated to HPV, herpes virus, intraepithelial neoplasia, or any other known pathogen. This phenomenon typically occurs on a background of chronically irritated skin in young adult women, is usually focal, and is thought to represent a reactive process. The multinucleated cells are composed of aggregates of uniform nuclei that exhibit distinct nucleoli and no significant hyperchromasia or contour abnormalities (Fig. 1.28). These nuclear aggregates are often surrounded by a clear zone. The histologic features are sufficiently distinctive to enable the separation of multinucleated epithelial atypia from koilocytosis/condyloma, herpes virus infection, and VIN. To avoid overtreatment or undue concern, the presumed reactive nature of this process should be emphasized in the pathology report.

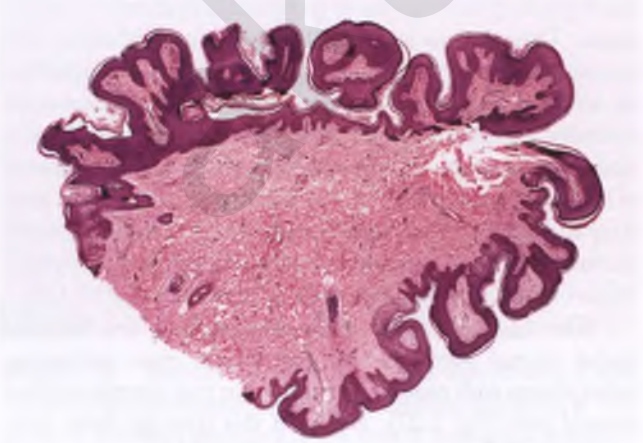

FIGURE 1.26. Fibroepithelial polyp with pronounced and repetitive pattern of papillomatosis (the so-called squamous papilloma).

Multinucleated Stromal Giant Cells

The presence of multinucleated stromal giant cells within the superficial stroma of the vulva (Fig. 1.29) is a common incidental finding that is also seen occasionally in the cervix (Fig. 3.93) and vagina.[20]

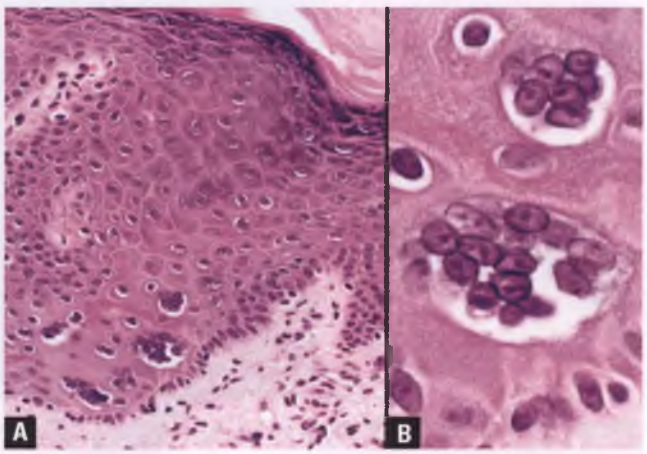

FIGURE 1.28. Multinucleated epithelial atypia. **A**: A localized focus of multinucleated cells is present within the lower portion of the epithelium, which elsewhere shows evidence of chronic irritation. **B**: High-magnification view of two of the multinucleated cells. Note the smooth nuclear contours, lack of chromatin abnormalities, nuclear uniformity, distinct nucleoli, and surrounding clear zone.

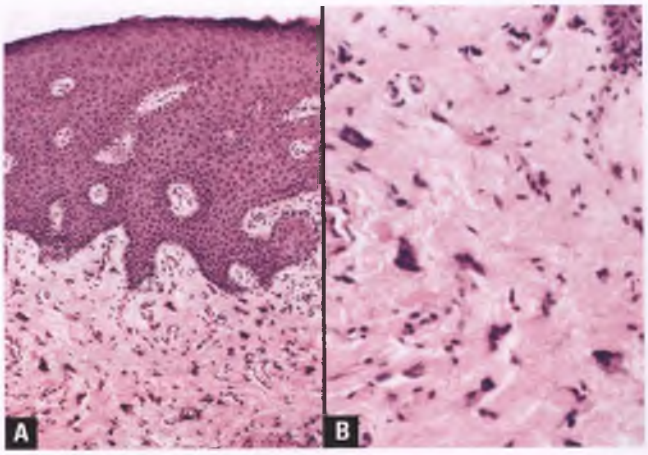

FIGURE 1.29. **A**: Scattered multinucleated stromal giant cells are present within the vulvar stroma beneath acanthotic squamous epithelium. **B**: Higher magnification view of multinucleated stromal giant cells.

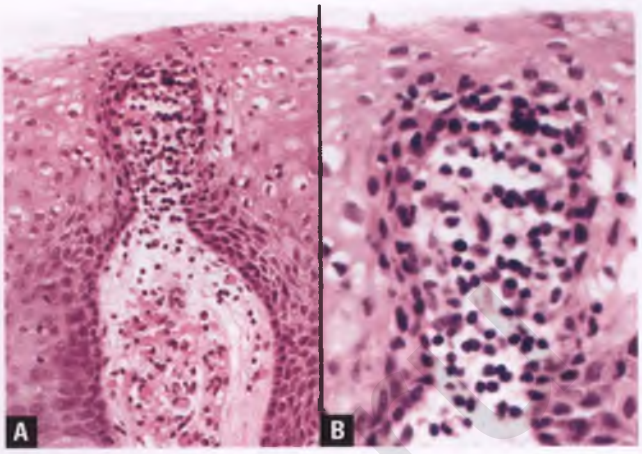

FIGURE 1.30. Tissue from the vulvar vestibule of a 29-year-old woman with dyspareunia. The chronic inflammatory infiltrate is nonspecific, and is not necessarily indicative of clinical "vestibulitis."

Provoked Vestibulodynia (Formerly Vulvar Vestibulitis)[21]

Provoked vestibulodynia is the term used in the 2003 version of the ISSVD classification of vulvar pain for what was formerly referred to as vulvar vestibulitis. Women with this controversial clinical disorder of unknown etiology are generally in the reproductive age group and present with discomfort or pain localized to the vulvar vestibule that is triggered by physical contact and is not related to a specific infectious, inflammatory, neoplastic, or neurologic cause. Although vestibular erythema and nonspecific chronic inflammation of the vestibule have often been considered to represent findings supportive of the diagnosis of "vestibulitis," more recent studies have found these features do not reliably distinguish patients with provoked vestibular pain from normal, asymptomatic women.

The vulvar vestibule is normally lined by nonkeratinizing squamous epithelium that is associated with minor vestibular glands composed of small aggregates of tubular glands lined by columnar mucinous epithelium. The pathologist examining tissue from this site should report the presence of an associated chronic inflammatory infiltrate (Fig. 1.30) or squamous metaplasia of the vestibular ducts and glands, but should indicate that the significance of these findings is unknown and that the diagnosis of provoked vestibulodynia is based upon clinical rather than pathologic features.

BENIGN MELANOCYTIC LESIONS

Lentigo Simplex/Vulvar Melanosis[22,23]

Lentigo simplex is a common disorder of hyperpigmentation that presents as a small, brown, well-demarcated macule measuring only a few millimeters in diameter. In the vulva, either hair-bearing or glabrous skin of patients who are usually adult Caucasian women may be involved. Histologically, these lesions feature elongated rete ridges associated with basilar hyperpigmentation and an increased number of normal-appearing melanocytes arranged as single cells within the basal layer (Fig. 1.31).

Vulvar melanosis is a related form of melanotic macule that shares the property of a hyperpigmented basal layer with lentigo simplex, but ranges up to 2 cm in size, shows only a slight to inapparent increase in the number of basal melanocytes, and does not exhibit elongated rete ridges. Melanosis is histologically similar to the common freckle (ephelis), but differs in that freckles are related to sun exposure and do not occur on mucous membranes. Although lentigo simplex and vulvar melanosis are clinically innocuous lesions, pathologists may encounter them in biopsies performed to exclude malignant melanoma.

Common Melanocytic Nevi[22,24]

The common melanocytic nevus ("mole") consists of a benign proliferation of melanocytes that typically features cells with variable amounts of melanin pigment and uniform, round to oval, mitotically inactive nuclei, often with visible nucleoli. These nevi are divided into three different types depending

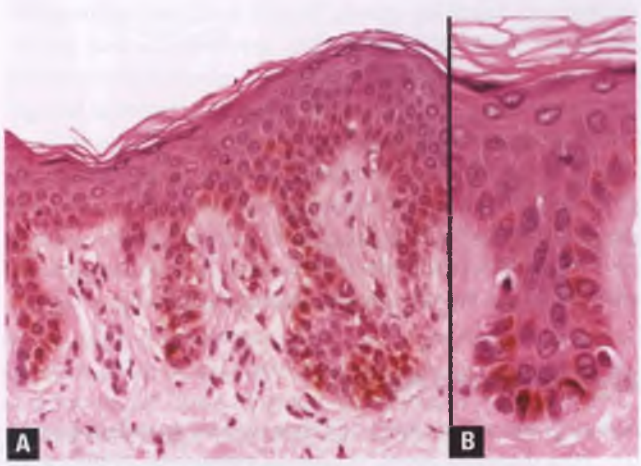

FIGURE 1.31. **A,B**: Lentigo simplex.

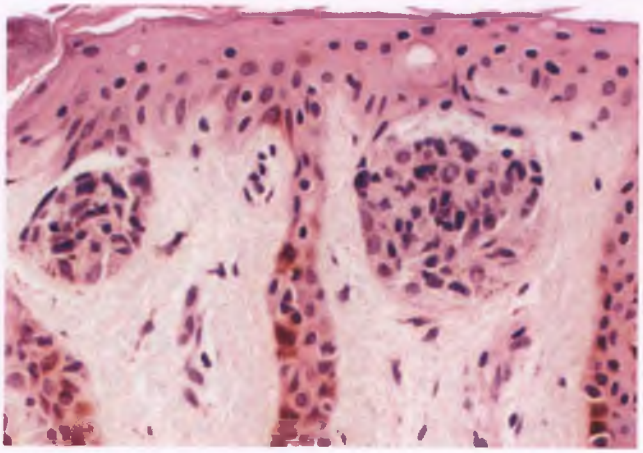

FIGURE 1.32. Lentiginous junctional nevus. Against a backdrop of a lentigo simplex are two nests of melanocytes at the dermoepidermal junction.

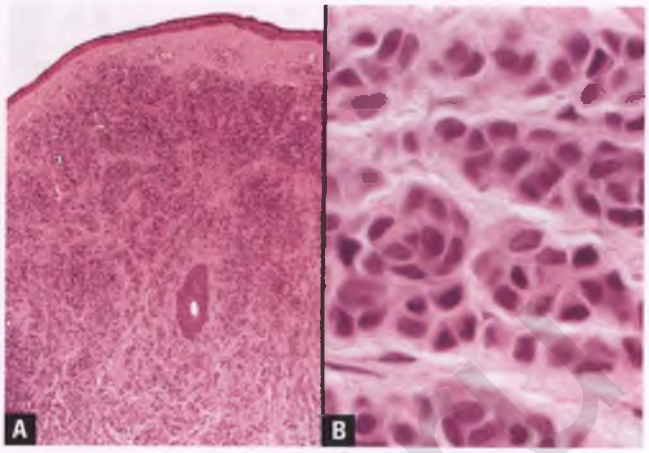

FIGURE 1.33. Intradermal melanocytic nevus. **A**: Low-magnification view demonstrating the presence of a dermal nodule formed by a proliferation of nevus cells. **B**: Nevus cell nests at high magnification.

upon the architecture of the lesion. In junctional nevi, small nests of melanocytes appear within the lower epidermis and often straddle the dermoepidermal *junction* (Fig. 1.32). Once junctional nevi have progressed to involve the dermis with persistence of a junctional component, they are referred to as compound nevi. Compound nevi evolve into intradermal nevi, which lack a junctional component and consist solely of intradermal melanocytes, often in the form of closely aggregated nests and cords (Fig. 1.33). Since classification of nevi into one of these three cell types is of no clinical significance, diagnoses such as "predominantly intradermal melanocytic nevus" or "predominantly junctional melanocytic nevus" are acceptable and preferable to agonizing over whether or not a focal junctional or intradermal component is present.

Most melanocytic nevi are <1 cm, well circumscribed, and a shade of brown, with lesions progressing from dark and macular to light and dome shaped as they mature from junctional into intradermal forms. The deeper aspect of the intradermal component of benign melanocytic nevi typically exhibits maturation, with the melanocytic nuclei becoming smaller and more hyperchromatic, and they may also exhibit neurotization, with melanocytes acquiring spindle-shaped nuclei and eosinophilic cytoplasm. Areas of a melanocytic proliferation that exhibit maturation, neurotization, and lack of mitotic activity within the dermal component can comfortably be regarded as benign. Other commonly seen features of melanocytic nevi are the presence of intranuclear cytoplasmic inclusions within occasional nevus cells (which can be helpful in suggesting the melanocytic nature of the lesion), the presence of scattered multinucleated nevus cells within the dermal component, and the formation of cleft-like spaces surrounding the dermal nevus nests.

Atypical Genital Nevus[24–26]

Although the vast majority of vulvar nevi are mundane nevi of the types discussed above, occasional vulvar nevi exhibit worrisome histologic features that often occur in women in the 20- to 30-year-old age group. These nevi, which are referred to as atypical melanocytic nevi of genital type or atypical genital nevi, pursue a benign clinical course and are usually separable from dysplastic nevi, which are discussed in the following section.

Atypical genital nevi usually have a compound architecture, but can be entirely intraepidermal. The dominant histologic feature of these lesions is a closely packed proliferation of enlarged junctional nests that vary in size, shape, and position (Fig. 1.34). These nests may exhibit retraction artifact and/or cellular dyscohesion, and the neighboring melanocytic proliferation often assumes a lentiginous pattern. In addition to the unusual nested pattern, features that can cause concern for the possibility of superficial spreading melanoma include varying degrees of nuclear atypia, focal pagetoid spread into the epidermis, and rare cases with isolated dermal mitoses. An indication of its benign nature is the constant presence of maturation in those lesions with a dermal component.

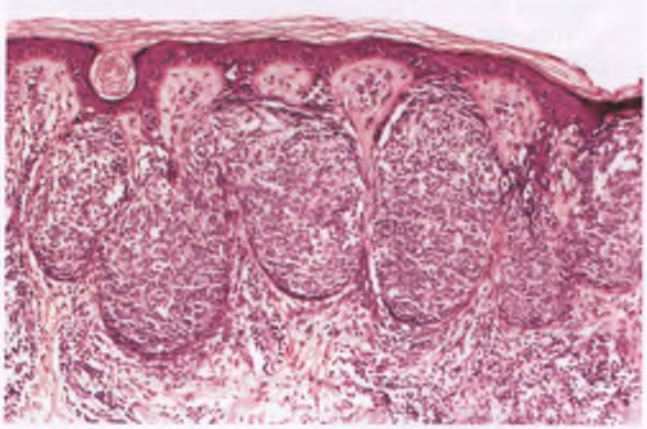

FIGURE 1.34. Atypical genital nevus. The presence of numerous enlarged, crowded, variably dyscohesive nests of melanocytes along the dermoepidermal junction is characteristic of this lesion.

In the differential diagnosis with melanoma, it should be kept in mind that patients with atypical genital nevi are usually young adults, whereas vulvar melanoma is generally a disease of postmenopausal women and is not usually of the superficial spreading type. Histologically, melanoma lacks maturation of the dermal component, usually shows a predominance of single cells rather than nests, and generally exhibits more overt nuclear atypia, more extensive pagetoid spread, more readily apparent dermal mitotic activity, and more asymmetry than atypical genital nevi.

Dysplastic Nevus[25,26]

The controversial dysplastic nevus also occurs on the vulva, although these lesions appear to be less common than atypical genital nevi. Dysplastic nevi often have irregular outlines and abnormal coloration, and in classic cases are characterized by bridging of melanocytic nests across adjacent rete ridges, a "shoulder effect" in which the junctional component extends beyond the dermal component, a lentiginous proliferation of single melanocytes, mild to moderate nuclear atypia, and distinctive patterns of stromal fibrosis (concentric eosinophilic fibroplasia and lamellar fibroplasia). Although atypical genital nevi are usually separable from dysplastic nevi, some cases have overlapping histologic features.

BENIGN EPITHELIAL TUMORS AND TUMOR-LIKE LESIONS

Seborrheic Keratosis

Seborrheic keratosis is a benign squamoproliferative lesion that exhibits a wide variety of patterns due to variable degrees of hyperkeratosis, acanthosis, papillomatosis, and horn cyst formation. Seborrheic keratoses typically occur on the trunk and face of adults, but can also be seen in other sites such as hair-bearing vulvar skin. These lesions are sharply demarcated from neighboring skin, are typically a shade of light to dark brown, and generally have a "stuck-on" appearance due to the well-defined squamous proliferation occurring almost exclusively at or above the level of the normal epidermis (Fig. 1.35). Depending on their degree of pigmentation, which is most commonly due to accumulation of melanin within keratinocytes (Fig. 1.36A), seborrheic keratoses may clinically simulate a melanocytic nevus or melanoma. Overgrowths of variable proportions of basaloid and mature squamous cells are responsible for the epithelial proliferation, which in the distinctive reticulated (adenoid) pattern assumes a branching trabecular architecture (Fig. 1.36B). Some condylomas exhibit seborrheic keratosis–like features, and their definitive recognition may require identification of HPV nucleic acids.[15]

Benign Tumors of Skin Appendage Origin

In the vulva, these tumors range from uncommon to rare. Hidradenoma papilliferum is the most likely tumor in this group to be encountered in the routine practice of surgical pathology, followed by syringoma. Accordingly, these two tumors are presented in some detail. Other benign tumors of skin appendage derivation that may be seen in the vulva on rare occasions are the trichogenic (hair follicle–related) tumors that include proliferating trichilemmal tumor, trichoepithelioma, trichofolliculoma, keratoacanthoma, and inverted follicular keratosis,[27–31] along with miscellaneous tumors of sweat gland origin, such as clear cell hidradenoma and apocrine cystadenoma.[32,33] The histologic features of trichoepithelioma are briefly discussed and depicted in the section on vulvar basal cell carcinoma, since these two neoplasms can be confused with one another. For analogous reasons, keratoacanthoma is also briefly described and illustrated in the section on the differential diagnosis of vulvar squamous cell carcinoma.

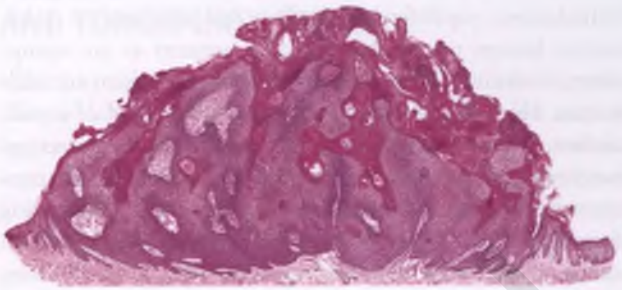

FIGURE 1.35. Seborrheic keratosis. This low-magnification view highlights the "stuck-on" appearance of this hyperkeratotic, acanthotic, papillomatous lesion.

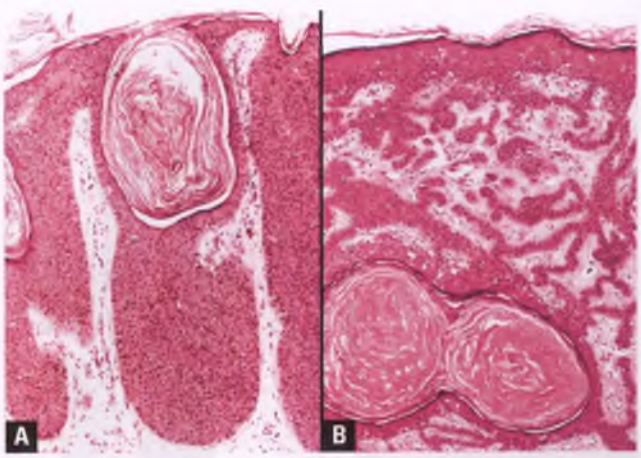

FIGURE 1.36. Seborrheic keratosis. **A**: In this hyperpigmented lesion, many of the keratinocytes contain melanin. **B**: Reticulated (adenoid) variant. Note: Keratin-filled cystic spaces are present in both of these images. These structures may represent cross sections of hyperkeratotic invaginations (pseudohorn cysts) or true horn cysts that are actually formed within the tumor.

Hidradenoma Papilliferum[34]

Hidradenoma papilliferum (papillary hidradenoma) is a distinctive benign tumor that typically presents as an asymptomatic, small (<1 cm) nodule in the labial region of adult women. Histologically, these tumors are composed of a well-circumscribed, subepithelial nodule that exhibits architectural complexity due to a papillary proliferation that may also contain tubular glands and/or solid areas (Fig. 1.37A). Reflecting its presumed derivation from anogenital sweat glands, hidradenoma papilliferum exhibits apocrine-like differentiation, which includes apical snouts related to decapitation secretion (Fig. 1.37B). Like the virtually identical intraductal papilloma of the breast, hidradenoma papilliferum features papillary structures lined by a single layer of epithelial cells with an underlying layer of myoepithelial cells, although the presence of myoepithelium ranges from obvious to inapparent in various areas of routinely stained sections. Mild degrees of nuclear atypia and occasional mitotic figures can be seen.

Local excision is adequate treatment for these benign lesions. The sharp circumscription of the neoplasm, the lack of significant nuclear atypia, the presence of two cell layers, and the overall resemblance to intraductal papilloma of the breast all help to avoid misinterpreting hidradenoma as an adenocarcinoma.

Syringoma[35]

Syringomas are most commonly encountered on the eyelid, but also occur in the vulva and other sites. Vulvar syringomas typically present in young adult women as multiple, tan to brown, 1- to 3-mm labial papules that may be either asymptomatic or pruritic.

Syringomas are benign tumors that are derived from eccrine ducts, and consist of a well-demarcated proliferation of microcystic sweat duct-like structures embedded within a sclerotic stroma (Fig. 1.38). These microcysts are lined by a double layer of compressed, mitotically inactive epithelium. Characteristically, curved epithelial strands are attached to some of the microcysts, creating a tadpole or comma-like appearance. The lumen of many of the microcysts contains eosinophilic material that is PAS positive and resistant to diastase pretreatment.

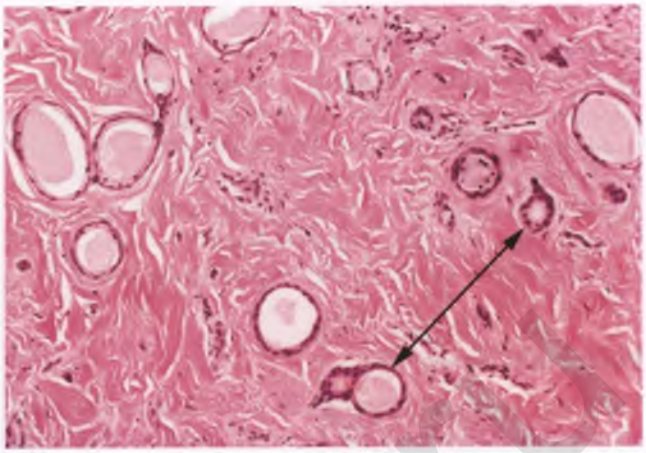

FIGURE 1.38. Syringoma. Scattered microcysts with pink-staining luminal contents are embedded within a fibrotic stroma. *Arrows* mark two of the characteristic tadpole or comma-like structures.

Nodular Hyperplasia of Bartholin's Gland[36]

This lesion is characterized by closely packed acini within lobules of Bartholin's glands that are increased in size and number, which results in the formation of a mass with an average size of about 2 cm (Fig. 1.39). These masses are usually solid, occur in women of reproductive age, and clinically simulate a Bartholin cyst. The acini are lined by cells with bland, basally oriented nuclei and abundant intracytoplasmic mucin and are individually

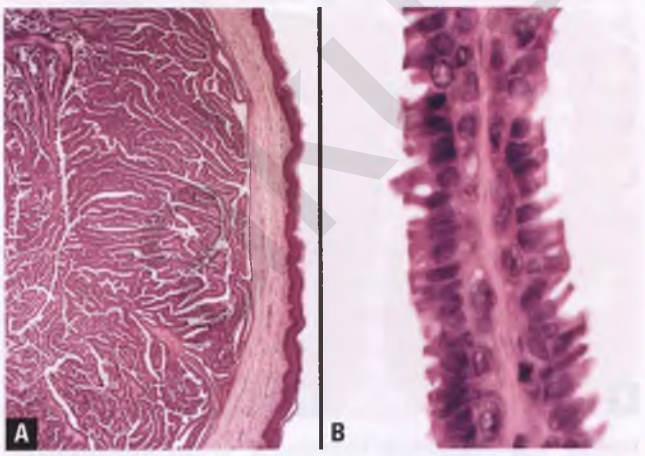

FIGURE 1.37. Hidradenoma papilliferum. **A**: A well-circumscribed, complex papillary proliferation is present beneath the skin surface. **B**: At high magnification, the apocrine-like nature of the epithelial cells lining the papillae is apparent, as is the presence of a discontinuous basal layer of myoepithelial cells.

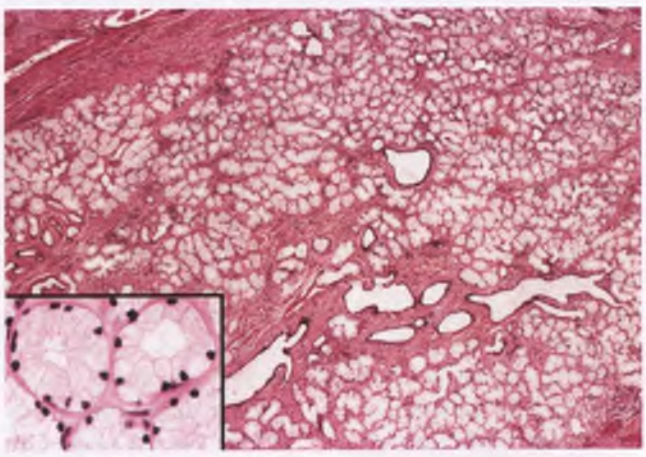

FIGURE 1.39. Nodular hyperplasia of Bartholin's gland. The lesion features large, lobulated aggregates of closely packed acini with interspersed dilated ducts. The inset highlights the bland, basally oriented nuclei, and abundant intracytoplasmic mucin of the cells lining the acini.

indistinguishable from those of the normal gland. Mild chronic inflammation, squamous metaplasia of the ducts, and small cysts are common associated findings. In contrast to the virtually nonexistent adenoma of Bartholin's gland, the peripheral border of nodular hyperplasia is lobulated or slightly irregular rather than well circumscribed or encapsulated, and hyperplasia also features maintenance of the normal duct–acinar relationship.

ECTOPIC BREAST TISSUE AND MAMMARY-TYPE TUMORS

Glands that are histologically similar to those found in the breast are identified within the vulva on rare occasions.[37,38] Although these glands have traditionally been regarded as ectopic breast tissue related to remnants of the embryonic milk line, it has also been proposed that they may represent normally occurring mammary-like glands that can be found within the anogenital region.[38] Whatever be their origin, these glands are usually found in the labia majora, and can give rise to a variety of lesions analogous to those that occur in the breast, such as fibrocystic change (Fig. 1.40), lactational change, sclerosing adenosis, pseudoangiomatous stromal hyperplasia, intraductal papilloma, fibroadenoma, phyllodes tumor, and mammary-type adenocarcinoma.[38–42]

"Fibroadenoma phyllodes" is a term that has been applied to a tumor that exhibits the combination of paucicellular, fibroadenoma-like stroma with the leaf-like architecture of a phyllodes tumor (Fig. 1.41).[43] Although this combination is unusual in the breast, a disproportionate number of vulvar fibroadenomas seem to have this appearance.[39,43] Limited experience with these benign tumors indicates that they have the capacity for local recurrence if incompletely excised, which matches the expected biologic behavior of conventional phyllodes tumors on the benign end of the spectrum.[40]

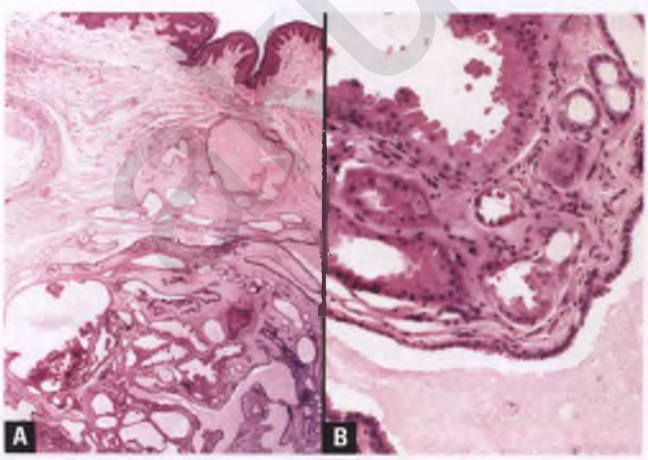

FIGURE 1.40. Ectopic breast tissue. **A**: A prominent focus of fibrocystic change is present beneath the squamous epithelium of a labium majus. **B**: Higher magnification highlighting an area with apocrine metaplasia and dilated ducts.

MESENCHYMAL TUMORS AND TUMOR-LIKE LESIONS

Mesenchymal tumors and tumor-like lesions of the vulva that are largely restricted to the vulvovaginal region such as aggressive angiomyxoma, angiomyofibroblastoma, cellular angiofibroma, and the larger, stromal-predominant version of fibroepithelial polyp are presumably derived from the hormonally responsive, specialized mesenchyme of the lower female genital tract. Other mesenchymal vulvar masses may represent soft tissue tumors or reactive proliferations similar to those found at other sites (e.g., tumors derived from muscular, adipose, vascular, fibrous, or neural tissue). The combination of (a) the morphologic overlap of the lesional stromal cells, which on the benign end of the spectrum tend to be bland and spindle shaped, (b) the rarity of vulvar-based tumors of this type, (c) the large number of diagnostic possibilities, and (d) the limited utility of immunohistochemistry in this situation conspire to make this an area of diagnostic difficulty. In addition to textbooks and the primary journal articles that describe and illustrate these lesions, several reviews have also been published on this topic.[44–47] Emphasis is herein placed upon the relatively site-specific mesenchymal tumors and selected other mass-forming soft tissue lesions about which there are more than isolated case reports describing vulvar involvement.

Aggressive Angiomyxoma[48,49]

Aggressive angiomyxoma is a rare soft tissue tumor with a propensity for local recurrence that is most commonly seen in the vulva, perineum, and pelvis of young adult women who have an average age of approximately 35 years. Grossly, these tumors are large, vaguely circumscribed, unencapsulated masses that are rarely <5 cm. Their cut surface is gelatinous, rubbery, and

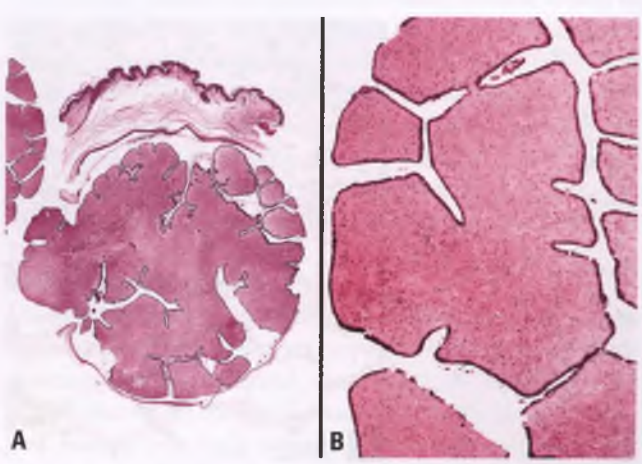

FIGURE 1.41. Fibroadenoma phyllodes. **A**: In this low-magnification view, an encysted, mixed epithelial and stromal neoplasm is present beneath the vulvar skin. **B**: The stroma of the neoplasm is hypocellular and forms blunt, epithelial-lined papillary structures that project into cystic spaces, which creates the leaf-like architecture.

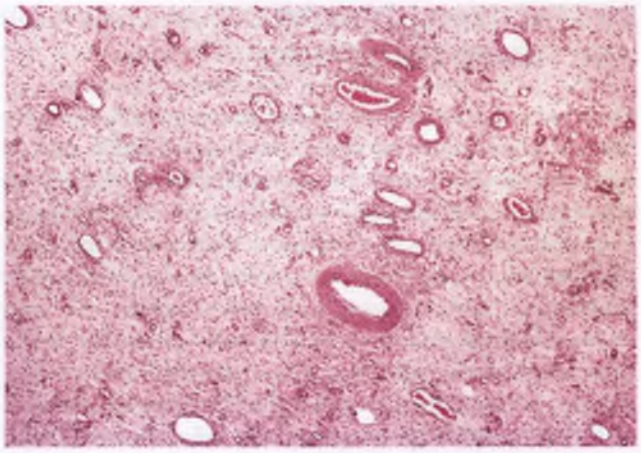

FIGURE 1.42. Aggressive angiomyxoma. Low-magnification view demonstrating a paucicellular myxomatous stroma that contains a haphazard arrangement of vessels of varying wall thickness and widely patent lumens.

homogeneous. Histologically, aggressive angiomyxomas consist of bland, spindle-shaped cells that are widely separated by a loose myxoid stroma that contains numerous small to medium-sized vessels that are randomly distributed throughout the tumor (Figs. 1.42 and 1.43A). The thickness of the vessel walls is typically quite variable, and the vessel lumens are generally widely patent. An arborizing network of capillary-like vessels, such as that seen in myxoid liposarcoma, is conspicuously absent. Aggressive angiomyxomas are locally infiltrative, and extension into fat characteristically consists of tumor encasing residual adipocytes found singly and in small clusters (Fig. 1.43B). The myxoid stroma, which stains weakly with Alcian blue, often harbors interspersed mast cells, and may also contain entrapped nerve twigs, extravasated red blood cells,

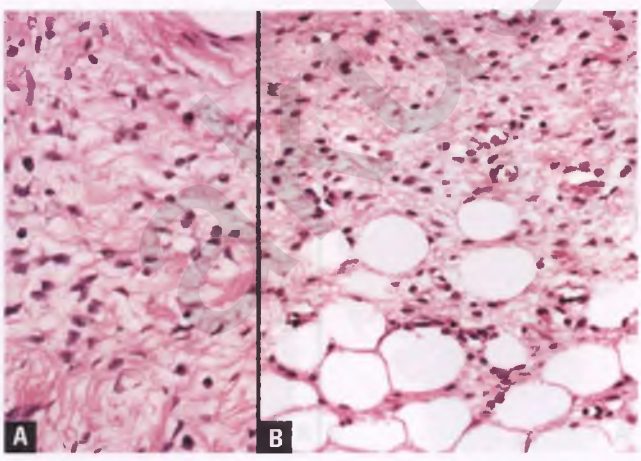

FIGURE 1.43. Aggressive angiomyxoma. **A**: The lesional cells have bland nuclei that are small and spindle to oval shaped. Occasional mast cells are also present. **B**: The tumor infiltrates adipose tissue in a characteristic fashion, percolating in between adipocytes and leaving stranded fat cells in its wake.

and strands of perivascular smooth muscle. These tumors are mitotically inactive and do not contain foci of tumor necrosis. The tumor cells are usually immunoreactive for estrogen and progesterone receptors, and at least focal reactivity for desmin is expected. Given the tendency of aggressive angiomyxoma to recur locally, wide local excision is the treatment of choice. Malignant behavior with distant metastases is extraordinarily rare, but has been reported.[50]

Differential Diagnosis

The differential diagnosis of aggressive angiomyxoma includes fibroepithelial stromal polyp with edema, superficial angiomyxoma, massive vulval edema, and angiomyofibroblastoma. Aggressive angiomyxoma is distinguished from fibroepithelial stromal polyp with edema by (a) its more deep-seated location without formation of an exophytic polyp; (b) its larger size; (c) its infiltrative growth pattern; (d) its myxoid, weakly Alcian blue–positive rather than edematous, Alcian blue–negative stroma; (e) its monotonous, bland spindle cell morphology that lacks a multinucleated component; and (f) its more prominent and widely distributed vascular component. The sections on superficial angiomyxoma, massive vulval edema, and angiomyofibroblastoma include a listing of features that help to differentiate these processes from aggressive angiomyxoma. It has recently been shown that nuclear immunoreactivity for HMGA2 is seen more often in aggressive angiomyxoma than in its mimics, and that this marker also has utility in identifying foci of tumor extending to resection margins and lurking within reexcision specimens.[51]

A variety of other tumors may enter the differential diagnosis by virtue of their myxoid stroma, but can usually be differentiated by the presence of a contrasting vascular pattern. Moreover, malignant myxoid tumors will generally exhibit greater cellularity, nuclear atypia, and mitotic activity than that seen in aggressive angiomyxoma.

Superficial Angiomyxoma[52,53]

Superficial angiomyxomas typically occur in the trunk and head/neck region, but can also involve the vulva of young women. These benign, slow-growing, painless masses are generally under 5 cm, and have a nodular or polypoid appearance. They usually involve both the dermis and subcutis, but may be limited to skin or subcutaneous adipose tissue (skeletal muscle involvement may be seen in facial tumors).

The sectioned surface of superficial angiomyxomas consists of one or more nodules of gelatinous tissue that are fairly well circumscribed (Fig. 1.44). At low magnification, histologic sections of these tumors show nodules of paucicellular myxoid stroma (Fig. 1.45) that can be highlighted with an Alcian blue stain. The vessels within superficial angiomyxomas are characteristically elongated and thin walled, may be congested, and often assume curvilinear shapes (Fig. 1.46A). The tumor cells are stellate or spindle shaped with no significant nuclear atypia, and often have dark, smudged chromatin (Fig. 1.46B). Mitotic figures are usually not evident. Additional findings may include the presence of

FIGURE 1.44. Superficial angiomyxoma. The sectioned surface of the tumor reveals its multinodular, lobulated contour, and gelatinous nature. The tumor has formed a polypoid lesion beneath the skin surface (top) and involves the dermis and subcutis. This example, which is from the back, is larger than most such tumors.

mucin-laden macrophages (Fig. 1.46B), acellular pools of mucin, an interspersed mixed inflammatory infiltrate that includes neutrophils, and incorporated cystic epithelial inclusions that are presumably derived from skin adnexal structures. The tumor cells lack immunoreactivity for desmin, estrogen receptors, and progesterone receptors, which can be of some diagnostic utility (see below). If incompletely excised, these tumors may recur, but they do not do so in a destructive fashion.

Differential Diagnosis

The main differential diagnostic consideration is aggressive angiomyxoma, which is distinguished by its (a) more deep-seated location; (b) larger size; (c) more indistinct interface with adjacent tissue; (d) lack of interspersed neutrophils; (e) widely patent vessels of varying wall thickness; (f) interdigitating pattern of involvement of adipose tissue, which contrasts with the bulging, nodular pattern of extension into subcutaneous fat that is seen in superficial angiomyxoma; and (g) usual immunoreactivity for desmin, estrogen receptors, and progesterone receptors.

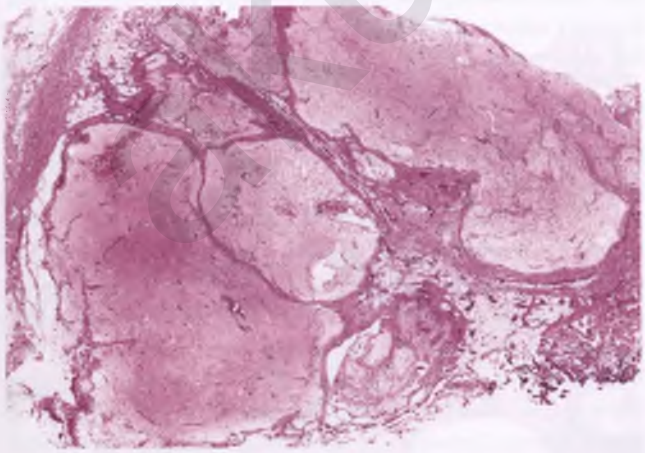

FIGURE 1.45. Superficial angiomyxoma. This low-magnification view highlights the coalescing lobules of myxoid stroma within the subcutaneous adipose tissue.

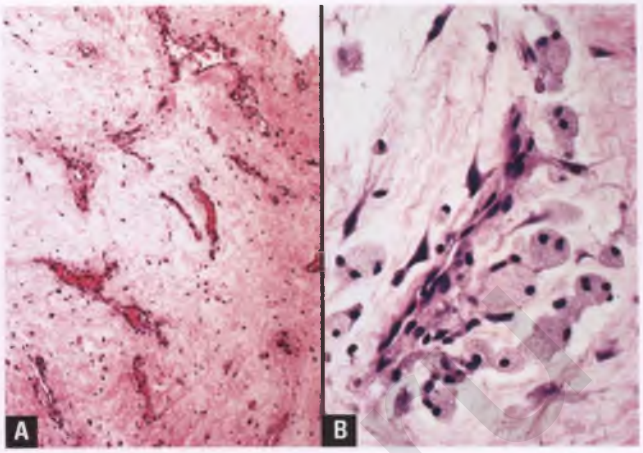

FIGURE 1.46. Superficial angiomyxoma. **A**: The vessels within the tumor are thin walled, and are often congested with arc-shaped outlines. **B**: Several muciphages are present adjacent to a thin-walled vessel. Stellate and spindle-shaped tumor cells are also present.

Massive Vulval Edema[54]

Patients who are obese or wheelchair bound are predisposed to bilateral vulvar swelling related to stromal edema from presumed chronic lymphatic obstruction. Mass lesions may form that can grossly and histologically simulate aggressive angiomyxoma or fibroepithelial stromal polyp. The edematous sectioned surface of resected specimens may resemble myxomatous tissue due to its glistening, pseudo-gelatinous appearance (Fig. 1.47A). Microscopic examination of this tissue reveals edematous connective tissue, dilated vessels of varying caliber and wall thickness, and a subset of vessels with perivascular lymphoplasmacytic cuffs (Figs. 1.47B and 1.48A). Most of the stromal cells are bland, spindle-shaped, mitotically inactive fibroblasts, but multinucleated forms are often admixed with the spindle cells (Fig. 1.48B). Since stromal edema is the dominant histologic finding, it is not surprising that there are no distinct lesional boundaries.

Differential Diagnosis

Massive vulval edema is distinguished from aggressive angiomyxoma by (a) its bilateral and superficial presentation, which contrasts with the unilateral, deep-seated nature of aggressive angiomyxoma; (b) the usual presence of scattered multinucleated stromal cells (as a consequence of their common presence in normal vulvar connective tissue) as opposed to the monotonous, bland spindle cell morphology of aggressive angiomyxoma; (c) its edematous, Alcian blue–negative rather than myxoid, weakly Alcian blue–positive stroma; and (d) the presence of perivascular lymphoplasmacytic infiltrates. Lack of immunoreactivity of the stromal cells in massive vulval edema

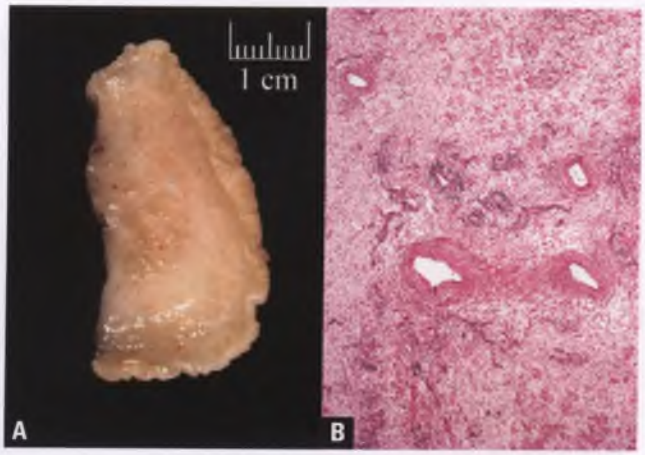

FIGURE 1.47. Massive vulval edema. **A**: The sectioned surface beneath the skin of this polypoid resection specimen consists of glistening, pale yellow stromal tissue that resembles a myxoid lesion. **B**: In this low-magnification image, note the splaying apart of collagen fibers by stromal edema, scattered vessels of varying caliber and wall thickness, and patchy perivascular chronic inflammatory infiltrates.

for desmin and estrogen receptors may also help to distinguish this process from aggressive angiomyxoma, although experience is limited in this regard.

Massive vulval edema shares with edematous fibroepithelial stromal polyps the histologic findings of stromal edema, lack of well-defined lesional borders, and multinucleated stromal cells. Features that favor massive vulval edema over fibroepithelial stromal polyp include (a) bilaterality, (b) clinical history of obesity and/or immobilization, (c) perivascular lymphoplasmacytic cuffs, and (d) incorporated nerve twigs.

Angiomyofibroblastoma[55–57]

Angiomyofibroblastoma is a rare tumor of adult women that typically presents as a painless vulvar mass that clinically mimics

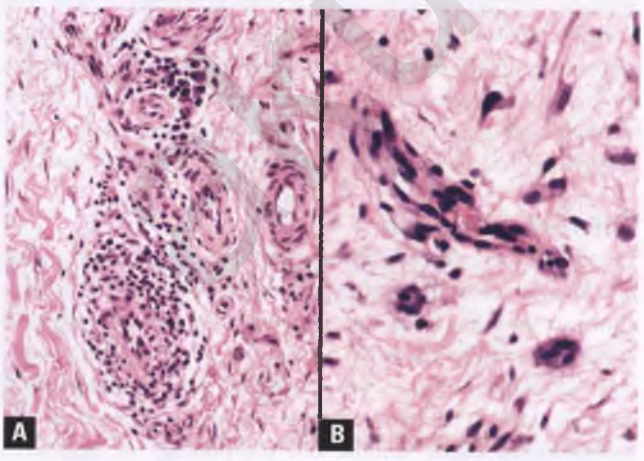

FIGURE 1.48. Massive vulval edema. **A**: Perivascular lymphoplasmacytic infiltrates are a helpful diagnostic feature. **B**: Scattered multinucleated stromal cells are present within the edematous connective tissue, similar to those that can be seen in fibroepithelial stromal polyps.

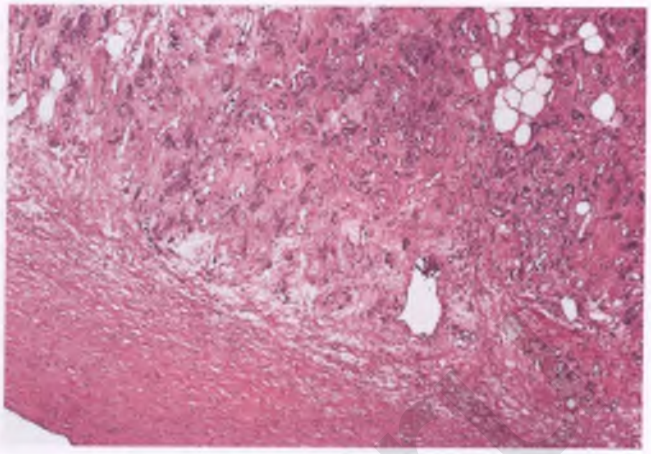

FIGURE 1.49. Angiomyofibroblastoma. The tumor is circumscribed and has a rim of fibrous tissue at its periphery. Hypercellular and hypocellular regions are present, and scattered islands of adipose tissue are incorporated into the substance of the tumor. (Courtesy of Dr. Harris S. Goodman.)

a Bartholin's cyst. Most angiomyofibroblastomas measure <5 cm, but they have been reported to be up to 12 cm. These tumors are well circumscribed and have a sectioned surface that is solid, rubbery, and tan to grayish pink, although the lipomatous variant may be yellow. At low magnification, zones of varying cellularity can be appreciated within the sharply demarcated tumor (Fig. 1.49). Thin-walled, capillary-like vessels of small to medium caliber are irregularly distributed throughout the tumor, some of which may exhibit a surrounding rim of sclerosis. The lesional stromal cells generally have bland nuclear features, show little to no mitotic activity, assume a variety of shapes (spindled, round, oval, plasmacytoid, multinucleate), are often found in nests and cords surrounding blood vessels, and typically exhibit immunoreactivity for desmin, estrogen receptors, and progesterone receptors (Fig. 1.50). Occasional

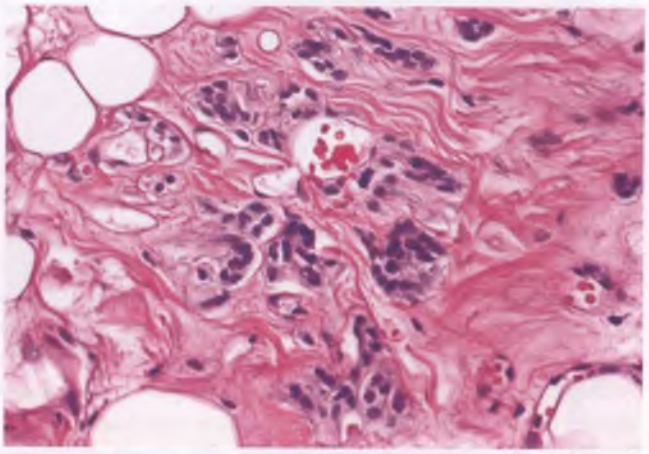

FIGURE 1.50. Angiomyofibroblastoma. Clusters of epithelioid tumor cells with a perivascular distribution are a characteristic feature. (Courtesy of Dr. Harris S. Goodman.)

mast cells and lymphocytes are often present within the loosely collagenous stroma, and intratumoral mature adipose tissue may also be present in variable amounts.

Differential Diagnosis

Before angiomyofibroblastoma was recognized as a distinct entity, it was often misdiagnosed as a cellular variant of aggressive angiomyxoma. Angiomyofibroblastoma is distinguished from aggressive angiomyxoma by its well-circumscribed borders, patches of increased cellularity, absence or paucity of thick-walled vessels, perivascular clusters of tumor cells with epithelioid or plasmacytoid morphology, absence of entrapped nerve twigs (with the exception of one reported case),[56] tendency to be smaller and more superficially located, and lack of recurrence following simple excision. The other major differential diagnostic consideration is cellular angiofibroma, which is more uniformly cellular than angiomyofibroblastoma, lacks a predilection for perivascular tumor cell aggregates, and typically contains numerous vessels with walls that are characteristically thick and hyalinized rather than thin and delicate. As discussed in Chapter 2, superficial myofibroblastoma usually arises in the vagina and resembles angiomyofibroblastoma in many respects. Examples of superficial myofibroblastoma involving the vulvar region are extraordinarily rare.[58]

Behavior

Angiomyofibroblastomas are benign tumors that are adequately treated by local excision. Malignant transformation into an angiomyofibrosarcoma is exceedingly rare, but has been reported.[59]

Cellular Angiofibroma[60,61]

Cellular angiofibroma is yet another rare, fairly recently described benign mesenchymal tumor with a predilection for involvement of the vulva. Tumors with identical histologic features can also occur in the vagina and in the inguinoscrotal region of men. As is the case for angiomyofibroblastoma, cellular angiofibroma typically presents as a painless, superficial vulvar mass centered in the dermis or subcutaneous tissue of adult women. Most tumors are <3 cm, well circumscribed, and have a solid, rubbery, light tan cut surface.

Histologically, cellular angiofibromas are composed of a sharply demarcated, cellular proliferation of spindle-shaped cells with bland nuclear features that often form short, intersecting fascicles (Figs. 1.51 and 1.52A). These cells are set in a fibrillary collagenous matrix that contains numerous vessels of small to medium caliber that characteristically have thick, rounded walls with striking hyalinization (Fig. 1.52B). Scattered lymphocytes and mast cells are commonly present. Mature adipose tissue is present in approximately 25% of cellular angiofibromas, and is usually found focally and peripherally. Mitoses are generally infrequent, although three of the first reported cases had brisk mitotic activity. In rare instances, cellular angiofibromas may contain scattered foci with marked nuclear atypia or sharply demarcated areas of frank sarcomatous transformation.[62] Based upon limited follow-up information on a small number of patients, it does not appear that these worrisome histologic findings are of any clinical significance.[62] Approximately half of vulvar cellular angiofibromas are immunoreactive for CD34, only 5% to 10% are desmin positive, and most are positive for estrogen and/or progesterone receptors. These unusual mesenchymal tumors are adequately treated by local excision.

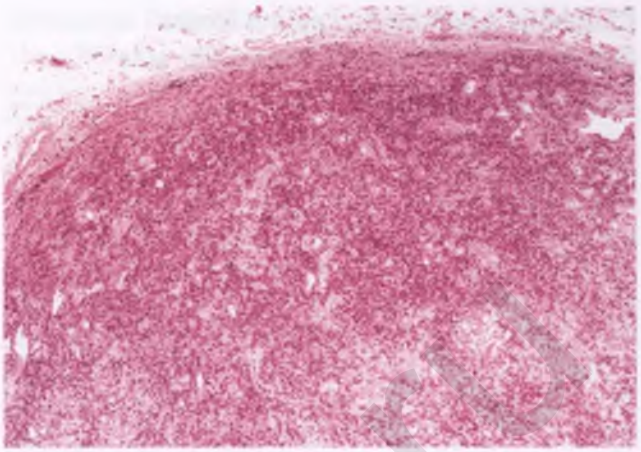

FIGURE 1.51. Cellular angiofibroma. This low-magnification view highlights the well-circumscribed, cellular nature of the typical form of this tumor.

Differential Diagnosis

The main differential diagnostic consideration is angiomyofibroblastoma. In contrast to cellular angiofibroma, angiomyofibroblastoma features alternating hypocellular and hypercellular zones, lacks thick-walled vessels with hyalinization, often exhibits perivascular aggregates of rounded tumor cells, and is usually immunoreactive for desmin. In some cases, it may be difficult to separate cellular angiofibroma from angiomyofibroblastoma, but this distinction is for "style points" only and is of no clinical significance.

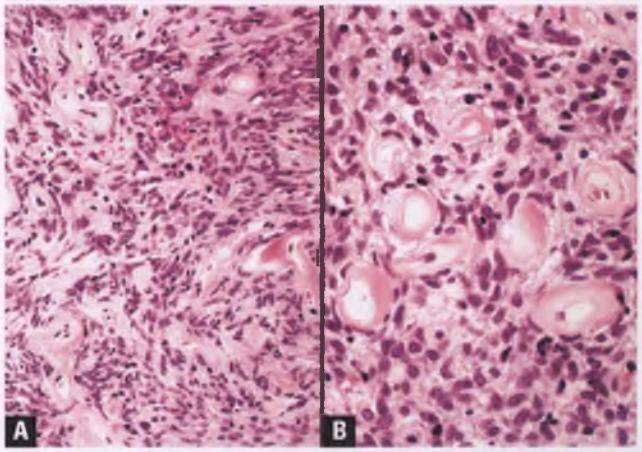

FIGURE 1.52. Cellular angiofibroma. **A**: The bland, spindle-shaped cells form short, intersecting fascicles. **B**: Numerous vessels of small to medium caliber with thick, hyalinized walls are characteristic.

Childhood Asymmetric Labium Majus Enlargement/Prepubertal Vulval Fibroma[63,64]

Attention has recently been focused upon a fairly common, previously underreported process that typically presents as an ill-defined, unilateral soft tissue mass within the labia majora of young girls (median age of 8 years). One group has interpreted this process as an aberrant expansion of vulvar soft tissue induced by the prepubertal hormonal environment that they have termed childhood asymmetric labium majus enlargement, while another group considers these masses to represent a distinctive type of infiltrative, benign mesenchymal tumor that they have designated prepubertal vulval fibroma. The similarities of the clinicopathologic features in both series of cases indicate that the two groups are likely describing the same entity, as has been previously suggested.[63]

These lesions are poorly demarcated soft tissue masses that range from 2 to 8 cm in greatest dimension, and consist of interconnecting, expansive fibrous bands that encircle variable-sized lobules of adipose tissue and incorporate normal preexisting vascular and neural elements. The stroma of the dominant fibrous component is hypocellular and may be collagenous, myxoid, or edematous. Interspersed bundles of thick, wavy collagen fibers are a characteristic feature (Fig. 1.53). Within the stroma are bland, mitotically inactive, spindle-shaped fibroblasts that typically exhibit a CD34-positive, actin-negative, desmin-negative immunophenotype. In the series of prepubertal fibromas, the lesional cells were consistently found to be negative for estrogen and progesterone receptors, whereas the subsequent study that described asymmetric labium majus enlargement and equated these lesions with prepubertal fibromas found uniform estrogen receptor and frequent progesterone receptor positivity.

The most important entity in the differential diagnosis is aggressive angiomyxoma, which occurs in an older age group, tends to be larger, has a vascular component that is more prominent and widely distributed, has a stroma that is more diffusely myxoid with more delicate collagen fibrils, and usually exhibits desmin immunoreactivity. About 30% to 50% of these lesions recur locally after simple excision, but they do so in a nondestructive manner and may spontaneously regress.

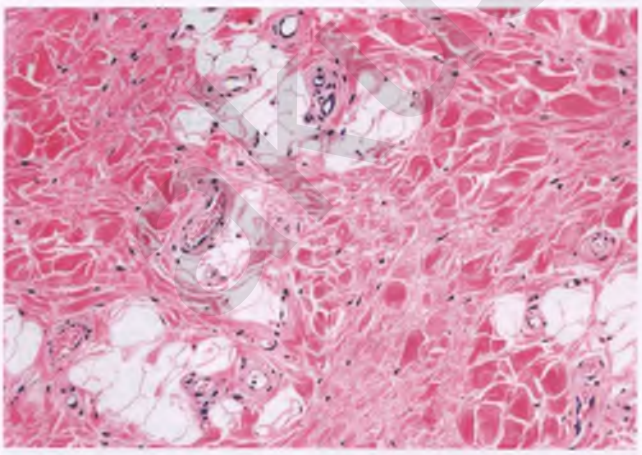

FIGURE 1.53. Childhood asymmetric labium majus enlargement/prepubertal vulval fibroma. The stromal matrix contains scattered fibroblasts and interspersed thick bundles of dense, brightly eosinophilic collagen fibers. Preexisting lobules of adipose tissue are embedded within the expanded fibrous compartment. (Courtesy of Dr. Deborah J. Gersell.)

Angiokeratoma[65]

Angiokeratomas of the vulva typically present as asymptomatic small papules that may be single, multiple, or coalesce into larger, warty lesions (Fig. 1.54A). In this site, they almost always represent an incidental finding and are not associated with metabolic disorders, in contrast to the widespread angiokeratomas that are seen in Fabry's disease. Histologically, angiokeratomas feature thin-walled, dilated vascular channels within the papillary dermis whose superficial aspects abut the epidermis (Fig. 1.54B). These ectatic vascular spaces may contain blood, blood plasma, or organizing thrombi, and are typically at least partially surrounded by elongated rete ridges. In established lesions, the epidermal surface is usually hyperkeratotic with patches of acanthosis.

Smooth Muscle Tumors[66,67]

Although leiomyoma and leiomyosarcoma are the most common benign and malignant mesenchymal tumors of the vulva, respectively, they are still relatively rare neoplasms. These tumors typically present in middle-aged adult women as a painless mass simulating a Bartholin's cyst. Their gross and microscopic features are similar to their much more common counterparts in the uterine corpus (see Chapter 4).

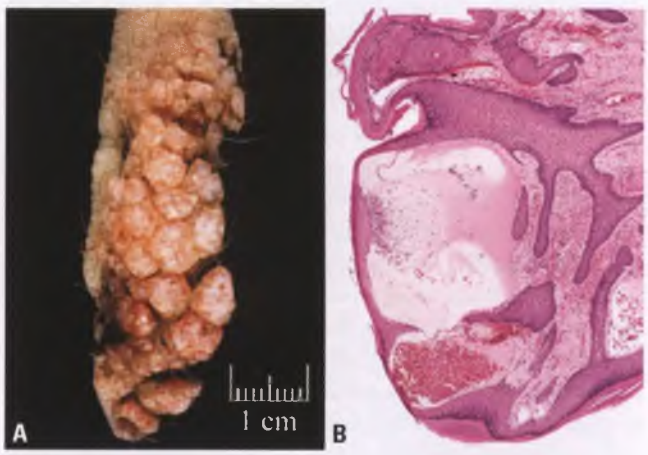

FIGURE 1.54. Vulvar angiokeratoma. **A**: This angiokeratoma, which is larger than most such lesions, consists of a conglomerate of papules that imparts a warty appearance. **B**: What appear to be small, reddish purple to pale yellow vesicles within the papules in the gross image at left are actually dilated subepithelial vascular channels filled with blood or blood plasma, respectively. The epidermis is hyperkeratotic with areas of acanthosis, and elongated rete ridges partially encompass the vascular spaces.

Vulvar leiomyomas tend to be <5 cm and well circumscribed, whereas most of the limited number of reported vulvar leiomyosarcomas have been >5 cm with microscopically infiltrative margins.

Most smooth muscle tumors of the vulva exhibit the usual pattern of intertwining fascicles of elongate cells with cigar-shaped nuclei and eosinophilic, fibrillar cytoplasm (Fig. 1.55). Epithelioid and/or myxoid variants are fairly common in the two major series of these neoplasms, but this may simply reflect an inherent selection bias related to a reliance upon consultation material. The presence of myxoid, hyaline, or myxohyaline stroma often occurs in the setting of epithelioid smooth muscle tumors, and may be associated with plexiform or other unusual patterns (Fig. 1.56).

The criteria used to separate benign from malignant smooth muscle tumors of the vulva are different from those used for the uterine corpus, and are based upon limited outcome data due to the rarity of these tumors. In the most recent large study of vulvar smooth muscle tumors, it is recommended that tumors with three or more of the following characteristics be classified as leiomyosarcoma: size ≥5 cm, infiltrative margins, ≥5 mitotic figures per 10 high power fields, and moderate to severe nuclear atypia.[67] In this study, tumors that exhibited only one of these four features were still considered leiomyomas, while tumors with two of these criteria were classified as atypical leiomyomas. However, other investigators take a more cautious approach, and consider vulvar smooth muscle tumors with isolated findings of infiltrative margins, significant nuclear atypia, or any mitotic activity to be atypical leiomyomas with recurring potential.[46] Tumor cell necrosis, as defined in the section on uterine smooth muscle tumors in Chapter 4, is an uncommon finding in vulvar smooth muscle tumors, but its presence is strongly associated with leiomyosarcoma.[67]

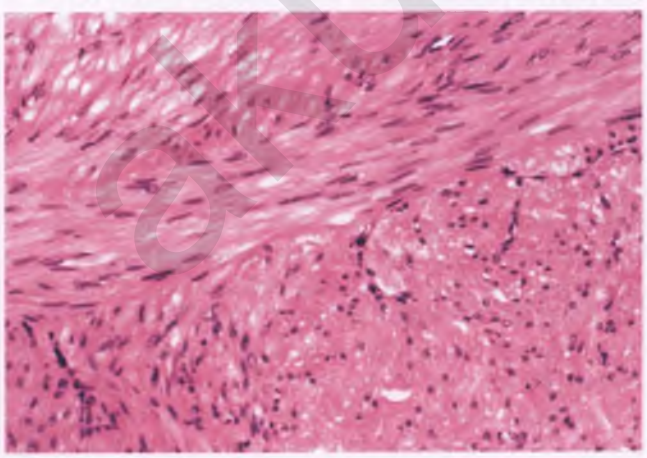

FIGURE 1.55. Leiomyoma of usual type. Note intertwining fascicles of elongated cells with cigar-shaped nuclei. Many of the nuclei in the bottom portion of the image have been cross-sectioned, resulting in their appearance as small, round to oval structures.

Differential Diagnosis

The differential diagnosis of vulvar smooth muscle tumors is broad and includes a variety of spindle cell and epithelioid tumors or tumor-like lesions. Most cases with the typical fascicular growth pattern of spindle cells with cigar-shaped nuclei and eosinophilic cytoplasm are readily recognized as smooth muscle tumors, and are further classified into benign, atypical, or malignant categories utilizing the criteria listed above. In those cases with unusual nuclear and/or stromal features, support for smooth muscle differentiation can be obtained by documenting immunoreactivity for actin, desmin, and h-caldesmon. Desmin positivity and the absence of numerous thick-walled vessels with hyalinized walls argue against the diagnosis of cellular angiofibroma, while S100 negativity helps to exclude the possibilities of neurofibroma, schwannoma, and malignant melanoma.

Granular Cell Tumor[68–70]

Granular cell tumor is an uncommon neoplasm, approximately 10% of which occur in the vulva. In this site, these tumors have a predilection for African Americans and typically present in adult women as an asymptomatic, solitary, 1 to 3 cm, circumscribed, firm nodule involving the labia majora. Occasional patients have more than one granular cell tumor of the vulva, typically in association with similar tumors in extravulvar sites.

The sectioned surface of granular cell tumors is solid and usually pale yellow. Histologically, vulvar granular cell tumors are located in the dermis and/or subcutis and although fairly well demarcated, they are often focally infiltrative along portions of their interface with neighboring tissue (Fig. 1.57A). These tumors consist of nests and sheets of large cells with nuclei that are small and uniform and cytoplasm that is abundant, eosinophilic, and granular (Fig. 1.57B). The background

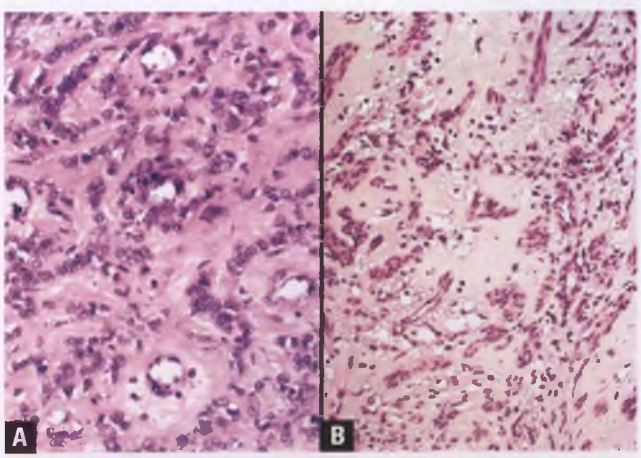

FIGURE 1.56. Leiomyomas with myxohyaline stroma. **A**: As is often the case in smooth muscle tumors with this type of stroma, the neoplastic cells exhibit an epithelioid morphology and a plexiform growth pattern. **B**: In this example, small fascicles of spindle-shaped smooth muscle cells are separated by myxohyaline stroma.

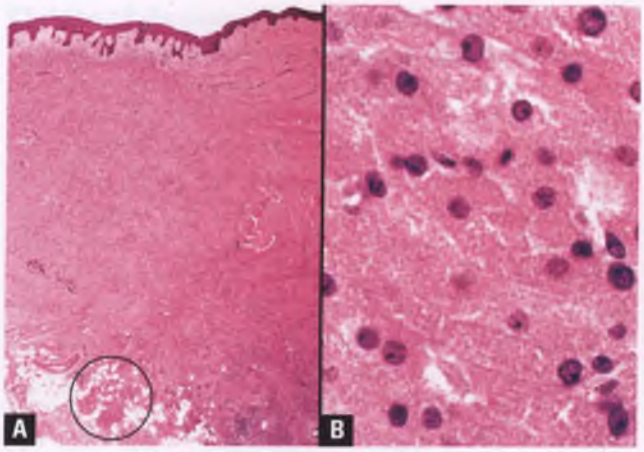

FIGURE 1.57. Granular cell tumor. **A**: The tumor has expanded and largely replaced the dermal compartment, and focally infiltrates subcutaneous adipose tissue (*circled*). **B**: High-magnification view of typical granular cells.

stroma is collagenous and varies from inconspicuous to prominent (Fig. 1.58). Roughly 20% of vulvar granular cell tumors are associated with pseudoepitheliomatous hyperplasia of the overlying squamous epithelium, which can lead to a misinterpretation of invasive well-differentiated squamous cell carcinoma (Fig. 1.59). To avoid this diagnostic pitfall, well-differentiated squamous carcinoma of the vulva should not be diagnosed in superficial biopsies unless there is adequate stromal tissue at the base of the lesion to exclude the possibility of a coexisting granular cell tumor.

Nearly all granular cell tumors pursue a benign clinical course. Malignant granular cell tumors do exist, but their histologic features overlap with benign tumors and as a practical matter are generally not diagnosed as malignant until aggressive clinical behavior has become apparent. Tumors with large size, high mitotic rates, foci of necrosis, and/or spindle cell morphology should be flagged as tumors with an increased likelihood of possible malignant behavior.

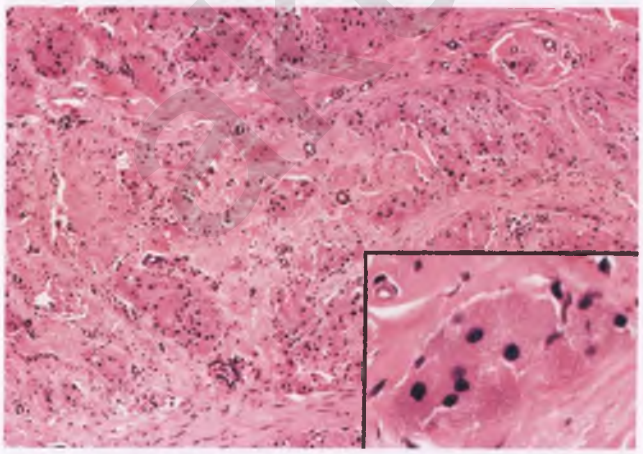

FIGURE 1.58. Granular cell tumor. Scattered nests of tumor cells are present within a densely sclerotic stroma.

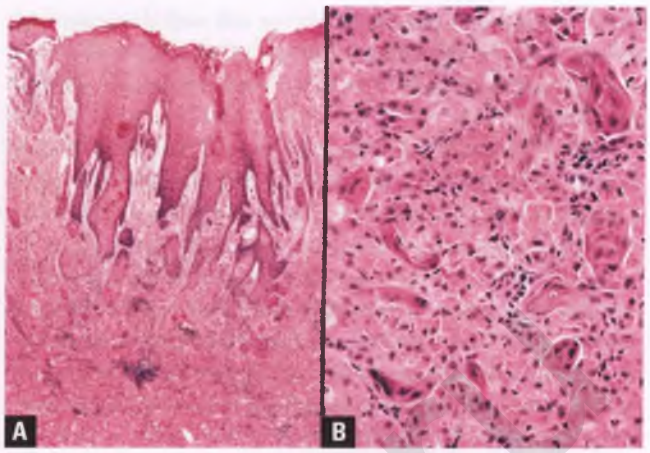

FIGURE 1.59. Granular cell tumor with pseudoepitheliomatous hyperplasia. **A**: The architecture of the hyperplastic squamous epithelium, which includes formation of jagged nests, mimics that of an invasive squamous cell carcinoma. In order to arrive at the correct diagnosis, the underlying granular cell tumor must be recognized. **B**: Nests of pseudoepitheliomatous squamous epithelium are seen in intimate association with a granular cell tumor.

Based upon the close relationship of some granular cell tumors to peripheral nerves, ultrastructural findings, and positive S100 immunohistochemistry, granular cell tumors are favored to be of peripheral nerve sheath origin. Electron microscopic studies have shown that the numerous intracellular granules seen at the light microscopic level correspond to lysosomes.

Nodular Fasciitis[71]

Although quite rare in the vulva, nodular fasciitis is presented in some detail due to the importance of its proper recognition in general surgical pathology. When it involves the vulva, this reactive proliferation of myofibroblasts usually occurs in the labial region of women of reproductive age, and has an average size of about 2.5 cm. Grossly, these lesions are solid nodules of variable color and consistency. Histologically, the nodular proliferation often extends into neighboring adipose tissue for short distances (Fig. 1.60). The lesional stromal cells consist of plump, mitotically active myofibroblasts with finely stippled chromatin and small nucleoli that are most often arranged in patterns that resemble myofibroblasts grown in tissue culture or found in granulation tissue (Fig. 1.61). These myofibroblasts typically form short, curved bundles within a loose, feathery background that contains extravasated erythrocytes and scattered lymphocytes. More cellular regions with a fascicular, storiform, or sheetlike architecture may also be present. Nodular fasciitis may also contain deposits of hyalinized collagen and small aggregates of multinucleated giant cells associated with foci of microhemorrhage (Fig. 1.62). Variable-sized cystic spaces also occur in some cases (Fig. 1.63). This pseudoneoplastic lesion is adequately treated by local excision.

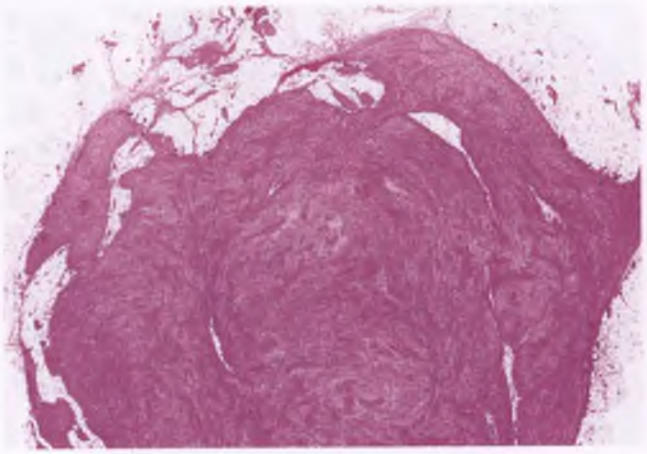

FIGURE 1.60. Nodular fasciitis. At scanning magnification, these lesions are seen to have a predominantly nodular configuration, but often extend into the adjacent adipose tissue for short distances.

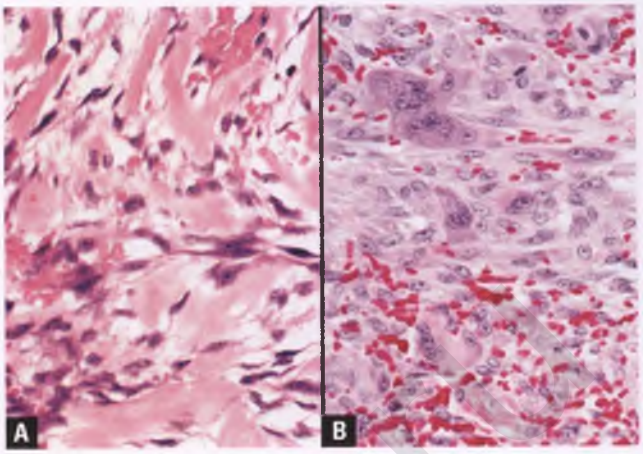

FIGURE 1.62. Nodular fasciitis. **A**: This example contains prominent hyalinized keloidal collagen. **B**: In this case, scattered osteoclast-like multinucleated giant cells are present in an area of microhemorrhage.

Differential Diagnosis

The differential diagnosis of nodular fasciitis is broad, and is more fully covered in textbooks of soft tissue pathology. In the vulva, half of the battle in arriving at the correct diagnosis is in recognizing that nodular fasciitis can occur in this site and including it in the list of possible diagnoses. Although the mitotic activity of nodular fasciitis can be eye-catching, the absence of atypical mitotic figures and the lack of significant nuclear atypia are clues that this lesion is not sarcomatous.

With specific reference to vulvar soft tissue tumors and tumor-like lesions that are in the differential diagnosis, the postoperative spindle cell nodule and aggressive angiomyxoma are the lesions most likely to be confused with nodular fasciitis. As discussed in Chapter 2, postoperative spindle cell nodules are associated with a previous recent operative procedure at the site of the lesion. Although they share many histologic features with nodular fasciitis, they have a distinctive clinical history, tend to be more uniformly cellular and less varied in their architectural patterns, and typically lack the secondary findings that cases of nodular fasciitis may exhibit, such as microcysts, multinucleated giant cells, and hyalinized collagen. Misinterpreting postoperative spindle cell nodule as nodular fasciitis, or vice versa, is of no clinical significance. In comparison with nodular fasciitis, aggressive angiomyxoma is usually a larger mass, has a much more distinctive and prominent vascular pattern with widely patent vessel lumens, is less cellular, and its stromal cells are mitotically inactive with inconspicuous nucleoli.

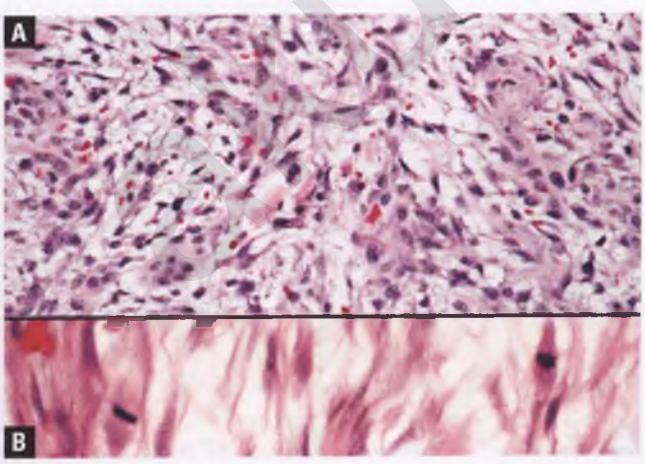

FIGURE 1.61. Nodular fasciitis. **A**: Loosely arranged, plump myofibroblasts are present in a feathery background that contains scattered extravasated erythrocytes. **B**: This image highlights the presence of two normal mitotic figures, which are typically scattered throughout the lesion and concentrated in the loosely textured, less cellular regions.

Epithelioid Sarcoma[72,73]

Epithelioid sarcoma is an extremely rare malignant neoplasm, but is worthy of discussion because of the predilection of its proximal variant to involve the vulva of women of reproductive age. Most vulvar tumors previously reported as malignant

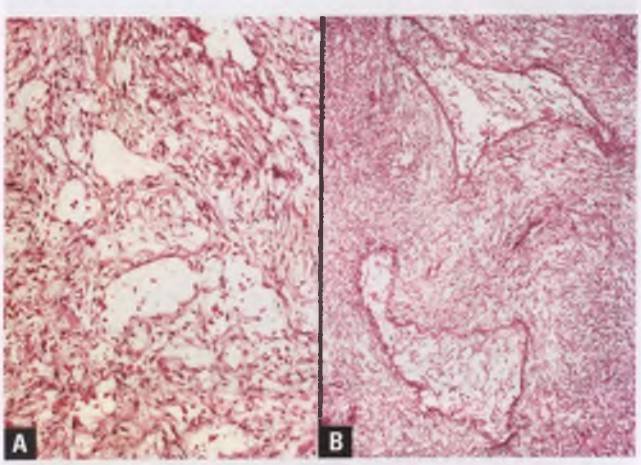

FIGURE 1.63. Nodular fasciitis. As these two images demonstrate, cysts of various sizes may be present.

rhabdoid tumor, such as cases 2 through 4 in the series by Perrone et al.,[74] would currently be classified as proximal-type epithelioid sarcoma, which was not described until 1997. Although the distinction between these two tumors is somewhat arbitrary and not presently of any clinical significance, recent evidence suggests that these tumors may have at least some immunohistochemical differences and may be separable.[75,76] Regardless of whether a tumor is diagnosed as proximal epithelioid sarcoma or malignant rhabdoid tumor, the most important observations are that these tumors pursue a more aggressive clinical course than the classic/conventional/distal type of epithelioid sarcoma that occurs most commonly in the soft tissue of the extremities, and that criteria exist to separate proximal-type from classic epithelioid sarcoma.

Both types of epithelioid sarcoma have the gross appearance of a nodular or multinodular, dermal and/or subcutaneous mass with a median size of 4 cm and a cut surface that is white, pale yellow, or tan with mottled areas of hemorrhage and necrosis (Fig. 1.64). The nodular growth pattern is often apparent in histologic sections at low magnification (Fig. 1.65). In contrast to classic epithelioid sarcoma, proximal-type epithelioid sarcoma seldom mimics a granulomatous process, exhibits a greater degree of nuclear enlargement and atypia of its epithelioid cells, and often contains numerous rhabdoid cells (Figs. 1.66 and 1.67). Rhabdoid cells are so named because of their resemblance to the rhabdomyoblasts of rhabdomyosarcoma. The rhabdoid cell is characterized by a large, globular, eosinophilic cytoplasmic inclusion that corresponds ultrastructurally to a paranuclear whorl of aggregated intermediate filaments. When these inclusions compress and displace nuclei, the tumor cells so affected take on a signet-ring appearance.

Epithelioid sarcomas are of unknown histogenesis, and have an immunophenotype that characteristically includes coexpression of cytokeratin, epithelial membrane antigen, and vimentin. Their lack of immunoreactivity for S100 and skeletal muscle markers help to exclude the differential diagnostic possibilities of malignant melanoma and rhabdomyosarcoma,

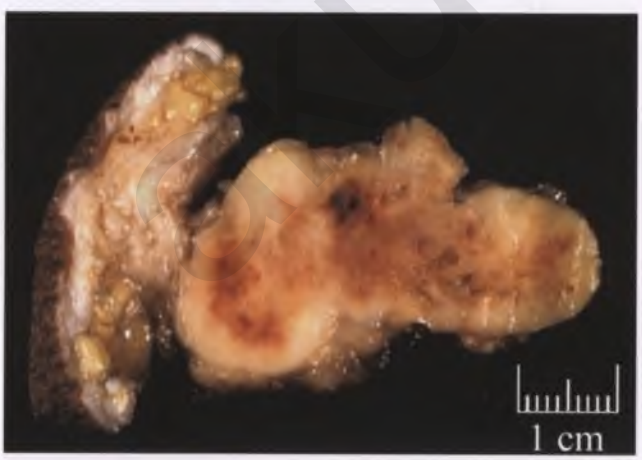

FIGURE 1.64. Epithelioid sarcoma. The cut surface of this subcutaneous nodule has a variegated appearance and contains foci of hemorrhage and necrosis.

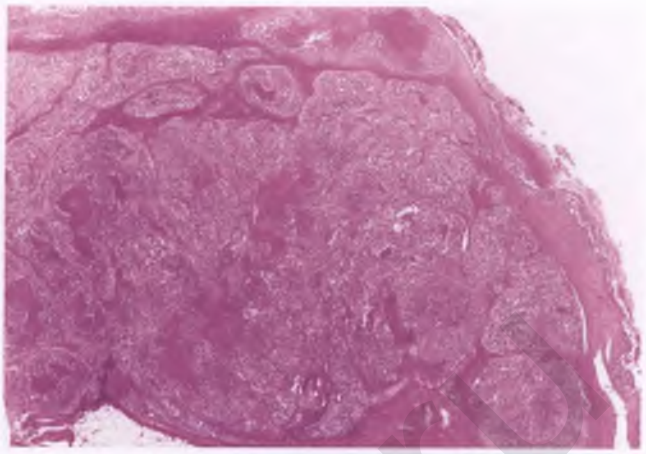

FIGURE 1.65. Epithelioid sarcoma. At scanning magnification, the multinodular growth pattern and randomly distributed foci of tumor necrosis are evident in this proximal-type tumor.

respectively. The reader is referred to the seminal article on proximal-type epithelioid sarcoma for a more in-depth discussion of the differential diagnosis of this unusual tumor.[72]

Miscellaneous Soft Tissue Tumors and Tumor-Like Lesions

The following is an incomplete listing of some other soft tissue tumors and tumor-like lesions that involve the vulva on rare occasions: postoperative spindle cell nodule (see Chapter 2),[77] fibromatosis,[78] dermal fibrous histiocytoma (dermatofibroma),[79] lipoma,[80] hemangioma,[79] lymphangioma,[81] glomus tumor,[82] paraganglioma,[83] neurofibroma,[84] schwannoma,[85] solitary fibrous tumor,[86] dermatofibrosarcoma protuberans,[87] malignant fibrous histiocytoma,[88] angiosarcoma,[89] Kaposi's sarcoma,[90] hemangiopericytoma,[91] liposarcoma,[92] synovial

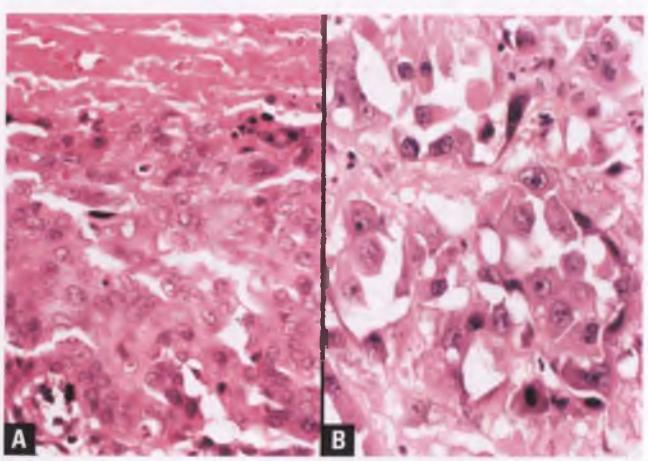

FIGURE 1.66. Epithelioid sarcoma. **A**: Classic type simulating a necrotizing granulomatous process. The tumor cells are epithelioid and are fairly uniform. **B**: Proximal type with marked nuclear atypia. Note: Both images were taken at the same magnification.

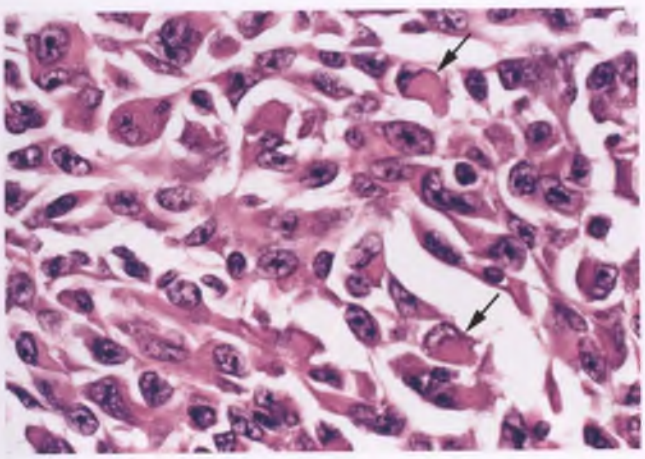

FIGURE 1.67. Epithelioid sarcoma with rhabdoid features. *Arrows* mark two of the rhabdoid tumor cells that have a signet-ring appearance.

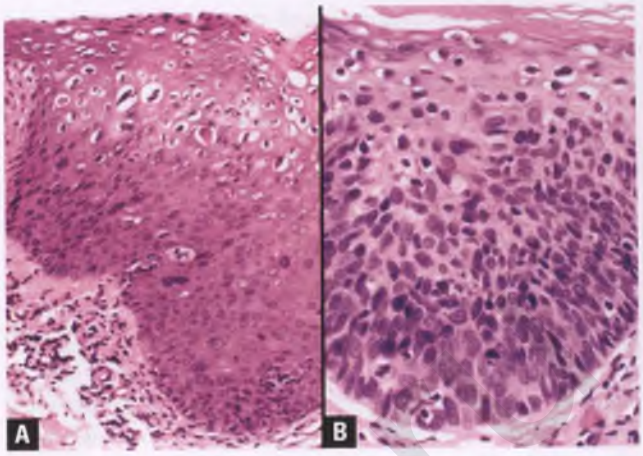

FIGURE 1.68. **A**: VIN 1 with koilocytosis. The lower third of the epithelium exhibits nuclear atypia and disordered maturation, while koilocytes predominate in the upper portion. **B**: VIN 2. The cells within the lower two-thirds of the epithelium are dysplastic, jumbled, and closely packed. The basal cells in usual VIN may exhibit a palisaded arrangement, as in this example.

sarcoma,[93] alveolar soft part sarcoma,[94] rhabdomyosarcoma,[95] malignant schwannoma,[96] and Ewing's sarcoma/peripheral primitive neuroectodermal tumor.[97,98] In general, these tumors have histologic features that are identical to their nonvulvar counterparts. The rarity of the sarcomas listed above is underscored by the fact that vulvar sarcomas collectively account for only about 2% of all vulvar malignancies.[89]

VULVAR INTRAEPITHELIAL NEOPLASIA

Lesions classified as VIN are thought to represent potential precursors of invasive squamous cell carcinoma. VIN is much less common than cervical intraepithelial neoplasia (CIN), but is more frequently encountered than vaginal intraepithelial neoplasia. There are two major types of VIN that will be discussed separately. Usual (classic, bowenoid) VIN is the dominant form, while the much less common type of VIN is referred to as differentiated (simplex) VIN.[99]

Usual VIN

Classification of usual VIN is currently in a state of flux. Traditionally, usual VIN has been divided into VIN 1, VIN 2, and VIN 3 (Figs. 1.68 and 1.69), analogous to the three grades of CIN as discussed in Chapter 3. However, as of 2004, the International Society for the Study of Vulvovaginal Disease (ISSVD) has recommended that lesions previously interpreted as VIN 1, which are quite uncommon in comparison to VIN 3, be regarded as flat condylomas rather than possible cancer precursors and that use of the term VIN 1 be discontinued.[100] In this classification system, usual VIN is equated with traditional forms of VIN 2 or VIN 3. The ISSVD's classification system has been met with resistance by some influential gynecologic pathologists. Some of these pathologists coauthored a 2006 study in which 42% of VIN 1 lesions were found to contain high-risk HPV, which has been taken as evidence that at least some cases of VIN 1 are at risk for the eventual development of VIN 2–3 and has led to the position that this risk is best conveyed by retaining the VIN 1 terminology.[101] Yet another classification system utilizes the Bethesda-like terminology of low-grade (condyloma/VIN 1) and high-grade (VIN 2/VIN 3) vulvar intraepithelial lesions.[102] This system has been criticized for including exophytic condylomas within the low-grade category when they have different HPV profiles from VIN 1 and are considered infectious lesions rather than potential cancer precursors, and for lumping VIN 2 with VIN 3 when some view VIN 2 as a biologically heterogeneous group of lesions with uncertain precancerous potential.[103] Given these controversies, I agree with the recommendation of Skapa et al. and McCluggage to continue using the traditional VIN 1 through VIN 3 classification system until a data-driven consensus emerges.[45,103]

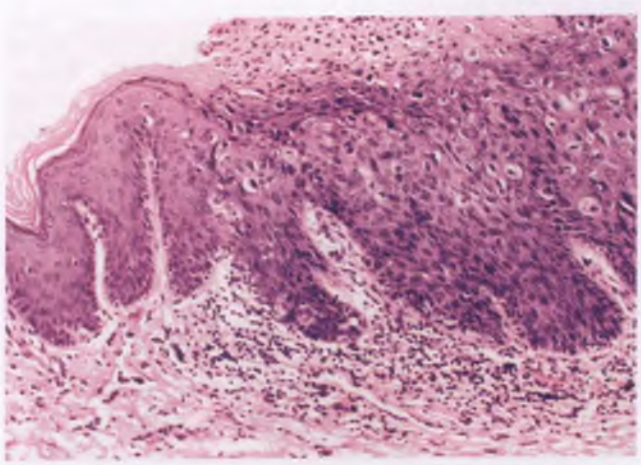

FIGURE 1.69. VIN 3. Compare the full-thickness atypia of the VIN 3 at right with the nondysplastic, hyperkeratotic squamous epithelium at left.

Usual VIN is most often found in young adult women and is associated with HPV infection; high-risk type HPV 16 predominates in the high-grade lesions (VIN 2–3).[101] Usual VIN has a variable clinical presentation, with lesions that may be (a) plaque-like, verruciform, polypoid, or papular; (b) white, pink, red, or brown; and (c) asymptomatic or pruritic.[99] These lesions are commonly multifocal and may occur within a condyloma. Patients with usual VIN are at high risk for HPV-related disease in the neighboring cervix, vagina, and perianal region.[99]

Basaloid and warty subtypes of usual VIN have been described.[104] The basaloid variant of VIN 3 resembles CIN 3 and is composed of atypical, closely packed, disorganized basaloid cells with scant cytoplasm occupying between the lower two-thirds and the full thickness of the epithelium (Fig. 1.70A). The surface is flat and variably hyperkeratotic or parakeratotic. In contrast, warty VIN 3 has a spiked or undulating surface with a conspicuous granular layer, exhibits prominent hyperkeratosis and/or parakeratosis, and is composed of larger cells with a greater degree of nuclear pleomorphism, more abundant eosinophilic cytoplasm, and more distinct cell membranes (Fig. 1.70B). Dyskeratotic cells, apoptotic bodies, and superficially located koilocytes are common in the warty variant. Scattered mitotic figures, including abnormal forms, are typically found throughout all levels of the epithelium in both basaloid and warty VIN 3. These subtypes are of use only to the extent that they assist in the recognition and description of VIN; their distinction is not clinically relevant and there is no need to specify the subtype in the pathology report (especially since these subtypes may coexist with one another or be difficult to separate due to the presence of overlapping features).[99] Other rare variants of usual VIN are pagetoid VIN and VIN with mucinous differentiation, which are discussed in the section on the differential diagnosis of Paget's disease. Pigmented VIN lesions that are a shade of brown typically have increased melanin in the basal layer and/or evidence of pigment incontinence within the upper dermis (Fig. 1.71).

In the vast majority of cases, usual VIN can be diagnosed by morphology alone. In selected instances, use of MIB-1 and p16 antibodies can facilitate the diagnosis, since both of these immunostains typically show diffuse, strong nuclear reactivity in VIN 3 that is lacking in normal and reactive processes.[7,105] MIB-1 can also be utilized to help distinguish VIN 1 from normal squamous epithelium with pseudokoilocytic changes, since the former will typically contain clusters of two or more positively stained nuclei in the upper two-thirds of the epithelium, whereas the latter will show staining only at or below the parabasal region (avoid counting immunoreactive parabasal cells lining loops of upwardly projecting papillary dermis or immunoreactive intraepithelial lymphocytes as staining patterns supportive of VIN).[106] MIB-1 and p16 are discussed in more detail in the section on squamous intraepithelial lesions in Chapter 3, since these antibodies are more commonly used in the evaluation of difficult cervical biopsies. It is recommended that the same conservative approach to the diagnosis of cervical LSIL as described in Chapter 3 be applied to VIN 1, which translates into classifying equivocal biopsies that might possibly represent a subtle form of VIN 1 as being within the range of normal without resorting to immunohistochemistry.

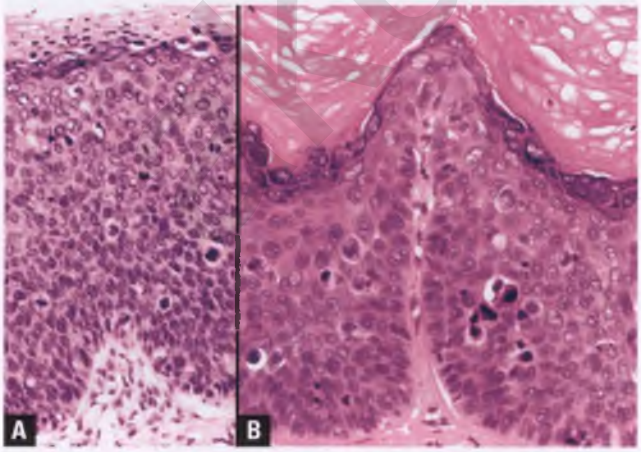

FIGURE 1.70. Histologic subtypes of usual VIN. **A**: VIN 3, basaloid type. **B**: VIN 3, warty type.

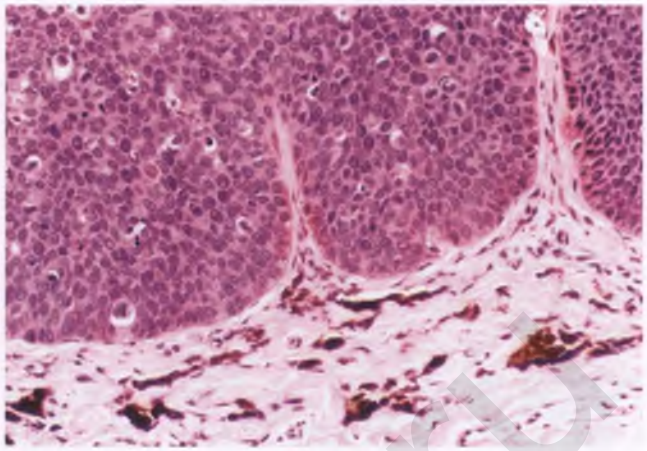

FIGURE 1.71. Pigmented VIN 3. The pigmentation of this lesion, which was dark brown clinically, is primarily due to pigment incontinence, as evidenced by melanophages and free melanin pigment within the dermis. Portions of the basal layer of the dysplastic epithelium are also hyperpigmented.

Usual VIN frequently extends into skin appendages.[107] Although this phenomenon is fairly easy to recognize in optimally oriented sections (Fig. 1.72), tangential sections of involved appendages can create the appearance of isolated nests of tumor cells within the stroma that may be misinterpreted as invasion (Fig. 1.73). The well-circumscribed nature of the nests of dysplastic cells, the lack of a desmoplastic host response, and the identification of residual elements of the skin appendage within or contiguous with the proliferation facilitate its recognition as extension of VIN into skin adnexal structures rather than stromal invasion. Associated chronic inflammation is common, and should not be taken as evidence supportive of invasion. Since legitimate stromal invasion is known to occur in roughly 10% to 20% of specimens excised

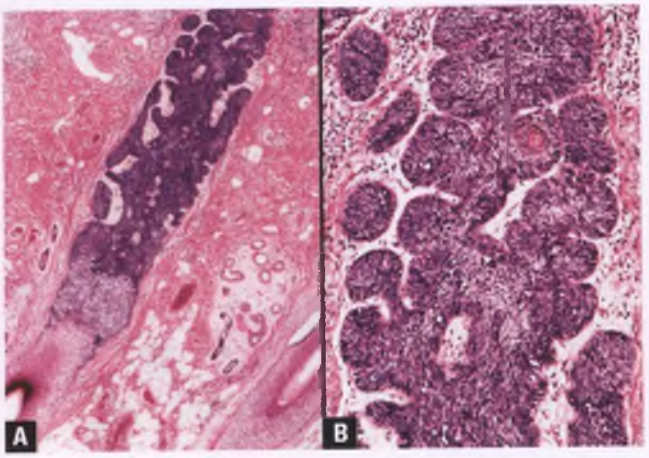

FIGURE 1.72. VIN 3 with skin appendage involvement. **A**: In this optimally oriented section, the basaloid dysplastic proliferation is clearly contiguous with the base of a hair follicle at lower left and remains confined within a narrow column related to the pilosebaceous unit. **B**: The nests of dysplastic cells in skin appendage involvement typically have smooth, rounded contours.

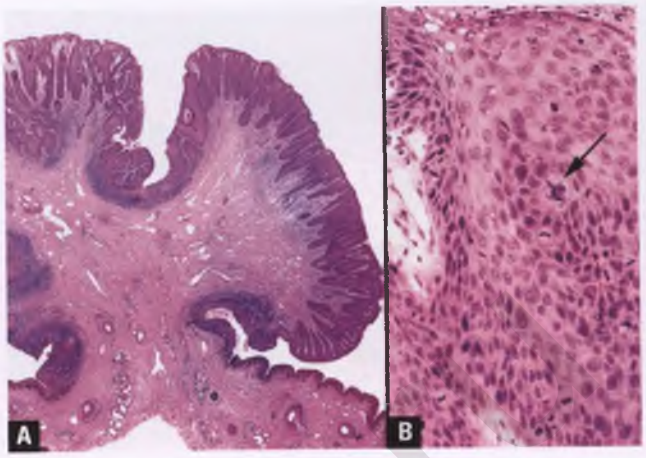

FIGURE 1.74. VIN 3 with papular architecture (formerly bowenoid papulosis). **A**: At low magnification, it is easy to understand why this polypoid papule would be submitted with a clinical diagnosis of condyloma or nevus. **B**: At high magnification, the epithelium shows features of VIN3, including brisk mitotic activity. The *arrow* marks an atypical mitotic figure.

for VIN, such specimens should be extensively sectioned and thoroughly examined.[99,108]

Usual VIN 3 may present in young adult women as one or more papules that clinically resemble condyloma or nevi (Fig. 1.74). In this situation, the term "bowenoid papulosis" has been applied, and it has been suggested that these lesions seldom progress to invasive squamous cell carcinoma and have the potential to spontaneously regress.[109] Currently, most investigators do not think that lesions of this type have sufficiently distinctive clinical or pathologic features to warrant their separation from the usual type of VIN 3.[99]

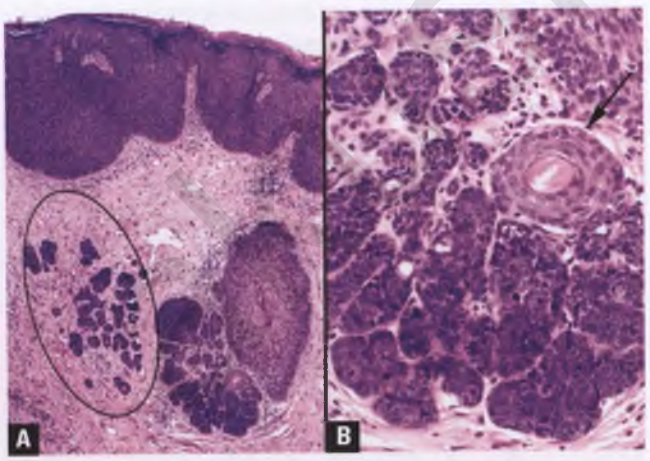

FIGURE 1.73. VIN 3 with skin appendage involvement. **A**: In this example, recognition of involvement of the hair follicle at lower right is facilitated by residual follicle elements. The circled nests are at higher risk of being misinterpreted as invasive carcinoma, but actually represent the edge of an involved hair follicle that has been tangentially sectioned. **B**: In this high-magnification view of the involved hair follicle in the lower right of the left-sided image, an *arrow* marks a residual component of the hair follicle.

Differentiated (Simplex) VIN

In contrast to usual VIN, differentiated VIN is not associated with HPV, occurs in an older age group (mean age of 67 years), and is commonly associated with lichen sclerosus or acanthotic squamous epithelium.[45,110,111] Differentiated VIN accounts for only about 2% to 10% of VIN, is considered to be high grade by definition (analogous to usual VIN 3), and is thought to be the precursor of most keratinizing squamous cell carcinomas of the vulva.[102,111,112]

Grossly, differentiated VIN appears as a gray-white roughened patch, plaque, or nodule that may blend in with a keratotic dermatosis in the background.[99,102] In contrast to usual VIN 3, recognition of differentiated VIN as a significant precursor lesion can be a challenge because of its lack of full-thickness or near full-thickness atypia and the need to become specifically educated about its subtle histologic features before it can be reliably diagnosed. Practice in identifying differentiated VIN can often be obtained by closely examining the epithelium adjacent to keratinizing squamous carcinomas of the vulva, where this lesion is commonly seen. The subtle gross and histologic features, coupled with its presumed rapid evolution to invasive carcinoma, conspire to make differentiated VIN an infrequent diagnosis in pure form.[45,99]

Differentiated VIN is recognized in histologic sections by a constellation of the following features: (a) parakeratosis overlying acanthotic squamous epithelium with rete ridges that are often elongated and/or branched; (b) hyperchromatic basal cells with a variable degree of nuclear atypia and some mitotic activity; (c) squamous cells in the parabasal to middle region

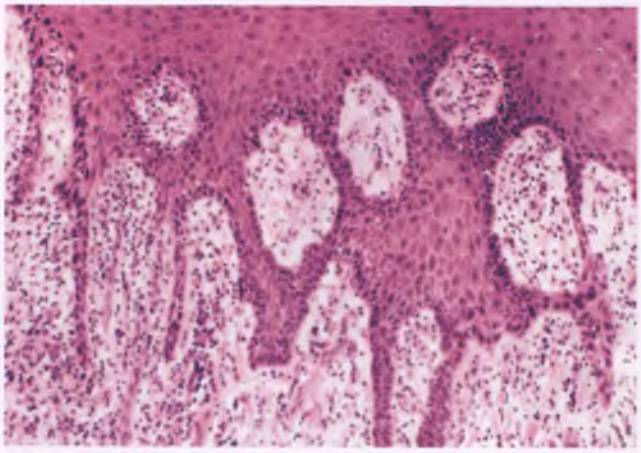

FIGURE 1.75. Differentiated VIN. As in this example, the rete ridges are often elongated, narrowed, and/or branched, and the dermis is frequently chronically inflamed.

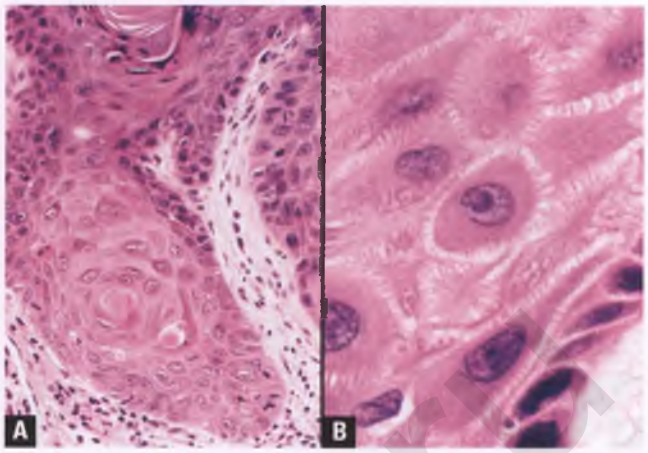

FIGURE 1.77. Differentiated VIN. **A**: A whorl of abnormal keratinocytes with early squamous pearl formation is present within an elongated and expanded rete ridge. A portion of a fully developed keratin pearl is present at top. **B**: Abnormally differentiated keratinocytes with dense eosinophilic cytoplasm, large vesicular nuclei, prominent nucleoli, and loss of cohesion with eye-popping intercellular bridges are found in the parabasal region of another case. Hyperchromatic basal cells are present in the lower right portion of the image.

of the epidermis with dense eosinophilic cytoplasm, large vesicular nuclei with prominent nucleoli, and loss of cohesion resulting in prominent intercellular bridges; and (d) whorls of keratinocytes within the rete ridges, sometimes with keratin pearl formation (Figs. 1.75–1.77).[99,110] Strong, continuous nuclear immunoreactivity for p53 within the basal layer with some degree of suprabasilar extension is seen in most cases of differentiated VIN (Fig. 1.78).[99,110,111]

Differential Diagnosis

Differentiated VIN at the lower end of the spectrum is subtle, subjective, and may be difficult to distinguish from the acanthotic squamous epithelium associated with reactive conditions such as lichen simplex chronicus or chronic lichen sclerosus. In contrast to differentiated VIN, these reactive conditions are generally associated with hyperkeratosis rather than parakeratosis, lack the population of enlarged keratinocytes with dense eosinophilic cytoplasm and prominent intercellular bridges, and do not have dysplastic cells within the basal layer.[99] For acanthotic lesions with questionable basal atypia and foci of parakeratosis in which a subtle form of differentiated VIN is a diagnostic consideration, a fungal stain should be performed to exclude a chronic fungal infection. Subacute spongiotic dermatitis and psoriasis, which are briefly discussed in the differential diagnosis of lichen simplex chronicus, can also resemble differentiated VIN.[102] Condyloma with podophyllin effect, as described earlier in this chapter, is an uncommon simulator of

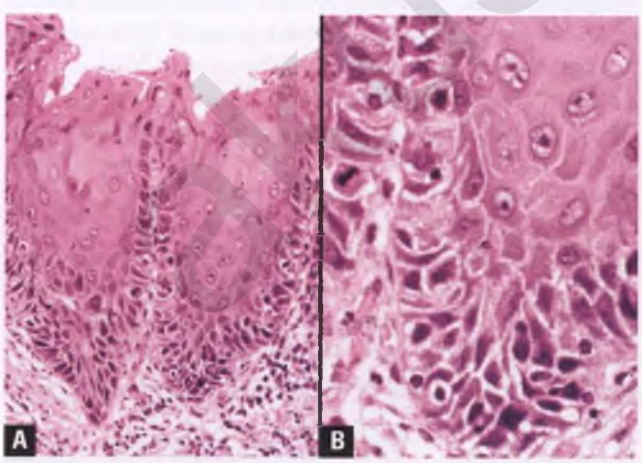

FIGURE 1.76. Differentiated VIN. **A**: This lesion features significant atypia of hyperchromatic keratinocytes in the basal region, where there is also loss of cohesion. **B**: Note the presence of a mitotic figure in this high-magnification image.

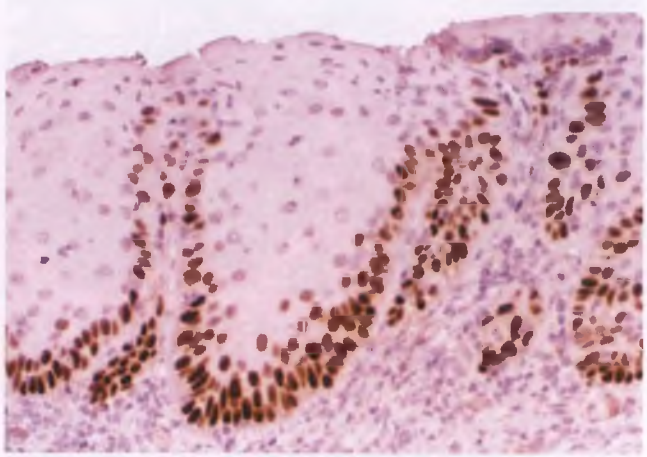

FIGURE 1.78. p53 immunostain of differentiated VIN. Strong, continuous nuclear staining of the basal layer with some suprabasilar extension is present in most examples of this lesion.

differentiated VIN whose recognition is obviously facilitated by the appropriate clinical history.[99]

Demonstration of the p53 staining pattern illustrated in Figure 1.78 provides some support for the diagnosis of differentiated VIN over reactive acanthotic lesions.[99,110,111] However, overlapping p53 staining patterns have been noted in some cases of lichen sclerosus, and p53 immunoreactivity is not currently viewed as necessary or sufficient for a diagnosis of differentiated VIN.[6,102,112] To complicate matters further, a small subset of differentiated VIN is histologically indistinguishable from the basaloid type of classic VIN, but is considered to be of differentiated type by virtue of its (a) tendency to occur in postmenopausal women, (b) association with keratinizing squamous cell carcinoma, (c) HPV negativity, and (d) p16-negative/p53-positive immunophenotype.[113]

SQUAMOUS CELL CARCINOMA AND ITS MAJOR VARIANTS

Conventional Squamous Cell Carcinoma

Conventional squamous cell carcinoma is the dominant malignant neoplasm of the vulva, accounting for approximately 90% of vulvar cancer.[114] The typical presentation is a postmenopausal woman (mean age of 65–70 years) with a vulvar mass that may be associated with pruritus, pain, bleeding, or a malodorous discharge. The staging system for vulvar carcinoma has recently been revised, and interested readers are referred to the primary articles on this topic.[115,116]

Grossly, squamous cell carcinoma of the vulva presents as a nodular, polypoid, or verrucous mass with a tan to red surface, with the latter color due to areas of ulceration and/or congestion (Fig. 1.79A). These tumors have a cut surface that is white to pale tan that may be punctuated by yellow areas of tumor necrosis or deposits of keratin (Fig. 1.79B).

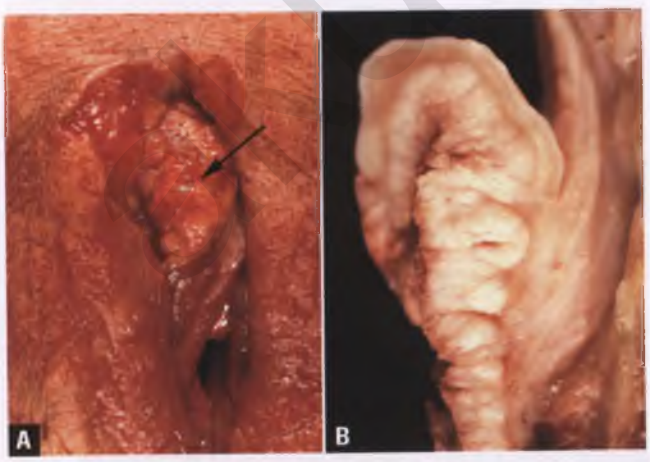

FIGURE 1.79. Gross appearance of invasive squamous cell carcinoma within two different vulvectomy specimens. **A**: The arrow marks a 2.5-cm nodular mass. **B**: The sectioned surface of this formalin-fixed, 5-cm polypoid mass varies from white to tan.

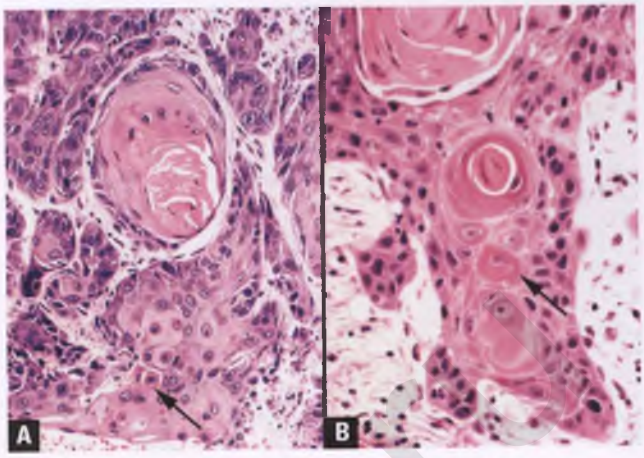

FIGURE 1.80. **A,B**: Invasive squamous cell carcinoma, keratinizing type. Both images feature keratin pearls, which are the histologic hallmark of keratinizing tumors. These pearls consist of concentric whorls of keratin that may be associated with pyknotic tumor cell nuclei. Individually keratinized cells are also evident, with representative examples marked with *arrows*.

HPV-Negative and HPV-Positive Squamous Cell Carcinomas

There are two basic types of invasive squamous cell carcinoma of the vulva. The dominant form is keratinizing squamous cell carcinoma, which represents 65% to 80% of cases, occurs in women on the older end of the age range, is not associated with HPV, and is often found within a background of differentiated VIN, lichen sclerosus, and/or lichen simplex chronicus.[4,104,117] The defining feature of keratinizing squamous cell carcinoma is the presence of keratin pearls (Fig. 1.80). Less commonly, HPV-associated squamous cell carcinoma arises from usual VIN in younger patients who are typically in the fifth and sixth decades of life. This group of squamous carcinomas has been subdivided into basaloid and warty types that are often associated with their corresponding type of usual VIN.[104] Basaloid squamous cell carcinoma infiltrates as nests and broad interconnecting bands of basaloid cells with scant cytoplasm that bear a strong resemblance to the cells of usual VIN 3 or cervical squamous cell carcinoma in situ (Fig. 1.81). Focal areas of squamous maturation and keratinization are allowed in this subtype of carcinoma. Warty squamous cell carcinoma often has a verrucous surface and is distinguished from the much more prevalent keratinizing squamous cell carcinoma by the presence of koilocyte-like tumor cells (Figs. 1.82 and 1.83).[104] Conventional squamous carcinoma of any type can exhibit pushing, infiltrative ("spray"), or mixed patterns of invasion, and there is some evidence that the "spray" pattern is associated with a worse prognosis (Figs. 1.82 and 1.84).[118]

There can be considerable overlap between the clinical and morphologic features of keratinizing, basaloid, and warty carcinoma.[45,117] p16 immunostaining can be utilized as a surrogate marker for high-risk HPV infection in this situation to help overcome the limitations of histology in

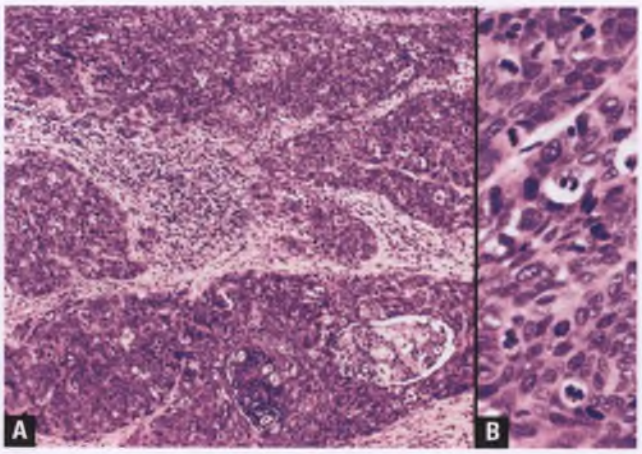

FIGURE 1.81. Invasive squamous cell carcinoma, basaloid type. **A**: Large nests of basaloid cells resembling VIN 3/CIN 3 infiltrate the stroma. **B**: Note the brisk mitotic activity in this example.

order to more accurately classify tumors with respect to their association with HPV.[117] However, given the current absence of any definite clinical significance of the HPV status of the tumor and its histologic subtype, pathologists should not agonize over these distinctions outside of a research setting.

Histologic Grade

Pathologists feel compelled to grade carcinoma, clinicians expect it, and in most organ systems, it has some prognostic significance. Unfortunately, there is no consensus on how to grade vulvar squamous carcinomas, and the significance of grade varies from study to study. In Kurman's grading system, keratinizing tumors with low nuclear grade that form large

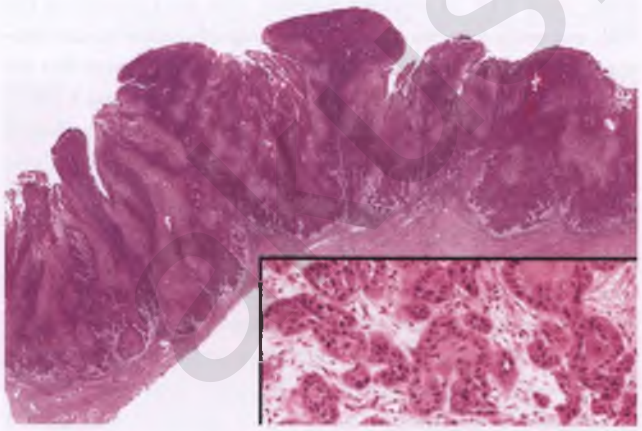

FIGURE 1.82. Invasive squamous cell carcinoma, warty type. The surface is partially verrucous. The advancing margin of the tumor is of the "pushing" type, is associated with an edematous stromal reaction, is indistinguishable from ordinary keratinizing squamous carcinoma, and is shown at higher magnification in the inset. Koilocyte-like tumor cells are scattered within the more pale-staining zones of the tumor, as illustrated in the next figure.

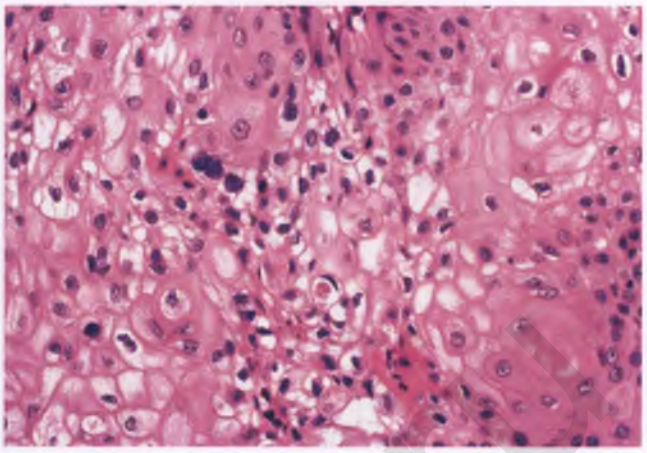

FIGURE 1.83. Invasive squamous cell carcinoma, warty type. Tumor cells that resemble koilocytes are the distinguishing feature of warty carcinoma, and are scattered throughout the pale-staining regions of the tumor.

rounded nests with numerous associated squamous pearls are considered well differentiated, whereas tumors with marked nuclear atypia consisting of small nests and cords with little keratinization are classified as poorly differentiated; moderately differentiated tumors are those with intermediate features.[104] The vast majority of keratinizing tumors are found to be well to moderately differentiated.[104] Since basaloid and warty carcinomas are sufficiently homogenous within their given subtypes that grading is impractical, Kurman does not grade these tumors.[104] The Gynecologic Oncology Group (GOG) takes a different approach, grading all subtypes of conventional squamous cell carcinoma of the vulva according to the percentage of the tumor that is composed of undifferentiated cells, which are defined as small cells with scant cytoplasm infiltrating in cords or small clusters (grade 1: no such cells; grade 2: 1%–33% undifferentiated cells; grade 3: 34%–50% undifferentiated

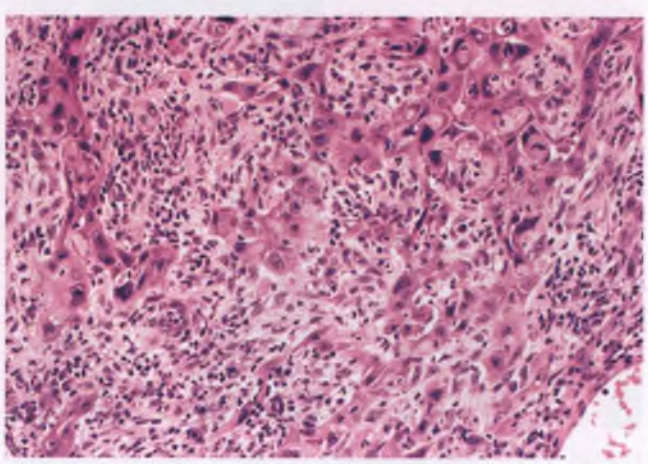

FIGURE 1.84. Squamous cell carcinoma with an infiltrative or "spray" pattern of growth. Tumor cells occurring singly and in irregular strands raggedly infiltrate the stroma.

cells; grade 4: more than 50% undifferentiated cells).[119] To add to the confusion, a major textbook of gynecologic pathology describes the GOG grading system, but cites significantly different percent ranges of undifferentiated cells for grades 2 through 4.[120]

Recognizing and Measuring Early Stromal Invasion

In some cases, it can be quite difficult, if not impossible, to distinguish architectural complexity within VIN due to tangential sectioning and/or involvement of skin adnexal structures from early stromal invasion. Features that facilitate recognition of actual stromal infiltration are (a) squamous maturation of the nests of infiltrating epithelium, which takes the form of an abrupt transition to cells with more abundant eosinophilic cytoplasm, sometimes with visible intercellular bridges and/or production of keratin; (b) an associated stromal reaction, with desmoplasia being more specific for invasion than edema and chronic inflammation; (c) tongues of infiltrating carcinoma with scalloped and/or jagged contours; and (d) atypical epithelium with highly complex, anastomosing growth patterns (Figs. 1.85 and 1.86). Note that the first criterion related to squamous maturation is applicable only to invasion originating from usual VIN, since maturation is a feature of differentiated VIN.

Once stromal invasion has been recognized, the depth of invasion is measured to the nearest tenth of a millimeter from the epithelial–stromal junction of the most superficial dermal papillae that is adjacent to the tumor to the deepest point of invasion.[121] In large tumors, it may be technically difficult or impossible to include adjacent noninvasive tissue and the deepest focus of invasion in the same section. However, this is not a critical issue, since the precision of the measurement of depth of invasion lessens in importance as the tumor advances deeply into the stroma. Some investigators prefer tumor thickness, which is measured to the nearest tenth of a millimeter from the surface of a nonkeratinized tumor or the granular layer of a keratotic tumor to the deepest point of invasion, as a more practical measurement.[119] Note that tumor thickness may underestimate the depth of invasion in ulcerated tumors and overestimate it in exophytic ones.[122]

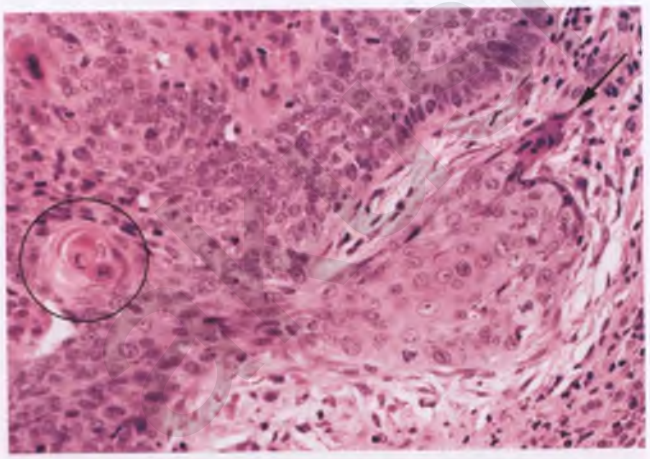

FIGURE 1.85. Nest of invasive squamous cell carcinoma arising within VIN 3. Squamous maturation within usual VIN, as seen in the circled area as a whorl of keratinized cells, often serves as a clue to impending or nearby invasion. The cells within the invasive nest also show maturation, with more abundant, eosinophilic cytoplasm than the focus of VIN, which exhibits palisading of basal layer nuclei near the top right. Note the jagged point of the invasive nest in an area with densely keratinized cytoplasm (*arrow*), and the edematous stromal reaction surrounding the area of invasion.

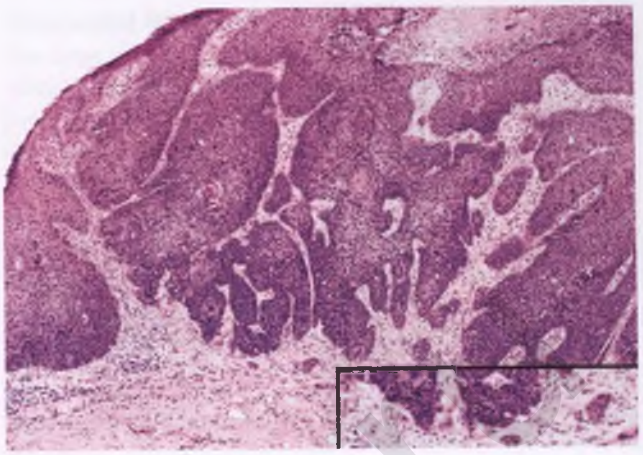

FIGURE 1.86. Invasive squamous cell carcinoma at an early stage of development. Stromal invasion is indicated by (a) central architectural complexity beyond what could be explained by tangential sectioning and/or skin appendage involvement, (b) an advancing margin composed of jagged nests of tumor cells, and (c) dropoff of scattered small clusters of tumor cells with squamous maturation associated with an edematous stromal reaction (see inset). Residual VIN 3 is most apparent at left.

Differential Diagnosis

As discussed in the section on usual VIN, tangential sectioning of skin adnexal structures involved by VIN can simulate invasive squamous cell carcinoma. The section on basal cell carcinoma lists features that help to distinguish it from basaloid squamous cell carcinoma. The distinction of warty squamous cell carcinoma from verrucous carcinoma is discussed in the section on verrucous carcinoma.

Keratoacanthoma is a controversial entity of presumed pilosebaceous origin that is generally regarded as a benign, well-differentiated squamous epithelial neoplasm. It rarely occurs on the vulva, and is distinguished from squamous cell carcinoma by its rapid growth, tendency for spontaneous regression, central keratin-filled crater, less infiltrative margins, lack of marked nuclear atypia, lack of atypical mitotic figures, and absence of adjacent VIN (Fig. 1.87).[30]

Prognosis and Initial Treatment

The prognosis of vulvar squamous cell carcinoma is largely driven by the stage of the tumor. Five-year survival rates drop significantly with increasing stage, and range from >90% for stage I

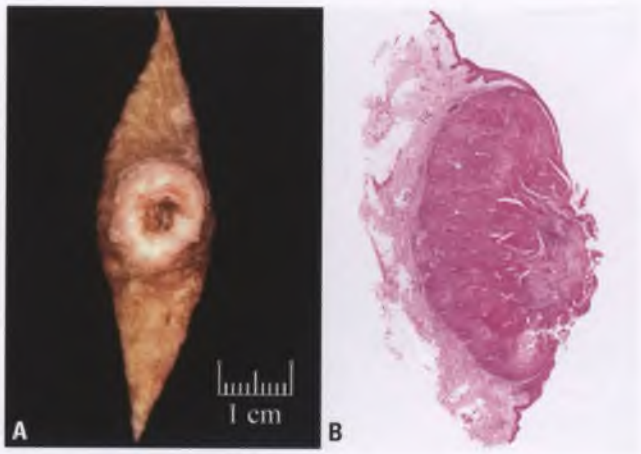

FIGURE 1.87. Keratoacanthoma. **A**: The nodule within this skin ellipse exhibits the typical gross appearance with a central keratin-filled crater. **B**: At low magnification, the presence of central keratinous material and the lack of jagged dermal infiltration can be appreciated (skin surface is at right).

to roughly 30% for stage IV.[123] Localized solitary tumors that are ≤ 2 cm in greatest dimension and invasive to a depth of ≤1 mm are referred to as superficially invasive and classified as stage Ia.[115,124] Patients with such tumors are at minimal (<1%) risk for inguinal lymph node metastasis, have an excellent prognosis, and can be treated by wide local excision.[122,124,125] As tumors invade more deeply, the incidence of nodal spread quickly becomes significant (approximately 15% for tumors that are 3 mm thick and 30% for those that have a thickness of 5 mm).[119,126] Accordingly, surgical treatment of tumors >1 mm deep may involve more extensive removal of vulvar tissue and generally includes a superficial inguinal lymph node dissection; patients with locally advanced tumors may be treated with preoperative chemoradiation.[114,127,128] Both pathologists and clinicians should be aware that negative superficial inguinal lymph nodes are highly predictive of the lack of involvement of deep pelvic nodes, whereas positive superficial inguinal nodes are associated with deep pelvic lymph node involvement in roughly one-third of cases.[129] Sentinel lymph node biopsy is increasingly being utilized in the staging of patients with squamous carcinoma of the vulva and hopefully will identify a subset of patients with localized disease that can be spared a lymph node dissection.[130,131]

The Pathology Report

The most important pathologic features to include in the pathology report of squamous cell carcinoma of the vulva are the size of the tumor, its depth of invasion, tumor grade, the presence or absence of angiolymphatic invasion, the status of the resection margins, and the status of any lymph nodes or other tissue submitted for staging purposes (the distinction of true angiolymphatic invasion from artifactual changes is discussed in the sections on retraction artifact and iatrogenic displacement of epithelium near the end of Chapter 3). Lymph node status should include the number of involved nodes, the total number of nodes examined, the greatest dimension of the largest involved node, and the presence or absence of extranodal extension, since these details provide additional prognostic information.[123,132–134] Not surprisingly, as the number of involved nodes and the size of the largest metastasis increases, the prognosis worsens; the presence of extranodal extension is also an adverse prognostic indicator. Recognition of the importance of these features has resulted in their incorporation into the subclassification of stage III tumors in the 2008 revised FIGO staging for carcinoma of the vulva.[115,116]

Verrucous Carcinoma

Verrucous carcinoma is a rare variant of well-differentiated squamous carcinoma that is locally destructive but does not possess metastatic potential.[135,136] Most investigators consider the giant condyloma of Buschke–Lowenstein to be an outmoded synonym for anogenital verrucous carcinoma. Most women with verrucous carcinoma of the vulva are postmenopausal and present with a large, exophytic, cauliflower-like mass. Superficial biopsies of these lesions are impossible to diagnose correctly and are likely to be misinterpreted as squamous papilloma or suggestive of condyloma. Accurate interpretation is facilitated by the clinician conveying the size of the lesion and submitting a representative sample that includes the epithelial–stromal interface.

The surface of verrucous carcinoma is hyperkeratotic, papillomatous, and acanthotic. These tumors characteristically exhibit no significant nuclear atypia, and are recognized by their downward penetration into the dermis in the form of tongues of squamous epithelium with pushing, rounded, bulbous contours (Figs. 1.88 and 1.89). Koilocytes are not present, and most recent studies have not found an association between HPV infection and verrucous carcinoma.[137,138] These tumors should be sampled extensively to exclude the possibility

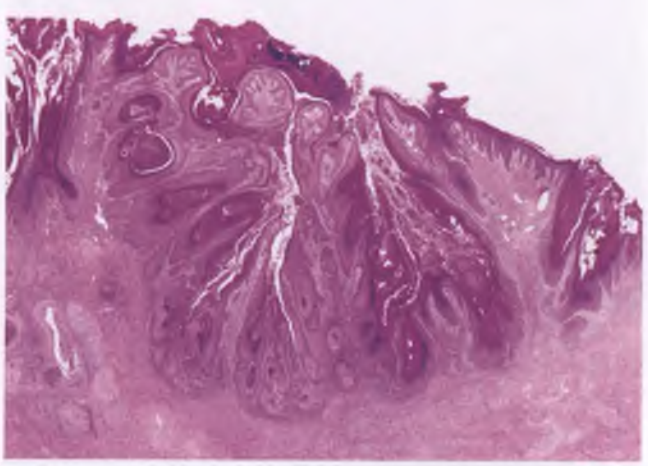

FIGURE 1.88. Verrucous carcinoma. This low-magnification image demonstrates a hyperkeratotic, papillomatous lesion with invasion into the dermis by extensions of squamous epithelium with a broad, pushing border.

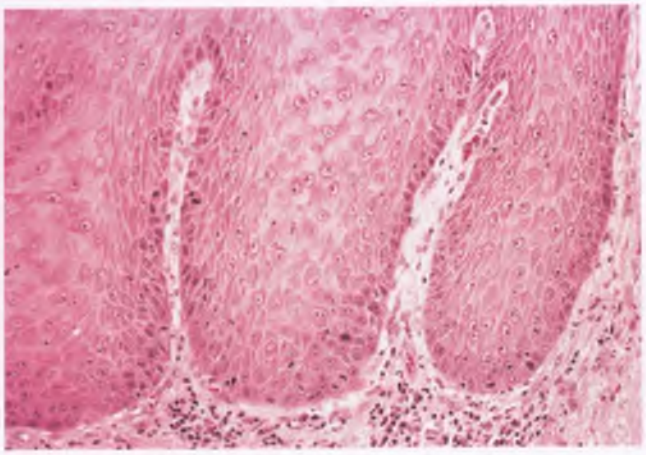

FIGURE 1.89. Verrucous carcinoma. Tongues of well-differentiated, mature squamous epithelium with bulbous contours infiltrate the dermis, which is chronically inflamed.

of a component of conventional squamous cell carcinoma, since the presence of conventional elements is indicative of a risk for metastatic disease.

A peculiar alteration of squamous differentiation that occurs within acanthotic squamous epithelium has recently been identified in association with some verrucous carcinomas and has been flagged as a possible precursor or marker of increased risk for development of this neoplasm.[138] This lesion, termed vulvar acanthosis with altered differentiation, features plaque-like layers of parakeratosis overlying thickened squamous epithelium with an absent or inconspicuous granular layer and superficial keratinocytes with pale-staining cytoplasm (Fig. 1.90). Although not considered a type of VIN, patients with this lesion should be followed closely so that any suspicious lesions that develop can be biopsied early in their clinical course.[138]

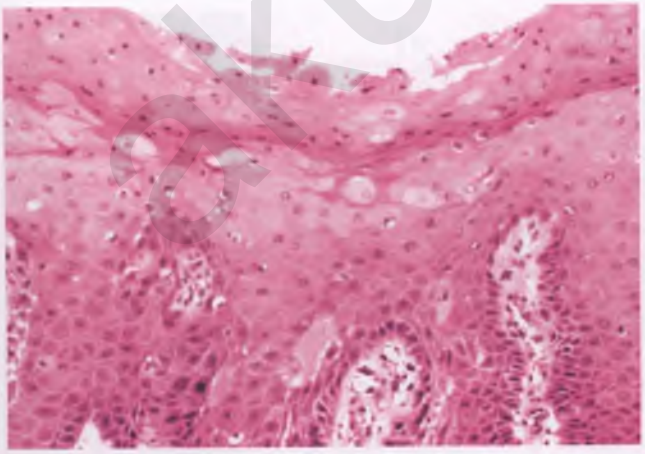

FIGURE 1.90. Vulvar acanthosis with altered differentiation. Note the plaque-like parakeratosis, loss of keratohyalin granules, and cytoplasmic pallor of the superficial keratinocytes.

Differential Diagnosis

The large size, solitary nature, tendency for occurrence in an older age group, lack of koilocytosis, and characteristic pushing pattern of downward ingrowth into the dermis of verrucous carcinoma facilitate its distinction from condyloma acuminatum. The features of warty squamous cell carcinoma that help to distinguish it from verrucous carcinoma are the presence of cells with HPV cytopathic effect within the central portion of some tumor cell nests, significant nuclear atypia and mitotic activity within the basal and parabasal regions of the nests, and a more infiltrative pattern at the base of the tumor.[104]

Sarcomatoid Squamous Cell Carcinoma

A few case reports of sarcomatoid squamous cell carcinoma of the vulva have been published.[139] The uterine cervical form of this aggressive tumor is similar to the vulvar form, and is described and illustrated in Chapter 3 (see Fig. 3.177).

Acantholytic Squamous Cell Carcinoma

Acantholytic squamous cell carcinoma is a rare variant that forms spaces that can result in the simulation of adenocarcinoma or angiosarcoma (Fig. 1.91).[140,141] Recognition of this variant is facilitated by finding areas of transition with more conventional squamous cell carcinoma or by identifying individually keratinized cells or intercellular bridges, which are indicative of squamous differentiation. If indicated, special stains can also be utilized (e.g., a mucin stain and an immunohistochemical panel that includes cytokeratin and the vascular markers CD31 and CD34).

BASAL CELL CARCINOMA[142]

Cutaneous basal cell carcinoma is the single most common malignant neoplasm and is seen on a daily basis in most

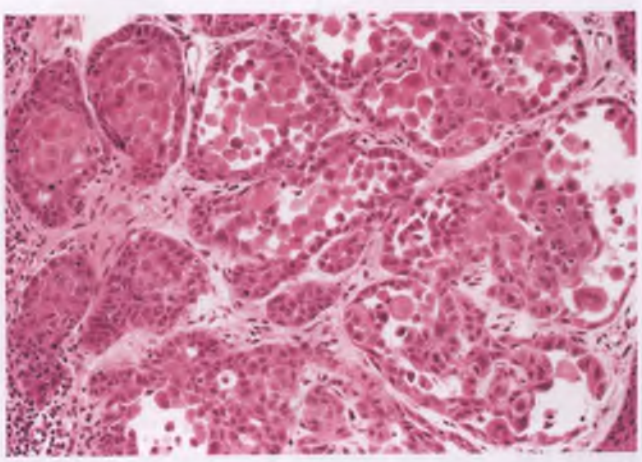

FIGURE 1.91. Acantholytic squamous cell carcinoma with a pseudoglandular pattern simulating adenocarcinoma. A few nests of conventional squamous carcinoma are at left. A small amount of surface epithelium is at right.

surgical pathology laboratories. However, this tumor represents only 3% to 5% of vulvar cancers, presumably due to the protection of this site from exposure to the sun. Vulvar basal cell carcinoma typically presents as a partially ulcerated nodule or plaque measuring up to a few centimeters on the labium majus of an elderly woman. Other than the absence of a background of actinic damage, the histologic features of vulvar basal cell carcinomas are identical to those that are commonly seen in sun-exposed skin (Fig. 1.92). Because of the low-grade behavior of basal cell carcinomas and their extremely low rate of lymph node metastases, wide local excision without lymphadenectomy is considered the treatment of choice.

Differential Diagnosis

Tumors that can be confused with basal cell carcinoma include trichoepithelioma, which is a benign tumor of hair follicle origin, and basaloid squamous cell carcinoma. Both trichoepithelioma and basal cell carcinoma are composed of basaloid cells whose nests exhibit peripheral palisading of nuclei, and both can contain horn cysts, exhibit areas in which the basaloid cells are interconnected by narrow strands in a lacelike pattern, and have lobules of tumor cells with invaginated contours. However, in contrast to basal cell carcinoma, trichoepithelioma rarely ulcerates, lacks the retraction artifact at the interface between the basaloid tumor nests and the stroma, and has a distinctive fibroblastic stroma that envelopes the tumor lobules (Fig. 1.93).[28] Unlike basal cell carcinoma, the basaloid variant of squamous cell carcinoma is usually associated with high-grade VIN, lacks palisading of the peripheral layer of cells within the basaloid tumor nests, and is composed of cells that exhibit a greater degree of nuclear atypia.[104] In addition, a tumor that exhibits a lobulated, circumscribed interface of its basaloid nests with the underlying stroma is more likely to be a basal cell carcinoma than a basaloid squamous cell carcinoma.[104]

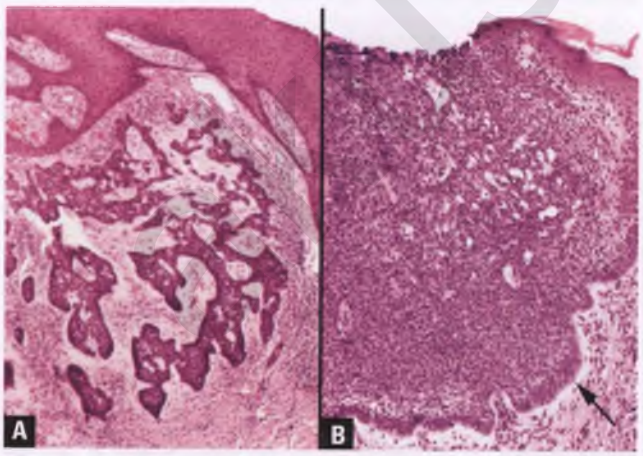

FIGURE 1.92. Basal cell carcinoma. **A**: Irregular nests of basaloid cells infiltrate the dermis. **B**: Superficial aspect of a vulvar basal cell carcinoma, highlighting the retraction artifact and peripheral palisading of nuclei along the epithelial–stromal interface that are characteristic of these tumors (*arrow*).

BARTHOLIN'S GLAND CARCINOMA[143–146]

Carcinoma of Bartholin's gland is rare and accounts for only a few percent of vulvar carcinomas. This tumor typically presents as a painless vulvar mass in a middle-aged adult woman, and is often clinically mistaken for a Bartholin's cyst. Squamous cell carcinoma is the dominant histologic subtype, followed by adenocarcinoma, adenoid cystic carcinoma, and other miscellaneous carcinomas. The most definitive cases exhibit a transition between the normal Bartholin's gland and the malignant neoplasm. However, most investigators do not require the presence of such a transition, and also accept as Bartholin's gland carcinomas those tumors that occur deep in a labium majus in the expected anatomic location, provided that there is no personal history of another primary tumor with similar histology.

PAGET'S DISEASE

Although Paget's disease of the vulva is the most common form of extramammary Paget's disease, it is rare and accounts for only about 1% of vulvar cancers. It typically presents as an erythematous, crusting, pruritic "rash" in an elderly woman (median age of 65 years).[147] In the vast majority of cases, this malignancy originates as a primary intraepidermal adenocarcinoma, with most investigators favoring derivation from the poral portion of the sweat ducts or from intraepidermal stem cells.[147,148] Only rare examples of vulvar Paget's disease represent secondary epidermotropic spread by a neighboring carcinoma, which is usually of anorectal or urinary bladder origin.[149] In contrast, nearly all cases of mammary Paget's disease are related to epidermotropic spread or direct extension of an underlying intraductal carcinoma (with or without an associated invasive component) that extends from one or more involved lactiferous ducts to the epidermis of the nipple.

Histologically, vulvar Paget's disease is characterized by the presence of malignant cells scattered throughout the epidermis,

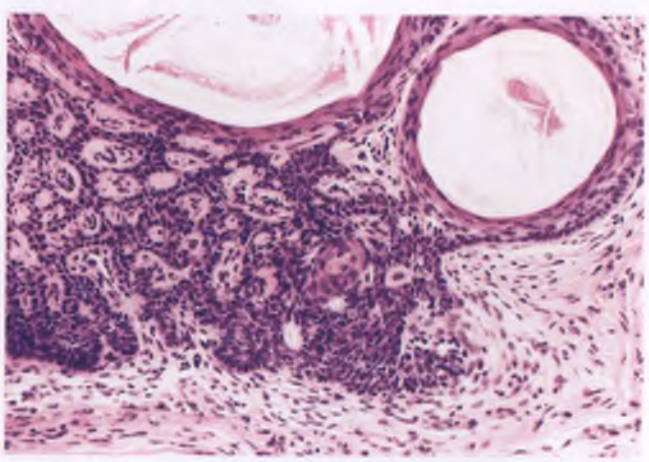

FIGURE 1.93. Trichoepithelioma. Note the horn cysts, invaginated contour of some of the tumor lobules, the partial lacelike architecture, the enveloping fibroblastic stroma, and the absence of retraction artifact.

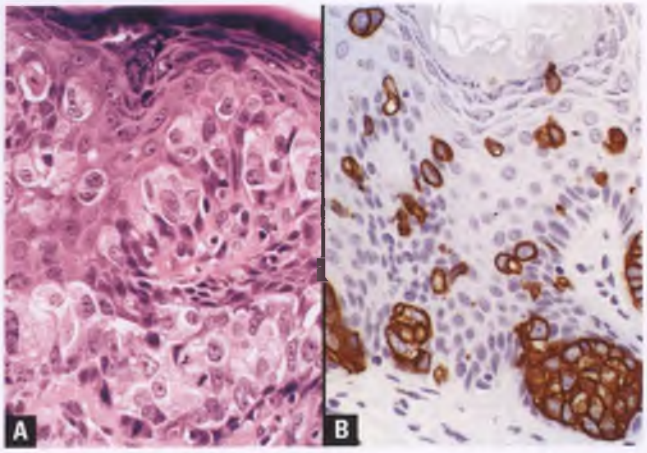

FIGURE 1.94. Paget's disease of the vulva. **A**: Tumor cells are concentrated in the basal region, but are present throughout all levels of the epithelium. **B**: In contrast to the native squamous epithelium, the tumor cells are strongly immunoreactive for cytokeratin 7.

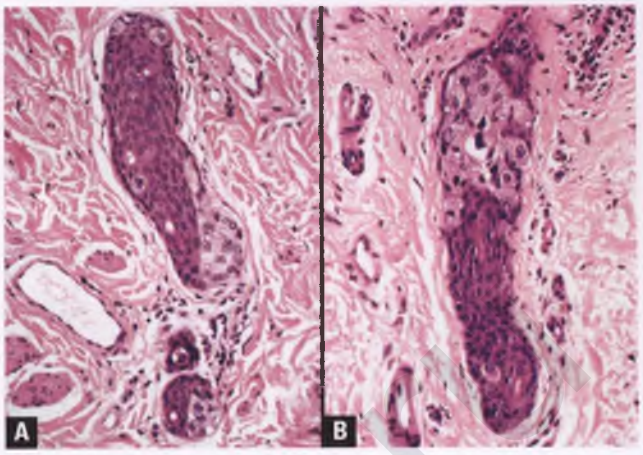

FIGURE 1.95. **A,B**: Paget's disease with adnexal involvement (two different cases). Large atypical cells with abundant pale cytoplasm, occurring both singly and in nests, are seen within hair follicles.

disposed singly and in small clusters and often concentrated within the lower aspect of the epithelium (Fig. 1.94A). Paget cells can be highlighted with a CK7 immunostain, which does not stain the native squamous epithelium and serves as a highly sensitive, although not specific, marker for these cells (Fig. 1.94B).[147,150,151] The neoplastic nuclei are generally vesicular and have prominent nucleoli, but it is the presence of abundant pale cytoplasm that allows for recognition of these cells at low magnification in routinely stained sections. Occasional signet-ring forms are often interspersed, and may rarely be dominant; intraepithelial glands may also be seen.[147,152] Extension of Paget cells into cutaneous adnexal structures is an expected finding that most often affects hair follicles (Fig. 1.95).[147,152]

In roughly one-third of cases, associated squamous hyperplasia occurs in acanthotic, papillomatous, or fibroepithelioma-like patterns.[153] The latter pattern, which resembles the variant of basal cell carcinoma known as the fibroepithelioma of Pinkus, is uncommon in vulvar as compared to perianal Paget's disease, but is worthy of illustration because of the ease at which it can be misinterpreted (Fig. 1.96).[153] Yet another pitfall is misinterpreting the papillomatous pattern of squamous hyperplasia that may be associated with Paget's disease as a condyloma, given its papillary architecture and the presence of scattered atypical cells with vacuolated cytoplasm that may be mistaken for koilocytes (Fig. 1.97).[153]

In addition to helping to confirm a diagnosis of vulvar Paget's disease, CK7 immunostaining can also assist in the detection and/or confirmation of foci of microinvasion, which is present in approximately 25% of cases.[147] Foci of microinvasive adenocarcinoma that are found within vulvar Paget's disease that measure ≤1mm in depth do not appear to have an adverse impact on prognosis when the possibility of foci of deeper invasion has been meticulously excluded.[147,154]

Although the CK7 immunostain has utility and generates oohs and aaahs during case presentations, the diagnosis

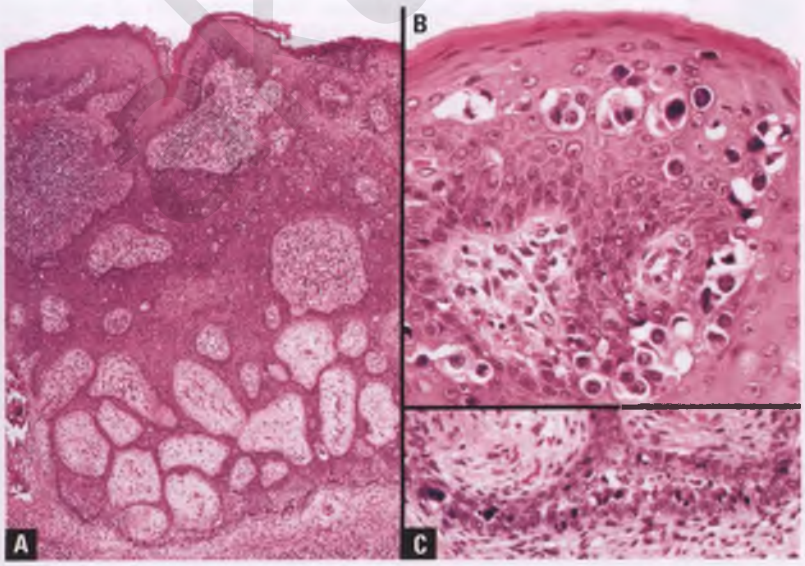

FIGURE 1.96. Paget's disease with fibroepithelioma-like hyperplasia. **A**: The squamous epithelium is hyperplastic, and forms lacelike anastomosing strands enveloping islands of pale-staining stroma at its deeper aspect. **B**: Classic Paget's disease found adjacent to the fibroepitheliomatous focus. **C**: Unlike typical cells of Paget's disease, those within fibroepithelioma-like areas often have pyknotic, shrunken nuclei.

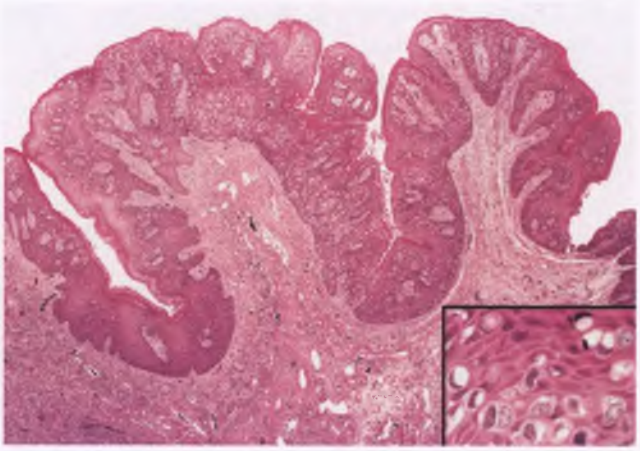

FIGURE 1.97. Paget's disease associated with papillomatous squamous hyperplasia. The lesion resembles a condyloma at low magnification. The inset shows the scattered vacuolated cells of Paget's disease rather than the koilocytes of HPV infection.

of vulvar Paget's disease often requires no more than a PAS with diastase or mucicarmine stain to confirm the presence of neutral mucin within the cytoplasm of some of the tumor cells (Fig. 1.98).[150] A positive mucin stain, which is almost always forthcoming in samples of adequate size, quickly and cost-effectively excludes most of the other entities in the differential diagnosis, as discussed below. In small samples, it is prudent to have several unstained sections cut in reserve for possible immunohistochemistry at the time the tissue is sectioned for the mucin stain, since one does not want to cut through the lesion and then realize that immunostains are warranted due to the absence of demonstrable intracytoplasmic mucin.

In addition to CK7, the immunoreactivity pattern of vulvar Paget's disease has been studied with a multitude of other antibodies.[147,148,150,154] For diagnostic purposes, expected

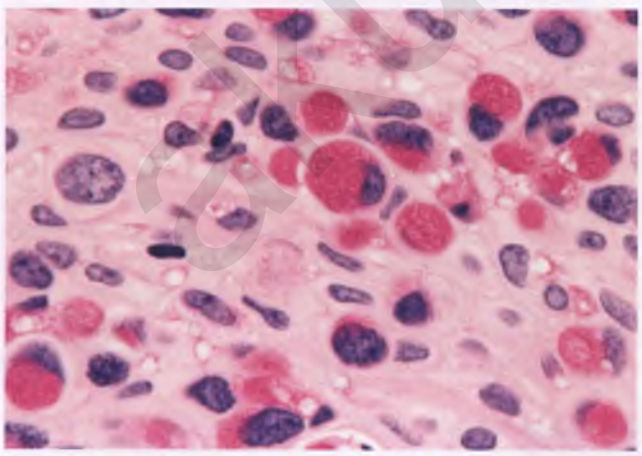

FIGURE 1.98. Paget's disease. In this example, many of the adenocarcinomatous cells infiltrating the squamous epithelium are signet-ring cells that contain PAS-positive, diastase-resistant intracytoplasmic mucin globules.

immunoreactivity with CK7 and carcinoembryonic antigen (CEA) and absence of staining with S100 are of greatest practical value when constructing a small antibody panel as part of the evaluation of a difficult pagetoid lesion. Although immunoreactivity of Paget cells with CAM 5.2 is expected, its staining pattern is mirrored by CK7 and its use is considered redundant in this situation (note that the most recent data sheet from Becton Dickinson for CAM 5.2 indicates that this antibody "cocktail" is directed against cytokeratins 7 and 8 rather than the originally reported reactivity against cytokeratins 8, 18, and 19). If the patient has a history of carcinoma of the anorectum or urinary bladder or there are other reasons to suspect secondary Paget's disease, immunostains for CK20 and GCDFP-15 should also be performed. Secondary Paget's disease will often have a CK20-positive and GCDFP-15-negative immunophenotype that is quite unusual for primary Paget's disease, and its staining pattern will match that of the internal regional cancer from which it has spread.[147,149]

Differential Diagnosis

The differential diagnosis of Paget's disease includes superficial spreading malignant melanoma, pagetoid squamous cell carcinoma in situ, VIN 3 with mucinous differentiation, and signet-ring artifact. For a more complete listing and discussion of processes with intraepithelial pagetoid cells, the reader is referred to the article by Kohler et al.[155]

- The presence of abundant intracytoplasmic melanin pigment that is readily apparent within intraepithelial malignant cells in routinely stained sections favors melanoma. However, such pigment can also occasionally be acquired by Paget cells, although it is generally present in lesser amounts within fewer cells, and often requires a Fontana–Masson stain for its identification.[156] Much more definitive in the distinction between melanoma and Paget's disease are mucin stains (negative in melanoma and usually positive in Paget's disease) and differences in immunohistochemical staining patterns. In contrast to Paget's disease, the tumor cells of melanoma are CK7 and CEA negative and typically express one or more of the melanoma markers S100, HMB-45, and Melan-A.
- Pagetoid squamous cell carcinoma in situ of the vulva is rare and features intraepithelial dysplastic keratinocytes with pale cytoplasm scattered singly and in nests throughout all levels of the squamous epithelium (Fig. 1.99).[157,158] The histologic appearance created by this pagetoid pattern of spread is quite similar to Paget's disease, and both processes may confusingly contain cells with intracytoplasmic melanin pigment.[155] Helpful clues to the squamous nature of the lesional cells include identification of single-cell keratinization, intercellular bridges, and cytoplasmic keratohyalin granules.[155] In addition, unlike typical extramammary Paget's disease, pagetoid squamous cell carcinoma in situ typically also has foci of conventional VIN 3, its constituent cells do not contain intracytoplasmic mucin, and it has a CEA-negative, p16-positive rather than CEA-positive, p16-negative immunophenotype.[158] Other immunostains also have some utility in this

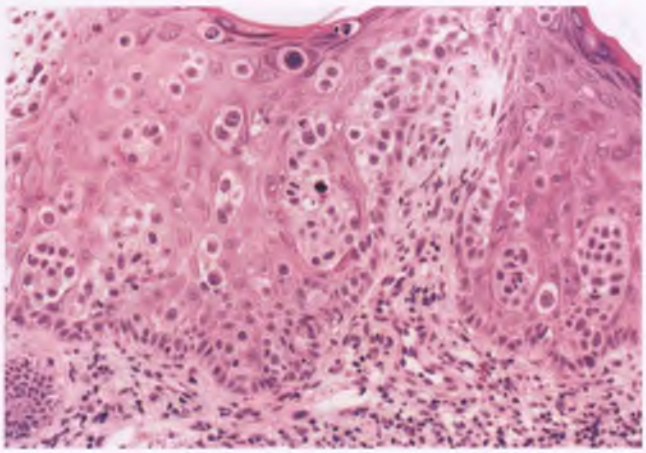

FIGURE 1.99. Pagetoid squamous cell carcinoma in situ. The resemblance to Paget's disease is striking.

setting: immunoreactivity with GFCDP-15 supports Paget's disease, while p63 immunoreactivity, with the pagetoid cells blending into the background of surrounding p63-positive keratinocytes, supports pagetoid squamous cell carcinoma in situ.[158] It is noteworthy that CK7 immunostaining does not help to resolve this differential diagnosis, since the neoplastic cells of both disorders are CK7 positive.[157,158]

- VIN 3 with mucinous differentiation is a recently described, rare phenomenon in which cells with abundant intracytoplasmic mucin and bland, eccentrically placed nuclei are scattered within an intraepithelial lesion that otherwise has the appearance of VIN 3.[159] These mucinous cells share with those of Paget's disease immunoreactivity for CK7, CAM5.2, and CEA, but can be distinguished by their bland morphology and their presence within a background of p16-positive dysplastic keratinocytes.[159] Although the histogenesis of the mucinous cells is unknown, a metaplastic origin is favored.[159]
- Signet-ring artifact, which is discussed in more detail in the section on artifacts in Chapter 3, can also mimic Paget's disease, but is distinguished by the presence of intercellular bridges between the vacuolated keratinocytes, the absence of formation of cell clusters, and the lack of intracytoplasmic mucin (Fig. 1.100).

Behavior

Paget's disease frequently recurs whether or not the resection margins are judged to be involved.[152,154] This unfortunate circumstance is due to a combination of the fact that the boundaries of Paget's disease are often difficult to delineate clinically, lesions may be multifocal, and it can be difficult to detect focal margin involvement histologically.

MALIGNANT MELANOMA

Clinical Features[160–163]

Approximately 5% to 10% of vulvar cancers are malignant melanomas, which occur predominantly in Caucasian women with a mean age of about 60 years. The typical presentation of these neoplasms is as a vulvar mass that may be associated with bleeding or pruritus. Most vulvar melanomas occur in the glabrous (smooth and bare) skin or along the border between glabrous and hair-bearing skin. Most are pigmented tumors that contain varying, mottled shades of brown, black, and other colors. However, approximately 30% of vulvar melanomas are macroscopically amelanotic (nonpigmented), and may clinically simulate a pyogenic granuloma (lobulated capillary hemangioma) or squamous cell carcinoma.

Histologic Types[160,164]

In sharp contrast to nonvulvar cutaneous melanomas, the most common type of vulvar melanoma in the largest series of these tumors resembles acral lentiginous melanoma, and is often

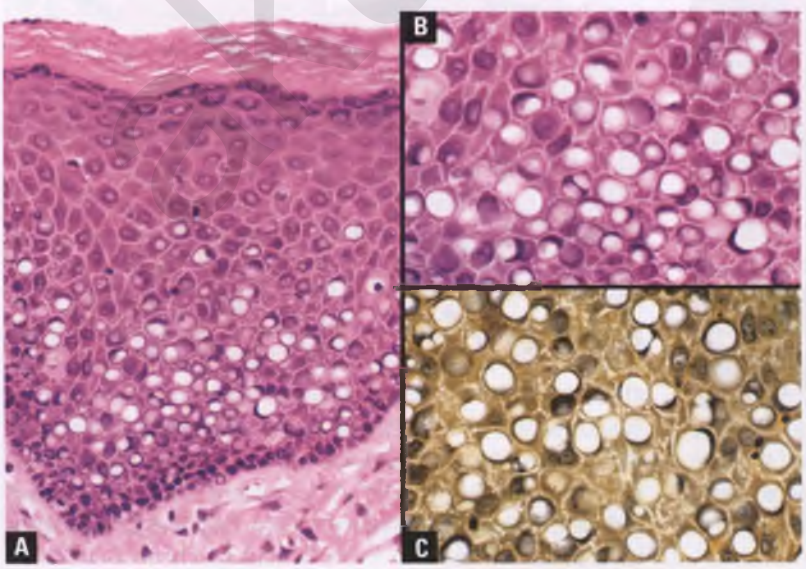

FIGURE 1.100. Signet-ring artifact in hyperkeratotic squamous epithelium of the vulva. **A**: Several vacuolated keratinocytes are present in the lower half of the epithelium. Note the absence of formation of cell clusters. **B**: Intercellular bridges, which are a marker of squamous differentiation, are present between many of the vacuolated keratinocytes. **C**: The vacuoles within the keratinocytes do not contain mucin, as evidenced by this negative mucicarmine stain.

referred to as malignant melanoma of mucosal lentiginous type to avoid the nonsensical use of the term "acral" in this situation.[160] Nodular and superficial spreading melanomas also occur in the vulvar region. Lentigo maligna melanoma is not seen in the vulva, since it is associated with sun exposure and is found within a background of actinically damaged skin.

Invasive mucosal lentiginous melanoma is characterized by (a) an in situ component composed of atypical melanocytes occurring singly and in small clusters in a concentrated linear arrangement along the basal region of elongated rete ridges with limited infiltration of the upper epidermis and (b) an invasive component within the dermis that usually exhibits a spindle cell morphology that may be associated with a desmoplastic response (Fig. 1.101). Nodular melanoma typically presents as a rapidly growing, nodular, polypoid, or plaque-like mass protruding above the skin surface, and may be either covered by squamous epithelium or ulcerated (Fig. 1.102). This variant may exhibit atypical junctional activity and/or transepidermal migration of tumor cells in the epidermis overlying the tumor, but by definition does not exhibit intraepidermal extension of malignant cells beyond the narrow distance encompassed by three rete ridges adjacent to the edge of the invasive component. Superficial spreading melanoma is distinguished by the prominence and peripheral extension of its in situ component, which characteristically shows transepidermal migration of large atypical melanocytes, both singly and in small nests, throughout all levels of the epithelium in what has been termed a pagetoid or buckshot distribution (Fig. 1.103). In all types of melanoma, dermal invasion is characterized by atypical melanocytes infiltrating as nests, cords, and individual cells, often in association with a lymphocytic response.

Cell Types

The invasive component of malignant melanoma may be epithelioid, spindle shaped, or a mixture of these two cell types, and exhibits a range of atypia that varies from subtle (with nevoid epithelioid cells or fibroblast-like spindle cells) to markedly anaplastic (Fig. 1.104). Epithelioid cells dominate most superficial spreading and nodular melanomas, whereas spindle-shaped cells predominate in the invasive component of acral/mucosal lentiginous melanomas.

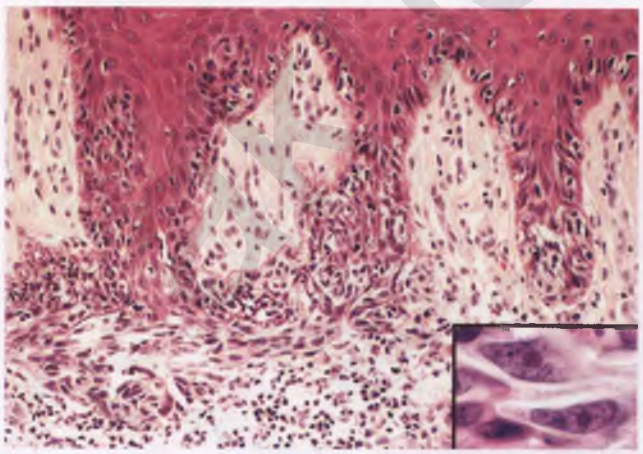

FIGURE 1.101. Malignant melanoma, mucosal lentiginous type. Atypical melanocytes are aligned along the basal portion of the elongated rete ridges, with a focus of dermal invasion by spindle-shaped melanocytes at lower left. The inset highlights the nuclear features of the invasive spindle cell component.

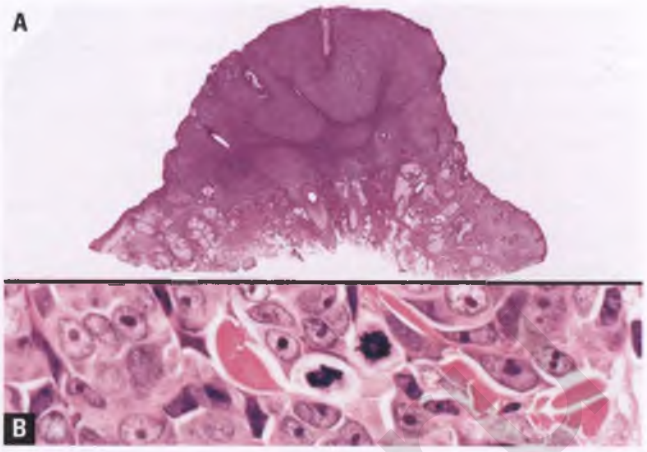

FIGURE 1.102. Malignant melanoma, nodular type. **A**: Scanning view demonstrating solid aggregates of tumor cells forming an elevated nodule. **B**: The tumor cells are epithelioid, amelanotic, mitotically active, and exhibit prominent nucleoli. The differential diagnosis of this nonvulvar melanoma includes immunoblastic lymphoma and lymphoepithelioma-like carcinoma.

Tumor Depth According to Skin Microanatomy versus Direct Measurement

In the approach developed by Clark, the depth of tumor invasion is divided into levels according to whether the melanoma is in situ (Level I), shows limited or extensive involvement of

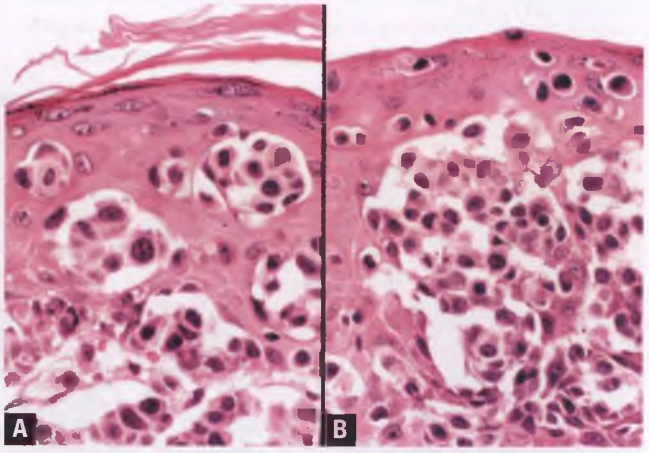

FIGURE 1.103. Malignant melanoma, superficial spreading type. Typical patterns of intraepithelial spread, with atypical melanocytes found individually and in nests throughout all levels of the squamous epithelium. **A**: Small nests of tumor cells predominate. **B**: Individual malignant melanocytes are present above a large nest of dyscohesive tumor cells.

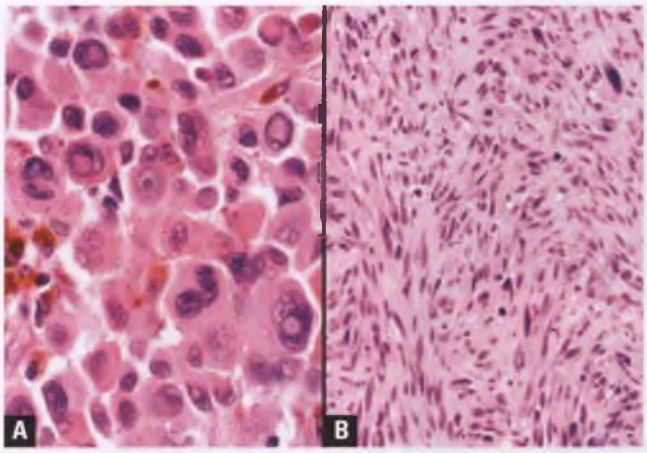

FIGURE 1.104. Malignant melanoma. **A**: Epithelioid tumor cells with marked nuclear pleomorphism. The presence of melanin pigment and intranuclear cytoplasmic inclusions within some of the tumor cells make this neoplasm easy to recognize as a melanoma. **B**: The growth of nonpigmented spindle cells in fascicles makes this melanoma difficult to distinguish from leiomyosarcoma in routinely stained sections.

the papillary dermis (Level II or III, respectively), invades the reticular dermis, which is recognized by the presence of discrete bundles of collagen that tend to be oriented parallel to the skin surface (Level IV), or extends into subcutaneous fat (Level V).[165] Not surprisingly, the higher (deeper) the level of invasion, the worse the prognosis. Breslow's method of measuring the thickness of an invasive melanoma takes a less subjective approach that involves using an optical micrometer to obtain a measurement in millimeters from the top of the granular layer (or the base of the ulcer in ulcerated tumors) to the deepest point of tumor invasion.[166] The Breslow measurement also has the advantage that it is fully applicable in sites such as the vagina and glabrous portions of the vulva that have a microanatomy in which there is no well-defined reticular layer. Melanomas with a tumor thickness of ≤ 0.75 mm have an excellent prognosis. Unfortunately, most vulvar melanomas have a thickness of ≥1.5 mm, which are associated with more aggressive behavior.[160–162]

Radial versus Vertical Growth Phase[167,168]

In recent years, the growth phase of malignant melanoma has attracted increasing attention, since only those melanomas in the vertical growth phase (and radial growth phase tumors with regression) have been shown to have metastatic potential. All the subtypes of melanoma except for the nodular variant have a radial growth phase and a prolonged period of in situ growth, which may be interrupted by development of a superimposed nodule of vertical growth phase melanoma. The radial growth phase refers to more than just horizontal, intraepithelial growth in pagetoid or lentiginous patterns, but also includes superficial invasion of the papillary dermis by similar-appearing cells disposed singly and in small nests in a platelike configuration. In contrast, the vertical growth phase is characterized by one or more large, expansile nests of dermal melanocytes that usually exhibit more nuclear atypia and more mitotic activity than the cells within the smaller nests of the overlying in situ component, and is more likely to be associated with tumor-infiltrating lymphocytes. Although the growth phase of a melanoma is an important prognostic factor, its independent utility in the vulva is limited, since nearly all melanomas with a thickness of >1 mm are in the vertical growth phase. Nevertheless, useful prognostic information can be obtained from the growth phase in the unusual circumstances in which a superficial (<0.75 mm) melanoma is found to be in the vertical growth phase (worse prognosis than would otherwise be expected) or a melanoma between 0.75 and 1 mm is found to still be in the radial growth phase (better prognosis than would otherwise be expected).

Reporting Pathologic Aspects of Malignant Melanoma[167,168]

The pathology report on malignant melanoma should include the tumor type, a measurement in millimeters of tumor thickness using Breslow's method, Clark's level when relevant, radial versus vertical growth phase, cell type, mitotic index of vertical growth phase tumors, the status of the resection margins (if negative, indicate distance from tumor to closest margin), and the presence or absence of (a) angiolymphatic invasion (unfavorable); (b) perineural invasion (unfavorable); (c) ulceration (unfavorable); (d) numerous tumor-infiltrating lymphocytes (favorable); (e) regression of the dermal component of a radial growth phase tumor, as characterized by vascular scar tissue associated with melanophages and scattered lymphocytes (unfavorable, since it implies a tumor of greater depth than currently apparent); and (f) satellite tumor nodules (unfavorable).

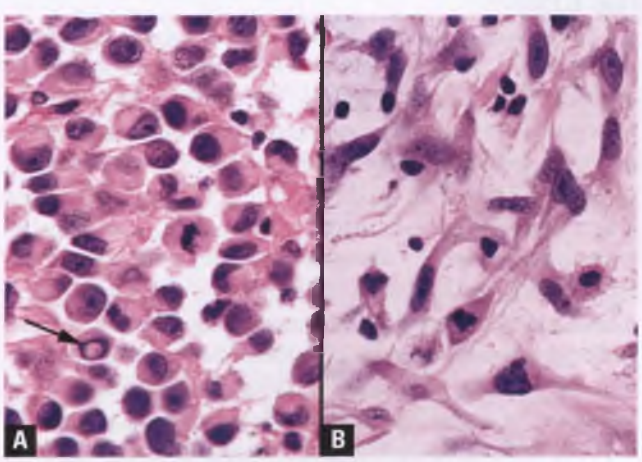

FIGURE 1.105. Unusual variants of malignant melanoma. **A**: Melanoma with signet-ring cells simulating signet-ring adenocarcinoma. The presence of an intranuclear cytoplasmic inclusion (*arrow*) is a clue to the correct diagnosis. **B**: Myxoid melanoma simulating a myxoid sarcoma. This focus was present in a metastasis that also contained more conventional areas of melanoma.

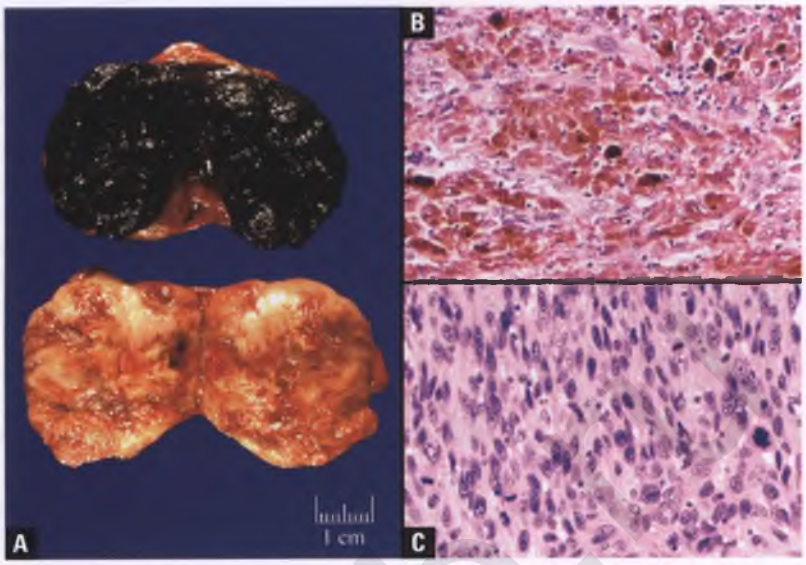

FIGURE 1.106. Malignant melanoma metastatic to lymph nodes. **A**: Bivalved lymph node metastases from the same patient. The top node is black due to heavy deposits of melanin pigment, whereas the bottom node is amelanotic with prominent areas of hemorrhage and necrosis. **B**: Histology of the pigmented node. **C**: Histology of the amelanotic node.

Differential Diagnosis and Immunophenotype

In one scenario, the pathologist struggles with the diagnosis of melanoma versus nevus. The most helpful features that favor melanoma over nevus are listed in the section on atypical genital nevi. In other situations, the tumor is obviously malignant, but its melanocytic nature is not immediately apparent. Such is the case for melanomas that appear to be nonpigmented histologically, which have a broad differential diagnosis that includes poorly differentiated carcinoma, extramammary Paget's disease, sarcoma, and large cell lymphoma. To add to its reputation as a great mimicker of other malignant neoplasms, nonpigmented signet-ring, myxoid, and other unusual forms of melanoma are also encountered on rare occasions (Fig. 1.105).[169]

Whenever a poorly differentiated malignant neoplasm of uncertain lineage is encountered, melanoma should be included amongst the diagnostic possibilities. Although the presence of brown granules of melanin pigment within tumor cells is a helpful clue to the melanocytic nature of the neoplasm, this feature varies from strikingly obvious to completely absent (Fig. 1.106). Melanoma can also be suspected if there is malignant junctional activity of pagetoid or lentiginous type involving the overlying squamous epithelium, provided that Paget's disease has been excluded as discussed earlier in this chapter. Although certainly not specific for melanocytic differentiation, the presence of intranuclear cytoplasmic inclusions or an admixture of epithelioid and spindle cell growth patterns in a poorly differentiated malignant neoplasm should prompt serious consideration for melanoma. Immunohistochemistry often plays an important role in arriving at the correct diagnosis, and a screening panel of S100, cytokeratin, and leukocyte common antigen can quickly narrow the diagnostic possibilities (isolated S100 positivity supports melanoma, isolated cytokeratin positivity supports carcinoma or epithelioid sarcoma, isolated leukocyte common antigen positivity supports lymphoma, and negative staining for all three markers suggests that additional immunostains are in order to further evaluate the possibilities of sarcoma and S100-negative melanoma). The melanoma markers HMB-45 and Melan-A (Mart-1) can be used to help confirm the diagnosis of melanoma, and are particularly useful in identifying those rare melanomas that are negative for S100.

MISCELLANEOUS TUMORS

In rare instances, the vulva may be involved by sweat gland carcinoma,[170] sebaceous carcinoma,[171] colonic-like "cloacogenic" adenocarcinoma,[172] Skene's gland adenocarcinoma resembling prostatic adenocarcinoma,[173] Merkel cell carcinoma,[174,175] non-Hodgkin's lymphoma,[176] Langerhans cell histiocytosis,[177] yolk sac (endodermal sinus) tumor,[178] giant cell tumor,[179] or metastatic carcinoma/melanoma.[180]

SUGGESTED READINGS

Clement PB, Young RH. *Atlas of Gynecologic Surgical Pathology*. 2nd ed. Philadelphia, PA: Elsevier Saunders; 2008.

Crum CP, Nucci, MR, Lee, K, eds. *Diagnostic Gynecologic and Obstetric Pathology*. 2nd ed. Philadelphia, PA: Elsevier Saunders; 2011.

Fu YS. *Pathology of the Uterine Cervix, Vagina, and Vulva*. 2nd ed. Philadelphia, PA: Saunders; 2002.

Kurman RJ, Ellenson LH, Ronnett BM, eds. *Blaustein's Pathology of the Female Genital Tract*. 6th ed. New York, NY: Springer; 2011.

Kurman RJ, Norris HJ, Wilkinson E. *Tumors of the Cervix, Vagina, and Vulva. Atlas of Tumor Pathology*. 3rd series, Fascicle 4. Washington, DC: Armed Forces Institute of Pathology; 1992:179–255.

Mills SE, ed. *Histology for Pathologists*. 3rd ed. Philadelphia, PA: Lippincott Williams & Wilkins; 2006.

Robboy, SJ, Mutter GL, Prat J, et al., eds. *Robboy's Pathology of the Female Reproductive Tract*. 2nd ed. Oxford, UK: Churchill Livingstone; 2009.

Tavassoli FA, Devilee P, eds. World Health Organization Classification of Tumors. In: *Pathology and Genetics of Tumours of the Breast and Female Genital Organs*. Lyon: IARC Press; 2003:313–334.

REFERENCES

1. Lynch PJ, Moyal-Barracco M, Bogliatto F, et al. 2006 ISSVD classification of vulvar dermatoses: pathologic subsets and their clinical correlates. *J Reprod Med.* 2007;52:3–9.
2. Ambros RA, Malfetano JH, Carlson JA, et al. Non-neoplastic epithelial alterations of the vulva: recognition assessment and comparisons of terminologies used among the various specialties. *Mod Pathol.* 1997;10:401–408.
3. Powell JJ, Wojnarowska F. Lichen sclerosus. *Lancet.* 1999;353:1777–1783.
4. Chiesa-Vottero A, Dvoretsky PM, Hart WR. Histopathologic study of thin vulvar squamous cell carcinomas and associated cutaneous lesions: a correlative study of 48 tumors in 44 patients with analysis of adjacent vulvar intraepithelial neoplasia types and lichen sclerosus. *Am J Surg Pathol.* 2006;30:310–318.
5. Carli P, De Magnis A, Mannone F, et al. Vulvar carcinoma associated with lichen sclerosus. Experience at the Florence, Italy, Vulvar Clinic. *J Reprod Med.* 2003;48:313–318.
6. Liegl B, Regauer S. p53 immunostaining in lichen sclerosus is related to ischaemic stress and is not a marker of differentiated vulvar intraepithelial neoplasia (d-VIN). *Histopatholog.* 2006;48:268–274.
7. Santos M, Montagut C, Mellado B, et al. Immunohistochemical staining for p16 and p53 in premalignant and malignant epithelial lesions of the vulva. *Int J Gynecol Pathol.* 2004;23:206–214.
8. Fung MA, LeBoit PE. Light microscopic criteria for the diagnosis of early vulvar lichen sclerosus: a comparison with lichen planus. *Am J Surg Pathol.* 1998;22:473–478.
9. Niamh L, Naveen S, Hazel B. Diagnosis of vulval inflammatory dermatoses: a pathological study with clinical correlation. *Int J Gynecol Pathol.* 2009;28:554–558.
10. Hammock LA, Barrett TL. Inflammatory dermatoses of the vulva. *J Cutan Pathol.* 2005;32:604–611.
11. Lynch PJ. Condylomata acuminata (anogenital warts). *Clin Obstet Gynecol.* 1985;28:142–151.
12. Aguilera-Barrantes I, Magro C, Nuovo GJ. Verruca vulgaris of the vulva in children and adults: a nonvenereal type of vulvar wart. *Am J Surg Pathol.* 2007;31:529–535.
13. Wade TR, Ackerman AB. The effects of resin of podophyllin on condyloma acuminatum. *Am J Dermatopathol.* 1984;6:109–122.
14. de Deus JM, Focchi J, et al. Histologic and biomolecular aspects of papillomatosis of the vulvar vestibule in relation to human papillomavirus. *Obstet Gynecol.* 1995;86:758–763.
15. Bai H, Cviko A, Granter S, et al. Immunophenotypic and viral (human papillomavirus) correlates of vulvar seborrheic keratosis. *Hum Pathol.* 2003;34:559–564.
16. Vanderhooft S, Kirby P. Genital herpes simplex virus infection: natural history. *Semin Dermatol.* 1992;11:190–199.
17. Smith KJ, Yeager J, Skelton H. Molluscum contagiosum: its clinical, histopathologic, and immunohistochemical spectrum. *Int J Dermatol.* 1999;38:664–672.
18. Robboy SJ, Ross JS, Prat J, et al. Urogenital sinus origin of mucinous and ciliated cysts of the vulva. *Obstet Gynecol.* 1978;51:347–351.
19. McLachlin CM, Mutter GL, Crum CP. Multinucleated atypia of the vulva. Report of a distinct entity not associated with human papillomavirus. *Am J Surg Pathol.* 1994;18:1233–1239.
20. Abdul-Karim FW, Cohen RE. Atypical stromal cells of lower female genital tract. *Histopathology.* 1990;17:249–253.
21. Moyal-Barracco M, Lynch PJ. 2003 ISSVD terminology and classification of vulvodynia: a historical perspective. *J Reprod Med.* 2004;49:772–777.
22. Rock B. Pigmented lesions of the vulva. *Dermatol Clin.* 1992;10:361–370.
23. Sison-Torre EQ, Ackerman AB. Melanosis of the vulva. A clinical simulator of malignant melanoma. *Am J Dermatopathol.* 1985;7(suppl):51–60.
24. Christensen WN, Friedman KJ, Woodruff JD, et al. Histologic characteristics of vulvar nevocellular nevi. *J Cutan Pathol.* 1987;14:87–91.
25. Clark WH Jr, Hood AF, Tucker MA, et al. Atypical melanocytic nevi of the genital type with a discussion of reciprocal parenchymal-stromal interactions in the biology of neoplasia. *Hum Pathol.* 1998;29:S1–S24.
26. Gleason BC, Hirsch MS, Nucci MR, et al. Atypical genital nevi. A clinicopathologic analysis of 56 cases. *Am J Surg Pathol.* 2008;32:51–57.
27. Avinoach I, Zirkin HJ, Glezerman M. Proliferating trichilemmal tumor of the vulva. Case report and review of the literature. *Int J Gynecol Pathol.* 1989;8:163–168.
28. Regauer S, Nogales FF. Vulvar trichogenic tumors: a comparative study with vulvar basal cell carcinoma. *Am J Surg Pathol.* 2005;29:479–484.
29. Peterdy GA, Huettner PC, Rajaram V, et al. Trichofolliculoma of the vulva associated with vulvar intraepithelial neoplasia: report of three cases and review of the literature. *Int J Gynecol Pathol.* 2002;21:224–230.
30. Chen W, Koenig C. Vulvar keratoacanthoma: a report of two cases. *Int J Gynecol Pathol.* 2004;23:284–286.
31. Roth LM, Look KY. Inverted follicular keratosis of the vulvar skin: a lesion that can be confused with squamous cell carcinoma. *Int J Gynecol Pathol.* 2000;19:369–373.
32. El Demellawy D, Daya D, Alowami S. Clear cell hidradenoma: an unusual vulvar tumor. *Int J Gynecol Pathol.* 2008;27:457–460.
33. Glusac EJ, Hendrickson MS, Smoller BR. Apocrine cystadenoma of the vulva. *J Am Acad Dermatol.* 1994;31:498–499.
34. Woodworth H Jr, Dockerty MB, Wilson RB, et al. Papillary hidradenoma of the vulva: a clinicopathologic study of 69 cases. *Am J Obstet Gynecol.* 1971;110:501–508.
35. Huang YH, Chuang YH, Kuo TT, et al. Vulvar syringoma: a clinicopathologic and immunohistologic study of 18 patients and results of treatment. *J Am Acad Dermatol.* 2003;48:735–739.
36. Koenig C, Tavassoli FA. Nodular hyperplasia, adenoma, and adenomyoma of Bartholin's gland. *Int J Gynecol Pathol.* 1998;17:289–294.
37. Garcia JJ, Verkauf BS, Hochberg CJ, et al. Aberrant breast tissue of the vulva. A case report and review of the literature. *Obstet Gynecol.* 1978;52:225–228.
38. van der Putte SCJ. Mammary-like glands of the vulva and their disorders. *Int J Gynecol Pathol.* 1994;13:150–160.
39. Sington JD, Manek S, Hollowood K. Fibroadenoma of the mammary-like glands of the vulva. *Histopathology.* 2002;41:563–565.
40. Tbakhi A, Cowan DF, Kumar D, et al. Recurring phyllodes tumor in aberrant breast tissue of the vulva. *Am J Surg Pathol.* 1993;17:946–950.
41. Abbott JJ, Ahmed I. Adenocarcinoma of mammary-like glands of the vulva: report of a case and review of the literature. *Am J Dermatopathol.* 2006;28:127–133.
42. Kazakov DV, Spagnolo DV, Stewart CJ, et al. Fibroadenoma and phyllodes tumors of anogenital mammary-like glands: a series of 13 neoplasms in 12 cases, including mammary-type juvenile fibroadenoma, fibroadenoma with lactation changes, and neurofibromatosis-associated pseudoangiomatous stromal hyperplasia with multinucleated giant cells. *Am J Surg Pathol.* 2010;34:95–103.
43. Tresserra F, Grases PJ, Izquierdo M, et al. Fibroadenoma phyllodes arising in vulvar supernumerary breast tissue: report of two cases. *Int J Gynecol Pathol.* 1998;17:171–173.
44. McCluggage WG. A review and update of morphologically bland vulvovaginal mesenchymal lesions. *Int J Gynecol Pathol.* 2005;24:26–38.
45. McCluggage WG. Recent developments in vulvovaginal pathology. *Histopathology.* 2009;54:156–173.
46. Nucci MR, Fletcher CDM. Vulvovaginal soft tissue tumours: update and review. *Histopathology.* 2000;36:97–108.
47. Nielsen GP, Young RH. Mesenchymal tumors and tumor-like lesions of the female genital tract: a selective review with emphasis on recently described entities. *Int J Gynecol Pathol.* 2001;20:105–127.
48. Steeper TA, Rosai J. Aggressive angiomyxoma of the female pelvis and perineum. Report of nine cases of a distinctive type of gynecologic soft-tissue neoplasm. *Am J Surg Pathol.* 1983;7:463–475.
49. Fetsch JF, Laskin WB, Lefkowitz M, et al. Aggressive angiomyxoma: a clinicopathologic study of 29 female patients. *Cancer.* 1996;78:79–90.
50. Blandamura S, Cruz J, Vergara LF, et al. Aggressive angiomyxoma: a second case of metastasis with patient's death. *Hum Pathol.* 2003;34:1072–1074.
51. McCluggage WG, Connolly L, McBride HA. HMGA2 is a sensitive but not specific immunohistochemical marker of vulvovaginal aggressive angiomyxoma. *Am J Surg Pathol.* 2010;34:1037–1042.
52. Fetsch JF, Laskin WB, Tavassoli FA. Superficial angiomyxoma (cutaneous myxoma): a clinicopathologic study of 17 cases arising in the genital region. *Int J Gynecol Pathol.* 1997;16:325–334.
53. Calonje E, Guerin D, McCormick D, et al. Superficial angiomyxoma: clinicopathologic analysis of a series of distinctive but poorly recognized cutaneous tumors with tendency for recurrence. *Am J Surg Pathol.* 1999;23:910–917.
54. McCluggage WG, Nielsen GP, Young RH. Massive vulval edema secondary to obesity and immobilization: a potential mimic of aggressive angiomyxoma. *Int J Gynecol Pathol.* 2008;27:447–452.
55. Fletcher CDM, Tsang WYW, Fisher C, et al. Angiomyofibroblastoma of the vulva. A benign neoplasm distinct from aggressive angiomyxoma. *Am J Surg Pathol.* 1992;16:373–382.
56. Laskin WB, Fetsch JF, Tavassoli FA. Angiomyofibroblastoma of the female genital tract: analysis of 17 cases including a lipomatous variant. *Hum Pathol.* 1997;28:1046–1055.

57. Nielsen GP, Rosenberg AE, Young RH, et al. Angiomyofibroblastoma of the vulva and vagina. *Mod Pathol.* 1996;9:284–291.
58. Ganesan R, McCluggage WG, Hirschowitz L, et al. Superficial myofibroblastoma of the lower female genital tract: report of a series including tumours with a vulval location. *Histopathology.* 2005;46:137–143.
59. Nielsen GP, Young RH, Dickersin GR, et al. Angiomyofibroblastoma of the vulva with sarcomatous transformation ("angiomyofibrosarcoma"). *Am J Surg Pathol.* 1997;21:1104–1108.
60. Nucci MR, Granter SR, Fletcher CDM. Cellular angiofibroma: a benign neoplasm distinct from angiomyofibroblastoma and spindle cell lipoma. *Am J Surg Pathol.* 1997;21:636–644.
61. Iwasa Y, Fletcher CDM. Cellular angiofibroma: clinicopathologic and immunohistochemical analysis of 51 cases. *Am J Surg Pathol.* 2004;28:1426–1435.
62. Chen E, Fletcher CD. Cellular angiofibroma with atypia or sarcomatous transformation: clinicopathologic analysis of 13 cases. *Am J Surg Pathol.* 2010;34:707–714.
63. Vargas SO, Kozakewich HP, Boyd TK, et al. Childhood asymmetric labium majus enlargement mimicking a neoplasm. *Am J Surg Pathol.* 2005;29:1007–1016.
64. Iwasa Y, Fletcher CDM. Distinctive prepubertal vulval fibroma: a hitherto unrecognized mesenchymal tumor of prepubertal girls: analysis of 11 cases. *Am J Surg Pathol.* 2004;28:1601–1608.
65. Cohen PR, Young AW Jr, Tovell HM. Angiokeratoma of the vulva: diagnosis and review of the literature. *Obstet Gynecol Surv.* 1989;44:339–346.
66. Tavassoli FA, Norris HJ. Smooth muscle tumors of the vulva. *Obstet Gynecol.* 1979;53:213–217.
67. Nielsen GP, Rosenberg AE, Koerner FC, et al. Smooth-muscle tumors of the vulva. A clinicopathological study of 25 cases and review of the literature. *Am J Surg Pathol.* 1996;20:779–793.
68. Horowitz IR, Copas P, Majmudar B. Granular cell tumors of the vulva. Am J *Obstet Gynecol.* 1995;173:1710–1714.
69. Wolber RA, Talerman A, Wilkinson EJ, et al. Vulvar granular cell tumors with pseudocarcinomatous hyperplasia: a comparative analysis with well-differentiated squamous carcinoma. *Int J Gynecol Pathol.* 1991;10:59–66.
70. Papalas JA, Shaco-Levy R, Robboy SJ, et al. Isolated and synchronous vulvar granular cell tumors: a clinicopathologic study of 17 cases in 13 patients. *Int J Gynecol Pathol.* 2010;29:173–180.
71. O'Connell JX, Young RH, Nielsen GP, et al. Nodular fasciitis of the vulva: a study of six cases and literature review. *Int J Gynecol Pathol.* 1997;16:117–123.
72. Guillou L, Wadden C, Coindre JM, et al. "Proximal-type" epithelioid sarcoma, a distinctive aggressive neoplasm showing rhabdoid features. Clinicopathologic, immunohistochemical, and ultrastructural study of a series. *Am J Surg Pathol.* 1997;21:130–146.
73. Argenta PA, Thomas S, Chura JC. Proximal-type epithelioid sarcoma vs. malignant rhabdoid tumor of the vulva: a case report, review of the literature, and an argument for consolidation. *Gynecol Oncol.* 2007;107:130–135.
74. Perrone T, Swanson PE, Twiggs L, et al. Malignant rhabdoid tumor of the vulva: is distinction from epithelioid sarcoma possible? A pathologic and immunohistochemical study. *Am J Surg Pathol.* 1989;13:848–858.
75. Izumi T, Oda Y, Hasegawa T, et al. Prognostic significance of dysadherin expression in epithelioid sarcoma and its diagnostic utility in distinguishing epithelioid sarcoma from malignant rhabdoid tumor. *Mod Pathol.* 2006;19:820–831.
76. Tholpady A, Lonergan CL, Wick MR. Proximal-type epithelioid sarcoma of the vulva: relationship to malignant extrarenal rhabdoid tumor. *Int J Gynecol Pathol.* 2010;29:600–604.
77. Manson CM, Hirsch PJ, Coyne JD. Post-operative spindle cell nodule of the vulva. *Histopathology.* 1995;26:571–574.
78. Nielsen GP, Young RH. Fibromatosis of soft tissue type involving the female genital tract: a report of two cases. *Int J Gynecol Pathol.* 1997;16:383–386.
79. Haley JC, Mirowski GW, Hood AF. Benign vulvar tumors. *Semin Cutan Med Surg.* 1998;17:196–204.
80. Kehagias DT, Smyrniotis VE, Karvounis EE, et al. Large lipoma of the vulva. *Eur J Obstet Gynecol Reprod Biol* 1999;84:5–6.
81. Vlastos AT, Malpica A, Follen M. Lymphangioma circumscriptum of the vulva: a review of the literature. *Obstet Gynecol.* 2003;101:946–954.
82. Sonobe H, Ro JY, Ramos M, et al. Glomus tumor of the female external genitalia: a report of two cases. *Int J Gynecol Pathol.* 1994;13:359–364.
83. Colgan TJ, Dardick I, O'Connell G. Paraganglioma of the vulva. *Int J Gynecol Pathol.* 1991;10:203–208.
84. Venter PF, Rohm GF, Slabber CF. Giant neurofibromas of the labia. *Obstet Gynecol.* 1981;57:128–130.
85. Huang HJ, Yamabe T, Tagawa H. A solitary neurilemmoma of the clitoris. *Gynecol Oncol.* 1983;15:103–110.
86. Biedrzycki OJ, Singh N, Habeeb H, et al. Solitary fibrous tumor of the female genital tract: a case report and review of the literature. *Int J Gynecol Pathol.* 2007;26:259–264.
87. Edelweiss M, Malpica A. Dermatofibrosarcoma protuberans of the vulva: a clinicopathologic and immunohistochemical study of 13 cases. *Am J Surg Pathol.* 2010;34:393–400.
88. Santala M, Suonio S, Syrjanen K, et al. Malignant fibrous histiocytoma of the vulva. *Gynecol Oncol.* 1987;27:121–126.
89. Nirenberg A, Ostor AG, Slavin J, et al. Primary vulvar sarcomas. *Int J Gynecol Pathol.* 1995;14:55–62.
90. Laartz BW, Cooper C, Degryse A, et al. Wolf in sheep's clothing: advanced Kaposi sarcoma mimicking vulvar abscess. *South Med J.* 2005;98:475–477.
91. Fakokunde A, Yoong W, Bajekal N. Vulva haemangiopericytoma: case report and literature review. *J Obstet Gynaecol.* 2004;24:94–95.
92. Nucci MR, Fletcher CDM. Liposarcoma (atypical lipomatous tumors) of the vulva: a clinicopathologic study of six cases. *Int J Gynecol Pathol.* 1998;17:17–23.
93. Nielsen GP, Shaw PA, Rosenberg AE, et al. Synovial sarcoma of the vulva: a report of two cases. *Mod Pathol.* 1996;9:970–974.
94. Shen JT, d'Ablaing G, Morrow CP. Alveolar soft part sarcoma of the vulva: report of first case and review of literature. *Gynecol Oncol.* 1982;13:120–128.
95. Andrassy RJ, Hays DM, Raney RB, et al. Conservative surgical management of vaginal and vulvar pediatric rhabdomyosarcoma: a report from the Intergroup Rhabdomyosarcoma Study III. *J Pediatr Surg* 1995;30:1034–1037.
96. Terada KY, Schmidt RW, Roberts JA. Malignant schwannoma of the vulva. A case report. *J Reprod Med.* 1988;33:969–972.
97. Fong YE, Lopez-Terrada D, Zhai QJ. Primary Ewing sarcoma/peripheral primitive neuroectodermal tumor of the vulva. *Hum Pathol* 2008;39:1535–1539.
98. McCluggage WG, Sumathi VP, Nucci MR, et al. Ewing family of tumours involving the vulva and vagina: report of a series of four cases. *J Clin Pathol.* 2007;60:674–680.
99. Hart WR. Vulvar intraepithelial neoplasia: historical aspects and current status. *Int J Gynecol Pathol.* 2001;20:16–30.
100. Sideri M, Jones RW, Wilkinson EJ, et al. Squamous vulvar intraepithelial neoplasia: 2004 modified terminology, ISSVD Vulvar Oncology Subcommittee. *J Reprod Med.* 2005;50:807–810.
101. Srodon M, Stoler MH, Baber GB, et al. The distribution of low and high-risk HPV types in vulvar and vaginal intraepithelial neoplasia (VIN and VaIN). *Am J Surg Pathol.* 2006;30:1513–1518.
102. Medeiros F, Nascimento AF, Crum CP. Early vulvar squamous neoplasia: advances in classification, diagnosis, and differential diagnosis. *Adv Anat Pathol.* 2005;12:20–26.
103. Skapa P, Zamecnik J, Hamsikova E, et al. Human papillomavirus (HPV) profiles of vulvar lesions: possible implications for the classification of vulvar squamous cell carcinoma precursors and for the efficacy of prophylactic HPV vaccination. *Am J Surg Pathol.* 2007;31:1834–1843.
104. Kurman RJ, Toki T, Schiffman MH. Basaloid and warty carcinomas of the vulva. Distinctive types of squamous cell carcinoma frequently associated with human papillomaviruses. *Am J Surg Pathol.* 1993;17:133–145.
105. Modesitt SC, Groben PA, Walton LA, et al. Expression of Ki-67 in vulvar carcinoma and vulvar intraepithelial neoplasia III: correlation with clinical prognostic factors. *Gynecol Oncol.* 2000;76:51–55.
106. Logani S, Lu D, Quint WG, et al. Low-grade vulvar and vaginal intraepithelial neoplasia: correlation of histologic features with human papillomavirus DNA detection and MIB-1 immunostaining. *Mod Pathol.* 2003;16:735–741.
107. Shatz P, Bergeron C, Wilkinson EJ, et al. Vulvar intraepithelial neoplasia and skin appendage involvement. *Obstet Gynecol.* 1989;74:769–774.
108. Husseinzadeh N, Recinto C. Frequency of invasive cancer in surgically excised vulvar lesions with intraepithelial neoplasia (VIN 3). *Gynecol Oncol.* 1999;73:119–120.
109. Patterson JW, Kao GF, Graham JH, et al. Bowenoid papulosis. A clinicopathologic study with ultrastructural observations. *Cancer.* 1986;57:823–836.
110. Yang B, Hart WR. Vulvar intraepithelial neoplasia of the simplex (differentiated) type: a clinicopathologic study including analysis of HPV and p53 expression. *Am J Surg Pathol.* 2000;24:429–441.
111. Mulvany NJ, Allen DG. Differentiated intraepithelial neoplasia of the vulva. *Int J Gynecol Pathol.* 2008;27:125–135.
112. Roma AA, Hart WR. Progression of simplex (differentiated) vulvar intraepithelial neoplasia to invasive squamous cell carcinoma: a prospective case study confirming its precursor role in the pathogenesis of vulvar cancer. *Int J Gynecol Pathol.* 2007;26:248–253.
113. Ordi J, Alejo M, Fuste V, et al. HPV-negative vulvar intraepithelial neoplasia (VIN) with basaloid histologic pattern: an unrecognized variant of simplex (differentiated) VIN. *Am J Surg Pathol.* 2009;33:1659–1665.

114. Stehman FB, Look KY. Carcinoma of the vulva. *Obstet Gynecol.* 2006;107:719–733.
115. FIGO Committee on Gynecologic Oncology. Revised FIGO staging for carcinoma of the vulva, cervix, and endometrium. *Int J Gynecol Obstet.* 2009;105:103–104.
116. Hacker NF. Revised FIGO staging for carcinoma of the vulva. *Int J Gynecol Obstet.* 2009;105:105–106.
117. Santos M, Landolfi S, Olivella A, et al. p16 overexpression identifies HPV-positive vulvar squamous cell carcinomas. *Am J Surg Pathol.* 2006;30:1347–1356.
118. Drew PA, al-Abbadi MA, Orlando CA, et al. Prognostic factors in carcinoma of the vulva: a clinicopathologic and DNA flow cytometric study. *Int J Gynecol Pathol.* 1996;15:235–241.
119. Sedlis A, Homesley H, Bundy BN, et al. Positive groin lymph nodes in superficial squamous cell vulvar cancer. A Gynecologic Oncology Group Study. Am J *Obstet Gynecol.* 1987;156:1159–1164.
120. Wilkinson EJ. Premalignant and malignant tumors of the vulva. In: Kurman RJ, ed. *Blaustein's Pathology of the Female Genital Tract.* 5th ed. New York, NY: Springer, 2002:112.
121. Wilkinson EJ. Protocol for the examination of specimens from patients with carcinomas and malignant melanomas of the vulva: a basis for checklists. Cancer Committee of the American College of Pathologists. *Arch Pathol Lab Med.* 2000;124:51–56.
122. Yoder BJ, Rufforny I, Massoll NA, et al. Stage IA vulvar squamous cell carcinoma: an analysis of tumor invasive characteristics and risk. *Am J Surg Pathol.* 2008;32:765–772.
123. Homesley HD, Bundy BN, Sedlis A, et al. Assessment of current International Federation of Gynecology and Obstetrics staging of vulvar carcinoma relative to prognostic factors for survival (a Gynecologic Oncology Group study). *Am J Obstet Gynecol.* 1991;164:997–1004.
124. Preti M, Rouzier R, Mariani L, et al. Superficially invasive carcinoma of the vulva: diagnosis and treatment. *Clin Obstet Gynecol.* 2005;48:862–868.
125. Magrina JF, Gonzalez-Bosquet J, Weaver AL, et al. Squamous cell carcinoma of the vulva stage IA: long-term results. *Gynecol Oncol.* 2000;76:24–27.
126. Homesley HD, Bundy BN, Sedlis A, et al. Prognostic factors for groin node metastasis in squamous cell carcinoma of the vulva (a Gynecologic Oncology Group study). *Gynecol Oncol.* 1993;49:279–283.
127. Gerszten K, Selvaraj RN, Kelley J, et al. Preoperative chemoradiation for locally advanced carcinoma of the vulva. *Gynecol Oncol.* 2005;99:640–644.
128. Moore DH. Chemotherapy and radiation therapy in the treatment of squamous cell carcinoma of the vulva: are two therapies better than one? *Gynecol Oncol.* 2009;113:379–383.
129. Andrews SJ, Williams BT, DePriest PD, et al. Therapeutic implications of lymph nodal spread in lateral T1 and T2 squamous cell carcinoma of the vulva. *Gynecol Oncol.* 1994;55:41–46.
130. Knopp S, Nesland JM, Trope C. SLNB and the importance of micrometastases in vulvar squamous cell carcinoma. *Surg Oncol.* 2008;17:219–225.
131. Van der Zee AGJ, Oonk MH, De Hullu JA, et al. Sentinel node dissection is safe in the treatment of early-stage vulvar cancer. *J Clin Oncol.* 2008;26:884–889.
132. Paladini D, Cross P, Lopes A, et al. Prognostic significance of lymph node variables in squamous cell carcinoma of the vulva. *Cancer.* 1994;74:2491–2496.
133. van der Velden J, van Lindert AC, Lammes FB, et al. Extracapsular growth of lymph node metastases in squamous cell carcinoma of the vulva. The impact on recurrence and survival. *Cancer.* 1995;75:2885–2890.
134. Origoni M, Sideri M, Garsia S, et al. Prognostic value of pathological patterns of lymph node positivity in squamous cell carcinoma of the vulva stage III and IVA FIGO. *Gynecol Oncol.* 1992;45:313–316.
135. Brisigotti M, Moreno A, Murcia C, et al. Verrucous carcinoma of the vulva. A clinicopathologic and immunohistochemical study of five cases. *Int J Gynecol Pathol.* 1989;8:1–7.
136. Japaze H, Van Dinh T, Woodruff JD. Verrucous carcinoma of the vulva: study of 24 cases. *Obstet Gynecol.* 1982;60:462–466.
137. Gualco M, Bonin S, Foglia G, et al. Morphologic and biologic studies on ten cases of verrucous carcinoma of the vulva supporting the theory of a discrete clinico-pathologic entity. *Int JGynecol Cancer.* 2003;13:317–324.
138. Nascimento AF, Granter SR, Cviko A, et al. Vulvar acanthosis with altered differentiation: a precursor to verrucous carcinoma? *Am J Surg Pathol.* 2004;28:638–643.
139. Choi DS, Lee JW, Lee SJ, et al. Squamous cell carcinoma with sarcomatoid features of the vulva: a case report and review of literature. *Gynecol Oncol.* 2006;103:363–367.
140. Giordano G, D'Adda T, Merisio C, et al. Vulvar acantholytic squamous carcinoma: a case report with immunohistochemical and molecular study. *Int J Gynecol Pathol.* 2005;24:303–306.
141. Horn LC, Liebert UG, Edelmann J, et al. Adenoid squamous carcinoma (pseudoangiosarcomatous carcinoma) of the vulva: a rare but highly aggressive variant of squamous cell carcinoma-report of a case and review of the literature. *Int J Gynecol Pathol.* 2008;27:288–291.
142. Feakins RM, Lowe DG. Basal cell carcinoma of the vulva: a clinicopathologic study of 45 cases. *Int J Gynecol Pathol.* 1997;16:319–324.
143. Copeland LJ, Sneige N, Gershenson DM, et al. Bartholin gland carcinoma. *Obstet Gynecol.* 1986;67:794–801.
144. Cardosi RJ, Speights A, Fiorica JV, et al. Bartholin's gland carcinoma: a 15-year experience. *Gynecol Oncol.* 2001;82:247–251.
145. Yang SYV, Lee JW, Kim WS, et al. Adenoid cystic carcinoma of the Bartholin's gland: report of two cases and review of the literature. *Gynecol Oncol.* 2006;100:422–425.
146. McCluggage WG, Aydin NE, Wong NA, et al. Low-grade epithelial-myoepithelial carcinoma of Bartholin gland: report of 2 cases of a distinctive neoplasm arising in the vulvovaginal region. *Int J Gynecol Pathol.* 2009;28:286–291.
147. Goldblum JR, Hart WR. Vulvar Paget's disease: a clinicopathologic and immunohistochemical study of 19 cases. *Am J Surg Pathol.* 1997;21:1178–1187.
148. Liegl B, Leibl S, Gogg-Kamerer M, et al. Mammary and extramammary Paget's disease: an immunohistochemical study of 83 cases. *Histopathology.* 2007;50:439–447.
149. Wilkinson EJ, Brown HM. Vulvar Paget disease of urothelial origin: a report of three cases and a proposed classification of vulvar Paget disease. *Hum Pathol.* 2002;33:549–554.
150. Battles OE, Page DL, Johnson JE. Cytokeratins, CEA, and mucin histochemistry in the diagnosis and characterization of extramammary Paget's disease. Am J Clin Pathol 1997;108:6–12.
151. Lundquist K, Kohler S, Rouse RV. Intraepidermal cytokeratin 7 expression is not restricted to Paget cells but is also seen in Toker cells and Merkel cells. *Am J Surg Pathol.* 1999;23:212–219.
152. Shaco-Levy R, Bean SM, Vollmer RT, et al. Paget disease of the vulva: a histologic study of 56 cases correlating pathologic features and disease course. *Int J Gynecol Pathol.* 2010;29:69–78.
153. Brainard JA, Hart WR. Proliferative epidermal lesions associated with anogenital Paget's disease. *Am J Surg Pathol.* 2000;24:543–552.
154. Crawford D, Nimmo M, Clement PB, et al. Prognostic factors in Paget's disease of the vulva: a study of 21 cases. *Int J Gynecol Pathol.* 1999;18:351–359.
155. Kohler S, Rouse RV, Smoller BR. The differential diagnosis of pagetoid cells in the epidermis. *Mod Pathol.* 1998;11:79–92.
156. Helwig EB, Graham JH. Anogenital (extramammary) Paget's disease. A clinicopathological study. *Cancer.* 1963;16:387–403.
157. Raju RR, Goldblum JR, Hart WR. Pagetoid squamous cell carcinoma in situ (pagetoid Bowen's disease) of the external genitalia. *Int J Gynecol Pathol.* 2003;22:127–135.
158. Armes JE, Lourie R, Bowlay G, et al. Pagetoid squamous cell carcinoma in situ of the vulva: comparison with extramammary paget disease and nonpagetoid squamous cell neoplasia. *Int J Gynecol Pathol.* 2008;27:118–124.
159. McCluggage WG, Jamison J, Boyde A, et al. Vulval intraepithelial neoplasia with mucinous differentiation: report of 2 cases of a hitherto undescribed phenomenon. *Am J Surg Pathol.* 2009;33:945–949.
160. Ragnarsson-Olding BK, Kanter-Lewensohn LR, Lagerlof B, et al. Malignant melanoma of the vulva in a nationwide, 25-year study of 219 Swedish females: clinical observations and histopathologic features. *Cancer.* 1999;86:1273–1284.
161. Raber G, Mempel V, Jackisch C, et al. Malignant melanoma of the vulva. Report of 89 patients. *Cancer.* 1996;78:2353–2358.
162. Phillips GL, Bundy BN, Okagaki T, et al. Malignant melanoma of the vulva treated by radical hemivulvectomy. A prospective study of the Gynecologic Oncology Group. *Cancer.* 1994;73:2626–2632.
163. Johnson TL, Kumar NB, White CD, et al. Prognostic features of vulvar melanoma: a clinicopathologic analysis. *Int J Gynecol Pathol.* 1986;5:110–118.
164. Smoller BR. Histologic criteria for diagnosing primary cutaneous malignant melanoma. *Mod Pathol.* 2006;19(suppl 2):S34–S40.
165. Clark WH Jr, From L, Bernardino EA, et al. The histogenesis and biologic behavior of primary human malignant melanomas of the skin. *Cancer Res.* 1969;29:705–727.
166. Breslow A. Thickness, cross-sectional areas and depth of invasion in the prognosis of cutaneous melanoma. *Ann Surg.* 1970;172:902–908.
167. Wick MR. Prognostic factors for cutaneous melanoma. *Am J Clin Pathol.* 1998;110:713–718.
168. Crowson AN, Magro CM, Mihm MC. Prognosticators of melanoma, the melanoma report, and the sentinel lymph node. *Mod Pathol.* 2006;19(suppl 2):S71–S87.

169. Magro CM, Crowson AN, Mihm MC. Unusual variants of malignant melanoma. *Mod Pathol.* 2006;19(suppl 2):S41–S70.
170. Wick MR, Goellner JR, Wolfe JT 3rd, et al. Vulvar sweat gland carcinomas. *Arch Pathol Lab Med.* 1985;109:43–47.
171. Khan Z, Misra G, Fiander AN, et al. Sebaceous carcinoma of the vulva. *BJOG* 2003;110:227–228.
172. Willen R, Bekassy, Carlen B, et al. Cloacogenic adenocarcinoma of the vulva. *Gynecol Oncol.* 1999;74:298–301.
173. Pongtippan A, Malpica A, Levenback C, et al. Skene's gland adenocarcinoma resembling prostatic adenocarcinoma. *Int J Gynecol Pathol.* 2004;23: 71–74.
174. Gil-Moreno A, Garcia-Jimenez A, Gonzalez-Bosquet J, et al. Merkel cell carcinoma of the vulva. *Gynecol Oncol.* 1997;64:526–532.
175. Hierro I, Blanes A, Matilla A, et al. Merkel cell (neuroendocrine) carcinoma of the vulva. A case report with immunohistochemical and ultrastructural findings and review of the literature. *Pathol Res Pract.* 2000;196:503–509.
176. Vang R, Medeiros LJ, Malpica A, et al. Non-Hodgkin's lymphoma involving the vulva. *Int J Gynecol Pathol.* 2000;19:236–242.
177. Padula A, Medeiros LJ, Silva EG, et al. Isolated vulvar Langerhans cell histiocytosis: report of two cases. *Int J Gynecol Pathol.* 2004;23: 278–283.
178. Flanagan CW, Parker JR, Mannel RS, et al. Primary endodermal sinus tumor of the vulva: a case report and review of the literature. *Gynecol Oncol.* 1997;66:515–518.
179. El Demellawy D, Saleh R, Daya D, et al. Malignant giant cell tumor of the vulva. *Int J Gynecol Pathol.* 2010;29:93–97.
180. Neto AG, Deavers MT, Silva EG, et al. Metastatic tumors of the vulva: a clinicopathologic study of 66 cases. *Am J Surg Pathol.* 2003;27: 799–804.

CHAPTER 2

Pathology of the Vagina

OVERVIEW OF VAGINAL HISTOLOGY

In the estrogen-stimulated state of the reproductive years, the normal vagina exhibits a pattern of rugal folds that results in an undulating appearance at low magnification, and is lined by nonkeratinized, well-glycogenated stratified squamous epithelium (Fig. 2.1). In situations of low to absent estrogen levels, such as before puberty and after menopause, the rugal folds are lost or diminished and the vaginal epithelium is atrophic. Atrophic vaginal epithelium histologically resembles atrophic exocervical epithelium, as illustrated in Chapter 3 (Fig. 3.145). Beneath the squamous epithelium, the vaginal wall consists of a highly vascular lamina propria that is normally devoid of glands. Together, the squamous epithelial lining and the lamina propria constitute what is referred to as the vaginal mucosa. Deep to the lamina propria are interlacing bundles of smooth muscle that are continuous with those of the uterus, with longitudinally oriented fibers predominating in the outer region. The adventitia, which is the outermost layer of connective tissue, merges with the soft tissue of surrounding structures.

VAGINAL ADENOSIS

The presence of glandular epithelium within the vagina is referred to as vaginal adenosis. At least one-third of women who have been exposed to diethylstilbestrol (DES) in utero develop adenosis, which usually becomes apparent in their teenage years.[1] DES, which is an orally active, synthetic, nonsteroidal estrogen, was commonly used in high-risk pregnancies between 1947 and the discovery of its association with clear cell carcinoma in 1971.[2] Vaginal adenosis also occurs in women who have not been exposed to DES, but in an older age group and at a much lower rate.[3] Now that the DES era has past, vaginal adenosis is rarely encountered.

Vaginal adenosis is usually asymptomatic, and is detected during colposcopic examination as iodine-negative patches that are red and granular if the glandular epithelium is on the mucosal surface or gray-white with small vessels that may be perceived as abnormal if covered by squamous metaplasia. Adenosis may also present as small cysts within the lamina propria, and is most commonly seen in the upper portions of the vagina.

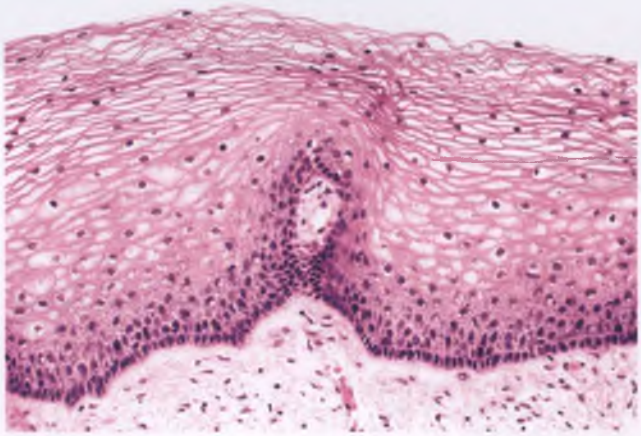

FIGURE 2.1. Nonkeratinized stratified squamous epithelium from a normal, estrogen-primed vagina. Note the single layer of basal cells with palisaded "picket fence" nuclei with ascending maturation toward parabasal cells, intermediate cells, and superficial cells. Perinuclear clearing in the central region is due to the presence of abundant intracytoplasmic glycogen.

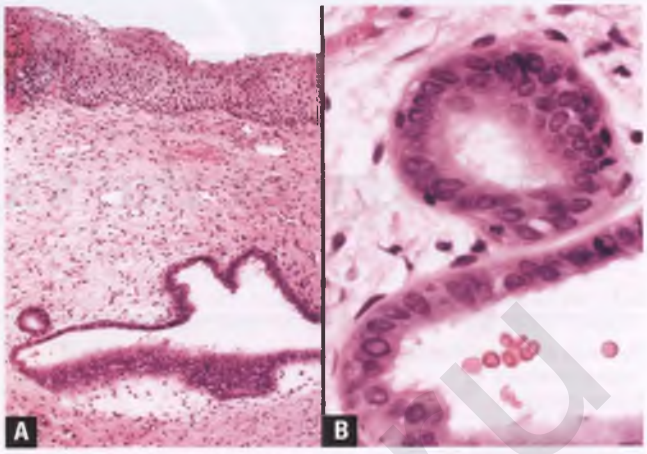

FIGURE 2.3. Vaginal adenosis, tuboendometrioid type. **A**: The bottom portion of the tuboendometrioid gland has been dissociated from its stroma and tangentially cut, creating the artifactual appearance of nuclear stratification. **B**: Some ciliated cells are evident, particularly in the lower left portion of the image.

The most common form of adenosis is the mucinous variant, with mucinous columnar cells of endocervical-type lining portions of the epithelial surface and/or forming glands lined by a single layer of epithelium within the lamina propria (Fig. 2.2). The other major type of adenosis is the tuboendometrioid variant, in which a portion of the cells are ciliated and resemble the lining cells of the fallopian tube or endometrium (Fig. 2.3). Mixtures of these two types of adenosis may be encountered.[3] The tuboendometrioid variant does not usually involve the mucosal surface, but rather is seen as glands within the lamina propria, and is the form of adenosis that is associated with clear cell carcinoma.[4] Whatever the type of adenosis, there is usually some degree of associated squamous metaplasia, which is the mechanism by which adenosis regresses (Fig. 2.4).[1] In advanced cases of squamous metaplasia, residual mucin droplets within the squamous epithelium detected with a mucicarmine stain may be the only evidence of prior adenosis.[1]

Atypical adenosis is the term used to describe tuboendometrioid variants whose glandular lining cells exhibit nuclear enlargement, pleomorphism, and prominent nucleoli.[4] This form of adenosis is closely linked to clear cell carcinoma, being found in close proximity to the cancer in 80% of thoroughly examined resections of tumor-containing specimens.[4]

Differential Diagnosis

Features that help to distinguish tuboendometrioid adenosis from endometriosis are discussed in the section on vaginal endometriosis. As discussed in the section on tubulosquamous polyps, this recently described entity can mimic vaginal adenosis that has undergone extensive squamous metaplasia. Rarely, microglandular hyperplasia can be superimposed on the

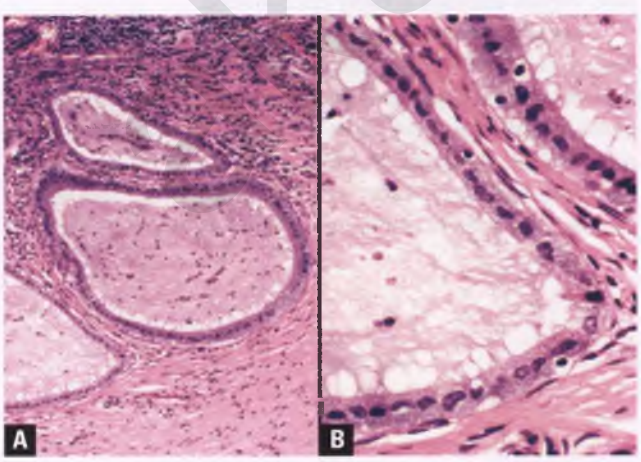

FIGURE 2.2. **A,B**: Vaginal adenosis, mucinous type. The glands resemble those of the endocervix.

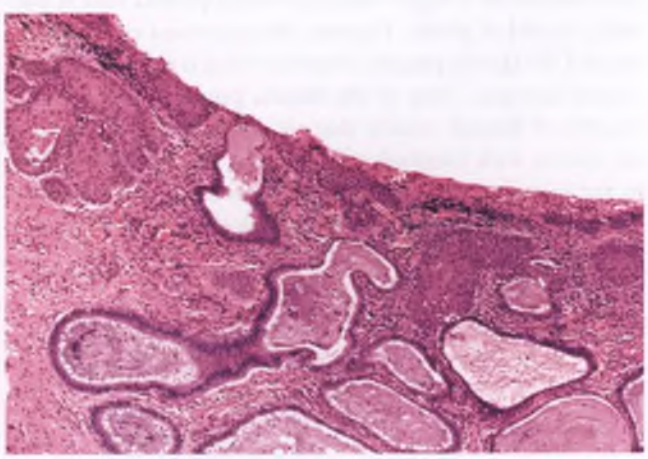

FIGURE 2.4. Adenosis with squamous metaplasia of portions of its superficial aspect.

mucinous type of vaginal adenosis, creating a pattern that can be confused with clear cell carcinoma.[5] The orderly arrangement of the closely packed glands, the lack of significant nuclear atypia, and interspersed areas of squamous metaplasia facilitate recognition of this process as microglandular hyperplasia.[5]

ENDOMETRIOSIS

The general features and extragenital manifestations of endometriosis are discussed in Chapter 8. In the vagina, endometriosis is an uncommon lesion that may be found within the superficial stroma in sites of previous trauma or within the deep aspects of the stroma in association with pelvic endometriosis[6] (Fig. 2.5). Rare cases of polypoid endometriosis of the vagina have been reported in which polypoid lesions protrude from the surface of the vaginal mucosa.[7] In exceptional circumstances, vaginal endometriosis may be found in association with an endometrioid adenocarcinoma, adenosarcoma, or endometrial stromal sarcoma, in which case the presence of coexisting endometriosis in the adjacent tissue can serve as supportive evidence of a primary vaginal tumor rather than a metastasis from another site.[8–10]

The major differential diagnostic consideration of vaginal endometriosis is the tuboendometrioid variant of vaginal adenosis. In contrast to this form of adenosis, vaginal endometriosis features a periglandular rim of endometriotic stroma that is often accompanied by evidence of old hemorrhage, is usually more deeply situated within the stroma, and has glands that more closely resemble those of the endometrium than the fallopian tube.

CYSTS[11]

Vaginal cysts are uncommon lesions that generally present in adult women as a vaginal mass that may be associated with discomfort, pain, or dyspareunia. The most common vaginal cysts are müllerian and epithelial inclusion cysts, followed by mesonephric (Gartner's duct) cysts. Cysts of these types are usually ≤2 cm in diameter. Bartholin cysts may be described as having a vaginal location, but are more appropriately considered lesions of the vulvar vestibule (see Chapter 1). Small endometriotic cysts can also be seen as part of the spectrum of vaginal endometriosis.

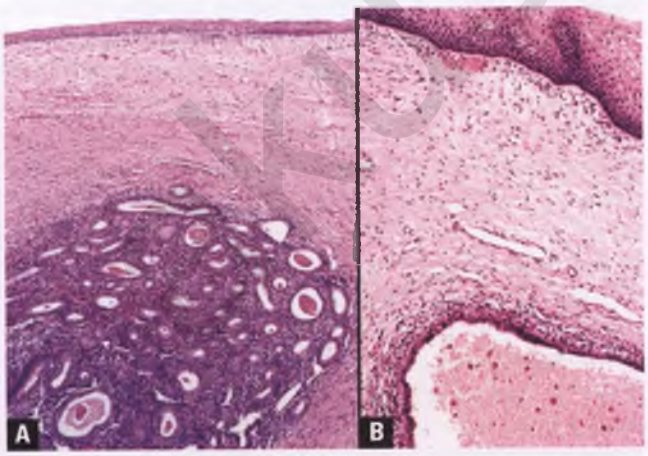

FIGURE 2.5. Vaginal endometriosis. **A**: A nodular aggregate of endometriotic glands and stroma is present within the vaginal connective tissue. **B**: This image depicts a portion of a cystically dilated endometriotic gland within the superficial vaginal stroma. Note the narrow periglandular rim of endometriotic stroma and the hemorrhagic luminal contents.

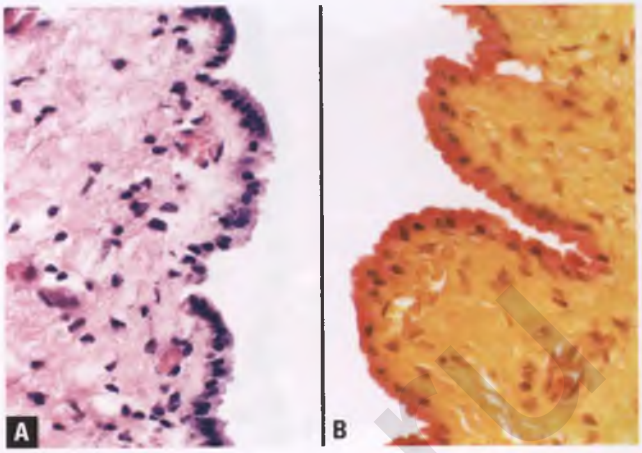

FIGURE 2.6. Müllerian cyst, mucinous type. **A**: The cyst is lined by a single layer of mucinous epithelium. **B**: A mucicarmine stain facilitates recognition of the mucinous nature of this vaginal cyst.

Müllerian cysts are usually lined by a single layer of mucinous epithelium of the type seen in the endocervix, but the lining may also consist of tubal (ciliated) and/or endometrioid-type epithelium (Figs. 2.6 and 2.7). Most of these cysts are presumably derived from vaginal adenosis.

Epithelial inclusion cysts are usually found within sites of previous vaginal trauma, such as in episiotomy scars. These cysts are lined by stratified squamous epithelium and contain keratinous debris. If these cysts rupture prior to removal,

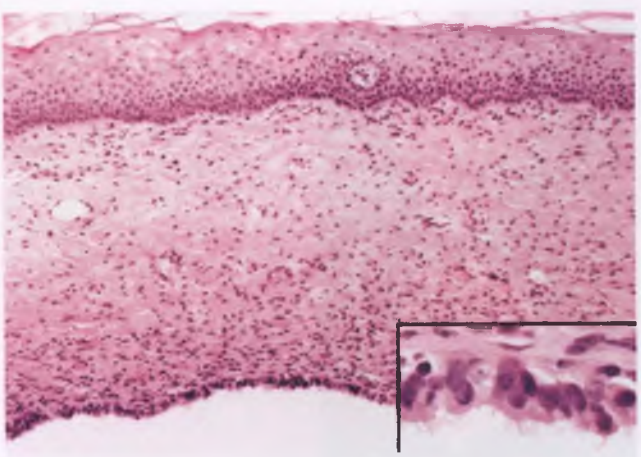

FIGURE 2.7. Müllerian cyst, tubal type. The epithelial lining of the cyst is present within the lamina propria along the bottom portion of the image. The inset highlights the ciliated nature of some of the epithelial cells lining the cyst.

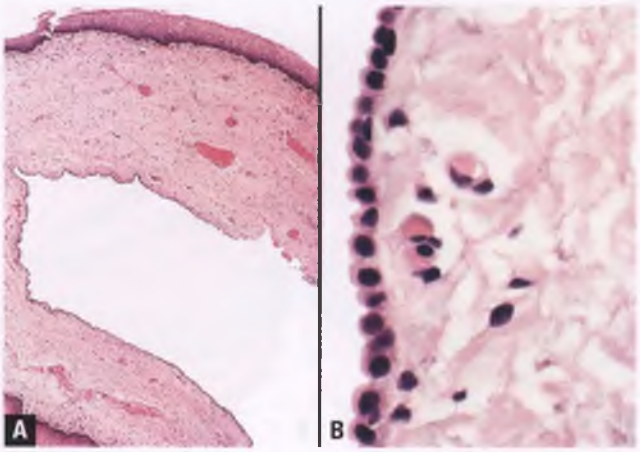

FIGURE 2.8. **A,B**: Mesonephric (Gartner's duct) cyst. The cyst is lined by a layer of cuboidal epithelium that lacks cilia and intracytoplasmic mucin.

chronic inflammation and a foreign body giant cell reaction are seen in the neighboring tissue.

Mesonephric (Gartner's duct) cysts are typically found in the lateral vaginal walls and are thought to represent cystically dilated mesonephric duct remnants. They are lined by a single layer of flattened to cuboidal epithelial cells that are nonciliated and devoid of intracytoplasmic mucin (Fig. 2.8).

FIBROEPITHELIAL POLYP[12–14]

Fibroepithelial polyps of the lower female genital tract are most commonly found in the vagina of adult women, sometimes in association with pregnancy or hormonal therapy. The polyps are usually single, average about 2 cm in diameter, have a smooth external surface, and have a tan, rubbery sectioned surface (Fig. 2.9A). The surface of occasional polyps can exhibit finger-like projections.

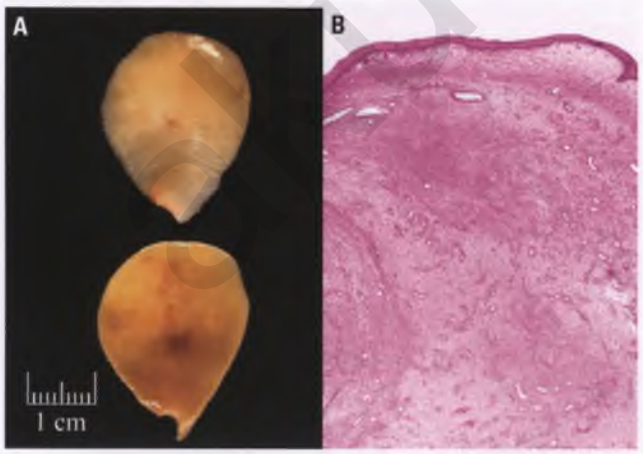

FIGURE 2.9. Fibroepithelial polyp. **A**: Gross appearance (top: external surface; bottom: sectioned surface). **B**: Low-magnification view, demonstrating prominent fibrovascular stroma with an overlying layer of unremarkable squamous epithelium.

The epithelium that covers these polyps is a continuation of the nonkeratinized, stratified squamous epithelium that lines normal portions of the vagina, and is generally unremarkable. The fibrovascular stroma of fibroepithelial polyps is usually hypocellular, may be loose and edematous or dense and fibrotic, blends with that of adjacent normal tissue, and abuts the basement membrane of the epidermis without a zone of uninvolved stroma (Fig. 2.9B). The vasculature ranges from thin-walled, dilated capillaries to medium-sized, thick-walled vessels, with the latter sometimes preferentially located within the core of the polyp.

The stromal cells within fibroepithelial polyps are usually spindle- or stellate-shaped cells with bland nuclear features. They usually exhibit no appreciable mitotic activity, and are typically immunoreactive for desmin, estrogen receptors, and progesterone receptors.[15] However, roughly half of vaginal fibroepithelial polyps contain scattered atypical stromal cells that exhibit nuclear enlargement, pleomorphism, hyperchromasia, and/or multinucleation (Fig. 2.10). Even more concerning are the subset of cases that typically occur in pregnant patients that mimic sarcomas by virtue of their hypercellularity, more diffuse nuclear atypia, and considerable mitotic activity, which may include atypical division figures (Fig. 2.11).[13] These pseudosarcomatous lesions are recognized as being within the family of fibroepithelial polyps by their lack of distinct lesional margins, the absence of a grenz zone of native stroma interposed between the squamous epithelium and the atypical stromal proliferation, and the presence of scattered multinucleated stromal cells.[13]

Differential Diagnosis

The potential to confuse fibroepithelial polyp with aggressive angiomyxoma is more of an issue in the vulva, and is discussed in Chapter 1. The features that help to distinguish fibroepithelial polyp from superficial myofibroblastoma are listed in the section on the latter entity. In contrast to vaginal sarcoma botryoides, cellular fibroepithelial polyps with mitotic activity and marked stromal atypia occur outside of the setting of early childhood

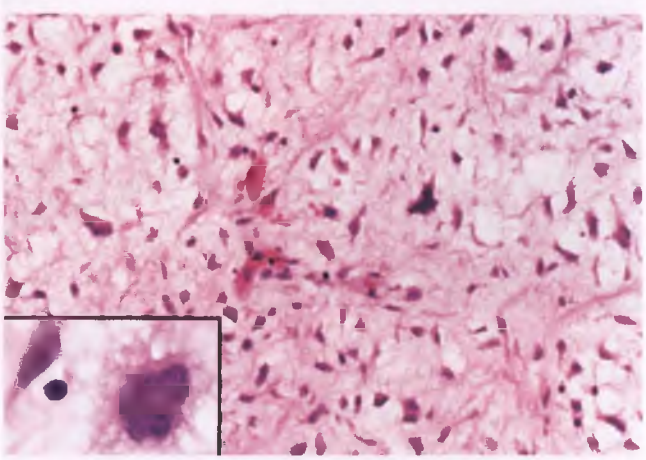

FIGURE 2.10. Fibroepithelial polyp with scattered atypical stromal cells.

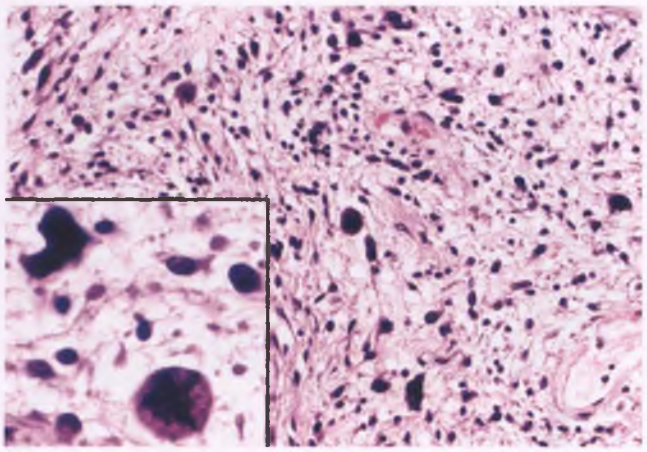

FIGURE 2.11. Cellular fibroepithelial polyp with pseudosarcomatous stroma from a pregnant teenager.

in patients who are often pregnant, lack a subepithelial zone of condensed tumor cells (the so-called cambium layer), do not contain rhabdomyoblasts with cross-striations, and do not stain with skeletal muscle markers such as myoglobin or myogenin.

Despite their occasional worrisome histologic appearance, fibroepithelial polyps are benign lesions that are adequately treated by simple excision. In rare cases, nondestructive local recurrences have been reported.[13]

TUBULOSQUAMOUS POLYP[16]

Tubulosquamous polyp is a rare, recently described entity that most often presents as a small polyp in the upper vagina of a postmenopausal woman. This lesion is lined by unremarkable vaginal mucosa and is characterized by an admixture of islands of benign squamous epithelium and small tubules that are embedded within a fibrous stroma (Fig. 2.12). The squamous elements often contain central foci of necrotic keratinous debris, and the fibrous component is hypocellular, mitotically inactive, and indistinguishable from normal vaginal connective tissue. The tubules, which are lined by cuboidal to columnar cells with bland nuclear features, are often present within the squamous nests, and are concentrated at their periphery (Fig. 2.13). The tubules can also be found in isolation in a minority of cases, and may be lined by cells with appreciable intracytoplasmic mucin. Peripheral palisading of basaloid cells is usually present at the edge of at least some of the epithelial nests, and occasionally basaloid differentiation can be prominent.[17] Sebaceous gland differentiation has also been reported.[18] An intriguing finding that is present in some cases is the immunoreactivity of a subset of the tubules for prostatic acid phosphatase and/or prostate-specific antigen, which raises the possibility of derivation from paraurethral (Skene's) glands (the female homologue of the prostate gland).

Differential Diagnosis

The main differential diagnostic consideration of tubulosquamous polyp is benign mixed tumor (spindle cell epithelioma),

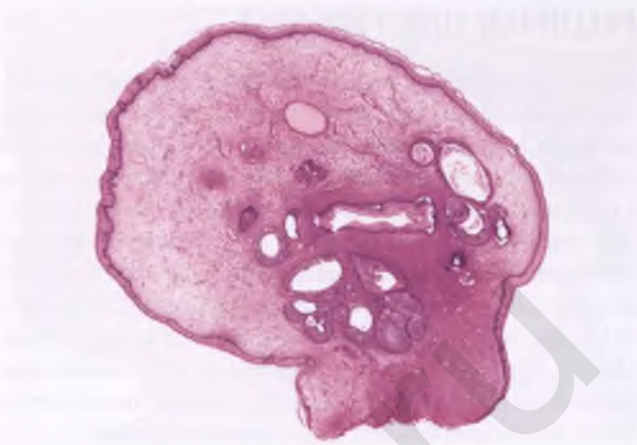

FIGURE 2.12. Tubulosquamous polyp. Nests of squamous epithelium are embedded within fibrous stroma. Some of the nests (top right) contain necrotic keratinous debris. A cystically dilated tubule is present near the top of the polyp in the center of the image.

which is recognized by its more prominent and more cellular stromal component, its typical location near the hymenal ring, its usual occurrence in a younger age group, and the cytokeratin immunoreactivity of its stroma. Tubulosquamous polyp may also be confused with vaginal adenosis with florid squamous metaplasia, but the latter lesion typically is not polypoid and its epithelial elements usually do not extend into the stroma to a depth that is seen in tubulosquamous polyps. Although basaloid differentiation within a tubulosquamous polyp can result in a resemblance to adenoid basal carcinoma of the uterine cervix, tumors of this type have yet to be reported in the vagina and are usually associated with a high-grade squamous intraepithelial lesion (see Chapter 3). Lesions previously reported as Brenner tumors of the vagina are now considered to be within the spectrum of tubulosquamous polyps.

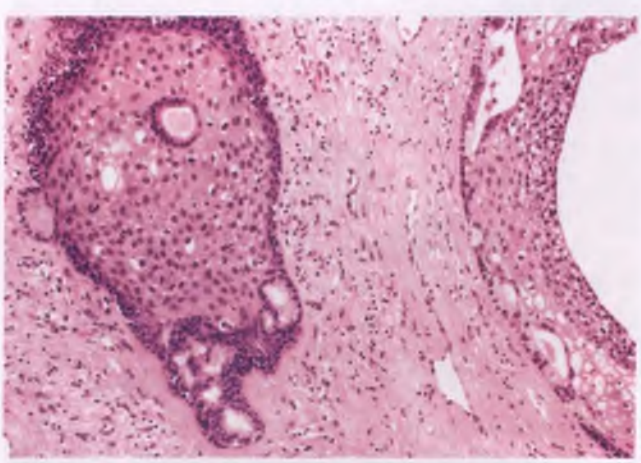

FIGURE 2.13. Tubulosquamous polyp. Tubules are concentrated at the periphery of the squamous nests. The epithelium lining the tubules varies from cuboidal to columnar, and in some areas is overtly mucinous.

FALLOPIAN TUBE PROLAPSE

Following hysterectomy, one or both fallopian tubes may descend into the pelvic floor, where tubal tissue may abut the sutured vaginal apex. On rare occasions, this barrier may be breached weeks to several years later, resulting in a prolapsed tube that appears as a red, granular, polypoid mass in the vaginal apex that may clinically resemble granulation tissue.[19,20] It is tempting to speculate that the tubal fimbriae, which are normally motile structures, play an active role in burrowing through the vaginal cuff. Symptoms of fallopian tube prolapse may include vaginal discharge, vaginal bleeding, pelvic pain, and/or dyspareunia. This complication occurs about four times more frequently in vaginal hysterectomies than it does in uteri removed via an abdominal approach.

When an adequate amount of intact tissue from a prolapsed fallopian tube is evaluated, a plical or fimbrial architecture can usually be appreciated (Fig. 2.14). In longstanding lesions, portions of the tubal tissue merge imperceptibly with vaginal stroma. In some cases, fallopian tube prolapse is associated with stromal reactions that can mimic aggressive angiomyxoma[21] (Fig. 2.15) or angiomyofibroblastoma.[22] The prolapsed tubal tissue is usually chronically inflamed and may exhibit reactive epithelial changes that can be misinterpreted as adenocarcinoma in both Pap smears and tissue samples (Fig. 2.16). The clinical history, the presence of some ciliated cells, the low mitotic rate, and an architectural pattern consistent with tubal plicae or fimbriae facilitate recognition of this process.

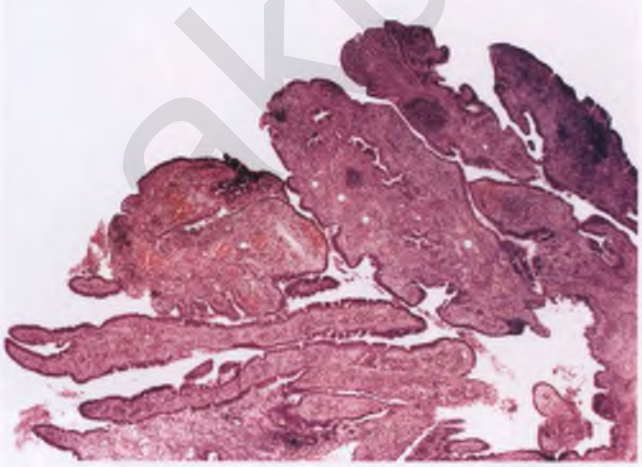

FIGURE 2.14. Prolapsed fallopian tube taken from vaginal apex. Fimbrial architecture can be appreciated at low magnification.

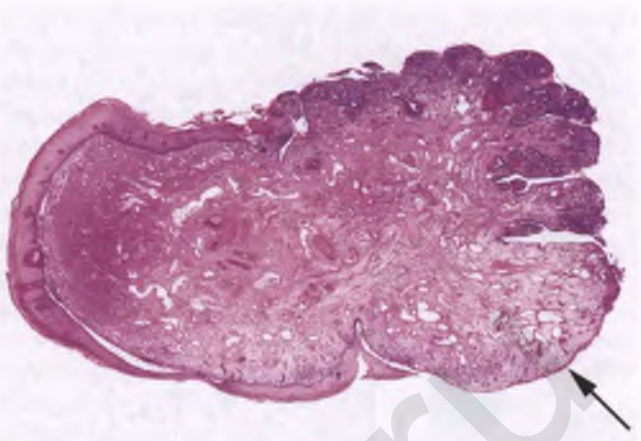

FIGURE 2.15. Prolapsed fallopian tube. Eroded and inflamed tubal tissue is recognizable at the upper right, vaginal mucosa is at left, and a polypoid piece of vascular, edematous stroma that in a small biopsy could be mistaken for aggressive angiomyxoma is marked by an *arrow*.

POSTOPERATIVE SPINDLE CELL NODULE[23]

Within the female genital tract, the vagina is the most common site of this rare pseudosarcomatous lesion that occurs at the site of a recent surgical procedure. The operation is usually a vaginal hysterectomy or episiotomy that has taken place 5 to 10 weeks prior to the identification of a superficially ulcerated, polypoid nodule that is generally <4 cm in greatest dimension. Histologically, postoperative spindle cell nodules are composed of a cellular proliferation of mitotically active, nucleoli-containing, spindle-shaped fibroblasts and/or myofibroblasts arranged in intersecting fascicles that are associated with a delicate network of capillary-like vessels (Fig. 2.17). These lesions are usually superficially ulcerated and contain scattered acute and chronic inflammatory cells and microhemorrhages. Although mitotic activity may be brisk, atypical mitotic figures are not present, and there is no significant nuclear atypia. An immunohistochemical study of two similar lesions from the urinary tract demonstrated immunoreactivity for vimentin, desmin, actin, and cytokeratin, the significance of which is discussed in the following paragraph.[24]

Differential Diagnosis

The distinction of postoperative spindle cell nodule from nodular fasciitis, which is vanishingly rare in the vagina, is based

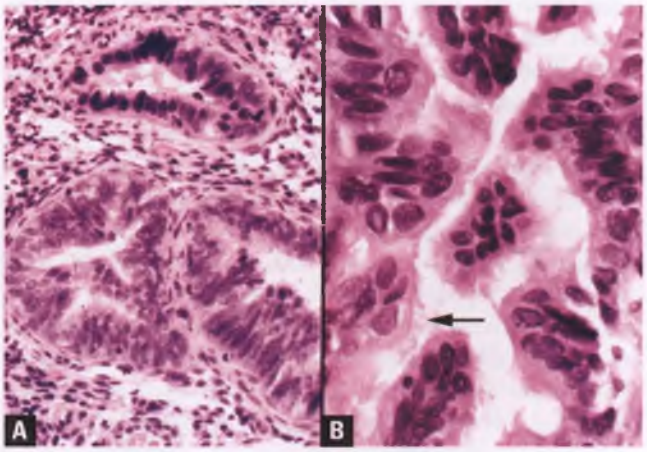

FIGURE 2.16. **A,B**: Prolapsed fallopian tube with reactive epithelial atypia. Note the presence of cilia and terminal bars (*arrow*). The Pap smear correlate of this case is shown in Figure 3.265.

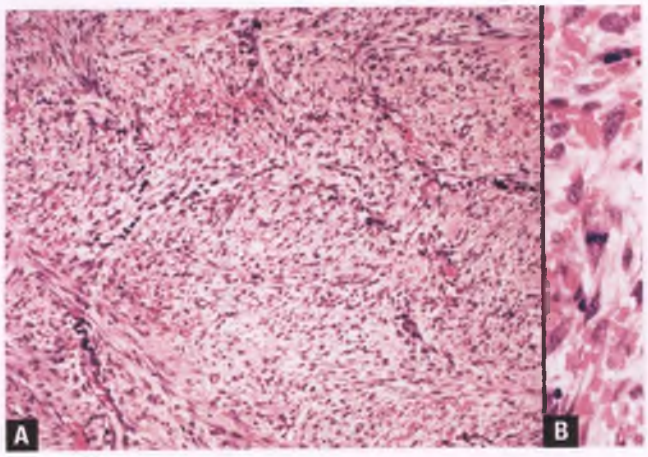

FIGURE 2.17. Postoperative spindle cell nodule. **A**: The lesion consists of intertwining fascicles of spindle-shaped cells with interspersed thin-walled vessels, inflammatory cells, and aggregates of extravasated erythrocytes. **B**: Normal mitotic figures, such as the one seen centrally, are an expected finding. Note the nucleoli within some of the spindle-shaped cells.

primarily on the distinctive clinical history of the former, and is of no clinical significance. The subtle histologic differences between these two lesions are discussed in the section on nodular fasciitis in Chapter 1. Much more important differential diagnostic considerations are spindle cell (sarcomatoid) carcinoma and leiomyosarcoma. The unexpected cytokeratin positivity of at least some postoperative spindle cell nodules may lead to a misdiagnosis of spindle cell carcinoma. This diagnostic pitfall may be avoided if attention is paid to the recent history of an operative procedure at the site of the lesion, if the absence of transitional areas between spindle cells and a more conventional squamous cell carcinoma is noted, and if a panel of immunostains that includes epithelial membrane antigen, actin, and desmin is used. Spindle cell carcinomas are expected to be immunoreactive for epithelial membrane antigen and to lack expression of actin and desmin, whereas the converse is true for postoperative spindle cell nodules.[24] Leiomyosarcomas on the well-differentiated end of the spectrum share many histologic features with postoperative spindle cell nodules. One subtle histologic difference is the prominent network of capillary-like vessels in the postoperative spindle cell nodule that is usually absent in leiomyosarcoma, but the overriding diagnostic clue to the true nature of the reactive nodule is the characteristic clinical setting in which it is found.

VAGINITIS EMPHYSEMATOSA[25]

Vaginitis emphysematosa is a rare, benign, self-limited lesion of unknown etiology that occurs in adult women, many of whom are pregnant. Histologically, one finds variable-sized, gas-filled, subepithelial cysts that are partially lined by multinucleated giant cells of the foreign body type (Fig. 2.18). These cysts may rupture under pressure and produce an audible popping sound, and will eventually regress spontaneously if left untreated.

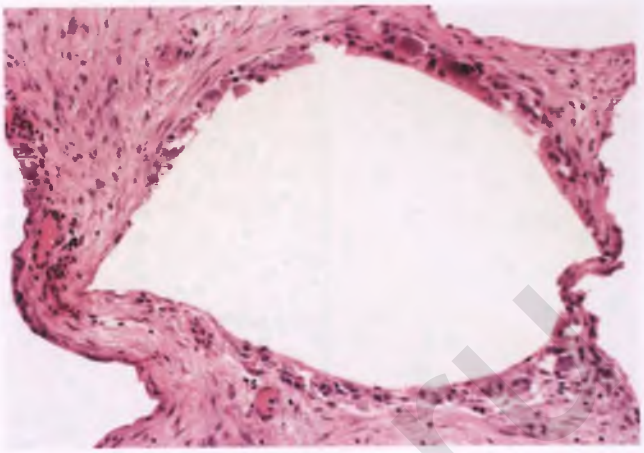

FIGURE 2.18. Vaginitis emphysematosa. The gas-filled cystic spaces within the stroma are partially lined by multinucleated foreign body–type giant cells.

MALAKOPLAKIA

Although the pathologist is most familiar with this uncommon chronic inflammatory lesion as it occurs in the urinary bladder, it also rarely involves the vagina and other sites within the female genital tract.[26,27] The pathogenesis of malakoplakia is thought to be related to an acquired defect in the ability of macrophages to destroy ingested bacteria, which usually represent *Escherichia Coli* organisms.[28]

In the vagina, yellow nodules or plaques may be found, sometimes in association with a vaginal discharge. Microscopically, malakoplakia typically consists of sheets of histiocytes with abundant eosinophilic cytoplasm admixed with a sprinkling of lymphocytes and plasma cells (Fig. 2.19). The characteristic

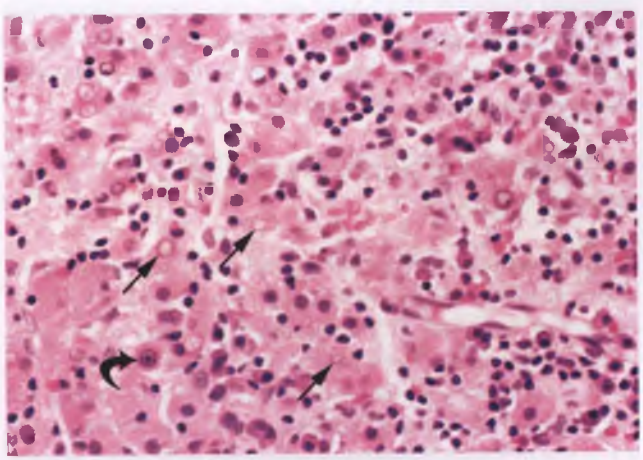

FIGURE 2.19. Malakoplakia. Numerous histiocytes with abundant eosinophilic cytoplasm are present in association with scattered lymphocytes and plasma cells. The *arrows* highlight the variable size and appearance of some of the Michaelis-Gutmann bodies within this lesion. Note the bull's-eye appearance of the Michaelis-Gutmann body marked by the *curved arrow*.

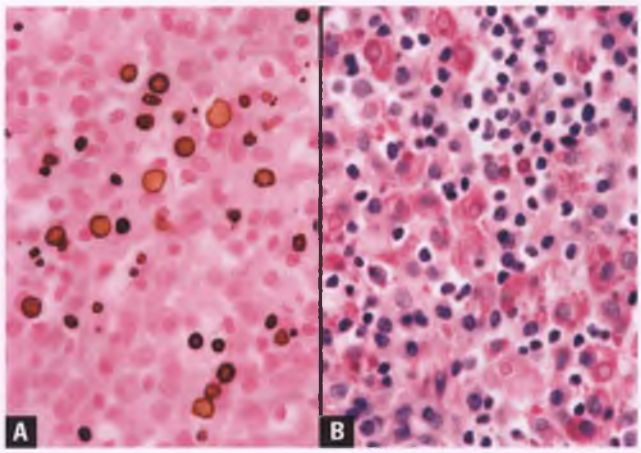

FIGURE 2.20. Malakoplakia. **A**: Michaelis-Gutmann bodies appear as brown spherules with the von Kossa stain. **B**: A PAS with diastase stain highlights the Michaelis-Gutmann bodies as well as the granular cytoplasm of the histiocytes.

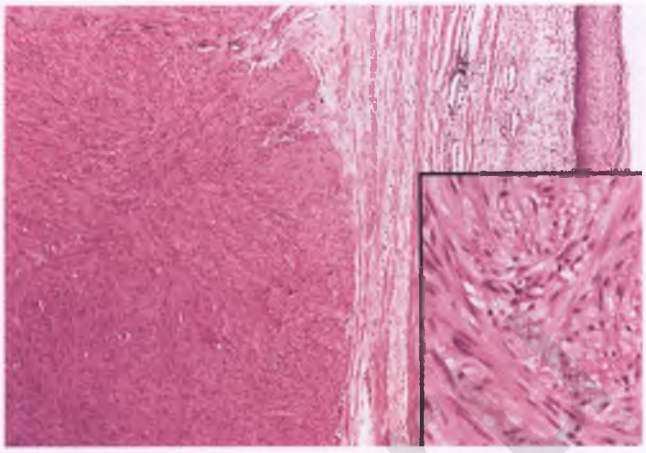

FIGURE 2.21. Vaginal leiomyoma. A well-circumscribed mass of benign smooth muscle lies beneath the vaginal mucosa, which is at right. The inset highlights the typical pattern of intertwining fascicles of spindle-shaped cells with bland nuclear features and eosinophilic cytoplasm.

feature of malakoplakia is the renowned Michaelis-Gutmann body, which is a favorite of pathology board examiners. These bodies are calcific spherules that range from roughly one-half to twice the size of a red blood cell that may be found either within the cytoplasm of the histiocytes or extracellularly, sometimes with a targetoid or bull's-eye appearance. Michaelis-Gutmann bodies can be highlighted with either the von Kossa or PAS with diastase stains, with the latter also staining the granular cytoplasm of the histiocytes (Fig. 2.20).

MULTINUCLEATED STROMAL GIANT CELLS

Multinucleated stromal giant cells are occasionally found scattered within the superficial stroma of the vagina and represent an incidental finding.[29] This phenomenon occurs throughout the lower female genital tract and is illustrated in Figures 1.29 (vulva) and 3.93 (cervix). Similar-appearing cells are also often present in fibroepithelial polyps, as discussed earlier in this chapter.

MESONEPHRIC REMNANTS AND HYPERPLASIAS

Benign glandular remnants and hyperplasias that originate from incomplete degeneration of the paired mesonephric (Wolffian) ducts may be found within the vaginal stroma, particularly in the lateral walls. The characteristic tubules and/or elongated ducts of the various forms of this incidental finding are described and illustrated in Chapter 3, since the uterine cervix is the site in which mesonephric elements most often present potential diagnostic difficulties. Mesonephric adenocarcinoma of the vagina occurs at a case-reportable frequency.[30,31]

LEIOMYOMA[32]

Although the leiomyoma is the most common benign mesenchymal tumor of the vagina, it is still a relatively rare neoplasm. These tumors typically present in adult women as a firm, well-demarcated, submucosal mass with a median size of 3 cm that may either be asymptomatic or cause pain or vaginal bleeding. Their gross and microscopic features are similar to those that have been described in the vulva (Chapter 1) and to those of their much more common counterparts in the uterine corpus that are discussed and extensively illustrated in Chapter 4. An example of a typical vaginal leiomyoma is shown in Figure 2.21. Distinction from vaginal leiomyosarcoma is based on the degree of mitotic activity and nuclear atypia, as discussed in the section on leiomyosarcoma.

RHABDOMYOMA[33,34]

Rhabdomyomas are rare benign tumors that exhibit skeletal muscle differentiation. In the vagina, they typically present in adult women as a small, solitary, polypoid mass with intact overlying squamous mucosa. The sectioned surface of these lesions is solid, tan, and rubbery. Histologically, unremarkable nonkeratinizing stratified squamous epithelium is seen covering loose connective tissue that is remarkable for the presence of intermingled skeletal muscle cells with abundant eosinophilic cytoplasm (Fig. 2.22). Cross-striations are easily visible in a subset of these cells, obviating the need for immunostains to document skeletal muscle differentiation. The nuclei of the skeletal muscle cells generally have a single prominent nucleolus, but they do not exhibit nuclear atypia or mitotic activity. Elongated "strap" cells are the predominant shape, but these cells can appear round or oval when cut in cross section.

Rhabdomyomas are adequately treated by local excision. Although these tumors can clinically and grossly be confused with fibroepithelial polyps, the latter lack skeletal muscle differentiation. The distinction between sarcoma botryoides and rhabdomyoma is made on both clinical and histologic grounds, as discussed later in this chapter.

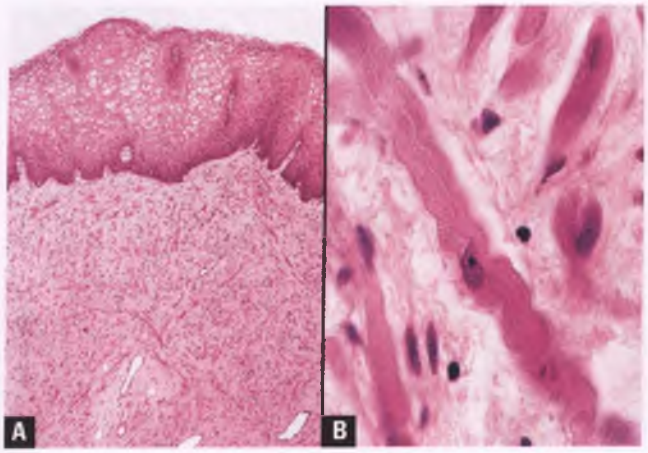

FIGURE 2.22. Vaginal rhabdomyoma. **A**: Squamous epithelium overlies elongated mature skeletal muscle cells, which are cut in various planes of section and separated by ample amounts of connective tissue. **B**: Cross-striations are readily apparent in the markedly elongated strap cell that courses diagonally across the image.

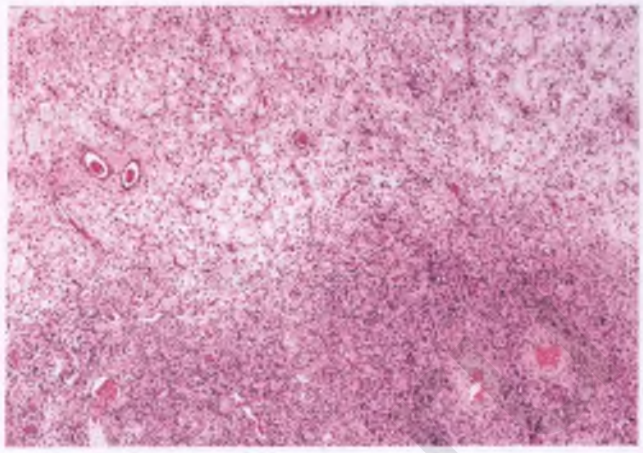

FIGURE 2.23. Superficial myofibroblastoma. The hypercellular region at bottom blends with the more superficially located, edematous, hypocellular zone at top. Several thin-walled vessels of small to medium caliber are scattered throughout the tumor.

ANGIOMYOFIBROBLASTOMA

Angiomyofibroblastoma is a rare benign mesenchymal tumor that has been reported to occur in the vagina, but is most commonly encountered in the vulva (see Chapter 1).[35] Some investigators have asserted that the purported vaginal examples of this tumor more likely represent superficial myofibroblastomas.[36]

SUPERFICIAL MYOFIBROBLASTOMA[36,37]

Superficial myofibroblastoma is a rare benign mesenchymal tumor that typically presents as a polypoid or nodular mass in the vagina of adult women. These are small, well-circumscribed tumors that rarely exceed 5 cm, and are adequately treated by local excision.

The sectioned surface of superficial myofibroblastoma is usually rubbery and tan. Histologically, these tumors are fairly well demarcated from the neighboring superficial vaginal stroma, and typically exhibit a grenz zone of uninvolved native stroma immediately beneath the overlying squamous epithelium. Characteristically, superficial myofibroblastomas have variegated growth patterns, in terms of both cellularity and architecture. Hypocellular zones, which may be edematous and/or myxoid, are commonly seen in the superficial aspects of the tumor, whereas regions of hypercellularity are likely to be found more centrally (Fig. 2.23). The lesional stromal cells are mitotically inactive, have bland, ovoid to spindle-shaped nuclei, and are embedded within a finely collagenous background with interspersed mast cells (Fig. 2.24). Intervening rounded accumulations of matrix material may result in a lace-like pattern, or the tumor cells may assume a fascicular architecture in its cellular regions. These tumors contain numerous thin-walled vessels, but the prefix "angio" has not been included in their name, presumably in an effort to help separate them from angiomyofibroblastomas. Superficial myofibroblastomas are typically immunoreactive for desmin, estrogen receptors, and progesterone receptors. CD34 immunoreactivity is also commonly found.

Differential Diagnosis

In contrast to angiomyofibroblastomas, superficial myofibroblastomas do not exhibit perivascular clusters of epithelioid or plasmacytoid cells, only rarely exhibit corded and nested patterns of tumor cell growth, are more likely to express CD34, and are typically vaginal rather than vulvar in location. The distinction between these two neoplasms can be difficult, as evidenced by one group's interpretation that many of the vaginal angiomyofibroblastomas that have been previously reported in the literature are actually superficial myofibroblastomas.[36] Fortunately, whether or not one is able to make this distinction

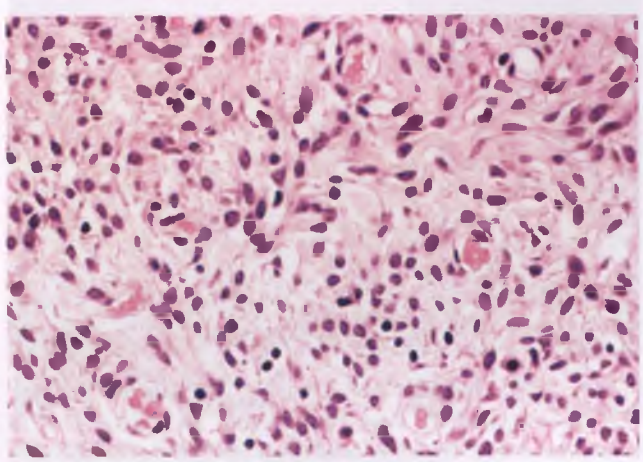

FIGURE 2.24. Superficial myofibroblastoma. The tumor cells have bland, ovoid to spindle-shaped nuclei. Note the fine fibrillary collagen in the background.

is of no clinical significance. The other main differential diagnostic consideration of superficial myofibroblastoma is fibroepithelial polyp, which lacks the nodular growth pattern, better defined margins, uninvolved grenz zone, and variegated architecture of superficial myofibroblastoma, and also commonly contains multinucleated stromal cells.

BENIGN MIXED TUMOR (SPINDLE CELL EPITHELIOMA)

Benign mixed tumors of the vagina are rare neoplasms of uncertain histogenesis.[38–40] They typically occur near the hymenal ring and are usually painless and asymptomatic.[38,39] In the largest reported series, patients had a mean age of 40 years and the tumors averaged 2.6 cm in diameter.[39] These tumors are optimally treated by local excision, but may recur if inadequately excised.[39]

Grossly, benign mixed tumors are solid nodules whose most superficial aspect comes to within a few millimeters of the overlying squamous epithelium. Their sectioned surface is white to pale gray, rubbery, and occasionally somewhat mucoid. Histologically, these tumors are well circumscribed, unencapsulated, and variably cellular (Fig. 2.25), and are composed predominantly of bland cells with ovoid to spindle-shaped nuclei with little to no mitotic activity. This stromal-like component may exhibit a fascicular, sheet-like, whorled, or corded architecture, and usually contains focal epithelial elements in the form of small nests of mature, well-glycogenated squamous epithelium (Fig. 2.26) and/or glands lined by cuboidal to columnar epithelium. The glandular elements may undergo squamous metaplasia, which at least in some cases appears to be the source of the squamous nests.

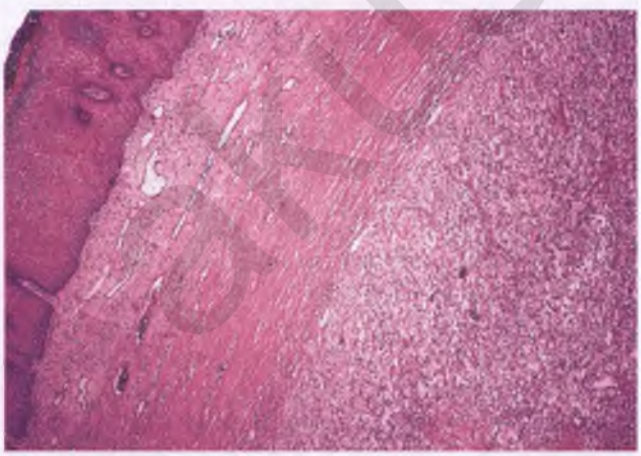

FIGURE 2.25. Benign mixed tumor (spindle cell epithelioma). This low-magnification view demonstrates the presence of a well-circumscribed, unencapsulated tumor (at right) that is separated from the surface squamous epithelium by a band of compressed vaginal stroma. (Courtesy of Dr. Harris S. Goodman.)

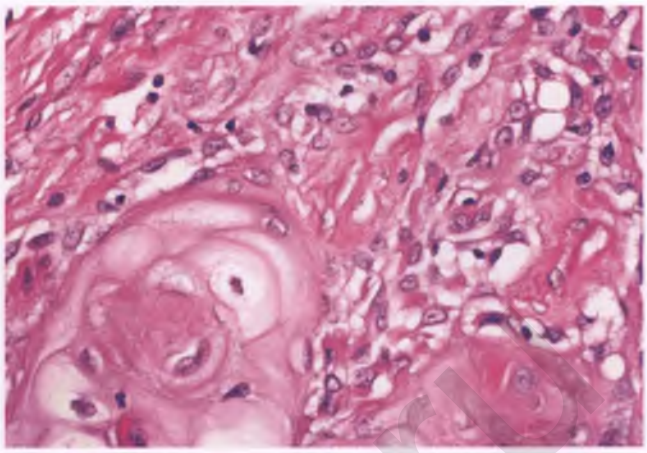

FIGURE 2.26. Benign mixed tumor (spindle cell epithelioma). The presence of small nests of well-glycogenated squamous epithelium within a background of bland cells with ovoid to spindle-shaped nuclei is characteristic. (Courtesy of Dr. Harris S. Goodman.)

The spindle and epithelial components of benign mixed tumors are both typically immunoreactive for cytokeratin, and ultrastructural analysis also supports an entirely epithelial process, prompting some investigators to favor the designation "spindle cell epithelioma" as a more accurate descriptor for this lesion.[39] The spindle cell component also typically demonstrates immunoreactivity for actin and CD10 and exhibits variable staining with a host of other markers.[40] Aside from the cytokeratin immunoreactivity of the spindle cell population facilitating the distinction of this tumor from tubulosquamous polyp, the immunoprofile of benign mixed tumor is not too helpful in distinguishing it from other entities in the differential diagnosis (tumors derived from smooth muscle and endometrial stroma may also express actin, CD10, and cytokeratin, as discussed in Chapter 4).[40] Fortunately, recognition of most benign mixed tumors can be accomplished based upon their distinctive location and histologic appearance.[40]

MÜLLERIAN PAPILLOMA

Müllerian papilloma of the vagina is an extraordinarily rare benign lesion that typically presents with intermittent vaginal bleeding in a child who is <5 years old.[41] This tumor can clinically simulate sarcoma botryoides, but its histologic features are distinctly different. Local excision is adequate treatment, although occasional recurrences have been reported.

Müllerian papilloma is composed of complex branching papillae with variably cellular and often superficially edematous stromal cores that at low magnification resemble an aggregate of chorionic villi (Fig. 2.27A). The papillae are usually lined by a single layer of bland, mitotically inactive, cuboidal to columnar epithelial cells (Fig. 2.27B). Interspersed foci of squamous metaplasia may be present. Although most reported cases have been exophytic tumors that protrude from the

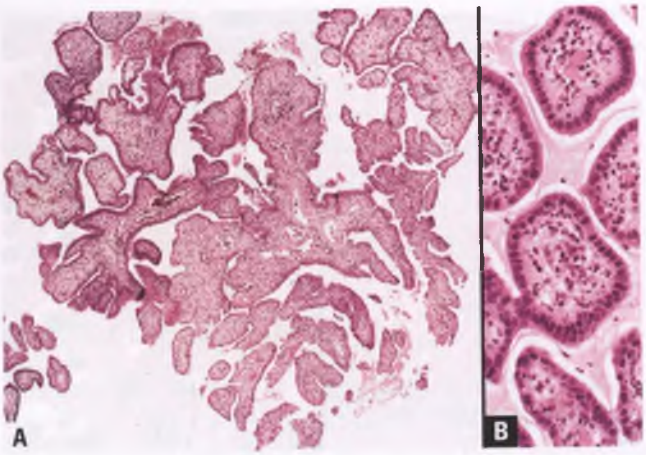

FIGURE 2.27. Müllerian papilloma. **A**: At low magnification, a papillary proliferation is seen that resembles an aggregate of chorionic villi. **B**: The papillae are lined by a single layer of epithelium with bland nuclear features. (Courtesy of Dr. Deborah J. Gersell.)

mucosal surface, a few examples of an intramural version of this lesion have also been published.[42,43] In contrast to sarcoma botryoides, müllerian papilloma lacks both a cambium layer and rhabdomyoblasts, and does not contain a primitive population of malignant, mitotically active cells.

CONDYLOMA ACUMINATUM

Exophytic condylomas occur on occasion in the vagina, and resemble their counterparts in the vulva and cervix (see Chapters 1 and 3). In the so-called spiked condyloma, which bridges the gap between condyloma acuminatum and flat condyloma, colposcopic examination reveals minute, elongated white spikes projecting from the surface of the vaginal mucosa whose histologic correlate is shown in Figure 2.28. Most condylomatous lesions in the vagina are flat condylomas, which are discussed in the following section.

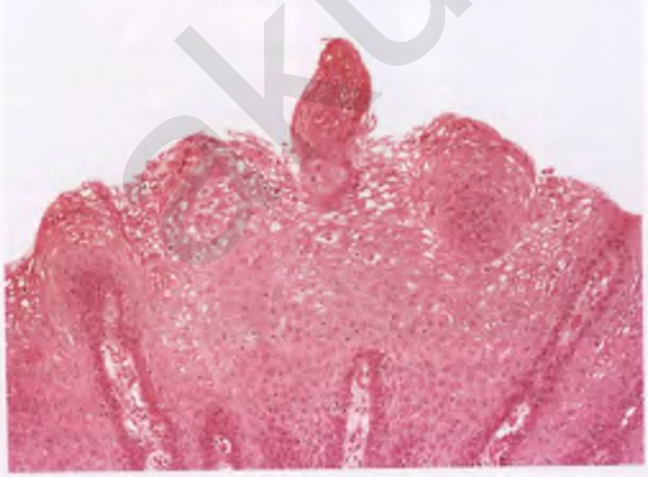

FIGURE 2.28. Spiked condyloma. A prominent, centrally located epithelial spike projects from the surface of a condylomatous lesion that exhibits koilocytosis in the superficial layers of the epithelium.

VAGINAL INTRAEPITHELIAL NEOPLASIA

Lesions classified as vaginal intraepithelial neoplasia (VaIN) are considered potential precursors of invasive squamous cell carcinoma. VaIN is about 100 times less common than cervical intraepithelial neoplasia (CIN), and is about three times less frequent than vulvar intraepithelial neoplasia (VIN).[44,45] Patients with VaIN typically are asymptomatic and present with an abnormal Pap smear. Although the mean age has been reported as 50 years,[46] more recent studies have found VaIN in a younger group of patients with a mean age of 35 years.[47] Patients with VaIN often have concurrent or previously treated human papillomavirus (HPV)-related disease in the form of CIN, VIN, or invasive squamous carcinoma of the lower genital tract.[45,46] About 80% to 90% of VaIN lesions are found within the upper vagina, and they are often multifocal.[46–48] Their subtle gross features are best appreciated under colposcopic visualization, where the presence of acetowhite epithelium is the most commonly observed abnormality.[47]

VaIN is subdivided into grades 1 through 3 in a manner directly analogous to CIN (Chapter 3). Examples of various grades of VaIN are presented in Figures 2.29–2.31. As in the vulva and cervix, some pathologists refer to grade 1 lesions as low-grade and combine grades 2 and 3 into a high-grade category. Most VaIN 1 and nearly all VaIN 3 lesions are associated with high-risk HPV.[49,50] Flat condylomas are not appreciably different from VaIN 1 of the type with mild dysplasia in the lower third of the epithelium in terms of mean age, frequency of past history of HPV infection, HPV profiles, MIB-1 staining patterns, biologic behavior, and clinical management, and they can be difficult to distinguish from one another histologically.[50] For these reasons, flat condylomas are considered to be within the spectrum of or indistinguishable from VaIN 1 by most investigators.

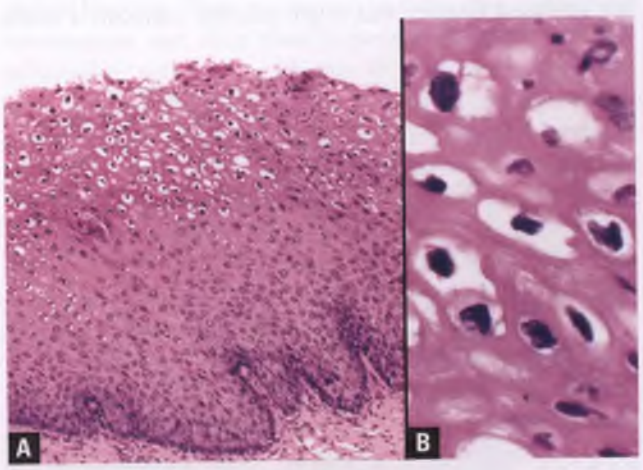

FIGURE 2.29. VaIN 1/flat condyloma. **A**: Koilocytes are prominent in the superficial portion of the epithelium. **B**: High-magnification view of koilocytes.

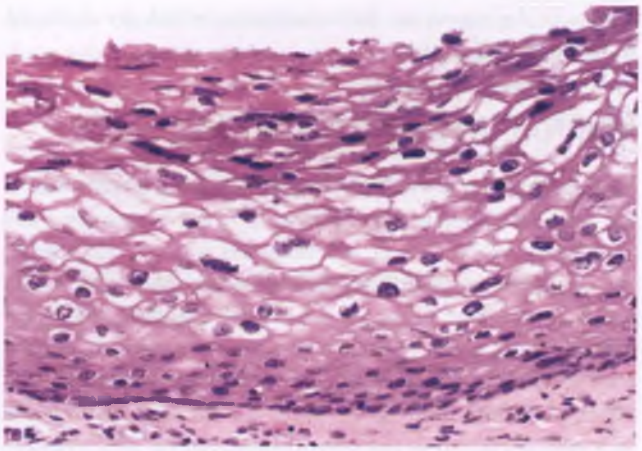

FIGURE 2.30. VaIN 1/flat condyloma. In this example, koilocytes are present throughout all but the bottom few layers of cells.

Differential Diagnosis

The most common differential diagnostic dilemma involves distinguishing variants of normal from viral cytopathic effect (koilocytosis) at the lower end of the spectrum. An example of vaginal squamous epithelium with perinuclear halos that should be regarded as being within the range of normal is illustrated in Figure 2.32. Although probably not cost-effective, MIB-1 immunostaining can be utilized to assist with this distinction. VaIN 1 will typically contain clusters of two or more MIB-1–positive nuclei in the upper two-thirds of the epithelium, whereas normal squamous epithelium with pseudokoilocytic changes will show staining only at or below the parabasal region (avoid counting immunoreactive parabasal cells lining loops of upwardly projecting stroma or immunoreactive intraepithelial lymphocytes as staining patterns supportive of VaIN).[50] It is recommended that the same conservative approach to the diagnosis of cervical LSIL as described in Chapter 3 be applied to VaIN 1, which translates into classifying equivocal biopsies that might possibly represent a subtle

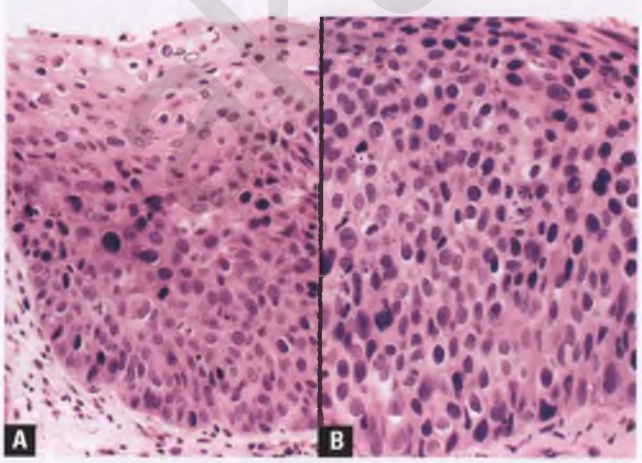

FIGURE 2.31. High-grade VaIN. **A**: VaIN 2. **B**: VaIN 3.

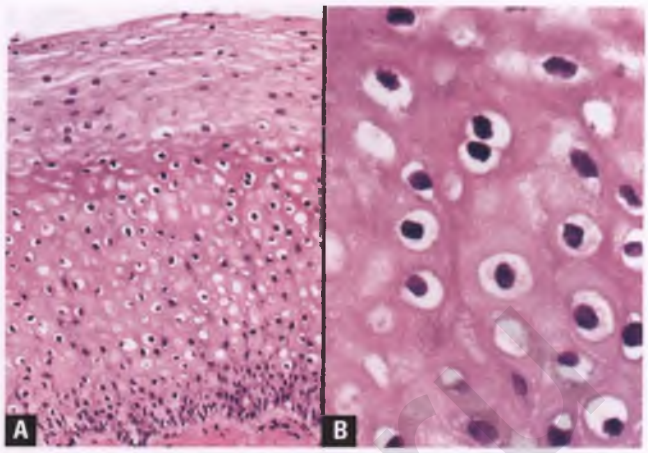

FIGURE 2.32. **A,B**: Vaginal squamous epithelium with no significant abnormality. The cells within the intermediate zone have prominent perinuclear halos, but the other features of koilocytosis as described in the section on flat condyloma/CIN 1 in Chapter 3 are lacking.

form of VaIN 1 as being within normal limits without resorting to immunohistochemistry. The section on the differential diagnosis of squamous intraepithelial lesions in Chapter 3 further addresses mimics of koilocytosis, and also discusses how to distinguish epithelial atrophy from high-grade dysplasia.

Behavior

Due to its rarity, the natural history of VaIN is not well characterized, but the following broad generalizations can be made: (a) spontaneous regression appears to be frequent, particularly in low-grade lesions, (b) some patients develop persistent or recurrent disease (particularly those with multifocal or more conservatively treated lesions), and (c) progression to invasive carcinoma occurs in approximately 5% of cases.[45,47,51]

SQUAMOUS CELL CARCINOMA

Squamous cell carcinoma of the vagina is a rare disease, but still accounts for the vast majority of malignant neoplasms in this site.[52,53] The typical presentation is a postmenopausal woman (mean age 67 years) with vaginal bleeding due to the presence of an ulcerated, exophytic, or endophytic vaginal mass.[54] About 20% to 30% of patients with vaginal squamous cell carcinoma have a history of CIN or cervical cancer, and these patients tend to present at a younger age.[53,55] In a recent study, approximately 80% of vaginal squamous cell carcinomas were found to contain detectable HPV-DNA.[56] In addition to behavior that increases the risk of exposure to HPV[55] (see section on the role of HPV in SIL in Chapter 3), other possible cofactors that may particularly play a role in the development of vaginal squamous cell carcinoma in older patients are low estrogen levels and history of vaginal trauma.[53]

Histologically, conventional squamous cell carcinoma of the vagina is indistinguishable from its counterpart in the uterine cervix (see Chapter 3). Verrucous, warty, sarcomatoid, and

lymphoepithelioma-like variants of squamous cell carcinoma are also uncommonly seen in the vagina.

Not surprisingly, the prognosis of vaginal squamous cell carcinoma is largely driven by the stage of the tumor, with 5-year survival rates being significantly worse for advanced-stage tumors in comparison with tumors limited to the vaginal wall.[52,54] Advanced patient age and large tumor size (≥4 cm) have also been found to be predictive of poor disease-specific survival.[54]

CLEAR CELL CARCINOMA

Women with a history of in utero exposure to DES have an estimated 1 in 1,000 chance of developing clear cell carcinoma of the vagina or cervix, with nearly all such tumors occurring between ages 15 and 35 years (median age 19 years).[2] Shortly after the association between DES and clear cell carcinoma became apparent in 1971,[57] physicians were warned to stop prescribing DES to pregnant women (to add insult to injury, DES had been shown many years earlier to be ineffective in preventing miscarriages and premature births, for which it was often prescribed).[58] The peak incidence of DES-related clear cell carcinomas occurred in the United States in 1975.[2] Now that the wave of DES-related clear cell carcinomas has past, vaginal tumors of this type have once again become quite rare and typically occur in postmenopausal women. When confined to the vaginal wall (Stage I), clear cell carcinoma is associated with a good prognosis.[59]

Vaginal clear cell carcinoma usually presents with abnormal vaginal bleeding or an abnormal Pap smear, and was sometimes found by screening of high-risk patients during the DES era.[59] Tumors vary from microscopic to huge, and may be polypoid, nodular, flat, or ulcerated (Fig. 2.33).[1] An example of the histologic appearance of vaginal clear cell carcinoma is presented in Figure 2.34. These tumors exhibit the same nuclear, cytoplasmic, and architectural features as clear cell carcinomas of the cervix, endometrium, and ovary, which are illustrated in Chapters 3, 4, and 7, respectively. When extensively sampled, vaginal clear cell carcinoma can usually be found in association with atypical adenosis, which may represent a transitional form between adenosis and carcinoma.[4]

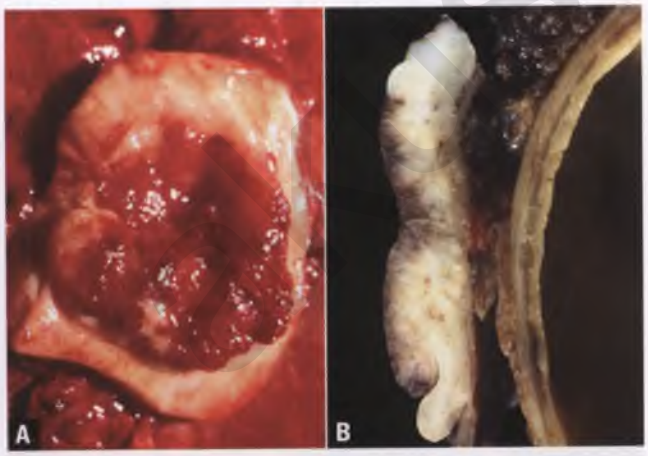

FIGURE 2.33. Clear cell carcinoma. **A**: The tumor appears as an elevated plaque in this fresh partial vaginectomy specimen. Its red, granular surface is largely due to the presence of overlying adenosis. The tissue in the background is an attached segment of rectum. **B**: In this cross section through the tumor after formalin fixation, the white to pale yellow clear cell carcinoma is seen deeply infiltrating the vaginal wall, but does not extend into the soft tissue of the rectovaginal septum or muscularis propria of the bowel. (Courtesy of Dr. Deborah J. Gersell.)

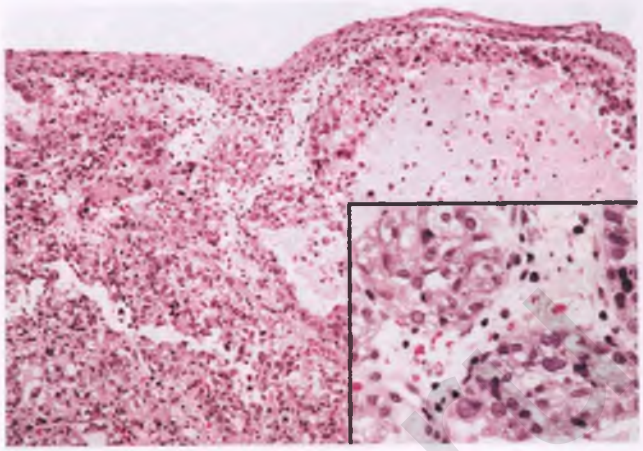

FIGURE 2.34. Clear cell carcinoma. The tumor is seen infiltrating vaginal stroma beneath intact squamous epithelium. The inset highlights the nuclear pleomorphism and pale to clear cytoplasm of the malignant cells within tumor cell nests.

The distinction of clear cell carcinoma from adenosis with microglandular hyperplasia is discussed in the section on adenosis.

ENDOMETRIOID ADENOCARCINOMA[8]

Primary vaginal endometrioid adenocarcinomas typically occur in adult women (mean age 60 years) who present with vaginal bleeding. These rare tumors resemble their endometrial counterparts, and share their propensity to exhibit a variety of histologic patterns (see Chapter 4). A potentially confusing pattern that is worth highlighting features prominent spindle cell growth thought to be secondary to abortive squamous metaplasia that results in a predominantly solid tumor with a biphasic appearance (Fig. 2.35). The discussion regarding the appropriate grading of these biphasic tumors and their distinction from carcinosarcoma in the section in Chapter 3 on endometrioid carcinoma with a prominent spindle cell component is equally relevant for vaginal tumors of this type.

Primary vaginal endometrioid adenocarcinomas are usually associated with endometriosis, from which they presumably arise, and whose identification helps to differentiate a primary tumor from the much more common situation of metastatic endometrioid carcinoma of endometrial origin. Metastatic colorectal adenocarcinoma can also simulate endometrioid carcinoma, but can be suspected by virtue of (a) a history of a colon cancer of similar histology or synchronous intestinal mass, (b) the absence of associated endometriosis,

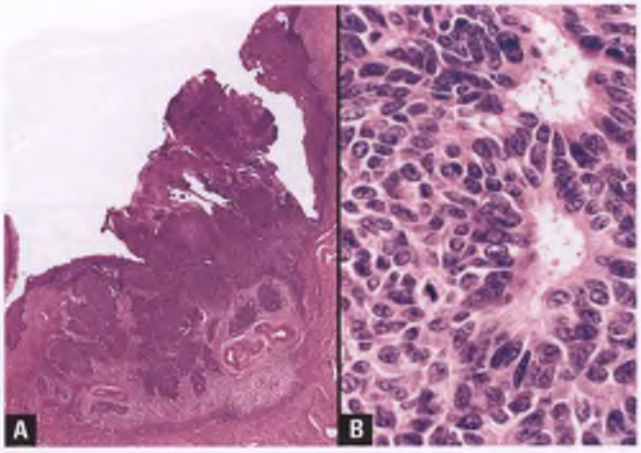

FIGURE 2.35. Vaginal endometrioid carcinoma with a prominent spindle cell component. **A**: At low magnification, a cellular, predominantly solid-appearing tumor is seen infiltrating the superficial vaginal stroma. **B**: At high magnification, scattered neoplastic glands of endometrioid type are seen merging with a proliferation of bland cells with ovoid to spindle-shaped nuclei that are thought to represent an abortive form of squamous differentiation.

and (c) its typical $CK7^-/CK20^+/CDX2^+$ immunophenotype, which contrasts with the $CK7^+/CK20^-/CDX2^-$ immunophenotype that is expected for endometrioid carcinomas of the female genital tract.[60]

INTESTINAL-TYPE EPITHELIAL NEOPLASMS

Isolated cases of tubulovillous adenoma and intestinal-type adenocarcinoma of the vagina have been reported.[61–63] The histologic differential diagnosis includes prolapse of the fimbriated portion of the fallopian tube, metastatic colorectal adenocarcinoma, and both primary and metastatic endometrioid adenocarcinoma.

PAPILLARY CARCINOMA WITH TRANSITIONAL OR SQUAMOTRANSITIONAL FEATURES

A few cases of vaginal carcinoma with papillary architecture have been reported that exhibit either pure transitional or squamotransitional differentiation.[64,65]

SMALL CELL NEUROENDOCRINE CARCINOMA

Primary small cell neuroendocrine carcinoma of the vagina is very rare, occurs in women with a mean age of 59 years, often presents with vaginal bleeding and spread beyond the vagina, pursues an aggressive clinical course, and has a histologic appearance similar to its counterparts in other sites such as the lung and uterine cervix.[66] The cervical version of this tumor is discussed and illustrated in Chapter 3.

CARCINOSARCOMA (MALIGNANT MIXED MÜLLERIAN TUMOR)

A limited number of primary vaginal carcinosarcomas have been reported.[67] These tumors typically occur in postmenopausal women, may be associated with a prior history of radiation therapy, and often pursue an aggressive course. In contrast to their much more common counterpart in the uterine corpus, vaginal carcinosarcomas (a) have a carcinomatous component that usually consists of squamous cell carcinoma rather than adenocarcinoma, (b) may be associated with VaIN 3, and (c) may contain HPV-DNA. Carcinosarcomas of the uterine cervix have a tendency to exhibit similar characteristics, and should be included in the differential diagnosis (see Chapter 3). The possibility of an endometrial or ovarian source should be considered in all cases of vaginal carcinosarcoma, but particularly in those whose malignant epithelial component is adenocarcinoma.

SARCOMA BOTRYOIDES (EMBRYONAL RHABDOMYOSARCOMA)[68]

Sarcoma botryoides is named for its clinical and gross appearance that resembles a conglomerate of soft, edematous, grape-like structures (botryoid = grape-like in Greek) that often protrudes through the vaginal introitus (Fig. 2.36). This malignant tumor with skeletal muscle differentiation is a subtype of embryonal rhabdomyosarcoma that acquires a botryoid growth pattern as a consequence of growing beneath an epithelial-lined cavity into which the tumor can expand. Although this tumor is the most common vaginal sarcoma, it is still quite rare. In this location, the vast majority of cases occur in patients <5 years of age who present with a vaginal mass and/or vaginal bleeding.

Histologically, sarcoma botryoides is composed of aggregates of papillary and polypoid structures lined by native

FIGURE 2.36. Sarcoma botryoides. **A**: Botryoid formations at Meramec Caverns in Stanton, Missouri. (With permission of Mr. Lester Turilli.) **B**: Red, edematous, polypoid tumor with a smooth and glistening surface protruding from the vaginal mucosa of a young girl. (Vaginal gross photograph courtesy of Dr. Deborah J. Gersell.)

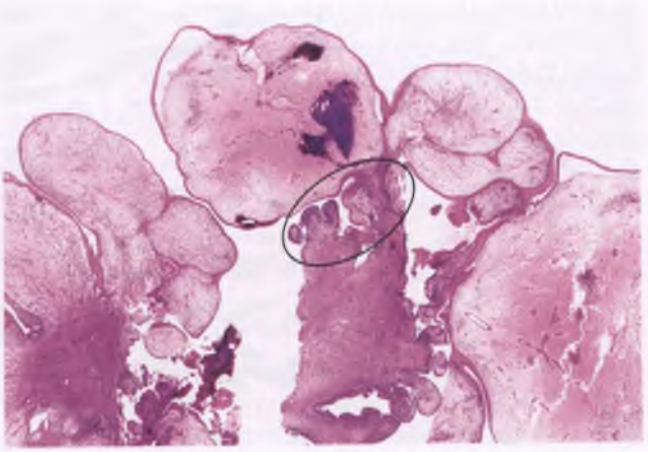

FIGURE 2.37. Sarcoma botryoides. These tumors are often deceptively bland at low magnification and resemble benign polyps with a squamous epithelial lining. In the edematous polypoid fragments, the cambium layer is inapparent or subtle. However, this hypercellular subepithelial zone is more visible in the central tissue fragment with a papillary contour, particularly within the *circled* region.

squamous epithelium that is often attenuated and/or focally ulcerated (Fig. 2.37). The major clue to the correct diagnosis at low magnification is the identification of a cambium layer, which is a densely cellular subepithelial band of primitive cells that overlies a less cellular edematous region (Fig. 2.38). The cambium layer is typically most apparent in the smaller papillary fragments with scalloped contours, and is often subtle or absent in the larger polypoid fragments with rounded contours and edematous stromal cores (Fig. 2.37). Samples in which these large polypoid fragments with edematous, paucicellular stroma predominate are at high risk for being misinterpreted as benign polyps. Once the cambium layer has been at least focally identified, examination at high magnification should confirm that this region is composed of primitive cells with mitotic activity (Fig. 2.39A), and a search for rhabdomyoblasts should

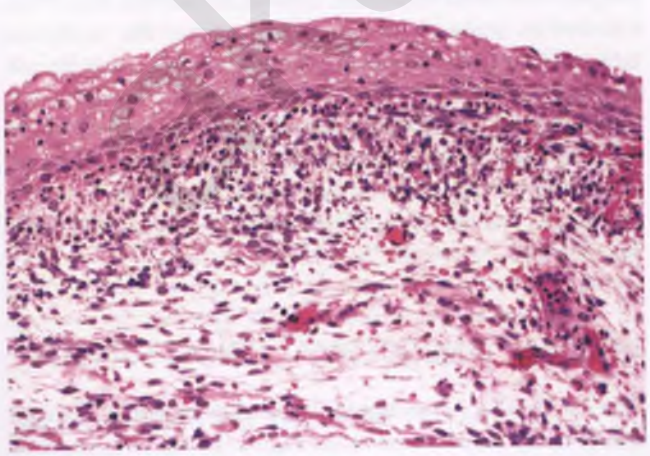

FIGURE 2.38. Sarcoma botryoides. This image is from an area where the subepithelial cambium layer is readily apparent.

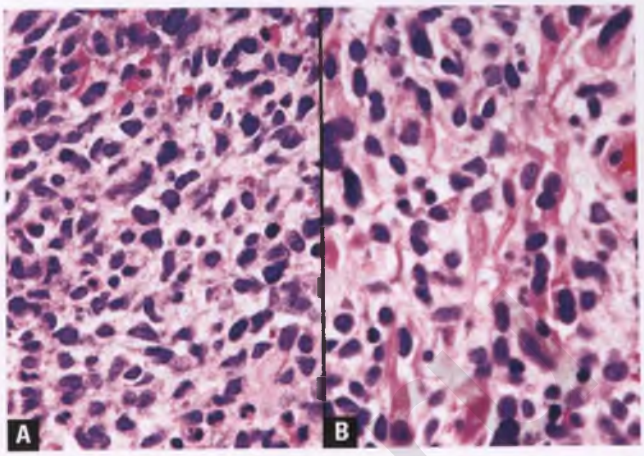

FIGURE 2.39. Sarcoma botryoides. **A**: Primitive malignant cells from the cambium layer. **B**: Several strap-shaped rhabdomyoblasts are present in this portion of the tumor.

commence. Rhabdomyoblasts are often found in the less cellular regions, and are recognized by their abundant eosinophilic cytoplasm and round to strap-shaped forms (Fig. 2.39B). Cross-striations may be found within some of the rhabdomyoblasts, but are not essential for their recognition. Although desmin immunoreactivity can help to highlight rhabdomyoblasts, nuclear staining with myogenin and/or myoD1 provides more specific evidence of skeletal muscle differentiation, but may not be present in all such cases.[69] An interesting and potentially confusing finding that may be present in sarcoma botryoides is infiltration of the overlying squamous epithelium by tumor cells in a pagetoid fashion (Fig. 2.40).

Differential Diagnosis

In the vagina, the main differential diagnostic considerations are cellular fibroepithelial polyp with atypical stromal

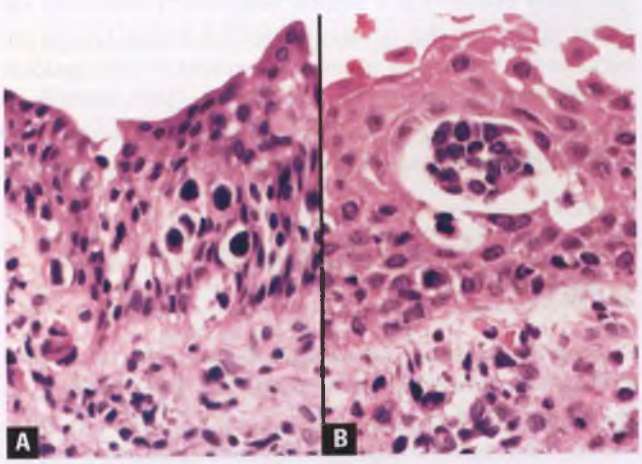

FIGURE 2.40. Sarcoma botryoides with pagetoid spread. **A**: Individual malignant cells are present within the squamous epithelium. **B**: In this example, there is an intraepithelial nest of embryonal rhabdomyosarcoma.

cells, rhabdomyoma, and müllerian papilloma. Features that distinguish an "uppity" fibroepithelial polyp from sarcoma botryoides have been discussed earlier in this chapter. In contrast to sarcoma botryoides, rhabdomyomas occur in adults rather than infants and young children, have a slow growth rate, lack a cambium layer, are composed of mature skeletal muscle cells, and do not contain a mitotically active, primitive-appearing component. Although the clinical setting and age range of patients with müllerian papilloma overlaps with that of sarcoma botryoides, the müllerian papilloma is distinguished by its lack of a cambium layer, absence of rhabdomyoblasts, bland stroma, and epithelial lining, which is dominated by a single layer of flattened, cuboidal, or columnar rather than squamous epithelial cells.[41]

Treatment and Prognosis

Before the advent of effective multiagent chemotherapy, vaginal sarcoma botryoides was treated with radical surgery and had a dismal prognosis. Currently, most patients are effectively treated by combination chemotherapy following their biopsy diagnosis or local excision, with organ removal reserved for patients with persistent or recurrent disease.[70]

LEIOMYOSARCOMA[32,71]

Vaginal leiomyosarcoma is a rare tumor that typically presents in adult women as a vaginal mass that may be associated with pain or vaginal bleeding. Based on limited outcome data, vaginal smooth muscle tumors are considered leiomyosarcomas if they exhibit moderate to severe nuclear atypia and ≥5 mitotic figures per 10 high power fields. Infiltrating tumor margins are also a potentially ominous finding, and tumors with recurring or metastatic potential are generally at least 3 cm in diameter. Tumor cell necrosis in these neoplasms is rare and has not been specifically evaluated as a possible prognostic factor. With the recent recognition that extragastrointestinal stromal tumors can occur in the vagina and rectovaginal septum,[72,73] it is prudent to screen potential vaginal leiomyosarcomas (particularly those that are >4 cm and mitotically active without marked nuclear atypia) with desmin and c-KIT immunostains (see next section).

EXTRAGASTROINTESTINAL STROMAL TUMOR[72,73]

Although quite rare, pathologists need to be aware that extragastrointestinal stromal tumors can present as a nodular mass within the vagina or rectovaginal septum. In this site, these tumors are generally composed of interlacing fascicles of spindle-shaped cells, and usually have a size and mitotic rate that warrant classification as a high-risk extragastrointestinal stromal tumor, which can also be referred to as extragastrointestinal stromal sarcoma or malignant extragastrointestinal stromal tumor (Fig. 2.41). These tumors bear a strong resemblance to smooth muscle tumors, and this difficult differential diagnosis

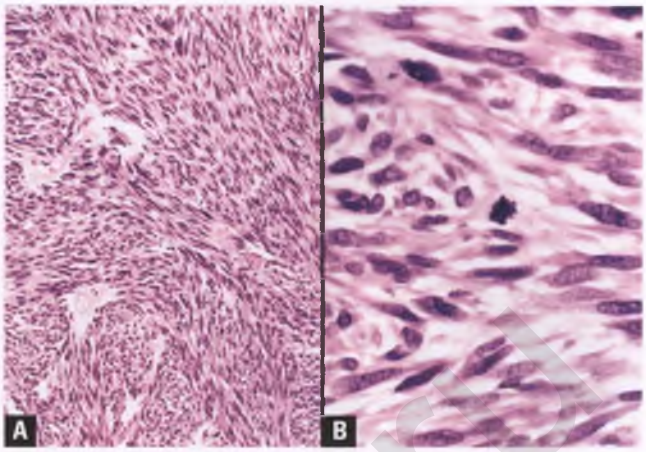

FIGURE 2.41. **A,B**: Extragastrointestinal stromal sarcoma. Note the resemblance of this spindle cell tumor to a smooth muscle neoplasm.

is best resolved by immunohistochemistry. Vaginal smooth muscle tumors typically exhibit a desmin-positive, c-KIT (CD117)-negative immunophenotype, whereas extragastrointestinal stromal tumors can be expected to be desmin negative and c-KIT positive. If both markers yield negative results, S100 should be added to the panel to exclude amelanotic spindle cell melanoma (additional immunostains may be necessary in complicated cases). In an era in which high-risk and recurrent/metastatic extragastrointestinal stromal tumors may be treated with tyrosine kinase inhibitors, proper recognition of these tumors takes on additional importance.

MALIGNANT MELANOMA[74]

Melanoma accounts for approximately 3% of malignant vaginal tumors, and typically presents as vaginal bleeding or as a vaginal mass in postmenopausal women with a mean age of 60 years. Most tumors are nodular or polypoid, ulcerated, pigmented, and deeply invasive, and are associated with a poor prognosis. Nodular melanoma is the dominant histologic type, followed by mucosal lentiginous melanoma. The malignant cells infiltrating the dermis may be of epithelioid, spindle cell, or mixed cell types, and may be pigmented or amelanotic. The discussion of the various aspects of melanoma and its differential diagnosis that is presented in the section on vulvar melanoma in Chapter 1 is also largely applicable to vaginal melanoma, and the reader is referred to this discussion for further details.

YOLK SAC (ENDODERMAL SINUS) TUMOR[75]

Yolk sac tumor is a primitive form of malignant germ cell tumor that is rarely encountered in the vagina. In this site, nearly all patients are young girls under 3 years of age who present with vaginal bleeding related to the presence of a polypoid or sessile vaginal mass that is usually <5 cm. In most cases, the serum α-fetoprotein (AFP) is elevated, and in this group of patients

this marker can be periodically measured to monitor the efficacy of treatment or to screen for recurrent disease.

Grossly, yolk sac tumors are soft and easily fragmented and have a sectioned surface that is white to pale tan with interspersed areas of hemorrhage and necrosis. Histologically, these tumors show the same set of patterns that are seen in their more common counterparts in the ovary (see Chapter 7 for a detailed discussion).

Differential Diagnosis

Clinically, the main differential diagnostic consideration is sarcoma botryoides, which is also quite rare but nevertheless represents the most common malignant vaginal tumor of young children. Prior to biopsy, an elevated serum AFP and an absence of grape-like structures would favor yolk sac tumor. Once a tissue sample has been taken, yolk sac tumor and sarcoma botryoides are easily distinguished from one another on histologic grounds. A much more difficult differential diagnosis at the microscopic level is clear cell carcinoma, but this tumor has not been reported to occur in the <3-year-old age group that typifies yolk sac tumor. Clear cell carcinoma can also be separated from yolk sac tumor on the basis of a normal serum AFP and a variety of histologic and immunologic features as discussed in Chapter 7.

Treatment and Prognosis

Prior to the advent of effective multiagent chemotherapy, the prognosis of vaginal endodermal sinus tumor was poor despite radical surgical procedures to remove the primary tumor. Currently, most patients are cured by the use of preoperative and/or postoperative chemotherapy in conjunction with conservative surgery.[76,77]

LYMPHOMA[78]

Non-Hodgkin's lymphomas that are localized to the vaginal region are considered primary vaginal tumors, and typically present in adult women with vaginal bleeding related to a vaginal mass. These rare tumors are usually of the diffuse large B-cell type, are often associated with areas of sclerosis, and are at risk for being misdiagnosed as nonlymphoid tumors such as poorly differentiated carcinoma, epithelioid leiomyosarcoma, or melanoma. Once lymphoma is considered in the differential diagnosis and the appropriate immunostains are performed, the correct diagnosis is usually readily apparent. Primary vaginal lymphomas are generally treated with combined radiotherapy and chemotherapy and have a favorable prognosis.

METASTASES TO VAGINA[79]

Most invasive carcinomas of the vagina are secondary rather than primary malignancies. In addition to direct extension of tumors from the uterine cervix or vulva, metastases from endometrial, ovarian, and colorectal carcinomas also occur at appreciable frequencies. In the era prior to more effective treatment of uterine choriocarcinoma, this tumor would often metastasize to the vagina. Vaginal metastases from renal cell carcinoma are rare, but create the potential for misinterpretation as primary clear cell carcinoma.[80] Knowledge of the clinical history is helpful in this situation (presence of a renal mass or a history of a renal tumor with similar histology and the absence of a history of vaginal adenosis or in utero exposure to DES would be expected). In addition, the absence of admixed tubulocystic and papillary patterns and immunoreactivity of the tumor cells with CD10 and renal cell carcinoma marker would also support a renal origin.[60] Other tumors that have rarely been reported to metastasize to the vagina include transitional cell carcinoma of the urinary tract, breast carcinoma, and malignant melanoma.[79,81]

SUGGESTED READINGS

Clement PB, Young RH. *Atlas of Gynecologic Surgical Pathology*. 2nd ed. Philadelphia, PA: Elsevier Saunders; 2008.

Crum CP, Nucci, MR, Lee, K., eds. *Diagnostic Gynecologic and Obstetric Pathology*. 2nd ed. Philadelphia, PA: Elsevier Saunders; 2011.

Fu YS. *Pathology of the Uterine Cervix, Vagina, and Vulva*. 2nd ed. Philadelphia, PA: Saunders; 2002.

Kurman RJ, Ellenson LH, Ronnett BM, eds. *Blaustein's Pathology of the Female Genital Tract*. 6th ed. New York, NY: Springer; 2011.

Kurman RJ, Norris HJ, Wilkinson E. *Tumors of the Cervix, Vagina, and Vulva. Atlas of Tumor Pathology*. 3rd series, Fascicle 4. Washington, DC: Armed Forces Institute of Pathology; 1992:141–178.

Robboy, SJ, Mutter GL, Prat J, et al., eds. *Robboy's Pathology of the Female Reproductive Tract*. 2nd ed. Oxford, UK: Churchill Livingstone; 2009.

Tavassoli FA, Devilee P, eds. World Health Organization Classification of Tumors. In: *Pathology and Genetics of Tumours of the Breast and Female Genital Organs*. Lyon, France: IARC Press; 2003:291–311.

REFERENCES

1. Robboy SJ, Scully RE, Welch WR, et al. Intrauterine diethylstilbestrol exposure and its consequences: pathologic characteristics of vaginal adenosis, clear cell adenocarcinoma, and related lesions. *Arch Pathol Lab Med*. 1977;101:1–5.
2. Melnick S, Cole P, Anderson D, et al. Rates and risks of diethylstilbestrol-related clear-cell adenocarcinoma of the vagina and cervix. An update. *N Engl J Med*. 1987;316:514–516.
3. Robboy SJ, Hill EC, Sandberg EC, et al. Vaginal adenosis in women born prior to the diethylstilbestrol era. *Hum Pathol*. 1986;17:488–492.
4. Robboy SJ, Young RH, Welch WR, et al. Atypical vaginal adenosis and cervical ectropion. Association with clear cell adenocarcinoma in diethylstilbestrol-exposed offspring. *Cancer*. 1984;54:869–875.
5. Robboy SJ, Welch WR. Microglandular hyperplasia in vaginal adenosis associated with oral contraceptives and prenatal diethylstilbestrol exposure. *Obstet Gynecol*. 1977;49:430–434.
6. Clement PB. The pathology of endometriosis: a survey of the many faces of a common disease emphasizing diagnostic pitfalls and unusual and newly appreciated aspects. *Adv Anat Pathol*. 2007;14:241–260.
7. Parker RL, Dadmanesh F, Young RH, et al. Polypoid endometriosis: a clinicopathologic analysis of 24 cases and a review of the literature. *Am J Surg Pathol*. 2004;28:285–297.
8. Staats PN, Clement PB, Young RH. Primary endometrioid adenocarcinoma of the vagina: a clinicopathologic study of 18 cases. *Am J Surg Pathol*. 2007;31:1490–1501.
9. Berkowitz RS, Ehrmann RL, Knapp RC. Endometrial stromal sarcoma arising from vaginal endometriosis. *Obstet Gynecol*. 1978;51:34s–37s.
10. Liu L, Davidson S, Singh M. Mullerian adenosarcoma of vagina arising in persistent endometriosis: report of a case and review of the literature. *Gynecol Oncol*. 2003;90:486–490.
11. Pradhan S, Tobon H. Vaginal cysts: a clinicopathological study of 41 cases. *Int J Gynecol Pathol*. 1986;5:35–46.

12. Norris HJ, Taylor HB. Polyps of the vagina. A benign lesion resembling sarcoma botryoides. *Cancer.* 1966;19:227–232.
13. Nucci MR, Young RH, Fletcher CDM. Cellular pseudosarcomatous fibroepithelial stromal polyps of the lower female genital tract: an underrecognized lesion often misdiagnosed as sarcoma. *Am J Surg Pathol.* 2000;24:231–240.
14. Chirayil SJ, Tobon H. Polyps of the vagina: a clinicopathologic study of 18 cases. *Cancer.* 1981;47:2904–2907.
15. Hartmann CA, Sperling M, Stein H. So-called fibroepithelial polyps of the vagina exhibiting an unusual but uniform antigen profile characterized by expression of desmin and steroid hormone receptors but no muscle-specific actin or macrophage markers. *Am J Clin Pathol.* 1990;93:604–608.
16. McCluggage WG, Young RH. Tubulo-squamous polyp: a report of ten cases of a distinctive hitherto uncharacterized vaginal polyp. *Am J Surg Pathol.* 2007;31:1013–1019.
17. Stewart CJ. Tubulo-squamous vaginal polyp with basaloid epithelial differentiation. *Int J Gynecol Pathol.* 2009;28:563–566.
18. Chaturvedi A, Padel A. Tubulo-squamous polyp of the vagina with sebaceous glands: novel features in an uncommon recently described entity. *Int J Gynecol Pathol.* 2010;29:494–496.
19. Wheelock JB, Schneider V, Goplerud DR. Prolapsed fallopian tube masquerading as adenocarcinoma of the vagina in a postmenopausal woman. *Gynecol Oncol.* 1985;21:369–375.
20. Sapan IP, Solberg NS. Prolapse of the uterine tube after abdominal hysterectomy. *Obstet Gynecol.* 1973;42:26–32.
21. Varnholt H, Otis CN, Nucci MR, et al. Fallopian tube prolapse mimicking aggressive angiomyxoma. *Int J Gynecol Pathol.* 2005;24:292–294.
22. Michal M, Rokyta Z, Mejchar B, et al. Prolapse of the fallopian tube after hysterectomy associated with exuberant angiomyofibroblastic stroma response: a diagnostic pitfall. *Virchows Arch.* 2000;437:436–439.
23. Proppe KH, Scully RE, Rosai J. Postoperative spindle cell nodules of genitourinary tract resembling sarcomas. A report of eight cases. *Am J Surg Pathol.* 1984;8:101–108.
24. Wick MR, Brown BA, Young RH, et al. Spindle-cell proliferations of the urinary tract. An immunohistochemical study. *Am J Surg Pathol.* 1988;12:379–389.
25. Kramer K, Tobon H. Vaginitis emphysematosa. *Arch Pathol Lab Med.* 1987;111:746–749.
26. Chalvardjian A, Picard L, Shaw R, et al. Malacoplakia of the female genital tract. *Am J Obstet Gynecol.* 1980;138:391–394.
27. Chen KT, Hendricks EJ. Malakoplakia of the female genital tract. *Obstet Gynecol.* 1985;65:84S–87S.
28. Kogulan PK, Smith M, Seidman J, et al. Malakoplakia involving the abdominal wall, urinary bladder, vagina, and vulva: case report and discussion of malakoplakia-associated bacteria. *Int J Gynecol Pathol.* 2001;20:403–406.
29. Abdul-Karim FW, Cohen RE. Atypical stromal cells of lower female genital tract. *Histopathology.* 1990;17:249–253.
30. Bague S, Rodriguez IM, Prat J. Malignant mesonephric tumors of the female genital tract: a clinicopathologic study of 9 cases. *Am J Surg Pathol.* 2004;28:601–607.
31. Ersahin C, Huang M, Potkul RK, et al. Mesonephric adenocarcinoma of the vagina with a 3-year follow-up. *Gynecol Oncol.* 2005;99:757–760.
32. Tavassoli FA, Norris HJ. Smooth muscle tumors of the vagina. *Obstet Gynecol.* 1979;53:689–693.
33. Gold JH, Bossen EH. Benign vaginal rhabdomyoma: a light and electron microscopic study. *Cancer.* 1976;37:2283–2294.
34. Lin GY, Sun X, Badve S. Pathologic quiz case. Vaginal wall mass in a 47-year-old woman. Vaginal rhabdomyoma. *Arch Pathol Lab Med.* 2002;126:1241–1242.
35. Nielsen GP, Rosenberg AE, Young RH, et al. Angiomyofibroblastoma of the vulva and vagina. *Mod Pathol.* 1996;9:284–291.
36. Laskin WB, Fetsch JF, Tavassoli FA. Superficial cervicovaginal myofibroblastoma: fourteen cases of a distinctive mesenchymal tumor arising from the specialized subepithelial stroma of the lower female genital tract. *Hum Pathol.* 2001;32:715–725.
37. Ganesan R, McCluggage WG, Hirschowitz L, et al. Superficial myofibroblastoma of the lower female genital tract: report of a series including tumours with a vulval location. *Histopathology.* 2005;46:137–143.
38. Sirota RL, Dickersin GR, Scully RE. Mixed tumors of the vagina. A clinicopathological analysis of eight cases. *Am J Surg Pathol.* 1981;5:413–422.
39. Branton PA, Tavassoli FA. Spindle cell epithelioma, the so-called mixed tumor of the vagina. A clinicopathologic, immunohistochemical, and ultrastructural analysis of 28 cases. *Am J Surg Pathol.* 1993;17:509–515.
40. Oliva E, Gonzalez L, Dionigi A, et al. Mixed tumors of the vagina: an immunohistochemical study of 13 cases with emphasis on the cell of origin and potential aid in differential diagnosis. *Mod Pathol.* 2004;17:1243–1250.
41. Mierau GW, Lovell MA, Wyatt-Ashmead J, et al. Benign mullerian papilloma of childhood. *Ultrastruct Pathol.* 2005;29:209–216.
42. Ulbright TM, Alexander RW, Kraus FT. Intramural papilloma of the vagina: evidence of Mullerian histogenesis. *Cancer.* 1981;48:2260–2266.
43. McCluggage WG, Nirmala V, Radhakumari K. Intramural mullerian papilloma of the vagina. *Int J Gynecol Pathol.* 1999;18:94–95.
44. Robboy SJ, Welch WR. Selected topics in the pathology of the vagina. *Hum Pathol.* 1991;22:868–876.
45. Sillman FH, Fruchter RG, Chen YS, et al. Vaginal intraepithelial neoplasia: risk factors for persistence, recurrence, and invasion and its management. *Am J Obstet Gynecol.* 1997;176:93–99.
46. Audet-Lapointe P, Body G, Vauclair R, et al. Vaginal intraepithelial neoplasia. *Gynecol Oncol.* 1990;36:232–239.
47. Dodge JA, Eltabbakh GH, Mount SL, et al. Clinical features and risk of recurrence among patients with vaginal intraepithelial neoplasia. *Gynecol Oncol.* 2001;83:363–369.
48. Diakomanolis E, Stefanidis K, Rodolakis A, et al. Vaginal intraepithelial neoplasia: report of 102 cases. *Eur J Gynaecol Oncol.* 2002;23:457–459.
49. Srodon M, Stoler MH, Baber GB, et al. The distribution of low and high-risk HPV types in vulvar and vaginal intraepithelial neoplasia (VIN and VaIN). *Am J Surg Pathol.* 2006;30:1513–1518.
50. Logani S, Lu D, Quint WG, et al. Low-grade vulvar and vaginal intraepithelial neoplasia: correlation of histologic features with human papillomavirus DNA detection and MIB-1 immunostaining. *Mod Pathol.* 2003;16:735–741.
51. Aho M, Vesterinen E, Meyer B, et al. Natural history of vaginal intraepithelial neoplasia. *Cancer.* 1991;68:195–197.
52. Creasman WT, Phillips JL, Menck HR. The National Cancer Data Base report on cancer of the vagina. *Cancer.* 1998;83:1033–1040.
53. Hellman K, Silfversward C, Nilsson B, et al. Primary carcinoma of the vagina: factors influencing the age at diagnosis. The Radiumhemmet series 1956–96. *Int J Gynecologic Cancer.* 2004;14:491–501.
54. Hellman K, Lundell M, Silfversward C, et al. Clinical and histopathologic factors related to prognosis in primary squamous cell carcinoma of the vagina. *Int J Gynecologic Cancer.* 2006;16:1201–1211.
55. Daling JR, Madeleine MM, Schwartz SM, et al. A population-based study of squamous cell vaginal cancer: HPV and cofactors. *Gynecol Oncol.* 2002;84:263–270.
56. Ferreira M, Crespo M, Martins L, et al. HPV DNA detection and genotyping in 21 cases of primary invasive squamous cell carcinoma of the vagina. *Mod Pathol.* 2008;21:968–972.
57. Herbst AL, Ulfelder H, Poskanzer DC. Adenocarcinoma of the vagina. Association of maternal stilbestrol therapy with tumor appearance in young women. *N Engl J Med.* 1971;284:878–881.
58. Dieckmann WJ, Davis ME, Rynkiewicz LM, et al. Does the administration of diethylstilbestrol during pregnancy have therapeutic value? *Am J Obstet Gynecol.* 1953;66:1062–1081.
59. Hanselaar AG, Van Leusen ND, De Wilde PC, et al. Clear cell adenocarcinoma of the vagina and cervix. A report of the Central Netherlands Registry with emphasis on early detection and prognosis. *Cancer.* 1991;67:1971–1978.
60. Baker PM, Oliva E. Immunohistochemistry as a tool in the differential diagnosis of ovarian tumors: an update. *Int J Gynecol Pathol.* 2005;24:39–55.
61. Fox H, Wells M, Harris M, et al. Enteric tumours of the lower female genital tract: a report of three cases. *Histopathology.* 1988;12:167–176.
62. Lee SE, Park NH, Park IA, et al. Tubulo-villous adenoma of the vagina. *Gynecol Oncol.* 2005;96:556–558.
63. Heller DS, Merrell M, Sama J, et al. Periurethral vaginal adenocarcinoma of the intestinal type: report of two cases and review of the literature. *Gynecol Oncol.* 2000;77:478–481.
64. Rose PG, Stoler MH, Abdul-Karim FW. Papillary squamotransitional cell carcinoma of the vagina. *Int J Gynecol Pathol.* 1998;17:372–375.
65. Singer G, Hohl MK, Hering F, et al. Transitional cell carcinoma of the vagina with pagetoid spread pattern. *Hum Pathol.* 1998;29:299–301.
66. Bing Z, Levine L, Lucci JA, et al. Primary small cell neuroendocrine carcinoma of the vagina: a clinicopathologic study. *Arch Pathol Lab Med.* 2004;128:857–862.
67. Sebenik M, Yan Z, Khalbuss WE, et al. Malignant mixed mullerian tumor of the vagina: case report with review of the literature, immunohistochemical study, and evaluation for human papilloma virus. *Hum Pathol.* 2007;38:1282–1288.

68. Hilgers RD, Malkasian GD Jr, Soule EH. Embryonal rhabdomyosarcoma (botryoid type) of the vagina. A clinicopathologic review. *Am J Obstet Gynecol* 1970;107:484–502.
69. Riedlinger WF, Kozakewich HP, Vargas SO. Myogenic markers in the evaluation of embryonal botryoid rhabdomyosarcoma of the female genital tract. *Pediatr Dev Pathol.* 2005;8:355–361.
70. Andrassy RJ, Wiener ES, Raney RB, et al. Progress in the surgical management of vaginal rhabdomyosarcoma: a 25-year review from the Intergroup Rhabdomyosarcoma Study Group. *J Pediatr Surg.* 1999;34:731–735.
71. Ciaravino G, Kapp DS, Vela AM, et al. Primary leiomyosarcoma of the vagina. A case report and literature review. *Int J Gynecol Cancer.* 2000;10:340–347.
72. Lam MM, Corless CL, Goldblum JR, et al. Extragastrointestinal stromal tumors presenting as vulvovaginal/rectovaginal septal masses: a diagnostic pitfall. *Int J Gynecol Pathol.* 2006;25:288–292.
73. Molina I, Seamon LG, Copeland LJ, et al. Reclassification of leiomyosarcoma as an extra-gastrointestinal stromal tumor of the gynecologic tract. *Int J Gynecol Pathol.* 2009;28:458–463.
74. Gupta D, Malpica A, Deavers MT, et al. Vaginal melanoma: a clinicopathologic and immunohistochemical study of 26 cases. *Am J Surg Pathol.* 2002;26: 1450–1457.
75. Young RH, Scully RE. Endodermal sinus tumor of the vagina: a report of nine cases and review of the literature. *Gynecol Oncol.* 1984;18: 380–392.
76. Mauz-Korholz C, Harms D, Calaminus G, et al. Primary chemotherapy and conservative surgery for vaginal yolk-sac tumour. Maligne Keimzelltumoren Study Group. *Lancet.* 2000;355:625.
77. Hwang EH, Han SJ, Lee MK, et al. Clinical experience with conservative surgery for vaginal endodermal sinus tumor. *J Pediatr Surg.* 1996;31: 219–222.
78. Vang R, Medeiros LJ, Silva EG, et al. Non-Hodgkin's lymphoma involving the vagina: a clinicopathologic analysis of 14 patients. *Am J Surg Pathol.* 2000;24:719–725.
79. Mazur MT, Hsueh S, Gersell DJ. Metastases to the female genital tract. Analysis of 325 cases. *Cancer.* 1984;53:1978–1984.
80. Allard JE, McBroom JW, Zahn CM, et al. Vaginal metastasis and thrombocytopenia from renal cell carcinoma. *Gynecol Oncol.* 2004;92:970–973.
81. Gupta D, Neto AG, Deavers MT, et al. Metastatic melanoma to the vagina: clinicopathologic and immunohistochemical study of three cases and literature review. *Int J Gynecol Pathol.* 2003;22:136–140.

CHAPTER 3

Pathology of the Uterine Cervix with Pap Smear Correlation

OVERVIEW OF ANATOMY, HISTOLOGY, AND CYTOLOGY OF THE NORMAL CERVIX

Anatomy

The cervix is the cylindrical inferior portion of the uterus, and consists of the exocervix (also referred to as the ectocervix) and the endocervix. The exocervix protrudes into the vagina, whereas the endocervix extends from the external cervical os (the opening of the endocervical canal that is located in the central portion of the exocervix) to the indistinct region of the isthmus known as the internal cervical os. The normal exocervix can exhibit a range of appearances, depending upon the parity of the patient and the presence and extent of cervical ectropion, which is everted endocervical mucinous mucosa (Fig. 3.1). The red, velvety gross appearance of this everted tissue is sometimes incorrectly referred to as an "erosion" because of its resemblance to superficial ulceration, but its histologic correlate is simply villous projections of highly vascular endocervical-type mucosa.

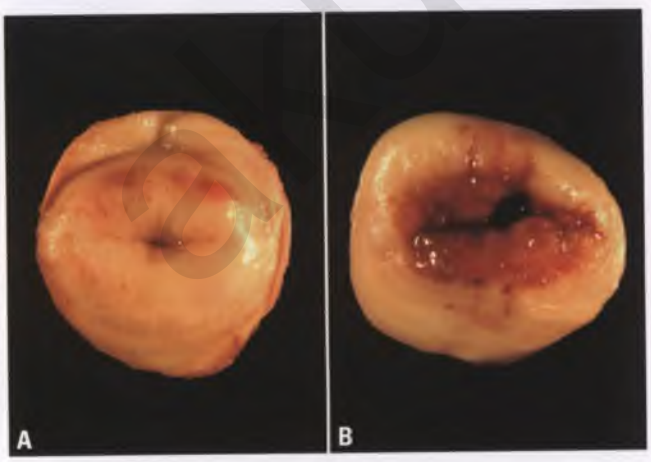

FIGURE 3.1. Varying normal appearances of the uterine cervix. **A**: Nulliparous cervix with small, round to oval external os. An asymmetric rim of vaginal cuff mucosa is also present. **B**: Parous cervix with slit-like, "fishmouth" external os and prominent ectropion.

Histology

The histologic features of normal exocervical stratified squamous epithelium are illustrated in Figure 3.2. The presence of perinuclear clearing in the intermediate cells, which is due to the presence of abundant glycogen, can lead to their misinterpretation as koilocytes, which are squamous cells with human papillomavirus (HPV)-related viral cytopathic effect (see section on squamous intraepithelial lesions). The endocervical canal is lined by a single layer of columnar mucinous epithelial cells that is contiguous with the lining of the underlying endocervical glands, which are actually cross sections of elongated clefts and their side channels rather than true glands (Figs. 3.3 and 3.4).

Starting at the original squamocolumnar junction (Fig. 3.5), columnar mucinous epithelium of the endocervix of postpubertal women is gradually replaced by squamous epithelium through a normal physiologic process known as squamous metaplasia.

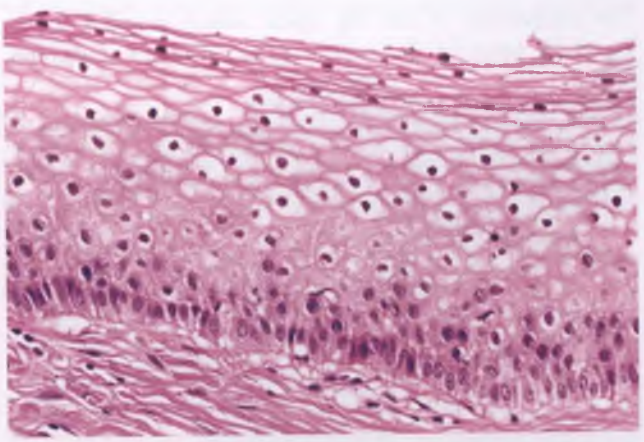

FIGURE 3.2. Nonkeratinized stratified squamous epithelium from the normal exocervix of a woman of reproductive age. Note the single layer of basal cells with palisaded "picket fence" nuclei with ascending maturation toward parabasal cells, intermediate cells, and superficial cells. Many of the intermediate cells exhibit perinuclear clearing, which is due to the presence of abundant glycogen rather than HPV-related viral cytopathic effect.

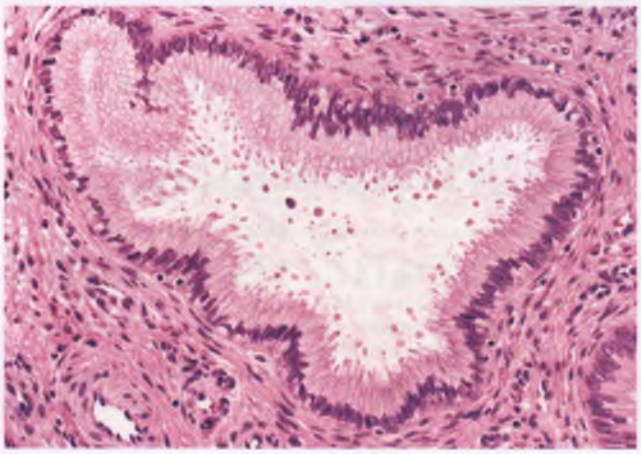

FIGURE 3.3. Normal endocervical gland lined by columnar mucinous epithelium with basally oriented nuclei.

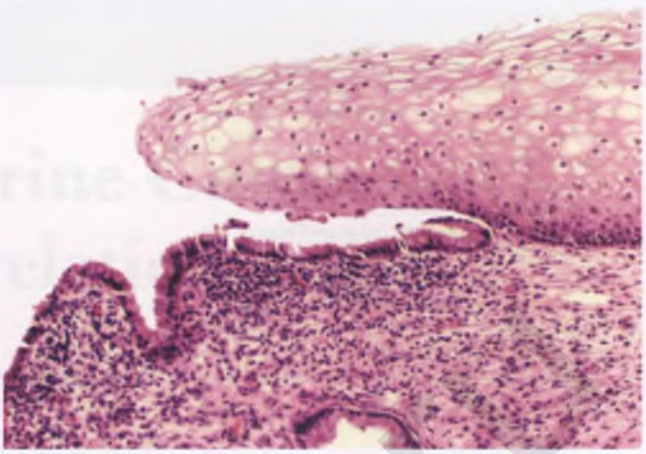

FIGURE 3.5. Normal original squamocolumnar junction. There is a sharp transition between the squamous epithelium of the exocervix and the mucinous columnar epithelium of the endocervix.

The functional squamocolumnar junction is the point at which endocervical epithelium is being actively replaced by squamous epithelium, and the area between the original and functional squamocolumnar junctions is referred to as the transformation zone (or T-zone) (Fig. 3.6). It is within the region of the transformation zone that cervical carcinomas and their precursors most frequently arise.

The cervical stroma consists predominantly of fibroelastic tissue admixed with occasional strands of smooth muscle. Superficially, this stroma gradually blends with the highly cellular endometrial stroma in the region of the lower uterine segment (in routine H&E sections, normal cervical stroma is pink, whereas normal endometrial stroma is blue).

Cytology

The composition of the Pap smear reflects sampling of the superficial layers of the cervicovaginal squamous epithelium, the transformation zone, and the endocervical canal, along with spontaneously shed elements that come into contact with the sampling device. Pap smears from estrogen-stimulated epithelium contain numerous superficial squamous cells, which are large, plate-like cells with polygonal outlines and small, dark, pyknotic nuclei that resemble inkspots (Fig. 3.7A). The nuclear features of the intermediate squamous cell are what distinguish it from the superficial cell. Intermediate squamous cell nuclei are vesicular, approximately twice as large as superficial cell nuclei in terms of nuclear area, and have a finely granular chromatin distribution

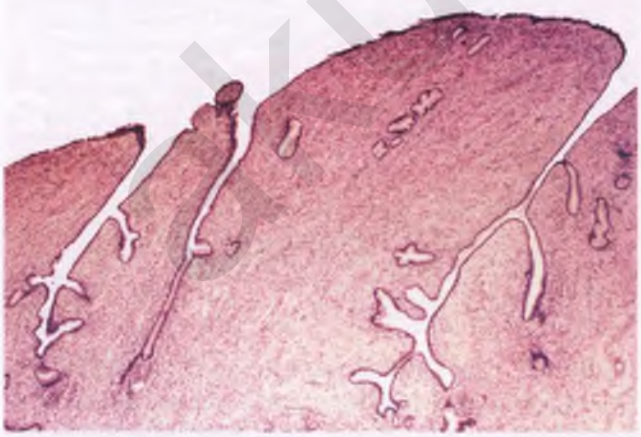

FIGURE 3.4. Tangential section of endocervical canal, taken to demonstrate the true architectural pattern of the endocervical papillary mucosal folds and epithelial-lined clefts. "Endocervical glands" are actually cross sections of outpouchings of the endocervical clefts.

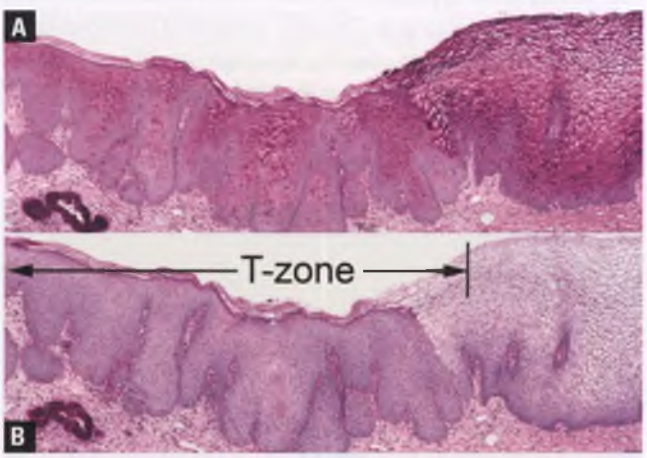

FIGURE 3.6. Cervix in region of transformation zone in woman of reproductive age. **A,B**: PAS stains without **(A)** and with **(B)** diastase pretreatment demonstrate the distribution of intraepithelial glycogen, which stains red and is digested by diastase. Squamous metaplastic epithelium, which is not as extensively glycogenated as the native exocervical mucosa toward the right, has replaced the visible portion of the transformation zone (T-zone), which extends further into the endocervical canal to the point where squamous epithelium meets endocervical mucinous epithelium (not shown). The endocervical gland in the lower left contains PAS-positive, diastase-resistant, intracytoplasmic mucin.

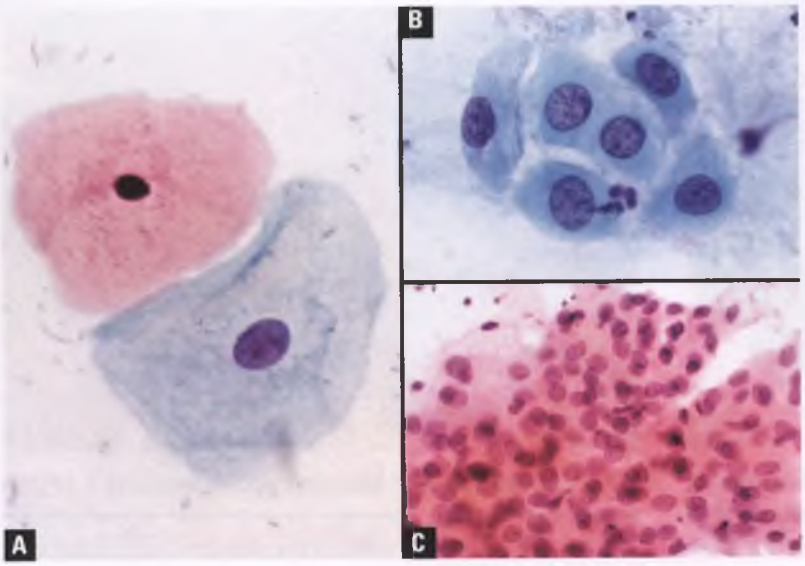

FIGURE 3.7. Normal squamous elements in Pap smear. **A**: Superficial squamous cell located above intermediate squamous cell. Note the differences in nuclear size and chromatin pattern. **B**: Parabasal cells in loose aggregate. **C**: Sheet of parabasal cells.

(Fig. 3.7A). To facilitate recognition of cytologic abnormalities in Pap smears, it is useful to utilize the nucleus of the intermediate squamous cell as an internal reference for nuclear size and chromatin normalcy. As a rule of thumb, virtually all epithelial cell abnormalities exhibit nuclear enlargement to a degree that is at least 1.5 times the nuclear area of the intermediate squamous cell nucleus, which represents at least a 20% increase in the nuclear diameter as compared to this internal size standard.

Parabasal cells have nuclei that are slightly larger than those of the intermediate cells, but their overall size is much smaller, their cytoplasm is more dense, and their cell boundaries are often ovoid or rounded rather than polygonal (Fig. 3.7B,C). The presence of numerous parabasal cells in a Pap smear indicates epithelial atrophy.

The presence of endocervical cells in a Pap smear is one means of documenting that the transformation zone has been sampled (the identification of squamous metaplastic cells also serves this purpose). Normal endocervical cells are seen most commonly in Pap smears as honeycomb sheets (Fig. 3.8) or small groups, but can also be found as epithelial strips or individual columnar cells. Their nuclear size is similar to that of the parabasal cell. When sampled high in the endocervical canal, closer to the lower uterine segment, they exhibit features that may lead to a diagnosis of atypical glandular cells (Fig. 3.9). Although these cells do have high nuclear to cytoplasmic ratios, appear densely packed, and lack a honeycomb architecture, their nuclei are round, bland, and mitotically inactive.

EPITHELIAL METAPLASIAS

Squamous Metaplasia

The process of squamous metaplasia begins with proliferation of endocervical "reserve cells" beneath the mucinous epithelium, which then stratify and gradually acquire dense, squamoid cytoplasm, distinct cell borders, and intercellular bridges as they proceed through the phases of immature and mature squamous metaplasia. The stages of reserve cell hyperplasia, immature squamous metaplasia, and mature squamous metaplasia represent a continuum with blurred rather than distinct boundaries. The histology of immature squamous metaplasia is illustrated in Figure 3.10, and is further discussed in the section detailing the differential diagnosis of high-grade squamous intraepithelial lesions (HSILs). In mature squamous metaplasia, the squamoid cytoplasm, distinct cell borders, and intercellular bridges are well developed (Fig. 3.11).

Florid squamous metaplasia, particularly when tangentially sectioned, can create an architecturally complex pattern that can be mistaken for invasive squamous cell carcinoma (Fig. 3.12). However, the nests of squamous metaplasia that have replaced endocervical glands have smooth rather than jagged outlines, do not elicit a fibroinflammatory stromal response, often have residual microcysts or mucinous epithelium in various stages of resorption, lack the nuclear atypia and mitotic activity of

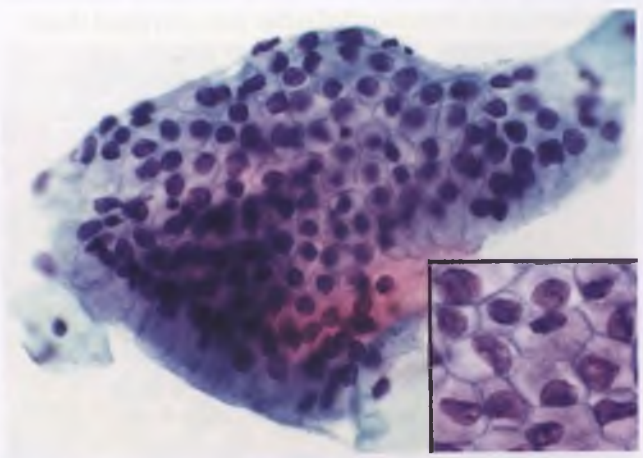

FIGURE 3.8. Normal endocervical cells in Pap smear. Note cohesive sheet with honeycomb appearance when viewed en face (central region), and columnar shape when viewed from the side (lower left edge of sheet). Cytoplasmic vacuoles may impinge upon and indent the nuclear membranes (inset).

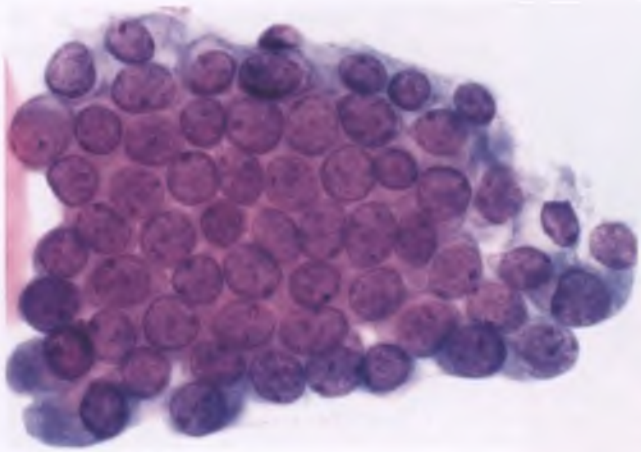

FIGURE 3.9. Normal endocervical cells in Pap smear, sampled from deeper in endocervical canal (toward lower uterine segment). The cells have higher nuclear to cytoplasmic ratios and appear more densely packed than endocervical cells closer to the transformation zone, and do not exhibit a honeycomb pattern.

squamous cell carcinoma, and typically occur in a setting that does not include neighboring squamous dysplasia.

In Pap smears, immature squamous metaplastic cells are typically found in loose aggregates with sharply defined cell borders, the combination of which results in a cobblestone pattern (Fig. 3.13). The individual metaplastic cells have a rounded shape and dense cytoplasm that may be vacuolated and/or have spidery processes. Nuclei are round to oval and slightly larger than those of intermediate squamous cells, the chromatin is finely granular, and nuclear contours are smooth to slightly irregular. Small nucleoli may be present. Mature squamous metaplastic cells are difficult to distinguish from native mature squamous epithelial cells in Pap smears, differing only by the presence in the former of slightly more dense cytoplasm and a more rounded rather than polygonal shape.

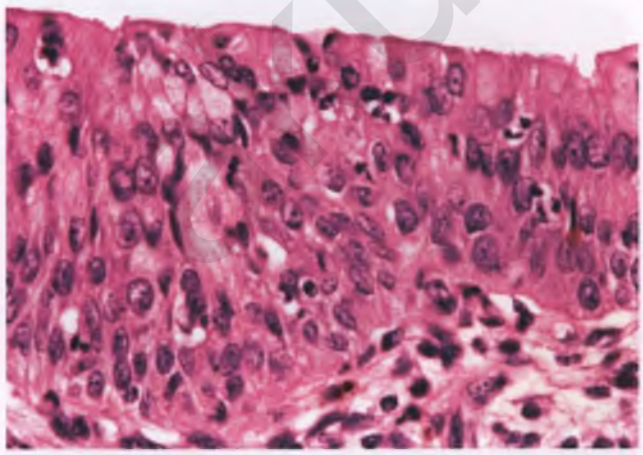

FIGURE 3. 10. Immature squamous metaplasia. Note the uniformity of the chromatin pattern of the metaplastic cells and the presence of residual mucinous endocervical cells near the surface.

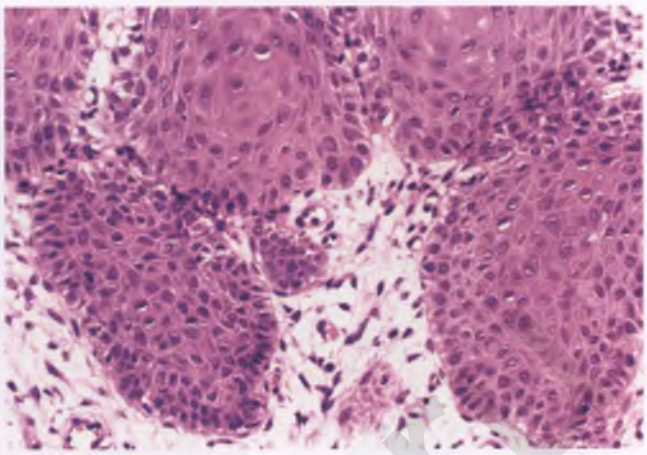

FIGURE 3.11. Mature squamous metaplasia.

Tubal, Tuboendometrioid, and Endometrioid Metaplasia

The fairly common process in which portions of the endocervical glandular epithelium are replaced by epithelium of the type normally seen lining the fallopian tubes is referred to as tubal metaplasia (Fig. 3.14).[1] This is an innocuous, incidental microscopic finding in its usual form, whose major significance lies in its potential to be confused with dysplastic endocervical lesions, including adenocarcinoma in situ (AIS). Tubal metaplasia features replacement of portions of the epithelial lining of the endocervical canal and/or a subset of endocervical glands by variable proportions of ciliated, secretory, and intercalated ("peg") cells (Fig. 5.1 illustrates these different cell types in their native state). Architecturally, the involved glands are typically similar to normal endocervical glands in terms of size, shape, and placement, although there are exceptions in which the metaplastic glands can be deep within the cervical stroma, irregularly shaped, variably sized, or pseudoinfiltrative.[2,3] In some cases, the stroma surrounding the metaplastic glands

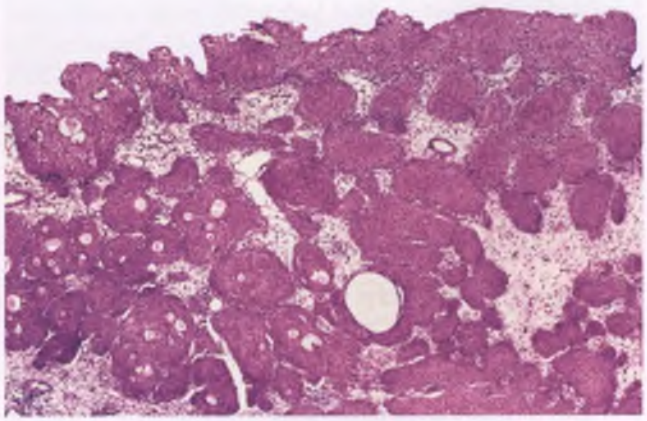

FIGURE 3.12. Florid squamous metaplasia simulating an invasive squamous cell carcinoma.

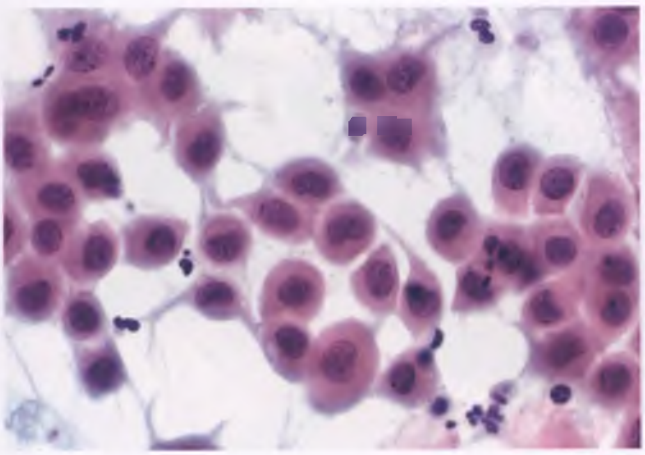

FIGURE 3.13. Conventional Pap smear with immature squamous metaplastic cells. Note the loose aggregates of cells with a cobblestone pattern, the ample amounts of dense cytoplasm with spider-like extensions, and the nuclei with uniform chromatin and only slight irregularities in contour.

may be hypercellular or edematous.[2] The metaplastic epithelium consists of a single layer, but may appear stratified due to oblique sectioning. Mitotic figures are scarce, and there is no significant nuclear atypia. Uncommon ciliated metaplasias that exhibit a level of nuclear enlargement, atypia, crowding, stratification, and mitotic activity that is intermediate in degree between usual tubal metaplasia and AIS are referred to as atypical tubal metaplasia (Fig. 3.15), and have been postulated to be a precursor of the rare ciliated variant of AIS.[4]

In tuboendometrioid metaplasia, the metaplastic epithelium contains fewer ciliated cells than seen in tubal metaplasia and exhibits blended features of both tubal and endometrioid epithelial types (Fig. 3.16). Rarely, the metaplastic process so closely resembles endometrial epithelium that it warrants classification as endometrioid metaplasia (Fig. 3.17).[5]

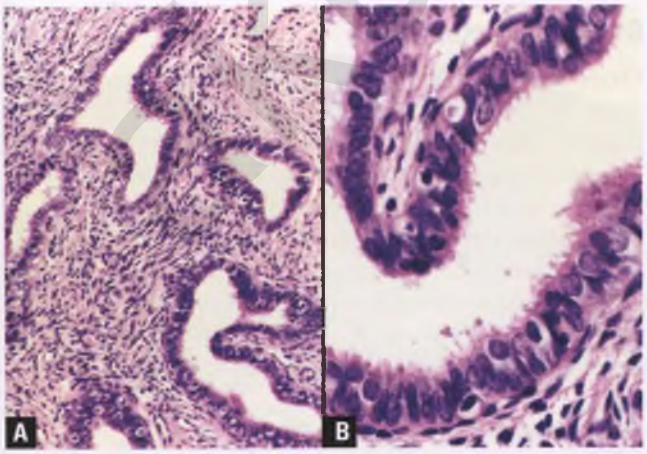

FIGURE 3.14. **A,B**: Tubal metaplasia. Note the presence of numerous ciliated cells and the lack of mitotic activity. In this example, the periglandular stroma is hypercellular.

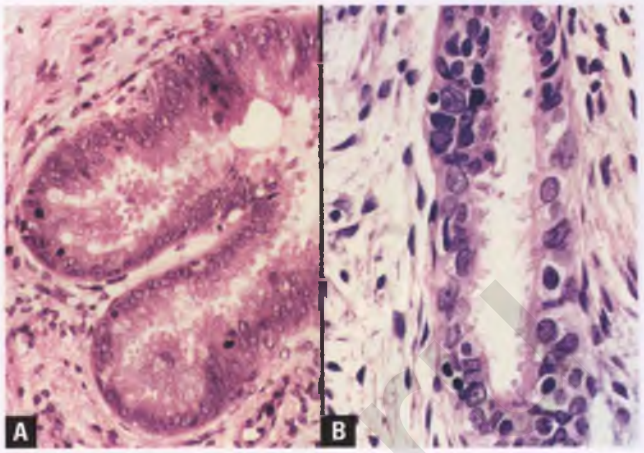

FIGURE 3.15. Atypical tubal metaplasia (two separate examples). **A**: This lesion exhibits some nuclear chromatin abnormalities and has significant mitotic activity. **B**: The top portion of this gland exhibits nuclear atypia, stratification, and crowding. Interpretation of lesions such as these is subjective, and their clinical significance is uncertain.

Differential Diagnosis

Histologically, the differential diagnosis of this group of metaplasias includes AIS, invasive endocervical adenocarcinoma, endometriosis, and mural endosalpingiosis.

- The usual types of metaplasia with a tubal component are distinguished from AIS by the presence in the former of an admixture of the three tubal cell types (ciliated, secretory, and intercalated), inconspicuous mitotic figures/apoptotic bodies, and the lack of significant nuclear atypia. MIB-1 and p16 immunohistochemistry can also be helpful, insofar as typical examples of tubal and tuboendometrioid metaplasia usually have only scattered MIB-1 positive nuclei (<10%) and at most focal p16 immunoreactivity, whereas in AIS generally >30% of nuclei are MIB-1 positive and p16 immunoreactivity is

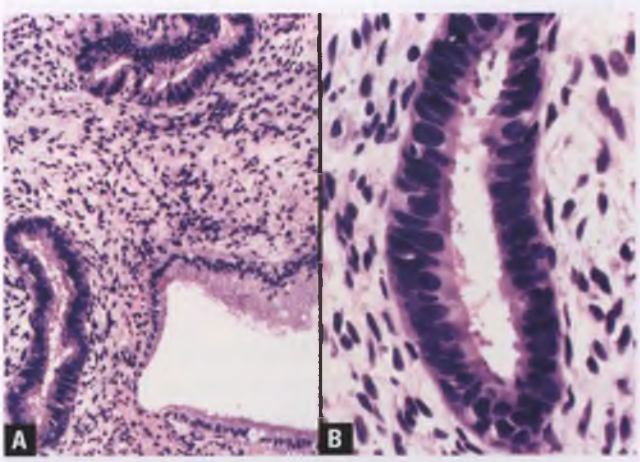

FIGURE 3.16. Tuboendometrioid metaplasia. **A**: Compare the two metaplastic glands with the normal endocervical gland at lower right. **B**: In comparison to tubal metaplasia, the number of ciliated cells is decreased, which results in a more hyperchromatic appearance.

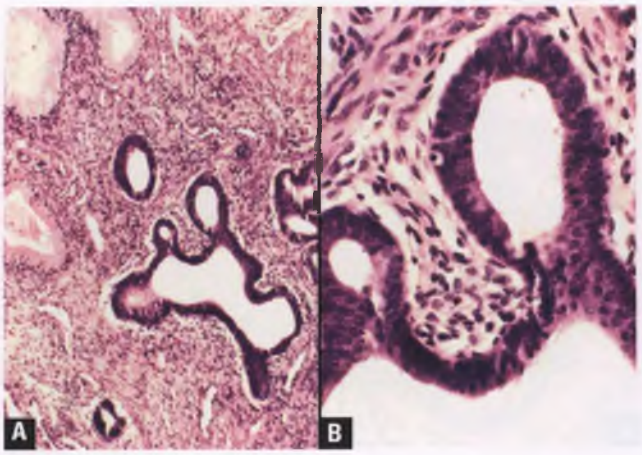

FIGURE 3.17. Endometrioid metaplasia. **A**: The metaplastic glands closely resemble those seen in proliferative endometrium, and contrast with the normal endocervical glands at top left. **B**: Endometrioid metaplasia at higher magnification.

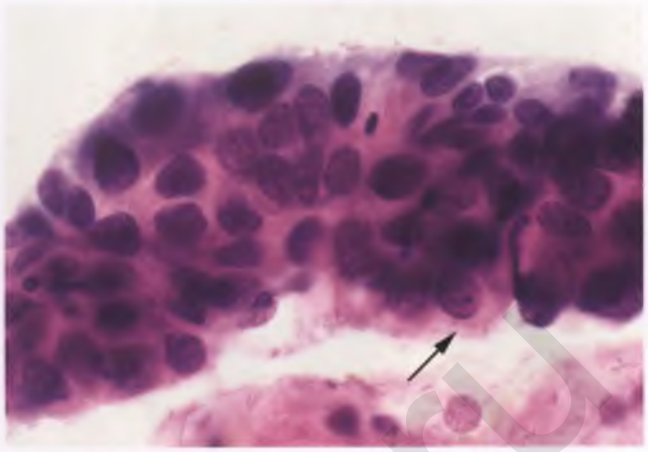

FIGURE 3.18. Tubal metaplasia in conventional Pap smear. An *arrow* marks a cell with cilia and an apical terminal bar. The variability in nuclear size, shape, and degree of hyperchromasia is a reflection of the admixture of cell types.

typically strong and diffuse.[6] To avoid overinterpretation of tubal metaplasia and atypical tubal metaplasia as the exceedingly rare ciliated variant of AIS, overtly malignant nuclear features should be present before such a diagnosis is rendered.

- Invasive endocervical adenocarcinoma is unlikely to be confused with this group of metaplasias, given that it is typically a mass-forming, symptomatic lesion with stromal invasion, nuclear atypia, and considerable mitotic activity.
- Of less significance is the distinction of tubal, tuboendometrioid, and endometrioid metaplasia from the usually incidental finding of superficial cervical endometriosis. This distinction is particularly difficult when the metaplastic glands are surrounded by hypercellular stroma, although the stroma in these instances is usually more fibroblastic than endometriotic stroma and tends to blend with the neighboring endocervical stroma.[2] The presence of numerous small vessels, extravasated red blood cells, and hemosiderin-laden macrophages within the stromal component favors endometriosis over metaplasia.
- Very rarely, florid examples of cystic endosalpingiosis involve the cervical wall (endosalpingiosis is discussed in Chapter 8). Although these lesions share with tubal metaplasia the presence of cytologically bland, tubal-type epithelium, they differ in their presentation with tumor-like symptoms, their grossly visible, multiple, transmural cysts, and their involvement of subserosal or paracervical tissue.[7]

Cytologic Features of Tubal Metaplasia and its Distinction from Adenocarcinoma In Situ

Although textbook cytologic examples of tubal metaplasia often show obvious cilia with terminal bars, cilia are delicate structures that are easily traumatized and are difficult to discern in practice. Tubal metaplasia typically presents in cytologic preparations as crowded sheets of glandular cells that exhibit nuclear enlargement, high nuclear to cytoplasmic ratios, hyperchromaticity, and mild degrees of nuclear pleomorphism (Fig. 3.18). Nuclei are usually round to oval with evenly distributed, finely granular chromatin.

The presence of tubal metaplastic cells in Pap smears may result in a diagnosis of atypical endocervical cells or AIS. In contrast to tubal metaplasia, palisaded, cigar-shaped nuclei typically predominate at the periphery of the cell groups in AIS, and the chromatin is usually more coarsely granular. The feathered edges, mitotic activity, and microacinar/rosette structures that are often seen in AIS are absent or inconspicuous in tubal metaplasia. Close inspection of the edges of groups of tubal metaplastic cells may reveal focal evidence of ciliation in the form of terminal bars and/or actual cilia. In addition, the presence of an admixture of ciliated, secretory, and intercalated cells imparts a heterogeneity to the sheets of metaplastic cells that contrasts with the more monotonous appearance of the sheets of neoplastic cells in AIS.

Oxyphilic Metaplasia

Oxyphilic metaplasia is a rare, inconsequential, focal microscopic finding in which the endocervical glandular epithelium possesses densely eosinophilic cytoplasm (Fig. 3.19).[9] The cells lining these glands often have enlarged, hyperchromatic nuclei, but there is no associated nuclear stratification or mitotic activity. Although these nuclear abnormalities have prompted this unusual metaplasia to be reported as atypical oxyphilic metaplasia, it is recommended that it simply be reported as oxyphilic metaplasia with a note referring to its incidental nature, so as to avoid undue clinical concern.

Transitional Cell Metaplasia

Transitional cell metaplasia is an uncommon form of metaplasia that usually presents in postmenopausal women as an incidental finding. It features a multilayered epithelium composed of uniform, spindle-shaped cells with evenly

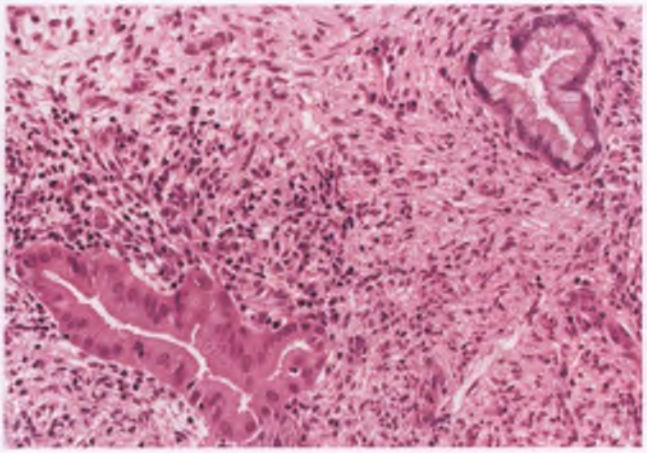

FIGURE 3.19. Oxyphilic metaplasia. The eosinophilic cytoplasm of the metaplastic gland in the lower left contrasts with cytoplasmic appearance of the normal endocervical gland in the upper right.

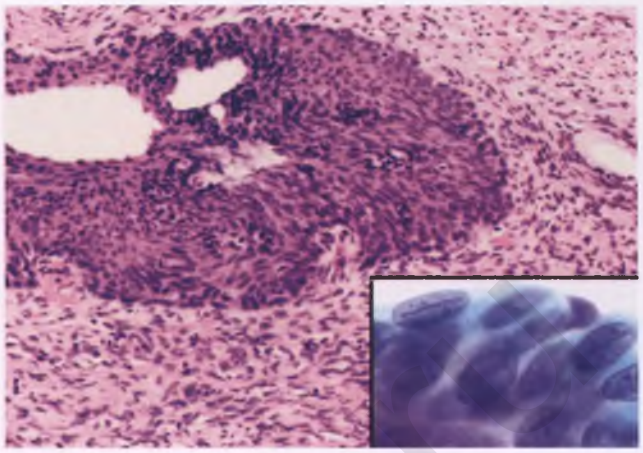

FIGURE 3.21. Endocervical gland replaced by transitional cell metaplasia. The inset shows a Pap smear with metaplastic transitional cells with characteristic longitudinal nuclear grooves.

dispersed chromatin, inconspicuous nucleoli, and frequent longitudinal nuclear grooves (Figs. 3.20 and 3.21).[10,11] Although the nuclei may be vertically oriented near the basement membrane, they typically transition to streaming and swirling patterns in the more superficial layers. Mitotic figures are usually absent.

The high nuclear to cytoplasmic ratios and lack of maturation seen in transitional metaplasia produce a low-power pattern that may suggest a HSIL. However, the streaming/swirling nuclear patterns and readily apparent nuclear grooves of transitional cell metaplasia, coupled with the lack of nuclear atypia and the virtual absence of mitotic activity, help to distinguish this process from HSIL. Although p16 and Ki-67 staining patterns have not been reported in a large series of transitional cell metaplasias, one would expect negative to limited staining with these biomarkers, which would be another distinguishing feature. In Pap smears, transitional cell metaplasia may be recognized as streaming groups of cohesive, spindle-shaped cells with bland nuclear features and longitudinal nuclear grooves (Fig. 3.21 inset).[12]

NABOTHIAN CYSTS

Nabothian (retention) cysts are common incidental findings related to endocervical crypt dilatation following obstruction of the crypt outlet, which may be due to fibrosis, squamous metaplasia, or mucus plugging. Grossly, they are yellowish white, dome-shaped cysts measuring up to 1.5 cm in diameter that often occur in aggregates (Fig. 3.22). The cysts are usually filled with translucent, mucoid material, but the contents may occasionally be purulent (Fig. 3.23). The cyst lining most commonly consists of a single layer of columnar mucinous

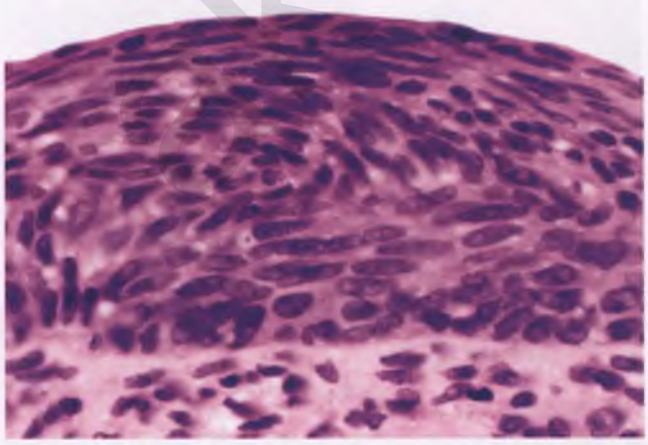

FIGURE 3.20. Transitional cell metaplasia. Note the streaming and swirling of the elongated nuclei.

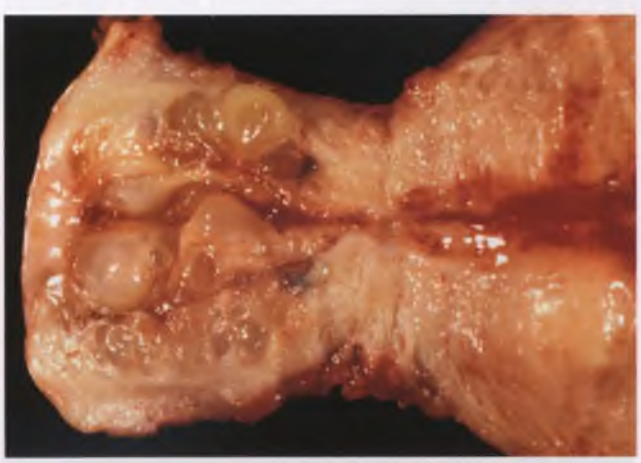

FIGURE 3.22. A conglomerate of superficially located Nabothian cysts is seen distorting the endocervical canal in the left half of the image.

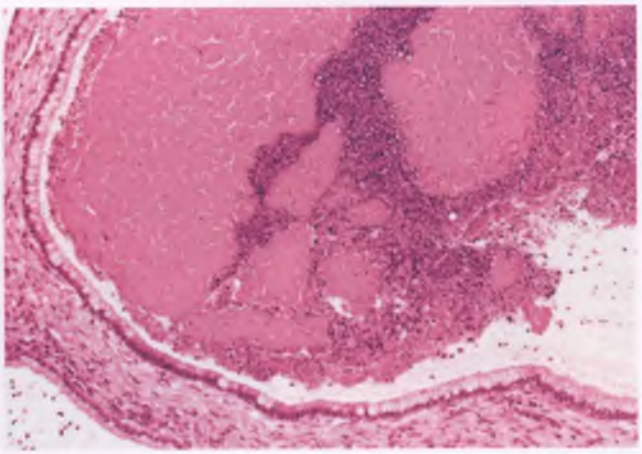

FIGURE 3.23. Nabothian cyst. This example is lined by columnar mucinous epithelium and contains purulent debris. More commonly, these cysts contain mucoid material.

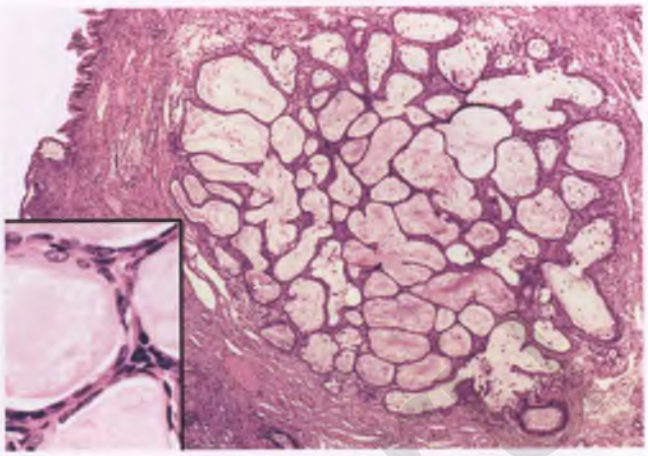

FIGURE 3.25. Cystic (type B) tunnel cluster. The aggregate of microcystic tubules has a lobular configuration. The inset shows a high-magnification view of the epithelial lining of the tubules.

epithelium, but may also exhibit tuboendometrioid or squamous metaplasia or be flattened due to pressure atrophy.

Although usually located in the superficial cervical stroma, Nabothian cysts can rarely be found deep within the cervical wall, where they can raise concern for adenoma malignum (minimal deviation adenocarcinoma) (Fig. 3.24).[13] In contrast to deep Nabothian cysts, adenoma malignum features (a) glands with more architectural complexity in which cyst formation is not usually a prominent finding, (b) an infiltrative pattern that is best appreciated at scanning magnification, and (c) focal areas in which nuclear atypia and a periglandular stromal reaction can be appreciated.

TUNNEL CLUSTERS

Tunnel clusters were first described by Fluhmann,[14] and are sometimes referred to as "Fluhmann's lumens." They almost always occur in multiparous women, prompting the suggestion that they represent a subinvolutional change within endocervical glands that have previously undergone physiologic hyperplasia.[15] They represent incidental findings that are usually multifocal, with each cluster averaging only a few millimeters in greatest dimension.

Cystic (type B) tunnel clusters are much more common than the noncystic (type A) variant, and are composed of closely packed, variably sized, mucin-filled microcystic tubules that form lobular aggregates (Fig. 3.25). The microcystic tubules in the cystic variant are lined by a single layer of flattened to cuboidal epithelial cells that are devoid of significant nuclear atypia or mitotic activity. By contrast, noncystic tunnel clusters are characterized by lobulated aggregates of closely packed, small, round to oval, variably compressed glands that often surround a larger endocervical cleft (Figs. 3.26 and 3.27). Frequently, noncystic tunnel clusters are found in association with those of the cystic type.

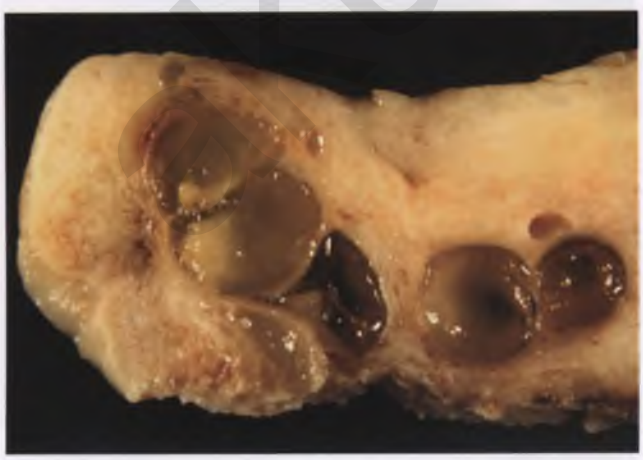

FIGURE 3.24. Deep Nabothian cysts. Cysts span the full thickness of the cervical wall in this longitudinal section (exocervix is at left).

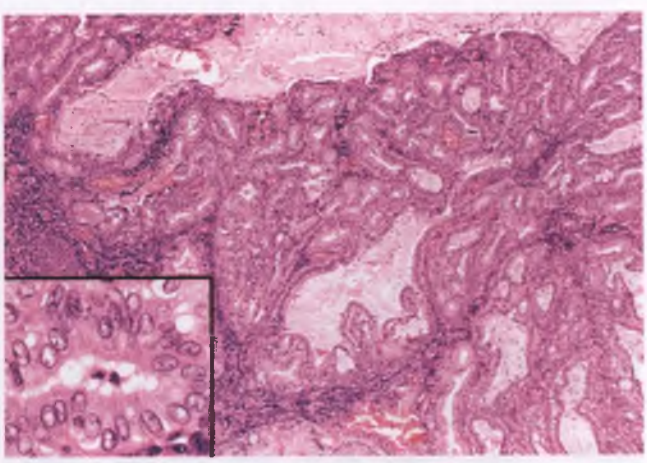

FIGURE 3.26. Noncystic (type A) tunnel cluster. This lesion consists of lobulated aggregates of predominantly small, closely packed glands with non-infiltrative borders. The inset shows the nuclear features of a representative gland.

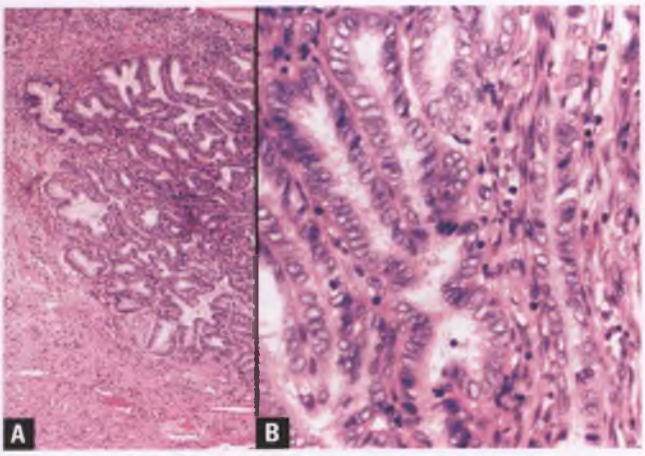

FIGURE 3.27. Noncystic (type A) tunnel cluster. **A**: At low magnification, a circumscribed proliferation of small glands is evident. **B**: In this example, the nuclear features resemble those of papillary carcinoma of the thyroid.

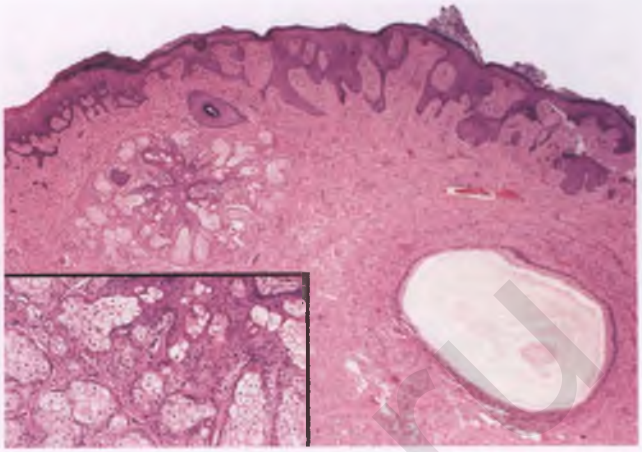

FIGURE 3.28. Cutaneous heterotopia (epidermidalization) of the cervix. Note the presence of hyperkeratosis, hypergranulosis, rete ridges, and sebaceous glands. A dilated endocervical gland is present in the right lower corner. The inset shows the sebaceous glands at higher magnification.

The glands of noncystic tunnel clusters are lined by cuboidal to columnar epithelium that may exhibit moderate nuclear atypia that is of no clinical significance.[16] The atypia is usually manifested by nuclear enlargement, nuclear overlapping, chromatin clearing, and distinct nucleoli. These nuclear changes are somewhat reminiscent of those seen in papillary carcinoma of the thyroid, albeit without prominent nuclear grooves or pseudoinclusions. The absence of a symptomatic cervical mass, its superficial location within the cervical stroma, the absence of a periglandular stromal reaction, and its noninfiltrative, lobular architecture help to differentiate noncystic tunnel clusters with nuclear atypia from the usual type of endocervical adenocarcinoma and adenoma malignum (minimal deviation adenocarcinoma).

HETEROTOPIAS

Heterotopias are microscopically normal cells or tissues that are present in abnormal locations.

Cutaneous Heterotopia

On rare occasions, the presence of sebaceous glands and hair follicles has been noted as an incidental finding within the cervix (Fig. 3.28).[17,18] This phenomenon is best referred to as cutaneous heterotopia or epidermidalization of the cervix, since it is invariably accompanied by other features of skin such as hyperkeratosis, the presence of a granular cell layer, and rete ridges.

Prostatic Heterotopia (Ectopia)

A rare, intriguing finding is the presence of prostatic glands within the uterine cervix.[19,20] These glands resemble those found in the male prostate, with the exception of the nearly universal presence of squamous metaplasia within some of the glands. The combination of benign glands with papillary infoldings with patches of squamous metaplasia should raise this possibility, which can be confirmed with immunostains for prostate-specific antigen and prostatic acid phosphatase.

Heterotopia of Adipose Tissue

Adipose tissue is generally not regarded as a normal constituent of the uterine cervix. However, a recent study has suggested that fat is present in approximately 15% of specimens of excised cervical tissue, and that its presence should be considered a normal finding.[21] However, the authors of this study acknowledged that adipocyte nuclei were not frequently discerned, and that only one of eight cases with fat demonstrated the typical S100 immunoreactivity of adipocytes.[21] If cervical fat were as common as that claimed in this study, then surgical pathologists would encounter its presence on a regular basis and it would be well described in histology textbooks, neither of which is the case. If the histologic features suggest the presence of adipose tissue within the cervical stroma, a more likely possibility that should first be excluded is pseudolipomatosis (see section on artifacts in cervical samples).

INFLAMMATORY PROCESSES

Noninfectious Cervicitis of Usual Type

Noninfectious cervicitis of the usual type is typically due to some nonspecified mechanical or chemical irritation. The stromal inflammatory infiltrate may be acute (neutrophils) and/or chronic (lymphocytes and plasma cells), and may extend into the epithelium (Fig. 3.29). When intraepithelial inflammatory cells are present, there is commonly some associated reactive/reparative epithelial atypia (see section on reactive and reparative processes). Some cases of so-called acute cervicitis may be

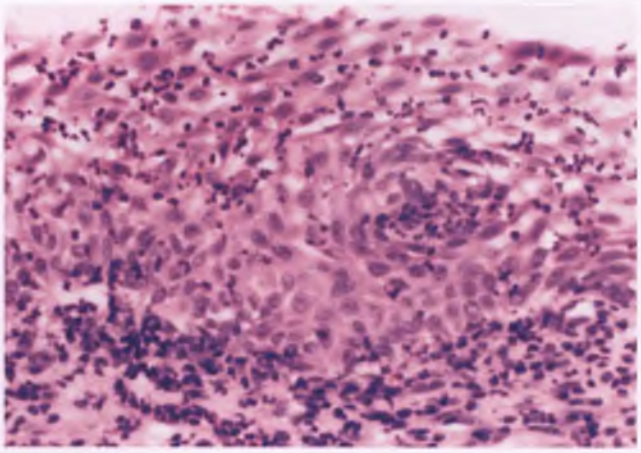

FIGURE 3.29. Active chronic cervicitis (acute and chronic cervicitis). A mixed acute and chronic inflammatory infiltrate is present within the superficial stroma and metaplastic squamous epithelium.

associated with a clinically swollen cervix and a purulent discharge, but many cases do not have acute symptoms and are probably more accurately described as active chronic cervicitis (analogous to active chronic gastritis), where the neutrophilic infiltrate serves as an indication that the nonspecific inflammatory process is active. Since scattered lymphocytes are a normal component of the endocervical stroma, the diagnosis of chronic cervicitis should be reserved for situations in which the number of chronic inflammatory cells is noteworthy and includes the presence of numerous plasma cells.

Papillary Endocervicitis

On occasion, chronic inflammation of the endocervix takes the form of micropapillae that project into the endocervical canal. This process is referred to as papillary endocervicitis.[22] The stroma of the papillae contains a dense infiltrate of lymphocytes and plasma cells, and the lining epithelium consists of a single layer of endocervical mucinous epithelium (Fig. 3.30).

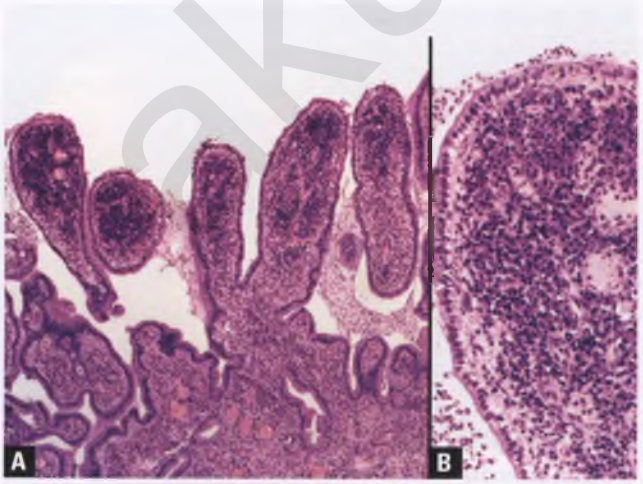

FIGURE 3.30. **A,B**: Papillary endocervicitis.

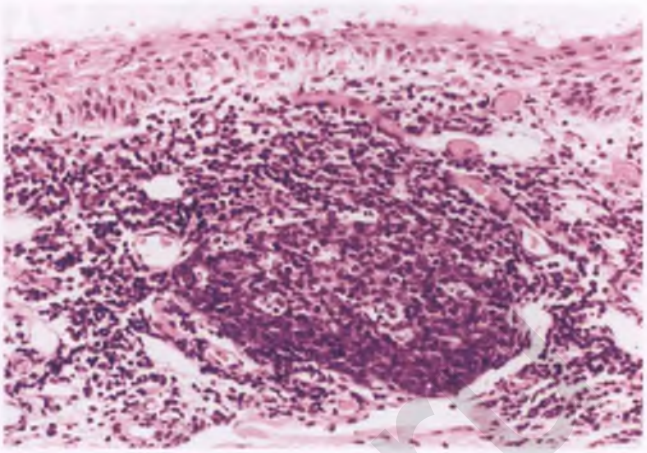

FIGURE 3.31. Follicular cervicitis with ill-defined germinal center that contains tingible-body macrophages.

The lining epithelium lacks both cellular stratification and nuclear atypia, which helps to distinguish this incidental chronic inflammatory process from well-differentiated villoglandular adenocarcinoma.

Follicular Cervicitis

An uncommon form of chronic cervicitis is follicular cervicitis, in which germinal centers (secondary lymphoid follicles) form in the superficial stroma as part of the chronic inflammatory infiltrate (Fig. 3.31). This type of cervicitis may be found in association with a chlamydial infection. When the lymphoid cells from the follicles of follicular cervicitis appear in Pap smears, their high nuclear to cytoplasmic ratios and coarsely clumped chromatin may cause them to be mistaken for HSIL (Fig. 3.32). The presence of tingible-body macrophages, the lack of cellular cohesion, the smooth nuclear contours, and the variability in size of the lymphocytes help to distinguish this process from HSIL.

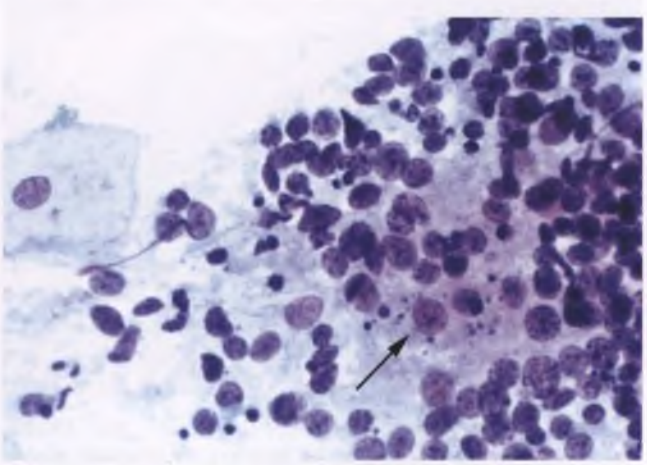

FIGURE 3.32. Pap smear with follicular cervicitis. Note the presence of tingible-body macrophages (*arrow*).

Reactive Polymorphous Lymphoid Infiltrates that Simulate Malignant Lymphoma

Rarely, florid reactive lymphoid lesions of the uterine cervix occur with a component of large lymphoid cells in a pattern that can simulate malignant lymphoma (Fig. 3.33).[23,24] They are distinguished from lymphoma by the absence of a gross mass or associated sclerosis, the superficial, band-like, polymorphous nature of the lymphoid infiltrate, and the frequent occurrence of surface ulceration with associated neutrophils. The large lymphoid cells are mitotically active, and some have the appearance of immunoblasts, with single, centrally located macronucleoli. Intermixed with the large lymphoid cells are small lymphocytes and plasma cells, and immunophenotypic studies demonstrate an admixture of B and T cells with polyclonal plasma cells.[24,25] Surprisingly, these reactive lymphoid lesions may show evidence of a clonal rearrangement of the immunoglobulin heavy chain gene, which in this setting does not warrant a diagnosis of lymphoma.[25] Given that this expensive, esoteric test for clonality has no bearing on the diagnosis, it is recommended that immunoglobulin gene rearrangement studies not be performed on this spectrum of lymphoid lesions outside of a research setting. If the pathologist is confident that the lesion is benign, a descriptive diagnosis such as "reactive polymorphous lymphoid infiltrate" or "florid reactive lymphoid hyperplasia" is preferable to "lymphoma-like lesion" or "pseudolymphoma," since the latter terms are more likely to provoke patient and clinician anxiety and result in unnecessarily close follow-up, additional clinical tests, and/or a request for expert consultation.

Arteritis

Necrotizing arteritis with features resembling polyarteritis nodosa rarely occurs within the female genital tract; when it does, it tends to preferentially involve the cervix.[26–28] Histologically, small to medium-sized arteries exhibit inflammation (predominantly chronic with a minor acute component) and prominent fibrinoid necrosis (Fig. 3.34). Although this is usually an isolated, localized finding in patients who lack symptoms related to vasculitis, such patients should be evaluated for the possibility of generalized disease.

Giant cell arteritis may also rarely involve the ovaries, fallopian tubes, and uterus.[28–30] As in its more typical presentation in the temporal arteries, this arteritis features (a) luminal narrowing/obliteration secondary to intimal proliferation; (b) a concentric inflammatory infiltrate composed primarily of an admixture of lymphocytes, plasma cells, epithelioid histiocytes, and multinucleated giant cells; (c) fragmentation of the internal elastic lamina; and (d) no appreciable fibrinoid necrosis (Fig. 3.35). Patients are typically postmenopausal, and their arteritis may be isolated and asymptomatic or associated with systemic disease. Clinical correlation is indicated in order to identify those patients who have generalized vasculitis.

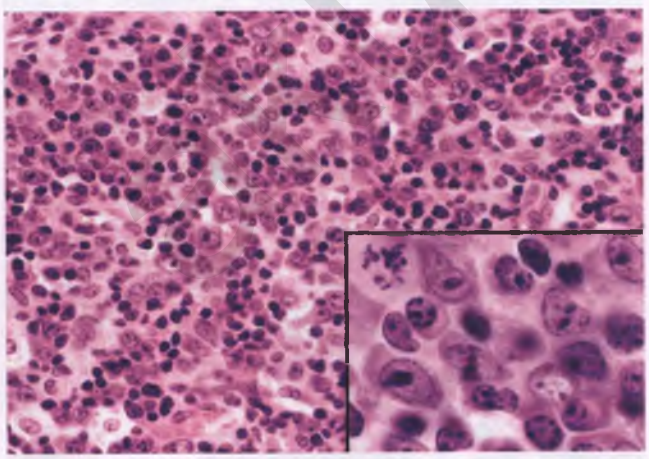

FIGURE 3.33. Reactive polymorphous lymphoid infiltrate (so-called "lymphoma-like lesion"). This process consists of an admixture of large lymphoid cells/immunoblasts with mitotic activity, small lymphocytes, and plasma cells.

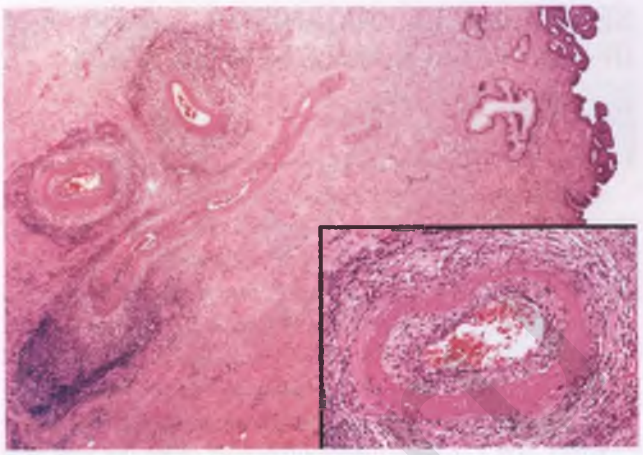

FIGURE 3.34. Isolated necrotizing arteritis within the stroma of the uterine cervix. The endocervical canal is at upper right. The inset shows an involved vessel with fibrinoid necrosis and an associated inflammatory infiltrate.

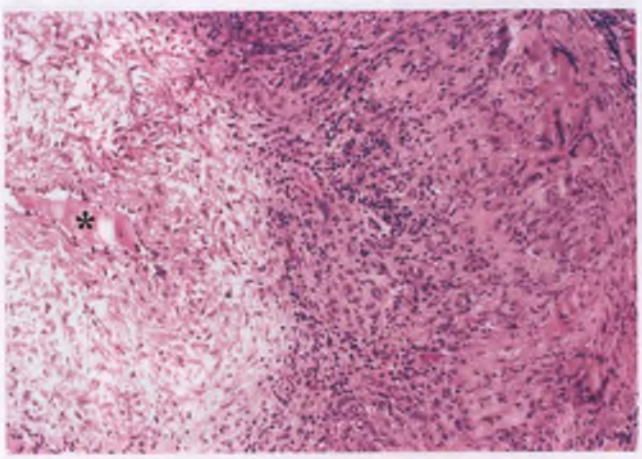

FIGURE 3.35. Giant cell arteritis. Scattered multinucleated giant cells are present within the vessel wall, which is also chronically inflamed. There is marked narrowing of vessel lumen (*asterisk*).

SELECTED MICROORGANISMS OF THE LOWER FEMALE GENITAL TRACT

Notes:

1. Since HPV infection is closely associated with the development of squamous intraepithelial lesions (SILs), endocervical AIS, and most forms of cervical cancer, it is discussed with these topics elsewhere in this chapter.
2. The microorganisms discussed in this section may cause no symptoms or produce disease that may be based in the vulvovaginal region or other extracervical site, but are presented here because evidence of their presence may be found in Pap smears. Emphasis is placed on those microorganisms that either have a characteristic morphology or induce relatively specific epithelial alterations.

Herpes

Herpes simplex virus (HSV) is a DNA virus that may infect the cervix (HSV type 2 is the usual cause of genital herpes infections). Infected cervical tissue rarely exhibits vesicles, since they are rapidly transformed into shallow ulcers. Since the diagnosis is often based on the clinical evaluation, cytology, and/or culture of lesions in the vulvovaginal region, cervical tissue samples with evidence of herpetic infection are uncommon. When cervical biopsies are obtained, viral inclusions are most likely to be identified within altered squamous cells from the margins of the ulcerated tissue (Fig. 3.36). There are two different types of herpetic intranuclear inclusions, both of which share the "3 M's": multinucleation, margination, and molding. To elaborate, the infected cells are often multinucleated, there is margination (pushing to the periphery) of the more darkly stained host chromatin, and the shape of the tightly packed nuclei of the multinucleated giant cells conforms to the contours of the neighboring nuclei (nuclear molding). In the most common form of herpetic inclusion, the bulk of the nucleus is replaced by homogeneous "ground glass" material. Less common is the Cowdry type A intranuclear herpetic inclusion, which features a large, centrally located, eosinophilic or purple inclusion surrounded by a clear halo and a peripheral rim of marginated chromatin (Fig. 3.37). This type of inclusion appears to represent a later stage in which virus particles are further concentrated within the nucleus.

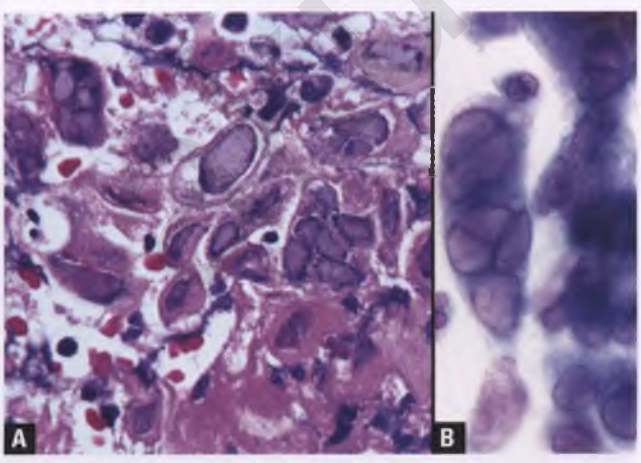

FIGURE 3.36. Herpes virus infection. **A**: Characteristic "ground glass" herpetic inclusions are present within several squamous epithelial cells from the margin of an ulcer. **B**: Pap smear with herpetic inclusions.

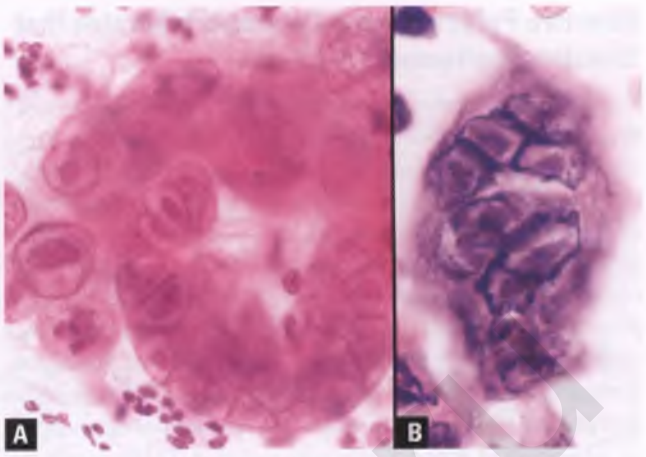

FIGURE 3.37. Herpes virus infection. **A**: Pap smear with multinucleated cells with several Cowdry type A herpetic inclusions. **B**: High-magnification view of a histologic section of a multinucleated cell with Cowdry type A inclusions.

Cytomegalovirus

Cytomegalovirus (CMV) is a member of the herpesvirus group that on rare occasions can produce an endocervicitis associated with characteristic viral inclusions (Fig. 3.38).[31,32] These inclusions are most often found within endocervical columnar epithelial cells as large, round to oval, purple structures surrounded by a thin halo. They are identical to the intranuclear inclusions of CMV found elsewhere in the body, but their

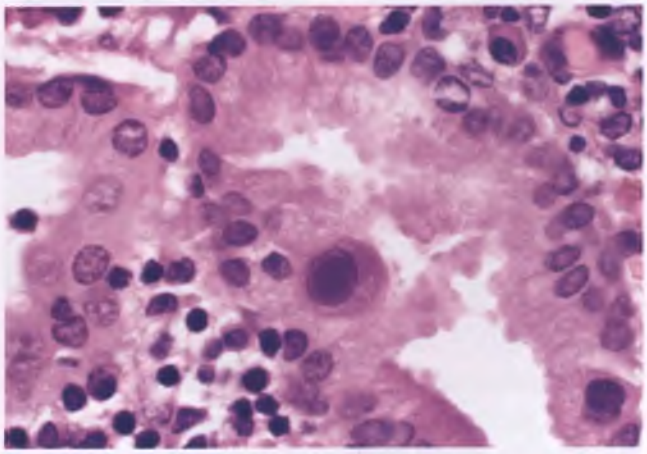

FIGURE 3.38. Cytomegaloviral endocervicitis. A single characteristic viral inclusion body is present within one of the endocervical cells. The neighboring stroma is chronically inflamed.

presence near the apical end of the endocervical cells, where they are often seen protruding into gland lumens, gives these inclusions the appearance of an intracytoplasmic location.

If the patient is asymptomatic and immunocompetent, as is usually the case, then no treatment is necessary. However, since a minority of patients may be immunocompromised, the finding of CMV endocervicitis should prompt an immunological evaluation that includes determination of human immunodeficiency virus status.

Candida Species

Fungal infection of the cervix by *Candida albicans* and closely related organisms such as *Candida glabrata* (*Torulopsis*) generally represents an extension of vulvovaginal disease. In Pap smears, *C. albicans* appears as an admixture of pseudohyphae and oval, budding yeast forms ("spaghetti and meatballs") (Fig. 3.39A). True septate hyphae may also be present. In contrast to other *Candida* organisms, *Torulopsis* is devoid of hyphal elements and consists exclusively of small, round to oval yeast-like cells that are often surrounded by a clear halo (Fig. 3.39B). In liquid-based preparations, squamous epithelial cells may appear to be skewered by the pseudohyphae of the more conventional *Candida* species, creating *Candida* "shish kabobs" (Fig. 3.40). *Candida* can induce changes in squamous and metaplastic cells in Pap smears that include slight nuclear enlargement, small perinuclear halos, cytoplasmic orangeophilia, and vacuolated cytoplasm; these reactive changes should not prompt a diagnosis of atypical squamous cells of undetermined significance (ASC-US).[33]

Cervical biopsy is not used to diagnose Candidiasis. However, fungal organisms may be identified in association with cervical tissue within a layer of desquamated squamous cells that is loosely adherent to the cervical mucosa (Fig. 3.41) or within the outermost aspect of the squamous epithelium, which is often infiltrated by neutrophils. Since *Candida* organisms can be recovered from the vagina of asymptomatic women, the diagnosis of Candidiasis should be made only in the appropriate clinical context.

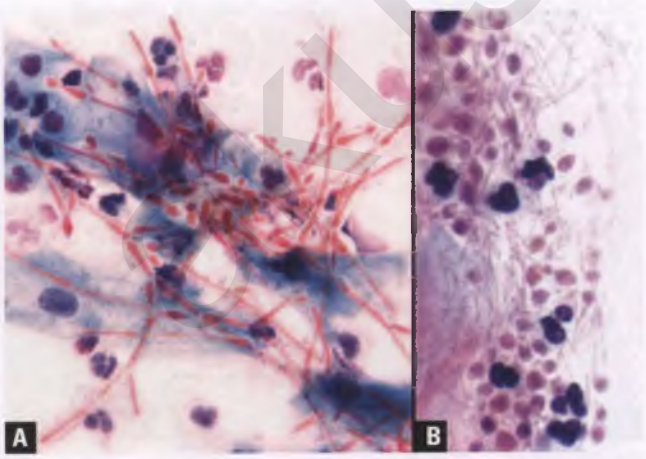

FIGURE 3.39. *Candida* organisms in Pap smears. **A**: Presumed *C. albicans*. Note pseudohyphae composed of chains of elongated yeast-like cells that are segmentally constricted at points of attachment. **B**: Only yeast forms are present in this example of presumed *Torulopsis (C. glabrata)*. The associated filamentous bacteria should not be mistaken for pseudohyphae.

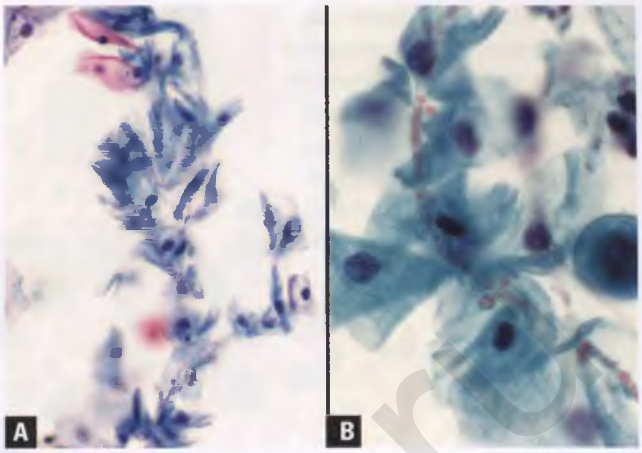

FIGURE 3.40. **A,B**: *Candida* "shish kabobs" in liquid-based Pap smears. These structures represent an important clue to the presence of *Candida* organisms that can be appreciated at low magnification.

Trichomonas Vaginalis

Trichomonads are flagellate parasites that are a common cause of sexually transmitted vaginitis. In Pap smears, they are recognized as faint-staining, pear/kite-shaped organisms with gray to green cytoplasm with red granules and small nuclei that are oval to elongate with pointed ends (Fig. 3.42). Since these organisms are often poorly preserved and their flagella do not usually survive the slide preparation process, their cytoplasmic granules are often not apparent and flagella are only rarely visualized. Leptothrix bacteria, which are long, thin, filamentous,

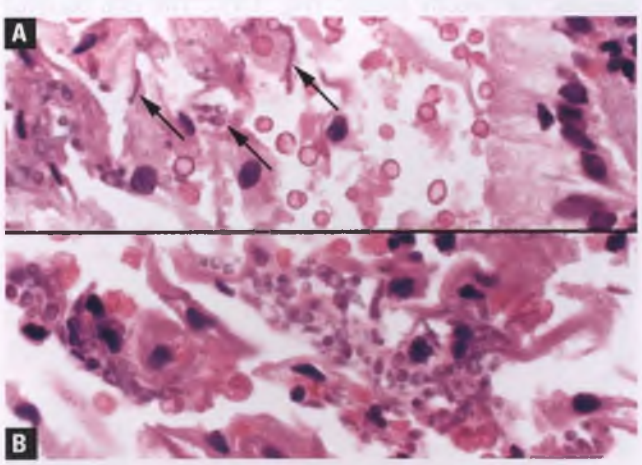

FIGURE 3.41. *Candida* organisms in tissue sections. **A**: Occasional fungal organisms consistent with *Candida* species (*arrows*) are comingled with shed squamous cells and red blood cells. Endocervical mucosa is at right. **B**: Focus with more numerous *Candida* fungal elements associated with shed squamous cells.

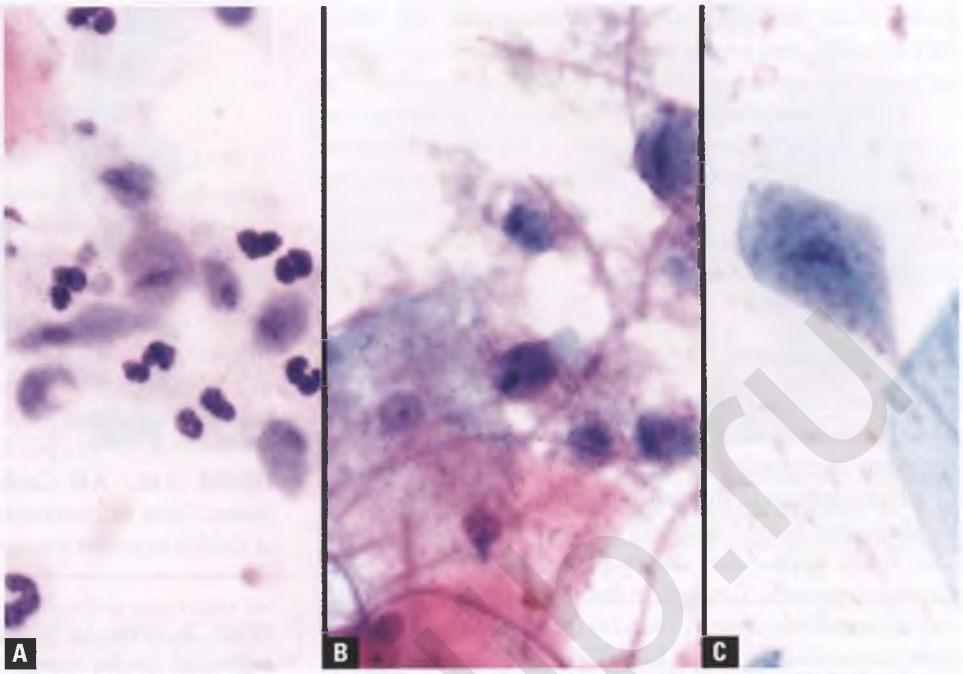

FIGURE 3.42. *T. vaginalis.* **A**: Loose aggregate of trichomonads admixed with more darkly stained neutrophils. Cytoplasmic granules and flagella are not visible. **B**: Few trichomonads associated with Leptothrix bacteria. **C**: Kite-shaped trichomonad with visible cytoplasmic granules and flagellum.

hair-like rods, are often seen in association with trichomonads. There may also be associated alterations in mature squamous cells that can mimic koilocytosis, as depicted in Figure 3.140.

Actinomyces

Actinomyces are anaerobic, gram-positive, filamentous bacteria whose identification in Pap smears is often associated with use of an intrauterine contraceptive device (IUD). They may be found as commensal microorganisms in asymptomatic women, but on rare occasions can also be responsible for pelvic inflammatory disease. In Pap smears, fuzzy aggregates of actinomyces organisms have been likened to cotton balls, "dust bunnies," or "woolly bodies" (Fig. 3.43). The thin bacterial filaments are best seen at the periphery of the tangled clusters of organisms, where they are seen radiating from the dense core in a sunburst pattern, often in association with neutrophils. Eosinophilic, club-like, Splendore-Hoeppli material may also be identified rimming the periphery of the actinomycotic granules, although this is more commonly seen in actinomycotic abscesses (Fig. 3.44).

The differential diagnosis of actinomyces includes pseudoactinomycotic radiate granules (PAMRAGs)[34–36] and cockleburrs.[37] Histologically, PAMRAGs are glassy fragments and strips composed of various minerals and cellular

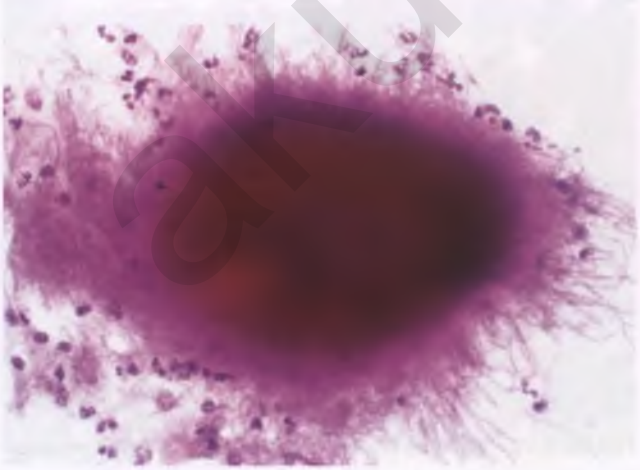

FIGURE 3.43. Pap smear with bacteria morphologically consistent with Actinomyces. Filamentous bacteria are seen radiating from the periphery of the aggregate of microorganisms.

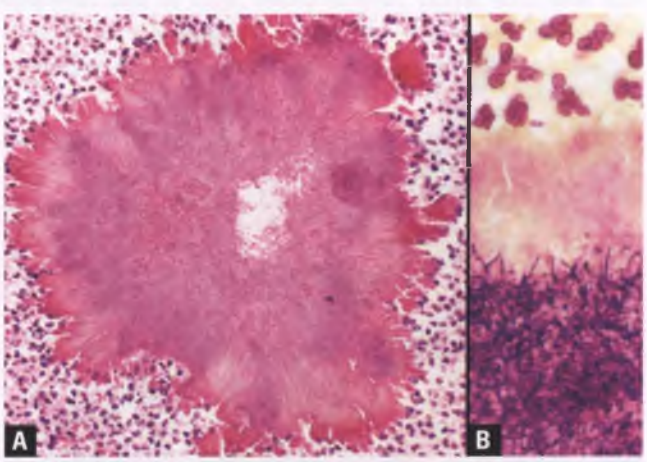

FIGURE 3.44. Actinomycosis. **A**: Tissue section of an actinomycotic granule found within an abscess. Note the prominent peripheral rim of Splendore-Hoeppli material. **B**: In this Gram-stained section of an actinomycotic granule, gram-positive, branching filamentous bacteria (bottom) are surrounded by a rim of gram-negative Splendore-Hoeppli material (middle) and suppurative exudate (top).

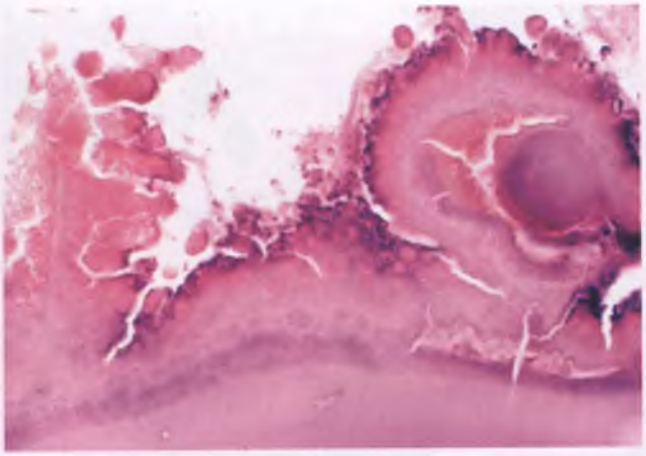

FIGURE 3.45. PAMRAG that was found in association with a small amount of tissue that was adherent to a removed IUD.

degradation products. They exhibit radiating, peripheral club-like projections due to a coating of Splendore-Hoeppli material, and often contain peripheral laminations that have been referred to as "tide-water" marks (Fig. 3.45). In contrast to the finely granular cores of actinomycotic granules, the cores of PAMRAGs are smooth and refractile. In addition, Gram stains of PAMRAGs demonstrate an absence of the thin, branching, gram-positive filaments characteristic of actinomyces. PAMRAGs are typically identified in samples of endometrial tissue that are closely associated with removed IUDs. Most PAMRAGs that occur in patients without a history of IUD use are found incidentally within endocervical Nabothian cysts that contain cellular debris and neutrophils (Fig. 3.46). Cockleburrs also have radiating club-like structures that appear to be related to the Splendore-Hoeppli phenomenon (Fig. 3.47). They may be found in Pap smears or within sites that harbor stagnating secretions and cellular debris, such as infected Nabothian cysts.

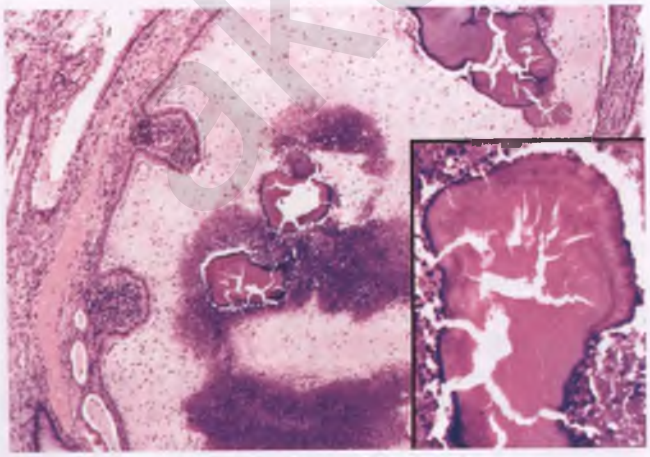

FIGURE 3.46. PAMRAGs within a Nabothian cyst in a patient with no history of IUD use.

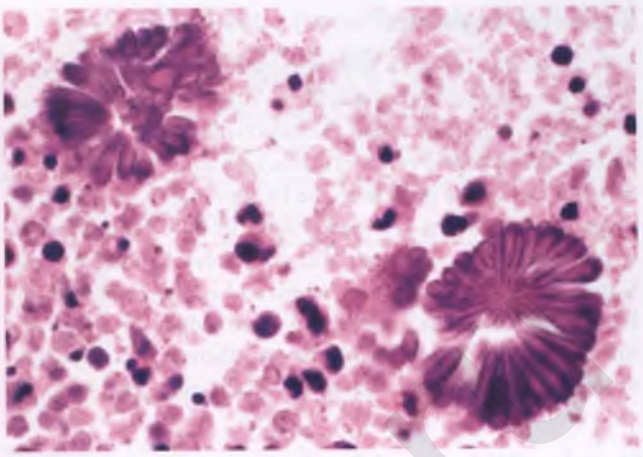

FIGURE 3.47. Two cockleburrs found in association with degenerating cellular debris within a Nabothian cyst.

Chlamydia Trachomatis

Chlamydial organisms are obligate intracellular bacteria that are a common cause of sexually transmitted disease. Chlamydial infection may be associated with chronic follicular cervicitis. In Pap smears, variably sized intracytoplasmic vacuoles with targetoid inclusions may be present within endocervical and squamous metaplastic cells, which often are multinucleated (Fig. 3.48). The frequent absence of such changes in documented case of *Chlamydia*, the difficulty in distinguishing these vacuolated inclusions from mucin vacuoles or degenerative vacuoles, and the availability of more accurate means of diagnosis via culture or immunologic/molecular techniques have led to the decision not to mention changes suggestive of *Chlamydia* when using The Bethesda System of Pap smear reporting. Nevertheless, those who examine Pap smears should be familiar with the changes that can sometimes be attributed to this infection, particularly since they often include nuclear alterations that can mimic dysplasia.

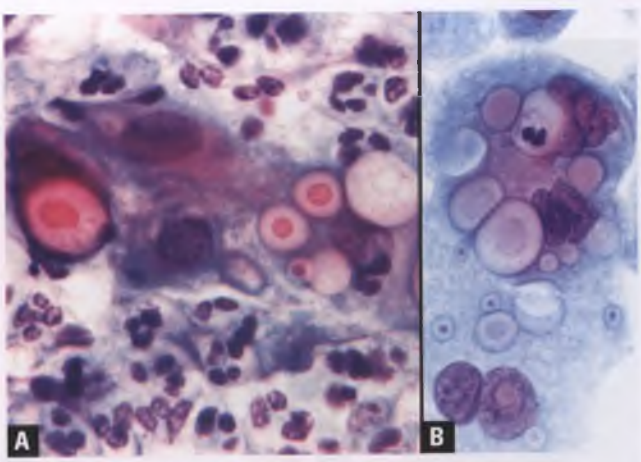

FIGURE 3.48. **A,B**: Cytologic changes suggestive of Chlamydial infection. Several intracytoplasmic targetoid inclusions of varying sizes are present. Also note the associated nuclear changes that could be mistaken for dysplasia.

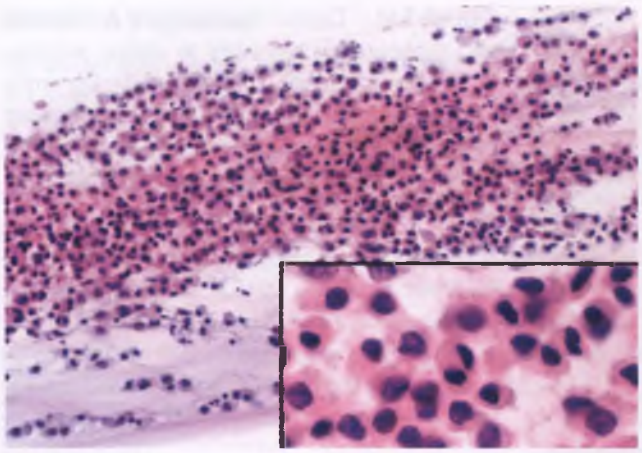

FIGURE 3.54. Pseudoparakeratosis in a Pap smear related to the degeneration of endocervical cells. The patient had a history of oral contraceptive use.

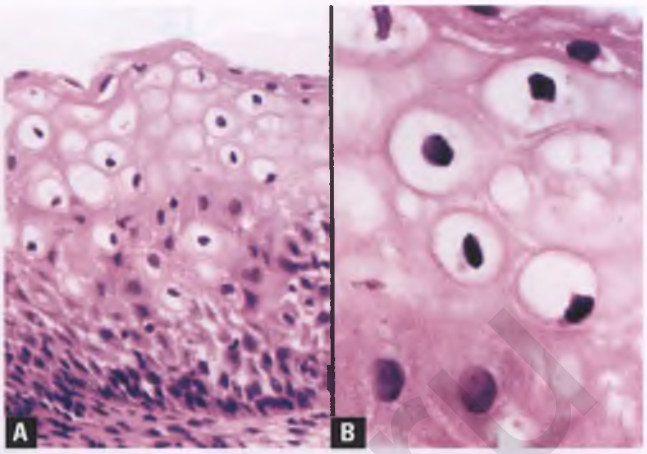

FIGURE 3.56. **A,B**: Pagetoid dyskeratosis. The scattered large pagetoid cells have pyknotic nuclei, perinuclear halos, and intercellular bridges with adjacent keratinocytes.

"basket-weave" appearance of glycogen-rich squamous cells (Fig. 3.2), pagetoid dyskeratotic cells are scattered singly in a splotchy distribution. The nuclei of koilocytes, unlike those of pagetoid dyskeratotic cells, are enlarged and irregularly shaped, and may be bi- or multinucleated. The absence of intracytoplasmic mucin, the lack of nuclear atypia, and the presence of intercellular bridges between the vacuolated cells and other keratinocytes help to distinguish pagetoid dyskeratosis from the extraordinarily rare examples of extramammary Paget's disease extending into the exocervix or adenocarcinoma spreading in a pagetoid fashion.

Note: Since most clinicians have never heard of pagetoid dyskeratosis, the pathology report should indicate that this is an incidental finding of no clinical significance.

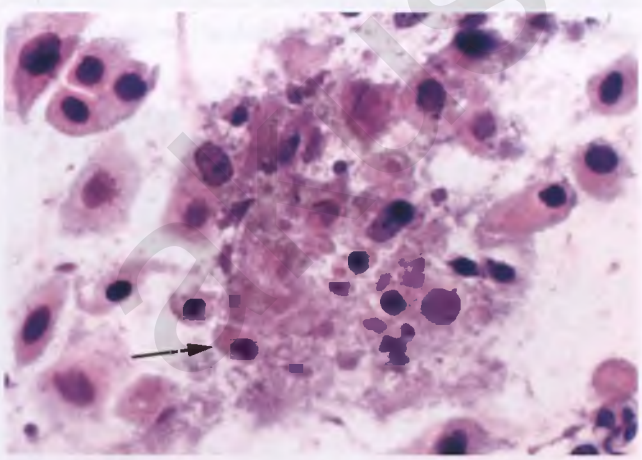

FIGURE 3.55. Pseudoparakeratosis in a Pap smear related to the degeneration of parabasal cells in a postmenopausal patient with atrophy. The *arrow* marks a representative pseudoparakeratotic cell. A "dirty background" is present, which is common in atrophic smears and needs to be distinguished from a true tumor diathesis (see section on squamous cell carcinoma).

Reactive Squamous Metaplastic Changes

When squamous metaplasia becomes inflamed, parabasal-type cells may proliferate and their occupation of the lower half of the epithelium may simulate an HSIL (Fig. 3.57). Recognition of the reactive nature of this process is facilitated by the presence of regularly spaced nuclei with only mild variations in size and shape, distinct nucleoli, intercellular edema, distinct cell borders, intraepithelial neutrophils, and surface maturation.

Reactive Endocervical Glandular Changes

In response to inflammation, erosion, or other causes of epithelial injury such as curettage, the lining epithelium of the endocervical canal and the underlying endocervical glands can exhibit reactive changes. These changes typically include (a) scattered cells with variably enlarged nuclei and smudged, dark chromatin, (b) mucin depletion and cytoplasmic eosinophilia,

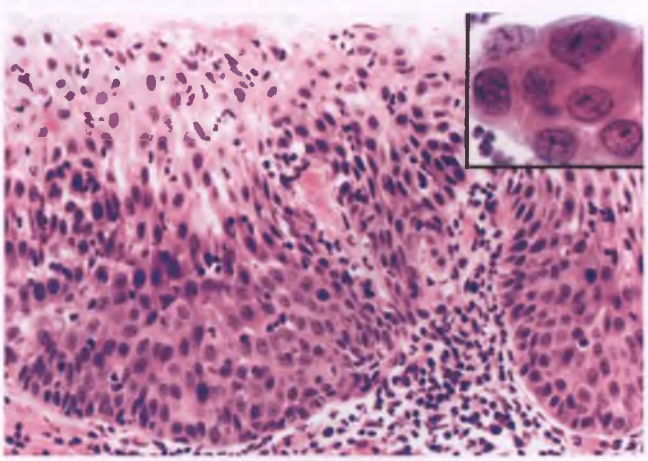

FIGURE 3.57. Squamous metaplasia with superimposed reactive changes associated with inflammation. The inset shows the Pap smear correlate of reactive squamous metaplastic cells.

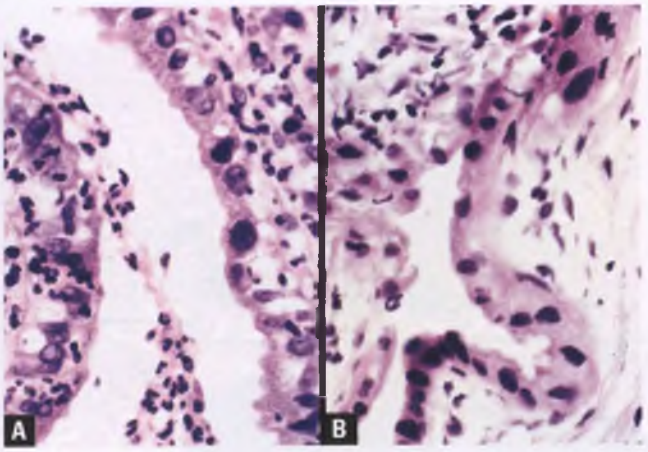

FIGURE 3.58. **A,B**: Endocervical glandular epithelium with reactive changes. Note the acute inflammation that is associated with the reactive gland in **A**.

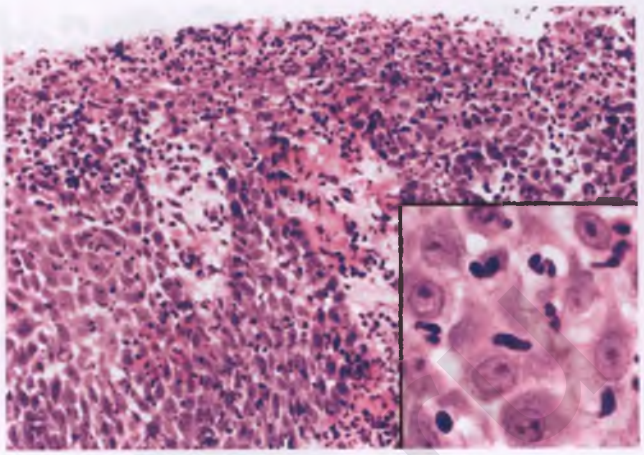

FIGURE 3.60. Reparative squamous changes in acute erosive cervicitis. Reactive epithelial cells with enlarged, vesicular nuclei and prominent nucleoli are present.

and (c) an associated inflammatory infiltrate (Fig. 3.58). In response to a curettage-related injury, the regenerating surface endocervical epithelium may also show nuclear stratification and formation of micropapillary structures.[40]

In Pap smears, aggregates of reactive endocervical cells exhibit a variable degree of nuclear enlargement and hyperchromasia, and it is not uncommon for multinucleated cells to be present (Fig. 3.59). Features that support their reactive nature include variably sized nuclei with preservation of smooth, round to oval nuclear contours with evenly distributed chromatin, minimal nuclear crowding/overlapping due to the presence of ample amounts of cytoplasm, and numerous acute inflammatory cells in the background.

Tissue Repair

In response to epithelial injury related to processes such as extensive inflammation, surface erosion, tissue sampling, or prior radiotherapy, reparative changes manifested by epithelial cells with enlarged nuclei and one or more macronucleoli may become prominent (Fig. 3.60). Mitotic activity may be present within this regenerating cell population. These changes may involve endocervical, immature squamous metaplastic, or squamous epithelium.

In Pap smears, the reactive epithelial cells in typical repair exhibit nuclear enlargement, prominent nucleoli, smooth nuclear membranes, and chromatin that is usually evenly dispersed and pale (Fig. 3.61). These cells form cohesive, monolayered sheets, with nonoverlapping nuclei streaming in the same direction. The typical scarcity of isolated reparative cells, bland chromatin, nonoverlapping nuclei within the sheets of cells, smooth nuclear membranes, and lack of a tumor diathesis help to distinguish repair from invasive squamous cell carcinoma. Although typical repair is classified as a negative cytologic finding, cases with any atypical reparative features such as nuclear

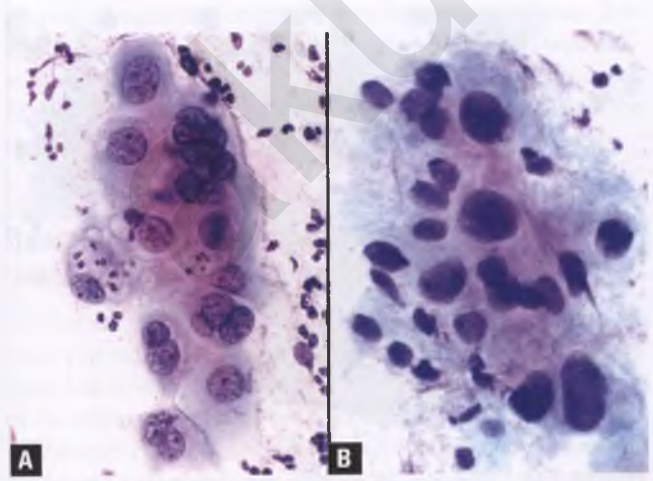

FIGURE 3.59. Reactive endocervical cells in Pap smears. **A**: Multinucleated cells and a few cells with ingested neutrophils are present. **B**: Note the marked variation in nuclear size; dysplastic/cancerous endocervical lesions tend to be much more monomorphic.

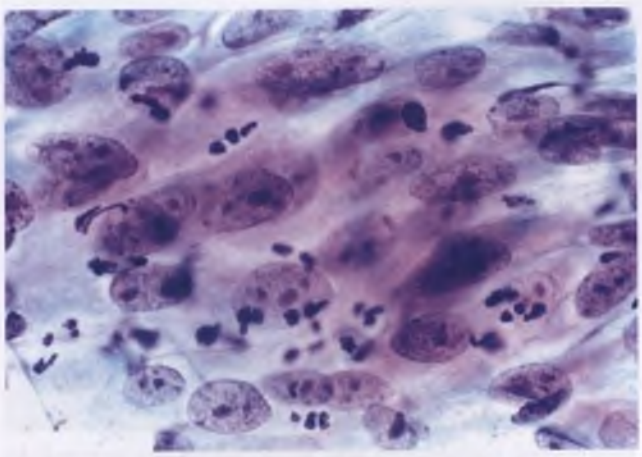

FIGURE 3.61. Typical reparative changes in presumed endocervical cells (Pap smear). The reactive cells form a monolayered sheet and exhibit prominent nucleoli and streaming nuclei. Intermingled acute inflammatory cells are also present.

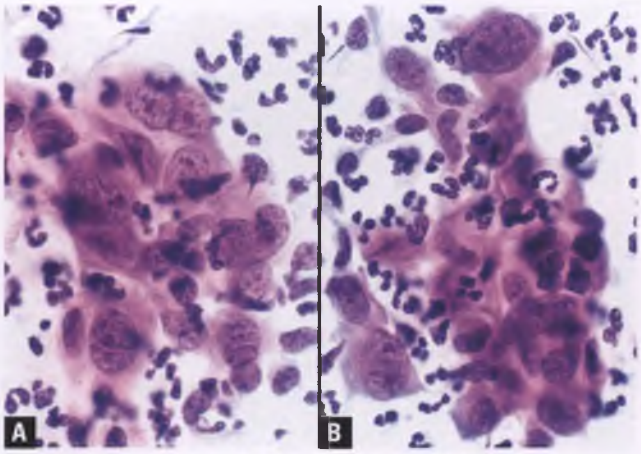

FIGURE 3.62. **A,B**: Pap smear with atypical reparative features in presumed squamous metaplastic cells.

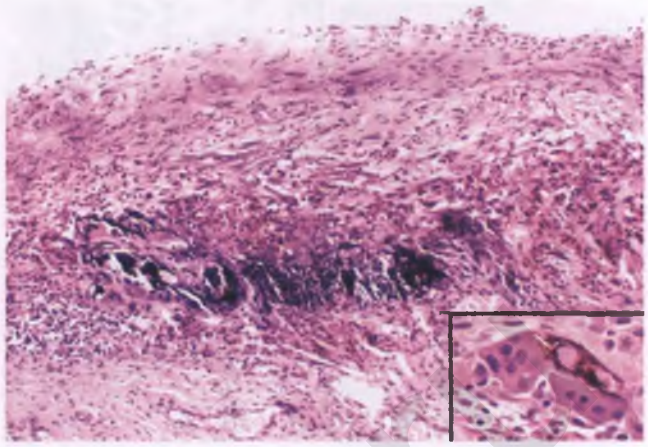

FIGURE 3.63. Cervix with biopsy site changes (chronic reparative phase). A layer of granulation tissue overlies a zone of brown to black pigment admixed with inflammatory cells. The inset highlights the presence of a foreign body giant cell reaction to the pigmented material.

crowding/overlapping, considerable variation in nuclear shape, an abnormal chromatin pattern, nuclear contour abnormalities, or significant loss of cohesion are classified as atypical glandular cells or ASC with reparative features whenever possible, recognizing that it is often difficult to determine the presumed cell type of origin (Fig. 3.62). In view of the fact that the major differential diagnostic consideration of atypical repair is invasive cancer, patients with a cytologic diagnosis of atypical repair should undergo colposcopy with tissue sampling.

Biopsy Site Changes and Postoperative Granulomas

Surgical procedures and associated maneuvers to achieve hemostasis result in traumatic injury to the cervix and can also generate a variety of artifactual changes (see section on artifacts near the end of this chapter). Tissue damage may be caused by a sharp knife, biopsy forceps, curette, laser, cryosurgical instrument, electrocautery device, or hemostatic agent. In the first few weeks following the procedure, superficial necrosis is the dominant histologic finding. As the lesion heals, granulation tissue, chronic inflammation, and hemosiderin-laden macrophages become prominent. In lesions in which a laser, electrocautery device, or Monsel's solution was used, brown to black pigment may be present, often in association with foreign body giant cells (Fig. 3.63).

The vast majority of cervical granulomas are localized, nonnecrotizing, foreign body–type granulomas related to a previous surgical procedure.[41] If pigmented or polarizable foreign material is present within these granulomas, special stains for microorganisms are not indicated. Rarely, biopsy/curettage-related necrobiotic granulomas that resemble rheumatoid nodules can also occur within the cervix.[42] In the absence of deposits of pigment or foreign material, these necrotizing granulomas should be examined with special stains to exclude the possibility of an infection with fungi or acid-fast bacilli.

Radiation Effect

Radiation therapy results in a spectrum of nuclear and cytoplasmic alterations that collectively are referred to as radiation effect. Since this effect is much more commonly seen in Pap smears than in tissue sections, the features of radiation-induced changes in cytologic preparations will be emphasized. The most characteristic alterations occur within cells that are thought to be of squamous origin, although similar changes can also take place within endocervical cells.

Cells with radiation effect may have bizarre shapes, and their cytoplasm often exhibits polychromatic staining (Figs. 3.64 and 3.65). Nuclei become enlarged, but there is a concomitant increase in cytoplasm such that the normal nuclear to cytoplasmic ratio is maintained (cytomegaly). Binucleation and multinucleation are common. Nuclear chromatin may be

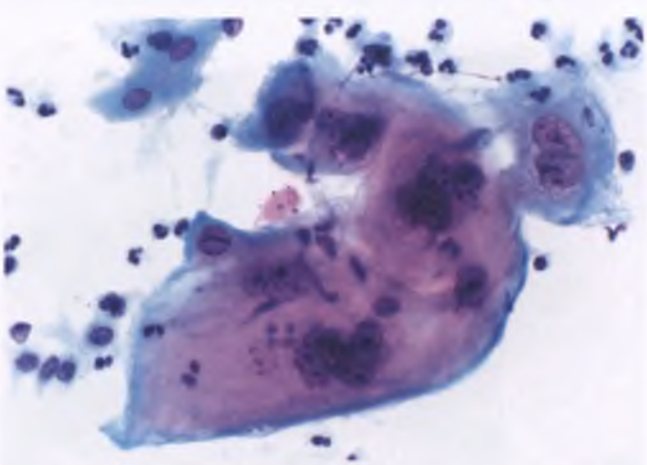

FIGURE 3.64. Radiation effect. Note the macrocytes with unusual cell shapes, multinucleation, and polychromatic cytoplasm. The presence of prominent nucleoli is related to the reparative process that takes place during the first few months following treatment.

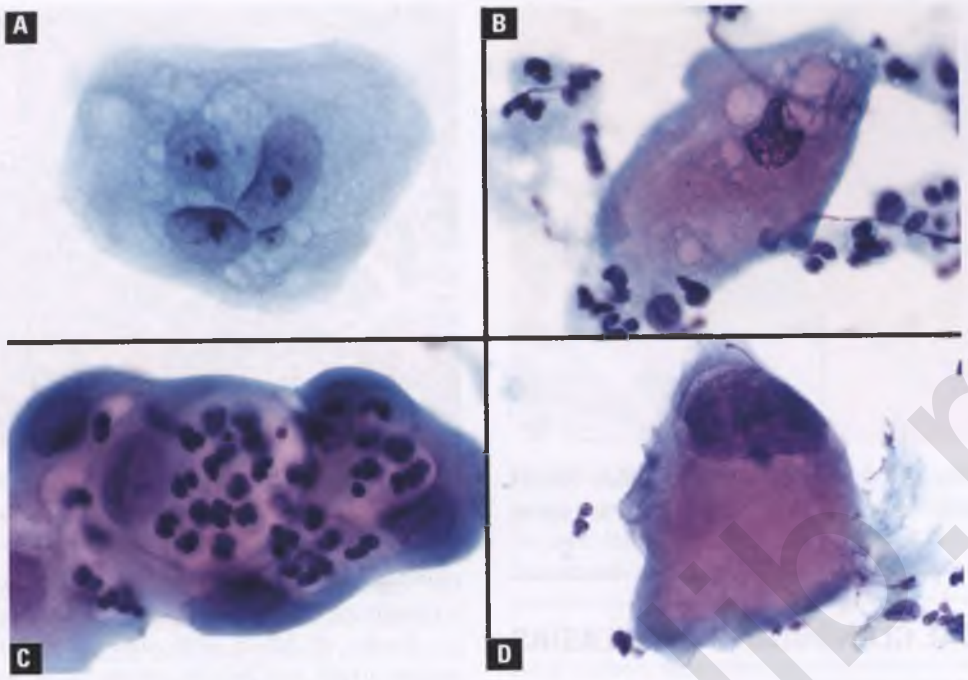

FIGURE 3.65. Radiation effect. **A**: Multinucleated macrocyte with cytoplasmic vacuolization and prominent nucleoli (acute phase). **B**: Macrocyte with cytoplasmic vacuolization and polychromatic cytoplasm (acute phase). **C**: Cell cluster with ingested neutrophils within cytoplasmic vacuoles (acute phase). **D**: Macrocyte with polychromatic cytoplasm (chronic phase).

finely granular or smudged, and ranges from hypochromatic to mildly hyperchromatic. Prominent nucleoli may be present during the first few months following radiation, when there is coexisting repair. Cytoplasmic vacuolization also occurs as part of the acute phase (first 6 months) of radiation damage, and these vacuoles may contain engulfed neutrophils. In some cases, chronic radiation-induced changes manifested primarily by the presence of macrocytes with unusual shapes and polychromatic cytoplasm develop that may persist for the life of the patient. Changes similar to radiation effect can be observed in patients who are administered chemotherapeutic agents or who are deficient in folic acid. Histologically, endocervical glands with radiation effect are widely spaced and lined by mitotically inactive, flattened to cuboidal epithelial cells, some of which exhibit the cytoplasmic and nuclear alterations described above.[43]

Reactive Changes in Pap Smears Associated with Intrauterine Contraceptive Devices

IUD-related irritation of the uterine lining may result in exfoliation of small clusters of atypical glandular cells with large cytoplasmic vacuoles that compress the nuclei to the periphery of the cells, creating an appearance that can simulate an adenocarcinoma (Fig. 3.66). Nucleoli may be prominent, and the vacuolated cytoplasm may contain phagocytosed neutrophils. Although these glandular clusters are reactive, the difficulty in excluding an adenocarcinoma often leads to their classification as atypical glandular cells, with a comment indicating that they are likely IUD related.

Another IUD-related finding in Pap smears is the occasional presence of a few isolated single cells of endometrial origin (nicknamed "ding cells") that can mimic squamous cell carcinoma in situ (CIS) (Fig. 3.67). In addition to the history of IUD use, cytologic features that help to distinguish ding cells from those of CIS are their occurrence exclusively as single cells, their lack of association with a morphologic spectrum of more obviously dysplastic squamous cells elsewhere in the smear, their scarcity, and their less pronounced nuclear contour abnormalities.

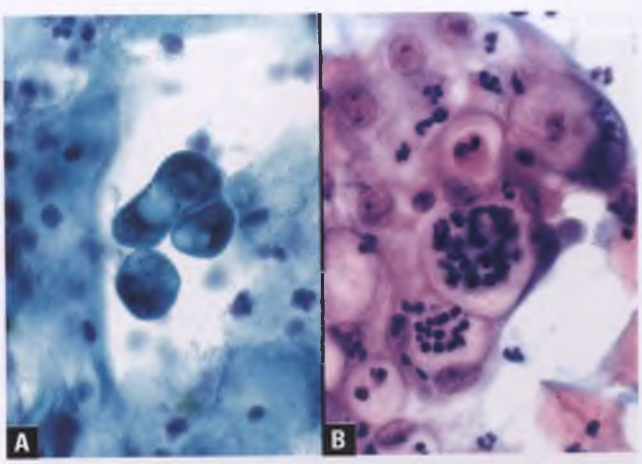

FIGURE 3.66. **A,B**: Atypical glandular cells associated with IUD. Reactive nuclear changes and prominent cytoplasmic vacuoles are present. In (**B**), some of these vacuoles contain engulfed neutrophils. Follow-up was negative in both cases.

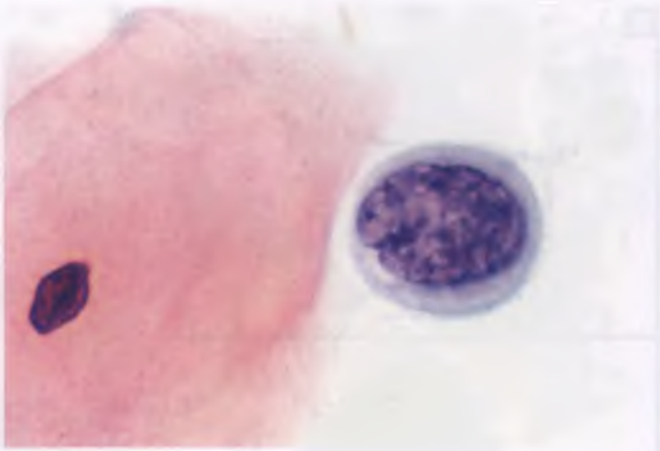

FIGURE 3.67. "Ding cell" in a Pap smear from a patient with an IUD. These are isolated benign cells of endometrial origin that can be mistaken for CIS.

ENDOCERVICAL GLANDULAR HYPERPLASIAS

Microglandular Hyperplasia

MGH is a microacinar proliferation of altered benign endocervical glands that typically occurs in women of reproductive age who often have a history of recent oral contraceptive use or pregnancy.[22] Although usually an incidental microscopic finding, florid examples of MGH can present as small polyps that may produce symptoms of abnormal vaginal bleeding or discharge (Fig. 3.68). The closely packed glands of MGH are of variable sizes and shapes, and their lumens often contain pale-staining mucinous secretions with scattered neutrophils (Fig. 3.69). The epithelium lining the glands may be columnar, cuboidal, or flattened, with the columnar cells often containing subnuclear vacuoles that result in cytoplasmic clearing (Fig. 3.70). Mitotic figures are scarce, and the epithelial cells typically have bland nuclear features. The stroma is scant and usually contains an admixture of neutrophils and lymphocytes. Associated

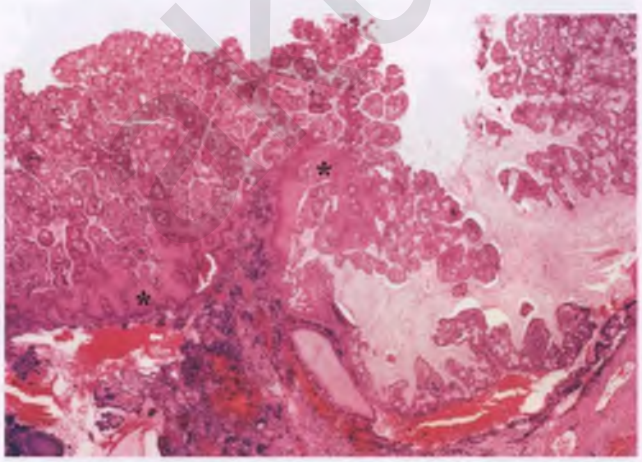

FIGURE 3.68. Florid MGH presenting as an endocervical polyp. Portions of the lesion have undergone squamous metaplasia *(asterisks)*.

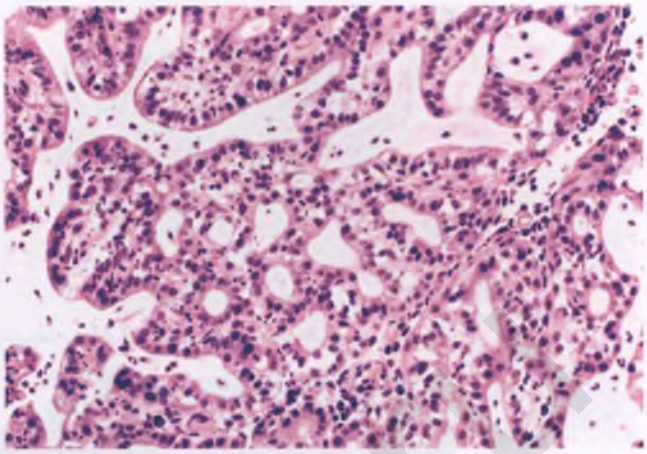

FIGURE 3.69. MGH, usual type.

squamous metaplasia is common (Fig. 3.71), and its presence is thought to indicate a later stage in the evolution of MGH.[44]

Forms of MGH with unusual architectural patterns, nuclear atypia, and peculiar stroma occur, some of which can simulate clear cell or MGH-like adenocarcinoma.[45,46] The lack of stromal invasion evident at low magnification, the scarcity of mitotic figures, the absence of marked nuclear atypia, the presence of a transition to more usual forms of MGH, and the absence of a clinically malignant mass help to distinguish MGH from adenocarcinoma.[45] In Pap smears, MGH with nuclear atypia can serve as a source of atypical glandular cells (Figs. 3.72 and 3.73).[47]

Diffuse Laminar Endocervical Glandular Hyperplasia

Diffuse laminar endocervical glandular hyperplasia is a rare incidental finding that occurs in women of reproductive age, the significance of which lies in its potential confusion with

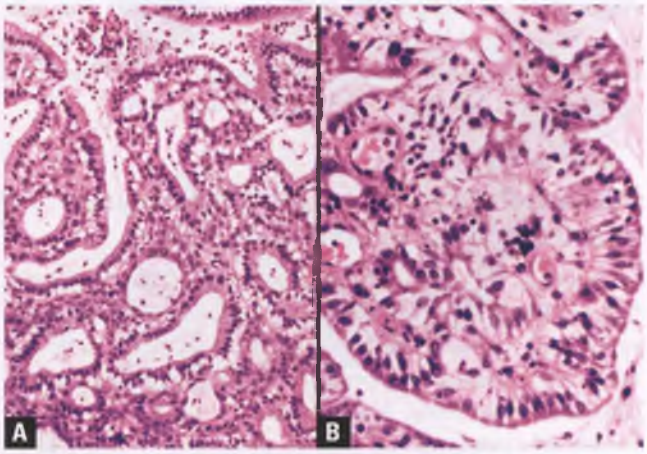

FIGURE 3.70. Microglandular hyperplasia. **A**: Note the prominent subnuclear vacuoles. **B**: The marked extent of cytoplasmic clearing results in a resemblance to clear cell carcinoma.

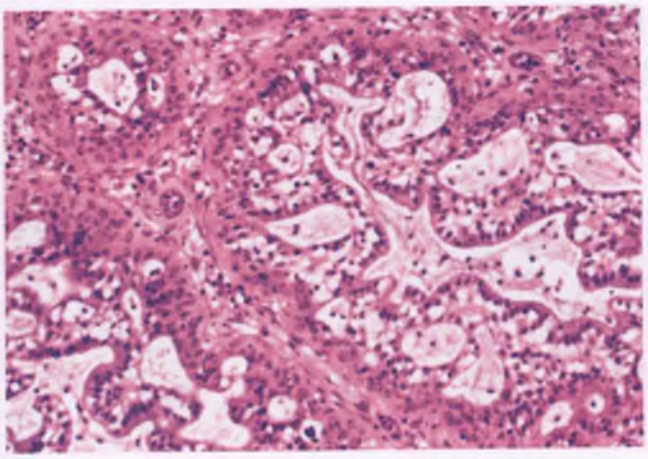

FIGURE 3.71. MGH composed of lobular glandular aggregates rimmed by immature squamous metaplasia.

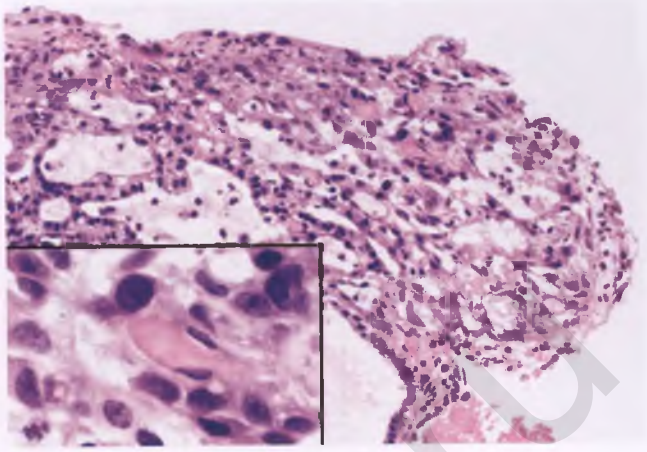

FIGURE 3.73. Histologic correlate to Pap smear in Figure 3.72 demonstrates the presence of endocervical MGH with nuclear atypia. The inset shows cells with nuclear features that are quite similar to those found in the corresponding Pap smear.

adenoma malignum (minimal deviation adenocarcinoma). The characteristic histologic finding is a diffuse band-like proliferation of crowded, evenly spaced, benign-appearing endocervical glands lined by columnar mucinous epithelium that is sharply demarcated from the underlying cervical stroma (Fig. 3.74).[48] There is typically an associated prominent chronic inflammatory infiltrate. The glandular proliferation usually does not extend beyond the inner third of the cervical wall. Reactive nuclear changes and periglandular stromal edema may be present, and should not be taken as evidence of malignancy. The absence of a symptomatic mass and the sharply demarcated border with uninvolved stroma are the most important features that differentiate this innocuous lesion from adenoma malignum.

Lobular Endocervical Glandular Hyperplasia

Lobular endocervical glandular hyperplasia is another rare type of benign endocervical glandular proliferation that occurs in adult women, most often as an incidental finding or associated with a cervicovaginal discharge.[49] The defining feature of this lesion is the distinctly lobular architecture of the glandular proliferation, which has a lining epithelium composed of benign-appearing columnar mucinous cells. The glands are of small to medium size and the lobular aggregates tend to cluster around larger glands (Fig. 3.75). Some of the glands exhibit a pyloric phenotype, prompting some investigators to refer to this process as pyloric gland or gastric metaplasia.[50,51] Most examples of this benign glandular proliferation are confined to the inner half of the cervical wall.

The combination of superficial location, lobular architecture, and tall columnar mucinous cells lining the glands allows distinction of lobular endocervical glandular hyperplasia from other entities in the differential diagnosis, such as tunnel clusters, mesonephric hyperplasia, MGH, diffuse laminar

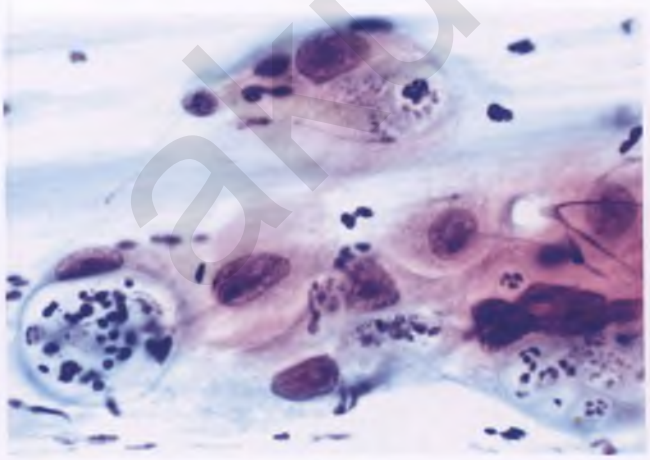

FIGURE 3.72. Pap smear with glandular atypia attributed to atypical form of MGH. The reactive glandular cells exhibit nuclear enlargement, prominent nucleoli, and phagocytosis of neutrophils. These changes are not specific for MGH and resemble tissue repair.

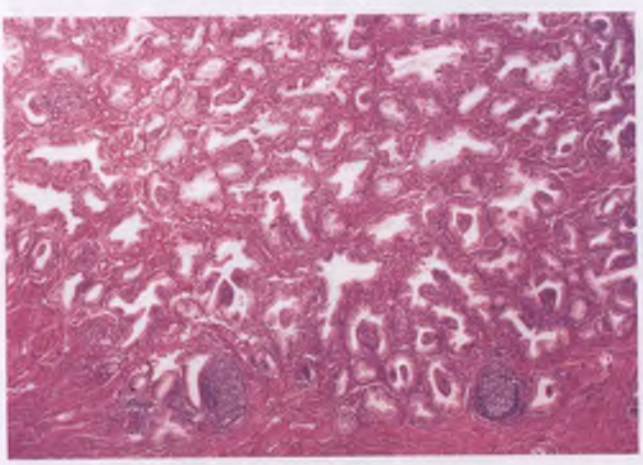

FIGURE 3.74. Diffuse laminar endocervical glandular hyperplasia. Note the sharp demarcation of the hyperplastic endocervical glands from the underlying stroma, and the associated chronic inflammation.

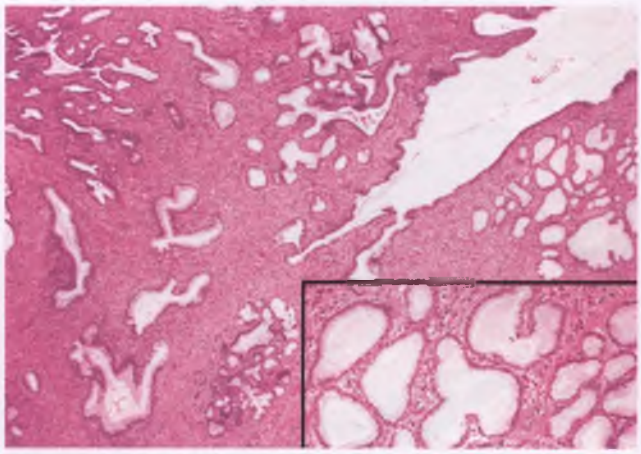

FIGURE 3.75. Lobular endocervical glandular hyperplasia.

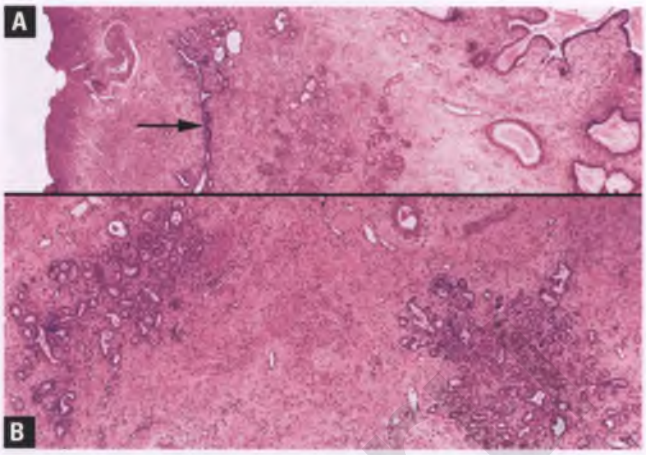

FIGURE 3.76. Lobular mesonephric hyperplasia. **A**: A lobular cluster of tubules (center) lies adjacent to a cleft-like duct *(arrow)*. Note the typical location of this process in the deep cervical stroma (overlying endocervical glands are at right). **B**: Two lobular aggregates of mesonephric tubules are present. Some of these tubules contain intraluminal eosinophilic secretions.

endocervical glandular hyperplasia, and adenoma malignum. In a few cases that have been interpreted as atypical lobular endocervical glandular hyperplasia due to the presence of epithelial tufting, pseudostratification, and nuc lear atypia, molecular evidence has been presented that suggests that an atypical form of this lesion may serve as a precursor of adenoma malignum.[52]

MESONEPHRIC REMNANTS AND HYPERPLASIAS

Benign mesonephric processes that originate from incompletely degenerated mesonephric (wolffian) ducts are typically found in the deep stroma of the lateral cervical walls. They are incidental microscopic findings in the vast majority of cases, and are composed of characteristic small tubules and/or elongated ducts that vary in extent and architecture.[53,54] On those unusual occasions when the mesonephric elements are superficially located and within reach of an endocervical sampling device, they can serve as the source of atypical glandular cells in Pap smears.[55,56]

Lobular proliferations of mesonephric tubules, with or without an associated duct, are referred to as **mesonephric remnants** when <6 mm in greatest extent, and arbitrarily classified as **lobular mesonephric hyperplasia** when they exceed this size limit (Fig. 3.76).[53,54] Although most mesonephric proliferations have a predominantly lobular architecture, approximately 20% exhibit a mainly diffuse pattern (Fig. 3.77). These diffuse processes typically span a distance of 10 to 25 mm and are referred to as **diffuse mesonephric hyperplasia**. The tubules of either type of mesonephric hyperplasia do not elicit a stromal reaction, and are typically small and round. These tubules are lined by a single layer of cuboidal to flattened, mitotically inactive, mucin-negative, nonciliated epithelial cells with bland nuclear features, and often contain an eosinophilic, colloid-like intraluminal secretion that is periodic acid-Schiff (PAS)-positive and diastase resistant (Fig. 3.78A). On occasion, the tubules may be lined by cells with "activated" nuclei with readily apparent nucleoli, but this finding is of no consequence in the context of an architecturally benign mesonephric proliferation (Fig. 3.78B). In contrast to the glands of the normal endocervix, tunnel clusters, MGH, tuboendometrioid metaplasia, and endometriosis, a variable proportion of the apical aspects of the glandular elements and eosinophilic luminal secretions of benign mesonephric proliferations typically exhibit strong CD10 immunoreactivity (Fig. 3.79).[57,58]

Mesonephric hyperplasia should not be confused with adenoma malignum (minimal deviation adenocarcinoma), since the latter typically features a symptomatic mass, tall columnar epithelial cells that contain abundant intracytoplasmic mucin, and irregularly shaped glands that infiltrate the superficial and deep aspects of the cervical wall. Although the tubulocystic pattern of clear cell carcinoma bears some resemblance to hyperplastic mesonephric tubules, other architectural patterns (solid,

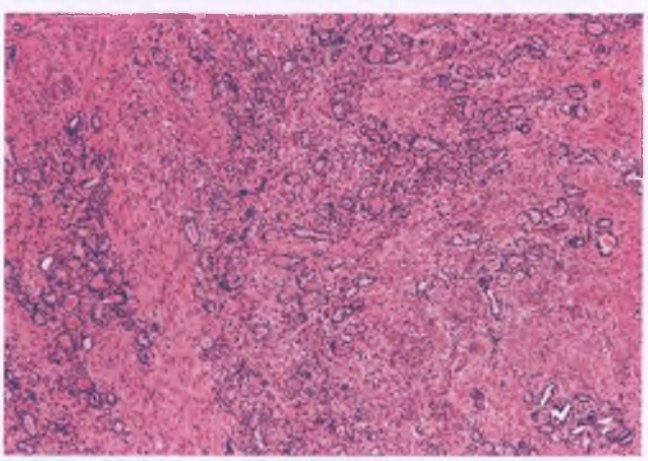

FIGURE 3.77. Diffuse mesonephric hyperplasia. Mesonephric tubules, many of which contain eosinophilic secretions, are scattered throughout this portion of the deep cervical stroma in a predominantly diffuse pattern.

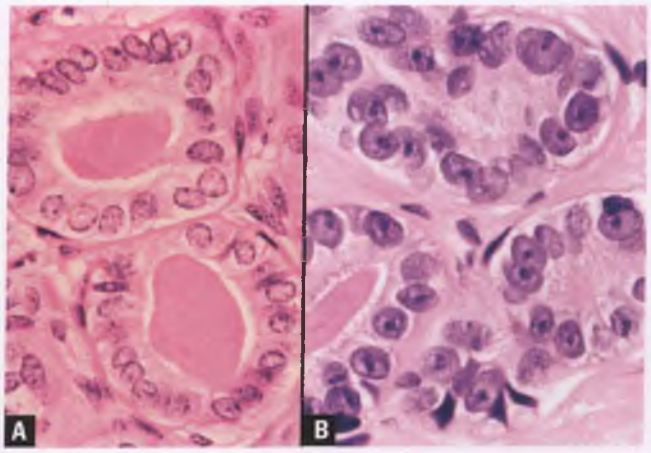

FIGURE 3.78. Tubules of mesonephric remnant/hyperplasia. **A**: Typical bland nuclei and eosinophilic, colloid-like intraluminal secretions. **B**: Mesonephric tubules are occasionally lined by cells that contain prominent nucleoli.

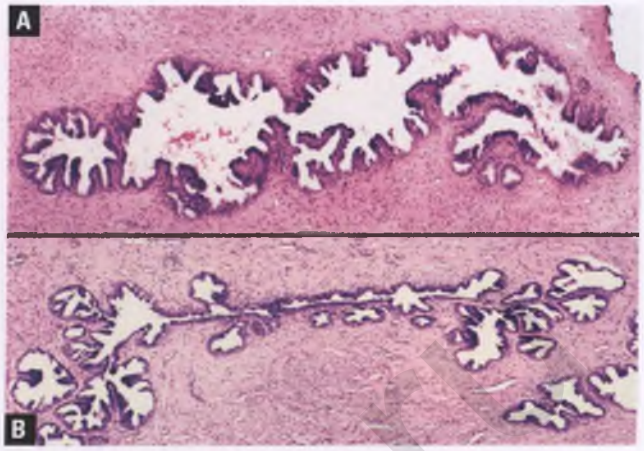

FIGURE 3.80. **A,B**: Mesonephric ductal hyperplasia. The hyperplastic duct in **A** is slightly dilated, whereas the duct in **B** is elongated, centrally compressed, and cleft-like.

papillary) are also usually present in these neoplasms. Moreover, clear cell carcinoma is a frankly malignant tumor, with significant nuclear atypia and mitotic activity, and also contains glycogen-rich clear cells and hobnail cells. Distinction of florid mesonephric hyperplasia from mesonephric adenocarcinoma is discussed in the section on the latter entity.

In contract to mesonephric tubules, mesonephric ducts typically are elongated structures that may have compressed or slightly dilated lumens and micropapillary epithelial tufts. When these ducts contain hyperplastic papillae and are found unassociated with a significant proliferation of mesonephric tubules, the process is classified as **mesonephric ductal hyperplasia** (Fig. 3.80).[53] The nuclei lining these ducts are often elongated, hyperchromatic, and oriented perpendicular to the basement membrane (Fig. 3.81). Distinction from endocervical AIS is facilitated by the absence of mitotic activity, the lack of significant nuclear atypia, the limitation of the hyperplastic micropapillary process to the elongated duct and its immediate vicinity, and its isolated location in the deep aspect of the cervical stroma unassociated with normal endocervical glands.

POLYPS

Endocervical Polyps

Endocervical polyps are common localized overgrowths of endocervical tissue that are usually small (<1 cm) and solitary. Although often asymptomatic, they may also be the cause of abnormal vaginal bleeding/discharge. Grossly, the polyps project from the endocervical canal and are nodular or elongated and pink to red due to their prominent vascularity (Fig. 3.82).

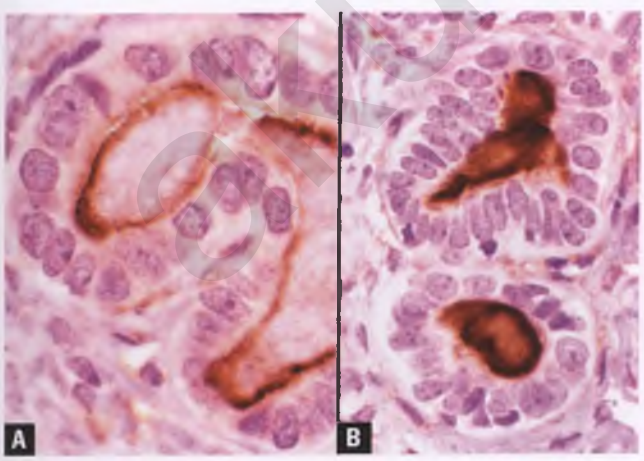

FIGURE 3.79. Mesonephric remnant/hyperplasia. **A**: CD10 positivity of the apical aspects of the cells lining a gland, resulting in a ring of positive staining surrounding the lumen. **B**: Intense CD10 positivity of an intraluminal secretory product.

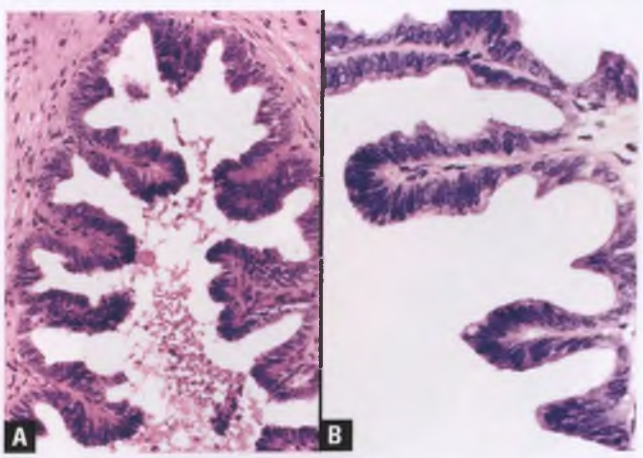

FIGURE 3.81. **A,B**: Mesonephric ductal hyperplasia. The cells lining the papillae tend to have elongated, hyperchromatic nuclei oriented perpendicular to the basement membrane (images taken from the two separate cases depicted in preceding figure).

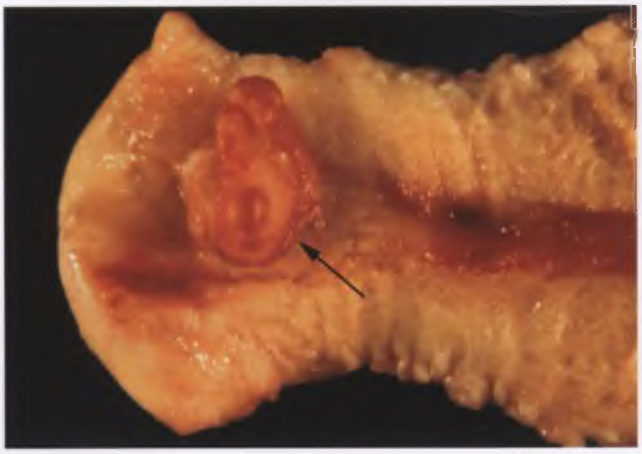

FIGURE 3.82. Endocervical polyp *(arrow)* projecting from the surface of the endocervical canal.

Histologically, endocervical polyps exhibit a wide range of patterns, depending on the relative proportions of the glandular and stromal components. In the usual type of endocervical polyp, mucinous endocervical-type epithelium lines the surface and the underlying crypts, and the core of the polyp consists of ample fibrous stroma with numerous thick-walled blood vessels (Fig. 3.83). Features that are commonly seen within these polyps are dilated glands, chronic inflammation of the superficial stroma, and squamous metaplasia. A pseudoneoplastic pattern may result on those occasions in which the glandular element predominates within these polyps (Fig. 3.84). A feature that helps to differentiate this lesion from a well-differentiated adenocarcinoma is that the hyperplastic glands recapitulate the architecture of the normal endocervix (elongated clefts with side channels) rather than exhibiting the haphazard architecture of infiltrating glands. In other endocervical polyps, the fibrous stroma or vascular component may predominate (stromal or vascular polyps, respectively).

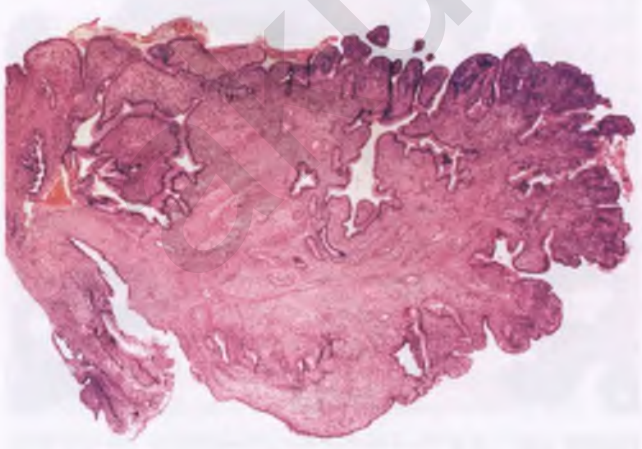

FIGURE 3.83. Endocervical polyp (usual type). Portions of the superficial stroma are chronically inflamed, and the stromal core contains several thick-walled blood vessels.

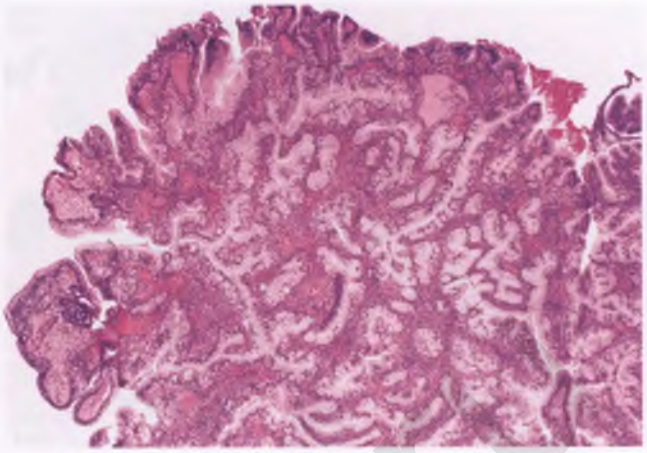

FIGURE 3.84. Endocervical polyp. The glands in this example are hyperplastic and recapitulate the architecture of the normal endocervix, with side channels branching from elongated clefts.

In endocervical polyps with surface erosion, the underlying stroma typically consists of inflamed granulation tissue (Fig. 3.85). Surface trauma and inflammation can also result in reparative/degenerative atypia within the overlying endocervical/metaplastic epithelium (Fig. 3.86), which can be the source of atypical epithelial cells in Pap smears (Fig. 3.87). Approximately 1 of every 200 endocervical polyps harbors an SIL; the Pap smears in such cases are typically nondiagnostic due to the less accessible nature of the lesional cells.[59]

Fibroepithelial Polyps

Fibroepithelial polyps (mesodermal stromal polyps) are more commonly seen in the vagina, but may also arise within the exocervix on rare occasions. The frequent finding of atypical stromal cells may cause concern for sarcoma. These lesions are invariably benign, and are discussed in more detail in Chapter 2.

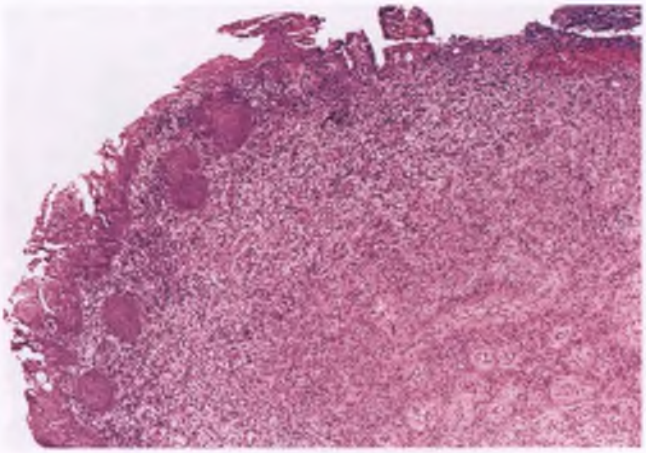

FIGURE 3.85. Endocervical polyp with a prominent fibrovascular component. A zone of erosion-related, inflamed granulation tissue is interposed between the surface squamous metaplastic epithelium and the vessel-rich stromal core.

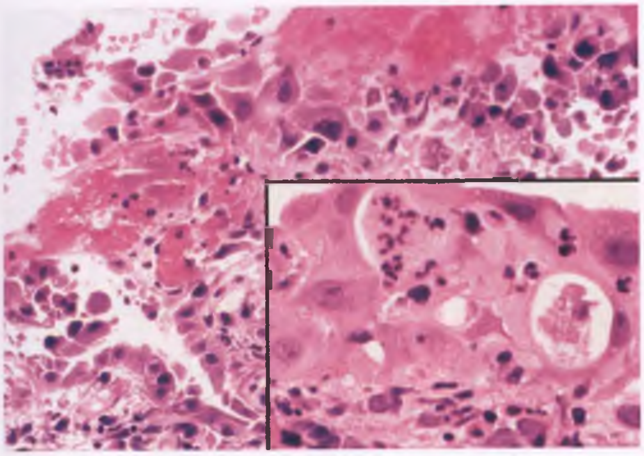

FIGURE 3.86. Surface of two different endocervical polyps with surface trauma and inflammation. The main image shows predominantly degenerative atypia, with variably sized, hyperchromatic, degenerating nuclei. The inset shows squamoid cells with reparative atypia that are the histologic correlate of the cells in the right-sided image in Figure 3.87.

MISCELLANEOUS NONNEOPLASTIC PROCESSES

Ectopic Decidua

Decidualization of the superficial cervical stroma occurs commonly during late pregnancy, and may present as an incidental microscopic finding, a plaque-like lesion, a pseudopolyp, or in association with endometriosis (Fig. 3.88).[60] This process can be distinguished from squamous cell carcinoma by its mitotic inactivity, lack of nuclear atypia, and cytokeratin negativity.

The presence of decidual cells in Pap smears is seen on occasion, where they are found singly and in small aggregates. Cytologically, decidual cells are large with a wide variation in

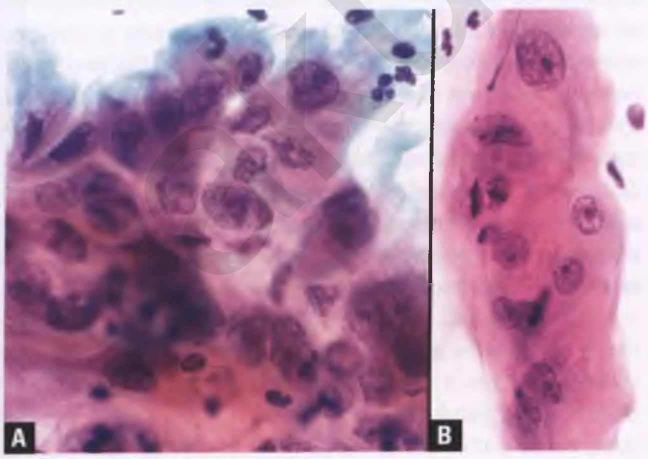

FIGURE 3.87. **A,B**: Pap smears from patients with biopsy-proven endocervical polyps with surface trauma and inflammation. Reparative features are evident in these aggregates of endocervical **(A)** and squamoid **(B)** cells.

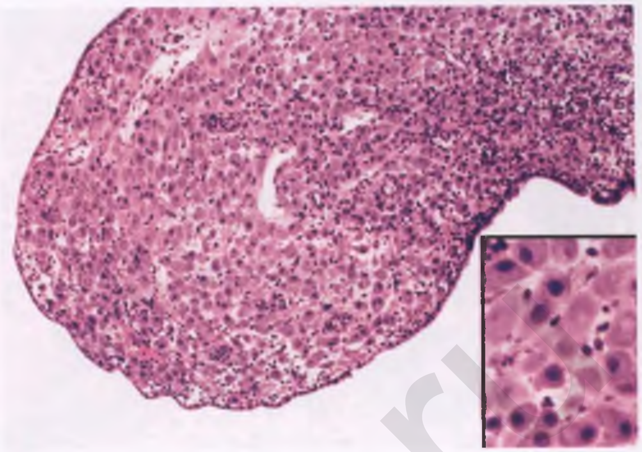

FIGURE 3.88. Decidual pseudopolyp. This polypoid cervical lesion is composed of decidualized stromal cells admixed with chronic inflammatory cells, and is lined by attenuated endocervical epithelium. The inset shows decidual cells with abundant cytoplasm and distinct cell borders.

nuclear size, finely granular chromatin, variably prominent nucleoli, and abundant cytoplasm (Fig. 3.89). The cytologic differential diagnosis of decidual cells includes moderate dysplasia, tissue repair, and carcinoma.

Arias-Stella Reaction

Although the pathologist is accustomed to recognizing the Arias-Stella reaction (ASR) in endometrial glands, this process may be misdiagnosed when found outside of its usual location. Nearly, all patients with endocervical gland involvement by the ASR are either pregnant or taking oral contraceptives, and the involved glands represent an incidental finding that may be either within otherwise normal endocervical mucosa or within an endocervical polyp.[61] The nuclear abnormalities are as described for endometrial ASR (see Chapter 4). Features that are often present in endocervical ASR include clear

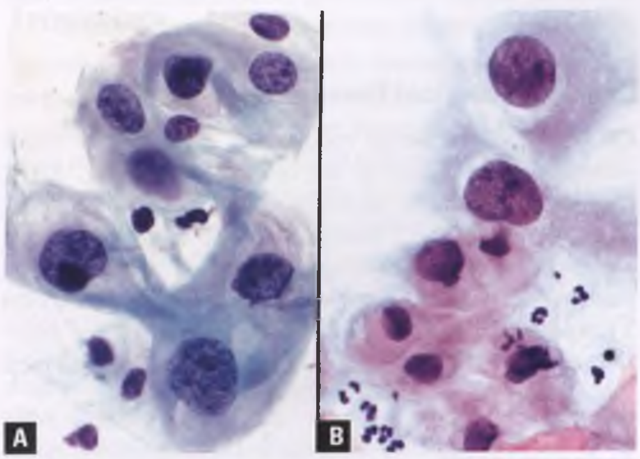

FIGURE 3.89. Decidual cells in Pap smears from two different patients. Without a history of pregnancy, these cells could be mistaken for a significant lesion.

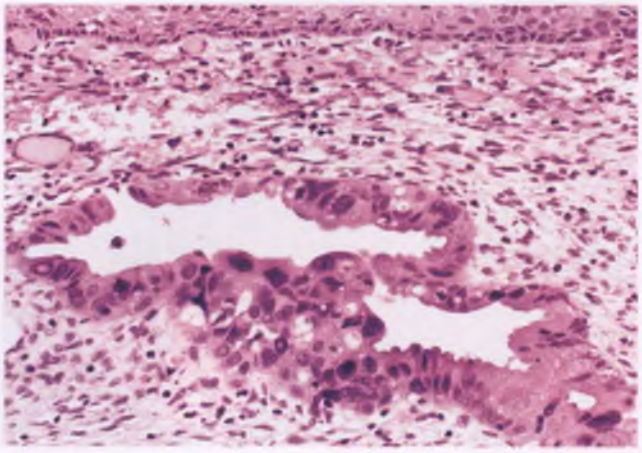

FIGURE 3.90. Endocervical gland with ASR. In this example, there is partial involvement of the gland. The lesional cells have enlarged nuclei with smudged chromatin, oxyphilic cytoplasm, occasional clear cytoplasmic vacuoles, and a few intranuclear pseudoinclusions (most visible at far left). Mitotic figures are conspicuously absent.

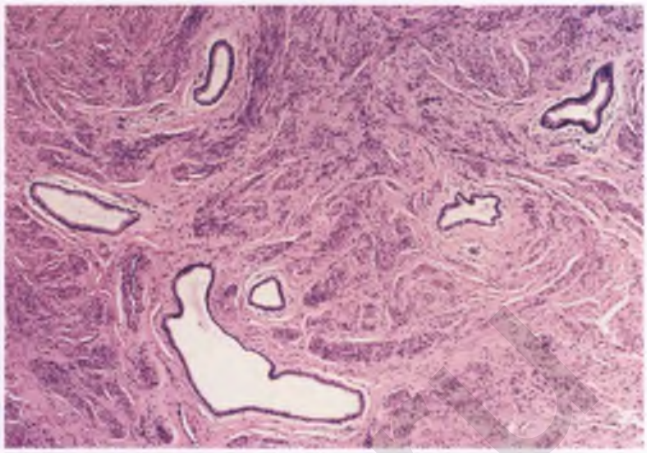

FIGURE 3.91. Deep endocervical glands. Scattered endocervical glands appear to be wandering through the deep portion of the cervical stroma.

cytoplasmic vacuoles, intraglandular epithelial tufts, hobnail cells, oxyphilic cytoplasm, delicate papillae, intranuclear pseudoinclusions, and partial gland involvement (Fig. 3.90).[61]

Differential Diagnosis

In contrast to endocervical AIS, the ASR does not feature easily recognizable mitotic figures, apoptotic bodies, a more uniform population of atypical cells, a high Ki-67 proliferative index, or strong immunoreactivity for p16. Features that favor the ASR over clear cell carcinoma include the absence of a mass, a scanning magnification architectural pattern that is consistent with involvement of preexisting benign glandular elements, the lack of stromal infiltration or an associated stromal reaction, the wide range of nuclear atypia, and the lack or rarity of mitotic figures within the involved glands. As one might imagine, glandular cells with ASR may be misinterpreted as dysplastic or malignant cells in Pap smears, underscoring the need for correlation with clinical history, physical examination, and biopsy material.

Deep Endocervical Glands

On rare occasions, benign endocervical glands can be found within the deep aspect of the cervical stroma (Fig. 3.91), prompting concern for adenoma malignum (minimal deviation adenocarcinoma).[62] Features that help to distinguish this process from a bland-appearing adenocarcinoma include (a) its presentation as an incidental microscopic finding rather than a symptomatic mass, (b) the widely spaced nature and architectural simplicity of the glands, and (c) the lack of even focal nuclear atypia or periglandular stromal reaction.

Endocervicosis

Endocervicosis is a very rare phenomenon that refers to the presence of benign endocervical-type glands in unusual sites such as the urinary bladder, abdominopelvic lymph nodes, and peritoneum. This process has been reported to involve the outer aspect of the cervical wall, where its irregularly shaped glands, pseudoinfiltrative pattern, and occasional reaction to mucin within the stroma can result in confusion with adenoma malignum.[63] Unlike the latter neoplasm, endocervicosis typically features a zone of uninvolved cervical stroma between the deep-seated lesion and the normal endocervical glands and contains a more prominent cystic component. In addition, cervical endocervicosis often has glands that are lined by low/mid columnar to flattened epithelial cells, which contrasts with the aberrantly tall, mucin-rich cells often present in adenoma malignum.

Endometriosis

The general features and extragenital manifestations of endometriosis are discussed in Chapter 8. In the cervix, endometriosis is usually superficially located beneath the exocervical epithelium or within the endocervical canal, where it most often represents an incidental finding.[64] Superficial endometriosis is typically unassociated with generalized pelvic endometriosis, and often occurs in patients whose cervix has been previously traumatized by a surgical procedure or birth-related injury. Endometriosis may also be located deep within the cervical stroma in occasional cases, where it is thought to represent an extension of symptomatic pelvic endometriosis. Whether superficial or deep, the area of endometriosis resembles an ectopic focus of disordered proliferative or weakly proliferative endometrium (Fig. 3.92).

The elongated, hyperchromatic nuclei of the cells lining the endometriotic glands, coupled with occasional glandular mitoses, may result in a misdiagnosis of a dysplastic/neoplastic endocervical glandular lesion if the endometriotic stromal component is attenuated, obscured, or not recognized.[64] Given these glandular features, it is not surprising that superficial endometriosis may also serve as an uncommon source of atypical glandular cells in Pap smears.[65]

In contrast to endometriosis in most other sites, CD10 immunostaining is not helpful in identifying cervical endometriosis

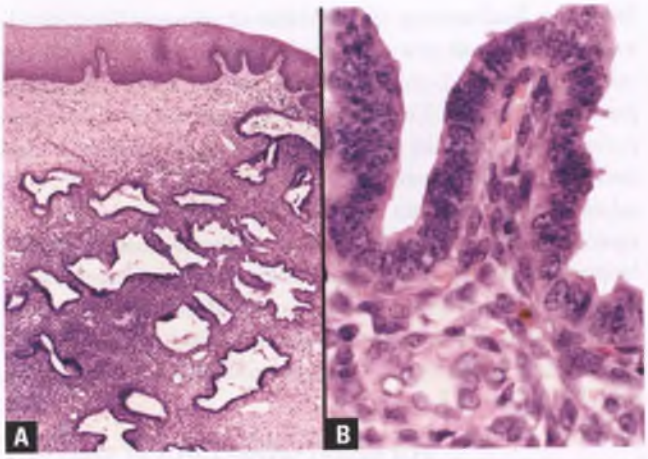

FIGURE 3.92. Superficial cervical endometriosis. **A**: An aggregate of endometrial glands and stroma resembling disordered proliferative endometrium is present beneath the squamous lining of the exocervix. **B**: High-magnification view of the focus of endometriosis.

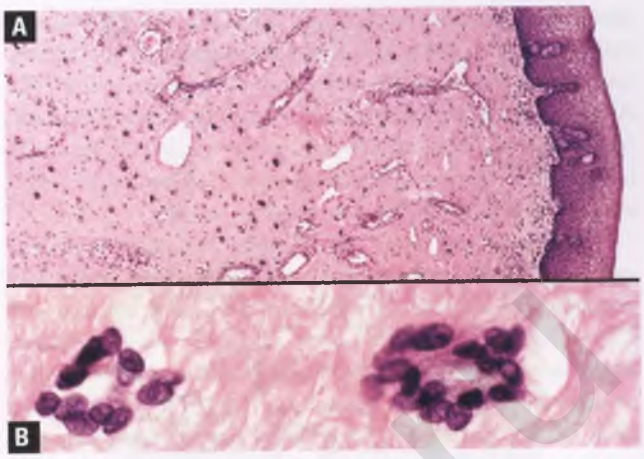

FIGURE 3.93. **A**: Multinucleated stromal giant cells scattered throughout the superficial stroma of the exocervix. **B**: Multinucleated giant cells with nuclei in a jumbled, wreathlike pattern.

because both endometriotic stroma and periglandular endocervical stroma are immunoreactive for this marker.[58] However, trichrome and reticulin stains can be utilized to facilitate recognition of endometriotic stroma within the cervix. With the trichrome stain, the collagen-sparse endometriotic stroma stains red, while the collagen-rich cervical stroma stains blue; the reticulin stain highlights the delicate network of fibers that surrounds the individual endometriotic stromal cells in a pattern that contrasts with the largely nonreactive cervical stroma.[66]

In rare cases of cervical endometriosis, there are no identifiable endometriotic glands. This unusual process, termed **stromal endometriosis**, is distinguished from low-grade endometrial stromal sarcoma on the basis of its small size, superficial location, circumscription, occasional evidence of old hemorrhage in the form of hemosiderin-laden macrophages, and lack of angiolymphatic invasion.[67] Another very rare lesion that is sometimes associated with cervical endometriosis is formation of a so-called **ceroid granuloma**, which is a nodular collection of sheets of histiocytes that contain ceroid (lipofuscin) pigment.[68] This light brown, finely granular pigment exhibits a positive reaction with the PAS with diastase stain and a negative reaction with iron stains such as Prussian blue, which facilitate its distinction from the more coarsely granular deposits of hemosiderin.[68] In gynecologic pathology, ceroid pigment is most commonly encountered in pseudoxanthomatous lesions of the fallopian tube and ovary, which are also often related to endometriosis and are illustrated in Chapters 5 and 6.

Multinucleated Stromal Giant Cells

The finding of scattered multinucleated stromal giant cells within the superficial stroma beneath the squamous mucosa of the exocervix represents an incidental microscopic finding (Fig. 3.93).[69,70] The arrangement of the nuclei within the multinucleated cells is often in a jumbled, wreathlike pattern, and the nuclei are variably hyperchromatic. Mitotic figures are absent, there is no stromal reaction, and there is no associated foreign material.

MISCELLANEOUS BENIGN TUMORS

Cervical leiomyomas are uncommon,[71] and exhibit the same histologic features as the much more common smooth muscle tumors of the uterine corpus (see Chapter 4). Other benign tumors that rarely occur in the cervix that resemble their counterparts in more usual sites are hemangiomas,[72] blue nevi,[73] glomus tumors,[74] inverted transitional cell papillomas,[75] and müllerian papillomas.[76] Superficial myofibroblastomas are rare tumors that usually involve the vagina (see Chapter 2), but a few reported cases have arisen within the uterine cervix.[77]

SQUAMOUS INTRAEPITHELIAL LESIONS

Terminology

The terminology of the Bethesda System is widely used for both cytologic and histologic classification of precursors of squamous cell carcinoma. Under this system, low-grade squamous intraepithelial lesion (LSIL) encompasses exophytic condylomas (condyloma acuminatum and immature condyloma), flat condylomas, and cervical intraepithelial neoplasia (CIN) 1/mild dysplasia, whereas HSIL includes CIN 2 and CIN 3 (moderate dysplasia, severe dysplasia, and CIS). Given that the older terminology is ingrained in the minds of many physicians and that the CIN terminology is still commonly used for tissue diagnoses, it is recommended that at least one of the equivalent older designations be listed in the pathology report in parentheses following the SIL diagnosis to minimize confusion.

Koilocytosis is the descriptive term used for the viral cytopathic effect of squamous cells that have been infected with HPV in a productive manner (i.e., with generation of large numbers of infectious virions), and is manifested primarily by

perinuclear cytoplasmic clearing ("halos") and nuclear abnormalities, as discussed below. Koilocytes are seen in condylomatous lesions, but may also be present on the surface of HSILs. Although the term "koilocytosis" is not used in the Bethesda System for reporting of cytologic specimens, it still has utility in succinctly conveying the finding of viral cytopathic effect associated with HPV infection in tissue samples.

In years past, some investigators separated koilocytosis/condylomatous change/flat condyloma from koilocytic/condylomatous atypia, with the latter often being equated with CIN 1. Koilocytic atypia demonstrated more extensive nuclear abnormalities than seen in typical koilocytosis, and was often associated with mild atypia and mitotic activity in the lower third of the epithelium. Since distinction of these lesions is poorly reproducible and they share similar HPV types, biologic behavior, and clinical management, more recent classifications have included all these lesions under the umbrella of LSIL.

Role of HPV

Infection of squamous epithelium with HPV is a necessary, but not sufficient, step in the development of the vast majority of cervical squamous cell carcinomas and their precursors.[78–80] Most of the risk factors for SIL and cervical carcinoma, such as multiple sex partners, first coitus at a young age, and history of sexual relations with males who have had penile warts or multiple sex partners, relate to behavior that increases the risk of exposure to HPV. Since this exposure usually occurs in young adult women, it is not surprising that the incidence of LSIL and HSIL peaks in the 20- to 24- and 25- to 29-year-old age groups, respectively.[81]

HPV may be found intracellularly as a free circular form known as an episome, integrated into the host DNA, or as both episomal and integrated forms.[80] Integration into the host DNA greatly facilitates the development of carcinoma. It is conceptually expedient to think of LSILs that are likely to regress as harboring virus in an episomal form, while HSILs and invasive cancer contain integrated virus, but this appears to be an oversimplification.[80] HPV is subclassified into low-risk and high-risk groups, depending upon the potential of the lesions with which they are associated to progress to carcinoma. Classic high-risk types found in cancer precursors and many carcinomas are HPV 16 and HPV 18, while prototypical low-risk types often found in exophytic condylomas are HPV 6 and HPV 11.[79,82]

Rationale for Screening Guidelines, Treatment Recommendations, Diagnostic Thresholds, and Subdivisions of SIL

In the recent past, it was standard to treat all biopsy-proven LSILs. However, it is now well established that most cases of LSIL behave like infectious rather than preneoplastic processes and will regress spontaneously, with the rare event of progression of LSIL to invasive cancer almost always being preceded by HSIL and taking several years to develop.[83,84] Attention has also recently been focused on the downside of identifying, following, and treating all HPV-related abnormalities, which includes increased cost, increased patient anxiety, and physical damage to the cervix that has been linked to increased premature births.[85] This information, coupled with the high prevalence of HPV in sexually active teenagers, has led to the development of updated guidelines that recommend that cervical cancer screening not be initiated until the age of 21 years, that it occur every 2 to 3 years rather than annually, and that biopsy-proven LSIL generally be followed conservatively rather than ablated or excised.[86,87] Since false-positive diagnoses of LSIL are not uncommon,[88] the implementation of these guidelines should markedly diminish overtreatment of patients with both legitimate and overcalled LSIL.

Even though a tissue diagnosis of LSIL may no longer prompt therapeutic intervention, the pathologist still needs to be cognizant of the potentially serious psychosocial implications of diagnoses of HPV-related lesions, given that they are sexually transmitted. In this environment, it is logical to use stringent criteria for a histologic diagnosis of LSIL to reduce the incidence of false-positives. Equivocal biopsies that are suggestive of a subtle form of LSIL should be diagnosed as being within the range of normal. In selected instances, such as when using a case for quality assurance, teaching, or research purposes, tissue from equivocal cases can be submitted for HPV-DNA analysis and/or an assessment of proliferative activity via MIB-1 immunohistochemistry,[89] but this is not cost-effective from the standpoint of patient management. This conservative approach to the diagnosis of LSIL should reduce stress for the pathologist, gynecologist, and patient when confronted with this commonplace, challenging, and subjective differential diagnosis.

In contrast to LSIL, HSIL (particularly CIN 3) is more likely to persist or progress to invasive cancer and requires treatment.[83,90] Although some studies have suggested that CIN 2 behaves more like CIN 1 than CIN 3, the diagnosis of CIN is subjective, and the reproducibility/validity of biopsy diagnoses of CIN 1 and CIN 2 is less than optimal.[88,91,92] There is evidence that CIN 2 represents a hodgepodge of both HPV-related lesions that are likely to regress and potential cancer precursors, rather than representing a distinct entity.[91] It is thought that combining CIN 2 with CIN 3 within the category of HSIL for diagnostic and management purposes provides a margin of safety, since approximately 25% of cases interpreted as CIN 2 will be upgraded to CIN 3 upon expert review.[91] Since such a review is equally likely to result in a downgrade to CIN 1,[91,92] the subjective diagnosis of CIN 2 in a cervical biopsy should be confirmed by intradepartmental consensus opinion.[93] The rationale for such a cautious approach to the diagnosis of CIN 2 is that with the revised treatment recommendations, the most clinically relevant histologic cut point in terms of treatment has shifted from negative versus LSIL to LSIL versus HSIL, which typically translates to attempting to distinguish the upper end of CIN 1 from the lower end of CIN 2.

Although the current recommendation is to follow histologic LSIL conservatively, LSIL diagnosed by Pap smear should prompt colposcopy except under special circumstances, since approximately 15% of cervical biopsies performed for

a cytologic diagnosis of LSIL result in a tissue diagnosis of HSIL.[94] The reasons for this cytologic/histologic discordance include (a) sampling error, (b) subjective differences in interpretation, and (c) masking of an underlying HSIL by surface koilocytosis or an atypical keratotic reaction.

The division of SILs into two rather than three or four categories is supported by the limited number of clinical management options, advances in the understanding of the biology of these conditions (LSIL often representing a viral infection likely to regress vs. HSIL representing a potential cancer precursor), and realistic expectations in terms of the diagnostic reproducibility of these categories.

The Role of Ki-67 (MIB-1) and p16 Immunohistochemistry in the Diagnosis of SIL

Fortunately, the vast majority of cervical biopsies can be interpreted on the basis of morphology alone. However, a small percentage of problematic cases can benefit from the use of immunohistochemistry. The most common difficult differential diagnoses of clinical significance that are related to SILs are (a) atrophy versus HSIL and (b) immature squamous metaplasia with reactive atypia versus metaplastic HSIL. The utility of MIB-1 and p16 immunohistochemistry in these and other related situations is discussed in the following paragraphs (these biomarkers are also useful in helping to distinguish endocervical AIS from its mimics, as discussed later in this chapter). ProExC is a recently developed biomarker that is also useful in the diagnosis of HSIL and AIS,[95–97] but protocols regarding how to best utilize this marker are still evolving.

Ki-67 (MIB-1)

Detection of the cell proliferation-associated Ki-67 antigen in formalin-fixed, paraffin-embedded tissue with the monoclonal antibody MIB-1 enables assessment of the proliferative activity of the cell population under study. In the normal exocervix, only scattered cells just above the basal layer and rare basal cells demonstrate MIB-1 positivity, which is a nuclear staining reaction (Fig. 3.94A).[98] Atrophic squamous epithelium shows even less MIB-1–detected proliferative activity that is also confined to the basal and parabasal region[98,99] (see separate section on atrophy). As alluded to in the previous section, MIB-1 can be utilized to help distinguish LSIL from normal squamous epithelium with pseudokoilocytic changes, although this is not encouraged. LSIL will typically contain clusters of two or more positively stained nuclei in the upper two-thirds of the epithelium, whereas variants of normal will show staining only at or below the parabasal region (avoid counting immunoreactive parabasal cells lining loops of upwardly projecting cervical stroma or immunoreactive intraepithelial lymphocytes as staining patterns supportive of LSIL).[89] MIB-1 staining of LSIL also shows many positive cells within the lower third of the epithelium.[89,98] Although this staining pattern overlaps with that of immature squamous metaplasia,[98] this form of metaplasia is much more easily confused with HSIL than LSIL, and the pattern of MIB-1 immunoreactivity in HSIL is one in which

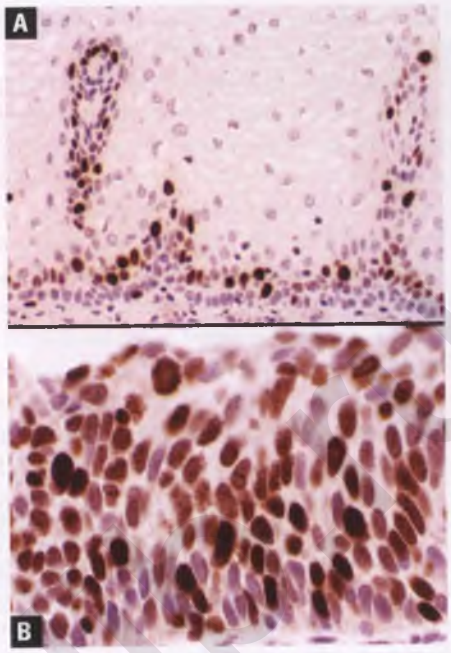

FIGURE 3.94. Typical patterns of MIB-1 immunoreactivity. **A**: Normal exocervical squamous epithelium, with positive nuclear staining confined to scattered cells within the parabasal and basal region, which includes cells in close proximity to the loop-shaped vertical projections of vascular cervical stroma. **B**: HSIL, with numerous cells with positive nuclear staining throughout all levels of the epithelium.

an average of approximately 60% of cells show positive nuclear staining throughout all layers of the epithelium (Fig. 3.94B).

Operationally, MIB-1 staining can be considered supportive of a diagnosis of HSIL (positive HSIL pattern) when nuclear staining of >30% of the epithelial cells present in the upper two-thirds of the cervical squamous epithelium is present.[100] The degree of staining in the bottom third of the epithelium is disregarded, and staining involving <30% of the epithelial cells in the upper two-thirds of the epithelium is considered to be a negative HSIL pattern. For proper evaluation, sections should be well oriented and without surface denudation or significant numbers of intraepithelial inflammatory cells.

MIB-1 staining also has utility in evaluating cauterized resection margins, since the usual patterns of immunoreactivity of dysplastic and nondysplastic epithelium are retained despite the artifactual changes that may make routine histologic assessment impossible[101] (see section on cautery artifact at the end of this chapter).

p16

p16 is a cell cycle regulatory protein. The mechanism by which infection of cervical squamous or glandular epithelial cells with high-risk HPV leads to p16 overexpression involves complex interactions between molecules that regulate the cell cycle and viral-encoded gene products,[82] and is beyond the scope of this work. For the practicing surgical pathologist, it is the differential patterns of p16 expression in the various squamous and

glandular lesions of the cervix, rather than the details of the molecular biology, that are of practical value.

When dealing with carcinoma of the cervix and its precursors, p16 overexpression as manifested by diffuse, strong, nuclear, and/or cytoplasmic immunostaining can generally be used as a surrogate marker for the presence of high-risk HPV-DNA, which otherwise would require in situ hybridization or polymerase chain reaction for its detection.[102] As expected, there is no significant p16 staining in normal, atrophic, inflamed, or metaplastic squamous epithelium of the cervix.[6,102] p16 immunoreactivity in LSIL is variable, but is often confined to the lower third to half of the epithelium (Fig. 3.95), whereas in HSIL the pattern is typically diffuse, continuous, and strong immunoreactivity extending from the basement membrane into the upper third of the epithelium or involving its full thickness (Fig. 3.96).[6,102] However, overlap in these staining patterns is sufficiently common to make this feature unreliable in distinguishing LSIL from HSIL.[102–104]

p16 immunohistochemistry is often used in conjunction with MIB-1 in ambiguous cervical biopsies, since the combination of an HSIL pattern of p16 immunoreactivity with a high Ki-67 proliferation index is strongly supportive of a diagnosis of HSIL. As a note of caution, it is important to remember when interpreting p16 immunostains that there are both HPV-dependent and non–HPV-related mechanisms of p16 overexpression, with the latter phenomenon exemplified by the frequent p16 positivity of lobular endocervical glandular hyperplasia, a subset of the superficial columnar cells of MGH, serous carcinoma of the endometrium, and uterine leiomyosarcoma.[102,105–108]

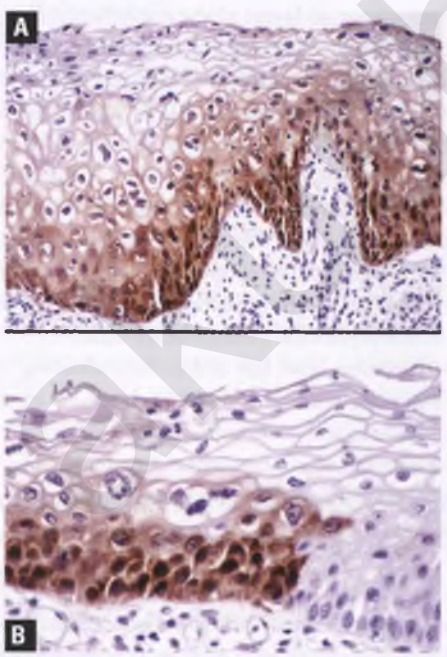

FIGURE 3.95. **A,B**: Typical pattern of p16 immunoreactivity in LSIL. Positive staining is present in the lower third to half of the HPV-infected epithelium. In **B**, note the absence of staining of the normal squamous epithelium on the right side of the image. (p16 immunostains courtesy of Dr. Steve Kargas.)

Low-Grade Squamous Intraepithelial Lesions

Exophytic Condylomas

In the cervix, the different forms of HPV-induced condylomas are considered subtypes of LSIL. Although uncommon, cervical **condyloma acuminata** with the typical exophytic papillary architecture do occur (Fig. 3.97). On occasion, epithelial hyperplasia within a condylomatous LSIL can take the form of small superficial spikes that can be visualized colposcopically, which has prompted some colposcopists to refer to these lesions as spiked condyloma (Fig. 3.98). As is the case for condyloma acuminatum, **immature condyloma**, which is also referred to as papillary immature metaplasia, is the product of a low-risk HPV infection (type 6 or 11).[109] This lesion is composed of papillary projections of immature parabasal-type squamous cells supported by slender fibrovascular stalks, and tends to arise within the deeper (more proximal) portions of the transformation zone (Fig. 3.99). The squamous cells of immature condyloma have bland nuclear features and show little to no mitotic activity, but are slightly crowded together. Koilocytosis is not well developed in these lesions, since viral cytopathic effect is manifested in mature rather than immature squamous epithelium. There is often preservation of overlying endocervical mucinous epithelium, although usually in an attenuated state.

Despite its name, immature condyloma does not appear to develop into the more mature condyloma acuminatum,

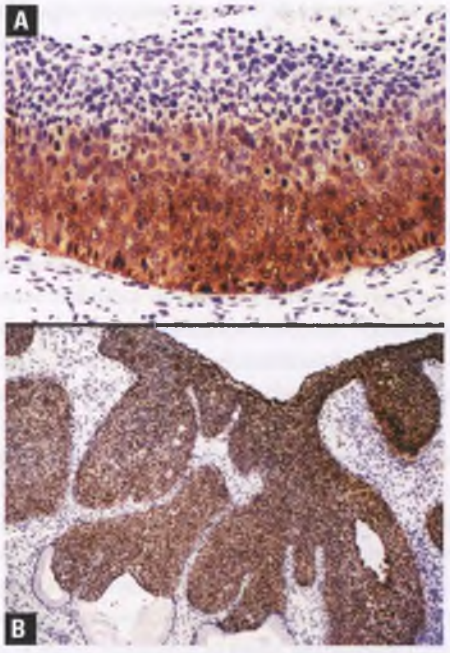

FIGURE 3.96. **A,B**: Typical patterns of p16 immunoreactivity in HSIL. The extent of positive staining of the dysplastic epithelial surface varies from involving the lower two-thirds of the epithelium **(A)** to involving its full thickness **(B)**. In **B**, also note the p16 positivity of the endocervical glands in those portions that have been replaced by HSIL, and the non-reactivity of the uninvolved glands. (p16 immunostains courtesy of Dr. Steve Kargas.)

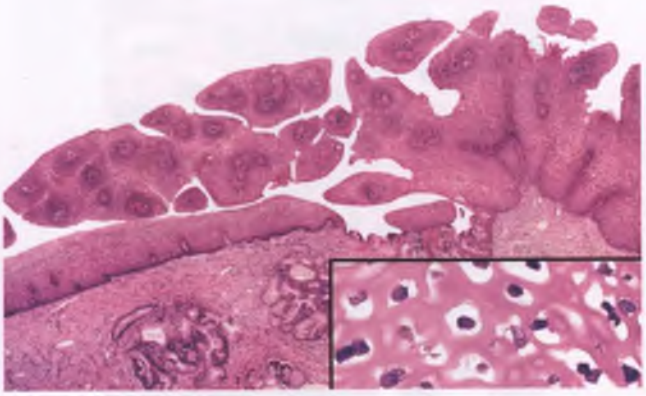

FIGURE 3.97. Condyloma acuminatum arising in cervical transformation zone. The inset shows koilocytosis of condylomatous squamous epithelium.

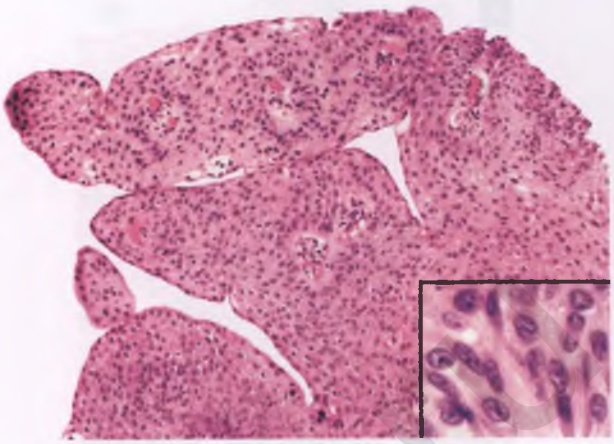

FIGURE 3.99. Immature condyloma (papillary immature metaplasia). An attenuated layer of endocervical mucinous epithelium envelopes the papillary projections. The inset shows the bland nuclear features of this lesion.

which is less cellular and exhibits squamous maturation with abundant amounts of eosinophilic cytoplasm and patches of overt koilocytosis. Immature condyloma also needs to be distinguished from papillary squamous cell carcinoma, which displays significant nuclear atypia and a high mitotic rate.

Flat Condyloma/CIN 1

In contrast to the vulva and perianal region, the vast majority of cervical condylomatous lesions are flat rather than papillary. Since (a) the morphologic features of flat condyloma (flat squamous epithelium with koilocytosis/koilocytic atypia) are difficult to distinguish from and merge with those of CIN 1, (b) both flat condyloma and CIN 1 usually harbor intermediate to high-risk rather than low-risk HPV,[100] and (c) their biologic behavior and clinical management are similar, they are considered to be within the same subgroup of LSIL.

Multiple features are assessed when evaluating a cervical biopsy for the presence of koilocytosis. True koilocytosis is usually apparent at low to medium magnification, presenting as a discrete alteration in the superficial to midzonal regions of the epithelium (Figs. 3.100–3.102). These alterations are due to variable combinations of nuclear enlargement, nuclear hyperchromasia, a jumbled distribution of cells with varying nuclear density, prominence and variability in the size and shape of perinuclear halos, and abnormal surface keratinization with hypereosinophilia. When examined under high magnification, the nuclei of koilocytes will generally have at least three times the nuclear area of normal intermediate squamous

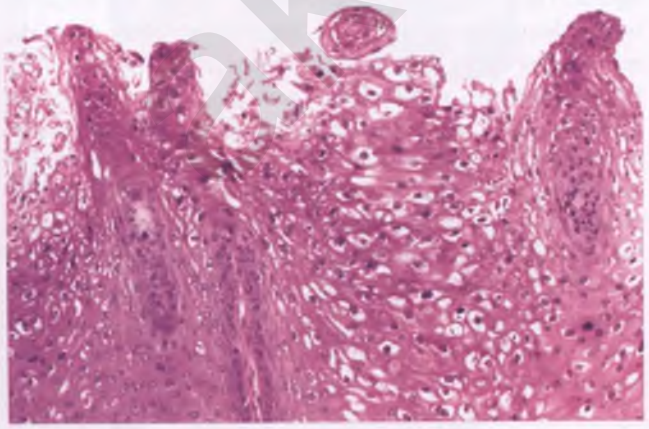

FIGURE 3.98. LSIL with features of the so-called spiked condyloma. This lesion is characterized by epithelial spikes and koilocytosis.

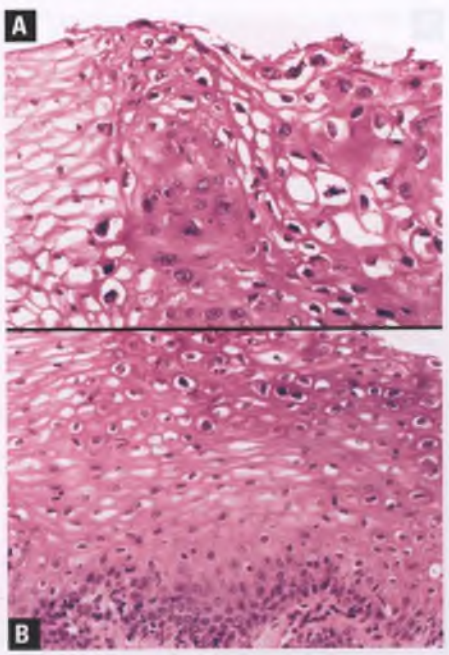

FIGURE 3.100. **A,B:** LSIL (flat condyloma/koilocytosis). Discrete alterations are evident in the superficial half of the epithelium at low to medium magnification.

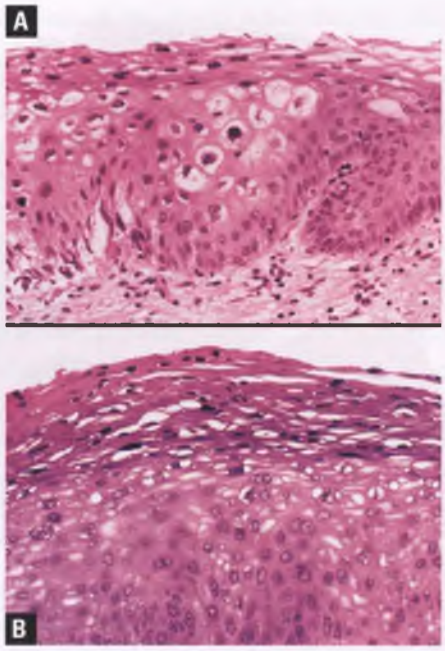

FIGURE 3.101. LSIL (flat condyloma/koilocytosis). **A**: Koilocytes are prominent, but atypia in the lower third of the epithelium is not impressive. **B**: Koilocytes with pyknotic nuclei are embedded within an atypical parakeratotic plaque.

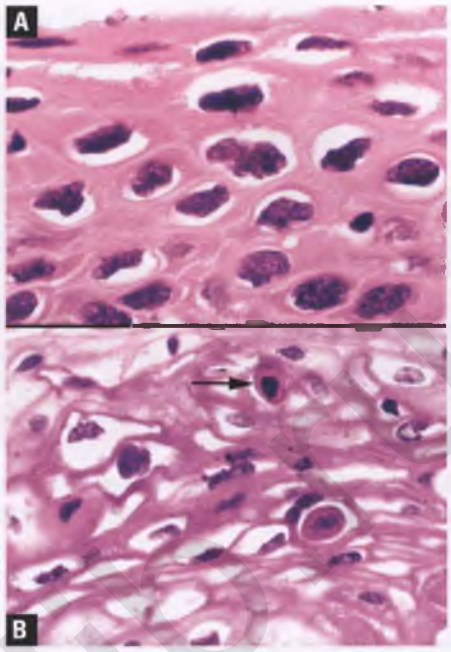

FIGURE 3.103. Low-grade squamous intraepithelial lesion. **A**: This image illustrates koilocytic atypia, which was previously distinguished from koilocytosis in some earlier classification schemes. **B**: An *arrow* marks a dyskeratocyte associated with koilocytosis.

cell nuclei, which corresponds to at least a 70% increase in nuclear diameter as compared to this reference cell. However, koilocytes may exhibit a range of nuclear sizes, and failure to meet this size criterion should not preclude a diagnosis of LSIL in an otherwise obvious case. The nuclei often exhibit dense, smudged chromatin and crinkled ("raisinoid") contours (Fig. 3.103A). Binucleation and multinucleation are common, and dyskeratotic cells may be present (Fig. 3.103B).

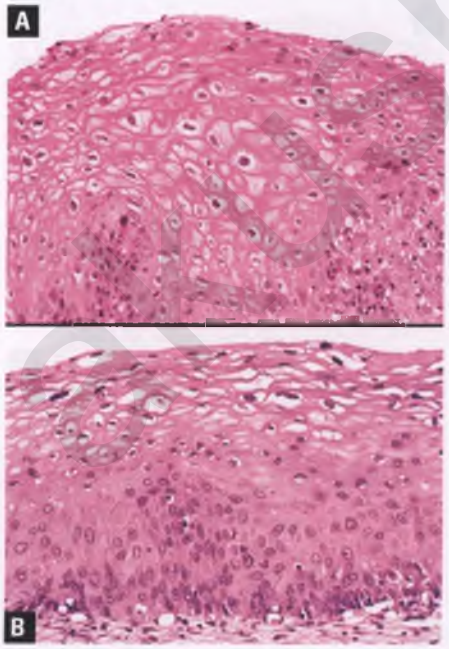

FIGURE 3.102. **A,B**: LSIL (flat condyloma/koilocytosis). The lesion in **A** is subtle, and represents the lower end of the spectrum of recognizable koilocytosis.

The nuclear and cytoplasmic features of koilocytes outlined above also apply to their identification within Pap smears (Figs. 3.104–3.106). The rim of dense cytoplasm at the periphery of the koilocytes may exhibit polychromatic blends of orange, pink, and blue-green with the Pap stain.

HPV-related lesions associated with or indistinguishable from CIN 1/mild dysplasia exhibit nuclear atypia within the lower third of the epithelium, often accompanied by some mitotic activity in this region that can include atypical division figures (Figs. 3.107 and 3.108). In Pap smears, the nuclei of mildly dysplastic squamous cells have at least three times the nuclear area of an intermediate squamous cell (at least 70% greater diameter), which makes them larger than most nuclei of higher grade squamous dysplasias (Fig. 3.109). However, mildly dysplastic squamous cells retain significant amounts of cytoplasm, which results in a lower nuclear to cytoplasmic ratio than that seen in HSIL. Whereas the nuclei of koilocytes often have dark, smudged chromatin, mildly dysplastic nuclei tend to be less hyperchromatic and exhibit a crisp, finely granular, evenly distributed chromatin pattern. The nuclear contours of mildly dysplastic squamous cells are smooth to only slightly irregular, and their cytoplasmic borders are well defined.

In an effort to prospectively identify the small proportion of cases of biopsy-proven LSIL that will eventually progress to HSIL or invasive carcinoma, some investigators have focused attention upon the roughly 5% to 10% of LSILs that feature

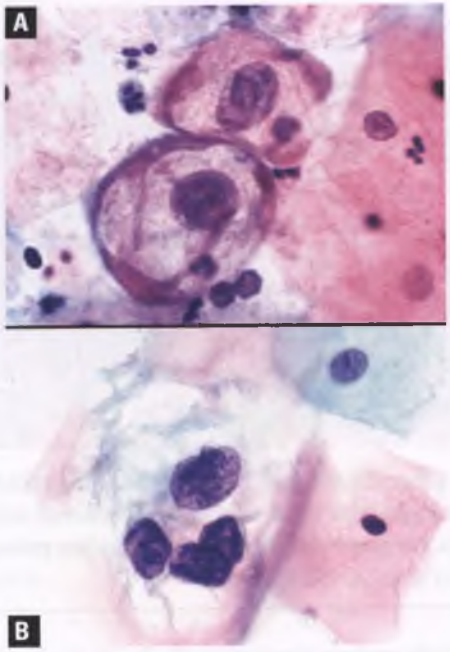

FIGURE 3.104. **A,B**: LSIL in Pap smears. Koilocytes with perinuclear cavitation, nuclear abnormalities, and a peripheral rim of polychromatic cytoplasm are present.

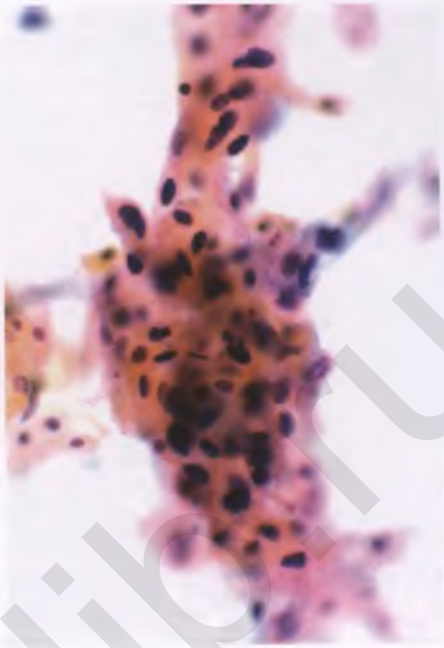

FIGURE 3.106. LSIL in Pap smear. Haphazardly arranged, atypical, orangeophilic dyskeratocytes with small, opaque nuclei are generally indicative of an HPV infection, although similar examples of "atypical parakeratosis" are sometimes classified as ASC-US.

scattered cells with marked nuclear atypia within the mature portions of the squamous epithelium. Although one group found that patients with cervical biopsies with LSIL of this type had a much higher incidence of HSIL on follow-up than did patients with ordinary LSIL,[110] another group found no such difference between these two types of LSIL and speculated that marked nuclear atypia in this setting is a degenerative phenomenon.[111]

In addition to the inherent subjective nature of interpreting potentially dysplastic lesions of the cervix, reproducible classification is hindered by the interpretation of some pathologists of lesions with significant (HSIL-like) nuclear atypia confined to the lower third of the epithelium as HSIL rather than LSIL (Fig. 3.110),[100] and by the lack of consensus as to the significance of

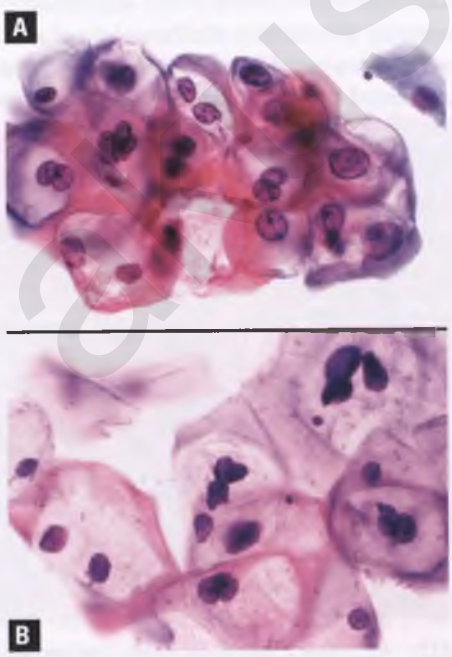

FIG 3.105. **A,B**: LSIL in Pap smears. Additional images of koilocytes.

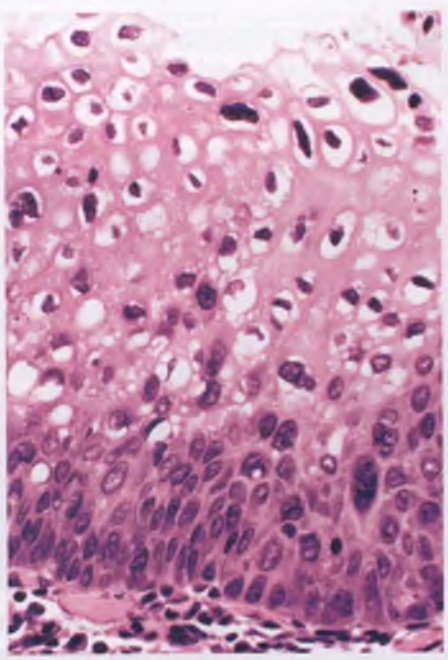

FIGURE 3.107. LSIL (CIN 1 with koilocytosis).

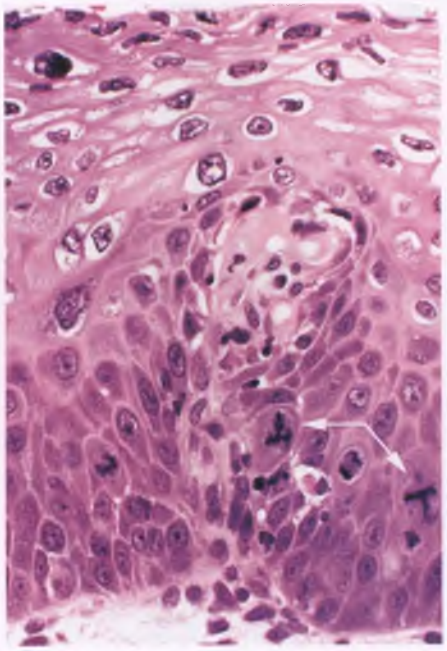

FIGURE 3.108. LSIL (CIN 1 with koilocytosis). Four mitoses are present in the lower third of the epithelium, two of which are abnormal *(arrows)*.

finding atypical mitotic figures within a lesion that would otherwise be classified as CIN 1. Atypical mitotic figures are considered a marker of aneuploidy, and their presence justifies classification as CIN 2 for some pathologists. However, others allow atypical mitotic figures in CIN 1, and recognizing what constitutes these structures in an individual case can be problematic.

High-Grade Squamous Intraepithelial Lesions

Conventional (Nonkeratinizing) HSIL

Nearly all HSILs contain high-risk HPV, often in an integrated form.[80,100] HSIL of the usual type features cells with obvious

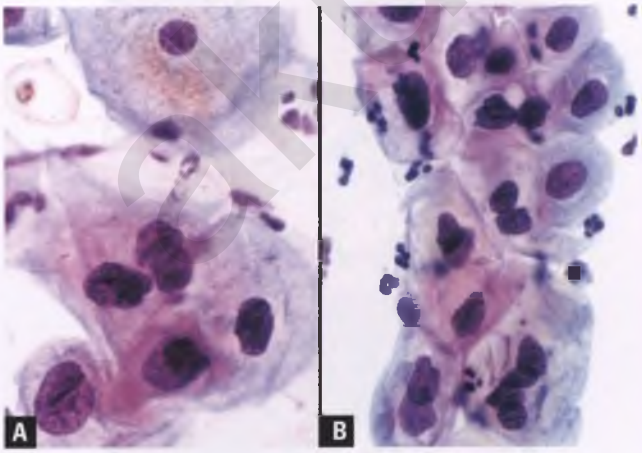

FIGURE 3.109. **A,B**: LSIL in Pap smears (mild dysplasia). In **A**, compare the nuclear features of the dysplastic cells to the nucleus of the normal intermediate squamous cell in the top mid-portion of the image.

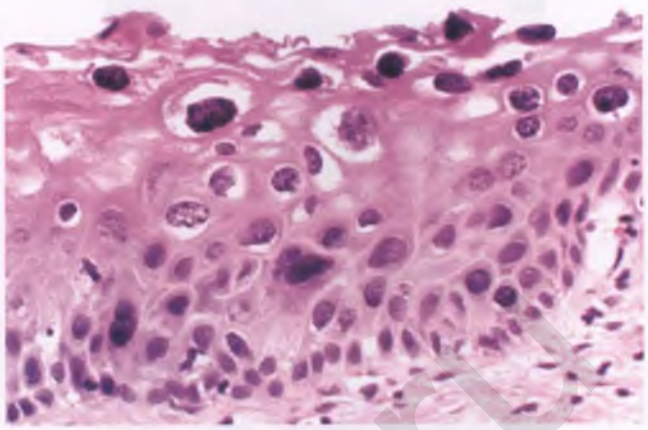

FIGURE 3.110. LSIL (CIN 1 with koilocytosis). The presence of some cells in the lower third of the epithelium with nuclear atypia of the degree typically seen in HSIL would prompt some pathologists to upgrade this lesion to HSIL (CIN 2).

nuclear atypia replacing more than the lower third of the squamous epithelium. In the older CIN terminology, CIN 2 refers to lesions in which between one-third and two-thirds of the lower aspect of the epithelium has been replaced by these dysplastic cells (Fig. 3.111), whereas CIN 3 encompasses those dysplasias that extend into the upper third of the epithelium, including the full-thickness lesion formerly referred to as CIS. As mentioned earlier, some pathologists also designate lesions that are architecturally CIN 1 as HSIL if there is HSIL-like nuclear atypia in the lower third of the epithelium (Fig. 3.110).

The atypical nuclei in HSIL are characterized by hyperchromasia, enlargement, variability in size and shape, irregular contours, and interspersed clumps of coarse chromatin (Fig. 3.112). Nuclei are crowded and haphazardly oriented, and often overlap one another. Cell membranes are indistinct, and there is often a variably prominent component of elongated cells oriented perpendicular to the basement membrane.

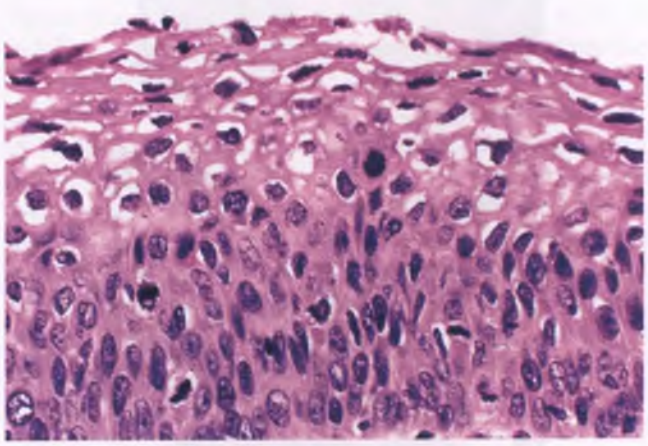

FIGURE 3.111. HSIL (CIN 2 with koilocytosis). The apparent "surface maturation" in CIN 2 is usually related to the presence of koilocytosis.

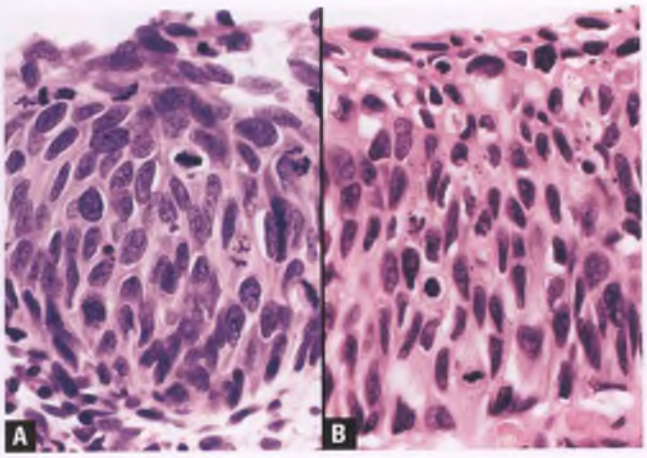

FIGURE 3.112. **A,B**: HSIL (CIN 3). In these two separate examples, note the full-thickness atypia and crowding of the dysplastic nuclei and the presence of scattered mitotic figures throughout all levels of the epithelium.

Scattered mitotic figures are present throughout the dysplastic portion of the epithelium, and atypical mitoses are usually readily apparent. Abnormal vascular patterns are associated with HSIL, which are useful colposcopic clues whose histologic correlate is seen on occasion (Fig. 3.113). HSIL typically originates in the transformation zone and grows via replacement of the lining of the endocervical canal with extension into endocervical glands (Fig. 3.114). Replacement of the surface glandular epithelium is usually complete, but there may be an overlying layer of mucinous endocervical epithelium in rare instances (Fig. 3.115).

Care should be taken not to misinterpret the smooth-contoured, distended nests of endocervical glands that have been replaced by HSIL as invasive carcinoma; this distinction may be difficult when such nests are closely aggregated rather than discrete (Fig. 3.116). Extensive gland involvement by

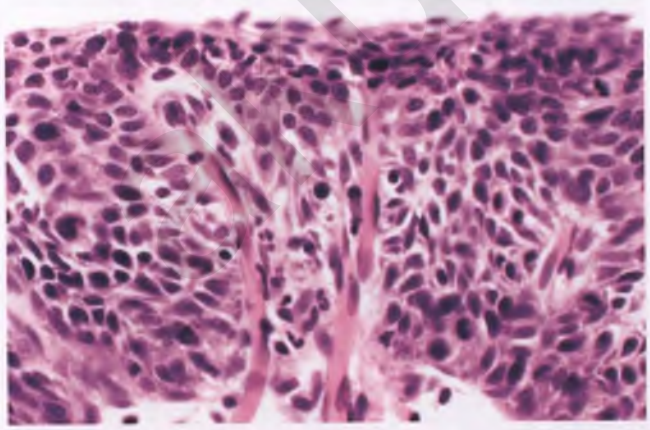

FIGURE 3.113. HSIL (CIN 3). Although not often well-visualized histologically, this section demonstrates the presence of vertically oriented, slender capillary loops extending very close to the epithelial surface, which is the correlate of the red dots (punctation) seen in HSIL via the colposcope.

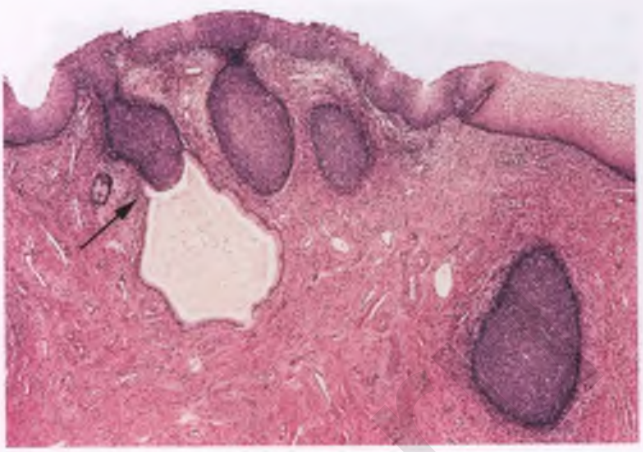

FIGURE 3.114. HSIL (CIN 3) replacing the surface lining of the endocervical canal along with some endocervical glands. The exocervical squamous epithelium at the upper right is uninvolved. Note the discrete, smooth-contoured nature of the replaced glands, and the partial involvement of the gland at left *(arrow)*.

HSIL maintains a depth and distribution of involved glands that is consistent with a noninvasive lesion, serial sections will usually demonstrate partial gland involvement by HSIL, and squamous maturation is typically absent.

The uncommon finding of either squamous maturation or central necrosis within endocervical glands replaced by HSIL serves as a clue to impending or nearby invasion (Fig. 3.117); multiple sections of such lesions should be examined to exclude microinvasion.[112] Extensive glandular involvement by HSIL with expansile growth, which is often accompanied by central necrosis, is also cited as another risk factor for microinvasion.[112] However, this phenomenon may be difficult to distinguish from a pattern of invasive squamous cell carcinoma that mimics endocervical crypt involvement by CIN 3, which is discussed later in this chapter and depicted in Figures 3.156–3.159.

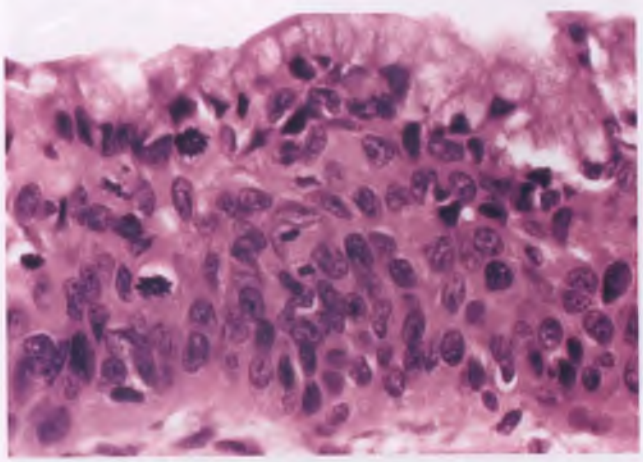

FIGURE 3.115. HSIL with preservation of surface layer of endocervical columnar mucinous epithelium. This finding is unusual in HSIL and is more typical of immature squamous metaplasia.

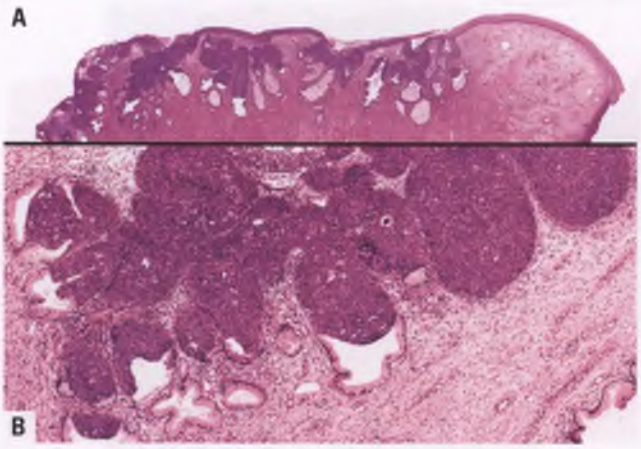

FIGURE 3.116. **A,B**: High-grade squamous intraepithelial lesion (CIN 3) with extensive endocervical glandular involvement. This lesion is characterized by superficial aggregates of closely packed endocervical glands that are partially to completely replaced by HSIL. The smooth epithelial-stromal interface, foci of partial glandular involvement, lack of squamous maturation, and absence of a stromal reaction all support this being a non-invasive process. Compare this pattern with that of superficial invasion that mimics endocervical glandular involvement by CIN 3 in Figs. 3.156 to 3.159.

When found in endocervical curettings, HSIL typically presents as randomly oriented, detached strips of dysplastic squamous epithelium (Fig. 3.118). Grading of these strips may not be possible, although features of HSIL are usually apparent despite the suboptimal orientation. Regardless of the degree of dysplasia, the detection of dysplastic squamous epithelium in an endocervical curettage necessitates a cone biopsy or loop electrosurgical excision procedure (LEEP) to ablate the lesion and exclude the possibility of

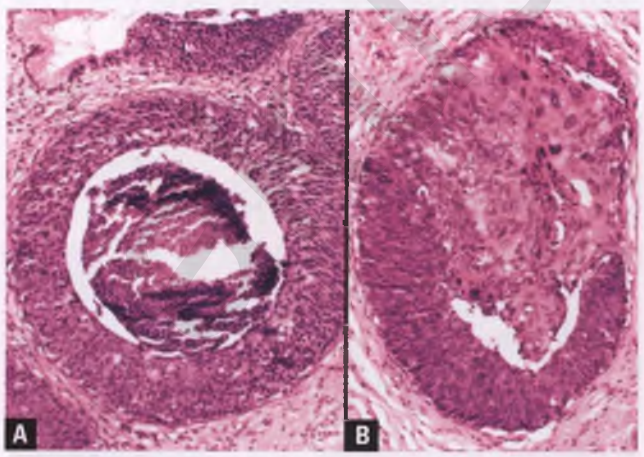

FIGURE 3.117. Endocervical glands replaced by HSIL (CIN 3) with features worrisome for impending/nearby invasion. **A**: Central necrosis of involved gland. **B**: Involved gland with squamous maturation (cells with abundant eosinophilic cytoplasm, sometimes in association with keratinization and/or intercellular bridges).

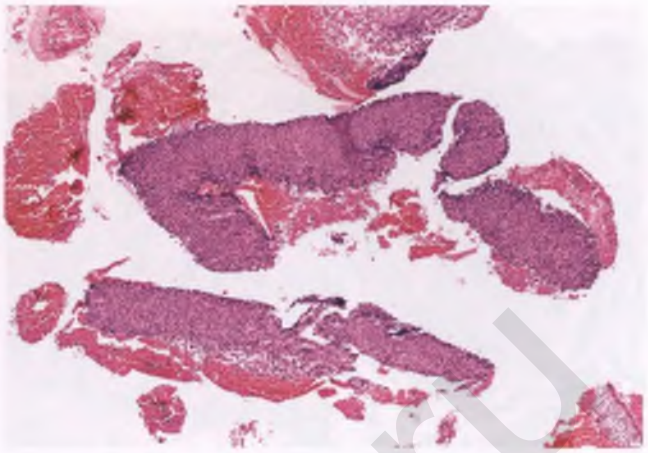

FIGURE 3.118. Detached strips of HSIL in an endocervical curettage.

an underlying invasive cancer (unless clinicopathologic correlation can confidently attribute the dysplastic epithelium to "contamination" from a lesion closer to the external os). On rare occasions, HSIL extends beyond the endocervical canal and replaces portions of the lining of the endometrial cavity and even the fallopian tube by direct extension (Fig. 3.119).[113] However, in the vast majority of endometrial samples in which detached strips of HSIL are identified, contamination of the sample by HSIL dislodged from the endocervical canal is the explanation (Fig. 3.120).

In Pap smears, the main features of HSIL that help to distinguish it from LSIL are the presence of smaller dysplastic cells with higher nuclear to cytoplasmic ratios, more pronounced irregularities in the contour of the nuclear membrane, and the tendency for HSIL to exhibit more hyperchromaticity, more granules of coarsely clumped chromatin, and more irregularly distributed chromatin than LSIL (Figs. 3.121 and 3.122). In some forms of CIS, the evenly distributed, coarsely granular chromatin imparts a speckled pattern that conveys a shimmer and sparkle to the nuclei that is quite characteristic

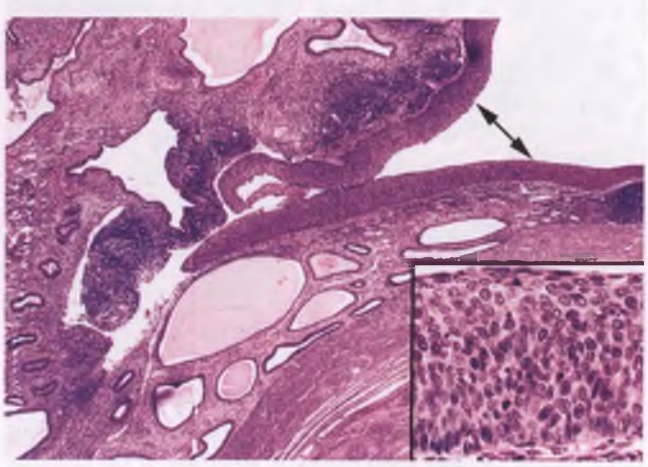

FIGURE 3.119. HSIL replacing the lining of the endometrium *(arrows)*. The inset shows the nuclear features of this HSIL.

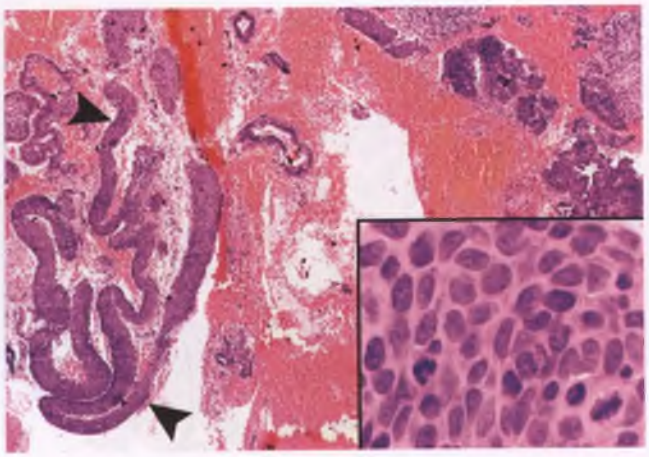

FIGURE 3.120. Convoluted strips of HSIL (*arrowheads*) found within an endometrial curettage. The inset shows a high-magnification view of the HSIL, which represents a "contaminant" originating from the endocervical canal.

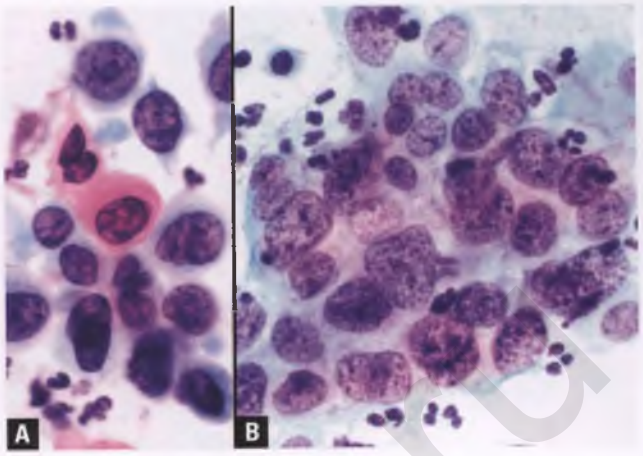

FIGURE 3.122. **A,B**: HSIL (severe dysplasia/CIS) in two separate Pap smears. The dysplastic cells in both cases have high nuclear to cytoplasmic ratios, but exhibit different types of chromatin abnormalities.

of this lesion (Fig. 3.123). CIS may also feature sheets of three-dimensional syncytial-like aggregates that are often referred to as hyperchromatic crowded groups (HCGs) (Fig. 3.124).

When extension of CIS into endocervical glands presents as HCGs in Pap smears, distinction from endocervical AIS may be difficult, since recognizable residual columnar cells and/or palisaded nuclei may be present at the edges of these cellular aggregates (Fig. 3.125).[114] The feature that is most helpful in characterizing the lesion as squamous rather than glandular is the presence of occasional flattened cells with elongated nuclei at the periphery of the cell clusters, which results in smooth, abrupt edges rather than the feathered edges typical of AIS. The histologic correlate of these occasional spindle-shaped cells are most likely the flattened residual endocervical lining cells that are undergoing pressure atrophy as they are being displaced by HSIL (Fig. 3.126). The nuclei of CIS are also more jumbled than those of AIS, and the rosettes and microacinar structures that may be seen in AIS are absent in CIS.

Metaplastic HSIL

The most difficult and subjective types of HSIL to diagnose are those that share features with immature squamous metaplasia. In the usual type of metaplastic HSIL, there is typically sufficient full-thickness nuclear atypia, hyperchromasia, crowding, and disorganization to distinguish this lesion from immature squamous metaplasia, although the degree of nuclear crowding and disorganization is less impressive than that in the conventional type of HSIL (Fig. 3.127). The finding of mitotic figures at various levels throughout the epithelium can make the diagnosis easier, although mitoses are often frustratingly rare in these lesions. Obtaining the HSIL pattern of results with p16 and Ki-67 immunostains may be necessary in order to make a definitive diagnosis.

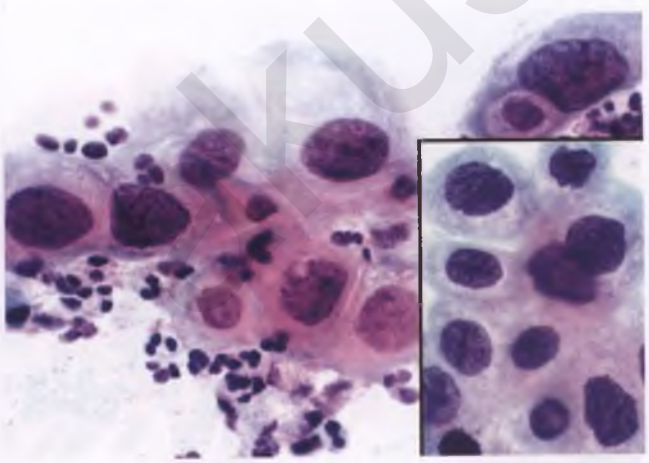

FIGURE 3.121. HSIL (moderate dysplasia) in two separate Pap smears. In comparison to the mildly dysplastic cells of LSIL, the dysplastic cells in HSIL are smaller, have higher nuclear to cytoplasmic ratios, and usually exhibit more pronounced nuclear contour and/or chromatin abnormalities.

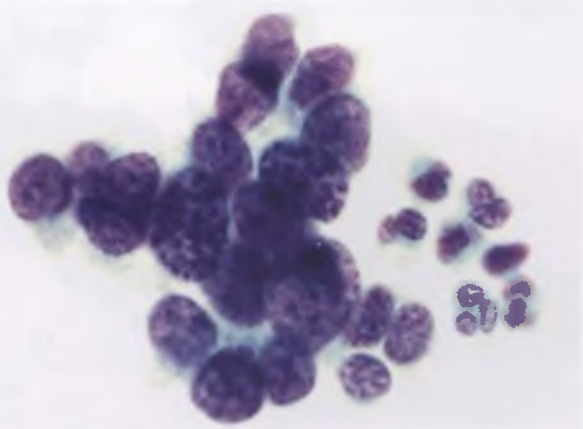

FIGURE 3.123. HSIL (CIS) in Pap smear. Some of the cells have a coarsely granular, evenly distributed, speckled chromatin pattern that is characteristic of CIS. The nuclear to cytoplasmic ratio is extremely high, nuclei are overlapping, and cell borders are indistinct.

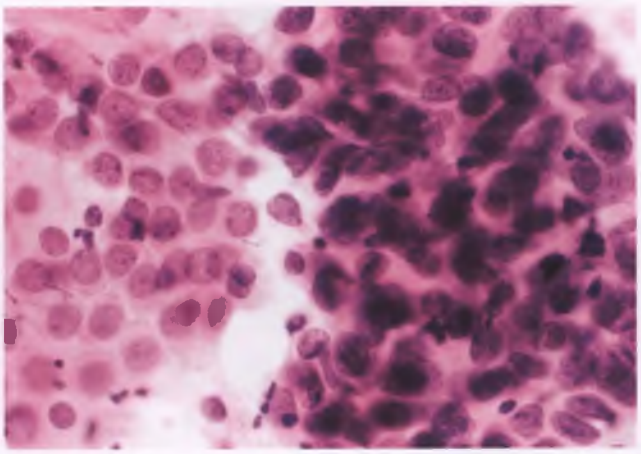

FIGURE 3.124. HSIL (CIS) in Pap smear. The "hyperchromatic crowded group," which in this case is CIS, contrasts with the sheet of endocervical cells on the left side of the image.

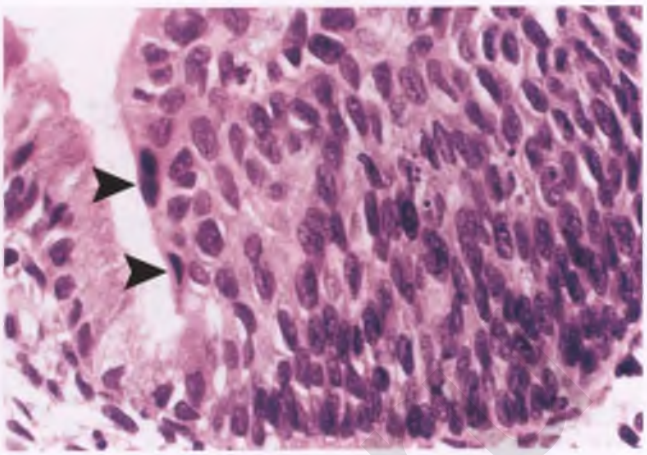

FIGURE 3.126. HSIL (CIN 3) with endocervical gland involvement. *Arrowheads* mark the flattened nuclei of attenuated endocervical lining cells, whose presence in Pap smears is a useful clue to the correct diagnosis. Also note peripheral palisading of nuclei along the bottom portion of the involved gland, which is the histologic correlate to the palisading shown in the Pap smear in Figure 3.125.

When there are significant nuclear contour and chromatin abnormalities, metaplastic HSILs are a recognizable form of HSIL in Pap smears (Fig. 3.128). However, these lesions can be subtle and pose diagnostic difficulties in cytologic preparations, just as they do in histologic sections. When metaplastic HSIL presents as a few small, isolated cells, they are easy to overlook or misinterpret (Fig. 3.129). In conventional smears, the cells of metaplastic HSIL may also form single-file, linear streaks within mucoid material that may be mistaken for histiocytes at low magnification (Fig. 3.130).

In the so-called "eosinophilic dysplasia" variant of metaplastic HSIL, metaplastic-type epithelial cells with abundant eosinophilic cytoplasm, distinct cell borders, mild nuclear atypia, and occasionally distinct nucleoli are crowded together throughout the full thickness of the epithelium (Figs. 3.131 and 3.132).[115] There is preservation of cell polarity and the nuclei are regularly spaced from one another. Isolated cells with recognizable dysplastic nuclear features are usually present. Mitotic figures are typically sparse. The vast majority of such cases show diffuse p16 positivity and a Ki-67 staining pattern similar to conventional HSIL, which supports their classification as a variant of HSIL. To avoid confusion, examples of eosinophilic dysplasia should be diagnosed first and foremost as HSIL, with a note indicating that it has features of this particular variant. Approximately 70% of cases of eosinophilic dysplasia are associated with a conventional SIL, which facilitates its recognition. In those cases in which the

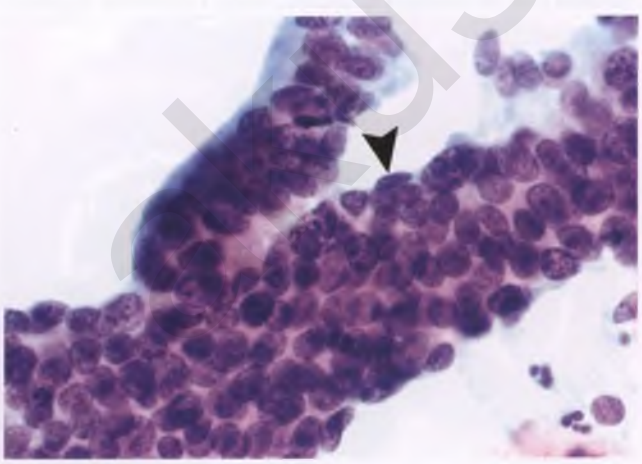

FIGURE 3.125. HSIL (CIS) in Pap smear. Features of endocervical gland involvement are present, as characterized by occasional cells with flattened nuclei at the periphery of the cellular aggregate (*arrowhead*) and smooth, abrupt edges. The partially detached epithelial strip to the left of the *arrowhead* shows nuclear palisading.

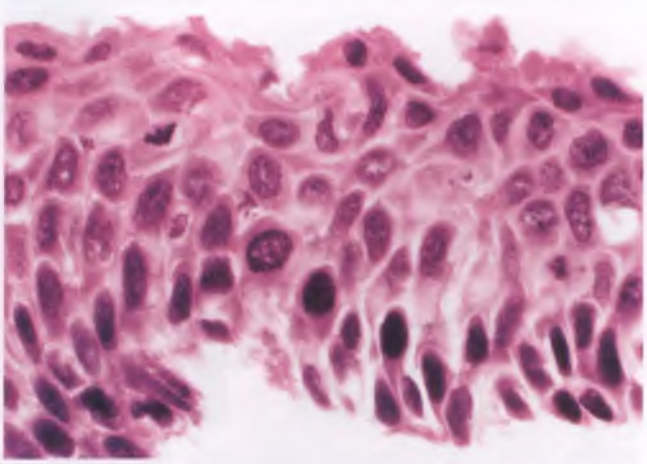

FIGURE 3.127. HSIL, metaplastic type. In comparison to conventional HSIL, the dysplastic cells of metaplastic HSIL are less densely packed, have more cytoplasm, exhibit less architectural disarray, and have a lower mitotic rate.

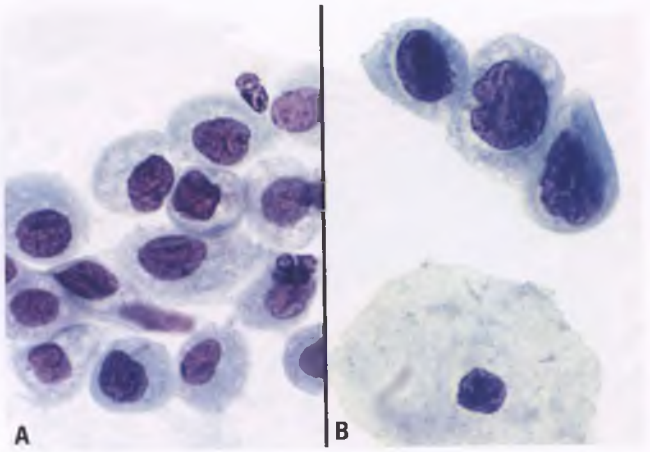

FIGURE 3.128. **A,B**: Pap smears with HSIL, metaplastic type. High nuclear to cytoplasmic ratios, chromatin abnormalities, and irregular nuclear contours are helpful diagnostic features. In **B**, a normal intermediate squamous cell is present in the bottom portion of the image.

diagnosis is being considered without a neighboring SIL that is more obvious, p16 and Ki-67 immunostains are recommended.

Keratinizing HSIL

A small subset of HSIL referred to as keratinizing HSIL exhibits abnormal surface keratinization (Fig. 3.133A). In Pap smears, severely dysplastic cells with extremely hyperchromatic nuclei, at least some of which have dense, orangeophilic cytoplasm, are characteristic of this lesion (Fig. 3.133B). The background often contains keratinous debris that may simulate a tumor diathesis, and dysplastic cells with spindle and tadpole shapes may be present. As discussed in the section on the Pap smear diagnosis of invasive squamous cell carcinoma, the resulting cytologic appearance can be virtually indistinguishable from invasive keratinizing tumors. In addition to the potential problem of overcalling keratinizing HSIL as invasive carcinoma in cytologic preparations, some cases can also be undercalled due to a surface layer of hyperkeratosis and/or parakeratosis that can mask the high-grade nature of these lesions in Pap smears (Fig. 3.134).

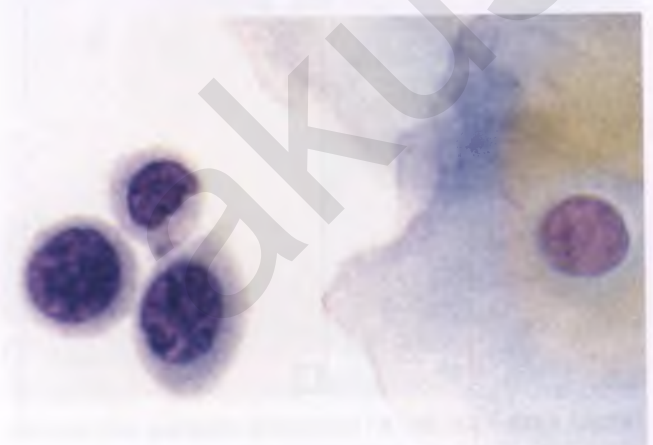

FIGURE 3.129. HSIL, metaplastic type (severe dysplasia). This loosely aggregated group of three severely dysplastic squamous cells lurking in the "white spaces" of a liquid-based Pap smear may be overlooked or misinterpreted as immature metaplasia, histiocytes, exfoliated endometrial cells, or "ding cells" related to IUD use.

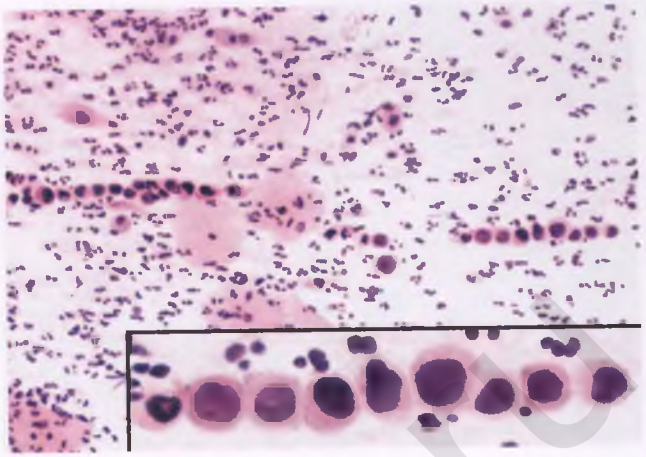

FIGURE 3.130. HSIL, metaplastic type (severe dysplasia). In this conventional Pap smear, linear streams of severely dysplastic squamous cells have formed that could be mistaken for histiocytes at low magnification.

ATYPICAL SQUAMOUS CELLS IN PAP SMEARS

In the Bethesda System, Pap smears that are suggestive of SIL are diagnosed as ASC. In the vast majority of these cases, the main differential diagnosis is with a low-grade or borderline SIL, and these Pap smears are further qualified as being of undetermined significance (ASC-US). In about 10% of ASC cases, the differential diagnosis is with HSIL, and these Pap smears are designated ASC-H to indicate that HSIL cannot be excluded. Ideally, ASC-US cases are triaged with same-specimen testing for high-risk HPV (positive → colposcopy; negative → follow-up in 1 year),

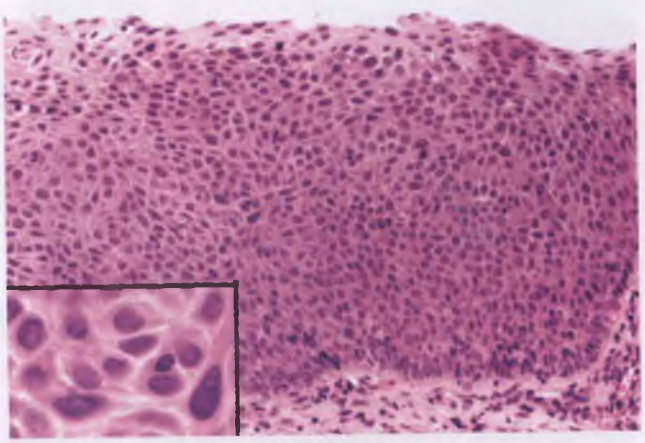

FIGURE 3.131. Eosinophilic dysplasia variant of metaplastic HSIL. Distinction from squamous metaplasia with reactive atypia can be difficult.

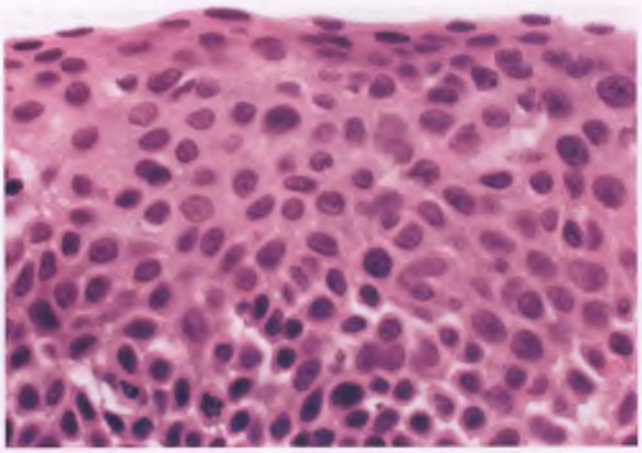

FIGURE 3.132. Eosinophilic dysplasia variant of metaplastic HSIL.

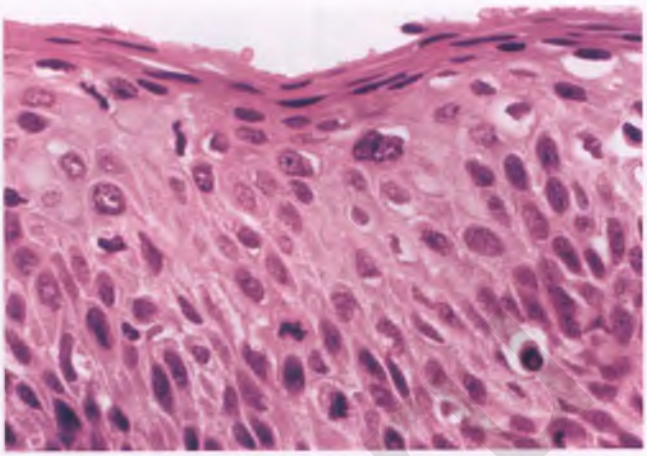

FIGURE 3.134. HSIL (CIN 2 with a few koilocytes). The overlying layer of parakeratosis may prevent cytologic sampling of the dysplastic squamous cells in the deeper layers and result in a false negative Pap smear.

while patients with ASC-H diagnoses proceed directly to colposcopy.[94,116] In a recent survey of several hundred laboratories, the median rate of ASC-US was 4.3%, and the median ASC to SIL ratio, which is commonly used as a quality improvement monitor, was 1.5.[117] Approximately 40% to 50% of ASC-US cases are positive for high-risk HPV, and this figure can be used as a quality assurance benchmark.[117,118] Although some cases of ASC-US will ultimately be shown to be associated with biopsy-proven SIL, many cases are due to reactive inflammatory/degenerative changes, atrophy, air-drying artifact, and other undefined processes.

Criteria for a diagnosis of ASC-US include nuclear enlargement (at least 2.5 times the nuclear area of a normal intermediate squamous cell, which corresponds to at least a 60% increase in nuclear diameter compared to this reference standard), a slight increase in nuclear to cytoplasmic ratio, and mild abnormalities in nuclear chromatin pattern and nuclear contour. Some cases achieve ASC-US status by virtue of the presence of atypical parakeratosis or by the rarity of the atypical cells, which if more numerous would be diagnostic of a low-grade or borderline (low- vs. high-grade) SIL. Not surprisingly, the diagnosis of ASC-US is subjective and poorly reproducible, and attempts to illustrate representative examples are often met with thoughts from the viewers of "looks negative to me" or "I'd call that LSIL" (Fig. 3.135). The most common reasons for classification of a Pap smear as ASC-H are (a) the presence of a small number of atypical immature metaplastic cells worrisome for metaplastic HSIL (Fig. 3.136) and (b) HCGs of cells with presumed squamous differentiation that are difficult to visualize.

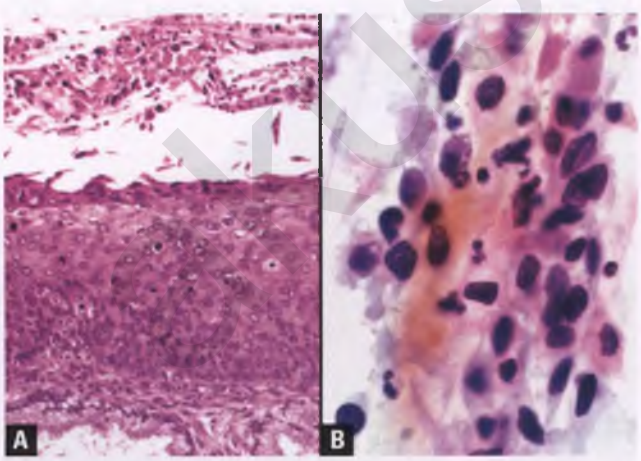

FIGURE 3.133. Keratinizing HSIL (CIN 3). **A**: This histologic section demonstrates the abnormal surface keratinization, which is associated with loosely adherent keratinous debris that contains dysplastic squamous cells. **B**: The corresponding Pap smear shows the cytologic features of a keratinizing HSIL. Note how the keratinous debris in the background simulates a tumor diathesis.

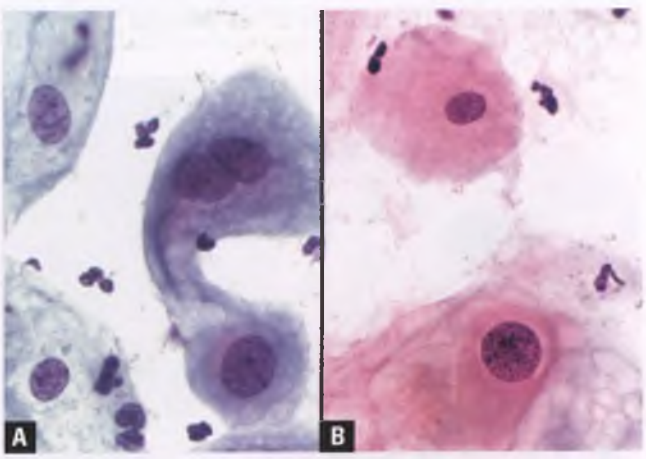

FIGURE 3.135. ASC-US. **A**: Two atypical squamous cells are present, one of which is binucleated. Note the enlarged nuclei, slightly hyperchromatic chromatin, and smooth nuclear contours of these cells. **B**: The squamous cell in the bottom of the image exhibits mild nuclear enlargement, grainy chromatin of the type often seen in dysplasia, and a slender perinuclear halo. However, the nuclear contour is smooth and this was one of only a few abnormal cells present in the smear.

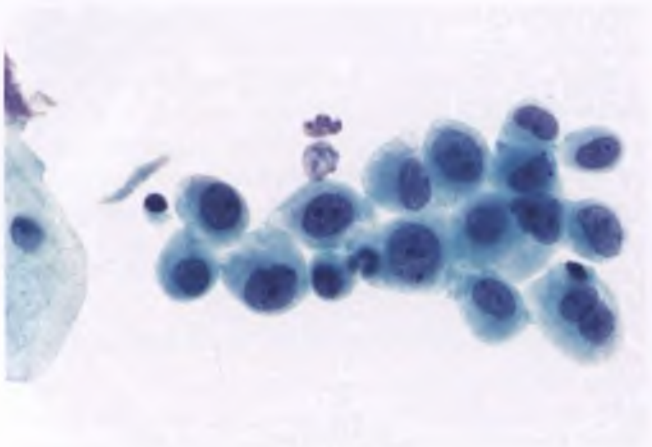

FIGURE 3.136. ASC-H. Atypical squamous metaplastic cells, a few of which exhibit nuclear contour abnormalities, are present in this liquid-based Pap smear. Follow-up biopsy showed HSIL.

THE DIFFERENTIAL DIAGNOSIS OF SQUAMOUS INTRAEPITHELIAL LESIONS

Perinuclear Halos

Without a doubt, misinterpretation of cervical squamous cells with perinuclear halos and mild nonspecific nuclear alterations as koilocytes is the single most overdiagnosed entity in gynecologic surgical pathology. In one study sponsored by the National Cancer Institute, 41% of cervical biopsies with an initial diagnosis of LSIL were reclassified as within normal limits by the panel of reviewing pathologists.[88] Cervical biopsies that feature large, uniform areas with perinuclear halos and mild nuclear abnormalities represent glycogenated epithelium with mild disturbances in maturation, reactive changes related to inflammation, or artifacts due to tissue processing and fixation (Figs. 3.137 and 3.138). Distinction of koilocytosis from pagetoid dyskeratosis is discussed in the section on reactive and reparative processes.

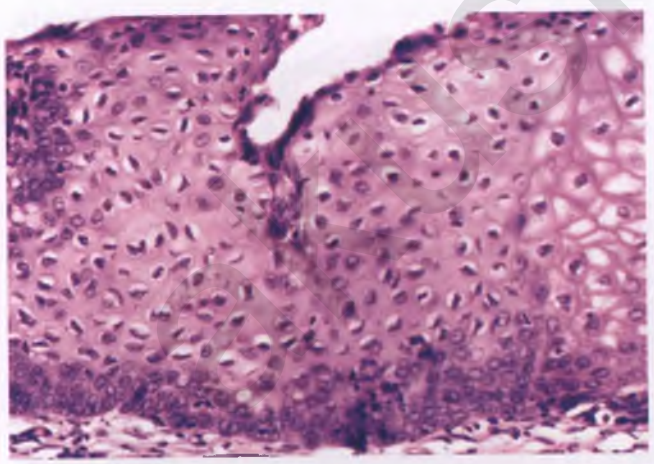

FIGURE 3.137. Mild nonspecific changes resulting in resemblance to koilocytosis (no significant abnormality). Perinuclear halos and irregular nuclear contours may result in an interpretation of koilocytosis. However, there is no nuclear enlargement (compare with normal intermediate cell nuclei at right), peripheral condensation of cytoplasm is absent, much of the apparent nuclear irregularity is due to compression of nuclear membranes by cytoplasmic contents, and the uniformity of the area of potential abnormality would be unusual for viral cytopathic effect.

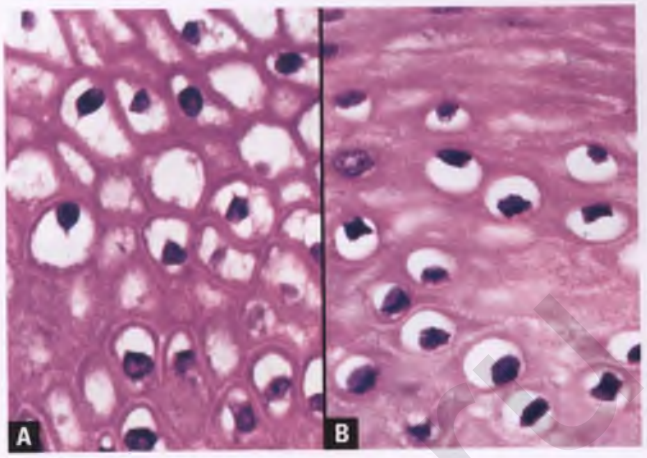

FIGURE 3.138. **A,B**: Pseudokoilocytosis (no significant abnormality). These high-magnification images of two different cervical biopsies highlight the common finding of glycogenated squamous cells with perinuclear halos. Although not apparent at this magnification, the nuclei are of comparable size to that of normal intermediate cells, and these histologic features were present over continuous, large portions of squamous epithelium.

In Pap smears, well-glycogenated squamous cells or cells with perinuclear halos without accompanying nuclear enlargement and atypia should be considered variants of normal and not overdiagnosed as ASC or LSIL (Fig. 3.139). In patients with a *Trichomonas vaginalis* infection, it is not uncommon for some of the mature squamous cells in Pap smears to exhibit

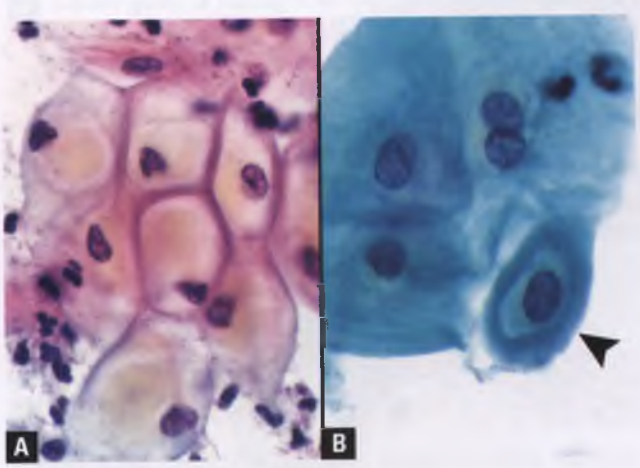

FIGURE 3.139. **A,B**: Pseudokoilocytes in Pap smears (negative cytology). Perinuclear halos are present, but without associated nuclear abnormalities. As shown in **A**, cytoplasmic clearing due to glycogen often has a golden-yellow tinge and is not as transparent as the halos seen in viral cytopathic effect.

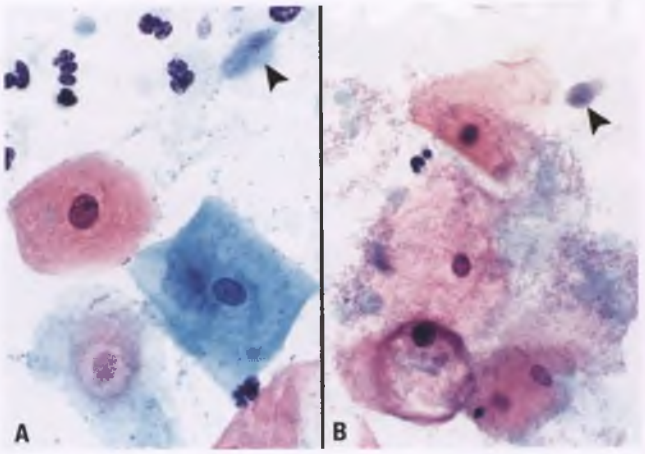

FIGURE 3.140. **A,B**: Pap smears showing *Trichomonas* infection associated with squamous cells with reactive perinuclear halos. The organisms are marked by *arrowheads*.

perinuclear halos (Fig. 3.140). The absence of nuclear enlargement and atypia distinguishes these reactive cells from HPV-related koilocytes.

Atypia of Maturity

In Pap smears from perimenopausal and postmenopausal women with mature squamous epithelium, isolated squamous cells may show some degree of nuclear enlargement that prompts consideration for a diagnosis of ASC or LSIL (Fig. 3.141). However, the threshold for a nonnegative diagnosis in such cases should be raised, since the vast majority of these cases do not harbor high-risk HPV or represent biopsy-proven SIL.[119] Unless there are nuclear contour and chromatin abnormalities that accompany the nuclear enlargement, these "atypias of maturity" should be regarded as being within normal limits.

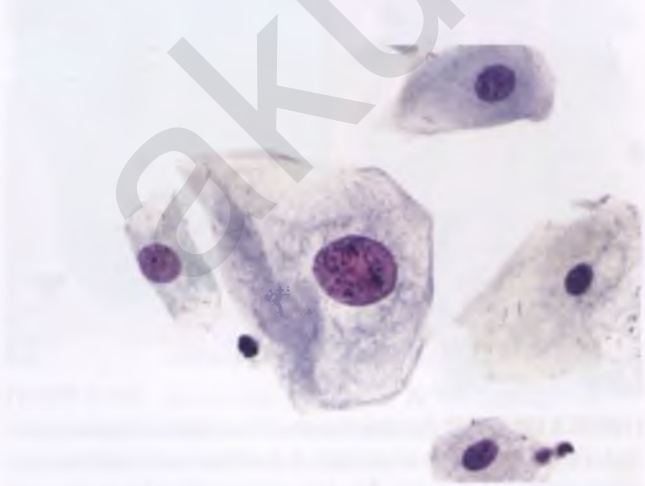

FIGURE 3.141. Nuclear enlargement of isolated mature squamous cells in a Pap smear from a postmenopausal woman. This so-called "atypia of maturity" is best interpreted as being within normal limits.

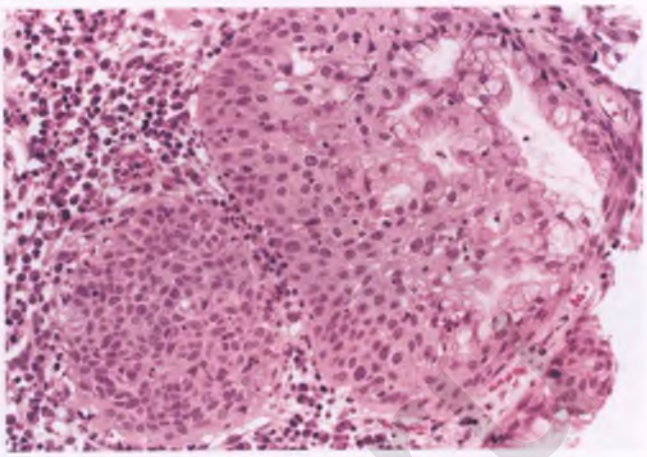

FIGURE 3.142. Immature squamous metaplasia with involvement of endocervical glands. Tangential sectioning through the basal region of a metaplastic gland accounts for the solid cellular nodule of metaplastic cells in the lower left portion of the image.

Immature Squamous Metaplasia

In immature squamous metaplasia, there is a gradual replacement of endocervical columnar mucinous epithelium by parabasal-type squamous cells. This is a normal finding that is commonly seen on the surface of the endocervical canal and within superficially located endocervical glands (Fig. 3.142). The presence of mild degrees of variation in nuclear size and shape, relatively high nuclear to cytoplasmic ratios, tendency for vertically oriented nuclei, and the lack of surface maturation can lead to confusion with HSIL (Fig. 3.143). Occasional mitotic figures may be seen, particularly in the lower levels of the epithelium, but atypical

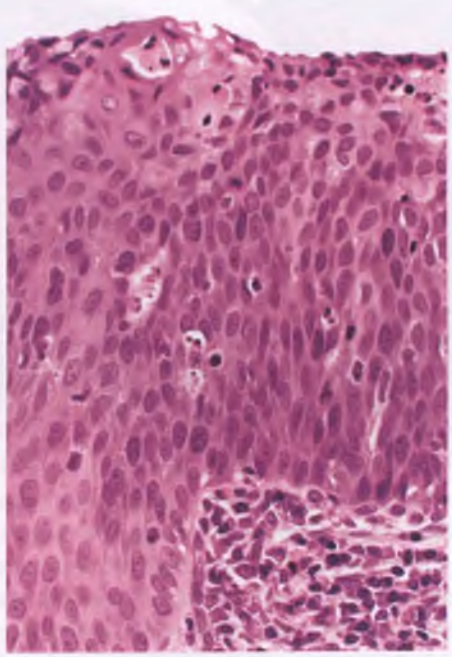

FIGURE 3.143. HSIL on the right merges with immature squamous metaplasia toward the left.

division figures are not present. Although the nuclear chromatin may appear mildly abnormal in immature squamous metaplasia, it is fairly uniform throughout, and does not exhibit more significant chromatin abnormalities such as the hyperchromatic, coarsely clumped chromatin often seen in HSIL. The regularity in the spacing of nuclei and the presence of nucleoli also favor a metaplastic process, as does the presence of residual mucinous epithelial cells on the surface (Fig. 3.10). However, this latter phenomenon can also rarely be seen in HSIL (Fig. 3.115).

Atypical Immature Squamous Metaplasia

There exists a subset of borderline squamous metaplastic lesions that blends reactive and potentially dysplastic features that confounds even experts in the field. The term atypical immature squamous metaplasia (AIM) was coined in 1983 to describe a "distinct histologic entity" with features of immature squamous metaplasia with increased cellularity, mild nuclear atypia, and a low mitotic rate with an absence of atypical division figures (Fig. 3.144).[120] It is associated with abnormal Pap smears that have usually been interpreted as ASCUS or ASC-H. Subsequent studies have shown poor reproducibility for the diagnosis of AIM, which actually represents a heterogeneous group of lesions that includes squamous metaplasia with reactive atypia, AIM, LSIL, and metaplastic HSIL.[103,121–124] Cases recognized as having AIM-like features should be reviewed with colleagues and critically evaluated with additional sections and considered for biomarker analysis with p16 and Ki-67 in an effort to more precisely characterize these lesions. Patients with problematic lesions that remain difficult to subcategorize should receive close clinical follow-up. Although the AIM terminology persists in the literature, its use as a diagnostic term has fallen out of favor in view of the wide range of processes that it represents.

Atrophy

Atrophy of exocervical and vaginal squamous epithelium is due to estrogen deprivation and is characterized by a thin layer of mitotically inactive basal and parabasal cells with oval to elongate nuclei (Fig. 3.145). There is some overlap between the histologic features of atrophy and transitional cell metaplasia. Atrophic squamous epithelium lacks surface maturation and may exhibit increased nuclear density and hyperchromatic nuclei, which can lead to the false impression of HSIL. However, the mitotic inactivity, uniformity in nuclear size and shape, and horizontal cellular arrangement of the subset of parabasal-type cells with spindle-shaped nuclei help to distinguish atrophy from HSIL. Immunostains for Ki-67, perhaps in conjunction with p16, can be helpful in difficult cases. In sharp contrast to HSIL with an atrophic pattern (Fig. 3.146), atrophic epithelium is p16 negative and has a Ki-67 proliferative

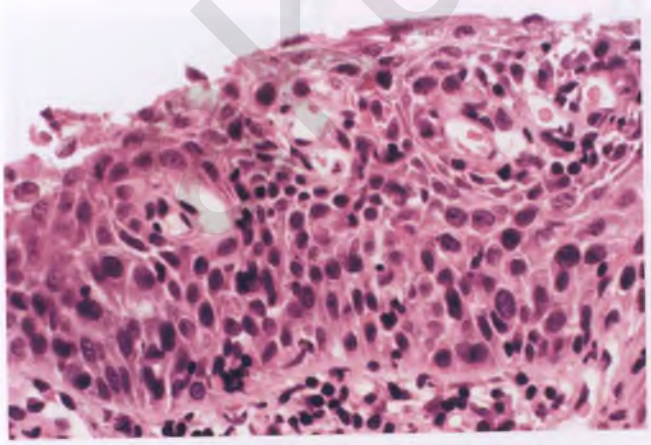

FIGURE 3.144. Atypical squamous intraepithelial process with AIM-like features. This lesion probably represents HSIL, but a definitive diagnosis is difficult on morphologic grounds alone.

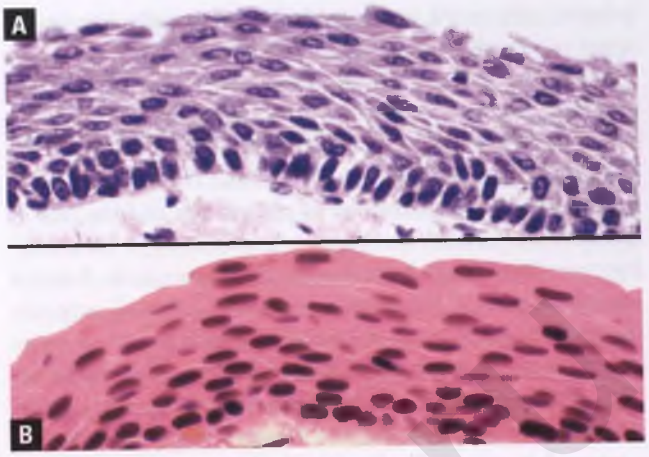

FIGURE 3.145. **A,B**: Atrophic exocervical squamous epithelium from two different postmenopausal women. Note the horizontal orientation of the elongated parabasal-type nuclei. The basal layer has a "picket fence" arrangement in **A**, but not in **B**.

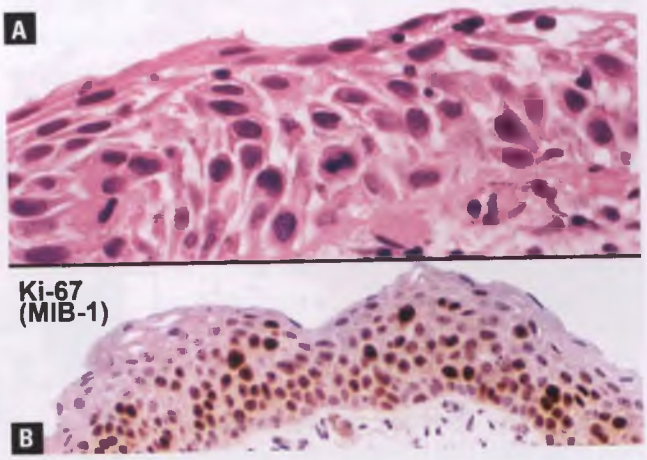

FIGURE 3.146. HSIL that resembles atrophy in routine histologic sections. **A**: Despite the thin epithelium and lack of cellular crowding, a suspicion for HSIL is raised by the mitotic figure and nuclear atypia. **B**: The Ki-67 (MIB-1) staining pattern, with nuclear staining of numerous cells throughout all but the uppermost level of the epithelium, supports the diagnosis of HSIL.

index of <3% in the basal one-third and virtually zero in the upper two-thirds of the epithelium.[6,98,99]

The Pap smear correlate of atrophy is the presence of numerous parabasal cells, which is illustrated in Figure 3.7B,C. When the sheets of parabasal cells are thick or cellular, they represent a form of HCG that can mimic HSIL (Fig. 3.147). Recognition of the uniformity of nuclear size and the lack of abnormalities in nuclear chromatin and contour in the monolayer portion of these sheets facilitates this distinction. Another possible source of misdiagnosis in some inflamed, atrophic smears is the presence of "blue blobs," which appear to represent mummified parabasal cells with precipitated hematoxylin (Fig. 3.147 inset). In postmenopausal women with atypical atrophic smears, a short course of estrogen therapy followed by a repeat Pap smear will often clarify the situation, since atrophic cells will show maturation, whereas dysplastic cells will persist.

Nodular Aggregates of Endometrial Histiocytes

As noted earlier in this chapter, HSIL can be found in endometrial samples on rare occasions, either due to contamination from dysplastic epithelium originating within the endocervical canal or related to replacement of portions of the endometrial lining by HSIL. One potential mimic of HSIL within endometrial samples is the presence of nodular aggregates of endometrial histiocytes, which can also mimic a variety of other histiocytic and nonhistiocytic processes (Fig. 3.148).[125] These nodules are commonly associated with blood and fibrin. The haphazard arrangement of cells that are closely packed, the variability of nuclear contours, and the presence of mitotic activity can lead to a misdiagnosis of HSIL (Fig. 3.149A). Immunohistochemistry can be of assistance, since the histiocytic aggregates are positive for the macrophage marker KP-1 (Fig. 3.149B) and negative for cytokeratin, whereas the opposite is true of the constituent cells of HSIL.

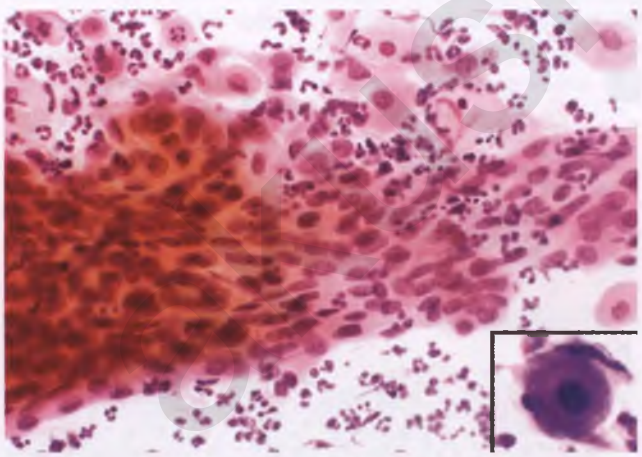

FIGURE 3.147. Squamous epithelial atrophy in a Pap smear. A sheet of parabasal cells is present within an inflammatory background. The sheet is thicker in the left side of the image, where it gives the false impression of nuclear crowding, hyperchromasia, and cytoplasmic orangeophilia. The inset shows a "blue blob" from a different atrophic smear, with the centrally located, small nucleus of a degenerated parabasal cell mimicking a macronucleolus within what falsely appears to be a large, atypical naked nucleus.

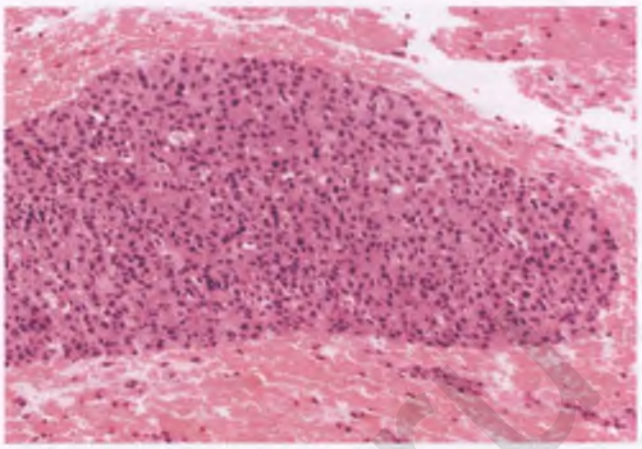

FIGURE 3.148. Nodular aggregate of endometrial histiocytes within an endometrial curettage. Aggregates of this type can be misinterpreted as fragments of HSIL originating in the endocervix that have been inadvertently admixed with the endometrial sample.

Other Entities

In tissue sections, HSIL also needs to be distinguished from squamous metaplasia with reactive changes, transitional metaplasia, and microinvasive squamous cell carcinoma. In Pap smears, additional entities/cell types that enter the differential diagnosis of HSIL include endometrial cells from the lower uterine segment, histiocytes, radiation effect, IUD-related "ding cells," follicular cervicitis, decidua, and trophoblastic cells. These topics are considered elsewhere in this chapter.

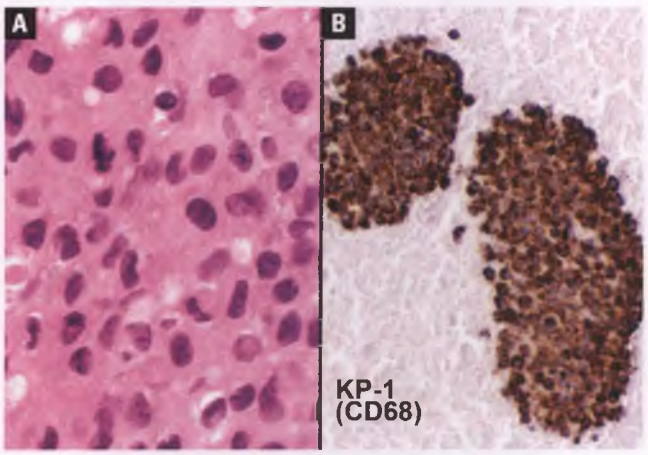

FIGURE 3.149. Endometrial histiocytes mimicking HSIL. **A**: Note the jumbled nuclei with variable shapes and mitotic activity. **B**: A KP-1 immunostain confirms the histiocytic nature of these aggregates.

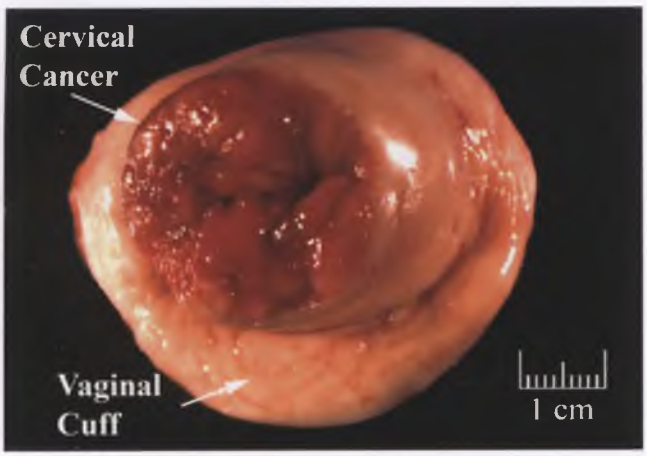

FIGURE 3.150. Invasive squamous cell carcinoma. This exophytic tumor protrudes from the external cervical os (the cervix has been amputated from a radical hysterectomy specimen).

INVASIVE SQUAMOUS CELL CARCINOMA AND ITS VARIANTS[126]

Squamous cell carcinoma and its variants account for approximately 75% of invasive carcinomas of the cervix. As is true for HSIL, the vast majority of squamous cell carcinomas are associated with high-risk HPV types. Although the mean age at presentation is 50 to 55 years, approximately 25% of tumors occur in patients under 35 years of age. Patients usually present with abnormal vaginal bleeding and/or an abnormal Pap smear; those with small tumors may be asymptomatic.

Grossly, squamous cell carcinoma almost always involves the transformation zone and may be polypoid, papillary, nodular, diffusely infiltrative, or ulcerated (Figs. 3.150–3.152). The sectioned surface of squamous cell carcinoma is usually gray-white and is sometimes punctuated by numerous minute specks of soft, pale yellow, paste-like material. This speckled pattern may be due to keratinous debris within nests of keratinizing squamous cell carcinoma and/or punctate foci of tumor necrosis (Fig. 3.153).

Microinvasive Squamous Cell Carcinoma[127,128]

Microinvasion is defined by the Society of Gynecologic Oncologists (SGO) as a depth of invasion of ≤3 mm and an absence of angiolymphatic invasion. In contrast, the International Federation of Gynecologic Oncologists (FIGO) 2008 revised staging system for carcinoma of the cervix has reaffirmed its prior policy of subdividing microinvasive squamous cell carcinomas according to whether the depth of invasion is ≤3 mm (stage Ia1) or >3 but ≤5 mm (stage Ia2).[129] For both FIGO stages, the tumor must be detected only microscopically rather than clinically, and its width must also be ≤7 mm; angiolymphatic invasion is reported but does not alter staging in this system.

When the origin of the invasive carcinoma can be pinpointed, the depth of invasion is measured from the basement membrane of the originating epithelium to the deepest point of invasion (Fig. 3.154).[127] In those situations in which the origin of invasion is indeterminate, the depth of invasion is measured from the epithelial–stromal interface of the surface to the deepest point of invasion. Microinvasion is identified in approximately 7% of conization specimens that are evaluated for CIN 3/CIS.[130] There are several histologic features that are helpful in recognizing stromal microinvasion: (a) squamous maturation within nests or finger-like protrusions of infiltrating epithelium that takes the form of a fairly abrupt transition from the originating dysplasia (which is usually an extensive HSIL with prominent involvement of endocervical glands) to cells with more abundant eosinophilic cytoplasm, sometimes with visible intercellular bridges and/or evidence of keratin production, (b) an associated stromal reaction, which may consist of edema and chronic inflammation or desmoplasia (exclude biopsy-related displacement of epithelium into fibroblastic stroma), (c) tongues of infiltrating carcinoma with scalloped contours, and (d) atypical epithelium with complex

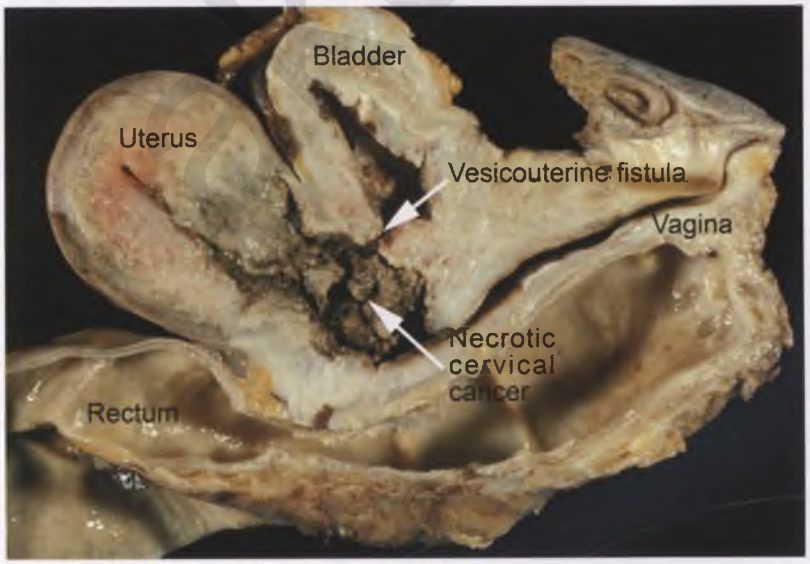

FIGURE 3.151. Invasive squamous cell carcinoma of the cervix (pelvic exenteration). This sagittal section through a necrotic cervical cancer demonstrates involvement of the bladder anteriorly and the rectal wall posteriorly. Note the formation of a vesicouterine fistula. (Courtesy of Dr. Enrique Higa.)

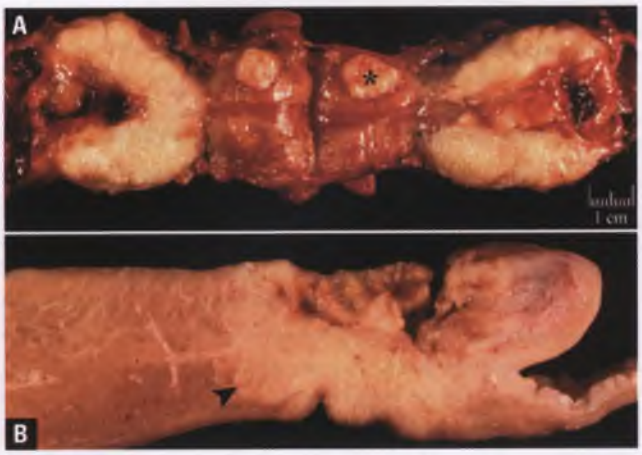

FIGURE 3.152. Invasive squamous cell carcinoma. **A**: This bivalved uterus exhibits diffuse replacement of the cervical wall by tumor. In its uncut state, circumferential involvement of the cervix resulted in a "barrel-shaped" configuration. An asterisk marks an incidental leiomyoma adjacent to the endometrial cavity. **B**: This longitudinal section through a fixed uterus demonstrates an ulceroinfiltrative tumor involving the full thickness of the cervical wall. An *arrowhead* marks a tumor-stromal interface. The vaginal cuff is in the lower right corner of the image. The sectioned surfaces of both carcinomas have some pale yellow specks, which were more easily visualized in the actual surgical specimens.

anastomosing growth patterns (Fig. 3.155; exclude tangentially cut squamous metaplasia).

A particularly deceptive pattern of stromal invasion mimics endocervical crypt involvement by CIN 3 and is distinguished by a constellation of features that include (a) expanded epithelial nests that have predominantly smooth, wavy contours with bulges and branches that result in the formation of unusual shapes, (b) the typical presence of central necrosis

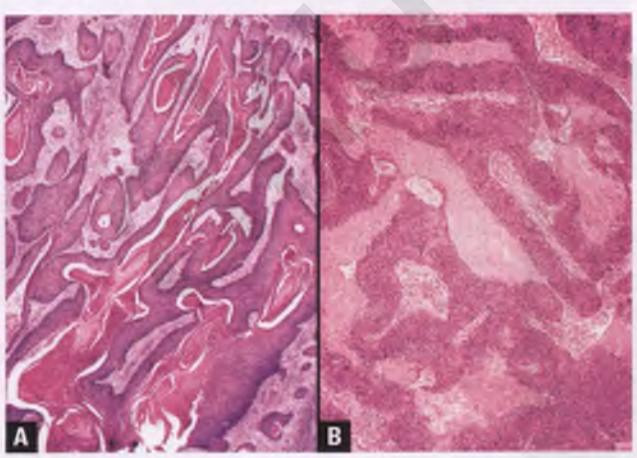

FIGURE 3.153. The pale yellow specks that are grossly visible on the sectioned surface of some squamous cell carcinomas are due to keratinous debris within nests of keratinizing squamous cell carcinoma **(A)** and/or foci of tumor necrosis **(B)**.

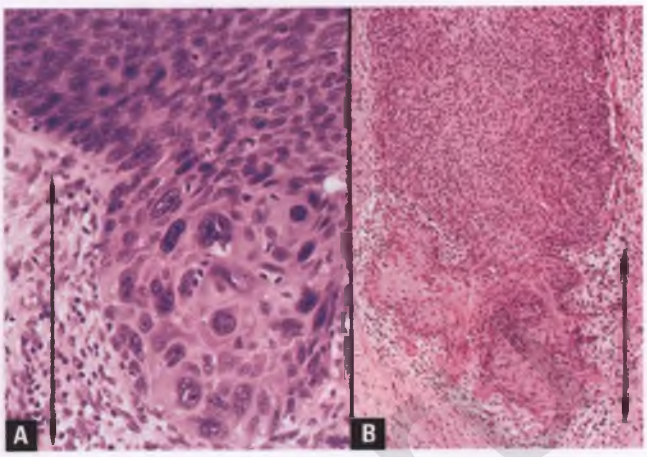

FIGURE 3.154. **A,B**: Microinvasive squamous cell carcinoma. Both microinvasive foci exhibit squamous maturation and are seen budding off of endocervical glands that have been replaced by HSIL. In **B,** the microinvasive focus also has scalloped contours and has elicited a stromal response manifested by edema and chronic inflammation. The measurements for depth of invasion are indicated by the *arrows*.

within many of the nests, (b) some degree of squamous maturation, usually in the form of a modest increase in the amount of eosinophilic cytoplasm (more pink and less blue at low magnification than endocervical glands replaced by CIN 3; compare with Fig. 3.116), (d) absence of residual partial gland involvement within the invasive nests, which are often found beneath the level of normal endocervical glands, (e) a variable stromal response that usually consists of edema and chronic inflammation, and (f) more conventional invasion at the advancing edge of some of the nests, which can easily be misinterpreted as minute foci of invasion budding off of endocervical glands replaced by CIN 3 (Figs. 3.156–3.159; several examples are shown because this is an underrecognized and frequently misinterpreted entity).[131]

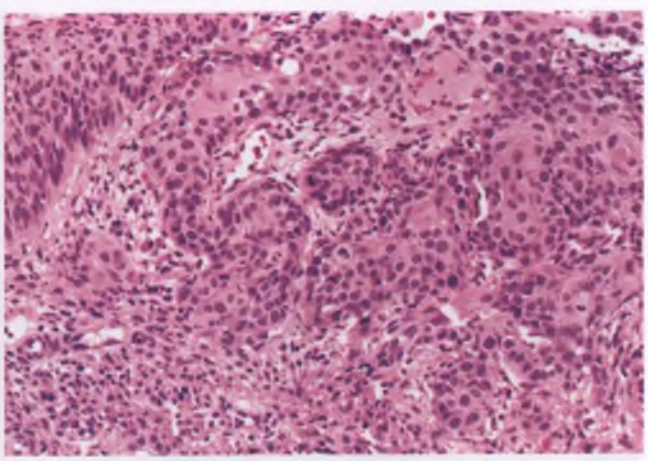

FIGURE 3.155. Microinvasive squamous cell carcinoma. This complex anastomosing growth pattern is indicative of stromal invasion. Residual surface HSIL is present in the upper left corner.

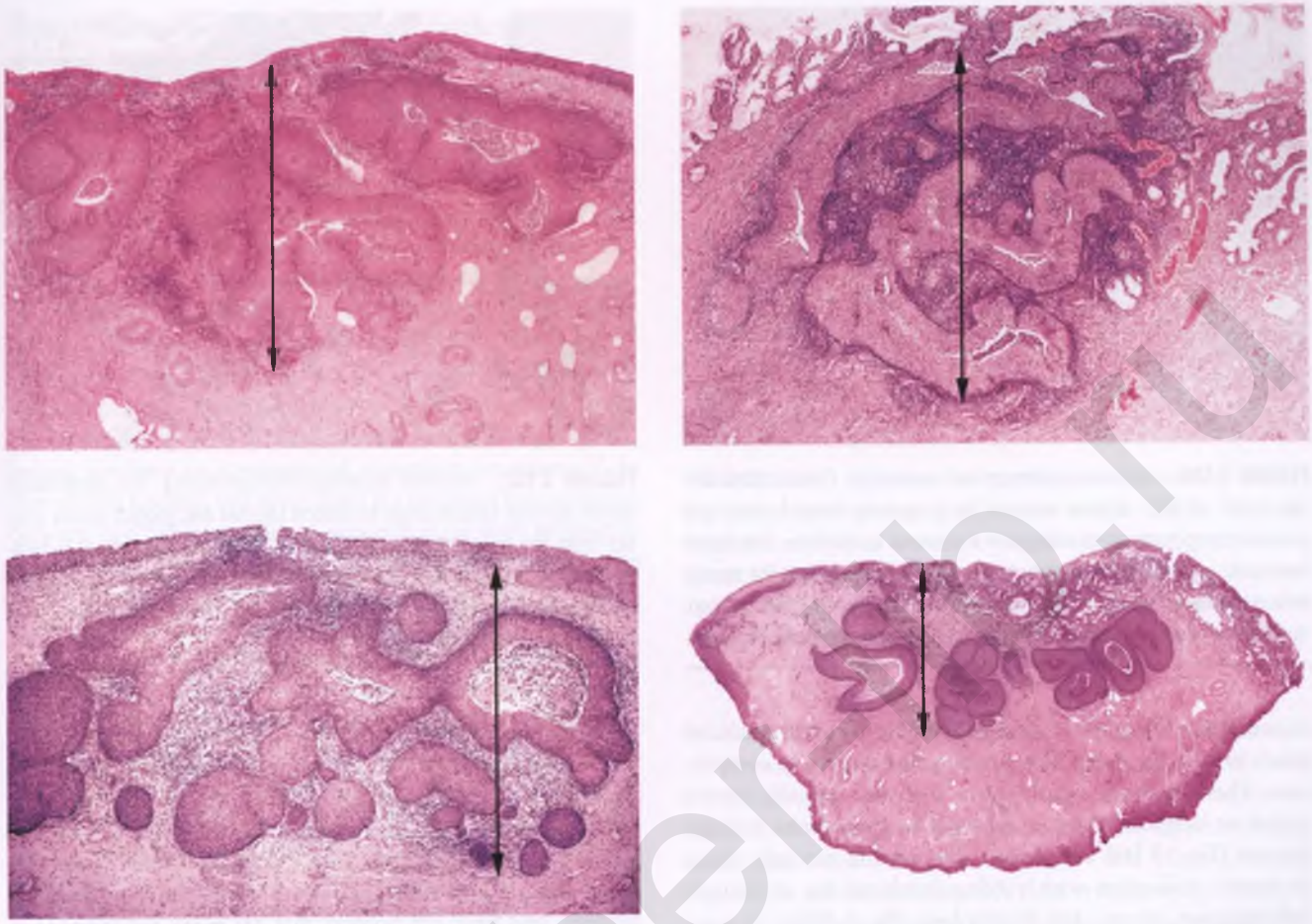

FIGS 3.156–3.159. Four separate examples of superficially invasive squamous cell carcinoma mimicking endocervical crypt involvement by CIN 3. An invasive process is indicated by the combination of (a) irregular tongues of epithelium projecting from large crypt-like structures, (b) squamous maturation, (c) central necrosis within some of the nests, (d) associated chronic inflammation and edema, and (e) in some cases, finding the abnormal epithelial nests located beneath the level of normal endocervical glands. Since the point of origin of these tumors is generally inapparent, the depth of invasion is measured from the basement membrane of the surface epithelium to the deepest point of invasion (*arrows*). In the lower right image, the lack of a connection between the abnormal epithelial nests and the overlying epithelium implies that the tumor seen in this section represents an extension of tumor located out of the plane of sectioning that has burrowed into the cervical stroma.

A diagnosis of microinvasion requires that the entire lesion is present for evaluation, since a transected microinvasive focus or a small biopsy with superficial invasion may represent the "tip of the iceberg" of a much more aggressive tumor. Whenever stromal invasion is identified, the presence or absence of angiolymphatic invasion should be indicated in the pathology report (see section on retraction artifact near the end of this chapter for a discussion of the distinction between true angiolymphatic invasion and artifactual clefts surrounding tumor cell nests). In addition to the status of angiolymphatic invasion, reports of specimens with microinvasion should indicate the depth of stromal invasion, the greatest horizontal extent of the invasive focus, and the status of the resection margins.

Treatment and Prognosis

The risk of lymph node metastases in stage Ia1 disease without angiolymphatic invasion is negligible (<1%),[128] such that it may be adequately treated by cone biopsy with documented negative resection margins in those patients who wish to preserve their fertility. Stage Ia1 tumors with angiolymphatic invasion and stage Ia2 tumors with or without angiolymphatic invasion have about an 8% risk of lymph node metastasis, which supports the use of pelvic lymphadenectomy as part of the treatment plan for these patients.[128] Prognosis is excellent, with only about 0.5% of patients with stage Ia1 and 2.5% of patients with stage Ia2 squamous cell carcinoma dying from recurrent tumor.[128]

Conventional Squamous Cell Carcinoma

For descriptive purposes, conventional invasive squamous cell carcinomas are divided into keratinizing and nonkeratinizing types. These tumors exhibit significant architectural heterogeneity, with tumor cells of both types infiltrating cervical stroma

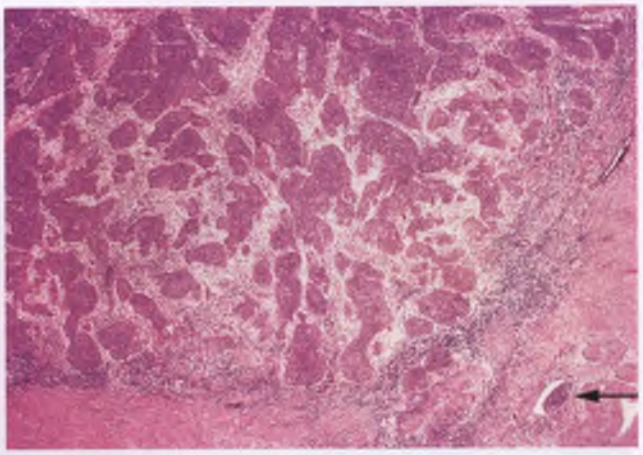

FIGURE 3.160. Invasive squamous cell carcinoma. This nonkeratinizing tumor exhibits stromal invasion by irregularly shaped nests and anastomosing tongues of malignant squamous epithelium. The tumor has a pushing interface with the uninvolved stroma, whereas the stroma within the tumor shows a combination of edema, chronic inflammation, and desmoplasia. The *arrow* marks a focus of angiolymphatic invasion.

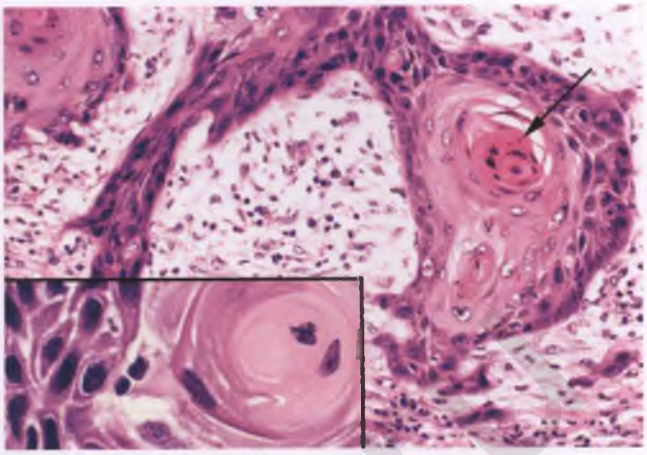

FIGURE 3.162. Invasive squamous cell carcinoma. This keratinizing tumor exhibits keratin pearl formation (*arrow*) and jagged points project from the nests of infiltrating tumor. Inset: To the left of a keratin pearl is a cluster of tumor cells that exhibits spinous intercellular bridges. Keratin formation and intercellular bridges are hallmarks of squamous differentiation.

as complex admixtures of nests and interconnecting epithelial bands of variable shapes, thicknesses, and degrees of compaction. The tumor cell nests vary in size, and typically have a jagged or irregular contour, although rounded nests can also be seen (Figs. 3.160 and 3.161). The stroma generally reacts to tumor infiltration with varying combinations of chronic inflammation, edema, and desmoplasia (Fig. 3.160).

The distinguishing feature of keratinizing squamous cell carcinoma, which is three to four times less common than the nonkeratinizing type, is the presence of "keratin pearls" within the tumor cell nests. Keratin pearls are typically found within the center of the nests, and consist of concentric whorls of keratin that in this context are often associated with pyknotic tumor cell nuclei (Fig. 3.162). Both keratinizing and nonkeratinizing tumor cells may show keratinization at the level of the individual cell. Infiltrative growth patterns, prominent intercellular bridges, and distinct cell borders are more typical of keratinizing tumors (Fig. 3.162), whereas nonkeratinizing tumors often grow with a pushing, expansile advancing margin (Fig. 3.160), exhibit less conspicuous intercellular bridges, and have cell borders that are more indistinct (Fig. 3.163). The nuclear features of these tumors are illustrated in Figures 3.162 and 3.163 and are described below as part of the discussion of the Pap smear findings of squamous carcinoma. Nonkeratinizing tumors generally exhibit a higher mitotic rate than keratinizing tumors, whose mitotic activity is concentrated toward the periphery of the tumor cell nests. In some cases, the distinction between keratinizing and

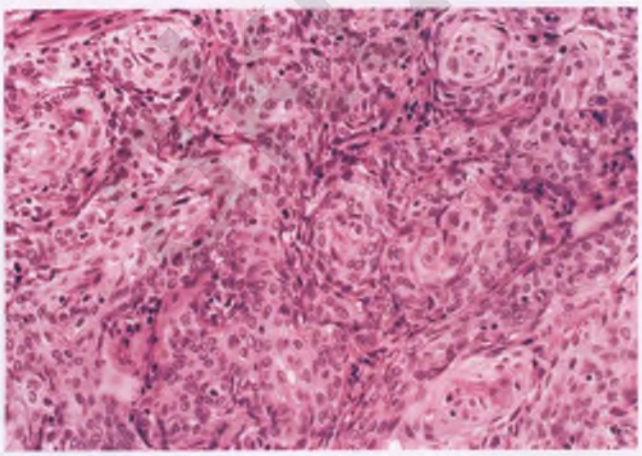

FIGURE 3.161. Invasive squamous cell carcinoma. This nonkeratinizing tumor infiltrates as closely packed anastomosing nests with rounded contours.

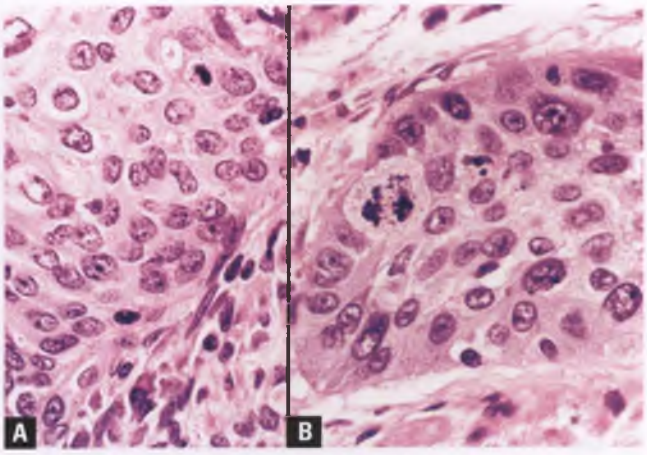

FIGURE 3.163. **A,B**: Invasive squamous cell carcinoma. This composite image highlights the nuclear features of two separate nonkeratinizing tumors.

nonkeratinizing tumors may be blurred due to an admixture or blending of cell types.

A rare, highly differentiated form of keratinizing squamous cell carcinoma has been reported that exhibits extensive keratinization, an inverted and infiltrative growth pattern with spread by local extension, minimal nuclear atypia, neighboring hyperkeratosis/parakeratosis, and a lack of association with HPV or SIL.[132] This rare variant shares many features with HPV-negative vulvar squamous cell carcinomas.

Rare nonkeratinizing tumors, referred to by some as small cell squamous carcinoma, consist of discrete nests of small HSIL-like cells with scant cytoplasm and only subtle evidence of squamous differentiation. Tumors with these features, when rigorously separated from small cell neuroendocrine carcinoma, behave similarly to conventional squamous carcinoma.[133] In view of this finding, and since there is a potential for confusion between two different types of tumor that are both referred to as small cell carcinoma (squamous and neuroendocrine), the WHO classification does not recognize small cell squamous carcinoma as a separate type of squamous carcinoma.

Approximately 20% of ordinary-appearing squamous cell carcinomas have been shown to harbor tumor cells with incidental PAS-positive, diastase-resistant, and/or mucicarmine-positive intracytoplasmic mucin droplets;[134] this finding should be neither searched for nor considered significant. The diagnosis of adenosquamous carcinoma is reserved for tumors with both malignant squamous and glandular differentiation that is readily apparent in routinely stained sections.

Squamous cell carcinomas are often divided into well, moderately, and poorly differentiated forms. Most keratinizing tumors, by virtue of the presence of abundant keratin and a low mitotic rate, are considered well differentiated, whereas most nonkeratinizing tumors are classified as moderately differentiated. However, it should be noted that both grade and tumor type (keratinizing vs. nonkeratinizing) do not appear to be of prognostic significance, since prognosis is largely determined by the stage of the tumor. Sentinel lymph node biopsy, which is considered standard of care in the treatment of selected invasive breast carcinomas and cutaneous melanomas, is increasingly being utilized in the staging of patients with invasive carcinoma of the cervix.[135]

Frankly invasive squamous cell carcinomas can exhibit unusual or deceptive patterns of stromal invasion. The pattern of invasion that mimics endocervical gland involvement by CIN 3 that was illustrated in the previous section can also be found deep within the cervical stroma, often with associated retraction artifact, a surrounding rim of desmoplasia, and/or central necrosis within the epithelial nests (Fig. 3.164). However, some or all of these diagnostic clues to an invasive process may be absent in an individual case, whereupon one must rely on low-magnification architectural features to recognize stromal invasion (Fig. 3.165).

Differential Diagnosis

As discussed elsewhere in this chapter, the histologic differential diagnosis of typical invasive squamous cell carcinoma includes florid squamous metaplasia, iatrogenic displacement of squamous epithelium, ectopic decidua, and HSIL with involvement of endocervical glands. Placental site nodule and epithelioid trophoblastic tumor also enter the differential diagnosis, and are discussed in Chapters 4 and 10, respectively. Squamous cell carcinomas with clear cytoplasm due the presence of abundant glycogen (Fig. 3.166) can be confused with clear cell carcinoma, although the latter will lack more typical areas of squamous carcinoma and will usually contain foci with the characteristic tubulocystic and/or papillary patterns and hobnail cells of clear cell carcinoma. Poorly differentiated forms of squamous cell carcinoma can exhibit sheet-like growth and

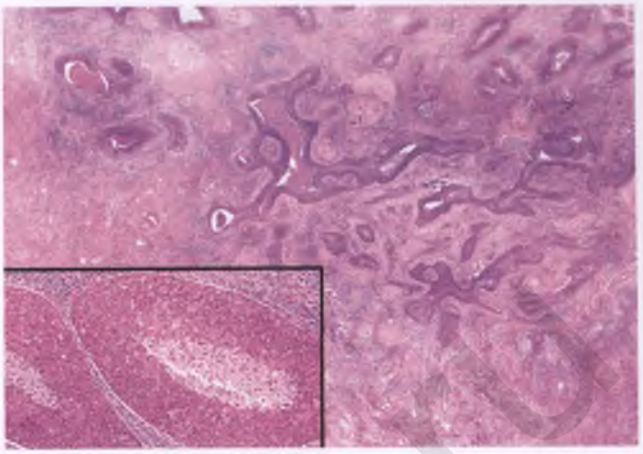

FIGURE 3.164. Squamous cell carcinoma with pattern of invasion that mimics endocervical gland involvement by CIN 3. The tumor infiltrates primarily as smooth-contoured nests with central necrosis, some of which branch and elongate to form unusual shapes. A stromal reaction is present. The inset shows a lymph node metastasis with recapitulation of this pattern (note the thin rim of retraction artifact).

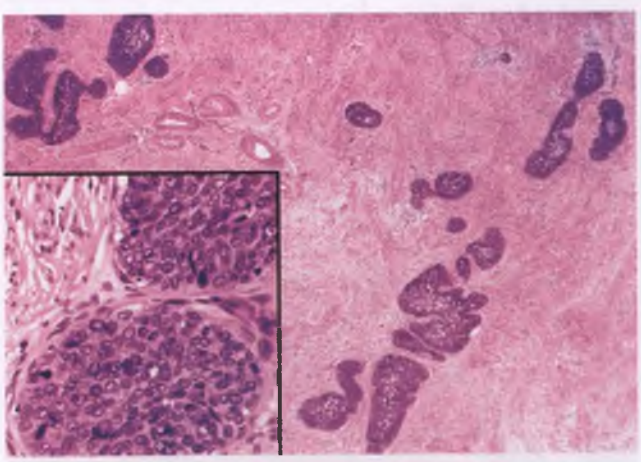

FIGURE 3.165. Squamous cell carcinoma with deceptive pattern of stromal invasion. The extent and depth of this process at low magnification indicates an invasive lesion, but the sharply demarcated tumor cell nests have rounded rather than jagged contours and elicit only a mild and focal stromal response.

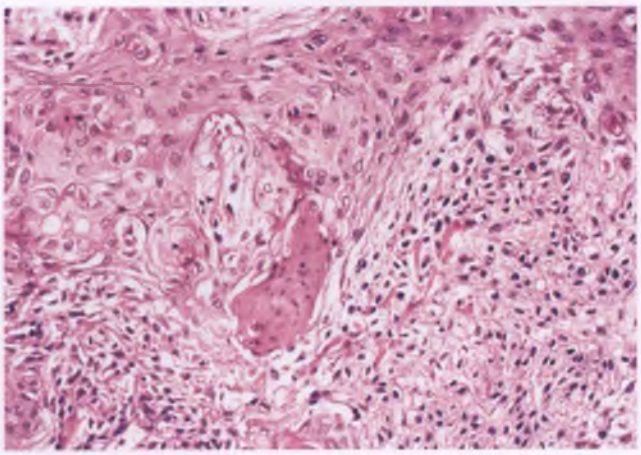

FIGURE 3.166. Invasive squamous cell carcinoma with clear cell areas due to the presence of abundant intracytoplasmic glycogen.

resemble malignant lymphoma, sarcoma, and melanoma; in such cases, a panel of immunohistochemical stains is indicated.

Cytologic Features of Squamous Cell Carcinoma

In Pap smears, the malignant cells of frankly invasive squamous cell carcinoma are found both singly and in clusters. These cells are often associated with a tumor diathesis ("dirty background"), which is more commonly seen and more extensive in nonkeratinizing tumors. The components of a tumor diathesis include broken down blood products and necrosis-related granular debris associated with proteinaceous fluid. Although similar backgrounds can also be seen in benign conditions such as severe *Trichomonas* infection or atrophic vaginitis, dirty backgrounds devoid of malignant cells can also be a clue to the presence of a suboptimally sampled malignant neoplasm (Fig. 3.167). Therefore, an explanation for these backgrounds should be sought. In liquid-based smears, the granular debris of a tumor diathesis, which has been likened to blue-green cotton candy, tends to be

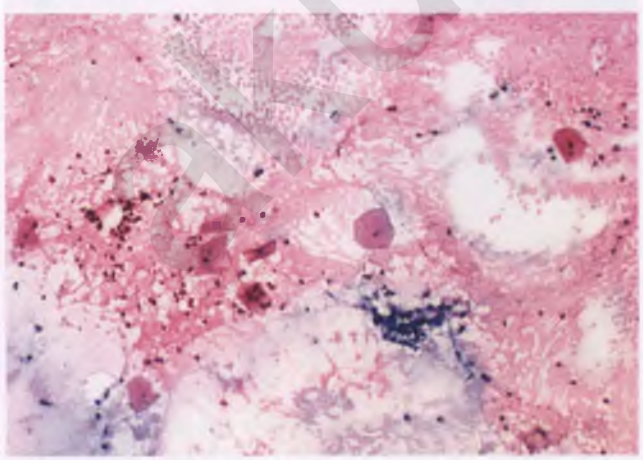

FIGURE 3.167. Conventional Pap smear with tumor diathesis. No definite tumor cells were found in this smear, but subsequent evaluation revealed invasive squamous cell carcinoma.

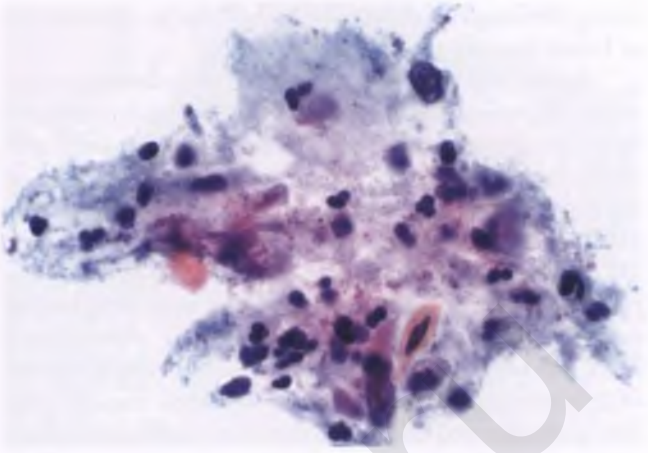

FIGURE 3.168. Invasive squamous cell carcinoma in liquid-based Pap smear. The blue-green, granular material that represents a tumor diathesis clings to scattered malignant squamous cells.

loosely adherent to and intermingled with tumor cells in a pattern that has been referred to as a clinging diathesis (Fig. 3.168).

Since (a) there is often not a sharp cytologic distinction between keratinizing and nonkeratinizing tumors (both of which can show individual cell keratinization) and (b) a given smear may show features of both tumor types, the Bethesda System has chosen not to subdivide squamous cell carcinomas into keratinizing and nonkeratinizing types. Nevertheless, it is instructive to discuss their general cytologic features separately. In keratinizing squamous cell carcinoma, the malignant squamous cells are quite variable in size and shape, and some elongated forms (spindle and tadpole cells) with keratinized, brightly orangeophilic cytoplasm may be present (Fig. 3.169). These cells typically represent only a minor

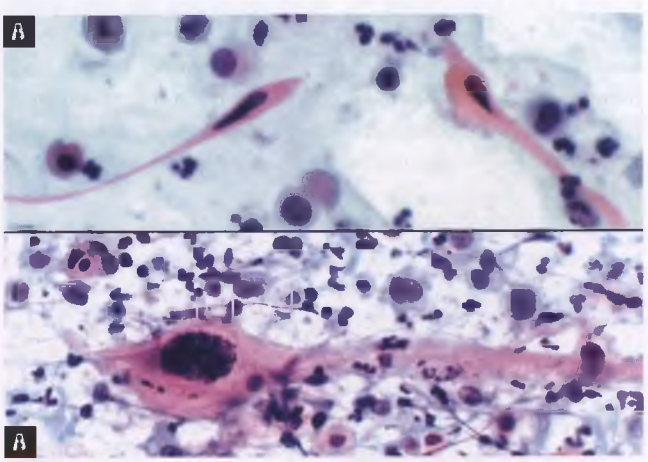

FIGURE 3.169. Keratinizing invasive squamous cell carcinoma (conventional Pap smears). **A**: Two elongated, wispy, orangeophilic cells with spindle-shaped, pyknotic nuclei are present. **B**: This image shows a monstrous orangeophilic tadpole cell with a large, intensely hyperchromatic nucleus located at the wider end of the cell. A tumor diathesis is present in the background of both smears.

component of the malignant cells in the smear. Nuclear detail is often obscured by intense hyperchromasia or pyknosis, but some tumor cells with enlarged nuclei, coarsely granular chromatin, and nuclear contour abnormalities are usually apparent, and prominent nucleoli are seen occasionally. The tumor cells of nonkeratinizing squamous cell carcinoma also have enlarged nuclei with coarsely clumped chromatin, but are more likely to exhibit round nuclear contours, prominent nucleoli, cyanophilic cytoplasm, and lesser degrees of nuclear pleomorphism than keratinizing tumors (Fig. 3.170).

Cytologic Differential Diagnosis

The differential diagnosis of invasive squamous cell carcinoma in Pap smears includes atrophic vaginitis, keratinizing HSILs, HSILs with "grungy" backgrounds, and benign reparative processes.

- In severely atrophic smears from postmenopausal women, there is often debris and granular precipitate that results from cellular degeneration and inflammation that creates a "dirty background" that must be distinguished from a true tumor diathesis (Fig. 3.55). The presence of "blue blobs" in smears of atrophic vaginitis heightens the potential for misinterpretation as a malignant process (Fig. 3.147).
- Keratinizing HSIL can be difficult to distinguish from keratinizing squamous cell carcinoma by virtue of the presence in this subtype of HSIL of bizarre orangeophilic cells and keratinous debris that can simulate a tumor diathesis. Cytologic smears of keratinizing HSIL lack a true tumor diathesis, but invasive keratinizing squamous cell carcinoma may also lack this feature, and both these lesions commonly lack prominent nucleoli. Although Pap smears of keratinizing lesions that contain an overwhelming number of severely dysplastic cells and an extensive tumor diathesis are indicative of an invasive process, some keratinizing HSILs are indistinguishable from invasive keratinizing squamous cell carcinoma and should be reported as HSIL with features suspicious for invasion.[136]
- Further complicating the differential diagnosis of HSIL versus invasive squamous cell carcinoma in Pap smears for both keratinizing and nonkeratinizing lesions is the occasional presence of comedo-type necrosis within superficial endocervical glands that have been replaced by HSIL that can result in small amounts of material indistinguishable from a tumor diathesis.[136]
- Features of benign reparative processes that facilitate their distinction from nonkeratinizing squamous cell carcinoma are discussed in the section on repair.

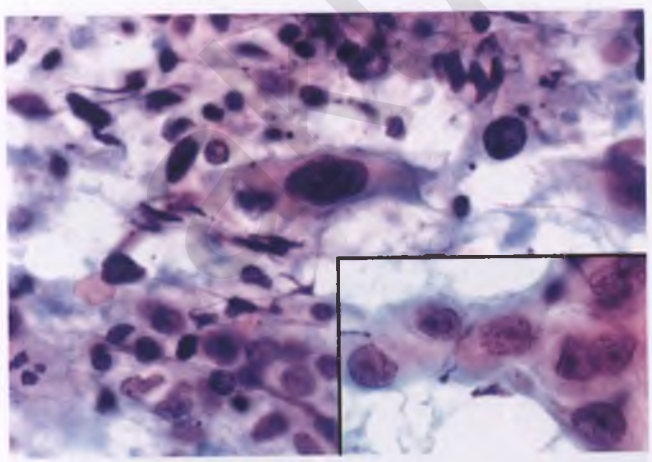

FIGURE 3.170. Nonkeratinizing squamous cell carcinoma (conventional Pap smears). Malignant squamous cells, occurring both singly and in clusters, are present in association with a tumor diathesis. The inset shows tumor cells from a different case in which prominent nucleoli are evident.

Basaloid Squamous Cell Carcinoma

Basaloid squamous cell carcinoma of the cervix is rare, but is probably underreported.[137] This tumor is composed of large, solid nests of variably sized, mitotically active, HSIL-like cells with high nuclear to cytoplasmic ratios that characteristically exhibit peripheral palisading (Fig. 3.171).[137] Keratinization may be present toward the center of some tumor cell islands.

Basaloid squamous cell carcinoma may resemble adenoid basal carcinoma, but its epithelial nests are larger and more infiltrative, and its constituent cells exhibit significantly more nuclear atypia and mitotic activity. Distinction from small cell carcinoma, large cell neuroendocrine carcinoma, and the solid variant of adenoid cystic carcinoma are discussed with these entities elsewhere in this chapter. To avoid confusion with the much less aggressive adenoid basal carcinoma, the ambiguous term "basaloid carcinoma" should not be used. Although cervical carcinosarcomas are quite rare, it is not uncommon for these tumors to contain a component of basaloid squamous cell carcinoma.[138,139]

Verrucous Carcinoma

Verrucous carcinoma is a rare variant of squamous carcinoma with a warty gross appearance that is composed of very well-differentiated, mature squamous epithelium.[140] Cervical verrucous carcinomas are histologically identical to their more common vulvar counterparts (see section on verrucous carcinoma in

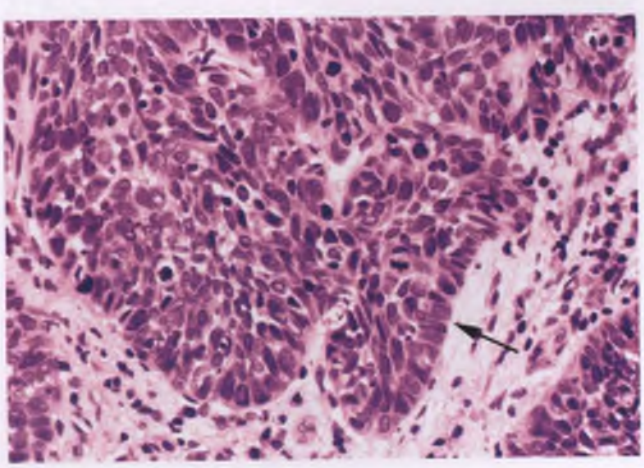

FIGURE 3.171. Basaloid squamous cell carcinoma. Palisading of nuclei is present at the periphery of the tumor cell nests (*arrow*).

Chapter 1). These tumors may recur locally, but do not metastasize if strict histologic criteria are used for their diagnosis. Reports of metastasizing verrucous carcinomas, such as case 2 in the report by Degefu et al.,[140] are invariably due to the presence of a component of conventional squamous cell carcinoma with infiltrative borders that contrasts with the broad, pushing advancing front that is characteristic of verrucous carcinoma.

Warty (Condylomatous) Carcinoma

Warty (condylomatous) carcinoma is another rare variant of squamous carcinoma with a warty surface that exhibits mature squamous differentiation. These tumors are distinguished from verrucous carcinoma by the presence of invasive tumor cell nests that display (a) scattered central foci of koilocytosis and (b) significant nuclear atypia and mitotic activity in the cell layers near the epithelial–stromal interface (Figs. 3.172 and 3.173). As is the case for verrucous carcinoma, there is more experience in the literature with vulvar tumors of this unusual type.

Papillary Squamous Cell Carcinoma and Related Tumors with Transitional Features

Papillary squamous cell carcinoma is an uncommon variant that features papillae lined by dysplastic epithelium that resembles HSIL (Figs. 3.174 and 3.175).[141,142] Grossly, the tumors are polypoid exophytic masses. The papillae are usually thin and delicate, but can also be thick and broad. When deep biopsies are obtained, there is usually an underlying invasive squamous cell carcinoma of conventional (large cell nonkeratinizing) type, although in situ forms of this lesion have been described. HPV is presumably involved in the pathogenesis of this tumor, since detectable HPV-DNA is often present.[142]

Other rare cervical tumors with a papillary architecture resemble papillary transitional cell carcinoma of the urinary bladder to varying degrees by virtue of the presence or predominance of stratified elongated cells that have their long axes oriented perpendicular to the basement membrane with abrupt flattening of the superficial cell layer. Such tumors may be designated papillary transitional cell carcinoma[75] or papillary squamotransitional cell carcinoma,[143] recognizing that classification of these various subtypes of papillary carcinomas is a subjective exercise. More important is differentiating these malignant papillary tumors from immature condyloma and condyloma acuminatum, which are distinguished by their lack of significant nuclear atypia, low mitotic rate, and low Ki-67 proliferation index. Verrucous and warty carcinomas are also differential diagnostic considerations. Verrucous carcinoma is distinguished from papillary squamous cell carcinoma by its bland nuclei and broad, pushing interface with the underlying stroma, whereas warty carcinoma features prominent koilocytosis that is lacking in papillary squamous cell carcinoma.

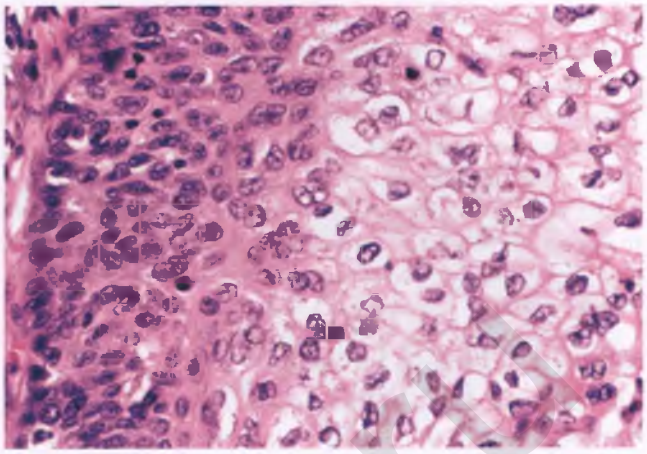

FIGURE 3.173. Warty (condylomatous) carcinoma. At higher magnification, some of the tumor cell nests are found to exhibit peripheral nuclear atypia with mitotic activity (left) and central koilocytosis (right).

Lymphoepithelioma-Like Carcinoma

Rare cervical carcinomas that bear a strong resemblance to the lymphoepitheliomatous type of nasopharyngeal carcinoma

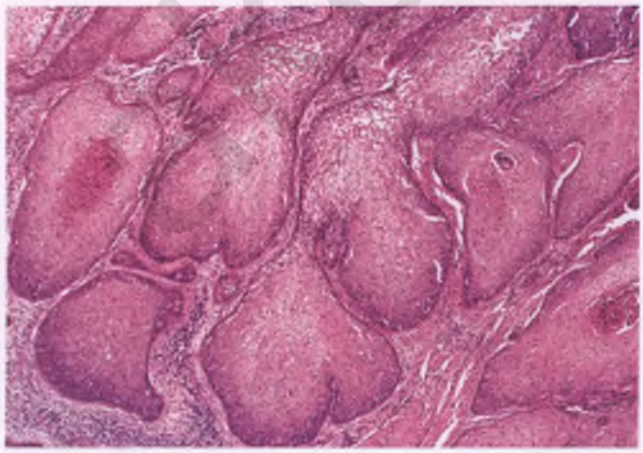

FIGURE 3.172. Warty (condylomatous) carcinoma. Confluent nests of well-differentiated squamous epithelium infiltrate the cervical stroma.

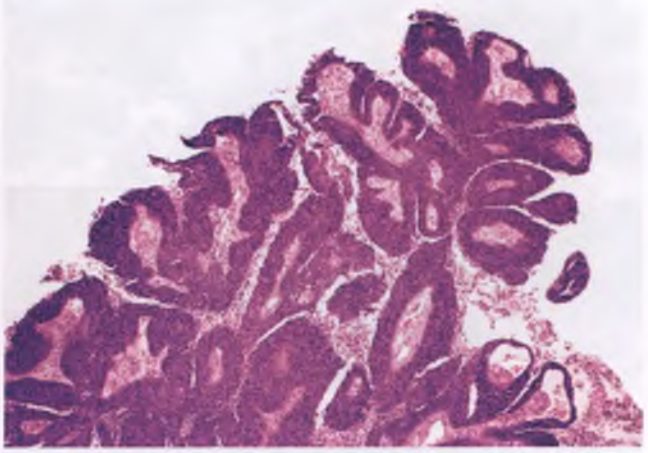

FIGURE 3.174. Papillary squamous cell carcinoma. There is no evidence of stromal invasion in this superficial portion of the tumor.

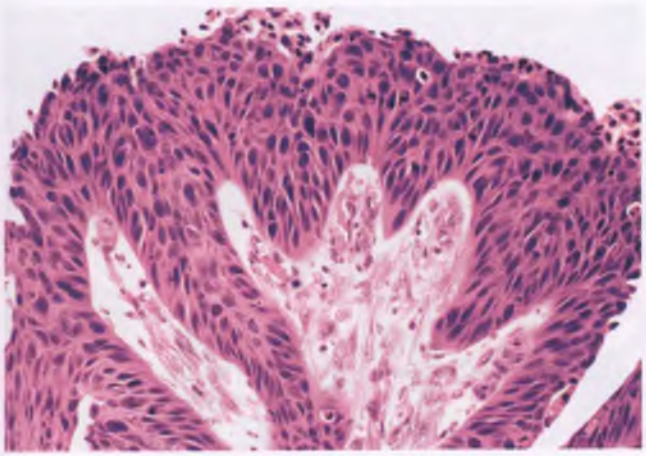

FIGURE 3.175. Papillary squamous cell carcinoma. The nuclear features resemble those seen in HSIL.

have been referred to as lymphoepithelioma-like carcinomas.[144] The malignant epithelial cells, which occur singly and in nests, have large nuclei that are uniform and vesicular with peripherally marginated chromatin, distinct nucleoli, and round to oval contours (Fig. 3.176). The cell borders are indistinct, which imparts a syncytial appearance to the nests of tumor. A prominent lymphoplasmacytic infiltrate is intimately associated with the tumor cells.

The neoplastic cells of lymphoepithelioma-like carcinoma are immunoreactive for cytokeratin and negative for leukocyte common antigen, which distinguishes this tumor from large cell lymphoma and reactive immunoblastic proliferations. Differentiating features of glassy cell carcinoma are its distinct cell membranes, abundant "ground-glass" cytoplasm, and more prominent nucleoli. Inflamed squamous cell carcinomas of the usual type will typically exhibit more nuclear pleomorphism and hyperchromaticity than lymphoepithelioma-like carcinoma, and will often show some light microscopic evidence of squamous differentiation (intercellular bridges or focal keratinization).

The Epstein-Barr virus (EBV) is presumed to play a role in the pathogenesis of the lymphoepitheliomatous type of nasopharyngeal carcinoma, but its potential role as a causative agent in the lookalike cervical tumors is controversial.[145,146] A recent study found lymphoepithelioma-like carcinomas of the cervix to be associated with high-risk HPV, and that weakly positive EBV DNA signals were due to scattered EBV-positive lymphocytes rather than to EBV-positive tumor cells.[146]

Patients with lymphoepithelioma-like carcinomas have been reported to have a better prognosis than those with the usual type of squamous cell carcinoma of the cervix.[145,146]

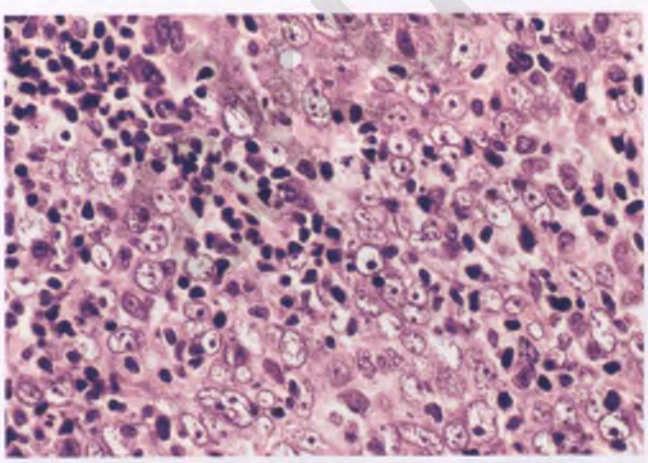

FIGURE 3.176. Lymphoepithelioma-like carcinoma. The ill-defined nests of malignant epithelial cells resemble immunoblasts from a lymphoma or florid reactive lymphoid process, and there are intermingled lymphocytes and plasma cells.

Spindle Cell (Sarcomatoid) Squamous Cell Carcinoma

Spindle cell (sarcomatoid) squamous cell carcinomas occur in the cervix on rare occasions, and typically pursue an aggressive course.[147,148] The identification of squamous differentiation (intercellular bridges and/or individual cell keratinization) in epithelioid tumor cells that blend with a malignant spindle cell component is the major diagnostic feature of tumors of this type (Fig. 3.177).

Differential Diagnosis

The differential diagnosis includes other rare entities such as cervical carcinosarcoma, leiomyosarcoma, and spindle cell melanoma.

- The transition between malignant squamous and spindle components, as well as the absence of basaloid differentiation in spindle cell carcinoma, facilitates differentiation of this tumor from most cervical carcinosarcomas. In addition, carcinosarcomas may contain heterologous elements or

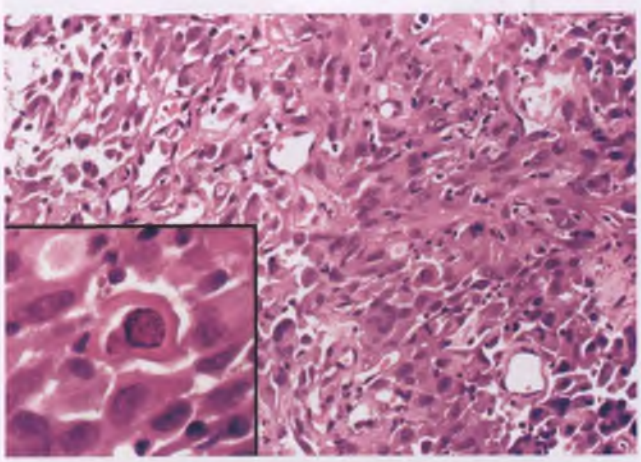

FIGURE 3.177. Spindle cell (sarcomatoid) squamous cell carcinoma. In this area of transition that contains an admixture of spindle and epithelioid cells, tumor cells with recognizable squamous differentiation are evident. The inset highlights a focus with individual cell keratinization and faint intercellular bridges; the latter are better visualized through fine focusing with a microscope.

exhibit malignant glandular differentiation, which are findings that are absent in spindle cell carcinomas. In general, strong and diffuse staining for cytokeratin within the spindle cell component favors spindle cell squamous cell carcinoma over carcinosarcoma, although immunohistochemical results need to be interpreted in the context of the histologic findings. It should be noted that separation of these tumors from one another is controversial, with some investigators considering carcinosarcoma a form of sarcomatoid carcinoma.[139]

- Leiomyosarcoma lacks an epithelial component and will typically show immunoreactivity for the muscle markers desmin and h-caldesmon.
- Spindle cell melanoma, which may be amelanotic and primary or metastatic, is also a differential diagnostic consideration when squamous differentiation is subtle or inapparent in routine sections; a panel of immunostains that includes cytokeratin and melanoma-associated markers such as S100, Melan-A, and HMB-45 should be applied in this situation.

ADENOCARCINOMA IN SITU[149,150]

AIS is causally linked to infection with high-risk HPV (usually type 18). Tissue diagnosis of AIS is typically preceded and prompted by an abnormal Pap smear. Most examples of AIS arise near the functional squamocolumnar junction and involve both the surface columnar epithelium and underlying glands (Fig. 3.178), but there are exceptions to this generalization. For example, AIS presents on rare occasions as a superficial lesion confined to the endocervical surface epithelium that may be both focal and subtle.[151] More typically, AIS involves both surface epithelium and glands in more than one quadrant and may extend for several millimeters into the endocervical canal; isolated separate foci of AIS are uncommon.[150]

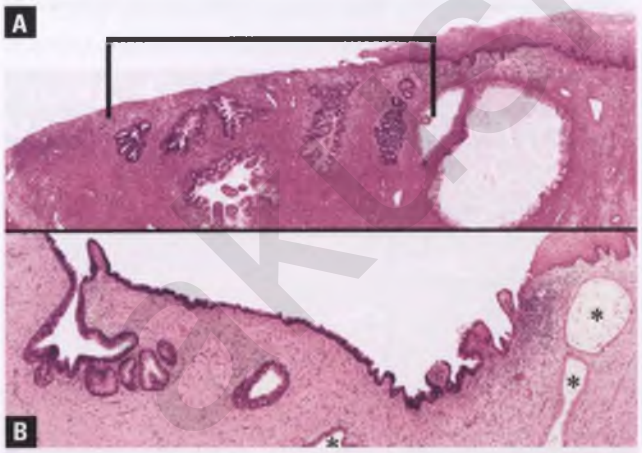

FIGURE 3.178. Adenocarcinoma in situ. **A**: This low-magnification image demonstrates the typical location of AIS (within brackets) in the superficial stroma on the glandular side of the squamocolumnar junction. Note that AIS involves preexisting glands, and that its hyperchromaticity suggests the diagnosis even at scanning magnification. **B**: In this example, AIS has replaced both the endocervical surface epithelium and some glands near the squamocolumnar junction. The asterisks mark uninvolved endocervical glands.

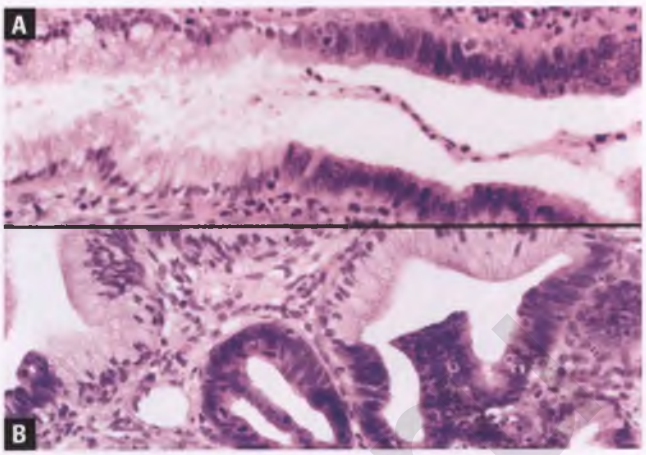

FIGURE 3.179. **A,B**: Adenocarcinoma in situ. Partial gland involvement, with an abrupt transition between involved (*dark*) and uninvolved (*pale*) gland segments, is a common finding in AIS. In **B,** the neoplastic portions of the glands in the left half of the image contain scattered juxtaluminal mitotic figures.

In contrast to invasive adenocarcinoma, the location, shape, and density of the glands involved by AIS are consistent with replacement of preexisting glands by malignant glandular epithelial cells. Partial glandular involvement is often present in AIS, which characteristically shows an abrupt transition between involved and uninvolved gland segments (Fig. 3.179). There is coexistent squamous dysplasia or squamous carcinoma in roughly 50% of cases of AIS,[150] with the vast majority of these associated squamous lesions being HSIL/CIN III (Fig. 3.180). Intraluminal micropapillary projections or cribriform structures may be seen in AIS (Fig. 3.181), and undulating gland contours can result in bud-like glandular protrusions extending into the stroma. However, most of the involved glands retain their lobulated configuration, the overall

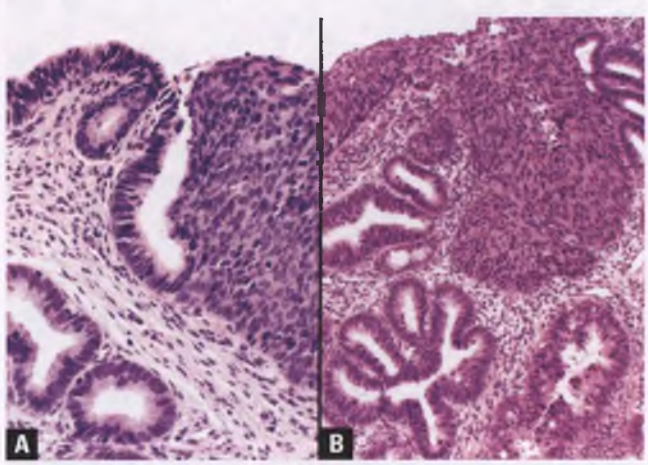

FIGURE 3.180. **A,B**: AIS with coexistent HSIL.

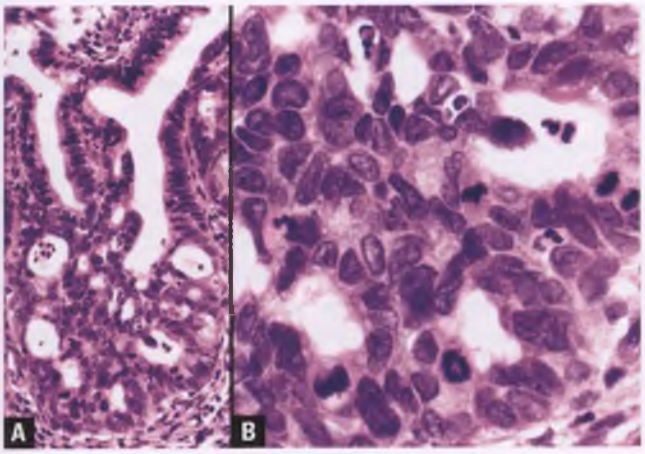

FIGURE 3.181. Adenocarcinoma in situ. **A**: AIS with a focal cribriform architecture. **B**: High-magnification view of the cribriform focus. Note the brisk mitotic activity.

pattern remains consistent with gland replacement, and the involved glands do not extend beyond the depth at which normal endocervical glands are found. The stroma surrounding glands involved by AIS remains unaltered, unless some of the superficially involved glands are coincidentally associated with inflammation related to cervicitis or biopsy-related changes.

The neoplastic cells in AIS are variably stratified or pseudostratified, with nuclei that are enlarged, oval to cigar shaped, hyperchromatic, and oriented perpendicular to the basement membrane of the glands (Fig. 3.179). Chromatin is evenly distributed with fine to moderate granularity, nucleoli are usually inconspicuous or absent, and the amount of cytoplasm is significantly diminished compared to normal endocervical cells (Fig. 3.179). Mitoses are typically easily found in AIS, and preferentially exhibit a juxtaluminal location (Fig. 3.179). Another characteristic finding of AIS is the presence of apoptotic bodies, which are shrunken, fragmented remnants of

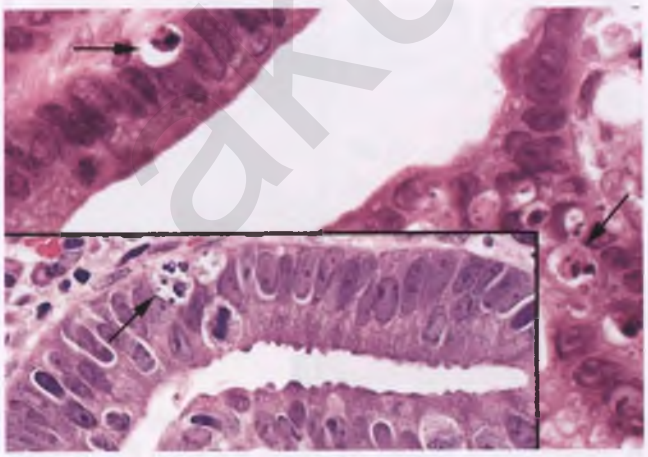

FIGURE 3.182. Adenocarcinoma in situ. Apoptotic bodies are marked by *arrows*. The lesion within the inset is unusual in that distinct nucleoli are visible and the chromatin is pale.

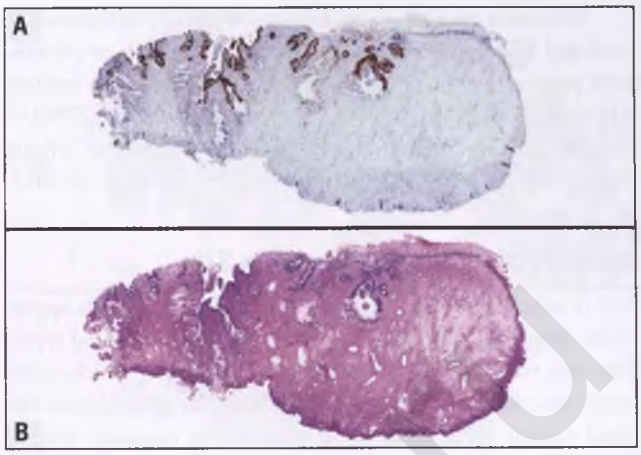

FIGURE 3.183. p16 immunoreactivity in AIS. **A**: This whole mount view demonstrates intense p16 immunoreactivity that is limited to foci of AIS involving surface epithelium, glands, and portions of glands. **B**: Serial whole mount section (H&E stain). Note the correlation between the darkly stained glands of AIS and the p16-positive glands. (p16 immunostain courtesy of Dr. Steve Kargas.)

agglutinated chromatin and cytoplasmic debris, often incorporated into a phagocytic vacuole with a peripheral clear zone (Fig. 3.182).[152,153] Apoptotic bodies need to be distinguished from intraepithelial lymphocytes and neutrophils, both of which can also be surrounded by a clear space.[152]

Although immunostains are rarely necessary for diagnostic purposes, AIS typically demonstrates diffuse and strong immunoreactivity for p16 (Figs. 3.183 and 3.184A) and a Ki-67 proliferative index as assessed with the MIB-1 antibody of >30% (Fig. 3.184B).[6,154,155]

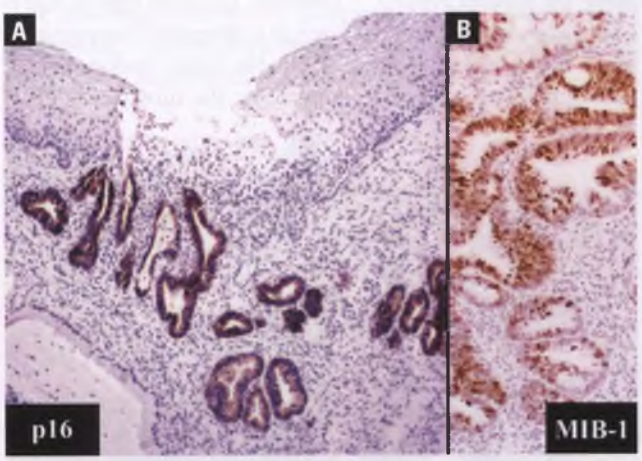

FIGURE 3.184. p16 and MIB-1 immunoreactivity in AIS. **A**: Most glands involved by AIS exhibit strong nuclear and cytoplasmic immunoreactivity for p16, whereas normal endocervical glands and squamous epithelium are nonreactive. **B**: AIS typically has a high Ki-67 proliferative index, as indicated by the strong nuclear staining reaction of many of the lesional cells with the MIB-1 antibody. (p16 immunostain courtesy of Dr. Steve Kargas.)

Whenever possible, the margin status should be reported in cone and LEEP specimens containing AIS, since those patients with positive margins have a higher risk of harboring residual AIS than do patients with negative margins (59% vs. 27%),[150] and are also at risk for an invasive adenocarcinoma lurking deeper within the unsampled portion of the endocervical canal.

Variants of Adenocarcinoma In Situ

AIS is subclassified into two variants that occur with appreciable frequency: the usual (endocervical) and intestinal types. The vast majority of cases are of the usual type, which is the entity described in the preceding section. The cytoplasm in the usual variant often gives the impression in routinely stained sections that at least some intracytoplasmic mucin is present, although mucin stains yield variable results.

The intestinal type of AIS is recognized by the presence of goblet cells (Fig. 3.185), which may also be accompanied by argentaffin and Paneth cells. Intestinal-type AIS is typically admixed with AIS of usual type and rarely, if ever, occurs in pure form.[156] Although most cases share the cytokeratin-7 positive, cytokeratin-20 negative, CEA positive, and p16 positive immunophenotype of usual-type AIS, intestinal-type AIS is much more likely than usual-type AIS to express the intestinal marker CDX2.[156] A diagnosis of intestinal metaplasia of the uterine cervix should be met with a heavy dose of skepticism, since the compressed nuclei of the goblet cells in intestinal-type AIS often do not show appreciable cytologic atypia and could easily be confused with intestinal metaplasia.[156]

The so-called endometrioid type of AIS is defined as showing more pronounced nuclear stratification than the usual variant and having scant cytoplasm that is devoid of stainable mucin (some investigators allow a "small amount" of stainable mucin along the luminal border).[149] However, the usual type of AIS is also mucin depleted and can have an endometrioid appearance, often being virtually indistinguishable from "endometrioid" AIS in routinely stained sections. Since the subtype of AIS is irrelevant from a biologic and clinical standpoint at the current time, performance of mucin stains in an attempt to help make this distinction would be an academic exercise, and would also be subject to sampling error and differences in interpretation. Until the endometrioid variant of AIS can be more precisely defined and shown to have some relevant difference from the usual type of AIS, it is recommended that AIS with endometrioid-like features be included under the umbrella of the usual variant.

Other rare variants of AIS include ciliated (tubal) AIS[4] (distinction from atypical tubal metaplasia is discussed in the section on tubal metaplasia), serous AIS,[157] stratified mucin-producing intraepithelial lesion (SMILE), and adenosquamous CIS. SMILE resembles HSIL, except that there are scattered foci with cytoplasmic vacuoles or clearing related to the presence of mucin (Fig. 3.186).[158] It is uncertain whether these rare lesions should be considered a form of adenosquamous CIS (Fig. 3.187) or a stratified variant of AIS. SMILEs are often seen in association with conventional AIS and HSIL, and associated invasive neoplasms are most frequently of adenosquamous type. Although occasional HSILs may have a layer of residual mucinous epithelial cells on their surface, they do not demonstrate the SMILE attribute of mucin-containing cells throughout various levels of the epithelium. The presence of dysplastic epithelial cells and a high Ki-67 proliferative index helps to differentiate SMILE from immature squamous metaplasia. Since SMILE is a rare entity and its moniker does not convey its high-grade nature, it is recommended that such lesions be diagnosed as "unusual in situ carcinoma with a component of glandular differentiation (so-called SMILE)."

Cytologic Diagnosis of Adenocarcinoma In Situ

In Pap smears, AIS is recognized by a constellation of features. Architecturally, classic examples present as HCGs with nuclear overlapping, feathered edges, peripheral palisading, microacini/

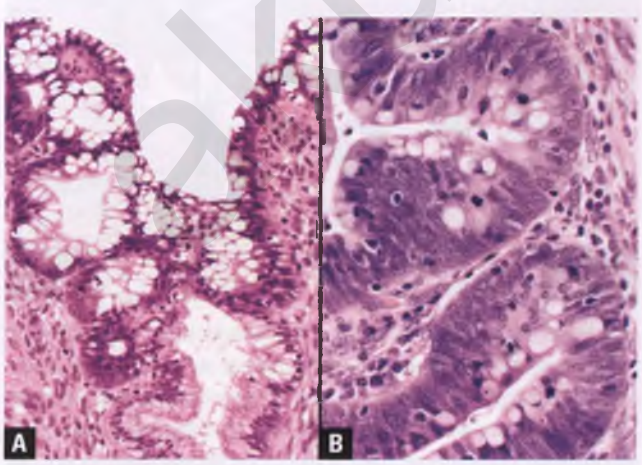

FIGURE 3.185. **A,B**: AIS, intestinal type, with numerous goblet cells. In **A**, there is partial gland involvement.

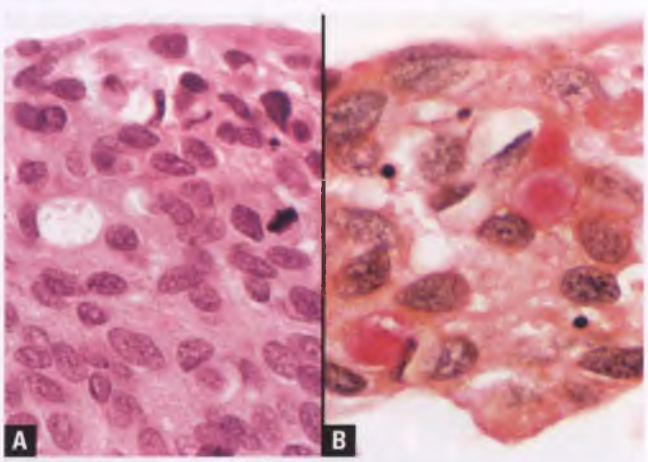

FIGURE 3.186. Stratified mucin-producing intraepithelial lesion. **A**: Intracytoplasmic vacuoles are present in a lesion that otherwise resembles HSIL. **B**: A mucicarmine stain confirms that some of these vacuoles contain mucin. This particular lesion was associated with an invasive adenosquamous carcinoma.

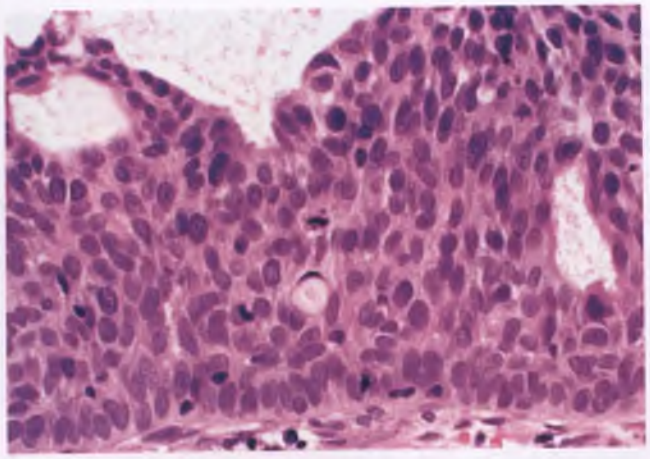

FIGURE 3.187. Adenosquamous carcinoma in situ. This very rare lesion resembles HSIL, but also exhibits intraepithelial glandular formations.

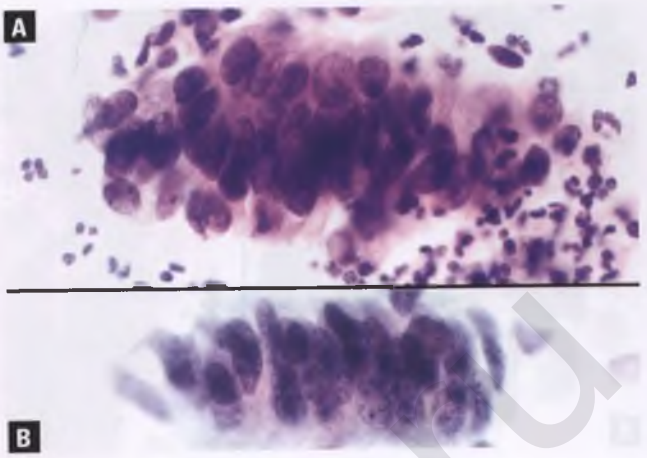

FIGURE 3.189. **A,B:** AIS (conventional Pap smears). Short strips of columnar epithelial cells with nuclear atypia, crowding, palisading, pseudostratification, and feathering are characteristic of AIS.

rosettes, and loss of the normal honeycomb pattern (Fig. 3.188).[159] Epithelial strips with crowded, overlapping, palisaded, pseudostratified nuclei are also often present (Fig. 3.189), and may show preferential congregation of nuclei toward the side opposite the luminal border of the strip. Feathered edges refer to varying degrees of protrusion of radially oriented, elongated nuclei and/or cytoplasmic tags along the edges of cell groups, which results in an uneven picket fence appearance rather than a smooth border (Fig. 3.190). Microacini are miniature gland formations (Fig. 3.191A), whereas rosettes in this context are gland-like structures composed of small, circular groups of cells that are radially arranged around central spaces (Fig. 3.190). The presence of large cytoplasmic vacuoles suggests goblet cell differentiation due to a component of AIS of the intestinal type (Fig. 3.191B).

The nuclei of AIS are enlarged, hyperchromatic, and oval to cigar shaped. They have absent to inconspicuous nucleoli and evenly distributed chromatin that varies from finely to moderately granular. The elongated shape of the neoplastic nuclei is best appreciated at the periphery of the cell groups where the cells lie flat (nuclei viewed *en face* within the center of these groups appear more rounded). Mitoses and apoptotic bodies may be seen. In liquid-based preparations, the crowded cell groups are more three-dimensional, the architectural clues of AIS (feathering, cell strips, and rosettes) may be more subtle, the chromatin pattern may be more open, and nucleoli may be more visible (Fig. 3.192).

Features that are helpful in distinguishing AIS in Pap smears from tubal metaplasia, abraded cells from the lower uterine segment, CIS with endocervical gland involvement, and invasive endocervical adenocarcinoma are discussed elsewhere in this chapter.

Differential Diagnosis

The histologic differential diagnosis of AIS includes tubal metaplasia, tuboendometrioid metaplasia, endometrioid metaplasia, endometriosis, reactive glandular atypia, ASR,

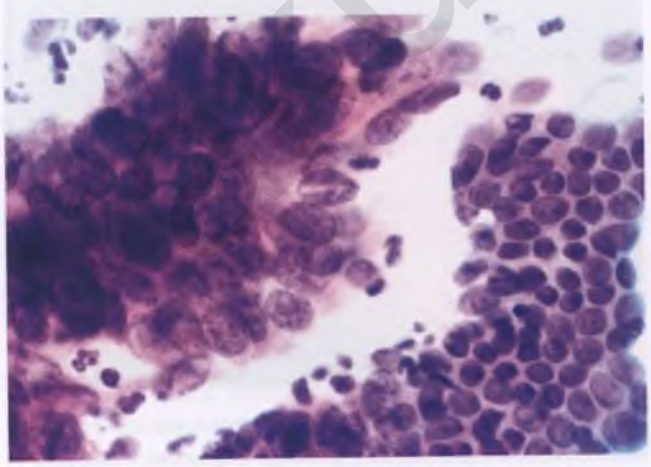

FIGURE 3.188. AIS (conventional Pap smear). Compare the nuclear and architectural features of AIS on the left with the sheet of normal endocervical cells on the right.

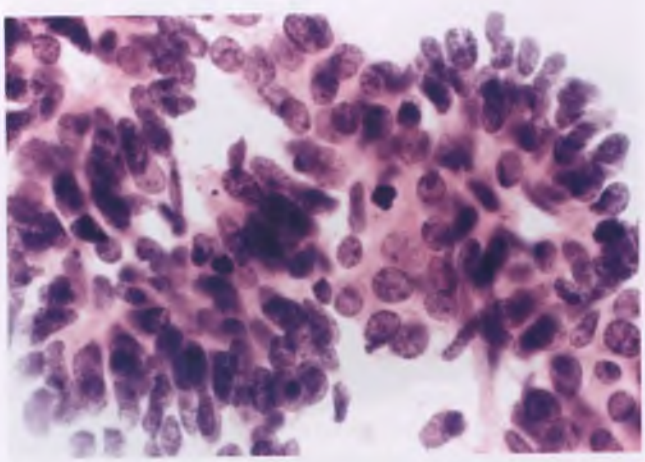

FIGURE 3.190. AIS (conventional Pap smear). Feathered edges are prominent in the upper right and lower left portions of this image. Some ill-defined rosette-like structures are also present.

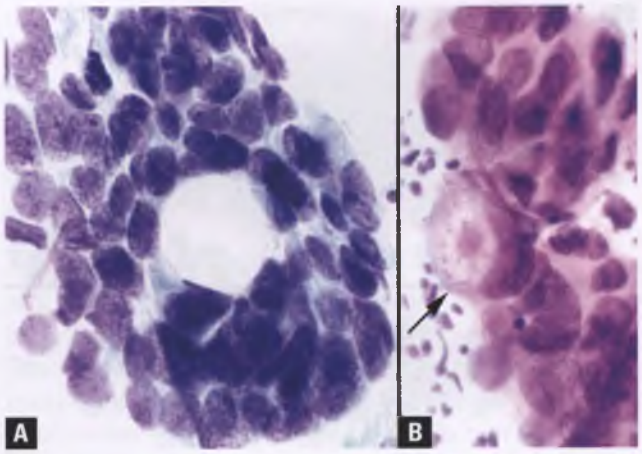

FIGURE 3.191. AIS (conventional Pap smears). **A,B**: A central microacinar structure is present. **B**: The presence of the cell with a large intracytoplasmic vacuole compressing its nucleus to the periphery (*arrow*) suggests goblet cell differentiation related to a component of intestinal-type AIS.

hematoxylin overstaining artifact, mesonephric ductal hyperplasia, dysplastic glandular changes that fall short of AIS (so-called endocervical glandular dysplasia [EGD]), and early invasive adenocarcinoma.

In the differential diagnosis with nondysplastic glandular lesions, AIS is distinguished by nuclear atypia that is contiguous and monotonous rather than patchy and variable, a high mitotic rate, readily apparent apoptotic bodies, and positive immunostaining with MIB-1 and p16 as previously described. Preliminary results suggest that lack of immunoreactivity of AIS for PAX2 can also be helpful in distinguishing it from benign mesonephric and müllerian glandular lesions, nearly all of which express PAX2.[160]

EGD[149] is a controversial and poorly reproducible entity that may not even exist.[150,152] The lower end of the spectrum of EGD cannot reliably be distinguished from tuboendometrioid metaplasia or reactive atypia, whereas the higher end of the spectrum is indistinguishable from AIS. If low-grade EGD were truly a precursor of AIS, then it should contain HPV-DNA, but this has rarely been shown to be the case.[161] Given the uncertainty surrounding the diagnostic criteria, biologic behavior, treatment, and existence of EGD, its use as a diagnostic term should be avoided.

Distinction of AIS from early invasive adenocarcinoma is discussed in the section on microinvasive adenocarcinoma.

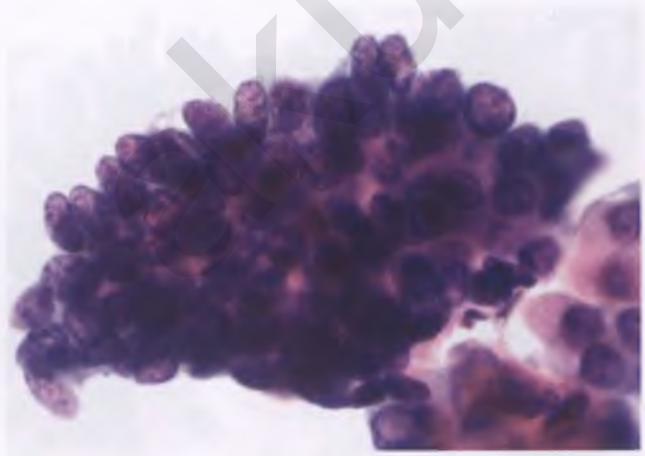

FIGURE 3.192. AIS (liquid-based Pap smear). This crowded, three-dimensional group of atypical glandular cells exhibits feathering and palisading along its top edge.

INVASIVE ADENOCARCINOMA AND ITS VARIANTS

The various types of adenocarcinoma account for approximately 20% of invasive cervical carcinomas. As is true for AIS, the vast majority of adenocarcinomas are associated with high-risk HPV types, especially type 18. Typical patients are approximately 50 years old and present with abnormal vaginal bleeding and/or an abnormal Pap smear. Grossly, the tumors may be polypoid, papillary, nodular, diffusely infiltrative, or ulcerated (Fig. 3.193). In a minority of cases, the tumor may not be appreciated grossly or the findings may be subtle (Fig. 3.194).

The subtypes of endocervical adenocarcinoma are described below. If at least 10% of a tumor consists of a subtype that is different from the dominant tumor type, the tumor is designated a mixed carcinoma, with an indication as to the approximate proportions of each subtype. There are considerable differences in the estimated frequencies of usual versus endometrioid endocervical adenocarcinoma, which relates to the inherent subjectivity in distinguishing these subtypes. I concur with Dr. Young's approach, which considers the common form of endocervical adenocarcinoma that contains little or no intracytoplasmic mucin to be of "usual" rather than endometrioid type.[162,163]

FIGURE 3.193. Invasive endocervical adenocarcinoma. This deeply invasive, nodular tumor has been sectioned longitudinally. Hemorrhage in the superficial portion of the tumor is related to a previous biopsy. The vaginal cuff is at lower left, and portions of the tumor-stromal interface are marked with *arrowheads*.

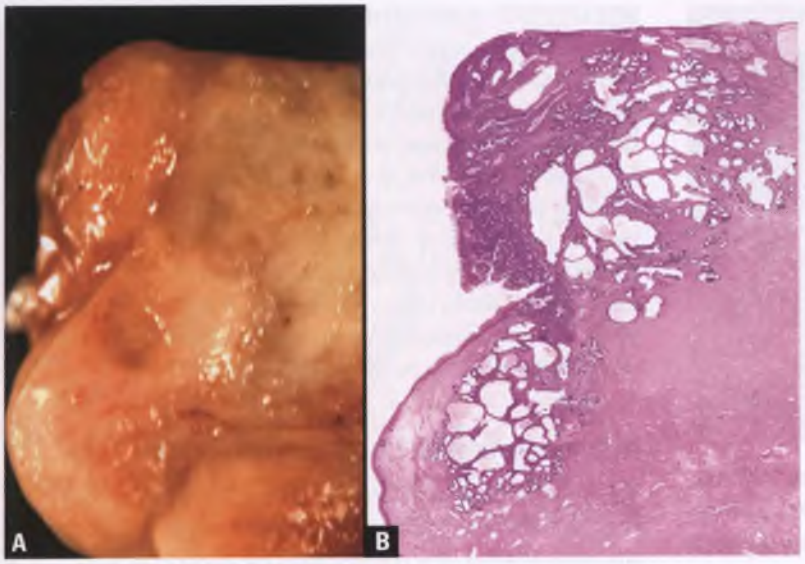

FIGURE 3.194. Invasive endocervical adenocarcinoma of usual type with a prominent microcystic pattern. **A**: The gross findings in the microcytic areas are subtle. **B**: This corresponding whole mount section demonstrates the large areas of invasive adenocarcinoma.

Microinvasive Adenocarcinoma[150,164,165]

It can be difficult and subjective to distinguish examples of AIS from AIS associated with microinvasive adenocarcinoma. The definition of microinvasion is the same as that used for squamous cell carcinoma. For the SGO, microinvasion indicates a depth of invasion of ≤3 mm and an absence of angiolymphatic invasion. In contrast, the FIGO 2008 revised staging system for carcinoma of the cervix has reaffirmed its prior policy of subdividing microinvasive adenocarcinomas according to whether the depth of invasion is ≤3 mm (stage Ia1) or >3 mm but ≤5 mm (stage Ia2).[129] For both FIGO stages, the tumor must be detected only microscopically rather than clinically, and its width must also be ≤7 mm; angiolymphatic invasion is reported but does not alter staging in this system. Since merely recognizing microinvasion is difficult, it is not surprising that measuring the depth of invasion from the basement membrane of the originating epithelium to the deepest point of invasion is a subjective exercise. As a practical matter, the thickness of the tumor, which is measured from the basement membrane of the overlying surface epithelium to the deepest point of invasion, is a more reproducible measurement and is often used for staging purposes.[166]

In a minority of microinvasive cases, invasion is recognized by (a) incomplete, malignant-appearing glands budding off of AIS or (b) small malignant glands, small aggregates of tumor cells, and/or individual malignant cells within the stroma in the immediate vicinity of AIS (Fig. 3.195). In these situations, there is usually an associated stromal reaction that may take the form of desmoplasia and/or chronic inflammation and edema. The microinvasive tumor cells may acquire more abundant, eosinophilic cytoplasm and exhibit nuclear alterations such as enlargement, rounding, chromatin clearing, and nucleolar prominence.

In most cases of early invasion, malignant glands are recognized as infiltrative by architectural abnormalities within AIS-like glands that are best appreciated at low magnification, such as (a) marked complexity of numerous crowded glands with a diffuse rather than lobular growth pattern, (b) glandular confluence, (c) formation of expansile, smooth-contoured, macroglandular structures with complex internal architecture that features cribriform and/or villous formations, and/or (d) neoplastic glands extending into the cervical stroma, beyond the level of normal endocervical glands or adjacent areas of AIS (Figs. 3.196 and 3.197). Although a periglandular stromal reaction is helpful in recognizing invasion, it is absent, subtle, or focal in a significant proportion of cases of this type. Additional findings that may be present that would corroborate

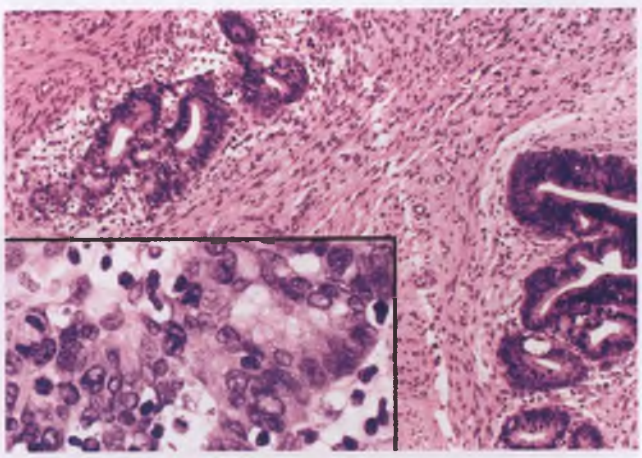

FIGURE 3.195. Microinvasive adenocarcinoma is present within the cluster of glands in the upper left corner. The inset shows the invasive portion of these glands at high magnification. Note the chronic inflammation and edema in the invasive focus, and the associated nuclear changes (chromatin clearing, rounding, and nucleolar prominence). A focus of AIS is at right.

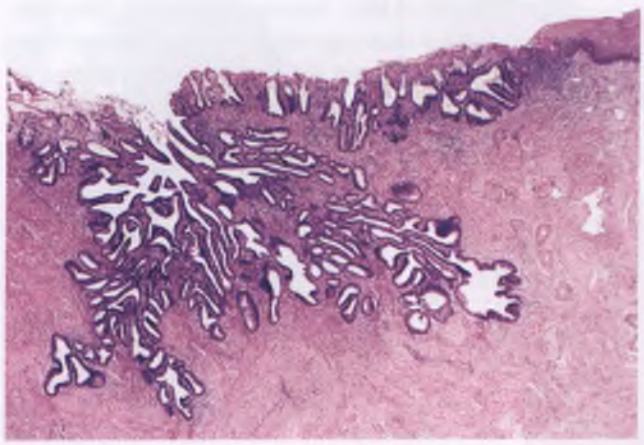

FIGURE 3.196. Microinvasive endocervical adenocarcinoma. A tongue of invasive adenocarcinoma is seen extending into the cervical stroma with more superficial foci of AIS on both sides. Although the stromal reaction to the invasive component is inconspicuous, the architecture of the glands is indicative of invasion (crowded glands that are nearly confluent that would not be consistent with replacement of preexisting glands).

stromal invasion include neoplastic glands in close proximity to thick-walled blood vessels (Fig. 3.198)[167] and angiolymphatic invasion.

Patients with microinvasive endocervical adenocarcinomas have an excellent prognosis, with a long-term survival of >98%.[168] Since the rate of pelvic lymph node metastases is approximately 1%, which is significantly lower than the rate of lymphadenectomy-related lymphedema, the routine use of lymph node dissections in patients without angiolymphatic invasion has been called into question.[166]

Rarely, endocervical adenocarcinomas are found in association with low-grade mucinous or endometrioid-appearing ovarian tumors with features that suggest a shared etiology related to HPV.[169,170] Some of these endocervical adenocarcinomas are superficially invasive and would qualify for microinvasive adenocarcinomas that would ordinarily be expected to have an excellent prognosis, and a few even represent AIS.[171] However, their shared expression of identical high-risk HPV types and p16 immunoreactivity have led to the interpretation that the ovarian tumors are metastases from the cervical adenocarcinomas.[169–171] The use of circumstantial HPV-related evidence to trump a lengthy list of more traditional features that are more in keeping with dual primary tumors has generated some controversy,[172,173] as discussed in more detail in the section on cervical carcinoma metastatic to the ovary in Chapter 7.

Adenocarcinoma, Usual (Endocervical) Type

The usual type of endocervical adenocarcinoma accounts for roughly 80% of endocervical adenocarcinomas.[163] In some classification systems, it is referred to as the endocervical variant of mucinous adenocarcinoma, although mucin is often absent or inconspicuous. In most cases, the individual glands are well formed and resemble AIS in their moderate degree of nuclear atypia, numerous mitotic figures with a predilection for a juxtaluminal location, and scattered apoptotic bodies (Fig. 3.199). Although there is a tendency to classify such tumors as well differentiated, Dr. Young cautions that these lesions are full-fledged malignancies, most of which he would categorize as moderately differentiated.[162,163] Some cases with well-formed glands exhibit more significant nuclear atypia, manifested by nuclear rounding, chromatin clearing, and prominent nucleoli. Poorly differentiated adenocarcinomas with these nuclear features combined with a more solid architecture occur, but are uncommon (Fig. 3.200).

The infiltrative pattern of stromal invasion is characterized by haphazardly and diffusely distributed malignant glands that often have irregular angulations or branches (Fig. 3.201). These glands may be closely packed or widely spaced from one another. The macroglandular (expansile) pattern of invasion features

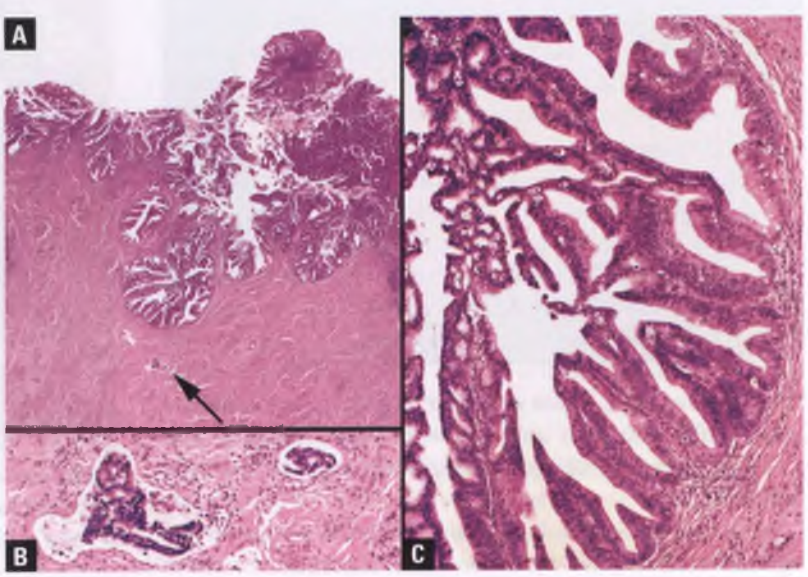

FIGURE 3.197. Endocervical adenocarcinoma with a macroglandular (expansile) pattern of invasion. **A**: Deep to a superficially invasive macrogland, there is a focus of angiolymphatic invasion (*arrow*). **B**: The angioinvasive focus is highlighted in this image. **C**: The internal architecture of the invasive macroglands consists of villous and cribriform structures. Although microinvasive in terms of depth of invasion, this tumor had a horizontal extent of 2 cm and was associated with a pelvic lymph node metastasis.

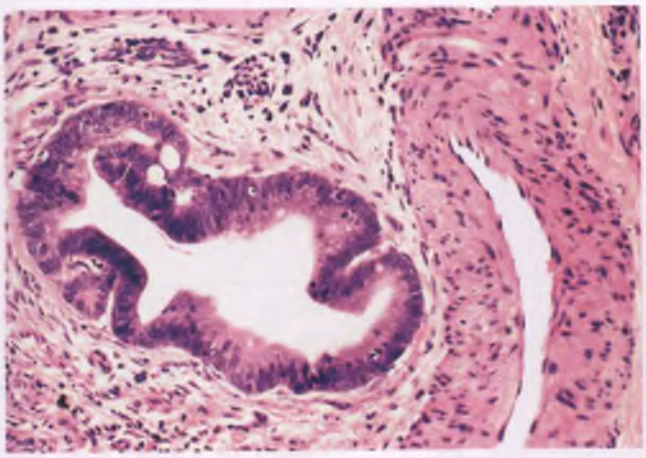

FIGURE 3.198. Endocervical adenocarcinoma. The presence of neoplastic glands adjacent to thick-walled blood vessels is supportive evidence of stromal invasion.

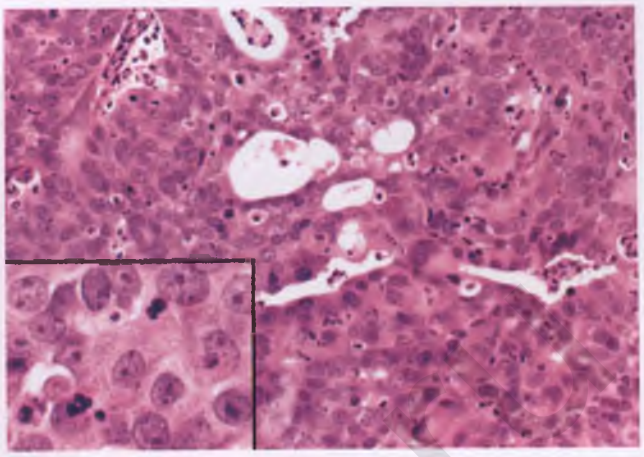

FIGURE 3.200. Poorly differentiated invasive endocervical adenocarcinoma of usual type. The tumor exhibits sheet-like growth punctuated by occasional glandular structures.

large, rounded, architecturally complex glands with internal villous and cribriform structures (Fig. 3.202).[164,165] As illustrated in the section on microinvasive adenocarcinoma, this pattern may be difficult to distinguish from AIS when superficial (Fig. 3.197). Although a stromal response is helpful in confirming invasion and may be primarily inflammatory (Fig. 3.203) or fibroblastic (Fig. 3.204), it is often subtle or absent.

The usual type of endocervical adenocarcinoma may contain a variable number of papillary or villous structures projecting from the surface of the tumor (Fig. 3.205). In these cases, the degree of nuclear and architectural atypia is beyond that which is seen in well-differentiated villoglandular adenocarcinoma, but falls short of that present in serous carcinoma. In another unusual pattern, variably dilated neoplastic glands form microcystic structures that can be mistaken for tunnel clusters or other benign endocervical glandular lesions, especially when there is pressure-related atrophy or denudation of the neoplastic epithelium lining the cystic spaces (Figs. 3.194 and 3.206).[174]

In addition to tunnel clusters and the variants of carcinoma mentioned in the preceding paragraph, the histologic differential diagnosis of the usual type of endocervical adenocarcinoma includes MGH, AIS, and cervical endometrioid adenocarcinoma. The distinguishing features of these entities are discussed elsewhere in this chapter. In addition, distinction of endocervical from endometrial adenocarcinoma has received much attention in the literature, and is discussed shortly.

Cytologic Features of Endocervical Adenocarcinoma, Usual Type

In Pap smears, the most common feature of endocervical adenocarcinoma is the presence of numerous clusters of cells with enlarged, crowded nuclei that are haphazardly arranged and overlapping (Fig. 3.207). There is considerable variability from case

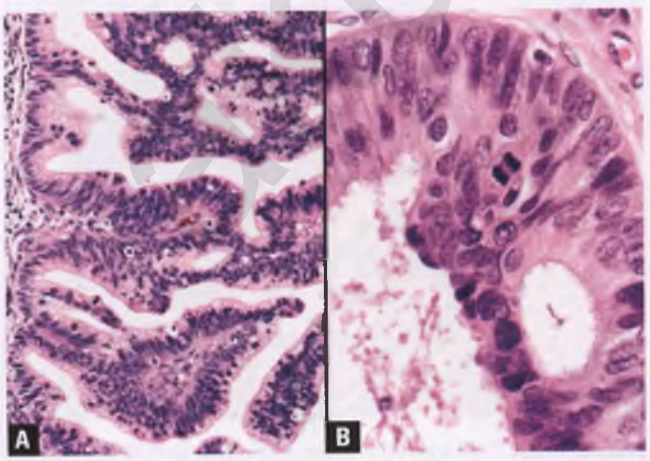

FIGURE 3.199. **A,B**: Endocervical adenocarcinoma of usual type. Well-formed glandular structures, moderate nuclear atypia, and brisk mitotic activity are typical.

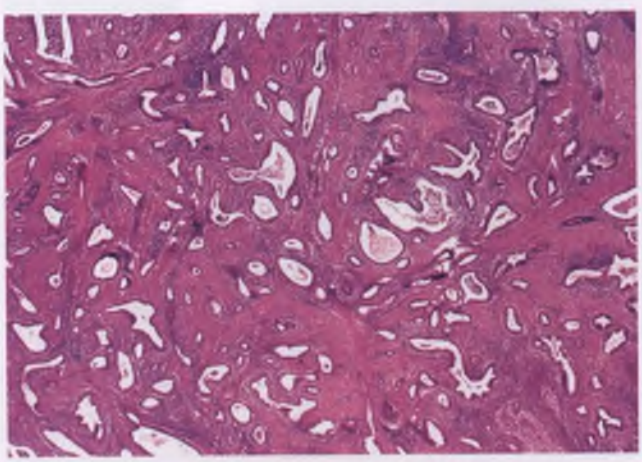

FIGURE 3.201. Endocervical adenocarcinoma of usual type with infiltrative pattern of stromal invasion.

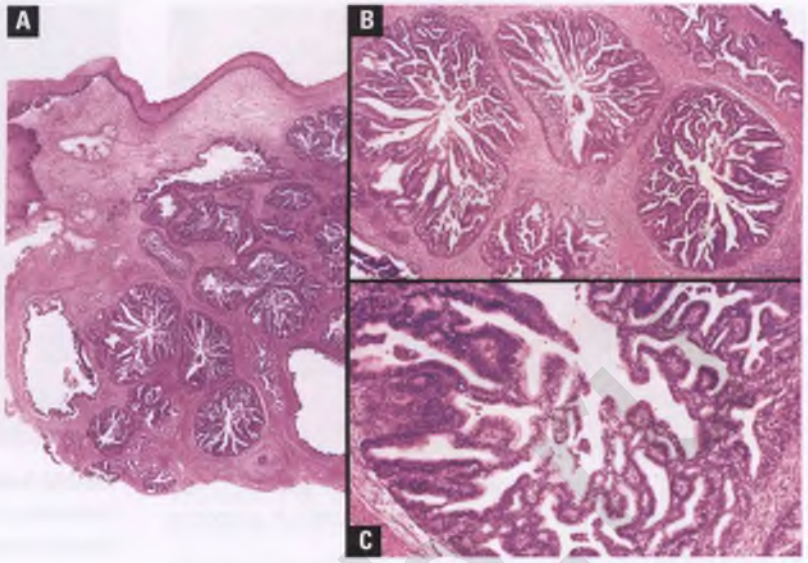

FIGURE 3.202. Endocervical adenocarcinoma of usual type with a macroglandular (expansile) pattern of invasion. **A**: Although well-circumscribed and associated with little to no stromal response, the architecural complexity of the glands, their large size, and their location deep within the cervical stroma all support an invasive process. **B,C**: The macroglandular structures have an internal villous and cribriform architecture.

to case in chromatin pattern, degree of nucleolar prominence, extent of nuclear contour abnormalities, mitotic rate, formation of rosettes/microacini, amount of cytoplasm, cytoplasmic vacuolization, and extent of tumor diathesis. However, within a given case, the nuclear features are more monomorphous than what is typically encountered in reactive endocervical processes.

In liquid-based preparations, the three-dimensional nature of the cell clusters can make it difficult to impossible to visualize cells that are centrally located, but nuclear detail at the periphery is well preserved (Fig. 3.208). Assessment of cells that border the "white spaces" will often reveal chromatin that appears more open or cleared than it does in conventional Pap smears, which also results in more readily apparent nucleoli. As in liquid-based preparations of squamous carcinoma, the tumor diathesis resembles blue-green cotton candy and may cling to the neoplastic cell groups.

There is some overlap in the cytologic features of AIS and invasive endocervical adenocarcinoma. Features favoring the latter include the presence of a tumor diathesis, a chromatin pattern that is open or unevenly distributed, and the presence of prominent nucleoli. In distinguishing endocervical from endometrial adenocarcinoma in Pap smears, the major features that favor an endocervical origin are a premenopausal rather than postmenopausal patient and the presence of abundant, well-preserved neoplastic cells (directly sampled from the endocervix) rather than a few groups of often degenerated neoplastic cells (spontaneously shed from the endometrium).

Differential Diagnosis with Endometrial Adenocarcinoma

It can be difficult to distinguish usual endocervical from endometrioid endometrial adenocarcinoma in biopsy and curettage material, and rarely even within hysterectomy specimens when tumors straddle the lower uterine segment and upper

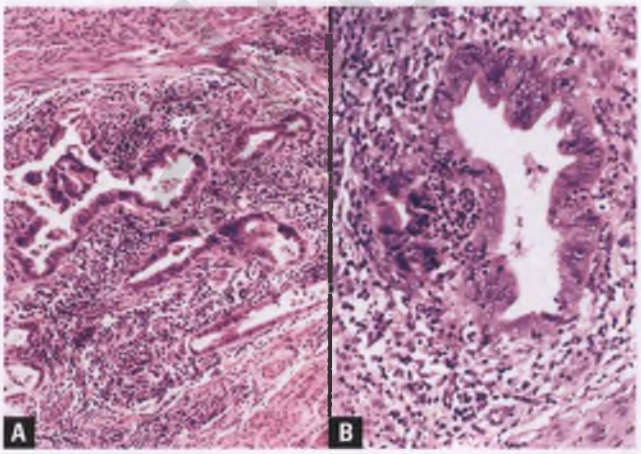

FIGURE 3.203. **A,B**: Endocervical adenocarcinoma with inflammatory and edematous stromal reaction to infiltrating glands.

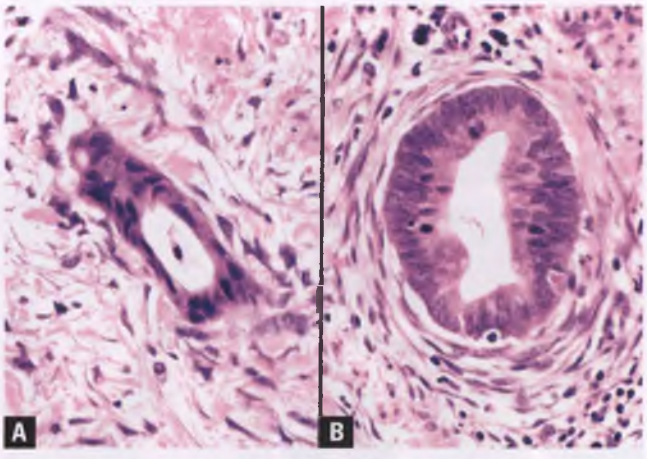

FIGURE 3.204. Endocervical adenocarcinoma with a fibroblastic stromal reaction. **A**: Fibroblasts are embedded in a loose, edematous stroma surrounding the infiltrating gland. **B**: Fibroblasts are concentrically arranged around the invasive gland.

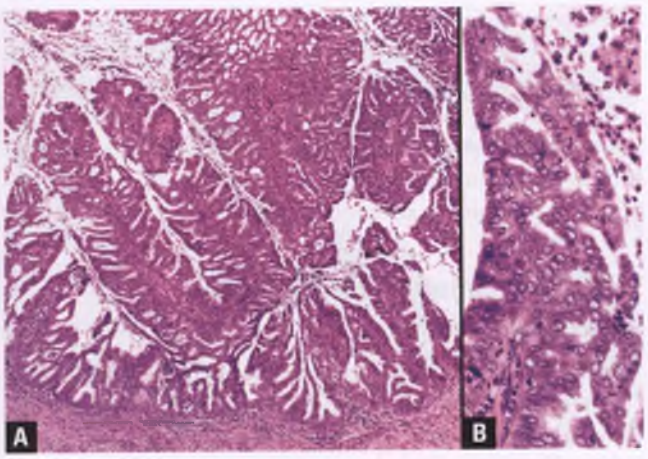

FIGURE 3.205. **A,B**: Foliaceous exophytic surface growth of endocervical adenocarcinoma of usual type. Stromal invasion is not present in these images, but was demonstrated in other sections. Although serous carcinoma is a consideration, it features arborizing papillae of greater thickness, prominent epithelial tufting, more numerous mitoses, and higher nuclear grade.

endocervical canal.[175] There are some significant differences in the initial and adjuvant treatment options for endocervical and endometrial adenocarcinoma, so this distinction is clinically relevant.[175,176]

In the vast majority of potentially problematic cases in which an adenocarcinoma is present in both the endocervical and endometrial portions of a fractional curettage, the distinction between endocervical and endometrial adenocarcinoma can be made by evaluating a combination of clinical and histologic parameters.[162,177] These include (a) statistical aspects of these tumors: endometrial adenocarcinoma occurs at an older age (mean age of 60 years vs. mean age of 50 years for endocervical adenocarcinoma), is roughly three times more common

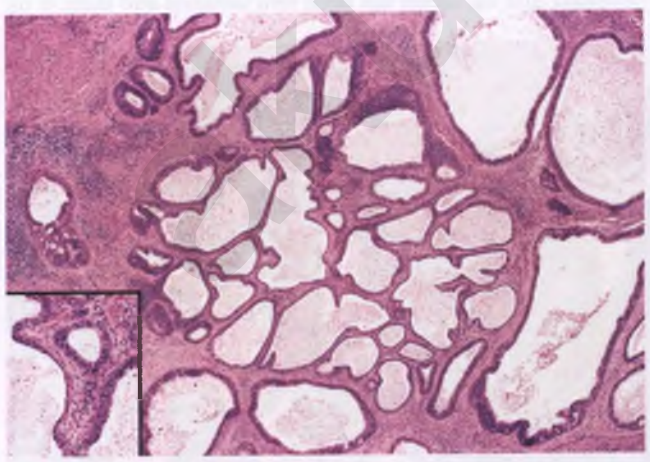

FIGURE 3.206. Endocervical adenocarcinoma with a microcystic pattern. Note how the central portion of this tumor resembles a tunnel cluster. The inset highlights a focus with epithelial flattening due to pressure atrophy.

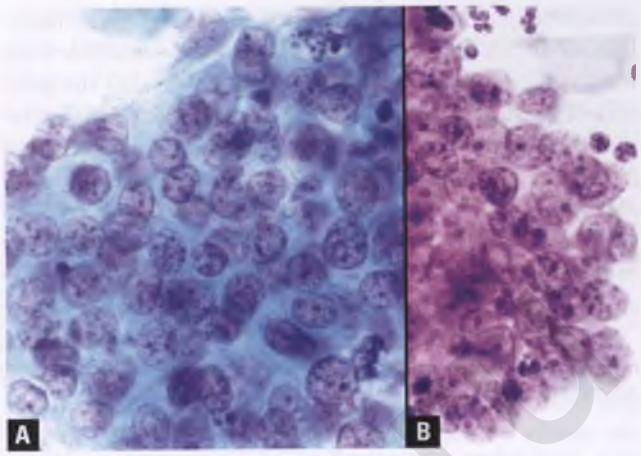

FIGURE 3.207. **A,B**: Invasive endocervical adenocarcinoma in two different conventional Pap smears. The nuclei are monotonous, crowded, and overlapping. In **A**, there is some mitotic activity and a microacinar structure is present at the top left of the cell group.

than endocervical adenocarcinoma,[176] involves the cervix in approximately 20% of cases[178] (endocervical adenocarcinoma is rarely associated with significant involvement of the endometrial cavity),[179] and is highly unlikely to coexist with a separate primary endocervical adenocarcinoma; (b) location of the dominant mass, as determined via variable combinations of hysteroscopy, colposcopy, and the relative amounts of tumor in the endometrial and endocervical portions of the fractional curettage; (c) the presence of subtle differences in histologic appearance between the usual type of endocervical adenocarcinoma and the usual (endometrioid) type of endometrial adenocarcinoma, with the former typically containing more

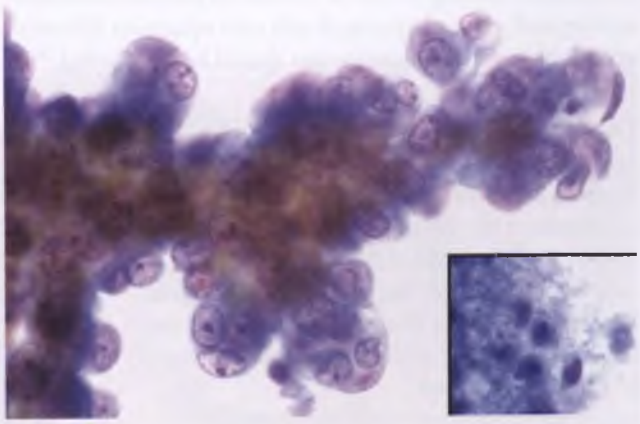

FIGURE 3.208. Invasive endocervical adenocarcinoma in liquid-based Pap smear. The protruding, rounded nubbins of neoplastic cells are indicative of glandular differentiation. Note that the central core of cells is thick and not interpretable, but many of the well-visualized cells along the periphery exhibit chromatin clearing and distinct nucleoli. The inset shows the granular necrotic debris of a tumor diathesis that was present elsewhere in the smear.

numerous apoptotic bodies in association with frequent juxtaluminal mitotic figures (generally useful, but not infallible since there is some overlap in histologic appearance); (d) the presence of associated squamous (particularly morular) differentiation and stromal foam cells, which are much more commonly present in endometrioid endometrial adenocarcinoma than they are in endocervical adenocarcinoma; (e) the presence of associated atypical endometrial hyperplasia, which would favor endometrial adenocarcinoma; and (f) the presence of associated AIS, which would favor endocervical adenocarcinoma.

In endocervical curettage specimens with documented adenocarcinoma invading cervical stroma, the definitive distinction between endocervical and endometrial adenocarcinoma can usually be deferred to the resection specimen. This is because the initial surgical treatment of endocervical and endometrial cancer with invasion of cervical stroma is generally the same, with radical hysterectomy (en bloc resection of the uterus with associated parametrium and at least 2 cm of the upper vagina) often being the treatment of choice in those patients who can tolerate an aggressive surgical approach.[180,181]

For those ambiguous cases in which distinction between endocervical adenocarcinoma of usual or endometrioid type and endometrioid endometrial adenocarcinoma would provide clinically useful information, ancillary studies can be helpful. Diffuse, strong staining with p16 and/or ProExC, detectable HPV-DNA, vimentin negativity, CEA positivity, and estrogen/progesterone receptor negativity favor endocervical adenocarcinoma, whereas negative or focal staining for p16, ProExC, and CEA, undetectable HPV-DNA, and positive immunoreactivity for vimentin and estrogen/progesterone receptors favor endometrial adenocarcinoma.[175,176,182–187] To optimize the performance of the CEA immunostain, a monoclonal rather than polyclonal antibody should be used, the tissue sample should include several fragments or a large piece of tumor, only cytoplasmic staining should be considered positive immunoreactivity, and positive staining of cells with squamous differentiation within the adenocarcinomas should be disregarded.[182,184] A 3-marker panel usually suffices, with recent studies recommending either estrogen receptor, vimentin, and CEA[188] or estrogen receptor, vimentin, and an HPV marker (either p16 or ProExC).[187] It should be emphasized that exceptions to the typical staining patterns of these endocervical and endometrial tumors occur, and that these immunoprofiles often do not pertain to special variant adenocarcinomas.

Well-Differentiated Villoglandular Adenocarcinoma

This uncommon variant of the usual type of cervical adenocarcinoma, originally described by Young and Scully in 1989 as villoglandular papillary adenocarcinoma, is associated with a favorable prognosis and typically presents as an exophytic, polypoid endocervical mass in a young woman (mean age of 35 years).[189,190] The noninvasive, exophytic portion of the tumor exhibits a prominent papillary architecture, with inflamed fibrovascular cores of variable thickness lined by one to several layers of columnar cells with elongated, hyperchromatic nuclei oriented perpendicular to the basement membrane (Figs. 3.209 and 3.210). Nuclear atypia is mild to moderate, analogous to the level of atypia seen in the well-differentiated end of the spectrum of endocervical AIS, which is often present in the neighboring cervical tissue. The columnar cells typically contain little to no mucin, although significant amounts of mucin can be present, prompting some investigators to subdivide these tumors into endometrioid, endocervical, and intestinal types.[190] Mitotic activity is usually evident. The presence of DNA from high-risk HPV types 16 and 18 has been demonstrated in these tumors, which implicates HPV in their pathogenesis.[191]

Invasion of the superficial cervical stroma (inner third) by a well-differentiated adenocarcinoma with an elongated, branching glandular pattern is often present in these tumors. However, this finding does not preclude treatment by cone biopsy in those patients who wish to preserve their fertility, provided that the lesion has been well sampled and there is no

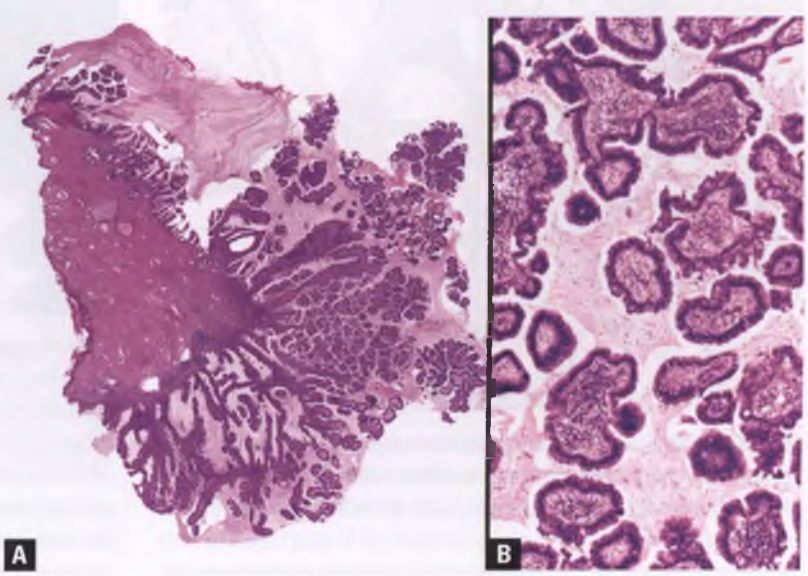

FIGURE 3.209. Well-differentiated villoglandular adenocarcinoma. **A**: This low-magnification view highlights the papillary architecture of this tumor, which is noninvasive in this section. **B**: In these cross sections through several papillae, note the virtual absence of detached cellular buds, the variability in the degree of stratification of the lining columnar cells, and the prominent acute and chronic inflammatory infiltrate within the stromal cores.

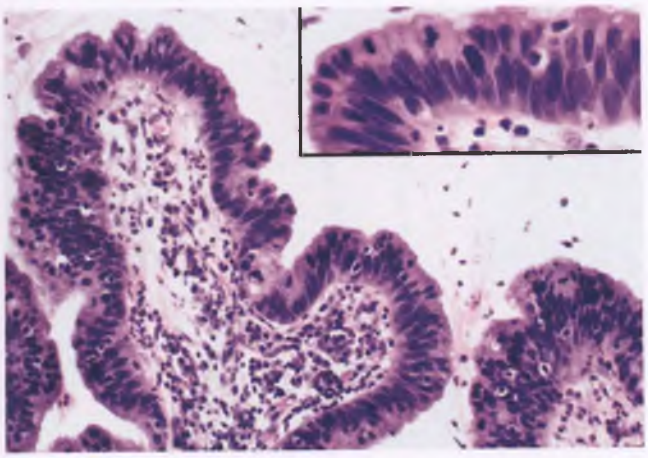

FIGURE 3.210. Well-differentiated villoglandular adenocarcinoma. Papillae are lined by variably stratified cells with elongated, hyperchromatic nuclei with low-grade atypia and occasional mitotic figures.

angiolymphatic invasion or involvement of the resection margins. Underscoring the need for extensive sampling is the occasional presence of deep invasion or an underlying moderately or poorly differentiated adenocarcinoma (Fig. 3.211), which are findings that prompt more aggressive surgery and worsen the patient's prognosis.

Differential Diagnosis

The differential diagnosis of well-differentiated villoglandular adenocarcinoma includes papillary endocervicitis, müllerian papilloma, and müllerian adenofibroma, all of which are lined by a single layer of benign, mitotically inactive epithelium. The latter two neoplasms are quite rare, and the müllerian papilloma is seen almost exclusively in young children. On the malignant side, usual endocervical adenocarcinoma with a villous component, serous carcinoma, and papillary clear cell carcinoma need to be distinguished from well-differentiated villoglandular adenocarcinoma. The usual type of endocervical adenocarcinoma may have a component of well-differentiated villoglandular adenocarcinoma or may have villous structures that are lined by cells with architectural and nuclear atypia beyond that which is acceptable for this special variant (Fig. 3.205). Serous carcinoma is distinguished on the basis of both architecture and cytology. The papillae of serous carcinoma are more architecturally complex and sprout numerous detached buds of neoplastic epithelium, and also feature round to oval, high-grade nuclei rather than elongated, low-grade nuclei. Papillary clear cell carcinomas have hyalinized stromal cores, the papillae are lined by clear cells and hobnail cells with nuclear atypia, and other patterns of clear cell carcinoma (tubulocystic, solid) are also usually present.

Note: As is the case for villoglandular endometrial adenocarcinomas, the term "papillary" is avoided as a diagnostic descriptor to help prevent confusion with the more aggressive uterine serous carcinomas, which were initially described and still often diagnosed as papillary serous carcinomas.

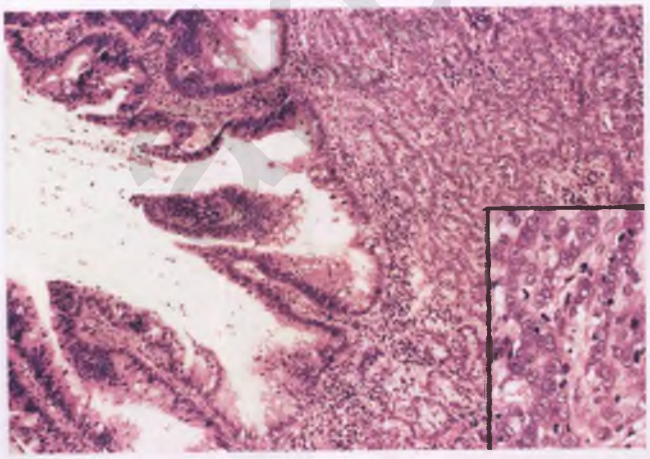

FIGURE 3.211. Aggressive adenocarcinoma (right and inset) lurking beneath a surface component of well-differentiated villoglandular adenocarcinoma (left).

Mucinous Adenocarcinoma

Given the abundance of mucin in normal endocervical cells, it is surprising that cervical cancers with a preponderance of mucin-rich cells are so uncommon. These mucinous adenocarcinomas may be distinguished from the usual type of endocervical adenocarcinoma solely by the presence of abundant intracytoplasmic mucin (Fig. 3.212), or they may exhibit additional characteristics that lead to their classification as one of the mucinous variants discussed below (adenoma malignum, intestinal-type adenocarcinoma, signet-ring adenocarcinoma, or colloid-type adenocarcinoma).[163] Whenever mucinous endocervical adenocarcinoma is encountered, cervical involvement by an endometrial mucinous adenocarcinoma should be excluded (if both sites are involved, the location with the dominant mass

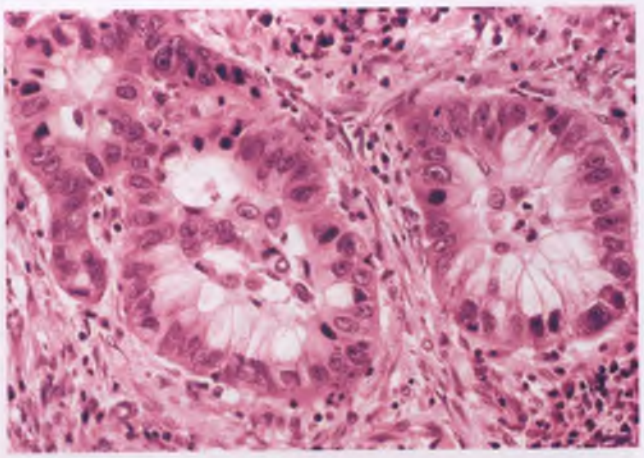

FIGURE 3.212. Mucinous adenocarcinoma of the endocervix. Most of the tumor cells contain abundant, pale-staining intracytoplasmic mucin, the presence of which could be confirmed by mucin stains (PAS with diastase or mucicarmine).

is the probable primary site). Some consideration should also be given to the possibility of a metastatic lesion, which would be more likely if there was a history of a primary mucinous carcinoma elsewhere, the tumor was "bottom heavy," and/or there was prominent angiolymphatic invasion.

Adenoma Malignum (Minimal Deviation Adenocarcinoma)

This rare variant of endocervical mucinous adenocarcinoma is worthy of special categorization because of its potential to be misdiagnosed as a benign process. These tumors typically present in adult women as cervical wall thickening and induration that produces abnormal vaginal bleeding or a mucoid discharge.[192] The mucosal surface is usually friable and mucoid, and sectioning through the tumor typically reveals a pale-tan, glistening, mucoid mass punctuated by cystic spaces (Fig. 3.213).[192] The diagnosis of adenoma malignum should be made with extreme caution and with the assistance of an expert consultant in an asymptomatic patient with a grossly normal cervix. The finding of adenoma malignum should prompt a thorough investigation of the ovaries, which may also harbor a mucinous tumor (either a separate primary tumor or a metastasis from the cervix).[193]

Histologically, architectural glandular abnormalities such as marked variation in size and shape with bizarre branching patterns, a subset of glands with undulating epithelium and papillary infoldings, glands adjacent to thick-walled blood vessels,[167] and irregular extension of glands deep into the cervical stroma are paramount in establishing the diagnosis of adenoma malignum, since the vast majority of the neoplastic cells lining the glands masquerade as mitotically inactive, benign-appearing endocervical-type cells with abundant intracytoplasmic mucin and bland, basally oriented nuclei (Figs. 3.214 and 3.215).[192] Accordingly, adenoma malignum can be difficult or impossible to diagnose in small biopsy samples.

FIGURE 3.213. Adenoma malignum (minimal deviation adenocarcinoma, mucinous type). The uterus has been bivalved in the sagittal plane, revealing an expansile cervical mass with a mucoid cut surface and scattered cysts that extends deeply into the cervical wall. (Courtesy of Dr. Richard L. Payne.)

The type of mucin in adenoma malignum (neutral) differs from the type present in normal endocervical glands (both neutral and acidic). This difference can be detected by an Alcian blue (AB)/PAS stain, which results in red staining of adenoma malignum glands and purple staining of normal endocervical glands (Fig. 3.216).[194] However, it is important to note that benign endocervical glands with pyloric metaplasia/lobular endocervical glandular hyperplasia are also red with this stain,[50] which must be interpreted in the context of the histologic findings. More traditional features that facilitate recognition of adenoma malignum are the findings of a periglandular stromal reaction, significant nuclear atypia (Fig. 3.217), angiolymphatic/perineural invasion, and strong cytoplasmic staining for CEA, all of which may be absent or present only focally in a given case. In view of the often focal nature of these

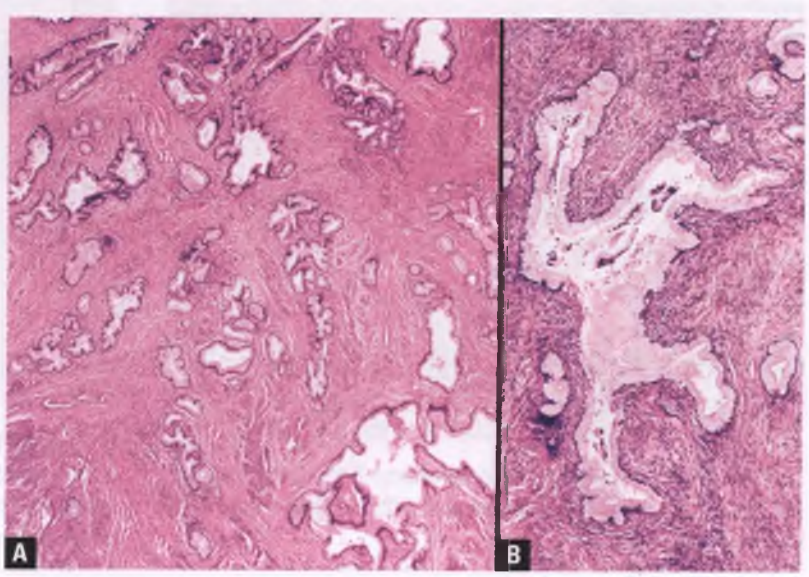

FIGURE 3.214. Adenoma malignum (minimal deviation adenocarcinoma, mucinous type). **A**: This low-magnification view highlights the prominent variability in gland size and shape and the extension of the haphazardly distributed abnormal glands deep into the cervical stroma. **B**: Malignant gland with "lobster claw" configuration.

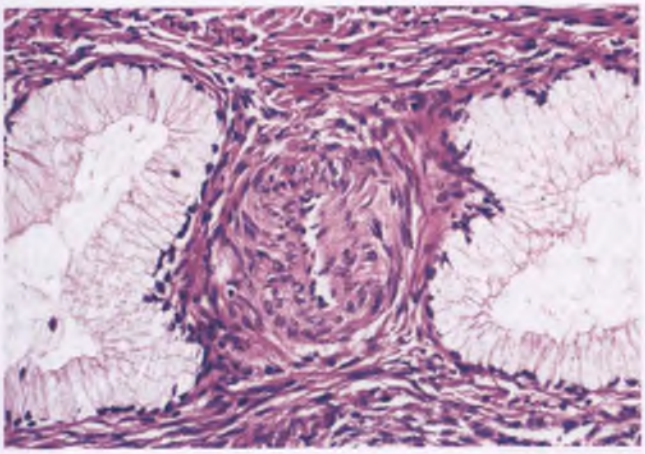

FIGURE 3.215. Adenoma malignum. The presence of these benign-appearing glands adjacent to a thick-walled blood vessel is supportive evidence of an invasive endocervical adenocarcinoma.

findings, extensive sampling is suggested when adenoma malignum is a diagnostic consideration. Note that the periglandular stromal reaction, which may consist of granulation tissue and/or edema and chronic inflammation, can be related to either stromal infiltration or disrupted glands that have leaked their mucinous contents into the neighboring tissue (Fig. 3.218). Since benign glands may also rupture and induce a stromal response, this finding should not be interpreted in isolation as evidence of malignancy.

Differential Diagnosis

Benign glandular processes that can be mistaken for adenoma malignum include deep Nabothian cysts, deep endocervical glands, lobular and diffuse laminar endocervical glandular hyperplasia, MGH, tunnel clusters, mesonephric hyperplasia, endocervicosis, and endocervical adenomyoma (see separate discussions of these entities). Preliminary results suggest that lack

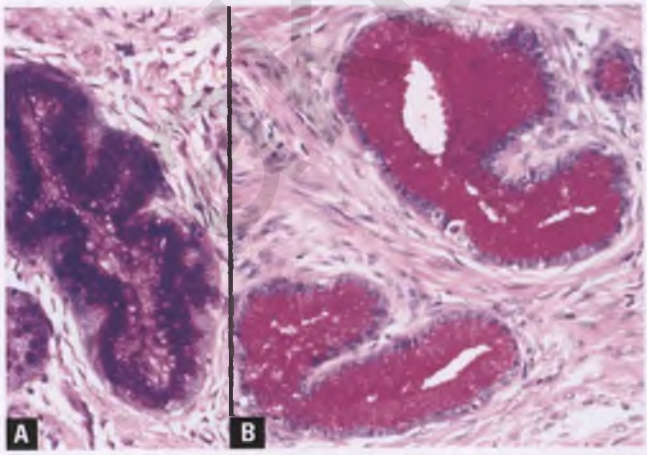

FIGURE 3.216. Adenoma malignum. With the AB/PAS stain, normal endocervical glands stain purple **(A)**, whereas the neoplastic glands of adenoma malignum stain red **(B)**.

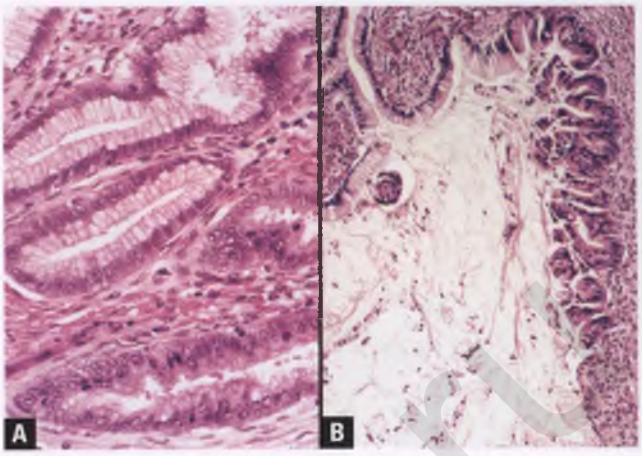

FIGURE 3.217. A,B: Adenoma malignum. Focal areas with more apparent cytologic atypia and mitotic activity are characteristic, either adjacent to the benign-appearing glands (bottom of **A**) or transitionally within portions of glands (right of **B**).

of immunoreactivity of adenoma malignum for PAX2 can assist in distinguishing it from a variety of benign mesonephric and müllerian glandular lesions, nearly all of which express PAX2.[160]

Intestinal-Type Adenocarcinoma

Rare variants of invasive endocervical mucinous adenocarcinoma contain goblet cells, which is evidence of intestinal differentiation.[163] The very well-differentiated tumors of this subtype could be considered intestinal variants of minimal deviation adenocarcinoma (Fig. 3.219). Distinction from AIS of intestinal type is made on the basis of features of stromal invasion, which include the presence of numerous, abnormally shaped glands in a haphazard arrangement deep to the level in which endocervical glands are normally found. Invading glands also often produce a stromal response in the form of periglandular edema, chronic inflammation, and granulation

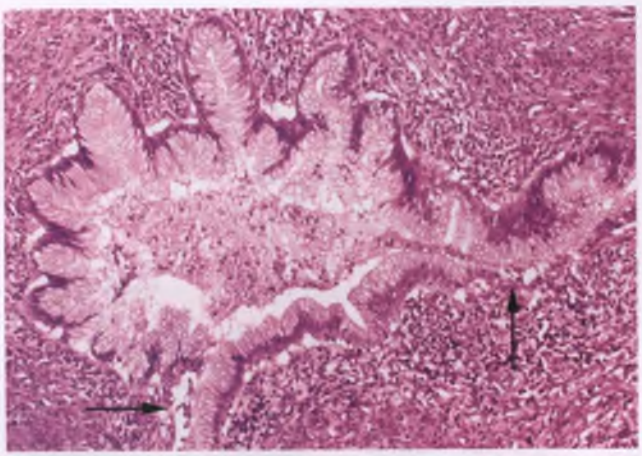

FIGURE 3.218. Adenoma malignum. This peculiar-shaped neoplastic gland is associated with a periglandular stromal reaction, which in this case is related to gland disruption (note loss of epithelial lining at *arrows*).

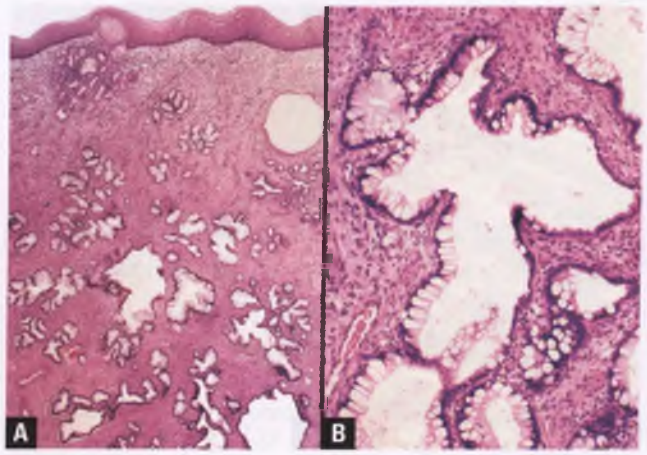

FIGURE 3.219. Intestinal-type adenocarcinoma. **A**: Abnormally shaped, mucinous glands infiltrate deeply into the cervical stroma. **B**: Several of these glands contain numerous goblet cells, which is indicative of intestinal differentiation.

tissue, but this may be focal and subtle. Similar to their in situ counterpart, most invasive endocervical adenocarcinomas of intestinal type express the intestinal marker CDX2.[195]

Signet-Ring Adenocarcinoma

Mucin-containing signet-ring cells may be found as a focal component of poorly differentiated endocervical carcinomas with glandular differentiation, and may rarely be the predominant or only cell type present (Fig. 3.220).[163,196] The possibility of the cervix harboring a metastatic signet-ring adenocarcinoma from a breast or gastrointestinal primary site should be considered whenever a cervical signet-ring cell tumor is not accompanied by a more recognizable form of primary cervical adenocarcinoma.

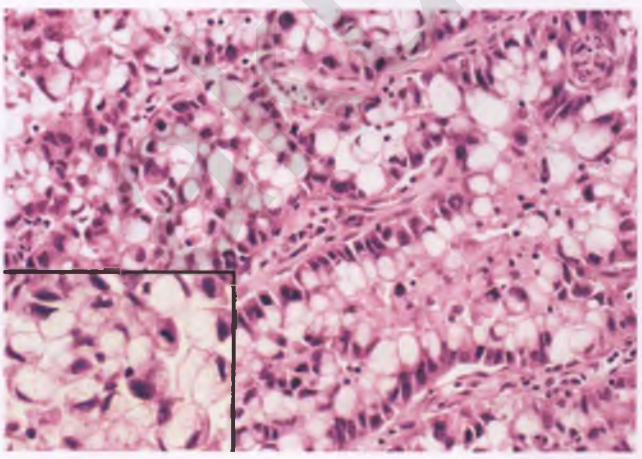

FIGURE 3.220. Poorly differentiated endocervical mucinous adenocarcinoma with areas with signet-ring differentiation. The inset shows a focus where signet-ring cells predominate.

Colloid-Type Adenocarcinoma

Colloid-type adenocarcinoma is another rare variant of endocervical mucinous adenocarcinoma.[197] This tumor resembles colloid carcinoma of the colon and features malignant glands that may be cystically dilated, incomplete, or irregularly shaped in association with large pools of extracellular mucin (Fig. 3.221). Some of the mucin pools contain strips and aggregates of malignant epithelial cells. Care should be taken not to confuse colloid-type adenocarcinoma with a reaction to stromal mucin related to rupture of benign glands, which is characterized by the presence of foreign body giant cells, a lack of nuclear atypia, the absence of more obvious invasive adenocarcinoma in the vicinity, and the lack of a clinically apparent mass.

Endometrioid Adenocarcinoma

Distinction of the usual type of endocervical adenocarcinoma from endometrioid adenocarcinoma can be a subjective exercise, given that the usual endocervical adenocarcinoma is mucin depleted and may have a pseudoendometrioid appearance.[163] Cervical tumors that truly resemble endometrioid adenocarcinomas of the endometrium are rare and typically feature tubular rather than irregularly branching glands (Fig. 3.222). An exception to this tendency toward a tubular glandular architecture is the extraordinarily rare minimal deviation variant of endometrioid adenocarcinoma, which shares with adenoma malignum the prominent variability in gland size and shape.[198] Conventional endometrioid adenocarcinomas of the cervix need to be distinguished from a primary endometrial adenocarcinoma of the usual type with secondary spread (see earlier discussion regarding distinguishing endocervical from endometrial adenocarcinoma).

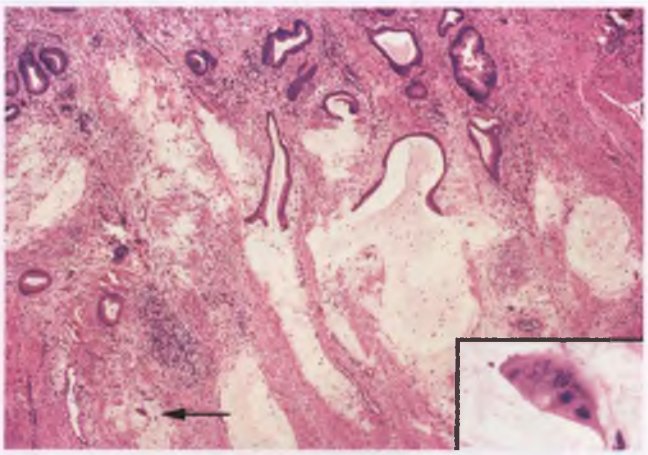

FIGURE 3.221. Colloid-type adenocarcinoma of the cervix. Incomplete neoplastic glands are present in association with pools of extracellular mucin. A component of adenocarcinoma of the usual type is also present, with colloid-type adenocarcinoma preferentially located at the advancing edge of the tumor. The inset shows a strip of tumor cells floating in mucin, which is marked by an *arrow* in the main image.

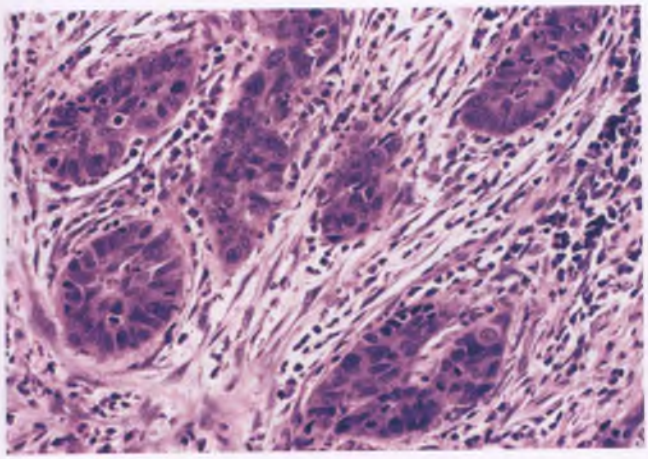

FIGURE 3.222. Endometrioid adenocarcinoma of the cervix.

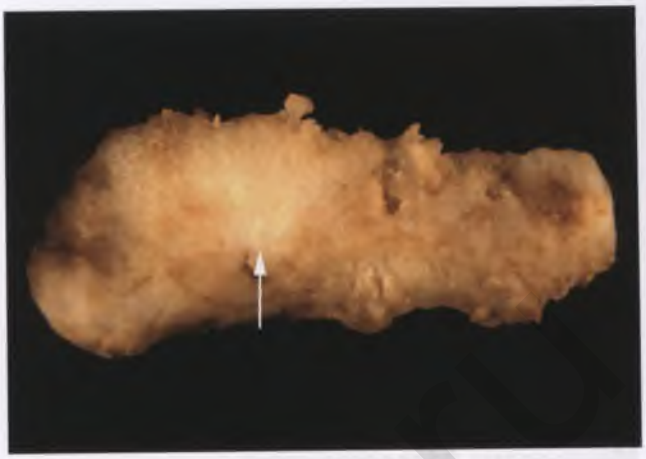

FIGURE 3.224. Clear cell carcinoma of the cervix. This longitudinal section through a formalin-fixed cervix reveals a tumor with a pale yellow cut surface. The *arrow* marks the deepest point of invasion, which is in the outer half the cervical wall. The exocervix is at left.

Clear Cell Adenocarcinoma

Clear cell carcinoma related to in utero exposure to diethylstilbestrol (DES) tends to occur at a young age (median age of 19 years).[199] In contrast, most cervical tumors of this type that are unrelated to DES occur in women over 45 years of age, although one-third of such tumors are also found in teenagers and young adults.[200] Since the warning to stop prescribing DES to pregnant women was issued in 1971, nearly all cases that are currently encountered are unrelated to DES exposure, and account for about 4% of cervical adenocarcinomas.

Grossly, clear cell carcinoma may be polypoid and nodular or eroded and indurated with a pale yellow cut surface (Figs. 3.223 and 3.224). The neoplastic cells of clear cell carcinoma typically have a high nuclear grade and abundant glycogen-rich cytoplasm, with the latter resulting in cytoplasmic clearing in routinely stained sections (Fig. 3.225). The presence of glycogen can be confirmed with PAS stains; mucin may be present within gland lumens but is only rarely encountered within the tumor cell cytoplasm. The various architectural patterns of clear cell carcinoma (solid, tubulocystic, and papillary) and the tendency of its cells to form hobnail structures are illustrated in the sections on clear cell carcinoma of the endometrium and ovary in Chapters 4 and 7, respectively.

In Pap smears, clear cell carcinoma is characterized by clusters of malignant cells that exhibit haphazard orientation, nuclear pleomorphism, variably prominent nucleoli, and cytoplasm that is delicate, finely vacuolated, pale, and usually abundant (Fig. 3.226).

The differential diagnosis of clear cell carcinoma includes MGH and ASR (see sections on these topics earlier in this chapter).

FIGURE 3.223. Clear cell carcinoma of the cervix. The tumor consists of polypoid nodules of yellow tissue partially coated by glistening mucoid material.

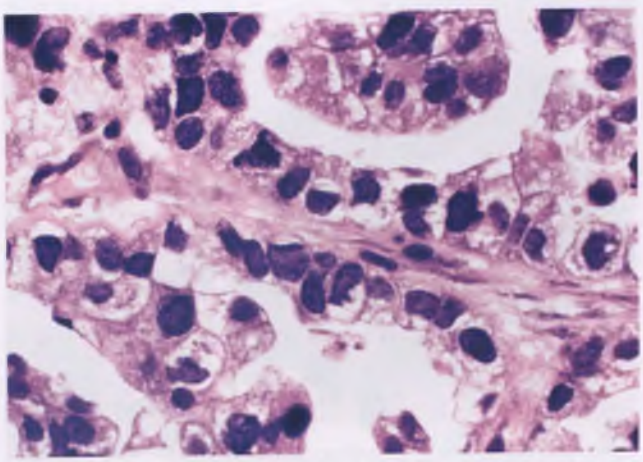

FIGURE 3.225. Clear cell carcinoma. Note the high grade nuclear features and abundant clear cytoplasm.

Serous Adenocarcinoma

On rare occasions, serous carcinoma occurs as a primary tumor of the cervix (Fig. 3.227).[201] Histologically, this tumor is identical to its better known and more common counterpart in the endometrium (see Chapter 4). In the cervix, approximately 40% of these tumors are associated with a tumor of different histologic type, which is most commonly well-differentiated villoglandular adenocarcinoma (Fig. 3.228). Whenever a diagnosis of a primary serous carcinoma of the cervix is being considered, it is necessary to exclude the possibility of spread of a serous carcinoma from the endometrium (or less commonly, the ovary, fallopian tube, or peritoneum).

Mesonephric Adenocarcinoma

Mesonephric adenocarcinoma is derived from mesonephric duct remnants, and is exceedingly rare.[202–204] It typically presents in middle-aged women as a cervical mass that produces abnormal vaginal bleeding. Glandular (ductal), tubular, retiform, solid, and sex-cord–like patterns may be encountered, some of which are illustrated in Figures 3.229 and 3.230. The glandular pattern is most commonly observed and resembles a well-differentiated endometrioid adenocarcinoma. The tubular pattern is distinctive and consists of back-to-back, small tubules that often contain eosinophilic secretions. In the retiform pattern, elongated, slit-like branching tubules with intraluminal papillae are present, whereas the sex-cord–like pattern features trabeculae and cords of tumor cells or tubules that are elongated and compressed. It is not uncommon for a given tumor to exhibit an admixture of these various patterns. Some cases, which are referred to as malignant mixed mesonephric tumors, contain an associated homologous or heterologous sarcomatous component.[202,204]

The recognition that an adenocarcinoma is of mesonephric origin can be difficult, especially in the minority of cases in which there is no associated mesonephric hyperplasia.

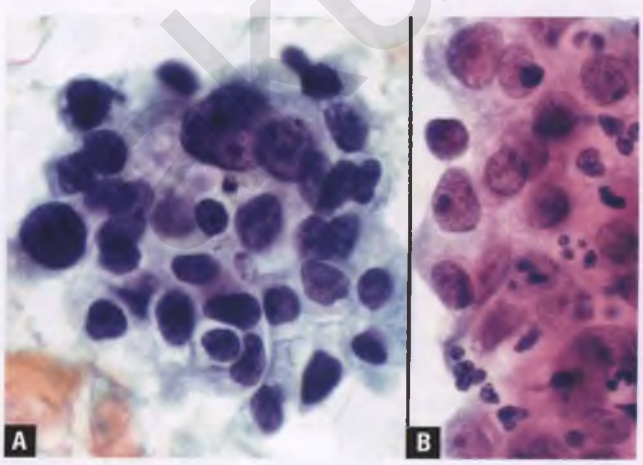

FIGURE 3.226. **A,B**: Clear cell carcinoma in conventional Pap smears (two different cases).

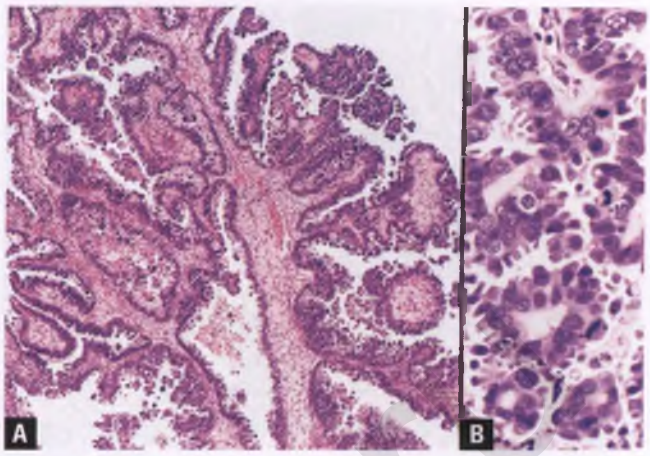

FIGURE 3.227. **A,B**: Serous carcinoma. In these low **(A)** and high-magnification **(B)** images of the exophytic surface component of the tumor, note the characteristic complex papillary architecture, epithelial budding with formation of detached cellular tufts, brisk mitotic rate, and high nuclear grade.

The role of immunohistochemistry as a diagnostic aid in this situation is currently limited and controversial. Although one group of investigators has found the usual finding of focal luminal staining with CD10 to be helpful in distinguishing mesonephric adenocarcinoma from other types of endocervical adenocarcinoma,[57] another group has not.[58] Distinction of a predominantly tubular mesonephric adenocarcinoma from florid diffuse mesonephric hyperplasia can be a diagnostic challenge, and is facilitated by the presence in the former of a symptomatic mass lesion, a more densely packed distribution of neoplastic tubules, nuclear atypia and mitotic activity beyond what is normally found in hyperplastic lesions, intermixed nontubular patterns of mesonephric adenocarcinoma, and the occasional finding of angiolymphatic or perineural invasion.

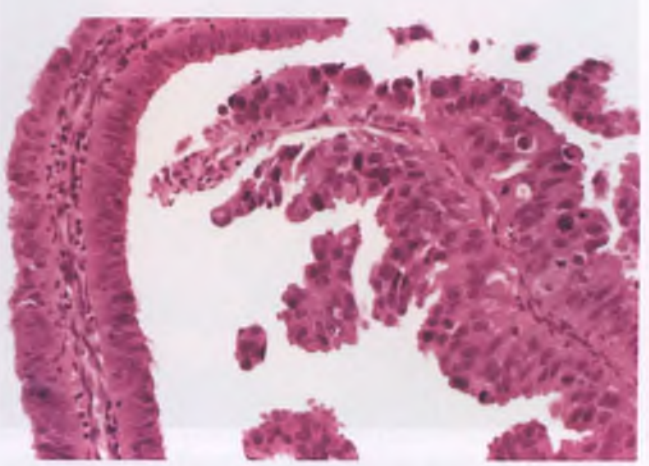

FIGURE 3.228. Serous carcinoma (*right*) admixed with well-differentiated villoglandular adenocarcinoma (*left*).

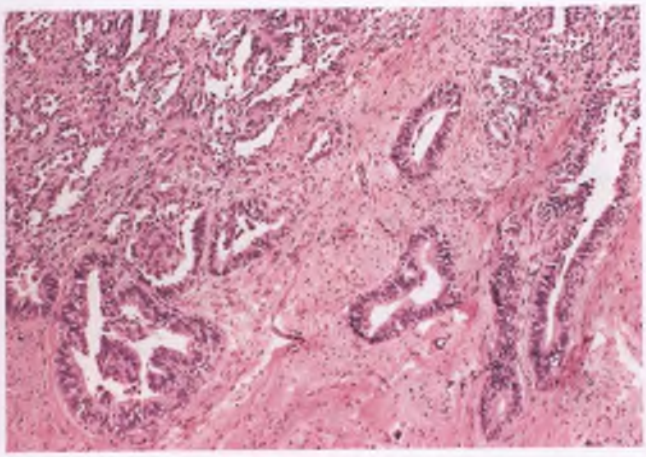

FIGURE 3.229. Mesonephric adenocarcinoma. The large glands infiltrating the cervical stroma resemble well-differentiated endometrioid carcinoma. The upper left portion of the image exhibits a retiform pattern consisting of angulated, branching, slit-like tubules. (Courtesy of Dr. Deborah J. Gersell.)

OTHER PRIMARY MALIGNANT EPITHELIAL TUMORS

Adenosquamous Carcinoma

Adenosquamous carcinoma is composed of an admixture of malignant glandular and squamous elements and accounts for roughly 5% of all cervical cancers. It occurs in adult women over a broad age range, and does not differ in gross appearance or clinical presentation from other types of cervical carcinoma. Reproducibility of this diagnosis is improved if it is restricted to tumors that exhibit squamous and glandular differentiation in routinely stained sections. Mucin stains are either not necessary or used only to confirm mucinous differentiation, rather than to detect it. The malignant glandular and squamous components may be side by side or intimately admixed with one another (Figs. 3.231 and 3.232).

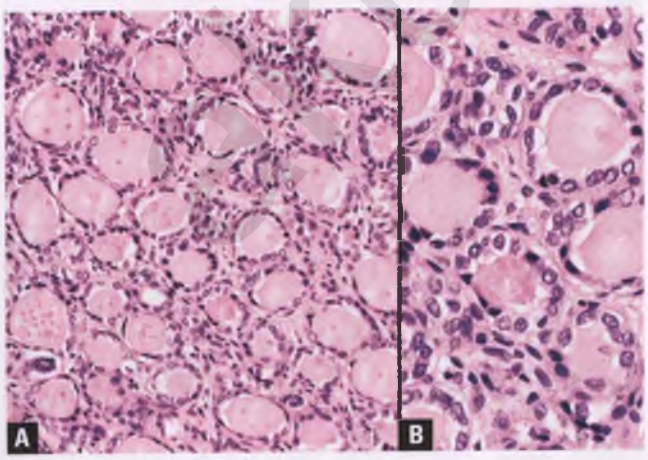

FIGURE 3.230. **A,B**: Tubular pattern of mesonephric adenocarcinoma. The neoplasm consists of closely packed tubules that contain a colloid-like secretion. (Courtesy of Dr. Deborah J. Gersell.)

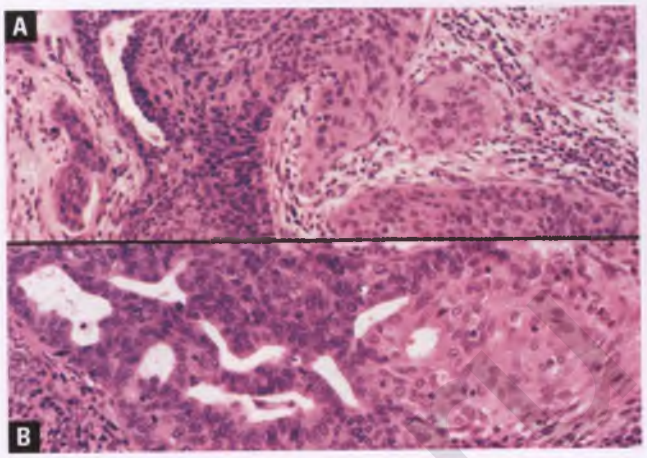

FIGURE 3.231. **A,B**: Adenosquamous carcinoma. Malignant glands are seen abutting and merging with nests of squamous cell carcinoma.

Adenosquamous carcinomas toward the well-differentiated end of the spectrum may resemble the much less aggressive adenoid basal carcinoma. However, adenosquamous carcinomas are clinically malignant masses rather than incidental findings, and exhibit more nuclear atypia, mitotic activity, architectural complexity, and stromal response than adenoid basal carcinomas. Cases in which the squamous component consists of sheets of cells with clear, glycogen-rich cytoplasm have been referred to as clear cell adenosquamous carcinoma, which is distinguished from clear cell carcinoma by the absence of admixed tubulocystic and papillary architectural patterns and the lack of hobnail cells.[205] Utilizing the histologic criteria for salivary gland mucoepidermoid carcinoma to identify similar tumors in the uterine cervix and to distinguish them from adenosquamous carcinoma, a recent study has provided molecular genetic

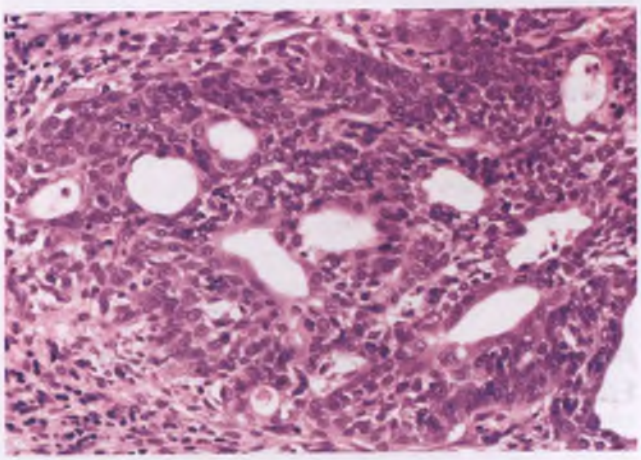

FIGURE 3.232. Adenosquamous carcinoma. Scattered discrete glands are embedded within a squamoid nest of infiltrating tumor. This portion of the tumor bears some resemblance to adenoid basal carcinoma.

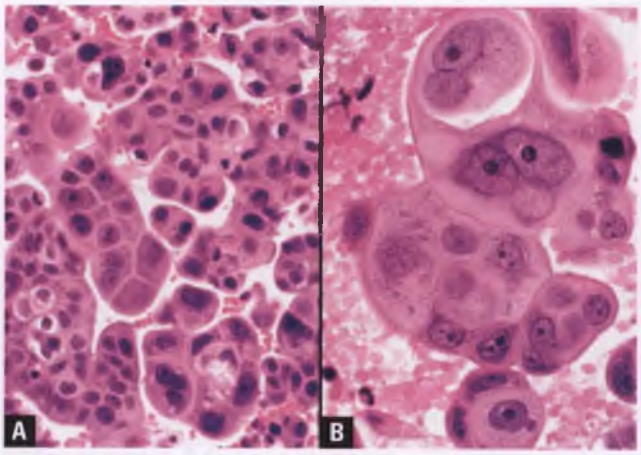

FIGURE 3.233. Glassy cell carcinoma. **A**: Nests of tumor cells are present in this superficial sample of an exophytic cervical mass. **B**: This high-magnification view highlights the macronucleoli and ground glass cytoplasm of the malignant cells.

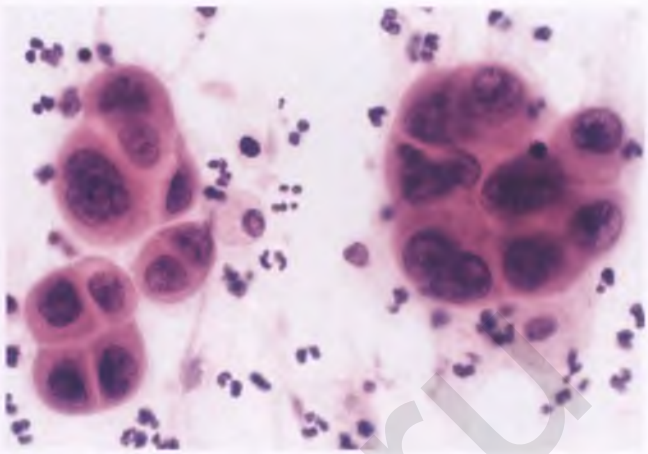

FIGURE 3.234. Pap smear with clusters of tumor cells from a glassy cell carcinoma. The cytoplasm has a "glassy" appearance, cell borders are often distinct, and nuclei tend to be large with prominent nucleoli.

evidence that supports recognition of mucoepidermoid carcinoma as an entity distinct from adenosquamous carcinoma.[206]

Glassy Cell Carcinoma[207,208]

Glassy cell carcinoma is a large cell carcinoma with a distinctive histologic appearance that is thought by some to represent a poorly differentiated adenosquamous carcinoma. It typically presents as an exophytic cervical mass that produces abnormal vaginal bleeding in an adult woman who usually is 25 to 50 years old.

Histologically, glassy cell carcinoma features nests of mitotically active large cells that often have distinct cell borders, macronucleoli, and abundant cytoplasm that has either a characteristic "ground glass"* or finely granular appearance (Fig. 3.233). The tumor cell nests are partitioned by strands of fibrovascular stroma that usually contain lymphocytes, plasma cells, and eosinophils. Evidence of squamous and glandular differentiation is either absent or focal by light microscopy, but is more apparent at the ultrastructural level. The immunoprofile of glassy cell carcinoma is variable and not specific, but usually provides confirmatory evidence of a component of squamous differentiation, and molecular studies have shown an association with high-risk HPV in approximately two-thirds of cases.[209,210] In Pap smears, clusters of large atypical cells with prominent nucleoli and glassy cytoplasm are present that may be difficult to distinguish from an atypical reparative process (Fig. 3.234).[208]

Adenoid Basal Carcinoma (Adenoid Basal Epithelioma)[211,212]

Adenoid basal carcinoma is a rare neoplasm that is typically an unsuspected microscopic finding located in the endocervical canal of a postmenopausal woman. The neoplasm is generally found during evaluation of cervical tissue removed for treatment of HSIL, which is an associated finding in nearly all cases.

The tumor consists of small nests of uniform basaloid cells, and these nests usually are widely spaced from one another within the cervical stroma (Fig. 3.235A). The nests have a round, oval, or lobulated configuration and fail to elicit a stromal reaction. Gland lumens of variable sizes are often present within the nests and are lined by epithelium that may be mucinous, cuboidal, or flattened (Figs. 3.235B and 3.236). The basaloid cells are mitotically inactive and often exhibit peripheral palisading (Fig. 3.236). Metaplastic squamous and transitional-like changes can also occur within the nests (Figs. 3.235B and 3.237), and squamous differentiation can also take the form of extensive replacement of the nests by severely dysplastic squamous epithelium. In this latter situation, a peripheral rim of basaloid cells persists

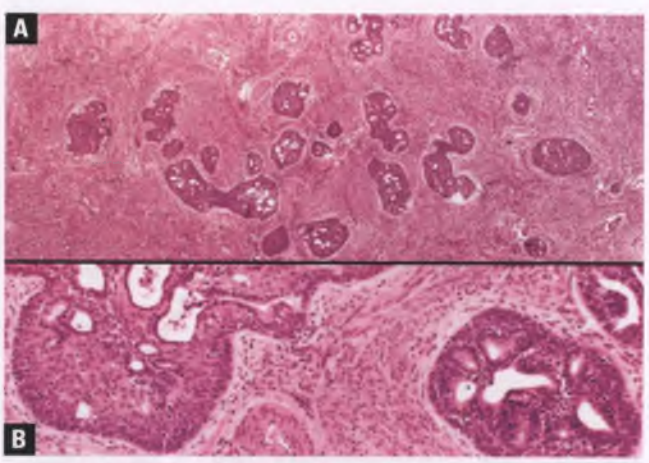

FIGURE 3.235. Adenoid basal carcinoma. **A**: Basaloid nests of tumor cells infiltrate the wall of the cervix without a stromal reaction. **B**: Gland lumens are present within the tumor cell nests, and the large nest at the left also shows patches of squamous metaplasia.

*For those of you who haven't ground any glass recently, ground glass cytoplasm is pale, waxy, eosinophilic to amphophilic, and homogeneous.

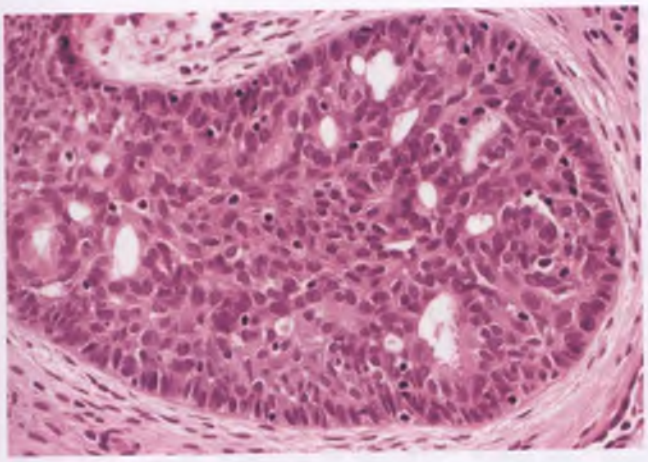

FIGURE 3.236. Adenoid basal carcinoma. This nest shows characteristic peripheral palisading, bland nuclear features, gland lumens, and mitotic inactivity.

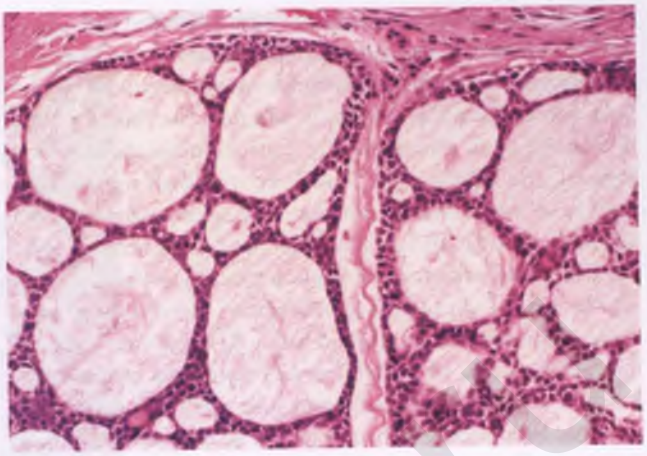

FIGURE 3.238. Adenoid cystic carcinoma. This portion of the tumor contains nests of tumor cells that exhibit a cribriform pattern, with the gland lumens containing pale-staining mucinous material.

that can be highlighted by a CAM 5.2 cytokeratin immunostain, which helps to distinguish this process from a synchronous invasive squamous cell carcinoma.[212] Small, superficial adenoid basal proliferations that remain in contact with or in close proximity to the epithelium from which they originate have been designated adenoid basal hyperplasias.[137,212]

Since pure, typical adenoid basal carcinomas have not behaved in a malignant fashion, some investigators have suggested the designation of adenoid basal epithelioma.[212] However, rare adenoid basal carcinomas have been documented to coexist with a histologically more aggressive carcinoma,[213] and this possibility must be considered when evaluating this special variant. The contrasting features of adenoid cystic carcinoma, basaloid squamous cell carcinoma, and adenosquamous carcinoma, all of which are much more aggressive neoplasms, are discussed with those entities elsewhere in this chapter.

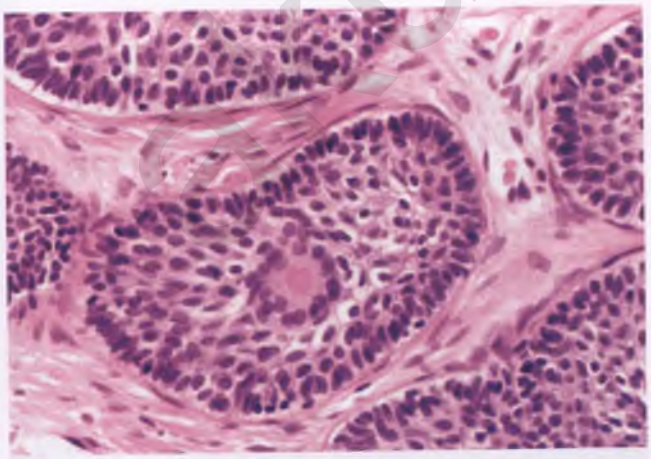

FIGURE 3.237. Adenoid basal carcinoma. The metaplastic process within these nests has transitional features, with elongated nuclei and occasional longitudinal nuclear grooves.

Adenoid Cystic Carcinoma

Adenoid cystic carcinoma of the cervix is a rare malignant neoplasm that resembles its counterpart in salivary gland tissue, although the cervical form of this tumor (a) lacks a predilection for perineural invasion, (b) does not have easily demonstrable myoepithelial cells, (c) often exhibits more prominent necrosis, (d) may contain foci with squamous differentiation, and (e) is more likely to have features of the solid variant.[211,214] It typically presents as a cervical mass in a postmenopausal woman, and histologically displays cribriform, sheet-like, trabecular, and cordlike architectural patterns (Fig. 3.238).[211,215] In the cribriform areas, the glandular lumens contain pale-staining mucin (Fig. 3.238) or hyalinized basement membrane-like material (Fig. 3.239).

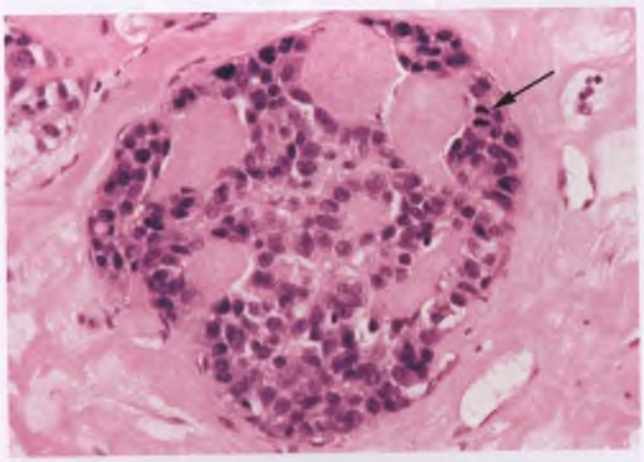

FIGURE 3.239. Adenoid cystic carcinoma. The tumor cells surround spherules of hyalinized basement membrane-like material. Nuclear atypia is not striking, but is more pronounced than that usually present in adenoid basal carcinoma. The stroma is hyalinized, and the *arrow* marks a mitotic figure.

The characteristic cribriform component and the deposition of basement membrane-like material are the most important features that help to distinguish adenoid cystic carcinoma from adenoid basal carcinoma. In addition, the neoplastic cells of adenoid cystic carcinoma are mass forming, slightly more atypical, and exhibit more mitotic activity than those of adenoid basal carcinoma. In contrast to adenoid basal carcinoma, adenoid cystic carcinoma also often has foci of necrosis and a reactive stroma that may be desmoplastic, hyalinized, or myxoid. In view of the aggressive behavior of adenoid cystic carcinoma, distinction from adenoid basal cell carcinoma is critical. The solid variant of adenoid cystic carcinoma can resemble basaloid squamous cell carcinoma and small cell neuroendocrine carcinoma, but can be recognized by the presence of small amounts of basement membrane-like material within the solid nests of tumor (Fig. 3.240).[214,215]

Note: The images of adenoid cystic carcinoma are from extrauterine examples of this tumor.

Neuroendocrine Carcinoma

Neuroendocrine tumors of the cervix are rare, and the histologic subtypes are the same as those more commonly found in the lung.[216] In most studies, the vast majority of these tumors exhibit at least focal immunoreactivity for chromogranin and/or synaptophysin, which are the most commonly used markers of neuroendocrine differentiation.[217–221] Although rarely necessary, ultrastructural examination will reveal dense core neurosecretory granules in most cases.

Typical and atypical carcinoid tumors of the cervix are extraordinarily rare, and will be discussed only briefly. Typical carcinoids are composed of trabeculae or organoid nests of small, uniform cells with minimal mitotic activity and no tumor necrosis. They are regarded as well-differentiated neuroendocrine carcinomas with the potential for malignant behavior. Atypical carcinoids (moderately differentiated neuroendocrine carcinomas) retain the architecture of typical carcinoids, but exhibit more nuclear atypia, increased mitotic activity, and central necrosis within some of the tumor cell nests.

Poorly differentiated neuroendocrine carcinomas are subdivided into small cell carcinoma and large cell neuroendocrine carcinoma, both of which are highly aggressive malignancies that generally resemble other types of aggressive cervical cancer in terms of their clinical and gross presentation. Small cell carcinoma is about three times more common than large cell neuroendocrine carcinoma, and accounts for approximately 2% of cervical carcinomas. Both tumor types are associated with the presence of high-risk HPV and are typically immunoreactive with p16.[221–223]

Small Cell Carcinoma

Histologically, small cell carcinoma is a highly cellular, loosely cohesive neoplasm that typically raggedly infiltrates the cervical stroma as sheets, irregular nests, trabeculae, and single cells without associated inflammation (Fig. 3.241).[217,220,224] The constituent cells exhibit finely and evenly dispersed chromatin, hyperchromatic nuclei with absent to inconspicuous nucleoli, scant cytoplasm resulting in a high nuclear to cytoplasmic ratio, nuclear molding, crush artifact, brisk mitotic activity, and foci of necrosis. In the classic "oat cell" variant, the neoplastic cells have small, round to oval, uniform nuclei and resemble lymphocytes (Fig. 3.242A). A subset of these tumor cells may have their nuclear detail obscured by smudged, dark chromatin. The so-called intermediate variant of small cell carcinoma features cells that have a chromatin pattern that is slightly more coarse than that of oat cell carcinoma, and its cells contain more cytoplasm than oat cells, have larger nuclei with polygonal or fusiform shapes, exhibit less crush artifact, and may contain more readily apparent small nucleoli (Fig. 3.242B). In practice, these two patterns are frequently blended within a given tumor, and their distinction is not clinically relevant.

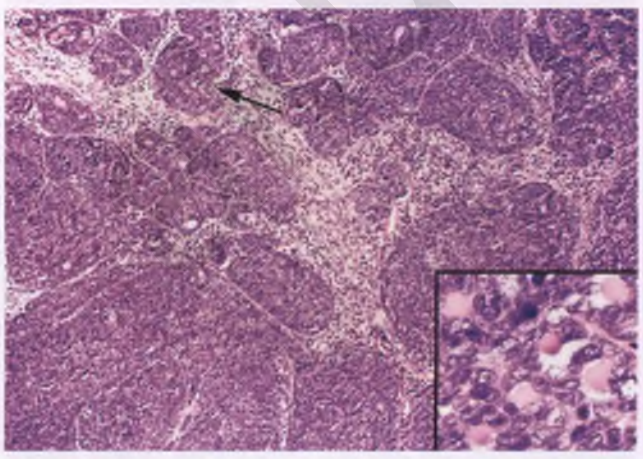

FIGURE 3.240. Adenoid cystic carcinoma, solid variant. The inset highlights the presence of basement membrane-like material within the tumor cell nest that is marked with an *arrow*.

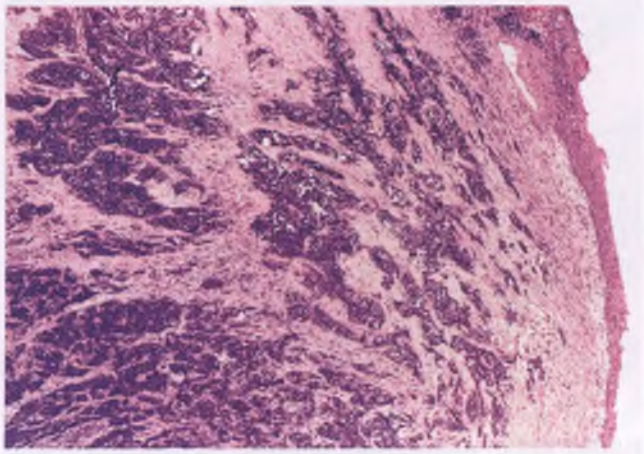

FIGURE 3.241. Small cell carcinoma raggedly infiltrating the cervical stroma.

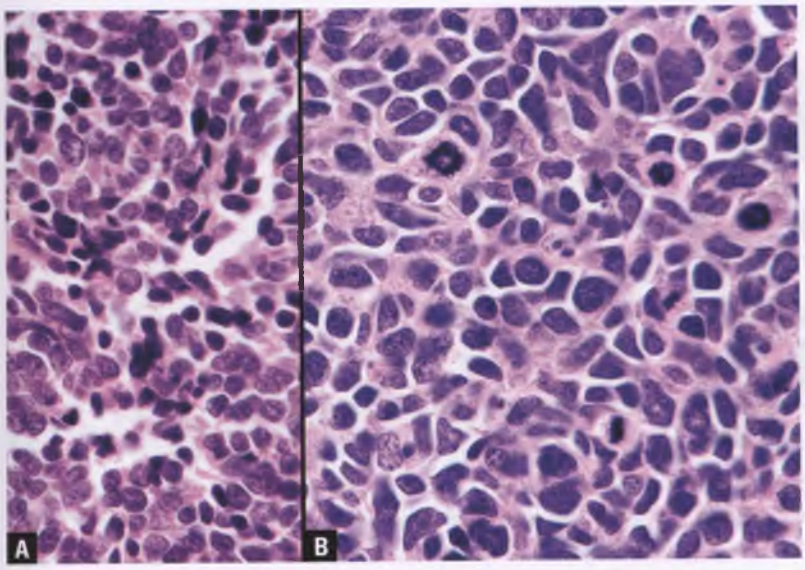

FIGURE 3.242. Small cell carcinoma. **A**: Oat cell variant. **B**: Intermediate variant.

In a minority of cases of small cell carcinoma, chromatin released from necrotic tumor cells is deposited along blood vessel walls. These vessels are intensely hematoxyphilic, creating the so-called Azzopardi effect. This phenomenon, along with an example of small cell carcinoma with crush artifact, is shown in Figure 3.243.

Small cell carcinomas of the cervix often contain a component of adenocarcinoma or squamous cell carcinoma, which may be in situ, invasive, or both (Fig. 3.244).[217]

In Pap smears from patients with small cell carcinoma, loosely cohesive clusters of malignant cells with nuclear features as described above are present, which may be difficult to distinguish from HSIL or lymphoma (Fig. 3.245).

Differential Diagnosis

The differential diagnosis of small cell carcinoma includes basaloid squamous cell carcinoma, leukemia/lymphoma, and endometrial stromal sarcoma.

- Basaloid squamous cell carcinomas often have foci with more obvious squamous differentiation (intercellular bridges and/or keratinization), nests of infiltrating tumor cells with HSIL-like nuclear features and an associated inflammatory response, peripheral palisading of nuclei, inconspicuous crush artifact, no significant nuclear molding, and a lack of staining for neuroendocrine markers.
- Chloroacetate esterase stains and immunostains for lymphoid markers will help to exclude leukemia/lymphoma.
- In contrast to small cell carcinoma, most endometrial stromal sarcomas consist of cells with minimal nuclear atypia and a low mitotic rate that lack nuclear molding and individual cell necrosis. These tumors have a characteristic vasculature and permeative pattern of stromal invasion, and large plugs of tumor within vessels are often present. In difficult cases, a panel of immunohistochemical stains can facilitate separation of small cell carcinoma from endometrial stromal sarcoma.

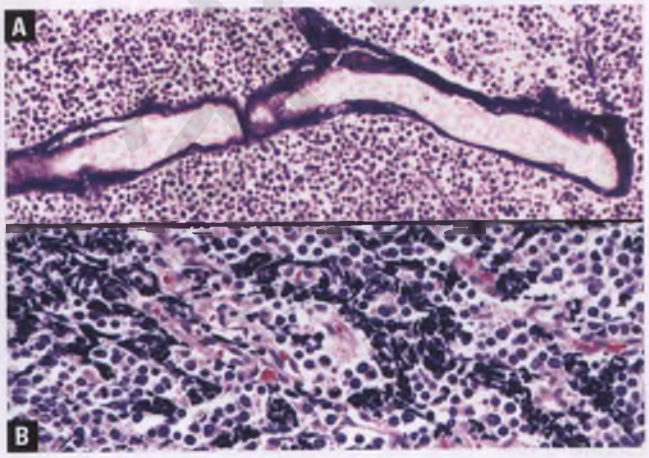

FIGURE 3.243. Small cell carcinoma. **A**: Intense staining of vessel walls with hematoxylin (Azzopardi effect). **B**: Crush artifact.

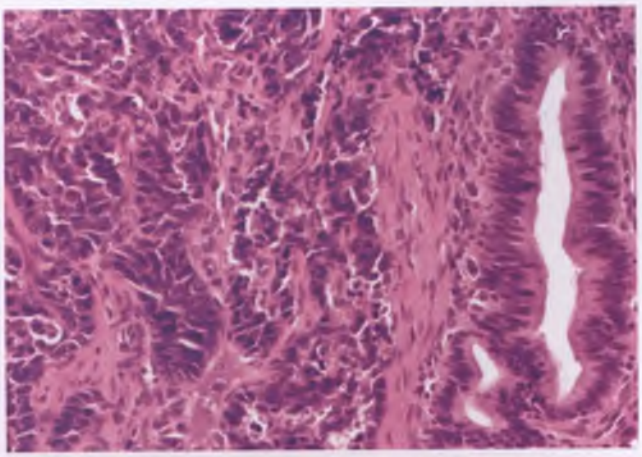

FIGURE 3.244. Small cell carcinoma with focus of endocervical AIS at right. Note the nuclear molding and focal crush artifact within the small cell component.

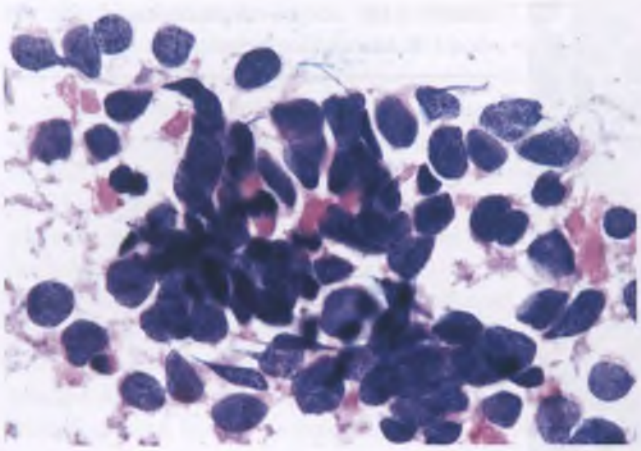

FIGURE 3.245. Touch preparation of small cell carcinoma, which simulates a Pap smear. Note the chromatin pattern, nuclear molding, crush artifact, and minimal amount of cytoplasm.

Large Cell Neuroendocrine Carcinoma

Large cell neuroendocrine carcinoma is composed of sheets, nests, and trabeculae of large cells that often exhibit peripheral palisading of nuclei, geographic areas of tumor necrosis, and prominent angiolymphatic invasion (Fig. 3.246).[218,219] The neoplastic cells have vesicular nuclei, prominent nucleoli, and abundant eosinophilic cytoplasm, and there is brisk mitotic activity (Fig. 3.247A). An additional frequent finding that is a helpful diagnostic clue is the presence of intracytoplasmic eosinophilic granules.[219]

Differential Diagnosis

Large cell neuroendocrine carcinoma may be associated with in situ and/or invasive adenocarcinoma, which can result in confusion with adenocarcinoma.[219] The presence of sheets and nests of malignant cells with abundant eosinophilic cytoplasm can also lead to the mistaken impression of conventional squamous cell carcinoma, and tumor cell nests with peripheral palisading can also result in a resemblance to basaloid squamous cell carcinoma. In these situations, other areas of the tumor with more characteristic neuroendocrine morphology, the absence of features of squamous differentiation (keratin production and intercellular bridges), and positive immunoreactivity for neuroendocrine markers (Fig. 3.247B) facilitate recognition of this tumor.

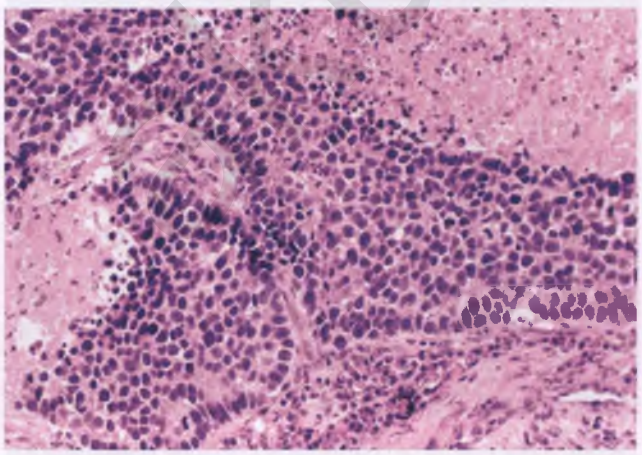

FIGURE 3.246. Large cell neuroendocrine carcinoma. Peripheral palisading and tumor cell necrosis are present.

MIXED EPITHELIAL AND MESENCHYMAL TUMORS

Endocervical Adenomyoma

Endocervical adenomyoma is an unusual benign tumor that typically presents in an adult woman as a well-circumscribed, polypoid mass protruding into the endocervical canal.[225] The sectioned surface often contains mucin-filled cysts. Histologically, the tumor is composed of benign endocervical-type glands embedded within myomatous smooth muscle (Fig. 3.248). Fibrous tissue is an additional minor stromal element.

Some of the glands within endocervical adenomyomas may have papillary infoldings and irregular shapes, which can result in a resemblance to adenoma malignum. However, endocervical adenomyoma is distinguished by its well-circumscribed nature, the tendency of its glands to exhibit a lobular rather than haphazard growth pattern, its myomatous stroma, and the absence of a periglandular stroma reaction. Lobular aggregates of endocervical glands are also seen in lobular endocervical glandular hyperplasia, but this process lacks a myomatous stroma and is usually an incidental microscopic finding.

Müllerian Adenofibroma/Adenosarcoma

Approximately 10% of uterine adenofibromas/adenosarcomas originate in the endocervix, with the remainder arising from the endometrium.[226] Accordingly, these tumors are considered in

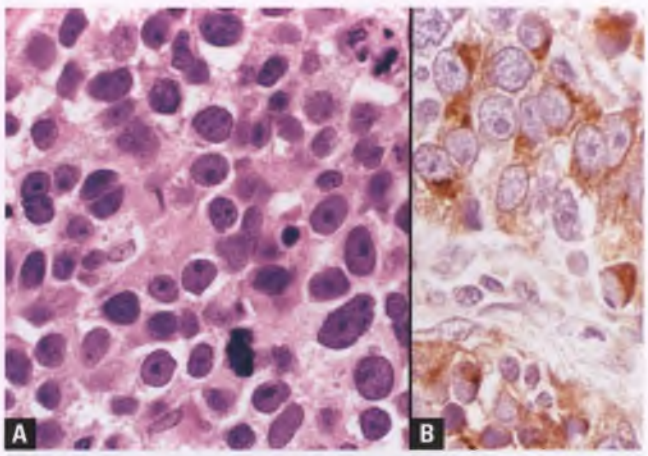

FIGURE 3.247. Large cell neuroendocrine carcinoma. **A**: High-magnification view. **B**: Many of the tumor cells are immunoreactive for synaptophysin.

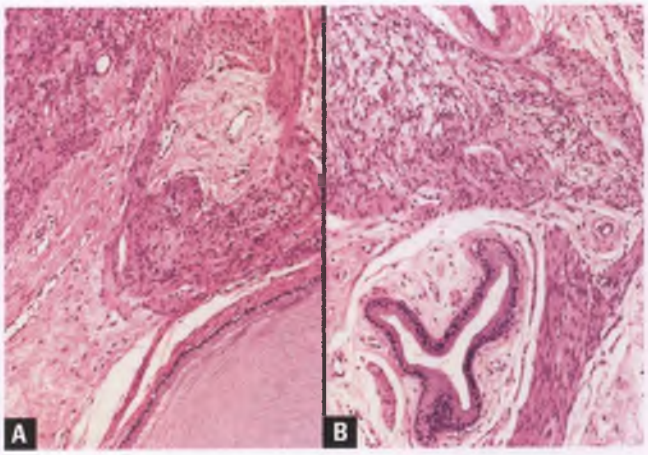

FIGURE 3.248. **A,B**: Endocervical adenomyoma. Benign endocervical glands, which may be cystically dilated or irregularly shaped, are embedded in stroma that consists predominantly of myomatous smooth muscle.

more detail in Chapter 4. Endocervical adenofibromas are quite rare, and typically present as firm, endocervical-based papillary/polypoid lesions in women who are 60 to 70 years of age.[227] Histologically, these benign tumors are composed of broad papillae that project from the surface or into glands that are cystically dilated (Fig. 3.249). The cores of these papillae are composed of bland fibromatous stroma that is not hypercellular or mitotically active (<2 mitotic figures per 10 high power fields). The condensation of stroma beneath the surface epithelium and around dilated glands that is characteristic of adenosarcoma is typically absent or inconspicuous in adenofibromas. In endocervical tumors, the epithelial lining may be of endocervical mucinous type or may be flattened or cuboidal (Fig. 3.250).

Multiple sections of these tumors should be examined histologically, since significant stromal cell atypia, marked stromal cellularity, or a stromal mitotic rate ≥2 mitotic figures per 10 high power fields warrant the diagnosis of adenosarcoma (Fig. 3.251), which is a tumor of low malignant potential.[226]

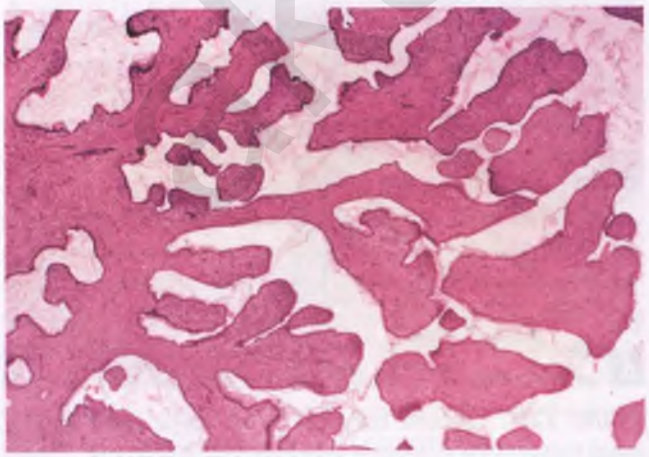

FIGURE 3.249. Endocervical müllerian adenofibroma. Note the broad, polypoid fronds and fibromatous stroma.

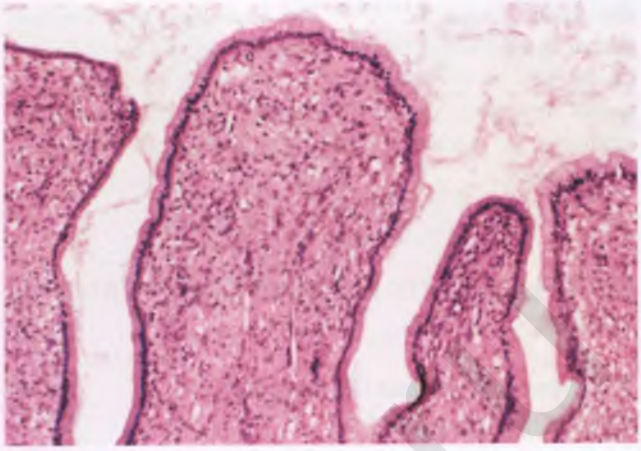

FIGURE 3.250. Endocervical müllerian adenofibroma. A single layer of epithelium that varies from flattened/cuboidal (far left) to mucinous endocervical columnar type lines broad papillae whose cores consist of mitotically inactive, bland fibromatous stroma.

Carcinosarcoma (Malignant Mixed MüllerianTumor)

As is the case for tumors in the adenofibroma/adenosarcoma group, carcinosarcomas are much more often found in the uterine corpus than in the cervix and are discussed in more detail in Chapter 4. However, it is noteworthy that in addition to conventional carcinosarcoma of the type that resembles its endometrial counterpart, cervical carcinosarcoma can exhibit some features that are characteristic of this site, such as (a) the presence of an associated HSIL, (b) HPV-DNA positivity, and (c) a carcinomatous component that consists of squamous cell carcinoma, basaloid squamous cell carcinoma, adenoid cystic carcinoma, adenoid basal carcinoma, or mesonephric carcinoma instead of the typical high-grade adenocarcinoma of endometrioid or serous type that is found in such tumors in

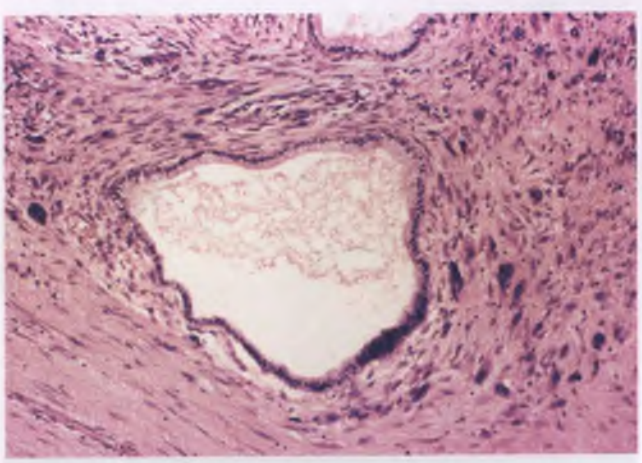

FIGURE 3.251. Endocervical müllerian adenosarcoma. The presence of significant nuclear atypia of the stromal cells warrants a diagnosis of adenosarcoma.

the uterine corpus.[138,139,202,204] The possibility of an endometrial or ovarian source should be considered in cases of cervical carcinosarcoma of conventional type. The controversial separation of cervical carcinosarcoma from spindle cell (sarcomatoid) squamous cell carcinoma is discussed in the section on spindle cell carcinoma.

MISCELLANEOUS PRIMARY MALIGNANT TUMORS

Sarcoma Botryoides (Embryonal Rhabdomyosarcoma)

Sarcoma botryoides is a rare malignant tumor with skeletal muscle differentiation that represents a subtype of embryonal rhabdomyosarcoma. In the uterine cervix, this tumor is five times less common than its vaginal counterpart.[228] Although vaginal sarcoma botryoides characteristically presents in children <5 years of age, the cervical version typically occurs in young women with a mean age of 18 years.[229]

Grossly, sarcoma botryoides of the cervix typically presents as smooth, glistening, red polypoid mass protruding from the external os (Fig. 3.252). Microscopically, a densely cellular subepithelial band of primitive cells, referred to as the cambium layer, overlies a less cellular edematous region (Fig 3.253). This edematous zone is often incorrectly referred to as having a myxoid quality, but AB stains for acidic mucopolysaccharides are negative.[229] Superficial vascular congestion is often prominent, which accounts for the red gross appearance that mimics hemorrhage or mucosal erosion. Variable numbers of round to strap-shaped rhabdomyoblasts are present, usually within the less cellular regions (Fig. 3.254A). These rhabdomyoblasts have abundant eosinophilic cytoplasm that may contain visible cross striations. Rare micronodules of fetal-type hyaline cartilage are present in almost half of the cases (Fig. 3.254B).[229] The primitive malignant cells of sarcoma botryoides may be detected in Pap smears (Fig. 3.255), but it is unlikely that the type of malignancy will be correctly suggested unless strap cells are also encountered. Although desmin staining is expected, nuclear immunoreactivity with myogenin and/or myoD1 provides more specific evidence of skeletal muscle differentiation, but is not detectable in all cases.[230]

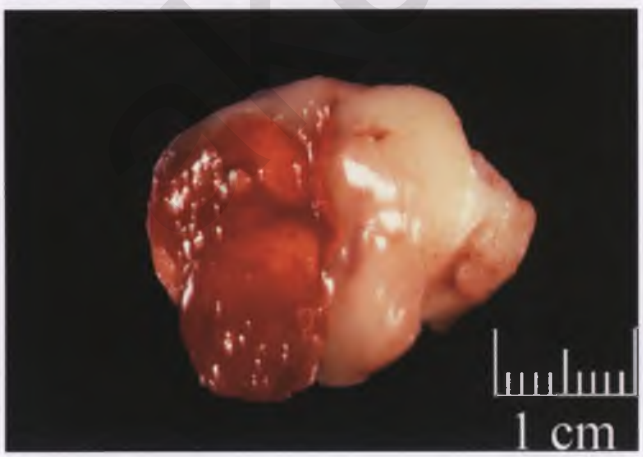

FIGURE 3.252. Sarcoma botryoides of the uterine cervix presenting as a smooth, red, polypoid mass protruding from the external os.

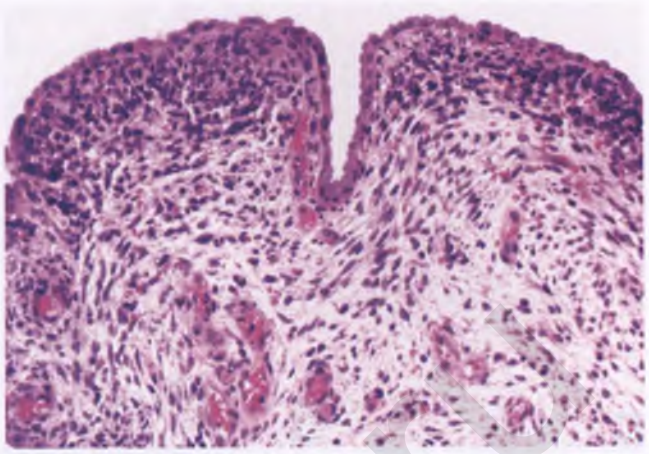

FIGURE 3.253. Sarcoma botryoides of the uterine cervix. A cellular subepithelial cambium layer overlies an edematous less cellular zone that contains congested vessels.

Differential Diagnosis

In the cervix, the major differential diagnostic considerations are benign endocervical polyps and adenosarcoma. The presence of a cambium layer, primitive cells with mitotic activity, and rhabdomyoblasts distinguish sarcoma botryoides from benign endocervical polyps, with the cambium layer serving as the low-power clue that these lesions need close examination under high magnification. Since adenosarcomas also

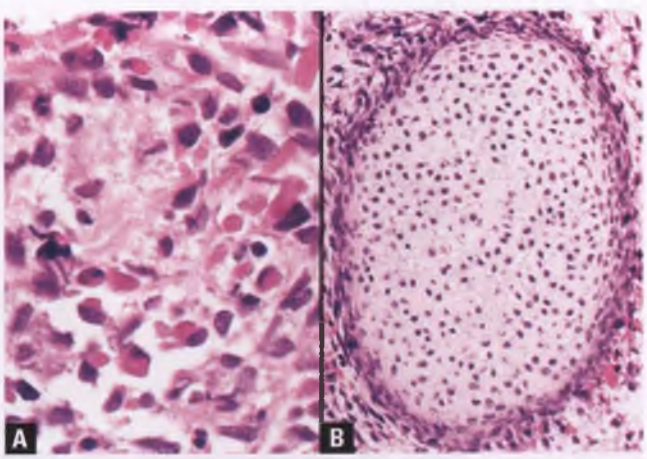

FIGURE 3.254. Sarcoma botryoides of the uterine cervix. **A**: This image highlights the presence of several round to strap-shaped rhabdomyoblasts with abundant eosinophilic cytoplasm. **B**: Micronodules of fetal-type hyaline cartilage are commonly present in these neoplasms.

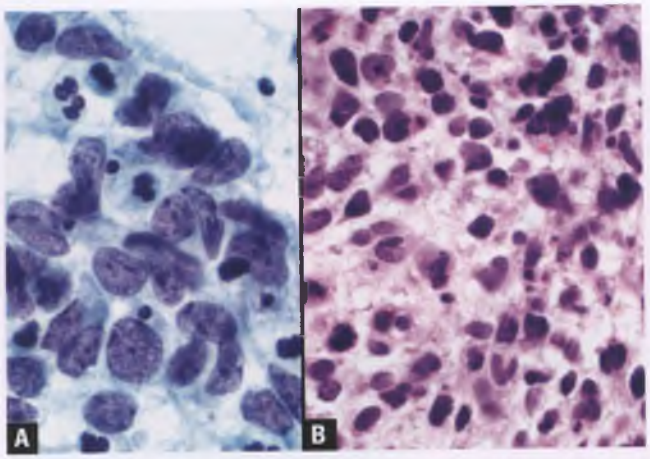

FIGURE 3.255. Sarcoma botryoides of the uterine cervix. **A**: Primitive malignant cells of embryonal rhabdomyosarcoma in a Pap smear. **B**: Histologic correlate.

exhibit a cambium-like layer beneath glandular epithelium and can rarely originate in the cervix and contain heterologous elements such as embryonal rhabdomyosarcoma and fetal-type cartilage,[231] they can also be confused with sarcoma botryoides. However, benign glands that often exhibit cystic dilatation are scattered throughout the sarcomatous component of adenosarcomas, whereas glands are an uncommon feature of sarcoma botryoides, and when present represent entrapped endocervical glands.

Treatment and Prognosis

Most patients with sarcoma botryoides of the uterine cervix present with localized disease without deep stromal invasion and can be treated with organ-preserving surgery.[228] Such patients have a favorable prognosis; adjuvant chemotherapy is of questionable value in this setting.[228]

Lymphoma

Rarely, the uterine cervix may be involved by lymphoma, either as a manifestation of primary extranodal lymphoma or secondary involvement by disseminated disease.[232–235] The typical presentation of a primary lymphoma of the uterine cervix is a 40- to 45-year-old woman with vaginal bleeding. In some cases, abnormal cells are present in a Pap smear that may be suggestive of lymphoma. Grossly, there is often circumferential cervical involvement by fleshy, rubbery, tan tissue that may result in a barrel-shaped cervix, although cervical lymphoma may also present as a polyp or solitary mass. The lymphoma typically extends deep into the wall and the overlying epithelium is usually intact (Fig. 3.256). In the exocervical region, there is often a thin subepithelial zone of nonneoplastic tissue that may contain lymphocytes and plasma cells.

Diffuse large B-cell lymphoma is the most common lymphoma of the cervix, followed by follicular lymphoma. In the exocervix, sclerosis is common, which can result in dense collagenous

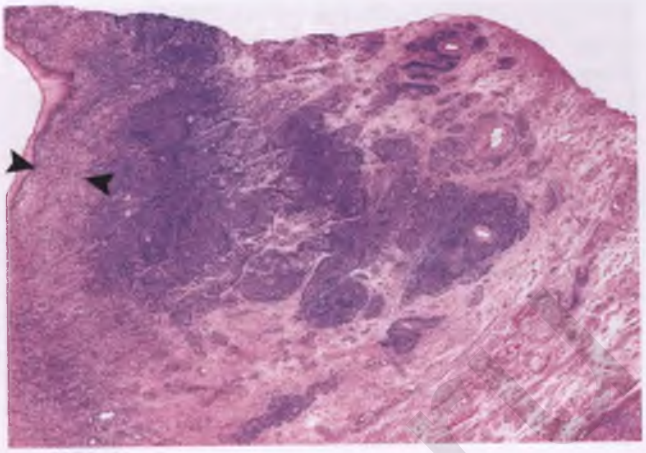

FIGURE 3.256. Malignant lymphoma of the uterine cervix with both diffuse and vaguely follicular architecture (the mucosal surface is along the left side near the top of the image). There is a narrow band of non-lymphomatous subepithelial tissue between the *arrowheads*. The lymphoma extends into outer half of cervical wall, and there is a tendency for the follicular component to exhibit perivascular extension at the tumor periphery.

bands outlining the periphery of neoplastic lymphoid follicles (Fig. 3.257) or hyalinized fibrils partitioning lymphoma cells into nests and cords in a pattern that can resemble carcinoma (Fig. 3.258). When diffuse lymphoma involves the endocervix, the endocervical glands are typically entrapped rather than destroyed.

Cognizance of the fact that lymphomas can occur in the uterine cervix can help avoid their misdiagnosis, with immunohistochemistry serving as a useful aid in distinguishing them from mimics such as poorly differentiated carcinoma,

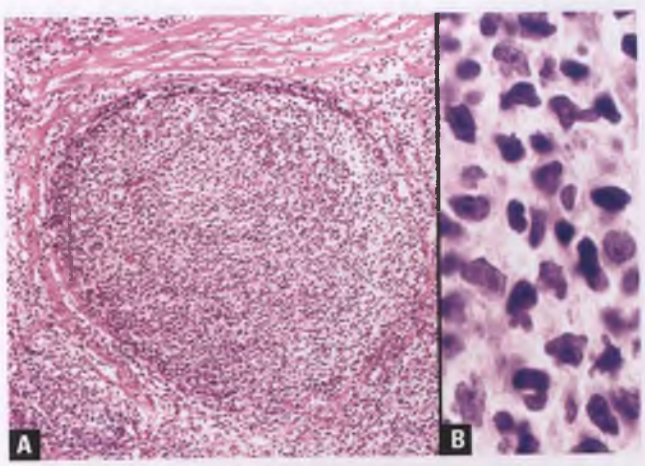

FIGURE 3.257. Follicular lymphoma with sclerosis. **A**: The lymphomatous nodule is partially outlined by a collagenous band. In contrast to reactive follicles with germinal centers, neoplastic lymphoid follicles typically have inconspicuous to absent mantle zones and lack tingible-body macrophages. **B**: High-magnification view of Grade I follicular lymphoma (previously referred to as predominantly small cleaved cell type, where "cleaved" connotes an irregular nuclear contour with variable combinations of angulations, clefts, indentations, and infoldings).

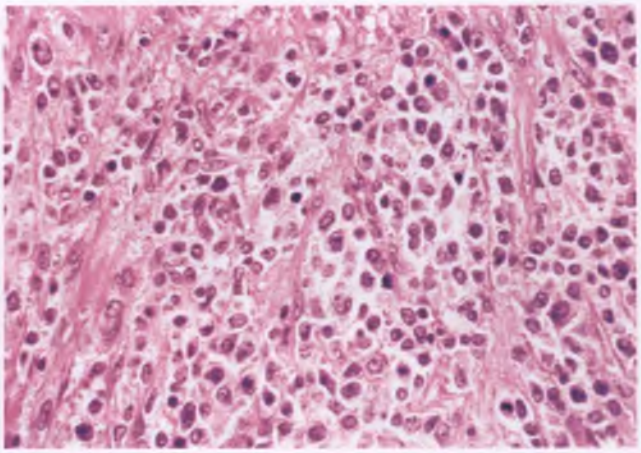

FIGURE 3.258. Diffuse large cell lymphoma with sclerosis.

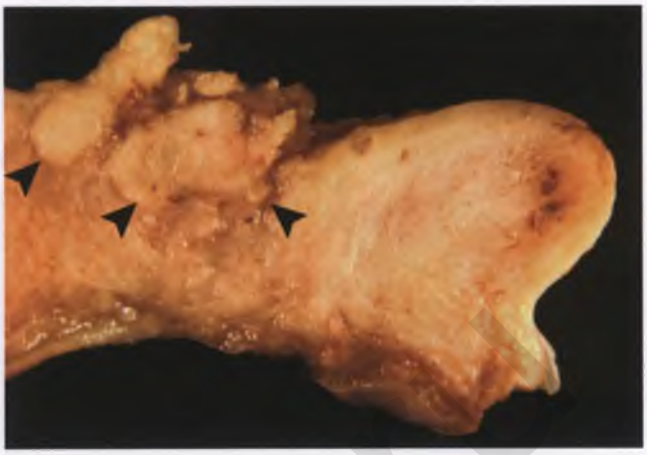

FIGURE 3.259. Cervical involvement by endometrial adenocarcinoma. The endometrial tumor has extended into the endocervical canal in this longitudinal section of a fixed uterus. The deep aspect of the tumor is marked by *arrowheads*.

melanoma, and primitive neuroectodermal tumor. Distinction from reactive lymphoid infiltrates is discussed in the section on inflammatory and infectious lesions earlier in this chapter.

Malignant Melanoma

Primary malignant melanoma of the cervix occurs, but is quite rare.[236] In the absence of in situ melanoma within the overlying epithelium, exclusion of melanoma metastatic to the cervix may not be possible. The presence of intracytoplasmic, finely granular, brown melanin pigment within the tumor cells is a clue to the diagnosis of melanoma, but it is not uncommon for melanoma to lack this pigment (amelanotic melanoma).

Due to its variety of architectural patterns (diffuse sheets, nests, fascicles), different tumor cell shapes (epithelioid, spindle cell), and its occasional amelanotic nature, melanoma has the ability to mimic poorly differentiated carcinoma, sarcoma, and lymphoma. For this reason, whenever confronted with a poorly differentiated malignant neoplasm, melanoma should be included in the differential diagnosis. In addition to searching for the presence of melanin pigment or the occasional finding of an associated in situ melanoma, an immunohistochemical panel that includes the melanoma markers S100, Melan-A, and HMB-45 will help to establish the correct diagnosis.

CERVICAL INVOLVEMENT BY ENDOMETRIAL ADENOCARCINOMA

Cervical involvement by endometrial adenocarcinoma occurs in roughly 20% of cases and is generally a result of direct extension.[178,237] Less commonly, the endometrial tumor may spread to the cervix via invasion of lymphatic channels or be inadvertently transplanted onto the surface of the endocervical mucosa during endometrial curettage.[238] Cervical involvement may be grossly obvious, subtle, or inapparent (Figs. 3.259 and 3.260). In the FIGO staging system that was utilized between 1988 and 2008, endometrial carcinomas that were confined to the uterus and involved the cervix were classified as stage II and subdivided into those whose cervical involvement was limited to the endocervical glands (stage IIa) and those that invaded the cervical stroma (stage IIb).[239] However, in most studies, only the latter were associated with a prognosis worse than stage I endometrial carcinoma (this worsened prognosis may have been due in large part to other associated high-risk factors such as high tumor grade, deep myometrial invasion, and/or angiolymphatic invasion).[240,241] In the 2008 revised FIGO staging system for endometrial carcinoma, the similarity in prognosis between patients with stage I disease (limited to the uterine corpus) and stage IIa disease prompted the merging of stage IIa with stage I, leaving stage II solely for those carcinomas that invade the cervical stroma while remaining confined to the uterus.[129]

To assess the status of the endocervical canal, the gynecologist may submit a fractional curettage (separate samples of endometrial and endocervical tissue, with the endocervical sample taken first). Unfortunately, it is not uncommon for the endocervical sample to be "contaminated" artifactually by a variable number of detached fragments of endometrial tumor. The lack of contiguity of these tumor fragments with cervical tissue should alert the pathologist that contamination is the most likely possibility, although this finding can also reflect true cervical involvement. Even when endometrial carcinoma is found in direct association with endocervical tissue, it is generally not possible to distinguish carcinoma limited to endocervical glands from carcinoma infiltrating stroma in the small, randomly oriented tissue fragments of an endocervical curettage,[237] and there is also the possibility of unsampled stromal invasion deep to disease that appears to be limited to the level of the endocervical glands.

Endometrial adenocarcinomas with cervical involvement limited to endocervical glands are typically well differentiated, and their endocervical involvement is confined to a superficial level where endocervical glands are normally found. They are

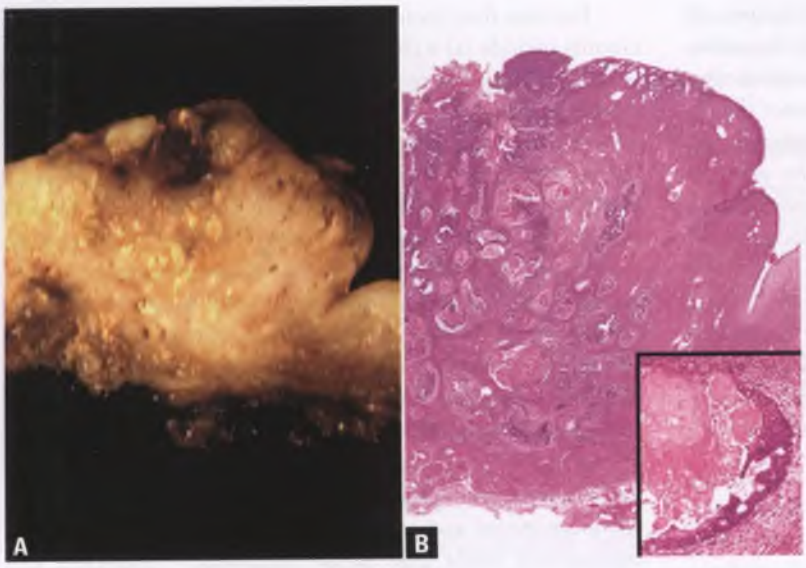

FIGURE 3.260. Cervical involvement by endometrial adenocarcinoma. **A**: This longitudinal section of a fixed uterus in the region of the cervix (with vaginal cuff at right) demonstrates the presence of a deeply invasive endometrial adenocarcinoma with prominent squamous differentiation. Without the yellow plugs of keratinous debris, cervical involvement would be difficult to appreciate grossly (foci of tumor necrosis could result in a similar gross appearance). **B**: Corresponding whole mount section and inset. Note the prominent eosinophilic keratinous debris within several of the cystically dilated tumor cell nests.

not associated with a desmoplastic stromal response (unless the tumor is embedded in a curettage-related implantation site of inflammatory cells and granulation tissue), their interface with the underlying stroma is smooth, and occasionally there are compressed, elongated endocervical glands underlying the tumor (Fig. 3.261). These compressed glands are oriented roughly parallel to the mucosal surface, and their shape and orientation are presumably secondary to pressure-related tumor encroachment.

In a subtle pattern of stromal-invasive disease that is typically grossly inapparent, widely spaced, well-differentiated glands that are contiguous with an endometrial tumor are found deeply infiltrating the cervical stroma without an appreciable stromal response (Fig. 3.262).[242] This pattern of involvement of cervical stroma by endometrial adenocarcinoma can be mistaken for diffuse mesonephric hyperplasia (in those cases that feature tubular glands with eosinophilic luminal secretions), a primary endometrioid minimal deviation adenocarcinoma of the cervix, or tuboendometrioid metaplasia. A recent study has suggested that some such cases and others in which the histologic appearance of the endocervical and endometrial endometrioid adenocarcinomas differ may actually represent separate primary tumors.[243] Although this may be true in rare instances, I am reluctant to broadly accept this conclusion because (a) the apparent histologic differences between the endometrial and endocervical tumors can often be explained by the different growth patterns that an adenocarcinoma assumes depending upon whether it is growing into the

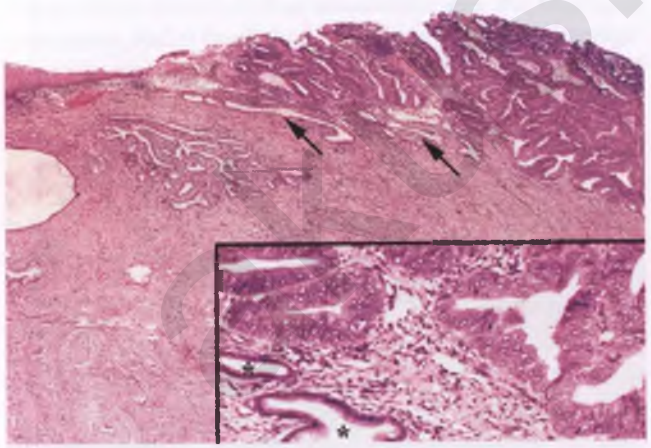

FIGURE 3.261. Endometrial adenocarcinoma with involvement of endocervical glands. Endometrial adenocarcinoma has replaced portions of the region where endocervical glands normally reside without invading the cervical stroma. In close proximity to the deep aspect of the endometrial adenocarcinoma are compressed, elongated endocervical glands oriented parallel to the mucosal surface (*arrows*). The inset shows two benign endocervical glands (marked by asterisks) adjacent to glands of endometrial adenocarcinoma.

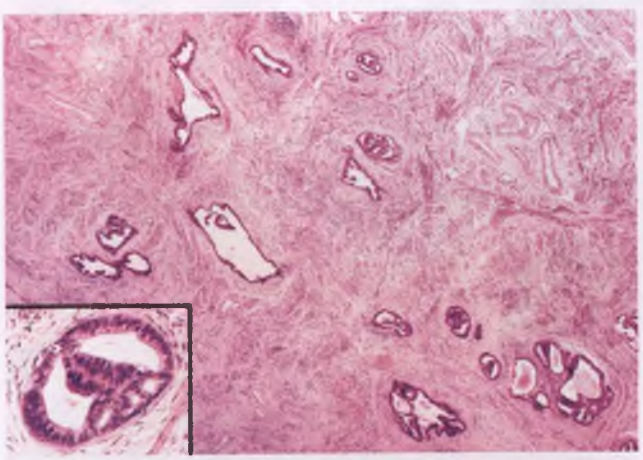

FIGURE 3.262. Cervical involvement by endometrial adenocarcinoma with subtle pattern of stromal invasion. The infiltrative glands are widely spaced, well-differentiated, and lack a stromal response. The inset highlights a gland with a cribriform pattern. Contiguity of this process with an endometrial adenocarcinoma was demonstrated (not shown).

endometrial cavity or invading the fibromuscular stroma of the endocervix, (b) AIS is typically not identified in the endocervical tumors, (c) the authors attribute the endometrial-type immunophenotype of the endocervical-based tumors that is generally considered supportive of endometrial origin as being related to endometrioid differentiation within the primary endocervical tumors, (d) the only endocervical tumor in their study in which the presence of HPV-DNA was documented was an example of a primary endocervical adenocarcinoma with extension into the lower uterine segment, and (e) their conclusions rely heavily upon clonality studies that utilize loss of heterozygosity technology, which cannot reliably distinguish between two independent tumors and the same tumor in two separate sites with genetic differences related to tumor heterogeneity.[244–246]

THE UTERINE CERVIX AS SITE OF METASTATIC CARCINOMA

Metastatic involvement of the cervix by genital tract carcinomas is most commonly due to spread of papillary serous carcinoma of the ovary[247] (cervical involvement by endometrial carcinoma is not classified as metastatic disease and is discussed in the preceding section). Locally advanced tumors from the rectum, bladder, or vagina may also involve the cervix by direct extension. Extragenital tumors from distant sites (most commonly the breast, stomach, and colon)[248] may also spread to the cervix on rare occasions, usually as part of widespread disease. A disproportionate number of breast cancers that are metastatic to this site are of lobular rather than ductal origin (Figs. 3.263 and 3.264),[249] and most gastric carcinomas with spread to the cervix are of signet-ring type.[250]

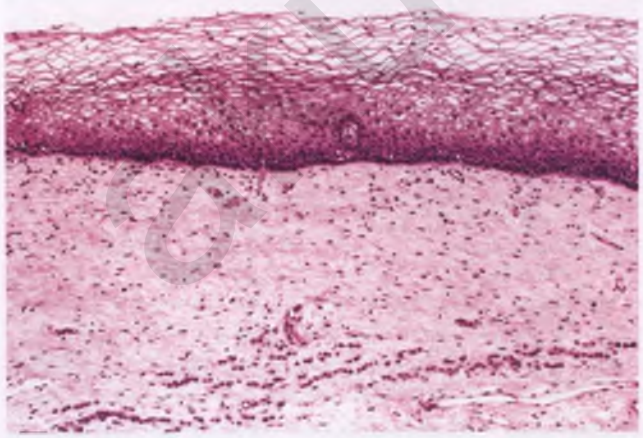

FIGURE 3.263. Infiltrating lobular carcinoma of the breast metastatic to the exocervix. At scanning magnification, the cords of infiltrating carcinoma within the stroma in the bottom portion of the image could be easily overlooked or assumed to be inflammatory cells.

Features that favor a metastatic origin for a cervical carcinoma include (a) a clinical history of an extracervical tumor with similar histology, (b) stromal infiltration, with or without a stromal reaction, with sparing of the native epithelium, (c) extensive angiolymphatic invasion, (d) lack of associated AIS or HSIL, (e) a "bottom heavy" distribution of carcinoma related to direct spread from tumor that has made its way into the cul de sac, and (f) presence of a histologic pattern that would be unusual for primary cervical carcinoma (such as the single-file infiltration pattern of metastatic lobular carcinoma of the breast or signet-ring cells in metastatic gastric carcinoma). With regard to this last feature, it should be noted that rare primary cervical adenocarcinomas can have a low-grade component that mimics the architectural patterns of metastatic lobular carcinoma of the breast, but these primary tumors have at least focal elements of usual endocervical adenocarcinoma and an immunophenotype that is typical of endocervical rather than breast carcinoma.[251] Moreover, primary signet-ring carcinomas of the cervix exist, although they are very rare.[196] Yet another potential pitfall is the rare cervical metastasis, usually originating from presumed transtubal spread of an ovarian serous carcinoma, that mimics endocervical AIS or a superficially invasive primary endocervical adenocarcinoma.[252]

Immunohistochemical stains may be helpful in cases of metastases to the cervix if a primary cervical tumor is a serious differential diagnostic consideration, the epithelial nature of the process is in doubt, or additional information that may support a specific site of origin is desired. The markers of greatest utility for a given situation are as discussed in the sections on specific sites of origin under the heading of "The Ovary as Site of Metastatic Tumor" in Chapter 7.

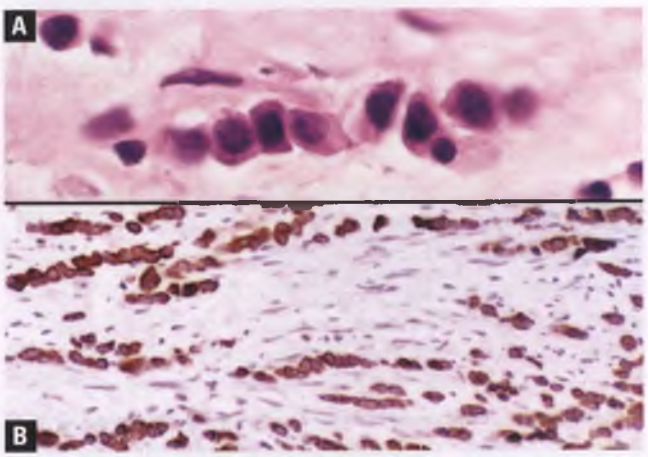

FIGURE 3.264. Infiltrating lobular carcinoma of the breast metastatic to the exocervix. **A**: A cord of malignant cells in characteristic single-file arrangement is present within the cervical stroma. Note the absence of a stromal response. **B**: A cytokeratin immunostain highlights the infiltrating cords of tumor cells. A GCDFP-15 immunostain was also positive (not shown).

PAP SMEAR DETECTION OF ABNORMALITIES BEYOND THOSE OF CERVICOVAGINAL ORIGIN

Fallopian Tube Prolapse

An unusual postoperative complication of hysterectomy is prolapse of the fallopian tube into the vaginal apex (see Chapter 2). There is often associated inflammation and reactive epithelial atypia of the retained tube, which is reflected in Pap smears by the presence of atypical glandular cells that can arouse suspicion for adenocarcinoma (Fig. 3.265).[253] The clinical history and the presence of glandular cells analogous to tubal metaplasia with reactive atypia help to suggest the true origin of these cells.

Psammoma Bodies in Pap Smears

Psammoma bodies are dark, spherical, concentrically laminated concretions composed of calcium apatite that are rarely found in Pap smears, with a reported incidence that varies from 1 in 10,000 to <1 in 100,000 cases (Fig. 3.266).[254] Psammoma bodies may occur with or without adherent epithelial elements. They may have no recognizable clinicopathologic correlate, be related to incidental psammomatous calcifications of the endocervical/endometrial glands and stroma, or be associated with endosalpingiosis, IUD/oral contraceptive use, or the full spectrum of serous tumors from the uterus, fallopian tube, ovary, or peritoneum.[254] Patients who are more likely to harbor a malignancy are those whose Pap smears also contain abnormal glandular cells, those who are postmenopausal, and those who have abnormal vaginal bleeding or a pelvic mass.[254] The overall incidence of an associated malignancy varies widely from study to study, but probably is on the order of 10% to 30%. Given this incidence, it is recommended that the finding of psammoma bodies in a Pap smear prompts a clinical investigation in an attempt to determine the source, with the extent of the evaluation guided by the degree of suspicion of malignancy as assessed by the presence or absence of worrisome glandular cells in the smear and the patient's age and symptoms.

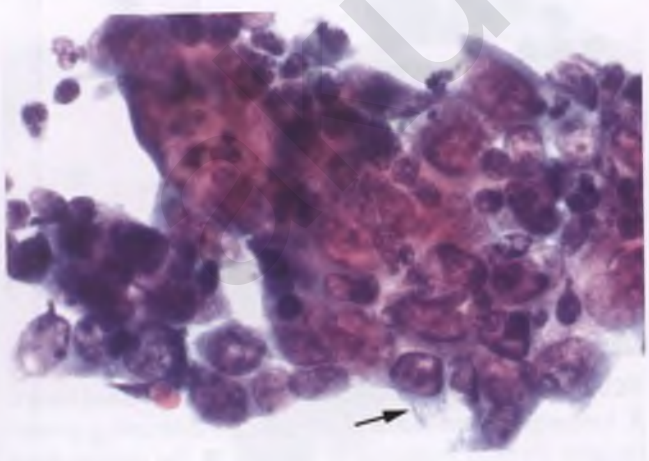

FIGURE 3.265. Pap smear from patient with fallopian tube prolapse. Atypical glandular cells are present and are admixed with inflammatory cells. The *arrow* marks a ciliated cell. The corresponding histology is illustrated in Figure 2.16.

Endometrial Adenocarcinoma

Pap smears from patients with endometrial adenocarcinoma may be entirely negative, may contain only a few groups of endometrial cells judged to be slightly atypical on the basis of a minor increase in nuclear size and subtle chromatin abnormalities, or may contain cells suspicious for or diagnostic of adenocarcinoma. Not surprisingly, the more tumor cells that are exfoliated and the higher the nuclear grade, the easier the adenocarcinoma is to recognize. When present in Pap smears, the neoplastic cells of endometrial adenocarcinoma usually occur in small, disorganized clusters or as single cells (Figs. 3.267 and 3.268). The nuclei are enlarged to a variable degree, and there are abnormal chromatin patterns that often include patches of chromatin clearing. The cytoplasm is usually blue-green (cyanophilic), and may contain vacuoles or ingested neutrophils. There is often an associated "watery tumor diathesis" that tends to be pale, cyanophilic, and finely granular (compare with the less subtle tumor diathesis of squamous cell carcinoma). In poorly differentiated endometrial adenocarcinomas, sheets of tumor cells with prominent nucleoli can be seen. The aggressive uterine serous carcinoma features papillary clusters of malignant glandular cells with prominent nucleoli, occasionally in association with psammoma bodies (Fig. 3.269).[255] Since malignant cells may be easily shed from the tufted surface papillae of this tumor, there may not be an associated tumor diathesis. Serous carcinomas of ovarian, tubal, or primary peritoneal origin can exfoliate cells that can result in Pap smears with a similar appearance (see below).

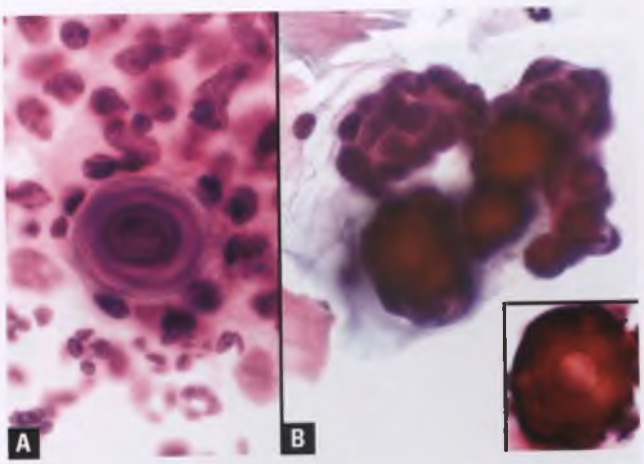

FIGURE 3.266. Psammoma bodies in Pap smears. **A**: Laminated psammoma body with a few adherent benign-appearing cells. Follow-up was benign, with no clinicopathologic correlate. **B**: Psammoma bodies associated with slightly atypical glandular cells. The inset shows a psammoma body with the focus set to visualize laminations. Follow-up was peritoneal serous micropapillomatosis of low malignant potential.

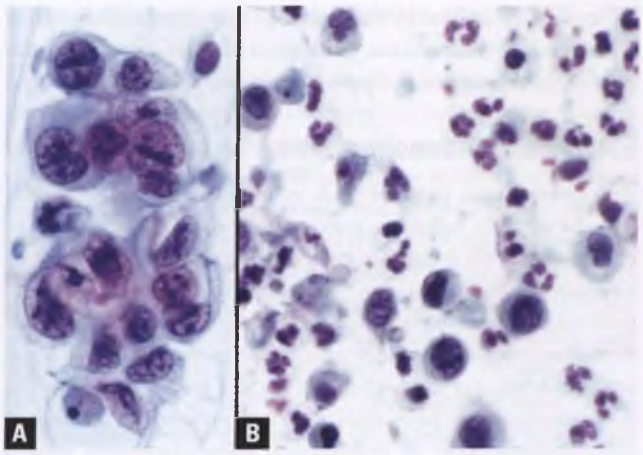

FIGURE 3.267. Endometrial adenocarcinoma in conventional Pap smears. **A**: A jumbled cluster of malignant glandular cells is present, and consists of cells with variable nuclear size and chromatin abnormalities. Note the watery tumor diathesis in the background. **B**: Single malignant glandular cells are present in association with some fragments and granules of cellular debris and some acute inflammatory cells.

In liquid-based Pap smears, three-dimensional "balling up" of cell clusters makes it difficult to view the nuclear features of centrally located cells, although nuclear detail is better appreciated at the periphery of the cell clusters (Fig. 3.270A). The watery tumor diathesis may be more difficult to discern, consisting of aggregates of finely granular debris in the background (Fig. 3.270B) or clinging to the surface of the abnormal cell groups.

The differential diagnosis of endometrial versus endocervical adenocarcinoma in Pap smears is discussed in the section on endocervical adenocarcinoma.

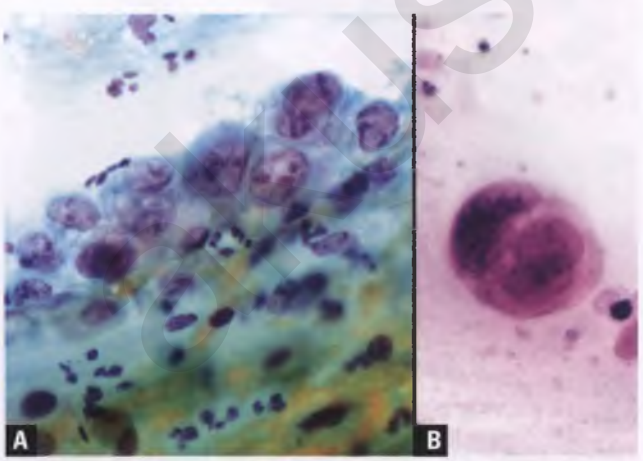

FIGURE 3.268. Endometrial adenocarcinoma in conventional Pap smears. **A**: This cluster of malignant glandular cells is associated with a tumor diathesis that includes erythrocyte degradation products with orange-yellow pigmentation consistent with hematoidin. **B**: A small, tight cluster of malignant glandular cells from a high-grade adenocarcinoma is present. A watery tumor diathesis is present in the background.

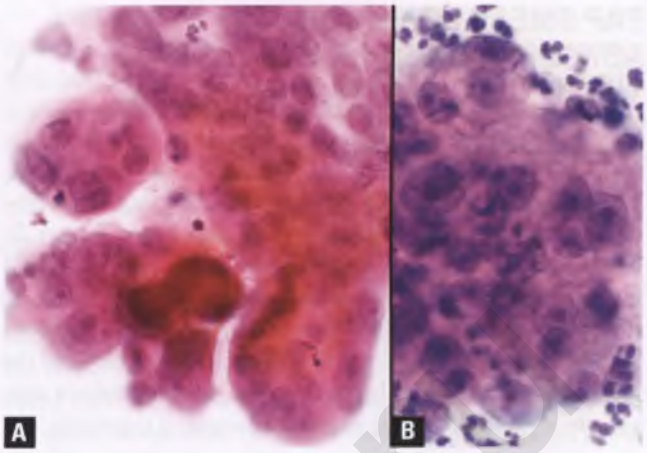

FIGURE 3.269. **A,B**: Uterine serous carcinoma in conventional Pap smears. Note the enlarged, vesicular nuclei and prominent nucleoli that are characteristic of this aggressive neoplasm. **A** also demonstrates the commonly present papillary configuration of the cell groups, and two amorphous structures that may represent psammoma bodies.

Extrauterine Adenocarcinoma

On rare occasions, adenocarcinomas from the ovary, gastrointestinal tract, fallopian tube, peritoneum, or other miscellaneous sites shed malignant cells that subsequently pass through the fallopian tube into cervicovaginal secretions, where they may be sampled for Pap smear analysis. Many such tumors are papillary serous carcinomas and are often of ovarian origin. The major clues in the Pap smear that one may be dealing with an extrauterine source are (a) the often degenerated appearance of the malignant glandular cells, which is not surprising in view

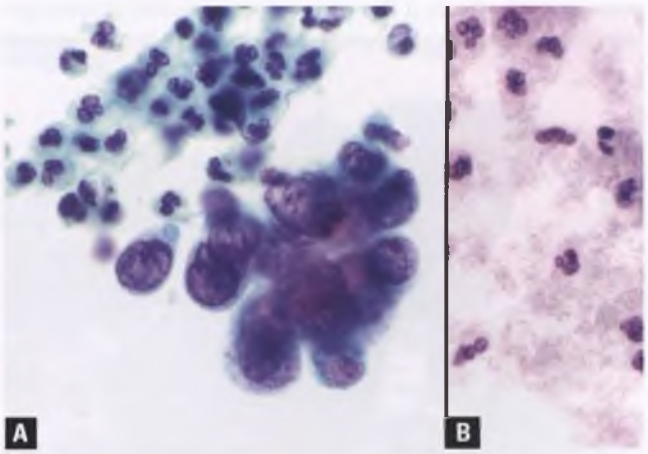

FIGURE 3.270. Endometrial adenocarcinoma in liquid-based smears. **A**: A three-dimensional cluster of malignant glandular cells is present. No tumor diathesis is apparent in this case. **B**: The granular debris in the background, incidentally admixed with neutrophils, represents a tumor diathesis from another endometrial carcinoma. The finding of such granular debris should prompt a thorough search for its cause, which will often be related to the presence of a malignant tumor.

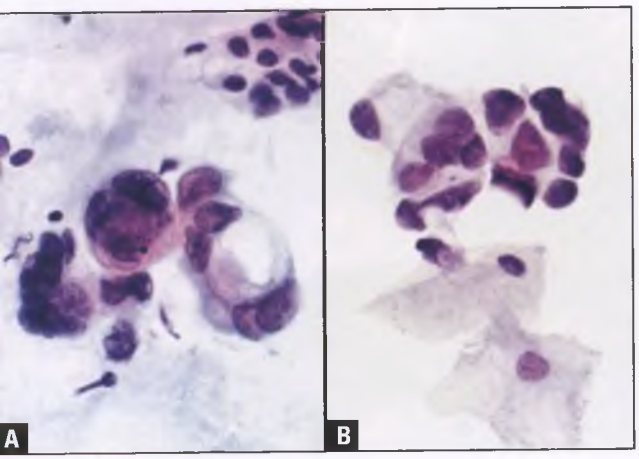

FIGURE 3.271. Ovarian **(A)** and tubal **(B)** serous carcinomas presenting in conventional Pap smears. The malignant glandular cells exhibit variable degrees of degeneration. Although the background in **B** is clean, the example of ovarian cancer in **A** is associated with a faint, watery diathesis that is not typically present in this situation.

of the distance traveled and the time elapsed between exfoliation from their extrauterine parent tumor and recovery from cervicovaginal secretions, and (b) the usual lack of an associated tumor diathesis, which can be explained by the passive intraluminal/intracavitary journey of the tumor cells (Figs. 3.271 and 3.272). In such situations, the report should indicate the possibility of extrauterine carcinoma and provide some guidance as to likely primary sites, but care should be taken not to interpret these findings as evidence of cervical involvement by metastatic disease. In those cases of actual metastasis to the uterus or vagina from genital tract or extragenital carcinomas, there is often associated tissue destruction and ulceration that is usually reflected in the Pap smear by the presence of a tumor diathesis. Although most such cases will be cytologically indistinguishable from primary uterine adenocarcinoma, the combination of clinical history, radiologic findings, and tissue sampling will eventually lead to the correct interpretation.

MISCELLANEOUS PAP SMEAR FINDINGS

Exfoliated Benign-Appearing Endometrial Cells

Spontaneously shed clusters of benign-appearing endometrial cells are a common finding in Pap smears, particularly during the first 10 days of the menstrual cycle.[256] These clusters may be of glandular, stromal, or mixed glandular and stromal origin. Those clusters that exhibit a double-contoured appearance are of mixed glandular and stromal origin, and consist of a central dark aggregate of condensed stromal cells, often with nuclear molding, surrounded by a rim of larger, more pale-staining glandular cells (Fig. 3.273). The mixed stromal and glandular nature of the double-contoured clusters has been confirmed immunohistochemically, using CD10 as a marker for the stromal cells and cytokeratin as a marker for the glandular cells.[257] Compact, monocontoured groups of endometrial cells, which are more common than the double-contoured clusters, consist of three-dimensional ball-like clusters of cells with scant cytoplasm and a nuclear area similar to that of normal intermediate squamous cells (Fig. 3.274). These monocontoured clusters may be of purely stromal, purely glandular, or mixed stromal and glandular origin, as has been confirmed with CD10 and cytokeratin antibodies, and their composition cannot be reliably determined by routine assessment in Pap smears.[257]

The Bethesda 2001 reporting system recommends the reporting of exfoliated, benign-appearing endometrial cells in all women who are ≥40 year of age, since this may be an indication of endometrial pathology on rare occasions in this age group. Using an age cutoff is a response to the fact that many Pap smears are submitted with absent or inaccurate information about the patient's menopausal status, date of last

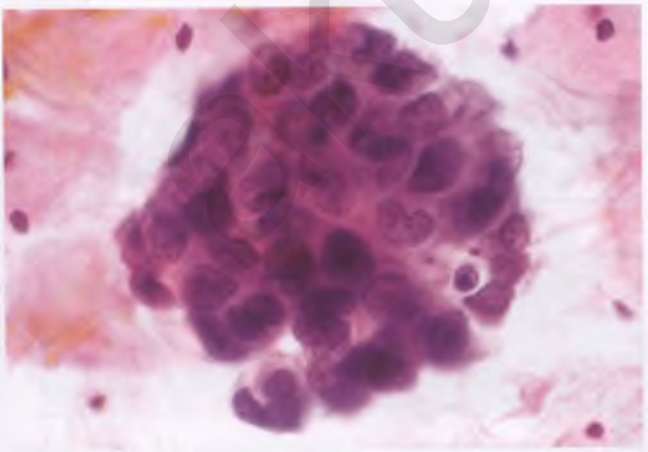

FIGURE 3.272. Primary peritoneal serous carcinoma presenting in a conventional Pap smear. The malignant glandular cells in this example are fairly well-preserved, and the background is clean.

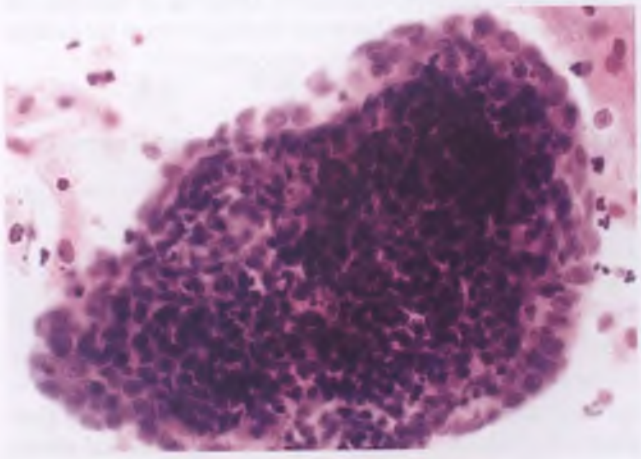

FIGURE 3.273. Double-contoured cluster of exfoliated endometrial cells consisting of a core of condensed endometrial stromal cells surrounded by a rim of glandular cells.

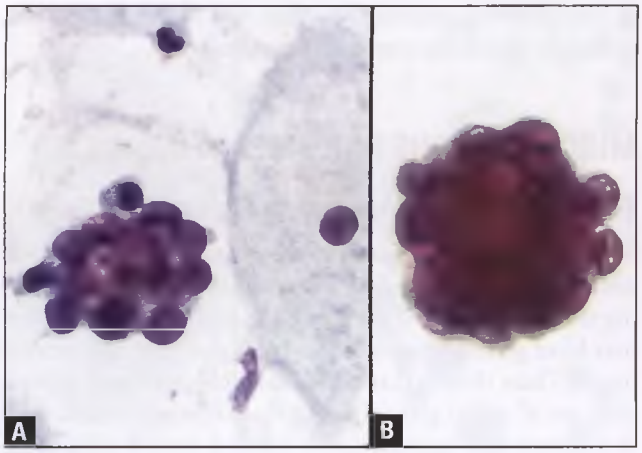

FIGURE 3.274. Monocontoured clusters of exfoliated endometrial cells. **A**: Note the similarity in nuclear size between the endometrial cells within the cell cluster and the intermediate squamous cell at the right of the image (conventional Pap smear). **B**: Compact three-dimensional cluster of endometrial cells in a clean background (liquid-based preparation).

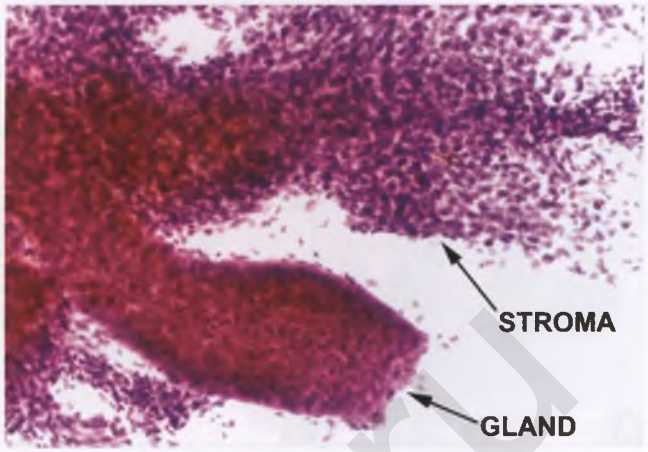

FIGURE 3.275. Large tissue fragment of abraded lower uterine segment endometrium consisting of an endometrial gland and its associated stroma.

menstrual period, symptoms, use of contraceptives or other hormonal agents, and risk factors for endometrial carcinoma. This method of reporting leaves interpretation of the significance of exfoliated, benign-appearing endometrial cells in Pap smears in this group of women to the clinicians, who need to be aware of the near-zero incidence of significant pathology in endometrial samples taken from asymptomatic, premenopausal patients, whether the endometrial cells are in phase or out of phase with the menstrual cycle.[258,259] In contrast to this group of patients, postmenopausal women with benign-appearing endometrial cells in their Pap smears will have significant endometrial pathology in approximately 10% of cases and should undergo endometrial sampling.[256] Although most of these postmenopausal patients with significant endometrial pathology will also have abnormal vaginal bleeding that would independently prompt endometrial sampling, a minority are asymptomatic and their Pap smear finding serves as the catalyst for discovery of the endometrial abnormality.[256]

Endometrial Cells from Lower Uterine Segment

Inadvertent sampling of endometrial cells from the lower uterine segment, which correlates with the use of the cytobrush as the device for sampling the endocervical canal, results in Pap smears with cellular fragments that can be quite concerning to the uninitiated.[260] These endometrial cells are abraded rather than spontaneously exfoliated, and are of no clinical significance, although they represent a form of "hyperchromatic crowded groups" that may be misinterpreted as atypical glandular cells, endocervical AIS, endometrial/endocervical adenocarcinoma, or squamous cell CIS.

The most easily recognized abraded endometrial samples consist of large biphasic tissue fragments that contain tubular endometrial glands in close association with a cellular, spindle cell stroma (Fig. 3.275). When examined under high magnification, the nuclei of the stromal component tend to be oval with finely granular chromatin (Fig. 3.276). The identification of elongated, slender capillary nuclei coursing through these stromal fragments facilitates their recognition. The appearance of some endometrial glandular fragments can be more worrisome, since the nuclei can be extremely crowded, the nuclear to cytoplasmic ratio is very high, and the chromatin is granular. If peripheral palisading is present, AIS or CIS involving endocervical glands may be considered (Fig. 3.277); if peripheral palisading is absent, these glandular fragments may be difficult to distinguish from CIS (Fig. 3.278). The presence in the smear of other fragments that are more obviously derived from the lower uterine segment, the intimate association of glandular and stromal elements, and the absence of isolated dysplastic squamous cells (in the

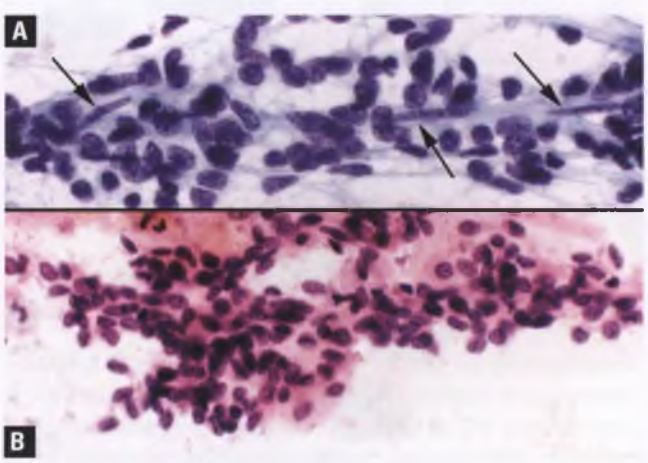

FIGURE 3.276. **A,B**: Abraded endometrial stromal cells. Note the presence of capillary nuclei streaming through the stromal fragment in **A** (*arrows*).

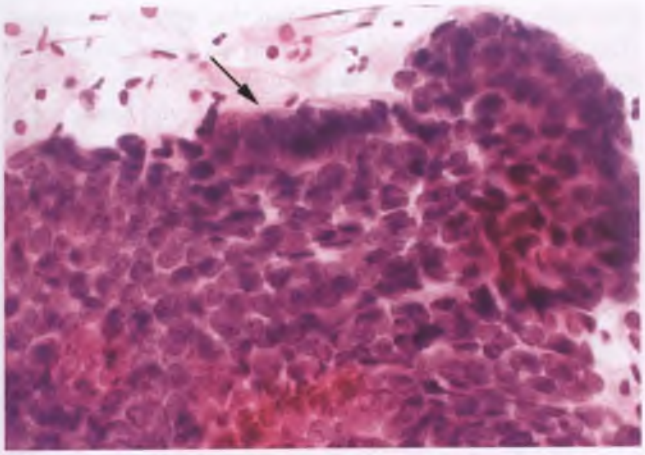

FIGURE 3.277. This crowded sheet of endometrial glandular cells from the lower uterine segment resembles AIS. Some of the cells that exhibit pseudostratified, palisaded nuclei (*arrow*) are associated with blurred, hair-like structures suggestive of cilia, which are normally found in a subset of these glandular cells.

differential diagnosis with CIS) can aid in their recognition as benign endometrial glandular tissue.[261]

Histiocytes

In Pap smears, histiocytes are found as single cells or in loose aggregates, and are recognized by (a) nuclei that are often eccentrically located, at least some of which are bean shaped, (b) finely vacuolated cytoplasm, and (c) fine, pale chromatin (Fig. 3.279). Mitotic figures may be present. Histiocytes may also be multinucleated, in which case the multiple nuclei typically closely resemble one another (Fig. 3.280). Attention to the nuclear and cytoplasmic features of the usual type of histiocyte allows distinction from HSIL and other types of epithelial cells.

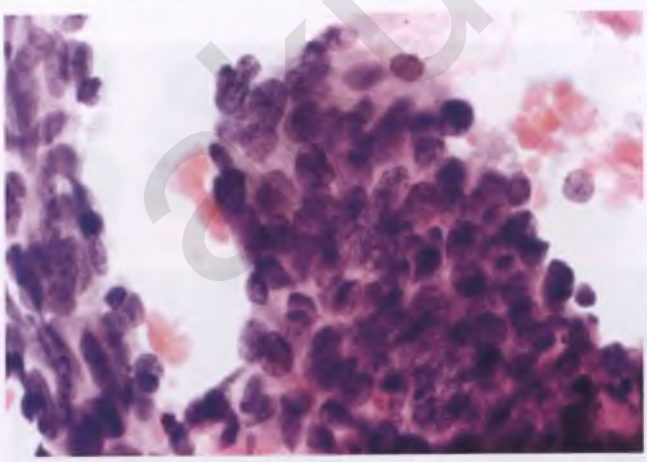

FIGURE 3.278. In isolation, this HCG of endometrial glandular cells from the lower uterine segment is difficult to distinguish from CIS. Recognition of its association with the endometrial stromal fragment at the far left assists in making the correct interpretation.

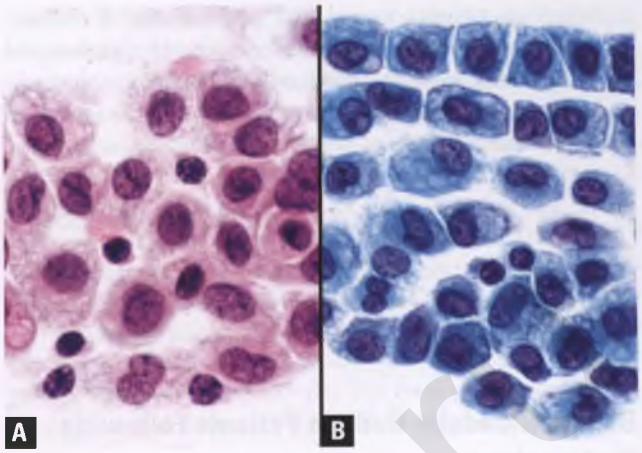

FIGURE 3.279. **A,B**: Histiocytes in Pap smears.

Note: Cytopathologists have traditionally divided endometrial stromal cells into superficial and deep types, and have attributed the "exodus" of "sticky histiocytes" on days 6 to 10 of the menstrual cycle to the shedding of superficial endometrial stromal cells. There is no evidence that these "superficial endometrial stromal cells" are anything other than histiocytes. Although histiocytes may be found within the normal endometrial stroma, they should not be regarded as one of its integral components. The "deep endometrial stromal cells" are the stromal cells discussed and illustrated in the previous section, and are present throughout the full thickness of the normal proliferative and lower uterine segment endometrium. Although the division of the endometrium into compact, spongy, and basal layers is both histologically and functionally justifiable, the separation of endometrial stromal cells into superficial and deep types based on cytologic grounds seems to be an artificial and invalid concept.

Foam Cells

The presence of foam cells in Pap smears has been thought by some to be an indirect indicator of possible endometrial

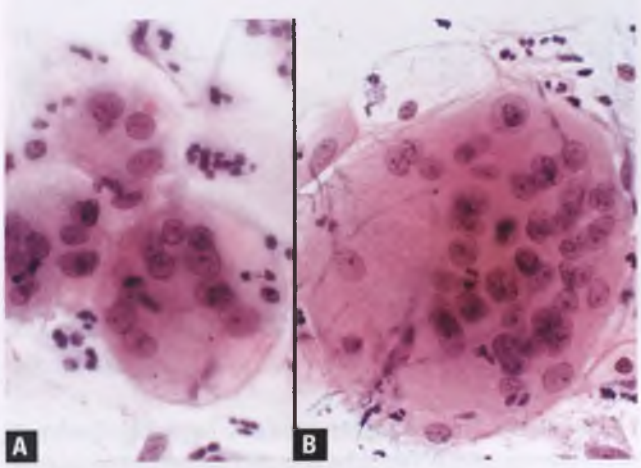

FIGURE 3.280. **A,B**: Multinucleated histiocytes in Pap smears.

pathology in perimenopausal and postmenopausal women, since these cells are often present in endometrial hyperplasia and carcinoma (see Chapter 4). Foam cells express histiocytic markers, and are thought to represent lipid-laden histiocytes.[262] In contrast to the usual type of histiocyte seen during the "exodus," foam cells are larger with more voluminous, foamy, pale cytoplasm, and are more likely to contain ingested cellular debris (Fig. 3.281). Most recent studies have shown that the isolated presence of histiocytes in a Pap smear of an asymptomatic postmenopausal woman, whether foamy or otherwise, is a nonspecific finding that does not warrant endometrial sampling.[263,264]

Benign Glandular Cells in Patients Following Hysterectomy

There are several possible explanations for the presence of benign glandular cells in Pap smears of patients who have previously undergone a hysterectomy.[265] In those situations in which the cells in question are truly glandular, these explanations include (a) an incorrect clinical history—the patient either never had her uterus removed or had undergone a supracervical hysterectomy, (b) prolapse of the fallopian tube into the vaginal apex, (c) vaginal endometriosis, (d) vaginal adenosis, (e) traumatized vaginal wall cysts of müllerian or mesonephric type, (f) superficial mesonephric duct remnants, and (g) rectovaginal fistula. On other occasions, pseudoglandular cells related to the presence of occasional goblet-like cells within groups of parabasal cells[266] or glandular mimicry by histiocytic cells may be the source of the apparently paradoxical glandular cells.

Trophoblastic Cells from Pregnant Patients

Trophoblastic cells can rarely be seen in Pap smears from patients who are pregnant or during the postpartum period.[267,268] If present in large numbers, trophoblastic disease or an abortion should be suspected. Syncytiotrophoblasts are multinucleated giant cells with abundant cytoplasm that may be vacuolated (Fig. 3.282A). Cytotrophoblastic cells are found singly or in small groups and may be mistaken for severely dysplastic or malignant cells, given their high nuclear to cytoplasmic ratios, nuclear atypia, and variably prominent nucleoli (Fig. 3.282B). Both types of trophoblastic cells can show degenerative changes. The cytologic diagnosis of malignancy should be made with caution during pregnancy and following delivery, given the many possible diagnostic pitfalls (exfoliated trophoblastic cells, ectopic decidua, and ASR).

Sperm

Spermatozoa have small, oval to teardrop-shaped heads and long, thin flagella (tails). In Pap smears, the basal portion of the sperm head stains more darkly than the apical region, and the sperm may be found intact or without their tails (Fig. 3.283). Except under medicolegal circumstances, the presence of sperm is not considered a reportable finding.

Starch Granules

Starch granules derived from glove powder may be found as a contaminant in Pap smears. These granules have a characteristic "Maltese cross" pattern of birefringence when examined under polarized light (Fig. 3.284).

PROCESSING TIPS FOR CERVICAL SAMPLES

Cervical Biopsies

The prosector should recognize the portion of the biopsies covered by epithelium and bisect samples ≥4 mm with a sharp scalpel in the correct plane, so that orientation is maintained and diagnostic tissue is not buried deep within the paraffin block. The histotechnologist must orient the specimen for sectioning perpendicular to

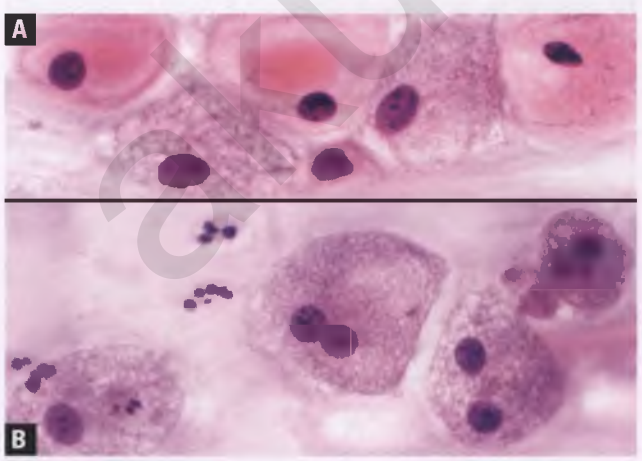

FIGURE 3.281. Foam cells in Pap smears. **A**: Two foam cells admixed with squamous cells. **B**: Two of the foam cells are binucleated, whereas the other two have ingested fragments of neutrophil-derived nuclei.

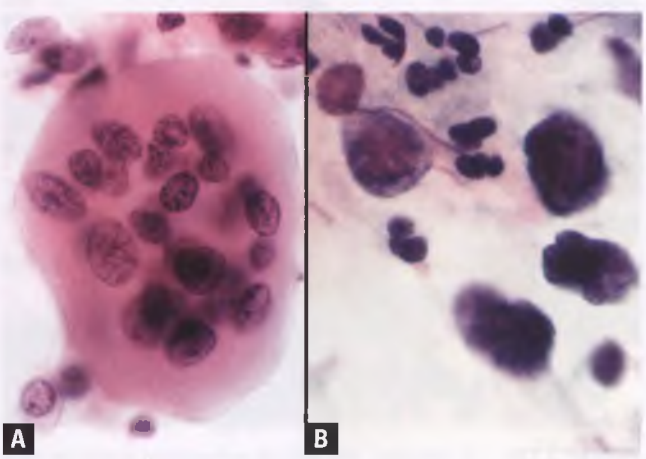

FIGURE 3.282. Trophoblastic cells in Pap smears from two different pregnant patients. **A**: Multinucleated syncytiotrophoblastic cell. **B**: Degenerated cytotrophoblastic cells.

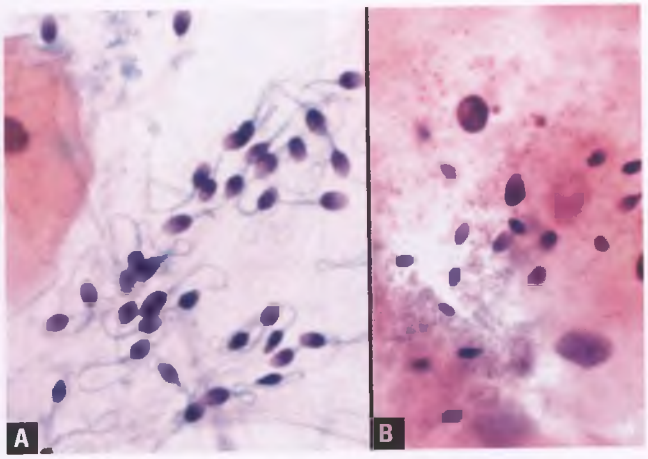

FIGURE 3.283. Sperm in Pap smears. **A**: Sperm are more easily recognized when they have retained their tails. **B**: It is not uncommon for sperm heads to be found in Pap smears without their tails.

the mucosal surface, so that epithelial maturation and the epithelial–stromal interface can be properly evaluated. Most laboratories initially evaluate ribbons of tissue sections from three different levels in the paraffin block. Since cervical abnormalities can be focal, additional sections should be prepared and evaluated in all cases in which the initial sections do not account for the abnormality noted in the Pap smear that prompted the biopsy.

If the cervical biopsy is being performed because of a Pap smear diagnosis of ASC-H, it is recommended that the biopsy be cut using an "immuno protocol" in which unstained slides are cut between the routinely stained slides and reserved for possible immunohistochemistry. This is prudent because (a) ASC-H smears often correspond to cervical epithelium with questionable metaplastic high-grade dysplasia in which p16 and MIB-1 immunostaining can be quite helpful in arriving at the correct diagnosis, and (b) the candidate lesion may be small and not available for further analysis in ordinary recuts. When requesting immunohistochemistry on a focal lesion in which unstained slides have not been prepared in advance, it is recommended that an additional H&E-stained slide be prepared as the last recut and that it be evaluated for specimen adequacy prior to actual performance of the immunostains.

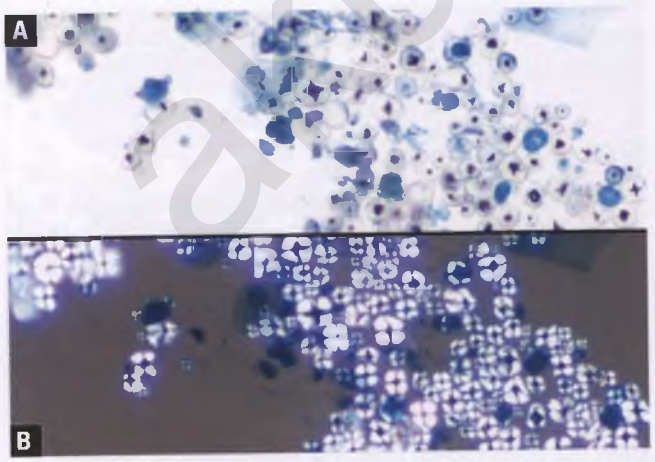

FIGURE 3.284. Starch granules. **A**: Appearance of the granules in a Pap smear. **B**: When viewed under polarized light, these granules exhibit a characteristic "Maltese cross" pattern of birefringence.

Endocervical Curettings

The gynecologist should place the sample on a Telfa pad or other suitable smooth surface before placing the specimen into formalin, so that the minute and fragmented specimen can be gently scraped from the pad, molded into a mucoid tissue aggregate, wrapped in lens paper that has been premoistened with formalin, and submitted in a cassette for further processing.

Cervical Cone Biopsy/Loop Electrosurgical Excision Procedure

Ideally, cone biopsies should be received in an intact, fresh state in a saline-filled container, with a suture placed by the gynecologist marking the 12:00 position (Fig. 3.285A). LEEP specimens are often smaller, more irregularly shaped, more difficult to orient, and fragmented. The exocervical and endocervical resection margins of intact specimens are inked (some prosectors prefer to use different-colored inks for the exocervical and endocervical margins, since orientation may not be obvious in all of the microscopic sections). If the specimen is received in more than one piece, the exocervical and endocervical specimen edges may still be inked for orientation purposes, but the distinction between a specimen edge and a true surgical margin must be kept in mind at the time of microscopic examination.

An intact specimen is opened by inserting one blade of a sharp-pointed scissors into the endocervical canal and cutting longitudinally along the 12 o'clock position. If the specimen has not been oriented as to position, it may be opened at any

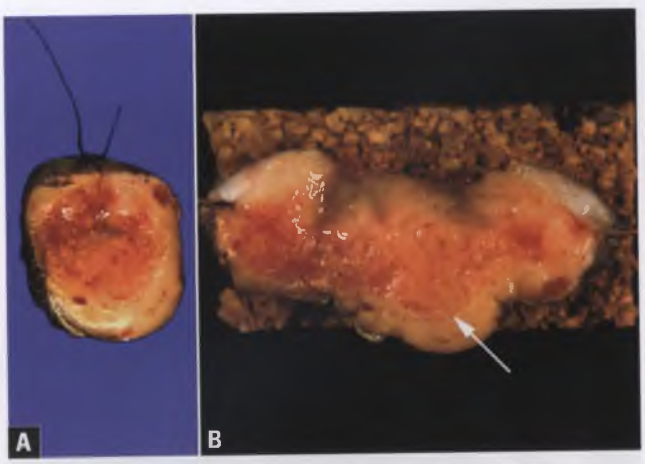

FIGURE 3.285. **A**: Intact, fresh cervical conization specimen. An orientating suture placed by the gynecologist marks the 12:00 position. The resection margins have been marked with black ink. **B**: The fresh conization specimen has been opened at the 12:00 position and pinned to a corkboard. An *arrow* marks the squamocolumnar junction.

site. The specimen is pinned to a piece of corkboard that is slightly larger than the tissue, with the mucosal surface facing up and taking care to pass pins through the stroma rather than the epithelium (Fig. 3.285B). The corkboard is then flipped over and placed in a formalin-filled container, where the tissue is allowed to fix for a minimum of 3 hours. The specimen is then removed from the corkboard and submitted entirely as sequential 2- to 3-mm thick parallel sections taken perpendicular to the mucosal surface in a manner that will optimally display the transformation zone. By convention, sectioning begins at the 12 o'clock position (the right-hand end of the opened, fixed specimen when viewed with the mucosal surface upward and the exocervix rimming the bottom aspect) and proceeds clockwise (from right to left). Since two to three tissue slices typically fit in a single cassette, it is usually feasible to submit a conization specimen in four cassettes, each of which represents tissue from one specific quadrant (Fig. 3.286).

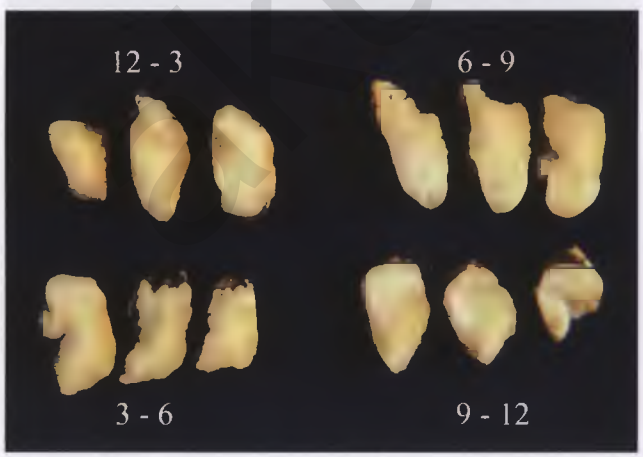

FIGURE 3.286. Fixed sections of a cervical conization specimen grouped into their quadrants (12 to 3 o'clock, 3 to 6 o'clock, 6 to 9 o'clock, and 9 to 12 o'clock) prior to placement within four cassettes.

ARTIFACTS IN CERVICAL SAMPLES

Tangential Sectioning

When tissue is suboptimally oriented in the paraffin block, tangential sectioning may occur that can result in confusing architectural patterns. A clue that the tissue has been tangentially cut is the presence of peculiar bridging connections of epithelium at the epithelial–stromal interface (Fig. 3.287). If sufficient tissue remains in the paraffin block and the diagnosis is unclear, reorientation and re-embedding of the tissue is recommended prior to obtaining additional sections.

Cautery Artifact

The LEEP (which when performed with a large loop may also be referred to as large loop excision of transformation zone or LLETZ) and laser conization induce characteristic cautery-related alterations in epithelial and stromal tissues. The epithelial

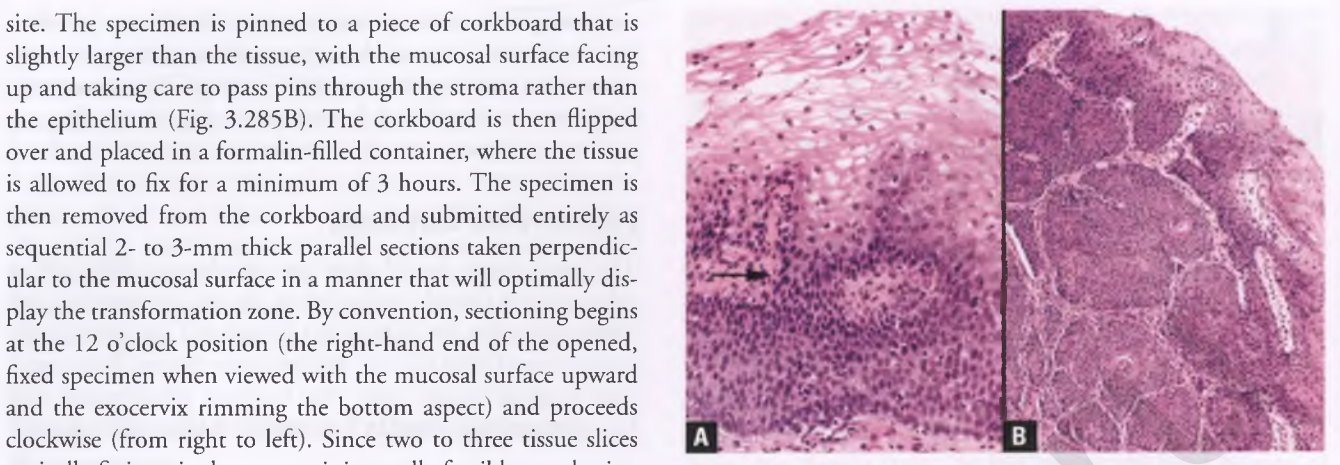

FIGURE 3.287. Tangential sectioning artifacts. **A**: Portions of the lower aspects of the epithelium appear thickened, and there is an artifactual epithelial bridge at the epithelial-stromal interface (*arrow*). Samples such as this could be misinterpreted as basal cell hyperplasia or LSIL. **B**: Tangential sectioning of squamous metaplasia has increased its architectural complexity, increasing its resemblance to invasive squamous cell carcinoma.

architecture becomes distorted, and the epithelial nuclei become compressed, hyperchromatic, and elongated, with a tendency to stream in a particular direction (Fig. 3.288). The stroma at the cauterized specimen edges, which may or may not represent true surgical margins, shows increased eosinophilia (as seen along the periphery of the image in the lower right of the quartet of images depicted in Figs. 3.156-3.159). Since significant squamous and glandular lesions of the cervix may also feature elongated cells with hyperchromatic nuclei, cautery artifact may interfere with proper interpretation. When obvious dysplasia is present elsewhere, it is often not important whether a particular cauterized focus is dysplastic. However, cautery artifact may interfere with definitive assessment of the surgical margins, which is desirable in view of the fact that patients with positive margins are more likely to have persistent or recurrent disease. In this situation, MIB-1 immunohistochemistry can be of assistance, since cauterized epithelium retains its usual patterns of immunoreactivity with the MIB-1 antibody (Fig. 3.289).[101]

Retraction Artifact

In situations where tissue fixation is delayed or inadequate, there is often prominent autolysis-related retraction of epithelial nests and glands away from their associated stroma, creating clusters of epithelial cells or glands surrounded by clear spaces in a pattern that can mimic widespread angiolymphatic invasion (Fig. 3.290). The global nature of this artifact, the presence of other features of autolysis such as epithelial sloughing, and the absence of an endothelial lining around the clear spaces help to distinguish this phenomenon from true angiolymphatic invasion.[†]

[†]Angiolymphatic invasion (also referred to as capillary-lymphatic space invasion, lymphovascular invasion, or vascular space invasion) connotes tumor invasion of either lymphatics or small vascular spaces (capillaries or venules), which are often not distinguishable from one another in routinely-stained sections.

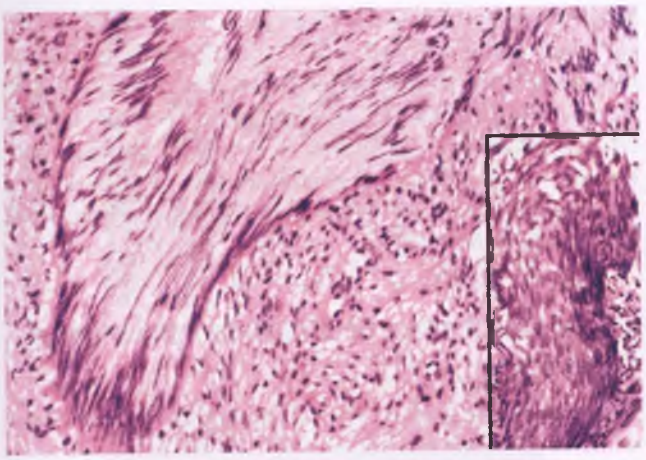

FIGURE 3.288. Endocervical gland with cautery artifact. The inset shows similar thermal-related damage to squamous epithelium.

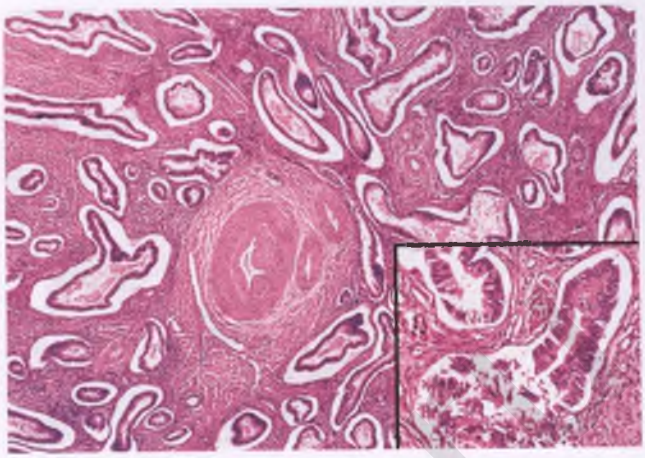

FIGURE 3.290. Invasive endocervical adenocarcinoma with autolysis-induced retraction artifact. The lower half of the inset highlights a focus of epithelial sloughing, which is another autolysis-related artifact.

In other situations, retraction artifact around nests of invasive cancer seems to reflect an altered relationship between tumor cell nests and stroma rather than simply representing a fixation-related artifact.[269] Distinguishing true angiolymphatic invasion from this type of retraction artifact is a common problem in surgical pathology. Features that help in the recognition of true angiolymphatic invasion include (a) intraluminal nests of tumor cells partially attached to the vessel wall, (b) smooth-surfaced nests of intraluminal tumor that may be covered by endothelium, (c) tumor cells associated with intravascular thrombotic material (in cases of blood vessel involvement), (d) the involved spaces being sharply demarcated, lined by endothelium, and devoid of an associated desmoplastic stromal reaction, and (e) the involved spaces being located in the tissues surrounding rather than within the tumor, preferably in association with other nearby vascular structures (Fig. 3.291). In ambiguous cases, immunohistochemical confirmation that the involved spaces are lymphatic (positive for a lymphatic marker such as D2-40/podoplanin)[270,271] or vascular (CD-31 positivity in conjunction with lymphatic marker negativity)[271] can be quite helpful, although sometimes the candidate lesion may be too focal to assess immunohistochemically. Some cases of legitimate angiolymphatic invasion do not demonstrate attachment of the tumor plug to the vessel wall and have spaces with an inconspicuous endothelial lining, which can heighten the resemblance to retraction artifact (Fig. 3.292). Another differential diagnostic consideration is artifactual displacement of dysplastic/malignant epithelium into angiolymphatic spaces (see below). When the assessment of angiolymphatic invasion is not definitive, the pathologist should describe the finding, indicate the differential diagnoses and their various likelihoods, and categorize this prognostic indicator as equivocal.

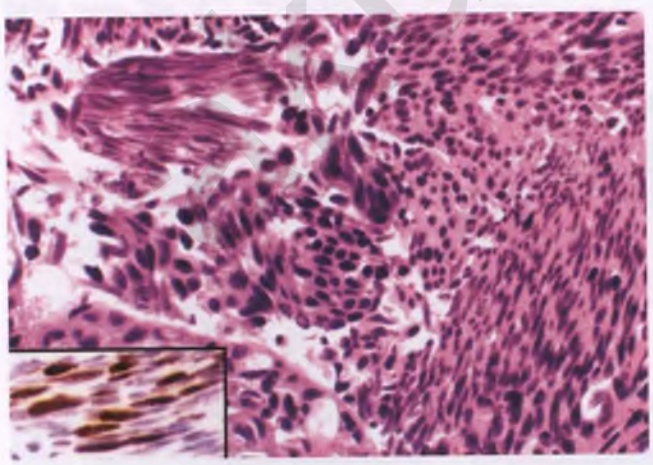

FIGURE 3.289. HSIL with variable degrees of cautery artifact. The inset shows several cauterized dysplastic epithelial cells with retained immunoreactivity for MIB-1.

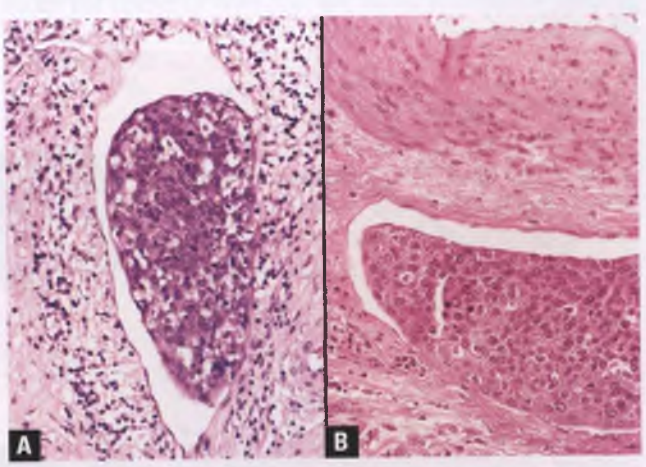

FIGURE 3.291. **A,B**: Lymphatic invasion in cervical squamous cell carcinoma. Note (a) the partial attachment of tumor plugs to the vessel walls, (b) the thin, flattened layer of endothelium partially enveloping the nests of tumor, and (c) the expected location of a lymphatic channel in close proximity to a thick-walled vessel in **B**.

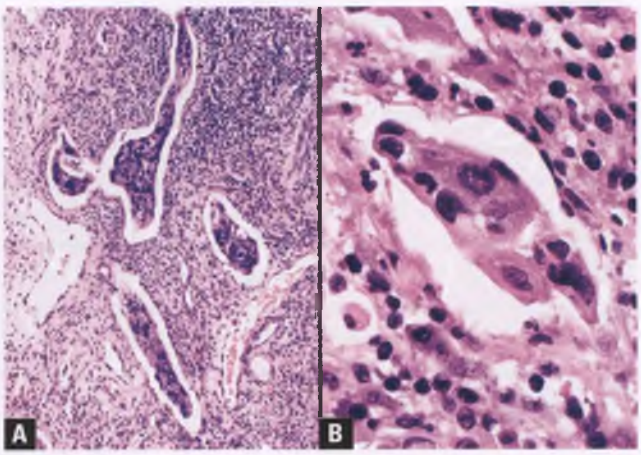

FIGURE 3.292. Lymphatic invasion in cervical squamous cell carcinoma **(A)** versus retraction artifact **(B)**. **A**: The nests of intraluminal tumor cells are surrounded by clear spaces with an inconspicuous endothelial lining, mimicking retraction artifact. However, these nests are located at the tumor periphery, there are other nearby uninvolved vessels, and the stroma, although chronically inflamed, lacks a desmoplastic response. **B**: Nest of invasive squamous cell carcinoma with retraction artifact. Neither the tumor cell nest nor the surrounding artifactually created clear space are completely smooth-surfaced, and the lining of a true angiolymphatic space is not evident.

Iatrogenic Displacement of Epithelium

An unusual finding related to cervical biopsy, increased intracavitary pressure, or injection of local anesthetic is artifactual displacement of epithelium (which may be malignant, dysplastic, metaplastic, reactive, or normal) into the cervical stroma or into vascular spaces (Fig. 3.293).[272] Depending on the type of displaced epithelium and its location, this artifact may mimic invasive cancer or vascular invasion by tumor. This artifact should be considered when (a) the epithelial abnormality is focal, (b) the potentially malignant focus seems out of context with the neighboring tissue, and (c) there are associated biopsy-site changes (hemorrhage, granulation tissue, fibrosis, and/or foreign body reaction). In the setting of an associated invasive cervical carcinoma, the finding of dysplastic/malignant epithelium within a vessel is generally assumed to represent true angiolymphatic invasion, unless a nearby biopsy site or needle tract can be demonstrated.

Signet-Ring Artifact in Squamous Epithelium of Exocervix

On occasion, an artifact that is presumably fixation related results in cells resembling signet-ring cells within the squamous epithelium of the exocervix (Fig. 3.294). Empty intracytoplasmic vacuoles compress the nuclei to the periphery of the cells, creating the signet-ring morphology. These vacuolated keratinocytes are joined to other keratinocytes by intercellular bridges, which is a clue to their squamous rather than glandular nature. If indicated, PAS with diastase or mucicarmine stains can be performed to confirm the absence of mucin within the vacuolated cells. A negative mucin stain helps to exclude extramammary Paget's disease, which is exceedingly rare in the cervix. Little attention has been paid to this artifact in the gynecologic pathology literature, but it is similar to the signet-ring artifact that has been documented in skin specimens.[273]

Artifact Induced by Lugol's Solution

The dehydration artifact associated with the application of a strong iodine (Lugol's) solution to the cervix in the Schiller test is most well documented in HSIL as a superficial band-like zone in which the nuclei appear intensely hyperchromatic with loss of chromatic detail and presence of visible intercellular space (Fig. 3.295A).[274] When this "Lugol effect" involves

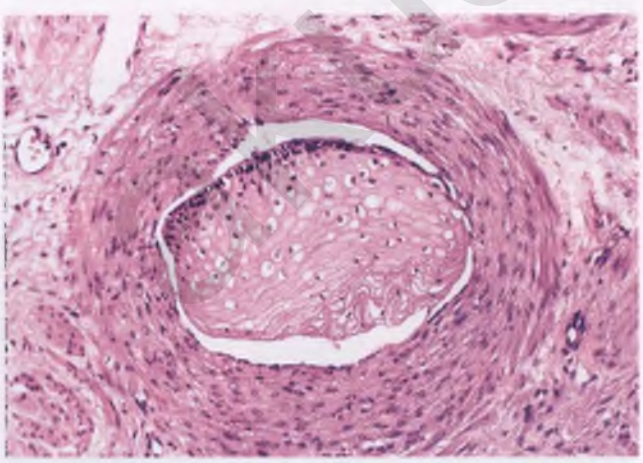

FIGURE 3.293. Displaced fragment of normal exocervical epithelium within a uterine vessel. The lack of epithelial atypia, the absence of associated thrombosis, and the absence of attachment of the epithelial fragment to the vessel wall all support the artifactual nature of this finding.

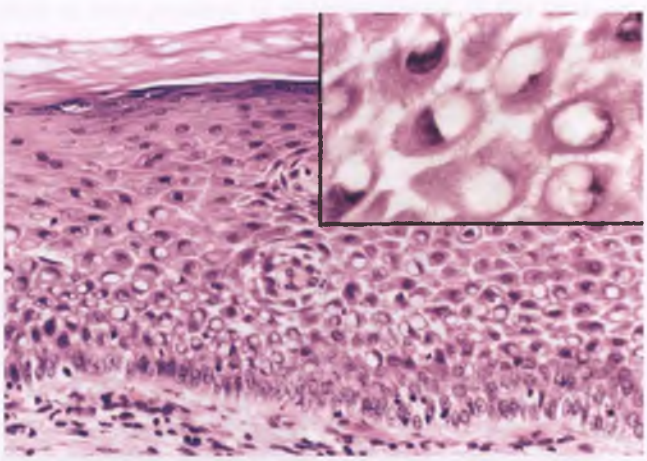

FIGURE 3.294. Signet-ring artifact in exocervical squamous epithelium that is also hyperkeratotic and spongiotic. The inset shows some of the vacuolated cells at high magnification (note the intercellular bridges, which are a feature of squamous differentiation).

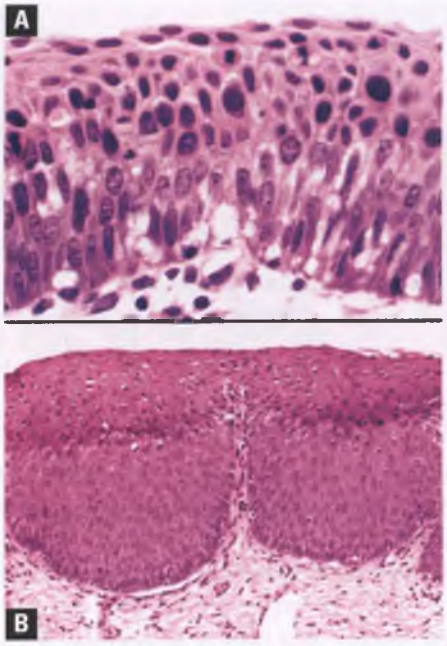

FIGURE 3.295. Lugol effect involving HSIL **(A)** and squamous metaplasia **(B)**. The superficial, band-like nature of this artifact is characteristic.

squamous metaplasia, it can induce changes that mimic koilocytosis (Fig. 3.295B). The resemblance to koilocytosis is due to the presence of a superficial zone of cytoplasmic eosinophilia and nuclear pyknosis that is readily apparent at low magnification. However, the band-like nature of this region, the absence of nuclear enlargement/atypia, and confirmation from the gynecologist regarding the application of Lugol's solution facilitate recognition of this artifact.

Artifact Induced by Monsel's Solution

Monsel's solution (ferric subsulfate) is a topical hemostatic agent that may be used following cervical biopsy or uterine curettage to control bleeding. If additional tissue is obtained within the first few weeks following application of Monsel's solution, the epithelium, superficial stroma, and associated clots of blood may exhibit diffuse iron deposition that can be highlighted with a Prussian blue stain (Fig. 3.296).[275,276] Necrosis of the superficial stroma underlying denuded mucosa is also present and has been attributed to the ability of Monsel's solution to denature and agglutinate proteins.[275,276] During the acute phase (the first 7–10 days), iron deposition may be so extensive as to cast a brown hue over the blood clots and tissue fragments, rendering the epithelium in such samples difficult or impossible to interpret (Fig. 3.297). It may take up to 3 months for these artifact-related changes to resolve, during which time pigmented macrophages, granulation tissue, and foreign body giant cells may be seen. However, superficial changes that can potentially hinder recognition and interpretation of epithelial abnormalities typically resolve within 3 weeks of the application of Monsel's solution.

Artifact Induced by Silver Nitrate

Silver nitrate cautery sticks are sometimes used to control the bleeding in cervical biopsies, which can result in deposition of silver in the epithelium and superficial stroma.[277] In the exocervix, silver deposits penetrate various depths of the epithelium corresponding to the length of time in which the tissue has been subjected to silver nitrate treatment, and there is usually associated spongiosis (intercellular edema). When there is full-thickness involvement, the silver deposits tend to congregate in the basal and parabasal regions (Fig. 3.298A). The silver deposits are golden brown granules that are found both within and between epithelial cells. In contrast to the brown deposits in the artifact related to Monsel's solution, these deposits are negative with the Prussian blue iron stain. In the columnar mucosa of the endocervix, most of the silver deposits penetrate the epithelial layer and are found in a narrow band in the superficial stroma (Fig. 3.298B). The silver deposits can be

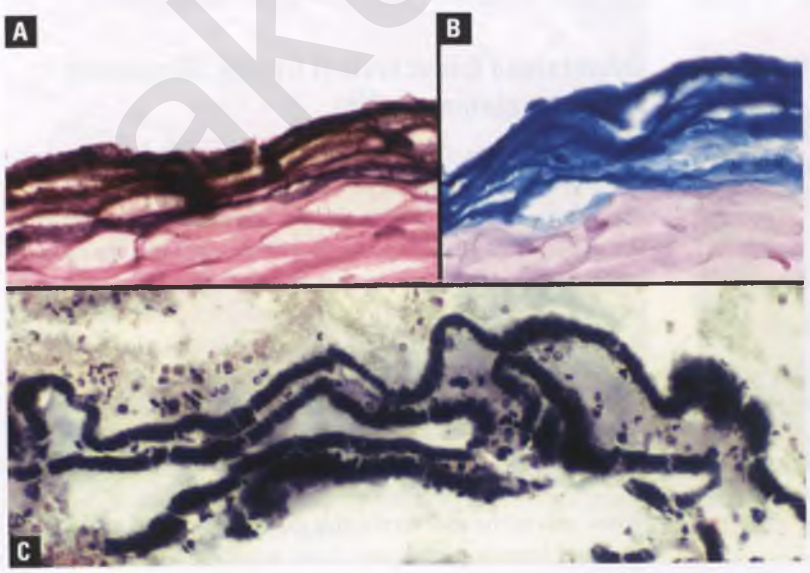

FIGURE 3.296. Artifact induced by Monsel's solution. **A**: There is encrustation of iron pigment in the superficial layers of the exocervical epithelium. **B**: The encrusted iron pigment is intensely positive with the Prussian's blue iron stain. **C**: These strips of endocervical epithelium are impossible to evaluate due to superimposed heavy pigmentation.

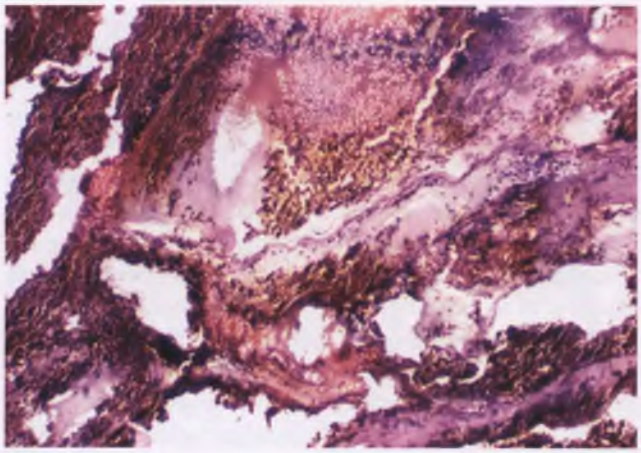

FIGURE 3.297. Endocervical curettage obscured by artifact induced by the recent application of Monsel's solution. There is extensive pigmentation due to the deposition of iron, most of which is in fragments of coagulated blood.

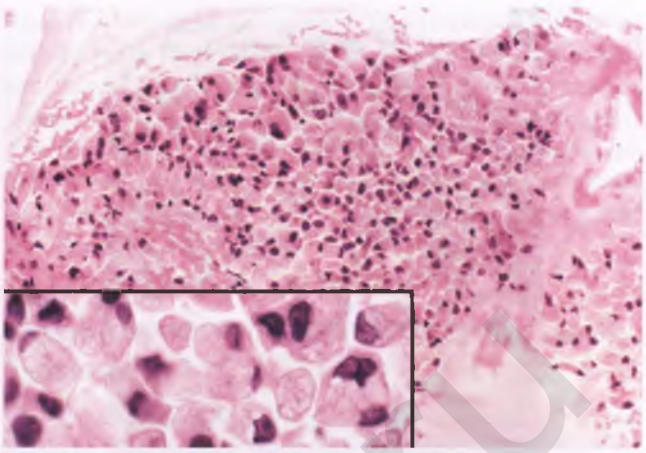

FIGURE 3.299. Degenerated endocervical cells from an endocervical curettage, some of which resemble signet-ring cells from an adenocarcinoma.

removed by treatment with a sodium thiosulphate/potassium ferrocyanide solution if they are obscuring morphologic detail of the involved epithelial cells.

Degenerated Endocervical Cells Simulating Signet-Ring Adenocarcinoma

When endocervical cells degenerate, they have a tendency to form loose aggregates, assume rounded shapes, and maintain the eccentric location of their nuclei. In histologic sections from endocervical curettings, this can result in an appearance that resembles signet-ring adenocarcinoma (Fig. 3.299). In contrast to carcinoma, these aggregates represent an incidental microscopic finding, and there is no evidence of tissue invasion. This finding is associated with oral contraceptives and MGH, and cells near the end stage of this process account for the pseudoparakeratosis seen in Pap smears that is related to endocervical cell degeneration (Fig. 3.54). Benign signet-ring cell change of presumed degenerative origin has also been reported within the mucosa of an endocervical polyp.[278]

Given that nonneoplastic signet-ring cell change and signet-ring adenocarcinoma both consist of cells that contain abundant neutral mucin and often have overlapping nuclear features, the identification of differentially expressed immunomarkers would be desirable to help distinguish these morphologically similar processes from one another. Toward this end, it has been shown that nonneoplastic signet-ring cell change within the gastrointestinal tract exhibits a p53 negative, Ki-67 negative immunophenotype, which contrasts with the presence of numerous p53 and Ki-67 positive cells in gastrointestinal signet-ring adenocarcinoma.[279] Similar studies of signet-ring lesions of the uterine cervix have not yet been reported.

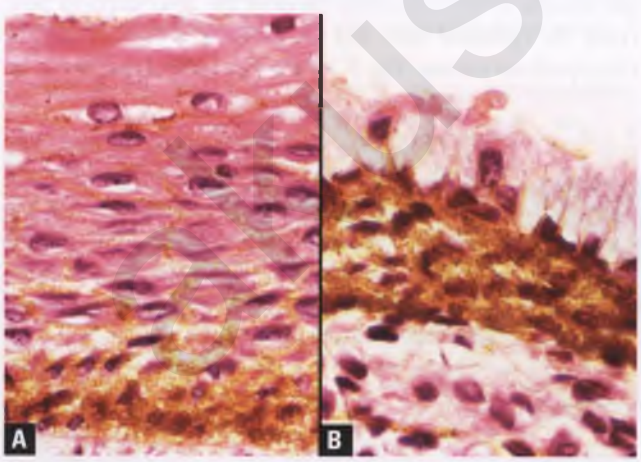

FIGURE 3.298. Artifact induced by silver nitrate. **A**: Granules of golden brown pigment within spongiotic exocervical epithelium are seen congregating in the basal/parabasal region. **B**: In this image, there are similar-appearing granules within endocervical tissue. The bulk of these granules are located in a band within the stroma immediately beneath the surface epithelium.

Overstained Endocervical Glands Simulating Adenocarcinoma in Situ

In some instances, the mucin within endocervical glands stains too heavily with hematoxylin, resulting in glands that can simulate endocervical AIS (Fig. 3.300). Personal experience with this artifact has found it to be associated with the use of Gill's rather than Harris hematoxylin, or when the slides were subjected to prolonged exposure to hematoxylin. Since this artifact makes screening for glandular abnormalities at low magnification impossible and obscures cellular detail, slides with this problem should be decolorized and properly restained.

Pseudolipomatosis

When seen in the endocervix, this gas bubble-related artifact that simulates heterotopic adipose tissue may be related to exposure

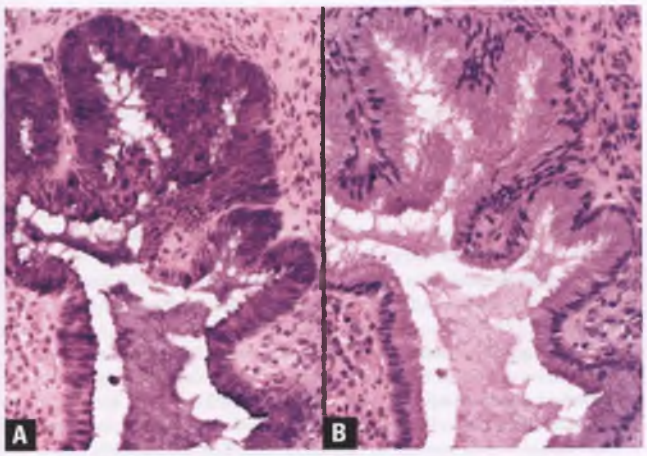

FIGURE 3.300. Hematoxylin overstaining artifact simulating endocervical AIS. **A**: This overstained normal endocervical gland is at risk for being misinterpreted as AIS. **B**: This image shows the same gland after decolorization and restaining, which reveals its unremarkable nature.

to pressurized gas during hysteroscopy[280] or, as recently demonstrated for colonic pseudolipomatosis,[281] as a consequence of exposure to instruments tainted with the disinfectant hydrogen peroxide. Adipocyte nuclei are not present, but can be mimicked by stromal cells that are compressed by the dissecting gas bubbles, which have a wide range of sizes and shapes and tend to track along pathways of least resistance (Fig. 3.301). A similar gas bubble-related artifact is commonly seen in endometrial samples that are obtained with devices that employ suction or removed during a hysteroscopic procedure (see Chapter 4).

Crush Artifact (Pap Smears)

If too much force is applied when sampled cells are spread on the slide of a conventionally prepared Pap smear, crush artifact

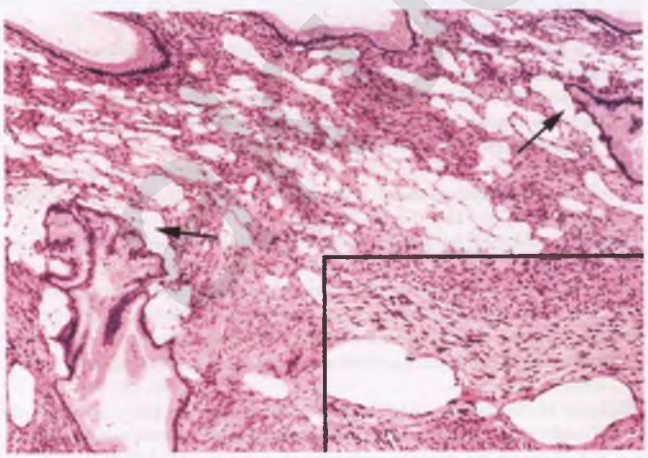

FIGURE 3.301. Endocervix with pseudolipomatosis. The sizes and shapes of the gas bubbles are more variable than the cells of adipose tissue. These bubbles also tend to track along pathways of least resistance, which include glandular-stromal interfaces (*arrows*) and spaces surrounding nerves (inset) and vessels.

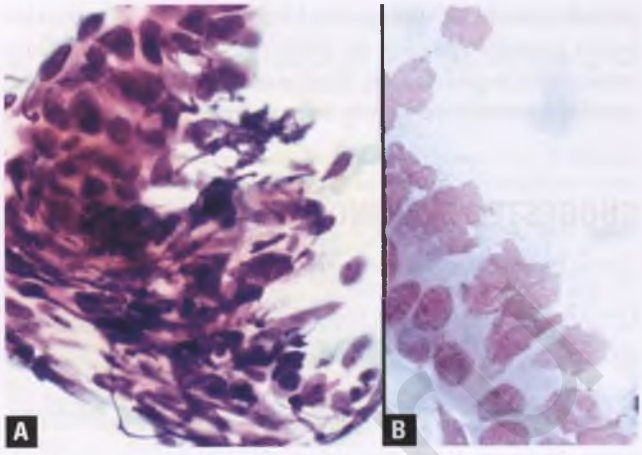

FIGURE 3.302. Crush **(A)** and air-drying **(B)** artifacts in conventional Pap smears.

may result. The affected cells are distorted, and nuclei are transformed into elongated streaks of basophilic material, rendering interpretation of the traumatized areas impossible (Fig. 3.302A).

Air-Drying Artifact (Pap Smears)

Air-drying artifact results when fixation of the cells smeared on the slide of a conventional Pap smear is delayed for more than a few seconds. The air-dried cells appear distorted and washed out, with hazy, indistinct chromatin and artifactually enlarged and irregular nuclei (Fig. 3.302B). Interpretation of Pap smears with extensive air-drying artifact is difficult to impossible. Air-drying artifact is not an issue when liquid-based technology is used.

"Cornflakes" (Pap Smears)

Innumerable, miniscule air bubbles are occasionally trapped on top of squamous cells during coverslipping, creating the so-called "cornflake" artifact. The air bubbles appear as golden brown, refractile granules that preferentially form on the cytoplasm of intermediate squamous cells (Fig. 3.303). Cornflake

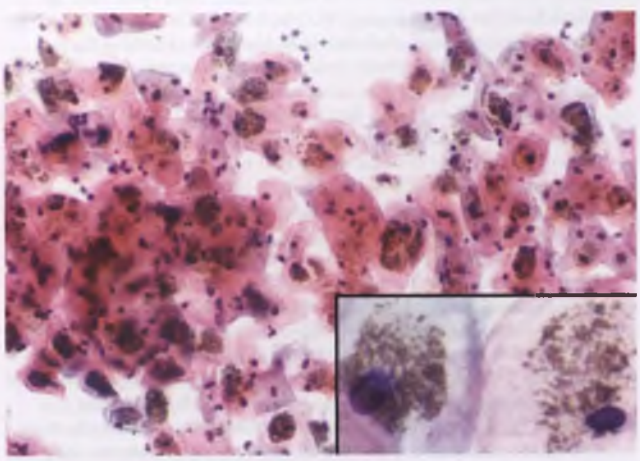

FIGURE 3.303. Cornflake artifact in Pap smear.

granules should be distinguished from the dark blue keratohyalin granules that may be present in squamous cells from smears with hyperkeratosis. If cellular detail is obscured by the cornflake artifact, it may help to recoverslip the slide.

SUGGESTED READINGS

Clement PB, Young RH. *Atlas of Gynecologic Surgical Pathology*. 2nd ed. Philadelphia, PA: Elsevier Saunders; 2008.

Crum CP, Nucci MR, Lee K, eds. *Diagnostic Gynecologic and Obstetric Pathology*. 2nd ed. Philadelphia, PA: Elsevier Saunders; 2011.

DeMay RM. *The Art and Science of Cytopathology*. Chicago, IL: ASCP Press; 1996:61–205.

Fu YS. *Pathology of the Uterine Cervix, Vagina, and Vulva*. 2nd ed. Philadelphia, PA: Saunders; 2002.

Kurman RJ, Ellenson LH, Ronnett BM, eds. *Blaustein's Pathology of the Female Genital Tract*. 6th ed. New York, NY: Springer; 2011.

Kurman RJ, Norris HJ, Wilkinson E. *Tumors of the Cervix, Vagina, and Vulva. Atlas of Tumor Pathology*. Third series, Fascicle 4. Washington, DC: Armed Forces Institute of Pathology; 1992:37–139.

Robboy, SJ, Mutter GL, Prat J, et al., eds. *Robboy's Pathology of the Female Reproductive Tract*. 2nd ed. Oxford, UK: Churchill Livingstone; 2009.

Solomon D, Nayar R, eds. *The Bethesda System for Reporting Cervical Cytology*. 2nd ed. New York, NY: Springer; 2004.

Tavassoli FA, Devilee P, eds. *World Health Organization Classification of Tumors. Pathology and Genetics of Tumours of the Breast and Female Genital Organs*. Lyon, France: IARC Press; 2003:259–289.

Wilbur DC, Henry MR, eds. *College of American Pathologists Practical Guide to Gynecologic Cytopathology: Morphology, Management, and Molecular Methods*. Northfield, IL: CAP Press; 2008.

REFERENCES

1. Suh KS, Silverberg SG. Tubal metaplasia of the uterine cervix. *Int J Gynecol Pathol*. 1990;9:122–128.
2. Oliva E, Clement PB, Young RH. Tubal and tubo-endometrioid metaplasia of the uterine cervix. Unemphasized features that may cause problems in differential diagnosis: a report of 25 cases. *Am J Clin Pathol*. 1995;103:618–623.
3. Vang R, Vinh TN, Burks RT, et al. Pseudoinfiltrative tubal metaplasia of the endocervix: a potential form of in utero diethylstilbestrol exposure-related adenosis simulating minimal deviation adenocarcinoma. *Int J Gynecol Pathol*. 2005;24:391–398.
4. Schlesinger C, Silverberg SG. Endocervical adenocarcinoma in situ of tubal type and its relation to atypical tubal metaplasia. *Int J Gynecol Pathol*. 1999;18:1–4.
5. Yeh IT, Bronner M, LiVolsi VA. Endometrial metaplasia of the uterine endocervix. *Arch Pathol Lab Med*. 1993;117:734–735.
6. Mittal K, Soslow R, McCluggage WG. Application of immunohistochemistry to gynecologic pathology. *Arch Pathol Lab Med*. 2008;132:402–423.
7. Clement PB, Young RH. Florid cystic endosalpingiosis with tumor-like manifestations: a report of four cases including the first reported cases of transmural endosalpingiosis of the uterus. *Am J Surg Pathol*. 1999;23:166–175.
8. Novotny DB, Maygarden SJ, Johnson DE, et al. Tubal metaplasia. A frequent potential pitfall in the cytologic diagnosis of endocervical glandular dysplasia on cervical smears. *Acta Cytol*. 1992;36:1–10.
9. Jones MA, Young RH. Atypical oxyphilic metaplasia of the endocervical epithelium: a report of six cases. *Int J Gynecol Pathol*. 1997;16:99–102.
10. Weir MM, Bell DA, Young RH. Transitional cell metaplasia of the uterine cervix and vagina: an underrecognized lesion that may be confused with high-grade dysplasia. A report of 59 cases. *Am J Surg Pathol*. 1997;21:510–517.
11. Egan AJ, Russell P. Transitional (urothelial) cell metaplasia of the uterine cervix: morphological assessment of 31 cases. *Int J Gynecol Pathol*. 1997;16:89–98.
12. Weir MM, Bell DA. Transitional cell metaplasia of the cervix: a newly described entity in cervicovaginal smears. *Diagn Cytopathol*. 1998;18:222–226.
13. Clement PB, Young RH. Deep nabothian cysts of the uterine cervix. A possible source of confusion with minimal-deviation adenocarcinoma (adenoma malignum). *Int J Gynecol Pathol*. 1989;8:340–348.
14. Fluhmann CF. The nature and development of the so-called glands of the cervix uteri. *Am J Obstet Gynecol*. 1957;74:753–768.
15. Segal GH, Hart WR. Cystic endocervical tunnel clusters. A clinicopathologic study of 29 cases of so-called adenomatous hyperplasia. *Am J Surg Pathol*. 1990;14:895–903.
16. Jones MA, Young RH. Endocervical type A (noncystic) tunnel clusters with cytologic atypia. A report of 14 cases. *Am J Surg Pathol*. 1996;20:1312–1318.
17. Ramdial PK, Bagratee JS. Cutaneous heterotopia of the cervix. *Pathology (Phila)*. 2003;35:258–260.
18. Ionescu DN, Mohan D, Carter G, et al. Epidermoid metaplasia of the cervix. *Arch Pathol Lab Med*. 2004;128:1052–1053.
19. Nucci MR, Ferry JA, Young RH. Ectopic prostatic tissue in the uterine cervix: a report of four cases and review of ectopic prostatic tissue. *Am J Surg Pathol*. 2000;24:1224–1230.
20. McCluggage WG, Ganesan R, Hirschowitz L, et al. Ectopic prostatic tissue in the uterine cervix and vagina: report of a series with a detailed immunohistochemical analysis. *Am J Surg Pathol*. 2006;30:209–215.
21. Doldan A, Otis CN, Pantanowitz L. Adipose tissue: a normal constituent of the uterine cervical stroma. *Int J Gynecol Pathol*. 2009;28:396–400.
22. Young RH, Clement PB. Pseudoneoplastic glandular lesions of the uterine cervix. *Semin Diagn Pathol*. 1991;8:234–249.
23. Young RH, Harris NL, Scully RE. Lymphoma-like lesions of the lower female genital tract: a report of 16 cases. *Int J Gynecol Pathol*. 1985;4:289–299.
24. Ma J, Shi QL, Zhou XJ, et al. Lymphoma-like lesion of the uterine cervix: report of 12 cases of a rare entity. *Int J Gynecol Pathol*. 2007;26:194–198.
25. Geyer JT, Ferry JA, Harris NL, et al. Florid reactive lymphoid hyperplasia of the lower female genital tract (lymphoma-like lesion): a benign condition that frequently harbors clonal immunoglobulin heavy chain gene rearrangements. *Am J Surg Pathol*. 2010;34:161–168.
26. Crow J, McWhinney N. Isolated arteritis of the cervix uteri. *Br J Obstet Gynaecol*. 1979;86:393–398.
27. Francke ML, Mihaescu A, Chaubert P. Isolated necrotizing arteritis of the female genital tract: a clinicopathologic and immunohistochemical study of 11 cases. *Int J Gynecol Pathol*. 1998;17:193–200.
28. Ganesan R, Ferryman SR, Meier L, et al. Vasculitis of the female genital tract with clinicopathologic correlation: a study of 46 cases with follow-up. *Int J Gynecol Pathol*. 2000;19:258–265.
29. Bell DA, Mondschein M, Scully RE. Giant cell arteritis of the female genital tract. A report of three cases. *Am J Surg Pathol*. 1986;10:696–701.
30. Marrogi AJ, Gersell DJ, Kraus FT. Localized asymptomatic giant cell arteritis of the female genital tract. *Int J Gynecol Pathol*. 1991;10:51–58.
31. McGalie CE, McBride HA, McCluggage WG. Cytomegalovirus infection of the cervix: morphological observations in five cases of a possibly underrecognised condition. *J Clin Pathol*. 2004;57:691–694.
32. Byard RW, Mikhael NZ, Orlando G, et al. The clinicopathological significance of cytomegalovirus inclusions demonstrated by endocervical biopsy. *Pathology (Phila)*. 1991;23:318–321.
33. Miguel NL Jr, Lachowicz CM, Kline TS. Candida-related changes and ASCUS: a potential trap! *Diagn Cytopathol*. 1997;16:83–86.
34. O'Brien PK, Roth-Moyo LA, Davis BA. Pseudo-sulfur granules associated with intrauterine contraceptive devices. *Am J Clin Pathol*. 1981;75:822–825.
35. Bhagavan BS, Ruffier J, Shinn B. Pseudoactinomycotic radiate granules in the lower female genital tract: relationship to the Splendore-Hoeppli phenomenon. *Hum Pathol*. 1982;13:898–904.
36. Pritt B, Mount SL, Cooper K, et al. Pseudoactinomycotic radiate granules of the gynaecological tract: review of a diagnostic pitfall. *J Clin Pathol*. 2006;59:17–20.
37. DeMay RM. *The Art and Science of Cytopathology*. Chicago, IL: ASCP Press; 1996:135.
38. Williamson BA, DeFrias D, Gunn R, et al. Significance of extensive hyperkeratosis on cervical/vaginal smears. *Acta Cytol*. 2003;47:749–752.
39. Val-Bernal JF, Pinto J, Garijo MF, et al. Pagetoid dyskeratosis of the cervix: an incidental histologic finding in uterine prolapse. *Am J Surg Pathol*. 2000;24:1518–1523.
40. Scott M, Lyness RW, McCluggage WG. Atypical reactive proliferation of endocervix: a common lesion associated with endometrial carcinoma and likely related to prior endometrial sampling. *Mod Pathol*. 2006;19:470–474.
41. Almoujahed MO, Briski LE, Prysak M, et al. Uterine granulomas: clinical and pathologic features. *Am J Clin Pathol*. 2002;117:771–775.
42. Evans CS, Goldman RL, Klein HZ, et al. Necrobiotic granulomas of the uterine cervix. A probable postoperative reaction. *Am J Surg Pathol*. 1984;8:841–844.

43. Lesack D, Wahab I, Gilks CB. Radiation-induced atypia of endocervical epithelium: a histological, immunohistochemical and cytometric study. Int J *Gynecol Pathol.* 1996;15:242–247.
44. Witkiewicz AK, Hecht JL, Cviko A, et al. Microglandular hyperplasia: a model for the de novo emergence and evolution of endocervical reserve cells. *Hum Pathol.* 2005;36:154–161.
45. Young RH, Scully RE. Atypical forms of microglandular hyperplasia of the cervix simulating carcinoma. A report of five cases and review of the literature. *Am J Surg Pathol.* 1989;13:50–56.
46. Young RH, Scully RE. Uterine carcinomas simulating microglandular hyperplasia. A report of six cases. *Am J Surg Pathol.* 1992;16:1092–1097.
47. Valente PT, Schantz HD, Schultz M. Cytologic atypia associated with microglandular hyperplasia. *Diagn Cytopathol.* 1994;10:326–331.
48. Jones MA, Young RH, Scully RE. Diffuse laminar endocervical glandular hyperplasia. A benign lesion often confused with adenoma malignum (minimal deviation adenocarcinoma). *Am J Surg Pathol.* 1991;15:1123–1129.
49. Nucci MR, Clement PB, Young RH. Lobular endocervical glandular hyperplasia, not otherwise specified: a clinicopathologic analysis of thirteen cases of a distinctive pseudoneoplastic lesion and comparison with fourteen cases of adenoma malignum. *Am J Surg Pathol.* 1999;23:886–891.
50. Mikami Y, Hata S, Melamed J, et al. Lobular endocervical glandular hyperplasia is a metaplastic process with a pyloric gland phenotype. *Histopathology.* 2001;39:364–372.
51. Ishii K, Ota H, Katsuyama T. Lobular endocervical glandular hyperplasia represents pyloric gland metaplasia? [Letter]. *Am J Surg Pathol.* 2000;24:325.
52. Kawauchi S, Kusuda T, Liu X-P, et al. Is lobular endocervical glandular hyperplasia a cancerous precursor of minimal deviation adenocarcinoma?: a comparative molecular-genetic and immunohistochemical study. *Am J Surg Pathol.* 2008;32:1807–1815.
53. Ferry JA, Scully RE. Mesonephric remnants, hyperplasia, and neoplasia in the uterine cervix. A study of 49 cases. *Am J Surg Pathol.* 1990;14:1100–1111.
54. Seidman JD, Tavassoli FA. Mesonephric hyperplasia of the uterine cervix: a clinicopathologic study of 51 cases. *Int J Gynecol Pathol.* 1995;14:293–299.
55. Hejmadi RK, Gearty JC, Waddell C, et al. Mesonephric hyperplasia can cause abnormal cervical smears: report of three cases with review of literature. *Cytopathology.* 2005;16:240–243.
56. Welsh T, Fu YS, Chan J, et al. Mesonephric remnants or hyperplasia can cause abnormal pap smears: a study of three cases. *Int J Gynecol Pathol.* 2003;22:121–126.
57. Ordi J, Romagosa C, Tavassoli FA, et al. CD10 expression in epithelial tissues and tumors of the gynecologic tract: a useful marker in the diagnosis of mesonephric, trophoblastic, and clear cell tumors. *Am J Surg Pathol.* 2003;27:178–186.
58. McCluggage WG, Oliva E, Herrington CS, et al. CD10 and calretinin staining of endocervical glandular lesions, endocervical stroma and endometrioid adenocarcinomas of the uterine corpus: CD10 positivity is characteristic of, but not specific for, mesonephric lesions and is not specific for endometrial stroma. *Histopathology.* 2003;43:144–150.
59. Chin N, Platt AB, Nuovo GJ. Squamous intraepithelial lesions arising in benign endocervical polyps: a report of 9 cases with correlation to the Pap smears, HPV analysis, and immunoprofile. *Int J Gynecol Pathol.* 2008;27:582–590.
60. Schneider V, Barnes LA. Ectopic decidual reaction of the uterine cervix: frequency and cytologic presentation. *Acta Cytol.* 1981;25:616–622.
61. Nucci MR, Young RH. Arias-Stella reaction of the endocervix: a report of 18 cases with emphasis on its varied histology and differential diagnosis. *Am J Surg Pathol.* 2004;28:608–612.
62. Daya D, Young RH. Florid deep glands of the uterine cervix. Another mimic of adenoma malignum. *Am J Clin Pathol.* 1995;103:614–617.
63. Young RH, Clement PB. Endocervicosis involving the uterine cervix: a report of four cases of a benign process that may be confused with deeply invasive endocervical adenocarcinoma. *Int J Gynecol Pathol.* 2000;19:322–328.
64. Baker PM, Clement PB, Bell DA, et al. Superficial endometriosis of the uterine cervix: a report of 20 cases of a process that may be confused with endocervical glandular dysplasia or adenocarcinoma in situ. *Int J Gynecol Pathol.* 1999;18:198–205.
65. Szyfelbein WM, Baker PM, Bell DA. Superficial endometriosis of the cervix: A source of abnormal glandular cells on cervicovaginal smears. *Diagn Cytopathol.* 2004;30:88–91.
66. Kim KR. Utility of trichrome and reticulin stains in the diagnosis of superficial endometriosis of the uterine cervix. *Int J Gynecol Pathol.* 2001;20:173–176.
67. Clement PB, Young RH, Scully RE. Stromal endometriosis of the uterine cervix. A variant of endometriosis that may simulate a sarcoma. *Am J Surg Pathol.* 1990;14:449–455.
68. Pikarsky E, Maly B, Maly A. Ceroid granuloma of the uterine cervix. *Int J Gynecol Pathol.* 2002;21:191–193.
69. Clement PB. Multinucleated stromal giant cells of the uterine cervix. Arch Pathol *Lab Med.* 1985;109:200–202.
70. Hariri J, Ingemanssen JL. Multinucleated stromal giant cells of the uterine cervix. *Int J Gynecol Pathol.* 1993;12:228–234.
71. Tiltman AJ. Leiomyomas of the uterine cervix: a study of frequency. *Int J Gynecol Pathol.* 1998;17:231–234.
72. Kondi-Pafiti A, Kairi-Vassilatou E, Spanidou-Carvouni H, et al. Vascular tumors of the female genital tract: a clinicopathological study of nine cases. *Eur J Gynaecol Oncol.* 2003;24:48–50.
73. Patel DS, Bhagavan BS. Blue nevus of the uterine cervix. *Hum Pathol.* 1985;16:79–86.
74. Albores-Saavedra J, Gilcrease M. Glomus tumor of the uterine cervix. *Int J Gynecol Pathol.* 1999;18:69–72.
75. Albores-Saavedra J, Young RH. Transitional cell neoplasms (carcinomas and inverted papillomas) of the uterine cervix. A report of five cases. *Am J Surg Pathol.* 1995;19:1138–1145.
76. Hollowell ML, Goulart RA, Gang DL, et al. Cytologic features of mullerian papilloma of the cervix: mimic of malignancy. *Diagn Cytopathol.* 2007;35: 607–611.
77. Laskin WB, Fetsch JF, Tavassoli FA. Superficial cervicovaginal myofibroblastoma: fourteen cases of a distinctive mesenchymal tumor arising from the specialized subepithelial stroma of the lower female genital tract. *Hum Pathol.* 2001;32:715–725.
78. Bosch FX, Lorincz A, Munoz N, et al. The causal relation between human papillomavirus and cervical cancer. *J Clin Pathol.* 2002;55:244–265.
79. Munger K, Baldwin A, Edwards KM, et al. Mechanisms of human papillomavirus-induced oncogenesis. *J Virol.* 2004;78:11451–11460.
80. Woodman CB, Collins SI, Young LS. The natural history of cervical HPV infection: unresolved issues. *Nat Rev Cancer.* 2007;7:11–22.
81. Insinga RP, Glass AG, Rush BB. Diagnoses and outcomes in cervical cancer screening: a population-based study. *Am J Obstet Gynecol.* 2004;191: 105–113.
82. Thomison J, 3rd, Thomas LK, Shroyer KR. Human papillomavirus: molecular and cytologic/histologic aspects related to cervical intraepithelial neoplasia and carcinoma. *Hum Pathol.* 2008;39:154–166.
83. Ostor AG. Natural history of cervical intraepithelial neoplasia: a critical review. *Int J Gynecol Pathol.* 1993;12:186–192.
84. Moscicki AB, Shiboski S, Hills NK, et al. Regression of low-grade squamous intra-epithelial lesions in young women. *Lancet.* 2004;364:1678–1683.
85. Jakobsson M, Gissler M, Paavonen J, et al. Loop electrosurgical excision procedure and the risk for preterm birth. *Obstet Gynecol.* 2009;114:504–510.
86. Wright TC, Jr., Massad LS, Dunton CJ, et al. 2006 consensus guidelines for the management of women with cervical intraepithelial neoplasia or adenocarcinoma in situ. *Am J Obstet Gynecol.* 2007;197:340–345.
87. ACOG Practice Bulletin. Clinical Management Guidelines for Obstetrician-Gynecologists. Number 109, December 2009. Cervical cytology screening. *Obstet Gynecol.* 2009;114:1409–1420.
88. Stoler MH, Schiffman M. Interobserver reproducibility of cervical cytologic and histologic interpretations: realistic estimates from the ASCUS-LSIL Triage Study. *JAMA.* 2001;285:1500–1505.
89. Pirog EC, Baergen RN, Soslow RA, et al. Diagnostic accuracy of cervical low-grade squamous intraepithelial lesions is improved with MIB-1 immunostaining. *Am J Surg Pathol.* 2002;26:70–75.
90. McCredie MR, Sharples KJ, Paul C, et al. Natural history of cervical neoplasia and risk of invasive cancer in women with cervical intraepithelial neoplasia 3: a retrospective cohort study. *Lancet Oncol.* 2008;9:425–434.
91. Castle PE, Stoler MH, Solomon D, et al. The relationship of community biopsy-diagnosed cervical intraepithelial neoplasia grade 2 to the quality control pathology-reviewed diagnoses: an ALTS report. *Am J Clin Pathol.* 2007;127:805–815.
92. Carreon JD, Sherman ME, Guillen D, et al. CIN2 is a much less reproducible and less valid diagnosis than CIN3: results from a histological review of population-based cervical samples. *Int J Gynecol Pathol.* 2007;26:441–446.
93. Crum CP. Laboratory management of CIN 2: the consensus is consensus. *Am J Clin Pathol.* 2008;130:162–164.
94. Wright TC, Jr., Massad LS, Dunton CJ, et al. 2006 consensus guidelines for the management of women with abnormal cervical cancer screening tests. *Am J Obstet Gynecol.* 2007;197:346–355.
95. Pinto AP, Schlecht NF, Woo TY, et al. Biomarker (ProEx C, p16(INK4A), and MiB-1) distinction of high-grade squamous intraepithelial lesion from its mimics. *Mod Pathol.* 2008;21:1067–1074.
96. Walts AE, Bose S. p16, Ki-67, and BD ProEx C immunostaining: a practical approach for diagnosis of cervical intraepithelial neoplasia. *Hum Pathol.* 2009;40:957–964.

97. Sanati S, Huettner P, Ylagan LR. Role of ProExC: a novel immunoperoxidase marker in the evaluation of dysplastic squamous and glandular lesions in cervical specimens. *Int J Gynecol Pathol.* 2010;29:79–87.
98. McCluggage WG, Buhidma M, Tang L, et al. Monoclonal antibody MIB1 in the assessment of cervical squamous intraepithelial lesions. *Int J Gynecol Pathol.* 1996;15:131–136.
99. Mittal K, Mesia A, Demopoulos RI. MIB-1 expression is useful in distinguishing dysplasia from atrophy in elderly women. *Int J Gynecol Pathol.* 1999;18:122–124.
100. Nucci MR, Crum CP. Redefining early cervical neoplasia: recent progress. *Adv Anat Pathol.* 2007;14:1–10.
101. Mittal K. Utility of MIB-1 in evaluating cauterized cervical cone biopsy margins. *Int J Gynecol Pathol.* 1999;18:211–214.
102. O'Neill CJ, McCluggage WG. p16 expression in the female genital tract and its value in diagnosis. *Adv Anat Pathol.* 2006;13:8–15.
103. Kong CS, Balzer BL, Troxell ML, et al. p16INK4A immunohistochemistry is superior to HPV in situ hybridization for the detection of high-risk HPV in atypical squamous metaplasia. *Am J Surg Pathol.* 2007;31:33–43.
104. Keating JT, Cviko A, Riethdorf S, et al. Ki-67, cyclin E, and p16INK4 are complimentary surrogate biomarkers for human papilloma virus-related cervical neoplasia. *Am J Surg Pathol.* 2001;25:884–891.
105. Hashi A, Xu JY, Kondo T, et al. p16INK4a overexpression independent of human papillomavirus infection in lobular endocervical glandular hyperplasia. *Int J Gynecol Pathol.* 2006;25:187–194.
106. Atkins KA, Arronte N, Darus CJ, et al. The use of p16 in enhancing the histologic classification of uterine smooth muscle tumors. *Am J Surg Pathol.* 2008;32:98–102.
107. Roh MH, Agoston E, Birch C, et al. P16 immunostaining patterns in microglandular hyperplasia of the cervix and their significance. *Int J Gynecol Pathol.* 2009;28:107–113.
108. Yemelyanova A, Ji H, Shih IM, et al. Utility of p16 expression for distinction of uterine serous carcinomas from endometrial endometrioid and endocervical adenocarcinomas. Immunohistochemical analysis of 201 cases. *Am J Surg Pathol.* 2009;33:1504–1514.
109. Ward BE, Saleh AM, Williams JV, et al. Papillary immature metaplasia of the cervix: a distinct subset of exophytic cervical condyloma associated with HPV-6/11 nucleic acids. *Mod Pathol.* 1992;5:391–395.
110. Park K, Ellenson LH, Pirog EC. Low-grade squamous intraepithelial lesions of the cervix with marked cytological atypia-clinical follow-up and human papillomavirus genotyping. *Int J Gynecol Pathol.* 2007;26:457–462.
111. Fadare O, Rodriguez R. The significance of marked nuclear atypia in grade 1 cervical intraepithelial neoplasia. *Hum Pathol.* 2009;40:1487–1493.
112. al-Nafussi AI, Hughes DE. Histological features of CIN3 and their value in predicting invasive microinvasive squamous carcinoma. *J Clin Pathol.* 1994;47:799–804.
113. Kanbour AI, Stock RJ. Squamous cell carcinoma in situ of the endometrium and fallopian tube as superficial extension of invasive cervical carcinoma. *Cancer.* 1978;42:570–580.
114. Selvaggi SM. Cytologic features of squamous cell carcinoma in situ involving endocervical glands in endocervical cytobrush specimens. *Acta Cytol.* 1994;38:687–692.
115. Ma L, Fisk JM, Zhang RR, et al. Eosinophilic dysplasia of the cervix: a newly recognized variant of cervical squamous intraepithelial neoplasia. *Am J Surg Pathol.* 2004;28:1474–1484.
116. Sherman ME, Castle PE, Solomon D. Cervical cytology of atypical squamous cells-cannot exclude high-grade squamous intraepithelial lesion (ASC-H): characteristics and histologic outcomes. *Cancer.* 2006;108:298–305.
117. Eversole GM, Moriarty AT, Schwartz MR, et al. Practices of participants in the College of American Pathologists interlaboratory comparison program in cervicovaginal cytology, 2006. *Arch Pathol Lab Med.* 2010;134:331–335.
118. Ko V, Nanji S, Tambouret RH, et al. Testing for HPV as an objective measure for quality assurance in gynecologic cytology: positive rates in equivocal and abnormal specimens and comparison with the ASCUS to SIL ratio. *Cancer.* 2007;111:67–73.
119. Cibas ES, Browne TJ, Bassichis MH, et al. Enlarged squamous cell nuclei in cervical cytologic specimens from perimenopausal women ("PM Cells"): a cause of ASC overdiagnosis. *Am J Clin Pathol.* 2005;124:58–61.
120. Crum CP, Egawa K, Fu YS, et al. Atypical immature metaplasia (AIM). A subset of human papilloma virus infection of the cervix. *Cancer.* 1983;51:2214–2219.
121. Geng L, Connolly DC, Isacson C, et al. Atypical immature metaplasia (AIM) of the cervix: is it related to high-grade squamous intraepithelial lesion (HSIL)? *Hum Pathol.* 1999;30:345–351.
122. Duggan MA, Akbari M, Magliocco AM. Atypical immature cervical metaplasia: immunoprofiling and longitudinal outcome. *Hum Pathol.* 2006;37:1473–1481.
123. Regauer S, Reich O. CK17 and p16 expression patterns distinguish (atypical) immature squamous metaplasia from high-grade cervical intraepithelial neoplasia (CIN III). *Histopathology.* 2007;50:629–635.
124. Iaconis L, Hyjek E, Ellenson LH, et al. p16 and Ki-67 immunostaining in atypical immature squamous metaplasia of the uterine cervix: correlation with human papillomavirus detection. *Arch Pathol Lab Med.* 2007;131:1343–1349.
125. Kim KR, Lee YH, Ro JY. Nodular histiocytic hyperplasia of the endometrium. *Int J Gynecol Pathol.* 2002;21:141–146.
126. Cannistra SA, Niloff JM. Cancer of the uterine cervix. *N Engl J Med.* 1996;334:1030–1038.
127. Ostor AG. Studies on 200 cases of early squamous cell carcinoma of the cervix. *Int J Gynecol Pathol.* 1993;12:193–207.
128. Benedet JL, Anderson GH. Stage IA carcinoma of the cervix revisited. *Obstet Gynecol.* 1996;87:1052–1059.
129. FIGO Committee on Gynecologic Oncology. Revised FIGO staging for carcinoma of the vulva, cervix, and endometrium. *Int J Gynecol Obstet.* 2009;105:103–104.
130. Robert ME, Fu YS. Squamous cell carcinoma of the uterine cervix—a review with emphasis on prognostic factors and unusual variants. *Semin Diagn Pathol.* 1990;7:173–189.
131. al-Nafussi AI, Monaghan H. Squamous carcinoma of the uterine cervix with CIN 3-like growth pattern: an under-diagnosed lesion. *Int J Gynecol Cancer.* 2000;10:95–99.
132. Morrison C, Catania F, Wakely P Jr, et al. Highly differentiated keratinizing squamous cell cancer of the cervix: a rare, locally aggressive tumor not associated with human papillomavirus or squamous intraepithelial lesions. *Am J Surg Pathol.* 2001;25:1310–1315.
133. Ambros RA, Park JS, Shah KV, et al. Evaluation of histologic, morphometric, and immunohistochemical criteria in the differential diagnosis of small cell carcinomas of the cervix with particular reference to human papillomavirus types 16 and 18. *Mod Pathol.* 1991;4:586–593.
134. Colgan TJ, Auger M, McLaughlin JR. Histopathologic classification of cervical carcinomas and recognition of mucin-secreting squamous carcinomas. *Int J Gynecol Pathol.* 1993;12:64–69.
135. Euscher ED, Malpica A, Atkinson EN, et al. Ultrastaging improves detection of metastases in sentinel lymph nodes of uterine cervix squamous cell carcinoma. *Am J Surg Pathol.* 2008;32:1336–1343.
136. Levine PH, Elgert PA, Mittal K. False-positive squamous cell carcinoma in cervical smears: cytologic-histologic correlation in 19 cases. *Diagn Cytopathol.* 2003;28:23–27.
137. Grayson W, Cooper K. A reappraisal of "basaloid carcinoma" of the cervix, and the differential diagnosis of basaloid cervical neoplasms. *Adv Anat Pathol.* 2002;9:290–300.
138. Clement PB, Zubovits JT, Young RH, et al. Malignant mullerian mixed tumors of the uterine cervix: a report of nine cases of a neoplasm with morphology often different from its counterpart in the corpus. *Int J Gynecol Pathol.* 1998;17:211–222.
139. Grayson W, Taylor LF, Cooper K. Carcinosarcoma of the uterine cervix: a report of eight cases with immunohistochemical analysis and evaluation of human papillomavirus status. *Am J Surg Pathol.* 2001;25:338–347.
140. Degefu S, O'Quinn AG, Lacey CG, et al. Verrucous carcinoma of the cervix: a report of two cases and literature review. *Gynecol Oncol.* 1986;25:37–47.
141. Randall ME, Andersen WA, Mills SE, et al. Papillary squamous cell carcinoma of the uterine cervix: a clinicopathologic study of nine cases. *Int J Gynecol Pathol.* 1986;5:1–10.
142. Brinck U, Jakob C, Bau O, et al. Papillary squamous cell carcinoma of the uterine cervix: report of three cases and a review of its classification. *Int J Gynecol Pathol.* 2000;19:231–235.
143. Koenig C, Turnicky RP, Kankam CF, et al. Papillary squamotransitional cell carcinoma of the cervix: a report of 32 cases. *Am J Surg Pathol.* 1997;21:915–921.
144. Mills SE, Austin MB, Randall ME. Lymphoepithelioma-like carcinoma of the uterine cervix. A distinctive, undifferentiated carcinoma with inflammatory stroma. *Am J Surg Pathol.* 1985;9:883–889.
145. Tseng CJ, Pao CC, Tseng LH, et al. Lymphoepithelioma-like carcinoma of the uterine cervix: association with Epstein-Barr virus and human papillomavirus. *Cancer.* 1997;80:91–97.
146. Chao A, Tsai CN, Hsueh S, et al. Does Epstein-Barr virus play a role in lymphoepithelioma-like carcinoma of the cervix? *Int J Gynecol Pathol.* 2009;28:279–285.
147. Brown J, Broaddus R, Koeller M, et al. Sarcomatoid carcinoma of the cervix. *Gynecol Oncol.* 2003;90:23–28.

148. Steeper TA, Piscioli F, Rosai J. Squamous cell carcinoma with sarcoma-like stroma of the female genital tract. Clinicopathologic study of four cases. *Cancer.* 1983;52:890–898.
149. Jaworski RC. Endocervical glandular dysplasia, adenocarcinoma in situ, and early invasive (microinvasive) adenocarcinoma of the uterine cervix. *Semin Diagn Pathol.* 1990;7:190–204.
150. Zaino RJ. Symposium part I: adenocarcinoma in situ, glandular dysplasia, and early invasive adenocarcinoma of the uterine cervix. *Int J Gynecol Pathol.* 2002;21:314–326.
151. Witkiewicz A, Lee KR, Brodsky G, et al. Superficial (early) endocervical adenocarcinoma in situ: a study of 12 cases and comparison to conventional AIS. *Am J Surg Pathol.* 2005;29:1609–1614.
152. Biscotti CV, Hart WR. Apoptotic bodies: a consistent morphologic feature of endocervical adenocarcinoma in situ. *Am J Surg Pathol.* 1998;22:434–439.
153. Moritani S, Ioffe OB, Sagae S, et al. Mitotic activity and apoptosis in endocervical glandular lesions. *Int J Gynecol Pathol.* 2002;21:125–133.
154. Riethdorf L, Riethdorf S, Lee KR, et al. Human papillomaviruses, expression of p16, and early endocervical glandular neoplasia. *Hum Pathol.* 2002;33:899–904.
155. Negri G, Egarter-Vigl E, Kasal A, et al. p16INK4a is a useful marker for the diagnosis of adenocarcinoma of the cervix uteri and its precursors: an immunohistochemical study with immunocytochemical correlations. *Am J Surg Pathol.* 2003;27:187–193.
156. McCluggage WG, Shah R, Connolly LE, et al. Intestinal-type cervical adenocarcinoma in situ and adenocarcinoma exhibit a partial enteric immunophenotype with consistent expression of CDX2. *Int J Gynecol Pathol.* 2008;27:92–100.
157. Nofech-Mozes S, Khalifa MA. Endocervical adenocarcinoma in situ, serous type. *Int J Gynecol Pathol.* 2009;28:140–141.
158. Park JJ, Sun D, Quade BJ, et al. Stratified mucin-producing intraepithelial lesions of the cervix: adenosquamous or columnar cell neoplasia?[see comment]. *Am J Surg Pathol.* 2000;24:1414–1419.
159. Ayer B, Pacey F, Greenberg M, et al. The cytologic diagnosis of adenocarcinoma in situ of the cervix uteri and related lesions. I. Adenocarcinoma in situ. *Acta Cytol.* 1987;31:397–411.
160. Rabban JT, McAlhany S, Lerwill MF, et al. PAX2 distinguishes benign mesonephric and mullerian glandular lesions of the cervix from endocervical adenocarcinoma, including minimal deviation adenocarcinoma. *Am J Surg Pathol.* 2010;34:137–146.
161. Lee KR, Sun D, Crum CP. Endocervical intraepithelial glandular atypia (dysplasia): a histopathologic, human papillomavirus, and MIB-1 analysis of 25 cases. *Hum Pathol.* 2000;31:656–664.
162. Young RH. Simple clefts, complex problems: reflections on glandular lesions of the uterine cervix (editorial). *Int J Gynecol Pathol.* 2002;21:212–216.
163. Young RH, Clement PB. Endocervical adenocarcinoma and its variants: their morphology and differential diagnosis. *Histopathology.* 2002;41:185–207.
164. Ostor AG. Early invasive adenocarcinoma of the uterine cervix. *Int J Gynecol Pathol.* 2000;19:29–38.
165. Lee KR, Flynn CE. Early invasive adenocarcinoma of the cervix. *Cancer.* 2000;89:1048–1055.
166. Ceballos KM, Shaw D, Daya D. Microinvasive cervical adenocarcinoma (FIGO stage 1A tumors): results of surgical staging and outcome analysis. *Am J Surg Pathol.* 2006;30:370–374.
167. Wheeler DT, Kurman RJ. The relationship of glands to thick-wall blood vessels as a marker of invasion in endocervical adenocarcinoma. *Int J Gynecol Pathol.* 2005;24:125–130.
168. Smith HO, Qualls CR, Romero AA, et al. Is there a difference in survival for IA1 and IA2 adenocarcinoma of the uterine cervix? *Gynecol Oncol.* 2002;85:229–241.
169. Elishaev E, Gilks CB, Miller D, et al. Synchronous and metachronous endocervical and ovarian neoplasms: evidence supporting interpretation of the ovarian neoplasms as metastatic endocervical adenocarcinomas simulating primary ovarian surface epithelial neoplasms. *Am J Surg Pathol.* 2005;29:281–294.
170. Ronnett BM, Yemelyanova AV, Vang R, et al. Endocervical adenocarcinomas with ovarian metastases: analysis of 29 cases with emphasis on minimally invasive cervical tumors and the ability of the metastases to simulate primary ovarian neoplasms. *Am J Surg Pathol.* 2008;32:1835–1853.
171. Chang MC, Nevadunsky NS, Viswanathan AN, et al. Endocervical adenocarcinoma in situ with ovarian metastases: a unique variant with potential for long-term survival. *Int J Gynecol Pathol.* 2010;29:88–92.
172. Reichert RA. Synchronous and metachronous endocervical and ovarian neoplasms: a different interpretation of HPV data [Letter to Editor]. *Am J Surg Pathol.* 2005;29:1686–1687.
173. Reichert RA. The endocervical origin of HPV-positive mucinous/endometrioid ovarian tumors remains unproven [Letter to Editor]. *Int J Gynecol Pathol.* 2010;29:298–300.
174. Tambouret R, Bell DA, Young RH. Microcystic endocervical adenocarcinomas: a report of eight cases. *Am J Surg Pathol.* 2000;24:369–374.
175. Zaino RJ. The fruits of our labors: distinguishing endometrial from endocervical adenocarcinoma. *Int J Gynecol Pathol.* 2002;21:1–3.
176. Kamoi S, AlJuboury MI, Akin MR, et al. Immunohistochemical staining in the distinction between primary endometrial and endocervical adenocarcinomas: another viewpoint. *Int J Gynecol Pathol.* 2002;21:217–223.
177. Young RH, Scully RE. Invasive adenocarcinoma and related tumors of the uterine cervix. *Semin Diagn Pathol.* 1990;7:205–227.
178. Nofech-Mozes S, Ghorab Z, Ismiil N, et al. Endometrial endometrioid adenocarcinoma: a pathologic analysis of 827 consecutive cases. *Am J Clin Pathol.* 2008;129:110–114.
179. Yemelyanova A, Vang R, Seidman JD, et al. Endocervical adenocarcinomas with prominent endometrial or endomyometrial involvement simulating primary endometrial carcinomas: utility of HPV DNA detection and immunohistochemical expression of p16 and hormone receptors to confirm the cervical origin of the corpus tumor. *Am J Surg Pathol.* 2009;33:914–924.
180. Mariani A, Webb MJ, Keeney GL, et al. Role of wide/radical hysterectomy and pelvic lymph node dissection in endometrial cancer with cervical involvement. *Gynecol Oncol.* 2001;83:72–80.
181. Cohn DE, Woeste EM, Cacchio S, et al. Clinical and pathologic correlates in surgical stage II endometrial carcinoma. *Obstet Gynecol.* 2007;109:1062–1067.
182. Castrillon DH, Lee KR, Nucci MR. Distinction between endometrial and endocervical adenocarcinoma: an immunohistochemical study. *Int J Gynecol Pathol.* 2002;21:4–10.
183. Staebler A, Sherman ME, Zaino RJ, et al. Hormone receptor immunohistochemistry and human papillomavirus in situ hybridization are useful for distinguishing endocervical and endometrial adenocarcinomas. *Am J Surg Pathol.* 2002;26:998–1006.
184. McCluggage WG, Sumathi VP, McBride HA, et al. A panel of immunohistochemical stains, including carcinoembryonic antigen, vimentin, and estrogen receptor, aids the distinction between primary endometrial and endocervical adenocarcinomas. *Int J Gynecol Pathol.* 2002;21:11–15.
185. McCluggage WG, Jenkins D. p16 immunoreactivity may assist in the distinction between endometrial and endocervical adenocarcinoma. *Int J Gynecol Pathol.* 2003;22:231–235.
186. Ansari-Lari MA, Staebler A, Zaino RJ, et al. Distinction of endocervical and endometrial adenocarcinomas: immunohistochemical p16 expression correlated with human papillomavirus (HPV) DNA detection. *Am J Surg Pathol.* 2004;28:160–167.
187. Kong CS, Beck AH, Longacre TA. A panel of 3 markers including p16, Pro-ExC, or HPV ISH is optimal for distinguishing between primary endometrial and endocervical adenocarcinomas. *Am J Surg Pathol.* 2010;34:915–926.
188. Han CP, Lee MY, Kok LF, et al. Adding the p16(INK4a) marker to the traditional 3-marker (ER/Vim/CEA) panel engenders no supplemental benefit in distinguishing between primary endocervical and endometrial adenocarcinomas in a tissue microarray study. *Int J Gynecol Pathol.* 2009;28:489–496.
189. Young RH, Scully RE. Villoglandular papillary adenocarcinoma of the uterine cervix. A clinicopathologic analysis of 13 cases. *Cancer.* 1989;63:1773–1779.
190. Jones MW, Silverberg SG, Kurman RJ. Well-differentiated villoglandular adenocarcinoma of the uterine cervix: a clinicopathological study of 24 cases. *Int J Gynecol Pathol.* 1993;12:1–7.
191. Jones MW, Kounelis S, Papadaki H, et al. Well-differentiated villoglandular adenocarcinoma of the uterine cervix: oncogene/tumor suppressor gene alterations and human papillomavirus genotyping. *Int J Gynecol Pathol.* 2000;19:110–117.
192. Gilks CB, Young RH, Aguirre P, et al. Adenoma malignum (minimal deviation adenocarcinoma) of the uterine cervix. A clinicopathological and immunohistochemical analysis of 26 cases. *Am J Surg Pathol.* 1989;13:717–729.
193. Young RH, Scully RE. Mucinous ovarian tumors associated with mucinous adenocarcinomas of the cervix. A clinicopathological analysis of 16 cases. *Int J Gynecol Pathol.* 1988;7:99–111.
194. Hayashi I, Tsuda H, Shimoda T. Reappraisal of orthodox histochemistry for the diagnosis of minimal deviation adenocarcinoma of the cervix. *Am J Surg Pathol.* 2000;24:559–562.
195. Saad RS, Ismiil N, Dube V, et al. CDX-2 expression is a common event in primary intestinal-type endocervical adenocarcinoma. *Am J Clin Pathol.* 2009;132:531–538.
196. Balci S, Saglam A, Usubutun A. Primary signet-ring cell carcinoma of the cervix: case report and review of the literature. *Int J Gynecol Pathol.* 2010;29:181–184.
197. Walker AN, Mills SE. Unusual variants of uterine cervical carcinoma. *Pathol Annu.* 1987;22 (pt1):277–310.

198. Young RH, Scully RE. Minimal-deviation endometrioid adenocarcinoma of the uterine cervix. A report of five cases of a distinctive neoplasm that may be misinterpreted as benign. *Am J Surg Pathol.* 1993;17:660–665.
199. Melnick S, Cole P, Anderson D, et al. Rates and risks of diethylstilbestrol-related clear-cell adenocarcinoma of the vagina and cervix. An update. *N Engl J Med.* 1987;316:514–516.
200. Kaminski PF, Maier RC. Clear cell adenocarcinoma of the cervix unrelated to diethylstilbestrol exposure. *Obstet Gynecol.* 1983;62:720–727.
201. Zhou C, Gilks CB, Hayes M, et al. Papillary serous carcinoma of the uterine cervix: a clinicopathologic study of 17 cases. *Am J Surg Pathol.* 1998;22:113–120.
202. Clement PB, Young RH, Keh P, et al. Malignant mesonephric neoplasms of the uterine cervix. A report of eight cases, including four with a malignant spindle cell component. *Am J Surg Pathol.* 1995;19:1158–1171.
203. Silver SA, Devouassoux-Shisheboran M, Mezzetti TP, et al. Mesonephric adenocarcinomas of the uterine cervix: a study of 11 cases with immunohistochemical findings. *Am J Surg Pathol.* 2001;25:379–387.
204. Bague S, Rodriguez IM, Prat J. Malignant mesonephric tumors of the female genital tract: a clinicopathologic study of 9 cases. *Am J Surg Pathol.* 2004;28:601–607.
205. Fujiwara H, Mitchell MF, Arseneau J, et al. Clear cell adenosquamous carcinoma of the cervix. An aggressive tumor associated with human papillomavirus-18. *Cancer.* 1995;76:1591–1600.
206. Lennerz JK, Perry A, Mills JC, et al. Mucoepidermoid carcinoma of the cervix: another tumor with the t(11;19)-associated CRTC1-MAML2 gene fusion. *Am J Surg Pathol.* 2009;33:835–843.
207. Ulbright TM, Gersell DJ. Glassy cell carcinoma of the uterine cervix. A light and electron microscopic study of five cases. *Cancer.* 1983;51:2255–2263.
208. Pak HY, Yokota SB, Paladugu RR, et al. Glassy cell carcinoma of the cervix. Cytologic and clinicopathologic analysis. *Cancer.* 1983;52:307–312.
209. Kato N, Katayama Y, Kaimori M, et al. Glassy cell carcinoma of the uterine cervix: histochemical, immunohistochemical, and molecular genetic observations. *Int J Gynecol Pathol.* 2002;21:134–140.
210. Kim SK, Shim HS, Lee KG, et al. Glassy cell carcinoma predominantly commits to a squamous lineage and is strongly associated with high-risk type human papillomavirus infection. *Int J Gynecol Pathol.* 2009;28:389–395.
211. Ferry JA, Scully RE. "Adenoid cystic" carcinoma and adenoid basal carcinoma of the uterine cervix. A study of 28 cases. *Am J Surg Pathol.* 1988;12:134–144.
212. Brainard JA, Hart WR. Adenoid basal epitheliomas of the uterine cervix: a reevaluation of distinctive cervical basaloid lesions currently classified as adenoid basal carcinoma and adenoid basal hyperplasia. *Am J Surg Pathol.* 1998;22:965–975.
213. Parwani AV, Smith Sehdev AE, Kurman RJ, et al. Cervical adenoid basal tumors comprised of adenoid basal epithelioma associated with various types of invasive carcinoma: clinicopathologic features, human papillomavirus DNA detection, and P16 expression. *Hum Pathol.* 2005;36:82–90.
214. Albores-Saavedra J, Manivel C, Mora A, et al. The solid variant of adenoid cystic carcinoma of the cervix. *Int J Gynecol Pathol.* 1992;11:2–10.
215. Grayson W, Taylor LF, Cooper K. Adenoid cystic and adenoid basal carcinoma of the uterine cervix: comparative morphologic, mucin, and immunohistochemical profile of two rare neoplasms of putative 'reserve cell' origin. *Am J Surg Pathol.* 1999;23:448–458.
216. Albores-Saavedra J, Gersell D, Gilks CB, et al. Terminology of endocrine tumors of the uterine cervix: results of a workshop sponsored by the College of American Pathologists and the National Cancer Institute. *Arch Pathol Lab Med.* 1997;121:34–39.
217. Gersell DJ, Mazoujian G, Mutch DG, et al. Small-cell undifferentiated carcinoma of the cervix. A clinicopathologic, ultrastructural, and immunocytochemical study of 15 cases. *Am J Surg Pathol.* 1988;12:684–698.
218. Sato Y, Shimamoto T, Amada S, et al. Large cell neuroendocrine carcinoma of the uterine cervix: a clinicopathological study of six cases. *Int J Gynecol Pathol.* 2003;22:226–230.
219. Gilks CB, Young RH, Gersell DJ, et al. Large cell neuroendocrine carcinoma of the uterine cervix: a clinicopathologic study of 12 cases. *Am J Surg Pathol.* 1997;21:905–914.
220. Ishida GM, Kato N, Hayasaka T, et al. Small cell neuroendocrine carcinomas of the uterine cervix: a histological, immunohistochemical, and molecular genetic study. *Int J Gynecol Pathol.* 2004;23:366–372.
221. McCluggage WG, Kennedy K, Busam KJ. An immunohistochemical study of cervical neuroendocrine carcinomas: neoplasms that are commonly TTF1 positive and which may express CK20 and P63. *Am J Surg Pathol.* 2010;34:525–532.
222. Grayson W, Rhemtula HA, Taylor LF, et al. Detection of human papillomavirus in large cell neuroendocrine carcinoma of the uterine cervix: a study of 12 cases. *J Clin Pathol.* 2002;55:108–114.
223. Stoler MH, Mills SE, Gersell DJ, et al. Small-cell neuroendocrine carcinoma of the cervix. A human papillomavirus type 18-associated cancer. *Am J Surg Pathol.* 1991;15:28–32.
224. Conner MG, Richter H, Moran CA, et al. Small cell carcinoma of the cervix: a clinicopathologic and immunohistochemical study of 23 cases. *Ann Diagn Pathol.* 2002;6:345–348.
225. Gilks CB, Young RH, Clement PB, et al. Adenomyomas of the uterine cervix of of endocervical type: a report of ten cases of a benign cervical tumor that may be confused with adenoma malignum. *Mod Pathol.* 1996;9:220–224.
226. Clement PB, Scully RE. Uterine tumors with mixed epithelial and mesenchymal elements. *Semin Diagn Pathol.* 1988;5:199–222.
227. Abell MR. Papillary adenofibroma of the uterine cervix. *Am J Obstet Gynecol.* 1971;110:990–993.
228. Zeisler H, Mayerhofer K, Joura EA, et al. Embryonal rhabdomyosarcoma of the uterine cervix: case report and review of the literature. *Gynecol Oncol.* 1998;69:78–83.
229. Daya DA, Scully RE. Sarcoma botryoides of the uterine cervix in young women: a clinicopathological study of 13 cases. *Gynecol Oncol.* 1988;29:290–304.
230. Riedlinger WF, Kozakewich HP, Vargas SO. Myogenic markers in the evaluation of embryonal botryoid rhabdomyosarcoma of the female genital tract. *Pediatr Dev Pathol.* 2005;8:355–361.
231. Clement PB, Scully RE. Mullerian adenosarcoma of the uterus: a clinicopathologic analysis of 100 cases with a review of the literature. *Hum Pathol.* 1990;21:363–381.
232. Harris NL, Scully RE. Malignant lymphoma and granulocytic sarcoma of the uterus and vagina. A clinicopathologic analysis of 27 cases. *Cancer.* 1984;53:2530–2545.
233. Kosari F, Daneshbod Y, Parwaresch R, et al. Lymphomas of the female genital tract: a study of 186 cases and review of the literature. *Am J Surg Pathol.* 2005;29:1512–1520.
234. Lagoo AS, Robboy SJ. Lymphoma of the female genital tract: current status. *Int J Gynecol Pathol.* 2006;25:1–21.
235. Vang R, Medeiros LJ, Fuller GN, et al. Non-Hodgkin's lymphoma involving the gynecologic tract: a review of 88 cases. *Adv Anat Pathol.* 2001;8:200–217.
236. Clark KC, Butz WR, Hapke MR. Primary malignant melanoma of the uterine cervix: case report with world literature review. *Int J Gynecol Pathol.* 1999;18:265–273.
237. Bigelow B, Vekshtein V, Demopoulos RI. Endometrial carcinoma, stage II: route and extent of spread to the cervix. *Obstet Gynecol.* 1983;62:363–366.
238. Fanning J, Alvarez PM, Tsukada Y, et al. Cervical implantation metastasis by endometrial adenocarcinoma. *Cancer.* 1991;68:1335–1339.
239. Creasman WT. New gynecologic cancer staging. *Obstet Gynecol.* 1990;75:287–288.
240. Morrow CP, Bundy BN, Kurman RJ, et al. Relationship between surgical-pathological risk factors and outcome in clinical stage I and II carcinoma of the endometrium: a Gynecologic Oncology Group study. *Gynecol Oncol.* 1991;40:55–65.
241. Zaino RJ. FIGO Staging of endometrial adenocarcinoma: a critical review and proposal. *Int J Gynecol Pathol.* 2009;28:1–9.
242. Tambouret R, Clement PB, Young RH. Endometrial endometrioid adenocarcinoma with a deceptive pattern of spread to the uterine cervix: a manifestation of stage IIb endometrial carcinoma liable to be misinterpreted as an independent carcinoma or a benign lesion. *Am J Surg Pathol.* 2003;27:1080–1088.
243. Jiang L, Malpica A, Deavers MT, et al. Endometrial endometrioid adenocarcinoma of the uterine corpus involving the cervix: some cases probably represent independent primaries. *Int J Gynecol Pathol.* 2010;29:146–156.
244. Szych C, Staebler A, Connolly DC, et al. Molecular genetic evidence supporting the clonality and appendiceal origin of Pseudomyxoma peritonei in women. *Am J Pathol.* 1999;154:1849–1855.
245. Matias-Guiu X, Lagarda H, Catasus L, et al. Clonality analysis in synchronous or metachronous tumors of the female genital tract. *Int J Gynecol Pathol.* 2002;21:205–211.
246. Chang KH, Albarracin C, Luthra R, et al. Discordant genetic changes in ovarian and endometrial endometrioid carcinomas: a potential pitfall in molecular diagnosis. *Int J Gynecol Cancer.* 2006;16:178–182.
247. Mazur MT, Hsueh S, Gersell DJ. Metastases to the female genital tract. Analysis of 325 cases. *Cancer.* 1984;53:1978–1984.
248. Lemoine NR, Hall PA. Epithelial tumors metastatic to the uterine cervix. A study of 33 cases and review of the literature. *Cancer.* 1986;57:2002–2005.

249. Manci N, Marchetti C, Esposito F, et al. Late breast cancer recurrence to the uterine cervix with a review of the literature. *Int J Gynecol Pathol.* 2008;27:113–117.
250. Imachi M, Tsukamoto N, Amagase H, et al. Metastatic adenocarcinoma to the uterine cervix from gastric cancer. A clinicopathologic analysis of 16 cases. *Cancer.* 1993;71:3472–3477.
251. Mansor S, McCluggage WG. Cervical adenocarcinoma resembling breast lobular carcinoma: a hitherto undescribed variant of primary cervical adenocarcinoma. *Int J Gynecol Pathol.* 2010;29:594–599.
252. McCluggage WG, Hurrell DP, Kennedy K. Metastatic carcinomas in the cervix mimicking primary cervical adenocarcinoma and adenocarcinoma in situ: report of a series of cases. *Am J Surg Pathol.* 2010;34:735–741.
253. Hellen EA, Coghill SB, Clark JV. Prolapsed fallopian tube after abdominal hysterectomy: a report of the cytological findings. *Cytopathology.* 1993;4:181–185.
254. Fadare O, Chacho MS, Parkash V. Psammoma bodies in cervicovaginal smears: significance and practical implications for diagnostic cytopathology. *Adv Anat Pathol.* 2004;11:250–261.
255. Kuebler DL, Nikrui N, Bell DA. Cytologic features of endometrial papillary serous carcinoma. *Acta Cytol.* 1989;33:120–126.
256. Fadare O, Ghofrani M, Chacho MS, et al. The significance of benign endometrial cells in cervicovaginal smears. *Adv Anat Pathol.* 2005;12:274–287.
257. Chang BS, Pinkus GS, Cibas ES. Exfoliated endometrial cell clusters in cervical cytologic preparations are derived from endometrial stroma and glands. *Am J Clin Pathol.* 2006;125:77–81.
258. Simsir A, Carter W, Elgert P, et al. Reporting endometrial cells in women 40 years and older: assessing the clinical usefulness of Bethesda 2001. Am *J Clin Pathol.* 2005;123:571–575.
259. Kapali M, Agaram NP, Dabbs D, et al. Routine endometrial sampling of asymptomatic premenopausal women shedding normal endometrial cells in Papanicolaou tests is not cost effective. *Cancer.* 2007;111:26–33.
260. de Peralta-Venturino MN, Purslow MJ, Kini SR. Endometrial cells of the "lower uterine segment" (LUS) in cervical smears obtained by endocervical brushings: a source of potential diagnostic pitfall. *Diagn Cytopathol.* 1995;12:263–268; discussion 268–271.
261. Lee KR, Genest DR, Minter LJ, et al. Adenocarcinoma in situ in cervical smears with a small cell (endometrioid) pattern: distinction from cells directly sampled from the upper endocervical canal or lower segment of the endometrium. *Am J Clin Pathol.* 1998;109:738–742.
262. Silver SA, Sherman ME. Morphologic and immunophenotypic characterization of foam cells in endometrial lesions. *Int J Gynecol Pathol.* 1998;17:140–145.
263. Nassar A, Fleisher SR, Nasuti JF. Value of histiocyte detection in Pap smears for predicting endometrial pathology. An institutional experience. *Acta Cytol.* 2003;47:762–767.
264. Tambouret R, Bell DA, Centeno BA. Significance of histiocytes in cervical smears from peri/postmenopausal women. *Diagn Cytopathol.* 2001;24:271–275.
265. Ponder TB, Easley KO, Davila RM. Glandular cells in vaginal smears from posthysterectomy patients. *Acta Cytol.* 1997;41:1701–1704.
266. Koike N, Higuchi T, Sakai Y. Goblet-like cells in atrophic vaginal smears and their histologic correlation. Possible confusion with endocervical cells. *Acta Cytol.* 1990;34:785–788.
267. Frank TS, Bhat N, Noumoff JS, et al. Residual trophoblastic tissue as a source of highly atypical cells in the postpartum cervicovaginal smear. *Acta Cytol.* 1991;35:105–108.
268. Fiorella RM, Cheng J, Kragel PJ. Papanicolaou smears in pregnancy. Positivity of exfoliated cells for human chorionic gonadotropin and human placental lactogen. *Acta Cytol.* 1993;37:451–456.
269. Acs G, Dumoff KL, Solin LJ, et al. Extensive retraction artifact correlates with lymphatic invasion and nodal metastasis and predicts poor outcome in early stage breast carcinoma. *Am J Surg Pathol.* 2007;31:129–140.
270. Kahn HJ, Marks A. A new monoclonal antibody, D2-40, for detection of lymphatic invasion in primary tumors. *Lab Invest.* 2002;82:1255–1257.
271. Mohammed RA, Martin SG, Gill MS, et al. Improved methods of detection of lymphovascular invasion demonstrate that it is the predominant method of vascular invasion in breast cancer and has important clinical consequences. *Am J Surg Pathol.* 2007;31:1825–1833.
272. McLachlin CM, Devine P, Muto M, et al. Pseudoinvasion of vascular spaces: report of an artifact caused by cervical lidocaine injection prior to loop diathermy. *Hum Pathol.* 1994;25:208–211.
273. Mehregan AH, Alberta E, Pinkus H. Artifacts in dermal histopathology. *Arch Dermatol.* 1966;94:218–225.
274. Benda JA, Lamoreaux J, Johnson SR. Artifact associated with the use of strong iodine solution (Lugol's) in cone biopsies. *Am J Surg Pathol.* 1987;11:367–374.
275. Davis JR, Steinbronn KK, Graham AR, et al. Effects of Monsel's solution in uterine cervix. *Am J Clin Pathol.* 1984;82:332–335.
276. Spitzer M, Chernys AE. Monsel's solution-induced artifact in the uterine cervix. *Am J Obstet Gynecol.* 1996;175:1204–1207.
277. Lowe DG, Levison DA, Crocker PR, et al. Silver deposition in the cervix after application of silver nitrate as a cauterising agent. *J Clin Pathol.* 1988;41:871–874.
278. Ragazzi M, Carbonara C, Rosai J. Nonneoplastic signet-ring cells in the gallbladder and uterine cervix. A potential source of overdiagnosis. *Hum Pathol.* 2009;40:326–331.
279. Wang K, Weinrach D, Lal A, et al. Signet-ring cell change versus signet-ring cell carcinoma: a comparative analysis. *Am J Surg Pathol.* 2003;27:1429–1433.
280. Unger ZM, Gonzalez JL, Hanissian PD, et al. Pseudolipomatosis in hysteroscopically resected tissues from the gynecologic tract: pathologic description and frequency. *Am J Surg Pathol.* 2009;33:1187–1190.
281. Cammarota G, Cesaro P, Cazzato A, et al. Hydrogen peroxide-related colitis (previously known as "pseudolipomatosis"): a series of cases occurring in an epidemic pattern. *Endoscopy.* 2007;39:916–919.

CHAPTER 4

Pathology of the Uterine Corpus

ORIENTATION OF AN ADULT HYSTERECTOMY SPECIMEN

The uterus is located between the bladder anteriorly and the rectum posteriorly (Fig. 3.151), and is largely covered by peritoneum. The posterior peritoneal covering of the uterus extends further inferiorly than the peritoneum on the anterior aspect. This difference in the level of peritoneal reflection is maintained in the hysterectomy specimen, and is one of four clues that help to determine the anterior and posterior aspects of a surgically removed uterus. Proper orientation is important for the pathologist, since it not only enables the identification of the anterior and posterior halves of the uterus but also allows for proper assignment of the laterality of the ovaries and fallopian tubes without assistance from the surgeon. The clues to uterine orientation are as follows:

- The posterior peritoneal covering of the uterus extends further inferiorly than the peritoneum on the anterior aspect (Fig. 4.1A,B)
- The attachment of the round ligament to the uterus is anterior (and inferior) to the uterotubal junction (Fig. 4.1C)
- The attachment of the ovarian ligament to the uterus is posterior (and inferior) to the uterotubal junction (Fig. 4.1C)
- A cesarean section scar may be present in the anterior wall of the lower uterine segment or endocervical canal (Fig. 4.1D)

A mnemonic for the positions of the round and ovarian ligaments in relation to the uterotubal junction is OPRA (as in "Oprah" or "opera"), for **O**varian ligament **P**osterior; **R**ound ligament **A**nterior. Once orientation has been established, it is helpful to mark the posterior aspect of the uterus with ink or a scalpel blade ("P"), so that orientation is easily recalled when returning to the fixed specimen for sectioning.

SELECTED CONGENITAL UTERINE ABNORMALITIES

Most congenital uterine abnormalities encountered in the surgical pathology laboratory are due to defects in the fusion of the paired müllerian (paramesonephric) ducts or postfusion septal wall resorption that normally occur during embryogenesis.[1] If only one müllerian duct develops properly, while the other duct undergoes agenesis or aplasia, a one-sided, banana-shaped uterus is formed. This anomaly is termed a unicornuate uterus (uterus unicornis), which may be associated with a rudimentary horn if the abnormal duct develops in a hypoplastic fashion (Fig. 4.2A). In a bicornuate uterus (uterus bicornis), the upper portions of both müllerian ducts develop but fail to fuse, resulting in a heart-shaped uterus that has two horns that enter a common vagina (Fig. 4.2B). If the dividing myometrial tissue of a bicornuate uterus extends only to the level of the internal cervical os, it is a bicornuate unicollis (bicornuate partial), whereas if this dividing tissue extends to the level of the external cervical os, creating two endocervical canals and two external cervical ostia, it is a bicornuate bicollis (bicornuate complete). If both müllerian ducts develop but fail to fuse along their entire lengths, a double uterus with two cervices is formed that is known as a uterus didelphys (Fig. 4.2C). In most cases of uterus didelphys, there is also a septate vagina, but the vagina may also be single and normal.

A septate uterus (uterus septus) results when the müllerian ducts fuse, but the wall separating the two cavities persists rather than degenerates. The septum may be of variable length and thickness, and consists of myometrial and/or fibrous tissue. The lack of a prominent fundal cleft helps to distinguish a septate uterus from a bicornuate uterus. The mildest form of a septate uterus is the arcuate uterus (uterus arcuatus), in which the fundus is more flat than normal with a slight midline indentation. The partial septate uterus has a V-shaped endometrial cavity (Fig. 4.2D), whereas the complete septate uterus features partitioning into two separate endometrial cavities, division of the endocervical canal in two, and a septate vagina. In some circumstances, the partitioned endometrial cavities of malformed uteri communicate with each other in the region of the lower uterine segment for a short distance before branching back out into separate endocervical canals (Fig. 4.2E), adding a degree of complexity to the nomenclature (e.g., uterus communicans septus with cervical and vaginal septa).[2] Figure 4.2F shows an amputated double cervix (cervix duplex) separated by a vaginal septum, which is seen in uterine didelphys and some variants of uteri communicans. Note the distinction between a true double cervix (as in Fig. 4.2C,F) and a cervical septum that results in the formation of two endocervical canals and two external ostia (as in Fig. 4.2B,E).

ENDOMETRIUM OF THE MENSTRUAL CYCLE

Overview of Endometrial Architecture

The endometrium beneath the surface epithelium is divided into the functionalis and basalis. The functionalis is composed of the zona compactum, which is an indistinct, thin, superficial layer, and a broad, intermediate region known as the zona spongiosum. The basalis is the deepest layer, and is located adjacent to the myometrium (Fig. 4.3).

Unlike the functionalis, the basalis is not shed during menstruation. The morphology of the basalis stays relatively constant throughout the menstrual cycle, consisting of a densely cellular, spindle cell stroma that contains weakly proliferative glands that may be closely packed. In contrast, the functionalis exhibits the characteristic hormone-dependent changes of the menstrual cycle. In both the proliferative and secretory phases, the glands of the functionalis are oriented perpendicular to the surface epithelium. Glands tend to be regularly distributed during the proliferative phase, but secretory glands may be seen in aggregates. As discussed elsewhere in this chapter, endometrial hyperplasia can be simulated by both late secretory and basalis endometrium when encountered as fragments within an endometrial sample, and fragments of basalis that are associated with thick-walled blood vessels may be misinterpreted as tissue derived from an endometrial polyp.

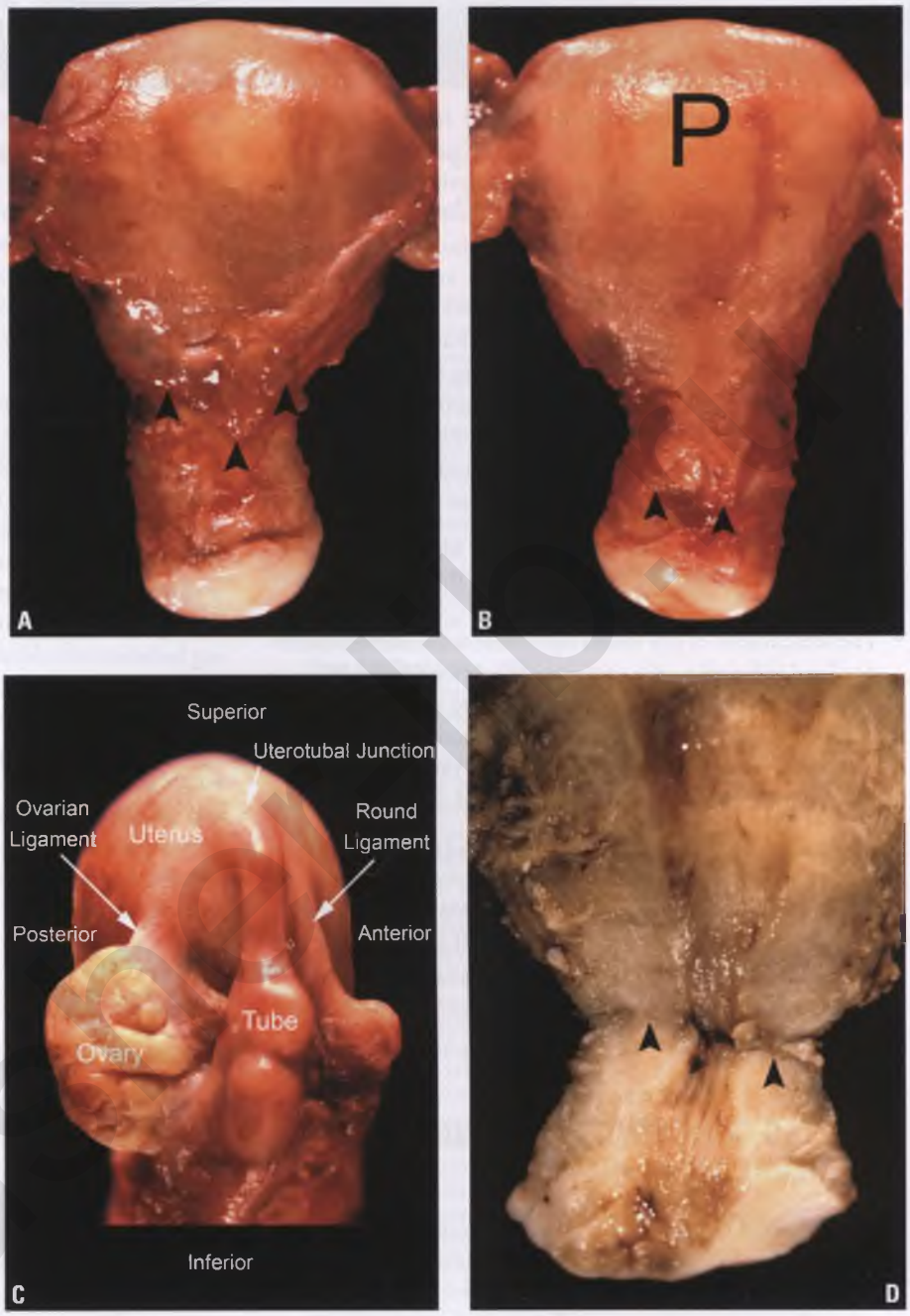

FIGURE 4.1. Anatomical landmarks for orienting a hysterectomy specimen. **A**: External anterior aspect of a surgically removed uterus, demonstrating the inferior limit of the incised peritoneal covering (*arrowheads*). **B**: External posterior aspect of the uterus shown in **(A)**. Note that the inferior limit of the incised peritoneal covering (*arrowheads*) is at a level below that seen anteriorly. **C**: Right side of uterus with attached ovary and tube. The positions of round ligament and ovarian ligament in relation to uterotubal junction help to orient a hysterectomy specimen. **D**: C-section scar (*arrowheads*) in the endocervical canal, indicating that this is the anterior half of this opened, formalin-fixed uterus.

The normal endometrial–myometrial junction is often irregular. This irregularity can lead to an overdiagnosis of adenomyosis or, in the presence of an endometrial adenocarcinoma, to misinterpretation of a nonmyoinvasive tumor as one with superficial myometrial invasion (see section on endometrioid adenocarcinoma).

Endometrial Dating: Guidelines and Limitations

From the foregoing, it is clear that the basalis should be avoided when evaluating the phase of the endometrium. This can be accomplished by restricting such analysis to well-oriented tissue fragments that possess surface epithelium. Tissue from the lower uterine segment, which is also limited in its hormonal responsiveness, should also be avoided. The histology of the basalis and lower uterine segment is presented in the discussion of the differential diagnosis of endometrial polyps. An additional caveat is that an assessment of the cycle date should not be performed in the presence of endometritis, since the inflammatory reaction alters the normal hormonal responsiveness of the endometrium.

For histologically unremarkable endometrial samples submitted for abnormal uterine bleeding, simply specifying whether the endometrium is in the proliferative or secretory phase and noting that there is no evidence of polyp, hyperplasia, or malignancy is sufficient. When endometrial tissue from the secretory phase of the cycle is submitted as part of an infertility evaluation, the pathologist is typically

expected to provide an estimate of the cycle date, which in turn will address the issues of whether or not ovulation has occurred and if the stage of maturation matches the clinical expectation. This date is typically provided as a 2-day range to reflect the imprecision of this evaluation, and is based upon the most histologically advanced degree of maturation that is present in the sample. Date reporting is accomplished either by referring to cycle days from a prototypical 28-day cycle in which day 1 is defined as the first day of menstrual bleeding and day 15 as the first day following ovulation or by referring to postovulatory days (the postovulatory day = the particular cycle day of the secretory phase of a presumed 28-day menstrual cycle − 14; e.g., cycle day 23 = postovulatory day 9). The method of reporting should be standardized within a given pathology group after taking into account any possible preferences of the local gynecologists (my personal preference is to use the postovulatory day terminology).

Once confident that the tissue being evaluated is representative of the functionalis, the analysis of multiple variables that will lead to an estimate of the cycle date can begin. During the first 6 days of the secretory phase, the features of the glandular component are paramount in estimating the cycle date, particularly the extent and location of intracellular secretory vacuoles, the pseudostratified versus basal location of the nuclei, the progressive decrease in epithelial mitoses, and the development of luminal secretions. Beginning with postovulatory day 7, the stromal changes of edema, progressive development of predecidual change, and the appearance of an infiltrate of

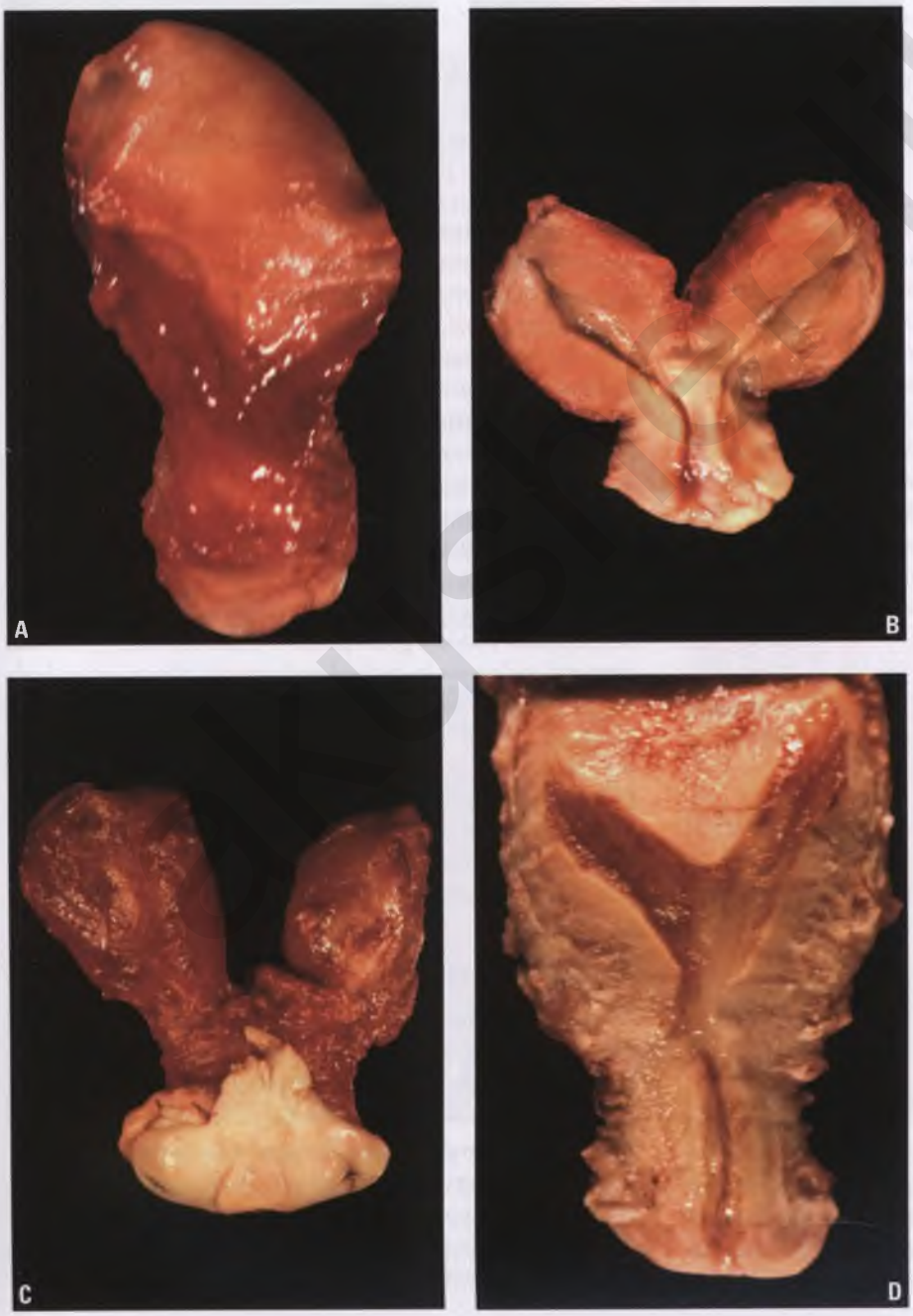

FIGURE 4.2. Congenital uterine abnormalities. **A**: Unicornuate uterus (unopened). **B**: Bicornuate uterus bicollis, opened to reveal partitioned endometrial cavities and separate endocervical canals. **C**: Uterus didelphys (unopened). **D**: Partial septate uterus with V-shaped endometrial cavity. (*continued*)

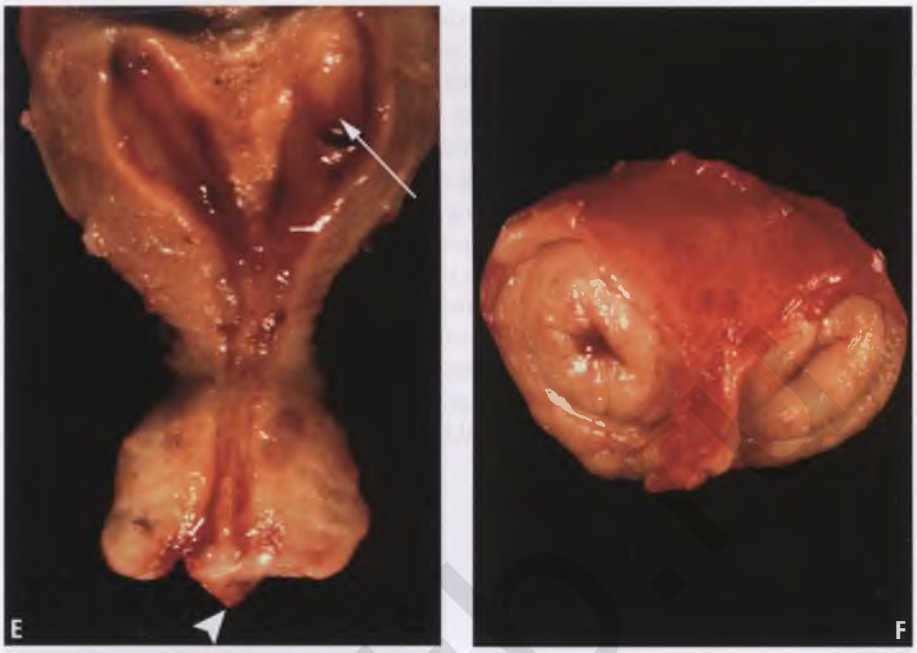

FIGURE 4.2. (*continued*) **E**: Uterus communicans septus with cervical and vaginal septa. *Arrowhead* marks vaginal septum; *arrow* marks an endometrial polyp. **F**: End-on view of double cervix separated by vaginal septum. (**C**: Courtesy of Dr. Julio A. Lagos.)

granular lymphocytes are the key features used in determining the approximate cycle date. Instead of reprinting the standard tables, charts, and graphs of these and other parameters as they vary during the course of the menstrual cycle, emphasis here is placed upon visual correlates.

It should be noted that the foundation of our knowledge of endometrial dating was laid in 1950, using a population of infertile women and using an imprecise method to estimate the time of ovulation that was based upon the onset of the following menses.[3] A contemporary study using normal volunteers that defined the day of ovulation as the day following the urinary luteinizing hormone surge has concluded that the traditional dating criteria are less temporally distinct and of lesser utility than originally described.[4] There are several confounding factors that make histologic dating of the secretory endometrium an imprecise exercise. Menstrual cycles rarely have the idealized length of 28 days, and although most of the variability is due to a longer or shorter ovarian follicular (proliferative endometrial) phase, the ovarian luteal (secretory endometrial) phase can also range from 12 to 16 days.[5] Note that a luteal phase length of anything other than 14 days introduces an element of inaccuracy when histologic dates are crosswalked to chronologic dates of an individual patient's cycle. Other possible sources of inaccuracy are (a) the inherent subjectivity of the dating process, which is associated with both interobserver and intraobserver variability, (b) regional variation in secretory development within a given patient's endometrium, (c) normal temporal variations in cyclical endometrial alterations at both the population level and between cycles of a given individual, (d) samples with an insufficient amount of tissue obtained from the cycling portion of the endometrium, and (e) samples with suboptimal fixation, processing, orientation, sectioning, or staining.[4,5] Despite these limitations, the pathologist is still obligated to respond to the clinician's request to provide the best estimate possible for the cycle date of secretory endometria.

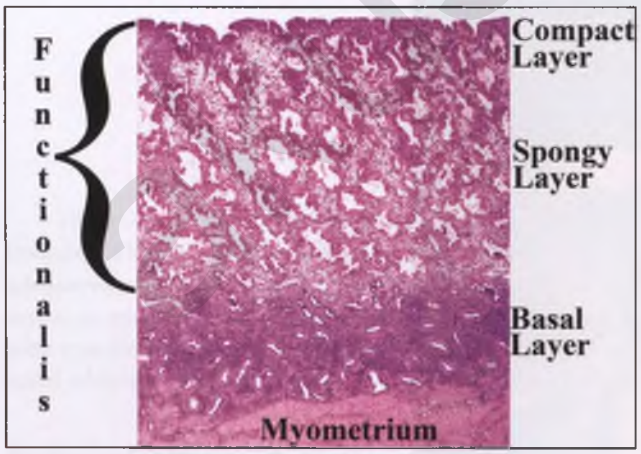

FIGURE 4.3. Endometrial architecture. This low-magnification view of a late secretory endometrium demonstrates the compact, spongy, and basal layers (zona compactum, zona spongiosum, and zona basalis). The functional layer (functionalis) is composed of the compact and spongy layers.

Proliferative Phase

As the proliferative phase progresses following the cessation of menstruation, the glands gradually become more tortuous and their lining cells become more pseudostratified and mitotically active. Since these changes are subtle, not easily quantified, and do not correlate well with specific days of the cycle, proliferative endometrium is generally not "dated." For descriptive purposes, the proliferative phase can be broadly divided into early (cycle days 4–7), mid (cycle days 8–10), and late (cycle days 11–14) stages. Throughout the proliferative phase, the glands appear

dark blue at low magnification. In early proliferative endometrium, the glands form tubules that are straight and narrow, and the stroma is abundant (Fig. 4.4). The glands are lined by low columnar cells that show mild degrees of pseudostratification and mitotic activity. In late proliferative endometrium, the glands are more tortuous and in optimally oriented sections exhibit a sinuous pattern (Fig. 4.5). In comparison to the early proliferative phase, the glandular lining cells are more elongated, pseudostratified, and mitotically active, and are more likely to possess small nucleoli. Although stromal edema is purported to be more apparent in the mid proliferative than in the late proliferative phase, this is an unreliable and subjective criterion for their separation. In practice, mid proliferative and late proliferative endometria are quite similar histologically.

Secretory Phase

Interval Phase (Postovulatory Days 1–2; Cycle Days 15–16)

During the first two postovulatory days, referred to as the interval phase, the endometrial glands and stroma resemble late proliferative endometrium, with the notable exception of scattered clear subnuclear vacuoles within the cells lining the glands (Fig. 4.6). The epithelial nuclei are pseudostratified and glandular mitoses are common during this period. Although most patients with interval phase endometria have likely ovulated, this pattern is not diagnostic of ovulation.

Early Secretory Phase (Postovulatory Days 3–5; Cycle Days 17–19)

Postovulatory day 3 has been attained when at least 50% of the glands contain uniformly distributed subnuclear vacuoles (Fig. 4.7). At this stage, there is unequivocal morphologic evidence that ovulation has occurred. Nuclear pseudostratification and mitotic activity of the glandular lining cells are markedly diminished in comparison to interval phase endometrium. Over the course of the next few days, there is a shift in the location of the vacuoles from a predominantly subnuclear to an apical position (Fig. 4.8). Discharge of secretory contents begins on postovulatory day 4, and is initially manifested by cytoplasmic apical blebs and/or a frayed appearance to the luminal surface. By postovulatory day 5, cytoplasmic vacuoles are infrequent and the glandular diameter increases as secretions appear within the lumens.

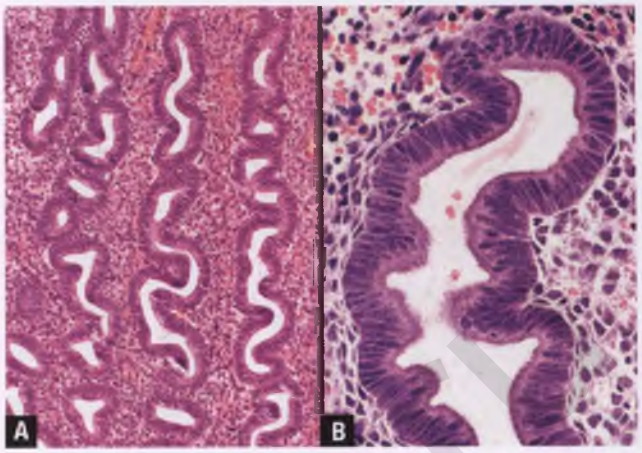

FIGURE 4.5. Late proliferative endometrium. **A**: Parallel arrays of coiled, tubular glands are oriented perpendicular to the epithelial surface, which is beyond the top of this image. **B**: High-magnification view of a serpentine, late-proliferative gland lined by pseudostratified cells with cigar-shaped nuclei and small nucleoli. Although not prominent in this gland, mitotic figures are frequent in the late-proliferative phase.

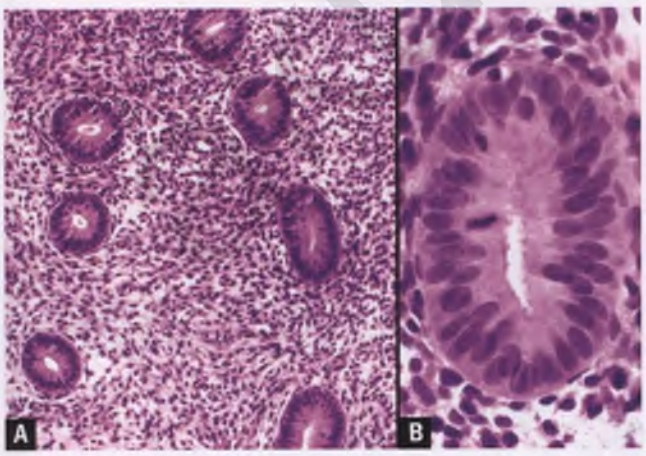

FIGURE 4.4. Early proliferative endometrium. **A**: The tubular glands are straight and narrow, and are seen here in cross section within a background of abundant stroma. **B**: The glands are lined by low columnar cells with mild pseudostratification and occasional mitotic figures.

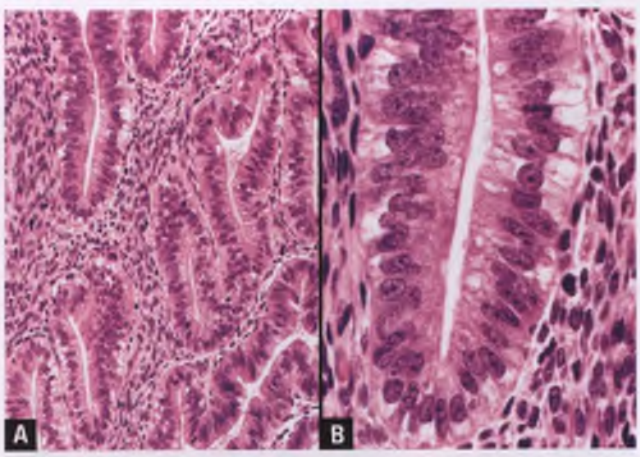

FIGURE 4.6. **A,B**: Interval phase endometrium. The cells lining the glands are pseudostratified, contain scattered subnuclear vacuoles, and exhibit some mitotic activity. The stroma resembles that of proliferative endometrium. Ovulation may have occurred, but development at or beyond the stage of postovulatory day 3 endometrium is necessary for definitive morphologic evidence of ovulation.

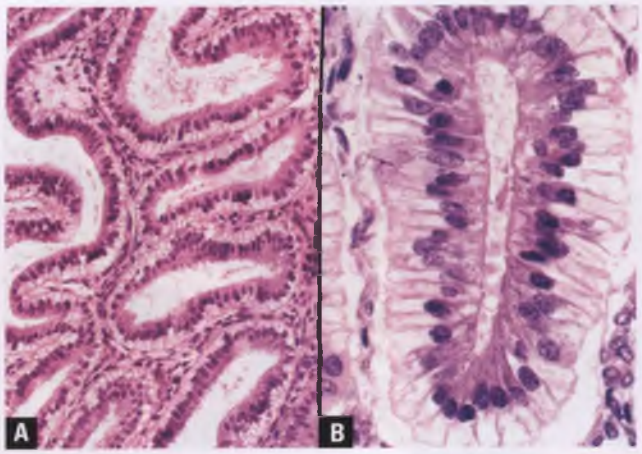

FIGURE 4.7. **A,B**: Early secretory endometrium, postovulatory day 3. Wavy glands with uniform subnuclear vacuoles characterize this phase of development.

Mid-Secretory Phase (Postovulatory Days 6–8; Cycle Days 20–22)

Postovulatory day 6 is characterized by peak intraluminal secretions and dilated glands that are lined by cells with a single layer of basally oriented nuclei and a few residual cytoplasmic vacuoles (Fig. 4.9). Secretion-related apical blebs may be prominent. There is little stromal edema and no predecidual reaction. Stromal edema becomes more prominent on postovulatory day 7, and reaches its maximum on postovulatory day 8 (Fig. 4.10). In view of the paucity of objective distinguishing morphologic features during the mid-secretory phase, it is not surprising that there is a high degree of observer variability in estimating a cycle date during this period. Note that in the event of fertilization, implantation occurs within the setting of a mid-secretory endometrium.

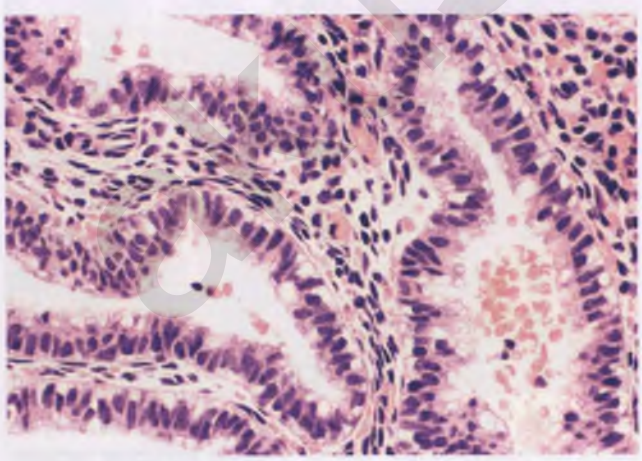

FIGURE 4.8. Early secretory endometrium, postovulatory day 4. Some glandular cells have persistent subnuclear vacuoles, but apical secretory vacuoles are now also evident. Portions of the luminal surface have a frayed appearance due to secretory activity.

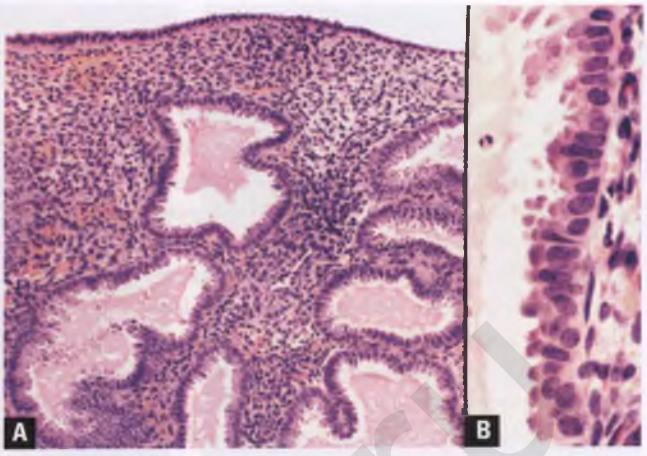

FIGURE 4.9. Mid-secretory endometrium, postovulatory day 6. **A**: The glands are dilated and contain eosinophilic secretions. Stromal edema is not yet prominent, and there is no predecidual change. **B**: Due to decapitation secretion, the cells lining the glands exhibit numerous apical cytoplasmic blebs.

Late Secretory Phase (Postovulatory Days 9–14; Cycle Days 23–28)

The hallmark of the postovulatory day 9 endometrium is the prominence of spiral arterioles due to the periarteriolar condensation of predecidua (Fig. 4.11). Since spiral arterioles are highly coiled structures, their sectioning typically results in clustered vascular profiles in various planes. In addition to their initial periarteriolar location, predecidualized stromal cells can be recognized by their accumulation of amphophilic cytoplasm, nuclear enlargement, pale chromatin, indistinct cell borders, and oval to polygonal shapes. By postovulatory day 10, the predecidual periarteriolar cuffs are thick (Fig. 4.12). By postovulatory day 11, scattered well-formed islands of predecidua are present. Postovulatory day 12 features

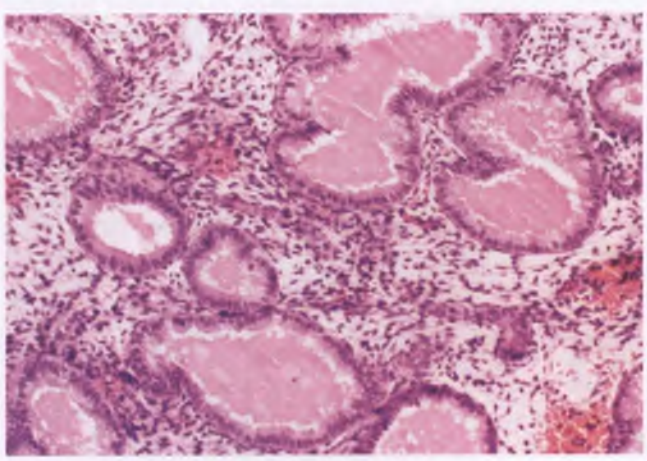

FIGURE 4.10. Mid-secretory endometrium, postovulatory day 7 to 8. Prominent luminal secretions and stromal edema characterize this period. The dilated glands are lined by basally oriented, round to oval, mitotically inactive nuclei. Predecidual changes are absent.

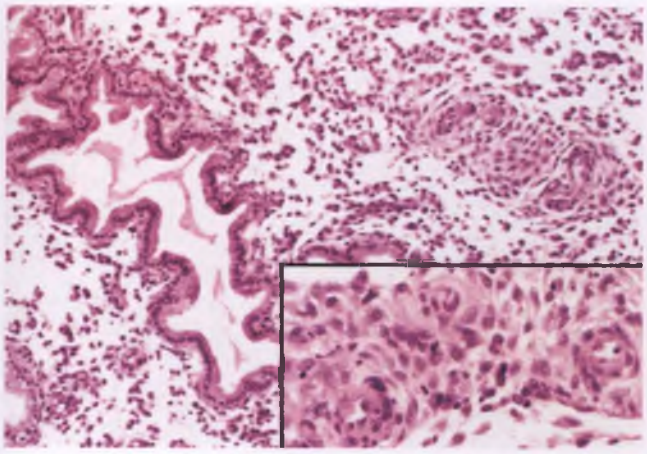

FIGURE 4.11. Late-secretory endometrium, postovulatory day 9. The distinctive feature of this cycle date is the prominence of clustered profiles of spiral arteries due to periarterial predecidual transformation (upper right and inset). Stromal edema persists, and the glands exhibit papillary infoldings.

continuation of the predecidualization process as manifested by formation of a linear band of predecidualized stromal cells beneath the epithelial surface and the early stages of coalesce of the predecidualized islands (Fig. 4.13). By postovulatory day 13, the upper portion of the functionalis is completely predecidualized (Fig. 4.14).

The timing and degree of stromal infiltration by granular lymphocytes roughly parallels the predecidualization process, such that these cells are conspicuous by postovulatory day 12 and increase in numbers during the last few days of the cycle (Fig. 4.15). The extent of glandular papillary infolding also gradually increases during the late secretory phase and peaks at

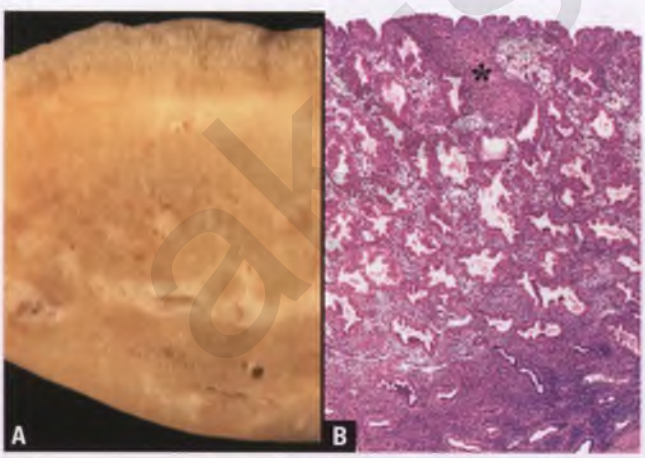

FIGURE 4.12. Late-secretory endometrium, postovulatory day 10. **A**: This section through a formalin-fixed uterine wall demonstrates a lush layer of secretory endometrium (5-mm thick at top) overlying the myometrium. **B**: In this corresponding histologic section through the endometrium, islands of predecidualized stroma surround clusters of spiral arterioles (*asterisk*) in a background of secretory glands with serrated contours. Note the nonresponsive basalis at the bottom of the image.

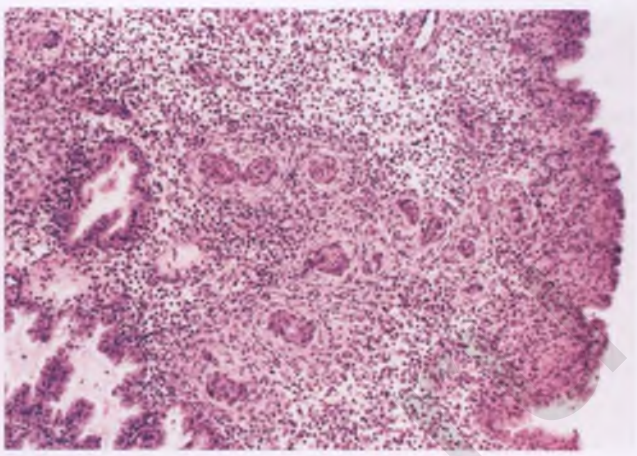

FIGURE 4.13. Late-secretory endometrium, postovulatory day 11 to 12. In addition to the thick periarteriolar cuffs of predecidua that are seen in POD 10 endometria, there is a linear band of predecidualized stromal cells just beneath the epithelial surface (at right). The glands are dilated and have a serrated architecture. Scattered granular lymphocytes, recognized only as small, dark blue cells at this magnification, are present.

postovulatory day 12 to 13, during which time glands with a serrated, "saw-toothed" appearance are prominent. Aggregates of these serrated glands may be crowded together within the deeper aspects of the functionalis and simulate endometrial hyperplasia (Fig. 4.16). However, in contrast to endometrial hyperplasia, these late secretory glands appear as closely packed columns of tortuous glands that are oriented perpendicular to the endometrial surface, lack mitotic activity, possess cytoplasmic vacuoles, and are associated with adjacent or nearby areas of predecidualized stroma. In addition, the regular and repetitive micropapillary architecture of late secretory endometrium is a constant feature, whereas a similar pattern is only occasionally present in endometrial hyperplasia.

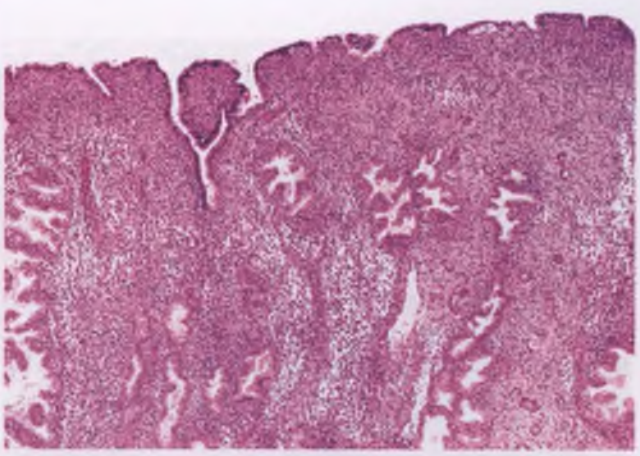

FIGURE 4.14. Late-secretory endometrium, postovulatory day 12 to 13. In addition to the continuous layer of predecidua beneath the surface that characterizes postovulatory day 12, there are large patches of predecidual confluence within the upper portion of the functionalis (most apparent at right).

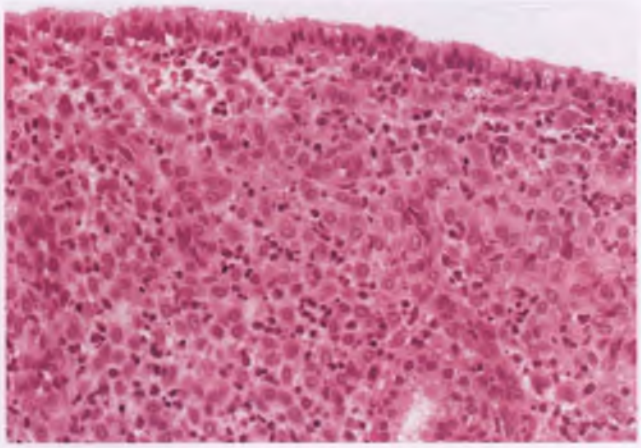

FIGURE 4.15. Late-secretory endometrium, postovulatory day 13. Several granular lymphocytes are scattered amongst the confluent predecidualized stromal cells beneath the endometrial surface.

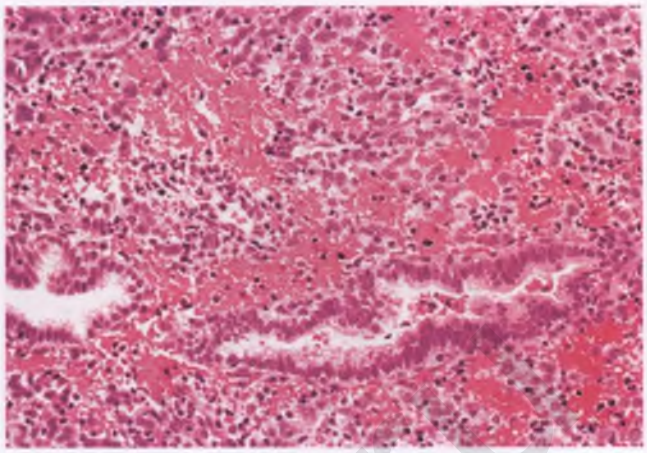

FIGURE 4.17. Late-secretory endometrium, postovulatory day 14. The predecidualized stroma is dissociating and thrombi-induced hemorrhage has resulted in stromal extravasation of erythrocytes. Tissue surrounding this area was intact and had not been spontaneously shed, but this particular field is virtually indistinguishable from early menstrual tissue.

Postovulatory day 14 is characterized by early signs of stromal dissociation and patches of interstitial hemorrhage, which heralds the onset of menstruation (Fig. 4.17).

Menstrual Phase

Endometrium in the menstrual phase is dark red, owing to the presence of interstitial hemorrhage. In addition to pools of blood, the process of endometrial dissolution also features formation of cords and aggregates of predecidualized cells with diminished amounts of cytoplasm, an infiltrate of leukocytes (predominantly neutrophils), fibrin thrombi, and glands with varying degrees of fragmentation and secretory exhaustion (Figs. 4.18 and 4.19). Another indicator of ongoing endometrial shedding, which may be menstrual or nonmenstrual in origin, is the presence of microfragments of nuclear debris ("nuclear dust") within the cytoplasm of the cells lining the endometrial glands (Fig. 4.20). Most, if not all, of the functionalis is shed during menstruation, whereas the basalis remains histologically unaltered by this process.

In the later stages of menstrual endometrium, the necrotic predecidual cells have lost virtually all of their cytoplasm, resulting in a pattern of stromal breakdown that overlaps with that related to anovulation (Fig. 4.21). However, distinction of these two processes is usually possible, as discussed in the section on nonphysiologic glandular and stromal breakdown. Collapse of the stroma during menstruation can result in close

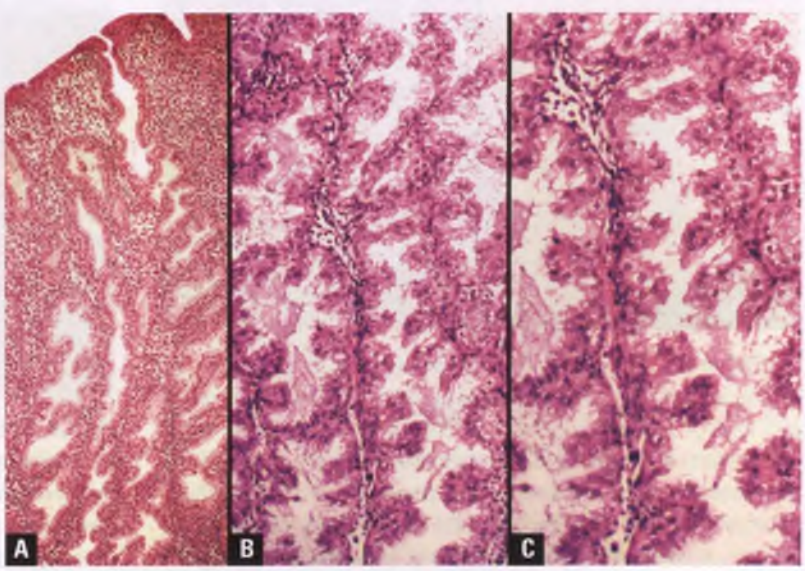

FIGURE 4.16. Late-secretory endometrium, postovulatory day 12 to 13, with crowded aggregates of serrated glands within the deeper aspects of the functionalis that could be mistaken for endometrial hyperplasia. **A**: Note the simplification of the glandular architecture near the endometrial surface at the top of the image. The function of this portion of the glands is primarily related to delivering rather than producing secretory products. **B,C**: Note the regular and repetitive nature of the micropapillary structures that are responsible for the serrated architecture of the glands.

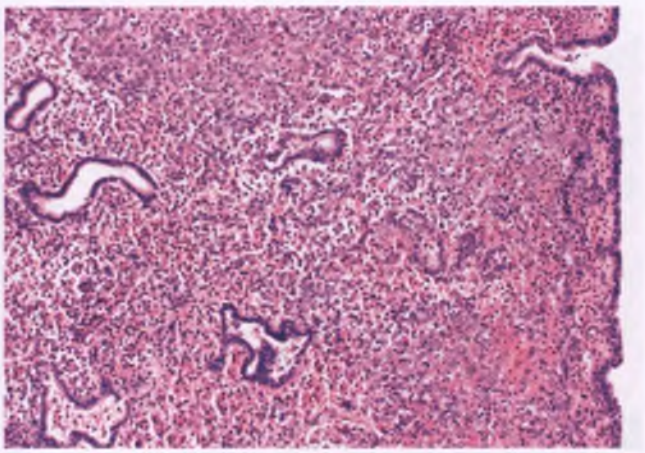

FIGURE 4.18. Menstrual endometrium. The predecidualized stroma has broken down into cords and aggregates of cells with diminished amounts of cytoplasm. There is an admixture of red blood cells and leukocytes, and the glands demonstrate secretory exhaustion. Note the diffuse nature of process. The endometrial surface is at right, and the plane of cleavage in the lower functionalis is beyond the field of view at left.

approximation of fragmented endometrial glands and surface epithelium, which can simulate hyperplasia or, in the presence of extensive tissue necrosis and inflammation, an adenocarcinoma. Attention to the degenerative appearance of the process, focal areas of recognizable secretory activity within the glands, the lack of significant nuclear atypia, an absence of glandular mitotic activity, and adherence to the general principle of not making a definitive interpretation on the basis of degenerated tissue should prevent such diagnostic errors.

Yet another potential pitfall in the interpretation of menstrual endometrium is the rare finding of its presence within myometrial and parametrial vessels in hysterectomy specimens (Figs. 4.22 and 4.23).[6] The involved vessels, which are usually recognizable as thin-walled veins, may contain tissue aggregates composed solely of collapsed stroma, solely of epithelial elements, or an admixture of the two components. These cases are usually recognized by the double-contoured appearance of some of the intravascular endometrial aggregates, the lack of overt features of malignancy, and correlation with the menstrual history, but immunohistochemistry using stromal and epithelial markers (e.g., CD10 and cytokeratin) may be necessary in selected instances.

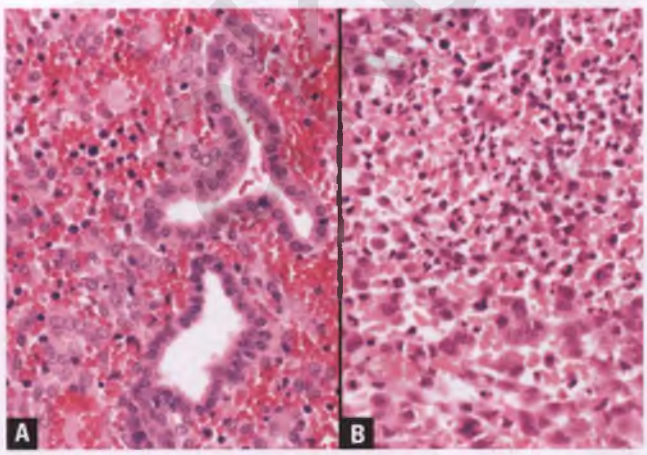

FIGURE 4.19. **A,B**: Menstrual endometrium. Higher magnification view of two different examples, with features as described in the preceding figure.

ENDOMETRIAL ATROPHY

Usual Atrophic Pattern

Endometrial atrophy is a normal, expected finding in postmenopausal women who are not on hormone replacement therapy. In addition to a lack of hormonal stimulation, pressure from an impinging mass lesion such as a submucosal leiomyoma can also result in an atrophic endometrial lining. Atrophic endometrium is thin, and typically features glands and surface epithelium lined by a single layer of flattened to cuboidal, mitotically inactive epithelial cells (Fig. 4.24). The simple, widely spaced glands are usually oriented parallel to the endometrial surface, in contrast to the perpendicular orientation of normal proliferative or secretory glands. The endometrial stroma is often partially to extensively collagenized (Fig. 4.25), which results in a resemblance to the stroma of the lower uterine segment of women in their reproductive years. In some cases, the epithelium that lines the surface and glands contains columnar-shaped and occasional ciliated cells, but the architecture, mucosal thinness, mitotic inactivity, and stromal features of endometrial atrophy are retained.

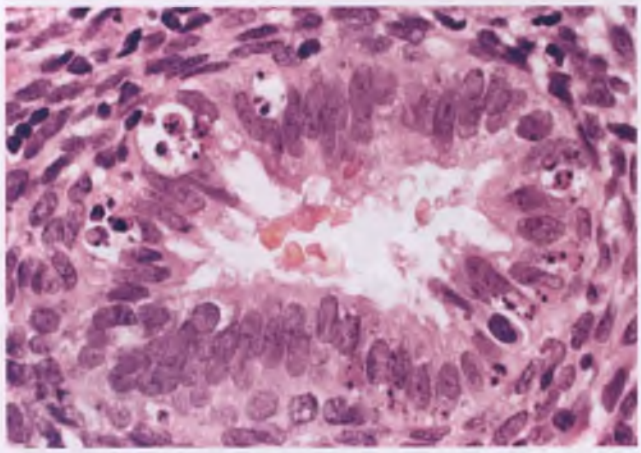

FIGURE 4.20. The presence of nuclear debris ("nuclear dust") within the cytoplasm of cells lining endometrial glands is evidence of shedding, even in the absence of stromal breakdown in the tissue available for histologic examination.

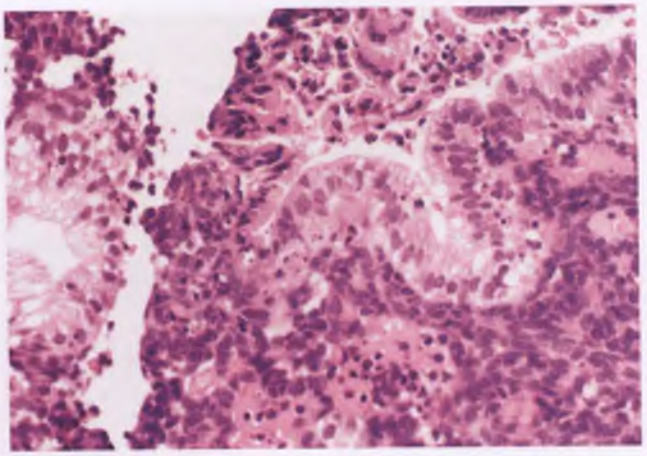

FIGURE 4.21. Menstrual endometrium. In this field, the pattern of stromal breakdown is indistinguishable from that seen in anovulation. However, the clear, vacuolated cytoplasm of the endometrial glands is indicative of secretory activity, which points to this process as being related to menstruation.

Samples of atrophic endometrium often consist only of scant strips of surface epithelium, sometimes in association with a minimal amount of stroma. These specimens should not be dismissed as being insufficient for histologic evaluation, since the scant nature of the tissue recovered may simply be a reflection of an atrophic endometrial lining. A descriptive pathology report that conveys these sentiments should be issued, an example of which is as follows:

Microscopic:

Sections show scant strips of benign surface endometrial epithelium. There is no evidence of hyperplasia or malignancy in this limited, superficial sample. The scant amount of tissue available for evaluation may be related to endometrial atrophy. Clinical correlation is suggested.

Diagnosis:

Uterus, endometrium, curettage –

Scant strips of benign surface endometrial epithelium (see Microscopic)

Although endometrial atrophy is often cited as a cause of postmenopausal bleeding, it probably is an epiphenomenon. Instead, vascular abnormalities such as myometrial arteriolosclerosis or rupture of congested, dilated veins that form either secondary to uterine prolapse or impingement by cystically dilated glands are more likely to play a primary role in the symptomatology.[7,8]

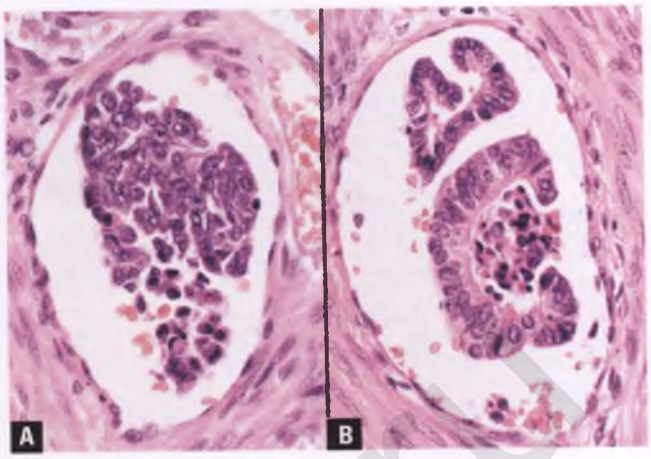

FIGURE 4.23. Menstrual endometrium within myometrial veins. **A**: Aggregate of condensed endometrial stromal cells within a vein. **B**: Strips of endometrial glandular epithelium and a few degenerated cells within a vein.

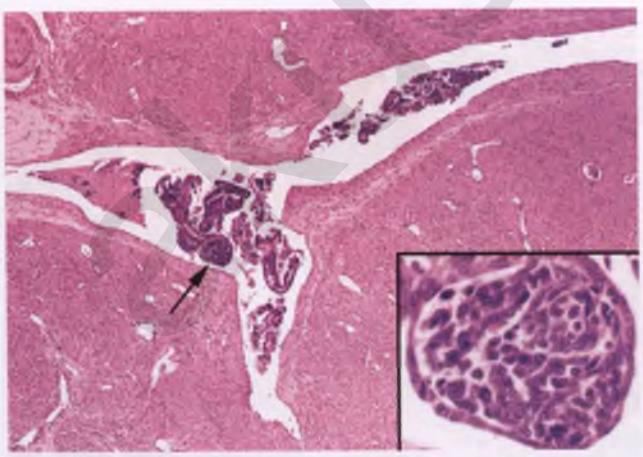

FIGURE 4.22. Menstrual endometrium within myometrial veins. The inset shows an aggregate of collapsed stroma with a peripheral rim of epithelial cells, which is marked by an arrow in the main image.

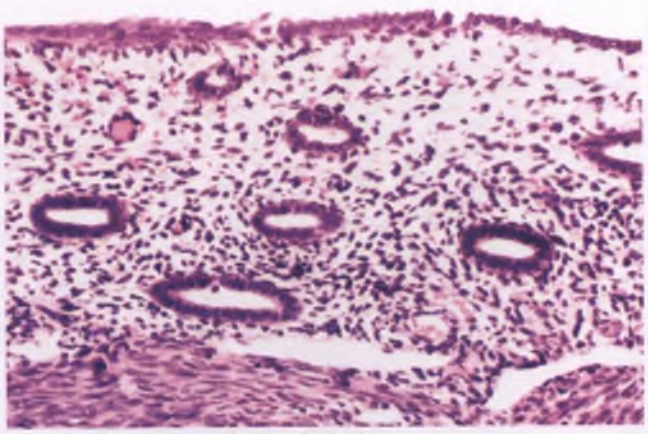

FIGURE 4.24. Endometrial atrophy. The endometrium is thin and the glands are lined by a single layer of cuboidal, mitotically inactive epithelial cells. Note that the glands tend to be simple, widely spaced, and oriented parallel to the surface.

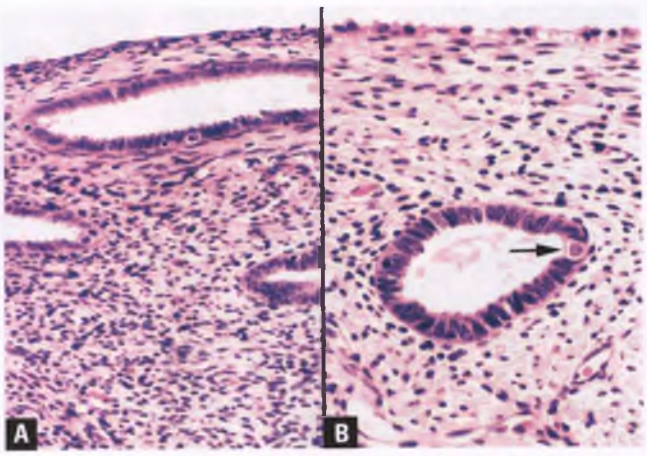

FIGURE 4.25. Endometrial atrophy. **A**: The stroma is partially collagenized and the glands are oriented parallel to the surface. **B**: In this example, the stroma is more prominently collagenized. The atrophic gland is lined by columnar epithelium and contains a cell with a rounded nucleus and a perinuclear halo (*arrow*), which are features that are often present in ciliated cells.

It is worth noting two potential diagnostic pitfalls when presented with a sample of atrophic endometrial tissue. First, it is important to evaluate these detached epithelial strips at high magnification to exclude the possibility of marked nuclear atypia that may be related to endometrial intraepithelial carcinoma (EIC), which is the putative precursor of serous carcinoma.[9] Second, strips of atrophic surface epithelium are predisposed to coiling artifact, which may mimic endometrial hyperplasia (see section on endometrial artifacts).

Cystic Atrophy

In this common variant of atrophy, aggregates of cystically dilated endometrial glands that are lined by a single layer of flattened, mitotically inactive epithelial cells replace portions of the endometrium. The stroma is typically fibrotic. When florid, cystic atrophy is grossly visible as a thickened endometrium with a "Swiss-cheese" appearance (Fig. 4.26). Although cystic atrophy and some forms of simple hyperplasia have overlapping architectural features, the flattened, amitotic nature of the epithelium of cystic atrophy contrasts with the columnar, mitotically active, stratified epithelium of simple hyperplasia.

WEAKLY PROLIFERATIVE (INACTIVE) ENDOMETRIUM

When the endometrial glands exhibit borderline atrophic changes in the setting of an endometrium of near-normal thickness and in association with a dense, spindle cell, basalis-like stroma, the terms weakly proliferative or inactive endometrium may be used to indicate an intermediate position in the spectrum between the normal proliferative phase and atrophy (Fig. 4.27).

ENDOMETRIUM AND MYOMETRIUM IN PREGNANCY, ABORTION, AND THE POSTPARTUM PERIOD

Gestational Endometrium

The endometrium is in the mid-secretory phase of the cycle when the implantation of the blastocyst occurs.[10] Implantation triggers the gradual conversion from secretory to gestational endometrium, with the latter initially featuring persistence of stromal edema, development of hypersecretory glands, and additional formation of predecidua.[11] However, these changes in the secretory phase of the cycle of conception are subtle and inconstant, and cannot be used as an indication of pregnancy. Hypersecretory glands feature

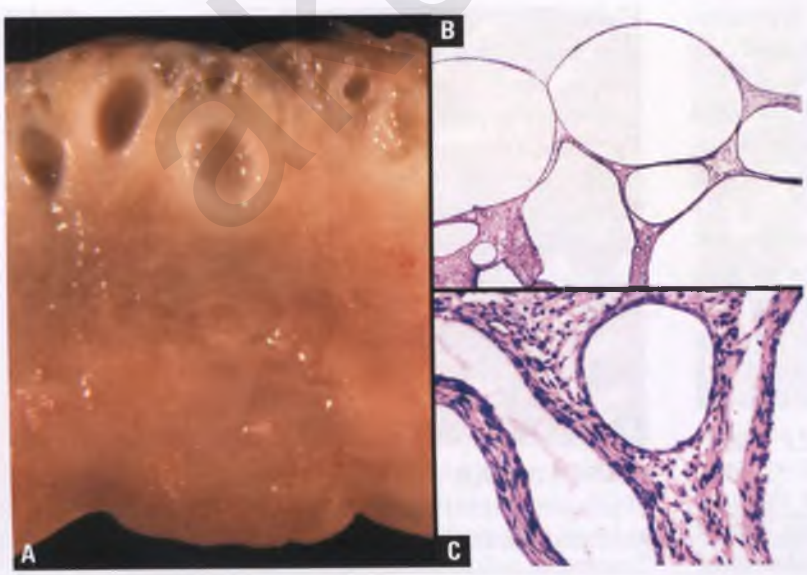

FIGURE 4.26. Cystic atrophy. **A**: This cross section through the uterine wall reveals a thickened endometrium with a "Swiss cheese" appearance. **B,C**: The histologic correlate is a conglomerate of cystically dilated endometrial glands lined by a flattened layer of atrophic epithelium associated with a fibrotic stroma.

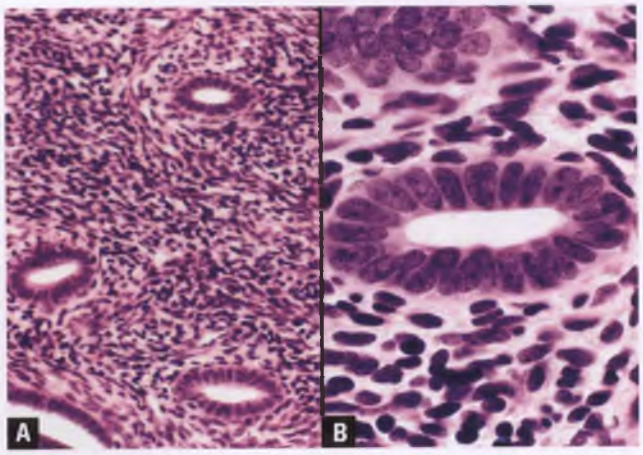

FIGURE 4.27. **A,B**: Weakly proliferative endometrium. Mitotically inactive, nonstratified or pseudostratified, columnar-shaped cells line the tubular glands, which are set within a dense, spindle cell stroma that resembles that normally found within the basalis. The nuclei of weakly proliferative glands are shrunken versions of those of the normal proliferative phase and exhibit a more densely basophilic chromatin pattern.

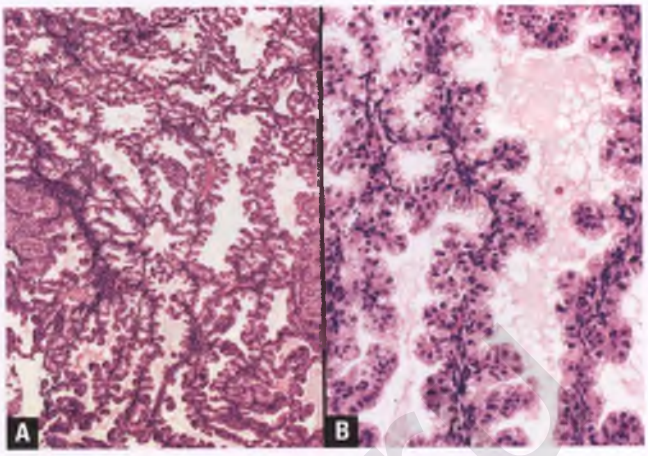

FIGURE 4.28. **A,B**: Gestational endometrium with hypersecretory glandular pattern. If taken out of context, the crowded, architecturally complex glands could be misinterpreted as endometrial hyperplasia.

prominent luminal secretions, cytoplasmic vacuolization with variable degrees of cytoplasmic clearing, and a serrated architecture due to the presence of numerous intraluminal micropapillary projections (Fig. 4.28). Decidual change is typically absent or inconspicuous in areas with hypersecretory glands.

The glands-to-stroma ratio is markedly elevated in some examples of gestational endometrium, creating the potential for confusion with endometrial hyperplasia. In addition to the clinical setting and the usual comingling with trophoblastic elements and fragments of decidua in histologic sections, features that help to distinguish hypersecretory endometrium from endometrial hyperplasia are similar to those previously described for the crowded glands of late secretory endometrium.

Occasionally, glandular epithelial cells within hypersecretory endometrium can exhibit focal patches of optically clear nuclei that can simulate herpes virus infection (Fig. 4.29).[12] Awareness of this phenomenon, the lack of an associated history of herpes cervicitis/vaginitis, and the lack of associated inflammation or necrosis facilitate recognition of this incidental finding.[12]

Over the course of the first month of an intrauterine gestation, the true decidua of pregnancy is established in the zona compactum and in islands surrounding spiral arteries. This stromal decidual reaction is indistinguishable from that seen in most patients with ectopic pregnancy or those treated with progestational agents. True decidual cells are about twice the size of predecidualized stromal cells, and form sheets of epithelioid stromal cells with abundant cytoplasm, distinct cell membranes, and round to oval, centrally placed nuclei that may contain small nucleoli (Fig. 4.30). Glands within the areas of decidualization are widely spaced and atrophic. Decidual spiral arteries in early gestation appear more prominent than their nongestational counterparts because of increased wall thickness. So-called stromal granulocytes, which are actually granular lymphocytes that express the natural killer marker CD56, are numerous in first-trimester decidua.[13]

As the pregnancy progresses, hypersecretory glands regress, and decidua dominates by the end of the first trimester. Note that endometrial tissue in spontaneous abortion specimens often seems to be a disparate admixture of fragments of hypersecretory endometrium and decidua with atrophic glands. This can be explained by fragmentation of the superficial zona compactum (decidua, often partially lined by cuboidal surface epithelium) and the underlying zona spongiosum (hypersecretory glands) during the curettage, as well as by the presence of islands of decidualization around spiral arteries within the zona spongiosum. The presence of variably necrotic and acutely inflamed fragments of decidua within abortion specimens is an expected finding that should not be misinterpreted as evidence of endometritis.

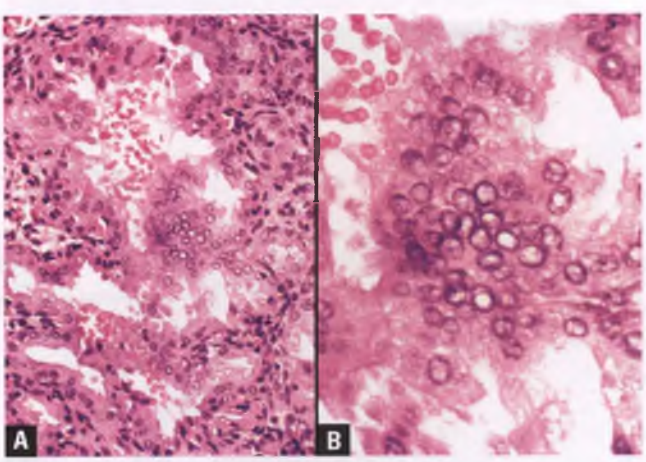

FIGURE 4.29. **A,B**: Hypersecretory endometrium with aggregates of cells with optically clear nuclei that simulate herpetic inclusions. Associated inflammation and necrosis are conspicuously absent.

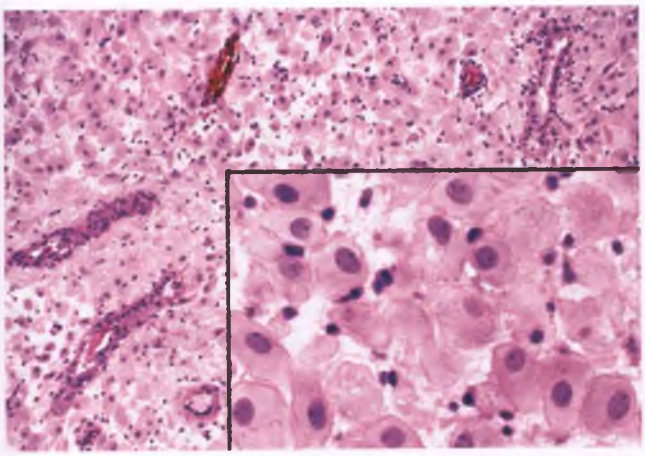

FIGURE 4.30. Gestational endometrium with a stromal decidual reaction, prominent spiral arteries, an atrophic gland (in upper right corner), and scattered granular lymphocytes ("stromal granulocytes"). The inset highlights the nuclear features and distinct cell borders of decidual cells.

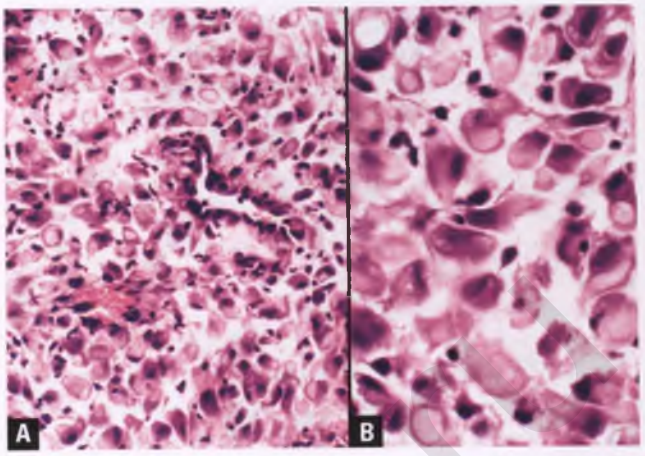

FIGURE 4.31. **A,B**: Endometrium with a decidual reaction that consists predominantly of loose aggregates of signet-ring cells. An atrophic endometrial gland is also present in **A**. Mucin and cytokeratin stains were negative in the signet-ring component, excluding the possibility of signet-ring carcinoma. The patient was a 69 year old female who was being treated with a high-dose progestational agent.

On rare occasions, loose aggregates of decidual cells become vacuolated and develop signet-ring forms, resulting in an appearance that resembles metastatic adenocarcinoma (Fig. 4.31).[14] This phenomenon can occur in either progestin-induced or pregnancy-related decidua. In contrast to signet-ring adenocarcinoma, this unusual decidual reaction lacks immunoreactivity for epithelial markers such as cytokeratin and epithelial membrane antigen, typically blends with more recognizable decidua, and lacks intracytoplasmic mucin.[14] Mucin stains are not recommended as a standalone discriminator in this situation, since muciphagic histiocytes can rarely produce a similar appearance, and ectopic decidua with signet-ring forms has been reported to contain acidic mucin that reacts with Alcian blue.[14,15]

Arias-Stella Reaction

The Arias-Stella reaction is a distinctive benign glandular change that is associated with intrauterine or extrauterine pregnancy and gestational trophoblastic disease,[16–18] and can also rarely be seen in nonpregnant patients on hormonal therapy.[19] It has been suggested by Dr. Arias-Stella that this reaction is dependent upon the simultaneous stimuli of estrogen-driven cellular proliferation and progesterone-driven secretory differentiation.[18] This phenomenon is most commonly encountered in endometrial glands, where it is characterized by intraglandular papillary epithelial tufts composed of cells with enlarged, hyperchromatic, pleomorphic nuclei and abundant cytoplasm that may be either densely eosinophilic or clear and vacuolated (Figs. 4.32 and 4.33). A hobnail growth pattern, with nuclei placed at the bulbous-shaped apical portion of the cytoplasm, is prominent in some cases, and intranuclear cytoplasmic invaginations resulting in pseudoinclusions can be seen. When meticulously searched for, mitotic figures have been found in 10% to 15% of cases, and can rarely be atypical or numerous.[20]

Differential Diagnosis

Not surprisingly, some examples of the Arias-Stella reaction can be confused with adenocarcinoma, particularly clear cell carcinoma. Features of the Arias-Stella reaction that help to distinguish it from endometrial carcinoma are (a) its usual association with a stromal decidual reaction and/or hypersecretory glands, (b) the absence of glandular mitotic figures in the vast majority of cases, (c) the lack of stromal invasion, and (d) its typical presentation as an incidental, focal microscopic finding in a premenopausal woman rather than as a mass lesion in a postmenopausal woman with vaginal bleeding. Distinction from EIC can also be problematic, since the Arias-Stella

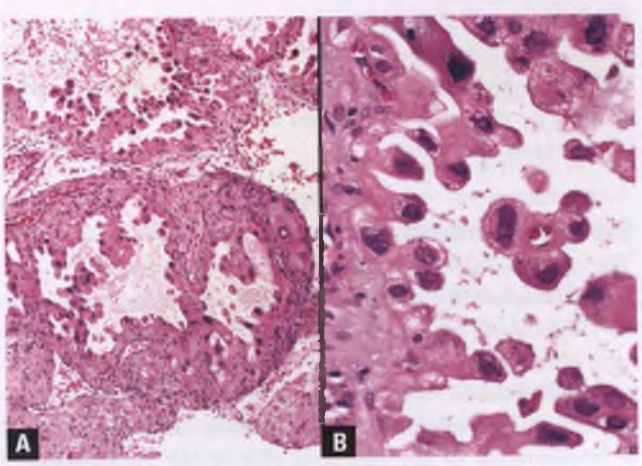

FIGURE 4.32. **A,B**: Arias-Stella reaction. This example features prominent hobnailing and a predominance of cells with eosinophilic cytoplasm. Note the lack of stromal invasion and the presence of a stromal decidual reaction.

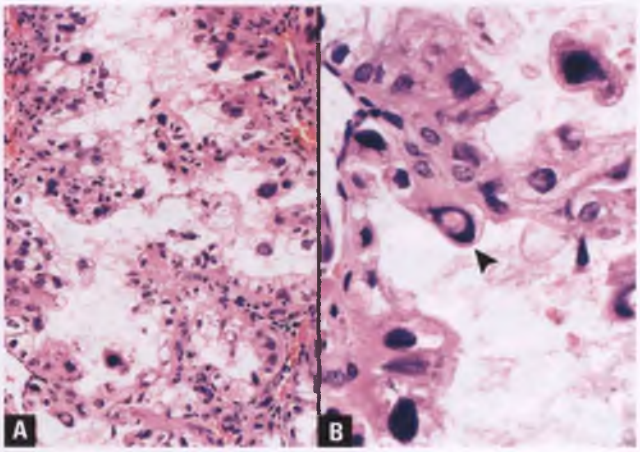

FIGURE 4.33. **A,B**: Arias-Stella reaction. Many of the cells in this example have clear, vacuolated cytoplasm. Note the dark, smudged chromatin of the atypical cells and the presence of an intranuclear pseudoinclusion (*arrowhead*).

reaction can occur on the endometrial surface, and both processes are microscopic findings that lack stromal invasion. In most cases, the clinical history and the status of the endometrial stroma are quite informative: a lesion of this ilk in a pregnant patient with decidualized endometrium almost assuredly represents the Arias-Stella reaction, whereas a similar lesion in an elderly patient with no decidual reaction is worrisome for EIC. In difficult cases, immunohistochemical stains for Ki-67 and p53 can be helpful, since these markers stain many fewer cells at a lower intensity in the Arias-Stella reaction than in EIC (or, for that matter, in other high-grade carcinomas in the differential diagnosis).[21]

Trophoblast and Chorionic Villi

When interpreting tissue from abortion specimens, it is essential to be able to recognize the different types of trophoblast and the various appearances of chorionic villi, and to not be alarmed by the tissue invasiveness and nuclear atypia of some trophoblastic elements.

Subtypes of Trophoblast

The subtypes of trophoblastic cells are the cytotrophoblast, syncytiotrophoblast, and intermediate trophoblast. Intermediate trophoblasts have been subdivided by location, morphology, and immunohistochemistry into villous, implantation site, and chorionic types.[22] It is the syncytiotrophoblast that attaches to and penetrates the endometrial surface at the time of implantation of the blastocyst (Fig. 4.34). As mentioned above, implantation takes place in the mid-secretory phase, but on those occasions when the implantation site is encountered by pathologists, it is typically weeks after the pregnancies have gone awry. This explains the presence of decidua rather than secretory endometrium at the implantation site in abortion specimens that have been under the influence of the hormones of pregnancy.

The actively proliferating cytotrophoblast and villous-type intermediate trophoblast, along with the terminally differentiated syncytiotrophoblast, are the trophoblastic elements associated with chorionic villi (Fig. 4.35). Cytotrophoblastic cells are mononucleate, small, uniform cells with nucleoli and distinct cell borders. They form the inner trophoblastic lining at the periphery of the villi, but gradually disappear by 4 months of gestation. The villous-type intermediate trophoblastic cells are found in the trophoblastic columns of villi that help to anchor the developing placenta to the maternal basal plate. Villous-type intermediate trophoblastic cells are larger and have more abundant clear cytoplasm than cytotrophoblastic cells, and there are also some immunophenotypic differences between these two cell types.[22,23] Syncytiotrophoblastic cells form the outermost trophoblastic envelopment of the chorionic villi, and exhibit multinucleation and abundant amphophilic cytoplasm that is often vacuolated.

The implantation type of intermediate trophoblast infiltrates the decidua, myometrium, and spiral arteries of the placental site (Fig. 4.36), and plays a critical role in establishing implantation and the uteroplacental circulation.[24] At least some of the cells of this type of intermediate trophoblast can be distinguished from decidua in routinely stained sections by virtue of their large, hyperchromatic nuclei with irregular contours and more darkly staining cytoplasm[25,26] (herein referred to as the hyperchromatic variant). However, other implantation-type intermediate trophoblasts bear a closer resemblance to decidua, with pale cytoplasm and more vesicular nuclei (the "deciduoid" variant).

Chorionic-type intermediate trophoblast is found within the subamniotic stripe of trophoblastic cells in the chorion laeve of the fetal membranes (see Chapter 9).

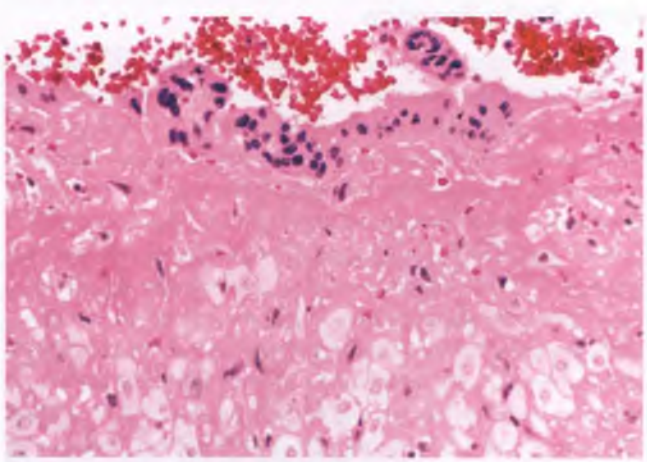

FIGURE 4.34. Implantation site in curettage from a missed abortion. Note the syncytiotrophoblastic cells overlying a layer of fibrinoid material and decidua.

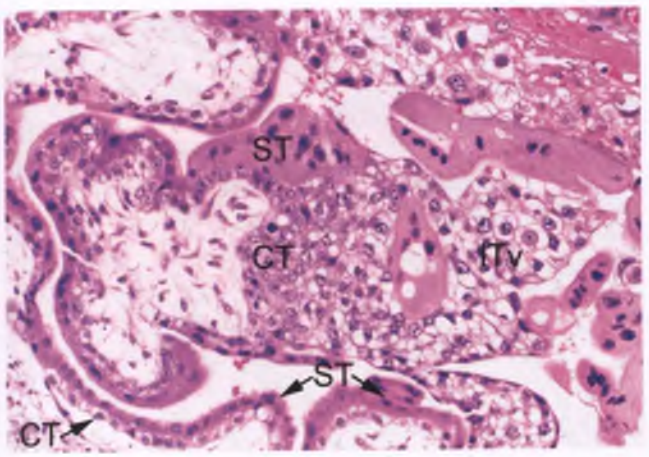

FIGURE 4.35. Immature chorionic villi lined by an inner layer of mononucleate cytotrophoblast (CT) and an outer layer of multinucleate syncytiotrophoblast (ST) that interfaces with maternal blood. The trophoblastic column emanating from one pole of the central villus is composed of germinative CT and intermediate trophoblast of villous type (ITv), capped by ST. The vacuolated ST cell in between the CT and ITv labels has been artifactually displaced into this position during processing.

Early Stages of Development of Chorionic Villi

Primary stem villi are formed beginning on approximately the 13th day of gestation, and are composed of a core of cytotrophoblast enveloped by a layer of syncytiotrophoblast (Fig. 4.37).[10] These villi are closely associated with lacunae filled with maternal blood, which are the forerunners of the intervillous space. The cores of primary stem villi are filled by plugs of extraembryonic mesoderm in the days that follow, whereupon they become known as secondary stem villi (Fig. 4.38). By this point, there is a solid rim of trophoblastic elements that surrounds the developing villi that is termed the trophoblastic shell. By the end of the third week of gestation, inconspicuous capillaries have begun to form within the villus cores, which are a defining feature of tertiary stem villi. At this stage of development, ramifying villous branches are seen radiating outward as they surround the centrally located embryo (Fig. 4.39). Over the course of the following weeks, the villi opposite the implantation site regress. In contrast, those on the embryonic pole continue to proliferate and mature to form the chorion frondosum, which eventually becomes the disc-shaped placenta. The morphology of normal chorionic villi as seen in grossly recognizable placental tissue is discussed in Chapter 9.

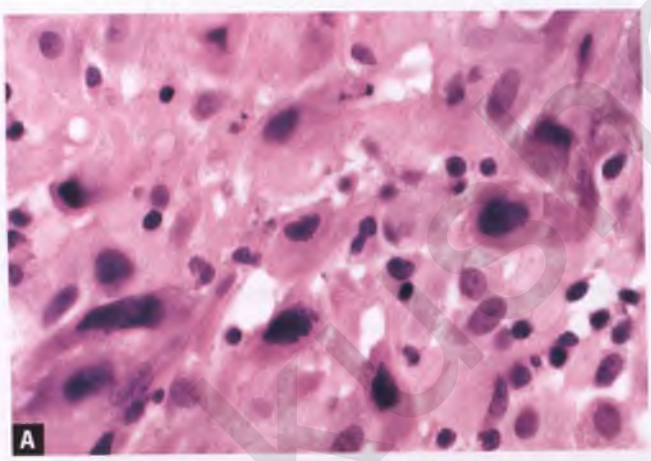

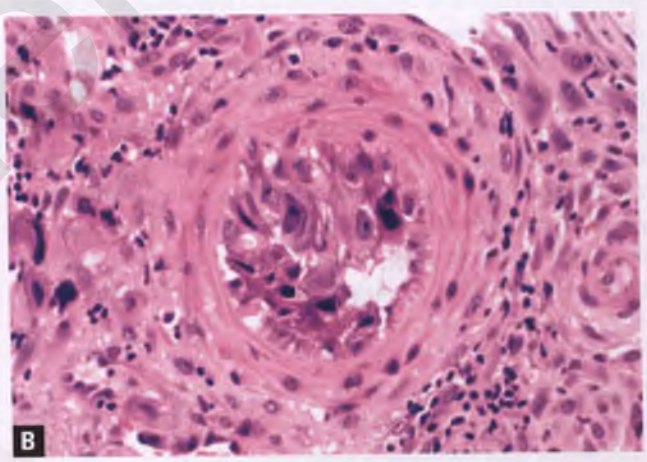

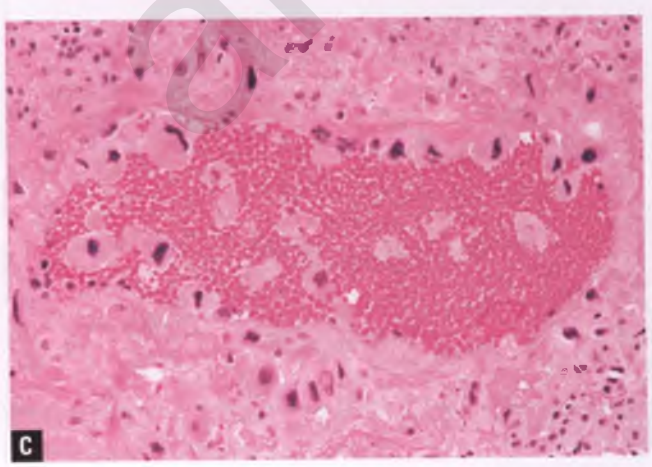

FIGURE 4.36. Implantation type of intermediate trophoblast. **A**: The scattered intermediate trophoblastic cells that are present within decidua are recognized by their large, hyperchromatic nuclei with irregular contours. Lymphocytes are also present. **B**: Vascular invasion of a decidual spiral artery by intermediate trophoblasts at the stage of an endovascular plug. **C**: Spiral arteries that are invaded by intermediate trophoblasts are eventually transformed into dilated, flaccid vessels whose endothelial lining is largely replaced by intermediate trophoblasts. The smooth muscle coat of the involved arteries is replaced by hyalinized fibrinoid material.

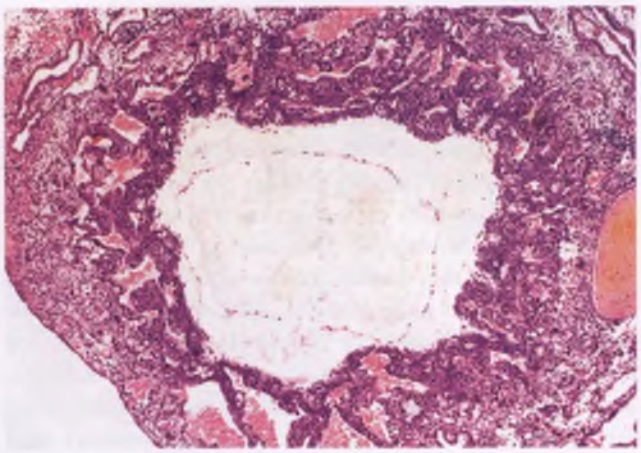

FIGURE 4.37. Implantation site at approximately 2 weeks of gestation. The finger-like trophoblastic projections represent primary stem villi, and are closely associated with lacunae filled with maternal blood. Note that the endometrial surface has been reepithelialized by this stage of development (lower left).

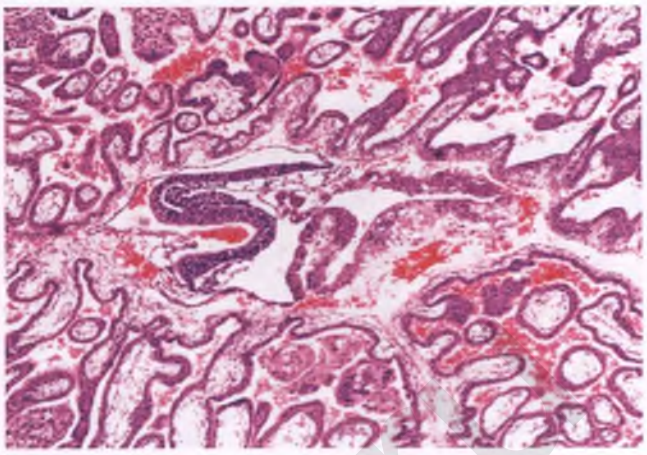

FIGURE 4.39. Embryo (centrally positioned) and nascent placenta at approximately the end of the third week of gestation.

Exaggerated Placental Site

Invasion of the inner third of the myometrium underlying the implantation site by intermediate trophoblastic cells is a normal and constant finding in the gravid uterus. When this finding is prominent, it has been referred to as an exaggerated placental site or exaggerated placental site reaction.[23,27] However, the distinction of an exaggerated from normal implantation site is subjective, and in the absence of gestational trophoblastic disease may be more of a function of the stage of gestation and how vigorously the myometrial tissue beneath the implantation site was sampled than any perceived increase in the number, size, or degree of atypia of the infiltrating trophoblastic cells. The infiltrating cells may be either decidua-oid or hyperchromatic (Fig. 4.40), and multinucleated intermediate trophoblasts may be present in significant numbers (Fig. 4.41).

When seen in only a few myometrial fragments of a curettage, it is best to recognize this phenomenon as a normal physiologic process and to not mention it in the pathology report, since it may cause confusion and undue concern. When the extent is such that it raises the differential diagnosis of a placental site trophoblastic tumor (PSTT), differentiating features of the exaggerated placental site are the usual presence of chorionic villi, the virtual absence of mitotic activity, the lack of a confluent growth pattern, a Ki-67 proliferation index of near zero,[28] and its presentation as a microscopic finding rather than a mass-forming lesion (PSTT is discussed in Chapter 10).

FIGURE 4.38. Implantation site at the stage of secondary stem villi formation. Note the circumferential trophoblastic shell that helps to firmly attach the villi to the endometrium.

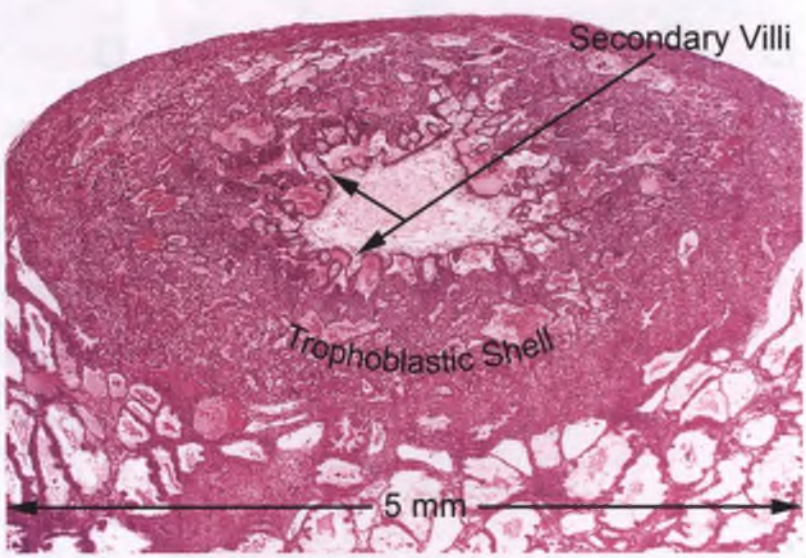

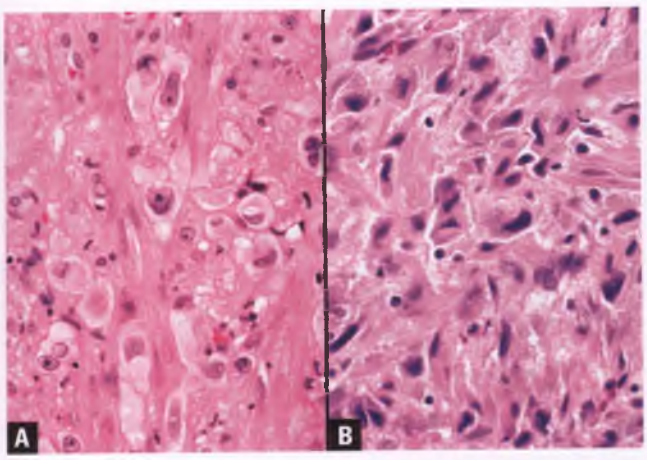

FIGURE 4.40. Exaggerated placental site with intermediate trophoblastic cells dissecting between myometrial muscle fibers. **A**: In this example, the intermediate trophoblastic cells have a deciduoid appearance. **B**: This example features hyperchromatic intermediate trophoblastic cells. Microscopic fields such as these are indistinguishable from PSTT.

Processing and Evaluating Early Gestational Tissue

For endometrial curettage specimens submitted as "products of conception," the primary responsibilities of the pathologist are to document the presence of an intrauterine pregnancy and to exclude the possibility of gestational trophoblastic disease. Evidence of an intrauterine pregnancy includes finding chorionic villi, embryonic/fetal tissue, or trophoblastic elements from an implantation site within the curettage. When evaluating the submitted jumble of tissue fragments, it is important for the pathologist, as well as those responsible for selecting tissue in instances when cytogenetic analysis is warranted, to be able to distinguish between decidua and chorionic villi. Decidual fragments are typically tan, solid, and rubbery, whereas nonmolar chorionic villi are light tan to pale yellow, granular, delicate,

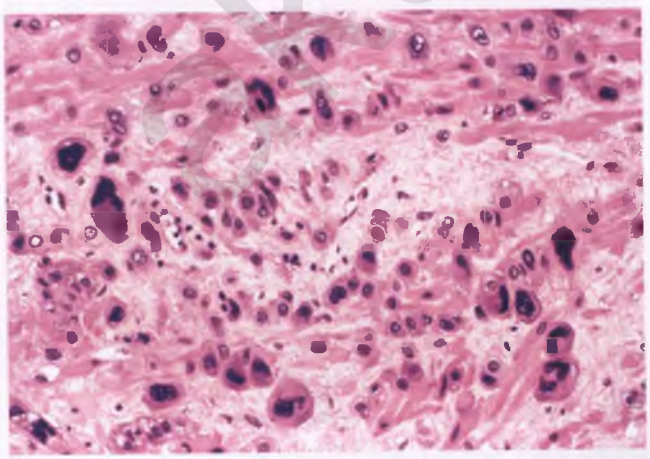

FIGURE 4.41. Exaggerated placental site with a component of multinucleated intermediate trophoblasts.

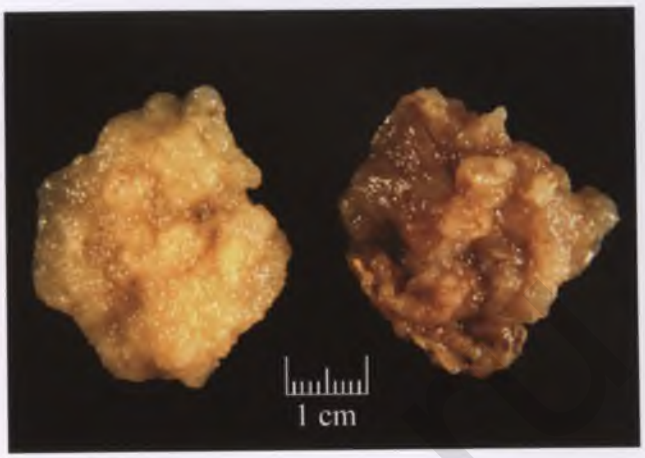

FIGURE 4.42. Gross appearance of chorionic villi (left) and decidua (right) in endometrial curettings.

and loosely aggregated (Fig. 4.42). Although rarely necessary, examination of tissue suspended in fluid using a dissecting microscope can assist in the recognition of villi.

If chorionic villi or embryonic/fetal tissues are identified grossly within a "products of conception" specimen and no hydropic villi suggestive of a molar pregnancy are present, submission of a single representative cassette is suggested. In the vast majority of cases, this will be sufficient to document an intrauterine pregnancy and exclude gestational trophoblastic disease. If embryonic/fetal tissue or villi are not grossly identified, submit three cassettes initially. Whether or not grossly recognizable chorionic villi and embryonic/fetal tissues are present should be clearly stated in the gross description (general guidelines related to the description and submission of endometrial tissue are provided in the section entitled "Processing Tips for Endometrial Samples" at the end of this chapter). If no chorionic villi or embryonic/fetal tissue are identified in the initial sections, search for the implantation site composed of syncytiotrophoblasts and decidua with an interposed layer of fibrinoid material (Fig. 4.34). If documentation of an intrauterine pregnancy is still lacking and examination of deeper sections does not resolve the issue, submit the remainder of the tissue and focus attention on the fragments of clotted blood, since this is where isolated syncytiotrophoblastic cells from early failed gestations are most likely to be found (Fig. 4.43). Although uncommonly needed, cytokeratin immunohistochemistry can be utilized to highlight the presence of cytokeratin-positive intermediate trophoblasts associated with cytokeratin-negative decidua, thereby documenting an intrauterine pregnancy in cases in which chorionic villi and embryonic/fetal tissues are absent (Fig. 4.44).[29]

If efforts to document an intrauterine pregnancy prove unsuccessful, direct communication with the patient's physician is necessary to alert him/her to the possibility of an ectopic pregnancy, since an ectopic pregnancy that progresses to the point of rupture can be a medical emergency. The date and time of this conversation should be documented in the surgical pathology report. It is also important for pathologists and gynecologists to be aware that in a minority of cases of

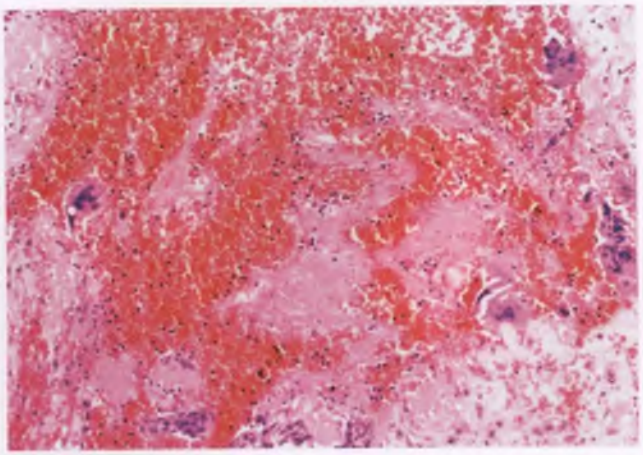

FIGURE 4.43. Isolated syncytiotrophoblastic cells embedded in hemorrhagic material, which in this case constituted the only evidence of an intrauterine pregnancy.

ectopic pregnancy, the endometrial tissue sample may show proliferative or secretory patterns devoid of stromal decidualization, hypersecretory change, or Arias-Stella reaction, leaving no histologic clues of pregnancy.[30]

Although finding trophoblastic tissue in an endometrial curettage can, for practical purposes, be taken as evidence excluding the possibility of an ectopic pregnancy, some cautionary notes are in order: (a) some thought should be given to cases with isolated chorionic villi—if their presence is not associated with gestational endometrium, or if they are small and mature with the appearance of third trimester villi, then they may be contaminants ("floaters") from another case; (b) although quite rare, it appears that isolated chorionic villi within an endometrial curettage may originate from sloughing from a tubal ectopic pregnancy into the endometrial cavity;[31] and (c) simultaneous intrauterine and ectopic pregnancies can occur, although they are extraordinarily rare (about 1 in 30,000 pregnancies).[32]

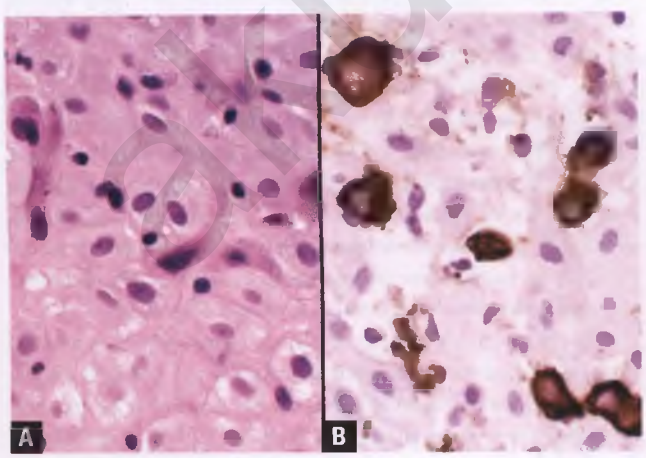

FIGURE 4.44. Scattered intermediate trophoblastic cells within decidua. **A**: Routinely stained section. **B**: The intermediate trophoblastic cells are immunoreactive for cytokeratin, whereas the decidual cells do not stain.

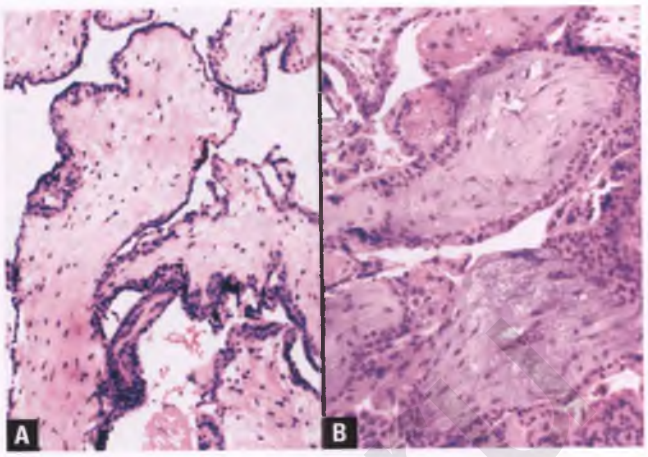

FIGURE 4.45. Villous changes associated with embryonic death. **A**: Avascular villous sclerosis. **B**: Myxoid degeneration.

Degenerative changes of no clinical significance are often seen in chorionic villi in the days following the demise of the embryo (Fig. 4.45). These changes include villous edema, avascular villous sclerosis, and myxoid degeneration. The presence of grossly hydropic villi raises the possibility of a molar pregnancy, and degenerative myxoid change needs to be distinguished from the myxoid stroma of some early complete hydatidiform moles (see Chapter 10).

Retained Placental Tissue

When placental tissue is retained in utero, the chorionic villi eventually become degenerated and hyalinized, and their ghost outlines may be difficult to recognize microscopically. In this situation, recognition of their villous nature may be facilitated by the use of a trichrome stain (Fig. 4.46). If the fragments of retained placental tissue are polypoid, the lesion is designated a placental polyp.

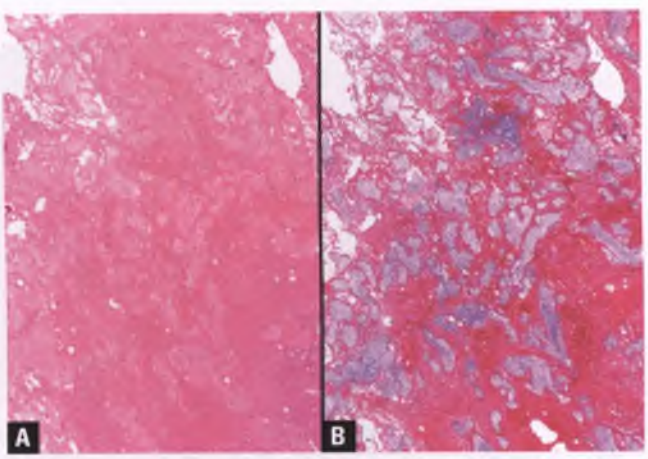

FIGURE 4.46. Retained placental tissue. **A**: Ghost outlines of chorionic villi from placental tissue that had been retained in utero for 10 weeks. **B**: Although these structures may be overlooked in routinely stained sections, a trichrome stain highlights the collagenous (*blue-stained*) villi.

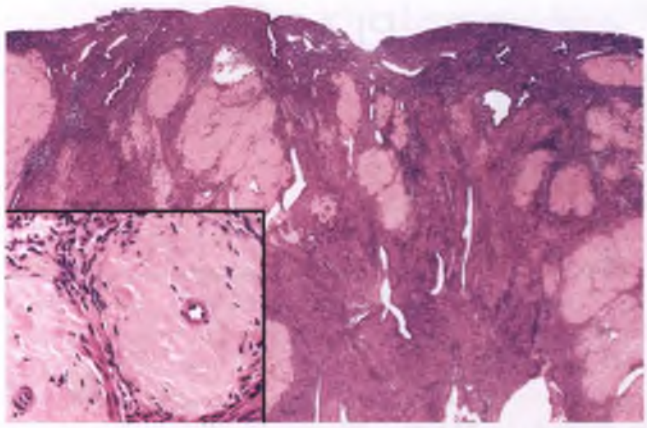

FIGURE 4.47. Normal involution of placental site vessels at nine weeks postpartum. Aggregated fibrohyaline nodules have formed in the endometrium and superficial myometrium. Inset: Fibrohyaline nodules with centrally located vascular lumens, indicative of their vascular origin.

Involution and Subinvolution of the Placental Site

Following delivery, the altered endometrial and myometrial arteries at the implantation site normally undergo involution, which involves thrombosis and, over a period of weeks to months, conversion into fibrohyaline nodules (Fig. 4.47).[33] Some cases of delayed postpartum uterine bleeding that occur between 1 week and several months postpartum are due to subinvolution of the placental site, which features clusters of dilated superficial myometrial arteries with variably aged thrombi and persistent intermediate trophoblast within the vessel walls and/or neighboring myometrium (Fig. 4.48).[33] Cytokeratin immunohistochemistry may be helpful in identifying the persistent

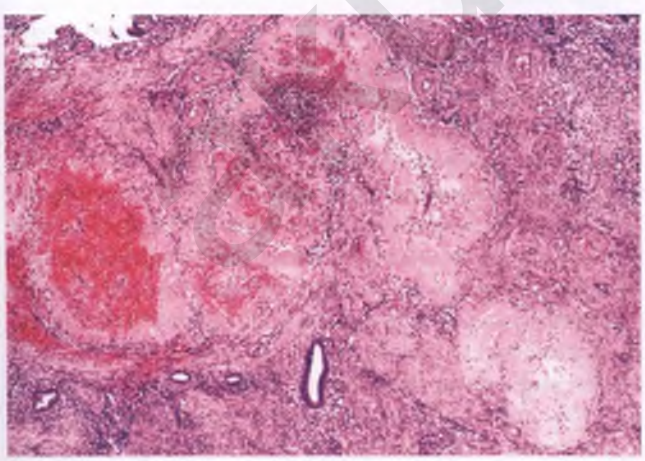

FIGURE 4.48. Subinvolution of the placental site. A cluster of dilated vessels with variably-aged thrombi is present in this patient who presented with postpartum bleeding 3 weeks after delivery. The vessel in the lower right corner has undergone normal involution.

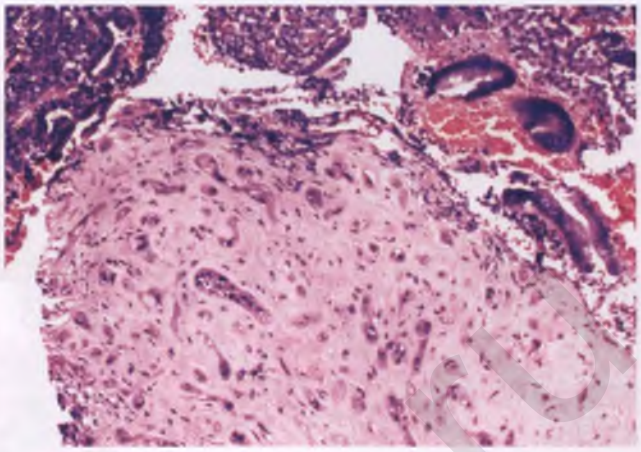

FIGURE 4.49. Placental site nodule in an endometrial curettage presenting as a small, circumscribed, hyalinized focus of degenerated intermediate trophoblastic cells.

trophoblastic cells, which can be difficult to recognize with confidence in routine sections in this setting.[33]

Placental Site Nodule

Occasionally, small nodular remnants of hyalinized implantation site composed of chorionic-type intermediate trophoblasts are retained in utero for a period of months to up to several years (Fig. 4.49).[34,35] These lesions, termed placental site nodules, are usually discovered at the time of endometrial curettage and represent an incidental indication of a remote pregnancy. The entrapped trophoblastic cells often show degenerative atypia (Fig. 4.50), but mitotic figures are generally absent.

Differential Diagnosis

Placental site nodules should not be confused with benign processes such as the fibrohyaline nodules that result from vascular involution of the placental site, pieces of hyalinized

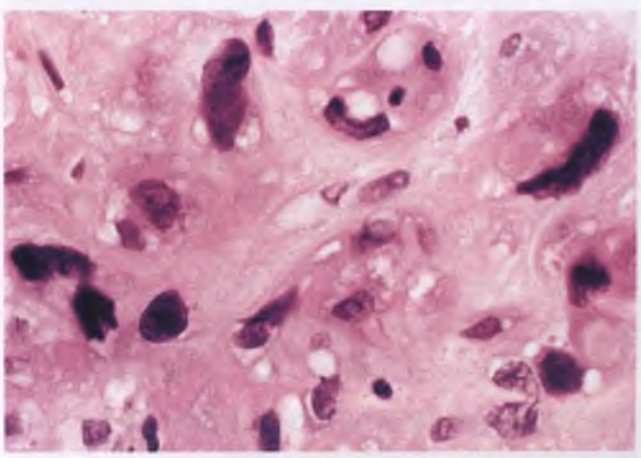

FIGURE 4.50. Placental site nodule. Note the degenerative nuclear atypia and cytoplasmic vacuolization.

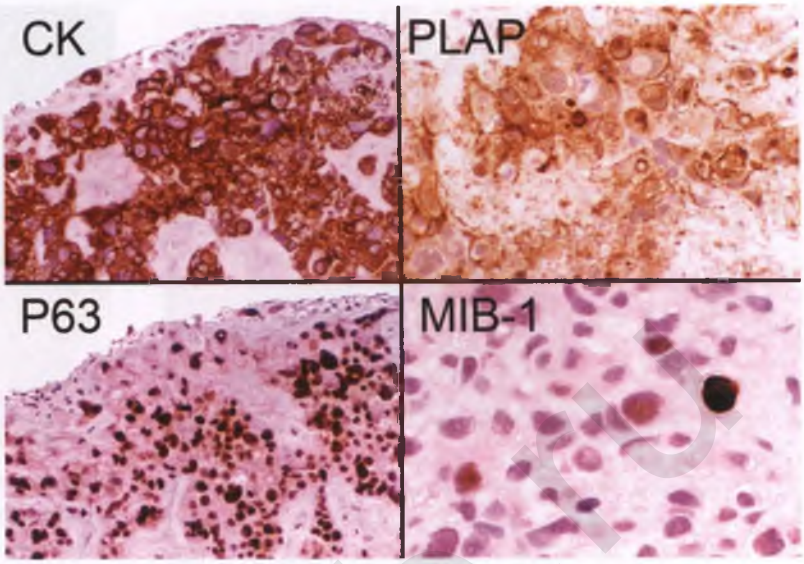

FIGURE 4.51. Placental site nodules are immunoreactive for cytokeratin (CK), placental alkaline phosphatase (PLAP), and p63, and have a Ki-67 proliferative index (as assessed by MIB-1 immunostaining) of <10%.

decidua, and exaggerated placental site, and also need to be distinguished from PSTT, epithelioid trophoblastic tumor, and squamous cell carcinoma of the cervix. Their small size, circumscription, degenerative appearance, and near-zero mitotic index generally allow for their recognition. In selected instances, immunohistochemistry may serve as an aid in diagnosis. As demonstrated in Figure 4.51, placental site nodules are typically immunoreactive for cytokeratin, placental alkaline phosphatase (PLAP), and p63, and have a low Ki-67 proliferative index (<10%).[22,34–36] Cytokeratin immunoreactivity facilitates elimination of most stromal lesions from the differential diagnosis, PLAP and p63 positivity help to exclude exaggerated placental site and PSTT, and a Ki-67 proliferative index of <10% helps to exclude a neoplastic process.[22,36] Note that p63 expression is determined by the degree of nuclear staining, and that p63 immunoreactivity is seen in lesions derived from chorionic-type intermediate trophoblast (placental site nodule and epithelioid trophoblastic tumor), whereas lesions derived from implantation site intermediate trophoblast (exaggerated placental site and PSTT) are typically p63 negative.[36] Distinction of placental site nodule from epithelioid trophoblastic tumor is discussed in more detail in the section on the latter entity in Chapter 10. In the differential diagnosis of either placental site nodule or epithelioid trophoblastic tumor with cervical squamous cell carcinoma, a p16-negative, HSD3B1-positive immunophenotype supports trophoblastic differentiation (see section on epithelioid trophoblastic tumors in Chapter 10).

ENDOMETRIUM IN DYSFUNCTIONAL UTERINE BLEEDING AND INFERTILITY

Deciphering the Clinical History in Patients with Abnormal Uterine Bleeding

Clinicians jot an array of terms and abbreviations on the surgical pathology requisition form to convey the clinical history of their patients to the pathologist. The following terms are the ones used most frequently:

Amenorrhea: Absence of menstruation.

Dysmenorrhea: Painful menstruation.

Hypermenorrhea: Uterine bleeding that occurs at the regular intervals of menstruation and for the usual duration, but that is excessive in amount.

Menorrhagia: Uterine bleeding that occurs at the regular intervals of menstruation, but is excessive in both amount and duration.

Metrorrhagia: Uterine bleeding, usually normal in amount, that occurs at irregular intervals.

Menometrorrhagia ("Menomet"): Excessive uterine bleed that occurs during the menses as well as at irregular intervals.

Postmenopausal Bleeding: Abnormal uterine bleeding that occurs at least one year following the cessation of menstruation (menopause).

Abnormal Uterine Bleeding (AUB): Any form of bleeding that originates from the uterus that occurs outside of the context of a normal menstrual period. Given its point of exit, AUB is often referred to as abnormal vaginal bleeding.

Dysfunctional Uterine Bleeding (DUB): This term is most properly used to indicate that the etiology of abnormal uterine bleeding in a woman in her reproductive years is due to ovulatory dysfunction that stems from an endogenous hormonal imbalance. In practice, clinicians use the term less rigorously to refer to abnormal uterine bleeding prior to the determination of its cause.

Breakthrough versus Withdrawal Bleeding: These confusing terms allude to the mechanism that produces some forms of abnormal uterine bleeding, with "breakthrough" indicating a relative hormonal imbalance and "withdrawal" indicating a rapid drop in hormone levels due to the removal of its source or a sudden decrease in its production. They have been variously defined by different investigators, which limits their utility.[30,37] In estrogen breakthrough bleeding,

the term "breakthrough" implies the eventual failure of estrogen levels to meet the increasingly demanding needs of an altered endometrium, which results in patchy endometrial breakdown. Examples of estrogen breakthrough bleeding are (a) partial shedding of disordered proliferative endometrium in anovulatory patients whose estrogen production cannot keep pace with endometrial requirements and (b) light uterine bleeding (spotting) in patients taking low-dose oral contraceptives. Partial shedding of endometrium with progestin effect in patients taking high-dose progestational agents is an example of progesterone breakthrough bleeding, which is due to an inordinately high ratio of progesterone to estrogen. In estrogen withdrawal bleeding, endometrial breakdown is due to a precipitous drop in estrogen, such as following cessation of estrogen replacement therapy, removal of the ovaries, or as may occur in midcycle spotting. Patients with anovulatory cycles whose cohort of estrogen-producing follicles undergoes synchronized atresia represent an additional example of estrogen withdrawal bleeding (note that anovulatory cycles can be associated with estrogen-related bleeding of either the breakthrough or withdrawal types). Exposure, followed by withdrawal, of an estrogen-primed endometrium to progestin results in progesterone withdrawal bleeding, which may be seen in sequential hormonal replacement therapy.

Notation Used to Indicate Pregnancy History: Gravida (G) refers to the number of pregnancies, including any current pregnancy. Para (P) refers to the number of previous deliveries of infants that weigh at least 500 g, which is often followed by a subscripted series of four numbers that indicates their various outcomes. The mnemonic FPAL for Florida Power And Light is useful in remembering that these four numbers sequentially signify the number of F = Full-term deliveries, P = Premature deliveries, A = Abortions, and L = Living children. For example, a patient who is G4, P_{2012} is currently pregnant, has had two previous full-term pregnancies and one abortion, and both of her children are currently alive.

Nonphysiologic Glandular and Stromal Breakdown

By definition, endometrial samples from patients with DUB show no evidence of an organic lesion, but they often show patches of glandular and stromal breakdown. The most common cause of DUB is anovulatory cycles (no ovulation → no corpus luteum → insufficient progesterone coupled with persistent production of estrogen by ovarian follicles → stimulation of proliferative-type endometrial growth → cohort of follicles eventually either becomes atretic (withdrawal bleed related to rapid drop in estrogen) or is unable to meet the increasing estrogen needs of the endometrial proliferation (breakthrough bleed) → breakdown that is patchy and irregular). Histologically, this translates into a proliferative or disordered proliferative phase pattern with patches of stromal breakdown that are characterized by distinctive tight aggregates of collapsed and condensed stroma that are occasionally rimmed by epithelial cells (Fig. 4.52). In this setting, it is common to see epithelial caps of papillary/surface syncytial change (see section on endometrial epithelial metaplasias).

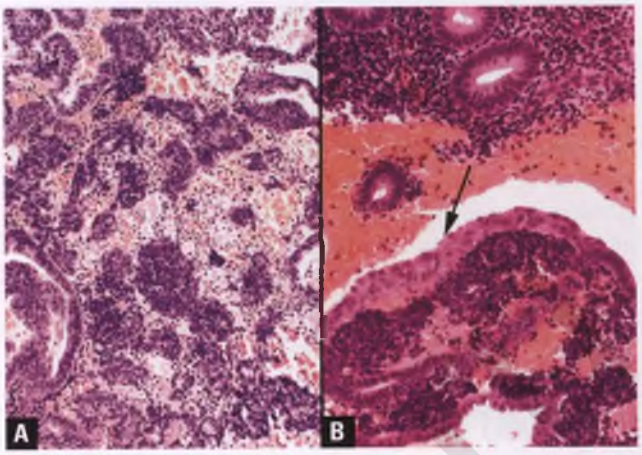

FIGURE 4.52. Glandular and stromal breakdown related to anovulatory cycles. **A**: Several *dark blue* aggregates of collapsed stroma are admixed with winding strips of disrupted glands. **B**: A piece of proliferative endometrium overlies a focus with stromal breakdown that is partially blanketed by surface syncytial change (*arrow*).

When examined at high magnification, the stromal aggregates of nonmenstrual endometrial breakdown are found to be composed of cells with hyperchromatic nuclei with scant cytoplasm, molded nuclear contours, and associated karyorrhectic debris (Fig. 4.53). As discussed in the section on small cell carcinoma, these findings can be misconstrued by the uninitiated as evidence of malignancy. Another potential diagnostic error is to misinterpret the presence of fragmented endometrial tissue in association with fresh blood as evidence of stromal breakdown related to dysfunctional uterine bleeding, when this is a ubiquitous finding in endometrial samples that is related to the procedure itself.

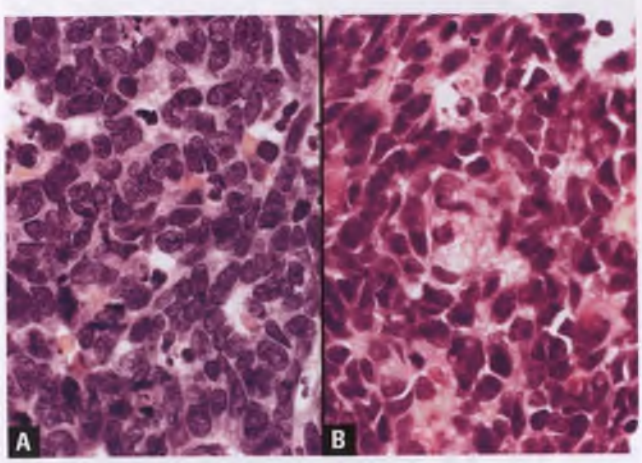

FIGURE 4.53. **A,B**: Stromal breakdown related to anovulatory cycles. At high magnification, the resemblance of collapsed and condensed endometrial stromal cells to small cell carcinoma in these two different examples is striking.

Portions of the collapsed stroma of menstrual endometrium can appear histologically indistinguishable from that seen in breakdown related to anovulatory cycles. However, menstrual-related stromal breakdown is usually recognized by the diffuse rather than patchy/focal nature of the collapsed stroma, evidence of secretory activity (crumbling predecidua and/or glands with vacuolated, clear cytoplasm, which may be focal findings), an absence of proliferative-type glands, the usual absence of papillary syncytial change (PSC), and the date of the last menstrual period being consistent with menstruation at the time of the sampling.[37]

Disordered Proliferation

The usual histologic correlate of sporadic anovulatory cycles, which are normal and expected as a woman transitions into menopause, is a disordered proliferative pattern. Other settings in which this pattern is seen include patients with polycystic ovary syndrome and women who are receiving unopposed estrogen therapy, which seldom occurs in current practice. The term "disordered proliferation" was coined and defined by Hendrickson and Kempson in their classic textbook from 1980, and serves as a useful "buffer zone" between normal proliferative endometrium and simple hyperplasia.[38]

Disordered proliferative endometrium is characterized by a hodgepodge of variably shaped glands, some of which are cystically dilated, that are set within an ample amount of proliferative-type stroma (Fig. 4.54). The glands are lined by cells whose mitotic rate and nuclear characteristics are indistinguishable from normal proliferative endometrium. The glandular contour abnormalities include mild branching and budding, but do not approach the degree of complexity seen in complex hyperplasia. The glands-to-stroma ratio is usually near unity, but can reach 2 to 1. Some investigators have arbitrarily modified the definition of disordered proliferation to require that such changes be focal; if similar changes are present diffusely, these pathologists diagnose simple hyperplasia without atypia.[30] However, what is herein considered disordered proliferation and what has been described as such by Drs. Hendrickson and Kempson is often seen throughout the endometrial sample.

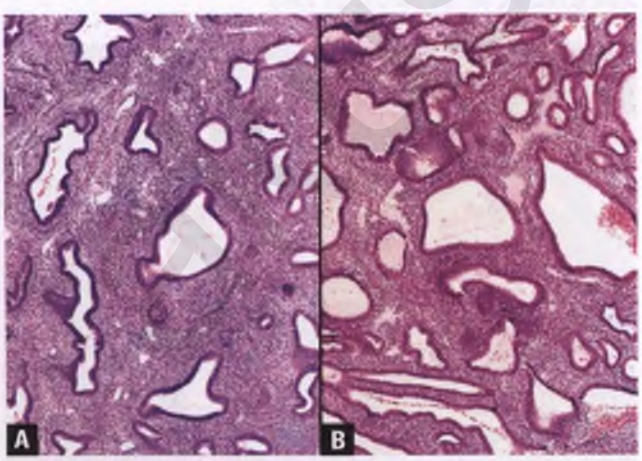

FIGURE 4.54. A,B: Disordered proliferative endometrium. The variably-shaped glands are haphazardly distributed and exhibit mild degrees of cystic dilatation. The glands-to-stroma ratio is <2:1. For reasons outlined in the text, it is recommended that endometria with these features not be diagnosed as simple hyperplasia without atypia.

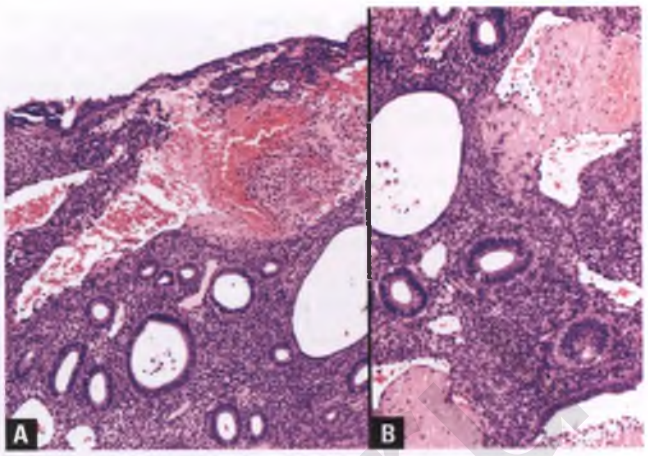

FIGURE 4.55. A,B: Disordered proliferative endometrium. Fibrin thrombi are present within thin-walled, ectatic vessels.

In the typical setting of a perimenopausal woman who is having irregular bleeding related to anovulatory cycles, the disordered endometrium will often exhibit patches of stromal breakdown, sometimes in association with dilated, thin-walled venules that contain fibrin thrombi (Fig. 4.55). In cases with the architectural and nuclear features of disordered proliferation in which the glands-to-stroma ratio exceeds 2 to 1, a diagnosis of simple hyperplasia without atypia is rendered. By utilizing this approach, the lower end of the spectrum of what constitutes simple hyperplasia without atypia for some investigators is incorporated into the disordered proliferative category. This is justifiable, given that there is no evidence that disordered proliferation is associated with an increased risk for the subsequent development of endometrial carcinoma.[39] Avoidance of the use of the charged term "hyperplasia" in these endometria with mild architectural alterations is also appropriate, since it helps to reduce patient anxiety and prevent overtreatment.

Sample microscopic and diagnosis sections of a pathology report for disordered proliferative endometrium with breakdown are as follows.

Microscopic:

Sections show numerous fragments of disordered proliferative endometrium, as characterized by haphazardly distributed, cystically dilated endometrial glands with mild degrees of branching and budding. There is ample endometrial stroma, and there is no evidence of polyp, hyperplasia, or malignancy. Patchy areas of stromal breakdown are also present, sometimes in association with ectatic, thin-walled vessels that contain fibrin thrombi. Disordered proliferative endometrium is not a cancer precursor, and is an expected finding in perimenopausal women who are having anovulatory cycles and in patients

receiving unopposed estrogen therapy. Clinical correlation is suggested.

Diagnosis:

Uterus, endometrium, curettage–

Disordered proliferative with patchy stromal breakdown (see Microscopic).

Luteal Phase Defect and Related Abnormalities

Luteal phase defect (LPD), which is also known as inadequate luteal phase, is a controversial entity whose defining features, clinical significance, and very existence have been questioned.[40] It is generally regarded as a rare cause of infertility or abnormal uterine bleeding related to insufficient production of progesterone by the corpus luteum, although other mechanisms such as an insufficient endometrial response to progesterone may play a role in some cases.[40] Traditionally, LPD is defined as a maturational delay that results in a normal secretory pattern that is at least 2 days earlier than expected in two consecutive cycles. Many investigators currently recommend requiring a 3-day rather than 2-day lag in secretory development for the diagnosis of an out-of-phase endometrium that would be consistent with LPD, having found this threshold to be of greater specificity.[40]

In addition to the lag in maturation of the secretory phase, a variety of abnormal secretory patterns have been attributed to LPD and other closely related hormonal imbalances.[37] In one form that is descriptively termed **uneven maturation**, the endometrial glands and stroma develop synchronously but to different degrees in different areas, which makes it impossible to assign a postovulatory histologic date within the usual 2-day range. For example, there may be an admixture of early secretory and mid to late secretory patterns (Fig. 4.56). In another abnormal secretory pattern related to hormonal imbalances, there is **glandular–stromal asynchrony**, such that the glands and stroma develop to different degrees within the same region (e.g., early secretory glands may be found embedded within a late secretory stroma that contains clusters of spiral arterioles). In yet another pattern of abnormal secretory differentiation referred to as **insufficient development**, the glands may exhibit secretory changes, but be of narrow caliber and fail to develop the expected degree of tortuosity. Knowledge of the patient's clinical history should be utilized to help distinguish this pattern from the simple tubular glands with subnuclear vacuoles that can be seen in oral contraceptive effect (see section on endometrium altered by exogenous hormones).

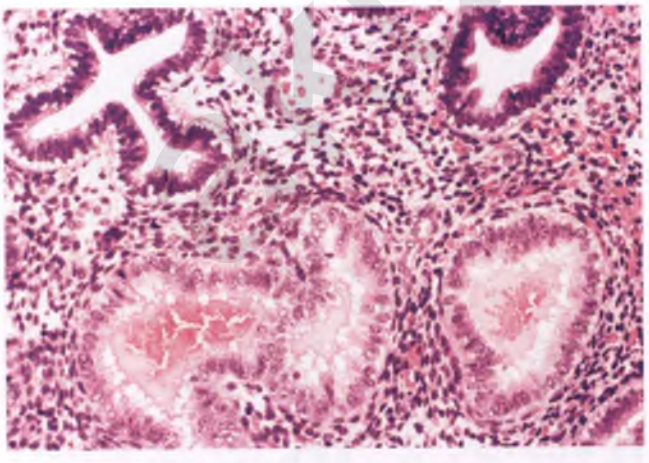

FIGURE 4.56. Abnormal secretory endometrium with uneven maturation. Early secretory type glands with subnuclear vacuoles (top) are seen adjacent to mid-secretory-type glands with intraluminal secretions (bottom).

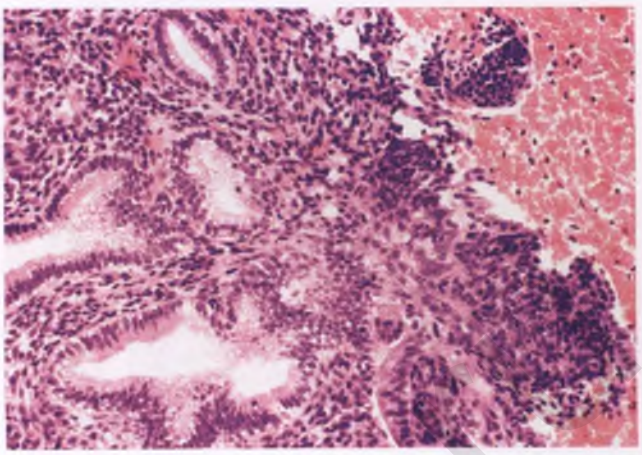

FIGURE 4.57. Underdeveloped secretory endometrium with premature stromal breakdown. Secretory differentiation is indicated by cytoplasmic vacuolization and the presence of basally oriented nuclei devoid of mitotic activity. The right side of the image shows stromal breakdown, as evidenced by condensed aggregates of dark blue stromal cells.

Associated stromal breakdown may or may not be readily apparent in all of these abnormal secretory patterns (Fig. 4.57), which usually do not have a clinically obvious etiology. However, their recognition helps to assure the patient and her physician that the patient's symptomatology is not due to an organic cause of endometrial origin. It should be noted that a recent study highlighted the lack of precision of endometrial dating and the inherent variations in secretory maturation, and asserted that many of these perceived patterns of abnormal secretory development may be within the range of normal.[4]

Irregular Shedding

Irregular shedding is a rare cause of abnormal uterine bleeding that is thought to be due to prolonged exposure to progesterone secondary to its production by a persistent corpus luteum cyst. It is defined as the presence of an admixture of proliferative and secretory patterns in an endometrium obtained at least 5 days following the onset of uterine bleeding (Fig. 4.58). Associated stromal breakdown is usually evident, but may be focal. When entertaining a diagnosis of irregular shedding, be sure to evaluate endometrium from near the surface so as to

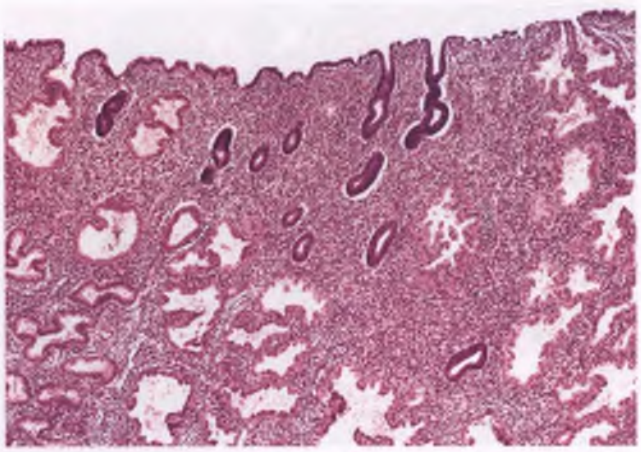

FIGURE 4.58. Irregular shedding. Mixed proliferative and secretory glandular elements are present in this endometrium from a patient with a persistent corpus luteum cyst.

avoid misinterpreting the weakly proliferative glands of the basalis as being an aberrant proliferative component in an otherwise secretory endometrium. In addition, the possibility of fragments of lower uterine segment and nonfunctional endometrial polyps occurring within a background of secretory endometrium should be considered (note how a fragmented sample of the endometrium present in Figure 4.74B could simulate irregular shedding).

ENDOMETRIUM ALTERED BY EXOGENOUS HORMONES

Women are often treated with various forms of estrogen and/or progesterone, most commonly for oral contraception and postmenopausal hormone replacement therapy. Most oral contraceptives (birth control pills) are low-dose combinations of estrogen and progesterone. Unopposed estrogen replacement therapy (estrogen without a counterbalancing progesterone-related preparation) is now uncommon in postmenopausal patients with a uterus, due to the increased risk of endometrial hyperplasia and carcinoma found in patients treated with this regimen.[41,42] Current hormone replacement therapy in the typical postmenopausal woman with a uterus utilizes estrogen and progesterone either in combination or sequentially at low doses and for a short duration. Progesterone and related synthetic hormones, which are referred to as progestins or progestogens, are used without estrogens in the empiric management of dysfunctional uterine bleeding and in the treatment of endometrial hyperplasia. Progestins are also used in the treatment of selected malignancies, such as well-differentiated endometrial carcinoma in nonsurgical candidates or those who wish to preserve their fertility, breast carcinoma, and endometrial stromal sarcoma. The histology of progestin-treated endometrial lesions within the spectrum of atypical hyperplasia and well-differentiated carcinoma is discussed in the section on endometrial hyperplasia.

The nonsteroidal drug tamoxifen is commonly used in the treatment and prophylaxis of breast carcinoma, and exerts its antiestrogen effect via estrogen receptor blockade. In the endometrium, the binding of tamoxifen to estrogen receptors mimics the effect of estrogen to some degree.[41] Patients who have received long-term tamoxifen therapy have a predilection for the development of endometrial polyps, and are more likely than the general population to develop endometrial hyperplasia, endometrial carcinoma, adenosarcoma, and carcinosarcoma.[43–45]

The effect of exogenous hormones on the endometrium is dependent upon the particular hormone or hormones prescribed, their dosages, the duration of therapy, the relative proportions of estrogen and progesterone, whether dual hormone preparations are administered in combined form or sequentially, the pretreatment histology of the endometrium, and the hormonal responsiveness of the patient. As might be expected, the endometrium can react to this altered hormonal environment in a wide variety of ways. This can be confusing for the pathologist, particularly in the common situation in which the gynecologist has neglected to provide the history of hormone therapy. Fortunately, the major histologic patterns induced by these hormones are fairly distinctive, as discussed below. The less commonly encountered and less well-documented endometrial patterns of response to progesterone receptor modulators, gonadotropin releasing hormone agonists, and ovulation induction agents are beyond the scope of this overview.[41,46,47]

Oral Contraceptive Effect

In patients taking oral contraceptives composed of an estrogen–progestin combination, the most common histologic pattern is the appearance of small caliber, tubular, inactive glands set within a dominant stroma that is composed of plump spindle cells (Fig. 4.59).[41] In some cases, the glands exhibit variable degrees of subnuclear vacuolization. The glands-to-stroma ratio is very low, and spiral arterioles are poorly developed or absent.

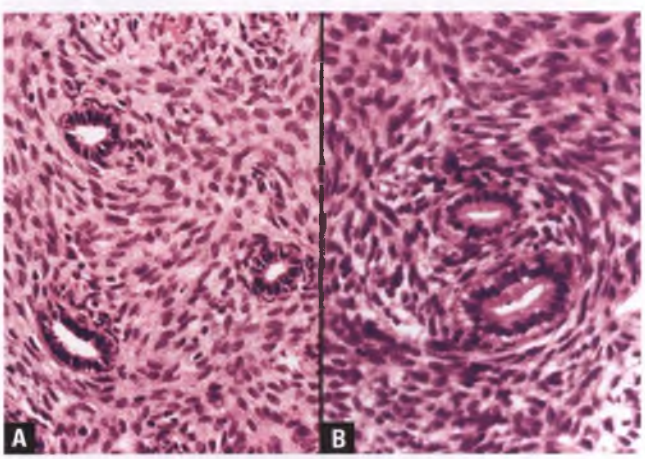

FIGURE 4.59. Oral contraceptive effect (two different examples). **A**: The stroma is dominant and composed of plump spindle cells. The glands are small, tubular, and inactive. **B**: Note the presence of scattered subnuclear vacuoles within the epithelial cells lining the glands.

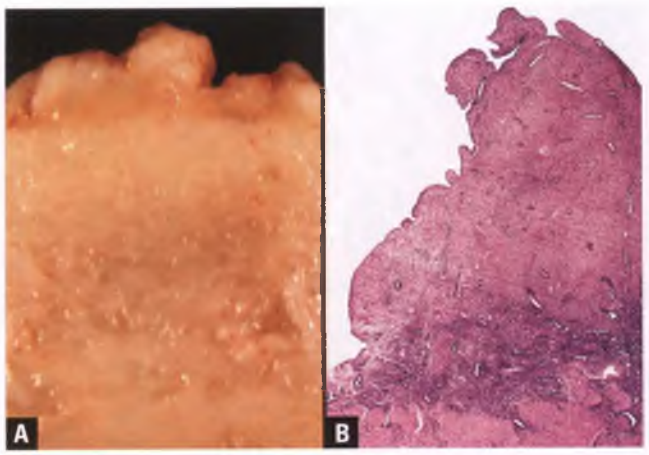

FIGURE 4.60. Progestin effect. **A**: Section through a formalin-fixed uterine wall, demonstrating an irregular endometrial surface due to the presence of polypoid projections. **B**: Corresponding histologic section of one of these polypoid areas. The functionalis exhibits a marked decidual reaction, which spares the basalis. The glands are atrophic and widely spaced. Features of a true polyp are not evident.

In the presence of the appropriate clinical history, which should be sought if not provided, a diagnosis of "consistent with oral contraceptive effect" can be rendered.

Progestin Effect

In cases in which progestins are given in high doses, the endometrium typically responds with a marked decidual reaction. Grossly, polypoid folds of endometrial tissue are formed, which may become quite prominent (Figs. 4.60 and 4.61). The decidual reaction is indistinguishable from that seen in pregnancy, and the endometrial glands are sparse and atrophic (Fig. 4.62). Thin-walled, ectatic venules are often present that

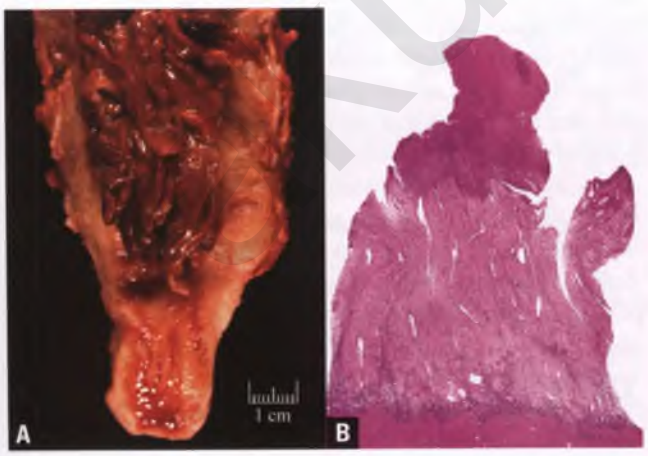

FIGURE 4.61. Exaggerated progestin effect with stromal breakdown. **A**: The endometrial cavity of this opened uterus is filled with hemorrhagic folds of polypoid tissue that could be mistaken for a neoplastic process. **B**: Histology reveals a marked decidual reaction with hemorrhagic necrosis of the superficial portions of the polypoid structures.

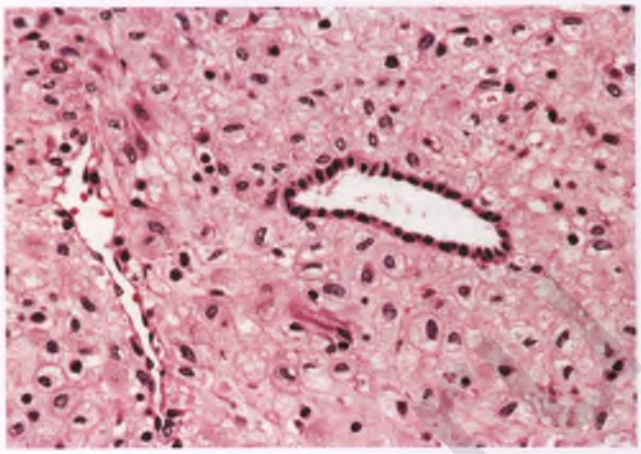

FIGURE 4.62. Progestin effect. The stroma exhibits marked decidual change, and there is also an atrophic gland lined by a single layer of cuboidal epithelium. An ectatic venule is present at left.

may thrombose, producing stromal breakdown that is manifested clinically as breakthrough bleeding (Fig. 4.63). In cases with stromal breakdown, neutrophils are an expected finding in the areas of tissue necrosis, and should not be misinterpreted as evidence of acute endometritis. Similarly, scattered lymphocytes are a normal finding in progestin-induced decidua, and are not indicative of chronic endometritis. The ability of marked decidual reactions to develop histologic changes that can mimic metastatic signet-ring adenocarcinoma has been discussed in the section on the endometrium in pregnancy.

Hormone Replacement Therapy

In the markedly diminished number of postmenopausal women with uteri whose hormone replacement therapy consists of

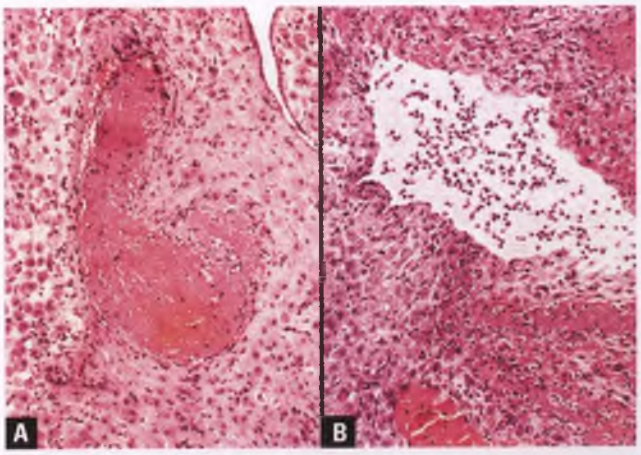

FIGURE 4.63. Progestin effect in two different patients with breakthrough bleeding. **A**: A fibrin thrombus is present within an ectatic venule. **B**: Several neutrophils and strands of fibrin are present in this focus of decidualized stroma with impending breakdown.

unopposed estrogen, the proliferative effect upon the endometrium results in the full spectrum of histologic changes that includes a normal proliferative pattern, disordered proliferation (the most common finding), hyperplasia, and occasional carcinomas. With the more standard replacement therapy that utilizes a combined regimen of low-dose estrogen–progestin preparations, weakly proliferative to atrophic patterns tend to be produced, sometimes with a few cytoplasmic vacuoles within the glandular epithelium.[42] Progestin-related subnuclear vacuolization in the cells lining the tubular glands are more likely to be seen in biopsies from patients on sequential estrogen–progestin regimens whose samples are taken during the period of progestin treatment.[42]

ENDOMETRITIS

Chronic Endometritis

Chronic endometritis may be associated with a recent abortion or pregnancy, salpingitis, intrauterine device, prior uterine instrumentation, or necrotic tissue. When a specific infectious agent is identified, it is often *Chlamydia trachomatis* or *Neisseria gonorrhoeae*.[48] Actinomyces-related infection, which is associated with use of an intrauterine device, and its differential diagnosis is discussed in Chapter 3, since these organisms are typically identified in Pap smears. Patients with chronic endometritis may be either asymptomatic or present with menometrorrhagia, cervical discharge, pelvic pain, and/or infertility.

Before embarking upon a discussion of the histology of chronic endometritis, it is important to acknowledge the normal presence of lymphoid cells within the endometrium. Lymphoid aggregates, including an occasional follicle with or without germinal center formation, are a normal finding in the endometrium, particularly in the basalis (Fig. 4.64).[38] Scattered granular lymphocytes are also normally present throughout the stroma, and are particularly prominent in the late secretory phase, in decidua, and in endometria with progestin effect. Although chronic endometritis also features a lymphocytic infiltrate, its principal distinguishing feature is the presence of plasma cells (Fig. 4.65A), which are conspicuously absent in the circumstances listed above. Predecidualized endometrial stromal cells and granular lymphocytes may have eccentric nuclei and be mistaken for plasma cells, but can be distinguished by their absence of a paranuclear pale zone and their lack of clumped, "clockface" chromatin that characterize bona fide plasma cells (Fig. 4.65B).

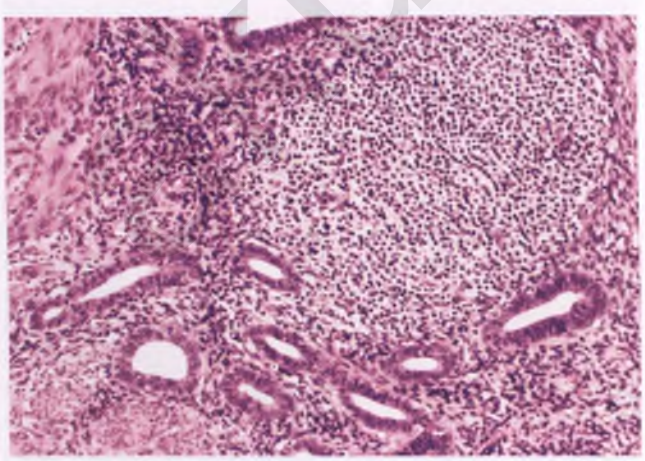

FIGURE 4.64. Innocuous lymphoid nodule within the basalis. Myometrium is at left.

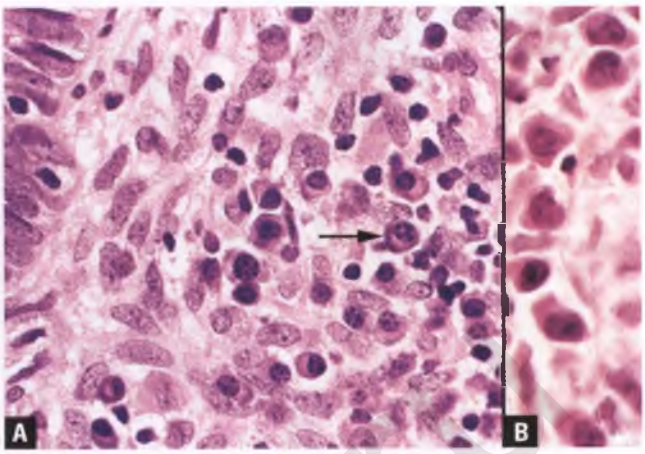

FIGURE 4.65. Chronic endometritis. **A**: In this example of chronic endometritis, several plasma cells are present within the stroma, one of which is marked by an *arrow*. **B**: Granular lymphocytes can sometimes have eccentric nuclei and simulate plasma cells. Note that these lymphocytes have eosinophilic cytoplasm and lack the clumped, "clockface" chromatin and paranuclear pale zone that are characteristic of true plasma cells.

In addition to a lymphoplasmacytic infiltrate, chronic endometritis is also often associated with reactive stromal changes that feature elongated, fibroblast-like stromal cells swirling around glands and/or forming pinwheel patterns (Fig. 4.66). This low-magnification clue to the diagnosis of chronic endometritis should prompt a careful search for plasma cells, as should cases with inflammatory cells in gland lumens, stromal eosinophils,[49] endometrial patterns that are difficult to assign to a particular phase of the menstrual cycle, or lymphoid infiltrates outside the setting of late secretory endometria. The glands typically appear weakly proliferative, but may exhibit reactive atypia; assignment of a cycle date to inflamed endometria is not reliable and should not be attempted.[38] By analogy to active chronic gastritis, cases of chronic endometritis that also feature an infiltrate of neutrophils can be considered examples of active chronic (rather than acute and chronic) endometritis (Fig. 4.67).

There is no doubt that the detection rate of plasma cells within endometrial stroma can be significantly increased by more careful scrutiny of routinely stained sections,[50] methyl green pyronin staining,[51] or immunostaining with the plasma cell marker CD138 (syndecan-1).[49] Indeed, these methods result in a reinterpretation of about 15% of control endometrial biopsies as "chronic endometritis" due to the identification

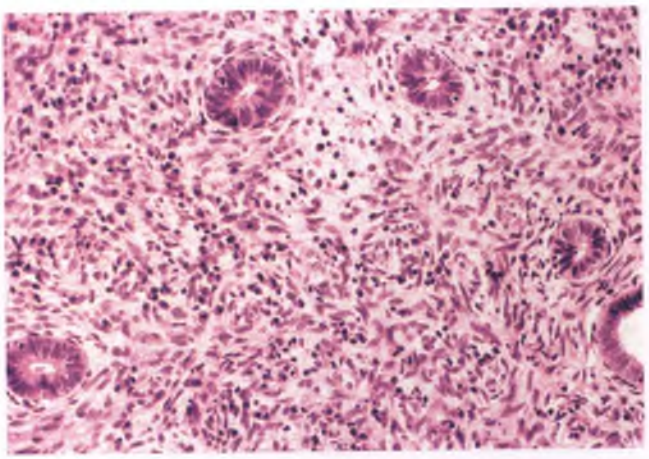

FIGURE 4.66. Chronic endometritis. The stroma contains several lymphocytes and plasma cells, and consists of swirling patterns of fibroblast-like spindle cells.

of plasma cells that were previously overlooked.[49,50] Not surprisingly, patients identified in this fashion typically have none of the risk factors or more characteristic symptoms of chronic endometritis, and it is doubtful that a course of antibiotic therapy in this group of patients would be of any benefit. In my opinion, there has recently been too much emphasis on the identification of a few plasma cells as a defining feature of chronic endometritis. In legitimate cases of chronic endometritis, plasma cells are easily recognized in routinely stained sections without an exhaustive search or the need to resort to special stains, other acute and chronic inflammatory cells are almost always present, and the spindle cell alteration of the stroma is usually evident. When diagnosed using these more strict and conventional criteria, chronic endometritis is an uncommon entity that is much more likely to fit with the clinical context and be worthy of antibiotic therapy. In support of the position that there are some situations in which the presence of plasma cells within the endometrium is best ignored, it has been shown that plasma cells can often be detected within the stroma of conventional endometrial polyps, disordered proliferative endometrium, and proliferative endometrium with stromal breakdown, and rare plasma cells can also be found in almost 20% of biopsies of normal proliferative endometrium.[51–53]

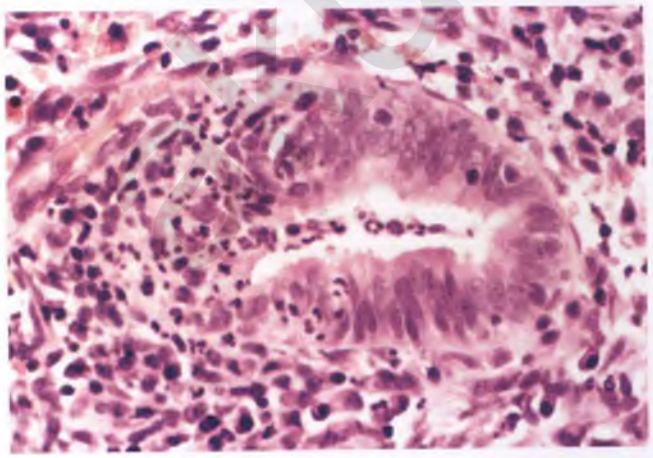

FIGURE 4.67. Active chronic endometritis. In addition to the lymphoplasmacytic stromal infiltrate, neutrophils are also present. As is typical, the acute inflammatory component is focused on the glandular epithelium and extends into the gland lumen.

Aside from the issue of the potential significance of plasma cells in endometrial samples, it is important to recognize contamination of an endometrial sample with chronically inflamed endocervical tissue. In this situation, the endocervical plasma cell infiltrate may be misinterpreted as evidence of chronic endometritis. This error can be avoided by noting the presence of cervical stroma and mucinous endocervical cells that are often accompanied by variable degrees of squamous metaplasia.

Acute Endometritis

Acute endometritis typically occurs in postpartum or postabortal settings, rarely requires submission of tissue for diagnosis, and is characterized by microabscess formation, intraepithelial neutrophils, glandular destruction, and intraluminal aggregates of neutrophils. The presence of stromal microabscesses helps to distinguish acute endometritis from neutrophilic infiltrates that are unrelated to infection that are found within the endometrium in areas of stromal breakdown, just prior to and during menses, and in association with tissue necrosis.

Menstrual endometrium is typically the most problematic differential diagnostic consideration. Recall that the neutrophils seen in menstrual endometrium are associated with glands with secretory differentiation and predecidualized stroma; acute endometritis is improbable in this setting. Correlation with the clinical findings is also quite helpful in avoiding the overinterpretation of menstrual endometrium as acute endometritis. If the patient is a few days removed from delivery or an abortion and has a fever, uterine tenderness, purulent vaginal discharge, and leukocytosis, acute endometritis is likely. On the other hand, if the patient's only complaint is abnormal uterine bleeding and the date of her last menstrual period is consistent with tissue having been sampled during menstruation, the diagnosis is almost certainly menstrual phase endometrium rather than acute endometritis.

Accumulation of neutrophil-rich, exudative material within the lumens of mid-secretory glands in the absence of other evidence of endometritis is an unusual, nonspecific finding of no known clinical significance, and should not be interpreted as acute endometritis (Fig. 4.68).[30]

Granulomatous Endometritis

True granulomatous endometritis is uncommon in the United States. It raises the possibility of tuberculous endometritis, which is associated with tuberculous salpingitis, systemic disease, and infertility.[54] Unlike pulmonary tuberculosis,

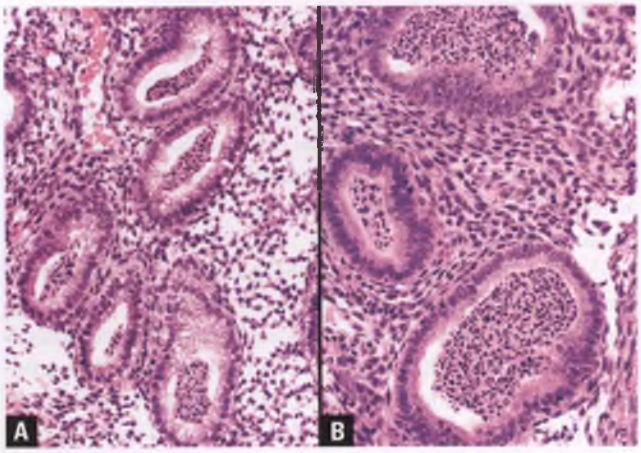

FIGURE 4.68. **A,B**: Mid-secretory endometrium with neutrophil-rich luminal contents (two different examples). This isolated finding is of no known significance, and should not be interpreted as acute endometritis.

endometrial tuberculous granulomas are typically nonnecrotizing (Fig. 4.69). Since granulomatous endometritis can also be caused by fungal infections, special stains for both acid-fast bacilli and fungi should be performed, although organisms of any kind are unlikely to be identified in histologic sections. Definitive diagnosis usually requires identification of the microorganism in cultures of fresh tissue or via molecular methods on paraffin-embedded material.

Endometrial granulomas that are associated with a history of previous endometrial sampling or ablation are typically focal, feature a foreign body giant cell reaction, and are not worthy of the designation of granulomatous endometritis (see section on histologic findings following thermal ablative therapy and hysteroscopic resection).[55] However, in the absence of an obvious foreign body etiology, endometrial granulomatous inflammation

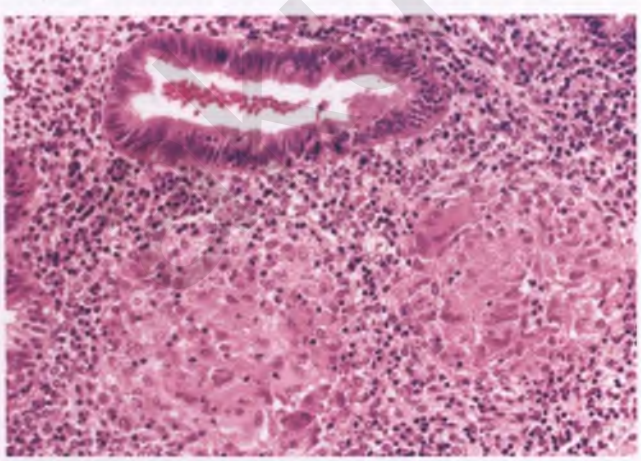

FIGURE 4.69. Tuberculous endometritis. Two nonnecrotizing granulomas are present beneath an endometrial gland. The stroma is also chronically inflamed.

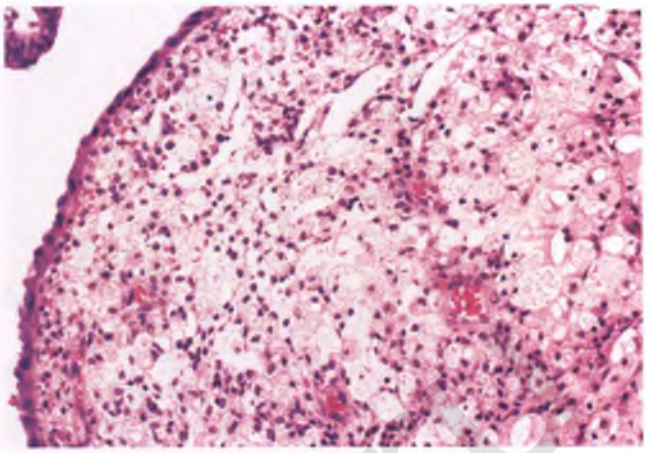

FIGURE 4.70. Xanthogranulomatous endometritis. Sheets of foamy histiocytes are present beneath the endometrial surface epithelium.

needs to be carefully evaluated to exclude infection and other causes of granulomatous disease such as sarcoidosis.

Distinction of endometrial-based granulomas from squamous morules is discussed in the section on morular/squamous metaplasia.

Xanthogranulomatous Endometritis

Xanthogranulomatous endometritis is an unusual inflammatory reaction that currently occurs primarily in postmenopausal women with pyometra or hematometra associated with cervical stenosis; an association of this process with irradiated endometrial adenocarcinoma is mainly of historical interest.[56,57] It features partial replacement to complete obliteration of the endometrial stroma by sheets of macrophages with abundant foamy to eosinophilic cytoplasm admixed with variable numbers of lymphocytes, plasma cells, and neutrophils (Fig. 4.70).[56,57] In addition, cholesterol clefts and foreign body giant cells may be present, along with a variety of pigmented cellular degradation products such as lipofuscin (ceroid), hemosiderin, and hematoidin (Fig. 4.71). Curetted tissue fragments are often an admixture of yellow and brown material due to the high content of foam cells and pigment, respectively.

The differential diagnosis of xanthogranulomatous endometritis includes the foam cells seen in endometrial hyperplasia and adenocarcinoma, which generally consist of a pure population of foamy macrophages that occur in smaller aggregates than the obliterative sheets of foam and inflammatory cells seen in xanthogranulomatous endometritis. Endometrial malakoplakia, which is extraordinarily rare, is also a differential diagnostic consideration, and is distinguished mainly by the presence of Michaelis-Gutmann bodies. The occasional finding of nodular aggregates of histiocytes within an endometrial sample is distinguished by the less-abundant, nonfoamy, eosinophilic nature of the histiocytic cytoplasm, the lack of associated pigmented material, and their occurrence as incidental small nodules (see Chapter 3).[58]

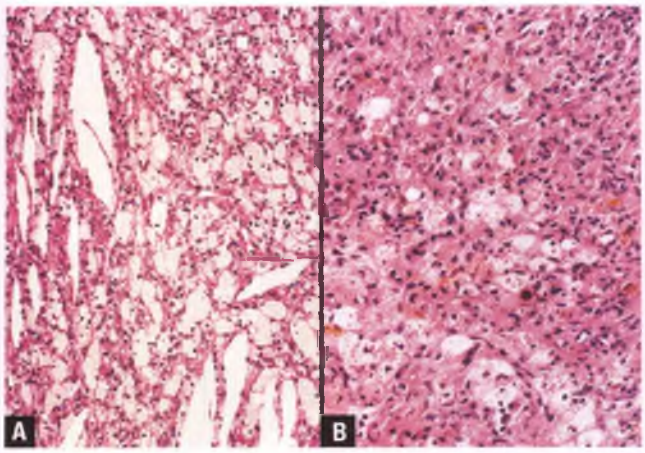

FIGURE 4.71. Xanthogranulomatous endometritis. **A**: Foamy histiocytes associated with cholesterol clefts. **B**: Numerous histiocytes with abundant foamy to eosinophilic cytoplasm obliterate the normal endometrial architecture. Clumps of refractile, *golden brown* hematoidin pigment are also present, which are shown at high magnification in Figure 4.95.

Cytomegalovirus and Herpes Endometritis

These rare, viral-related forms of endometritis can be recognized by their characteristic intracellular viral inclusions, as illustrated in Chapter 3.

ENDOMETRIAL POLYPS

Endometrial polyps are localized overgrowths of endometrial glands and stroma that are commonly found in uteri of adult women. Although often asymptomatic, these polyps can cause abnormal uterine bleeding when their surfaces have been traumatized or when they have undergone some degree of hemorrhagic infarction related to torsion of their stalks. Endometrial polyps are also an occasional cause of infertility.

Endometrial polyps may be pedunculated or sessile, and range in size from a few millimeters to several centimeters. Their external surface is smooth with occasional lobulations, and their cut surface is tan and rubbery and may exhibit scattered cysts or varying degrees of hemorrhage (Figs. 4.72 and 4.73A). In curettage specimens, most polyps are fragmented and admixed with other pieces of endometrium; in such cases, the polyps are often grossly recognizable as firm, polypoid fragments whose presence should be noted in the gross description.

Histologically, the appearance of endometrial polyps is quite variable, depending on the characteristics of the glands and stroma and the degree of prominence of the supporting vasculature. The glands of endometrial polyps have an altered architecture characterized by variation in size, shape, extent of crowding, and degree of cystic dilatation, and are lined by cells that range from atrophic to pseudostratified and mitotically active. For most endometrial polyps, the glandular component has a low-magnification appearance similar to that of disordered

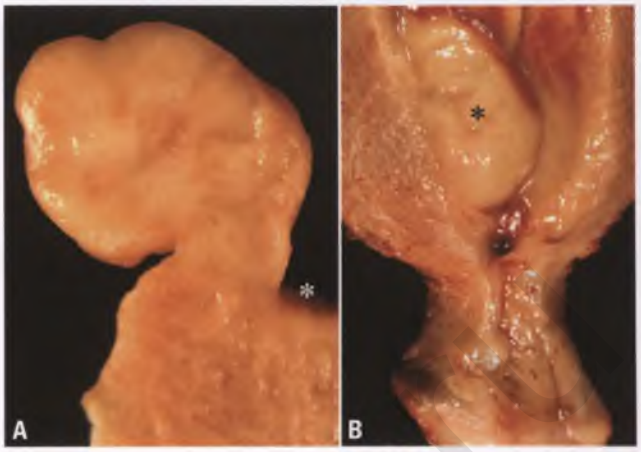

FIGURE 4.72. Endometrial polyps. **A**: Cut surface of a formalin-fixed, 2.3-cm pedunculated endometrial polyp. The endometrial surface is marked by a *white asterisk*, beneath which is unremarkable myometrium. **B**: A broad-based, sessile endometrial polyp, marked by a *black asterisk*, protrudes into the endometrial cavity of this lightly fixed uterus.

proliferative endometrium, and it is generally accepted to allow endometrial polyps to exhibit architectural glandular changes that would otherwise be considered within the spectrum of simple hyperplasia without atypia or low-end complex hyperplasia without flagging these polyps as being out of the range of normal. The stroma is often at least partially hypocellular and fibrotic, which is typical of polyps from postmenopausal women (Fig. 4.73B). Alternatively, the stroma may resemble that of the normal proliferative phase or a hypercellular version thereof (Figs. 4.74); in these cases, there may be some stromal mitotic activity.[59] A characteristic and diagnostically useful feature of endometrial polyps is the presence of clusters of

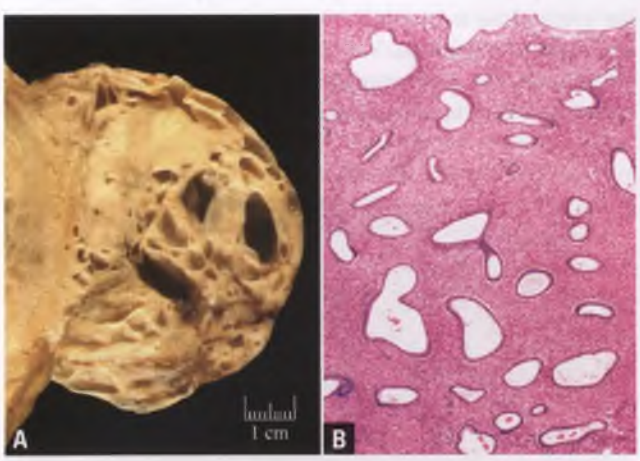

FIGURE 4.73. Endometrial polyp. **A**: Cross section through a formalin-fixed, 7-cm sessile polypoid mass (myometrium is at left). The large size, broad base, and spongy appearance of this polyp raise the possibility of an adenofibroma, adenosarcoma, or carcinosarcoma. **B**: Histologic examination of this well-sampled lesion shows an endometrial polyp composed of dilated glands set within a fibrous stroma.

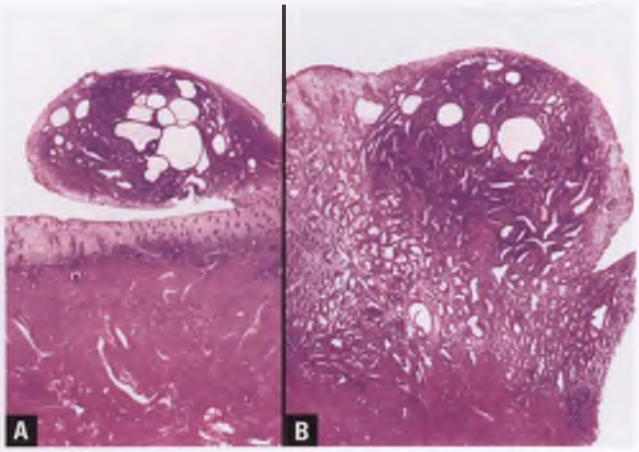

FIGURE 4.74. Endometrial polyps. **A**: Pedunculated endometrial polyp (0.6 cm) composed of mildly crowded glands with altered architecture set within a cellular endometrial stroma. Although difficult to appreciate at this magnification, a few clusters of thick-walled vessels are also present. **B**: Incipient endometrial polyp composed of a nodular, intraendometrial overgrowth of glands and stroma similar to that described above. Note the secretory phase of the surrounding endometrium.

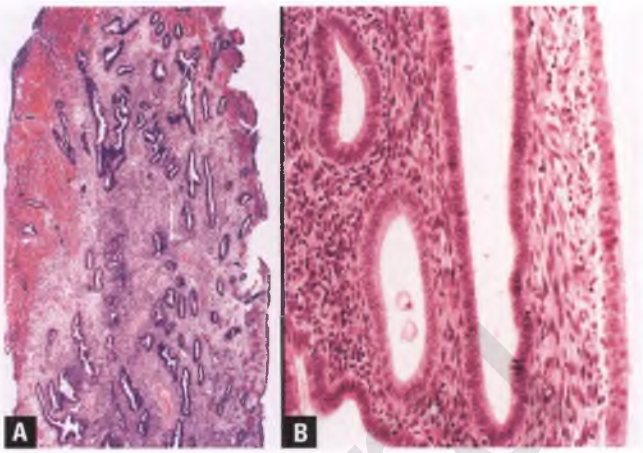

FIGURE 4.76. Endometrial polyps. **A**: Pedunculated endometrial polyp with superficial hemorrhagic areas. This polyp has predominantly endometrial-type stroma and exhibits the feature of elongated endometrial glands oriented parallel to the surface epithelium. **B**: High-magnification view of a different pedunculated endometrial polyp, demonstrating a combination of endometrial and fibroblastic stroma and an elongated endometrial gland oriented parallel to the epithelial surface, which is at right.

thick-walled blood vessels within the base, stalk, and/or body of the polyp (Fig. 4.75). In addition to the presence of the triad of thick-walled vessels, altered stroma, and altered glandular architecture, the presence of elongated glands oriented parallel to the surface epithelium is also a useful clue that aids in the recognition of fragmented endometrial polyps in curettings, particularly those that are pedunculated (Fig. 4.76).[60]

Functional polyps with secretory differentiation are uncommon, and typically show disorganized secretory glands in a stroma that is often dense and inactive rather than edematous or predecidualized (Fig. 4.77). Polyps originating near the internal os may exhibit hybrid features of endocervical and endometrial polyps. Very rarely, mitotically inactive atypical stromal cells with smudged chromatin (analogous to the bizarre cells seen in atypical leiomyomas) may be found within otherwise ordinary endometrial polyps.[61] As shown in Figure 4.119, infarcted polyps may exhibit papillary syncytial change with reactive atypia that needs to be distinguished from endometrial intraepithelial carcinoma.

Foci of complex atypical hyperplasia (CAH) and endometrioid adenocarcinoma are found within polyps on rare occasions (Fig. 4.78); patients with such lesions have a significant risk for the presence of CAH or adenocarcinoma in the adjacent nonpolypoid endometrium and are generally treated with hysterectomy.[62] Other types of carcinoma can also arise within endometrial polyps; serous carcinomas presenting within polyps are of particular interest and are discussed later in this chapter.

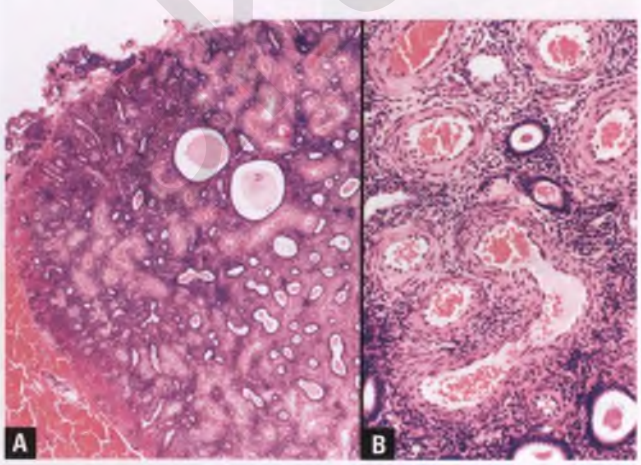

FIGURE 4.75. **A,B**: Endometrial polyp. Prominent thick-walled blood vessels are evident.

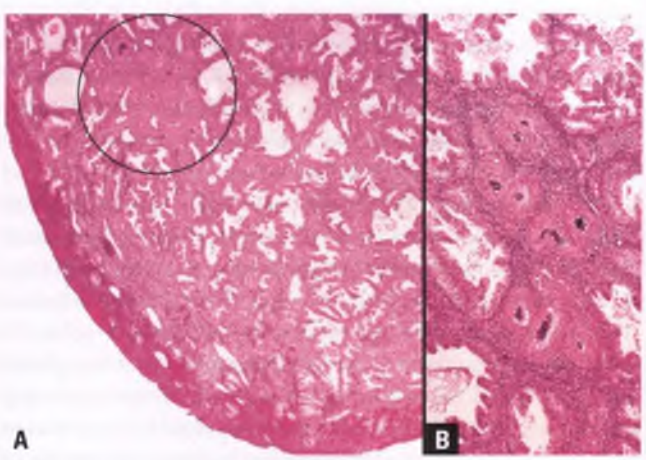

FIGURE 4.77. Functional endometrial polyp with secretory differentiation. **A**: Clusters of thick-walled vessels (*circled*) that are larger and thicker than spiral arterioles help to distinguish this polyp from a polypoid piece of secretory endometrium. The surface of the polyp is hemorrhagic. **B**: Cluster of thick-walled vessels at higher magnification.

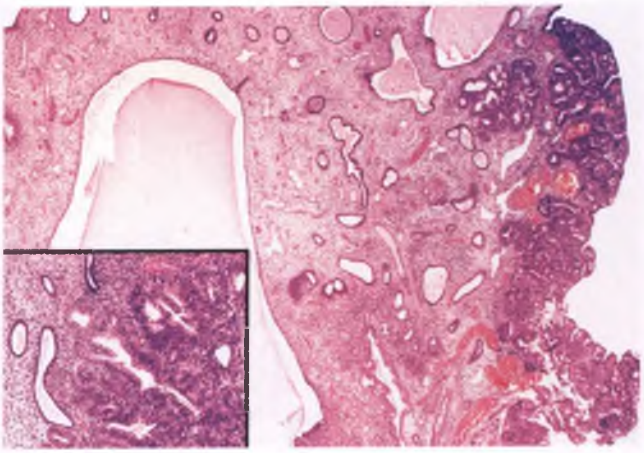

FIGURE 4.78. Endometrioid adenocarcinoma replacing the superficial portion of an endometrial polyp (inset and far right of image).

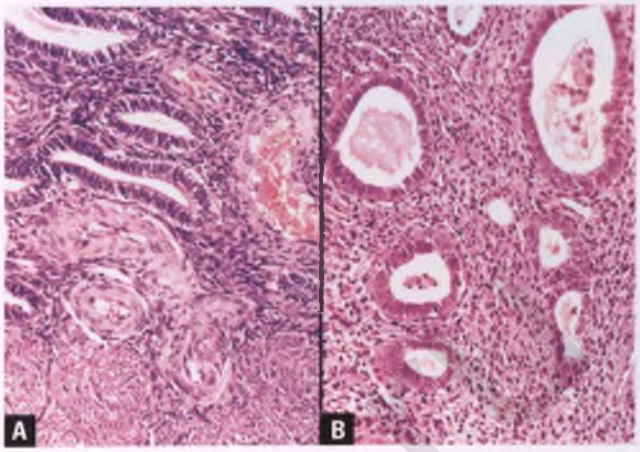

FIGURE 4.79. Features of the normal endometrium that can mimic an endometrial polyp. **A**: Clusters of thick-walled blood vessels within the basalis, which is composed of weakly proliferative glands and a densely cellular, spindle-cell stroma. Myometrium is at bottom. **B**: The endometrial stroma of the lower uterine segment is less cellular and more fibrotic than that of proliferative endometrium from the uterine body or fundus.

On occasion, endometrial samples are submitted with a clinical diagnosis of endometrial polyp, but the presence of a polyp cannot be documented histologically, even after thorough examination of deeper sections. Possible explanations of this phenomenon are (a) sampling of polypoid mucosa rather than a true endometrial polyp, (b) excessive fragmentation of the polyp, rendering it unrecognizable, and (c) superficial sampling of nondiagnostic portions of a polyp. In this circumstance, the pathologist should indicate that histologic features of a polyp are not evident, and that clinical correlation is suggested to determine if any of the aforementioned explanations apply.

Differential Diagnosis

The differential diagnosis of endometrial polyps includes polypoid pieces of normal endometrium, fragments of basalis or lower uterine segment, adenofibroma, and subtle forms of adenosarcoma. Although intact polyps are polypoid and covered by surface epithelium, a similar appearance can be generated when undulating, polypoid endometrial tissue is curetted, embedded, and cut in a plane parallel to the endometrial surface (see Fig. 4.111 in section on common endometrial artifacts). In addition to having a polypoid appearance, true polyps exhibit two or more of the following features: (a) clusters of thick-walled vessels, (b) an altered glandular pattern that stands out from the other fragments of nonpolypoid endometrium, (c) stroma that is abnormally dense or fibrotic, and (d) elongated glands oriented parallel to the epithelial surface. To avoid the mistake of confusing the presence of the normal finding of thick-walled vessels within the basalis (Fig. 4.79A) as evidence in favor of an endometrial polyp, the surface of the candidate polyp should be identified. Another pitfall is misinterpreting the stroma of the lower uterine segment, which is normally less cellular and more fibrotic than that of proliferative endometrium from the uterine body or fundus (Fig. 4.79B), as the altered stroma of a polyp. Distinction of endometrial polyps from adenofibromas and adenosarcomas is discussed later in this chapter.

ADENOMYOSIS

Adenomyosis is defined as the presence of endometrial glands and stroma within the myometrium at some distance from the typically irregular endometrial–myometrial junction such that tangential cutting of basalis can be excluded. This distance has not been standardized, and varies from 1 to 2.5 mm. In premenopausal patients, bona fide adenomyosis is often accompanied by smooth muscle hypertrophy, which is typically grossly recognizable as thickened, trabeculated areas of the myometrium (Fig. 4.80). Not uncommonly, these trabeculated areas are punctuated by small cysts that contain fluid related to recent (red) or remote (brown) accumulation of blood products (Fig. 4.81). Although superficial adenomyosis detected solely on the basis of histologic examination is often a focal and incidental finding, grossly detectable adenomyotic foci are more likely to be associated with the nonspecific symptoms of menorrhagia or dysmenorrhea.

The glands and stroma within the islands of adenomyosis usually have the appearance of basalis or proliferative endometrium, and generally do not show secretory changes during the luteal phase of the cycle. A potential pitfall associated with extensive adenomyosis is the occasional finding of intravascular endometrial tissue, which may consist of an admixture of glands and stroma or be composed solely of stromal cells (Fig. 4.82).[63,64] This is an incidental finding that should not be misinterpreted as evidence of malignancy.

As discussed elsewhere in this chapter, endometrial hyperplasia and endometrial adenocarcinoma may involve foci of adenomyosis, and distinguishing this phenomenon from true myometrial invasion is clinically relevant.

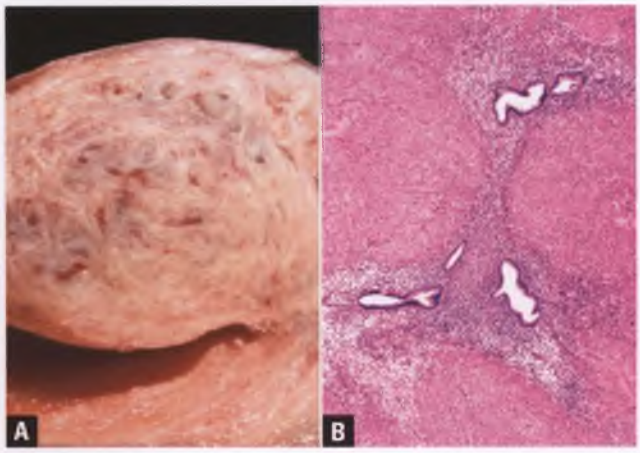

FIGURE 4.80. Florid adenomyosis. **A**: In this sagittal section through a formalin-fixed uterus, note the diffuse thickening, trabeculation, and scattered small cysts in the adenomyotic myometrium above the endometrial cavity. The myometrium of the opposite wall beneath the endometrial cavity is normal. **B**: Islands of endometrial glands and stroma of weakly proliferative type are surrounded and partially compressed by hypertrophic smooth muscle.

Differential Diagnosis

Usual adenomyosis can rarely be confused with low-grade endometrial stromal sarcoma with endometrioid glandular differentiation, but the latter neoplastic process usually involves the endometrium as well as the myometrium, has a dominant stromal component with widely spaced glands and areas in which the glands are rare to absent, lacks associated myometrial hypertrophy, may show considerable stromal mitotic activity and/or a host of morphologic variations characteristic

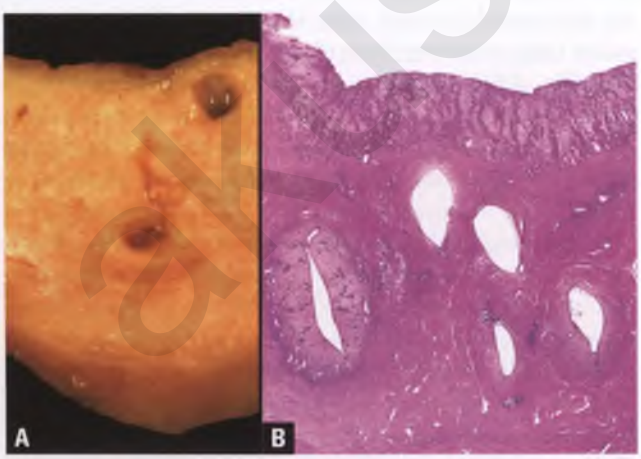

FIGURE 4.81. Adenomyosis. **A**: Cross section through the wall of a formalin-fixed uterus, revealing adenomyosis within the inner half of the myometrium. In the involved area, the myometrium is trabeculated and contains scattered cysts. **B**: Corresponding histologic section showing proliferative endometrium overlying cystic foci of adenomyosis.

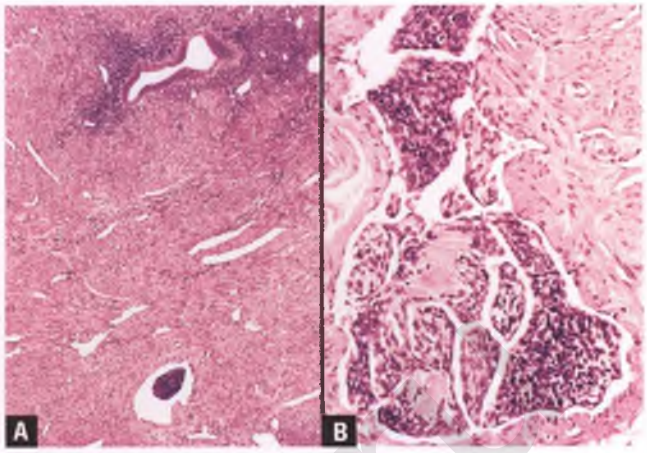

FIGURE 4.82. Adenomyosis with vascular intrusion. **A**: An intravascular aggregate of endometrial stroma lies beneath a focus of adenomyosis. **B**: Endometrial stroma within a dilated, thin-walled vessel in a patient with adenomyosis.

of endometrial stromal tumors, and often exhibits widespread, expansile vascular involvement.[65,66]

In rare instances, particularly in postmenopausal patients, adenomyosis may have sparse glands, resulting in an appearance that resembles the usual type of low-grade endometrial stromal sarcoma (Fig. 4.83).[67] In this situation, adenomyosis is favored by the incidental nature and microscopic size of this process (i.e., no mass lesion), the presence of typical adenomyosis elsewhere in the uterus, the postmenopausal age of the patient, a characteristic concentric zonal arrangement of the adenomyotic foci with a central pale area of stromal cells surrounded by a hypercellular darker rim of stromal and/or smooth muscle cells, stromal mitotic inactivity, and lack of widespread vascular involvement.[67] Conversely, the stromal component of adenomyosis may be atrophic and fibrotic, resulting in scattered glands within the myometrium with an appearance that may be difficult to distinguish from myometrial invasion by a very

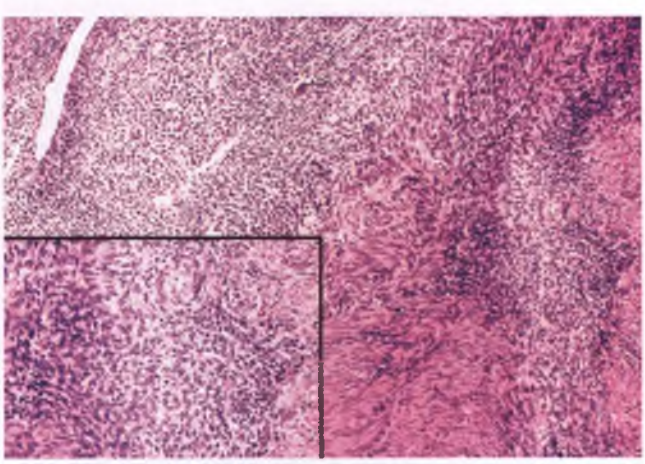

FIGURE 4.83. Adenomyosis with sparse glands. The inset highlights the tendency for the central zone of this form of adenomyosis to be more pale than the hypercellular peripheral zone.

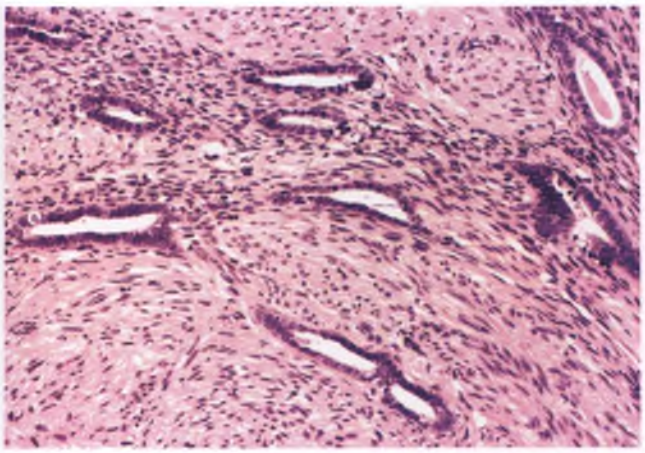

FIGURE 4.84. Adenomyosis with atrophic and fibrotic stroma. This process could be confused with a well differentiated endometrioid adenocarcinoma with myoinvasion.

well-differentiated endometrioid adenocarcinoma (Fig. 4.84). When confronted with this problem, features that favor adenomyosis include the atrophic appearance of the glands, the absence of a low-magnification infiltrative pattern, recognizable wisps of endometrial stroma around some of the glands, typical adenomyosis elsewhere in the uterus, the lack of a host reaction to the glands, and the usual absence of an associated endometrial adenocarcinoma.

ADENOMYOMA

Adenomyoma is the term used to describe grossly nodular, leiomyoma-like foci composed of smooth muscle with interspersed islands of endometrial glands and stroma (Fig. 4.85).[68,69] Most of the intramural examples of this lesion are probably circumscribed forms of adenomyosis, although the submucosal polypoid variant is more likely neoplastic (Figs. 4.86 and 4.87).

FIGURE 4.85. Adenomyoma. This cross section through a formalin-fixed uterus reveals a 9 cm fairly well circumscribed adenomyoma with prominent trabeculations and scattered cysts.

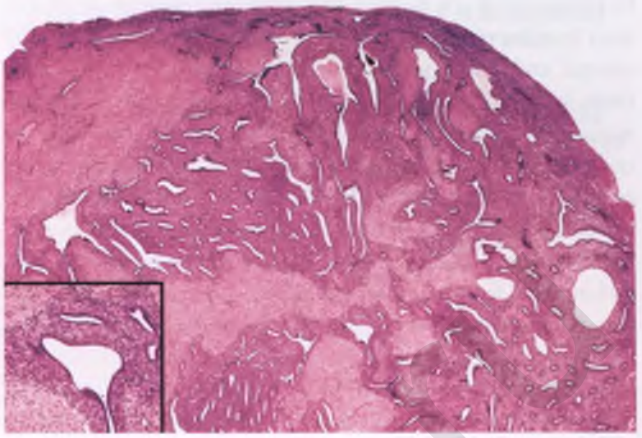

FIGURE 4.86. Submucosal polypoid adenomyoma consisting of islands of endometrial glands and stroma embedded within a prominent smooth muscle stroma. Note the resemblance to adenosarcoma imparted by the elongated, compressed, and/or clefted glands surrounded by endometrial stroma. The inset highlights the abrupt transition between endometrial stroma and smooth muscle.

Although some investigators cite a distinction between the myometrial muscle of adenomyosis and the leiomyomatous muscle of adenomyomas, the hypertrophic, intersecting fascicles of myometrial smooth muscle that surround foci of adenomyosis are often indistinguishable from those seen in leiomyomas.

Differential Diagnosis

Submucosal polypoid adenomyomas, also referred to as adenomyomatous polyps, need to be distinguished from typical endometrial polyps, adenofibromas, adenosarcomas, and atypical polypoid adenomyomas (APAs). Although typical endometrial polyps may contain a minor component of smooth muscle, their mesenchymal elements are dominated

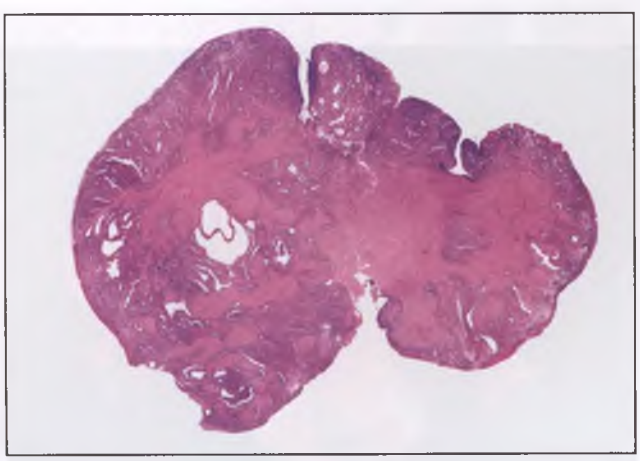

FIGURE 4.87. Submucosal polypoid adenomyoma. Note that a superficial biopsy of this lesion would likely yield only proliferative or disordered proliferative endometrium.

by endometrial stroma and fibrous tissue rather than prominent bundles of smooth muscle. Compression of endometrial stroma and elongated endometrial glands by myomatous tissue within a polypoid adenomyoma may result in the formation of leaf-like, clefted glands surrounded by cuffs of endometrial stroma, leading to simulation of an adenofibroma or adenosarcoma (Fig. 4.86). However, tumors in the adenofibroma/adenosarcoma group do not have a prominent smooth muscle stroma and may form papillary fronds, which is an architectural feature not seen in adenomyomas. Moreover, the low-grade sarcomatous stroma of adenosarcoma often exhibits hypercellular periglandular cuffs that blend with less cellular sarcomatous stroma away from the glands, whereas the periglandular endometrial stroma of polypoid adenomyomas is sharply demarcated from its smooth muscle component. The clinically important distinction between the similarly named polypoid adenomyoma and APA is discussed later in this chapter.

MISCELLANEOUS NONNEOPLASTIC PROCESSES

Endometriosis of the Uterine Serosa

The uterine serosa of hysterectomy specimens should be closely inspected for evidence of endometriosis, which is typically manifested by the presence of hemorrhagic adhesions or brown "powder burns" on the posterior serosal surface (Figs. 4.88 and 4.89). In classic examples of this lesion, the triad of endometriotic glands, endometriotic stroma, and hemosiderin-laden macrophages is present (Fig. 4.90). The main differential diagnostic consideration of endometriosis in this location is endosalpingiosis, which is usually an incidental microscopic finding that features benign, tubal-type glands lined by ciliated epithelium that lack a periglandular rim of endometrial stroma and may be seen in association with psammoma bodies (see Chapter 8 for a more complete discussion of endometriosis and endosalpingiosis).

FIGURE 4.88. Endometriosis. Numerous hemorrhagic adhesions related to endometriosis are present on the posterior uterine serosa and ovaries of this lightly fixed specimen.

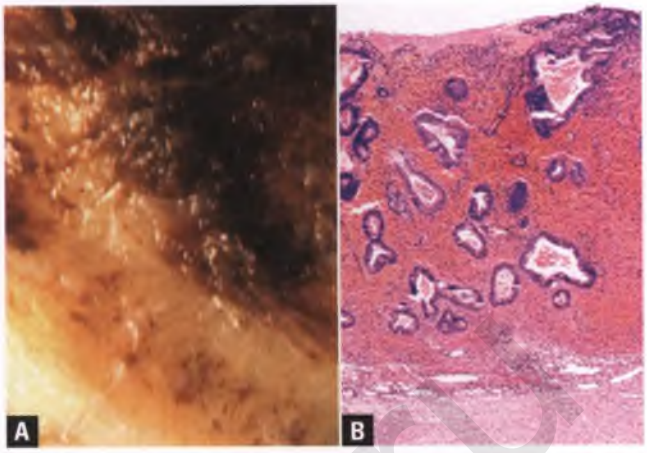

FIGURE 4.89. Endometriosis. **A**: High-magnification view of a formalin-fixed specimen with prominent endometriosis of the uterine serosa. **B**: The corresponding histologic section shows extensive involvement of the uterine serosa in a pattern that simulates disordered proliferative endometrium with stromal hemorrhage.

Uterine Prolapse

In uterine prolapse, weakened pelvic support results in an abnormal protrusion of the uterus into or beyond the vagina. In some cases, there is associated cervical elongation, which may be striking (Fig. 4.91). Histologically, the exocervix in uterine prolapse often shows irritation/friction-related hyperkeratosis and/or parakeratosis, and may also show pagetoid dyskeratosis (see Chapter 3).

Histologic Findings Following Thermal Ablative Therapy and Hysteroscopic Resection

Endometrial ablation is sometimes performed in women with prolonged, heavy uterine bleeding unrelated to hyperplasia or malignancy that is refractory to hormonal treatment and for

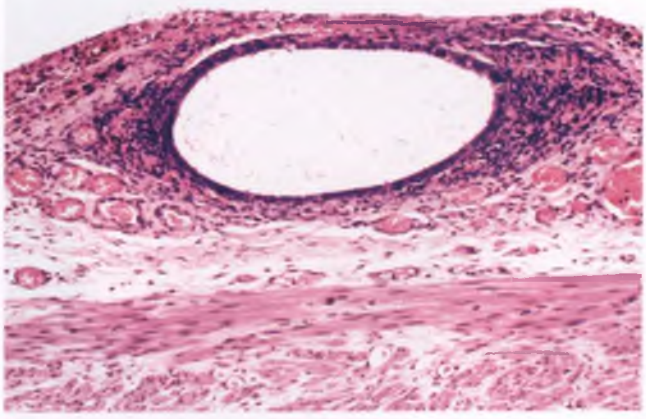

FIGURE 4.90. Endometriosis. Uterine serosal adhesion with focus of endometriosis characterized by a cystically dilated endometrial-type gland that is surrounded by endometrial stroma and aggregates of hemosiderin-laden macrophages.

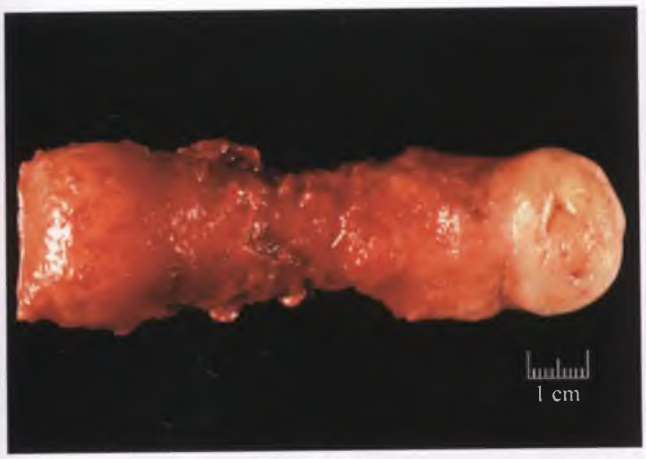

FIGURE 4.91. Hysterectomy specimen from a patient with uterine prolapse with striking cervical elongation. The cervix protruded beyond the vaginal introitus. Corpus is at left; cervix is at right.

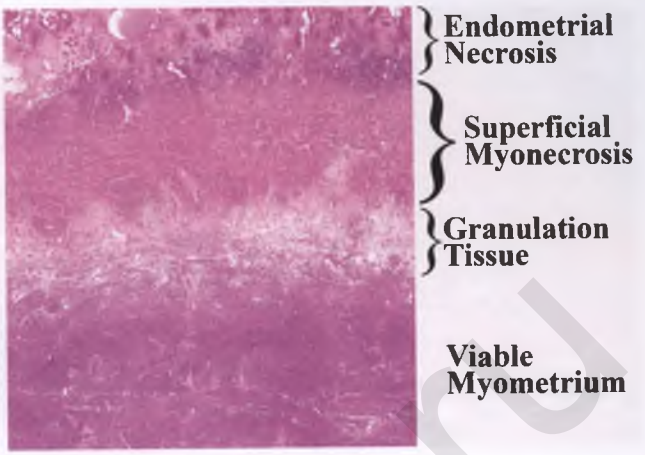

FIGURE 4.92. Subacute post-thermal ablation tissue reaction. Necrotic endometrial tissue is present in the superficial zone, but pockets of viable basalis persist in this case despite the presence of an underlying band of necrotic, hyalinized myometrial tissue. A band of granulation tissue separates the deep, viable myometrium from the inner, necrotic myometrium.

whom hysterectomy is not preferred or otherwise indicated.[70] A variety of methods are employed to ablate the endometrium, including laser thermal ablation, thermal balloon ablation using heated saline, and thermal ablation using electrosurgical coagulation or vaporization current that is applied via a rollerball or other specialized device.[71] Prior to rollerball treatment, a resectoscope with a loop electrode is sometimes used that creates shavings of endometrium and superficial myometrium. The goal of these different ablative methods is heat-induced destruction/removal of the entire endometrial lining, with a successful outcome defined as amenorrhea or conversion to light menstrual periods.

In failed endometrial ablations, endomyometrial tissue samples or hysterectomy specimens may be submitted for histologic evaluation. The endometrium may be entirely absent, patches of basalis may survive beneath coagulated tissue, relatively normal endometrium may be present, or a thin layer of glandless endometrium lined by surface epithelium may be found.[72] In the areas of significant thermal damage, there is an acute necrotic phase during the first month postablation that features endometrial and inner myometrial bands of necrosis (Fig. 4.92).[72] Within a few weeks, a zone of granulation tissue also forms at the interface between necrotic and viable myometrium (Fig. 4.92).[72]

The acute necrotic phase gradually transitions to a chronic reparative phase characterized by varying amounts of fibrosis, hyalinization, and granulation tissue associated with irregular clumps of golden-brown and/or black pigment (Fig. 4.93).[72–74] This pigment typically incites a multinucleated giant cell reaction that may contribute to granuloma formation, and may be seen whenever and wherever tissue is subjected to fulguration or laser treatment, such as following hysteroscopic resections of polyps or submucosal leiomyomas (Fig. 4.94) or diathermy ablation of endometriosis[72–76] (see section on postoperative carbon pigment granulomas in Chapter 8). This pigment does not represent hemosiderin, as evidenced by both its histologic appearance and negative iron stains.[75] Unlike many types of foreign material such as suture and starch granules, it does not exhibit birefringence when examined under polarized light.[75] The black pigment is often attributed to carbon particles formed within charred tissue,[70,75] but similar-appearing material has also been shown to be related to metal deposits originating from the laser tip, wire loop, or electrode of the device used for ablation.[73,77] The golden-brown pigment is also often regarded as a variant of carbon particle,[75] although some investigators have suggested that this pigment may represent hematoidin, which is a breakdown product of hemoglobin.[73] However, in most examples of this ablation-related phenomenon, the brown pigment lacks the characteristic golden-yellow, refractile, crystalline appearance of hematoidin that typically includes formation of rhomboid plates. A comparison of hematoidin versus hemosiderin pigment is provided in Figure 4.95.

Whatever the nature of ablation-associated pigments, their presence indicates previous laser or fulguration surgery, and special stains to exclude an infectious granulomatous etiology are not

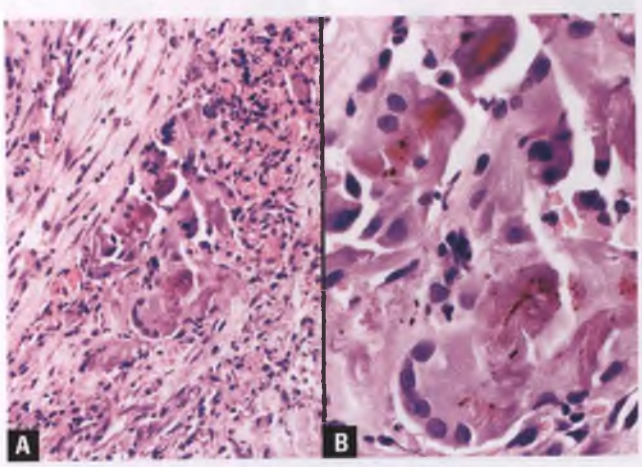

FIGURE 4.93. **A,B**: Postablation tissue reaction in chronic reparative phase following thermal ablation of the endometrium. Note the presence of fibrosis, inflamed granulation tissue, and a multinucleated giant cell reaction to pigmented material.

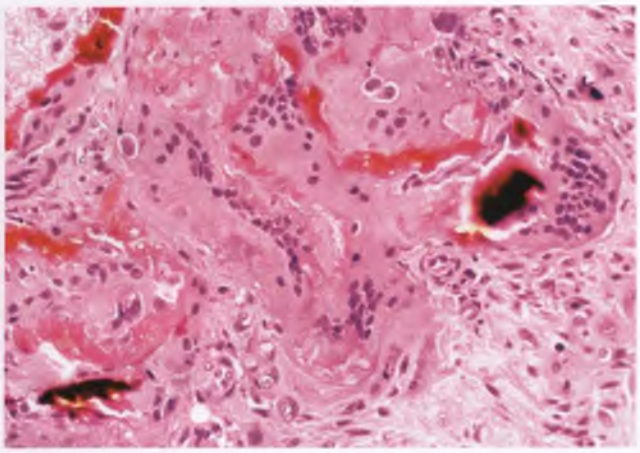

FIGURE 4.94. Foreign body giant cell reaction to pigmented material, 2 months following hysteroscopic resection of a submucosal leiomyoma.

indicated. However, necrotizing granulomas with palisading histiocytes that produce patterns reminiscent of rheumatoid nodules have been reported as a rare consequence of thermal ablation.[77,78] In the absence of characteristic deposits of pigment, these granulomas should be examined with special stains as part of an evaluation to exclude the possibility of an infection with fungi or acid-fast bacilli.

Idiopathic Granulomatous Inflammation of the Uterine Stroma

On rare occasions, the myometrium or cervical stroma contains nonnecrotizing granulomas that appear to be unrelated to foreign material, previous surgical intervention, infection, or systemic granulomatous disease.[79] These granulomas have a predilection for proximity to thin-walled vascular channels, but there is no evidence of an associated vasculitis.[79] Although these granulomas likely represent an incidental microscopic finding of unknown cause, they should be evaluated with special stains for acid-fast bacilli and fungi. After these stains have been confirmed as negative, the pathology report should mention the unlikely possibility of systemic granulomatous disease, and note that negative "bug" stains do not entirely exclude an infectious etiology.

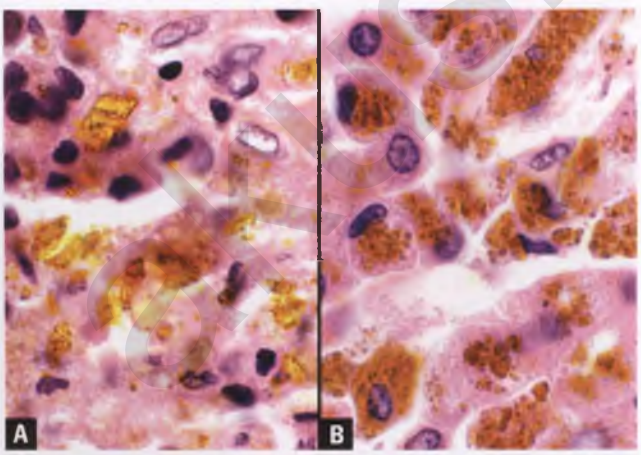

FIGURE 4.95. Hematoidin versus hemosiderin. **A**: *Golden yellow*, refractile, crystalline deposits of hematoidin in a case of xanthogranulomatous endometritis from a patient with a history of hematometra. Hematoidin crystals are iron negative (not shown). **B**: Brown, coarsely granular, intracellular particles of hemosiderin within hepatic tissue in a patient with hemochromatosis. Hemosiderin granules are iron positive (not shown). Both images were taken at the same magnification.

Histologic Evidence of Iatrogenic Uterine Perforation in Endometrial Samples

The presence of adipose tissue within an endometrial sample is presumptive evidence of a uterine perforation. In some cases, yellow tissue fragments consistent with fat can be grossly identified within the specimen, which help to exclude the possibility of tissue contamination from another case. Distinction of adipose tissue from pseudolipomatosis/bubble artifact is discussed in the section on endometrial artifacts. In addition to adipose tissue, other pieces of tissue originating from the bowel, bladder, or other abdominopelvic sites may be inadvertently sampled through a perforated uterus and found admixed with endometrial fragments (Fig. 4.96). Upon microscopic confirmation of the presence of any of the aforementioned extrauterine tissue, the clinician should be notified that the histologic findings are best explained by the presence of a uterine perforation. The pathology report should document the details of this notification along with the type and amount of extrauterine tissue.

Postoperative Spindle Cell Nodule

Within the female genital tract, this unusual lesion is most commonly found in the vagina (see Chapter 2). Rarely, postoperative spindle cell nodules involve the endometrium/superficial myometrium in the weeks to months following curettage (Fig. 4.97).[80]

Malakoplakia

Rare cases of endometrial malakoplakia have been reported in women with postmenopausal bleeding.[81] As seen in more typical sites such as the urinary bladder, malakoplakia features sheets of histiocytes with abundant eosinophilic cytoplasm and occasional Michaelis-Gutmann bodies (Fig. 4.98). Malakoplakia is discussed in more detail in Chapter 2, since the vagina is the most common site of involvement within the female genital tract.

Histiocytic Nodules

See Chapter 3.

Pseudoactinomycotic Radiate Granules

See Chapter 3.

Osseous Metaplasia

So-called osseous metaplasia of the endometrium is quite rare (Fig. 4.99). Most cases are due to retention and implantation of fetal bones in women of childbearing age who have a history of an abortion occurring at >3 months gestation, which is

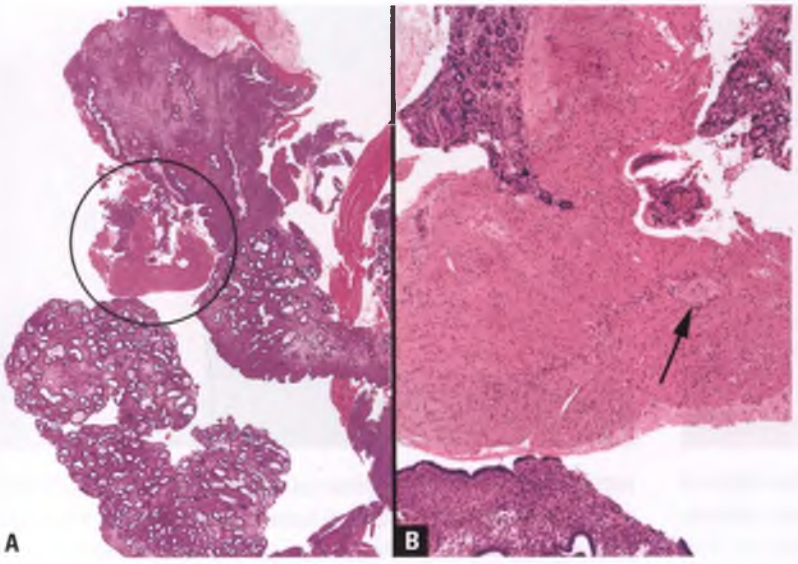

FIGURE 4.96. Endometrial curettage complicated by perforation of the uterus and small bowel. **A**: The curettings contain a full-thickness fragment of small bowel (*circled*) lurking amongst fragments of benign endometrial tissue, some of which represent pieces of endometrial polyp. **B**: This higher magnification view of the piece of small bowel shows myenteric plexus (*arrow*) in the smooth muscle wall, fragmented villi, and small bowel crypts with Paneth cells.

after the period of fetal bone formation.[82,83] Secondary infertility is the most common clinical presentation. Less often, true osseous metaplasia of endometrial stromal cells may occur as a response to inflammation or trauma.

Uterine Lithiasis

Stone formation within the endometrial cavity is extremely uncommon. When it occurs, the stones are typically small (0.2–0.5 cm), white, starlike structures composed of calcium carbonate (Fig. 4.100).[84]

Mönckeberg's Medial Calcific Sclerosis

This form of arteriosclerosis is commonly seen within the medium-sized uterine arteries of elderly patients, and is not thought to be of any clinical significance (Fig. 4.101).[85] The calcified, sclerotic vessels may be visible both grossly and radiologically.

COMMON ENDOMETRIAL ARTIFACTS

Dissociation and Close Approximation of Endometrial Glands

By its very nature, the act of sampling the endometrium results in a fragmented specimen. In some instances, endometrial glands are stripped from their associated stroma and aggregated in a compacted manner that can simulate endometrial hyperplasia (Fig. 4.102). In other cases, lesser degrees of trauma result in artifactual clustering and compaction of glands surrounded by relatively intact stroma, creating an appearance that mimics microaggregates of hyperplastic glands (Fig. 4.103). The key feature that allows for recognition of these dissociation artifacts is the fact that at least some of the traumatized glands are lacking or deficient in stromal support, and often appear to be free floating. Such tissue is not suitable for an assessment of the

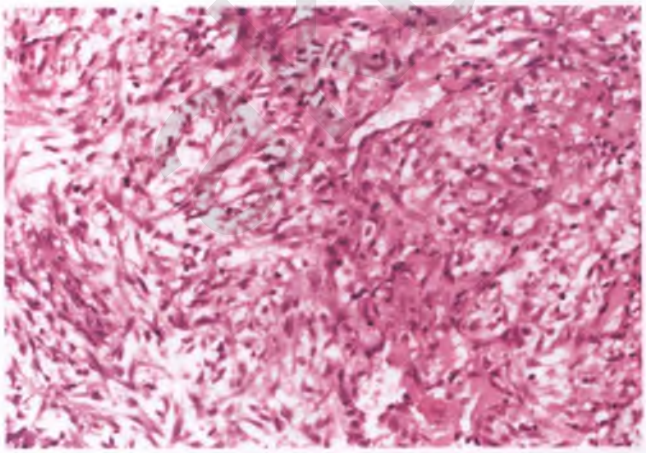

FIGURE 4.97. Postoperative spindle cell nodule in a patient 2 months after endometrial curettage. The lesion resembles inflamed granulation tissue and nodular fasciitis, and typically has a mitotically active spindle cell component of probable fibroblastic origin.

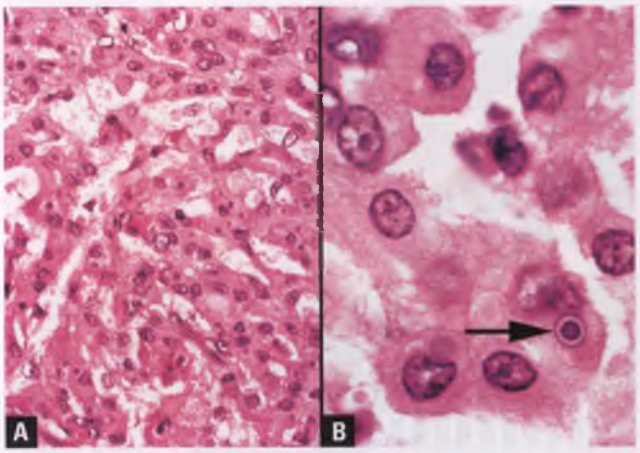

FIGURE 4.98. Malakoplakia. **A**: Sheets of histiocytes with abundant eosinophilic cytoplasm are present, some of which contain Michaelis-Gutmann bodies. **B**: This high-magnification view highlights the presence of a Michaelis-Gutmann body with a "bull's-eye" appearance (*arrow*).

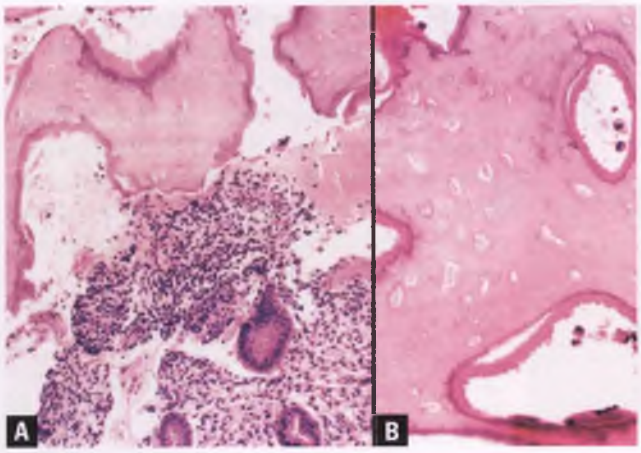

FIGURE 4.99. **A,B**: So-called osseous metaplasia. Fragments of devitalized bone are admixed with pieces of proliferative endometrium. The patient was a 28-year old woman with infertility.

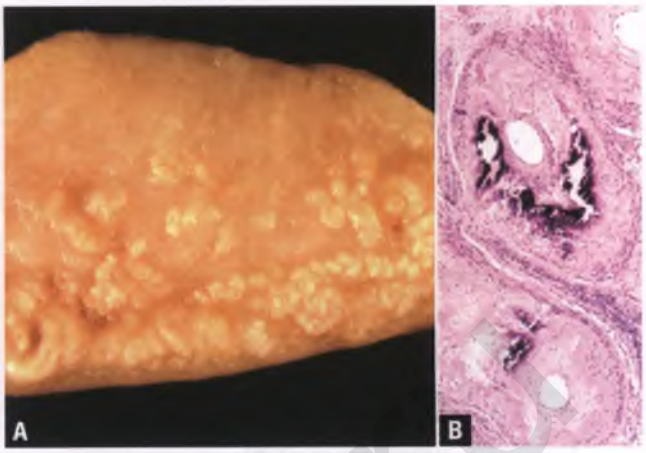

FIGURE 4.101. Mönckeberg's medial calcific sclerosis. **A**: Cross section through the uterine wall, revealing numerous abnormal vessels located predominantly within the outer half of the myometrium. **B**: Cluster of myometrial arteries with sclerosis and calcification of the media.

presence or absence of endometrial hyperplasia, which must be based on intact tissue where the architectural relationship of the glands to one another can be evaluated. Fortunately, this artifact is rarely so extensive that it compromises the adequacy of the specimen.

Endometrial Surface Epithelial Coiling Artifact

Scant strips of benign surface endometrial epithelium may be all that are obtained in some endometrial samples. This is particularly common in postmenopausal women with endometrial atrophy. When such strips form coiled aggregates, the resulting histologic sections can mimic endometrial hyperplasia (Fig. 4.104). If the coiled epithelial strips originate from contaminating superficial endocervical elements, a mucinous lesion may be simulated (see section on mucinous metaplastic hyperplasia).

Autolysis-Induced Artifacts

When a tissue sample or hysterectomy specimen is left for prolonged periods without being adequately fixed, the ensuing autolysis results in a retraction artifact in which the glands are separated from their associated stroma by a clear space. As depicted and discussed in the section on artifacts in Chapter 3, this phenomenon should not be mistaken for angiolymphatic invasion.

Another potential autolysis-related pitfall is misinterpreting an autolyzed hyperplasia or grade 1 endometrioid carcinoma as a grade 3 neoplasm. In these cases, an apparent solid architectural pattern is created by collapse and epithelial sloughing of the architecturally complex glandular structures that are supported by minimal amounts of stroma (Fig. 4.105). In addition to the presence of epithelial sloughing, recognition of this artifact is

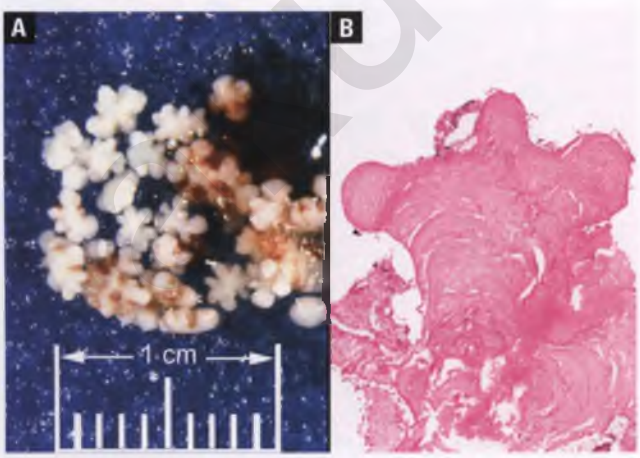

FIGURE 4.100. Uterine lithiasis. **A**: Numerous small starlike concretions are present in this endometrial curettage. **B**: Corresponding representative histologic section shows amorphous calcified material in a starlike configuration.

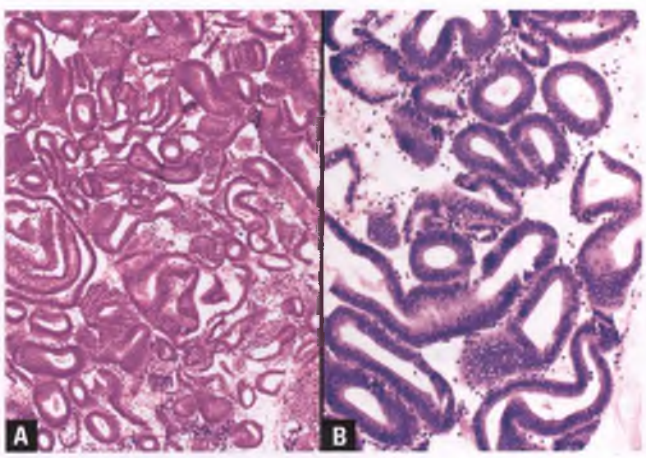

FIGURE 4.102. **A,B**: Dissociation artifact (two different examples). Artifactually crowded aggregates of proliferative endometrial glands have been dissociated from their stroma, creating a free-floating appearance.

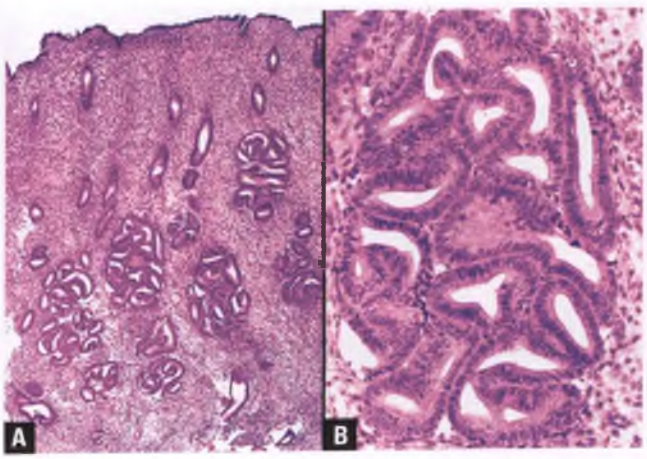

FIGURE 4.103. **A,B**: Dissociation artifact. In this less traumatized example, clusters of collapsed proliferative endometrial glands simulate islands of endometrial hyperplasia. An architectural pattern such as this would be most unusual for true hyperplasia, which is typically either unifocal or diffuse.

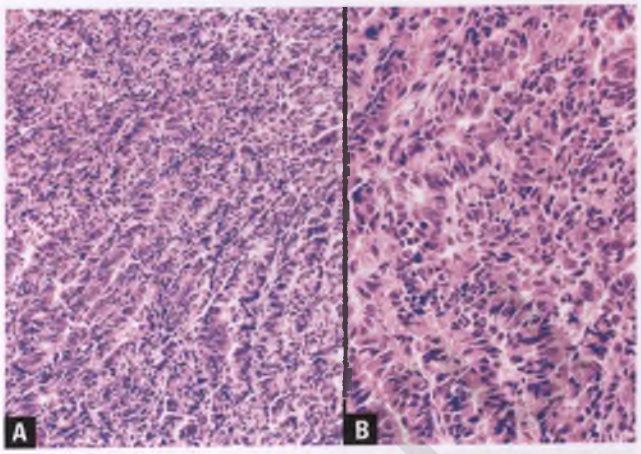

FIGURE 4.105. **A,B**: Grade 1 endometrioid carcinoma with autolysis-related artifact. The collapse of the neoplastic glands, coupled with the sloughing of their epithelial lining, results in a solid-appearing lesion that can be misinterpreted as a grade 3 endometrioid carcinoma. Note the partial preservation of the gland architecture and the low-grade nuclear features.

facilitated by the partially preserved outlines of the glands, the usual low-grade nuclear features of the neoplastic cells (which would be unusual for areas with nonsquamous solid differentiation), and the presence of retraction artifact elsewhere in the tissue where glands are embedded in ample amounts of stroma. This artifact is much more likely to be found in hysterectomy specimens than in endometrial samples, since the latter are routinely placed in fixative, whereas a late-afternoon hysterectomy specimen may be inadvertently left overnight on the gross room counter in an unfixed state or arrive from a distant location with inadequate fixation. When autolysis-related artifacts are encountered in uteri, it is also helpful to compare the histologic features of the hysterectomy specimen with that of any recent endometrial samples.

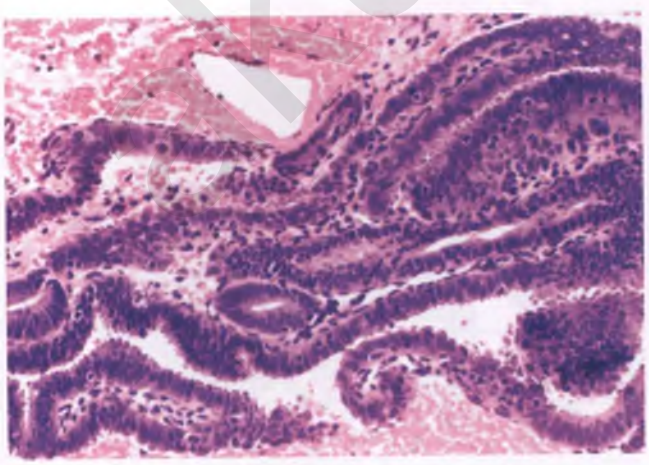

FIGURE 4.104. Coiling artifact. The section of this winding aggregate of endometrial surface epithelium results in a crowded appearance that simulates endometrial hyperplasia.

Pseudolipomatosis/Bubble ("Swiss Cheese") Artifact

Gas bubbles generated during application of suction when obtaining an endometrial sample can become embedded within endometrial stroma or loosely clotted blood. Histologic sections of tissue and blood obtained in this fashion can result in what is referred to as pseudolipomatosis or bubble ("Swiss cheese") artifact (Fig. 4.106). Although this phenomenon has been recognized for many years,[38] it has only recently been systematically studied and reported in the literature.[86]

Pseudolipomatosis may also occur in tissue removed during a hysteroscopic procedure.[87] In this situation,

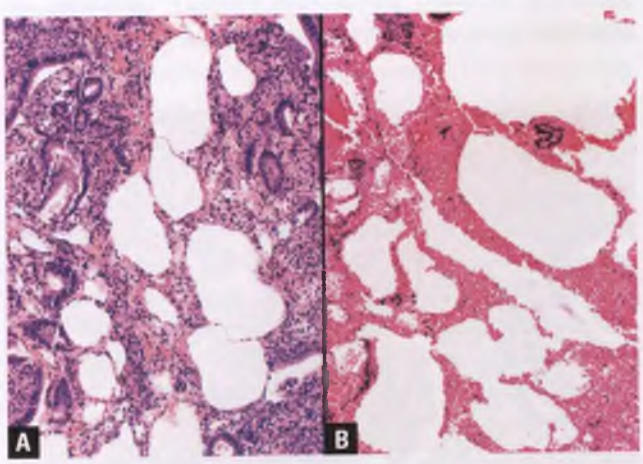

FIGURE 4.106. Pseudolipomatosis. **A**: Involvement of endometrial stroma. **B**: Involvement of clotted blood. The misinterpretation of this artifact as adipose tissue will result in the incorrect assumption that the endometrial sampling procedure was complicated by a uterine perforation.

pseudolipomatosis may be produced by exposure to pressurized gas or, as recently demonstrated for colonic pseudolipomatosis, as a consequence of exposure to instruments tainted with the disinfectant hydrogen peroxide.[87,88]

Whatever its cause, it is important to distinguish pseudolipomatosis from adipose tissue, since the finding of adipose tissue in an endometrial sample is presumptive evidence of a uterine perforation if tissue contamination from another specimen can be excluded. In contrast to pseudolipomatosis, adipose tissue is much more uniform in the size and spherical shape of the clear spaces that it produces in histologic sections, its vacuoles do not exceed 120 μm in diameter, it typically demonstrates S100 immunoreactivity, its constituent cells contain identifiable ellipsoidal adipocyte nuclei rimming the periphery of their lipid droplets, and there may be associated mesothelium.[86,87]

An extraordinarily rare entity in the differential diagnosis with pseudolipomatosis is the incidental finding of endometrial pneumatosis (so-called pneumopolycystic endometritis), which is distinguished by preoperative radiologic findings consistent with gas-filled endometrial cysts that are found histologically to have occasional histiocytes rimming their periphery.[89] There will also be an absence of cystic spaces within fragments of clotted blood in endometrial pneumatosis, except in the unlikely circumstance of coexistent pseudolipomatosis.

Telescoping Artifact

This common artifact, which results from cross-sectioning of intussuscepted glands recoiling from the trauma of the sampling procedure, creates the impression of glands within the lumens of other glands (Fig. 4.107). It tends to occur in straight glands, which may be of either proliferative or secretory type. This phenomenon is of no clinical significance, and should not be confused with endometrial hyperplasia.

Bridging Artifact

Sectioning of coiled glands with papillary infoldings can create the appearance of epithelial bridges (Fig. 4.108). If this phenomenon occurs within an aggregate of hyperplastic glands in a repetitive manner, it can mimic a cribriform pattern and be misinterpreted as evidence in favor of adenocarcinoma. This artifact should be expected whenever prominent papillary infoldings are present that approach the size of the luminal diameter of the glands.

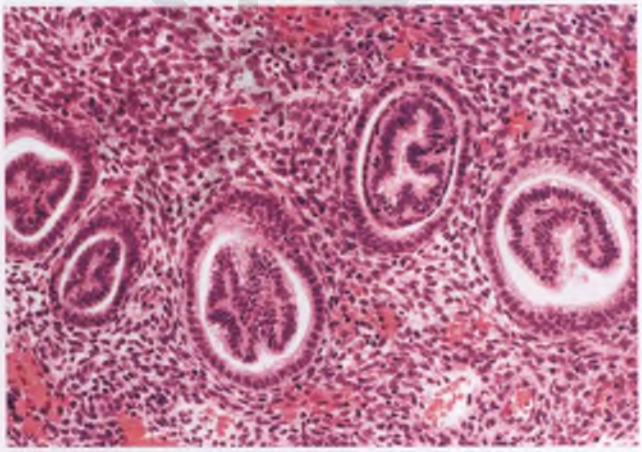

FIGURE 4.107. Telescoping artifact. The gland-in-gland appearance is an artifact of endometrial sampling.

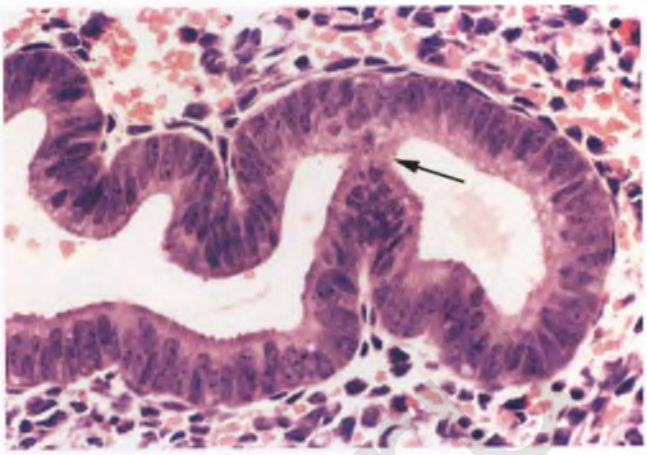

FIGURE 4.108. Bridging artifact. Sectioning of this late proliferative gland with papillary infoldings has resulted in an artifactual epithelial bridge (*arrow*). When this phenomenon occurs repeatedly within a hyperplastic endometrial proliferation, it can be misinterpreted as a cribriform pattern.

Tangential Sectioning

Tangential sectioning of randomly oriented fragments of endometrium can create the appearance of increased architectural complexity or result in structures that simulate cysts or polyps. It is very common for some endometrial glands to be tangentially cut, which creates the false impression of increased nuclear stratification (Fig. 4.109). Superficial sections parallel

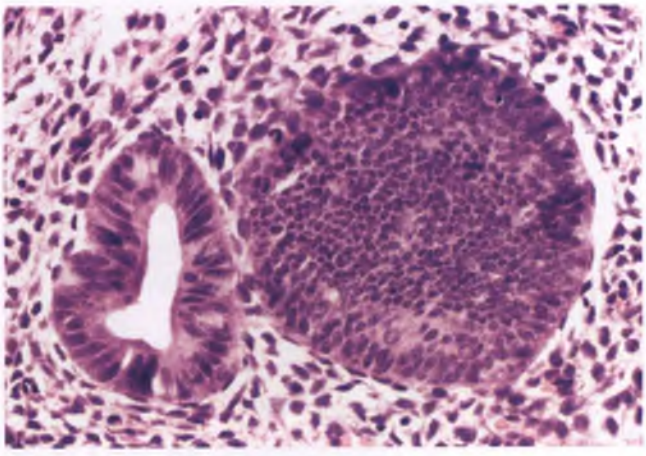

FIGURE 4.109. Tangential sectioning has resulted in the false impression of marked nuclear stratification in the gland at right. Compare this appearance with the properly oriented proliferative gland at left.

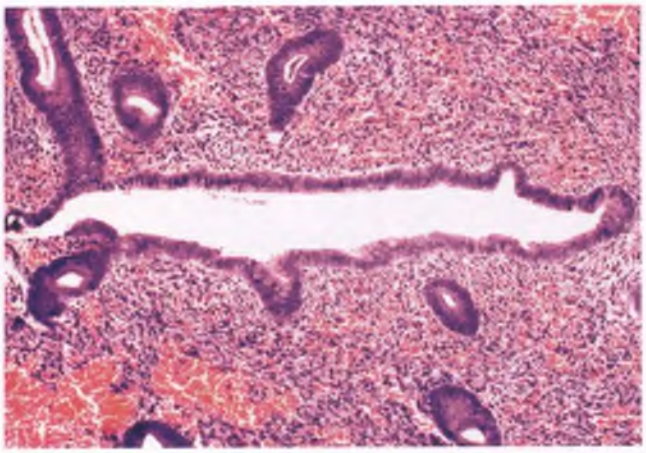

FIGURE 4.110. This apparently cystic space actually represents a dip in the endometrial lining that has been sectioned parallel to and just beneath the surface. Although not readily apparent at this magnification, many of the cells lining the surface epithelium (the pseudocyst) have apical blebs or cilia, whereas the neighboring glands are of the normal proliferative type.

to an indentation in an undulating endometrial surface can result in the formation of a pseudocystic space (Fig. 4.110), whereas a similarly maloriented section through an elevated portion of endometrium generates a piece of endometrium that is circumferentially rimmed by surface epithelium that can be mistaken for an endometrial polyp (Fig. 4.111). As discussed in the section on the differential diagnosis of endometrial hyperplasia, glands within the basalis are often normally crowded, and tangential sections through this area can accentuate the resemblance to a hyperplastic process.

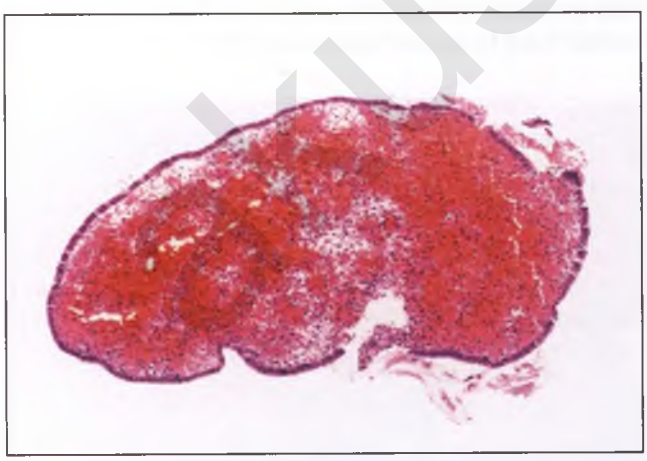

FIGURE 4.111. This polypoid fragment of normal endometrium, whose stroma is dominated by biopsy-related hemorrhage, is the product of sectioning parallel to the endometrial surface near the tip of an elevated portion of endometrium. Although polypoid in appearance and surrounded by epithelium, this tissue fragment should not be interpreted as an endometrial polyp.

Vascular Pseudoinvasion and Other Artifacts Related to Utilization of a Uterine Manipulator during Total Laparoscopic Hysterectomy

Total laparoscopic hysterectomy, which is a procedure that is distinct from laparoscopic-assisted vaginal hysterectomy, utilizes a uterine manipulator and positive intrauterine pressure. Caution should be exercised when diagnosing angiolymphatic invasion in low-risk endometrial carcinomas that have been removed with this technique, since intravascular tumor in most of these cases represents artifactual mechanical transport into vascular spaces rather than true vascular involvement.[90–92] This type of vascular pseudoinvasion, which in one study was associated with total laparoscopic hysterectomies of polypoid tumors,[91] should be suspected when (a) vascular involvement is restricted to large vessels, (b) apparent widespread vascular invasion is present in a grade 1 tumor that is confined to the uterus, (c) tumor is found within artifactual clefts in addition to vascular spaces, (d) tumor does not adhere to vessel walls and is not admixed with fibrin, and (e) intravascular tumor is associated with stromal tissue.[90,91] In addition to vascular pseudoinvasion and endomyometrial cleft artifact, the use of a uterine manipulator is associated with disruption of the endometrial lining, nuclear crush artifact, displacement of tumor into the tubal lumens, and, in some series, an increased incidence of malignant cells within peritoneal washings.[92] The potential clinical significance of these findings has yet to be determined.

ENDOMETRIAL EPITHELIAL METAPLASIAS AND RELATED ALTERATIONS

Endometrial epithelium can undergo a variety of nonneoplastic alterations that are collectively loosely referred to as metaplasias.[93] Since most of these lesions do not fit the strict definition of a metaplastic process, many investigators prefer the use of the less restrictive term "change." Some metaplasias and related processes have overlapping features, and it is common to see more than one type of metaplasia within a given sample. These lesions may occur in polyps or be seen in association with ordinary, hyperplastic, or malignant endometrial proliferations. In many cases, the altered differentiation results in an appearance that does not raise any concern for a clinically significant lesion. In other situations, reactive nuclear atypia can result in a resemblance to a premalignant process. Yet another subset of these lesions features metaplastic glandular proliferations with varying degrees of architectural complexity, some of which can be difficult to distinguish from carcinoma. These "metaplastic hyperplasias" are discussed separately in the section on endometrial hyperplasia.

Morular/Squamous Metaplasia

The most common form of endometrial squamous metaplasia is morular metaplasia, which is named for its berry-like appearance (morule = Latin for mulberry). Morular metaplasia is characterized by nests of epithelial cells with round,

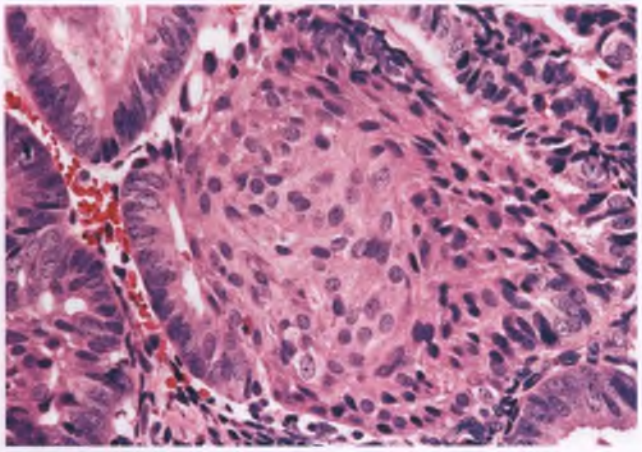

FIGURE 4.112. Squamous morule associated with endometrial hyperplasia.

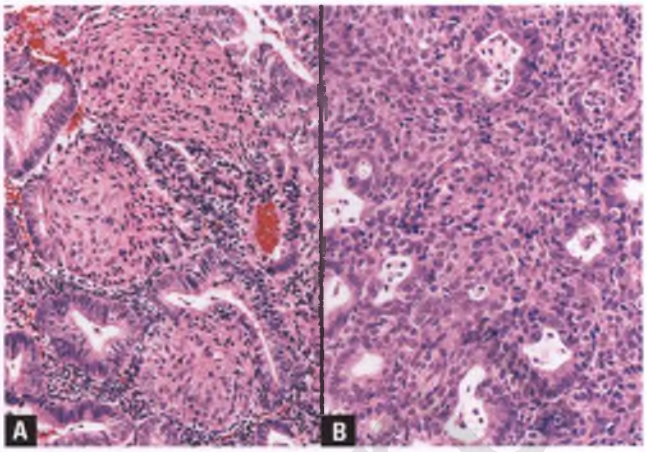

FIGURE 4.114. Morular metaplasia associated with endometrial hyperplasia. **A**: Typical pattern with three discrete morules. **B**: Less common pattern with morular metaplastic cells blending with hyperplastic glands and occupying the interglandular spaces.

oval, or spindle-shaped nuclei and indistinct cell borders that are usually in continuity with the lining of endometrial glands (Fig. 4.112).[93] These glands are often part of a proliferative lesion that ranges from endometrial hyperplasia to well-differentiated adenocarcinoma.

Morules represent an immature form of squamous differentiation that lack keratinization, abundant eosinophilic cytoplasm, and recognizable intercellular bridges.[93] They are composed of mitotically inactive cells with bland nuclear features. When morules occupy a central gland lumen, a wreath of punched-out spaces can be formed along the junction where morular and glandular epithelium converge that should not be mistaken for the cribriform architecture of an adenocarcinoma (Fig. 4.113). Although most morules are discrete structures, they can occasionally exhibit a more meandering and/or confluent architectural pattern (Fig. 4.114). As morules enlarge and impinge upon one another, they can create an alarming low-magnification appearance, particularly when there is associated central necrosis (Fig. 4.115). Other than the potential for these findings to be misinterpreted as evidence of carcinoma, morular enlargement, crowding, confluence, and central necrosis are of no pathologic significance. When evaluating the malignant potential of an endometrial sample with morules, it is the nature of the glandular component that determines whether the process is hyperplasia, carcinoma, or the occasional case of morular metaplasia within normal or disordered proliferative endometrium.

More mature forms of squamous metaplasia with keratinization, abundant eosinophilic cytoplasm, and intercellular bridges also occur within the endometrium (Fig. 4.116), and morules may be seen merging with such foci.[93] A rare form of squamous metaplasia, termed ichthyosis uteri, is associated with pyometra and features extensive replacement of the endometrial lining by mature squamous epithelium.

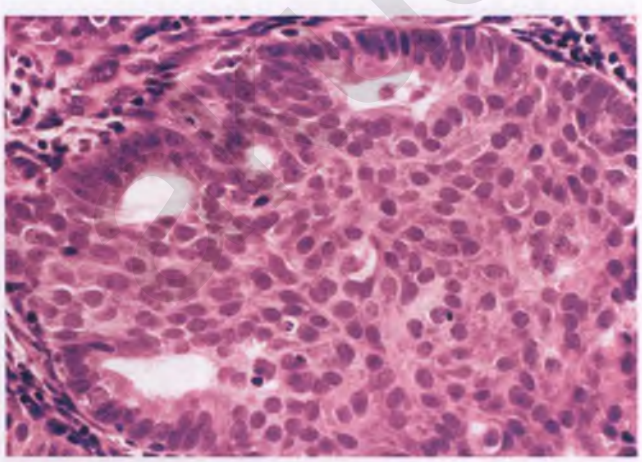

FIGURE 4.113. Morular metaplasia. Note the formation of a peripheral rim of punched-out spaces where glandular and morular epithelium converge. This common phenomenon should not be confused with the cribriform pattern that may be seen in endometrial adenocarcinoma.

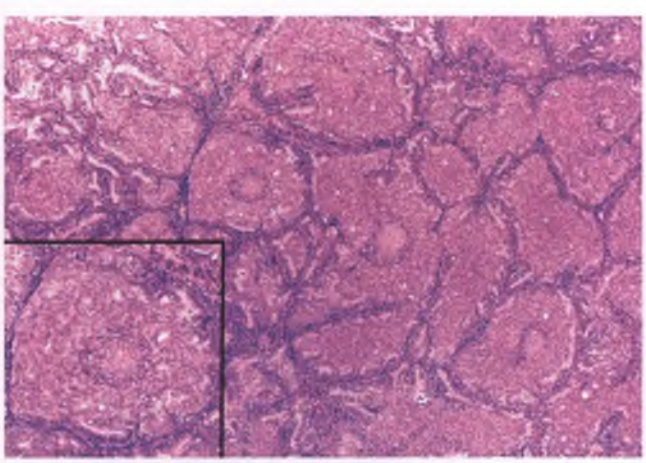

FIGURE 4.115. Florid morular metaplasia associated with endometrial hyperplasia. Four of the nearly back-to-back morules exhibit central necrosis, one of which is shown at higher magnification in the inset.

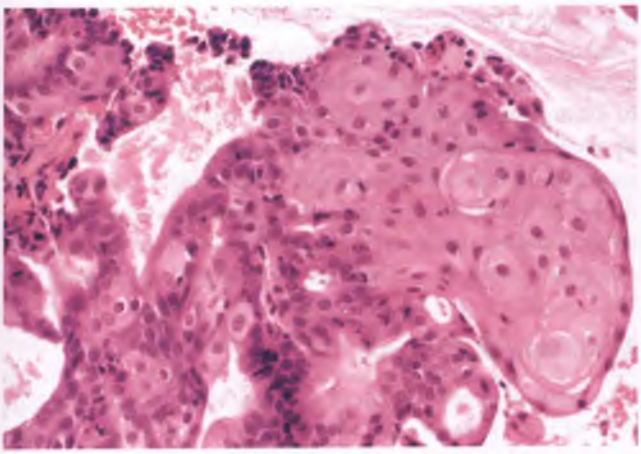

FIGURE 4.116. Mature form of squamous metaplasia (right) associated with endometrial hyperplasia.

Granulomas are sometimes confused with squamous morules, but the former are distinguished by their association with at least occasional multinucleated giant cells and a surrounding lymphocytic infiltrate of variable prominence. Moreover, morules are typically found in the setting of endometrial hyperplasia or well-differentiated adenocarcinoma, whereas granulomatous inflammation is rarely associated with a hyperplastic/malignant endometrial glandular lesion other than keratin-induced granulomas in adenocarcinomas with squamous differentiation. Although rarely necessary, cytokeratin immunohistochemistry could be utilized to discriminate between these two processes (cytokeratin positive → morules; cytokeratin negative → granulomas).

Papillary Syncytial Change

PSC was originally described as papillary (syncytial) metaplasia, and is now also referred to as surface syncytial change or eosinophilic syncytial change.[93–96] PSC features epithelial cells with eosinophilic cytoplasm and indistinct cell borders that aggregate on the endometrial surface, often forming small papillary structures without fibrovascular cores (Fig. 4.117). PSC is primarily a surface phenomenon, and only rarely extends into superficial endometrial glands. It is a commonly encountered lesion that is characteristically associated with nonphysiologic endometrial breakdown (Fig. 4.118), and is only infrequently found in menstrual endometrium.[94] PSC may also be seen on the surface of infarcted endometrial polyps (Fig. 4.119). Small aggregates of neutrophils, sometimes located within microcystic spaces, are often associated with this process. The cells of PSC are generally bland and may exhibit a squamoid appearance, although reactive nuclear atypia and hobnail patterns are seen occasionally (Fig. 4.120).

PSC has been found to have a very low Ki-67 proliferative index (mean of 1.3%), which is supportive evidence of the

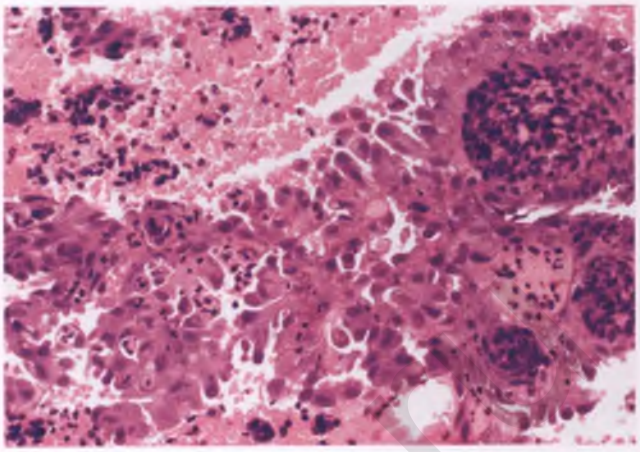

FIGURE 4.118. Papillary syncytial change. Note the intermingled neutrophils, some hobnailing, and the associated rounded aggregates of endometrial stroma with features of breakdown.

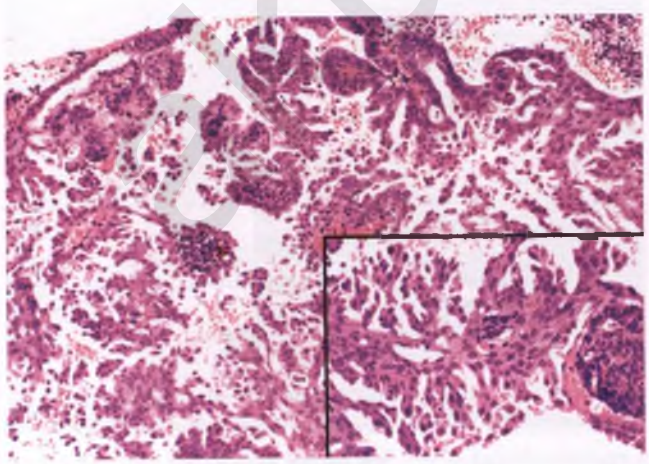

FIGURE 4.117. Florid example of PSC. The inset highlights the bland nuclear features and its association with condensed, rounded aggregates of crumbling endometrial stroma.

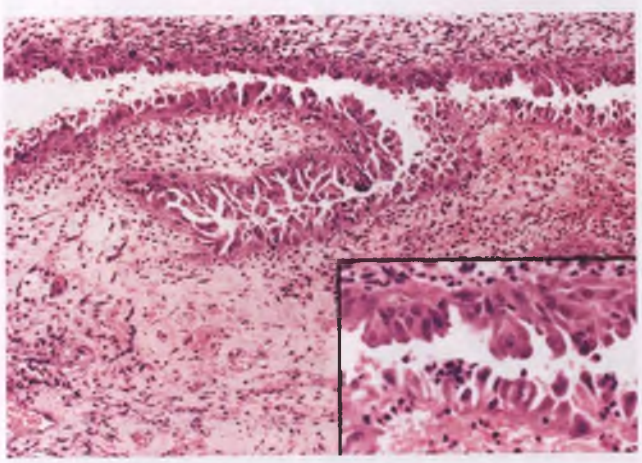

FIGURE 4.119. Partially infarcted endometrial polyp with PSC. Inset: Portions of this process have a squamoid appearance, and hobnail cells are evident.

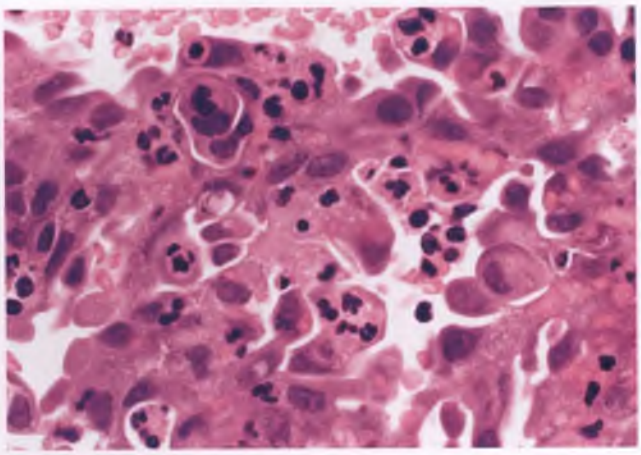

FIGURE 4.120. Papillary syncytial change with reactive epithelial atypia.

postulate that this lesion represents a regressive process related to stromal collapse with ensuing coalescence of associated surface epithelium rather than an actively proliferating, regenerative phenomenon.[96] PSC with superimposed reactive atypia can simulate endometrial intraepithelial carcinoma (EIC), and florid examples need to be distinguished from serous carcinoma. The strong association of PSC with nonphysiologic endometrial breakdown or ischemically damaged endometrial tissue facilitates distinction of this lesion from EIC/serous carcinoma, as does the less impressive degree of nuclear atypia, the absence or scarcity of mitotic activity without atypical division figures, and a low Ki-67 proliferative index. In addition, this phenomenon can be distinguished from EIC/serous carcinoma by its expected lack of diffuse and strong immunoreactivity for p53, although the p53 results should be interpreted within the context of all of the clinical and pathologic findings.

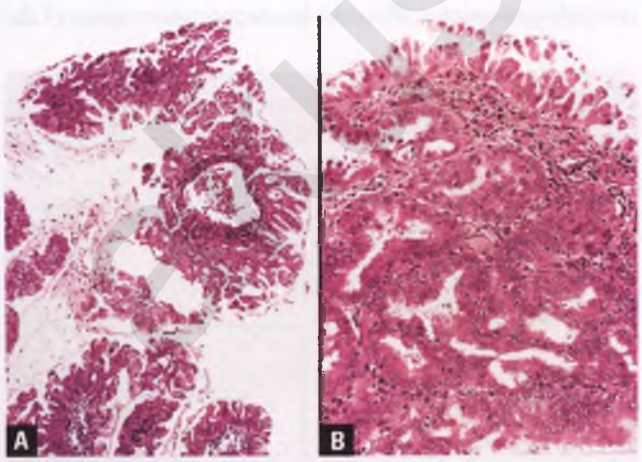

FIGURE 4.121. Surface epithelial alteration simulating PSC in a patient with an underlying grade 1 endometrioid adenocarcinoma. **A**: Fragments of surface of tumor that resemble PSC. **B**: Surface papillary syncytial-like change (top) in close proximity to the adenocarcinoma, which was myoinvasive.

Scant, superficial samples of endometrial tissue in which a diagnosis of PSC is being considered, especially in the setting of a postmenopausal woman whose tissue does not show evidence of stromal breakdown, should be viewed with suspicion in light of the known tendency for some grade 1 to 2 endometrioid carcinomas to be associated with such surface changes (Fig. 4.121).[97] In this situation, clinical correlation with consideration for repeat curettage is suggested if careful examination of multiple sections fails to disclose an associated carcinoma.

Mucinous Metaplasia

Mucinous metaplasia refers to the replacement of all or a portion of one or more endometrial glands and/or part of the surface epithelium by columnar, mucin-rich, endocervical-like epithelium.[93] Intestinal metaplasia with recognizable goblet cells is an extraordinarily rare variant of mucinous metaplasia.[98] Although cytologically bland mucinous metaplastic changes occurring within a setting of minimal architectural abnormalities such as occasional intraluminal papillary tufts can comfortably be regarded as benign (Fig. 4.122), lesions with similar nuclear features that exhibit complex microacinar or papillary formations are associated with a significant risk of low-grade adenocarcinoma and should be managed as a form of atypical hyperplasia (see section on metaplastic hyperplasia).[99,100]

Ciliated Cell Change (Ciliated Metaplasia)

Since occasional ciliated cells are a component of the surface lining of the endometrium and some proliferative phase glands, the diagnosis of ciliated cell change is reserved for cases in which altered benign glands are dominated by ciliated epithelium (Fig.

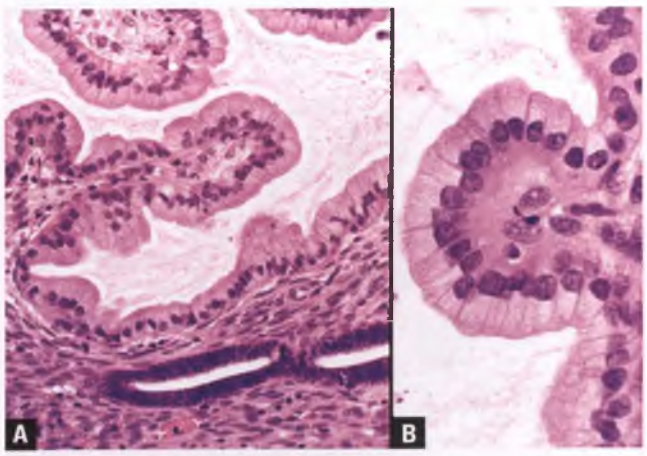

FIGURE 4.122. Mucinous metaplasia. **A**: The altered gland shows mild architectural changes, with a few simple papillae projecting into a cystically dilated lumen. Two weakly proliferative glands are present beneath the metaplastic gland. **B**: This high-magnification view demonstrates the bland nuclear features and abundant mucinous cytoplasm of the metaplastic epithelium.

4.123).[93] The nuclei of ciliated cells are typically round and slightly larger than conventional endometrial epithelial cells. The cytoplasm is usually eosinophilic, except for a distinctive rim of perinuclear clearing that is often present in a subset of these cells. There is commonly an alignment of the terminal bars of the ciliated cells that creates the appearance of a cuticle along the luminal border.[93] All of these features help to distinguish true ciliated cells from cells to which intraluminal threadlike secretions have been loosely attached. Some abnormalities in gland architecture and mild degrees of nuclear atypia are common findings in ciliated cell change. However, once the altered glands exhibit hyperplastic features over a span of ≥1 mm, they should be flagged as a metaplastic hyperplasia (see below).

Eosinophilic Cell Change

Eosinophilic cell change is characterized by the presence of endometrial glands that are partially to completely lined by nonciliated, nonstratified cells with abundant eosinophilic cytoplasm (Fig. 4.124).[93] Nuclei are generally round, uniform, centrally placed, and mitotically inactive. Since cytoplasmic eosinophilia can be seen across the full spectrum of benign, hyperplastic, and malignant endometrial glandular processes, attention to the nuclear and architectural features both within and away from the areas of altered differentiation is necessary for proper classification. Eosinophilic cell change is commonly seen in the glands of endometrial hyperplasias and well-differentiated carcinomas that have been treated with progestins[101] (see section on endometrial hyperplasia).

Clear Cell Change

Clear cell change refers to the uncommon finding of benign endometrial glands that are lined by cells with abundant clear cytoplasm (Fig. 4.125).[93] This phenomenon may be idiopathic

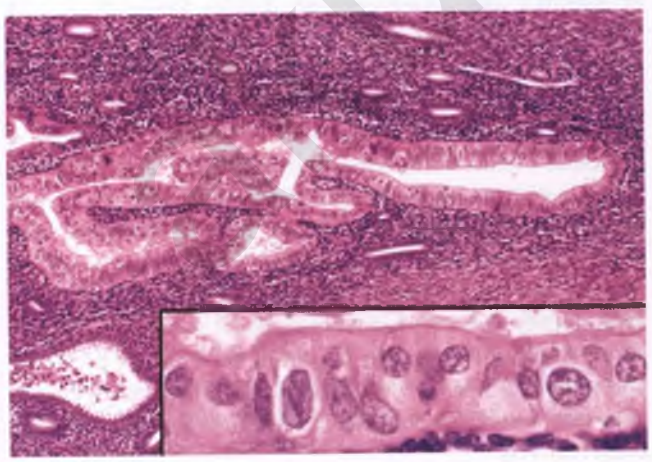

FIGURE 4.123. Ciliated cell change in a small focus of glands within the basalis endometrium. The inset highlights the bland nuclear features, occasional perinuclear halos, and tufts of luminal cilia with their associated terminal bars.

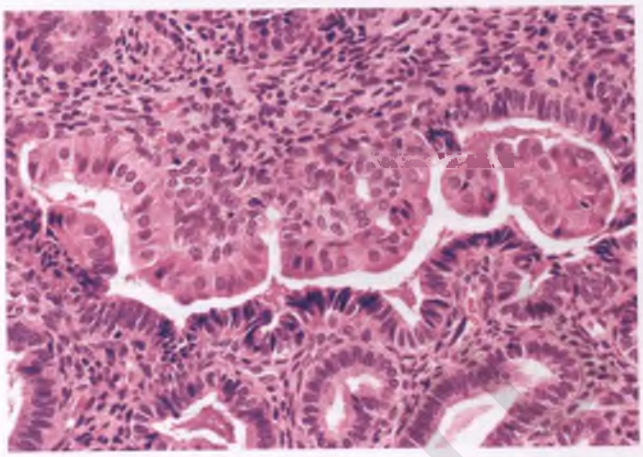

FIGURE 4.124. Eosinophilic cell change involving a portion of an endometrial gland. Note that the cells that exhibit cytoplasmic eosinophilia have round, bland, centrally placed nuclei.

or associated with pregnancy, and generally represents a focal finding that involves a small cluster of glands. The cytoplasmic clearing is usually due to the presence of glycogen. The bland nuclear features, absence of mitotic activity, microscopic size, and lack of stromal invasion distinguish this incidental finding from clear cell carcinoma. In pregnant patients, the absence of striking nuclear atypia allows for the distinction of clear cell change from the Arias-Stella reaction.

Postcurettage Regenerative Atypia

Following endometrial curettage, the reepithelialization of the denuded endometrial surface can result in formation of a

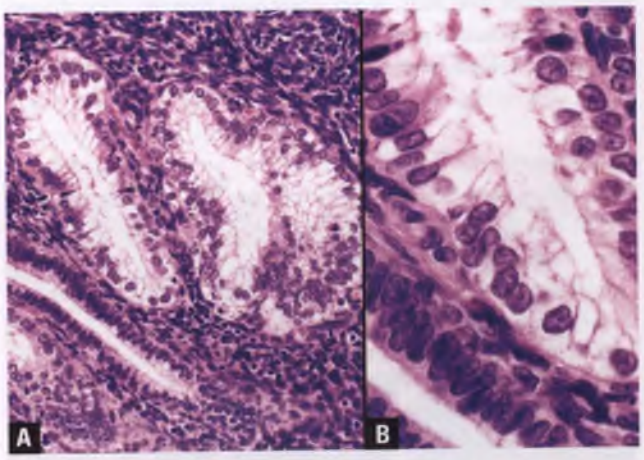

FIGURE 4.125. Clear cell change. **A**: A small cluster of benign endometrial glands is lined by cells with abundant clear cytoplasm. The right half of the altered gland on the right has been tangentially sectioned, creating the false impression of nuclear stratification. **B**: The nuclei of the cells lining the altered glands are bland and mitotically inactive. Compare the nuclear and cytoplasmic features with the weakly proliferative gland at lower left.

jumbled, variably stratified epithelial lining whose constituent cells may exhibit nuclear enlargement, nuclear hyperchromasia, prominent nucleoli, and hobnail formations (Fig. 4.126). The resulting histology can simulate EIC (see section on serous carcinoma). The clinical history of an endometrial curettage in the weeks preceding an endometrial sample that contains worrisome cells lining the surface epithelium and superficial glands can assist in the recognition of postcurettage regenerative atypia. In addition, this phenomenon can be distinguished from EIC by its inconspicuous mitotic activity, absence of atypical mitoses, and expected lack of diffuse and strong immunoreactivity for p53, although the p53 results should be interpreted within the context of all of the clinical and pathologic findings.

Hobnail Cell Change

Hobnail morphology is a reference to the shape of hobnails used in boot repair. A hobnail cell has a slender cytoplasmic stalk at its base and a bulbous apex that harbors a protruding nucleus. Most examples of hobnail cell change affect the endometrial surface and are related to postcurettage regenerative atypia (Fig. 4.126), infarction of an endometrial polyp (Fig. 4.119), or nonphysiologic surface ischemic damage (Fig. 4.127). As illustrated by the example shown occurring in a partially infarcted polyp, some of these lesions can be considered to be within the spectrum of PSC.

The presence of hobnail cells in an architecturally complex glandular lesion outside of the setting of the Arias-Stella reaction should be viewed as a potentially ominous sign, as exemplified by the oxyphilic clear cell carcinoma illustrated in Figure 4.241. The Arias-Stella reaction is distinguished from hobnail cell change by its usual association with a stromal decidual reaction and/or hypersecretory glands in a patient who is either pregnant or on hormonal therapy. The discussions on PSC and postcurettage regenerative atypia address the distinction of these lesions from EIC; this discussion is applicable to hobnail cell change as well. The clinical setting, presentation as a surface-based microscopic finding rather than an architecturally complex mass lesion, lack of marked nuclear atypia, absent to inconspicuous mitotic activity, and absence of stromal invasion help to distinguish hobnail cell change from clear cell carcinoma.

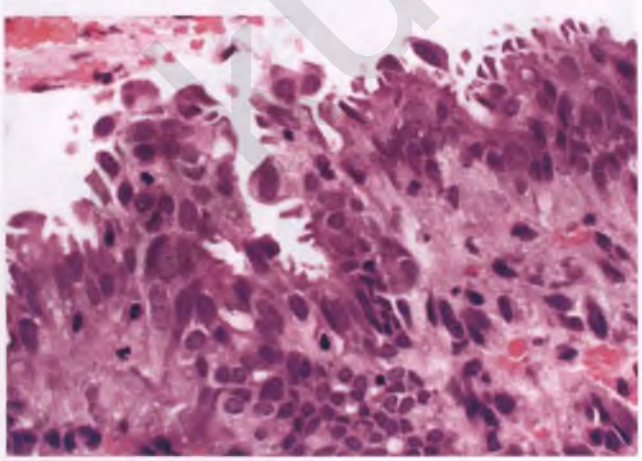

FIGURE 4.126. Postcurettage regenerative atypia of the epithelium lining the endometrial surface.

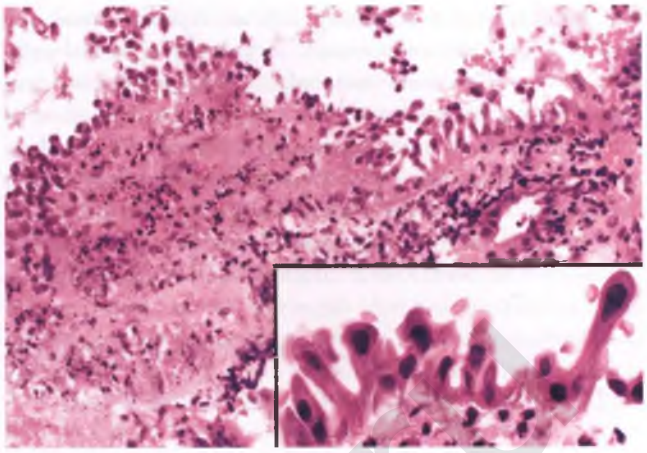

FIGURE 4.127. Hobnail cell change associated with surface necrosis of the endometrium.

ENDOMETRIAL HYPERPLASIA

Terminology

The most widely used and accepted classification system for endometrial hyperplasia is the one recommended by the World Health Organization (WHO) and International Society of Gynecologic Pathologists (ISGP) that dates back to 1994.[102] This system is based upon the pioneering work of Kurman and colleagues and divides hyperplasias into atypical and nonatypical forms according to the presence or absence of cytologic (nuclear) atypia of the epithelial cells lining the glands.[103] These hyperplasias are further subclassified as simple or complex according to the degree of glandular architectural complexity. Although four different diagnoses are possible (simple hyperplasia without atypia, complex hyperplasia without atypia, simple hyperplasia with atypia, and complex hyperplasia with atypia), it is the determination of whether or not the proliferation is considered cytologically atypical that drives clinical management decisions. Atypical hyperplasia is considered a cancer precursor and is usually treated with hysterectomy, whereas hyperplasia without atypia is considered self-limited and is managed conservatively.

As discussed below, the WHO/ISGP classification system has significant limitations, which have spawned alternative approaches. The most viable competing classification system employs the "endometrial intraepithelial neoplasia"

(EIN) nomenclature. Whereas the WHO/ISGP system emphasizes the importance of nuclear atypia, the EIN system places its emphasis upon abnormalities in glandular architecture. The objective of the EIN system is to separate those endometrial hyperplasias that are solely related to the proliferative effects of unopposed estrogen from those that have undergone additional alterations and progressed to a monoclonal, premalignant state (EIN). While approximately 50% to 65% of examples of EIN correspond to cases of atypical hyperplasia, 45% to 60% of cases considered by either the EIN investigators or other experienced gynecologic pathologists to represent complex hyperplasia without atypia and 5% to 10% of simple hyperplasias without atypia combine to form the remainder of EIN diagnoses.[104,105] Although the EIN classification system has its loyal advocates, it also has its own set of limitations (see below). My approach to this difficult, subjective, and controversial area is to retain the hyperplasia/atypical hyperplasia terminology, but to incorporate many of the concepts of EIN and some other recommendations by prominent gynecologic pathologists into a hybrid classification system, as discussed later in this section.

Defining Features and Limitations of WHO/ISGP Endometrial Hyperplasia

In order to use the WHO/ISGP classification system, one needs to understand (a) what is meant by the terms "simple" and "complex" as they are applied in the description of glandular architecture and (b) what constitutes cytologic atypia.

Simple architecture implies prominent glandular tubule formation with variable degrees of cystic dilatation, with outpouches and infoldings being absent, inconspicuous, or focal. In contrast, complex architecture features abnormal glandular configurations in which branching channels, irregular budding, papillary infoldings, and foci with back-to-back glands are commonplace. Simple and complex architectural patterns often coexist, and while easily separable at their extremes, there is considerable overlap between the upper end of simple architecture and the lower end of complex architecture. The subjective distinction between simple and complex architectural patterns has not been aided by their various and loose definitions. In their seminal article from 1985, Kurman and colleagues vaguely describe the architecture of simple hyperplasia as an increase in the number of glands resulting in crowding that ranges from mild to short of back-to-back, and glandular shapes that may be altered due to cystic dilatation or mild irregularities in outline.[103] In contrast, they describe complex hyperplasia as exhibiting back-to-back crowding of markedly complex glands with highly irregular outlines.[103] Presumably motivated by a desire for increased reproducibility in this separation, Dr. Kurman's definitions of simple and complex architecture have evolved over the years, such that he has recently advocated using solely the amount of stroma separating the glands to distinguish simple and complex forms of hyperplasia; in simple hyperplasia, the glands are separated by "abundant" or "considerable" stroma, whereas complex hyperplasia features glands that are more densely crowded and often back-to-back with only small amounts of intervening stroma.[30] Although there is no doubt that this approach reduces interobserver variability, it sacrifices the potential discriminating power of glandular complexity. Just as a villous adenoma with areas of cribriforming is at a much higher risk for the development of colonic adenocarcinoma than the architecturally simple tubular adenoma, endometrial lesions with increasing architectural complexity are associated with an increasing risk of myoinvasion[106,107] (see section on endometrioid adenocarcinoma). I agree with those who continue to distinguish simple from complex architectural patterns based upon the degree of contour abnormalities of the constituent glands as described at the beginning of this paragraph, despite the more subjective nature of this approach.

Although assignment of a given hyperplastic process to a simple versus complex category can be problematic, this descriptive feature is not what drives clinical management in this classification system. Instead, it is the assessment of cytologic (nuclear) atypia within a hyperplastic glandular proliferation that determines whether a diagnosis of atypical hyperplasia is rendered. Cytologic atypia is recognized by variable combinations of nuclear enlargement, loss of polarity, stratification, rounding, contour irregularities, prominent nucleoli, and chromatin abnormalities that are most often manifested as chromatin clearing.[103,108] In contrast, the nuclei in nonatypical hyperplasia are oval to elongate, oriented perpendicular to the basement membrane, pseudostratified, and have a more dense and uniform chromatin distribution with absent to inconspicuous nucleoli. Some investigators have attempted to grade the degree of cytologic atypia as mild, moderate, or severe, but these subdivisions are not reproducible, lose relevance in a biologic system in which some well-differentiated carcinomas exhibit less cytologic atypia than some examples of atypical hyperplasia, and have not been shown to further stratify risk of progression to carcinoma.[103]

There is a strong correlation between increasing architectural complexity and the likelihood that the proliferation will be designated an atypical hyperplasia, which results in simple hyperplasia without atypia and complex hyperplasia with atypia being significantly more common that simple hyperplasia with atypia and complex hyperplasia without atypia. Whether consciously or subconsciously, officially or unofficially, you know, I know, and the American people know that most pathologists use a "sliding scale" when making the subjective assessment of cytologic atypia, requiring only focal and mild atypia (of the smoke and mirrors, wave of a hand, kind that can't be photographed variety) for lesions with significant architectural complexity and more obvious and diffuse atypia for lesions with simple architecture. I think that this sliding scale is perfectly appropriate and should be brought out of the closet and recognized as an essential tool in the evaluation of endometrial hyperplasia, rather than following guidelines

that expect pathologists to assess cytologic atypia totally independent of glandular architecture (see section on hybrid classification of endometrial hyperplasia).

Determination of the presence or absence of cytologic atypia is subjective and poorly reproducible, which has a direct and adverse impact on the ability to reliably separate abnormal endometrial proliferations into the clinically relevant categories of atypical versus nonatypical hyperplasia.[109–114] Cytologic atypia is likely more reproducible and meaningful if it is not subtle and identified in most of the cells that line the hyperplastic glands.[30] Unfortunately, the WHO/ISGP system statically defines cytologic atypia without reference to an internal standard. I concur with those investigators who emphasize the importance of nuclear atypia *relative* to the nuclear features of nonhyperplastic endometrial glands elsewhere in the specimen.[115,116] It is not uncommon for normal proliferative glands to be lined by cells with "activated" nuclei that possess prominent nucleoli or other worrisome features (Fig. 4.128). Artifacts related to fixation and processing can also result in perceived nuclear abnormalities such as chromatin clearing. Whenever possible, a conscious comparison of the nuclear features of the potentially atypical glandular proliferation should be made to what passes for normal in a given sample, which will help to avoid the overdiagnosis of cytologic atypia. This exercise is particularly important when considering a diagnosis of simple atypical hyperplasia, which is a rare entity that upon review often represents an overcall of one of the mimics of hyperplasia, such as fragments of basalis or endometrial polyp with activated nuclei or nuclear changes related to fixation artifact. Since the diagnosis of simple atypical hyperplasia is fraught with difficulty and may result in hysterectomy, this diagnosis should be made with extreme caution and preferably only after consultation with an experienced gynecologic pathologist.

In addition to the problems of reproducibly distinguishing simple from complex hyperplastic proliferations and the static and subjectively applied definition of cytologic atypia, further limitations of the WHO/ISGP system include (a) many innocuous proliferations with a glands-to-stroma ratio of <2:1 that are related to anovulatory cycles that are more appropriately classified as disordered proliferative endometrium are diagnosed in this system as simple hyperplasia without atypia, (b) the extent of glandular crowding as expressed in terms of a minimal glands-to-stroma ratio required for a diagnosis of hyperplasia is not specified, and (c) there is no specified minimum lesional size, which increases the probability that an incidental metaplastic proliferation or a small focus of artifactually crowded glands will be misinterpreted as a hyperplastic process.

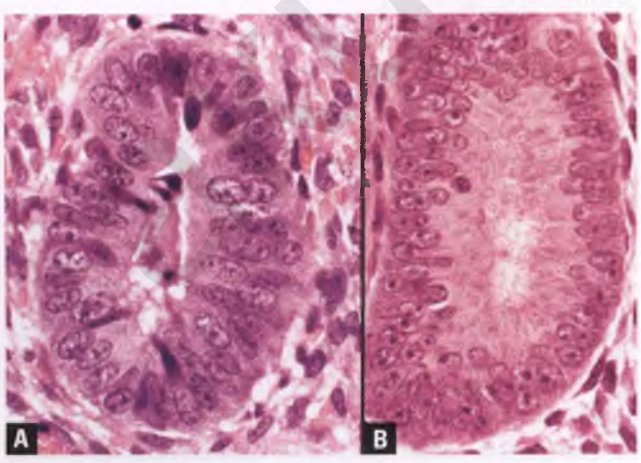

FIGURE 4.128. **A,B**: Proliferative endometrial glands with "activated" nuclei. Both of these examples were taken from architecturally unremarkable proliferative endometria, and the nuclear features depicted were present throughout all of the glands.

Defining Features and Limitations of EIN

Although rooted in computer-based morphometric measurements and molecular studies with microdissected tissues that have demonstrated monoclonality of lesions classified as EIN, its proponents have developed criteria to diagnose EIN lesions that can be applied to routinely stained and examined histologic sections.[115] The diagnostic features of EIN, all of which must be present, include (a) crowded glands with a glands-to-stroma ratio of >1:1 (areas of cystic atrophy and the dilated glands of disordered proliferation/simple hyperplasia are avoided in this assessment), (b) altered cytology ("cytologic demarcation") of the crowded glandular foci relative to the background endometrial epithelium, which may include either nuclear or cytoplasmic (metaplastic) changes (if no normal tissue is available for comparison, cytologic atypia of the type required in conventional atypical hyperplasia is necessary), and (c) the lesion size must be >1 mm within a single tissue fragment.[115] Mimics of EIN, such as artifactually crowded glands, disordered proliferative endometrium, secretory endometrium, basalis, endometrial polyps, PSC, and the more architecturally complex adenocarcinomas need to be excluded.[115] Note that the subjective assessment of EIN without the application of special equipment emphasizes glandular crowding without regard for the degree of glandular complexity, and is subject to the same criticism applied to those who rely solely on the extent of glandular crowding to separate simple from complex hyperplasia (see above).

A 2005 study by EIN proponents that used morphometry to diagnose EIN compared the risk of progression to adenocarcinoma of EIN to internally diagnosed WHO/ISGP equivalents, and found a relative risk for EIN of 45 (EIN vs. non-EIN hyperplasias) versus a relative risk of only 7 for atypical hyperplasia as compared to hyperplasias without atypia.[117] However, a subsequent, more rigorous joint study by pathologists with expertise in using the WHO/ISGP system and EIN proponents who rendered EIN diagnoses solely on the basis of histology found relative risks for EIN and atypical hyperplasia of 7.8 and 9.2, respectively.[105] This same study demonstrated that although EIN has a higher sensitivity than atypical hyperplasia in its ability to predict progression to adenocarcinoma, this comes at the price of lower specificity.[105] The results of this study suggest that the EIN system is a comparable alternative to the WHO/ISGP system, but that claims of EIN's superiority in predicting disease progression are unwarranted. Furthermore, the utility and reproducibility of the EIN classification system

has not yet been tested with large numbers of cases with multiple pathologists of different backgrounds who have not been associated with or directly trained by its original proponents.

Another problem with EIN lies with the terminology itself, which leaves significant room for potential confusion with other lesions of endometrial glandular epithelium. Over the course of decades, pathologists and clinicians have been indoctrinated with the terms hyperplasia and atypical hyperplasia, and clinicians are comfortable making treatment decisions based upon this classification system. EIN, on the other hand, is relatively new terminology that is easily confused with the terms EIC and endometrial glandular dysplasia (EmGD), which refer to potential precursor lesions of serous carcinoma. I suspect that pathologists have difficulty keeping these terms straight, let alone clinicians. Like those who may have found a better way to rearrange the letters of the alphabet on a keyboard, EIN has a minority group of ardent supporters, but this terminology faces an uphill battle against tradition and inertia. The effort required to convert pathologists and clinicians to this terminology, with its attendant risks for confusion and inappropriate clinical management, should not be underestimated. Unless it can be shown to be vastly superior rather than merely comparable to the WHO/ISGP classification in the hands of community pathologists, the EIN system is unlikely to make significant inroads into the lexicon of pathologists and gynecologists beyond the circle of influence of its initial descriptors and their disciples.

Hybrid Classification of Endometrial Hyperplasia

I use a hybrid classification system that incorporates elements of the WHO/ISGP system, the EIN system, and recommendations from the Stanford group. Although this system has not been validated, it represents a logical amalgamation of what I interpret as the most desirable features of each system. Highlights of this hybrid classification system are outlined below:

- As advocated by the Stanford group, a glands-to-stoma ratio of >2:1 is required for a diagnosis of hyperplasia. When estimating this ratio, the space occupied by the gland lumens and villoglandular structures is included in the glandular compartment.[39]
- Endometrial hyperplasias do not include those processes whose glands are crowded but lined by atrophic or weakly proliferative epithelium, such as cystic atrophy.[39]
- To help avoid overdiagnosis of a few clustered glands as a hyperplastic process and to ensure that a sufficient number of altered glands are present for evaluation, the same size limitation that is used to diagnose EIN has been incorporated into this hybrid classification system; namely, that the hyperplastic focus must measure at least 1 mm in a single tissue fragment.[115] If a lesion is of lesser size, it can be descriptively diagnosed as a minute focus of nondiagnostic glandular crowding, with a recommendation for follow-up or rebiopsy.
- Cytologic (nuclear) atypia is evaluated on a "sliding scale" based on the degree of glandular architectural complexity. Architecturally complex lesions in which back-to-back glands with minimal or inapparent cytologic atypia are separated by threadlike wisps of stroma are designated "complex atypical hyperplasia (based on architecture)." The traditional nuclear features that define cytologic atypia are not required for this form of CAH. However, readily apparent cytologic atypia usually accompanies complex glandular proliferations, accounting for the conventional category of CAH. For moderately complex endometrial glandular proliferations with more appreciable amounts of intervening stroma, a moderate degree of cytologic atypia is necessary for a diagnosis of CAH. For lesions with simple architecture, obvious and diffuse atypia is necessary before the process is categorized as atypical. To summarize, the degree of cytologic atypia required for an "atypical" designation is inversely proportional to the degree of glandular architectural complexity.
- In lesions that would otherwise qualify as hyperplasia on the basis of an increased glands-to-stroma ratio, there is an upper limit for cytologic atypia, beyond which a diagnosis of malignancy is more appropriate.[106,107] Although most of these unusual cases with marked cytologic atypia represent endometrioid adenocarcinoma, other considerations include EIC with involvement of superficial glands and the glandular pattern of serous carcinoma. The degree of atypia that triggers a malignant diagnosis is depicted in discussions of these entities. In exceptionally rare circumstances, metastatic carcinoma may also produce this histologic appearance.
- Disordered proliferative endometrium is the term used for the lower end of the spectrum of what is termed simple hyperplasia without atypia in the WHO/ISGP system.[39] Disordered proliferative endometrium can have a glands-to-stroma ratio of up to 2:1, and is usually a diffuse rather than focal pattern.
- *Diagnostic categories of hyperplasia* (Figs. 4.129–4.136*)*:
  - Simple Hyperplasia without Atypia (exclude disordered proliferation)
  - Simple Atypical Hyperplasia (very rare; exclude mimics)

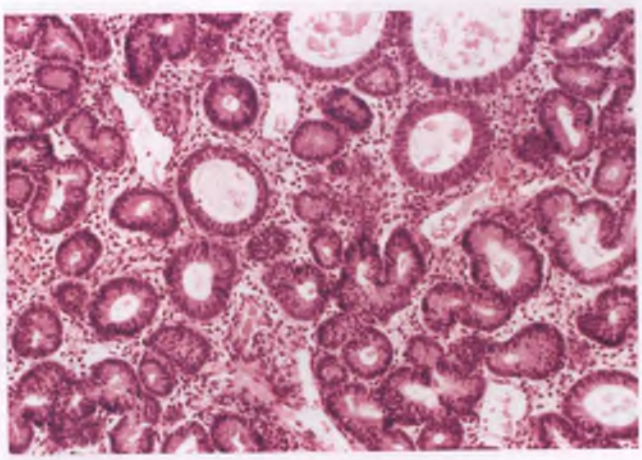

FIGURE 4.129. Simple hyperplasia without atypia. The glands are predominantly tubular, exhibit some cystic dilatation, and are lined by pseudostratified cells without nuclear atypia. There is ample stroma separating the glands, but the glands-to-stoma ratio exceeds 2 to 1.

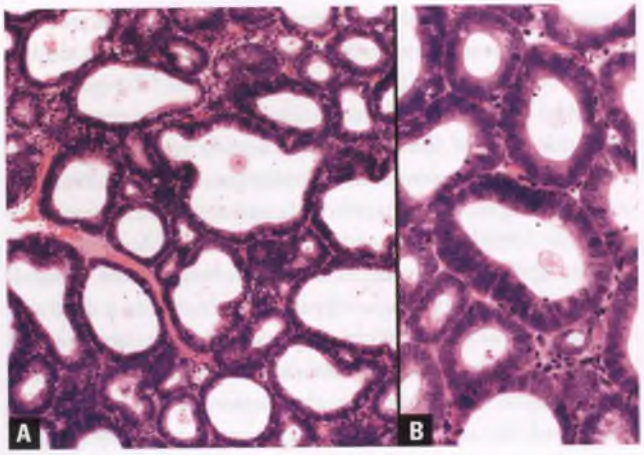

FIGURE 4.130. **A,B**: Simple hyperplasia without atypia. This example consists of closely packed tubular glands of varying caliber that lack cytologic atypia and demonstrate a simple rather than complex architectural pattern. Although many of the glands exhibit a back-to-back configuration, they are predominantly tubular-shaped and are enveloped by threadlike strands of stroma. Some pathologists would classify this lesion as complex hyperplasia without atypia on the basis of high gland density with scant intervening stroma.

- Complex Hyperplasia without Atypia (uncommon; exclude CAH)
- Complex Atypical Hyperplasia (based on architecture)
- Complex Atypical Hyperplasia (traditional WHO/ISGP version)

- Clinicians can continue to regard the various forms of hyperplasia dichotomously as either with or without atypia, but should be skeptical of a diagnosis of simple atypical hyperplasia and realize that sufficient outcome data for this rare lesion does not yet exist.

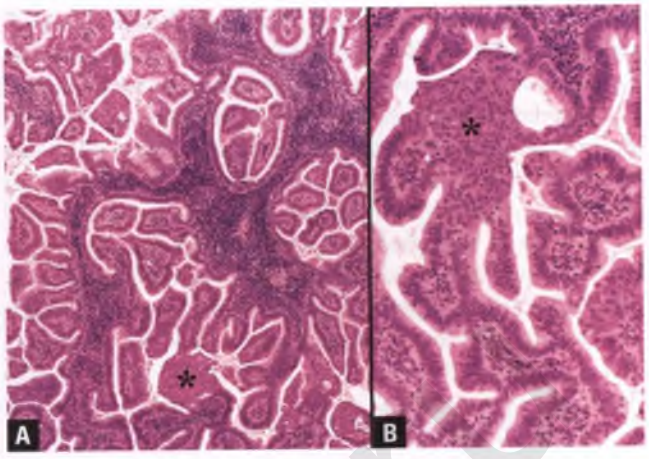

FIGURE 4.132. **A,B**: Complex hyperplasia without atypia. The macroglandular units of this hyperplastic proliferation are separated by variable amounts of stroma and contain internal papillary structures that lack second or third degree branching. Cytologic atypia is absent. A few squamous morules accompany this hyperplastic process (*asterisks*).

- Metaplastic hyperplasias are held to the same size requirements and are evaluated primarily by their degree of glandular crowding and architectural complexity (see below).

The Battleground: Classification of Complex Hyperplasia without Atypia

Approximately 80% of cases with a WHO/ISGP diagnosis of atypical hyperplasia translate into an actionable diagnosis in the EIN classification system of either EIN or well-differentiated adenocarcinoma, which is a reasonably good correlation.[104,105] However, complex hyperplasia without atypia is another story, with differences in categorization of this subjective lesion

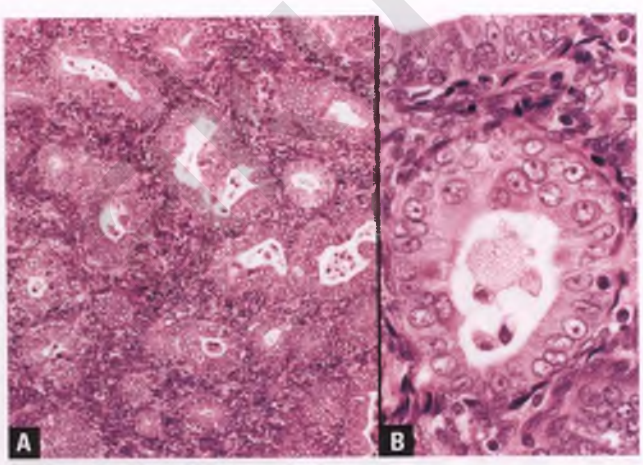

FIGURE 4.131. Simple atypical hyperplasia. **A**: The crowded glands have a predominantly tubular configuration. **B**: At high magnification, cytologic atypia is evident, as manifested by nuclear enlargement, nuclear rounding, chromatin clearing, and prominent nucleoli.

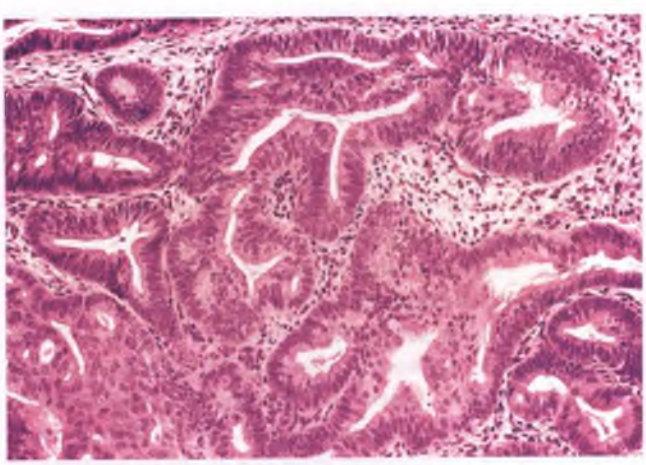

FIGURE 4.133. Complex hyperplasia without atypia. This complex glandular proliferation lacks cytologic atypia and the glands are surrounded by a moderate amount of stroma. A focus of morular metaplasia is present at lower left.

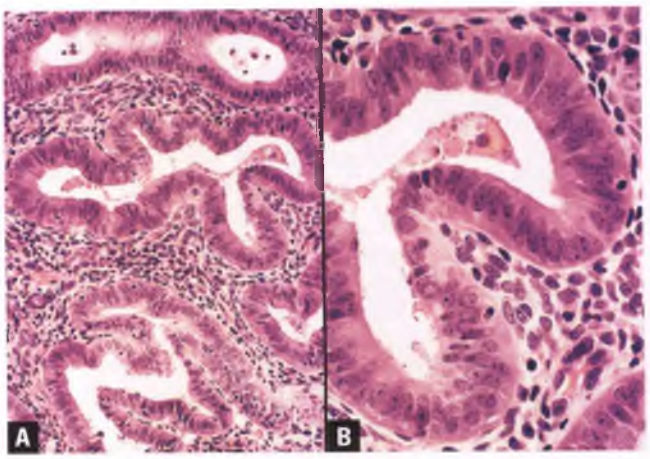

FIGURE 4.134. **A,B**: Complex hyperplasia without atypia. For this modest degree of glandular crowding, there is insufficient nuclear atypia to warrant a diagnosis of CAH.

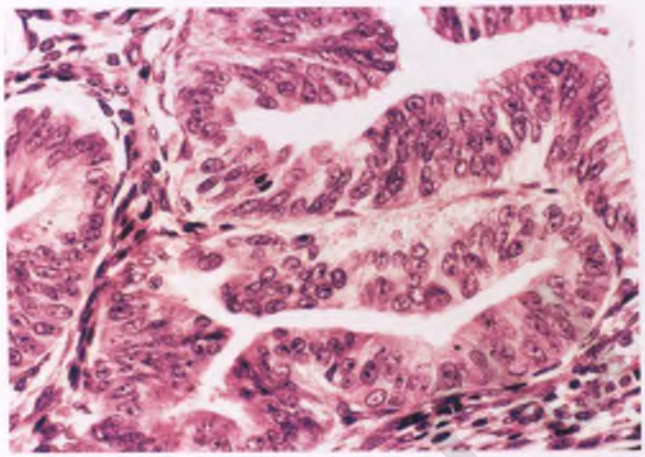

FIGURE 4.136. Complex atypical hyperplasia. In this lesion, cytologic atypia is manifested by nuclear rounding, nuclear enlargement, distinct nucleoli, chromatin clearing, and epithelial stratification. This high magnification view is from the same case as in Figs. 4.138 and 4.139.

accounting for most of the translational discrepancies between the two classification systems. It is not surprising that a system that emphasizes nuclear atypia (WHO/ISGP) would place these lesions in a low-risk category, whereas a system that emphasizes aberrant architecture (EIN) would categorize most of these lesions as being of higher risk and worthy of an EIN diagnosis. In the study by Lacey et al.,[105] a whopping 61% of lesions interpreted by a panel of experienced gynecologic pathologists as complex hyperplasia without atypia were interpreted by the EIN proponents as EIN, and an additional 15% of these lesions were interpreted by the EIN proponents as full-fledged adenocarcinoma. Although the rate of progression to carcinoma reported in the 1985 study by Kurman et al.[103] for complex hyperplasia without atypia was only 3% (1 of 29 patients), three other studies from that era summarized by Silverberg yield an aggregate progression rate of 18.3% (30 of 164 patients),[116] and more recent studies have indicated an intermediate progression rate of 10% (8 of 80 patients).[104,117] Taken together, these studies indicate a progression rate for complex hyperplasia without atypia of 14.3% (39 of 273 patients), which exceeds the estimated progression rate of simple atypical hyperplasia. These data provide strong support for upgrading the substantial proportion of cases that would traditionally be considered complex hyperplasia without atypia to "complex atypical hyperplasia (based on architecture)" when there are back-to-back, architecturally complex glands that are separated from one another by only threadlike strands of stroma, despite their bland nuclear features (Fig. 4.135).

Topography of Endometrial Hyperplasia

Endometrial hyperplasia may present as a focal abnormality (Fig. 4.137) or as a diffuse process that produces a thickened endometrium and abundant tissue in curettings (Figs. 4.138 and 4.139). Most advocates of the WHO/ISGP system state that hyperplasia is generally diffuse, but may be focal, whereas

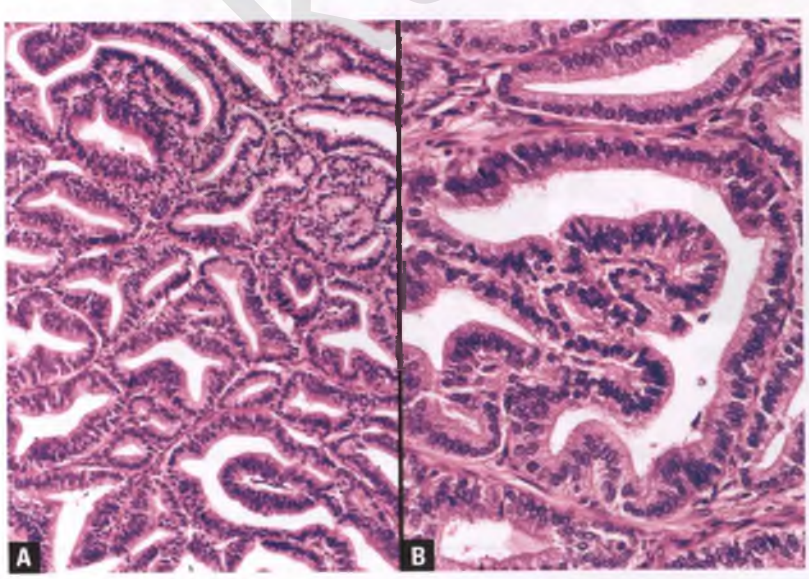

FIGURE 4.135. **A,B**: Complex atypical hyperplasia (based on architecture). These lesions lack conventional features of cytologic atypia and are composed of architecturally complex, back-to-back glands with threadlike strands of intervening stroma. Although the glands are complex, the mazelike, labyrinthine pattern of adenocarcinoma is absent. Classification of proliferations of this type is subjective and controversial. In the WHO/ISGP system, most would be classified as complex hyperplasia without atypia, whereas EIN proponents would consider many of these to be EIN.

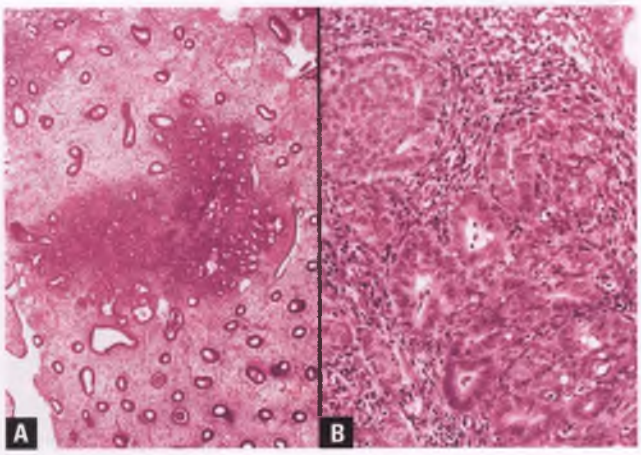

FIGURE 4.137. Focal endometrial hyperplasia with atypia. **A**: An island of hyperplasia is present within a background of proliferative endometrium. **B**: The hyperplastic focus exhibits some cytologic atypia and consists of an admixture of simple and complex architectural patterns with focal morular metaplasia.

EIN proponents have found that most EIN lesions are focal, but may be diffuse. These descriptive differences probably relate to the fact that the commonly seen lesions on the lower end of the hyperplasia spectrum, which do not qualify as EIN, are typically diffuse processes, whereas CAH and its EIN analog are more likely to be localized. In addition, the terms focal and diffuse lack precision and are subjectively applied to endometrial lesions.

Foam Cells in Endometrial Hyperplasia

Aggregates of stromal foam cells are most often seen in the setting of endometrial hyperplasia or well-differentiated adenocarcinoma.[118] These foam cells have small, pyknotic nuclei and abundant cytoplasm that is filled with microvesicles of lipid, which imparts a foamy appearance (Fig. 4.140A). Although originally thought to represent a modified stromal cell, the consistent immunoreactivity of foam cells with the macrophage marker KP-1 (CD68) is strong evidence that these cells are derived from macrophages/histiocytes (Fig. 4.140B).[118]

It is easy to underestimate the biologic potential of an endometrial glandular lesion whose stroma has been expanded by aggregates of foam cells, since the glands-to-stroma ratio

FIGURE 4.138. Complex atypical hyperplasia. In this longitudinal section through the wall of a formalin-fixed uterus, the endometrium is diffusely thickened by an off-white to pale yellow hyperplastic process that measures up to 1 cm in thickness. Hyperplastic glands with cystic dilatation impart a spongy appearance to portions of the lesion. The cervix is at left.

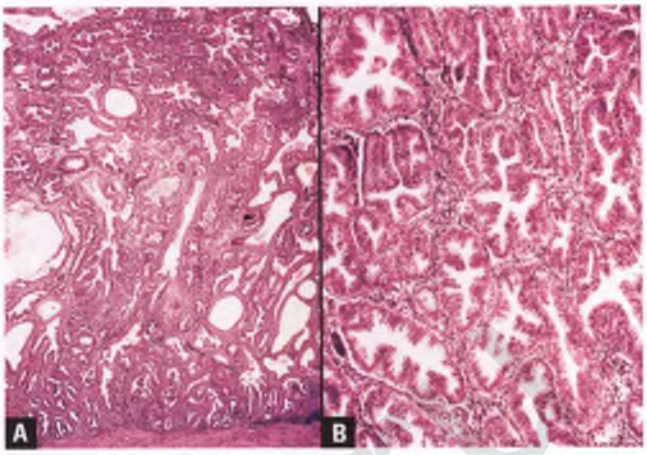

FIGURE 4.139. Complex atypical hyperplasia (histologic correlate to preceding figure). **A**: This low-magnification view demonstrates a markedly thickened endometrium composed of crowded glands with a variety of sizes and shapes. The myometrium is at the bottom of the image. **B**: Numerous papillary infoldings in these crowded glands creates a pattern of architectural complexity. There is a limited amount of stroma, but it is readily apparent.

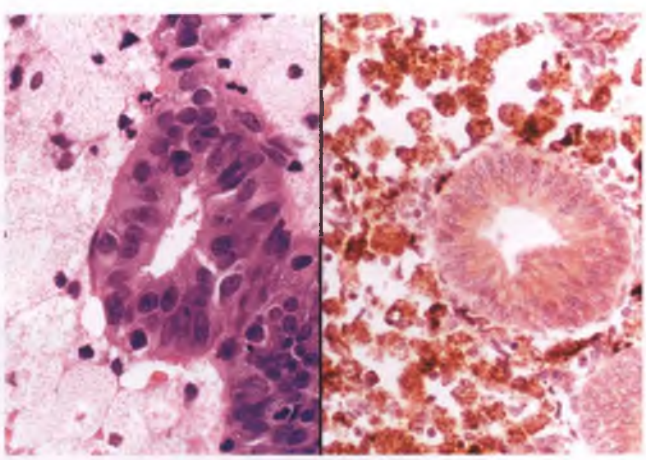

FIGURE 4.140. Endometrial hyperplasia with stromal foam cells. **A**: Note the abundant, microvesicular cytoplasm of the clusters of lipid-laden foam cells in this example, which elsewhere showed features of CAH. **B**: The foam cells exhibit intense, granular, cytoplasmic immunoreactivity for the macrophage marker KP-1 (CD68).

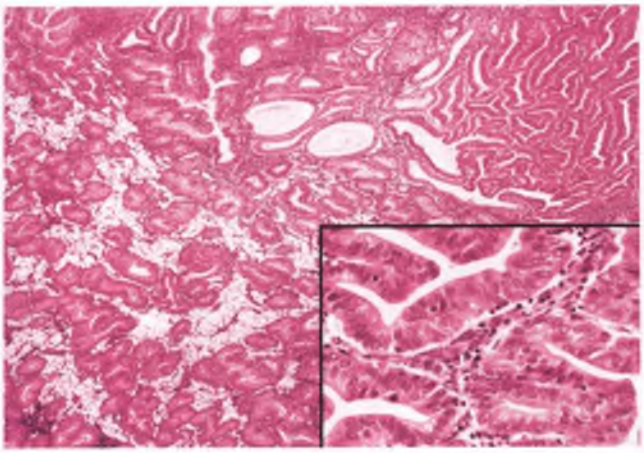

FIGURE 4.141. Endometrial hyperplasia with stromal foam cells. The glands-to-stroma ratio cannot be properly evaluated in areas where the stroma has been expanded by aggregates of foam cells, such as in the left side of the image. An area devoid of foam cells exhibits features of CAH (upper right and inset).

cannot be properly evaluated in these areas (Fig. 4.141). Whenever possible, the diagnosis should be based upon areas where stromal foam cells are absent or inconspicuous; if the architecture of the entire sample is altered by clusters of foam cells, the report should include a cautionary note about the possibility of underdiagnosis with a recommendation for close follow-up with consideration for resampling.

Behavior of Endometrial Hyperplasia

The risk of progression of simple hyperplasia without atypia to carcinoma is negligible and within the range seen in the general population as a whole.[103] The risk of progression of complex hyperplasia without atypia is controversial and has been discussed above. The behavior of simple atypical hyperplasia is often inappropriately lumped together with the much more well-characterized behavior of CAH in the blanket statement that 23% (often rounded to 25%) of atypical hyperplasias progress to adenocarcinoma.[103] In reality, the natural history of simple atypical hyperplasia is basically unknown. In the study by Kurman et al. that forms the basis of the WHO/ISGP classification, the stated risk of simple hyperplasia with atypia developing into adenocarcinoma is 8%. However, this percentage is based upon the experience of *a single patient* out of 13 similarly diagnosed patients who progressed to well-differentiated adenocarcinoma over a 5-year period.[103] The often cited 23% risk of progression for atypical hyperplasia of either simple or complex types is calculated by adding together the risk of patients with CAH of 29% (10 of 35 patients) to the 1 of 13 patients with simple atypical hyperplasia to obtain progression in a total of 11 of 48 patients = 23%.[103] There are clearly insufficient outcome data on simple atypical hyperplasia to make a statement about its risk of progression to adenocarcinoma, and its comingling with CAH for this purpose has been done purely as a matter of convenience. In a recent large study, the risk of progression of atypical hyperplasia (almost all of which were presumably of the complex type) to endometrial carcinoma was confirmed to be approximately 30% over a 20-year period.[119]

The incidence of adenocarcinoma in uteri removed shortly after a diagnosis of CAH has been found to be approximately 40%.[120,121] This disappointingly high percentage, which includes both nonmyoinvasive and myoinvasive adenocarcinomas, represents concurrent disease, yet is on par with the rate of presumed progression of CAH in many of the studies designed to determine the rate of disease progression after many years of follow-up.[103,116,119] The similarity of these rates raises the possibility that some adenocarcinomas thought to represent disease progression may actually be persistent lesions that have gone undetected for long periods of time.[116] In the largest of the recent reports that have evaluated the incidence of concurrent carcinomas, the percentage of myoinvasive tumors was 31% of the total number of adenocarcinomas and 13% of the total number of cases of community-diagnosed atypical hyperplasia.[121] Some of the high incidence of unexpected adenocarcinoma can be explained by sampling error in which either a localized lesion is not sampled by the initial procedure or the sampling is limited to the superficial aspects of a tumor that appears less aggressive on its surface than it does near the endomyometrial junction.

In stark contrast to these data, Longacre and colleagues claim an incidence of myoinvasion in hysterectomies performed ≤8 weeks after their diagnosis of CAH of <1 in 2,000 (<0.05%).[106,107] Although the subjective application of variable sets of diagnostic criteria between different groups of investigators may play some role in generating this wide discrepancy, features of the Longacre study that also contribute to their apparent near-zero rate of misclassification are (a) their circumvention of the issue of sampling error by assessing morphologic features that may predict myoinvasion solely in the hysterectomy specimens of those cases in which the matched endometrial sample was not representative of the lesion within the uterus, (b) their exclusion of hysterectomies with nonmyoinvasive adenocarcinomas from being considered misclassifications, (c) their exclusion of hysterectomies with equivocal myometrial invasion from the study group, (d) their restriction of myoinvasive cases to those associated with a granulation tissue response, excluding those with a diffusely infiltrative, "adenoma malignum" pattern of invasion whose deceptively bland features may be more likely to be associated with endometrial samples that are difficult to distinguish from CAH, (e) their use of computer-assisted analysis of approximately 150 cases of CAH to calculate rather than directly measure their reported incidence of <1 in 2,000 cases of CAH having myometrial invasion in the resected uteri, which takes into account the low incidence of myoinvasion in their experience with lesions that fall within the spectrum of CAH/well-differentiated adenocarcinoma, and (f) their use of a "borderline" group with a calculated incidence of myoinvasion of 5.5%, which no doubt includes cases that other investigators would interpret as CAH.[106]

Gynecologists are expected to be familiar with the studies that have shown a significant risk of concurrent/subsequent adenocarcinoma following a biopsy or curettage diagnosis of CAH. However, in some practice settings, endometrial samples may be submitted by general practitioners or family medicine physicians, in which case it is prudent to include a comment in the pathology report that conveys the clinical significance of this diagnosis.

Differential Diagnosis of Endometrial Hyperplasia

The differential diagnosis of endometrial hyperplasia includes (a) dissociation, coiling, and telescoping artifacts, (b) endometrial polyps, (c) disordered proliferative endometrium, (d) late secretory or hypersecretory endometrium, (e) basalis endometrium, (f) cystic atrophy, (g) epithelial metaplasias and related alterations, (h) forms of hyperplasia other than the subtype diagnosed, (i) atypical polypoid adenomyoma, and (j) well-differentiated adenocarcinoma. The distinguishing features of these processes are discussed elsewhere in this chapter, but a few points deserve reiteration. Whenever contemplating a diagnosis of localized hyperplasia on the low end of the spectrum or a localized disordered proliferative pattern, closely evaluate the stroma and blood vessels for features of an endometrial polyp, and remember that the glands within endometrial polyps are given considerable leeway in terms of crowding, budding, and cystic dilatation before a diagnosis of endometrial hyperplasia within an endometrial polyp is rendered. Another potential mimic of a localized endometrial hyperplasia relates to the common finding of increased glandular density within the basalis (Fig. 4.142). Although generally not given more than a passing glance in hysterectomy specimens, this phenomenon can be misinterpreted as hyperplasia (with atypia in cases of "activated" nuclei) when encountered in fragments of tangentially cut endometrial samples. Attention to the dense stroma of the basalis, the tendency of glands in this location to be small and tubular, and limiting definitive diagnoses of abnormalities within this spectrum to samples that include properly oriented fragments with recognizable surface epithelium facilitate correct interpretation of this variant of normal.

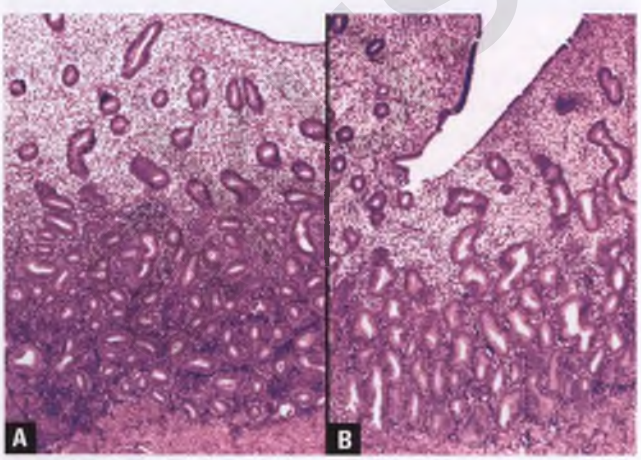

FIGURE 4.142. **A,B**: Proliferative endometrium. In these two variants of normal, the tubular glands of the basalis, which are associated with dense stroma, are significantly more crowded than those of the functionalis. Note how tangential sections through fragments of basalis could simulate endometrial hyperplasia.

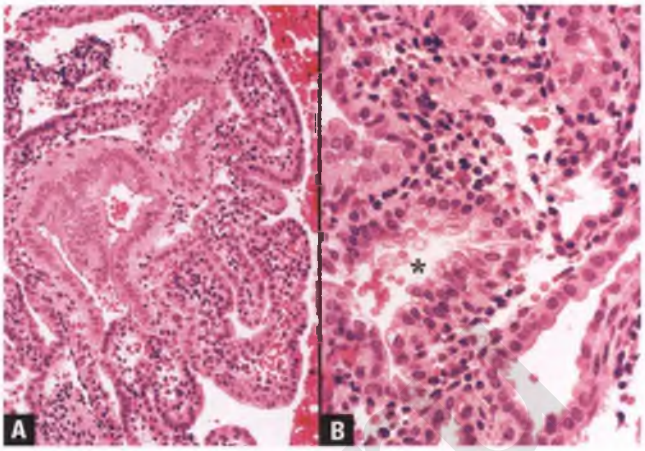

FIGURE 4.143. **A,B**: Complex hyperplasia with progestin effect. Note the bland nuclear features, lack of nuclear stratification, patches of eosinophilic cell change with homogenized nuclear chromatin, and focus with cytoplasmic vacuolization (in cells lining the gland with an *asterisk*). The pretreatment biopsy contained an admixture of CAH and well-differentiated endometrioid carcinoma.

Progestin-Induced Changes

CAH and well-differentiated endometrioid carcinoma are sometimes treated with progestin therapy rather than hysterectomy, with response rates that range from 40% to 70%.[101] The most common histologic changes related to this hormonal treatment are patches of stromal decidualization, decreased glands-to-stroma ratio, a variety of metaplastic changes, and decreased glandular cellularity with loss of nuclear stratification, decreased mitotic activity, loss of nuclear atypia, decreased nuclear-to-cytoplasmic ratio, and a homogenized chromatin pattern.[101] Eosinophilic cell change is almost invariably present, and secretory change, as manifested by cytoplasmic vacuolization, is seen in roughly one-third of cases (Fig. 4.143).[101] In the areas of persistent hyperplasia/carcinoma, stromal decidualization is typically absent or muted. In the study by Wheeler et al.,[101] the persistence of nuclear and/or architectural atypia in endometrial samples taken >6 months after initiation of hormonal therapy were predictive of treatment failure.

Metaplastic Hyperplasias

Metaplastic hyperplasias could just as easily be referred to as hyperplastic metaplasias, but use of the former term is preferred to emphasize that these processes should be regarded as a form of hyperplasia. As for hyperplasias of the usual type, it is recommended that metaplastic hyperplasias measure at least 1 mm in a single tissue fragment before being diagnosed.

Metaplastic hyperplasias can be divided into two categories: those with and without atypia. Unlike the traditional WHO/ISGP classification of endometrial hyperplasia in which atypia applies only to cytologic (nuclear) atypia, atypical metaplastic hyperplasias can achieve this status by virtue of cytologic and/*or* significant architectural abnormalities.

Metaplastic hyperplasias without atypia are not thought to be clinically significant lesions, and can be considered to be within the spectrum of ordinary metaplasia. Although there are limited outcome data on atypical metaplastic hyperplasias, they may be associated with low-grade adenocarcinoma elsewhere in the endometrium. When there is significant glandular crowding and complexity with scant intervening stroma, it seems prudent to manage sizable (>1 mm) lesions of this type as a form of CAH, even in the absence of nuclear atypia.[93] Without the degree of nuclear atypia as a reliable guide to help classify these metaplastic hyperplasias, we must rely upon a subjective assessment of how much architectural complexity and glandular crowding is allowed within each category along the morphologic continuum between ordinary metaplasia and similarly differentiated variants of well-differentiated carcinoma. The figures in this section will help to convey my approach to this difficult area. It should be noted that this discussion is not applicable to extensive PSC in the setting of endometrial breakdown or to florid morular metaplasia, which in and of themselves are not associated with an increased risk of carcinoma.

Some metaplastic proliferations fit the definition of a hyperplasia by virtue of a glands-to-stroma ratio of >2 to 1, but exhibit little architectural complexity, have bland nuclear morphology, and are composed of glands that are separated by ample amounts of stroma. Lesions of this type are best regarded as metaplastic hyperplasias without atypia. Mucinous and ciliated examples of such lesions are presented in Figures 4.144 and 4.145.

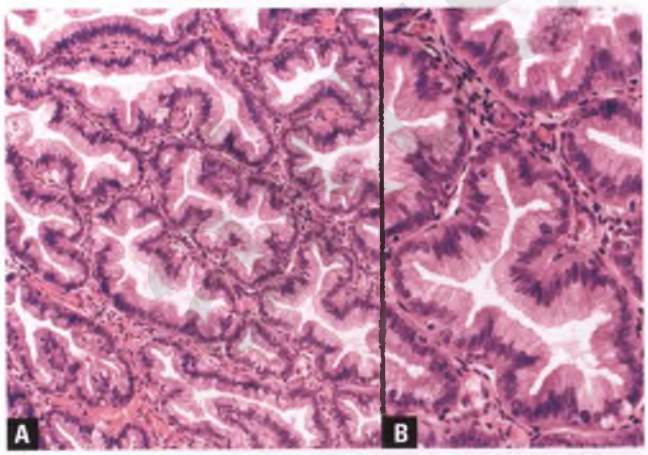

FIGURE 4.144. **A,B**: Metaplastic mucinous hyperplasia without atypia. These moderately crowded metaplastic glands represent a form of mucinous metaplasia that is not thought to be associated with a significant risk of concurrent or subsequent carcinoma. Glandular complexity is minimal and manifested primarily by undulating folds of mucinous epithelium without nuclear atypia. Microacinar and complex papillary structures are absent.

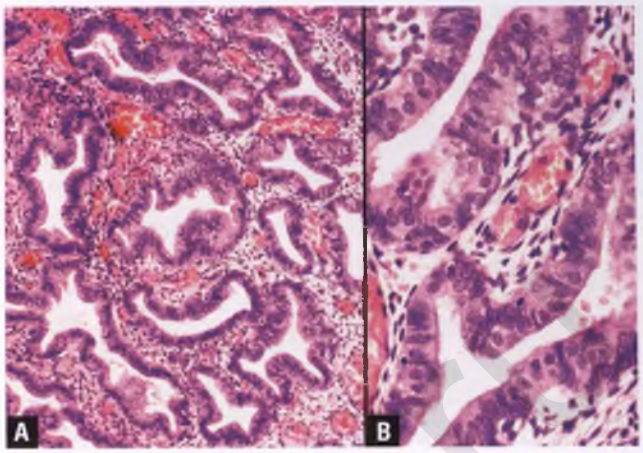

FIGURE 4.145. **A,B**: Metaplastic ciliated hyperplasia without atypia. Glands lined by ciliated cells exhibit an architecture similar to that of the mucinous lesion in the preceding figure. There is no nuclear atypia.

As metaplastic hyperplasias increase in architectural complexity, their classification becomes more controversial. As a practical matter, the presence of numerous ciliated cells in an endometrial proliferation is strong evidence in favor of a benign process, since adenocarcinomas composed predominantly of ciliated cells are quite rare.[122] Nevertheless, such carcinomas do occur, and the presence of ciliated endometrial proliferations with marked architectural complexity may be an indication of an endometrium that is at an increased risk for the development of atypical hyperplasia/well-differentiated carcinoma.[93] For these reasons, it is recommended that endometrial ciliated proliferations with the degree of architectural complexity as illustrated in Figures 4.146 and 4.147 be considered forms of CAH, even in the absence of appreciable nuclear atypia.

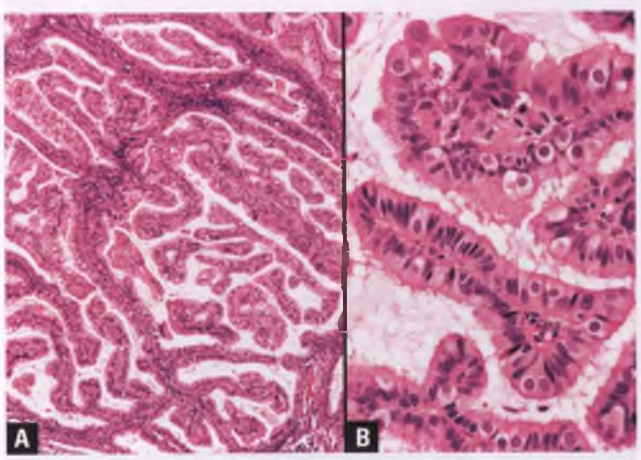

FIGURE 4.146. **A,B**: Metaplastic CAH with ciliated cells. The ciliated cells have round to oval, bland nuclei, some of which surrounded by a clear halo. Despite the bland nuclear features, the architectural complexity suggests that this lesion is best managed as an atypical hyperplasia.

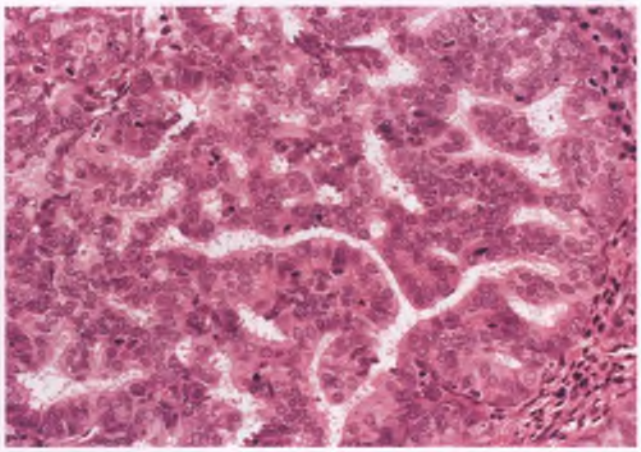

FIGURE 4.147. Metaplastic CAH with ciliated cells. As in the preceding figure, complex architecture warrants treatment as an atypical hyperplasia.

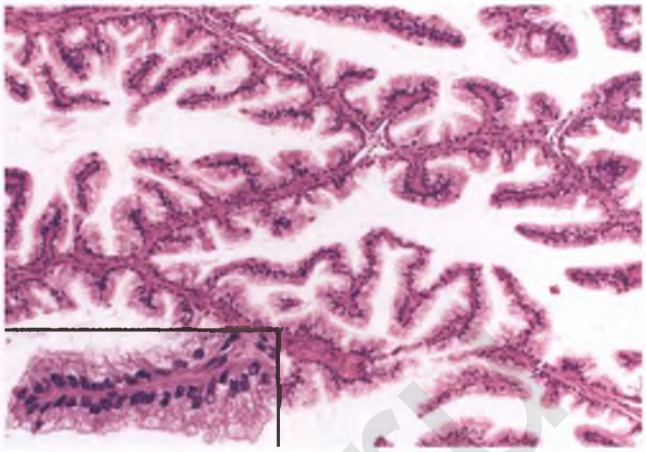

FIGURE 4.149. Atypical hyperplastic papillary proliferation with mucinous metaplasia. As in the preceding figure, the finely papillary architecture is worrisome for an associated low-grade mucinous carcinoma. The inset highlights the lack of nuclear atypia.

Classification of cytologically bland mucinous endometrial proliferations with marked architectural complexity manifested by microacinar, villoglandular, and finely papillary patterns is particularly problematic (Figs. 4.148 and 4.149).[99,100,123] Although often not morphologically diagnostic of adenocarcinoma in and of themselves, these lesions may be associated with an underlying low-grade mucinous carcinoma with overlapping histologic features. Emblematic of the difficulty in classifying these lesions is the fact that quite similar lesions with finely papillary architecture have been illustrated as examples of complex papillary hyperplasia without atypia by one group and as well-differentiated adenocarcinoma by another.[106,123] Given this state of uncertainty, it is recommended that nonlocalized, complex papillary proliferations of this type, even with no appreciable nuclear atypia, be regarded as a form of CAH that should be managed with either hysterectomy or close follow-up with repeat curettage. The pathology report should indicate that the findings are suspicious for low-grade mucinous carcinoma, or that this possibility cannot be excluded.

In terms of differential diagnosis, mucinous metaplastic lesions of the endometrium with a microacinar architecture need to be distinguished from contaminating fragments of microglandular hyperplasia curetted from the endocervix, which often exhibit subnuclear vacuoles and reserve cell hyperplasia and are not found in continuity with recognizable endometrial stroma (Figs. 3.69–3.71). Endometrial curettings may also be contaminated by shredded, compacted strips of benign endocervical mucinous epithelium that may be mistaken for architecturally complex mucinous lesions of endometrial origin (Fig. 4.150); the awareness of the existence of

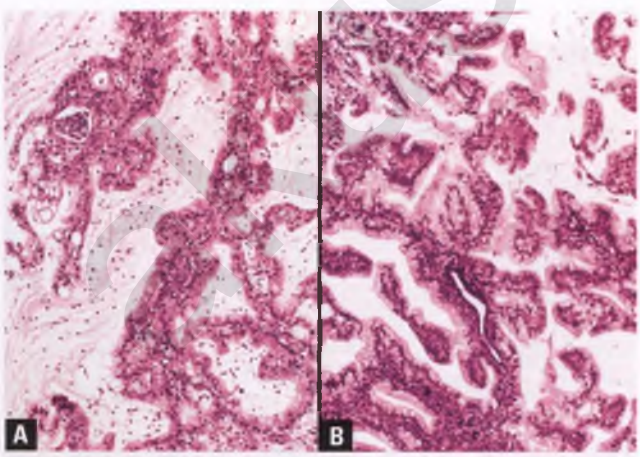

FIGURE 4.148. **A,B**: Atypical hyperplastic papillary proliferations with mucinous metaplasia. Both of these lesions presented as nonlocalized findings within endometrial curettings. In this setting, the finely papillary and focally microacinar architecture is a worrisome feature, despite the bland nuclear features.

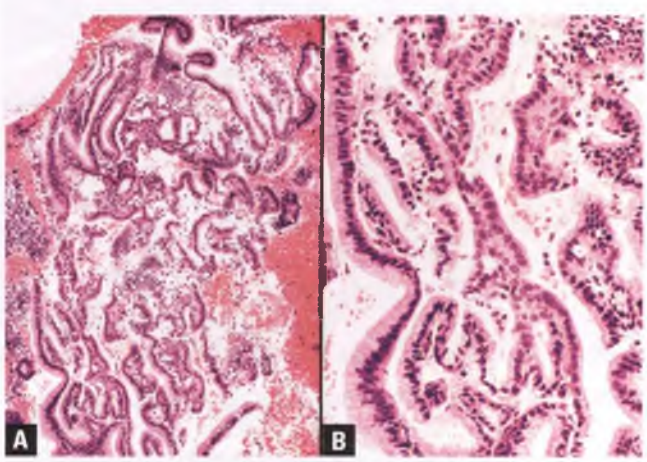

FIGURE 4.150. **A,B**: Compacted, shredded strips of normal surface endocervical mucinous epithelium within an endometrial curettage. These epithelial strips simulate a hyperplastic mucinous lesion. Note the lack of stromal support.

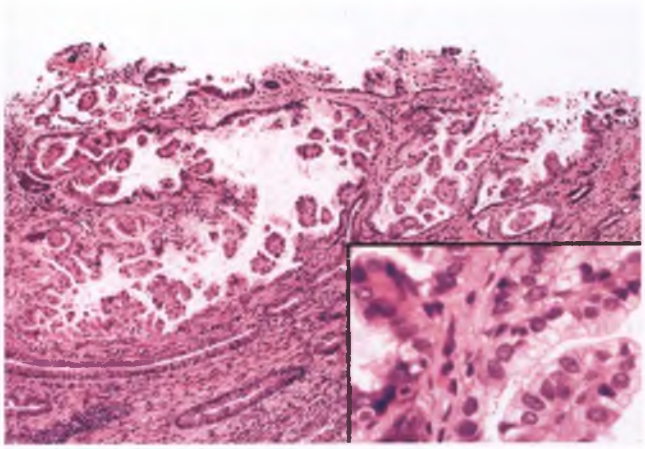

FIGURE 4.151. Localized hyperplastic papillary proliferation with mucinous metaplasia involving the endometrial surface. Note the fibrovascular cores within most of the papillary structures and the bland nuclear features. A lesion such as this can comfortably be regarded as an incidental finding.

this phenomenon and the absence of stromal support facilitates its recognition.

Lehman and Hart have described a localized hyperplastic proliferation that features a papillary architecture and associated metaplastic epithelial changes, which are usually of mucinous, eosinophilic, and/or ciliated cell type (Figs. 4.151 and 4.152).[123] These lesions usually project into one or more cystically dilated glands, but may also involve the endometrial surface. Nuclear atypia is absent or mild. When small and localized, and particularly when confined to an endometrial polyp as is often the case, these lesions can be regarded as incidental findings. Architecturally simple and cytologically bland papillary proliferations that some have referred to

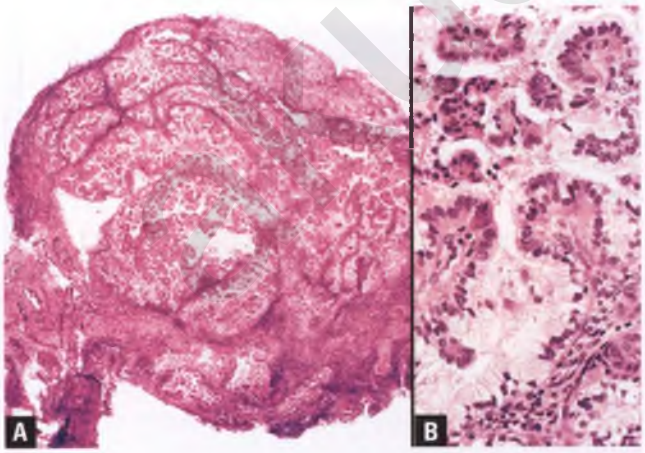

FIGURE 4.152. **A,B**: Localized hyperplastic papillary proliferation with mucinous metaplasia. Although this is a larger and more architecturally complex lesion than the one in the preceding figure, it is confined to an endometrial polyp and has bland nuclear features. Polypectomy is considered adequate treatment.

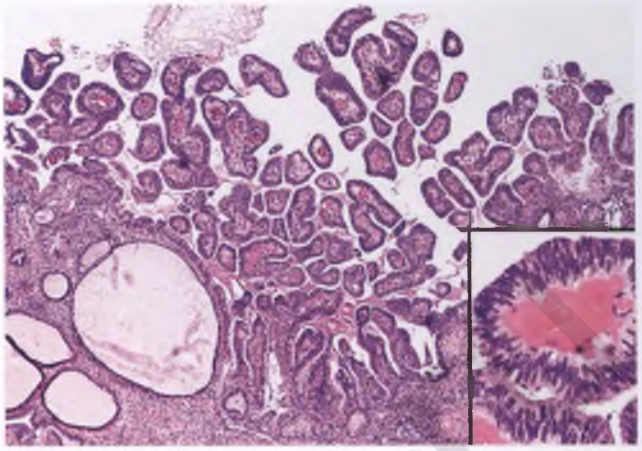

FIGURE 4.153. Papillary/villoglandular hyperplasia. Note the simple papillary architecture and bland nuclear features of this surface lesion, which facilitate its distinction from villoglandular endometrioid adenocarcinoma.

as villoglandular hyperplasias or simply "papillary proliferations" may also be considered to be within this group of lesions (Fig. 4.153).[124] These unusual proliferations are generally limited to the endometrial surface and occasional superficial glands, show no more than mild nuclear atypia, lack appreciable mitotic activity, may have superimposed mucinous or ciliated metaplasia, and have a less complex architectural pattern than villoglandular endometrioid adenocarcinoma (compare with Fig. 4.189). As these various types of papillary proliferations increase in architectural complexity and become less localized, their classification becomes more subjective and controversial, and data on their natural history are limited. The recommendations outlined earlier in the discussion of architecturally complex mucinous endometrial proliferations apply to this situation as well.

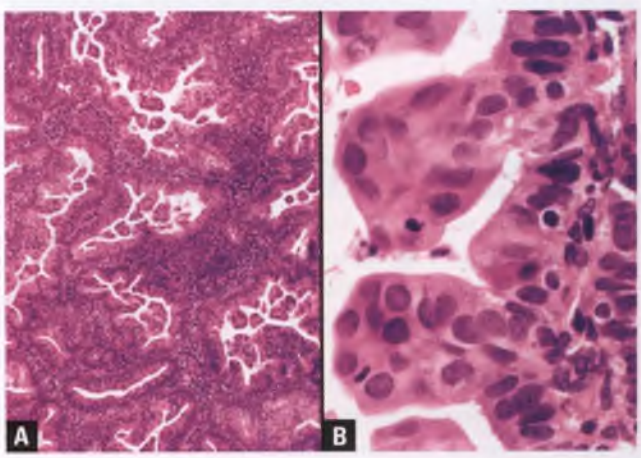

FIGURE 4.154. **A,B**: Metaplastic hyperplasia with small nonvillous papillae without atypia. The papillae impart some architectural complexity, but there is ample stroma separating the glands and there is no cytologic atypia. This lesion could also be referred to as metaplastic hyperplasia with papillary eosinophilic cell change without atypia.

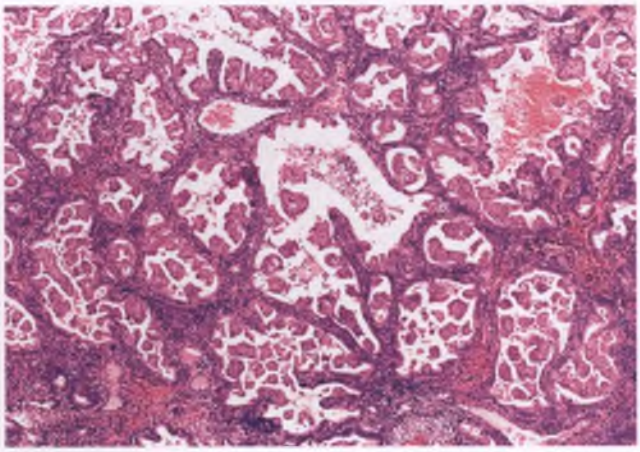

FIGURE 4.155. Metaplastic CAH with small nonvillous papillae (metaplastic complex atypical hyperplasia with papillary eosinophilic cell change). Although the nuclear features of this lesion are similar to those illustrated in the preceding figure, the more crowded architectural pattern warrants the designation "atypical."

In yet another form of metaplastic hyperplasia, the architecture of crowded endometrial glands is complicated by the presence of numerous small papillary epithelial buds that project into the gland lumens (Figs. 4.154 and 4.155). These buds lack fibrovascular cores and have eosinophilic cytoplasm and are identical to those found in the variant of endometrioid adenocarcinoma that bears the appellation "with small nonvillous papillae," as described in the section on variants of endometrioid carcinoma. When seen in endometrial proliferations that are not worthy of a diagnosis of adenocarcinoma, the descriptive term "papillary eosinophilic cell change" has also been applied to these proliferations.

OVERVIEW AND GENETIC ASPECTS OF ENDOMETRIAL CARCINOMA

Overview

Thanks to the success of the Pap smear in markedly reducing the incidence of cancer of the uterine cervix, endometrial carcinoma is now the most common malignancy of the female genital tract in the United States.[125] The usual type of endometrial carcinoma is an adenocarcinoma that is referred to as endometrioid carcinoma, which accounts for approximately 80% of all endometrial carcinomas.[126] The typical clinical presentation is a postmenopausal woman (mean age of 60 years) with abnormal uterine bleeding. Endometrioid carcinomas are "Type I" tumors that are related to exposure to increased levels of estrogenic substances, which may be associated with one or more of the following: obesity, diabetes, infertility, nulliparity, unopposed estrogen replacement therapy, tamoxifen therapy, polycystic ovary syndrome, stromal hyperthecosis, or an estrogen-secreting ovarian tumor.[127] Type I tumors are often preceded by or associated with endometrial hyperplasia, roughly 80% are confined to the uterus at presentation, and the prognosis is generally favorable.[127–129] The major type II endometrial tumors are serous and clear cell carcinoma, which are aggressive, estrogen-independent tumors.

Genetic Aspects[128,130,131]

Type I and type II endometrial carcinomas appear to arise via different molecular genetic pathways, as evidenced by their different mutational patterns.Type I tumors are more likely to exhibit PTEN, KRAS, and β-catenin gene mutations and have a higher frequency of microsatellite instability than serous carcinoma (the prototypical type II carcinoma), which is much more likely to harbor a p53 gene mutation.

Hereditary nonpolyposis colorectal cancer, also known as HNPCC and Lynch syndrome, is an autosomal dominant disorder that is associated with a heritable mutation in one of four DNA mismatch repair genes. This defect results in a predilection for the early onset of several different forms of carcinoma, most notably of colorectal and endometrial origin. It is estimated that roughly half of women with HNPCC will develop endometrial cancer over the course of their lifetime, and that about 2% of endometrial carcinomas are due to this inherited genetic defect. Pathologists can play a role in identifying those patients with endometrial cancer who have HNPCC either by using immunohistochemistry to screen for loss of expression of one or more of the DNA mismatch repair proteins or by requesting a test that utilizes polymerase chain reaction technology to identify those tumors with a high frequency of microsatellite instability (whether or not the 25% of endometrioid carcinomas that are associated with a high frequency of microsatellite instability have characteristic histologic features or a different prognosis is controversial). Endometrial cancer patients who are most likely to benefit from such studies include those (a) younger than 50 years of age, (b) with a personal or family history suggestive of HNPCC, or (c) with prominent intratumoral and peritumoral lymphocytic infiltrates. Such studies should be performed only at the request of the clinician and after patient consent has been obtained. Follow-up of an abnormal result involves genetic counseling and further testing to identify the roughly 10% of such patients who actually have HNPCC, which in turn would lead to increased cancer surveillance of other organ systems for the individual patient and shed light upon the increased risk of cancer for some of their relatives.

ENDOMETRIOID ADENOCARCINOMA: USUAL PATHOLOGIC FEATURES, GRADING CRITERIA, AND INTRAOPERATIVE CONSULTATIONS

Aspects related to the typical gross and microscopic appearances of endometrioid carcinoma are presented in this section. Clinical and pathologic features that help to distinguish endometrial endometrioid adenocarcinoma from the usual type of endocervical adenocarcinoma are discussed in Chapter 3, as are the different patterns of cervical involvement by endometrial carcinoma. The special situation in which dual endometrioid carcinomas of the endometrium and ovary are found is addressed in the section on ovarian endometrioid carcinomas

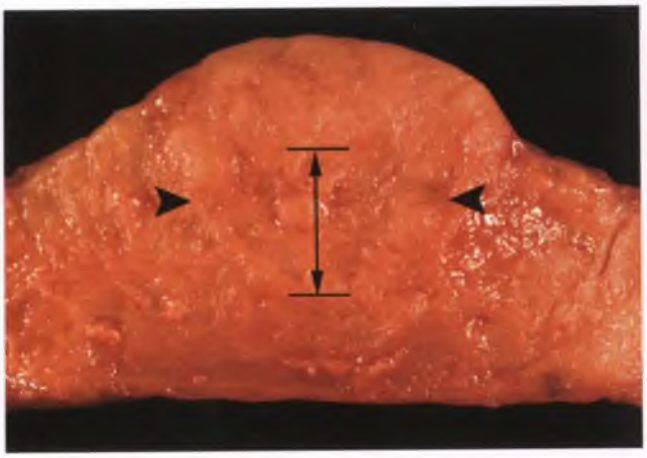

FIGURE 4.156. Gross appearance of an endometrioid carcinoma in the fresh state. This longitudinal section through the tumor reveals an elevated, tan nodule as demarcated by the *arrowheads*. Gross detection of myometrial invasion is often more difficult in fresh as opposed to fixed specimens. The depth of invasion, as indicated by the vertical arrow, does not include the portion of the tumor that protrudes above the normal endometrial–myometrial junction (see section on myometrial invasion).

in Chapter 7. The pathology report of resected endometrial carcinomas should include the following information: tumor type, tumor grade, depth of myometrial invasion, presence or absence of angiolymphatic invasion, status of the cervix, and presence or absence of involvement of any other submitted tissues (ovaries, fallopian tubes, lymph nodes, etc.).

Gross Features

Endometrioid carcinomas vary from polypoid masses to infiltrative plaques to carpets of shaggy tissue (Figs. 4.156–4.159).

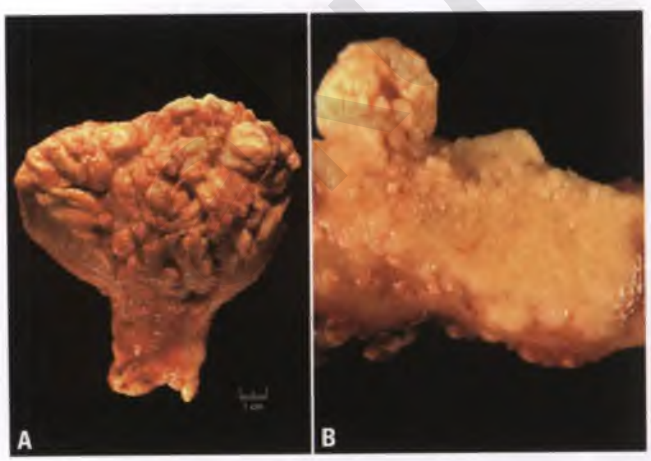

FIGURE 4.157. Gross appearance of endometrioid carcinoma. **A**: A large, polypoid tumor bulges into the distended endometrial cavity of this unfixed specimen. **B**: Longitudinal section of a different endometrioid carcinoma following formalin fixation with polypoid (upper left) and deeply invasive (lower right) components.

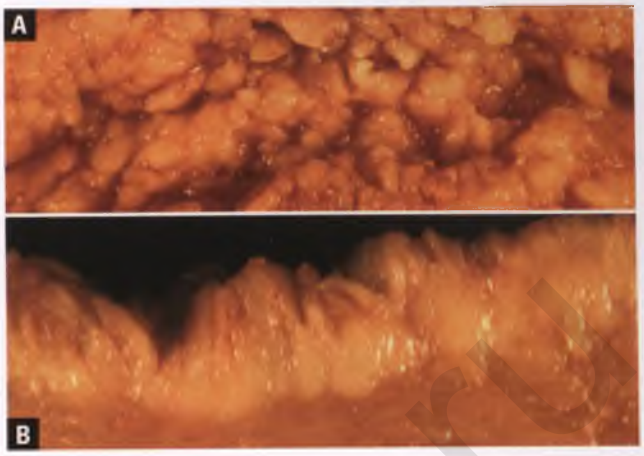

FIGURE 4.158. Gross appearance of endometrioid carcinoma. **A**: Tumor viewed from above. **B**: View of sectioned surface after light formalin fixation. This superficial tumor resembles a shag carpet.

Their superficial aspects are typically friable, soft, fleshy, light tan, light yellow, and/or off-white. Specks and/or geographic islands of pasty yellow material may represent either foci of necrosis or keratin related to squamous differentiation (Fig. 4.160). Foci of hemorrhage may also be evident. In those tumors with myometrial infiltration, the blending of tumor with muscle often results in a rubbery texture. Myometrial invasion may be grossly recognizable in sections of the fresh specimen, but is often more readily apparent after formalin fixation.

Microscopic Features

This discussion is restricted primarily to the histology of the superficial aspects of well-differentiated endometrioid carcinomas as encountered in endometrial biopsies and curettings.

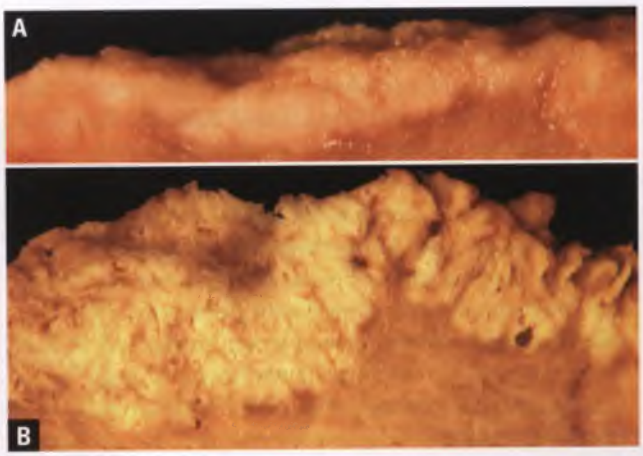

FIGURE 4.159. Gross appearance of endometrioid carcinoma. **A**: Lightly fixed section of plaque-like tumor with superficial myometrial invasion. **B**: This section through a formalin-fixed tumor demonstrates invasion into the inner half of the myometrium at left. Undulating, superficial tumor at right represents noninvasive tumor with involvement of an irregular endometrial–myometrial junction.

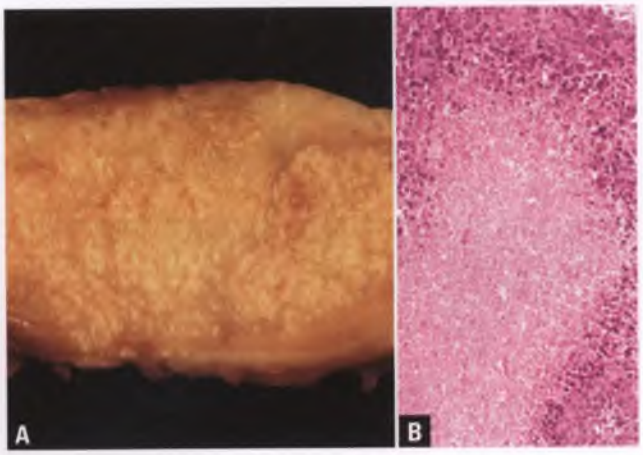

FIGURE 4.160. Gross appearance of endometrioid carcinoma. **A**: This longitudinal section through a formalin-fixed uterus reveals near full-thickness involvement by a tumor with prominent geographic islands of yellow material. **B**: In this case, the yellow material represents tumor necrosis in a grade 3 carcinoma (keratin related to squamous differentiation can result in a similar gross appearance).

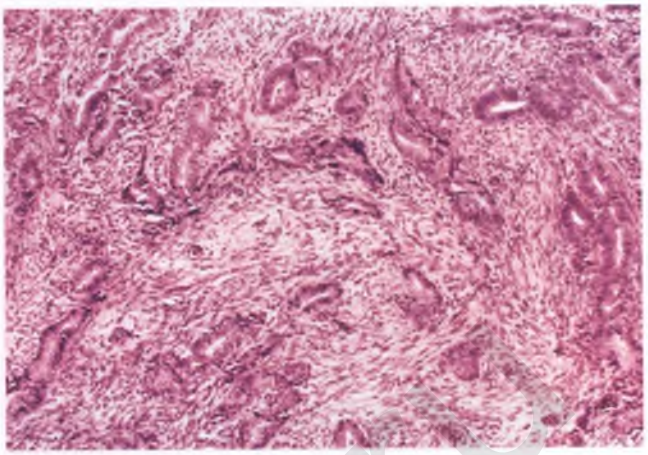

FIGURE 4.161. Desmoplasia of endometrial stroma in an endometrioid carcinoma. This image, taken from an endometrial curettage, demonstrates haphazardly distributed endometrial glands, some with angulated contours, embedded within a fibroblastic, spindle cell stroma. Follow-up hysterectomy showed myometrial invasion 30% into the uterine wall.

The histologic features of progestin-treated well-differentiated endometrioid carcinoma are similar to those seen in similarly treated CAH, and are discussed in the section on endometrial hyperplasia. The separation of CAH from grade 1 endometrioid carcinoma is difficult, and relies upon a subjective assessment of the extent of architectural glandular complexity and the degree of nuclear atypia of the cells lining the glands. This assessment is sometimes complicated by overlying or admixed metaplastic changes, as discussed in other sections of this chapter. The histology of grades 2 and 3 endometrioid carcinomas is illustrated in the section on grading, and patterns of myometrial invasion are addressed separately.

Endometrial Stromal Invasion

Actual invasion of endometrial stroma by endometrioid carcinoma is an uncommon histologic finding. When present, a haphazard glandular arrangement associated with an altered stroma composed of spindle-shaped fibroblasts that resembles granulation tissue may be seen (Fig. 4.161).[106,132] Although this pattern is a good predictor of myometrial invasion, a similar type of stroma may be seen during the postbiopsy reparative period, and an overlapping pattern that consists of fibromatous stroma that is dense, cellular, and eosinophilic can be found in both endometrial adenocarcinomas and benign entities such as endometrial polyps, atypical polypoid adenomyoma, lower uterine segment, and inactive endometrium.[106,133] Moreover, virtually any endometrial proliferation with a villoglandular architecture, whether malignant, hyperplastic, or metaplastic, can contain this latter type of fibromatous stroma within its supporting framework, and the compressed endometrial stroma between the crowded glands of some endometrial hyperplasias can have a similar appearance (Fig. 4.162). Given these numerous potential pitfalls, caution should be exercised when using a desmoplastic stromal reaction to diagnose adenocarcinoma in endometrial samples. In an even less common form of recognizable stromal invasion, unequivocal carcinoma is found meandering within the endometrial stroma (Fig. 4.163). In this situation, the possibility of metastatic carcinoma should be considered (see section on the uterine corpus as site of metastatic carcinoma).

In the vast majority of cases of well-differentiated endometrial carcinoma, the presence of endometrial stromal invasion is inferred by the marked crowding and architectural complexity of the glands rather than directly observed.[132] In an effort to make recognition of this inferred form of stromal invasion more reproducible and objective, Kurman and Norris have developed guidelines to assist the pathologist in this exercise. Their guidelines, as modified from their original work

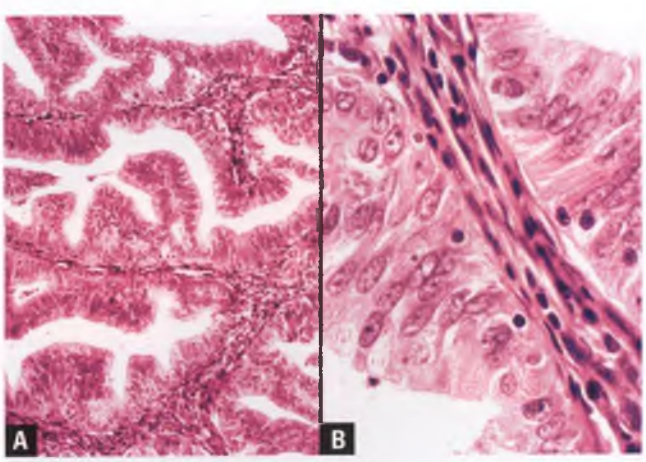

FIGURE 4.162. **A,B**: Complex atypical hyperplasia with fibromatous stroma. Glandular crowding has compressed the stromal cells, resulting in formation of spindle cells with some fibroblastic differentiation and collagenization. This type of stroma should not be interpreted as evidence of endometrial stromal invasion.

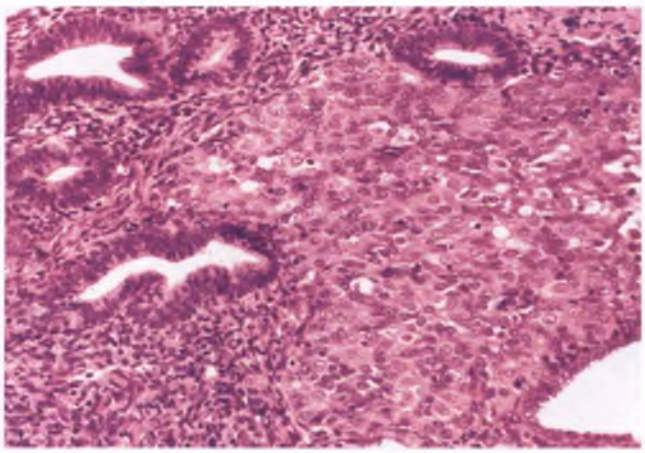

FIGURE 4.163. Unusual pattern of endometrial stromal invasion by endometrioid carcinoma. A tongue-like sheet of malignant epithelium that is punctuated by occasional glandular structures has replaced a portion of the endometrial stroma. The carcinoma impinges upon, but does not destroy, the native proliferative glands in a pattern that mimics a metastatic lesion. This tumor was confined to the endometrium and was associated with CAH.

from 1982, describe this form of stromal invasion as (a) the presence of confluent, architecturally complex, interconnected, back-to-back glands with a complete absence of intervening stroma (which, in practical terms, translates into not easily visible stroma) or (b) an extensive papillary pattern.[30,132] Diagnostic accuracy is increased when the confluent or extensive papillary patterns are present over a distance of at least 2 mm, which corresponds to the diameter of a microscopic field when using 10× eyepieces (field number 20) and a 10× objective lens, but this is not an absolute requirement. The confluent and extensive papillary patterns are largely captured by the high-risk architectural patterns described by Longacre and colleagues, which are discussed in the following section.

Well-Differentiated Architectural Patterns Associated with a Significant Risk of Myoinvasion

In contrast to the approach of Kurman and Norris, Longacre and colleagues do not rely upon inferred "endometrial stromal invasion" in order to identify well-differentiated endometrial adenocarcinoma. Instead, they utilize a pictorial gallery that conveys the many different architectural patterns of endometrial glandular proliferations along the spectrum between hyperplasia and well-differentiated adenocarcinoma, and divide these patterns according to their risk for concurrent myometrial invasion into negligible risk (hyperplasia with or without atypia), intermediate risk (borderline; cannot exclude well-differentiated adenocarcinoma), and high-risk (well-differentiated adenocarcinoma).[106,107]

Longacre and colleagues recommend use of a "multidirectional 150× test" in cases with closely packed glands to assess whether the degree of glandular branching and budding is sufficient for a diagnosis of adenocarcinoma.[106,107] If a 150× microscopic field of crowded glands (15× eyepieces with 10× objective) can be traversed in more than one direction without encountering stroma, then the glandular proliferation is of sufficient architectural complexity to warrant a diagnosis of adenocarcinoma. With the exception of the labyrinthine and complex papillary patterns, they also impose a requirement that at least 30% of the problematic endometrial proliferation exhibit one of the high-risk architectural patterns before a diagnosis of adenocarcinoma is rendered.

Although the pattern of small, crowded, back-to-back, interconnected glands with budding and branching is the most common one seen in well-differentiated adenocarcinoma (Figs. 4.164 and 4.165), other high-risk architectural patterns include (a) exophytic, complex papillary patterns with delicate or broad stromal cores (Figs 4.166–4.168) and (b) macroglands with marked internal complexity with apparent cribriform structures (Fig. 4.169). The less controversial papillary patterns that qualify for well-differentiated adenocarcinoma are diffuse rather than localized processes,

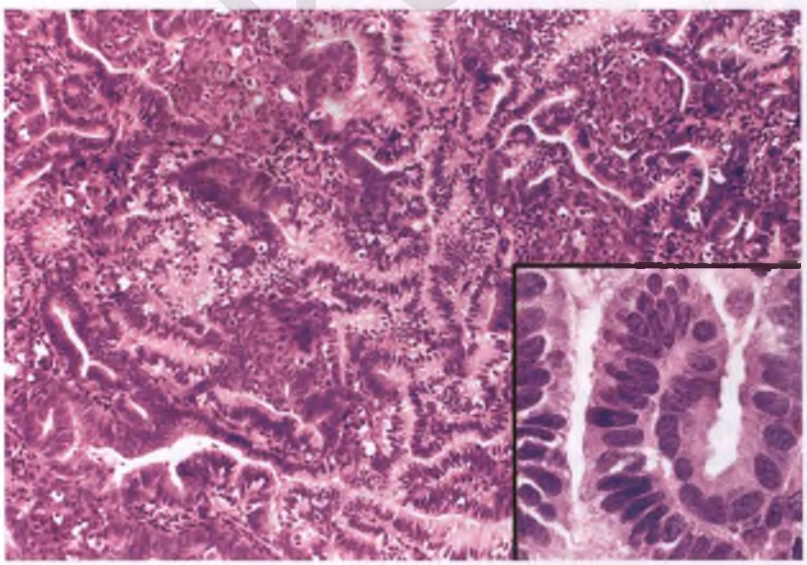

FIGURE 4.164. Well-differentiated endometrioid adenocarcinoma with a labyrinthine, maze-like architectural pattern and a few squamous morules. The inset highlights the absence of appreciable cytologic atypia. Lesions with this degree of architectural complexity with miniscule amounts of stroma enveloping the glands should be diagnosed as adenocarcinoma, even in the apparent absence of cytologic atypia. Follow-up hysterectomy revealed a grade 1 adenocarcinoma with myometrial invasion 40% into the wall.

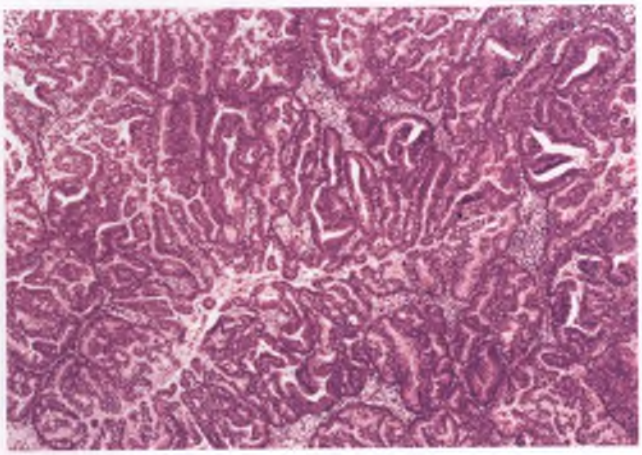

FIGURE 4.165. Well-differentiated endometrioid adenocarcinoma. This degree of glandular crowding and maze-like architectural complexity is diagnostic of adenocarcinoma.

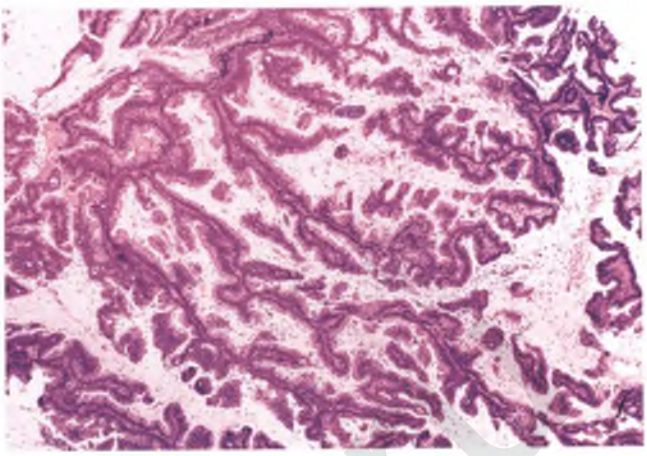

FIGURE 4.167. Well-differentiated adenocarcinoma with a finely papillary pattern that is diffuse, complex, and exophytic. This example is from a mucinous carcinoma of the endometrium.

have fibrovascular cores, and exhibit complex second- and third-order branching. Most of the tumors in which a finely papillary architecture predominates have characteristics of villoglandular or low-grade mucinous carcinoma (Figs. 4.166 and 4.167). Uterine serous carcinoma is distinguished from these low-grade papillary proliferations by its high-grade nuclei and epithelial tufting.

It should be noted that true cribriform areas, in which a glandular space or epithelial sheet is subdivided into smaller glandular spaces by arching struts of glandular epithelial cells with no stromal support, are actually fairly uncommon in grade 1 adenocarcinoma and are more common in grade 2 tumors, but facilitate the diagnosis of malignancy when more than focally present.[133] In grade 1 tumors, it is much more common to see large gland-like spaces (macroglands) with a complex internal structure formed by back-to-back glands that are separated by a barely perceptible, fine tracery of supporting stromal fibrils (Figs. 4.170–4.172).[133] It is not critical to separate this latter gland-within-gland pattern from true cribriforming, since both patterns are indicative of a high degree of architectural complexity and are associated with malignancy. However, these patterns do need to be distinguished from the pseudocribriform spaces formed by glandular epithelium abutting intraluminal morules that may be seen in either well-differentiated adenocarcinomas or hyperplastic processes (see Fig. 4.113).

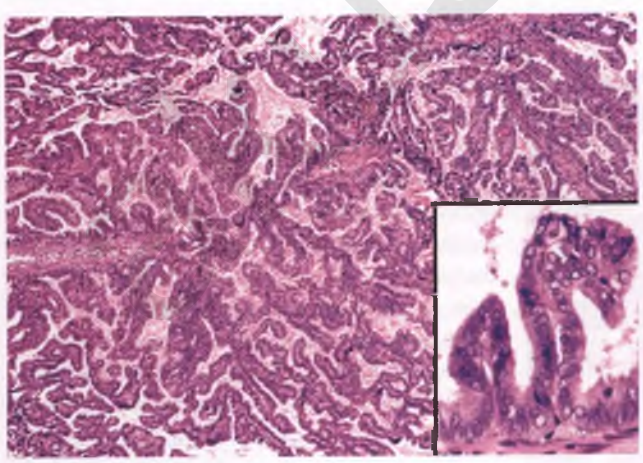

FIGURE 4.166. Well-differentiated endometrioid adenocarcinoma with a diffuse, complex papillary pattern. With the exception of the major supporting branches, the papillary structures in this example have thin and delicate fibrovascular cores. The inset highlights the low nuclear grade of this villoglandular adenocarcinoma.

Cytologic Features of Well-Differentiated Adenocarcinoma

In approximately 70% of well-differentiated endometrial adenocarcinomas, the degree of nuclear atypia is minimal, mild,

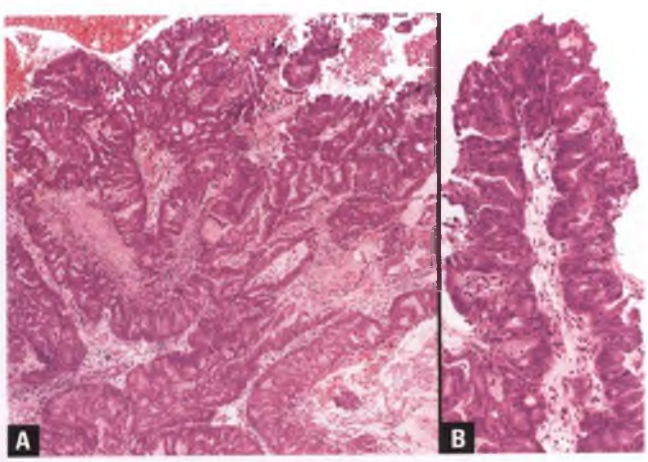

FIGURE 4.168. **A,B**: Well-differentiated endometrioid adenocarcinoma with a high-risk, coarsely papillary pattern. The glandular architecture of these exophytic structures is complicated by a garland of neoplastic epithelium of relatively uniform thickness that is composed of a repetitive winding pattern of short papillary processes and occasional cribriform spaces. The high-grade nuclear features of serous carcinoma are absent.

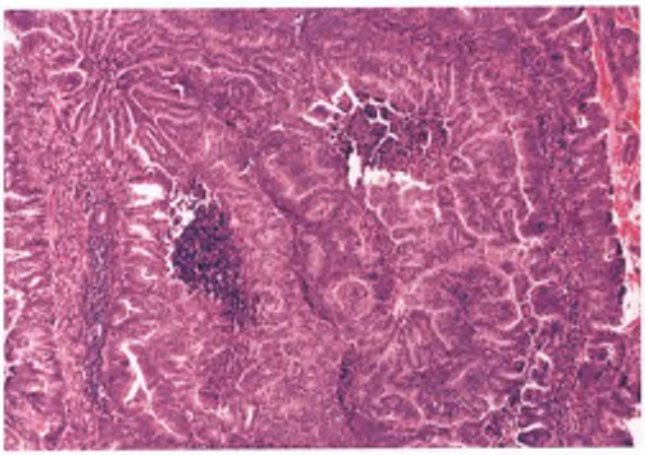

FIGURE 4.169. Well-differentiated endometrioid adenocarcinoma. This tumor features a prominent macroglandular pattern with a markedly complex internal architecture due primarily to numerous and closely packed papillary infoldings. Foci of central necrosis are also present within the two macroglands.

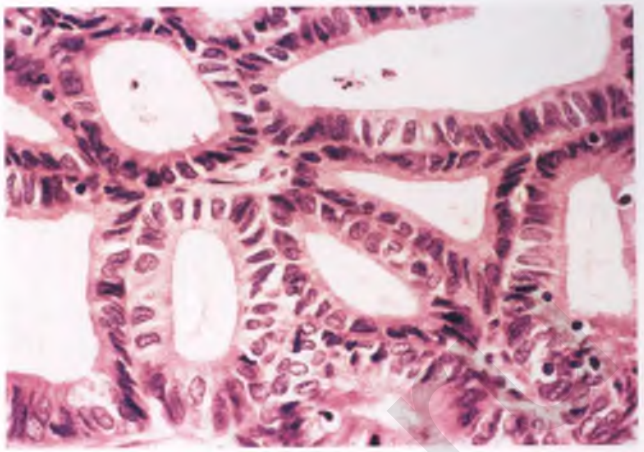

FIGURE 4.171. Well-differentiated endometrioid adenocarcinoma (high-magnification image of tumor in Fig. 4.170). What appears to be true cribriforming at low-magnification is actually found to be closely aggregated glands that are separated by wisps of stroma. Even in areas where stroma is difficult to visualize and consists of no more than apposed basal laminae, its presence can be inferred by the orientation of the nuclei of the individual glands.

or moderate, and it is the high-risk architectural features found in endometrial samples that allow recognition of these lesions as malignant (see Figs. 4.164–4.169).[106] Most of the remaining adenocarcinomas will have both high-risk architecture and easily recognizable cytologic atypia (Fig. 4.173). The degree of nuclear atypia may be focally severe; indeed, a small percentage of cases of adenocarcinoma have less than diagnostic architectural abnormalities, but are recognized as malignant by virtue of their marked cytologic atypia.[106,107] When used as an indicator of adenocarcinoma, marked cytologic atypia is defined by Longacre and colleagues as the presence of prominent nucleoli and/or significant nuclear pleomorphism that are visible at 150× and beyond what is usually seen in atypical hyperplasia (Fig. 4.174).[106,107] For practical purposes, this marked degree of cytologic atypia can be equated with the "notable" (grade 3) nuclear atypia in the Federation of Gynecology and Obstetrics (FIGO) grading system that prompts an increase in the grade of a grade 1 or 2 tumor by one level.[39] However, in the experience of the Stanford group, this degree of atypia is often focal in this setting, and does not warrant an upgrading of the tumor to a grade 2 carcinoma.[39] Before making a diagnosis of endometrioid adenocarcinoma on a focal and superficial lesion primarily on the basis of marked cytologic atypia, one must also consider the possibility of EIC, which is discussed in the section on serous carcinoma.

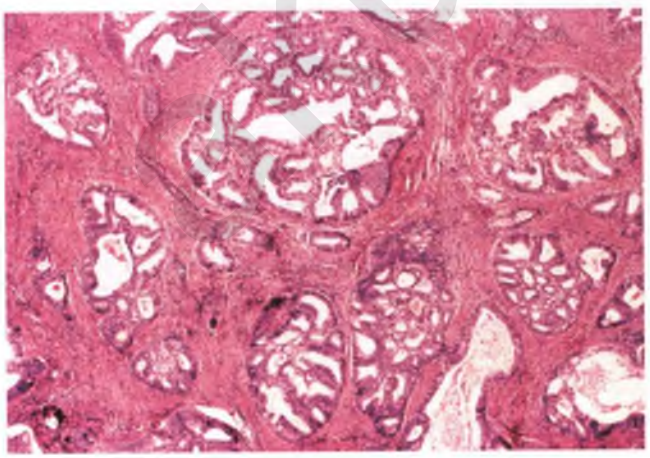

FIGURE 4.170. Well-differentiated endometrioid adenocarcinoma with myometrial invasion. At this magnification, the predominant growth pattern appears to be macroglandular with an internal cribriform architecture.

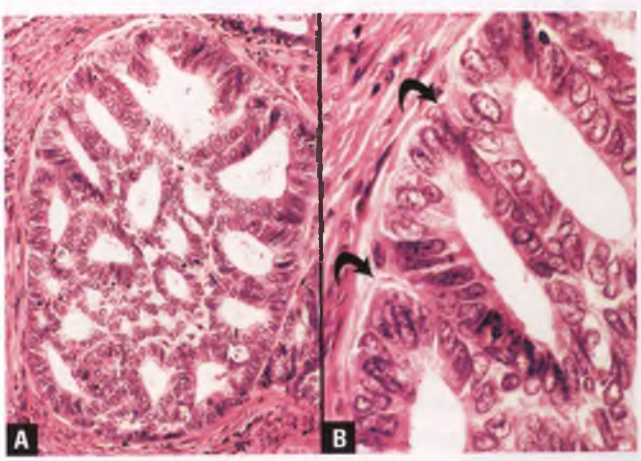

FIGURE 4.172. Well-differentiated endometrioid adenocarcinoma (high-magnification images of tumor in Fig. 4.170). **A**: Apparent macroglandular structure. **B**: In this particular tumor, the peripheral rim of most of these "macroglands" is actually formed by the tight apposition and smooth contouring of neighboring glands rather than by a contiguous band of epithelium (*arrows mark* junction of closely apposed glands).

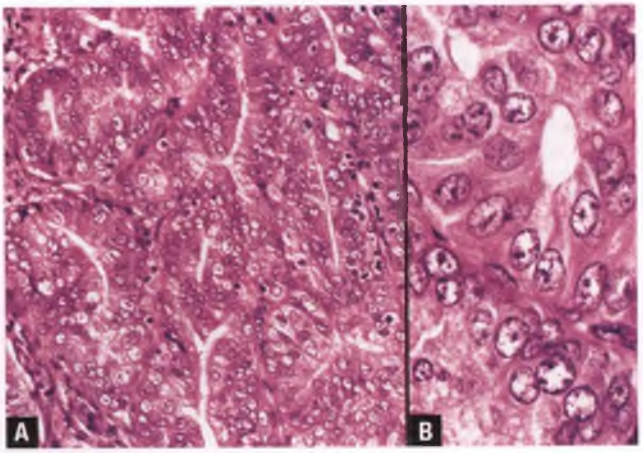

FIGURE 4.173. Well-differentiated endometrioid adenocarcinoma. **A**: Back-to-back, architecturally complex glands with barely discernible amounts of intervening stroma are lined by cells with cytologic atypia. Compressed glandular lumens have been reduced to slits, which results in an appearance that mimics a more solid growth pattern. **B**: Obvious cytologic atypia is present, with nuclear rounding, chromatin clearing, and prominent nucleoli. However, this degree of cytologic atypia can also be seen in atypical hyperplasia.

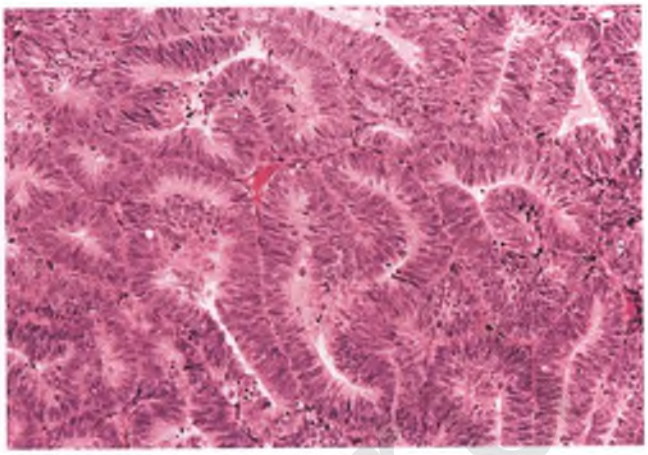

FIGURE 4.175. Borderline lesion: CAH versus well-differentiated adenocarcinoma. This problematic endometrial proliferation features back-to-back glands with moderate degrees of architectural complexity and cytologic atypia, and is often interpreted as adenocarcinoma. However, since each glandular prolife is invested by a fine tracery of eosinophilic stroma that includes compressed stromal cell nuclei in addition to apposed basal laminae, this lesion does not meet the definition of endometrial carcinoma by either the Kurman and Norris or Stanford criteria.

Borderline Lesions

Given the subjective nature of evaluating lesions within the morphologic continuum that exists between CAH and well-differentiated adenocarcinoma, it is inevitable that borderline cases will be encountered that are difficult to dogmatically place into one of these categories (Fig. 4.175). Of course, one pathologist's borderline lesion may be an example of atypical hyperplasia or well-differentiated adenocarcinoma to another pathologist, which should be expected given the lack of precision and standardization of phrases such as "glandular confluence," "glands uninterrupted by stroma," and "complete absence of stroma" that conjure up the images that we use to make these distinctions.

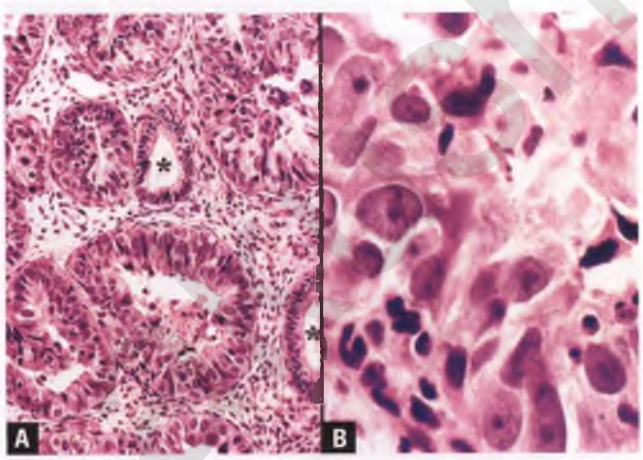

FIGURE 4.174. Endometrial adenocarcinoma. **A**: In this example, the diagnosis of adenocarcinoma is based upon the presence of a cluster of glands with marked nuclear atypia. Two glands that are lined by nonatypical epithelium are also present (*asterisks*). **B**: This high-magnification image demonstrates the prominent nucleoli, nuclear enlargement, and significant nuclear pleomorphism of the cells lining a malignant gland with intraluminal necrotic debris. In a lesion such as this, additional sampling may be indicated to exclude a nearby serous carcinoma or more aggressive endometrioid carcinoma.

Incidental Associated Findings

In some endometrial adenocarcinomas, there is prominent intraluminal mucinous material within glands whose lining epithelium has an endometrioid appearance (Fig. 4.176). In the absence of abundant intracytoplasmic mucin, these cases are referred to as mucin-rich endometrioid carcinomas and should not be interpreted as mucinous carcinomas.[134]

Aggregates of foamy histiocytes may be found within the stroma of endometrial adenocarcinoma (Fig. 4.177), as previously noted during the more in-depth discussion of the presence of these cells in endometrial hyperplasia. In most such cases, the endometrial tumor is a well-differentiated endometrioid carcinoma.[118] In cases where both the endometrial and endocervical compartments are involved by tumor, the presence of stromal foam cells can be taken as evidence supportive of an endometrial origin.

Histologic Grade

The 1988 International Federation of Gynecology and Obstetrics (FIGO) system is the most commonly utilized

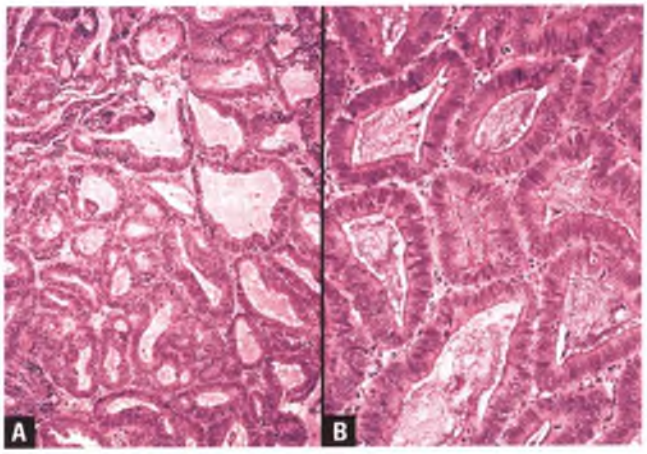

FIGURE 4.176. **A,B**: Mucin-rich endometrioid carcinoma (grade 1). Note the prominent accumulation of intraluminal mucinous material in a tumor whose glandular epithelium retains its endometrioid appearance.

method for grading endometrioid and mucinous carcinomas.[135] Details of this system, which relies heavily upon the architecture of the malignant glandular elements and includes a set of three explanatory notes, are outlined below (my comments are in italics). Several examples of grade 1 endometrioid carcinoma have already been presented; examples of grade 2 and grade 3 endometrioid carcinomas are depicted in Figures 4.178–4.180.

FIGO Histologic Grade

Grade 1 (well-differentiated; low-grade): ≤5% solid growth pattern*

Grade 2 (moderately differentiated; intermediate grade): 6% to 50% solid growth pattern*

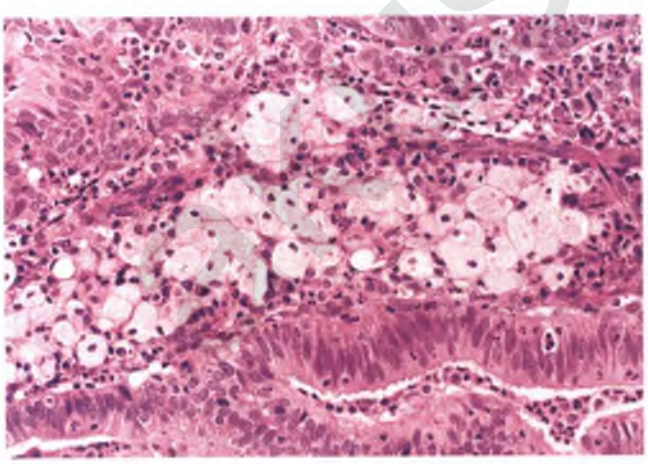

FIGURE 4.177. Grade 1 endometrioid carcinoma with an aggregate of stromal foam cells.

*Areas of squamous differentiation, morular or otherwise, are excluded from this assessment. *Nonsolid growth may be gland forming, villoglandular, or papillary. Within the setting of an endometrioid carcinoma, solid epithelial foci that lack recognizable glandular or squamous differentiation are considered to be of glandular origin for grading purposes.*[136]

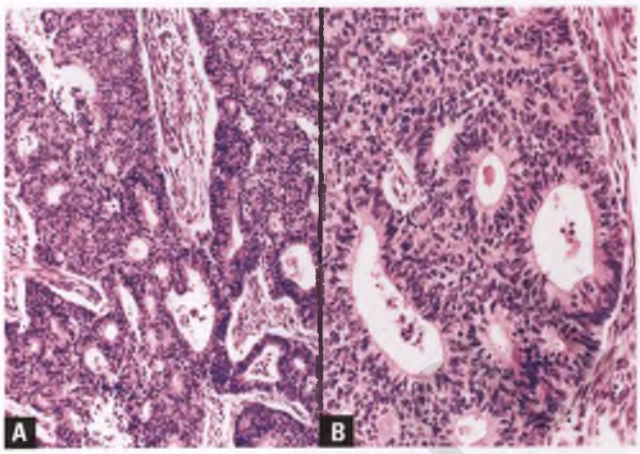

FIGURE 4.178. Grade 2 endometrioid carcinoma. **A**: This tumor exhibits a true cribriform growth pattern, and its nonsquamous solid component falls within the range of 6% to 50% that defines grade 2 neoplasms. **B**: Portion of a partially solid macrogland punctuated by cribriform glandular structures.

Grade 3 (poorly differentiated; high-grade): >50% solid growth pattern*

FIGO Notes on Grading

1. Notable nuclear atypia that is inappropriate for the architectural grade raises the grade of a grade 1 or grade 2 tumor by one level. *"Notable" has since been defined as grade 3 nuclear atypia in the majority of the neoplastic cells* (Fig. 4.180).[137] *Nuclear grade is based largely upon the degree of nuclear pleomorphism and the prominence of nucleoli.*[30,106,137] *Grade 1 nuclei are round to oval and have finely distributed chromatin with inconspicuous nucleoli, whereas grade 3 nuclei exhibit marked pleomorphism, prominent nucleoli, and abnormally coarse or cleared chromatin patterns.*[30,137] *Grade 2 nuclei have intermediate features. There is a tendency for the mitotic rate to increase in parallel with the nuclear grade. In the FIGO grading system,*

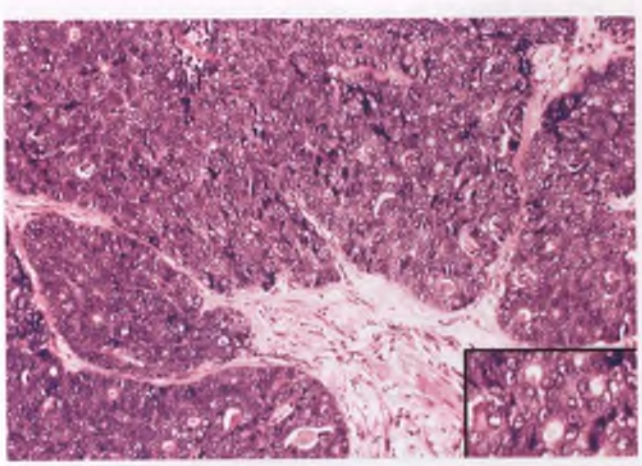

FIGURE 4.179. Grade 3 endometrioid carcinoma. This tumor features solid nests and sheets of malignant glandular epithelium with occasional microglandular formations, as highlighted in the inset.

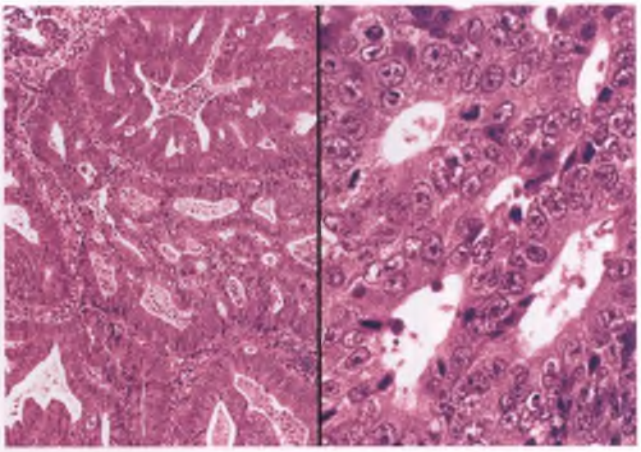

FIGURE 4.180. Grade 2 endometrioid carcinoma. This tumor is architecturally grade 1, but is upgraded to grade 2 on the basis of a high nuclear grade. The possibility of a serous carcinoma with glandular differentiation should be considered in tumors of this type (see section on serous carcinoma).

note that there is no significance attached to the subjective distinction between nuclear grades 1 versus 2. Upgrading tumors that are architecturally grade 1 to grade 2 on the basis of high-grade nuclei is very uncommon (2% of architecturally grade 1 cases in the series by Zaino and colleagues).[137] *It is now recognized that many endometrial tumors with the unusual combination of well-formed glands and high nuclear grade are actually serous carcinomas with glandular differentiation, so this possibility should be considered whenever contemplating an upgrade of an endometrioid carcinoma based on marked nuclear atypia.*[9,138] *Upgrading of tumors that are architecturally grade 2 to grade 3 based on high nuclear grade occurs in approximately 15% of architecturally grade 2 cases.*[137]

2. Nuclear grading takes precedence in serous, clear cell, and squamous cell carcinoma. *Most investigators consider serous and clear cell carcinomas to be high grade by definition. Primary squamous cell carcinomas of the endometrium are extraordinarily rare, and there are no outcome data to support nuclear grading of these tumors over conventional grading based on a combination of nuclear atypia, keratin production, and mitotic rate.*
3. Adenocarcinomas with squamous differentiation are graded according to the nuclear grade of the glandular component. *Although there is nearly universal agreement that adenocarcinomas with squamous differentiation should be graded according to the features of the glandular component, most investigators currently recommend that such grading be based upon glandular architecture in the same way that it is done for usual endometrioid carcinomas, with nuclear grade having an impact only when grade 3 atypia prompts an increase in the grade of a grade 1 or grade 2 tumor by one level.*[30,136,137]

Additional Comments on FIGO Grading

1. Undifferentiated carcinoma shows a complete lack of glandular formation and pursues a more aggressive course than FIGO grade 3 adenocarcinoma.[139,140] The FIGO grading system was formulated prior to detailed reporting of undifferentiated carcinoma and classifies both of these tumors as grade 3 carcinomas. Given their prognostic differences, these two tumors should be separated from one another.
2. On rare occasions, a low-grade adenocarcinoma may be found side by side with an undifferentiated carcinoma.[141] When the high-grade component represents at least 20% of the tumor, these malignancies behave as high-grade tumors and should be diagnosed as a form of mixed carcinoma, with a note emphasizing their aggressive behavior. Grading such tumors based on an overall estimate of their degree of solid architecture will often result in an underestimate of their malignant potential.
3. In most series, the frequency of grade 1 tumors exceeds that of grade 2 tumors, which in turn exceeds that of grade 3 tumors. Taken together, grade 1 and grade 2 tumors, which some investigators combine into a low-grade category, comprise approximately 80% of endometrioid carcinomas.[126,129,142–144]

Utility and Prognostic Significance of the FIGO Grading System

Primarily due to issues related to tumor heterogeneity and sampling error, it is not uncommon for the final grade of the tumor in the hysterectomy specimen to be different from that in the diagnostic endometrial sample.[145,146] The lower the grade of the tumor in the endometrial sample, the higher the likelihood of a discrepancy with the final tumor grade in the resected uterus (particularly if the initial diagnosis is based upon biopsy rather than curettage material).[145,146] Intraoperative consultations for situations in which the surgeon would like to spare the patient with a presumed low-grade tumor a staging procedure can help to address this issue, as well as provide additional information to guide surgical management (see below).

The 5-year survival of surgical stage I tumors with grades 1, 2, and 3 endometrioid carcinoma is approximately 90% to 95%, 85%, and 70% to 75%, respectively,[143,147] although some studies have not found there to be a statistically significant survival difference between grade 1 versus grade 2 tumors.[148] In endometrioid carcinomas that are confined to the uterus, the impact of histologic grade as an independent prognostic factor is diminished by the positive correlation between adverse prognostic factors such as deep myometrial invasion, angiolymphatic invasion, and involvement of the uterine cervix with increasing tumor grade.[126,129,144,149,150] Another important positive correlation with increasing tumor grade is the associated higher incidence of lymph node metastases.[149]

As is the case for almost all malignancies, the stage of the tumor at the time of definitive treatment is the single most important prognostic factor, although the 5-year survival rate of those patients with metastatic deposits of low-grade tumor is superior to those with high-grade metastatic disease.[128,147] In 2008, important changes were made to the FIGO staging system for endometrial carcinoma,[151] some of which are discussed in the section on cervical involvement by endometrial adenocarcinoma in Chapter 3 and in the section on the reporting of myometrial invasion later in this chapter.

Alternatives to the FIGO Grading System

Attempts to improve upon the reproducibility and clinical relevance of the three-grade FIGO system have resulted in the proposal of several different two-grade systems.[142,148,152,153] Some of the approaches that have been utilized include using 20% as the cutoff for the amount of nonsquamous solid component to distinguish low- from high-grade tumors,[153] collapsing grades 1 and 2 tumors into a single low-grade category,[129,148] doing away with the need to distinguish squamous from nonsquamous solid growth,[142,152] and placing emphasis on other variables such as the pattern of tumor infiltration,[152] the presence or absence of tumor necrosis,[152] nuclear grade,[148] and the mitotic index.[148] Some of these proposals are based solely on experience with hysterectomy specimens, and their utility in biopsy material remains unproven.[142,148,152] Although the current FIGO grading system has its flaws and can be improved, more experience with these various two-tier systems is necessary before any of them can be recommended as a possible successor.

Intraoperative Consultations

In cases in which the pathologist is called for an intraoperative consultation to examine a uterus that harbors endometrial carcinoma, the primary issue is whether or not the surgeon should perform a staging procedure. If the preoperative diagnosis is grade 3 endometrioid, undifferentiated, serous, or clear cell carcinoma, then the high risk of extrauterine disease should prompt the surgeon to proceed with staging regardless of the findings in the uterus. For endometrioid carcinomas, a rough assessment of the depth of myometrial invasion (superficial = inner half; deep = outer half), approximate tumor grade (grade 1–2 vs. high grade), and gross status of the endocervical canal is sufficient information to guide intraoperative management. Intraoperative consultations with frozen sections have been shown to result in appropriate surgical management in almost 95% of cases.[154,155] In situations where the gross examination reveals obvious deep myometrial invasion by biopsy-proven adenocarcinoma, the frozen section may be omitted at the pathologist's discretion.

The intraoperative consultation should be phrased in such a way as to tell the surgeon the relevant information without providing details that may need to be revised or retracted in the final report. For example, "Low or intermediate grade endometrial carcinoma with no evidence of deep myometrial invasion or endocervical involvement" is preferable to "grade 1 endometrioid carcinoma with no evidence of myometrial invasion or endocervical involvement." In this example, if review of the permanent sections results in a final diagnosis of grade 2 endometrioid carcinoma with invasion 10% into the uterine wall, the final diagnosis is fully compatible with the more broadly worded intraoperative consultation. On the other hand, the more specific intraoperative consultation disagrees with both the tumor grade and the degree of myometrial invasion, could be scored by a "bean counter" as an intraoperative consultation disagreement, and also serves as a potential source of confusion for readers of the report.

ENDOMETRIOID ADENOCARCINOMA: VARIANTS AND UNUSUAL PATTERNS

Endometrioid Carcinoma with Squamous Differentiation

Although squamous differentiation is found in approximately 25% of endometrioid carcinomas,[136,156] this diagnostic category is intended for those endometrioid carcinomas in which squamous differentiation comprises at least 10% of the epithelial component. In endometrioid carcinomas with extensive squamous differentiation, deposits of keratin may be grossly visible (see Fig. 3.260). The squamous elements may be overt, subtle, focal, or widespread, and may have an appearance that is histologically benign, malignant, or indeterminant.[156] Obvious examples of mature squamous differentiation feature cells with abundant eosinophilic cytoplasm, polygonal shapes, distinct cell membranes, intercellular bridges, and keratin production, although intercellular bridges and keratin production are not required in this context.[156] The discrete form of morular metaplasia is fairly easy to recognize, but morules with spindle cell morphology, sheet-like growth, confluence, and/or central necrosis can lead to misinterpretation of a hyperplastic process as malignant or a grade 1 endometrioid carcinoma with squamous differentiation as a higher grade tumor (Figs. 4.181 and 4.182). The more benign-appearing forms of squamous differentiation tend to be intimately associated with the neoplastic glands, whereas nests of malignant squamous epithelium are typically found independently infiltrating stroma with an associated desmoplastic response.[136,156,157]

In general, the degree of squamous atypia parallels that of the glandular component, such that the grade of the glandular component sufficiently reflects the prognostic significance associated with tumor grade.[136,156,157] In other words,

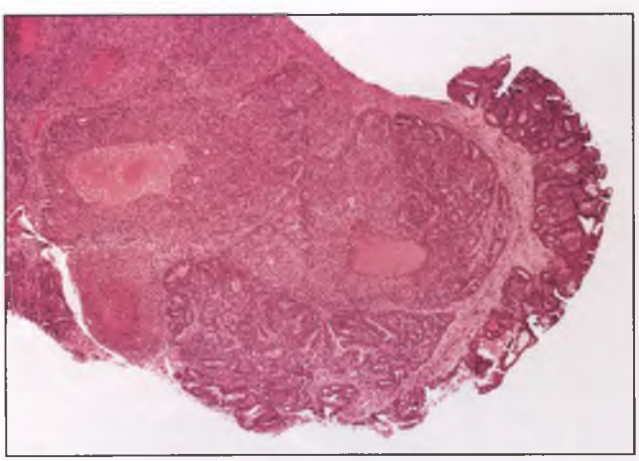

FIGURE 4.181. This grade 1 endometrioid carcinoma with squamous differentiation exhibits prominent morules, many of which contain foci of central necrosis. The tumor is graded on the basis of its glandular component, which is well differentiated.

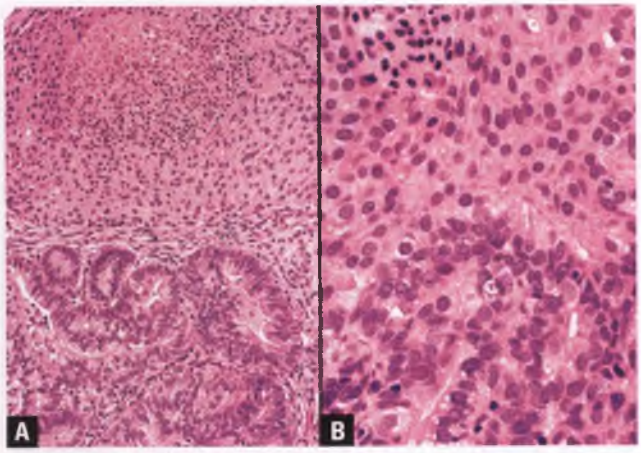

FIGURE 4.182. **A,B**: Grade 1 endometrioid carcinoma with squamous differentiation (same case as preceding figure). Note the bland nuclear features of the squamous morules, which are partially necrotic.

benign-appearing squamous morules, identical to those seen in endometrial hyperplasia and metaplasia, are typically associated with grade 1 endometrioid carcinomas, whereas malignant-appearing squamous elements are usually seen in association with grade 3 endometrioid carcinomas (Figs. 4.183–4.185). Traditionally, the former tumors were designated adenoacanthomas, whereas the latter were termed adenosquamous carcinomas, but the current recommendation is to refer to all such tumors as endometrioid carcinomas with squamous differentiation, and to grade them according to the features of the glandular component.

Although not diagnostic of carcinoma, endometrial samples that contain masses of squamous epithelium and/or sheets of keratin should be viewed with suspicion, since this finding often represents superficial sampling of the squamous component of an endometrioid carcinoma with extensive squamous differentiation (Fig. 4.186).

In some cases of endometrioid carcinoma with squamous differentiation, solid patches of squamous cells have clear cytoplasm due to the presence of abundant glycogen, which results in an appearance that could be mistaken for a component of clear cell carcinoma (Fig. 4.187). In contrast to the almost invariably solid, sheet-like architecture of these glycogen-rich squamous cells, clear cell carcinoma typically exhibits a distinctive admixture of solid, papillary, and tubulocystic patterns, and is also generally composed of cells with a greater degree of nuclear atypia that often display hobnail features.

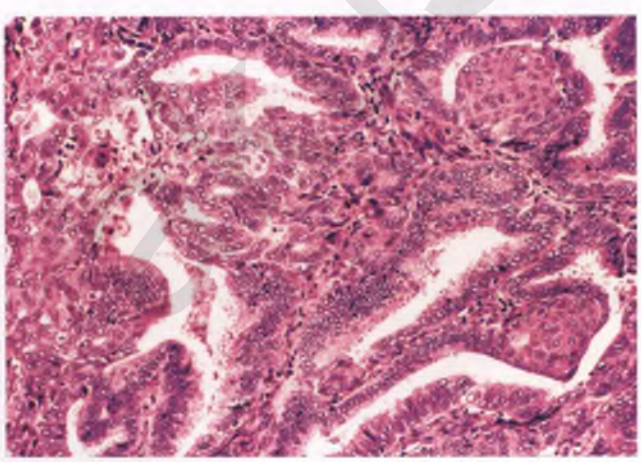

FIGURE 4.183. Grade 1 endometrioid carcinoma with squamous differentiation. Two benign-appearing, well-formed morules are present on the right side of the image. On the left side, less discrete forms of squamous differentiation with bland nuclear features are evident.

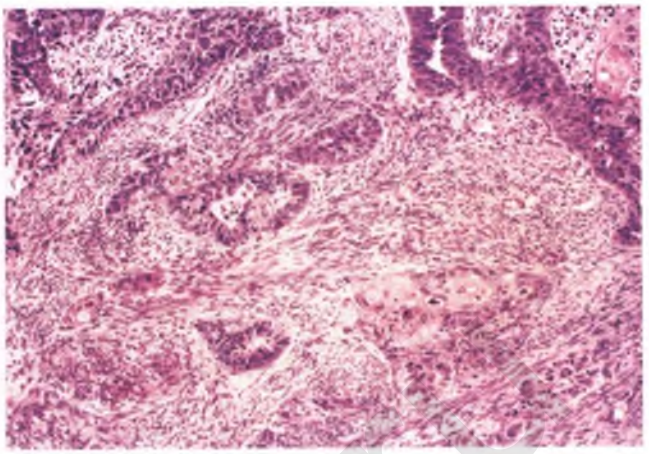

FIGURE 4.184. Myoinvasive grade 3 endometrioid carcinoma with squamous differentiation. Squamous elements are scattered throughout this aggressive adenocarcinoma, which is grade 3 by virtue of its glandular component having an architecture that is >50% solid.

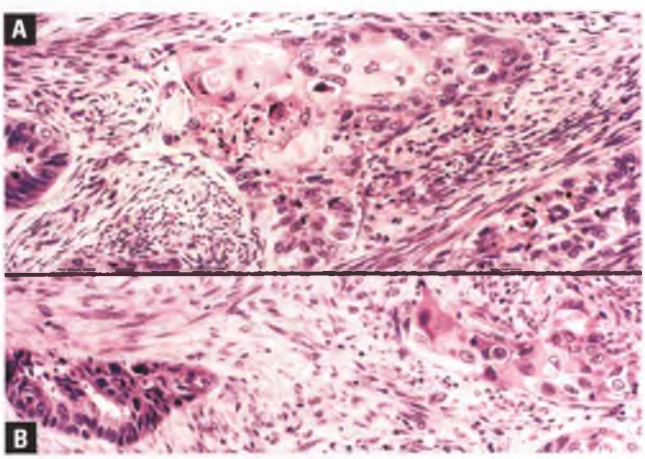

FIGURE 4.185. **A,B**: Myoinvasive grade 3 endometrioid carcinoma with squamous differentiation. These two high-magnification views of the tumor in the preceding figure highlight the cytologically malignant squamous component (at center in **A** and at right in **B**) that invades the myometrium.

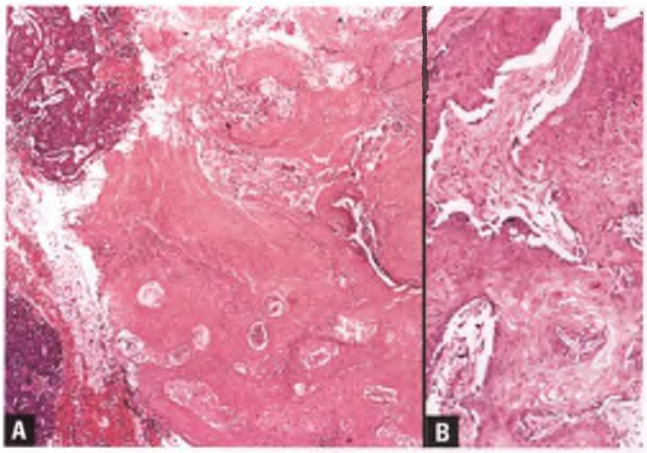

FIGURE 4.186. Beware of masses of squamous epithelium and/or sheets of keratin within endometrial samples. **A**: This curettage contains sheets of keratin associated with benign-appearing squamous cells and small fragments of endometrioid carcinoma (upper and lower left). **B**: This curettage contains irregular masses of indeterminate squamous epithelium and some desmoplastic stroma. A Grade 1 endometrioid carcinoma was present in other tissue fragments.

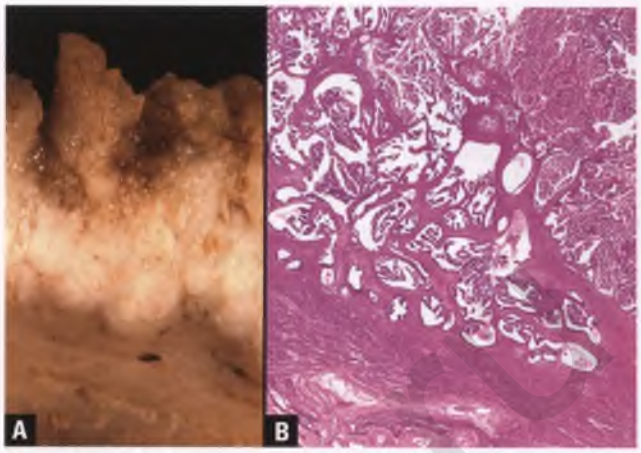

FIGURE 4.188. Villoglandular endometrioid carcinoma. **A**: Section through a formalin-fixed tumor with superficial myometrial invasion. Note the resemblance to a villous adenoma of the large intestine. **B**: This low-magnification view documents the presence of myometrial invasion along the deep aspect of the tumor. In this example, villoglandular architecture is present in both the invasive and noninvasive components, and there is no stromal reaction in the myoinvasive foci.

Villoglandular Endometrioid Carcinoma

Pure villoglandular endometrioid carcinoma (VGEC) has a gross appearance that resembles a villous adenoma of the colon, with shaggy, friable, fingerlike fronds projecting from the surface of the tumor (Fig. 4.188A). This resemblance extends to the histologic features of these fronds, which consist of closely packed, branching arrays of long, slender papillae with delicate fibrovascular cores (Fig. 4.188B).[158,159] These structures are lined by pseudostratified columnar epithelial cells with mild to moderate nuclear atypia that tend to be oriented perpendicular to their basement membranes (Fig. 4.189).[158,159] The apical aspects of the neoplastic cells form a predominantly smooth border with the interposed crevice-like spaces, although occasional apical cytoplasmic blebs can be seen.[158] Although some degree of villoglandular differentiation can be seen in as many as 31% of endometrioid adenocarcinomas,[159] most investigators reserve the diagnosis of VGEC for the approximately 10% of such tumors in which the dominant pattern is villoglandular. When typical endometrioid adenocarcinoma and VGEC are admixed with one another, the conventional component is usually located at the base of the neoplasm. Although the prevailing opinion is that VGECs behave similarly to ordinary low-grade endometrioid adenocarcinomas,[158] one study suggested that those VGECs whose villoglandular architecture is preserved in the areas of myoinvasion pursue a more aggressive course.[159]

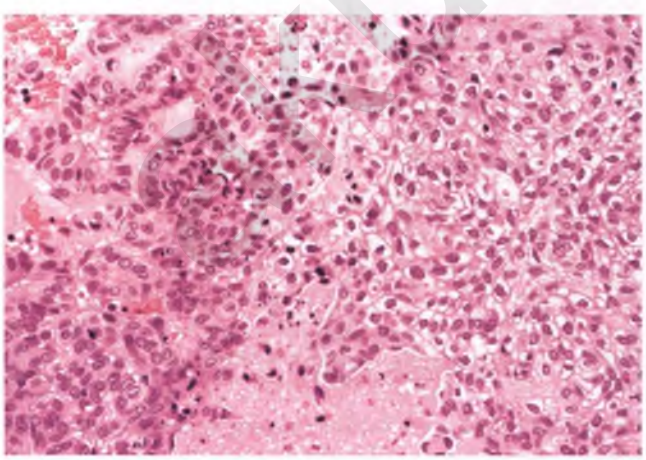

FIGURE 4.187. Endometrioid carcinoma with squamous differentiation. In this example, the squamous elements at right have clear cytoplasm due to the presence of abundant glycogen, which results in some resemblance to clear cell carcinoma.

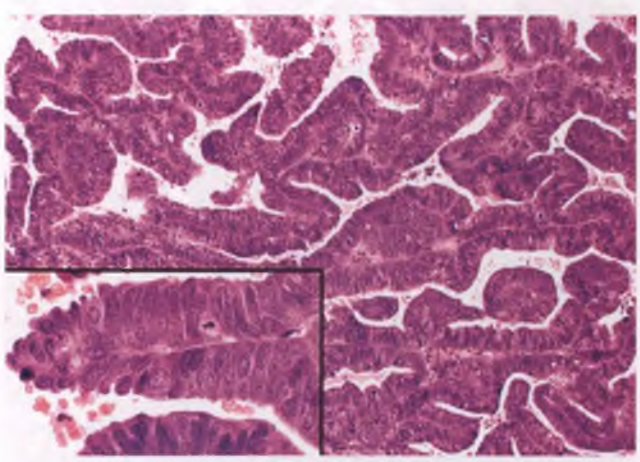

FIGURE 4.189. Villoglandular endometrioid carcinoma. Neoplastic columnar epithelial cells with mild to moderate nuclear atypia line winding villous structures with slender, delicate fibrovascular cores and predominantly smooth apical aspects.

Differential Diagnosis

The differential diagnosis of VGEC includes serous carcinoma, endometrioid carcinoma with small nonvillous papillae, and lesions within the spectrum of the benign endometrial papillary proliferations described by Lehman and Hart.[123,124,160,161]

- Serous carcinomas often have a papillary architecture, but classic examples are distinguished from VGEC by the combination of high rather than low to intermediate nuclear grade, round to oval rather than elongate and radially arranged nuclei, broad rather than slender papillary stalks, a more complex and arborizing architecture, small detached papillary epithelial clusters in the vicinity of the larger papillae ("epithelial tufting"), and a scalloped rather than smooth surface contour. Rare endometrial carcinomas represent an admixture of VGEC and serous carcinoma (as illustrated for endocervical tumors in Figure 3.228), and there are occasional cases that exhibit architectural and nuclear features intermediate between VGEC and serous carcinoma (Fig. 4.190). When these situations arise in curettage specimens, it is recommended that patients be treated using the protocol for serous carcinoma (i.e., undergo a careful staging procedure at the time of hysterectomy). Anecdotal experience with intermediate (as opposed to mixed) forms suggests that they do not behave as aggressively as full-fledged serous carcinomas.
- In some endometrial carcinomas with a villoglandular architecture, papillary eosinophilic buds project from a significant proportion of the slender villi, as illustrated in the next section. It is arbitrary whether such tumors are regarded as VGECs with superimposed small nonvillous papillae or considered as being within the spectrum of endometrioid adenocarcinomas with small nonvillous papillae. Although these papillary buds are of no clinical significance, their importance lies in the fact that their presence heightens the resemblance of these villoglandular tumors to serous carcinomas.
- The distinction of benign endometrial papillary proliferations from VGEC is discussed in the section on metaplastic hyperplasias.

Note: Although VGEC could legitimately be referred to as a papillary neoplasm, the term "papillary" is avoided as a diagnostic descriptor to help prevent confusion with the more aggressive uterine serous carcinoma, which was initially described and is still often diagnosed as papillary serous carcinoma.

Endometrioid Carcinoma with Small Nonvillous Papillae

Some endometrioid adenocarcinomas are characterized by the presence of small eosinophilic papillary buds that lack fibrovascular cores. These projections are typically found within closely packed glands of otherwise ordinary grade 1 to 2 endometrioid adenocarcinomas (Figs. 4.191A and 4.192). Occasionally, buds with these features are also seen emanating from villous structures similar to those seen in villoglandular endometrioid adenocarcinoma (Fig. 4.191B). Those endometrioid carcinomas in which papillary buds of this type are present in ≥25% of the tumor have been dubbed endometrioid carcinomas with small nonvillous papillae.[161] When so defined, such tumors account for approximately 8% of endometrioid adenocarcinomas, and are associated with a behavior and prognosis similar to that of the usual type of non–high-grade endometrioid adenocarcinoma.[161] The adjacent endometrium frequently contains endometrial hyperplasia with similar-appearing papillary buds.[161]

The distinction between the upper end of a metaplastic hyperplasia with papillary eosinophilic budding and an endometrioid adenocarcinoma with small nonvillous papillae is difficult

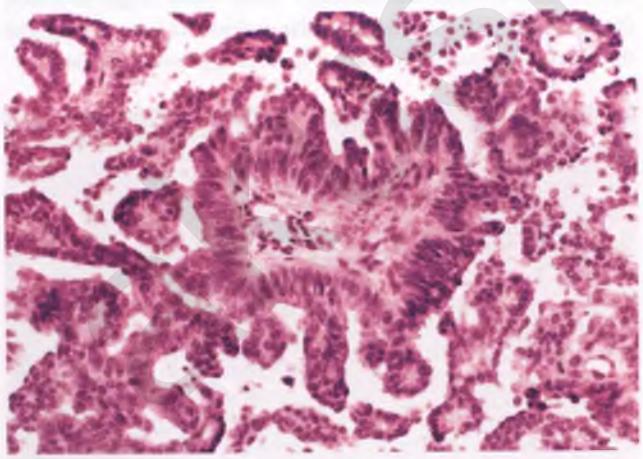

FIGURE 4.190. Adenocarcinoma with features intermediate between villoglandular endometrioid adenocarcinoma and serous carcinoma. In this endometrial sample, the architectural features favor serous carcinoma, but the nuclear features are more in keeping with VGEC. The elderly patient was staged as if she had serous carcinoma, found to have tumor invading the outer half of the myometrium with no extrauterine spread, and died seven years later of unrelated causes. (Glass slide kindly provided by Dr. Cheryl M. Reichert.)

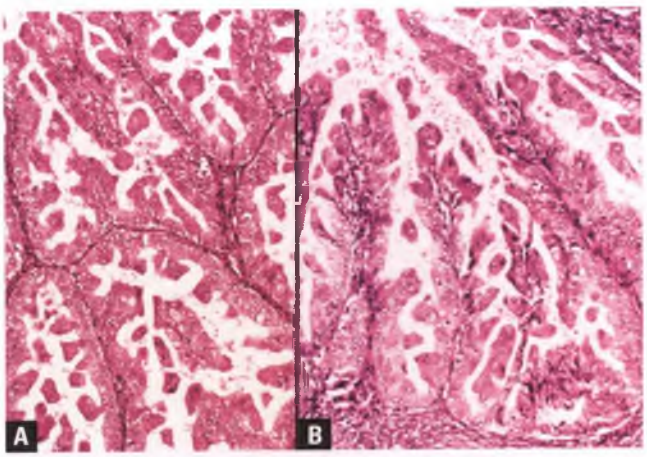

FIGURE 4.191. Grade 1 endometrioid adenocarcinoma with small nonvillous papillae. **A**: The papillae have eosinophilic cytoplasm, lack fibrovascular cores, and are found budding from back-to-back glands of a usual endometrioid adenocarcinoma, which showed less stromal support in adjacent fields. **B**: Occasionally, these papillary buds can also be seen projecting from villous structures similar to those seen in villoglandular endometrioid adenocarcinoma.

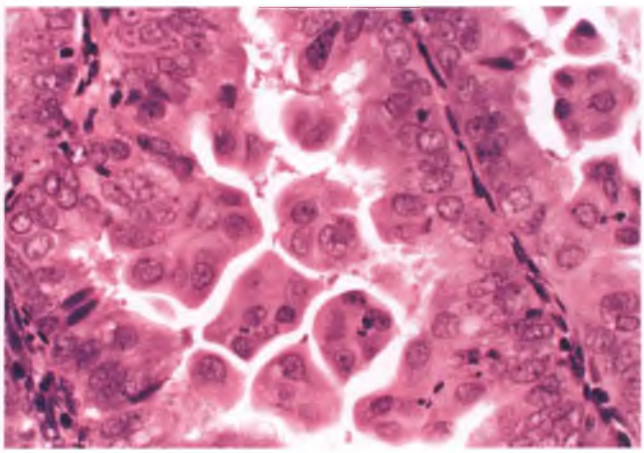

FIGURE 4.192. Grade 1 endometrioid adenocarcinoma with small nonvillous papillae. Several papillae are seen projecting into gland lumens in an area of back-to-back glands.

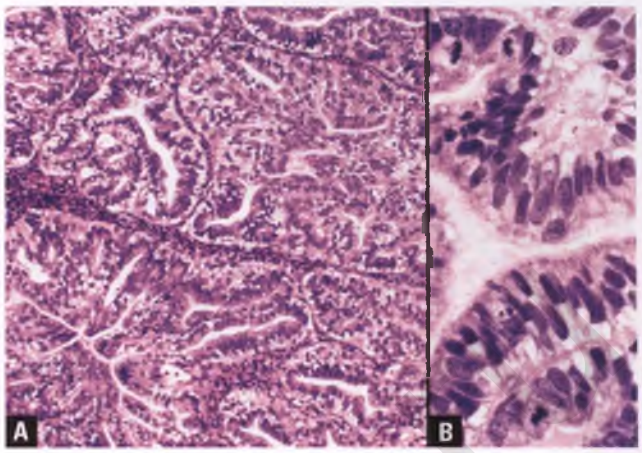

FIGURE 4.193. Grade 1 secretory carcinoma. **A**: This tumor is characterized by markedly complex glands with scant intervening stroma and prominent subnuclear and supranuclear vacuoles. **B**: High-magnification view of columnar cells with cytoplasmic vacuolization, low-grade nuclear atypia, and mitotic activity.

and subjective, as discussed in the section on metaplastic hyperplasias. The other major differential diagnostic consideration is serous carcinoma, which is a more aggressive tumor that is distinguished mainly by its high-grade nuclear features. Serous carcinoma is also more likely to have psammoma bodies, invade angiolymphatic spaces, present with extrauterine disease, and lack associated hyperplasia in the neighboring endometrium.[161]

Secretory Carcinoma

Secretory carcinoma is a rare variant of endometrioid carcinoma that is characterized by architecturally complex, markedly crowded glands that bear some resemblance to postovulatory day 3 to 4 secretory endometrium due to the prominence of clear subnuclear and/or supranuclear cytoplasmic vacuoles (Fig. 4.193).[162,163] These tumors generally exhibit minimal epithelial stratification, are almost always well differentiated, and have a prognosis similar to grade 1 endometrioid carcinoma. The cytoplasmic vacuolization is sometimes due to a recognizable source of progesterone, in which case the secretory differentiation may be a transient phenomenon. However, many cases occur in postmenopausal women with no history of hormonal therapy, for which there is no explanation for the secretory appearance.

It is important to distinguish secretory carcinoma from the more aggressive clear cell carcinoma, which is accomplished by noting the low nuclear grade of secretory carcinoma and its lack of architectural tricks that are found within the repertoire of clear cell carcinomas (admixed papillary, tubulocystic, and solid patterns).[162–164] Secretory carcinoma should also be distinguished from CAH with secretory differentiation, which shows low-grade nuclear atypia accompanied by lesser degrees of architectural complexity and glandular crowding (Fig. 4.194).

Endometrioid Carcinoma with Benign-Appearing Surface Epithelial Changes

It is not uncommon for grade 1 to 2 endometrioid carcinomas from hysterectomy specimens to exhibit focal to prominent surface epithelial changes that resemble papillary syncytical change and/or endocervical microglandular hyperplasia.[97] In this setting, these findings are usually given only a passing glance. However, in some endometrial samples where tissue is limited or only the surface of the lesion is available for analysis, these surface epithelial changes can be the predominant or sole element and lead to diagnostic difficulties. The papillary syncytial aspect of this issue has been addressed and illustrated in the section on endometrial metaplasias. The histologic features that result in a resemblance to microglandular hyperplasia include a prominent microglandular architecture associated with an intraluminal mucinous secretion, numerous neutrophils located within gland lumens and the stroma, glands lined by cells with round to oval nuclei with a degree of nuclear atypia that ranges from inapparent to moderate, and inconspicuous mitotic activity (Fig. 4.195).[97] It is not known

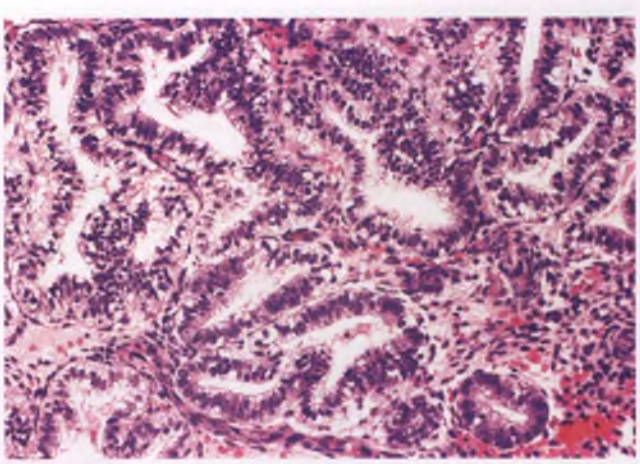

FIGURE 4.194. CAH with secretory differentiation. In comparison to secretory carcinoma, the glands are less complex and less crowded, but exhibit a similar degree of nuclear atypia.

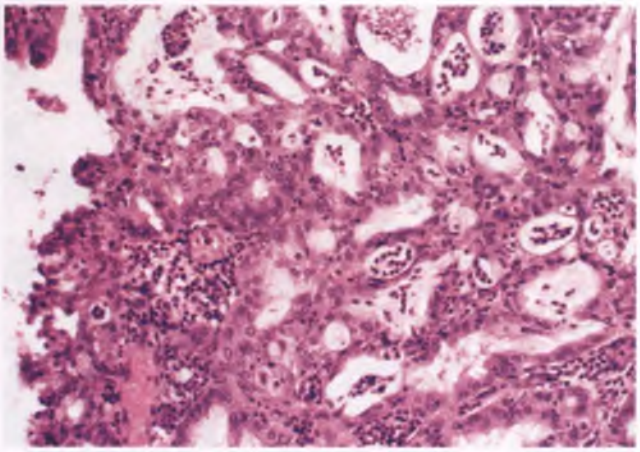

FIGURE 4.195. Endometrioid carcinoma with surface epithelial change simulating microglandular hyperplasia. Note the microglandular pattern, bland nuclear features, and intraluminal/stromal neutrophils. This field is not diagnostic of carcinoma, but should raise the possibility of an associated malignancy in this postmenopausal patient. At hysterectomy, there was an underlying grade 1 endometrioid carcinoma with superficial myometrial invasion.

whether the bland forms of these surface epithelial changes represent a morphologically uninformative portion of the carcinoma or a coexisting form of metaplastic hyperplasia.

In addition to occurring as a surface phenomenon, endometrial adenocarcinomas can simulate microglandular hyperplasia throughout all or major portions of their superficial and deep aspects.[165,166] Since most such carcinomas represent forms of mucinous or mixed mucinous and endometrioid carcinoma, they are discussed in the section on mucinous carcinoma.

Corded and Hyalinized Endometrioid Carcinoma

This rare, unusual variant of endometrioid carcinoma has a peculiar low-magnification appearance due to the presence of cords, clusters, and/or trabeculae of epithelioid and spindle cells embedded within a hyalinized matrix (Fig. 4.196).[134,167] Typical grade 1 to 2 endometrioid adenocarcinoma is also present in variable amounts. Most cases also exhibit squamous differentiation, which is occasionally associated with the formation of osteoid.[167] The corded component exhibits variable immunoreactivity for cytokeratin, and is negative for the muscle markers actin and desmin, the endometrial stromal marker CD10, and the sex-cord marker inhibin.[167] This immunophenotype, coupled with the occasionally seen gradual merging of the corded and squamous elements (Fig. 4.197), supports an epithelial rather than stromal origin for the cells in these cords. In a small percentage of cases, the corded architecture is unassociated with hyalinized stroma (Fig. 4.197); in this situation, the designation "endometrioid adenocarcinoma with cord-like differentiation" is more appropriate.

The biphasic appearance of the corded and hyalinized endometrioid carcinoma imparts a resemblance to carcinosarcoma, and there is no doubt that these tumors account for a significant proportion of neoplasms previously placed in the tenuous category of "low-grade" carcinosarcoma/malignant mixed müllerian tumor. In contrast to carcinosarcoma, the glandular and pseudo-stromal components are of low to intermediate rather than high grade, patients tend to be younger (mean age of 52 years), nearly all patients present with disease confined to the uterus, and the prognosis is generally favorable.[167] Although various rare uterine tumors with sex-cord–like growth patterns are also differential diagnostic considerations, the coexistence of endometrioid adenocarcinoma and the usual association with squamous differentiation in corded and hyalinized endometrial carcinoma generally allow for its distinction.

Endometrioid Carcinoma with a Prominent Spindle Cell Component

Although better documented for ovarian rather than endometrial endometrioid tumors,[168] rare uterine endometrioid carcinomas can exhibit prominent spindle cell differentiation (Fig. 4.198).[134] These tumors are not worthy of the ominous-sounding

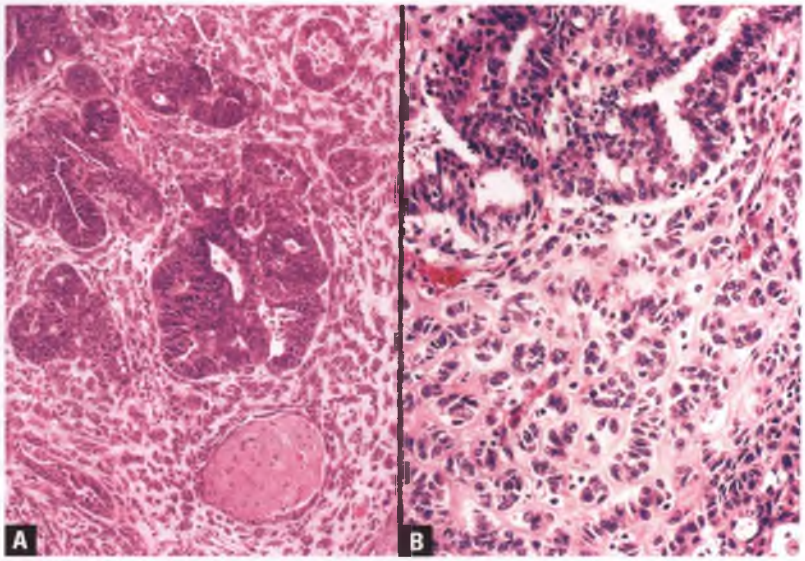

FIGURE 4.196. **A,B**: Characteristic biphasic appearance of corded and hyalinized endometrioid adenocarcinoma. Note the focus of squamous differentiation at the lower right in **A**.

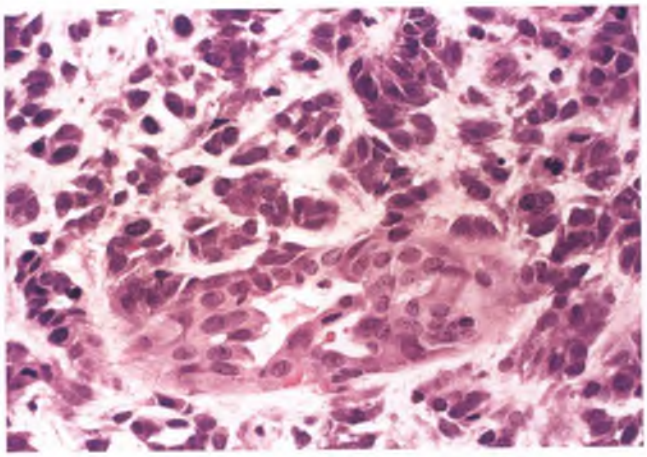

FIGURE 4.197. Endometrioid adenocarcinoma with cord-like differentiation. Note the merging of the corded and squamous elements (typical low-grade endometrioid carcinoma was present in adjacent tissue). In this example, stromal hyalinization is absent.

designation of "sarcomatoid carcinoma," since both the glandular and spindle cell components appear well to moderately differentiated and the expected behavior is no different than ordinary grade 1 to 2 endometrioid carcinoma. The spindle cells in these tumors are uniform and do not exhibit the high nuclear grade and brisk mitotic activity that is seen in the spindle cell component of carcinosarcoma, and appear to represent an abortive form of squamous differentiation. As such, the spindle cell component in these endometrioid carcinomas should not be considered a solid growth pattern for grading purposes. Instead, these tumors should be graded based upon the architectural and nuclear features of the glandular component. In addition to the differences in nuclear grade and mitotic activity noted above, these tumors are also distinguished from carcinosarcoma by

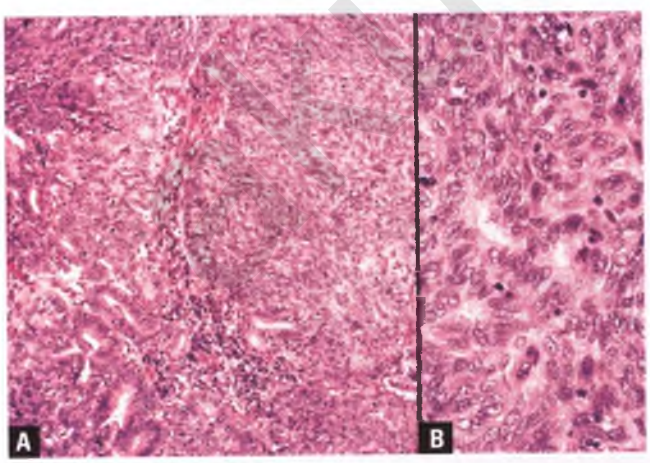

FIGURE 4.198. Endometrial endometrioid carcinoma with a prominent spindle cell component. **A**: An area of well-differentiated endometrioid adenocarcinoma is seen in association with a spindle cell proliferation. **B**: The spindle cells are uniform, bland, mitotically inactive, and merge imperceptibly with some of the neoplastic glands.

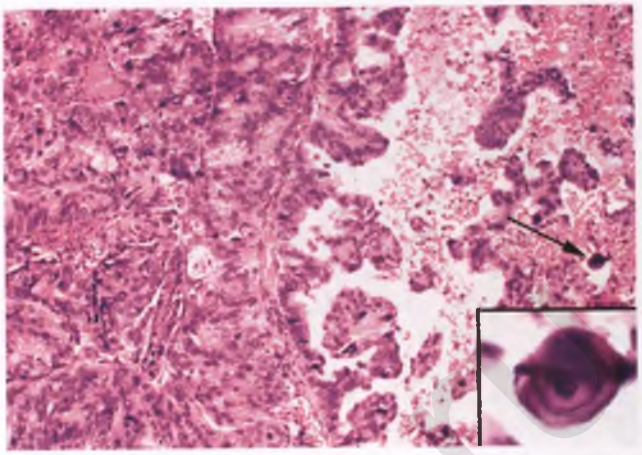

FIGURE 4.199. Endometrioid carcinoma with rare psammoma bodies (*arrow* and inset). These concretions are laminated and basophilic.

their gradual blending of the epithelial and spindle cell components and by the frequent finding of diffuse immunoreactivity of the spindle cells for cytokeratin.[168]

Endometrioid Carcinoma with Psammoma Bodies

Although most endometrial adenocarcinomas that are associated with psammoma bodies are serous carcinomas, these structures can rarely be encountered in endometrioid carcinomas of usual type, particularly in association with areas of inflammation and necrosis (Fig. 4.199).[169]

Oxyphilic/Oncocytic Endometrioid Carcinoma

Rare oxyphilic endometrioid carcinomas are composed predominantly or entirely of cells with large amounts of granular, eosinophilic cytoplasm (Fig. 4.200).[170] When examined ultrastructurally, some of these tumors have been found to be composed of cells with abundant mitochondria; the term oncocytic

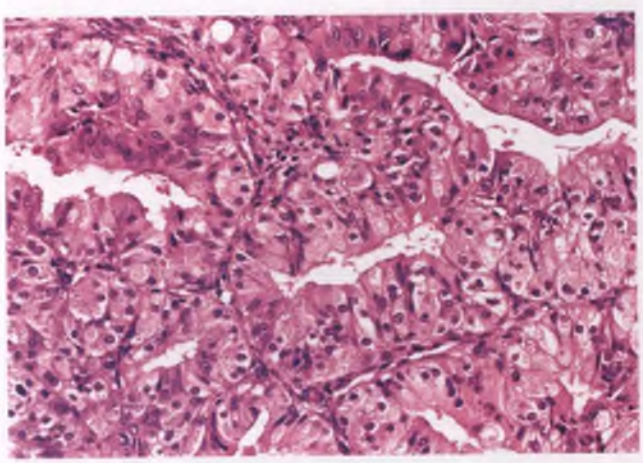

FIGURE 4.200. Oxyphilic endometrioid carcinoma. The neoplastic cells of this back-to-back glandular proliferation have abundant amounts of granular, eosinophilic cytoplasm.

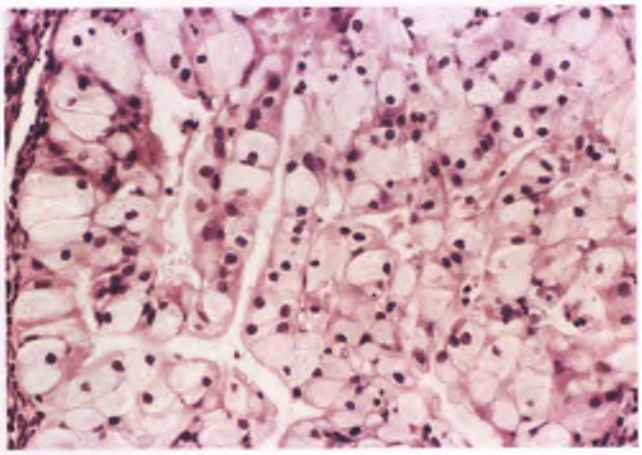

FIGURE 4.201. Lipid-rich endometrioid carcinoma. Note the abundant amount of foamy cytoplasm within the neoplastic cells. These cells resemble foamy histiocytes, but are recognized as epithelial by their cohesiveness and their ability to form glandular structures.

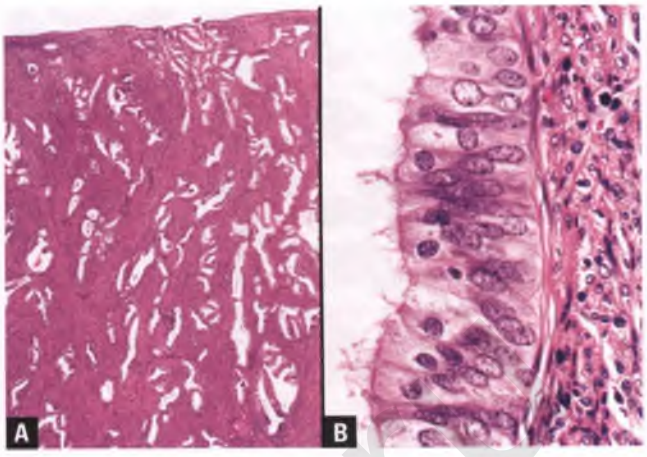

FIGURE 4.202. Ciliated adenocarcinoma. **A**: The diffusely infiltrative ("adenoma malignum") pattern of myoinvasion is the only indicator of malignancy in this case. There is no stromal reaction to the well-differentiated, myoinvasive glands. **B**: The infiltrating glands are lined by ciliated cells with bland nuclear features that in other settings would pass for ciliated cell change. Myometrium is at right.

carcinoma has been applied in this situation.[171] Oxyphilic carcinomas are generally grade 1 or 2 and have a presentation and behavior that does not differ from grade and stage-matched endometrioid carcinomas of conventional type.

Lipid-Rich Endometrioid Carcinoma

Rare endometrioid carcinomas contain a significant component of cells with large amounts of foamy, microvesicular cytoplasm that can presumably be attributed to the presence of lipid (Fig. 4.201). Although there is more experience with ovarian versions of these endometrioid carcinomas with clear cells of nonsecretory type, they do occur in endometrial forms as well.[172]

Sertoliform Endometrioid Carcinoma

The presence within endometrioid carcinomas of columnar to cuboidal cells with bland nuclei that form uniform, hollow to solid tubules and trabecular structures can result in an appearance that resembles ovarian Sertoli cell tumors. This phenomenon is better documented for ovarian endometrioid carcinomas (see Figs. 7.108 and 7.109), but has been shown to occur in endometrial tumors on very rare occasions.[173] These tumors are differentiated from endometrial stromal sarcomas with sex-cord–like elements and uterine tumors resembling ovarian sex-cord tumors by their association with endometrioid carcinoma of usual type, and are further distinguished from endometrial stromal sarcoma with sex-cord–like elements by their lack of a malignant mesenchymal component and absence of a permeative growth pattern.[173]

Ciliated Carcinoma

The vast majority of endometrial glandular processes that consist predominantly of ciliated cells represent ciliated cell change or a form of metaplastic hyperplasia. However, very rare endometrioid adenocarcinomas have been documented to be composed predominantly of cells that bear cilia that are recognizable with a conventional microscope. Most of these cases are ciliated versions of well-differentiated endometrioid adenocarcinoma (Fig. 4.202), although another more readily identifiable form has been described in which sheets of cells with malignant (grade 1 to 2) nuclear features are punctuated by small extracellular lumens lined by ciliated cells.[122] Unless the well-differentiated form of ciliated adenocarcinoma is admixed with conventional endometrioid adenocarcinoma or contains foci with appreciable nuclear atypia and mitotic activity within an area of architectural complexity, its true nature is unlikely to be recognized in an endometrial curettage. Flagging of the process as at least a form of atypical hyperplasia should lead to appropriate treatment; definitive diagnosis may need to be deferred until a hysterectomy specimen can be evaluated.

ENDOMETRIOID ADENOCARCINOMA: MYOMETRIAL AND VASCULAR INVASION

Myometrial Invasion: Frequency and Prognostic Significance

Grade 1 endometrioid carcinomas have a reported incidence of myometrial invasion that ranges widely from 16% to 75%,[106,126,149] which suggests interpretive issues in the evaluation of superficial myoinvasion and different diagnostic thresholds in making the subjective distinction between CAH and well-differentiated adenocarcinoma (e.g., a pathologist with a low threshold for a diagnosis of carcinoma who utilizes strict criteria for myoinvasion will have a much lower incidence of myoinvasive carcinomas than a pathologist who has a higher

threshold for a diagnosis of carcinoma who uses lax criteria for myoinvasion). Deep (outer half) myometrial invasion is more likely to occur in high-grade tumors, although occasionally one will encounter grade 1 tumors with deep myoinvasion or grade 3 tumors that are confined to the endometrium.[129,149] Not surprisingly, there is a positive correlation between increasing depth of myometrial invasion and the incidence of pelvic lymph node metastases.[149] Although stage of the tumor dominates prognosis, the depth of myometrial invasion is probably the most important prognostic factor in endometrioid carcinomas that are confined to the uterus.[128,136]

Myometrial Invasion: Issues Related to Sectioning, Measuring, and Reporting

Given its prognostic significance, it is important to accurately measure the depth of myometrial invasion and to indicate the percentage of myometrial penetration, so that the patient can be accurately staged. The measurement is a histologic one that is made from the nearest normal endometrial–myometrial junction to the deepest point of microscopically confirmed myoinvasion. Whenever topographically feasible, a full-thickness section that includes a portion of the normal endometrial–myometrial junction and the deepest point of invasion should be submitted for histologic evaluation. If the uterine wall is too thick to submit such a section, the myometrium should be cut in the horizontal plane at its midpoint and a bisected version of a full-thickness section should be submitted in two cassettes, with the serosal surface inked to facilitate orientation and notes included in the gross description that provide sufficient information to reconstruct how the sections were prepared (dividing the superficial and deep sections so that they fit together like a simple jigsaw puzzle allows for quick recognition of proper orientation).[9] If submission of sections that include the normal endometrial–myometrial junction is not possible due to the topography of the tumor, a small notch should be cut at the edge of the sections of tumor at the gross level of the endometrial–myometrial junction for use as a marker when measuring depth of invasion. In an exophytic tumor, care should be taken to measure the depth of myometrial invasion as described above rather than measuring the thickness of the tumor, which would include the noninvasive portion of the tumor that protrudes into the endometrial cavity.[174] Plugs of tumor found within angiolymphatic spaces beyond the deepest point of myoinvasion should not be taken into account when measuring the depth of myometrial invasion.

In the FIGO staging system of endometrial carcinoma, tumors that are confined to the uterine corpus are stage I and are subdivided based upon the depth of myometrial invasion. In the system that was utilized between 1988 and 2008, stage Ia indicated that the tumor was limited to the endometrium, stage Ib indicated invasion of <50% of the myometrium, and stage Ic indicated invasion of >50% of the myometrium.[135] The 2008 revised FIGO staging system for endometrial carcinoma has condensed the previous stage Ia and Ib categories into a new stage Ia with no or <50% myometrial invasion, with the new stage Ib for tumors with ≥50% myoinvasion.[151] The rationale for this change was twofold: (a) distinction between endometrial carcinomas that are confined to the endometrium (the old stage Ia) from those that are superficially invasive (the old stage Ib) is difficult and subjective and (b) there are no appreciable differences in survival for patients with grade 1 or 2 tumors with these stages of disease, with 5-year survivals in the range of 90% to 93%.[147,175]

The diagnosis line of the pathology report should succinctly indicate the percentage of myometrial penetration, depth of myometrial invasion, and myometrial thickness at the point of deepest invasion, and should also indicate which slide demonstrates the deepest focus of myoinvasion to facilitate subsequent slide review. For example, the depth of myoinvasion can be reported as 75% (1.5/2.0 cm) into myometrium (slide M). Until pathologists and clinicians become thoroughly familiar with the new staging system, it is recommended that if the pathology report indicates the tumor stage, then it should be specified that the 2008 FIGO system is being used and that the equivalent former stage be provided (the above example would be reported as revised FIGO 2008 stage Ib, formerly stage Ic).

Patterns of Myometrial Invasion

Usual Pattern

The conventional form of myometrial invasion is easily recognized by the presence of irregularly shaped, sharply angulated glands dissecting through the myometrium with an associated stromal reaction (Fig. 4.203). In addition to glandular structures, the epithelial elements may also be represented by sheets, nests, cords, or isolated neoplastic cells. Most commonly, the stromal reaction takes the form of loose granulation tissue with interspersed lymphocytes, although a desmoplastic response can also be seen.

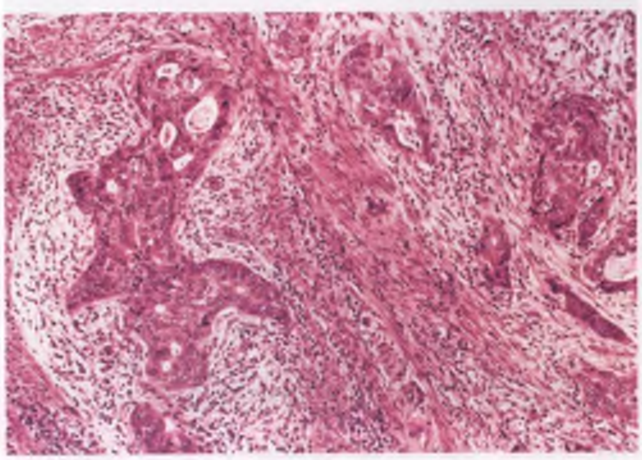

FIGURE 4.203. Endometrioid adenocarcinoma demonstrating the usual pattern of myometrial invasion. Note the jagged contours of the infiltrating epithelial elements and the associated stromal reaction.

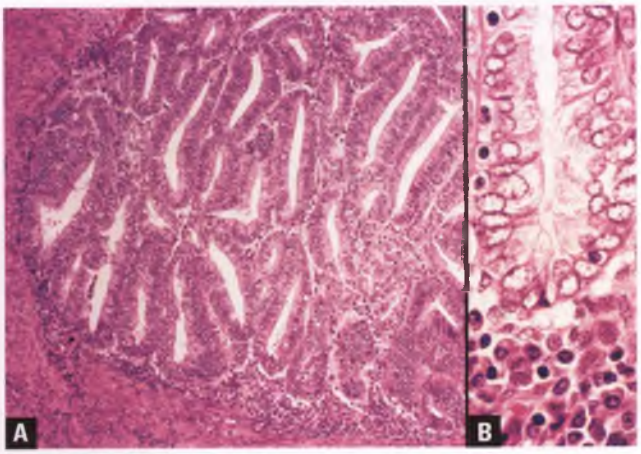

FIGURE 4.204. **A,B**: Expansile, pushing pattern of myometrial invasion in a grade 1 endometrioid adenocarcinoma. The interpretation of myoinvasion is supported by the combination of the absence of incorporated benign glands, the lack of adenomyosis in the vicinity, and the presence of a thin band of lymphocytes and plasma cells at the interface between the tumor and myometrium (highlighted in **B**).

Expansile, Pushing Pattern

The advancing margin of some myoinvasive carcinomas is characterized by a broad, expansile, pushing front with a mild to absent stromal reaction (Figs. 4.204–4.206). In such cases, it is particularly important to submit histologic sections that employ one of the methods outlined above for indicating the level of the normal endometrial–myometrial junction to facilitate recognition and measurement of myometrial invasion. Distinction of this form of myoinvasion from tumor involvement of an irregular endometrial–myometrial junction or tumor extension into adenomyosis can be difficult, and is discussed in the section on mimics of myometrial invasion.

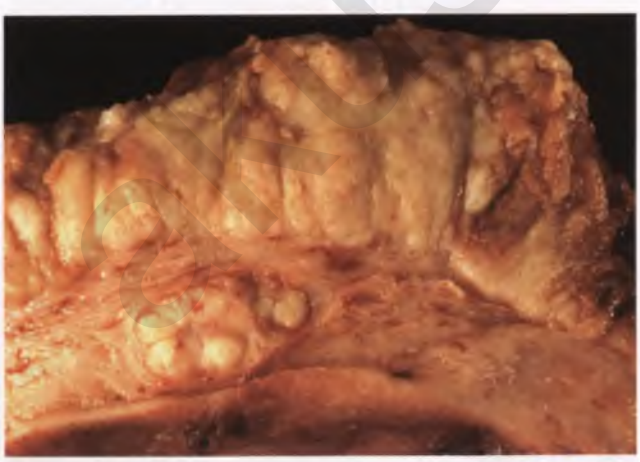

FIGURE 4.205. Expansile, pushing pattern of myometrial invasion in a high-grade endometrioid adenocarcinoma. This longitudinal section through a formalin-fixed uterus reveals a pale yellow tumor infiltrating the inner portion of the myometrium as a broad front with a pushing margin. The multinodular lesion within the myometrium is a leiomyoma.

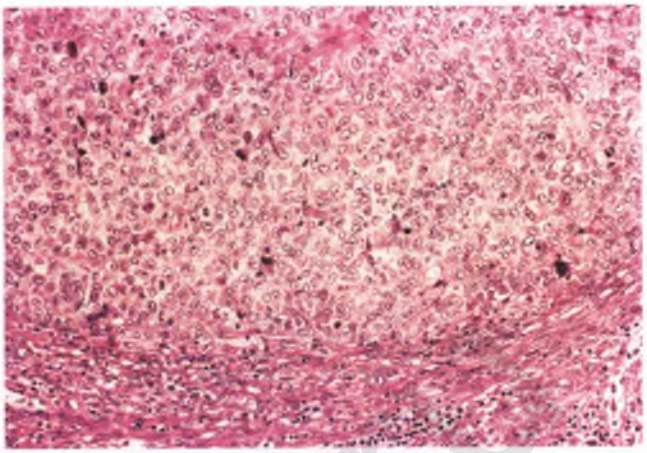

FIGURE 4.206. Expansile, pushing pattern of myometrial invasion in a high-grade endometrioid adenocarcinoma. The subtle stromal reaction consists of interspersed myometrial lymphocytes along the advancing border of the tumor.

Diffusely Infiltrative Pattern

This pattern, also referred to as an "adenoma malignum" form of myoinvasion, is characterized by individual, well-formed glands with mild to occasionally moderate nuclear atypia that diffusely infiltrate the myometrium with an inconspicuous or absent stromal reaction.[176] In most cases of this type, there is widespread infiltration of the myometrium that is readily apparent at low magnification (Fig. 4.207). Recognition of the diffusely infiltrative pattern of myometrial invasion is based largely upon these low-power architectural features, since the architecture and nuclear features of the individual glands are not diagnostic of malignancy (Fig. 4.208). Given this situation, it is not surprising that it can be difficult to distinguish

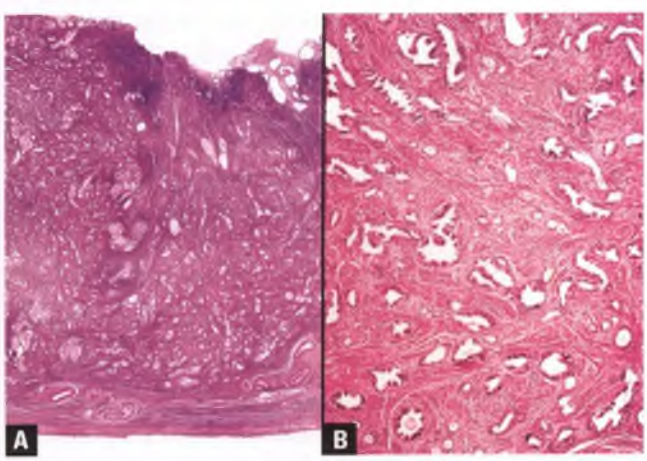

FIGURE 4.207. Grade 1 endometrioid adenocarcinoma with a diffusely infiltrative pattern of myoinvasion. **A**: This low-magnification view demonstrates diffuse permeation of the myometrium to within 2 mm of the uterine serosa. Some partially involved foci of adenomyosis are also present centrally. **B**: Well-formed glands "melt" through the myometrium without eliciting a stromal reaction.

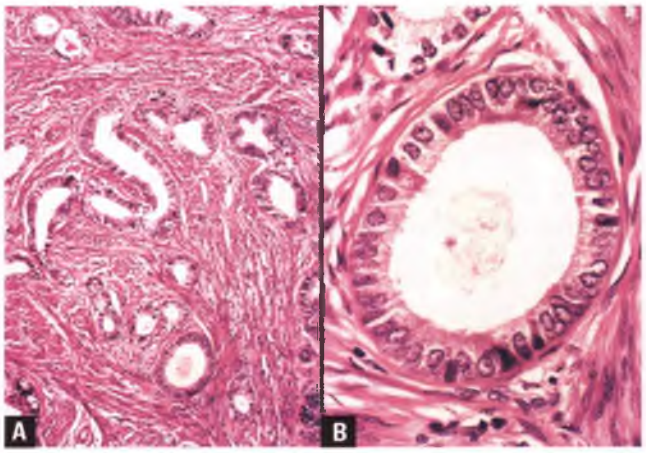

FIGURE 4.208. **A,B**: Grade 1 endometrioid adenocarcinoma with a diffusely infiltrative pattern of myoinvasion. The cells lining the glands are of low nuclear grade, and are recognized as malignant only by their collective architecture, location within the myometrium, and lack of associated endometrial stroma.

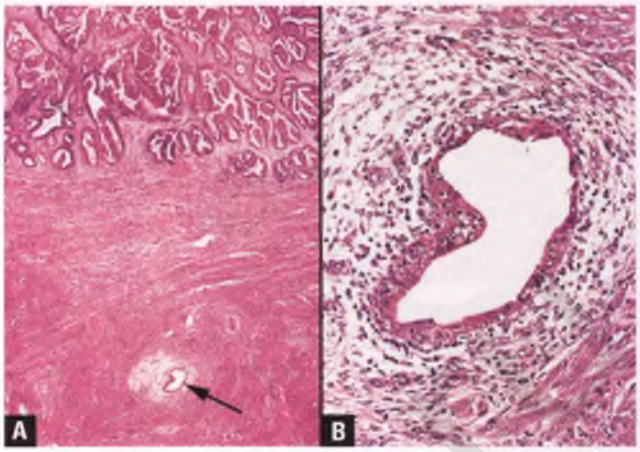

FIGURE 4.209. "MELF" pattern of myometrial invasion. **A**: An isolated microcystic gland (*arrow*) lies deep to a conventional invasive endometrioid adenocarcinoma. Note the prominent loose granulation tissue surrounding the microcystic gland, which serves as a useful low-magnification marker of this form of invasion. **B**: High-magnification view of the microcystic gland with surrounding loose granulation tissue. This type of myoinvasion can be easily overlooked.

superficial myometrial invasion of this type from well-differentiated endometrial carcinoma involving an irregular endometrial–myometrial junction or extending into adenomyosis with atrophic and fibrotic stroma. When agonizing over this differential diagnosis, it is comforting to know that stage I tumors with a diffusely infiltrative pattern of growth have a 98% recurrence-free survival across the entire spectrum of myoinvasion,[176] so an inability to definitively recognize superficial myometrial invasion of this type is highly unlikely to be clinically significant.

MELF (Microcystic, Elongated, and Fragmented) Pattern

This distinctive pattern of myometrial invasion is characterized by variable combinations of microcystic, elongated, and fragmented glands that are associated with a prominent fibromyxoid stromal reaction.[177] It is not uncommon for subtle epithelial elements from this form of myoinvasion to be lurking within islands of edematous fibromyxoid tissue several millimeters deep to more conventional forms of invasive adenocarcinoma (Fig. 4.209). Invasive endometrioid glands of the usual type may be seen transitioning into those with MELF features (Fig. 4.210A). The microcystic and elongated glands of the MELF pattern of invasion are often lined by flattened cells with eosinophilic, squamoid cytoplasm, with slit-like versions resulting in an endothelioid pattern that simulate vascular spaces (Fig. 4.210B). The lumens of these unusual-appearing glandular structures often contain aggregates of neutrophils, and the altered stroma typically contains an admixture of lymphocytes, neutrophils, and eosinophils. The endothelioid

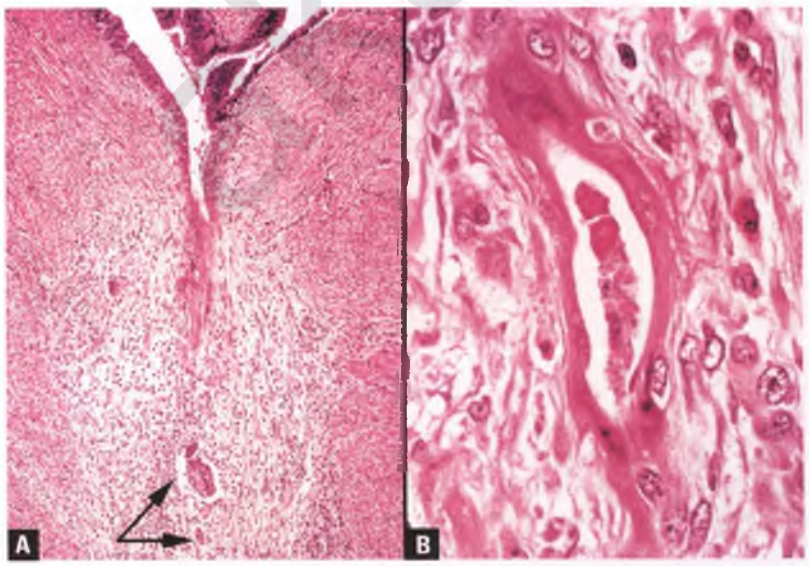

FIGURE 4.210. "MELF" pattern of myometrial invasion. **A**: Conventional invasive endometrioid adenocarcinoma (top) is seen transitioning to elongated and fragmented patterns of MELF-type invasion. Note the retraction artifact surrounding some of the small aggregates of tumor cells (*arrows*). **B**: This elongated, malignant "endothelioid" gland is lined by flattened cells with eosinophilic cytoplasm and could be mistaken for a vessel.

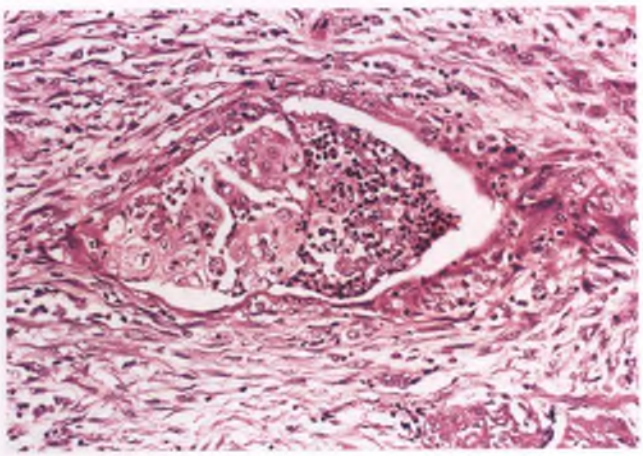

FIGURE 4.211. Endothelioid pattern of MELF-type invasion. The presence of inflammatory cells and squamoid tumor cells within the gland lumen mimics angiolymphatic invasion by carcinoma.

pattern can mimic vascular invasion when there are sloughed tumor cells within the gland lumens (Fig. 4.211). In the fragmented form, tumor cells occur singly or in small aggregates within loose granulation tissue, sometimes accompanied by retraction artifact (Fig. 4.210A and Fig. 4.212A). Cytokeratin immunohistochemistry can be utilized as indicated to detect small numbers of tumor cells within suspicious foci of altered stroma (Fig. 4.212B) or to confirm the epithelial nature of the elongated (endothelioid) pattern of invasion.

Vascular Invasion: Frequency and Prognostic Significance

Angiolymphatic invasion occurs in approximately 15% to 25% of endometrioid carcinomas, and is significantly more likely to be found in high-grade tumors.[129,149,178] Most studies have found angiolymphatic invasion to be an important adverse prognostic factor in endometrial carcinomas that are confined to the uterus.[128,178] Accordingly, the presence or absence of this feature should be indicated in the diagnosis line of the pathology report.

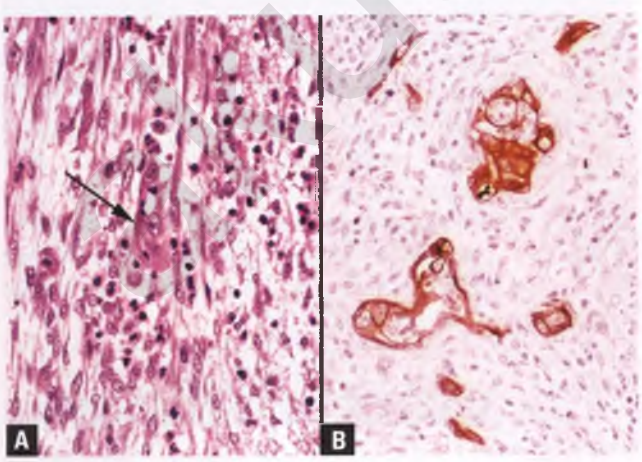

FIGURE 4.212. Fragmented pattern of MELF-type invasion. **A**: Tumor cells, occurring singly and in small clusters (*arrow*), may be difficult to recognize within the altered stroma. **B**: The fragmented epithelial elements are highlighted by cytokeratin immunohistochemistry.

Patterns of Vascular Invasion

Usual Pattern

In the usual type of angiolymphatic invasion, cohesive, sharply demarcated nests of tumor cells are found within vascular spaces (Fig. 4.213). Distinction of true angiolymphatic invasion from retraction artifact is discussed in the section on artifacts in Chapter 3. The additional differential diagnostic considerations of intravascular menstrual endometrium, intravascular endometrial tissue associated with adenomyosis, the elongated/endothelioid "MELF" pattern of myometrial invasion, and vascular pseudoinvasion related to total laparoscopic hysterectomy are discussed elsewhere in this chapter.

Histiocytoid Pattern

This subtle form of angiolymphatic invasion features discohesive tumor cells with eosinophilic cytoplasm that may be intermingled with red and/or white blood cells (Fig. 4.214).[179] The tumor cells bear some resemblance to histiocytes, and this resemblance is maintained in associated lymph node metastases. Although easily overlooked, the presence of this form of vascular invasion should be suspected if the candidate vessel harbors loosely associated cells with significant nuclear atypia and/or small clusters of cohesive cells. In difficult cases in which definitive vascular invasion cannot be identified elsewhere in the specimen, the epithelial nature of the abnormal intravascular cells can be confirmed by documenting their immunoreactivity for cytokeratin.

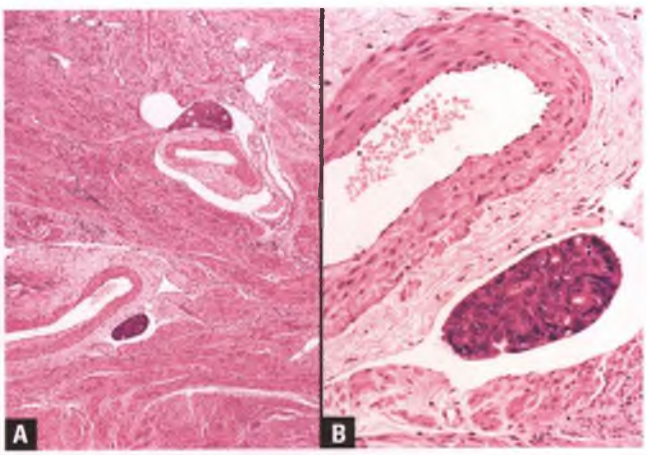

FIGURE 4.213. **A,B**: Endometrioid adenocarcinoma with angiolymphatic invasion. Since veins are expected adjacent to lymphatics, their presence serves as supportive evidence that the spaces surrounding the plugs of tumor represent true lymphatic channels rather than retraction artifact, as does the location of the involved vessels being in tissue adjacent to rather than within the main tumor mass.

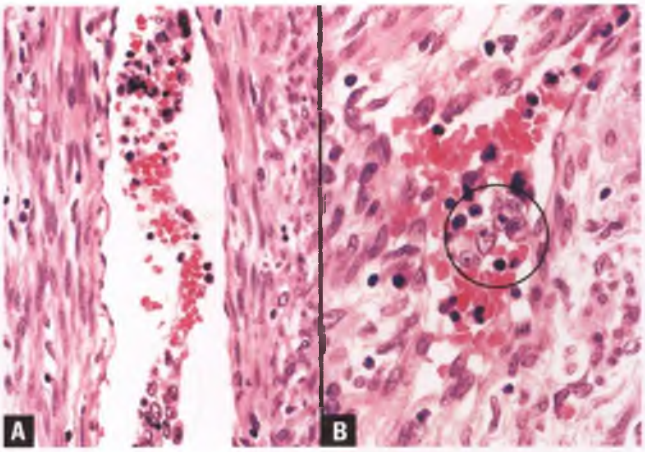

FIGURE 4.214. Histiocytoid pattern of vascular invasion. **A**: This thin-walled myometrial vein contains loose aggregates of tumor cells derived from an endometrioid adenocarcinoma. The tumor cells, which are located at the top and bottom of the image, are partially enmeshed in fibrin and are admixed with inflammatory cells and erythrocytes. **B**: This venous space, which was adjacent to the vessel in **A**, contains a small cluster of malignant cells (*circled*).

ENDOMETRIOID ADENOCARCINOMA: MIMICS OF MYOMETRIAL INVASION

Simulation of Myoinvasion by Endometrioid Adenocarcinoma Involving Adenomyosis

The presence and extent of myometrial invasion are often overestimated by pathologists, which in some cases is due to the misinterpretation of involvement of adenomyosis by adenocarcinoma as true myometrial invasion.[174,180] Such involvement occurs in about 20% to 25% of cases in which endometrial adenocarcinoma coexists with adenomyosis, is associated with low-grade endometrioid adenocarcinoma in the vast majority of cases, and in cases that lack foci of legitimate myometrial invasion is associated with a prognosis that is equivalent to noninvasive endometrial adenocarcinoma.[181,182] Limited data also suggest that the presence of tumor-involved adenomyosis deeper within the myometrium than conventional invasive adenocarcinoma does not worsen the prognosis and should not influence staging (e.g., an adenocarcinoma with inner half myoinvasion and involvement of adenomyosis that extends into the outer half of the myometrium should still be staged as invading only the inner half).[183] Regarding the rare and difficult to diagnose situation in which myoinvasive foci of adenocarcinoma emerge from foci of tumor-involved adenomyosis at a depth that is significantly deeper than the component of conventional invasive adenocarcinoma, insufficient outcome data exist to determine if this finding is of any prognostic significance.[183]

Although extension of endometrial adenocarcinoma into adenomyosis is usually a microscopic finding, in occasional cases it can be recognized grossly as well-circumscribed, intramural nodules of pale tan to off-white, solid tumor with scattered slit-like spaces or minute cysts (Fig. 4.215A). The correct diagnosis is suggested by the low-magnification appearance of tumor islands with smooth, rounded contours that are usually located within the inner third of the myometrium (Fig. 4.215B).[182] Evidence that is further supportive of this diagnosis includes the presence of (a) residual benign endometrial "marker" glands and/or endometrial stromal cells that are entrapped within the carcinomatous foci (Figs. 4.216 and 4.217), (b) a tumor–myometrial interface that shows no evidence of desmoplasia, edema, or inflammation, and (c) neighboring areas of uninvolved adenomyosis.[182] In the very rare cases in which there is no overlying endometrial adenocarcinoma, the adenocarcinoma is considered to have arisen from within the foci of adenomyosis.[184]

Simulation of Myoinvasion by Endometrioid Adenocarcinoma Involving an Irregular Endometrial–Myometrial Junction

Although interpretation of adenocarcinoma extending into adenomyosis can be problematic, the most common cause

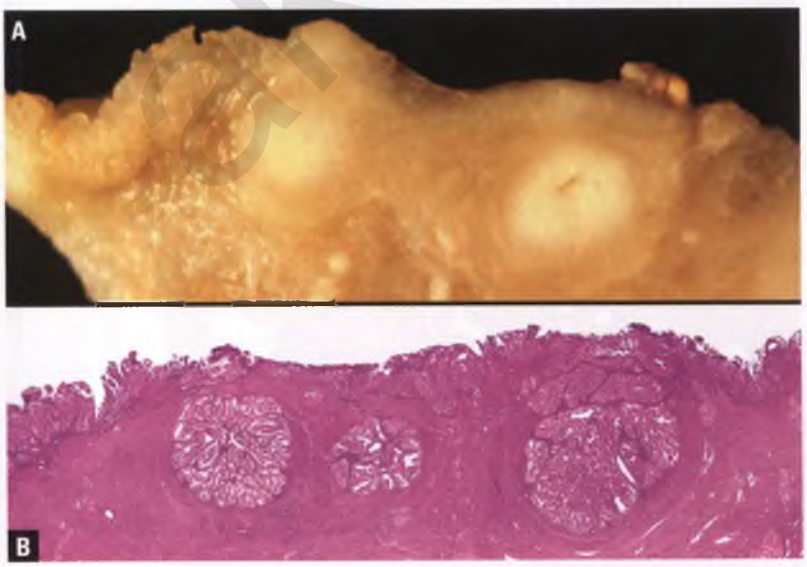

FIGURE 4.215. Noninvasive grade 1 endometrioid adenocarcinoma with involvement of adenomyosis. **A**: This section through a formalin-fixed uterus reveals a shaggy, superficial endometrial carcinoma at left and two nodules within the superficial myometrium that represent extension of adenocarcinoma into adenomyosis. Note the slit-like space in the nodule at right. **B**: This low-magnification view of a corresponding histologic section shows noninvasive carcinoma at far left and nodules of adenocarcinoma within adenomyosis.

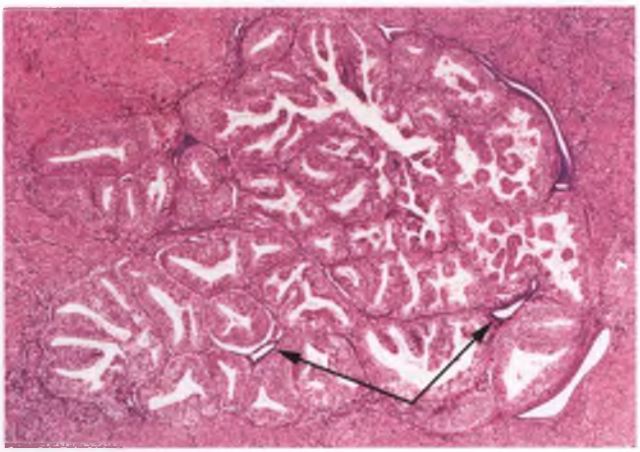

FIGURE 4.216. Noninvasive grade 1 endometrioid adenocarcinoma involving a nodular focus of adenomyosis. Note the smooth contour of the nodule, the absence of a stromal response, and the presence of several compressed, benign "marker" glands located both within and at the periphery of the neoplastic glandular proliferation (two of these glands are marked by *arrows*).

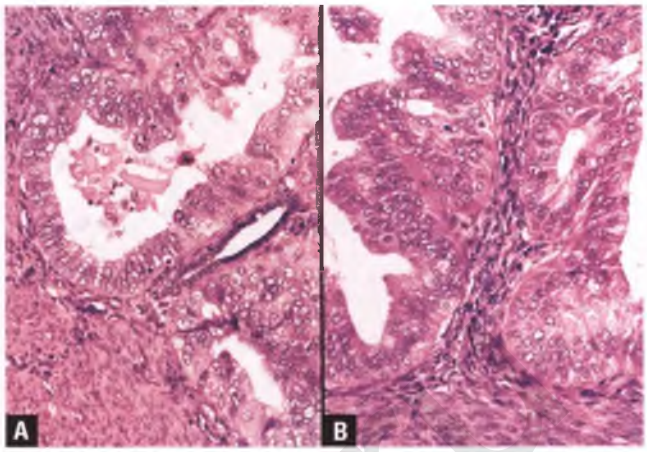

FIGURE 4.217. Noninvasive grade 1 endometrioid adenocarcinoma involving adenomyosis. **A**: This image demonstrates adenocarcinomatous glands impinging upon a benign "marker" gland. **B**: This image shows a narrow band of recognizable endometrial stroma between the neoplastic glands. Note: Both images were taken from the edge of involved foci of adenomyosis.

of overdiagnosis of myometrial invasion is involvement of an irregular endometrial–myometrial junction by endometrial adenocarcinoma.[174,180] The normal endometrial–myometrial junction typically has some undulations due to interdigitations of endometrial glands and stroma with myometrium (Fig. 4.218). Endometrial incursions into the myometrium usually measure only a few mm, but the endometrial–myometrial junction may occasionally dip into the outer half of the myometrium.[176] The gross correlate of endometrioid carcinoma involving an irregular endometrial–myometrial junction is depicted in the right side of Figure 4.159B. In an analogous phenomenon, an endometrial carcinoma that involves a cornual aspect of the uterus can also simulate myometrial invasion by extending into the intramural portion of the fallopian tube.

When the interface of an irregular endometrial–myometrial junction is replaced by adenocarcinoma, distinction from myometrial invasion can be difficult. The features that help to recognize this process as noninvasive are similar to those discussed above for identifying adenocarcinoma involving adenomyosis—the contours of the interface of the neoplastic glands and myometrium are smooth and well circumscribed, residual benign endometrial glands and/or endometrial stromal cells are present, and there is no obvious stromal reaction (Fig. 4.219).[174,180] When evaluating these features, one should not require noninvasive carcinoma to possess a continuous, obvious peripheral rim of endometrial stroma, since (a) the impinging adenocarcinoma may severely compress and attenuate the underlying stroma and (b) the endometrial stroma of

FIGURE 4.218. Irregular endometrial–myometrial junction. **A**: A tongue-like extension of benign endometrial glands and stroma is seen protruding into the myometrium. This is a common finding that represents a variant of normal. **B**: This higher magnification view shows the deep aspect of the portion of the endometrium that interdigitates with the myometrium.

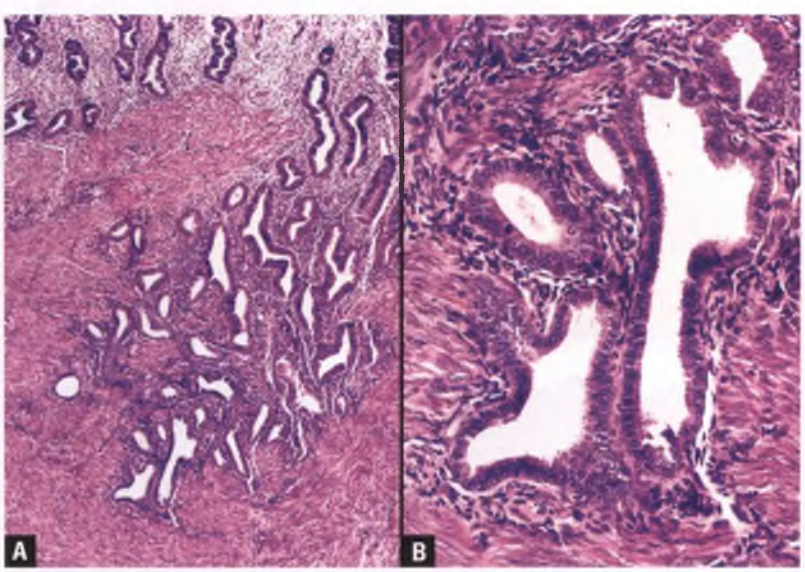

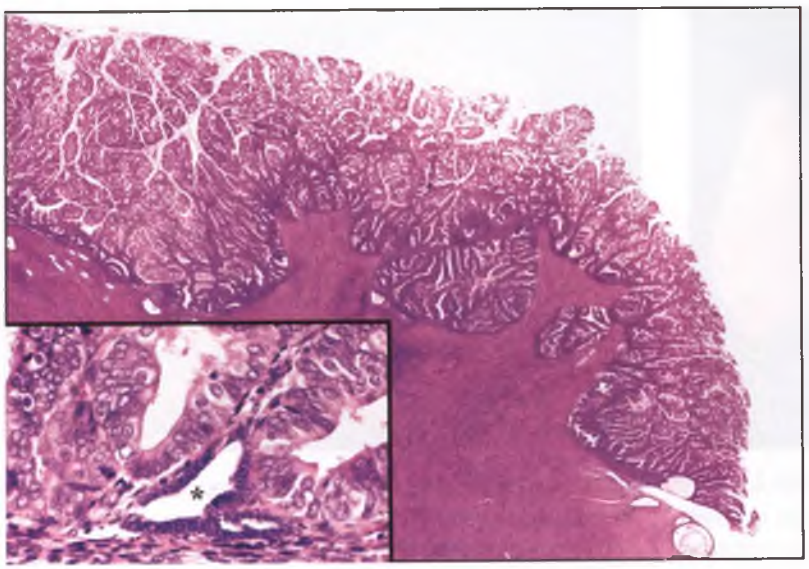

FIGURE 4.219. Nonmyoinvasive endometrial adenocarcinoma with an undulating interface with the myometrium due to involvement of an irregular endometrial–myometrial junction. The inset highlights the presence of occasional residual benign glands (*asterisk*) at the interface between the tumor and the myometrium.

postmenopausal women is often atrophic, eosinophilic, and fibrotic. Moreover, since lymphocytes normally reside within the basalis and since a lymphocytic infiltrate may be part of the endometrial stromal response to adenocarcinoma, the mere presence of a few lymphocytes at the tumor–myometrial interface is not necessarily indicative of a stromal response to myometrial invasion (Fig. 4.220).

Soon after it was first recognized that CD10 reliably stained endometrial stromal cells,[185,186] it was hoped that this finding would be of utility in distinguishing myoinvasive adenocarcinoma from adenocarcinoma with involvement of an irregular endometrial–myometrial junction or with extension into adenomyosis. Unfortunately, immunostaining of straightforward cases of myoinvasive adenocarcinoma has shown that the stromal cells that immediately surround the myoinvasive glands are typically CD10 positive.[187] Since all three of the entities in the differential diagnosis are associated with peritumoral CD10-positive stromal cells, this immunostain is of no assistance in helping to make this distinction.[187]

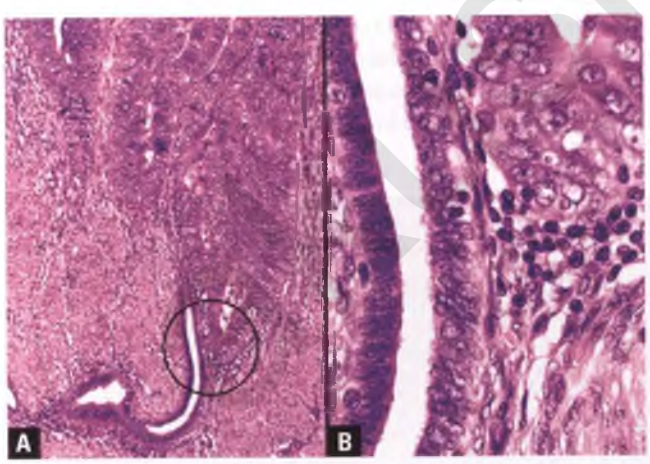

FIGURE 4.220. Nonmyoinvasive endometrial adenocarcinoma with involvement of an irregular endometrial–myometrial junction. **A**: Note the presence of an elongated, benign endometrial gland at the deep aspect of the tumor. **B**: High-magnification view of the area circled in **A**. Occasional lymphocytes can be present without indicating myoinvasion. The lymphoid rather than endometrial stromal nature of the aggregate of small blue cells is supported by the intraepithelial location of a few of these cells.

Simulation of Myoinvasion by Lesions Containing Metaplastic Smooth Muscle or Altered Stroma

The distinction of atypical polypoid adenomyoma from myoinvasive endometrioid adenocarcinoma is discussed later in this chapter. Some foci of adenomyosis or uterine adenomyomas may contain an unconventional stromal component that exhibits atrophy, fibrosis, or smooth muscle/fibroblastic metaplasia, which can result in an appearance that mimics well-differentiated endometrioid adenocarcinoma infiltrating myometrium (see section on adenomyosis).[174]

ENDOMETRIAL CARCINOMA: SPECIAL VARIANTS (INCLUDING CARCINOSARCOMA)

Serous Carcinoma

Serous carcinoma is the major "type II" (estrogen-independent) endometrial carcinoma.[188] In contrast to the much more common "type I" (estrogen-dependent) endometrioid carcinomas, serous carcinomas lack an association with endometrial hyperplasia, tend to occur in an older age group, and often behave in an aggressive fashion.[188] These tumors were originally referred to as uterine papillary serous carcinoma (UPSC), reflecting their typical complex papillary architecture.[160] However, with

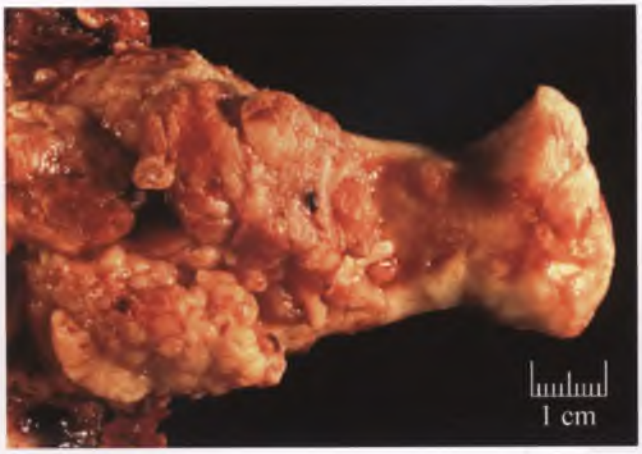

FIGURE 4.221. Serous carcinoma. This opened half of a lightly formalin-fixed uterus demonstrates the presence of a shaggy, polypoid tumor mass that fills the endometrial cavity and approaches the lower uterine segment.

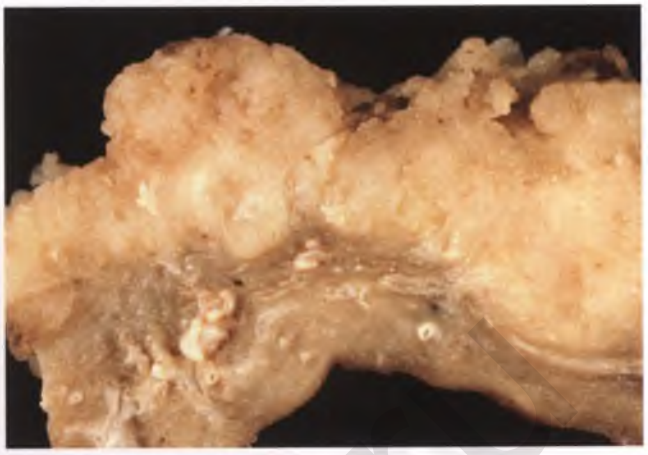

FIGURE 4.222. Serous carcinoma. This section through a formalin-fixed uterine wall demonstrates a *light tan* to *pale yellow* serous carcinoma with myometrial invasion. The papillary architecture of the tumor imparts a shaggy and/or granular appearance to its cut surface.

the recognition that occasional cases have a predominantly glandular or solid rather than papillary architecture, the less restrictive term "serous carcinoma" has been adopted.

Serous carcinomas represent 5% to 10% of endometrial carcinomas.[189] The typical presentation is a 65- to 70-year-old woman with postmenopausal uterine bleeding who also often has high-grade adenocarcinomatous or otherwise worrisome cells in her Pap smear (Fig. 3.269).[190] It is fairly typical for the patient to have a small, atrophic uterus that harbors a bulky tan tumor that fills the endometrial cavity (Fig. 4.221). Careful gross examination will often reveal a granular or shaggy appearance due to the presence of papillations (Fig. 4.222), although this finding can also be seen in villoglandular, clear cell, and other types of endometrial carcinoma. Myoinvasive foci of serous carcinoma may be grossly inconspicuous and require numerous sections for identification.

Serous carcinomas are not graded, since they are considered high grade by definition. They typically have an arborizing, complex papillary architecture with fibrovascular cores that are usually more substantial than those seen in VGECs, although thin papillae may also be encountered (Fig. 4.223A,B).[191] The cells lining the papillae are variably stratified and are characteristically of high nuclear grade, which classically translates to enlarged, round to oval nuclei with cleared chromatin and macronucleoli (Fig. 4.224). Scattered monstrous, pleomorphic nuclear forms with dark, smudged chromatin are often present, typically simulating an "umbrella cell layer" or protruding into gland lumens in a hobnail fashion (Fig. 4.225). There is brisk mitotic activity, and atypical division figures are usually readily identified. A characteristic feature that further complicates the architectural pattern is the exfoliation of small papillary clusters and individual tumor cells in the vicinity of the

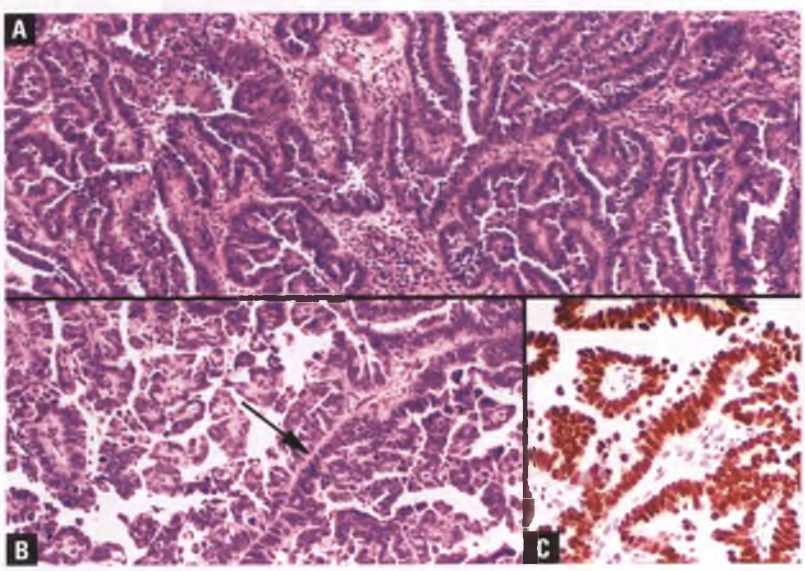

FIGURE 4.223. Serous carcinoma. **A**: Broad papillae are characteristic. **B**: Slender papillae may also be seen in serous carcinoma (*arrow*). **C**: Typical pattern of diffuse strong nuclear immunoreactivity of serous carcinoma for p53.

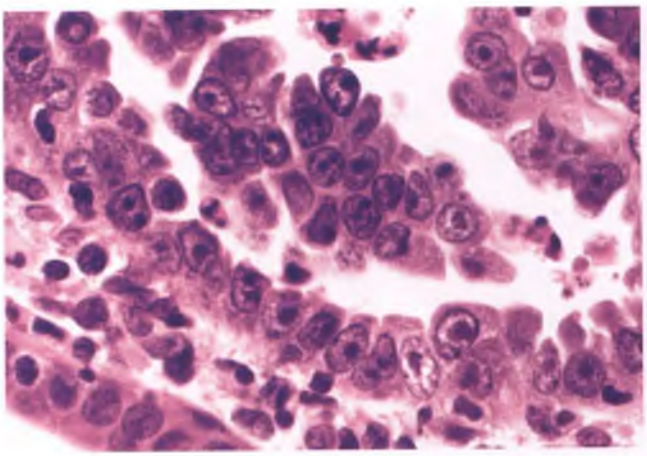

FIGURE 4.224. Serous carcinoma. Compare the high-grade nuclear features of this tumor with the strip of nonneoplastic endometrial epithelium in the lower left corner.

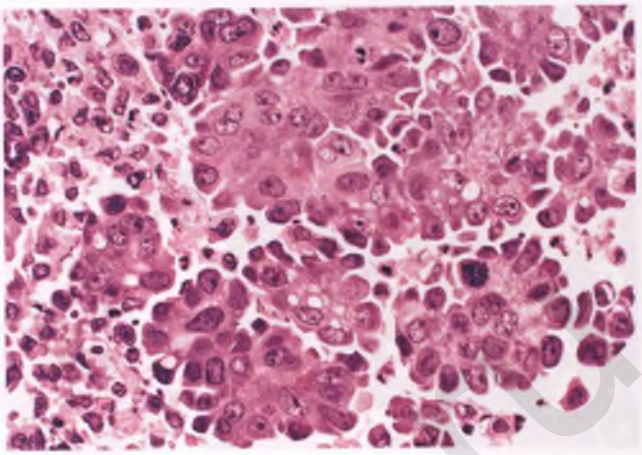

FIGURE 4.226. Serous carcinoma in an area of prominent epithelial tufting.

larger papillae, which is a phenomenon referred to as epithelial tufting (Fig. 4.226). Psammoma bodies are present in approximately 30% of the cases, but are not entirely specific for this type of carcinoma.[169] The papillary pattern predominates on the surface where the tumor can grow into an expandable cavity, but myoinvasive serous carcinoma is usually characterized by a "gaping glands" pattern (Fig. 4.227).[160] In some cases, slit-like glandular spaces may be a dominant feature (Fig. 4.228).

Occasionally, serous carcinomas exhibit prominent glandular differentiation that takes the form of tubular spaces (Fig. 4.229), or the tumor may grow predominantly as sheets of high-grade cells (Fig. 4.230). In these cases, it is the presence of high-grade nuclear features, coupled with supportive evidence of serous differentiation (focal papillae and/or slit-like spaces) and/or an immunophenotype that includes p16 positivity, p53 positivity, and progesterone receptor negativity, that helps to establish a diagnosis of serous carcinoma.[138,192,193] Diffuse, moderate to strong p16 immunoreactivity has recently been demonstrated to be a nearly universal finding in uterine serous carcinomas, whereas endometrioid endometrial adenocarcinomas display patchy p16 immunoreactivity of weak to moderate intensity.[193] The utility of p53 immunostaining lies in the fact that approximately 85% of uterine serous carcinomas exhibit diffuse, strong, nuclear immunoreactivity for p53 (Fig. 4.223C), whereas only about 20% of endometrioid carcinomas show such a staining pattern.[194] Most recently, immunoreactivity for the oncofetal protein IMP3 has been shown to be an effective marker for endometrial serous carcinoma in this situation and may be used in place of some of these other markers.[195,196] With the progress that has been made in

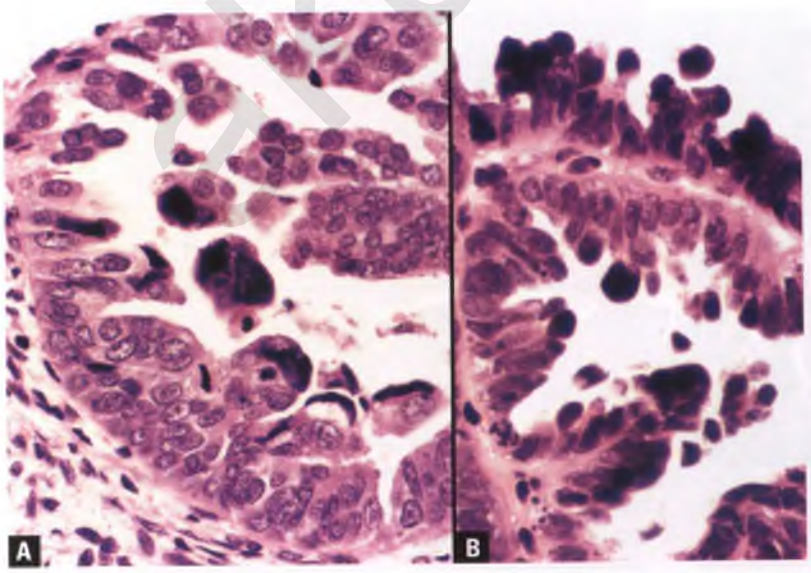

FIGURE 4.225. A,B: Serous carcinoma. The presence of cells with large, bizarre nuclei with smudged, dark chromatin is a common finding. Note how these cells tend to form an "umbrella cell layer" overlying the other tumor cells **(A)** or protrude into gland lumens in a hobnail fashion **(B)**.

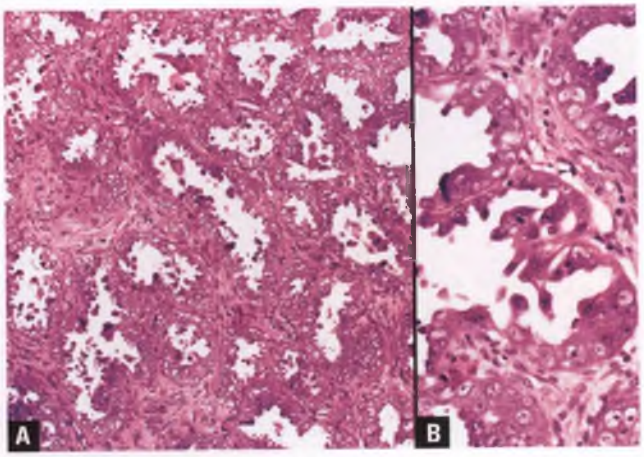

FIGURE 4.227. **A,B**: Serous carcinoma. The malignant glands in areas of myoinvasion often exhibit a "gaping gland" pattern with intraluminal hobnail cells and micropapillary projections.

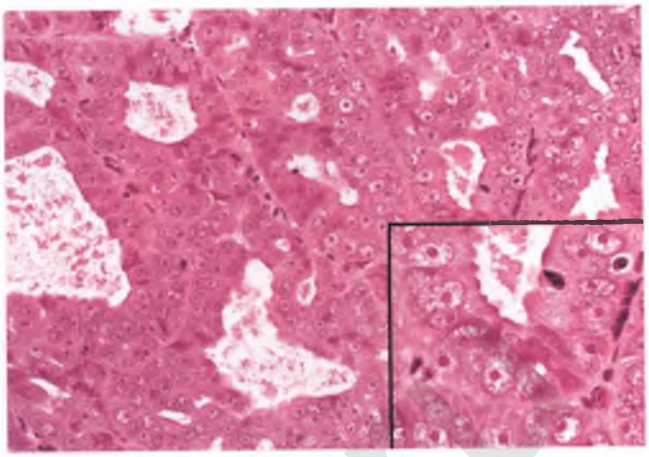

FIGURE 4.229. Serous carcinoma, glandular pattern. Although architecturally well differentiated, the epithelial cells lining the glands are of high nuclear grade and are identical to that seen in classic forms of serous carcinoma. Hysterectomy revealed deep myometrial invasion, and pelvic lymph node metastases were present.

recognizing the complete spectrum of serous differentiation in recent years, it is apparent that some cases of "endometrioid" carcinoma that have previously been upgraded based upon the presence of significant nuclear atypia actually represent serous carcinomas according to current criteria and supplemental immunohistochemistry.[197]

Serous carcinomas exhibit a peculiar propensity to arise within endometrial polyps of postmenopausal women (Fig. 4.231).[191,198–201] Even when of microscopic size and confined to the polyp, these serous carcinomas are often associated with extrauterine disease. Given this situation, it is recommended that (a) endometrial polyps, particularly those from postmenopausal women, be submitted for histologic evaluation in their entirety whenever practical and (b) patients with a prehysterectomy diagnosis of serous carcinoma within a polyp undergo a thorough staging procedure.

Uterine serous carcinomas have been previously reported to be frequently admixed with other types of carcinoma, usually of endometrioid or clear cell type.[189,191,198] Although "mixed" tumors with as little as 25% typical serous histology have been found to behave as aggressively as conventional serous carcinomas,[191,198] it is probable that some of these tumors would now be considered to be within the spectrum of the recently expanded definition of serous carcinoma that includes tumors with glandular or solid architecture under circumstances as discussed above. True mixed serous and endometrioid tumors certainly exist (Fig. 4.232), but they are undoubtedly less common than previously reported. The clinical outcome of tumors with <25% serous histology is not well defined; given the potential

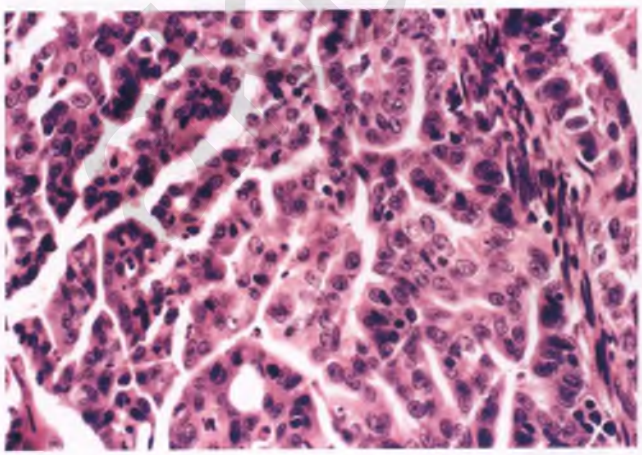

FIGURE 4.228. Serous carcinoma in an area where slit-like glandular spaces are a prominent feature.

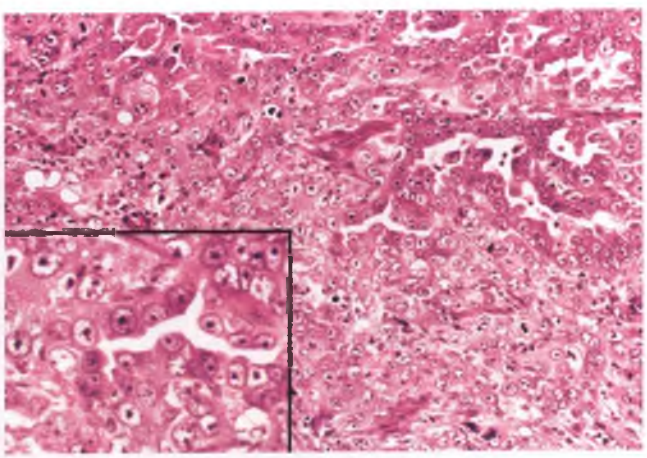

FIGURE 4.230. Serous carcinoma. In this tumor, areas of solid, sheet-like growth blend with glands with slit-like spaces. The inset highlights the similarity in the nuclear features between the glandular and solid components.

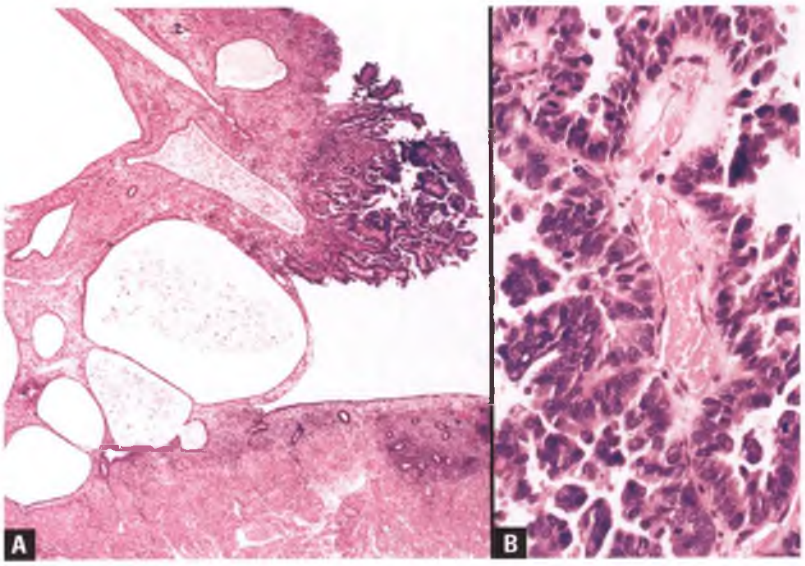

FIGURE 4.231. Serous carcinoma arising within an endometrial polyp of an elderly woman. **A**: The carcinoma involves the tip of the polyp. **B**: This image shows the malignant focus at higher magnification.

aggressive behavior of EIC and minimal serous carcinoma, it is recommended that any degree of unequivocal serous differentiation be noted in the pathology report.

Some serous carcinomas have areas with clear cell differentiation, but many investigators allow foci that would otherwise qualify as clear cell carcinoma within tumors that are diagnosed as serous carcinoma.[160,191] The rationale for this approach is that (a) clear cell and serous carcinomas have some overlapping histologic features (papillary architecture, high nuclear grade, and hobnail cells), (b) both tumors are considered aggressive variants of endometrial carcinoma, and (c) there is no known clinical significance to the presence of a clear cell component within a serous carcinoma.

Endometrial Intraepithelial Carcinoma

In approximately 90% of cases of uterine serous carcinoma, so-called EIC is an associated finding.[191,202,203] Against a backdrop of what is usually atrophic endometrium, EIC features an abrupt replacement of the surface and/or superficial glandular epithelium by cells that are similar to those of full-fledged serous carcinoma in their high-grade nuclear features, mitotic activity, high Ki-67 proliferative index, and propensity for p53 immunoreactivity (Figs. 4.233–4.235).[194,202,204] Although EIC is thought to serve as a precursor of serous carcinoma, it is frequently associated with extrauterine disease even when found as a standalone entity, and managerially should be regarded as an early form of serous carcinoma.[197,204,205] Since it can be difficult to distinguish early stromal invasion from EIC involving clusters of superficial glands, and both of these processes have a similar clinical behavior, the term "minimal serous carcinoma" has been applied to encompass both EIC and superficial serous carcinomas limited to invasion of the endometrium and measuring ≤1 cm in greatest dimension.[197,203] EIC is also commonly referred to as noninvasive serous carcinoma,

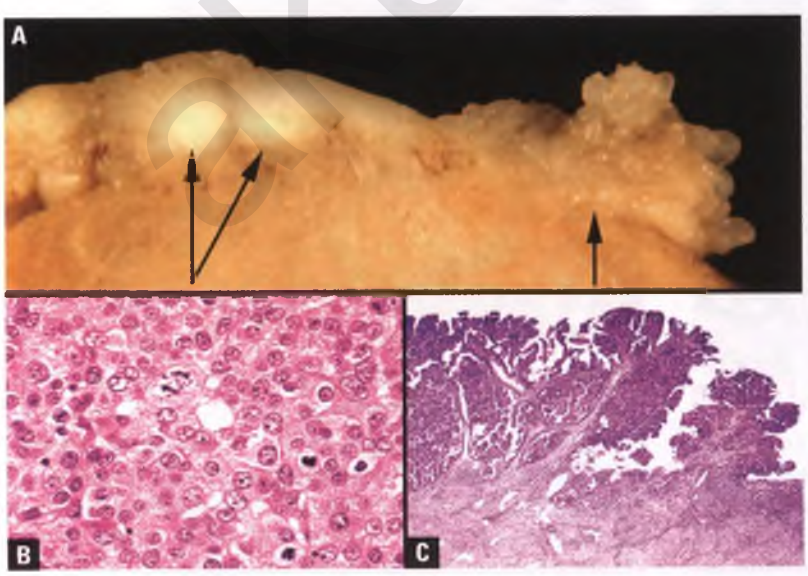

FIGURE 4.232. Gross and microscopic correlates of a mixed uterine serous carcinoma and grade 3 endometrioid adenocarcinoma. **A**: This section through the uterus reveals two white nodules of endometrioid adenocarcinoma (*V-shaped arrows*) and a separate superficial papillary focus of classic serous carcinoma (*single arrow*). **B**: Histologic correlate of grade 3 endometrioid adenocarcinoma. **C**: Histologic correlate of papillary serous carcinoma.

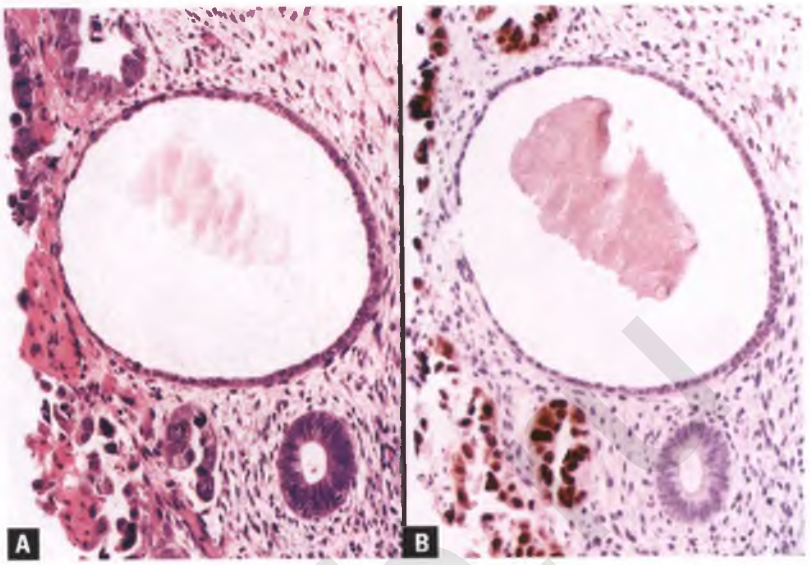

FIGURE 4.233. Endometrial intraepithelial carcinoma (intraepithelial serous carcinoma). **A**: The surface epithelium (at left) and a few superficial glands have been replaced by malignant cells similar to those present in full-fledged serous carcinoma. One gland with cystic atrophy and a smaller proliferative-type gland are also present. **B**: This p53 immunostain of a serial section demonstrates immunoreactivity limited to the foci of EIC.

serous surface carcinoma, and intraepithelial serous carcinoma.[201,206,207] Whatever terminology is used, this lesion should not be confused with EIN, which is the term employed as an alternative for the endometrial hyperplasia nomenclature (see section on endometrial hyperplasia).

Atypical glands thought to represent possible precursor lesions to EIC have been identified, to which the term endometrial glandular dysplasia (EmGD) has been applied.[208,209] Although interesting from a research standpoint, it is premature to prospectively diagnose lesions within endometrial samples with features that fall short of EIC as premalignant, with its attendant risks of confusion with incidental reactive processes, patient and clinician anxiety over proper therapy, and potential overtreatment. I suspect that EmGD will suffer the same reproducibility issues as endocervical glandular dysplasia, with high-grade lesions being inseparable from EIC and low-grade lesions not being reliably distinguishable from reactive processes. Taking the hunt for precursors of uterine serous carcinomas one step further, researchers have identified isolated, benign-appearing endometrial glands that strongly express p53 (so-called p53 signatures), although the significance of this finding when encountered in benign conditions is unknown.[209,210]

Stage-Related Issues and Patterns of Spread in Serous Carcinoma

As is true of most malignant neoplasms, stage is the most important prognostic factor. Serous carcinomas have a propensity for deep infiltration of the myometrium, angiolymphatic invasion (Fig. 4.236), and extrauterine spread. In recent years, more meticulous staging by gynecologic oncologists and more thorough sampling

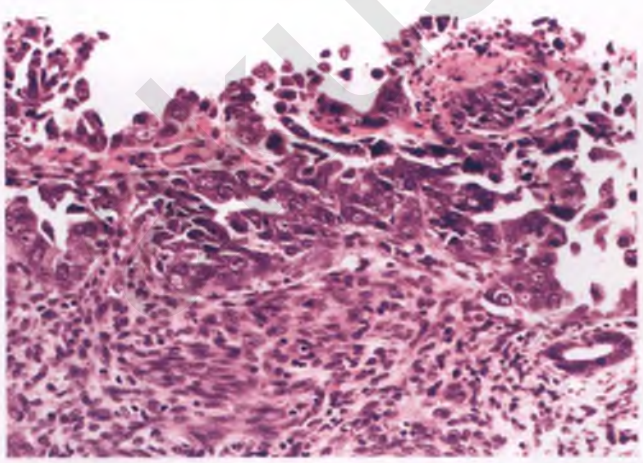

FIGURE 4.234. Endometrial intraepithelial carcinoma (intraepithelial serous carcinoma) involving the endometrial surface and a few superficial glands. Compare the nuclear features of EIC with those of the atrophic gland at lower right.

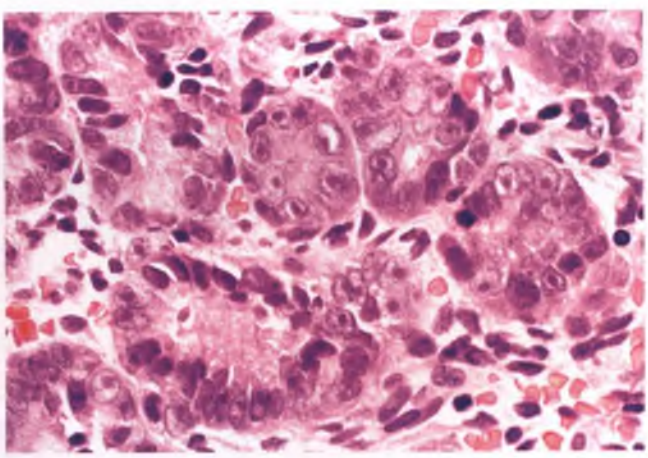

FIGURE 4.235. Endometrial intraepithelial carcinoma (intraepithelial serous carcinoma). This focus of superficial glandular involvement could be misinterpreted as simple atypical hyperplasia, but the macronucleoli as seen here are beyond the degree of nucleolar prominence found in atypical hyperplasia. Frank serous carcinoma was present in neighboring tissue.

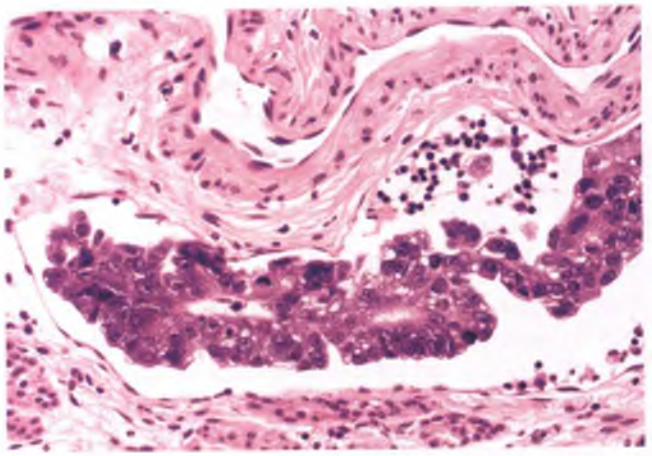

FIGURE 4.236. Lymphatic invasion by serous carcinoma. The lymphatic space that harbors the papillary cluster of serous carcinoma is located away from the main tumor mass, is lined by endothelium, contains small aggregates of lymphocytes, and is located beneath a thin-walled vein, all of which help to document that this represents true tumor involvement rather than retraction artifact.

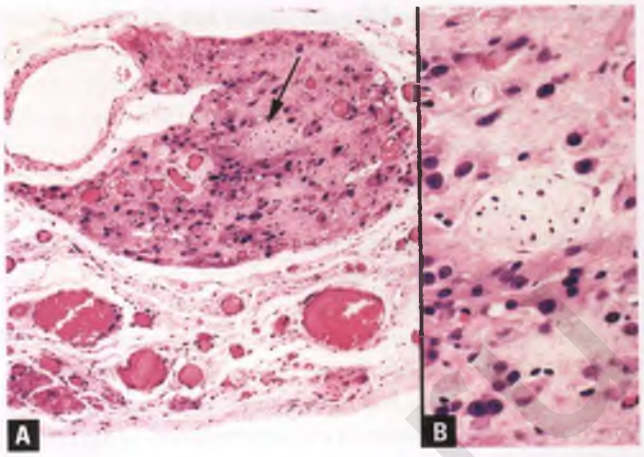

FIGURE 4.237. Hilus cell nest within the ovarian ligament mimicking microscopic involvement by serous carcinoma. **A**: The *arrow* marks a nerve twig that could be misconstrued as evidence of perineural invasion. **B**: High-magnification view of the area marked by the *arrow*. Some of the hilus cells have prominent nucleoli.

of extrauterine tissues by pathologists have led to a more accurately defined subset of patients with stage I disease. Long-term survival rates for such patients are now roughly 80%,[189] which is a significant improvement in comparison to studies of presumed stage I patients from years past and contrasts with a much lower survival rate of patients with stage III to IV disease. Unlike usual endometrioid carcinoma, most studies have not shown a correlation between the depth of myometrial invasion of serous carcinoma and the incidence of extrauterine disease.[191,211]

Serous carcinomas share the tendency of their ovarian counterpart to spread over peritoneal surfaces, which can lead to omental and bowel implants, malignant ascites, and abdominal carcinomatosis. Since serous carcinomas are commonly clinically understaged, a prehysterectomy diagnosis of EIC or serous carcinoma of minimal or conventional type should prompt not only a total abdominal hysterectomy/bilateral salpingo-oophorectomy but also a thorough staging procedure that includes omentectomy, pelvic and paraaortic lymph node sampling, peritoneal washings, and biopsies of any suspicious lesions in the pelvis and abdomen.[188,203,211] The sectioning protocol should include rigorous sampling of serosal surfaces, connective tissue, omentum, lymph nodes, ovaries, and fallopian tubes (particularly the fimbriae) in an effort to identify extrauterine disease that is not grossly apparent.

One caveat in the search for microscopic disease within connective tissue is to be careful not to misinterpret nests of hilus cells associated with small nerve twigs within the ovarian ligament or mesovarium as micronodules of serous carcinoma tracking along peripheral nerves (Fig. 4.237). Once attuned to the presence of hilus cell nests in this type of tissue, this normal finding is usually readily recognized; if difficulties are encountered, their true nature could be confirmed by demonstrating an inhibin-positive, cytokeratin-negative immunophenotype.[212]

Grossly inapparent spread of serous carcinoma is often manifested as small peritoneal implants, nests of tumor cells within capillary/lymphatic spaces, or tumor cell clusters lurking within the lumens of the fallopian tubes (Fig. 4.238). The finding of cells derived from serous carcinoma within the tubal lumens is highly predictive of peritoneal metastases, and retrograde transtubal spread is the mechanism that most likely accounts for the not uncommon finding of noninvasive serous carcinoma or EIC presenting with peritoneal disease.[213] Further supporting this mechanism over synchronous, multifocal disease are the findings of (a) monoclonality as assessed by p53 mutational patterns in cases of extrauterine disease associated with minimal serous

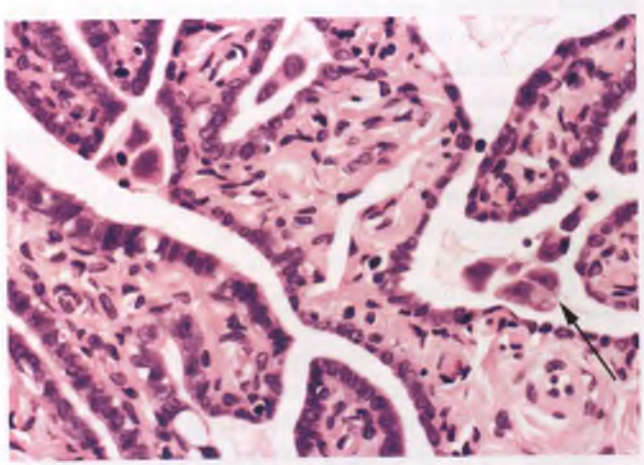

FIGURE 4.238. Detached clusters of malignant cells from a serous carcinoma found within the lumen of the fallopian tube (*arrow* marks one of three clusters). Such a finding could be associated with transtubal spread into the peritoneal cavity, and explain the malignant behavior of some cases of EIC and nonmyoinvasive serous carcinoma.

carcinoma or EIC[214] and (b) concordant lack of WT-1 expression in matched pairs of serous carcinomas from patients that have both peritoneal involvement and uterine serous carcinoma apparently confined to an endometrial polyp (WT-1 is typically expressed in primary peritoneal, ovarian, and tubal serous carcinomas, but not in serous carcinomas of endometrial origin).[215]

In a minority of superficial serous carcinomas of the endometrium with apparent extrauterine spread, serous tubal intraepithelial carcinoma may actually be the source of the neoplastic process, rather than a mucosal site of tumor implantation or separate primary lesion.[216] In addition to the fallopian tube serving as a conduit for or potential source of endometrial serous carcinoma, inconspicuous lymphatic invasion (for which myometrial invasion is not a prerequisite) or multifocal carcinogenesis may still serve as the causative mechanism of some cases of minimal serous carcinoma of the endometrium associated with synchronous extrauterine disease.

Commonly encountered features of serous carcinoma can be summarized by the mnemonic "UPSC DASE" (pronounced "up′sə; dā′zē" as in upsy-daisy) for **U**terine **P**apillary **S**erous **C**arcinoma → **D**eep myometrial invasion, **A**ngiolymphatic invasion, **S**pread beyond the uterus at presentation, and **E**IC.

Differential Diagnosis

As discussed earlier in this chapter, the differential diagnosis of EIC includes the Arias-Stella reaction and reactive epithelial atypia associated with either papillary syncytial change (PSC) or regeneration of the endometrial lining following curettage. In addition, some cases of EIC can mimic simple atypical endometrial hyperplasia (Fig. 4.235), which is a rare form of endometrial hyperplasia and a diagnosis that should be made with caution. The degree of nuclear atypia is much more marked in EIC than in atypical hyperplasia, with the former usually exhibiting high-grade nuclei with macronucleoli.[197] In addition, EIC features an atrophic background that is seldom associated with atypical hyperplasia, and typically occurs in patients who are a decade older than those with atypical hyperplasia.[197] EIC is also usually a localized microscopic finding, whereas most endometrial hyperplasias are more widespread processes. Although diffuse and strong p53 immunoreactivity of a surface/superficial glandular lesion with significant nuclear atypia supports a diagnosis of EIC, there is insufficient experience with this immunostain on mimics of EIC to rely too heavily on this finding in isolation. Additional supportive evidence for a diagnosis of EIC is the finding of a high (>50%) Ki-67 proliferative index.[204]

Processes that need to be distinguished from serous carcinoma include florid PSC, villoglandular endometrioid carcinoma (VGEC), the occasional endometrial carcinoma with features that are intermediate between VGEC and serous carcinoma, endometrioid carcinoma with small nonvillous papillae, endometrioid carcinoma with high-grade nuclei, and clear cell carcinoma. The differentiating features of most of these entities have been discussed earlier in this chapter. As mentioned, there is some overlap in the histologic features of serous carcinoma and some forms of clear cell carcinoma, although classic forms of the latter entity are readily recognized by more prominent zones with clear cytoplasm, an admixture of solid, papillary, and tubulocystic architectural patterns, and a papillary component with hyalinized stromal cores. Metastatic high-grade serous carcinoma originating from the fallopian tubes, ovaries, or peritoneum may be histologically indistinguishable from primary uterine serous carcinoma in a curettage specimen, and requires clinicopathologic correlation for its identification.

Clear Cell Carcinoma

Clear cell carcinoma and serous carcinoma account for the vast majority of type II (estrogen-independent) endometrial carcinomas. Clear cell carcinoma is less common than serous carcinoma, accounting for 1% to 3% of endometrial carcinomas, and is not appreciably different from serous carcinoma in its gross and presenting clinical characteristics.[189,217] Unlike cervical and vaginal clear cell carcinoma, these tumors are not associated with in utero exposure to diethylstilbestrol.

The same histologic patterns (solid, papillary, tubulocystic) and cell shapes (polygonal, hobnail, and flattened) that are encountered in vaginal, cervical, and ovarian clear cell carcinomas are seen in the endometrial version as well, although the tubulocystic pattern is infrequent in this site (Figs. 4.239 and 4.240). There is a tendency for different architectural patterns to be found in different areas of the tumor, and for polygonal clear cells to predominate in solid areas, hobnail or clear cells to line tubules and papillae, and flattened or hobnail cells to line cystic spaces.[164,218] The stromal cores in the papillary areas of clear cell carcinoma often have a hyalinized appearance, which can be a useful diagnostic feature. The neoplastic cells of clear cell carcinoma typically have an intermediate to high nuclear grade, although the degree of nuclear atypia and nucleolar prominence are often not as striking as in serous carcinoma.

The presence of abundant glycogen-rich cytoplasm accounts for the cytoplasmic clearing that is characteristic of most clear cell carcinomas, although occasional tumors of this type have a variable and sometimes dominant component of cells with oxyphilic rather than clear cytoplasm (Fig. 4.241).[217] Mucin may be present within gland lumens, but is only rarely

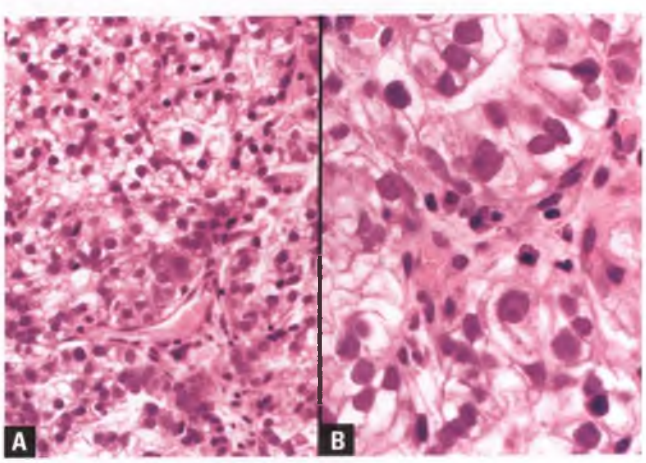

FIGURE 4.239. **A,B**: Clear cell carcinoma with a predominantly solid pattern.

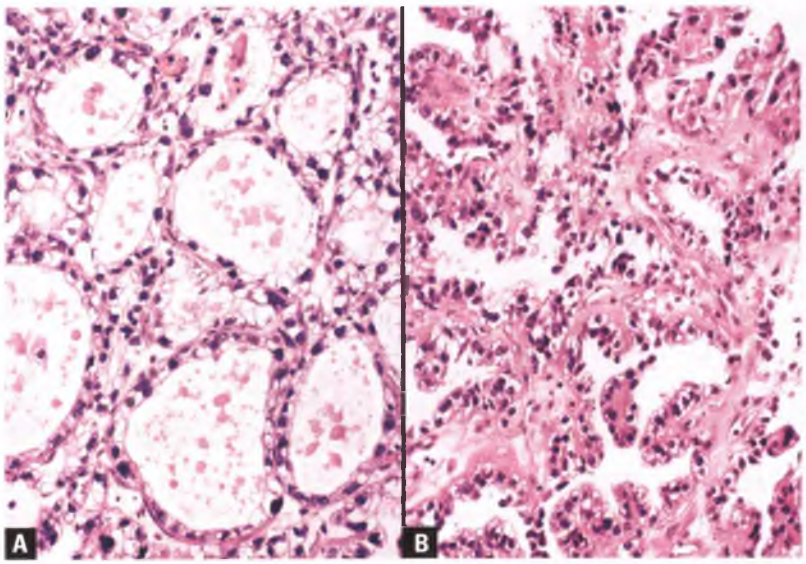

FIGURE 4.240. Clear cell carcinoma. **A**: Tubulocystic pattern. **B**: Papillary pattern. Note the characteristic hyalinization of the fibrovascular cores.

encountered within the tumor cell cytoplasm. Psammoma bodies have been reported in a small percentage of tumors with a papillary architecture,[164] which may in part be related to the difficulty in separating this pattern of clear cell carcinoma from serous carcinoma. A lesion analogous to EIC that is a putative precursor to endometrial clear cell carcinoma has been described (Fig. 4.242).[219] About 15% to 30% of clear cell carcinomas have a minor component of endometrioid adenocarcinoma of the usual type.

Most studies have shown that clear cell carcinoma is an aggressive form of endometrial carcinoma, behaving similarly to or worse than stage-matched grade 3 endometrioid adenocarcinoma.[162,218,220,221] Histologic grading of endometrial clear cell carcinomas is not a useful exercise, since there is no correlation between nuclear grade or architectural pattern and outcome. As is the case for serous carcinoma, a prehysterectomy diagnosis of clear cell carcinoma should prompt a thorough staging procedure at the time of surgical treatment, regardless of the intraoperative assessment of the extent of myometrial invasion.

Differential Diagnosis

The differential diagnosis of clear cell carcinoma includes clear cell metaplasia, the Arias-Stella reaction, serous carcinoma, the secretory variant of endometrioid carcinoma, and endometrioid carcinomas with squamous differentiation that takes the form of glycogenated clear cells, all of which have been discussed earlier in this chapter. In addition, those epithelioid smooth muscle tumors and perivascular epithelioid cell tumors with a predominance of clear cells can simulate clear cell carcinomas, but are distinguished by their myometrial origin, lack of glandular differentiation, and immunoprofile.

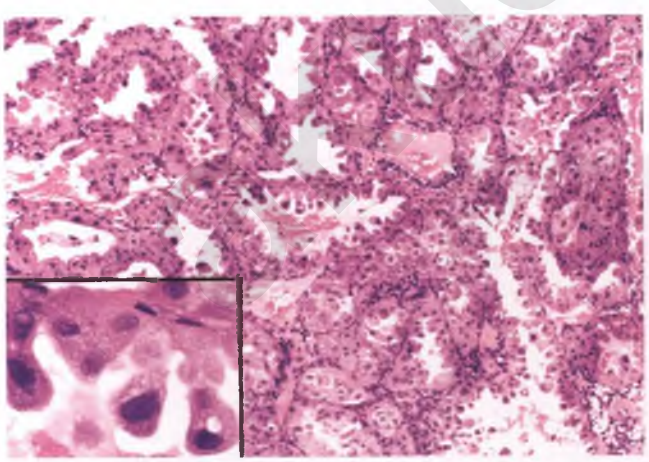

FIGURE 4.241. Oxyphilic clear cell carcinoma. The inset highlights an area with hobnailing. Scattered mitotic figures and tumor cells with prominent nucleoli were also present (not shown). This lesion was not myoinvasive, but lymphatic invasion was present and the patient developed malignant ascites due to metastatic clear cell carcinoma 3 years posthysterectomy.

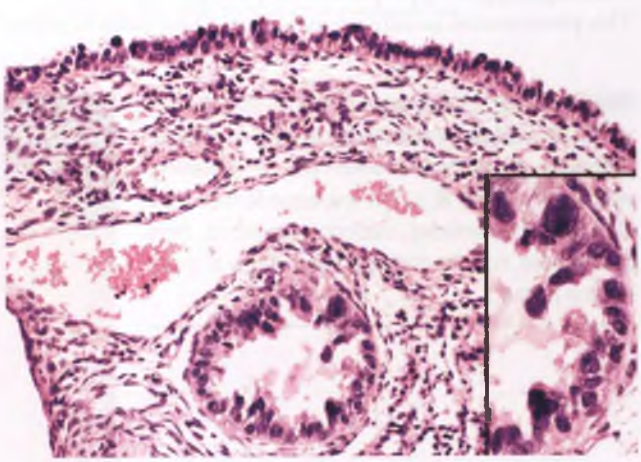

FIGURE 4.242. Putative precursor lesion of clear cell carcinoma involving the endometrial surface and a superficial gland. The inset highlights the high-grade nuclear features of this lesion. Fully developed clear cell carcinoma was present in neighboring tissue.

Mucinous Carcinoma

The incidence of mucinous carcinoma ranges from 1% to 9% of endometrial carcinomas, with much of this variation due to differences in diagnostic criteria.[189,222] In the largest reported series of mucinous carcinomas, tumors with a dominant (>50%) mucinous component were considered mucinous carcinomas,[222] whereas others may require a higher proportion of the tumor to be mucinous in order to qualify as this special variant. It is my preference that cases with a nonmucinous (usually endometrioid) component that accounts for at least 10% of the neoplasm be classified as mixed carcinomas. The vast majority of mucinous carcinomas are grade 1 or 2 and confined to the uterus, and have a prognosis similar to stage and grade-matched endometrioid carcinomas.[222]

Many mucinous carcinomas, particularly those that are well differentiated and purely mucinous, have a mucoid cut surface (Fig. 4.243A). Most endometrial mucinous carcinomas have at least a partial villous or villoglandular architecture, particularly on their surface where these patterns can blossom within the endometrial cavity (Fig. 4.243B).[222] Mucinous differentiation within endometrial carcinoma is defined by the presence of abundant intracytoplasmic mucin. Mucinous cells are usually recognizable as such in routinely stained sections by the presence of abundant, pink-tinged, granular or bubbly cytoplasm; if necessary, their mucinous nature can be confirmed with stains for neutral mucin. Architectural complexity is generally marked in terms of crowding and formation of an array of glandular, villoglandular, and papillary structures, but the degree of epithelial stratification is typically quite limited in most areas (Fig. 4.244).[222] An example of a mixed endometrioid and mucinous carcinoma is presented in Figure 4.245.

In mucinous carcinomas, neutrophils are often present within extracellular pools of mucin that may be located within cystically dilated glands or loosely associated with strands of neoplastic epithelium.[222] This finding, when coupled with a microacinar architecture and bland nuclear features, produces a **microglandular hyperplasia-like pattern** (Fig. 4.246).[165,166] This phenomenon usually occurs within a mucinous or mixed mucinous and endometrioid carcinoma, and, as discussed earlier, may also be seen on the surface of some endometrioid carcinomas. Although endometrial samples with this pattern that contain abundant abnormal tissue with moderate nuclear atypia are recognizable as carcinoma, more often than not it is a limited amount of cytologically bland microglandular tissue that is encountered in curettings. In the latter situation, a definitive diagnosis is often not possible without obtaining additional endometrial tissue, which is usually forthcoming following a conversation with the clinician and a descriptive diagnosis that conveys the concern about the possibility of malignancy.

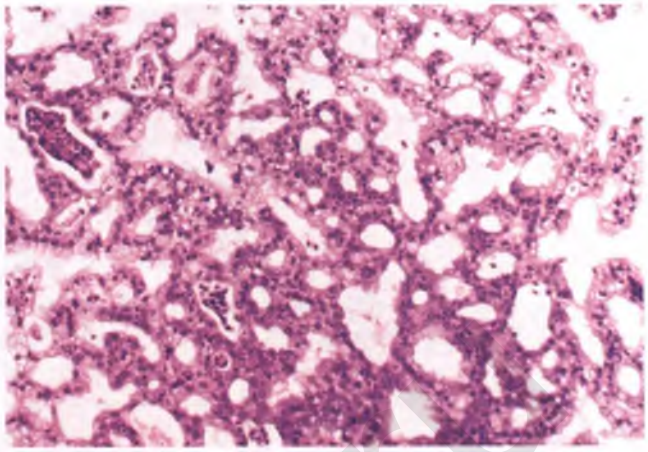

FIGURE 4.244. Mucinous carcinoma. This architecturally complex proliferation exhibits little to no nuclear stratification. Note the presence of neutrophils, which are dispersed singly and in small intraluminal aggregates throughout the tumor.

Differential Diagnosis

The differential diagnosis of endometrial mucinous carcinoma includes endocervical mucinous carcinoma, metaplastic mucinous hyperplasia, microglandular hyperplasia, metastatic mucinous carcinoma, and compacted, shredded strips of benign endocervical mucinous epithelium.

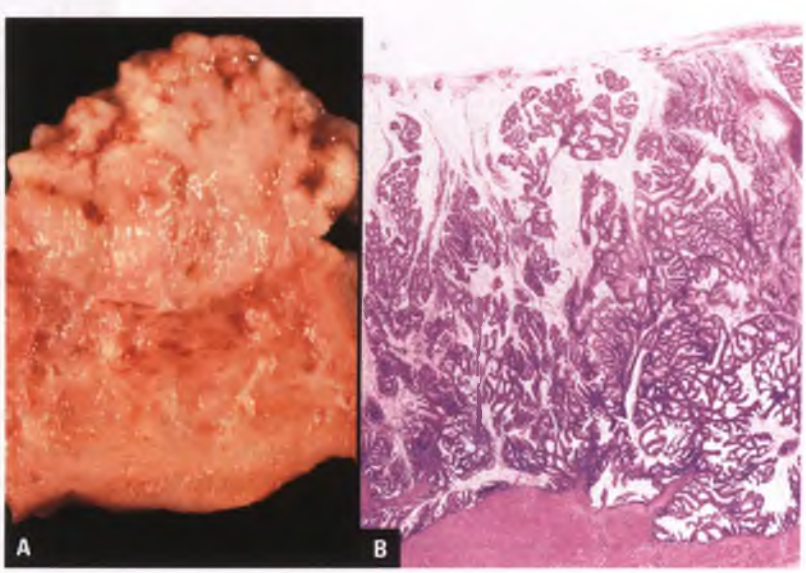

FIGURE 4.243. Mucinous carcinoma. **A**: This polypoid, well-differentiated mucinous carcinoma with superficial myometrial invasion has a glistening, mucoid cut surface. **B**: In this low-magnification view of a well-differentiated mucinous carcinoma from another case, note the complexity and variety of architectural patterns.

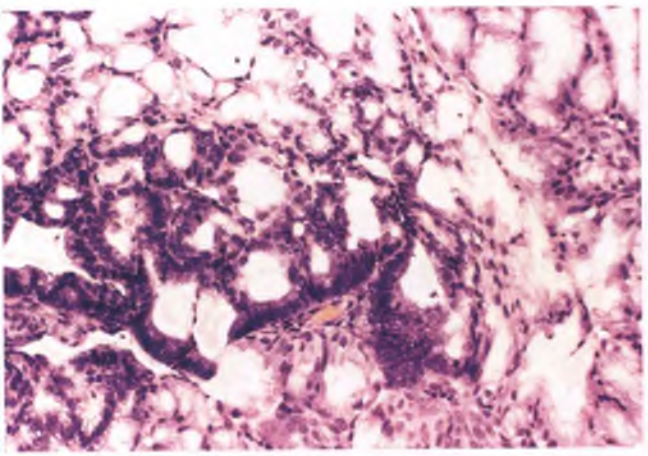

FIGURE 4.245. Mixed endometrioid and mucinous carcinoma.

- Since there are some significant differences in the treatment options for endocervical and endometrial adenocarcinoma, the site of origin of the mucinous carcinoma is clinically relevant. Features that favor an endometrial origin include (a) associated endometrial epithelium and/or stroma, (b) stromal foam cells, (c) associated endometrial hyperplasia or mucinous metaplasia, (d) minor foci of endometrioid carcinoma, (e) a prominent villous or villoglandular surface component, and (f) a fractional curettage and/or other clinical evidence that the neoplasm is located within the endometrial cavity.[222] As discussed in Chapter 3, an immunohistochemical panel can help to distinguish endometrioid endometrial adenocarcinoma from the usual type of endocervical adenocarcinoma, but this approach is of little utility in the differential diagnosis of endometrial versus endocervical mucinous carcinoma.[223] When confronted with this problem, it should also be remembered that authentic mucinous endocervical carcinomas are rare neoplasms that are unlikely to be found in appreciable amounts within endometrial samples, and occur within women who on average are a decade younger than patients with endometrial carcinoma (see Chapter 3).
- The determination of whether an architecturally complex and cytologically bland mucinous proliferation encountered in an endometrial sample is better classified as being within the spectrum of metaplastic hyperplasia or well-differentiated mucinous carcinoma is difficult, and sometimes impossible. Conspiring to reduce the pathologist's diagnostic skills to educated guesswork in this situation are (a) the benign-appearing nature of portions of mucinous carcinomas, which can include foci of myoinvasion and metastases (Fig. 4.247), (b) the tendency of these benign-appearing foci to predominate superficially, where they represent the tissue most likely to be recovered during endometrial sampling, and (c) the commonplace finding within mucinous carcinomas of significant heterogeneity of architectural patterns and only focal areas with nuclear atypia (Figs. 4.248 and 4.249). The most useful histologic features that facilitate recognition of mucinous carcinoma in this setting are the presence of epithelial stratification, loss of nuclear polarity, and moderate nuclear atypia, all of which may require abundant tissue for identification.[222] In instances in which an atypical mucinous proliferation cannot be definitively diagnosed as mucinous carcinoma within an endometrial biopsy or curettage, phrasing of the pathology report should indicate the concern for the possibility of carcinoma (see section on mucinous metaplastic hyperplasia).
- Features of microglandular hyperplasia-like endometrial carcinoma that facilitate its distinction from contaminating fragments of endocervical microglandular hyperplasia include (a) the postmenopausal status of the patient, (b) foci with significant nuclear atypia and mitotic activity, (c) an absence of associated reserve cell hyperplasia and subnuclear vacuoles, (d) a Ki-67 proliferative index of >5%, (e) a CD10 strong/CD34 negative to weak stromal staining pattern (in those samples with ample stroma), (f) the uncommon finding of associated stromal foam cells, and (g) a sample of sufficient size with associated areas of typical endometrioid or mucinous carcinoma.[165,224–226] The utility of p16 and vimentin immunohistochemistry in this situation is controversial.[224,225,227]

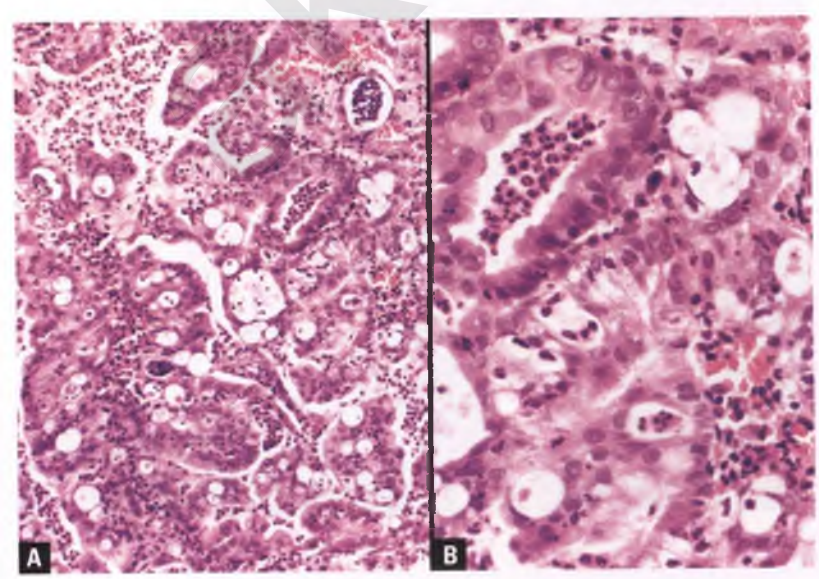

FIGURE 4.246. **A,B**: Microglandular hyperplasia-like area in a grade 1 mucinous carcinoma.

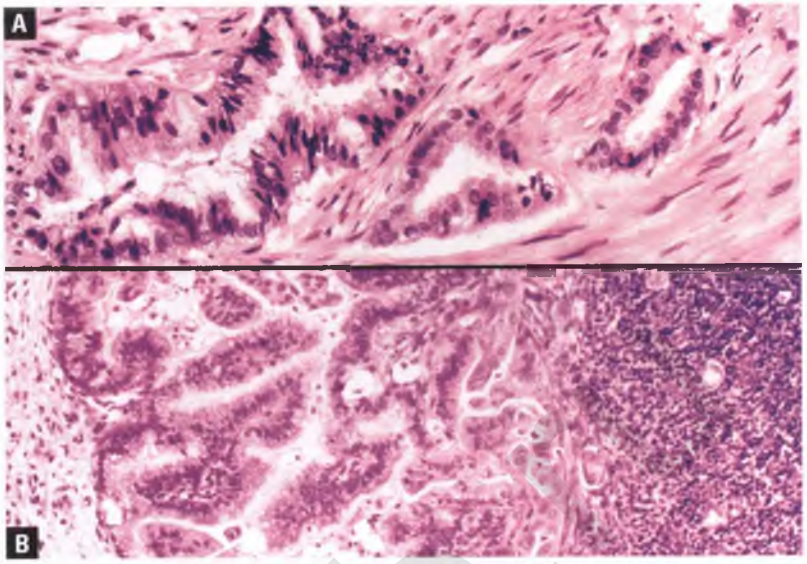

FIGURE 4.247. Myoinvasive and metastatic mucinous carcinoma with a deceptively bland appearance. **A**: Myometrial invasion by a very well-differentiated mucinous carcinoma. The glands resemble benign endocervical glands, and there is no stromal reaction. **B**: Well-differentiated mucinous carcinoma within a pelvic lymph node. The tumor deposit is architecturally complex with inapparent to focally moderate nuclear atypia. This patient developed lung metastases 4 years later.

- Very rarely, the uterus harbors a metastatic mucinous carcinoma. These tumors are distinguished from primary mucinous carcinoma by the clinical history of an extrauterine tumor with similar histology, a "bottom heavy" distribution of tumor that is concentrated in the myometrium, prominent angiolymphatic invasion, and signet-ring or colloid patterns that would be unusual for primary uterine tumors.[189]
- The ability of artifactually aggregated and coiled strips of benign endocervical mucinous epithelium to mimic a significant mucinous lesion is discussed in the section on metaplastic hyperplasias and illustrated in Figure 4.150.

Small Cell (Neuroendocrine) Carcinoma

Small cell carcinomas represent approximately 1% of endometrial carcinomas.[189] They share the histologic appearance and aggressive behavior of their more common counterparts in the uterine cervix (Fig. 4.250).[228,229] The characteristic nuclear features and variants of small cell carcinoma are discussed in Chapter 3.

Differential Diagnosis

Roughly half of endometrial small cell carcinomas are associated with an endometrioid carcinoma, which can lead to their misinterpretation as carcinosarcomas.[228,229] Further complicating this differential diagnosis is the fact that occasional carcinosarcomas can have small cell carcinoma as one of their components (Fig. 4.251).[229] The sarcomatous component of most carcinosarcomas is composed of pleomorphic, spindle-shaped cells rather than cells that could be confused with a small cell malignancy. If indicated, immunohistochemistry or ultrastructural studies could be performed in biphasic tumors composed of adenocarcinoma and a small cell malignancy in an effort to document that the small cell component exhibits neuroendocrine rather than sarcomatous differentiation.

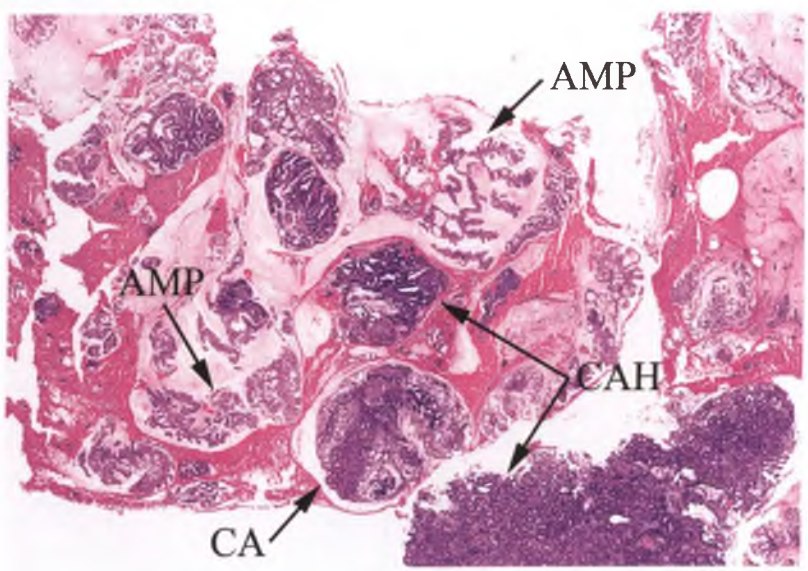

FIGURE 4.248. Heterogeneity within an endometrial curettage that contains a mixed endometrioid/mucinous carcinoma. Fragments of a nondiagnostic atypical mucinous proliferation (AMP) are admixed with pieces of CAH and carcinoma (CA). AMPs tend to predominate in limited, superficial samples, and often mask more readily recognizable portions of an underlying carcinoma.

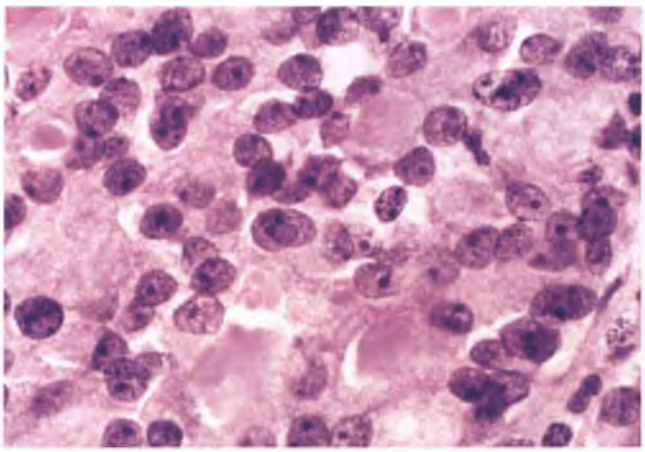

FIGURE 4.249. Mucinous carcinoma with moderate nuclear atypia in an area with a vaguely microacinar growth pattern. Note the prominent nucleoli within some of the tumor cells.

The differential diagnosis of pure endometrial small cell carcinoma includes lymphoma, low-grade endometrial stromal sarcoma, primitive neuroectodermal tumor (PNET), secondary involvement by a cervical small cell carcinoma, and benign endometrium with nonmenstrual breakdown.

- Immunohistochemical stains for lymphoid markers will help to exclude or establish the lymphoid nature of a small cell lesion; if lymphoid, a separate assessment is necessary to determine whether the process is malignant.
- In contrast to small cell carcinoma, low-grade endometrial stromal sarcoma tends to be composed of cells with minimal nuclear atypia and a low mitotic rate that lack nuclear molding and individual cell necrosis. These tumors have a characteristic vasculature and permeative pattern of myoinvasion, and large plugs of tumor within vessels are a common finding.
- Most PNETs exhibit evidence of neuroectodermal differentiation, typically in the form of a fibrillary matrix or rosettes/pseudorosettes, and are cytokeratin negative, synaptophysin positive, neurofilament positive, and CD99 positive.[230,231] This combination of features helps to distinguish uterine PNETs from small cell carcinoma.
- If the endometrial involvement by a small cell carcinoma is secondary to extension from a primary cervical tumor, this should be obvious on clinical grounds.
- It is almost a rite of passage for pathology residents to mistake endometrial samples with nonmenstrual shedding related to anovulatory cycles for small cell carcinoma. The resemblance can be striking, since the compacted aggregates of endometrial stromal cells have hyperchromatic nuclei, scant cytoplasm, and molded nuclear contours (Fig. 4.53). The absence of a mass lesion, a clinical history consistent with dysfunctional uterine bleeding, a double-contoured appearance of some of the fragments of crumbling endometrium (due to an outer rim of epithelial cells surrounding the condensed stromal cells), associated papillary syncytial change, and an absence of mitotic activity within the compact cell aggregates are features that aid in the recognition of benign endometrium with nonmenstrual breakdown. The degenerating stroma of some examples of menstrual endometrium can also raise this differential diagnostic consideration.

Undifferentiated Carcinoma (Non–Small Cell)

This tumor, which represents up to 9% of all endometrial carcinomas, was recently separated from and found to be more aggressive than grade 3 endometrioid carcinoma.[139,140] It is distinguished from grade 3 endometrioid carcinoma by virtue of its complete absence of glandular structures, and is composed of diffuse sheets of monotonous, medium-sized cells with moderate nuclear atypia (Fig. 4.252).[139] There is brisk mitotic activity, and foci of necrosis are typically present. Evidence of

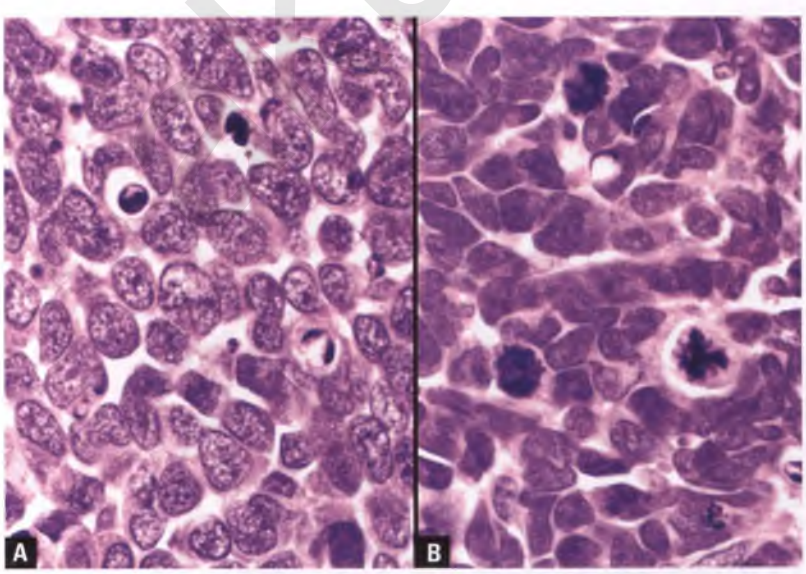

FIGURE 4.250. Endometrial small cell carcinoma. **A**: Many of these tumor cells fit the description of the oat cell variant. **B**: Intermediate variant. Note: these images were taken from different areas of the same tumor.

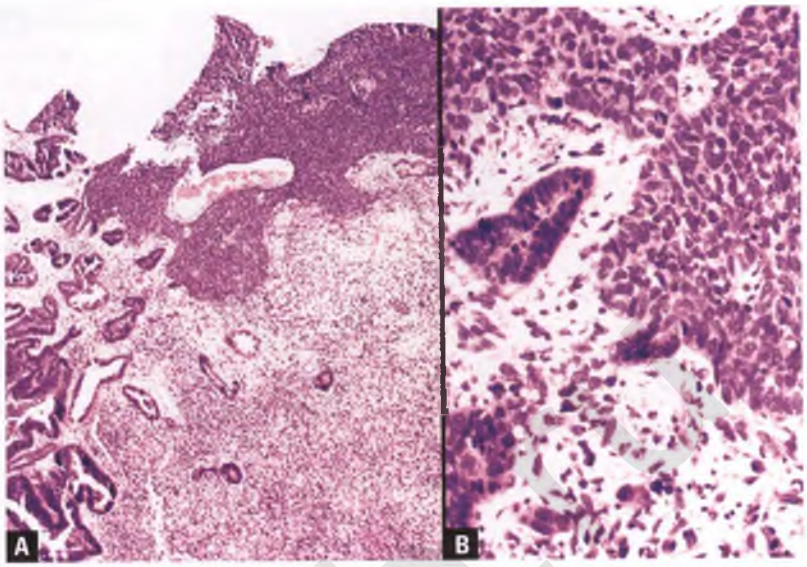

FIGURE 4.251. Small cell carcinoma as a component of carcinosarcoma. **A**: In addition to the small cell carcinoma (top), components of adenocarcinoma and spindle cell sarcoma are also present. **B**: This high-magnification view includes all three malignant components.

neuroendocrine differentiation is usually absent or only focally present, and its presence or absence has no impact on the dismal prognosis of patients with this tumor.[232] At least focal immunoreactivity for cytokeratin and epithelial membrane antigen is almost always present.[139] To avoid confusion with small cell carcinoma, which is often referred to as a form of undifferentiated carcinoma, the pathology report should specify that these tumors represent a non–small cell variant of undifferentiated carcinoma.

Occasional endometrial carcinomas are composed of an admixture of low-grade (grade 1 or 2) endometrioid carcinoma and undifferentiated carcinoma (Fig. 4.253).[141] These tumors have an aggressive behavior, even when the undifferentiated component comprises as little as 20% of the tumor.[141] Note that a strict application of the FIGO grading system for these tumors would result in a diagnosis of a grade 2 or grade 3 endometrioid carcinoma, depending on whether the undifferentiated component comprised ≤50% or >50% of the tumor, respectively. This undergrading would underestimate the probability of an adverse outcome, particularly in those cases that were misclassified as grade 2 endometrioid carcinomas. It is more appropriate to diagnose these tumors as a form of mixed carcinoma, with a note emphasizing their aggressive behavior.

Differential Diagnosis

The differential diagnosis of undifferentiated carcinoma includes grade 3 endometrioid carcinoma, hematopoietic malignancies (lymphoma and granulocytic sarcoma), undifferentiated endometrial sarcoma, epithelioid leiomyosarcoma, and endometrial involvement by a large cell neuroendocrine carcinoma originating from the uterine cervix.

- As indicated above, grade 3 endometrioid carcinoma features the presence of at least focal glandular differentiation that is lacking in undifferentiated carcinoma.
- The focal immunoreactivity of undifferentiated carcinoma with cytokeratin and epithelial membrane antigen can help to

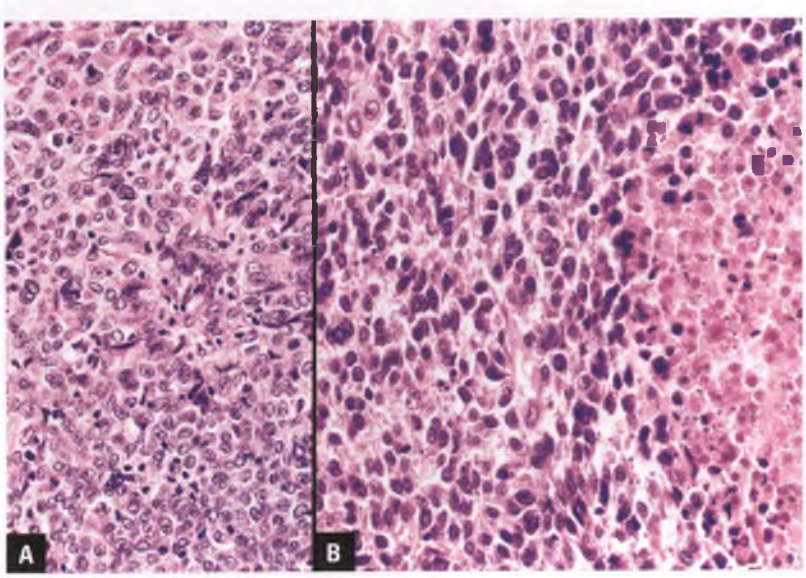

FIGURE 4.252. **A,B**: Undifferentiated carcinoma. In these two different examples, note the diffuse sheets of monotonous tumor cells with moderate nuclear atypia and an absence of gland formation. The tumor in **B** is partially necrotic.

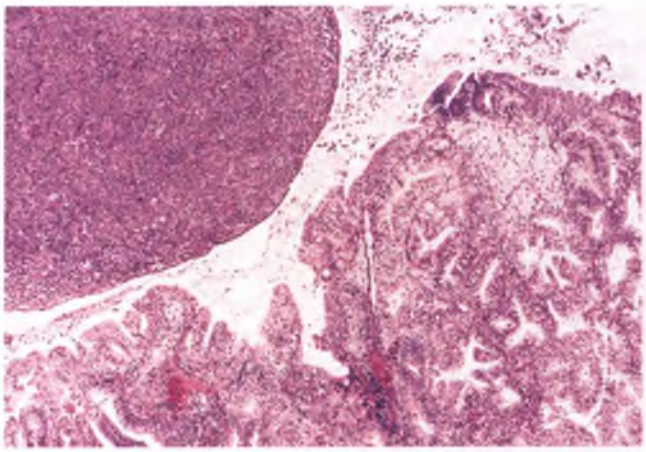

FIGURE 4.253. Mixed low-grade endometrioid adenocarcinoma and undifferentiated carcinoma. Misclassification of this tumor as a grade 2 endometrioid carcinoma would significantly underestimate its malignant potential.

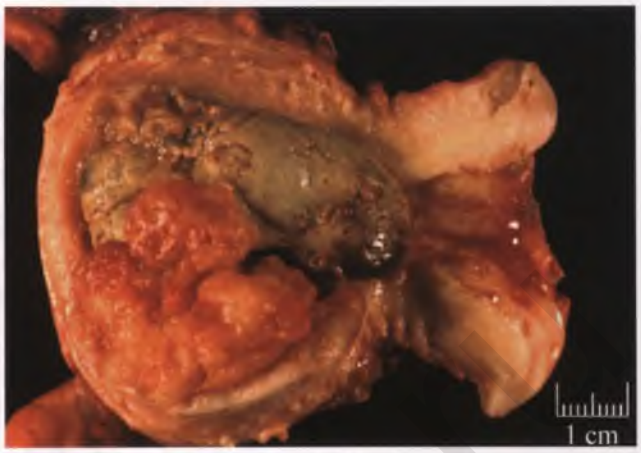

FIGURE 4.254. Carcinosarcoma. The polypoid tumor fills and expands the endometrial cavity and protrudes into the isthmic region of the uterus. The tannish-gray portion of the tumor is extensively necrotic, and is also focally hemorrhagic at its tip.

distinguish it from large cell lymphoma and granulocytic sarcoma, which will express one or more hematopoietic markers.

- Undifferentiated endometrial sarcoma is distinguished from undifferentiated carcinoma largely on the basis of a panel of immunohistochemical stains that focuses on detecting epithelial vs. mesenchymal differentiation.
- In contrast to undifferentiated carcinomas, epithelioid leiomyosarcomas are myometrial-based tumors. Although epithelioid leiomyosarcomas may be immunoreactive for cytokeratin,[233] they usually have areas that transition to a more conventional spindle cell morphology and express one or more mesenchymal markers such as actin, desmin, or h-caldesmon.[189]
- Endometrial involvement by a large cell neuroendocrine carcinoma of the cervix should be recognizable by the presence of a cervical mass and immunoreactivity for neuroendocrine markers.

Mixed Carcinomas

By definition, mixed carcinomas contain two histologic patterns in which the minor component constitutes at least 10% of the tumor.[189] The relative proportions of each component should be indicated in the pathology report. The most common types of mixed carcinomas are endometrioid carcinomas that are admixed with a component of mucinous, serous, small cell, or undifferentiated carcinoma.[189] Representative examples of these tumors have been illustrated earlier in this chapter.

Carcinosarcoma

Carcinosarcoma is also referred to as malignant mixed müllerian tumor, malignant mixed mesodermal tumor, or more succinctly as MMMT or "Triple M" T. It is a biphasic neoplasm composed of an admixture of epithelial and mesenchymal elements, both of which are malignant. Carcinosarcomas represent approximately 2% of primary uterine malignancies, and account for about half of uterine cancers with a malignant mesenchymal component. These tumors have traditionally been considered a subtype of uterine sarcoma, and as such have often been cited as the most common primary uterine sarcoma. However, since mounting clinical, histologic, immunologic, and molecular data strongly support the concept that these tumors represent metaplastic carcinomas,[234–236] they are herein considered a special variant of endometrial adenocarcinoma.

Carcinosarcomas typically occur in postmenopausal women who present with abnormal vaginal bleeding and/or abdominopelvic pain, with the latter symptom suggesting extrauterine spread. Grossly, carcinosarcomas are most often large, bulky, broad-based, polypoid tumors that fill and distend the endometrial cavity (Fig. 4.254). The tumor may protrude through the external os, and myometrial invasion is often grossly evident. The sectioned surface of the tumor is usually fleshy with areas of hemorrhage and necrosis.

Eighty to ninety percent of carcinosarcomas are monoclonal.[237] It is tempting to speculate that careful gross examination

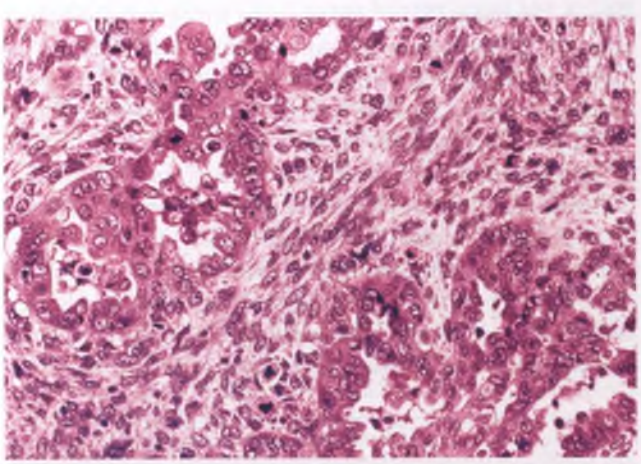

FIGURE 4.255. Carcinosarcoma. In this example, the malignant glandular component is high-grade serous carcinoma, whereas the sarcomatous component is of the high-grade homologous type and exhibits brisk mitotic activity. Note that although the two components are intimately admixed, they are sharply demarcated from one another.

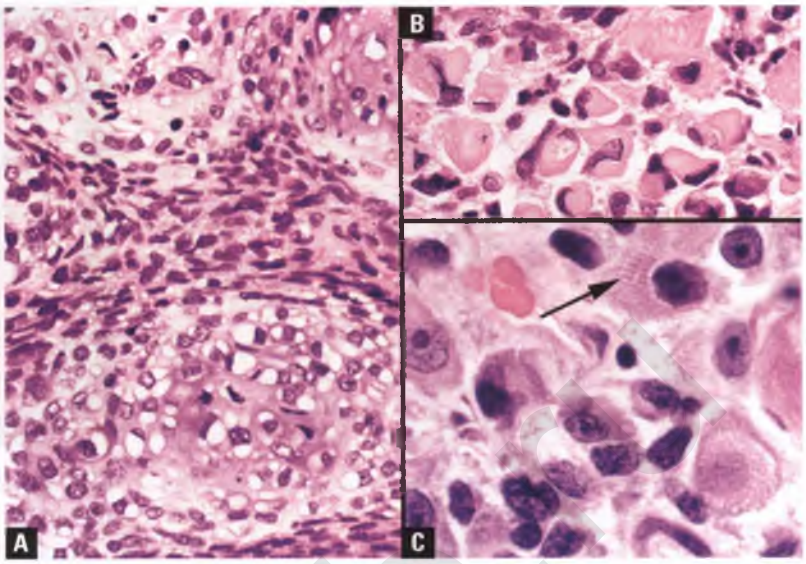

FIGURE 4.256. Carcinosarcoma with heterologous elements. **A**: Mesenchymal area composed of micronodules of chondrosarcoma embedded within a cellular, spindle cell sarcoma. **B,C**: Rhabdomyoblasts from rhabdomyosarcomatous foci within the mesenchymal component of two different carcinosarcomas. Note the cytoplasmic cross-striations in **C** (*arrow*).

of the 10% to 20% of biclonal (collision) tumors would reveal at least some areas where the sarcomatous and carcinomatous components are topographically distinct, as exemplified by the ovarian carcinosarcoma in Figure 7.116.

Histologically, the carcinomatous component of carcinosarcoma is typically a high-grade adenocarcinoma with endometrioid or serous differentiation, with clear cell or other rare carcinomas being seen less commonly (Fig. 4.255).[238] The sarcomatous component is also usually high grade and cases are roughly evenly split between homologous and heterologous types.[238†] Homologous sarcoma is usually composed of nondescript spindle, oval, or round cells with significant nuclear atypia and mitotic activity in patterns that are consistent with sarcoma derived from endometrial stroma, fibrosarcoma, or rarely leiomyosarcoma.[238] Heterologous sarcomatous elements are usually found in association with homologous sarcoma, and in descending order of frequency are represented by rhabdomyosarcoma, chondrosarcoma, osteosarcoma, and liposarcoma (Figs. 4.256 and 4.257).[238] Although the sarcomatous and carcinomatous elements are usually intimately admixed, they may be topographically distinct. However, in either situation, they are histologically generally sharply demarcated from one another.[238]

Immunohistochemistry plays a limited role in the diagnosis of carcinosarcomas, where it can confirm the identification of rhabdomyoblasts via the demonstration of immunoreactivity with skeletal muscle markers (myoglobin, myoD1, or myogenin), confirm chondroid over squamous differentiation by demonstrating positivity for S100, or provide evidence that favors carcinosarcoma over sarcomatoid carcinoma by demonstrating diffuse immunoreactivity for actin or desmin within the sarcomatous component. Cytokeratin can be utilized to highlight the biphasic nature of carcinosarcomas for tumor board presentations (carcinoma → cytokeratin positive; sarcoma → cytokeratin negative), although many cases show at least focal cytokeratin positivity of the sarcomatous component.[235,236,239]

Differential Diagnosis

The differential diagnosis of carcinosarcomas includes endometrioid adenocarcinoma with a prominent spindle cell component, the so-called corded and hyalinized endometrioid carcinoma, and endometrial adenocarcinoma with benign heterologous elements. In endometrioid carcinomas with a prominent spindle cell component, the spindle cells only *simulate* a sarcoma. In contrast,

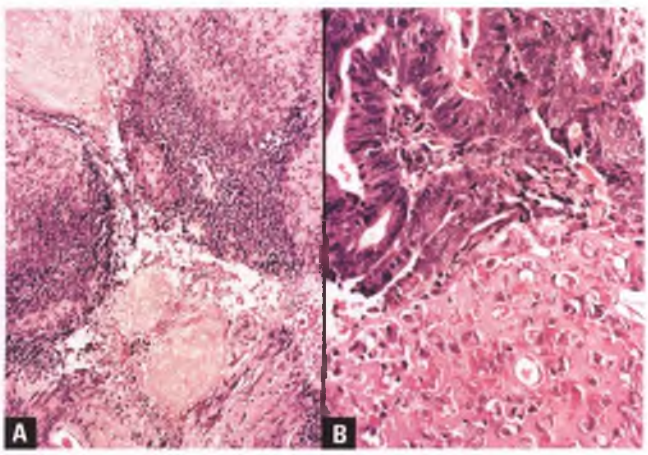

FIGURE 4.257. Carcinosarcoma with heterologous elements. **A**: Osteosarcoma merges with the cellular spindle cell sarcomatous component of a carcinosarcoma. The pale foci of squamous differentiation with keratin formation are related to a nearby endometrioid adenocarcinoma. **B**: The aforementioned endometrioid adenocarcinoma (top) is seen adjacent to a focus of osteosarcoma (bottom). The malignant-appearing osteoid in these images is recognized by its eosinophilic, glassy, homogeneous nature and its association with cells resembling osteoblasts.

† In the older literature, use of the term carcinosarcoma was restricted to tumors with homologous sarcomatous elements, whereas MMMT indicated that heterologous tissue (i.e., tissue of a type not normally found in the uterus) comprised a portion of the sarcomatous component. Currently, all tumors of this type are referred to as carcinosarcomas (or MMMTs), and are further subclassified as being of homologous type or as containing heterologous elements. If the latter, the type(s) and approximate amount(s) of the heterologous tissue should be specified in the pathology report.

carcinosarcomas are legitimately partly sarcomatous, which is particularly apparent in those cases with heterologous elements. The distinction of these two tumors from one another, as well as the separation of carcinosarcoma from the corded and hyalinized endometrioid carcinoma, are discussed in the section on unusual patterns in endometrioid adenocarcinoma. Focal areas of benign heterologous tissue can rarely be seen in otherwise ordinary endometrial adenocarcinomas;[240] the absence of a sarcomatous component distinguishes these tumors from carcinosarcoma.

Behavior and Prognosis

Carcinosarcomas are aggressive neoplasms that as a group have a prognosis that is worse than both high-grade endometrial adenocarcinoma and the high-risk subtypes of serous and clear cell carcinoma.[241–243] The presence of a sarcomatous component appears to serve as a marker of increased aggressiveness,[234] which is manifested by carcinosarcomas having an increased incidence of extrauterine spread of tumor at the time of clinical presentation as compared to high-grade endometrial adenocarcinomas.[241]

Although there is no doubt that tumor stage is the most powerful prognostic predictor for carcinosarcomas (5-year survival for stage I disease of 50%–60% vs. 0%–25% for stage III–IV disease),[242] numerous studies have sought to identify prognostic indicators within the subset of these tumors that are confined to the uterus. In a recent study of stage I patients who had undergone comprehensive surgical staging, the presence of heterologous sarcomatous elements was found to be a powerful negative prognostic factor.[242] However, the potential prognostic significance of heterologous elements is controversial and has a long and checkered past, and this finding needs to be confirmed by similarly designed studies that also use patients who have undergone rigorous surgical staging, since this tumor is notorious for its high incidence of being clinically understaged. Some other purported adverse prognostic factors in low-stage disease that are also not universally accepted are the presence of high-grade serous/clear cell carcinoma, deep myometrial invasion, and angiolymphatic invasion.[238]

Carcinosarcomas have a pattern of spread that is similar to ovarian cancer, with the most common sites of extrauterine spread being the pelvis, abdomen, and regional lymph nodes.[241,243] Metastatic lesions are typically purely carcinomatous, occasionally both carcinomatous and sarcomatous (exclude cellular, reactive desmoplastic stroma mimicking sarcoma), and rarely purely sarcomatous.[236,238,244]

Miscellaneous Rare Carcinomas

Rare cases of primary squamous cell carcinoma of the endometrium have been reported.[245] Before making such a diagnosis, the possibilities of secondary spread from a cervical squamous cell carcinoma and an endometrial endometrioid carcinoma that has been overrun by extensive squamous differentiation must be excluded.

Additional neoplasms that occur at case-reportable frequencies as primary endometrial tumors are transitional cell carcinoma,[246] giant cell carcinoma,[247,248] glassy cell carcinoma,[249] lymphoepithelioma-like carcinoma,[250] hepatoid carcinoma,[251] signet-ring carcinoma,[252,253] and carcinomas with trophoblastic/choriocarcinomatous elements.[254–256]

UTERINE SMOOTH MUSCLE TUMORS

Evaluating and Predicting Behavior of Uterine Smooth Muscle Tumors

Uterine smooth muscle tumors, specifically leiomyomas ("uterine fibroids"), are common everyday specimens in the surgical pathology laboratory. It is recommended that pathologists follow the strategy of the Stanford group[39,257] for evaluating and classifying myomatous tumors of the uterus:

1. *Confirm the smooth muscle nature of the tumor.*

   Typical uterine smooth muscle tumors are composed of intertwining fascicles of spindle-shaped cells with elongated and blunt-ended (cigar-shaped) nuclei and eosinophilic, fibrillary cytoplasm. With the trichrome stain, the cytoplasmic fibrils have a brick-red appearance. These features are characteristic of normal and most neoplastic smooth muscle cells in all sites, and are illustrated at high magnification in an example of an ovarian leiomyoma in Figure 7.304. The constituent cells of epithelioid smooth muscle tumors have rounded and centrally placed nuclei with eosinophilic or clear cytoplasm, and are often compartmentalized by hyalinized stroma. In the rare myxoid smooth muscle tumors, stellate smooth muscle cells are widely separated by myxoid material. Tumors that exhibit usual smooth muscle differentiation follow one set of classification guidelines, whereas separate guidelines exist for epithelioid and myxoid smooth muscle tumors. A small subset of pure mesenchymal neoplasms of the uterine corpus exhibits ambiguous features in which it is difficult or impossible to determine smooth muscle vs. endometrial stromal differentiation (see section on cellular leiomyomas).
2. *Use a multivariate approach to assign a diagnosis that reflects the malignant potential of the tumor.*

   Once the smooth muscle nature of the neoplasm has been established, one can set about determining its malignant potential and assigning it to a particular subtype. The Stanford classification system for tumors with usual smooth muscle differentiation utilizes a multivariate approach, with less reliance on mitotic activity than earlier classification schemes.[39,257] The major features to assess initially are the presence or absence of necrosis and the degree of nuclear atypia, followed in a small proportion of cases by a formal assessment of the mitotic rate. Definitions and clarifications of these three variables are discussed below.

Necrosis

If necrosis is present, it is critical to determine whether it represents tumor cell necrosis[258] (referred to as coagulative tumor cell necrosis by the Stanford group),[39,259] infarct-type necrosis[258]

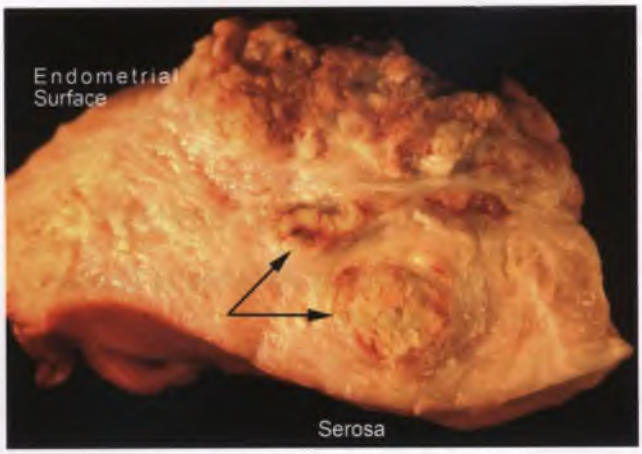

FIGURE 4.258. Longitudinal section through a uterine leiomyosarcoma with extensive tumor cell necrosis. Note the plugs of intravascular necrotic tumor distending myometrial veins (*arrows*).

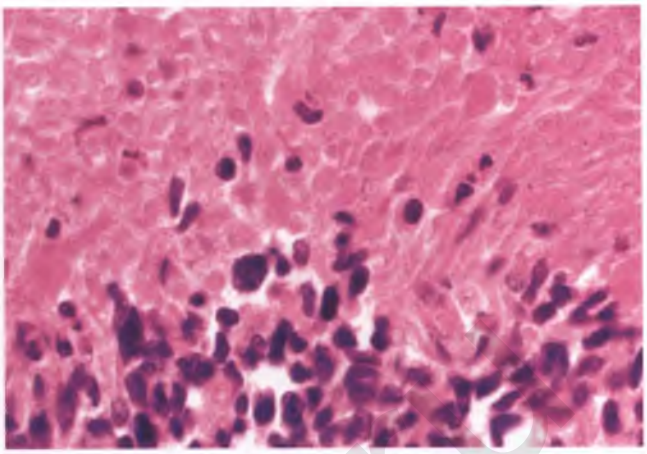

FIGURE 4.260. Tumor cell necrosis in leiomyosarcoma. Note the abrupt transition between viable tumor (bottom) and focus of tumor necrosis (top).

(referred to as hyalin necrosis, hyaline necrosis, or hyalinizing necrosis by the Stanford group),[39,259] or ulcerative necrosis.

Tumor cell necrosis, which is presumably a reflection of a tumor outstripping its blood supply, often has geographic outlines and when grossly visible resembles a yellow paste with the consistency of paté (Fig. 4.258). It is often seen in leiomyosarcoma and features an abrupt transition between necrotic cells and preserved cells (Figs. 4.259 and 4.260). Ghost outlines of pleomorphic nuclei are often visible within the murky background of cellular debris within tumor cell necrosis, and there may be selective viability of perivascular tumor (analogous to that shown for choriocarcinoma in Fig. 10.36). Tumor cell necrosis is an ominous finding, and was the most powerful univariate predictor of an adverse clinical outcome in the landmark 1994 Stanford study.[259]

In contrast to tumor cell necrosis, the typical case of infarct-type necrosis is circumscribed, yellow with variable amounts of hemorrhage, and soft or rubbery with a consistency analogous to that of tofu or brie cheese (Fig. 4.261). Microscopically, typical infarct-type necrosis exhibits a characteristic zone of hyalinized collagen interposed between the dead cells, which appear pale and mummified, and the preserved cells (Fig. 4.262A). In infarcts that are more recent, this band may consist of granulation tissue rather than hyalinized collagen. It may be absent altogether in acute infarcts, which can make the distinction between tumor cell and infarct-type necrosis difficult. Multiple sections may be needed to identify a focal, incomplete band of hyalin in infarct-type necrosis, the identification of which may be aided by a trichrome stain (Fig. 4.262B). Correlation with clinical history can also be quite helpful, since recent infarction simulating tumor cell necrosis can occur following treatment for menorrhagia with the antifibrinolytic agent tranexamic acid (cyklokapron),[260] and has also been reported in the setting of recent uterine artery embolization.[261–264] In the latter situation, foreign embolic material may be identified. In a small

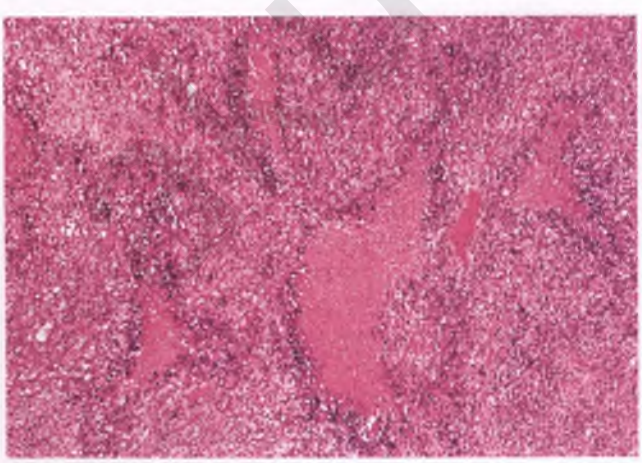

FIGURE 4.259. Tumor cell necrosis in uterine sarcoma. Sharply demarcated zones of necrotic tumor are present in a "geographic" pattern, resembling islands on a map.

FIGURE 4.261. Section through a leiomyoma with central focus of infarct-type necrosis.

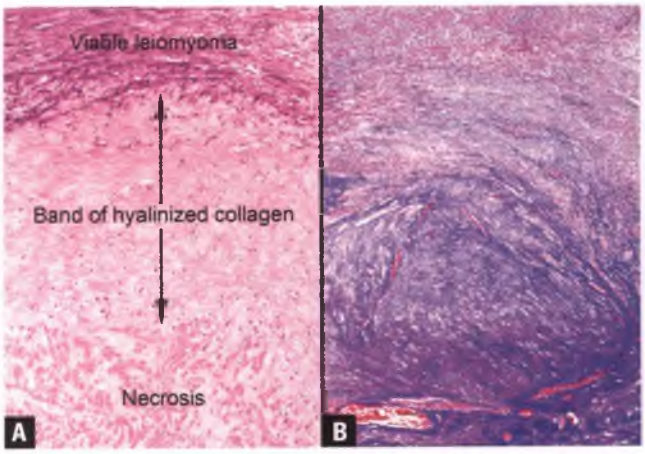

FIGURE 4.262. Infarct-type necrosis in a leiomyoma. **A**: Note the band of hyalinized collagen separating viable from necrotic smooth muscle cells. **B**: With a trichrome stain, this band appears as a blue-stained layer of fibrous tissue.

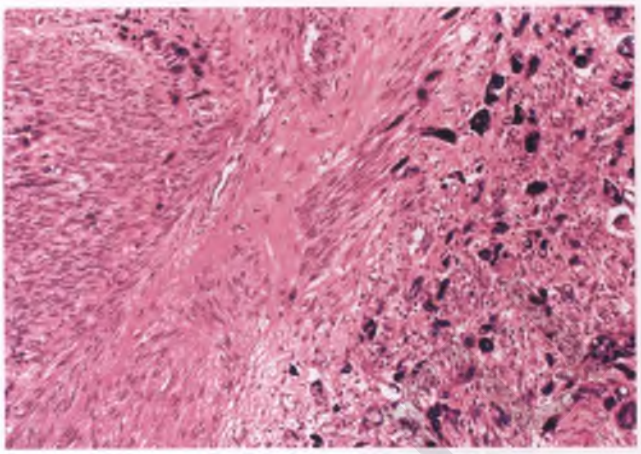

FIGURE 4.264. Uterine smooth muscle tumor (atypical leiomyoma) with patches of severe nuclear atypia.

percentage of leiomyomas, usually in patients who are pregnant or on oral contraceptives, massive infarction produces so-called red degeneration, which appears to be due to hemorrhagic infarction followed by hemolysis (Fig. 4.263).

Ulcerative necrosis may be seen in submucosal tumors, and features the presence of numerous inflammatory cells (particularly neutrophils), as one would expect in an ulcerative process. It is worth noting that inflammatory cells are not common in either tumor cell necrosis or infarct-type necrosis.

Nuclear Atypia

Another major parameter in the evaluation of uterine smooth muscle tumors is the presence or absence of moderate to severe ("significant") nuclear atypia (often referred to as cytologic atypia). If present, it should be determined whether the atypia is focal, multifocal, or diffuse. This degree of atypia is easily recognized at scanning magnification, and is manifested by variable combinations of nucleomegaly, hyperchromatic chromatin (with varying degrees of degenerative smudging), pleomorphism, nucleolar prominence, giant cell formation, multilobulation, multinucleation, and cytoplasmic pseudonuclear inclusions (Fig. 4.264). Mild atypia, manifested by mild nuclear pleomorphism, possibly with small nucleoli, is considered insignificant and is included within the group with no atypia.[259] Unfortunately, some leiomyosarcomas have atypia in the low-moderate range (Fig. 4.265), which can cause some classification difficulties.

Mitotic Index (MI)

The vast majority of uterine smooth muscle tumors are leiomyomas in which there is no tumor cell necrosis and no significant nuclear atypia, rendering a formal mitotic count unnecessary in the absence of an unavoidably high mitotic rate. Tumors that exhibit both tumor cell necrosis and significant nuclear atypia are interpreted as leiomyosarcomas

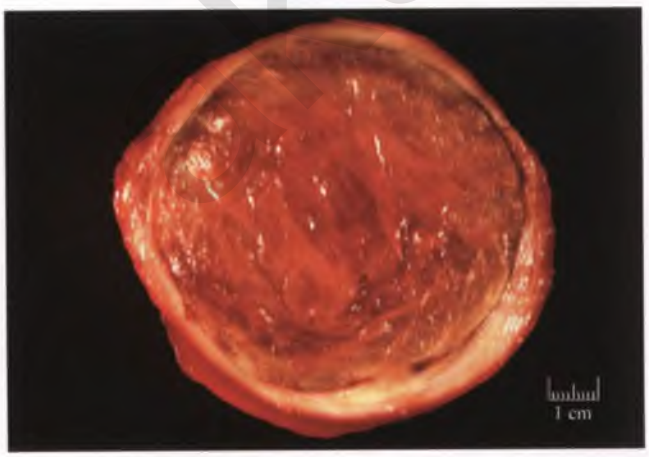

FIGURE 4.263. Section through a leiomyoma with massive red degeneration.

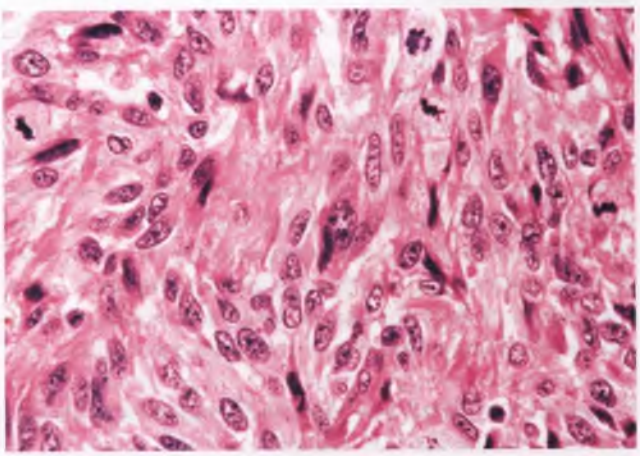

FIGURE 4.265. Leiomyosarcoma with brisk mitotic activity (four mitoses in this field) and nuclear atypia in the low-moderate range.

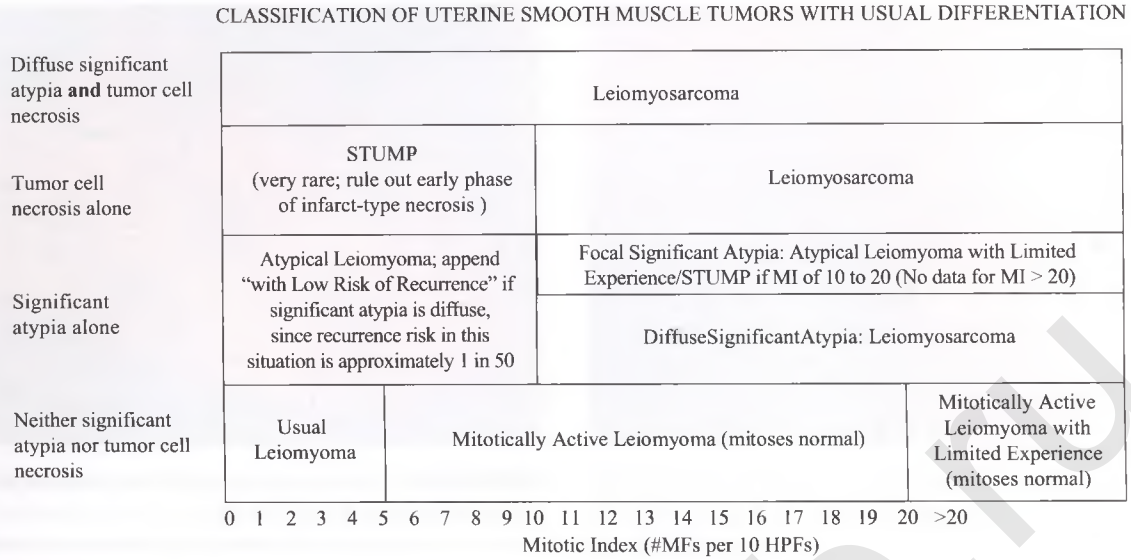

FIGURE 4.266. This diagram, which is based upon the classification system of Bell et al.,[259] can be used to diagnose uterine smooth muscle tumors with usual differentiation once the key histologic features discussed in the text have been evaluated. STUMP: Smooth Muscle Tumor of Uncertain Malignant Potential; Significant Atypia: Moderate to severe nuclear atypia; MFs: mitotic figures; HPFs: high power fields (40× objective with 15× ocular lens).

regardless of their mitotic rate.[259] In those instances in which one of these worrisome features is present in the absence of the other, the MI (defined as the number of mitotic figures per 10 high power fields) influences the diagnosis as depicted in Figure 4.266. When evaluating mitotic activity, mitotic counts should be performed using the methodology of Bell et al. (in the most mitotically active area of tumor, count the number of unequivocal mitotic figures in at least four sets of 10 high power fields, defined as the field of view obtained with a 15× ocular lens and 40× objective, and report the highest MI obtained).[259] It should be emphasized that this classification system applies only to uterine smooth muscle tumors with usual differentiation.

Other Parameters

Note that tumor hypercellularity, myometrial infiltration, intravascular growth, and extrauterine spread do not play a direct role in assessing the malignant potential of uterine smooth muscle tumors. This is because although one or more of these features are commonly present in leiomyosarcomas, there are variants of benign uterine smooth muscle tumors that can also exhibit these findings, either singly or in combination (see below). Nevertheless, the presence of any of these features in what appears to be a benign uterine smooth muscle tumor should prompt reexamination of the gross specimen and submission of additional sections for histologic examination.

Requests for Frozen Sections on Unusual-Appearing Uterine Smooth Muscle Tumors

Some uterine smooth muscle tumors have an unusual gross appearance that may prompt a request for intraoperative consultation. Although a frozen section diagnosis can be made with confidence in some situations, evaluating a fleshy, necrotic uterine smooth muscle tumor by frozen section has its limitations, as set forth below:

1. Accurate diagnosis of problematic smooth muscle tumors requires thorough sampling (e.g., 1 section per cm of tumor) that is not practical in the setting of an intraoperative consultation.
2. Tumor cell necrosis may not be readily distinguishable from infarct-type necrosis in frozen sections.
3. Mitotic figures cannot be reliably identified in frozen sections.
4. Atypical leiomyomas with diffuse severe atypia will look malignant in frozen sections.
5. Karyorrhectic nuclear debris within an atypical leiomyoma, as illustrated later in this section, cannot be reliably distinguished from abnormal mitotic figures in frozen sections.

Despite these limitations, it may still be worthwhile to perform a frozen section to evaluate the possibility that one is dealing with a carcinosarcoma, the diagnosis of which would prompt surgical staging. Given the more likely scenario of finding a presumed smooth muscle neoplasm that is not frankly malignant, it is appropriate to issue a descriptive intraoperative diagnosis (e.g., smooth muscle neoplasm with extensive necrosis), and defer the final diagnosis to permanent sections. In a hysterectomy specimen, not much is at stake, since leiomyosarcomas are not typically treated with lymph node dissection unless there are nodes that are clinically suspicious for metastatic disease.[265] In myomectomy specimens, because of the limitations outlined above, it is better to render the diagnosis on permanent sections and then make the appropriate treatment plans.

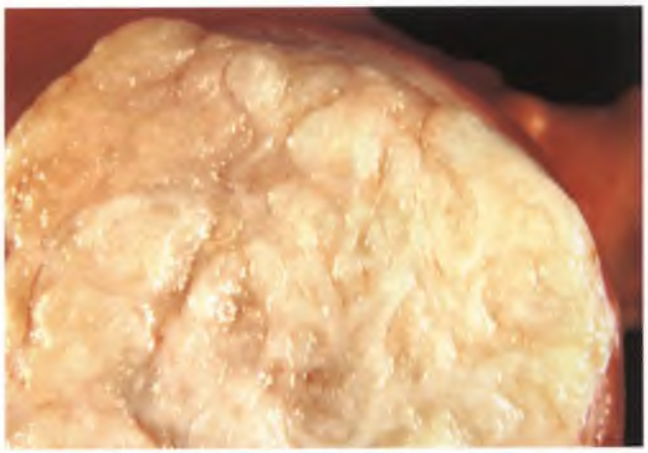

FIGURE 4.267. Uterine leiomyoma. Note the characteristic whorled pattern and the bulging of tumor above the cut surface.

Usual Leiomyoma

The usual type of uterine leiomyoma is often multiple and has a firm, white to light gray, whorled cut surface (Fig. 4.267). Leiomyomas are well circumscribed, protrude from the adjacent myometrium when sectioned, and may be easily enucleated. They may be subserosal (bulging outward from just beneath the serosal surface), intramural (within the myometrium), or submucosal (protruding into the endometrial cavity) (Fig. 4.268). Leiomyomas are tumors of adult women, and only a minority produce symptoms such as pelvic pain, a pelvic mass, or abnormal vaginal bleeding.

Histologically, usual leiomyomas are composed of intertwining fascicles of cytologically bland, spindle-shaped smooth muscle cells with a cellularity similar to that of the adjacent myometrium (Fig. 4.269A). It is very common for portions of leiomyomas to be replaced by deposits of collagen,

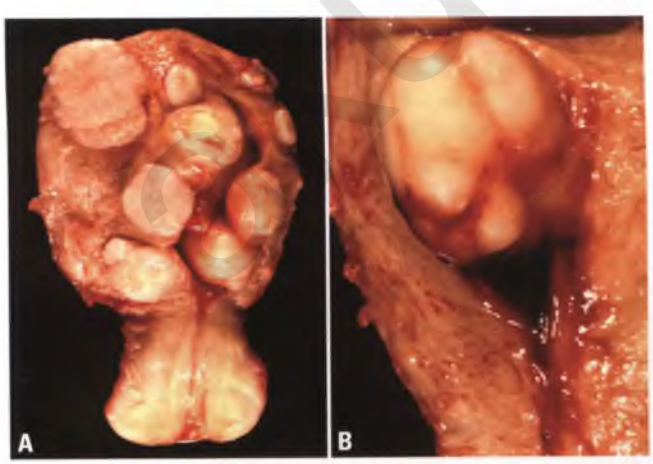

FIGURE 4.268. Uterine leiomyomas. **A**: Intramural and submucosal leiomyomas impinging upon and distorting the endometrial cavity. **B**: Submucosal polypoid leiomyoma protruding into the endometrial cavity.

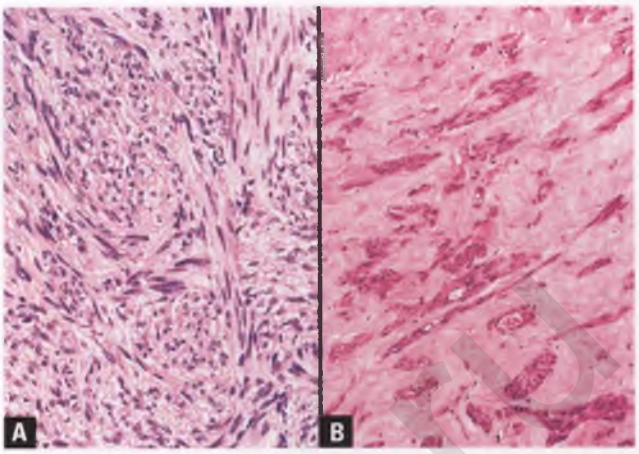

FIGURE 4.269. Uterine leiomyomas. **A**: Leiomyoma of usual type. **B**: Hyalinized leiomyoma.

and this hyalinization can create peculiar patterns resulting from compartmentalization of nests and cords of tumor cells (Fig. 4.269B). Dystrophic calcification may also be present.

In an attempt to shrink their uterine leiomyomas, some patients are treated with the gonadotropin releasing hormone agonist leuprolide acetate. It is controversial whether such treatment has any impact on tumor cellularity, incidence of infarct-type necrosis or hemorrhage, mitotic rate, or the frequency of various degenerative changes.[266–268]

Cellular Leiomyoma

Grossly, cellular leiomyomas may look similar to usual leiomyomas, although they often are more soft and fleshy and exhibit varying shades of yellow. Histologically, cellular leiomyomas resemble leiomyomas of the usual type, except that they are significantly more cellular than normal myometrium (Fig. 4.270A). Cellular leiomyomas often interdigitate with the neighboring myometrium in a pattern that simulates invasion.

When highly cellular and composed of cells with scant cytoplasm and oval rather than spindle-shaped nuclei, cellular leiomyomas can be confused with endometrial stromal tumors (Fig. 4.270B). Although this distinction is not critical for well-circumscribed tumors with a differential diagnosis of highly cellular leiomyoma vs. endometrial stromal nodule (ESN), the diagnostic considerations for such tumors with infiltrating margins are highly cellular leiomyoma and low-grade endometrial stromal sarcoma. Histologic clues that one is dealing with a highly cellular leiomyoma are (a) the merging of densely cellular areas with foci with a discernible fascicular growth pattern and (b) the presence of thick-walled blood vessels or thin-walled cleft-like spaces (Fig. 4.271).[269] If necessary, immunohistochemistry can be performed to aid in this distinction. In contrast to most endometrial stromal tumors, highly cellular leiomyomas are typically immunoreactive for the smooth muscle markers desmin, h-caldesmon, and histone deacetylase 8.[269–273] CD10 is also helpful when used as part of an antibody panel to address this differential diagnosis, since almost all endometrial stromal tumors are CD10 positive, whereas most

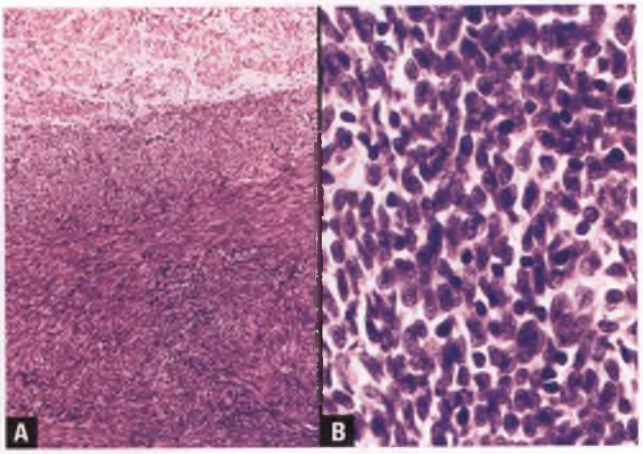

FIGURE 4.270. Cellular leiomyomas. **A**: Note the hypercellularity of the neoplasm as compared to the overlying myometrium and the fascicular growth pattern of the spindle-shaped cells. **B**: This highly cellular leiomyoma is difficult to distinguish from an endometrial stromal tumor in this particular field.

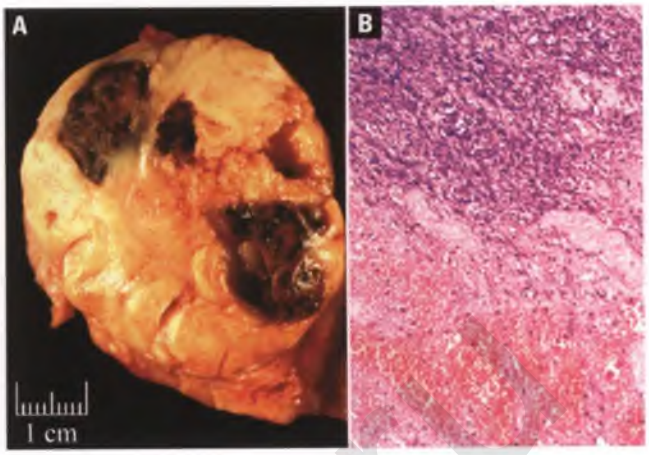

FIGURE 4.272. Hemorrhagic cellular leiomyoma. **A**: Like many cellular leiomyomas, the cut surface of this tumor is yellow. Scattered hemorrhagic foci are evident. **B**: Histologic correlate showing recent hemorrhage adjacent to a hypercellular spindle cell neoplasm.

highly cellular leiomyomas are CD10 negative.[185,270,274] If, after thorough study, the tumor has irregular borders and is judged to have ambiguous differentiation, it should be treated as if it were of endometrial stromal origin.[39]

Hemorrhagic Cellular ("Apoplectic") Leiomyoma

Hemorrhage can occur within cellular leiomyomas that are under the influence of oral contraceptives or pregnancy, and produce abnormal uterine bleeding and abdominal pain.[275,276] A variable number of hemorrhagic nodules are apparent when these leiomyomas are sectioned, which histologically correlate with recent hemorrhage and edema (Fig. 4.272). Infarct-type necrosis may also be present, but is generally inconspicuous. It seems likely that the abnormal vessels that are often present in cellular leiomyomas, particularly the ones that create dilated, thin-walled, cleft-like spaces, are at risk for rupture when subjected to the effects of reproductive hormones.

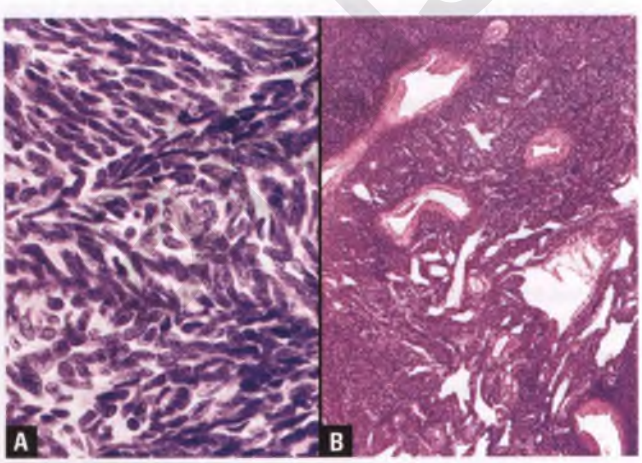

FIGURE 4.271. Histologic features of highly cellular leiomyomas that are helpful in their distinction from endometrial stromal tumors. **A**: Fascicular growth pattern. **B**: Presence of thick-walled blood vessels and thin-walled, cleft-like spaces.

Mitotically Active Leiomyoma

Mitotically active leiomyomas are defined as usual or cellular leiomyomas with a mitotic index of between 5 and up to 20 mitotic figures per 10 high power fields.[259,277–279] These tumors are often submucosal and usually occur in women of reproductive age in association with the secretory phase of the menstrual cycle, pregnancy, or hormonal therapy. They pursue a benign course, and are adequately treated by myomectomy. Most investigators require an absence of atypical mitotic figures, but rare atypical mitotic figures were allowed in the study by Perrone and Dehner.[278] Hypercellularity, mild nuclear atypia, and infarct-type necrosis may be seen in mitotically active leiomyomas.

Extensive sampling of mitotically active leiomyomas is indicated in an effort to identify any exclusionary features such as significant nuclear atypia, atypical mitotic figures, or tumor cell necrosis. One should exercise caution when diagnosing a hypercellular uterine smooth muscle tumor with brisk mitotic activity as a mitotically active leiomyoma, since some leiomyosarcomas with similar features show only subtle degrees of nuclear atypia (Fig. 4.265). Experience with tumors that are otherwise similar to mitotically active leiomyomas except that their mitotic index exceeds 20 is so limited that pathology reports should include a disclaimer reflecting the lack of outcome data in this subset of patients.

Hydropic Leiomyoma

When leiomyomas accumulate significant amounts of edema fluid, they develop peculiar gross and microscopic characteristics

FIGURE 4.273. Hydropic leiomyoma. The edematous sectioned surface may be misinterpreted as being myxoid or gelatinous.

that may result in misdiagnosis as angiomyxoma, intravenous leiomyomatosis (IVL), or a myxoid smooth muscle tumor.[280] Grossly, the edematous sectioned surfaces of these hydropic leiomyomas may be misinterpreted as myxoid or gelatinous (Fig. 4.273). Microscopically, the zones of edematous connective tissue dominate the architecture of the leiomyoma, relegating residual smooth muscle cells to thin cords (Fig. 4.274). Thick-walled blood vessels are often prominent, sometimes mimicking a primary vascular tumor. In some cases, the edema is distinctly perinodular (Fig. 4.275). This pattern, when associated with retraction artifact that results in pseudovascular spaces surrounding the nodules, can be mistaken for IVL.

The accumulation of edema fluid within hydropic leiomyomas should not be referred to as "myxoid degeneration." The term "myxoid" should be reserved for the situation in which the stroma contains pools of acidic mucopolysaccharides that are highlighted by Alcian blue or colloidal iron stains, which is quite uncommon in uterine smooth muscle tumors.

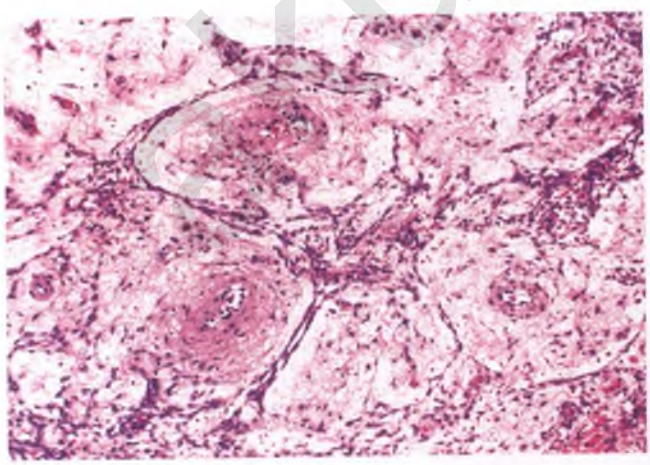

FIGURE 4.274. Hydropic leiomyoma. These tumors typically feature edematous stroma, thick-walled blood vessels, and thin strands of residual smooth muscle cells.

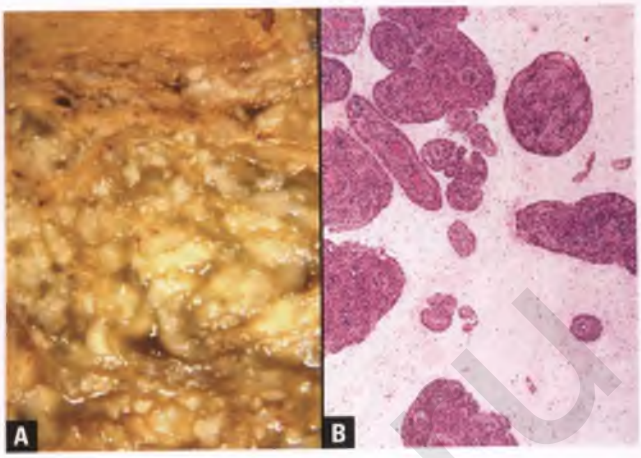

FIGURE 4.275. Hydropic leiomyoma, perinodular pattern. **A**: The sectioned surface demonstrates the presence of multiple nodules embedded within edematous tissue. **B**: Numerous small leiomyomatous nodules are surrounded by edematous stroma.

Cystic Leiomyoma

Leiomyomas may become cystic as a result of extensive hydropic degeneration or following necrosis (Fig. 4.276).

Epithelioid Leiomyoma

When ≥50% of a benign uterine smooth muscle tumor consists of round or polygonal cells with abundant eosinophilic or clear cytoplasm, it takes on an epithelial-like appearance and is referred to as an epithelioid leiomyoma (Fig. 4.277).[281,282] The constituent cells are often loosely arranged in sheets, but may also form nests or plexiform cords separated by a hyalinized matrix. Small epithelioid leiomyomas <1 cm that exhibit cellular arrangements in trabecular cords or small nests set within hyalinized stroma are termed plexiform tumorlets (Fig. 4.278).[283] Grossly, epithelioid leiomyomas may be

FIGURE 4.276. Cystic leiomyoma. The large central cavity of this sectioned leiomyoma was filled with fluid.

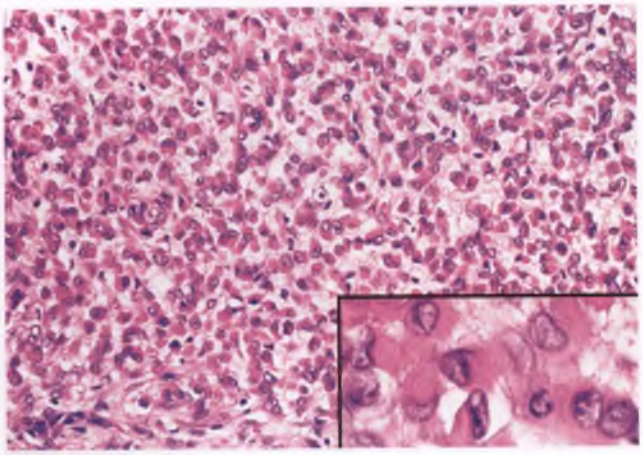

FIGURE 4.277. Epithelioid leiomyoma composed of loosely arranged epithelioid cells with dense eosinophilic cytoplasm and intermediate grade nuclei.

indistinguishable from the usual type of leiomyoma, but are often fleshy and light yellow to tan (Fig. 4.279).

Recognition of an epithelioid leiomyoma is assisted by the frequent finding of a transition from epithelioid to more typical spindled smooth muscle cells in tumors that are well sampled. Most epithelioid leiomyomas exhibit a myogenous immunophenotype, which is additional evidence in favor of this diagnosis.[273] A diagnostic pitfall worth noting is that roughly one-third of epithelioid leiomyomas are cytokeratin positive, which creates the potential for confusion with epithelial neoplasms.[233] Care should also be taken not to mistake hyalinized leiomyomas with compartmentalized nests and cords of tumor cells or tumors with cells that appear rounded due to cross-sectioning of fascicles composed of plump spindle cells as epithelioid leiomyomas.

To qualify as an epithelioid leiomyoma rather than a potentially more aggressive neoplasm, there should be minimal mitotic activity (mitotic index ≤ 2), no more than moderate nuclear atypia, and no tumor cell necrosis (see section on epithelioid leiomyosarcoma).[282] Note that the threshold

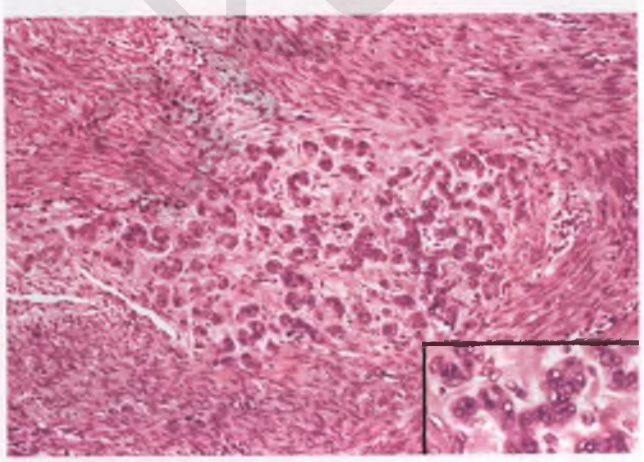

FIGURE 4.278. Plexiform tumorlet. Small nests and trabeculae of epithelioid smooth muscle cells are embedded within a hyalinized matrix.

FIGURE 4.279. Epithelioid leiomyoma. The sectioned surface of this neoplasm is *pale yellow* and fleshy with focal hemorrhagic areas.

for mitotic activity that corresponds to potentially malignant behavior in epithelioid neoplasms of the uterus (like that of myxoid neoplasms) is much lower than that used for uterine smooth muscle tumors with usual differentiation.

Some investigators consider the uterine perivascular epithelioid cell tumor to be part of the spectrum of epithelioid uterine smooth muscle tumors rather than being a distinct entity (see PEComa below). The term "leiomyoblastoma" was formerly used to describe an epithelioid leiomyoma with eosinophilic cytoplasm and cytoplasmic vacuolization, but such terminology is not recommended because it conjures up images of a primitive malignant neoplasm.

Myxoid Leiomyoma

True myxoid change within a uterine smooth muscle tumor is unusual, and needs to be distinguished from hydropic degeneration, which is much more common (see hydropic leiomyoma). Grossly, myxoid leiomyomas may be gelatinous when there is extensive deposition of myxoid material. Microscopically, the smooth muscle cells are separated by pale-staining myxomatous stroma, whose myxoid nature should be confirmed with Alcian blue or colloidal iron stains (Fig. 4.280).

Distinction of myxoid leiomyoma from myxoid leiomyosarcoma can be difficult, and this problem is exacerbated by the absence of detailed reports on large series of these rare tumors. Per guidelines published in abstract form, myxoid leiomyomas can occasionally have infiltrating borders, but must exhibit no more than mild nuclear atypia, lack tumor cell necrosis, and have a mitotic index of <2 mitotic figures per 10 high power fields.[284] Partial involvement of a leiomyoma by myxoid change can simulate myometrial invasion by an infiltrating myxoid leiomyosarcoma if it is not appreciated that the areas with usual smooth muscle differentiation are part of the leiomyoma rather than myometrium.

Lipoleiomyoma

A leiomyoma that contains more than just an occasional mature adipocyte is designated a lipoleiomyoma (Fig. 4.281).[285] When the amount of fat is considerable, the sectioned surface of these

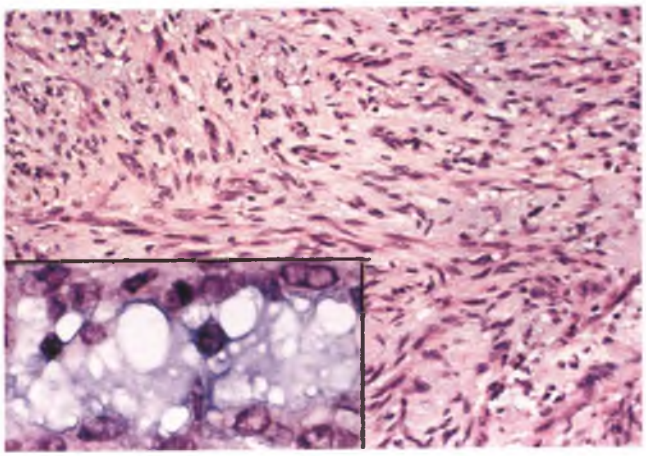

FIGURE 4.280. Myxoid leiomyoma. The inset shows positive staining of the myxoid material with Alcian blue.

tumors may have soft and yellow areas. Although extraordinarily rare, a few cases of liposarcoma arising within uterine lipoleiomyoma have been reported.[286]

Neurilemoma (Schwannoma)-Like Leiomyoma

These leiomyomas feature nuclear palisading, which results in a strong resemblance to benign nerve sheath tumors (Fig. 4.282). However, ultrastructural examination has confirmed their smooth muscle nature.[287] Although generally not necessary, smooth muscle differentiation could also be confirmed immunohistochemically, since these tumors would be expected to be positive for muscle markers and negative for S100, in contrast to neurilemomas.

Leiomyoma with Hematopoietic Cells

Rarely, a massive lymphoid infiltrate is found within a leiomyoma, which can raise the possibility of malignant lymphoma (Fig. 4.283).[288,289] Features that help to distinguish this benign

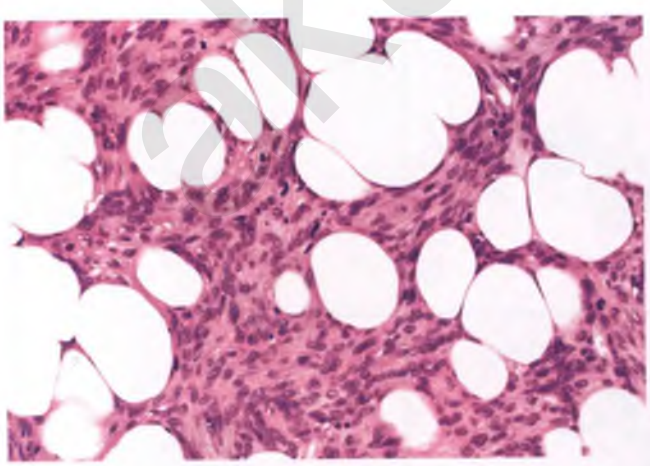

FIGURE 4.281. Lipoleiomyoma composed of an admixture of mature adipocytes and smooth muscle cells.

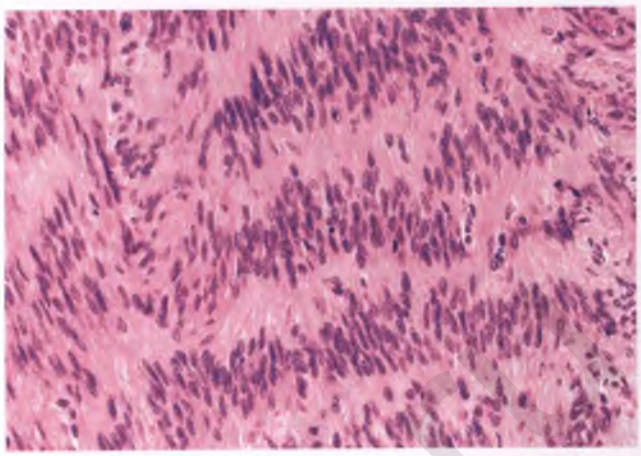

FIGURE 4.282. Neurilemoma-like leiomyoma with prominent nuclear palisading.

process from lymphoma are (a) the lymphoid infiltrate remains within the confines of the leiomyoma, which often is at least partially sclerotic, and (b) the lymphoid infiltrate is polymorphous, consisting of a preponderance of small lymphocytes admixed with occasional larger lymphoid cells, plasma cells, and histiocytes.

Leiomyomas may also contain appreciable numbers of mast cells or eosinophils (Fig. 4.284).[290,291] These tumors do not differ from ordinary leiomyomas in their clinical presentation. The same can be said for leiomyomas that contain foci of extramedullary hematopoiesis[292] or increased numbers of histiocytes.[293]

Atypical Leiomyoma

In 2003, the WHO adopted the term "atypical leiomyoma" for those unusual smooth muscle tumors that have also been termed symplastic leiomyoma, bizarre leiomyoma, leiomyoma with bizarre nuclei, and pleomorphic leiomyoma.[294] As these

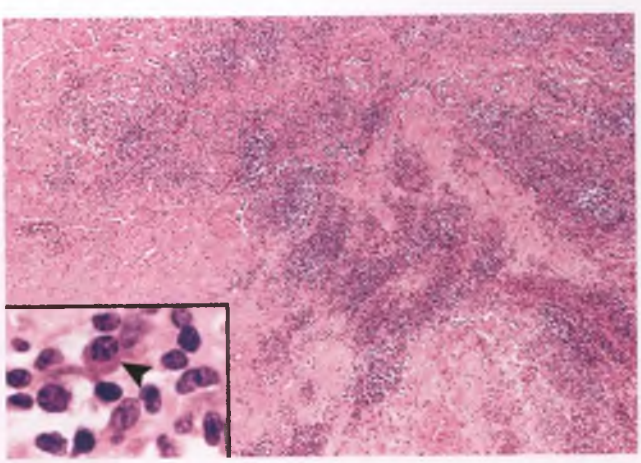

FIGURE 4.283. Sclerotic leiomyoma containing a dense lymphoid infiltrate. The inset documents the polymorphous nature of this benign process, which includes plasma cells (*arrowhead*).

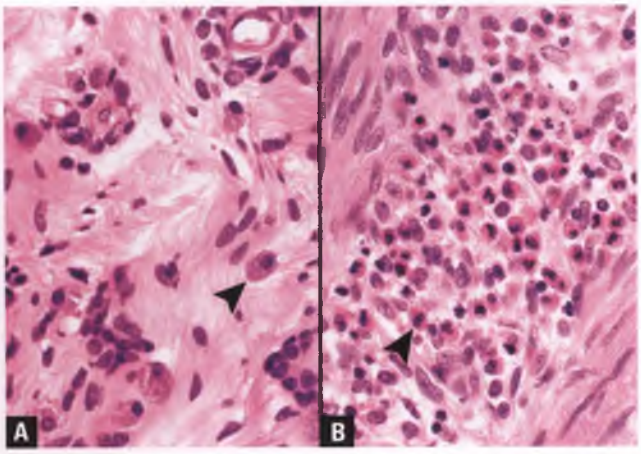

FIGURE 4.284. **A**: Leiomyoma with mast cells. **B**: Leiomyoma with eosinophils. *Arrowheads* point to representative cells of interest.

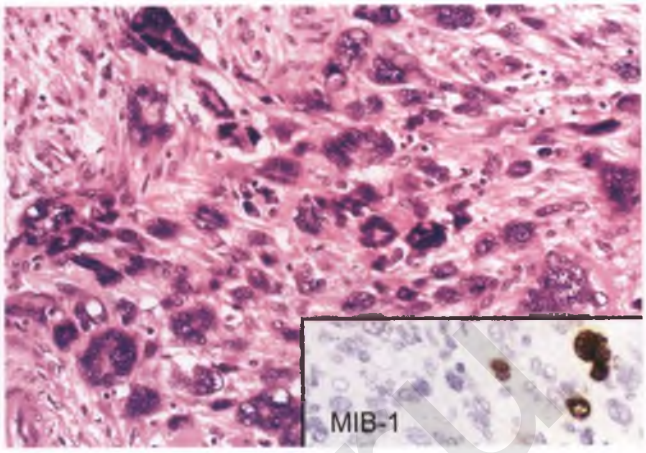

FIGURE 4.285. Severe nuclear atypia within an atypical leiomyoma. Inset: This MIB-1 immunostain shows a low proliferative rate, which supports a diagnosis of atypical leiomyoma over that of leiomyosarcoma.

names suggest, the key histologic feature of these tumors is the presence of moderate to severe nuclear atypia that may be focal, multifocal, or diffuse (Figs. 4.264 and 4.285). Typically, these tumors grossly resemble leiomyomas of the usual type. True tumor cell necrosis ("coagulative tumor cell necrosis") is not present, but infarct-type (hyaline) necrosis may be seen (see previous discussion of the different types of necrosis). The extent of the areas with significant nuclear atypia and the mitotic index influence whether a uterine smooth muscle tumor with bizarre nuclei and no tumor cell necrosis is classified as an atypical leiomyoma, atypical leiomyoma with low risk of recurrence, or leiomyosarcoma, as diagramed in Figure 4.266.

Both noteworthy and problematic is the not infrequent finding of karyorrhectic nuclear debris in atypical leiomyomas that can take forms resembling atypical mitotic figures (Fig. 4.286).[295,296] Caution should be exercised in interpreting such structures, keeping in mind the standard guidelines that only unequivocal mitotic figures should be tallied in mitotic counts. Evidence that favors an atypical leiomyoma with karyorrhectic debris over a potentially more aggressive smooth muscle tumor with atypical mitotic figures includes (a) the paucity or lack of typical division figures elsewhere in the tumor (it would be most peculiar for the few mitotic figures in a tumor to all be of such bizarre type), (b) the absence of intact cytoplasm surrounding these bizarre structures, (c) a proliferative rate, as assessed by MIB-1 immunostaining, of <10% that is characteristic of atypical leiomyomas and most smooth muscle tumors of uncertain malignant potential (Fig. 4.285 inset) rather than the >30% proliferative rate that is seen in most leiomyosarcomas,[297–299] and (d) absence of staining of these structures with the mitosis-specific marker phospho-histone H3.[300]

Since a leiomyosarcoma can harbor areas that are indistinguishable from an atypical leiomyoma, extensive sampling is indicated when patches of significant nuclear atypia are encountered (e.g., submit the entire tumor if it can fit in up to five cassettes, or submit at least one section per centimeter for larger tumors). Patients with atypical leiomyomas can be

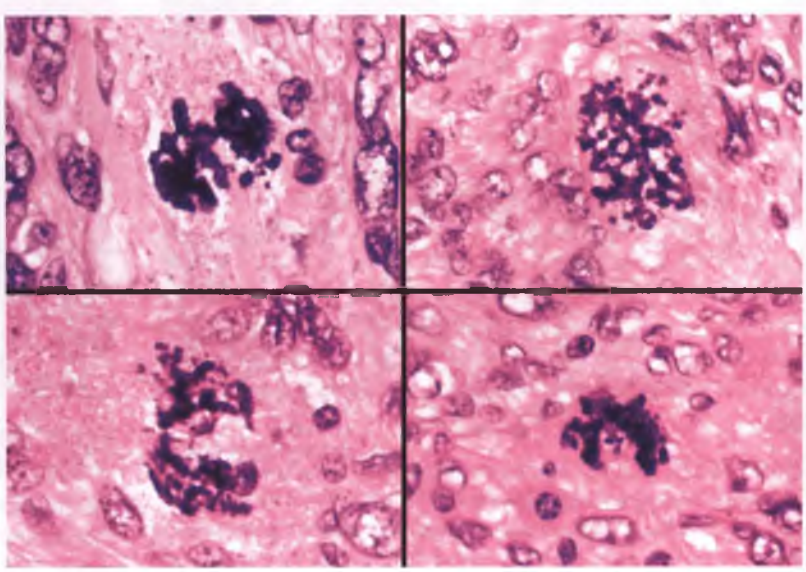

FIGURE 4.286. Atypical leiomyoma with a low risk of recurrence with four examples of karyorrhectic nuclear debris mimicking abnormal mitotic figures. The patient is alive and well five years posthysterectomy.

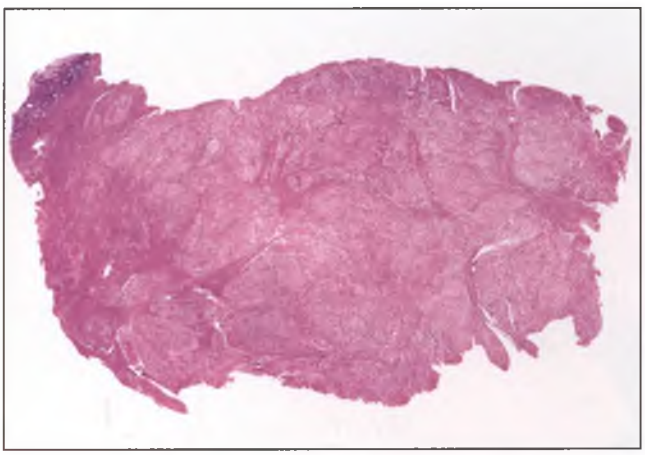

FIGURE 4.287. Low-magnification view of diffuse leiomyomatosis. A small amount of proliferative endometrium is present at upper left.

considered to have a benign tumor for management purposes, although approximately one in fifty with diffuse atypia will experience an extrauterine recurrence.[‡259]

Benign Metastasizing Leiomyoma

Benign metastasizing leiomyoma is the term used to describe the extremely rare circumstance in which single or multiple extrauterine (usually pulmonary) nodules of histologically benign smooth muscle are found in women with a history of uterine leiomyomas. Typically, the uterus has been removed many years previously. In pulmonary lesions, smooth muscle often entraps native bronchiolar epithelial structures, perhaps reflective of the slow-growing nature of this process. Benign metastasizing leiomyoma is a diagnosis of exclusion, and other alternatives such as a metastasis from a bland extrauterine (e.g., gastrointestinal or retroperitoneal) sarcoma with a low mitotic index, a primary pulmonary smooth muscle tumor, lymphangioleiomyomatosis, and origin from IVL or leiomyoma with vascular invasion need to be considered. Two studies have found the pulmonary and associated uterine tumors to be clonally related, which supports a uterine origin for the pulmonary tumors.[302,303]

Recently, five benign metastasizing leiomyomas were all reported to have the same cytogenetic abnormalities (19q and 22q terminal deletions).[304] This cytogenetic profile, which is shared by 3% of uterine leiomyomas, may aid in the diagnosis of benign metastasizing leiomyoma and provides support that this unusual process is a distinct entity.

Diffuse Leiomyomatosis

On rare occasions, the myometrium may contain innumerable, small, benign, coalescing myomatous nodules that result in symmetrical uterine enlargement (Fig. 4.287).[305] This process is referred to as diffuse leiomyomatosis.

Intravenous Leiomyomatosis and Leiomyoma with Vascular Invasion

IVL is an uncommon benign uterine smooth muscle tumor that features intravenous tumor growth beyond the confines of a leiomyoma.[306,307] Tumor may grow into the pelvic veins, and on rare occasions can extend into the inferior vena cava or right side of the heart. Grossly, IVL classically presents in a myomatous uterus as convoluted, wormlike plugs of myomatous tissue distending myometrial veins (Fig. 4.288), although it may also be identified as a microscopic finding. Rare cases of IVL are predominantly or

[‡]The incidence of extrauterine recurrence of atypical leiomyomas with diffuse significant atypia may actually be less than one in fifty. This figure is based upon the experience of a single patient with a uterine smooth muscle tumor of unknown size that contained scattered atypical mitotic figures and for which only four slides were available for review,[259] raising the possibility that it was an undersampled leiomyosarcoma. In a separate study reported in abstract form, the extrauterine recurrence rate of atypical leiomyomas was also 2% and was also based upon the experience of a single patient, but details related to this tumor such as its size, extent of atypia, presence or absence of atypical mitotic figures, and number of slides reviewed were not provided.[301]

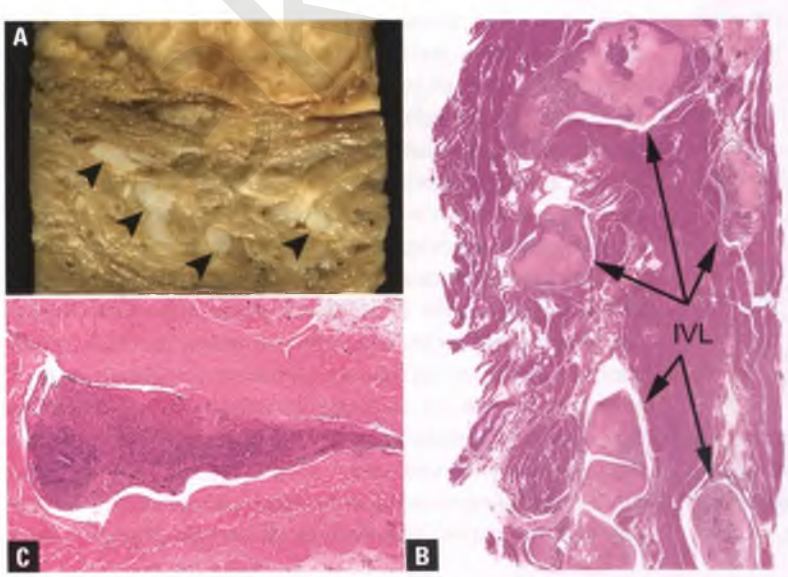

FIGURE 4.288. Intravenous leiomyomatosis (IVL). **A**: This section through a formalin-fixed leiomyoma (top) demonstrates the presence of wormlike plugs of intravascular tumor within the underlying myometrium (*arrowheads*). **B**: This low-magnification view of the myometrium shows several plugs of intravascular tumor surrounded by cleft-like spaces. **C**: A focus of IVL is shown at higher magnification.

entirely intravascular, in which case its origin is presumably from smooth muscle cells within the walls of vessels.

Histologically, the intravascular tumor is ensheathed by a thin layer of endothelium and resembles a usual leiomyoma or leiomyoma variant, sometimes with hyalinization, hydropic degeneration, or aggregates of thick-walled blood vessels.[308] The intravascular tumor plugs are typically partially or completely surrounded by a cleft-like space that follows the contour of the involved veins, and this should be distinguished from leiomyomas with retraction artifact or leiomyomas that are partially surrounded by compressed vascular spaces. If indicated, immunostains for endothelial antigens can be performed to highlight the lining of the involved veins in IVL as well as the endothelial coat that covers the intravascular tumor plugs.

A distinction is made between IVL and a leiomyoma in which intravascular growth is microscopic and found only within the confines of the tumor, which has been termed a leiomyoma with vascular invasion. This latter phenomenon is rare and generally thought to be an incidental finding.[296] However, rare examples of both IVL and leiomyomas with vascular invasion have been noted in association with benign metastasizing leiomyoma,[308,309] and it has been theorized that leiomyomas with vascular invasion may represent an incipient form of IVL.[309]

Cellular variants of IVL can resemble vascular involvement by low-grade endometrial stromal sarcoma. However, the previously discussed vascular and immunophenotypic differences between highly cellular leiomyomas and endometrial stromal tumors hold true in this situation as well, and the characteristic permeative pattern of myometrial invasion and commonplace replacement of portions of the endometrium by the extravascular component of low-grade endometrial stromal sarcoma are not features of the leiomyomata associated with IVL.[308]

Dissecting Leiomyoma

A very rare subset of benign uterine smooth muscle tumors exhibits tongue-like extensions that dissect into the neighboring myometrium for a significant distance (arbitrarily defined as ≥5 mm).[310] Grossly, these dissecting leiomyomas have lobulated, indistinct borders. Recognized as a specific subtype is the cotyledonoid dissecting leiomyoma, which features an exophytic, bulky, reddish-purple, placental-like component that extends in continuity from the myometrial tumor into the region of the broad ligament.[311] The bulbous processes of the exophytic component show degenerative changes and vascular congestion.

Disseminated (Diffuse) Peritoneal Leiomyomatosis

See Chapter 8.

Leiomyosarcoma

Leiomyosarcomas are highly malignant neoplasms that demonstrate smooth muscle differentiation, either histologically or immunohistochemically. Most occur in patients over 40 years

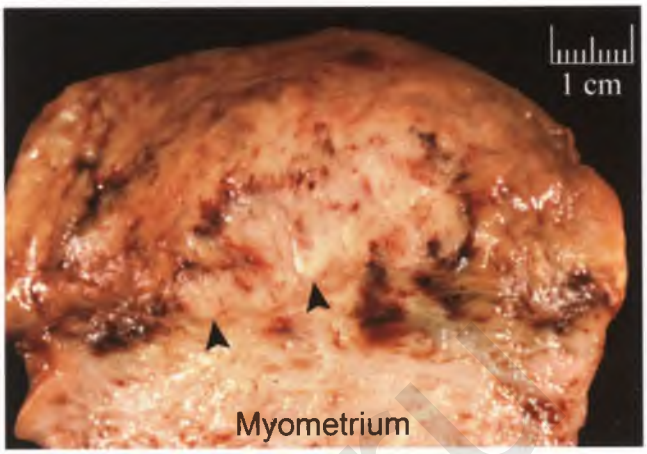

FIGURE 4.289. Leiomyosarcoma. Only the central region of the tumor has been sectioned, and this area demonstrates the off-white, "fish-flesh" appearance of the tumor (*arrowheads*), along with splotchy areas of hemorrhagic and necrosis.

of age and produce symptoms such as abnormal uterine bleeding, pelvic pain, and uterine enlargement that are indistinguishable from those of a large "fibroid uterus." Leiomyosarcomas are generally thought to arise *de novo*, but recent molecular genetic evidence suggests that some of these tumors may evolve from preexisting leiomyomas.[312] Although leiomyosarcomas represent only about 1% of all uterine malignancies, they are the most common pure uterine sarcoma, outnumbering endometrial stromal sarcoma by a margin of approximately 2.5 to 1.

Leiomyosarcomas are typically solitary tumors of appreciable size (mean 10 cm) with a soft, fleshy, off-white, light gray, or tan cut surface with intermixed foci of hemorrhage and necrosis (Figs. 4.258 and 4.289). Two-thirds of leiomyosarcomas are intramural, and they are typically less well circumscribed than leiomyomas.

Microscopically, the classic leiomyosarcoma is a hypercellular spindle cell neoplasm that exhibits diffuse significant nuclear atypia, a high mitotic rate that includes the presence of atypical division figures, infiltration the neighboring myometrium, and geographic foci of tumor cell necrosis (Fig. 4.290). Ten to twenty percent also demonstrate vascular invasion. More subtle forms of leiomyosarcoma also exist, such as those that exhibit only increased cellularity, borderline nuclear atypia, and brisk mitotic activity (Fig. 4.265).Tumor size >5 cm correlates with more aggressive behavior, and there has yet to be a reported instance of a uterine leiomyosarcoma <3 cm that has metastasized.[313,314] The importance of tumor size is reflected in the 2008 FIGO staging system that is specifically designed for uterine leiomyosarcoma, in which tumors confined to the uterus that are ≤5 cm are designated stage IA and those >5 cm are categorized as stage IB.[315] There is no well-established grading system for uterine leiomyosarcoma that correlates with outcome.

Note: For a discussion of the relative importance of nuclear atypia, mitotic rate, and tumor cell necrosis in rendering a

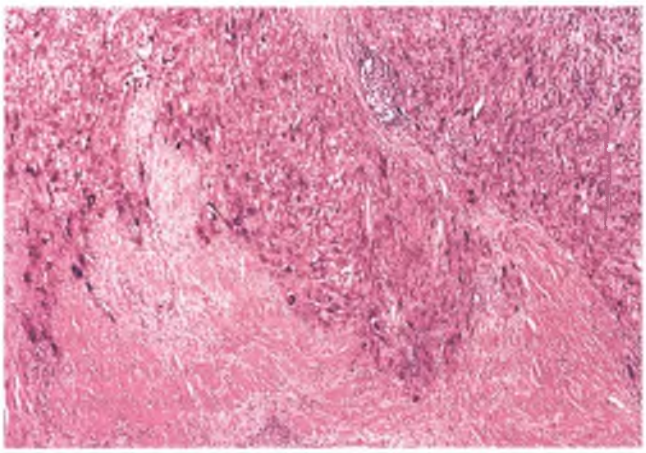

FIGURE 4.290. Leiomyosarcoma exhibiting hypercellularity, nuclear pleomorphism, and an infiltrating margin with the neighboring myometrium. This tumor also had a high mitotic index and contained foci of tumor cell necrosis.

diagnosis of the usual type of leiomyosarcoma, as well as for additional gross and microscopic images depicting its features, please see the section on evaluating and predicting behavior of uterine smooth muscle tumors.

Epithelioid Leiomyosarcoma

Characteristics of epithelioid histology are discussed in the section describing epithelioid leiomyomas. Features associated with aggressive behavior of epithelioid uterine smooth muscle tumors are tumor cell necrosis, severe nuclear atypia, and a mitotic index of >2, usually in combination.[282] However, guidelines predictive of malignant behavior of these tumors are still evolving, with more recent reports not having gone beyond the abstract stage.[316,317] Although a diagnosis of malignancy can be made when at least two of the three adverse prognostic findings are present, experts using their own personal experience differ on whether a diagnosis of epithelioid smooth muscle tumor of uncertain malignant potential (STUMP) or epithelioid leiomyosarcoma is more appropriate for those cases in which only tumor cell necrosis, severe nuclear atypia, or mitotic activity in the MI = 3 to 5 range is present as an isolated finding. Examples of two different epithelioid leiomyosarcomas are shown in Figures 4.291 and 4.292.

The usual immunoreactivity of epithelioid leiomyosarcomas with at least some smooth muscle markers and the identification of areas of transition to more typical smooth muscle differentiation with spindle cell morphology facilitate its distinction from poorly differentiated carcinoma, placental site trophoblastic tumor, and other entities with an epithelioid appearance. When interpreting a panel of immunostains in this context, it is important to recall that cytokeratin immunoreactivity may be seen in epithelioid smooth muscle tumors of the uterus.[233]

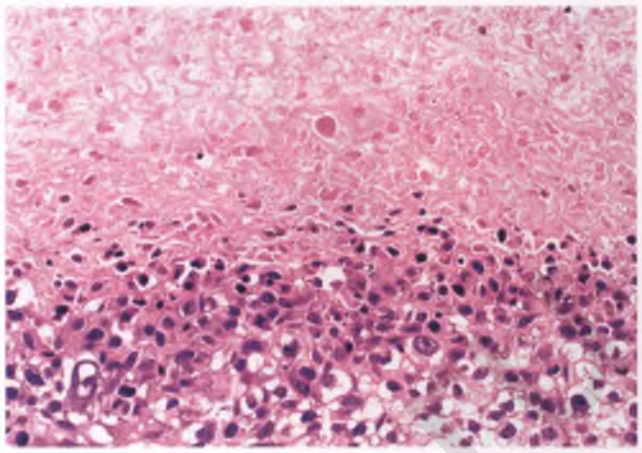

FIGURE 4.291. Epithelioid leiomyosarcoma. Note the nuclear pleomorphism, clear cell component, and tumor cell necrosis.

Myxoid Leiomyosarcoma

On gross examination, the rare myxoid leiomyosarcoma is typically large, gelatinous, and well circumscribed (Fig. 4.293A), but microscopic evaluation demonstrates infiltration of neighboring myometrium.[318] In contrast to myxoid leiomyomas, myxoid leiomyosarcomas exhibit either significant nuclear atypia (Fig. 4.293B), tumor cell necrosis, and/or a mitotic index of >2 mitotic figures per 10 high power fields.[284] The tumors are characteristically paucicellular, which probably accounts for their low mitotic index.

Leiomyosarcoma with Osteoclast-Like Giant Cells

Rarely, uterine leiomyosarcomas may contain significant numbers of osteoclast-like giant cells, resulting in a resemblance to

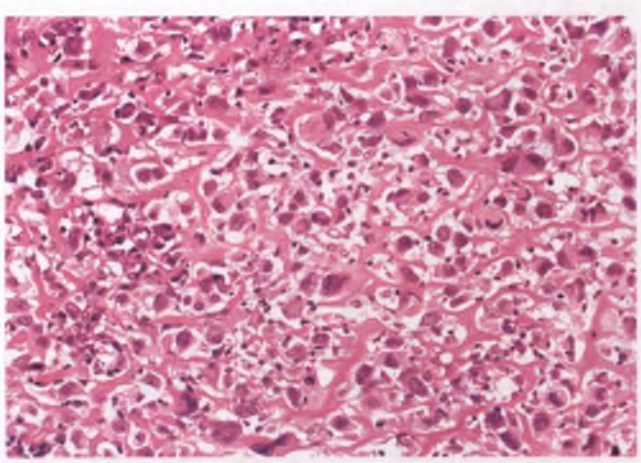

FIGURE 4.292. Epithelioid leiomyosarcoma. This example features sheets of epithelioid tumor cells with significant nuclear atypia and mitotic activity embedded within a hyalinized matrix.

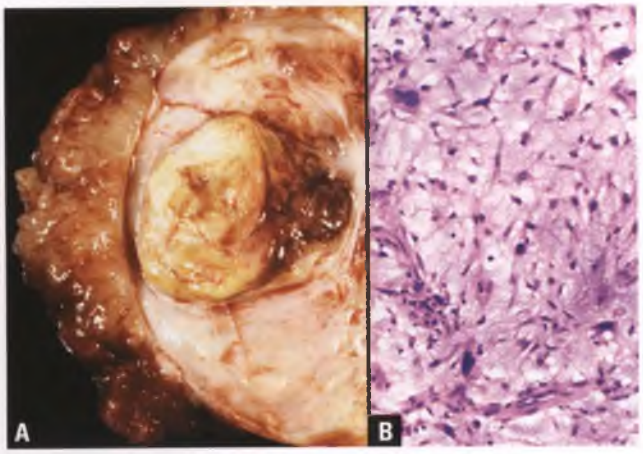

FIGURE 4.293. Myxoid leiomyosarcoma. **A**: Sectioned surface of a large myxoid leiomyosarcoma where the myxoid areas, which are glistening and gelatinous, are most prominent at the periphery and within a central nodular area. **B**: The smooth muscle cells in these tumors are widely separated by abundant myxoid stroma. As in this example, some cells may exhibit significant nuclear atypia. (**A**: courtesy of Dr. Deborah J. Gersell.)

giant cell tumor of bone or the giant cell variant of malignant fibrous histiocytoma (Fig. 4.294).[319,320] Immunohistochemical evidence suggests that these giant cells within uterine tumors are a reactive component derived from macrophages.[320]

Smooth Muscle Tumor of Uncertain Malignant Potential

When a tumor has histologic features that approach that of leiomyosarcoma, but fails to meet established criteria for full-fledged malignancy, the term STUMP is used. The terms UMP (uncertain malignant potential) and LMP (low malignant potential) should not be used interchangeably. Tumors classified as being of low malignant potential, such as the ovarian serous borderline tumor, are sufficiently common to have been studied in detail, and are known to have a low potential for an unfavorable outcome. In contrast, we have very limited experience with tumors of uncertain malignant potential, and can only make an educated guess as to their future behavior. Different investigators use the STUMP designation in different ways, such that some would include a leiomyoma that has diffuse significant atypia and an estimated risk of recurrence of only 1 in 50 in the STUMP category, whereas others think that this minimal degree of risk of an adverse outcome deserves its own special designation of atypical leiomyoma with low risk of recurrence.

STUMPs are a heterogeneous group of rare tumors with various constellations of worrisome features in which insufficient outcome data are available, or perhaps a few similar tumors have behaved in a malignant fashion. Examples of how a tumor may achieve STUMP status include the following: (a) The tumor has a moderately high mitotic rate and some nuclear atypia, but it is unclear as to which set of classification guidelines to use because the type of smooth muscle differentiation (usual, myxoid, or epithelioid) is not readily apparent; (b) the tumor exhibits diffuse significant atypia, but the mitotic index is borderline between atypical and malignant categories; (c) the tumor is hypercellular, lacks tumor cell necrosis, has an MI >10, and exhibits borderline nuclear atypia; (d) the tumor has focal significant atypia, an MI > 10, and no tumor cell necrosis; (e) tumor cell necrosis is present in a hypercellular neoplasm, but there is no significant atypia and the mitotic index is <10 (Fig. 4.295); and (f) the tumor has diffuse significant atypia or an MI > 10, and has necrosis of ambiguous type. Categorizing tumors that are otherwise ordinary leiomyomas as STUMPs based solely on the presence of *possible* tumor cell necrosis is discouraged, since virtually all such tumors represent leiomyomas with early infarct-type necrosis.

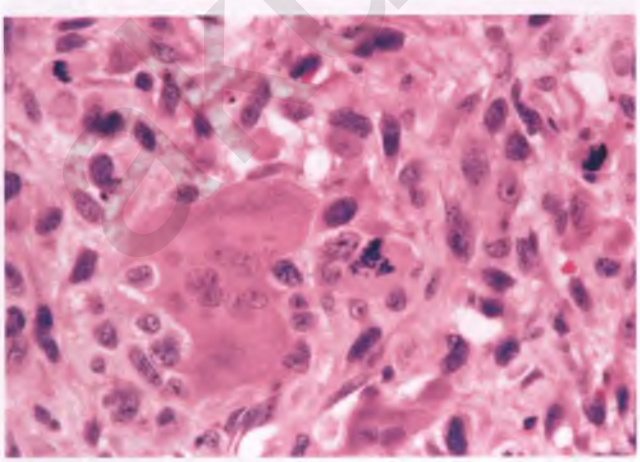

FIGURE 4.294. Uterine leiomyosarcoma with osteoclast-like giant cells.

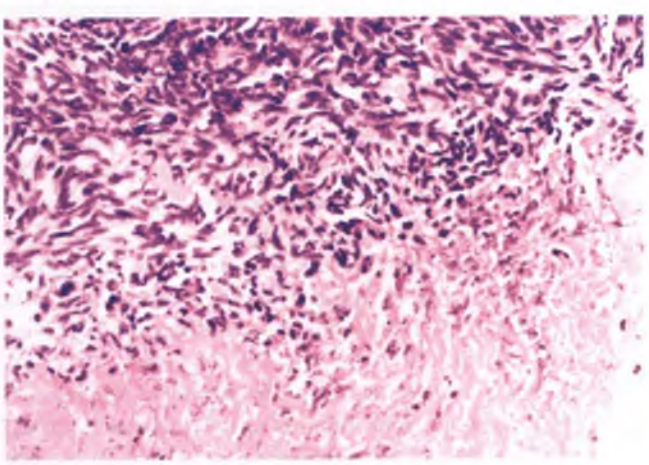

FIGURE 4.295. STUMP. This hypercellular neoplasm exhibits no significant nuclear atypia, sparse mitotic activity, and tumor cell necrosis. The distinction from cellular leiomyoma is based on the presence of tumor cell necrosis, which is often an ominous finding. The patient experienced several recurrences, beginning at 3 years posthysterectomy.

Some recent studies have suggested that diffuse and strong immunoreactivity for p16 and/or p53 may help identify a subset of STUMPs that are at an increased risk of aggressive behavior.[298,299,321] However, other investigators have found significant overlap in p16 and p53 expression patterns in uterine smooth muscle tumors in the atypical leiomyoma to leiomyosarcoma spectrum,[322,323] suggesting that it is premature to recommend routine use of these antibodies in this setting. As mentioned in the section on atypical leiomyomas, most studies have found that MIB-1 immunostaining can help to differentiate atypical leiomyomas and STUMPs from leiomyosarcoma. When the differential diagnosis is between STUMP and leiomyosarcoma, STUMP should be favored when the tumor is small, since malignant behavior in a primary uterine smooth muscle tumor <3 cm has yet to be reported.

A STUMP diagnosis in a myomectomy specimen allows for flexibility in management that would not be available to patients with leiomyosarcoma (e.g., a patient with a STUMP who understands the risks may opt to postpone hysterectomy in the hopes of becoming pregnant). Following hysterectomy, patients with STUMPs are managed expectantly and need long-term follow-up.

ENDOMETRIAL STROMAL TUMORS

Endometrial stromal tumors, which are quite uncommon, are currently classified by the WHO as endometrial stromal nodule (ESN), low-grade endometrial stromal sarcoma (low-grade ESS; formerly known as endolymphatic stromal myosis), and undifferentiated endometrial sarcoma.[324]

Based upon the work of Norris and Taylor in 1966,[325] malignant endometrial stromal tumors were subclassified for many years into low-grade and high-grade ESSs according to their degree of mitotic activity (<10 mitotic figures per 10 high power fields → low grade; ≥10 mitotic figures per 10 high power fields → high grade). However, a subsequent larger study of uterine sarcomas with recognizable endometrial stromal differentiation failed to confirm the prognostic relevance of this separation based upon mitotic activity, and found surgical stage to be the most powerful predictor of clinical outcome.[326] What followed was the demise of the high-grade ESS category based upon a high mitotic rate, and the subsequent widespread tendency to refer to low-grade ESS simply as ESS.

Although acknowledging the foregoing, many investigators favor acceptance of a modern-day version of high-grade ESS, albeit using criteria different than those originally put forth by Norris and Taylor (see below). This revived category serves as a buffer zone between low-grade ESS and undifferentiated endometrial sarcoma, providing an alternative designation for those ESSs whose subjective assessment of cytologic atypia marginally exceeds the limits of that allowed for low-grade ESS without having to resort to equating them with the more aggressive undifferentiated endometrial sarcomas. Given the resurgence of interest in using the term high-grade ESS for this small subset of endometrial stromal tumors, it is recommended that the low-grade vs. modern-day high-grade nature of ESSs be specified in pathology reports to avoid confusion.

Up until recently, the FIGO staging system for uterine sarcomas and endometrial carcinomas were one and the same. However, the 2008 FIGO staging system has developed specific staging systems for leiomyosarcoma and for endometrial stromal sarcoma combined with adenosarcoma (since carcinosarcoma is regarded as a form of metaplastic carcinoma, it continues to be staged as an endometrial carcinoma).[315] For endometrial stromal sarcoma, the change most likely to impact pathologists is that involvement of the endocervix in tumors limited to the uterus is now considered within the spectrum of stage I rather than stage II disease.

Endometial Stromal Nodule and Low-Grade Endometrial Stromal Sarcoma: Similarities and Differences

ESNs are very rare, accounting for only 10% to 20% of endometrial stromal tumors. Although ESSs are the most common form of endometrial stromal tumor, they are also rare, representing only about 1 in 200 of all primary uterine malignancies. The lack of significant infiltration of the myometrium and an absence of angiolymphatic invasion in ESNs are the only features that are used to distinguish them from low-grade ESSs. It follows that if multiple fragments of a well-differentiated endometrial stromal proliferation devoid of glands are encountered in endometrial curettings, a diagnosis of "endometrial stromal proliferation, nodule vs. low-grade sarcoma" should be rendered, with a note suggesting imaging studies to confirm the presence of a mass lesion and indicating that hysterectomy with evaluation of the margins of the tumor would be necessary for definitive diagnosis.

Although ESNs are benign and stage I low-grade ESSs are low-grade malignancies, their clinical presentation, gross appearance of their sectioned surfaces, histologic appearance of their constituent cells, immunophenotype, and even some aspects of their molecular genetics are identical. Patients with both types of tumor are commonly under 50 years of age, and typically present with abnormal vaginal bleeding or pelvic/abdominal pain. The sectioned surfaces of these tumors are fleshy and yellow or tan, with the neoplasm bulging above the neighboring myometrium and lacking the whorled appearance of smooth muscle tumors. Cysts of variable size and foci of necrosis may be present. ESNs have an average size of 5 to 6 cm and are most often intramural lesions, but may also present as endometrial polyps or involve both the endometrium and myometrium.[327,328] They are typically solitary, well-circumscribed, round to oval nodules (Fig. 4.296). Low-grade ESSs have a similar topography and may have a similar gross appearance, although classic cases show one or more tumor nodules associated with worm-like cords within the myometrium, which often represent plugs of tumor within distended vessels (Fig. 4.297).

ESNs and low-grade ESSs are composed of diffuse sheets of uniform, round to oval cells with scant cytoplasm that resemble those of normal proliferative phase endometrial stroma. Although these tumors are usually densely cellular, varying

FIGURE 4.296. Endometrial stromal nodule. This tumor has been bisected, revealing its typical fleshy, yellow, well circumscribed cut surface that bulges above the neighboring myometrium. Typical leiomyomas are also present. (Courtesy of Dr. Julio A. Lagos.)

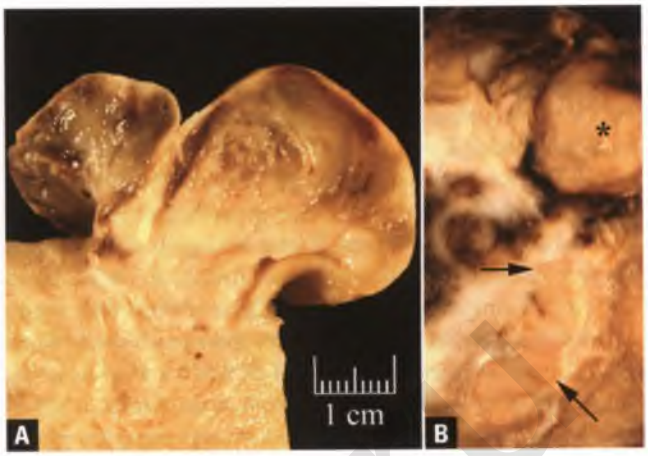

FIGURE 4.297. Low-grade endometrial stromal sarcoma. **A**: This intracavitary, polypoid tumor has gelatinous, hemorrhagic, and small cystic areas superficially. At its base, the tumor is fleshy and extends into the inner portion of the myometrium. **B**: The tan nodule marked with the *asterisk* is a low-grade ESS, and the arrows point to a serpentine cord of ESS within the myometrium. A larger leiomyoma with central hemorrhage is also present.

amounts of stromal edema may result in a less cellular appearance, and patches of hyalinized collagen can also alter the architecture (Fig. 4.298). ESNs and low-grade ESSs are supported by a characteristic vasculature composed of regularly spaced, thin-walled, elongated, compressed, branching capillaries and/or numerous small arterioles, although it is usually the latter that are emphasized in the literature (Fig. 4.299). The arterioles resemble the spiral arterioles of normal late secretory endometrium, and may be surrounded by concentric whorls of tumor cells (Fig. 4.300). ESNs and low-grade ESSs generally have a low mitotic rate, but occasional tumors may exceed 10 mitotic figures per 10 high power fields. Atypical mitotic figures are not seen in ESNs, and are distinctly uncommon in low-grade ESS.

In addition to edema and hyalinization, endometrial stromal tumors can also have myxoid areas, fibrous foci, interspersed foamy histiocytes, and exhibit sex-cord–like, endometrioid glandular, or smooth muscle differentiation, along with several other case-reportable variations (Figs. 4.301–4.307).[65,66,329–335] Recognition of tumors with myxoid and/or fibrous areas as being of endometrial stromal rather than smooth muscle, neural, or fibroblastic origin is dependent upon ancillary features such as coexistent endometrial stromal tumor of conventional type, a preserved vascular pattern of the type typically seen in endometrial stromal tumors, a permeative pattern of myoinvasion characteristic of low-grade ESS, and a CD10-positive/h-caldesmon–negative immunophenotype of tumor cells that histologically appear to be of endometrial stromal origin.[330,333]

The sex-cord–like elements that occur in some endometrial stromal tumors appear as cords, trabeculae, nests, and

FIGURE 4.298. Impact of varying degrees of edema and hyalinization on the appearance of endometrial stromal tumors. **A–D**: Although usually densely cellular, as in **A**, variable amounts of stromal edema can result in reduced cellularity **(B,C)**. Patches of hyalinized collagen are a common finding in these tumors **(D)**.

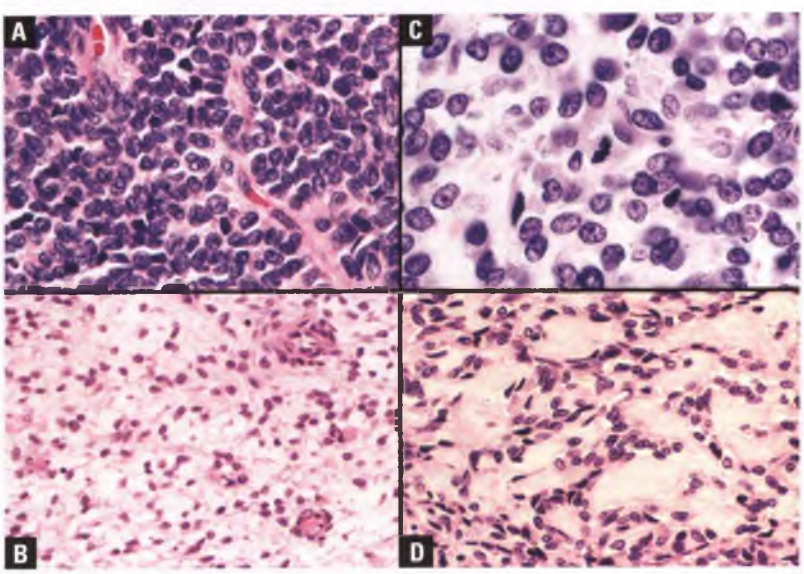

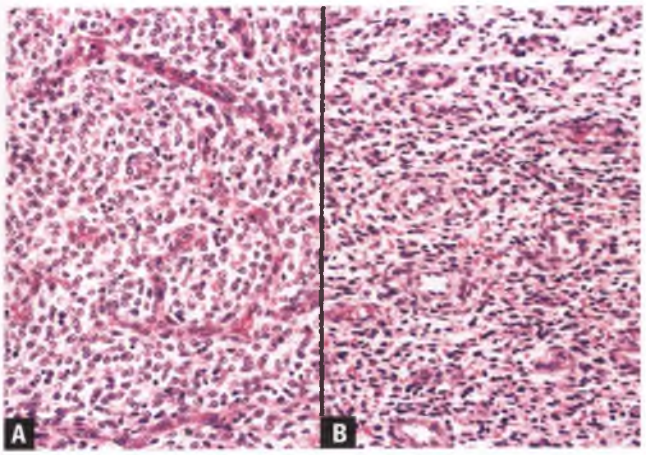

FIGURE 4.299. Characteristic vascular patterns of endometrial stromal tumors. **A**: Branching, compressed, interconnected capillaries. **B**: Network of small arterioles.

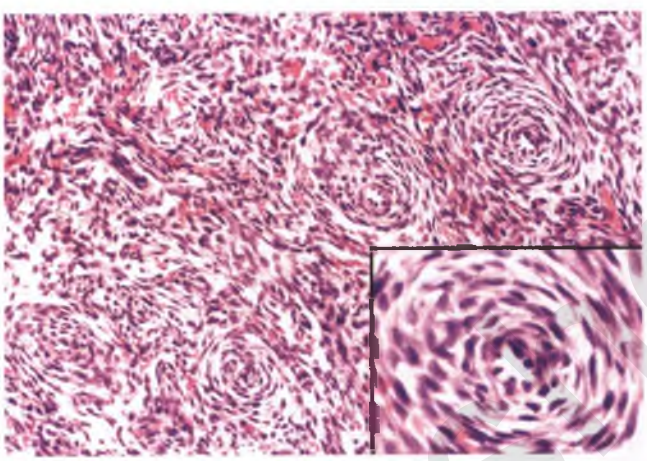

FIGURE 4.300. Endometrial stromal tumor. Note the concentric whorls of tumor cells swirling around the arterioles, as highlighted in the inset.

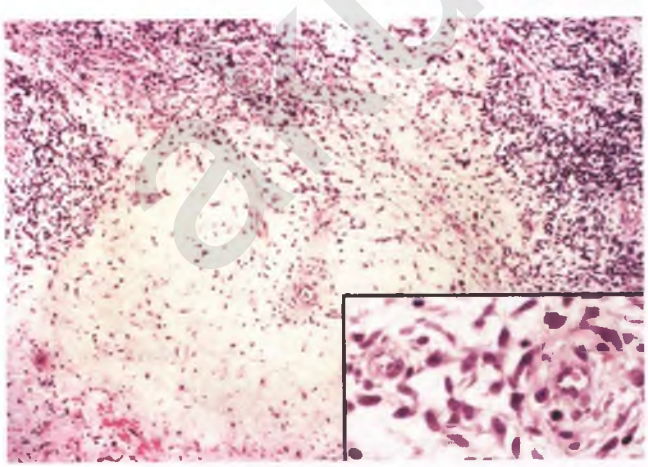

FIGURE 4.301. Myxoid areas within a low-grade endometrial stromal sarcoma. Hypocellular myxoid stroma is seen adjacent to islands of more cellular tumor with recognizable endometrial stromal differentiation. The inset highlights the vasculature within a myxoid area that is consistent with endometrial stromal origin.

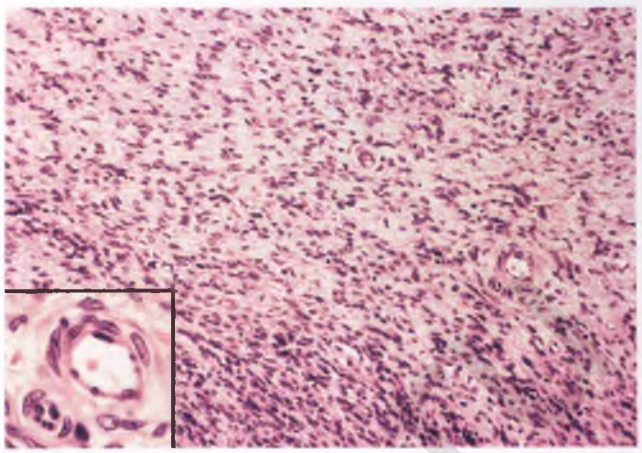

FIGURE 4.302. Fibrous areas within a low-grade endometrial stromal sarcoma. Spindle cells resembling fibroblasts are set within a collagenous matrix. Clues to endometrial stromal origin are arterioles with partial perivascular whorls of tumor cells (inset) and merging of the fibrous areas with more conventional low-grade ESS in the lower portion of the field.

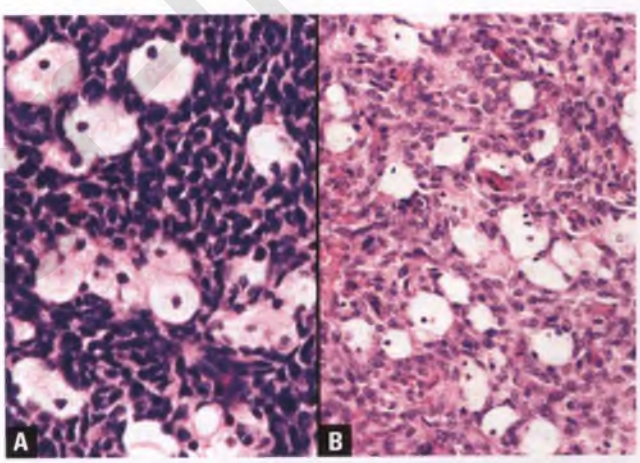

FIGURE 4.303. **A,B**: Low-grade endometrial stromal sarcoma with interspersed foamy histiocytes (two separate cases).

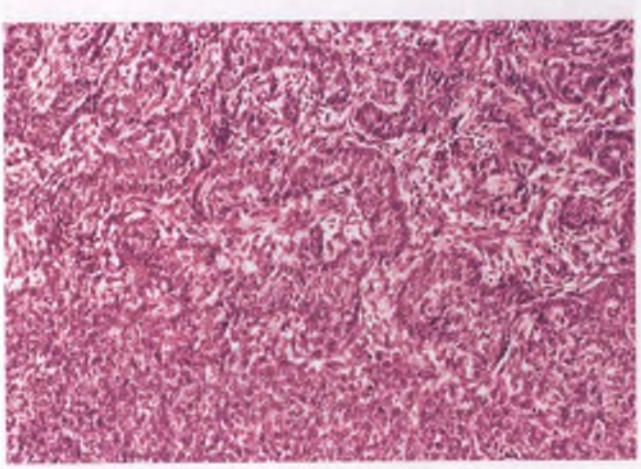

FIGURE 4.304. Low-grade endometrial stromal sarcoma with sex-cord–like elements composed of winding, interconnected trabecular bands (top) adjacent to conventional low-grade ESS (bottom).

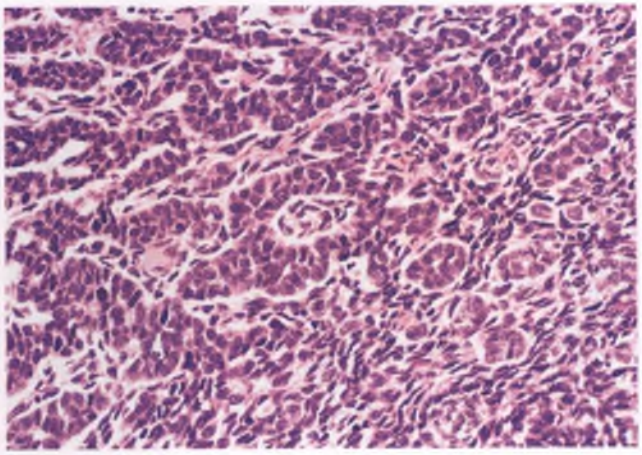

FIGURE 4.305. Low-grade endometrial stromal sarcoma with sex-cord–like elements. In this example, the sex-cord–like elements appear as trabeculae, nests, and small tubules with miniscule lumens.

solid or hollow tubules, as illustrated in Figures 4.304 and 4.305 and in the section on uterine tumors resembling ovarian sex-cord tumors.

Endometrioid glandular differentiation in endometrial stromal tumors is usually manifested by sparsely distributed, well-formed, benign-appearing glands resembling the type seen in normal proliferative endometrium, although exceptions occur.[65,66] Although occasional endometrial stromal tumors may incorporate a few nonneoplastic glands from the endometrium or foci of endometriosis or adenomyosis, most of these cases appear to represent true divergent differentiation of primitive stroma into glands.

Endometrial stromal tumors with smooth muscle differentiation were arbitrarily defined by Oliva et al as containing more than 30% of each component.[331] However, recognition that infiltrating uterine tumors with even minimal endometrial

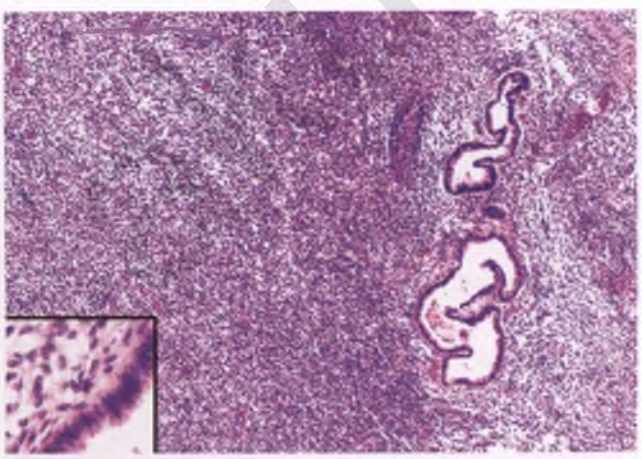

FIGURE 4.306. Low-grade endometrial stromal sarcoma with endometrioid glandular differentiation. A few well-formed, benign-appearing, endometrioid glands are embedded within a sheet of otherwise typical low-grade ESS. The inset highlights a portion of one of the glands.

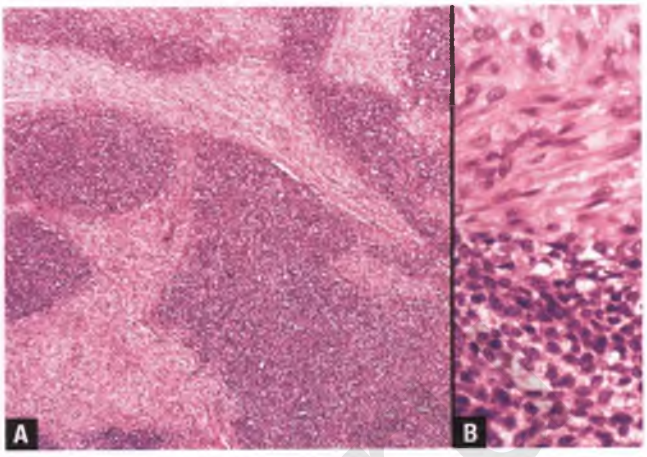

FIGURE 4.307. Endometrial stromal nodule with smooth muscle differentiation. **A**: Irregular islands of leiomyomatous smooth muscle interdigitate with tumor cells that exhibit endometrial stromal differentiation. Note how this pattern could be misconstrued as invasion of myometrium by a low-grade endometrial stromal sarcoma, when this is actually a section from the central aspect of a sharply circumscribed tumor. **B**: This high-magnification view shows the smooth muscle (top) and endometrial stromal (bottom) components.

stromal differentiation that contain a smooth muscle component infiltrate and behave like low-grade ESSs has prompted omission of a formal quantitative requirement for the endometrial stromal component.[329,333] In some endometrial stromal tumors with smooth muscle differentiation, the admixture of soft, tan to yellow endometrial stromal tissue with rubbery, grayish white, whorled myomatous tissue can be recognized grossly. Approximately 60% of endometrial stromal tumors with smooth muscle differentiation are well circumscribed and lack angiolymphatic invasion, and are therefore considered variants of ESN (referred to by some as "stromomyomas"), whereas the infiltrative features of other such tumors warrants their classification as variants of low-grade ESS.[329,331] Smooth muscle differentiation, which can be confirmed immunohistochemically, is typically recognized as an abrupt transition to irregular islands of spindle cells with usual leiomyomatous morphology (Fig. 4.307) or paucicellular nodules with central hyalinization that produces a "starburst" pattern (Fig. 4.308). A potential pitfall in the interpretation of endometrial stromal tumors with smooth muscle differentiation is misinterpreting the haphazard interdigitations of the endometrial stromal and smooth muscle components that occur within the tumor as representing an endometrial stromal tumor with myometrial invasion (Fig. 4.307).[329] This problem underscores the need for familiarity with the gross aspects of the tumor and a knowledge of which sections truly represent the interface of the tumor with the myometrium.

Although most ESNs have a smooth, expansile, noninfiltrative border with the neighboring myometrium (Fig. 4.309), the definition of these tumors allows for focal finger-like projections into the myometrium as long as they do not exceed 3 mm and there is no evidence of angiolymphatic invasion.[327,328] Similar tumors with extensions into the myometrium of up

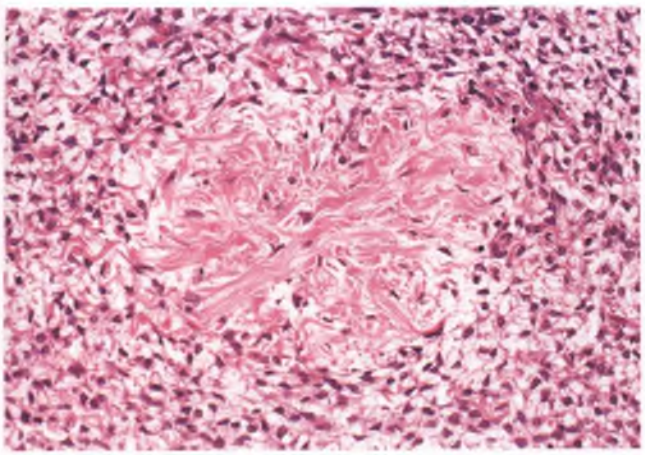

FIGURE 4.308. Endometrial stromal tumor with smooth muscle differentiation. A radiating focus of central hyalinization within a paucicellular nodule of smooth muscle generates a "starburst" pattern. (Courtesy of Dr. Deborah J. Gersell.)

to 9 mm have been termed endometrial stromal tumors with limited infiltration; although no meaningful follow-up is available for this rare subset of tumors, the expectation is that most, if not all, will also behave in a benign fashion.[328]

Low-grade ESS characteristically permeates the myometrium as broad, branching islands of variable sizes and shapes, often with pointed edges (Fig. 4.310). In approximately half of the cases, there are associated intrauterine worm-like plugs of tumor within thin-walled, distended vessels that usually represent veins rather than lymphatics (Fig. 4.310 inset). In the minority of cases that present with disease extending beyond the uterus, cords of tumor may be palpated within the extrauterine veins.

ESN and low-grade ESS both express CD10, vimentin, epidermal growth factor receptor, and estrogen and progesterone receptors, and may yield positive staining results for cytokeratin, actin, and occasionally desmin.[186,329,336–339] The smooth

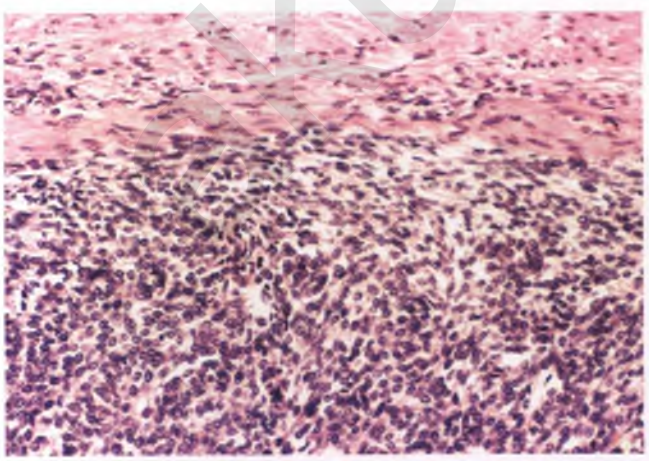

FIGURE 4.309. Endometrial stromal nodule composed of cells that closely resemble those of normal endometrial stroma from the proliferative phase. Note the sharp demarcation of the endometrial stromal proliferation from the adjacent myometrium (top).

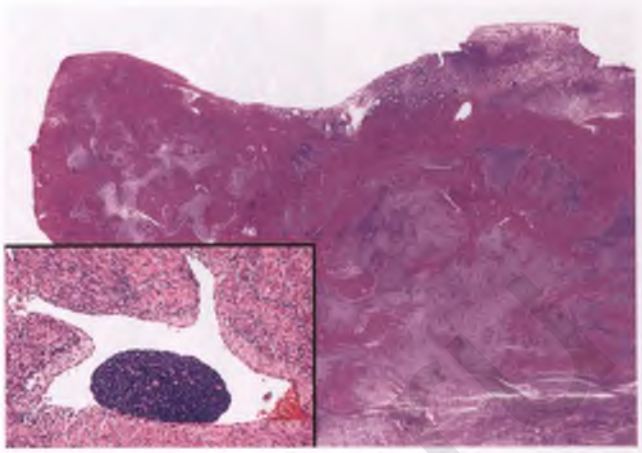

FIGURE 4.310. Low-grade endometrial stromal sarcoma. Low-magnification view demonstrating tumor replacing a portion of the endometrium (upper right) and infiltrating the myometrium in its characteristic jagged, interdigitating pattern. The inset shows invasion of a thin-walled, dilated vein in a different case of low-grade ESS.

muscle marker h-caldesmon is reliably negative in these tumors (except in areas of smooth muscle metaplasia).[270–272] The presence of a translocation between chromosomes 7 and 17 (JAZF1-JJAZ1 gene fusion) in many ESNs and low-grade ESSs may have some diagnostic utility, although the biologic role of this translocation is not yet understood.[340]

Low-grade ESS is well-known for its indolent behavior and tendency for late recurrences, which not uncommonly occur more than 10 years after initial treatment. Favored sites of recurrences are the pelvis, abdomen, and vagina, although metastases are occasionally found in distant sites such as the lung.[341] Lung metastases tend to be solid and well circumscribed, and entrapment of nonneoplastic respiratory epithelium may result in simulation of a biphasic neoplasm (Fig. 4.311).[341] The classic tongue-like infiltration pattern of low-grade ESS is often recapitulated in abdominal and extraovarian pelvic recurrences (Fig. 4.312). A potential pitfall in the identification of metastases from low-grade ESS is the not uncommon finding of the metastases exhibiting prominent smooth muscle or fibromyxoid differentiation even when these features are not apparent in the primary tumors.[333] Low-grade ESS metastatic to the ovary is discussed in Chapter 7.

Differential Diagnosis

In addition to the need to distinguish ESN and low-grade ESS from one another, other entities can be confused with endometrial stromal tumors. The main differential diagnostic consideration of both tumors is the highly cellular leiomyoma, distinction from which was discussed earlier in this chapter. Previously discussed in the section on IVL is the potential for its cellular variant to simulate vascular involvement by low-grade ESS. Some endometrial polyps with cellular stroma may simulate an ESN, but a core of thick-walled blood vessels and scattered glands usually allows for their recognition.

Low-grade ESS with endometrioid glandular differentiation can be confused with adenosarcoma, endometriosis

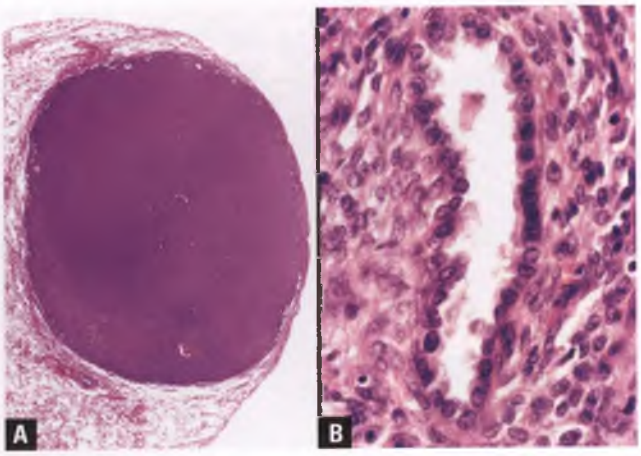

FIGURE 4.311. Low-grade endometrial stromal sarcoma metastatic to the lung 14 years posthysterectomy. **A**: Note the well-circumscribed nature of this metastasis, which is typical for low-grade ESS in this site. **B**: Entrapment of nonneoplastic respiratory epithelium can mistakenly suggest the presence of an intrinsic glandular component. (Glass slide kindly provided by Dr. Cheryl M. Reichert.)

(if encountered in an extrauterine site), and adenomyosis. The glandular component of adenosarcomas is more regularly distributed and features periglandular stromal condensation and/or formation of epithelial-lined, stromal polypoid structures that project into cystically dilated glands or into the endometrial cavity. Adenosarcoma would also not be expected to exhibit the permeative pattern of myoinvasion or the propensity for vascular invasion that often characterizes low-grade ESS. In contrast to endometriosis, low-grade ESS with endometrioid glandular differentiation is mass forming and contains areas of more typical ESS that may exhibit significant stromal mitotic activity, plugs of tumor within vessels, and/or one or more of the other morphologic variations that are commonly seen in these tumors (note that most lesions formerly described as "aggressive endometriosis" would probably now be considered low-grade ESSs with endometrioid glandular differentiation).[65,66] Distinction of usual adenomyosis and adenomyosis with sparse glands from ESS is discussed in the section on adenomyosis.

Endometrial stromal tumors with sex-cord–like elements can be misinterpreted as carcinosarcomas, but the latter tumors typically feature high-grade carcinomatous and sarcomatous components. Distinction of endometrial stromal tumors with sex-cord–like elements from uterine tumors resembling ovarian sex-cord tumors is based upon the absence or inconspicuous nature of an endometrial stromal component in the latter.

A role for a category of modern-day high-grade ESS was mentioned earlier, and is discussed later in this section.

Undifferentiated Endometrial Sarcoma

Undifferentiated endometrial sarcoma and its synonym undifferentiated uterine sarcoma are the terms currently employed by the WHO for those rare sarcomas that have a more aggressive histologic appearance than allowed for low-grade ESS, but whose topography indicates an endometrial origin.[§] These tumors generally occur in the postmenopausal rather than perimenopausal age group, present with abnormal vaginal bleeding and uterine enlargement, and are associated with a poor prognosis.

Grossly, undifferentiated endometrial sarcomas are usually bulky, polypoid, intracavitary, fleshy, grayish-white tumors with prominent areas of hemorrhage and necrosis (Fig. 4.313). Myometrial invasion is usually in the form of a broad front of tumor that replaces rather than interdigitates with the myometrium. Angiolymphatic invasion is often present, but the macroscopic plugs of intravascular tumor that often characterize low-grade ESS are usually absent. These tumors do not exhibit the characteristic vascular pattern of low-grade ESS, and their constituent cells bear no resemblance to those of the normal proliferative phase endometrial stroma. The tumors grow as cellular sheets that may

[§] Note that the "poorly differentiated endometrial sarcomas" described by Evans were aggressive malignancies whose only link to endometrial differentiation was a topographical one, and correspond to what is currently termed undifferentiated endometrial sarcoma.[342]

FIGURE 4.312. Low-grade endometrial stromal sarcoma metastatic to the colon. Note the permeative pattern of infiltration by geographic islands of tumor, which in this case demonstrate transmural involvement and formation of "colon polyps" that could be sampled by a gastroenterologist.

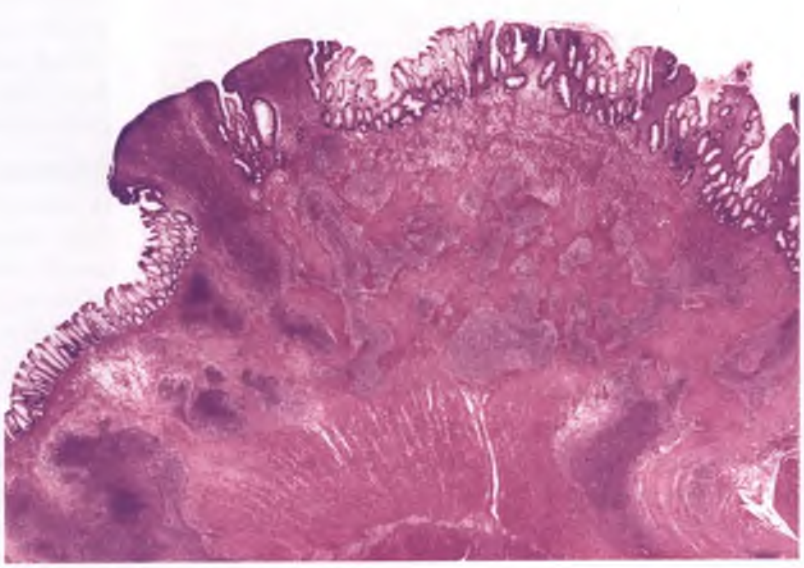

FIGURE 4.313. Undifferentiated endometrial sarcoma. The sectioned surface of this fixed specimen demonstrates a large, polypoid, intracavitary, fleshy tumor with prominent areas of hemorrhage and necrosis. The tumor is firmly attached to and impinges upon a thinned myometrium, which it invaded superficially.

exhibit either marked nuclear pleomorphism or retain a degree of uniformity in their anaplasia (Fig. 4.314). There is brisk mitotic activity, and abnormal division figures are usually found with ease.

Since undifferentiated endometrial sarcomas may have histologic features that are indistinguishable from the sarcomatous component of a carcinosarcoma, thorough sampling should be undertaken to search for carcinomatous elements. Examination of numerous sections will also help to exclude poorly differentiated/undifferentiated carcinoma, leiomyosarcoma, rhabdomyosarcoma, large cell lymphoma, and granulocytic sarcoma, which are also differential diagnostic considerations. In most cases, immunohistochemistry will be required to arrive at the correct diagnosis.

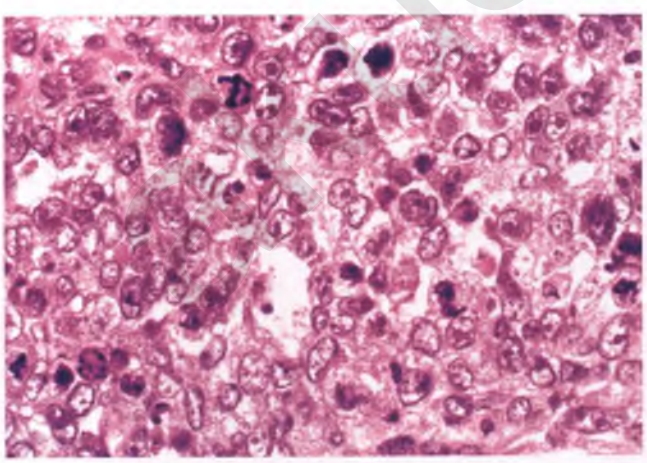

FIGURE 4.314. Undifferentiated endometrial sarcoma. Note the high nuclear grade, macronucleoli, individual tumor cell necrosis, brisk mitotic activity that includes atypical division figures, and lack of resemblance to endometrial stroma. There is relative nuclear uniformity in this example, which is the histologic correlate of the tumor shown in the preceding figure.

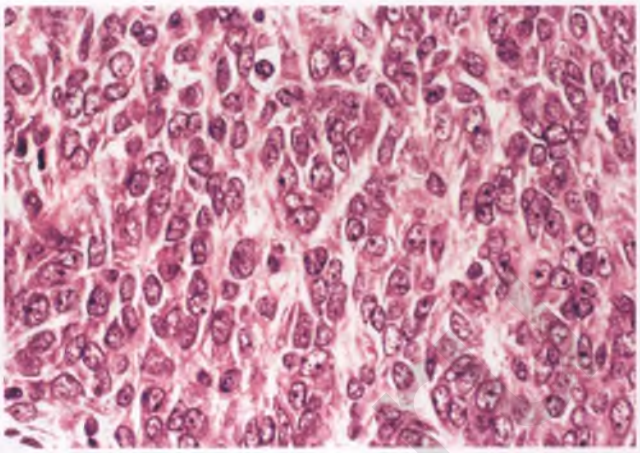

FIGURE 4.315. Modern-day high-grade endometrial stromal sarcoma. In comparison to typical ESS, the nuclei are slightly larger with more open chromatin and more readily apparent nucleoli.

Modern-Day High-Grade Endometrial Stromal Sarcoma

The distinction between undifferentiated endometrial sarcoma and low-grade ESS is usually obvious. However, a small number of cases exhibit more than the usual degree of nuclear atypia seen in low-grade ESS, often in conjunction with considerable mitotic activity that includes the presence of atypical division figures, but maintain both a degree of nuclear uniformity and some evidence of endometrial stromal differentiation. Although the nuclei of the neoplastic cells retain their round to ovoid shape in these cases, they are slightly larger with more open chromatin and often exhibit more readily apparent nucleoli as compared to the nuclei of typical cases of low-grade ESS (Figs. 4.315 and 4.316). Classification of such tumors is controversial, but they are considered by many investigators to represent modern-day high-grade ESSs. Due to their rarity and the variable inclusion criteria utilized for such cases, limited follow-up information is available for this subgroup of tumors, although there is anecdotal evidence that they often present at high stage, with recurrences and tumor-related deaths occurring more often and more rapidly than typical cases of low-grade ESS.

It should be noted that although a minority of ESSs in the Chang series were reported to have "grade 2 or 3" nuclear atypia, this assessment of atypia was on a relative scale within the spectrum of fairly uniform cells that still demonstrated recognizable endometrial stromal differentiation; neoplasms with marked nuclear pleomorphism were specifically excluded from that study.[326] The grade 3 subset of such tumors appears to fit the above definition of the modern-day high-grade ESS. Despite the statement by Chang and coworkers that they require nuclear atypia beyond that seen in their grade 3 tumors for a diagnosis of undifferentiated endometrial sarcoma (see their Figure 2 legend),[326] others have included tumors with grade 2 or 3 nuclear atypia as defined in the Chang study

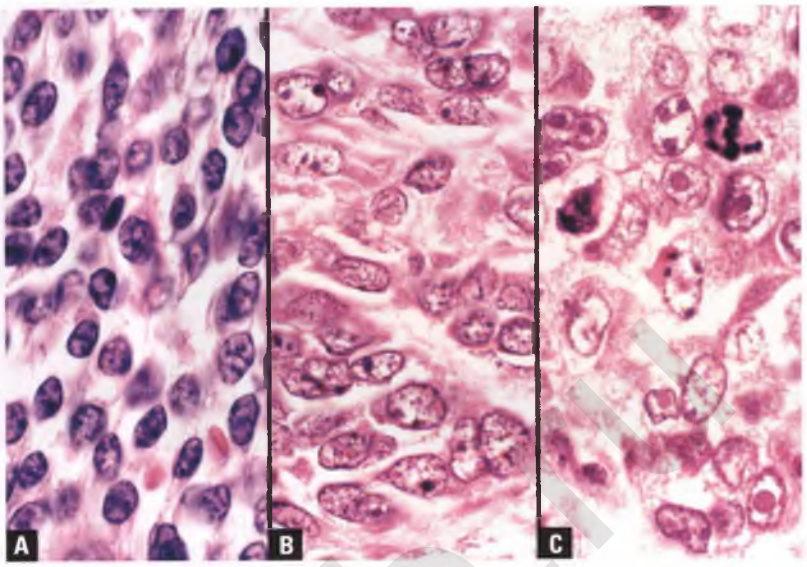

FIGURE 4.316. Comparison of the nuclear features of a typical low-grade endometrial stromal sarcoma **(A)**, a modern-day high-grade endometrial stromal sarcoma **(B)**, and an undifferentiated endometrial sarcoma that retains an element of nuclear uniformity **(C)**. All three images were taken at the same magnification.

within their undifferentiated endometrial sarcoma category.[343] Clearly, there are subclassification issues within the more aggressive end of the spectrum of endometrial sarcomas that remain unresolved.

ATYPICAL POLYPOID ADENOMYOMA

First described by Mazur in 1981, the APA is a polypoid proliferation of abnormal endometrial glands embedded within a cellular myomatous or myofibromatous stroma.[344–346] Patients with APA are typically premenopausal (mean age of 39 years) and present with abnormal vaginal bleeding. APAs have an average size of about 2 cm and have a gross appearance similar to that of endometrial polyps, albeit with a more firm or rubbery cut surface. They are typically sharply demarcated from the adjacent endometrium and myometrium.

The glands of APAs may be either haphazardly arranged or clustered in lobular configurations, and typically are crowded, irregularly shaped, and accompanied by morular metaplasia (Fig. 4.317). The architectural abnormalities and degree of cytologic atypia of the glandular component range from that seen in endometrial hyperplasia with borderline atypia to well-differentiated adenocarcinoma. The squamous morules are often prominent and may contain foci of central necrosis. The stromal component consists of interwoven fascicles of cellular, bland smooth muscle, and/or myofibromatous tissue (Fig. 4.318); hence the alternative designation atypical polypoid adenomyofibroma.[346] A trichrome stain that demonstrates the presence of spindle cells with red, fibrillar cytoplasm within the stromal component can be used to confirm smooth muscle differentiation. In roughly 80% of cases, the uninvolved endometrium exhibits normal histology (usually an unremarkable

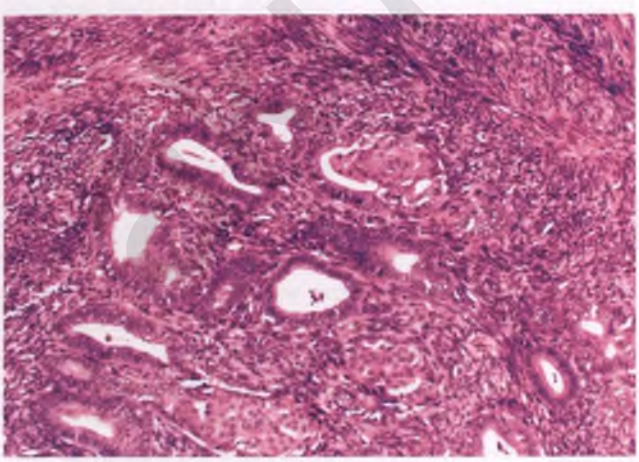

FIGURE 4.317. Atypical polypoid adenomyoma. This example contains a lobulated cluster of crowded endometrial glands with scattered squamous morules. Note the cellular fibromuscular stroma.

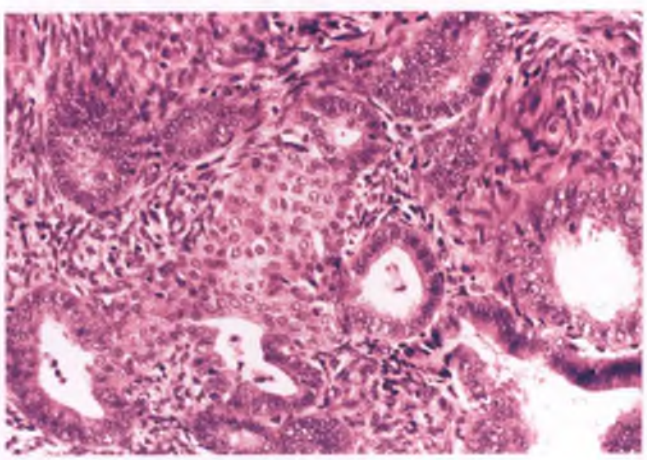

FIGURE 4.318. Atypical polypoid adenomyoma. Atypical endometrial glands and a squamous morule are embedded within a cellular fibromuscular stroma.

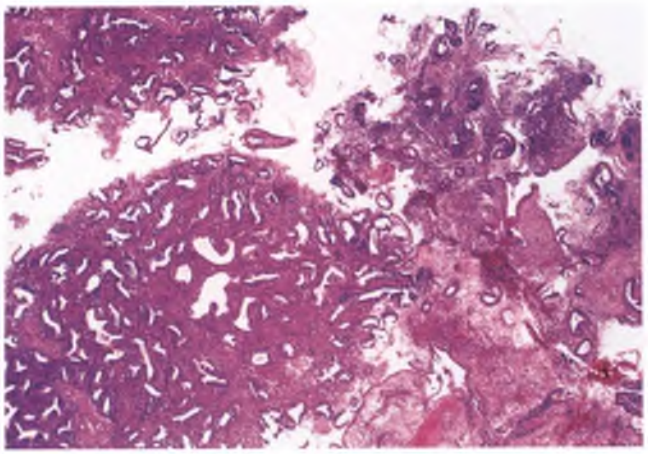

FIGURE 4.319. Atypical polypoid adenomyoma. This curettage specimen contains fragments of atypical polypoid adenomyoma (left) and proliferative endometrium (right).

proliferative pattern), which results in a low-magnification dimorphic appearance in curettings due to the admixture of involved and uninvolved endometrial fragments (Fig. 4.319).

APAs that feature glandular abnormalities that correspond to a type of endometrial hyperplasia have no appreciable risk of myoinvasion and can be treated by local excision, although approximately one-third of such cases will subsequently be shown to have persistent or recurrent disease.[346] However, those APAs that contain foci that are indistinguishable from well-differentiated adenocarcinoma (Fig. 4.320), designated APAs of low malignant potential, are associated with an approximately 60% chance of persistence/recurrence if managed conservatively and a 15% to 20% chance of harboring superficial myometrial invasion.[346]

Differential Diagnosis

The principal differential diagnostic consideration for APA in curettage specimens is a well-differentiated endometrial adenocarcinoma with myometrial invasion. At the outset, one should be biased against the possibility of a myoinvasive endometrial adenocarcinoma in a premenopausal woman, since this is an uncommon situation. Moreover, it is distinctly uncommon for myometrium invaded by adenocarcinoma to be sampled by curettage devices, and when present these fragments are typically associated with a host response to the infiltrating glands that consists of inflamed granulation tissue. In addition, tissue samples that contain myoinvasive endometrial adenocarcinoma typically also harbor easily recognizable adenocarcinoma/atypical hyperplasia in other tissue fragments that lack a myomatous stromal component. In contrast, the glands within APAs do not elicit a host reaction and uninvolved endometrium is typically normal. Although the stroma of APAs and myoinvasive endometrial adenocarcinomas does not have an appreciably different immunophenotype with respect to actin, desmin, and CD34,[347] recent studies support the utility of CD10 and h-caldesmon in helping to make this distinction (APA → CD10-negative and h-caldesmon–negative stromal cells; myoinvasive adenocarcinoma → CD10-positive fringe of stromal cells rimming many of the myoinvasive glands and positive immunoreactivity of the neighboring myometrium for h-caldesmon).[348,349]

Polypoid submucosal adenomyomas of the usual type (adenomyomatous polyps) also share some similarities with APAs, but are distinguished by (a) minimal glandular crowding of disordered proliferative-type glands that lack cytologic atypia, (b) investment of many of the glands by collars of normocellular endometrial stroma, (c) a prominent smooth muscle component that is less cellular and more obviously of smooth muscle origin than that typically seen in APAs, and (d) an absence of morular metaplasia.

The APA may also be mistaken for an adenosarcoma if the cellular stroma of the APA is misinterpreted as being sarcomatous. Although smooth muscle is occasionally found focally within the mesenchymal component of an adenosarcoma, smooth muscle differentiation is seldom as prominent in adenosarcomas as it is in APAs.[350] Moreover, the periglandular stromal cuffs and papillary projections of adenosarcomas are

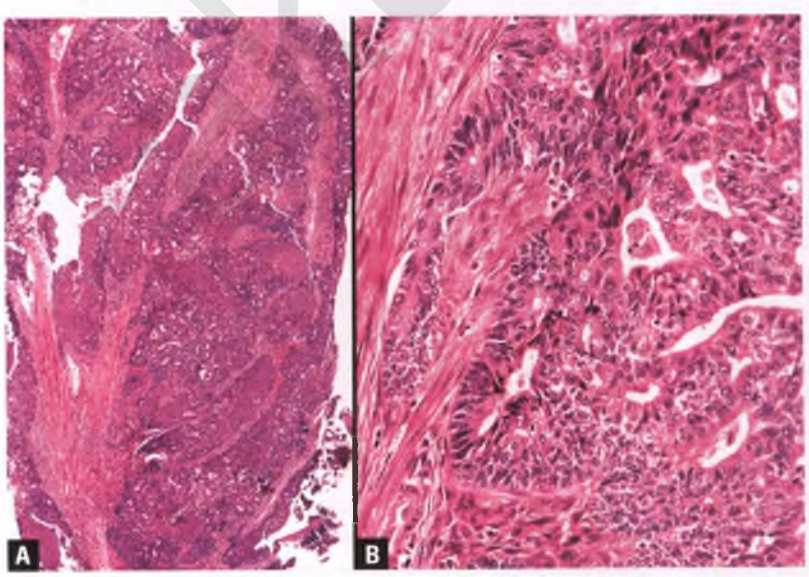

FIGURE 4.320. Atypical polypoid adenomyoma of low malignant potential. **A**: This low-magnification view shows a polypoid fragment that features marked architectural complexity of the glandular component. The solid appearance of patchy epithelial areas is due to morular metaplasia. **B**: The glandular component has architectural and nuclear features that are indistinguishable from well differentiated endometrioid adenocarcinoma. Note the smooth muscle component at left. A hysterectomy showed no myometrial invasion.

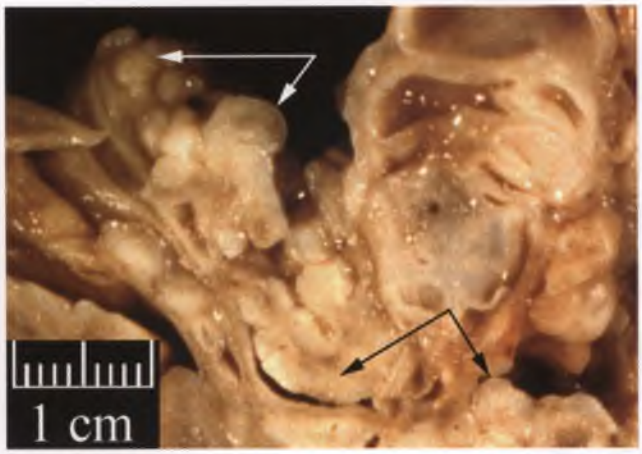

FIGURE 4.321. Adenosarcoma. This section through a formalin-fixed adenosarcoma demonstrates the presence of scattered cysts as well as polypoid projections extending from the surface of the tumor (*white arrows*) and into cystic spaces (*black arrows*). The largest intracystic polypoid projection measures 1 cm and occupies all but the peripheral rim of the cystic space; its formation is analogous to a fist punched deeply into a balloon. (Courtesy of Dr. Julio A. Lagos.)

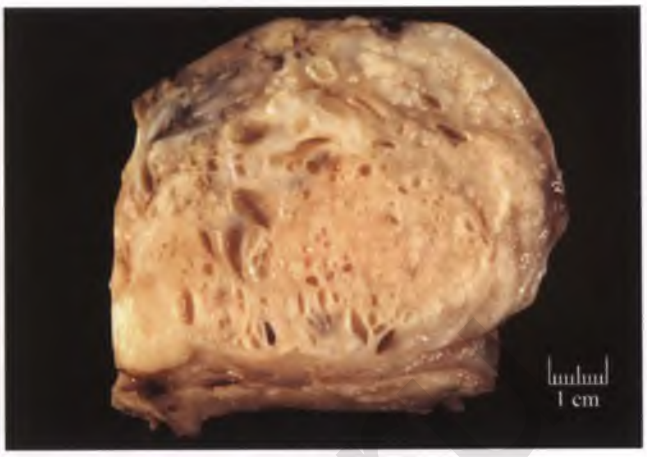

FIGURE 4.322. Adenosarcoma. This section through a formalin-fixed adenosarcoma demonstrates a broad-based, polypoid neoplasm with a spongy appearance due to the presence of scattered, variable-sized cysts. The tumor is sharply demarcated from the underlying myometrium, as is typically the case.

not seen in APAs, and the atypical, hyperplastic, generally noncystic glands accompanied by squamous morules that are characteristic of APAs would be unusual findings in adenosarcoma.

ADENOSARCOMA AND ADENOFIBROMA

Adenosarcoma

Adenosarcoma is a biphasic neoplasm composed of a benign epithelial component associated with malignant stroma.[350] It is a rare tumor that accounts for only about 8% of uterine tumors with a malignant mesenchymal component,[351] which corresponds to approximately one of every 300 primary uterine malignancies. Adenosarcoma occurs in women across a wide age range, and typically presents with abnormal uterine bleeding related to a large polypoid tumor (mean diameter of 5 cm) that projects into the endometrial cavity and may protrude through the external os.[350] Patients with repeated episodes of "recurrent endometrial polyps" should be carefully evaluated for the possibility of adenosarcoma, since areas with nondiagnostic or subtle histologic features are common.[350] Although most tumors within the adenosarcoma/adenofibroma group arise from the endometrium, approximately 10% have an endocervical origin.[350,352] Per the 2008 FIGO staging system for uterine sarcomas, involvement of the endocervix in tumors limited to the uterus is still within the spectrum of stage I disease.[315]

Grossly, adenosarcoma is typically a broad-based tumor that may have polypoid projections extending from its surface or into cystic spaces (Fig. 4.321). Myometrial invasion is present in only about 15% of cases, and is rarely grossly evident.[350] The sectioned surface is usually tan to off-white and may have a spongy appearance due to the presence of multiple small cysts (Fig. 4.322). These cysts correspond to cystically dilated glands (Fig. 4.323), which is the most nondescript glandular pattern in adenosarcomas. More characteristic are glands that form elongated, curved, slit-like clefts in patterns that resemble the outline of a leaf or the mouth of a shark (Figs. 4.324 and 4.325). These clefted patterns, which are similar to those seen in phyllodes tumor of the breast, are due to impingement upon and compression of the cystic glandular spaces by polypoid projections of sarcomatous stroma. The histology of the polypoid or papillary structures that form the surface or project into cystic spaces of some adenosarcomas is illustrated in Figure 4.326.

Characteristically, at least some of the glandular spaces in adenosarcomas, whether cystic or clefted, are surrounded by a cuff of condensed stroma (Figs. 4.323–4.325), which is typically the site of greatest mitotic activity. The glands are usually lined by endometrioid epithelium, although a variety of

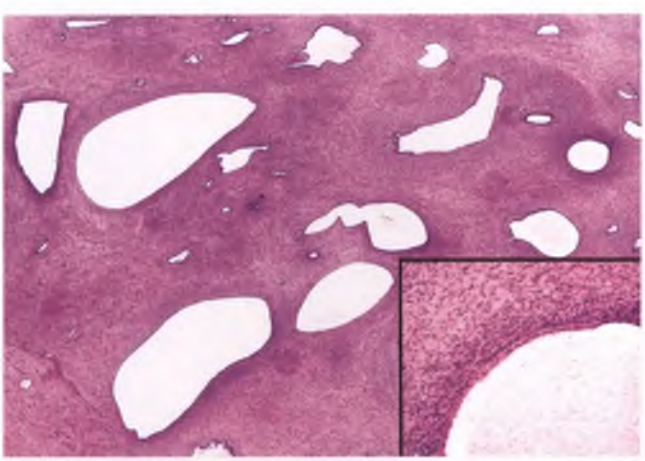

FIGURE 4.323. Adenosarcoma. This image represents the histologic correlate of the large, spongy tumor in the preceding figure. The glands are cystically dilated, and the periglandular stromal cuffs range from absent to subtle to readily apparent. The inset depicts a portion of a gland with one of the more obvious periglandular cuffs from this tumor.

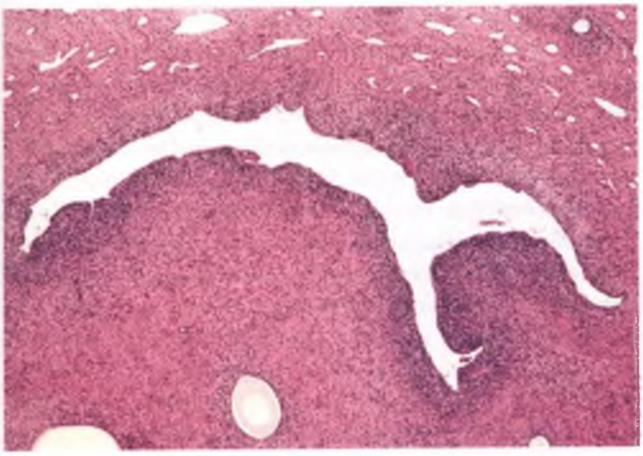

FIGURE 4.324. Adenosarcoma. The shape of this elongated, leaf-like gland is due to partial compression by protrusions of sarcomatous stroma. Note the characteristic periglandular cuff of stromal cells.

other types of epithelia may be seen, and the glands may be focally atypical in a minority of cases.[350,353] The sarcomatous component usually resembles low-grade endometrial stromal sarcoma (Fig. 4.327), but elements of fibrosarcoma may also be present or dominant.[350] Heterologous elements are identified in approximately 20% of cases, and are usually represented by embryonal rhabdomyosarcoma, although isolated rhabdomyoblasts, occasional micronodules of fetal cartilage, or focal patches of adipose tissue may also be present.[350] Another unusual finding, seen in <10% of adenosarcomas, is the presence of sex-cord–like elements.[354]

Adenosarcoma with Sarcomatous Overgrowth

A minority of adenosarcomas demonstrate the prognostically significant feature of sarcomatous overgrowth, which is arbitrarily defined as the presence of a pure sarcoma representing at least 25% of an otherwise typical adenosarcoma (Fig. 4.328).[355] In these cases, the areas of pure sarcoma are much more likely to exhibit higher nuclear grade, more tumor necrosis, increased mitotic activity, a higher Ki-67 proliferation index, and loss of immunoreactivity for markers commonly expressed by endometrial stromal cells (CD10, ER, and PR) than the sarcomatous component of typical adenosarcomas, and in some series are more likely to be myoinvasive and associated with rhabdomyosarcomatous elements.[353,355–357] Not surprisingly, adenosarcomas with sarcomatous overgrowth have been found to be more aggressive tumors than typical adenosarcomas, with recurrences, metastases, and tumor-related deaths occurring at rates similar to leiomyosarcoma or carcinosarcoma.

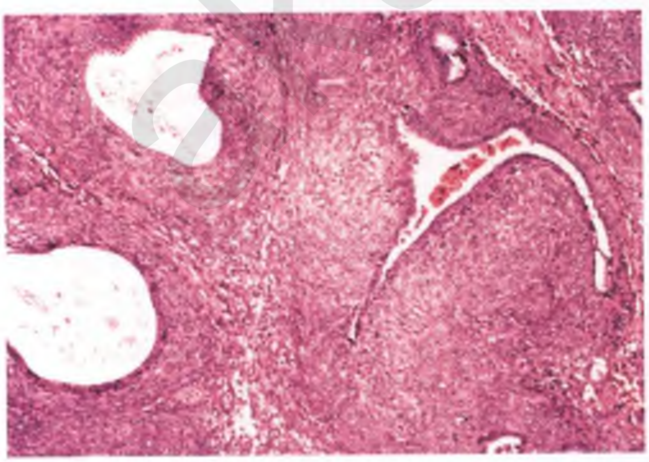

FIGURE 4.325. Adenosarcoma. This example has two thick periglandular cuffs of stromal cells (left) and a compressed gland in a "shark mouth" configuration (right).

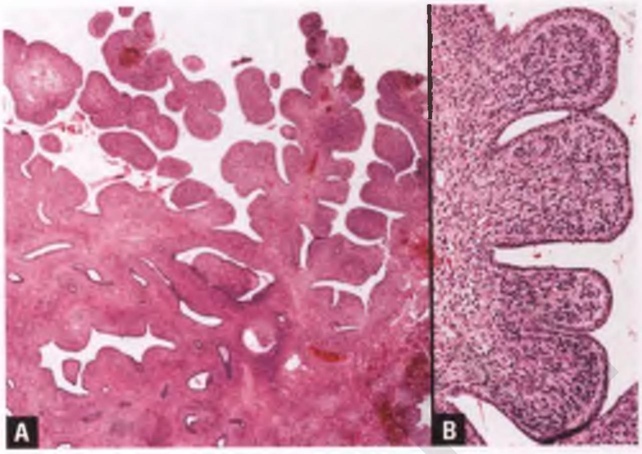

FIGURE 4.326. Adenosarcoma. **A**: This tumor has a papillary surface component that could be appreciated grossly. The contour of some of the glands at the base of the papillary structures has been altered in characteristic leaf-like fashion by polypoid protrusions of sarcomatous stroma. **B**: Higher magnification view of the papillae.

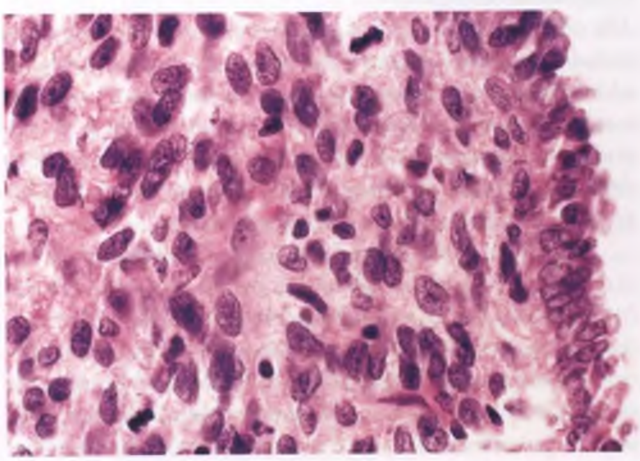

FIGURE 4.327. Adenosarcoma. As in this example, the sarcomatous component typically resembles endometrial stromal sarcoma and is most mitotically active in the more cellular region beneath the glandular epithelium, which is at right. Two mitotic figures are present in this image.

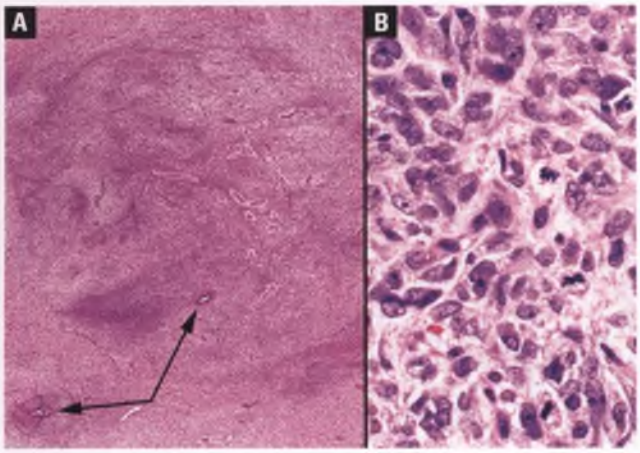

FIGURE 4.328. Adenosarcoma with sarcomatous overgrowth. **A**: In this area of transition to sarcomatous overgrowth, only two small glands with periglandular stromal cuffs remain (*arrows*). **B**: Sarcomatous overgrowth typically consists of a high-grade sarcoma with brisk mitotic activity, as shown here.

Behavior

Adenosarcomas of usual type are considered low-grade malignancies. The tumor recurs in approximately 25% of cases, usually within the vagina, pelvis, or abdomen.[350] Most recurrences of adenosarcomas are composed solely of the sarcomatous element, although metastases with a preserved biphasic pattern of adenosarcoma also occur.[350] Tumors with extrauterine spread, myometrial invasion, and sarcomatous overgrowth are associated with a higher risk of recurrence and tumor-related death, but it should be noted that adenosarcomas can recur despite an absence of myometrial invasion.[350,353] Since it is not uncommon for the initial recurrence of adenosarcoma to occur more than 5 years following hysterectomy, long-term follow-up is indicated.[350]

Differential Diagnosis

The differential diagnosis of endometrial-based adenosarcoma includes endometrial polyp, adenofibroma, atypical polypoid adenomyoma, and endometrial stromal sarcoma with endometrioid glandular differentiation. Features that help to distinguish adenosarcomas from the latter two lesions have been discussed earlier in this chapter, and distinction from adenofibroma is discussed in the following section.

The dividing line between an "uppity" endometrial polyp and the lower limit of adenosarcoma is not well defined. Although the typical endometrial polyp has a prominent central vasculature with thick-walled vessels and does not raise concern for adenosarcoma, occasional endometrial polyps are encountered that exhibit one or more worrisome features, such as a cellular stroma, some stromal mitotic activity, focal stromal atypia, a few glands with a clefted architecture, or a rare periglandular stromal cuff.[59,61] Some such lesions are comfortably recognizable as benign, but the only thing separating a subset of these problematic polyps from low-grade adenosarcoma is the subjective opinion of an expert consultant. Fortunately, typical adenosarcomas are low-grade malignancies to begin with, so aggressive behavior from tumors at the low end of the spectrum that mimic endometrial polyps is extremely rare. The usual outcome of these tumors diagnosed in curettings is a hysterectomy with no residual tumor, so a diagnosis of "endometrial polyp with atypical features" with a recommendation for monitoring of the endometrial cavity for recurrence may be more prudent than diagnosing and treating these lesions as if they were full-fledged adenosarcomas.

Adenofibroma

Uterine adenofibroma is an extremely rare biphasic neoplasm whose epithelial and mesenchymal elements are both benign.[358] It occupies a small and very subjective niche between endometrial polyps on the one hand and the low end of the spectrum of adenosarcoma on the other.

The clinical and gross features of adenofibroma are similar to those of adenosarcoma, which is not surprising in view of the fact that rigorous sampling of a purported adenofibroma will often reveal at least focal features that prompt its placement within the adenosarcoma category. In the Clement and Scully series, only about 5% of tumors in the adenofibroma/adenosarcoma group were classified as adenofibromas.[350]

The epithelial component of an adenofibroma is similar to that of adenosarcoma. The stromal component has the appearance of a proliferation of fibroblasts or endometrial stromal cells, or an admixture thereof. Broad, epithelial-lined papillae emanate from the surface of the tumor and/or project into cystic spaces,[358] as illustrated in an endocervical example of this tumor in Chapter 3 (Figs. 3.249 and 3.250). As previously described for adenosarcoma, cleft-like gland formations are also commonly seen in adenofibroma.[358] In contrast to adenosarcoma, the stromal component of adenofibroma exhibits a very low mitotic rate (<2 mitotic figures per 10 high power fields) and absent or inconspicuous periglandular cuffs of condensed stroma.[350] The stromal component of adenofibroma is also described as being variably cellular, although less cellular than adenosarcoma, and exhibiting minimal, if any, nuclear atypia.[350,352]

When confronted with a tumor in the adenofibroma/adenosarcoma group, minimal criteria for adenosarcoma include any one or more of the following: (a) a stromal mitotic index ≥2 mitotic figures per 10 high power fields, (b) "marked" stromal hypercellularity, and (c) more than mild nuclear atypia of the stromal component.[350] In practice, these differentiating features are of little use in borderline cases, since (a) a mitotic index of 1 vs. 2 mitotic figures per 10 high power fields is unlikely to be a reproducible or biologically significant difference, (b) there is considerable overlap in the subjective assessment of stromal cellularity between adenofibromas, adenosarcomas, and even endometrial polyps, and the degree of hypercellularity required for a diagnosis of adenosarcoma at its lower limit is impossible to define, and (c) the sarcomatous component of adenosarcomas at the low end of the spectrum is

well differentiated and resembles low-grade endometrial stromal sarcoma. Despite these limitations, most adenosarcomas are recognizable by virtue of their periglandular stromal cuffs, presence of at least moderate stromal atypia in 70% of cases, and a mean mitotic index of 9 mitotic figures per 10 high power fields.[350]

Since the everyday endometrial polyp and the vanishingly rare adenofibroma both consist of benign endometrial glands and stroma, their distinction from one another is problematic and arbitrary unless the papillary and/or cleft-like architectural features of the adenofibroma, which are highly unusual for endometrial polyps, are accepted as a definitional requirement for a diagnosis of adenofibroma.

When strictly defined, adenofibromas are benign, noninfiltrative tumors. It should be noted that the two reported cases of uterine adenofibromas with myometrial invasion do not fit the definition of an adenofibroma that requires the presence of cleft-like gland formations or broad papillary structures.[359] An alternative explanation for these myoinvasive "adenofibromas" is that they represent very low-grade adenosarcomas, and that adenosarcomas at the low end of the spectrum may have large areas with a deceptively bland appearance, even in foci of myoinvasion. A recent report of two additional cases of myoinvasive tumors that were initially interpreted as adenofibromas demonstrated subsequent malignant behavior,[357] which supports the view that adenofibroma should not be diagnosed in the presence of myometrial invasion, no matter how bland and mitotically inactive the tumor appears.

MISCELLANEOUS MESENCHYMAL TUMORS

A variety of rare benign and malignant mesenchymal tumors can arise within the uterine corpus. This section provides a selective review of some of these tumors. To put the incidence of uterine sarcomas in perspective, roughly 4% of uterine cancers contain a malignant mesenchymal component, and of these, about half are carcinosarcomas, 25% to 30% are leiomyosarcomas, 10% to 15% are endometrial stromal sarcomas, roughly 8% are adenosarcomas, and <5% are miscellaneous sarcomas such as rhabdomyosarcoma, PNET, angiosarcoma, osteosarcoma, chondrosarcoma, malignant perivascular epithelioid cell tumor, liposarcoma, alveolar soft part sarcoma, and malignant rhabdoid tumor.[286,360,361]

Inflammatory Myofibroblastic Tumor

Inflammatory myofibroblastic tumor (IMT), formerly referred to as inflammatory pseudotumor, is a myofibroblastic proliferation associated with a lymphoplasmacytic infiltrate that has been reported to involve the uterus on rare occasions.[362] The spindle cell population of all uterine IMTs tested thus far, and many of those from other sites, demonstrate immunohistochemical expression of the ALK protein that is also expressed in anaplastic large cell lymphoma.[362] ALK protein expression is due to clonal translocations involving the ALK gene, and

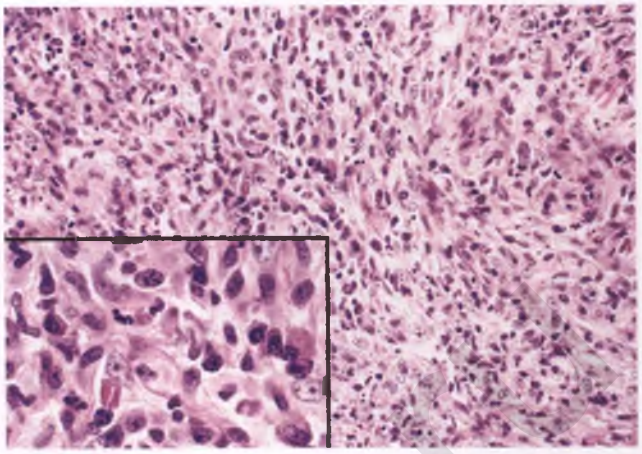

FIGURE 4.329. IMT composed of a proliferation of spindle-shaped myofibroblasts associated with interspersed small lymphocytes and plasma cells.

these abnormalities indicate that IMT is a neoplastic rather than reactive process.

Grossly, IMTs resemble intramural leiomyomas that may have focally irregular margins or polypoid submucosal leiomyomas that may protrude through the cervical os. Histologically, the spindle cells may exhibit hypocellular, fascicular, or hyalinized patterns, all of which are associated with a sprinkling of lymphocytes and plasma cells (Fig. 4.329). The spindle cells have a bland nuclear morphology, the mitotic rate is low (typically ≤2 mitotic figures per 10 high power fields), and tumor necrosis is absent. ALK expression, coupled with the usually unimpressive staining for actin and desmin, helps to differentiate IMTs from leiomyomas and leiomyosarcomas. These benign lesions are adequately treated by complete excision.

Perivascular Epithelioid Cell Tumor ("PEComa")

This rare, controversial entity has the appearance of an epithelioid smooth muscle tumor with cytoplasm that may be clear or eosinophilic and granular, but is given special recognition by some because of the potential significance of its focal to diffuse HMB-45 positivity.[363,364] The genesis of the name PEComa stems from the belief that these tumors are part of the family of tumors derived from perivascular epithelioid cells that includes epithelioid angiomyolipoma, clear cell sugar tumor of the lung, and lymphangioleiomyomatosis, which in some instances are associated with the tuberous sclerosis complex.

PEComas can be well circumscribed and grossly resemble an epithelioid leiomyoma, or their margins may be more ill-defined. One growth pattern of the uterine PEComa features tongue-like infiltration similar to that seen in low-grade endometrial stromal sarcoma. Somewhat confusing for the uninitiated is the fact that the cells comprising these tumors in the uterus usually do not have a perivascular distribution. Although spindle cells may predominate in some extrauterine PEComas, epithelioid morphology with a nested or sheet-like

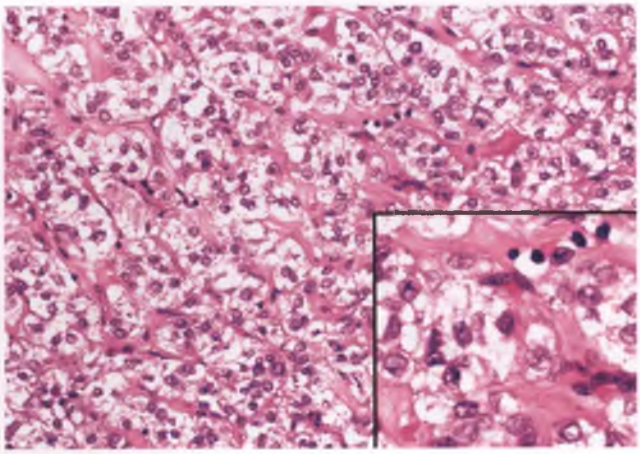

FIGURE 4.330. Perivascular epithelioid cell tumor. Nests of epithelioid cells with clear cytoplasm are partitioned by a delicate, branching capillary network that is incorporated into hyalinized stroma. The inset highlights the presence of partially sclerotic capillaries with residual hematopoietic elements.

architectural pattern is most typical of the uterine cases.[365] PEComas typically exhibit a prominent capillary network that is often incorporated into delicate, arborizing, hyalinized stroma in a pattern that suggests ongoing sclerosis of small vessels (Fig. 4.330). This contrasts with the hyaline matrix that is often present in epithelioid smooth muscle tumors, which is devoid of such residual vascular structures (Fig. 4.292).

In the limited reported experience with uterine PEComas, about 40% have behaved in a malignant fashion.[364] However, this is probably an underestimate, given the short average follow-up of only 2 years in the collective literature.[364] Since uterine tumors that qualify for PEComa status are extraordinarily rare, it is not surprising that well-established criteria for separating them into benign and malignant categories have yet to be formulated. One study suggested that PEComas with two or more of the following features should be classified as malignant: size >5 cm, infiltrative borders, high nuclear grade, mitotic rate ≥ 1 mitotic figure per 50 high power fields, tumor cell necrosis, and vascular invasion.[365] However, only 6 of the 26 tumors in that study were of uterine origin, and it is quite possible that site-specific differences exist when correlating tumor characteristics with malignant potential, as is the case with some other soft tissue tumors such as smooth muscle and gastrointestinal stromal tumors. In Fadare's review that was confined to uterine PEComas, it was noted that malignant tumors were often larger than their benign counterparts (mean size of 10 vs. 5 cm), and were much more likely to exhibit tumor necrosis and a mitotic rate of >1 mitotic figure per 10 high power fields.[364] The criteria that are emerging to assess the malignant potential of uterine PEComas closely resemble those that have evolved for uterine epithelioid smooth muscle tumors, which is further indicative of the close relationship and overlapping features of these two tumors.

Since its initial description, investigators skeptical of the existence of uterine PEComas have demonstrated at least focal HMB-45 staining in the clear cell component of uterine epithelioid leiomyosarcomas[366] and in 36% of conventional uterine leiomyosarcomas,[367] and lobbied against recognizing PEComa as a diagnostic entity. At the present time, it is recommended to perform HMB-45 staining on all uterine epithelioid smooth muscle tumors, and to diagnose PEComa in those tumors that exhibit both the morphology of PEComas as described above and HMB-45 positivity, with a note indicating the possible infrequent association of these tumors with tuberous sclerosis and/or lymphangioleiomyomatosis.

Pleomorphic Rhabdomyosarcoma

Uterine pleomorphic rhabdomyosarcoma is a rare, highly aggressive, heterologous sarcoma of middle-aged to elderly women.[368,369] These tumors tend to be bulky, fleshy, and partially necrotic. Histologically, skeletal muscle differentiation is evidenced by the presence of rhabdomyoblasts scattered amongst cells of variable shapes and sizes that exhibit a range of nuclear atypia. In rare instances, strap cells with cross-striations are evident (Fig. 4.331). Although desmin staining is expected, nuclear immunoreactivity with myogenin and/or myoD1 provides more specific evidence of skeletal muscle differentiation.[369] These tumors should be well sampled in order to exclude the possibility of a carcinosarcoma in which rhabdomyosarcoma is the dominant element.

Primitive Neuroectodermal Tumor

PNETs have been reported to involve the uterus on rare occasions, either in pure form or mixed with another type of malignancy.[230,231,370] The typical presentation is a postmenopausal woman with vaginal bleeding and an enlarged uterus due to a polypoid, endometrial-based mass. Rearrangement of Ewing's sarcoma gene is characteristic of Ewing's sarcoma and

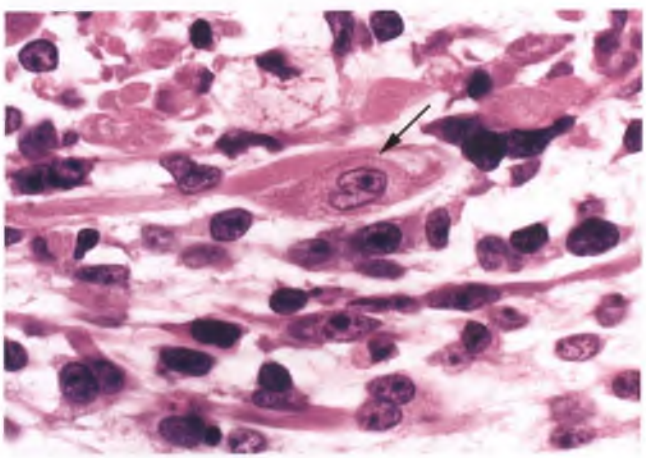

FIGURE 4.331. Pleomorphic rhabdomyosarcoma with strap cells, one of which exhibits visible cross-striations (*arrow*).

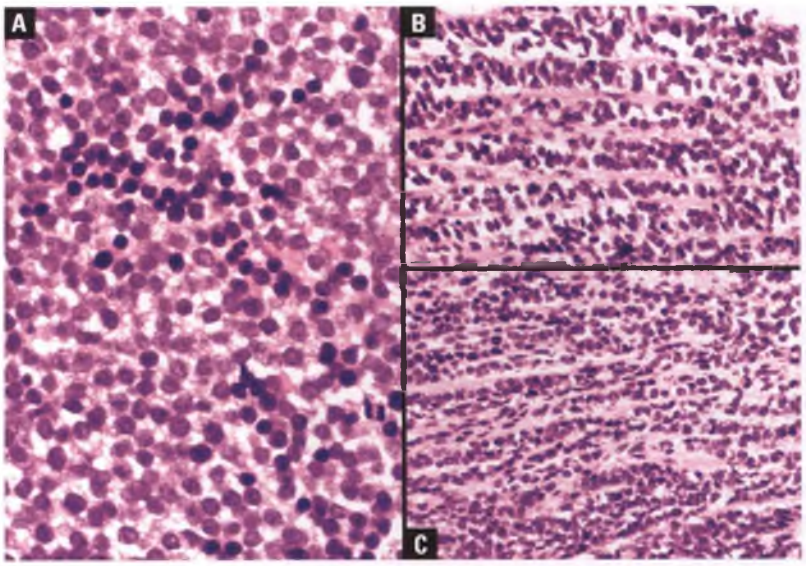

FIGURE 4.332. Primitive neuroectodermal tumor. **A**: Diffuse sheet of primitive malignant cells ("small round blue cell" pattern). **B**: Trabecular pattern. **C**: Cordlike pattern.

peripheral PNETs, whereas central-type PNETs (medulloblastoma and neuroblastoma) and most uterine PNETs lack this rearrangement.[231] Despite this genetic difference and multiple different sites of origin, peripheral and central PNETs have overlapping histologic and immunohistochemical features.

PNETs exhibit a cellular, primitive, "small round blue cell" component with a diffuse architecture, but may also grow in trabeculae and cords (Fig. 4.332). Evidence of neuroectodermal differentiation, most commonly a fibrillary matrix or rosettes/pseudorosettes (Fig. 4.333), is present at least focally in the vast majority of uterine cases. A subset of PNETs contains larger cells with more appreciable nuclear atypia and more abundant cytoplasm (Fig. 4.334). Most PNETs are cytokeratin negative, synaptophysin positive, neurofilament positive, and CD99 positive.[231] This immunophenotype, coupled with the foci of neuroectodermal differentiation, helps to distinguish uterine PNETs from small cell carcinoma and lymphoma. Uterine PNETs often present with advanced stage disease, which is a poor prognostic sign.

Note: PNET images are from extrauterine examples of this tumor.

OTHER MISCELLANEOUS PRIMARY TUMORS

Adenomatoid Tumor

Adenomatoid tumor is a benign tumor of mesothelial origin that typically presents as an incidental subserosal or intramural nodule that is solitary, solid, and <4 cm in diameter (mean 2.1 cm).[371,372] In contrast to ordinary leiomyoma, its sectioned surface is often tan, gray, or tinged with yellow (Fig. 4.335A). On rare occasions, adenomatoid tumors can be cystic and/or spongy.

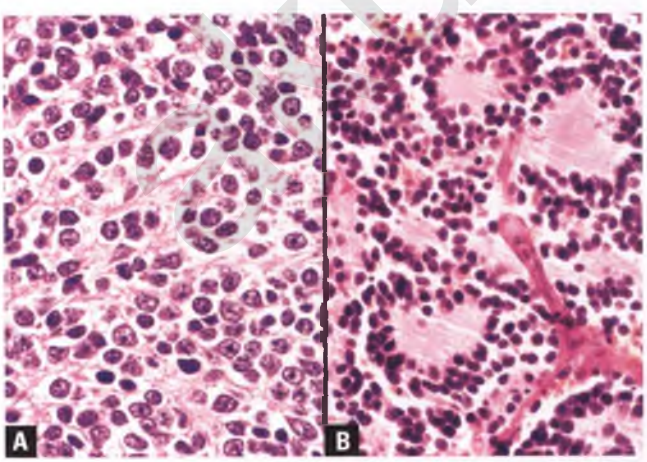

FIGURE 4.333. Primitive neuroectodermal tumor. **A**: PNET with a recognizable fibrillary matrix. **B**: Homer-Wright rosettes (cells radiate outward from a central, solid core of fibrillar material).

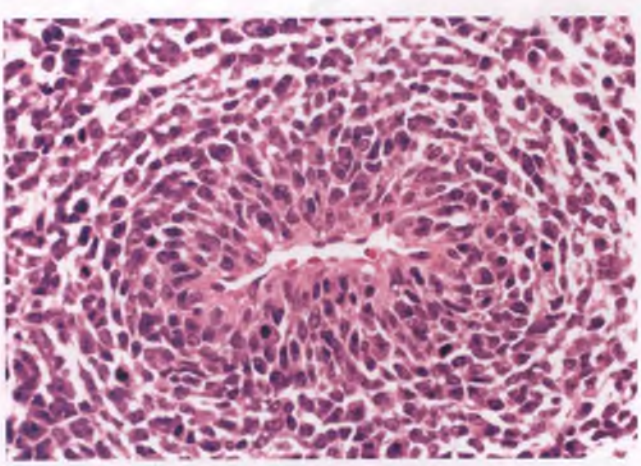

FIGURE 4.334. Primitive neuroectodermal tumor with nuclear atypia and more appreciable cytoplasm forming a perivascular pseudorosette (cells radiate outward from a centrally-located blood vessel).

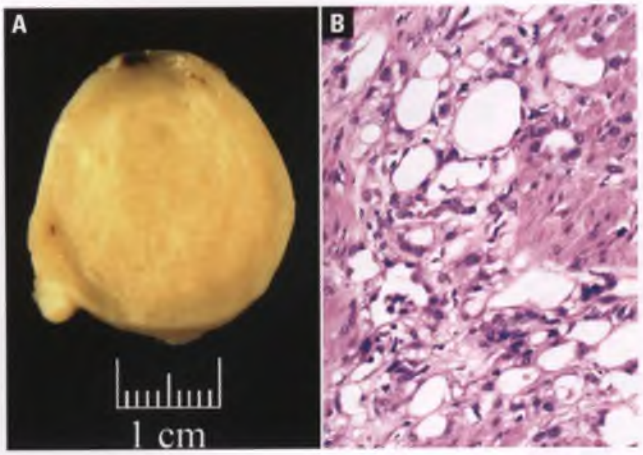

FIGURE 4.335. Adenomatoid tumor. **A**: The sectioned surface of this formalin-fixed nodular tumor is tannish yellow. **B**: Adenomatoid tumor in area with pseudoglandular and pseudovascular spaces lined by cuboidal and flattened mesothelial cells, respectively. The background stroma is myometrial smooth muscle.

Microscopically, adenomatoid tumors exhibit a variety of distinctive patterns, the most common of which are cuboidal cells lining anastomosing pseudoglandular spaces (the adenoid pattern) and flattened cells lining aggregates of pseudovascular spaces (the angiomatoid pattern)[372] (Fig. 4.335B). Less commonly, solid, cystic, and papillary patterns may be observed. An additional characteristic feature of adenomatoid tumors is the presence of "thread-like bridging strands" of attenuated tumor cell cytoplasm that traverse the pseudovascular spaces in angiomatoid areas (Fig. 4.336).[373] Mitotic figures are typically absent within adenomatoid tumors, and there is no significant nuclear atypia. The mesothelial elements are embedded within

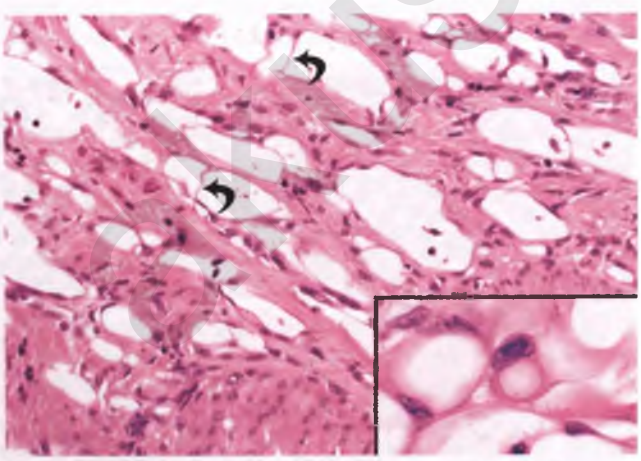

FIGURE 4.336. Adenomatoid tumor with angiomatoid pattern. Arrows mark representative thread-like bridging strands, which are a characteristic feature of adenomatoid tumors. The inset shows a vacuolated mesothelial cell from a different adenomatoid tumor that mimics a signet-ring cell from a metastatic adenocarcinoma.

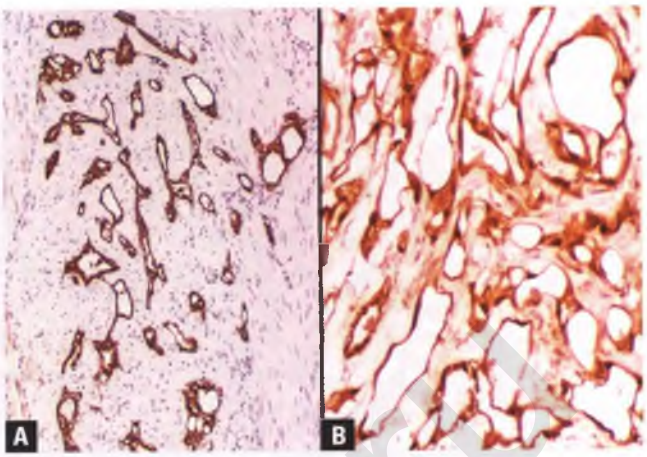

FIGURE 4.337. Adenomatoid tumor. The mesothelial elements are intensely positive for cytokeratin **(A)** and calretinin **(B)**.

myometrial smooth muscle of variable prominence, which is thought to be induced to become hyperplastic by the mesothelial proliferation.

The cytoplasm of the cuboidal mesothelial cells in adenomatoid tumors is often vacuolated, which may result in a resemblance to signet-ring cells from a metastatic adenocarcinoma (Fig. 4.336 inset). In contrast to the signet-ring cells derived from metastatic adenocarcinomas, the signet-ring cells in adenomatoid tumors do not contain mucins of the type that react with the PAS and mucicarmine stains, although they may contain acid mucins that show reactivity with the Alcian blue and colloidal iron stains.[372,374] One must not make the mistake of using cytokeratin immunostains as a potential differentiating feature when presented with this differential diagnosis, since adenocarcinomas and the mesothelial cells from adenomatoid tumors are both intensely positive for cytokeratin (Fig. 4.337A).[371] In addition to cytokeratin, the mesothelial elements within an adenomatoid tumor are positive for the mesothelial marker calretinin (Fig. 4.337B) and WT1.[371,375]

Uterine Tumor Resembling Ovarian Sex-Cord Tumor (UTROSCT)

UTROSCTs are rare neoplasms that were initially described by Clement and Scully in 1976.[376] Their "Group I" UTROSCTs exhibited prominent endometrial stromal differentiation and are currently classified as endometrial stromal nodules or endometrial stromal sarcomas with sex-cord–like elements, as discussed in the section on endometrial stromal tumors.[329,377] Tumors initially categorized as belonging to Group II consist predominantly or exclusively of sex-cord–like elements with no conspicuous endometrial stromal differentiation, and it is this group of tumors that continues to be classified as UTROSCTs.

The clinical and gross presentation of UTROSCTs does not differ significantly from that of endometrial stromal

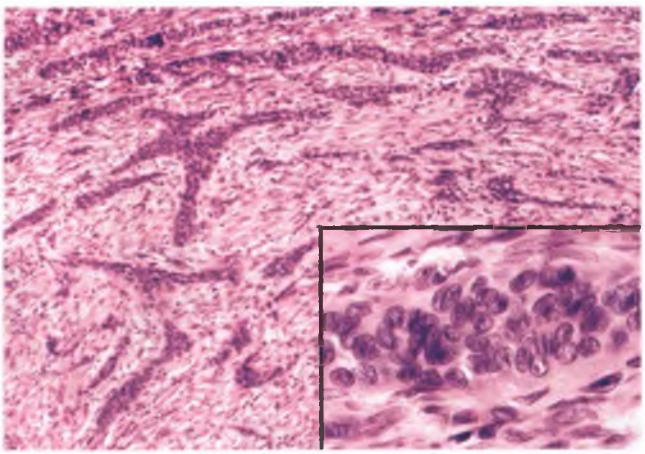

FIGURE 4.338. Uterine tumor resembling ovarian sex-cord tumor. Anastomosing cords and trabeculae of cells are set within a prominent myofibroblastic stroma. The inset highlights the nuclear features of the sex-cord–like elements, which in this case include occasional nuclear grooves that further heighten the resemblance of this tumor to a granulosa cell tumor.

nodules. Histologically, they represent a heterogeneous group of tumors whose sex-cord–like differentiation results in a resemblance to ovarian granulosa cell tumor and/or Sertoli cell tumor. The sex-cord–like patterns formed by the constituent cells of these tumors include interconnecting thin cords, anastomosing broad trabeculae, small nests, solid or hollow tubules, retiform patterns, glomeruloid structures, and solid areas of monotonous cells resembling the diffuse pattern of ovarian adult granulosa cell tumor (Figs. 4.338–4.341).[329,376,377] The nuclei typically are closely packed and overlapping with pale chromatin, small nucleoli, and only minor variations in their round to oval nuclear contour. Nuclear grooves may be seen in occasional cells, but are not nearly as conspicuous as in ovarian

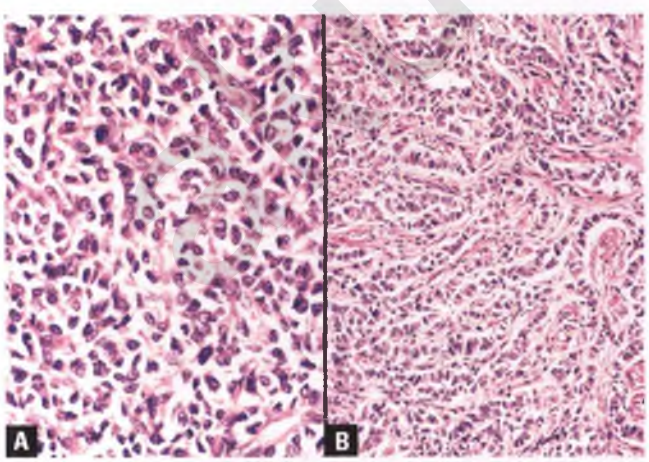

FIGURE 4.339. Uterine tumor resembling ovarian sex-cord tumor. This tumor has scant stroma, and exhibits solid **(A)** and trabecular/corded **(B)** architectural patterns simulating those that can be seen in granulosa cell tumors.

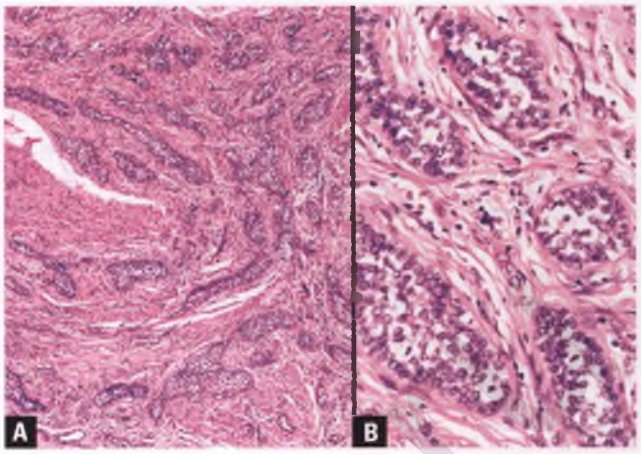

FIGURE 4.340. **A,B**: Uterine tumor resembling ovarian sex-cord tumor. This sertoliform tumor consists predominately of solid tubules embedded within an abundant stroma that contains considerable amounts of smooth muscle.

adult granulosa cell tumor (Fig. 4.338 inset). UTROSCTs also lack legitimate Call-Exner bodies, which further distinguishes them from true adult granulosa cell tumors. Mitotic figures are rare, and tumor necrosis is generally absent or inconspicuous. The cytoplasm is usually scant, but some epithelioid cells may contain abundant, lipid-rich, foamy cytoplasm (Fig. 4.341B). The stroma is usually fibrous and varies from scant to abundant, but occasionally there may be a prominent component of smooth muscle that has the appearance of incorporated myometrium (Fig. 4.340).

Immunohistochemically, the sex-cord–like elements of UTROSCTs have a diverse immunophenotype that usually includes staining for at least one marker of sex-cord differentiation, such as calretinin, inhibin, WT1, CD99 (O13, MIC2), or Melan A (A103).[377–380] Areas with sex-cord–like differentiation

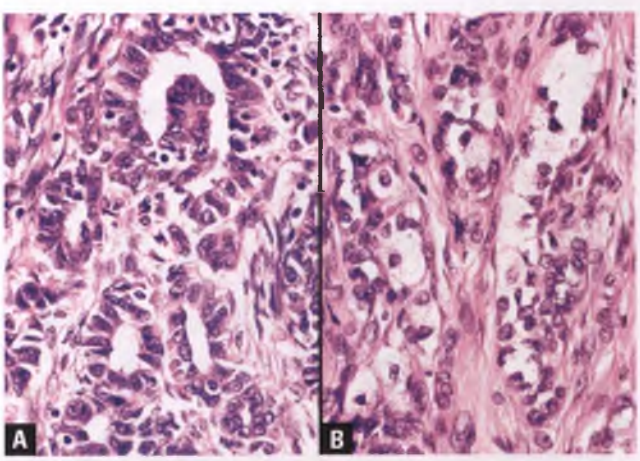

FIGURE 4.341. Uterine tumor resembling ovarian sex-cord tumor. **A**: Hollow sertoliform tubules associated with a glomeruloid structure. **B**: Aggregates of epithelioid cells with foamy, lipid-rich cytoplasm.

are also immunoreactive for estrogen and progesterone receptors and vimentin, and exhibit variable positivity for keratin, actin, desmin, and other smooth muscle markers.[378,380]

Given the histologic resemblance of UTROSCTs to endometrial stromal tumors with sex-cord–like elements, most investigators have presumed that UTROSCTs are related to endometrial stromal tumors. However, a recent study has demonstrated that UTROSCTs uniformly lack the specific translocation between chromosomes 7 and 17 (the JAZF1-JJAZ1 gene fusion) that is present in approximately 60% of endometrial stromal tumors, which suggests that UTROSCT is a separate and distinct entity (hence its placement in the "miscellaneous primary tumors" category).[381]

Differential Diagnosis

The differential diagnosis of UTROSCTs includes endometrial stromal tumors with sex-cord–like elements, epithelioid smooth muscle tumors, and metastatic carcinoma. Unlike endometrial stromal tumors with sex-cord–like elements, UTROSCTs have an absent or inconspicuous endometrial stromal component. Although epithelioid smooth muscle tumors may grow in nests and cords, they usually exhibit areas where they transition to more typical spindle cell tumors, they do not form tubules or contain cells with foamy cytoplasm, and they generally lack expression of sex-cord markers. Metastatic carcinoma, particularly of breast origin, enters the differential diagnosis when UTROSCTs exhibit prominent tubular or cord-like growth, which can simulate metastatic infiltrating ductal or lobular carcinoma, respectively.[379] In addition to correlation with clinical history and slide review of any previous malignancies, immunohistochemistry for sex-cord markers and the breast marker GCDFP-15 can facilitate correct interpretation (if the patient has a history of breast carcinoma, these studies should ideally be run in parallel on both the candidate UTROSCT and tissue from her previous cancer).

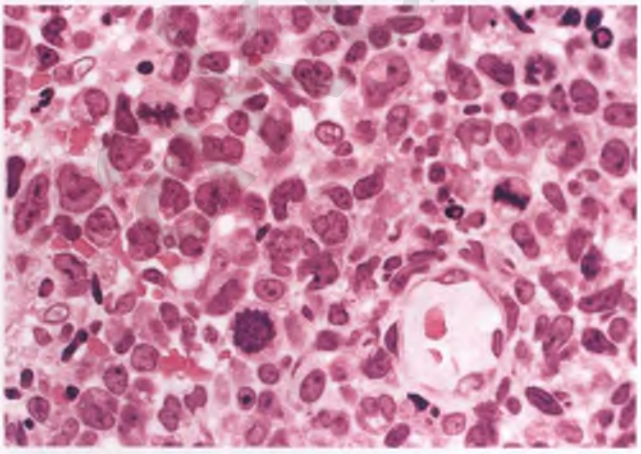

FIGURE 4.342. Malignant lymphoma, diffuse large B-cell type, involving the endometrium.

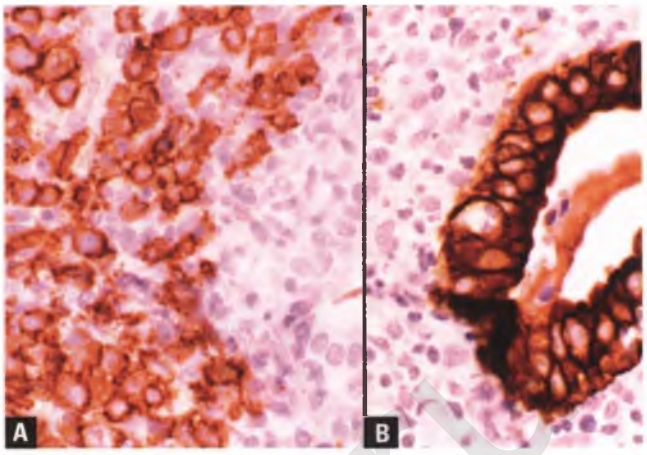

FIGURE 4.343. Malignant lymphoma, diffuse large B-cell type, involving the endometrium. **A**: The lymphoma cells express the B-cell marker CD-20, which does not stain the endometrial gland. **B**: The endometrial gland is positive for cytokeratin, but the lymphoma cells are negative.

Behavior

UTROSCTs are considered to be neoplasms of low malignant potential, although those that are small and well circumscribed can be regarded as benign.

Lymphoma

Rarely, the uterine corpus may be involved by lymphoma, either as a manifestation of primary extranodal lymphoma or secondary involvement due to disseminated disease.[382–385] The typical presentation of a primary uterine lymphoma is a postmenopausal woman with vaginal bleeding. Grossly, there may be a polypoid endometrial mass or diffuse thickening of the endometrium. The myometrium is usually spared.

Most primary uterine lymphomas are diffuse large B-cell lymphomas that infiltrate the endometrium with preservation of the endometrial glands (Figs. 4.342 and 4.343). Unlike their cervical counterparts, prominent sclerosis is not commonly seen in endometrial-based lymphomas. Cognizance of the fact that lymphomas can occur at this site can help avoid their misdiagnosis, with immunohistochemistry serving as a useful aid in distinguishing them from mimics such as poorly differentiated carcinoma, endometrial stromal sarcoma, melanoma, and PNET. Distinction of lymphoma from a reactive lymphoid infiltrate is discussed in the section on inflammatory and infectious lesions of the uterine cervix (Chapter 3).

THE UTERINE CORPUS AS SITE OF METASTATIC CARCINOMA

On rare occasions, carcinomas from extrauterine sites spread to the uterine corpus by direct extension, intratubal migration, or via angiolymphatic routes. Genital tract tumors with

such behavior are most commonly of ovarian origin, whereas breast, colon, gastric, and pancreatic carcinomas (in descending order of frequency) account for over 80% of extragenital carcinomas with this pattern of spread.[386,387] Although not as well documented as for tumors that have spread to the uterine cervix, there seems to be a disproportionate number of breast carcinomas of infiltrating lobular type and gastric carcinomas of signet-ring type that exhibit this behavior (involvement of the uterine cervix by metastatic carcinoma is considered in Chapter 3).

In most cases, involvement of the uterine corpus by an extrauterine carcinoma is a manifestation of widespread disease, and does not represent a diagnostic dilemma.[386] In the small number of cases in which a primary uterine carcinoma is a serious differential diagnostic consideration, the following features favor a metastatic origin: (a) a clinical history of an extrauterine tumor with similar histology, (b) a "bottom heavy" distribution of tumor that is concentrated in the myometrium, (c) a pattern of endometrial involvement in which there is sparing of geographic areas of endometrial stroma and/or entrapment of native endometrial glands (Figs. 4.344 and 4.345), (d) prominent angiolymphatic invasion, (e) lack of associated atypical endometrial hyperplasia in an endometrioid-like tumor or lack of EIC in a serous tumor, and (f) the presence of cord-like, colloidal, or signet-ring architectural patterns that would be unusual for primary endometrial carcinoma. With regard to the latter feature, a potential diagnostic pitfall that may be encountered within endometrial samples is the occasional presence of loose aggregates of decidual cells with signet-ring morphology in women who are either pregnant or who have been treated with high-dose progestational agents (see section on the endometrium and myometrium in pregnancy, abortion, and the postpartum period).

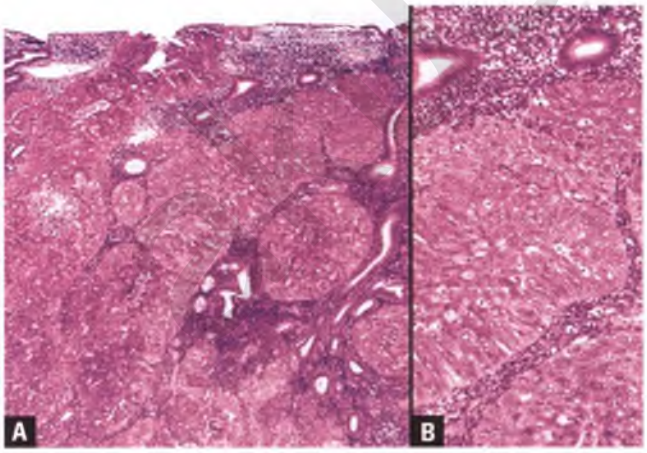

FIGURE 4.344. **A,B**: Serous carcinoma of the ovary metastatic to the endometrium. Sheets and nodules of high-grade serous carcinoma with characteristic slit-like glandular spaces partially replace the endometrium. This pattern of partial replacement of endometrial tissue favors a metastatic over a primary process. The myometrium and numerous angiolymphatic spaces were also infiltrated by this tumor.

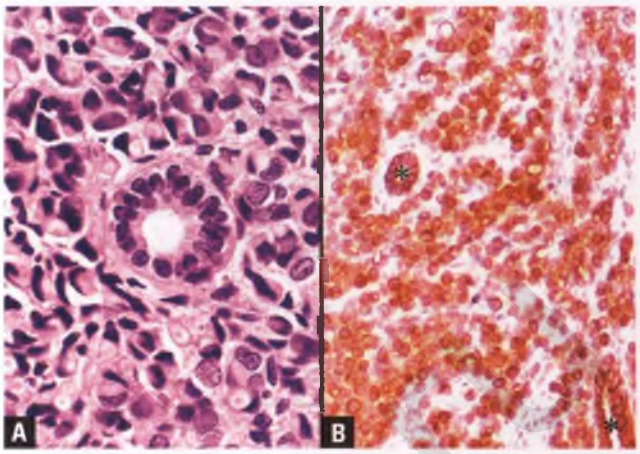

FIGURE 4.345. Breast carcinoma metastatic to the endometrium. **A**: A centrally-located native endometrial gland is surrounded by malignant cells, many of which have a signet-ring morphology. **B**: Both the residual endometrial glands (*asterisks* × 2) and the signet-ring cells are immunoreactive for cytokeratin, which excludes the possibility of signet-ring cell change within decidualized stromal cells. Metastatic gastric carcinoma can have a similar appearance and immunophenotype.

PROCESSING TIPS FOR ENDOMETRIAL SAMPLES

- Specify a standard amount (such as 3 cc) to signify that a cassette is full of curettings. This will allow quick recognition of any discordance with the amount of tissue present on the slide due to tissue wash-off or superficial sampling by the histotechnologist.
- Describe color and proportion of tissue in relation to amount of admixed hemorrhagic and/or mucoid material.
- If any of the tissue fragments are polypoid, include this finding in the gross description as a prompt to be on guard for the presence of polyp(s), which can be difficult to recognize microscopically when fragmented and randomly oriented. If no explanation for the polypoid tissue is found with the initial sections, the polyp may be deeper in the paraffin block and recuts are indicated.
- If any of the tissue fragments are yellow and suspected to be adipose tissue, this finding should be noted in the gross description and the clinician should be alerted to the possibility of a uterine perforation. Upon microscopic confirmation of the presence of fat, the clinician should be notified that the histologic findings are best explained by the presence of a uterine perforation. Documentation of this notification and the presence of adipose tissue should be included in the pathology report.
- For biopsies and diagnostic curettages, submit all tissue. For recommendations regarding processing of "products of conception," see the section on the endometrium in abortions.

- Submit all tissue between sponges or in fine mesh sacs to (a) prevent loss of tissue and (b) prevent minute tissue fragments from migrating out of the cassette and becoming extraneous tissue ("floaters" or "cutting board carcinomas") in other cases.
- Clean and rinse forceps and strainer carefully between cases to avoid contamination. Use of smooth rather than serrated forceps reduces the risk of transfer of small amounts of tissue between cases.
- Sample gross description: Received as "endometrial curettings" are multiple fragments of tan tissue admixed with a small amount of hemorrhagic and mucoid material with aggregate volume of 3 cc. A few of the fragments are polypoid. Submitted entirely in A.
- In most laboratories, endometrial samples have traditionally been examined utilizing sections taken from three different levels of the paraffin block. However, two sections cut at different levels have been found to be sufficient for diagnosis in the vast majority of cases.[388] This is not surprising, since endometrial pathology is not often a submillimeter microscopic finding. In cases with large amounts of tissue that require 3 or more cassettes, one section per block is probably adequate for the initial evaluation. Regardless of the number of initial sections, recuts are indicated when there is a discordance with the gross description or clinical impression.
- Using a microscope with a 2× objective helps to ensure that all tissue fragments are viewed at scanning magnification.

PROCESSING TIPS FOR HYSTERECTOMY SPECIMENS

Since detailed discussions of how to describe and process hysterectomy specimens can be found in several other pathology texts, I will focus only on selected issues.

- *Orientation:* Anatomic landmarks that are used to distinguish the anterior from posterior aspects of resected uteri are discussed at the beginning of this chapter.
- *Uterine weight:* The weight of the uterus is a basic piece of information that should be included in every report. The pathologist should also be aware that uterine weight impacts the gynecologist in terms of procedure coding and reimbursement for vaginal hysterectomies and myomectomies; reimbursement is significantly higher for these procedures when the specimen weighs >250 g. The gynecologist often realizes that this information is missing several weeks after the pathology report has been issued, and will not be pleased if the weight cannot be determined because the specimen has been discarded.
- *Adequate Fixation Time:* At least 3 hours to overnight. Properly sectioned and fixed uteri that have been received by early afternoon can be processed in the late afternoon without compromising section quality.
- *Routine Sections:* For hysterectomies with no gross abnormalities, recommended sections include anterior cervix, posterior cervix, one full-thickness section from the posterior fundic region that includes endometrium, myometrium, and serosa, and one cassette with 2 to 3 sections of fundic endometrium that are contiguous with the inner third of the myometrium.
- *Endometrial Polyps:* Submit in their entirety or in up to 10 cassettes, whichever comes first (recall the occasional occurrence of atypical hyperplasia or carcinoma within endometrial polyps, and the propensity of EIC to occur focally within endometrial polyps of elderly patients).
- *Multiple Grossly Typical Leiomyomas:* Submit one section of the largest tumor and one other cassette of randomly selected smaller tumors.
- *Serosal Adhesions:* Adhesions, particularly when hemorrhagic and located on the posterior uterine serosa, should be generously sampled to document their presence and to search for foci of endometriosis.
- *Grossly Apparent Myoinvasive Endometrial Carcinoma:* Submit 3 sections, including the area of deepest invasion. Recommendations regarding optimal submission of tissue sections when evaluating uteri with myoinvasive endometrial carcinoma are given in the section on myometrial invasion.
- *Atypical Endometrial Hyperplasia/Endometrial Carcinoma with No Grossly Obvious Myoinvasion:* Extensive sampling is needed in this situation to exclude the possibility of subtle myometrial invasion. Submit one full-thickness section of abnormal endometrium with associated myometrium, and then submit the remainder of the endometrium with inner myometrium as 2 to 3 sections per cassette (label the anterior and posterior halves separately).

SUGGESTED READINGS

Clement PB, Young RH. *Atlas of Gynecologic Surgical Pathology*. 2nd ed. Philadelphia, PA: Elsevier Saunders; 2008.

Crum CP, Nucci MR, Lee K (eds). *Diagnostic Gynecologic and Obstetric Pathology*. 2nd ed. Philadelphia, PA: Elsevier Saunders; 2011.

Hendrickson MR, Kempson RL. Surgical Pathology of the Uterine Corpus. In: Bennington JL (ed). *Major Problems in Pathology*. Vol. 12. Philadelphia, PA: WB Saunders, 1980.

Kurman RJ, Ellenson LH, Ronnett BM, eds. *Blaustein's Pathology of the Female Genital Tract*. 6th ed. New York, NY: Springer; 2011.

Longacre, TA, Atkins, KA, Kempson, RL, et al. The uterine corpus (Chapter 53). In: Mills SE, ed. *Sternberg's Diagnostic Surgical Pathology*. 5th ed. Philadelphia, PA: Lippincott Williams & Wilkins; 2009.

Mazur MT, Kurman RJ. *Diagnosis of Endometrial Biopsies and Curettings*. 2nd ed. New York, NY: Springer; 2005.

Mills SE, ed. *Histology for Pathologists*. 3rd ed. Philadelphia, PA: Lippincott Williams & Wilkins; 2006.

Robboy, SJ, Mutter GL, Prat J, et al., eds. *Robboy's Pathology of the Female Reproductive Tract*. 2nd ed. Oxford, UK: Churchill Livingstone; 2009.

Silverberg SG, Kurman RJ. *Tumors of the Uterine Corpus and Gestational Trophoblastic Disease. Atlas of Tumor Pathology*. Third series, Fascicle 3. Washington, DC: Armed Forces Institute of Pathology; 1992:1–218.

Tavassoli FA, Devilee P, eds. *World Health Organization Classification of Tumors. Pathology and Genetics of Tumours of the Breast and Female Genital Organs*. Lyon, France: IARC Press; 2003:217–257.

Zaino RJ. *Interpretation of Endometrial Biopsies and Curettings*. Philadelphia, PA: Lippincott-Raven; 1996.

REFERENCES

1. The American Fertility Society. The American Fertility Society classifications of adnexal adhesions, distal tubal occlusion, tubal occlusion secondary to tubal ligation, tubal pregnancies, mullerian anomalies and intrauterine adhesions. *Fertil Steril.* 1988;49:944–955.
2. Toaff R. A major genital malformation—communicating uteri. *Obstet Gynecol.* 1974;43:221–231.
3. Noyes RW, Hertig AT, Rock J. Dating the endometrial biopsy. *Fertil Steril.* 1950;1:3–25.
4. Murray MJ, Meyer WR, Zaino RJ, et al. A critical analysis of the accuracy, reproducibility, and clinical utility of histologic endometrial dating in fertile women. *Fertil Steril.* 2004;81:1333–1343.
5. Zaino RJ. *Interpretation of Endometrial Biopsies and Curettings.* Philadelphia, PA: Lippincott-Raven; 1996:53–99.
6. Banks ER, Mills SE, Frierson HF Jr. Uterine intravascular menstrual endometrium simulating malignancy. *Am J Surg Pathol.* 1991;15:407–412.
7. Meyer WC, Malkasian GD, Dockerty MB, et al. Postmenopausal bleeding from atrophic endometrium. *Obstet Gynecol.* 1971;38:731–738.
8. Choo YC, Mak KC, Hsu C, et al. Postmenopausal uterine bleeding of nonorganic cause. *Obstet Gynecol.* 1985;66:225–228.
9. Silverberg SG. The endometrium. Pathologic principles and pitfalls. *Arch Pathol Lab Med.* 2007;131:372–382.
10. Sadler TW. *Langman's Medical Embryology.* 10th ed. Philadelphia, PA: Lippincott Williams & Wilkins; 2006.
11. Hertig AT. Gestational hyperplasia of endometrium. A morphologic correlation of ova, endometrium, and corpora lutea during early pregnancy. *Lab Invest.* 1964;13:1153–1191.
12. Mazur MT, Hendrickson MR, Kempson RL. Optically clear nuclei. An alteration of endometrial epithelium in the presence of trophoblast. *Am J Surg Pathol.* 1983;7:415–423.
13. Bulmer JN, Longfellow M, Ritson A. Leukocytes and resident blood cells in endometrium. *Ann N Y Acad Sci.* 1991;622:57–68.
14. Iezzoni JC, Mills SE. Nonneoplastic endometrial signet-ring cells. Vacuolated decidual cells and stromal histiocytes mimicking adenocarcinoma. *Am J Clin Pathol.* 2001;115:249–255.
15. Clement PB, Young RH, Scully RE. Nontrophoblastic pathology of the female genital tract and peritoneum associated with pregnancy. *Semin Diagn Pathol.* 1989;6:372–406.
16. Arias-Stella J. Atypical endometrial change associated with the presence of chorionic tissue. *Arch Pathol Lab Med.* 1954;58:112–128.
17. Arias-Stella J. Atypical endometrial changes produced by chorionic tissue. *Hum Pathol.* 1972;3:450–453.
18. Arias-Stella J. The Arias-Stella reaction: facts and fancies four decades after. *Adv Anat Pathol.* 2002;9:12–23.
19. Huettner PC, Gersell DJ. Arias-Stella reaction in nonpregnant women: a clinicopathologic study of nine cases. *Int J Gynecol Pathol.* 1994;13:241–247.
20. Arias-Stella J Jr, Arias-Velasquez A, Arias-Stella J. Normal and abnormal mitoses in the atypical endometrial change associated with chorionic tissue effect. *Am J Surg Pathol.* 1994;18:694–701.
21. Vang R, Barner R, Wheeler DT, et al. Immunohistochemical staining for Ki-67 and p53 helps distinguish endometrial Arias-Stella reaction from high-grade carcinoma, including clear cell carcinoma. *Int J Gynecol Pathol.* 2004;23:223–233.
22. Shih IM, Seidman JD, Kurman RJ. Placental site nodule and characterization of distinctive types of intermediate trophoblast. *Hum Pathol.* 1999;30:687–694.
23. Kurman RJ. The morphology, biology, and pathology of intermediate trophoblast: a look back to the present. *Hum Pathol.* 1991;22:847–855.
24. Meekins JW, Luckas MJ, Pijnenborg R, et al. Histological study of decidual spiral arteries and the presence of maternal erythrocytes in the intervillous space during the first trimester of normal human pregnancy. *Placenta.* 1997;18:459–464.
25. O'Connor DM, Kurman RJ. Intermediate trophoblast in uterine curettings in the diagnosis of ectopic pregnancy. *Obstet Gynecol.* 1988;72:665–670.
26. Wan SK, Lam PW, Pau MY, et al. Multiclefted nuclei. A helpful feature for identification of intermediate trophoblastic cells in uterine curetting specimens. *Am J Surg Pathol.* 1992;16:1226–1232.
27. Young RH, Kurman RJ, Scully RE. Proliferations and tumors of intermediate trophoblast of the placental site. *Semin Diagn Pathol.* 1988;5:223–237.
28. Shih IM, Kurman RJ. Ki-67 labeling index in the differential diagnosis of exaggerated placental site, placental site trophoblastic tumor, and choriocarcinoma: a double immunohistochemical staining technique using Ki-67 and Mel-CAM antibodies. *Hum Pathol.* 1998;29:27–33.
29. Daya D, Sabet L. The use of cytokeratin as a sensitive and reliable marker for trophoblastic tissue. *Am J Clin Pathol.* 1991;95:137–141.
30. Mazur MT, Kurman RJ. *Diagnosis of Endometrial Biopsies and Curettings.* 2nd ed. New York: Springer; 2005.
31. Gruber K, Gelven PL, Austin RM. Chorionic villi or trophoblastic tissue in uterine samples of four women with ectopic pregnancies. *Int J Gynecol Pathol.* 1997;16:28–32.
32. Reece EA, Petrie RH, Sirmans MF, et al. Combined intrauterine and extrauterine gestations: a review. *Am J Obstet Gynecol.* 1983;146:323–330.
33. Weydert JA, Benda JA. Subinvolution of the placental site as an anatomic cause of postpartum uterine bleeding: a review. *Arch Pathol Lab Med.* 2006;130:1538–1542.
34. Young RH, Kurman RJ, Scully RE. Placental site nodules and plaques. A clinicopathologic analysis of 20 cases. *Am J Surg Pathol.* 1990;14:1001–1009.
35. Huettner PC, Gersell DJ. Placental site nodule: a clinicopathologic study of 38 cases. *Int J Gynecol Pathol.* 1994;13:191–198.
36. Shih IM, Kurman RJ. p63 expression is useful in the distinction of epithelioid trophoblastic and placental site trophoblastic tumors by profiling trophoblastic subpopulations. *Am J Surg Pathol.* 2004;28:1177–1183.
37. Zaino RJ. *Interpretation of Endometrial Biopsies and Curettings.* Philadelphia, PA: Lippincott-Raven; 1996:120–142.
38. Hendrickson MR, Kempson RL. Surgical pathology of the uterine corpus. In: Bennington JL, ed. *Major Problems in Pathology.* Vol 12. Philadelphia, PA: W.B. Saunders; 1980.
39. Longacre TA, Atkins KA, Kempson RL, et al. The uterine corpus (Chapter 53). In: Mills SE, ed. *Sternberg's Diagnostic Surgical Pathology.* 5th ed. Philadelphia, PA: Lippincott Williams & Wilkins, 2009.
40. Fadare O, Zheng W. Histologic dating of the endometrium: accuracy, reproducibility, and practical value. *Adv Anat Pathol.* 2005;12:39–46.
41. Deligdisch L. Hormonal pathology of the endometrium. *Mod Pathol.* 2000;13:285–294.
42. Feeley KM, Wells M. Hormone replacement therapy and the endometrium. *J Clin Pathol.* 2001;54:435–440.
43. Swerdlow AJ, Jones ME; British Tamoxifen Second Cancer Study G. Tamoxifen treatment for breast cancer and risk of endometrial cancer: a case-control study. *J Natl Cancer Inst.* 2005;97:375–384.
44. Cohen I. Endometrial pathologies associated with postmenopausal tamoxifen treatment. *Gynecol Oncol.* 2004;94:256–266.
45. Clement PB, Oliva E, Young RH. Mullerian adenosarcoma of the uterine corpus associated with tamoxifen therapy: a report of six cases and a review of tamoxifen-associated endometrial lesions. *Int J Gynecol Pathol.* 1996;15:222–229.
46. Mutter GL, Bergeron C, Deligdisch L, et al. The spectrum of endometrial pathology induced by progesterone receptor modulators. *Mod Pathol.* 2008;21:591–598.
47. Benda JA. Clomiphene's effect on endometrium in infertility. *Int J Gynecol Pathol.* 1992;11:273–282.
48. Eckert LO, Hawes SE, Wolner-Hanssen PK, et al. Endometritis: the clinical-pathologic syndrome. *Am J Obstet Gynecol.* 2002;186:690–695.
49. Adegboyega PA, Pei Y, McLarty J. Relationship between eosinophils and chronic endometritis. *Hum Pathol.* 2010;41:33–37.
50. Smith M, Hagerty KA, Skipper B, et al. Chronic endometritis: a combined histopathologic and clinical review of cases from 2002 to 2007. *Int J Gynecol Pathol.* 2010:29:44–50.
51. Gilmore H, Fleischhacker D, Hecht JL. Diagnosis of chronic endometritis in biopsies with stromal breakdown. *Hum Pathol.* 2007;38:581–584.
52. Euscher E, Nuovo GJ. Detection of kappa- and lambda-expressing cells in the endometrium by in situ hybridization. *Int J Gynecol Pathol.* 2002;21:383–390.
53. Crum CP, Hornstein MD, Nucci MR, et al. Hertig and beyond: a systematic and practical approach to the endometrial biopsy. *Adv Anat Pathol.* 2003;10:301–318.
54. Bazaz-Malik G, Maheshwari B, Lal N. Tuberculous endometritis: a clinicopathological study of 1000 cases. *Br J Obstet Gynaecol.* 1983;90:84–86.
55. Almoujahed MO, Briski LE, Prysak M, et al. Uterine granulomas: clinical and pathologic features. *Am J Clin Pathol.* 2002;117:771–775.
56. Ladefoged C, Lorentzen M. Xanthogranulomatous inflammation of the female genital tract. *Histopathology.* 1988;13:541–551.
57. Russack V, Lammers RJ. Xanthogranulomatous endometritis. Report of six cases and a proposed mechanism of development. *Arch Pathol Lab Med.* 1990;114:929–932.
58. Kim KR, Lee YH, Ro JY. Nodular histiocytic hyperplasia of the endometrium. *Int J Gynecol Pathol.* 2002;21:141–146.
59. Hattab EM, Allam-Nandyala P, Rhatigan RM. The stromal component of large endometrial polyps. *Int J Gynecol Pathol.* 1999;18:332–337.

60. Kim KR, Peng R, Ro JY, et al. A diagnostically useful histopathologic feature of endometrial polyp: the long axis of endometrial glands arranged parallel to surface epithelium. *Am J Surg Pathol.* 2004;28:1057–1062.
61. Tai LH, Tavassoli FA. Endometrial polyps with atypical (bizarre) stromal cells. *Am J Surg Pathol.* 2002;26:505–509.
62. Mittal K, Da Costa D. Endometrial hyperplasia and carcinoma in endometrial polyps: clinicopathologic and follow-up findings. *Int J Gynecol Pathol.* 2008;27:45–48.
63. Sahin AA, Silva EG, Landon G, et al. Endometrial tissue in myometrial vessels not associated with menstruation. *Int J Gynecol Pathol.* 1989;8:139–146.
64. Meenakshi M, McCluggage WG. Vascular involvement in adenomyosis: report of a large series of a common phenomenon with observations on the pathogenesis of adenomyosis. *Int J Gynecol Pathol.* 2010;29:117–121.
65. Clement PB, Scully RE. Endometrial stromal sarcomas of the uterus with extensive endometrioid glandular differentiation: a report of three cases that caused problems in differential diagnosis. *Int J Gynecol Pathol.* 1992;11: 163–173.
66. McCluggage WG, Ganesan R, Herrington CS. Endometrial stromal sarcomas with extensive endometrioid glandular differentiation: report of a series with emphasis on the potential for misdiagnosis and discussion of the differential diagnosis. *Histopathology.* 2009;54:365–373.
67. Goldblum JR, Clement PB, Hart WR. Adenomyosis with sparse glands. A potential mimic of low-grade endometrial stromal sarcoma. *Am J Clin Pathol.* 1995;103:218–223.
68. Gilks CB, Clement PB, Hart WR, et al. Uterine adenomyomas excluding atypical polypoid adenomyomas and adenomyomas of endocervical type: a clinicopathologic study of 30 cases of an underemphasized lesion that may cause diagnostic problems with brief consideration of adenomyomas of other female genital tract sites. *Int J Gynecol Pathol.* 2000;19:195–205.
69. Tahlan A, Nanda A, Mohan H. Uterine adenomyoma: a clinicopathologic review of 26 cases and a review of the literature. *Int J Gynecol Pathol.* 2006;25:361–365.
70. Goldrath MH, Fuller TA, Segal S. Laser photovaporization of endometrium for the treatment of menorrhagia. *Am J Obstet Gynecol.* 1981;140:14–19.
71. Munro MG. Abnormal uterine bleeding: surgical management—part III. *J Am Assoc Gynecol Laparosc.* 2001;8:20–44.
72. Davis JR, Maynard KK, Brainard CP, et al. Effects of thermal endometrial ablation. Clinicopathologic correlations. *Am J Clin Pathol.* 1998;109: 96–100.
73. Silvernagel SW, Harshbarger KE, Shevlin DW. Postoperative granulomas of the endometrium: histological features after endometrial ablation. *Ann Diagn Pathol.* 1997;1:82–90.
74. Colgan TJ, Shah R, Leyland N. Post-hysteroscopic ablation reaction: a histopathologic study of the effects of electrosurgical ablation. *Int J Gynecol Pathol.* 1999;18:325–331.
75. Tatum ET, Beattie JF Jr, Bryson K. Postoperative carbon pigment granuloma: a report of eight cases involving the ovary. *Hum Pathol.* 1996;27:1008–1011.
76. Clarke TJ, Simpson RH. Necrotizing granulomas of peritoneum following diathermy ablation of endometriosis. *Histopathology.* 1990;16:400–402.
77. Reid PC, Thurrell W, Smith JH, et al. Nd:YAG laser endometrial ablation: histological aspects of uterine healing. *Int J Gynecol Pathol.* 1992;11:174–179.
78. Ferryman SR, Stephens M, Gough D. Necrotising granulomatous endometritis following endometrial ablation therapy. *Br J Obstet Gynaecol.* 1992;99:928–930.
79. Kelly P, McCluggage WG. Idiopathic uterine granulomas: report of a series with morphological similarities to idiopathic ovarian cortical granulomas. *Int J Gynecol Pathol.* 2006;25:243–246.
80. Clement PB. Postoperative spindle-cell nodule of the endometrium. *Arch Pathol Lab Med.* 1988;112:566–568.
81. Kawai K, Fukuda K, Tsuchiyama H. Malacoplakia of the endometrium. An unusual case studied by electron microscopy and a review of the literature. *Acta Pathol Jpn.* 1988;38:531–540.
82. Lainas T, Zorzovilis I, Petsas G, et al. Osseous metaplasia: case report and review. *Fertil Steril.* 2004;82:1433–1435.
83. Onderoglu LS, Yarali H, Gultekin M, et al. Endometrial osseous metaplasia: an evolving cause of secondary infertility. *Fertil Steril.* 2008;90:2013. e9–2013.e11.
84. Alpert LC, Haufrect EJ, Schwartz MR. Uterine lithiasis. *Am J Surg Pathol.* 1990;14:1071–1075.
85. Atri M, de Stempel J, Senterman MK, et al. Diffuse peripheral uterine calcification (manifestation of Monckeberg's arteriosclerosis) detected by ultrasonography. *J Clin Ultrasound.* 1992;20:211–216.
86. Deshmukh-Rane SA, Wu ML. Pseudolipomatosis affects specimens from endometrial biopsies. *Am J Clin Pathol.* 2009;132:374–377.
87. Unger ZM, Gonzalez JL, Hanissian PD, et al. Pseudolipomatosis in hysteroscopically resected tissues from the gynecologic tract: pathologic description and frequency. *Am J Surg Pathol.* 2009;33:1187–1190.
88. Cammarota G, Cesaro P, Cazzato A, et al. Hydrogen peroxide-related colitis (previously known as "pseudolipomatosis"): a series of cases occurring in an epidemic pattern. *Endoscopy.* 2007;39:916–919.
89. Val-Bernal JF, Villoria F, Cagigal ML, et al. Pneumopolycystic endometritis. *Am J Surg Pathol.* 2006;30:258–261.
90. Logani S, Herdman AV, Little JV, et al. Vascular "pseudo invasion" in laparoscopic hysterectomy specimens: a diagnostic pitfall. *Am J Surg Pathol.* 2008;32:560–565.
91. Kitahara S, Walsh C, Frumovitz M, et al. Vascular pseudoinvasion in laparoscopic hysterectomy specimens for endometrial carcinoma: a grossing artifact? *Am J Surg Pathol.* 2009;33:298–303.
92. Krizova A, Clarke BA, Bernardini MQ, et al. Histologic artifacts in abdominal, vaginal, laparoscopic, and robotic hysterectomy specimens: a blinded, retrospective review. *Am J Surg Pathol.* 2011;35:115–126.
93. Hendrickson MR, Kempson RL. Endometrial epithelial metaplasias: proliferations frequently misdiagnosed as adenocarcinoma. Report of 89 cases and proposed classification. *Am J Surg Pathol.* 1980;4:525–542.
94. Zaman SS, Mazur MT. Endometrial papillary syncytial change. A nonspecific alteration associated with active breakdown. *Am J Clin Pathol.* 1993;99:741–745.
95. Silverberg SG, Kurman RJ. Tumors of the Uterine Corpus and Gestational Trophoblastic Disease. Atlas of Tumor Pathology, Third series, Fascicle 3. Washington, DC: Armed Forces Institute of Pathology, 1992:200–204.
96. Shah SS, Mazur MT. Endometrial eosinophilic syncytial change related to breakdown: immunohistochemical evidence suggests a regressive process. *Int J Gynecol Pathol.* 2008;27:534–538.
97. Jacques SM, Qureshi F, Lawrence WD. Surface epithelial changes in endometrial adenocarcinoma: diagnostic pitfalls in curettage specimens. *Int J Gynecol Pathol.* 1995;14:191–197.
98. Wells M, Tiltman A. Intestinal metaplasia of the endometrium. *Histopathology.* 1989;15:431–433.
99. Nucci MR, Prasad CJ, Crum CP, et al. Mucinous endometrial epithelial proliferations: a morphologic spectrum of changes with diverse clinical significance. *Mod Pathol.* 1999;12:1137–1142.
100. Vang R, Tavassoli FA. Proliferative mucinous lesions of the endometrium: analysis of existing criteria for diagnosing carcinoma in biopsies and curettings. *Int J Surg Pathol.* 2003;11:261–270.
101. Wheeler DT, Bristow RE, Kurman RJ. Histologic alterations in endometrial hyperplasia and well-differentiated carcinoma treated with progestins. *Am J Surg Pathol.* 2007;31:988–998.
102. Scully RE, Bonfiglio TA, Kurman RJ, et al. Uterine corpus. In: *World Health Organization: HIstological Typing of Female Genital Tract Tumors.* New York: Springer-Verlag; 1994:13–31.
103. Kurman RJ, Kaminski PF, Norris HJ. The behavior of endometrial hyperplasia. A long-term study of "untreated" hyperplasia in 170 patients. *Cancer.* 1985;56:403–412.
104. Hecht JL, Ince TA, Baak JP, et al. Prediction of endometrial carcinoma by subjective endometrial intraepithelial neoplasia diagnosis. *Mod Pathol.* 2005;18:324–330.
105. Lacey JV Jr, Mutter GL, Nucci MR, et al. Risk of subsequent endometrial carcinoma associated with endometrial intraepithelial neoplasia classification of endometrial biopsies. *Cancer.* 2008;113:2073–2081.
106. Longacre TA, Chung MH, Jensen DN, et al. Proposed criteria for the diagnosis of well-differentiated endometrial carcinoma. A diagnostic test for myoinvasion. *Am J Surg Pathol.* 1995;19:371–406.
107. McKenney JK, Longacre TA. Low-grade endometrial adenocarcinoma: a diagnostic algorithm for distinguishing atypical endometrial hyperplasia and other benign (and malignant) mimics. *Adv Anat Pathol.* 2009;16:1–22.
108. Mazur MT. Endometrial hyperplasia/adenocarcinoma. a conventional approach. *Ann Diagn Pathol.* 2005;9:174–181.
109. Kendall BS, Ronnett BM, Isacson C, et al. Reproducibility of the diagnosis of endometrial hyperplasia, atypical hyperplasia, and well-differentiated carcinoma. *Am J Surg Pathol.* 1998;22:1012–1019.
110. Zaino RJ, Kauderer J, Trimble CL, et al. Reproducibility of the diagnosis of atypical endometrial hyperplasia: a Gynecologic Oncology Group study. *Cancer.* 2006;106:804–811.
111. Bergeron C, Nogales FF, Masseroli M, et al. A multicentric European study testing the reproducibility of the WHO classification of endometrial hyperplasia with a proposal of a simplified working classification for biopsy and curettage specimens. *Am J Surg Pathol.* 1999;23:1102–1108.
112. Soslow RA. Problems with the current diagnostic approach to complex atypical endometrial hyperplasia. *Cancer.* 2006;106:729–731.

113. Allison KH, Reed SD, Voigt LF, et al. Diagnosing endometrial hyperplasia: why is it so difficult to agree? *Am J Surg Pathol.* 2008;32:691–698.
114. Sherman ME, Ronnett BM, Ioffe OB, et al. Reproducibility of biopsy diagnoses of endometrial hyperplasia: evidence supporting a simplified classification. *Int J Gynecol Pathol.* 2008;27:318–325.
115. Mutter GL, Zaino RJ, Baak JP, et al. Benign endometrial hyperplasia sequence and endometrial intraepithelial neoplasia. *Int J Gynecol Pathol.* 2007;26: 103–114.
116. Silverberg SG. Problems in the differential diagnosis of endometrial hyperplasia and carcinoma. *Mod Pathol.* 2000;13:309–327.
117. Baak JP, Mutter GL, Robboy S, et al. The molecular genetics and morphometry-based endometrial intraepithelial neoplasia classification system predicts disease progression in endometrial hyperplasia more accurately than the 1994 World Health Organization classification system. *Cancer.* 2005;103:2304–2312.
118. Silver SA, Sherman ME. Morphologic and immunophenotypic characterization of foam cells in endometrial lesions. *Int J Gynecol Pathol.* 1998;17:140–145.
119. Lacey JV Jr, Sherman ME, Rush BB, et al. Absolute risk of endometrial carcinoma during 20-year follow-up among women with endometrial hyperplasia. *J Clin Oncol.* 2010;28:788–792.
120. Shutter J, Wright TC Jr. Prevalence of underlying adenocarcinoma in women with atypical endometrial hyperplasia. *Int J Gynecol Pathol.* 2005;24: 313–318.
121. Trimble CL, Kauderer J, Zaino R, et al. Concurrent endometrial carcinoma in women with a biopsy diagnosis of atypical endometrial hyperplasia: a Gynecologic Oncology Group study. *Cancer.* 2006;106:812–819.
122. Hendrickson MR, Kempson RL. Ciliated carcinoma—a variant of endometrial adenocarcinoma: a report of 10 cases. *Int J Gynecol Pathol.* 1983;2:1–12.
123. Lehman MB, Hart WR. Simple and complex hyperplastic papillary proliferations of the endometrium: a clinicopathologic study of nine cases of apparently localized papillary lesions with fibrovascular stromal cores and epithelial metaplasia. *Am J Surg Pathol.* 2001;25:1347–1354.
124. Silverberg SG, Kurman RJ. Tumors of the Uterine Corpus and Gestational Trophoblastic Disease. Atlas of Tumor Pathology, Third series, Fascicle 3. Washington, DC: Armed Forces Institute of Pathology, 1992:204–205.
125. American Cancer Society. *Cancer Facts & Figures 2010.* Atlanta, GA: American Cancer Society; 2010.
126. Hendrickson M, Ross J, Eifel PJ, et al. Adenocarcinoma of the endometrium: analysis of 256 cases with carcinoma limited to the uterine corpus. Pathology review and analysis of prognostic variables. *Gynecol Oncol.* 1982;13:373–392.
127. Bokhman JV. Two pathogenetic types of endometrial carcinoma. *Gynecol Oncol.* 1983;15:10–17.
128. Prat J. Prognostic parameters of endometrial carcinoma. *Hum Pathol.* 2004;35:649–662.
129. Nofech-Mozes S, Ghorab Z, Ismiil N, et al. Endometrial endometrioid adenocarcinoma: a pathologic analysis of 827 consecutive cases. *Am J Clin Pathol.* 2008;129:110–114.
130. Gwin K, Wilcox R, Montag A. Insights into selected genetic diseases affecting the female reproductive tract and their implication for pathologic evaluation of gynecologic specimens. *Arch Pathol Lab Med.* 2009;133:1041–1052.
131. Karamurzin Y, Rutgers JK. DNA mismatch repair deficiency in endometrial carcinoma. *Int J Gynecol Pathol.* 2009;28:239–255.
132. Kurman RJ, Norris HJ. Evaluation of criteria for distinguishing atypical endometrial hyperplasia from well-differentiated carcinoma. *Cancer.* 1982;49:2547–2559.
133. Hendrickson MR, Ross JC, Kempson RL. Toward the development of morphologic criteria for well-differentiated adenocarcinoma of the endometrium. *Am J Surg Pathol.* 1983;7:819–838.
134. Clement PB, Young RH. Endometrioid carcinoma of the uterine corpus: a review of its pathology with emphasis on recent advances and problematic aspects. *Adv Anat Pathol.* 2002;9:145–184.
135. Creasman WT. New gynecologic cancer staging. *Obstet Gynecol.* 1990;75: 287–288.
136. Zaino RJ, Kurman R, Herbold D, et al. The significance of squamous differentiation in endometrial carcinoma. Data from a Gynecologic Oncology Group study. *Cancer.* 1991;68:2293–2302.
137. Zaino RJ, Kurman RJ, Diana KL, et al. The utility of the revised International Federation of Gynecology and Obstetrics histologic grading of endometrial adenocarcinoma using a defined nuclear grading system. A Gynecologic Oncology Group study. *Cancer.* 1995;75:81–86.
138. Darvishian F, Hummer AJ, Thaler HT, et al. Serous endometrial cancers that mimic endometrioid adenocarcinomas: a clinicopathologic and immunohistochemical study of a group of problematic cases. *Am J Surg Pathol.* 2004;28:1568–1578.
139. Altrabulsi B, Malpica A, Deavers MT, et al. Undifferentiated carcinoma of the endometrium. *Am J Surg Pathol.* 2005;29:1316–1321.
140. Silva EG, Deavers MT, Malpica A. Undifferentiated carcinoma of the endometrium: a review. *Pathology (Phila).* 2007;39:134–138.
141. Silva EG, Deavers MT, Bodurka DC, et al. Association of low-grade endometrioid carcinoma of the uterus and ovary with undifferentiated carcinoma: a new type of dedifferentiated carcinoma? *Int J Gynecol Pathol.* 2006;25:52–58.
142. Scholten AN, Smit VT, Beerman H, et al. Prognostic significance and interobserver variability of histologic grading systems for endometrial carcinoma. *Cancer.* 2004;100:764–772.
143. Jones HW, 3rd. The importance of grading in endometrial cancer. *Gynecol Oncol.* 1999;74:1–2.
144. Zaino RJ, Kurman RJ, Diana KL, et al. Pathologic models to predict outcome for women with endometrial adenocarcinoma: the importance of the distinction between surgical stage and clinical stage—a Gynecologic Oncology Group study. *Cancer.* 1996;77:1115–1121.
145. Petersen RW, Quinlivan JA, Casper GR, et al. Endometrial adenocarcinoma—presenting pathology is a poor guide to surgical management. *Aust N Z J Obstet Gynaecol.* 2000;40:191–194.
146. Larson DM, Johnson KK, Broste SK, et al. Comparison of D&C and office endometrial biopsy in predicting final histopathologic grade in endometrial cancer. *Obstet Gynecol.* 1995;86:38–42.
147. Zaino RJ. FIGO staging of endometrial adenocarcinoma: a critical review and proposal. *Int J Gynecol Pathol.* 2009;28:1–9.
148. Alkushi A, Abdul-Rahman ZH, Lim P, et al. Description of a novel system for grading of endometrial carcinoma and comparison with existing grading systems. *Am J Surg Pathol.* 2005;29:295–304.
149. Creasman WT, Morrow CP, Bundy BN, et al. Surgical pathologic spread patterns of endometrial cancer. A Gynecologic Oncology Group study. *Cancer.* 1987;60:2035–2041.
150. Morrow CP, Bundy BN, Kurman RJ, et al. Relationship between surgical-pathological risk factors and outcome in clinical stage I and II carcinoma of the endometrium: a Gynecologic Oncology Group study. *Gynecol Oncol.* 1991;40:55–65.
151. FIGO Committee on Gynecologic Oncology. Revised FIGO staging for carcinoma of the vulva, cervix, and endometrium. *Int J Gynecol Obstet.* 2009;105:103–104.
152. Lax SF, Kurman RJ, Pizer ES, et al. A binary architectural grading system for uterine endometrial endometrioid carcinoma has superior reproducibility compared with FIGO grading and identifies subsets of advance-stage tumors with favorable and unfavorable prognosis. *Am J Surg Pathol.* 2000;24:1201–1208.
153. Taylor RR, Zeller J, Lieberman RW, et al. An analysis of two versus three grades for endometrial carcinoma. *Gynecol Oncol.* 1999;74:3–6.
154. Noumoff JS, Menzin A, Mikuta J, et al. The ability to evaluate prognostic variables on frozen section in hysterectomies performed for endometrial carcinoma. *Gynecol Oncol.* 1991;42:202–208.
155. Quinlivan JA, Petersen RW, Nicklin JL. Accuracy of frozen section for the operative management of endometrial cancer. *Br J Obstet Gynaecol.* 2001;108:798–803.
156. Zaino RJ, Kurman RJ. Squamous differentiation in carcinoma of the endometrium: a critical appraisal of adenoacanthoma and adenosquamous carcinoma. *Semin Diagn Pathol.* 1988;5:154–171.
157. Abeler VM, Kjorstad KE. Endometrial adenocarcinoma with squamous cell differentiation. *Cancer.* 1992;69:488–495.
158. Zaino RJ, Kurman RJ, Brunetto VL, et al. Villoglandular adenocarcinoma of the endometrium: a clinicopathologic study of 61 cases: a gynecologic oncology group study [see comment]. *Am J Surg Pathol.* 1998;22:1379–1385.
159. Ambros RA, Ballouk F, Malfetano JH, et al. Significance of papillary (villoglandular) differentiation in endometrioid carcinoma of the uterus. *Am J Surg Pathol.* 1994;18:569–575.
160. Hendrickson M, Ross J, Eifel P, et al. Uterine papillary serous carcinoma: a highly malignant form of endometrial adenocarcinoma. *Am J Surg Pathol.* 1982;6:93–108.
161. Murray SK, Young RH, Scully RE. Uterine endometrioid carcinoma with small nonvillous papillae: an analysis of 26 cases of a favorable-prognosis tumor to be distinguished from serous carcinoma. *Int J Surg Pathol.* 2000;8:279–289.
162. Christopherson WM, Alberhasky RC, Connelly PJ. Carcinoma of the endometrium: I. A clinicopathologic study of clear-cell carcinoma and secretory carcinoma. *Cancer.* 1982;49:1511–1523.

163. Tobon H, Watkins GJ. Secretory adenocarcinoma of the endometrium. *Int J Gynecol Pathol.* 1985;4:328–335.
164. Kurman RJ, Scully RE. Clear cell carcinoma of the endometrium: an analysis of 21 cases. *Cancer.* 1976;37:872–882.
165. Young RH, Scully RE. Uterine carcinomas simulating microglandular hyperplasia. A report of six cases. *Am J Surg Pathol.* 1992;16:1092–1097.
166. Zaloudek C, Hayashi GM, Ryan IP, et al. Microglandular adenocarcinoma of the endometrium: a form of mucinous adenocarcinoma that may be confused with microglandular hyperplasia of the cervix. *Int J Gynecol Pathol.* 1997;16:52–59.
167. Murray SK, Clement PB, Young RH. Endometrioid carcinomas of the uterine corpus with sex cord-like formations, hyalinization, and other unusual morphologic features: a report of 31 cases of a neoplasm that may be confused with carcinosarcoma and other uterine neoplasms. *Am J Surg Pathol.* 2005;29:157–166.
168. Tornos C, Silva EG, Ordonez NG, et al. Endometrioid carcinoma of the ovary with a prominent spindle-cell component, a source of diagnostic confusion. A report of 14 cases. *Am J Surg Pathol.* 1995;19:1343–1353.
169. Parkash V, Carcangiu ML. Endometrioid endometrial adenocarcinoma with psammoma bodies. *Am J Surg Pathol.* 1997;21:399–406.
170. Pitman MB, Young RH, Clement PB, et al. Endometrioid carcinoma of the ovary and endometrium, oxyphilic cell type: a report of nine cases. *Int J Gynecol Pathol.* 1994;13:290–301.
171. Silver SA, Cheung AN, Tavassoli FA. Oncocytic metaplasia and carcinoma of the endometrium: an immunohistochemical and ultrastructural study. *Int J Gynecol Pathol.* 1999;18:12–19.
172. Silva EG, Young RH. Endometrioid neoplasms with clear cells: a report of 21 cases in which the alteration is not of typical secretory type. *Am J Surg Pathol.* 2007;31:1203–1208.
173. Eichhorn JH, Young RH, Clement PB. Sertoliform endometrial adenocarcinoma: a study of four cases. *Int J Gynecol Pathol.* 1996;15:119–126.
174. Ali A, Black D, Soslow RA. Difficulties in assessing the depth of myometrial invasion in endometrial carcinoma. *Int J Gynecol Pathol.* 2007;26:115–123.
175. Creasman W. Revised FIGO staging for carcinoma of the endometrium. *Int J Gynecol Obstet.* 2009;105:109.
176. Longacre TA, Hendrickson MR. Diffusely infiltrative endometrial adenocarcinoma: an adenoma malignum pattern of myoinvasion. *Am J Surg Pathol.* 1999;23:69–78.
177. Murray SK, Young RH, Scully RE. Unusual epithelial and stromal changes in myoinvasive endometrioid adenocarcinoma: a study of their frequency, associated diagnostic problems, and prognostic significance. *Int J Gynecol Pathol.* 2003;22:324–333.
178. Nofech-Mozes S, Ackerman I, Ghorab Z, et al. Lymphovascular invasion is a significant predictor for distant recurrence in patients with early-stage endometrial endometrioid adenocarcinoma. *Am J Clin Pathol.* 2008;129:912–917.
179. McKenney JK, Kong CS, Longacre TA. Endometrial adenocarcinoma associated with subtle lymph-vascular space invasion and lymph node metastasis: a histologic pattern mimicking intravascular and sinusoidal histiocytes. *Int J Gynecol Pathol.* 2005;24:73–78.
180. Jacques SM, Qureshi F, Munkarah A, et al. Interinstitutional surgical pathology review in gynecologic oncology: II. Endometrial cancer in hysterectomy specimens. *Int J Gynecol Pathol.* 1998;17:42–45.
181. Hall JB, Young RH, Nelson JH Jr. The prognostic significance of adenomyosis in endometrial carcinoma. *Gynecol Oncol.* 1984;17:32–40.
182. Jacques SM, Lawrence WD. Endometrial adenocarcinoma with variable-level myometrial involvement limited to adenomyosis: a clinicopathologic study of 23 cases. *Gynecol Oncol.* 1990;37:401–407.
183. Hanley KZ, Dustin SM, Stoler MH, et al. The significance of tumor involved adenomyosis in otherwise low-stage endometrioid adenocarcinoma. *Int J Gynecol Pathol.* 2010;29:445–451.
184. Koshiyama M, Suzuki A, Ozawa M, et al. Adenocarcinomas arising from uterine adenomyosis: a report of four cases. *Int J Gynecol Pathol.* 2002;21:239–245.
185. Chu PG, Arber DA, Weiss LM, et al. Utility of CD10 in distinguishing between endometrial stromal sarcoma and uterine smooth muscle tumors: an immunohistochemical comparison of 34 cases. *Mod Pathol.* 2001;14:465–471.
186. McCluggage WG, Sumathi VP, Maxwell P. CD10 is a sensitive and diagnostically useful immunohistochemical marker of normal endometrial stroma and of endometrial stromal neoplasms. *Histopathology.* 2001;39:273–278.
187. Srodon M, Klein WM, Kurman RJ. CD10 imunostaining does not distinguish endometrial carcinoma invading myometrium from carcinoma involving adenomyosis. *Am J Surg Pathol.* 2003;27:786–789.
188. Hendrickson MR, Longacre TA, Kempson RL. Uterine papillary serous carcinoma revisited. *Gynecol Oncol.* 1994;54:261–263.
189. Clement PB, Young RH. Non-endometrioid carcinomas of the uterine corpus: a review of their pathology with emphasis on recent advances and problematic aspects. *Adv Anat Pathol.* 2004;11:117–142.
190. Kuebler DL, Nikrui N, Bell DA. Cytologic features of endometrial papillary serous carcinoma. *Acta Cytol.* 1989;33:120–126.
191. Sherman ME, Bitterman P, Rosenshein NB, et al. Uterine serous carcinoma. A morphologically diverse neoplasm with unifying clinicopathologic features. *Am J Surg Pathol.* 1992;16:600–610.
192. O'Neill CJ, McCluggage WG. p16 expression in the female genital tract and its value in diagnosis. *Adv Anat Pathol.* 2006;13:8–15.
193. Yemelyanova A, Ji H, Shih IM, et al. Utility of p16 expression for distinction of uterine serous carcinomas from endometrial endometrioid and endocervical adenocarcinomas. Immunohistochemical analysis of 201 cases. *Am J Surg Pathol.* 2009;33:1504–1514.
194. Sherman ME, Bur ME, Kurman RJ. p53 in endometrial cancer and its putative precursors: evidence for diverse pathways of tumorigenesis. *Hum Pathol.* 1995;26:1268–1274.
195. Zheng W, Yi X, Fadare O, et al. The oncofetal protein IMP3: a novel biomarker for endometrial serous carcinoma. *Am J Surg Pathol.* 2008;32:304–315.
196. Mhawech-Fauceglia P, Herrmann FR, Rai H, et al. IMP3 distinguishes uterine serous carcinoma from endometrial endometrioid adenocarcinoma. *Am J Clin Pathol.* 2010;133:899–908.
197. Wheeler DT, Bell KA, Kurman RJ, et al. Minimal uterine serous carcinoma: diagnosis and clinicopathologic correlation. *Am J Surg Pathol.* 2000;24 :797–806.
198. Carcangiu ML, Chambers JT. Uterine papillary serous carcinoma: a study on 108 cases with emphasis on the prognostic significance of associated endometrioid carcinoma, absence of invasion, and concomitant ovarian carcinoma. *Gynecol Oncol.* 1992;47:298–305.
199. Trahan S, Tetu B, Raymond PE. Serous papillary carcinoma of the endometrium arising from endometrial polyps: a clinical, histological, and immunohistochemical study of 13 cases. *Hum Pathol.* 2005;36:1316–1321.
200. Silva EG, Jenkins R. Serous carcinoma in endometrial polyps. *Mod Pathol.* 1990;3:120–128.
201. Hui P, Kelly M, O'Malley DM, et al. Minimal uterine serous carcinoma: a clinicopathological study of 40 cases. *Mod Pathol.* 2005;18:75–82.
202. Ambros RA, Sherman ME, Zahn CM, et al. Endometrial intraepithelial carcinoma: a distinctive lesion specifically associated with tumors displaying serous differentiation. *Hum Pathol.* 1995;26:1260–1267.
203. Rabban JT, Zaloudek CJ. Minimal uterine serous carcinoma: current concepts in diagnosis and prognosis. *Pathology (Phila).* 2007;39:125–133.
204. Soslow RA, Pirog E, Isacson C. Endometrial intraepithelial carcinoma with associated peritoneal carcinomatosis. *Am J Surg Pathol.* 2000;24:726–732.
205. Zheng W, Schwartz PE. Serous EIC as an early form of uterine papillary serous carcinoma: recent progress in understanding its pathogenesis and current opinions regarding pathologic and clinical management. *Gynecol Oncol.* 2005;96:579–582.
206. Zheng W, Khurana R, Farahmand S, et al. p53 immunostaining as a significant adjunct diagnostic method for uterine surface carcinoma: precursor of uterine papillary serous carcinoma. *Am J Surg Pathol.* 1998;22:1463–1473.
207. Carcangiu ML, Tan LK, Chambers JT. Stage IA uterine serous carcinoma: a study of 13 cases. *Am J Surg Pathol.* 1997;21:1507–1514.
208. Zheng W, Liang SX, Yi X, et al. Occurrence of endometrial glandular dysplasia precedes uterine papillary serous carcinoma. *Int J Gynecol Pathol.* 2007;26:38–52.
209. Zheng W, Xiang L, Fadare O, et al. A proposed model for endometrial serous carcinogenesis. *Am J Surg Pathol.* 2011;35:e1–e14.
210. Jarboe EA, Pizer ES, Miron A, et al. Evidence for a latent precursor (p53 signature) that may precede serous endometrial intraepithelial carcinoma. *Mod Pathol.* 2009;22:345–350.
211. Goff BA, Kato D, Schmidt RA, et al. Uterine papillary serous carcinoma: patterns of metastatic spread. *Gynecol Oncol.* 1994;54:264–268.
212. Rabban JT, Barnes M, Chen LM, et al. Ovarian pathology in risk-reducing salpingo-oophorectomies from women with BRCA mutations, emphasizing the differential diagnosis of occult primary and metastatic carcinoma. *Am J Surg Pathol.* 2009;33:1125–1136.
213. Snyder MJ, Bentley R, Robboy SJ. Transtubal spread of serous adenocarcinoma of the endometrium: an underrecognized mechanism of metastasis. *Int J Gynecol Pathol.* 2006;25:155–160.
214. Baergen RN, Warren CD, Isacson C, et al. Early uterine serous carcinoma: clonal origin of extrauterine disease. *Int J Gynecol Pathol.* 2001;20:214–219.

215. Euscher ED, Malpica A, Deavers MT, et al. Differential expression of WT-1 in serous carcinomas in the peritoneum with or without associated serous carcinoma in endometrial polyps. *Am J Surg Pathol.* 2005;29:1074–1078.
216. Jarboe EA, Miron A, Carlson JW, et al. Coexisting intraepithelial serous carcinomas of the endometrium and fallopian tube: frequency and potential significance. *Int J Gynecol Pathol.* 2009;28:308–315.
217. Lax SF, Pizer ES, Ronnett BM, et al. Clear cell carcinoma of the endometrium is characterized by a distinctive profile of p53, Ki-67, estrogen, and progesterone receptor expression. *Hum Pathol.* 1998;29:551–558.
218. Malpica A, Tornos C, Burke TW, et al. Low-stage clear-cell carcinoma of the endometrium. *Am J Surg Pathol.* 1995;19:769–774.
219. Fadare O, Liang SX, Ulukus EC, et al. Precursors of endometrial clear cell carcinoma. *Am J Surg Pathol.* 2006;30:1519–1530.
220. Carcangiu ML, Chambers JT. Early pathologic stage clear cell carcinoma and uterine papillary serous carcinoma of the endometrium: comparison of clinicopathologic features and survival. *Int J Gynecol Pathol.* 1995;14:30–38.
221. Abeler VM, Kjorstad KE. Clear cell carcinoma of the endometrium: a histopathological and clinical study of 97 cases. *Gynecol Oncol.* 1991;40:207–217.
222. Ross JC, Eifel PJ, Cox RS, et al. Primary mucinous adenocarcinoma of the endometrium. A clinicopathologic and histochemical study. *Am J Surg Pathol.* 1983;7:715–729.
223. Kamoi S, AlJuboury MI, Akin MR, et al. Immunohistochemical staining in the distinction between primary endometrial and endocervical adenocarcinomas: another viewpoint. *Int J Gynecol Pathol.* 2002;21:217–223.
224. Qiu W, Mittal K. Comparison of morphologic and immunohistochemical features of cervical microglandular hyperplasia with low-grade mucinous adenocarcinoma of the endometrium. *Int J Gynecol Pathol.* 2003;22:261–265.
225. Chekmareva M, Ellenson LH, Pirog EC. Immunohistochemical differences between mucinous and microglandular adenocarcinomas of the endometrium and benign endocervical epithelium. *Int J Gynecol Pathol.* 2008;27:547–554.
226. Barroeta JE, Pasha TL, Acs G, et al. Immunoprofile of endocervical and endometrial stromal cells and its potential application in localization of tumor involvement. *Int J Gynecol Pathol.* 2007;26:76–82.
227. Mittal K. Distinguishing mucinous adenocarcinoma of the endometrium from benign endocervical epithelium [Letter to Editor]. *Int J Gynecol Pathol.* 2009;28:479.
228. Huntsman DG, Clement PB, Gilks CB, et al. Small-cell carcinoma of the endometrium. A clinicopathological study of sixteen cases. *Am J Surg Pathol.* 1994;18:364–375.
229. van Hoeven KH, Hudock JA, Woodruff JM, et al. Small cell neuroendocrine carcinoma of the endometrium. *Int J Gynecol Pathol.* 1995;14:21–29.
230. Daya D, Lukka H, Clement PB. Primitive neuroectodermal tumors of the uterus: a report of four cases. *Hum Pathol.* 1992;23:1120–1129.
231. Euscher ED, Deavers MT, Lopez-Terrada D, et al. Uterine tumors with neuroectodermal differentiation: a series of 17 cases and review of the literature. *Am J Surg Pathol.* 2008;32:219–228.
232. Taraif SH, Deavers MT, Malpica A, et al. The significance of neuroendocrine expression in undifferentiated carcinoma of the endometrium. *Int J Gynecol Pathol.* 2009;28:142–147.
233. Rizeq MN, van de Rijn M, Hendrickson MR, et al. A comparative immunohistochemical study of uterine smooth muscle neoplasms with emphasis on the epithelioid variant. *Hum Pathol.* 1994;25:671–677.
234. McCluggage WG. Uterine carcinosarcomas (malignant mixed Mullerian tumors) are metaplastic carcinomas. *Int J Gynecol Cancer.* 2002;12:687–690.
235. de Brito PA, Silverberg SG, Orenstein JM. Carcinosarcoma (malignant mixed mullerian (mesodermal) tumor) of the female genital tract: immunohistochemical and ultrastructural analysis of 28 cases. *Hum Pathol.* 1993;24:132–142.
236. Bitterman P, Chun B, Kurman RJ. The significance of epithelial differentiation in mixed mesodermal tumors of the uterus. A clinicopathologic and immunohistochemical study. *Am J Surg Pathol.* 1990;14:317–328.
237. Jin Z, Ogata S, Tamura G, et al. Carcinosarcomas (malignant mullerian mixed tumors) of the uterus and ovary: a genetic study with special reference to histogenesis. *Int J Gynecol Pathol.* 2003;22:368–373.
238. Silverberg SG, Major FJ, Blessing JA, et al. Carcinosarcoma (malignant mixed mesodermal tumor) of the uterus. A Gynecologic Oncology Group pathologic study of 203 cases. *Int J Gynecol Pathol.* 1990;9:1–19.
239. George E, Manivel JC, Dehner LP, et al. Malignant mixed mullerian tumors: an immunohistochemical study of 47 cases, with histogenetic considerations and clinical correlation. *Hum Pathol.* 1991;22:215–223.
240. Nogales FF, Gomez-Morales M, Raymundo C, et al. Benign heterologous tissue components associated with endometrial carcinoma. *Int J Gynecol Pathol.* 1982;1:286–291.
241. George E, Lillemoe TJ, Twiggs LB, et al. Malignant mixed mullerian tumor versus high-grade endometrial carcinoma and aggressive variants of endometrial carcinoma: a comparative analysis of survival. *Int J Gynecol Pathol.* 1995;14:39–44.
242. Ferguson SE, Tornos C, Hummer A, et al. Prognostic features of surgical stage I uterine carcinosarcoma. *Am J Surg Pathol.* 2007;31:1653–1661.
243. Amant F, Cadron I, Fuso L, et al. Endometrial carcinosarcomas have a different prognosis and pattern of spread compared to high-risk epithelial endometrial cancer. *Gynecol Oncol.* 2005;98:274–280.
244. Sreenan JJ, Hart WR. Carcinosarcomas of the female genital tract. A pathologic study of 29 metastatic tumors: further evidence for the dominant role of the epithelial component and the conversion theory of histogenesis. *Am J Surg Pathol.* 1995;19:666–674.
245. Goodman A, Zukerberg LR, Rice LW, et al. Squamous cell carcinoma of the endometrium: a report of eight cases and a review of the literature. *Gynecol Oncol.* 1996;61:54–60.
246. Ahluwalia M, Light AM, Surampudi K, et al. Transitional cell carcinoma of the endometrium: a case report and review of the literature. *Int J Gynecol Pathol.* 2006;25:378–382.
247. Jones MA, Young RH, Scully RE. Endometrial adenocarcinoma with a component of giant cell carcinoma. *Int J Gynecol Pathol.* 1991;10:260–270.
248. Mulligan AM, Plotkin A, Rouzbahman M, et al. Endometrial giant cell carcinoma: a case series and review of the spectrum of endometrial neoplasms containing giant cells. *Am J Surg Pathol.* 2010;34:1132–1138.
249. Mhawech P, Dellas A, Terracciano LM. Glassy cell carcinoma of the endometrium: a case report and review of the literature. *Arch Pathol Lab Med.* 2001;125:816–819.
250. Vargas MP, Merino MJ. Lymphoepitheliomalike carcinoma: an unusual variant of endometrial cancer. A report of two cases. *Int J Gynecol Pathol.* 1998;17:272–276.
251. Toyoda H, Hirai T, Ishii E. Alpha-fetoprotein producing uterine corpus carcinoma: a hepatoid adenocarcinoma of the endometrium. *Pathol Int.* 2000;50:847–852.
252. Mooney EE, Robboy SJ, Hammond CB, et al. Signet-ring cell carcinoma of the endometrium: a primary tumor masquerading as a metastasis. *Int J Gynecol Pathol.* 1997;16:169–172.
253. Boyd C, Cameron I, McCluggage WG. Endometrial adenocarcinoma with signet ring cells: report of two cases of an extremely rare phenomenon. *Int J Gynecol Pathol.* 2010;29:579–582.
254. Bradley CS, Benjamin I, Wheeler JE, et al. Endometrial adenocarcinoma with trophoblastic differentiation. *Gynecol Oncol.* 1998;69:74–77.
255. Kalir T, Seijo L, Deligdisch L, et al. Endometrial adenocarcinoma with choriocarcinomatous differentiation in an elderly virginal woman. *Int J Gynecol Pathol.* 1995;14:266–269.
256. Pesce C, Merino MJ, Chambers JT, et al. Endometrial carcinoma with trophoblastic differentiation. An aggressive form of uterine cancer. *Cancer.* 1991;68:1799–1802.
257. Hendrickson MR, Kempson RL. A diagnostic approach to smooth muscle tumors of the uterus. *Curr Diagn Pathol.* 2000;6:21–30.
258. Hart WR. Problematic uterine smooth muscle neoplasms. *Am J Surg Pathol.* 1997;21:252–253.
259. Bell SW, Kempson RL, Hendrickson MR. Problematic uterine smooth muscle neoplasms. A clinicopathologic study of 213 cases. *Am J Surg Pathol.* 1994;18:535–558.
260. Ip PPC, Lam KW, Cheung CL, et al. Tranexamic acid-associated necrosis and intralesional thrombosis of uterine leiomyomas: a clinicopathologic study of 147 cases emphasizing the importance of drug-induced necrosis and early infarcts in leiomyomas. *Am J Surg Pathol.* 2007;31:1215–1224.
261. McCluggage WG, Ellis PK, McClure N, et al. Pathologic features of uterine leiomyomas following uterine artery embolization. *Int J Gynecol Pathol.* 2000;19:342–347.
262. Colgan TJ, Pron G, Mocarski EJ, et al. Pathologic features of uteri and leiomyomas following uterine artery embolization for leiomyomas. *Am J Surg Pathol.* 2003;27:167–177.
263. Weichert W, Denkert C, Gauruder-Burmester A, et al. Uterine arterial embolization with tris-acryl gelatin microspheres: a histopathologic evaluation. *Am J Surg Pathol.* 2005;29:955–961.
264. Maleki Z, Kim HS, Thonse VR, et al. Uterine artery embolization with trisacryl gelatin microspheres in women treated for leiomyomas: a clinicopathologic analysis of alterations in gynecologic surgical specimens. *Int J Gynecol Pathol.* 2010;29:260–268.
265. Leitao MM, Sonoda Y, Brennan MF, et al. Incidence of lymph node and ovarian metastases in leiomyosarcoma of the uterus. *Gynecol Oncol.* 2003;91:209–212.

266. Sreenan JJ, Prayson RA, Biscotti CV, et al. Histopathologic findings in 107 uterine leiomyomas treated with leuprolide acetate compared with 126 controls. *Am J Surg Pathol.* 1996;20:427–432.
267. Demopoulos RI, Jones KY, Mittal KR, et al. Histology of leiomyomata in patients treated with leuprolide acetate. *Int J Gynecol Pathol.* 1997;16: 131–137.
268. Colgan TJ, Pendergast S, LeBlanc M. The histopathology of uterine leiomyomas following treatment with gonadotropin-releasing hormone analogues. *Hum Pathol.* 1993;24:1073–1077.
269. Oliva E, Young RH, Clement PB, et al. Cellular benign mesenchymal tumors of the uterus. A comparative morphologic and immunohistochemical analysis of 33 highly cellular leiomyomas and six endometrial stromal nodules, two frequently confused tumors. *Am J Surg Pathol.* 1995;19:757–768.
270. Oliva E, Young RH, Amin MB, et al. An immunohistochemical analysis of endometrial stromal and smooth muscle tumors of the uterus: a study of 54 cases emphasizing the importance of using a panel because of overlap in immunoreactivity for individual antibodies. *Am J Surg Pathol.* 2002;26:403–412.
271. Nucci MR, O'Connell JT, Huettner PC, et al. h-Caldesmon expression effectively distinguishes endometrial stromal tumors from uterine smooth muscle tumors. *Am J Surg Pathol.* 2001;25:455–463.
272. Rush DS, Tan J, Baergen RN, et al. h-Caldesmon, a novel smooth muscle-specific antibody, distinguishes between cellular leiomyoma and endometrial stromal sarcoma. *Am J Surg Pathol.* 2001;25:253–258.
273. de Leval L, Waltregny D, Boniver J, et al. Use of histone deacetylase 8 (HDAC8), a new marker of smooth muscle differentiation, in the classification of mesenchymal tumors of the uterus. *Am J Surg Pathol.* 2006;30: 319–327.
274. Agoff SN, Grieco VS, Garcia R, et al. Immunohistochemical distinction of endometrial stromal sarcoma and cellular leiomyoma. *Appl Immunohistochem Mol Morphol.* 2001;9:164–169.
275. Myles JL, Hart WR. Apoplectic leiomyomas of the uterus. A clinicopathologic study of five distinctive hemorrhagic leiomyomas associated with oral contraceptive usage. *Am J Surg Pathol.* 1985;9:798–805.
276. Norris HJ, Hilliard GD, Irey NS. Hemorrhagic cellular leiomyomas ("apoplectic leiomyoma") of the uterus associated with pregnancy and oral contraceptives. *Int J Gynecol Pathol.* 1988;7:212–224.
277. O'Connor DM, Norris HJ. Mitotically active leiomyomas of the uterus. *Hum Pathol.* 1990;21:223–227.
278. Perrone T, Dehner LP. Prognostically favorable "mitotically active" smooth-muscle tumors of the uterus. A clinicopathologic study of ten cases. *Am J Surg Pathol.* 1988;12:1–8.
279. Prayson RA, Hart WR. Mitotically active leiomyomas of the uterus. *Am J Clin Pathol.* 1992;97:14–20.
280. Clement PB, Young RH, Scully RE. Diffuse, perinodular, and other patterns of hydropic degeneration within and adjacent to uterine leiomyomas. Problems in differential diagnosis. *Am J Surg Pathol.* 1992;16:26–32.
281. Kurman RJ, Norris HJ. Mesenchymal tumors of the uterus. VI. Epithelioid smooth muscle tumors including leiomyoblastoma and clear-cell leiomyoma: a clinical and pathologic analysis of 26 cases. *Cancer.* 1976;37:1853–1865.
282. Prayson RA, Goldblum JR, Hart WR. Epithelioid smooth-muscle tumors of the uterus: a clinicopathologic study of 18 patients. *Am J Surg Pathol.* 1997;21:383–391.
283. Kaminski PF, Tavassoli FA. Plexiform tumorlet: a clinical and pathologic study of 15 cases with ultrastructural observations. *Int J Gynecol Pathol.* 1984;3:124–134.
284. Atkins K, Bell S, Kempson R, et al. Myxoid smooth muscle tumors of the uterus (abstract). *Mod Pathol.* 2001;14:132A.
285. Wang X, Kumar D, Seidman JD. Uterine lipoleiomyomas: a clinicopathologic study of 50 cases. *Int J Gynecol Pathol.* 2006;25:239–242.
286. McDonald AG, Cin PD, Ganguly A, et al. Liposarcoma arising in uterine lipoleiomyoma: a report of 3 cases and review of the literature. *Am J Surg Pathol.* 2011;35:221–227.
287. Gisser SD, Young I. Neurilemoma-like uterine myomas: an ultrastructural reaffirmation of their non-Schwannian nature. *Am J Obstet Gynecol.* 1977;129:389–392.
288. Ferry JA, Harris NL, Scully RE. Uterine leiomyomas with lymphoid infiltration simulating lymphoma. A report of seven cases. *Int J Gynecol Pathol.* 1989;8:263–270.
289. Botsis D, Koliopoulos C, Kondi-Pafitis A, et al. Frequency, histological, and immunohistochemical properties of massive inflammatory lymphocytic infiltration of leiomyomas of the uterus: an entity causing diagnostic difficulties. *Int J Gynecol Pathol.* 2005;24:326–329.
290. Maluf HM, Gersell DJ. Uterine leiomyomas with high content of mast cells. *Arch Pathol Lab Med.* 1994;118:712–714.
291. Vang R, Medeiros LJ, Samoszuk M, et al. Uterine leiomyomas with eosinophils: a clinicopathologic study of 3 cases. *Int J Gynecol Pathol.* 2001;20: 239–243.
292. Schmid C, Beham A, Kratochvil P. Haematopoiesis in a degenerating uterine leiomyoma. *Arch Gynecol Obstet.* 1990;248:81–86.
293. Adany R, Fodor F, Molnar P, et al. Increased density of histiocytes in uterine leiomyomas. *Int J Gynecol Pathol.* 1990;9:137–144.
294. Hendrickson MR, Tavassoli FA, Kempson RL, et al. Mesenchymal tumours and related lesions. In: Tavassoli FA, Devilee P, eds. *World Health Organization Classification of Tumours. Pathology and Genetics of Tumours of the Breast and Female Genital Organs.* Lyon, France: IARC Press; 2003:241.
295. Downes KA, Hart WR. Bizarre leiomyomas of the uterus: a comprehensive pathologic study of 24 cases with long-term follow-up. *Am J Surg Pathol.* 1997;21:1261–1270.
296. Kempson RL, Hendrickson MR. Smooth muscle, endometrial stromal, and mixed Mullerian tumors of the uterus. *Mod Pathol.* 2000;13:328–342.
297. Mittal K, Demopoulos RI. MIB-1 (Ki-67), p53, estrogen receptor, and progesterone receptor expression in uterine smooth muscle tumors. *Hum Pathol.* 2001;32:984–987.
298. O'Neill CJ, McBride HA, Connolly LE, et al. Uterine leiomyosarcomas are characterized by high p16, p53 and MIB1 expression in comparison with usual leiomyomas, leiomyoma variants and smooth muscle tumours of uncertain malignant potential. *Histopathology.* 2007;50:851–858.
299. Ip PPC, Cheung ANY, Clement PB. Uterine smooth muscle tumors of uncertain malignant potential (STUMP): a clinicopathologic analysis of 16 cases. *Am J Surg Pathol.* 2009;33:992–1005.
300. Veras E, Malpica A, Deavers MT, et al. Mitosis-specific marker phosphohistone H3 in the assessment of mitotic index in uterine smooth muscle tumors: a pilot study. *Int J Gynecol Pathol.* 2009;28:316–321.
301. Ly A, McKenney JK, Longacre TA, et al. Atypical leiomyoma of the uterus: a clinicopathologic study of 46 cases [Abstract]. *Mod Pathol.* 2009;22:225A.
302. Patton KT, Cheng L, Papavero V, et al. Benign metastasizing leiomyoma: clonality, telomere length and clinicopathologic analysis. *Mod Pathol.* 2006;19:130–140.
303. Tietze L, Gunther K, Horbe A, et al. Benign metastasizing leiomyoma: a cytogenetically balanced but clonal disease. *Hum Pathol.* 2000;31:126–128.
304. Nucci MR, Drapkin R, Cin PD, et al. Distinctive cytogenetic profile in benign metastasizing leiomyoma: pathogenetic implications. *Am J Surg Pathol.* 2007;31:737–743.
305. Clement PB, Young RH. Diffuse leiomyomatosis of the uterus: a report of four cases. *Int J Gynecol Pathol.* 1987;6:322–330.
306. Clement PB. Intravenous leiomyomatosis of the uterus. *Pathol Annu.* 1988;23(pt 2):153–183.
307. Mulvany NJ, Slavin JL, Ostor AG, et al. Intravenous leiomyomatosis of the uterus: a clinicopathologic study of 22 cases. *Int J Gynecol Pathol.* 1994; 13:1–9.
308. Clement PB, Young RH, Scully RE. Intravenous leiomyomatosis of the uterus. A clinicopathological analysis of 16 cases with unusual histologic features. *Am J Surg Pathol.* 1988;12:932–945.
309. Canzonieri V, D'Amore ES, Bartoloni G, et al. Leiomyomatosis with vascular invasion. A unified pathogenesis regarding leiomyoma with vascular microinvasion, benign metastasizing leiomyoma and intravenous leiomyomatosis. *Virchows Arch.* 1994;425:541–545.
310. Roth LM, Reed RJ. Dissecting leiomyomas of the uterus other than cotyledonoid dissecting leiomyomas: a report of eight cases. *Am J Surg Pathol.* 1999;23:1032–1039.
311. Roth LM, Reed RJ, Sternberg WH. Cotyledonoid dissecting leiomyoma of the uterus: the Sternberg tumor. *Am J Surg Pathol.* 1996;20:1455–1461.
312. Mittal KR, Chen F, Wei JJ, et al. Molecular and immunohistochemical evidence for the origin of uterine leiomyosarcomas from associated leiomyoma and symplastic leiomyoma-like areas. *Mod Pathol.* 2009;22: 1303–1311.
313. Evans HL, Chawla SP, Simpson C, et al. Smooth muscle neoplasms of the uterus other than ordinary leiomyoma. A study of 46 cases, with emphasis on diagnostic criteria and prognostic factors. *Cancer.* 1988;62:2239–2247.
314. Jones MW, Norris HJ. Clinicopathologic study of 28 uterine leiomyosarcomas with metastasis. *Int J Gynecol Pathol.* 1995;14:243–249.
315. FIGO Committee on Gynecologic Oncology. FIGO staging for uterine sarcomas. *Int J Gynecol Obstet.* 2009;104:179.
316. Atkins K, Bell S, Kempson R, et al. Epithelioid smooth muscle tumors of the uterus (abstract). *Mod Pathol.* 2001;14:132A.

317. Oliva E, Nielsen GP, Clement PB, et al. Epithelioid smooth muscle tumors of the uterus. A clinicopathologic analysis of 80 cases (abstract). *Lab Invest.* 1997;76:107A.
318. King ME, Dickersin GR, Scully RE. Myxoid leiomyosarcoma of the uterus. A report of six cases. *Am J Surg Pathol.* 1982;6:589–598.
319. Darby AJ, Papadaki L, Beilby JO. An unusual leiomyosarcoma of the uterus containing osteoclast-like giant cells. *Cancer.* 1975;36:495–504.
320. Marshall RJ, Braye SG, Jones DB. Leiomyosarcoma of the uterus with giant cells resembling osteoclasts. *Int J Gynecol Pathol.* 1986;5:260–268.
321. Atkins KA, Arronte N, Darus CJ, et al. The use of p16 in enhancing the histologic classification of uterine smooth muscle tumors. *Am J Surg Pathol.* 2008;32:98–102.
322. Chen L, Yang B. Immunohistochemical analysis of p16, p53, and Ki-67 expression in uterine smooth muscle tumors. *Int J Gynecol Pathol.* 2008;27:326–332.
323. Sung CO, Ahn G, Song SY, et al. Atypical leiomyomas of the uterus with long-term follow-up after myomectomy with immunohistochemical analysis for p16INK4A, p53, Ki-67, estrogen receptors, and progesterone receptors. *Int J Gynecol Pathol.* 2009;28:529–534.
324. Tavassoli FA, Devilee P, eds. *World Health Organization Classification of Tumors. Pathology and Genetics of Tumours of the Breast and Female Genital Organs.* Lyon, France: IARC Press; 2003.
325. Norris HJ, Taylor HB. Mesenchymal tumors of the uterus. I. A clinical and pathological study of 53 endometrial stromal tumors. *Cancer.* 1966;19:755–766.
326. Chang KL, Crabtree GS, Lim-Tan SK, et al. Primary uterine endometrial stromal neoplasms. A clinicopathologic study of 117 cases. *Am J Surg Pathol.* 1990;14:415–438.
327. Tavassoli FA, Norris HJ. Mesenchymal tumours of the uterus. VII. A clinicopathological study of 60 endometrial stromal nodules. *Histopathology.* 1981;5:1–10.
328. Dionigi A, Oliva E, Clement PB, et al. Endometrial stromal nodules and endometrial stromal tumors with limited infiltration: a clinicopathologic study of 50 cases. *Am J Surg Pathol.* 2002;26:567–581.
329. Oliva E, Clement PB, Young RH. Endometrial stromal tumors: an update on a group of tumors with a protean phenotype. *Adv Anat Pathol.* 2000;7:257–281.
330. Oliva E, Young RH, Clement PB, et al. Myxoid and fibrous endometrial stromal tumors of the uterus: a report of 10 cases. *Int J Gynecol Pathol.* 1999;18:310–319.
331. Oliva E, Clement PB, Young RH, et al. Mixed endometrial stromal and smooth muscle tumors of the uterus: a clinicopathologic study of 15 cases. *Am J Surg Pathol.* 1998;22:997–1005.
332. Oliva E, Clement PB, Young RH. Epithelioid endometrial and endometrioid stromal tumors: a report of four cases emphasizing their distinction from epithelioid smooth muscle tumors and other oxyphilic uterine and extrauterine tumors. *Int J Gynecol Pathol.* 2002;21:48–55.
333. Yilmaz A, Rush DS, Soslow RA. Endometrial stromal sarcomas with unusual histologic features: a report of 24 primary and metastatic tumors emphasizing fibroblastic and smooth muscle differentiation. *Am J Surg Pathol.* 2002;26:1142–1150.
334. Baker PM, Moch H, Oliva E. Unusual morphologic features of endometrial stromal tumors: a report of 2 cases. *Am J Surg Pathol.* 2005;29:1394–1398.
335. McCluggage WG, Young RH. Endometrial stroma sarcomas with true papillae and pseudopapillae. *Int J Gynecol Pathol.* 2008;27:555–561.
336. Toki T, Shimizu M, Takagi Y, et al. CD10 is a marker for normal and neoplastic endometrial stromal cells. *Int J Gynecol Pathol.* 2002;21:41–47.
337. Sabini G, Chumas JC, Mann WJ. Steroid hormone receptors in endometrial stromal sarcomas. A biochemical and immunohistochemical study. *Am J Clin Pathol.* 1992;97:381–386.
338. Moinfar F, Gogg-Kamerer M, Sommersacher A, et al. Endometrial stromal sarcomas frequently express epidermal growth factor receptor (EGFR, HER-1): potential basis for a new therapeutic approach. *Am J Surg Pathol.* 2005;29:485–489.
339. Adegboyega PA, Qiu S. Immunohistochemical profiling of cytokeratin expression by endometrial stroma sarcoma. *Hum Pathol.* 2008;39:1459–1464.
340. Nucci MR, Harburger D, Koontz J, et al. Molecular analysis of the JAZF1-JJAZ1 gene fusion by RT-PCR and fluorescence in situ hybridization in endometrial stromal neoplasms. *Am J Surg Pathol.* 2007;31:65–70.
341. Aubry MC, Myers JL, Colby TV, et al. Endometrial stromal sarcoma metastatic to the lung: a detailed analysis of 16 patients. *Am J Surg Pathol.* 2002;26:440–449.
342. Evans HL. Endometrial stromal sarcoma and poorly differentiated endometrial sarcoma. *Cancer.* 1982;50:2170–2182.
343. Kurihara S, Oda Y, Ohishi Y, et al. Endometrial stromal sarcomas and related high-grade sarcomas: immunohistochemical and molecular genetic study of 31 cases. *Am J Surg Pathol.* 2008;32:1228–1238.
344. Mazur MT. Atypical polypoid adenomyomas of the endometrium. *Am J Surg Pathol.* 1981;5:473–482.
345. Young RH, Treger T, Scully RE. Atypical polypoid adenomyoma of the uterus. A report of 27 cases. *Am J Clin Pathol.* 1986;86:139–145.
346. Longacre TA, Chung MH, Rouse RV, et al. Atypical polypoid adenomyofibromas (atypical polypoid adenomyomas) of the uterus. A clinicopathologic study of 55 cases. *Am J Surg Pathol.* 1996;20:1–20.
347. Soslow RA, Chung MH, Rouse RV, et al. Atypical polypoid adenomyofibroma (APA) versus well-differentiated endometrial carcinoma with prominent stromal matrix: an immunohistochemical study. *Int J Gynecol Pathol.* 1996;15:209–216.
348. Ohishi Y, Kaku T, Kobayashi H, et al. CD10 immunostaining distinguishes atypical polypoid adenomyofibroma (atypical polypoid adenomyoma) from endometrial carcinoma invading the myometrium. *Hum Pathol.* 2008;39:1446–1453.
349. Horita A, Kurata A, Maeda D, et al. Immunohistochemical characteristics of atypical polypoid adenomyoma with special reference to h-caldesmon. *Int J Gynecol Pathol.* 2011;30:64–70.
350. Clement PB, Scully RE. Mullerian adenosarcoma of the uterus: a clinicopathologic analysis of 100 cases with a review of the literature. *Hum Pathol.* 1990;21:363–381.
351. Piura B, Rabinovich A, Meirovitz M, et al. Mullerian adenosarcoma of the uterus: case report and review of literature. *Eur J Gynaecol Oncol.* 2000;21:387–390.
352. Clement PB, Scully RE. Uterine tumors with mixed epithelial and mesenchymal elements. *Semin Diagn Pathol.* 1988;5:199–222.
353. Kaku T, Silverberg SG, Major FJ, et al. Adenosarcoma of the uterus: a Gynecologic Oncology Group clinicopathologic study of 31 cases. *Int J Gynecol Pathol.* 1992;11:75–88.
354. Clement PB, Scully RE. Mullerian adenosarcomas of the uterus with sex cord-like elements. A clinicopathologic analysis of eight cases. *Am J Clin Pathol.* 1989;91:664–672.
355. Clement PB. Mullerian adenosarcomas of the uterus with sarcomatous overgrowth. A clinicopathological analysis of 10 cases. *Am J Surg Pathol.* 1989;13:28–38.
356. Soslow RA, Ali A, Oliva E. Mullerian adenosarcomas: an immunophenotypic analysis of 35 cases. *Am J Surg Pathol.* 2008;32:1013–1021.
357. Gallardo A, Prat J. Mullerian adenosarcoma: a clinicopathologic and immunohistochemical study of 55 cases challenging the existence of adenofibroma. *Am J Surg Pathol.* 2009;33:278–288.
358. Zaloudek CJ, Norris HJ. Adenofibroma and adenosarcoma of the uterus: a clinicopathologic study of 35 cases. *Cancer.* 1981;48:354–366.
359. Clement PB, Scully RE. Mullerian adenofibroma of the uterus with invasion of myometrium and pelvic veins. *Int J Gynecol Pathol.* 1990;9:363–371.
360. Moinfar F, Azodi M, Tavassoli FA. Uterine sarcomas. *Pathology (Phila).* 2007;39:55–71.
361. Fadare O. Heterologous and rare homologous sarcomas of the uterine corpus: a clinicopathologic review. *Adv Anat Pathol.* 2011;18:60–74.
362. Rabban JT, Zaloudek CJ, Shekitka KM, et al. Inflammatory myofibroblastic tumor of the uterus: a clinicopathologic study of 6 cases emphasizing distinction from aggressive mesenchymal tumors. *Am J Surg Pathol.* 2005;29:1348–1355.
363. Vang R, Kempson RL. Perivascular epithelioid cell tumor ('PEComa') of the uterus: a subset of HMB-45-positive epithelioid mesenchymal neoplasms with an uncertain relationship to pure smooth muscle tumors. *Am J Surg Pathol.* 2002;26:1–13.
364. Fadare O. Perivascular epithelioid cell tumor (PEComa) of the uterus: an outcome-based clinicopathologic analysis of 41 reported cases. *Adv Anat Pathol.* 2008;15:63–75.
365. Folpe AL, Mentzel T, Lehr HA, et al. Perivascular epithelioid cell neoplasms of soft tissue and gynecologic origin: a clinicopathologic study of 26 cases and review of the literature. *Am J Surg Pathol.* 2005;29:1558–1575.
366. Silva EG, Deavers MT, Bodurka DC, et al. Uterine epithelioid leiomyosarcomas with clear cells: reactivity with HMB-45 and the concept of PEComa. *Am J Surg Pathol.* 2004;28:244–249.
367. Simpson KW, Albores-Saavedra J. HMB-45 reactivity in conventional uterine leiomyosarcomas. *Am J Surg Pathol.* 2007;31:95–98.
368. Ordi J, Stamatakos MD, Tavassoli FA. Pure pleomorphic rhabdomyosarcomas of the uterus. *Int J Gynecol Pathol.* 1997;16:369–377.
369. Fadare O, Bonvicino A, Martel M, et al. Pleomorphic rhabdomyosarcoma of the uterine corpus: a clinicopathologic study of 4 cases and a review of the literature. *Int J Gynecol Pathol.* 2010;29:122–134.

370. Varghese L, Arnesen M, Boente M. Primitive neuroectodermal tumor of the uterus: a case report and review of literature. *Int J Gynecol Pathol.* 2006;25:373–377.
371. Nogales FF, Isaac MA, Hardisson D, et al. Adenomatoid tumors of the uterus: an analysis of 60 cases. *Int J Gynecol Pathol.* 2002;21:34–40.
372. Quigley JC, Hart WR. Adenomatoid tumors of the uterus. *Am J Clin Pathol.* 1981;76:627–635.
373. Hes O, Perez-Montiel DM, Alvarado Cabrero I, et al. Thread-like bridging strands: a morphologic feature present in all adenomatoid tumors. *Ann Diagn Pathol.* 2003;7:273–277.
374. Goddard MJ, Grant JW. Adenomatoid tumours: a mucin histochemical and immunohistochemical study. *Histopathology.* 1992;20:57–61.
375. Schwartz EJ, Longacre TA. Adenomatoid tumors of the female and male genital tracts express WT1. *Int J Gynecol Pathol.* 2004;23:123–128.
376. Clement PB, Scully RE. Uterine tumors resembling ovarian sex-cord tumors. A clinicopathologic analysis of fourteen cases. *Am J Clin Pathol.* 1976;66:512–525.
377. Czernobilsky B. Uterine tumors resembling ovarian sex cord tumors: an update. *Int J Gynecol Pathol.* 2008;27:229–235.
378. Krishnamurthy S, Jungbluth AA, Busam KJ, et al. Uterine tumors resembling ovarian sex-cord tumors have an immunophenotype consistent with true sex-cord differentiation. *Am J Surg Pathol.* 1998;22:1078–1082.
379. Baker RJ, Hildebrandt RH, Rouse RV, et al. Inhibin and CD99 (MIC2) expression in uterine stromal neoplasms with sex-cord-like elements. *Hum Pathol.* 1999;30:671–679.
380. de Leval L, Lim GS, Waltregny D, et al. Diverse phenotypic profile of uterine tumors resembling ovarian sex cord tumors: an immunohistochemical study of 12 cases. *Am J Surg Pathol.* 2010;34:1749–1761.
381. Staats PN, Garcia JJ, Dias-Santagata DC, et al. Uterine tumors resembling ovarian sex cord tumors (UTROSCT) lack the JAZF1-JJAZ1 translocation frequently seen in endometrial stromal tumors. *Am J Surg Pathol.* 2009;33:1206–1212.
382. Harris NL, Scully RE. Malignant lymphoma and granulocytic sarcoma of the uterus and vagina. A clinicopathologic analysis of 27 cases. *Cancer.* 1984;53:2530–2545.
383. Kosari F, Daneshbod Y, Parwaresch R, et al. Lymphomas of the female genital tract: a study of 186 cases and review of the literature. *Am J Surg Pathol.* 2005;29:1512–1520.
384. Lagoo AS, Robboy SJ. Lymphoma of the female genital tract: current status. *Int J Gynecol Pathol.* 2006;25:1–21.
385. Vang R, Medeiros LJ, Fuller GN, et al. Non-Hodgkin's lymphoma involving the gynecologic tract: a review of 88 cases. *Adv Anat Pathol.* 2001;8:200–217.
386. Kumar NB, Hart WR. Metastases to the uterine corpus from extragenital cancers. A clinicopathologic study of 63 cases. *Cancer.* 1982;50:2163–2169.
387. Mazur MT, Hsueh S, Gersell DJ. Metastases to the female genital tract. Analysis of 325 cases. *Cancer.* 1984;53:1978–1984.
388. Hill CB, Prihoda TJ, Sharkey FE. Number of levels needed for diagnosis of endometrial biopsies. *Histopathology.* 2005;47:225–226.

CHAPTER 5

Pathology of the Fallopian Tube and Broad Ligament

FALLOPIAN TUBE

OVERVIEW OF ANATOMY AND HISTOLOGY OF THE NORMAL FALLOPIAN TUBE

The two fallopian tubes extend from the uterine cornua to the lateral aspects of their corresponding ovaries. The normal fallopian tube typically measures about 10 cm in length and 0.5 cm in diameter. The ovarian end of each tube is composed of *fimbriae*, which are motile, finger-like extensions that serve to guide ova released from the ovary during ovulation into the tubal lumen. The fimbriae are contiguous with the short, expanded end of the fallopian tube known as the *infundibulum*, which in turn merges medially with the *ampulla*. The ampullary segment, which is of smaller diameter than the infundibulum, is somewhat tortuous, and accounts for roughly half of the length of the tube. The ampulla blends medially with the *isthmus*, which is a short segment of the tube that is continuous with the intramural portion that opens into the endometrial cavity.

The extrauterine portion of the tube is enveloped by the mesosalpinx, which is lined by mesothelium and represents the superior portion of the broad ligament. The smooth muscle wall of the fallopian tube (*myosalpinx* or muscularis) is composed of an inner circular and less conspicuous outer longitudinal layer. The isthmic and intramural segments also possess an innermost longitudinal muscular layer. The mucosa (epithelium and supporting lamina propria) of the fallopian tube is thrown into branching folds known as *plicae*, which project into the lumen (Fig. 5.1A). The plicae increase in number, height, and complexity proceeding from the medial to lateral segments of the tube, and terminate in the fimbriae. The nonstratified epithelial lining of the fallopian tube consists of an admixture of ciliated, secretory, and intercalated (peg) cells (Fig. 5.1B). In addition to cilia, ciliated cells have visible apical terminal bars and round to oval nuclei. Secretory cells have more elongated nuclei, and may have short apical cytoplasmic snouts. Intercalated (peg) cells, which are thought to be morphologic variants of secretory cells, have thin, dark, elongated

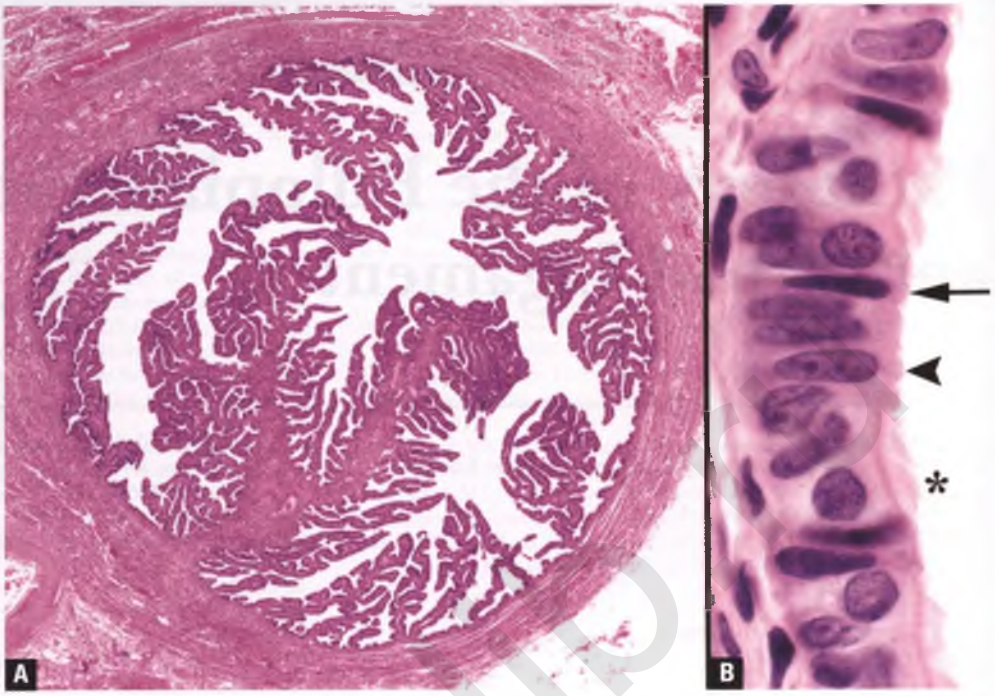

FIGURE 5.1. Normal fallopian tube. **A:** Cross section through the ampullary region of a fallopian tube from a woman of reproductive age. Note the architectural complexity of the branching plicae. **B:** High-magnification view of tubal epithelium. An *asterisk* marks a ciliated cell, an *arrowhead* marks a secretory cell, and an *arrow* marks an intercalated (peg) cell.

nuclei and scant cytoplasm. The lamina propria of the mucosal folds consists of fibrovascular tissue that may become fibrotic and blunted in postmenopausal women (Fig. 5.2). Note that the lamina propria directly abuts the muscular wall of the fallopian tube (i.e., there is no interposed layer of submucosa).

SALPINGITIS

Background Clinical Information Related to Infectious Salpingitis

Pelvic inflammatory disease (PID) is typically centered in the fallopian tubes as a form of salpingitis. This common disorder is most often caused by a sexually transmitted agent such as *Neisseria gonorrhoeae, Chlamydia trachomatis*, or *Mycoplasma genitalium* that ascends from the vagina and cervix. Although most cases of PID occur in young, sexually active women, a variety of other PID-producing organisms can also be introduced into the female genital tract as a consequence of instrumentation or use of a contraceptive intrauterine device (IUD). Symptoms of PID vary widely in severity, and are often vague and nonspecific. Most patients present with some degree of lower abdominal pain, and may also have a fever, adnexal tenderness, leukocytosis, dyspareunia, dysuria, and/or a malodorous vaginal discharge. Patients may have repeated bouts of PID, which can result in acute inflammatory changes superimposed upon chronic ones. If left untreated, salpingitis can cause irreparable damage to the fallopian tubes that can lead to ectopic pregnancy, infertility, and chronic pelvic pain.

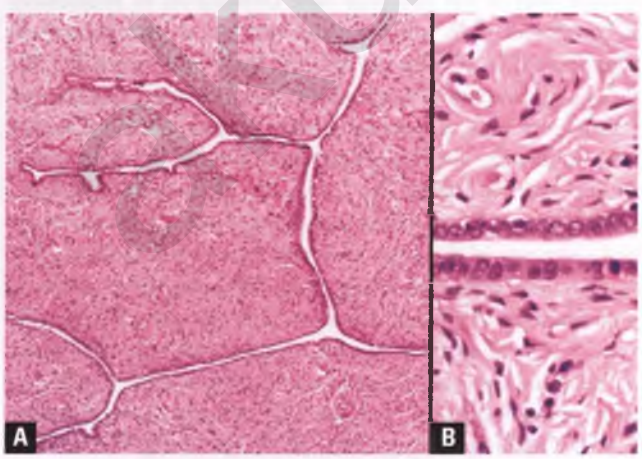

FIGURE 5.2. **A,B:** Fallopian tube of a postmenopausal woman. Note the fibrotic stroma with a pseudoneuritized appearance.

Nongranulomatous Infectious Salpingitis and Its Derivatives

The natural evolution of the usual form of bacterial salpingitis begins as *acute salpingitis*, which is characterized by a swollen tube with acute inflammation of the mucosa and a lumen filled with a purulent exudate. With time, lymphocytes and plasma cells join the inflammatory infiltrate within the lamina propria (Fig. 5.3). As discussed below, the subsequent form of progression is dependent in large part on whether or not the tubal ostia become closed, and when in the course of the disease such closure occurs.

If the tubal ostium remains patent, luminal distension is limited by the release of tubal contents into the peritoneal cavity, allowing damaged plicae that are closely approximated to fuse with one another. Eventually, the inflammation subsides, leaving a network of compartmentalized, epithelial-lined

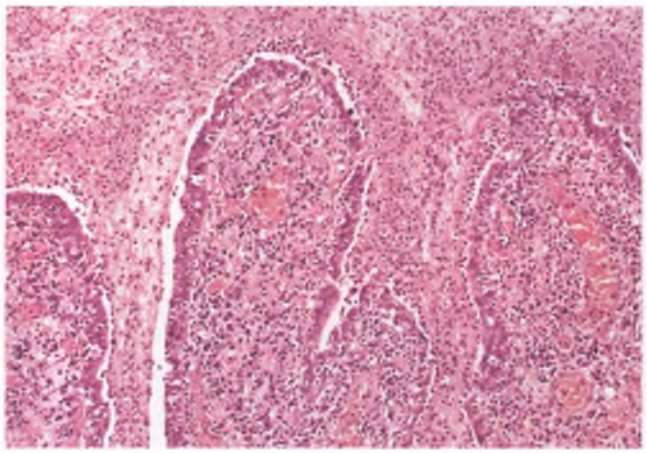

FIGURE 5.3. Active chronic salpingitis (acute and chronic salpingitis). The plicae are expanded by a mixed population of lymphocytes, plasma cells, and occasional neutrophils. The lumen contains fibrinopurulent debris.

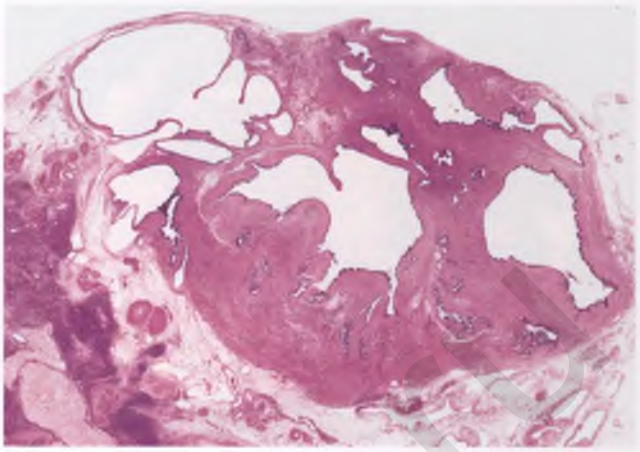

FIGURE 5.5. Hydrosalpinx follicularis. This compartmentalized cystic lesion is densely adherent to the ovary at left and could be mistaken for an ovarian serous cystadenofibroma, were it not for the prominent smooth muscle stroma derived from the myosalpinx, structures consistent with residual plicae, and history of PID.

spaces in its wake (Fig. 5.4). This stage of healed salpingitis is referred to as *follicular salpingitis* due to the presence of follicle-like spaces (note that this designation has nothing to do with lymphoid follicles). If fluid subsequently accumulates within the spaces of follicular salpingitis and expands the tube to a minor degree, the resulting lesion is designated *hydrosalpinx follicularis*. As illustrated in Figure 5.5, such lesions can fuse with the neighboring ovary and mimic benign serous ovarian tumors. In some cases of *chronic salpingitis*, plical fusion is not a prominent feature, and the lesion is characterized by a dense infiltrate of lymphocytes and plasma cells within the plical lamina propria (Fig. 5.6).

Another possible consequence of a patent tubal ostium is the spread of the inflammatory process to the ipsilateral ovary, resulting in the formation of a *tubo-ovarian abscess*. These lesions are usually bilateral, and often form masses in which ovarian and tubal tissue have fused due to intense inflammation and dense tubo-ovarian adhesions (Fig. 5.7). Some tubo-ovarian abscesses are due to actinomycosis, which is associated with longstanding IUD use and is recognized by the identification of characteristic actinomycotic (sulfur) granules within the inflammatory exudates, as illustrated in Figure 3.44.

If the inflammatory process results in closure of the fimbriated ends of the tubes relatively early in the course of the disease, inflammation may not spread beyond the fallopian tubes. Instead, pus may continue to accumulate within the lumen, whose expansion results in the formation of a *pyosalpinx*

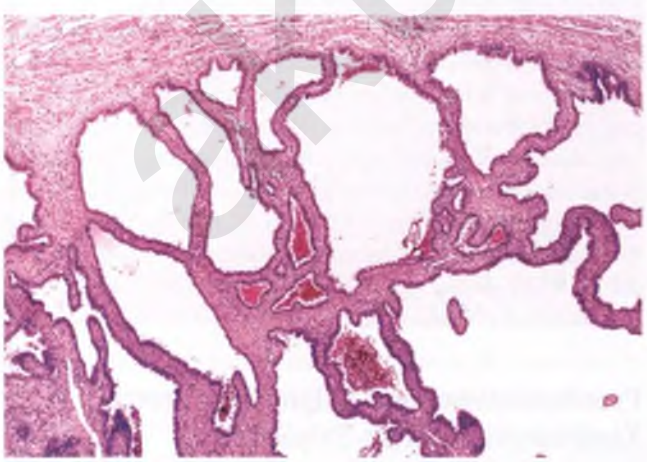

FIGURE 5.4. Chronic follicular salpingitis. The inflammatory infiltrate is sparse and plical fusion has resulted in the formation of several follicle-like spaces.

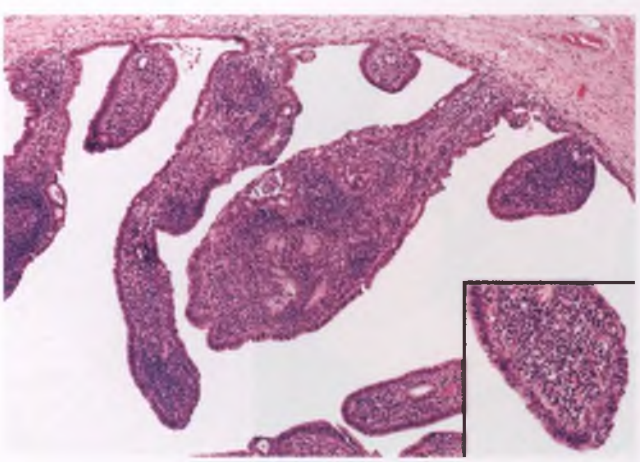

FIGURE 5.6. Chronic salpingitis. In this example, the plicae are distended with an infiltrate of lymphocytes and plasma cells, but plical fusion is not present.

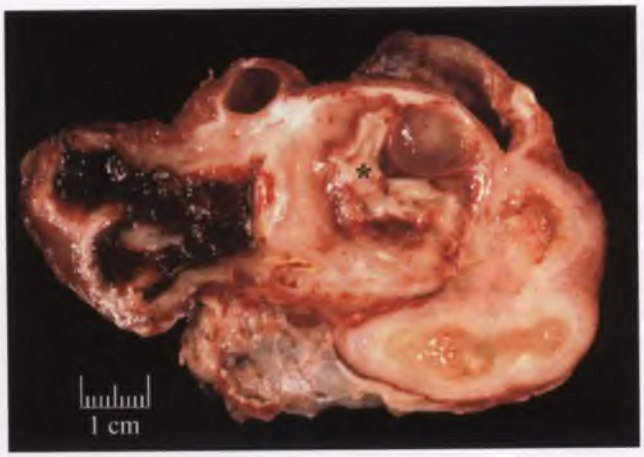

FIGURE 5.7. Tubo-ovarian abscess. The sectioned fallopian tube at lower right has a thickened wall and a lumen that contains pus. It is densely adherent to the ovary, which contains a geographic area of pale yellow necrotic material with a hemorrhagic border (*asterisk*).

(Fig. 5.8). Eventually, the pus is reabsorbed and replaced by clear fluid and the mucosal inflammation becomes quiescent, resulting in a *hydrosalpinx* (Fig. 5.9A). The shape of a hydrosalpinx has been likened to a chemist's retort, which is a piece of glassware with a spherical vessel that is contiguous with a long, progressively narrowing neck. The wall of a hydrosalpinx is thin and consists of attenuated layer of smooth muscle and connective tissue with only a few remaining plical folds (Fig. 5.9B). The epithelial lining varies from flattened to normal appearing with interspersed ciliated cells. As discussed above for hydrosalpinx follicularis, the usual forms of hydrosalpinx can also become adherent to the ovary and mimic ovarian serous cystadenomas.

Some cases of salpingitis are associated with a pronounced form of reactive epithelial hyperplasia that can be confused

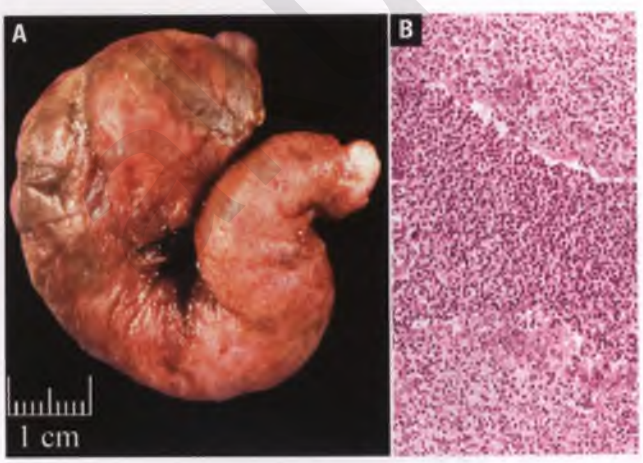

FIGURE 5.8. Pyosalpinx. **A:** The fallopian tube is swollen, discolored, and has some serosal adhesions. **B:** The plicae (top and bottom) are inflamed, and the lumen is full of pus.

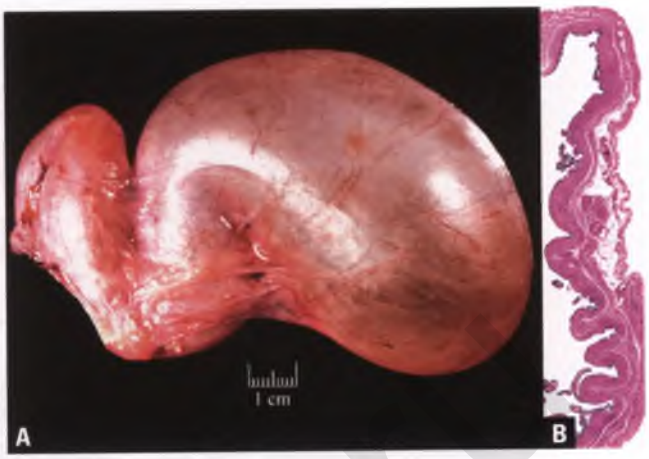

FIGURE 5.9. Hydrosalpinx. **A:** The occluded distal portion of the tube at right is markedly dilated and progressively narrows along its convoluted course toward the isthmic end at left. Note the fibrous adhesions between the kinked segments of the tube. **B:** The wall of a hydrosalpinx consists of an attenuated layer of smooth muscle and connective tissue, with few residual plical elements projecting into the lumen. Although not apparent at this magnification, the epithelial lining varies from flattened to unaltered from normal tubal epithelium.

with carcinoma. This issue is addressed in the section on epithelial hyperplasia.

Granulomatous Salpingitis[1]

Most cases of granulomatous salpingitis are due to tuberculosis and are associated with infertility, although tuberculosis of the female genital tract is rare in developed countries. In contrast to the ascending route of infection of usual bacterial salpingitis, tuberculous infection of the female genital tract occurs via hematogenous or lymphatic routes. Tuberculous salpingitis is usually bilateral and is characterized by granulomas within the lamina propria of the plicae. Caseous necrosis within the granulomas is a helpful diagnostic clue, but is often focal or absent. The diagnosis is best confirmed by bacterial culture, since special stains for acid-fast bacilli in tissue sections seldom result in identification of the organisms in this situation. Examples of granulomas related to tuberculous endometritis and peritonitis are illustrated in Figures 4.69 and 8.14, respectively. Other unusual causes of granulomatous salpingitis include sarcoidosis, Crohn's disease, parasitic infection, and a foreign body granulomatous reaction.

Pseudoxanthomatous Salpingiosis versus Xanthogranulomatous Salpingitis

Pseudoxanthomatous salpingiosis, which is also known as pseudoxanthomatous salpingitis, melanosis tubae, and pigmentosis tubae, is an uncommon lesion that grossly presents as a swollen fallopian tube whose mucosal surface

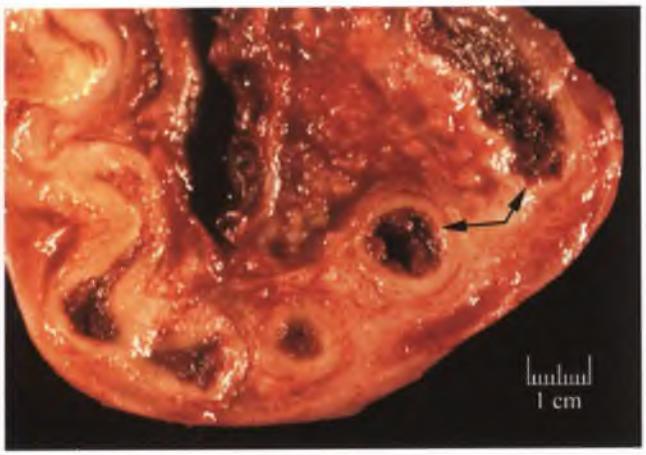

FIGURE 5.10. Pseudoxanthomatous salpingiosis. In this longitudinal section, note the brown discoloration of the mucosa of the swollen fallopian tube (*arrows*), which has a serpentine shape that comes in and out of the plane of view.

consists of polypoid projections with a brown discoloration (Fig. 5.10).[2–4] The combination of a denuded epithelial surface related to an active salpingitis and exposure to intratubal blood whose source is usually actively bleeding ovarian endometriosis is thought to set the stage for the development of pseudoxanthomatous salpingiosis.[2] The macrophages within the lamina propria of the inflamed tubal plicae are initially stuffed with material derived from degraded erythrocytes, which as the salpingitis resolves is gradually converted from hemosiderin and lipid to lipofuscin (ceroid) pigment (Fig. 5.11).[2] In most cases, this material is recognized as finely granular, light brown pigment that exhibits a positive reaction with the periodic acid Schiff (PAS) with diastase stain and a negative reaction with iron stains such as Prussian blue.[2,3] These staining properties facilitate the distinction of this pigment from the more coarsely granular deposits of hemosiderin. In practice, some hemosiderin-laden macrophages often persist, which results in focally positive iron stains.[2,3] As is true for the necrotic pseudoxanthomatous nodules of the ovary and peritoneum that are also related to longstanding endometriosis (see Chapter 6),[5] some examples of pseudoxanthomatous salpingiosis contain pseudoxanthoma cells with abundant eosinophilic cytoplasm in which pigment is difficult to discern (Fig. 5.12).

Pseudoxanthomatous salpingiosis is distinguished from xanthogranulomatous salpingitis on the basis of its (a) usual association with a history of endometriosis, (b) brown, polypoid, mucosal projections, (c) presence of lipofuscin within the aggregates of histiocytes, and (d) near pure population of histiocytes within the lamina propria.[3] In contrast, xanthogranulomatous salpingitis is associated with (a) PID that may be manifested by the presence of a xanthogranulomatous, tubo-ovarian mass, (b) yellow, polypoid, mucosal projections, (c) histiocytes with abundant, foamy cytoplasm that contain microvesicles of lipid, and (d) numerous admixed lymphocytes, plasma cells, and neutrophils (Figs. 5.13 and 5.14).[3]

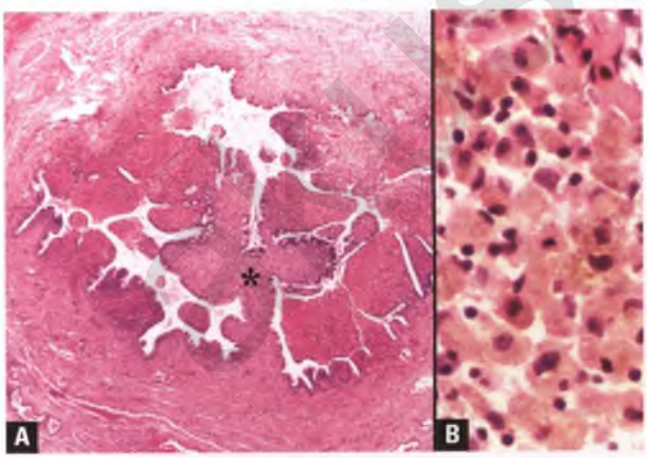

FIGURE 5.11. Pseudoxanthomatous salpingiosis. **A:** The lamina propria of the polypoid mucosal folds is distended with histiocytes that contain finely granular, light brown, lipofuscin (ceroid) pigment. The plicae that are lined by intact, healthy, ciliated epithelium (*asterisk*) are more impervious to the luminal contents and tend to incorporate much less pigmented material. **B:** High-magnification view of the pigmented histiocytes.

SALPINGITIS ISTHMICA NODOSA[6]

Salpingitis isthmica nodosa (SIN) is an uncommon lesion of the isthmic portion of the fallopian tube that occurs in young women. It is often bilateral, and is associated with infertility and ectopic pregnancy. Grossly, SIN appears as a small nodular swelling of the tube that on cut section consists of rubbery, light tan to pale yellow

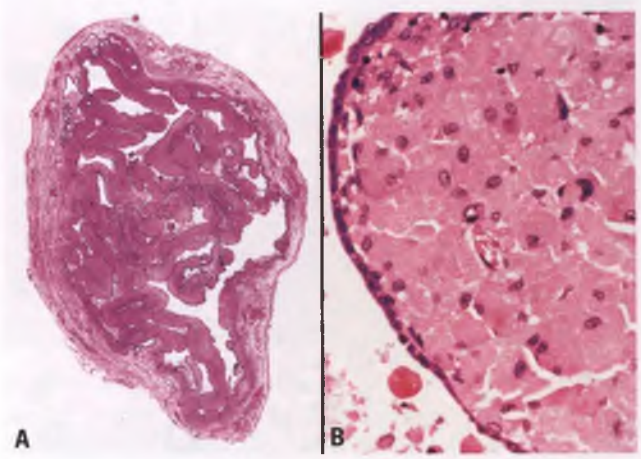

FIGURE 5.12. **A,B:** Pseudoxanthomatous salpingiosis. In this example, the pseudoxanthoma cells that distend the tubal plicae are eosinophilic and lipofuscin pigment is difficult to discern.

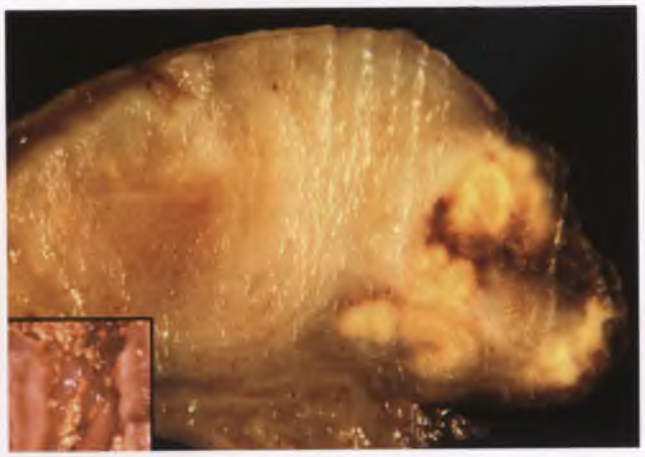

FIGURE 5.13. Xanthogranulomatous salpingitis. In this solid mass of inflamed adnexal tissue with obscured anatomy, the yellow tissue at right represents xanthogranulomatous salpingitis. The inset shows an opened segment of fallopian tube from another case with yellow, polypoid projections studding the mucosal surface.

tissue punctuated by small cysts that surround the original tubal lumen. Histologically, channels ("glands") of variable shapes and sizes that are lined by normal tubal epithelium are seen embedded within hypertrophic smooth muscle of the tubal wall and usually are found throughout its full thickness (Fig. 5.15). These channels communicate with the original tubal lumen, which is recognizable within the central portion of the lesion.

The absence of a desmoplastic, inflammatory, or edematous stromal reaction to the glands, the bland nuclear features of the cells lining the glands, and the presence of ciliated glandular cells facilitate the distinction of SIN from adenocarcinoma. In contrast to endometriosis, SIN lacks the presence of endometrial-type stroma surrounding the glands, and the glands of SIN

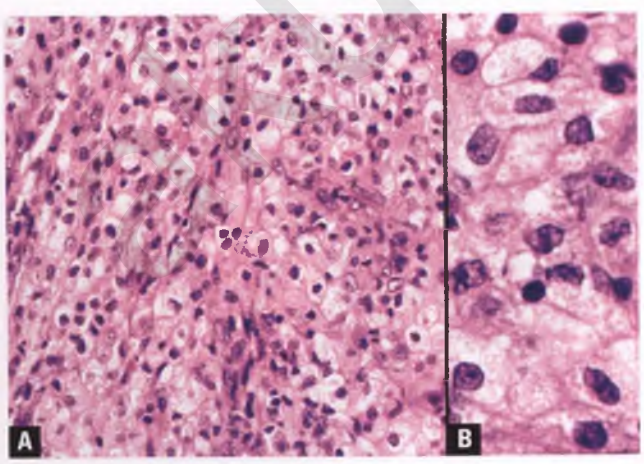

FIGURE 5.14. **A,B:** Xanthogranulomatous salpingitis. Although the lesion is dominated by foamy histiocytes, other inflammatory cells are also present.

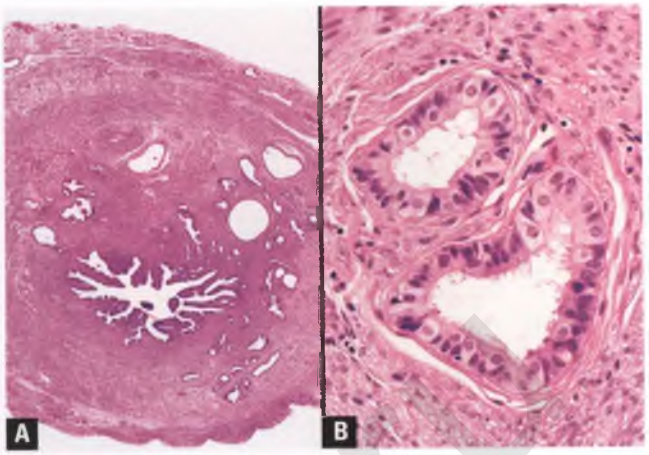

FIGURE 5.15. Salpingitis isthmica nodosa. **A:** At low magnification, channels of tubal-type epithelium, which appear as glands when cross sectioned, surround the original lumen and are scattered throughout the full thickness of the wall. **B:** The glands are lined by tubal-type epithelium with bland nuclear features and readily apparent cilia. Note that the glands are in direct contact with the smooth muscle of the tubal wall without interposed endometrial stroma or a host reaction.

have a tubal rather than endometrioid appearance, with more numerous ciliated cells. Although the pathogenesis of SIN is uncertain, it appears to be analogous to uterine adenomyosis.

EPITHELIAL HYPERPLASIA

Epithelial hyperplasia of uninflamed mucosa, also referred to as mucosal epithelial proliferation, is a subjective entity of unknown significance for which reproducible diagnostic criteria have not been established. Mild forms of epithelial hyperplasia, which exhibit mild degrees of stratification, some cell crowding, and no significant nuclear atypia are so common as to be considered variants of normal (Fig. 5.16).[7,8] At least some of the epithelial hyperplasias that exhibit more prominent cellular stratification and/or nuclear atypia ("moderate to marked mucosal epithelial proliferation") may be precursors of tubal intraepithelial carcinoma (TIC), and are discussed later in this chapter.

In some cases of salpingitis, particularly those that are active and chronic or tuberculous, the tubal epithelium may exhibit a form of hyperplasia that can be confused with carcinoma.[9] Complex pseudoglandular architectural patterns, including the formation of cribriform structures, are seen emanating from the tubal plicae in these hyperplastic areas (Figs. 5.17 and 5.18). Recognition of this process as reactive rather than neoplastic is facilitated by (a) the absence of a mass lesion, (b) the typical clinical setting of a young woman with PID as opposed to a postmenopausal woman with no such history, (c) the absence of high-grade nuclear atypia, (d) the low mitotic rate with an absence of atypical division figures, (e) the lack of a solid epithelial growth pattern, and (f)

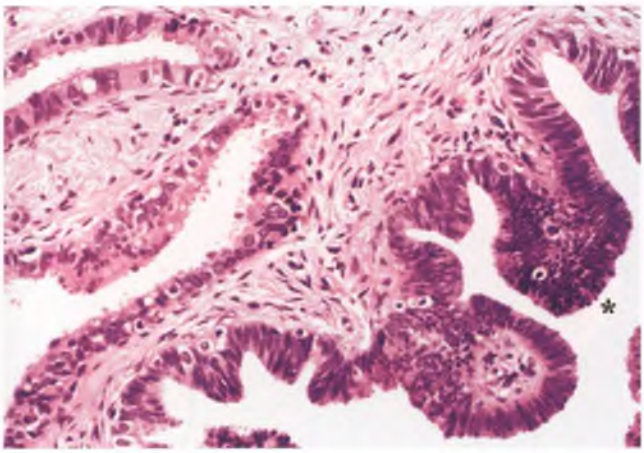

FIGURE 5.16. Innocuous epithelial hyperplasia (no significant abnormality). In this common variant of normal that simulates endometrial epithelium, the tubal epithelium at right is crowded and mildly stratified, but exhibits no nuclear atypia and contains interspersed ciliated cells. The nuclei have a monotonous, elongated shape and maintain their orientation perpendicular to the basement membrane. The epithelial fold marked by an *asterisk* has been cut tangentially. Normal tubal epithelium is at left.

the prominent associated inflammatory component.[9] Since occasional tubal carcinomas are associated with significant inflammation (Fig. 5.19), not too much emphasis should be placed on the last criterion. Once confidently recognized as nonneoplastic, it is preferable to describe lesions within this spectrum as florid reactive epithelial hyperplasia rather than pseudocarcinomatous hyperplasia, since the latter term is more likely to produce undue anxiety on the part of the patient and clinician.

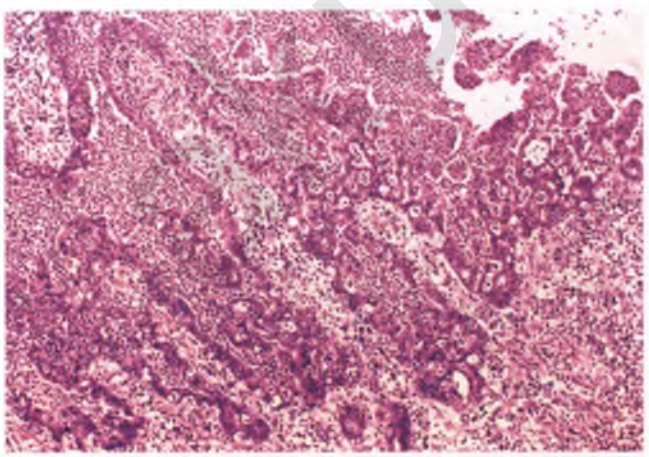

FIGURE 5.17. Active chronic salpingitis with florid reactive epithelial hyperplasia. The tubal mucosa is edematous and inflamed, and there is pus within the lumen. The epithelial proliferation has produced areas with a cribriform pattern, but solid sheets of epithelium are absent.

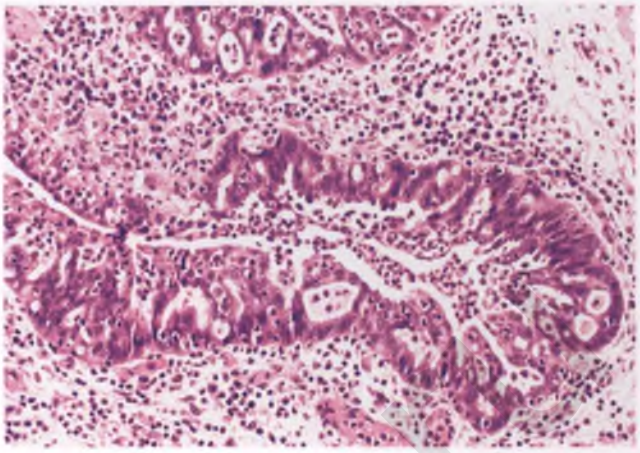

FIGURE 5.18. Active chronic salpingitis with florid reactive epithelial hyperplasia. Although a cribriform pattern is present, mitotic activity is inconspicuous and there is an absence of severe nuclear atypia.

CAUTERY ARTIFACT

Cautery induces characteristic artifactual changes in the epithelium and stroma of the fallopian tube. The traumatized epithelium may be torn away from its supporting stroma, and the epithelial nuclei become compressed, hyperchromatic, and elongated, with a tendency to stream in a particular direction (Fig. 5.20). Detached epithelial fragments can create the appearance of an intraluminal papillary proliferation. The stroma often shows increased eosinophilia. Similar changes have been reported when the fallopian tube is exposed to the heat from a steam radiator.[10] Awareness of this heat-related artifact

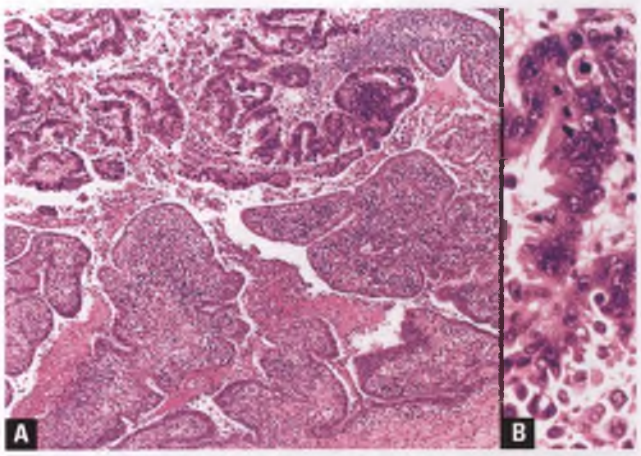

FIGURE 5.19. Serous carcinoma associated with salpingitis. **A:** At low magnification, the foci of adenocarcinoma at the top of the image stand out by virtue of the nuclear hyperchromasia of the malignant cells. This tumor is intraluminal and noninvasive, but the presence of detached carcinomatous tufts places this patient at high risk for peritoneal spread. **B:** In this high-magnification view of the carcinoma, severe nuclear atypia and brisk mitotic activity are evident.

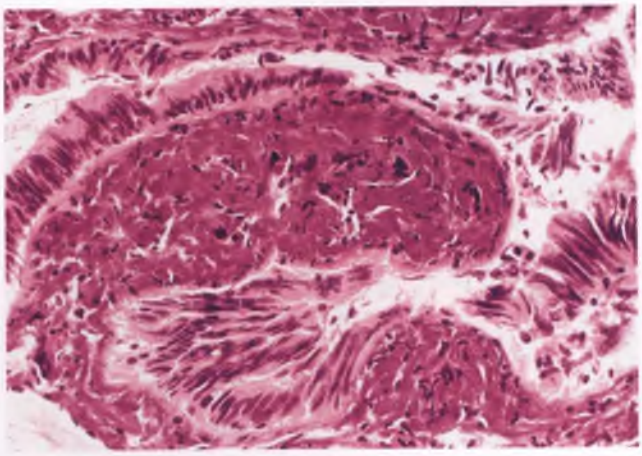

FIGURE 5.20. Cautery artifact of tubal mucosa. The distorted epithelial nuclei are elongated, compressed, and hyperchromatic. Portions of the epithelium have been detached from the stroma, which is hypereosinophilic.

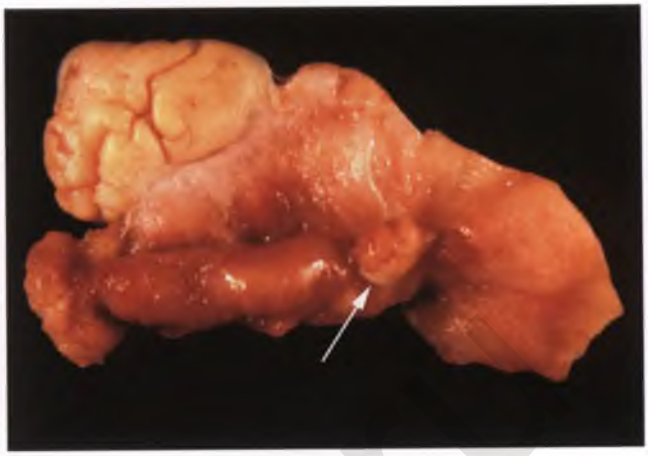

FIGURE 5.21. Salpingo-oophorectomy specimen from a patient who had undergone a previous tubal ligation. Note the presence of a ring-like device that is covered by a thin layer of peritoneal tissue (*arrow*).

is important, since dysplastic/malignant tubal epithelium can also feature elongated cells with hyperchromatic nuclei, albeit with mitotic activity and more appreciable nuclear atypia.

TUBAL LIGATION

Segments of bilateral fallopian tubes are commonly resected for sterilization purposes and are submitted to the surgical pathology laboratory for documentation that complete segments of tubal tissue have been removed. This is most efficiently accomplished by inking the serosa of one of the tubes, specifying which tube has been inked in the gross description, and submitting two to three representative cross sections from each tube in a single cassette. In the usual situation, the diagnosis line of the pathology report is simply "fallopian tubes, left and right, tubal ligation—full cross sections identified." If full cross sections are not documented in the initial sections, the tissue may need to be reoriented in the block prior to obtaining additional sections, and any remaining tubular tissue should be processed for histology. In the final analysis, if full cross sections of both tubes cannot be documented or if tissue other than fallopian tube is present (such as vascular fibromuscular tissue from the round ligament), this information needs to be conveyed directly to the clinician. Both the absence of complete cross sections and the communication with the clinician need to be clearly documented in the pathology report.

When evaluating fallopian tubes that have been incidentally removed during other surgical procedures, a routine part of that evaluation should be to note whether or not there is evidence of a prior tubal ligation. Such evidence includes absence of a segment of the mid-portion of the tube, absence of the fimbriated end, or the presence of a tubal clip or ring. The tissue that has been compressed by a clip or ring undergoes pressure necrosis, and after a period of time the clip or ring may either drop off or be held in position only by a thin layer of peritoneal tissue that has grown over the device (Fig. 5.21). The pathologist typically encounters post-sterilization tubes many years after the procedure, and the proximal tubal stumps in these specimens commonly exhibit mild luminal dilatation, plical attenuation, and chronic inflammation with formation of small pseudopolyps (Fig. 5.22).[11] In the diagnosis section of the pathology report, any of these gross or microscopic findings can simply be reported as "status post tubal ligation."

Patients who have undergone tubal sterilization can still become pregnant on rare occasions. Sterilization failures can be due to faulty technique, recanalization of the tubal lumen, or

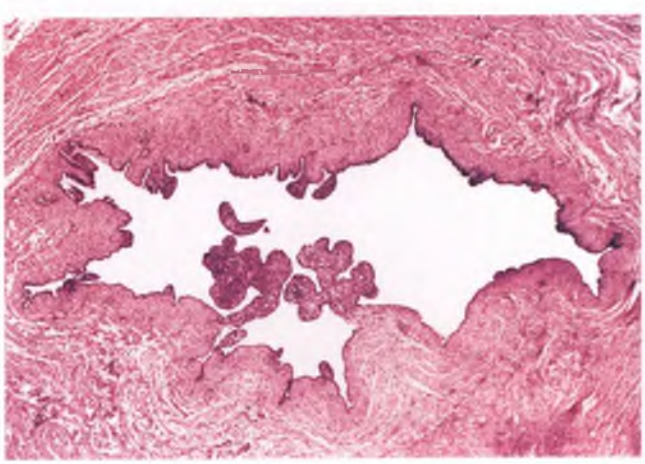

FIGURE 5.22. Proximal fallopian tube with chronic post-sterilization changes. The lumen is slightly dilated, the plical architecture varies from blunted and simplified to flattened, and the lamina propria of the few residual polypoid fronds is chronically inflamed.

tuboperitoneal fistula. If a fallopian tube is submitted for pathologic evaluation following a failed sterilization, it is imperative that the clinician provides the pathologist with the appropriate clinical information, so that the gross specimen can be photographed and carefully examined for sterilization device placement and tuboperitoneal fistula. Histologic sections should be taken to detect lumen recanalization or residual intact lumen in an area where a clip has been improperly placed.[11]

TORSION[12,13]

Tubal torsion is usually an innocent bystander phenomenon related to torsion of a cystically enlarged ipsilateral ovary, but may also occur as an isolated finding in the setting of hydrosalpinx, hematosalpinx, pyosalpinx, ectopic pregnancy, previous tubal surgery, tubal neoplasm, or other tubal disorders. Rarely, isolated tubal torsion occurs without an apparent predisposing factor. Patients usually present with acute abdominal pain, and the twisted structures appear swollen and hemorrhagic. In the early stages of torsion, venous congestion and stromal edema are the major histologic findings, but this is soon followed by interstitial hemorrhage and hemorrhagic infarction (Fig. 5.23).

FALLOPIAN TUBE PROLAPSE

See Chapter 2.

ECTOPIC PREGNANCY

Up to 2% of pregnancies are ectopic, and nearly all of these are located in the fallopian tube.[14,15] Any process that distorts the tubal architecture or otherwise damages the tube, such as PID or SIN, may impair the transport of the fertilized ovum to the uterus and predispose to the development of an ectopic pregnancy.[14,15] In the typical case, there is a sausage-like expansion

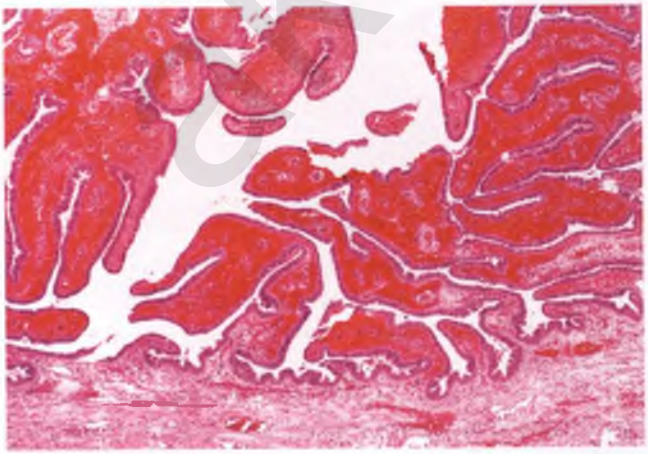

FIGURE 5.23. Torsion of the fallopian tube. In this example, there is marked interstitial hemorrhage in the lamina propria.

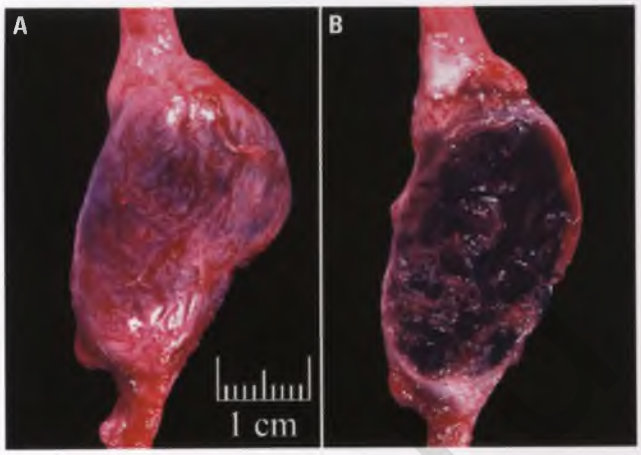

FIGURE 5.24. Tubal ectopic pregnancy. **A:** In this fresh salpingectomy specimen, the ampullary segment is bulging and the serosal surface is hyperemic. **B:** As is typically the case, this longitudinal section demonstrates the dominance of clotted blood, which obscures the presence of products of conception that are only detectable microscopically. (Courtesy of Dr. Richard L. Payne.)

of the ampullary segment of the tube, and the serosa is hyperemic (Fig. 5.24A). In most cases, gross examination of the ectopic pregnancy reveals only blood clot (Fig. 5.24B), although chorionic villi and/or an embryo may be grossly apparent.

The hemorrhage that so often dominates the gross and microscopic findings of a tubal ectopic pregnancy is produced by destructive infiltration of maternal blood vessels by intermediate trophoblast. The combination of blood and trophoblastic tissue may be predominantly intraluminal (Fig. 5.25),

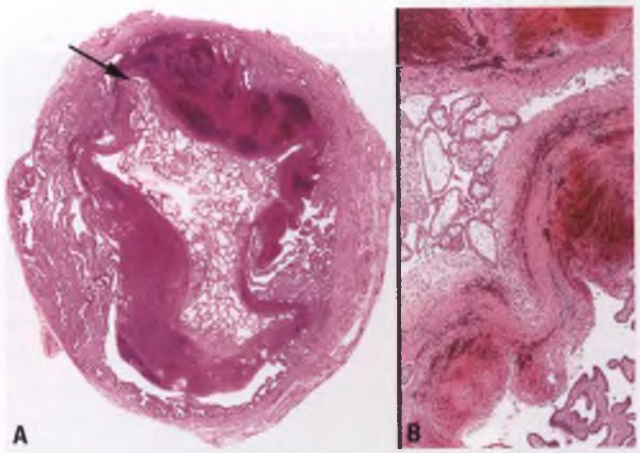

FIGURE 5.25. Tubal ectopic pregnancy. **A:** Low-magnification view of an early ectopic pregnancy. Chorionic villi are confined to the lumen and are surrounded by a convoluted rim of organizing hemorrhage, beyond which are variably compressed tubal plicae. The *arrow* marks a focal area where intermediate trophoblasts have invaded plical tissue, which is sufficient to produce significant hemorrhage. The myosalpinx is thin, but portions have been artifactually torn away. **B:** At higher magnification, chorionic villi are easily distinguished from the tubal plicae at lower right.

FIGURE 5.26. Ruptured tubal ectopic pregnancy. The extruded hemorrhagic material has clotted and remains loosely attached to the tube.

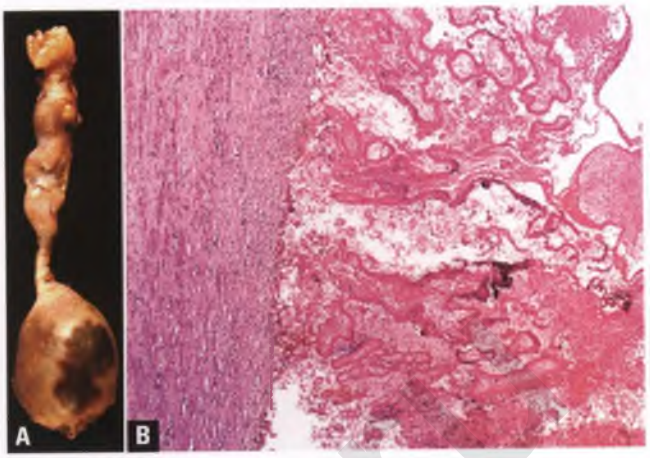

FIGURE 5.27. Remote tubal ectopic pregnancy. **A:** The 2.5 cm nodule at the bottom of the image represents an old ectopic pregnancy of the isthmic region. Note that torsion of the tube has occurred just above the nodule, blocking potential expulsion of the ectopic pregnancy from the fimbriated end of the tube. **B:** The tubal lumen in the region of the remote ectopic pregnancy contains ghost outlines of necrotic villi and hemorrhagic material. Note that the myosalpinx in this area has been partially replaced by fibrous tissue and contains scattered chronic inflammatory cells.

or invasion of the myosalpinx by intermediate trophoblast may be present.[14,16] Ectopic pregnancies with mural invasion by trophoblastic tissue are more prone to rupture, although rupture can also occur as a consequence of an ever-expanding mass within a tube of limited distensibility (Fig. 5.26).[14,16] Rupture of a tubal ectopic pregnancy is often a medical emergency that can be life threatening. Another possible outcome that occurs in an unknown proportion of tubal ectopic pregnancies is spontaneous abortion. Tissue from failed pregnancies of this type may be expelled from the tube via the fimbrial ostium, expelled via the uterus, or retained within the tube. In the latter situation, the pathologist may encounter evidence of a remote tubal pregnancy in the form of ghost outlines of necrotic chorionic villi (Fig. 5.27).[17]

When documenting the presence of an ectopic pregnancy in the absence of grossly apparent chorionic villi or embryonic tissue, the pathologist should focus attention on the clotted blood. In particular, areas within the clot that are tan and granular should be submitted for histologic evaluation, since these foci are most likely to contain chorionic villi. Sections of the tube should also be taken medial to the ectopic pregnancy in an effort to identify any underlying disorder that predisposed to its development. When evaluating tubal tissue for the presence of chronic salpingitis, keep in mind that chronically inflamed plicae near the implantation site may be part of a reaction to the pregnancy itself rather than a manifestation of preexisting inflammatory disease.

Ectopic pregnancies are often removed at a time of gestation when the trophoblastic shell is prominent and trophoblastic proliferation along one pole of the chorionic villi is florid; these findings, which may be seen in association with intermediate trophoblasts infiltrating the myosalpinx and associated vessels, can lead to misinterpretation as a molar pregnancy (Fig. 5.28).[18] This issue is discussed further in the section on the differential diagnosis of molar pregnancy in Chapter 10. For the purposes of the current discussion, suffice it to say that tubal molar pregnancy is very rare and should be diagnosed using strict criteria.[18]

Surgical treatment options for ectopic pregnancy are salpingostomy (incision of the tube followed by removal of the products of conception) and salpingectomy, both of which are usually accomplished via a laparoscopic approach.[19] The chemotherapeutic agent methotrexate is a nonsurgical alternative

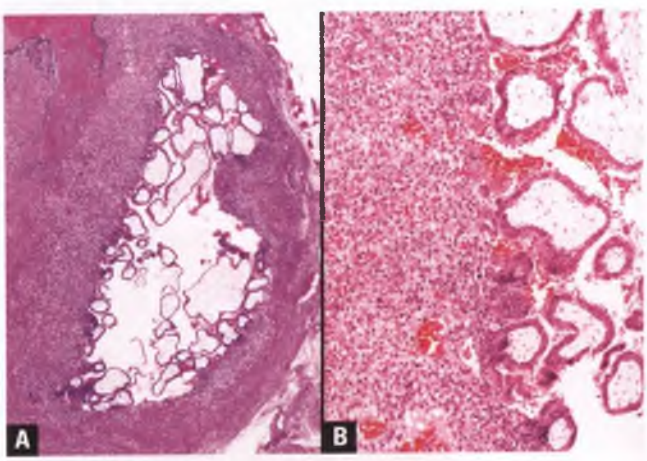

FIGURE 5.28. Tubal ectopic pregnancy. **A:** In this specimen, invading intermediate trophoblasts have destroyed most of the tubal plicae (residual plical elements are at upper left). The intermediate trophoblast also extends into the myosalpinx and vessels, although not evident in this image. Sheets of trophoblast from the trophoblastic shell are present, which should not be misinterpreted as evidence of a molar pregnancy. **B:** Closer view of chorionic villi associated with the trophoblastic shell.

that may be administered systemically to treat early, unruptured ectopic pregnancies.[19] On occasion, trophoblastic elements inadvertently left behind following salpingostomy can persist within the tube or implant on peritoneal surfaces,[20] and methotrexate can also be used to eradicate residual trophoblastic tissue in this circumstance.

ECTOPIC DECIDUA

In the setting of pregnancy, it is not uncommon for the lamina propria of the fallopian tube to undergo decidual change. Rarely, similar findings may be seen in patients who have been treated with progestins.[21] These decidual reactions range from focal with minimal architectural changes to florid with marked expansion, blunting, and distortion of some or all of the tubal plicae (Fig. 5.29). The epithelium overlying the decidual reaction is typically atrophic. The nuclear and cytologic features of the decidualized cells are identical to normal decidua, as described and illustrated in the section on gestational endometrium in Chapter 4. Decidualization of the subserosal paratubal tissue is part of the spectrum of decidual change within the peritoneum, which is discussed in Chapter 8. Distinction of ectopic decidua from placental site nodule is discussed later in this chapter.

ENDOMETRIOSIS

The most common form of tubal endometriosis involves the serosal surface and subserosal tissue and often represents only one of several sites of pelvic involvement. As such, it does not differ appreciably from endometriosis involving peritoneal surfaces, which is discussed in Chapter 8.

Replacement of the lining of the interstitial and isthmic portions of the fallopian tube by endometrial glands and stroma is not uncommon (Fig. 5.30). Rather than being a true form of endometriosis, this phenomenon is considered a variant of normal in which the transition from endometrial to tubal mucosa has shifted further into the fallopian tube. Nevertheless, when bilateral and occlusive of the tubal lumens, the presence of endometrial-type mucosa can result in infertility. Rarely, mucosal replacement by endometrial-type tissue extends beyond the isthmus, at which point a diagnosis of mucosal endometriosis appears justified. An unusual manifestation of mucosal endometriosis is the formation of a hematosalpinx (Fig. 5.31). Endometrial-type mucosa within the fallopian tube can also give rise to endometrioid polyps that

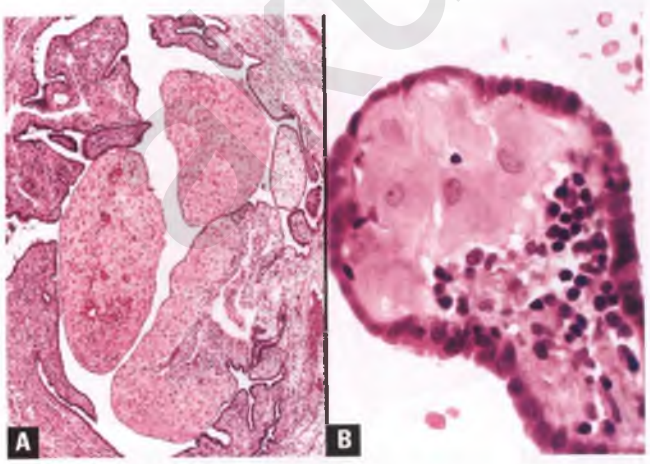

FIGURE 5.29. Ectopic decidua. **A:** Portions of the lamina propria have undergone decidual change, which has distorted the plical architecture. **B:** High-magnification view of a partially decidualized tubal plica.

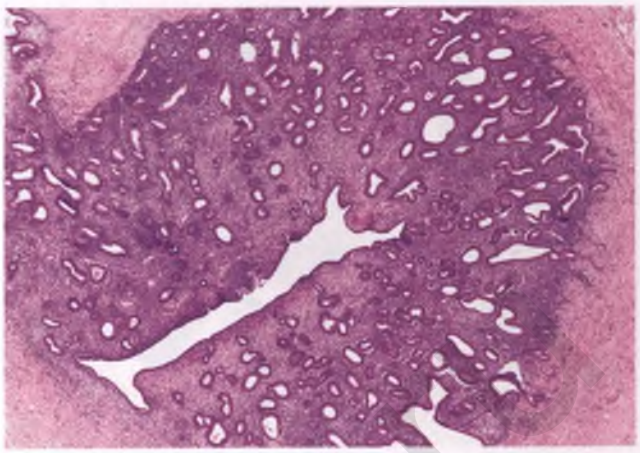

FIGURE 5.30. Replacement of tubal mucosa by proliferative-type endometrial tissue. In this example, the tubal lumen persists as an elongated slit.

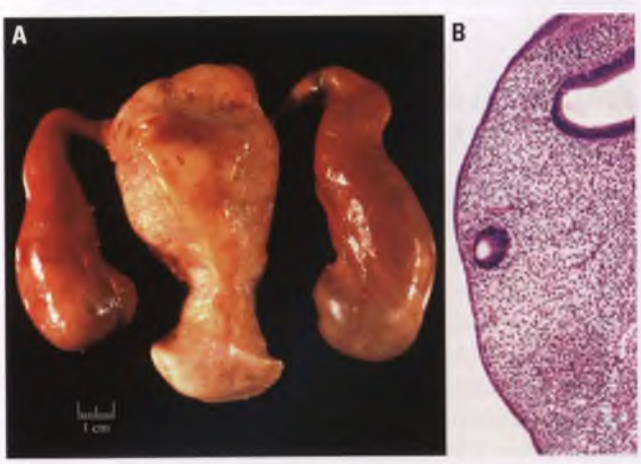

FIGURE 5.31. Bilateral hematosalpinx associated with mucosal endometriosis. **A:** Both fallopian tubes, which are attached to the anterior half of the uterus, exhibit hydrosalpinx-like enlargement, but were filled with chocolate-colored rather than serous fluid. **B:** Representative section of the tubal lining, demonstrating replacement of the mucosa by endometrial-type glands and stroma.

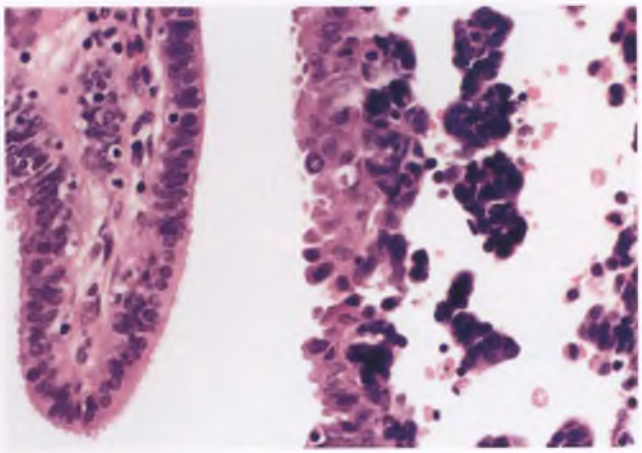

FIGURE 5.32. Endometrial breakdown with retrograde transport into fallopian tube. The tubal lumen contains small fragments of crumbling endometrial tissue composed of epithelium (central vertical strip) and compacted stromal aggregates. Normal tubal mucosa is at left.

FIGURE 5.33. Several small Walthard nests stud the serosal surface of this segment of fallopian tube.

typically have the same stromal and vascular changes as uterine endometrial polyps; such lesions have also been reported as polypoid endometriosis.[22]

The finding of fragments of crumbling endometrial stroma within the tubal lumen, sometimes in association with endometrial glandular epithelium, is due to retrograde transport from the uterine cavity (Fig. 5.32). These fragments are usually generated during menstruation or uterine bleeding related to anovulatory cycles. This phenomenon is one of the theoretical causes of pelvic endometriosis, but should not be considered endometriosis per se. Repeated episodes of retrograde menstruation are presumably the mechanism by which the proximal tubal stumps become involved by endometriosis following salpingectomy.[23]

WALTHARD NESTS/TRANSITIONAL METAPLASIA

The term Walthard nests (or Walthard rests) refers to the common incidental finding of small foci of transitional cell metaplasia on the tubal serosa. These foci are often multiple, may be solid or cystic, and can also involve the broad ligament. Their appearance as small, pale-tan nodules studding the serosal surface of the fallopian tube may result in the clinical or gross impression of metastatic carcinoma (Fig. 5.33). Histologically, the stratified transitional epithelium is mitotically inactive and has bland nuclear features with occasional longitudinal nuclear grooves (Fig. 5.34). Portions of the lining of the cystic form of Walthard nests often have a flattened appearance, which may possibly reflect a mesothelial origin or be related to pressure atrophy. Eosinophilic material is often found within these cystic spaces.

When examined carefully, it is not uncommon to find one or more small foci of transitional metaplasia in the tubal fimbriae.[24] The nuclear features of transitional metaplasia, as described above, generally allow for its distinction from tubal intraepithelial carcinoma. In problematic cases, p53 and MIB-1 immunostains can provide useful information, since transitional metaplasia is negative for p53 and has a near-zero MIB-1 labeling index, whereas intraepithelial carcinoma exhibits diffuse and strong nuclear p53 staining and has a high MIB-1 labeling index.[24] As is the case for Walthard nests, transitional cell metaplasia of the tubal fimbriae is of no clinical significance.

MUCINOUS METAPLASIA

Mucinous metaplasia is a rare phenomenon in which some or all of the tubal epithelial lining is replaced by tall columnar mucinous epithelium (Fig. 5.35).[25,26] Although this may represent an isolated finding, it may be associated with Peutz-Jeghers syndrome

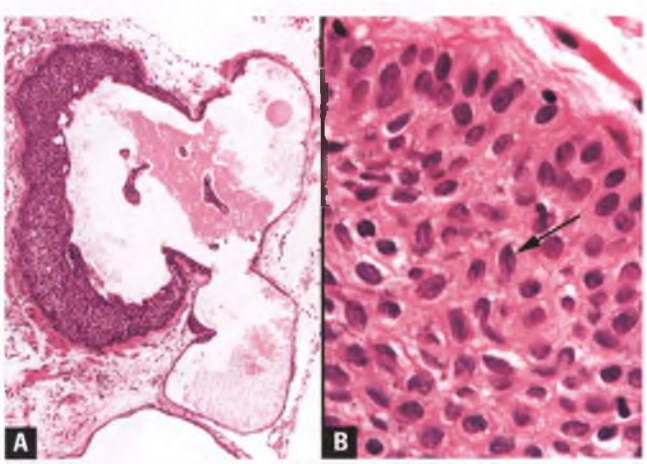

FIGURE 5.34. Walthard nests. **A:** Cystic form containing eosinophilic material and partially lined by transitional epithelium. **B:** High-magnification view of a solid Walthard nest. Note the presence of longitudinal nuclear grooves within some of the cells (*arrow*).

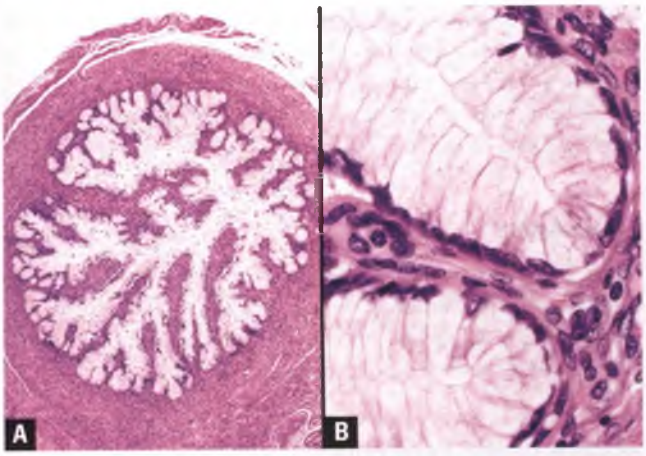

FIGURE 5.35. **A,B:** Mucinous metaplasia. In this portion of the fallopian tube, the native epithelial lining has been completely replaced by tall columnar mucinous epithelium.

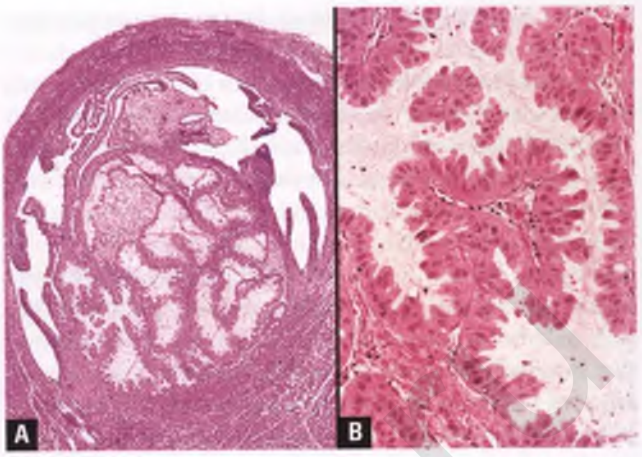

FIGURE 5.36. Metaplastic papillary tumor. **A:** At low-magnification, the lesion is seen occupying a rounded portion of the tubal lumen. Note that it is partially surrounded by a crescent of uninvolved tubal mucosa, and that the luminal diameter is unaltered by the proliferation. **B:** This higher magnification view highlights the papillary architecture, nuclear pseudostratification, cellular buds, oncocytic cytoplasm, and pale-staining intraluminal mucinous material. A mitotic figure is present in the central portion of the image.

and/or mucinous tumors of the endocervix or ovary. In patients with pseudomyxoma peritonei, the possibility of colonization of the tubal epithelium by neoplastic mucinous epithelium, typically derived from a ruptured low-grade mucinous neoplasm of the appendix, should be considered before rendering a diagnosis of mucinous metaplasia (see section on Secondary Tumors).

METAPLASTIC PAPILLARY TUMOR

Metaplastic papillary tumor is a rare benign lesion that occurs almost exclusively as an incidental microscopic finding within a grossly normal fallopian tube of a postpartum woman.[27] This lesion replaces a portion of the tubal lumen without expanding the tubal diameter, and is characterized by a papillary proliferation that exhibits an architecture that is similar to serous borderline tumors of the ovary, including formation of detached cellular buds (Fig. 5.36). The epithelial cells lining the papillae are nonciliated, exhibit areas of nuclear pseudostratification, and have abundant eosinophilic cytoplasm that imparts an oncocytic appearance. Nuclear atypia is mild, and rare mitotic figures may be present. Occasional cells may contain intracytoplasmic mucin, and intraluminal mucin may also be found. Although reported as a neoplasm, some pathologists think that this lesion represents an exuberant, localized form of oncocytic metaplasia. It is distinguished form the tubal form of serous borderline tumor by its microscopic size, lack of tubal distension, and association with pregnancy.[28]

ADENOMATOID TUMOR

Adenomatoid tumors are benign neoplasms of mesothelial origin. Although rare, these tumors have generally been regarded as the most common benign tumor of the fallopian tube, but small incidental adenofibromas of the tubal fimbriae have recently been found to be much more prevalent.[29] Tubal adenomatoid tumor typically presents in an adult woman as an incidental, small, firm, mural-based nodule that has a pale yellow to off-white sectioned surface. The tumor impinges upon neighboring structures and replaces tissue as it expands, but does not show evidence of destructive invasion (Fig. 5.37).

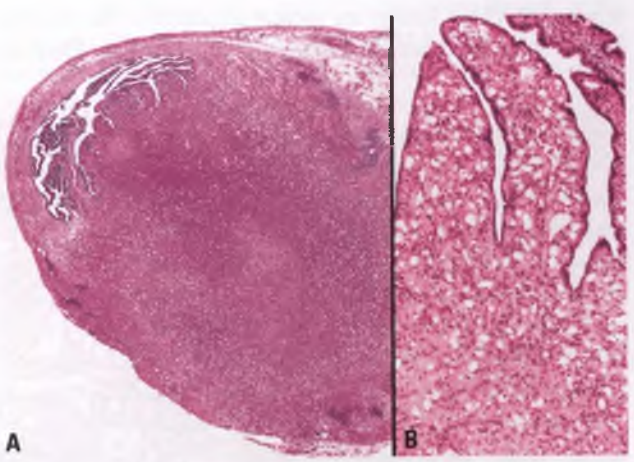

FIGURE 5.37. Adenomatoid tumor. **A:** At low magnification, a nodular tumor is seen expanding and replacing a large portion of the tubal wall and compressing the lumen into a thin crescent. **B:** At higher magnification, the microcystic nature of the tumor is evident in an area where the tumor extends into the lamina propria of some of the tubal plicae.

The most common histologic patterns of adenomatoid tumor are ones in which pseudovascular or pseudoglandular spaces are created due to the presence of microcystic spaces that are lined by either flattened or cuboidal cells, respectively (Fig. 5.38). Cells with vacuolated cytoplasm, sometimes imparting a signet-ring appearance, are also often present. The tumor cells have bland nuclear features and virtually no mitotic activity, which help to differentiate these innocuous lesions from malignant tumors. Adenomatoid tumors are immunoreactive for cytokeratin and the mesothelial marker calretinin, and fail to stain with endothelial markers. There is little in the recent literature that specifically addresses adenomatoid tumors of the fallopian tube, but studies on the histologic and immunologic features of adenomatoid tumors in one site generally apply to those in other sites (see references on adenomatoid tumors in Chapter 4).

ADENOFIBROMA

These tumors are located preferentially at the fimbriated end of the tube and are histologically identical to their ovarian counterparts, which are discussed in Chapter 7. The vast majority of tubal adenofibromas are of the serous type, although endometrioid adenofibromas may also be encountered in this location. Tubal adenofibromas that are of a size such that they are appreciable grossly are rare, but a recent study has demonstrated the presence of small incidental adenofibromas or their precursors in 30% of fallopian tubes that were submitted entirely for histologic evaluation.[29]

MISCELLANEOUS BENIGN PROCESSES

Papilloma

Tubal papillomas are extraordinarily rare, but have been reported.[30] These lesions are loosely attached to the mucosa, project into the lumen, and consist of a papillary proliferation with fibrovascular cores lined by tubal-type epithelium. Papillomas are distinguished from normal tubal plicae by their discrete nature and more impressive architectural complexity, and from serous borderline tumors by their bland nuclear features and lack of epithelial tufting.

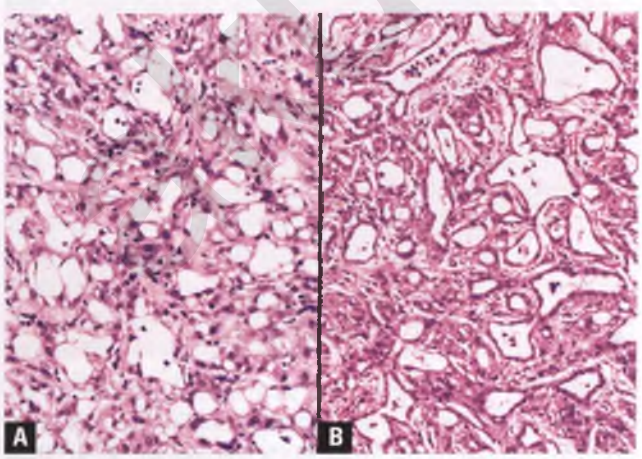

FIGURE 5.38. Adenomatoid tumor. **A:** Predominantly pseudovascular pattern, with spaces lined mainly by flattened cells. **B:** Predominantly pseudoglandular pattern, with spaces lined mainly by cuboidal cells.

Leiomyoma

Tubal leiomyomas are rare, but represent the most common benign soft tissue tumor in this site.[31] They usually present as a small, solitary, incidental nodule, but may rarely be associated with or simulate an ectopic pregnancy.

Mature Cystic Teratoma

Rare mature cystic teratomas (dermoid cysts) of the fallopian tube have been reported.[32]

Arias-Stella Reaction

The Arias-Stella reaction is most commonly seen within endometrial glandular epithelium during early pregnancy, and is described and illustrated in Chapter 4. On very rare occasions, tubal epithelium can also exhibit features of the Arias-Stella reaction.[33] The absence of a mass lesion, its incidental presentation as a focal finding in a patient who is harboring an intrauterine or ectopic pregnancy, the lack of mitotic activity, the absence of stromal invasion, and the dark, smudged chromatin of the involved cells facilitate its distinction from carcinoma.

Clear Cell Hyperplasia

Clear cell hyperplasia of tubal epithelium is a very rare finding that has been reported in association with ectopic pregnancy.[34] This lesion lacks the nuclear atypia, mitotic activity, stromal invasion, and variety of architectural patterns of clear cell carcinoma, and is further distinguished by its association with pregnancy.

Placental Site Nodule

Placental site nodules are small remnants of hyalinized implantation site that contain intermediate trophoblasts and represent an incidental indication of a remote pregnancy. These lesions are usually found within endometrial samples, and are discussed and illustrated in Chapter 4. Placental site nodule has been reported in the fallopian tube on rare occasions, and presumably represents a manifestation of an old ectopic pregnancy.[35]

Placental site nodule may be misinterpreted as a nodule of ectopic decidua, which is a diagnostic error of no clinical significance. The correct diagnosis can usually be made by paying attention to the morphologic differences between decidual cells and intermediate trophoblast (see section on subtypes of trophoblast in Chapter 4); if desired, immunohistochemistry can be utilized to distinguish cytokeratin-positive intermediate trophoblast from cytokeratin-negative decidua.

Ovarian Hilus Cell Heterotopia

Small nests and cords of cells that are morphologically similar to ovarian hilus cells are a rare finding within the lamina propria of the fallopian tube, particularly in the fimbrial region, and may also be encountered within the perisalpinx.[36,37]

Calcification[38]

Calcifications within the tubal lumen or mucosa that are unassociated with frankly malignant epithelium are referred to as salpingoliths. Many of these calcifications have the concentric laminations of psammoma bodies, and the vast majority are surrounded by a simple layer of bland epithelium. Salpingoliths are most likely to be found in the settings of salpingitis and ovarian serous neoplasia (particularly serous borderline tumors of usual and micropapillary types).

Intraluminal Keratin

The presence of clumps of keratin within the lumen of the fallopian tube is rare, and most often originates from an endometrial carcinoma that exhibits prominent squamous differentiation (Fig. 5.39).[39] Other potential sources of this keratinous material include ruptured mature cystic teratomas of the ovary or ovarian endometrioid tumors with squamous differentiation with a breached capsule. The intraluminal aggregated flakes of keratin are typically unassociated with viable tumor cells, and are of no known prognostic significance. Intratubal retrograde transport of endometrial-derived keratin fragments through the fimbrial ostia can result in the formation of peritoneal keratin granulomas, just as can occur with keratin more directly deposited within the peritoneal cavity from the types of ovarian tumors mentioned above (see Chapter 8).

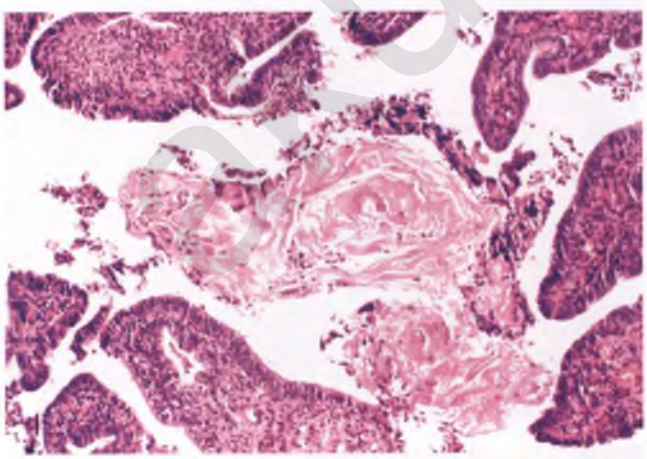

FIGURE 5.39. Eosinophilic clumps of keratin are present within the lumen of the fallopian tube. The patient had concurrent endometrioid adenocarcinoma of the endometrium with prominent squamous differentiation.

BORDERLINE EPITHELIAL TUMORS

Borderline tumors of serous, endometrioid, and mucinous types are extraordinarily rare neoplasms of the fallopian tube, but have been reported.[25,28,40] These tumors histologically resemble their more common ovarian counterparts (see Chapter 7).

GENERAL FEATURES OF TUBAL CARCINOMA[41]

As currently defined, primary carcinoma of the fallopian tube is a rare entity. By convention, the presence of bulky tumor in the ovary is considered evidence of primary ovarian neoplasia whenever the ovary and tube are both involved by tumor. The peritoneum is given similar priority when assigning the site of origin when tubal carcinoma is associated with extensive peritoneal disease with absent or only superficial ovarian involvement. Although these conventions are entrenched in the literature, evidence continues to mount that many high-stage serous tumors that are classified using traditional criteria as primary ovarian or peritoneal serous carcinomas actually originate within the tubal fimbriae (see below).

Women with tubal carcinoma have a mean age of 55 to 58 years and present with abnormal vaginal bleeding, a watery vaginal discharge, an abdominal mass, and/or abdominal pain.[42] Cells that are suspicious for or diagnostic of adenocarcinoma may be present in the patient's Pap smear.[42,43] In a large study using combined cancer registry data, 8% of tubal carcinomas were bilateral.[44] Tubal carcinoma has a variable gross appearance, as depicted in the section on serous carcinoma, which is by far the most common type of tubal cancer.

In the International Federation of Gynecology and Obstetrics (FIGO) staging system for fallopian tube carcinoma, stage 0 refers to carcinoma in situ, stage I to carcinoma limited to the fallopian tube, stage II to carcinoma that has spread locally to the uterus, ovaries, or other pelvic tissues, stage III to carcinoma with peritoneal implants outside of the pelvis and/or involvement of regional lymph nodes, and stage IV to carcinoma with distant metastases.[45] As discussed previously by others,[42] FIGO's use of inaccurate terminology for tubal histology is a potential source of confusion. When used appropriately, the term "mucosa" refers to *both* the epithelial lining and its supporting lamina propria; hence, FIGO's definition of carcinoma in situ as being limited to the tubal mucosa is misleading and could potentially include carcinomas that invade the lamina propria.[42] FIGO's intent is to include tumors that invade the lamina propria within the stage Ia category, where their reference to "submucosal" invasion presumably refers to the lamina propria (the fallopian tube has no submucosa).[42] In addition to clarifying this issue, Alvarado-Cabrero et al.[42] have recommended further subdivisions within the stage I category based upon the more aggressive clinical behavior of (a) a stage I intraluminal tumor mass that is noninvasive as compared to carcinoma in situ, (b) a stage I myoinvasive carcinoma as compared to one that has not progressed beyond the lamina

propria, and (c) a stage I fimbrial carcinoma (which has direct exposure to the peritoneal cavity) as compared to a nonfimbrial tumor.

Stage is the dominant factor in the prognosis of fallopian tube carcinoma, with 5-year survival of roughly 70% for stage I disease progressively decreasing to about 10% for stage IV.[43] In low-stage disease, closure of the fimbriated end has been associated with an improvement in survival, presumably due to the prevention of direct seeding of the peritoneal cavity by luminal-based tumor.[42,43] As discussed in the section on tubal intraepithelial carcinoma, occasional patients with carcinoma in situ (stage 0) may recur and die of disease.[43]

There is no standard grading system for carcinoma of the fallopian tube, and grade is only of marginal, if any, independent prognostic significance.[42,43,46] That said, most fallopian tube carcinomas that present at high stage are high-grade tumors.[42] My preference is to use the two-tier grading system of ovarian serous carcinoma as described in Chapter 7 for tubal serous carcinoma and the three-tier grading scheme that is applied to endometrial carcinoma as described in Chapter 4 for tubal endometrioid carcinoma. The less common types of tubal carcinoma can be graded similarly to their corresponding type of ovarian carcinoma.

The most important aspects to include in the pathology report of resection specimens that contain tubal carcinoma are tumor size, tumor location (particularly whether or not of fimbrial origin), closed versus patent nature of the fimbrial ostium, histologic tumor type, tumor grade, extent of invasion of the tubal wall (with regard to lamina propria, muscularis, and serosa), presence or absence of angiolymphatic invasion, and presence or absence of tumor involvement of extratubal structures.[46]

TUBAL INTRAEPITHELIAL CARCINOMA AND ITS PRECURSORS

TIC is analogous to endometrial intraepithelial carcinoma (EIC), and is also referred to as adenocarcinoma in situ or carcinoma in situ. Unless otherwise specified, it is assumed to be of the serous type. This lesion is not apparent grossly, and has a strong predilection for a fimbrial location.[47,48] TIC features replacement of the tubal epithelium by a crowded and jumbled proliferation of malignant epithelial cells that exhibit marked nuclear atypia with hyperchromasia, prominent nucleoli, high proliferative rates, and an absence of cilia (Fig. 5.40).[49,50] Stratified nuclei and fragile micropapillary epithelial struts with nearby clusters of exfoliated tumor cells are often present, although more subtle examples with minimal stratification also occur.[49] TIC usually exhibits diffuse and strong nuclear immunoreactivity for p53 *and* has a high MIB-1 proliferative index, which help to distinguish it from reactive atypias and innocuous hyperplasias.[47,49,50]

On occasion, one encounters a mucosal epithelial proliferation with histologic features that fall between that of ordinary hyperplasia and TIC. These lesions have been variously termed

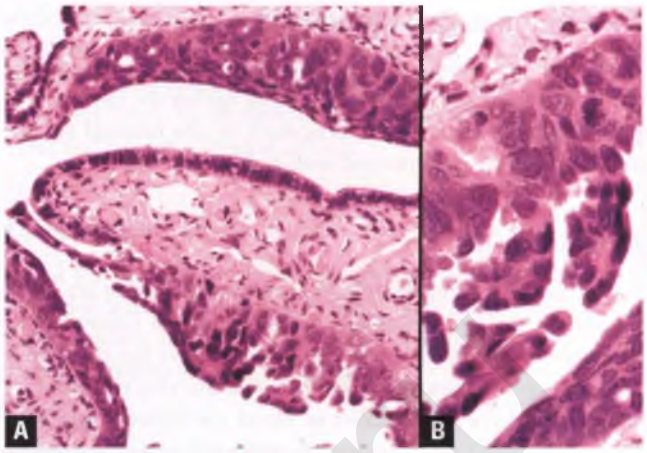

FIGURE 5.40. Tubal intraepithelial carcinoma. **A:** Portions of the tubal epithelium have been replaced by a jumbled, stratified proliferation of markedly atypical cells. **B:** This high-magnification view highlights the micropapillary epithelial struts and exfoliated tumor cells that are commonly present in this lesion, which may result in peritoneal dissemination ("shed and spread"). Also note the significant nuclear atypia and the presence of a mitotic figure at upper right.

moderate to severe dysplasia, moderate to marked mucosal epithelial proliferation, atypical hyperplasia, or tubal epithelial atypia (Fig. 5.41).[7,50,51] Some of these proliferations, dubbed "tubal intraepithelial lesions in transition" (TILTs), may represent precursors of TIC.[49] TILTs are p53 positive and have a MIB-1 proliferation index that is higher than normal, but the proliferation index and the degree of nuclear atypia are less than that seen in full-fledged TIC.[49] The earliest step in serous carcinogenesis may be the production of the so-called p53 signatures, which are short stretches of normal-appearing tubal

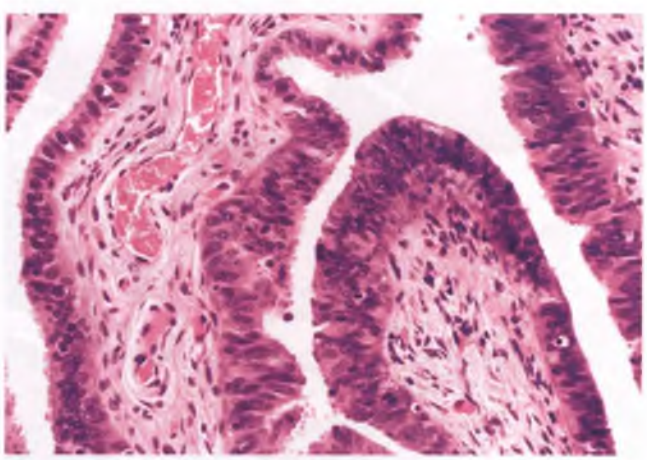

FIGURE 5.41. Moderate to severe dysplasia (atypical hyperplasia). The tubal epithelium in this patient with a strong family history of ovarian cancer is stratified and shows some nuclear atypia, but polarity is preserved and there are occasional interspersed ciliated cells. Normal tubal epithelium is at left.

epithelium of secretory type that are characterized by strong expression of p53 in conjunction with a low proliferative index.[49,52–54] p53 signatures can be identified in roughly one-third of fallopian tubes from women both with and without known BRCA mutations.[52–54] TILTs, which have also recently been designated proliferative p53 signatures, and ordinary p53 signatures are currently of no known clinical significance, and are not recommended as diagnostic terms.[50]

In contrast to in situ carcinomas of most other organ systems, TIC (like EIC) can be lethal, since its cells may be shed into the peritoneal cavity or onto the nearby ovarian surface, where their growth can lead to findings that are indistinguishable from primary peritoneal or ovarian serous carcinoma.[43,55] Thus, many ovarian and peritoneal serous carcinomas that are considered primaries by conventional criteria related to where the bulk of the tumor is located and the surface versus parenchymal nature of the ovarian involvement may actually originate from cells shed from TICs or tubal serous carcinomas that have since been overrun by tumor or overlooked by the pathologist.[55–57] Such a mechanism would certainly explain why most high-grade "primary" ovarian serous carcinomas do not have a recognizable precursor lesion within the ovary and present with widespread abdominal and pelvic involvement, and does not bode well for developing strategies to detect and treat this disease in its early stages.

SEROUS CARCINOMA[42]

Serous carcinoma is the most common type of primary tubal carcinoma. When nonconsultation material is classified by experts, it accounts for approximately 70% of cases. The gross appearance of tubal serous carcinoma typifies that of tubal carcinoma in general. Most tumors produce a fusiform swelling involving most or all of the tube, sometimes producing an external appearance that is indistinguishable from a hydrosalpinx, hematosalpinx, or ectopic pregnancy (Figs. 5.42 and 5.43). When tubal carcinomas occur in patients with a genetic predisposition for their development, they often originate in the fimbriated end and may be overlooked if specific attention is not paid to this area (Fig. 5.44A).

Histologically, serous carcinomas of the fallopian tube resemble their ovarian counterparts. Tumors consist of variable combinations of papillae, slit-like spaces, and diffuse sheets of neoplastic cells, which usually exhibit considerable nuclear pleomorphism and mitotic activity (Figs. 5.44B, 5.45, and 5.46). Psammoma bodies, foci of tumor necrosis, and scattered tumor giant cells may be present. Extension of tumor into preexisting epithelial invaginations that have been tangentially sectioned should not be misinterpreted as evidence of myoinvasion (Fig. 5.47). As mentioned above, my preference is to grade tubal serous carcinoma in the same manner as ovarian serous carcinoma (see Chapter 7). Whatever grading system is used, the architectural, nuclear, and proliferative features of the vast majority of tubal serous carcinomas should result in their classification as high-grade tumors.

LESSONS LEARNED FROM PATIENTS WITH BRCA MUTATIONS

The treatment of patients with BRCA gene mutations or a strong family history of breast/ovarian cancer with risk-reducing bilateral salpingo-oophorectomy has sparked a wave of research that is revolutionizing our concepts of pelvic (tubal, ovarian, and peritoneal) serous carcinoma. When thoroughly

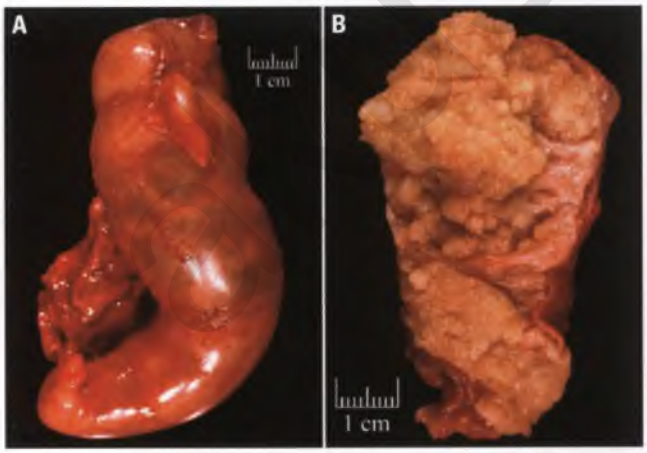

FIGURE 5.42. Serous carcinoma of the fallopian tube. **A:** The tube exhibits a sausage-like distension and has an external appearance similar to that of an ectopic pregnancy or hematosalpinx. **B:** Opening of the tube reveals an inner lining studded with multiple soft, friable, tan to pale yellow tumor nodules that appear granular due to their papillary nature.

FIGURE 5.43. Serous carcinoma of the fallopian tube simulating a hydrosalpinx. During its evolution, growth of the main tumor nodule at the apex of this opened, cystically dilated tube (*arrow*) presumably led to closure of the fimbriated end, which in turn led to intraluminal accumulation of fluid.

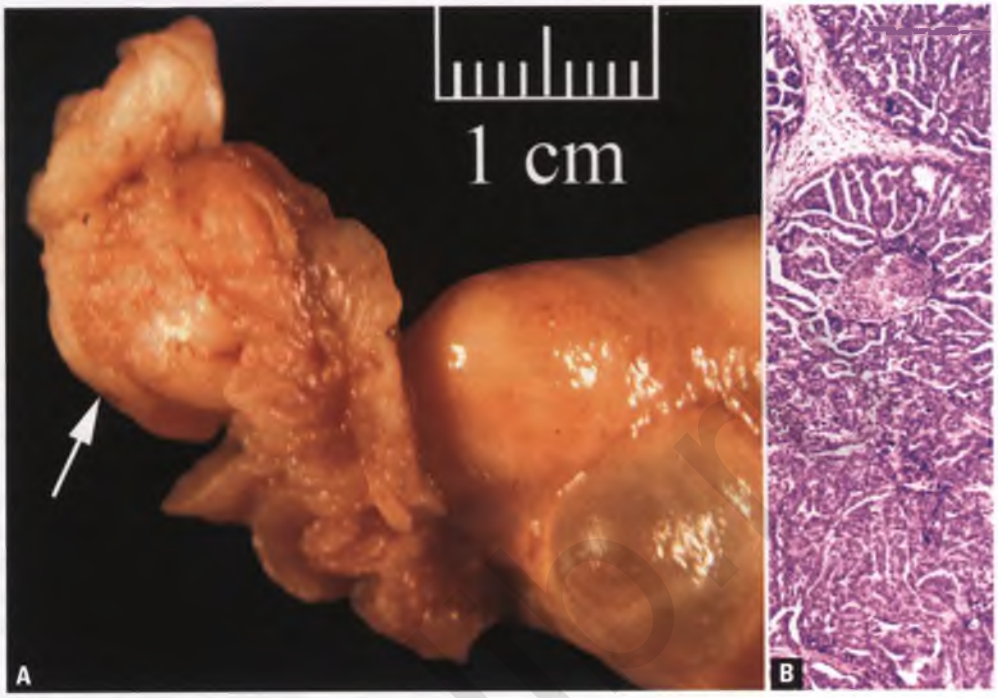

FIGURE 5.44. Occult tubal carcinoma from a total abdominal hysterectomy/bilateral salpingo-oophorectomy specimen of a patient with a strong family history of ovarian cancer. **A:** The small tumor at the fimbriated end (*arrow*) was not detected until examination in the pathology laboratory. **B:** Histology of this nodule reveals a serous carcinoma with papillae, slit-like spaces, and foci of necrosis. *Note*: A subsequent staging procedure showed omental metastases. Had the fimbrial carcinoma gone unnoticed, this patient would have presented with "primary peritoneal serous carcinoma" a few months or years later.

examined, approximately 10% of fallopian tubes from patients with BRCA gene mutations will have TIC or occult serous carcinoma, and most of these lesions are of fimbrial origin.[58,59] Although initially documented in women with BRCA mutations, the key role played by the tubal fimbriae in the pathogenesis of pelvic serous carcinoma has since been shown to hold true for sporadic carcinomas of this type as well.[55–57]

In order to maximize detection of these tiny serous lesions, evaluation of prophylactic salpingo-oophorectomy specimens in high-risk patients should employ the so-called SEE-FIM or similar sectioning protocol after tissue has been adequately fixed in formalin for at least 4 hours. Using these protocols, 2- to 3-mm thick sections of the entire specimen are examined histologically, with the tubal fimbriae sectioned longitudinally to optimize visualization of their plical folds.[47,59] A better understanding of the true origin of "primary" ovarian and peritoneal serous carcinomas will also be obtained if rigorous processing of the fallopian tube is utilized in these situations as well.[57] Expanding the potential significance of TIC one step further, a recent study has suggested that TIC may actually

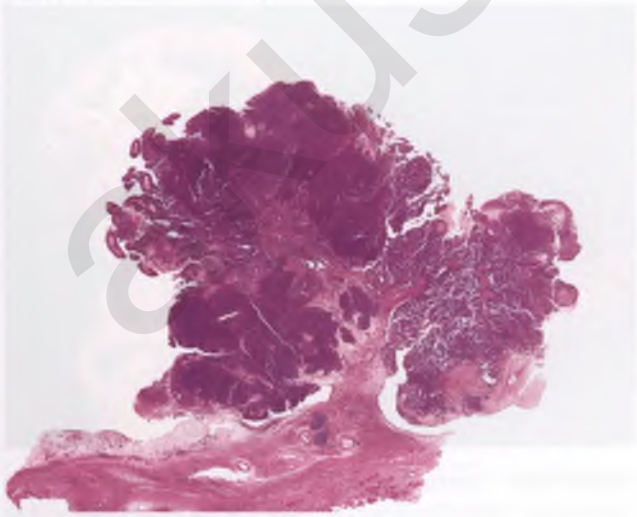

FIGURE 5.45. Serous carcinoma of the fallopian tube. This polypoid tumor on a stalk represents the histologic correlate of the tumor nodule in Figure 5.43.

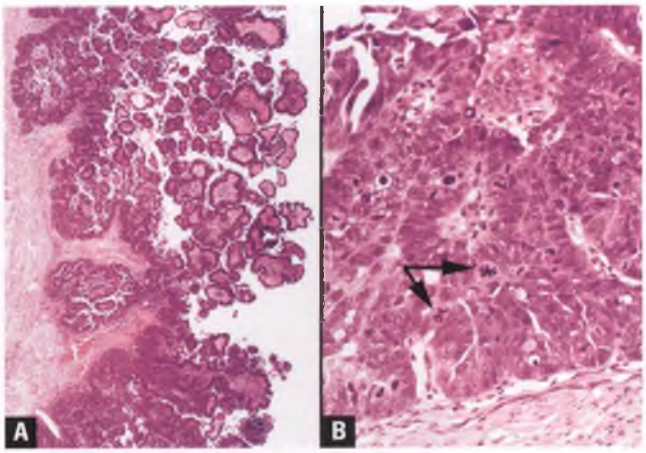

FIGURE 5.46. Serous carcinoma of the fallopian tube (histologic correlate to the tumor in the Fig. 5.42). **A:** The papillary architecture of the tumor is readily apparent at low magnification. No definite myoinvasion is present. **B:** High-magnification view of an area with a partially solid architecture. Note the brisk mitotic activity, which includes two atypical division figures (*arrows*).

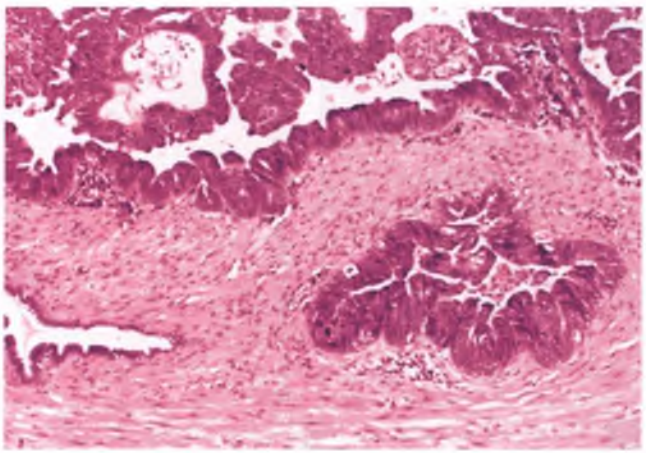

FIGURE 5.47. Nonmyoinvasive serous carcinoma of the fallopian tube. The epithelial invagination at lower left is unaltered from its native state, whereas the size, placement, and undulating margin of the island of tumor at lower right is indicative of replacement of what was once a similar epithelial invagination rather than tumor invading the myosalpinx.

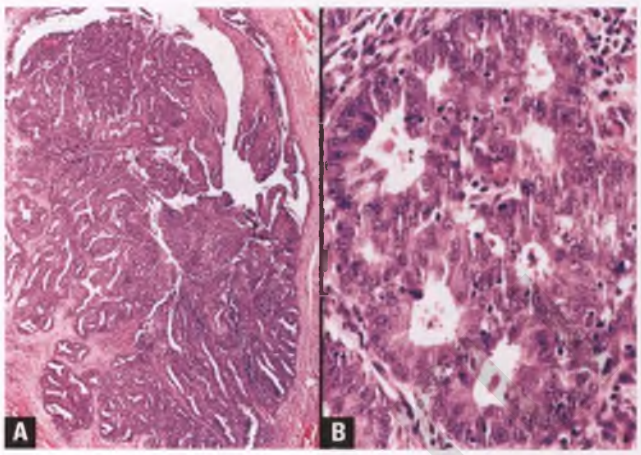

FIGURE 5.48. Endometrioid carcinoma of the fallopian tube. **A:** At low magnification, an endometrioid tumor is seen replacing most of the lumen and superficially infiltrating the tubal wall. **B:** Higher magnification reveals a glandular pattern with features that are typical of endometrioid carcinoma.

be the source of a minority of endometrial serous carcinomas, and that the SEE-FIM protocol should also be applied to these tumors.[60] At this point, it is clear that the tenet that the bulk of a pelvic carcinoma must be located within the fallopian tube before such a cancer is accepted as a primary tubal carcinoma is not valid and should be abandoned.

ENDOMETRIOID CARCINOMA

Tubal endometrioid carcinoma is the second most common type of tubal carcinoma, accounting for roughly 10% of nonconsultation cases interpreted by experts.[42] This type of carcinoma resembles its much more common endometrial counterpart (Fig. 5.48), and is graded using the same criteria (see Chapter 4). Since tubal endometrioid carcinoma is often luminal based and seldom infiltrates deeply into the myosalpinx, it tends to have a favorable prognosis.[61]

Tubal endometrioid carcinomas occasionally contain areas with prominent microcystic and/or diffuse spindle cell patterns that can result in a resemblance to female adnexal tumors of probable wolffian origin (FATPWO),[62] which are discussed in the section on the broad ligament at the end of this chapter. Although FATPWOs are known to occur on rare occasions as primary ovarian tumors (see Chapter 7), they have yet to be reported as luminal-based primary tumors of the fallopian tube. In addition to the intraluminal location of tubal endometrioid tumors, features that favor endometrioid carcinoma include (a) foci in which the glands are more characteristic of usual endometrioid adenocarcinoma, (b) associated squamous differentiation, (c) small amounts of mucicarmine-positive intraluminal mucin, and (d) immunoreactivity for epithelial membrane antigen.[62]

When found in conjunction with an endometrial or ovarian endometrioid carcinoma, tubal endometrioid carcinoma can either represent an independent primary tumor or be related to direct extension or metastasis from the nontubal carcinoma. Several criteria for distinguishing between primary and secondary carcinoma of the fallopian tube have been put forth,[42,61] with discontinuity between the luminal-based tubal tumor and the nontubal tumor(s) being the most important finding that is supportive of independent primary malignancies. Synchronous tubal and endometrial endometrioid carcinomas that have been selected for features of two independent primary neoplasms tend to be grade 1 or 2, confined to their organs of origin, associated with a favorable prognosis, and found in obese women.[63]

MISCELLANEOUS PRIMARY MALIGNANT TUMORS

Primary tubal malignancies other than serous and endometrioid carcinoma range from uncommon to vanishingly rare, and include transitional cell carcinoma,[64] undifferentiated carcinoma,[28] squamous cell carcinoma,[65] clear cell carcinoma,[66] mucinous carcinoma,[67] glassy cell carcinoma,[68] malignant mixed müllerian tumor (carcinosarcoma),[69] adenosarcoma,[70] leiomyosarcoma,[71] choriocarcinoma,[72] placental site trophoblastic tumor,[35] epithelioid trophoblastic tumor,[73] immature teratoma,[74] and lymphoma.[75]

SECONDARY TUMORS

As currently defined, primary tubal carcinomas are outnumbered by secondary ones by a considerable margin.[76] It is fairly common for the fallopian tube to be involved by carcinoma

when a mass-forming carcinoma is present in the ipsilateral ovary; in this situation, the tubal tumor has traditionally been attributed to direct spread from the ovarian tumor, even when the tubal tumor is represented only by apparent carcinoma in situ.[76] In the latter situation, it has been proposed that carcinoma in situ is simulated by implantation and luminal surface growth of the extratubal carcinoma.[76] However, evidence continues to mount that the fallopian tube mucosa is quite resistant to this type of implantation, perhaps due to the constant sweeping motion of its cilia, and that TICs and small serous carcinomas that originate in the tubal fimbriae may shed cells onto the ovary or into the peritoneal cavity and serve as the primary source, rather than a metastatic deposit, of a significant proportion of tumors that have conventionally been interpreted as primary ovarian or peritoneal serous carcinomas.[53,55,56,77]

Involvement of the fallopian tube by endometrial carcinoma is best documented by direct extension of tumor from the endometrial cavity into the tubal lumen. Theoretically, endometrial carcinoma can also involve the fallopian tube via intracavitary detachment and reimplantation within the tubal mucosa, although this mechanism is considered unlikely for reasons as mentioned above, and would be virtually impossible to distinguish histologically from an independent primary tubal carcinoma. Very rarely, the in situ component of cervical squamous cell carcinoma has been documented to coat the lining of the endometrium and extend in contiguous fashion to replace the epithelium of the fallopian tube, where it may invade anywhere along its course.[78,79]

Other than serosal implants from peritoneal carcinomatosis or mesothelioma, metastases to the fallopian tube from extragenital carcinomas are very rare, and have been reported to originate from the breast, gastrointestinal tract, and urinary bladder.[76,80] Histologic features that support secondary involvement of the fallopian tube by carcinoma include microscopic clusters of intraluminal carcinomatous epithelial cells within an otherwise normal tube (Fig. 5.49), normal tubal epithelium overlying lamina propria that has been undermined by nests of carcinoma (Fig. 5.50), histology that is not typical of primary tubal carcinoma and/or that matches the histology of a known previous carcinoma of the patient, and extensive vascular invasion of the tubal plicae.

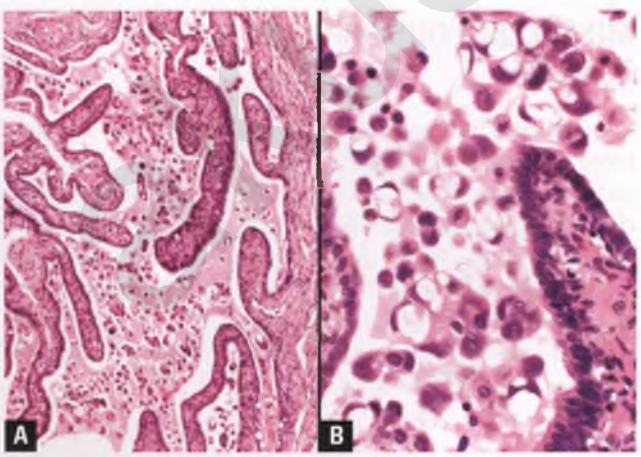

FIGURE 5.49. **A,B:** Detached clusters of carcinomatous cells are present within the lumen of the fallopian tube. These malignant cells are most likely derived from a neoplasm of the ovary, peritoneum, endometrium, or elsewhere within the tube.

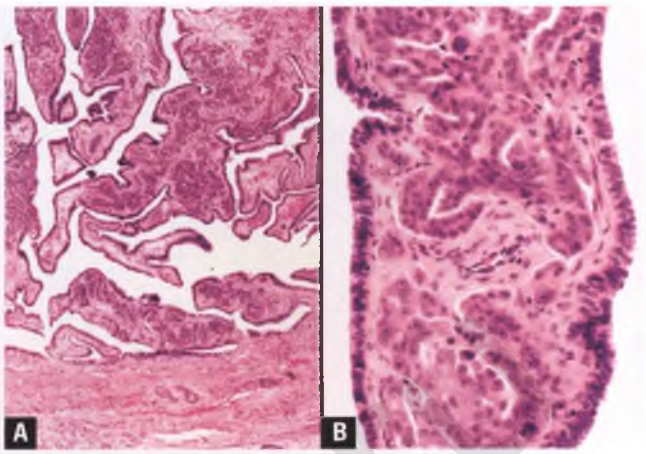

FIGURE 5.50. **A,B:** Fallopian tube with metastatic serous carcinoma of ovarian origin. The lamina propria of the tubal plicae is partially replaced by tumor, but the surface epithelium is spared.

Intraluminal Spread from Pseudomyxoma Peritonei versus Mucinous Metaplasia

One potential diagnostic pitfall is misinterpreting replacement of the tubal epithelial lining by slightly atypical mucinous epithelium as mucinous metaplasia or a primary low-grade mucinous tumor without considering the unlikely possibility of colonization related to pseudomyxoma peritonei, which is most commonly due to a ruptured low-grade mucinous neoplasm of the appendix.[25,76,81] In this situation, the ciliary-based defense mechanisms of the fallopian tube that normally prevent implantation may be thwarted by the gelatinous material that accompanies the free-floating strips of neoplastic mucinous epithelium of appendiceal origin that wander into the tubal lumen.

Two cases of tubal mucosa with mucinous change that were associated with appendiceal mucinous neoplasms that had spread to the ovaries have recently been analyzed immunohistochemically.[26] It is difficult to draw conclusions on the basis of only two cases and in the absence of a comparative analysis of the immunophenotype of several cases of unequivocal mucinous metaplasia of the fallopian tube, but the coordinate expression of the gastrointestinal markers cytokeratin 20, CDX2, and MUC2 in the mucinous epithelium of the fallopian tube and the appendiceal tumors in both cases suggests to me that these markers may have utility in supporting an appendiceal origin for the tubal mucinous epithelium, especially in the setting of accompanying pseudomyxoma peritonei and/or ovarian involvement.

In addition to matching immunoprofiles, there are two other points that argue against the notion that the fallopian tubes and appendix of some women may be predisposed to the formation of separate and similar primary mucinous epithelial lesions. First, it appears to be more than just coincidence that the only appendiceal mucinous lesions that seem to be associated with mucinous epithelium within the tube are those that have spread beyond the appendix. Second, it does not make sense embryologically for an organ of mesodermal origin (the fallopian tube) to be predisposed to the development of a histologically similar epithelial process in an organ of endodermal origin (the appendix).

It should be noted that the differential diagnosis of mucinous metaplasia versus colonization of tubal epithelium by a low-grade mucinous neoplasm of the appendix is only of academic interest, since the colonizing neoplastic appendiceal epithelium appears incapable of invasion of the tube and the overall clinical behavior is dominated by the extent and epithelial content of the associated pseudomyxoma peritonei (see Chapter 8).

BROAD LIGAMENT

MESONEPHRIC REMNANTS

In the broad ligament, vestigial remnants of the mesonephric (wolffian) duct take the form of small hollow tubules that are lined by cuboidal epithelial cells that are surrounded by prominent cuffs of smooth muscle (Fig. 5.51). Whether or not some of the cells lining these tubules may be ciliated varies from text to text, which may be related to difficulty in distinguishing coexistent patches of endosalpingiosis (see Chapter 8). There is no need to mention these incidental structures in the pathology report.

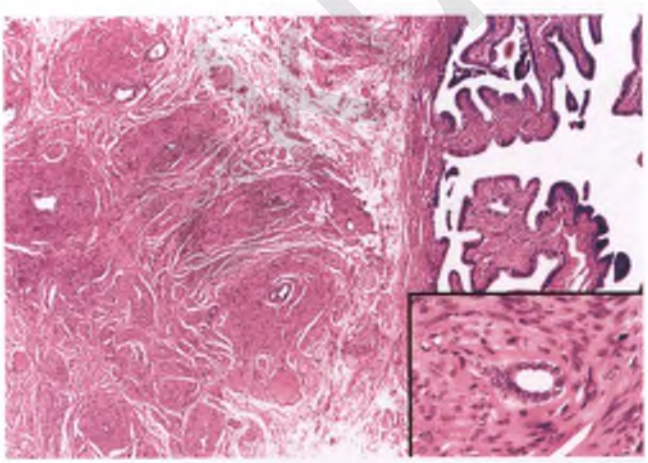

FIGURE 5.51. Mesonephric remnants within the soft tissue adjacent to the fallopian tube. The inset highlights the bland nuclear features of the cuboidal epithelial cells lining the tubules and the surrounding smooth muscle.

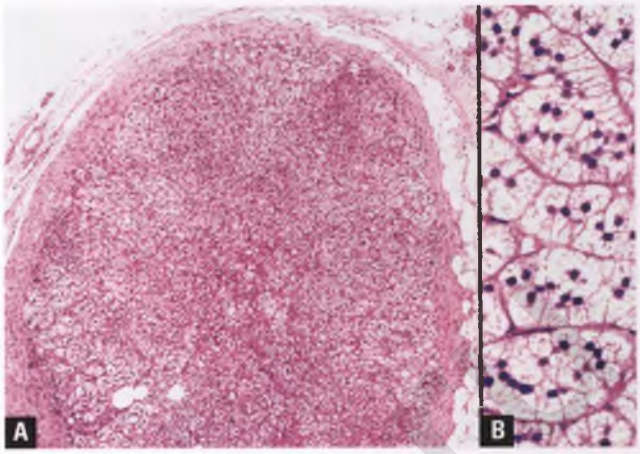

FIGURE 5.52. Adrenal cortical rest within the broad ligament. **A:** The 0.3 cm nodule appears to consist largely of clear cells, but this is related to tangential sectioning of a nodule whose dominant layer recapitulates that of the zona fasciculata. **B:** High-magnification view of the clear cells that are indistinguishable from those of the normal zona fasciculata.

ADRENAL CORTICAL RESTS

An adrenal cortical rest is occasionally found within the broad ligament, and typically presents as an incidental small yellow nodule. In some cases, the typical zonation of the three cortical layers is recognizable. However, tangential sectioning through other examples results in an apparent clear cell lesion that is dominated by cells identical to those within the zona fasciculata, which is the thickest layer of the adrenal cortex (Fig. 5.52). Recognition of the clear cell component as being of adrenal cortical nature is facilitated by noting the microvesicular appearance of the abundant cytoplasm and the clustered arrangement of the clear cells.

PARATUBAL CYSTS[82]

Paratubal cysts are common findings that may be derived from mesonephric, paramesonephric (müllerian), or mesothelial elements (cystic Walthard nests are discussed earlier in this chapter). Although usually incidental, torsion or torsion-related infarction of paratubal cysts can produce abdominal pain. The most common müllerian cyst is the hydatid cyst of Morgagni, which characteristically dangles from the fimbriated end of the fallopian tube via a thin stalk, whereas other types of cysts occur in a variety of paratubal locations (Fig. 5.53). Hydatid cysts are filled with serous fluid and have a thin, translucent wall that histologically corresponds to an attenuated layer of fibromuscular tissue and a tubal-type mucosal lining with ciliated cells whose folds occasionally form simplified plical-like structures. Similar-appearing cysts can be sessile and found within the broad ligament.

A small hydatid cyst of Morgagni can be mistaken histologically for fallopian tube, and a larger cyst of this type can

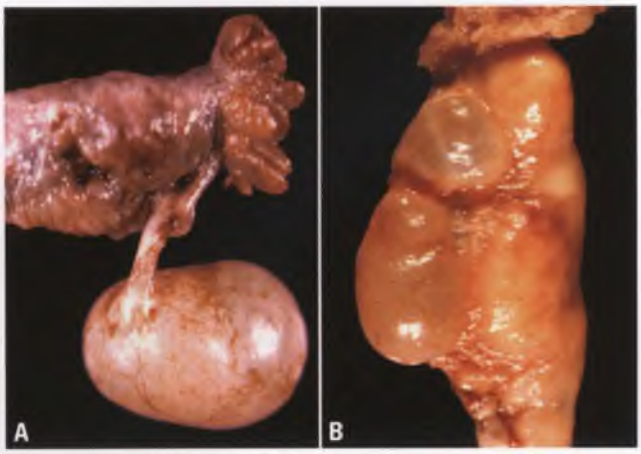

FIGURE 5.53. Paratubal cysts. **A:** A hydatid cyst of Morgagni dangles from its stalk near the fimbriated end of this formalin-fixed fallopian tube. **B:** A paratubal cyst bulges from one aspect of the fallopian tube in this fresh specimen. A portion of the fimbriated end of the tube is at top.

mimic a hydrosalpinx. Distinguishing features of the hydatid cyst include its typical gross appearance and the much more limited amount of smooth muscle within its paper-thin wall. The other main differential diagnostic consideration of the hydatid cyst is a serous cystadenoma, whose main distinguishing features are the absence of plical-like folds and a thicker wall that is either collagenized or reminiscent of ovarian stroma.

The occasional mesothelial cysts that occur in this location are typically lined by a single layer of flattened mesothelial cells. Mesonephric cysts are lined by cuboidal epithelium with absence to rare ciliated cells, but are very rare (perhaps because the thick muscular coats of mesonephric remnants inhibit cystic dilatation of their epithelial elements). Distinction of mesonephric, müllerian, and unilocular mesothelial cysts from one another can be problematic, since pressure atrophy of the lining epithelium often results in a nonspecific, flattened appearance. Although hydatid cysts of Morgagni can usually be recognized by their gross appearance and ciliated lining, all of the various types of innocuous cysts that occur in this region are adequately diagnosed as paratubal cysts without fretting over their precise classification.

ENDOMETRIOSIS AND ENDOSALPINGIOSIS

Foci of endometriosis and endosalpingiosis are common within the broad ligament, and have histologic features as discussed and illustrated in Chapter 8.

MÜLLERIAN-TYPE EPITHELIAL TUMORS

Benign and Borderline Serous Tumors[83]

Although the literature on serous cystadenomas of the broad ligament is scant, they are said to be the most common type of müllerian-derived epithelial tumor in this location. Distinction of serous cystadenoma from the much more common paratubal cyst is discussed in the section on the latter entity.

Several cases of serous borderline tumor arising within the broad ligament have been reported. These tumors occur in patients with an average age of 33 years, and form smooth-surfaced, unilocular, unilateral cysts with an average size of 6 cm. The internal lining of the cysts exhibits one or more papillary projections that are identical to those seen in endophytic serous borderline tumors of the ovary (see Chapter 7). However, unlike their ovarian counterparts, serous borderline tumors of the broad ligament have not been reported to be associated with peritoneal implants (perhaps because of their exclusively endophytic architecture). Although the histogenesis of these broad ligament tumors is not known with certainty, origin from endosalpingiosis seems most plausible.

Carcinoma[84]

Primary carcinoma of the broad ligament is very rare. Most such tumors are of endometrioid or clear cell type, and are thought to arise from foci of endometriosis (Figs. 5.54 and 5.55). Broad ligament carcinomas, particularly those of the serous type, may also originate from endosalpingiosis.

FEMALE ADNEXAL TUMOR OF PROBABLE WOLFFIAN ORIGIN[85-87]

The FATPWO is a rare tumor of adult women that is thought to be derived from the mesonephric remnants that are universally present within the broad ligament. These tumors are typically unilateral with a smooth, bosselated external surface and may be as small as a pea or as large as a cantaloupe. Their sectioned surface is tan to pale yellow, lobulated, rubbery, and predominantly solid, although small cysts may be present.

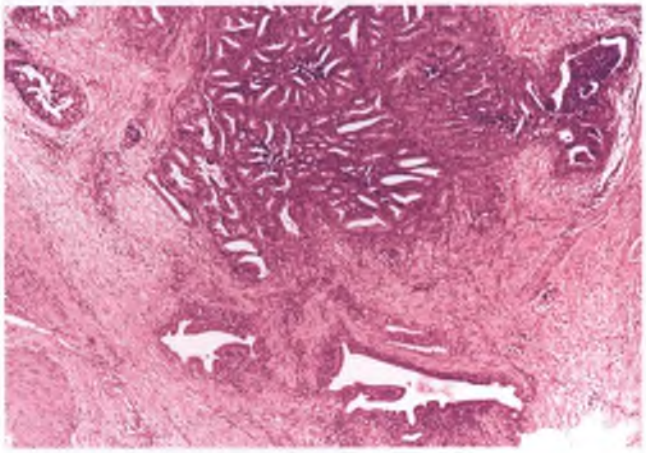

FIGURE 5.54. Primary endometrioid carcinoma of the broad ligament. Note the association with endometriosis at the bottom of the image.

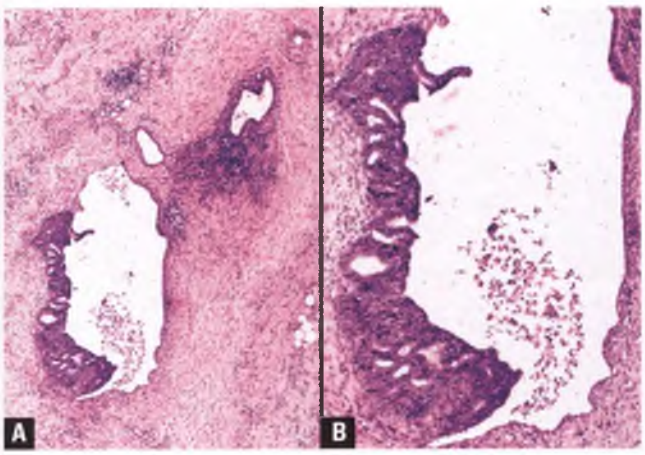

FIGURE 5.55. Early stage of development of primary endometrioid carcinoma of the broad ligament. **A:** Within these foci of endometriosis, a portion of the lining is transitioning to endometrioid carcinoma. **B:** Close-up view of the area of transition.

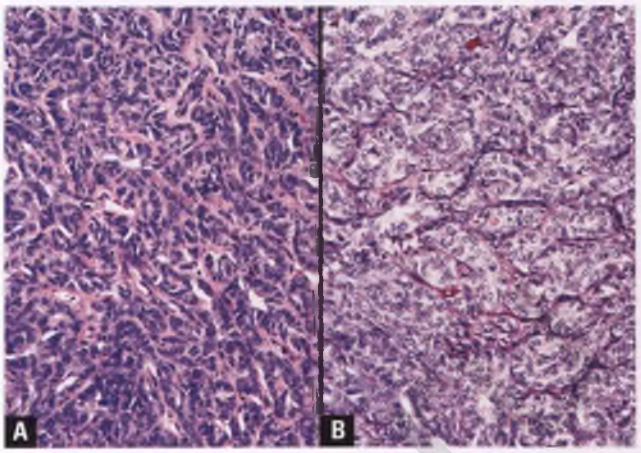

FIGURE 5.57. **A,B:** Female adnexal tumor of probable wolffian origin. Closely packed tubules with absent to inconspicuous lumens impart a predominantly solid appearance.

Winding, interconnected, small tubules usually dominate the histology of FATPWOs, generating a variety of patterns at low magnification depending on whether they are solid versus hollow and densely versus loosely packed (Fig. 5.56). Areas that appear solid can usually be resolved as closely packed solid tubules upon closer inspection (Figs. 5.57 and 5.58), particularly with the aid of reticulin or PAS stains or a laminin immunostain. However, diffuse areas of spindle-shaped cells may also be present and sometimes comprise a significant portion of the neoplasm. In areas where hollow tubules predominate, a characteristic sieve-like pattern is often formed that may have a retiform appearance (Fig. 5.59). With rare exceptions, the tumor cells exhibit bland nuclear features and little to no mitotic activity. The tubular elements in FATPWO are frequently immunoreactive for cytokeratin, vimentin, inhibin, and calretinin; unlike the glands of endometrioid carcinoma, they usually lack expression of epithelial membrane antigen. Although this immunoprofile can be of some utility in selected instances, the diagnosis of FATPWO is largely based upon its distinctive histologic patterns and location.

Only a few FATPWO have been reported to be clinically malignant, and these have generally been tumors with significant nuclear atypia and high mitotic rates. However, the correlation between bland appearance and benign clinical outcome is not absolute, necessitating long-term monitoring of all patients with FATPWO for potential malignant behavior.

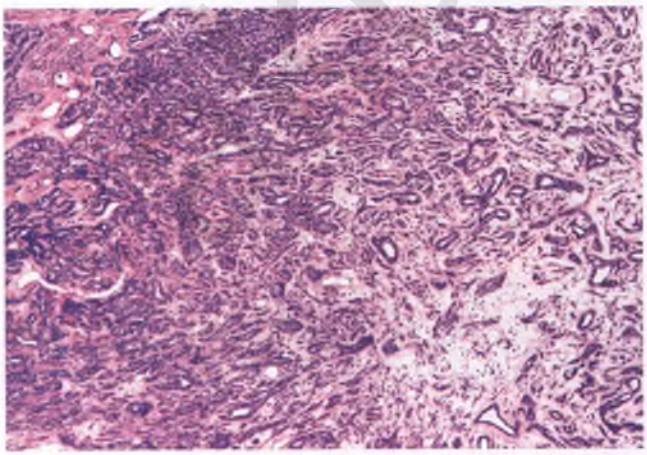

FIGURE 5.56. Female adnexal tumor of probable wolffian origin. An area of closely packed solid tubules at left merges with an area of widely spaced hollow tubules at right.

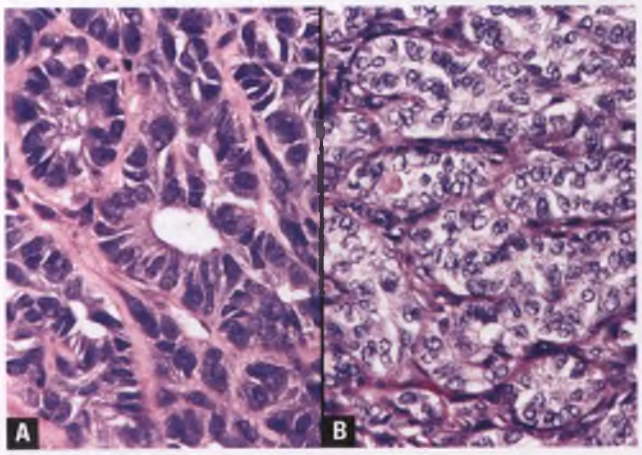

FIGURE 5.58. **A,B:** Female adnexal tumor of probable wolffian origin. At high magnification, tubular differentiation within "solid" areas is usually evident.

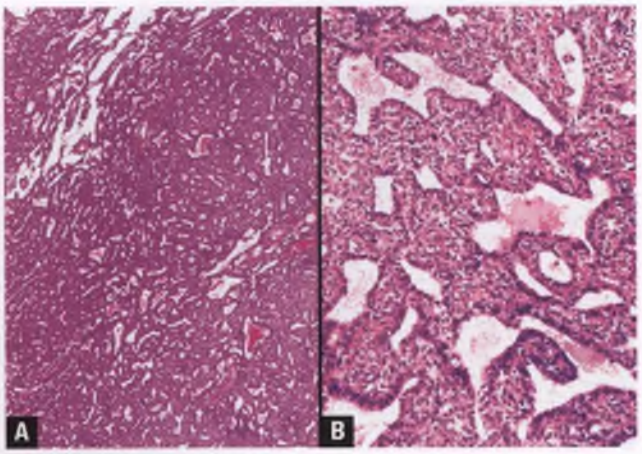

FIGURE 5.59. Female adnexal tumor of probable wolffian origin. **A:** Low-magnification view of a region where numerous hollow tubules and microcystic spaces separated by areas of solid growth result in a sieve-like pattern. **B:** The branching tubules often have angulated contours and papillary structures projecting into their lumens. Note the resemblance to rete ovarii (compare with Fig. 6.22).

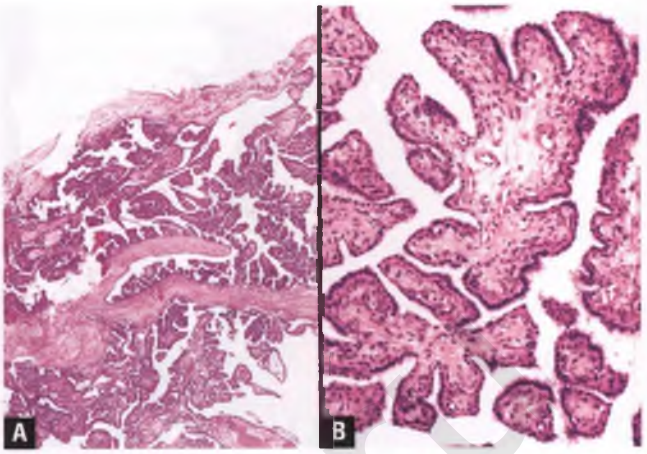

FIGURE 5.60. Papillary cystadenoma of broad ligament associated with von Hippel-Lindau disease. **A:** This low-magnification view highlights the complex papillary architecture of this benign tumor. **B:** The papillae are lined by a single layer of cuboidal epithelial cells with bland nuclear features. (Glass slide kindly provided by Dr. Peter A. Humphrey.)

PAPILLARY CYSTADENOMA[88]

Von Hippel-Lindau disease is a rare, autosomal dominant genetic disorder characterized by the development in young adulthood of one or more of a variety of tumors that include retinal angioma, cerebellar hemangioblastoma, renal cell carcinoma, pheochromocytoma, and papillary cystadenoma of the epididymis. Rarely, female patients with von Hippel-Lindau disease develop a benign tumor in the broad ligament that is histologically identical to the epididymal papillary cystadenoma that is found in roughly 10% of male patients with this disorder.

In the handful of reported cases, the broad ligament form of papillary cystadenoma has measured up to 3 cm in diameter. These tumors are loculated cysts with internal papillary excrescences that branch in a complex arborizing pattern similar to that of serous borderline tumors (Fig. 5.60A), but are thought to be of wolffian rather than müllerian origin. The papillae consist of fibrovascular stalks lined by a single layer of cuboidal, nonciliated, mitotically inactive epithelial cells with bland nuclear features (Fig. 5.60B) and glycogen-rich cytoplasm (Fig. 5.61). Portions of the cyst wall may be calcified, which is a finding that may be noted radiologically. The absence of nuclear stratification, nuclear atypia, cilia, and epithelial tufting along with the presence of glycogen-rich cytoplasm and the association with von Hippel-Lindau disease facilitate distinction of these benign tumors from serous borderline tumors.

EPENDYMOMA[89,90]

Rare cases of primary ependymoma of the broad ligament have been reported. These tumors are of unknown histogenesis in this site and have malignant potential. The features that are most helpful in recognizing these unusual tumors are the combination of low-grade histology, anuclear perivascular zones that result in the formation of pseudorosettes (Fig. 5.62), and immunoreactivity for glial fibrillary acidic protein (note that the latter can rarely be seen in high-grade serous carcinoma). Extra-axial ependymomas exhibit more architectural diversity than their central nervous system counterparts, and also differ in their patterns of immunoreactivity with respect to several markers.

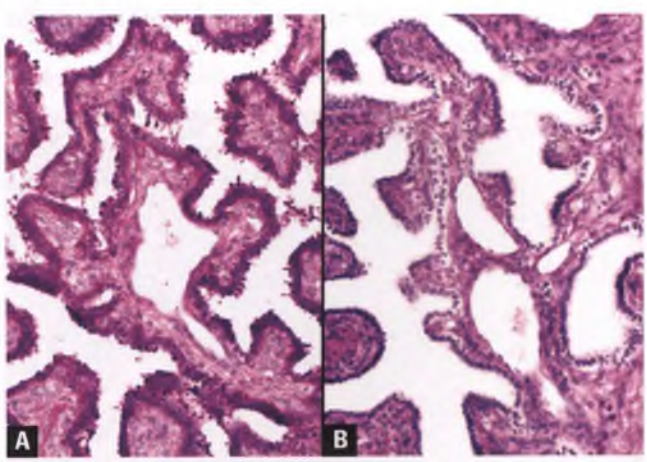

FIGURE 5.61. Papillary cystadenoma of broad ligament associated with von Hippel-Lindau disease. **A:** The tumor cells contain abundant PAS-positive glycogen within their cytoplasm. **B:** This section has been treated with diastase prior to PAS staining, and demonstrates the complete removal of the glycogen granules. (Glass slides kindly provided by Dr. Peter A. Humphrey.)

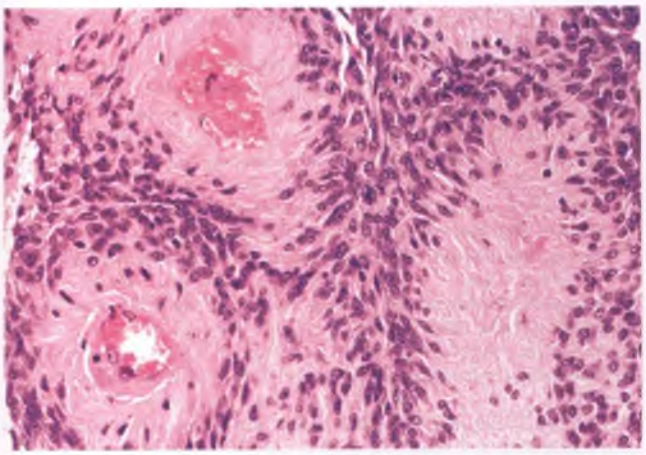

FIGURE 5.62. Ependymoma. Perivascular pseudorosettes are a characteristic feature.

LEIOMYOMA[91]

Of the variety of soft tissue tumors that can be found within the broad ligament on rare occasions, the leiomyoma is the most common. Leiomyoma of the broad ligament typically presents as a bulging, nodular mass that is clearly separated from the fallopian tube, ovary, and uterus (Fig. 5.63). The range of gross and microscopic appearances of these benign smooth muscle tumors is similar to that of their much more common counterpart in the uterus, which is discussed in Chapter 4.

LEIOMYOSARCOMA[92]

Although quite rare, leiomyosarcoma is the most common sarcoma of the broad ligament. These tumors typically present

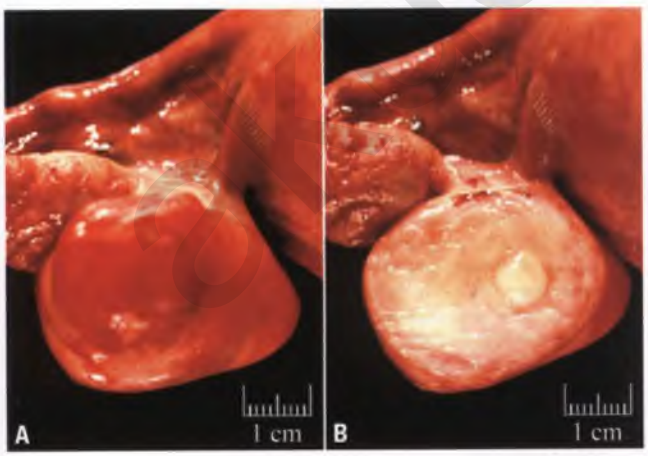

FIGURE 5.63. Leiomyoma of the broad ligament. **A:** This tumor presented as a 4 cm nodular mass arising from ligamentous tissue. A portion of the uterus is at top right, the fallopian tube is at top, and the ovary is at left of center. **B:** The sectioned surface of the leiomyoma is rubbery and off-white to pale yellow.

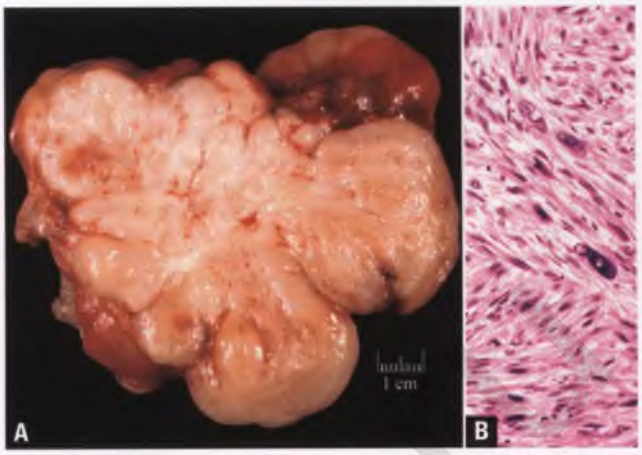

FIGURE 5.64. Leiomyosarcoma of the broad ligament. **A:** This image represents the sectioned surface of a large, fleshy tumor with lobulated margins. **B:** The spindle-shaped tumor cells exhibit a fascicular growth pattern, eosinophilic cytoplasm, and an element with significant nuclear atypia. A mitotic figure is also present in this field.

as a large, fleshy, lobulated mass that may contain areas of hemorrhage or necrosis (Fig. 5.64). Histologically, obvious examples of this neoplasm show discernible smooth muscle differentiation and exhibit marked nuclear atypia, brisk mitotic activity with atypical division figures, and foci of tumor cell necrosis. Given that the rarity of these tumors precludes development of their own site-specific set of diagnostic criteria to help distinguish the low end of the spectrum of leiomyosarcoma from leiomyoma variants and smooth muscle tumors of uncertain malignant potential, it is recommended that broad ligament smooth muscle tumors be classified using the criteria that have been established for uterine tumors of this type (see Chapter 4).

SUGGESTED READINGS

Clement PB, Young RH. *Atlas of Gynecologic Surgical Pathology*. 2nd ed. Philadelphia, PA: Elsevier Saunders; 2008.

Crum CP, Nucci MR, Lee K, eds. *Diagnostic Gynecologic and Obstetric Pathology*. 2nd ed. Philadelphia, PA: Elsevier Saunders; 2011.

Kurman RJ, Ellenson LH, Ronnett BM, eds. *Blaustein's Pathology of the Female Genital Tract*. 6th ed. New York: Springer; 2011.

Robboy, SJ, Mutter GL, Prat J, et al., eds. *Robboy's Pathology of the Female Reproductive Tract*. 2nd ed. Oxford, UK: Churchill Livingstone; 2009.

Scully RE, Young, RH, Clement PB. Tumors of the ovary, maldeveloped gonads, fallopian tube, and broad ligament. *Atlas of Tumor Pathology*, 3rd series, Fascicle 23. Washington, DC: Armed Forces Institute of Pathology; 1998:457–511.

Tavassoli FA, Devilee P, eds. *World Health Organization Classification of Tumors. Pathology and Genetics of Tumours of the Breast and Female Genital Organs*. Lyon, France: IARC Press; 2003:203–216.

REFERENCES

1. Nogales-Ortiz F, Tarancon I, Nogales FF Jr. The pathology of female genital tuberculosis. A 31-year study of 1436 cases. *Obstet Gynecol*. 1979;53:422–428.
2. Seidman JD, Oberer S, Bitterman P, et al. Pathogenesis of pseudoxanthomatous salpingiosis. *Mod Pathol*. 1993;6:53–55.

3. Furuya M, Murakami T, Sato O, et al. Pseudoxanthomatous and xanthogranulomatous salpingitis of the fallopian tube: a report of four cases and a literature review. *Int J Gynecol Pathol.* 2002;21:56–59.
4. Zorzi MG, Pusiol T, Piscioli F. Melanosis tubae: histogenesis and appropriate terminology. *Int J Gynecol Pathol.* 2010;29:248–251.
5. Clement PB, Young RH, Scully RE. Necrotic pseudoxanthomatous nodules of ovary and peritoneum in endometriosis. *Am J Surg Pathol.* 1988;12:390–397.
6. Jenkins CS, Williams SR, Schmidt GE. Salpingitis isthmica nodosa: a review of the literature, discussion of clinical significance, and consideration of patient management. *Fertil Steril.* 1993;60:599–607.
7. Yanai-Inbar I, Siriaunkgul S, Silverberg SG. Mucosal epithelial proliferation of the fallopian tube: a particular association with ovarian serous tumor of low malignant potential? *Int J Gynecol Pathol.* 1995;14:107–113.
8. Yanai-Inbar I, Silverberg SG. Mucosal epithelial proliferation of the fallopian tube: prevalence, clinical associations, and optimal strategy for histopathologic assessment. *Int J Gynecol Pathol.* 2000;19:139–144.
9. Cheung AN, Young RH, Scully RE. Pseudocarcinomatous hyperplasia of the fallopian tube associated with salpingitis. A report of 14 cases. *Am J Surg Pathol.* 1994;18:1125–1130.
10. Cornog JL, Currie JL, Rubin A. Heat artifact simulating adenocarcinoma of fallopian tube. *JAMA.* 1970;214:1118–1119.
11. Stock RJ. Histopathologic changes in fallopian tubes subsequent to sterilization procedures. *Int J Gynecol Pathol.* 1983;2:13–27.
12. Bernardus RE, Van der Slikke JW, Roex AJ, et al. Torsion of the fallopian tube: some considerations on its etiology. *Obstet Gynecol.* 1984;64:675–678.
13. Antoniou N, Varras M, Akrivis C, et al. Isolated torsion of the fallopian tube: a case report and review of the literature. *Clin Exp Obstet Gynecol.* 2004;31:235–238.
14. Green LK, Kott ML. Histopathologic findings in ectopic tubal pregnancy. *Int J Gynecol Pathol.* 1989;8:255–262.
15. Ramirez NC, Lawrence WD, Ginsburg KA. Ectopic pregnancy. A recent five-year study and review of the last 50 years' literature. *J Reprod Med.* 1996;41:733–740.
16. Pauerstein CJ, Croxatto HB, Eddy CA, et al. Anatomy and pathology of tubal pregnancy. *Obstet Gynecol.* 1986;67:301–308.
17. Jacques SM, Qureshi F, Ramirez NC, et al. Retained trophoblastic tissue in fallopian tubes: a consequence of unsuspected ectopic pregnancies. *Int J Gynecol Pathol.* 1997;16:219–224.
18. Sebire NJ, Lindsay I, Fisher RA, et al. Overdiagnosis of complete and partial hydatidiform mole in tubal ectopic pregnancies. *Int J Gynecol Pathol.* 2005;24:260–264.
19. Carson SA, Buster JE. Ectopic pregnancy. *N Engl J Med.* 1993;329:1174–1181.
20. Doss BJ, Jacques SM, Qureshi F, et al. Extratubal secondary trophoblastic implants: clinicopathologic correlation and review of the literature. *Hum Pathol.* 1998;29:184–187.
21. Mills SE, Fechner RE. Stromal and epithelial changes in the fallopian tube following hormonal therapy. *Hum Pathol.* 1980;11:583–585.
22. Parker RL, Dadmanesh F, Young RH, et al. Polypoid endometriosis: a clinicopathologic analysis of 24 cases and a review of the literature. *Am J Surg Pathol.* 2004;28:285–297.
23. Stock RJ. Postsalpingectomy endometriosis: a reassessment. *Obstet Gynecol.* 1982;60:560–570.
24. Rabban JT, Crawford B, Chen LM, et al. Transitional cell metaplasia of fallopian tube fimbriae: a potential mimic of early tubal carcinoma in risk reduction salpingo-oophorectomies from women with BRCA mutations. *Am J Surg Pathol.* 2009;33:111–119.
25. Seidman JD. Mucinous lesions of the fallopian tube. A report of seven cases. *Am J Surg Pathol.* 1994;18:1205–1212.
26. Wong AK, Seidman JD, Barbuto DA, et al. Mucinous metaplasia of the fallopian tube: a diagnostic pitfall mimicking metastasis. *Int J Gynecol Pathol.* 2011;30:36–40.
27. Saffos RO, Rhatigan RM, Scully RE. Metaplastic papillary tumor of the fallopian tube—a distinctive lesion of pregnancy. *Am J Clin Pathol.* 1980;74:232–236.
28. Alvarado-Cabrero I, Navani SS, Young RH, et al. Tumors of the fimbriated end of the fallopian tube: a clinicopathologic analysis of 20 cases, including nine carcinomas. *Int J Gynecol Pathol.* 1997;16:189–196.
29. Bossuyt V, Medeiros F, Drapkin R, et al. Adenofibroma of the fimbria: a common entity that is indistinguishable from ovarian adenofibroma. *Int J Gynecol Pathol.* 2008;27:390–397.
30. Gisser SD. Obstructing fallopian tube papilloma. *Int J Gynecol Pathol.* 1986;5:179–182.
31. Schust D, Stovall DW. Leiomyomas of the fallopian tube. A case report. *J Reprod Med.* 1993;38:741–742.
32. Hurd JK Jr. Benign cystic teratoma of the fallopian tube. *Obstet Gynecol.* 1978;52:362–364.
33. Milchgrub S, Sandstad J. Arias-Stella reaction in fallopian tube epithelium. A light and electron microscopic study with a review of the literature. *Am J Clin Pathol.* 1991;95:892–895.
34. Tziortziotis DV, Bouros AC, Ziogas VS, et al. Clear cell hyperplasia of the fallopian tube epithelium associated with ectopic pregnancy: report of a case. *Int J Gynecol Pathol.* 1997;16:79–80.
35. Baergen RN, Rutgers J, Young RH. Extrauterine lesions of intermediate trophoblast. *Int J Gynecol Pathol.* 2003;22:362–367.
36. Honore LH, O'Hara KE. Ovarian hilus cell heterotopia. *Obstet Gynecol.* 1979;53:461–464.
37. Hirschowitz L, Salmons N, Ganesan R. Ovarian hilus cell heterotopia. *Int J Gynecol Pathol.* 2011;30:46–52.
38. Seidman JD, Sherman ME, Bell KA, et al. Salpingitis, salpingoliths, and serous tumors of the ovaries: is there a connection? *Int J Gynecol Pathol.* 2002;21:101–107.
39. Kim KR, Scully RE. Peritoneal keratin granulomas with carcinomas of endometrium and ovary and atypical polypoid adenomyoma of endometrium. A clinicopathological analysis of 22 cases. *Am J Surg Pathol.* 1990;14:925–932.
40. Zheng W, Wolf S, Kramer EE, et al. Borderline papillary serous tumour of the fallopian tube. *Am J Surg Pathol.* 1996;20:30–35.
41. Young RH. Neoplasms of the fallopian tube and broad ligament: a selective survey including historical perspective and emphasizing recent developments. *Pathology (Phila).* 2007;39:112–124.
42. Alvarado-Cabrero I, Young RH, Vamvakas EC, et al. Carcinoma of the fallopian tube: a clinicopathological study of 105 cases with observations on staging and prognostic factors. *Gynecol Oncol.* 1999;72:367–379.
43. Baekelandt M, Jorunn Nesbakken A, Kristensen GB, et al. Carcinoma of the fallopian tube. *Cancer.* 2000;89:2076–2084.
44. Stewart SL, Wike JM, Foster SL, et al. The incidence of primary fallopian tube cancer in the United States. *Gynecol Oncol.* 2007;107:392–397.
45. FIGO Committee on Gynecologic Oncology. Current FIGO staging for cancer of the vagina, fallopian tube, ovary, and gestational trophoblastic neoplasia. *Int J Gynecol Obstet.* 2009;105:3–4.
46. Longacre TA, Oliva E, Soslow RA, et al. Recommendations for the reporting of fallopian tube neoplasms. *Hum Pathol.* 2007;38:1160–1163.
47. Medeiros F, Muto MG, Lee Y, et al. The tubal fimbria is a preferred site for early adenocarcinoma in women with familial ovarian cancer syndrome. *Am J Surg Pathol.* 2006;30:230–236.
48. Crum CP, Drapkin R, Kindelberger D, et al. Lessons from BRCA: the tubal fimbria emerges as an origin for pelvic serous cancer. *Clin Med Res.* 2007;5:35–44.
49. Jarboe E, Folkins A, Nucci MR, et al. Serous carcinogenesis in the fallopian tube: a descriptive classification. *Int J Gynecol Pathol.* 2008;27:1–9.
50. Mehrad M, Ning G, Chen EY, et al. A pathologist's road map to benign, precancerous, and malignant intraepithelial proliferations in the fallopian tube. *Adv Anat Pathol.* 2010;17:293–302.
51. Carcangiu ML, Radice P, Manoukian S, et al. Atypical epithelial proliferation in fallopian tubes in prophylactic salpingo-oophorectomy specimens from BRCA1 and BRCA2 germline mutation carriers. *Int J Gynecol Pathol.* 2004;23:35–40.
52. Lee Y, Miron A, Drapkin R, et al. A candidate precursor to serous carcinoma that originates in the distal fallopian tube. *J Pathol.* 2007;211:26–35.
53. Folkins AK, Jarboe EA, Roh MH, et al. Precursors to pelvic serous carcinoma and their clinical implications. *Gynecol Oncol.* 2009;113:391–396.
54. Crum CP. Intercepting pelvic cancer in the distal fallopian tube: theories and realities. *Mol Oncol.* 2009;3:165–170.
55. Kindelberger DW, Lee Y, Miron A, et al. Intraepithelial carcinoma of the fimbria and pelvic serous carcinoma: evidence for a causal relationship. *Am J Surg Pathol.* 2007;31:161–169.
56. Przybycin CG, Kurman RJ, Ronnett BM, et al. Are all pelvic (nonuterine) serous carcinomas of tubal origin? *Am J Surg Pathol.* 2010;34:1407–1416.
57. Roh MH, Kindelberger D, Crum CP. Serous tubal intraepithelial carcinoma and the dominant ovarian mass: clues to serous tumor origin? *Am J Surg Pathol.* 2009;33:376–383.
58. Powell CB, Kenley E, Chen LM, et al. Risk-reducing salpingo-oophorectomy in BRCA mutation carriers: role of serial sectioning in the detection of occult malignancy. *J Clin Oncol.* 2005;23:127–132.
59. Rabban JT, Krasik E, Chen LM, et al. Multistep level sections to detect occult fallopian tube carcinoma in risk-reducing salpingo-oophorectomies from women with BRCA mutations: implications for defining an optimal specimen dissection protocol. *Am J Surg Pathol.* 2009;33:1878–1885.

60. Jarboe EA, Miron A, Carlson JW, et al. Coexisting intraepithelial serous carcinomas of the endometrium and fallopian tube: frequency and potential significance. *Int J Gynecol Pathol.* 2009;28:308–315.
61. Navani SS, Alvarado-Cabrero I, Young RH, et al. Endometrioid carcinoma of the fallopian tube: a clinicopathologic analysis of 26 cases. *Gynecol Oncol.* 1996;63:371–378.
62. Daya D, Young RH, Scully RE. Endometrioid carcinoma of the fallopian tube resembling an adnexal tumor of probable wolffian origin: a report of six cases. *Int J Gynecol Pathol.* 1992;11:122–130.
63. Culton LK, Deavers MT, Silva EG, et al. Endometrioid carcinoma simultaneously involving the uterus and the fallopian tube: a clinicopathologic study of 13 cases. *Am J Surg Pathol.* 2006;30:844–849.
64. Koshiyama M, Konishi I, Yoshida M, et al. Transitional cell carcinoma of the fallopian tube: a light and electron microscopic study. *Int J Gynecol Pathol.* 1994;13:175–180.
65. Cheung AN, So KF, Ngan HY, et al. Primary squamous cell carcinoma of fallopian tube. *Int J Gynecol Pathol.* 1994;13:92–95.
66. Voet RL, Lifshitz S. Primary clear cell adenocarcinoma of the fallopian tube: light microscopic and ultrastructural findings. *Int J Gynecol Pathol.* 1982;1:292–298.
67. Jackson-York GL, Ramzy I. Synchronous papillary mucinous adenocarcinoma of the endocervix and fallopian tubes. *Int J Gynecol Pathol.* 1992;11:63–67.
68. Herbold DR, Axelrod JH, Bobowski SJ, et al. Glassy cell carcinoma of the fallopian tube. A case report. *Int J Gynecol Pathol.* 1988;7:384–390.
69. Carlson JA Jr, Ackerman BL, Wheeler JE. Malignant mixed mullerian tumor of the fallopian tube. *Cancer.* 1993;71:187–192.
70. Gollard R, Kosty M, Bordin G, et al. Two unusual presentations of mullerian adenosarcoma: case reports, literature review, and treatment considerations. *Gynecol Oncol.* 1995;59:412–422.
71. Jacoby AF, Fuller AF Jr, Thor AD, et al. Primary leiomyosarcoma of the fallopian tube. *Gynecol Oncol.* 1993;51:404–407.
72. Muto MG, Lage JM, Berkowitz RS, et al. Gestational trophoblastic disease of the fallopian tube. *J Reprod Med.* 1991;36:57–60.
73. Parker A, Lee V, Dalrymple C, et al. Epithelioid trophoblastic tumour: report of a case in the fallopian tube. *Pathology (Phila).* 2003;35:136–140.
74. Baginski L, Yazigi R, Sandstad J. Immature (malignant) teratoma of the fallopian tube. *Am J Obstet Gynecol.* 1989;160:671–672.
75. Lagoo AS, Robboy SJ. Lymphoma of the female genital tract: current status. *Int J Gynecol Pathol.* 2006;25:1–21.
76. Scully RE, Young RH, Clement PB. Tumors of the ovary, maldeveloped gonads, fallopian tube, and broad ligament. *Atlas of Tumor Pathology*, 3rd series, Fascicle 23. Washington, DC: Armed Forces Institute of Pathology; 1998:482–484.
77. Carlson JW, Miron A, Jarboe EA, et al. Serous tubal intraepithelial carcinoma: its potential role in primary peritoneal serous carcinoma and serous cancer prevention. *J Clin Oncol.* 2008;26:4160–4165.
78. Kanbour AI, Stock RJ. Squamous cell carcinoma in situ of the endometrium and fallopian tube as superficial extension of invasive cervical carcinoma. *Cancer.* 1978;42:570–580.
79. Pins MR, Young RH, Crum CP, et al. Cervical squamous cell carcinoma in situ with intraepithelial extension to the upper genital tract and invasion of tubes and ovaries: report of a case with human papilloma virus analysis. *Int J Gynecol Pathol.* 1997;16:272–278.
80. Mazur MT, Hsueh S, Gersell DJ. Metastases to the female genital tract. Analysis of 325 cases. *Cancer.* 1984;53:1978–1984.
81. Young RH. Pseudomyxoma peritonei and selected other aspects of the spread of appendiceal neoplasms. *Semin Diagn Pathol.* 2004;21:134–150.
82. Samaha M, Woodruff JD. Paratubal cysts: frequency, histogenesis, and associated clinical features. *Obstet Gynecol.* 1985;65:691–694.
83. Aslani M, Ahn GH, Scully RE. Serous papillary cystadenoma of borderline malignancy of broad ligament. A report of 25 cases. *Int J Gynecol Pathol.* 1988;7:131–138.
84. Aslani M, Scully RE. Primary carcinoma of the broad ligament. Report of four cases and review of the literature. *Cancer.* 1989;64:1540–1545.
85. Kariminejad MH, Scully RE. Female adnexal tumor of probable wolffian origin. A distinctive pathologic entity. *Cancer.* 1973;31:671–677.
86. Devouassoux-Shisheboran M, Silver SA, Tavassoli FA. Wolffian adnexal tumor, so-called female adnexal tumor of probable Wolffian origin (FATWO): immunohistochemical evidence in support of a Wolffian origin. *Hum Pathol.* 1999;30:856–863.
87. Sivridis E, Giatromanolaki A, Koutlaki N, et al. Malignant female adnexal tumour of probable Wolffian origin: criteria of malignancy. *Histopathology.* 2005;46:716–718.
88. Gersell DJ, King TC. Papillary cystadenoma of the mesosalpinx in von Hippel-Lindau disease. *Am J Surg Pathol.* 1988;12:145–149.
89. Bell DA, Woodruff JM, Scully RE. Ependymoma of the broad ligament. A report of two cases. *Am J Surg Pathol.* 1984;8:203–209.
90. Idowu MO, Rosenblum MK, Wei XJ, et al. Ependymomas of the central nervous system and adult extra-axial ependymomas are morphologically and immunohistochemically distinct—a comparative study with assessment of ovarian carcinomas for expression of glial fibrillary acidic protein. *Am J Surg Pathol.* 2008;32:710–718.
91. Honore LH. Parauterine leiomyomas in women: a clinicopathologic study of 22 cases. *Eur J Obstet Gynecol Reprod Biol.* 1981;11:273–279.
92. Murialdo R, Usset A, Guido T, et al. Leiomyosarcoma of the broad ligament: a case report and review of literature. *Int J Gynecol Cancer.* 2005;15:1226–1229.

CHAPTER 6

Pathology of the Nonneoplastic Ovary and Maldeveloped Gonad

HISTOLOGY OF THE OVARY

Basic Microanatomy

Details regarding the embryology and gross anatomy of the ovary can be found in several of the references listed in the Suggested Readings at the end of this chapter. Histologically, the substance of the ovary is divided into a peripheral cortex and a central medulla, although the boundary between these two regions is often indistinct. However, in the atrophic ovary of the postmenopausal woman, the cellular cortex is usually more sharply demarcated from the less cellular and highly vascular medulla (Fig. 6.1). Blood vessels, lymphatics, and nerves enter the ovary through the hilus, which merges imperceptibly with the medulla. In the atrophic ovaries of postmenopausal women, the medulla may be occupied mainly by contorted masses of thick-walled blood vessels that may have calcified walls and/or mural deposits of hyalinized material that resemble amyloid (Fig. 6.2).

Surface Lining and Cortical Stroma

The surface of the ovary is lined by a single layer of modified mesothelial cells (Fig. 6.3A), which are immunoreactive for the mesothelial marker calretinin and fail to stain with the müllerian marker PAX8.[1] This lining is easily denuded when the ovary is handled, and so is often not apparent in histologic sections. The surface lining of the ovary is often loosely referred to as surface epithelium.

The cortex is composed predominantly of densely cellular, spindle-shaped stromal cells that often exhibit an irregularly whorled (storiform) pattern (Fig. 6.3B). The stromal cells are surrounded by a network of reticulin fibers and separated by a variable amount of collagen, which may be most prominent immediately beneath the surface. It is within the cortex that the ova-containing ovarian follicles can be found, with their numbers and stages of development dictated by the patient's age (see below).

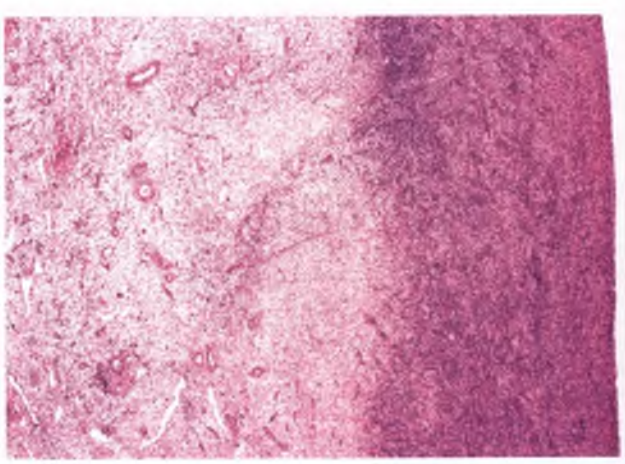

FIGURE 6.1. Ovarian microanatomy. In this postmenopausal ovary, a densely cellular cortex (right) overlies a more sparsely cellular medulla (left) that contains several blood vessels.

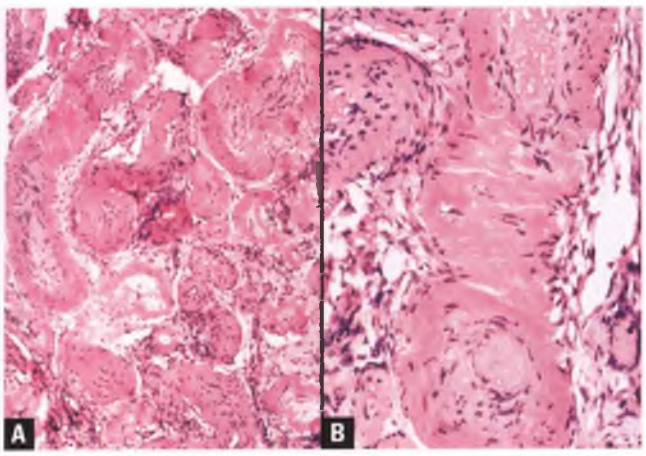

FIGURE 6.2. **A,B:** This conglomeration of thick-walled medullary vessels exhibits mural deposits of amorphous, eosinophilic material. This is a common incidental finding in the ovaries of postmenopausal women. A Congo red stain for amyloid was negative (not shown).

Epithelial Inclusions

Traditionally, it has been thought that formation of epithelial inclusion glands or cysts occurs via the invagination of the ovarian surface lining followed by the metaplastic acquisition of serous epithelial characteristics. However, it is also possible, and perhaps even more likely, that these epithelial inclusions originate from dislodged epithelial cells from the fimbria of the fallopian tube that implant on the surface of the ovary at the site of ovulation-induced disruption.[1] In this model, subsequent epithelial proliferation, invagination, and encystation lead to the formation of epithelial inclusions.[1] The importance of these structures lies in their probable role as the site of origin of some tumors within the epithelial–stromal group, although this role appears to be more limited than previously thought (see Chapter 7).

By convention, inclusion "glands" are a purely microscopic finding, whereas "cysts" are grossly visible but <1 cm. Cysts that are ≥1 cm are considered cystadenomas. Epithelial inclusion glands and cysts are frequent incidental findings that are more common in middle age and beyond. They are typically found

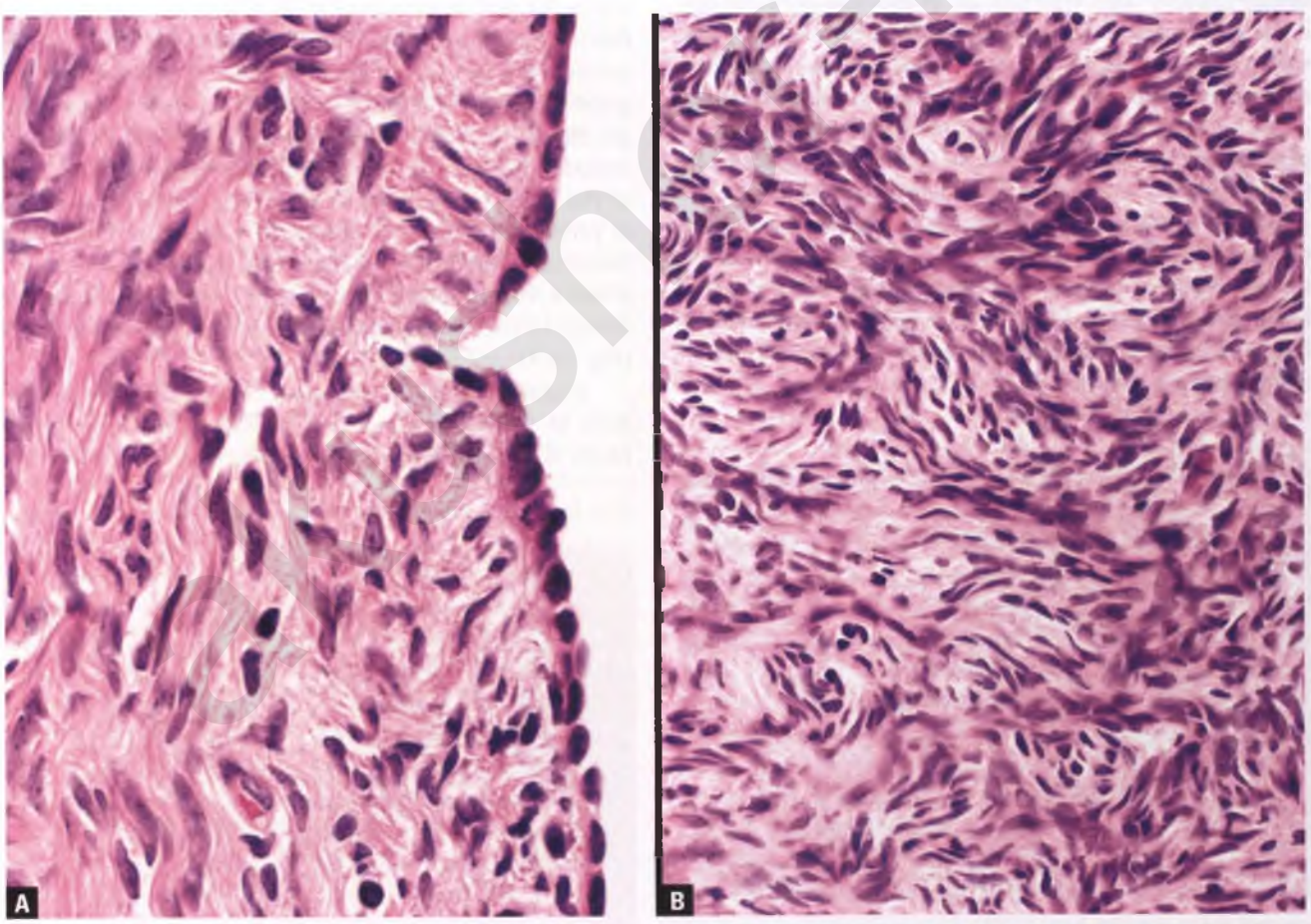

FIGURE 6.3. Ovarian surface lining and cortical stroma. **A:** The cells lining the ovarian surface are usually flattened to cuboidal and form a single layer, as seen along the right side of the image. In some ovaries, the lining may include columnar-shaped cells. **B:** The spindle-shaped stromal cells in the cortex are typically arranged in a storiform pattern.

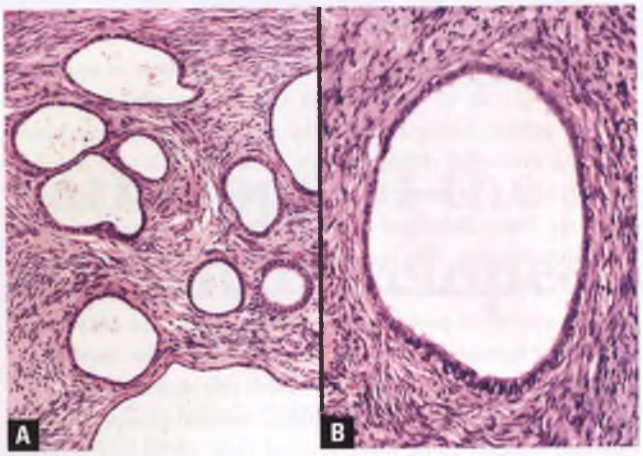

FIGURE 6.4. Epithelial inclusion glands. **A:** Cluster of glands within the ovarian cortex with variably dilated lumens. **B:** Closer view of an inclusion gland lined by tubal-type epithelium. Scattered ciliated cells are responsible for the fuzzy lining seen at this magnification.

scattered singly or in small clusters in the ovarian cortex, are usually lined by tubal-type (serous) or tuboendometrioid epithelium (i.e., ciliated cells are present), and may be associated with psammoma bodies (Fig. 6.4). The histologic appearance of these inclusions is identical to what is termed "endosalpingiosis" within sites such as the peritoneal surface, omentum, or pelvic lymph nodes (see Chapter 8). Rarely, inclusions may be lined by endometrioid or mucinous epithelium.

Small transitional-type epithelial inclusions also rarely occur within the substance of the ovary. These metaplastic inclusions are usually solid, feature cells with occasional longitudinal nuclear grooves, and are termed Walthard nests (Fig. 6.5), just like their more common counterparts found in the tubal serosa (see Chapter 5).

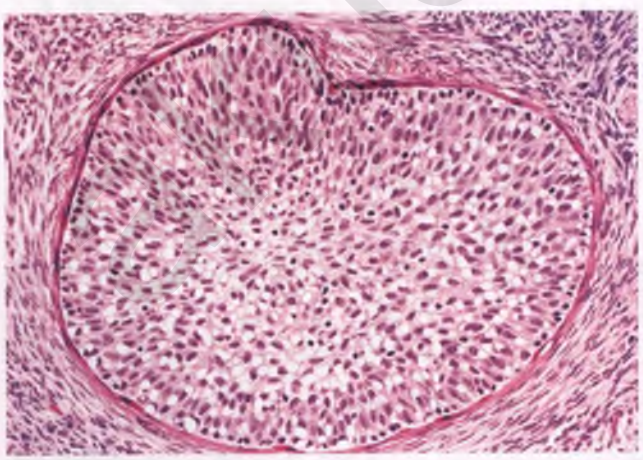

FIGURE 6.5. Solid Walthard nest surrounded by ovarian stroma. Note the bland nuclear features. Although difficult to appreciate at this magnification, scattered cells with longitudinal nuclear grooves are present.

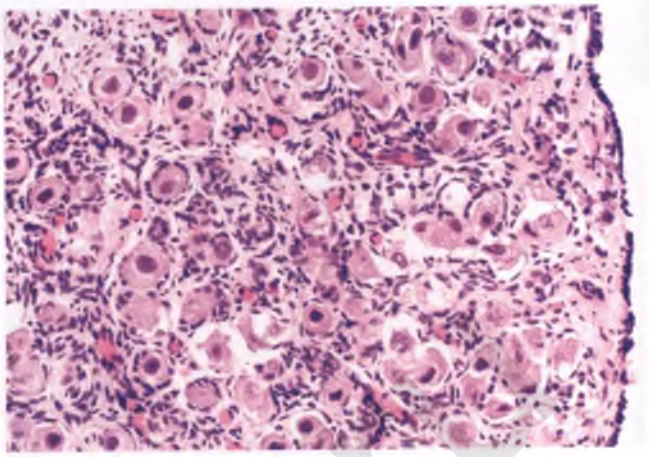

FIGURE 6.6. Infant ovary with numerous primordial follicles within the ovarian cortex. The oocytes have large vesicular nuclei with variably visible nucleoli.

Ovarian Follicles and Their Derivatives

The earliest form of ovarian follicle is the *primordial follicle*, which consists of an oocyte surrounded by a single layer of flattened granulosa cells. These structures are most numerous in the cortex of the newborn ovary (Fig. 6.6), and progressively decrease in number throughout life, such that they are absent to rare in postmenopausal ovaries. During the reproductive years, primordial follicles cluster within a band in the superficial portion of the cortex (Fig. 6.7). A cohort of primordial follicles is stimulated to develop during each menstrual cycle. These follicles are initially transformed into *primary follicles*, which feature slightly enlarged oocytes and a single layer of cuboidal rather than flattened granulosa cells (Fig. 6.8A).

Proliferation of the granulosa cells and further enlargement of the oocyte result in a *secondary (preantral) follicle*, which is characterized by the presence of several layers of

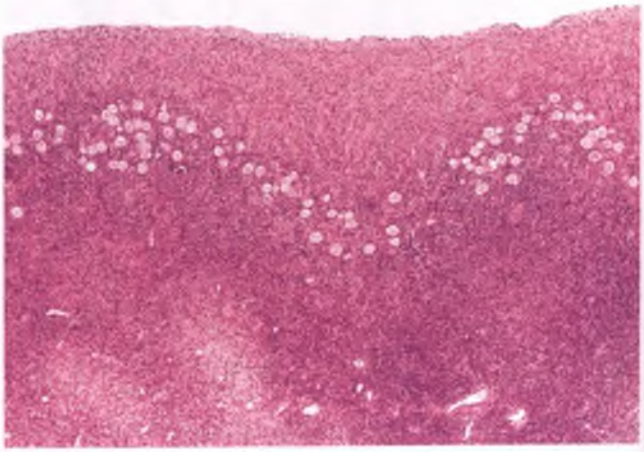

FIGURE 6.7. Undulating band of primordial follicles within the ovarian cortex of a 30 year old woman.

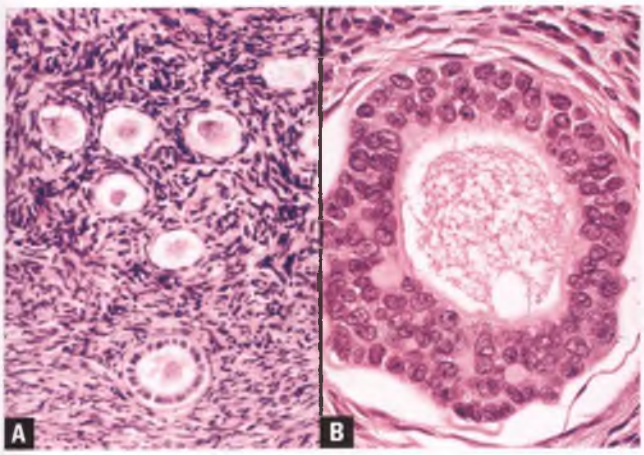

FIGURE 6.8. Primordial, primary, and secondary (preantral) follicles. **A:** Compare the primary follicle at bottom with the primordial follicles above it. **B:** Secondary follicle in an early stage of atresia with degenerated oocyte surrounded by several layers of granulosa cells (the zona granulosa). A few Call-Exner bodies are present within the granulosa layer.

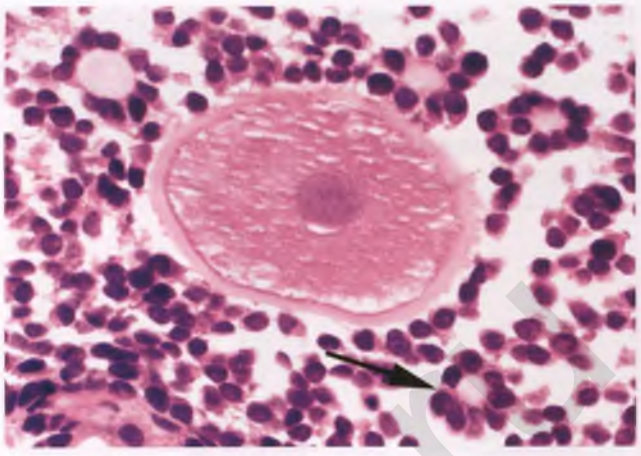

FIGURE 6.9. High-magnification view of a secondary follicle with an oocyte surrounded by a well-developed zona pellucida and four Call-Exner bodies, one of which is marked by an *arrow*.

granulosa cells (the zona granulosa) surrounding the oocyte (Fig. 6.8B). The egg nucleus may or may not be visible, depending on the plane of the section and whether or not it has degenerated. The zona pellucida, which is a circumferential band of eosinophilic glycoprotein that encases the oocyte, and Call-Exner bodies, which are small, spherical cavities containing eosinophilic material that are surrounded by granulosa cells, also develop at this stage (Fig. 6.9). As discussed in Chapter 7, Call-Exner bodies are a useful diagnostic feature of adult granulosa cell tumors. Interestingly, nuclear grooves, which are another characteristic feature of adult granulosa cell tumors, are typically absent within the granulosa cells of nonneoplastic follicles.

In the *tertiary (antral) follicle*, accumulation of fluid produced by the granulosa cells results in the formation of a crescentic cavity (antrum). The theca interna and theca externa develop from the surrounding ovarian stromal cells and begin to become apparent at this stage (proceeding from the inside of the follicle outward, the three layers are the zona granulosa, theca interna, and theca externa). The two theca layers can usually be distinguished from one another by the at least partial luteinization of the steroid-producing theca interna cells. As illustrated in the section on follicle cysts and elsewhere in this chapter, luteinized stromal cells have polygonal to round contours, round rather than spindle-shaped nuclei, distinct nucleoli, and abundant vacuolated cytoplasm that may be eosinophilic or clear. Unlike the cells of the zona granulosa, thecal cells are enmeshed in a delicate network of reticulin fibers, which is also demonstrated in the section on follicle cysts.

In the *mature (Graafian) follicle*, the antrum has progressively enlarged, and the oocyte has become situated in an eccentric position in a thickened area of granulosa cells termed the cumulus oophorus (Fig. 6.10). The thin rim of granulosa cells that remains circumferentially attached to the oocyte is referred to as the corona radiata. As the follicle destined for ovulation enlarges, it attains a size of approximately 2 cm and bulges from the ovarian surface. At ovulation, its wall ruptures and the oocyte (with its attached corona radiata) is released into the peritoneal cavity, where the tubal fimbriae assist in its passage into the lumen of the ipsilateral fallopian tube.

Following ovulation and under the influence of the surge in luteinizing hormone from the anterior pituitary, the ruptured follicle is transformed into the *corpus luteum*. The granulosa layer is thrown into undulating folds, a blood clot forms in the central cavity, and both the granulosa and theca interna cells become luteinized (Figs. 6.11 and 6.12). The framework of the corpus luteum includes curvilinear vascular septa that extend into the center of its lining; these septa are often ensheathed by theca interna cells. The major function of the corpus luteum is to produce progesterone, although it also synthesizes estrogens and androgens in lesser amounts.

If fertilization does not occur, the corpus luteum of menstruation lacks the persistent hormonal stimulus necessary for its maintenance, and it begins to degenerate in the latter part of the secretory phase of the menstrual cycle. As the corpus luteum regresses, its granulosa cells develop pyknotic nuclei and accumulate large amounts of intracytoplasmic lipid, imparting a foamy appearance (Fig. 6.13). Over the course of months, progressive involutional changes result in the formation of a small white scar known as the *corpus albicans* (Fig. 6.14). Over time, corpora albicantia migrate toward the center of the ovary and are gradually resorbed.

If fertilization occurs, the corpus luteum is maintained by human chorionic gonadotropin (and perhaps other factors) produced by the trophoblastic cells of the developing placenta. In this situation, the *corpus luteum of pregnancy* produces an adequate amount of steroid hormones until that function can be assumed by the placenta near the 12th week of gestation.

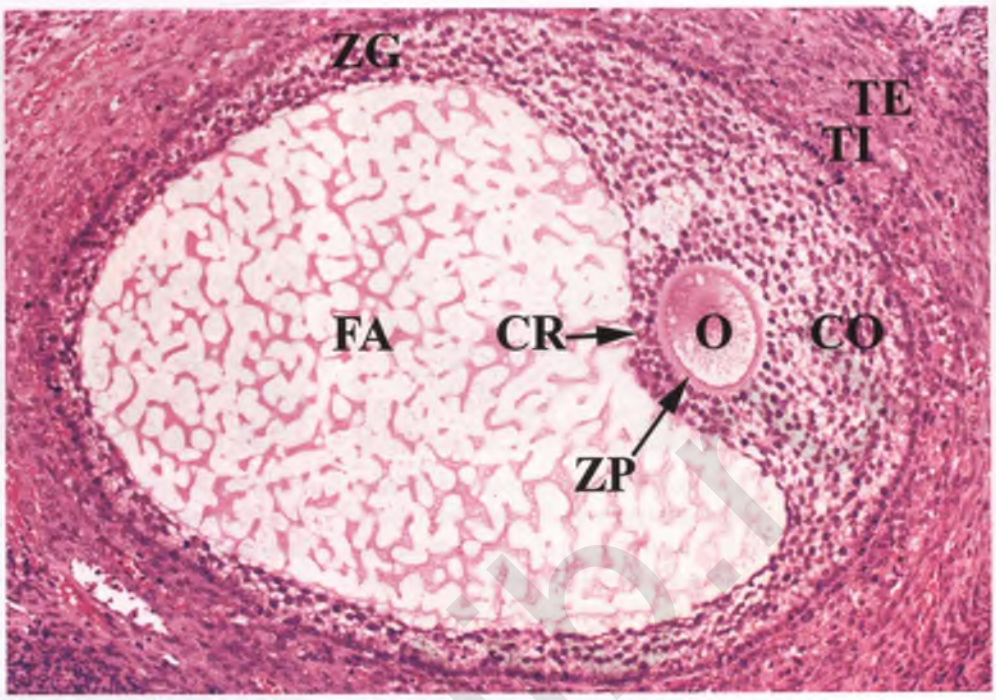

FIGURE 6.10. Mature (Graafian) follicle. FA, follicular antrum; O, oocyte; ZP, zona pellucida; ZG, zona granulosa; CO, cumulus oophorus; CR, corona radiata; TI, theca interna; TE, theca externa.

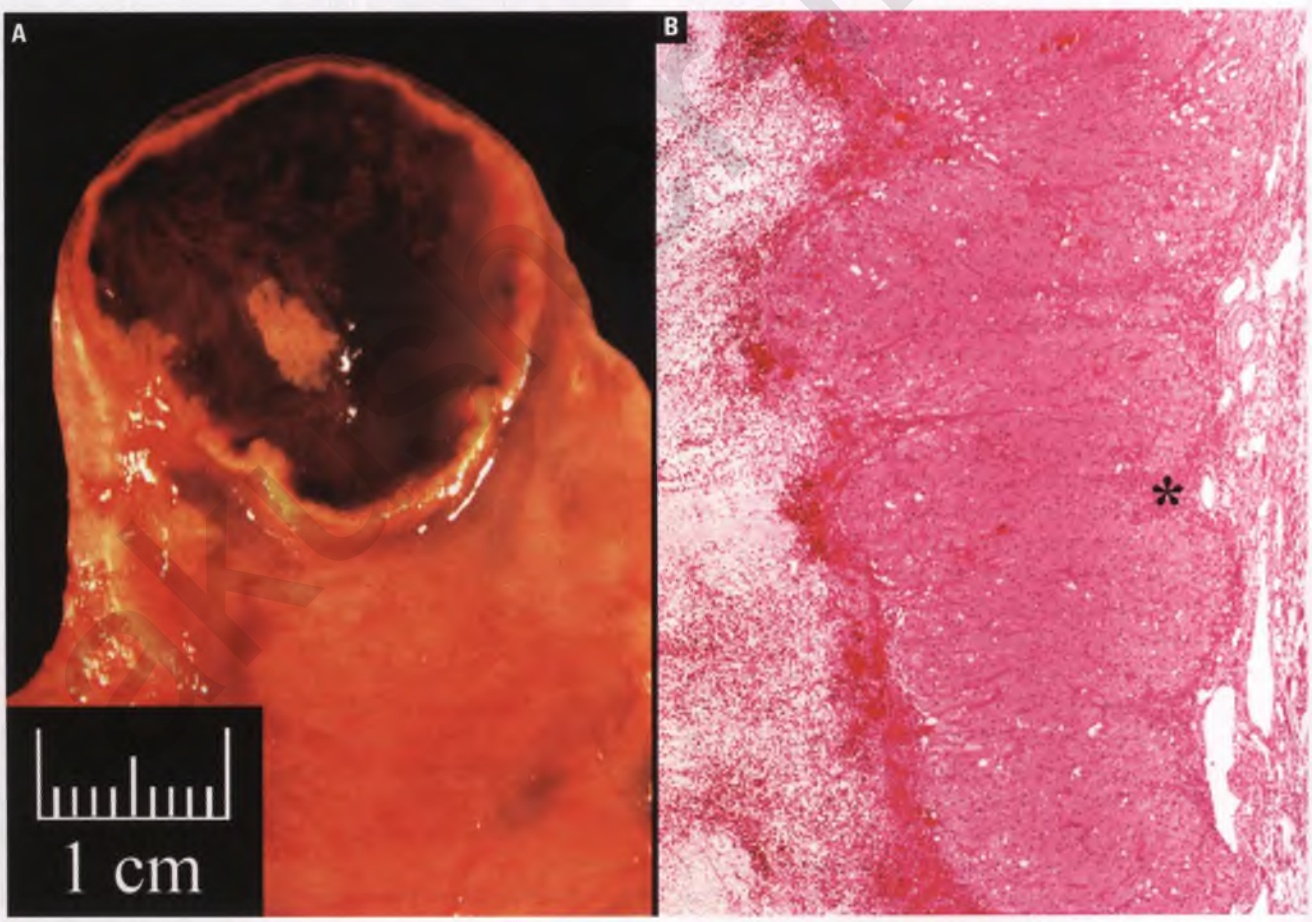

FIGURE 6.11. Corpus luteum of menstruation. **A:** As seen in this sectioned ovary, the corpus luteum bulges from the surface and characteristically has a convoluted, orange-yellow peripheral rim surrounding a central blood clot. **B:** The wall of the corpus luteum is dominated by the undulating layer of luteinized granulosa cells, which is largely responsible for the orange-yellow rim seen in gross specimens. Also note the surrounding wedge-shaped aggregates of theca interna cells that appear at periodic intervals, one of which is marked by an *asterisk*. The cavity (at left) contains fibrin and erythrocytes.

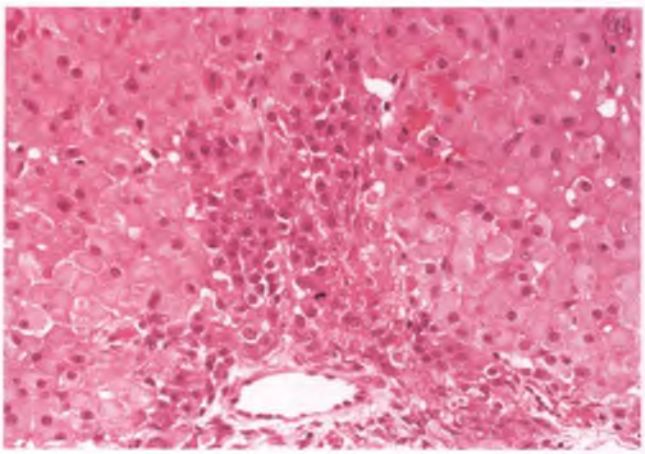

FIGURE 6.12. Corpus luteum of menstruation. At high magnification, the luteinized granulosa cells appear as large polygonal cells with abundant eosinophilic cytoplasm, round nuclei, and prominent nucleoli. This image also highlights one of the wedges of luteinized theca interna, whose cells are recognized by the shape of their aggregates and their location, smaller size, and more darkly stained cytoplasm.

During its period of peak functioning in the first trimester, the corpus luteum of pregnancy is larger than its menstrual counterpart, has a fluid or blood-filled central cavity, and has a wall that is bright yellow rather than orange-yellow. Characteristic histologic features of the corpus luteum of pregnancy are the further enlargement of the luteinized granulosa cells and the presence of eosinophilic hyaline droplets, which eventually calcify to form microcalcifications (Fig. 6.15). The cystic cavity of the corpus luteum of pregnancy begins to regress in mid-gestation, and is usually absent by the time of delivery. A solid, late-gestation corpus luteum of pregnancy may mimic a small pregnancy luteoma (Fig. 6.16), but is distinguished by its convoluted rather than rounded contour, lack of mitotic

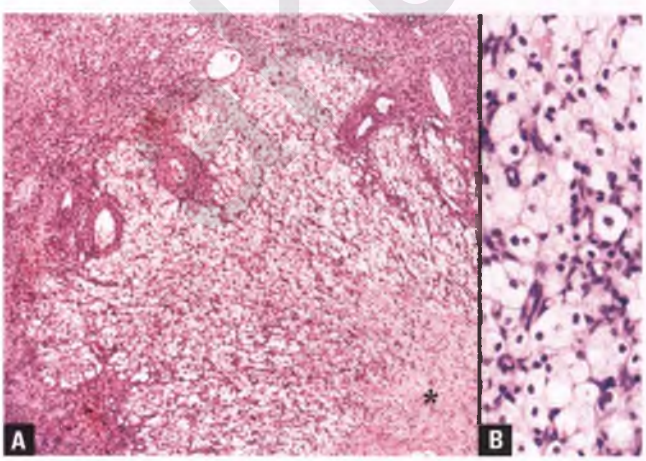

FIGURE 6.13. **A,B:** Degenerating corpus luteum of menstruation. The granulosa cells have been converted into cells with foamy, lipid-rich cytoplasm and shrunken nuclei. Note the beginning of scar formation in the core of the involuting corpus luteum (*asterisk*).

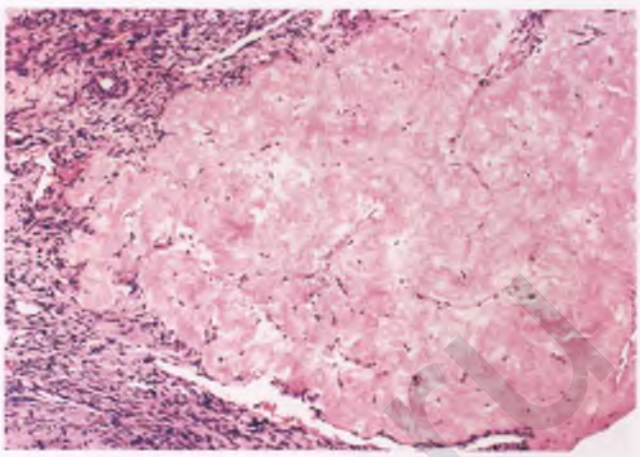

FIGURE 6.14. Corpus albicans. What was once a corpus luteum is now a small scar.

activity, absence of follicle-like spaces, and presence of hyaline droplets and microcalcifications.

In the usual menstrual cycle, only one follicle completes the entire maturation sequence that results in ovulation; the remaining follicles in its cohort undergo atresia (degeneration) at various stages in their development and over various time intervals. Atretic follicles display a variety of changes. In those at a more advanced stage, common findings include partial to complete loss of the granulosa cells, cystic dilatation with eventual replacement of the follicular cavity by vascularized connective tissue, prominence of the theca interna (which is often luteinized), and transformation of the basement membrane that separates the zona granulosa from the theca interna into a thick, undulating, hyalinized eosinophilic band that is referred to as the glassy membrane (Fig. 6.17). A diameter of ≤3 cm is the sole criterion that arbitrarily distinguishes atretic

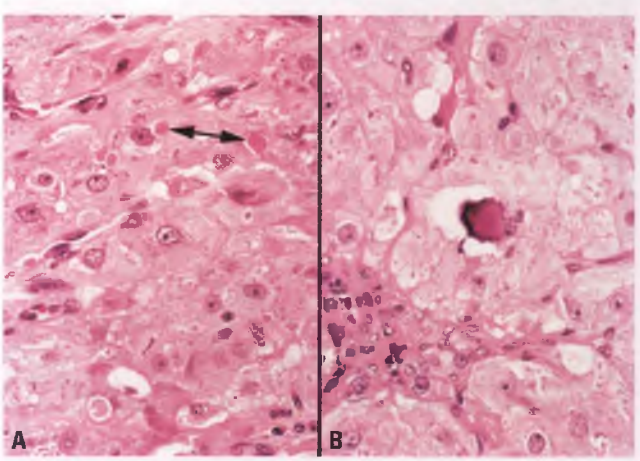

FIGURE 6.15. Corpus luteum of pregnancy. **A:** Note the presence of two hyaline droplets, which are marked by the *arrow*. **B:** This image highlights a centrally located, purple microcalcification. Both of these histologic features are characteristic of the corpus luteum of pregnancy.

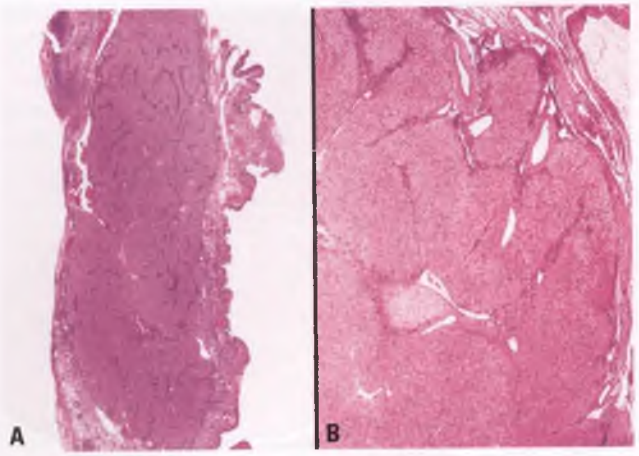

FIGURE 6.16. Corpora lutea of pregnancy from term gestations. **A:** In this low-magnification view, an oblong, solid corpus luteum is present within the wall of a mucinous cystadenoma. Within the corpus luteum are prominent vascular septa with curvilinear shapes that account for its convoluted architecture. **B:** All that remains of the central cavity of this corpus luteum is a small scar. Note the cerebriform contour, which contrasts with the rounded outline of a pregnancy luteoma.

cystic follicles from follicle cysts, whose histologic features are further illustrated later in this chapter. The process of atresia eventually results in the obliterated follicle being represented only by a serpentine band of hyalinized tissue known as the corpus fibrosum (Fig. 6.18), which is presumably ultimately resorbed by the ovarian stroma.

One potential diagnostic pitfall related to ovarian follicles is the occasional enlarged follicle that has been tangentially sectioned through the theca externa, producing the appearance of a small solid nodule composed of a cellular proliferation of plump, spindle-shaped cells with brisk mitotic activity

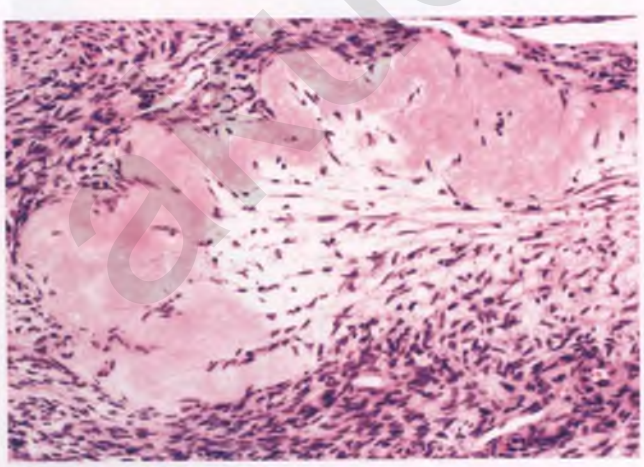

FIGURE 6.17. Portion of an atretic follicle in which the central cavity has been replaced by loose connective tissue. Note the characteristic undulating, hyalinized, thickened basement membrane that is referred to as the glassy membrane.

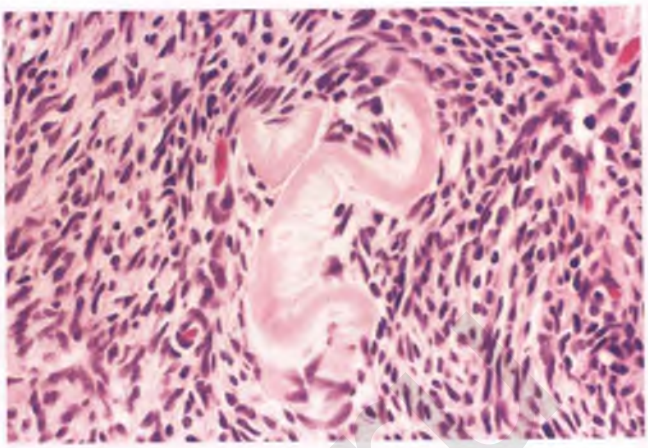

FIGURE 6.18. Corpus fibrosum.

(Figs. 6.19 and 6.20). Such a nodule could be misinterpreted as an incipient fibrosarcoma, but its true nature can be established by (a) being aware of this artifact of sectioning and the small size of the "nodules" that it produces, (b) obtaining additional sections that may disclose its relationship to a follicle, (c) finding mitotically active cells with identical nuclear features within the theca externa of adjacent follicles that are properly oriented, and (d) noting the gradual blending of the thecal cells from the worrisome nodule with the neighboring ovarian stroma.

Hilus Cells

Ovarian hilus cells are capable of producing androgenic steroid hormones and are virtually identical to Leydig cells of the testis.They are typically found in aggregates within the hilum, adjacent mesovarium, and ovarian ligament, often in intimate association with nonmyelinated nerves and/or adjacent to

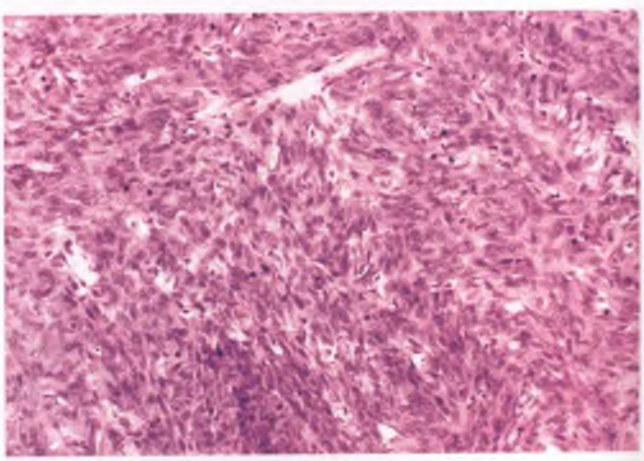

FIGURE 6.19. Appearance of tangentially sectioned theca externa. This image is from the center of what appeared to be a 3 mm solid nodule. The cellular pattern of intertwining fascicles of plump, spindle-shaped cells with significant mitotic activity results in a resemblance to fibrosarcoma.

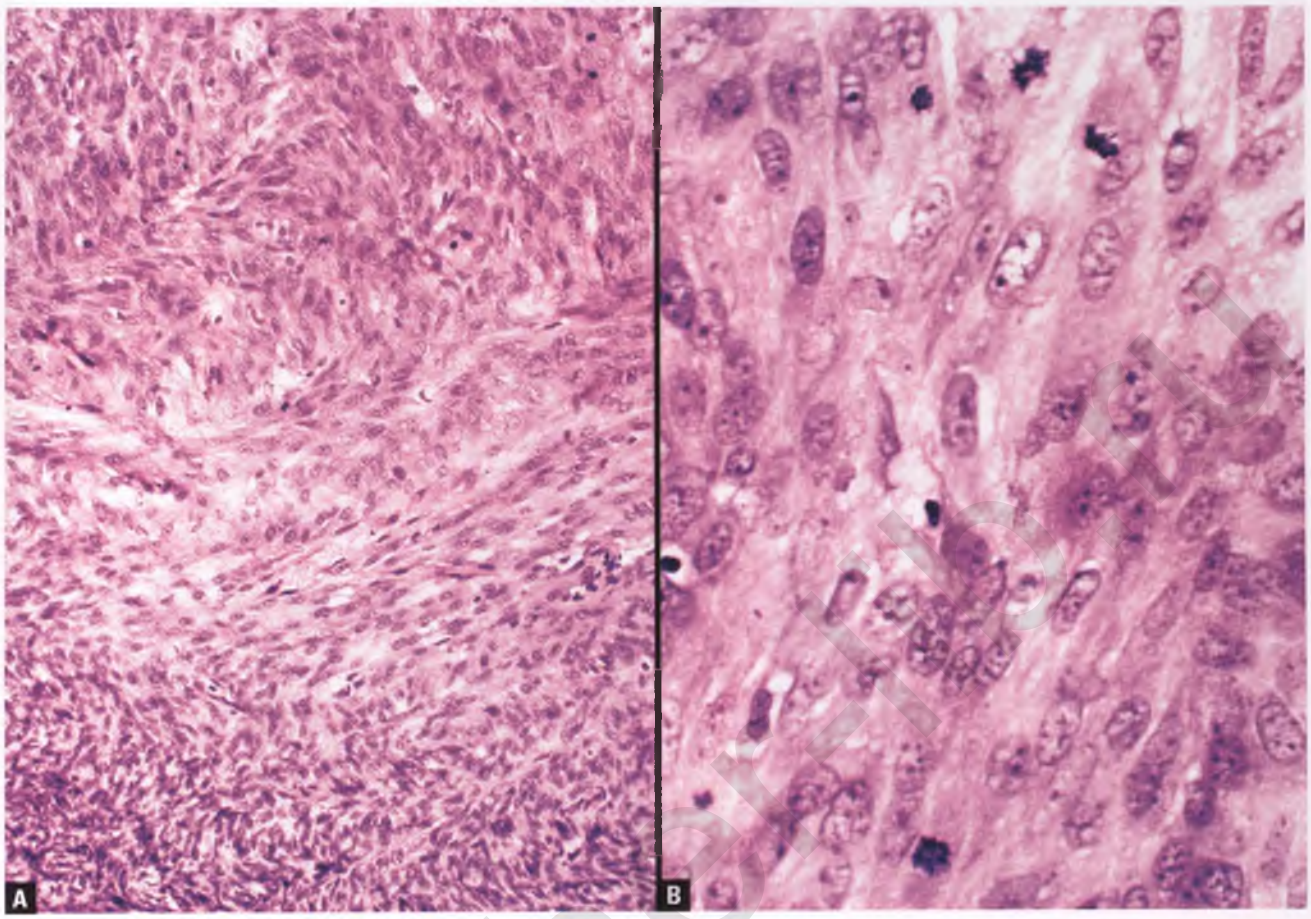

FIGURE 6.20. Theca externa. **A:** The edge of the "nodule" depicted in the preceding figure is shown at top. Note how the theca externa gradually blends with the normal ovarian stroma at bottom. **B:** This high-magnification view of the plump, spindle-shaped cells of the theca externa highlights their brisk mitotic activity.

large, thin-walled venous and lymphatic channels (Fig. 6.21A). Hilus cells have abundant eosinophilic cytoplasm and vesicular nuclei with distinct nucleoli (Fig. 6.21B). Some degree of nuclear atypia is not uncommon. Close inspection may result in the identification of occasional crystals of Reinke, which are considered pathognomonic for Leydig-type cells. Examples of these eosinophilic, rod-shaped structures, which should not be confused with elongated, compressed erythrocytes within capillary spaces, are shown in Figure 7.224.

Heterotopic hilus cells are rarely found in the subcapsular ovarian cortex, perisalpinx, and lamina propria of the fallopian tube, and may form either rounded aggregates or cords.[2,3] The morphology of hilus cells, their architectural patterns, their association with nerve twigs, and their occurrence in unfamiliar locations may lead to misinterpretation as metastatic carcinoma (see Fig. 4.237). In difficult cases, such as in a prophylactic oophorectomy specimen from a patient with a history of breast cancer, this differential diagnosis can be resolved using immunohistochemistry (see the section on hilus cell hyperplasia near the end of this chapter).

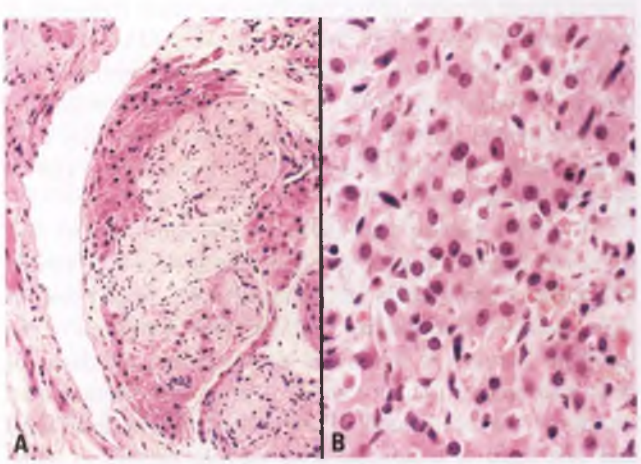

FIGURE 6.21. Hilus cells. **A:** Nests of hilus cells are seen adjacent to a large, thin-walled vessel and in close association with a small nerve. **B:** High-magnification view of hilus cells.

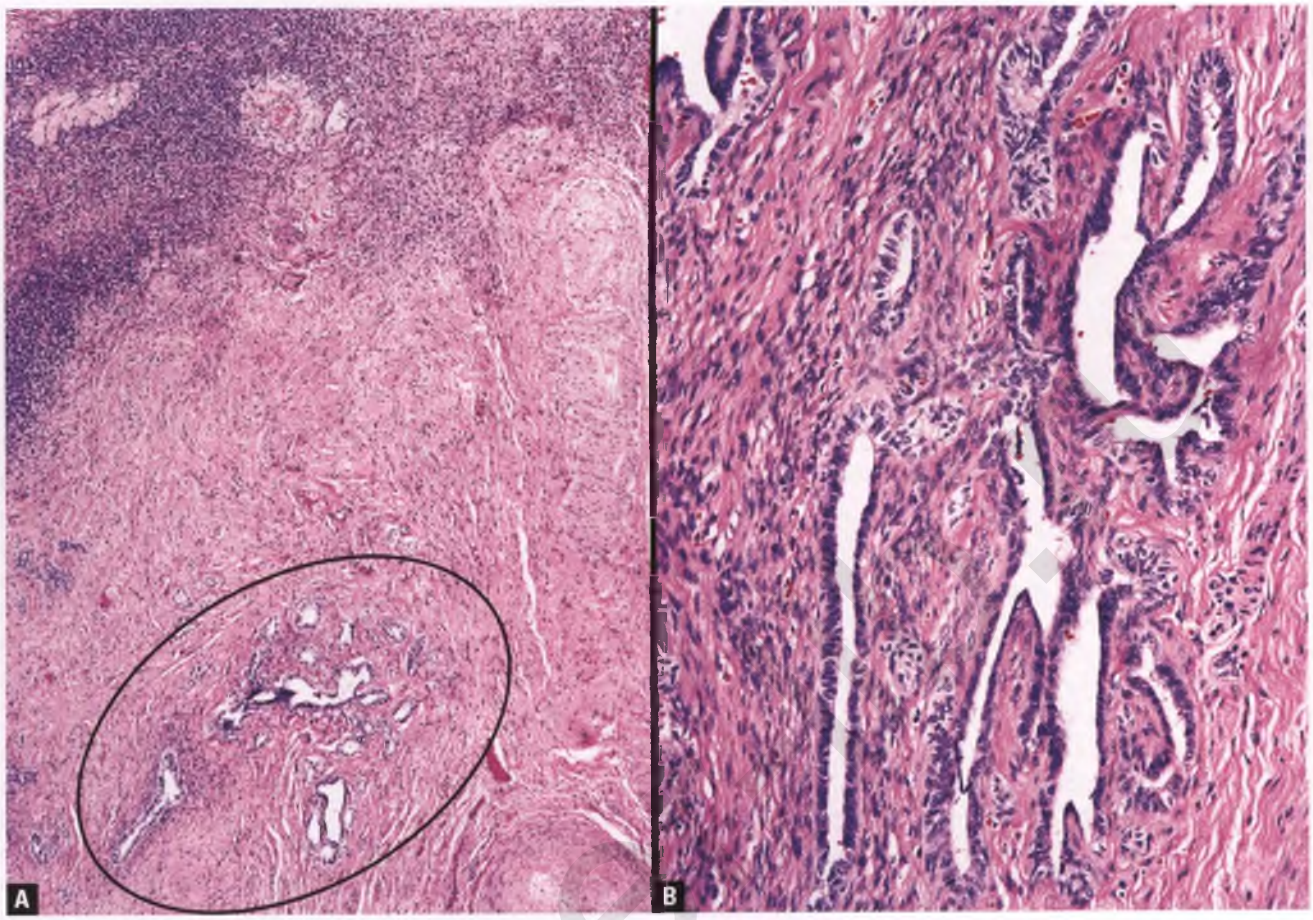

FIGURE 6.22. Rete ovarii. **A:** At low magnification, the rete ovarii (*circled*) is seen in its characteristic location within the ovarian hilum. **B:** At higher magnification, the typical architectural features of the rete tubules can be appreciated.

Rete Ovarii

The rete ovarii is a normal constituent of the ovarian hilus and represents the counterpart of the rete testis of the male, occurring as a form of mesonephric (wolffian) remnant. It consists of a localized network of branching, interconnected tubules variably lined by flattened to cuboidal to columnar epithelial cells (Fig. 6.22). Small papillary structures are often seen projecting into the tubular lumens, and some of the tubules may have pointed ends. The tubules are often surrounded by a cuff of spindly, ovarian-type stroma.

The characteristic location and architecture of rete ovarii, as well as the lack of surrounding endometrial-type stroma or associated hemosiderin-laden macrophages, should prevent their confusion with ovarian endometriosis. Awareness of the histologic features of rete ovarii also facilitates avoidance of their misinterpretation as a small focus of well-differentiated metastatic adenocarcinoma. The histology of the rete ovarii and rete testis is recapitulated to varying degrees in some Sertoli-Leydig cell tumors, female adnexal tumors of probable wolffian origin, and mesonephric adenocarcinomas, which are then referred to as exhibiting a retiform pattern. Actual tumors of the rete ovarii are very rare (see Chapter 7).

TUBO-OVARIAN ABSCESS

See section on Salpingitis in Chapter 5.

FOLLICLE CYST[4]

When a cystic follicle attains a size of ≥3 cm, it is designated a follicle cyst. These cysts are rarely larger than 8 cm and are typically solitary. They are most commonly encountered in nonpregnant women in the reproductive age group. Follicle cysts may be asymptomatic, produce estrogen-related menstrual irregularities, or present acutely with symptoms related to rupture.

Grossly, follicle cysts are smooth surfaced and unilocular with thin walls and a cavity filled with watery to bloody fluid (Fig. 6.23). Classic examples are lined by one or more layers of mildly luteinized granulosa cells with an underlying layer of more prominently luteinized theca cells (Fig. 6.24). Follicle cysts in which the granulosa cell layer has been partially or completely denuded are more difficult to recognize, but a clue to the correct diagnosis is the at least focal persistence of the luteinized theca layer.

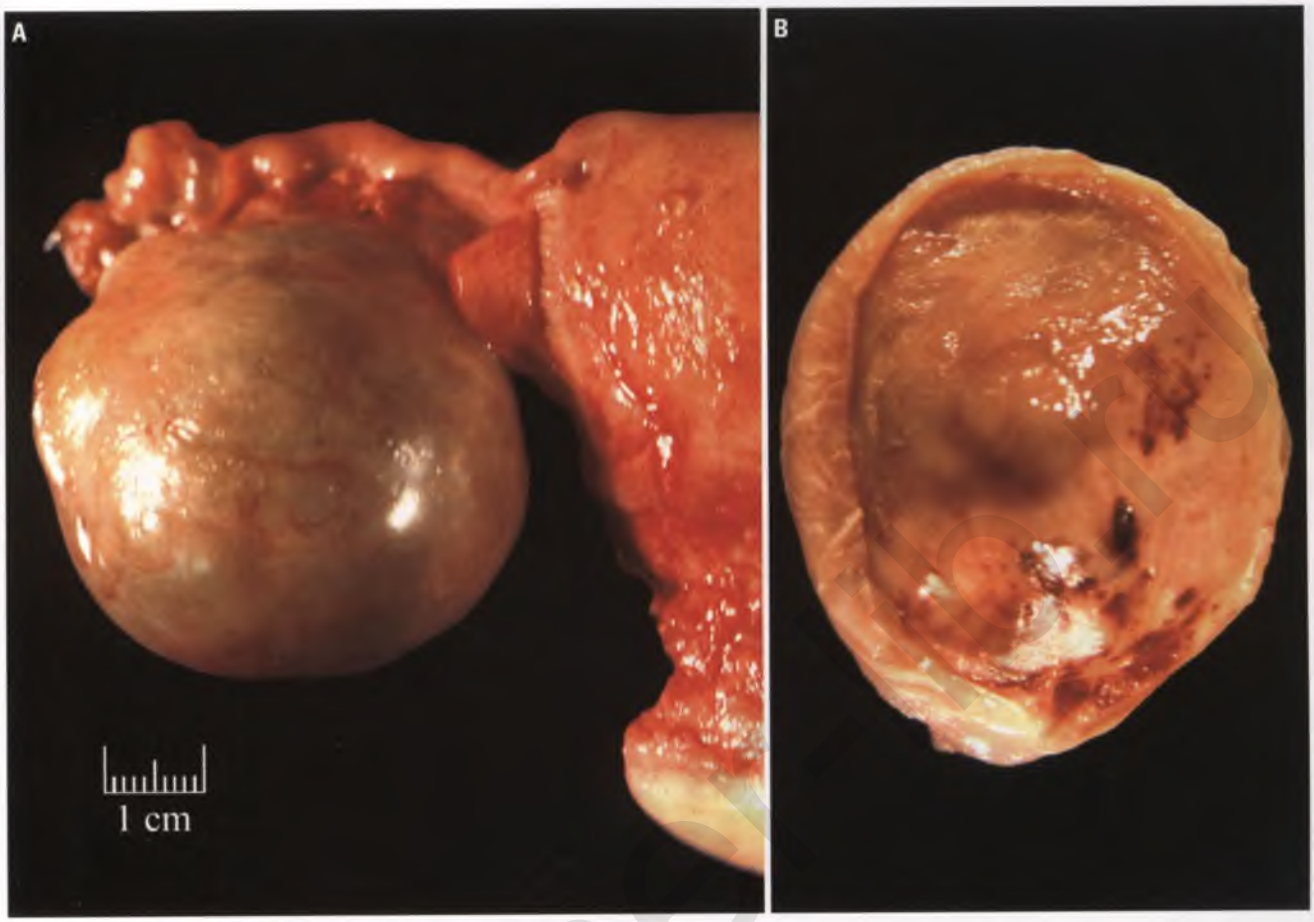

FIGURE 6.23. Follicle cyst. **A:** This 5 cm follicle cyst has a smooth external surface. **B:** The wall of this unilocular cyst is thin and its inner lining is smooth with patchy hemorrhagic areas. The cyst contained watery, dark brown fluid.

Follicle cysts are usually easily recognized as benign, but two potential pitfalls are worth mentioning. First, before rendering a diagnosis of a large follicle cyst, some consideration should be given to a cystic granulosa cell tumor (see Chapter 7). Second, exfoliated granulosa cells can be quite numerous in cytologic preparations of aspirates of follicle cysts, which can lead to a worrisome appearance for the uninitiated (Fig. 6.25).[5] The uniformity of the granulosa cells and an awareness that the cells were sampled from a unilocular cyst rather than a solid mass facilitate correct interpretation.

Since follicle cysts typically regress within 2 months, cystic lesions that are clinically and radiologically consistent with this diagnosis should be managed conservatively, with cystectomy reserved for cysts that persist or enlarge.

CORPUS LUTEUM CYST[4]

In their early stages, corpus luteum cysts resemble their normal counterparts, except that by definition they have reached a size of at least 3 cm. Symptoms, if present, are related to menstrual irregularities or cyst rupture. The typical corpus luteum cyst contains congealed blood and has an orange-yellow lining that corresponds to the layer of luteinized cells (Fig. 6.26). In its later stages, an involuting corpus luteum cyst may have only a thin band of residual luteinized cells and can be difficult to distinguish from an involuting follicle cyst (Fig. 6.27). Features that favor a corpus luteum cyst in this situation are the gross recognition of the orange-yellow band of luteal tissue, the partial retention of an undulating pattern of the luteinized cells, and the innermost lining of the cyst consisting of organizing hemorrhage and/or fibrous tissue related to resolution of the hematoma. To facilitate the diagnosis, histologic sections should focus on areas where the orange-yellow band is the thickest. As is the case for follicle cysts, corpus luteum cysts tend to regress spontaneously if left untreated.

SIMPLE CYST[4]

Simple cyst is a diagnosis of exclusion used for those instances in which a benign cyst is not classifiable due to the absence or atrophic and nonspecific nature of its lining. Such cysts are usually solitary, unilocular, smooth surfaced, and <10 cm in

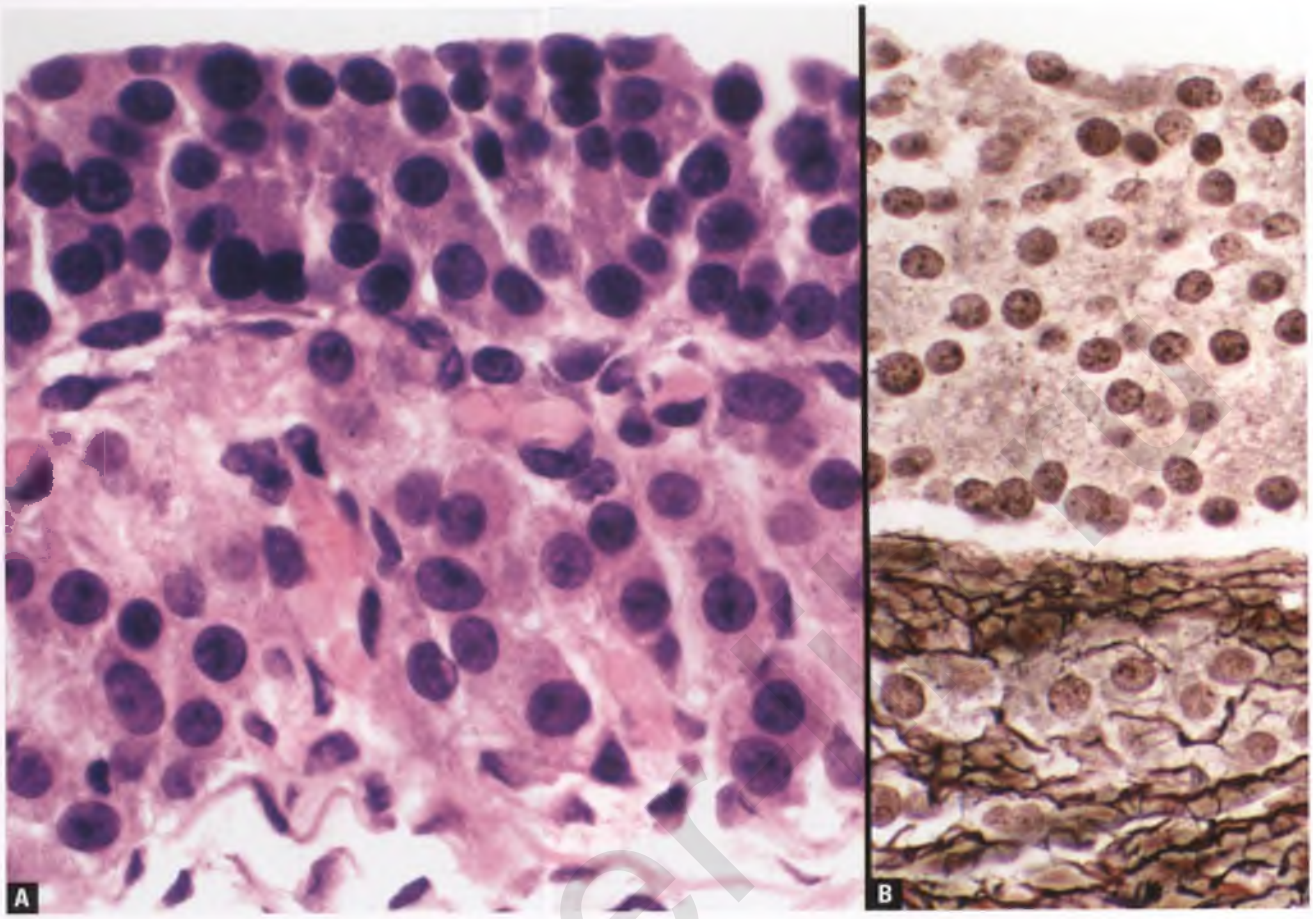

FIGURE 6.24. Follicle cyst. **A:** This high-magnification view of the cyst lining demonstrates the luteinized granulosa and theca cell layers at top and bottom, respectively. **B:** As demonstrated in this reticulin stain of a different follicle cyst with a thicker granulosa cell layer, the individual cells of the theca layer and ovarian stroma are enmeshed in reticulin fibers (bottom) that are absent in the granulosa cell layer (top).

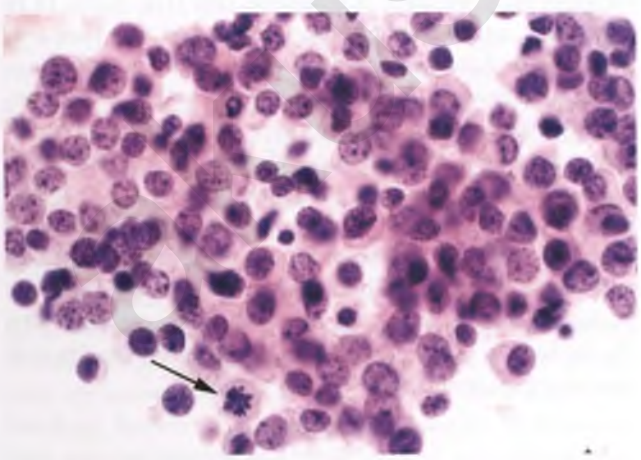

FIGURE 6.25. Aspirated contents of a follicle cyst. These specimens can be cellular and contain mitotic figures (*arrow*). If the pathologist is unfamiliar with the appearance of exfoliated granulosa cells in samples of this type, there may be undue concern for the possibility of malignancy.

diameter (Fig. 6.28). Simple cysts are commonly derived from cysts of follicular origin that are removed in their late stages of involution or small serous cystadenomas whose lining has become flattened and mesothelial–like as a result of pressure atrophy (Fig. 6.29). Although some pathologists are taught that a diagnosis of simple cyst is for those with simple minds, this diagnosis is appropriate for benign cysts that defy precise classification due to their absent or flattened lining.

ENDOMETRIOSIS[4]

The general features and extragenital manifestations of endometriosis are discussed in Chapter 8. The ovary is the most common site of endometriosis, where it may present as a superficial lesion on or near the surface, an endometriotic cyst, or a necrotic pseudoxanthomatous nodule. In the discussion that follows, the section on endometriotic cysts includes a review of the many different alterations that can occur in the epithelium, stroma, wall, and contents of these cysts that can cause diagnostic difficulty.

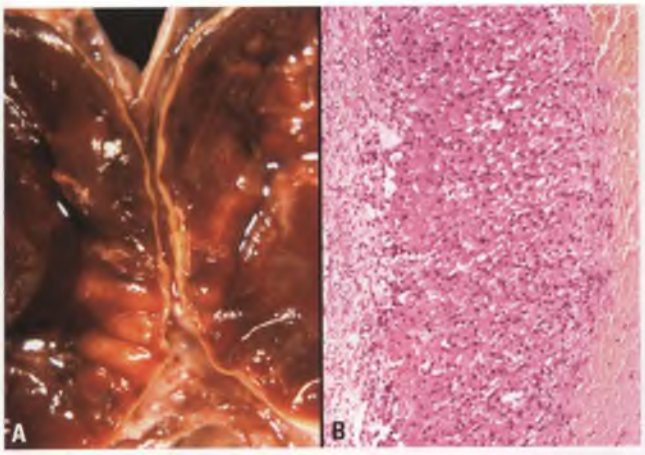

FIGURE 6.26. Corpus luteum cyst. **A:** The cyst has been bisected, revealing congealed blood surrounded by a rim of orange-yellow tissue. **B:** The cyst wall is dominated by a layer of luteinized granulosa cells. Occasional luteinized theca cells are present at the interface between the granulosa cells and the ovarian stroma near the left edge of the image. The innermost layer (right) consists of recent organizing hemorrhage.

Superficial Endometriosis

Surface endometriosis may be grossly recognized by its association with hemorrhagic adhesions or by the presence of patchy brown discolorations referred to as "powder burns" (Fig. 6.30). An example of endometriosis involving the ovarian cortex is presented in Figure 6.31. Classic cases of endometriosis feature endometriotic glands enveloped by a layer of endometriotic stroma, often accompanied by aggregates of pigmented histiocytes and hemorrhagic luminal material. In contrast to superficial ovarian endometriosis, cortical inclusion glands and cysts lack associated endometriotic stroma and sequelae of hemorrhage.

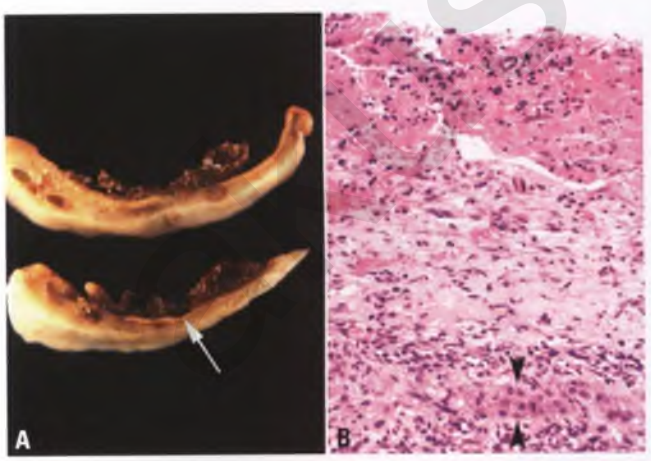

FIGURE 6.27. Corpus luteum cyst, late stage. **A:** Sections through the wall of this hemorrhagic cyst reveal an attenuated orange-yellow rim of luteinized tissue as marked by the *arrow*. **B:** The innermost lining of the cyst (top) consists of recent organizing hemorrhage, beneath which is a fibrous layer. The *arrowheads* mark a narrow and incomplete band of involuting luteinized cells that corresponds to the orange-yellow rim of tissue noted grossly.

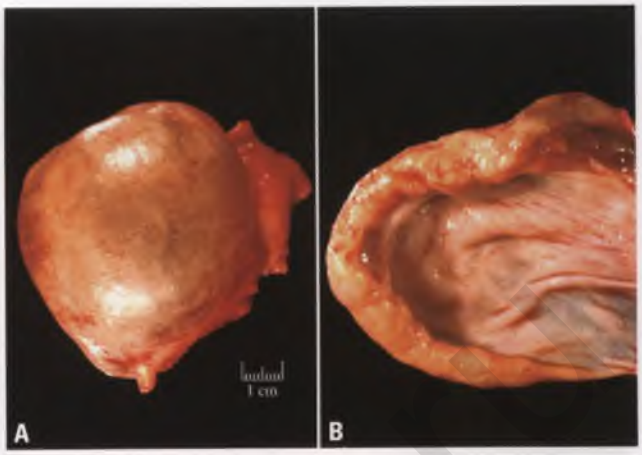

FIGURE 6.28. Simple cyst. **A:** The cyst has a smooth external surface. A segment of attached fallopian tube is at right. **B:** The internal lining of the cyst is smooth.

Endometriotic Cyst (Endometrioma)

Foci of endometriosis may extend into the substance of the ovary and cystically enlarge as the central cavity accumulates blood and its breakdown products. The result is an endometriotic cyst, which is also referred to as an endometrioma or "chocolate cyst" (owing to the chocolate color of the semiliquid cyst contents). These unilocular cysts are frequently bilateral and often have adhesions on their external surface. Their internal lining is tan and smooth in areas where the endometrial epithelial lining persists, and brown and shaggy with adherent hemorrhagic material

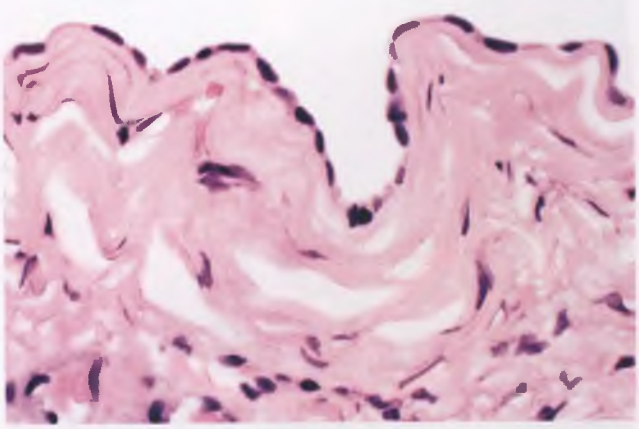

FIGURE 6.29. Simple cyst. This cyst is lined by a single layer of flattened cells of uncertain lineage that resembles mesothelium. Most ovarian cysts with this appearance probably represent serous cystadenomas with pressure atrophy of the lining related to the accumulation of fluid within the cyst.

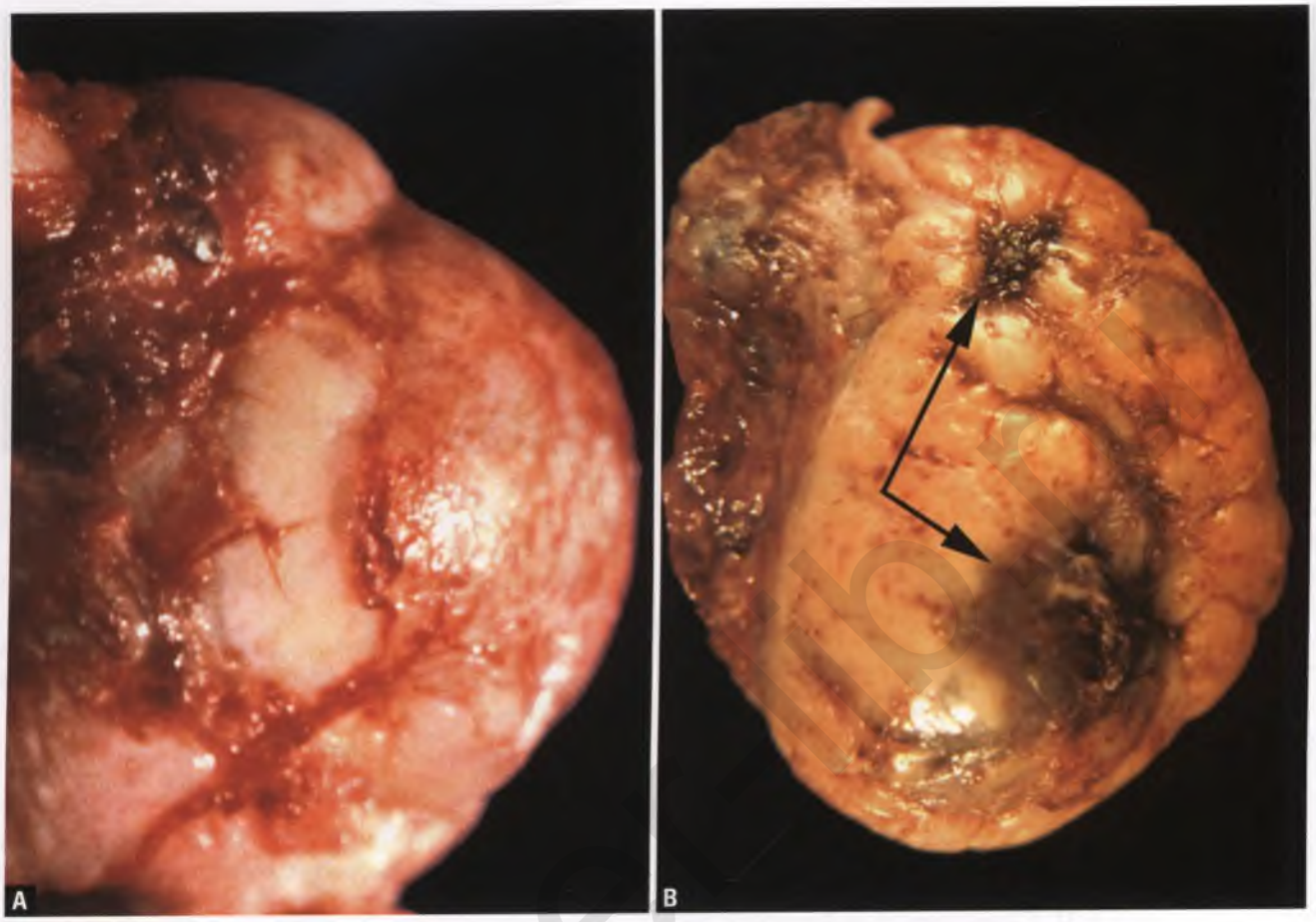

FIGURE 6.30. Involvement of the ovarian surface by endometriosis. **A:** Hemorrhagic adhesions associated with red lesions of serosal endometriosis. **B:** Two "powder burns" are marked by *arrows*.

in areas where it has been obliterated (Figs. 6.32–6.34). Since malignant neoplasms arise within endometriotic cysts in approximately 1% of cases, these cysts should be examined carefully.[6]

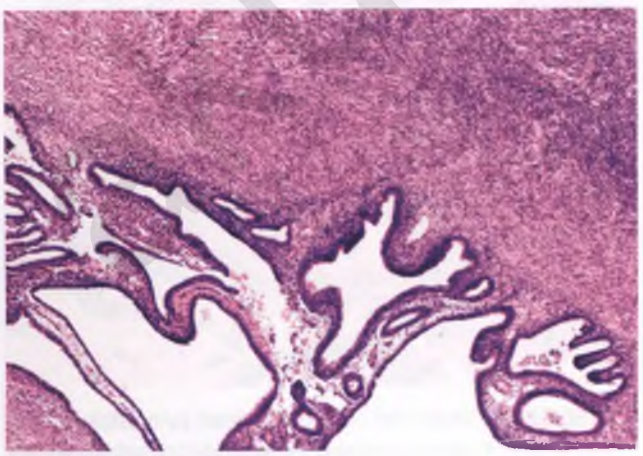

FIGURE 6.31. Ovarian endometriosis. A conglomeration of endometriotic glands with associated endometriotic stroma is present within the ovarian cortex. Some of the glands are cystically dilated.

Grossly, suspicious areas in need of histologic sampling include any intraluminal polypoid projections or regions of the cyst wall that are thickened or nodular. The vast majority of malignant tumors arising within endometriotic cysts are endometrioid or clear cell carcinomas (see Figs. 7.96, 7.123, and 7.155).[7]

Histologically, the classic endometriotic cyst is at least partially lined by endometriotic epithelium with a subjacent layer of endometriotic stromal cells and variable numbers of pigmented histiocytes (Fig. 6.35). The cyst wall is typically fibrotic. Commonly, the lining of the cyst is at least partially eroded (Fig. 6.36). Old endometriotic cysts may have no residual endometriotic lining whatsoever, with the lining replaced by a combination of degraded blood products, fibrous tissue, and pigmented histiocytes (Fig. 6.37). In this situation, a diagnosis of "benign hemorrhagic cyst most consistent with endometriotic cyst" is appropriate.

Progestational Changes

Endometriotic cysts take on a different histologic appearance in patients who are pregnant or being treated with progestational agents. The subepithelial endometriotic stroma becomes decidualized (Fig. 6.38), and the endometriotic glands may become atrophic.[8]

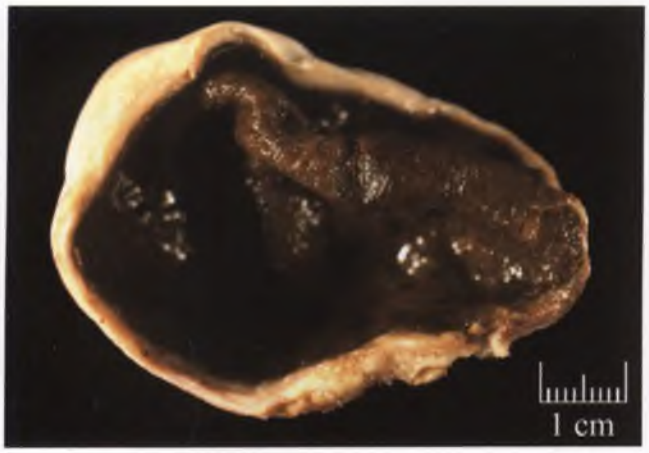

FIGURE 6.32. Endometriotic cyst. This cyst, which was filled with chocolate-colored fluid and has a dark brown lining, is unlikely to have areas with a residual endometrial epithelial lining.

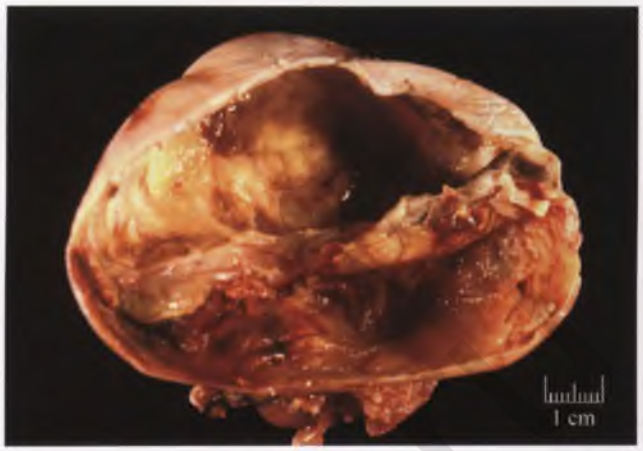

FIGURE 6.33. Endometriotic cyst (top) fused with a corpus luteum cyst (bottom). The endometriotic cyst was filled with chocolate-colored fluid.

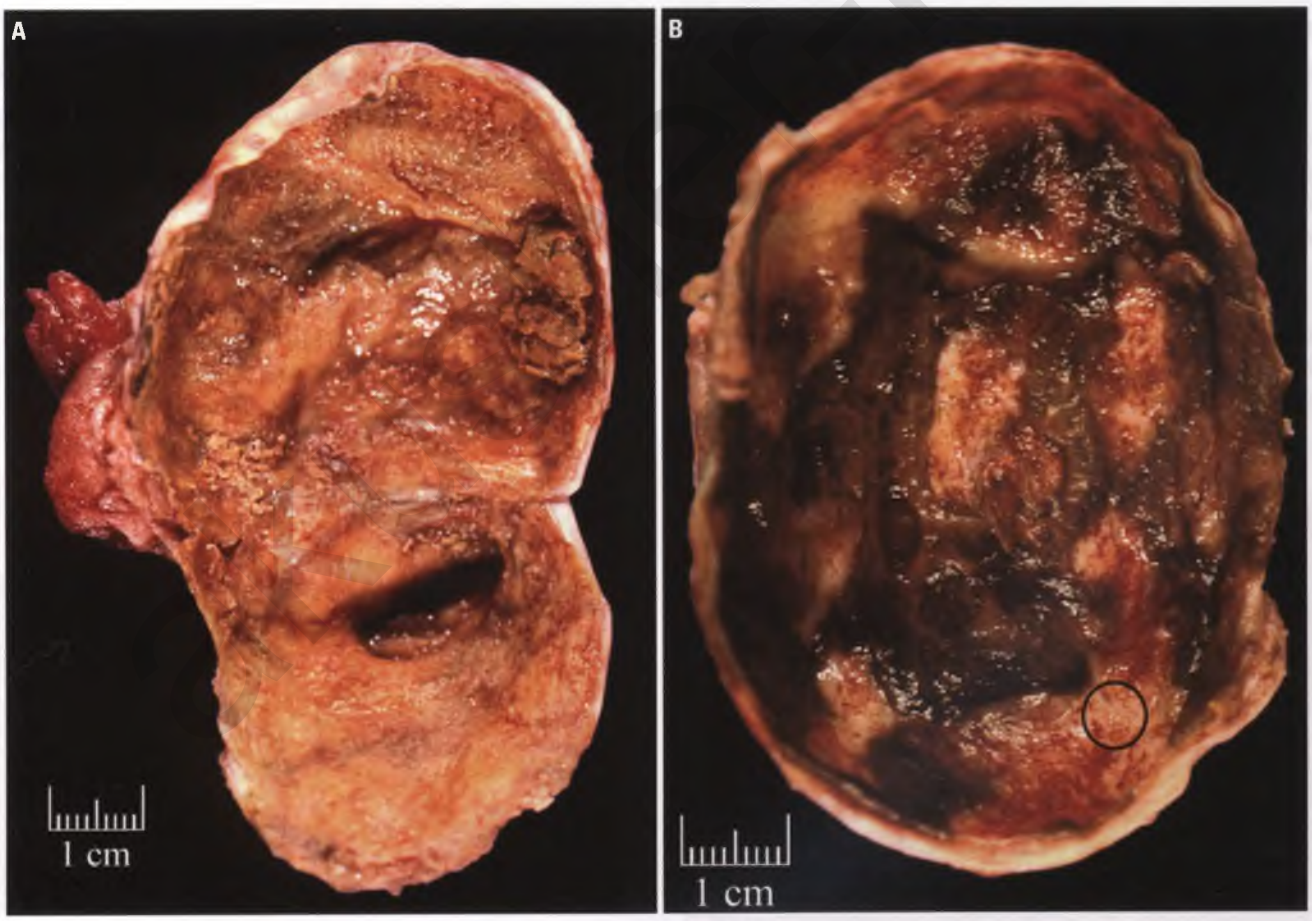

FIGURE 6.34. Endometriotic cysts. **A:** In this bivalved cyst, the inner lining is tan and granular with patches of adherent hemorrhagic material. **B:** The inner lining of this endometriotic cyst features a haphazard distribution of darkly hemorrhagic areas. A residual intact lining with diagnostic endometriotic glands and stroma is most likely to be found in the interspersed tannish pink foci (*circled*).

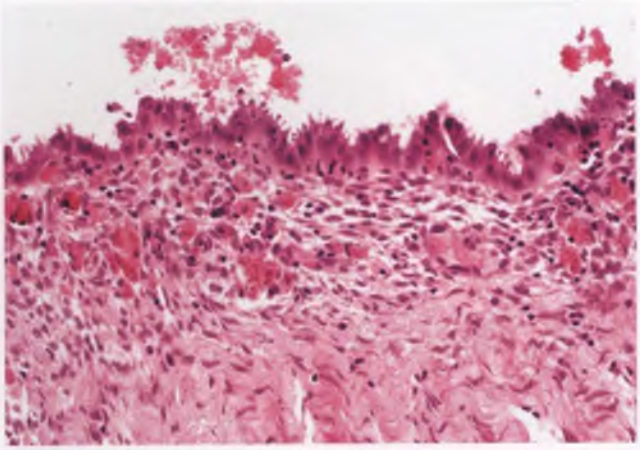

FIGURE 6.35. Endometriotic cyst. In this classic example, the cyst is lined by endometriotic epithelium with subjacent endometriotic stroma and interspersed pigmented histiocytes. As in this case, the lining epithelium often takes on an apocrine-like appearance, with eosinophilic cytoplasm and apical snouts.

Metaplastic Changes

Ciliated, mucinous, squamous (morular), clear cell, and hobnail forms of metaplasia have been described within the lining epithelium and glands of endometriotic cysts, analogous to the changes that can take place in the eutopic endometrium (Fig. 6.39).[8] Cases with atypical lining cells are considered separately under the section Endometriotic Cysts with Nuclear Atypia, although many of these lesions could also be classified as atypical metaplasias. Papillary forms of mucinous metaplasia may be the precursors of endocervical-like mucinous borderline tumors, some of which are known to arise within endometriotic cysts (see Chapter 7).

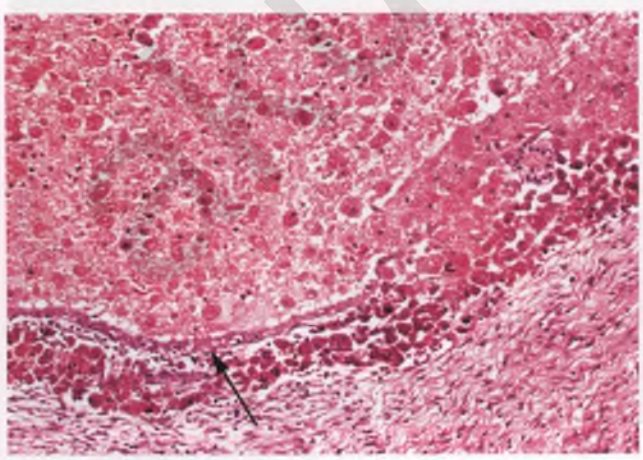

FIGURE 6.36. Endometriotic cyst with a partially eroded lining. Some residual epithelium (*arrow*) is present just above a band of pigmented histiocytes.

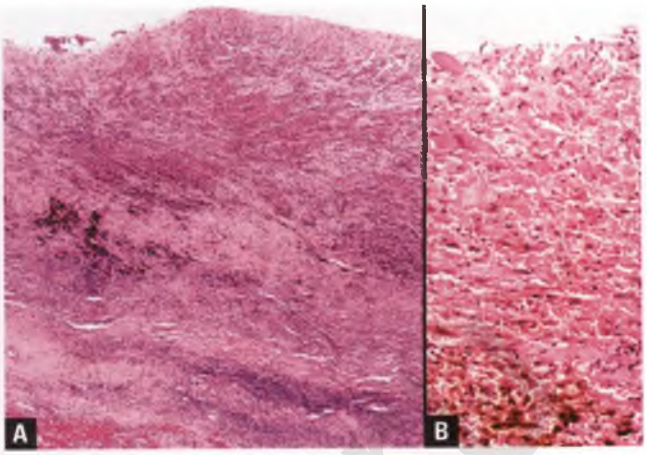

FIGURE 6.37. **A,B:** Old endometriotic cysts. The cyst linings are eroded in these two different examples. **B** is the histologic correlate of the endometriotic cyst in Figure 6.32.

Hyperplastic Changes[8,9]

Roughly 5% of endometriotic cysts are associated with hyperplastic glandular changes. As in the endometrium, these changes range from simple hyperplasia without atypia to complex atypical hyperplasia (Fig. 6.40). These cases are too infrequent to obtain meaningful data on the risk of the various forms of hyperplasia transforming into endometrioid carcinoma, but it can be presumed that the risk increases with the degree of architectural and nuclear atypia on a scale analogous to that seen in the endometrium. Whenever hyperplastic foci are encountered within endometriotic lesions, reexamination of the gross specimen and submission of additional tissue for histologic evaluation are indicated to exclude the possibility of coexistent carcinoma. The native endometrium should also be carefully examined for concurrent endometrial pathology in this situation.

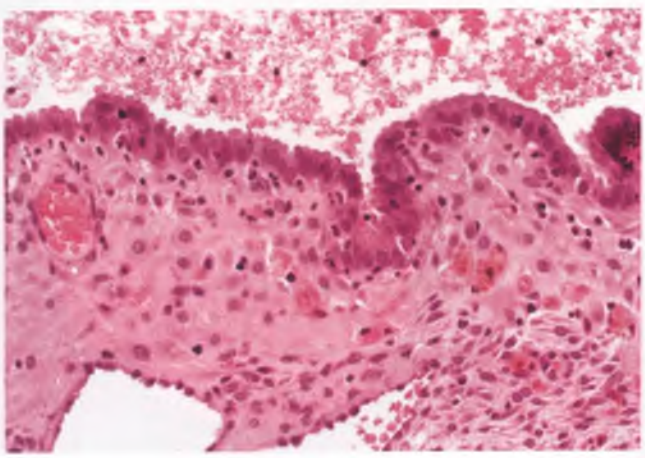

FIGURE 6.38. Endometriotic cyst with superimposed progestogen effect. The subepithelial layer of endometriotic stroma is decidualized in this cyst, which is from a patient who has been treated with a progestational agent.

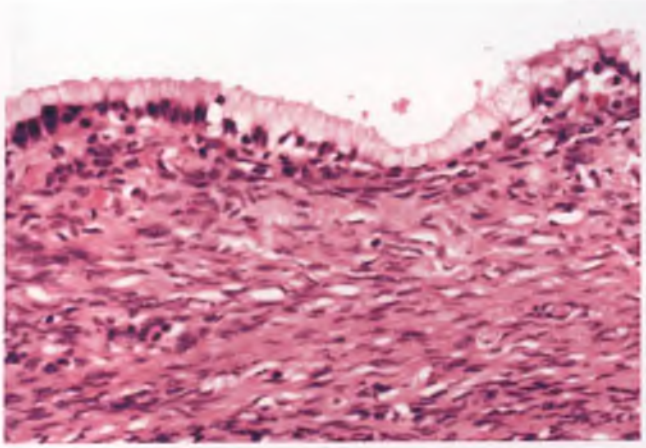

FIGURE 6.39. Endometriotic cyst with mucinous metaplasia. The lining epithelium in this portion of the cyst consists of tall columnar mucinous epithelium with basally oriented nuclei. Although the subepithelial layer of endometriotic stroma is inconspicuous, a few pigmented histiocytes are present in this region. Other portions of this cyst contained the epithelial and stromal layers of a conventional endometriotic cyst.

Endometriotic Cysts with Nuclear Atypia[9]

In occasional endometriotic cysts, focal areas of the lining epithelium are composed of cells that exhibit significant nuclear atypia, often in association with abundant eosinophilic cytoplasm (Fig. 6.41). These atypical areas have a predilection for the invaginated crevices of the lining epithelium, which may also be the only areas in which the epithelial lining has been preserved. Epithelial stratification is present in half of the cases, and may take the form of micropapillary projections. Some degree of acute inflammation is usually intimately associated with the foci of epithelial atypia.

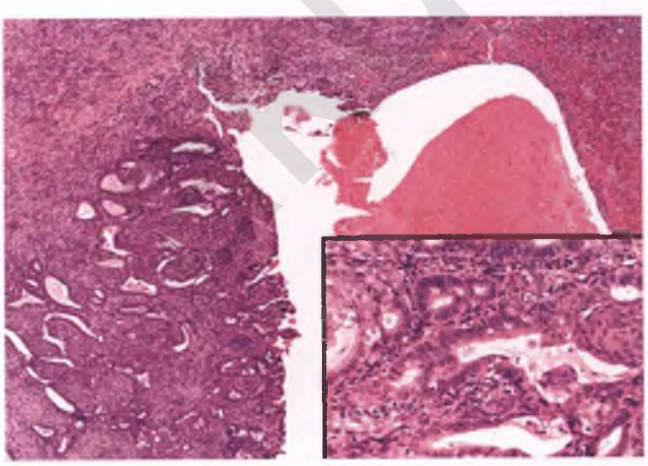

FIGURE 6.40. Hyperplasia arising within endometriosis. There is a nodular focus of complex atypical hyperplasia with morular metaplasia arising within the wall of an endometriotic cyst. The inset shows a portion of the hyperplastic focus at higher magnification.

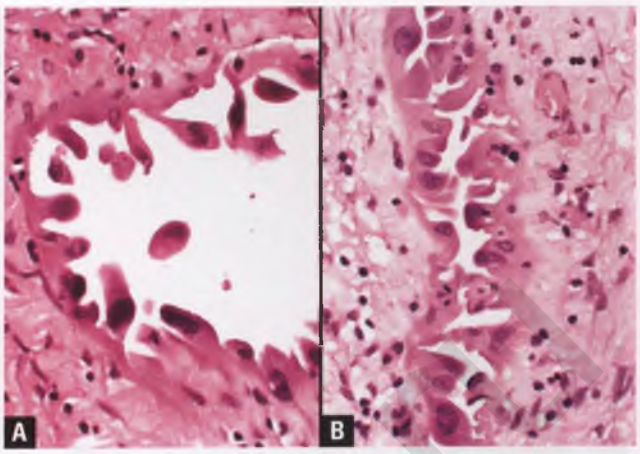

FIGURE 6.41. **A,B:** Endometriotic cyst with nuclear atypia of the lining epithelium. The invaginated epithelial surface in both images is lined by cells with abundant eosinophilic cytoplasm, significant nuclear atypia, and some hobnailing. Also note the presence of occasional neutrophils both within the epithelium and in the adjacent stroma.

Although many of these lesions presumably represent reactive atypia, others appear to be premalignant, as evidenced by cases in which atypia of this type is seen merging with carcinoma (Fig. 6.42).[8] Managerially, the finding of nuclear atypia within an endometriotic cyst can be regarded as an incidental finding if it is not associated with a cancer at the time of diagnosis, since even those cases that are premalignant have been widely and completely excised and would not be expected to recur (analogous to cervical squamous cell carcinoma in situ treated with hysterectomy).

Mesothelial Hyperplasia

Endometriotic cysts may incorporate hyperplastic mesothelial elements into their walls, which may simulate invasive adenocarcinoma.[8] Mesothelial hyperplasia is discussed in Chapter 8.

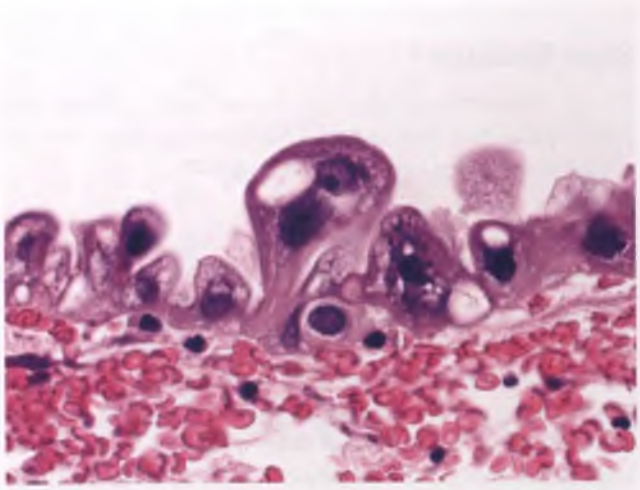

FIGURE 6.42. Endometriotic cyst with nuclear atypia of the lining epithelium. Mixed hobnail, clear cell and eosinophilic features are evident, and there is significant nuclear atypia. Clear cell carcinoma was present adjacent to this focus.

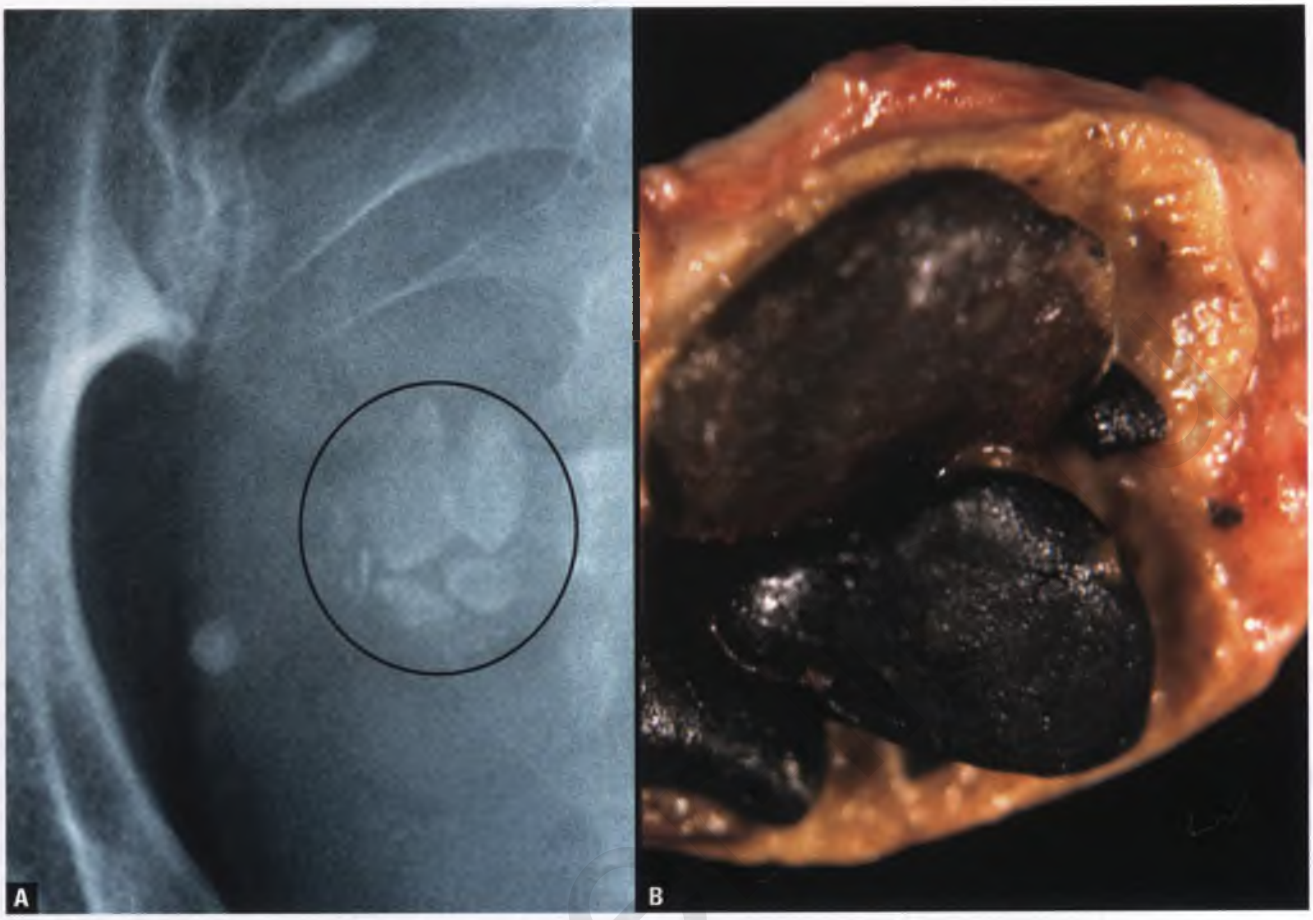

FIGURE 6.43. "Ovarian stones" within an old endometriotic cyst. **A:** Pelvic radiograph demonstrating the presence of an aggregate of stones (*circled*) in an ovarian location. **B:** The endometriotic cyst has been opened, revealing a conglomeration of black stones that were composed of old, densely clotted blood in a partially calcified matrix.

Stone Formation

In old endometriotic cysts, the hemorrhagic contents may rarely agglutinate and undergo calcification and/or osseous metaplasia, forming ovarian stones (Fig. 6.43).[10]

Liesegang Rings[11,12]

Very rarely, Liesegang rings are found with the lumen and/or wall of an endometriotic cyst. These acellular, eosinophilic to amber-colored, variably sized, ring-like structures represent an incidental microscopic finding (Fig. 6.44). Liesegang rings are nonbirefringent when viewed under polarized light, can be highlighted with a periodic acid-Schiff (PAS) stain, and may exhibit an internal lamination. An awareness of their potential presence within endometriotic cysts and their variable size help to prevent confusion with cross sections of parasitic organisms, and their lack of birefringence facilitates distinction from many types of foreign material.

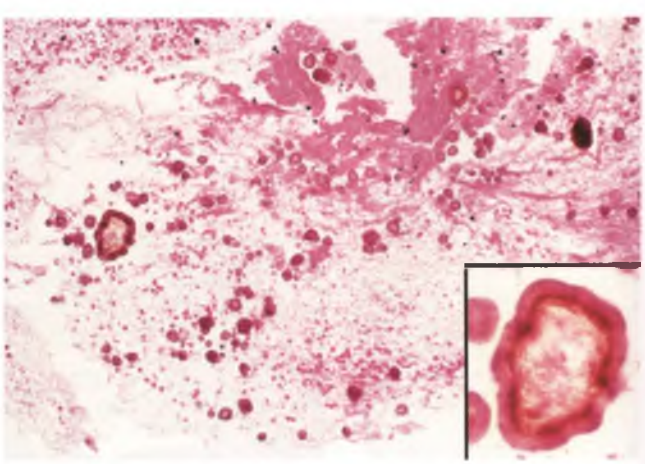

FIGURE 6.44. Liesegang rings. Numerous variably-sized ring-like structures are present within a background of old hemorrhagic material. The inset shows the largest ring with an internal lamination at high magnification.

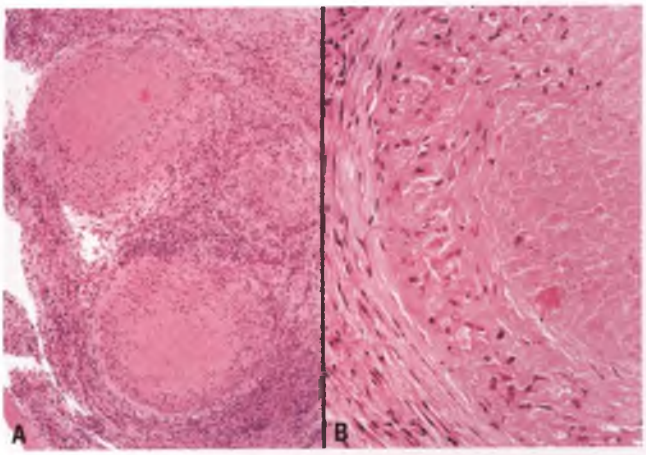

FIGURE 6.45. Necrotic pseudoxanthomatous nodules. **A:** Two small nodules are present within the ovary. **B:** This high-magnification view demonstrates the inner rim of pseudoxanthoma cells and the outer rim of fibrous tissue that surround the necrotic core of this nodule.

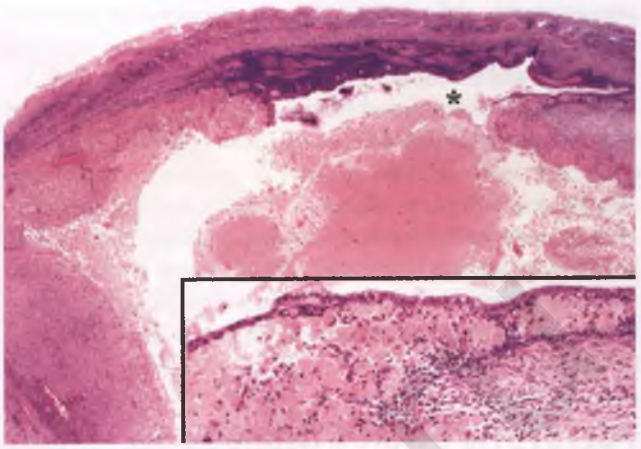

FIGURE 6.47. Endometriotic cyst in transition to a necrotic pseudoxanthomatous nodule. Most of the epithelial lining of the cyst has been denuded and the interface with the hemorrhagic cyst contents consists largely of a layer of pseudoxanthoma cells. Residual endometriotic cyst lining and associated stroma are present in the region of the *asterisk*. The inset highlights the area to the right of the *asterisk* with a residual epithelial lining.

Necrotic Pseudoxanthomatous Nodule[13]

Necrotic pseudoxanthomatous nodules represent an unusual manifestation of long-standing endometriosis that are typically found in perimenopausal or postmenopausal women. They present as small nodules (usually <2 cm) either within the ovary, attached to peritoneal surfaces, or free floating within the peritoneal cavity. These nodules are composed of a central core of necrotic tissue that often contains calcified debris and scattered remnants of pseudoxanthoma cells. Surrounding this necrotic core is a rim of pseudoxanthoma cells, a rim of hyalinized fibrous tissue, or an inner rim of pseudoxanthoma cells and an outer rim of fibrous tissue (Fig. 6.45). Portions of these nodules may be lined by palisading histiocytes, producing a pattern that resembles necrotizing granulomatous inflammation (Fig. 6.46). Although the nodules themselves are not obviously endometriotic in nature, occasional cases exhibit transitional features and foci of recognizable endometriosis are usually apparent in adjacent tissue (Fig. 6.47).

The pseudoxanthoma cells that are found in these nodules are histiocytes that have abundant cytoplasm that may be either eosinophilic or filled with finely granular, light brown lipofuscin (ceroid) pigment (Fig. 6.48). The staining properties of this

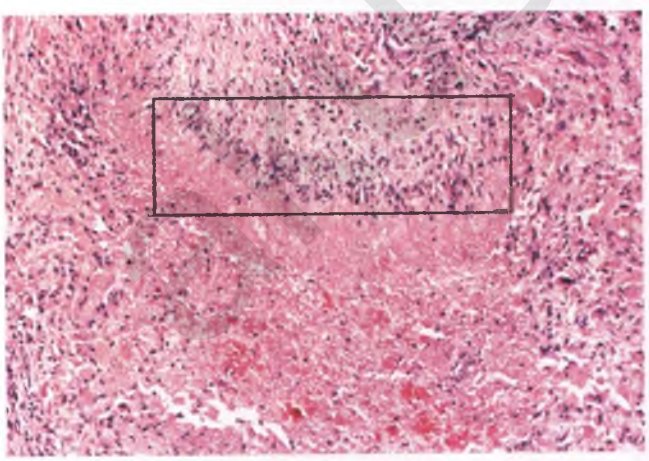

FIGURE 6.46. Necrotic pseudoxanthomatous nodule. The portion of this nodule within the *rectangle* is lined by palisading histiocytes in a pattern that is indistinguishable from granulomatous inflammation. However, most of the nodule is lined by typical pseudoxanthomatous cells, and necrotic forms of these cells are present within the core of the lesion.

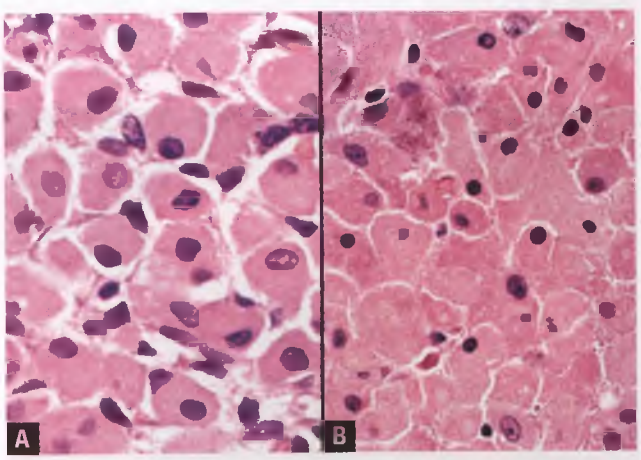

FIGURE 6.48. Pseudoxanthoma cells in necrotic pseudoxanthomatous nodules. **A:** In some cases, the pseudoxanthoma cells have abundant eosinophilic cytoplasm with absent to subtle deposits of pigment. **B:** More commonly, the pseudoxanthoma cells are filled with finely granular, light brown lipofuscin (ceroid) pigment.

pigment and its differentiation from hemosiderin are discussed in the sections on ceroid granuloma of the uterine cervix in Chapter 3 and pseudoxanthomatous salpingitis in Chapter 5.

The reader is referred to the original article from 1988 that describes these lesions for a discussion of their differential diagnosis, which includes nodules of metastatic tumor, necrotizing granulomas of infectious etiology, isolated noninfectious granulomas of the ovary, foreign body granulomas, and infarcted appendices epiploicae.[13] An additional lesion that can resemble necrotic pseudoxanthomatous nodules is the postoperative carbon pigment granuloma, which was described in the 1990s (see Chapter 8).[14,15]

POLYCYSTIC OVARY SYNDROME[16,17]

Polycystic ovary syndrome (PCOS), also known as polycystic ovary disease and Stein-Leventhal syndrome, is a common endocrine disorder of unknown etiology that affects approximately 5% of the female population. Patients are typically in the 20- to 40-year-old age group and present with irregular uterine bleeding, amenorrhea/oligomenorrhea, infertility, and/or hirsutism, which are related to chronic anovulation and hyperandrogenism. Most patients are also obese and resistant to insulin. The increased incidence of endometrial hyperplasia and low-grade endometrial adenocarcinoma in women with PCOS is explained by the development of hyperestrogenism related to (a) peripheral conversion of the elevated levels of androgens into estrogens by the often overabundant adipose tissue and (b) the lack of cyclical progesterone opposition to the effects of estrogen because of chronic anovulation.

Since the diagnosis of PCOS is based upon the clinical findings and the usual treatments for anovulation and hirsutism do not involve removal of the ovaries, pathologists are most likely to encounter polycystic ovaries when they are incidentally removed during a hysterectomy. Characteristically, the ovaries in PCOS are bilaterally enlarged (2–5 times normal size) and have smooth external surfaces(Fig. 6.49). Translucent

FIGURE 6.49. Polycystic ovary syndrome. The ovary is enlarged and has a smooth external surface.

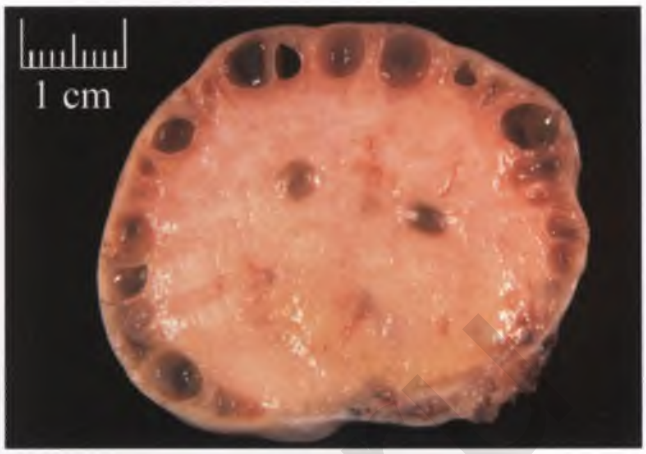

FIGURE 6.50. Polycystic ovary syndrome. The sectioned surface of the ovary exhibits multiple cystic follicles, most of which are located in the superficial cortex. Note the absence of stigmata of previous ovulatory cycles (corpora lutea and corpora albicantia).

cystic areas that are small and spherical may be externally visible. When sectioned, these ovaries are found to contain multiple small cysts within the superficial cortex that are typically of similar size and <1 cm in diameter (Fig. 6.50). Since this is a disorder of chronic anovulation, corpora lutea and corpora albicantia are absent or infrequent.

Histologically, the most superficial aspect of the cortex in PCOS is typically more collagenized and bandlike than normal, sometimes creating the appearance of a capsule. The cysts represent atretic cystic follicles that are usually lined by an inconspicuous layer of nonluteinized granulosa cells and a more prominent layer of luteinized cells from the theca interna (Fig. 6.51). The diagnosis of PCOS should not be made solely on the basis of the pathologic findings; typical clinical features must also be present.

HYPERREACTIO LUTEINALIS[18,19]

Hyperreactio luteinalis represents an ovarian reaction to inordinately high levels of human chorionic gonadotropin, such as occurs in hydatidiform mole, choriocarcinoma, and multiple gestations. Regimens used to induce ovulation can also produce this reaction (ovarian hyperstimulation syndrome). The ovaries are bilaterally enlarged due to a conglomeration of thin-walled cysts that contain fluid that varies from clear to hemorrhagic (Fig. 6.52A). Although usually asymptomatic, abdominal pain may occur if torsion, internal hemorrhage, or rupture occurs.

The cysts in hyperreactio luteinalis represent multiple luteinized cystic follicles (Fig. 6.52B). Since the theca interna is typically more prominently luteinized than the granulosa layer, these cysts are often referred to as theca lutein cysts (Fig. 6.53). The ovarian stroma between the cystic follicles is often edematous, and may contain clusters of luteinized cells. Once the source of the elevated human chorionic gonadotropin is removed, these cysts regress over a period of weeks to months.

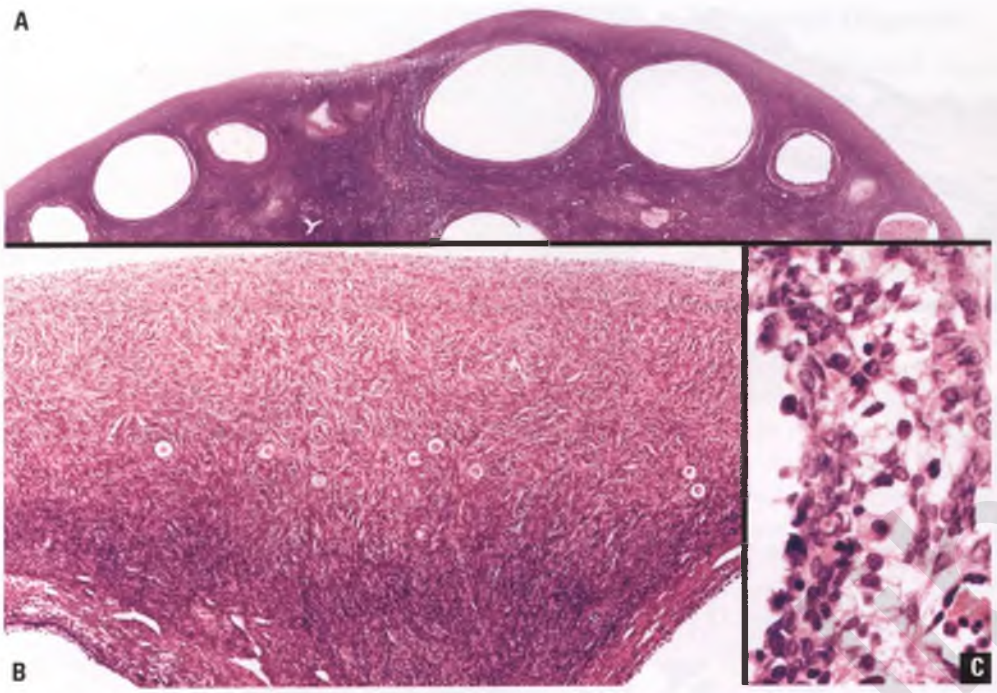

FIGURE 6.51. Polycystic ovary syndrome. **A:** Low-magnification view of the multiple small cystic follicles within the superficial cortex. **B:** The collagenized band of superficial cortex is highlighted in this image. **C:** Portion of the lining of one of the cystic follicles. Note the innermost thin layer of nonluteinized granulosa cells and the outer luteinized layer of theca interna cells with cytoplasm that is abundant, clear to lightly eosinophilic, and vacuolated.

LARGE SOLITARY LUTEINIZED FOLLICLE CYST OF PREGNANCY AND PUERPERIUM[20,21]

This rare and distinctive type of follicle cyst presents during pregnancy or the first several weeks after delivery as a palpable adnexal mass, a cystic lesion on ultrasound, or an incidental finding during cesarean section. These cysts have a median diameter of 25 cm, and are solitary, unilocular, thin walled, and filled with watery fluid. Their external and internal surfaces are smooth.

Histologically, the cyst lining consists of one to multiple layers of luteinized granulosa and theca cells that exhibit significant variation in size and shape and have abundant eosinophilic to clear cytoplasm. Unlike the lining of ordinary solitary follicle cysts, the lining of these large cysts cannot usually be easily separated into granulosa and theca cell layers, and the constituent cells typically display at least focal marked nuclear enlargement, pleomorphism, and hyperchromasia (Fig. 6.54). The lining cells lack mitotic activity, which is a reassuring feature. Cytologic preparations of aspirated cyst contents can cause alarm when the pleomorphic luteinized cells are encountered, but the characteristic clinical setting and the simple nature of the cyst on ultrasound should facilitate the diagnosis.

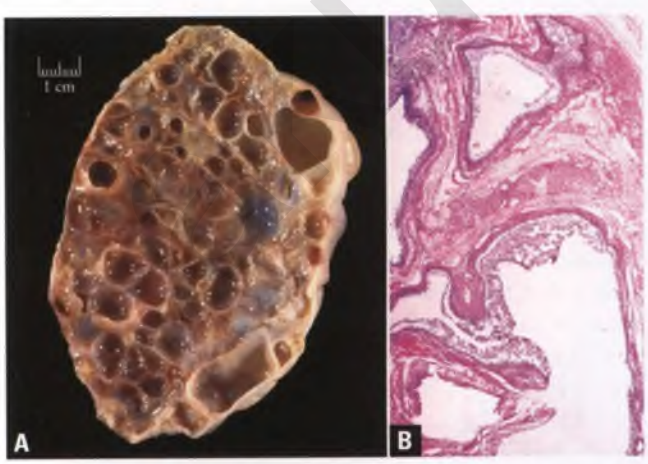

FIGURE 6.52. Hyperreactio luteinalis. **A:** The sectioned surface of this enlarged ovary has a honeycomb appearance due to the presence of multiple cystic follicles. **B:** Low-magnification view of representative cystic follicles. (Gross image courtesy of Dr. Richard L. Payne.)

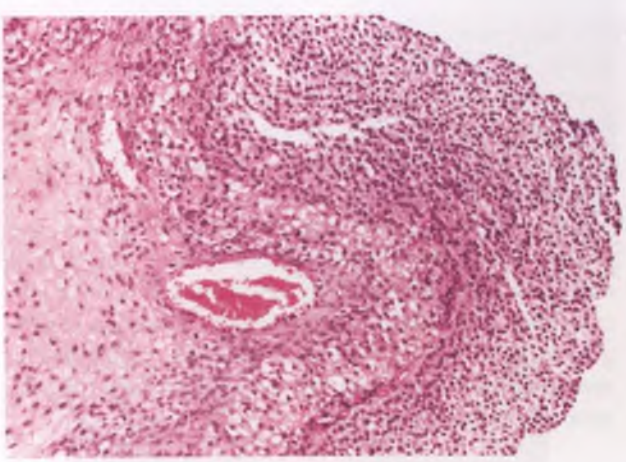

FIGURE 6.53. Hyperreactio luteinalis. In this view of a portion of the lining of a cystic follicle, note how the serpentine band of theca interna cells that lies beneath the granulosa cell layer shows prominent luteinization.

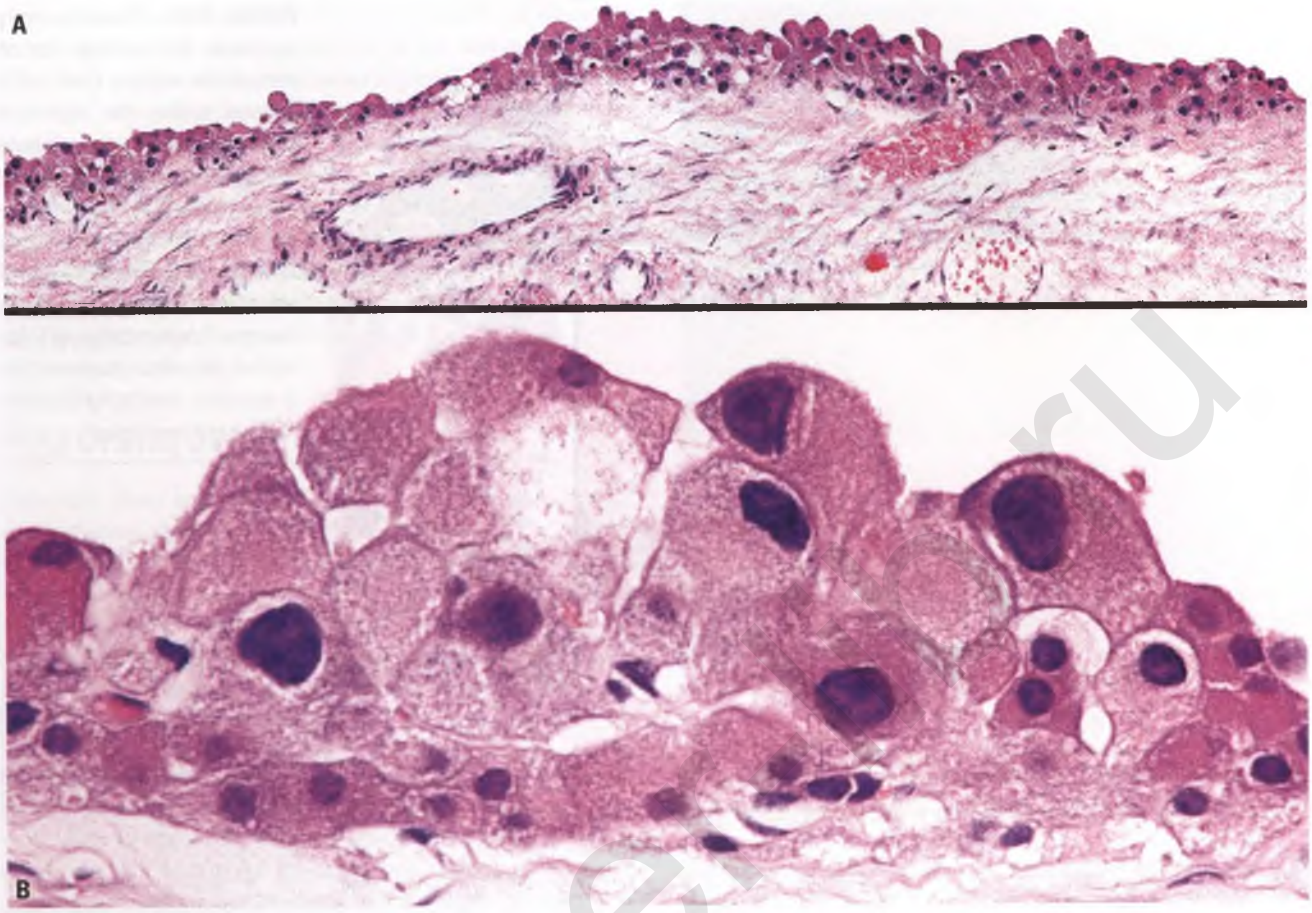

FIGURE 6.54. Large solitary luteinized follicle cyst of pregnancy. **A:** The cyst is lined by one to several layers of luteinized cells with abundant eosinophilic cytoplasm. **B:** This high-magnification view highlights an area of the cyst lining that exhibits nuclear enlargement, pleomorphism, and hyperchromasia. (Courtesy of Dr. Colin J. R. Stewart.)

Differential Diagnosis

The principal differential diagnostic considerations are the unilocular cystic forms of adult and juvenile granulosa cell tumors.

- The adult version of cystic granulosa cell tumor lacks the lining cells with marked nuclear pleomorphism and abundant eosinophilic cytoplasm. In addition, other diagnostic features of adult granulosa cell tumor (nuclear grooves, Call-Exner bodies) are typically present within groups of tumor cells within the cyst wall.
- The juvenile form of cystic granulosa cell tumor more closely mimics the large solitary luteinized follicle cyst because its tumor cells may also contain abundant eosinophilic cytoplasm and exhibit nuclear atypia. However, juvenile granulosa cell tumors, cystic or otherwise, should exhibit appreciable mitotic activity and form at least focal follicular structures of microscopic size.

STROMAL HYPERTHECOSIS[22]

Stromal hyperthecosis features a variable degree of hyperplasia of the ovarian stroma coupled with the presence of numerous luteinized stromal cells of thecal origin dispersed throughout the stroma in a variety of architectural patterns. Stromal hyperthecosis most commonly occurs in postmenopausal women, where it may be associated with endometrial pathology related to elevated estrogen levels (endometrial hyperplasia and well-differentiated adenocarcinoma). When encountered in the reproductive age group, virilization is more common and symptoms overlap clinically with PCOS. In either situation, the luteinized stromal cells of hyperthecosis produce androgenic hormones, but in postmenopausal women there is significant conversion of androgens to estrogens in adipose tissue.

The ovaries in stromal hyperthecosis are bilaterally enlarged to up to twice normal size and have a sectioned surface that is predominantly solid and yellow, off-white, or tan. The stromal proliferation may result in grossly diffuse or multinodular patterns (Figs. 6.55 and 6.56). The hyperplastic spindle-cell stroma replaces the cortex and medulla to variable degrees, usually incorporating some follicular derivatives (most commonly corpora albicantia). The luteinized stromal cells typically have round nuclei with distinct nucleoli and abundant cytoplasm that ranges from eosinophilic (lipid-poor) to bubbly and clear (lipid-rich). They are usually widely dispersed as single cells and small nests, but can also be found in single-file patterns and small nodules (Figs. 6.57 and 6.58).

FIGURE 6.55. Stromal hyperthecosis. The sectioned surface of this mildly enlarged ovary is solid and varying shades of yellow. Scattered off-white corpora albicantia and an involuting corpus luteum are also present.

Differential Diagnosis

The major differential diagnostic considerations of stromal hyperthecosis are stromal luteoma, luteinized thecoma, and metastatic carcinoma.

- The distinction between one or more dominant nodules within nodular hyperthecosis and stromal luteoma is based solely upon an arbitrary minimum size criterion for stromal luteoma that has ranged between 2.5 mm and 1 cm in the literature.
- Areas of stromal hyperthecosis can be histologically indistinguishable from luteinized thecoma when examined under high magnification. However, the vast majority of luteinized thecomas are unilateral rather than bilateral and show more impressive ovarian enlargement. Moreover, these tumors form a discrete mass that obliterates or displaces normal ovarian structures, whereas stromal hyperthecosis typically features partial preservation and incorporation of ovarian follicles and their derivatives.
- In instances where the histologic pattern raises the possibility of metastatic carcinoma, such as when the single-file pattern of luteinized stromal cells mimics metastatic lobular carcinoma of the breast, demonstration of an inhibin-positive,

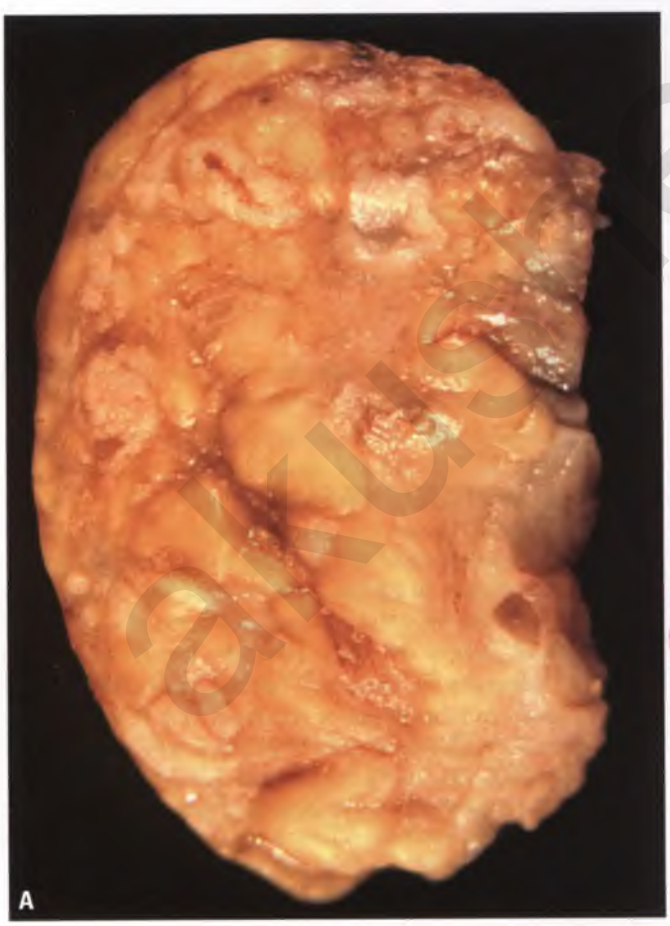

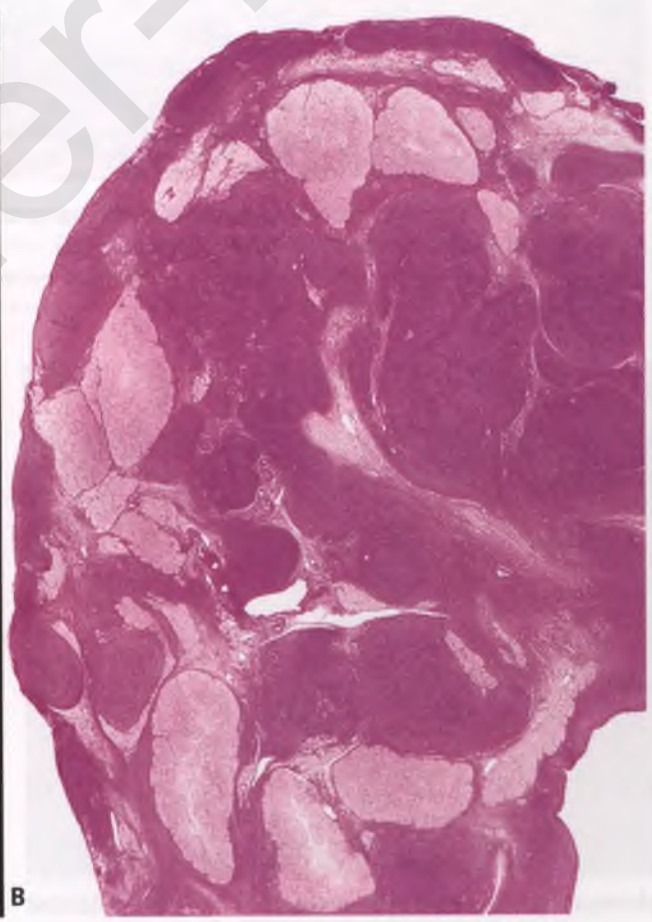

FIGURE 6.56. Stromal hyperthecosis. **A:** The sectioned surface of this 3 cm ovary from an elderly woman has a multinodular yellow appearance. Note the presence of several corpora albicantia that are resistant to being displaced by the hyperplastic stromal cells. **B:** Cellular nodules of stromal cells weave their way in between scattered corpora albicantia and replace both cortex and medulla.

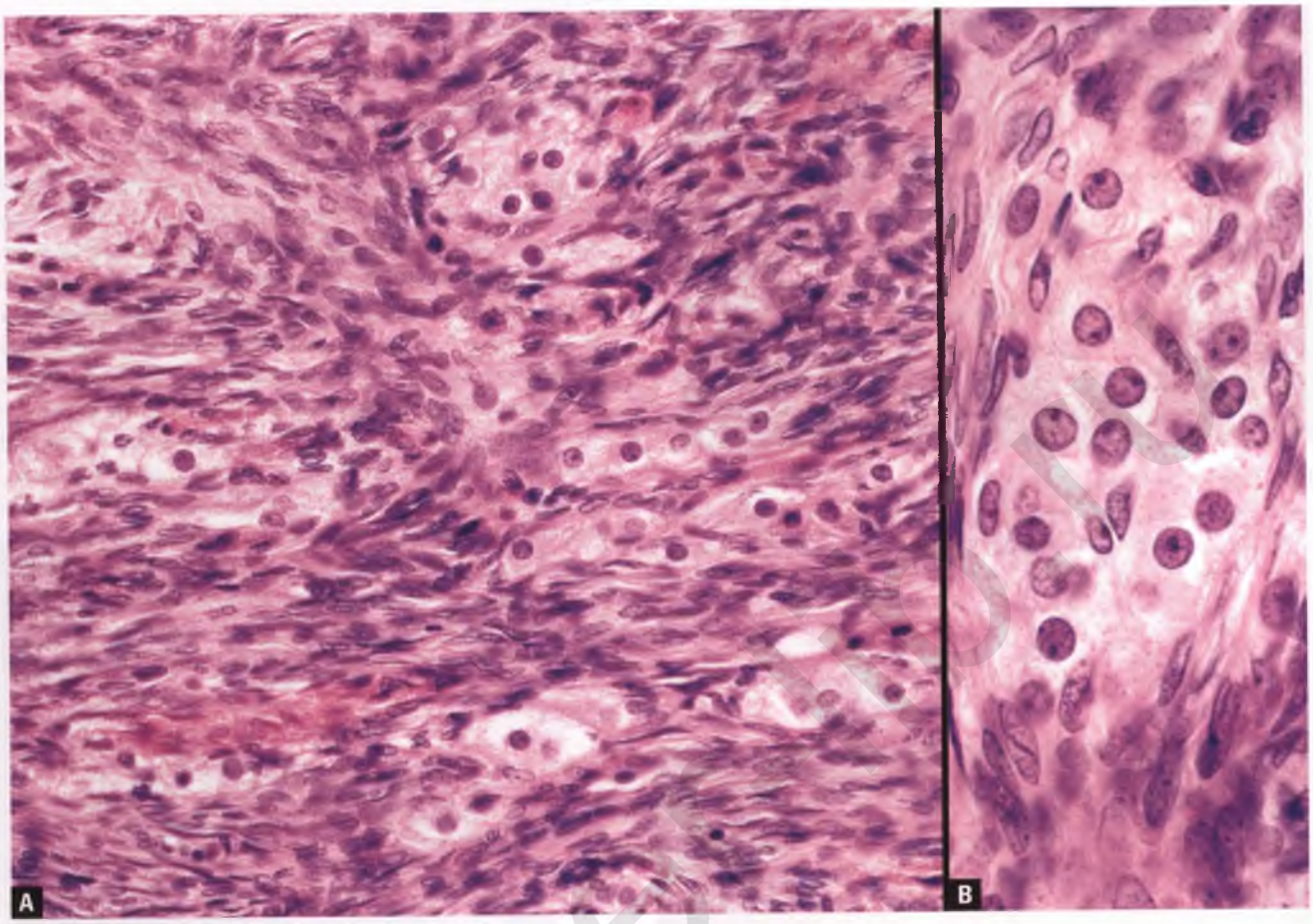

FIGURE 6.57. **A,B:** Stromal hyperthecosis. Small aggregates of luteinized stromal cells are present within a cellular background of spindle-shaped stromal cells.

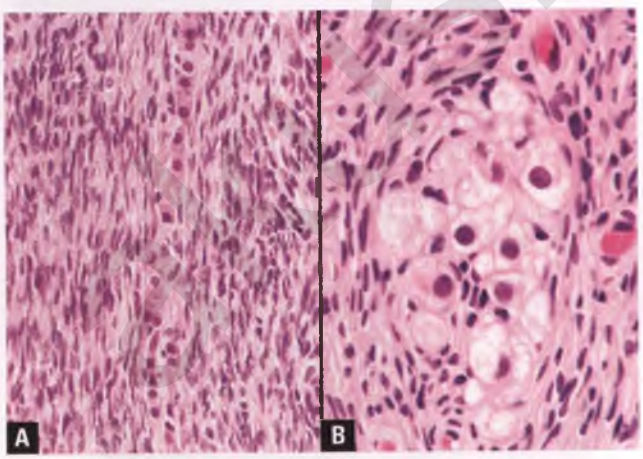

FIGURE 6.58. Stromal hyperthecosis. **A:** Luteinized stromal cells with eosinophilic cytoplasm in a single-file arrangement reminiscent of metastatic lobular carcinoma of the breast. **B:** Nest of luteinized stromal cells with abundant cytoplasm that is clear and vacuolated, which is indicative of a high lipid content.

cytokeratin-negative immunophenotype can help to confirm the diagnosis of stromal hyperthecosis.[23]

STROMAL HYPERPLASIA

Stromal hyperplasia is identical in its gross and histologic appearance to those cases of stromal hyperthecosis with hyperplastic stroma, except that hyperthecosis also features scattered aggregates of luteinized stromal cells. The bilaterally hyperplastic stroma blurs or obliterates the distinction between cortex and medulla and/or results in some degree of nodularity (Fig. 6.59). Stromal hyperplasia is typically an incidental finding in the ovaries of postmenopausal women, but is occasionally associated with symptoms related to an imbalance in androgens or estrogens.

Differential Diagnosis

In addition to stromal hyperthecosis, the differential diagnosis of stromal hyperplasia includes fibroma and low-grade endometrioid stromal sarcoma. In contrast to stromal hyperplasia,

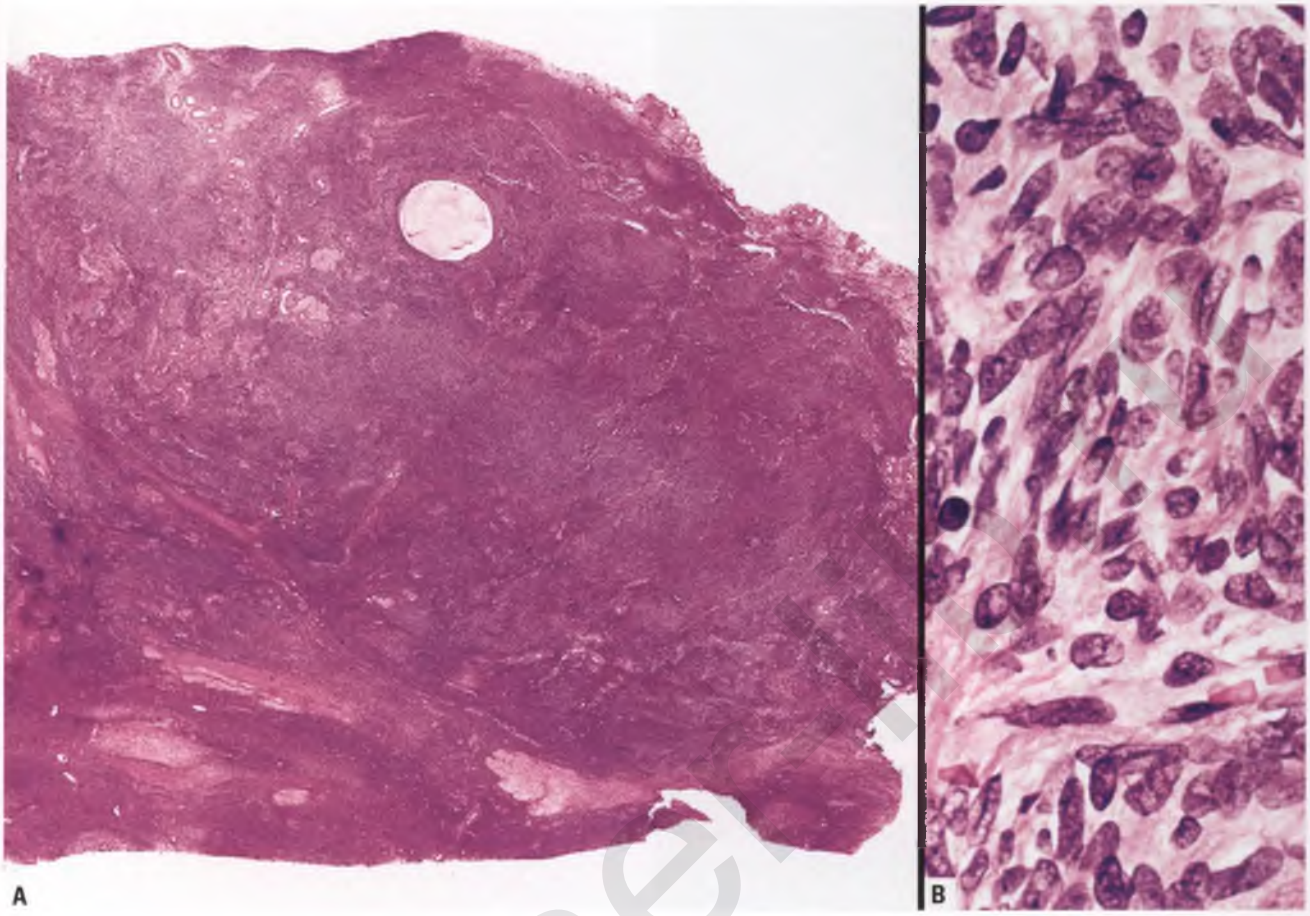

FIGURE 6.59. Stromal hyperplasia. **A:** The ovarian cortex and medulla are diffusely replaced by a cellular proliferation of stromal cells, expanding both regions and blurring their distinction. **B:** The stroma consists of mitotically inactive cells with bland, overlapping, spindle-shaped nuclei devoid of luteinized cells.

ovarian fibromas and low-grade endometrioid stromal sarcomas are discrete, mass-forming tumors that are usually unilateral and do not incorporate follicles and their derivatives. Low-grade endometrioid stromal sarcoma is further differentiated from stromal hyperplasia by the usual presence of at least some mitotic activity and its characteristic vascular pattern.

OVARIAN TORSION[24,25]

In the usual situation, ovarian/adnexal torsion occurs in the setting of an adnexal mass that is cystic and benign, although exceptions occur. Patients typically present with acute abdominal pain, and surgical exploration reveals a swollen, dark red adnexal mass with a twisted fibrovascular pedicle (Fig. 6.60). Interstitial hemorrhage usually dominates the histologic picture, although frank tissue necrosis indicative of infarction may also be present. Careful gross examination with submission of several sections for histologic evaluation is indicated to exclude the possibility of a neoplasm.

FIGURE 6.60. Torsion-related hemorrhage in a benign, cystically dilated ovary and its associated fallopian tube (at bottom). The adnexa are diffusely swollen and a mottled dark red.

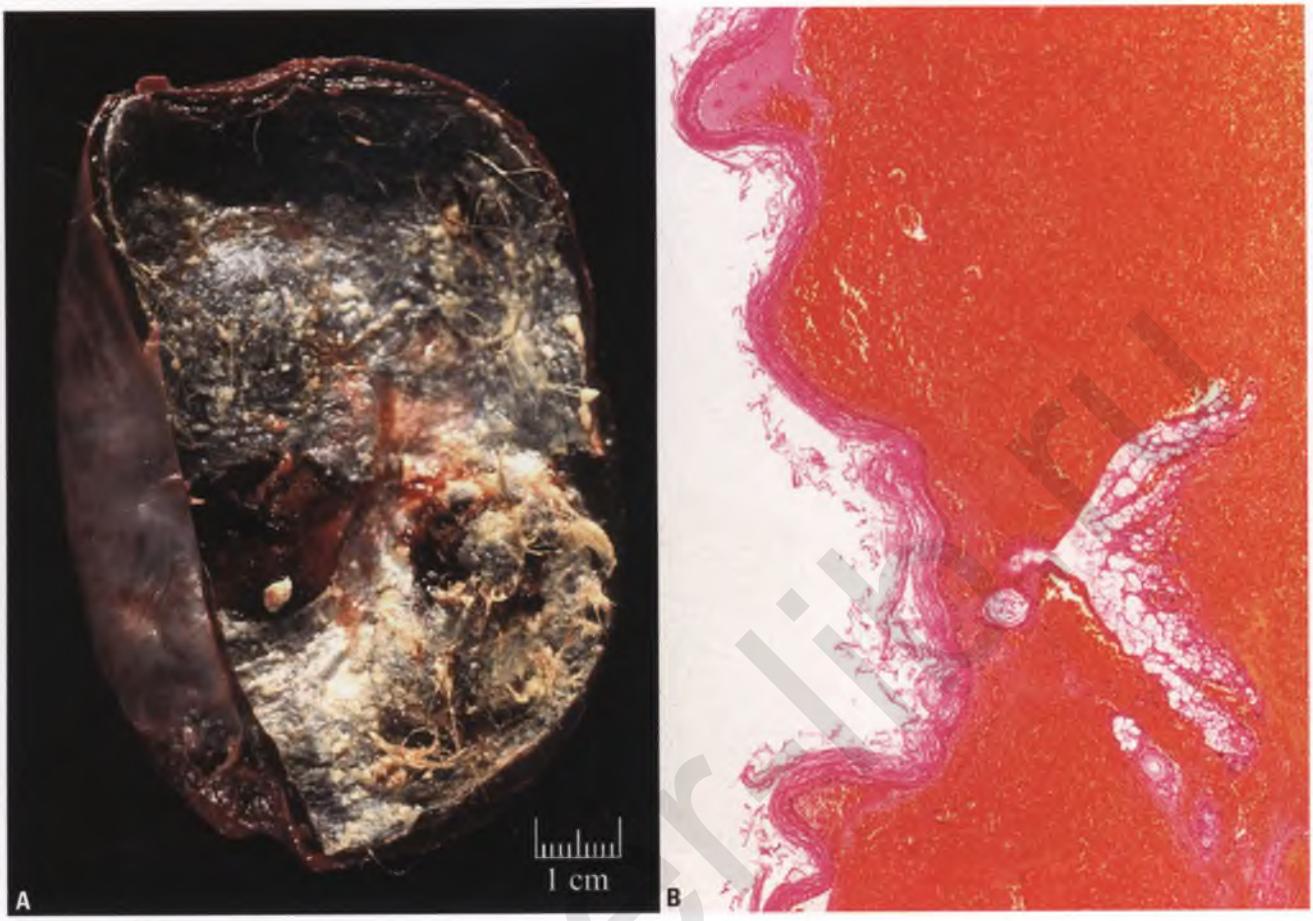

FIGURE 6.61. Torsion-related hemorrhage in a mature cystic teratoma. **A:** The sectioned surface of the cyst wall is dark red. The cyst contains sebaceous material and matted hair, most of which was removed prior to photography. **B:** The cyst wall is diffusely hemorrhagic, but an attenuated squamous epithelial lining with adherent keratinous debris and some underlying sebaceous glands are still apparent.

When extensive, the hemorrhage and infarction can obscure the precise nature of the underlying lesion, although in such cases the presence of a benign type of hemorrhagic cyst that cannot be further characterized can usually be confirmed (a reticulin stain may be utilized to highlight the framework of a preexisting cyst or tumor). Neoplasms most likely to be identified in association with ovarian torsion are mature cystic teratomas (dermoid cysts) and serous or mucinous cystadenomas (Figs. 6.61–6.63).

MASSIVE EDEMA[26,27]

Massive ovarian edema is an uncommon condition that can simulate an ovarian neoplasm. This phenomenon typically occurs in young women (mean age of ~20 years) who usually present with abdominal pain that is sometimes accompanied by menstrual irregularities and/or virilization. Evaluation reveals an ovarian mass with a smooth external surface that averages about 10 cm in diameter and often exhibits some degree of torsion of its pedicle. Bilateral ovarian involvement occurs in about 10% of cases. Involved ovaries are predominantly solid, but cystic follicles measuring up to 4 cm are often present, and may be evident on external examination (Fig. 6.64). The cut surface of these enlarged ovaries ranges from off-white to pale yellow to tan, typically exudes edema fluid, and has a glistening appearance that may be misinterpreted as myxoid or gelatinous (Fig. 6.65).

Histologically, massive edema is characterized by ovarian stroma that is markedly edematous, hypocellular, and pale staining, although the outermost rim of cortical tissue is characteristically spared and remains dense and collagenized (Fig. 6.66A). Clusters of luteinized stromal cells may be present (Fig. 6.66B), particularly in those patients with evidence of androgen excess. Development of these luteinized stromal cells may somehow be promoted by the edematous microenvironment, although the superimposition of stromal edema upon preexistent stromal hyperthecosis is another possible explanation. A diagnostically useful feature of massive edema is the manner in which it surrounds rather than displaces normal ovarian structures, which helps to distinguish this condition from an edematous ovarian fibroma and other neoplasms with a dominant spindle cell component.

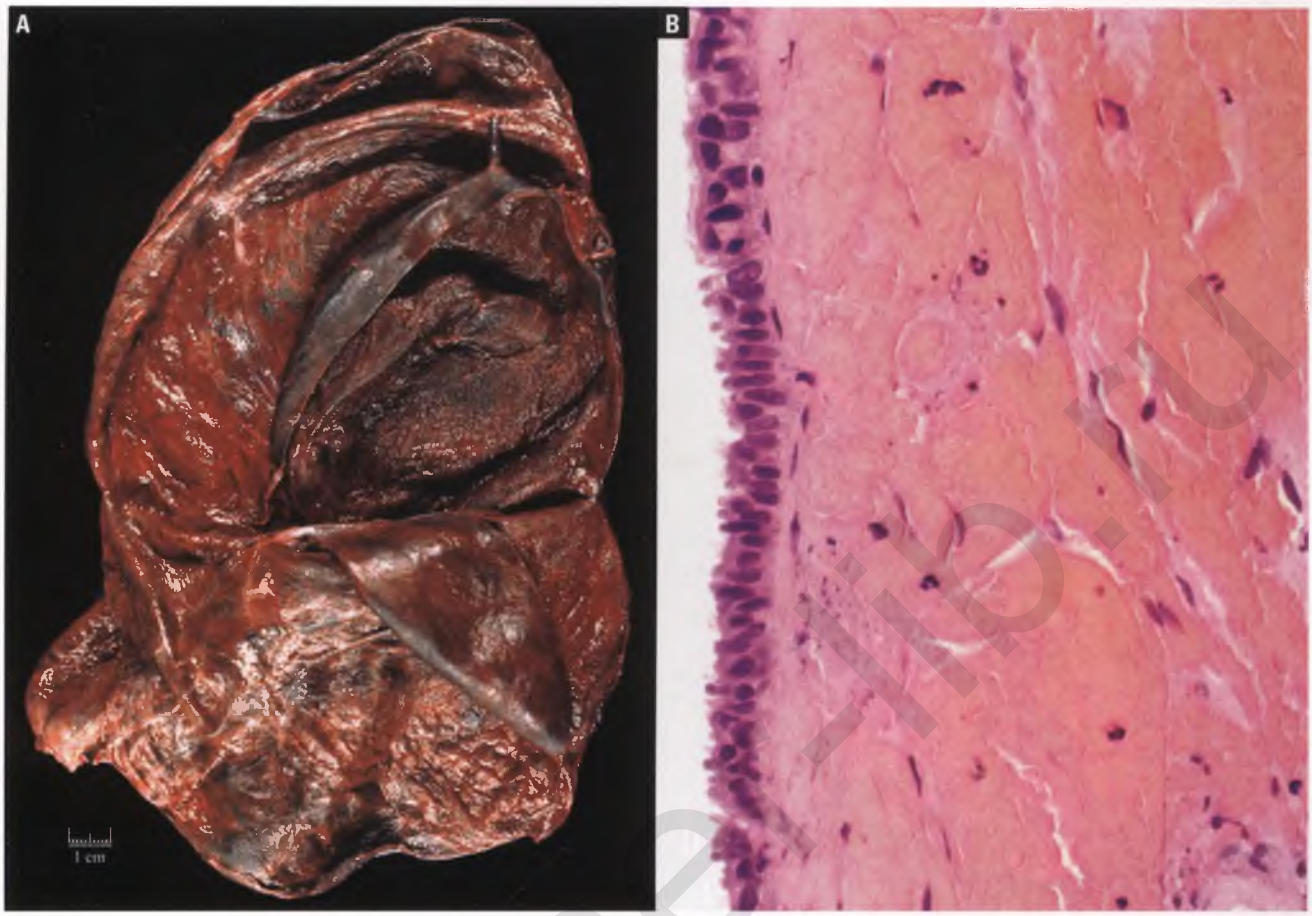

FIGURE 6.62. Torsion-related hemorrhage in a serous cystadenoma. **A:** The inner lining of this loculated cystic mass is diffusely hemorrhagic. **B:** In areas where the epithelial lining has been preserved, it consists of a thin layer of tubal-type epithelium that overlies hemorrhagic stroma. Ciliated cells are most apparent near top left.

The usual explanation for the formation of a massively edematous ovary is partial torsion that is sufficient to interfere with venous and lymphatic drainage, but not of a degree that would produce interstitial hemorrhage or infarction. It has also been proposed that some cases of massive edema represent preexisting ovarian fibromatosis that have undergone partial torsion with subsequent accumulation of edema fluid.

OVARIAN FIBROMATOSIS[27]

Ovarian fibromatosis is a rare tumor-like condition that typically occurs in young women (mean age of 25 years) who usually present with menstrual irregularities. The involved ovaries are enlarged to an average of 8 cm, have a smooth or lobulated external surface, and have a predominantly solid, firm, off-white sectioned surface. Bilateral ovarian involvement is present in approximately 20% of cases. Histologically, there is prominent overgrowth of spindle-shaped cells in a collagenized background, with primordial follicles and their derivatives entrapped within the fibrous proliferation (Fig. 6.67).

The diagnosis of ovarian fibromatosis should be reserved for cases that cause a significant gross abnormality, and not be used in the fairly common situation in which the cortical stroma is incidentally and mildly expanded by a fibrosing proliferation of stromal cells. Although portions of an ovarian fibroma may be histologically indistinguishable from fibromatosis, fibromas tend to occur in an older age group and displace rather than incorporate native ovarian structures. Ovarian fibromatosis should be distinguished from the soft tissue type of fibromatosis involving the ovary, which infiltrates neighboring tissue and is virtually nonexistent.[28]

PREGNANCY LUTEOMA[18,19]

As its name suggests, pregnancy luteoma occurs exclusively during pregnancy and represents a hormone-dependent, pseudoneoplastic lesion composed of luteinized stromal cells. Pregnancy luteoma is rare, and has a predilection for multiparous, African-American women. It is usually found incidentally at the time of cesarean section, but may be associated with

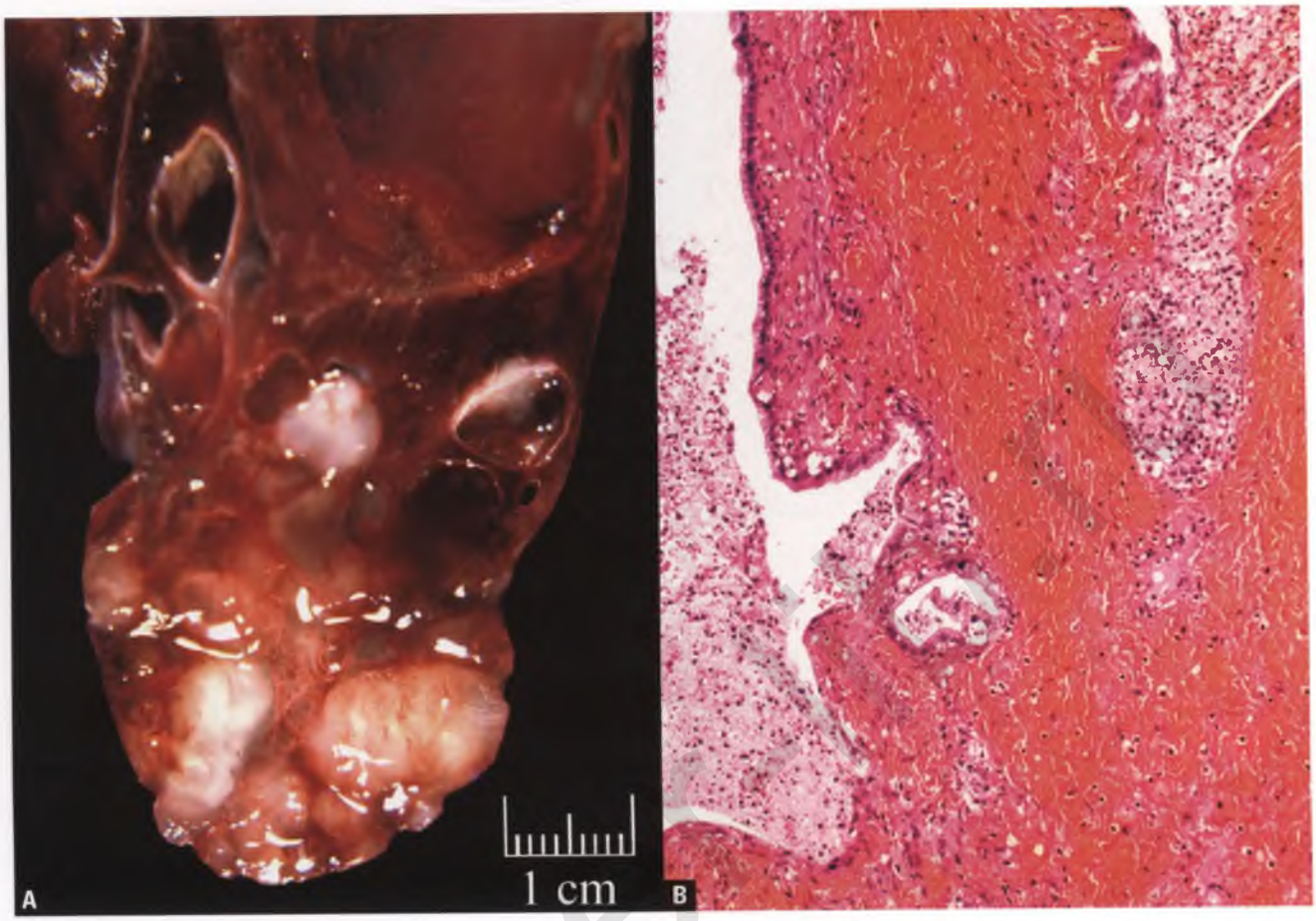

FIGURE 6.63. Torsion-related hemorrhage in a mucinous cystadenoma. **A:** The sectioned surface of this multiloculated neoplasm is hemorrhagic, and some of the locules are distended with mucoid material. **B:** Portions of the epithelial lining of the cystic spaces have sloughed, but some benign mucinous epithelium persists. Note the extensive interstitial hemorrhage.

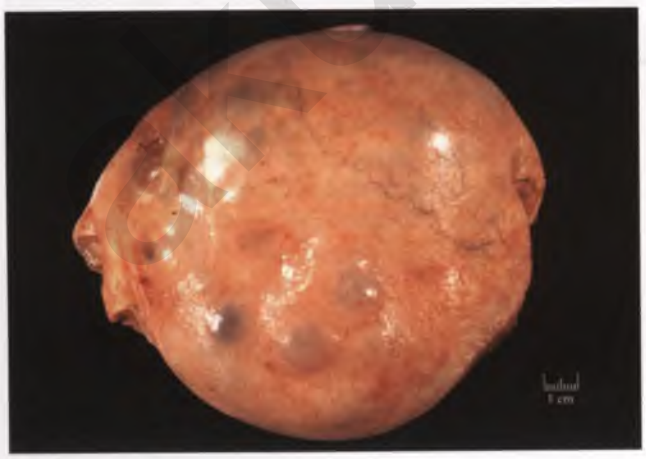

FIGURE 6.64. Massive edema. The external surface of the enlarged ovary is smooth, with scattered blue-domed cysts representing cystic follicles located just beneath the surface.

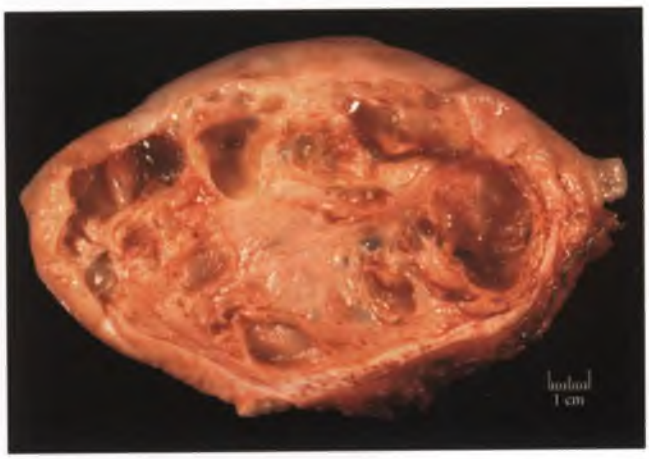

FIGURE 6.65. Massive edema. The sectioned surface shows a solid and partially cystic ovarian mass. Cystic follicles of various sizes are concentrated around the periphery of the enlarged ovary and account for the cystic component. The exudation of watery fluid results in a glistening cut surface.

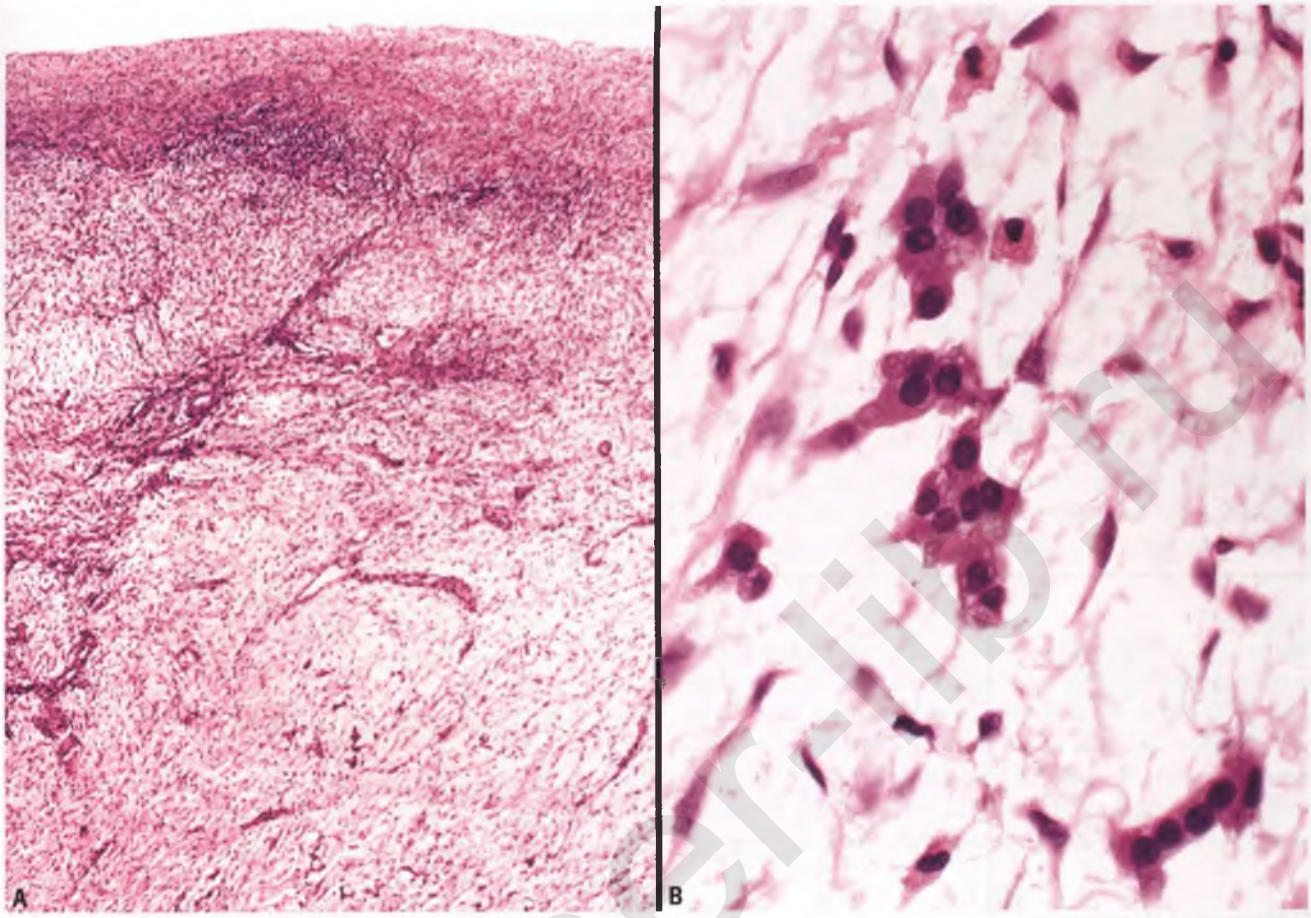

FIGURE 6.66. Massive edema. **A:** The ovarian stroma beneath the outermost rim is markedly edematous. **B:** Clusters of luteinized stromal cells are present within a stroma whose other elements are splayed apart by edema fluid.

virilization. The nodules of pregnancy luteoma may be solitary or multiple and can also be bilateral. Excision is not necessary, since these lesions spontaneously regress following delivery. Hence, it is important to be able to recognize pregnancy luteomas intraoperatively.

Grossly, the ovary is enlarged (median size of 7 cm) and contains one or more solid, red to brown, focally hemorrhagic, well-circumscribed nodules (Fig. 6.68). These nodules are composed of luteinized cells with abundant eosinophilic cytoplasm, round nuclei, distinct nucleoli, and occasional mitotic

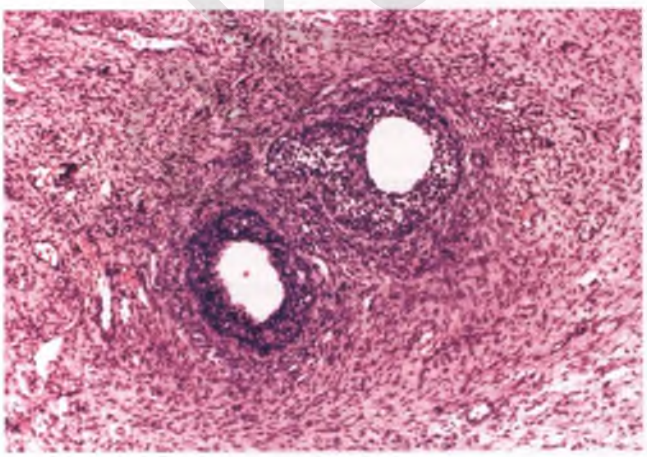

FIGURE 6.67. Ovarian fibromatosis. Fibrous tissue surrounds two ovarian follicles.

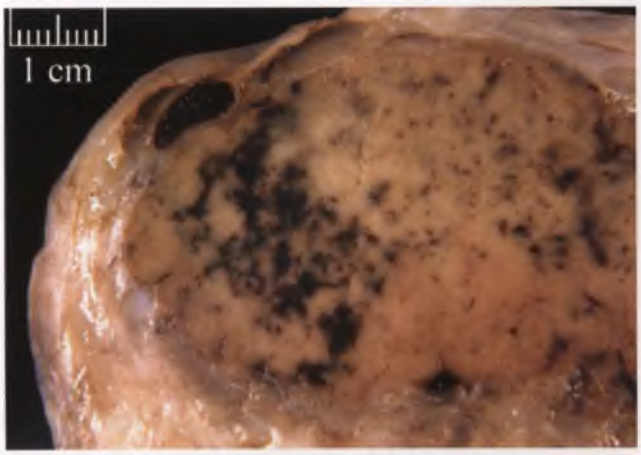

FIGURE 6.68. Pregnancy luteoma. This well-circumscribed nodule has a tannish-brown sectioned surface and scattered hemorrhagic foci.

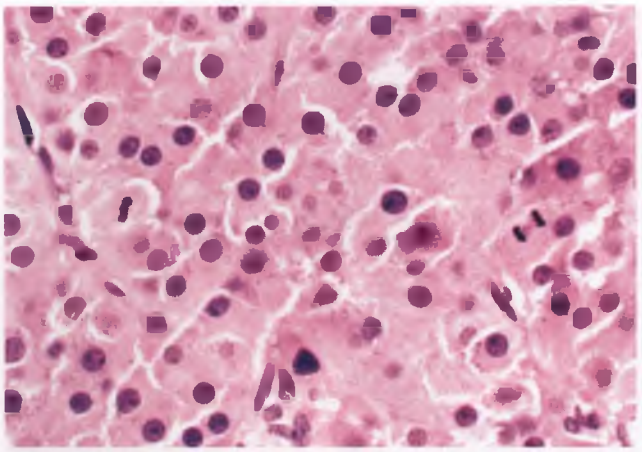

FIGURE 6.69. Pregnancy luteoma. Note the abundant eosinophilic cytoplasm, round nuclei, and distinct nucleoli. Two mitotic figures are present in this field.

figures (Fig. 6.69). Follicle-like spaces containing pink fluid may be present, imparting a resemblance to thyroid tissue (Fig. 6.70). As is the case for true neoplasms of steroid-type cells, the lesional cells of pregnancy luteomas are typically immunoreactive for inhibin[29,30] (immunoreactivity for calretinin is also expected, but formal studies of the expression of this marker in pregnancy luteomas have yet to be reported).

Differential Diagnosis

The differential diagnosis of pregnancy luteoma includes metastases, steroid cell tumor, juvenile granulosa cell tumor, and an involuting corpus luteum of pregnancy.

- In those cases that are multiple and/or bilateral, the clinician may be concerned about the possibility of metastatic tumor. Histologic examination is generally all that is required to exclude the possibility of metastatic carcinoma. Immunoreactivity with inhibin and/or calretinin and S100 negativity should be confirmed in pregnancy luteomas from patients in which melanoma is considered either on the basis of clinical history or histology, since metastatic amelanotic melanoma can form follicle-like spaces and closely mimic these tumor-like lesions.[31]
- Although pregnancy luteomas and steroid cell tumors can have overlapping histologic features, lesions of this ilk that lack crystals of Reinke are generally considered pregnancy luteomas when encountered in the setting of pregnancy, particularly when bilateral or multiple or when follicle-like spaces are present.
- Pregnancy luteomas with follicle-like spaces can mimic juvenile granulosa cell tumors, but the former have more monotonous nuclear and architectural features, are often multiple and/or bilateral, and their association with pregnancy is more than just coincidental.
- The distinction between pregnancy luteoma and a late-gestation corpus luteum of pregnancy is discussed in the section on ovarian follicles and their derivatives.

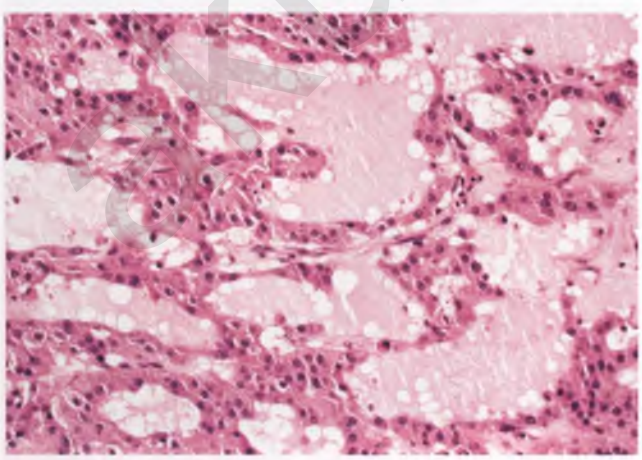

FIGURE 6.70. Pregnancy luteoma. This image highlights the presence of follicle-like spaces filled with pink fluid.

HILUS CELL HYPERPLASIA[4]

Hilus cells, whose characteristics are described at the beginning of this chapter, may become more prominent during pregnancy and following menopause. At some subjective, arbitrary point, the number of hilus cells is deemed excessive and a diagnosis of hilus cell hyperplasia is rendered. At the other end of the spectrum, distinction of a nodule of hilus cell hyperplasia from a hilus cell tumor is also arbitrary; the latter is diagnosed when the nodule is larger than 1 cm.

Hilus cell hyperplasia may be associated with virilization. It usually takes the form of several microscopic nodules within the hilar region, but may also occur in a sheet-like pattern (Fig. 6.71). Its constituent cells may exhibit some nuclear atypia, and hilus cell hyperplasia may occasionally be difficult to distinguish from small foci of metastatic carcinoma. If necessary, confirmation of the hilus cell nature of the proliferation can be obtained by demonstrating an inhibin-positive, cytokeratin-negative immunophenotype, which is the opposite of what one would expect for metastatic carcinoma.[23]

SELECTED DISORDERS OF GONADAL DEVELOPMENT

A complete discussion of the pathology of abnormal sexual development and its causes was recently published[32] and is beyond the scope of this work. However, those disorders that produce distinctive gonadal abnormalities in patients with ambiguous or female external genitalia are described in this section. It is important to recall from embryology that the female phenotype occurs in the absence of testicular influences (e.g., testosterone produced by Leydig cells and müllerian-inhibiting hormone produced by embryonic Sertoli cells), which explains

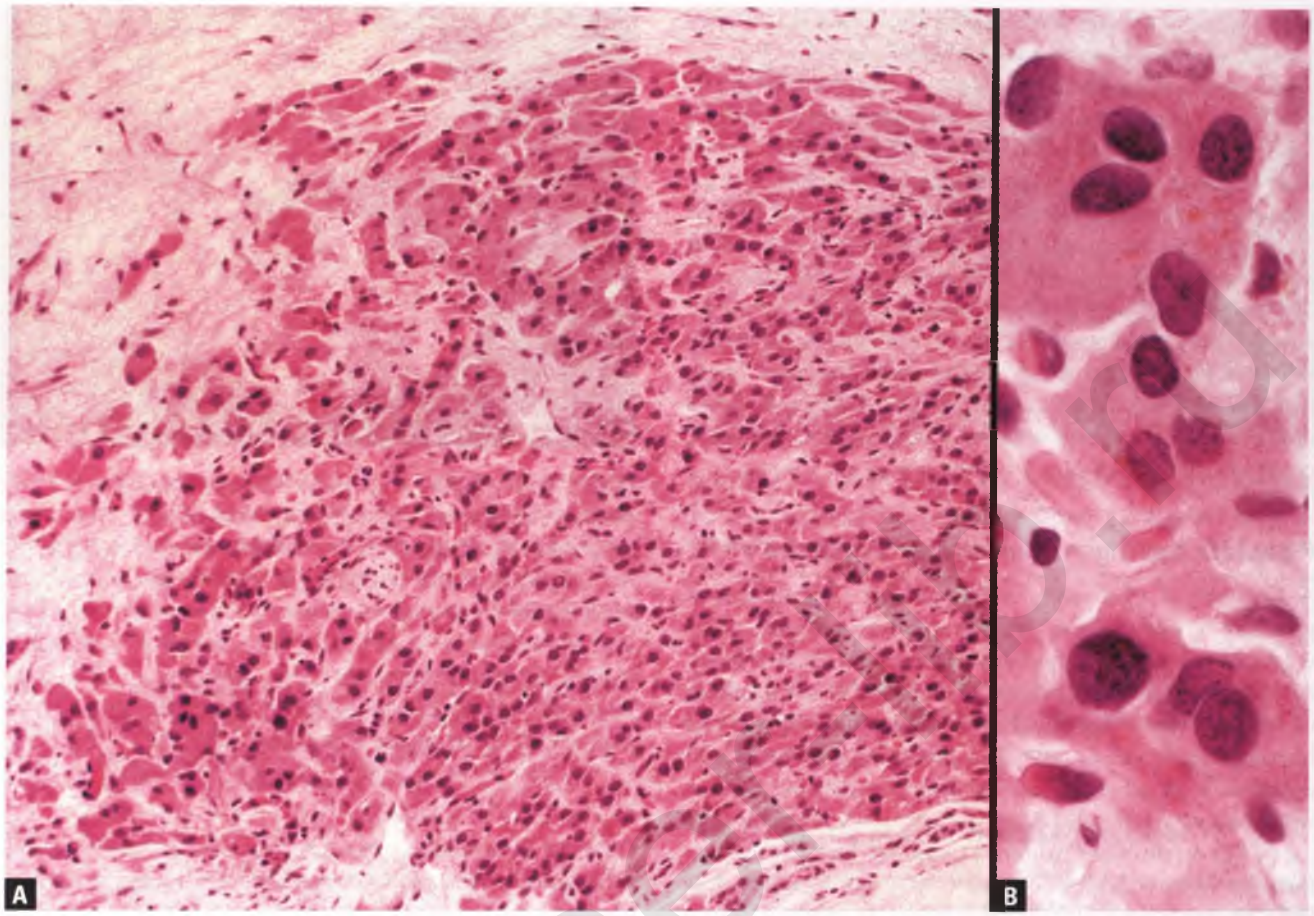

FIGURE 6.71. Hilus cell hyperplasia. **A:** There is a prominent, vaguely nodular proliferation of hilus cells within the ovarian hilum. **B:** High-magnification view of the hilus cells.

why patients with nonfunctional gonads or complete androgen insensitivity have female external genitalia.

Disorders Associated with Streak Gonads[33,34]

A streak gonad is a small elongated structure (roughly 0.5 × 0.5 × 2–3 cm) that has the gross appearance of a white fibrous streak. The cortical region of this maldeveloped gonad is composed of ovarian-type stroma. Although oocytes are present in streak gonads during gestation, they rapidly disappear and are rarely seen after early childhood. Streak gonads removed at puberty consist of cortical ovarian-type stroma devoid of germ cells and a hilar region with hilus cell hyperplasia and a rete-type formation (Fig. 6.72).

Patients with *pure gonadal dysgenesis* have a normal karyotype (46,XY or 46,XX), but have gene defects that result in bilateral streak gonads. The best characterized of these defects is an abnormality in the sex-determining region Y gene (SRY) that is located on the Y chromosome. A defect in this gene, which encodes the testis-determining factor that plays a key role in directing the bipotential embryonic gonad toward testicular differentiation, results in some cases of 46, XY pure gonadal dysgenesis (*Swyer's syndrome*). Patients with pure gonadal dysgenesis are phenotypic females who typically present with failure of development of secondary sex characteristics at the time of puberty. Patients with *Turner's syndrome* (45, XO

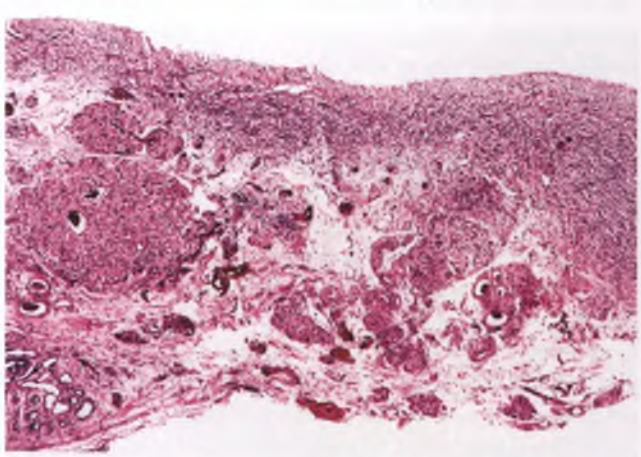

FIGURE 6.72. Streak gonad. The thin layer of ovarian-type cortical stroma at top is devoid of germ cells, and the hilar region contains nodules of hyperplastic hilus cells. A rete structure is present in the lower left portion of the image.

karyotype) also typically have bilateral streak gonads. In *mixed gonadal dysgenesis*, defective gonadal development is due to a variety of chromosomal mosaic patterns that result in partial sex chromosome monosomy, the most common of which is 45,X/46,XY. Most such patients have ambiguous external genitalia, rudimentary müllerian duct structures, a unilateral streak gonad, and a contralateral testis that is usually cryptorchid.

Since streak gonads associated with karyotypes that include Y chromosomal material have an approximately 25% chance of developing a malignant germ cell tumor by age 25, it is recommended that Y chromosome–associated streak gonads be removed shortly after recognition of their presence. Most malignant tumors that arise within dysgenetic gonads are gonadoblastomas, which can be thought of as a type of in situ malignant germ cell tumor, or gonadoblastoma-associated dysgerminomas (see Chapter 7).

Complete Androgen Insensitivity Syndrome[33,35–37]

A spectrum of phenotypic and functional abnormalities is produced by mutations in the androgen receptor gene, which is located on the X chromosome. Depending upon the specific nature of these mutations, of which there are hundreds of different types, the degree of androgen insensitivity may be complete, partial, or mild. This discussion is limited to the complete form of androgen insensitivity syndrome (CAIS), which was previously also known as testicular feminization.

CAIS is the most common cause of male pseudohermaphroditism, which is a condition in which a genetic male (46, XY karyotype) with testes exhibits an external female phenotype. Approximately 70% of cases of CAIS are inherited in an X-linked recessive fashion, whereas the remaining 30% occur as sporadic, *de novo* mutations. Patients with CAIS have an end-organ defect in their ability to respond to androgenic hormones that results in external genitalia that are phenotypically female. Patients typically present at puberty with primary amenorrhea, or less commonly with an inguinal hernia during childhood. Evaluation of pubertal patients reveals normal female breast development, scant pubic and axillary hair, a shortened vagina that ends in a blind pouch, an absent uterus, and cryptorchid testes. Since these patients have a risk of developing a malignant germ cell neoplasm (most frequently seminoma) in their abnormally located testes that is negligible in the early teenage years but increases to 30% to 40% by age 50, removal of the cryptorchid testes is recommended after puberty. Following orchiectomy, patients are treated with estrogen replacement therapy and other means to support their female gender identity.

Grossly, cryptorchid testes removed from patients with CAIS usually contain solid Sertoli cell nodules that are light tan to yellow, 1 mm to 4 cm in diameter, and typically multiple and bilateral (Fig. 6.73). A 1- to 2-cm nodule of tannish white smooth muscle is also often present at one testicular pole, and has been theorized to represent either a hypertrophic gubernaculum (the ligament that attaches the testis to the abdominal wall during its development) or a rudimentary uterus (Figs. 6.73 and 6.74).

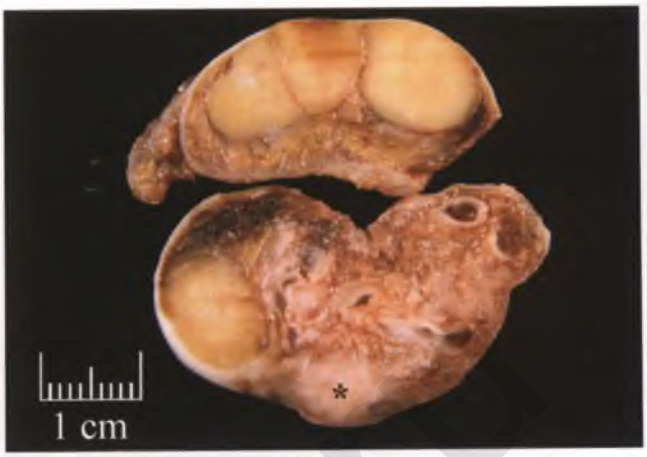

FIGURE 6.73. Testes of complete androgen insensitivity syndrome (testicular feminization). The sectioned surface of both testes reveals the presence of one or more solid, tannish yellow Sertoli cell nodules. Fig. 6.74 documents that the light tan to off-white nodular area marked by an *asterisk* is composed predominantly of smooth muscle, and that most of the tissue to the right of the Sertoli cell nodule in the bottom image is nontesticular stromal tissue. The yellow specks of golden yellow tissue that are most apparent in the bottom portion of the top testicle correspond to lobular aggregates of Leydig and Sertoli cells (see Fig. 6.77).

The Sertoli cell nodules are composed primarily of solid to minimally patent tubules that are lined by Sertoli cells and separated by fibromatous stroma (Fig. 6.75). The genesis of these benign nodules is uncertain, as is reflected in their various descriptions as hamartomas, adenomas, or nodular hyperplasias. (I prefer the noncommittal term benign Sertoli cell nodules). Although a purported distinction between hamartomas and Sertoli cell adenomas is an abundance of Leydig cells in the former, this criterion seems artificial when many of these nodules lack a Leydig cell component and yet are small, multiple, and

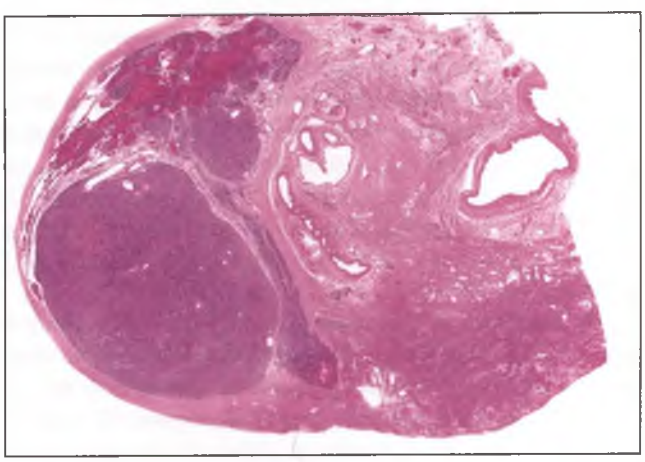

FIGURE 6.74. Testis of complete androgen insensitivity syndrome (testicular feminization). Low-magnification view of the testis in the bottom half of the preceding image.

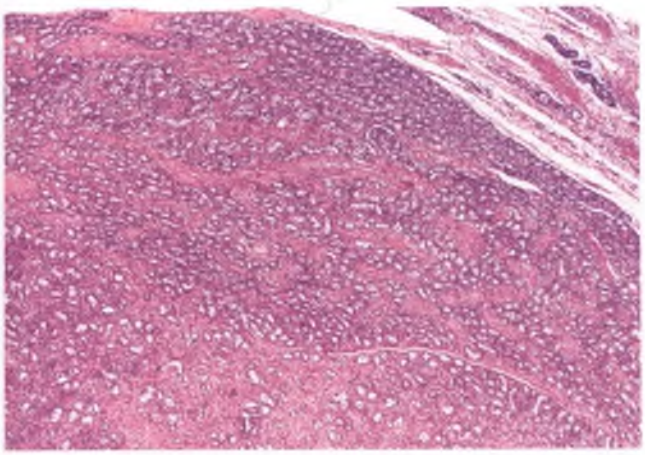

FIGURE 6.75. Sertoli cell nodule in a patient with complete androgen insensitivity syndrome (testicular feminization). In this low-magnification view, the nodule is seen to be composed of numerous Sertoli cell tubules set within a fibromatous stroma.

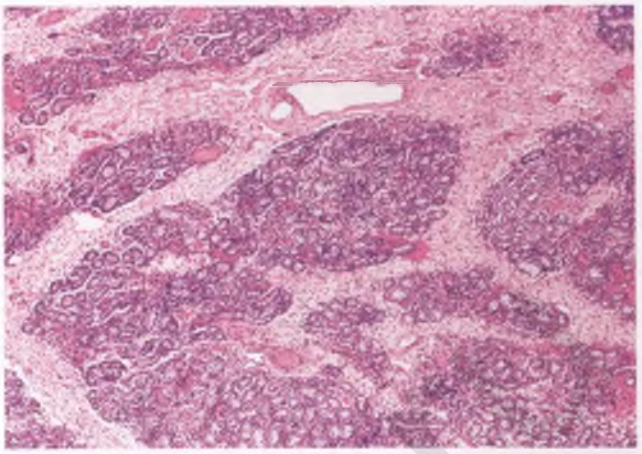

FIGURE 6.77. Testis of complete androgen insensitivity syndrome (testicular feminization). Testicular parenchyma with a lobular tubulostromal pattern.

bilateral as would be expected for a nonneoplastic process. However, when these nodules are solitary and unilateral, contain no to rare Leydig cells, and attain a diameter of more than 4 cm, it seems reasonable to dignify them as Sertoli cell adenomas.

The background testicular parenchyma in patients with CAIS consists of a diffuse pattern composed of immature Sertoli cell tubules admixed with numerous Leydig cells (Fig. 6.76), a lobular tubulostromal pattern (Fig. 6.77), or a mixed pattern. The lobular pattern corresponds to the golden yellow specks that are sometimes evident within this tissue (Fig. 6.73). In some cases, stroma resembling that of the ovarian cortex can be found within either the nodular or background testicular tissue (Fig. 6.78). If this type of stroma is present diffusely throughout the testis, it can be misinterpreted as an ovary, although the clinical history and the absence of ovarian follicles and their derivatives should facilitate this distinction.

The Ovotestis of True Hermaphroditism[33,34]

True hermaphroditism is the rarest form of intersexuality and its pathogenesis is poorly understood. True hermaphrodites possess both ovarian and testicular tissue that is readily identifiable, either in the form of separate gonads or unilateral or bilateral ovotestes, and most have ambiguous external genitalia. An ovotestis is a maldeveloped gonad that contains both ova and immature seminiferous tubules, and is usually biopsied early in life when primordial follicles predominate within the ovarian

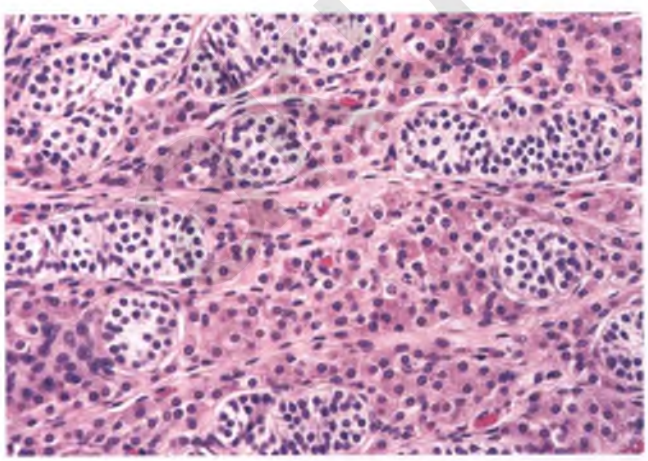

FIGURE 6.76. Testis of complete androgen insensitivity syndrome (testicular feminization). In this example, the nonnodular parenchyma consists largely of a diffuse admixture of immature Sertoli cells forming solid tubules and numerous Leydig cells.

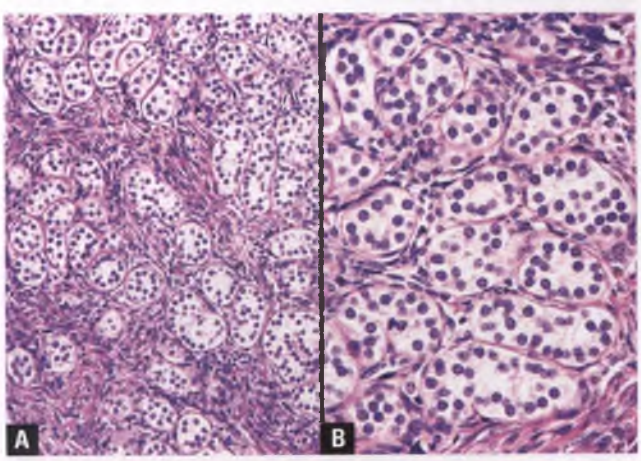

FIGURE 6.78. **A,B:** Sertoli cell nodule in a patient with complete androgen insensitivity syndrome (testicular feminization). In this example, the stroma resembles ovarian stroma.

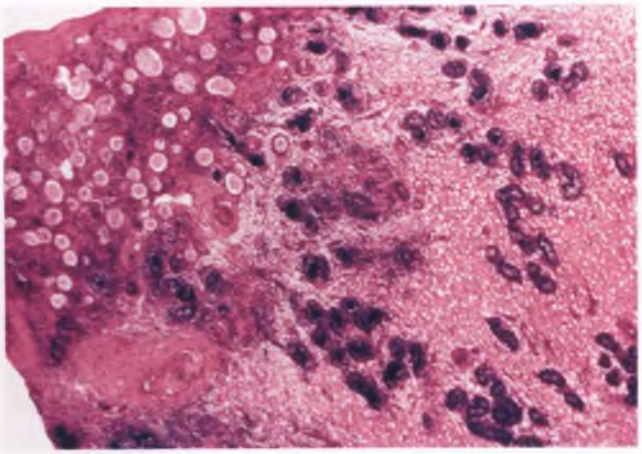

FIGURE 6.79. Ovotestis of patient with true hermaphroditism. The ovarian component at upper left contains numerous primordial follicles, and is fairly sharply demarcated from the testicular component that is punctuated by darkly stained, immature seminiferous tubules. (Glass slide kindly provided by Dr. Michael R. Hendrickson.)

component (Fig. 6.79). Development of malignant germ cell tumors in these patients is rare. Management typically includes gender assignment, removal of conflicting gonadal tissue, genital reconstruction as necessary, and hormonal supplementation. Some true hermaphodites raised as females have ovulated and successfully borne children.

MISCELLANEOUS NONNEOPLASTIC PROCESSES

Surface Papillary Stromal Proliferation[4]

Small papillary excrescences composed of stromal tissue enveloped by a single layer of surface lining cells may project from the ovarian surface, particularly in women beyond 40 years of age (Fig. 6.80). By definition, this incidental finding is smaller

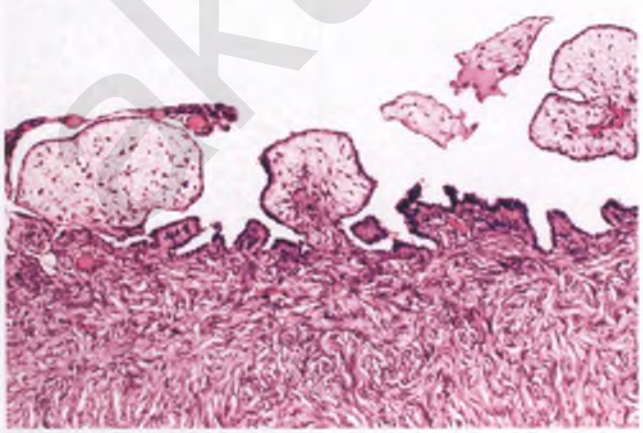

FIGURE 6.80. Papillary stromal proliferation emanating from the ovarian surface. This is an incidental histologic finding.

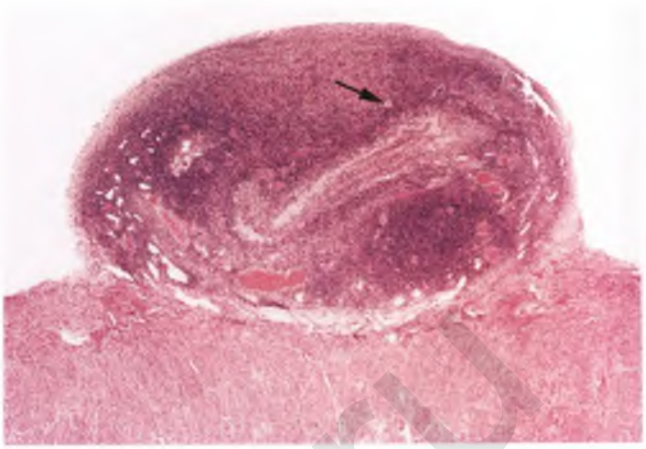

FIGURE 6.81. Supernumerary ovary adherent to the uterine serosa. The nodule consists largely of ovarian-type stroma, and contains a primordial follicle (*arrow*).

than 1 cm, although such foci are often multiple. Surface papillomas have a similar histologic appearance, but are ≥1 cm.

Supernumerary Ovary[4]

A supernumerary ovary occurs at a distance from the normal ovaries and is composed of ordinary ovarian tissue. Supernumerary ovaries are rare and may be found in a variety of pelvic or abdominal sites, such as within the omentum or mesentery or adherent to the uterine serosa, bladder, or pelvic wall (Fig. 6.81). Most supernumerary ovaries are <1 cm, but possess the functional and pathologic potential of normal ovaries.

Ovarian Remnant Syndrome[38]

On occasion, patients who have previously undergone a procedure that had the intent of removing both ovaries develop symptoms related to the presence of persistent ovarian tissue. Such patients typically have a history of ovarian surgery that was complicated by the presence of dense fibrous adhesions, and complain of pelvic pain and that may be associated with a small pelvic mass. When removed, this mass is found to represent residual ovarian tissue that often contains one or more follicle or corpus luteum cysts surrounded by chronically inflamed fibrous tissue.

Autoimmune Oophoritis[39]

Autoimmune oophoritis is very rare and is associated with a minority of cases of premature ovarian failure. Its main histologic feature is the presence of a chronic inflammatory infiltrate that is largely limited to the wall and lining of developing ovarian follicles.

Ectopic Ovarian Pregnancy[40]

Only 1% to 3% of ectopic pregnancies involve the substance of the ovary. Patients typically present with abdominal pain

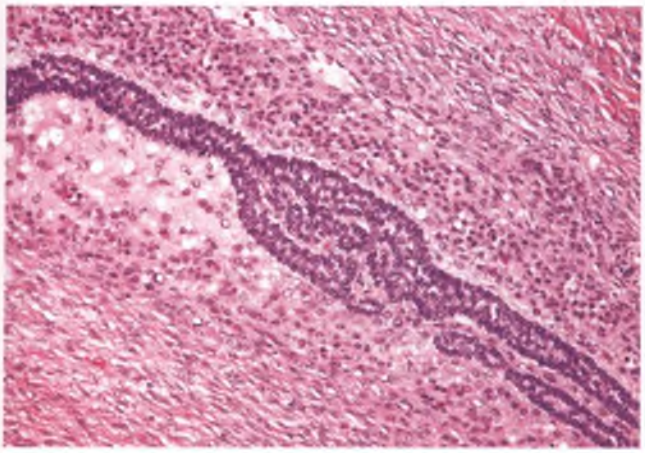

FIGURE 6.82. Granulosa cell proliferation of pregnancy. This elongated granulosa cell proliferation is located within the center of an atretic follicle and is surrounded by a mantle of luteinized theca interna cells. (Courtesy of Dr. Colin J. R. Stewart.)

and hemoperitoneum related to rupture of an enlarged, hemorrhagic ovarian mass that contains products of conception.

Granulosa Cell Proliferations of Pregnancy[41]

Within the atretic follicles of pregnant women may be incidental and often multiple granulosa cell proliferations that mimic microscopic granulosa cell tumors by virtue of their architectural patterns (solid, insular, microfollicular, or trabecular) and the nuclear grooves and scant cytoplasm of their constituent cells (Figs. 6.82 and 6.83). Their confinement to atretic follicles, association with pregnancy, miniscule size, and multifocality are all supportive of a nonneoplastic, hormonally induced etiology.

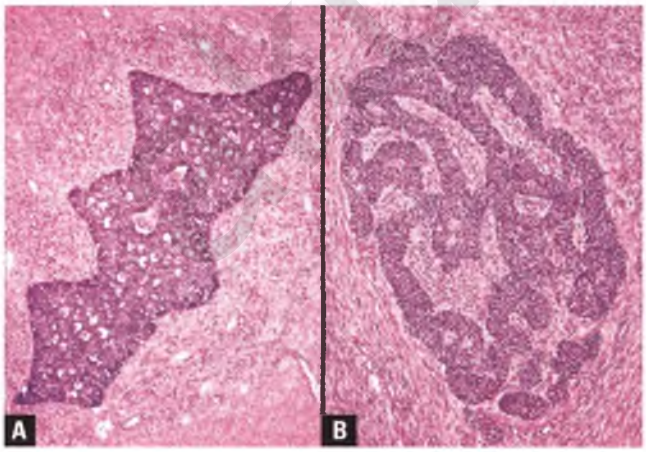

FIGURE 6.83. Granulosa cell proliferations of pregnancy. **A:** Microfollicular pattern. **B:** Trabecular pattern. These incidental proliferations mimic microscopic granulosa cell tumors. (Courtesy of Dr. Colin J. R. Stewart.)

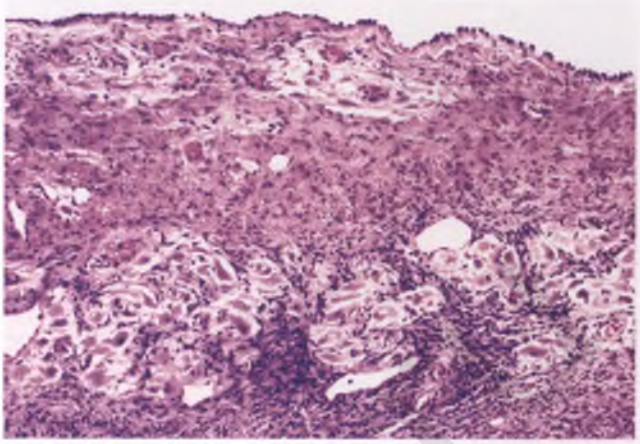

FIGURE 6.84. Ectopic decidua. In the lower portion of this image, a horizontal band of loosely arranged decidualized cells is present within the superficial ovarian cortex.

Artifactual Displacement of Granulosa Cells[42,43]

A rare incidental finding is the artifactual displacement of granulosa cells into vascular channels or the ovarian stroma. When superimposed crush artifact is present, these cells may resemble small cell carcinoma. In other situations, displaced luteinized granulosa cells may mimic nests of carcinoid tumor or metastatic breast carcinoma. Recognition of this phenomenon is facilitated by an awareness that this artifact can occur, the presence of neighboring follicles lined by similar cells, the absence of an associated ovarian tumor, and inhibin immunoreactivity of the displaced cells.

Ectopic Decidua[4]

A focal decidual reaction occurring on the ovarian surface or within the superficial ovarian cortex is an expected and usually incidental microscopic finding in term pregnancies (Fig. 6.84). The decidua is histologically similar to that normally found in gestational endometrium (Chapter 4) and in other ectopic sites such as the fallopian tube (Chapter 5) and peritoneum (Chapter 8).

Arteritis[44,45]

Arteritis of the ovarian vessels is rare and may occur as either an isolated finding or a manifestation of systemic vasculitis (Fig. 6.85). Necrotizing arteritis and giant cell arteritis have both been reported to involve the ovary. Since the most common site of arteritis within the female genital tract is the cervix, these forms of arteritis are discussed in more detail in Chapter 3.

Ovarian Granulomas

Ovarian granulomas are uncommon and are associated with a variety of causes, the most frequent of which in developed countries is a foreign body reaction to suture material.[46]

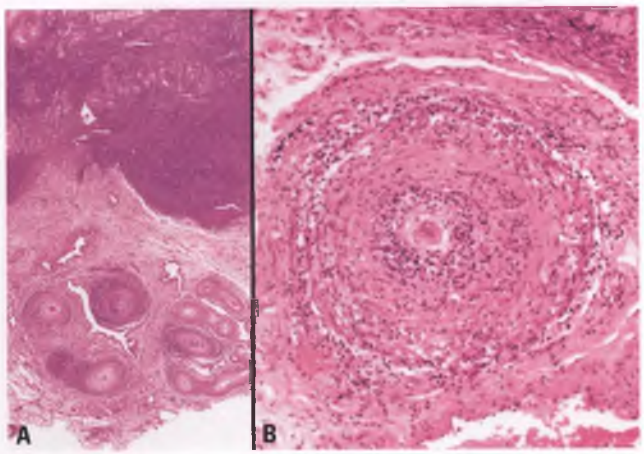

FIGURE 6.85. Ovarian arteritis. **A:** Inflammation of several of the medium-sized hilar vessels has resulted in obliterated lumens. **B:** This view of one of the involved vessels demonstrates the presence of a nonnecrotizing lymphocytic arteritis.

An example of one of these suture-related lesions, which are often referred to as suture granulomas, is illustrated in Figure 8.15.

A granulomatous reaction to previous laser or fulguration surgery, referred to as a postoperative carbon pigment granuloma or postcautery granuloma, is most commonly seen on the peritoneal and ovarian surfaces and is discussed in Chapter 8.

On occasion, the ovaries have been found to harbor necrotizing granulomas that appear to be isolated and not related to an infectious process (Fig. 6.86).[47] The core of these granulomas may be hyalinized and acellular, but can also consist of fibrinoid necrosis or necrotic cellular debris.[47] Cultures of such lesions are generally unavailable, but special stains for acid-fact bacilli and fungi should be performed in an attempt to identify microorganisms. In addition to these special stains, sections should be examined under polarized light as part of a search for foreign material. In the absence of a specific etiology, the lesions may be reported as "necrotizing granulomatous inflammation (see comment)," with a note stating that although consistent with isolated noninfectious granulomas, the negative "bug" stains do not entirely exclude infection and that clinical correlation and follow-up are indicated. In addition to tuberculous and fungal disease, the differential diagnosis of these lesions includes postoperative carbon pigment granulomas (see Chapter 8) and necrotic pseudoxanthomatous nodules (see section on ovarian endometriosis). In most cases, these isolated granulomas probably represent a response to a prior surgical procedure.[46,47] If a history of previous ovarian surgery is obtained and special stains for microorganisms are negative, a diagnosis of necrotizing granulomatous inflammation consistent with postoperative reaction can be rendered. It is noteworthy that the only distinguishing feature between the version of these granulomas with fibrinoid necrotic centers and postoperative carbon pigment granulomas is the presence of pigment in the latter lesions, which may disappear over a period of years.

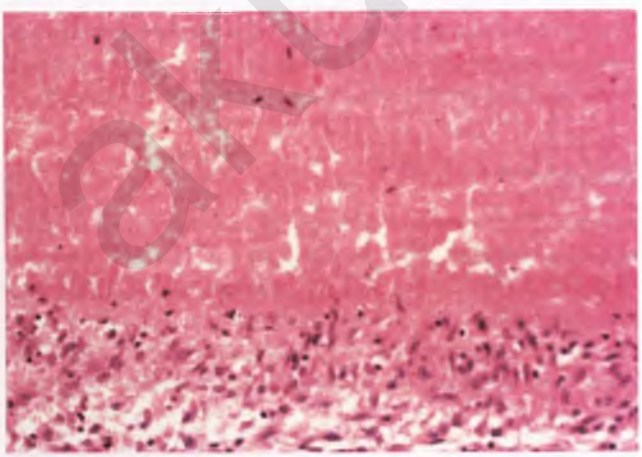

FIGURE 6.86. Necrotizing granulomatous inflammation. A rim of palisaded histiocytes is present adjacent to the eosinophilic necrotic debris.

In developed countries, tuberculosis is a rare cause of ovarian granulomas and is almost always associated with tuberculous salpingitis. Other situations in which ovarian granulomas occur include Crohn's disease, sarcoidosis, and cases without a known or presumed etiology. In Crohn's disease, the ovaries may become adherent to involved segments of bowel and develop granulomatous inflammation as a result of direct extension of the inflammatory bowel disease.[46] Nonnecrotizing granulomatous inflammation secondary to sarcoidosis has been reported to involve the ovaries on rare occasions, but this usually occurs in the setting of systemic sarcoidosis. Idiopathic granulomas are usually few in number, small, confined to the ovarian cortex, and nonnecrotizing.[46]

SUGGESTED READINGS

Clement PB, Young RH. *Atlas of Gynecologic Surgical Pathology*. 2nd ed. Philadelphia, PA: Elsevier Saunders; 2008.

Crum CP, Nucci MR, Lee K, eds. *Diagnostic Gynecologic and Obstetric Pathology*. 2nd ed. Philadelphia, PA: Elsevier Saunders; 2011.

Kurman RJ, Ellenson LH, Ronnett BM, eds. *Blaustein's Pathology of the Female Genital Tract*. 6th ed. New York: Springer; 2011.

Mills SE, ed. *Histology for Pathologists*. 3rd ed. Philadelphia, PA: Lippincott Williams & Wilkins; 2006.

Prat J. *Pathology of the Ovary*. Philadelphia, PA: Saunders; 2004.

Robboy SJ, Mutter GL, Prat J, et al., eds. *Robboy's Pathology of the Female Reproductive Tract*. 2nd ed. Oxford, UK: Churchill Livingstone; 2009.

Scully RE, Young, RH, Clement PB. Tumors of the ovary, maldeveloped gonads, fallopian tube, and broad ligament. *Atlas of Tumor Pathology*. 3rd series, Fascicle 23. Washington, DC: Armed Forces Institute of Pathology; 1998.

REFERENCES

1. Kurman RJ, Shih IeM. The origin and pathogenesis of epithelial ovarian cancer: a proposed unifying theory. *Am J Surg Pathol*. 2010;34:433–443.
2. Honore LH, O'Hara KE. Ovarian hilus cell heterotopia. *Obstet Gynecol*. 1979;53:461–464.

3. Hirschowitz L, Salmons N, Ganesan R. Ovarian hilus cell heterotopia. *Int J Gynecol Pathol.* 2011;30:46–52.
4. Scully RE, Young RH, Clement PB. Tumors of the ovary, maldeveloped gonads, fallopian tube, and broad ligament. *Atlas of Tumor Pathology.* 3rd series, Fascicle 23. Washington, DC: Armed Forces Institute of Pathology; 1998.
5. Stanley MW, Horwitz CA, Frable WJ. Cellular follicular cyst of the ovary: fluid cytology mimicking malignancy. *Diagn Cytopathol.* 1991;7:48–52.
6. Stern RC, Dash R, Bentley RC, et al. Malignancy in endometriosis: frequency and comparison of ovarian and extraovarian types. *Int J Gynecol Pathol.* 2001;20:133–139.
7. Mostoufizadeh M, Scully RE. Malignant tumors arising in endometriosis. *Clin Obstet Gynecol.* 1980;23:951–963.
8. Clement PB. The pathology of endometriosis: a survey of the many faces of a common disease emphasizing diagnostic pitfalls and unusual and newly appreciated aspects. *Adv Anat Pathol.* 2007;14:241–260.
9. Seidman JD. Prognostic importance of hyperplasia and atypia in endometriosis. *Int J Gynecol Pathol.* 1996;15:1–9.
10. Lanzafame S, Nicolosi AG, Caltabiano R. Bilateral massive osseous metaplasia in ovaries: "ovarian stones." *Gynecol Surg.* 2007;4:191–193.
11. Clement PB, Young RH, Scully RE. Liesegang rings in the female genital tract. A report of three cases. *Int J Gynecol Pathol.* 1989;8:271–276.
12. Perrotta PL, Ginsburg FW, Siderides CI, et al. Liesegang rings and endometriosis. *Int J Gynecol Pathol.* 1998;17:358–362.
13. Clement PB, Young RH, Scully RE. Necrotic pseudoxanthomatous nodules of ovary and peritoneum in endometriosis. *Am J Surg Pathol.* 1988;12:390–397.
14. Tatum ET, Beattie JF Jr, Bryson K. Postoperative carbon pigment granuloma: a report of eight cases involving the ovary. *Hum Pathol.* 1996;27:1008–1011.
15. Clarke TJ, Simpson RH. Necrotizing granulomas of peritoneum following diathermy ablation of endometriosis. *Histopathology.* 1990;16:400–402.
16. Franks S. Polycystic ovary syndrome. *N Engl J Med.* 1995;333:853–861.
17. Guzick DS. Polycystic ovary syndrome. *Obstet Gynecol.* 2004;103:181–193.
18. Clement PB, Young RH, Scully RE. Nontrophoblastic pathology of the female genital tract and peritoneum associated with pregnancy. *Semin Diagn Pathol.* 1989;6:372–406.
19. Clement PB. Tumor-like lesions of the ovary associated with pregnancy. *Int J Gynecol Pathol.* 1993;12:108–115.
20. Clement PB, Scully RE. Large solitary luteinized follicle cyst of pregnancy and puerperium: a clinicopathological analysis of eight cases. *Am J Surg Pathol.* 1980;4:431–438.
21. Fang YM, Gomes J, Lysikiewicz A, et al. Massive luteinized follicular cyst of pregnancy. *Obstet Gynecol.* 2005;105:1218–1221.
22. Sasano H, Fukunaga M, Rojas M, et al. Hyperthecosis of the ovary. Clinicopathologic study of 19 cases with immunohistochemical analysis of steroidogenic enzymes. *Int J Gynecol Pathol.* 1989;8:311–320.
23. Rabban JT, Barnes M, Chen LM, et al. Ovarian pathology in risk-reducing salpingo-oophorectomies from women with BRCA mutations, emphasizing the differential diagnosis of occult primary and metastatic carcinoma. *Am J Surg Pathol.* 2009;33:1125–1136.
24. Hibbard LT. Adnexal torsion. *Am J Obstet Gynecol.* 1985;152:456–461.
25. Houry D, Abbott JT. Ovarian torsion: a fifteen-year review. *Ann Emerg Med.* 2001;38:156–159.
26. Roth LM, Deaton RL, Sternberg WH. Massive ovarian edema. A clinicopathologic study of five cases including ultrastructural observations and review of the literature. *Am J Surg Pathol.* 1979;3:11–21.
27. Young RH, Scully RE. Fibromatosis and massive edema of the ovary, possibly related entities: a report of 14 cases of fibromatosis and 11 cases of massive edema. *Int J Gynecol Pathol.* 1984;3:153–178.
28. Nielsen GP, Young RH. Fibromatosis of soft tissue type involving the female genital tract: a report of two cases. *Int J Gynecol Pathol.* 1997;16:383–386.
29. Kommoss F, Oliva E, Bhan AK, et al. Inhibin expression in ovarian tumors and tumor-like lesions: an immunohistochemical study. *Mod Pathol.* 1998;11:656–664.
30. Rishi M, Howard LN, Bratthauer GL, et al. Use of monoclonal antibody against human inhibin as a marker for sex cord-stromal tumors of the ovary. *Am J Surg Pathol.* 1997;21:583–589.
31. Young RH, Scully RE. Malignant melanoma metastatic to the ovary. A clinicopathologic analysis of 20 cases. *Am J Surg Pathol.* 1991;15:849–860.
32. Robboy SJ, Jaubert F. Neoplasms and pathology of sexual developmental disorders (intersex). *Pathology (Phila).* 2007;39:147–163.
33. Rutgers JL. Advances in the pathology of intersex conditions. *Hum Pathol.* 1991;22:884–891.
34. Kim KR, Kwon Y, Joung JY, et al. True hermaphroditism and mixed gonadal dysgenesis in young children: a clinicopathologic study of 10 cases. *Mod Pathol.* 2002;15:1013–1019.
35. Rutgers JL, Scully RE. The androgen insensitivity syndrome (testicular feminization): a clinicopathologic study of 43 cases. *Int J Gynecol Pathol.* 1991;10:126–144.
36. Galani A, Kitsiou-Tzeli S, Sofokleous C, et al. Androgen insensitivity syndrome: clinical features and molecular defects. *Hormones.* 2008;7:217–229.
37. Oakes MB, Eyvazzadeh AD, Quint E, et al. Complete androgen insensitivity syndrome—a review. *J Pediatr Adolesc Gynecol.* 2008;21:305–310.
38. Magtibay PM, Magrina JF. Ovarian remnant syndrome. *Clin Obstet Gynecol.* 2006;49:526–534.
39. Bannatyne P, Russell P, Shearman RP. Autoimmune oophoritis: a clinicopathologic assessment of 12 cases. *Int J Gynecol Pathol.* 1990;9:191–207.
40. Itoh H, Ishihara A, Koita H, et al. Ovarian pregnancy: report of four cases and review of the literature. *Pathol Int.* 2003;53:806–809.
41. Clement PB, Young RH, Scully RE. Ovarian granulosa cell proliferations of pregnancy: a report of nine cases. *Hum Pathol.* 1988;19:657–662.
42. McCluggage WG, Young RH. Non-neoplastic granulosa cells within ovarian vascular channels: a rare potential diagnostic pitfall. *J Clin Pathol.* 2004;57:151–154.
43. Clarke B, McCluggage WG. Iatrogenic lesions and artefacts in gynaecological pathology. *J Clin Pathol.* 2009;62:104–112.
44. Onuma K, Chu CT, Dabbs DJ. Asymptomatic giant-cell (temporal) arteritis involving the bilateral adnexa: case report and literature review. *Int J Gynecol Pathol.* 2007;26:352–355.
45. Francke ML, Mihaescu A, Chaubert P. Isolated necrotizing arteritis of the female genital tract: a clinicopathologic and immunohistochemical study of 11 cases. *Int J Gynecol Pathol.* 1998;17:193–200.
46. McCluggage WG, Allen DC. Ovarian granulomas: a report of 32 cases. *J Clin Pathol.* 1997;50:324–327.
47. Herbold DR, Frable WJ, Kraus FT. Isolated noninfectious granulomas of the ovary. *Int J Gynecol Pathol.* 1984;2:380–391.

CHAPTER 7

Pathology of Ovarian Tumors

OVERVIEW AND STAGING OF OVARIAN TUMORS

The vast majority of primary ovarian tumors, about 75% of which are benign, occur in the 20 to 65 year old age group.[1] Typical symptoms include abdominal distension and/or pain in the abdominopelvic region. Less commonly, patients present with endocrine manifestations due to functioning stroma, acute abdominal pain related to torsion or rupture, or paraneoplastic syndromes. Some tumors, particularly those that are small and benign, are asymptomatic. The current classification of ovarian tumors is morphology-based and predicated upon the presumed cell type of origin whenever possible, which results in three major subtypes (epithelial-stromal, sex cord-stromal, and germ cell) along with some miscellaneous tumors.

Most primary ovarian cancers are carcinomas, and the extent of disease at presentation, as indicated by the surgical stage of the tumor, is the most important prognostic factor (the higher the stage, the worse the prognosis).[2–4] In brief, staging of ovarian carcinoma is as follows: stage I tumors are limited to the ovaries (one ovary → Ia; both ovaries → Ib; one or both ovaries with surface involvement,* rupture, or malignant cells in ascites/peritoneal washings → Ic), stage II tumors have spread to the pelvic region only, stage III tumors involve the abdomen and/or regional lymph nodes, and stage IV tumors have distant metastases.[5] Intuitively, it would seem that patients with stage Ic disease related to the presence of malignant cells within the peritoneal cavity would have a worse prognosis than other stage I patients, but studies that have addressed this issue have yielded inconsistent and conflicting results.[6]

Patients with stage I ovarian carcinoma have an 85% to 90% 5-year survival rate, which is even higher if the patient has undergone a comprehensive surgical staging procedure to minimize the chance of understaging.[6] However, most patients with ovarian carcinoma present with advanced stage disease that is difficult or impossible to completely resect, and have a poor prognosis.[2,3] In the United States, ovarian cancer is the fifth most common cause of cancer-related death in women, trailing lung, breast, intestinal, and pancreatic cancer in descending order of frequency.[7]

*Although the presence or absence of surface involvement impacts the substage of a stage I ovarian tumor, I am not a proponent of routinely inking the tumor surface as an aid in this assessment or as part of the evaluation of ovarian tumor resection margins for the following reasons: (a) the ovarian surface does not represent a true surgical margin, since it is surrounded by peritoneal space rather than tissue, (b) surface involvement by ovarian tumors is usually obvious on gross examination and is easily confirmed using uninked histologic sections, (c) many ovarian tumors are evaluated intraoperatively, and the inking process increases the turnaround time of the intraoperative consultation, (d) it can be tedious and/or messy to ink the surface of a large ovarian tumor, and (e) the result is not photogenic. However, in selected instances in which a focal and subtle area of surface involvement by tumor is suspected, inking of that specific area prior to sectioning can be helpful in documenting the presence of an exophytic component.

NEW VIEWS ON THE PATHOGENESIS OF EPITHELIAL-STROMAL OVARIAN TUMORS

It has long been held that the epithelial component of epithelial-stromal tumors of the ovary originates from the surface epithelium (actually modified mesothelium) through a process of invagination, formation of inclusion cysts, metaplasia, and neoplastic transformation, despite the rarity of the identification of dysplastic precursor lesions or early superficial carcinomas.[8,9] Recently, it has become apparent that many high-grade serous carcinomas previously assumed to be of ovarian or peritoneal origin actually originate in the distal fallopian tube (see Chapter 5).[10–13] By analogy, it has also been postulated that shedding of benign epithelial cells from the tubal fimbriae can result in their implantation in the ovary at the site of ovulation, where they can develop into epithelial inclusions and serve as fertile ground for subsequent development of benign, borderline, and low-grade malignant serous tumors.[14] Implantation of benign serous cells of tubal origin could also explain the phenomenon of endosalpingiosis (see Chapter 8).

In addition to the mounting evidence that most serous tumors of the ovary and peritoneum have roots in the fallopian tube, it has also become more widely accepted that ovarian endometriosis serves as the precursor of most endometrioid and clear cell tumors.[14] Although the origin of mucinous and transitional cell tumors is more obscure, the proposal that most such tumors originate from microscopic transitional cell (Walthard) nests rather than the ovarian surface epithelium is favored by an increasing number of investigators.[14,15] According to this theory, many of the mucinous tumors are the result of cystic overgrowth of the mucinous metaplastic component that is commonly present in Brenner tumors (the most common type of ovarian transitional cell tumor), which in turn arise from Walthard nests.[15] Mucinous or squamous elements within an ovarian teratoma are yet another potential source of primary ovarian tumors with a dominant epithelial component. Given the lack of direct evidence that the ovarian surface epithelium is ever the source of epithelial tumors and the accumulating evidence in favor of alternative explanations, I have intentionally dropped the word "surface" from the category of ovarian tumors that has traditionally been referred to as surface epithelial-stromal neoplasms.

EPITHELIAL-STROMAL TUMORS OF THE OVARY

General Features[9]

Tumors in this category account for 50% to 60% of all primary ovarian tumors and about 90% of primary ovarian cancers.[1,16] In addition to the defining epithelial element, these tumors also contain an ovarian-derived stromal component that is present in variable amounts, justifying inclusion of the word "stromal" in the classification of this group of tumors.

The five most common types of tumor in this category in descending order of frequency are serous, mucinous, endometrioid, clear cell, and transitional tumors. Each of these tumor types are further subdivided into benign, borderline, and malignant categories. The terms "neoplasms of low malignant potential" and "atypical proliferative tumors" are synonymous with borderline tumors, which account for about 5% of ovarian neoplasms.[1,16] Borderline tumors are noninvasive (or no more than microinvasive) tumors that exhibit a degree of epithelial proliferation and nuclear atypia that bridges the gap between straightforward benign and malignant tumors. The prototypical borderline tumor is the serous borderline tumor, which actually has a clinical behavior befitting of its name; the other types of borderline tumor are essentially benign neoplasms with a somewhat worrisome histologic appearance.

For descriptive purposes, the prefix "cyst" and/or the suffix "fibroma" are applied when serous, mucinous, endometrioid, or clear cell tumors are grossly at least partially cystic or contain a prominent fibrous stromal component, respectively. This nomenclature results in designations such as serous cystadenofibroma, mucinous cystadenoma, endometrioid cystadenocarcinoma, and clear cell adenofibroma. The pathology report should indicate the location of the neoplastic elements (surface = exophytic, intracystic = endophytic, or both), and this is sometimes reflected in the name of the tumor (e.g., serous surface papillary adenofibroma).

Because of the similarity of ovarian adenosarcoma, carcinosarcoma, and endometrioid stromal sarcoma to their more common endometrial counterparts, they are all considered to be within the spectrum of endometrioid tumors.

Histologic Grading of Ovarian Carcinoma

In most studies, the histologic grade of ovarian carcinoma has been shown to be a univariate prognostic factor, with higher grade tumors having a worse prognosis.[2–4,17,18] However, the strength of the predictive value of tumor grade independent of stage is debatable, at least for non-serous tumors, and the method used to arrive at the grade of these tumors has not been standardized.[2,18–20] Most grading systems are three-tiered (low grade = well differentiated = grade 1; intermediate grade = moderately differentiated = grade 2; high grade = poorly differentiated = grade 3);[2,4,19] for serous carcinomas, a two-tier grading system (low grade vs. high grade) has also been proposed.[17] Some grading systems emphasize the architecture of the tumor (extent of glandular vs. papillary vs. solid tumor growth), whereas others emphasize the degree of nuclear atypia or a combination of architectural and nuclear features, sometimes in conjunction with the mitotic rate.[19] Some grading systems are meant to be applied to all the different types of ovarian carcinoma, whereas others are more suited to specific types.[17,19]

In general, the tumor grade increases as the carcinomatous component of the tumor becomes more solid architecturally and exhibits greater degrees of nuclear pleomorphism and mitotic activity. The histologic heterogeneity of ovarian carcinomas, the occasional discordance of architectural and nuclear features (e.g., high-grade nuclei with low-grade architecture), and the subjective application of sometimes underspecified grading criteria often conspire to make histologic grading a poorly reproducible exercise,[2,18] although excellent reproducibility has recently been reported for the two-tier system for grading ovarian serous carcinoma.[21]

Although a three-tier grading system that is applicable to all types of ovarian carcinoma is appealing in its universality and lack of dependence upon assigning a tumor to the correct histologic type, its acceptance is unlikely in view of (a) the accumulating evidence that serous carcinomas develop via two distinct pathways and are best segregated into two groups rather than three,[14,20,22] (b) the heterogeneity of ovarian carcinomas, and (c) the lack of prognostic significance of the histologic grade of clear cell carcinoma.[3,4]

My approach to histologic grading of ovarian carcinomas is type-specific: serous carcinomas are graded as low-grade or high-grade as per the criteria of Malpica et al.,[17] endometrioid carcinoma is graded using the same criteria as endometrial endometrioid carcinoma (see Chapter 4), mucinous and transitional cell carcinomas are graded using the three-tier grading system of Shimizu and Silverberg that is patterned after the grading system for breast carcinoma,[4] and clear cell carcinomas are considered high-grade by definition.

Serous Tumors

Serous tumors represent about 30% of all ovarian neoplasms.[1,16] Of these tumors, about 60% to 65% are benign, 10% are borderline, and 25% to 30% are malignant.[1,16] At the benign end of the spectrum, the epithelium of serous neoplasms strongly resembles the epithelial lining of the fallopian tube, whereas the identification of complex papillary growth with epithelial budding and tufting, slit-like glandular spaces, and psammoma bodies assist in the recognition of less differentiated serous tumors.

Benign Serous Tumors[9]

Benign serous tumors (cystadenomas, adenofibromas, and cystadenofibromas) are commonly encountered tumors, trailing only mature cystic teratomas in frequency.[1,16] They are most often found in adult women of reproductive age, and generally are asymptomatic. These tumors are usually <15 cm, and about 10% to 20% are bilateral.

Serous cystadenomas typically have a smooth external surface and consist of one or more thin-walled cysts filled with watery fluid (Figs. 7.1 and 7.2A). Their inner lining may be smooth or studded with polypoid excrescences that may be fibrotic or edematous. The cystic spaces and polypoid projections are lined by tubal-type epithelium that usually includes ciliated cells (Fig. 7.2B). Fluid-filled cysts may be associated with varying degrees of pressure atrophy of the epithelial lining, which can result in cuboidal to flattened epithelium and

FIGURE 7.1. Serous cystadenoma. External view of intact tumor.

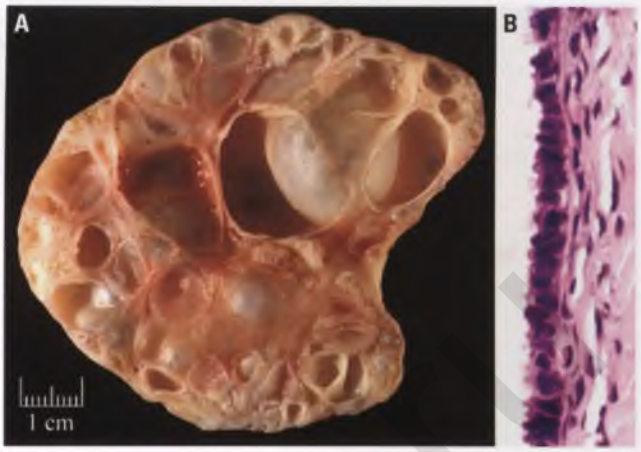

FIGURE 7.2. Serous cystadenoma. **A:** Sectioned surface of multiloculated tumor. **B:** The cysts are lined by tubal-type epithelium with interspersed ciliated cells.

loss of cilia that when widespread may prompt a diagnosis of simple cyst (see Fig. 6.29).

When fibrotic polypoid protuberances are a prominent feature or when a predominantly solid adenofibromatous component is present, a diagnosis of serous cystadenofibroma is appropriate (Figs. 7.3 and 7.4). Those adenofibromatous serous tumors in which cysts represent an inconspicuous or minor component are referred to as serous adenofibromas (Fig. 7.5) and can be further designated as serous surface papillary adenofibromas when surface involvement is prominent. In the latter situation, epithelial cells and/or psammoma bodies derived from these benign tumors can exfoliate into the peritoneal cavity, which can result in cytologic preparations that are at risk for being overcalled as involved by a serous borderline tumor (SBT) or low-grade serous carcinoma (Fig. 7.6).

Benign-appearing ovarian serous cystadenomas with an endophytic architecture that contain one or more small foci aggregating to <10% of the tumor in which the papillae meet the histologic criteria for a SBT are best referred to as "focally proliferative" serous cystadenomas rather than subtle examples of SBTs, since such tumors are virtually guaranteed to pursue a benign clinical course (Fig. 7.7).[23] Exophytic tumors with this feature are treated less leniently and diagnosed as SBTs, since

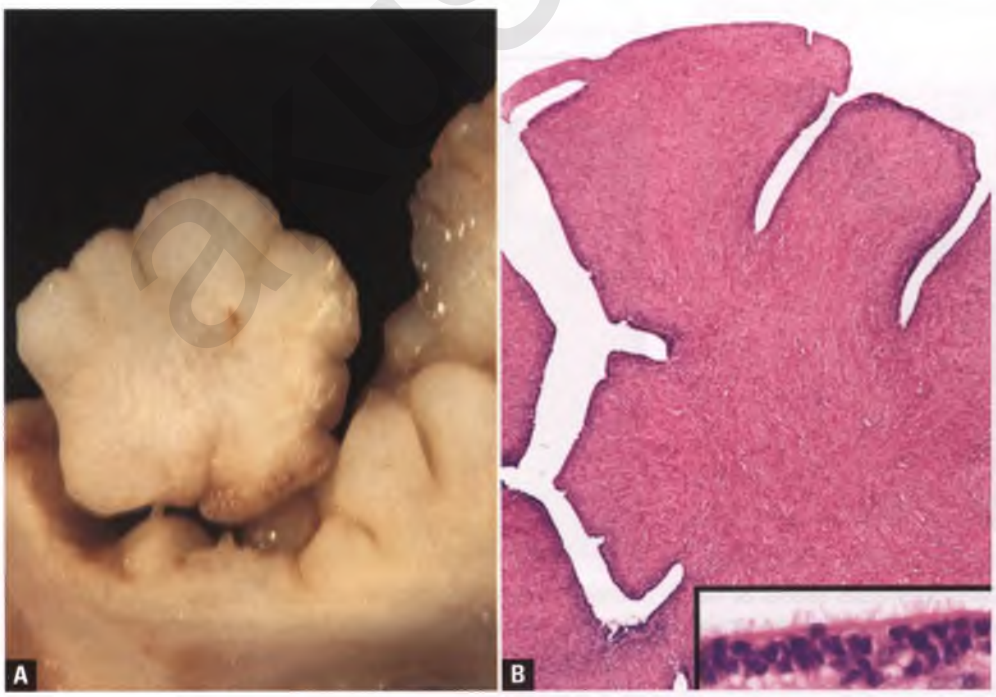

FIGURE 7.3. Serous cystadenofibroma. **A:** Sectioned surface of stubby polyps with clefts projecting into a cystic cavity. Such projections are composed of firm to rubbery, off-white to pale yellow tissue and are characteristic of this tumor. **B:** The polypoid projections have dense fibrous stromal cores with a clefted architecture, and are lined by a thin layer of tubal-type epithelium (inset).

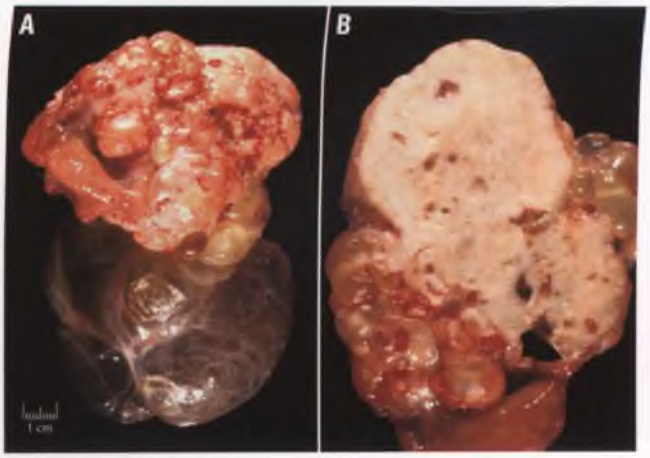

FIGURE 7.4. Serous cystadenofibroma. **A:** This tumor has both solid (top) and cystic (bottom) components. Some papillary excrescences protrude from the surface of the solid component. **B:** This image highlights the fibrotic appearance of the sectioned surface of the solid component.

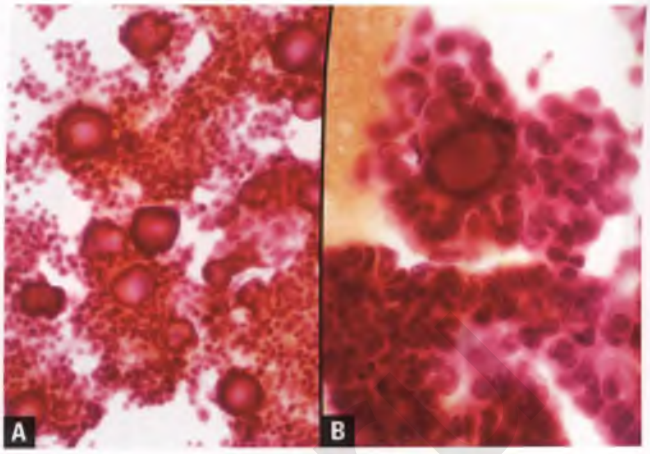

FIGURE 7.6. Pelvic wash from patient with serous surface papillary adenofibroma (Pap-stained cytologic preparation). **A:** At low magnification, the high cellularity and the presence of several psammoma bodies are the most striking findings. **B:** At high magnification, note the bland nuclear features of the epithelial cells associated with the psammoma bodies. Definitive distinction from peritoneal involvement by serous borderline tumor or low-grade serous carcinoma requires correlation with the resected ovarian tumor.

such tumors are theoretically at an increased risk for seeding of the peritoneal cavity.

Serous cystadenomas are one of the more common tumor types to undergo torsion-related hemorrhage, as illustrated in Figure 6.62.

Differential Diagnosis

Small serous cystadenomas are distinguished from epithelial inclusion cysts solely and arbitrarily on the basis of size; if such lesions are ≥1 cm in diameter, then they are diagnosed as serous cystadenomas. The distinction between serous cystadenoma and rete cystadenoma and that between serous cystadenoma and cystic struma ovarii are discussed in the corresponding sections elsewhere in this chapter, and the distinction between surface papillomas and incidental surface papillary stromal proliferations is discussed in Chapter 6. The previous discussion of focally proliferative serous cystadenomas addresses the issue of where to draw the line between the upper end of a cystadenoma and the lower end of a borderline tumor.

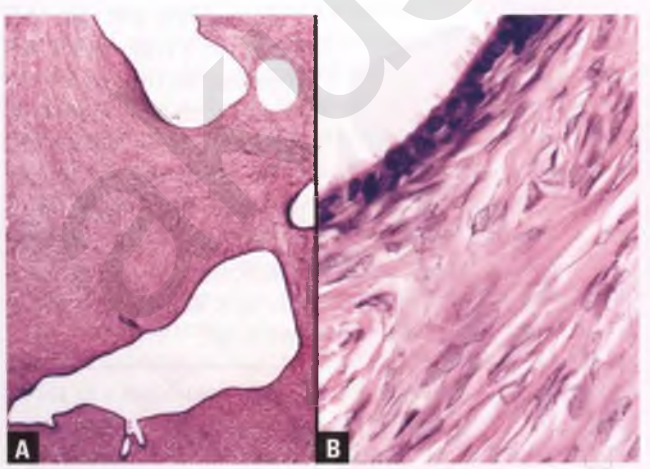

FIGURE 7.5. Serous adenofibroma. **A:** Scattered epithelial-lined cysts and glands are embedded within a fibromatous stroma. **B:** The cysts and glands are lined by tubal-type epithelium (note surface ciliation).

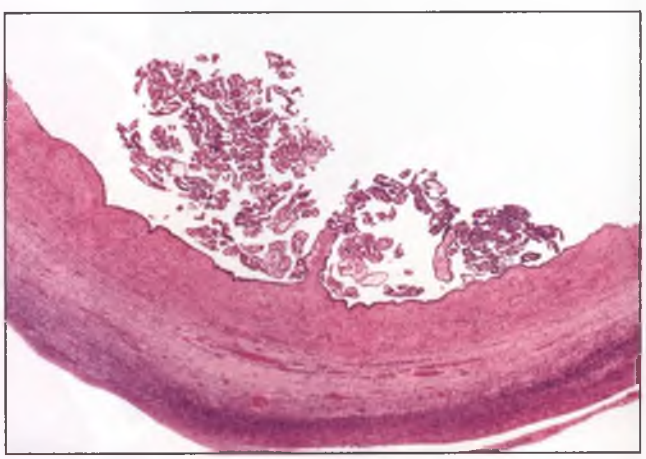

FIGURE 7.7. Serous cystadenoma, focally proliferative. This serous borderline-like papillary proliferation is a focal finding protruding from the inner lining of an intracystic serous neoplasm. Tumors such as this are not diagnosed as borderline tumors, since they are not thought to have any malignant potential.

Serous Borderline Tumor and Its Extraovarian Manifestations

This section discusses the many interesting and important aspects of SBTs and their extraovarian manifestations, some of which have provoked considerable controversy.[24–29]

Serous Borderline Tumor, Usual Type

SBTs are also known as serous tumors of low malignant potential, and are referred to by some as atypical proliferative serous tumors.[25,30] These tumors exhibit a greater degree of architectural and nuclear atypia than benign serous tumors, but lack the frank stromal invasion of serous carcinoma. SBTs are found in women over a wide age range, with an average age of 40 to 45 years.[30,31] About two-thirds of patients have stage I disease, and the other third are stage II or III; stage IV disease occurs at case-reportable rates.[25,30,31] Note that studies with a heavy bias toward consultation cases are likely to report higher rates of greater than stage I disease, since it is the assessment of peritoneal implants that often prompts the consultation.

Combined data from two of the larger and more recent series on SBTs indicates that they have an average size of 11 cm and a nearly 50% incidence of bilaterality.[30,31] Tumors are most commonly smooth-surfaced, unilocular or multilocular cysts with a variably prominent intracystic papillary proliferation (Fig. 7.8).[30,31] Mixtures of intracystic and exophytic (surface) growth are also fairly frequent, and occasional tumors are exclusively exophytic (Fig. 7.9).[30,31] The papillae are typically soft, edematous, and tan to pale yellow. Fluid within the cystic spaces is usually watery, but may be mucinous (see below), and a solid fibromatous component may also be present.

Histologically, SBTs are characterized by a complex arborizing architecture with hierarchical branching of papillary structures; in other words, large stem papillae progressively divide into smaller papillae in a gradual and orderly fashion (Fig. 7.10). This process culminates in the formation of small detached papillary epithelial clusters in the vicinity of the larger papillae ("epithelial tufts") (Fig. 7.11). The extent of actual tumor cell exfoliation may be less than it appears in histologic sections, since narrow attachments of cells near the tips of papillae may not be in the plane of section. The presence on the surface of the papillae of undulating epithelial-lined clefts results in a scalloped rather than smooth interface of the epithelium with the underlying stroma. Sectioning through randomly oriented papillary stalks, whose stromal cores contain these epithelial invaginations, results in a blunted, regular branching pattern without an associated stromal reaction, which should not be misinterpreted as evidence of invasion (Fig. 7.12).

The tumor cells of SBT exhibit mild to moderate nuclear atypia and a low mitotic rate, and a subpopulation of these cells

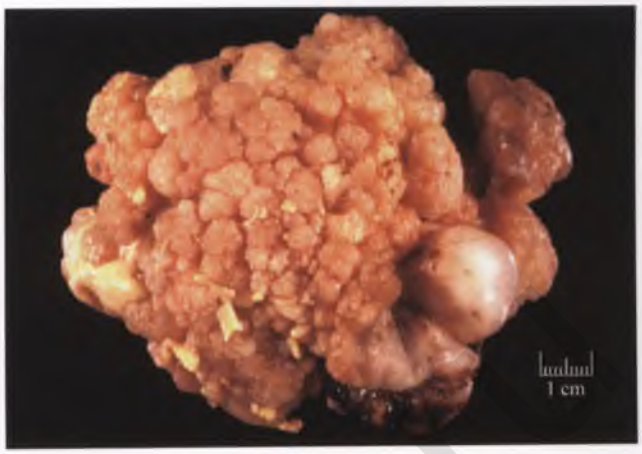

FIGURE 7.9. Serous borderline tumor. This exophytic tumor consists of a conglomeration of tan papillae projecting from the surface of the ovarian mass.

FIGURE 7.8. Serous borderline tumor. Opening of this smooth-surfaced, endophytic tumor reveals several locules, some of which contain numerous papillae that are pale yellow and edematous.

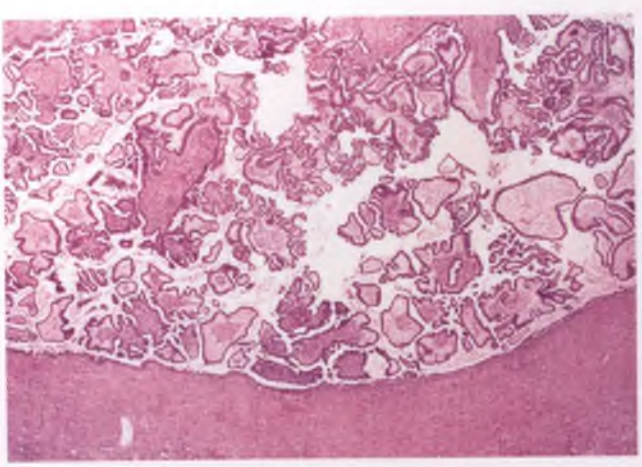

FIGURE 7.10. Serous borderline tumor. At low-magnification, this tumor typically appears as a complex aggregate of scalloped papillae of varying sizes and shapes with cores that range from edematous to fibrotic.

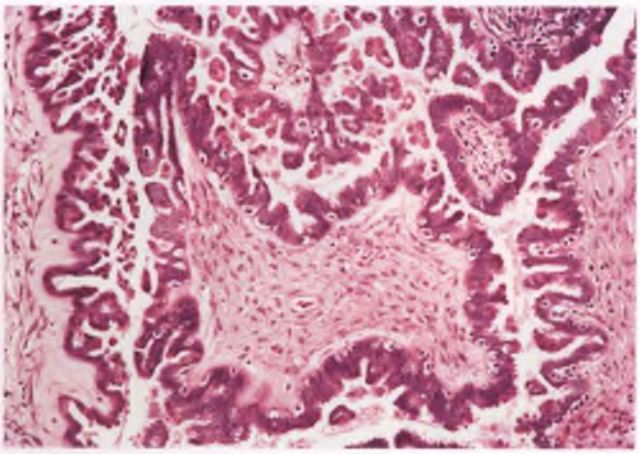

FIGURE 7.11. Serous borderline tumor. This image highlights the budding of tumor cells from the surface of the papillae and the detached epithelial tufts that are characteristic of this neoplasm.

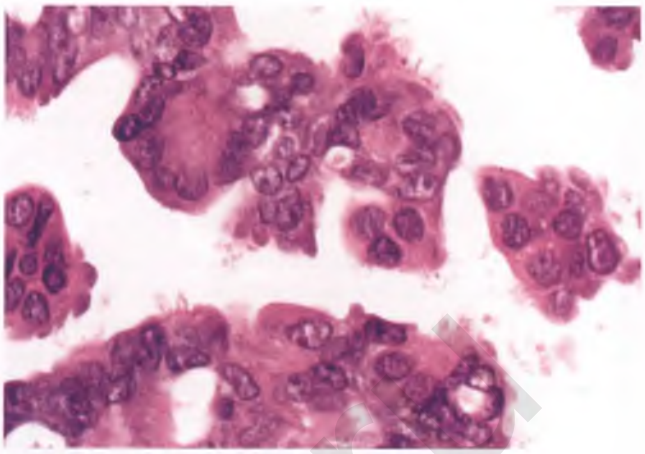

FIGURE 7.13. Serous borderline tumor. This example features moderate nuclear atypia, with several of the tumor cells displaying distinct nucleoli. The mitotic rate is low, and some of the tumor cells are ciliated.

is usually ciliated (Fig. 7.13). It is common for psammoma bodies to be present and for some of the tumor cells, particularly those in the epithelial tufts, to have abundant eosinophilic cytoplasm. In some cases, mucin-rich luminal contents are present that may grossly suggest the presence of a mucinous tumor, but the tumor cells themselves either contain no mucin or mucin is limited to their apical borders (Figs. 7.14 and 7.15).

Serous Borderline Tumor, Micropapillary Type

Serous borderline tumors of micropapillary type (SBTs-MP) represent about 12% of SBTs, as estimated from the combined results of three studies that included consecutive hospital cases of all stages, thereby eliminating consultation referral selection bias and the bias of studies that are limited to advanced-stage SBTs.[31–33] Variable amounts of typical SBT are usually found within SBTs-MP, and the latter is not diagnosed unless at least one focus with pure micropapillary features measures ≥5 mm in diameter.[34] In comparison to SBTs of usual type, SBTs-MP occur in a slightly younger age group, tend to be slightly smaller, and are more likely to be bilateral, at least partially exophytic, and associated with peritoneal implants even when entirely intracystic (Fig. 7.16).[31,32,35] SBTs with a micropapillary pattern should be sampled extensively, since they are more likely to harbor foci of stromal invasion than usual SBTs.[35]

Histologically, SBT-MP is characterized by numerous slender micropapillae (at least five times as long as they are wide) with absent to inconspicuous stromal cores that circumferentially emanate from large fibrous cores, resulting

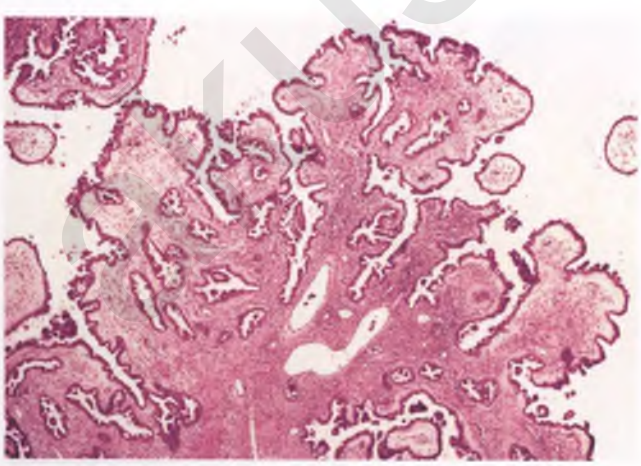

FIGURE 7.12. Serous borderline tumor. The branching epithelial invaginations of these architecturally complex tumors are often cut tangentially or in cross section, creating gland-like structures within the stroma that should not be misinterpreted as evidence of stromal invasion.

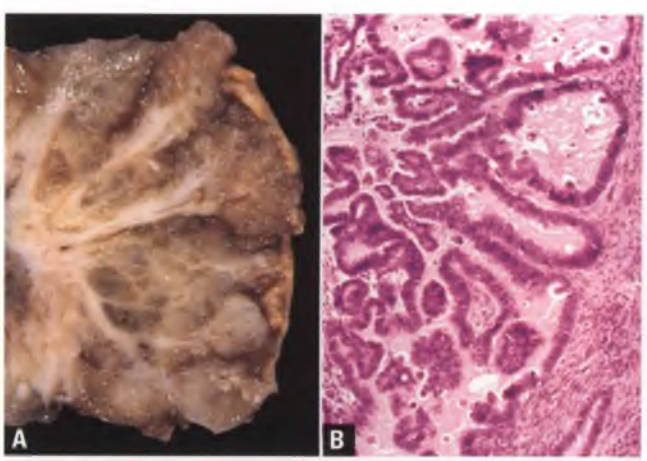

FIGURE 7.14. Serous borderline tumor with mucin-rich luminal contents. **A:** The sectioned surface of the tumor has a glistening, mucoid, and partially papillary appearance. **B:** Pale eosinophilic mucinous material is present within the crevices and dilated cystic spaces that communicate with the luminal aspects of the tumor.

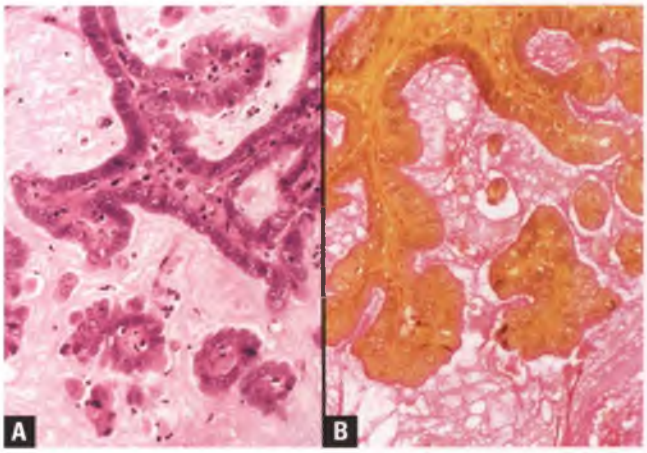

FIGURE 7.15. Serous borderline tumor with mucin-rich luminal contents. **A:** High-magnification view of a routinely-stained section from the tumor in the preceding figure. **B:** A mucicarmine stain highlights the presence of the intraluminal mucinous material; staining of the tumor cells is restricted to their apical borders. The distinction of serous versus mucinous differentiation in an ovarian tumor is based upon the nature of the tumor cells rather than the presence or absence of luminal mucin.

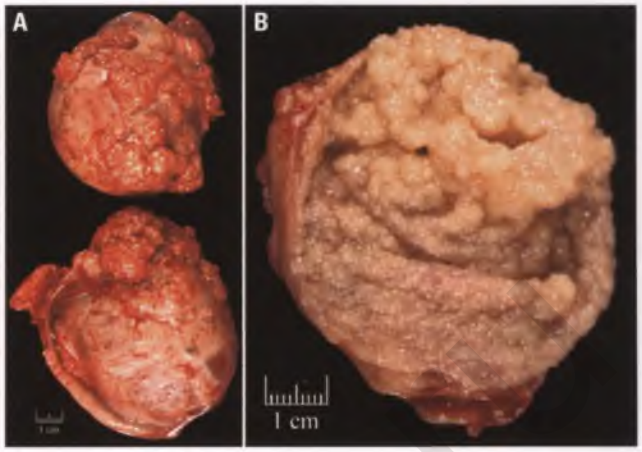

FIGURE 7.16. Serous borderline tumor with micropapillary pattern. **A:** As is typical of these tumors, there is bilateral ovarian involvement and an exophytic surface component is present. **B:** The internal aspect of this cystic tumor is lined by innumerable papillae that range from granular to polypoid in appearance.

in a pattern that has been likened to the head of Medusa (Figs. 7.17 and 7.18).[32,34] In contrast to usual SBTs, the branching pattern of the papillae is non-hierarchical and the interface between the epithelial proliferation and the large fibrous stalks is smooth rather than scalloped.[34] The neoplastic cells tend to be monomorphic, lack cilia, and exhibit mild to moderate nuclear atypia with inconspicuous mitotic activity (Fig. 7.19). By definition, high-grade nuclear atypia is not present. Since fusion of micropapillae may be one mechanism by which a surface cribriform pattern is formed, this pattern is also considered to be within the spectrum of SBT-MP (Fig. 7.20). The surface cribriform pattern is rarely more than a minor and focal finding in SBTs, with cases with at least one such focus measuring ≥5 mm being even less common than those with similar amounts of the micropapillary pattern.[32]

Although noninvasive, SBT-MP was originally described as micropapillary serous carcinoma, stemming from the belief that these tumors are more aggressive than usual SBTs and behave like low-grade carcinomas.[34,36] However, subsequent studies have failed to demonstrate significant differences in survival between usual SBT and SBT-MP when controlled for the presence and type of implant, and have emphasized that it is the invasive versus noninvasive nature of the associated peritoneal implants, rather than the presence of micropapillary architecture per se, that is the major prognostic determinant in advanced-stage SBTs.[26,27,30–33,37]

Serous Borderline Tumor with Autoimplants[30,38]

Autoimplants are found in about 10% of SBTs and are strongly associated with the presence of peritoneal implants in the pelvis and/or abdomen, but do not adversely impact the prognosis. They are typically found on the surface of the neoplasm or between exophytic papillae as discrete, plaque-like lesions. Histologically, they are identical to noninvasive desmoplastic implants, as described in the section on peritoneal implants of serous borderline tumor (Fig. 7.21).

Serous Borderline Tumor with Microinvasion

Microinvasion occurs in about 10% to 15% of patients with SBTs.[30,31,39] The upper size limit for microinvasion in ovarian borderline tumors is arbitrary and has not been standardized; it varies from 3 to 5 mm in linear extent to an area of

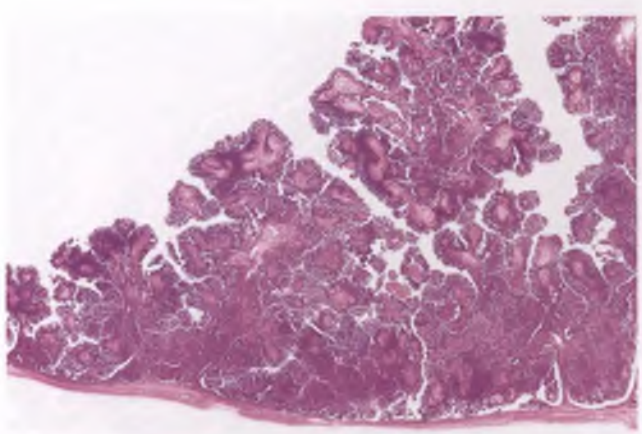

FIGURE 7.17. Serous borderline tumor with micropapillary pattern. At low magnification, these tumors appear as papillary neoplasms with marked complexity and cellularity.

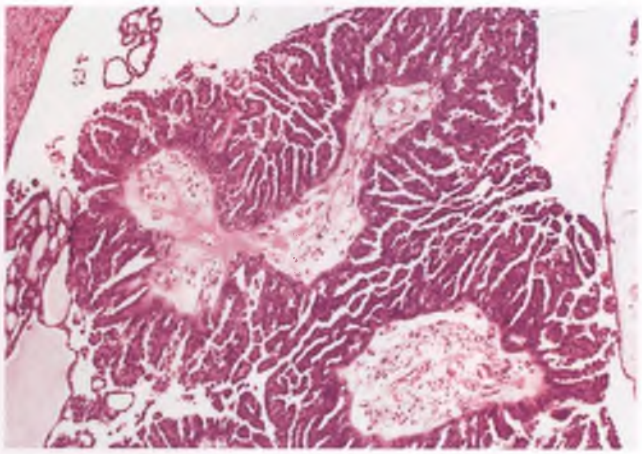

FIGURE 7.18. Serous borderline tumor with micropapillary pattern. The appearance of the long, slender micropapillae emanating from thick and fibrotic stromal cores has been likened to the snaky-haired head of Medusa from Greek mythology. The micropapillae themselves have minimal to absent stromal support.

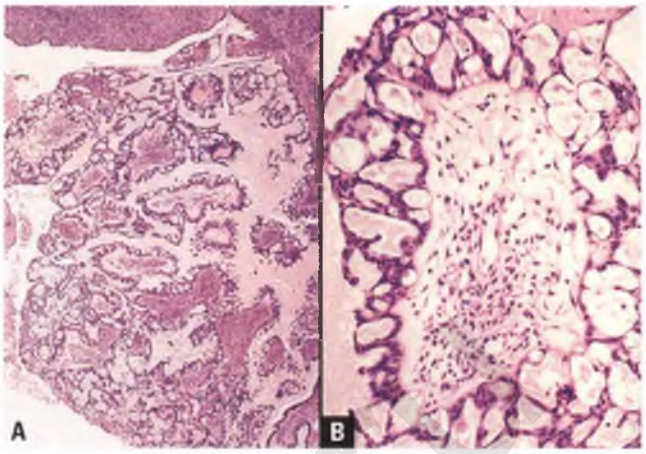

FIGURE 7.20. **A,B:** Serous borderline tumor with surface cribriform pattern.

10 mm^2.[23,27] Multiple separate foci of microinvasion are often present, and their individual sizes are not added together when making a determination of whether the extent of infiltration qualifies as microinvasion. For unknown reasons, microinvasion appears to be more common in SBTs removed from pregnant patients.[39–41]

In the most common type of microinvasion, the stromal cores of the papillary tumor are infiltrated by neoplastic cells with abundant eosinophilic cytoplasm that are disposed singly, in small clusters, and as simple papillae (Figs. 7.22 and 7.23). These infiltrating cells and tumor aggregates do not elicit a significant stromal reaction and are typically at least partially surrounded by a clear space or cleft, which may represent either retraction artifact or lymphatic invasion.[39,40] Recently, the lymphatic endothelial marker D2-40 has been utilized to document the presence of intratumoral lymphatic invasion in 60% of microinvasive SBTs, although such involvement is not associated with an increased risk of tumor spreading to regional lymph nodes.[42]

In the less common forms of microinvasion, inverted macropapillae surrounded by cleft-like spaces (Figs. 7.24 and 7.25), cribriform glands, and complex micropapillae focally infiltrate the stroma.[39,41] Some investigators make a distinction between SBTs with microinvasion and SBTs with microinvasive carcinoma, with the latter more closely resembling the complex micropapillary pattern seen in invasive low-grade serous carcinomas,[23,27] but there is insufficient outcome data to endorse this potentially confusing distinction at this time.

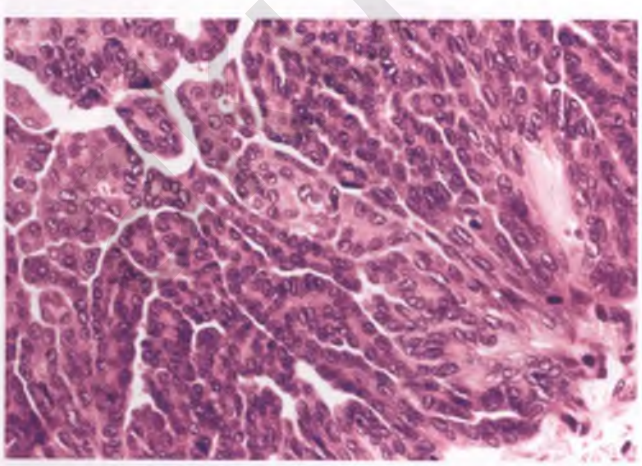

FIGURE 7.19. Serous borderline tumor with micropapillary pattern. The neoplastic cells are monomorphic and exhibit mild to moderate nuclear atypia with small nucleoli. Mitoses are infrequent.

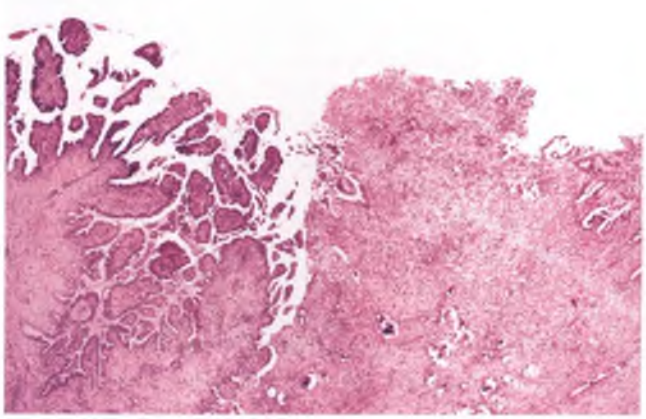

FIGURE 7.21. Exophytic serous borderline tumor (left) associated with an autoimplant that resembles a peritoneal implant of the noninvasive desmoplastic type (right).

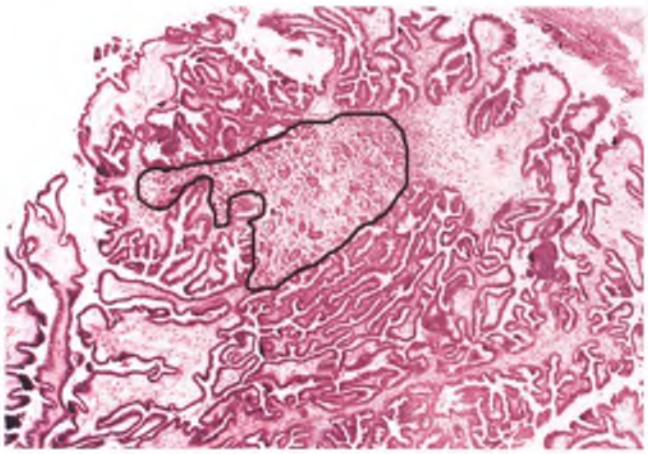

FIGURE 7.22. Serous borderline tumor with microinvasion. The focus of microinvasion, which is outlined in *black,* is located within the connective tissue core of the papillary tumor and is composed of an admixture of single cells, cell clusters, and simple papillae.

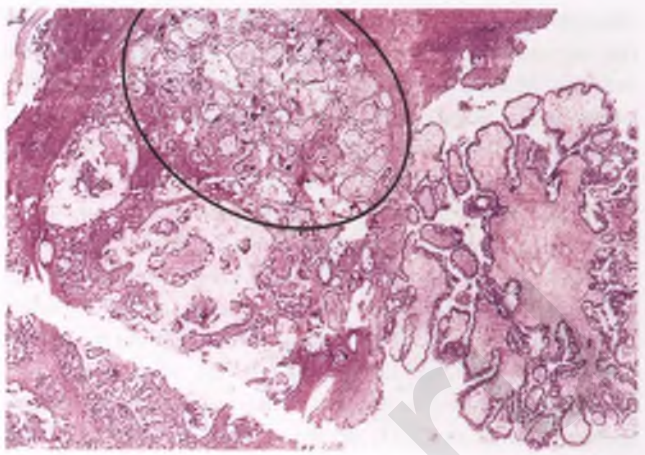

FIGURE 7.24. Serous borderline tumor with microinvasion. The *circled area* represents a focus of the inverted macropapillary pattern of stromal invasion, with bland macropapillae often surrounded by cleft-like spaces haphazardly distributed within the ovarian stroma. Small foci of conventional microinvasion are admixed and nearby, as shown more clearly in Figure 7.25. No invasion is present within the focus of serous borderline tumor at right.

The presence of microinvasion has traditionally been thought to not adversely impact the prognosis,[25,27,31,39,40] but a recent study of a large group of patients has suggested that this finding may be a long-term, low-level risk factor for disease progression to low-grade serous carcinoma in nonpregnant patients.[41]

Peritoneal Implants of Serous Borderline Tumor[27,43,44]

About one-third of SBTs are associated with peritoneal implants.[25,31] These implants are found much more frequently in SBTs with an exophytic component (i.e., surface papillations) than in completely endophytic tumors, which supports a mechanism whereby neoplastic epithelial cells are shed from surface papillae of the ovary and implanted on peritoneal surfaces (the implantation theory).[30,45] However, this need not be the sole mechanism for the development of peritoneal implants; some such lesions may arise independently from foci of endosalpingiosis within the peritoneum (the multifocal field effect theory).[46] In the latter circumstance, these serous epithelial proliferations would not actually be implants, but they are still referred to as such as a matter of convenience.

Whatever their origin, peritoneal implants of SBT are divided into noninvasive and invasive types, and this

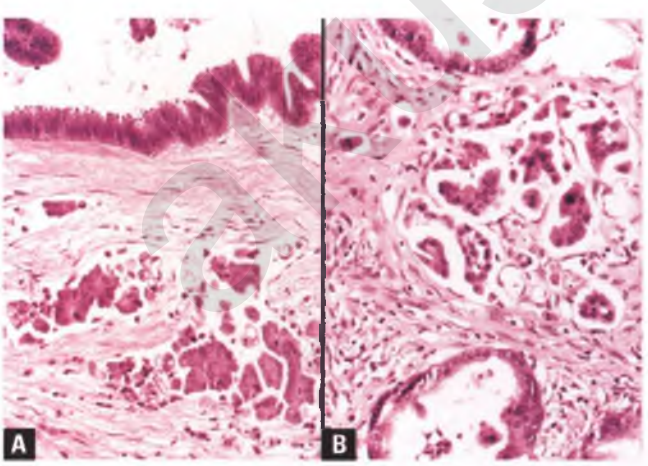

FIGURE 7.23. **A,B:** Serous borderline tumor with microinvasion. The microinvasive foci are surrounded by clear spaces and consist of individual cells and small papillary clusters of cells with abundant eosinophilic cytoplasm, which contrasts with the larger glands and cysts of the noninvasive portion of the neoplasm.

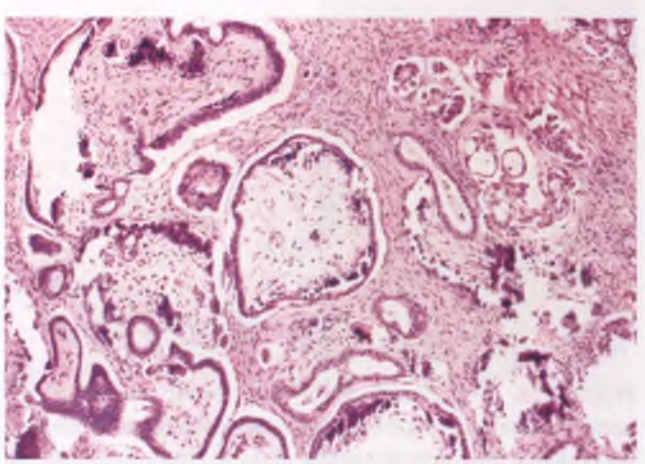

FIGURE 7.25. Serous borderline tumor with microinvasion. In addition to the invasive macropapillae surrounded by cleft-like spaces, a focus of conventional microinvasion is present in the upper right portion of the image.

distinction is of prognostic and therapeutic significance (see section on behavior and prognosis of serous borderline tumors). As discussed below, noninvasive implants are further categorized as being of epithelial or desmoplastic type.[43] When diagnosed using conventional criteria, invasive implants are found in only 10% to 15% of patients with peritoneal involvement by SBT.[30,31,43,47] Although invasive implants are uncommon, they are frequently admixed with noninvasive implants, which necessitates a careful gross examination and adequate sampling of cases that fail to demonstrate invasion in the initial sections. Whether an invasive implant represents a metastasis from an undersampled SBT with occult foci of invasion, development of a peritoneal carcinoma that is independent of the SBT, or is the result of a proliferation of implanted neoplastic cells in a microenvironment that is more conducive to the development of stromal invasion is a matter of speculation.[46]

Noninvasive implants of epithelial type are often not detectable with the naked eye, but may appear as small granular lesions. In contrast, noninvasive implants of desmoplastic type are often recognized as small plaques or nodules on the surface of the peritoneum, and within the omentum may appear as a tracery of white fibrous tissue representing expanded septa between fat lobules (Fig. 7.26). Most invasive implants are found in the omentum and are often grossly apparent as small stellate masses akin to small breast carcinomas.

Histologically, noninvasive implants of epithelial type are composed of well-delimited aggregates of tufted papillary projections that are usually found within mesothelial-lined invaginations or between lobules of omental fat (Fig. 7.27). The cells lining the invaginations have been shown to be immunoreactive for calretinin, which supports their mesothelial nature.[48]

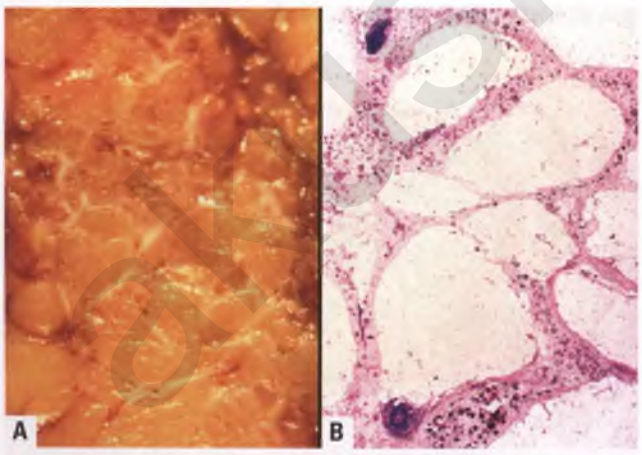

FIGURE 7.26. Implant of serous borderline tumor, noninvasive desmoplastic type, involving the omentum. **A:** The sectioned surface of the omentum exhibits a fine tracery of white fibrous tissue. **B:** The preexisting septa between omental fat lobules are expanded by noninvasive desmoplastic implants that are associated with numerous psammoma bodies and two lymphoid aggregates, but invasion of adipose tissue is not present.

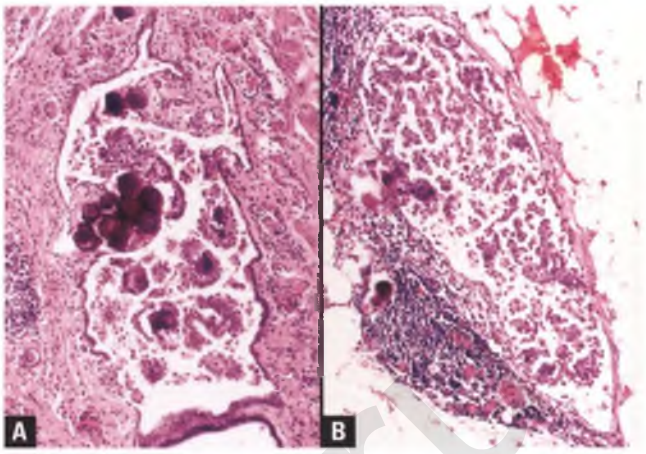

FIGURE 7.27. Implants of serous borderline tumor, noninvasive epithelial type. **A:** Peritoneum. **B:** Omentum. In both examples, a single layer of flattened to cuboidal mesothelial cells encircles a proliferation of delicately branching papillae associated with psammoma bodies. There is no desmoplastic or granulation tissue-like response to the serous implants.

The papillary epithelial cells exhibit mild nuclear atypia, are mitotically inactive, and are often associated with psammomatous calcifications. The presence of this type of implant does not provoke a fibroblastic response.

The plaques, nodules, and expanded omental septa related to noninvasive implants of the desmoplastic type consist of a minor epithelial element that may take the form of glands, papillae, small epithelial nests, and isolated single cells that is dominated by a stromal component that is often studded with psammoma bodies (Figs. 7.26B and 7.28). The stroma typically has a loose, granulation tissue-like appearance that is

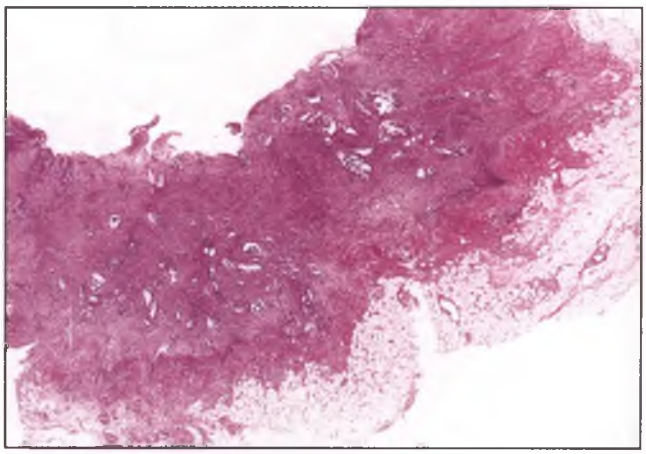

FIGURE 7.28. Implant of serous borderline tumor, noninvasive desmoplastic type. This 4 mm thick peritoneal plaque contains scattered gland-forming serous epithelial elements embedded within a fibroblastic stroma that is inflamed and partially hemorrhagic. There is no invasion of the underlying adipose tissue.

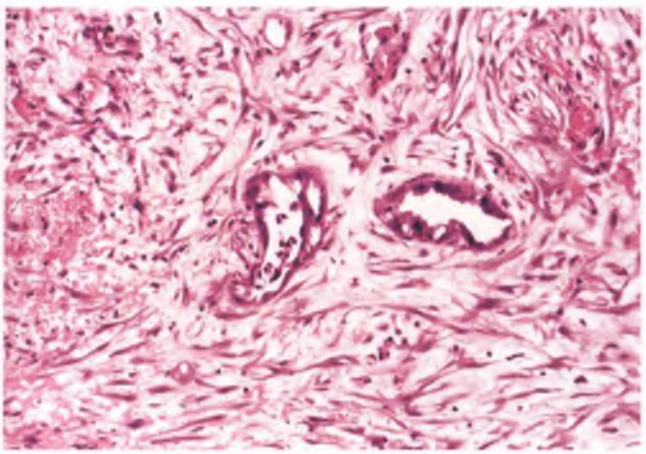

FIGURE 7.29. Implant of serous borderline tumor, noninvasive desmoplastic type. Two glands lined by epithelial cells with mild to moderate nuclear atypia are present within a loose, granulation tissue-like stroma that contains a focus of fibrin deposition at left.

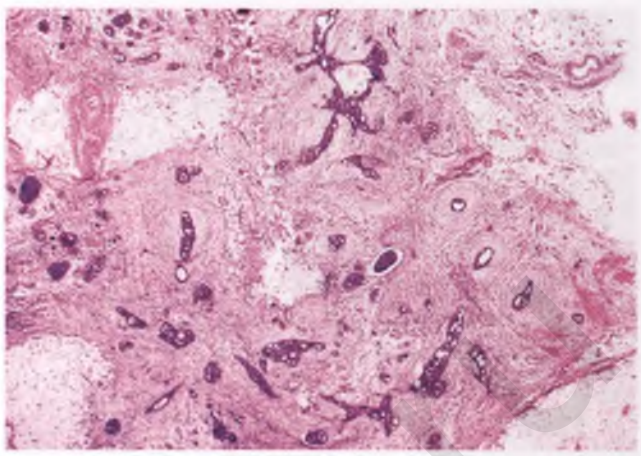

FIGURE 7.31. Invasive implants of serous borderline tumor. Neoplastic glands, often with pointed ends or a cribriform pattern, raggedly infiltrated omental adipose tissue with an associated desmoplastic response.

often associated with inflammation, recent hemorrhage, and/or fibrin deposition (Fig. 7.29). These implants are generally easily stripped off of the peritoneal surface, and this feature can be used to presume the noninvasive nature of the implant when underlying tissue is absent.[32,43,49] When associated tissue is present, it is the sharp demarcation of the noninvasive implant from the adjacent stroma that more definitively distinguishes it from an invasive implant.

Invasive implants classically feature an irregular, haphazardly infiltrative border with involved tissue, which is usually the omentum (Fig. 7.30). They typically resemble metastatic low-grade serous carcinoma, often with a greater amount of neoplastic epithelium and a greater degree of nuclear atypia than that seen in noninvasive implants, a cribriform glandular component, and a desmoplastic stroma (Figs. 7.31 and 7.32). Occasionally, peritoneal implants are composed of obviously malignant cells without definitive stromal invasion, as can occur in frank serous carcinoma; such lesions are fully malignant and should be considered metastatic carcinoma.[32]

In addition to the established features of invasive implants as described in the preceding paragraph, the group at Johns Hopkins has proposed expanding the invasion criteria to include the findings of solid epithelial nests

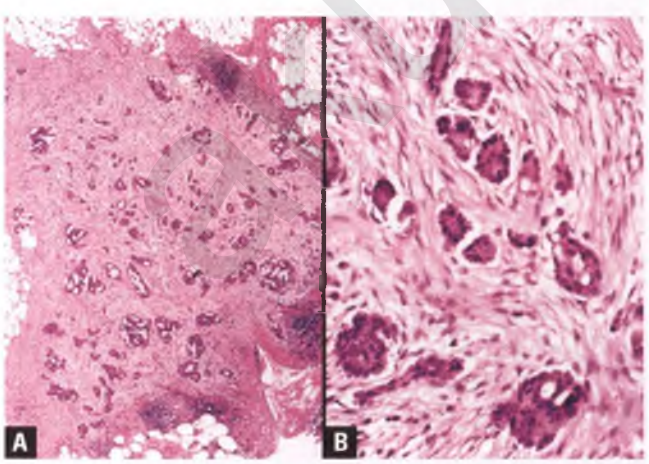

FIGURE 7.30. Invasive implant of serous borderline tumor. **A:** This stellate mass is beyond what could be explained by tangential sectioning or septal expansion by a noninvasive process. **B:** In this example, the degree of nuclear atypia is similar to that seen in most noninvasive implants.

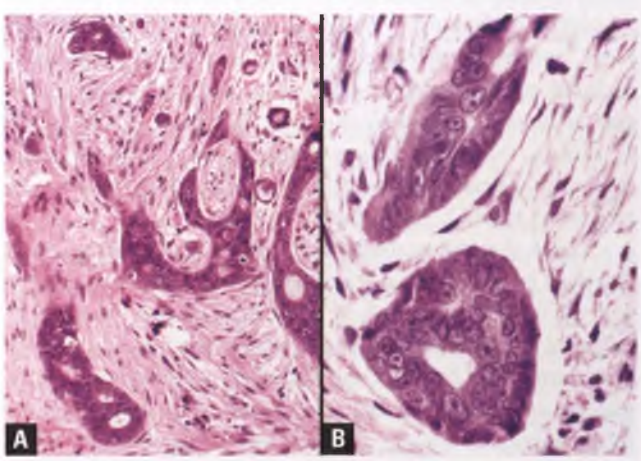

FIGURE 7.32. Invasive implants of serous borderline tumor. **A:** Glands with pointed ends, peculiar shapes, and intraglandular bridges are associated with a fibroblastic stromal reaction. **B:** This degree of nuclear atypia, with chromatin clearing and prominent nucleoli, is often seen in invasive implants and exceeds that usually seen in noninvasive implants.

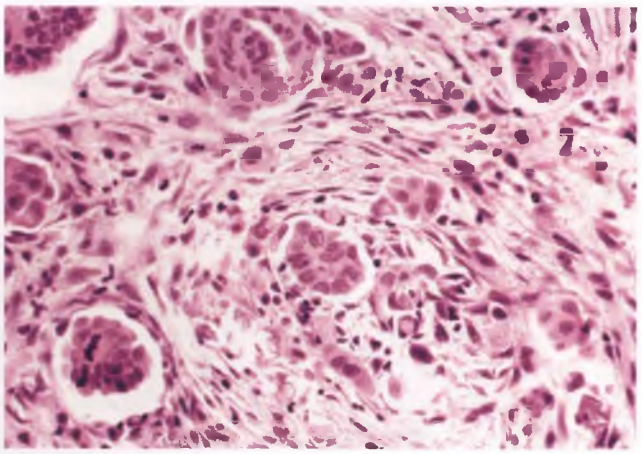

FIGURE 7.33. Implants of serous borderline tumor composed of small nests of low-grade neoplastic epithelium surrounded by clefts. A few isolated tumor cells, which can be seen in noninvasive desmoplastic implants, are also present within the reactive fibroblastic stroma. Some investigators classify lesions with epithelial nests surrounded by clefts as invasive implants solely on the basis of this finding, but this is a minority viewpoint (see text).

surrounded by clefts (Fig. 7.33) and implants with micropapillary architecture.[44†] Although there is no doubt that these clefted and micropapillary patterns are often seen in invasive implants, their validity as standalone indirect markers of stromal invasion has not been confirmed in other studies,[31,49] and these more liberal criteria have not been widely accepted. It is noteworthy that in the study advocating the use of these additional criteria that their presence is not associated with a statistically significant increased death rate as compared to patients with noninvasive implants, but rather with a dramatically increased incidence of patients who are alive with what the authors term "progressive disease," which subjectively and circularly includes patients with residual or recurrent "invasive" disease as loosely defined by the investigators.[44] To add to the confusion, the identification of single tumor cells within an implant has been used as a criterion for invasive implants by the group at M.D. Anderson.[46,50]

Given that the established criteria for invasive implants as described by D. Bell et al.[43] identifies a small subset of patients with SBTs with a high risk of death from disease, whereas the proposed addition of other criteria for invasion (solid epithelial nests surrounded by clefts, micropapillary architecture, and the presence of single tumor cells) only serves to needlessly increase the frequency of invasive implants and to significantly dilute their prognostic significance, it is recommended that invasive implants not be diagnosed unless they meet the established criteria.[27] It should be noted that it is not always possible to definitively classify an implant as invasive or noninvasive, such as when the interface between the implant and adjacent tissue is neither obviously rounded nor frankly infiltrative. In this situation, classifying the implant as indeterminate for invasion is appropriate.[30]

Fallopian Tube Involvement in Serous Borderline Tumor[51,52]

The tubal lumens of patients with ovarian SBTs have a propensity to contain papillary fragments of tumor. This finding tends to occur in patients with advanced-stage disease, and is often associated with psammomatous calcifications.

Lymph Node Involvement in Serous Borderline Tumor[53,54]

About 20% to 30% of patients with SBTs have involvement of regional lymph nodes; such involvement is usually associated with peritoneal implants. Endosalpingiosis is commonly found adjacent to or seemingly as part of lymph node deposits of SBT, which has led to the proposal that some intranodal foci of SBT may arise within endosalpingiosis.[55] Since conventional types of lymph node involvement by SBT are not an independent adverse prognostic factor[25,30] and SBT may develop within the lymph node, a statement in the pathology report that simply documents such involvement is preferred over use of the term "metastatic SBT."

Histologically, lymph node involvement by SBT is manifested by aggregates of serous epithelial cells with mild to moderate nuclear atypia in various patterns that include individual cells, small papillary clusters, cribriforming glands, and intraglandular proliferations within the sinuses and/or parenchyma of the lymph node (Figs. 7.34 and 7.35). In a less common

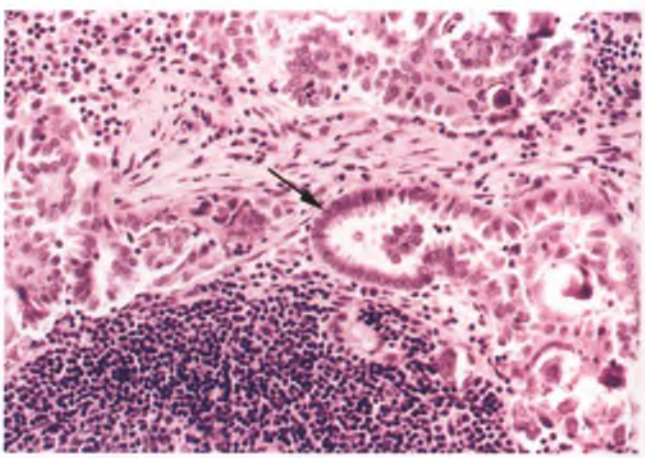

FIGURE 7.34. Serous borderline tumor involving pelvic lymph node. The lesion is composed of aggregates of small papillary clusters and individual tumor cells with intermingled psammoma bodies. The edge of one of these aggregates may represent a focus of preexisting endosalpingiosis (*arrow*).

†For whom the Bell toiled: Dr. Karen A. Bell worked with Dr. Robert Kurman at Johns Hopkins and was the lead author on the article espousing expanded criteria for invasive implants; Dr. Debra A. Bell worked with Dr. Robert Scully at Harvard and was the lead author on the article that described the classic criteria for invasive implants.

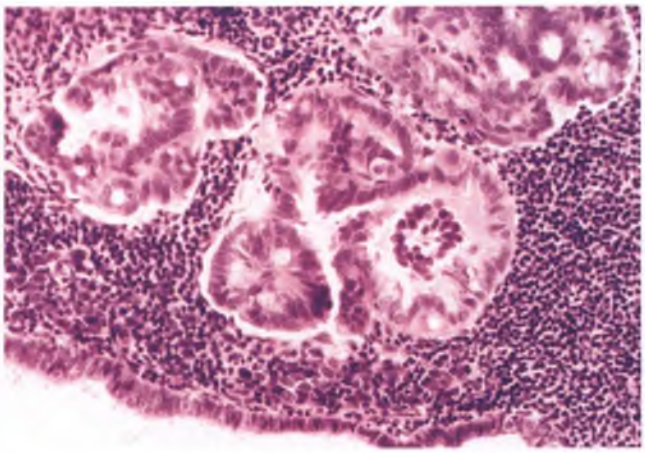

FIGURE 7.35. Serous borderline tumor involving pelvic lymph node. In addition to the cribriforming glandular aggregates of serous borderline tumor, a portion of a cystically dilated focus of endosalpingiosis is present at the bottom.

pattern, aggregates are formed by tumor cells with abundant eosinophilic cytoplasm that are found as closely packed single cells and as small cohesive units (Fig. 7.36). These eosinophilic cells resemble those seen in foci of microinvasion, from which they may be derived in some cases. When pure, this pattern may require immunohistochemistry to distinguish it from intranodal hyperplastic mesothelial cells; in this situation, calretinin can be used as a marker for mesothelial cells and Ber-EP4 or PAX8 as a marker for SBT. The only pattern of lymph node involvement that may adversely impact prognosis (via increased likelihood of disease recurrence) is one in which the intranodal tumor forms a noncystic mass >1 mm without intervening lymphoid tissue, often in association with a desmoplastic stroma and a micropapillary architecture that results in a

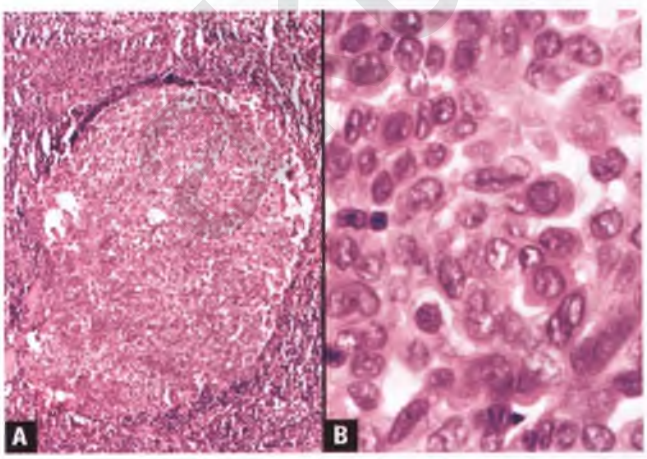

FIGURE 7.36. **A,B:** Serous borderline tumor involving pelvic lymph node. This pattern features nested aggregates of tumor cells with eosinophilic cytoplasm.

histologic appearance that to some observers (myself included) fulfills the criteria for metastatic low-grade serous carcinoma.

When lymph nodes are involved in recurrent SBT, tumor may rarely be found in supradiaphragmatic (e.g., supraclavicular or cervical) locations and/or may have undergone progression to a more aggressive histologic pattern.[30,56-59]

Differential Diagnosis of Serous Borderline Tumor

Features that help to distinguish SBT from focally proliferative serous cystadenoma, clear cell carcinoma with a prominent papillary pattern, serous carcinoma, and retiform Sertoli-Leydig cell tumor are discussed in the sections on these other entities. Endocervical-like mucinous borderline tumor contains papillae that are predominantly lined by mucinous epithelial cells that are inconspicuous or absent in SBT, and borderline tumors of mixed cell type contain various admixtures of serous, mucinous, endometrioid, and/or squamous elements.

Behavior and Prognosis of Serous Borderline Tumor

Patients with stage I SBTs with adequate follow-up have a 95% to 98% survival rate, with recurrences eventually developing in about 10% of these patients.[30,60] Literature that reports 99% to 100% survival and much lower recurrence rates for stage I SBTs is largely based upon studies in which patients were followed for too short a time interval.[25] Many of the recurrences in stage I SBTs are low-grade serous carcinomas, which may occur many years and even decades after the initial diagnosis, and often ultimately result in the death of these patients.[30,37,57,60] Recurrences of SBTs as high-grade serous carcinoma also occur, but are rare.[56,59] Because of the frequently long time interval between treatment for the primary tumor and the detection of recurrent disease, it is uncertain how many cases of newly detected serous carcinoma actually represent progression of an SBT, recurrence of an ovarian serous neoplasm that had occult foci of invasion, or development of an independent primary tumor from foci of endosalpingiosis.[60]

For stage II and stage III SBTs with noninvasive implants, recurrences and disease-related deaths also often occur well beyond 5 years after the initial diagnosis, resulting in deceptive 5-year survival rates on the order of 95%.[25,47] In one of the few studies that followed patients for an adequate period of time, almost half of such patients eventually recurred, with less than a quarter of these recurrences occurring in the first 5 years and about a third occurring 10 or more years after the resection of the primary tumor.[61] In that study, 25% of patients with stage II to III SBTs eventually died of recurrent disease, which in most cases represented low-grade serous carcinoma (transformed SBT vs. recurrence of undersampled serous carcinoma vs. second primary tumor).[61]

It is generally agreed that patients with stage I SBTs and SBTs with noninvasive implants should be treated surgically, followed for the long-term, and only treated with chemotherapy if their disease recurs as invasive carcinoma.[26,31,36] In most studies, the presence of invasive implants of conventional type[32,43] in SBTs is a significant adverse prognostic factor, with at least half

of such patients dying of disease.[30,31,43,47] It is these patients who may potentially benefit from adjuvant chemotherapy.

Low-Grade Serous Carcinoma[14,17,20,35,62–64]

Low-grade serous carcinoma comprises only about 10% of ovarian serous carcinomas, and typically presents as a pelvic mass in women with an average age of 45 to 50 years. Most such tumors involve both ovaries, and the vast majority of patients have extraovarian disease at the time of presentation. There is strong evidence for a dualistic pathway of ovarian serous carcinogenesis, which supports a division of serous carcinomas into two rather than three grades. Briefly, low-grade serous carcinomas are thought to arise at a leisurely pace from SBTs (particularly the micropapillary variant), frequently harbor a mutation of the KRAS, BRAF, or ERBB2 genes, and only rarely have a p53 mutation. As discussed below, high-grade serous carcinomas are thought to arise via an independent pathway and exhibit a different mutational pattern. The distinction of low-grade versus high-grade serous carcinoma is clinically relevant, since the disease course of high-stage, low-grade serous carcinoma is considerably more indolent than it is for high-grade serous carcinoma of similar stage.

Low-grade serous carcinoma has an average size of 8 cm and commonly has a grossly recognizable noninvasive papillary component. Histologically, these tumors often contain numerous psammoma bodies with an invasive component that is typically composed of epithelial nests and micropapillae that are haphazardly dispersed within the stroma and often surrounded by clear spaces (Figs. 7.37). A much less common pattern of stromal invasion is one that is dominated by inverted macropapillae surrounded by cleft-like spaces.[65] This pattern can mimic a serous adenofibroma and is illustrated in the section on microinvasive SBTs (see Fig. 7.24). An example of a low-grade serous carcinoma arising in association with the micropapillary variant of SBT is illustrated in Figure 7.38. It should be noted that the prominent nested and micropapillary architectural patterns that are typical of low-grade serous carcinoma can also be seen in the high-grade form,[66] which is distinguished primarily by its nuclear features.

Within the context of low-grade serous carcinoma, the concept of what constitutes "low-grade" nuclear atypia does not correlate directly with nuclear grading of other carcinomas, such as those of breast origin. In the two-tier grading system of Malpica et al.,[17] low-grade serous carcinomas can have nuclei with up to moderate atypia and nucleoli can be conspicuous (Fig. 7.39), which are features that would not be allowed in breast carcinoma of low nuclear grade. In this system, the presence of only mild variation in nuclear size and shape and the

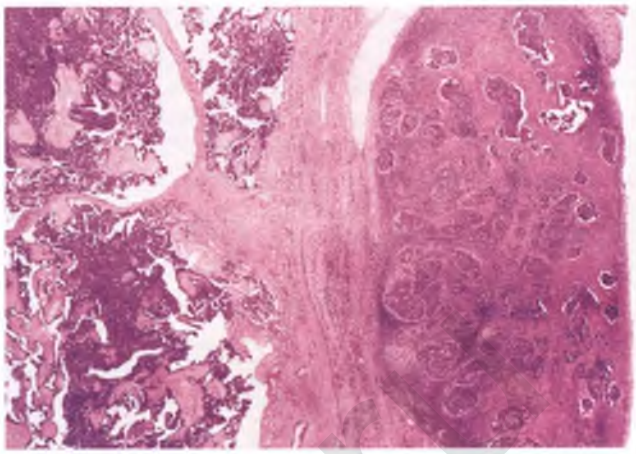

FIGURE 7.38. Low-grade serous carcinoma infiltrates the ovarian stroma at right, and is seen arising adjacent to the micropapillary variant of serous borderline tumor.

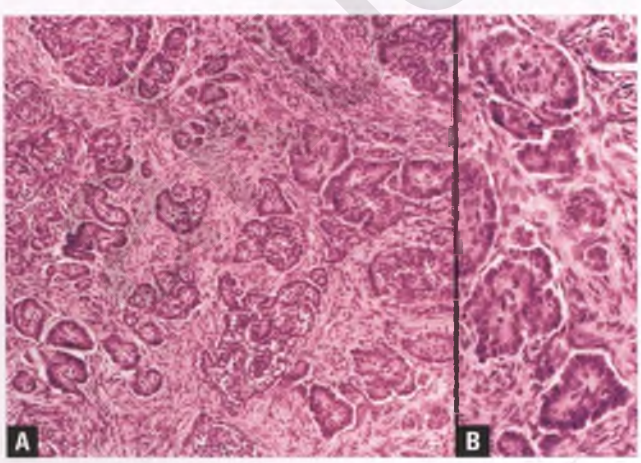

FIGURE 7.37. Serous carcinoma, low-grade. **A:** Nests and micropapillary groups of neoplastic epithelial cells that are often surrounded by clear spaces infiltrate the ovarian stoma. **B:** The neoplastic cells have low-grade nuclear features and a low mitotic rate.

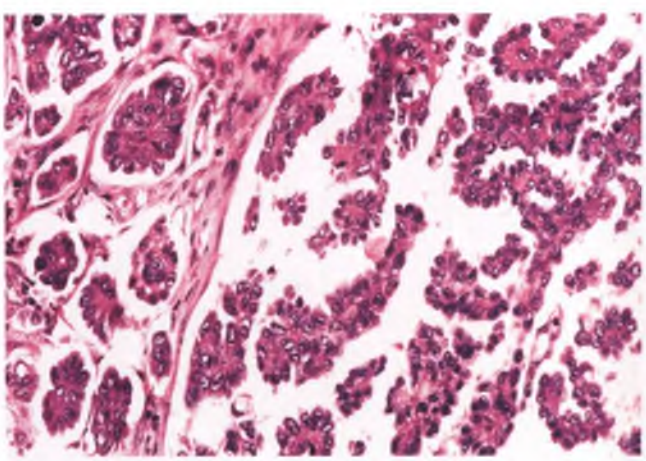

FIGURE 7.39. Serous carcinoma, low-grade. In this example, haphazardly oriented micropapillae are surrounded by clear spaces. Although many of the neoplastic cells have easily visible nucleoli, they are considered low grade because of their mild variation in size and shape, low mitotic rate, and uniform chromatin pattern.

evenly distributed chromatin pattern are important determinants of low-grade status.

In those cases in which it is difficult to determine whether the nuclei are low or high grade, the mitotic rate comes into play. Malpica et al.[17] have proposed that "tweener" serous carcinomas with ≤12 mitotic figures per 10 high power fields be designated as low grade, whereas another group's experience has led them to propose a lower threshold of 5 mitotic figures per 10 high power fields.[67]

In addition to less impressive nuclear atypia and mitotic activity, the absence of tumor necrosis and an immunoprofile in which the Ki-67 proliferation index is low and reactivity for p53 and p16 is not strong and diffuse can be used to support a diagnosis of low-grade over high-grade serous carcinoma.[62] Another method of double-checking the low-grade versus high-grade status of a serous carcinoma is to grade it using the three-tiered Shimizu-Silverberg system, since virtually all cases of grade 1 tumors translate into low grade and the vast majority of grade 2 or 3 tumors can be considered high grade.[17] Other tumors that can be confused with serous carcinomas of either grade are discussed in the section on the differential diagnosis of high-grade serous carcinoma.

Serous psammocarcinoma, which is a variant of low-grade serous carcinoma that occurs in the ovary and peritoneum, is discussed and illustrated in the section on peritoneal serous carcinoma in Chapter 8.

High-Grade Serous Carcinoma[9,14,62]

High-grade serous carcinoma is the most common type of ovarian cancer, and represents about 90% of ovarian serous carcinomas. Its clinical presentation is similar to that of low-grade serous carcinoma, except that it tends to present in older women (mean age of 60 years). Unlike low-grade serous carcinoma, high-grade serous carcinoma is an aggressive neoplasm that evolves rapidly and whose major developmental pathway is thought to involve a p53 mutation rather than a mutation in the KRAS, BRAF, or ERBB2 genes. The actual origin of many ovarian high-grade serous carcinomas is probably intraepithelial carcinoma of the distal fallopian tube, although de novo development via transformation of ovarian epithelial inclusion cysts (which may also ultimately be of tubal origin) is another possibility.[11,13] The surface epithelial origin of these tumors that was favored for so many years is now considered unlikely.

Grossly, high-grade serous carcinomas average about 8 cm in diameter and are predominantly solid tumors with foci of hemorrhage and necrosis, which is an appearance that is indistinguishable from many other types of poorly differentiated ovarian cancer (Fig. 7.40). Occasionally, the tumor may consist entirely or predominantly of a conglomeration of exophytic, tan to red, papillary excrescences or plaques on the surface of the ovary (Fig. 7.41). When ovarian involvement represents the bulk of a tumor with this appearance, the neoplasm is conventionally classified as a serous surface carcinoma of ovarian origin, although with our current understanding it is likely that many such tumors actually originate within the fimbriae of the fallopian tube. Although uncommon, some high-grade serous carcinomas appear to develop from adenomatous, borderline,

FIGURE 7.40. Serous carcinoma, high-grade. The sectioned surface demonstrates an admixture of solid tumor, geographic areas of necrosis, and cystic degeneration with associated hemorrhage.

or low-grade malignant serous tumors.[68] In such cases, careful gross examination and adequate sampling play an important role in making an accurate diagnosis, particularly at the time of an intraoperative consultation (Figs. 7.42 and 7.43).

Histologically, high-grade serous carcinoma usually exhibits at least focal areas of destructive stromal invasion and architecturally frequently consists of sheets of tumor cells with some differentiation into slit-like glandular spaces admixed with variably prominent papillae, solid nests, and tubules (Fig. 7.44). In this context, massive replacement of the ovarian stroma by a neoplastic epithelial proliferation of this type is considered sufficient evidence of stromal invasion. In the grading system

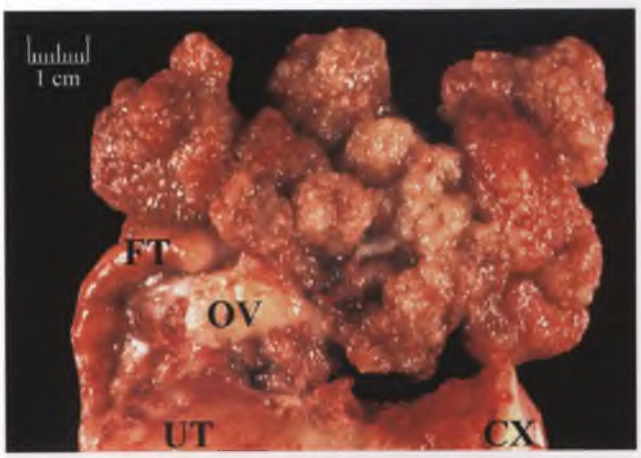

FIGURE 7.41. Serous surface carcinoma, high-grade. Attached to the ovarian surface are polypoid aggregates composed of granular-appearing papillae. Although currently classified as ovarian carcinoma, it is easy to see how such a tumor could have originated from the fimbriae of the fallopian tube. FT, fallopian tube; OV, ovary; UT, uterine corpus; CX, cervix.

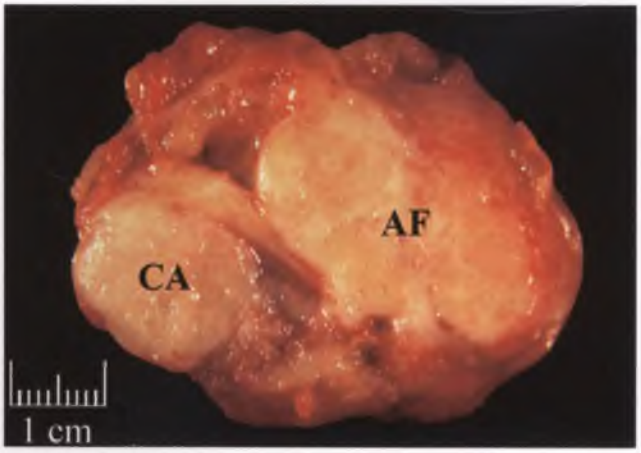

FIGURE 7.42. Serous carcinoma associated with serous adenofibroma. The nodule of carcinoma (CA) is soft and fleshy, whereas the larger adenofibromatous nodule (AF) is firm and trabeculated. In an intraoperative setting, both areas should be sampled for frozen section analysis.

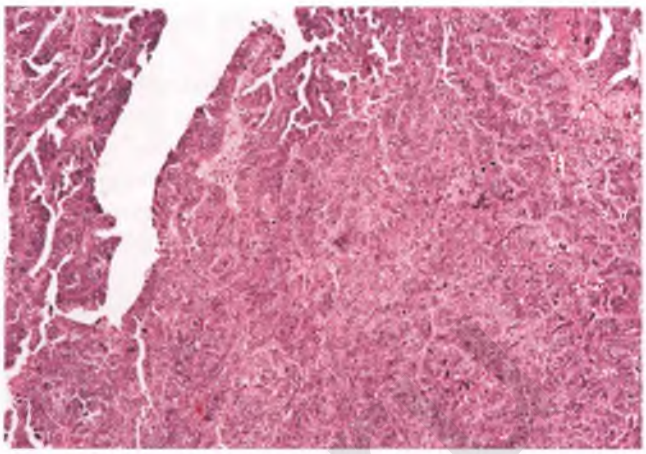

FIGURE 7.44. Serous carcinoma, high-grade. Although the solid growth pattern predominates in this image, papillae and slit-like spaces are also evident.

of Malpica et al., it is the marked variation in nuclear size and shape, irregular chromatin distribution, and variable presence of macronucleoli that define the high-grade nuclei that characterize high-grade serous carcinoma (Figs. 7.45 and 7.46). Mitotic activity is brisk, and atypical division figures are usually readily identified. Psammoma bodies, foci of tumor necrosis, and bizarre tumor giant cells are commonly present.

As indicated above, some serous carcinomas lack classic destructive stromal invasion, but can be confidently diagnosed as fully malignant by virtue of confluent carcinomatous elements. More difficult is the infrequent situation in which papillary serous tumors exhibit the combination of numerous high-grade nuclei in conjunction with a lack of both carcinomatous confluence and obvious stromal invasion (Fig. 7.47). Such tumors will usually have abnormally cellular papillae and should be sampled extensively in an attempt to find foci of destructive infiltration; even if invasion is not identified, many experts diagnose such tumors as high-grade serous carcinoma.[23] Until outcome data on a large number of well-sampled tumors of this type becomes available, it is not clear whether this approach is correct or whether it may be more appropriate to label such tumors as SBTs with intraepithelial carcinoma. Based upon the assumption that an exophytic tumor with this feature is more likely to seed the peritoneal cavity than a similar tumor that is completely intracystic, my preference is to

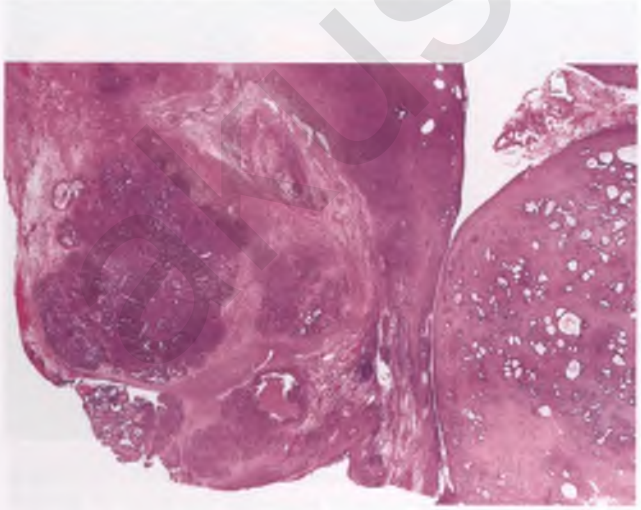

FIGURE 7.43. Serous carcinoma associated with serous adenofibroma. This low-magnification view of the tumor in the preceding figure shows the nodule of grade 3 serous carcinoma (left) adjacent to the serous adenofibroma (right).

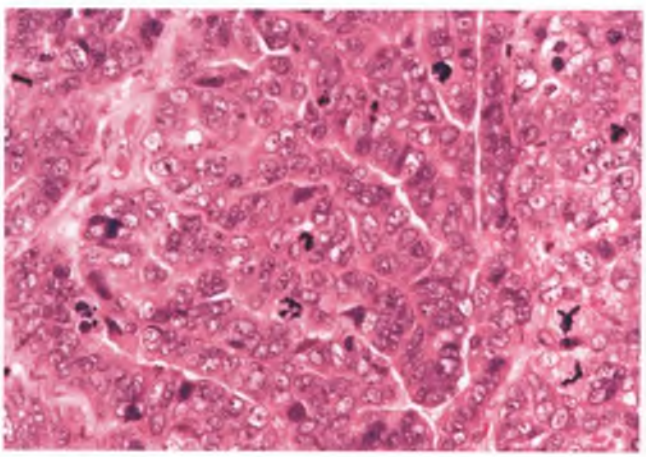

FIGURE 7.45. Serous carcinoma, high-grade. In this high-magnification view, the tumor cells exhibit significant nuclear pleomorphism and brisk mitotic activity with atypical mitotic figures. Note the presence of slit-like spaces, which is characteristic of tumors with serous differentiation.

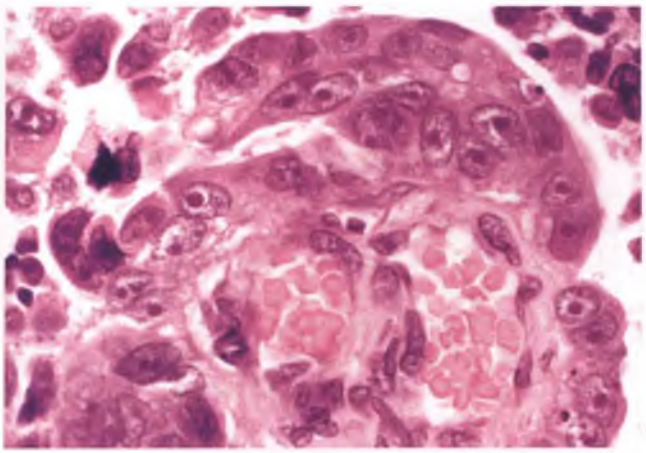

FIGURE 7.46. Serous carcinoma, high-grade. This example features tumor cells with macronucleoli.

diagnose the former as high-grade serous carcinoma and the latter as an SBT with intraepithelial carcinoma.

Immunohistochemically, ovarian serous carcinoma of any grade typically demonstrates nuclear immunoreactivity for WT-1, and high-grade serous carcinoma generally exhibits significantly higher levels of p53, p16, and MIB-1 immunoreactivity than the low-grade variant.[62,69]

Differential Diagnosis[9]

As discussed in the section on low-grade serous carcinoma, distinction of high-grade serous carcinoma from its low-grade counterpart is based primarily upon nuclear features and secondarily upon mitotic activity, with occasional assistance from immunohistochemistry.

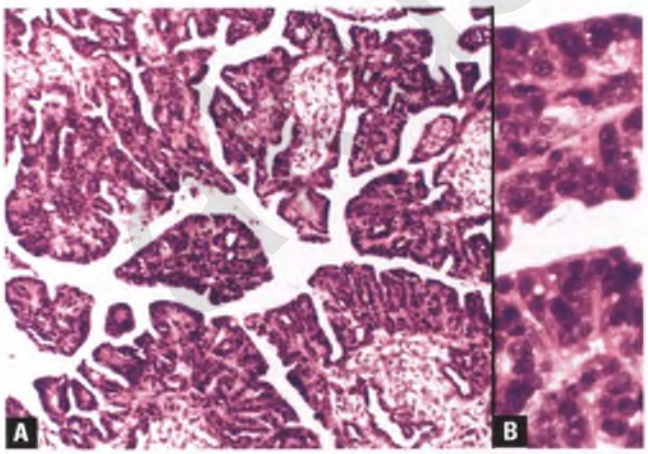

FIGURE 7.47. High-grade serous carcinoma without identifiable stromal invasion (serous borderline tumor with intraepithelial carcinoma). **A:** The papillae are cellular, but stromal invasion is not identified. **B:** This high-magnification view demonstrates the presence of numerous high-grade nuclei with macronucleoli.

Other entities in the differential diagnosis include SBT, endometrioid carcinoma, clear cell carcinoma, malignant epithelioid mesothelioma, metastatic serous carcinoma of endometrial or peritoneal origin, and metastatic breast carcinoma.

- In contrast to serous carcinoma, SBT features less impressive nuclear atypia, an orderly architectural pattern, and a lack of stromal invasion (other than possible microinvasion). The issue of how to handle a serous tumor with borderline-like architecture and high-grade nuclear features is addressed in the above discussion.
- Endometrioid carcinoma may have a papillary architecture, but these structures are more villiform and less complex than the papillae of serous carcinoma, and are not typically associated with epithelial budding and tufting. The presence of patches of squamous differentiation, tubular rather than slit-like glands, and associated endometriosis also favor endometrioid carcinoma, whereas the presence of psammoma bodies favors serous carcinoma. Immunoreactivity for WT-1 also supports serous over endometrioid differentiation.[18]
- Clear cell carcinoma with papillary architecture can resemble serous carcinoma, but the presence of an admixed tubulocystic pattern, tumor cells with clear cytoplasm, hobnail cells, and papillae with hyalinized stromal cores facilitate recognition of the clear cell nature of the tumor. In addition, high-grade serous carcinoma also almost always exhibits a much higher mitotic rate than clear cell carcinoma.[70] In difficult cases, immunohistochemical staining for WT-1, estrogen receptor (ER), and hepatocyte nuclear factor (HNF)-1β can be a useful diagnostic aid. Serous carcinomas are typically WT-1 positive, ER positive, and HNF-1β negative, whereas clear cell carcinomas generally have the opposite immunophenotype.[71]
- The differential diagnosis of serous carcinoma versus malignant mesothelioma applies equally to ovarian and peritoneal-based tumors, and is discussed in the section on mesothelioma in Chapter 8.
- In the presence of a known endometrial serous carcinoma, an ovarian serous carcinoma is likely to be a metastasis when the endometrial tumor exhibits deep myometrial invasion and/or widespread angiolymphatic invasion, but in some cases the distinction between dual primary tumors versus a primary in one site and a metastasis in the other is nothing more than an educated guess. The distinction between high-stage ovarian serous carcinoma and primary peritoneal serous carcinoma with ovarian involvement is discussed in Chapter 8.‡
- In cases of metastatic breast carcinoma with serous-like features, the clinical history and a comparative slide review should facilitate the correct interpretation. This diagnosis

‡The differential diagnosis of ovarian serous carcinoma with metastatic tubal serous carcinoma has been intentionally omitted, since it appears that many "ovarian" serous carcinomas actually originate in the fallopian tube.

can be further substantiated by demonstrating lack of immunoreactivity for WT-1 and PAX8, which are markers that are typically expressed in ovarian serous carcinoma and absent in breast carcinoma.[72,73] Although gross cystic disease fluid protein-15 and mammaglobin are fairly specific markers for carcinomas of breast origin and can be added to the immunohistochemical panel, their suboptimal sensitivity limits their utility.[72,74,75]

Pattern of Spread and Prognosis

As is true for ovarian carcinoma in general, intraabdominal spread is typically manifested as nodules studding the peritoneal surface, replacement of portions of the omentum, and involvement of regional lymph nodes. When visceral organs are involved, it almost always represents growth of metastatic carcinoma that began on the serosal surface. That said, parenchymal metastases to the liver and spleen do occur on rare occasions (Fig. 7.48).[76,77]

The prognosis of patients with advanced stage high-grade serous carcinoma is poor.

Mucinous Tumors

Mucinous ovarian tumors form cysts, glands, or papillae whose epithelial lining contains a significant number of cells with abundant intracytoplasmic mucin exhibiting endocervical-like or gastrointestinal features.[78] These tumors account for about 15% of all primary ovarian tumors.[1,16] Using data from unselected series from the 1980s, about 75% are considered mucinous cystadenomas, 10% borderline tumors, and 15% carcinomas.[1,16] However, current criteria would shift some borderline tumors into the benign category and some carcinomas into the borderline group, such that these percentages are probably on the order of 85%, 10% and 5%, respectively (see below). Tumors of gastrointestinal type far outnumber those resembling endocervical cells.

FIGURE 7.48. High-grade serous carcinoma of ovarian origin with parenchymal metastasis to the spleen (sectioned surface).

Mucinous ovarian tumors have many controversial aspects, treacherous simulators, and interesting associations, which are outlined below and further discussed either in this section or later in this chapter:

- Criteria for mucinous carcinoma from the 1970s were too liberal and were even more liberally applied in practice, and have since been revised.
- Many of the older studies on borderline and malignant mucinous ovarian tumors inadvertently included tumors of extraovarian origin in their database, which falsely increased the rate of malignant behavior of mucinous borderline tumors of gastrointestinal type and some presumed stage I mucinous carcinomas.
- The determination of endocervical-like versus gastrointestinal type is often not a straightforward exercise.
- Mucin granulomas and pseudomyxoma ovarii may be found within the stroma.
- The high frequency of gastrointestinal differentiation in ovarian mucinous tumors results in an immunophenotype that is distinct from that of other primary ovarian epithelial-stromal tumors.
- Mucinous ovarian tumors may be associated with mature cystic teratomas, as discussed later in this section, or with Brenner tumors (see section on mixed epithelial tumors).
- Functioning stromal steroid cells may be present in mucinous cystadenomas (see Fig. 7.305); this is a particularly common occurrence in those patients who are pregnant.[79]
- Mucinous cystadenomas are one of the more common tumor types to undergo torsion-related hemorrhage, as illustrated in Figure 6.63.
- Nodules within the walls of mucinous cystic neoplasms may represent a variety of benign or malignant processes, including sarcoma-like reactive lesions, anaplastic carcinoma, and true sarcoma.
- Ovarian mucinous neoplasms of gastrointestinal type are known for their heterogeneity; some sections may show only mucinous cystadenoma, whereas nearby areas or other sections of the same tumor may show a spectrum of abnormalities up to and including invasive carcinoma (see Figure 7.83). This feature, coupled with the ability of the ovaries involved by metastatic mucinous tumors to simulate primary ovarian neoplasia, makes adequate sampling especially important in this group of tumors and creates unique challenges in the setting of an intraoperative consultation.

Revised Criteria for Benign, Borderline, and Malignant Categories

The genesis for criteria formulated in the 1970s to separate mucinous carcinomas from borderline tumors was the observation that some mucinous ovarian tumors have the ability to metastasize without exhibiting a destructive pattern of stromal invasion within the ovary. In order to better identify those tumors with a likelihood of malignant behavior, Hart and Norris[80] developed a classification scheme in which mucinous

tumors that exhibited either destructive stromal invasion, confluent sheets of malignant-appearing glands with no intervening stroma, *or* glands and cysts lined by cells with severe nuclear atypia[§] and stratified to at least 4 cells in thickness qualified as mucinous carcinomas. It was not specified how widespread the stratification and nuclear atypia needed to be in order to qualify for the latter type of mucinous carcinoma. In addition, many pathologists ignored the requirement for severe nuclear atypia, which was underemphasized in the original report.[80]

The practice of diagnosing mucinous carcinoma solely on the basis of perceived excessive nuclear stratification is strongly discouraged; most such tumors are more appropriately diagnosed as borderline tumors or mucinous cystadenomas. Although the Hart and Norris method of categorizing mucinous ovarian tumors captured the few legitimate mucinous carcinomas with an expansile type of stromal invasion (see section on mucinous carcinoma), many of the carcinomas diagnosed solely on the basis of stratification and atypia have since been shown to have an excellent prognosis and are currently classified as mucinous borderline tumors with intraepithelial carcinoma.[81–85] A separate category of mucinous borderline tumors with microinvasion is also recognized and is associated with an equally excellent prognosis.[81–85]

Just as there has been justification for taking the lower end of mucinous carcinomas and placing them within specialized categories of borderline tumor, there are compelling reasons for reinterpreting the lower end of mucinous borderline tumors as mucinous cystadenomas. Virtually all of the malignant behavior that has been previously attributed to occasional cases of ovarian mucinous borderline tumors of gastrointestinal type is due to one of four situations: (a) misdiagnosis of a secondary tumor derived from a ruptured appendiceal mucinous cystadenoma (major source), (b) misdiagnosis of a deceptively benign-appearing metastatic tumor from an occult primary tumor originating in sites such as the pancreas, biliary tract, and endocervix (minor source), (c) an undersampled primary ovarian tumor with occult foci of invasion (minor source), and (d) misdiagnosis of an endocervical-like mucinous borderline tumor that subsequently recurs in an aggressive fashion (rare source).[81,86]

Thus, it appears that once the "contaminants" cited above have been culled from the group of mucinous borderline tumors of gastrointestinal type, we are left with a group of benign stage I tumors.[81,82,87,88] This revelation has prompted some to relabel the entire group of mucinous borderline tumors as "atypical proliferative" tumors, which is intended to indicate that these are benign tumors with an uppity epithelial proliferation.[81,85,89] However, others prefer to retain the "borderline" terminology, since (a) these mucinous neoplasms are often notoriously heterogeneous, (b) even extensively sampled borderline tumors may contain occult foci of intraepithelial or invasive carcinoma or areas where the diagnosis of intraepithelial carcinoma is difficult and subjective, and (c) no evidenced-based, valid sampling protocol exists that can exclude the presence of intraepithelial or invasive carcinoma with 100% certainty.[82,88,90]

My approach, which is modeled after that of Drs. Hendrickson and Kempson,[91] expands the category of mucinous cystadenoma to include those stage I tumors with a degree of architectural complexity seen in the old-style borderline tumors as long as they have been well sampled, show maturation of the villous tips in at least 90% of villoglandular structures (see below), and show no more than mild to focally moderate nuclear atypia. Such tumors generally do not show impressive stratification, but stratification is not used as a criterion because it is subjective, plagued by issues related to tangential sectioning, and has never been shown to be of prognostic significance in and of itself.[81] I include a note in my report indicating that tumors of this type have been previously referred to as borderline tumors or neoplasms of low malignant potential, but that anything other than a benign clinical course for a completely resected stage I tumor would be an extraordinary event worthy of a case report (after exclusion of the four more likely possibilities outlined above). In those stage I old-style borderline tumors that have been suboptimally sampled, lack tip maturation in at least 10% of their epithelial area, or exhibit more than focal moderate nuclear atypia, I retain the "borderline" or "low malignant potential" terminology as a hedge against the possibility of something worse lurking within unsampled areas of the tumor.

Drs. Hendrickson and Kempson have championed the concept of "maturation of the tips" as an indication of the benign nature of an ovarian mucinous proliferation when present throughout the tumor.[91] This phenomenon, in which active crypts at the base of a villous epithelial proliferation merge with mature tips composed of mucin-rich, mitotically inactive cells (Fig. 7.49), can be used as a criterion to distinguish

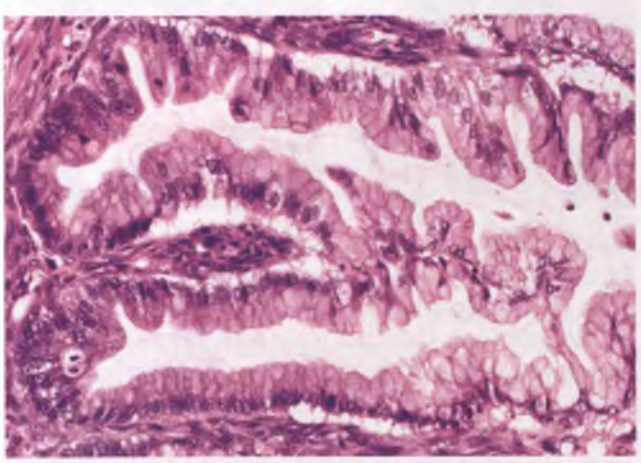

FIGURE 7.49. Maturation of a villous tip in an ovarian mucinous cystadenoma. The villous structure coursing horizontally through the center of the image has an active base with some nuclear stratification, hyperchromasia, and mitotic activity (at lower left), but demonstrates maturation of its tip.

[§]Cells with severe nuclear atypia have nuclei that are enlarged and rounded with prominent nucleoli and coarsely clumped chromatin, and are often found in association with atypical mitotic figures.

a mucinous cystadenoma that has villoglandular complexity from a mucinous borderline tumor.[91] Additional examples of architecturally complex mucinous neoplasms with tip maturation are presented in the section on mucinous cystadenomas.

The Imprecision of Histologic Subtyping

Ovarian mucinous tumors have historically been categorized as exhibiting intestinal (more accurately gastrointestinal), endocervical, or mixed endocervical-intestinal differentiation. However, the distinction between endocervical-like (müllerian) and gastrointestinal differentiation in ovarian mucinous neoplasms is more subjective and less obvious than many standard textbooks of gynecologic pathology would indicate. In routinely-stained sections, it is usually not possible to definitively determine whether a mucinous cystadenoma is lined by endocervical-like or gastric type superficial/foveolar cells with pyloric differentiation. When such tumors are subjected to histochemical, immunologic, and ultrastructural analysis, the vast majority are found to exhibit gastric differentiation.[92,93]

In the context of histologic subtyping of ovarian mucinous tumors, it is instructive to recall the normal histology of the stomach and small intestine. The superficial/foveolar mucinous cells that line the gastric mucosa are commonly distended with mucin and goblet-shaped, but these are not true goblet cells (Fig. 7.50).[94] If one applies the same strict definition of a goblet cell used when diagnosing Barrett's esophagus or gastric mucosa with intestinal metaplasia, then most examples of mucinous cystadenomas with "goblet cell differentiation" would be reclassified as mucinous cystadenomas with gastric differentiation containing pseudogoblet cells (Fig. 7.51). Ironically, those pathologists with a loose definition of goblet cells who interpret any goblet-shaped mucinous cell as evidence of intestinal differentiation would be correct in their classification of nearly all mucinous cystadenomas as being of gastrointestinal type, but for the wrong reasons, whereas those who appropriately have more rigid goblet cell criteria are at risk for misclassifying many of these tumors as being of endocervical type.

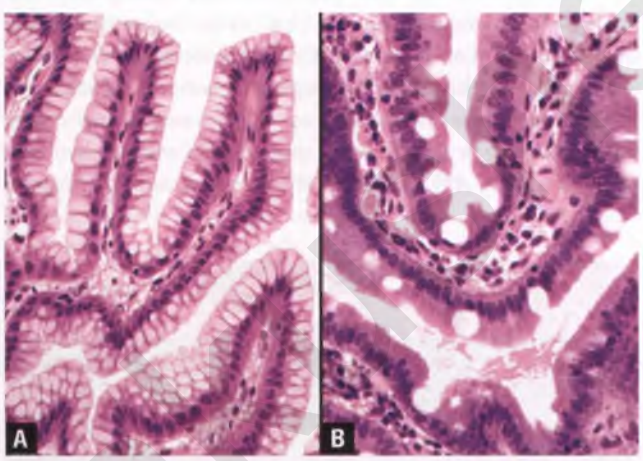

FIGURE 7.50. Gastrointestinal examples of "pseudogoblet" cells and true goblet cells. **A:** In this sample from the gastric pylorus, many of the superficial/foveolar lining cells are distended with mucin and simulate goblet cells. Unlike true goblet cells, they have a light pink, homogeneous cytoplasmic blush, are often arranged in back-to-back fashion uninterrupted by columnar cells, and would stain weakly or negatively with Alcian blue at pH 2.5. **B:** In this sample from the duodenum, true goblet cells are present, which stand out as scattered barrel-shaped cells with clear cytoplasm. The cytoplasm of these cells may be light blue and bubbly in preparations that utilize Gill's rather than Harris hematoxylin, and would stain strongly with Alcian blue at pH 2.5.

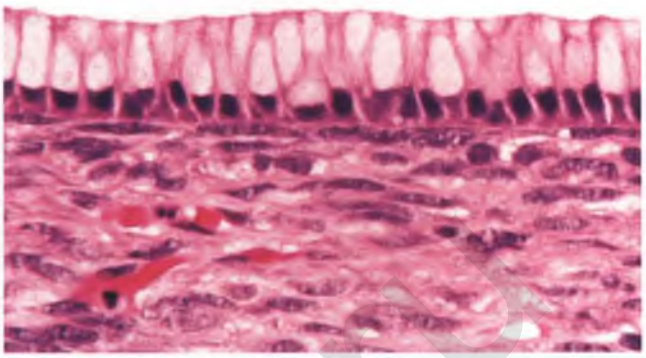

FIGURE 7.51. Ovarian mucinous cystadenoma. One can appreciate the difficulty in definitively classifying the type of epithelial differentiation based solely upon routine histology. Although foci such as this are often attributed to goblet cell intestinal differentiation, it is more likely that they represent mucinous epithelium of gastric superficial/foveolar type.

In practice, subtyping of mucinous cystadenomas and mucinous carcinomas is not usually mentioned because it is only of academic interest and because it is usually not obvious in routinely-stained sections. However, nearly all such tumors would be found to exhibit some degree of gastrointestinal differentiation if thoroughly investigated. It is important to note that the gastrointestinal versus endocervical-like distinction is relevant and more apparent in the subtyping of ovarian mucinous borderline tumors. Most of these borderline tumors are of gastrointestinal type and frequently contain true goblet cells (Fig. 7.52), although a distinct minority shows legitimate endocervical-like differentiation (see below).

True mixed gastrointestinal and endocervical-like mucinous ovarian tumors are probably close to nonexistent, with the vast majority of such tumors actually being composed of an admixture of goblet-cell containing epithelium of intestinal type and pseudoendocervical epithelium of gastric foveolar type.

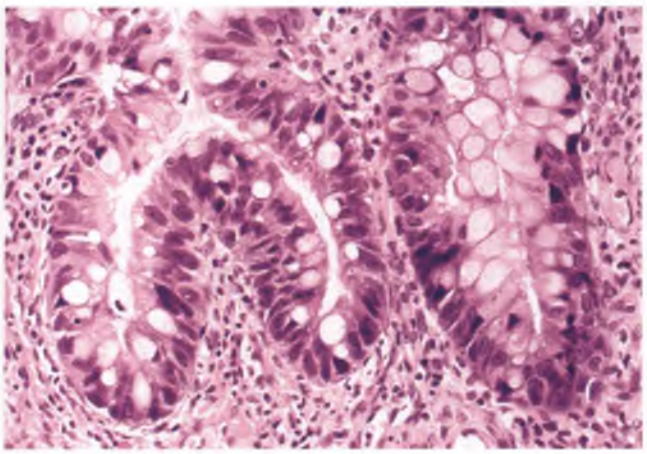

FIGURE 7.52. Ovarian mucinous borderline tumor of gastrointestinal type. The most obvious goblet cells are those scattered cells with barrel-shaped, clear cytoplasmic vacuoles in the bifid gland at left. The numerous goblet-shaped cells with light pink cytoplasm in the gland at right most likely represent distended mucinous cells of gastric superficial/foveolar type.

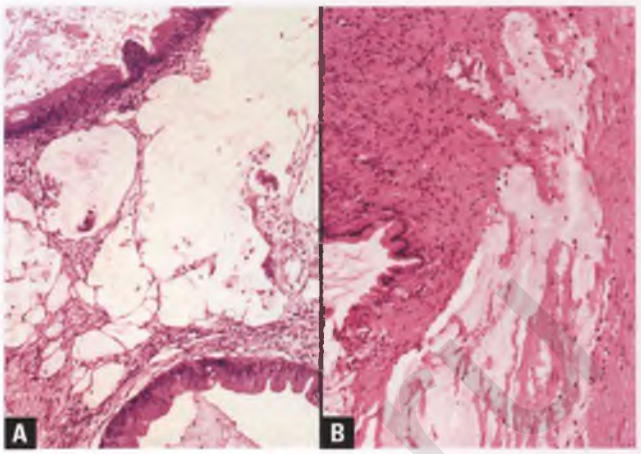

FIGURE 7.54. Mucinous ovarian tumors with pseudomyxoma ovarii. **A,B:** In these two different examples, mucin dissects through the ovarian stroma with nearby mucinous cysts. **(A)** contains a few strips and clusters of neoplastic epithelial cells floating within the mucin, which may be due to either secondary involvement by a low-grade mucinous appendiceal neoplasm or pseudomyxomatous stromal microinvasion. **(B)** is devoid of epithelial cells and represents an incidental finding.

Mucin Granulomas Versus Pseudomyxoma Ovarii

On occasion, dilated mucinous glands within a mucinous ovarian tumor rupture and release mucin into the neighboring stroma. The term "mucin granuloma" is applied when a histiocytic reaction ensues that organizes the pools of mucin into small, rounded, well-defined, mucin-rich nodules (Fig. 7.53).[95] Mucin granulomas are typically devoid of easily recognizable epithelial cells in routinely-stained sections; when tumor cells are present, they are usually scant and have a degenerative appearance.[96,97] Although most mucin granulomas represent incidental findings, those with epithelial cells that are found in association with mucinous borderline tumors are difficult to distinguish from foci of stromal microinvasion,[96,97] and some investigators consider all such foci to represent microinvasion.[83]

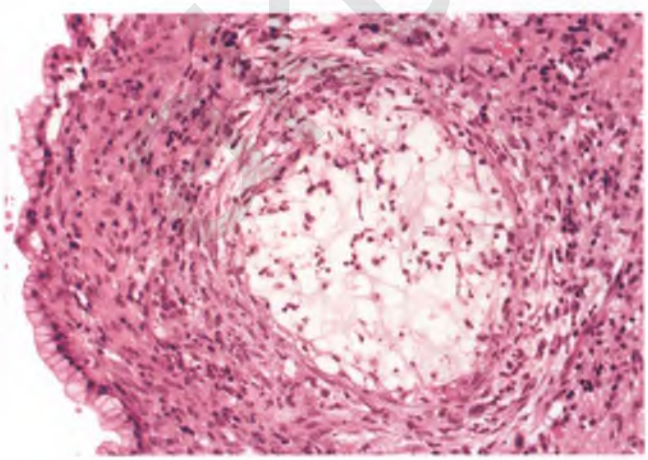

FIGURE 7.53. Mucinous cystadenoma with mucin granuloma related to nearby rupture of a mucinous gland with escape of its contents into the stroma.

In pseudomyxoma ovarii, large mucin pools with irregular margins and an absent to inconspicuous stromal response dissect through the ovarian stroma, sometimes with clusters of tumor cells within the mucin (Fig. 7.54).[82,95] Pseudomyxoma ovarii is usually absent or only a focal finding in mucinous cystadenomas and mucinous borderline tumors, although it can be prominent in about 10% of the latter tumors.[88,98] This phenomenon is more commonly encountered in mucinous tumors associated with mature cystic teratomas,[99,100] and is a prominent finding in most secondary ovarian tumors that originate from a low-grade mucinous neoplasm (ruptured cystadenoma) of the appendix.[95,98,101]

In years past, there was concern about pseudomyxoma ovarii being an independent risk factor in primary mucinous tumors for extraovarian spread and the development of pseudomyxoma peritonei,[91] such that prominent pseudomyxoma ovarii in what was otherwise a mucinous borderline tumor was sufficient for some to warrant an upgrade to mucinous carcinoma[102] or if prominent within a mucinous cystadenoma, would lead to an upgrade to a borderline tumor. However, this concern was based upon data that was actually measuring the behavior of comingled appendiceal-derived tumors rather than true primary mucinous tumors with pseudomyxoma ovarii (see the section on low-grade appendiceal mucinous tumors near the end of this chapter). It now appears that the isolated finding of pseudomyxoma ovarii devoid of tumor cells in a properly diagnosed stage I mucinous cystadenoma or borderline tumor is an incidental finding of no clinical significance.[88] However, those cases of pseudomyxoma ovarii in which tumor

cells are identified within the pools of mucin are at high risk for either representing foci of pseudomyxomatous stromal microinvasion[97] (if focal) or secondary tumors of appendiceal origin (if diffuse).

Immunohistochemistry of Mucinous Ovarian Tumors

Cytokeratin 7 (CK7) and cytokeratin 20 (CK20) immunostains are widely used in the evaluation of the primary versus metastatic nature of ovarian involvement by tumors with mucinous or endometrioid histology. In this context, it is important to realize that primary mucinous ovarian tumors often do not express the standard CK7+/CK20– immunophenotype that is seen in other types of primary ovarian epithelial-stromal tumors. Although consistently CK7+, these mucinous tumors also express CK20 to a variable degree (Figs. 7.55 and 7.56).[103,104]

CK 20 immunoreactivity, which in this setting implies gastrointestinal differentiation, preferentially localizes to the superficial aspects of gastrointestinal-type epithelium, and in tumors is often quite regionally distributed.[105] Moreover, within a region of CK20 positivity, isolated and clustered intensely positive cells are often juxtaposed with negative cells in a mosaic pattern.[105] These staining properties create opportunities for error when interpreting CK20 immunoreactivity, with a significant chance for a false negative result in small samples such as the tissue cores utilized in microarray studies. If sections of resected ovarian tumors are used, approximately 85% of ovarian mucinous borderline tumors of gastrointestinal type and about 60% of primary ovarian mucinous carcinomas are CK7+/CK20+.[104] Some mucinous cystadenomas are also CK7+/CK20+,[105] although these tumors have not been extensively studied.

In addition to the common coexpression of CK 7 and CK 20 in primary ovarian mucinous tumors of gastrointestinal type, anywhere from 40% to 100% of these tumors exhibit at least some immunoreactivity for CDX2, which is another marker of intestinal differentiation.[106–108] In keeping with their müllerian nature, endocervical-like mucinous borderline tumors are CK7+, CK20–, CDX2–, and frequently express estrogen and progesterone receptors, which contrasts with the CK7+, CK20+, CDX2±, ER–, and PR– immunophenotype of most mucinous borderline tumors of gastrointestinal type.[109]

The CK7/CK20 immunophenotype of primary ovarian mucinous tumors that arise in association with mature cystic teratomas deserves specific attention, and is discussed in the separate section on these tumors.

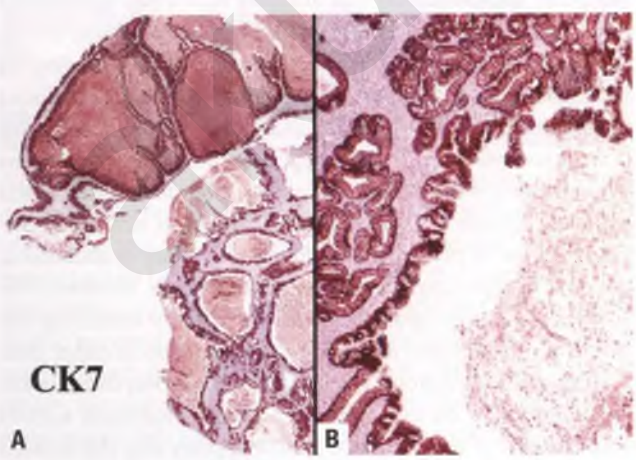

FIGURE 7.55. **A,B:** CK7 immunohistochemistry of ovarian mucinous borderline tumor of gastrointestinal type. In this typical example, nearly all of the tumor cells are intensely immunoreactive for CK7.

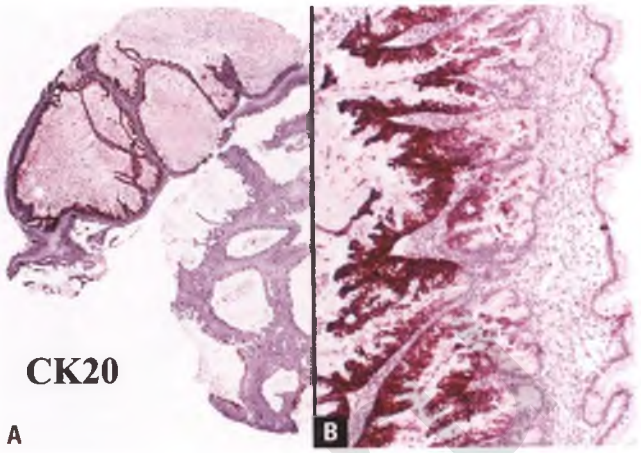

FIGURE 7.56. CK20 immunohistochemistry of ovarian mucinous borderline tumor of gastrointestinal type. **A:** Note the regional differences in staining of the two different sections of tumor. Depending on the piece of tissue examined, CK20 immunoreactivity could be scored as diffusely positive (upper left) or focally positive (lower right), and it is possible that if tissue from the lower right sample had been core biopsied for microarray analysis it would have been scored as negative. **B:** In this case, CK20 tends to stain the superficial, more architecturally complex aspects of the epithelium. In most scoring systems, a staining pattern such as this would somewhat confusingly be referred to as diffusely positive because more than half of the epithelial cells are immunoreactive.

Mucinous Cystadenoma

Mucinous cystadenomas typically present as a pelvic or abdominal mass in an adult woman (mean age of 40–45 years). As discussed above, the vast majority of these tumors are of the gastrointestinal type by virtue of their extensive gastric pyloric-type differentiation. Mucinous cystadenomas, in either pure form or combined with mature cystic teratoma, have bragging rights when it comes to the ability to form tumors of massive size. Tumors in the neighborhood of 30 cm are not uncommon, and one tumor measured an astonishing 1 m in diameter (see Fig. 7.67). The external surface of mucinous cystadenomas is smooth, with nodular bulges present in loculated tumors

FIGURE 7.57. Mucinous cystadenoma. The smooth surface and externally visible locules are typical of these neoplasms, which are often quite large. The locule at the bottom is yellow because it is filled with inspissated mucus.

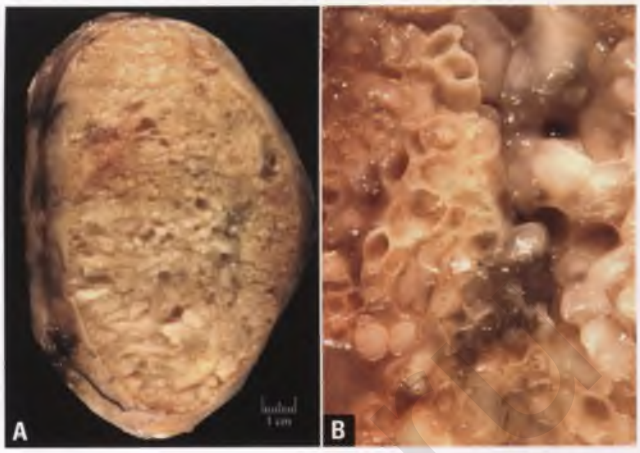

FIGURE 7.59. Mucinous cystadenoma. **A:** At first glance, this tumor has an ominous-appearing, predominantly solid cut surface that is worrisome for mucinous carcinoma. **B:** Closer inspection reveals a honeycomb pattern of simple cysts, many of which are filled with inspissated mucus.

(Fig. 7.57), and their cyst contents vary from mucin-tinged fluid to inspissated mucoid material. Less than five percent of these tumors are bilateral, and they may be either unilocular or multilocular (Fig. 7.58). In addition to representative sections of the cyst wall, solid and spongy areas should be searched for and sampled, since they may represent a conglomeration of cysts with inspissated mucus (Figs. 7.59 and 7.60), a fibromatous component, an admixed Brenner tumor or teratoma, a borderline or carcinomatous element, or a mural nodule of benign or malignant etiology.

Histologically, the classic mucinous cystadenoma is composed of glands and cysts that are lined by a single layer of columnar mucinous cells with bland, basally-oriented nuclei (Fig. 7.61). As discussed in the section on the revised criteria for mucinous ovarian tumors, the presence of papillary formations should not lead to an automatic diagnosis of a borderline tumor without an assessment of the degree of tip maturation and nuclear atypia (Fig. 7.62). As advocated by Drs. Hendrickson and Kempson, global or near-global maturation of the villous tips in association with mild nuclear atypia is considered within the spectrum of mucinous cystadenomas, even if it occurs within an extensive, architecturally complex proliferation (Figs. 7.63 and 7.64).[91] When particularly florid or when containing very minor elements that would qualify for a borderline tumor, such tumors can be diagnosed as mucinous cystadenoma with epithelial hyperplasia or mucinous cystadenoma with focal atypia, respectively.

FIGURE 7.58. Mucinous cystadenoma. The sectioned surface of this tumor exhibits multiple, variable-sized locules that contain mucinous material.

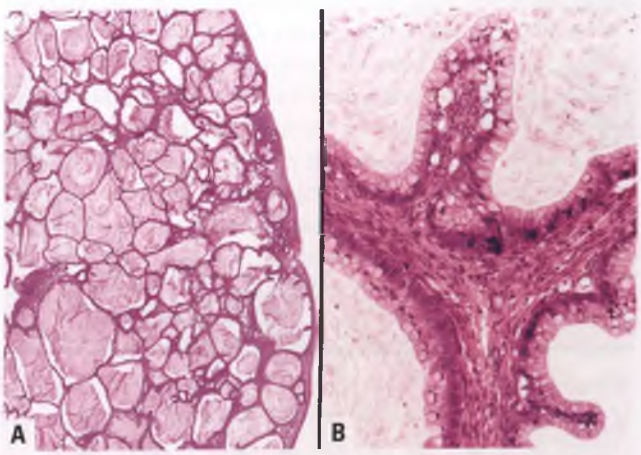

FIGURE 7.60. **A,B:** Mucinous cystadenoma. Histologic correlate of the tumor in the preceding figure. The mucin-filled cysts are lined by simple to undulating mucinous epithelium with mild nuclear atypia and virtually no stratification.

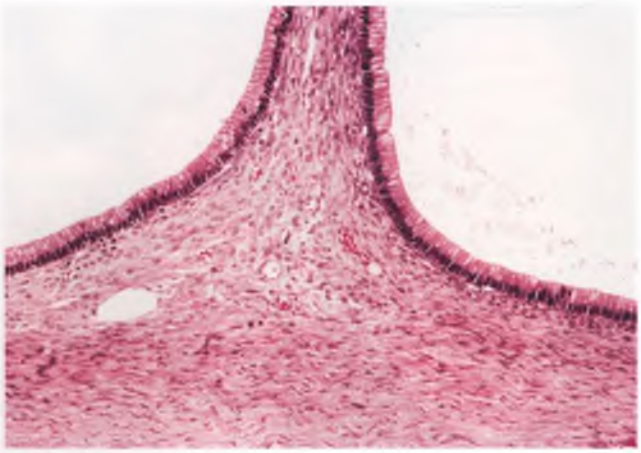

FIGURE 7.61. Mucinous cystadenoma. Portions of two locules are lined by a single layer of bland mucinous columnar epithelial cells with basally-oriented nuclei and no architectural complexity. In some textbooks, an image similar to this one is the sole example provided for mucinous cystadenomas, which can give readers the mistaken impression that papillary/villoglandular growth is not allowed in these neoplasms.

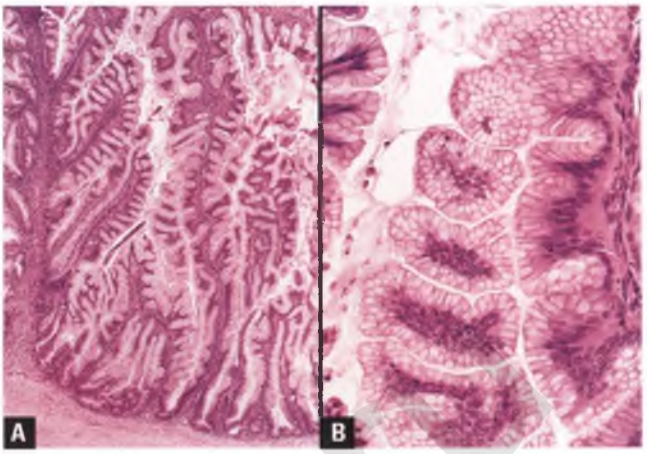

FIGURE 7.63. **A,B:** Mucinous cystadenoma. Despite the apparent architectural complexity related to prominent papillary infolding, this tumor should be classified as a mucinous cystadenoma rather than a mucinous borderline tumor because of its mild nuclear atypia and global tip maturation.

Mucinous Adenofibroma[110]

This is a rare benign tumor that is less common than adenofibromas of serous and endometrioid types. Mucinous adenofibromas typically present in an adult woman as a unilateral ovarian mass with an average diameter of 7 cm. They are predominantly solid tumors with scattered small cysts, and have a pale yellow to light tan sectioned surface that may appear mucoid (Fig. 7.65). Histologically, mucinous adenofibromas are composed of widely-spaced glands that are lined by a single layer of tall columnar mucinous epithelial cells with basally-oriented nuclei that are set within a fibromatous stroma (Fig. 7.66), which commonly contains calcified plaques. Tumors of this type whose glands are focally crowded and lined by minimally stratified cells with mild to moderate nuclear atypia have been referred to as mucinous adenofibromas with epithelial atypia, but this represents an incidental microscopic finding.

Since mucinous adenocarcinoma metastatic to the ovary that originates from sites such as the uterine cervix, pancreas, and biliary tract can be extremely well differentiated and mimic

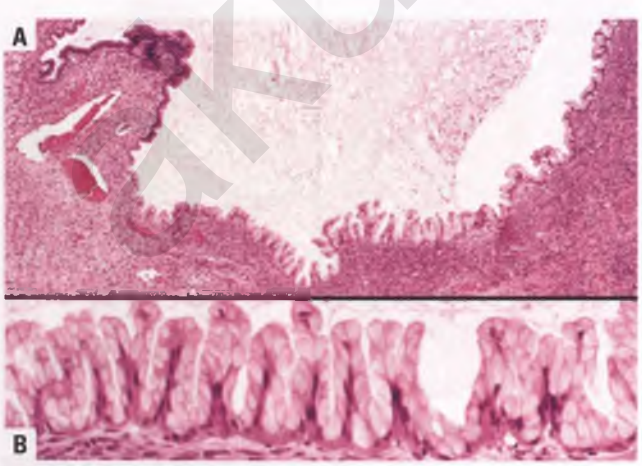

FIGURE 7.62. **A,B:** Mucinous cystadenoma with patches of bland micropapillary growth.

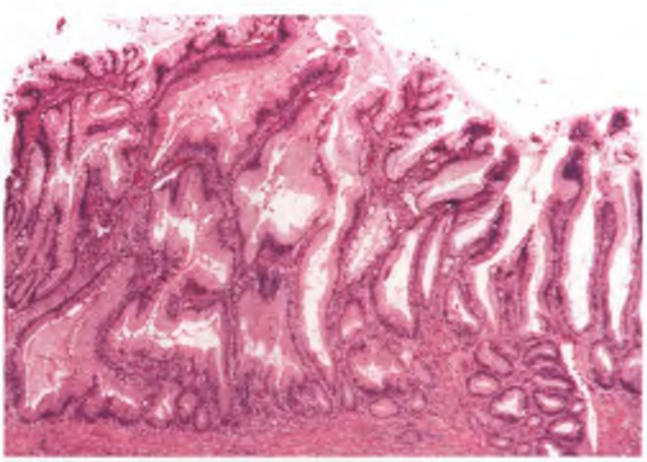

FIGURE 7.64. Mucinous cystadenoma. This old-style borderline tumor has an arborizing villoglandular architectural pattern that exhibits the benign feature of maturation of the villous tips. Many of the glands at the base of the proliferation are basophilic and contain scattered normal mitotic figures, but these "active crypts" are associated with mature tips composed of mucin-rich, mitotically inactive cells (compare with Fig. 7.69).

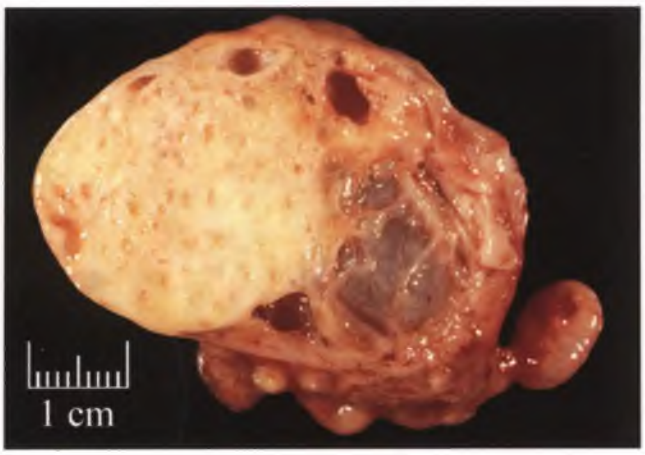

FIGURE 7.65. Mucinous cystadenofibroma. The sectioned surface is predominantly solid with scattered cystic areas. The dominant adenofibromatous component at left is pale yellow, glistening, mucoid, and punctuated with multiple small cysts. (Courtesy of Dr. Enrique Higa.)

primary mucinous adenofibroma, the possibility of metastatic disease should be given serious consideration whenever one or more of the following are present: history of an extraovarian primary mucinous carcinoma, bilateral ovarian involvement, high-stage disease, an infiltrative glandular pattern with an associated host reaction, and angiolymphatic or perineural invasion.

Primary Mucinous Neoplasms Arising in Association with Mature Cystic Teratomas[99,100]

About 5% of primary mucinous ovarian tumors are associated with a mature cystic teratoma. This finding, in conjunction with the common presence of cells with gastrointestinal-type

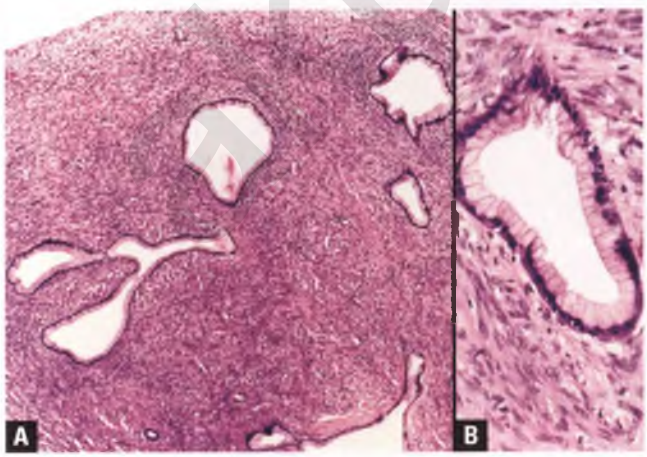

FIGURE 7.66. **A,B:** Mucinous adenofibroma. Abundant fibromatous stroma separates dilated glands lined by columnar mucinous epithelial cells with bland nuclear features.

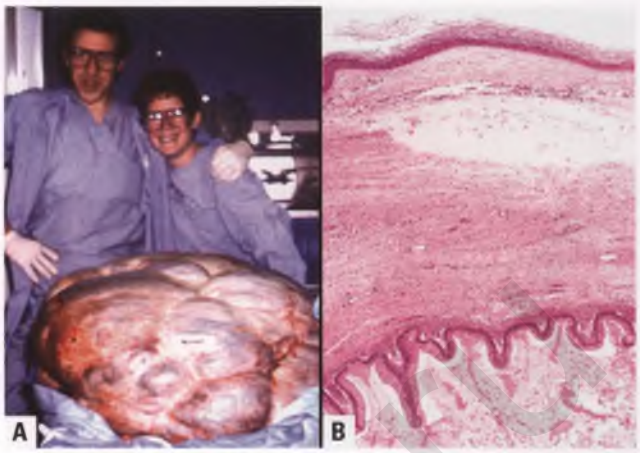

FIGURE 7.67. Gargantuan mucinous cystadenoma associated with mature cystic teratoma. **A:** The multiloculated tumor measures approximately 1 m in diameter and weighs 137.6 kg (303.2 lb). Its external surface is smooth, glistening, and gray, and the locule-related mounds resemble moguls on a ski slope. **B:** Histologically, these tumors consist of adjoining locules of benign teratomatous tissue (keratin-producing squamous epithelium at top) and mucinous cystadenoma (bottom), with the latter generally predominating. (Gross photograph courtesy of Drs. Matt van de Rijn and Julie Desch.)

differentiation in mucinous ovarian tumors, lends credence to the theory that some of these tumors may actually be monodermal teratomas that have overgrown their teratomatous elements rather than neoplasms derived from Walthard nests or the surface epithelium. Teratoma-associated mucinous tumors occur in patients with a mean age of about 40 years, and run the full spectrum from mucinous cystadenoma to mucinous carcinoma. The teratomatous elements are typically a minor component of the neoplasm. Almost all of these tumors are unilateral, although a contralateral mature cystic teratoma is present in about 10% of cases. Teratoma-associated mucinous tumors can be quite large; one of the largest ovarian tumors on record is a tumor of this type (Fig. 7.67).[111]

About half of teratoma-associated mucinous ovarian tumors show features of pseudomyxoma ovarii, and some are associated with pseudomyxoma peritonei as well (see Chapter 8).** The ovarian tumors that are associated with pseudomyxoma peritonei have almost always ruptured and typically contain prominent areas of pseudomyxoma ovarii. The tumors that are associated with these pseudomyxomatous processes tend to express the lower intestinal CK7−/CK20+ immunophenotype, and also usually express other intestinal markers such as CDX2, MUC2, and villin. Although this lower intestinal immunophenotype can create confusion with metastatic colorectal or appendiceal adenocarcinoma, the presence of at

**Many of the peritoneal mucinous deposits in reported examples of pseudomyxoma peritonei associated with these tumors do not contain neoplastic epithelial cells,[82,100,112] and may represent examples of organizing mucinous ascites as discussed in the section on the differential diagnosis of pseudomyxoma peritonei in Chapter 8.

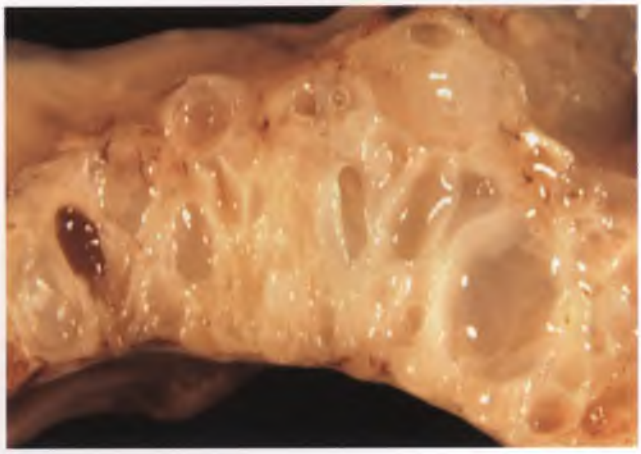

FIGURE 7.68. Mucinous borderline tumor, gastrointestinal type. In this cross section of a tumor whose wall measures up to 2 cm in thickness, multiple internal mucinous cysts are evident.

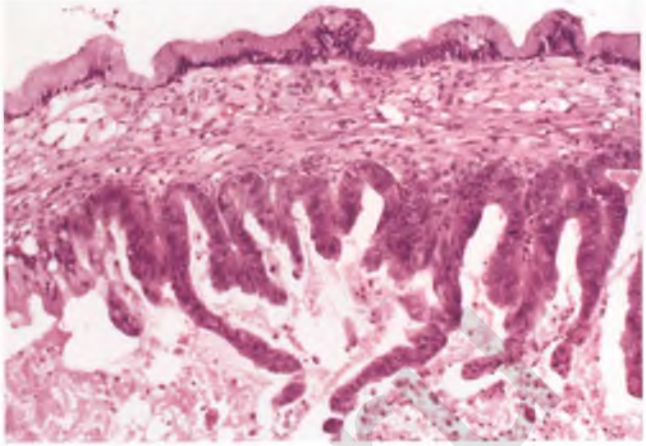

FIGURE 7.70. Mucinous borderline tumor, gastrointestinal type. The diagnosis is justified by the presence of papillae that are lined by cells with moderate nuclear atypia and some stratification that lack tip maturation (bottom locule). This image also highlights the heterogeneity that is often present in mucinous ovarian tumors, with the top locule only showing features of a mucinous cystadenoma.

least focal teratomatous elements and clinicopathologic correlation allow for proper recognition of these primary mucinous ovarian tumors, which presumably have arisen from gastrointestinal-type elements within the teratoma.[99]

Mucinous Borderline Tumor, Gastrointestinal Type[81,82,86,87]

These tumors, which represent about 85% of mucinous borderline tumors, occur in patients with a mean age of 45 to 50 years and have an average size of about 20 cm. Only about 5% are bilateral, and the presence of bilateral involvement should prompt serious consideration for a metastatic process. Their gross appearance overlaps with that of mucinous cystadenomas, with diagnostic areas being located in solid or spongy foci (Fig. 7.68). In contrast to the endocervical-like variant of mucinous borderline tumors, those of gastrointestinal type do not usually have grossly evident papillae and instead feature villoglandular structures of microscopic size emanating from cystically dilated glands. Architectural complexity and nuclear stratification up to 6 cells in thickness are commonplace, but it is the presence of moderate nuclear atypia and/or the incomplete maturation of the villous tips that are most helpful in establishing the diagnosis (Figs. 7.69 and 7.70). Cribriform growth confined to cystic spaces is an acceptable architectural pattern in these tumors as long as severe nuclear atypia is absent (Fig. 7.71).

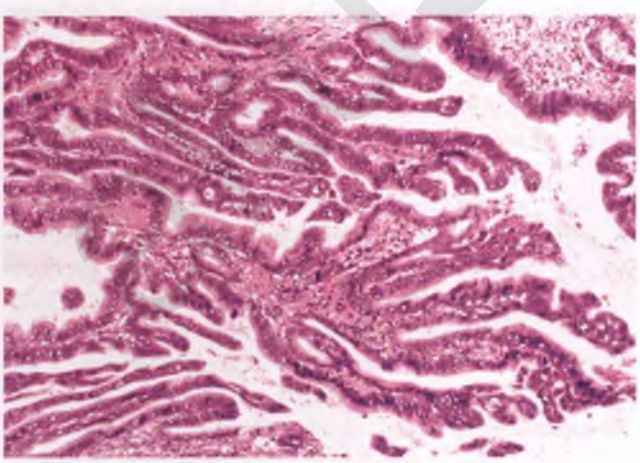

FIGURE 7.69. Mucinous borderline tumor, gastrointestinal type. Neoplastic cells with moderate nuclear atypia line the entire length of the long, slender papillae. This failure to show maturation of the villous tips helps to distinguish this tumor from a mucinous cystadenoma with architectural complexity (compare with Fig. 7.64).

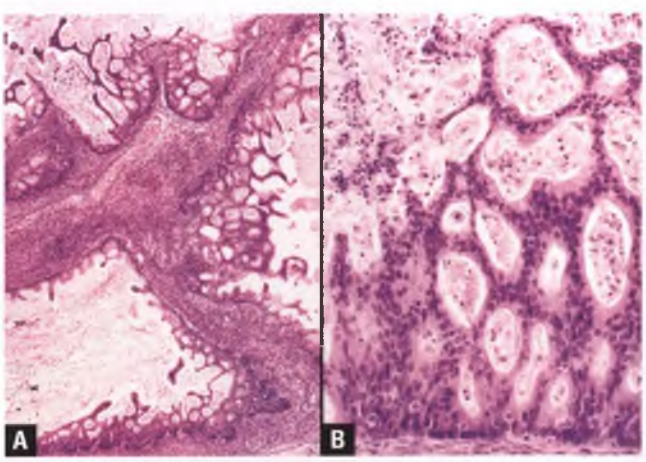

FIGURE 7.71. **A,B:** Mucinous borderline tumor, gastrointestinal type. Cribriform growth *confined to cystic spaces* is allowed in these tumors. However, this finding should prompt extensive sampling to exclude marked nuclear atypia (intraepithelial carcinoma) and stromal invasion.

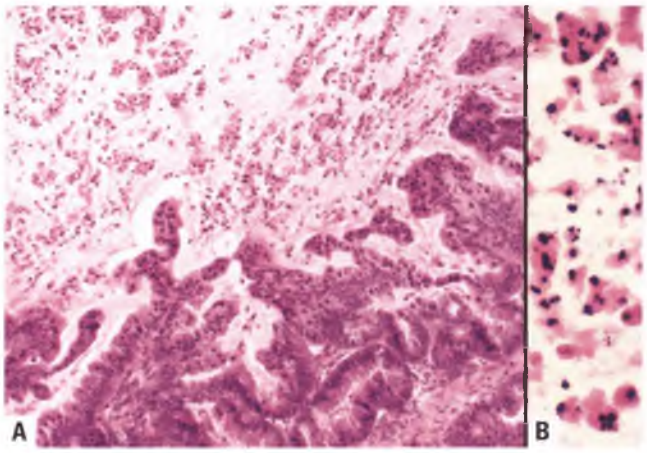

FIGURE 7.72. **A,B:** Mucinous borderline tumor, gastrointestinal type. Degenerated neutrophils and histiocytes are suspended within intraluminal inspissated mucus, as shown at higher magnification in **B**. This finding should not be misconstrued as "dirty necrosis."

Cystic spaces within mucinous borderline tumors and primary ovarian mucinous tumors in general may contain mucus with an accumulation of degenerated neutrophils, histiocytes, and occasional sloughed tumor cells (Fig. 7.72).[113] This type of intraluminal material should be distinguished from the "dirty necrosis" that is illustrated and discussed in the section on metastatic intestinal adenocarcinoma.

The minimal amount of borderline features (however defined) that should be present in order to label a mucinous tumor on the lower end of the proliferative spectrum as borderline is impossible to determine, given that mucinous cystadenomas and the lower end of mucinous borderline tumors are both entirely benign, but suggestions have ranged from 5% to 10% of the epithelial area.[84,85,114]

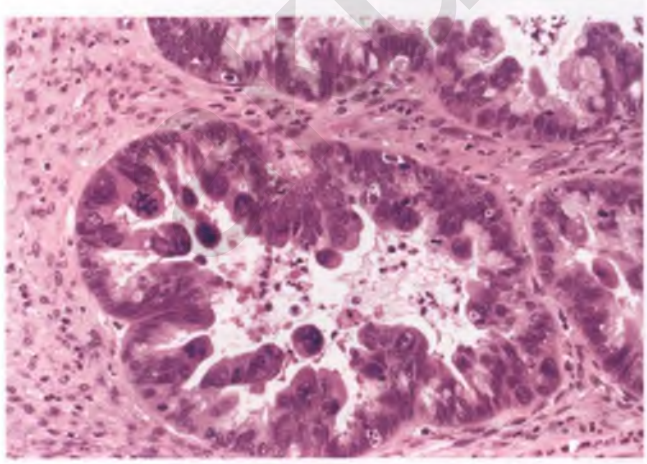

FIGURE 7.73. Mucinous borderline tumor, gastrointestinal type, with intraepithelial carcinoma. In this straightforward example involving the featured gland, some of the cells exhibit severe nuclear atypia and an atypical mitotic figure is present.

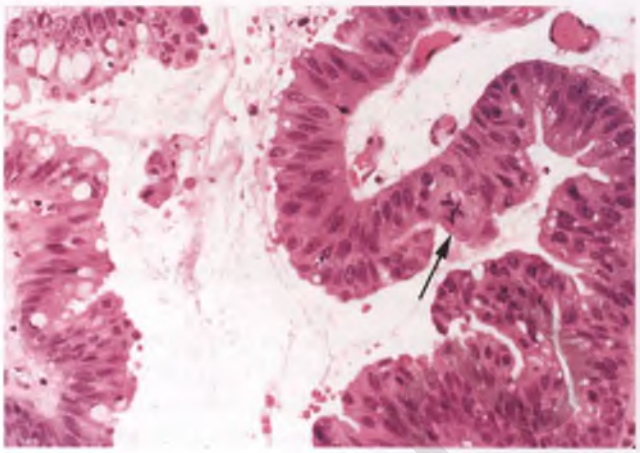

FIGURE 7.74. Mucinous borderline tumor, gastrointestinal type, with intraepithelial carcinoma. The glandular proliferation in the right side of the image exhibits moderate nuclear atypia and some degree of stratification. This lesion contained several atypical mitotic figures, one of which is shown (*arrow*), which was the deciding factor in issuing a diagnosis of intraepithelial carcinoma.

Mucinous Borderline Tumor, Gastrointestinal Type, with Intraepithelial Carcinoma[81,83–85]

In classic examples of these tumors, which would qualify as a form of mucinous carcinoma using the 1973 criteria of Hart and Norris,[80] stratified epithelial cells with severe nuclear atypia line cysts and glands (Fig. 7.73). Finger-like micropapillary projections without stromal cores, cribriform glandular proliferations, and brisk mitotic activity are often apparent. When several atypical mitotic figures are present, most pathologists lower the threshold for what constitutes severe nuclear atypia (Fig. 7.74) or keep sampling the tumor until more obvious

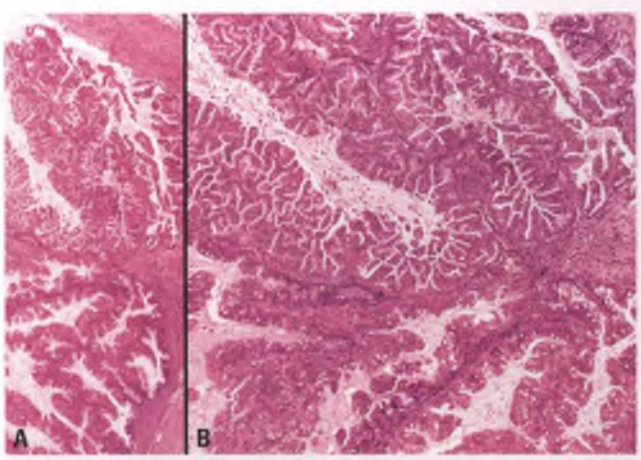

FIGURE 7.75. **A,B:** Mucinous borderline tumor, gastrointestinal type, with florid intraepithelial carcinoma. The extensive architectural complexity is recognizably occurring along villous structures and within the confines of dilated glands that are separated by appreciable amounts of intervening stroma, which distinguishes this entity from the expansile form of invasive mucinous carcinoma.

atypia is encountered. Some examples are more florid than others (Fig. 7.75), and in some cases the distinction from the expansile form of invasive carcinoma may be difficult and subjective. Only about 5% of patients with these tumors die of their disease, which in most cases is presumably related to the behavior of an undetected frankly invasive component in a large, heterogeneous tumor.

Mucinous Borderline Tumor, Gastrointestinal Type, with Microinvasion[81–84,96]

Stromal microinvasion is identified in 5% to 10% of mucinous borderline tumors of gastrointestinal type, and is more likely to occur in cases with intraepithelial carcinoma. Microinvasion may take the form of (a) tumor cells disposed singly and in small clusters within the stroma, often surrounded by clear spaces (Fig. 7.76), (b) jagged glands associated with desmoplastic or edematous stroma, (c) small foci of expansile invasion as discussed in the section on mucinous carcinoma, or (d) tiny nests or strips of tumor cells associated with small pools of mucin (similar to that shown in Figs. 7.54 and 7.86) or a vaguely granulomatous reaction. As detailed in a recent study, the distinction between the latter type of microinvasion and mucocele-like stromal reactions or mucin granulomas can be problematic.[97]

The upper size limit for microinvasion in ovarian borderline tumors is arbitrary and has not been standardized; it varies from 3 to 5 mm in linear extent to an area of 10 mm^2. Multiple separate foci of microinvasion are often present, and their individual sizes are not added together when making a determination of whether the extent of infiltration qualifies as microinvasion. Some investigators recommend distinguishing microinvasive borderline tumors in which the invasive foci exhibit mild to moderate nuclear atypia from microinvasive carcinomas that are defined by the presence of invasive foci with severe nuclear atypia.[84] Since this distinction between microinvasive borderline tumor and microinvasive carcinoma serves as a source of confusion and the limited data available in the literature suggests that the prognosis of microinvasion in mucinous borderline tumors is excellent and indistinguishable from those with intraepithelial carcinoma regardless of nuclear grade, my preference is to consider all such lesions mucinous borderline tumors with microinvasion.

Mucinous Borderline Tumor, Endocervical-Like[115–117]

These tumors, which are also referred to as müllerian mucinous borderline tumors and are considered by some to be within the spectrum of seromucinous borderline (atypical proliferative) tumors, represent about 15% of mucinous borderline tumors. They typically present in young women (mean age of 35–40 years) with an ovarian mass (average size of 8 cm) that is bilateral in roughly 25% of patients. Concurrent endometriosis is present in about one-third of cases, and the tumor may arise within an endometriotic cyst. Although the external aspect of most of these tumors is smooth, about 10% to 15% have an exophytic component composed of grossly visible papillae projecting from the surface.[115] Internally, these tumors are composed of one or more cysts filled with mucoid fluid, at least some of which contain pale yellow, papillary excrescences with a gelatinous sectioned surface (Fig. 7.77). At the time of presentation, the tumor has spread beyond the ovary in only about 10% of patients, and limited data suggests that this is more likely to occur in patients with an exophytic component.

Endocervical-like mucinous borderline tumors have many features in common with SBTs, such as their distinctive papillary architecture (Fig. 7.78), tendency to spread as peritoneal implants or lymph node deposits, and excellent prognosis.

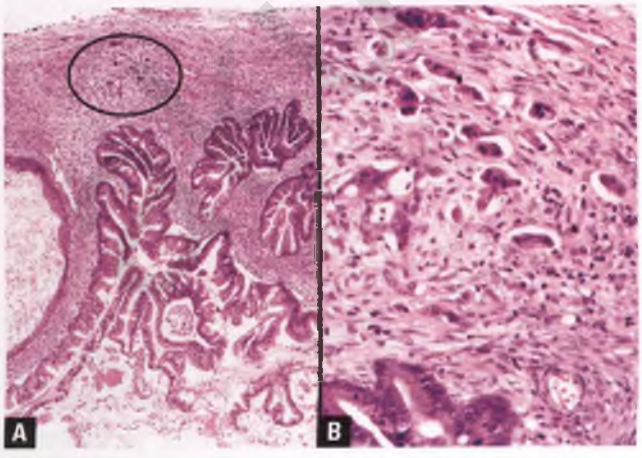

FIGURE 7.76. Mucinous borderline tumor, gastrointestinal type, with microinvasion. **A:** In this low-magnification view, the focus of microinvasion is *circled*. **B:** As is typically the case, the microinvasive nests of carcinoma are surrounded by clear spaces.

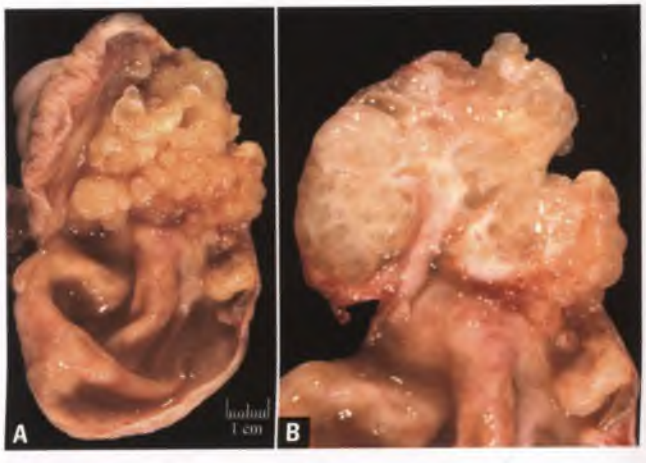

FIGURE 7.77. Endocervical-like mucinous borderline tumor. **A:** Opening of this cystic tumor reveals mucoid cyst contents and a conglomerate of pale yellow papillary excrescences. **B:** The sectioned surface of the papillary region has a glistening, gelatinous appearance.

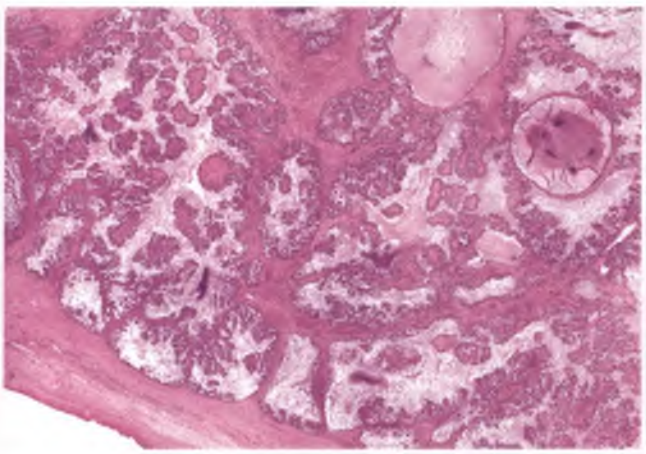

FIGURE 7.78. Endocervical-like mucinous borderline tumor. This low-magnification view highlights the papillary architecture that is indistinguishable from that seen in serous borderline tumors.

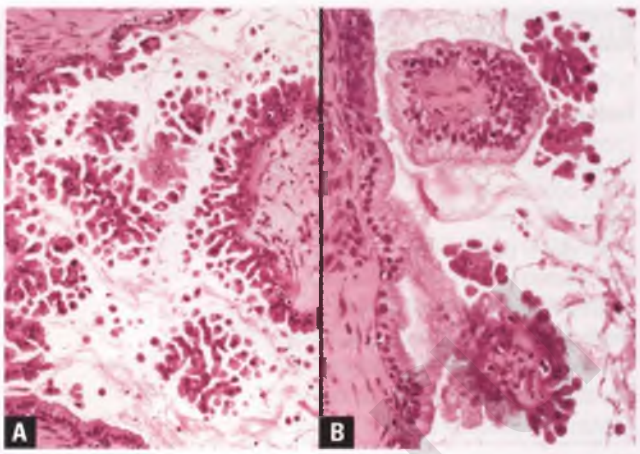

FIGURE 7.80. A,B: Endocervical-like mucinous borderline tumor. So-called indifferent cells with abundant eosinophilic cytoplasm are often present, particularly at the tips of the papillae and in the detached epithelial tufts.

Their papillae are lined by endocervical-like mucinous cells that do not form goblet cells or show other evidence of gastrointestinal differentiation, and detached epithelial tufts are a constant feature (Fig. 7.79). In addition to endocervical-like mucinous cells, most cases also contain so-called indifferent cells, which are nonciliated cells with abundant eosinophilic cytoplasm that are found preferentially at the tips of the papillae and as epithelial tufts (Fig. 7.80). Nuclear stratification of these indifferent cells can be impressive (up to 20 cells in thickness), but is of no significance. Nuclear atypia is generally mild to moderate, and the mitotic rate is low. Other characteristic features of these tumors are the presence of edematous papillae and the identification of acute inflammatory cells within both the stromal cores and the intracystic mucin (Fig. 7.81). As previously discussed in the section on the immunohistochemistry of mucinous ovarian tumors, endocervical-like mucinous borderline tumors have a müllerian rather than gastrointestinal immunophenotype.

Intraepithelial, microinvasive, and invasive carcinomas have been reported in a small proportion of cases of endocervical-like mucinous borderline tumors.[116–119] The presence of intraepithelial or microinvasive carcinoma in these endocervical-like tumors does not appear to adversely impact the prognosis, but some patients with associated invasive mucinous carcinomas have died of tumor-related disease. Analogous to the situation illustrated in Fig. 7.12 for SBTs, the gland-like structures that are commonly present within the stroma of endocervical-like mucinous borderline tumors that are related to randomly

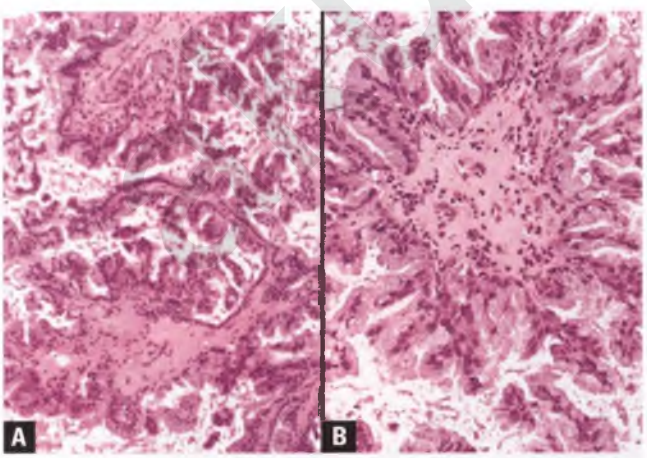

FIGURE 7.79. A,B: Endocervical-like mucinous borderline tumor. The arborizing papillae are lined by mucinous cells that resemble those found in the endocervix. Note the presence of detached tufts of mucinous cells in the background.

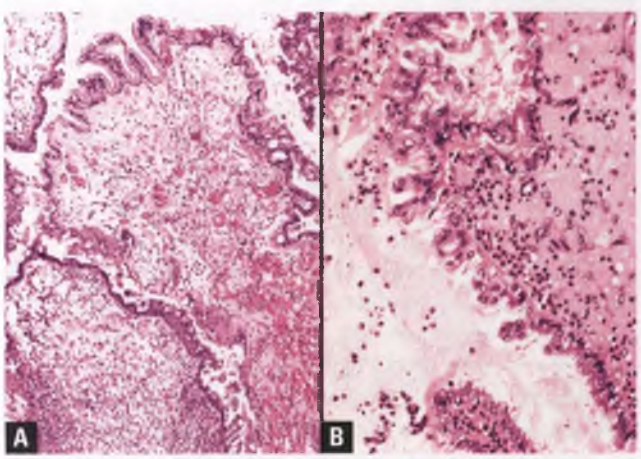

FIGURE 7.81. A,B: Endocervical-like mucinous borderline tumor. Some of the papillae are typically edematous, and acute inflammatory cells are often present within the stromal cores and intracystic mucin.

TABLE 7.1 Comparison of Ovarian Mucinous Borderline Tumors of Endocervical-Like vs. Gastrointestinal Types

Endocervical-like (15% of cases)	Gastrointestinal (85% of cases)
No goblet cells or other evidence of GI diff	Goblet cells or other evidence of GI diff
Mean age: 35–40 y	Mean age: 45–50 y
Mean size: 8 cm	Mean size: 20 cm
Unilocular or paucilocular	Multilocular
25% bilateral	5% bilateral
Grossly visible papillae (SBT-like)	Microscopic villoglandular structures
Stromal acute inflammation prominent	Stromal acute inflammation inconspicuous
Usually ER+ and PR+; CK20– (müllerian)	ER– and PR–; usually CK20+ (GI diff)
One-third associated with endometriosis	No special association with endometriosis
Incidence of pseudomyxoma peritonei: 0	Incidence of pseudomyxoma peritonei: 0[a]

[a]The previously reported rate of 17% was based upon the experience of three patients who in retrospect almost assuredly had misclassified ovarian tumors that were actually secondary to low-grade mucinous appendiceal tumors.[115] The current thinking is that the only primary ovarian mucinous tumors that are capable of producing pseudomyxoma peritonei are a subset of intestinal-type mucinous tumors that arise in association with mature cystic teratomas.[99,120]

oriented sections through branched epithelial invaginations should not be mistaken for actual stromal invasion.

A summary of the differences between endocervical-like and gastrointestinal type mucinous borderline tumors is presented in Table 7.1. Note that in comparison with gastrointestinal type mucinous borderline tumors, those of endocervical-like type are more likely to (a) occur in younger patients, (b) be of smaller size, (c) be bilateral, (d) have grossly recognizable papillae, and (e) be associated with endometriosis.

Mucinous Carcinoma[81–84,87]

Similar to the situation with mucinous cystadenomas and mucinous borderline tumors being "contaminated" by treacherous low-grade mucinous neoplasms of appendiceal origin, the older literature no doubt includes cases of ovarian involvement by metastatic mucinous carcinomas that have been misinterpreted as primary mucinous carcinomas. When these extraovarian sources are rigorously excluded, frankly invasive primary ovarian mucinous carcinomas are outnumbered by metastatic ones, and probably account for only about 3% of primary ovarian carcinomas.[121]

Primary ovarian mucinous carcinomas have similar clinical and gross pathologic features to that described for gastrointestinal-type mucinous borderline tumors, although solid tissue is generally more prominent in the carcinomas (Fig. 7.82). Only about 20% of patients have extraovarian spread at the time of presentation.

There are two types of stromal invasion that are frequently admixed with one another that, when present in greater than microinvasive amounts, qualify a mucinous neoplasm as frankly invasive. In the expansile (or confluent) pattern of invasion, an architecturally complex conglomeration of glands and/or papillae with significant nuclear atypia and minimal to no intervening stroma occupies a region that is incompatible with mere involvement of glands and papillae by intraepithelial carcinoma (Figs. 7.83–7.85). Cribriform, labyrinthine, and serpiginous patterns may be encountered. The infiltrative pattern is easier to recognize and features haphazard invasion of stroma by neoplastic glands, solid epithelial nests, and cords of cells in association with a reactive stroma (Fig. 7.86).

The cytoplasm of the neoplastic epithelial cells in mucinous carcinomas becomes increasingly mucin-depleted as they become more poorly differentiated, and their mucinous nature may have to be inferred from their association with recognizable mucinous differentiation elsewhere in the tumor. Nearly all ovarian mucinous carcinomas are considered to be of gastrointestinal type, although this is generally not specified in the pathology report and sometimes this determination is more of an act of faith than a histologic assessment.

Differential Diagnosis

The most important differential diagnostic considerations of intestinal-type mucinous tumors that may simulate the full

FIGURE 7.82. Mucinous carcinoma. The sectioned surface is solid, glistening, and gelatinous with focal hemorrhagic areas.

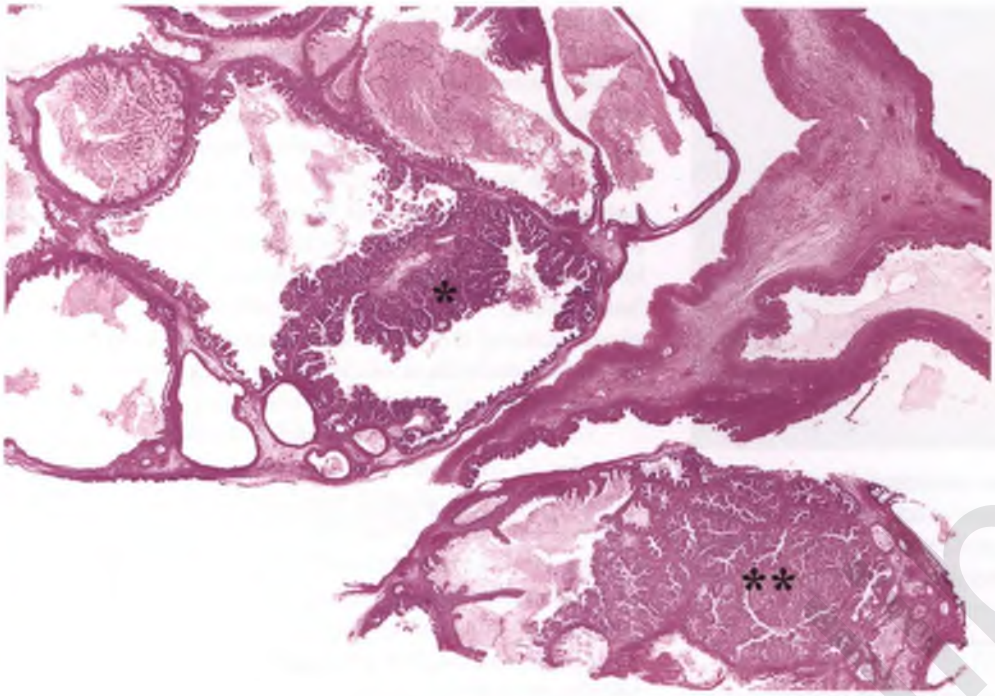

FIGURE 7.83. Mucinous carcinoma. This low-magnification view demonstrates the striking heterogeneity that is often present in mucinous ovarian tumors. In addition to benign and borderline areas, there is a focus of borderline tumor with intraepithelial carcinoma (*asterisk*) and an area that represents mucinous carcinoma on the basis of expansile invasion (*double asterisks*).

spectrum of mucinous tumors from cystadenoma to carcinoma are (a) metastatic adenocarcinomas from such sites as the colon, appendix, pancreas, biliary tract, stomach, small bowel, and endocervix, and (b) ovarian involvement by a low-grade mucinous adenomatous neoplasm of appendiceal origin. Bilateral mucinous tumors, those associated with high-stage disease, and those with an infiltrative pattern of stromal invasion should be considered metastases until proven otherwise. The strategies that are employed to distinguish primary from secondary mucinous ovarian tumors are presented in the section on the ovary as site of metastatic tumor near the end of this chapter. Although the presence of mucin-containing signet-ring cells in an ovarian tumor is highly suggestive of a metastatic signet-ring carcinoma, such cells may rarely be present in primary ovarian neoplasms.[122–124]

Prognosis

Carcinomas with an infiltrative pattern of stromal invasion behave more aggressively than those with expansile invasion in most studies, but stage is the most important prognostic factor. Only about 15% of stage I mucinous carcinomas recur, and most of these are tumors with an infiltrative pattern of invasion. In most studies, the histologic grade of the mucinous carcinoma has not been shown to be of prognostic significance in

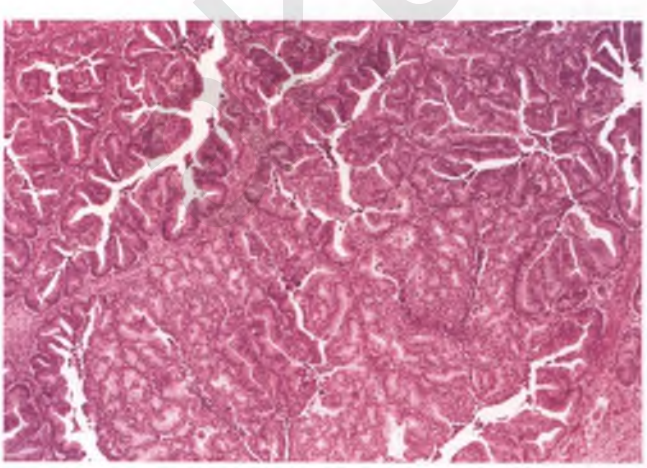

FIGURE 7.84. Mucinous carcinoma with expansile pattern of stromal invasion. Marked glandular complexity is present without an apparent preexisting architectural framework.

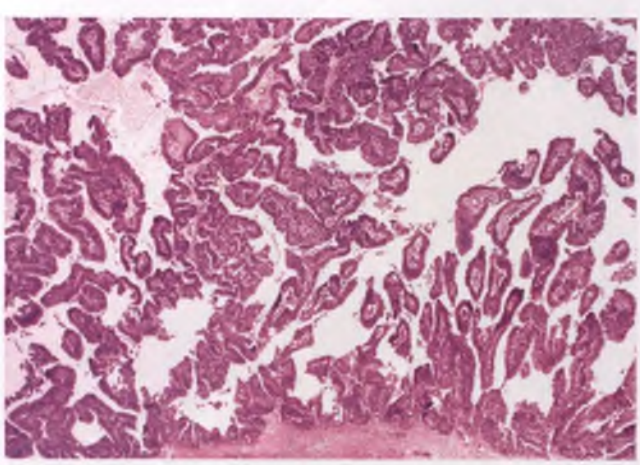

FIGURE 7.85. Mucinous carcinoma with expansile pattern of stromal invasion. The extent and complexity of this papillary proliferation, in conjunction with significant nuclear atypia that is not apparent at this magnification, warrant a diagnosis of mucinous carcinoma.

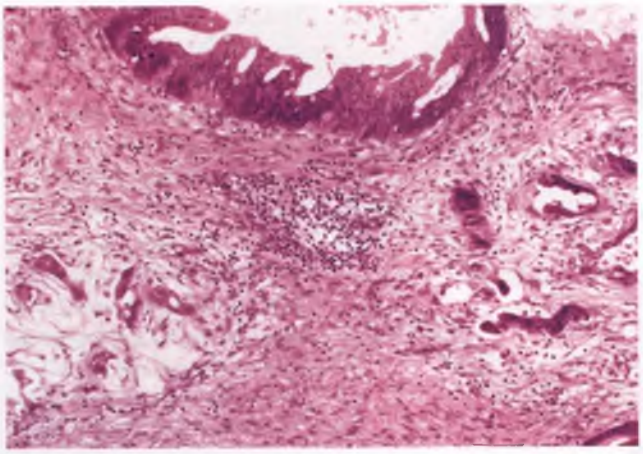

FIGURE 7.86. Mucinous carcinoma with infiltrative pattern of stromal invasion. The two adjacent clusters of infiltrating tumor beneath the borderline focus are associated with a stromal reaction that varies from small pools of mucin (left) to chronically inflamed granulation tissue (right).

stage I tumors. The 20% of patients with mucinous carcinoma who present with high-stage disease have a dismal prognosis.

Mucinous Tumors with Mural Nodules

Mural nodules of several different types may rarely be encountered in cystic mucinous neoplasms. A presumably reactive lesion referred to as a sarcoma-like mural nodule (SLMN) is the most common variant.[125,126] SLMNs are small, well-circumscribed, often multiple, and usually have a reddish-brown sectioned surface. Histologically, they are typically composed of a heterogeneous admixture of osteoclast-like giant cells and mitotically active spindle cells with varying degrees of nuclear atypia (Fig. 7.87). Extravasated erythrocytes and scattered inflammatory cells are present in the background, and the invariable association with the former suggests that an unusual reaction to mural hemorrhage may play a role in the formation of SLMNs. The spindle cells are strongly immunoreactive for vimentin, and cytokeratin staining varies from negative to focally and weakly positive.[126] The presence of SLMNs does not impact the prognosis of the tumor, which is dependent upon the benign, borderline, or malignant nature of the mucinous epithelial component and the tumor stage. Since the term "sarcoma-like" may arouse concern on the part of the clinician or patient, the pathology report should emphasize that the SLMN component of the tumor should be regarded as a benign, incidental finding.

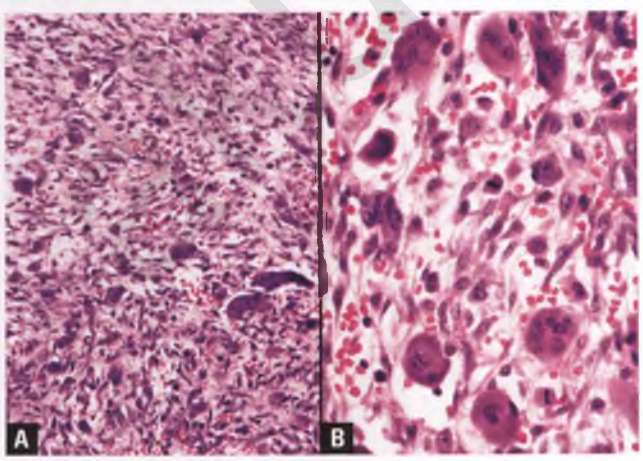

FIGURE 7.87. **A,B:** Sarcoma-like mural nodule. The nodule is composed of a mitotically active population of atypical spindle cells and osteoclast-like giant cells. Scattered extravasated red blood cells are also present.

In addition to SLMNs, nodules of anaplastic carcinoma may also be encountered within the wall of mucinous ovarian tumors.[127–129] Rhabdoid, spindled (sarcomatoid), and pleomorphic patterns have been described.[128] Although the mere presence of these carcinomatous nodules was initially thought to be associated with a poor outcome,[127] more recent data has demonstrated that unruptured stage I tumors with this finding still have an excellent prognosis.[128] In contrast to SLMNs, nodules of anaplastic carcinoma are poorly circumscribed at the level of their histologic interface with stroma, are more commonly necrotic, may be seen invading angiolymphatic spaces, generally lack osteoclast-like giant cells and extravasated erythrocytes, often exhibit at least focal frankly carcinomatous differentiation, and typically exhibit strong cytokeratin immunoreactivity.[128]

Rounding out the field of mural nodules within mucinous ovarian tumors are very rare examples of legitimate sarcoma, anaplastic carcinoma combined with reactive elements similar to those seen in SLMN, and leiomyoma.[128–130]

Guidelines for Histologic Sampling and Intraoperative Consultations[91]

As emphasized earlier in this section, mucinous ovarian tumors are notoriously heterogeneous, and must be well sampled. As in other areas of pathology, 1 section per cm of tumor is the usual guideline,[80] but this should be adjusted using common sense. It is of no value to submit 30 sections of a 30 cm unilocular, thin-walled mucinous cystadenoma; a few blocks that each contain 2 to 3 sections through the wall will suffice. On the other end of the spectrum, when presented with a 20 cm mucinous ovarian tumor that is largely solid, it is most cost effective to submit about 5 pilot sections to get an idea of the process, and then resort to submitting up to one section per cm of *solid/spongy* tumor in those cases where the additional sampling is likely to impact the diagnosis. Cases with intraepithelial carcinoma, microinvasion, and expansile invasion are at particularly high risk for harboring foci of frank stromal invasion, and should be extensively sampled in excess of the 1 section per cm guideline.[86,131]

The heterogeneity of mucinous neoplasms increases the possibility of sampling error at the time of an intraoperative consultation, since only a small portion of the tumor can be examined by frozen section. If the tumor has a significant solid or spongy component

and the frozen section from the most solid area looks benign or borderline, it is prudent to report only the presence of a mucinous neoplasm and defer the final diagnosis to permanent sections. Whether the tumor has a benign, borderline, or malignant appearance on frozen section, the surgeon should be told of the possibility of a metastatic lesion mimicking a primary ovarian tumor, especially if the tumor is bilateral and/or pseudomyxoma peritonei is present. If present, the appendix should be removed, and the stomach, bowel, and pancreas should be inspected. The surgeon should be warned of the possibility of finding mucinous carcinoma on the permanent sections, so that any staging procedure can be tailored to the patient's age and fertility status. Of course, all of these caveats are not necessary when confronted with a unilateral ordinary mucinous cystadenoma without solid or spongy components.

Endometrioid Adenofibromatous Neoplasms and Endometrioid Carcinoma[9]

This group of tumors is recognized by the presence of an epithelial component that resembles that found in proliferative, hyperplastic, or carcinomatous endometrium, and accounts for about 3% of all ovarian tumors.[1,16] Benign and borderline endometrioid tumors are rare, whereas endometrioid carcinoma is the second most common type of ovarian carcinoma, representing about 15% of the tumors in this group.[1,16] As is also the case for clear cell tumors, endometrioid tumors are frequently associated with endometriosis, and in some cases a transition between endometriotic and neoplastic epithelium can be demonstrated.

For practical purposes, endometrioid cystadenomas do not exist, since nearly all cystic lesions lined by benign endometrioid epithelium are at least focally associated with endometrial-type stroma, in which case a diagnosis of endometriotic cyst is more appropriate. Adenofibromatous endometrioid tumors tend to be quite heterogeneous from one area to another, which necessitates careful gross examination and extensive sampling of putative benign and borderline tumors to exclude foci of carcinoma (Fig. 7.88).

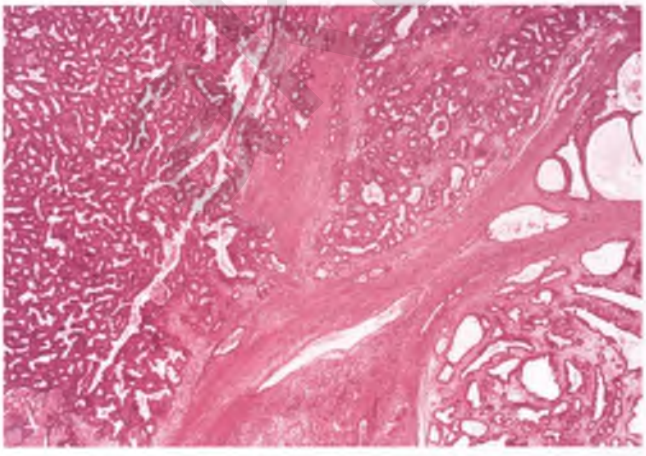

FIGURE 7.88. Endometrioid tumor with neighboring foci of benign (far right), borderline (mid upper right), and grade I carcinomatous (left) elements.

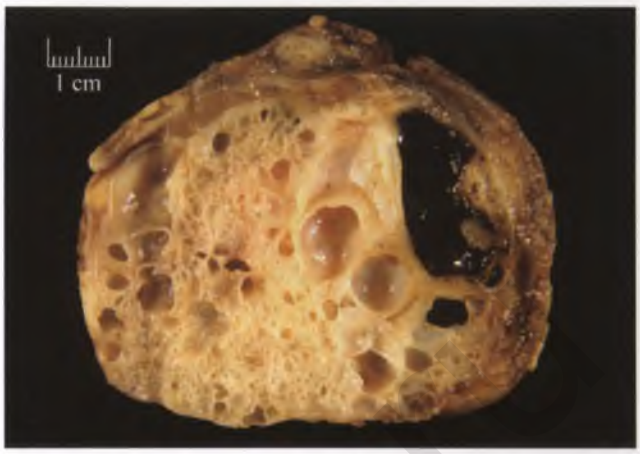

FIGURE 7.89. Endometrioid cystadenofibroma arising in association with an endometriotic cyst. The sectioned surface of this tumor has a honeycombed appearance due to the presence of innumerable cysts. The large cyst filled with dark "motor oil" fluid is an endometriotic cyst.

Endometrioid Adenofibroma[132–135]

Almost all of the rare endometrioid tumors that are classified as benign are adenofibromatous or cystadenofibromatous, and usually present in adult women as an incidental finding or a pelvic mass. These tumors are typically unilateral, range from 1 to 20 cm in diameter, and have a smooth external capsule. The sectioned surface is solid or spongy and pale yellow to off-white (Fig. 7.89). Endometrioid adenofibromas are composed of widely-spaced endometrioid glands with open lumens and varying degrees of cystic dilatation that are set within a prominent fibromatous stroma (Fig. 7.90). The glands are lined by columnar, nonciliated cells that resemble those seen in disordered proliferative endometria or within endometrial polyps,

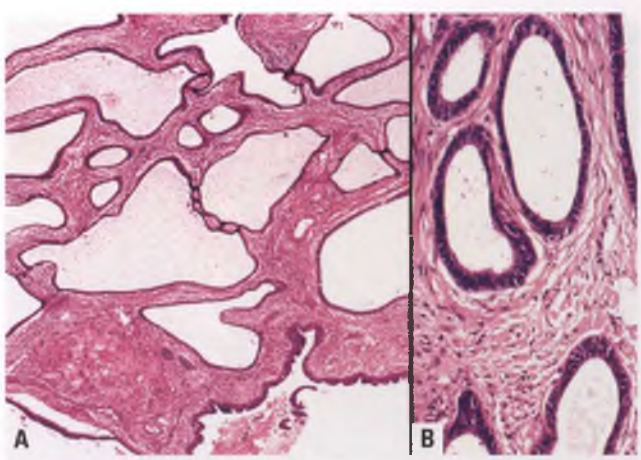

FIGURE 7.90. **A,B:** Endometrioid cystadenofibroma. The cystically dilated glands, some of which contain hemorrhagic material, are lined by endometrioid-type epithelium and embedded within a fibromatous stroma. Note: This is the histologic correlate of the tumor in the preceding figure.

except that mitotic figures are typically absent within the lining cells. Squamous differentiation, often in the form of morules, is commonly present.

To accommodate those tumors with a degree of epithelial proliferation and/or nuclear atypia that falls between that present in the usual adenofibroma and the borderline tumor, some pathologists use an additional category that has been variously termed "proliferative endometrioid tumor"[134] or "atypical endometrioid adenofibroma."[133] However, the terms "atypical proliferative endometrioid tumor" and "proliferating endometrioid tumor" have also been used as synonyms for borderline endometrioid tumors, rendering use of the terms "atypical" and "proliferative" hopelessly confusing in this context. Since both benign and borderline endometrioid tumors pursue a benign clinical course, one approach is to "fuhgeddaboudit" and lump such tumors into either the adenofibroma or borderline tumor category depending on whatever ill-defined criteria one chooses to use. For those pathologists who would like to convey the presence of a somewhat uppity, but clinically inconsequential, epithelial proliferation, I suggest using the term "endometrioid adenofibroma with epithelial hyperplasia." Such tumors feature glands that are more closely packed and irregularly shaped than those found in the usual type of endometrioid adenofibroma (Fig. 7.91). Cribriform and villoglandular proliferations, if present, are focal. The lining epithelium exhibits mild to moderate nuclear atypia with occasional mitotic figures. As rough guidelines, the upper range of architectural complexity and nuclear atypia exhibited in endometrioid adenofibromas with epithelial hyperplasia corresponds to that seen in mid-level complex atypical hyperplasia of the endometrium, and any single focus with such features should not exceed 5 mm.

Borderline Endometrioid Tumors[133–137]

Borderline endometrioid tumors occur in adult women (mean age of about 50 years) who may be asymptomatic or present with symptoms related to a pelvic mass or abnormal vaginal bleeding from concurrent endometrial hyperplasia or carcinoma. These ovarian tumors are solid, spongy, and/or cystic, typically unilateral, usually adenofibromatous, and have an average diameter of roughly 10 cm (Fig. 7.92). By definition, these tumors lack frank stromal invasion, although microinvasive foci analogous to those discussed in the sections on serous and mucinous borderline tumors may be found. Diagnostic criteria vary for this entity. Although endometrioid borderline tumors have a name that implies low malignant potential, the limited number of cases reported thus far (including those with microinvasion) have been clinically benign. In fact, the 5-year survival rate for grade 1, stage I endometrioid carcinoma is >95%.[136] Thus, there are virtually no outcome data to test the validity of the different criteria used to distinguish benign, borderline, and localized grade 1 malignant endometrioid tumors from one another.

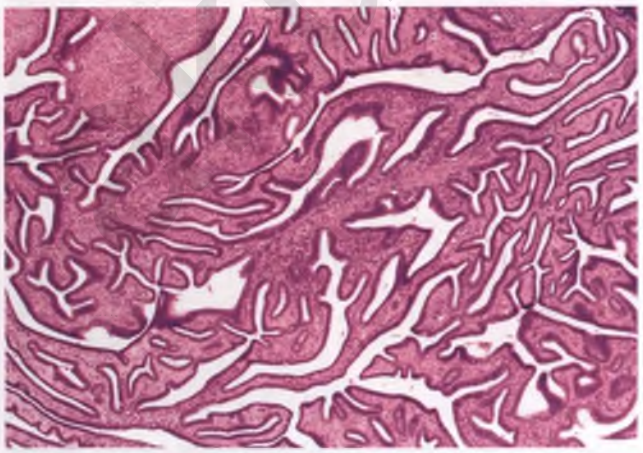

FIGURE 7.91. Endometrioid adenofibroma with epithelial hyperplasia. The elongated and irregularly branched glands are closely spaced and of endometrioid type.

FIGURE 7.92. Borderline endometrioid adenofibroma. Multiple polypoid nodules with a spongy sectioned surface protrude into a cystic cavity.

One pattern of borderline endometrioid tumor is characterized by an intracystic epithelial proliferation with a relatively simple villoglandular architecture that exceeds 5 mm in at least one focus.[134,137] More commonly, borderline endometrioid tumors are partially or entirely adenofibromatous. Before rendering a diagnosis of a borderline tumor when evaluating a noninvasive adenofibromatous endometrioid neoplasm, my approach is to require either (a) a significant (>5 mm in at least one focus) complex epithelial proliferation with closely approximated glands corresponding to endometrial lesions within the spectrum of mid-range complex atypical hyperplasia to those in which well-differentiated carcinoma cannot be excluded, or (b) at least somewhat crowded glands with low-grade malignant nuclear features in the range of that seen in well-differentiated endometrial adenocarcinoma (Fig. 7.93). Severe nuclear atypia analogous to the grade 3 nuclei of endometrial carcinoma of the uterine corpus may be seen, which warrants a diagnosis of borderline endometrioid tumor with intraepithelial carcinoma if it is more than a focal finding. As is the case for all endometrioid tumors, squamous differentiation, morular or otherwise, is often present,

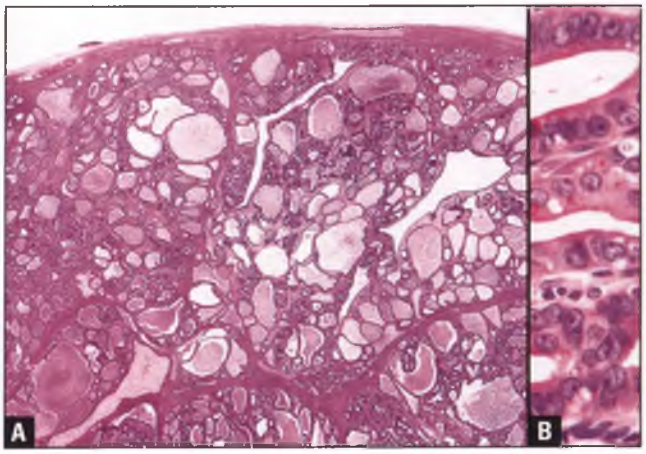

FIGURE 7.93. Borderline endometrioid adenofibroma. **A:** In this histologic correlate of the tumor in the preceding figure, cystically dilated glands are seen to account for the spongy gross appearance. **B:** Clusters of glands with low-grade malignant nuclear features (nuclear rounding, chromatin clearing, and distinct nucleoli) are present.

and some of the morules are likely to contain central plugs of necrotic debris (Fig. 7.94).[136]

Differential Diagnosis

In contrast to endometrioid adenofibromas with epithelial hyperplasia and borderline endometrioid tumors, endometriosis with superimposed epithelial hyperplasia usually occurs as a localized microscopic finding within an endometriotic cyst and features endometrial-type stroma that is closely associated with the crowded glands. The distinction of borderline endometrioid tumor from endometrial carcinoma is discussed in the following section.

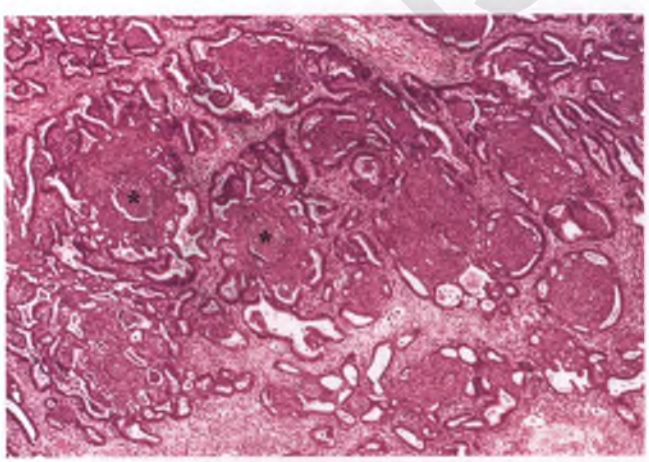

FIGURE 7.94. Borderline endometrioid adenofibroma. The solid areas of this crowded glandular proliferation represent squamous morules. Two of the morules have central necrosis (*asterisks*), which is a common incidental finding in these tumors. Stromal invasion is absent.

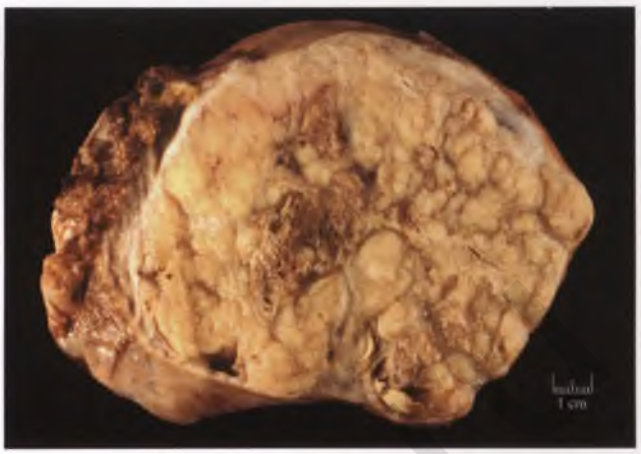

FIGURE 7.95. Endometrioid carcinoma. The sectioned surface of this formalin-fixed ovarian tumor is solid and lobulated and has central areas of necrosis. Hemorrhagic adhesions with some incorporated adipose tissue are present along the left surface of the tumor, which should be sampled to determine if they are related to endometriosis.

Endometrioid Carcinoma—Typical Pathologic Features[9,136–139]

Endometrioid carcinoma typically presents in an adult woman (mean age of 50–55 years) with symptoms related to a pelvic mass. About 45% of ovarian endometrioid carcinomas are confined to the ovary at presentation (stage I), as compared to the approximately 15% incidence of stage I serous carcinoma.[136,140] Of the endometrioid carcinomas that are stage I, about 15% are bilateral.

Grossly, endometrioid carcinoma has a rounded external surface and an average diameter of about 12 cm. The sectioned surface has a solid or mixed solid and cystic appearance that is not distinctive (Fig. 7.95). Some tumors may form a mass that thickens the wall and/or protrudes into the cavity of an endometriotic cyst (Figs. 7.96 and 7.97).

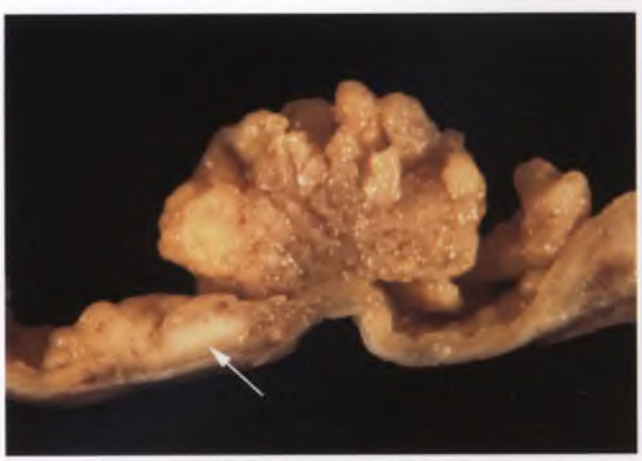

FIGURE 7.96. Endometrioid carcinoma arising within an endometriotic cyst. In this cross section through the wall of the cyst, the intraluminal polypoid projections and solid, off-white, thickened area in the wall (*arrow*) represent foci of carcinoma.

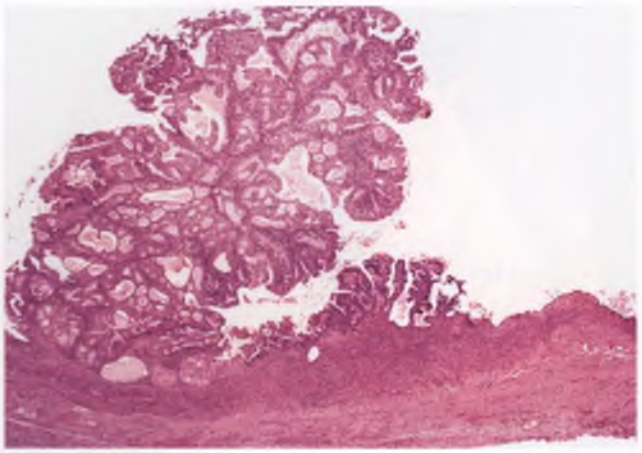

FIGURE 7.97. Endometrioid carcinoma arising within an endometriotic cyst. The intraluminal polypoid projections depicted in the preceding figure represent grade I endometrioid carcinoma. Residual endometriotic cyst is present at lower right.

Histologically, recognizably adenocarcinomatous areas of endometrioid carcinoma typically consist of masses of closely packed glands that are round, oval, tubular, and branched, which are often admixed with more complex villoglandular and cribriform patterns (Figs. 7.98–7.101). This appearance is referred to as a confluent or expansile pattern of stromal invasion. In this pattern, invasion is inferred by the extent and complexity of the epithelial proliferation rather than by directly visualizing carcinoma destructively and raggedly infiltrating connective tissue, which is seen in only a small proportion of these tumors. Squamous differentiation is often present (Fig. 7.102), and there may be associated endometriosis. Mucinous material within gland lumens is common, but intracytoplasmic mucin is definitionally absent or present in <10% of the tumor cells.

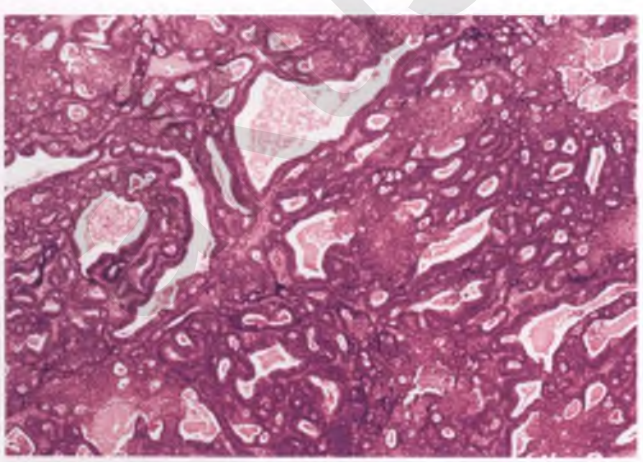

FIGURE 7.98. Endometrioid carcinoma, grade 1. Extensive confluent glandular proliferations such as this are diagnostic of carcinoma. The interspersed solid and more eosinophilic areas represent foci of squamous differentiation.

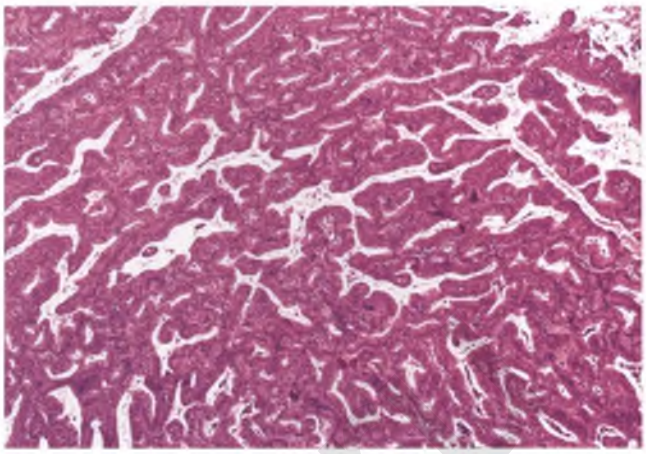

FIGURE 7.99. Endometrioid carcinoma, grade 1. This confluent glandular proliferation has a villoglandular architecture.

A spectrum of nuclear atypia may be seen in endometrioid carcinoma. Low-grade nuclei are oval to elongate with inconspicuous nucleoli and tend to be oriented perpendicular to the basement membrane of the glands and papillae that they line, whereas higher grade nuclei are rounded with prominent nucleoli and cleared or clumped chromatin. Similar to what can be seen in the endometrium, some well-differentiated endometrioid carcinomas feature marked architectural complexity with virtually non-existent nuclear atypia (Fig. 7.103). Most pathologists grade endometrioid carcinoma using the same FIGO criteria that are utilized when grading endometrial endometrioid carcinoma, as detailed in Chapter 4. Several examples of grade 1 endometrioid carcinoma have already been presented; an example of a grade 2 endometrioid carcinoma is depicted in Figure 7.104.

Endometrioid carcinomas are commonly associated with an adenofibromatous component, which can help to document the primary rather than metastatic nature of the

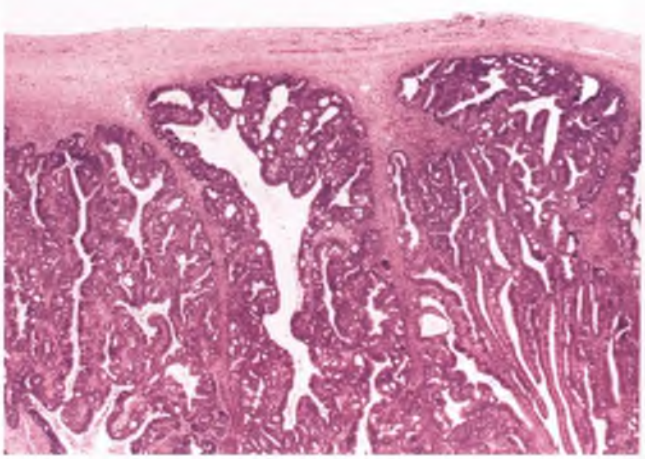

FIGURE 7.100. Endometrioid carcinoma, grade 1. This neoplasm exhibits an admixture of cribriform and villoglandular patterns.

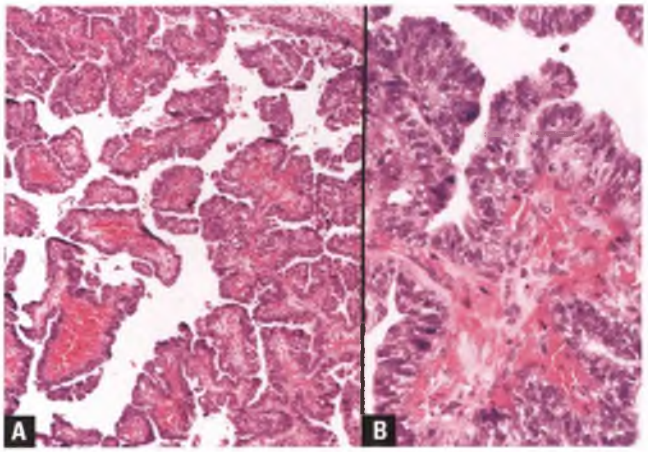

FIGURE 7.101. **A,B:** Endometrioid carcinoma with a papillary architecture.

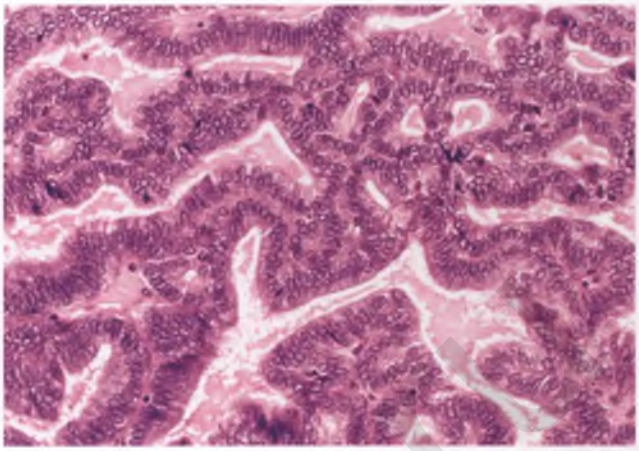

FIGURE 7.103. Endometrioid carcinoma, grade 1. The complex villoglandular architecture trumps the bland nuclear features and is indicative of carcinoma when present in sizable (>5 mm) amounts. Note how the nuclei tend to be elongated and oriented perpendicular to the basement membrane.

neoplasm.[132,133] In most such cases, the carcinoma is adjacent to a benign or borderline adenofibromatous tumor (Fig. 7.105), whereas rarely the adenofibromatous component itself has a malignant appearance (Figs. 7.106 and 7.107).[133]

Differential Diagnosis

Since most endometrioid carcinomas exhibit the less obvious expansile/confluent rather than infiltrative pattern of stromal invasion,[136] the lack of destructive infiltrative growth cannot be used to distinguish endometrioid borderline tumor from endometrioid carcinoma. To avoid undercalling endometrioid carcinoma as a borderline tumor, tumors with sizable (>5 mm) confluent epithelial proliferations analogous to that seen in endometrial adenocarcinoma are best interpreted as frankly invasive carcinomas. The pathologist also needs to be aware of the existence of adenofibromatous endometrioid carcinomas such as the one illustrated in Fig. 7.107, which feature a jagged and haphazard pattern of infiltration of fibromatous stroma by glands and solid epithelial nests; such tumors should not be misinterpreted as borderline endometrioid adenofibromas.[133]

The differential diagnoses of endometrioid carcinoma versus serous carcinoma, clear cell carcinoma (vs. the secretory pattern of endometrioid carcinoma), the endometrioid-like variant of yolk sac tumor, ovarian tumor of probable wolffian origin, and metastatic colorectal adenocarcinoma are discussed in the sections on these other entities. Specific attention is given to endometrioid carcinomas with sex cord-stromal-like areas and spindle cell differentiation and their differential diagnoses in the section on variants and unusual patterns in endometrioid carcinoma. The possibility of metastatic endometrial

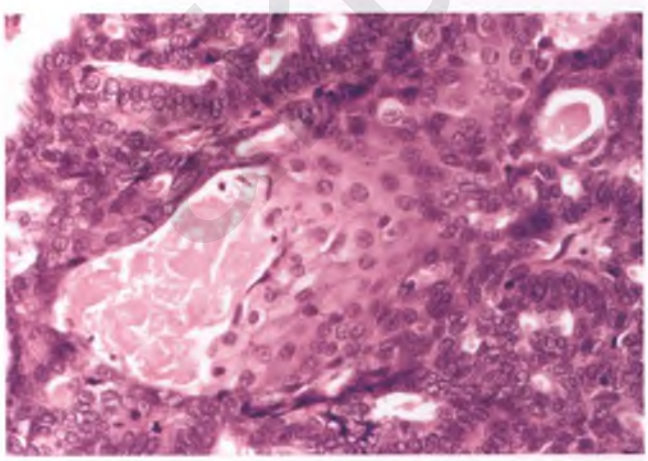

FIGURE 7.102. Endometrioid carcinoma. This high-magnification view highlights a central focus of squamous differentiation with keratin production.

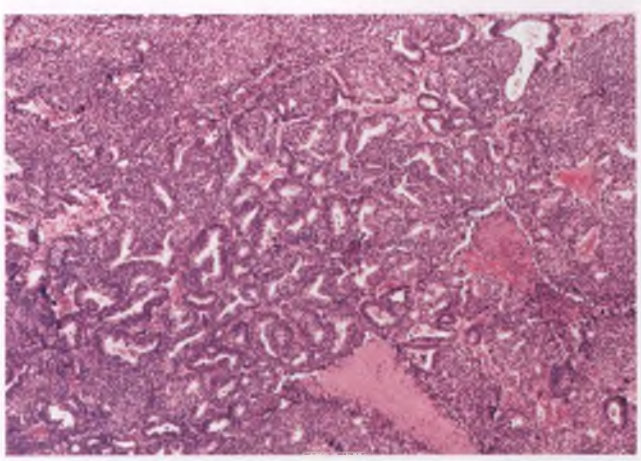

FIGURE 7.104. Endometrioid carcinoma, grade 2. The extent of the solid component, which does not show squamous or spindle cell differentiation, warrants the diagnosis of a grade 2 carcinoma. Note the presence of two foci of tumor cell necrosis.

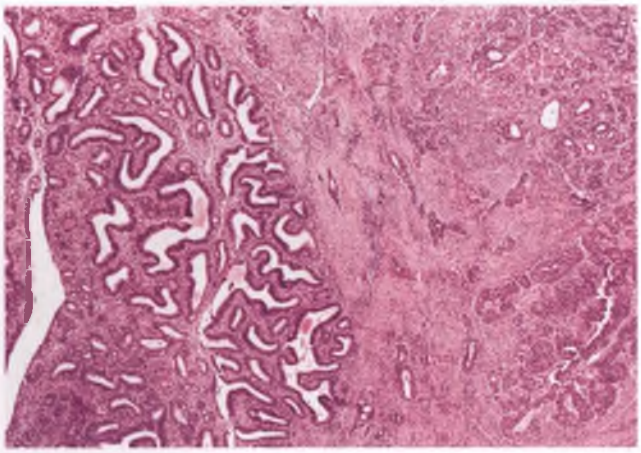

FIGURE 7.105. Endometrioid adenofibroma with epithelial hyperplasia (left) adjacent to endometrioid carcinoma with an infiltrative pattern of stromal invasion (right).

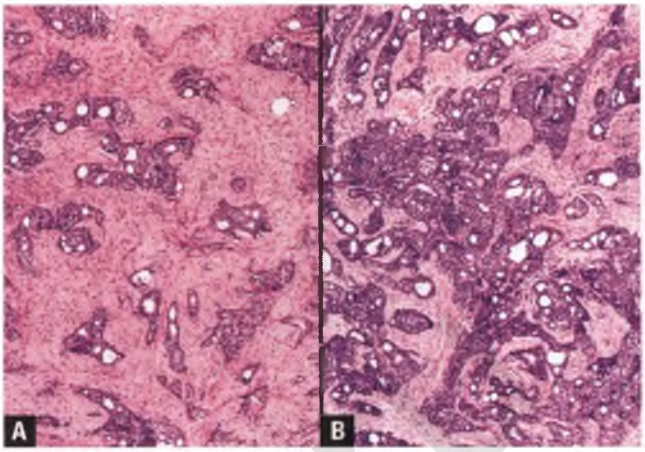

FIGURE 7.107. A,B: Adenofibromatous endometrioid carcinoma with varying degrees of cellularity of the carcinomatous component, which exhibits jagged and haphazard stromal infiltration by cribriforming glands and semisolid epithelial nests.

adenocarcinoma is addressed in the section on simultaneous endometrioid carcinoma of the ovary and endometrium.

Note: A parenchymal liver metastasis with pseudoendometrioid histology that is attributed to a primary ovarian endometrioid carcinoma is a red flag for misdiagnosed metastatic colorectal adenocarcinoma involving both sites.

Prognosis

Endometrioid carcinoma has a better prognosis than serous carcinoma, but it is commonly held that this is largely related to the higher incidence of low-stage tumors within the endometrioid group. However, a recent large study has shown that this survival advantage for endometrioid tumors holds true even when endometrioid and serous carcinomas are matched for stage (for stages II and III) and grade (for grades 2 and 3).[141]

Variants of Endometrioid Carcinoma

Endometrioid Carcinoma Resembling Sex Cord-Stromal Tumor[142–144]

This tumor constitutes a small proportion of endometrioid neoplasms, but has attracted attention because of the ease with which it can be misdiagnosed as a sex cord-stromal tumor. In most such cases, sertoliform architectural patterns result in a resemblance to Sertoli cell and Sertoli-Leydig cell tumors (SLCTs). These patterns include aggregates of small tubular glands with hollow lumens and solid anastomosing trabecular structures (Figs. 7.108 and 7.109). It is not uncommon for such cases to contain luteinized stromal cells that can be highlighted by their inhibin immunoreactivity, which heightens the resemblance to SLCTs.[144] A few tumors within

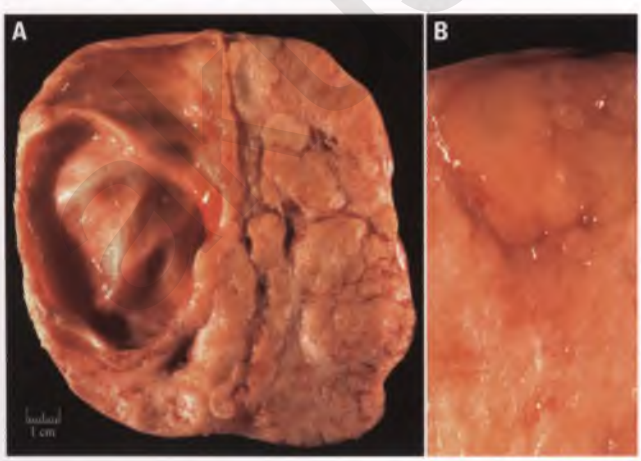

FIGURE 7.106. A,B: Endometrioid carcinoma with cystic and adenofibromatous components. Foci such as the fleshy yellow nodule at the top of **(B)** represent carcinoma dominated by its epithelial element, whereas the more fibrotic and rubbery areas are adenofibromatous.

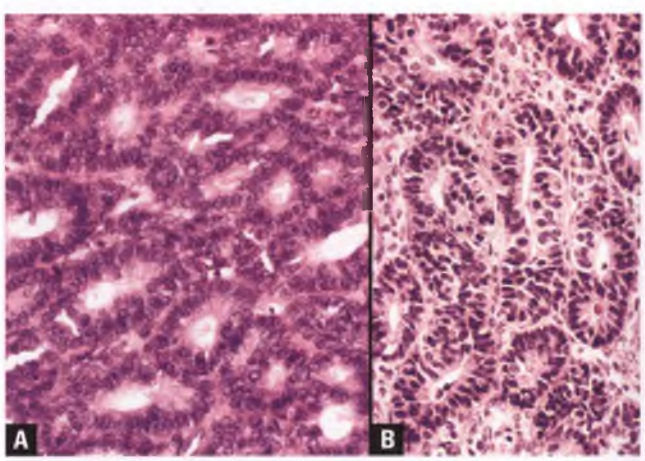

FIGURE 7.108. A,B: Sertoliform endometrioid carcinoma. The presence of closely packed, fairly uniform tubules that are small caliber results in a resemblance to sex cord-stromal tumors that are composed of tubules lined by Sertoli cells.

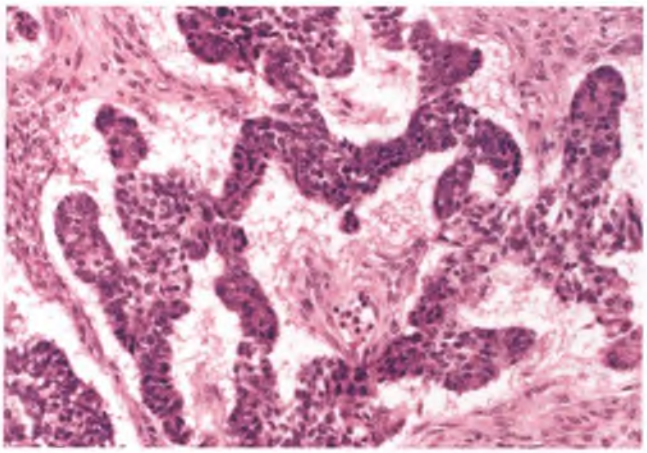

FIGURE 7.109. Sertoliform endometrioid carcinoma. The anastomosing trabecular architecture of this tumor can be misinterpreted as evidence of Sertoli cell differentiation.

this category mimic adult granulosa cell tumors (AGCT) by virtue of the presence of epithelial islands with microfollicular spaces containing eosinophilic material that results in formation of Call-Exner-like bodies (Fig. 7.110). Most of these tumors exhibit only mild to moderate nuclear atypia and low mitotic rates, and should be regarded as well-differentiated even when the sex cord-like elements exhibit a solid architectural pattern.

There are several clinical and pathologic features that can help to distinguish ovarian endometrioid carcinomas that resemble sex cord-stromal tumors from actual sex cord-stromal tumors. The endometrioid carcinomas in question (a) occur in an older age group (mean age 60–70 years) than patients with Sertoli and SLCTs (mean age 25–30 years), (b) are only rarely associated with clinical evidence of hormone production, (c) have areas of conventional endometrioid carcinoma with glands that exhibit more variability in size and shape and that contain luminal mucin, (d) may be associated with endometriosis or endometrioid endometrial adenocarcinoma, and (e) may contain an adenofibromatous component or foci of squamous differentiation. The lack of nuclear grooves is also a helpful differentiating feature in those cases that architecturally mimic an AGCT. In addition, the glands of endometrioid carcinomas typically show immunoreactivity for CK7 and epithelial membrane antigen but not for inhibin and calretinin, which is the exact opposite immunophenotype of that expected for the cords and tubules of sex cord-stromal tumors.[144–146] It should be noted that a positive result with pan-cytokeratin antibodies does not provide useful information in this situation, since both carcinomas and a significant proportion of granulosa cell tumors, Sertoli cell tumors, and SLCTs exhibit cytokeratin immunoreactivity.[147–149]

Endometrioid carcinomas resembling sex cord-stromal tumors have an excellent prognosis when limited to the ovary, as is usually the case.

Endometrioid Carcinoma with Spindle Cell Differentiation[150]

Another unusual finding in endometrioid carcinoma is the presence of a prominent spindle cell component. Tumors with this feature typically have a lobulated appearance when viewed at low magnification and are composed of an intimate admixture of spindle cells and endometrioid glands (Fig. 7.111). The nuclei of the glandular and spindle cell components share many features, and are of low to intermediate grade. The

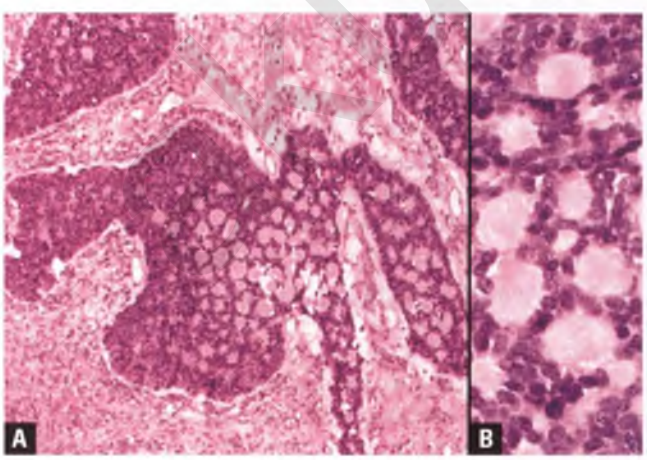

FIGURE 7.110. **A:** Endometrioid carcinoma resembling a granulosa cell tumor by virtue of the presence of a microfollicular architecture with Call-Exner-like bodies. **B:** In this high-magnification view of the microfollicular structures, note the absence of nuclear grooves.

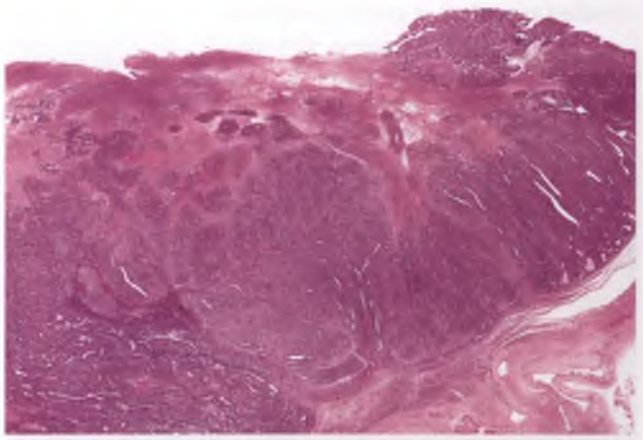

FIGURE 7.111. Endometrioid carcinoma with spindle cell differentiation. In this low-magnification view, note the lobulated architecture and the regional differences in the prominence of the spindle cell component. Typical grade 1 endometrioid carcinoma is present in the lower left and upper right portions of the image. Despite the predominantly solid architecture, this tumor is considered a grade 1 endometrioid carcinoma (see text).

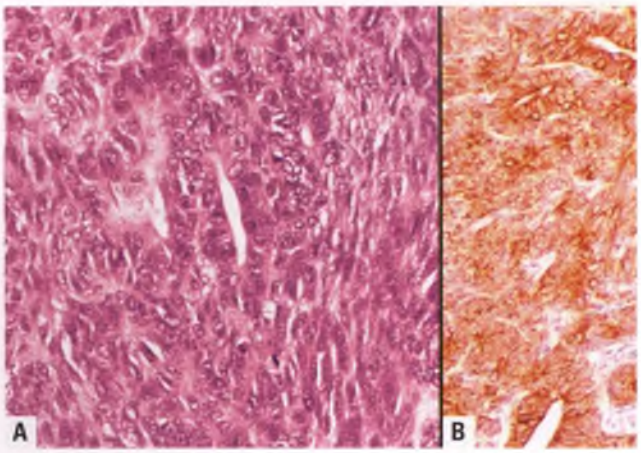

FIGURE 7.112. Endometrioid carcinoma with spindle cell differentiation. **A:** The spindle cell and glandular components have intermediate grade nuclei and merge with one another. **B:** Both the glands and the spindle cells are immunoreactive for cytokeratin.

spindle cells, which are thought to represent an abortive form of squamous differentiation, typically exhibit areas in which they merge imperceptibly with the glandular component (Fig. 7.112A). Further supportive of epithelial differentiation in the spindle cell component is the frequent finding of cytokeratin immunoreactivity in these cells (Fig. 7.112B). Because the solid growth pattern of the spindle cell component is best regarded as a metaplastic phenomenon, these areas should not be considered a pattern of solid growth for grading purposes. Instead, it is recommended that tumors of this type be graded according to the architectural and nuclear features of the glandular component, which results in nearly all such tumors being classified as grade 1 or grade 2 neoplasms.

Endometrioid carcinomas with spindle cell differentiation can be misinterpreted as a variety of other tumors, most of which can be excluded by thorough sampling with identification of at least focal endometrioid carcinoma of conventional type. In contrast to spindly endometrioid carcinomas, carcinosarcomas feature high-grade carcinomatous and sarcomatous components, and often contain heterologous elements. Moreover, the carcinomatous and sarcomatous components of a carcinosarcoma are usually haphazardly admixed with one another and gradual transitions between these elements are absent or inconspicuous, whereas such transitions are a characteristic feature of endometrioid carcinoma with spindle cell differentiation. Although there is significant overlap in immunohistochemical staining patterns between these two tumors, diffuse and strong immunoreactivity for cytokeratin within the spindle cell component is more commonly seen in this variant of endometrioid carcinoma than in carcinosarcoma. At low magnification, endometrioid carcinoma with spindle cell differentiation may resemble small cell carcinoma of pulmonary type when the latter tumor is associated with endometrioid carcinoma. However, the small cell component of this form of carcinoma features more primitive-appearing cells with nuclear molding, brisk mitotic activity, nuclear pyknosis, and geographic foci of tumor necrosis.[151]

Miscellaneous Variants

The presence of clear cells within endometrioid carcinomas can result in both secretory and non-secretory patterns.[152] The secretory pattern is characterized by the presence of subnuclear and/or supranuclear clear vacuoles, similar to that more commonly seen in the secretory variant of endometrial endometrioid adenocarcinoma (see Fig 4.193). Non-secretory clear cell patterns may result in abundant foamy, vacuolated, or pale cytoplasm, but an architecture that is typical of endometrioid carcinoma and an absence of hobnail cells facilitate their distinction from clear cell carcinoma.[152]

Other rare variants of endometrioid carcinoma include those in which ciliated or oxyphilic cells predominate or that contain a component of yolk sac tumor.[153–156] Although the aforementioned subgroup of ciliated tumors is provisionally classified within the endometrioid category for reasons discussed when initially described,[153] evaluation of a recent case of ovarian ciliated adenocarcinoma with immunohistochemical and molecular genetic techniques suggests serous differentiation.[157]

Simultaneous Endometrioid Carcinoma of the Ovary and Endometrium[9,158–163]

In 15% to 20% of ovarian endometrioid carcinomas, there is an associated endometrioid carcinoma of the endometrium. These patients have an average age of about 50 years and usually present with abnormal uterine bleeding. Most such cases represent dual primary malignancies, some represent endometrial tumors that have metastasized to one or both ovaries, and only a few of these cases represent ovarian carcinoma metastatic to the uterus. Obviously, whether the two tumors are dual primary malignancies or have a primary-metastatic relationship has significant therapeutic and prognostic implications.

In the usual case of independent primary malignancies, the ovary and the uterus are the only sites involved, the endometrioid tumors are of similar histologic appearance and grade (usually grade 1 or 2), the endometrial carcinoma is either noninvasive or only superficially invades the myometrium, coexistent atypical hyperplasia is present in the endometrium, and angiolymphatic invasion is absent. The presence of ovarian endometriosis, unilateral involvement of the substance of the ovary, and an associated adenofibromatous component constitute additional evidence supportive of a primary ovarian tumor. The excellent prognosis of these patients, which is similar to patients with stage I tumors in either site, is strong evidence in favor of the dual primary nature of these tumors. Patients with primary endometrioid carcinomas of both the ovary and endometrium tend to be about 10 years younger than patients with typical ovarian and endometrial cancer, and are more likely to be obese and nulliparous. These findings suggest that a hormonal "field effect" may play a role in the etiology of these tumors. Only about 5% of such cases can be attributed to hereditary nonpolyposis colorectal cancer syndrome.

Cases in which the uterine tumor exhibits lymphatic and/or deep myometrial invasion, the tumors are high grade, the ovarian involvement is bilateral and/or multinodular, ovarian vascular invasion is present, and cancer has spread beyond the uterus and ovaries are almost assuredly primary endometrial carcinomas with secondary ovarian involvement. More problematic are cases in which only one or a few of these features are present, such as when a uterine tumor exhibits deep myometrial invasion, but the only other site of involvement is a single ovary. In cases of this type, low-grade tumors probably represent separate primary malignancies, whereas the ovarian tumor in high-grade tumors is more likely to be a metastasis from the endometrial carcinoma.

The unusual cases of metastases from the ovary to the uterus are not likely to pose a diagnostic dilemma, since (a) there is typically metastatic disease elsewhere in the peritoneal cavity in addition to the ovarian and uterine involvement, (b) the entry point of the carcinoma is often the uterine serosa, which results in a "bottom heavy" distribution that is concentrated in the myometrium, (c) the tumor is likely to be a grade 3 carcinoma with invasion of uterine lymphatics, (d) atypical endometrial hyperplasia is absent, and (e) the resulting pattern of partial endometrial involvement is highly suggestive of a metastatic lesion.

Utilization of DNA ploidy and molecular genetic studies to sort out the issue of dual primary tumors versus tumors with a primary-metastatic relationship may be helpful in selected instances, but is usually not necessary and has its limitations.[164–166] Specifically, obtaining different results in the two different sites does not necessarily indicate that the two tumors arose independent of one another; these results could be related to heterogeneity of a tumor when compared to its metastatic site. Conversely, the finding of the same genetic abnormality in tumors from two different sites does not necessarily indicate that one tumor is a metastasis from the other, since the milieu that induced two independent tumors may be responsible for their sharing the same genetic alteration. Immunohistochemistry may have some utility in determining the relationship between simultaneous endometrial and ovarian endometrioid carcinomas, since nuclear as opposed to membranous staining for β-catenin holds promise as an indicator of independent tumors in this situation, but further experience with this marker is needed.[167] If ancillary studies are performed in an attempt to facilitate the diagnosis, they should always be interpreted in the context of the other clinicopathologic findings, which by themselves are usually sufficient to guide clinical management in ambiguous cases.

Carcinosarcoma (Malignant Mixed Mesodermal Tumor)[††168–171]

Carcinosarcomas are biphasic neoplasms that are composed of an admixture of epithelial and mesenchymal elements, both of which are malignant. In homologous tumors, the sarcomatous component typically has the appearance of a high-grade spindle cell sarcoma of no special type, whereas heterologous tumors have sarcomatous elements that are associated with tissue types that are not ordinarily found in the ovary (most commonly chondrosarcoma or rhabdomyosarcoma, followed by osteosarcoma and liposarcoma). In most series, heterologous tumors outnumber homologous ones. Carcinosarcomas account for about 1% of all malignant primary ovarian tumors and typically present as a pelvic mass in a postmenopausal woman (mean age of roughly 65 years). The vast majority of these tumors have spread beyond the ovary at the time of presentation. Some cases are bilateral, but it is often difficult to determine if involvement of both ovaries is simply a manifestation of pelvic spread or truly represents dual primary neoplasms.

Grossly, carcinosarcomas are typically smooth-surfaced with some bosselations and have an average size of about 15 cm. Their sectioned surface is predominantly solid with a variably prominent cystic component. The solid tissue has a variegated off-white, pale yellow, tan, and brown appearance with patches of hemorrhage and necrosis, and cartilage or bone may be grossly apparent in some heterologous tumors (Figs. 7.113 and 7.114). Their high-grade epithelial component is usually a serous, endometrioid, or undifferentiated carcinoma, and their mesenchymal component is as described above. Heterologous foci are generally found embedded within areas of homologous sarcoma. The proportions of carcinoma and sarcoma can vary widely from case to case, and thorough sampling may be necessary to identify both components. In areas where the carcinomatous and sarcomatous elements are intimately admixed, they are sharply demarcated and transitions of one component into the other are uncommon (Fig. 7.115A). The carcinomatous component of carcinosarcoma is strongly and diffusely immunoreactive for cytokeratin, whereas the sarcomatous

FIGURE 7.113. Carcinosarcoma with heterologous (chondrosarcomatous) elements. The sectioned surface shows a mainly solid tumor with areas of hemorrhage and necrosis. Scattered foci with cartilaginous differentiation are grossly recognizable, such as the area marked by the *arrow*.

[††]Note that the term malignant mixed müllerian tumor is often used incorrectly as a synonym for ovarian tumors of this type; unlike the uterus, fallopian tubes, and upper portion of the vagina, the ovary is not embryologically related to the müllerian duct.

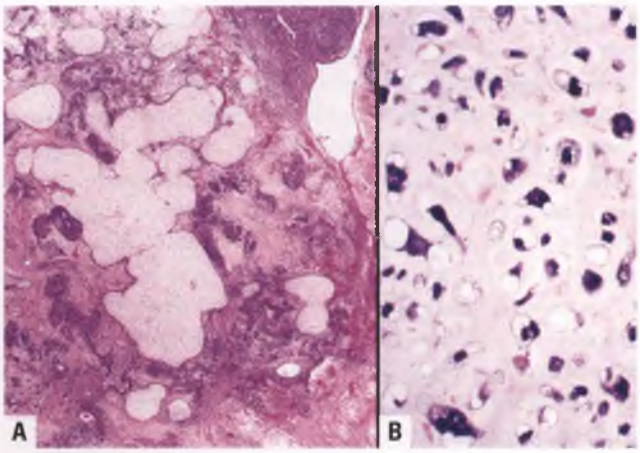

FIGURE 7.114. Carcinosarcoma with heterologous (chondrosarcomatous) elements. **A:** Islands of malignant cartilage are present within a partially necrotic tumor that also contains cellular blue foci of spindle cell sarcoma admixed with adenocarcinoma. **B:** Although not apparent at low power, this high-magnification view highlights the increased cellularity, nuclear atypia, bi- and multinucleation, and mitotic activity of the chondrosarcomatous component.

elements are usually either negative or only focally positive for this marker of epithelial differentiation (Fig. 7.115B).[172,173] However, there are cases of carcinosarcoma in which most of the sarcomatous cells are cytokeratin-positive.[172,173]

Although most carcinosarcomas are of monoclonal origin and are thought to represent a form of metaplastic carcinoma,[174] those in which the carcinomatous and sarcomatous components are topographically distinct may be biclonal and represent so-called "collision tumors" (Figs. 7.116 and 7.117).

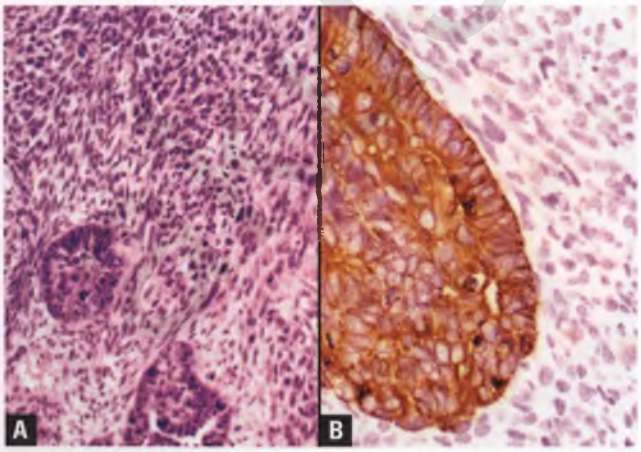

FIGURE 7.115. Carcinosarcoma. **A:** Two malignant glands are admixed with a spindle cell sarcoma, but the two components are sharply demarcated from one another. **B:** The island of carcinoma is strongly immunoreactive for cytokeratin, whereas the spindle cell sarcoma is nonreactive.

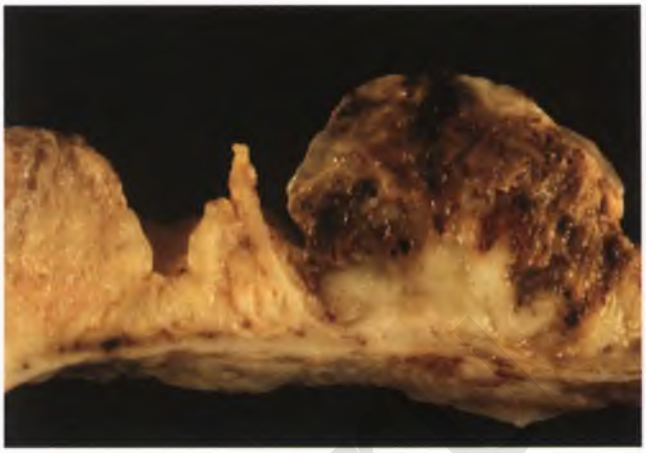

FIGURE 7.116. Cross section through the wall of a cystic ovarian carcinosarcoma. The left half of the image is carcinoma, and the right half is sarcoma. The carcinomatous component is tan, homogeneous, and partially papillary, whereas the sarcomatous component is grayish-white and fleshy with prominent areas of hemorrhage and necrosis.

Additional images of carcinosarcoma are provided in the section on their more common uterine counterpart in Chapter 4.

Differential Diagnosis

The differential diagnosis of carcinosarcoma includes poorly differentiated carcinoma with associated spindle cells, immature teratoma, endometrioid carcinoma with spindle cell differentiation, and poorly differentiated Sertoli-Leydig cell tumor (SLCT).

- The distinction of carcinosarcoma from a poorly differentiated carcinoma with either a reactive spindle cell stroma

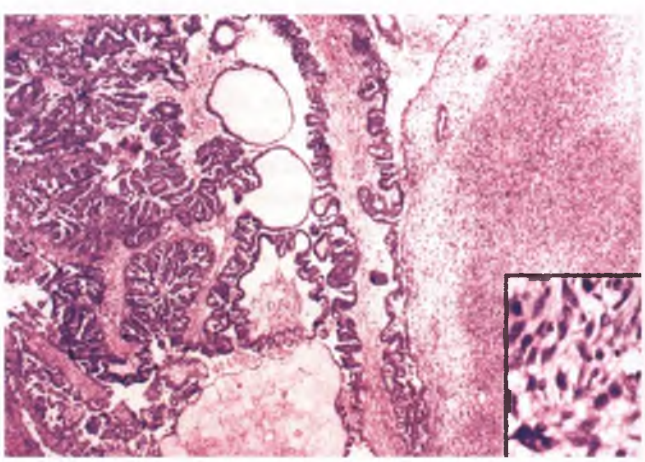

FIGURE 7.117. Carcinosarcoma (histologic correlate of preceding image). The left side of the image shows features of a high-grade papillary serous carcinoma, and the right side and inset document the presence of a spindle cell sarcoma.

or spindle cell differentiation can be problematic, and rests upon the identification of true sarcomatous elements. Although reactive stroma can be cellular and mitotically active, its distinction from frank sarcoma is usually possible on morphologic grounds. The presence of a sharp interface between the purported sarcomatous element and the carcinoma supports the diagnosis of carcinosarcoma over poorly differentiated carcinoma with spindle cell differentiation (sarcomatoid carcinoma). Fortunately, these difficult distinctions are of little, if any, clinical significance.

- In contrast to carcinosarcomas, immature teratomas occur in a younger age group, are much more likely to present with disease confined to the ovary, feature tissues derived from the ectoderm and endoderm in addition to the mesoderm, have a malignant component that consists predominantly of neuroepithelial elements, and have epithelial and stromal components that generally lack the frankly malignant appearance that characterizes carcinosarcoma.
- The differential diagnoses of carcinosarcoma with endometrioid carcinoma with spindle cell differentiation and poorly differentiated SLCT are discussed in the sections on these other entities.

Prognosis

Carcinosarcomas are aggressive tumors with a poor prognosis. Most recent series have not demonstrated a prognostic difference based upon whether the mesenchymal component is homologous or heterologous. As is true for ovarian cancer in general, the chances of survival are improved in those patients whose tumors are optimally debulked at the time of initial surgery.

Adenosarcoma[175]

Primary ovarian adenosarcomas are very rare and are analogous to their more common uterine counterparts. They typically present in adult women as a unilateral solid mass with a mean size of 14 cm that may have cystic or exophytic components. The appearance of the sectioned surface and histology of these tumors does not differ from uterine adenosarcoma, which are illustrated in Figures 4.321–4.328. It should be noted that mitotic counts in ovarian adenosarcoma can be very low and a given threshold of mitotic activity should not be used as one of the defining features of this neoplasm. These tumors are prone to rupture, particularly intraoperatively, which contributes to the more aggressive behavior of ovarian as compared to uterine adenosarcomas (75% vs. 25% recurrence rate, respectively, with a correspondingly higher incidence of tumor-related deaths).

Differential Diagnosis

The keys to correctly identifying ovarian adenosarcoma are an awareness that this tumor can originate in the ovary and thorough sampling to identify the characteristic architectural features of this neoplasm, which are (a) glandular spaces surrounded by hypercellular cuffs of sarcomatous stroma and (b) polypoid protrusions of cellular stroma that project into dilated glands that result in the formation of "shark mouth" or leaf-like patterns. Identification of these features helps to distinguish ovarian adenosarcoma from endometrioid adenofibroma and polypoid endometriosis, which are the main differential diagnostic considerations.

Endometrioid Stromal Sarcoma[176,177]

Clinicopathologic data on primary ovarian endometrioid stromal sarcoma (ESS) is difficult to extract from the literature, since the only large series of these extremely rare tumors[176] reported in a partially combined fashion 14 cases of apparent primary ovarian ESS with 9 additional cases that at some point also had uterine ESS, 4 of which were subsequently reported as ovarian metastases of primary uterine ESS.[178] Primary ovarian ESS tends to present in adult women with abdominal swelling or pain related to an ovarian mass. These tumors have a smooth external surface, average about 10 cm in size, are typically either solid or solid and cystic, and have a sectioned surface that is tan to pale yellow that may contain foci of hemorrhage and/or necrosis. Associated endometriosis is present in about half of the cases and may have been obliterated by tumor overgrowth in others, and is theorized to be the most common source of the endometrioid stromal cells that undergo neoplastic transformation to produce this type of tumor in this site.

Primary ovarian ESSs have a histologic appearance that is similar to their much more common uterine counterparts and share the potential to exhibit focal sex cord-like differentiation, endometrioid glandular differentiation, and interspersed foam cells. In typical cases, diffuse sheets of uniform cells that resemble endometrial stromal cells of the normal proliferative phase are supported by a characteristic network of capillaries and/or arterioles (Fig. 7.118). In areas where this vascular

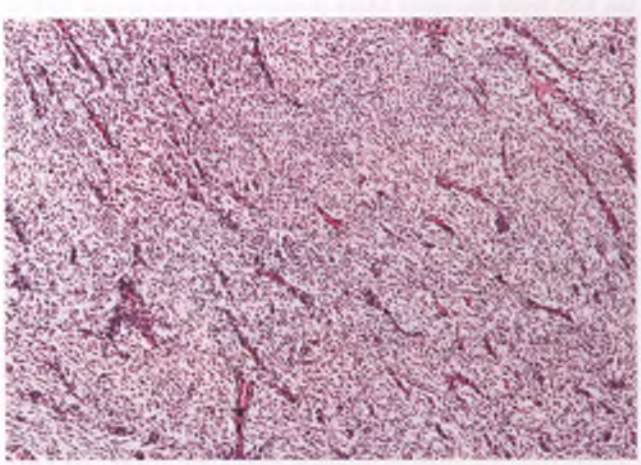

FIGURE 7.118. Endometrioid stromal sarcoma. A prominent network of capillaries and/or arterioles is typically present in at least a portion of the tumor, which exhibits a sheet-like growth pattern.

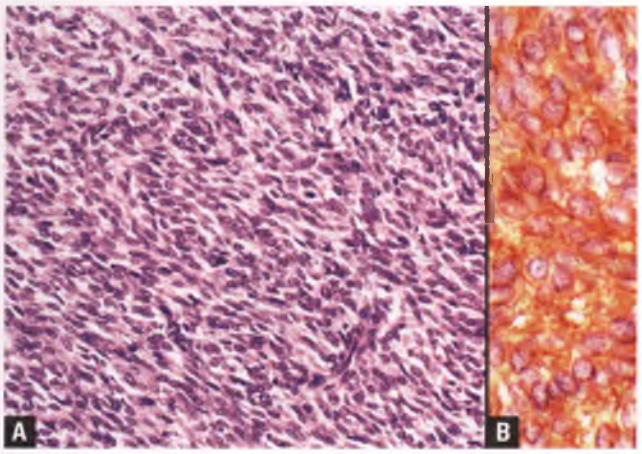

FIGURE 7.119. Endometrioid stromal sarcoma. **A:** In areas where the classic vascular pattern is lacking, the tumor can resemble a cellular fibroma or diffuse adult granulosa cell tumor. **B:** The tumor is diffusely and strongly immunoreactive for CD10, which supports endometrial stromal differentiation in this setting.

pattern is lacking or inconspicuous, primary ovarian ESS may resemble a cellular fibroma or an AGCT with a diffuse or sarcomatoid pattern of growth (Fig. 7.119A). In about half of the cases, the mimicry of an ovarian fibroma is accentuated by the presence of fibromatous areas with a storiform pattern. Diffuse and strong CD10 immunoreactivity, which is typical of ESS, can facilitate distinction of this tumor from its mimics (Fig. 7.119B).[179] Note that whereas the tongue-like pattern of stromal infiltration that is characteristic of uterine ESS is often seen in areas of extraovarian involvement, the ovary itself usually does not exhibit this feature.

Differential Diagnosis

Efforts must be made to attempt to distinguish primary ovarian ESS from the more likely possibility of metastatic ESS of uterine origin. Before a definitive diagnosis of primary ovarian ESS is rendered in a case with convincing endometrial stromal differentiation, the possibility of a primary uterine ESS should be excluded by review of prior or concurrent histologic material from the patient's uterus, with a cautionary note regarding the uncertainty of the primary site appended to those cases in which the uterus has not yet been removed. In addition to documenting the lack of uterine involvement, the diagnosis of primary ovarian ESS is further bolstered by (a) the presence of a unilateral ovarian tumor that has not spread beyond the ovary at the time of presentation and (b) associated endometriosis.

The differential diagnosis of primary ovarian ESS with cellular fibroma and AGCTs of diffuse and sarcomatoid types that was touched upon above is discussed further in the sections on these entities. In contrast to adenosarcoma, the variant of ESS with endometrioid glands has a focal rather than widespread glandular distribution and lacks periglandular stromal condensation and polypoid protrusions into cystically dilated glands. ESS with an endometrioid glandular component may also raise the possibility of endometriosis, but is distinguished by the presence of a sizeable mass that is predominantly solid, other areas that are more typical of ESS, and occurrence in women who are usually beyond their reproductive years.

Prognosis

Primary ovarian ESS tends to behave similarly to high-stage uterine ESS and commonly presents with extraovarian disease in the abdomen and pelvis. Recurrences are common, may occur several years after the initial presentation, and can either cause death or be compatible with long-term survival. Although high mitotic counts were predictive of poor outcome in one series,[176] they were not in another study of primary extrauterine ESSs that were followed for a longer period of time (mean of 83 months).[177] Sorting through the issue of the potential importance of the mitotic index in these tumors is further complicated by the fact that the upper end of nuclear atypia that is allowed before an ESS is interpreted as an undifferentiated sarcoma is subjective and tumors with significant nuclear atypia are more likely to have brisk mitotic activity. As discussed in Chapter 4 for uterine ESS, there may be a role for a category of ovarian modern-day high-grade ESS that serves as a buffer zone between the usual low-grade form of ESS and undifferentiated sarcoma.

Clear Cell Tumors

Nearly all ovarian clear cell tumors are clear cell carcinomas, which account for 5% to 10% of ovarian carcinomas.[1,16,140] Clear cell tumors are generally recognized by the dominance of cells with clear cytoplasm, which is related to the presence of abundant intracytoplasmic glycogen. Hobnail cells with bulbous nuclei that protrude into luminal spaces are commonly seen lining cysts and tubules, and are another characteristic feature of these tumors. As discussed below, other less common cell types may also be present. A significant proportion of clear cell tumors are associated with, and presumably arise from, endometriosis or endometriotic cysts.[14,180,181]

Benign and Borderline Clear Cell Adenofibromas[182,183]

Almost all of the rare clear cell tumors that are benign or borderline have an adenofibromatous architectural pattern, and usually present in adult women as a pelvic mass or are found during evaluation of abnormal uterine bleeding related to endometrial hyperplasia. These tumors are typically unilateral, average 10 to 15 cm in diameter, have a smooth external surface, and have a sectioned surface that is solid or spongy and pale yellow to off-white. By definition, these tumors lack frank stromal invasion, although microinvasive foci analogous to those discussed in the sections on serous and mucinous borderline tumors may be found within the borderline variant.

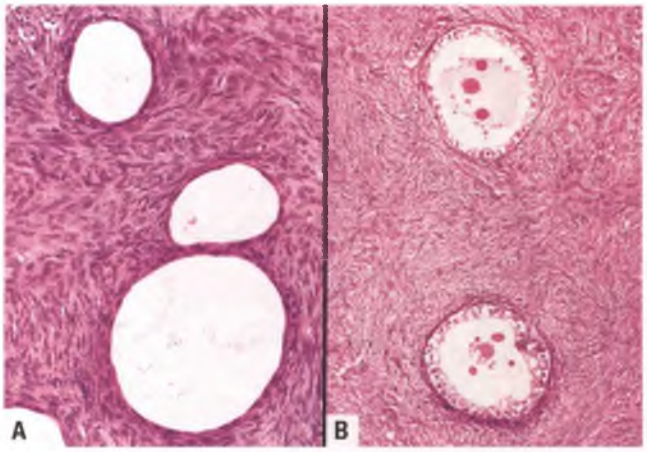

FIGURE 7.120. Clear cell adenofibroma. **A:** Simple and slightly dilated glands are lined by flattened cells. This appearance suggests clear cell differentiation, which should be sought in other areas of the tumor. **B:** Clear cell adenofibroma with glands lined by bland cells with abundant clear cytoplasm.

Histologically, clear cell adenofibroma is composed of simple glands that are widely spaced and embedded within a fibromatous stroma. The round to oval glands are slightly dilated and are variably lined by flattened, cuboidal, eosinophilic, clear, and hobnail cells (Fig. 7.120). The epithelial component exhibits absent to minimal mitotic activity and no significant nuclear atypia. Clear cell adenofibromas should be sampled extensively to exclude the presence of a borderline or malignant clear cell component.

A clear cell adenofibroma is designated as "borderline" when the cells lining the glands exhibit significant nuclear atypia, as characterized by chromatin clumping, irregular nuclear contours, and prominent nucleoli (Fig. 7.121). In tandem with the nuclear changes, the glands may become focally crowded and may exhibit some budding and branching, and the lining cells may be stratified to up to 3 cells in thickness. Occasional small, solid nests of epithelial cells may also be present. Hobnail cells are typically prominent. Mitotic activity remains inconspicuous, unless there is superimposed intraepithelial carcinoma. Extensive sampling is necessary to exclude microinvasion or a coexisting clear cell carcinoma, with particular attention paid to areas that are grossly fleshy rather than fibromatous. Nearly all borderline clear cell adenofibromas that have been adequately sampled pursue a benign clinical course, but experience with these rare tumors is limited.

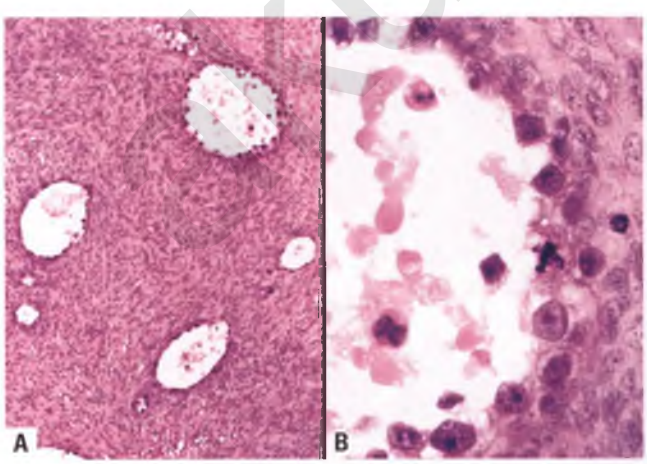

FIGURE 7.121. **A,B:** Borderline clear cell adenofibroma. Some investigators append the phrase "with intraepithelial carcinoma" for borderline tumors with lining epithelial cells with this degree of atypia.

Clear Cell Carcinoma[9]

Clear cell carcinoma typically presents in an adult woman (mean age of 50–55 years) with symptoms related to a unilateral pelvic mass. About half of patients with clear cell carcinoma present with stage I disease, which is significantly more frequent than the incidence of stage I serous carcinoma.[70,140,184]

Grossly, clear cell carcinoma has a smooth external surface and an average size of roughly 15 cm. Most commonly, the tumor consists of one or more cysts with areas of pale yellow tumor that thicken the wall and protrude as polypoid masses into the cyst lumen (Fig. 7.122). Occasional tumors have a nonspecific solid or mixed solid and cystic appearance. Tumors that arise in association with endometriotic cysts have dark-colored luminal fluid and there is similar discoloration of portions of the cyst lining (Fig. 7.123).

Histologically, the three main patterns of clear cell carcinoma are solid, tubulocystic, and papillary (Figs. 7.124–7.126).[70] These patterns are often present within different areas of the same tumor, with papillary architecture predominating in grossly polypoid areas. The papillae may have hyalinized stromal cores, which can help to suggest the diagnosis of clear cell carcinoma (Fig. 7.127), and psammoma bodies may be present. The most common cell types are the glycogen-rich

FIGURE 7.122. Clear cell carcinoma. This intracystic tumor contains numerous masses and polypoid tumor nodules arising from the inner cyst wall. Histologically, a papillary pattern predominated.

FIGURE 7.123. **A,B:** Clear cell carcinoma arising within an endometriotic cyst. In these sections through the wall of a portion of an endometriotic cyst, solid yellow nodules of clear cell carcinoma are seen projecting into the cyst lumen.

clear cell and the hobnail cell. Clear cells are usually the exclusive cell type in the solid areas and are seen in the other patterns as well, whereas hobnail cells are preferentially found lining tubules and cysts (Fig. 7.128). The tubules and cysts of clear cell carcinomas may contain luminal mucin, but intracytoplasmic mucin is generally not present beyond that in the apical cytoplasm of the lining cells. Less common cell types, which are also less diagnostic of clear cell tumors, are (a) flattened to cuboidal cells that tend to line small cysts, (b) oxyphilic cells that have abundant eosinophilic cytoplasm usually seen forming sheets, solid nests, or trabeculae (Fig. 7.129),[185] and

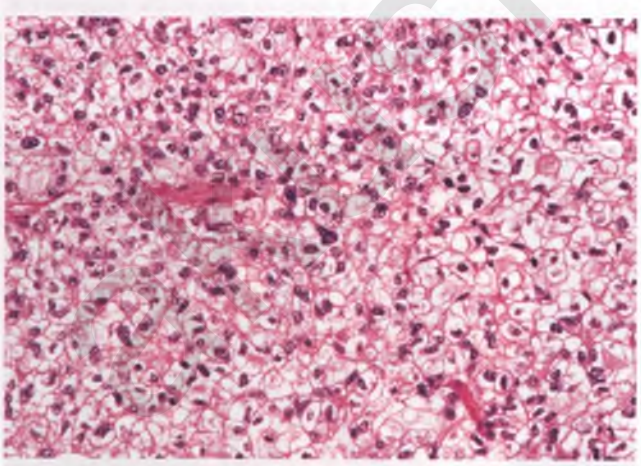

FIGURE 7.124. Clear cell carcinoma with solid architecture. This pattern features sheets of tumor cells, many of which have polyhedral shapes. Note the significant variability in the size and shape of the tumor cells and the low mitotic rate. The cells appear clear due to the presence of abundant intracytoplasmic glycogen. In contrast to metastatic renal cell carcinoma, the vascular pattern is inconspicuous (compare with Fig. 7.341).

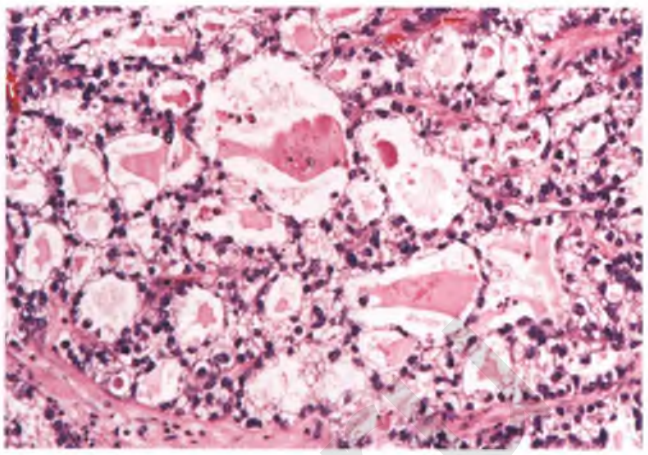

FIGURE 7.125. Clear cell carcinoma with tubulocystic architecture.

(c) cells with a signet-ring appearance. The latter is due to the targetoid accumulation of inspissated mucinous material, and appears to represent miniaturization of small cysts associated with condensed luminal contents rather than true signet-ring cells. Clear cell carcinomas generally exhibit at least some areas with high-grade nuclear features, but this is often a focal finding.[70,181] The mitotic index is generally low, averaging only about 4 mitotic figures per 10 high power fields.[70]

Fifteen to twenty percent of clear cell carcinomas have an associated adenofibromatous component (Fig. 7.130), which underscores the need for extensive sampling of presumed benign or borderline clear cell tumors.[180,181] In comparison to clear cell tumors without an adenofibromatous component, these tumors are less likely to be associated with endometriosis, and their carcinomatous elements exhibit a mixed or tubulocystic histologic pattern rather than the predominantly papillary pattern that is often seen in cystic clear cell carcinomas. Whether the presence

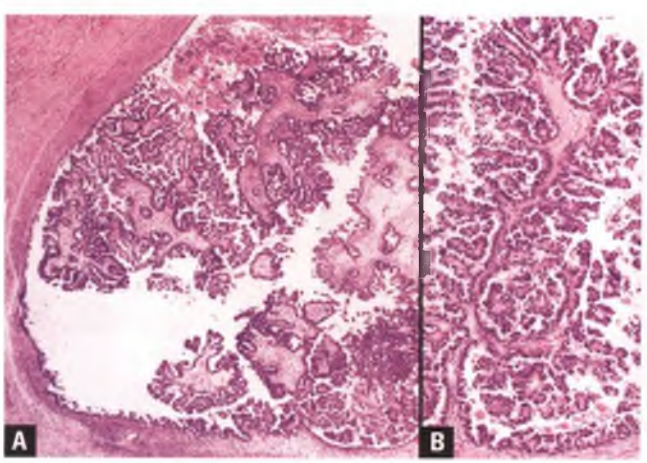

FIGURE 7.126. **A,B:** Intracystic clear cell carcinoma with a complex papillary architecture. Note the resemblance to the usual type of serous borderline tumor at low magnification.

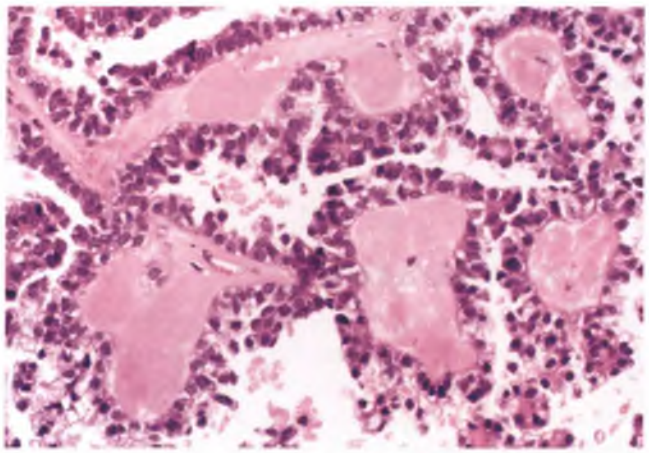

FIGURE 7.127. Clear cell carcinoma with papillary architecture. Hyalinization of the stromal cores of the papillae is a characteristic, but not a pathognomonic, feature. Note the relatively monomorphic neoplastic epithelial cells lining the papillae, many of which have clear cytoplasm.

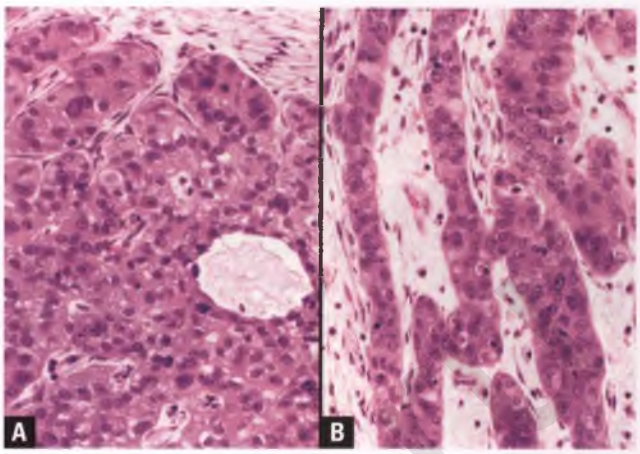

FIGURE 7.129. **A,B:** Clear cell carcinoma, oxyphil type. In this example, the oxyphilic cells form coalescing nests **(A)** and trabeculae **(B)**. Other regions of the tumor exhibited conventional patterns of clear cell carcinoma.

of an adenofibromatous component within a clear cell carcinoma is of any prognostic significance is controversial.[180,181]

Clear cell carcinoma is commonly admixed with foci of endometrioid carcinoma (see Fig. 7.155), which reflects the ability of both of these tumors to arise from endometriosis.

Immunohistochemically, most clear cell carcinomas are immunoreactive for HNF-1β and fail to stain for ER and WT1.[70,71]

Differential Diagnosis

Some intracystic clear cell carcinomas with papillary architecture can mimic the usual, micropapillary, or surface cribriform patterns of SBT (Figs. 7.126 and 7.131) Recognition of the former is aided by the identification of the tubulocystic and/or solid patterns of clear cell carcinoma elsewhere in the neoplasm, cells with clear cytoplasm, and papillae with hyalinized stromal cores.[186] In contrast to SBTs, clear cell carcinomas with a papillary pattern also tend to be unilateral, are often associated with endometriosis, and usually exhibit at least focal high-grade nuclear atypia.[186] The presence of psammoma bodies is not a useful differentiating feature, since these structures may be found in either serous or clear cell neoplasms. In problematic cases that are not resolved by extensive tissue sampling, the lack of immunoreactivity of clear cell carcinoma for WT-1 and ER, along with its typical expression of HNF-1β, can be utilized to help distinguish this tumor from SBT.[71]

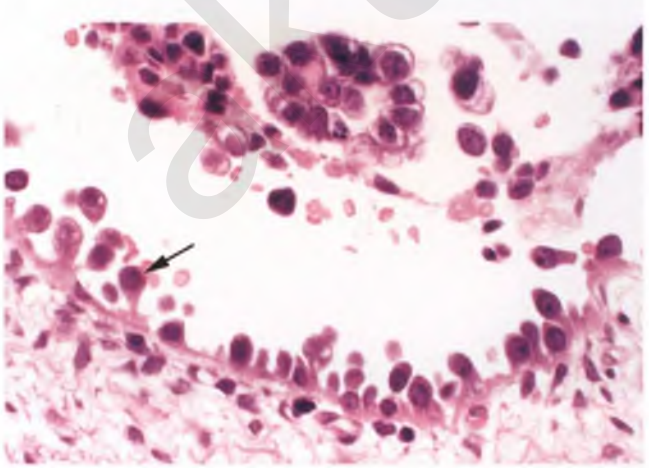

FIGURE 7.128. Clear cell carcinoma. Several hobnail cells, such as the one marked by the *arrow*, line the neoplastic cyst.

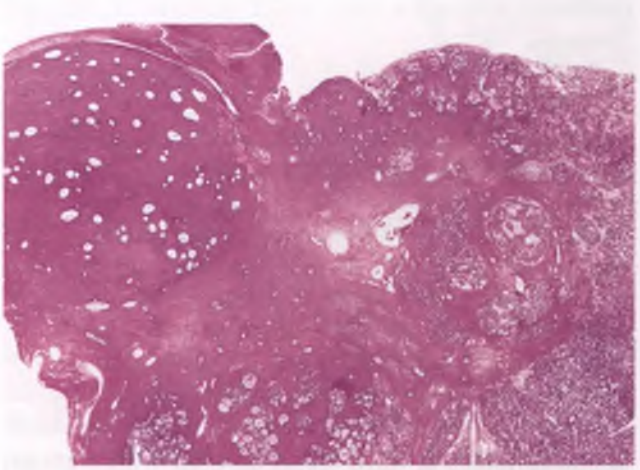

FIGURE 7.130. Clear cell carcinoma with adenofibromatous component. The adenofibromatous component, which is most prominent in the upper left portion of the image, gradually blends with clear cell carcinoma.

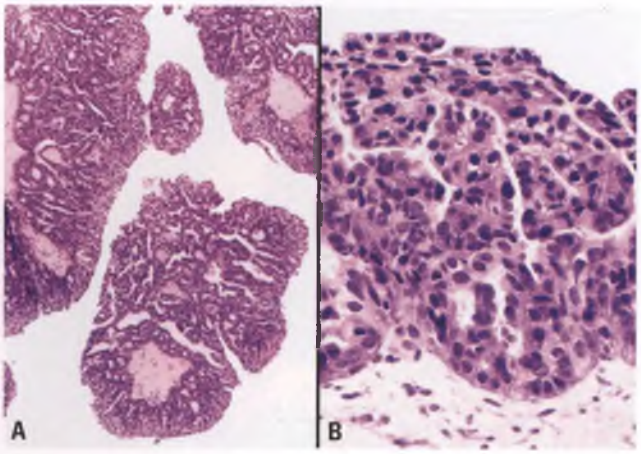

FIGURE 7.131. **A,B:** Clear cell carcinoma with papillary architecture mimicking the micropapillary/surface cribriform patterns of serous borderline tumor. Note the hyalinization of some of the stromal cores, the degree of nuclear atypia that is beyond that seen in serous borderline tumors, and the presence of some cells with pale-staining cytoplasm.

Although the secretory pattern of endometrioid carcinoma features cells with clear cytoplasm, the clear vacuoles are seen in columnar cells in subnuclear and/or supranuclear locations. This produces a distinctly different appearance from clear cell carcinoma, with its admixture of polyhedral clear cells, hobnail cells, and various architectural patterns.

The differential diagnosis of clear cell carcinoma also includes serous carcinoma, dysgerminoma, yolk sac tumor, steroid cell tumor, juvenile granulosa cell tumor, and metastatic renal cell carcinoma, all of which are discussed in the sections on these other entities. The oxyphil variant of clear cell carcinoma is most easily distinguished from tumors such as hepatoid carcinoma and steroid cell tumor by its association with other more typical patterns of clear cell carcinoma.[185]

Prognosis

As is true for all ovarian carcinomas, stage is the dominant prognostic factor. Recent studies have demonstrated a >90% 5-year survival rate for patients with stage Ia disease, whereas 5-year survival rates drop to 60% to 75% for stage Ic patients.[140,184] The prognosis for the specific subset of stage Ic patients with malignant cells in their ascites or peritoneal washings may be significantly worse.[187] Five-year survival rates for stages II, III, and IV are approximately 60%, 30%, and 15%, respectively.[140] In comparison to serous carcinoma, clear cell carcinoma seems to have a significantly lower response rate to platinum-based chemotherapy, which indicates a need for alternative treatment approaches.[184]

The architectural pattern, nuclear grade, and overall histologic grade of clear cell carcinoma has not shown any consistent correlation with prognosis,[3,4,188] and I concur with those who regard clear cell carcinomas as high grade by definition. It is understandable that many clear cell carcinomas would not be scored as high grade using grading systems that place considerable weight on architecture and mitotic activity, since the tubulocystic and papillary patterns would receive low to intermediate scores and clear cell carcinomas tend to have low mitotic rates.

Transitional Cell Tumors[9]

More than 95% of the tumors in this category are benign Brenner tumors, which account for about 5% of benign epithelial-stromal tumors; the other neoplasms discussed in this section are rare.[1,16] By definition, the epithelial component of transitional cell tumors bears a histologic resemblance to neoplastic urothelium of the urinary bladder.

Benign Brenner Tumor[189,190]

Benign Brenner tumors are often found incidentally in adult women (mean age of 50 years) as a small, solid, well-circumscribed ovarian mass, about 5% to 10% of which are bilateral. Roughly half of benign Brenner tumors are <2 cm, and tumors of this type >10 cm are uncommon. Sectioning of these smooth-surfaced tumors typically reveals a solid, firm, off-white to pale yellow nodular mass that may have gritty calcific deposits (Fig. 7.132). Occasional tumors may have a variably prominent cystic component. About 20% of Brenner tumors are admixed with a tumor of another type, which is usually a mucinous cystadenoma (as illustrated in the section on mixed epithelial tumors) or less commonly a mature cystic teratoma or serous cystadenoma.

Histologically, benign Brenner tumors have a distinctive low-magnification appearance, with sharply demarcated islands of epithelium embedded within a

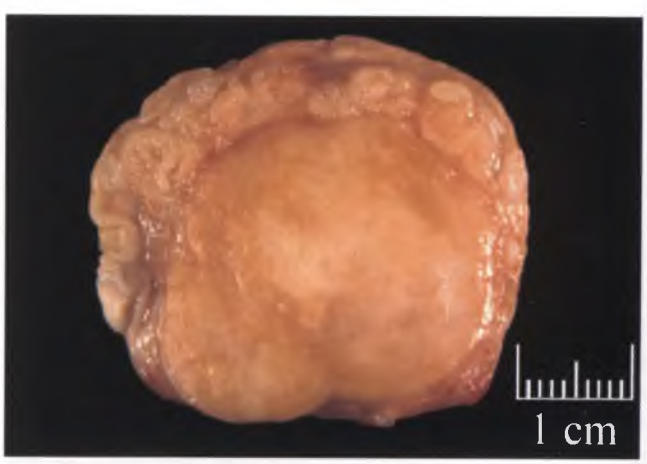

FIGURE 7.132. Benign Brenner tumor. The sectioned surface is solid and varying shades of *yellow*. Note how this small, well-circumscribed tumor abuts the peripheral rim of nonneoplastic ovarian tissue, which contains several corpora albicantia.

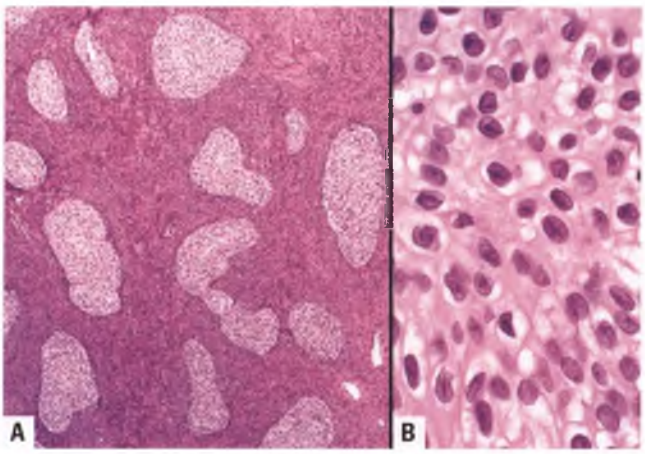

FIGURE 7.133. Benign Brenner tumor. **A:** Widely spaced nests of transitional cells are embedded within a prominent fibrous stroma. **B:** This high-magnification view highlights the bland nuclear features and the characteristic longitudinal nuclear grooves that are present in some of the tumor cells.

dominant fibrous stromal component (Fig. 7.133A). The neoplastic cells that comprise the epithelial nests have bland nuclei with finely dispersed chromatin, frequent longitudinal nuclear grooves, abundant clear to eosinophilic cytoplasm, and rare to absent mitotic figures (Fig. 7.133B). Although most of the epithelial nests are solid, the nests may contain one or more cystic spaces of various sizes that often contain inspissated material (Fig. 7.134). Some investigators refer to benign Brenner tumors with cystic spaces lined by stratified transitional cells that are capped by a layer of mucinous or ciliated cells as metaplastic Brenner tumors.[191]

Most Brenner tumors are immunoreactive with the urothelial markers uroplakin III and thrombomodulin, which supports true urothelial differentiation.[192]

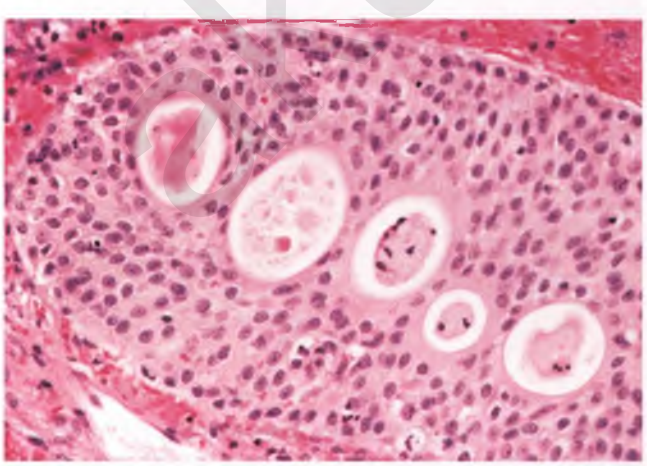

FIGURE 7.134. Benign Brenner tumor. One or more lumens may be present within some of the epithelial nests.

Differential Diagnosis

Adult granulosa cell tumors (AGCTs) with an insular pattern can resemble benign Brenner tumors because of their grooved nuclei and because the microcystic spaces present in some Brenner tumors can be mistaken for Call-Exner bodies. However, AGCTs typically have other more characteristic architectural patterns admixed with insular areas, and their neoplastic cells have less abundant cytoplasm and lack the mucinous epithelial component that is often at least focally present in Brenner tumors. The differential diagnosis of Brenner tumor with insular carcinoid tumor is discussed in the section on the latter entity.

Borderline Brenner Tumor[191,193]

Borderline Brenner tumors typically present in adult women (mean age of 60–65 years) with symptoms related to a unilateral pelvic mass. Although some investigators classify noninvasive transitional cell tumors with the papillary architecture of a borderline tumor as proliferative Brenner tumors if there is only low-grade nuclear atypia,[191] the WHO and other influential pathologists classify all such tumors, whether low or high grade, as borderline tumors.[9,194]

Grossly, borderline Brenner tumors are smooth-surfaced cystic masses that average 15 to 20 cm in diameter with interior polypoid or papillary cauliflower-like masses that protrude into one or more cystic cavities. Histologically, these tumors are characterized by florid noninvasive papillary epithelial growth into cystic spaces in a pattern that resembles papillary transitional cell carcinoma (TCC) of the bladder (Fig. 7.135). Benign Brenner elements are typically present at the periphery of the neoplasm, and foci of mucinous, squamous, and/or ciliated metaplasia may be seen (Fig. 7.136). As alluded to above, the degree of nuclear atypia of the epithelial cells lining the papillae ranges from mild to severe; in the latter situation, some pathologists render a

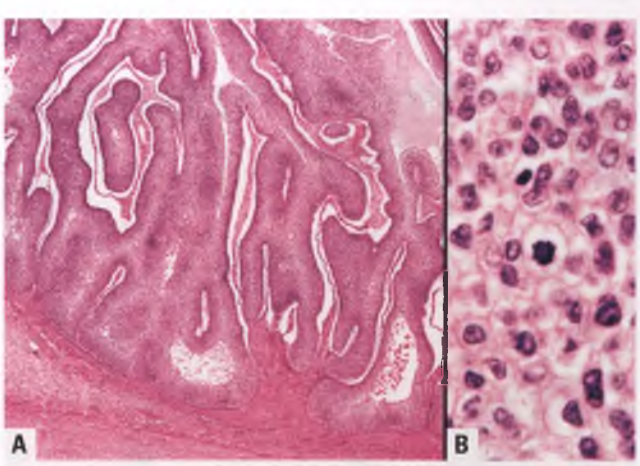

FIGURE 7.135. Borderline Brenner tumor. **A:** Interconnected papillary structures protrude into the cavity of a cystic mass. **B:** In this example, the transitional cells exhibit low-grade nuclear atypia and are mitotically active. Low-grade tumors such as this have also been referred to as proliferating Brenner tumors.

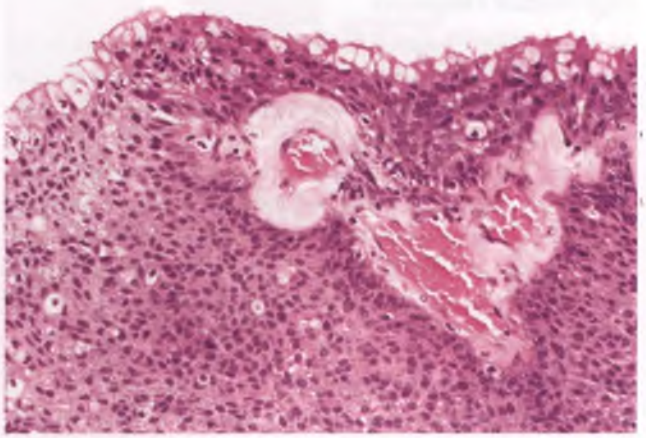

FIGURE 7.136. Borderline Brenner tumor. The surface of this papillary frond exhibits prominent mucinous and focal ciliated metaplasia.

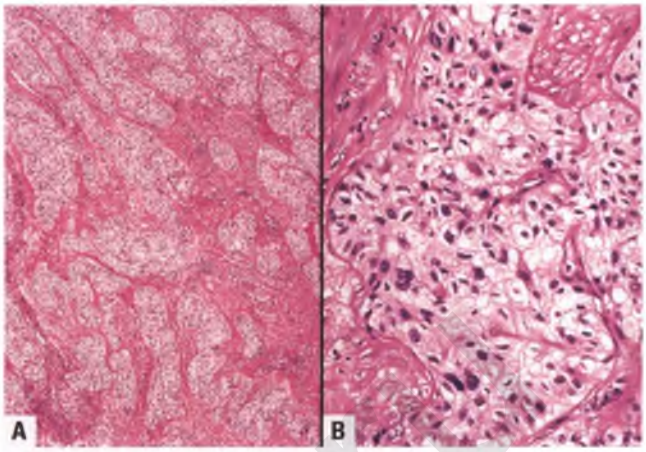

FIGURE 7.138. Malignant Brenner tumor. **A:** Crowded, anastomosing Brenner-like nests infiltrate fibrous stroma. **B:** Some of the nests contain cells with marked nuclear atypia. Benign Brenner tumor was present elsewhere in the neoplasm (not shown).

diagnosis of "borderline Brenner tumor with intraepithelial carcinoma." The mitotic rate of borderline Brenner tumors is highly variable, and foci of tumor necrosis may be present.

Prognosis

Although borderline Brenner tumors almost always behave in a benign fashion and the expectation is that they are cured by excision, a recent case with a uterine recurrence with myometrial invasion has been reported.[193]

Malignant Brenner Tumor[195,196]

Malignant Brenner tumors occur in adult women with a mean age of 60 to 64 years. These tumors average 15 cm in diameter, are bilateral in 5% to 10% of cases, and are similar in gross appearance to borderline Brenner tumors (Fig. 7.137). Eighty percent of these tumors are confined to the ovary at the time of presentation. By definition, malignant Brenner tumors contain invasive transitional cell aggregates in addition to at least focal areas of benign or borderline Brenner tumor (Fig. 7.138). In a significant number of cases, the invasive component contains elements of squamous cell carcinoma (Fig. 7.139).

Although often not addressed, the identification of stromal invasion in these tumors can be a subjective exercise. It may be difficult to apply the vague criteria of infiltration by confluent or crowded, irregularly-shaped nests of malignant transitional cells, especially in the usual situation in which there is no recognizable stromal response. In the presence of significant nuclear atypia in an otherwise possibly malignant case, it is prudent to lower the threshold for stromal invasion.

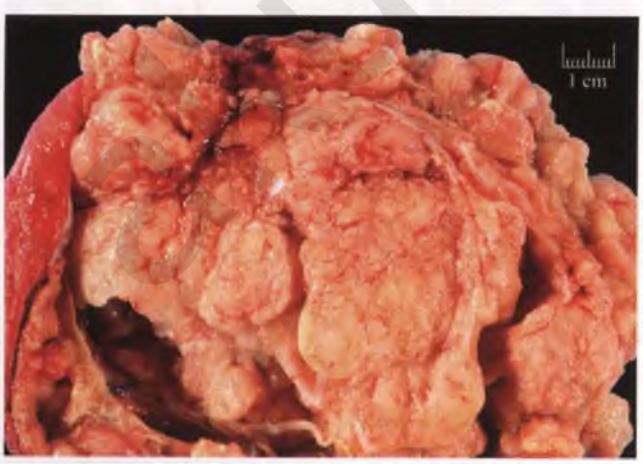

FIGURE 7.137. Malignant Brenner tumor. The internal solid areas of this solid and cystic tumor consist of light tan to pale yellow masses, nodules, and polypoid projections. (Courtesy of Dr. Colin J. R. Stewart.)

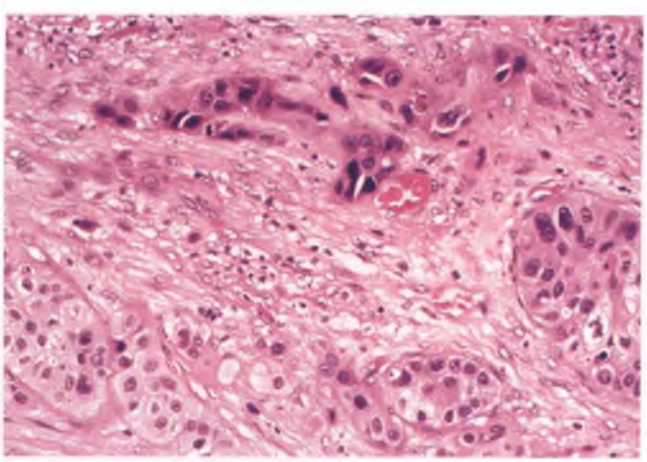

FIGURE 7.139. Malignant Brenner tumor. In addition to the Brenner-like nests, this area contains a jagged focus of invasive squamous cell carcinoma (top). Benign Brenner tumor was present elsewhere in the neoplasm (not shown).

Differential Diagnosis

The presence of a benign or borderline Brenner component distinguishes malignant Brenner tumor from ovarian TCC, and is also of great assistance in excluding undifferentiated carcinoma and metastatic carcinoma.

Prognosis

For the 80% of patients who present with stage I disease, the prognosis is favorable. Although data is limited, patients with high-stage malignant Brenner tumors appear to have a dismal prognosis.

Transitional Cell Carcinoma[197,198]

Ovarian TCC is an invasive malignant neoplasm that histologically resembles TCC of the urinary bladder. In contrast to malignant Brenner tumor, it definitionally does not contain elements of benign or borderline Brenner tumor. Ovarian TCC in pure form is rare, but it is not uncommon for mixed carcinomas to contain transitional cell elements.[197–200]

These neoplasms typically present in adult women in the 50 to 70 year age group with symptoms related to a pelvic mass that in more than half of the cases has spread beyond the ovaries. The tumors average about 10 cm in diameter and usually have both solid and cystic components. 15% of stage I tumors are bilateral.

Histologically, the most characteristic features of ovarian TCC are smooth-surfaced papillae protruding into large cystic spaces, undulating thick bands of neoplastic epithelium lining elongated and compressed cystic spaces with well-demarcated luminal borders, and rounded intraepithelial microspaces with a "punched out" appearance (Figs. 7.140–7.142).[198] Stromal invasion is present, and diffuse, insular, and trabecular patterns may also be seen. The neoplastic cells usually are fairly monomorphic, mitotically active, and of intermediate to high nuclear grade with prominent nucleoli. Tumors with low-grade nuclei are more likely to have cells with longitudinal nuclear grooves.

Unlike a significant number of bona fide urothelial carcinomas, ovarian TCCs typically are immunoreactive for WT-1 and do not express uroplakin III, thrombomodulin, and CK20.[192] In contrast to benign, borderline, and malignant Brenner tumors, ovarian TCCs frequently are immunoreactive for p53 and p16, which suggests that the latter tumors follow a high-grade tumorigenic pathway that is different from that followed by the tumors within the Brenner group.[193]

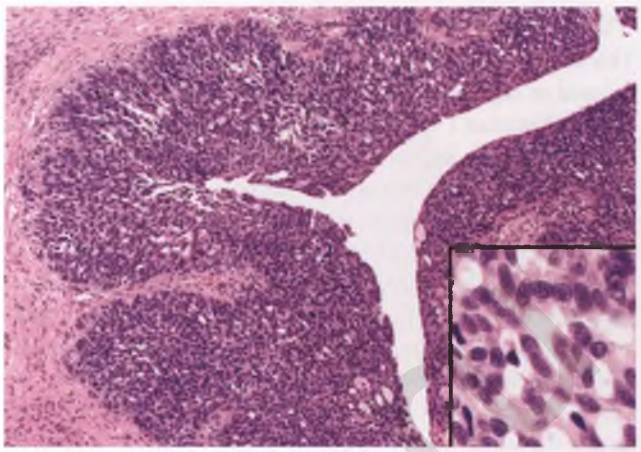

FIGURE 7.141. Transitional cell carcinoma. Undulating thick bands of neoplastic epithelium lining elongated and compressed cystic spaces with sharp luminal borders is a characteristic pattern. The inset highlights the presence of rounded microspaces, which is another common and useful diagnostic feature.

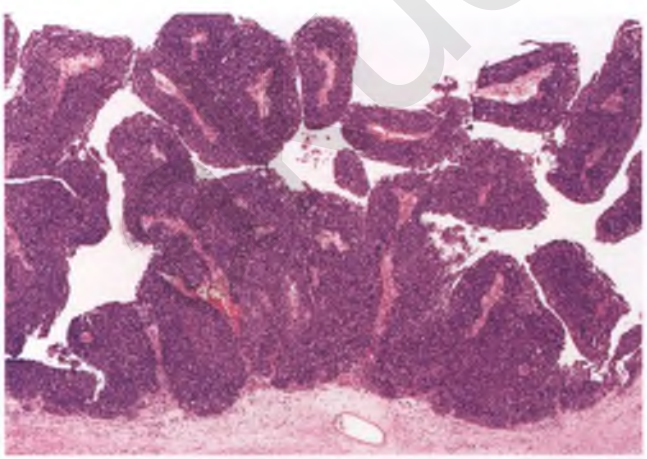

FIGURE 7.140. Transitional cell carcinoma. Epithelial-lined papillary structures with smooth luminal borders project into a cystic space. Note the resemblance to papillary transitional cell carcinoma of the urinary bladder. Stromal invasion was present elsewhere within the tumor.

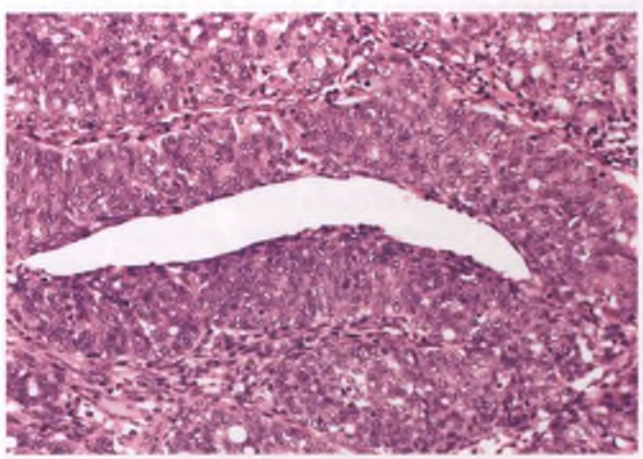

FIGURE 7.142. Transitional cell carcinoma. In areas with a more solid or nested architecture, the presence of scattered microspaces and elongated and compressed cystic spaces with sharp luminal borders are findings that are supportive of transitional cell differentiation.

Differential Diagnosis

This unusual tumor is underrecognized and is frequently misdiagnosed as high-grade serous or undifferentiated carcinoma.[201] Although ovarian TCC can have some overlapping features with serous carcinoma, such as slit-like spaces and bizarre tumor giant cells, these relatively nonspecific findings are seen within the context of what is otherwise typical transitional cell neoplasia.[198] Moreover, the papillae of serous carcinoma usually have scalloped contours, in contrast to the smooth luminal borders of the papillae in ovarian TCC. In undifferentiated carcinoma, a pseudopapillary architecture related to tumor cell necrosis can result in a resemblance to ovarian TCC, but the true papillary and undulating patterns of TCC are absent, and undifferentiated carcinoma usually exhibits a greater degree of nuclear atypia.

Clinicopathologic correlation can facilitate recognition of those rare ovarian metastatic squamous cell carcinomas that can form cysts and undulating bands of neoplastic cells that can result in a resemblance to primary TCC.[202] The same can be said for the rare TCCs of urothelial origin that metastasize to the ovary; their immunophenotypic differences with ovarian TCC as outlined above can also help to make this distinction.[192]

Prognosis

Although it is often stated that ovarian TCC is a more aggressive neoplasm than malignant Brenner tumor, much of this behavioral difference is due to the fact that malignant Brenner tumors are more likely than ovarian TCCs to present with disease limited to one ovary (stage Ia).[196] When only stage Ia tumors of these two types are compared with one another, the prognosis is relatively favorable and not appreciably different.[196] The confusion lies in the fact that the 1987 article by Austin and Norris that quotes a 43% versus 88% survival difference for stage IA ovarian TCC as compared to malignant Brenner tumor uses an old staging system wherein stage "IA" includes cases with ruptured tumor, which is now classified as stage Ic.[196] Three of the four patients with ovarian TCC who died of tumor that Austin and Norris staged as "IA" had ruptured tumors (really Ic), and the fourth had ascites but the results of her peritoneal cytology studies were not known (possibly Ic).[196] Therefore, there is currently insufficient data to support the claim that ovarian TCCs have a worse prognosis than stage-matched malignant Brenner tumors; rather, the data of Austin and Norris suggest that rupture of ovarian TCCs may be a bad prognostic indicator.

Whether ovarian TCC has a more favorable response to chemotherapy than other epithelial-stromal malignancies is also controversial.[197,199,200] Currently, it appears likely that the overall prognosis for ovarian TCC is not appreciably different from that of other types of primary ovarian carcinoma of similar stage and grade.

Squamous Tumors

Epidermoid Cyst[203–205]

The ovarian epidermoid cyst is a rare, keratin-producing, squamous-lined cyst of unknown histogenesis that is somewhat arbitrarily categorized as a squamous cell tumor. By definition, this benign lesion is not associated with skin adnexal structures or any other type of teratomatous element, the identification of which would result in reclassification as a mature cystic teratoma (dermoid cyst). Some examples may represent insufficiently sampled mature cystic teratomas, and others may be related to squamous metaplasia occurring in either cystic Brenner tumors or cysts of a variety of other origins.

Ovarian epidermoid cysts are typically small, unilateral, incidental lesions that are filled with creamy keratinous debris that may be yellow, white, or tan (Fig. 7.143). The stratified squamous epithelial lining is mature and contains a variably prominent granular layer (Fig. 7.144).

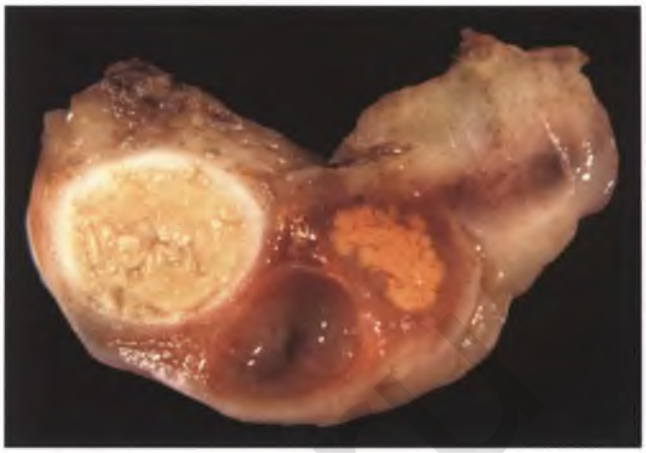

FIGURE 7.143. Epidermoid cyst. The ovary has been sectioned, revealing a 1 cm epidermoid cyst filled with tan, creamy material. Also present are a central cystic follicle and an involuting corpus luteum with characteristic *yellow-orange* convolutions.

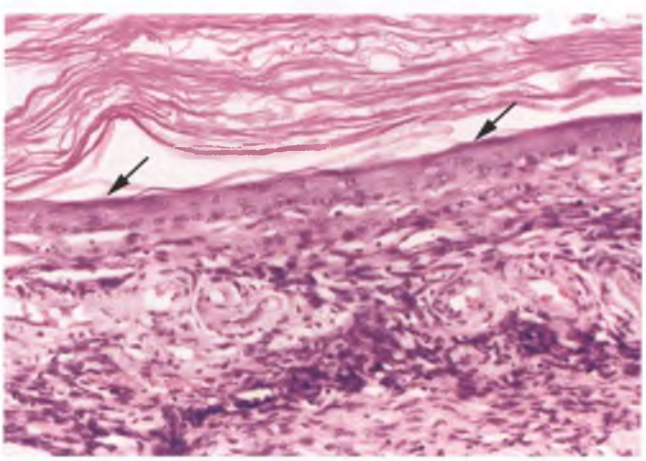

FIGURE 7.144. Epidermoid cyst. The cyst is filled with laminated layers of keratin (top). The squamous epithelial lining contains a granular layer (*arrows*). Unremarkable ovarian stroma lies beneath the epithelium.

Squamous Cell Carcinoma[206,207]

Squamous cell carcinomas of the ovary are rare. This type of carcinoma is most commonly found arising within a mature cystic teratoma (see Figs. 7.261 and 7.262), and may also be seen as a component of a malignant Brenner tumor (see Fig. 7.139). In addition, primary ovarian squamous cell carcinomas can occur in pure form (SCCP) or in association with endometriosis (SCCE), and it is these tumors that are discussed in this section.

SCCP and SCCE typically present in adult women as a pelvic mass that has usually spread beyond the ovary at the time of presentation. In a substantial proportion of cases of SCCP, there is an interesting association with a history of high-grade squamous intraepithelial lesion (HSIL) of the uterine cervix. SCCP and SCCE average about 10 cm in diameter and usually have both solid and cystic components (Fig. 7.145). Histologically, these tumors grow in a variety of architectural patterns and tend to be poorly differentiated (Figs. 7.146 and 7.147). In some cases, the cystic portion of the tumor is lined by squamous cell carcinoma in situ (Fig. 7.148).

The association of cervical HSIL with SCCP could be due to (a) contiguous retrograde spread of HSIL via the mucosal surface of the endometrium and fallopian tube onto the ovary, (b) occult invasive cervical squamous cell carcinoma that has metastasized to the ovary, (c) retrograde tubal transport of exfoliated cervical HSIL followed by implantation onto the ovarian surface, or (d) an HPV-related "field effect" that targets both the uterine cervix and the ovary. I agree with Pins et al. and Mai et al. that the "field effect" theory is the most plausible explanation for most examples of this phenomenon,[206,207] just as I think that an analogous field effect is responsible for the rare association of noninvasive or minimally invasive adenocarcinoma of the endocervix with ovarian tumors that have the appearance of borderline or well-differentiated carcinomas of endometrioid and/or mucinous type (see section on "metastatic" cervical carcinoma).

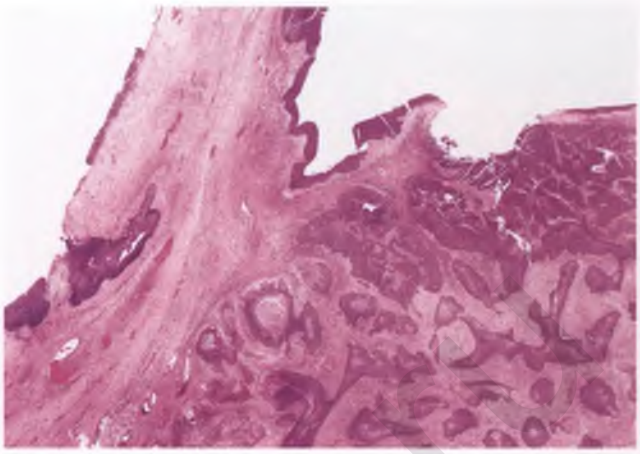

FIGURE 7.146. Squamous cell carcinoma. In this section taken from the edge of the nodule in the preceding figure, the solid mass is seen to consist of jagged and irregular nests of invasive squamous cell carcinoma. The adjacent cyst locules are lined by squamous cell carcinoma in situ.

Differential Diagnosis

The differential diagnosis of SCCP and SCCE includes metastatic squamous cell carcinoma, TCC (vs. squamous cell carcinoma with a prominent papillary architecture), and foci of squamous carcinoma or extensive squamous differentiation within malignant Brenner tumors and endometrioid carcinomas. A combination of clinicopathologic correlation, adequate histologic sampling of the tumor, and the identification of definite foci of squamous differentiation are helpful in making these distinctions.

FIGURE 7.145. Pure squamous cell carcinoma. This predominantly cystic ovarian mass has been opened, revealing the presence of a solid nodule of carcinoma (*arrow*) arising from one of the cyst walls. This patient had previously undergone a hysterectomy for HSIL of the cervix (Figs. 7.146–7.148 are from the same tumor).

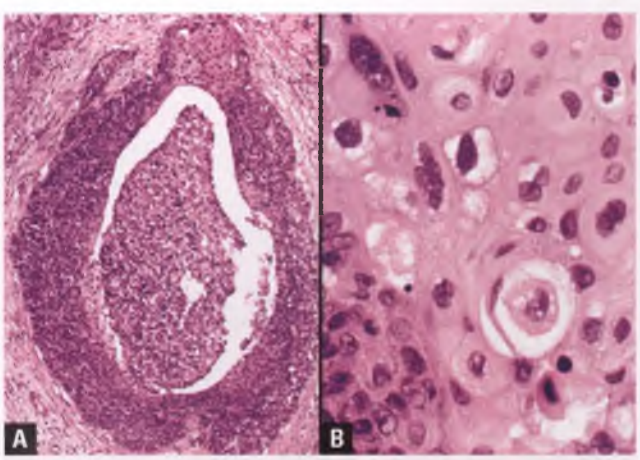

FIGURE 7.147. Squamous cell carcinoma. **A:** Infiltrative nest of squamous cell carcinoma with central necrosis. **B:** High-magnification image from a different area of the tumor documenting squamous differentiation.

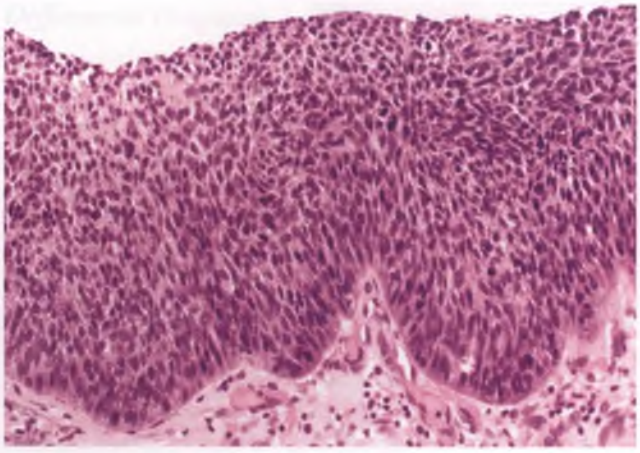

FIGURE 7.148. Squamous cell carcinoma. High-magnification view of the in situ component that lines the locules of the cyst.

Prognosis

The prognosis of both SCCP and SCCE is poor, except in those few patients who present with stage I disease.

Adenofibromatous Neoplasm with Mucin-Containing Signet-Ring Cells[123]

The descriptive name of this rare tumor that occurs in women of reproductive age reflects the uncertainty about its type of differentiation and degree of aggressiveness. On the basis of limited experience, these tumors are provisionally considered to be low-grade adenocarcinomas within the miscellaneous category of epithelial-stromal tumors.

These solid, well-circumscribed tumors have an adenofibromatous growth pattern and feature an epithelial component that includes an admixture of microcysts and mucin-containing signet-ring cells (Figs. 7.149 and 7.150).

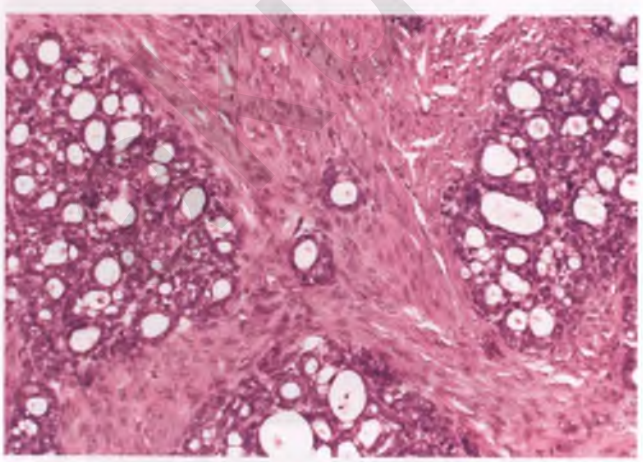

FIGURE 7.149. Adenofibromatous neoplasm with mucin-containing signet-ring cells. Lobulated islands of neoplastic epithelium with prominent microcysts are embedded within a fibromatous stroma.

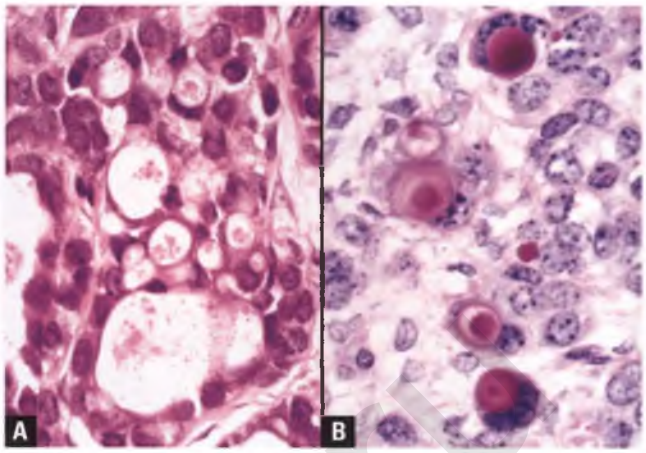

FIGURE 7.150. Adenofibromatous neoplasm with mucin-containing signet-ring cells. **A:** In addition to microcysts, the epithelial islands contain scattered signet-ring cells. **B:** The presence of intracytoplasmic mucin globules within the signet-ring cells is confirmed using a periodic acid-Schiff stain with diastase pretreatment.

They are often misdiagnosed as a form of metastatic adenocarcinoma with signet-ring cells (Krukenberg tumor). Although long-term follow-up is most helpful in excluding this possibility, the diagnosis of an adenofibromatous neoplasm with mucin-containing signet-ring cells can be suspected at the time of presentation in unilateral tumors with semiorganized epithelial and integral fibrous components that lack angiolymphatic invasion and occur in patients without a known extraovarian signet-ring carcinoma. Distinction of this tumor from the frankly malignant mixed carcinoma with microcystic and signet-ring components is discussed in the section on mixed epithelial tumors.

Hepatoid Carcinoma[208]

Primary hepatoid carcinomas are rare tumors of adult women (mean age of 63 years) that present with symptoms related to a nondescript ovarian mass. Most such tumors have spread beyond the ovary at the time of presentation, and are associated with a poor prognosis. Their defining features are (a) a resemblance to hepatocellular carcinoma imparted by sheets, cords, and trabeculae of cells with abundant eosinophilic cytoplasm and centrally placed, rounded nuclei with single prominent nucleoli (Fig. 7.151), and (b) immunoreactivity for alpha-fetoprotein (AFP). Most hepatoid carcinomas have high mitotic rates, foci of tumor necrosis, hyaline globules, and occasional cells with striking nuclear enlargement and atypia. Some of these tumors are associated with a carcinoma of serous, endometrioid, or mucinous type.[209]

Differential Diagnosis

The occasional undifferentiated carcinoma that has hepatoid features by routine histology is still diagnosed as undifferentiated carcinoma if the AFP immunostain is negative. Primary

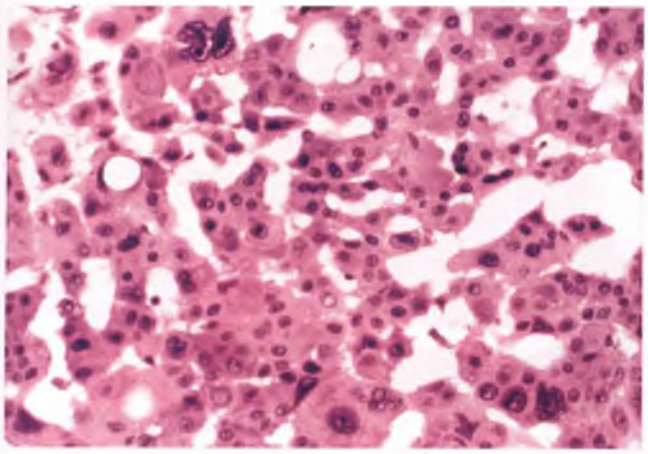

FIGURE 7.151. Hepatoid carcinoma. The tumor cells have abundant eosinophilic cytoplasm and form anastomosing trabecular structures. Note the scattered large cells with bizarre nuclei.

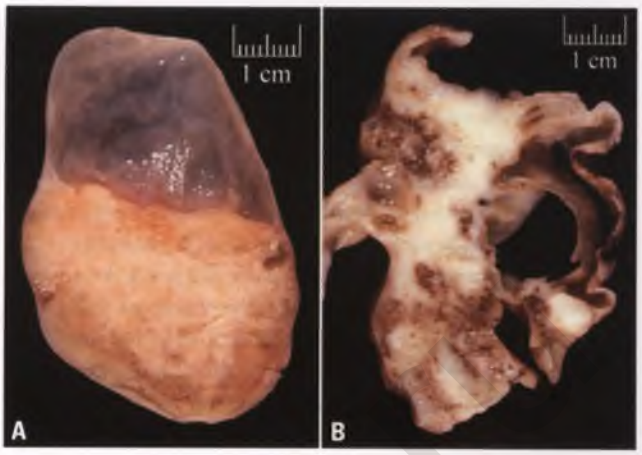

FIGURE 7.152. Combined Brenner tumor/mucinous cystadenoma (sectioned surfaces of two different examples). **A:** A unilocular mucinous cystadenoma sits atop a solid Brenner tumor. **B:** The solid, pale yellow tissue that expands the septa of this portion of a multilocular mucinous cystadenoma represents the Brenner component.

hepatocellular carcinoma metastatic to the ovary is extraordinarily rare and can usually be excluded on clinical grounds as well as by histology in the subset of hepatoid carcinomas that is associated with an epithelial-stromal tumor.[210] Hepatoid yolk sac tumor is distinguished by its occurrence in a younger age group, the presence of other foci of typical yolk sac tumor, and less variation in nuclear size and shape (note that the presence of hyaline globules is not a discriminating feature, since they are often seen in both hepatoid carcinoma and hepatoid yolk sac tumor).[208,211]

Adenoid Cystic Carcinoma and Basaloid Carcinoma[212]

These ovarian tumors are extraordinarily rare and resemble their salivary gland counterparts. Adenoid cystic carcinoma is often associated with a component of serous, endometrioid, or clear cell carcinoma, usually presents at high stage, and pursues an aggressive clinical course. In contrast, basaloid carcinoma is associated with an excellent prognosis.

Mixed Epithelial Tumors

To qualify as a mixed epithelial tumor, the minor component(s) must in aggregate represent at least 10% of the tumor or be grossly evident as a different tumor type.[194] Selected examples of mixed epithelial tumors are discussed below. A recent study of presumed mixed carcinomas with clear cell and serous components concluded on the basis of immunophenotype and clinicopathologic features that such tumors are more appropriately considered serous carcinomas with clear cell changes.[213] Moreover, in view of the fact that high-grade serous carcinoma frequently has poorly differentiated areas of no special type, I concur with those who consider such tumors to be of serous type, rather than categorizing them as mixed serous and undifferentiated tumors.[18]

Brenner Tumor with Mucinous Cystadenoma[190]

About 20% of Brenner tumors are associated with a tumor of another type, which is most frequently a mucinous cystadenoma. The Brenner component may either be found adjacent to the mucinous tumor or incorporated within its walls (Figs. 7.152 and 7.153). The commonly noted presence of mucinous epithelium lining the surface of transitional epithelial nests within a Brenner tumor, which has been referred to as metaplastic Brenner tumor,[191] is within the spectrum of ordinary Brenner tumor and is not considered a type of mixed epithelial tumor.

Mixed Epithelial Borderline Tumors

Classification of these tumors, which are noninvasive neoplasms that have the architecture of SBTs, is not standardized. One group defines mixed epithelial borderline tumor as containing

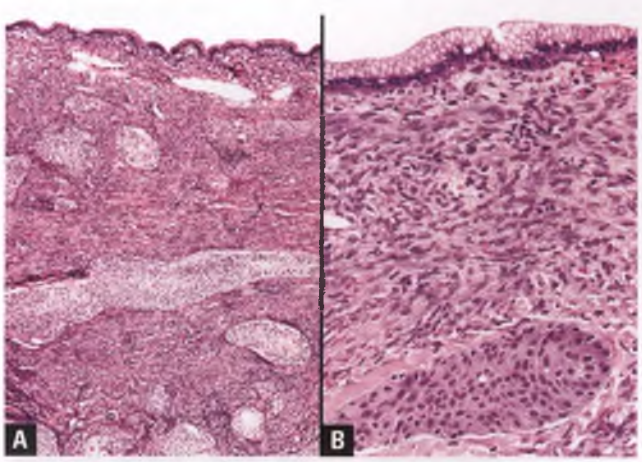

FIGURE 7.153. **A,B:** Combined Brenner tumor/mucinous cystadenoma. In these two different examples, nests of Brenner tumor embedded within fibromatous stroma lie beneath cysts lined by bland mucinous epithelium.

varying admixtures of two or more types of endocervical-like mucinous, ciliated serous, endometrioid, or squamous epithelium, with those other components present representing at least 10% of the tumor epithelium.[214] However, others consider tumors with an admixture of endocervical-type mucinous cells and serous cells to fall within the spectrum of endocervical-like mucinous borderline tumors, designate all such tumors as being of seromucinous type, and also include cases with endometrioid differentiation under this same diagnostic heading.[116] I concur with the former approach that maintains use of the term endocervical-like mucinous borderline tumor for those tumors that are dominated by endocervical-like mucinous epithelium with variably prominent indifferent cells, and refer to tumors of mixed cell type as mixed epithelial borderline tumors followed by a specification of the cell types present (e.g., "mixed epithelial borderline tumor, seromucinous type" for those cases with mixed mucinous and ciliated serous differentiation). An example of a mixed epithelial borderline tumor of seromucinous and endometrioid types is presented in Figure 7.154. Whatever terminology is used, these mixed tumors share many clinical and pathologic features with endocervical-like mucinous borderline tumors and can be managed similarly.[116,214]

Endometrioid Carcinoma Mixed with Clear Cell, Serous, or Undifferentiated Carcinoma

Admixtures of endometrioid and clear cell carcinoma may be seen, which typically occur in the setting of an endometriosis-associated tumor (Fig. 7.155). It is noteworthy that endometrioid carcinomas with a component of serous or undifferentiated carcinoma tend to behave more aggressively than carcinomas of pure endometrioid type.[215,216]

Mixed Carcinoma with Microcystic and Signet-Ring Components[122]

This rare tumor occurs in adult women (mean age of 58 years) and averages 7 cm in diameter. About one-third are bilateral, and the sectioned surface typically has both solid and cystic components. Histologically, this tumor is characterized by sheets of malignant epithelial cells with a prominent microcystic pattern and variable numbers of mucin-containing signet-ring cells (Fig. 7.156). Areas with serous or endometrioid differentiation are almost always present, but are often focal.

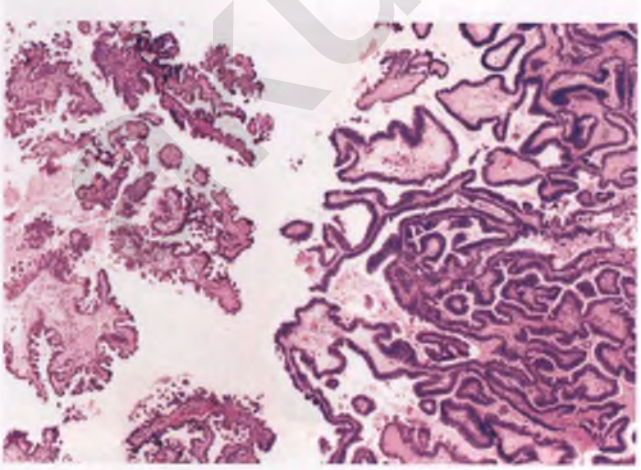

FIGURE 7.154. Mixed epithelial borderline tumor, seromucinous (left) and endometrioid (right) types.

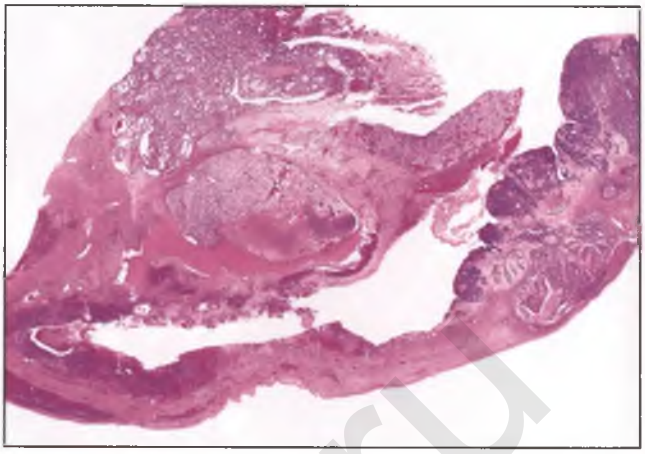

FIGURE 7.155. Mixed endometrioid carcinoma (right third) and partially necrotic clear cell carcinoma (left two-thirds) arising within an endometriotic cyst.

Differential Diagnosis

The main differential diagnostic consideration is metastatic signet-ring carcinoma (Krukenberg tumor), which typically does not have a prominent microcystic component, lacks foci of serous or endometrioid differentiation, is more likely to be bilateral, and is usually associated with a known extraovarian source. The lack of an adenofibromatous component, the presence of foci with recognizable serous or endometrioid differentiation, and the frankly malignant nature of these tumors help

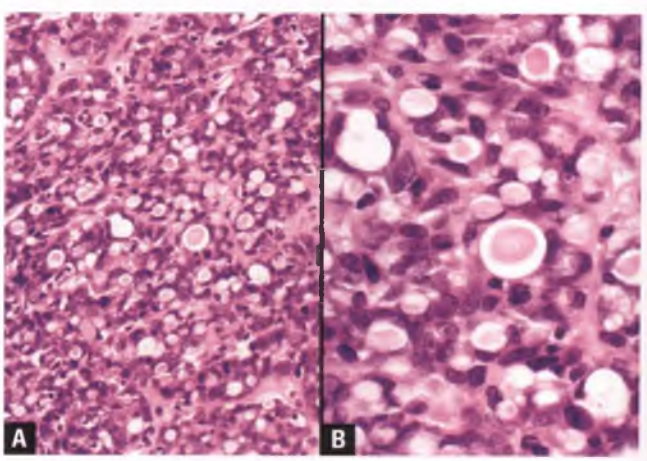

FIGURE 7.156. **A,B:** Carcinoma with a predominant microcystic pattern. Sheets of neoplastic epithelial cells are punctuated by microcysts and signet-ring cells.

to distinguish them from the so-called adenofibromatous neoplasm with mucin-containing signet-ring cells.[123] Some of these microcystic/signet-ring carcinomas may fit within the broad definition that some use for clear cell carcinoma that allows the presence of numerous mucin-containing signet-ring cells.[9]

Prognosis

Most patients with mixed carcinoma with microcystic and signet-ring components present with high-stage disease and have an unfavorable prognosis that is similar to those with other types of high-stage ovarian carcinoma.

Undifferentiated Carcinoma[217]

Only broad generalizations can be made about this group of tumors, since they are defined differently by different investigators. Undifferentiated carcinomas represent about 5% to 10% of epithelial-stromal tumors, occur in adult women, have typically spread beyond the ovary at the time of presentation, and are aggressive tumors with a poor prognosis. In their most typical form, they consist of sheets of poorly differentiated malignant cells with histologic and/or immunologic evidence of epithelial differentiation (Fig. 7.157). Mitotic activity is brisk, and there are often foci of tumor necrosis. Some pathologists allow up to 50% of specific types of ovarian carcinoma, which is usually of the serous variety, to be present in undifferentiated carcinoma.[217] I prefer the more rigid WHO criteria, in which undifferentiated carcinomas are either completely devoid of differentiated areas or contain only small foci of differentiated tumor.[194]

SEX CORD-STROMAL TUMORS

Sex cord differentiation refers to cells of the Sertoli or granulosa cell lineage that form epithelial structures, and "stroma" in this context refers to fibromatous, thecomatous, or steroid cell differentiation. Tumors within this category, which represent only about 6% of all primary ovarian neoplasms, may be composed of one or more of these various components, and are classified accordingly. Most sex cord-stromal tumors can be placed into one of four broad categories: granulosa cell tumors, tumors in the fibroma-thecoma group, Sertoli-stromal tumors, and steroid cell tumors, which is the order in which these tumors are discussed. Roughly 70% of sex cord-stromal tumors are fibromas; other tumors of this type that are likely to be encountered in an ordinary hospital-based practice are the occasional adult granulosa cell tumor (AGCT) and tumors in the thecoma/fibrothecoma group. All of the several other tumors in this category are very rare and collectively account for <1% of primary ovarian tumors.

Because of the rarity of many of these tumors and the presence of diverse histologic features that may overlap with other neoplasms, the diagnosis of sex cord-stromal tumors can be difficult. Immunohistochemistry can play an important role in resolving these diagnostic dilemmas. Of the variety of markers that have been shown to exhibit a reasonable degree of specificity and sensitivity for sex cord-stromal tumors, inhibin and calretinin are the most thoroughly studied and widely available (calretinin is more commonly used as a marker of mesothelial differentiation).[147,218–222] A few broad generalizations and caveats are in order that relate to their utility: (a) although most types of sex cord-stromal tumors are immunoreactive for inhibin and calretinin, fibromas are often negative for these markers, (b) the differential diagnosis often pits one sex cord-stromal tumor against another, and these markers are usually of little to no help in this situation, (c) neither inhibin nor calretinin is entirely sensitive or specific for sex cord-stromal differentiation, and are best utilized as part of an antibody panel, and (d) steroid-type cells can occasionally be found either scattered within or forming bands along the periphery of a variety of ovarian neoplasms and their presence, which will be highlighted by inhibin and calretinin immunostains, does not necessarily indicate that the tumor belongs to the sex cord-stromal category.[223,224]

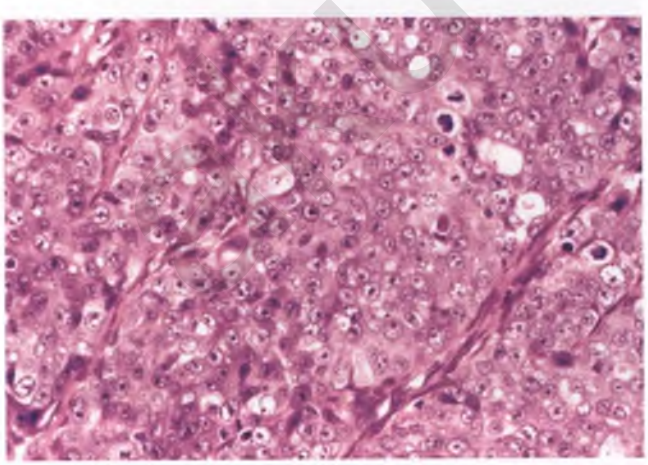

FIGURE 7.157. Undifferentiated carcinoma of the ovary. Thin bands of fibrous stroma separate aggregates of undifferentiated tumor cells with brisk mitotic activity. Rare foci of differentiation, in this case manifested by a few tiny glandular structures, are allowed in undifferentiated carcinoma.

Adult Granulosa Cell Tumor[225–228]

AGCTs account for roughly 10% of sex cord-stromal tumors and about 2% to 3% of all primary ovarian cancers. AGCTs are low-grade malignant tumors that typically present as an adnexal mass (mean size of 12 cm) in a 50 to 55 year old woman, although these neoplasms may occur at any age. They are commonly associated with estrogenic manifestations such as abnormal uterine bleeding, which are often associated with disordered proliferative endometrium or endometrial hyperplasia and in a small percentage of cases are due to the presence of well-differentiated endometrial endometrioid adenocarcinoma. Roughly 10% of cases present abruptly as a result of tumor rupture and hemoperitoneum. The vast majority of AGCTs are confined to the ovary at the time of presentation.

Approximately 95% of AGCTs are unilateral, and most are composed of a combination of solid yellow and cystic tissue

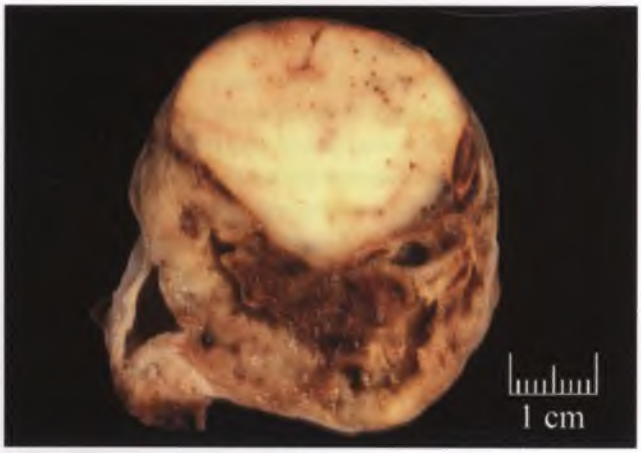

FIGURE 7.158. Adult granulosa cell tumor with two distinct components. A solid, pale yellow nodule sits atop tan tissue with multiple crevice-like spaces, some of which are filled with hemorrhagic material.

FIGURE 7.160. Adult granulosa cell tumor. This section through the solid and spongy portion of the ovarian tumor in the previous image demonstrates solid yellow tissue at left blending with spongy tissue at right. A portion of the cyst wall is shown at the extreme right.

(Figs. 7.158–7.160). Cysts may be filled with fluid or blood, and some examples are diffusely hemorrhagic (Fig. 7.161).

AGCTs exhibit a wide range of histologic patterns that are frequently admixed with one another. Before launching into a discussion of these various patterns, it is important to note that morphology at the cellular level plays a critical role in the diagnosis of AGCTs. The neoplastic cells typically have scant cytoplasm and angulated to oval, monotonous nuclei that appear to have been thrown together at random within the constraints of a given pattern. Occasional mitotic figures are an expected finding, but high mitotic counts and atypical mitoses are unusual. In classic cases, many of the tumor cells exhibit prominent **nuclear grooves**. Although such grooves are one of the most useful diagnostic features of AGCTs, they can also be seen in Brenner tumors and a few other ovarian tumors.

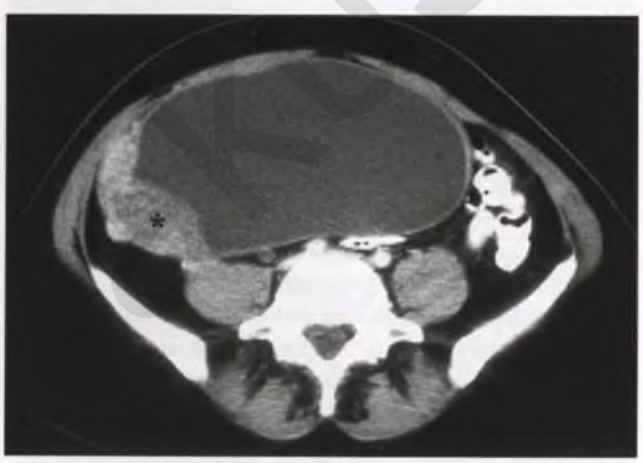

FIGURE 7.159. Adult granulosa cell tumor. CT scan of a predominantly cystic granulosa cell tumor that measures 29 cm in diameter. The *asterisk* marks a spongy portion of the tumor that blends superiorly with more solid tissue, as demonstrated in the following figure.

AGCTs rarely contain focal areas with bizarre nuclei, which is a finding of no prognostic significance.[229]

The nuclear features of AGCTs as described above are apparent in several of the images that are provided to illustrate the various histologic patterns, which are referred to as diffuse, microfollicular, trabecular, insular, macrofollicular, watered silk, gyriform, pseudopapillary, and sarcomatoid (in approximate decreasing order of frequency). Although some pathologists consider the diffuse and sarcomatoid patterns to be one and the same, I concur with those who separate these two patterns. In the diffuse pattern, cells grow as solid sheets, but their nuclear features are similar to those of typical

FIGURE 7.161. Adult granulosa cell tumor with prominent hemorrhagic areas. Sections through this cystic tumor reveal a thick hemorrhagic wall with scattered cysts and focal pale yellow areas. The resemblance to placental tissue with scattered infarcts is striking. Not surprisingly, the most diagnostic areas histologically are contained within the solid patches of pale yellow tissue.

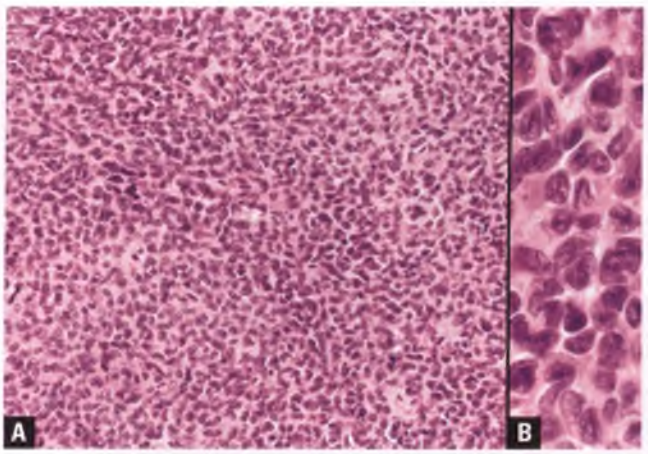

FIGURE 7.162. **A,B:** Adult granulosa cell tumor with a diffuse pattern. Note that the cells have the typical nuclear features of the usual granulosa cell tumor.

AGCTs (Fig. 7.162). In contrast, sarcomatoid AGCT features spindle-shaped cells with inconspicuous nuclear grooves, and can be easily confused with cellular fibroma or fibrosarcoma (Fig. 7.163). As illustrated in Figure 7.164, a reticulin stain can be of great assistance in excluding a tumor in the fibroma-thecoma group.

The microfollicular pattern of AGCT features characteristic **Call-Exner bodies**, which are small rounded cavities that usually contain eosinophilic material and/or a few degenerating nuclei (Figs. 7.165 and 7.166). In the trabecular pattern, the tumor forms anastomosing cords of cells of varying thickness (Fig. 7.167). The insular pattern is characterized by discrete nests of tumor cells separated by a variable amount of

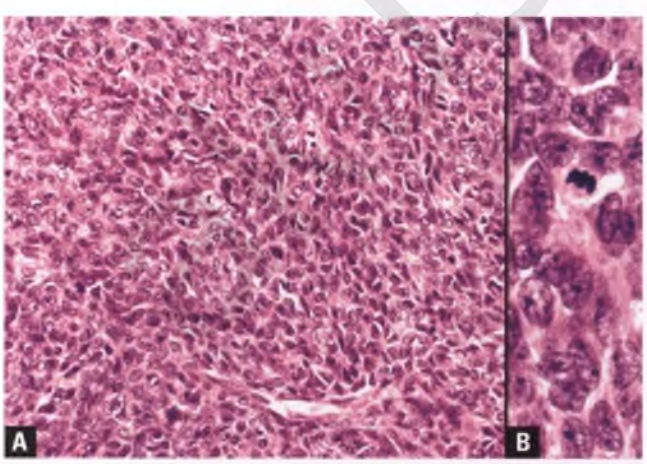

FIGURE 7.163. Adult granulosa cell tumor with a sarcomatoid pattern. **A:** Note the suggestion of a fascicular architecture and the presence of some plump spindle-shaped cells, which raise the possibility of fibrosarcoma or cellular fibroma. **B:** These tumors exhibit more nuclear atypia and higher mitotic rates than the typical granulosa cell tumor.

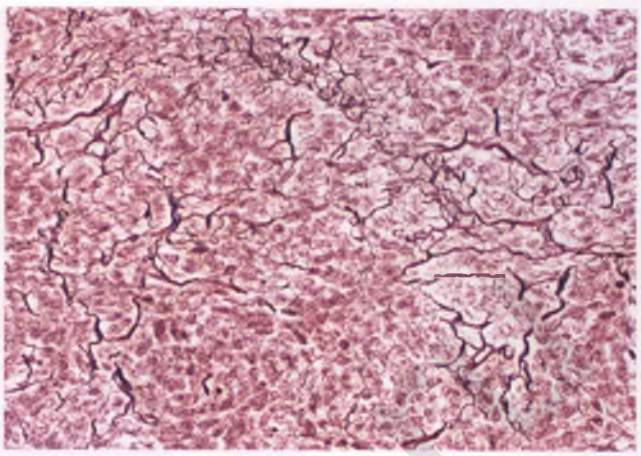

FIGURE 7.164. Adult granulosa cell tumor with a sarcomatoid pattern. A reticulin stain shows fibrils partially enveloping large aggregates of tumor cells. This pattern is very helpful in distinguishing granulosa cell tumors from those of a fibrothecomatous nature, which characteristically have reticulin fibrils surrounding cells individually or in groups of only a few cells.

stroma (Fig. 7.168). A macrofollicular pattern is created when neoplastic granulosa cells line a major or minor cystic component that is grossly apparent (Fig. 7.169). The pseudopapillary pattern is created as a result of cystic degeneration, and is often associated with hemorrhage and necrosis (Fig. 7.170).[230] The uncommon watered silk and gyriform patterns, which are described and illustrated in Figures 7.171 and 7.172, are often seen blending with one another. Formation of small hollow tubules is not common in AGCTs, but can be seen on rare occasions.

The rare luteinized variant of AGCT can cause diagnostic difficulties because the neoplastic granulosa cells acquire considerable amounts of eosinophilic cytoplasm,

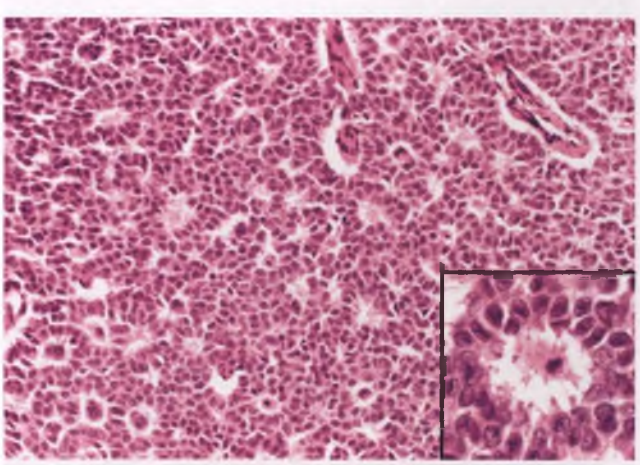

FIGURE 7.165. Adult granulosa cell tumor with a microfollicular pattern. The inset highlights a Call-Exner body whose cavity contains a degenerating nucleus.

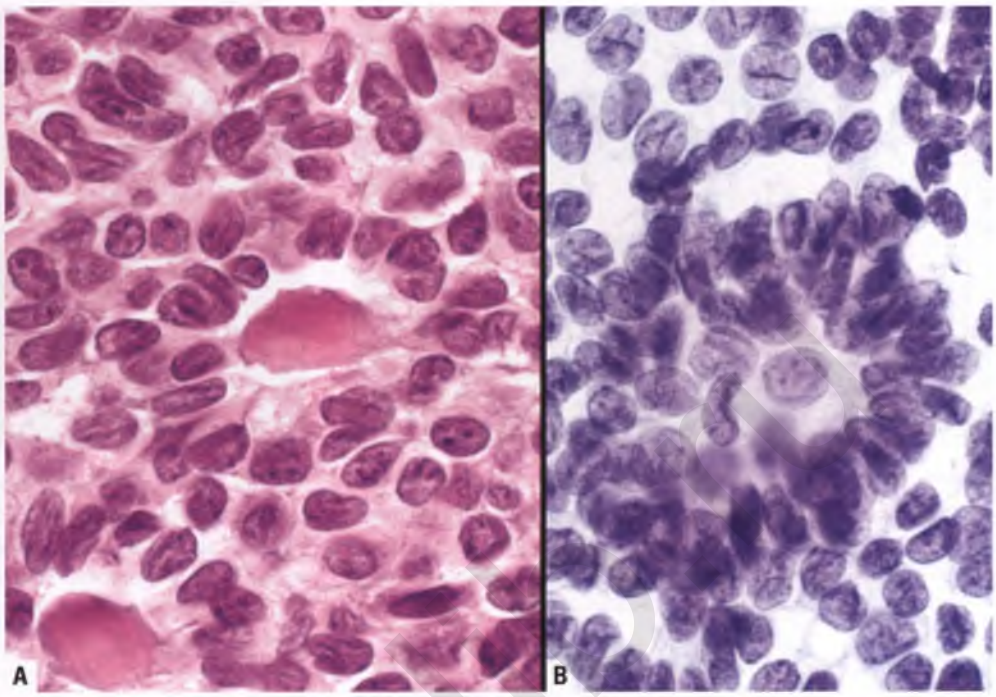

FIGURE 7.166. Adult granulosa cell tumor. **A:** High-magnification view of Call-Exner bodies with densely eosinophilic material within their cavities. The jumbled arrangement of the nuclei, their angulated contours, and prominent nuclear grooves are characteristic features of this tumor. **B:** Papanicolaou-stained scrape preparation that shows a Call-Exner body and scattered cells with nuclear grooves.

their nuclei become more rounded, nucleoli become more apparent, the dominant architectural pattern is diffuse, and nuclear grooves are less conspicuous than usual (Fig. 7.173).[231]

The stroma in AGCTs varies from barely discernible in tumors with a diffuse pattern of growth to prominent in some examples in which the tumor cells form nests and cords (Fig. 7.174). The stroma can be fibromatous or thecomatous, exhibits a range of cellularity, and may be highly vascular. Superimposed recent or remote hemorrhage may also alter the histologic appearance.

Like most sex cord-stromal tumors, AGCTs are typically immunoreactive for inhibin and calretinin, and lack expression of epithelial membrane antigen.[147] When constructing an antibody panel to help differentiate AGCT from a tumor outside of the sex cord-stromal group, these markers should be included (see below).

In a recent study, nearly all AGCTs were shown to have a single point mutation in FOXL2, which is a gene that encodes a transcription factor that is known to play a critical role in the development of granulosa cells.[232] Identification of this abnormality may serve as an additional diagnostic tool in selected cases. In addition, further study of the mutated FOXL2 gene and its associated protein may lead to a better understanding of the pathogenesis of AGCT and to targeted therapies in patients with recurrent disease.

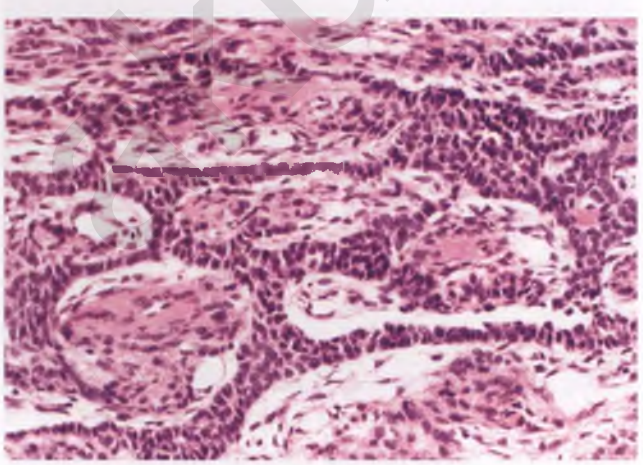

FIGURE 7.167. Adult granulosa cell tumor with a trabecular/corded pattern.

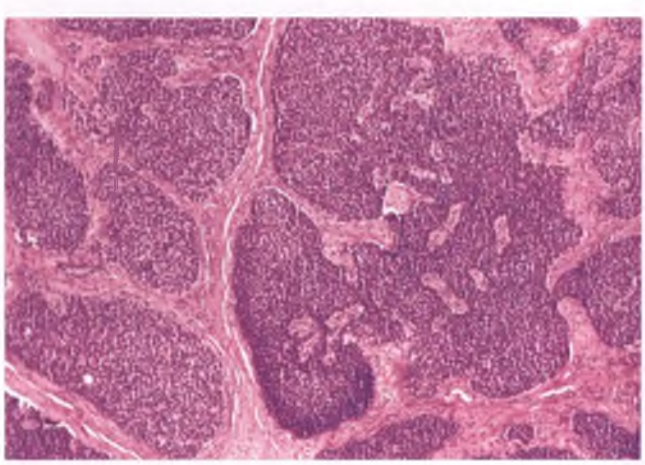

FIGURE 7.168. Adult granulosa cell tumor with an insular (nested) pattern.

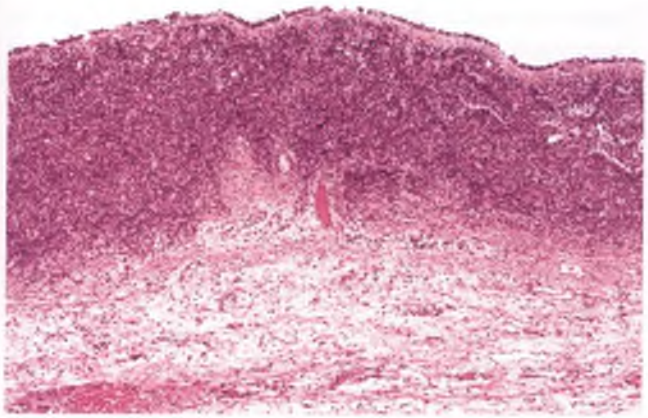

FIGURE 7.169. Adult granulosa cell tumor with a macrofollicular pattern. This representative portion of a large unilocular cyst is lined by a band of neoplastic granulosa cells. Tumors of this type need to be distinguished from follicle cysts.

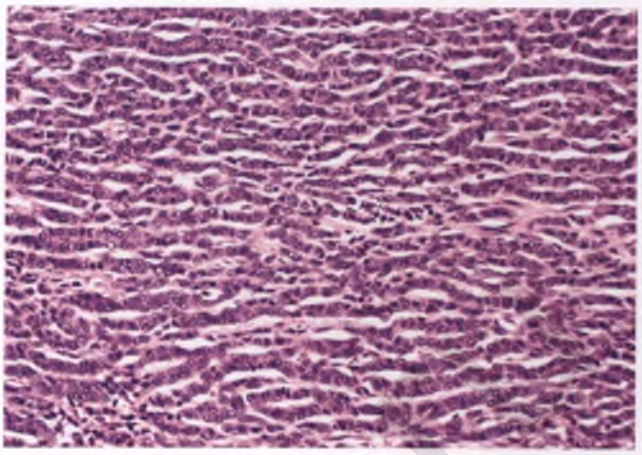

FIGURE 7.171. Adult granulosa cell tumor with a watered silk pattern formed by undulating parallel rows of tumor cells.

Differential Diagnosis

As should be expected for a tumor with such a wide spectrum of histologic patterns, the differential diagnosis of AGCT is broad and dependent upon the pattern encountered.

- Diffuse AGCTs can be misinterpreted as undifferentiated carcinoma or small cell carcinoma of hypercalcemic type (SCCHT), but these carcinomas often present with widespread disease, lack estrogenic manifestations, lack nuclear grooves, have high mitotic rates, lack inhibin immunoreactivity, and often express epithelial membrane antigen.[233] SCCHT is further differentiated by its occurrence in a younger age group and its frequent association with hypercalcemia.
- Primary endometrioid stromal sarcoma is a differential diagnostic consideration of AGCT of diffuse or sarcomatoid types. Its recognition is aided by its characteristic vascular pattern, lack of nuclear grooves, tongue-like pattern of infiltration in areas with extraovarian involvement, diffuse and strong immunoreactivity for CD10, lack of staining with inhibin and calretinin, absence of estrogenic manifestations, association with endometriosis, and the identification of reticulin fibrils enveloping individual tumor cells.[176,179,234]
- As previously discussed and illustrated, a reticulin stain is of value in distinguishing sarcomatoid AGCT from cellular fibroma and fibrosarcoma.
- Although some AGCTs can have a prominent fibromatous or thecomatous stroma, the granulosa cell component is still readily identifiable. If such a tumor has only focal and minor sex cord elements, then the designation of stromal tumor with minor sex cord elements is more appropriate.[235]

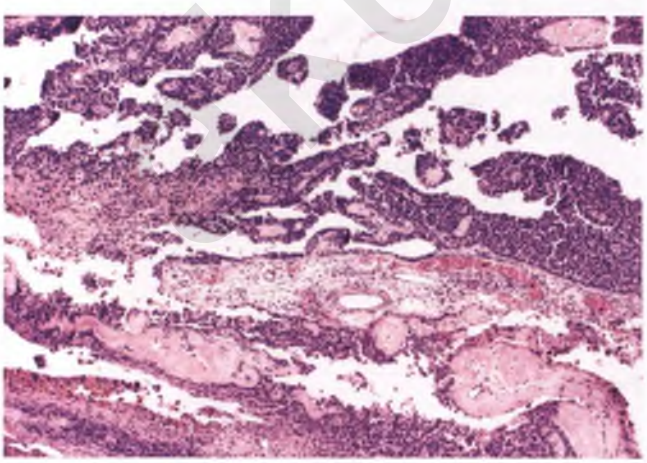

FIGURE 7.170. Adult granulosa cell tumor with a pseudopapillary pattern. Note: This image was taken from a section of the partially cystic and hemorrhagic tan tissue in Fig. 7.158.

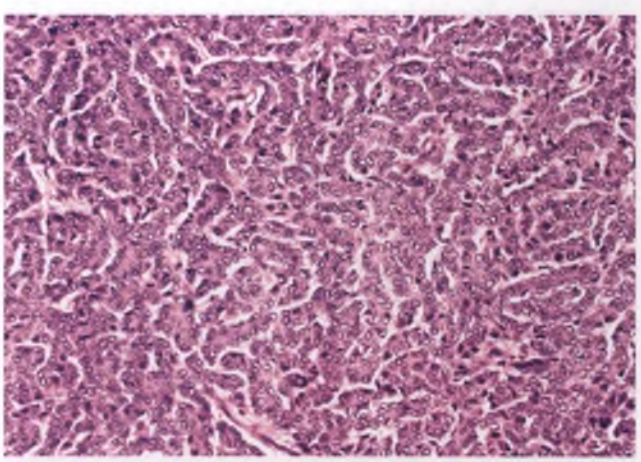

FIGURE 7.172. Adult granulosa cell tumor with a gyriform pattern formed by zigzag cords of tumor cells. This pattern creates an irregular network of clear crevice-like spaces in between the neoplastic granulosa cells.

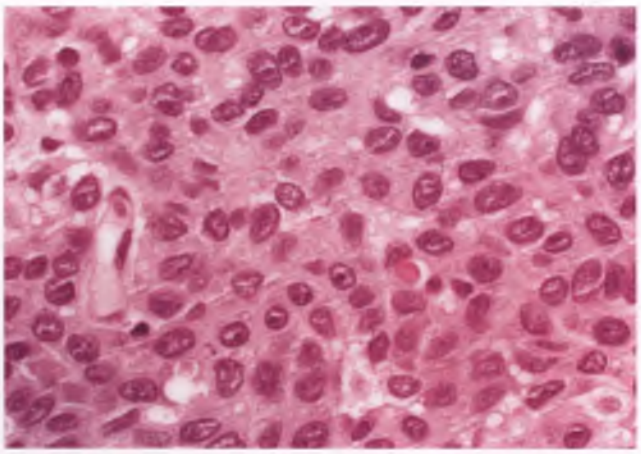

FIGURE 7.173. Adult granulosa cell tumor, luteinized variant. In contrast to the usual adult granulosa cell tumor, this variant features cells with abundant eosinophilic cytoplasm and a subpopulation of cells with rounded nuclei and prominent nucleoli. The jumbled cell arrangement and occasional cells with nuclear grooves are preserved features of granulosa cell differentiation.

- The differential diagnosis of the microfollicular pattern of AGCT with endometrioid carcinoma with sex cord-like patterns is discussed in the section on this variant of endometrioid carcinoma. It is worth reiterating that granulosa cell tumors are frequently immunoreactive for cytokeratin, rendering a positive result with this common marker of epithelial differentiation of no help in the distinction of AGCT from carcinoma of any type.[147,148]
- The starry sky pattern of Burkitt's lymphoma (see Fig. 7.290) can be confused with the microfollicular pattern of AGCT if the structures related to the phagocytic activity of histiocytes are misinterpreted as Call-Exner bodies.[236] In contrast to Burkitt's lymphoma, AGCT occurs in an older age group, is rarely bilateral, has distinctly different nuclear features, and does not stain with lymphoid markers.

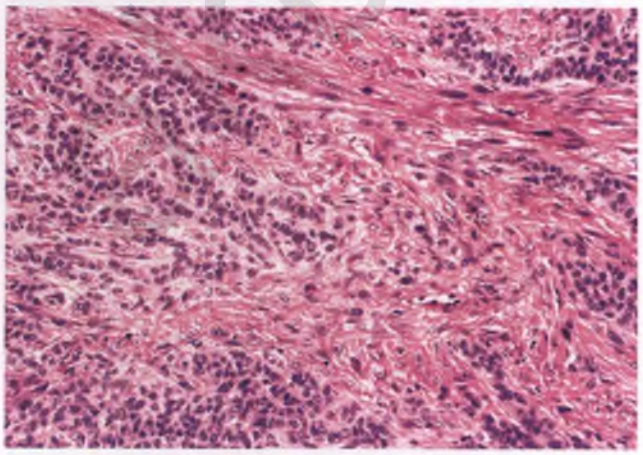

FIGURE 7.174. Adult granulosa cell tumor with a fibromatous stroma.

- The insular pattern of AGCT can mimic nests of carcinoid tumor. However, carcinoid tumors are composed of cells with nuclei that have stippled chromatin without grooves and cytoplasm that often contains visible eosinophilic granules. Moreover, metastatic carcinoid tumors are usually bilateral and primary insular carcinoid tumors are often found arising within a mature cystic teratoma.[237–239] In problematic cases, immunoreactivity for chromogranin and synaptophysin can confirm the diagnosis of carcinoid tumor.[146]
- The resemblance of AGCT with an insular pattern to benign Brenner tumor is discussed in the section on the latter entity.
- Macrofollicular AGCTs can resemble large follicle cysts or the large solitary luteinized follicle cyst of pregnancy and the puerperium. In contrast to these benign cysts, the granulosa cells lining cystic AGCTs and those within the cyst wall have the typical nuclear features of AGCTs. Moreover, the cells that line cystic AGCTs do not have the abundant eosinophilic cytoplasm and at least focal significant nuclear pleomorphism that characterizes the large follicle cyst associated with pregnancy.[240]
- Luteinized AGCTs can be difficult to distinguish from steroid cell tumors, but when sufficiently sampled should contain areas with the architectural and nuclear features of AGCTs of the usual type.[231] Luteinized AGCTs can also be confused with JGCTs and thecomas, as discussed in the sections on these entities.
- The distinction of a small AGCT from an incidental granulosa cell proliferation of pregnancy is discussed in Chapter 6.
- The cord-like pattern of metastatic lobular carcinoma of the breast can simulate the corded/trabecular pattern of AGCT, but is distinguished by the history of lobular breast carcinoma, high incidence of bilateral ovarian involvement, lack of nuclear grooves, presence of intracytoplasmic mucin, commonly present immunoreactivity for epithelial membrane antigen and gross cystic disease fluid protein-15, and lack of expression of inhibin.
- Rare metastatic melanomas that are composed of diffuse sheets of cells with small nuclei can resemble diffuse or luteinized AGCT. Features that favor melanoma include a prior history of melanoma, bilaterality, absent to infrequent nuclear grooves, intranuclear pseudoinclusions, identification of melanin pigment, frank nuclear anaplasia, and immunoreactivity for the melanoma markers HMB-45 and/or Melan-A in conjunction with negative staining for inhibin and calretinin (the expected, but not invariable, immunophenotype).[241,242] Note that while S100 normally serves as a good marker of melanocytic differentiation, the fact that about half of AGCTs are S100-positive limits its utility in this situation.[148]

Prognosis

AGCTs are notorious for their tendency to recur many years after removal, with recurrences eventually seen in about one-third of patients. Most recurrences are within the abdomen and pelvis, and are associated with a poor prognosis. Patients with tumor confined to the ovary (stage I) at the time of presentation have a 10-year survival of about 90%,

whereas higher stage patients have only about a 60% 10-year survival. Stage I tumors that have ruptured are more likely to recur than unruptured stage I tumors. Numerous studies have examined multiple potential prognostic factors such as tumor size, mitotic rate, degree of nuclear atypia, histologic pattern, DNA ploidy, and Ki-67 index with inconsistent results, and none with a significance that compares with tumor stage.[243]

Juvenile Granulosa Cell Tumor[244,245]

JGCTs are very rare neoplasms, representing only about 5% of tumors in the granulosa cell group. As their name indicates, the vast majority of these tumors present in young patients (mean age of 13 years), with prepubertal patients often exhibiting features of isosexual pseudoprecocity. JGCTs are rarely bilateral, have a mean size of 13 cm, and have a gross appearance that overlaps with that of AGCTs.

The most common histologic pattern of JGCTs features solid sheets and/or nodules of luteinized granulosa cells that are punctuated by haphazardly placed and variably prominent follicular spaces (Fig. 7.175). Theca cells may be seen surrounding some of the follicles, and are often admixed with granulosa cells in the solid areas. The follicles typically vary in size and shape, are lined by granulosa cells, usually contain eosinophilic to basophilic material within their lumens, and are an important diagnostic feature. The granulosa cells are usually mitotically active and have abundant eosinophilic to vacuolated cytoplasm, rounded nuclei with absent to rare grooves, and a variable degree of nuclear atypia (Fig. 7.176). It is noteworthy that about 15% of JGCTs exhibit severe nuclear atypia, but this has not been shown to worsen the prognosis. Hemorrhage and/or necrosis may be present. JGCTs are typically immunoreactive for inhibin and calretinin.[147,220,222]

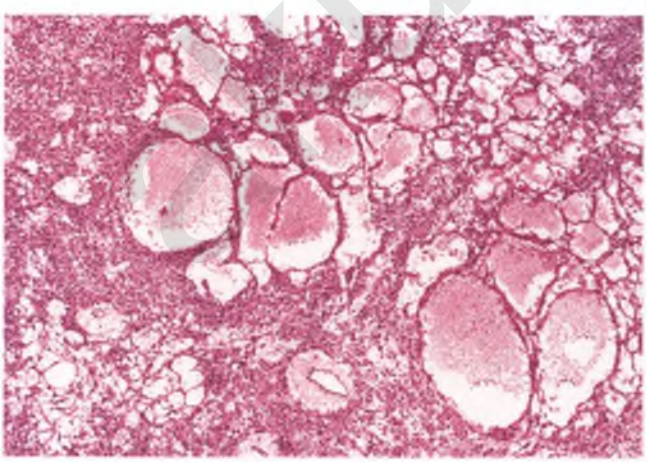

FIGURE 7.175. Juvenile granulosa cell tumor. At low magnification, several follicles of variable sizes and shapes are present. Note the presence of eosinophilic fluid within many of the follicles.

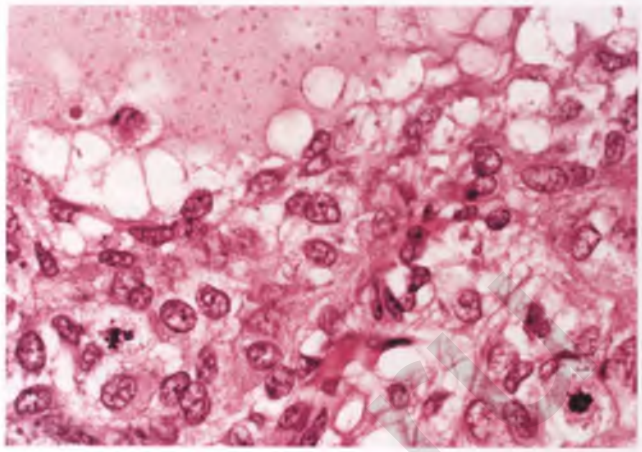

FIGURE 7.176. Juvenile granulosa cell tumor. As is typical, the neoplastic cells at the edge of this follicle have abundant eosinophilic to vacuolated cytoplasm, lack nuclear grooves, and are mitotically active.

Differential Diagnosis

- Distinction of JGCT from AGCT can be difficult, particularly when dealing with the luteinized variant of AGCT. However, JGCTs generally occur in a younger age group, have a characteristic follicular pattern, lack nuclear grooves, and typically have a high mitotic rate.
- Malignant germ cell tumors such as yolk sac tumor and embryonal carcinoma occur in a similar age group as JGCTs and can show some histologic similarities. In contrast to most JGCTs, these germ cell tumors have more frankly malignant-appearing nuclear features, do not form follicles, and typically have elevated serum levels of AFP and/or β-hCG. The diagnosis of yolk sac tumors is also often facilitated by the presence of a reticular pattern, Schiller-Duval bodies, and AFP immunoreactivity.
- The follicle-like spaces and frequent presence of a subset of cells with abundant eosinophilic cytoplasm in SCCHT can result in its confusion with JGCT, but these carcinomas often present with widespread rather than stage I disease, are frequently associated with elevated serum calcium levels, lack estrogenic manifestations, and lack inhibin immunoreactivity.[233] It should be noted that although this type of carcinoma is often immunoreactive for epithelial membrane antigen,[233] JGCT may also focally express this marker.[246]
- JGCTs with inapparent follicles can resemble thecomas, but extensive sampling of JGCTs will demonstrate at least focal areas with the characteristic follicular pattern. A reticulin stain is also helpful in identifying the scant fibrils that outline groups of granulosa cells in JGCT, which contrasts with the abundance of intercellular fibrils in thecomas and in areas with thecomatous differentiation. Usual thecomas also typically occur in an older age group and seldom exhibit the degree of mitotic activity seen in most JGCTs.

- The tubulocystic variant of clear cell carcinoma can be simulated by JGCT if the follicles are lined by hobnail-like cells. However, clear cell carcinomas occur in an older age group, often have admixed papillary and solid patterns, and have glycogen-rich rather than lipid-rich cytoplasm. A potential diagnostic pitfall is that some degree of inhibin immunoreactivity has been reported in a few ovarian clear cell carcinomas.[247]
- Although pregnancy luteomas with follicle-like spaces can mimic juvenile JGCTs, the former have more monotonous nuclear and architectural features, are often multiple and/or bilateral, and their association with pregnancy is more than just coincidental.
- Metastatic melanoma can consist of cells with abundant eosinophilic cytoplasm and form follicle-like spaces, imparting a resemblance to JGCT.[241,242] Features that favor metastatic melanoma include a previous history of melanoma, age over 20 years, tumor bilaterality, identification of melanin pigment, nuclear pseudoinclusions, and immunoreactivity for a panel of melanoma markers coupled with lack of staining for inhibin and calretinin.

Prognosis

Stage is the dominant prognostic factor in JGCT. Nearly all patients have stage I disease, and nearly all of these patients are cured by surgical removal of the tumor. Those few patients who have extraovarian spread at the time of operation often die of their disease, typically within the first 3 years following their diagnosis.

Fibroma

Fibromas are far and away the most common sex cord-stromal tumor, and account for about 4% of all primary ovarian tumors.[1,16] These benign collagen-producing tumors typically present as a pelvic mass (average size of 6 cm) in a middle-aged woman (mean age of 48 years). Ascites is present in roughly 10% of patients, and approximately 1% of cases are associated with Meigs' syndrome (ascites and pleural effusion that resolve after removal of the fibroma). Less than 10% of ovarian fibromas are bilateral or calcified. The presence of these features, particularly in combination and in young patients, suggests the presence of nevoid basal cell carcinoma (Gorlin) syndrome, whose more common manifestations include the early development of multiple basal cell carcinomas and odontogenic keratocysts.[248–250]

Grossly, fibromas typically have a smooth to bosselated, off-white external surface and a solid sectioned surface that is firm and whorled with a color that may be white, pale yellow, and/or tan (Fig. 7.177). Areas of cystic degeneration are seen on occasion. Those fibromas that are associated with nevoid basal cell carcinoma syndrome are often multinodular.

Histologically, fibromas are composed of a sparsely to moderately cellular population of spindle-shaped cells that form intertwining fascicles or storiform patterns within a collagenized matrix that may be hyalinized (Figs. 7.178–7.180). The

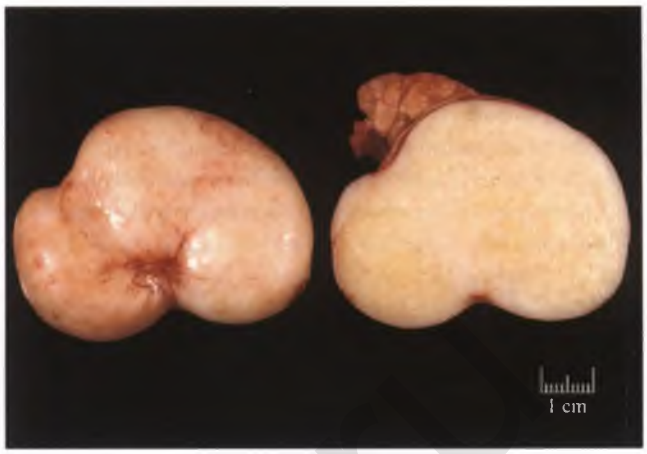

FIGURE 7.177. Fibroma. External surface (left) and sectioned surface (right). This tumor is solid and composed of firm, trabeculated, white to pale yellow tissue.

elongated nuclei do not exhibit significant cytologic atypia, and mitotic figures are uncommon. Patchy areas of edema are commonly present in fibromas and related tumors, as illustrated in the section on cellular fibroma. In some cases, the edematous areas can be difficult to distinguish from thecomatous differentiation, as discussed in the section on fibrothecoma. Small amounts of intracytoplasmic lipid can be seen in fibromas, which can cause further confusion with thecomatous tumors. An example of a calcified fibroma from a patient with nevoid basal cell carcinoma syndrome is shown in Figure 7.181.

Differential Diagnosis

- The distinction of fibroma from cellular fibroma, fibrothecoma, and usual thecoma can be subjective and arbitrary, as discussed in the following sections.

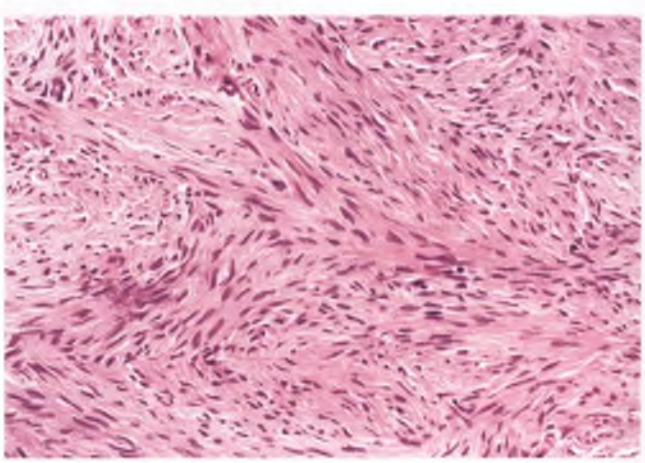

FIGURE 7.178. Fibroma. In this typical example, intertwining fascicles of bland, spindle-shaped cells are set within a collagenous stroma.

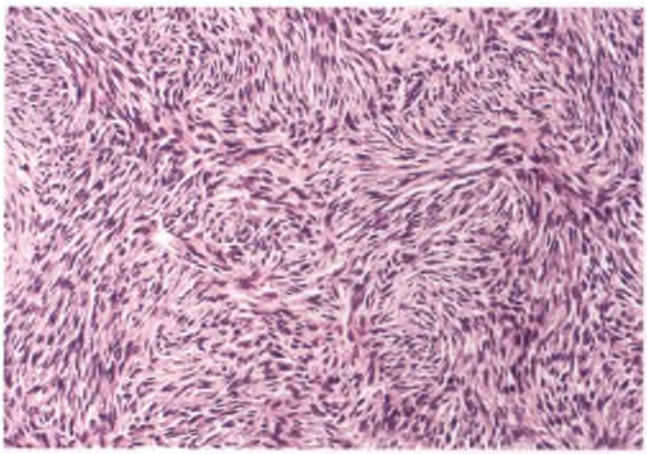

FIGURE 7.179. Fibroma with an irregularly and tightly whorled (storiform) pattern.

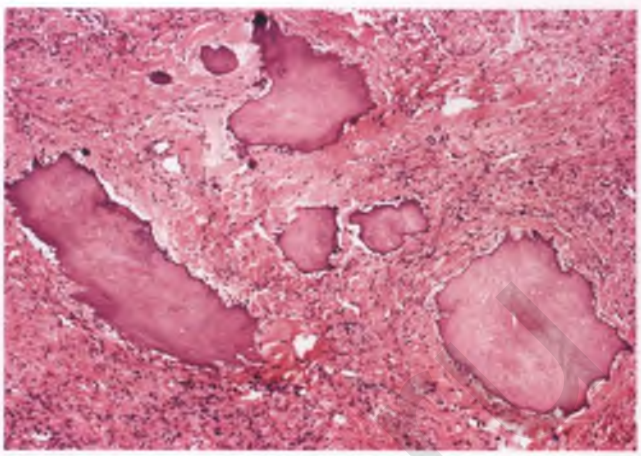

FIGURE 7.181. Fibroma with calcifications. Bilateral calcified fibromas were present in this 17 year-old patient with nevoid basal cell carcinoma (Gorlin) syndrome.

- A fibromatous tumor that contains significant numbers of luteinized stromal cells is considered a luteinized thecoma rather than a luteinized fibroma, as discussed in the section on luteinized thecomas.
- The pseudolobular pattern of sclerosing stromal tumor (SST) can be simulated by fibromas with patchy edema or those with sharply demarcated differences in cellularity, but fibromas have a less prominent vascular pattern than SSTs, lack the rounded vacuolated cells that are characteristic of the latter neoplasm, and tend to occur in an older patient population.
- Fibromas can resemble leiomyomas, which rarely occur in the ovary. This distinction is discussed in the section on ovarian leiomyomas, but it is worth noting here that about half of ovarian fibromas are at least focally immunoreactive for smooth muscle actin, rendering this stain of little use in the differentiation of fibroma from leiomyoma.[251]
- Since fibromas displace rather than incorporate ovarian follicles and their derivatives, they should not be confused with massive edema or ovarian fibromatosis.

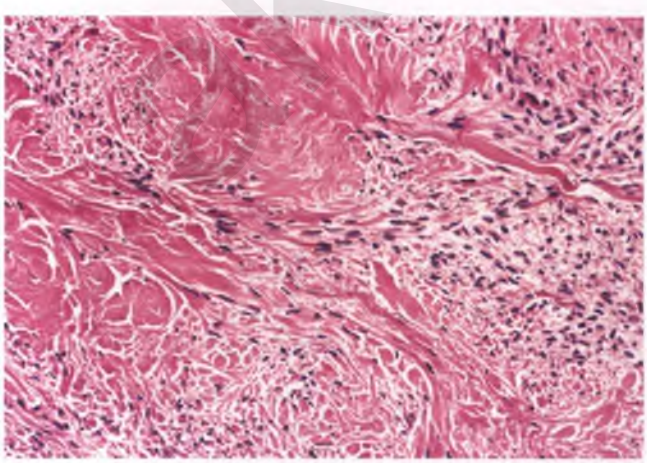

FIGURE 7.180. Fibroma with hyalinized stroma.

- Whether a small fibroma is dignified as such or designated a benign fibromatous nodule is a matter of personal preference.

Cellular Fibroma

Approximately 10% of benign ovarian fibromatous neoplasms are markedly cellular and are referred to as cellular fibromas.[252,253] Although there is significant overlap in the gross appearance of ordinary fibroma and cellular fibroma, the sectioned surface of the latter is more likely to contain shades of yellow and have a soft or rubbery texture that may be described as "fleshy" (Fig 7.182). Although these tumors can be intensely cellular, the mitotic rate is ≤3 mitotic figures per 10 high-power fields (MF/10 HPF), no atypical mitotic figures are present, and there is no significant nuclear atypia (Fig. 7.183A). Reticulin stains highlight fibrils surrounding individual tumor cells (Fig. 7.183B), which can be of diagnostic significance in

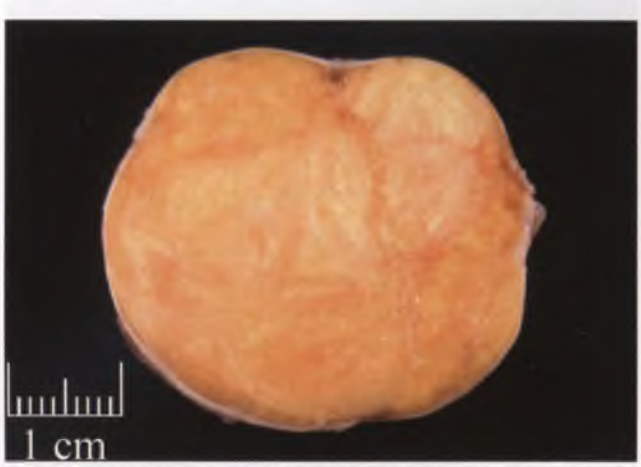

FIGURE 7.182. Cellular fibroma. As is often the case with this variant, the sectioned surface is yellow and rubbery.

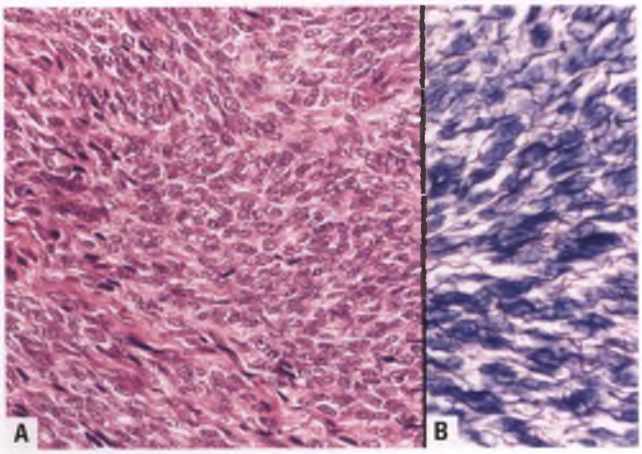

FIGURE 7.183. Cellular fibroma. **A:** The tumor is densely cellular, but does not exhibit significant nuclear atypia or mitotic activity. **B:** A reticulin stain highlights the delicate, darkly-stained fibrils that are present in between individual tumor cells, which helps to distinguish cellular fibroma from the diffuse variant of adult granulosa cell tumor (hematoxylin counterstain).

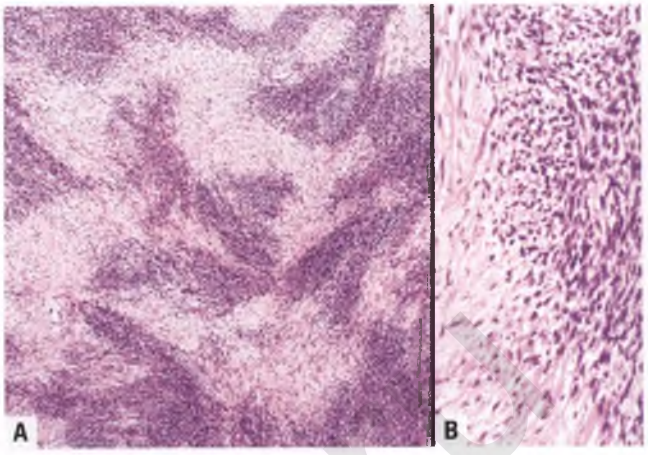

FIGURE 7.185. Cellular fibroma with edema (histologic correlate of preceding image). **A:** Hypercellular regions alternate with patchy hypocellular edematous zones. **B:** High-magnification view of a transition between edematous and cellular areas.

selected instances. As is true of fibromatous ovarian neoplasms in general, intercellular edema can alter the gross and microscopic appearance of cellular fibromas (Figs. 7.184 and 7.185). Necrosis is present in a minority of tumors, and is often seen in the setting of a pedunculated tumor that has undergone torsion.

An important modification in the classification of cellular fibromas was made in 2006 that provides a needed buffer zone between cellular fibroma and fibrosarcoma.[253] Using earlier guidelines, mitotic activity was of paramount importance in distinguishing these two tumors (≤3 MF/10 HPF → cellular fibroma; 4 or more MF/10 HPF → fibrosarcoma).[252] The degree of nuclear atypia played a secondary role, since both cellular fibromas and fibrosarcomas could exhibit a moderate degree of atypia in the Prat and Scully study.[252] In the more recent and larger study by Irving et al. the category of mitotically active cellular fibroma (MACF) was created to house those fibromatous tumors with mild nuclear atypia and increased numbers of normal mitoses (mitotic counts of ≥4 MF/10 HPF using the highest count method rather than the average count method of Prat and Scully) (Fig. 7.186).[253] Using this methodology, these tumors had mitotic counts that ranged from 4 to 19 MF/10 HPF and were found to behave no differently from their less mitotically active counterparts.[253]

Emblematic of the subjective nature of what constitutes moderate nuclear atypia in this group of tumors, Irving et al.

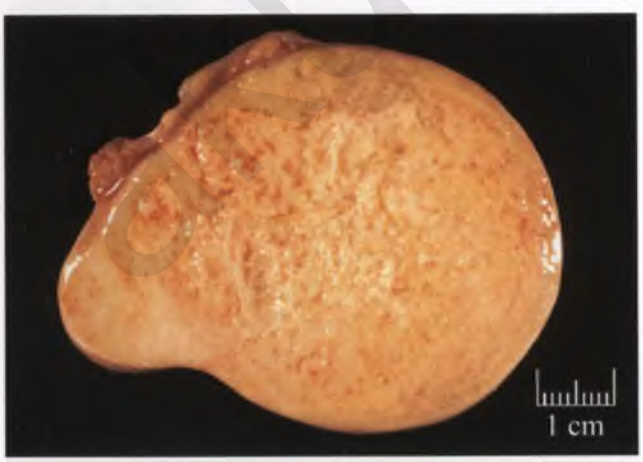

FIGURE 7.184. Cellular fibroma with edema. The sectioned surface of this tumor has a wet, mottled appearance due to the presence of multiple patches of intercellular edema.

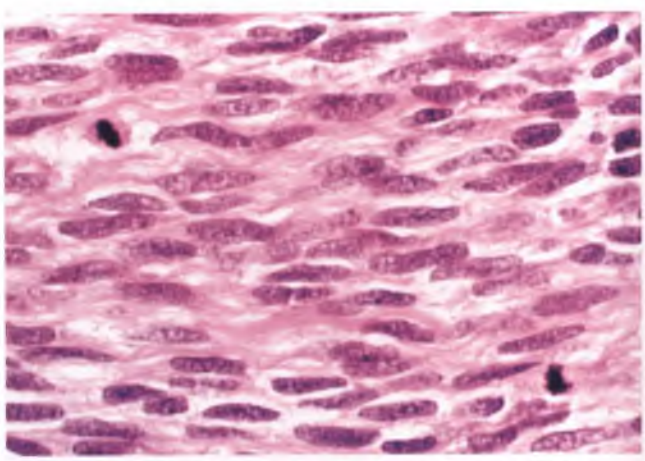

FIGURE 7.186. Mitotically active cellular fibroma. Two normal mitotic figures are present in this image. Although this cellular tumor had a mitotic count as high as 7 MF/10 HPF, the presence of only mild nuclear atypia distinguishes it from fibrosarcoma (compare with Fig. 7.187).

considered none of the 75 cellular fibromas and MACFs in their study to exhibit more than mild atypia (except for focal reactive atypia of moderate degree that bordered foci of necrosis in a few cases), whereas Prat and Scully considered 6 of their 11 cellular fibromas to exhibit moderate nuclear atypia.[252,253] Since the current guidelines are to categorize mitotically active fibromatous ovarian neoplasms as MACFs if they exhibit no more than mild atypia and to reserve the diagnosis of fibrosarcoma for those cases that exhibit the combination of moderate to severe atypia and a high mitotic rate, it is clear that there will be some cases where this distinction rests on the subjective opinion of the pathologist as to whether the degree of atypia is mild or moderate.

Both typical cellular fibromas and its mitotically active variant can be considered benign for management purposes, although some tumors that are adherent to adjacent structures or that have ruptured have recurred.[252]

Differential Diagnosis

- The degree of cellularity at which a fibroma becomes a cellular fibroma is in the eye of the beholder, and the current criteria used to distinguish cellular fibroma from MACF and fibrosarcoma have been discussed above.
- Stromal hyperplasia can have an appearance similar to cellular fibroma when viewed at high magnification, but is readily distinguished by its bilaterality, mild degree of ovarian enlargement, entrapment of normal ovarian structures, and less discrete nodularity.
- Luteinized thecomas often have a cellular fibromatous background, but are recognized by their clusters of luteinized cells.
- AGCTs of diffuse and sarcomatoid types may resemble cellular fibromas, but the presence of nuclear grooves and/or a pattern of reticulin fibrils surrounding cellular aggregates rather than individual tumor cells facilitate the recognition of the granulosa cell nature of these neoplasms.
- Just as ordinary fibroma can be confused with leiomyoma, cellular fibroma can be mistaken for cellular leiomyoma. This distinction is touched upon in the section on ovarian leiomyomas.
- Primary endometrioid stromal sarcoma and metastatic endometrial stromal sarcoma are distinguished by their characteristic vascular pattern and CD10 immunoreactivity; the former is also frequently associated with endometriosis and the latter is often bilateral and associated with a known primary uterine tumor.[176,179,253]
- A gastrointestinal stromal tumor (GIST) that has metastasized to the ovary can mimic a cellular fibroma.[254] The frequent bilaterality of these metastases, the clinical history of such a tumor, and immunoreactivity with c-KIT (CD117) and CD34 in conjunction with desmin negativity help to confirm the diagnosis and also exclude the additional possibility of a smooth muscle neoplasm.

Fibrosarcoma

Although fibrosarcomas are considered to be the most common ovarian sarcoma, these are very rare neoplasms. The typical presentation is that of a postmenopausal woman (mean age of 58 years) who presents with a large pelvic mass (average size of 17 cm).[252]

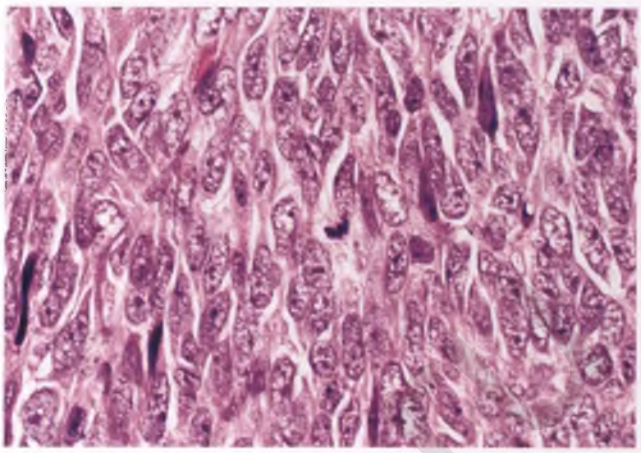

FIGURE 7.187. Fibrosarcoma. This tumor is mitotically active and features significant nuclear atypia in the form of plump, spindle-shaped cells with prominent nucleoli.

The sectioned surface of ovarian fibrosarcoma is usually solid, soft, and grayish-white to tan with interspersed areas of hemorrhage and necrosis. Histologically, the fascicular architecture of these hypercellular tumors may be difficult to appreciate, although herringbone or storiform patterns may be recognizable. At high magnification, nuclei are ovoid to spindle-shaped, often contain prominent nucleoli, and exhibit moderate to severe atypia (Fig. 7.187). Mitotic figures, including atypical forms, are readily identified, with mitotic counts of at least 4MF/10 HPF.[252]

Differential Diagnosis

The distinction of fibrosarcoma from MACF has been discussed in the previous section, and the comments made therein regarding the separation of cellular fibromas from endometrial stromal sarcomas and a subset of AGCTs are equally applicable to fibrosarcoma in its distinction from these tumors. As noted in Chapter 6, tangential cutting through a mitotically active zone of the theca externa of an ovarian follicle can produce a solid-appearing nodule that can be misinterpreted as a microscopic fibrosarcoma (see Figs. 6.19 and 6.20).

Thecoma, Usual Type[255–257]

Usual thecomas are rare stromal neoplasms that typically occur in postmenopausal women (mean age of 60 years), and are often associated with estrogenic manifestations similar to those described for AGCT. They are confined to the ovary at presentation and are almost always unilateral. For unknown reasons, no large series focusing on the pathologic features of the usual type of thecoma has been published for over 60 years.

Grossly, thecomas are solid, circumscribed neoplasms with a mean size of 7 cm, and their sectioned surface is typically yellow. Histologically, classic examples of thecoma are composed of sheets of cells resembling those of the theca interna

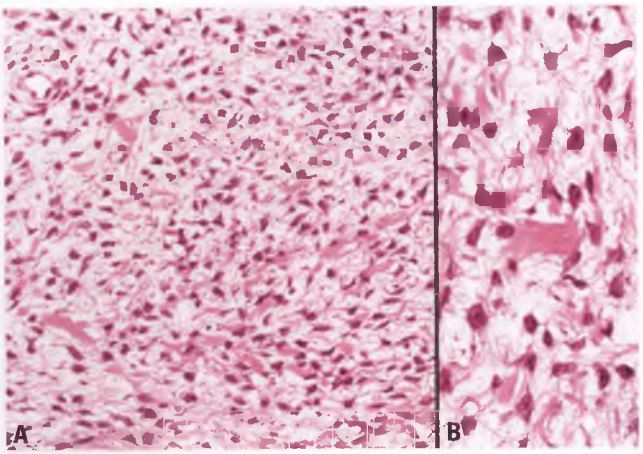

FIGURE 7.188. **A,B:** Thecoma. The tumor consists of sheets of cells with ovoid to spindle-shaped nuclei and clear, vacuolated cytoplasm. Scattered hyaline plaques are evident.

with abundant cytoplasm that is pale-staining and lipid-rich (Fig. 7.188). Nuclei vary in shape from round to oval to spindled and lack significant atypia. Mitotic figures are usually not apparent. Reticulin stains highlight the presence of delicate fibrils enveloping individual cells. A characteristic feature is the common presence of hyaline plaques, although these are also often seen in fibromas. Rare thecomas in young adult women may be extensively calcified.[258]

The subjectivity of the diagnosis of thecoma increases when non-classic cases that have predominantly spindle-shaped nuclei and/or dense cytoplasm are encountered. In these cases, the diagnosis is often heavily influenced by the presence of estrogenic manifestations, which favors thecoma over fibroma. In cases where a frozen sample of tumor is available, the presence of abundant intracytoplasmic lipid as detected with the oil red O stain is also supportive of a diagnosis of thecoma, and more than minimal immunoreactivity for inhibin has also been taken as evidence in favor of thecoma over fibroma.[9] In addition to being positive for inhibin, thecomas are typically immunoreactive for calretinin and fail to stain with cytokeratin.[147,220,221]

Differential Diagnosis

- In addition to the often subjective distinction of usual thecoma from fibroma as discussed above, thecoma can be confused with the luteinized variant of AGCT. In contrast to thecoma, a well-sampled granulosa cell tumor of this type contains some areas with nuclear grooves and the usual architectural patterns of AGCT, has scant rather than abundant intercellular fibrils as demonstrated with a reticulin stain, and may be immunoreactive for cytokeratin.[231]
- Some steroid cell tumors in the "not otherwise specified" category may be misinterpreted as usual thecomas because of their abundant lipid-rich cytoplasm and sheetlike architecture. However, these steroid tumors more frequently exhibit androgenic rather than estrogenic manifestations, lack the significant stromal component and hyaline plaques of thecomas, and have monotonous, round, centrally located nuclei, often with prominent nucleoli, that are quite different from the nuclei of usual thecomas.

Prognosis

The vast majority of thecomas are benign, and criteria for malignancy have not been established. Diagnoses such as fibrosarcoma and sarcomatoid granulosa cell tumor should be strongly considered before raising the possibility of malignant thecoma, of which there are only a few well-documented cases.[256,259] Given that identification of thecomatous differentiation is often a subjective exercise even in bland tumors, it is not surprising that those rare potentially malignant thecomas that exhibit brisk mitotic activity and marked nuclear atypia are not easily recognized as being of thecal origin.

Fibrothecoma

The typical fibroma is readily distinguished from the classic thecoma. However, many of the tumors within this group have overlapping features, and some have applied the term "fibrothecoma" in this situation. Drs. Scully, Young, and Clement do not use this term, and instead prefer to diagnose such tumors as fibromas unless lipid and/or inhibin stains provide supportive evidence for thecoma as discussed above.[9] In practice, frozen tissue is unlikely to be available to perform an oil red O lipid stain and it is not cost-effective to perform an inhibin immunostain in an effort to help distinguish one benign ovarian stromal tumor from another, making fibroma the usual default diagnosis for tumors with blended fibrothecomatous features. On the other hand, it seems appropriate to use the term fibrothecoma for those tumors that contain an admixture of separately recognizable fibromatous and thecomatous components (Figs. 7.189 and 7.190). Without a lipid stain, it can be difficult to distinguish

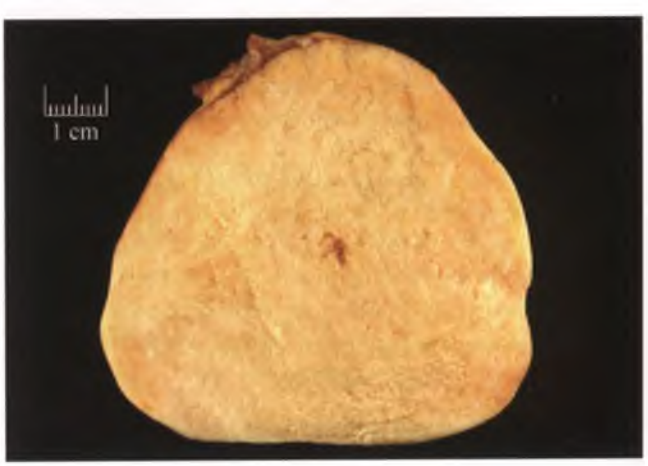

FIGURE 7.189. Fibrothecoma. The sectioned surface is solid with both light gray (fibromatous) and yellow (thecomatous) areas.

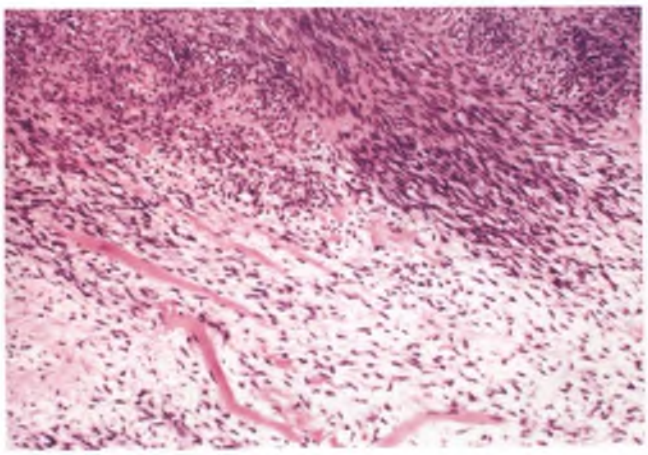

FIGURE 7.190. Fibrothecoma. An area of cellular fibroma (top) is adjacent to an area with thecomatous differentiation (bottom).

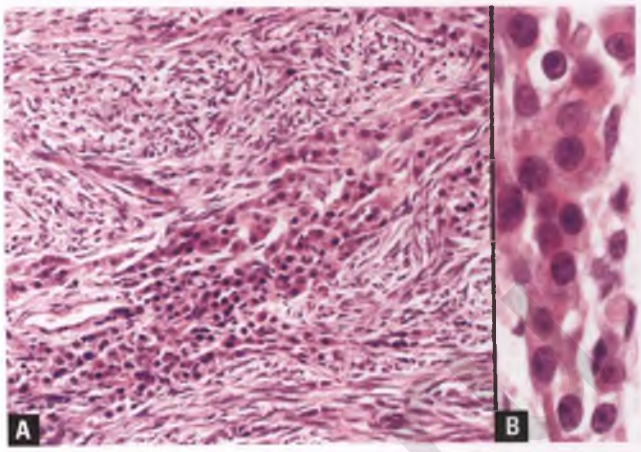

FIGURE 7.192. Luteinized thecoma. **A:** Aggregates of luteinized cells are present within a fibromatous background. **B:** In this high-magnification view of the luteinized cells, note the common presence of single prominent nucleoli.

fibrothecomas of this type from fibromas with edematous regions, but such a distinction is only of academic interest.

Luteinized Thecoma[260]

Luteinized thecomas occur at an average age of 46 years. About half of these tumors are associated with estrogenic manifestations, and another 10% exhibit androgenic changes. As is the case for usual thecomas, luteinized thecomas are solid neoplasms that have an average size of 7 cm, a smooth external surface, an often partially lobulated sectioned surface that is usually a shade of yellow, and are rarely bilateral (Fig. 7.191). Luteinized thecomas may have either a fibromatous or thecomatous background, with the former often being cellular and outnumbering the latter by a ratio of roughly 5 to 1. The distinguishing histologic feature of luteinized thecomas is the presence of aggregates of luteinized cells that are recognized by their abundant pale to eosinophilic cytoplasm and round nuclei that often contain single prominent nucleoli (Fig. 7.192). By definition, crystals of Reinke are not identified in these steroid-type cells (see below).

FIGURE 7.191. Luteinized thecoma. The sectioned surface of this tumor is solid, yellow, lobulated, and focally hypervascular.

Rare luteinized thecomas have a peculiar association with sclerosing peritonitis, and have a different set of clinical and pathologic features.[261,262] These lesions occur over a wide age range (median age of 27 years), are not associated with endocrine manifestations, and are almost always bilateral. They may be small to quite large (average size of 10 cm), and often exhibit a high mitotic rate within the spindle cell population, stromal edema with formation of microcysts, and entrapped follicular elements. Although occasional patients may die related to complications of sclerosing peritonitis, the ovarian masses have behaved in a benign fashion. The possibility that the ovarian lesions actually represent reactive stromal proliferations has recently been given serious consideration, and an alternative designation of thecomatosis has been proposed.[262] A nonneoplastic etiology is supported by the common finding of entrapped follicles, the sparing of the medullary region in involved ovaries that are small enough to have preserved architecture, and the nearly universal bilaterality of this process.

Differential Diagnosis

The differential diagnosis of luteinized thecoma includes other tumors in the fibroma-thecoma group, stromal-Leydig cell tumor, steroid cell tumor, and stromal hyperthecosis.

- The presence of significant numbers of luteinized cells is the determining factor in the distinction of luteinized thecoma from other tumors in the fibroma-thecoma group. In the usual situation, an ovarian tumor that otherwise has the histologic appearance of a fibroma or cellular fibroma is found to have several clusters of luteinized cells, at which point the tumor magically transforms into a luteinized thecoma. Although such

tumors can literally be thought of as "fibromas on steroids" and the diagnostic term luteinized fibroma may seem more appropriate, these tumors are classified as a variant of thecoma in deference to their endocrine nature, which is evidenced by the presence of cells of the type that secrete steroid hormones.

- In yet another twist of nomenclature, stromal-Leydig cell tumor is the diagnostic term used in the very rare situation in which crystals of Reinke are found within the steroid-type cells of a tumor that otherwise exhibits the histologic features of a luteinized thecoma.
- On occasion, the luteinized cells can come to dominate a case of luteinized thecoma, which results in a resemblance to a steroid cell tumor. By convention, a diagnosis of steroid cell tumor is not made unless the fibromatous or thecomatous component of such a case constitutes <10% of the tumor.[9]
- The differential diagnosis of luteinized thecoma with stromal hyperthecosis is discussed in the section on stromal hyperthecosis in Chapter 6.

Behavior

The vast majority of luteinized thecomas are benign, but those with the combination of high mitotic rates and significant nuclear atypia should be flagged as having recurring potential.

Stromal Tumor With Minor Sex Cord Elements[235]

Tumors in the fibroma-thecoma group may rarely contain focal sex cord elements that do not alter the behavior of these benign tumors. The sex cord component usually has an indifferent appearance (Fig. 7.193), but may also resemble neoplastic granulosa cells or immature Sertoli tubules.

Sclerosing Stromal Tumor[263–265]

SST is a rare benign tumor that typically presents in a young woman (mean age of 26 years) as a nonfunctional ovarian mass. Virtually all well-documented tumors of this type are unilateral.

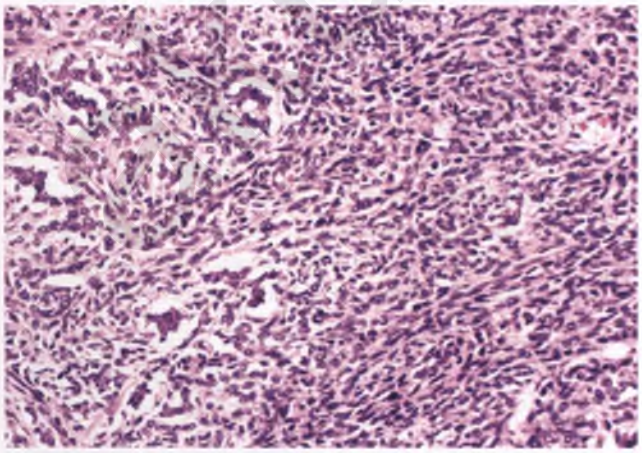

FIGURE 7.193. Cellular fibroma with minor sex cord elements. The focal nests of indifferent-appearing sex cord elements are associated with retraction artifact.

FIGURE 7.194. Sclerosing stromal tumor. This view of a bivalved tumor demonstrates a sharply circumscribed, off-white to tannish pink neoplasm with scattered cystic areas. (Courtesy of Dr. Colin J. R. Stewart)

SSTs average about 10 cm in diameter, and are nodular masses with a smooth external surface. The sectioned surface of most tumors is rubbery, predominantly solid, and off-white to pale yellow with edematous areas (Fig. 7.194). Scattered cysts are commonly present, and rare SSTs present as unilocular cysts.

Histologically, SSTs exhibit a characteristic pseudolobulation that is due to the presence of cellular nodules that are separated by edematous or sclerotic tissue (Figs. 7.195 and 7.196). Within the cellular islands is a prominent network of thin-walled vessels that are commonly dilated and irregularly shaped, imparting a resemblance to hemangiopericytoma (Fig. 7.197). When examined at high magnification, the cellular areas are found to be composed of a hodgepodge of rounded cells with vacuolated cytoplasm (theca-like luteinized cells that typically have little to no functionality) and spindle-shaped fibroblastic cells (Fig. 7.198). Occasionally, signet-ring-like cells may be present within these areas (Fig. 7.199). Reticulin fibrils are

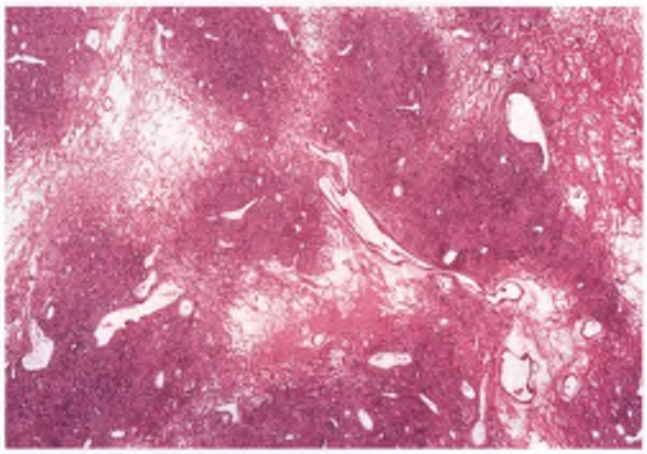

FIGURE 7.195. Sclerosing stromal tumor. This low-magnification view highlights the characteristic pseudolobular architecture that is formed by cellular islands separated by lacy edematous tissue.

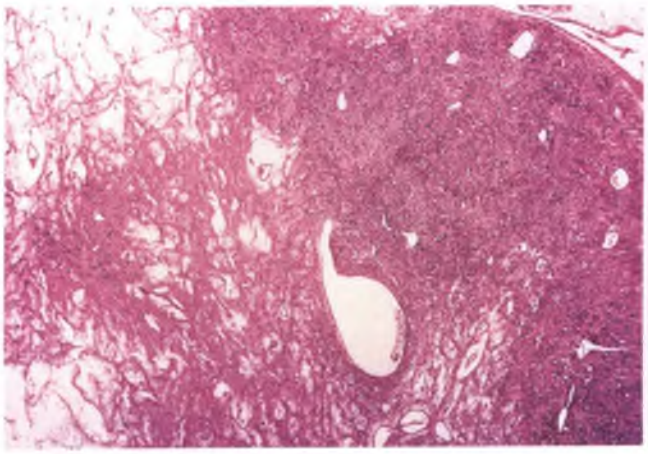

FIGURE 7.196. Sclerosing stromal tumor. An alternating sclerotic and edematous area at left merges with a lobulated cellular region at right.

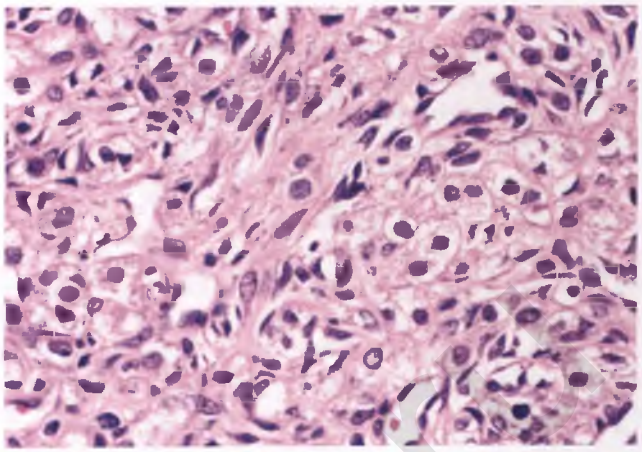

FIGURE 7.198. Sclerosing stromal tumor. There is an admixture of vacuolated cells with round contours and spindle-shaped cells within the cellular regions.

abundant and surround individual tumor cells. Mitotic figures are uncommon. The cysts in these tumors form as an exaggeration of stromal edema, and lack an epithelial lining. Most SSTs are immunoreactive for inhibin in the vacuolated theca-like component and also exhibit positive staining for actin and desmin in the spindle cell component.[265]

Differential Diagnosis

The distinction between SST and fibroma is discussed in the section on fibroma, and largely applies to thecoma as well. More important is the distinction from metastatic signet-ring adenocarcinoma (Krukenberg tumor), which may be simulated by SSTs with prominent signet-ring-like cells. Unlike SSTs, Krukenberg tumors are often bilateral, occur in an older age group, and have mucin rather than lipid-containing signet-ring cells that are immunoreactive for cytokeratin.

Signet-Ring Stromal Tumor[266,267]

This extraordinarily rare benign neoplasm is worthy of discussion because it can be mistaken for metastatic signet-ring carcinoma (Krukenberg tumor). These tumors are almost always unilateral and are composed of an admixture of spindle-shaped stromal cells with a variably-prominent signet-ring component (Fig. 7.200). In a minority of signet-ring stromal tumors, intracytoplasmic and extracellular hyaline globules are present. The signet-ring cells of these tumors have bland nuclei that are compressed into peripheral crescentic shapes by single, large vacuoles that do not contain mucin or lipid. In contrast, Krukenberg tumors harbor mucin-containing signet-ring cells that are usually admixed with more obvious epithelial elements. Krukenberg tumors are also likely to be bilateral, may be found in association with peritoneal implants and/or ascites, and may be associated with a known primary malignancy.

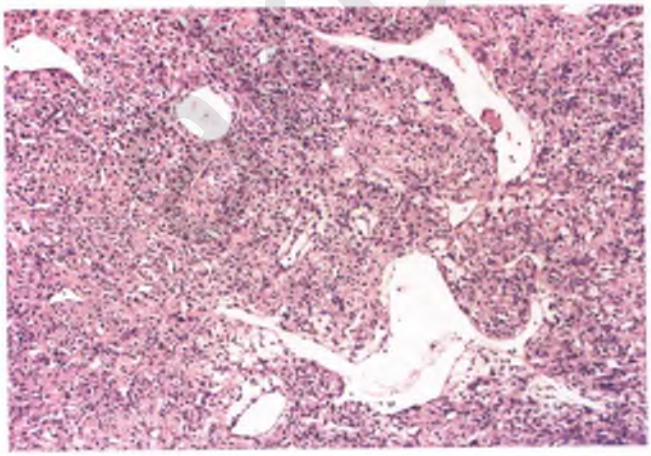

FIGURE 7.197. Sclerosing stromal tumor. Note the prominent thin-walled vessels, some of which have a staghorn configuration reminiscent of that seen in hemangiopericytomas.

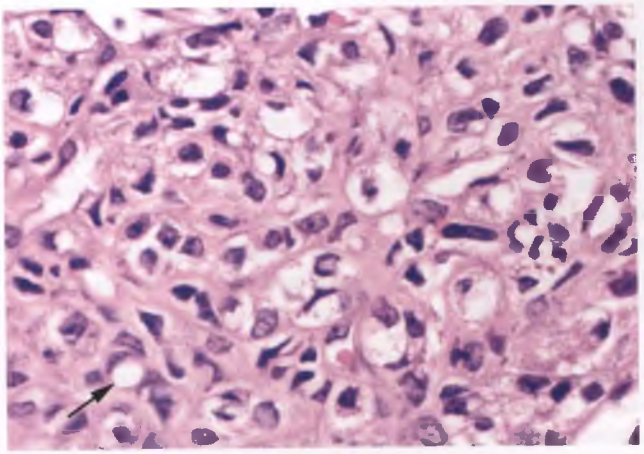

FIGURE 7.199. Sclerosing stromal tumor. Scattered signet-ring-like cells, such as the one marked by the *arrow*, can be seen in these tumors due to the presence of lipid-containing vacuoles.

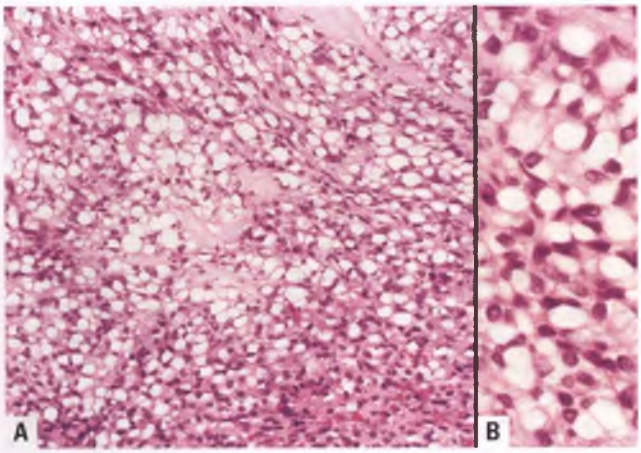

FIGURE 7.200. **A,B:** Signet-ring stromal tumor. The presence of numerous signet-ring cells can result in misdiagnosis as metastatic signet-ring carcinoma if the pathologist is unaware of the existence of this entity and mucin stains are not performed.

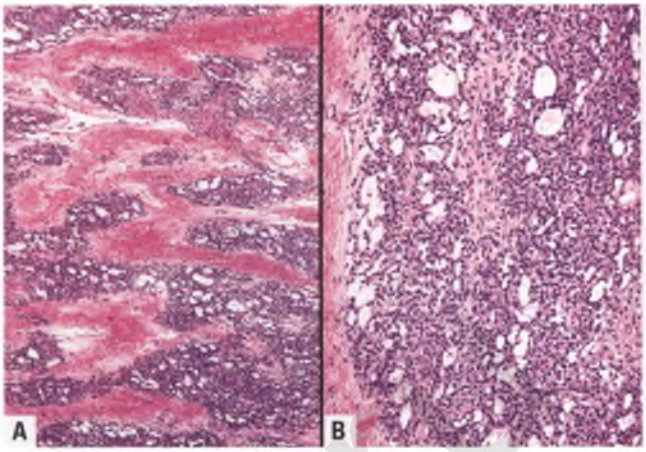

FIGURE 7.201. Microcystic stromal tumor. **A:** Lobulated cellular areas with interspersed microcysts are separated by hyalinized fibrous bands. **B:** At higher magnification, the microcystic pattern and bland nuclear features that are characteristic of this neoplasm are better appreciated. (Courtesy of Drs. Julie A. Irving and Robert H. Young)

Immunohistochemistry can also be utilized to help distinguish these two tumors, since signet-ring stromal tumors are typically immunoreactive for vimentin and fail to express cytokeratin and epithelial membrane antigen, which is the opposite phenotype of that expected for Krukenberg tumors.[‡‡]

Unlike most other tumors in the sex cord-stromal category, signet-ring stromal tumors are usually not immunoreactive for inhibin or calretinin. To my eye, these tumors bear a strong resemblance to the variant of gastrointestinal stromal tumor (GIST) that has exaggerated cytoplasmic vacuoles. It would be interesting to determine if ovarian signet-ring stromal tumors express the GIST-associated marker c-KIT (CD117). If so, then perhaps these tumors represent yet another form of extragastrointestinal GIST, such as those that occur in the vagina (Chapter 2) and omentum (Chapter 8).

Microcystic Stromal Tumor[268]

This recently described tumor is yet another example of an extremely rare benign ovarian stromal tumor. The typical presentation is that of a mostly solid, unilateral ovarian mass (mean size of 9 cm) in an adult woman (mean age of 45 years). The diagnosis is based upon the presence of lobulated cellular islands composed of cells with bland nuclear features and minimal mitotic activity that form a microcystic pattern (Fig. 7.201). These lobules are typically separated from one another by bands of hyalinized fibrous tissue or fibrous plaques. Approximately 60% of cases have focal areas with bizarre nuclei that appear to represent a degenerative phenomenon.

Microcystic stromal tumors are typically negative for epithelial membrane antigen and strongly and diffusely positive for CD10 and vimentin. Stains for inhibin, calretinin, and cytokeratin are generally negative, but focal and weak immunoreactivity for these markers is seen in a minority of cases. These tumors should be thoroughly sampled for histologic evaluation to exclude the possibility of a tumor of another type with microcystic change (e.g., luteinized thecoma associated with sclerosing peritonitis, Sertoli-Leydig cell tumor (SLCT), yolk sac tumor, struma ovarii, and ovarian carcinoma with a microcystic pattern).

Sertoli Cell Tumor[149]

These very rare tumors, which are far less common than the hardly commonplace SLCTs, tend to occur in young adult women (mean age 30 years). Sertoli cell tumors are usually nonfunctional, occasionally estrogenic, and uncommonly androgenic. Aside from possible hormonal manifestations, these tumors may present with abdominal swelling, abdominal pain, incidentally, or rarely in association with Peutz-Jeghers syndrome.

Sertoli cell tumors are unilateral neoplasms with an average size of 9 cm, and have a sectioned surface that is usually solid, lobulated, and yellow. Tubular differentiation is almost always present, at least focally, in the form of solid and/or hollow tubules (Figs. 7.202 and 7.203). Other common architectural patterns include formations of cords, trabeculae, and diffuse sheets of sertoliform cells. The fibrous stroma that separates the sertoliform elements ranges from virtually inapparent to thin and delicate to broad and hyalinized. In most cases, there is no significant nuclear atypia or mitotic activity, and the cells have moderate amounts of pale-staining cytoplasm. In one-third of cases, occasional nuclear grooves are identified.

[‡‡]To date, all well-documented signet-ring stromal tumors have been negative for cytokeratin. A single neoplasm reported along with three signet-ring stromal tumors as a "related tumor" exhibited epithelial differentiation as evidenced by cytokeratin immunoreactivity and numerous desmosomes ultrastructurally, and was theorized to represent an unusual granulosa cell tumor or unclassified sex cord-stromal tumor with signet-ring cells.[266] The immunophenotype of this tumor has sometimes been inappropriately considered evidence that signet-ring stromal tumors can occasionally be positive for cytokeratin.

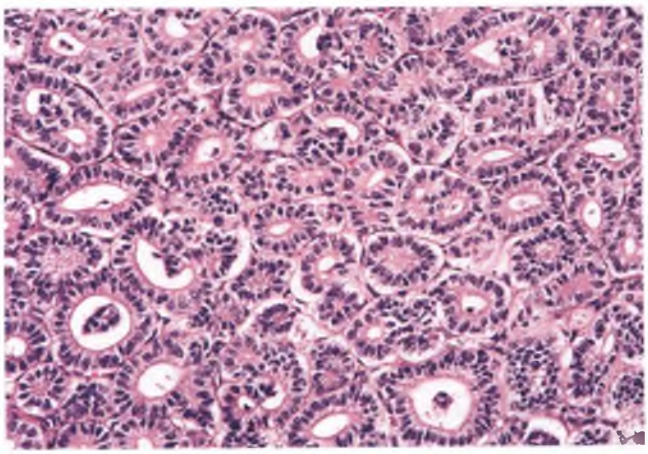

FIGURE 7.202. Sertoli cell tumor composed of closely packed hollow tubules that are lined by mitotically inactive cells with bland nuclear features.

Approximately 10% of Sertoli cell tumors qualify as the lipid-rich variant due to the presence of solid tubules with abundant intracytoplasmic lipid, which results in a clear, vacuolated appearance. Another 10% of cases have abundant eosinophilic cytoplasm and are referred to as oxyphil Sertoli cell tumors. Histologic features that are more likely to be present in those rare Sertoli cell tumors that pursue a malignant clinical course are significant nuclear atypia of a non-degenerative nature, brisk mitotic activity, and tumor cell necrosis, particularly when seen in combination.

Differential Diagnosis

The differential diagnosis of Sertoli cell tumor includes well-differentiated SLCT, AGCT, carcinoid tumor, tubular Krukenberg tumor, sertoliform endometrioid carcinoma, ovarian tumor of probable wolffian origin, and steroid cell tumor.

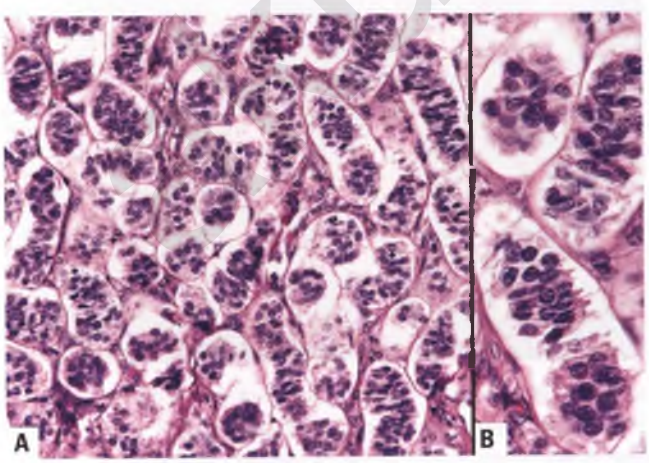

FIGURE 7.203. **A,B:** Sertoli cell tumor. This example features solid tubules surrounded by clear spaces that are related to retraction artifact.

Immunohistochemistry can play a vital role in evaluating Sertoli cell tumors, since inhibin and/or calretinin immunoreactivity will help place the tumor in the sex cord-stromal category, and the lack of staining with epithelial membrane antigen and neuroendocrine markers such as chromogranin help to exclude carcinomas and carcinoid tumors, respectively.

- Well-differentiated SLCT is distinguished by the presence of Leydig cells, although some investigators allow "rare" or "a few" Leydig cells within Sertoli cell tumors. However, the presence of a few such cells in a virilized patient is more likely to be related to undersampling of a SLCT.
- Sertoli cell tumors that have trabecular or diffuse patterns may mimic an AGCT, but the latter tumor tends to occur in an older age group, is less proficient at forming tubules, and has more prominent nuclear grooves.
- The discussion in the section on the differential diagnosis of SLCTs with carcinoid tumors and tubular Krukenberg tumors pertains to Sertoli cell tumors as well.
- The differential diagnosis with sertoliform endometrioid carcinoma, ovarian tumor of probable wolffian origin, and the lipid-rich variant of Sertoli cell tumor with steroid cell tumor are discussed in the sections on these other entities.

Sertoli-Leydig Cell Tumors

SLCTs, which are also known as androblastomas, have sex cord and stromal elements that exhibit testicular differentiation.[269] These rare tumors, which represent only about 1 of every 500 ovarian tumors, usually occur in young women (mean age of 25 years), almost half of whom have some evidence of virilization.[269] Nearly all patients present with unilateral, smooth-surfaced tumors that are confined to the ovary (mean size 13 cm). As discussed in the following paragraphs, SLCTs exhibit a wide range of histologic patterns, may contain heterologous elements, and have a prognosis that correlates with their degree of differentiation.

Notes:

1. In the setting of an associated Sertoli cell component, the steroid cells of SLCTs are presumed to represent Leydig cells, even without identification of crystals of Reinke. This convention simplifies the nomenclature of these tumors, since identification of such crystals in SLCTs is the exception rather than the rule.[269] An additional point of potential confusion is that the identification of steroid cells meeting this relaxed definition of Leydig cells is not required for the diagnosis of the intermediate and poorly differentiated forms of SLCT.[269]
2. The frequency of well differentiated, intermediate differentiated, and poorly differentiated SCLTs has been reported as 10%, 70%, and 20%, respectively (after reassignment of the heterologous cases according to the degree of differentiation of their homologous component).[269] However, nearly all tumors reviewed to obtain these frequencies were from consultation cases. Since it is considerably easier for general

FIGURE 7.204. Well-differentiated Sertoli-Leydig cell tumor. The sectioned surface is solid, yellow, and lobulated.

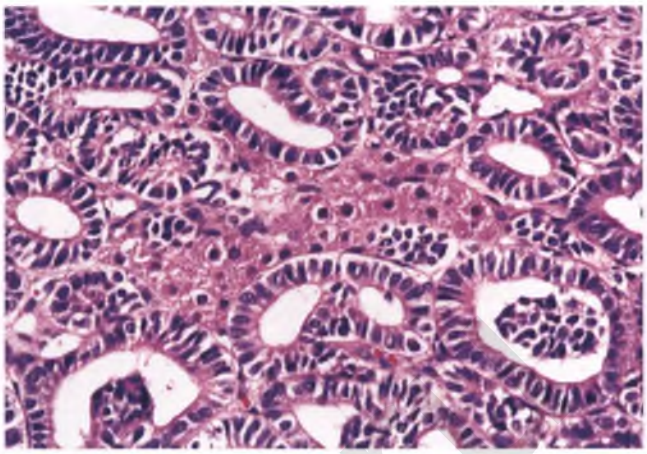

FIGURE 7.206. Well-differentiated Sertoli-Leydig cell tumor. In this example, the centrally located Leydig cell component consists of cells with abundant eosinophilic cytoplasm.

surgical pathologists to recognize well-differentiated SLCTs than intermediate and poorly differentiated forms, reports from referral centers probably have a significant selection bias that results in an underestimation of the proportion of SLCTs that are well differentiated (note that six of the seven *in-house* cases in the Harvard series were well-differentiated SLCTs).[269,270]

Well-differentiated SLCTs have an average size of 5 cm, and are typically solid, lobulated, and yellow (Fig. 7.204).[270] The lobules are formed by closely packed aggregates of hollow or solid tubules that are lined by mitotically inactive Sertoli cells with bland nuclear features (Fig. 7.205). Leydig cells, which have abundant cytoplasm that ranges from vacuolated to eosinophilic, are found in nests within the stroma (Figs. 7.205 and 7.206). The supporting stroma is variable in amount and consists of bands of mature fibrous tissue. Retiform patterns and heterologous elements are not present in well-differentiated SLCTs.

Since all well-differentiated tumors reported to date have followed a benign clinical course, unilateral salpingo-oophorectomy is appropriate treatment for a young woman who wishes to preserve her fertility.

SLCTs of intermediate differentiation typically have a yellow-tinged, lobulated solid component that is often admixed with scattered cysts (Fig. 7.207). The lobules are often dominated by largely nondescript, spindle-shaped cells that have been variously attributed to cellular proliferations of immature

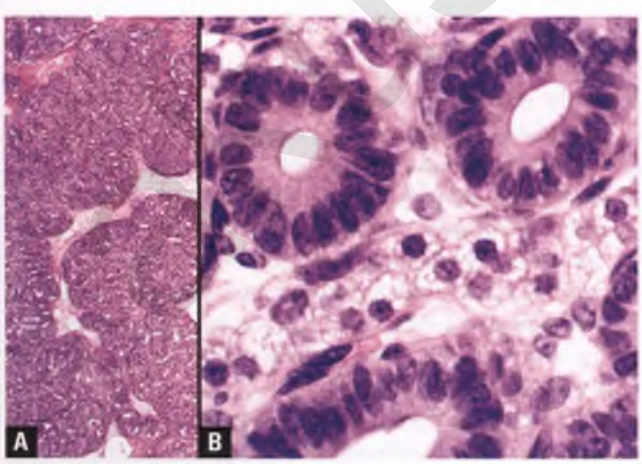

FIGURE 7.205. Well-differentiated Sertoli-Leydig cell tumor. **A:** The lobulated architecture is highlighted in this low-magnification view. **B:** At high magnification, nests of Leydig cells with vacuolated cytoplasm are seen in association with hollow tubules lined by Sertoli cells.

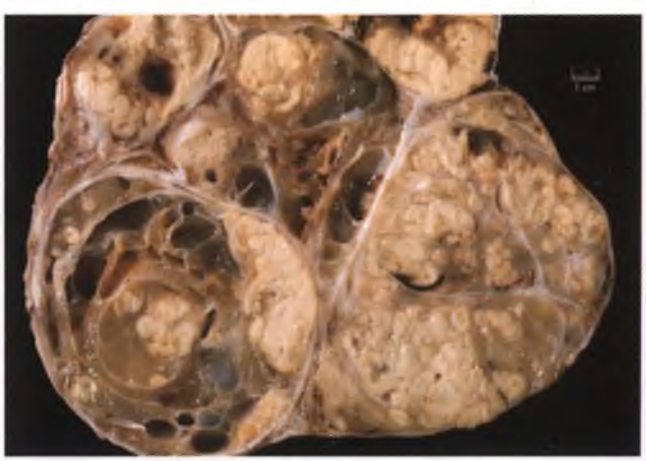

FIGURE 7.207. Sertoli-Leydig cell tumor of intermediate differentiation with heterologous mucinous elements. The sectioned surface of this formalin-fixed tumor from a 17 year-old virilized female is composed of pale yellow, lobulated tissue admixed with cystic spaces. Note the presence of inspissated, glistening mucoid material related to mucinous differentiation. (Courtesy of Dr. Julio A. Lagos.)

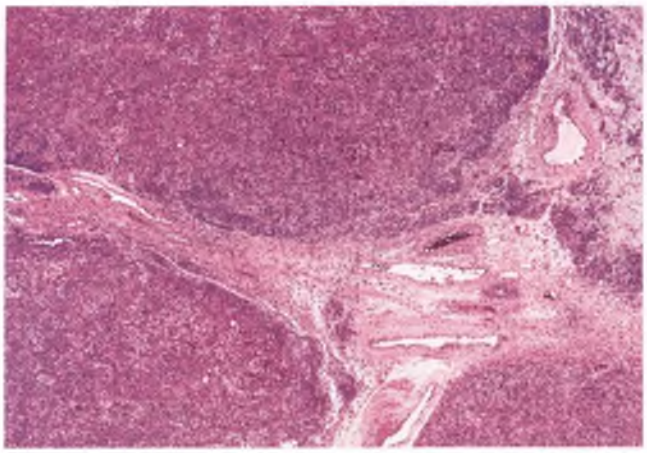

FIGURE 7.208. Sertoli-Leydig cell tumor of intermediate differentiation. This low-magnification view highlights the cellular lobules that are a prominent feature of most tumors of this type.

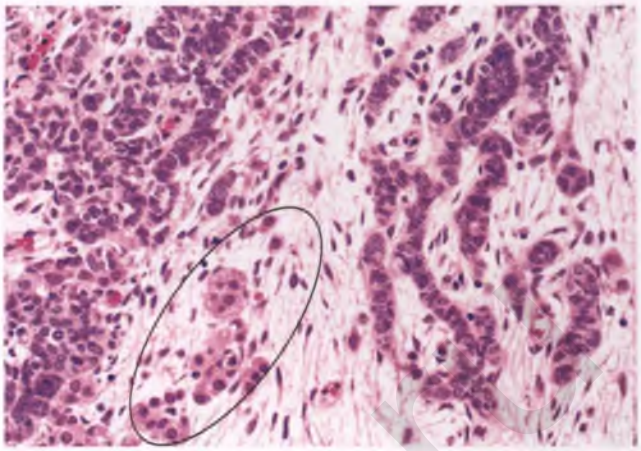

FIGURE 7.210. Sertoli-Leydig cell tumor of intermediate differentiation. In this example, many of the Sertoli cells form thin cordlike structures within an edematous stroma. Leydig cells, disposed singly and in small clusters, are also present, and are particularly evident in the *circled* region.

Sertoli cells[269] or primitive gonadal stromal cells[271] (Fig. 7.208). Subtle evidence of Sertoli and Leydig cell differentiation is often best appreciated at the periphery of these lobules (Fig. 7.209) or within the usually hypocellular and often edematous bands of connective tissue that separate the lobules (Fig. 7.210). For Sertoli cells, formation of epithelial ribbons, cords, and hollow or solid tubules constitute such evidence. Leydig cells have a similar appearance regardless of the degree of differentiation of the SLCT, which is in keeping with their presumed reactive rather than neoplastic nature.[272] Some degree of mitotic activity is usually evident within both the nondescript cellular and recognizably sertoliform components, and the degree of nuclear atypia in these cell types ranges from mild to moderate.

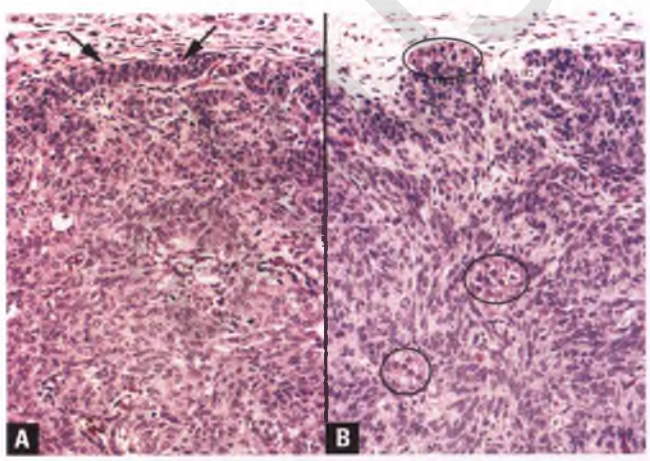

FIGURE 7.209. Sertoli-Leydig cell tumor of intermediate differentiation. Sertoli and Leydig cell differentiation is often most apparent at the periphery of cellular nodules. **A:** Sertoli cell differentiation in the form of focal corded growth (*arrows*). **B:** Nests of Leydig cells with eosinophilic and vacuolated cytoplasm (*circled*) are seen at or near the periphery of an otherwise nondescript spindle cell stromal nodule.

In rare cases, cells with bizarre nuclei of presumed degenerative nature are present that have no impact on the prognosis.[229]

Patients with SLCTs of intermediate differentiation have a favorable prognosis, with only about 10% of such tumors pursuing a malignant clinical course.[269] Adjuvant therapy is generally reserved for those few patients whose tumors have ruptured or been found to have spread beyond the ovary at the time of operation.

Poorly differentiated SLCTs often have extensive areas of hemorrhage and necrosis. They can be difficult to diagnose, since the viable areas typically consist predominantly of solid sheets of mitotically active cells that resemble a sarcoma of no special type (Fig. 7.211). In the setting of a young woman with

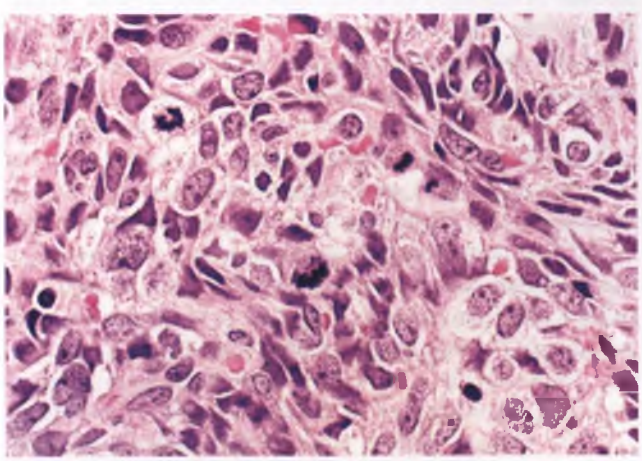

FIGURE 7.211. Sertoli-Leydig cell tumor, poorly differentiated (sarcomatoid). Large portions of these tumors are indistinguishable from sarcomas and other poorly differentiated malignant neoplasms with a spindle cell component. Note the brisk mitotic activity.

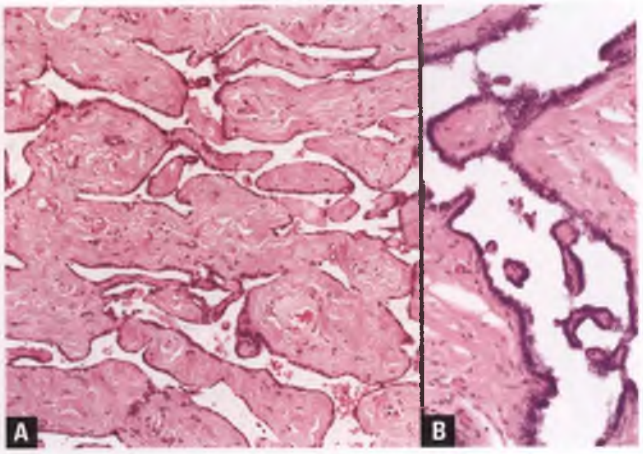

FIGURE 7.212. **A,B:** Histology of the normal rete testis. Epithelial-lined papillary projections protrude into slit-like spaces that are elongated and interconnected. Note the hyalinization of some of the stromal cores of the papillae.

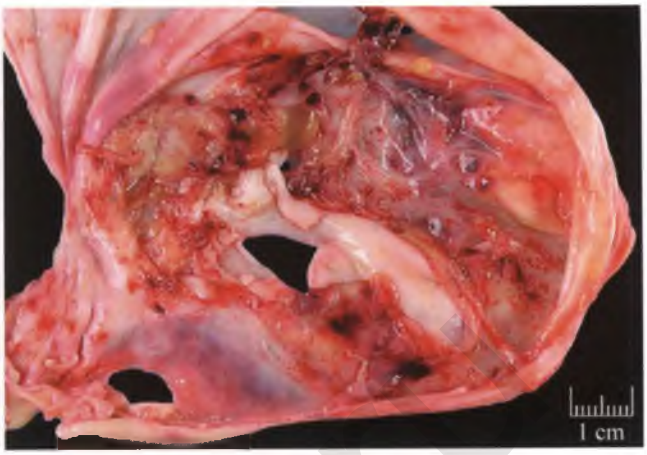

FIGURE 7.213. Sertoli-Leydig cell tumor, cystic retiform variant. The cystic mass has been opened, revealing scattered edematous polyps and redundant folds of tissue projecting from its inner lining. (Courtesy of Dr. Colin J. R. Stewart.)

virilization, a tumor with these features should be suspected of being of Sertoli-Leydig cell origin, and multiple sections should be examined to look for areas with recognizable Sertoli-Leydig cell differentiation. Poorly differentiated SLCTs are full-fledged malignancies, and account for most tumor-related deaths within the SLCT category.

SLCTs with retiform elements contain areas that architecturally resemble the normal rete testis (Fig. 7.212). In the landmark studies by Young and Scully, a retiform pattern only needed to be present in ≥5% of the tumor to fit into this category, which accounted for approximately 10% to 15% of SLCTs in their series.[269,273] In the most recent WHO classification, SLCTs with between 10% and 90% retiform elements are referred to as SLCTs with retiform elements, whereas those with ≥90% retiform elements are further dignified as retiform SLCTs.[194] Although this change was purportedly made to better segregate prognostically different tumor types,[256] virtually all of the variation in prognosis of SLCTs is captured by the stage of the tumor and its degree of differentiation.

In comparison to patients with SLCTs in general, those with SLCTs with a significant retiform component are more likely to present at an even younger age and are less likely to be virilized.[273–275] A significant retiform component is seen only in SLCTs in the intermediate to poorly differentiated spectrum, and most such tumors are at least partially cystic. Occasionally, retiform SLCTs feature large, edematous polyps that project into the lumen of a cystic neoplasm (Fig. 7.213). In this situation, large portions of the polyps show nonspecific findings, and thorough sampling is necessary to identify the retiform elements.

The retiform pattern consists of a network of interconnected, irregularly branched, slit-like tubular spaces or cysts with intraluminal papillary or polypoid projections (Figs. 7.214 and 7.215). These intraluminal structures usually take the form of microscopic papillae that may have hyalinized cores or a complex branching pattern with cellular budding. These patterns may result in a resemblance to clear cell carcinoma or a well-differentiated papillary serous carcinoma, respectively.

Most SLCTs with retiform elements that have pursued a malignant clinical course have been either poorly differentiated or poorly sampled, and the metastatic deposits in these tumors usually have a sarcomatoid pattern that lacks retiform elements.[273,274] Therefore, although it is sometimes stated that SLCTs with prominent retiform elements are more likely to behave aggressively than nonretiform SLCTs, it does not appear likely that the presence or dominance of the retiform pattern is a prognostic factor that is independent of the degree of differentiation.

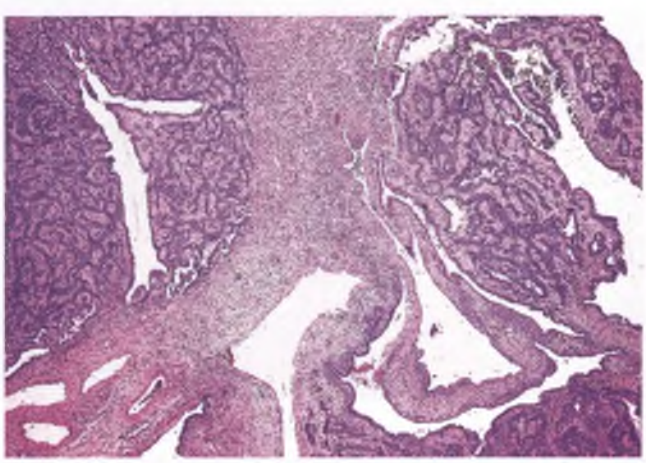

FIGURE 7.214. Sertoli-Leydig cell tumor of intermediate differentiation with retiform elements. The elongated retiform spaces are dilated with slit-like branches and occasional intraluminal papillary projections. (Courtesy of Dr. Colin J. R. Stewart.)

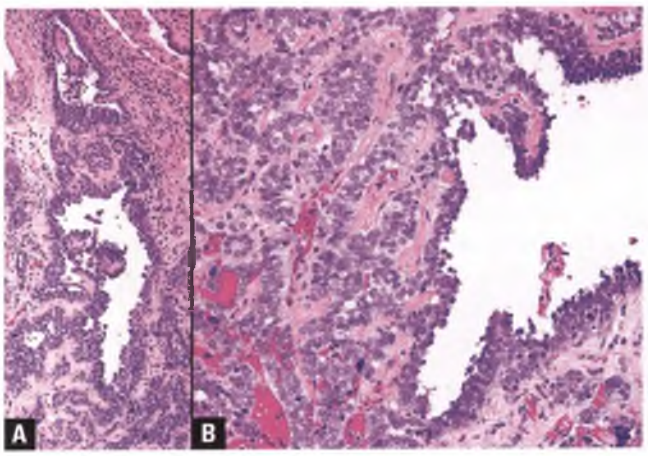

FIGURE 7.215. **A,B:** Sertoli-Leydig cell tumor of intermediate differentiation with retiform elements. Retiform areas are seen adjacent to cords of Sertoli cells. Note the hyalinization of the stromal cores of the papillae, which is a frequent finding. (Courtesy of Dr. Colin J. R. Stewart.)

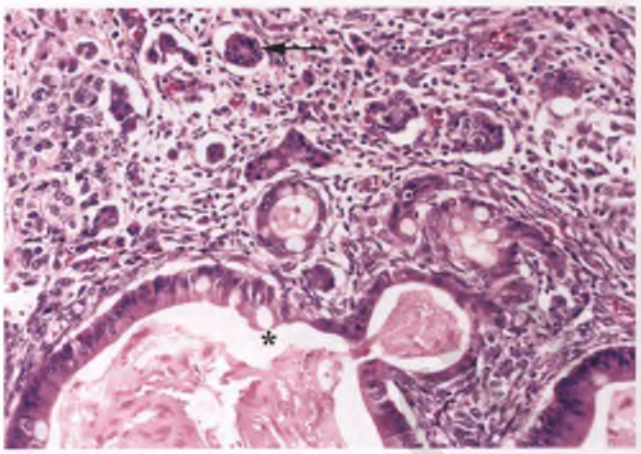

FIGURE 7.217. Sertoli-Leydig cell tumor of intermediate differentiation with heterologous elements. At high magnification, some of the mucinous glands are seen to be lined by epithelium that includes goblet cells (adjacent to *asterisk*). Note the presence of neighboring nests of carcinoid tumor surrounded by retraction artifact (*arrow*).

Heterologous elements are found within approximately 20% of SLCTs, all of which are either of intermediate differentiation or poorly differentiated.[276,277] The most common heterologous element, which is seen in roughly 80% of such cases, is mucinous epithelium of gastric or intestinal type. SLCTs with heterologous elements of this type are often composed of an admixture of solid and cystic components. Mucoid material may be grossly apparent when these tumors are sectioned, as shown in Figure 7.207. Histologically, the mucinous glands show varying degrees of cystic dilatation, and often have eosinophilic secretions within their lumens (Fig. 7.216). In most cases, goblet cells indicative of intestinal differentiation are identified at least focally within the mucinous epithelium, which otherwise often has abundant eosinophilic cytoplasm (Fig. 7.217). In other examples, the mucinous epithelium resembles that of the gastric pylorus and is devoid of goblet cells. The mucinous epithelium usually has a benign appearance, but can appear borderline or low-grade malignant. In some cases, mucinous epithelium may be associated with neuroendocrine cells that contain basally-located eosinophilic granules that can be highlighted with argentaffin (Fontana-Masson) or argyrophilic (Grimelius) stains, and Paneth cells are rarely evident. Of those cases with identifiable neuroendocrine cells, more than half are associated with microscopic and presumably incidental carcinoid tumors (Fig. 7.217).

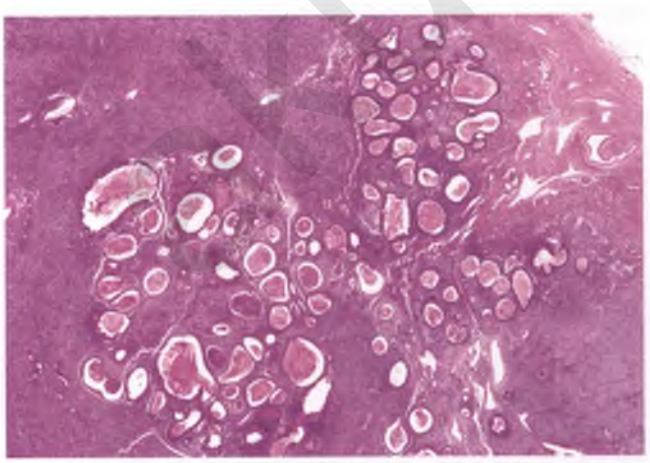

FIGURE 7.216. Sertoli-Leydig cell tumor of intermediate differentiation with heterologous elements. The cystically dilated glands that are filled with eosinophilic material are lined by mucinous epithelium, as illustrated in the following figure.

The other major heterologous elements that may be encountered in SLCTs are immature skeletal muscle and islands of fetal-type cartilage. In those rare SLCTs that are associated with elevated AFP levels, heterologous AFP-positive hepatocytes that resemble Leydig cells in routinely-stained sections may be present.[278] Such tumors also tend to have retiform elements.

Although the prognosis of SLCTs with gastrointestinal heterologous elements is excellent and survival of patients with SLCTs with mesenchymal heterologous elements is poor, much of this difference can be explained by the degree of differentiation of the SLCT. Cases with gastrointestinal epithelium are usually of intermediate differentiation, whereas cases with immature skeletal muscle or cartilage are almost always poorly differentiated.

Differential Diagnosis

The differential diagnosis of well-differentiated SLCT and those of intermediate differentiation includes Sertoli cell tumor, sertoliform endometrioid carcinoma, AGCT, trabecular carcinoid tumor, tubular Krukenberg tumor, and the ovarian tumor of probable wolffian origin.

- Sertoli cell tumors are distinguished from well-differentiated SLCTs by the absence of Leydig cells.
- Features that help to distinguish sertoliform endometrioid carcinomas from Sertoli cell tumors and SLCTs are discussed in the section on ovarian endometrioid carcinomas that resemble sex cord-stromal tumors. While on the topic of diagnostic difficulties caused by unusual endometrioid patterns, the converse problem should also be noted wherein occasional well to moderately differentiated SLCTs contain large numbers of pseudoendometrioid tubules that can result in misclassification as endometrioid carcinoma.[279]
- AGCTs with trabecular and cordlike patterns can resemble SLCTs, particularly when luteinized stromal cells are also present. However, AGCTs occur in an older age group and are often associated with estrogenic rather than androgenic manifestations. Histologically, most AGCTs are composed of cells with characteristic nuclear grooves that are lacking in SLCTs.
- Trabecular carcinoid tumors only rarely contain a steroid cell component, and are also distinguished from SLCTs by their stippled chromatin pattern, intracytoplasmic eosinophilic neurosecretory granules, and characteristic long ribbons of columnar cells.[237,269] The diagnosis of carcinoid tumor can be confirmed by demonstrating immunoreactivity for neuroendocrine markers such as chromogranin and synaptophysin and lack of staining for inhibin.[146] In addition, SLCTs are almost always unilateral and are not associated with germ cell elements, whereas metastatic carcinoid tumors are usually bilateral and primary carcinoid tumors are often found arising within a teratoma or in association with struma ovarii.[237,280]
- The resemblance of tubular Krukenberg tumors to SLCTs is heightened in cases with luteinized stromal cells and/or associated virilization. However, in contrast to SLCTs, tubular Krukenberg tumors are likely to be bilateral, may be found in association with peritoneal implants and/or ascites, may be associated with a known primary malignancy, and have tubules that are usually lined by cells that exhibit significant nuclear atypia and mitotic activity.[281] Most importantly, both the tubular lining and the involved stroma of tubular Krukenberg tumors contain scattered mucin-filled signet-ring cells that are absent in SLCTs.[281]
- Ovarian tumors of probable wolffian origin can form sertoliform solid tubules, but lack a Leydig cell component and are not associated with androgenic manifestations.[282] Further differentiating features of this tumor as discussed in its differential diagnosis with Sertoli cell tumor in the section on ovarian wolffian tumors are applicable to SLCTs as well.

In addition to sarcoma, poorly differentiated SLCTs can resemble carcinosarcoma (malignant mixed mesodermal tumor), particularly when heterologous mesenchymal elements are present. In contrast to most SLCTs, carcinosarcomas occur in an older age group, lack androgenic manifestations, have more pleomorphic epithelial and stromal elements, fail to stain with inhibin, and have an epithelial component that is immunoreactive for epithelial membrane antigen.[283,284] SLCTs with heterologous elements may also be misinterpreted as ovarian teratomas. However, teratomas are distinguished by their lack of Sertoli and Leydig cells and the common presence of skin, skin adnexal, and neuroectodermal elements.[269]

In resolving the differential diagnosis between retiform SLCT versus clear cell and serous papillary neoplasms, features that favor retiform SLCT include (a) age <30 years, (b) androgenic manifestations, (c) other areas of more typical SLCT, and (d) inhibin immunoreactivity.[273,285]

Stromal-Leydig Cell Tumor[260,286]

Luteinized thecomas and stromal-Leydig cell tumors have identical histologic features, except that the steroid-type cells of the latter contain crystals of Reinke. Experience with these extremely rare neoplasms is limited, but roughly half of the cases are virilizing and they have pursued a benign clinical course.

Gynandroblastoma[287,288]

As the first half of its name implies, this extraordinarily rare tumor is a combination of granulosa cell ("gyn") and Sertoli cell ("andro") sex cord elements (pay no attention to the ominous-sounding "blastoma" part of this tumor's name). By definition, both the granulosa and Sertoli cell components are well differentiated, and the lesser component must comprise at least 10% of the tumor so as to avoid overdiagnosis of gynandroblastoma. The granulosa cell component is usually of the adult type, but a juvenile granulosa cell pattern has also been reported, and Leydig cells may also be present.

Most patients with gynandroblastoma are young adults with manifestations of either excess androgens or estrogens who are found to have a predominantly solid, unilateral ovarian tumor. In the typical example, Sertoli cells line lobulated aggregates of well-formed, hollow tubules that abut or are adjacent to rounded nests of adult-type granulosa cells (Fig. 7.218). Although experience with these tumors is limited, nearly all patients present with tumors that have not spread beyond the ovary, and oophorectomy is considered sufficient treatment for these presumably benign neoplasms.

Sex Cord Tumor with Annular Tubules[289]

Sex cord tumors with annular tubules (SCTATs) are very rare neoplasms of presumed Sertoli cell origin that are classified separately because of their distinctive histologic and clinical features. They tend to occur in young adult women, and may be associated with symptoms related to elevated estrogen levels. One third of cases are seen in the setting of Peutz-Jeghers syndrome (PJS), where these incidentally discovered tumors almost invariably pursue a benign clinical course and are typically small, multifocal, bilateral, and calcified. In contrast, patients with SCTAT unassociated with PJS have unilateral tumors that

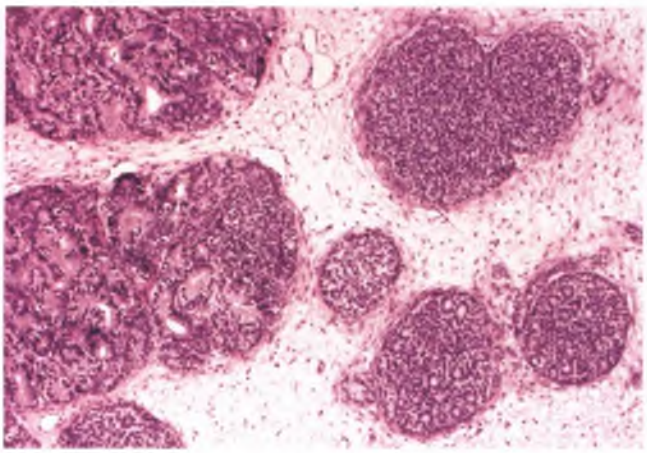

FIGURE 7.218. Gynandroblastoma. Lobulated aggregates of hollow tubules lined by Sertoli cells in the left portion of the image are seen in association with nests of adult-type granulosa cells with occasional Call-Exner bodies.

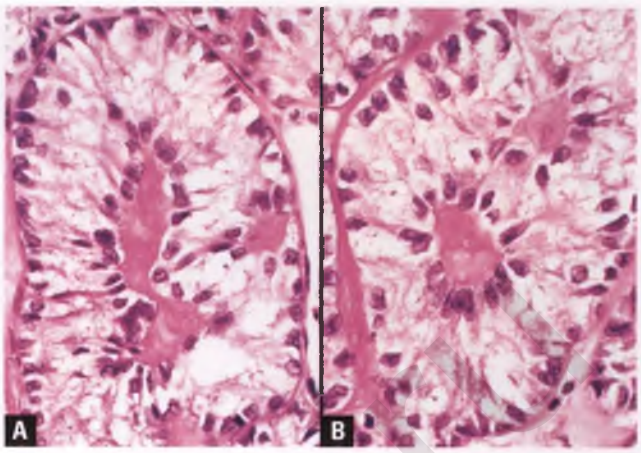

FIGURE 7.220. **A,B:** Sex cord tumor with annular tubules. Note the two rings of nuclei, with one immediately adjacent to the central hyaline core and the other rimming the periphery of the tubules. A clear cytoplasmic zone separates the two nuclear layers.

are often large enough to present as a palpable adnexal mass, and approximately 20% of these cases are clinically malignant.

Grossly visible SCTATs are smooth-surfaced, nodular masses that typically have a solid, yellow, firm sectioned surface. The histologic hallmark of the SCTAT is the annular tubule, which may occur as an isolated unit or, more commonly, serves as the building block for larger rounded epithelial islands composed of a network of tubules (Fig. 7.219). Cross sections of these tubules reveal a central core of hyalinized, basement membrane-like material surrounded by two ringed layers of nuclei with an interposed pale to clear cytoplasmic zone (Fig. 7.220). The bands of fibrous stroma that separate the tubular structures may become hyalinized. The calcification that is often seen in patients with PJS typically occurs within the intratubular cores of hyalinized material. Most SCTATs exhibit little nuclear atypia or mitotic activity. It is not uncommon for SCTATs in patients without PJS to harbor foci of Sertoli cell and/or granulosa cell tumor.

As is the case for most sex cord-stromal tumors, SCTATs are immunoreactive for inhibin and calretinin.[147,220] Since it is not possible to predict the behavior of the SCTATs that occur outside the setting of PJS and metastases may occur many years after excision, long-term follow-up is indicated in this group of patients.

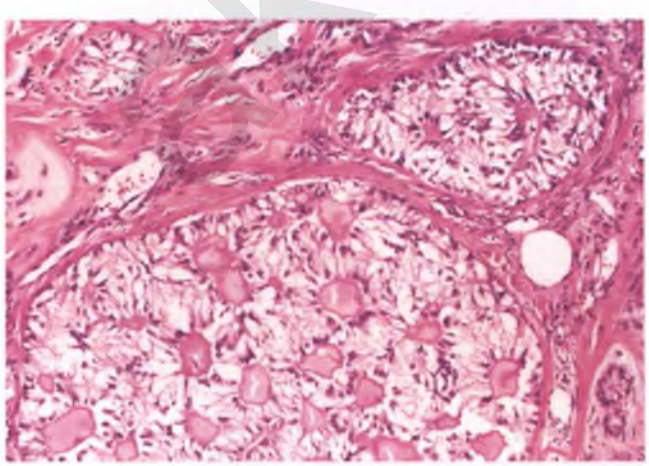

FIGURE 7.219. Sex cord tumor with annular tubules.

Differential Diagnosis

The differential diagnosis of SCTAT includes gonadoblastoma, Sertoli cell tumor, and granulosa cell tumor.

- Although gonadoblastomas also exhibit a nested architecture punctuated by hyaline bodies and often contain calcifications, many of the cells within the nests are of germ cell origin, resemble the cells of dysgerminoma, and are OCT4-positive.[290] Moreover, gonadoblastomas occur almost exclusively in patients with an underlying gonadal disorder.
- Sertoli cell tumors are composed of hollow and/or solid tubules rather than the distinctive annular tubules of SCTAT.
- Although annular tubules may be confused with Call-Exner bodies of the microfollicular variant of granulosa cell tumor, the hyaline bodies of SCTAT are frequently larger and more irregularly shaped than the eosinophilic material within Call-Exner bodies, and may be calcified or seen merging with thickened basement membranes. An additional distinguishing feature is that true ring-shaped tubules are not a feature of granulosa cell tumors.

Unclassified Sex Cord-Stromal Tumors[291,292]

Approximately 10% of ovarian sex cord-stromal tumors are not easily assigned to a specific diagnostic category, and are referred to as being of unclassified type. Most such tumors have sex cord elements with an indifferent or intermediate appearance

TABLE 7.2 Subclassification of Ovarian Steroid Cell Tumors

Location	Reinke Crystals	Diagnosis
Cortex and/or medulla (enveloped by ovarian stroma)	No	Stromal luteoma
Hilus	Yes	Leydig cell tumor (Hilus cell tumor)
Hilus	No	Steroid cell tumor, Probable Leydig cell type
Other than hilus (usually medullary-based)	Yes	Leydig cell tumor, Nonhilar type
Inconclusive	Yes	Leydig cell tumor, Not otherwise specified
Inconclusive	No	Steroid cell tumor, Not otherwise specified

that makes it difficult to determine if the tumor is exhibiting granulosa or Sertoli cell differentiation. Sex cord-stromal tumors that are removed during pregnancy are predisposed to rupture and are more likely to exhibit marked edema and more extensive luteinization. These superimposed changes can make precise classification of these pregnancy-associated tumors difficult, resulting in their placement within the unclassified category in about 20% of cases.

Steroid Cell Tumors

Steroid cell tumors are composed entirely or almost entirely of cells capable of synthesizing steroid hormones, and are derived principally from luteinized stromal cells or hilar Leydig cells. These rare tumors account for <1% of ovarian tumors and are often associated with symptoms related to an imbalance of androgens or estrogens. Steroid cell tumors are subclassified based upon their location and presence or absence of crystals of Reinke as outlined in Table 7.2.

Of the steroid cell tumors, stromal luteomas represent 20% of cases, the group of Leydig and probable Leydig cell tumors represents another 20%, and steroid cell tumors that are not otherwise specified account for the remaining 60%.[293–295] However, these often cited percentages were obtained largely from consultation-based cases, which are likely to be heavily biased in favor of tumors that are difficult to diagnose, large, and suspicious for malignancy (i.e., tumors that are likely to fall within the "steroid cell tumor, not otherwise specified" category).

Although certainly not specific for steroid cell tumors, immunoreactivity for inhibin and calretinin is expected and these markers can be utilized as part of a panel of immunostains if difficulty is encountered in placing a given tumor within the sex cord-stromal category.[218,219,221]

Stromal Luteoma[294]

Stromal luteomas are small and benign steroid cell tumors that are located within the ovarian stroma. They are presumed to be derived from luteinized stromal cells, which is an assumption that is supported by both their location and by the associated presence of stromal hyperthecosis in 90% of cases. Stromal luteomas occur in patients with a mean age of 58 years, 60% of whom present with abnormal uterine bleeding related to hyperestrogenism whose histologic correlate is often endometrial hyperplasia and occasionally well-differentiated endometrial adenocarcinoma. Virilization, which occurs in only approximately 10% of patients, is a much less common finding at presentation than is the case for most other subtypes of steroid cell tumors.

Grossly, stromal luteomas are almost always unilateral, <3 cm (mean diameter of 1.3 cm), and well-circumscribed. Their sectioned surface is solid and of a fairly uniform color, although that color varies by case from off-white to yellow to red to brown. In the only large reported series of these tumors, tumors were accepted as stromal luteomas rather than nodules of nodular hyperthecosis if they were grossly visible, which translates into tumors as small as 2.5 mm.[294] The distinction between one or more dominant nodules within nodular hyperthecosis and stromal luteoma is based upon an arbitrary minimum size criterion for stromal luteoma that has ranged between 2.5 mm and 1 cm in the literature.

Histologically, stromal luteomas are composed of a circumscribed, unencapsulated proliferation of luteinized cells that form sheets, nests, or cords (Fig. 7.221). The tumors are

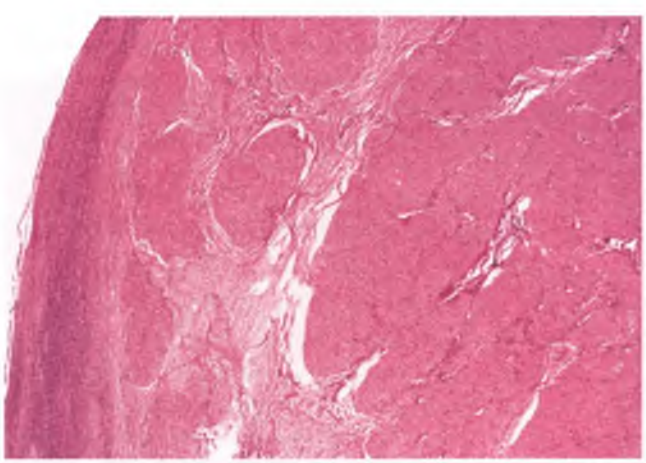

FIGURE 7.221. Stromal luteoma. The tumor is composed of sheets and nests of eosinophilic cells within a focally fibrotic background. The tumor is enveloped by ovarian stroma, which is partially seen near the ovarian surface at left.

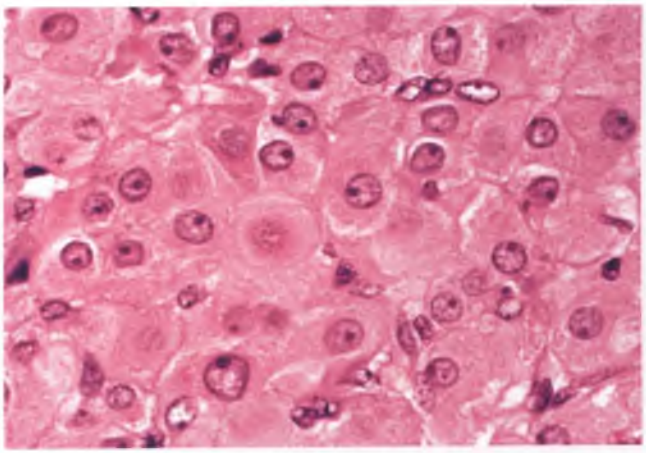

FIGURE 7.222. Stromal luteoma. The neoplastic cells have abundant eosinophilic cytoplasm, round nuclei, and single prominent nucleoli.

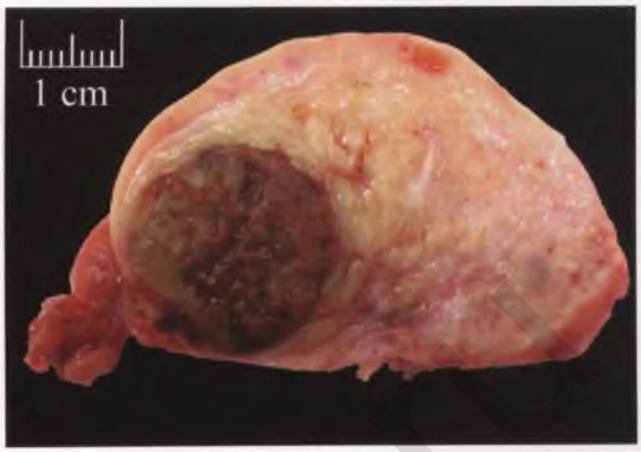

FIGURE 7.223. Leydig cell tumor. A section through the tumor reveals a well-circumscribed, brown nodule within the substance of the ovary. (Altered from Stewart C, Hammond I. Cytologic identification of Reinke crystalloids in ovarian Leydig cell tumor. *Arch Pathol Lab Med.* 2006;130(6):765–766. Altered and reprinted with permission from Dr. Colin J. R. Stewart and the Archives of Pathology and Laboratory Medicine. Copyright 2006. College of American Pathologists.)

small enough to be surrounded by ovarian stroma. Intratumoral supporting stroma is generally sparse, but may be fibrotic and/or hyalinized. The tumor cells have abundant eosinophilic cytoplasm that often contains lipochrome pigment and round nuclei with single prominent nucleoli (Fig. 7.222). There is minimal to no mitotic activity.

By definition, crystals of Reinke are not identified in stromal luteomas. If Reinke crystals are found in a tumor that otherwise has the features of a stromal luteoma, then it is classified as a Leydig cell tumor of nonhilar type. Stromal luteomas may also be difficult to distinguish histologically from pregnancy luteomas, but the latter lesions occur in younger patients in the setting of pregnancy, are often multiple and mitotically active, may have follicle-like spaces, and spontaneously involute following delivery (see Chapter 6).

Leydig Cell Tumor[293,296]

As Table 7.2 indicates, the Leydig cell group of tumors encompasses all of the steroid cell tumors except for stromal luteoma and steroid cell tumors that are not otherwise specified. Leydig cell tumors occur in adult women with a mean age of approximately 60 years, and are frequently associated with elevated levels of serum testosterone and virilization. All well-documented Leydig cell tumors reported thus far have pursued a benign clinical course.

Grossly, Leydig cell tumors are solid nodules with an average size of 2 cm whose sectioned surface is most often a shade of brown (Fig. 7.223). Most Leydig cell tumors are derived from hilar Leydig cells and are located within the ovarian hilus; hence the equivalent designation of hilus cell tumor for this subset of Leydig cell tumors.

Leydig cell tumors are composed of sheets and ill-defined nests of round to polygonal cells with abundant eosinophilic to vacuolated cytoplasm, round nuclei with single nucleoli, and absent to rare mitotic figures. Intracytoplasmic lipochrome pigment is often present. By definition, Leydig cell tumors contain at least one identifiable crystal of Reinke within the cytoplasm of their constituent cells. Reinke crystals are eosinophilic, elongated, rectangular to cigar-shaped inclusions that can be recognized in routinely-stained sections and highlighted with trichrome or PTAH stains (Fig. 7.224); cytologic examination of scrape preparations can also facilitate their identification.[297] Additional findings that are present in a subset of Leydig cell tumors include nuclear pseudoinclusions, degenerative nuclear atypia, stromal hyalinization (Fig. 7.225A), and supporting vessels with fibrinoid necrosis without an associated inflammatory infiltrate (Fig. 7.225B).

Those steroid cell tumors with crystals of Reinke that arise within the ovarian stroma are usually based in the medulla and are known as Leydig cell tumors, nonhilar type (Fig. 7.226). Leydig cell tumors in which the hilar versus ovarian stromal origin is uncertain are labeled Leydig cell tumors, not otherwise specified. Tumors of definite hilar origin that have the typical features of a steroid cell tumor in which a search for crystals of Reinke yields negative results are referred to as steroid cell tumors of probable Leydig cell type. If you find this subclassification a bit confusing and complex and you'd rather lump than split, just call any steroid cell tumor with crystals of Reinke and/or a hilar location a Leydig cell tumor, and move on to the next case.

Steroid Cell Tumor, Not Otherwise Specified[295]

These tumors tend to occur in a younger age group than other steroid cell tumors (mean age of 43 years), and exhibit malignant clinical behavior in about one-third of cases. Approximately half of the patients show some degree of virilization, although occasional patients exhibit hyperestrogenic manifestations or elevated cortisol levels with Cushing's syndrome. By

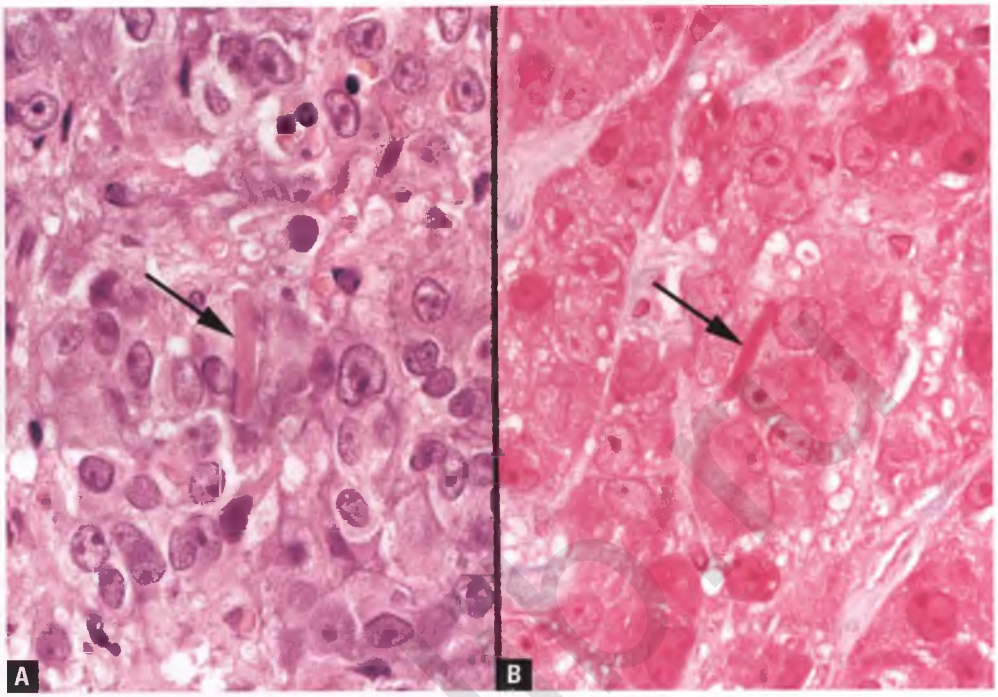

FIGURE 7.224. **A,B:** Leydig cell tumor. These high-magnification views highlight the nuclear features of the neoplastic Leydig cells and the presence of crystals of Reinke (*arrows*) in routine **(A)** and trichrome-stained **(B)** sections.

definition, tumors placed in this category do not contain identifiable crystals of Reinke and are not small enough to be surrounded by ovarian stroma; otherwise, they would be classified as Leydig cell tumors or stromal luteomas, respectively.

Although these tumors exhibit a wide size range, they typically are considerably larger than other steroid cell tumors (mean size of 8 cm), and are almost always unilateral. The tumors are usually solid, well-circumscribed, and vaguely lobulated. Lipid-rich tumors are yellow to orange, lipid-poor tumors are a shade of brown, and those tumors with abundant lipochrome pigment are dark brown to black (Fig. 7.227).

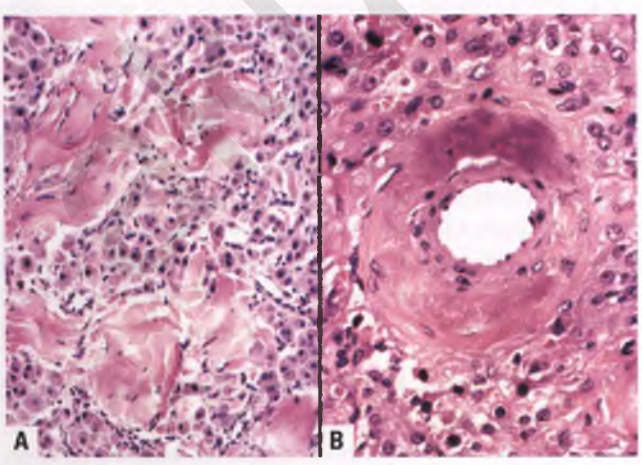

FIGURE 7.225. Leydig cell tumor. **A:** Clusters of neoplastic Leydig cells are separated by hyalinized stroma. **B:** Intratumoral vessel with its wall replaced by fibrinoid material.

Histologically, steroid cell tumors of no special type consist of cells with abundant eosinophilic cytoplasm (similar to that illustrated for stromal luteomas) or cells with clear vacuolated cytoplasm due to the presence of large amounts of lipid (Fig. 7.228). Tumors with mixtures of these two cell types can also be encountered. As is the case for other steroid tumors, intracytoplasmic lipochrome pigment is often present. The predominant architectural pattern is diffuse, although nests and cords of tumor cells may also be present. The nuclear features are generally as described for other steroid cell tumors.

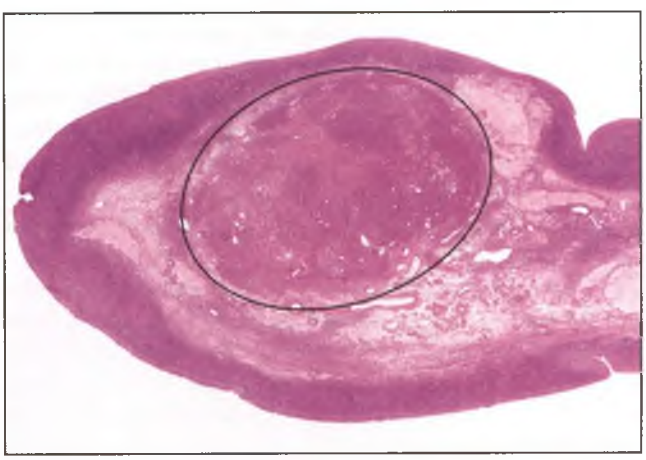

FIGURE 7.226. Leydig cell tumor, nonhilar type. At low magnification, the tumor is visible as a small nodule within the medullary region of the ovary (*circled*). Distinction from a stromal luteoma is based solely on the identification of crystals of Reinke within the cytoplasm of some of the tumor cells (not shown).

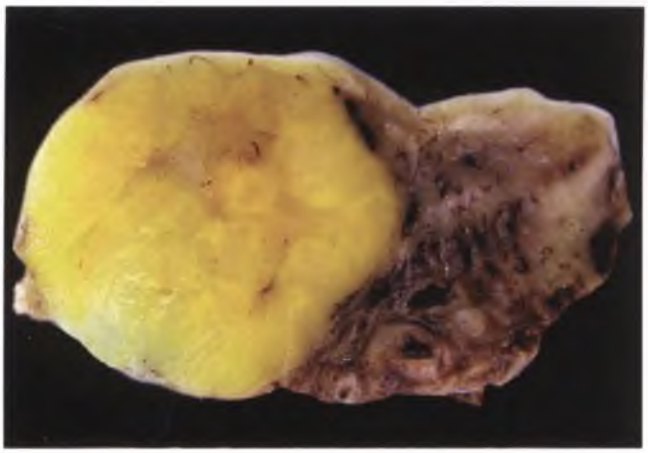

FIGURE 7.227. Steroid cell tumor, not otherwise specified. The sectioned surface of this 2.3 cm solid tumor nodule is bright yellow due to its high lipid content. (Courtesy of Dr. Colin J. R. Stewart.)

Mitotic activity is usually low, but is variable from case to case. The stroma is usually sparse, but may be fibrotic or hyalinized. Foci of hemorrhage and/or necrosis are occasionally present.

The malignant potential of these tumors may be difficult to predict, but features associated with malignancy include (a) size of at least 7 cm, (b) 2 or more mitotic figures per 10 high power fields, (c) significant nuclear atypia, (d) tumor cell necrosis, and (e) intratumoral hemorrhage.

Differential Diagnosis

Lipid-poor steroid cell tumors resemble pregnancy luteomas, but lesions of this type that are encountered during pregnancy should be regarded as pregnancy luteomas unless obvious malignant features are present.

Lipid-rich steroid cell tumors with clear cytoplasm may be confused with a variety of other clear cell or lipid-rich tumors. The distinction of this subset of steroid cell tumors from thecomas is discussed in the sections on usual and luteinized thecomas. Lipid-rich Sertoli cell tumors are distinguished from lipid-rich steroid cell tumors on the basis of at least focal tubular differentiation in adequately sampled tumors (the tubular architecture can be highlighted with a reticulin stain).[149] Moreover, the presence of intracytoplasmic lipochrome pigment favors a steroid cell tumor in this setting.[149] Primary ovarian clear cell carcinoma typically exhibits a variety of architectural patterns that are not within the repertoire of steroid cell tumors, and the clear cytoplasm of its constituent cells is due to periodic acid-Schiff (PAS)-positive, diastase-sensitive glycogen rather than lipid. Metastatic renal cell carcinoma of clear cell type usually has a prominent sinusoidal vascular framework, areas with tubular differentiation, cytoplasm that is rich in glycogen rather than lipid, a history of a prior or concurrent renal mass without endocrine abnormalities, and a CD10-positive, renal cell carcinoma marker-positive immunophenotype.[298,299]

Metastatic melanoma is also a differential diagnostic consideration, particularly when the tumor cells possess eosinophilic cytoplasm and lipochrome pigment that may simulate melanin both grossly and microscopically.[241] In contrast to steroid cell tumors, metastatic melanoma is bilateral in about 40% of the cases and is not associated with androgenic manifestations. Since steroid cell tumors often express Melan-A and may also be focally immunoreactive for S100 and HMB-45,[219] the unwary may be mistakenly trapped into thinking that positive staining with one or more of these "melanoma" markers favors a diagnosis of melanoma. In the differential diagnosis with melanoma and clear cell tumors other than those in the sex cord-stromal category, inhibin and/or calretinin immunoreactivity is supportive evidence of a diagnosis of steroid cell tumor.[219,300]

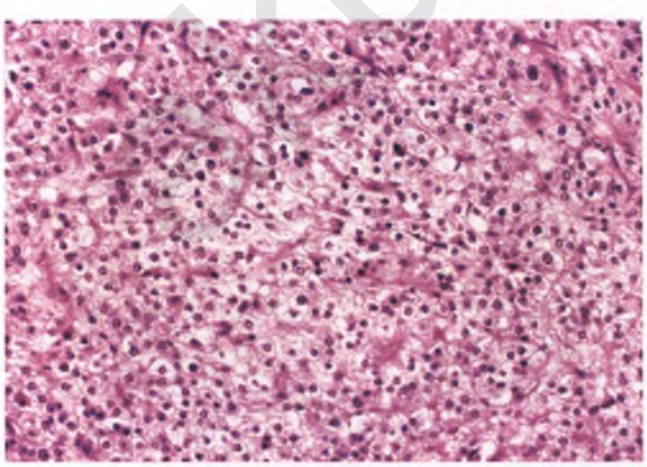

FIGURE 7.228. Steroid cell tumor, not otherwise specified. The cells of this particular tumor have abundant, pale-staining, lipid-rich cytoplasm.

GERM CELL TUMORS

Germ cell tumors collectively account for about 30% of all primary ovarian neoplasms, and roughly 95% of such tumors are mature cystic teratomas (dermoid cysts).[16] Of the remaining germ cell tumors, all are rare and most are malignant, with the malignant group collectively accounting for <2% of primary ovarian cancers.[1] However, malignant germ cell tumors have a striking predilection for young patients, such that they account for a majority of the primary ovarian cancers that occur during the first 20 years of life. In the WHO classification, most germ cell tumors are placed into one of three categories: (a) Biphasic or triphasic teratomas (as relates to the presence of tissues representative of the ectodermal, mesodermal, and/or endodermal germ cell layers), (b) Monodermal teratomas and somatic-type tumors associated with dermoid cysts, most of which represent a form of struma ovarii or carcinoid tumor, and (c) Primitive germ cell tumors (dysgerminoma, yolk sac tumor, embryonal carcinoma, polyembryoma, non-gestational choriocarcinoma, and mixed germ cell tumor).[194]

Immature Teratoma[301,302]

Immature teratomas are rare neoplasms that account for approximately 20% of malignant germ cell tumors. These tumors should not be referred to as malignant teratomas, since this is an ambiguous term that has been applied to immature teratomas as well as to dermoid cysts that have undergone malignant transformation of a somatic tissue type. Immature teratomas are largely tumors of children and young adults, with patients presenting at an average age of 20 years. Symptoms related to an ovarian mass are usually present, and serum AFP levels are often modestly elevated. Approximately 80% of patients present with disease confined to the ovary; when metastases are present, the omentum and peritoneum are common sites of involvement. These tumors are rarely bilateral.

Grossly, immature teratomas have a smooth outer surface and an average diameter of 16 cm. They are predominantly solid neoplasms that often contain scattered small cysts. The solid portion of their sectioned surface is fleshy, variably tan, gray, or pink, and contains interspersed areas of hemorrhage and/or necrosis (Fig. 7.229). Teratomatous elements such as cartilage, bone, and/or hair may be grossly apparent, and about 25% of cases are associated with a full-fledged dermoid cyst.[303] It is vital that immature teratomas are adequately sampled to facilitate accurate grading and to minimize the possibility that other types of malignant germ cell tumor are admixed with the teratomatous elements. One section per cm is the standard recommendation, with targeting of areas that are fleshy, encephaloid, and bordering hemorrhagic and necrotic foci.

Histologically, immature teratomas are characterized by the haphazard distribution of various tissue types that definitionally includes the presence of embryonic-type tissue, which corresponds to the primitive tissue seen during development of an embryo between 2 and 8 weeks post-fertilization.[304] When dealing with teratomas, the word "immature" should be used in a narrow sense to refer to the presence of such embryonic tissue, and should not be used to describe other tissues at a fetal stage of development (a fertilization age of >8 weeks), such as fetal cartilage or developing teeth. In addition to embryonic tissue, most immature teratomas also contain mature tissues that are derived from all three germ cell layers. The vast majority of immature teratomas are recognized as such on the basis of the presence of primitive neuroepithelial tissue that forms tubules, rosettes and/or cellular and mitotically active aggregates or sheets of glial tissue (Figs. 7.230 and 7.231). In some cases, the primitive neuroepithelial elements are associated with a proliferation of closely packed blood vessels, analogous to what can be seen in glioblastoma multiforme (Fig. 7.232).[305]

Rare cases of immature teratoma that lack identifiable neuroepithelial elements can be recognized by the presence of cellular immature mesenchyme surrounding embryonal

FIGURE 7.229. Immature teratoma. This predominantly solid tumor has been sectioned to reveal fleshy, tannish pink and focally hemorrhagic tissue. Some clotted blood is also in a cystic space in the upper left portion of the image. (Courtesy of Dr. Enrique Higa.)

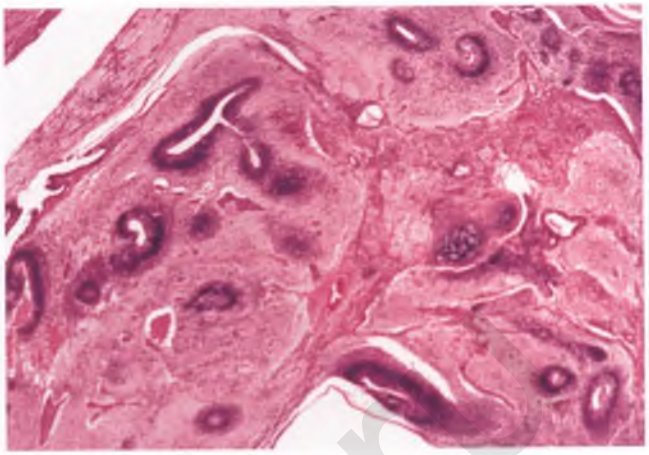

FIGURE 7.230. Immature teratoma. This low-magnification view demonstrates the presence of scattered neuroepithelial tubules with *dark blue outlines.*

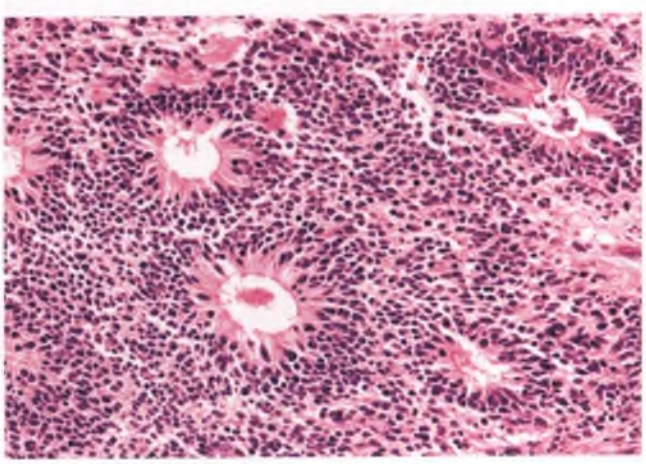

FIGURE 7.231. Immature teratoma. Neuroepithelial rosettes are seen in association with glial elements that are primitive and cellular.

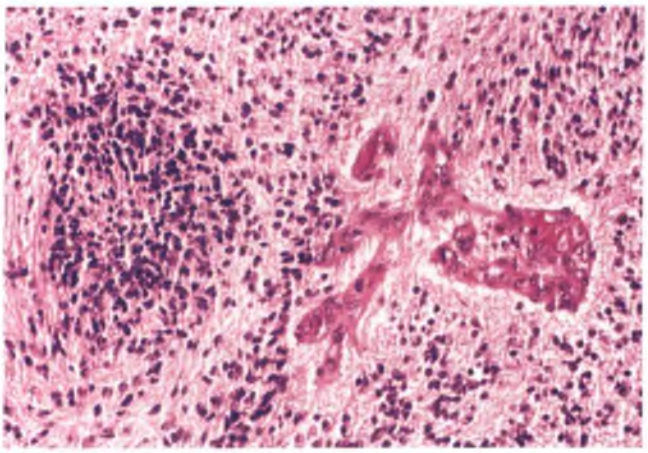

FIGURE 7.232. Immature teratoma with a focus of vascular proliferation to the right of a hypercellular area of primitive neural tissue.

endodermal epithelium, with the latter characteristically forming glands and microcysts that are lined by cells with prominent subnuclear and apical vacuoles similar to that commonly seen in the glandular structures of the endometrioid-like variant of ovarian yolk sac tumor (Fig. 7.233).[304,306,307] Although I favor the interpretation that these vacuolated glands and the foci of hepatocytic differentiation that often accompany them are reflective of endodermal differentiation within an immature teratoma, others have asserted that these findings represent microscopic foci of well-differentiated subtypes of yolk sac tumor.[308]

When considering a diagnosis of immature teratoma, it is recommended that the pathologist focuses on the identification and quantification of the aforementioned embryonal-type neuroepithelial elements and primitive endodermal

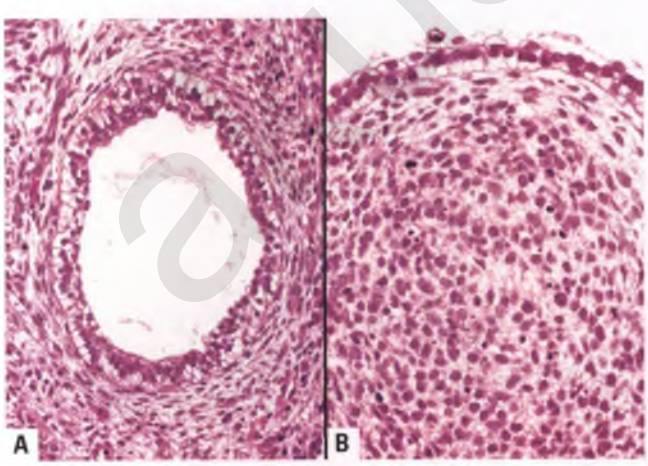

FIGURE 7.233. **A,B:** Immature teratoma with endodermal differentiation. Cellular, mitotically active mesenchyme is closely associated with immature endodermal epithelium with prominent cytoplasmic vacuoles.

epithelial-mesenchymal complexes. In this way, diagnostic errors related to the subjective assessment of the degree of immaturity of various tissue types, such as whether cellular micronodules of cartilage are of embryonal or fetal type, can be avoided.

As outlined below, immature teratomas and their implants should be assigned a histologic grade that is uniquely based upon the presence and extent of immature (embryonic-type) neuroepithelial tissue.

Grade 0: Composed entirely of mature elements, which generally consist of mitotically inactive glial tissue. This grade applies only to tumor implants, since grade 0 ovarian teratomas are benign by definition and are not considered to be within the spectrum of immature teratomas.

Grade 1: Tumors with rare foci of embryonic-type neuroepithelial tissue that occupy ≤1 40× low power field in any single slide (this translates into a 5 mm field of view diameter when evaluated using a standard 4× objective and 10× eyepiece).

Grade 2: Tumors with foci of embryonic-type neuroepithelial tissue that occupy >1 but ≤3 40× low power fields in any single slide.

Grade 3: Tumors with prominent foci of embryonic-type neuroepithelial tissue that exceed 3 40× low power fields in any single slide.

Notes on Grading:

1. Some pathologists prefer a condensed grading system in which grade 1 tumors are classified as low-grade and grades 2 and 3 are combined into a high-grade category.[302]
2. There is insufficient experience with the rare subtype of immature endodermal teratoma to make a definitive statement regarding grading criteria, but these tumors can tentatively be graded based upon an analogous assessment of the extent of embryonal tissue.
3. A recent study suggests that it is not simply a matter of there being more embryonic-type neuroepithelial tissue in high-grade immature teratomas than in low-grade ones, but that there are immunophenotypic differences as well. In particular, OCT4 appears to preferentially stain the immature neuroepithelium of grade 3 and a minority of grade 2 immature teratomas, whereas the immature neuroepithelium of grade 1 immature teratomas is not immunoreactive with this marker.[309]
4. Although there is a consensus that adults with stage I immature teratoma with grade 2 or 3 histology and all patients with high-grade implants/metastases should be treated with chemotherapy,[194,310] it is no longer automatic for children with grade 2 or 3 immature teratomas confined to the ovary to receive prophylactic chemotherapy. In the pediatric population, where the acute toxicity and possible long-term adverse effects of chemotherapy are more of an issue, the trend has been for those patients with completely resected stage I immature teratomas of all grades to be treated with curative intent by surgery alone.[308,311,312] In this scenario, chemotherapy is reserved for those few patients who relapse,

with the expectation being that these patients will be salvaged.[311]

Although most metastatic deposits of immature teratoma are also immature, an unusual phenomenon referred to as **gliomatosis peritonei** is rarely encountered in which the teratomatous implants consist of mature, mitotically inactive ("grade 0") nodules of glial tissue devoid of immature elements (Fig. 7.234).[313,314] These peritoneal or omental nodules are typically gray-white, small, superficial, and multiple, and may grossly simulate miliary tuberculosis or peritoneal carcinomatosis.[313,314] Lymph node involvement occurs in a small percentage of cases.[308] On occasion, the implants of gliomatosis peritonei are associated with mature epithelium, cartilage, foci of endometriosis, a chronic inflammatory infiltrate, fibrosis, or a benign vascular proliferation.[313–316] Although the glial nature of these nodules is usually readily apparent from the clinical setting and their histologic appearance, glial differentiation can be confirmed by obtaining positive immunoreactivity for glial fibrillary acidic protein.[314] Bona-fide examples of gliomatosis peritonei have been well-sampled to exclude the possibility of admixed immature elements, are not associated with a worse prognosis, and should not prompt treatment with chemotherapeutic agents.[301,308,313] Although some molecular studies have supported the nonintuitive notion that these glial implants have a peritoneal origin that is independent of their associated ovarian teratomas,[317,318] I concur with those who believe that this is extremely unlikely.[310]

Another peculiar phenomenon that occurs rarely in the setting of metastatic immature teratoma is the **growing teratoma syndrome**, which involves post-chemotherapeutic enlargement of metastatic deposits that have been histologically proven to have converted into pure mature teratoma.[319] Teratomatous nodules related to the growing teratoma syndrome usually appear within 2 years of the initial diagnosis of the ovarian tumor, typically remain confined to the pelvis, abdomen, and retroperitoneum, can recur repeatedly over the course of many years, may produce symptoms related to compression of adjacent structures, and in exceptional cases may develop secondary somatic neoplasms.[319]

Differential Diagnosis

The differential diagnoses of immature teratoma with mature cystic teratoma, mature solid teratoma, and carcinosarcoma are discussed in the sections on these other entities. Immature teratomas with dominant neuroepithelial elements may be confused with aggressive variants of ovarian neuroectodermal tumor, but the latter tumors do not contain significant amounts of tissue representative of all three germ cell layers and are more committed to a particular pattern of neuroepithelial differentiation.

Prognosis

The prognosis of patients with completely resected immature teratoma has improved dramatically since the advent of selective use of modern chemotherapeutic regimens, and is now excellent regardless of grade.[302,308,311]

Mature Solid Teratoma[320,321]

Very rarely, a predominantly solid teratoma is composed entirely of histologically benign, nonembryonic tissue that is representative of all three germ cell layers. These tumors, which are referred to as mature solid teratomas, tend to occur

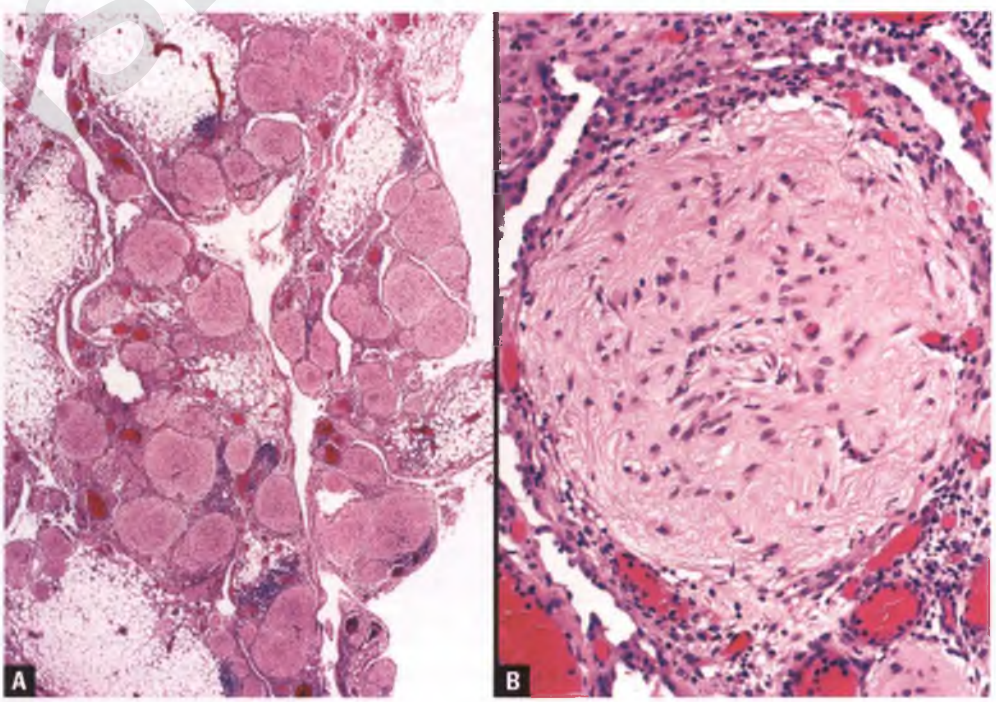

FIGURE 7.234. Gliomatosis peritonei involving the omentum. **A:** In this low-magnification view, multiple small glial nodules are present in a pattern that resembles the noncaseating granulomas of sarcoidosis. **B:** At high magnification, the fibrillary background, low cellularity, absence of nuclear atypia, and lack of mitotic activity are indicative of a mature glial implant. (Glass slide kindly provided by Dr. Reardon C. West.)

in children and young adults and have a gross appearance that is similar to that of immature teratoma, although hemorrhagic and necrotic areas are typically absent. Before a tumor is accepted as a mature solid teratoma, it should be extensively sampled to exclude the presence of minor foci of embryonic tissue that would warrant a diagnosis of immature teratoma. Well-documented mature solid teratomas pursue a benign clinical course, including those occasional tumors that are associated with gliomatosis peritonei or other mature implants.[313,320]

Mature Cystic Teratoma (Dermoid Cyst)[322,323]

The mature cystic teratoma is a benign germ cell neoplasm that has the distinction of being the most common ovarian tumor.[1,16] It is usually found in patients in the reproductive age group, but occurs over a wide age distribution. Patients may be asymptomatic or present with symptoms related to an ovarian mass. In some cases, the clinical course may be complicated by abdominal pain or an acute abdomen related to torsion or spontaneous rupture. Granulomatous peritonitis may be present if a mature cystic teratoma leaks its oily and keratinous contents into the peritoneal cavity.

Mature cystic teratomas are typically 5 to 10 cm in diameter, and about 10% to 15% are bilateral. Their external surface is smooth, glistening, and pearly gray to tan-pink. Most of these cystic neoplasms are unilocular and contain an admixture of oily sebaceous material and matted hair (Fig. 7.235A). The cyst contents are liquid at body temperature, but congeal into a vaseline-like consistency when left at room temperature. The Rokitansky protuberance, also known as the dermoid mamilla, dermoid protuberance, or Rokitansky's tubercle, is a nodular or polypoid solid mass of variable size that arises from the cyst wall and projects into the cavity (Fig. 7.235A). There is usually only one such protuberance, which most often consists of an outer layer of skin-like tissue with a fatty core (Fig. 7.235B). This area is a preferred site for formation of bone and teeth. In extraordinarily rare cases referred to as fetiform teratomas, a fetus-like structure is the dominant component of a mature teratoma.[324] An example of a mature cystic teratoma that has undergone torsion-related hemorrhage is shown in Figure 6.61.

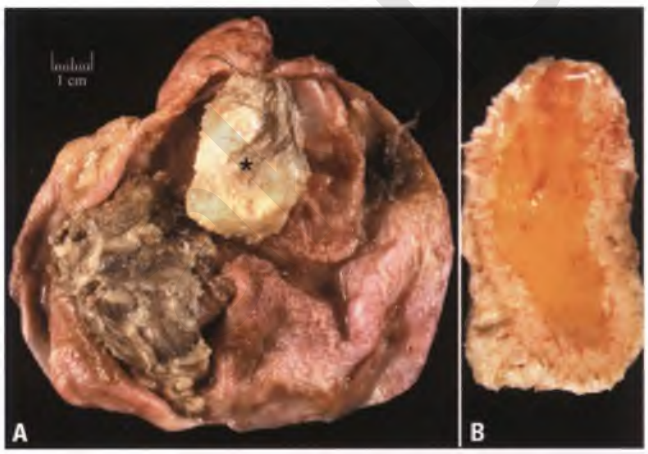

FIGURE 7.235. Mature cystic teratoma. **A:** The cyst has been opened, revealing the presence of sebaceous material and hair, some of which has been removed to expose the tannish-pink lining that resembles squamous mucosa. Note the prominent Rokitansky protuberance (*asterisk*). **B:** As is commonly the case, the core of this Rokitansky protuberance is composed of adipose tissue.

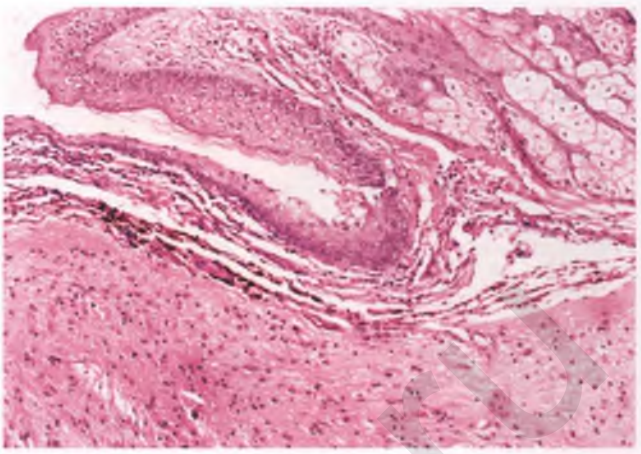

FIGURE 7.236. Mature cystic teratoma with the usual squamous epithelial lining and associated sebaceous glands. Note the underlying band of mature neuroglial tissue and the elongated layer of darkly pigmented dendritic cells that corresponds to an incidental meningothelial proliferation.

Histologically, mature cystic teratomas are composed of an organoid conglomerate of adult and occasionally fetal-type tissue, with the latter corresponding to the type seen during development of a fetus >8 weeks post-fertilization. All three germ cell layers are usually represented, with ectodermal-derived skin and skin appendages typically predominating. The cyst lining is usually composed of keratinized squamous epithelium associated with sebaceous glands (Fig. 7.236),

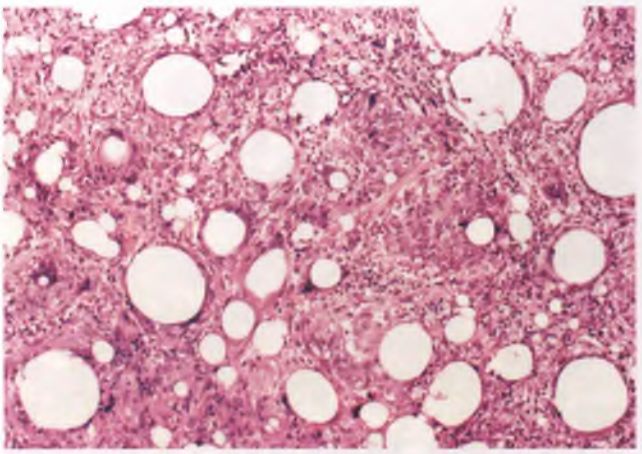

FIGURE 7.237. Lipogranulomatous reaction with sieve-like spaces. This pattern can result when the oily sebaceous contents of a dermoid cyst are released into the stroma.

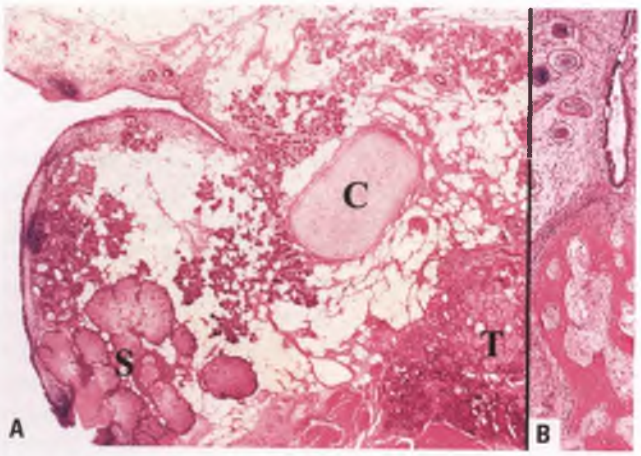

FIGURE 7.238. Mature cystic teratoma. **A:** In this low-magnification view, sebaceous glands (*S*), cartilage (*C*), thyroid (*T*), smooth muscle (lower right), and adipose tissue admixed with sweat glands are seen beneath the epithelial lining of the cyst. **B:** This example features bone beneath hair follicles and a glandular structure.

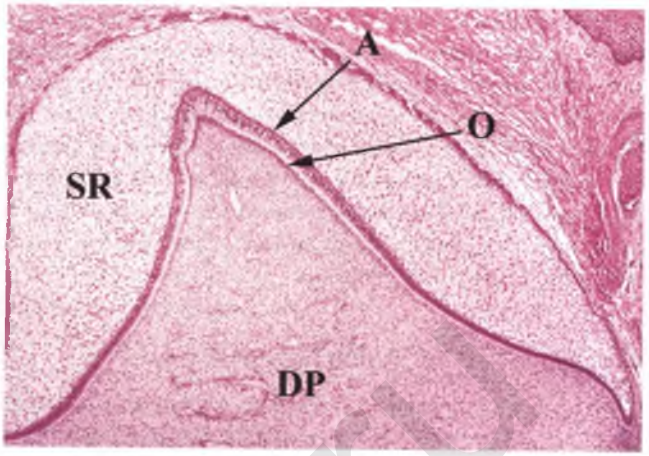

FIGURE 7.240. Mature cystic teratoma. A portion of a developing tooth at the bell stage is shown. A, ameloblasts; O, odontoblasts; SR, stellate reticulum; DP, dental papilla.

although endodermal-derived epithelium or glia may occasionally line portions of the cyst. In some cases, the cyst lining is partially eroded and replaced by a foreign body giant cell reaction (see Fig. 7.257). If an eroded cyst lining leads to the presence of sebaceous cyst contents within the stroma of the cyst wall, a lipogranulomatous reaction with a characteristic sieve-like architecture may occur (Fig. 7.237).[325]

In addition to keratinized squamous epithelium and sebaceous glands, other ectodermal tissues that are commonly present within mature cystic teratomas include sweat glands, hair follicles, and mature neuroectodermal elements such as glial tissue, cerebral cortex, cerebellum, and choroid plexus. Mesodermal derivatives (smooth muscle, cartilage, bone, and adipose tissue) and endodermal tissues (respiratory and gastrointestinal epithelium, thyroid, and salivary gland tissue) are also commonly present in varying proportions. Teeth may be present and are derived from a combination of ectodermal and mesodermal components. A rare and intriguing finding that can be encountered within these tumors is the presence of prostate tissue.[326,327] Examples of mature cystic teratomas that contain these various tissue types are presented in Figures 7.236 and 7.238–7.241.

As is also the case for immature teratomas and their implants, the neural component of dermoid cysts may be associated with a florid benign vascular proliferation.[305] Recently, it has also become apparent that microscopic meningothelial proliferations that feature anastomosing slit-like channels lined by EMA-positive meningothelial cells are a common incidental finding in mature cystic teratomas.[328] Characteristically,

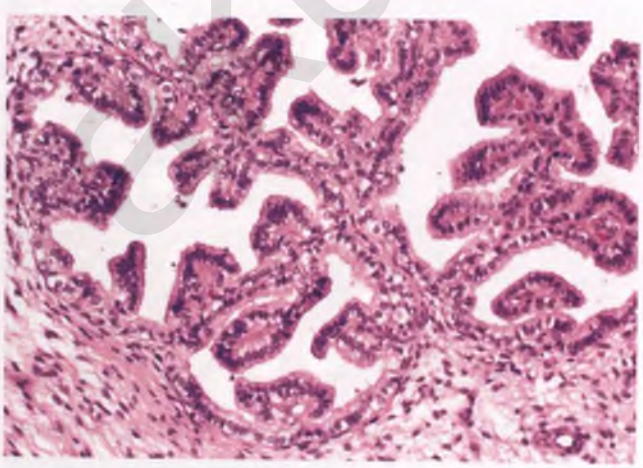

FIGURE 7.239. Choroid plexus in a mature cystic teratoma.

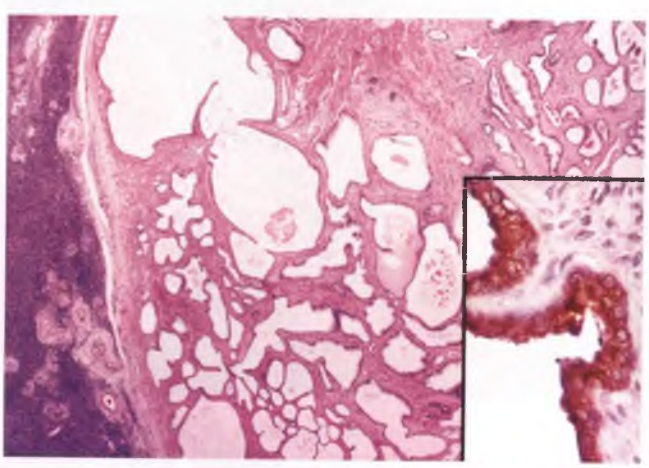

FIGURE 7.241. Prostatic tissue within a mature cystic teratoma. Nonneoplastic ovarian tissue is at left. The inset documents intense immunoreactivity of the glandular epithelium for prostate-specific antigen.

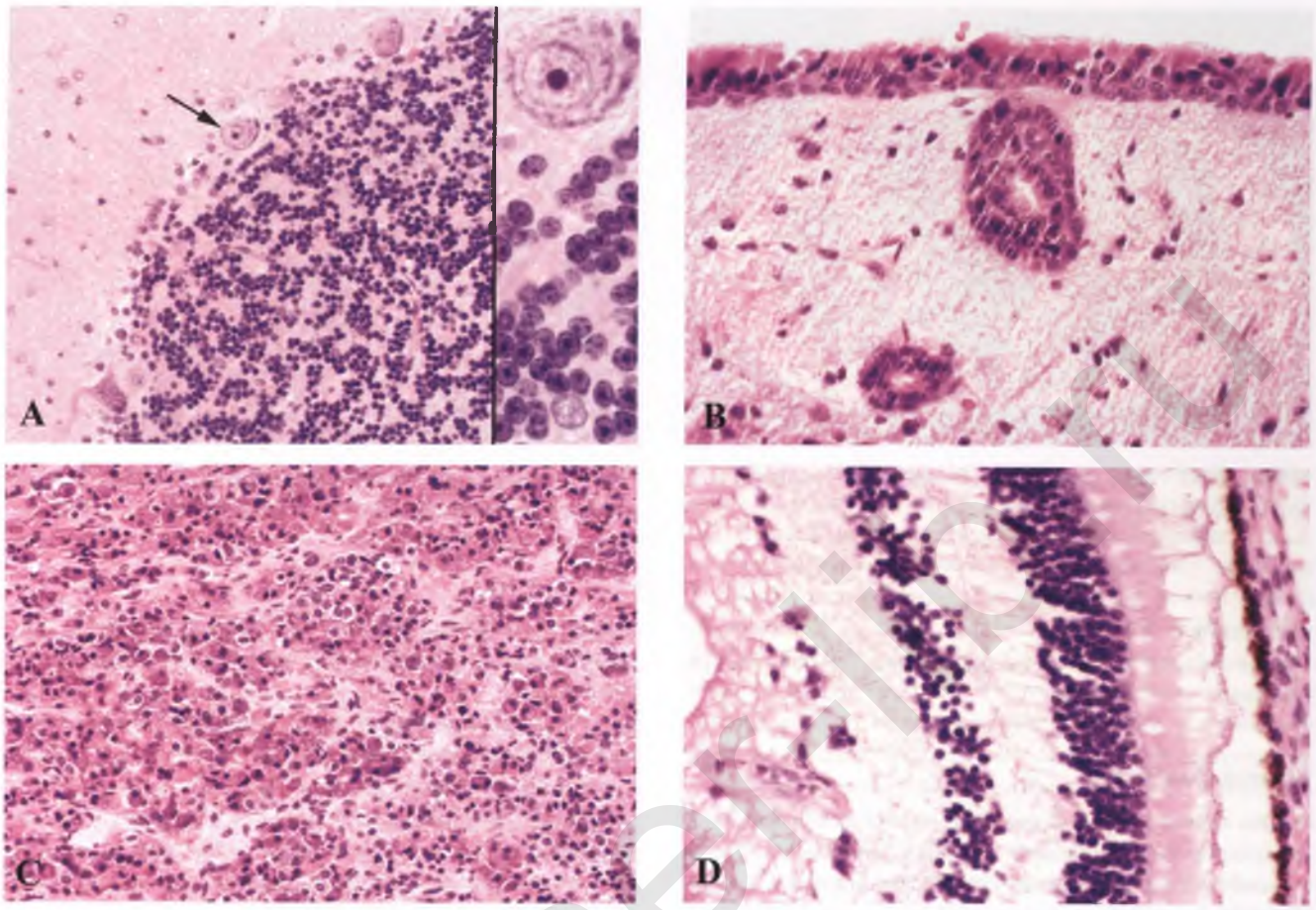

FIGURE 7.242. Components of mature cystic teratoma that may be misinterpreted as evidence of immaturity. **(A)** Cerebellar tissue. The densely populated granular layer can be misinterpreted as a malignant "small round blue cell tumor," but note the nuclear uniformity and mitotic inactivity of its constituent cells. Its association with a molecular layer and the presence of Purkinje cells (*arrow*) at the junction between these two zones confirm that this is normal cerebellar tissue. **(B)** Ciliated ependymal cells lining the surface of mature neural tissue and two associated tubules. **(C)** Anterior pituitary tissue. An admixture of chromophilic and chromophobic cells is present. **(D)** Retinal tissue from a 1-year old. This view of actual retinal tissue highlights the orderly arrangement of the three nuclear layers. The pigmented epithelium at right has been artifactually stripped away from the remainder of the retina.

proliferations of this type are in close proximity to skin with pilosebaceous units and glial tissue, are often found in association with pigmented dendritic cells, and may contain psammomatous calcifications (Fig. 7.236).[328]

Differential Diagnosis

The main differential diagnostic consideration is immature teratoma. One should be wary of making a diagnosis of immature teratoma in an ovarian tumor that grossly is an ordinary dermoid cyst, since immature teratomas typically are predominantly solid and fleshy with areas of hemorrhage and necrosis. Care should be taken not to confuse fetal-type tissue that may be found in mature cystic teratomas with the embryonic-type tissue of immature teratomas, which is most problematic when evaluating cartilage or other mesenchymal elements. Fetal-type tissue corresponds to a fertilization age of >8 weeks, whereas embryonic-type tissue corresponds to a fertilization age of 2 to 8 weeks.[304] As emphasized in the section on immature teratomas, an assessment of tissue immaturity should be based largely on neuroepithelial elements and secondarily on primitive endodermal epithelial-mesenchymal complexes. The pathologist should also be aware of the possible presence and histologic appearance of mature tissues such as cerebellum, ependymal tubules, pituitary, and retina, so that an encounter with these tissues does not result in misclassification of a mature cystic teratoma as an immature teratoma (Fig. 7.242).

Based upon limited experience, cases of otherwise typical mature cystic teratoma in which a few microscopic foci of immature tissue are identified pursue a benign clinical course and can be managed as ordinary dermoid cysts.[303] Note that this exception does not apply to solid teratomas, where even a small amount of embryonic-type tissue warrants a diagnosis of grade 1 immature teratoma because of their low malignant potential.[9]

FIGURE 7.243. Pure struma ovarii. Bivalved view of a tumor with solid and cystic components.

FIGURE 7.245. Cystic struma ovarii. The reddish brown tissue that expands some of the septa is a clue to the diagnosis.

Treatment

Mature cystic teratomas are adequately treated by ovarian cystectomy.

Struma Ovarii[329]

Struma ovarii is a type of ovarian teratoma in which thyroid tissue either predominates, is the sole component, or forms a grossly recognizable mass. Grossly, struma ovarii usually resembles normal thyroid tissue and is tan to reddish brown (Figs. 7.243 and 7.244). Scattered strumal cysts may contain straw-colored, brown, or green-tinged fluid (the latter is particularly suggestive of cystic thyroid tissue). Occasionally, struma ovarii is predominantly or entirely cystic (Fig. 7.245), in which case the tumor may be mistaken for a cystadenoma (see below).[330]

Histologically, struma ovarii typically consists of normal-appearing thyroid tissue, but may also resemble nodular hyperplasia or follicular adenoma (Fig. 7.246). In rare cases, unusual patterns (diffuse, microfollicular, pseudotubular, trabecular, oxyphilic, or clear cell) may predominate, resulting in a resemblance to a variety of tumors such as steroid cell tumor, Sertoli cell tumor, granulosa cell tumor, carcinoid tumor, paraganglioma, clear cell carcinoma, or melanoma (Fig. 7.247).[331] Evidence in favor of one of these unusual forms of struma ovarii includes the common association with a dermoid cyst, at least focal areas of typical struma ovarii, and immunoreactivity with thyroglobulin and/or thyroid

FIGURE 7.244. Struma ovarii arising within a dermoid cyst. In this bivalved view, the yellowish white sebaceous contents of the dermoid cyst contrast with the solid, tannish brown, lobulated thyroid tissue. For classification purposes, such tumors are loosely considered monodermal teratomas, even though they are derived from at least two different germ cell layers (thyroid tissue from endoderm, and dermoid cyst mainly from ectoderm).

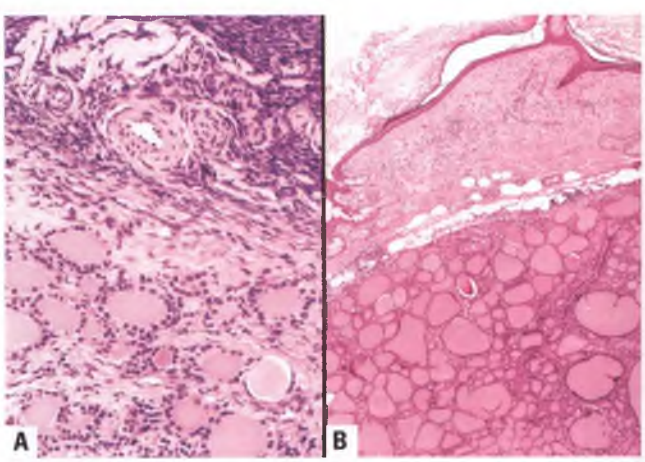

FIGURE 7.246. Struma ovarii. **A:** Pure struma ovarii, with thyroid follicles (bottom) adjacent to ovarian stroma (top). **B:** The variably-sized, colloid-filled follicles of struma ovarii (bottom) abut components of a dermoid cyst (top). This image is the histologic correlate of the tumor shown in Figure 7.244.

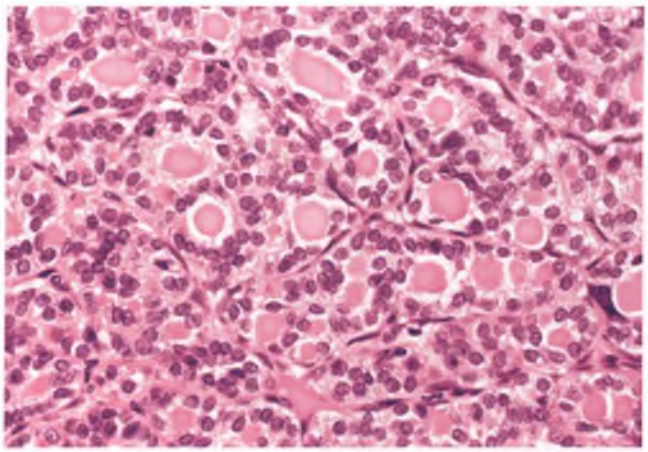

FIGURE 7.247. Struma ovarii. In this example, the presence of a microfollicular pattern imparts a resemblance to granulosa cell tumor.

transcription factor-1 (TTF1).[331,332] If one of these difficult patterns is encountered during an intraoperative frozen section, the identification of birefringent calcium oxalate crystals within the colloid of the follicles can serve as a clue to the correct diagnosis.[329,333]

With regard to the deceptive cystic form of struma ovarii, the identification of a few thyroid follicles within the cyst wall or connective tissue septa assists in its recognition (Fig. 7.248).[330] The epithelium lining the cysts in these cases is typically flattened to cuboidal and its thyroid-related nature can only be established with certainty by demonstrating immunoreactivity for thyroglobulin or TTF1 (Fig. 7.249).[330,332] Fortunately, mistaking cystic struma ovarii for a benign cystadenoma is of no clinical significance.

As illustrated in Figure 7.307, struma ovarii may be associated with a peripheral band of steroid cells.[223]

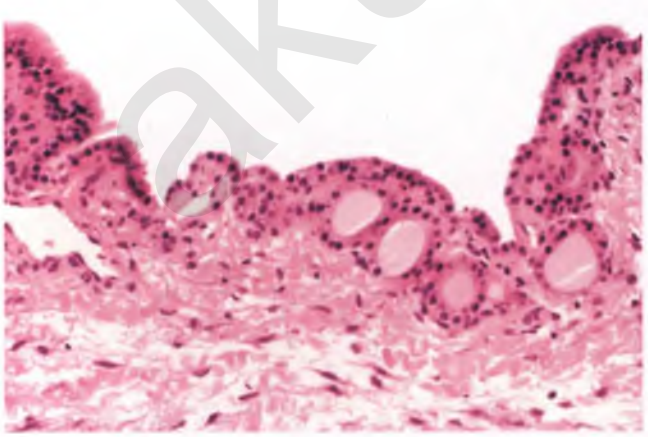

FIGURE 7.248. Cystic struma ovarii. In some cases of this type, the diagnosis is suggested by the presence of follicles consistent with thyroid origin within the cyst wall or connective tissue septa.

Carcinoma Associated with Struma Ovarii

Thyroid-type carcinoma may rarely develop within struma ovarii.[329,334–339] The term "malignant struma ovarii" should not be used as a specific diagnosis in this situation, since it is an imprecise term that in the older literature often referred to strumal carcinoid and currently may be applied in a general sense to struma-associated cancers that range from anaplastic carcinoma to innocuous-appearing lesions that histologically are indistinguishable from benign thyroid tissue (see below). Instead, the specific type of carcinoma, usually papillary or follicular, should be specified as originating within struma ovarii.

Since struma ovarii usually does not have a capsule, capsular invasion cannot be evaluated as a criterion for malignancy of most follicular carcinomas in this site. Instead, this diagnosis is typically based upon the presence of unequivocal vascular invasion (Fig. 7.250), frank infiltration of ovarian stroma, or documented metastases of appropriate histologic type.[329]

The diagnosis of struma-associated papillary carcinoma rests upon the widespread and characteristic nuclear features of this neoplasm, which include optically clear nuclei, nuclear grooves, nuclear overlapping, and nuclear pseudoinclusions (Figs. 7.251 and 7.252).[329,334,339] Analogous to the corresponding thyroid neoplasm, both a classic type of papillary carcinoma with a papillary architecture and a follicular variant are recognized.[334]

Despite histologic features characteristic of malignancy, thyroid-type carcinomas arising within struma ovarii seldom behave in a clinically aggressive manner.[329,339] When a thyroid-type carcinoma is encountered within the ovary without an associated dermoid cyst, the remote possibility of metastatic carcinoma of actual thyroid origin should be considered and excluded by clinicopathologic correlation.[340]

In the original study in which the term "proliferative struma ovarii" was first used to describe follicular adenoma-like changes, the authors noted that the associated risk of malignant behavior was nonexistent.[339] However, several recent studies with long-term follow-up have documented the ability of occasional cases of this type to metastasize, usually many years after removal of the primary tumor and with an indolent clinical course.[335–337] Terminology for this extraordinarily rare occurrence varies and includes the out-of-favor term "peritoneal strumosis" (when extraovarian spread is limited to peritoneal implants), struma ovarii with peritoneal dissemination, highly differentiated follicular carcinoma, and minimal deviation follicular thyroid-type carcinoma.[329,337] Bland-appearing strumas that are at increased risk for this type of behavior are those that are associated with adhesions, ≥1 L of ascites, and/or a serosal tear in the tumor.[335,336] It is important for patients, pathologists, gynecologists, and malpractice attorneys to understand that a diagnosis of this type of carcinoma can only be made once extraovarian spread has been documented. Histologically, the struma in both its primary and metastatic sites in these cases usually has proliferative or follicular adenoma-like features, but may also have the appearance of nodular hyperplasia or even normal thyroid tissue.[335–337] These cases differ from subtle papillary carcinomas that may not be recognized until subsequent extraovarian spread prompts retrospective review.[334]

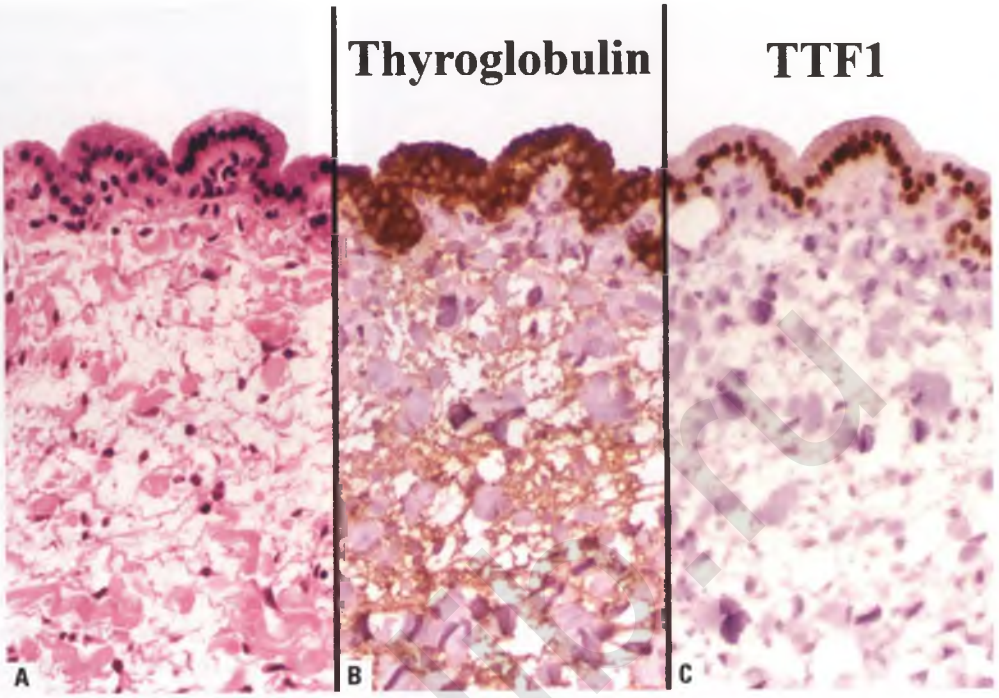

FIGURE 7.249. Cystic struma ovarii. When the epithelial lining has a nonspecific appearance **(A)**, identification of thyroid tissue via additional sampling or immunoreactivity with thyroglobulin **(B)** and/or TTF1 **(C)** is necessary to establish the diagnosis. Note that thyroglobulin reactivity is cytoplasmic, and TTF1 staining is nuclear.

Insular Carcinoid[237,239]

Of the four types of primary carcinoid tumor of the ovary (insular, trabecular, strumal, and mucinous), the insular variant is the most common. The typical presentation is a middle-aged to elderly adult woman who develops symptoms related to a unilateral mass that is confined to the ovary. The carcinoid syndrome is present in about one-third of patients, is more likely to occur in patients with large tumors, and occurs only rarely in other variants of primary ovarian carcinoid tumor.[§§]

Grossly, most tumors are associated with a mature cystic teratoma and present either as an area of wall thickening or as a nodule protruding into a cystic cavity. Pure tumors measure up to 20 cm in diameter and have a smooth exterior. Their sectioned surface is firm, predominantly solid, and tannish yellow.

Histologically, insular carcinoids are composed of solid tumor cell nests and small acinar structures that are separated from one another by variable amounts of fibromatous stroma (Fig. 7.253). Intraluminal secretions that are either homogeneous and eosinophilic or calcified and basophilic may be present (Fig. 7.254). In the latter situation, the calcific deposits may form psammomatous laminations. The neoplastic cells have the typical features of carcinoid tumors, with uniform round nuclei, stippled chromatin, and cytoplasm that contains neuroendocrine granules that are often concentrated in a characteristic distribution (Fig. 7.255). Mitotic figures are absent to inconspicuous, and tumor necrosis is not present in the absence of torsion-related infarction. As expected, the tumor cells are immunoreactive for the neuroendocrine markers chromogranin and/or synaptophysin.[146]

Differential Diagnosis

In most cases, the association of insular carcinoid with mature cystic teratoma narrows the differential diagnosis considerably, and the diagnosis can be made on the basis of histologic features

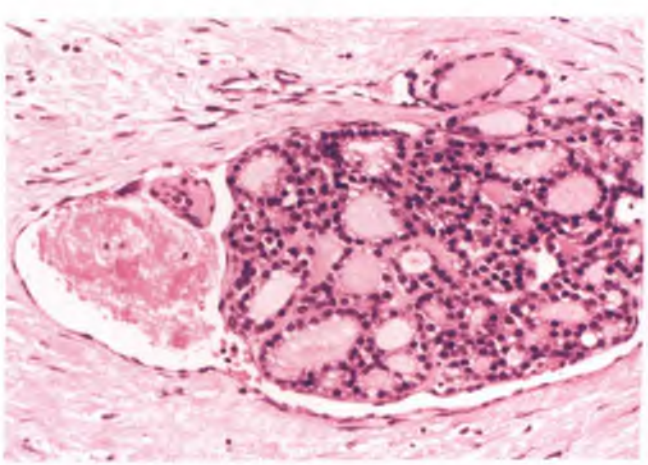

FIGURE 7.250. Well-differentiated follicular carcinoma. Despite the bland histologic features, the presence of angiolymphatic invasion is indicative of malignancy. This patient had documented metastases.

[§§]The most common symptoms of the carcinoid syndrome are diarrhea and flushing, with the latter not being related to frequent trips to the toilet, but rather representing a cutaneous reaction that is episodic, erythematous, typically confined to the face, and occasionally provoked by specific stimuli.[239] Note that the venous drainage of the ovary enters the systemic circulation directly, which deprives the liver of an opportunity to inactivate the vasoactive substances responsible for producing the carcinoid syndrome. In contrast, the venous blood of intestinal tumors enters the liver via the portal vein prior to entering the systemic circulation, where these substances undergo hepatic degradation. This anatomic difference explains why almost all intestinal carcinoid tumors need to metastasize to the liver and gain direct access to the systemic circulation before the carcinoid syndrome develops, whereas this is not the case for ovarian carcinoids.

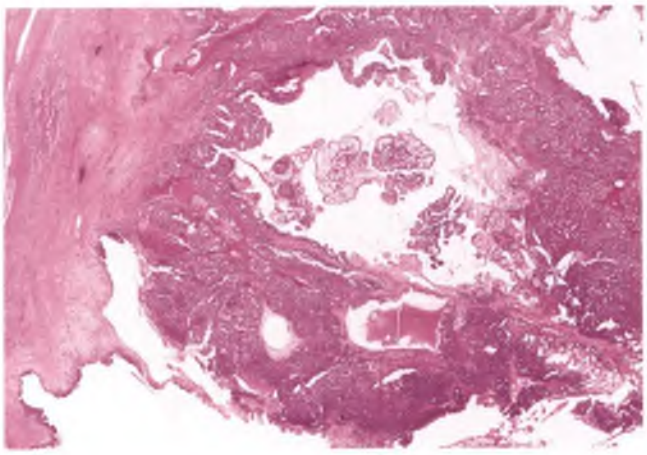

FIGURE 7.251. Papillary thyroid carcinoma arising from the inner lining of a cystic struma ovarii.

alone or confirmed by obtaining immunoreactivity with neuroendocrine markers within the carcinoid component. Pure insular carcinoid tumors of the ovary create more of a diagnostic challenge, since they cannot be distinguished on histologic grounds from metastatic carcinoid tumors of similar type that usually arise in the small intestine. Unfortunately, the intestinal marker CDX-2 is frequently expressed in both primary and metastatic insular carcinoid tumors of the ovary,[280] and other currently available immunohistochemical markers are also not helpful in making this distinction. However, the diagnosis of metastatic carcinoid tumor involving this site is usually readily apparent by virtue of the presence of a known carcinoid tumor elsewhere, bilateral ovarian involvement, multinodular growth, and high-stage disease.[238,280]

The nested architecture of the Brenner tumor results in some resemblance to pure insular carcinoid, but the former tumor is composed of transitional cells with characteristic nuclear grooves and does not stain with neuroendocrine markers.

The differential diagnosis of insular carcinoid tumor with AGCT is discussed in the section on the latter entity.

Behavior

The vast majority of patients with primary insular carcinoid tumors have tumors that are limited to the ovary at the time of diagnosis and are cured by removal of the tumor. Symptoms related to the carcinoid syndrome, if present, also typically resolve following surgical treatment.

Trabecular Carcinoid[341,342]

The clinical presentation and gross appearance of ovarian trabecular carcinoid is not significantly different from that of the insular variant, other than the rarity with which the former tumor is associated with the carcinoid syndrome. This similarity includes their unilateral nature and the propensity of both of these neoplasms to be associated with a dermoid cyst.

Histologically, trabecular carcinoids feature long winding ribbons of columnar cells with elongated nuclei that are oriented parallel to one another and perpendicular to the long axes of the ribbons. Moderate amounts of eosinophilic cytoplasm are present, nuclear chromatin is stippled, and the mitotic rate is low. These tumors have a fibromatous stroma, which is usually inconspicuous. An example of a trabecular carcinoid is illustrated in the following section on strumal carcinoid. Immunoreactivity with neuroendocrine markers is expected, and nearly all primary ovarian trabecular carcinoids are clinically benign.

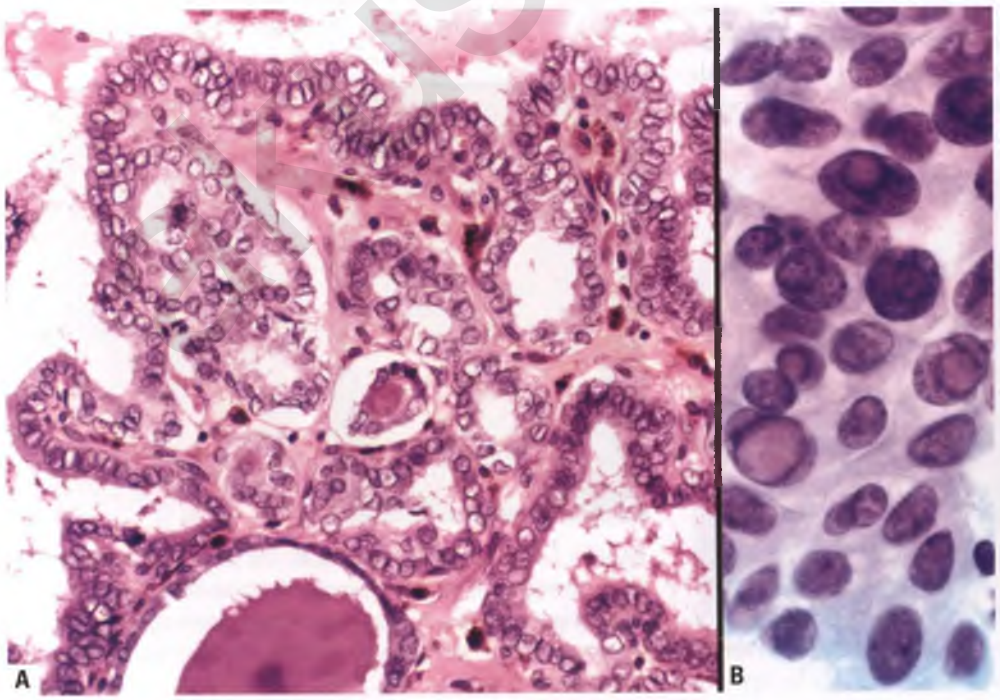

FIGURE 7.252. Papillary thyroid carcinoma. **A:** In addition to the partially papillary architecture, which is not essential for the diagnosis, note the optically clear, overlapping nuclei with occasional grooves that are characteristic of this neoplasm. **B:** This Papanicolaou-stained cytologic scrape preparation highlights the presence of intranuclear pseudoinclusions, which is another helpful diagnostic feature of papillary carcinoma.

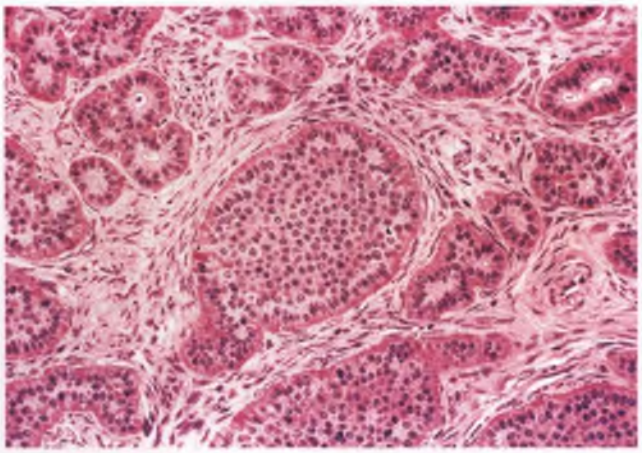

FIGURE 7.253. Insular carcinoid. Neuroendocrine cells form nests and acini and are embedded within a fibrous stroma. Note how the eosinophilic neurosecretory granules within the cytoplasm of the tumor cells are concentrated around the periphery of the nests and acini.

Differential Diagnosis

Metastatic trabecular carcinoid tumors involving the ovary are extraordinarily rare, and can be distinguished by their lack of association with teratomatous elements and high frequency of bilaterality, multinodularity, and presence of tumor elsewhere in the abdomen and/or pelvis. If thyroid follicles are identified in association with a trabecular carcinoid, then the tumor is classified as a strumal carcinoid. As discussed in the section on Sertoli-Leydig cell tumors, the trabeculae of trabecular carcinoid can simulate the sex cord formations that are found in this type of sex cord-stromal tumor.

Strumal Carcinoid[237,343]

Strumal carcinoid is a distinctive form of teratomatous germ cell tumor in which thyroid tissue is closely associated with a carcinoid tumor. It is the second most common type of primary ovarian carcinoid tumor, and typically presents as a unilateral adnexal mass in an adult woman. In spite of the fact that all carcinoid tumors have some potential for malignant behavior, virtually all patients with strumal carcinoid are cured by removal of their tumor.

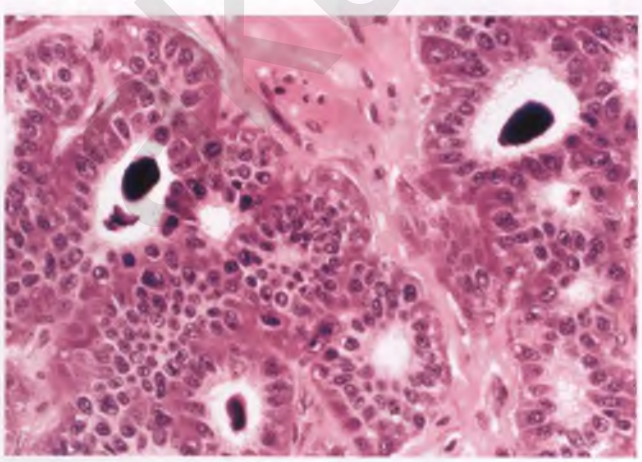

FIGURE 7.254. Insular carcinoid with calcified deposits within acinar spaces.

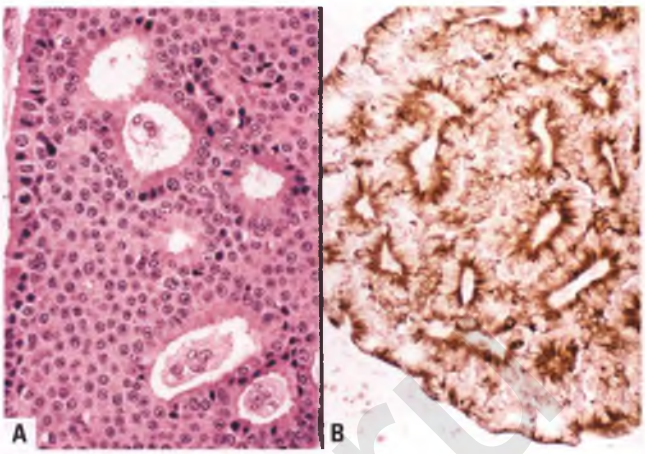

FIGURE 7.255. Insular carcinoid. **A:** This image highlights the uniform round nuclei and stippled chromatin of the tumor cells that are characteristic of this neoplasm. Note that when acinar structures are present within large nests, the eosinophilic neurosecretory granules are often concentrated along the luminal aspect of the acini. **B:** The distribution pattern of the neurosecretory granules in insular carcinoid tumors with internal acini is nicely demonstrated in this Grimelius stain.

Most cases of strumal carcinoid occur either as a nodule within the wall of a dermoid cyst or in pure form. Grossly, pure strumal carcinoids are solid nodules that are usually a fairly homogeneous yellow-brown color (Fig. 7.256), but may be composed of grossly recognizable thyroid (reddish brown)

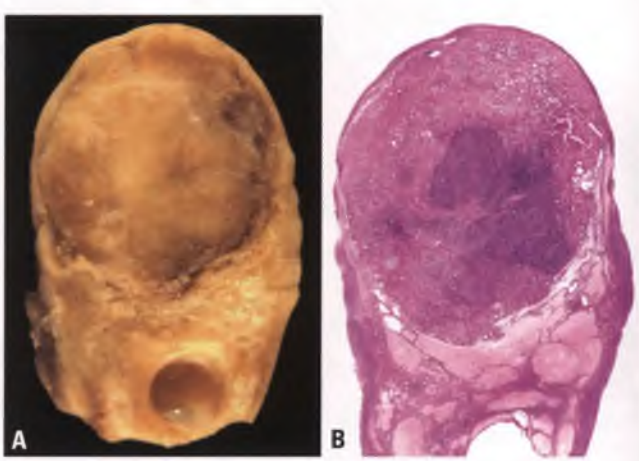

FIGURE 7.256. Strumal carcinoid. **A:** The sectioned surface of this ovary reveals a 1.8 cm solid yellow-brown nodule. **B:** Although fairly homogeneous grossly, this low-magnification view demonstrates the presence of geographic areas in which the dark blue-staining carcinoid tumor predominates.

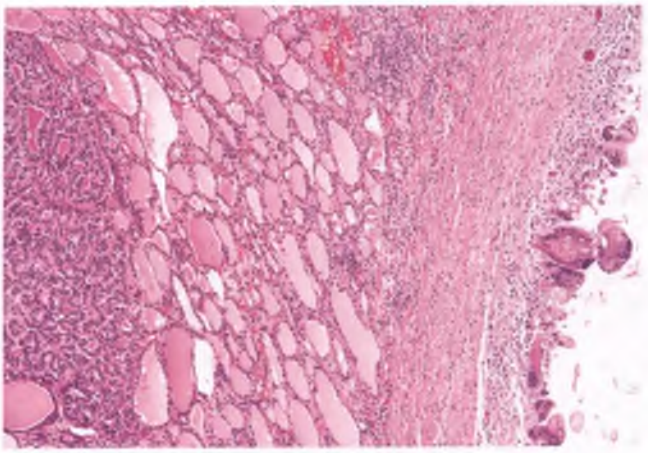

FIGURE 7.257. Strumal carcinoid. In this example, the carcinoid tumor (left) abuts thyroid tissue with only minor comingling of the two components. At right is the eroded lining of a dermoid cyst that has been replaced by foreign body giant cells.

and carcinoid (light gray to tannish yellow) components. It follows that most tumors will histologically be composed of an intimate admixture of thyroid tissue and carcinoid tumor, whereas in occasional tumors these two components are more segregated (Figs. 7.257 and 7.258). The carcinoid component is usually pure trabecular (Fig. 7.259) or of mixed trabecular and insular types. As is the case for other types of carcinoid tumor, immunoreactivity for chromogranin and/or synaptophysin is expected, and the strumal component expresses the thyroid markers TTF-1 and thyroglobulin.[332]

Mucinous Carcinoid[310,344]

Mucinous carcinoids, which bear a strong resemblance to goblet cell carcinoids of the appendix, account for only 1% to 2% of primary ovarian carcinoid tumors. These tumors are unilateral, usually confined to the ovary at the time of diagnosis, and commonly associated with a mature cystic teratoma or other cystic ovarian neoplasm. Mucinous carcinoids have also been seen in association with yolk sac tumors on rare occasions.[345]

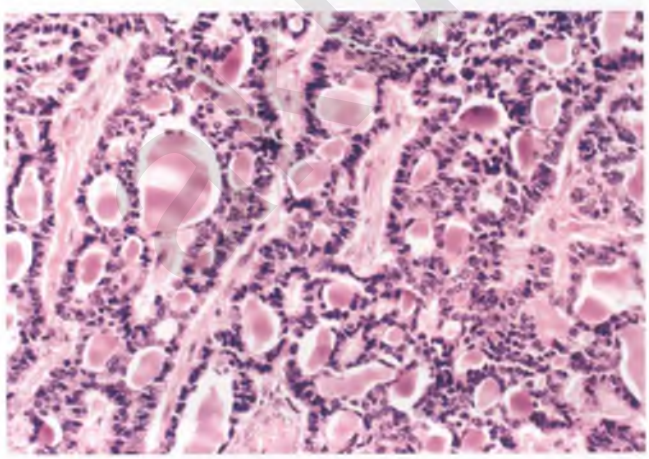

FIGURE 7.258. Strumal carcinoid. In this field, there is an intimate admixture of thyroid follicles and trabecular carcinoid. Note how carcinoid cells appear to have replaced the lining of portions of the colloid-filled spaces.

In well differentiated examples of mucinous carcinoid, discrete nests of minimally atypical tumor cells composed of an admixture of goblet cells and granulated neuroendocrine cells dissect fibrous stroma or float within pools of mucin. A mucicarmine stain highlights the presence of the mucin-containing goblet cells, whereas the neuroendocrine cells are immunoreactive for neuroendocrine markers such as chromogranin and/or synaptophysin. It is not uncommon for frank carcinoma to arise in this setting, and an atypical variant with an intermediate degree of architectural and cytologic abnormalities has also been described (Fig. 7.260). In limited experience with this spectrum of tumors, only those with a carcinomatous component that have spread beyond the ovary at the time of presentation have been clinically malignant.

Differential Diagnosis

The main differential diagnostic consideration is metastatic adenocarcinoma with goblet cell carcinoid-like features (see Fig. 7.331), which is most commonly of appendiceal origin and is a diagnosis that will often be apparent from the clinical history or concurrent surgical material.[346] Ovarian involvement by this form of Krukenberg tumor is likely to be bilateral, and tumor has often spread elsewhere within the abdomen and/or pelvis. Metastatic adenocarcinoma of this type lacks an association with a primary ovarian tumor, has a mucin-containing signet-ring component, and is associated with a poor prognosis.[346] Pure goblet cell carcinoids of the appendix that lack a more aggressive component could theoretically metastasize to the ovary and produce a histologic pattern that is virtually identical to that of a primary well-differentiated mucinous carcinoid. However, appendiceal tumors of this type, when carefully separated from goblet cell carcinoids that are admixed with adenocarcinoma, have an excellent prognosis.[347,348] In the experience of some experts, pure goblet cell carcinoids of the appendix have not been observed to metastasize to the ovary.[346] I concur with their position that most, if not all, of the several case reports in the literature that claim to describe this phenomenon are more accurately interpreted as examples of metastatic adenocarcinoma with goblet cell carcinoid-like features.[346]

Carcinomas Associated with Dermoid Cysts[206,349]

Malignant change in a somatic component of a dermoid cyst occurs in roughly 1% of cases. Most patients are in the 40 to 60 year-old age group, and the malignant tumor is usually a squamous cell carcinoma. Adenocarcinomas and other miscellaneous types of carcinoma have also been reported to arise in this setting on rare occasions. Whatever the type of superimposed malignant tumor, it may manifest

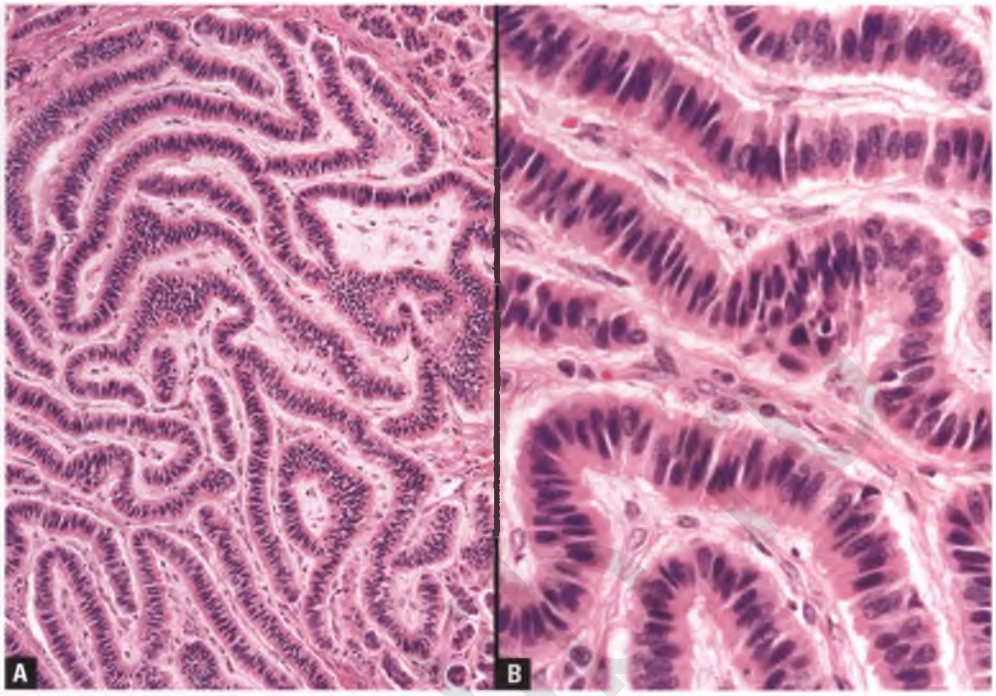

FIGURE 7.259. Strumal carcinoid. **A:** Classic trabecular carcinoid component composed of long, slender, wavy ribbons of tumor cells. **B:** The columnar-shaped tumor cells have elongated nuclei that are oriented parallel to one another and perpendicular to the long axes of the ribbons. The abundant eosinophilic cytoplasm contains neurosecretory granules that are detectable by special stains or electron microscopy.

itself grossly as an irregular thickening of the cyst wall, a mural nodule, a polypoid mass protruding into a cystic cavity, or a solid tumor mass (Figs. 7.261 and 7.262). For this reason, areas within dermoid cysts with gross features as described above should be adequately sampled for histologic examination.

Once a dermoid-associated carcinoma has spread beyond the ovary, the prognosis is generally poor. However, those patients with stage I tumors have a favorable prognosis, particularly when the tumor is well differentiated and there is no demonstrable angiolymphatic invasion.

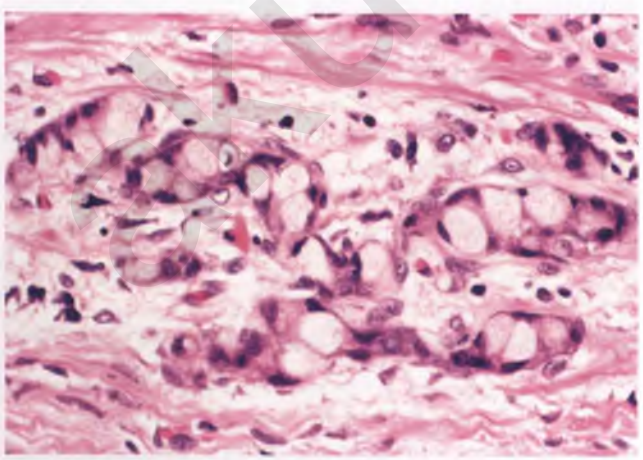

FIGURE 7.260. Atypical mucinous carcinoid with some fusion of the goblet cell nests, moderate nuclear atypia, and occasional signet-ring cells.

Melanocytic Tumors Associated with Dermoid Cysts

Very rarely, malignant melanoma may arise within a dermoid cyst, and it is the presence of associated teratomatous elements that establishes the primary nature of this tumor.[350] The absence of a prior history of melanoma and unilateral ovarian involvement are additional expected findings in this situation. Most primary ovarian melanomas have spread beyond the ovary at the time of presentation and can be expected to pursue an aggressive clinical course.

FIGURE 7.261. Squamous cell carcinoma arising within a mature cystic teratoma. In this section though a formalin-fixed ovarian tumor, the thick, solid, light-gray tissue of squamous cell carcinoma at right contrasts with the other elements of an ordinary dermoid cyst, including cysts with adherent yellow sebaceous material. (Courtesy of Dr. Deborah J. Gersell.)

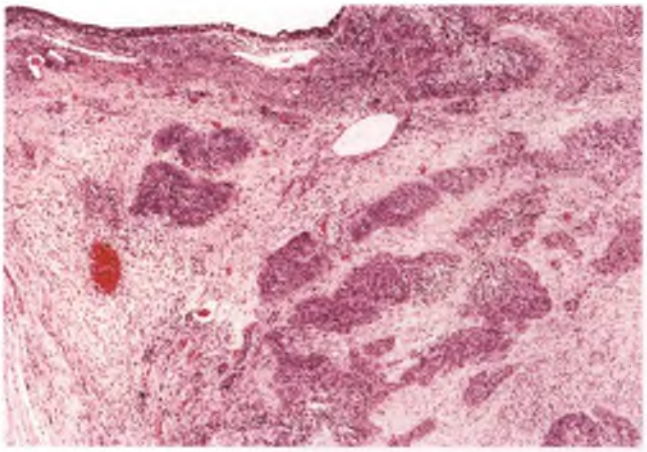

FIGURE 7.262. Squamous cell carcinoma arising within a mature cystic teratoma. In this histologic correlate of the tumor in the preceding figure, irregularly shaped nests of squamous cell carcinoma are seen raggedly infiltrating stromal tissue. A portion of the cyst lining is at top left. (Courtesy of Dr. Deborah J. Gersell.)

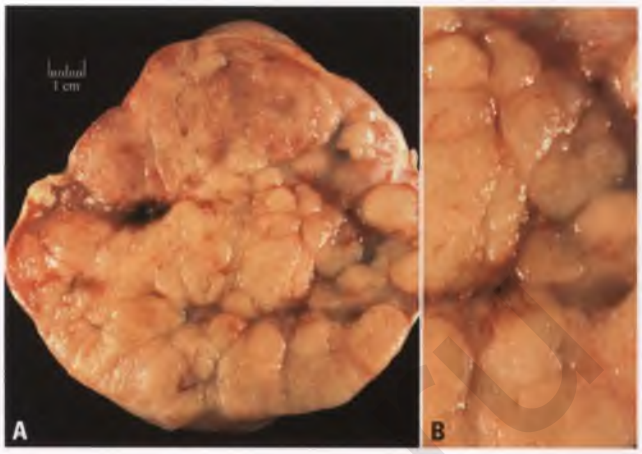

FIGURE 7.263. **A,B:** Dysgerminoma. The sectioned surface of this solid tumor is lobulated, cream-colored, and grossly indistinguishable from ovarian lymphoma (see Fig. 7.287).

Melanocytic nevi have also been reported to arise within dermoid cysts on rare occasions.[351]

Sarcomas Associated with Dermoid Cysts[310]

A variety of sarcomas have been reported to arise within dermoid cysts, and account for about 10% of malignant tumors of somatic type that occur in this setting. These are aggressive tumors with a poor prognosis.

Miscellaneous Monodermal Teratomas and Dermoid-Associated Somatic-type Tumors[310]

Miscellaneous tumors within this category that occur at case-reportable frequencies include neuroectodermal tumors ranging from ependymomas to anaplastic tumors resembling glioblastoma multiforme,[352] sebaceous adenomas and carcinomas,[353] pituitary-type tumors,[354] and the retinal anlage tumor.[355] Although some epidermoid cysts may be monodermal teratomas, they are considered a type of squamous tumor for classification purposes.

Dysgerminoma[310,356]

Dysgerminoma, which is the ovarian counterpart of the more common testicular seminoma, is a rare tumor that nevertheless is the most common malignant germ cell tumor of the ovary. It accounts for about half of such cases, which corresponds to roughly 1% of all primary ovarian malignancies. Dysgerminomas typically present in a child or young adult (mean age of roughly 20 years) with symptoms related to an ovarian mass. About one-third of patients are found to have extraovarian spread at the time of diagnosis. In rare cases, there may be hypercalcemia or an elevated serum β-hCG.[310,357] As discussed in Chapter 6, some patients with gonadal dysgenesis are at risk for the development of a dysgerminoma arising within a gonadoblastoma.

Dysgerminomas are grossly bilateral in approximately 10% of cases and have a median diameter of about 15 cm. Their external surface is smooth or nodular, and sectioning typically reveals cream-colored, fleshy, lobulated tissue that is grossly indistinguishable from lymphoma (Fig. 7.263). Foci of hemorrhage and/or necrosis may be present. Adequate sampling of putative dysgerminomas, with emphasis on areas with different gross appearances, is necessary to exclude the possibility of a mixed germ cell tumor with more aggressive components such as yolk sac tumor or choriocarcinoma.

Histologically, the neoplastic cells of dysgerminoma are typically arranged in sheets, nests, trabeculae, or cords in association with variably prominent strands of fibrous tissue that contain lymphocytes and occasional plasma cells (Fig. 7.264).

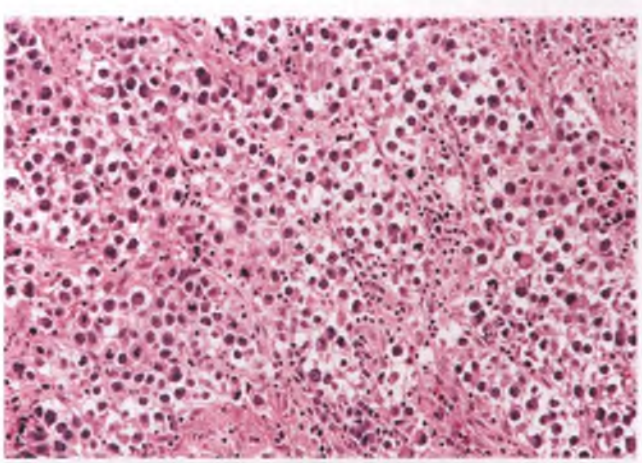

FIGURE 7.264. Dysgerminoma. Clusters of neoplastic germ cells are separated by thin bands of fibrous stroma that are associated with an infiltrate of mature lymphocytes. Note the brisk mitotic activity within the germ cell population.

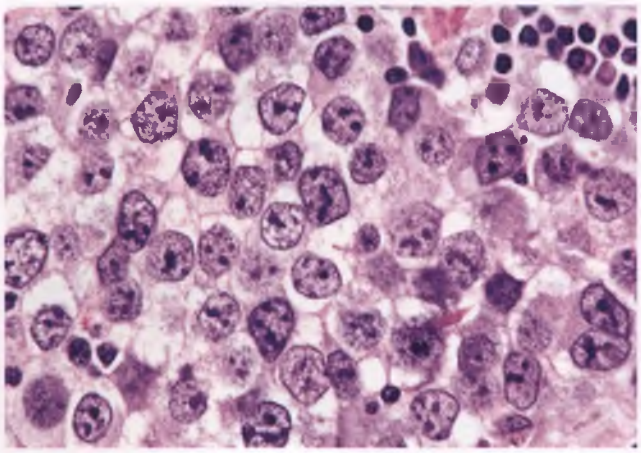

FIGURE 7.265. Dysgerminoma. The tumor cells have large vesicular nuclei that often contain one or more prominent nucleoli.

The tumor cells are large, rather monotonous, and mitotically active, with well-defined cell membranes, clear cytoplasm that contains abundant glycogen, and centrally located, rounded nuclei that contain one or more prominent nucleoli (Figs. 7.265 and 7.266). They bear a strong resemblance to the germ cells within primordial follicles. Optimal fixation is necessary to avoid artifacts such as cytoplasmic eosinophilia and loss of cellular cohesion, and can be obtained by preselecting at least one thinly sliced section of tumor for histology when the specimen is fresh and fixing it separately in a small jar of formalin. Granulomatous inflammation, which may be in the form of vague clusters of epithelioid histiocytes, scattered Langhans giant cells, or well-defined noncaseating granulomas, is seen in about 20% of cases (Fig. 7.267), and may occasionally obscure the presence of the malignant germ cells in the background. Syncytiotrophoblastic

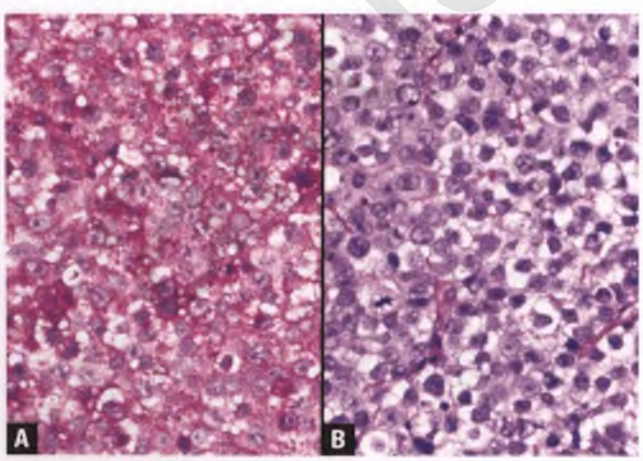

FIGURE 7.266. Dysgerminoma. **A:** The tumor cells contain abundant PAS-positive glycogen within their cytoplasm. **B:** This section has been pretreated with diastase prior to PAS staining, and demonstrates the complete removal of the glycogen granules.

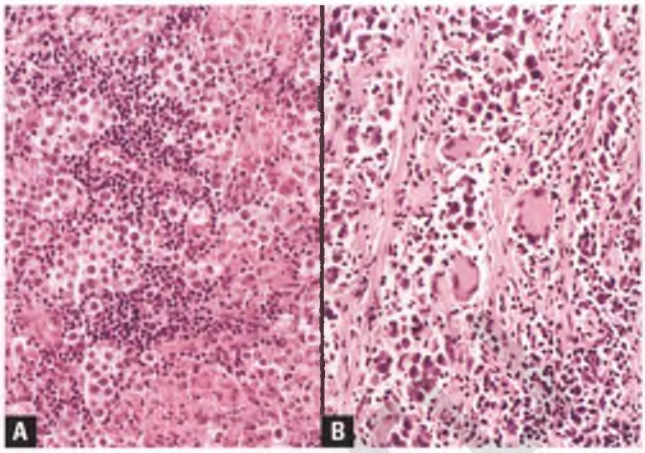

FIGURE 7.267. Dysgerminoma with granulomatous inflammation. **A:** Loosely aggregated clusters of epithelioid histiocytes with abundant eosinophilic cytoplasm are admixed with lymphocytes and islands of malignant germ cells. **B:** Dysgerminoma with scattered Langhans giant cells. Suboptimal fixation has resulted in cytoplasmic eosinophilia and loss of cohesion of the tumor cells.

giant cells that are immunoreactive for β-hCG are present in about 3% of cases, and are typically associated with elevated serum levels of this hormone.[357] Clusters of luteinized stromal cells are also occasionally present.[357] The finding of calcifications within a dysgerminoma, particularly if mulberry-shaped, suggests that the tumor originated within a gonadoblastoma.

Dysgerminomas typically demonstrate nuclear immunoreactivity for OCT4 and membranous positivity for CD117 (c-kit), are usually cytokeratin-negative, and do not express CD30.[290,358–360]

Differential Diagnosis

The major differential diagnostic considerations of dysgerminoma are embryonal carcinoma, clear cell carcinoma, large cell lymphoma, and the solid variant of yolk sac tumor.

- In contrast to dysgerminoma, embryonal carcinoma features tumor cells that have larger, more anaplastic nuclei and cytoplasm that is amphophilic rather than clear. Papillary or slit-like architectural patterns, an absence of fibrous septa with an associated lymphoplasmacytic infiltrate, and a CD30-positive, CD117-negative immunophenotype also favor embryonal carcinoma over dysgerminoma.
- Solid areas of clear cell carcinoma may resemble dysgerminoma, but are typically associated with tubulocystic and papillary patterns as well, and occur in an older age group. In contrast to dysgerminomas, clear cell carcinomas are also expected to be immunoreactive for epithelial membrane antigen and to be negative or only focally rather than diffusely positive for OCT4.[290,361]
- Large cell lymphomas share some gross and histologic features with dysgerminoma, but are easily distinguished by their lack of glycogen-rich cytoplasm and immunoreactivity

with leukocyte common antigen and other lymphocytic markers (nearly all such tumors are of B-cell lineage).[362]

- The differential diagnosis of dysgerminoma with the solid pattern of yolk sac tumor is discussed in the section on the latter entity.

A few other sources of potential diagnostic confusion are worth mentioning. When a dysgerminoma with syncytiotrophoblastic giant cells is encountered, it may be misinterpreted as choriocarcinoma. However, the biphasic admixture of cytotrophoblastic and syncytiotrophoblastic cells and prominent areas of hemorrhagic necrosis that are characteristic of choriocarcinoma are lacking in dysgerminomas.[357] Seminoma can also occur in the setting of a cryptorchid testis in a phenotypic female with androgen insensitivity syndrome and mimic an ovarian dysgerminoma.

Prognosis

The prognosis of dysgerminoma is excellent. Small amounts of residual disease are highly sensitive to either chemotherapy or radiation therapy, which accounts for high cure rates even in those patients with advanced disease or recurrent tumor.[312]

Yolk Sac Tumor[363,364]

Yolk sac tumor, which is the preferred term for the neoplasm also known as endodermal sinus tumor, accounts for approximately 20% of malignant germ cell neoplasms. This rare tumor typically presents in a child or young adult (median age of 19 years) with symptoms related to a unilateral pelvic mass that has often spread beyond the ovary at the time of diagnosis. Nearly all patients have an elevated serum AFP.

Grossly, yolk sac tumors have a smooth external surface and a median diameter of 15 cm. Their sectioned surface is predominantly solid with scattered cysts. The solid tissue may be light gray, tan, and/or yellow, and patches of hemorrhage and necrosis are typically present (Fig. 7.268). Polyvesicular vitelline areas may be apparent grossly as honeycombed, spongy foci.

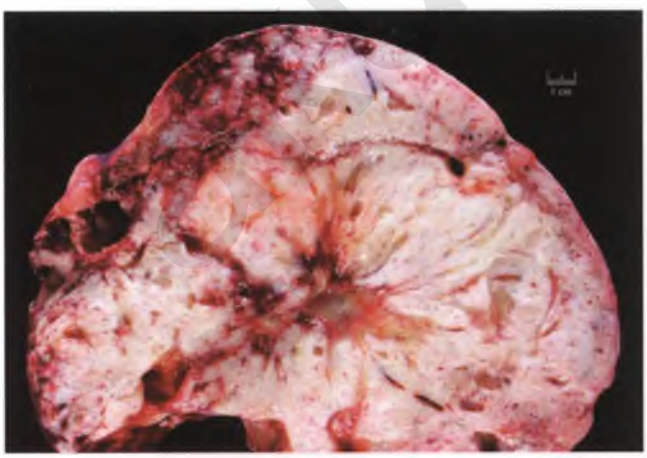

FIGURE 7.268. Yolk sac tumor. The sectioned surface is predominantly solid with scattered cysts. The solid areas are soft and gray with patches of hemorrhage and necrosis. (Courtesy of Dr. Colin J. R. Stewart.)

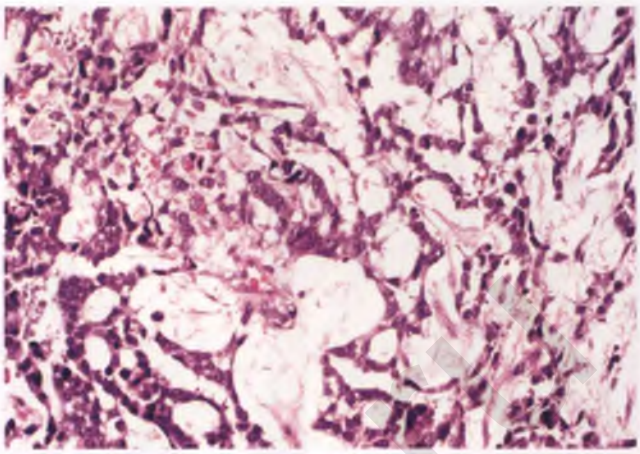

FIGURE 7.269. Yolk sac tumor with a reticular pattern.

Microscopically, yolk sac tumors are known for their variety of endodermal-related histologic patterns and their association with hyaline globules and Schiller-Duval bodies. The reticular/microcystic pattern is most common, and is characterized by a loose meshwork of interconnected spaces and small cysts that are lined by flattened to cuboidal tumor cells with a primitive appearance (Fig. 7.269). The pattern variously referred to as pseudopapillary, festoon, or endodermal sinus is the one in which pathognomonic **Schiller-Duval bodies** are found. These bodies, which are not required for a diagnosis of yolk sac tumor, consist of a small cystic space that partially to completely envelops a papillary structure that represents a cross section though a delicate fibrovascular core that is lined by a single layer of tumor cells (Fig. 7.270). Solid, polyvesicular vitelline, hepatoid, glandular (enteric or endometrioid-like), and nonspecific papillary patterns are seen less commonly (Figs. 7.271–7.275).[211,307,365] Many of these patterns are discussed in more detail in the section on differential diagnosis. In most cases, the reticular/microcystic pattern is admixed with one or more of the other patterns.

Although not specific for yolk sac tumors, **hyaline globules** are almost always present. These pink to light red globules may be intracellular or extracellular, range in size from 2 to 30 μm, are PAS-positive and diastase-resistant, and may be immunoreactive for AFP (Fig. 7.276). Extravasated red blood cells can be distinguished from hyaline globules by the presence of more obvious red blood cells in the vicinity, a more intense red color, a more uniform size, an exclusively extracellular location, and a contour that is not as smooth and round.

The distinctive immunophenotype of yolk sac tumors can greatly facilitate its recognition. In addition to at least focal immunoreactivity for AFP, these tumors are typically immunoreactive for glypican-3 and SALL4, and fail to stain for CK7, epithelial membrane antigen, CD117, CD30, and OCT4.[361,366–368]

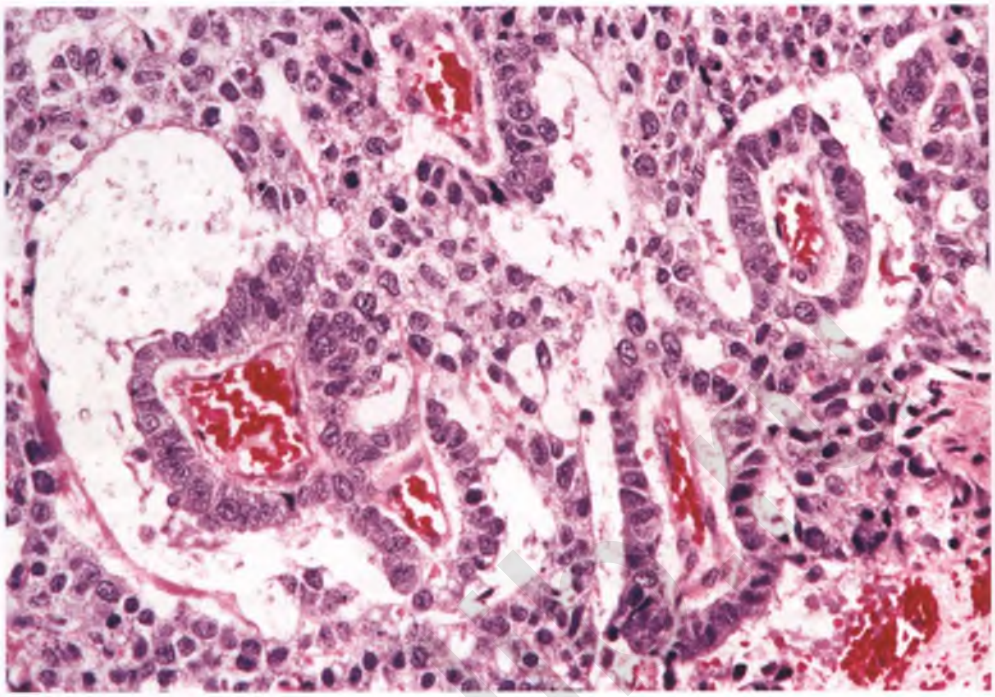

FIGURE 7.270. Yolk sac tumor with Schiller-Duval bodies.

Differential Diagnosis

The differential diagnosis is dependent upon the pattern of yolk sac tumor that predominates in a given case. Thorough sampling to identify typical areas of yolk sac tumor, rather than a battery of immunostains and expert consultation, may be all that is needed to make the correct diagnosis. Clinical findings, such as the young age of the patient and the presence of an elevated serum AFP, also help to exclude mimics of yolk sac tumor.

- Unlike yolk sac tumor, embryonal carcinoma is associated with an elevated serum β-hCG, does not have reticular, polyvesicular vitelline, hepatoid, or endometrioid-like patterns or the ability to form Schiller-Duval bodies in its repertoire, typically contains isolated syncytiotrophoblastic giant cells, has more "angry-appearing" nuclei, is immunoreactive for OCT4 and CD30, and fails to stain for glypican-3.[363,366,368]
- Dysgerminoma may enter the differential diagnosis when the solid growth pattern of yolk sac tumor predominates. In contrast to yolk sac tumor, the neoplastic cells of dysgerminoma are characteristically partitioned by delicate fibrous septa that are associated with a lymphoplasmacytic infiltrate, lack hyaline globules, and have an OCT4-positive, CD117-positive, AFP-negative immunophenotype.
- The microcystic, papillary, and solid patterns of yolk sac tumor often result in a resemblance to clear cell carcinoma. In contrast to clear cell carcinoma, yolk sac tumor occurs in a younger age

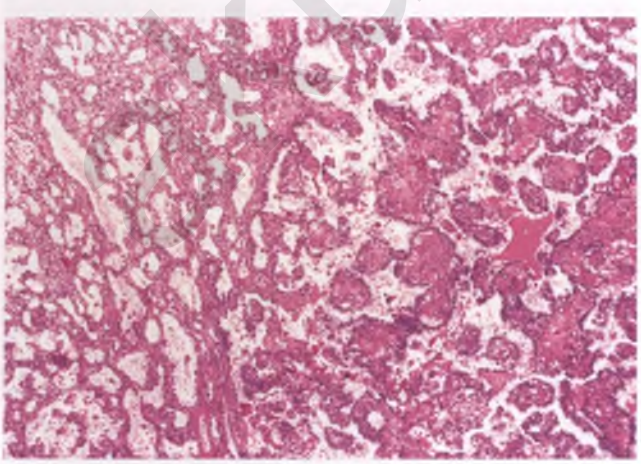

FIGURE 7.271. Yolk sac tumor with a nonspecific papillary pattern (right) adjacent to a microcystic area (left).

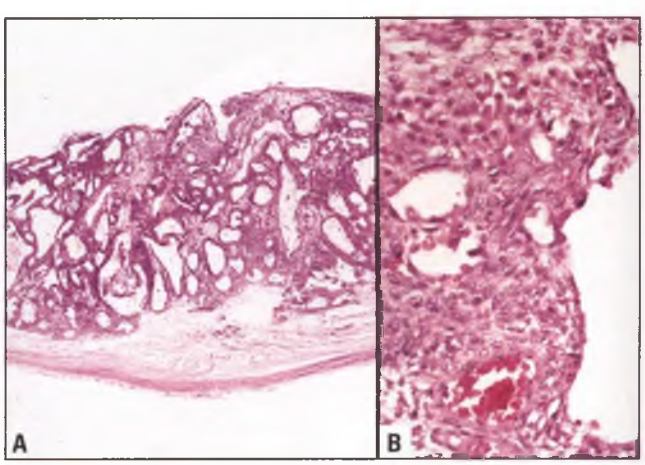

FIGURE 7.272. Yolk sac tumor with polyvesicular vitelline pattern. **A:** Multiple cystic spaces are present that are lined by flattened to cuboidal cells. **B:** This image highlights a focus with hepatoid differentiation.

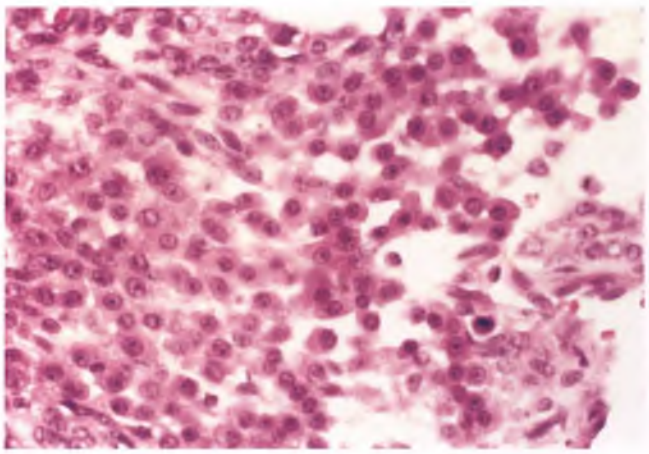

FIGURE 7.273. Yolk sac tumor with a hepatoid pattern.

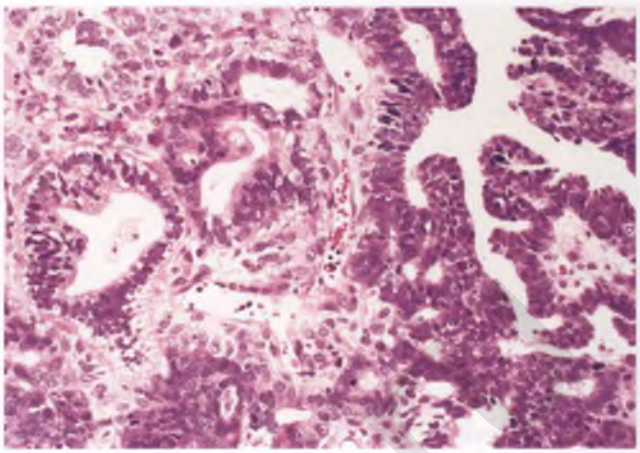

FIGURE 7.275. Yolk sac tumor with endometrioid-like glands. The glands at right exhibit a villoglandular pattern, and some of the glands at left are lined by cells with clear cytoplasmic vacuoles. When prominent, this latter pattern can result in a resemblance to endometrioid carcinoma with secretory differentiation.

group, is associated with an elevated serum AFP, often contains Schiller-Duval bodies, usually has areas that resemble a loosely constructed honeycomb network, has nonhyalinized papillary cores, is immunoreactive with AFP, glypican-3, and SALL4, and fails to stain for CK7 and epithelial membrane antigen.

- In contrast to endometrioid carcinoma, the endometrioid-like variant of yolk sac tumor occurs in a younger age group, is associated with an elevated serum AFP, is usually admixed with other patterns of more easily recognizable yolk sac tumor, frequently exhibits prominent subnuclear and/or supranuclear vacuoles, and lacks squamous morules, which should not be confused with islands of hepatoid differentiation.[307] Moreover, in keeping with its endodermal/yolk sac derivation, the endometrioid-like glands of this variant have an AFP-positive, CK7-negative, epithelial membrane antigen-negative immunophenotype, which is the exact opposite of that expected for endometrioid carcinoma. These immunostains can also be useful in identifying the combination of true endometrioid and yolk sac differentiation in those extraordinarily rare ovarian endometrioid carcinomas that occur in older women that contain a component of yolk sac tumor.[155,156]
- Hepatoid yolk sac tumors are so named because of their resemblance to tumors of hepatocytes that is imparted by a prominence of cells with abundant eosinophilic cytoplasm and centrally placed round nuclei with single large nucleoli. These cells are at least focally immunoreactive for AFP, and are often associated with hyaline globules. Hepatoid yolk sac tumors need to be distinguished from metastatic hepatocellular carcinoma, hepatoid carcinoma, oxyphilic clear cell carcinoma, steroid cell tumors, and metastatic melanoma. Clinical

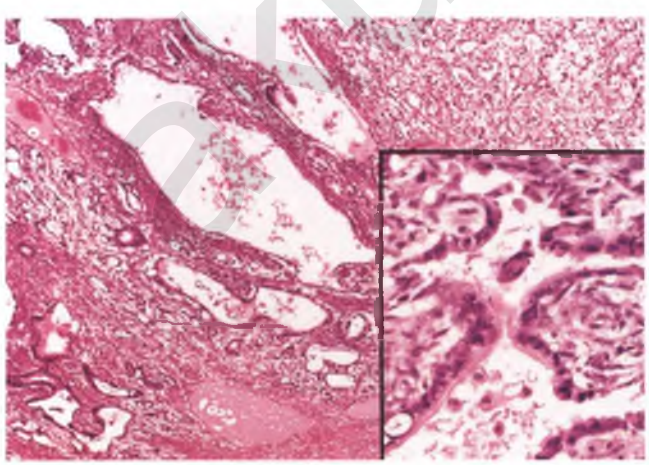

FIGURE 7.274. Yolk sac tumor with enteric-type glands admixed with a reticular pattern. The inset highlights a focus of glandular differentiation.

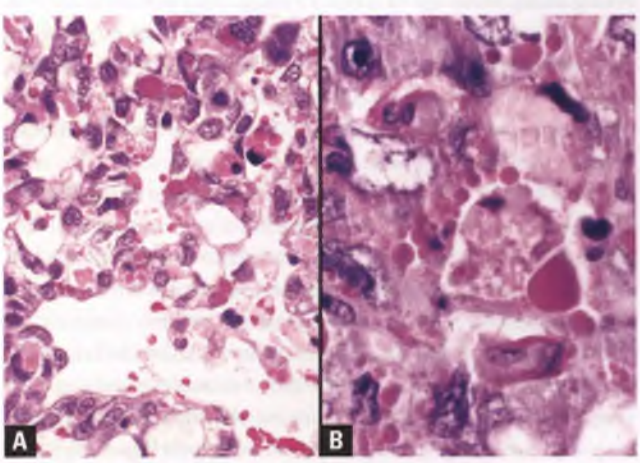

FIGURE 7.276. Yolk sac tumor. **A:** Multiple hyaline globules are evident, which need to be distinguished from the scattered red blood cells that are also in the vicinity. **B:** The hyaline globules are PAS-positive and diastase-resistant.

correlation that includes the age of the patient, prior oncologic history, association with hormonal abnormalities, and distribution of tumor will narrow the diagnostic possibilities considerably, with a focused panel of immunostains used in cases in which thorough sampling fails to reveal typical foci of yolk sac tumor (e.g., calretinin and/or inhibin to highlight steroid cells or CK7 and epithelial membrane antigen to confirm epithelial rather than germ cell origin). Without calretinin or inhibin immunohistochemistry, minor foci of hepatoid differentiation within a yolk sac tumor may be difficult to distinguish from clusters of luteinized stromal cells, but this distinction is only of academic interest.

- The polyvesicular vitelline variant of yolk sac tumor features the presence of multiple innocuous-appearing cysts, and may be mistaken for benign or borderline clear cell adenofibroma. However, other patterns of more typical yolk sac tumor are typically present, and the clinical and immunophenotypic features as discussed above assist in its recognition.

Prognosis

Stage is the most important prognostic factor. With modern chemotherapy, the vast majority of stage I tumors can now be cured, but the prognosis is less favorable for patients with stage III or IV disease and for those whose tumor cannot be optimally debulked.[369] Monitoring of serum AFP levels is useful to determine the efficacy of treatment and to detect disease recurrence. Limited experience with two extensively sampled yolk sac tumors with a *pure* polyvesicular vitelline pattern suggests that this variant may not behave in a malignant fashion.[365]

Embryonal Carcinoma[370]

The ovarian version of this tumor is much less common than its testicular counterpart, and is more often seen as a component of a mixed germ cell tumor than in pure form. It typically presents as a unilateral ovarian mass (mean size of nearly 16 cm) in children or young adults (mean age of about 15 years). Sixty percent of patients have symptoms related to excessive production of estrogens or androgens, and serum levels of AFP and β-hCG are usually elevated. At the time of presentation, tumor has spread beyond the ovary to other pelvic and/or abdominal sites in about 40% of cases. Although many patients died of disease in the only major series that has studied these tumors, this was prior to the era of modern chemotherapy.

Grossly, embryonal carcinoma has a smooth external surface and a predominantly solid sectioned surface that is soft and off-white to tan with interspersed areas of hemorrhage and/or necrosis. A variety of histologic growth patterns are usually present, with tumor cells forming solid sheets, nests, and papillae along with spaces that resemble glands or slits (Fig. 7.277). The tumor cells are mitotically active and have amphophilic cytoplasm with primitive-appearing nuclei that are large, rounded, pleomorphic, and in possession of one or more prominent nucleoli (Fig. 7.278). AFP-positive hyaline globules of the type commonly seen in yolk sac tumors may be present. The presence of occasional hCG-positive syncytiotrophoblastic giant cells within the stroma or in association with the tumor cell nests is a near-constant feature (Fig. 7.279).

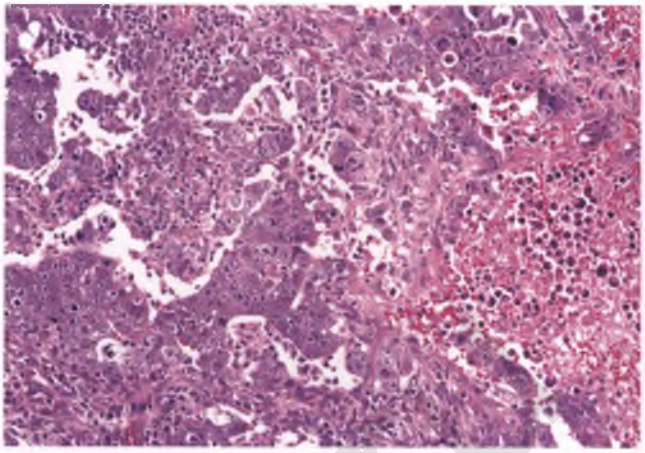

FIGURE 7.277. Embryonal carcinoma. Anaplastic tumor cells are seen forming papillae and slit-like spaces. An area of hemorrhage and necrosis is at right.

Although the immunoprofile of ovarian embryonal carcinoma is to some extent extrapolated from studies with testicular tumors of this type, the mononuclear embryonal cells can be presumed to exhibit a cytokeratin-positive, OCT4-positive, CD30-positive, SALL4-positive, hCG-negative, CD117-negative, epithelial membrane antigen-negative immunophenotype, which can help to distinguish this tumor from its mimics.[359,367,368,370,371] Such cells are also usually at least focally immunoreactive for AFP, whereas the syncytiotrophoblastic giant cells are AFP-negative.[372]

Differential Diagnosis

The differential diagnoses of embryonal carcinoma with dysgerminoma and yolk sac tumor are discussed in the sections on these other entities. Poorly differentiated adenocarcinomas occur in an older age group, lack evidence of AFP and hCG production, are more often bilateral, usually are immunoreactive

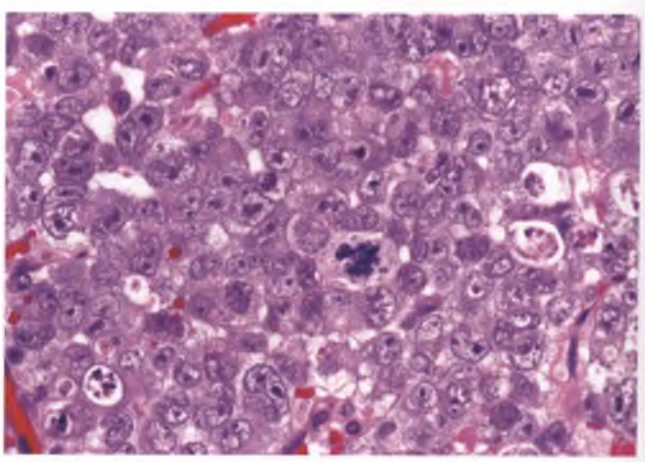

FIGURE 7.278. Embryonal carcinoma. This high-magnification view highlights the nuclear features, mitotic activity, and amphophilic cytoplasm of the malignant cells, and also shows the formation of a few gland-like spaces in an otherwise sheet-like area of solid growth.

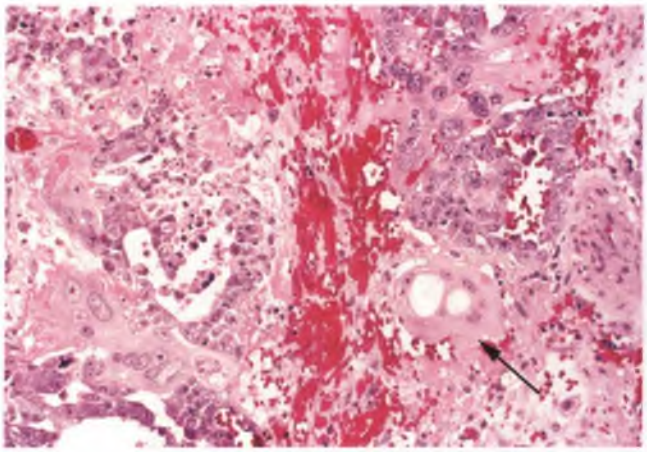

FIGURE 7.279. Embryonal carcinoma. Note the presence of occasional syncytiotrophoblastic giant cells, such as the vacuolated one marked by the *arrow*, in this partially hemorrhagic and necrotic neoplasm. These cells are characteristically immunoreactive for hCG (not shown), and are a common focal finding in these tumors.

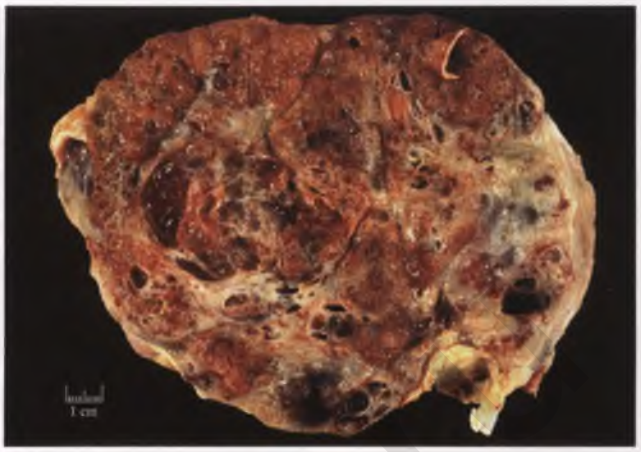

FIGURE 7.280. Polyembryoma. The sectioned surface is spongy and has a variegated reddish brown, tan, and light gray appearance. The bright yellow tissue at lower right represents a minor teratomatous component. (Altered from Jondle DM, Shahin MS, Benda JA. Ovarian mixed germ cell tumor with predominance of polyembryoma: a case report with literature review. *Int J Gynecol Pathol.* 2002;21:78–81. Altered and reprinted with permission from Dr. Jo Ann Benda and the International Journal of Gynecological Pathology.)

for epithelial membrane antigen, and have a less primitive appearance. Although the presence of syncytiotrophoblastic giant cells may suggest the diagnosis of choriocarcinoma, these cells in embryonal carcinoma are not abundant, are not associated with cytotrophoblast or intermediate trophoblast in the characteristic biphasic pattern of choriocarcinoma, and do not produce a frankly hemorrhagic mass like that typically seen in choriocarcinoma.

Polyembryoma

Polyembryoma is an extraordinarily rare malignant germ cell tumor that almost always occurs as the dominant component of a mixed germ cell tumor, with immature teratoma representing the most common other associated element.[373] These tumors typically present as a bulky ovarian mass in young adult women (mean age of 25 years) and are usually confined to the ovary at the time of diagnosis. Serum AFP and/or β-hCG may be elevated.

Grossly, polyembryomas have a mean size of about 17 cm and are composed of soft, tan to reddish brown tissue with interspersed spongy and hemorrhagic areas (Fig. 7.280). Histologically, polyembryomas are characterized by the presence of photogenic embryoid bodies, which recapitulate to varying degrees the bilaminar germ disc with associated amniotic and yolk sac cavities that are seen in embryos at approximately 2 weeks of development (Fig. 7.281).[373,374] Syncytiotrophoblastic giant cells are often seen in the vicinity of some of the embryoid bodies. The background stroma may be edematous, myxoid, or collagenous, and there are often admixed endodermal elements such as hepatic, intestinal, and pancreatic tissue (Fig. 7.282).

Polyembryomas are malignant tumors, presumably by virtue of their comingling with other primitive germ cell elements, but most patients are successfully treated with combination chemotherapy.

Nongestational Choriocarcinoma[375]

This is an extraordinarily rare tumor in pure form, but may occasionally be seen as a component of mixed germ cell tumor.[376] The few reported pure nongestational choriocarcinomas have occurred in children and young adults who present with symptoms and laboratory findings related to a β-hCG-producing ovarian mass (e.g., abdominal pain, vaginal bleeding, isosexual pseudoprecocity, and a false-positive pregnancy test).

As is typical of choriocarcinomas in all sites, these tumors are circumscribed, solid, and extensively hemorrhagic, and have not been reported to be bilateral. Histologically, choriocarcinomas feature a characteristic admixture of syncytiotrophoblastic cells and mononucleated trophoblast elements (Fig. 7.283), which is discussed and illustrated in more detail in Chapter 10.

Differential Diagnosis

The distinction of choriocarcinoma from a dysgerminoma or embryonal carcinoma that contains syncytiotrophoblastic giant cells is discussed in the sections on these other entities. Although histologically identical to gestational choriocarcinoma, nongestational choriocarcinoma can often be distinguished on the basis of other evidence, such as when (a) the patient is a premenarchal child, (b) extensive sampling reveals a mixed tumor with other germ cell elements, or (c) comparative DNA analysis fails to reveal the presence of paternally-derived gene sequences.[377] Note that although ovarian involvement by gestational choriocarcinoma is much more likely to represent a metastasis from a tumor of probable intrauterine origin, it can also be a primary tumor that is derived from an ectopic gestational event within

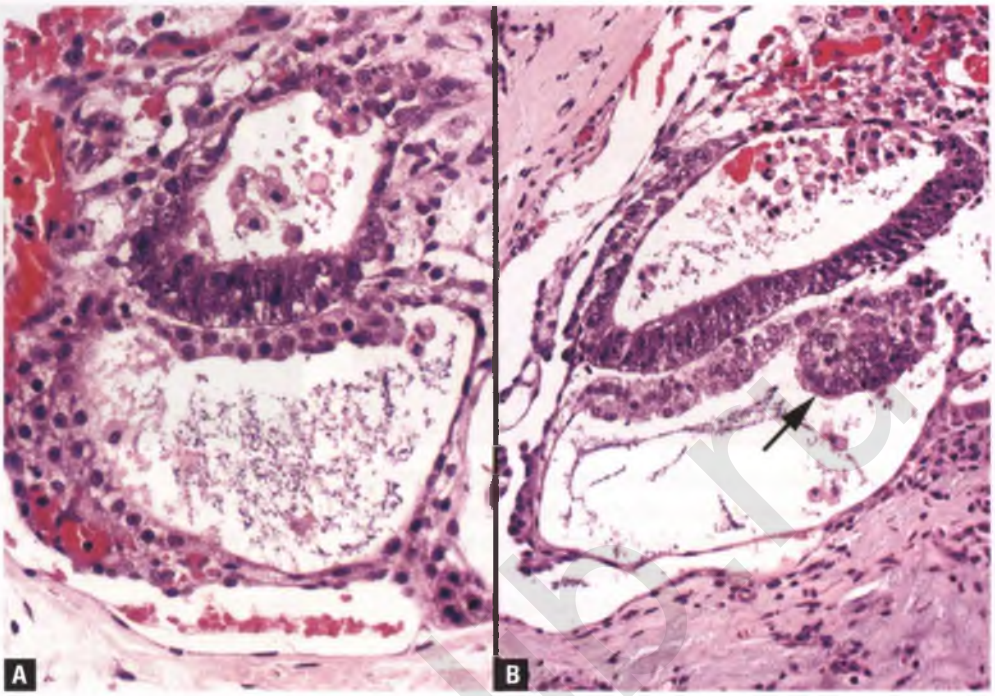

FIGURE 7.281. Polyembryoma. The classic embryoid body is composed of a bilaminar germ disc associated with two cavities. **A:** The amniotic cavity is on the side of the thicker and more darkly stained ectodermal cell layer, and the yolk sac cavity is on the side of the thinner endodermal cell layer. **B:** This embryoid body exhibits a focal nodular accumulation of cells within the endodermal cell layer (*arrow*). (Glass slide kindly provided by Dr. Jo Ann Benda.)

the ovary. Yet another extremely rare occurrence that is a differential diagnostic consideration is the presence of choriocarcinoma found in association with an ovarian epithelial-stromal tumor.[378] These tumors occur in an older age group and are readily distinguished by their other components.

Malignant Mixed Germ Cell Tumor[376]

Occasional ovarian tumors feature more than one type of germ cell malignancy (e.g., dysgerminoma admixed with yolk sac tumor). In such cases, a diagnosis of malignant mixed germ cell tumor is issued, and the type and approximate proportion of each component should be stated in the diagnosis line of the pathology report. Tumors of this type account for roughly 10% of malignant germ cell tumors of the ovary.

Gonadoblastoma[379,380]

Gonadoblastoma is a rare tumor composed of an admixture of germ cell and sex cord-stromal elements. It characteristically occurs in children and young adults who have pure or mixed gonadal dysgenesis and at least some Y chromosomal material (more specifically, the TSPY1 gene from the GBY locus), although there are occasional exceptions.[381] Most patients are

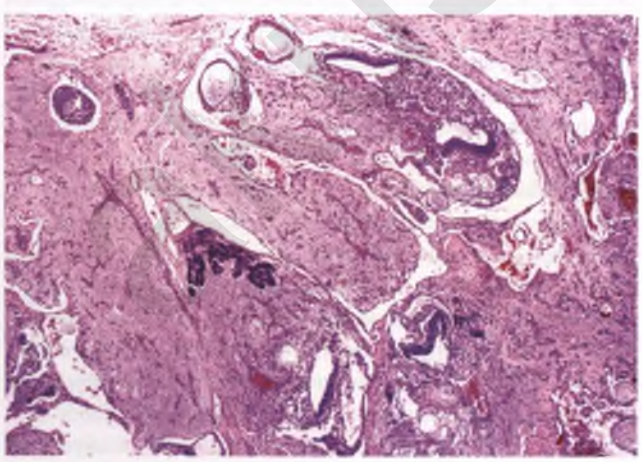

FIGURE 7.282. Polyembryoma. The background stroma is myxoid and contains scattered imperfectly formed embryoid bodies. The clustered cords of darkly-stained cells near left of center are fetal-type hepatocytes. (Glass slide kindly provided by Dr. Jo Ann Benda.)

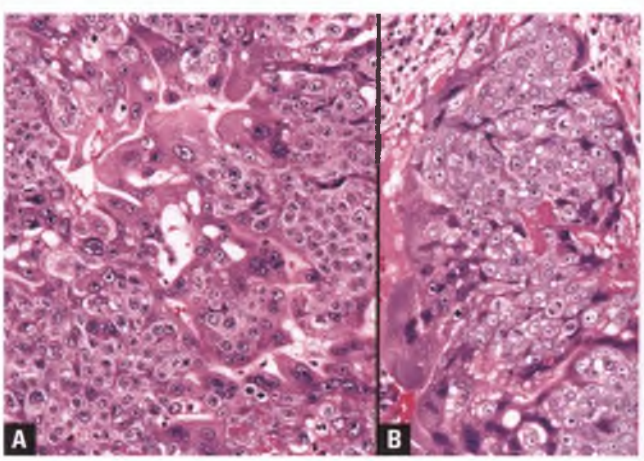

FIGURE 7.283. A,B: Choriocarcinoma. Note the characteristic biphasic pattern that is produced by the comingling of mononucleated cytotrophoblastic and multinucleated syncytiotrophoblastic cells.

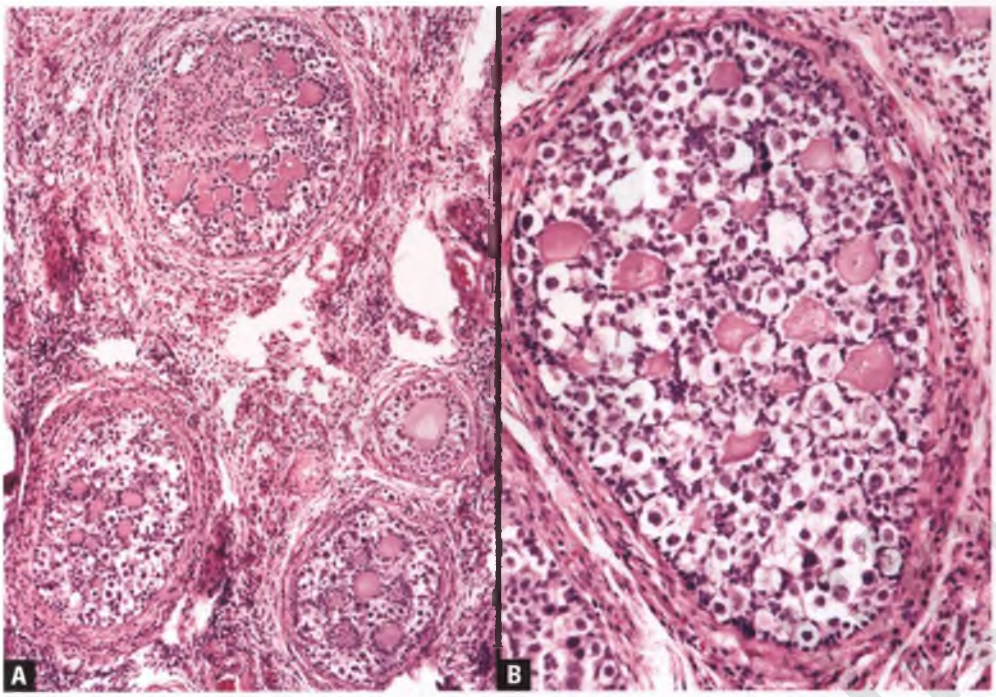

FIGURE 7.284. A,B: Gonadoblastoma. Discrete nests of tumor cells are present within a fibrous stroma. The nests are punctuated by rounded accumulations of eosinophilic hyaline material. The dysgerminoma-like germ cells have large vesicular nuclei, distinct nucleoli, and abundant clear cytoplasm, whereas the small, bland cells of sex cord origin are concentrated around the periphery of the nests and around the deposits of eosinophilic hyaline material. Although not easily visualized in these images, aggregates of luteinized or Leydig-like cells are present within the stroma.

phenotypic females with some degree of virilization. Approximately one-third of tumors are bilateral, and the size of pure gonadoblastoma ranges from an unsuspected microscopic finding to a tumor up to 8 cm in diameter. Calcification, which may be extensive, occurs in 80% of cases. Sixty percent of cases are complicated by overgrowth by an invasive germ cell component. Given these commonly present alterations, it is not surprising that the gross appearance of gonadoblastoma is quite variable.

Histologically, gonadoblastomas are composed of discrete cellular nests that represent an admixture of dysgerminoma-like germ cells and small, bland, mitotically inactive cells of sex cord type (Fig. 7.284). The sex cord cells are typically seen rimming the periphery of the nests (coronal pattern), encircling round spaces filled with eosinophilic hyaline material that are located within the internal aspect of the nests (Call-Exner-like pattern), and surrounding individual germ cells (follicular pattern reminiscent of the primary ovarian follicle). The tumor cell nests are separated by variable amounts of fibrous stroma, which often contain focal aggregates of luteinized or Leydig-like cells. The process of calcification can often be seen evolving from the hyalinization, expansion, and lamination of the internal rounded aggregates of eosinophilic material, which can result in the formation of mulberry-like structures (Fig. 7.285). As is the case for dysgerminoma, the neoplastic germ cells of gonadoblastoma demonstrate nuclear immunoreactivity for OCT4.[290]

Gonadoblastoma can be considered an in situ form of malignant germ cell tumor. Its distinctive pattern has never been observed in metastatic deposits. When associated with an invasive germ cell tumor, that tumor is a dysgerminoma in 80% of cases (Fig. 7.286).

Differential Diagnosis

The tumor that is most likely to be confused with gonadoblastoma is the SCTAT. As illustrated in Figures 7.219 and 7.220, SCTAT and gonadoblastoma have similar architectural patterns, but SCTAT lacks the germ cells and history of an underlying gonadal disorder that characterize gonadoblastoma. Moreover, the germ cell component of gonadoblastoma can be highlighted using OCT4 immunohistochemistry, whereas SCTATs are OCT4-negative.[290]

Mixed Germ Cell-Sex Cord-Stromal Tumor[380]

As is the case for gonadoblastoma, these extremely rare tumors are composed of an intimate admixture of germ cells and sex cord-stromal elements. However, the distinctive nested pattern,

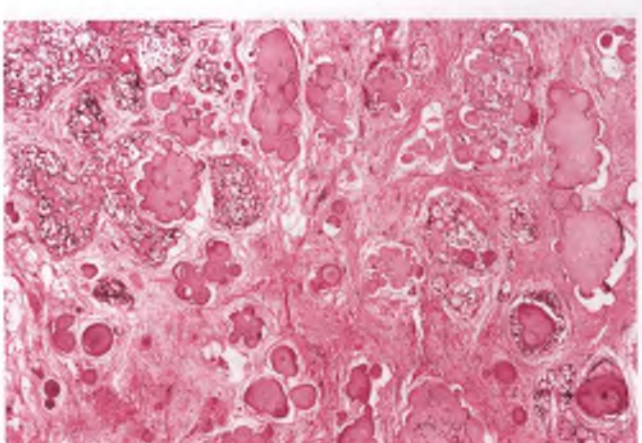

FIGURE 7.285. Gonadoblastoma with extensive hyalinization. Note the characteristic mulberry shape of many of these deposits, their origin from the smaller deposits within tumor cell nests, and their laminations as they evolve into calcifications.

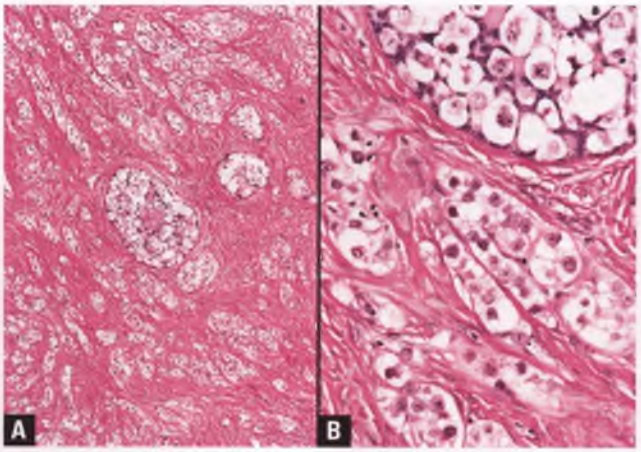

FIGURE 7.286. Gonadoblastoma associated with dysgerminoma. **A:** A few large nests of residual gonadoblastoma are present within a fibrous stroma that contains numerous smaller nests and clusters of invasive dysgerminoma. **B:** In this high-magnification view, small nests of invasive dysgerminoma are seen beneath a portion of a large nest of gonadoblastoma.

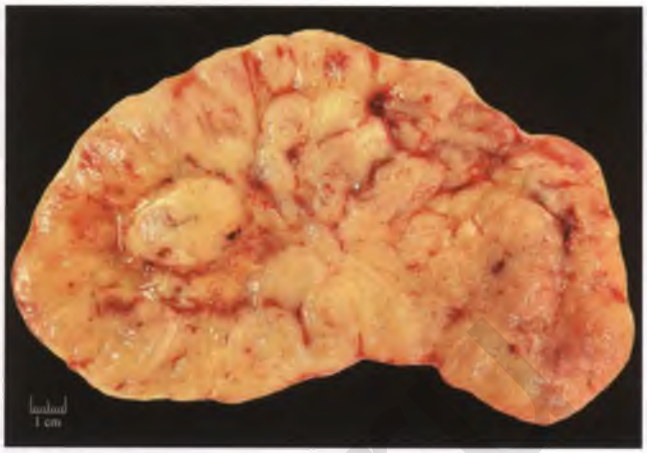

FIGURE 7.287. Ovarian lymphoma. The sectioned surface of this diffuse large cell lymphoma is solid, fleshy, lobulated, and light tan to pale yellow. (Courtesy of Dr. Colin J. R. Stewart.) Note: ovarian dysgerminomas have a similar macroscopic appearance (see Figure 7.263).

rounded aggregates of eosinophilic hyaline material, and calcifications of gonadoblastoma are absent, and the young patients (usually <10 years of age) are genetically normal females. Instead of nests, the tumor cells grow in trabecular, solid tubular, and/or diffuse patterns, and proliferative activity may be observed in the sex cord component. These tumors may be associated with dysgerminoma, or rarely another type of malignant germ cell tumor, but this is an uncommon finding. Unlike gonadoblastoma, the mixed germ cell-sex cord-stromal tumor occasionally exhibits malignant behavior in the absence of a superimposed malignant germ cell tumor of another type.

HEMATOPOIETIC TUMORS

Malignant Lymphoma[236,362,382,383]

Malignant lymphoma rarely presents as an ovarian mass. Even when it does so, most such cases are judged to be manifestations of systemic disease, as evidenced by the high frequency of bilaterality (>50%) and involvement of regional lymph nodes, fallopian tubes, omentum, peritoneum, and other miscellaneous sites. Most patients present with symptoms related to an ovarian mass in one of two settings: a middle-aged adult with diffuse large cell lymphoma or a child/young adult with Burkitt's lymphoma, although exceptions to these generalizations occur and other types of lymphoma are also seen on occasion.

Ovaries involved by malignant lymphoma have an average size of about 12 cm and have a gross appearance that is similar to that previously described for dysgerminoma (Fig. 7.287). As in some other extranodal sites, the diffuse large cell lymphomas tend to be associated with sclerosis, which can partition the tumor cells and create pseudoepithelial patterns. Nearly all lymphomas that involve the ovary, whether primary or secondary, are of B-cell lineage. Examples of diffuse large cell lymphoma, the immunoblastic variant of diffuse large cell lymphoma, and Burkitt's lymphoma are presented in Figures 7.288–7.290.

Differential Diagnosis

Once the possibility of malignant lymphoma enters the differential diagnosis, it can be readily confirmed or refuted with the use of immunostains for lymphoid markers. The most common differential diagnostic considerations are dysgerminoma, undifferentiated carcinoma, SCCHT, AGCT, metastatic breast carcinoma, and extramedullary granulocytic sarcoma, which are discussed elsewhere in this chapter.

Prognosis

Those few patients with disease confined to one ovary can be considered primary ovarian lymphomas, and these patients have a good prognosis (5-year survival of roughly 80%) when treated by surgical excision and chemotherapy.[383] With more extensive disease, the 5-year survival rate drops to about 33%.[383]

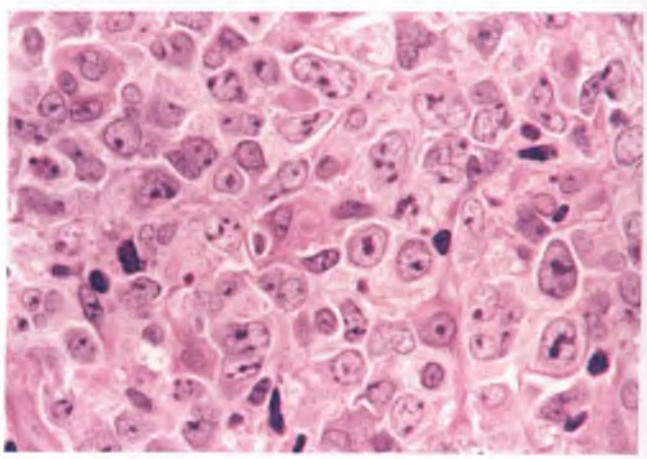

FIGURE 7.288. Diffuse large cell lymphoma.

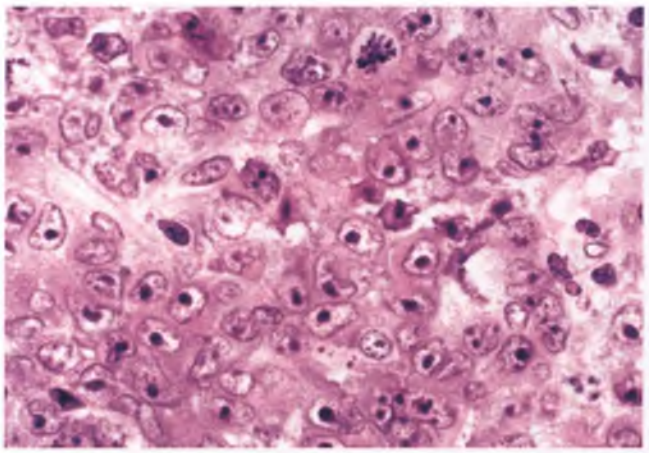

FIGURE 7.289. Immunoblastic lymphoma. Note the single prominent central nucleoli in many of the tumor cells.

Leukemia[384]

Very rarely, granulocytic sarcoma presents as an ovarian mass. When evaluated, most such patients have hematologic evidence of acute myelogenous leukemia or will develop this disease if left untreated. Although these tumors can be difficult to distinguish from malignant lymphoma, the presence of at least some cells that are recognizable as precursors of eosinophils is an important diagnostic clue (Fig. 7.291). Further confirmatory evidence of the granulocytic nature of the disease process can be obtained via a positive chloroacetate esterase stain or by demonstrating immunoreactivity for lysozyme or myeloperoxidase.

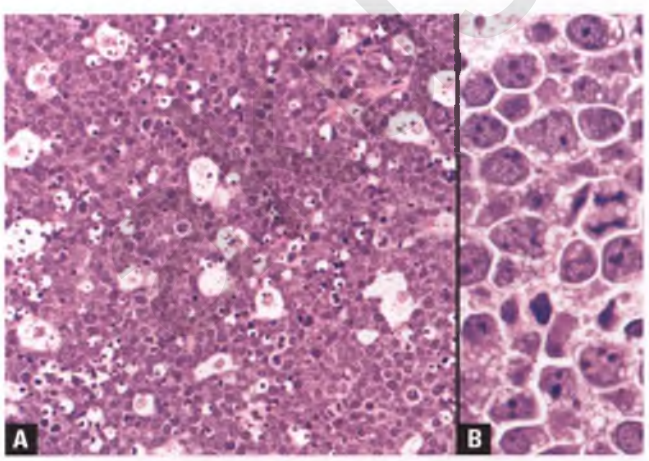

FIGURE 7.290. Burkitt's lymphoma. **A:** The presence of scattered tingible-body macrophages engulfing apoptotic debris produces the so-called starry sky pattern. **B:** The tumor cells are fairly uniform and of intermediate size. Note how many of the cells have (a) two or more small nucleoli, (b) squared-off cell borders that result in a pattern in which the cells fit together like pieces of a jigsaw puzzle, and (c) cytoplasmic vacuoles, which are often only apparent in touch preparations.

Although acute lymphoblastic leukemia has not been reported to present as an ovarian mass, the ovary is rarely the site of a clinically apparent recurrence (Fig. 7.292).

Plasmacytoma

A few cases of primary ovarian plasmacytoma have been reported.[385] The neoplasm is composed of sheets of plasma cells with a degree of maturity that varies from case to case (Fig. 7.293). Once the diagnosis is suspected, it can be confirmed by obtaining immunoreactivity for the plasma cell marker CD138 and demonstrating light chain restriction. Patients should be evaluated for the presence of multiple myeloma and monoclonal paraproteins in their blood and urine. Progression to myeloma has been reported.

MISCELLANEOUS OVARIAN TUMORS

These rare ovarian tumors are of diverse origin. In addition to the tumors discussed under this heading as outlined at the beginning of this chapter, other extraordinarily rare tumors within this group include adenomatoid tumor,[386,387] myxoma,[388] paraganglioma,[389] glomus tumor,[390] Wilms' tumor,[391] gestational choriocarcinoma[375,377] or hydatidiform mole[392] arising within an ectopic ovarian pregnancy, and placental site trophoblastic tumor.[393] Some of the tumors that the WHO includes in this category that are of definite or probable epithelial-stromal origin are discussed in the section on miscellaneous epithelial-stromal tumors.

Small Cell Carcinoma, Hypercalcemic Type[233,394]

SCCHT is a rare, aggressive tumor that typically presents as a unilateral ovarian mass (average size of 15 cm) in a young woman (mean age of 24 years). Two-thirds of patients have hypercalcemia, although symptoms related to hypercalcemia are rarely present. Serum calcium levels return to normal after removal of the tumor. It is noteworthy that rare familial cases of bilateral SCCHT have been reported.

The external surface of SCCHT is smooth or nodular, and sectioning reveals predominantly solid, light tan to pale yellow tissue with patches of hemorrhage, necrosis, and/or cystic degeneration (Fig. 7.294A). Histologically, classic cases feature sheets of small, monomorphic, closely packed, mitotically active cells with scant cytoplasm (Fig. 7.294B). The tumor cells may also form nests and cords in areas where there are appreciable amounts of stroma. A characteristic finding, which is seen at least focally in 80% of cases, is the presence of follicle-like spaces that usually contain lightly eosinophilic fluid (Fig. 7.295).

Somewhat confusingly, larger cells with more abundant eosinophilic cytoplasm and prominent nucleoli are frequently present in variable amounts in SCCHT, and rarely may predominate (at which point clinicians may be left scratching their heads when informed of the diagnosis of the large cell variant of SCCHT). Another potential source of confusion is the presence of cysts or glands that are lined by mucinous epithelium, which is seen in about 10% of cases.

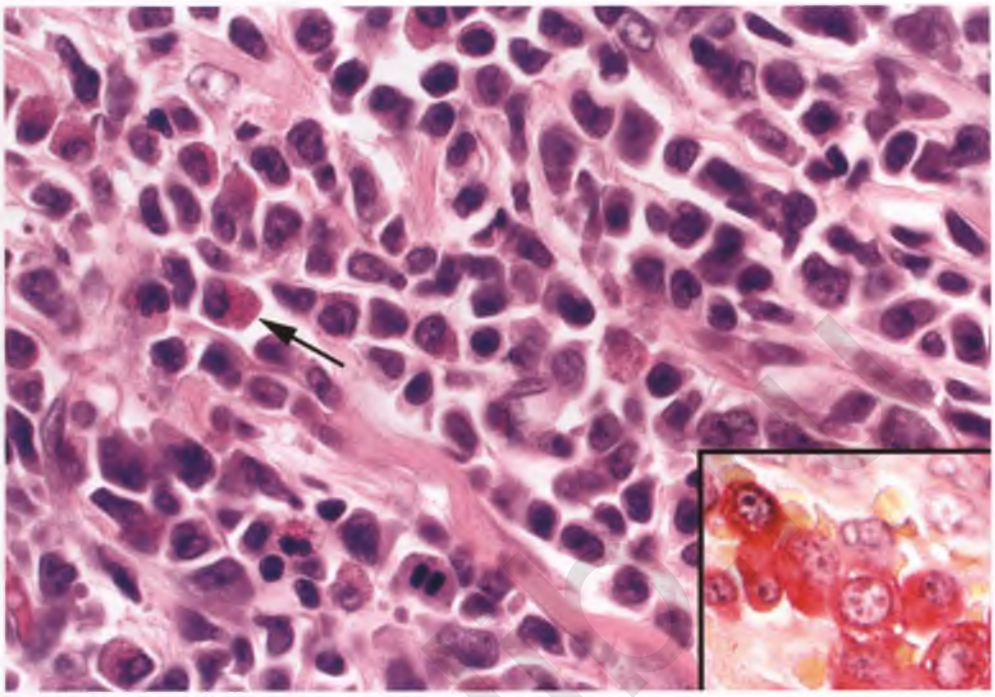

FIGURE 7.291. Extramedullary granulocytic sarcoma. The presence of cells with abundant eosinophilic granules, such as the one marked by the *arrow*, is an important diagnostic clue. The inset shows the result of a chloroacetate esterase stain, which highlights the presence of several cells with granulocytic differentiation.

SCCHTs are of presumed epithelial origin and often express cytokeratin, epithelial membrane antigen, and WT-1, and typically lack immunoreactivity for inhibin and TTF-1.[233,395,396]

Differential Diagnosis

The differential diagnosis of SCCHT is broad and includes the adult and juvenile types of granulosa cell tumor and small cell carcinoma of pulmonary type, as discussed in the sections on these other entities. Malignant lymphoma can be excluded by noting the presence of follicle-like spaces and the lack of immunoreactivity for leukocyte common antigen. Metastatic melanoma shares with SCCHT the ability to form follicle-like spaces, and can be particularly difficult to distinguish on morphologic grounds from the so-called large cell variant of SCCHT.[241,394] Features that favor metastatic melanoma include a prior history of melanoma, normal serum calcium levels, bilaterality, intranuclear pseudoinclusions, identification of melanin pigment, and immunoreactivity for one or more melanoma markers (S100, HMB-45, or Melan-A) in conjunction with negative staining for cytokeratin and epithelial membrane antigen.[233,241]

Behavior and Prognosis

When carefully staged, most patients with SCCHT are found to have extraovarian spread at the time of presentation, and the prognosis for such patients is dismal. Even those patients diagnosed initially with stage Ia disease have a recurrence rate of 67%.

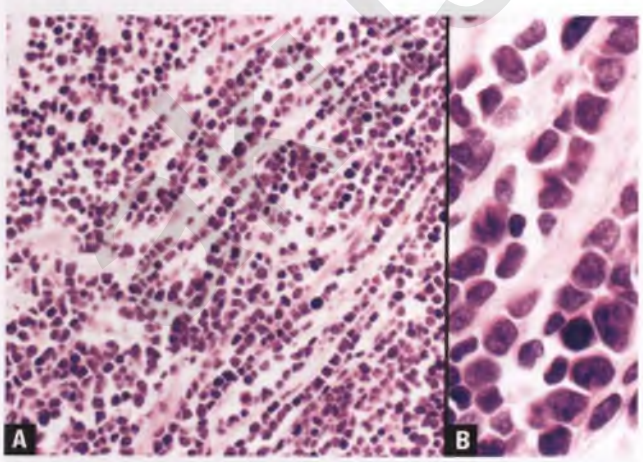

FIGURE 7.292. **A,B:** Ovary with relapsed acute lymphoblastic leukemia. Although the single-file pattern of portions of the leukemic infiltrate simulates metastatic lobular carcinoma of the breast, the latter diagnosis is easily excluded by clinical history, laboratory data, and immunohistochemical profile.

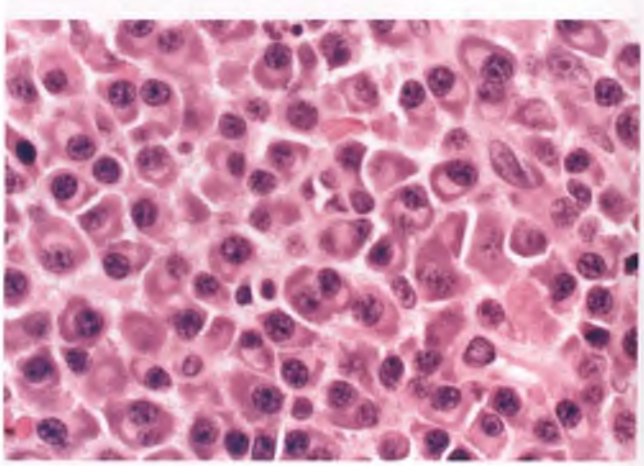

FIGURE 7.293. Plasmacytoma.

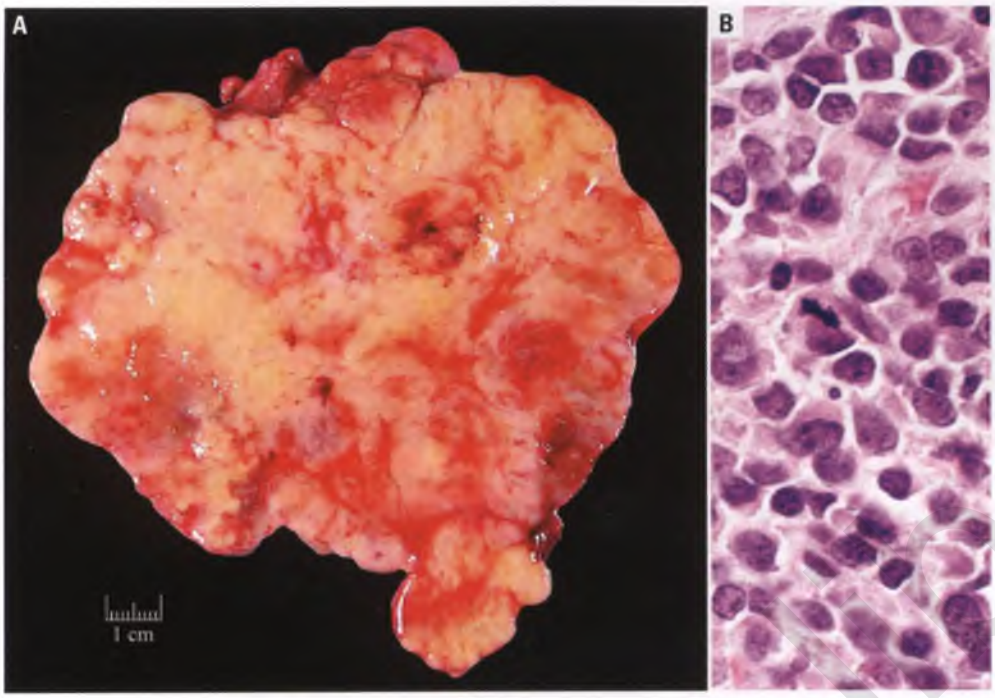

FIGURE 7.294. Small cell carcinoma, hypercalcemic type. **A:** The sectioned surface of this solid tumor is light tan to pale yellow with splotchy hemorrhagic areas. **B:** The tumor cells have a primitive appearance and are mitotically active. (Gross photograph courtesy of Dr. Colin J. R. Stewart.)

Small Cell Carcinoma, Pulmonary Type[151]

This rare type of ovarian cancer has a poor prognosis and usually presents as an ovarian mass (mean size of 14 cm) in an adult woman (mean age of 59 years). These tumors are frequently bilateral, and most have spread beyond the ovary at the time of presentation. The sectioned surface of involved ovaries is predominantly solid, gray-white to tan, and often exhibits foci of necrosis. Histologically, these tumors usually are associated with a component of an epithelial-stromal neoplasm, which is most commonly endometrioid carcinoma (Fig. 7.296). The small cell component resembles the intermediate variant of the much more commonly encountered small cell neuroendocrine carcinoma of the lung (Fig. 7.297).

Differential Diagnosis

In contrast to many small cell carcinomas of hypercalcemic type, these tumors occur in an older age group, are frequently bilateral, are not associated with hypercalcemia, are usually associated with a recognizable type of epithelial-stromal tumor, rarely form follicle-like spaces, lack a large cell component, and typically are immunoreactive for TTF-1 and fail to stain with WT-1.[396] Metastatic small cell carcinoma involving the ovary usually occurs in patients with a known history of a pulmonary or other extraovarian

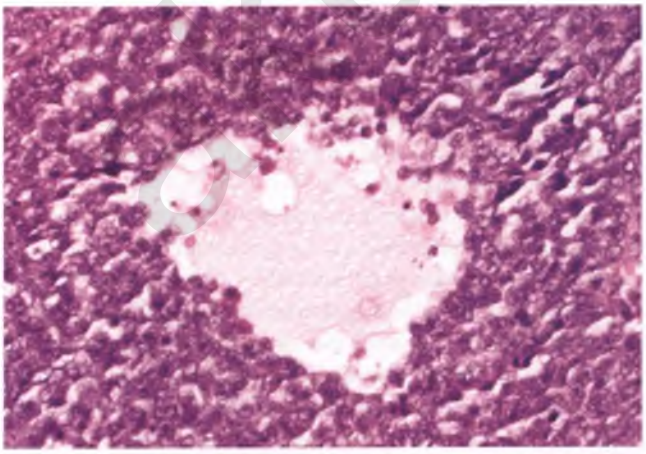

FIGURE 7.295. Small cell carcinoma, hypercalcemic type. The presence of follicle-like spaces is a characteristic feature of this neoplasm, but may be a focal finding.

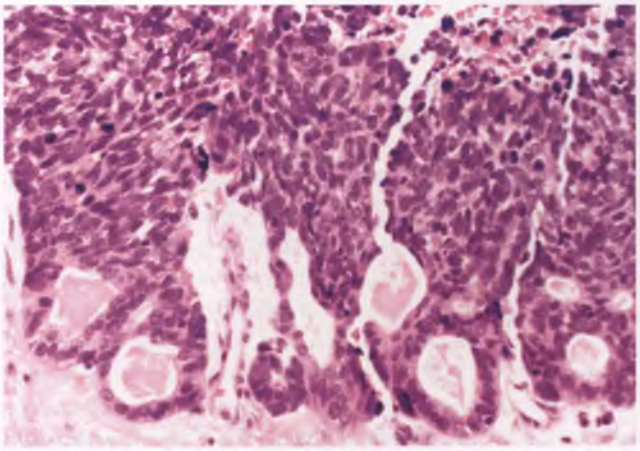

FIGURE 7.296. Ovarian small cell carcinoma, pulmonary type. The small cell component is seen merging with well-formed glands of endometrioid carcinoma near the bottom of the image.

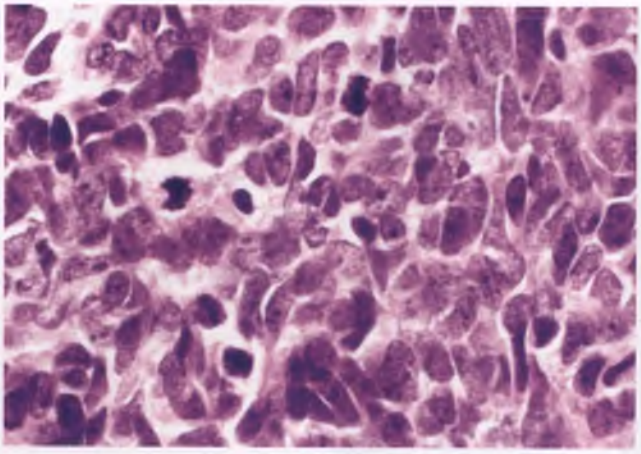

FIGURE 7.297. Ovarian small cell carcinoma, pulmonary type. The malignant cells of the small cell component vary in shape and have scant cytoplasm with stippled chromatin and nucleoli that are generally inconspicuous. Brisk mitotic activity and nuclear molding are additional characteristic features.

primary tumor of this type or radiologic evidence of a pulmonary mass, lacks a component of an epithelial-stromal neoplasm, and usually presents as part of widespread metastatic disease.[397,398] The section on endometrioid carcinoma with spindle cell differentiation discusses its distinction from small cell carcinoma of pulmonary type with associated endometrioid carcinoma.

Large (Nonsmall) Cell Neuroendocrine Carcinoma[399,400]

This tumor represents yet another rare type of aggressive ovarian cancer. It typically presents as a unilateral ovarian mass (mean size of about 15 cm) with extraovarian spread in an adult woman (mean age of roughly 50 years). The strong association of large cell neuroendocrine carcinoma with epithelial-stromal tumors (usually of mucinous or endometrioid type) and less frequent association with mature cystic teratomas suggest that it arises from the occasional neuroendocrine cells that are present within these other tumor types.

The sectioned surface of large cell neuroendocrine carcinoma has a variably prominent cystic component, and typically is extensively necrotic. Histologically, areas with sheet-like, nested, and/or trabecular patterns of growth with little intervening stroma are seen admixed with patches of necrosis (Fig. 7.298). The constituent cells are of intermediate to large size, have high mitotic rates, and typically have round to oval nuclei with prominent nucleoli and appreciable amounts of cytoplasm (Fig. 7.299). At least focal immunoreactivity with one or more neuroendocrine markers such as chromogranin or synaptophysin is a definitional feature. The frequent association of this tumor with an epithelial-stromal neoplasm, areas with nested and/or trabecular architecture, and high-grade nuclear features with extensive areas of necrosis should suggest the diagnosis, which can be confirmed by immunohistochemistry.

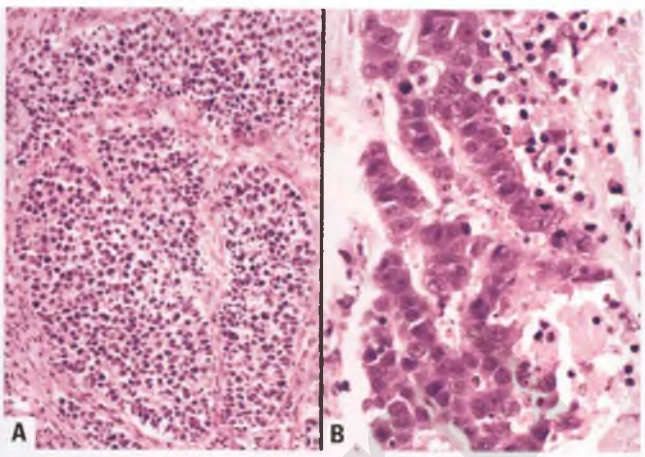

FIGURE 7.298. Large cell neuroendocrine carcinoma. **A:** Nested architecture. **B:** Trabecular pattern with adjacent necrosis.

Ovarian Tumor of Probable Wolffian Origin[282]

The ovarian version of this very rare tumor typically occurs in adult women who present with a unilateral ovarian mass that has an average size of 12 cm. The ovarian-based mesonephric (wolffian) remnants from which these tumors presumably arise are thought to correspond to the rete ovarii within the hilum. The gross appearance, microscopic features, and clinical behavior of this generally benign tumor are identical to its counterpart in the broad ligament (see Chapter 5).

Differential Diagnosis

When this tumor presents in the ovary, it has a wider differential diagnosis than corresponding tumors within the broad ligament. As presented below, tumors that can resemble ovarian wolffian tumors include Sertoli cell tumor, endometrioid carcinoma, cellular fibroma, granulosa cell tumor, and ependymoma.

- Ovarian wolffian tumors may be confused with Sertoli cell tumors due to the overlapping histologic features of the tubules present in these two neoplasms. However, the combination of diffuse, sieve-like, and tubular patterns in ovarian wolffian tumors usually allows for their distinction from Sertoli cell tumors, which tend to exhibit a more monotonous tubular pattern.
- Some endometrioid carcinomas that have areas in which small tubules predominate can resemble ovarian wolffian tumors, but are distinguished by the presence of small amounts of mucicarmine-positive intraluminal mucin, their common association with foci of squamous differentiation, the presence of other areas in which the glands are more characteristic of usual endometrioid adenocarcinoma, the absence of a sieve-like pattern, and by their immunoreactivity for epithelial membrane antigen.[401]
- Some ovarian wolffian tumors have prominent areas composed of sheets of densely cellular spindle cells that can result in misinterpretation as a cellular fibroma.[402] In sufficiently

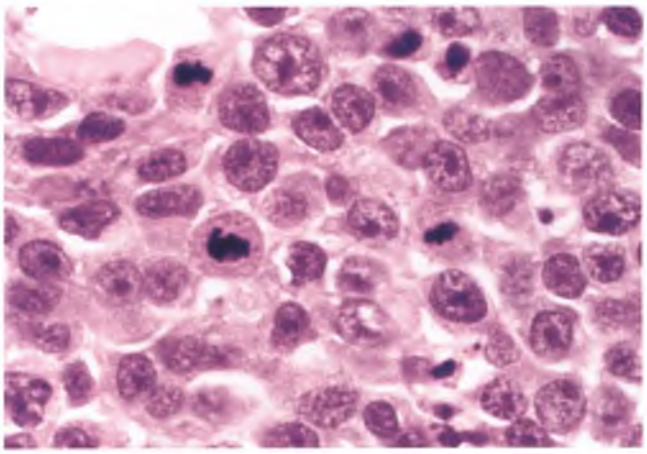

FIGURE 7.299. Large cell neuroendocrine carcinoma. As in most examples of this tumor, the cells are large and mitotically active with round to oval nuclei, prominent nucleoli, and appreciable amounts of cytoplasm.

sampled ovarian wolffian tumors, more diagnostic patterns will become apparent.

- Taken in isolation, foci of ovarian wolffian tumors with diffuse patterns of growth can also resemble AGCTs, but the constituent cells of wolffian tumors do not exhibit the prominent nuclear grooves that are characteristic of granulosa cell tumors and will form more characteristic patterns elsewhere in the neoplasm.
- Ovarian ependymoma can resemble an ovarian wolffian tumor, but is distinguished by the presence of perivascular pseudorosettes and immunoreactivity for glial fibrillary acidic protein.[352,403]

Tumors of the Rete Ovarii[404,405]

Tumors of the rete ovarii are uncommon. Most such tumors are cystadenomas, which are arbitrarily defined as rete cysts that have attained a diameter of ≥1 cm. They occur in adult women who usually present with a pelvic mass with an average size of 9 cm, sometimes in association with androgenic manifestations. These tumors are usually unilocular and are hilar-based, but may extend into the medulla. They are filled with clear to yellow fluid.

Histologically, rete cystadenomas have thin walls with a smooth internal surface that is lined by a single layer of epithelial cells that may have a flattened, cuboidal, or columnar appearance. Although often misdiagnosed as serous cystadenomas, rete cystadenomas can be recognized by their hilar location, the frequent presence of bundles of smooth muscle and bands of hyperplastic hilus cells within their walls, their characteristic formation of epithelial-lined crevices, an epithelial lining that either lacks or contains only rare ciliated cells, and the common finding of normal rete ovarii in the adjacent tissue (Fig. 7.300).

Adenomas and adenocarcinomas of the rete ovarii occur at case-reportable frequencies and are discussed further in the references provided.

Solid Pseudopapillary Neoplasm[406]

It has recently become apparent that this neoplasm, which is better known in the pancreas, can rarely occur as a primary ovarian tumor. In this site, this tumor tends to present in young adult women as a well-circumscribed pelvic mass that has both solid and cystic components. The ovarian solid pseudopapillary neoplasm is histologically and immunologically identical to its pancreatic counterpart, which is also quite uncommon. The name of the tumor is derived from the propensity of the cells within the solid and delicately vascular component of the tumor to partially dissociate, which results in the formation of pseudopapillae comprised of cells clinging to the vascular framework (Fig. 7.301). The nuclei of the neoplastic cells are monotonous, bland, round to oval, and mitotically inactive with pale chromatin, small nucleoli, and occasional longitudinal grooves. Cytoplasm is moderate in amount and may be pale, eosinophilic, vacuolated, or foamy. Variably-sized eosinophilic globules are usually present, at least focally (Fig. 7.302).

An awareness that solid pseudopapillary tumors can occur in the ovary, coupled with its characteristic immunophenotype (nuclear immunoreactivity with β-catenin and lack of staining for e-cadherin, inhibin, calretinin, thyroglobulin, and chromogranin), facilitates the distinction of this tumor from sex-cord stromal tumors, steroid cell tumors, struma ovarii, and carcinoid tumors. In the pancreas, these tumors are regarded as low-grade malignancies with an excellent prognosis; although the same can be expected for the ovarian version of these tumors, sufficient follow-up information is currently lacking.

Leiomyoma[407,408]

Ovarian leiomyomas are rare, and are generally thought to arise from the smooth muscle that is present within the walls of the hilar blood vessels. In keeping with this theory, many of the smaller leiomyomas that are removed when ovarian

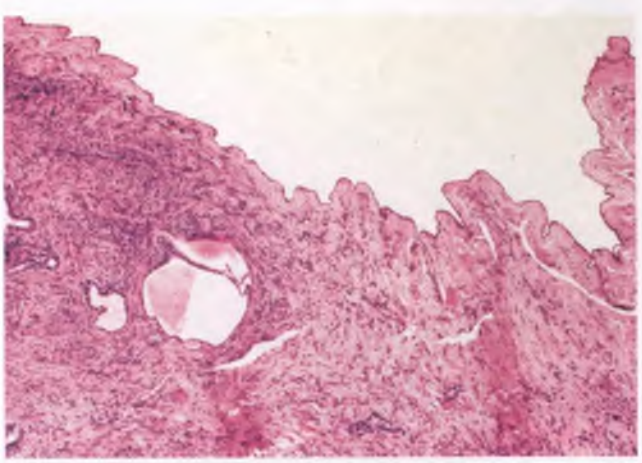

FIGURE 7.300. Rete cystadenoma. The cyst is lined by a flattened layer of undulating epithelium that forms shallow crevices. Rete ovarii are present in the adjacent tissue.

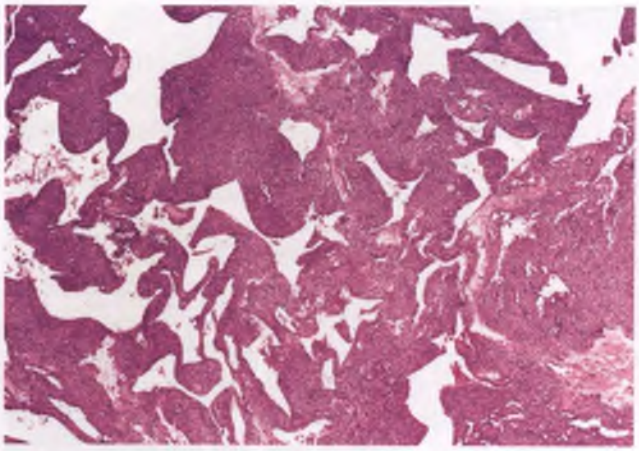

FIGURE 7.301. Solid pseudopapillary neoplasm. In this low-magnification view, the pseudopapillary pattern related to tumor dyscohesion is apparent.

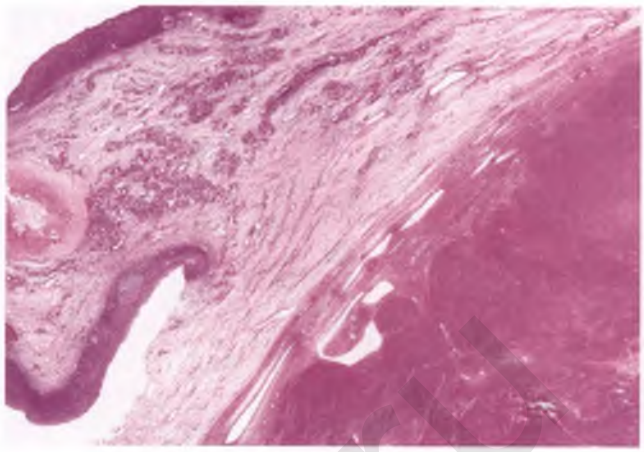

FIGURE 7.303. Leiomyoma. In this low-magnification view, a portion of an eosinophilic nodule of smooth muscle is present within the hilar region of the ovary. The hilar location is consistent with origin from the smooth muscle wall of hilar blood vessels.

architecture can still be appreciated are found in a hilar location (Fig. 7.303). Another possible origin for some of these tumors is ovarian stroma that has undergone smooth muscle metaplasia.

Ovarian leiomyomas are benign tumors that occur over a wide age range, are almost always unilateral, and may present as either an adnexal mass or as an incidental finding. These tumors exhibit the same spectrum of histologic features as their much more common uterine counterparts. Most ovarian leiomyomas that are encountered outside of a consultation-based setting are of the usual type and have an average size of 5 cm.

Differential Diagnosis

Ovarian fibromatous tumors can closely resemble smooth muscle tumors, and are the main differential diagnostic consideration. Since ovarian fibroma and its cellular variant are much more common than ovarian leiomyoma and cellular leiomyoma, the pathologist may not give serious consideration to smooth muscle differentiation when evaluating spindle cell neoplasms of the ovary. At the macroscopic level, spindle cell tumors with a hilar location are more likely to be leiomyomas than fibromas. Routine histologic features can also be of some assistance when attempting to distinguish leiomyomas from fibromas. Normal and most neoplastic smooth muscle cells generally have elongated and blunt-ended (cigar-shaped) nuclei (Fig. 7.304A), as opposed to the more tapered ends of the fusiform nuclei of fibromas. In addition, those bland ovarian spindle cell tumors with a storiform rather than fascicular growth pattern are more likely to be fibromas rather than leiomyomas. The trichrome stain can also be helpful in

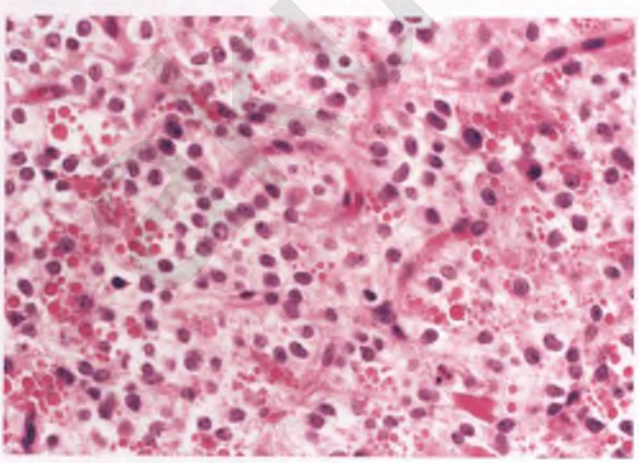

FIGURE 7.302. Solid pseudopapillary neoplasm. This image highlights the bland nuclear features, delicate vasculature, and eosinophilic globules that are characteristic of this tumor.

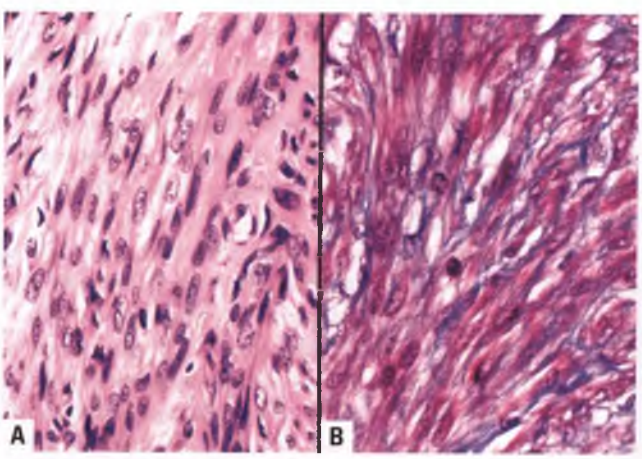

FIGURE 7.304. Leiomyoma. **A:** This high-magnification view highlights the cigar-shaped nuclei of many of the smooth muscle cells. **B:** In this trichrome-stained section, the fibrillar cytoplasm of the smooth muscle cells has a brick-red appearance. A small amount of blue-stained collagenous tissue is also present in the background.

this situation by demonstrating the brick-red fibrillar cytoplasm of smooth muscle cells (Fig. 7.304B), which contrasts with the often abundant blue-staining extracellular collagen present in fibromatous tumors. More conclusive evidence of smooth muscle differentiation in this setting is diffusely positive immunoreactivity for muscle markers such as desmin and h-caldesmon, but one could question the cost-effectiveness of using immunohistochemistry in an effort to distinguish one benign ovarian tumor from another. It should be noted that the smooth muscle actin positivity of leiomyomas is not helpful in differentiating leiomyomas from fibromas, since about half of ovarian fibromas are at least focally positive for this marker.[251]

As is the case for their uterine counterparts, most ovarian leiomyosarcomas can be distinguished from leiomyomas by the presence of various combinations of significant nuclear atypia, high mitotic rates, and foci of tumor cell necrosis.[408]

A rare mimic of cellular smooth muscle tumors is a gastrointestinal stromal tumor that has metastasized to the ovary.[254] The frequent bilaterality of these metastases, the clinical history of such a tumor, and a c-KIT (CD117)-positive, CD34-positive, and desmin-negative immunophenotype help to establish this diagnosis.

Miscellaneous Tumors of Soft Tissue Type

Fibrosarcoma is discussed in the section on sex cord-stromal tumors, and leiomyosarcoma is briefly mentioned in the section on ovarian leiomyoma. A variety of other types of benign and malignant soft tissue tumors are rarely encountered in the ovary and are discussed in more comprehensive texts of gynecologic pathology.

Ovarian Tumors with Functioning Stroma***[79,223,224]

A wide variety of ovarian tumors, whether benign, malignant, primary, or metastatic, occasionally contain steroid cells that may produce symptoms related to an excess of androgens or estrogens. The tumors most likely to exhibit this phenomenon are mucinous cystadenomas (particularly those from pregnant patients) (Fig. 7.305), metastatic gastrointestinal carcinomas (Fig. 7.306), struma ovarii (Fig. 7.307), and rete cystadenomas. The steroid cells usually correspond to luteinized stromal cells. However, they may also represent hyperplastic hilus cells, as most commonly seen within the wall of rete cystadenomas, and may rarely be of Leydig cell type with documented crystals of Reinke. In most cases, the steroid cells are scattered haphazardly throughout the neoplasm in small aggregates, but in struma ovarii and some other tumors these cells preferentially form discontinuous peripheral bands measuring up to 2 mm in thickness.[223] The histologic features of steroid cells are as noted in the legends to Figs. 7.305–7.307 and are further described and illustrated in Chapter 6 in the sections on hilus cells and stromal hyperthecosis.

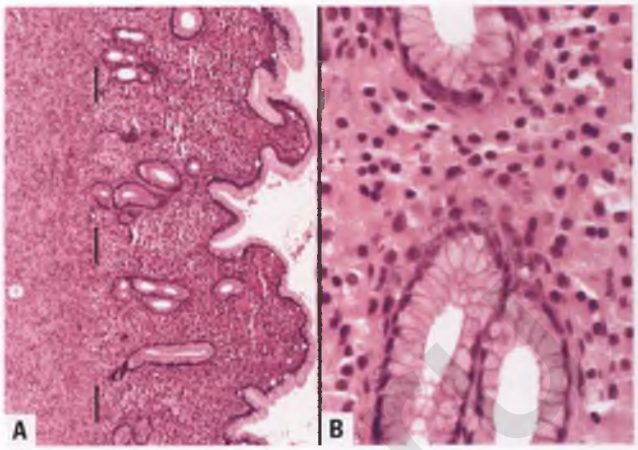

FIGURE 7.305. Mucinous cystadenoma with functioning stroma in a pregnant patient. **A:** A band of steroid cells extends from just beneath the mucinous epithelial lining of the cyst (at right) to the interface between the neoplastic mucinous glands and the normal ovarian stroma (as marked by the *dotted line*). **B:** The steroid cells within the stroma between the mucinous glands have abundant eosinophilic cytoplasm and round nuclei.

THE OVARY AS SITE OF METASTATIC TUMOR

General Considerations[202,409,410]

Roughly 5% to 10% of malignant ovarian tumors that are encountered by the surgical pathologist as clinically suspected primary neoplasms are actually of metastatic origin. Most

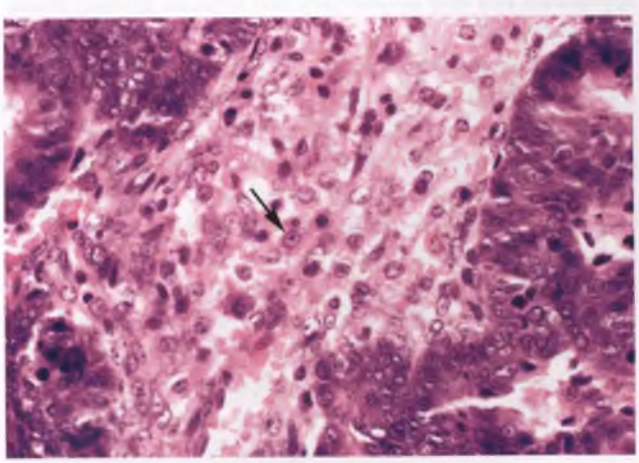

FIGURE. 7.306. Colonic adenocarcinoma metastatic to the ovary with functioning stroma. The stromal steroid cells, one of which is marked by an *arrow*, are recognized by their round nuclei, single prominent nucleoli, and abundant eosinophilic cytoplasm.

***The term "ovarian tumors with functioning stroma" is used loosely, with reports of these tumors with steroid-type stromal cells often including many patients who have no clinical or biochemical evidence of abnormal endocrine function. Moreover, in those patients with an endocrinologic abnormality, definitive evidence that the hormone-related changes are directly attributable to the ovarian tumor is often lacking. Also note that sex cord-stromal tumors are excluded from this category by convention, since they are expected to frequently possess functioning stroma.

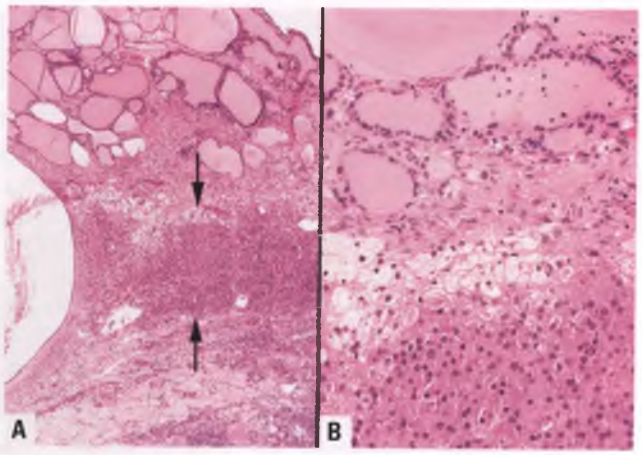

FIGURE 7.307. Struma ovarii with functioning stroma. **A:** A peripheral band of steroid cells (*arrows*) is interposed between the thyroid follicles (top) and ovarian stroma (bottom). **B:** At high magnification, a subset of the steroid cells is seen to have pale, lipid-rich cytoplasm, which when dominant can result in a grossly visible yellow rim.

commonly, these tumors originate from the large intestine, appendix, stomach, and breast, but malignant neoplasms from multiple other sites have been reported to metastasize to the ovary on occasion. Metastatic adenocarcinoma is well known for its ability to masquerade as a primary ovarian tumor, which is related to observations that (a) the primary tumor may be much smaller than the involved ovaries and may not be clinically apparent, as exemplified by some gastric carcinomas with this pattern of spread, (b) the ovarian metastasis may be partially or predominantly cystic, even when the primary tumor is solid, (c) metastatic mucinous carcinomas can have areas that closely resemble the glands and cysts of mucinous borderline tumors or even mucinous cystadenomas, and (d) metastatic colorectal adenocarcinoma often has an endometrioid-like appearance and may occasionally also simulate primary mucinous carcinoma.

The following features, particularly when seen in combination, favor ovarian involvement by a metastatic rather than primary tumor: (a) known history of an extraovarian malignancy with histologic features similar to the ovarian tumor (the possibility of synchronous primary tumors as often occurs with endometrial and ovarian endometrioid carcinomas must be excluded), (b) high-stage disease in a tumor whose differential diagnostic primary ovarian alternatives seldom present with extraovarian spread, or any tumor with parenchymal liver metastases, (c) bilaterality (there are many exceptions to this generalization, with some primary tumors being bilateral and some metastases being unilateral), (d) surface implants, (e) multinodular growth, (f) a histologic pattern that is unusual for primary ovarian neoplasia, (g) angiolymphatic invasion (most apparent in sections taken through the ovarian hilar region), and (h) spotty involvement of ovarian parenchyma. Many of these features are illustrated in the sections that follow on the various specific types of metastatic cancer. These sections will also highlight the selected instances in which mucin stains and immunohistochemistry serve as invaluable diagnostic tools.

Intraoperative Consultation

The pathologist is often called upon to evaluate ovarian tumors intraoperatively. If an ovarian malignancy is suspected and the surgeon does not volunteer information related to the patient's oncologic history, whether the tumor involves one or both ovaries, or if the tumor shows evidence of extraovarian spread, the pathologist should ask for this important data. Although 60% to 80% of ovarian metastases can be distinguished from primary ovarian tumors by frozen section, in some cases it can only be suggested as a differential diagnostic consideration.[411]

For mucinous carcinomas, a presumption can be made that unilateral tumors ≥13 cm are primary, whereas those that are either bilateral (any size) or unilateral and <13 cm are metastases, although there are exceptions to these general guidelines.[412†††]

Neoplastic ovarian tissue submitted for frozen section analysis should be selected with care. A firm, fibromatous area may represent a benign adenofibromatous component within a primary malignant tumor (see Fig. 7.42), or may be indicative of a stromal-predominant portion of the tumor in which malignant epithelial elements may be difficult to detect in a frozen section. The most malignant component of an ovarian tumor is likely to be soft or fleshy and may be associated with foci of hemorrhage and necrosis, and attention should be focused on these areas. Although surface implants should be sought, the common finding of cystic Walthard nests on the surface of the fallopian tubes should not be misinterpreted as evidence of tumor spread.

The pathologist should go through the list as outlined in (a) through (h) in the "General Considerations" section and make an assessment as to the probable primary versus metastatic nature of the tumor. Examples in which the intraoperative opinion of the pathologist may be instrumental in helping to identify an occult primary neoplasm include suggesting removal of the appendix in cases of mucinous ovarian tumors associated with pseudomyxoma peritonei, and recommending close evaluation of (a) the stomach and other less likely primary sites when numerous signet-ring cells are present, (b) the large bowel when the characteristic pseudoendometrioid pattern of metastatic colon cancer is encountered, and (c) the small bowel when the ovaries are involved by bilateral carcinoid tumors.

Intestinal Carcinoma[413–415]

Colorectal adenocarcinomas are the single most common source of ovarian metastases that simulate primary ovarian malignancies, accounting for about 40% to 45% of such cases.[416] Unless the pathologist has made a specific effort to become familiar with the gross and microscopic features of

†††In the initial study regarding tumor size and laterality, the size cutoff was 10 cm,[121] but a larger and more recent study from the same institution found that the performance of this algorithm was optimized at 13 cm.[412]

FIGURE 7.308. Colonic adenocarcinoma metastatic to the ovary (sectioned surface). Scattered cysts are present within this predominantly solid neoplasm, which contains prominent areas of grayish yellow necrosis.

FIGURE 7.310. Mucinous variant of colonic adenocarcinoma metastatic to ovary. This solid and cystic neoplasm has a glistening, gelatinous sectioned surface due to the presence of abundant mucin (see Fig. 7.315 for histologic correlate).

colonic adenocarcinoma metastatic to the ovary, there is a high probability that when confronted with this tumor it will be misinterpreted as a primary ovarian tumor. Although most patients have either a recent history of colon cancer or the two sites of involvement are found concurrently, there are occasional cases in which surgical treatment for presumed ovarian cancer precedes recognition of the colonic tumor. Most patients are middle-aged adults who present with abdominal pain and/or symptoms related to their colon cancer. The typical colon cancer that metastasizes to the ovary has (a) a rectosigmoid location, (b) extended through the bowel wall, and (c) spread to mesenteric lymph nodes.

Grossly, about half of colonic adenocarcinomas metastatic to the ovary are bilateral. They average 10 to 15 cm in diameter, and typically have a smooth external surface. Their sectioned surface is usually a conglomeration of solid and cystic areas, with the solid areas often dominated by mushy, grayish yellow necrotic tissue (Fig. 7.308). Less frequently, these metastatic lesions may form a multiloculated cyst (Fig. 7.309) or have a distinctly gelatinous cut surface due to their derivation from a mucinous variant of colonic adenocarcinoma (Fig. 7.310).

Histologically, the usual type of colonic adenocarcinoma produces a pseudoendometrioid appearance when it metastasizes to the ovary. Characteristic features of this pattern are glands with garland and cribriform growth patterns, intraluminal "dirty" necrosis, and segmental glandular destruction (Figs. 7.311 and 7.312). The garland growth pattern refers to a back-to-back wreath-like arrangement of rings of malignant glands encircling necrotic debris. In dirty necrosis, the presence of abundant tumor-related karyorrhectic debris within

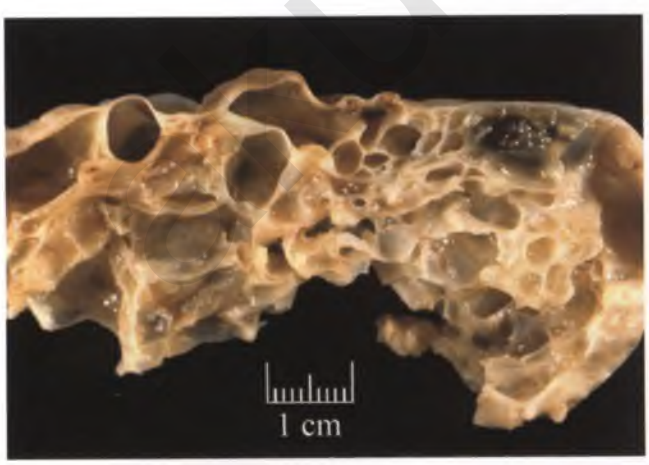

FIGURE 7.309. Colonic adenocarcinoma metastatic to the ovary. This multiloculated neoplasm has a honeycombed sectioned surface that mimics a primary mucinous cystadenoma (see Fig. 7.314 for histologic correlate).

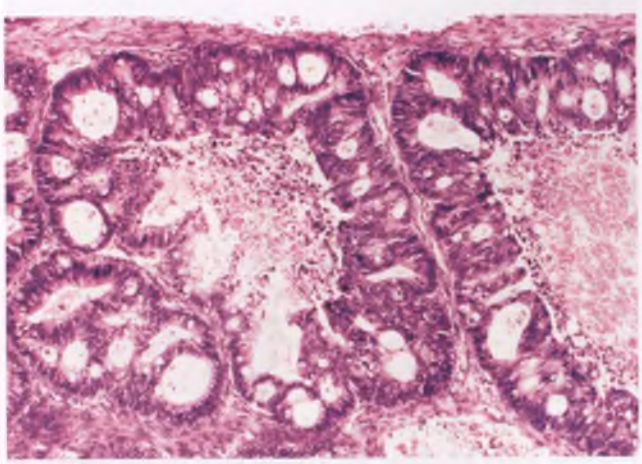

FIGURE 7.311. Colonic adenocarcinoma metastatic to ovary. Classic histologic appearance with garlands of malignant glandular epithelium encircling lumens filled with dirty necrosis. Also note the focus of glandular cribriforming at lower left.

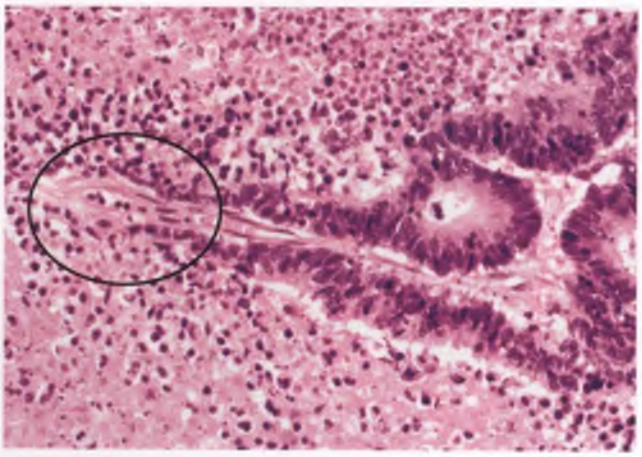

FIGURE 7.312. Colonic adenocarcinoma metastatic to ovary. Segmental destruction of glandular epithelium (*circled*) is another characteristic feature. Note the prominent dirty necrosis.

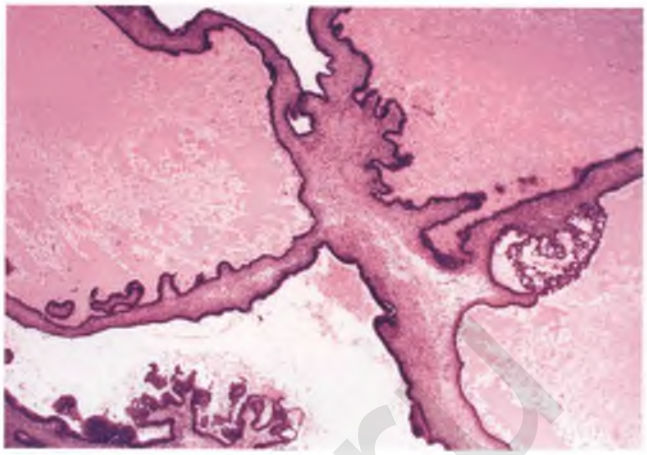

FIGURE 7.314. Colonic adenocarcinoma metastatic to ovary. The neoplastic glands are cystically dilated, but contain focal areas of glandular complexity. A tumor such as this is easily misinterpreted as a primary ovarian neoplasm.

cystic glandular structures results in granular basophilic deposits within a background of eosinophilic necrotic material, with the basophilic nuclear fragments often concentrated along the luminal periphery. This type of necrosis should be distinguished from the accumulation of degenerated neutrophils, histiocytes, and occasional sloughed tumor cells within inspissated mucus, which has a less densely eosinophilic background and is often seen within the cystically dilated glands of primary mucinous tumors (see Fig. 7.72).[113] Infiltrative glands with an associated desmoplastic stromal reaction may represent a portion of the tumor (Fig. 7.313), but this is not usually a prominent feature. When the cystic glandular spaces of metastatic colonic adenocarcinoma become macroscopic and the epithelial lining of the cysts becomes more simplified, the resemblance to primary ovarian neoplasia is heightened (Fig. 7.314). A treacherous tumor of this type requires thorough clinicopathologic correlation and adequate sampling with supplemental immunohistochemistry in order to avoid misinterpretation as a primary ovarian neoplasm.

In addition to the pitfalls presented by pseudoendometrioid metastatic colonic adenocarcinoma, malignant epithelium derived from some colonic adenocarcinomas is occasionally overtly mucinous or has hybrid endometrioid-mucinous features (Fig. 7.315). When overtly mucinous, it is not uncommon for foci within the tumor to resemble primary borderline or even benign mucinous tumors (Fig. 7.316). This finding should not be misconstrued as evidence of a primary neoplasm.

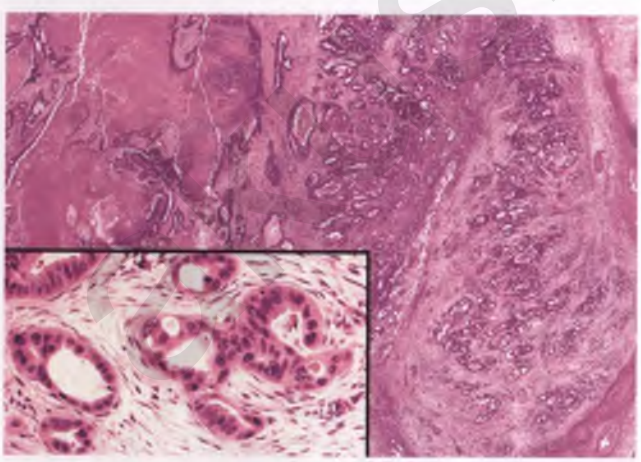

FIGURE 7.313. Colonic adenocarcinoma metastatic to ovary. Infiltrative glands associated with a desmoplastic stromal reaction, as shown at right and at higher magnification in the inset, are commonly present, although this is often a focal finding. Cystically dilated glands with intraluminal necrosis and segmental glandular destruction are also present in the upper left portion of the main image.

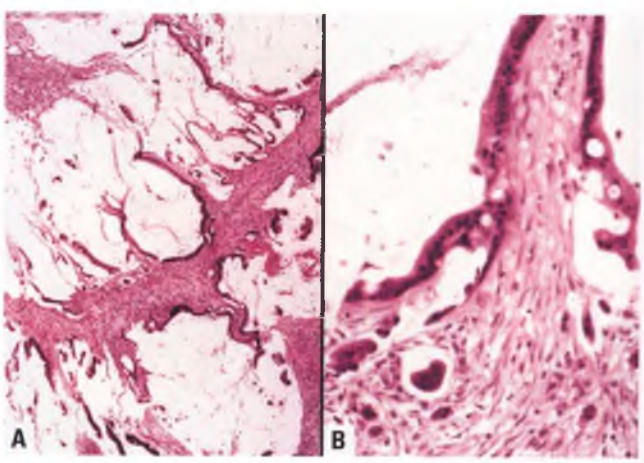

FIGURE 7.315. **A,B:** Mucinous variant of colonic adenocarcinoma metastatic to ovary. The abundant pale to clear-appearing material is extracellular mucin, which is associated with strips and clusters of neoplastic mucinous epithelium.

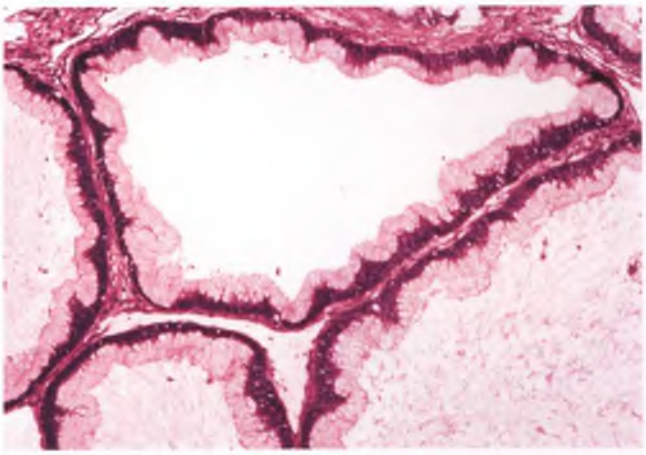

FIGURE 7.316. Mucinous variant of colonic adenocarcinoma metastatic to ovary. In this area of the tumor, the cystically dilated glands are lined by very well differentiated mucinous epithelium that has the potential to mislead the pathologist into thinking that this is a primary ovarian neoplasm.

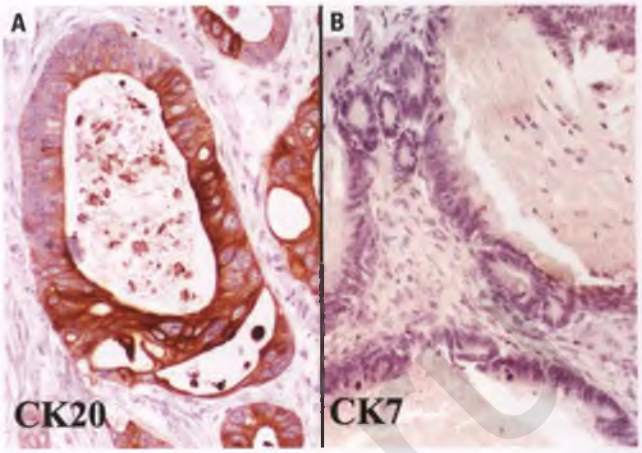

FIGURE 7.317. Characteristic immunophenotype of colonic adenocarcinoma metastatic to ovary. **A:** The neoplastic glands exhibit strong immunoreactivity for CK20 that is often in a patchy, mosaic-like pattern. **B:** CK7 staining is usually completely negative.

The stroma of metastatic colonic adenocarcinoma commonly contains scattered aggregates of steroid cells that may be associated with endocrine abnormalities (see Fig. 7.306). The immunoprofile of metastatic colonic adenocarcinoma is discussed within the context of the differential diagnosis.

Differential Diagnosis

In the most common scenario, the pseudoendometrioid pattern of colonic adenocarcinoma metastatic to the ovaries needs to be distinguished from primary endometrioid carcinoma. Features that in the aggregate help to establish the former diagnosis include (a) a clinical history of a previous or concurrent transmural colorectal adenocarcinoma, (b) bilateral ovarian involvement, (c) parenchymal liver metastases, (d) intraluminal dirty necrosis,[‡‡‡] (e) segmental glandular destruction, (f) absence of squamous metaplasia, (g) lack of an adenofibromatous component, (h) lack of associated endometriosis, and (i) the appropriate immunophenotype. Metastatic pseudoendometrioid colorectal adenocarcinomas are typically positive for CK20 and negative for CK7 (Fig. 7.317), and also exhibit nuclear immunoreactivity for the intestinal marker CDX2.[107,415,417–419] This immunophenotype is the exact opposite of that expected for primary endometrioid carcinoma.

Less frequently, colonic adenocarcinoma metastatic to the ovaries has mucinous features and needs to be distinguished from primary mucinous carcinomas and borderline tumors. Fortunately, mucinous tumors of colorectal origin typically have the same characteristic CK7−/CK20+ immunophenotype as their more common pseudoendometrioid counterparts, and this staining pattern is strong supportive evidence of an origin within the lower intestinal tract.[104] However, the role of immunohistochemistry in distinguishing metastases from pancreatic, gastric, and biliary adenocarcinomas from primary ovarian mucinous tumors is more complicated and less definitive, as discussed later in this section. Table 7.3 presents a summary of the characteristic patterns of expression of CK7 and CK20 that are associated with selected tumors involving the ovary that can be difficult to separate from one another on morphologic grounds alone.

For the sake of completeness, it is worth mentioning that rare variants of intestinal carcinoma have a clear cell morphology, and their metastases may simulate primary ovarian clear cell carcinoma or the secretory type of endometrioid carcinoma.[422]

Krukenberg Tumor (Metastatic Signet-Ring Carcinoma)[410,423,424]

The Krukenberg tumor is best defined as a metastatic adenocarcinoma of the ovary that contains an appreciable number of mucin-containing signet-ring cells.[§§§] As a guideline, it has

[‡‡‡]Although intraluminal dirty necrosis can be present in primary ovarian tumors,[418] its presence should prompt serious consideration of a diagnosis of metastatic intestinal carcinoma, which must then be excluded by clinical correlation and appropriate pathologic analysis.

[§§§]Thus defined, there is no such thing as a "primary Krukenberg tumor." However, it is appropriate to acknowledge the existence of rare primary ovarian tumors that mimic Krukenberg tumors, most notably mucinous carcinoids,[344] mixed carcinomas with microcystic and signet-ring components,[122] and adenofibromatous neoplasms with mucin-containing signet-ring cells.[123,124] Alternative definitions that do not require a Krukenberg tumor to be of metastatic origin or that demand classic histology with a preponderance of signet-ring cells in a cellular stroma only invite diagnostic confusion by being too inclusive or exclusive, which can lead to errors in prognostication and treatment. Because the term "Krukenberg tumor" is vague and its precise definition has not been standardized, it should not be used as a standalone diagnosis. Depending upon the degree of diagnostic certainty, diagnoses such as "metastatic signet-ring adenocarcinoma consistent with gastric origin (so-called Krukenberg tumor)" or "adenocarcinoma with signet-ring component, favor metastatic origin" are more appropriate.

TABLE 7.3 Characteristic Patterns of CK7 and CK20 Expression in Selected Tumors Involving the Ovary[a]

Primary non-mucinous ovarian carcinoma:[103,417–420]	CK7+/CK20–
Primary mucinous ovarian carcinoma:[103,104]	CK7+/CK20– or CK7+/CK20+
Metastatic colorectal carcinoma (pseudoendometrioid or mucinous):[104,415,417–419]	CK7–/CK20+
Ovarian involvement by low-grade mucinous neoplasm (ruptured adenoma) of appendiceal origin:[104,421]	CK7–/CK20+
Metastatic pancreatic/biliary carcinoma:[104]	CK7+/CK20+

[a]Although other staining patterns occur to varying degrees in these various tumor types, it is helpful to know the single most characteristic immunoprofile for these different situations. Most of these phenotypes can be deduced by knowing that (a) CK20 expression implies gastrointestinal differentiation in this setting,[105] (b) primary ovarian mucinous carcinomas frequently show evidence of gastrointestinal differentiation, which may be manifested by CK20 immunoreactivity,[84] and (c) nearly all primary ovarian carcinomas express CK7, as do many other carcinomas other than those of the lower gastrointestinal tract.[103,420] The major take-home lesson is that *an ovarian tumor with a CK7–/CK20+ immunophenotype is highly likely to be of extraovarian origin and most commonly derived from the colon or appendix*, although this pattern is also seen in some primary mucinous tumors of intestinal type that arise within a teratoma.[99,100]

recently been suggested that at least 10% of the tumor be composed of signet-ring cells in order to qualify as a Krukenberg tumor.[423] Presumably, this percentage applies only to the malignant epithelial elements and not to the entire tumor, which often contains considerable amounts of stroma. Most Krukenberg tumors are due to metastases from a primary gastric signet-ring carcinoma, but they can also originate from the colon, appendix, breast, gallbladder, biliary tract and other miscellaneous sites. The fame and lore of the Krukenberg tumor is far out of proportion to the frequency with which it is encountered. It should be clear from the above discussion that the Krukenberg tumor is not a single entity, but rather a collection of high-stage adenocarcinomas that share the ability to form signet-ring cells.

The clinical presentation of patients with Krukenberg tumor, who have an average age of only about 45 years, varies considerably. Most patients have complaints related to the presence of an ovarian mass, although symptoms due to the primary tumor or its other sites of metastatic disease may dominate the clinical picture. Stromal luteinization is occasionally seen in Krukenberg tumors, and may be associated with manifestations related to abnormal hormone production. The prognosis of this uncommon tumor is poor, with most patients dying within 1 to 2 years of diagnosis.

At least 80% of Krukenberg tumors as encountered fresh from the operating room are bilateral, although series based on difficult and unusual consultation cases in which a primary tumor is a serious diagnostic consideration understandably report a lower percentage of bilaterality. Grossly, Krukenberg tumors have an average size of about 10 cm and an external surface that is smooth and often bosselated. The usual lack of adhesions or implants on the surface of the tumor favors lymphatic over transperitoneal spread as the likely route of metastasis in most cases. Their sectioned surface is usually solid, but varies substantially in terms of its color (white, pale yellow, tan, or reddish brown), texture (firm, fleshy, edematous, or gelatinous), and degree of nodularity (Figs. 7.318 and 7.319).

Histologically, the classic Krukenberg tumor is composed of numerous mucin-containing signet-ring cells set within a cellular spindle-cell stroma (Figs. 7.320 and 7.321). The signet-ring component shows only minimal mitotic activity and its degree of nuclear atypia is often unimpressive. Angiolymphatic invasion is commonly identified, particularly within the hilar region. In order to avoid diagnostic error, it is important to use a mucicarmine or PAS with diastase stain to document the presence of intracytoplasmic mucin within the signet-ring cells.

As has been recently emphasized, Krukenberg tumors may stray from their classic appearance.[423] In addition to occurring singly, the signet-ring cells may aggregate to form nests or elongated pseudotubules (Fig. 7.322). A tubular variant of Krukenberg tumor is recognized, wherein solid tubules or those with small lumens predominate (Fig. 7.323).[281] In this variant, mucin-containing signet-ring cells are identifiable both within the tubular lining epithelium and within the stroma. In other Krukenberg tumors, small microcystic glands lined by flattened tumor cells (Fig. 7.324), intestinal-type glands, or

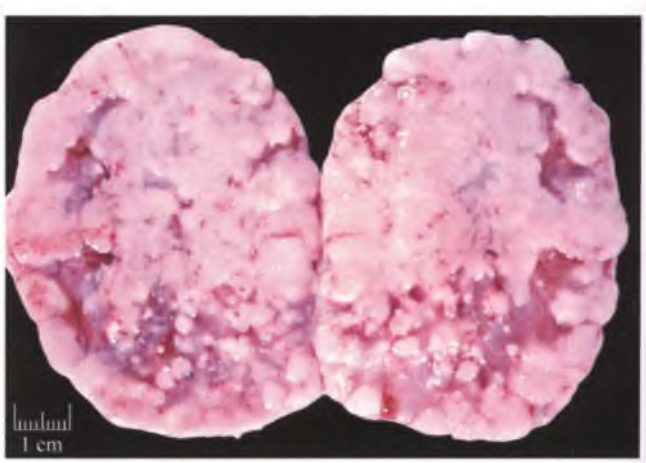

FIGURE 7.318. Krukenberg tumor. The sectioned surface of this bivalved ovarian tumor consists of multiple coalescing nodules, some of which are separated by edematous and hemorrhagic tissue. (Courtesy of Dr. Enrique Higa.)

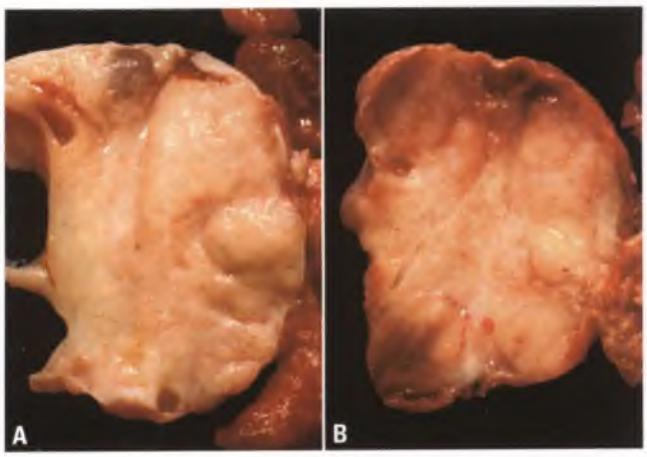

FIGURE 7.319. **A,B:** Krukenberg tumor. The sectioned surfaces of these bilateral 6 to 8 cm ovarian tumors exhibit only minimal nodularity and have a minor cystic component. The tumor in **(B)** also has a variably prominent rim of reddish brown tissue. (Courtesy of Dr. Enrique Higa.)

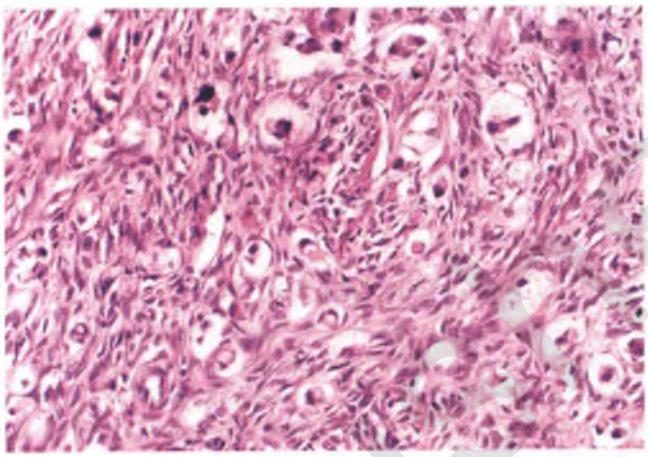

FIGURE 7.320. Krukenberg tumor, classic type. Scattered adenocarcinomatous cells, many of which have a signet-ring appearance, are set within a cellular spindle-cell stroma.

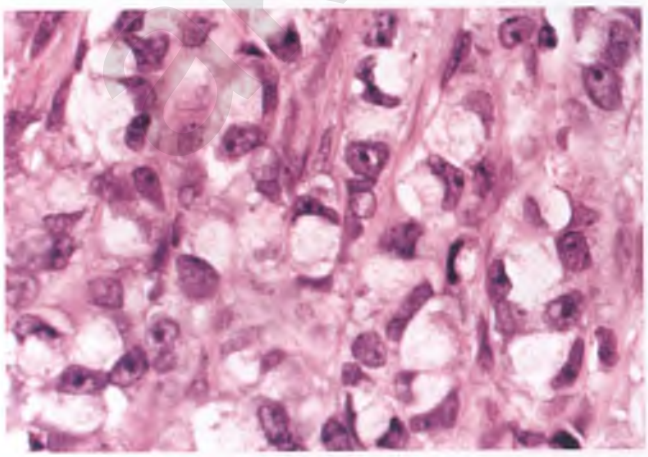

FIGURE 7.321. Krukenberg tumor, classic type. High-magnification view of several signet-ring cells.

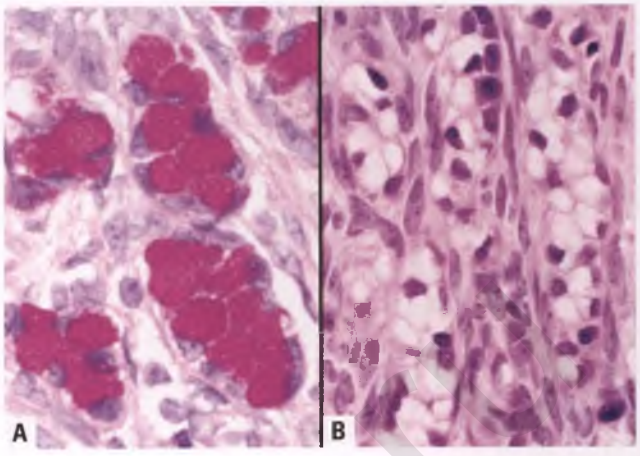

FIGURE 7.322. Krukenberg tumor. **A:** Nests of mucin-containing signet-ring cells highlighted with a PAS with diastase stain. **B:** Aggregates of signet-ring cells forming elongated pseudotubules.

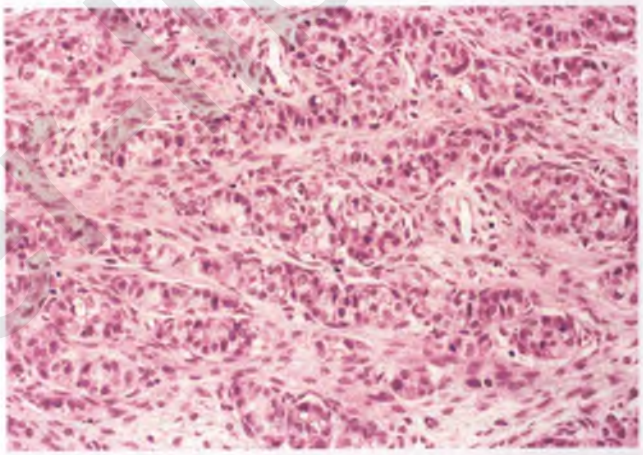

FIGURE 7.323. Krukenberg tumor, tubular variant. The tumor is composed of predominantly solid, elongated tubules. Note the presence of scattered signet-ring cells lining the tubules.

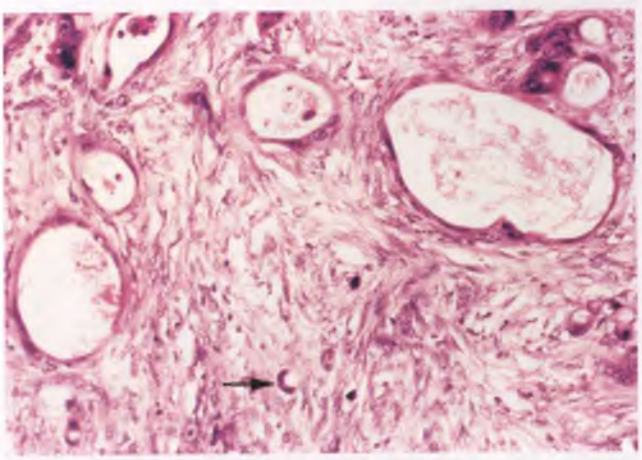

FIGURE 7.324. Krukenberg tumor. Small microcystic glands lined by flattened tumor cells are a frequent finding. Note the presence of occasional signet-ring cells in the background, such as the one marked by the *arrow*.

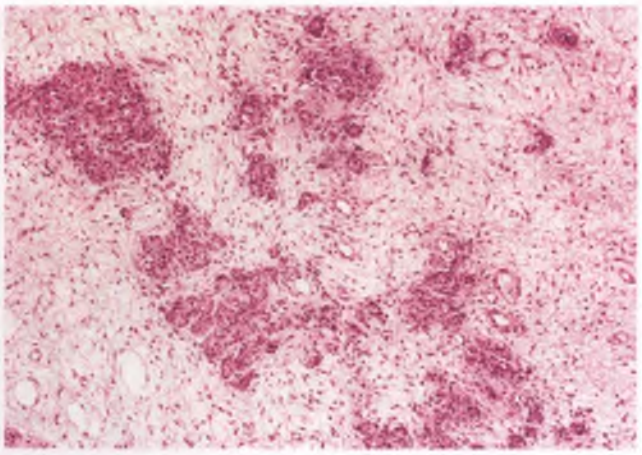

FIGURE 7.325. Krukenberg tumor. The markedly edematous stroma isolates islands of metastatic adenocarcinoma.

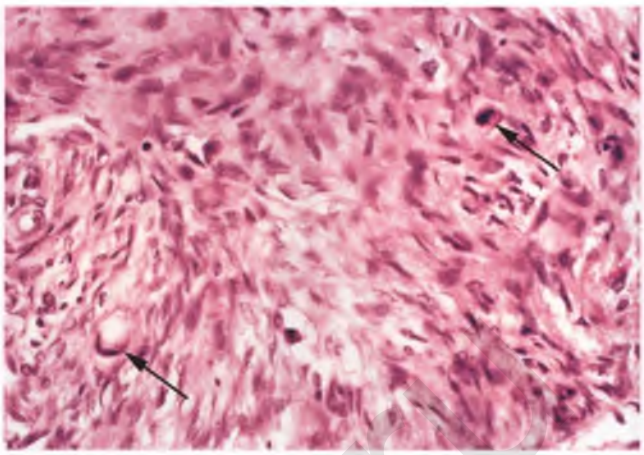

FIGURE 7.327. Krukenberg tumor. In microscopic fields such as this, the dominance of the fibromatous stroma can lead to a misdiagnosis of ovarian fibroma if the widely scattered tumor cells are not recognized (two tumor cells are marked by *arrows*, one of which is of the signet-ring type).

other tubuloglandular patterns may be present. On the stromal front, the stroma may be edematous (Fig. 7.325) or mucoid (Fig. 7.326) rather than cellular, and the cellular stroma that is classically present should not be required as part of the definition of the Krukenberg tumor. Stromal luteinization may also be present, and is much more likely to be seen in association with pregnancy. In cases in which the spindle cell stroma predominates and the epithelial component consists only of sparsely distributed signet-ring cells, the tumor may be misdiagnosed as an ovarian fibroma, particularly at the time of frozen section analysis (Fig. 7.327).

Differential Diagnosis

The differential diagnosis of Krukenberg tumors is broad, and has recently been reviewed in detail.[410,423] Various clinical and pathologic findings, such as a known primary source, high-stage disease, tumor bilaterality, confirmed presence of mucin within the signet-ring cells, and the presence of angiolymphatic invasion usually enable identification of the Krukenberg tumor. The sections on sclerosing stromal tumor, signet-ring stromal tumor, Sertoli-Leydig cell tumor, and mucinous carcinoid tumor elaborate on the differences between Krukenberg tumors and these other neoplasms.

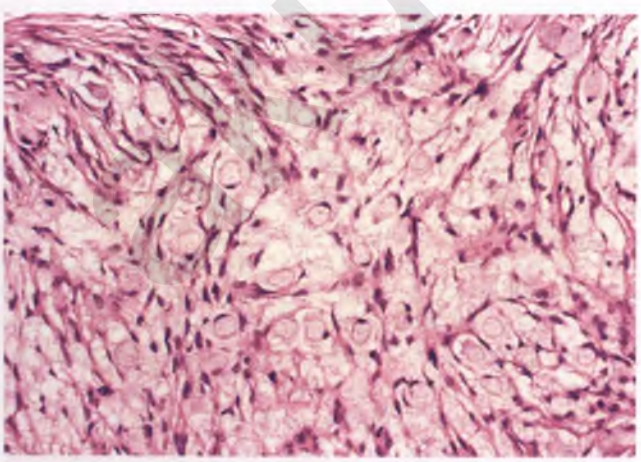

FIGURE 7.326. Krukenberg tumor. Mucinous material interdigitates with strands of collagen, creating a feathery appearance. Note the presence of several signet-ring cells lurking in the background.

Gastric Carcinoma, Intestinal Type[425]

The intestinal type of gastric carcinoma metastasizes to the ovary much less frequently than the signet-ring variant. It produces a pseudoendometrioid or mucinous appearance that is similar to the much more commonly encountered metastatic colorectal carcinoma. Since there is no dominant or distinctive pattern of expression of CK7 and CK20 in intestinal-type gastric carcinomas,[426] it follows that these markers cannot be expected to play a significant role in their identification at metastatic sites such as the ovary. Instead, ovarian metastases of intestinal type from this source are recognized largely on the basis of a pseudoendometrioid or mucinous tumor with some of the general features that are supportive of metastatic origin, the absence of a colorectal tumor, and the presence of a prior, concurrent, or subsequently identified gastric carcinoma.

Low-Grade Appendiceal Mucinous Tumors

In this section, attention is focused on the bland mucinous ovarian tumors that are produced when epithelial strips derived from ruptured appendiceal mucinous adenomas (also referred to as low-grade mucinous neoplasms) implant on the surface of the ovary and subsequently encyst. An alternative viewpoint is that what myself and others interpret as ruptured adenomas are actually very well-differentiated mucinous adenocarcinomas

with a deceptive pattern of invasion, which actively metastasize to the ovaries and peritoneum.[427] This issue, along with the saga of pseudomyxoma peritonei and other aspects of its common association with low-grade mucinous neoplasms of the appendix, are discussed in detail in Chapter 8.

For many years, it was controversial as to whether these bland mucinous ovarian tumors originated from the appendix or represented independent primary mucinous cystadenomas or borderline tumors.[95,98,101,428] However, the combination of careful clinicopathologic correlation, comparative immunohistochemistry (particularly the findings that most matched pairs of ovarian and appendiceal tumors express the gastrointestinal marker MUC2 and the identical lower gastrointestinal CK7-/CK20+ immunophenotype), and molecular genetic analysis have convincingly demonstrated that the vast majority of ovarian tumors that occur in association with mucinous neoplasms of the appendix are of appendiceal origin.[101,421,429–431]

Clinicopathologic Features[95,98,101,428,429]

Patients with these tumors have a mean age of 50 years and usually have associated pseudomyxoma peritonei, which accounts for the typical presenting symptoms of abdominal enlargement and/or abdominal pain. Grossly, the ovarian tumors have an average diameter of 16 cm and about 30% to 40% are bilateral when the common finding of mucoid implants on the surface of the contralateral ovary is not tabulated as evidence of bilaterality. The sectioned surface of the ovarian tumor typically exhibits a multilocular cyst filled with jelly-like mucoid material (Fig. 7.328). Some tumors resemble delicate bags of jelly, and are easily ruptured during their removal.

Histologic examination of these gelatinous masses reveals an appearance that usually resembles a primary mucinous borderline tumor or occasionally a mucinous cystadenoma, albeit with subtle differences that should suggest the correct diagnosis. A clue that is not emphasized in the literature is the prominence of partial separation of the mucinous epithelial lining of the cysts from the stroma (Fig. 7.329). The presence of surface implants, mucinous cysts lined by inordinately tall, hypermucinous epithelial cells with lightly-stained cytoplasm and indistinct apical borders (Fig. 7.330), and prominent pseudomyxoma ovarii (mucin pools dissecting within the ovarian stroma), particularly when seen in combination and in the setting of pseudomyxoma peritonei, are additional clues that the origin of the ovarian tumor is essentially a ruptured mucinous cystadenoma of the appendix. Because of this treacherous situation, whenever the pathologist encounters a mucinous ovarian tumor with pseudomyxoma ovarii or associated with

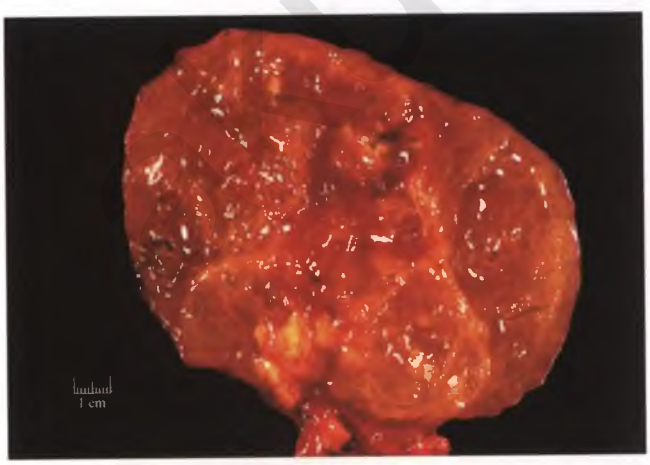

FIGURE 7.328. Ovaries involved by low-grade mucinous neoplasms of the appendix typically have a sectioned surface that is dominated by mucinous cyst contents with a glistening, translucent, jelly-like appearance.

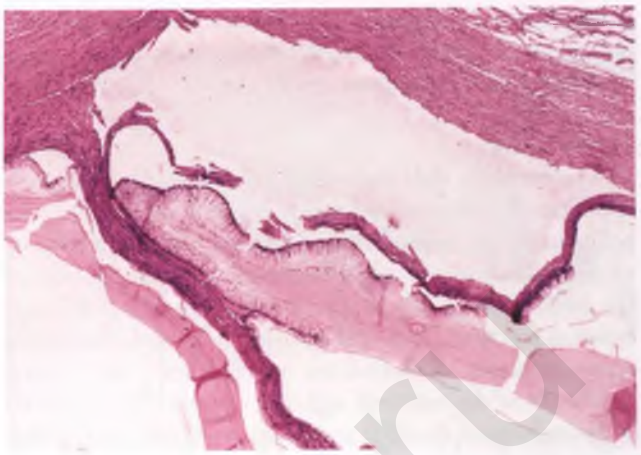

FIGURE 7.329. Ovarian involvement by low-grade mucinous neoplasm (ruptured adenoma) of appendiceal origin. Partial separation of the mucinous epithelial lining of the cysts from the stroma is commonly present, and is associated with pseudomyxoma ovarii once the fragile epithelial barrier has been breached.

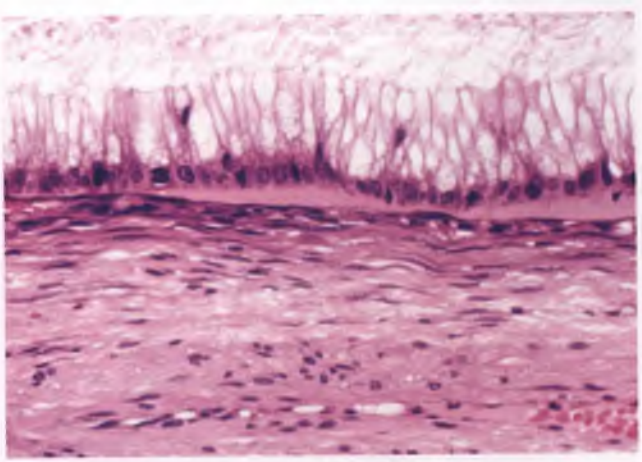

FIGURE 7.330. Ovarian involvement by low-grade mucinous neoplasm (ruptured adenoma) of appendiceal origin. As is often the case in this situation, the bland mucinous epithelial cells are inordinately tall ("hypermucinous") with lightly-stained cytoplasm, and have indistinct apical margins that blend with the luminal mucin.

pseudomyxoma peritonei in an intraoperative setting, it is prudent to inquire about the status of the appendix and to request its removal, even if it appears grossly normal.

Terminology

The terminology used for ovarian involvement by low-grade appendiceal mucinous neoplasms depends on whether one believes that the appendiceal tumors are ruptured adenomas or well-differentiated adenocarcinomas. For supporters of the latter position, the ovarian tumors can simply be diagnosed as metastatic well-differentiated (low-grade) mucinous adenocarcinoma of appendiceal origin. Since I am a strong proponent of the ruptured adenoma concept,[95,101,432] I prefer to avoid the more ominous and broad-brush diagnosis of metastatic adenocarcinoma and instead indicate that the ovary is involved by a low-grade mucinous neoplasm (ruptured adenoma) of appendiceal origin. Another approach is to use the word "metastasis" for the sake of convenience, even if it is agreed that these are not metastases in the usual sense of the word, and refer to the ovarian tumors as metastatic low-grade mucinous neoplasms of appendiceal origin.[433,434] Note that whatever terminology is used, in the backdrop of widespread pseudomyxoma peritonei of the usual (low-grade) type, the ovary is just one of many sites of involvement by this slowly progressive disease.

Differential Diagnosis

The clinical setting and pathologic features as described and illustrated should allow for the distinction of these tumors from primary ovarian mucinous cystadenomas and borderline tumors. In problematic cases, obtaining a CK7−/CK20+ immunophenotype can be used to provide additional support for an appendiceal origin.[421] In some primary ovarian mucinous neoplasms that occur in association with mature cystic teratomas, there is a striking similarity to the secondary ovarian tumors under discussion in terms of histology, immunophenotype, and clinical presentation.[100,112,120] Identification of the teratomatous elements, which may be focal, and the documentation of a histologically normal appendix aid in the recognition of these neoplasms as primary ovarian tumors.

Appendiceal Adenocarcinoma

Signet-ring adenocarcinoma is the most common type of overt appendiceal adenocarcinoma that metastasizes to the ovary, and frequently exhibits a nested architectural pattern that results in a goblet cell carcinoid-like appearance (Fig. 7.331).[346,348,435] As is the case for other Krukenberg tumors, the prognosis is poor. It is important not to confuse this aggressive malignancy with primary ovarian mucinous carcinoid and metastatic goblet cell carcinoid, as discussed in the sections on these other entities.

Adenocarcinoma of the ordinary colorectal and mucinous gland-forming or colloid types also occurs in the appendix and can metastasize to the ovary.[435] The endometrioid-like and mucinous ovarian tumors that are produced can be confused with primary ovarian tumors or metastases from other gastrointestinal sites. The ovarian and peritoneal metastases that are derived from invasive well-differentiated mucinous carcinomas of the appendix often have histologic features that overlap with tumors of these sites that are produced by ruptured appendiceal low-grade mucinous neoplasms (cystadenomas), although thorough sampling will reveal at least focal carcinomatous differentiation.[432,436] The strategies that are discussed in the section on metastatic intestinal carcinoma that facilitate correct interpretation are applicable to this situation as well. The mucinous ovarian carcinomas of appendiceal origin, including the signet-ring variant, share CK20 immunoreactivity with metastatic colorectal adenocarcinoma, but are more likely than their colorectal counterparts to at least focally express CK7.[104,435]

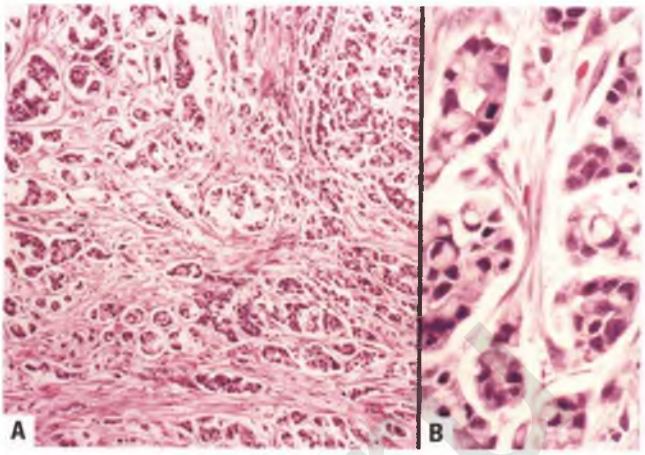

FIGURE 7.331. A,B: This goblet cell carcinoid-like nested pattern can be seen in appendiceal adenocarcinoma metastatic to the ovary. **B** highlights the presence of several signet ring cells within the nests of tumor cells.

Pancreatic and Biliary Adenocarcinoma[437–440]

Adenocarcinomas originating from the pancreas, bile ducts, and gallbladder occasionally metastasize to the ovary, where the major differential diagnostic consideration is often a benign, borderline, or malignant primary ovarian mucinous neoplasm. Patients are adult women who tend to be postmenopausal, and in most cases the primary tumor has either been detected prior to the ovarian metastases or discovered at the same time. Grossly, the ovarian tumors have an average size of about 10 cm may be either solid, mixed solid and cystic, or multicystic. Their metastatic nature is usually suggested by the high incidence of bilateral ovarian involvement, the common presence of surface implants, and the finding of tumor deposits throughout the peritoneal cavity (most primary ovarian mucinous carcinomas are unilateral, smooth-surfaced tumors that are confined to the ovary at the time of presentation). The frequent finding of tumor implants on the surface of the ovarian metastases, coupled with the low incidence of ovarian angiolymphatic invasion, suggests that the major mode of spread to

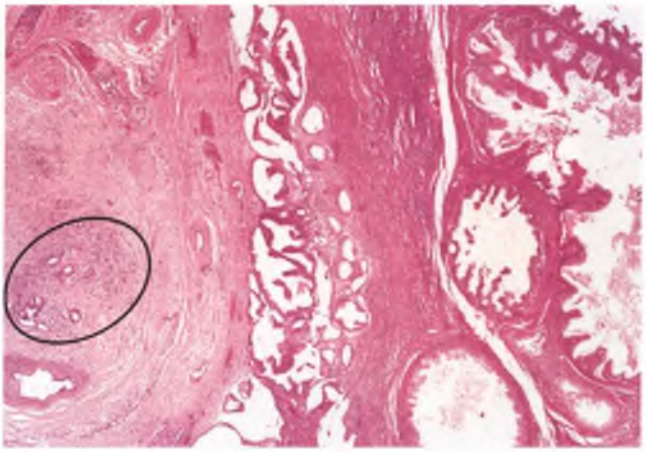

FIGURE 7.332. Pancreatic adenocarcinoma metastatic to ovary. The solid portion at left contains a cluster of small malignant glands infiltrating stroma and evoking a desmoplastic response (*circled*). At right are cystic glands reminiscent of a primary mucinous borderline tumor. Cases such as this are at risk for misinterpretation as primary borderline tumors with foci of microinvasion.

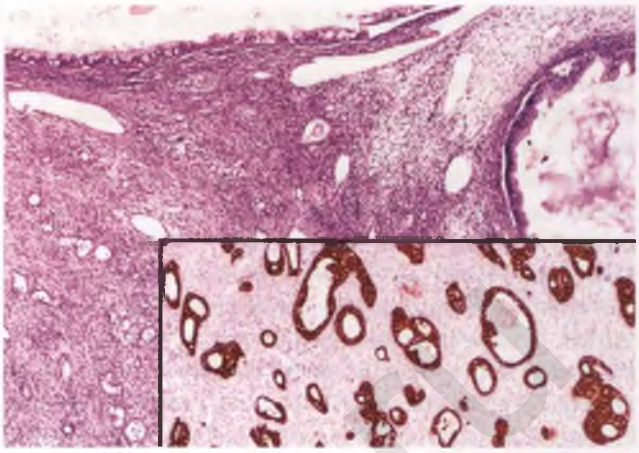

FIGURE 7.334. Biliary tract adenocarcinoma metastatic to ovary. The mucinous cysts and widely spaced glands lined by bland epithelium set within a fibromatous stroma conspire to simulate a mucinous adenofibroma. The CK7 immunostain shown in the inset highlights the glandular elements.

the ovary is transperitoneal rather than vascular in this subset of tumors.

Histologically, ovarian metastases from these sites have a variable appearance, ranging from small glands infiltrating within a desmoplastic stroma to cysts lined by mucinous epithelium with varying degrees of architectural complexity and nuclear atypia (Figs. 7.332 and 7.333). A well-documented pitfall is the presence of mucinous epithelium that can be so well differentiated that it is histologically indistinguishable from that seen in primary ovarian mucinous cystadenomas and borderline tumors (Figs. 7.334 and 7.335). When this component is abundant, it can lead to a misdiagnosis of a primary benign or borderline tumor (especially when dealing with limited clinical information and a limited tissue sample at the time of frozen section), and when focal can be misconstrued as evidence that the mucinous carcinoma is arising within a primary ovarian tumor.

The application of CK7 and CK20 immunostains that is so helpful in confirming colorectal adenocarcinoma metastatic to the ovary and ovarian involvement by adenomatous mucinous epithelium of appendiceal origin (both characteristically CK7−/CK20+) is unfortunately of no use in distinguishing primary ovarian mucinous carcinomas from adenocarcinomas of pancreatic or biliary origin, all of which typically express

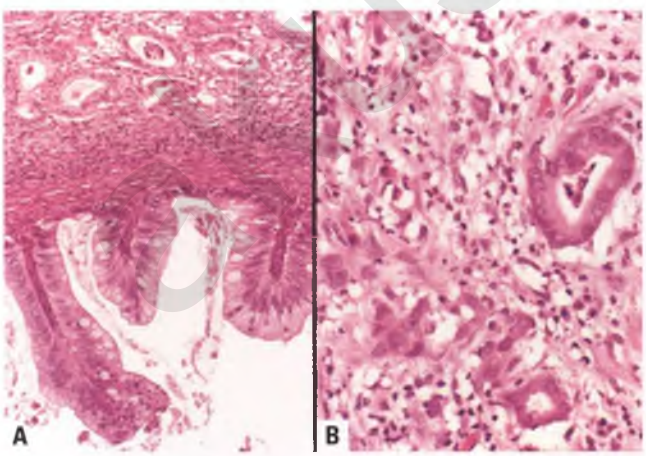

FIGURE 7.333. Pancreatic adenocarcinoma metastatic to ovary. **A:** Small infiltrative glands are present above a mucinous cyst that is lined by minimally atypical epithelium. **B:** High-magnification view of small infiltrative glands and single tumor cells with associated inflammation, edema, and fibroblastic proliferation.

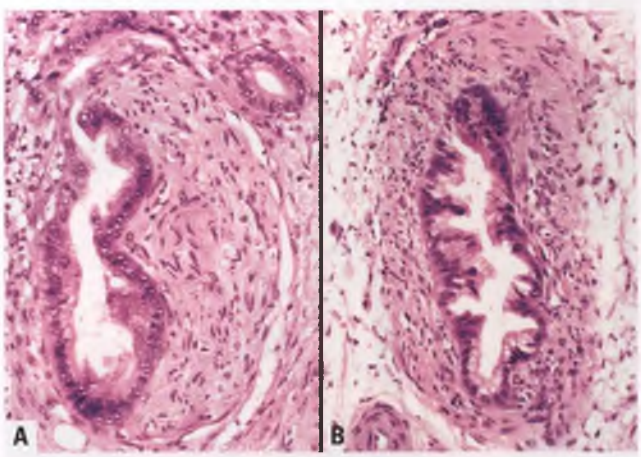

FIGURE 7.335. Biliary tract adenocarcinoma metastatic to cul-de-sac. The presence of extraovarian spread, perineural invasion **(A)**, and vascular invasion **(B)** facilitate recognition of the ovarian tumor as malignant and metastatic (same case as Fig. 7.334).

CK7.[104,441] Stated another way, if a mucinous ovarian carcinoma or borderline-like tumor is immunoreactive for CK7, then regardless of its CK20 staining pattern, the diagnostic possibilities include a primary ovarian mucinous tumor and metastases from the pancreas, gallbladder, biliary tract, stomach, and endocervix.[104,441] In about half of metastatic pancreatic carcinomas, the lack of immunoreactivity for Dpc4 can be used as supportive evidence of pancreatic origin.[440–442] However, anti-Dpc4 is not a widely available antibody because of its extremely limited utility in diagnostic surgical pathology, and the development of other markers to help identify carcinomas of pancreatic and biliary origin would be of value. Fortunately, the diagnosis of a mucinous ovarian metastasis can usually be made and its site of origin determined based upon a combination of the gross and histologic features of the ovarian tumor and correlation with the clinical history and radiologic findings.

Breast Carcinoma[443]

In patients with advanced breast cancer, it is not uncommon for the ovaries to contain small, asymptomatic nodules of metastatic carcinoma. Occasionally, metastatic breast carcinoma presents as an ovarian mass, which almost always occurs in women with a known history of breast cancer.

Ovarian involvement by metastatic breast carcinoma is bilateral in about two-thirds of cases, and when mass-forming typically produces solid, pale-tan to white coalescing nodules and modest ovarian enlargement that usually does not exceed 5 cm (Figs. 7.336–7.338). Cystic degeneration and necrosis are uncommon.

Metastases of infiltrating ductal carcinoma most commonly produce an admixture of tubular glands and solid epithelial nests, but may also exhibit papillary, cribriform, and solid patterns (Fig. 7.339). Cells derived from metastatic infiltrating lobular carcinoma typically form cords or diffuse sheets (Fig. 7.340). Rarely, signet-ring cells may predominate and serve as an uncommon source of the Krukenberg tumor.

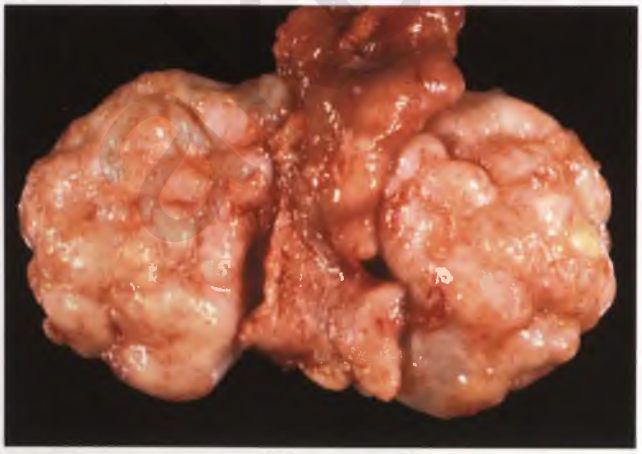

FIGURE 7.336. Breast carcinoma metastatic to ovary. Note the multinodular external surface of this bivalved tumor.

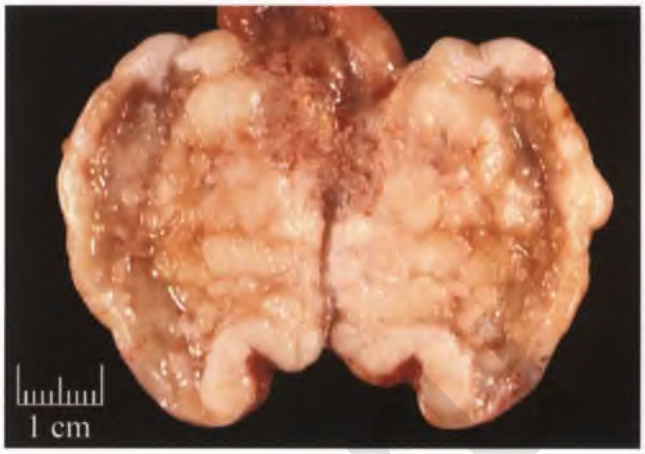

FIGURE 7.337. Breast carcinoma metastatic to ovary. The sectioned surface of the tumor in Figure 7.336 consists of multiple coalescing tumor nodules separated by edematous tissue.

In breast cancer patients who have undergone chemotherapy prior to a prophylactic salpingo-oophorectomy, pathologists need to be aware that in those rare instances of occult ovarian metastases that the tumor cells may exhibit superimposed chemotherapy-related alterations (foamy cytoplasm, less nuclear atypia, and decreased mitotic activity), and that the tumor will likely be unilateral, microscopic, and well-circumscribed.[444] In this situation, distinction from benign entities such as stromal hyperthecosis and hilus cell lesions may require immunohistochemistry. Expression of inhibin and lack of immunoreactivity for cytokeratin would be expected for these benign processes, whereas metastatic breast carcinoma should have the opposite immunophenotype.[444]

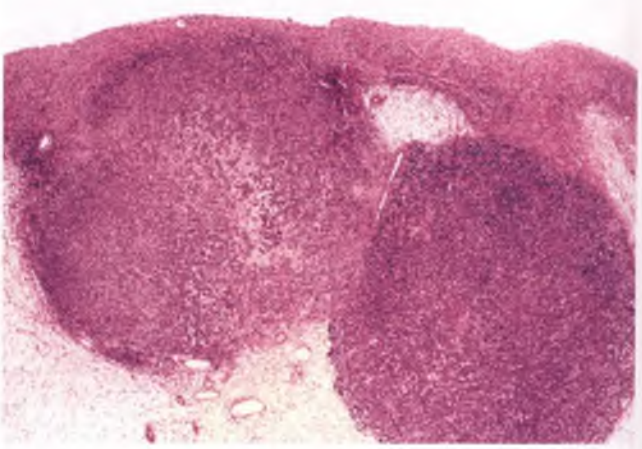

FIGURE 7.338. Breast carcinoma metastatic to ovary. Two coalescing nodules of metastatic carcinoma are present just beneath the ovarian surface. This nodular pattern of growth strongly favors metastatic over primary tumor.

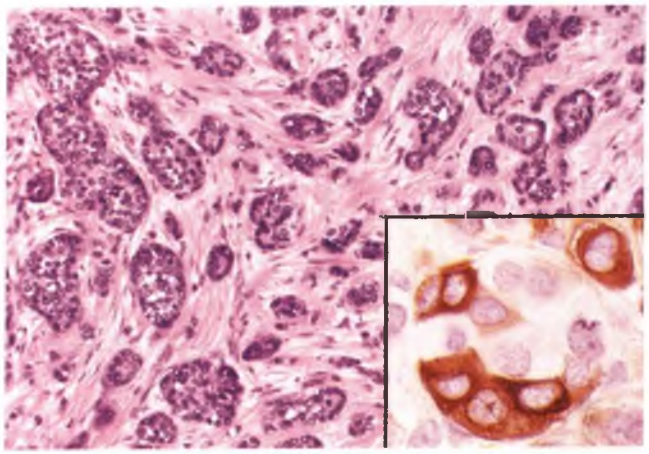

FIGURE 7.339. Breast carcinoma metastatic to ovary. This example of metastatic ductal carcinoma consists of epithelial nests and poorly formed tubules infiltrating the stroma. The inset shows strong cytoplasmic immunoreactivity in a subset of the tumor cells for gross cystic disease fluid protein-15, which helps to confirm breast origin.

Differential Diagnosis

Sizable ovarian metastases of breast carcinoma are most likely to be confused with serous carcinoma, carcinoid tumor, granulosa cell tumor, lymphoma, and leukemic infiltrates. A review of the clinical history and the slides of the previous breast cancer should be performed whenever metastatic breast carcinoma is a differential diagnostic consideration, and this may be all that is necessary to render a diagnosis. In this context, it is important to keep in mind that patients with breast cancer who have BRCA gene mutations are at an increased risk for the development of an independent primary tubo-ovarian carcinoma.[445] In cases of metastatic breast carcinoma with serous-like features, the diagnosis can be substantiated by demonstrating lack of immunoreactivity for WT-1 and PAX8, which are markers that are typically expressed in ovarian serous carcinoma and absent in breast carcinoma.[72,73] Gross cystic disease fluid protein-15 and mammaglobin are fairly specific markers for carcinomas of breast origin and can help to distinguish metastatic breast carcinoma from the above-listed entities in the differential diagnosis when immunoreactivity is demonstrated, but their suboptimal sensitivity limits their utility.[72,74,75]

The distinction of metastatic breast carcinoma from granulosa cell tumor and metastatic carcinoid tumor is discussed in the sections on these other entities. Corded and diffuse patterns derived from infiltrating lobular carcinoma can mimic lymphoma or leukemia, in which case the demonstration of cytokeratin immunoreactivity and an absence of staining for markers of lymphoid and myeloid differentiation will help to confirm the diagnosis.

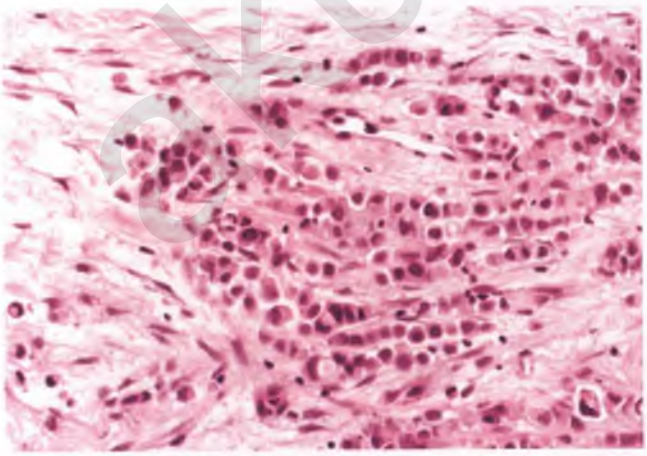

FIGURE 7.340. Breast carcinoma metastatic to ovary. The presence of a single file pattern of infiltration and occasional signet-ring cells suggest an origin from infiltrating lobular carcinoma.

Renal Cell Carcinoma[298]

Renal cell carcinoma metastatic to the ovary is rare and is easy to misinterpret because it is often unilateral, commonly presents before the renal tumor has been discovered, and histologically resembles primary ovarian clear cell carcinoma. Grossly, ovaries involved by metastatic renal cell carcinoma average about 12 cm in diameter, usually have both solid and cystic components, and may be partially hemorrhagic. The solid tissue is usually yellow or yellow-orange.

Histologically, renal cell carcinoma metastatic to the ovary is typically a clear cell carcinoma on the well to moderately differentiated end of the spectrum that grows as diffuse sheets, nests, and/or tubules. Two characteristic features are (a) a strikingly prominent lattice-like vascular pattern coursing its way between tumor cell nests and tubules (Fig. 7.341) and (b) the presence of eosinophilic, colloid-like material and/or blood within the lumens of occasional tubules (Fig. 7.342).

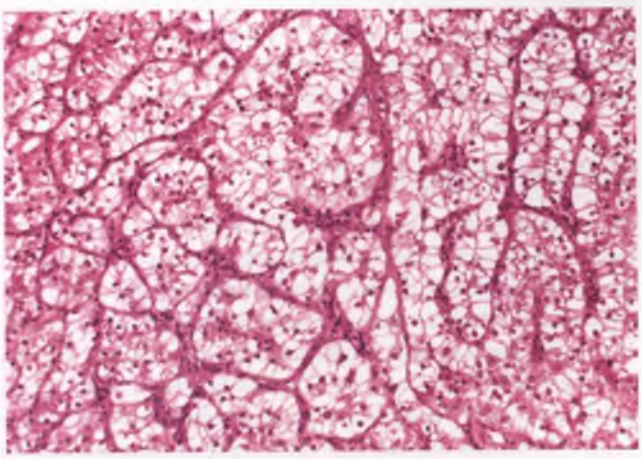

FIGURE 7.341. Metastatic renal cell carcinoma, clear cell type. A prominent lattice-like network of blood vessels supporting the nests of clear cells is a characteristic feature.

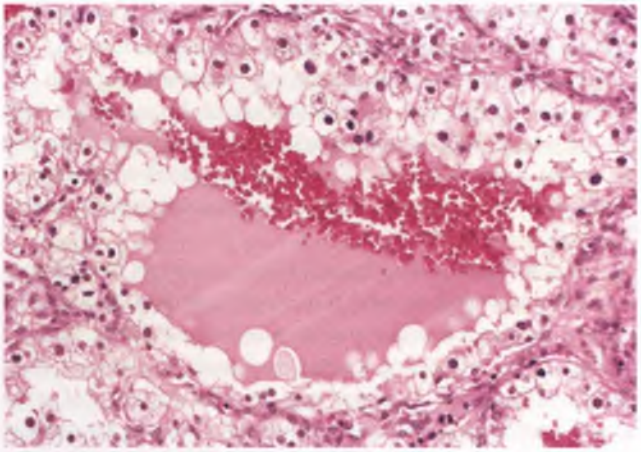

FIGURE 7.342. Metastatic renal cell carcinoma, clear cell type. In this example, the presence of occasional tubules containing colloid-like material and blood is a clue to the correct diagnosis.

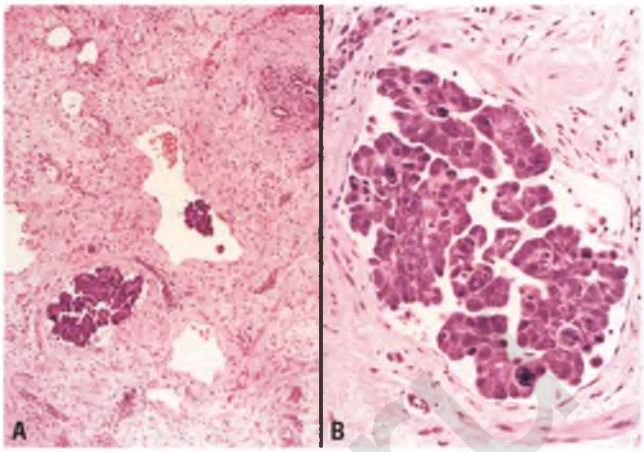

FIGURE 7.343. A,B: Uterine serous carcinoma metastatic to ovary with prominent invasion of hilar angiolymphatic spaces. Angiolymphatic invasion is more commonly present in metastatic than in primary ovarian tumors.

Differential Diagnosis

In contrast to the major differential diagnostic consideration of primary ovarian clear cell carcinoma, metastatic renal cell carcinoma (a) will have a detectable renal mass in those cases in which renal carcinoma has not already declared itself, (b) has a prominent vascular pattern, (c) is typically fairly homogeneous architecturally with an absence of admixed solid, papillary, and tubulocystic patterns, (d) does not have hobnail cells lining areas with tubular differentiation, (e) does not have papillae with hyalinized stromal cores, and (f) frequently has colloid-like material and/or blood rather than mucin within the lumen of some of its tubules. In problematic cases, immunohistochemistry can assist in distinguishing these two clear cell tumors from one another: primary ovarian clear cell carcinoma typically expresses CK7 and lacks immunoreactivity for CD10 and renal cell carcinoma marker, whereas the exact opposite immunophenotype is expected for metastatic renal cell carcinoma.[299] Since ovarian clear cell carcinoma frequently is immunoreactive for PAX-2, PAX-8, and hKIM-1, these newer and oftentimes superior markers for renal cell carcinoma do not have diagnostic utility in this particular situation.[446]

Endometrial Carcinoma

As discussed in the section on simultaneous endometrioid carcinoma of the ovary and endometrium, most such tumors that involve both of these sites are independent primary neoplasms. In those cases in which the endometrial tumor is deeply myoinvasive and/or has demonstrable angiolymphatic invasion, an ovarian metastasis should be suspected. The features listed under "general considerations" at the beginning of this section provide additional information that can facilitate making this determination.

Ovarian tumors that exhibit angiolymphatic invasion within the hilus or spotty involvement of ovarian parenchyma with encroachment upon preexisting normal structures should be suspected of being of metastatic origin. Examples of ovarian involvement by uterine serous carcinoma with these features are shown in Figures 7.343 and 7.344.

The presence of tumor cells within the lumen of the fallopian tube is most commonly seen in uterine serous rather than endometrioid carcinoma and suggests a tubal route of spread from the endometrium to the ovaries and peritoneal cavity (see Fig. 4.238).[447]

Cervical Carcinoma

Metastases to the ovary from the cervix are rare. Most cervical carcinomas with ovarian spread that create masses that simulate primary ovarian cancer are adenocarcinomas,[448,449] although

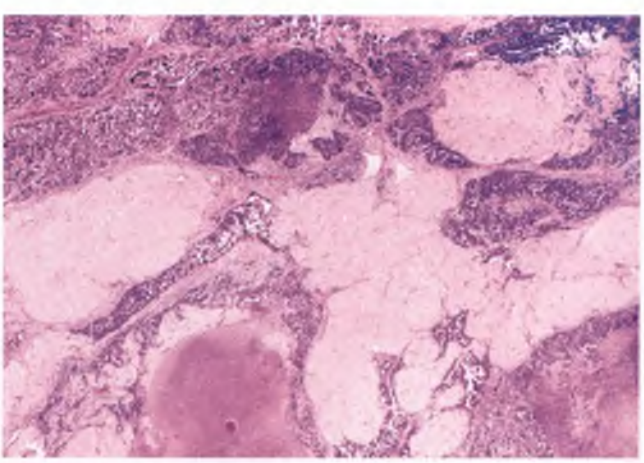

FIGURE 7.344. Uterine serous carcinoma metastatic to ovary. Note the manner in which the spotty foci of carcinoma take the path of least resistance, preferentially infiltrating stroma in between corpora albicantia rather than obliterating them. This pattern of ovarian involvement suggests metastatic disease.

squamous cell carcinoma and a variety of other less common cervical carcinomas can rarely present in a similar manner.[450]

Ovarian metastases from endocervical adenocarcinomas are often multiloculated cystic masses and may contain areas with a benign or borderline histologic appearance.[449] In some series, the cervical tumor is an adenoma malignum (minimal deviation adenocarcinoma) in a disproportionate number of cases.[449] The features that are most helpful in recognizing an endocervical adenocarcinoma that is metastatic to the ovary are (a) involvement of other sites in addition to the cervix and ovaries, (b) bilaterality of the ovarian tumors, (c) the presence of tumor implants on the surface of the ovary, (d) a deeply invasive endocervical tumor, and (e) the identification of angiolymphatic invasion within either tumor.[449]

HPV-Related Ovarian Tumors: Metastases or Separate Primaries?

When an ovarian tumor with mucinous or endometrioid-like histology has the appearance of a borderline tumor or well-differentiated carcinoma and exhibits numerous apoptotic bodies in association with frequent juxtaluminal mitotic figures, the possibility of an HPV-related tumor should be considered (especially if a pseudoendometrioid tumor with these characteristics lacks squamous differentiation and is not associated with endometriosis or an adenofibromatous component).[451,452] When such a tumor has been documented to contain HPV and is associated with a concurrent or prior HPV-positive endocervical adenocarcinoma, it may represent a metastasis from the endocervical tumor. An ovarian metastasis is particularly likely if several of the features itemized as (a)–(e) in the preceding paragraph are present.

More controversial are similar HPV-related ovarian tumors that are associated with minimally invasive or noninvasive endocervical adenocarcinomas in a setting with disease limited to these two sites. Using documentation of identical HPV types of the ovarian and cervical tumors as "rigorous, compelling, and definitive evidence," some investigators consider the endocervical origin of these ovarian tumors to be an established fact, and suggest that the tumor may spread from the endocervix to the ovaries via retrograde transtubal transport of exfoliated neoplastic cells.[452,453] I consider the HPV-related data to be circumstantial rather than compelling evidence, and have put forth an alternative explanation of independent primary endocervical and ovarian neoplasms generated by an HPV-related "field effect" that targets these two sites.[454,455] I also interpret the only example of tumor cells actually found within the tubal lumen in HPV-matched endocervical and ovarian tumors that has been reported thus far[456] as being related to an exophytic ovarian tumor of probable metastatic origin shedding cells that are traveling downstream rather than representing cells ascending from an endocervical adenocarcinoma.

An HPV-related "field effect" that targets the endocervix and ovaries would account for the selective involvement of these two sites, the lack of the usual features of ovaries that are involved by metastatic disease (angiolymphatic invasion, destructive stromal invasion, surface implants, and frequent bilaterality), the absence of any documented tumor-related deaths in patients whose HPV-matched disease at the time of detected ovarian involvement was limited to the endocervix and ovaries, and the lack of any recognizable clinical significance to the "misclassification" of these ovarian tumors as low-grade/borderline primary rather than metastatic tumors in the many years that preceded recognition of their shared HPV expression.[454,455] Long term follow-up information on significant numbers of such patients, determination of the frequency of HPV-positivity of tumors previously diagnosed as low-grade/borderline endometrioid/mucinous ovarian tumors proven by many years of uneventful follow-up to be primary rather than metastatic tumors, and additional molecular genetic analysis that might help to establish or refute a clonal relationship (such as comparing HPV integration sites in the pairs of endocervical and ovarian tumors) would help to resolve this controversy, but have yet to be reported.

On a related note, whether strong and diffuse immunoreactivity for p16 in ovarian tumors with endometrioid or mucinous histology supports an HPV-related etiology is also controversial.[457–459]

Fallopian Tube Carcinoma

As discussed in Chapter 5 and elsewhere in this chapter, it now appears that most serous carcinomas that we currently refer to as being of ovarian origin actually originate within the fallopian tube. This revelation will create some classification issues as we grapple with the problem of when to diagnose such ovarian tumors as metastases.

Carcinoid Tumors[238,460]

The source of most carcinoid tumors that are metastatic to the ovary is the small intestine, and this site (particularly the distal ileum) should be thoroughly examined intraoperatively if a pure carcinoid tumor is encountered at the time of frozen section. Ovarian metastases of this type are rare and occur in adult women, about one-third of whom have the carcinoid syndrome. Both ovaries are involved and tumor has spread to other abdominal and/or pelvic sites in nearly all such cases. The ovarian metastases have a smooth or multinodular external surface. Their sectioned surface is typically predominantly solid, firm, and tannish yellow.

Histologically, most carcinoid tumors that are metastatic to the ovary are indistinguishable from primary insular carcinoid tumors (see Figs. 7.253–7.255), although trabecular patterns are seen occasionally. A prominent fibromatous stromal reaction is often induced by the metastatic carcinoid tumor (Fig. 7.345). As is the case for neuroendocrine tumors in general, carcinoid tumors can demonstrate striking degenerative nuclear atypia that may cause an unwary pathologist to mistakenly consider other diagnostic possibilities or to have concerns about tumors with this feature exhibiting more aggressive behavior (Fig. 7.346). The occasional presence of follicle-like spaces can be another source of diagnostic confusion (Fig. 7.347). Making the correct diagnosis is important, since with modern treatment methods the 5-year survival rates

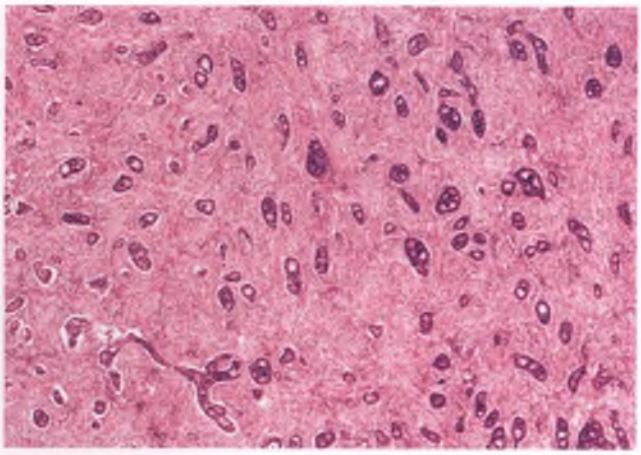

FIGURE 7.345. Ileal carcinoid tumor metastatic to ovary. Nests and acini of insular carcinoid tumor are embedded in a prominent fibromatous stroma.

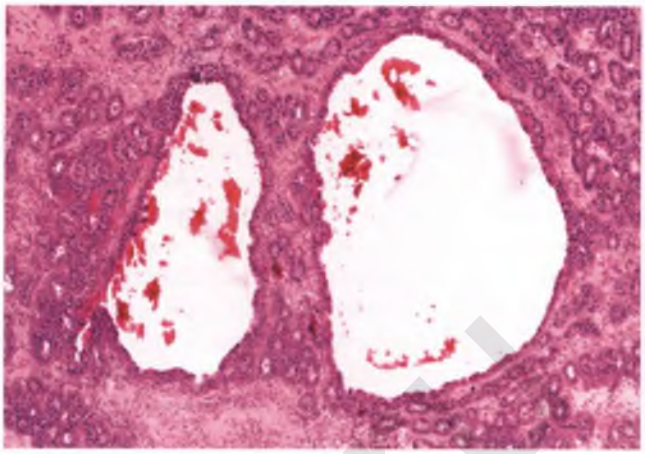

FIGURE 7.347. Ileal carcinoid tumor metastatic to ovary. This image highlights the presence of two follicle-like spaces.

for carcinoid tumor metastatic to the ovary have improved dramatically and can exceed 90%, which is far higher than the expected survival rates of the metastatic adenocarcinomas with which it can be confused.[460]

Differential Diagnosis

Features that favor metastatic over primary carcinoid tumor are the presence of a known primary carcinoid tumor within the gastrointestinal tract, bilateral ovarian involvement, a multinodular growth pattern, high-stage disease, and the absence of an associated primary ovarian tumor.[238,280] Other entities in the differential diagnosis such as adult granulosa cell tumor, Brenner tumor, endometrioid adenofibroma, and metastatic breast carcinoma are distinguished by their different nuclear and cytoplasmic features, low-stage disease (with the exception of metastatic breast carcinoma), and their usual lack of immunoreactivity with neuroendocrine markers such as synaptophysin and chromogranin.

In those rare instances in which a pattern resembling a goblet cell carcinoid is encountered and the tumor is considered to be a metastasis by virtue of its bilaterality and lack of association with a dermoid cyst or other primary cystic ovarian tumor, the appendix should be included on the short list of possible primary sites. The vast majority of such tumors of appendiceal origin contain areas with more infiltrative architectural patterns and more prominent signet-ring cells than well-differentiated goblet cell carcinoids, are associated with a poor prognosis, and should be diagnosed as full-fledged metastatic adenocarcinomas rather than metastatic goblet cell carcinoids even though they may focally express neuroendocrine markers.[346,435]

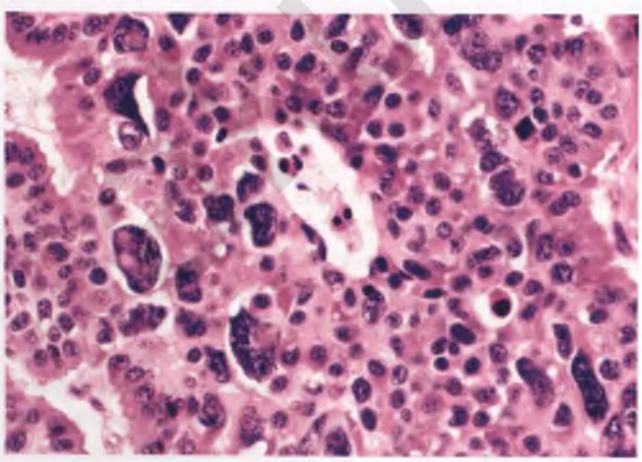

FIGURE 7.346. Ileal carcinoid tumor metastatic to ovary. Note the striking degenerative nuclear atypia that was a focal finding in this tumor.

Malignant Melanoma[241,242,461]

Ovarian involvement by metastatic melanoma is rarely encountered in a surgical setting, and occurs in patients with a mean age of about 35 to 40 years who usually have a recent or remote history of primary melanoma in another site. Although ovarian metastases in general are likely to be bilateral, metastatic melanoma is bilateral in only about 40% of cases. Ovaries involved by metastatic melanoma have an average size of 10 cm with a smooth and nodular external surface. The sectioned surface is predominantly solid in most cases, and the individual nodules of metastatic melanoma may or may not contain grossly visible quantities of melanin pigment (Fig. 7.348).

As illustrated in the section on vulvar melanoma (Figs. 1.101–1.106), melanoma is composed of epithelioid and/or spindle-shaped cells that produce a diverse spectrum of histologic patterns. In the ovary, metastatic melanoma often forms follicle-like spaces, which can lead to misinterpretation as a primary ovarian tumor (Fig. 7.349). Clues to the correct diagnosis

FIGURE 7.348. Malignant melanoma metastatic to ovary. The sectioned surface of this irregularly shaped ovarian mass exhibits multiple nodules of varying size and color. The multinodular growth pattern is characteristic of a metastatic tumor, and the tannish-brown appearance of the solid tissue within the large hemorrhagic nodule further suggests melanoma. (Courtesy of Dr. Richard L. Payne.)

of metastatic melanoma, which may or may not be present in an individual case, are (a) a known history of melanoma, (b) tumor bilaterality, (c) a multinodular growth pattern, (d) melanin pigment, (e) intranuclear pseudoinclusions, and (f) immunoreactivity with one or more melanoma markers (S100, HMB-45, and Melan-A) in conjunction with expected lack of staining for cytokeratin and inhibin. Although rarely needed, ultrastructural analysis with demonstration of melanosomes or premelanosomes can also help to establish the diagnosis of melanoma.

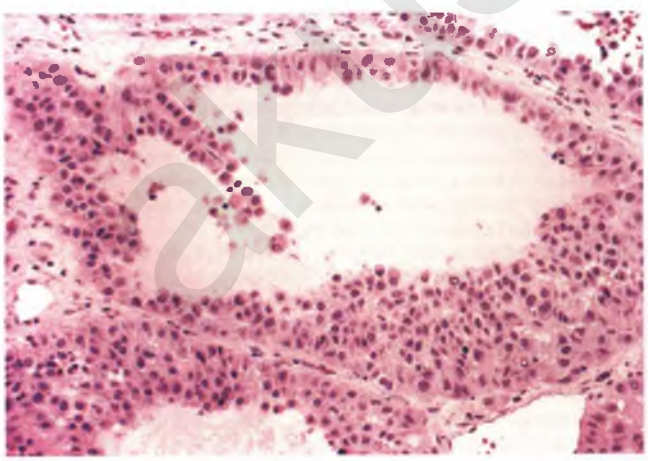

FIGURE 7.349. Malignant melanoma metastatic to ovary. The presence of follicle-like spaces can result in confusion with juvenile granulosa cell tumor or small cell carcinoma of hypercalcemic type. The presence of scattered cells with intranuclear pseudoinclusions is a clue to the correct diagnosis.

Differential Diagnosis

Primary malignant melanoma of the ovary is very rare, and the best documented cases are distinguished from metastatic melanoma by their association with teratomatous elements (dermoid cyst or struma ovarii), the lack of a prior history of melanoma, and unilateral ovarian involvement.[350] Most poorly differentiated carcinomas have a cytokeratin-positive, S100-negative immunophenotype, which is the opposite of that expected for metastatic melanoma. The differential diagnoses of metastatic melanoma with steroid cell tumor, granulosa cell tumor of adult and juvenile types, SCCHT, and pregnancy luteoma are discussed in the sections on these other entities.

Sarcomas

A wide variety of sarcomas have been reported to metastasize to the ovary on rare occasions, the most common of which is endometrial stromal sarcoma (ESS).[178] Metastatic ESS often involves both ovaries and other sites within the abdomen and pelvis, is typically associated with a known history of prior or concurrent uterine ESS, and lacks an association with endometriosis. These features help to distinguish metastatic from primary ovarian ESS.

Metastatic gastointestinal stromal tumor (GIST) has recently received attention because of the availability of targeted therapy and its ability to mimic tumors with a wide range of therapeutic implications (e.g., primary cellular fibroma, primary fibrosarcoma, metastatic leiomyosarcoma, or metastatic spindle cell melanoma).[254] In this site, metastatic GIST typically has either a spindle cell morphology similar to that depicted in Figure 2.41 or may have admixed spindle cell and epithelioid elements. Recognition of the true nature of this tumor is facilitated by correlation with clinical history, the high incidence of bilateral ovarian involvement, and the demonstration of a c-KIT (CD117)-positive, desmin-negative, S100-negative immunophenotype.

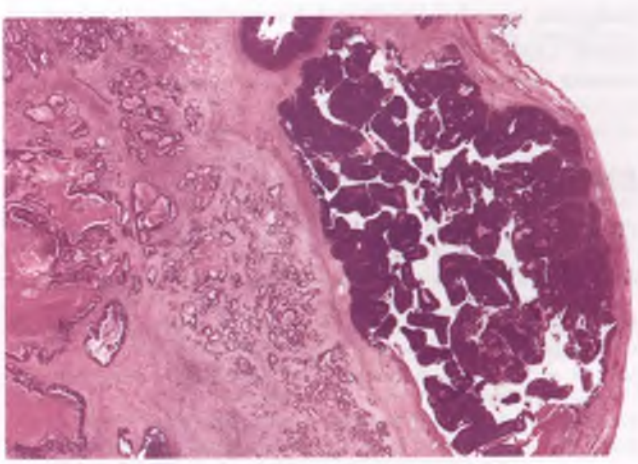

FIGURE 7.350. Colonic adenocarcinoma (left) metastatic to primary ovarian transitional cell carcinoma (right).

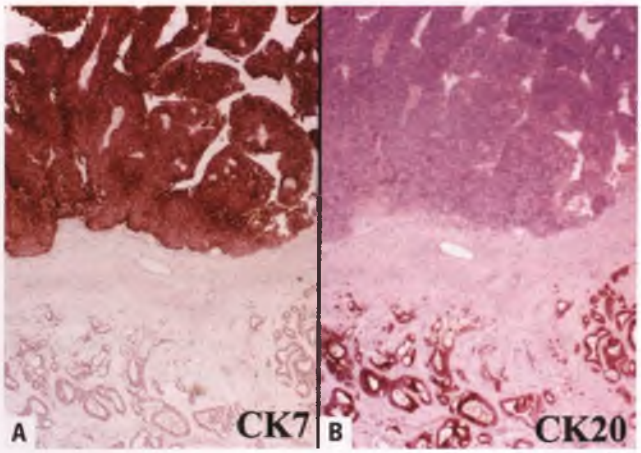

FIGURE 7.351. Colonic adenocarcinoma metastatic to primary ovarian transitional cell carcinoma. **A:** CK7 immunostain. **B:** CK20 immunostain. The metastatic colonic adenocarcinoma (bottom) is CK7–/CK20+, whereas the primary ovarian transitional cell carcinoma (top) is CK7+/CK20–.

Metastasis to a Primary Ovarian Tumor

Very rarely, a carcinoma may metastasize to an ovary that contains a preexisting primary ovarian tumor, which itself may be benign or malignant.[202,398] An example of a "collision tumor" composed of metastatic colonic adenocarcinoma and a primary ovarian transitional cell carcinoma (TCC) is illustrated in Figures 7.350 and 7.351.

Miscellaneous Tumors

Metastatic carcinomas that could conceivably be misinterpreted as primary ovarian neoplasms that occur at case-reportable frequencies include metastases from lung carcinoma,[398] small cell carcinomas of nonpulmonary origin,[397] hepatocellular carcinoma,[210] TCC of the renal pelvis and urinary bladder,[462] and acinar cell carcinoma of the pancreas.[463] In rare cases, malignant mesothelioma[464] and desmoplastic small round cell tumor[465] may present with dominant ovarian involvement in a manner that mimics primary ovarian neoplasia.

SUGGESTED READINGS

Clement PB, Young RH. *Atlas of Gynecologic Surgical Pathology*. 2nd ed. Philadelphia, PA: Elsevier Saunders; 2008.

Crum CP, Nucci MR, Lee K, eds. *Diagnostic Gynecologic and Obstetric Pathology*. 2nd ed. Philadelphia, PA: Elsevier Saunders; 2011.

Kurman RJ, Ellenson LH, Ronnett BM, eds. *Blaustein's Pathology of the Female Genital Tract*. 6th ed. New York: Springer; 2011.

Mills SE, ed. *Histology for Pathologists*. 3rd ed. Philadelphia, PA: Lippincott Williams & Wilkins; 2006.

Prat J. Pathology of the Ovary. Philadelphia, PA: Saunders, 2004.

Robboy SJ, Mutter GL, Prat J, et al., eds. *Robboy's Pathology of the Female Reproductive Tract*. 2nd ed. Oxford,UK: Churchill Livingstone; 2009.

Scully RE, Young, RH, Clement PB. *Tumors of the Ovary, Maldeveloped Gonads, Fallopian Tube, and Broad Ligament. Atlas of Tumor Pathology, Third series, Fascicle 23*. Washington, DC: Armed Forces Institute of Pathology; 1998.

Tavassoli FA, Devilee P, eds. *World Health Organization Classification of Tumors. Pathology and Genetics of Tumours of the Breast and Female Genital Organs*. Lyon, France: IARC Press. 2003: 113–196.

REFERENCES

1. Koonings PP, Campbell K, Mishell DR, Jr, et al. Relative frequency of primary ovarian neoplasms: a 10-year review. *Obstet Gynecol*. 1989;74:921–926.
2. Hendrickson MR, Longacre TA, Kempson RL. Clinicopathology of malignant surface epithelial neoplasms of the ovary. In: Hendrickson MR, ed. *Pathology: State of the Art Reviews—Surface Epithelial Neoplasms of the Ovary*. Philadelphia, PA: Hanley & Belfus, Inc.; 1993:367–410.
3. Sato Y, Shimamoto T, Amada S, et al. Prognostic value of histologic grading of ovarian carcinomas. *Int J Gynecol Pathol*. 2003;22:52–56.
4. Shimizu Y, Kamoi S, Amada S, et al. Toward the development of a universal grading system for ovarian epithelial carcinoma: testing of a proposed system in a series of 461 patients with uniform treatment and follow-up. *Cancer*. 1998;82:893–901.
5. FIGO Committee on Gynecologic Oncology. Current FIGO staging for cancer of the vagina, fallopian tube, ovary, and gestational trophoblastic neoplasia. *Int J Gynecol Obstet*. 2009;105:3–4.
6. Seidman JD, Yemelyanova AV, Khedmati F, et al. Prognostic factors for stage I ovarian carcinoma. *Int J Gynecol Pathol*. 2010;29:1–7.
7. American Cancer Society. *Cancer Facts & Figures 2010*. Atlanta, GA: American Cancer Society; 2010.
8. Bell DA, Scully RE. Early de novo ovarian carcinoma. A study of fourteen cases. *Cancer*. 1994;73:1859–1864.
9. Scully RE, Young RH, Clement PB. *Tumors of the Ovary, Maldeveloped Gonads, Fallopian Tube, and Broad Ligament. Atlas of Tumor Pathology, Third series, Fascicle 23*. Washington, DC: Armed Forces Institute of Pathology; 1998.
10. Crum CP, Drapkin R, Kindelberger D, et al. Lessons from BRCA: the tubal fimbria emerges as an origin for pelvic serous cancer. *Clin Med Res*. 2007;5:35–44.
11. Kindelberger DW, Lee Y, Miron A, et al. Intraepithelial carcinoma of the fimbria and pelvic serous carcinoma: evidence for a causal relationship. *Am J Surg Pathol*. 2007;31:161–169.
12. Crum CP. Intercepting pelvic cancer in the distal fallopian tube: theories and realities. *Mol Oncol*. 2009;3:165–170.
13. Przybycin CG, Kurman RJ, Ronnett BM, et al. Are all pelvic (nonuterine) serous carcinomas of tubal origin? *Am J Surg Pathol*. 2010;34:1407–1416.
14. Kurman RJ, Shih Ie M. The origin and pathogenesis of epithelial ovarian cancer: a proposed unifying theory. *Am J Surg Pathol*. 2010;34:433–443.
15. Seidman JD, Khedmati F. Exploring the histogenesis of ovarian mucinous and transitional cell (Brenner) neoplasms and their relationship with Walthard cell nests: a study of 120 tumors. *Arch Pathol Lab Med*. 2008;132:1753–1760.
16. Katsube Y, Berg JW, Silverberg SG. Epidemiologic pathology of ovarian tumors: a histopathologic review of primary ovarian neoplasms diagnosed in the Denver Standard Metropolitan Statistical Area, 1 July-31 December 1969 and 1 July-31 December 1979. *Int J Gynecol Pathol*. 1982;1:3–16.
17. Malpica A, Deavers MT, Lu K, et al. Grading ovarian serous carcinoma using a two-tier system. *Am J Surg Pathol*. 2004;28:496–504.
18. Gilks CB, Ionescu DN, Kalloger SE, et al. Tumor cell type can be reproducibly diagnosed and is of independent prognostic significance in patients with maximally debulked ovarian carcinoma. *Hum Pathol*. 2008;39:1239–1251.
19. Silverberg SG. Histopathologic grading of ovarian carcinoma: a review and proposal. *Int J Gynecol Pathol*. 2000;19:7–15.
20. Gershenson DM, Sun CC, Lu KH, et al. Clinical behavior of stage II-IV low-grade serous carcinoma of the ovary. *Obstet Gynecol*. 2006;108:361–368.
21. Malpica A, Deavers MT, Tornos C, et al. Interobserver and intraobserver variability of a two-tier system for grading ovarian serous carcinoma. *Am J Surg Pathol*. 2007;31:1168–1174.
22. Vang R, Shih Ie M, Salani R, et al. Subdividing ovarian and peritoneal serous carcinoma into moderately differentiated and poorly differentiated does not have biologic validity based on molecular genetic and in vitro drug resistance data. *Am J Surg Pathol*. 2008;32:1667–1674.
23. Seidman JD, Soslow RA, Vang R, et al. Borderline ovarian tumors: diverse contemporary viewpoints on terminology and diagnostic criteria with illustrative images. *Hum Pathol*. 2004;35:918–933.
24. Kurman RJ, Trimble CL. The behavior of serous tumors of low malignant potential: are they ever malignant? *Int J Gynecol Pathol*. 1993;12:120–127.
25. Seidman JD, Kurman RJ. Ovarian serous borderline tumors: a critical review of the literature with emphasis on prognostic indicators. *Hum Pathol*. 2000;31:539–557.

26. Kempson RL, Hendrickson MR. Ovarian serous borderline tumors: the citadel defended. *Hum Pathol.* 2000;31:525–526.
27. Bell DA, Longacre TA, Prat J, et al. Serous borderline (low malignant potential, atypical proliferative) ovarian tumors: workshop perspectives. *Hum Pathol.* 2004;35:934–948.
28. Kurman RJ, Seidman JD, Shih IM. Serous borderline tumours of the ovary. *Histopathology.* 2005;47:310–315.
29. Longacre TA, Kempson RL, Hendrickson MR. Serous tumours of low malignant potential (serous borderline tumours): moving toward detente. *Histopathology.* 2005;47:315–318.
30. Longacre TA, McKenney JK, Tazelaar HD, et al. Ovarian serous tumors of low malignant potential (borderline tumors): outcome-based study of 276 patients with long-term (≥5-year) follow-up. *Am J Surg Pathol.* 2005;29:707–723.
31. Prat J, De Nictolis M. Serous borderline tumors of the ovary: a long-term follow-up study of 137 cases, including 18 with a micropapillary pattern and 20 with microinvasion. *Am J Surg Pathol.* 2002;26:1111–1128.
32. Eichhorn JH, Bell DA, Young RH, et al. Ovarian serous borderline tumors with micropapillary and cribriform patterns: a study of 40 cases and comparison with 44 cases without these patterns. *Am J Surg Pathol.* 1999;23:397–409.
33. Slomovitz BM, Caputo TA, Gretz HF, et al. A comparative analysis of 57 serous borderline tumors with and without a noninvasive micropapillary component. *Am J Surg Pathol.* 2002;26:592–600.
34. Burks RT, Sherman ME, Kurman RJ. Micropapillary serous carcinoma of the ovary. A distinctive low-grade carcinoma related to serous borderline tumors. *Am J Surg Pathol.* 1996;20:1319–1330.
35. Smith Sehdev AE, Sehdev PS, Kurman RJ. Noninvasive and invasive micropapillary (low-grade) serous carcinoma of the ovary: a clinicopathologic analysis of 135 cases. *Am J Surg Pathol.* 2003;27:725–736.
36. Seidman JD, Kurman RJ. Subclassification of serous borderline tumors of the ovary into benign and malignant types. A clinicopathologic study of 65 advanced stage cases. *Am J Surg Pathol.* 1996;20:1331–1345.
37. Deavers MT, Gershenson DM, Tortolero-Luna G, et al. Micropapillary and cribriform patterns in ovarian serous tumors of low malignant potential: a study of 99 advanced stage cases. *Am J Surg Pathol.* 2002;26:1129–1141.
38. Rollins SE, Young RH, Bell DA. Autoimplants in serous borderline tumors of the ovary: a clinicopathologic study of 30 cases of a process to be distinguished from serous adenocarcinoma. *Am J Surg Pathol.* 2006;30:457–462.
39. Bell DA, Scully RE. Ovarian serous borderline tumors with stromal microinvasion: a report of 21 cases. *Hum Pathol.* 1990;21:397–403.
40. Tavassoli FA. Serous tumor of low malignant potential with early stromal invasion (serous LMP with microinvasion). *Mod Pathol.* 1988;1:407–414.
41. McKenney JK, Balzer BL, Longacre TA. Patterns of stromal invasion in ovarian serous tumors of low malignant potential (borderline tumors): a reevaluation of the concept of stromal microinvasion. *Am J Surg Pathol.* 2006;30:1209–1221.
42. Sangoi AR, McKenney JK, Dadras SS, et al. Lymphatic vascular invasion in ovarian serous tumors of low malignant potential with stromal microinvasion: a case control study. *Am J Surg Pathol.* 2008;32:261–268.
43. Bell DA, Weinstock MA, Scully RE. Peritoneal implants of ovarian serous borderline tumors. Histologic features and prognosis. *Cancer.* 1988;62:2212–2222.
44. Bell KA, Smith Sehdev AE, Kurman RJ. Refined diagnostic criteria for implants associated with ovarian atypical proliferative serous tumors (borderline) and micropapillary serous carcinomas. *Am J Surg Pathol.* 2001;25:419–432.
45. Segal GH, Hart WR. Ovarian serous tumors of low malignant potential (serous borderline tumors). The relationship of exophytic surface tumor to peritoneal "implants." *Am J Surg Pathol.* 1992;16:577–583.
46. Silva EG, Kurman RJ, Russell P, et al. Symposium: ovarian tumors of borderline malignancy. *Int J Gynecol Pathol.* 1996;15:281–302.
47. Gilks CB, Alkushi A, Yue JJ, et al. Advanced-stage serous borderline tumors of the ovary: a clinicopathological study of 49 cases. *Int J Gynecol Pathol.* 2003;22:29–36.
48. Lee ES, Leong ASY, Kim YS, et al. Calretinin, CD34, and alpha-smooth muscle actin in the identification of peritoneal invasive implants of serous borderline tumors of the ovary. *Mod Pathol.* 2006;19:364–372.
49. McKenney JK, Gilks CB, Longacre TA. Classification of extra-ovarian implants associated with ovarian serous tumors of low malignant potential (S-LMP): Clinicopathologic study of 181 cases. *Mod Pathol.* 2005;18:195A.
50. Gershenson DM, Silva EG, Levy L, et al. Ovarian serous borderline tumors with invasive peritoneal implants. *Cancer.* 1998;82:1096–1103.
51. Scully RE, Young RH, Clement PB. *Tumors of the Ovary, Maldeveloped Gonads, Fallopian Tube, and Broad Ligament. Atlas of Tumor Pathology, Third series, Fascicle 23.* Washington, DC: Armed Forces Institute of Pathology; 1998:482–484.
52. Seidman JD, Sherman ME, Bell KA, et al. Salpingitis, salpingoliths, and serous tumors of the ovaries: is there a connection? Int J Gynecol Pathol. 2002;21:101–107.
53. McKenney JK, Balzer BL, Longacre TA. Lymph node involvement in ovarian serous tumors of low malignant potential (borderline tumors): pathology, prognosis, and proposed classification. *Am J Surg Pathol.* 2006;30:614–624.
54. Djordjevic B, Malpica A. Lymph node involvement in ovarian serous tumors of low malignant potential: a clinicopathologic study of thirty-six cases. *Am J Surg Pathol.* 2010;34:1–9.
55. Djordjevic B, Clement-Kruzel S, Atkinson NE, et al. Nodal endosalpingiosis in ovarian serous tumors of low malignant potential with lymph node involvement: a case for a precursor lesion. *Am J Surg Pathol.* 2010;34:1442–1448.
56. Tan LK, Flynn SD, Carcangiu ML. Ovarian serous borderline tumors with lymph node involvement. Clinicopathologic and DNA content study of seven cases and review of the literature. *Am J Surg Pathol.* 1994;18:904–912.
57. Malpica A, Deavers MT, Gershenson D, et al. Serous tumors involving extra-abdominal/extra-pelvic sites after the diagnosis of an ovarian serous neoplasm of low malignant potential. *Am J Surg Pathol.* 2001;25:988–996.
58. Verbruggen MB, Verheijen RH, van de Goot FR, et al. Serous borderline tumor of the ovary presenting with cervical lymph node involvement: a report of 3 cases. *Am J Surg Pathol.* 2006;30:739–743.
59. Parker RL, Clement PB, Chercover DJ, et al. Early recurrence of ovarian serous borderline tumor as high-grade carcinoma: a report of two cases. *Int J Gynecol Pathol.* 2004;23:265–272.
60. Silva EG, Tornos C, Zhuang Z, et al. Tumor recurrence in stage I ovarian serous neoplasms of low malignant potential. *Int J Gynecol Pathol.* 1998;17:1–6.
61. Silva EG, Gershenson DM, Malpica A, et al. The recurrence and the overall survival rates of ovarian serous borderline neoplasms with noninvasive implants is time dependent. *Am J Surg Pathol.* 2006;30:1367–1371.
62. Vang R, Shih IM, Kurman RJ. Ovarian low-grade and high-grade serous carcinoma: pathogenesis, clinicopathologic and molecular biologic features, and diagnostic problems. *Adv Anat Pathol.* 2009;16:267–282.
63. Gilks CB, Prat J. Ovarian carcinoma pathology and genetics: recent advances. *Hum Pathol.* 2009;40:1213–1223.
64. Silva EG, Deavers MT, Malpica A. Patterns of low-grade serous carcinoma with emphasis on the nonepithelial-lined spaces pattern of invasion and the disorganized orphan papillae. *Int J Gynecol Pathol.* 2010;29:507–512.
65. Yemelyanova A, Mao TL, Nakayama N, et al. Low-grade serous carcinoma of the ovary displaying a macropapillary pattern of invasion. *Am J Surg Pathol.* 2008;32:1800–1806.
66. Singer G, Shih Ie M, Truskinovsky A, et al. Mutational analysis of K-ras segregates ovarian serous carcinomas into two types: invasive MPSC (low-grade tumor) and conventional serous carcinoma (high-grade tumor). *Int J Gynecol Pathol.* 2003;22:37–41.
67. Ayhan A, Kurman RJ, Yemelyanova A, et al. Defining the cut point between low-grade and high-grade ovarian serous carcinomas: a clinicopathologic and molecular genetic analysis. *Am J Surg Pathol.* 2009;33:1220–1224.
68. Dehari R, Kurman RJ, Logani S, et al. The development of high-grade serous carcinoma from atypical proliferative (borderline) serous tumors and low-grade micropapillary serous carcinoma: a morphologic and molecular genetic analysis. *Am J Surg Pathol.* 2007;31:1007–1012.
69. O'Neill CJ, Deavers MT, Malpica A, et al. An immunohistochemical comparison between low-grade and high-grade ovarian serous carcinomas: significantly higher expression of p53, MIB1, BCL2, HER-2/neu, and C-KIT in high-grade neoplasms. *Am J Surg Pathol.* 2005;29:1034–1041.
70. DeLair D, Oliva E, Kobel M, et al. Morphologic spectrum of immunohistochemically characterized clear cell carcinoma of the ovary: a study of 155 cases. *Am J Surg Pathol.* 2011;35:36–44.
71. Kobel M, Kalloger SE, Carrick J, et al. A limited panel of immunomarkers can reliably distinguish between clear cell and high-grade serous carcinoma of the ovary. *Am J Surg Pathol.* 2009;33:14–21.
72. Tornos C, Soslow R, Chen S, et al. Expression of WT1, CA 125, and GCDFP-15 as useful markers in the differential diagnosis of primary ovarian carcinomas versus metastatic breast cancer to the ovary. *Am J Surg Pathol.* 2005;29:1482–1489.
73. Nonaka D, Chiriboga L, Soslow RA. Expression of Pax8 as a useful marker in distinguishing ovarian carcinomas from mammary carcinomas. *Am J Surg Pathol.* 2008;32:1566–1571.
74. Kanner WA, Galgano MT, Stoler MH, et al. Distinguishing breast carcinoma from Mullerian serous carcinoma with mammaglobin and mesothelin. *Int J Gynecol Pathol.* 2008;27:491–495.
75. Sasaki E, Tsunoda N, Hatanaka Y, et al. Breast-specific expression of MGB1/mammaglobin: an examination of 480 tumors from various organs and clinicopathological analysis of MGB1-positive breast cancers. *Mod Pathol.* 2007;20:208–214.
76. Lim MC, Kang S, Lee KS, et al. The clinical significance of hepatic parenchymal metastasis in patients with primary epithelial ovarian cancer. *Gynecol Oncol.* 2009;112:28–34.

77. Otrock ZK, Seoud MA, Khalifeh MJ, et al. Laparoscopic splenectomy for isolated parenchymal splenic metastasis of ovarian cancer. *Int J Gynecol Cancer.* 2006;16:1933–1935.
78. Scully RE, Young RH, Clement PB. *Tumors of the Ovary, Maldeveloped Gonads, Fallopian Tube, and Broad Ligament. Atlas of Tumor Pathology, Third series, Fascicle 23.* Washington, DC: Armed Forces Institute of Pathology; 1998:81.
79. Ishikura H, Sasano H. Histopathologic and immunohistochemical study of steroidogenic cells in the stroma of ovarian tumors. *Int J Gynecol Pathol.* 1998;17:261–265.
80. Hart WR, Norris HJ. Borderline and malignant mucinous tumors of the ovary. Histologic criteria and clinical behavior. *Cancer.* 1973;31:1031–1045.
81. Riopel MA, Ronnett BM, Kurman RJ. Evaluation of diagnostic criteria and behavior of ovarian intestinal-type mucinous tumors: atypical proliferative (borderline) tumors and intraepithelial, microinvasive, invasive, and metastatic carcinomas. *Am J Surg Pathol.* 1999;23:617–635.
82. Lee KR, Scully RE. Mucinous tumors of the ovary: a clinicopathologic study of 196 borderline tumors (of intestinal type) and carcinomas, including an evaluation of 11 cases with 'pseudomyxoma peritonei'. *Am J Surg Pathol.* 2000;24:1447–1464.
83. Hoerl HD, Hart WR. Primary ovarian mucinous cystadenocarcinomas: a clinicopathologic study of 49 cases with long-term follow-up. *Am J Surg Pathol.* 1998;22:1449–1462.
84. Hart WR. Mucinous tumors of the ovary: a review. *Int J Gynecol Pathol.* 2005;24:4–25.
85. Ronnett BM, Kajdacsy-Balla A, Gilks CB, et al. Mucinous borderline ovarian tumors: points of general agreement and persistent controversies regarding nomenclature, diagnostic criteria, and behavior. *Hum Pathol.* 2004;35:949–960.
86. Siriaunkgul S, Robbins KM, McGowan L, et al. Ovarian mucinous tumors of low malignant potential: a clinicopathologic study of 54 tumors of intestinal and mullerian type. *Int J Gynecol Pathol.* 1995;14:198–208.
87. Rodriguez IM, Prat J. Mucinous tumors of the ovary: a clinicopathologic analysis of 75 borderline tumors (of intestinal type) and carcinomas. *Am J Surg Pathol.* 2002;26:139–152.
88. Chiesa AG, Deavers MT, Veras E, et al. Ovarian intestinal type mucinous borderline tumors: are we ready for a nomenclature change? *Int J Gynecol Pathol.* 2010;29:108–112.
89. Kurman RJ, Ronnett BM. Ovarian intestinal-type mucinous borderline tumors: a nomenclature change is long overdue [Letter to Editor]. *Int J Gynecol Pathol.* 2010;29:552–553.
90. Malpica A, Deavers MT, Silva E, et al. Ovarian intestinal-type mucinous borderline tumors: a nomenclature change is long overdue [Authors' Reply]. *Int J Gynecol Pathol.* 2010;29:553–554.
91. Hendrickson MR, Kempson RL. Well-differentiated mucinous neoplasms of the ovary. In: Hendrickson MR, ed. *Pathology: State of the Art Reviews—Surface Epithelial Neoplasms of the Ovary.* Philadelphia, PA: Hanley & Belfus, Inc., 1993:307–334.
92. Tenti P, Aguzzi A, Riva C, et al. Ovarian mucinous tumors frequently express markers of gastric, intestinal, and pancreatobiliary epithelial cells. *Cancer.* 1992;69:2131–2142.
93. Shiohara S, Shiozawa T, Shimizu M, et al. Histochemical analysis of estrogen and progesterone receptors and gastric-type mucin in mucinous ovarian tumors with reference to their pathogenesis. *Cancer.* 1997;80:908–916.
94. Younes M, Ertan A, Ergun G, et al. Goblet cell mimickers in esophageal biopsies are not associated with an increased risk for dysplasia. *Arch Pathol Lab Med.* 2007;131:571–575.
95. Prayson RA, Hart WR, Petras RE. Pseudomyxoma peritonei. A clinicopathologic study of 19 cases with emphasis on site of origin and nature of associated ovarian tumors. *Am J Surg Pathol.* 1994;18:591–603.
96. Khunamornpong S, Russell P, Dalrymple JC. Proliferating (LMP) mucinous tumors of the ovaries with microinvasion: morphologic assessment of 13 cases. *Int J Gynecol Pathol.* 1999;18:238–246.
97. Kim KR, Lee HI, Lee SK, et al. Is stromal microinvasion in primary mucinous ovarian tumors with "mucin granuloma" true invasion? *Am J Surg Pathol.* 2007;31:546–554.
98. Ronnett BM, Kurman RJ, Zahn CM, et al. Pseudomyxoma peritonei in women: a clinicopathologic analysis of 30 cases with emphasis on site of origin, prognosis, and relationship to ovarian mucinous tumors of low malignant potential. *Hum Pathol.* 1995;26:509–524.
99. Vang R, Gown AM, Zhao C, et al. Ovarian mucinous tumors associated with mature cystic teratomas: morphologic and immunohistochemical analysis identifies a subset of potential teratomatous origin that shares features of lower gastrointestinal tract mucinous tumors more commonly encountered as secondary tumors in the ovary. *Am J Surg Pathol.* 2007;31:854–869.
100. McKenney JK, Soslow RA, Longacre TA. Ovarian mature teratomas with mucinous epithelial neoplasms: morphologic heterogeneity and association with pseudomyxoma peritonei. *Am J Surg Pathol.* 2008;32:645–655.
101. Young RH, Gilks CB, Scully RE. Mucinous tumors of the appendix associated with mucinous tumors of the ovary and pseudomyxoma peritonei. A clinicopathological analysis of 22 cases supporting an origin in the appendix. *Am J Surg Pathol.* 1991;15:415–429.
102. Michael H, Sutton G, Roth LM. Ovarian carcinoma with extracellular mucin production: reassessment of "pseudomyxoma ovarii et peritonei". *Int J Gynecol Pathol.* 1987;6:298–312.
103. Wang NP, Zee S, Zarbo RJ, et al. Coordinate expression of cytokeratins 7 and 20 defines unique subsets of carcinomas. *Appl Immunohistochem.* 1995;3:99–107.
104. Vang R, Gown AM, Barry TS, et al. Cytokeratins 7 and 20 in primary and secondary mucinous tumors of the ovary: analysis of coordinate immunohistochemical expression profiles and staining distribution in 179 cases. *Am J Surg Pathol.* 2006;30:1130–1139.
105. Miettinen M. Keratin 20: immunohistochemical marker for gastrointestinal, urothelial, and Merkel cell carcinomas. *Mod Pathol.* 1995;8:384–388.
106. Fraggetta F, Pelosi G, Cafici A, et al. CDX2 immunoreactivity in primary and metastatic ovarian mucinous tumours. *Virchows Arch.* 2003;443:782–786.
107. Groisman GM, Meir A, Sabo E. The value of Cdx2 immunostaining in differentiating primary ovarian carcinomas from colonic carcinomas metastatic to the ovaries. *Int J Gynecol Pathol.* 2004;23:52–57.
108. Vang R, Gown AM, Wu LS, et al. Immunohistochemical expression of CDX2 in primary ovarian mucinous tumors and metastatic mucinous carcinomas involving the ovary: comparison with CK20 and correlation with coordinate expression of CK7. *Mod Pathol.* 2006;19:1421–1428.
109. Vang R, Gown AM, Barry TS, et al. Ovarian atypical proliferative (borderline) mucinous tumors: gastrointestinal and seromucinous (endocervical-like) types are immunophenotypically distinctive. *Int J Gynecol Pathol.* 2006;25:83–89.
110. Bell DA. Mucinous adenofibromas of the ovary. A report of 10 cases. *Am J Surg Pathol.* 1991;15:227–232.
111. O'Hanlan KA. Resection of a 303.2-pound ovarian tumor. *Gynecol Oncol.* 1994;54:365–371.
112. Stewart CJ, Tsukamoto T, Cooke B, et al. Ovarian mucinous tumour arising in mature cystic teratoma and associated with pseudomyxoma peritonei: report of two cases and comparison with ovarian involvement by low-grade appendiceal mucinous tumour. *Pathology (Phila).* 2006;38:534–538.
113. Lee KR, Young RH. The distinction between primary and metastatic mucinous carcinomas of the ovary: gross and histologic findings in 50 cases. *Am J Surg Pathol.* 2003;27:281–292.
114. Clement PB, Young RH. *Atlas of Gynecologic Surgical Pathology.* 2nd ed. Philadelphia, PA: Elsevier Saunders; 2008.
115. Rutgers JL, Scully RE. Ovarian mullerian mucinous papillary cystadenomas of borderline malignancy. A clinicopathologic analysis. *Cancer.* 1988;61:340–348.
116. Shappell HW, Riopel MA, Smith Sehdev AE, et al. Diagnostic criteria and behavior of ovarian seromucinous (endocervical-type mucinous and mixed cell-type) tumors: atypical proliferative (borderline) tumors, intraepithelial, microinvasive, and invasive carcinomas. *Am J Surg Pathol.* 2002;26:1529–1541.
117. Rodriguez IM, Irving JA, Prat J. Endocervical-like mucinous borderline tumors of the ovary: a clinicopathologic analysis of 31 cases. *Am J Surg Pathol.* 2004;28:1311–1318.
118. Lee KR, Nucci MR. Ovarian mucinous and mixed epithelial carcinomas of mullerian (endocervical-like) type: a clinicopathologic analysis of four cases of an uncommon variant associated with endometriosis. *Int J Gynecol Pathol.* 2003;22:42–51.
119. Dube V, Roy M, Plante M, et al. Mucinous ovarian tumors of Mullerian-type: an analysis of 17 cases including borderline tumors and intraepithelial, microinvasive, and invasive carcinomas. *Int J Gynecol Pathol.* 2005;24:138–146.
120. Ronnett BM, Seidman JD. Mucinous tumors arising in ovarian mature cystic teratomas: relationship to the clinical syndrome of pseudomyxoma peritonei. *Am J Surg Pathol.* 2003;27:650–657.
121. Seidman JD, Kurman RJ, Ronnett BM. Primary and metastatic mucinous adenocarcinomas in the ovaries: incidence in routine practice with a new approach to improve intraoperative diagnosis. *Am J Surg Pathol.* 2003;27:985–993.
122. Che M, Tornos C, Deavers MT, et al. Ovarian mixed-epithelial carcinomas with a microcystic pattern and signet-ring cells. *Int J Gynecol Pathol.* 2001;20:323–328.
123. Reichert RA. Primary ovarian adenofibromatous neoplasms with mucin-containing signet-ring cells: a report of 2 cases. *Int J Gynecol Pathol.* 2007;26:165–172.

124. McCluggage WG, Young RH. Primary ovarian mucinous tumors with signet ring cells: report of 3 cases with discussion of so-called primary Krukenberg tumor. *Am J Surg Pathol.* 2008;32:1373–1379.
125. Prat J, Scully RE. Ovarian mucinous tumors with sarcoma-like mural nodules: a report of seven cases. *Cancer.* 1979;44:1332–1344.
126. Bague S, Rodriguez IM, Prat J. Sarcoma-like mural nodules in mucinous cystic tumors of the ovary revisited: a clinicopathologic analysis of 10 additional cases. *Am J Surg Pathol.* 2002;26:1467–1476.
127. Prat J, Young RH, Scully RE. Ovarian mucinous tumors with foci of anaplastic carcinoma. *Cancer.* 1982;50:300–304.
128. Provenza C, Young RH, Prat J. Anaplastic carcinoma in mucinous ovarian tumors: a clinicopathologic study of 34 cases emphasizing the crucial impact of stage on prognosis, their histologic spectrum, and overlap with sarcomalike mural nodules. *Am J Surg Pathol.* 2008;32:383–389.
129. Nichols GE, Mills SE, Ulbright TM, et al. Spindle cell mural nodules in cystic ovarian mucinous tumors. A clinicopathologic and immunohistochemical study of five cases. *Am J Surg Pathol.* 1991;15:1055–1062.
130. Prat J, Scully RE. Sarcomas in ovarian mucinous tumors: a report of two cases. *Cancer.* 1979;44:1327–1331.
131. Ludwick C, Gilks CB, Miller D, et al. Aggressive behavior of stage I ovarian mucinous tumors lacking extensive infiltrative invasion: a report of four cases and review of the literature. *Int J Gynecol Pathol.* 2005;24:205–217.
132. Roth LM, Czernobilsky B, Langley FA. Ovarian endometrioid adenofibromatous and cystadenofibromatous tumors: benign, proliferating, and malignant. *Cancer.* 1981;48:1838–1845.
133. Bell DA, Scully RE. Atypical and borderline endometrioid adenofibromas of the ovary. A report of 27 cases. *Am J Surg Pathol.* 1985;9:205–214.
134. Snyder RR, Norris HJ, Tavassoli F. Endometrioid proliferative and low malignant potential tumors of the ovary. A clinicopathologic study of 46 cases. *Am J Surg Pathol.* 1988;12:661–671.
135. Norris HJ. Proliferative endometrioid tumors and endometrioid tumors of low malignant potential of the ovary. *Int J Gynecol Pathol.* 1993;12:134–140.
136. Bell KA, Kurman RJ. A clinicopathologic analysis of atypical proliferative (borderline) tumors and well-differentiated endometrioid adenocarcinomas of the ovary. *Am J Surg Pathol.* 2000;24:1465–1479.
137. Roth LM, Emerson RE, Ulbright TM. Ovarian endometrioid tumors of low malignant potential: a clinicopathologic study of 30 cases with comparison to well-differentiated endometrioid adenocarcinoma. *Am J Surg Pathol.* 2003;27:1253–1259.
138. Kline RC, Wharton JT, Atkinson EN, et al. Endometrioid carcinoma of the ovary: retrospective review of 145 cases. *Gynecol Oncol.* 1990;39:337–346.
139. Geyer JT, Lopez-Garcia MA, Sanchez-Estevez C, et al. Pathogenetic pathways in ovarian endometrioid adenocarcinoma: a molecular study of 29 cases. *Am J Surg Pathol.* 2009;33:1157–1163.
140. Chan JK, Teoh D, Hu JM, et al. Do clear cell ovarian carcinomas have poorer prognosis compared to other epithelial cell types? A study of 1411 clear cell ovarian cancers. *Gynecol Oncol.* 2008;109:370–376.
141. Storey DJ, Rush R, Stewart M, et al. Endometrioid epithelial ovarian cancer: 20 years of prospectively collected data from a single center. *Cancer.* 2008;112:2211–2220.
142. Young RH, Prat J, Scully RE. Ovarian endometrioid carcinomas resembling sex cord-stromal tumors. A clinicopathological analysis of 13 cases. *Am J Surg Pathol.* 1982;6:513–522.
143. Roth LM, Liban E, Czernobilsky B. Ovarian endometrioid tumors mimicking Sertoli and Sertoli-Leydig cell tumors: Sertoliform variant of endometrioid carcinoma. *Cancer.* 1982;50:1322–1331.
144. Ordi J, Schammel DP, Rasekh L, et al. Sertoliform endometrioid carcinomas of the ovary: a clinicopathologic and immunohistochemical study of 13 cases. *Mod Pathol.* 1999;12:933–940.
145. Guerrieri C, Franlund B, Malmstrom H, et al. Ovarian endometrioid carcinomas simulating sex cord-stromal tumors: a study using inhibin and cytokeratin 7. *Int J Gynecol Pathol.* 1998;17:266–271.
146. Zhao C, Bratthauer GL, Barner R, et al. Comparative analysis of alternative and traditional immunohistochemical markers for the distinction of ovarian sertoli cell tumor from endometrioid tumors and carcinoid tumor: A study of 160 cases. *Am J Surg Pathol.* 2007;31:255–266.
147. Deavers MT, Malpica A, Liu J, et al. Ovarian sex cord-stromal tumors: an immunohistochemical study including a comparison of calretinin and inhibin. *Mod Pathol.* 2003;16:584–590.
148. Costa MJ, DeRose PB, Roth LM, et al. Immunohistochemical phenotype of ovarian granulosa cell tumors: absence of epithelial membrane antigen has diagnostic value. *Hum Pathol.* 1994;25:60–66.
149. Oliva E, Alvarez T, Young RH. Sertoli cell tumors of the ovary: a clinicopathologic and immunohistochemical study of 54 cases. *Am J Surg Pathol.* 2005;29:143–156.
150. Tornos C, Silva EG, Ordonez NG, et al. Endometrioid carcinoma of the ovary with a prominent spindle-cell component, a source of diagnostic confusion. A report of 14 cases. *Am J Surg Pathol.* 1995;19:1343–1353.
151. Eichhorn JH, Young RH, Scully RE. Primary ovarian small cell carcinoma of pulmonary type. A clinicopathologic, immunohistologic, and flow cytometric analysis of 11 cases. *Am J Surg Pathol.* 1992;16:926–938.
152. Silva EG, Young RH. Endometrioid neoplasms with clear cells: a report of 21 cases in which the alteration is not of typical secretory type. *Am J Surg Pathol.* 2007;31:1203–1208.
153. Eichhorn JH, Scully RE. Endometrioid ciliated-cell tumors of the ovary: a report of five cases. *Int J Gynecol Pathol.* 1996;15:248–256.
154. Pitman MB, Young RH, Clement PB, et al. Endometrioid carcinoma of the ovary and endometrium, oxyphilic cell type: a report of nine cases. *Int J Gynecol Pathol.* 1994;13:290–301.
155. Rutgers JL, Young RH, Scully RE. Ovarian yolk sac tumor arising from an endometrioid carcinoma. *Hum Pathol.* 1987;18:1296–1299.
156. Nogales FF, Bergeron C, Carvia RE, et al. Ovarian endometrioid tumors with yolk sac tumor component, an unusual form of ovarian neoplasm. Analysis of six cases. *Am J Surg Pathol.* 1996;20:1056–1066.
157. Sciallis AP, Aubry MC, Bell DA. Ciliated adenocarcinoma of the ovary with evidence of serous differentiation: report of a case. *Int J Gynecol Pathol.* 2009;28:447–452.
158. Eifel P, Hendrickson M, Ross J, et al. Simultaneous presentation of carcinoma involving the ovary and the uterine corpus. *Cancer.* 1982;50:163–170.
159. Ulbright TM, Roth LM. Metastatic and independent cancers of the endometrium and ovary: a clinicopathologic study of 34 cases. *Hum Pathol.* 1985;16:28–34.
160. Zaino R, Whitney C, Brady MF, et al. Simultaneously detected endometrial and ovarian carcinomas–a prospective clinicopathologic study of 74 cases: a gynecologic oncology group study. *Gynecol Oncol.* 2001;83:355–362.
161. Singh N. Synchronous tumours of the female genital tract. *Histopathology.* 2010;56:277–285.
162. Soliman PT, Slomovitz BM, Broaddus RR, et al. Synchronous primary cancers of the endometrium and ovary: a single institution review of 84 cases. *Gynecol Oncol.* 2004;94:456–462.
163. Robboy SJ, Datto MB. Synchronous endometrial and ovarian tumors: metastatic disease or independent primaries? *Hum Pathol.* 2005;36:597–599.
164. Kaneki E, Oda Y, Ohishi Y, et al. Frequent microsatellite instability in synchronous ovarian and endometrial adenocarcinoma and its usefulness for differential diagnosis. *Hum Pathol.* 2004;35:1484–1493.
165. Matias-Guiu X, Lagarda H, Catasus L, et al. Clonality analysis in synchronous or metachronous tumors of the female genital tract. *Int J Gynecol Pathol.* 2002;21:205–211.
166. Chang KH, Albarracin C, Luthra R, et al. Discordant genetic changes in ovarian and endometrial endometrioid carcinomas: a potential pitfall in molecular diagnosis. *Int J Gynecol Cancer.* 2006;16:178–182.
167. Irving JA, Catasus L, Gallardo A, et al. Synchronous endometrioid carcinomas of the uterine corpus and ovary: alterations in the beta-catenin (CTNNB1) pathway are associated with independent primary tumors and favorable prognosis. *Hum Pathol.* 2005;36:605–619.
168. Dehner LP, Norris HJ, Taylor HB. Carcinosarcomas and mixed mesodermal tumors of the ovary. *Cancer.* 1971;27:207–216.
169. Harris MA, Delap LM, Sengupta PS, et al. Carcinosarcoma of the ovary. *Br J Cancer.* 2003;88:654–657.
170. Brown E, Stewart M, Rye T, et al. Carcinosarcoma of the ovary: 19 years of prospective data from a single center. *Cancer.* 2004;100:2148–2153.
171. Rutledge TL, Gold MA, McMeekin DS, et al. Carcinosarcoma of the ovary-a case series. *Gynecol Oncol.* 2006;100:128–132.
172. George E, Manivel JC, Dehner LP, et al. Malignant mixed mullerian tumors: an immunohistochemical study of 47 cases, with histogenetic considerations and clinical correlation. *Hum Pathol.* 1991;22:215–223.
173. de Brito PA, Silverberg SG, Orenstein JM. Carcinosarcoma (malignant mixed mullerian (mesodermal) tumor) of the female genital tract: immunohistochemical and ultrastructural analysis of 28 cases. *Hum Pathol.* 1993;24:132–142.
174. Jin Z, Ogata S, Tamura G, et al. Carcinosarcomas (malignant mullerian mixed tumors) of the uterus and ovary: a genetic study with special reference to histogenesis. *Int J Gynecol Pathol.* 2003;22:368–373.
175. Eichhorn JH, Young RH, Clement PB, et al. Mesodermal (mullerian) adenosarcoma of the ovary: a clinicopathologic analysis of 40 cases and a review of the literature. Am *J Surg Pathol.* 2002;26:1243–1258.
176. Young RH, Prat J, Scully RE. Endometrioid stromal sarcomas of the ovary. A clinicopathologic analysis of 23 cases. *Cancer.* 1984;53:1143–1155.
177. Chang KL, Crabtree GS, Lim-Tan SK, et al. Primary extrauterine endometrial stromal neoplasms: a clinicopathologic study of 20 cases and a review of the literature. *Int J Gynecol Pathol.* 1993;12:282–296.

178. Young RH, Scully RE. Sarcomas metastatic to the ovary: a report of 21 cases. *Int J Gynecol Pathol.* 1990;9:231–252.
179. Oliva E, Garcia-Miralles N, Vu Q, et al. CD10 expression in pure stromal and sex cord-stromal tumors of the ovary: an immunohistochemical analysis of 101 cases. *Int J Gynecol Pathol.* 2007;26:359–367.
180. Yamamoto S, Tsuda H, Yoshikawa T, et al. Clear cell adenocarcinoma associated with clear cell adenofibromatous components: a subgroup of ovarian clear cell adenocarcinoma with distinct clinicopathologic characteristics. *Am J Surg Pathol.* 2007;31:999–1006.
181. Veras E, Mao TL, Ayhan A, et al. Cystic and adenofibromatous clear cell carcinomas of the ovary: distinctive tumors that differ in their pathogenesis and behavior: a clinicopathologic analysis of 122 cases. *Am J Surg Pathol.* 2009;33:844–853.
182. Roth LM, Langley FA, Fox H, et al. Ovarian clear cell adenofibromatous tumors. Benign, of low malignant potential, and associated with invasive clear cell carcinoma. *Cancer.* 1984;53:1156–1163.
183. Bell DA, Scully RE. Benign and borderline clear cell adenofibromas of the ovary. *Cancer.* 1985;56:2922–2931.
184. Sugiyama T, Kamura T, Kigawa J, et al. Clinical characteristics of clear cell carcinoma of the ovary: a distinct histologic type with poor prognosis and resistance to platinum-based chemotherapy. *Cancer.* 2000;88:2584–2589.
185. Young RH, Scully RE. Oxyphilic clear cell carcinoma of the ovary. A report of nine cases. *Am J Surg Pathol.* 1987;11:661–667.
186. Sangoi AR, Soslow RA, Teng NN, et al. Ovarian clear cell carcinoma with papillary features: a potential mimic of serous tumor of low malignant potential. *Am J Surg Pathol.* 2008;32:269–274.
187. Kennedy AW, Biscotti CV, Hart WR, et al. Ovarian clear cell adenocarcinoma. *Gynecol Oncol.* 1989;32:342–349.
188. Yamamoto S, Kasajima A, Takano M, et al. Validation of the histologic grading for ovarian clear cell adenocarcinoma: a retrospective multi-institutional study by the Japan clear cell carcinoma study group. *Int J Gynecol Pathol.* 2011;30:129–138.
189. Silverberg SG. Brenner tumor of the ovary. A clinicopathologic study of 60 tumors in 54 women. *Cancer.* 1971;28:588–596.
190. Waxman M. Pure and mixed Brenner tumors of the ovary: clinicopathologic and histogenetic observations. Cancer 1979;43:1830–1839.
191. Roth LM, Dallenbach-Hellweg G, Czernobilsky B. Ovarian Brenner tumors. I. Metaplastic, proliferating, and of low malignant potential. *Cancer.* 1985;56:582–591.
192. Logani S, Oliva E, Amin MB, et al. Immunoprofile of ovarian tumors with putative transitional cell (urothelial) differentiation using novel urothelial markers: histogenetic and diagnostic implications. *Am J Surg Pathol.* 2003;27:1434–1441.
193. Cuatrecasas M, Catasus L, Palacios J, et al. Transitional cell tumors of the ovary: a comparative clinicopathologic, immunohistochemical, and molecular genetic analysis of Brenner tumors and transitional cell carcinomas. *Am J Surg Pathol.* 2009;33:556–567.
194. Tavassoli FA, Devilee P, eds. *World Health Organization Classification of Tumors. Pathology and Genetics of Tumours of the Breast and Female Genital Organs.* Lyon,France: IARC Press; 2003.
195. Roth LM, Czernobilsky B. Ovarian Brenner tumors. II. Malignant. *Cancer.* 1985;56:592–601.
196. Austin RM, Norris HJ. Malignant Brenner tumor and transitional cell carcinoma of the ovary: a comparison. *Int J Gynecol Pathol.* 1987;6:29–39.
197. Silva EG, Robey-Cafferty SS, Smith TL, et al. Ovarian carcinomas with transitional cell carcinoma pattern. *Am J Clin Pathol.* 1990;93:457–465.
198. Eichhorn JH, Young RH. Transitional cell carcinoma of the ovary: a morphologic study of 100 cases with emphasis on differential diagnosis. *Am J Surg Pathol.* 2004;28:453–463.
199. Hollingsworth HC, Steinberg SM, Silverberg SG, et al. Advanced stage transitional cell carcinoma of the ovary. *Hum Pathol.* 1996;27:1267–1272.
200. Costa MJ, Hansen C, Dickerman A, et al. Clinicopathologic significance of transitional cell carcinoma pattern in nonlocalized ovarian epithelial tumors (stages 2–4). *Am J Clin Pathol.* 1998;109:173–180.
201. Kommoss F, Kommoss S, Schmidt D, et al. Survival benefit for patients with advanced-stage transitional cell carcinomas vs. other subtypes of ovarian carcinoma after chemotherapy with platinum and paclitaxel. *Gynecol Oncol.* 2005;97:195–199.
202. Young RH. From Krukenberg to today: the ever present problems posed by metastatic tumors in the ovary. Part II. *Adv Anat Pathol.* 2007;14:149–177.
203. Young RH, Prat J, Scully RE. Epidermoid cyst of the ovary. A report of three cases with comments on histogenesis. *Am J Clin Pathol.* 1980;73:272–276.
204. Fan LD, Zang HY, Zhang XS. Ovarian epidermoid cyst: report of eight cases. *Int J Gynecol Pathol.* 1996;15:69–71.
205. Khedmati F, Chirolas C, Seidman JD. Ovarian and paraovarian squamous-lined cysts (epidermoid cysts): a clinicopathologic study of 18 cases with comparison to mature cystic teratomas. *Int J Gynecol Pathol.* 2009;28:193–196.
206. Pins MR, Young RH, Daly WJ, et al. Primary squamous cell carcinoma of the ovary. Report of 37 cases. *Am J Surg Pathol.* 1996;20:823–833.
207. Mai KT, Yazdi HM, Bertrand MA, et al. Bilateral primary ovarian squamous cell carcinoma associated with human papilloma virus infection and vulvar and cervical intraepithelial neoplasia. A case report with review of the literature. *Am J Surg Pathol.* 1996;20:767–772.
208. Ishikura H, Scully RE. Hepatoid carcinoma of the ovary. A newly described tumor. *Cancer.* 1987;60:2775–2784.
209. Tochigi N, Kishimoto T, Supriatna Y, et al. Hepatoid carcinoma of the ovary: a report of three cases admixed with a common surface epithelial carcinoma. *Int J Gynecol Pathol.* 2003;22:266–271.
210. Young RH, Gersell DJ, Clement PB, et al. Hepatocellular carcinoma metastatic to the ovary: a report of three cases discovered during life with discussion of the differential diagnosis of hepatoid tumors of the ovary. *Hum Pathol.* 1992;23:574–580.
211. Prat J, Bhan AK, Dickersin GR, et al. Hepatoid yolk sac tumor of the ovary (endodermal sinus tumor with hepatoid differentiation): a light microscopic, ultrastructural and immunohistochemical study of seven cases. *Cancer.* 1982;50:2355–2368.
212. Eichhorn JH, Scully RE. "Adenoid cystic" and basaloid carcinomas of the ovary: evidence for a surface epithelial lineage. A report of 12 cases. *Mod Pathol.* 1995;8:731–740.
213. Han G, Gilks CB, Leung S, et al. Mixed ovarian epithelial carcinomas with clear cell and serous components are variants of high-grade serous carcinoma: an interobserver correlative and immunohistochemical study of 32 cases. *Am J Surg Pathol.* 2008;32:955–964.
214. Rutgers JL, Scully RE. Ovarian mixed-epithelial papillary cystadenomas of borderline malignancy of mullerian type. A clinicopathologic analysis. *Cancer.* 1988;61:546–554.
215. Tornos C, Silva EG, Khorana SM, et al. High-stage endometrioid carcinoma of the ovary. Prognostic significance of pure versus mixed histologic types. *Am J Surg Pathol.* 1994;18:687–693.
216. Silva EG, Deavers MT, Bodurka DC, et al. Association of low-grade endometrioid carcinoma of the uterus and ovary with undifferentiated carcinoma: a new type of dedifferentiated carcinoma? *Int J Gynecol Pathol.* 2006;25:52–58.
217. Silva EG, Tornos C, Bailey MA, et al. Undifferentiated carcinoma of the ovary. *Arch Pathol Lab Med.* 1991;115:377–381.
218. Zhao C, Vinh TN, McManus K, et al. Identification of the most sensitive and robust immunohistochemical markers in different categories of ovarian sex cord-stromal tumors. *Am J Surg Pathol.* 2009;33:354–366.
219. Deavers MT, Malpica A, Ordonez NG, et al. Ovarian steroid cell tumors: an immunohistochemical study including a comparison of calretinin with inhibin. *Int J Gynecol Pathol.* 2003;22:162–167.
220. Kommoss F, Oliva E, Bhan AK, et al. Inhibin expression in ovarian tumors and tumor-like lesions: an immunohistochemical study. *Mod Pathol.* 1998;11:656–664.
221. Movahedi-Lankarani S, Kurman RJ. Calretinin, a more sensitive but less specific marker than alpha-inhibin for ovarian sex cord-stromal neoplasms: an immunohistochemical study of 215 cases. *Am J Surg Pathol.* 2002;26:1477–1483.
222. Rishi M, Howard LN, Bratthauer GL, et al. Use of monoclonal antibody against human inhibin as a marker for sex cord-stromal tumors of the ovary. *Am J Surg Pathol.* 1997;21:583–589.
223. Rutgers JL, Scully RE. Functioning ovarian tumors with peripheral steroid cell proliferation: a report of twenty-four cases. *Int J Gynecol Pathol.* 1986;5:319–337.
224. Matias-Guiu X, Prat J. Ovarian tumors with functioning stroma. An immunohistochemical study of 100 cases with human chorionic gonadotropin monoclonal and polyclonal antibodies. *Cancer.* 1990;65:2001–2005.
225. Stenwig JT, Hazekamp JT, Beecham JB. Granulosa cell tumors of the ovary. A clinicopathological study of 118 cases with long-term follow-up. *Gynecol Oncol.* 1979;7:136–152.
226. Fox H, Agrawal K, Langley FA. A clinicopathologic study of 92 cases of granulosa cell tumor of the ovary with special reference to the factors influencing prognosis. *Cancer.* 1975;35:231–241.
227. Bjorkholm E, Silfversward C. Prognostic factors in granulosa-cell tumors. *Gynecol Oncol.* 1981;11:261–274.
228. Villella J, Herrmann FR, Kaul S, et al. Clinical and pathological predictive factors in women with adult-type granulosa cell tumor of the ovary. *Int J Gynecol Pathol.* 2007;26:154–159.

229. Young RH, Scully RE. Ovarian sex cord-stromal tumors with bizarre nuclei: a clinicopathologic analysis of 17 cases. *Int J Gynecol Pathol.* 1983;1:325–335.
230. Irving JA, Young RH. Granulosa cell tumors of the ovary with a pseudopapillary pattern: a study of 14 cases of an unusual morphologic variant emphasizing their distinction from transitional cell neoplasms and other papillary ovarian tumors. *Am J Surg Pathol.* 2008;32:581–586.
231. Young RH, Oliva E, Scully RE. Luteinized adult granulosa cell tumors of the ovary: a report of four cases. *Int J Gynecol Pathol.* 1994;13:302–310.
232. Shah SP, Kobel M, Senz J, et al. Mutation of FOXL2 in granulosa-cell tumors of the ovary. *N Engl J Med.* 2009;360:2719–2729.
233. Oliva E. Small cell carcinoma of the ovary, hypercalcemic type: an update on an enigmatic neoplasm. *Pathol Case Rev.* 2006;11:43–49.
234. Shah VI, Freites ON, Maxwell P, et al. Inhibin is more specific than calretinin as an immunohistochemical marker for differentiating sarcomatoid granulosa cell tumour of the ovary from other spindle cell neoplasms. *J Clin Pathol.* 2003;56:221–224.
235. Young RH, Scully RE. Ovarian stromal tumors with minor sex cord elements: a report of seven cases. *Int J Gynecol Pathol.* 1983;2:227–234.
236. Osborne BM, Robboy SJ. Lymphomas or leukemia presenting as ovarian tumors. An analysis of 42 cases. *Cancer.* 1983;52:1933–1943.
237. Talerman A. Carcinoid tumors of the ovary. *J Cancer Res Clin Oncol.* 1984;107:125–135.
238. Robboy SJ, Scully RE, Norris HJ. Carcinoid metastatic to the ovary. A clinicopathologic analysis of 35 cases. *Cancer.* 1974;33:798–811.
239. Robboy SJ, Norris HJ, Scully RE. Insular carcinoid primary in the ovary. A clinicopathologic analysis of 48 cases. *Cancer.* 1975;36:404–418.
240. Clement PB, Scully RE. Large solitary luteinized follicle cyst of pregnancy and puerperium: A clinicopathological analysis of eight cases. *Am J Surg Pathol.* 1980;4:431–438.
241. Young RH, Scully RE. Malignant melanoma metastatic to the ovary. A clinicopathologic analysis of 20 cases. *Am J Surg Pathol.* 1991;15:849–860.
242. Gupta D, Deavers MT, Silva EG, et al. Malignant melanoma involving the ovary: a clinicopathologic and immunohistochemical study of 23 cases. *Am J Surg Pathol.* 2004;28:771–780.
243. Miller K, McCluggage WG. Prognostic factors in ovarian adult granulosa cell tumour. *J Clin Pathol.* 2008;61:881–884.
244. Young RH, Dickersin GR, Scully RE. Juvenile granulosa cell tumor of the ovary. A clinicopathological analysis of 125 cases. *Am J Surg Pathol.* 1984;8:575–596.
245. Zaloudek C, Norris HJ. Granulosa tumors of the ovary in children: a clinical and pathologic study of 32 cases. *Am J Surg Pathol.* 1982;6:503–512.
246. McCluggage WG. Immunoreactivity of ovarian juvenile granulosa cell tumours with epithelial membrane antigen. *Histopathology.* 2005;46:235–236.
247. Pelkey TJ, Frierson HF, Jr., Mills SE, et al. The diagnostic utility of inhibin staining in ovarian neoplasms. *Int J Gynecol Pathol.* 1998;17:97–105.
248. Fonseca RB, Grzeszczak EF. Case 128: Bilateral ovarian fibromas in nevoid basal cell carcinoma syndrome. *Radiology.* 2008;246:318–321.
249. Bosch-Banyeras JM, Lucaya X, Bernet M, et al. Calcified ovarian fibromas in prepubertal girls. *Eur J Pediatr.* 1989;148:749–750.
250. Howell CG, Jr., Rogers DA, Gable DS, et al. Bilateral ovarian fibromas in children. *J Pediatr Surg.* 1990;25:690–691.
251. He H, Luthringer DJ, Hui P, et al. Expression of CD56 and WT1 in ovarian stroma and ovarian stromal tumors. *Am J Surg Pathol.* 2008;32:884–890.
252. Prat J, Scully RE. Cellular fibromas and fibrosarcomas of the ovary: a comparative clinicopathologic analysis of seventeen cases. *Cancer.* 1981;47:2663–2670.
253. Irving JA, Alkushi A, Young RH, et al. Cellular fibromas of the ovary: a study of 75 cases including 40 mitotically active tumors emphasizing their distinction from fibrosarcoma. *Am J Surg Pathol.* 2006;30:929–938.
254. Irving JA, Lerwill MF, Young RH. Gastrointestinal stromal tumors metastatic to the ovary: a report of five cases. *Am J Surg Pathol.* 2005;29:920–926.
255. Bjorkholm E, Silfversward C. Theca-cell tumors. Clinical features and prognosis. *Acta Radiol Oncol Radiat Phys Biol.* 1980;19:241–244.
256. Roth LM. Recent advances in the pathology and classification of ovarian sex cord-stromal tumors. *Int J Gynecol Pathol.* 2006;25:199–215.
257. Irving JA, McCluggage WG. Ovarian spindle cell lesions: a review with emphasis on recent developments and differential diagnosis. *Adv Anat Pathol.* 2007;14:305–319.
258. Young RH, Clement PB, Scully RE. Calcified thecomas in young women. A report of four cases. *Int J Gynecol Pathol.* 1988;7:343–350.
259. Waxman M, Vuletin JC, Urcuyo R, et al. Ovarian low-grade stromal sarcoma with thecomatous features: a critical reappraisal of the so-called "malignant thecoma". *Cancer.* 1979;44:2206–2217.
260. Zhang J, Young RH, Arseneau J, et al. Ovarian stromal tumors containing lutein or Leydig cells (luteinized thecomas and stromal Leydig cell tumors)—a clinicopathological analysis of fifty cases. *Int J Gynecol Pathol.* 1982;1:270–285.
261. Clement PB, Young RH, Hanna W, et al. Sclerosing peritonitis associated with luteinized thecomas of the ovary. A clinicopathological analysis of six cases. *Am J Surg Pathol.* 1994;18:1–13.
262. Staats PN, McCluggage WG, Clement PB, et al. Luteinized thecomas (thecomatosis) of the type typically associated with sclerosing peritonitis: a clinical, histopathologic, and immunohistochemical analysis of 27 cases. *Am J Surg Pathol.* 2008;32:1273–1290.
263. Chalvardjian A, Scully RE. Sclerosing stromal tumors of the ovary. *Cancer.* 1973;31:664–670.
264. Kawauchi S, Tsuji T, Kaku T, et al. Sclerosing stromal tumor of the ovary: a clinicopathologic, immunohistochemical, ultrastructural, and cytogenetic analysis with special reference to its vasculature. *Am J Surg Pathol.* 1998;22:83–92.
265. Zekioglu O, Ozdemir N, Terek C, et al. Clinicopathological and immunohistochemical analysis of sclerosing stromal tumours of the ovary. *Arch Gynecol Obstet.* 2010;282:671–676.
266. Dickersin GR, Young RH, Scully RE. Signet-ring stromal and related tumors of the ovary. *Ultrastruct Pathol.* 1995;19:401–419.
267. Vang R, Bague S, Tavassoli FA, et al. Signet-ring stromal tumor of the ovary: clinicopathologic analysis and comparison with Krukenberg tumor. *Int J Gynecol Pathol.* 2004;23:45–51.
268. Irving JA, Young RH. Microcystic stromal tumor of the ovary: report of 16 cases of a hitherto uncharacterized distinctive ovarian neoplasm. *Am J Surg Pathol.* 2009;33:367–375.
269. Young RH, Scully RE. Ovarian Sertoli-Leydig cell tumors. A clinicopathological analysis of 207 cases. *Am J Surg Pathol.* 1985;9:543–569.
270. Young RH, Scully RE. Well-differentiated ovarian Sertoli-Leydig cell tumors: a clinicopathological analysis of 23 cases. *Int J Gynecol Pathol.* 1984;3:277–290.
271. Zaloudek C, Norris HJ. Sertoli-Leydig tumors of the ovary. A clinicopathologic study of 64 intermediate and poorly differentiated neoplasms. *Am J Surg Pathol.* 1984;8:405–418.
272. Mooney EE, Man YG, Bratthauer GL, et al. Evidence that Leydig cells in Sertoli-Leydig cell tumors have a reactive rather than a neoplastic profile. *Cancer.* 1999;86:2312–2319.
273. Young RH, Scully RE. Ovarian Sertoli-Leydig cell tumors with a retiform pattern: a problem in histopathologic diagnosis. A report of 25 cases. *Am J Surg Pathol.* 1983;7:755–771.
274. Roth LM, Slayton RE, Brady LW, et al. Retiform differentiation in ovarian Sertoli-Leydig cell tumors. A clinicopathologic study of six cases from a Gynecologic Oncology Group study. *Cancer.* 1985;55:1093–1098.
275. Talerman A. Ovarian Sertoli-Leydig cell tumor (androblastoma) with retiform pattern. A clinicopathologic study. *Cancer.* 1987;60:3056–3064.
276. Young RH, Prat J, Scully RE. Ovarian Sertoli-Leydig cell tumors with heterologous elements. I. Gastrointestinal epithelium and carcinoid: a clinicopathologic analysis of thirty-six cases. *Cancer.* 1982;50:2448–2456.
277. Prat J, Young RH, Scully RE. Ovarian Sertoli-Leydig cell tumors with heterologous elements. II. Cartilage and skeletal muscle: a clinicopathologic analysis of twelve cases. *Cancer.* 1982;50:2465–2475.
278. Mooney EE, Nogales FF, Tavassoli FA. Hepatocytic differentiation in retiform Sertoli-Leydig cell tumors: distinguishing a heterologous element from Leydig cells. *Hum Pathol.* 1999;30:611–617.
279. McCluggage WG, Young RH. Ovarian Sertoli-Leydig cell tumors with pseudoendometrioid tubules (pseudoendometrioid Sertoli-Leydig cell tumors). *Am J Surg Pathol.* 2007;31:592–597.
280. Rabban JT, Lerwill MF, McCluggage WG, et al. Primary ovarian carcinoid tumors may express CDX-2: a potential pitfall in distinction from metastatic intestinal carcinoid tumors involving the ovary. *Int J Gynecol Pathol.* 2009;28:41–48.
281. Bullon A Jr, Arseneau J, Prat J, et al. Tubular Krukenberg tumor. A problem in histopathologic diagnosis. *Am J Surg Pathol.* 1981;5:225–232.
282. Young RH, Scully RE. Ovarian tumors of probable wolffian origin. A report of 11 cases. *Am J Surg Pathol.* 1983;7:125–135.
283. Costa MJ, Morris RJ, Wilson R, et al. Utility of immunohistochemistry in distinguishing ovarian sertoli-stromal cell tumors from carcinosarcomas. *Hum Pathol.* 1992;23:787–797.
284. Cathro HP, Stoler MH. The utility of calretinin, inhibin, and WT1 immunohistochemical staining in the differential diagnosis of ovarian tumors. *Hum Pathol.* 2005;36:195–201.

285. Mooney EE, Nogales FF, Bergeron C, et al. Retiform Sertoli-Leydig cell tumours: clinical, morphological and immunohistochemical findings. *Histopathology.* 2002;41:110–117.
286. Sternberg WH, Roth LM. Ovarian stromal tumors containing Leydig cells. I. Stromal-Leydig cell tumor and non-neoplastic transformation of ovarian stroma to Leydig cells. *Cancer.* 1973;32:940–951.
287. Neubecker RD, Breen SL. Gynandroblastoma. A report of five cases, with a discussion of the histogenesis and classification of ovarian tumors. *Am J Clin Pathol.* 1962;38:60–69.
288. Broshears JR, Roth LM. Gynandroblastoma with elements resembling juvenile granulosa cell tumor. *Int J Gynecol Pathol.* 1997;16:387–391.
289. Young RH, Welch WR, Dickersin GR, et al. Ovarian sex cord tumor with annular tubules: review of 74 cases including 27 with Peutz-Jeghers syndrome and four with adenoma malignum of the cervix. *Cancer.* 1982;50:1384–1402.
290. Cheng L, Thomas A, Roth LM, et al. OCT4: a novel biomarker for dysgerminoma of the ovary. *Am J Surg Pathol.* 2004;28:1341–1346.
291. Seidman JD. Unclassified ovarian gonadal stromal tumors. A clinicopathologic study of 32 cases. *Am J Surg Pathol.* 1996;20:699–706.
292. Young RH, Dudley AG, Scully RE. Granulosa cell, Sertoli-Leydig cell, and unclassified sex cord-stromal tumors associated with pregnancy: a clinicopathological analysis of thirty-six cases. *Gynecol Oncol.* 1984;18:181–205.
293. Paraskevas M, Scully RE. Hilus cell tumor of the ovary. A clinicopathological analysis of 12 Reinke crystal-positive and nine crystal-negative cases. *Int J Gynecol Pathol.* 1989;8:299–310.
294. Hayes MC, Scully RE. Stromal luteoma of the ovary: a clinicopathological analysis of 25 cases. *Int J Gynecol Pathol.* 1987;6:313–321.
295. Hayes MC, Scully RE. Ovarian steroid cell tumors (not otherwise specified). A clinicopathological analysis of 63 cases. *Am J Surg Pathol.* 1987;11:835–845.
296. Roth LM, Sternberg WH. Ovarian stromal tumors containing Leydig cells. II. Pure Leydig cell tumor, non-hilar type. *Cancer.* 1973;32:952–960.
297. Stewart C, Hammond I. Cytologic identification of Reinke crystalloids in ovarian Leydig cell tumor. *Arch Pathol Lab Med.* 2006;130:765–766.
298. Young RH, Hart WR. Renal cell carcinoma metastatic to the ovary: a report of three cases emphasizing possible confusion with ovarian clear cell adenocarcinoma. *Int J Gynecol Pathol.* 1992;11:96–104.
299. Cameron RI, Ashe P, O'Rourke DM, et al. A panel of immunohistochemical stains assists in the distinction between ovarian and renal clear cell carcinoma. *Int J Gynecol Pathol.* 2003;22:272–276.
300. Portugal R, Oliva E. Calretinin: diagnostic utility in the female genital tract. *Adv Anat Pathol.* 2009;16:118–124.
301. Norris HJ, Zirkin HJ, Benson WL. Immature (malignant) teratoma of the ovary: a clinical and pathologic study of 58 cases. *Cancer.* 1976;37:2359–2372.
302. O'Connor DM, Norris HJ. The influence of grade on the outcome of stage I ovarian immature (malignant) teratomas and the reproducibility of grading. *Int J Gynecol Pathol.* 1994;13:283–289.
303. Yanai-Inbar I, Scully RE. Relation of ovarian dermoid cysts and immature teratomas: an analysis of 350 cases of immature teratoma and 10 cases of dermoid cyst with microscopic foci of immature tissue. *Int J Gynecol Pathol.* 1987;6:203–212.
304. Cho NH, Kim YT, Lee JH, et al. Diagnostic challenge of fetal ontogeny and its application on the ovarian teratomas. *Int J Gynecol Pathol.* 2005;24:173–182.
305. Baker PM, Rosai J, Young RH. Ovarian teratomas with florid benign vascular proliferation: a distinctive finding associated with the neural component of teratomas that may be confused with a vascular neoplasm. *Int J Gynecol Pathol.* 2002;21:16–21.
306. Nogales FF, Ruiz Avila I, Concha A, et al. Immature endodermal teratoma of the ovary: embryologic correlations and immunohistochemistry. *Hum Pathol.* 1993;24:364–370.
307. Clement PB, Young RH, Scully RE. Endometrioid-like variant of ovarian yolk sac tumor. A clinicopathological analysis of eight cases. *Am J Surg Pathol.* 1987;11:767–778.
308. Heifetz SA, Cushing B, Giller R, et al. Immature teratomas in children: pathologic considerations: a report from the combined Pediatric Oncology Group/Children's Cancer Group. *Am J Surg Pathol.* 1998;22:1115–1124.
309. Abiko K, Mandai M, Hamanishi J, et al. Oct4 expression in immature teratoma of the ovary: relevance to histologic grade and degree of differentiation. *Am J Surg Pathol.* 2010;34:1842–1848.
310. Roth LM, Talerman A. Recent advances in the pathology and classification of ovarian germ cell tumors. *Int J Gynecol Pathol.* 2006;25:305–320.
311. Cushing B, Giller R, Ablin A, et al. Surgical resection alone is effective treatment for ovarian immature teratoma in children and adolescents: a report of the pediatric oncology group and the children's cancer group. *Am J Obstet Gynecol.* 1999;181:353–358.
312. Gershenson DM. Management of ovarian germ cell tumors. *J Clin Oncol.* 2007;25:2938–2943.
313. Robboy SJ, Scully RE. Ovarian teratoma with glial implants on the peritoneum. An analysis of 12 cases. *Hum Pathol.* 1970;1:643–653.
314. Nielsen SN, Scheithauer BW, Gaffey TA. Gliomatosis peritonei. *Cancer.* 1985;56:2499–2503.
315. Nogales FF, Aguilar D. Florid vascular proliferation in grade 0 glial implants from ovarian immature teratoma [Letter to Editor]. *Int J Gynecol Pathol.* 2002;21:305–307.
316. Calder CJ, Light AM, Rollason TP. Immature ovarian teratoma with mature peritoneal metastatic deposits showing glial, epithelial, and endometrioid differentiation: a case report and review of the literature. *Int J Gynecol Pathol.* 1994;13:279–282.
317. Ferguson AW, Katabuchi H, Ronnett BM, et al. Glial implants in gliomatosis peritonei arise from normal tissue, not from the associated teratoma. *Am J Pathol.* 2001;159:51–55.
318. Kwan MY, Kalle W, Lau GT, et al. Is gliomatosis peritonei derived from the associated ovarian teratoma? *Hum Pathol.* 2004;35:685–688.
319. Djordjevic B, Euscher ED, Malpica A. Growing teratoma syndrome of the ovary: review of literature and first report of a carcinoid tumor arising in a growing teratoma of the ovary. *Am J Surg Pathol.* 2007;31:1913–1918.
320. Thurlbeck WM, Scully RE. Solid teratoma of the ovary. A clinicopathological analysis of 9 cases. *Cancer.* 1960;13:804–811.
321. Calame JJ, Schaberg A. Solid teratomas and mixed mullerian tumors of the ovary: a clinical, histological, and immunocytochemical comparative study. *Gynecol Oncol.* 1989;33:212–221.
322. Caruso PA, Marsh MR, Minkowitz S, et al. An intense clinicopathologic study of 305 teratomas of the ovary. *Cancer.* 1971;27:343–348.
323. Comerci JT Jr, Licciardi F, Bergh PA, et al. Mature cystic teratoma: a clinicopathologic evaluation of 517 cases and review of the literature. *Obstet Gynecol.* 1994;84:22–28.
324. Abbott TM, Hermann WJ Jr, Scully RE. Ovarian fetiform teratoma (homunculus) in a 9-year-old girl. *Int J Gynecol Pathol.* 1984;2:392–402.
325. Canzonieri V, Volpe R, Gloghini A, et al. Sieve-like areas in mature cystic teratomas of the ovary. A histochemical and immunohistochemical study of 7 cases. *Pathologica.* 1994;86:43–46.
326. McLachlin CM, Srigley JR. Prostatic tissue in mature cystic teratomas of the ovary. *Am J Surg Pathol.* 1992;16:780–784.
327. Halabi M, Oliva E, Mazal PR, et al. Prostatic tissue in mature cystic teratomas of the ovary: a report of four cases, including one with features of prostatic adenocarcinoma, and cytogenetic studies. *Int J Gynecol Pathol.* 2002;21:261–267.
328. Chen E, Fletcher CD, Nucci MR. Meningothelial proliferations in mature cystic teratoma of the ovary: evidence for the common presence of cranially derived tissues paralleling anterior embryonic plate development. An analysis of 25 consecutive cases. *Am J Surg Pathol.* 2010;34:1014–1018.
329. Roth LM, Talerman A. The enigma of struma ovarii. *Pathology (Phila).* 2007;39:139–146.
330. Szyfelbein WM, Young RH, Scully RE. Cystic struma ovarii: a frequently unrecognized tumor. A report of 20 cases. *Am J Surg Pathol.* 1994;18:785–788.
331. Szyfelbein WM, Young RH, Scully RE. Struma ovarii simulating ovarian tumors of other types. A report of 30 cases. *Am J Surg Pathol.* 1995;19:21–29.
332. Hamazaki S, Okino T, Tsukayama C, et al. Expression of thyroid transcription factor-1 in strumal carcinoid and struma ovarii: an immunohistochemical study. *Pathol Int.* 2002;52:458–462.
333. Isotalo PA, Lloyd RV. Presence of birefringent crystals is useful in distinguishing thyroid from parathyroid gland tissues. *Am J Surg Pathol.* 2002;26:813–814.
334. Garg K, Soslow RA, Rivera M, et al. Histologically bland "extremely well differentiated" thyroid carcinomas arising in struma ovarii can recur and metastasize. *Int J Gynecol Pathol.* 2009;28:222–230.
335. Robboy SJ, Shaco-Levy R, Peng RY, et al. Malignant struma ovarii: an analysis of 88 cases, including 27 with extraovarian spread. *Int J Gynecol Pathol.* 2009;28:405–422.
336. Shaco-Levy R, Bean SM, Bentley RC, et al. Natural history of biologically malignant struma ovarii: analysis of 27 cases with extraovarian spread. *Int J Gynecol Pathol.* 2010;29:212–227.
337. Roth LM, Karseladze AI. Highly differentiated follicular carcinoma arising from struma ovarii: a report of 3 cases, a review of the literature, and a reassessment of so-called peritoneal strumosis. *Int J Gynecol Pathol.* 2008;27:213–222.

338. Roth LM, Miller AW, 3rd, Talerman A. Typical thyroid-type carcinoma arising in struma ovarii: a report of 4 cases and review of the literature. *Int J Gynecol Pathol.* 2008;27:496–506.
339. Devaney K, Snyder R, Norris HJ, et al. Proliferative and histologically malignant struma ovarii: a clinicopathologic study of 54 cases. *Int J Gynecol Pathol.* 1993;12:333–343.
340. Young RH, Jackson A, Wells M. Ovarian metastasis from thyroid carcinoma 12 years after partial thyroidectomy mimicking struma ovarii: report of a case. *Int J Gynecol Pathol.* 1994;13:181–185.
341. Robboy SJ, Scully RE, Norris HJ. Primary trabecular carcinoid of the ovary. *Obstet Gynecol.* 1977;49:202–207.
342. Talerman A, Evans MI. Primary trabecular carcinoid tumor of the ovary. *Cancer.* 1982;50:1403–1407.
343. Robboy SJ, Scully RE. Strumal carcinoid of the ovary: an analysis of 50 cases of a distinctive tumor composed of thyroid tissue and carcinoid. *Cancer.* 1980;46:2019–2034.
344. Baker PM, Oliva E, Young RH, et al. Ovarian mucinous carcinoids including some with a carcinomatous component: a report of 17 cases. *Am J Surg Pathol.* 2001;25:557–568.
345. Nogales FF, Buritica C, Regauer S, et al. Mucinous carcinoid as an unusual manifestation of endodermal differentiation in ovarian yolk sac tumors. *Am J Surg Pathol.* 2005;29:1247–1251.
346. Hristov AC, Young RH, Vang R, et al. Ovarian metastases of appendiceal tumors with goblet cell carcinoidlike and signet ring cell patterns: a report of 30 cases. *Am J Surg Pathol.* 2007;31:1502–1511.
347. Burke AP, Sobin LH, Federspiel BH, et al. Goblet cell carcinoids and related tumors of the vermiform appendix. *Am J Clin Pathol.* 1990;94:27–35.
348. Tang LH, Shia J, Soslow RA, et al. Pathologic classification and clinical behavior of the spectrum of goblet cell carcinoid tumors of the appendix. *Am J Surg Pathol.* 2008;32:1429–1443.
349. Hirakawa T, Tsuneyoshi M, Enjoji M. Squamous cell carcinoma arising in mature cystic teratoma of the ovary. Clinicopathologic and topographic analysis. *Am J Surg Pathol.* 1989;13:397–405.
350. McCluggage WG, Bissonnette JP, Young RH. Primary malignant melanoma of the ovary: a report of 9 definite or probable cases with emphasis on their morphologic diversity and mimicry of other primary and secondary ovarian neoplasms. *Int J Gynecol Pathol.* 2006;25:321–329.
351. Kuroda N, Hirano K, Inui Y, et al. Compound melanocytic nevus arising in a mature cystic teratoma of the ovary. *Pathol Int.* 2001;51:902–904.
352. Kleinman GM, Young RH, Scully RE. Primary neuroectodermal tumors of the ovary. A report of 25 cases. *Am J Surg Pathol.* 1993;17:764–778.
353. Chumas JC, Scully RE. Sebaceous tumors arising in ovarian dermoid cysts. *Int J Gynecol Pathol.* 1991;10:356–363.
354. Axiotis CA, Lippes HA, Merino MJ, et al. Corticotroph cell pituitary adenoma within an ovarian teratoma. A new cause of Cushing's syndrome. *Am J Surg Pathol.* 1987;11:218–224.
355. Hameed K, Burslem MR. A melanotic ovarian neoplasm resembling the "retinal anlage" tumor. *Cancer.* 1970;25:564–567.
356. Bjorkholm E, Lundell M, Gyftodimos A, et al. Dysgerminoma. The Radiumhemmet series 1927–1984. *Cancer.* 1990;65:38–44.
357. Zaloudek CJ, Tavassoli FA, Norris HJ. Dysgerminoma with syncytiotrophoblastic giant cells. A histologically and clinically distinctive subtype of dysgerminoma. *Am J Surg Pathol.* 1981;5:361–367.
358. Sever M, Jones TD, Roth LM, et al. Expression of CD117 (c-kit) receptor in dysgerminoma of the ovary: diagnostic and therapeutic implications. *Mod Pathol.* 2005;18:1411–1416.
359. Leroy X, Augusto D, Leteurtre E, et al. CD30 and CD117 (c-kit) used in combination are useful for distinguishing embryonal carcinoma from seminoma. *J Histochem Cytochem.* 2002;50:283–285.
360. Cossu-Rocca P, Jones TD, Roth LM, et al. Cytokeratin and CD30 expression in dysgerminoma. *Hum Pathol.* 2006;37:1015–1021.
361. Ramalingam P, Malpica A, Silva EG, et al. The use of cytokeratin 7 and EMA in differentiating ovarian yolk sac tumors from endometrioid and clear cell carcinomas. *Am J Surg Pathol.* 2004;28:1499–1505.
362. Monterroso V, Jaffe ES, Merino MJ, et al. Malignant lymphomas involving the ovary. A clinicopathologic analysis of 39 cases. *Am J Surg Pathol.* 1993;17:154–170.
363. Kurman RJ, Norris HJ. Endodermal sinus tumor of the ovary: a clinical and pathologic analysis of 71 cases. *Cancer.* 1976;38:2404–2419.
364. Rabban JT, Zaloudek C. Ovarian yolk sac tumors. *Pathol Case Rev.* 2006;11:50–57.
365. Nogales FF Jr, Matilla A, Nogales O, et al. Yolk sac tumors with pure and mixed polyvesicular vitelline patterns. *Hum Pathol.* 1978;9:553–566.
366. Esheba GE, Pate LL, Longacre TA. Oncofetal protein glypican-3 distinguishes yolk sac tumor from clear cell carcinoma of the ovary. *Am J Surg Pathol.* 2008;32:600–607.
367. Cao D, Guo S, Allan RW, et al. SALL4 is a novel sensitive and specific marker of ovarian primitive germ cell tumors and is particularly useful in distinguishing yolk sac tumor from clear cell carcinoma. *Am J Surg Pathol.* 2009;33:894–904.
368. Cheng L, Zhang S, Talerman A, et al. Morphologic, immunohistochemical, and fluorescence in situ hybridization study of ovarian embryonal carcinoma with comparison to solid variant of yolk sac tumor and immature teratoma. *Hum Pathol.* 2010;41:716–723.
369. Nawa A, Obata N, Kikkawa F, et al. Prognostic factors of patients with yolk sac tumors of the ovary. *Am J Obstet Gynecol.* 2001;184:1182–1188.
370. Kurman RJ, Norris HJ. Embryonal carcinoma of the ovary: a clinicopathologic entity distinct from endodermal sinus tumor resembling embryonal carcinoma of the adult testis. *Cancer.* 1976;38:2420–2433.
371. Niehans GA, Manivel JC, Copland GT, et al. Immunohistochemistry of germ cell and trophoblastic neoplasms. *Cancer.* 1988;62:1113–1123.
372. Kurman RJ, Norris HJ. Mesenchymal tumors of the uterus. VI. Epithelioid smooth muscle tumors including leiomyoblastoma and clear-cell leiomyoma: a clinical and pathologic analysis of 26 cases. *Cancer.* 1976;37:1853–1865.
373. Jondle DM, Shahin MS, Sorosky J, et al. Ovarian mixed germ cell tumor with predominance of polyembryoma: a case report with literature review. *Int J Gynecol Pathol.* 2002;21:78–81.
374. Nakashima N, Murakami S, Fukatsu T, et al. Characteristics of "embryoid body" in human gonadal germ cell tumors. *Hum Pathol.* 1988;19:1144–1154.
375. Axe SR, Klein VR, Woodruff JD. Choriocarcinoma of the ovary. *Obstet Gynecol.* 1985;66:111–114.
376. Kurman RJ, Norris HJ. Malignant mixed germ cell tumors of the ovary. A clinical and pathologic analysis of 30 cases. *Obstet Gynecol.* 1976;48:579–589.
377. Lorigan PC, Grierson AJ, Goepel JR, et al. Gestational choriocarcinoma of the ovary diagnosed by analysis of tumour DNA. *Cancer Lett.* 1996;104:27–30.
378. Hirabayashi K, Yasuda M, Osamura RY, et al. Ovarian nongestational choriocarcinoma mixed with various epithelial malignancies in association with endometriosis. *Gynecol Oncol.* 2006;102:111–117.
379. Scully RE. Gonadoblastoma. A review of 74 cases. *Cancer.* 1970;25:1340–1356.
380. Talerman A, Roth LM. Recent advances in the pathology and classification of gonadal neoplasms composed of germ cells and sex cord derivatives. *Int J Gynecol Pathol.* 2007;26:313–321.
381. Hertel JD, Huettner PC, Dehner LP, et al. The chromosome Y-linked testis-specific protein locus TSPY1 is characteristically present in gonadoblastoma. *Hum Pathol.* 2010;41:1544–1549.
382. Lagoo AS, Robboy SJ. Lymphoma of the female genital tract: current status. *Int J Gynecol Pathol.* 2006;25:1–21.
383. Vang R, Medeiros LJ, Fuller GN, et al. Non-Hodgkin's lymphoma involving the gynecologic tract: a review of 88 cases. *Adv Anat Pathol.* 2001;8:200–217.
384. Oliva E, Ferry JA, Young RH, et al. Granulocytic sarcoma of the female genital tract: a clinicopathologic study of 11 cases. *Am J Surg Pathol.* 1997;21:1156–1165.
385. Emery JD, Kennedy AW, Tubbs RR, et al. Plasmacytoma of the ovary: a case report and literature review. *Gynecol Oncol.* 1999;73:151–154.
386. Young RH, Silva EG, Scully RE. Ovarian and juxtaovarian adenomatoid tumors: a report of six cases. *Int J Gynecol Pathol.* 1991;10:364–371.
387. Phillips V, McCluggage WG, Young RH. Oxyphilic adenomatoid tumor of the ovary: a case report with discussion of the differential diagnosis of ovarian tumors with vacuoles and related spaces. *Int J Gynecol Pathol.* 2007;26:16–20.
388. Eichhorn JH, Scully RE. Ovarian myxoma: clinicopathologic and immunocytologic analysis of five cases and a review of the literature. *Int J Gynecol Pathol.* 1991;10:156–169.
389. McCluggage WG, Young RH. Paraganglioma of the ovary: report of three cases of a rare ovarian neoplasm, including two exhibiting inhibin positivity. *Am J Surg Pathol.* 2006;30:600–605.
390. Slone SP, Moore GD, Parker LP, et al. Glomus tumor of the ovary masquerading as granulosa cell tumor: case report. *Int J Gynecol Pathol.* 2010;29:24–26.
391. Sahin A, Benda JA. Primary ovarian Wilms' tumor. *Cancer.* 1988;61:1460–1463.
392. D'Aguillo AF, Goldberg MI, Kamalamma M, et al. Primary ovarian hydatidiform mole. *Hum Pathol.* 1982;13:279–281.
393. Baergen RN, Rutgers J, Young RH. Extrauterine lesions of intermediate trophoblast. *Int J Gynecol Pathol.* 2003;22:362–367.

394. Young RH, Oliva E, Scully RE. Small cell carcinoma of the ovary, hypercalcemic type. A clinicopathological analysis of 150 cases. *Am J Surg Pathol.* 1994;18:1102–1116.
395. McCluggage WG, Oliva E, Connolly LE, et al. An immunohistochemical analysis of ovarian small cell carcinoma of hypercalcemic type. *Int J Gynecol Pathol.* 2004;23:330–336.
396. Carlson JW, Nucci MR, Brodsky J, et al. Biomarker-assisted diagnosis of ovarian, cervical and pulmonary small cell carcinomas: the role of TTF-1, WT-1 and HPV analysis. *Histopathology.* 2007;51:305–312.
397. Eichhorn JH, Young RH, Scully RE. Nonpulmonary small cell carcinomas of extragenital origin metastatic to the ovary. *Cancer.* 1993;71:177–186.
398. Irving JA, Young RH. Lung carcinoma metastatic to the ovary: a clinicopathologic study of 32 cases emphasizing their morphologic spectrum and problems in differential diagnosis. *Am J Surg Pathol.* 2005;29:997–1006.
399. Eichhorn JH, Lawrence WD, Young RH, et al. Ovarian neuroendocrine carcinomas of non-small-cell type associated with surface epithelial adenocarcinomas. A study of five cases and review of the literature. *Int J Gynecol Pathol.* 1996;15:303–314.
400. Veras E, Deavers MT, Silva EG, et al. Ovarian nonsmall cell neuroendocrine carcinoma: a clinicopathologic and immunohistochemical study of 11 cases. *Am J Surg Pathol.* 2007;31:774–782.
401. Daya D, Young RH, Scully RE. Endometrioid carcinoma of the fallopian tube resembling an adnexal tumor of probable wolffian origin: a report of six cases. *Int J Gynecol Pathol.* 1992;11:122–130.
402. Li F, Szallasi A, Young RH. Wolffian tumor of the ovary with a prominent spindle cell component: report of a case with brief discussion of unusual problems in differential diagnosis, and literature review. *Int J Surg Pathol.* 2008;16:222–225.
403. Takano T, Akahira J, Moriya T, et al. Primary ependymoma of the ovary: a case report and literature review. Int J Gynecol *Cancer.* 2005;15:1138–1141.
404. Rutgers JL, Scully RE. Cysts (cystadenomas) and tumors of the rete ovarii. *Int J Gynecol Pathol.* 1988;7:330–342.
405. Nogales FF, Carvia RE, Donn, et al. Adenomas of the rete ovarii. *Hum Pathol.* 1997;28:1428–1433.
406. Deshpande V, Oliva E, Young RH. Solid pseudopapillary neoplasm of the ovary: a report of 3 primary ovarian tumors resembling those of the pancreas. *Am J Surg Pathol.* 2010;34:1514–1520.
407. Doss BJ, Wanek SM, Jacques SM, et al. Ovarian leiomyomas: clinicopathologic features in fifteen cases. *Int J Gynecol Pathol.* 1999;18:63–68.
408. Lerwill MF, Sung R, Oliva E, et al. Smooth muscle tumors of the ovary: a clinicopathologic study of 54 cases emphasizing prognostic criteria, histologic variants, and differential diagnosis. *Am J Surg Pathol.* 2004;28:1436–1451.
409. Young RH, Scully RE. Metastatic tumors in the ovary: a problem-oriented approach and review of the recent literature. *Semin Diagn Pathol.* 1991;8:250–276.
410. Young RH. From Krukenberg to today: the ever present problems posed by metastatic tumors in the ovary. Part I. Historical perspective, general principles, mucinous tumors including the Krukenberg tumor. *Adv Anat Pathol.* 2006;13:205–227.
411. Stewart CJ, Brennan BA, Hammond IG, et al. Accuracy of frozen section in distinguishing primary ovarian neoplasia from tumors metastatic to the ovary. *Int J Gynecol Pathol.* 2005;24:356–362.
412. Yemelyanova AV, Vang R, Judson K, et al. Distinction of primary and metastatic mucinous tumors involving the ovary: analysis of size and laterality data by primary site with reevaluation of an algorithm for tumor classification. *Am J Surg Pathol.* 2008;32:128–138.
413. Lash RH, Hart WR. Intestinal adenocarcinomas metastatic to the ovaries. A clinicopathologic evaluation of 22 cases. *Am J Surg Pathol.* 1987;11:114–121.
414. Daya D, Nazerali L, Frank GL. Metastatic ovarian carcinoma of large intestinal origin simulating primary ovarian carcinoma. A clinicopathologic study of 25 cases. *Am J Clin Pathol.* 1992;97:751–758.
415. Lewis MR, Deavers MT, Silva EG, et al. Ovarian involvement by metastatic colorectal adenocarcinoma: still a diagnostic challenge. *Am J Surg Pathol.* 2006;30:177–184.
416. Mazur MT, Hsueh S, Gersell DJ. Metastases to the female genital tract. Analysis of 325 cases. *Cancer.* 1984;53:1978–1984.
417. Wauters CC, Smedts F, Gerrits LG, et al. Keratins 7 and 20 as diagnostic markers of carcinomas metastatic to the ovary. *Hum Pathol.* 1995;26:852–855.
418. DeCostanzo DC, Elias JM, Chumas JC. Necrosis in 84 ovarian carcinomas: a morphologic study of primary versus metastatic colonic carcinoma with a selective immunohistochemical analysis of cytokeratin subtypes and carcinoembryonic antigen. *Int J Gynecol Pathol.* 1997;16:245–249.
419. Loy TS, Calaluce RD, Keeney GL. Cytokeratin immunostaining in differentiating primary ovarian carcinoma from metastatic colonic adenocarcinoma. *Mod Pathol.* 1996;9:1040–1044.
420. Chu P, Wu E, Weiss LM. Cytokeratin 7 and cytokeratin 20 expression in epithelial neoplasms: a survey of 435 cases. *Mod Pathol.* 2000;13:962–972.
421. Ronnett BM, Shmookler BM, Diener-West M, et al. Immunohistochemical evidence supporting the appendiceal origin of pseudomyxoma peritonei in women. *Int J Gynecol Pathol.* 1997;16:1–9.
422. Young RH, Hart WR. Metastatic intestinal carcinomas simulating primary ovarian clear cell carcinoma and secretory endometrioid carcinoma: a clinicopathologic and immunohistochemical study of five cases. *Am J Surg Pathol.* 1998;22:805–815.
423. Kiyokawa T, Young RH, Scully RE. Krukenberg tumors of the ovary: a clinicopathologic analysis of 120 cases with emphasis on their variable pathologic manifestations. *Am J Surg Pathol.* 2006;30:277–299.
424. Holtz F, Hart WR. Krukenberg tumors of the ovary: a clinicopathologic analysis of 27 cases. *Cancer.* 1982;50:2438–2447.
425. Lerwill MF, Young RH. Ovarian metastases of intestinal-type gastric carcinoma: A clinicopathologic study of 4 cases with contrasting features to those of the Krukenberg tumor. *Am J Surg Pathol.* 2006;30:1382–1388.
426. Park SY, Kim HS, Hong EK, et al. Expression of cytokeratins 7 and 20 in primary carcinomas of the stomach and colorectum and their value in the differential diagnosis of metastatic carcinomas to the ovary. *Hum Pathol.* 2002;33:1078–1085.
427. Bradley RF, Cortina G, Geisinger KR. Pseudomyxoma peritonei: review of the controversy. *Curr Diagn Pathol.* 2007;13:410–416.
428. Seidman JD, Elsayed AM, Sobin LH, et al. Association of mucinous tumors of the ovary and appendix. A clinicopathologic study of 25 cases. *Am J Surg Pathol.* 1993;17:22–34.
429. Guerrieri C, Franlund B, Fristedt S, et al. Mucinous tumors of the vermiform appendix and ovary, and pseudomyxoma peritonei: histogenetic implications of cytokeratin 7 expression. *Hum Pathol.* 1997;28:1039–1045.
430. Szych C, Staebler A, Connolly DC, et al. Molecular genetic evidence supporting the clonality and appendiceal origin of Pseudomyxoma peritonei in women. *Am J Pathol.* 1999;154:1849–1855.
431. O'Connell JT, Hacker CM, Barsky SH. MUC2 is a molecular marker for pseudomyxoma peritonei. *Mod Pathol.* 2002;15:958–972.
432. Ronnett BM, Zahn CM, Kurman RJ, et al. Disseminated peritoneal adenomucinosis and peritoneal mucinous carcinomatosis. A clinicopathologic analysis of 109 cases with emphasis on distinguishing pathologic features, site of origin, prognosis, and relationship to "pseudomyxoma peritonei". *Am J Surg Pathol.* 1995;19:1390–1408.
433. Young RH. Pseudomyxoma peritonei and selected other aspects of the spread of appendiceal neoplasms. *Semin Diagn Pathol.* 2004;21:134–150.
434. Misdraji J, Yantiss RK, Graeme-Cook FM, et al. Appendiceal mucinous neoplasms: a clinicopathologic analysis of 107 cases. *Am J Surg Pathol.* 2003;27:1089–1103.
435. Ronnett BM, Kurman RJ, Shmookler BM, et al. The morphologic spectrum of ovarian metastases of appendiceal adenocarcinomas: a clinicopathologic and immunohistochemical analysis of tumors often misinterpreted as primary ovarian tumors or metastatic tumors from other gastrointestinal sites. *Am J Surg Pathol.* 1997;21:1144–1155.
436. Bradley RF, Stewart JHt, Russell GB, et al. Pseudomyxoma peritonei of appendiceal origin: a clinicopathologic analysis of 101 patients uniformly treated at a single institution, with literature review. *Am J Surg Pathol.* 2006;30:551–559.
437. Young RH, Hart WR. Metastases from carcinomas of the pancreas simulating primary mucinous tumors of the ovary. A report of seven cases. *Am J Surg Pathol.* 1989;13:748–756.
438. Khunamornpong S, Siriaunkgul S, Suprasert P, et al. Intrahepatic cholangiocarcinoma metastatic to the ovary: a report of 16 cases of an underemphasized form of secondary tumor in the ovary that may mimic primary neoplasia. *Am J Surg Pathol.* 2007;31:1788–1799.
439. Khunamornpong S, Lerwill MF, Siriaunkgul S, et al. Carcinoma of extrahepatic bile ducts and gallbladder metastatic to the ovary: a report of 16 cases. *Int J Gynecol Pathol.* 2008;27:366–379.
440. Meriden Z, Yemelyanova AV, Vang R, et al. Ovarian metastases of pancreaticobiliary tract adenocarcinomas: analysis of 35 cases, with emphasis on the ability of metastases to simulate primary ovarian mucinous tumors. *Am J Surg Pathol.* 2011;35:276–288.
441. Vang R, Ronnett BM. Distinction of primary ovarian mucinous tumors and mucinous tumors metastatic to the ovary: a practical approach with guidelines for prediction of primary site for metastases of uncertain origin. *Pathol Case Rev.* 2006;11:18–30.

442. Ji H, Isacson C, Seidman JD, et al. Cytokeratins 7 and 20, Dpc4, and MUC5AC in the distinction of metastatic mucinous carcinomas in the ovary from primary ovarian mucinous tumors: Dpc4 assists in identifying metastatic pancreatic carcinomas. *Int J Gynecol Pathol.* 2002;21:391–400.
443. Gagnon Y, Tetu B. Ovarian metastases of breast carcinoma. A clinicopathologic study of 59 cases. *Cancer.* 1989;64:892–898.
444. Rabban JT, Barnes M, Chen LM, et al. Ovarian pathology in risk-reducing salpingo-oophorectomies from women with BRCA mutations, emphasizing the differential diagnosis of occult primary and metastatic carcinoma. *Am J Surg Pathol.* 2009;33:1125–1136.
445. Metcalfe KA, Lynch HT, Ghadirian P, et al. The risk of ovarian cancer after breast cancer in BRCA1 and BRCA2 carriers. *Gynecol Oncol.* 2005;96:222–226.
446. Sangoi AR, Karamchandani J, Kim J, et al. The use of immunohistochemistry in the diagnosis of metastatic clear cell renal cell carcinoma: a review of PAX-8, PAX-2, hKIM-1, RCCma, and CD10. *Adv Anat Pathol.* 2010;17:377–393.
447. Snyder MJ, Bentley R, Robboy SJ. Transtubal spread of serous adenocarcinoma of the endometrium: an underrecognized mechanism of metastasis. *Int J Gynecol Pathol.* 2006;25:155–160.
448. LiVolsi VA, Merino MJ, Schwartz PE. Coexistent endocervical adenocarcinoma and mucinous adenocarcinoma of ovary: a clinicopathologic study of four cases. *Int J Gynecol Pathol.* 1983;1:391–402.
449. Young RH, Scully RE. Mucinous ovarian tumors associated with mucinous adenocarcinomas of the cervix. A clinicopathological analysis of 16 cases. *Int J Gynecol Pathol.* 1988;7:99–111.
450. Young RH, Gersell DJ, Roth LM, et al. Ovarian metastases from cervical carcinomas other than pure adenocarcinomas. A report of 12 cases. *Cancer.* 1993;71:407–418.
451. Elishaev E, Gilks CB, Miller D, et al. Synchronous and metachronous endocervical and ovarian neoplasms: evidence supporting interpretation of the ovarian neoplasms as metastatic endocervical adenocarcinomas simulating primary ovarian surface epithelial neoplasms. *Am J Surg Pathol.* 2005;29:281–294.
452. Ronnett BM, Yemelyanova AV, Vang R, et al. Endocervical adenocarcinomas with ovarian metastases: analysis of 29 cases with emphasis on minimally invasive cervical tumors and the ability of the metastases to simulate primary ovarian neoplasms. *Am J Surg Pathol.* 2008;32:1835–1853.
453. Chang MC, Nevadunsky NS, Viswanathan AN, et al. Endocervical adenocarcinoma in situ with ovarian metastases: a unique variant with potential for long-term survival. *Int J Gynecol Pathol.* 2010;29:88–92.
454. Reichert RA. Synchronous and metachronous endocervical and ovarian neoplasms: a different interpretation of HPV data [Letter to Editor]. *Am J Surg Pathol.* 2005;29:1686–1687.
455. Reichert RA. The endocervical origin of HPV-positive mucinous/endometrioid ovarian tumors remains unproven [Letter to Editor]. *Int J Gynecol Pathol.* 2010;29:298–300.
456. Stewart CJR, Dabner M, Khor TS, et al. Ovarian neoplasia associated with localized endocervical carcinoma [Letter to Editor]. Int J Gynecol Pathol 2011;30:62–63.
457. Vang R, Gown AM, Farinola M, et al. p16 expression in primary ovarian mucinous and endometrioid tumors and metastatic adenocarcinomas in the ovary: utility for identification of metastatic HPV-related endocervical adenocarcinomas. *Am J Surg Pathol.* 2007;31:653–663.
458. Wentzensen N, du Bois A, Kommoss S, et al. No metastatic cervical adenocarcinomas in a series of $p16^{INK4a}$-positive mucinous or endometrioid advanced ovarian carcinomas: an analysis of the AGO ovarian cancer study group. *Int J Gynecol Pathol.* 2008;27:18–23.
459. Phillips V, Kelly P, McCluggage WG. Increased p16 expression in high-grade serous and undifferentiated carcinoma compared with other morphologic types of ovarian carcinoma. *Int J Gynecol Pathol.* 2009;28:179–186.
460. Strosberg J, Nasir A, Cragun J, et al. Metastatic carcinoid tumor to the ovary: a clinicopathologic analysis of seventeen cases. *Gynecol Oncol.* 2007;106:65–68.
461. Fitzgibbons PL, Martin SE, Simmons TJ. Malignant melanoma metastatic to the ovary. *Am J Surg Pathol.* 1987;11:959–964.
462. Lee M, Jung YW, Kim SW, et al. Metastasis to the ovaries from transitional cell carcinoma of the bladder and renal pelvis: a report of two cases. *J Gynecol Oncol.* 2010;21:59–61.
463. Vakiani E, Young RH, Carcangiu ML, et al. Acinar cell carcinoma of the pancreas metastatic to the ovary: a report of 4 cases. *Am J Surg Pathol.* 2008;32:1540–1545.
464. Clement PB, Young RH, Scully RE. Malignant mesotheliomas presenting as ovarian masses. A report of nine cases, including two primary ovarian mesotheliomas. *Am J Surg Pathol.* 1996;20:1067–1080.
465. Young RH, Eichhorn JH, Dickersin GR, et al. Ovarian involvement by the intra-abdominal desmoplastic small round cell tumor with divergent differentiation: a report of three cases. *Hum Pathol.* 1992;23:454–464.

CHAPTER 8

Pathology of the Peritoneum and Extragenital Endometriosis

HISTOLOGY AND CYTOLOGY OF NORMAL AND REACTIVE MESOTHELIUM[1]

The peritoneum is composed of a thin strip of loose connective tissue that is normally covered by a single layer of flattened mesothelial cells (Fig. 8.1A). When injured or irritated, mesothelial cells become cuboidal and their nuclei acquire reactive features (Fig. 8.1B). The proliferation of reactive mesothelial cells may lead to cellular stratification and/or formation of papillae.

In cytologic preparations, mesothelial cells may be found singly, in clusters, or in sheets. The best opportunity to see normal mesothelial cells is in unremarkable peritoneal wash specimens, since mesothelial cells always show at least some reactive changes in effusions. In peritoneal washings, large orderly sheets of mesothelial cells are often present (Fig. 8.2). Normal mesothelial cells typically have round to oval nuclei that are centrally located, chromatin that is evenly dispersed and finely granular, micronucleoli, and moderate amounts of lightly stained cytoplasm (Fig. 8.3). Not all normal mesothelial cells follow their textbook description, with some having eccentric nuclei and others exhibiting nuclear membranes that are indented or folded.

In cytologic preparations of benign effusions, the mesothelial cell component is often dominated by individual cells, although groups of cells are also seen. The presence of abundant microvilli on the surface of mesothelial cells often results in clear spaces or "windows" between cells that occur in groups of two or more. Reactive mesothelial cells have a wider range of sizes and shapes than their normal counterparts, typically have dense cytoplasm, can exhibit minor chromatin abnormalities, may have nucleoli that are more prominent than usual, may be mitotically active, and can contain degenerative vacuoles (Fig. 8.4). In addition to intercellular windows, the presence of dense cytoplasm and cell groups with knobby, scalloped peripheral borders are the most helpful features that aid in the recognition of mesothelial differentiation. Clinical situations in which the presence of reactive mesothelial cells should be expected in peritoneal samples include longstanding ascites, chronic renal failure,

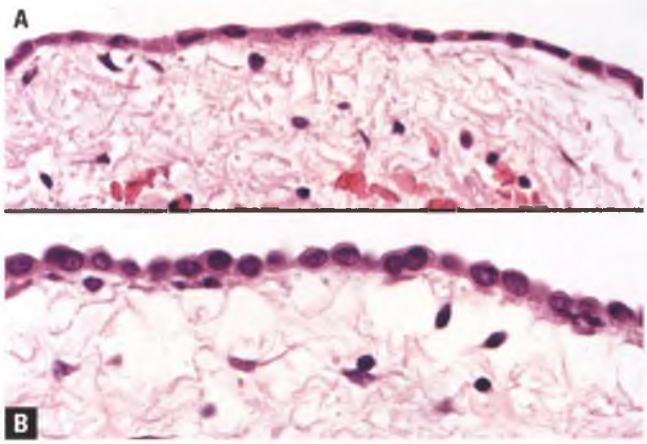

FIGURE 8.1. Normal and reactive mesothelial cells. **A:** The normal mesothelial cells that line the peritoneum and other types of serosal membranes (pleura and pericardium) typically have a flattened appearance. **B:** Reactive mesothelial cells are cuboidal and may contain prominent nucleoli.

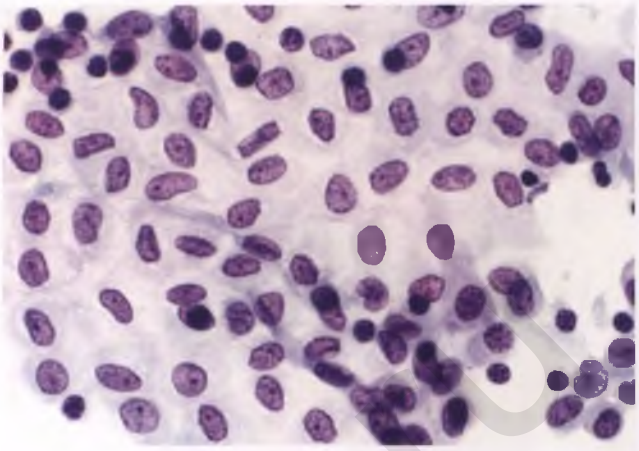

FIGURE 8.3. Normal mesothelial cells in a Papanicolaou-stained cytologic preparation. In this high-magnification view, the mesothelial cells are seen to have bland chromatin, small nucleoli, occasional indentations of the nuclear membrane, and moderate amounts of lightly-stained cytoplasm. Scattered small lymphocytes and a few histiocytes are also present.

cirrhosis of the liver, and patients with a history of radiotherapy or chemotherapy.

Differential Diagnosis

Distinction of mesothelial cells from histiocytes may be difficult, but the latter are usually recognizable by their eccentrically located nuclei, abundant bubbly cytoplasm that may contain engulfed particulate matter, failure to form cohesive groups, and lack of windows between adjacent cells (Fig. 8.5). Degenerative vacuoles may be present in either histiocytes or mesothelial cells. Histiocytes can be mitotically active; in fact, most cells in mitoses in benign effusions are of histiocytic origin. Histiocytes are often described as having nuclei that are the shape of beans or kidneys, but this is usually true of only a minority of any given population, and their nuclei may be in a central rather than eccentric position. Although rarely necessary, mesothelial cells and histiocytes can be distinguished by immunohistochemistry, with mesothelial cells being immunoreactive for cytokeratin and negative for the histiocytic marker CD68 (KP1), whereas the opposite is true of histiocytes.[2]

The distinction of reactive mesothelial cells from malignant mesothelioma and metastatic adenocarcinoma is discussed in the sections on these other entities.

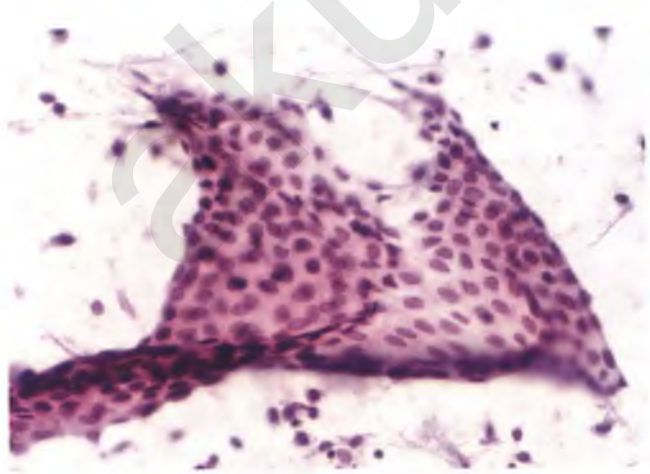

FIGURE 8.2. Partially folded-over sheet of normal mesothelial cells from a Papanicolaou-stained cytologic preparation of a peritoneal wash.

NONGRANULOMATOUS INFLAMMATION

Acute Peritonitis

The usual form of peritonitis encountered by pathologists is bacterial related and due to a perforated or transmurally inflamed area within the gastrointestinal tract (e.g., appendicitis, diverticulitis, or perforated peptic ulcer). A thin, cream-colored, fibrinopurulent exudate forms and is found adherent to the peritoneal surface (Fig. 8.6). A band of reactive mesothelial cells corresponding to the level of the original peritoneal lining can often be identified sandwiched between the superficial exudate and inflamed subserosal tissue (Fig. 8.7).

Nodular Histiocytic Hyperplasia

This nonspecific inflammatory reaction was initially reported as nodular mesothelial hyperplasia, which serves as a testament to the degree to which histiocytes can simulate mesothelial cells.[3] Peritoneal lesions of this type are usually incidental microscopic findings and are most commonly seen in hernia

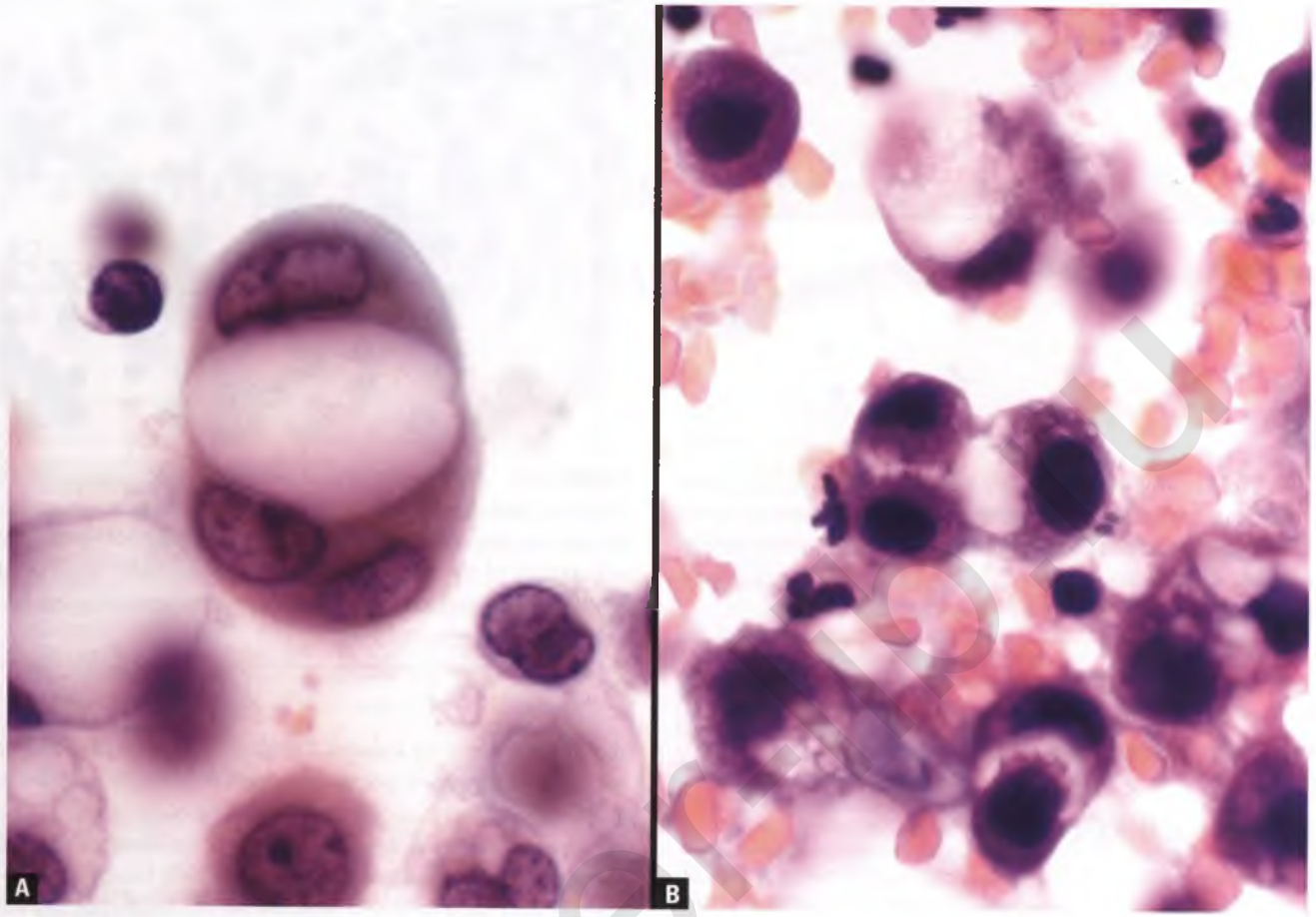

FIGURE 8.4. Reactive mesothelial cells with degenerative vacuoles. **A:** Cytologic preparation. **B:** Cell block of different case. Note how the vacuoles appear to originate within pairs or small groups of mesothelial cells in the area normally occupied by intercellular windows. When the vacuoles are fully developed, the cells that contain them can resemble those derived from metastatic signet-ring carcinoma.

sacs.[3]* In contrast to legitimate mesothelial hyperplasia, which typically consists of complex papillary proliferations, nests, cords, tubules, or scattered single cells near the peritoneal surface,[3,4] nodular histiocytic hyperplasia occurs exclusively as vague to distinct nodules composed of diffuse sheets of histiocytes (Fig. 8.8).[2] These histiocytes have a fairly monotonous appearance and may be mitotically active. Their histiocytic nature is confirmed by their strong and diffuse immunoreactivity with the histiocytic marker CD68 and their failure to stain with cytokeratin.[2] Not uncommonly, there are a few entrapped reactive mesothelial cells, occurring singly or in small groups, that can be highlighted with cytokeratin or calretinin immunostains.[2]

The importance of nodular histiocytic hyperplasia lies in its potential to be confused with metastatic carcinoma, metastatic granulosa cell tumor, or malignant mesothelioma. Once pathologists are aware of the existence of this phenomenon, the correct diagnosis can usually be made on the basis of routinely stained sections; when indicated, such as when a lesion of this

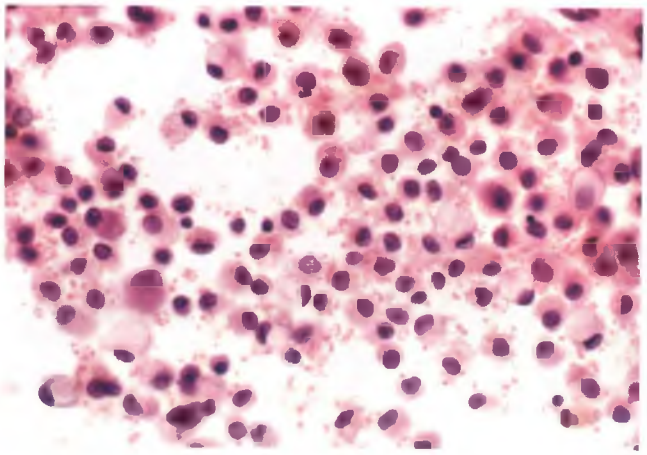

FIGURE 8.5. Histiocytes. Several of the cells contain engulfed particulate matter and/or hemosiderin, and some degenerative vacuoles are present.

*The report that conclusively demonstrated the dominance of histiocytes in these lesions included a case from the lamina propria of the urinary bladder;[2] before such a case can be accepted as an example of nodular histiocytic hyperplasia, the possibility of malakoplakia needs to be excluded.

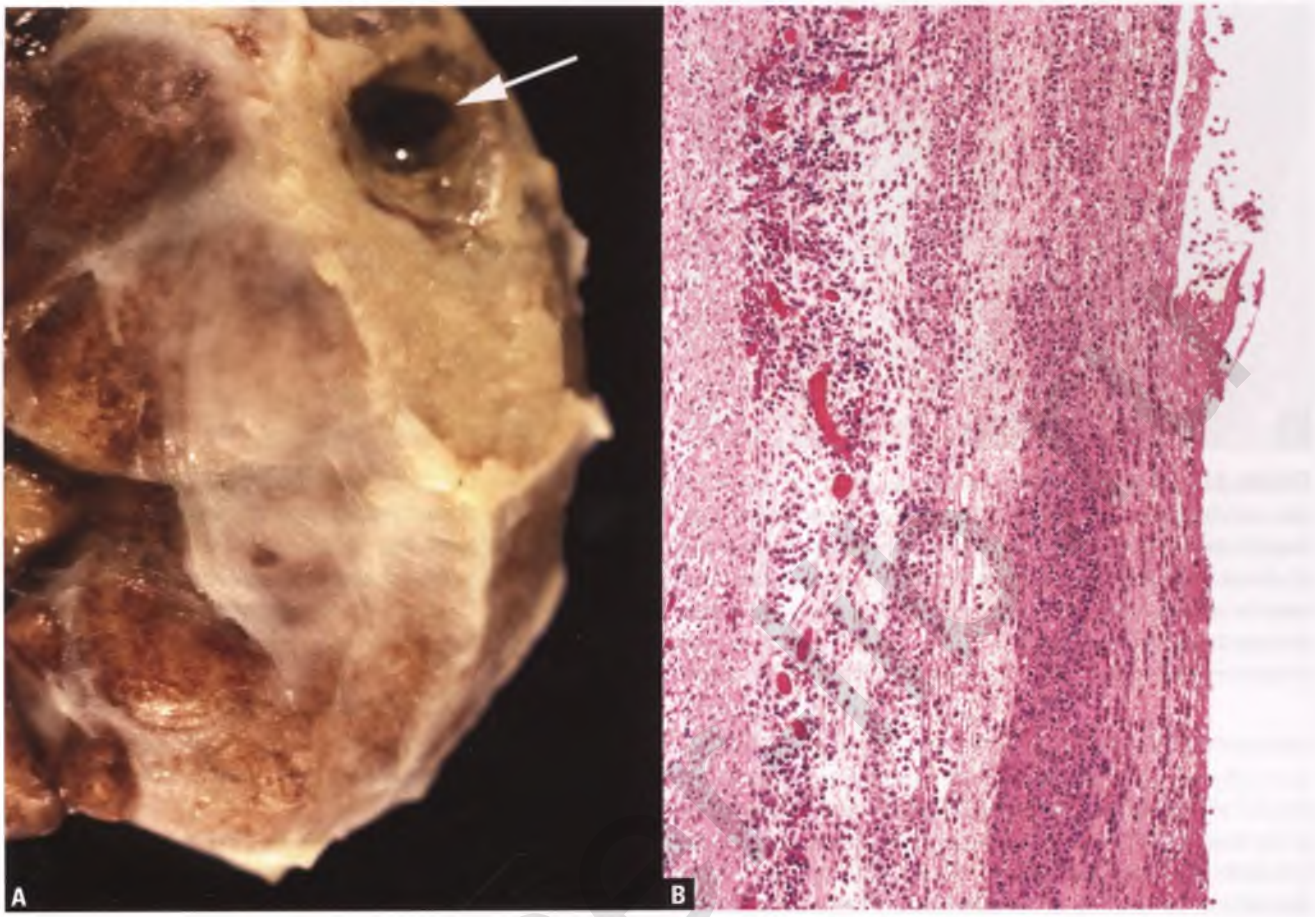

FIGURE 8.6. Acute peritonitis. **A:** A perforated appendix (*arrow*) has resulted in acute peritonitis, which appears grossly as a thin, *light gray* to *pale yellow* exudate covering portions of the peritoneal surface. **B:** In this low-magnification view, the exudate is seen to consist predominantly of neutrophils and fibrin.

type is found in a patient with a history of granulosa cell tumor, the diagnosis can be confirmed with immunohistochemistry.

Sclerosing Peritonitis[5,6]

Sclerosing peritonitis is a nonspecific fibroinflammatory reaction that occurs in response to a variety of stimuli.[5,6] It is typically most prominent in the omentum and small bowel serosa. Patients usually have ascites and abdominal pain/distension, often in conjunction with small bowel obstruction. There is an enigmatic association of sclerosing peritonitis with a particular form of luteinized thecoma.

Grossly, areas of omentum that are involved by sclerosing peritonitis are indurated, thickened, and nodular. Histologically, the lobular architecture of the omentum is accentuated due to a combination of expansion, fibrosis, and inflammation of the preexisting omental septa (Fig. 8.9). The bands of fibrosis contain proliferating fibroblasts and myofibroblasts, collections of chronic inflammatory cells, and linear arrangements of reactive mesothelial cells (Fig. 8.10).[7] In areas of small bowel involvement, the serosal surface often contains deposits of fibrin, and the thickening and fibrosis of the serosa results in kinking of loops of bowel with formation of adhesions.

Sclerosing Mesenteritis[8,9]

Sclerosing mesenteritis, which is a diagnostic term that also encompasses diseases that have been referred to as retractile

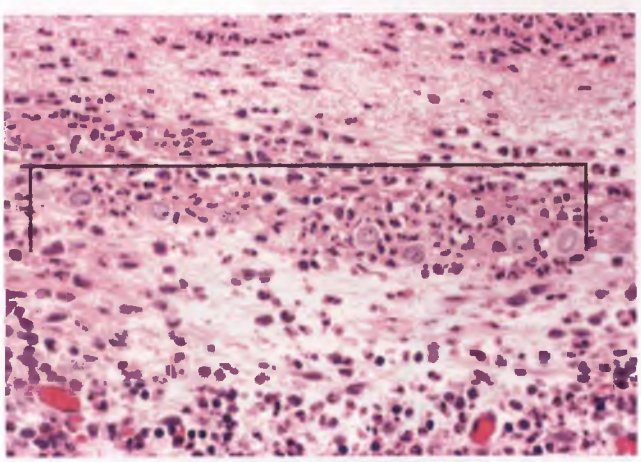

FIGURE 8.7. Acute peritonitis. There is often a recognizable linear band of reactive mesothelial cells that corresponds to the level of the native peritoneal surface (*brackets*).

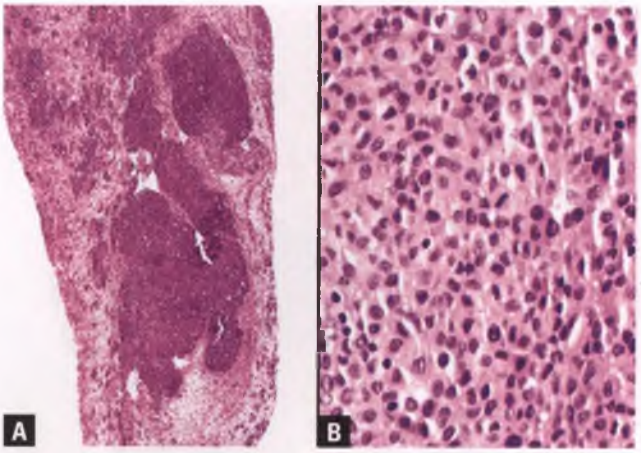

FIGURE 8.8. Nodular histiocytic hyperplasia. **A:** At low magnification, cellular nodules are seen within a pelvic adhesion. **B:** This high-magnification view of one of the nodules demonstrates the presence of sheets of histiocytes, which can be difficult to distinguish from mesothelial cells in routinely-stained sections. A mitotic figure is present near the center of the image.

mesenteritis, mesenteric panniculitis, and mesenteric lipodystrophy, is an uncommon fibroinflammatory process of unknown etiology that most commonly involves the mesentery of the small bowel. This mass-forming lesion typically presents in middle-aged or elderly men or women, and can cause bowel obstruction by binding down and kinking loops of intestine. The mass is most often solitary, averages 10 cm in diameter, and is firm with a grayish yellow discoloration (Fig. 8.11).

Histologically, sclerosing mesenteritis has an abrupt interface with the muscularis propria of the small bowel and is characterized by fibrosis, lobules of adipose tissue with varying degrees of fat necrosis, and chronic inflammation (Figs. 8.12 and 8.13). The chronic inflammatory component consists predominantly

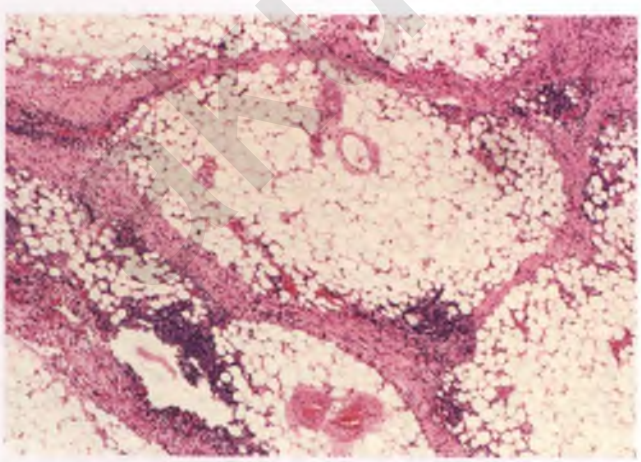

FIGURE 8.9. Sclerosing peritonitis involving the omentum. Fibrosis and chronic inflammation of the omental septa have resulted in accentuation of the lobular architecture.

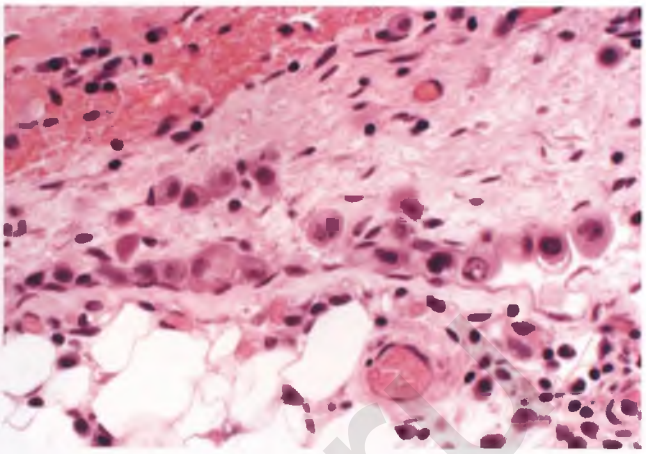

FIGURE 8.10. Sclerosing peritonitis involving the omentum. The fibrotic omental septa typically contain linear arrangements of reactive mesothelial cells that should not be mistaken for metastatic carcinoma or a neoplastic mesothelial proliferation.

of scattered and aggregated lymphocytes and plasma cells. Foci of dystrophic calcification are commonly present.

GRANULOMATOUS INFLAMMATION

Peritoneal granulomas may be formed in response to a variety of infectious and noninfectious agents. In some cases, the presence of multiple nodules may simulate peritoneal carcinomatosis. Tuberculosis is the most common cause of infectious granulomatous peritonitis, but fungal and parasitic infections can also produce this reaction. The lengthy list of noninfectious causes of peritoneal granulomas includes keratin derived from endometrial or ovarian tumors with squamous differentiation, contents of ruptured or slowly leaking mature cystic teratomas of the ovary (sebaceous material and keratin), amniotic fluid

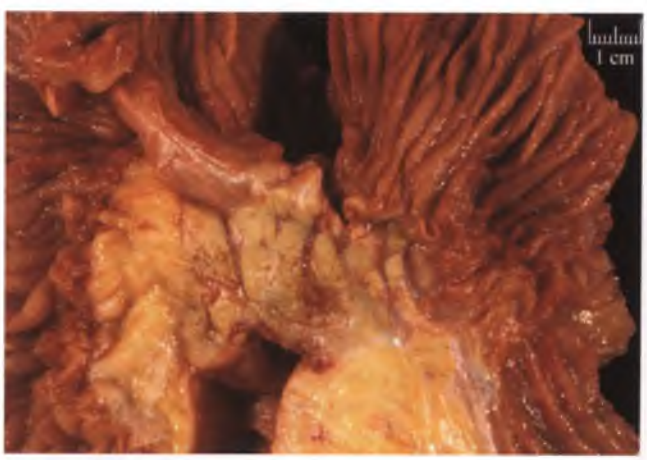

FIGURE 8.11. Sclerosing mesenteritis. The mass within the mesentery of the small bowel is discolored and lobulated due to a combination of fat necrosis and fibrosis, and contrasts with the normal yellow mesenteric adipose tissue.

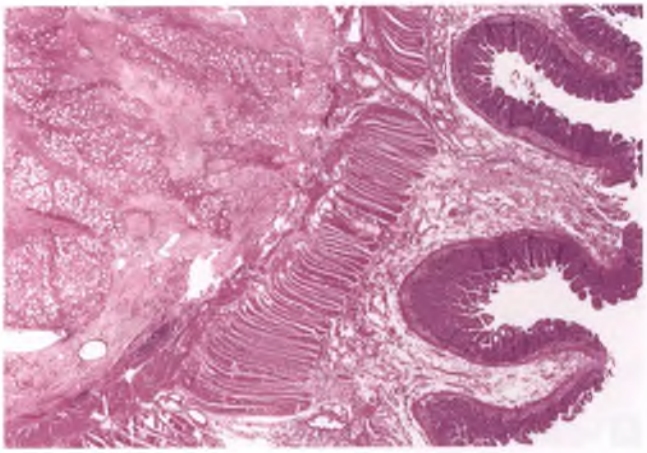

FIGURE 8.12. Sclerosing mesenteritis. In this low-magnification view of the small bowel and its mesentery, the mesenteric mass at left is seen to consist of fibrous bands outlining lobules of adipose tissue. Note the sharp demarcation between the fibrosing process and the muscularis propria of the small bowel.

spilled into the peritoneal cavity at cesarean section resulting in the production of vernix caseosa peritonitis, bowel contents introduced into the peritoneal cavity via perforation, and material such as starch granules, talc, suture, resorbable hemostatic agents, and carbon particles that are almost always associated with a history of prior abdominal surgery. A selection of these granuloma-inducing agents is discussed in further detail in the following sections.

Tuberculous Peritonitis[10]

Tuberculous peritonitis is rare in developed countries, and typically produces a fibroinflammatory surface coating that is studded with granulomas that range from minute to conglomerations that form visible nodules (Fig. 8.14A). This macroscopic appearance,

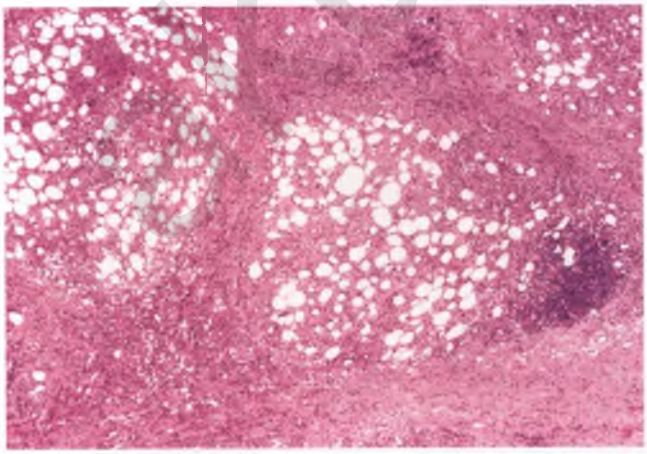

FIGURE 8.13. Sclerosing mesenteritis. Lobules of adipose tissue with fat necrosis are surrounded by fibrous bands and an admixed chronic inflammatory infiltrate.

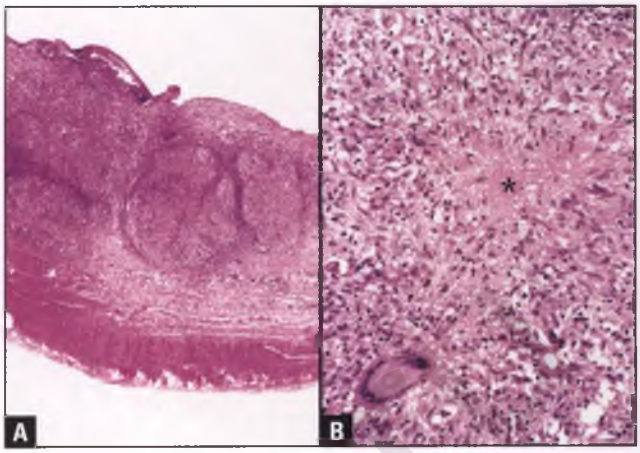

FIGURE 8.14. Tuberculous peritonitis. **A:** In this low-magnification view of markedly thickened peritoneum, nodular granulomas are seen within a layer of fibroinflammatory tissue (surface is at top; band of fascia is at bottom). **B:** This tuberculous granuloma features a focal area of caseous necrosis (*asterisk*) and a Langhans giant cell at lower left. The nuclei of Langhans giant cells congregate at the periphery of the cell in a wreath-like arrangement. (Glass slide kindly provided by Dr. Cheryl M. Reichert.)

coupled with the presence of ascites and an elevated CA-125, can lead to the clinical impression of metastatic ovarian cancer.[11] In most cases, some of the granulomas exhibit caseous necrosis and associated Langhans giant cells are typically present, although neither of these findings is specific for tuberculosis (Fig. 8.14B). In the setting of a granulomatous peritonitis of unknown etiology, microbiologic cultures and special stains for acid-fast bacilli and fungi should be performed, although acid-fast bacilli may be quite difficult to identify in peritoneal-based tuberculous disease.

Suture Granulomas

Suture material related to a previous operative procedure may incite a foreign body granulomatous reaction (Fig. 8.15).

Talc and Starch Granulomas

Talc granulomas in gynecologic pathology are mainly of historical interest, since problems due to the formation of these granulomas and their associated adhesions have led to the discontinuance of the use of talcum powder on surgical gloves, which was the main source of intraperitoneal talc.[12] Talc (hydrated magnesium silicate) induces noncaseating granulomas with a foreign body multinucleated giant cell reaction, with talc particles often found within the giant cells.[12] Talc particles may be difficult to visualize in conventionally examined routine sections, exhibit a variety of shapes and sizes (up to 30 μm), and are strongly birefringent when viewed under polarized light (Fig. 8.16). In current pathology practice, they are most likely to be encountered in the lungs of intravenous drug abusers whose narcotics have been "cut" with talcum powder.

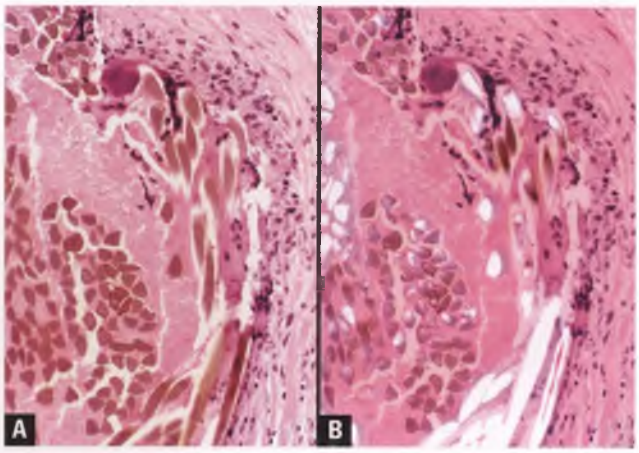

FIGURE 8.15. Foreign body reaction to suture. **A:** A granulomatous reaction that includes multinucleated giant cells surrounds suture material. **B:** Portions of the suture material are strongly birefringent when viewed under polarized light.

Starch granules, which have replaced talc as a surgical glove powder, are also known to elicit a granulomatous response and induce formation of adhesions, albeit to lesser degrees and with less significant clinical consequences.[13] An example of starch granules within a peritoneal adhesion is presented in Figure 8.47.

Postoperative Carbon Pigment Granulomas

Due to their discolored, punctate nature, postoperative carbon pigment granulomas formed on the peritoneal or ovarian surfaces as a reaction to previous laser or fulguration surgery grossly resemble foci of endometriosis and may be biopsied.[14,15] Histologically, these lesions typically have necrotic centers that contain clumps of brown to black pigmented material and a surrounding rim of palisaded histiocytes and multinucleated giant cells, although pigment-containing, nonnecrotizing granulomas or loose aggregates of pigment-containing multinucleated giant cells may also be seen (Figs. 8.17 and 8.18).[14,15] Although this pigment is generally assumed to represent carbon particles related to the process of carbonization that takes place during charring of tissue, there is evidence that the black pigment in similarly treated tissue may be derived from metal deposits from the laser tip or electrosurgical device.[16,17]

Postoperative carbon pigment granulomas are distinguished from necrotic pseudoxanthomatous nodules of endometriosis by the presence of clumps of brown and/or black pigment and the absence of pseudoxanthoma cells (see Chapter 6).

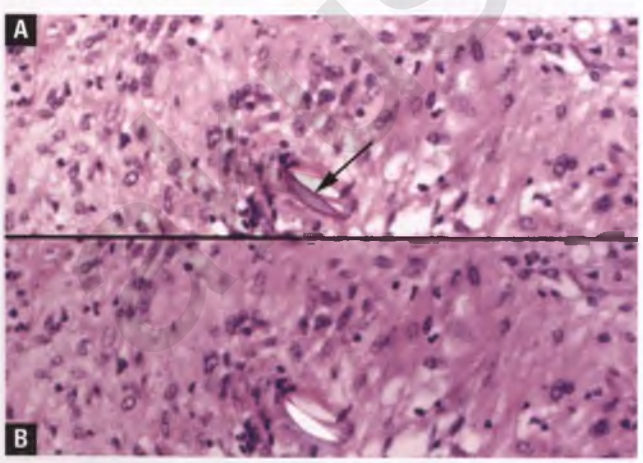

FIGURE 8.16. Talc granuloma. **A:** A talc particle (*arrow*) is surrounded by a proliferation of epithelioid histiocytes. The trauma of histologic sectioning has partially dislodged the particle from its original location within a multinucleated giant cell. **B:** Examination under partially polarized light highlights the strongly birefringent particle.

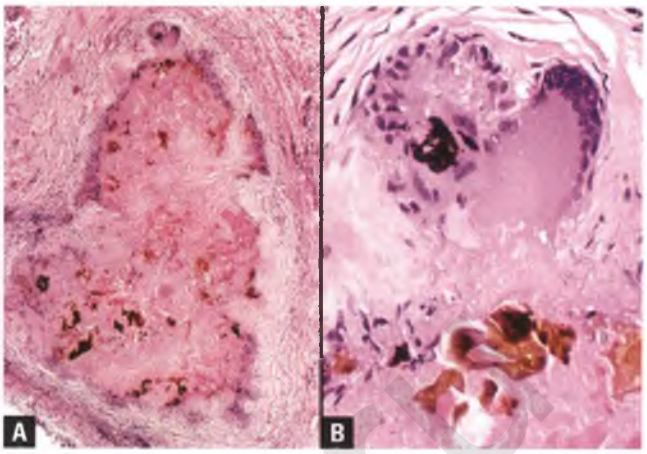

FIGURE 8.17. Postoperative carbon pigment granuloma. **A:** This 0.2 cm lesion has a necrotic center that contains irregularly shaped clumps of golden brown and black pigment, and is surrounded by a rim of palisading histiocytes and multinucleated giant cells. **B:** Some of the pigmented material has been ingested by the multinucleated giant cells.

Reaction to Resorbable Hemostatic Agents

Resorbable hemostatic agents composed of microfibrillar collagen (e.g., Avitene) can occasionally produce mass lesions

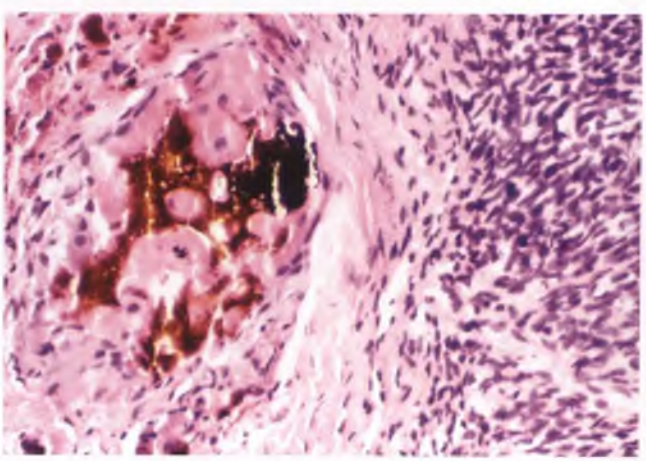

FIGURE 8.18. Postoperative carbon pigment granuloma. This example is nonnecrotizing and involves the ovarian surface (ovarian stroma is at right).

("textilomas") composed of an admixture of variable-sized collagen fibrils and a fibroinflammatory response. This response characteristically includes eosinophils, and these lesions take on a granulomatous appearance when associated with a foreign body multinucleated giant cell reaction (Fig. 8.19). In exceptional cases, a granulomatous response to microfibrillar collagen can be florid and mass producing.[18,19] Pathologists also encounter microfibrillar collagen in other organ systems, such as in breast biopsies following insertion of a metallic clip that is embedded within a collagen plug[20] or in intracranial tumors with a history of previous surgical intervention.[21]

Microfibrillar collagen should be distinguished from resorbable gelatin sponge (Gelfoam), which exhibits a characteristic branching architecture and purple hue in routine sections (Fig. 8.20).[21] Oxidized cellulose (Surgicel) is yet another type of resorbable hemostatic agent that can produce a histiocytic or foreign body granulomatous reaction.[22,23]

Keratin Granulomas[24]

The deposition of keratin on the peritoneal surface incites a foreign body granulomatous reaction. When present in large quantities, such deposits are usually derived from a mature cystic teratoma of the ovary that has ruptured. The surgical pathologist is more likely to encounter peritoneal keratin granulomas in the context of one or more nodular, pale yellow deposits measuring up to 1 cm that may be mistaken clinically for metastatic carcinoma or miliary tuberculosis. In this situation, keratin granulomas are most commonly related to keratin derived from an endometrial endometrioid adenocarcinoma with squamous differentiation whose shed keratinous debris has made its way through the fallopian tubes and into the peritoneal cavity (see Fig. 5.39 for an image of intratubal clumps of keratin). Less often, focal tearing, localized rupture, or penetration of the capsule of ovarian tumors of this type is the mechanism leading to small deposits of keratin within the peritoneal cavity. Rarely, squamous cell carcinoma of the cervix or atypical polypoid adenomyoma of the uterus is the source of the keratinous material.

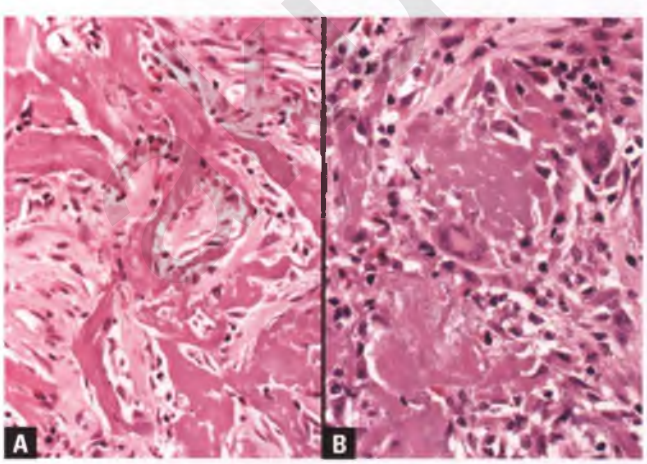

FIGURE 8.19. Reaction to microfibrillar collagen. **A:** Variable-sized collagen fibrils are embedded in a reactive stroma that contains scattered eosinophils. **B:** The presence of a multinucleated giant cell reaction to the fibrils imparts a granulomatous appearance.

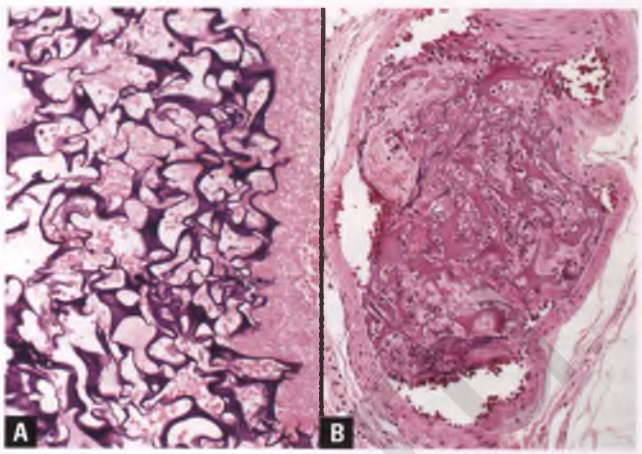

FIGURE 8.20. Gelfoam. **A:** Gelfoam exhibits a distinctive branching pattern and purple hue in histologic sections (fibrin and red blood cells are also present). **B:** Vessel with a gelfoam embolus.

Peritoneal keratin granulomas consist of a foreign body giant cell reaction to deposits of keratin or defunct, heavily keratinized squamous cells (Fig. 8.21). Variable amounts of fibrosis and inflammation are also present. In the absence of associated viable tumor cells, peritoneal keratin granulomas are of no prognostic significance and should not be considered spread of tumor beyond the organ of origin.

Vernix Caseosa Peritonitis[25,26]

Vernix caseosa is a white, cheesy substance that coats the skin of the fetus and newborn. It is composed primarily of flakes of

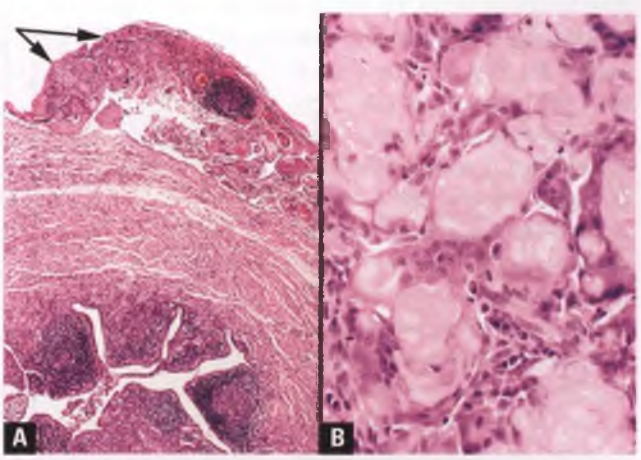

FIGURE 8.21. Keratin granulomas. **A:** Keratin granulomas (*arrows*) are seen in association with serosal adhesions in the paratubal tissue of this patient with endometrial endometrioid adenocarcinoma with squamous differentiation. The fallopian tube shows features of an active chronic salpingitis. **B:** High-magnification view of a keratin granuloma. The lesion consists largely of deposits of keratin surrounded by foreign-body giant cells.

keratin sloughed from the skin surface, oily sebaceous material, and shed lanugo hair. A rare complication of spillage of amniotic contents into the maternal peritoneal cavity at the time of cesarean section is vernix caseosa peritonitis. This inflammatory process typically presents with abdominal pain, fever, and a neutrophilic leukocytosis within the first 5 weeks following cesarean section.

Grossly, this form of peritonitis is characterized by scattered plaque-like deposits of white, cheesy material on the surface of the peritoneal cavity. The histologic features are characteristic, with an organizing peritonitis whose most prominent feature is a multinucleated giant cell reaction to loosely aggregated flakes of keratin (Fig. 8.22). Although classified as a granulomatous peritonitis, well-formed granulomas are usually not present and there is a mixed acute and chronic inflammatory infiltrate in the background.

The characteristic clinical setting of vernix caseosa peritonitis should make it easily distinguishable from the other causes of a peritoneal-based foreign body giant cell reaction to keratin that are discussed in the previous section. Although most cases of vernix caseosa peritonitis are self-limited, some are associated with complications such as adhesion-related bowel obstruction. Intraoperative diagnosis of this form of peritonitis via frozen section analysis helps to prevent unnecessary surgical removal of organs covered by the peritoneal exudates, which can clinically simulate the usual kind of peritonitis related to perforation of a viscus.

Meconium Peritonitis[27]

If the bowel of a developing fetus perforates prior to birth, meconium is released into the peritoneal cavity. The bile, pancreatic, and intestinal secretions that are contained within meconium produce a chemical peritonitis that is characterized by loose fibroblastic tissue that contains calcifications and aggregates of macrophages stuffed with bile pigment (Fig. 8.23). A foreign body giant cell reaction to the calcified material may be present, which is the reason for the inclusion of meconium peritonitis within the category of granulomatous inflammation. Bowel-obstructing conditions that predispose to the development of meconium peritonitis include cystic fibrosis, stricture, atresia, volvulus, and intussusception.

ECTOPIC DECIDUA[28,29]

Ectopic decidua, which in this site is also referred to as a peritoneal decidual reaction, is strongly associated with a concurrent pregnancy. Peritoneal-based ectopic decidua involves the submesothelial stroma of a variety of different tissues, and is most frequently seen on the outer aspect of the fallopian tubes, uterus, appendix, and omentum, as well as within pelvic adhesions (Figs. 8.24 and 8.25). Although often an incidental microscopic finding, florid examples of ectopic decidua are grossly visible as small grayish white to tan nodules, plaques, or polypoid projections emanating from the serosal surface. Histologically, the decidualized stromal cells of ectopic decidua are identical to their normal counterpart in gestational endometrium. They may be closely packed, but more often are widely spaced within an edematous stroma (Fig. 8.26).

On rare occasions, ectopic decidualized cells can be found within abdominal lymph nodes. In this situation, the association of these cells with pregnancy and the absence of

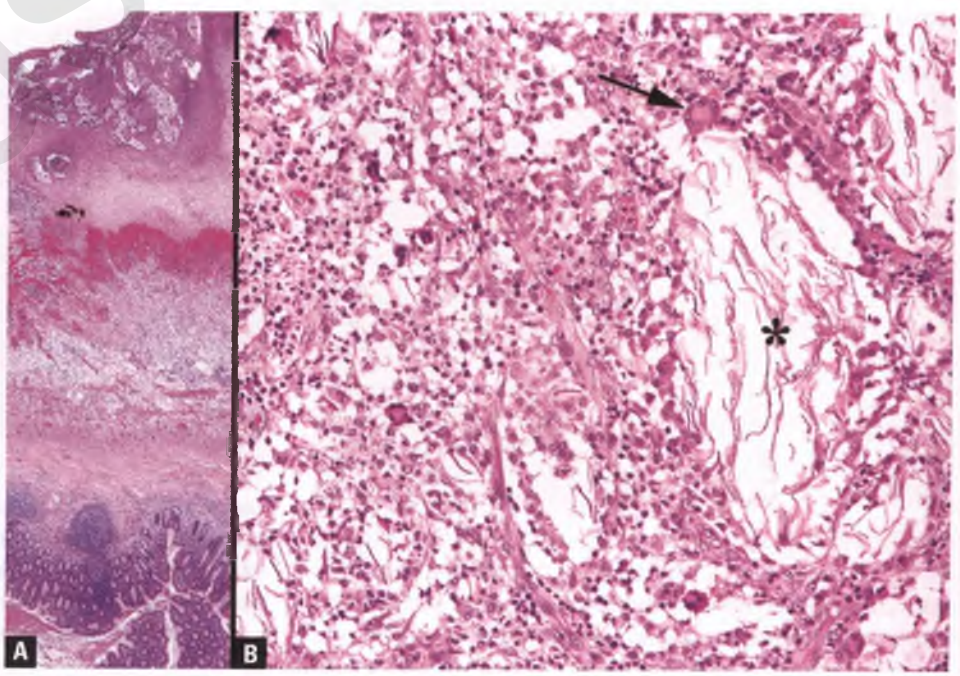

FIGURE 8.22. Vernix caseosa peritonitis. **A:** This low-magnification view demonstrates markedly thickened and inflamed peritoneal tissue (top half) that is densely adherent to the appendix (bottom half). Islands of keratin flakes with associated inflammation are located near the peritoneal surface at the top of the image. **B:** At high magnification, loosely aggregated keratin flakes (*asterisk*) are seen in association with a mixed inflammatory infiltrate that includes multinucleated giant cells (*arrow*). (Altered from Stuart OA, Morris AR, Baber RJ. Vernix caseosa peritonitis—no longer rare or innocent: a case series. *J Med Case Rep.* 2009;3:60. Reproduced and altered with permission of Dr. Olivia A. Stuart and BioMed Central, Ltd.)

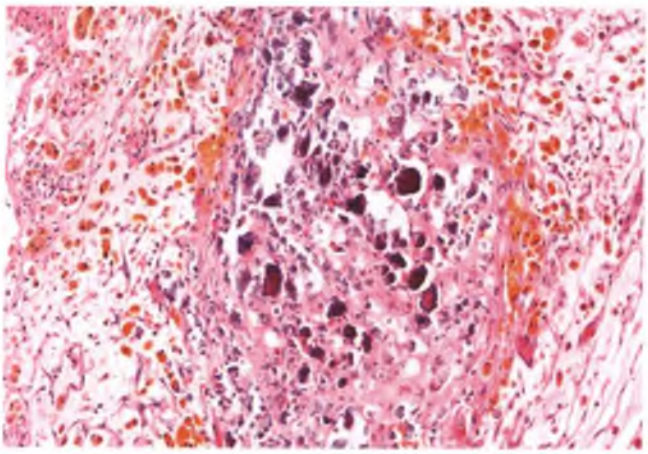

FIGURE 8.23. Meconium peritonitis. Within a background of loose granulation tissue are numerous dark purple calcifications and macrophages that have engulfed golden brown bile pigment. (Courtesy of Dr. Deborah J. Gersell.)

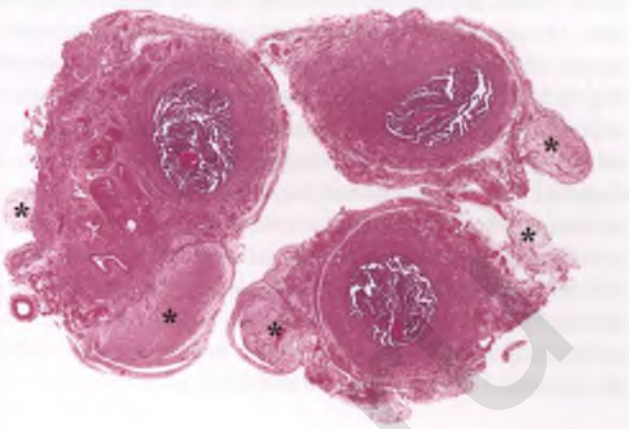

FIGURE 8.25. Florid paratubal decidual reaction. In these three cross sections of a fallopian tube from a postpartum tubal ligation, scattered nodules composed of decidualized tissue protrude from the serosal surface (*asterisks*). In cases such as this, the decidual reaction is grossly apparent to the astute observer.

cytokeratin immunoreactivity can help to exclude the diagnosis of metastatic carcinoma.

The distinction of ectopic decidua from deciduoid malignant mesothelioma is discussed in the section on malignant mesothelioma.

ENDOSALPINGIOSIS[30–32]

Endosalpingiosis is the term used to refer to the presence of benign glands lined by tubal-type epithelium within peritoneal tissues, the omentum, and regional lymph nodes. Endosalpingiotic glands are also referred to as benign müllerian glandular inclusions or müllerian inclusion cysts. Endosalpingiosis is most common in the reproductive age group, occurs almost exclusively in women, and is found in about 10% to 15% of pelvic lymph node dissections and surgically removed omenta. It is often found in association with inflammatory tubal disease and epithelial ovarian tumors, most notably serous borderline tumors. Endosalpingiosis may be derived from dislodged cells originating from the fimbria of the fallopian tube, as has been proposed for ovarian epithelial inclusions with a similar histologic appearance (see Chapter 6).[33] Alternatively, the peritoneal mesothelium and its subjacent mesenchyme, which in females are thought to represent part of the "secondary müllerian system" by virtue of their close embryonic relationship with the müllerian ducts, may produce findings such as endosalpingiosis as part of their müllerian repertoire.

The tubal-type glands of endosalpingiosis are of variable size and shape, may be dilated, and are often associated with psammoma bodies. The epithelial cells that line the glands have

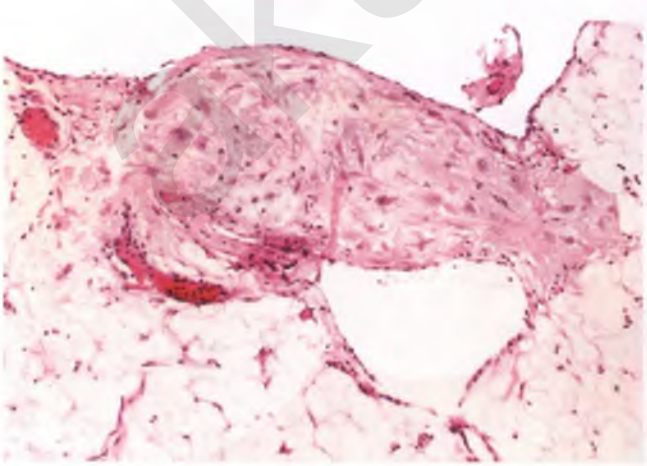

FIGURE 8.24. A small nodule of decidualized cells is present within submesothelial omental tissue.

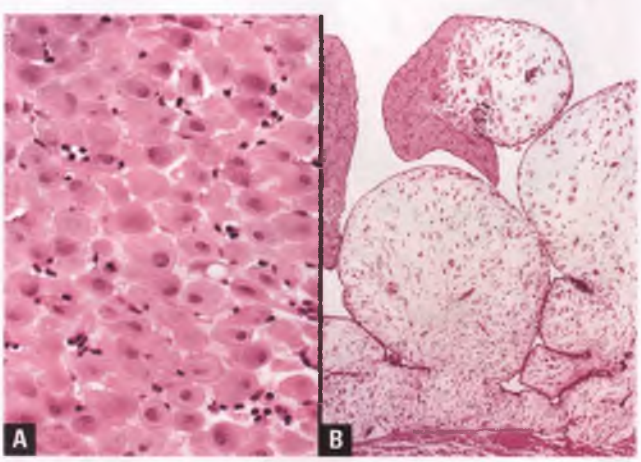

FIGURE 8.26. Ectopic decidua. **A:** Compact sheet of decidualized cells. **B:** Polypoid nodules of decidualized tissue with a predominantly edematous stroma.

bland, mitotically inactive nuclei and include scattered ciliated cells. The glands of endosalpingiosis tend to be architecturally simple, although minor papillary infoldings may be present (Fig. 8.27). When psammoma bodies are found intermingled with subserosal fibrous tissue in the absence of associated epithelial elements, "burned-out" endosalpingiosis is the presumptive diagnosis (Fig. 8.28). Endosalpingiosis is usually an incidental microscopic finding or visible as millimeter-sized cystic bumps on serosal surfaces, but can create a tumor-like mass when florid and cystic (Fig. 8.29).[34] When lymph nodes are involved, they are usually from the pelvic or paraaortic region, and the glands are typically located within the lymph node capsule or within the superficial cortex (Figs. 8.30 and 8.31).

Differential Diagnosis

In contrast to endometriosis, the glands of endosalpingiosis are not associated with endometrial-type stroma or evidence of prior hemorrhage. The mesonephric tubules of mesonephric remnants, which are typically found in the broad ligament, are distinguished from endosalpingiosis by their collarettes of smooth muscle and lack of ciliated cells (see Fig. 5.51). Examples of ectopic tubal-type glands with epithelial cells forming complex papillae and detached clusters have been labeled "atypical endosalpingiosis" by some investigators, but glandular inclusions with these features cannot be reliably distinguished from noninvasive implants of ovarian serous borderline tumors or from lesions related to serous borderline tumors of the peritoneum.[35] The bland nuclear features, architectural simplicity, mitotic inactivity, and usual location within the lymph node capsule rather than in subcapsular sinuses aid in the distinction of endosalpingiosis involving lymph nodes from involvement by serous borderline tumor and metastatic adenocarcinoma.

Although most investigators interpret the frequent association of endosalpingiosis and serous borderline tumor within a lymph node as evidence that the former may serve as an intranodal precursor of the latter,[32] one group has speculated that the endosalpingiotic glandular inclusions may represent morphologically uninformative metastases of serous borderline tumor.[31] In any case, it is certainly in the patient's best interest to continue to refer to these glandular inclusions as incidental foci of endosalpingiosis, especially in view of the fact that even *bona fide* lymph node involvement by serous borderline tumor is not an independent adverse prognostic factor.[36,37]

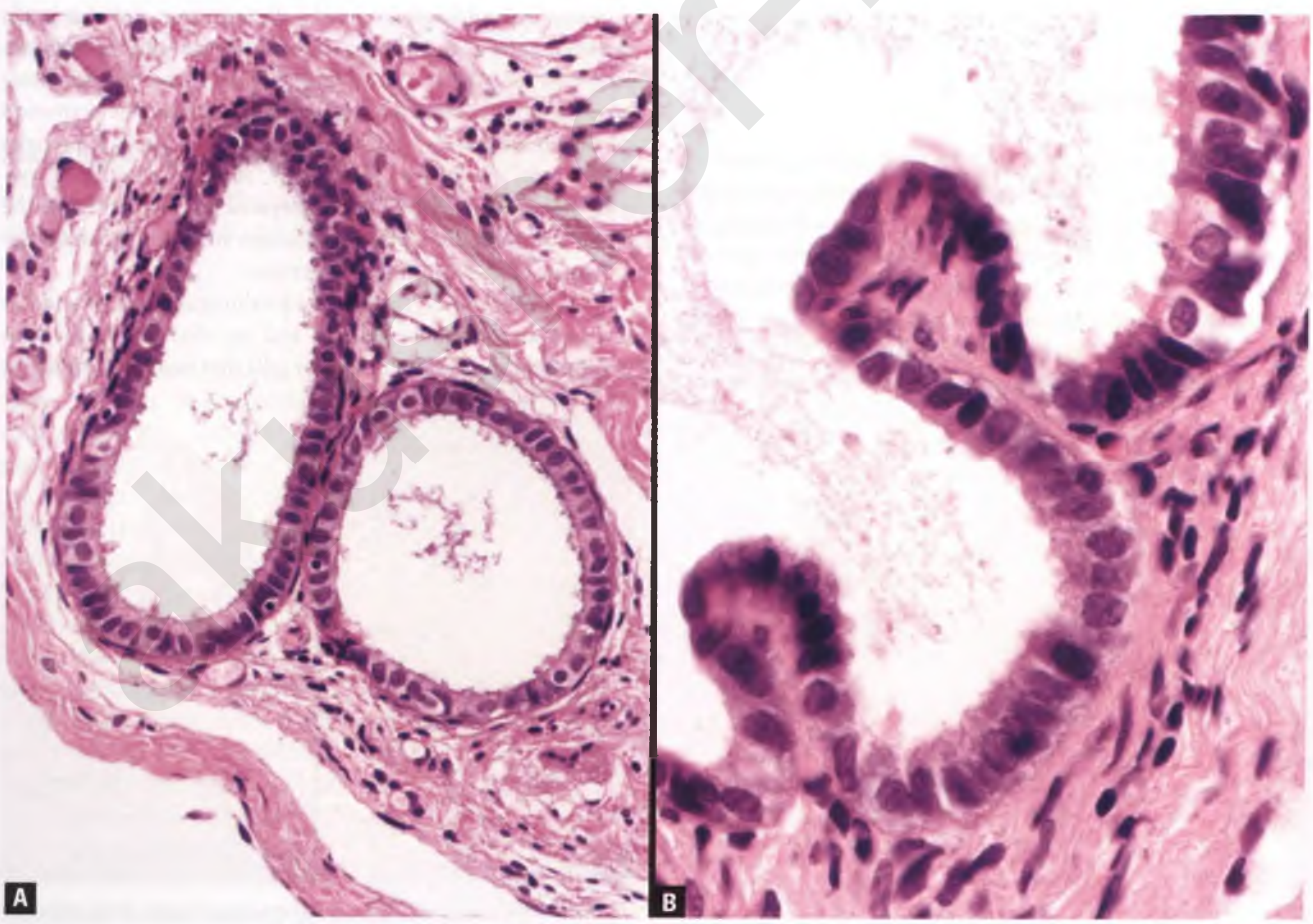

FIGURE 8.27. Endosalpingiosis. **A:** The benign glands have a simple architecture and are lined by tubal-type epithelium. **B:** The glandular epithelium may exhibit innocuous papillary infoldings. Note the presence of interspersed ciliated cells.

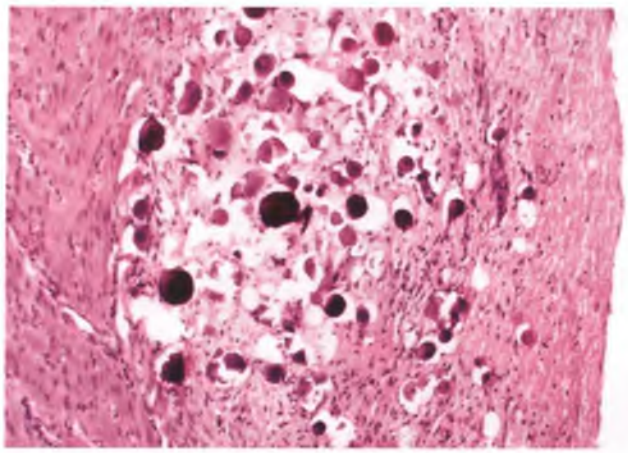

FIGURE 8.28. Endosalpingiosis. This "burned-out" focus in the uterine subserosa consists of fibrous tissue and psammoma bodies.

ENDOCERVICOSIS[38,39]

Endocervicosis, which is very rare in comparison to endosalpingiosis and endometriosis, is defined as the presence of benign endocervical-type epithelium in unusual sites such as the peritoneum, urinary bladder, outer wall of the cervix, and abdominopelvic lymph nodes. Endocervicosis typically occurs in women of reproductive age, may be associated with pelvic pain or site-specific symptoms, and may form a visible mass. Histologically, this nonneoplastic lesion consists of cysts and glands lined by columnar mucinous epithelium with bland to mildly atypical nuclear features. The glands may be irregularly shaped, surrounded by a reactive fibrous stroma, or ruptured, with the latter associated with extravasated stromal mucin. In addition to mucinous glands, there may also be interspersed glands of tubal or endometrioid type. An example of endocervicosis involving a paraaortic lymph node is depicted in Figure 8.32.

The awareness of the existence of endocervicosis, knowledge of its range of histologic features, and clinicopathologic correlation facilitate its distinction from metastatic well-differentiated mucinous adenocarcinoma. Features that help to distinguish endocervicosis involving the outer aspect of the uterine cervix from adenoma malignum are discussed in Chapter 3.

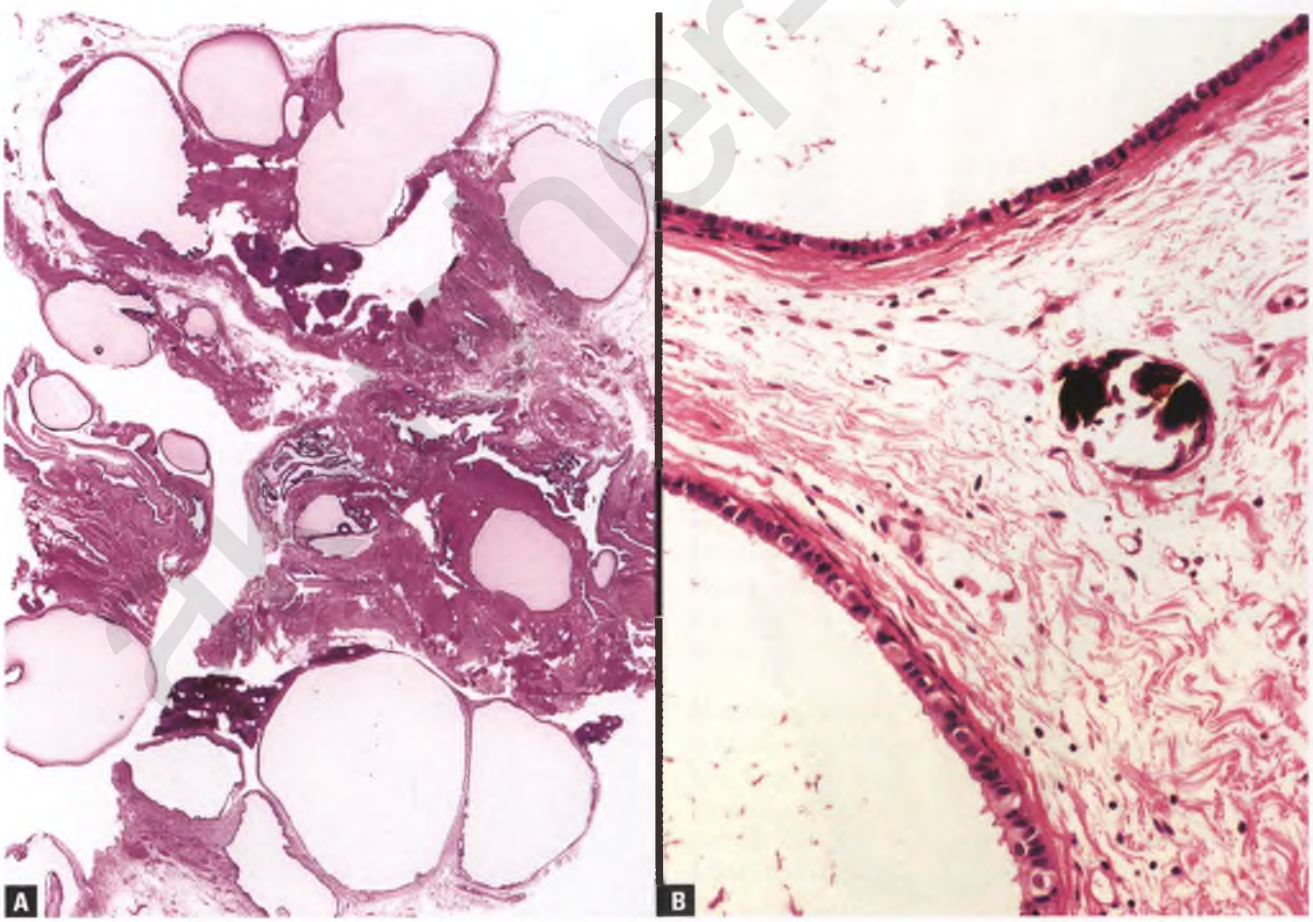

FIGURE 8.29. Florid cystic endosalpingiosis. **A:** The lesion consists of a conglomerate of variable-sized cysts. **B:** The cysts are lined by a single layer of cuboidal epithelial cells, some of which are ciliated with perinuclear haloes. Within the stroma, note the presence of a psammoma body that has been traumatized by the microtome blade.

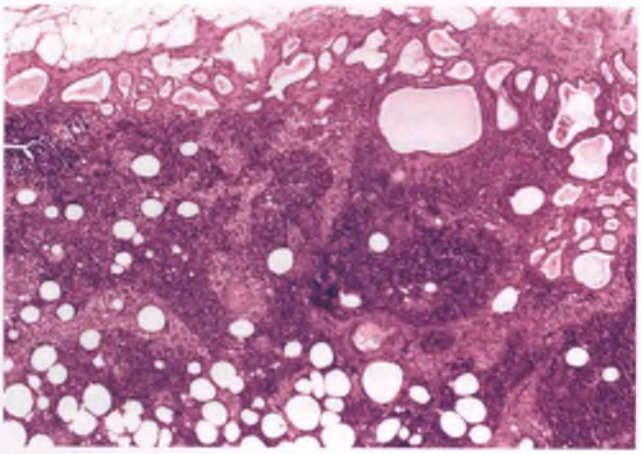

FIGURE 8.30. Endosalpingiosis within a pelvic lymph node. The glandular inclusions are preferentially located within the lymph node capsule.

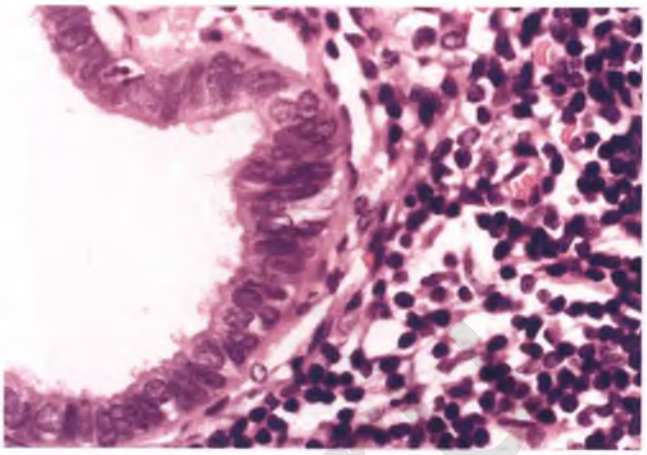

FIGURE 8.31. Endosalpingiosis within a pelvic lymph node. The glandular inclusion is lined by tubal-type epithelium with scattered ciliated cells.

ENDOMETRIOSIS[40]

Endometriosis refers to the presence of endometrial tissue beyond the confines of the endometrium and myometrium. The most common sites of involvement are the ovary, uterine ligaments, cul-de-sac (rectouterine pouch), and serosa of the uterus, fallopian tubes, and other pelvic organs. This overview is limited to the general features of endometriosis and selected

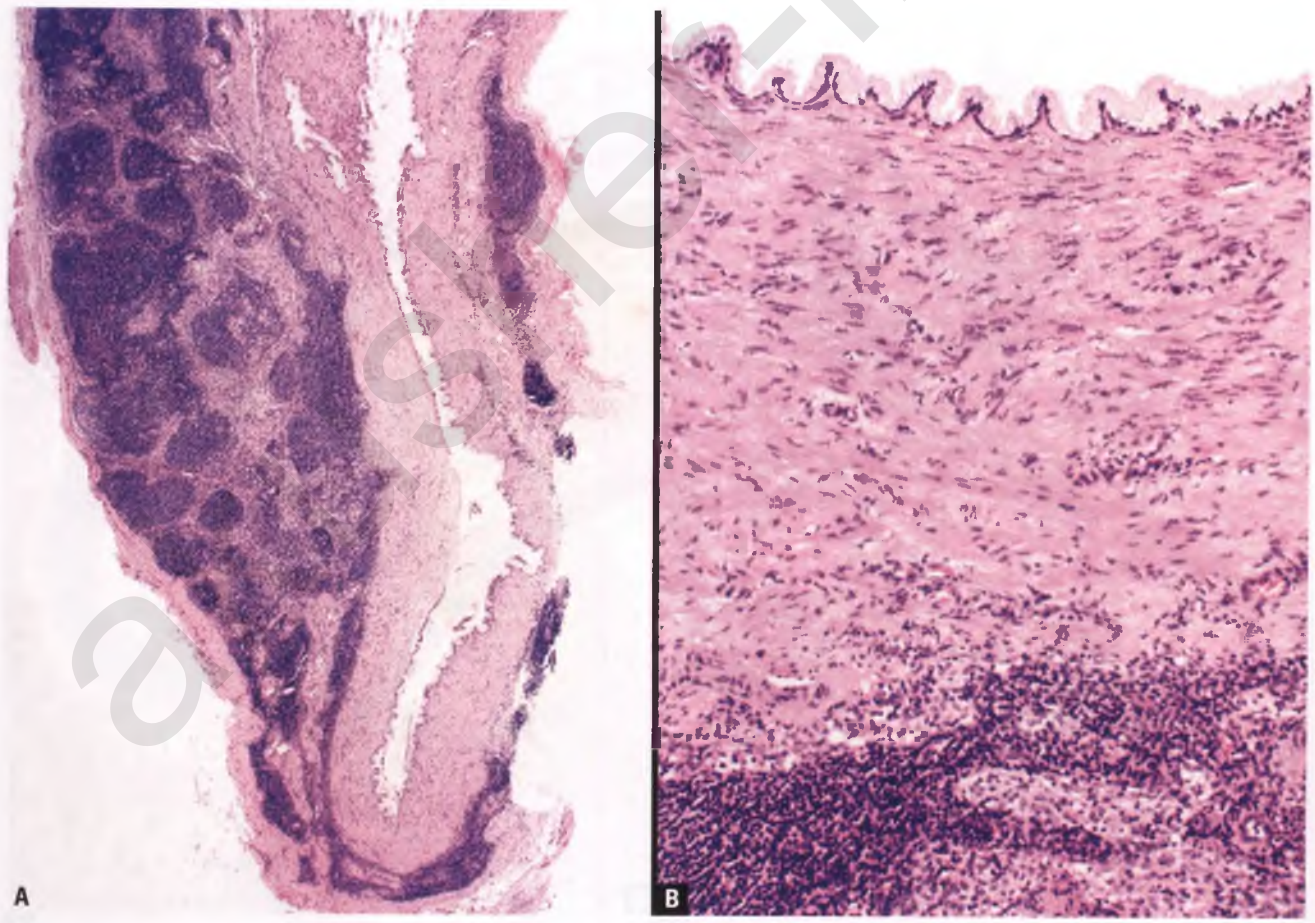

FIGURE 8.32. Endocervicosis involving a paraaortic lymph node. **A:** In this low-magnification image, the lesion is seen to consist of a compressed and pseudoencapsulated epithelial-lined cyst within a lymph node. **B:** At higher magnification, the mucinous, columnar nature of the cyst lining is apparent (top).

extragenital manifestations. Endometriosis of the vagina, cervix, uterine serosa, fallopian tubes, and ovaries is discussed in the chapters that correspond to these sites.

Endometriosis is a common disorder that usually affects women in the reproductive age group. Usual symptoms include dysmenorrhea, chronic pelvic/lower abdominal pain, dyspareunia, irregular uterine bleeding, and infertility. Symptoms may also correspond to the specific site of involvement, such as when intestinal endometriosis mimics inflammatory disorders of the bowel. Endometriosis may also be asymptomatic.

Endometriosis may result from retrograde menstruation and implantation of endometrial tissue, metaplasia of the mesothelial lining and subjacent mesenchyme of the pelvic and lower abdominal region, or iatrogenic implantation of endometrial tissue during a surgical procedure. The uncommon instances of endometriosis within regional lymph nodes or distant sites such as the lungs can be explained by transport of endometrial tissue via lymphatics and blood vessels, respectively.

Macroscopic Appearance

The gross features of peritoneal-based endometriosis are highly variable. The lesions may present as small serosal spots, puckered patches, plaques, cysts, or nodules that may be translucent, white, pink, dark red, blue, tan, brown, or black (Fig. 8.33). The color of a given focus of endometriosis is dependent upon the amount of associated blood, the extent of its breakdown, and the presence or absence of associated scar tissue or endometriosis-induced hypertrophy of smooth muscle. Some of the darker lesions are referred to as "powder burns."

In view of the ability of endometriosis to induce formation of pelvic adhesions, these thin bands of tissue should be generously sampled for histologic evaluation to document the presence or absence of endometriosis. This is particularly true when the adhesions are grossly hemorrhagic.

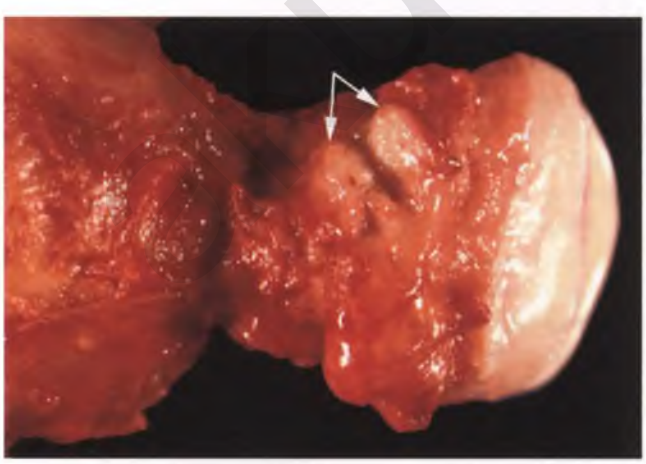

FIGURE 8.33. Endometriosis. In this posterior view of a hysterectomy specimen, a bisected tan nodule of endometriosis lies within the tissue corresponding to the cul-de-sac (*arrows*). Hemorrhagic adhesions are also present.

Histologic Features

In most cases, the diagnosis of endometriosis is straightforward, with ectopic endometrioid glands and stroma found in close association with one another. A familiarity with the range of appearances of endometriotic stroma facilitates the recognition of endometriosis. Endometriotic stroma usually has a periglandular distribution and is typically composed of a densely cellular population of small blue cells. These cells have round to oval nuclei with bland nuclear features, and are set within a supporting network of small blood vessels. The appearance of endometriotic stroma is typically identical to that of endometrial stroma during the proliferative phase of the menstrual cycle (see Chapter 4).

In occasional cases of endometriosis, the endometriotic stromal component is inconspicuous, obscured by histiocytes, spindly/fibroblastic, or decidualized. When the presence or identity of endometriotic stroma is in doubt, the diagnosis of endometriosis can still be suspected when extravasated red blood cells or evidence of previous hemorrhage in the form of pigmented histiocytes are found within the stroma near the endometrioid glands and/or within glandular lumens. Since endometriotic stroma shares the property of immunoreactivity with CD10 with native endometrial stroma, this marker can also be utilized in selected instances to support endometrial stromal differentiation. A notable exception regarding the utility of CD10 in diagnosing endometriosis is in cases of possible cervical involvement, since periglandular endocervical stromal cells are also normally CD10 positive.[41]

The wide range of histologic features that may be seen in endometriosis is discussed in more detail in the sections that follow.

Progestational Changes[40]

Foci of endometriosis take on a different histologic appearance in patients who are pregnant or being treated with progestational agents. The subepithelial endometriotic stroma becomes decidualized, and the endometriotic glands may become atrophic (Fig. 8.34). In rare cases, the Arias-Stella reaction may also be seen in this setting.

Atrophic Changes[40]

In women with endometriosis who are postmenopausal or who have been previously treated with anti-estrogenic hormonal agents, the endometriotic glands may be atrophic and the associated stroma may be fibrotic, making it difficult to render a definitive diagnosis.

Mesothelial Hyperplasia

As an irritant of the peritoneal surface, endometriosis may be associated with some degree of mesothelial hyperplasia, which is discussed later in this chapter.

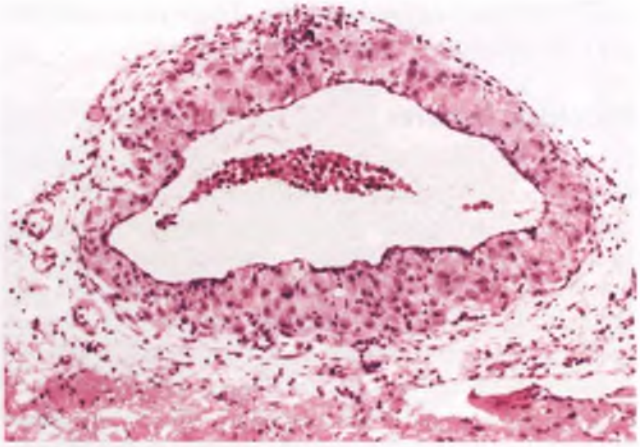

FIGURE 8.34. Endometriosis with superimposed progestogen effect. In this biopsy from the cul-de-sac, a small, cystic focus of endometriosis exhibits decidualized stroma and an atrophic epithelial lining. Note the presence of hemosiderin-laden macrophages within the gland lumen.

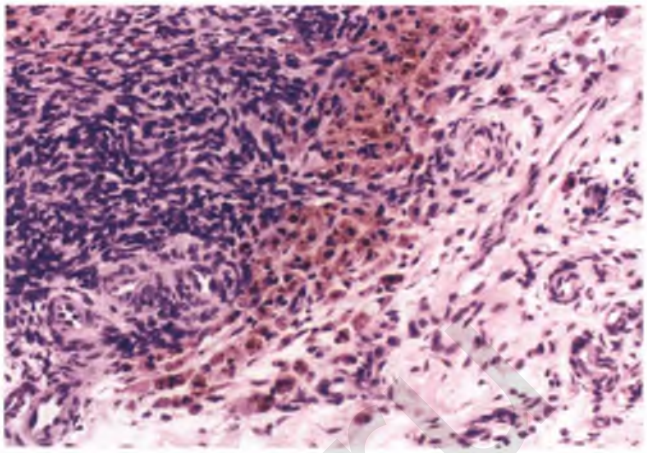

FIGURE 8.35. Stromal endometriosis. This peritoneal biopsy contains a densely cellular aggregate of endometriotic stroma associated with pigmented histiocytes. Endometriotic glands were not identified in this sample.

Necrotic Pseudoxanthomatous Nodules

Formation of necrotic pseudoxanthomatous nodules is an unusual manifestation of longstanding endometriosis that is seen in both the ovaries and the peritoneum, and is discussed in Chapter 6.

Stromal Endometriosis[40]

This term is used to indicate an endometriotic lesion in which glands are not identified. In peritoneal samples, this diagnosis is largely limited to small, suboptimal biopsies of presumptive endometriosis in which endometriotic stroma can be confidently identified (Fig. 8.35). In addition to its morphologic features, endometrial stromal differentiation in this location is supported by a leukocyte common antigen-negative/CD10-positive immunophenotype and an association with extravasated erythrocytes and/or pigmented histiocytes.

Metaplastic, Hyperplastic, and Atypical Nuclear Changes

Since the metaplastic, hyperplastic, and atypical nuclear changes that can occur within endometriosis are usually seen within ovarian endometriotic cysts, these abnormalities are discussed in the section on endometriosis in Chapter 6.

Malignancy Arising within Endometriosis

Most malignant tumors that arise within endometriosis do so within the ovary, where this occurs at an estimated frequency of roughly 1% of unselected cases.[42] Note that the phrase "arising within" requires direct continuity between the tumor and endometriosis, which is more stringent than "associated with," which only requires the presence of tumor and endometriosis within the same organ. There is no doubt that some malignant tumors that arise within endometriosis are not categorized as such because the focus of continuity was not sampled or because subsequent growth of the tumor obliterated the endometriotic focus from which it arose.

Endometrioid carcinoma is the most common histologic type of malignancy that arises within endometriosis, followed by clear cell carcinoma.[43] Examples of these tumors arising within ovarian endometriotic cysts are illustrated in Figures 7.96, 7.123, and 7.155. Although the ovary is the most common site for neoplastic transformation of endometriosis, this phenomenon can occur anywhere that endometriosis is present.[44] For example, a case of endometriosis transitioning to endometrioid carcinoma within the soft tissue of the broad ligament is presented in Figures 5.54 and 5.55. In addition to endometrioid and clear cell carcinomas, other malignant tumors that may be seen in association with endometriosis include endometrioid stromal sarcoma, carcinosarcoma, and adenosarcoma.[42–46]

Myxoid Change[40,47]

On rare occasions, the stromal tissue within a focus of endometriosis may undergo myxoid change (Fig. 8.36). This phenomenon tends to occur within foci of endometriosis in the skin and superficial soft tissue, often in patients with a history of concurrent or recent pregnancy. Pseudomyxoma peritonei (PMP) is a differential diagnostic consideration, but is excluded by the presence of nearby recognizable endometriosis, the absence of mucin-rich epithelial cells floating within the pools of mucin, and the absence of a known (usually appendiceal) mucinous neoplasm of the abdominopelvic region.

Skeletal Muscle Regeneration[48]

Abdominal wall endometriosis may be associated with skeletal muscle regeneration. This phenomenon, which features maturing myoblasts admixed with multinucleated myogenous cells, may be mistaken for a benign or malignant neoplasm with skeletal muscle or rhabdoid differentiation (Fig. 8.37). The presence of nearby endometriosis, the clinical setting, the presence

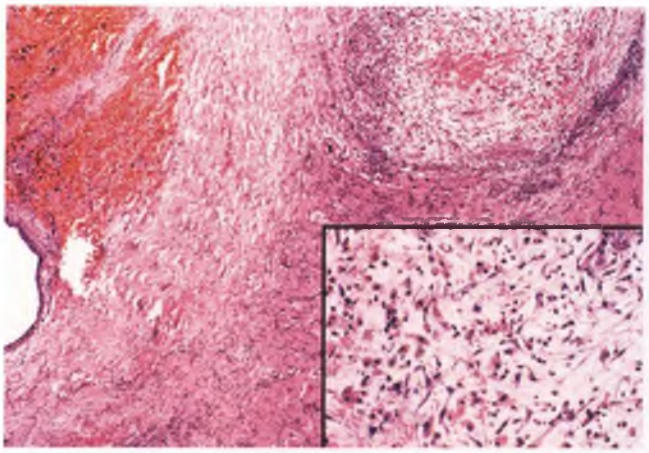

FIGURE 8.36. Endometriosis with myxoid change. In this soft tissue lesion from a cesarean section scar, there is typical endometriosis at left and a nodular focus of myxoid change at the upper right. The inset highlights the myxoid focus.

of skeletal muscle without regenerative features in adjacent areas and/or blending with the regenerative foci, and the absence of a mass related solely to the skeletal muscle component typically allow for the distinction of endometriosis-associated skeletal muscle regeneration from a neoplastic process.[48]

Involvement of Veins, Lymphatics, and Nerves[40]

The finding of endometriosis within venous and lymphatic spaces is a rare, well-documented phenomenon (Figs. 8.38 and 8.39). Venous and lymphatic involvement does not predict aggressive behavior, but may be associated with endometriosis in distant sites or regional lymph nodes, respectively. Perineural involvement is another rare manifestation of endometriosis, and does not appear to have any impact on the clinical course of the disease.

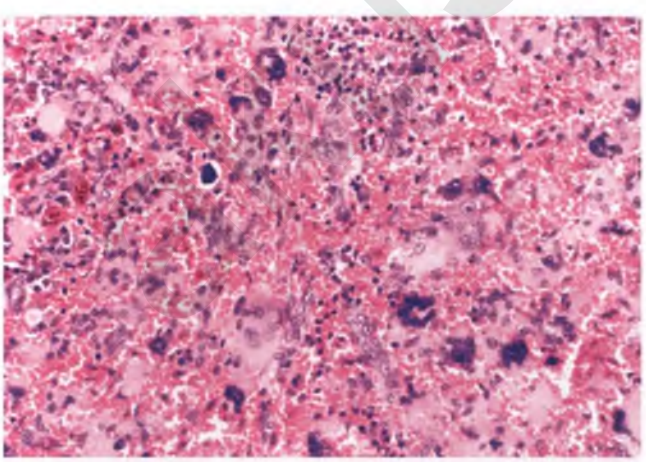

FIGURE 8.37. Endometriosis-associated skeletal muscle regeneration. The skeletal muscle of this abdominal wall tissue exhibits regenerative changes, with maturing myoblasts and scattered multinucleated myogenous cells. The accompanying recent and remote hemorrhage is due to nearby endometriosis, which is out of the field of view.

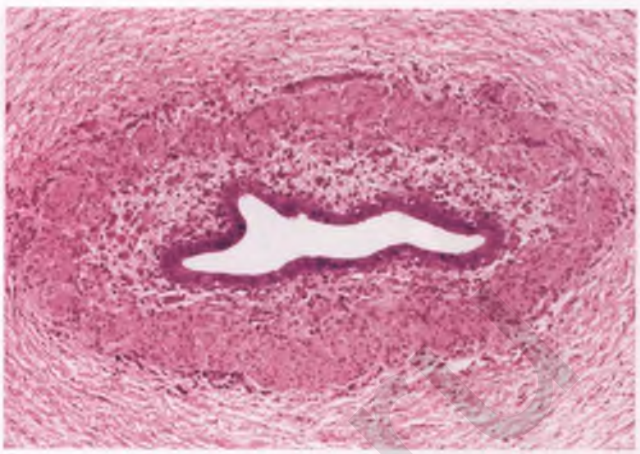

FIGURE 8.38. Intravenous endometriosis. The lumen of a vein from the ovarian ligament contains an endometriotic gland accompanied by endometriotic stroma and a few pigmented histiocytes.

Selected Extragenital Manifestations

Abdominopelvic Surgical Scars

Most cases of endometriosis involving surgical scars represent a complication of previous uterine surgery and are presumably a result of iatrogenic implantation of endometrial tissue at the time of operation. These lesions typically create a gray-white mass that usually involves the dermis and/or subcutaneous adipose tissue (Fig. 8.40). Focal areas of recent (red) or remote (brown) hemorrhage within the mass, coupled with the appropriate clinical history, allow for a presumptive diagnosis of endometriosis prior to evaluation of histologic sections.

Intestinal Tract[49]

The intestinal tract is the most frequent site of extrapelvic endometriosis. In many of these cases, the endometriosis is peritoneal based and just happens to be occurring on the serosa of the bowel in addition to elsewhere in the peritoneal cavity. Examples seen by pathologists tend to be those less common lesions that produce intestinal symptoms and deformities and usually involve the rectosigmoid colon or appendix. Endometriosis of this type usually spares the mucosa, but typically induces subserosal fibrosis and hypertrophy of the smooth muscle wall, which in turn produces kinking deformities (Figs. 8.41 and 8.42).

Occasionally, intestinal endometriosis results in the formation of intraluminal polypoid lesions that mimic carcinomas when large or tubular adenomas when small (Figs. 8.43 and 8.44).[49,50] Although rarely necessary, the CK7+/CK20– immunophenotype of the glands of endometriosis can be utilized to distinguish them from the CK7–/CK20+ glands of intestinal origin. These same immunophenotypic differences can also be of use in distinguishing those rare endometrioid carcinomas that arise within colonic endometriosis from primary colonic adenocarcinoma, although the former are usually recognizable by their association with endometriosis, absence of mucosal involvement, low nuclear grade, absence of necrotic luminal debris within the neoplastic

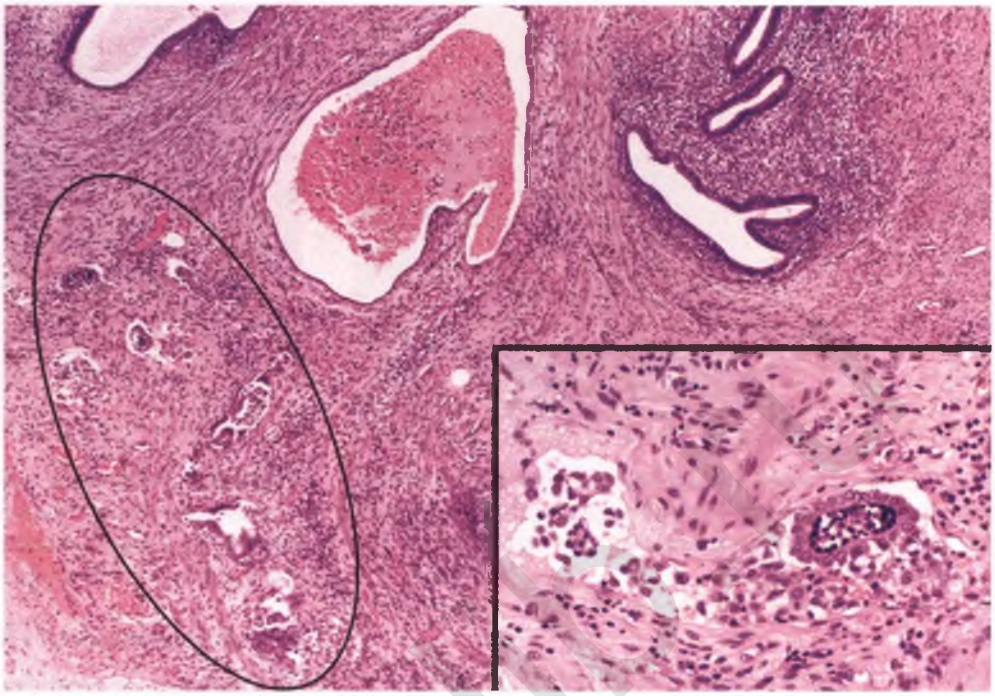

FIGURE 8.39. Endometriosis within appendiceal lymphatic spaces. Within a background of obvious endometriosis is a cluster of lymphatic spaces that contains endometriotic glands, stroma, and histiocytes (*circled*). The inset highlights one such lymphatic space.

tubules, and association with morular metaplasia.[45,46] This distinction is important, since endometrioid carcinoma arising within colonic endometriosis is managed differently after surgical resection and is associated with a better prognosis. Although most endometriosis-associated intestinal tumors are endometrioid carcinomas, tumors such as adenosarcoma, carcinosarcoma, endometrioid stromal sarcoma, and adenofibroma may also be encountered in this setting.[45,46]

Pelvic Lymph Nodes

Endometriosis within pelvic lymph nodes is uncommon, and needs to be distinguished from endosalpingiosis and metastatic carcinoma. It is the association of endometrioid glandular structures with endometrial-type stroma that is most helpful in distinguishing intranodal endometriosis from its mimics (Fig. 8.45).

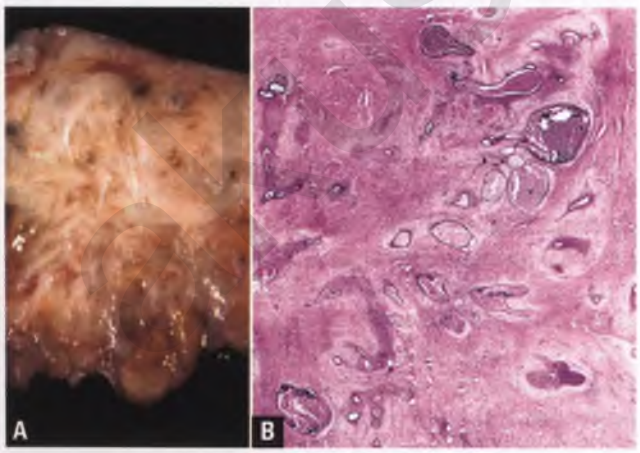

FIGURE 8.40. Endometriosis within a cesarean section surgical scar. **A:** Sectioned surface of a *gray-white* mass centered within the subcutaneous adipose tissue. Note the scattered punctate foci of old (*brown*) hemorrhage, which is a helpful diagnostic feature. **B:** Several foci of endometriosis, some cystically dilated and filled with old hemorrhagic material, are embedded within densely fibrotic tissue.

MISCELLANEOUS NONNEOPLASTIC PROCESSES

Adhesions

The presence of adhesions should not be overlooked or omitted from the pathology report, since they are often of clinical significance. Adhesions that are related to previous surgery, pelvic inflammatory disease, and inflammatory

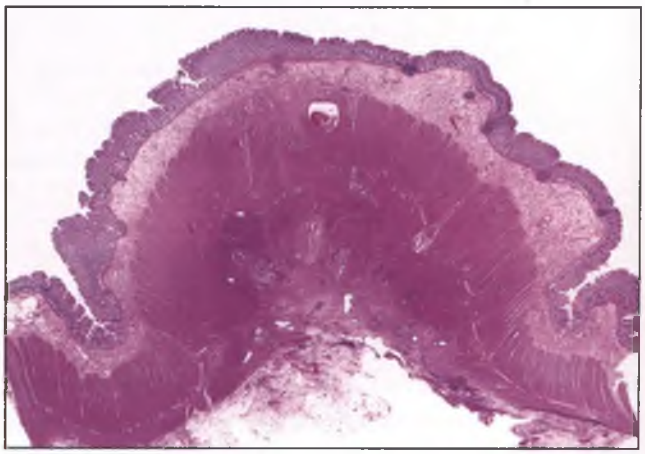

FIGURE 8.41. Endometriosis of colon. This low-magnification view highlights the ability of intestinal endometriosis to produce kinks in the bowel through a combination of muscular hypertrophy and subserosal fibrosis.

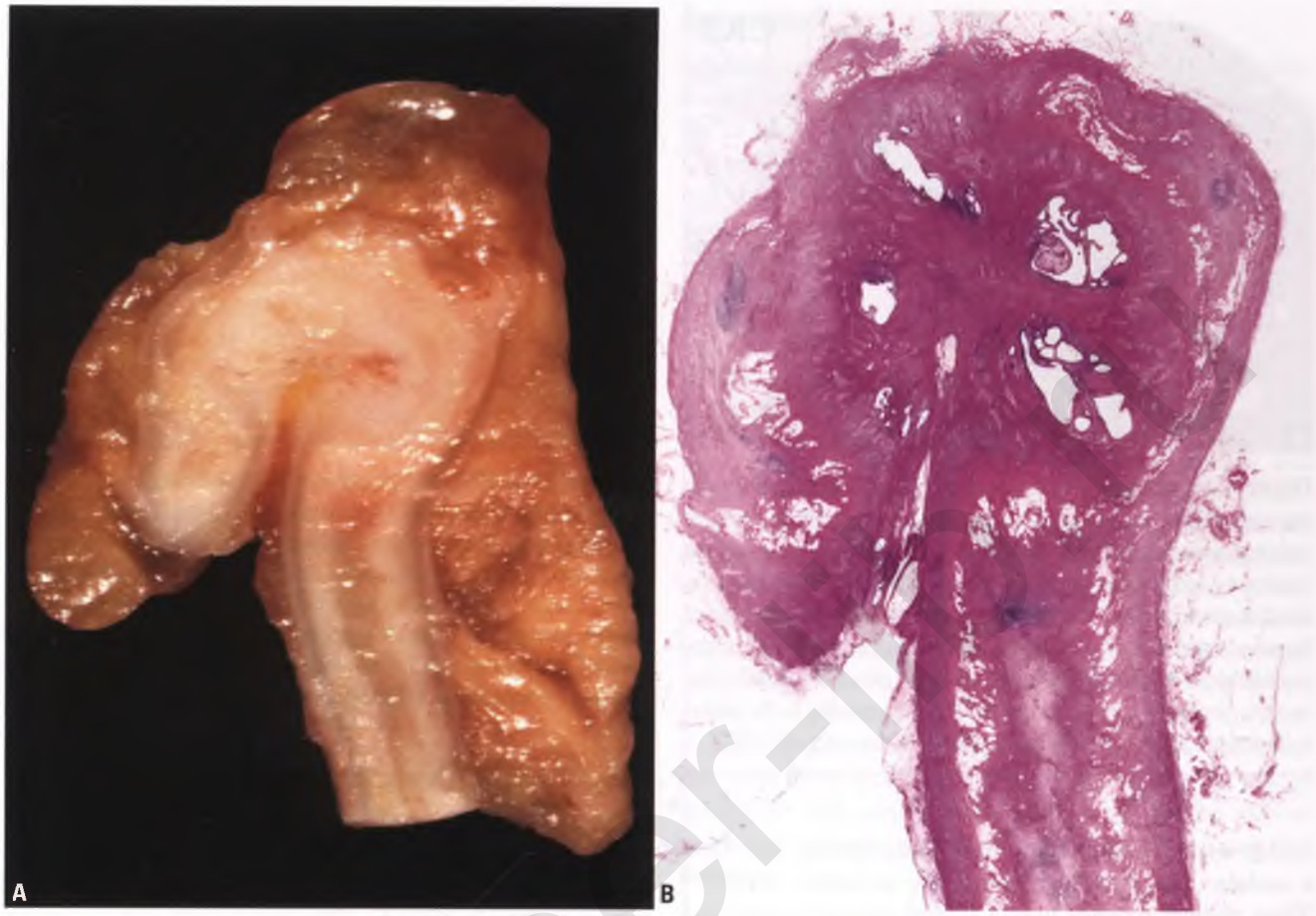

FIGURE 8.42. Endometriosis of the appendix. **A:** This longitudinal section reveals an area of appendiceal kinking and mural thickening, resulting in a question mark-shaped appendix. **B:** This low-magnification view demonstrates the presence of microcystic foci of endometriosis and muscular hypertrophy in the grossly abnormal area.

bowel disease consist of strands of mesothelial-lined fibrovascular tissue, generally without evidence of a specific etiology (Fig. 8.46). However, histologic examination of adhesions may reveal the agent that induced their formation, such as associated foci of endometriosis or a reaction to foreign material such as glove powder-related starch granules (Fig. 8.47).

Reactive Peritoneal Fibrosis

Reactive peritoneal fibrosis is a descriptive diagnosis that refers to a nonspecific reaction to peritoneal injury or irritation. This phenomenon is typically seen in the postoperative setting, longstanding peritonitis, and in patients with a history of endometriosis. Small fibrotic nodules may form that may be targeted for biopsy (Fig. 8.48).

Infarcted Appendix Epiploica

If one of the fatty appendages on the serosal surface of the large intestine known as appendices epiploicae undergoes

FIGURE 8.43. Polypoid endometriosis of colon. This section through a formalin-fixed, polypoid mass reveals radiating hypertrophy of the smooth muscle wall, white fibrotic areas, and intact overlying mucosa. The muscular hypertrophy, rubbery texture of the fibrous tissue, and intact mucosa are clues that this lesion represents endometriosis rather than carcinoma.

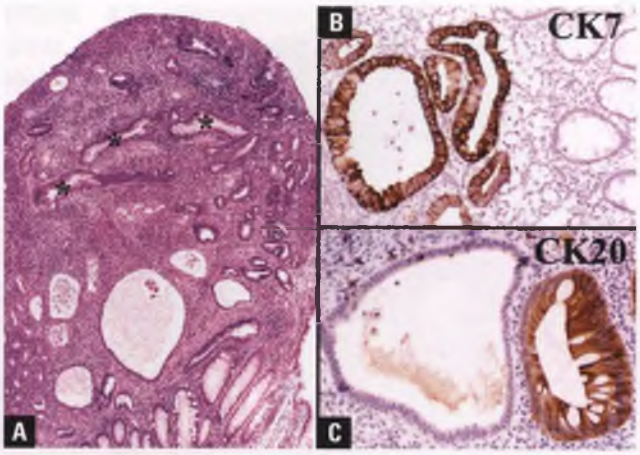

FIGURE 8.44. Polypoid endometriosis of colon mimicking a tubular adenoma. **A:** This polypoid lesion could easily be passed off as a tubular adenoma at low magnification. However, portions of the lamina propria are replaced by endometrial-type stroma (not apparent at this magnification). Residual colonic glands with goblet cells are present within the substance of the polyp (*asterisks*) and at lower right. Most of the other glands are of endometriotic origin. **B:** In contrast to the normal colonic glands at right, the endometriotic glands are immunoreactive for CK7. **C:** In contrast to the dilated endometriotic gland at left, the colonic gland is immunoreactive for CK20.

torsion-related infarction, it may autoamputate and form a nodular mass lying free within the peritoneal cavity.[51,52] These nodules typically have a smooth external surface and their fatty nature is usually apparent once they have been sectioned (Fig. 8.49A). These lesions are enveloped by a thin rim of hyalinized fibrous tissue. Dystrophic calcification is common, particularly within the fibrous shell and along the septa of the fat lobules (Fig. 8.49B,C). The infarcted adipose tissue has a mummified appearance, which differs from the typical histologic features of fat necrosis as commonly seen following biopsy or trauma in other sites such as the breast.

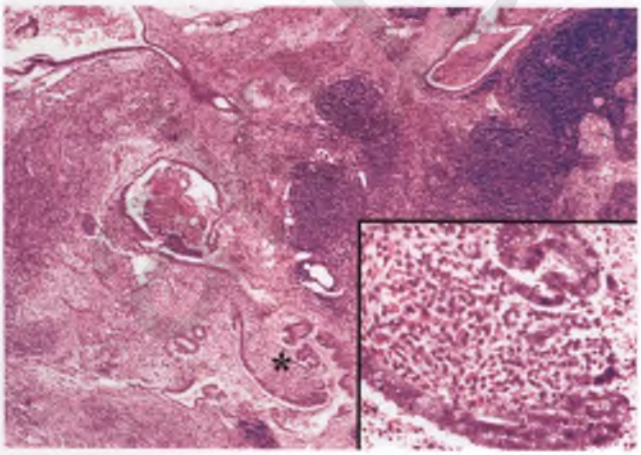

FIGURE 8.45. Endometriosis of pelvic lymph node. Several foci of endometriosis, some of which are cystic and filled with hemorrhagic material, are present. The focus of endometriotic glands and stroma marked by the *asterisk* is shown at higher magnification in the inset.

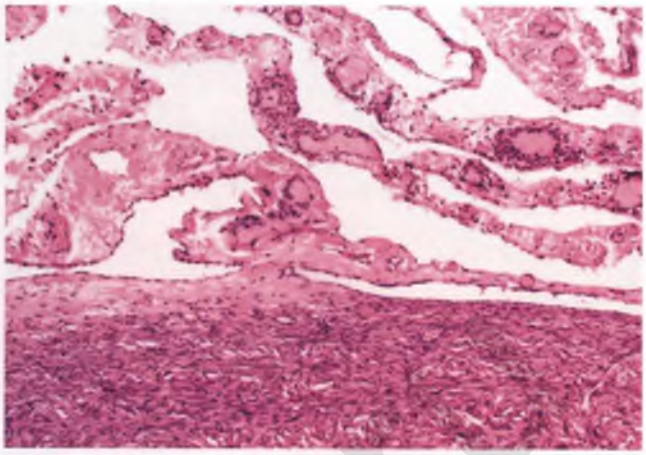

FIGURE 8.46. Nondescript adhesions on ovarian surface. Irritation of the ovary during its removal has resulted in cuffs of neutrophils surrounding some of the vessels within the adhesions.

Mucicarminophilic Histiocytosis[53]

This rare entity is mainly of historical interest, since it represents a histiocytic reaction to a substance (polyvinylpyrrolidone) that was previously used as a component of some blood plasma substitutes that has long since been replaced by other products. It has been reported to involve multiple sites, including the omentum, pelvic lymph nodes, vagina, cervix, uterus, and ovaries. The histiocytes of mucicarminophilic histiocytosis have vacuolated cytoplasm and eccentric nuclei, which results

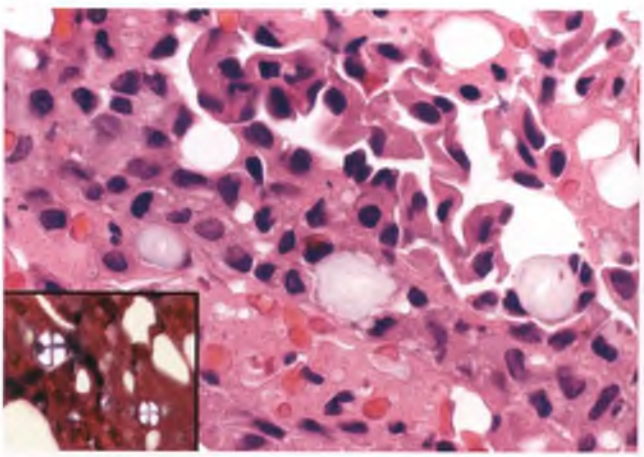

FIGURE 8.47. Adhesion with starch granules. In this high-magnification view, mesothelial cells and histiocytes are associated with three starch granules, which in routinely stained sections appear as rounded, pale bodies that are light *gray-blue* with clear central cores. The inset demonstrates the characteristic Maltese cross pattern of birefringence of these granules when viewed under polarized light.

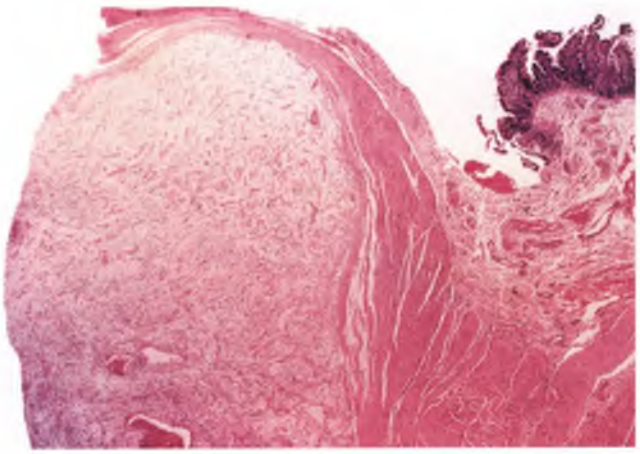

FIGURE 8.48. Reactive peritoneal fibrosis. The subperitoneal nodule of edematous fibrous tissue in the left half of the image was biopsied during a "second look" procedure for ovarian cancer. Note: The pathologist needs to be aware of the context in which this biopsy was taken, and that the presence of small bowel mucosa (upper right) signifies an inadvertent bowel perforation that the clinician needs to be informed of immediately.

in a resemblance to metastatic signet-ring carcinoma that is heightened by their shared positive reaction with the mucicarmine stain. However, these histiocytes are negative with the periodic acid-Schiff and cytokeratin stains, and are immunoreactive with histiocytic markers such as CD68 (KP1), which is the exact opposite staining pattern of that expected for signet-ring carcinoma.[54]

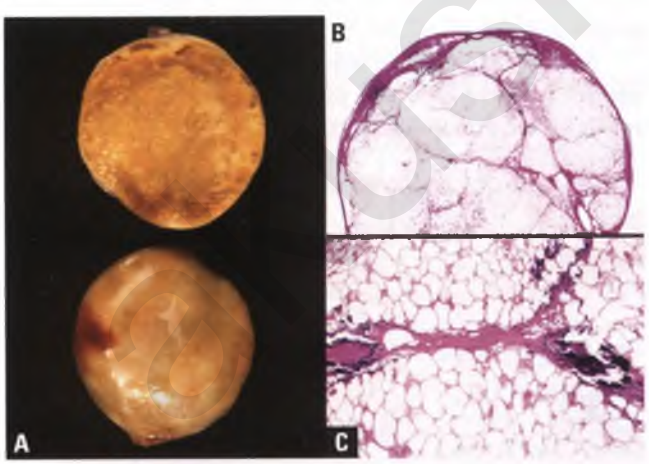

FIGURE 8.49. Infarcted appendix epiploica. **A:** Sectioned surface (top) and external surface (bottom) of a 1.4 cm infarcted appendix epiploica that was found loose within the peritoneal cavity. The yellow color of the sectioned surface is due to the high content of adipose tissue. **B:** This low-magnification view of a portion of the nodule shows a fibrotic and focally calcified peripheral rim encompassing lobules of adipose tissue. **C:** The infarcted adipose tissue has a mummified appearance, and portions of the fibrous septum are calcified.

Splenosis[55]

Splenosis is a term that refers to the implantation of splenic tissue following splenic injury. It is typically an incidental finding in which multiple reddish purple nodules are found on the peritoneal surface, omentum, and/or mesentery. These nodules may be biopsied with a differential diagnosis of endometriosis or vascular tumor, but the clinical history and histologic appearance of normal splenic tissue readily establishes the diagnosis.

Trophoblastic Implants[56]

During the course of surgical treatment for a tubal pregnancy, disrupted trophoblastic elements may escape removal and implant on the peritoneal surface or within the omentum. The risk for this complication is higher when a laparoscopic approach is utilized rather than laparotomy, and when the procedure is a salpingostomy rather than a salpingectomy. Post-procedure serum β-hCG levels are abnormally high, and these lesions may be associated with abdominal pain. The histologic documentation of viable or semiviable immature chorionic villi or other trophoblastic elements within the implants, the characteristic clinical history, and an awareness of this phenomenon allow for its recognition. Since most such cases are treated empirically with methotrexate, which eradicates the residual trophoblastic tissue, the pathologist is unlikely to encounter this lesion.

PRIMARY PERITONEAL SEROUS BORDERLINE TUMOR[35,57,58]

Most commonly, serous borderline tumors are encountered in the peritoneum as implants derived from ovarian tumors of this type, as discussed and illustrated in the section on serous borderline tumors in Chapter 7. On occasion, serous borderline tumors are thought to arise within the peritoneum in the absence of ovarian involvement, where they have also been referred to as primary peritoneal serous micropapillomatosis of low malignant potential. These peritoneal-based tumors presumably arise from foci of endosalpingiosis, which are identified in about 80% of cases.

Primary peritoneal serous borderline tumors typically occur in young adult women (mean age of 32 years) who may complain of abdominal or pelvic pain or be asymptomatic. In some instances, the patient presents with psammoma bodies and low-grade epithelial cells in a routine Pap smear (see Fig. 3.266B). The typical operative findings are widespread peritoneal adhesions and miliary granules.

By definition, the ovaries in primary peritoneal serous borderline tumors are either free of involvement or show only superficial implants of tumor and adhesions on their serosal surfaces (Fig. 8.50). The implants themselves, both on the ovary and on other peritoneal surfaces, are identical to the epithelial and/or desmoplastic types of noninvasive implants

of ovarian serous borderline tumors (Figs. 8.51–8.53). In the omentum, fibrovascular septa may be expanded when involved by this process, as is seen in ovarian-derived implants, but features of invasive implants are absent (see Fig. 7.26).

Differential Diagnosis

The main differential diagnostic consideration is low-grade peritoneal serous carcinoma, which usually forms sizable nodules, invades underlying tissues, and is generally more cellular than its borderline counterpart. Foci of endosalpingiosis are distinguished by a combination of their more open lumens, bland nuclear features, regularly interspersed ciliated cells, and simplified architecture. Immunohistochemistry utilizing the same markers discussed in the section on the differential diagnosis of serous carcinoma versus malignant mesothelioma may be indicated to facilitate exclusion of a papillary mesothelial lesion.

Prognosis and Treatment

The prognosis of patients with primary peritoneal serous borderline tumors is favorable and parallels that of patients with ovarian tumors of similar type with noninvasive implants. There is a small risk of progression to an invasive tumor that increases over time. Postoperative chemotherapy or radiotherapy is not recommended, but long-term follow-up is indicated.

EXTRAOVARIAN PERITONEAL SEROUS CARCINOMA

These tumors usually occur in postmenopausal women who present with abdominal pain and swelling due to carcinomatous involvement of the omentum and/or peritoneal-lined tissues.[59,60] They occur in low-grade and high-grade forms, with the latter being much more common.[59,60] By definition, the bulk of the tumor is located in the peritoneum, and ovarian involvement is absent, limited to the serosal surface, or only focally involves the ovarian parenchyma.[59]

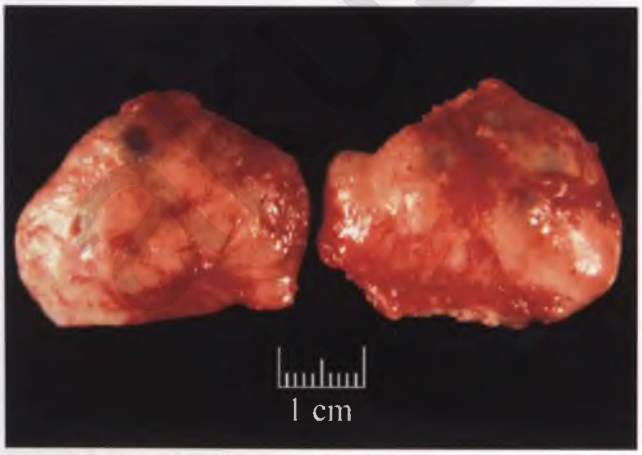

FIGURE 8.50. Primary peritoneal serous borderline tumor involving the ovarian surface. The ovary is of normal size, but its surface is partially covered by hemorrhagic adhesions associated with small yellow granules.

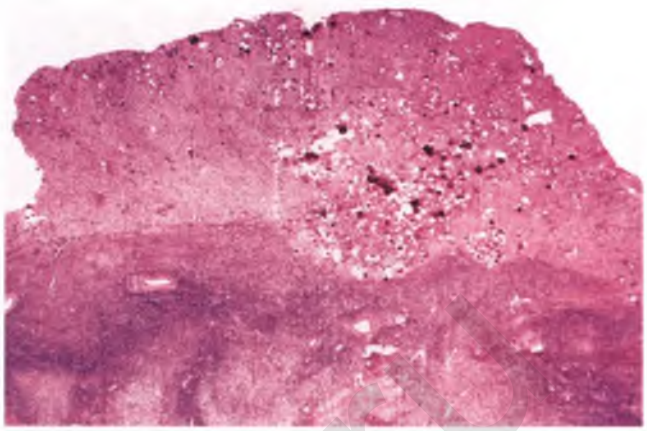

FIGURE 8.51. Primary peritoneal serous borderline tumor involving the ovarian surface. The densely adherent plaque is composed of fibrous tissue, psammoma bodies, and small papillary clusters of serous epithelium, and is sharply demarcated from the underlying ovarian stroma.

Low-Grade Peritoneal Serous Carcinoma

Low-grade peritoneal serous carcinoma usually forms sizable nodules and histologically resembles those invasive implants of ovarian serous borderline tumors that feature low- to intermediate-grade nuclear atypia (see Fig. 7.30).[58]

Serous psammocarcinoma is a variant of low-grade serous carcinoma in which psammoma bodies predominate and large nests or solid sheets of neoplastic epithelium are

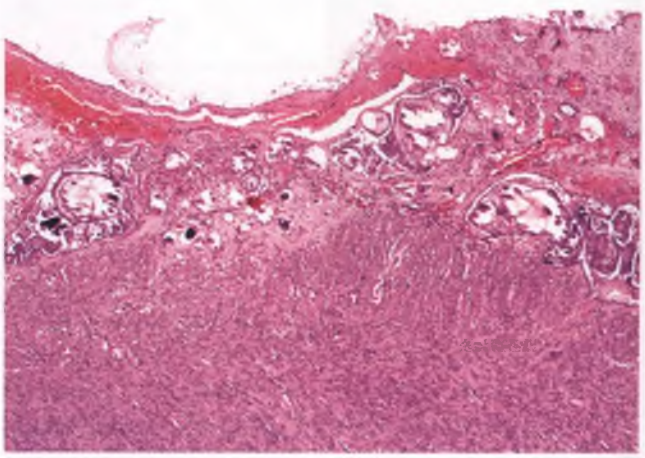

FIGURE 8.52. Primary peritoneal serous borderline tumor involving the uterine serosa. Note how the lesion appears to be plastered onto the serosal surface, without invasion of the underlying myometrium.

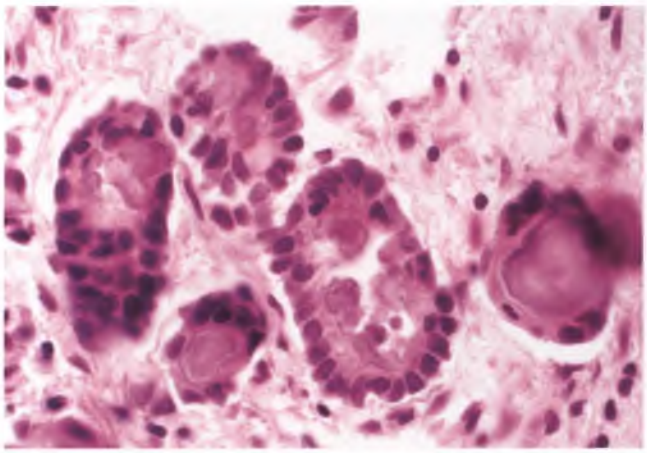

FIGURE 8.53. Primary peritoneal serous borderline tumor involving the ovarian surface. This high-magnification view highlights the low-grade nuclear features of the papillary serous epithelium and the associated psammoma bodies.

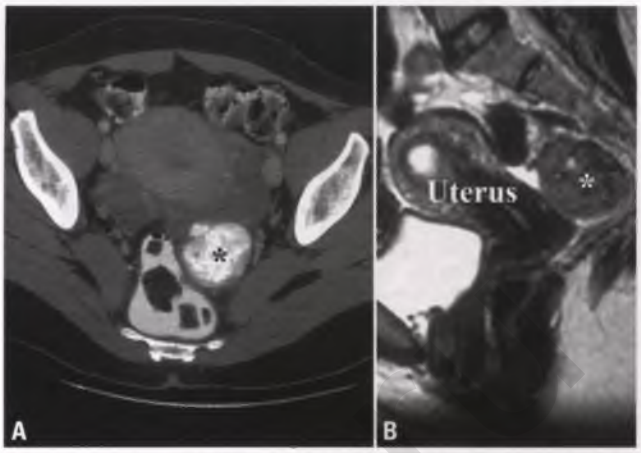

FIGURE 8.54. Peritoneal serous psammocarcinoma mimicking a pedunculated subserosal uterine leiomyoma with calcification. **A:** The CT scan demonstrates the presence of a nodular calcified mass (*asterisk*) in the pelvic region. **B:** In this sagittal MRI scan, the mass (*asterisk*) is localized to the region of the cul-de-sac and rectovaginal septum posterior to the uterus.

absent.[58,61] These tumors may be visibly calcified radiographically (Fig. 8.54), and typically have a gritty or granular sectioned surface (Fig. 8.55). The epithelium of serous psammocarcinoma is arranged in small nests and papillae and lacks high-grade nuclear features (Fig. 8.56). Some areas of these tumors may be completely replaced by psammoma bodies (Fig. 8.57).

Long-term prognostic information on low-grade peritoneal serous carcinomas is limited, but there is a suggestion that patients with serous psammocarcinoma have a prognosis that is similar to peritoneal serous borderline tumors and fare better than those with usual low-grade serous carcinoma, which in turn behaves less aggressively than high-grade serous carcinoma.[58,61] The presence of stromal invasion in low-grade serous carcinoma is the feature that distinguishes it from peritoneal serous borderline tumor.

High-Grade Peritoneal Serous Carcinoma

High-grade peritoneal serous carcinoma often presents with widespread and bulky peritoneal tumor (Figs. 8.58–8.60), and histologically resembles its ovarian counterpart (see Figs. 7.44–7.46). These are aggressive tumors that in most studies have been shown to behave similarly to high-grade, high-stage ovarian serous carcinomas.[59,60,62,63]

Bilateral prophylactic salpingo-oophorectomy in BRCA-mutated patients at high risk for tubal and ovarian cancer substantially reduces, but does not eliminate, the risk of subsequent peritoneal carcinomatosis, which is estimated to be on the order of 4% at 20 years following prophylactic surgery.[64,65] Development of peritoneal carcinoma in this situation may be related to either (a) the neoplastic potential of preexisting or subsequently formed foci of endosalpingiosis or (b) microscopic foci of tubo-ovarian carcinoma with metastatic potential that went undetected at the time of risk-reducing salpingo-oophorectomy.[64–66]

Differential Diagnosis

In addition to high-stage primary ovarian serous carcinoma, which is excluded on the basis of bulky peritoneal disease in conjunction with the ovarian component being absent, confined to the ovarian surface, or only focally involving the stroma,[59] attempts should be made to exclude metastases from similar-appearing serous carcinomas originating in the fallopian tube or endometrium. In the presence of an endometrial serous carcinoma, lack of WT-1 expression at both sites favors an endometrial origin.[67]

As discussed in the section on tubal carcinoma in Chapter 5, many high-grade serous carcinomas previously thought to originate in the peritoneum are likely derived from tubal intraepithelial carcinomas or small invasive carcinomas of the

FIGURE 8.55. Peritoneal serous psammocarcinoma. The sectioned surface has a grossly appreciable granular texture due to the presence of innumerable psammoma bodies.

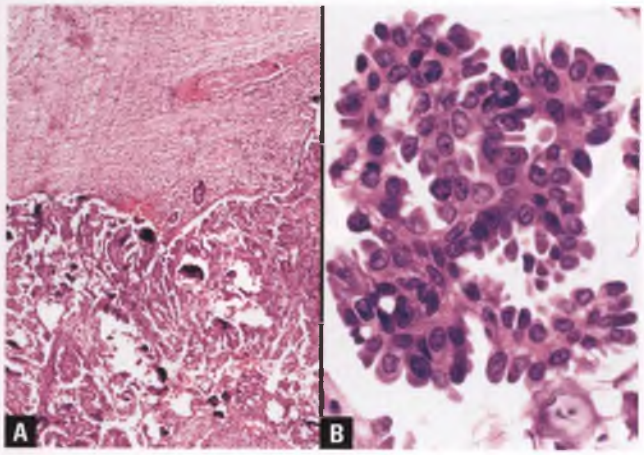

FIGURE 8.56. Peritoneal serous psammocarcinoma. **A:** At low magnification, a fibrous pseudocapsule is seen encasing papillary clusters of neoplastic cells that are associated with several darkly stained and fragmented psammoma bodies. **B:** The low-grade nature of the tumor cells is apparent in this high-magnification view.

distal fallopian tube.[68,69] Accordingly, whenever the diagnosis of primary peritoneal serous carcinoma is being considered, extensive histologic examination of the fallopian tubes is warranted, with particular attention focused on the fimbriae.

The differential diagnosis of peritoneal serous carcinoma and malignant mesothelioma is discussed in the section on the latter entity.

NONNEOPLASTIC MESOTHELIAL LESIONS

Mesothelial Hyperplasia[70]

Mesothelial cells may become hyperplastic in response to inflammation, endometriosis, mechanical irritation from a large ovarian mass, or other causes of serosal injury. This is usually an incidental microscopic finding in which mesothelial-derived nests, tubules, cords, papillary structures, and wandering single cells proliferate near the peritoneal surface (Fig. 8.61). The hyperplastic mesothelial cells may exhibit reactive nuclear atypia, some mitotic activity, and cytoplasmic vacuolization. Aggregates of hyperplastic mesothelial cells within fibrous tissue may be associated with retraction artifact, which can simulate angiolymphatic invasion. The sections on acute peritonitis and sclerosing peritonitis illustrate the tendency of proliferating mesothelial cells to form linear arrangements when they are entrapped within fibroinflammatory tissue.

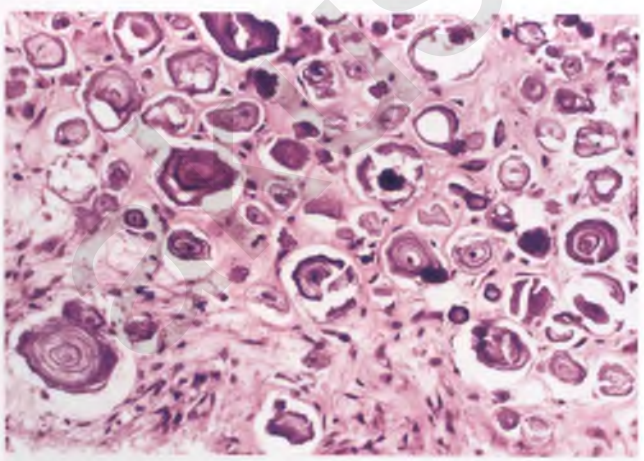

FIGURE 8.57. Peritoneal serous psammocarcinoma. In areas like this one, the tumor consists largely of concentrically laminated psammoma bodies embedded within fibrous tissue with inapparent epithelial elements. These calcific bodies fragment to varying degrees when sectioned.

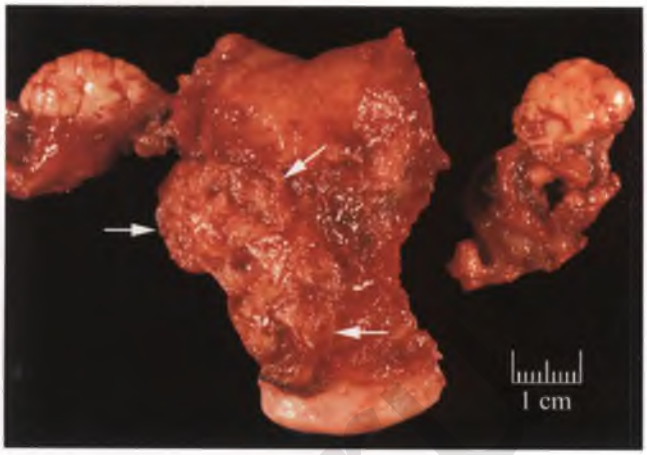

FIGURE 8.58. Uterine serosal involvement by high-grade peritoneal serous carcinoma. The peritoneal-based tumor (*arrows*) is adherent to the serosa of the uterus. Except for a few adhesions, the ovaries are grossly normal.

Differential Diagnosis

The main differential diagnostic considerations are malignant mesothelioma and well-differentiated papillary mesothelioma

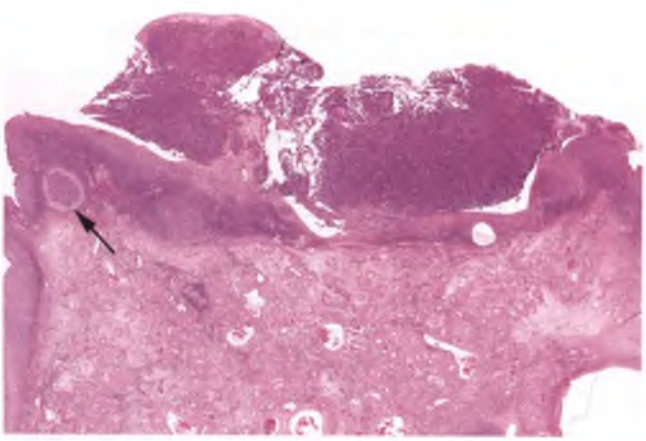

FIGURE 8.59. Ovarian involvement by high-grade peritoneal serous carcinoma. Ovarian involvement is largely confined to the serosal surface, with the exception of a small parenchymal nodule (*arrow*). Bulky disease was present in the omentum (see Fig. 8.60).

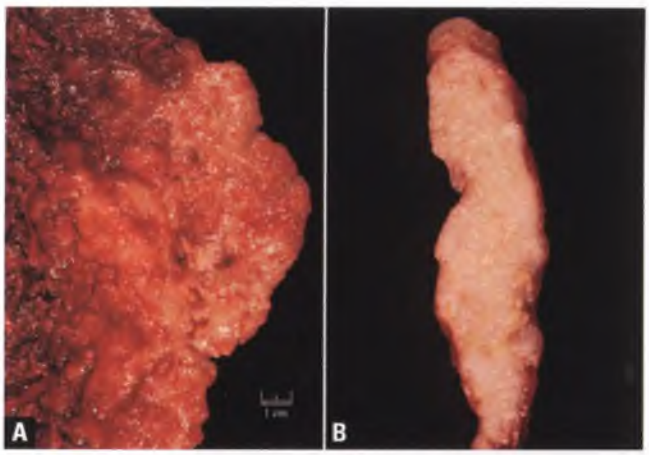

FIGURE 8.60. Omental involvement by high-grade peritoneal serous carcinoma. **A:** A large portion of the omentum has been replaced by tumor, forming an "omental cake." **B:** In this cross-sectional view of the omental cake, there is only a scant amount of residual adipose tissue.

(WDPM). In contrast to mesothelial hyperplasia, malignant mesothelioma typically forms multiple grossly visible nodules, frankly invades involved tissue, and may exhibit marked nuclear atypia, tumor necrosis, and atypical mitotic figures. The florid papillary architecture of WDPM, its lack of inflammation, and the absence of associated reactive nuclear atypia are features that help to distinguish this indolent tumor from mesothelial hyperplasia.

Hyperplastic mesothelial cells may be present within the walls of cystic ovarian tumors and endometriotic cysts, where they can be confused with foci of invasive carcinoma.[4,40] Awareness of the existence of this phenomenon and the identification of linearly arranged clusters of mesothelial cells can suggest the correct interpretation, which can be substantiated by obtaining immunohistochemical evidence of mesothelial differentiation as discussed elsewhere in this chapter.

"Nodular Mesothelial Hyperplasia"

See section on nodular histiocytic hyperplasia.

Intranodal Mesothelial Cells[71]

On rare occasions, mesothelial cells are found within the sinusoids of abdominal or mediastinal lymph nodes (Fig. 8.62). Patients with abdominal nodes that are involved by this incidental microscopic finding often have mesothelial hyperplasia of the peritoneum. The intranodal mesothelial cells may be found singly or as small cohesive nests or papillary structures, usually have abundant eosinophilic cytoplasm, and may form arc-shaped bands surrounding lymphoid follicles. Reactive nuclear features may be evident.

The importance of intranodal mesothelial cells lies in their potential to be misinterpreted as metastatic carcinoma, melanoma, or mesothelioma. An awareness of this phenomenon and its association with concurrent mesothelial hyperplasia, coupled with clinical correlation regarding the history of any of the aforementioned malignancies, will help the pathologist to avoid this diagnostic error. Stains for neutral mucin and immunohistochemistry can also facilitate making the correct diagnosis, except when nodal involvement by malignant mesothelioma is a realistic clinical consideration. Note that both mesothelial-related lesions and metastatic carcinoma are immunoreactive for cytokeratin. Mesothelial differentiation should be confirmed by demonstrating both nuclear and cytoplasmic immunoreactivity for calretinin (Fig. 8.63) and an absence of staining for markers usually expressed by metastatic adenocarcinoma, such as MOC-31 and Ber-EP4.

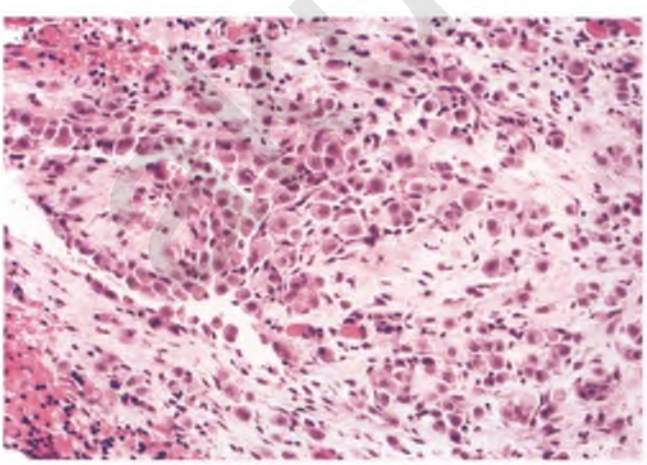

FIGURE 8.61. Mesothelial hyperplasia with reactive atypia. In this omental crevice, reactive mesothelial cells are seen forming a papillary structure, shedding into the peritoneal space, and meandering within the superficial stroma.

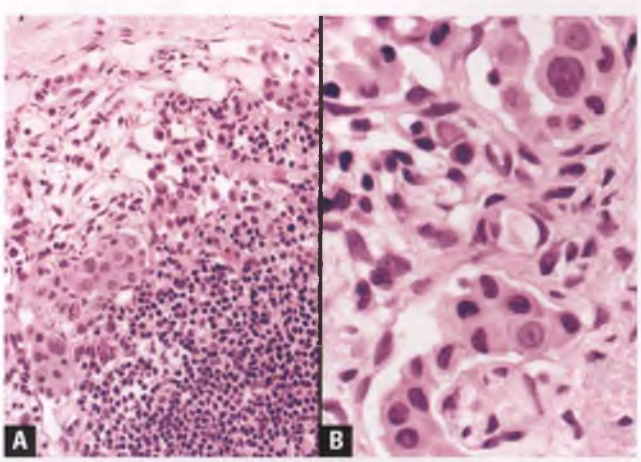

FIGURE 8.62. **A,B:** Intranodal mesothelial cells. Incidental clusters of reactive mesothelial cells are present within the subcapsular sinus of a lymph node, which could be easily mistaken for metastatic carcinoma.

Unilocular Peritoneal Inclusion Cyst

Cysts of this type usually occur in women of reproductive age and represent an incidental finding. They may be single or multiple and either free floating or attached to a peritoneal surface. The cysts typically contain watery fluid and have thin, translucent walls whose inner lining is composed of a single layer of flattened mesothelial cells.

In rare examples of this lesion, the wall may become inflamed and fibrotic and entrap mesothelial cells. These entrapped cells proliferate and may be found singly or forming glands, nests, and cords, which can result in misinterpretation as malignant mesothelioma or metastatic adenocarcinoma.[72] An awareness of this phenomenon and the tendency for entrapped mesothelial cells to proliferate in a zonal or linear arrangement can help the pathologist avoid this diagnostic pitfall.[72]

BENIGN CYSTIC MESOTHELIOMA (MULTILOCULAR PERITONEAL INCLUSION CYST)[73,74]

Benign cystic mesothelioma is rare and usually occurs in women of reproductive age. Most patients present with lower abdominal pain and/or one or more peritoneal-based masses that have a predilection for the pelvic region. Whether or not these cystic lesions are benign neoplasms or reactive mesothelial proliferations is controversial. The case for a reactive lesion is stronger in those patients who have a history of previous abdominal surgery, pelvic inflammatory disease, or endometriosis.[75]

Grossly, these lesions consist of one or more cysts that are smooth surfaced, thin walled, translucent, and multiloculated (Fig. 8.64). They are usually adherent to pelvic organs, and may extend to involve the upper abdomen. The cysts typically contain clear to yellow serous fluid and may form clusters that can exceed 20 cm in diameter. These lesions are often more impressive on imaging studies (Fig. 8.65) or intraoperatively, since the pathologist may receive only a sampling of the cystic masses, which after a laparoscopic procedure may arrive in the gross room ruptured or shredded. Regardless of the type of surgical treatment, recurrences are common.

Histologically, the benign cystic mesothelioma is composed of multiple cysts that are separated by delicate fibrovascular tissue (Fig. 8.66). The cysts are typically lined by a single layer of flattened to cuboidal mesothelial cells with little to no nuclear atypia (Fig. 8.67). Exfoliated clusters of mesothelial cells may be seen within the cyst lumens. Occasionally, the mesothelial cells undergo squamous metaplasia or proliferate in a pattern that resembles the mesothelial-derived adenomatoid tumor that most commonly occurs in the myometrium and fallopian tube. In some cases, the stroma is inflamed. As described for unilocular inclusion cysts, entrapped proliferating mesothelial cells may also be encountered within the cyst walls and be a source of diagnostic difficulty.

Differential Diagnosis

The main differential diagnostic consideration is intra-abdominal lymphangioma, which typically occurs in male children, is found outside the pelvis, contains chylous fluid, frequently contains stromal lymphoid aggregates and bundles of smooth muscle within its walls, and is lined by endothelial cells that are immunoreactive for CD31 and CD34. In contrast, mesothelial lesions are nonreactive for these endothelial markers, and are immunoreactive for cytokeratin and calretinin. Note that the lymphatic endothelial marker D2-40 is

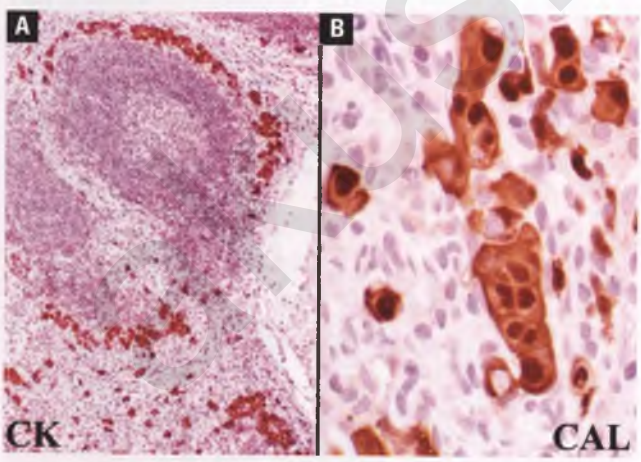

FIGURE 8.63. Immunohistochemistry of intranodal mesothelial cells. **A:** An arc-like band of cytokeratin-positive mesothelial cells surrounds a lymphoid follicle. Other mesothelial cells occurring singly and in small clusters are also highlighted by this immunostain. **B:** The combined nuclear and cytoplasmic immunoreactivity for calretinin shown here supports mesothelial differentiation.

FIGURE 8.64. Benign cystic mesothelioma (multilocular peritoneal inclusion cyst). This fluid-filled, internally loculated cystic mass has a paper-thin wall with a delicate vasculature. (Courtesy of Dr. Colin J. R. Stewart.)

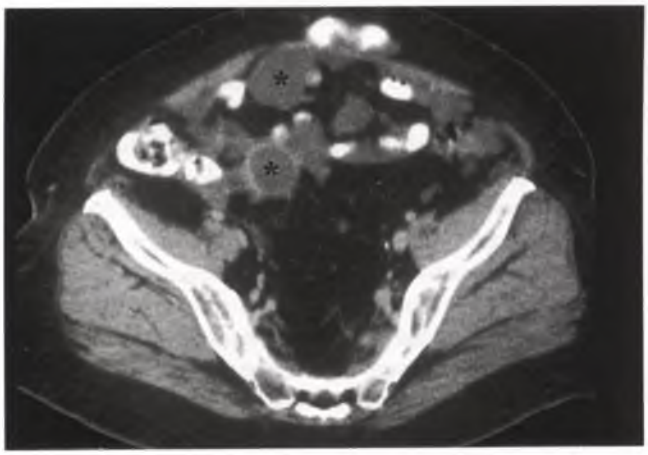

FIGURE 8.65. Benign cystic mesothelioma (multilocular peritoneal inclusion cyst). This axial CT image of the pelvis demonstrates several cystic locules, two of which are marked with asterisks. Oral contrast agent within the intestinal tract distinguishes white-appearing loops of bowel from these abnormal cystic structures. Incidental note is made of a ventral hernia containing bowel. (Courtesy of Dr. Valerie C. Reichert.)

not useful in this situation, since it stains both lymphangiomas and mesothelial-derived lesions.[76,77]

WELL-DIFFERENTIATED PAPILLARY MESOTHELIOMA[78–80]

WDPM is an uncommon tumor that is usually found in women of reproductive age. In most cases, it represents an unsuspected finding during exploration of the peritoneal cavity for an unrelated reason. In contrast to malignant mesothelioma of the pleura, a causative link between asbestos exposure and development of WDPM has not been established.

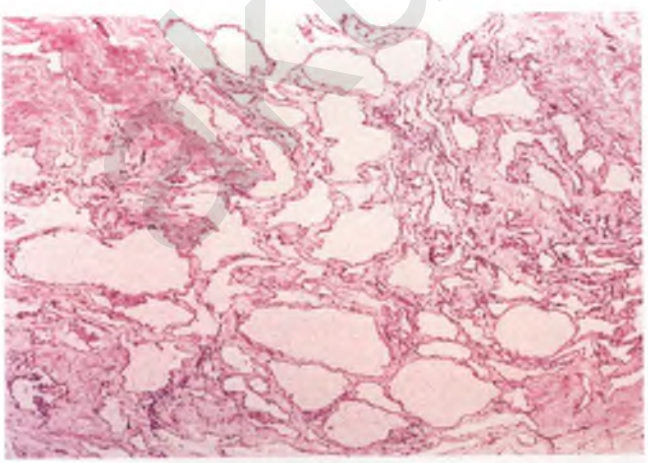

FIGURE 8.66. Benign cystic mesothelioma (multilocular peritoneal inclusion cyst). Multiple cystic spaces of varying sizes and shapes are separated by fibrous tissue.

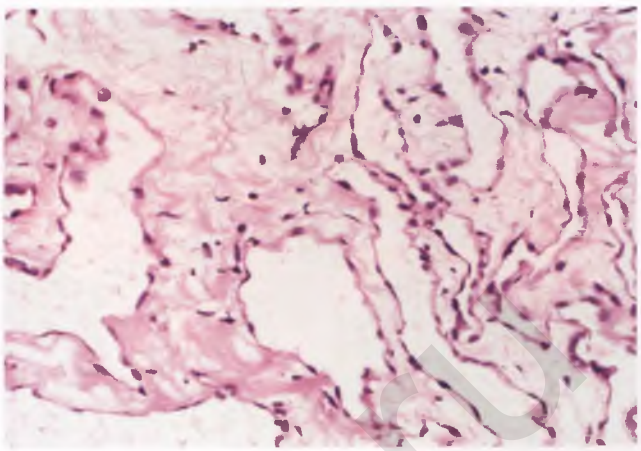

FIGURE 8.67. Benign cystic mesothelioma (multilocular peritoneal inclusion cyst). The cystic spaces are lined by a single layer of flattened to cuboidal mesothelial cells with bland nuclear features.

Grossly, WDPMs are solitary or multifocal lesions with a polypoid, papillary, or nodular appearance. Each individual tumor is usually <2 cm in greatest dimension, and may be seen projecting from the mesothelial surface or forming a nodule within the omentum (Fig. 8.68).

Histologically, classic WDPM is characterized by a purely papillary architectural pattern, with the fibrous-cored papillae lined by a single layer of flattened to cuboidal, mitotically inactive mesothelial cells with bland nuclear features (Fig. 8.69). Psammoma bodies are present in a minority of WDPMs. By definition, there is no invasion of the underlying tissue. Classification of cases that deviate from the purely papillary pattern, such as those with prominent tubulopapillary patterns, branching cords, or solid sheets, is controversial. Some tumors with these features may represent undersampled or subtle forms of malignant mesothelioma, especially when the disease process is multifocal.[81]

Differential Diagnosis

In contrast to malignant mesothelioma, WDPM are often small, may be solitary, do not invade tissue, and in their most common and widely accepted form consist entirely of papillae that are lined by a single layer of bland mesothelial cells.

The differential diagnosis of WDPM with mesothelial hyperplasia is discussed in the section on the latter entity.

Prognosis

As a group, WDPMs are often considered to be indolent tumors of low malignant potential. However, there is strong evidence that at least the solitary forms of this tumor that have classic, purely papillary architecture and low-grade nuclear features are clinically benign. It is likely that the few WDPMs that have been reported to behave in a malignant fashion were multifocal malignant mesotheliomas that were either undersampled

FIGURE 8.68. Well-differentiated papillary mesothelioma. The nodular tumor at left is attached to the serosal surface of the fallopian tube via a stalk. Note that the tumor has a velvety, granular surface, which is due to the presence of innumerable papillae.

or misclassified. Radiation and chemotherapy are not recommended for WDPMs that have been well sampled and diagnosed using strict criteria, since these treatments can cause significant complications and are of no proven benefit in this situation.

MALIGNANT MESOTHELIOMA[79,81–83]

Malignant mesothelioma of the peritoneum is a rare tumor that is less common than its pleural counterpart, and in women is much less frequently encountered than extraovarian peritoneal serous carcinoma. Peritoneal malignant mesothelioma typically presents in adults with abdominal pain, increasing abdominal girth, and ascites, and generally remains confined to the peritoneal cavity throughout its course. A rare clinical presentation that is relevant to gynecologic pathologists is one in which malignant mesothelioma exhibits extensive involvement of one or both ovaries to the extent that it mimics a primary ovarian tumor.[84] Most women with peritoneal malignant mesothelioma do not have a history of asbestos exposure. Nevertheless, the pathologist should keep in mind that every case of malignant mesothelioma is a potential medicolegal case, since any case in which an exposure to asbestos is eventually documented may become the subject of litigation.

Grossly, typical examples of peritoneal malignant mesothelioma are characterized by rind-like thickening of portions of the peritoneum, innumerable nodules and plaques studding the peritoneal surface, and varying degrees of encasement of visceral organs. In cross sections of some examples of involved omentum prior to complete obliteration of normal tissue, there may be swirls of rubbery white tumor tracking along preexisting fibrous septa in a pattern that imparts a resemblance to marble cake (Fig. 8.70). When this marbled pattern created by tumor with a rubbery texture is encountered, it should raise the index of suspicion for mesothelioma.

Histologically, most peritoneal malignant mesotheliomas are of the epithelioid type, a few are biphasic, and rare tumors are purely sarcomatous. The most common epithelioid variants typically consist of varying proportions of tubules, papillae, and solid areas (Figs. 8.71–8.74), but multiple other epithelioid subtypes exist. The degree of nuclear atypia ranges from mild to severe, varies from case to case, and may also vary within different areas of the same tumor. Severe nuclear atypia of epithelioid tumor cells is usually manifested by the presence of large vesicular nuclei with cleared chromatin and single macronucleoli (Fig. 8.75). Whatever the degree of atypia, the tumor cell nuclei generally have a monotonous rather than pleomorphic appearance. Some degree of mitotic activity is usually evident, but high mitotic rates are uncommon. Although stromal invasion is usually apparent (Fig. 8.76), it is not required for the diagnosis when features of otherwise obvious malignant mesothelioma

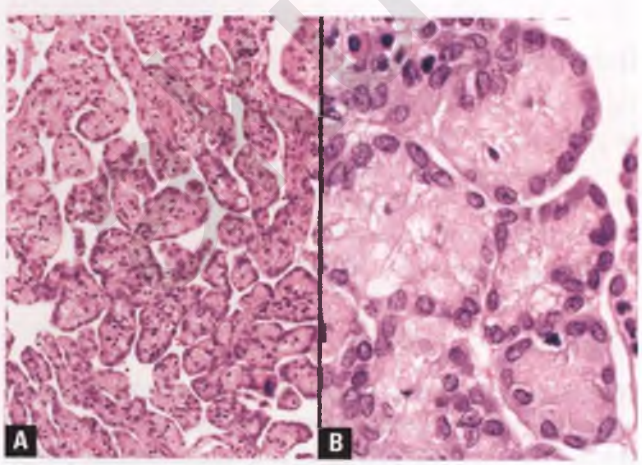

FIGURE 8.69. **A,B:** Well-differentiated papillary mesothelioma. The neoplasm consists of fibrous-cored papillae that are lined by a single layer of bland, mitotically inactive mesothelial cells.

FIGURE 8.70. Malignant mesothelioma. This cross section through the omentum demonstrates a "marble cake" pattern of involvement.

are identified. Psammoma bodies and foci of tumor necrosis are present in a minority of cases.

Selected Unusual Patterns

Deciduoid malignant mesothelioma is a rare subtype of the solid epithelioid variant that can occur in young women.[85] These tumors have a pseudodecidual appearance by virtue of their sheets of large cells with nuclei that are round and vesicular, nucleoli that are prominent and single, and cytoplasm that is abundant and eosinophilic (Fig. 8.77).[85,86]

Biphasic malignant mesotheliomas consist of an admixture of epithelioid and sarcomatous components (Fig. 8.78).

Sarcomatoid tumors with the gross, clinical, and radiologic characteristics of a peritoneal mesothelioma and a frankly sarcomatous appearance do not pose much of a diagnostic dilemma, and could only be confused with other malignant tumors with an equally dismal prognosis. However, those sarcomatoid malignant mesotheliomas whose spindle cells are neither densely packed nor overtly anaplastic can be difficult to distinguish from reactive fibrous tissue (Fig. 8.79A). In this situation, the identification of invasion of adipose tissue by cytokeratin-positive spindle cells in a characteristic insinuating pattern is of great help in recognizing these tumors as malignant (Fig. 8.79B).[7] This pattern of infiltration resembles that seen when the tumor cells of aggressive angiomyxoma and dermatofibrosarcoma protuberans extend into fat.

Differential Diagnosis

The differential diagnoses of epithelioid malignant mesothelioma with mesothelial hyperplasia and WDPM are discussed in the sections on these other entities.

The papillary and tubulopapillary patterns of epithelioid malignant mesothelioma may resemble papillary serous carcinoma involving the peritoneum either primarily or secondarily. Histologically, mesothelioma is favored when (a) the papillae do not exhibit a hierarchical branching pattern or cellular stratification, (b) small detached clusters of tumor cells are not prominent in the vicinity of the papillae, (c) the stromal cores of the papillae are hyalinized, (d) psammoma bodies and slit-like glandular spaces are infrequent, (e) nuclei are monomorphic and their degree of atypia is not striking, (f) eosinophilic cytoplasm is conspicuous, and (g) mitotic activity is unimpressive.[81]

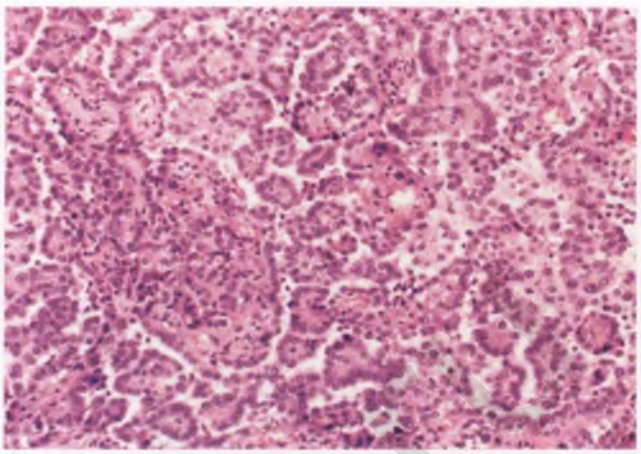

FIGURE 8.72. Malignant mesothelioma, papillary pattern.

In problematic or potential medicolegal cases, immunohistochemistry can facilitate or substantiate the diagnosis of malignant mesothelioma. Over the years, numerous immunostains have been evaluated for their utility in the differential diagnosis between mesothelioma and adenocarcinoma. Some antibodies that are effective in the distinction between pleural mesothelioma and lung adenocarcinoma are of limited or no use in discriminating between peritoneal mesothelioma and serous carcinoma. The value of immunohistochemistry in the latter situation has been recently reviewed, with the recommendation to use a panel of markers that includes estrogen receptor and either MOC-31 or Ber-EP4, all of which are commonly

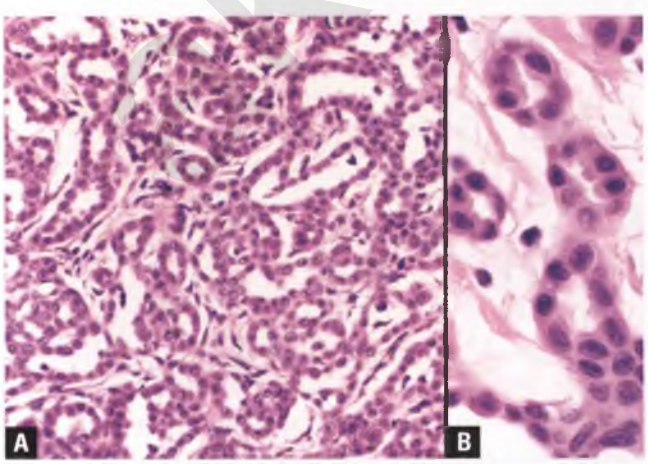

FIGURE 8.71. **A,B:** Malignant mesothelioma, tubular pattern.

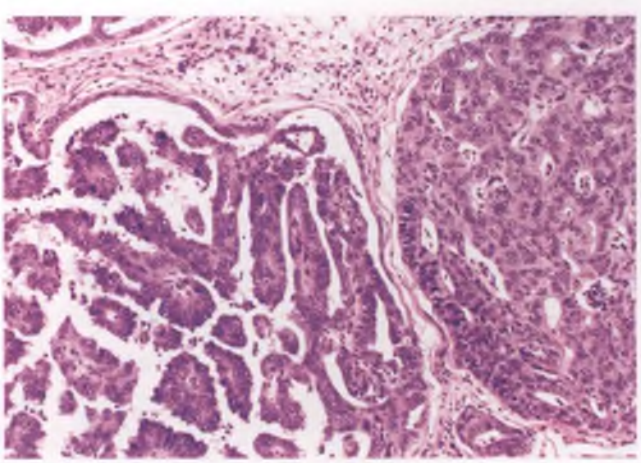

FIGURE 8.73. Malignant mesothelioma, tubulopapillary pattern. The papillary architecture at left contrasts with the aggregate of closely packed tubules at right. In other examples of this pattern, the tubules and papillae are intermingled with one another.

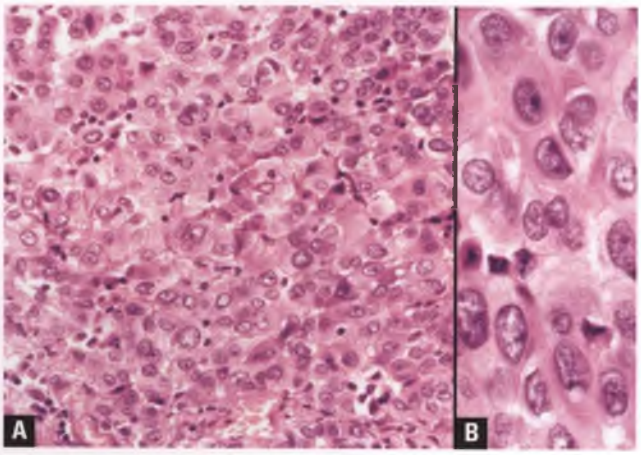

FIGURE 8.74. **A,B:** Malignant mesothelioma, solid pattern. This pattern consists of sheets of malignant mesothelial cells.

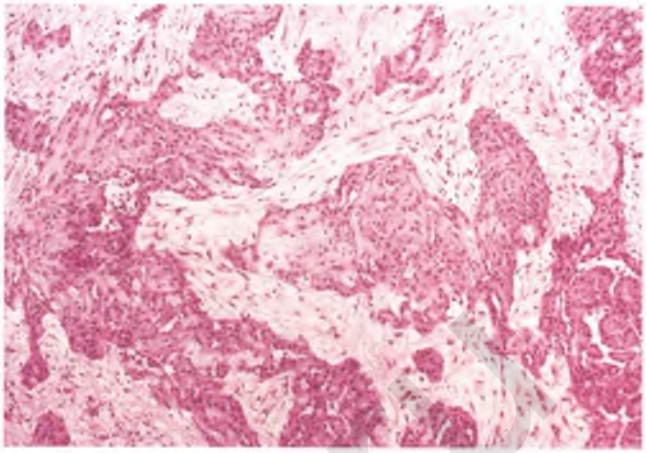

FIGURE 8.76. Malignant mesothelioma. Obvious stromal invasion is present in this region of the tumor.

expressed in serous carcinomas and only rarely expressed in mesotheliomas, in conjunction with the mesothelial marker calretinin.[87] Since that time, PAX8 has also been shown to be a valuable marker that typically stains serous carcinomas and only infrequently stains mesotheliomas.[88]

With current immunostains, electron microscopy is seldom needed, but the ultrastructural demonstration of tumor cells with numerous, long, slender microvilli along with other secondary features does provide additional support for a diagnosis of mesothelioma that can be useful in a medicolegal setting.[77]

When the differential diagnosis includes metastatic adenocarcinoma of gastric, pancreatic, colorectal, and breast origin, positive results within the cytoplasmic vacuoles of the tumor cells with a neutral mucin stain (mucicarmine or PAS with diastase) can be considered strongly supportive of metastatic adenocarcinoma. However, because of the rare cases of malignant mesothelioma that can show a similar staining reaction,[82] it is recommended that these stains be interpreted only within the context of the clinical history, routine histology, and immunohistochemical results.

In contrast to an exuberant peritoneal decidual reaction, deciduoid malignant mesothelioma is immunoreactive for cytokeratin and calretinin, usually exhibits more pronounced nuclear atypia than ectopic decidua, may be admixed with more conventional patterns of malignant mesothelioma, may have appreciable mitotic activity, and involves the peritoneal cavity to a much greater and grossly obvious extent.[85,86]

The distinction of bland forms of sarcomatoid malignant mesothelioma from reactive fibrous tissue is addressed in the section that pertains to this type of mesothelioma.

Prognosis

Although most patients with peritoneal malignant mesothelioma have a poor prognosis, a significant number of patients are

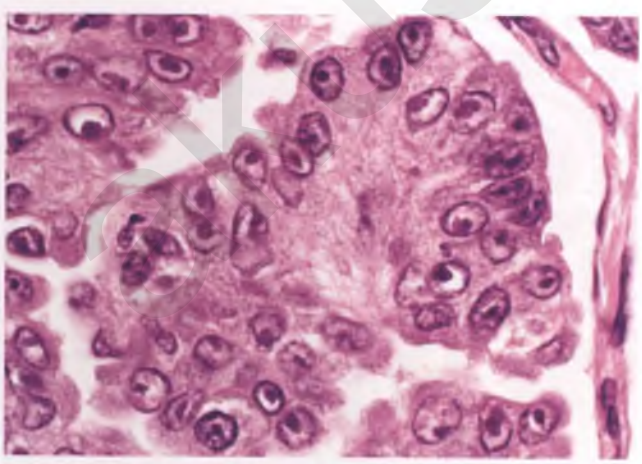

FIGURE 8.75. Malignant mesothelioma. Epithelioid tumors with high nuclear grade often feature large vesicular nuclei with single macronucleoli. Note how the tumor cells are relatively monomorphic, which is a common finding in mesotheliomas.

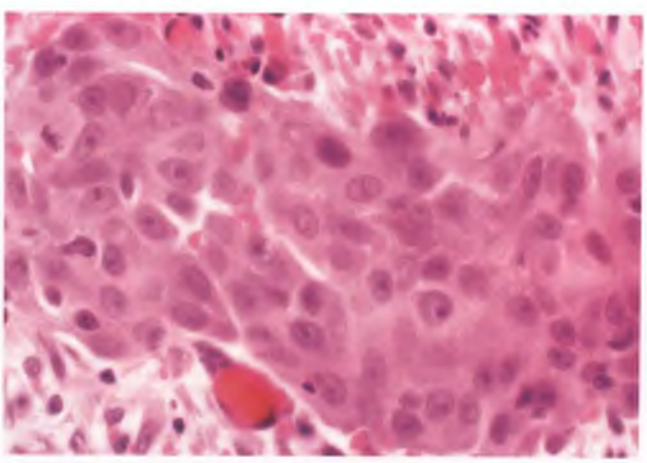

FIGURE 8.77. Malignant mesothelioma, deciduoid variant. The malignant mesothelial cells resemble decidualized stromal cells. Note the mitotic figure in the upper left portion of the image.

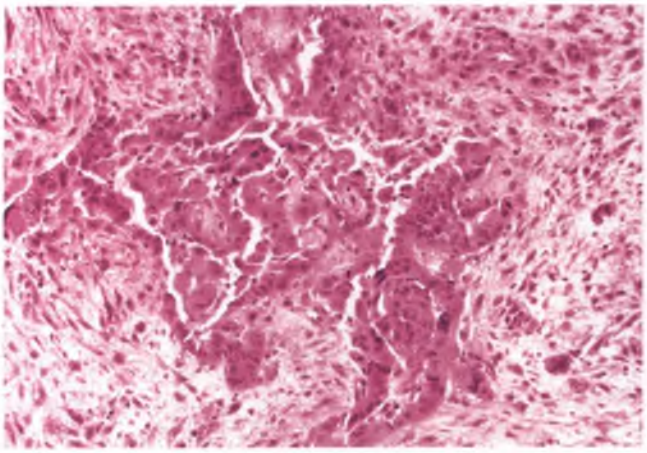

FIGURE 8.78. Malignant mesothelioma, biphasic variant. Both the epithelioid and spindle cell components are histologically malignant.

long-term survivors.[89,90] In one recent study, the features that correlated with a more favorable outcome were low nuclear grade, low mitotic index, and optimal cytoreduction.[90]

Cytologic Features of Epithelioid Malignant Mesothelioma in Peritoneal Fluid[1,83]

This discussion is limited to malignant mesotheliomas with an epithelioid component, since peritoneal sarcomatoid malignant mesotheliomas are rare and are rarely associated with ascites. Since it is difficult to make the initial diagnosis of malignant mesothelioma with certainty solely on the basis of cytologic material, and because much is at stake both medically and legally, it is recommended that an initial diagnosis of malignant mesothelioma that is made or suspected cytologically be confirmed by evaluation of a tissue sample.

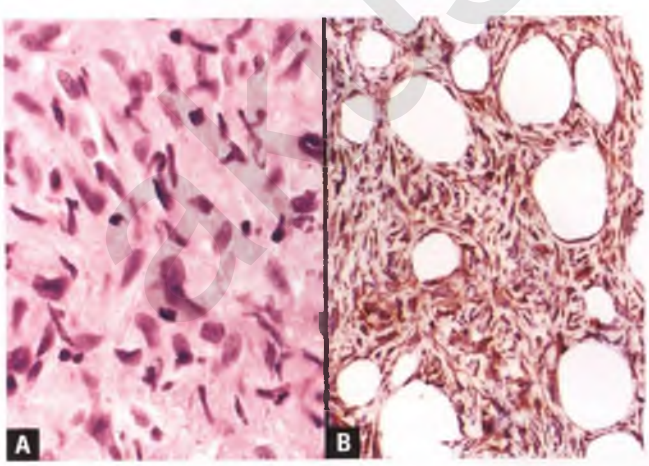

FIGURE 8.79. Malignant mesothelioma, sarcomatoid variant. **A:** The spindle cells are atypical, but not overtly malignant. **B:** The spindle cells, which are highlighted by a cytokeratin immunostain, infiltrate adipose tissue in a characteristic pattern that results in a honeycomb appearance.

An important clue to the cytologic diagnosis of malignant mesothelioma at scanning magnification is the presence of a highly cellular sample with numerous three-dimensional cell clusters of substantial size (>50 cells) (Fig. 8.80). Such a finding is highly suggestive of malignancy, and a diagnosis of malignant mesothelioma can be strongly favored when cells with a sufficient degree of nuclear atypia and evidence of mesothelial differentiation (intercellular windows, central nuclei, scalloped borders, and dense cytoplasm) are identified upon closer inspection (Fig. 8.81). In many cases of malignant mesothelioma, it is the large size of the tumor cells that is the first high-magnification feature that helps to substantiate the diagnosis (Fig. 8.82); this clue may be overlooked if one does not utilize the nonneoplastic cells in the background as an internal size standard. These large tumor cells often maintain a relatively normal nuclear to cytoplasmic ratio, but usually exhibit a combination of nuclear contour abnormalities, nuclear pleomorphism, hyperchromasia, prominent nucleoli, frequent bi- and multinucleation, and cell-in-cell arrangements that favor malignancy.

Differential Diagnosis

The exfoliated cells of malignant mesothelioma may closely resemble reactive mesothelial cells in cytologic preparations. In benign effusions, reactive mesothelial cells do not exhibit the marked cellularity and formation of large three-dimensional aggregates that typify most malignant mesotheliomas. Instead, reactive mesothelial cells occur singly, in small monolayered sheets, and in small clusters. The individual cells may exhibit some degree of nuclear enlargement, nuclear pleomorphism, bi- and multinucleation, hyperchromasia, nucleolar prominence, and mitotic activity, but usually not to the degree seen in malignant mesothelioma.

At the other end of the spectrum, the cytologic sample may be obviously malignant, but it may be difficult to determine whether the cells are derived from malignant mesothelioma or metastatic adenocarcinoma. This differential diagnosis

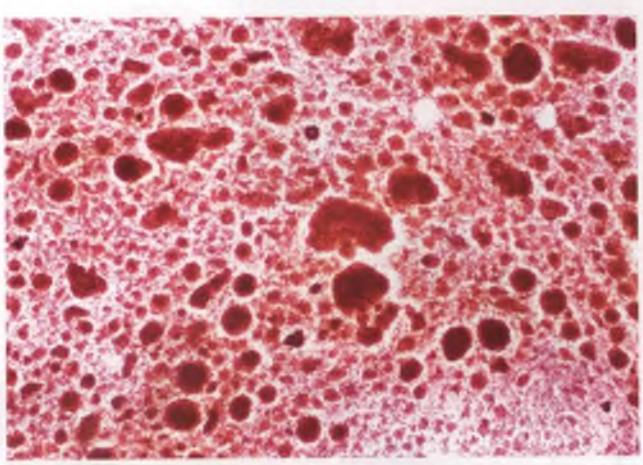

FIGURE 8.80. Malignant mesothelioma. In this low-magnification view of a cytologic preparation, the presence of innumerable rounded cell clusters of substantial size is highly suggestive of either metastatic adenocarcinoma or malignant mesothelioma.

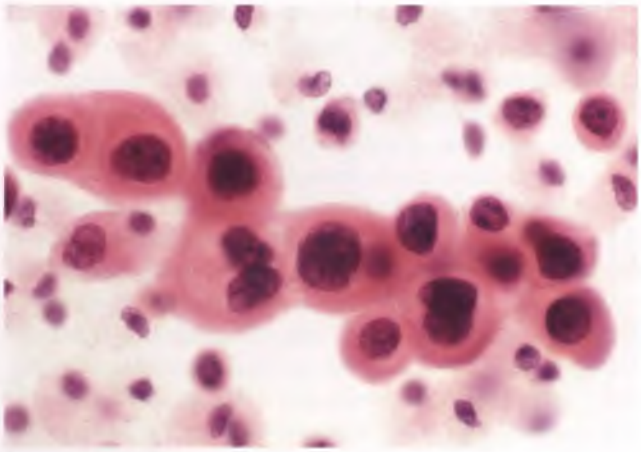

FIGURE 8.81. Malignant mesothelioma. These malignant mesothelial cells exhibit cytomegaly, nuclear atypia, and frequent binucleation. The knobby contour of the cell cluster and the dense cytoplasm, central nuclei, and faint intercellular windows exhibited by its constituent cells are evidence in favor of mesothelial differentiation.

is discussed in the section on the cytologic features of metastatic adenocarcinoma at the end of this chapter.

MESENCHYMAL AND OTHER RARE INTRA-ABDOMINAL TUMORS[91,92]

Disseminated Peritoneal Leiomyomatosis

Disseminated peritoneal leiomyomatosis (DPL) is a rare entity that occurs in women of reproductive age, most of whom are either pregnant or on oral contraceptives.Its major significance is its potential to be confused with metastatic leiomyosarcoma. The gross findings can be alarming to the surgeon, with numerous small (usually <1 cm) nodules studding the peritoneal surfaces in a pattern that mimics widespread metastatic disease (Fig. 8.83). Histologically, the nodules resemble typical leiomyomas (Fig. 8.84). Patches of decidual cells may be admixed with the smooth muscle proliferation, and coexisting endometriosis is found in about 10% of cases (Fig. 8.85).

Aggressive treatment of DPL is not necessary, since regression of these nodules is the rule. There have been a few reports of malignancy arising in DPL. However, most of these cases

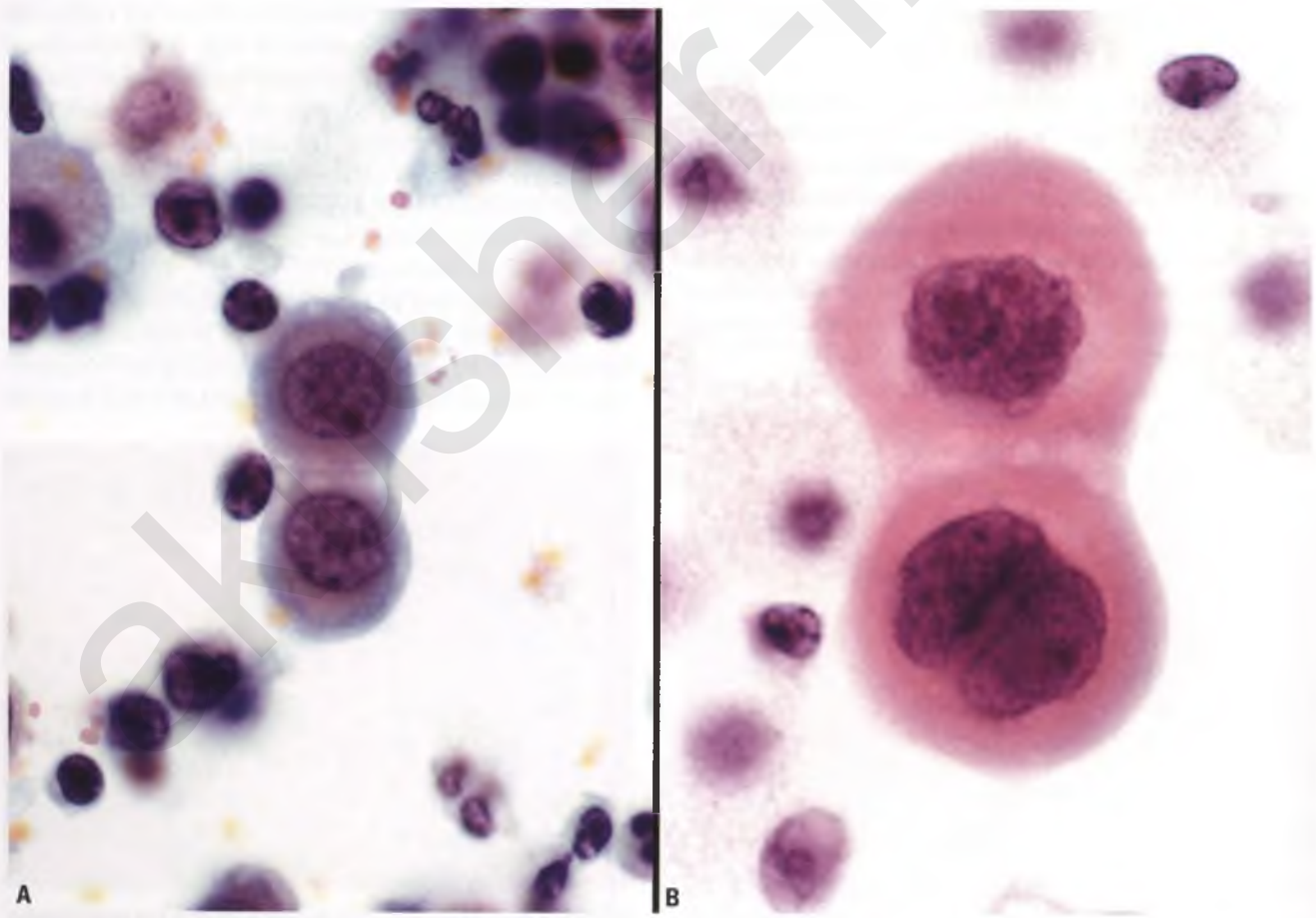

FIGURE 8.82. Reactive mesothelial cells **(A)** versus malignant mesothelioma **(B)**. Note how much larger the pair of malignant cells is in comparison with the pair of reactive cells, although their nuclear to cytoplasmic ratios are similar (both images were taken at the same magnification). Intercellular windows are present between both pairs of mesothelial cells. Inflammatory cells in the background serve as internal size reference points.

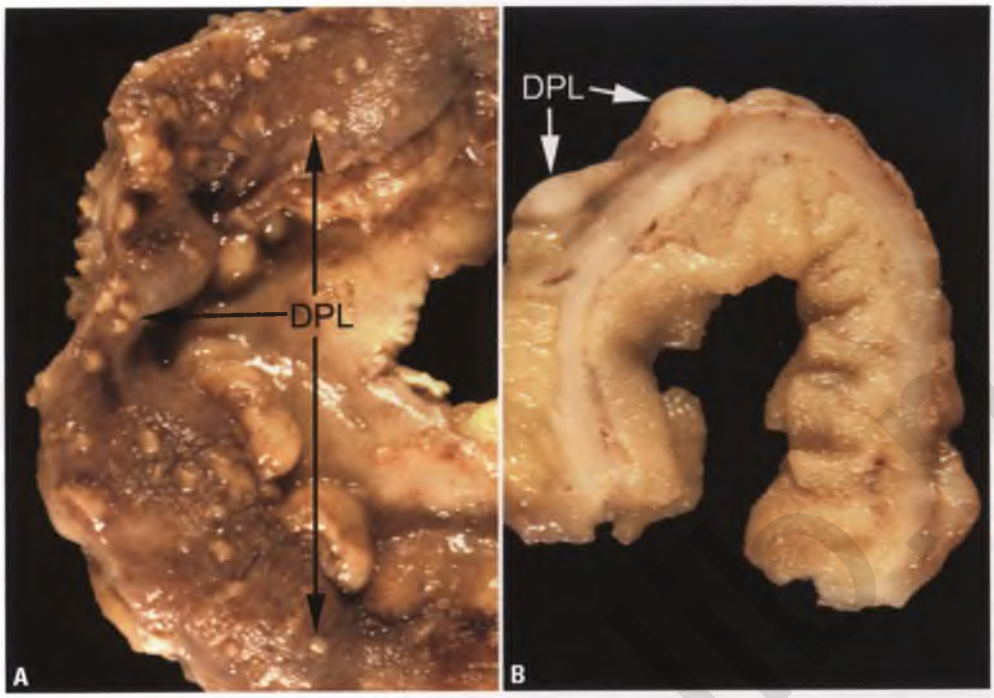

FIGURE 8.83. **A,B:** Disseminated peritoneal leiomyomatosis. Several small myomatous nodules stud the serosal surface of the small bowel. Lack of familiarity with this rare entity resulted in an unnecessary segmental resection.

have been shown to be quite different from typical DPL, with tumors failing to express estrogen and progesterone receptors and occurring without associated uterine leiomyomas in patients that lack a history of increased estrogen exposure. Since retroperitoneal and gastrointestinal stromal sarcomas can be composed of benign-appearing spindle cells and have very low mitotic rates, the possibility that these cases represent occult sarcomas with deceptively bland histology metastasizing to the peritoneum needs to be more rigorously excluded before malignant transformation of DPL can be accepted as a legitimate phenomenon.

Intra-Abdominal Fibromatosis[93]

Fibromatosis,which has been shown to be a clonal neoplasm,[94] can occur in the superficial or deep soft tissues. This discussion is limited to its intra-abdominal form. These tumors typically present as mass lesions in adults, sometimes in association with abdominal pain, and average 14 cm in diameter. Some cases of intra-abdominal fibromatosis are associated with Gardner's syndrome, which is a variant of familial adenomatous polyposis.

Fibromatosis classically has a sectioned surface that is firm, off-white to pale tan, and trabeculated, and lacks areas of necrosis or frank hemorrhage (Fig. 8.86). However, intra-abdominal fibromatosis differs in that it often has a mucoid cut surface with less appreciable trabeculations (Fig. 8.87). Although often well circumscribed grossly, fibromatosis characteristically has infiltrative margins when examined histologically.

The myofibroblastic tumor cells of fibromatosis form ill-defined, sweeping fascicles, and are embedded within a prominent matrix that varies from collagenous to mucoid. These cells are generally uniform, elongate, slender, and spindle shaped (Fig. 8.88). Nuclear features are bland, and mitotic figures are uncommon. The degree of cellularity may vary, and keloid-like hyalinization may be evident. Vascular support is usually in the form of thin-walled vessels, which are often congested and associated with stromal microhemorrhages. Inflammation is characteristically absent within the tumor, except

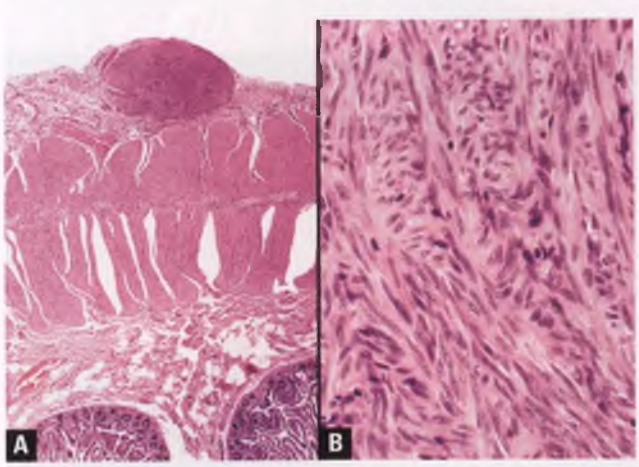

FIGURE 8.84. Disseminated peritoneal leiomyomatosis. **A:** In this low-magnification view, a small nodule protrudes from the serosal surface of the small bowel. **B:** When examined at high-magnification, the nodule is found to exhibit the histologic features of an ordinary leiomyoma.

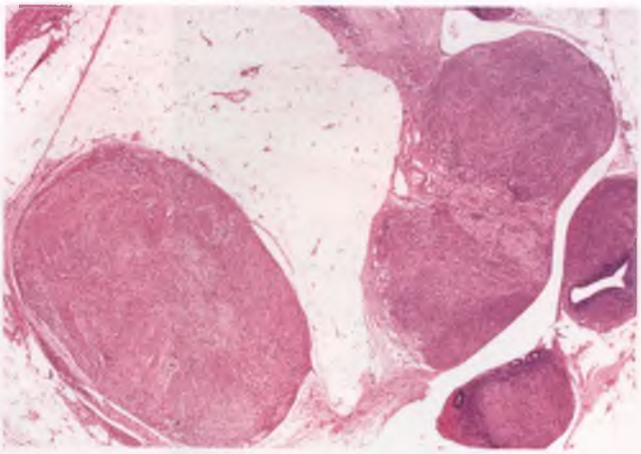

FIGURE 8.85. Disseminated peritoneal leiomyomatosis. Several small leiomyomatous nodules are present within the omentum. Note the coexisting foci of endometriosis in the lower right portion of the image.

when associated with bowel perforation, abscess formation, or erosion of the intestinal mucosa.

Fibromatosis versus Gastrointestinal Stromal Tumor

Although intra-abdominal fibromatosis generally involves the pelvis, mesentery, and retroperitoneum, it may encroach upon, insinuate into, or occasionally arise from the bowel wall (Fig. 8.89).[95] When intimately associated with bowel, fibromatosis may be misdiagnosed as a gastrointestinal stromal tumor (GIST), which in this site has significant metastatic potential. Whereas fibromatosis is a solid neoplasm that is characterized by elongated fascicles of monotonous spindle-shaped cells with bland nuclear features and a stroma devoid of frank hemorrhage or necrosis, GISTs feature spindle and/or epithelioid cells in a variety of architectural patterns, and may exhibit significant

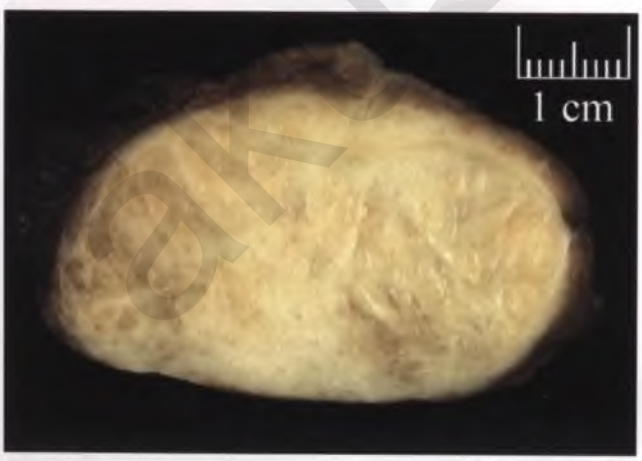

FIGURE 8.86. Fibromatosis. The sectioned surface of this formalin-fixed tumor is firm, pale tan, and trabeculated. Although grossly well circumscribed, the tumor infiltrates skeletal muscle at its edges.

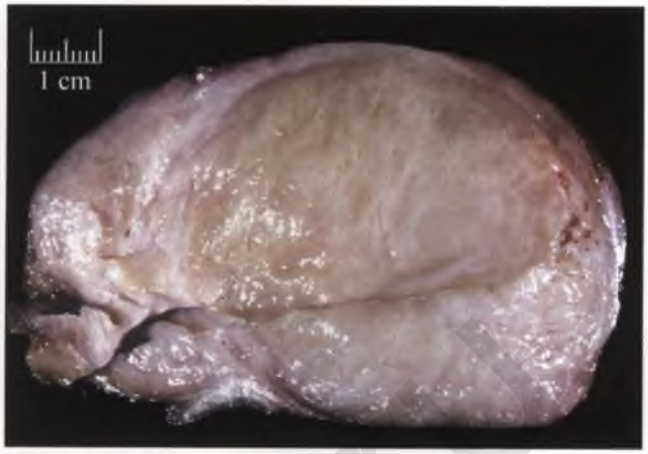

FIGURE 8.87. Fibromatosis. In this example, the sectioned surface has a mucoid appearance, which is commonly the case in intra-abdominal forms of this tumor.

nuclear atypia and grossly visible foci of hemorrhage, necrosis, or cystic degeneration. Although CD34 immunoreactivity favors GIST in this situation, a significant number of GISTs are CD34 negative.[95–97]

It is important to be aware that c-KIT (CD117) immunoreactivity should not be taken as strong evidence in support of GIST when fibromatosis is a differential diagnostic consideration, since fibromatosis is often positive for this marker when using a variety of staining protocols.[95,98,99] A better immunostain in this circumstance is β-catenin, since nuclear immunoreactivity with this marker is expected in deep fibromatosis and is typically absent in GIST.[98]

Behavior

Fibromatosis is a benign tumor that can locally recur if incompletely excised, but it does not have metastatic potential. In cases where the tumor is not resectable, it may cause death via intestinal obstruction.

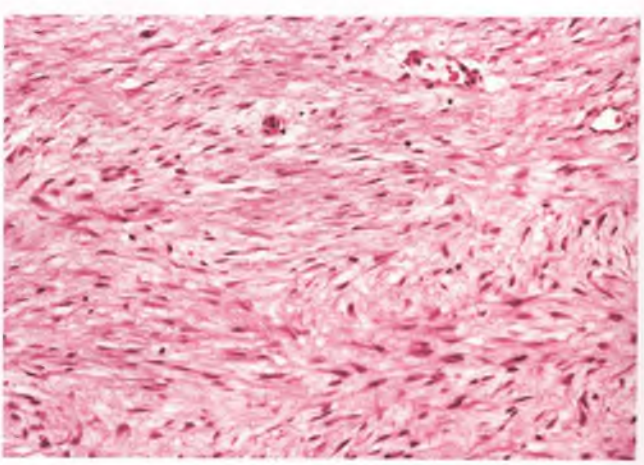

FIGURE 8.88. Fibromatosis. The tumor cells are slender, elongate, and bland.

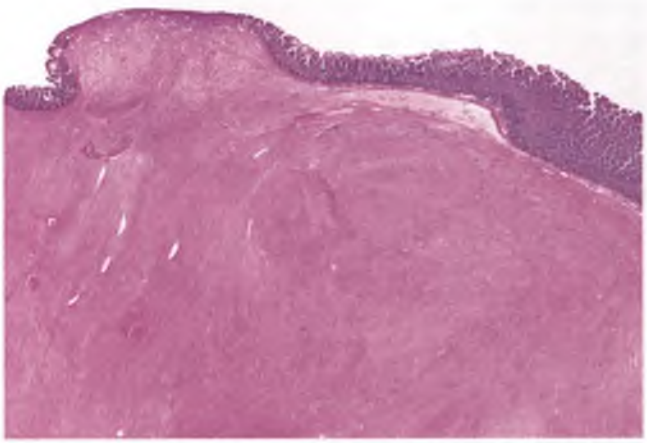

FIGURE 8.89. Fibromatosis involving small bowel. Fibromatosis has replaced this portion of the bowel wall and most of the submucosa, and has caused focal erosion of the mucosal surface.

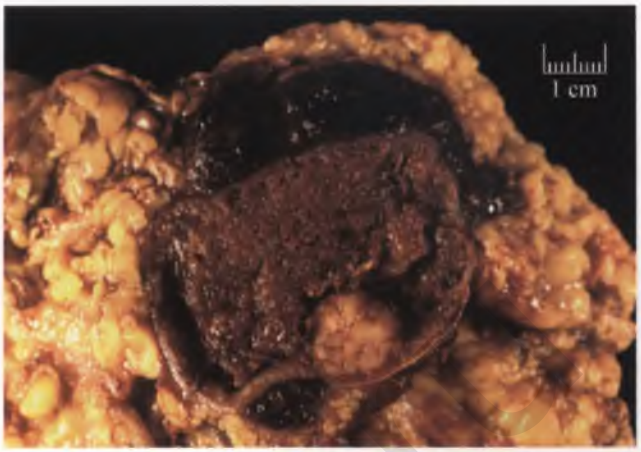

FIGURE 8.90. Solitary omental GIST. The tumor is well circumscribed, and its sectioned surface consists predominantly of friable reddish brown tissue along with a solid tan nodule. The tumor has bled into the neighboring tissue, where clotted blood has accumulated. The patient is alive and well 15 years after surgical resection.

Omental Gastrointestinal Stromal Tumor[96,97]

Although most GISTs originate in the wall of the stomach or small intestine, they also occur elsewhere in the gastrointestinal tract and rarely appear to arise in unusual sites such as the omentum. Solitary omental GISTs typically present in adults as an abdominal mass associated with vague abdominal pain. Grossly, these tumors are well circumscribed and have a sectioned surface that often contains both friable hemorrhagic tissue and solid nodules of tan to pale yellow tumor (Fig. 8.90). Varying degrees of cystic degeneration may be present, and foci of tumor necrosis may also be evident.

As is true for GISTs in general, these tumors may exhibit epithelioid, spindle cell, or mixed histologic patterns (Figs. 8.91–8.93). The expected c-KIT (CD117) immunoreactivity of GISTs is helpful in excluding other spindle cell neoplasms such as leiomyosarcoma, malignant peripheral nerve sheath tumor, and metastatic amelanotic spindle cell melanoma. The distinction of GIST from intra-abdominal fibromatosis is discussed in the section on the latter entity.

The prognosis of completely resected solitary omental GISTs is excellent. Patients with such tumors that have low mitotic rates, no tumor necrosis, and lack peritumoral infiltration of adipose tissue are particularly likely to be long-term survivors. In contrast, patients with multiple omental GISTs, regardless of their histologic features, have a poor prognosis. Most such cases probably represent metastases from occult GISTs elsewhere in the abdomen or malignant GISTs that have detached from their site of origin and taken up residence within the omentum.

Intra-Abdominal Desmoplastic Small Round-Cell Tumor[100,101]

Desmoplastic small round-cell tumor (DSRCT) is a rare malignant neoplasm of unknown histogenesis that has a dismal prognosis. Most patients are young (mean age of 20–25 years) and male, with a male to female ratio of roughly 4 to 1. DSRCT typically presents as an abdominal mass that is often associated with abdominal pain. Prominent involvement of the ovaries may simulate a primary ovarian tumor.[102]

Grossly, DSRCT typically consists of a multinodular tumor with a firm, off-white sectioned surface. The main tumor averages about 10 cm in diameter, and smaller satellite tumor nodules are typically present in other peritoneal locations. Histologic examination reveals a monotonous population of small, mitotically active, epithelioid tumor cells with scant cytoplasm that form irregularly shaped nests and cords within a prominent desmoplastic stroma that occasionally has

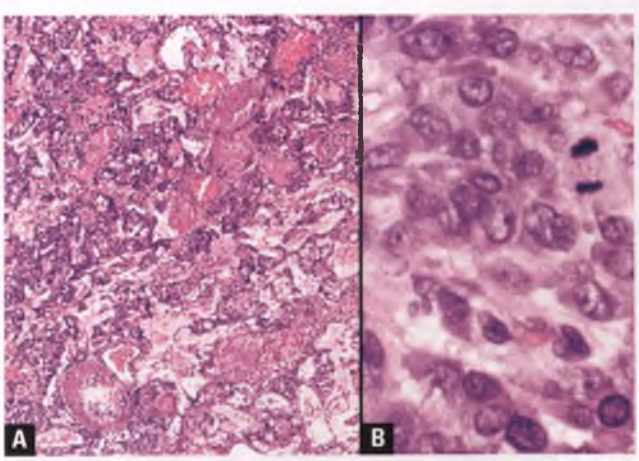

FIGURE 8.91. Solitary omental GIST (histologic correlate to tumor in preceding figure). **A:** Epithelioid tumor cells in the friable reddish area are loosely aggregated and are intermingled with numerous thin-walled vessels with recent organizing thrombi. **B:** The solid tan nodule is composed of sheets of tumor cells with an epithelioid morphology and occasional mitotic figures.

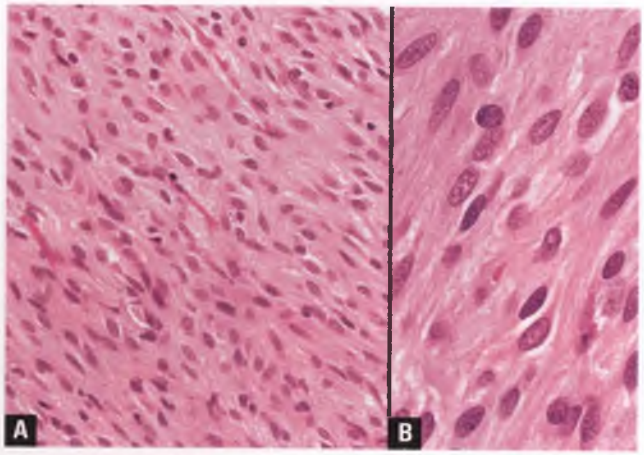

FIGURE 8.92. **A,B:** Gastrointestinal stromal tumor. In routinely-stained sections, the spindle cell morphology that is seen in many of these tumors can be easily misinterpreted as evidence of smooth muscle differentiation.

a myxoid appearance (Figs. 8.94 and 8.95). Patches of necrosis, particularly within the larger islands of tumor cells, are common. Unusual patterns, such as a predominance of spindle-shaped cells or formation of tubules, glands, rosettes, cysts, and trabeculae, can complicate the microscopic appearance of this tumor.[103] In addition, a small number of DSRCTs actually have inconspicuous amounts of desmoplastic stroma, despite their name. Nearly all DSRCTs have a reciprocal translocation between chromosomes 11 and 22 that fuses the Ewing's sarcoma gene (EWS1) and the Wilms' tumor suppressor gene (WT1), which can have diagnostic utility (see below).

DSRCT has a characteristic immunophenotype in which the tumor cells are reactive for cytokeratin, vimentin, desmin (paranuclear dot pattern), and WT1 (nuclear staining; an antibody that recognizes the carboxy rather than amino terminus of the human WT1 protein should be used in this situation).[100,104] This immunoprofile suggests divergent differentiation, and is quite helpful in distinguishing this tumor from its mimics (small cell carcinoma, EWS/primitive neuroectodermal tumor, lymphoma, neuroblastoma, and rhabdomyosarcoma). In difficult cases, demonstration of the EWS-WT1 gene fusion transcript that results from the translocation mentioned above can clinch the diagnosis of DSRCT.[101] This analysis can be performed on paraffin-embedded tissue.

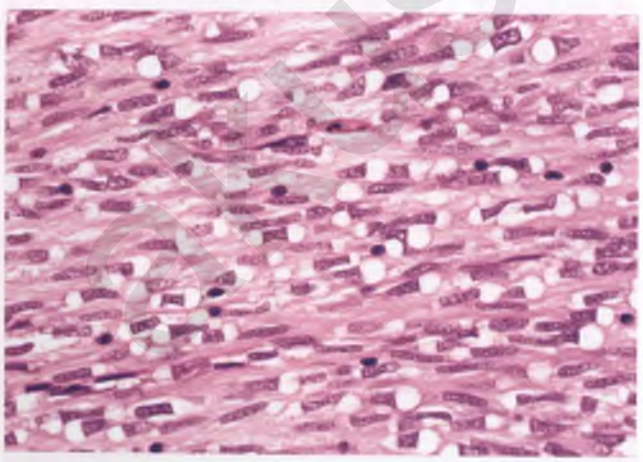

FIGURE 8.93. Gastrointestinal stromal tumor. In this spindle cell variant characteristic of some benign gastric tumors, one or two prominent perinuclear vacuoles are present at the ends of the elongated nuclei of many of the tumor cells. This pattern is recapitulated in some omental tumors.

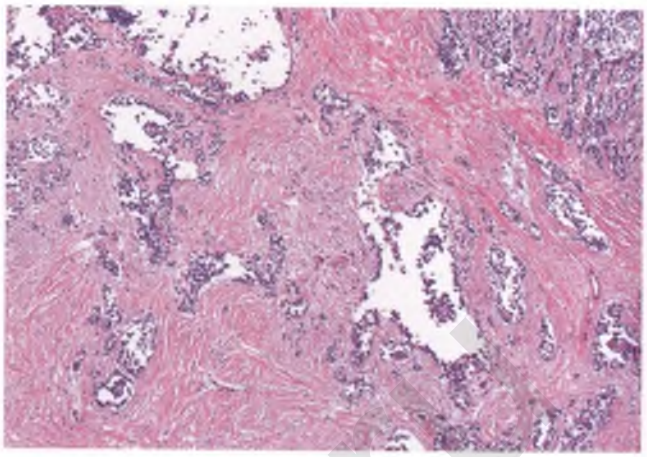

FIGURE 8.94. Intra-abdominal desmoplastic round cell tumor. Irregularly shaped nests and cords of tumor cells are embedded within a hypocellular desmoplastic stroma. Discohesion and/or tumor cell necrosis within the larger nests has resulted in degenerative cystic change. (Courtesy of Dr. Andrew E. Horvai.)

Miscellaneous Tumors

The reader is referred to standard pathology textbooks for a discussion of liposarcoma, leiomyosarcoma, and peripheral nerve

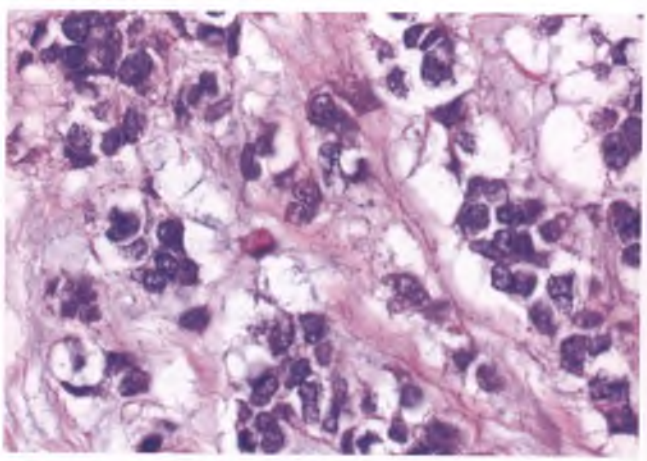

FIGURE 8.95. Intra-abdominal desmoplastic round cell tumor. This high-magnification view highlights the primitive appearance of the epithelioid tumor cells. In this example, the stroma is partially myxoid. (Courtesy of Dr. Andrew E. Horvai.)

sheath tumors that, although they may involve the abdomen, generally arise within the retroperitoneum or gastrointestinal tract. Other extraordinarily rare mesenchymal and miscellaneous intra-abdominal tumors include leiomyomatosis of pelvic lymph nodes,[105] solitary fibrous tumor,[106] inflammatory myofibroblastic tumor,[107] calcifying fibrous tumor,[108,109] malignant vascular tumors that mimic mesothelioma,[110] omental mesenteric myxoid hamartoma,[111] and retroperitoneal ovarian-like mucinous tumors.[112,113]

PSEUDOMYXOMA PERITONEI AND ASSOCIATED APPENDICEAL TUMORS

Background Information

PMP, also colloquially known as "jelly belly," is a descriptive clinical term that refers to the presence of grossly visible aggregates of gelatinous material within the peritoneal cavity. As used here, the term PMP does not apply to cases in which the rupture of a mucinous ovarian tumor results in the presence of mucinous ascites unassociated with gooey peritoneal deposits. In order to understand the pathogenesis of PMP, it is necessary to delve into the pathology of the appendiceal mucinous neoplasms that are the source of the vast majority of cases. This is a controversial topic that has been recently reviewed from different perspectives.[114–117]

I am convinced that the initiating event in most cases of PMP is the rupture of an appendiceal mucinous adenoma, and will make arguments and provide images to bolster this claim. Although many pathologists agree with this position,[118–120] others view the ruptured adenoma concept as flawed, and argue that these appendiceal tumors are actually very well-differentiated adenocarcinomas that invade in a broad-front, pushing pattern that is difficult to recognize.[117,121,122] Whatever the true nature of the appendiceal tumors, all would agree that whenever the pathologist encounters PMP or pseudomyxoma ovarii in an intraoperative setting that it is prudent to inquire about the status of the appendix and to request its removal, even if it appears grossly normal.

Classification of Appendiceal Mucinous Tumors

Before addressing the pathologic features of appendiceal mucinous neoplasms, a discussion of their nomenclature is in order. The terminology recommended herein is a slightly modified version of that espoused by Pai et al.[123] and the portion of this classification system that applies to noninvasive, low-grade mucinous neoplasms of the appendix is presented in Figure 8.96. To begin with, a significant number of these neoplasms (probably more than half in nonconsultation settings) are benign tumors that are confined to the appendix, and these tumors should be labeled "mucinous adenoma" when the strict diagnostic criteria that are outlined in Figure 8.96 are met.[123] In this system, the more nebulous diagnosis of "low-grade mucinous neoplasm" is reserved for those situations in which there is extra-appendiceal spread and some risk for recurrent disease, although others apply this term to mucinous adenomas as well.[124]

When extra-appendiceal mucin is present unaccompanied by neoplastic epithelium, there is a low risk of recurrence (roughly 5%) that is related to the possibility that scant amounts of neoplastic epithelium may go undetected, and this risk is present even when the extra-appendiceal mucin is localized to the periappendiceal region.[123,125] When neoplastic epithelium is identified within the extra-appendiceal mucin, there is a high risk of recurrence (about 40% when localized to the periappendiceal region and much higher when diffusely involving the peritoneal cavity).[123,125] Low-grade mucinous neoplasms with low and high risks of recurrence actually represent ruptured mucinous adenomas with varying proportions of mucus and neoplastic epithelial elements spread to variable degrees and proliferating to variable extents within the peritoneal cavity (see section on pathogenesis of PMP). Since a diagnosis of "ruptured mucinous adenoma" does not accurately reflect the expected clinical course of the disease, the terminology as outlined in Figure 8.96 is preferable, with "ruptured adenoma" relegated to a parenthetical phrase. Note that the presence of extra-appendiceal organizing mucin is sufficient evidence of rupture, whether or not an actual rupture site is identified.

All noninvasive low-grade mucinous neoplasms of the appendix can be placed into one of the three diagnostic categories outlined in Figure 8.96 unless hedge phrases need to be used because the tumor has been incompletely excised or there is a question of stromal invasion. The possibility of stromal invasion should not be raised solely on the basis of the presence of acellular mucin dissecting into the appendiceal wall. For the appendix, there should be no need to use confusing terms such as mucinous borderline tumor,[118] mucinous neoplasm of low malignant potential,[116] and mucinous neoplasm of uncertain malignant potential.[116,122] In fact, many of those who previously advocated one or more of these designations have since abandoned their use,[123,124] and there are more straightforward ways to convey uncertainty about whether or not stromal invasion is present (e.g., low-grade mucinous neoplasm most consistent with adenoma; focal stromal invasion cannot be excluded).

I concur with those who require conventional stromal invasion in order to diagnose invasive appendiceal adenocarcinoma.[123,126] In another approach advocated by some pathologists, an appendiceal mucinous neoplasm can attain the status of an adenocarcinoma by either meeting the usual criteria of stromal invasion or by virtue of its association with gelatinous peritoneal implants that contain viable neoplastic epithelial cells.[122,127] Many pathologists, including myself, object to diagnosing what appears to be an appendiceal mucinous adenoma as an adenocarcinoma solely on the basis of the presence of neoplastic cells within the peritoneum, whose identification is dependent upon the material submitted and the extent to which it is examined, and whose disease course rarely includes typical carcinomatous behavior such as spread to lymph nodes, extension beyond the peritoneal cavity, and destructive

CLASSIFICATION OF NONINVASIVE LOW-GRADE MUCINOUS NEOPLASMS OF THE APPENDIX

Extra-appendiceal mucin absent	**MUCINOUS ADENOMA** • Tumor confined to appendix with negative proximal resection margin • Entire appendix has been examined histologically to exclude high-grade dysplasia, invasion, and extra-appendiceal mucin • "Carry-over" mucin may be present on appendiceal serosa (in this sectioning/processing artifact, the globs of mucin are not associated with a granulation tissue-like response or neovascularization)
Extra-appendiceal mucin present WITHOUT neoplastic epithelium	**LOW-GRADE MUCINOUS NEOPLASM (RUPTURED ADENOMA) WITH LOW RISK OF RECURRENCE** • Examine all submitted extra-appendiceal mucin histologically to exclude presence of neoplastic epithelium • Exclude artifactual "carry-over" mucin
Extra-appendiceal mucin present WITH neoplastic epithelium	**LOW-GRADE MUCINOUS NEOPLASM (RUPTURED ADENOMA) WITH HIGH RISK OF RECURRENCE** • Exclude artifactual "carry-over" mucin • Widespread involvement of peritoneal sites by this process is equivalent to disseminated peritoneal adenomucinosis

FIGURE 8.96. This diagram, which is based upon the classification system of Pai et al., can be used to subdivide those mucinous appendiceal neoplasms with low-grade nuclear features and an absence of invasion into clinically relevant categories (see text). (Pai RK, Beck AH, Norton JA, et al. Appendiceal mucinous neoplasms: clinicopathologic study of 116 cases with analysis of factors predicting recurrence. *Am J Surg Pathol.* 2009;33:1425–1439.)

invasion of visceral organs.[119,123,126,128] Although some pathologists advocate this unique approach to tumor classification as a matter of convenience to indicate the expected course of the disease, the terminology outlined in Figure 8.96 also accomplishes this without resorting to referring to ruptured adenomas as adenocarcinomas, and segregates patients by their risk of recurrence.

Gross Appearance of Appendiceal Mucinous Neoplasms

Mucinous adenomas and mucinous adenocarcinomas often appear macroscopically as a cystically dilated appendix filled with gooey mucus (Figs. 8.97 and 8.98).[124,127] The term "mucocele" is often used to refer to this gross appearance, but it is the underlying cause of the mucocele that needs to be identified and reported as the specific pathologic diagnosis.[116,127] Appendiceal mucoceles are most commonly due to a mucinous adenoma, but may also be associated with mucosal hyperplasia, mucinous adenocarcinoma, or processes that result in luminal obstruction.[116,127] The external surface of the appendix should be carefully examined for the presence of mucus, and measures should be taken not to allow globs of "carry-over" mucus to artifactually adhere to the serosa of the appendix as a result of tissue sectioning and processing.[123] In those cases in which extra-appendiceal mucin is identified, efforts should be made to identify the site of rupture.

Histology of Appendiceal Mucinous Neoplasms

Mucinous Adenomas and their Differential Diagnosis

Appendiceal mucinous adenomas, which when cystically dilated may be referred to as mucinous cystadenomas, are lined by mucinous columnar epithelial cells with hyperchromatic nuclei that feature low-grade atypia, limited stratification, and a low mitotic rate. The epithelial lining may exhibit villous, undulating, flattened, or denuded architectural patterns that may vary from one area to another, with the nonvillous patterns largely related to varying degrees of pressure atrophy (Figs. 8.99 and 8.100).[116,122–124] Long, slender, closely packed villi are commonly seen in appendiceal adenomas, which when prominent may prompt subclassification as a villous adenoma. Loss of the normal complement of mucosal-associated lymphoid tissue is a near-constant feature.[122,123] Immunohistochemically, most appendiceal adenomas express the CK7–/CK20+ immunophenotype that is typical of epithelial neoplasms derived from the lower intestinal tract (Fig. 8.101).[129]

Cribriform architectural patterns and high-grade nuclear atypia (enlarged, vesicular nuclei with prominent nucleoli and brisk mitotic activity) are not features of the usual appendiceal adenoma, and their presence should prompt a careful evaluation to exclude an associated invasive adenocarcinoma. Even if invasion is not identified, the presence of severe dysplasia/

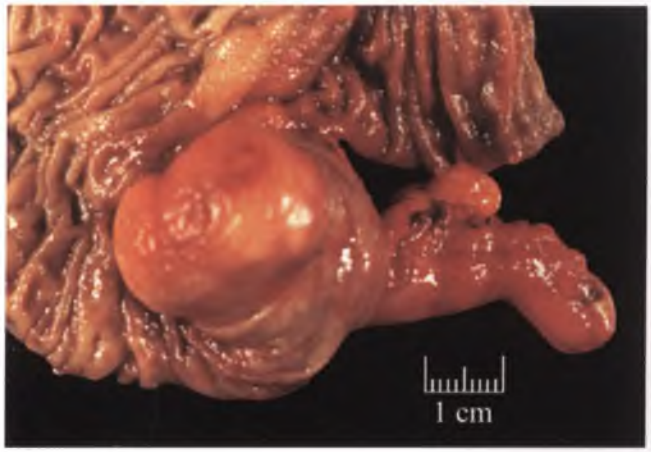

FIGURE 8.97. Mucinous cystadenoma of appendix. Although most of the appendix is only mildly dilated, its proximal portion bulges into the cecum, where it is covered by a thinned layer of cecal mucosa.

intramucosal adenocarcinoma is a potentially ominous sign in appendiceal adenomas, since fully malignant epithelium can spread throughout the peritoneal cavity when these tumors rupture.

The differential diagnosis of appendiceal mucinous adenoma includes mucosal hyperplasia, retention (simple) mucocele, and invasive well-differentiated adenocarcinoma arising within an adenoma. Mucosal hyperplasia is an incidental finding with cytoarchitectural features that are similar to the mucosa of colonic hyperplastic polyps (Fig. 8.102).[127] Localized hyperplastic polyps may also be found in the appendix, and may be difficult to distinguish from serrated adenomas.[116] Retention mucoceles secondary to luminal obstruction are an uncommon cause of appendiceal mucocele,[122] and should be extensively sampled to

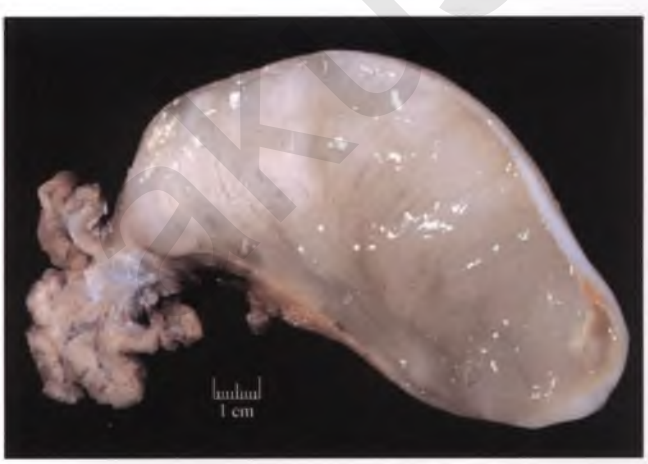

FIGURE 8.98. Mucinous cystadenoma of appendix. This longitudinal section demonstrates that the appendix is distended and filled with mucinous material (the so-called mucocele). At left is the sectioned surface of a neighboring villous adenoma of the cecum. (Courtesy of Dr. Enrique Higa.)

FIGURE 8.99. Mucinous cystadenoma of appendix. In areas unaffected by pressure atrophy, the neoplastic cells often form delicate villous structures. The tumor cells have abundant mucinous cytoplasm and basally located, elongated, hyperchromatic nuclei oriented parallel to one another.

exclude the possibility of a mucinous cystadenoma with extensive flattening or denudation of its epithelial lining related to pressure atrophy. As discussed below, the distinction of adenoma from invasive adenocarcinoma can be difficult and depends largely on the criteria that are used to identify stromal invasion.

Invasive Mucinous Adenocarcinomas

Primary appendiceal signet-ring carcinomas are not a focus of this discussion, since their pattern of invasion is generally easily recognized. In appendiceal mucinous adenocarcinomas of the non–signet-ring type, true stromal invasion is characterized

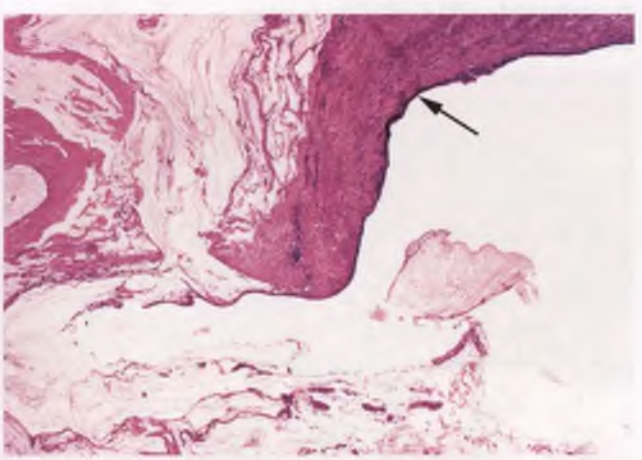

FIGURE 8.100. Low-grade mucinous neoplasm (ruptured adenoma) of appendix associated with PMP. In this example, pressure atrophy from intraluminal accumulation of mucinous contents has resulted in a tumor with a simple epithelial lining (*arrow*). The appendix eventually ruptured, releasing mucinous material and clusters of tumor cells into the peritoneal cavity.

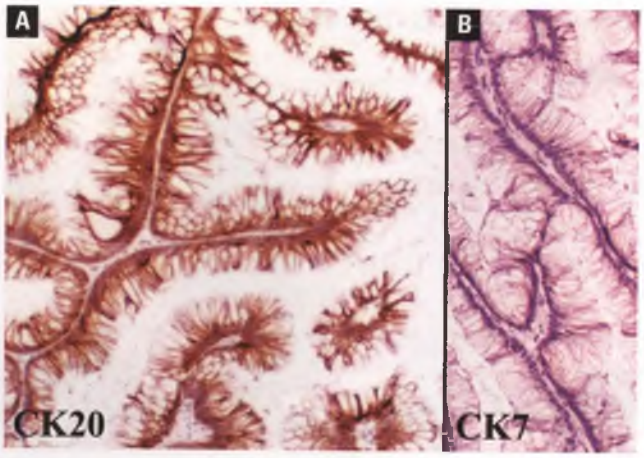

FIGURE 8.101. Mucinous cystadenoma of appendix. These tumors are typically diffusely immunoreactive for CK20 **(A)** and fail to express CK7 **(B)**. Note the inordinately tall, hypermucinous epithelium, which is commonly present in these neoplasms and can serve as a clue to the organ of origin when found in the peritoneum or ovary.

by either pools of mucin dissecting into the appendiceal wall in association with clusters and strips of neoplastic mucinous epithelium (Fig. 8.103) or the haphazard infiltration beneath the muscularis mucosa of small glands with appreciable mucinous differentiation that are often associated with desmoplastic stroma (Fig. 8.104).[123,124] These tumors may exhibit either low-grade or high-grade nuclear features.[123] I am not a proponent of the concept of broad-front invasion by adenomatous, well-differentiated mucinous epithelium that invades by pushing deeply into the appendiceal wall,[117] and would interpret nearly all such cases as mucinous adenomas extending into diverticular spaces or other weak spots in the wall as a consequence of increased intraluminal pressure (or when focal and superficial, as attributable to tangential sectioning).

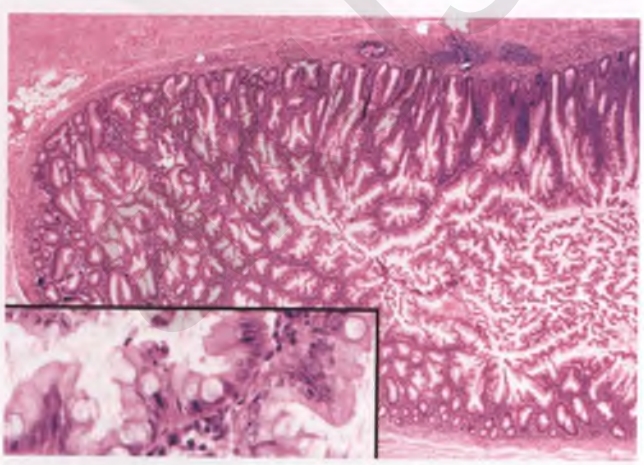

FIGURE 8.102. Mucosal hyperplasia of appendix. Unlike mucinous cystadenomas, this hyperplastic process resembles the common hyperplastic polyp of the large intestine, with repetitive intraluminal papillary infoldings creating serrated luminal profiles.

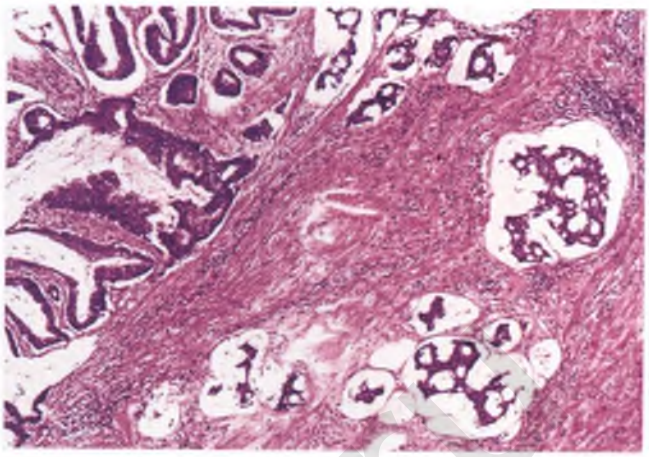

FIGURE 8.103. Invasive mucinous adenocarcinoma of appendix. The irregular chains of neoplastic epithelium that are floating within pools of mucin within the muscularis propria represent invasive adenocarcinoma. (Courtesy of Dr. Enrique Higa.)

Pathogenesis of Pseudomyxoma Peritonei

In most cases of PMP, the rupture of an appendiceal mucinous adenoma is the initiating event. A minority of cases of PMP are caused by invasive mucinous adenocarcinomas, the vast majority of which are of appendiceal or colorectal origin.[119,126]

The observation that rupture of an appendiceal mucinous adenoma may not be demonstrable in a variable proportion of cases associated with PMP can be explained on the basis of one or more of the following: (a) gross evidence of rupture may be subtle or inapparent, and may only be found after histologic examination of multiple sections, (b) following rupture, the appendix may be encased in mucinous material and fibrous adhesions, masking the rupture site and/or severely distorting the appendiceal anatomy, (c) following rupture and decompression of the appendiceal lumen, the healing process may result in resealing of the perforation site, (d) mucin and associated tumor cells may

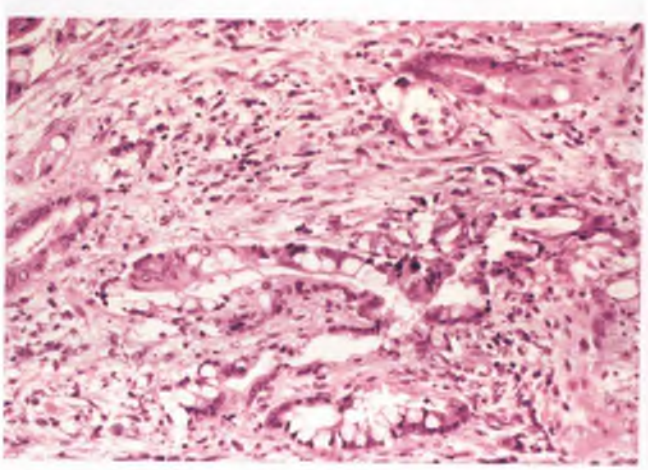

FIGURE 8.104. Invasive mucinous adenocarcinoma of appendix. Infiltrating mucin-rich glands are embedded within a desmoplastic stroma.

gradually dissect through the wall of the appendix without a dramatic burst of the appendiceal wall, and (e) most reports in the literature rely heavily upon consultation material and/or retrospective reviews in which the investigating pathologists have no control over the gross evaluation or sampling of the appendix, which no doubt results in some appendiceal ruptures going undetected.[118–120]

Favored sites for diverticular outpouchings and eventual rupture of appendiceal mucinous cystadenomas whose contents are under pressure due to the gradual accumulation of mucus are the points at which the muscularis propria has been penetrated by vessels (Figs. 8.105 and 8.106), analogous to what is seen in colonic diverticula.[130] Whereas appendiceal diverticula can thus form in association with an appendiceal adenoma, pathologists need to be aware that nonneoplastic appendiceal diverticula also occur, which when ruptured can simulate a ruptured mucinous adenoma.[128]

It appears that nearly all cases of PMP are caused by intestinal-type mucinous epithelial cells that express the gel-forming mucin MUC2, which is a mucin that is generally absent to only focally present in typical primary ovarian mucinous tumors.[131] Perhaps the presence of a different type of mucin (MUC5AC) in usual primary ovarian mucinous tumors,[131] coupled with absent to low levels of MUC2, accounts for the finding that benign and borderline mucinous ovarian tumors, even when ruptured, are rarely associated with PMP.[132,133] The only well-documented cases of primary ovarian mucinous tumors that cause classic PMP with identifiable neoplastic epithelial cells are a subset of those that occur in association with mature cystic teratomas.[134–136] Interestingly, this particular subset of primary ovarian mucinous tumors (a) has typically ruptured, (b) is strongly associated with pseudomyxoma ovarii, and (c) has been shown to most commonly express the lower gastrointestinal CK7–/CK20+ immunophenotype and to be strongly immunoreactive for MUC2, just like most PMP-associated appendiceal mucinous neoplasms.[134,136]

Gross Appearance of Pseudomyxoma Peritonei[115]

PMP typically forms gelatinous masses within the peritoneal cavity that on sectioning may appear translucent, pale yellow, gray, or tan. These masses may coat or encase pelvic and abdominal structures, and the omentum is often thickened from extensive involvement (Fig. 8.107). The ovarian tumors that are formed as a consequence of involvement by low-grade mucinous neoplasms of the appendix, which for many years were frequently misdiagnosed as benign or borderline primary ovarian mucinous tumors, are discussed in Chapter 7. Although the low-grade form of PMP rarely involves the parenchyma of organs other than the ovary, splenic involvement can occur and most commonly is manifested as a cystic mucinous mass that displaces splenic tissue (Fig. 8.108).[137]

Histology of Pseudomyxoma Peritonei[115,120]

PMP is dominated histologically by organizing pools of mucin that are separated by bands of fibrous connective tissue that contain patches of chronic inflammatory cells. Within the mucin pools are strands of fibroblastic tissue and recently formed vessels, which serve as evidence of organization and help to distinguish true PMP from mucin related to "carry-over" artifact from intraluminal appendiceal contents.

When evaluating samples of PMP, it is important to document the presence or absence of neoplastic epithelium,

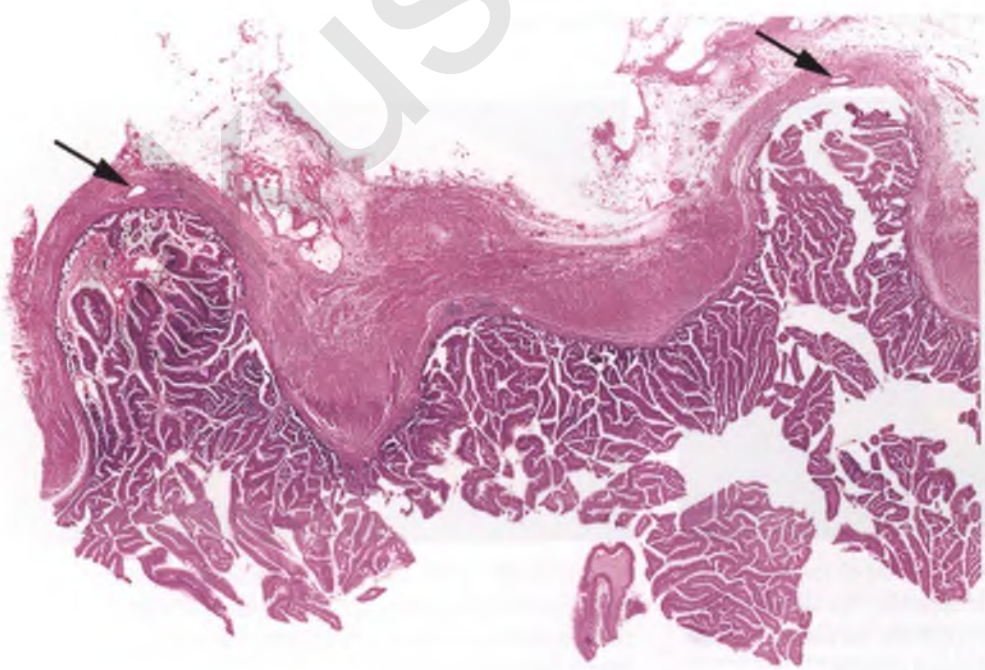

FIGURE 8.105. Mucinous cystadenoma of appendix. This low-magnification view of a longitudinal section through the appendix reveals outpouching of adenomatous epithelium into two diverticula. These diverticula occur at points of weakness within the wall, which correspond to points of vessel entry (*arrows* mark vessels at the diverticular tips).

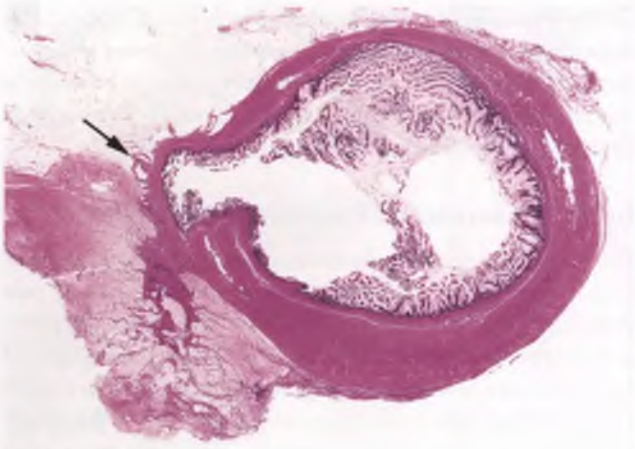

FIGURE 8.106. Low-grade mucinous neoplasm (ruptured adenoma) of appendix. This cross section also demonstrates an outpouching of adenomatous epithelium into a diverticulum at a point of vessel entry (*arrow*). In this case, there is diverticular rupture just out of the plane of section, which has resulted in the accumulation of periappendiceal mucinous material at lower left.

estimate its relative abundance when present, and note whether the degree of nuclear atypia is low grade or high grade. In the typical case of PMP, neoplastic mucin-producing epithelium is present but sparsely distributed, low grade, and found as strips partially lining or clusters floating within the pools of mucin (Figs. 8.109 and 8.110). Cases of PMP with high-grade nuclear atypia and/or mucinous adenocarcinoma with aggressive patterns of infiltration usually feature easily detectible malignant glands and/or signet-ring cells floating within pools of mucin (Fig. 8.111), and often exhibiting destructive patterns of invasion and lymph node metastases.[119] A destructive pattern of stromal invasion is not seen in the typical low-grade form of PMP, even when organs such as the ovary and spleen are involved.[115,137] The peritoneal metastases that are derived from invasive well-differentiated mucinous adenocarcinomas of the appendix often have histologic features that overlap with those produced by ruptured appendiceal adenomas, although thorough sampling will reveal at least focal carcinomatous differentiation.[119,121]

Given the prognostic significance of the presence or absence of neoplastic epithelial cells within peritoneal mucinous deposits, histologic sections of submitted material of this type should be examined until several sections that contain neoplastic epithelial cells have been reviewed or until all such material has been examined microscopically. Small strips and clusters of neoplastic epithelium are usually evident in routinely stained sections. However, for those appendiceal tumors with proven diffuse CK20 positivity, CK20 can also be utilized to identify or confirm the presence of scant epithelial elements derived from appendiceal mucinous tumors within large pools of mucin (Fig. 8.112). MUC2 and CDX2 can also be used for this purpose, although most laboratories do not stock antibodies against these markers of intestinal differentiation.

Diagnostic Terminology Utilized to Indicate Involvement by Pseudomyxoma Peritonei

There is general agreement that the pathologist should not use the clinically descriptive term PMP as a specific standalone pathologic diagnosis. However, the controversy regarding the terminology for appendiceal mucinous neoplasms is interwoven with any proposed classification system for PMP.[114,117,119] The best terminology should accurately reflect the pathogenesis of the disease and give an accurate indication as to the expected clinical course. For the most common appendiceal-related

FIGURE 8.107. PMP secondary to involvement by low-grade mucinous neoplasm (ruptured adenoma) of appendix. This section through an extensively involved omentum demonstrates the presence of multiple locules filled with glistening gelatinous material.

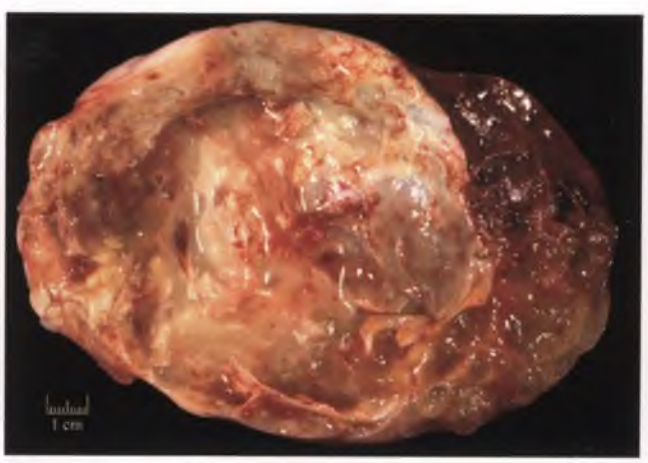

FIGURE 8.108. PMP with splenic involvement secondary to low-grade mucinous neoplasm (ruptured adenoma) of appendix. The sectioned surface is dominated by a large mucinous cyst. Normal residual splenic tissue is at upper right.

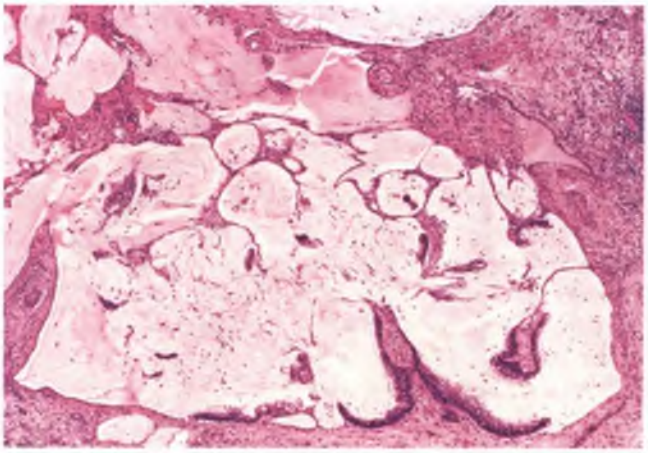

FIGURE 8.109. PMP secondary to involvement by low-grade mucinous neoplasm (ruptured adenoma) of appendix. Isolated strips and clusters of mucinous epithelium are suspended within mucinous material in addition to partially enveloping the mucin pools. Fibrous tissue, portions of which are chronically inflamed, course in between the aggregates of mucin.

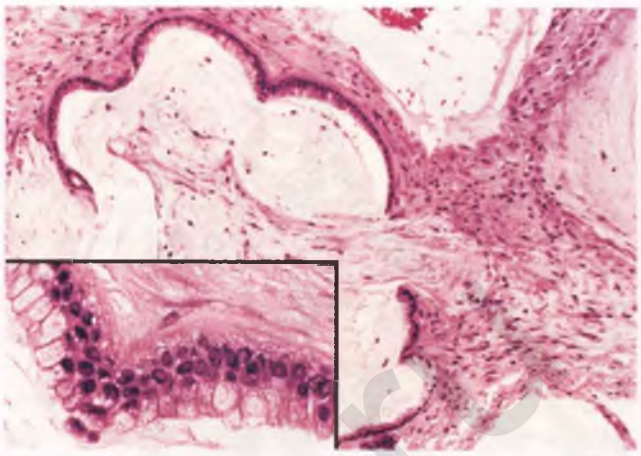

FIGURE 8.110. PMP secondary to involvement by low-grade mucinous neoplasm (ruptured adenoma) of appendix. This area features small pools of mucin, some of which are incompletely encircled by strips of mucinous epithelium. The highlights the bland nuclear features and abundant mucinous cytoplasm of the neoplastic cells.

situation conforming to classic PMP, it is recommended that sites of involvement be reported as "involved by low-grade mucinous neoplasm (ruptured adenoma) of appendiceal origin; neoplastic epithelial cells identified." When multiple peritoneal biopsies need to be itemized in the diagnosis, reporting for each site should list whether or not neoplastic epithelial cells are identified in that site. However, since the patient is at high risk of recurrence if any one of these biopsies contains neoplastic epithelial cells, the low-risk versus high-risk nature of *individual* sites should not be reported to avoid confusion. The diagnosis of the appendix should summarize the risk of recurrence based on the overall findings in the peritoneum, and it may also be helpful to include a comment such as "This is the most common and classic form of PMP that is associated with a high risk of recurrence and a 10-year survival of approximately 50%."

When multiple peritoneal sites are involved by an appendiceal low-grade mucinous neoplasm with high risk of recurrence, the disease process is equivalent to what has been referred to as disseminated peritoneal adenomucinosis (DPAM).[119,138] The DPAM terminology has been met with significant resistance both from those who agree that these lesions are derived from ruptured mucinous adenomas[115,123,124] and from those who consider any extra-appendiceal spread of tumor with identifiable neoplastic epithelial cells to be definitional of a primary appendiceal carcinoma with peritoneal metastases.[117,121] From my perspective, the major disadvantage of using DPAM as a pathologic diagnosis is that it does not convey the nature of the disease and the risk of recurrence to those who have not been specifically educated in the use of this terminology. I also do not favor branding all of the typical cases of PMP with identifiable neoplastic epithelial cells as metastatic mucinous adenocarcinoma or low-grade mucinous carcinoma peritonei,[117,121] since this does not reflect my view of the pathogenesis of the disease.

About 30% of cases of PMP are due to metastases of high-grade or signet-ring mucinous adenocarcinomas of appendiceal or intestinal origin.[119] In this situation, sites of involvement can simply be reported as metastatic mucinous adenocarcinoma, with a note indicating their frankly carcinomatous appearance and the expected aggressive clinical course. In other classification systems, these lesions are referred to as peritoneal mucinous carcinomatosis[119] or high-grade mucinous carcinoma peritonei.[121]

Occasionally, PMP associated with the fully malignant form of metastatic mucinous adenocarcinoma is derived from a ruptured appendiceal mucinous adenoma with foci of high grade dysplasia/intramucosal adenocarcinoma.[124] Although some of these cases with malignant behavior may actually be undersampled invasive adenocarcinomas, it is likely that most represent ruptured adenomas with high-grade dysplasia/intramucosal adenocarcinoma whose implantation on the peritoneum has resulted in spread of an aggressive adenocarcinoma that is both histologically and clinically worthy of the designation of involvement by mucinous adenocarcinoma.[124]

A small percentage of cases of PMP are due to metastases from invasive well-differentiated appendiceal adenocarcinomas with mucinous differentiation.[119,121,123] The inclusion criteria and whether their behavior more closely approximates that of typical low-grade PMP or those cases due to full-fledged mucinous adenocarcinoma, or somewhere in between, are controversial.[119,121,123] My preference is to report a case of this type as metastatic well-differentiated mucinous adenocarcinoma, indicate the high risk of recurrence, and suggest that over a 10-year period that the patient will likely fare worse than those with the usual type of low-grade PMP.

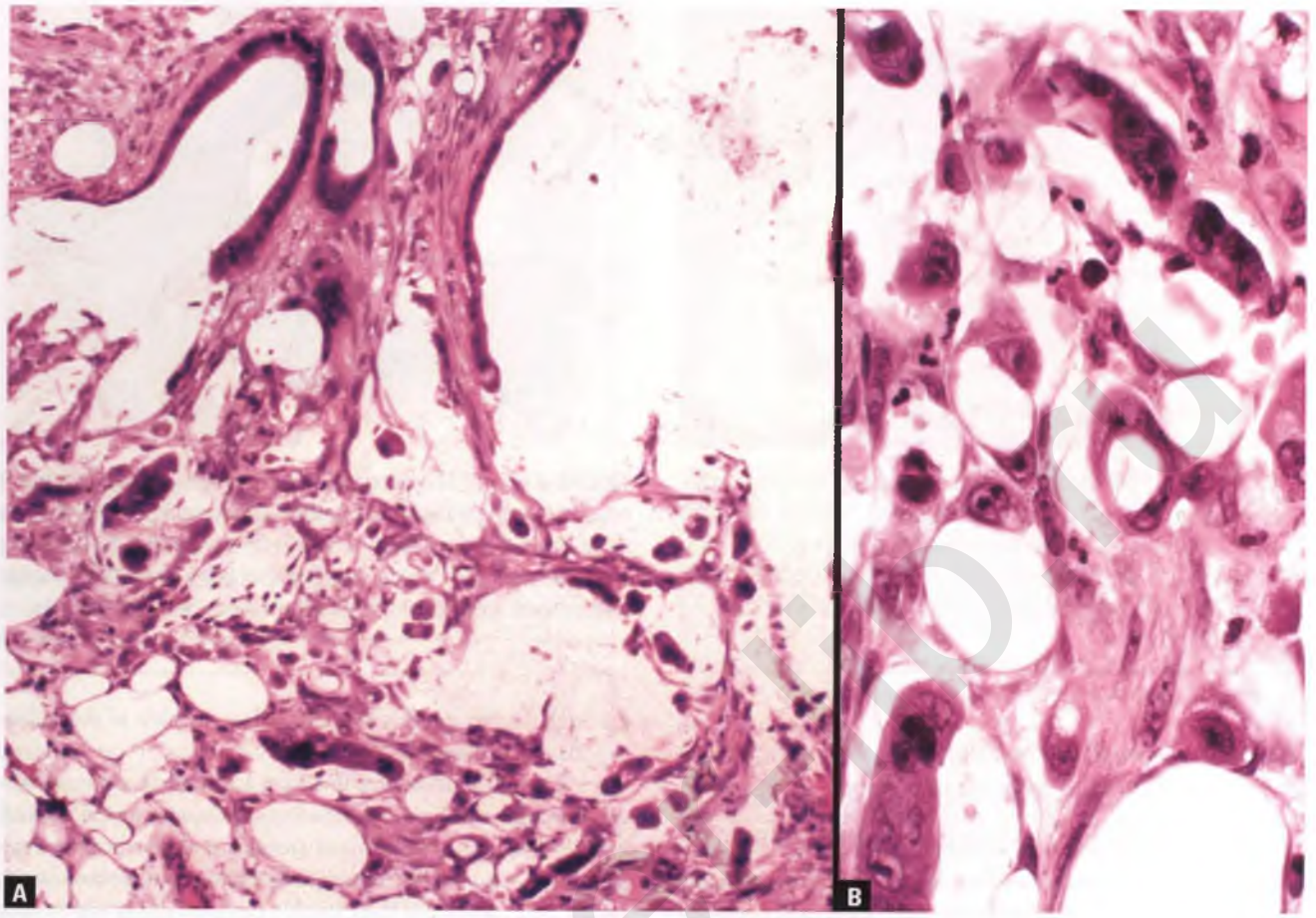

FIGURE 8.111. PMP of omentum secondary to an aggressive metastatic mucinous adenocarcinoma. **A:** Although a portion of the tumor is indistinguishable from the usual type of low-grade PMP (incomplete cystic glands at upper left), there is also ragged infiltration by mucin-producing cells with high-grade nuclear features. **B:** This high-magnification view highlights an area of full-fledged mucinous adenocarcinoma.

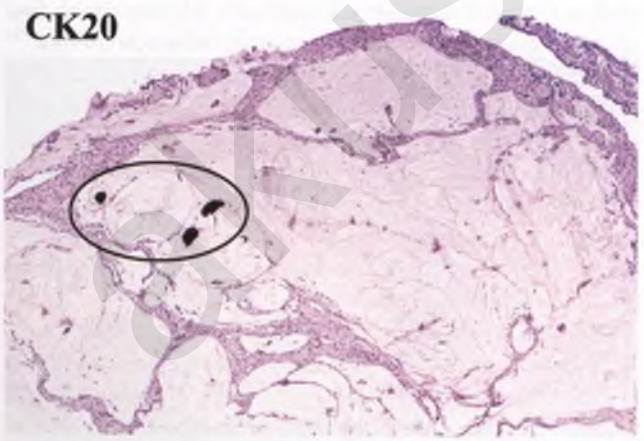

FIGURE 8.112. Pseudomyxomatous deposit secondary to involvement by low-grade mucinous neoplasm (ruptured adenoma) of appendix. This CK20 immunostain highlights the presence of three small clusters of neoplastic epithelium (*circled*) that are floating within large pools of mucin. In contrast to pan-cytokeratin, CK20 stains the cells of interest and does not react with mesothelial cells.

Reporting of peritoneal disease in those rare cases of PMP that are associated with a combined mucinous neoplasm/teratoma of the ovary should reflect the limited knowledge of the prognostic significance of its various forms (see below).

Differential Diagnosis of Pseudomyxoma Peritonei

Spillage of lightly concentrated mucinous fluid into the peritoneal cavity due to the rupture of an ovarian mucinous tumor prior to the operative procedure should not be classified as PMP. In these cases, the distinctive gelatinous masses of PMP are absent, there is superficial organization of the adherent mucin that is limited to the peritoneal surfaces, the mucinous ascites rarely contains neoplastic epithelial cells, and disease progression is very uncommon.[115] Many of the cases reported as PMP associated with combined mucinous/teratomatous ovarian tumors appear to fall into this category.[133,136,139]

Prognostic Significance of Different Forms of Pseudomyxoma Peritonei

The much improved prognosis of those patients whose gelatinous peritoneal deposits have undetectable amounts of associated neoplastic epithelium is better documented for those cases in which peritoneal involvement is limited to the periappendiceal region, but appears to apply to widespread disease as well.[118,123,125,127] Patients with PMP with these features should be designated as having a low risk of recurrence.[123] However, most cases of PMP, including the vast majority of those with disease that has spread throughout the abdomen, contain recognizable strips and clusters of low-grade mucinous epithelium that are associated with a high risk of recurrence.[119,123] When optimally debulked, PMP with these histologic features is an indolent and slowly progressive disease with 5- and 10-year survival rates of about 75% to 85% and 45% to 65%, respectively.[123,124,138] Recurrences in these patients are almost always confined to the peritoneal surface, with morbidity and mortality related to the reaccumulation of gelatinous material and the formation of adhesions that produce small bowel obstructions.[138]

In sharp contrast with patients with the typical low-grade form of PMP, those with frankly carcinomatous mucinous neoplasms that produce copious amounts of extracellular mucin pursue a much more aggressive clinical course. These patients have 5- and 10-year survival rates of roughly 15% to 40% and 5%, respectively, and do not benefit from an aggressive surgical approach.[123,124,138] Controversies related to the existence of an intermediate category that bridges the gap between the low-grade form of PMP and aggressive forms of metastatic mucinous adenocarcinoma have been discussed previously.

Very little data are available on the long-term prognosis of patients whose PMP is related to a primary ovarian mucinous neoplasm that is associated with a mature cystic teratoma. It is clear that those patients whose peritoneal disease has the appearance of full-fledged mucinous adenocarcinoma have a poor prognosis, and it appears that recurrence is very unlikely in those patients whose peritoneal disease is due to a low-grade mucinous ovarian neoplasm with benign or borderline histology when no detectable neoplastic epithelial cells are found in the extraovarian mucinous deposits.[135,136] Many of the latter patients may simply have organizing mucinous ascites, as described in the section on the differential diagnosis of PMP.[133] Currently, there is insufficient information to estimate the long-term recurrence rate of those patients whose peritoneal deposits contain low-grade mucinous epithelium. Preliminary data suggest that these patients may be less likely to recur than similar patients with appendiceal primary tumors.[135,136]

GLIOMATOSIS PERITONEI

Gliomatosis peritonei is discussed within the context of ovarian immature teratomas in Chapter 7.

METASTATIC CARCINOMA

Most metastatic carcinomas within the peritoneal cavity stud the serosal surface (Fig. 8.113), may form an omental cake as shown in Figure 8.60, and are easy to diagnose. The most common source in women is ovarian carcinoma, which is usually of serous type. This section focuses on a pattern of metastatic carcinoma that can pose diagnostic difficulty, along with the cytologic features of metastatic adenocarcinoma and its differential diagnosis. Since most cases of PMP are not considered metastatic carcinoma in the true sense, this entity is discussed in a separate section.

Histologically, the most deceptive form of metastatic carcinoma with peritoneal spread consists of widely scattered malignant cells and/or minute aggregates of small glands within a background that otherwise mimics sclerosing peritonitis (Fig. 8.114). Metastatic signet-ring carcinoma, usually of gastric origin, is prone to this type of behavior, and can be particularly difficult to diagnose in frozen section material. In this situation, knowledge of the clinical history is important, and recognition at scanning magnification of the pools of extracellular mucin that may accompany metastatic signet-ring carcinoma can serve as a clue to the correct diagnosis.

Cytologic Features of Metastatic Adenocarcinoma in Peritoneal Fluid[1]

The vast majority of metastatic tumors that produce ascites are adenocarcinomas. In the most common situation, the diagnosis in cytologic preparations is straightforward, with an obviously foreign population of tumor cells forming cell balls and/or papillae that clearly stand out at low magnification (Figs. 8.115 and 8.116). Papillae in ascitic fluids are most often seen in metastatic adenocarcinoma of ovarian or endometrial origin, but may also be seen in (a) metastatic adenocarcinomas from other sites, such as the breast and lung, (b) a spectrum of mesothelial lesions ranging from hyperplastic to malignant, and (c) washings from benign and borderline serous ovarian tumors. The

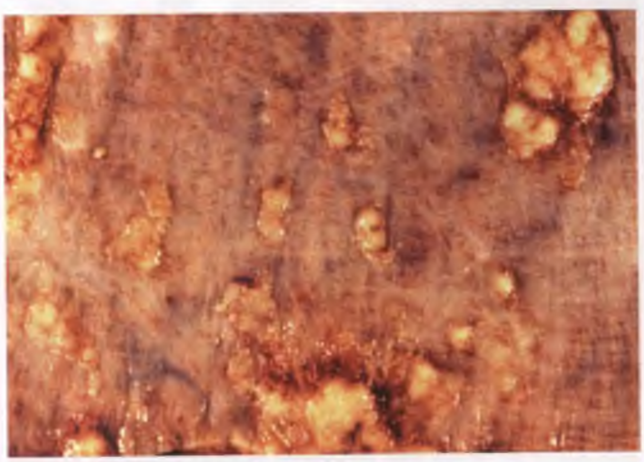

FIGURE 8.113. Multiple nodules of metastatic ovarian carcinoma measuring up to 1 cm stud the peritoneal surface of the diaphragm in this autopsy specimen.

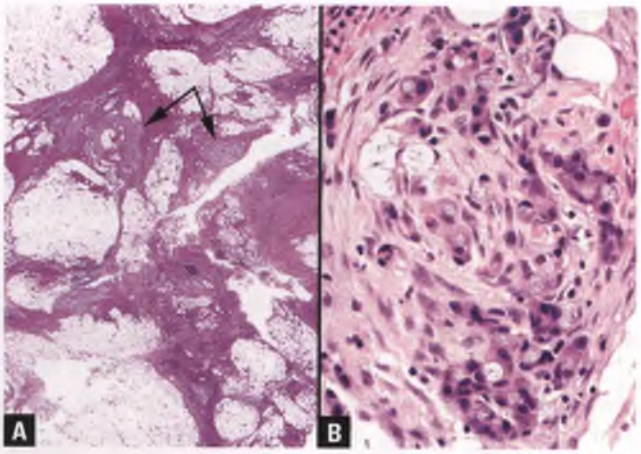

FIGURE 8.114. Omental involvement by metastatic mucin-producing adenocarcinoma with a signet-ring component. **A:** At low magnification, this process has an appearance similar to sclerosing peritonitis. However, recognition of scattered pools of extracellular mucin, which appear as islands of *grainy blue* material in this preparation, facilitates correct interpretation (representative mucin pools are marked by *arrows*). **B:** This field depicts the most cellular focus of metastatic adenocarcinoma identified in this sample.

cell balls and papillae of metastatic adenocarcinoma typically have smooth "community" borders and are three-dimensional, with different parts of the cell clusters being in focus at different focal planes.

The tumor cells in cytologic preparations of metastatic adenocarcinoma usually have pleomorphic, eccentric nuclei, and delicate cytoplasm. However, malignant nuclear features may be subtle, particularly in cases of metastatic breast carcinoma (Fig. 8.117). Cytoplasmic vacuoles are often present

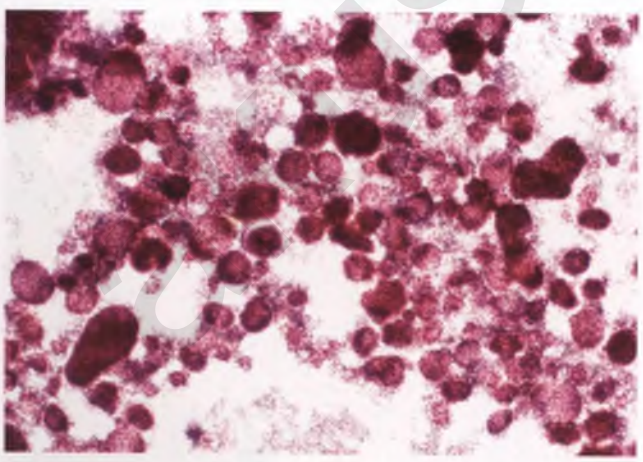

FIGURE 8.115. Metastatic adenocarcinoma of breast origin. Several sharply demarcated aggregates of tumor cells with smooth community borders are present. In a patient with a history of breast carcinoma, the diagnosis of malignancy can be made with confidence based upon the low-magnification "cannonball" pattern.

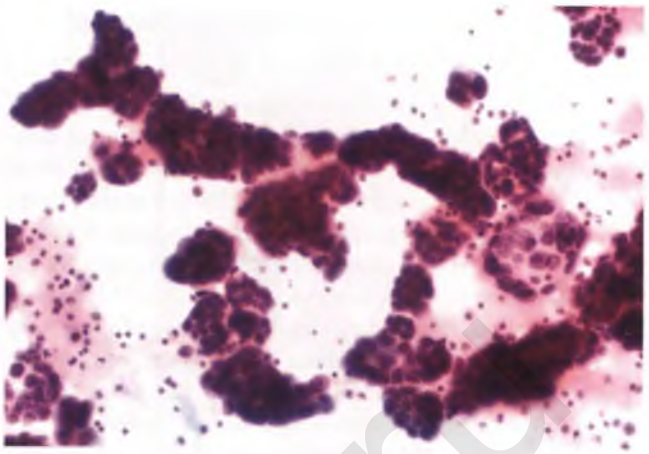

FIGURE 8.116. Metastatic adenocarcinoma. In this example of ovarian origin, aggregates of tumor cells with micropapillary shapes are present.

within malignant epithelial cells, which may represent either intracytoplasmic neutral mucin or nonspecific degenerative vacuoles (Fig. 8.118). Although psammoma bodies are most often present in cytologic preparations that contain cells derived from ovarian serous tumors, they can also be found in other entities such as mesothelioma.

The occasional examples of malignant ascites in which single tumor cells predominate or are the sole epithelial element, such as in the mesothelioid or histiocytoid patterns of metastatic infiltrating lobular carcinoma of the breast, can be extremely difficult to diagnose (Fig. 8.119). In such cases, close attention to the nuclear features, the identification of targetoid secretory vacuoles, and utilization of cell block material for mucin and immunohistochemical stains facilitate recognition of this subtle form of malignancy. Another example of metastatic adenocarcinoma with a single cell pattern is shown at higher magnification in Figure 8.120.

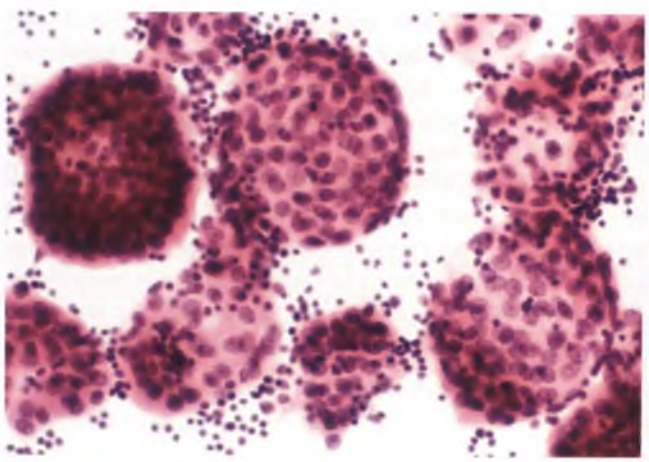

FIGURE 8.117. Metastatic adenocarcinoma of breast origin. The nuclear features of some metastatic adenocarcinomas, particularly those of breast origin, can be deceptively bland and uniform.

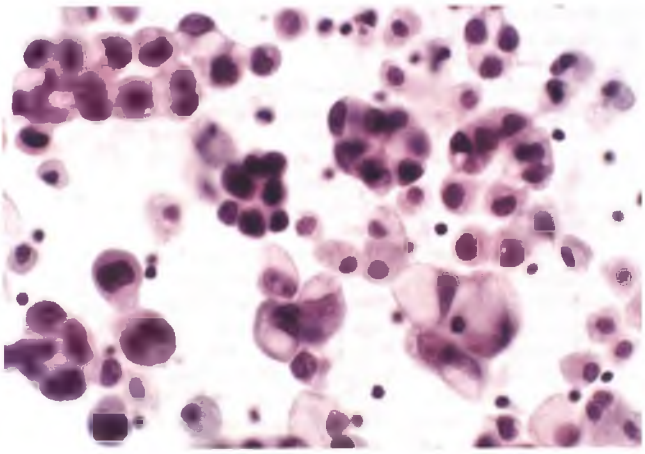

FIGURE 8.118. Metastatic adenocarcinoma. Several of the tumor cells contain intracytoplasmic degenerative vacuoles. Note how the pleomorphic tumor cells dwarf the nonneoplastic cells in the background.

Differential Diagnosis

Once a peritoneal fluid has been determined to contain malignant cells, the most common differential diagnostic difficulty is distinguishing metastatic adenocarcinoma from malignant mesothelioma. Clinicopathologic correlation is often of substantial help in this regard, such as when the patient has a history of ovarian carcinoma. Cytologically, metastatic adenocarcinoma is typically recognized by its foreign population of cells with pleomorphic, eccentric nuclei and delicate cytoplasm forming three-dimensional cell balls and/or papillae with smooth community borders, which contrasts with the classic malignant mesothelioma that is characterized by a spectrum of mesothelial cells with less pleomorphic, central nuclei and dense cytoplasm that form three-dimensional cell balls and/or papillae with knobby contours and intercellular windows (unfortunately, there are exceptions to these generalizations). In this setting, the identification of neutral mucin within intracytoplasmic vacuoles of the tumor cells with a mucicarmine or PAS with diastase stain strongly favors metastatic adenocarcinoma. When deemed necessary, immunohistochemical studies as outlined in the section on malignant mesothelioma can also be performed on cell block material to facilitate the distinction between metastatic adenocarcinoma and malignant mesothelioma.

Reactive mesothelial cells can also be confused with metastatic adenocarcinoma. However, these reactive cells lack frankly malignant nuclear features, and their recognition is further facilitated by the absence of a foreign population of cells and evidence of mesothelial differentiation (dense cytoplasm, central nuclei, knobby contours, and intercellular windows). In addition, clusters of reactive mesothelial cells in fluid samples tend to be monolayered, with all cells in focus within one plane, whereas clusters of metastatic adenocarcinoma usually have a three-dimensional appearance. The degenerative vacuoles that are commonly seen in reactive mesothelial cells may displace the nuclei into an eccentric position, resulting in a resemblance to the signet-ring cells of metastatic adenocarcinoma. In contrast to the latter, the degenerative vacuoles in reactive mesothelial cells do not contain the neutral mucins that are detectable with the mucicarmine and PAS with diastase stains. Clinical correlation can be very helpful, and it is worth noting that metastatic carcinoma is unlikely in fluids that are transudates rather than exudates and in those that contain marked inflammation. In difficult cases, support for mesothelial differentiation can also be obtained immunohistochemically.

In cytologic preparations of peritoneal washings, it is usually not possible to distinguish malignant cells at the lower

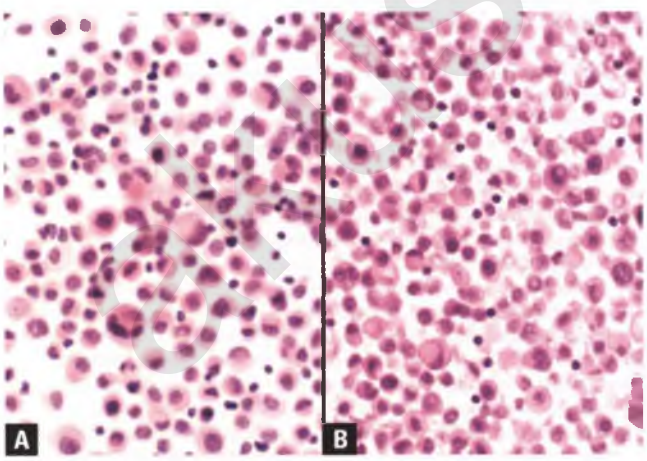

FIGURE 8.119. Metastatic adenocarcinoma originating from infiltrating lobular carcinoma of the breast. **A:** The tumor cells are present as relatively bland individual cells rather than cell clusters. **B:** Histologic section of corresponding cell block preparation. In both images, the presence of eosinophilic targetoid secretions within the cytoplasm of some of the tumor cells facilitates their distinction from reactive mesothelial cells.

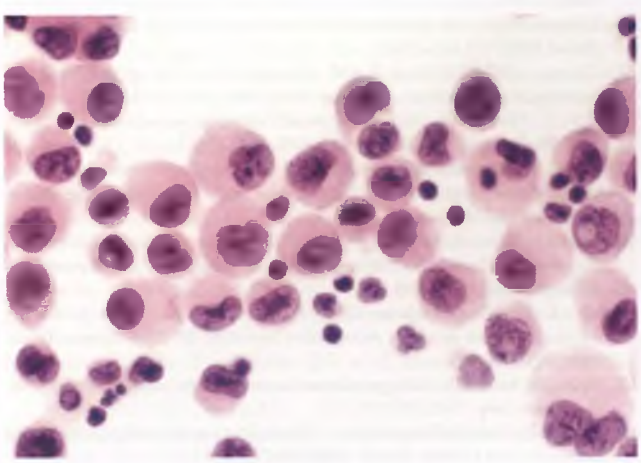

FIGURE 8.120. Metastatic adenocarcinoma, single cell pattern. The nuclear abnormalities are diagnostic of malignancy, and the eccentrically located nuclei and delicate cytoplasm support adenocarcinomatous differentiation.

end of the spectrum of low-grade serous carcinoma from cells derived from serous borderline tumor, exophytic serous adenofibroma, and endosalpingiosis (see Fig. 7.6). Ciliated cells can be seen in any of the latter three processes, and the presence of psammoma bodies is further supportive of serous differentiation. When a cytologic sample is encountered that spans the spectrum from endosalpingiosis to a low-grade malignant serous neoplasm, it is prudent to delay issuing a final diagnosis until this material can be correlated with tissue from the pelvic source of these cells.

SUGGESTED READINGS

Clement PB, Young RH. *Atlas of Gynecologic Surgical Pathology*. 2nd ed. Philadelphia, PA: Elsevier Saunders; 2008.

Crum CP, Nucci, MR, Lee, K, eds. *Diagnostic Gynecologic and Obstetric Pathology*. 2nd ed. Philadelphia, PA: Elsevier Saunders; 2011.

DeMay RM. *The Art and Science of Cytopathology*. Chicago, IL: ASCP Press; 1996:257–325.

Kurman RJ, Ellenson LH, Ronnett BM, eds. *Blaustein's Pathology of the Female Genital Tract*. 6th ed. New York, NY: Springer;2011.

Robboy SJ, Mutter GL, Prat J, et al., eds. *Robboy's Pathology of the Female Reproductive Tract*. 2nd ed. Oxford, UK: Churchill Livingstone; 2009.

REFERENCES

1. DeMay RM. *The Art and Science of Cytopathology*. Chicago, IL: ASCP Press; 1996:257–325.
2. Ordonez NG, Ro JY, Ayala AG. Lesions described as nodular mesothelial hyperplasia are primarily composed of histiocytes. *Am J Surg Pathol*. 1998;22:285–292.
3. Rosai J, Dehner LP. Nodular mesothelial hyperplasia in hernia sacs: a benign reactive condition simulating a neoplastic process. *Cancer*. 1975;35:165–175.
4. Clement PB, Young RH. Florid mesothelial hyperplasia associated with ovarian tumors: a potential source of error in tumor diagnosis and staging. *Int J Gynecol Pathol*. 1993;12:51–58.
5. Clement PB, Young RH, Hanna W, et al. Sclerosing peritonitis associated with luteinized thecomas of the ovary. A clinicopathological analysis of six cases. *Am J Surg Pathol*. 1994;18:1–13.
6. Staats PN, McCluggage WG, Clement PB, et al. Luteinized thecomas (thecomatosis) of the type typically associated with sclerosing peritonitis: a clinical, histopathologic, and immunohistochemical analysis of 27 cases. *Am J Surg Pathol*. 2008;32:1273–1290.
7. Churg A, Colby TV, Cagle P, et al. The separation of benign and malignant mesothelial proliferations. *Am J Surg Pathol*. 2000;24:1183–1200.
8. Kelly JK, Hwang WS. Idiopathic retractile (sclerosing) mesenteritis and its differential diagnosis. *Am J Surg Pathol*. 1989;13:513–521.
9. Emory TS, Monihan JM, Carr NJ, et al. Sclerosing mesenteritis, mesenteric panniculitis and mesenteric lipodystrophy: a single entity? *Am J Surg Pathol*. 1997;21:392–398.
10. Demir K, Okten A, Kaymakoglu S, et al. Tuberculous peritonitis—reports of 26 cases, detailing diagnostic and therapeutic problems. *Eur J Gastroenterol Hepatol*. 2001;13:581–585.
11. Koc S, Beydilli G, Tulunay G, et al. Peritoneal tuberculosis mimicking advanced ovarian cancer: a retrospective review of 22 cases. *Gynecol Oncol*. 2006;103:565–569.
12. Ross WB, Lubitz JM. Talc granuloma—a survey of its incidence and significance. *Ann Surg*. 1949;130:100–112.
13. Kirshen EJ, Naftolin F, Benirschke K. Starch glove powders and granulomatous peritonitis. *Am J Obstet Gynecol*. 1974;118:799–804.
14. Tatum ET, Beattie JF Jr, Bryson K. Postoperative carbon pigment granuloma: a report of eight cases involving the ovary. *Hum Pathol*. 1996;27:1008–1011.
15. Clarke TJ, Simpson RH. Necrotizing granulomas of peritoneum following diathermy ablation of endometriosis. *Histopathology*. 1990;16:400–402.
16. Reid PC, Thurrell W, Smith JH, et al. Nd:YAG laser endometrial ablation: histological aspects of uterine healing. *Int J Gynecol Pathol*. 1992;11:174–179.
17. Silvernagel SW, Harshbarger KE, Shevlin DW. Postoperative granulomas of the endometrium: histological features after endometrial ablation. *Ann Diagn Pathol*. 1997;1:82–90.
18. Nakajima M, Kamei T, Tomimatu K, et al. An intraperitoneal tumorous mass caused by granulomas of microfibrillar collagen hemostat (Avitene). *Arch Pathol Lab Med*. 1995;119:1161–1163.
19. Park SA, Giannattasio C, Tancer ML. Foreign body reaction to the intraperitoneal use of Avitene. *Obstet Gynecol*. 1981;58:664–667.
20. Guarda LA, Tran TA. The pathology of breast biopsy site marking devices. *Am J Surg Pathol*. 2005;29:814–819.
21. Ribalta T, McCutcheon IE, Neto AG, et al. Textiloma (gossypiboma) mimicking recurrent intracranial tumor. *Arch Pathol Lab Med*. 2004;128:749–758.
22. Kershisnik MM, Ro JY, Cannon GH, et al. Histiocytic reaction in pelvic peritoneum associated with oxidized regenerated cellulose. *Am J Clin Pathol* 1995;103:27–31.
23. Gao HW, Lin CK, Yu CP, et al. Oxidized cellulose (Surgicel) granuloma mimicking a primary ovarian tumor. *Int J Gynecol Pathol*. 2002;21:422–423.
24. Kim KR, Scully RE. Peritoneal keratin granulomas with carcinomas of endometrium and ovary and atypical polypoid adenomyoma of endometrium. A clinicopathological analysis of 22 cases. *Am J Surg Pathol*. 1990;14:925–932.
25. George E, Leyser S, Zimmer HL, et al. Vernix caseosa peritonitis. An infrequent complication of cesarean section with distinctive histopathologic features. *Am J Clin Pathol*. 1995;103:681–684.
26. Stuart OA, Morris AR, Baber RJ. Vernix caseosa peritonitis—no longer rare or innocent: a case series. *J Med Case Rep* [*Electronic Resource*]. 2009;3:60.
27. Forouhar F. Meconium peritonitis. Pathology, evolution, and diagnosis. *Am J Clin Pathol*. 1982;78:208–213.
28. Zaytsev P, Taxy JB. Pregnancy-associated ectopic decidua. *Am J Surg Pathol*. 1987;11:526–530.
29. Burnett RA, Millan D. Decidual change in pelvic lymph nodes: a source of possible diagnostic error. *Histopathology*. 1986;10:1089–1092.
30. Zinsser KR, Wheeler JE. Endosalpingiosis in the omentum: a study of autopsy and surgical material. *Am J Surg Pathol*. 1982;6:109–117.
31. Moore WF, Bentley RC, Berchuck A, et al. Some mullerian inclusion cysts in lymph nodes may sometimes be metastases from serous borderline tumors of the ovary. *Am J Surg Pathol*. 2000;24:710–718.
32. Djordjevic B, Clement-Kruzel S, Atkinson NE, et al. Nodal endosalpingiosis in ovarian serous tumors of low malignant potential with lymph node involvement: a case for a precursor lesion. *Am J Surg Pathol*. 2010;34:1442–1448.
33. Kurman RJ, Shih Ie M. The origin and pathogenesis of epithelial ovarian cancer: a proposed unifying theory. *Am J Surg Pathol*. 2010;34:433–443.
34. Clement PB, Young RH. Florid cystic endosalpingiosis with tumor-like manifestations: a report of four cases including the first reported cases of transmural endosalpingiosis of the uterus. *Am J Surg Pathol*. 1999;23:166–175.
35. Bell DA, Scully RE. Serous borderline tumors of the peritoneum. *Am J Surg Pathol*. 1990;14:230–239.
36. McKenney JK, Balzer BL, Longacre TA. Lymph node involvement in ovarian serous tumors of low malignant potential (borderline tumors): pathology, prognosis, and proposed classification. *Am J Surg Pathol*. 2006;30:614–624.
37. Djordjevic B, Malpica A. Lymph node involvement in ovarian serous tumors of low malignant potential: a clinicopathologic study of thirty-six cases. *Am J Surg Pathol*. 2010;34:1–9.
38. Clement PB, Young RH. Endocervicosis of the urinary bladder. A report of six cases of a benign müllerian lesion that may mimic adenocarcinoma. *Am J Surg Pathol*. 1992;16:533–542.
39. Young RH, Clement PB. Endocervicosis involving the uterine cervix: a report of four cases of a benign process that may be confused with deeply invasive endocervical adenocarcinoma. *Int J Gynecol Pathol*. 2000;19:322–328.
40. Clement PB. The pathology of endometriosis: a survey of the many faces of a common disease emphasizing diagnostic pitfalls and unusual and newly appreciated aspects. *Adv Anat Pathol*. 2007;14:241–260.
41. McCluggage WG, Oliva E, Herrington CS, et al. CD10 and calretinin staining of endocervical glandular lesions, endocervical stroma and endometrioid adenocarcinomas of the uterine corpus: CD10 positivity is characteristic of, but not specific for, mesonephric lesions and is not specific for endometrial stroma. *Histopathology* 2003;43:144–150.
42. Stern RC, Dash R, Bentley RC, et al. Malignancy in endometriosis: frequency and comparison of ovarian and extraovarian types. *Int J Gynecol Pathol*. 2001;20:133–139.
43. Mostoufizadeh M, Scully RE. Malignant tumors arising in endometriosis. *Clin Obstet Gynecol*. 1980;23:951–963.
44. Brooks JJ, Wheeler JE. Malignancy arising in extragonadal endometriosis: a case report and summary of the world literature. *Cancer*. 1977;40:3065–3073.

45. Yantiss RK, Clement PB, Young RH. Neoplastic and pre-neoplastic changes in gastrointestinal endometriosis: a study of 17 cases. *Am J Surg Pathol.* 2000;24:513–524.
46. Slavin RE, Krum R, Van Dinh T. Endometriosis-associated intestinal tumors: a clinical and pathological study of 6 cases with a review of the literature. *Hum Pathol.* 2000;31:456–463.
47. Clement PB, Granai CO, Young RH, et al. Endometriosis with myxoid change. A case simulating pseudomyxoma peritonei. *Am J Surg Pathol.* 1994;18:849–853.
48. Colella R, Mameli MG, Bellezza G, et al. Endometriosis-associated skeletal muscle regeneration: a hitherto undescribed entity and a potential diagnostic pitfall. *Am J Surg Pathol.* 2010;34:10–17.
49. Yantiss RK, Clement PB, Young RH. Endometriosis of the intestinal tract: a study of 44 cases of a disease that may cause diverse challenges in clinical and pathologic evaluation. *Am J Surg Pathol.* 2001;25:445–454.
50. Parker RL, Dadmanesh F, Young RH, et al. Polypoid endometriosis: a clinicopathologic analysis of 24 cases and a review of the literature. *Am J Surg Pathol.* 2004;28:285–297.
51. Elliott GB, Freigang B. Aspetic necrosis, calcification and separation of appendices epiploicae. *Ann Surg.* 1962;155:501–505.
52. Vuong PN, Guyot H, Moulin G, et al. Pseudotumoral organization of a twisted epiploic fringe or 'hard-boiled egg' in the peritoneal cavity. *Arch Pathol Lab Med.* 1990;114:531–533.
53. Kuo TT, Hsueh S. Mucicarminophilic histiocytosis. A polyvinylpyrrolidone (PVP) storage disease simulating signet-ring cell carcinoma. *Am J Surg Pathol.* 1984;8:419–428.
54. Clarke B, McCluggage WG. Iatrogenic lesions and artefacts in gynaecological pathology. *J Clin Pathol.* 2009;62:104–112.
55. Carr NJ, Turk EP. The histological features of splenosis. *Histopathology.* 1992;21:549–553.
56. Doss BJ, Jacques SM, Qureshi F, et al. Extratubal secondary trophoblastic implants: clinicopathologic correlation and review of the literature. *Hum Pathol.* 1998;29:184–187.
57. Biscotti CV, Hart WR. Peritoneal serous micropapillomatosis of low malignant potential (serous borderline tumors of the peritoneum). A clinicopathologic study of 17 cases. *Am J Surg Pathol.* 1992;16:467–475.
58. Weir MM, Bell DA, Young RH. Grade 1 peritoneal serous carcinomas: a report of 14 cases and comparison with 7 peritoneal serous psammocarcinomas and 19 peritoneal serous borderline tumors. *Am J Surg Pathol.* 1998;22: 849–862.
59. Bloss JD, Liao SY, Buller RE, et al. Extraovarian peritoneal serous papillary carcinoma: a case-control retrospective comparison to papillary adenocarcinoma of the ovary. *Gynecol Oncol.* 1993;50:347–351.
60. Jaaback KS, Ludeman L, Clayton NL, et al. Primary peritoneal carcinoma in a UK cancer center: comparison with advanced ovarian carcinoma over a 5-year period. *Int J Gynecologic Cancer.* 2006;16(suppl 1):123–128.
61. Gilks CB, Bell DA, Scully RE. Serous psammocarcinoma of the ovary and peritoneum. *Int J Gynecol Pathol.* 1990;9:110–121.
62. Dalrymple JC, Bannatyne P, Russell P, et al. Extraovarian peritoneal serous papillary carcinoma. A clinicopathologic study of 31 cases. *Cancer.* 1989;64:110–115.
63. Ben-Baruch G, Sivan E, Moran O, et al. Primary peritoneal serous papillary carcinoma: a study of 25 cases and comparison with stage III-IV ovarian papillary serous carcinoma. *Gynecol Oncol.* 1996;60:393–396.
64. Casey MJ, Synder C, Bewtra C, et al. Intra-abdominal carcinomatosis after prophylactic oophorectomy in women of hereditary breast ovarian cancer syndrome kindreds associated with BRCA1 and BRCA2 mutations. *Gynecol Oncol.* 2005;97:457–467.
65. Finch A, Beiner M, Lubinski J, et al. Salpingo-oophorectomy and the risk of ovarian, fallopian tube, and peritoneal cancers in women with a BRCA1 or BRCA2 Mutation. *JAMA.* 2006;296:185–192.
66. Rabban JT, Barnes M, Chen LM, et al. Ovarian pathology in risk-reducing salpingo-oophorectomies from women with BRCA mutations, emphasizing the differential diagnosis of occult primary and metastatic carcinoma. *Am J Surg Pathol.* 2009;33:1125–1136.
67. Euscher ED, Malpica A, Deavers MT, et al. Differential expression of WT-1 in serous carcinomas in the peritoneum with or without associated serous carcinoma in endometrial polyps. *Am J Surg Pathol.* 2005;29:1074–1078.
68. Kindelberger DW, Lee Y, Miron A, et al. Intraepithelial carcinoma of the fimbria and pelvic serous carcinoma: evidence for a causal relationship. *Am J Surg Pathol.* 2007;31:161–169.
69. Przybycin CG, Kurman RJ, Ronnett BM, et al. Are all pelvic (nonuterine) serous carcinomas of tubal origin? *Am J Surg Pathol.* 2010;34:1407–1416.
70. Daya D, McCaughey WT. Pathology of the peritoneum: a review of selected topics. *Semin Diagn Pathol.* 1991;8:277–289.
71. Clement PB, Young RH, Oliva E, et al. Hyperplastic mesothelial cells within abdominal lymph nodes: mimic of metastatic ovarian carcinoma and serous borderline tumor—a report of two cases associated with ovarian neoplasms. *Mod Pathol.* 1996;9:879–886.
72. McFadden DE, Clement PB. Peritoneal inclusion cysts with mural mesothelial proliferation. A clinicopathological analysis of six cases. *Am J Surg Pathol.* 1986;10:844–854.
73. Weiss SW, Tavassoli FA. Multicystic mesothelioma. An analysis of pathologic findings and biologic behavior in 37 cases. *Am J Surg Pathol.* 1988;12:737–746.
74. Ross MJ, Welch WR, Scully RE. Multilocular peritoneal inclusion cysts (so-called cystic mesotheliomas). *Cancer.* 1989;64:1336–1346.
75. Kurisu Y, Tsuji M, Shibayama Y, et al. Multicystic mesothelioma caused by endometriosis: 2 case reports and review of the literature. *Int J Gynecol Pathol.* 2011;30:163–166.
76. Kahn HJ, Bailey D, Marks A. Monoclonal antibody D2–40, a new marker of lymphatic endothelium, reacts with Kaposi's sarcoma and a subset of angiosarcomas. *Mod Pathol.* 2002;15:434–440.
77. Ordonez NG. The diagnostic utility of immunohistochemistry and electron microscopy in distinguishing between peritoneal mesotheliomas and serous carcinomas: a comparative study. *Mod Pathol.* 2006;19:34–48.
78. Daya D, McCaughey WT. Well-differentiated papillary mesothelioma of the peritoneum. A clinicopathologic study of 22 cases. *Cancer.* 1990;65:292–296.
79. Goldblum J, Hart WR. Localized and diffuse mesotheliomas of the genital tract and peritoneum in women. A clinicopathologic study of nineteen true mesothelial neoplasms, other than adenomatoid tumors, multicystic mesotheliomas, and localized fibrous tumors. *Am J Surg Pathol.* 1995;19:1124–1137.
80. Hoekstra AV, Riben MW, Frumovitz M, et al. Well-differentiated papillary mesothelioma of the peritoneum: a pathological analysis and review of the literature. *Gynecol Oncol.* 2005;98:161–167.
81. Baker PM, Clement PB, Young RH. Malignant peritoneal mesothelioma in women: a study of 75 cases with emphasis on their morphologic spectrum and differential diagnosis. *Am J Clin Pathol.* 2005;123:724–737.
82. Hammar SP. Macroscopic, histologic, histochemical, immunohistochemical, and ultrastructural features of mesothelioma. *Ultrastruct Pathol.* 2006;30:3–17.
83. Husain AN, Colby TV, Ord EZ, et al. Guidelines for pathologic diagnosis of malignant mesothelioma: a consensus statement from the International Mesothelioma Interest Group. *Arch Pathol Lab Med.* 2009;133:1317–1331.
84. Clement PB, Young RH, Scully RE. Malignant mesotheliomas presenting as ovarian masses. A report of nine cases, including two primary ovarian mesotheliomas. *Am J Surg Pathol.* 1996;20:1067–1080.
85. Nascimento AG, Keeney GL, Fletcher CD. Deciduoid peritoneal mesothelioma. An unusual phenotype affecting young females. *Am J Surg Pathol.* 1994;18:439–445.
86. Shanks JH, Harris M, Banerjee SS, et al. Mesotheliomas with deciduoid morphology: a morphologic spectrum and a variant not confined to young females. *Am J Surg Pathol.* 2000;24:285–294.
87. Ordonez NG. Value of immunohistochemistry in distinguishing peritoneal mesothelioma from serous carcinoma of the ovary and peritoneum: a review and update. *Adv Anat Pathol.* 2006;13:16–25.
88. Laury AR, Hornick JL, Perets R, et al. PAX8 reliably distinguishes ovarian serous tumors from malignant mesothelioma. *Am J Surg Pathol.* 2010;34:627–635.
89. Kerrigan SA, Turnnir RT, Clement PB, et al. Diffuse malignant epithelial mesotheliomas of the peritoneum in women: a clinicopathologic study of 25 patients. *Cancer.* 2002;94:378–385.
90. Nonaka D, Kusamura S, Baratti D, et al. Diffuse malignant mesothelioma of the peritoneum: a clinicopathological study of 35 patients treated locoregionally at a single institution. *Cancer.* 2005;104:2181–2188.
91. Tavassoli FA, Norris HJ. Peritoneal leiomyomatosis (leiomyomatosis peritonealis disseminata): a clinicopathologic study of 20 cases with ultrastructural observations. *Int J Gynecol Pathol.* 1982;1:59–74.
92. Bekkers RL, Willemsen WN, Schijf CP, et al. Leiomyomatosis peritonealis disseminata: does malignant transformation occur? A literature review. *Gynecol Oncol.* 1999;75:158–163.
93. Burke AP, Sobin LH, Shekitka KM, et al. Intra-abdominal fibromatosis. A pathologic analysis of 130 tumors with comparison of clinical subgroups. *Am J Surg Pathol.* 1990;14:335–341.
94. Li M, Cordon-Cardo C, Gerald WL, et al. Desmoid fibromatosis is a clonal process. *Hum Pathol.* 1996;27:939–943.
95. Yantiss RK, Spiro IJ, Compton CC, et al. Gastrointestinal stromal tumor versus intra-abdominal fibromatosis of the bowel wall: a clinically important differential diagnosis. *Am J Surg Pathol.* 2000;24:947–957.
96. Reith JD, Goldblum JR, Lyles RH, et al. Extragastrointestinal (soft tissue) stromal tumors: an analysis of 48 cases with emphasis on histologic predictors of outcome. *Mod Pathol.* 2000;13:577–585.

97. Miettinen M, Sobin LH, Lasota J. Gastrointestinal stromal tumors presenting as omental masses—a clinicopathologic analysis of 95 cases. *Am J Surg Pathol.* 2009;33:1267–1275.
98. Montgomery E, Torbenson MS, Kaushal M, et al. Beta-catenin immunohistochemistry separates mesenteric fibromatosis from gastrointestinal stromal tumor and sclerosing mesenteritis. *Am J Surg Pathol.* 2002;26:1296–1301.
99. Lucas DR, al-Abbadi M, Tabaczka P, et al. c-Kit expression in desmoid fibromatosis. Comparative immunohistochemical evaluation of two commercial antibodies. *Am J Clin Pathol.* 2003;119:339–345.
100. Gerald WL, Miller HK, Battifora H, et al. Intra-abdominal desmoplastic small round-cell tumor. Report of 19 cases of a distinctive type of high-grade polyphenotypic malignancy affecting young individuals. *Am J Surg Pathol.* 1991;15:499–513.
101. Lae ME, Roche PC, Jin L, et al. Desmoplastic small round cell tumor: a clinicopathologic, immunohistochemical, and molecular study of 32 tumors. *Am J Surg Pathol.* 2002;26:823–835.
102. Young RH, Eichhorn JH, Dickersin GR, et al. Ovarian involvement by the intra-abdominal desmoplastic small round cell tumor with divergent differentiation: a report of three cases. *Hum Pathol.* 1992;23:454–464.
103. Ordonez NG. Desmoplastic small round cell tumor I: a histopathologic study of 39 cases with emphasis on unusual histological patterns. *Am J Surg Pathol.* 1998;22:1303–1313.
104. Barnoud R, Sabourin JC, Pasquier D, et al. Immunohistochemical expression of WT1 by desmoplastic small round cell tumor: a comparative study with other small round cell tumors. *Am J Surg Pathol.* 2000;24:830–836.
105. Mazzoleni G, Salerno A, Santini D, et al. Leiomyomatosis in pelvic lymph nodes. *Histopathology.* 1992;21:588–589.
106. Young RH, Clement PB, McCaughey WT. Solitary fibrous tumors ('fibrous mesotheliomas') of the peritoneum. A report of three cases and a review of the literature. *Arch Pathol Lab Med.* 1990;114:493–495.
107. Coffin CM, Watterson J, Priest JR, et al. Extrapulmonary inflammatory myofibroblastic tumor (inflammatory pseudotumor). A clinicopathologic and immunohistochemical study of 84 cases. *Am J Surg Pathol.* 1995;19:859–872.
108. Fetsch JF, Montgomery EA, Meis JM. Calcifying fibrous pseudotumor. *Am J Surg Pathol.* 1993;17:502–508.
109. Nascimento AF, Ruiz R, Hornick JL, et al. Calcifying fibrous 'pseudotumor': clinicopathologic study of 15 cases and analysis of its relationship to inflammatory myofibroblastic tumor. *Int J Surg Pathol.* 2002;10:189–196.
110. Lin BT, Colby T, Gown AM, et al. Malignant vascular tumors of the serous membranes mimicking mesothelioma. A report of 14 cases. *Am J Surg Pathol.* 1996;20:1431–1439.
111. Gonzalez-Crussi F, deMello DE, Sotelo-Avila C. Omental-mesenteric myxoid hamartomas. Infantile lesions simulating malignant tumors. *Am J Surg Pathol.* 1983;7:567–578.
112. Mikami M, Tei C, Takehara K, et al. Retroperitoneal primary mucinous adenocarcinoma with a mural nodule of anaplastic tumor: a case report and literature review. *Int J Gynecol Pathol.* 2003;22:205–208.
113. Matsubara M, Shiozawa T, Tachibana R, et al. Primary retroperitoneal mucinous cystadenoma of borderline malignancy: a case report and review of the literature. *Int J Gynecol Pathol.* 2005;24:218–223.
114. Misdraji J. Appendiceal mucinous neoplasms: controversial issues. *Arch Pathol Lab Med.* 2010;134:864–870.
115. Young RH. Pseudomyxoma peritonei and selected other aspects of the spread of appendiceal neoplasms. *Semin Diagn Pathol.* 2004;21:134–150.
116. Pai RK, Longacre TA. Appendiceal mucinous tumors and pseudomyxoma peritonei: histologic features, diagnostic problems, and proposed classification. *Adv Anat Pathol.* 2005;12:291–311.
117. Bradley RF, Cortina G, Geisinger KR. Pseudomyxoma peritonei: review of the controversy. *Curr Diagn Pathol.* 2007;13:410–416.
118. Young RH, Gilks CB, Scully RE. Mucinous tumors of the appendix associated with mucinous tumors of the ovary and pseudomyxoma peritonei. A clinicopathological analysis of 22 cases supporting an origin in the appendix. *Am J Surg Pathol.* 1991;15:415–429.
119. Ronnett BM, Zahn CM, Kurman RJ, et al. Disseminated peritoneal adenomucinosis and peritoneal mucinous carcinomatosis. A clinicopathologic analysis of 109 cases with emphasis on distinguishing pathologic features, site of origin, prognosis, and relationship to "pseudomyxoma peritonei." *Am J Surg Pathol.* 1995;19:1390–1408.
120. Prayson RA, Hart WR, Petras RE. Pseudomyxoma peritonei. A clinicopathologic study of 19 cases with emphasis on site of origin and nature of associated ovarian tumors. *Am J Surg Pathol.* 1994;18:591–603.
121. Bradley RF, Stewart JHt, Russell GB, et al. Pseudomyxoma peritonei of appendiceal origin: a clinicopathologic analysis of 101 patients uniformly treated at a single institution, with literature review. *Am J Surg Pathol.* 2006;30:551–559.
122. Carr NJ, McCarthy WF, Sobin LH. Epithelial noncarcinoid tumors and tumor-like lesions of the appendix. A clinicopathologic study of 184 patients with a multivariate analysis of prognostic factors. *Cancer.* 1995;75:757–768.
123. Pai RK, Beck AH, Norton JA, et al. Appendiceal mucinous neoplasms: clinicopathologic study of 116 cases with analysis of factors predicting recurrence. *Am J Surg Pathol.* 2009;33:1425–1439.
124. Misdraji J, Yantiss RK, Graeme-Cook FM, et al. Appendiceal mucinous neoplasms: a clinicopathologic analysis of 107 cases. *Am J Surg Pathol.* 2003;27:1089–1103.
125. Yantiss RK, Shia J, Klimstra DS, et al. Prognostic significance of localized extra-appendiceal mucin deposition in appendiceal mucinous neoplasms. *Am J Surg Pathol.* 2009;33:248–255.
126. Ronnett BM, Kurman RJ, Zahn CM, et al. Pseudomyxoma peritonei in women: a clinicopathologic analysis of 30 cases with emphasis on site of origin, prognosis, and relationship to ovarian mucinous tumors of low malignant potential. *Hum Pathol.* 1995;26:509–524.
127. Higa E, Rosai J, Pizzimbono CA, et al. Mucosal hyperplasia, mucinous cystadenoma, and mucinous cystadenocarcinoma of the appendix. A re-evaluation of appendiceal "mucocele." *Cancer.* 1973;32:1525–1541.
128. Hsu M, Young RH, Misdraji J. Ruptured appendiceal diverticula mimicking low-grade appendiceal mucinous neoplasms. *Am J Surg Pathol.* 2009;33:1515–1521.
129. Ronnett BM, Shmookler BM, Diener-West M, et al. Immunohistochemical evidence supporting the appendiceal origin of pseudomyxoma peritonei in women. *Int J Gynecol Pathol.* 1997;16:1–9.
130. Lamps LW, Gray GF Jr, Dilday BR, et al. The coexistence of low-grade mucinous neoplasms of the appendix and appendiceal diverticula: a possible role in the pathogenesis of pseudomyxoma peritonei. *Mod Pathol.* 2000;13:495–501.
131. O'Connell JT, Hacker CM, Barsky SH. MUC2 is a molecular marker for pseudomyxoma peritonei. *Mod Pathol.* 2002;15:958–972.
132. Hart WR, Norris HJ. Borderline and malignant mucinous tumors of the ovary. Histologic criteria and clinical behavior. *Cancer.* 1973;31:1031–1045.
133. Lee KR, Scully RE. Mucinous tumors of the ovary: a clinicopathologic study of 196 borderline tumors (of intestinal type) and carcinomas, including an evaluation of 11 cases with 'pseudomyxoma peritonei'. *Am J Surg Pathol.* 2000;24:1447–1464.
134. Ronnett BM, Seidman JD. Mucinous tumors arising in ovarian mature cystic teratomas: relationship to the clinical syndrome of pseudomyxoma peritonei. *Am J Surg Pathol.* 2003;27:650–657.
135. Vang R, Gown AM, Zhao C, et al. Ovarian mucinous tumors associated with mature cystic teratomas: morphologic and immunohistochemical analysis identifies a subset of potential teratomatous origin that shares features of lower gastrointestinal tract mucinous tumors more commonly encountered as secondary tumors in the ovary. *Am J Surg Pathol.* 2007;31:854–869.
136. McKenney JK, Soslow RA, Longacre TA. Ovarian mature teratomas with mucinous epithelial neoplasms: morphologic heterogeneity and association with pseudomyxoma peritonei. *Am J Surg Pathol.* 2008;32:645–655.
137. Du Plessis DG, Louw JA, Wranz PA. Mucinous epithelial cysts of the spleen associated with pseudomyxoma peritonei. *Histopathology.* 1999;35:551–557.
138. Ronnett BM, Yan H, Kurman RJ, et al. Patients with pseudomyxoma peritonei associated with disseminated peritoneal adenomucinosis have a significantly more favorable prognosis than patients with peritoneal mucinous carcinomatosis. *Cancer.* 2001;92:85–91.
139. Stewart CJ, Tsukamoto T, Cooke B, et al. Ovarian mucinous tumour arising in mature cystic teratoma and associated with pseudomyxoma peritonei: report of two cases and comparison with ovarian involvement by low-grade appendiceal mucinous tumour. *Pathology (Phila).* 2006;38:534–538.

CHAPTER 9

Pathology of the Placenta

INTRODUCTION

The placenta is a highly vascular organ that develops during pregnancy to enable the exchange of gases and nutrients between the bloodstreams of the mother and fetus. The placenta is also involved in the production of hormones such as progesterone, estrogen, and human chorionic gonadotropin, and assists in the transfer of maternal antibodies to the fetus. The umbilical cord connects the vasculature of the fetus to the placenta. Shortly after delivery of the baby, the placenta normally separates from the uterine lining and is removed.

This chapter takes a targeted and practical approach to the placenta. It is directed at those who aspire to acquire more than a cursory knowledge of placental pathology, but who do not have the time to read a detailed textbook devoted solely to this subspecialty. I have omitted a discussion regarding recommendations for the gross examination and sampling of the placenta, since this information is readily available in standard textbooks of surgical pathology as well as in many of the texts listed in the Suggested Readings at the end of this chapter. Placental tissue as encountered during the evaluation of "products of conception" specimens is discussed in Chapter 4, and gestational trophoblastic disease and its differential diagnosis are discussed in Chapter 10.

BASIC PLACENTAL TERMINOLOGY

Amnion

The amnion is the innermost layer of the amniotic cavity, which is enveloped by the chorion laeve in fully developed extraplacental fetal membranes. In the region of the placenta, the amnion lines the fetal surface of the chorionic plate. The amnion is an avascular structure, the histology of which is discussed and illustrated later in this chapter.

Basal Plate

The basal plate refers to the maternal surface of the placenta, which normally consists of a thin rim of compressed decidua that is often associated with a haphazard admixture of fibrinoid material and intermediate trophoblastic cells.

Chorion

The chorion encompasses the embryo and becomes loosely adherent to the amnion at about 12 weeks of gestation, after the expanding amniotic cavity has obliterated the chorionic cavity. The chorion is also the site of continued development and proliferation of villi in the region of the embryonic pole that is destined to become the placenta, which is referred to as the chorion frondosum. The large vessels of the fetal vasculature course through the chorionic connective tissue in the region of the chorionic plate.

Chorion Laeve

The chorion laeve, accompanied by an inner layer of amnion, together constitute the extraplacental fetal membrane. In other words, the chorion laeve represents the outer layer of the sac that contains amniotic fluid. The histology of the chorion laeve is discussed and illustrated later in this chapter.

Chorionic Plate

Chorionic villi are anchored to and arise from the chorionic plate. In a normal placenta, the grayish purple chorionic plate and its numerous fetal stem vessels are visible on the fetal surface and are covered by a transparent and glistening layer of amnion. Since fetal surface chorionic arteries and veins are difficult to distinguish from one another histologically, it is helpful to know that fetal arteries cross over veins.

Cotyledons

Cotyledons represent subdivisions of the placenta that are formed as a result of formation of placental septa. There are typically 15 to 28 cotyledons, which are grossly visible when the placenta is viewed from its maternal surface.

Fetal Membranes

It is understood that this term refers to the extraplacental fetal membranes, which are composed of a combination of amnion and chorion laeve.

Hofbauer Cells

Villous macrophages.

Intervillous Space

This term refers to the space between the chorionic villi of the placenta. It is occupied by maternal blood that is derived from the spiral arteries that have been altered by invading trophoblastic cells. In this manner, the chorionic villi are bathed in oxygenated maternal blood that is eventually returned to the maternal circulation via the endometrial veins.

Placental Septa

Placental septa are extensions of maternal decidua, intermediate trophoblastic cells, and fibrinoid material that arise from the basal plate. They form pillars rather than complete septa, and are responsible for the cotyledonoid architecture of the placenta. In contrast to placental septa, so-called cell islands are composed of intermediate trophoblastic cells and fibrinoid material without a decidual component.

OVERVIEW OF DEVELOPMENT OF CHORIONIC VILLI[1]

The histology of chorionic villi as they develop during the first few weeks of gestation is discussed in Chapter 4 within the context of evaluating tissue from abortion specimens. As gestation proceeds, the villi proliferate and mature, with the terminal villi representing the final stage of development. First trimester villi consist predominantly of the so-called mesenchymal villi with abundant loose stroma enveloped by an inner layer of cytotrophoblast and an outer layer of syncytiotrophoblast (Fig. 9.1). Hofbauer cells may be a prominent stromal component at this stage.

With villous maturation, small vessels and capillaries become more apparent. At first, these structures are centrally located and inconspicuous. As differentiation proceeds toward terminal villi, capillaries gradually become more prominent and peripherally located and the germinative cytotrophoblastic layer is reduced to a few compressed cells. In addition to these changes, the most differentiated villi are characterized by the presence of apoptotic syncytiotrophoblastic nuclei that

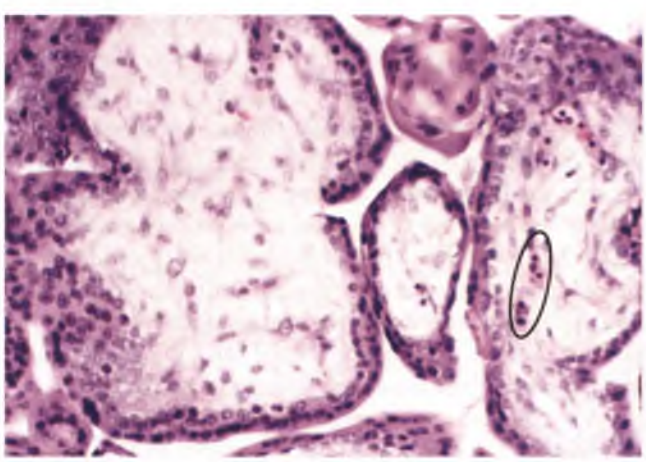

FIGURE 9.1. Mesenchymal villi. These villi predominate in the first trimester, and are characterized by abundant loose stroma and a surface bilayer composed of inner cytotrophoblast and outer syncytiotrophoblast. Once capillaries have formed, intraluminal nucleated red blood cells are normally found up until about the end of the first trimester (*circled*). In early gestation, villi of this type are often capped by a polar trophoblastic proliferation, as shown more dramatically in Figure 10.19.

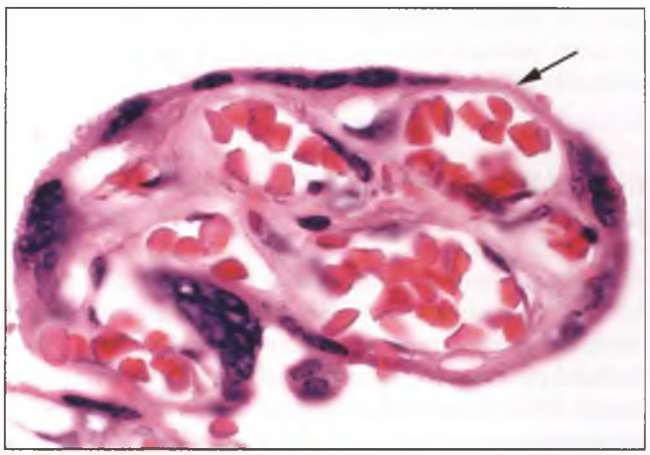

FIGURE 9.2. Third-trimester terminal villus. An *arrow* marks one of the regions where the fetal and maternal circulations are separated only by the vasculosyncytial membrane. In vivo, the white space outside the villus is filled with maternal blood. Note the aggregates of syncytiotrophoblastic nuclei ("syncytial knots").

have aggregated into knots, which are eventually shed into the intervillous space (maternal circulation). The net result of these events is the formation of the vasculosyncytial membrane, which consists only of attenuated syncytiotrophoblastic cytoplasm fused with capillary endothelium (Fig. 9.2). It is in these areas that most gas and nutrient exchange occurs between the maternal and fetal circulations.

Chorionic villi have a tree-like architecture, with stem villi being analogous to the major branches of the tree (Fig. 9.3). They provide structural support and transport blood, and their progressive division eventually results in the formation of the terminal villi that normally account for at least one-third of the villous volume of a term placenta. The placental unit that is referred to as a cotyledon is composed of a primary stem villus and all of the villi that emanate from it. As illustrated in Figure 10.23, stem villi that have been subjected to shearing forces during tissue extraction or processing often have central clear spaces that are of traumatic origin; such spaces should not be misinterpreted as cisterns related to a molar pregnancy.

For the sake of simplicity, I have omitted a discussion of two other subtypes of chorionic villi, which are referred to as immature and mature intermediate villi.

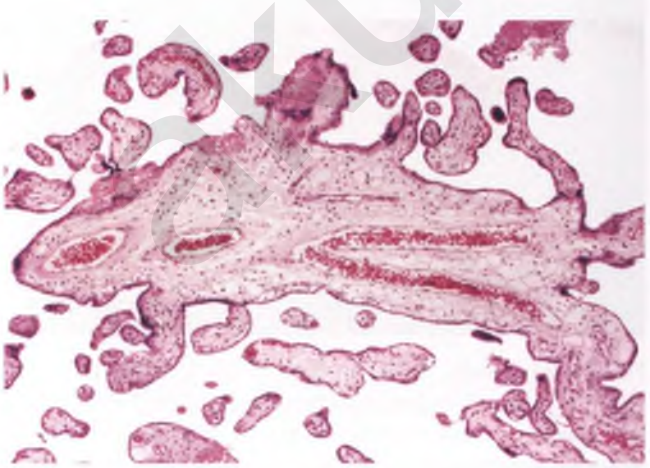

FIGURE 9.3. Stem villus. Large vessels course through the center of stem villi, which progressively branch to form the smaller villi that are involved in gas and nutrient exchange with the maternal circulation.

HISTOLOGY OF NORMAL FETAL MEMBRANES

The extraplacental fetal membranes are composed of an inner layer of amnion that is loosely adherent to the chorion laeve (Fig. 9.4). The most conspicuous components of the membranes are the amniotic epithelium and the band of intermediate trophoblastic cells within the chorion laeve. The latter may harbor remnants of chorionic villi that have undergone pressure atrophy (see Fig. 9.16). A thin rim of decidua is often adherent to the outer aspect of the chorion laeve. Decidua in this region usually has a flattened appearance with spindle-shaped nuclei streaming parallel to the amniotic epithelium, which is due to pressure from the fluid-filled amniotic cavity.

A thin layer of fibrin is normally present beneath the fetal membranes that are applied to the chorionic plate (Fig. 9.5). This layer, which may extend down along nearby stem villi, is of no clinical significance.

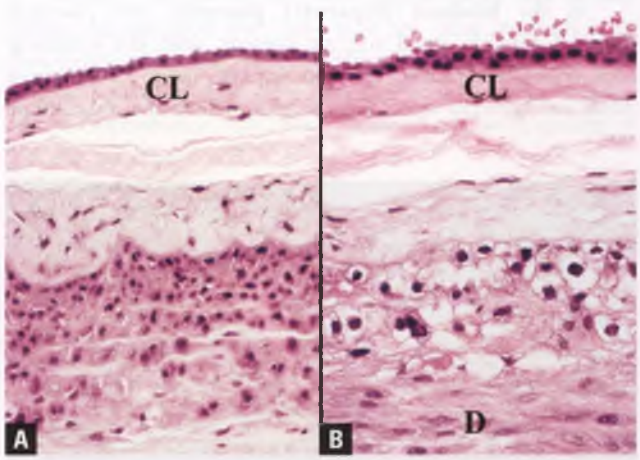

FIGURE 9.4. **A,B:** Normal fetal membranes (amnion juxtaposed to chorion laeve). Cuboidal amniotic epithelium at top is in contact with the amniotic fluid, and is densely adherent to the underlying compact layer of the amnion (CL). There is often an artifactual space where the amnion abuts the chorion laeve, as in these examples. The cellular band of chorionic-type intermediate trophoblasts within the chorion laeve contains cells whose cytoplasm may be eosinophilic **(A)**, clear **(B)**, or an admixture of these two phenotypes (not shown), and often exhibits some nuclear atypia that is presumably degenerative in nature. A rim of maternal decidua (*D*) lies beneath the trophoblastic cells.

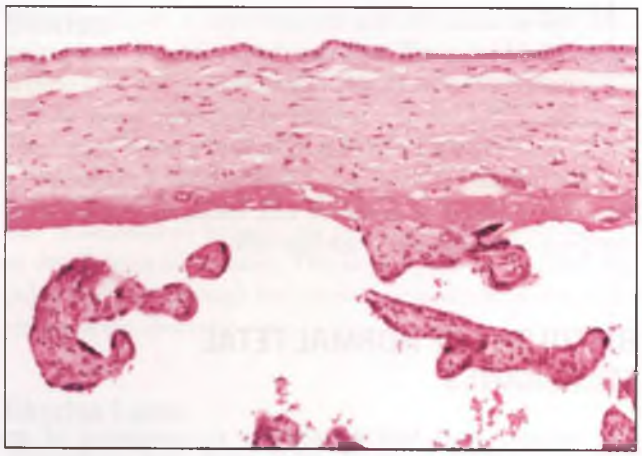

FIGURE 9.5. The membranes that cover the chorionic plate are normally underscored by a thin layer of fibrin, which is seen as an eosinophilic band coursing horizontally through the center of the image.

ABNORMALITES OF PLACENTAL SHAPE

The most common abnormality of placental shape is the presence of an **accessory (succenturiate) lobe**, which occurs in about 3% of placentas. In this condition, a separate mass of placental tissue is attached to the main disc by tissue that ranges from vessel-containing membranes without structural support to a narrow band of placental tissue (Fig. 9.6). In the usual situation, the umbilical cord inserts into the main placental disc.

In the **bilobate (bipartite) placenta**, two placental lobes of roughly equal size are present, with the umbilical cord typically inserting between the two lobes. Other more rarely encountered anomalous shapes include the multilobate placenta, placenta membranacea, ring-shaped placenta, and fenestrate placenta, which are described in more comprehensive books of placental pathology.

FIGURE 9.6. Accessory lobe. The smaller accessory lobe is present in the left side of the image. Note how segments of the fetal vessels at the junction between the accessory and main lobes are supported only by fetal membranous tissue, which puts them at an increased risk for traumatic injury during delivery.

CIRCUMVALLATE AND CIRCUMMARGINATE PLACENTAS

Circumvallate and circummarginate placentas represent two fairly common structural abnormalities. Unlike a normal placenta, the chorionic plate in these two entities is smaller than the basal plate and the chorionic plate does not extend to the margin of the placental disc. Circumvallate and circummarginate placentas are referred to as extrachorial placentas because a portion of the fetal side extends beyond the chorionic plate and consists of bare (extrachorial) placental tissue.

In the circumvallate placenta, the transition from the chorionic plate to the fetal membranes is raised and rolled where the membrane is reflected back upon itself, whereas this transitional area is flat in the circummarginate placenta. It is most likely that the formation of a circumvallate placenta is related to repeated episodes of hemorrhage of maternal veins at the margin of the placental disc, the extension of which beneath the chorionic plate results in elevation and central displacement of the membrane insertion site.[2] Evidence of recent and/or remote hemorrhage is commonly found in the reflected fold of membranous tissue and beneath the membrane of the chorionic plate (Fig. 9.7).

It is generally accepted that circummarginate placentation is of no clinical significance, but circumvallate placentation has been associated with a variety of complications.[3]

FIGURE 9.7. Circumvallate placenta. In this example, the membranes of the small, central chorionic plate of the fetal surface have been removed to reveal a compressed layer of old blood (*asterisk*) along with some recent blood clots. The fetal membranes have been wrapped around the placenta, but these membranes are not attached to the placenta beyond the abnormally small chorionic plate, which is raised and rolled at its peripheral margin. (Courtesy of Dr. Richard L. Payne.)

PLACENTA ACCRETA, INCRETA, AND PERCRETA[4,5]

Placenta accreta is a rare condition that refers to the abnormal adherence of chorionic villi to the myometrium, which is due to the absence of the interposed layer of decidua that is normally present (Fig. 9.8). In most examples of this phenomenon, there is a thin layer of fibrin that separates the villi from the smooth muscle cells of the myometrium. This abnormal adherence may be focal, partial, or complete, and results in a placenta that is difficult or impossible to remove following birth of the child. For the pathologist, the diagnosis is most straightforward when management of the accreta warrants hysterectomy. When only the placenta is available for examination, careful examination of the basal plate may demonstrate mild or focal forms of histologic placenta accreta, although correlation with the clinical history is required to determine its significance.[5,6]

The most common predisposing factors of placenta accreta are previous cesarean section and placenta previa. In the latter situation, implantation of the placenta in the poorly decidualized lower uterine segment is the explanation for the association.

Placenta increta is much less common than placenta accreta. In this variant, the abnormally adherent villi extend into the myometrium (Figs. 9.9 and 9.10). The "invading" villi are histologically normal and do not infiltrate the myometrium in the same manner as a carcinoma. Instead, these villi take the path of least resistance as they find and exploit points of weakness in the wall. These points of weakness are usually related to previous cesarean section or repeated aggressive endometrial sampling.

Placenta percreta is the rarest form of abnormal placental adherence. In this situation, there is at least focal extension of the villi through the myometrium to the serosal surface of the uterus, which may result in uterine rupture.

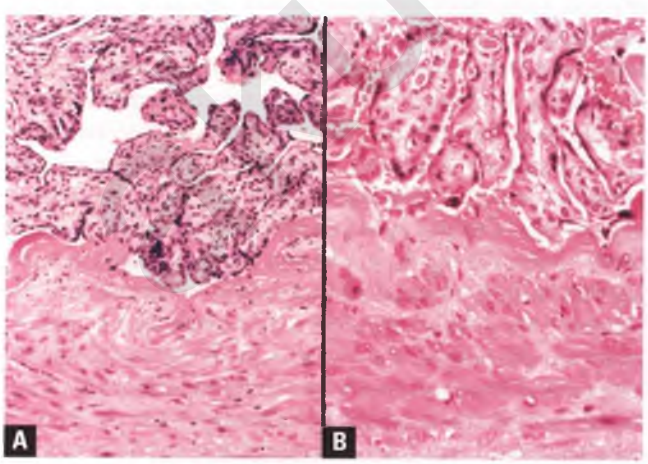

FIGURE 9.8. **A,B:** Placenta accreta. These two different examples show chorionic villi separated from the myometrium by only a thin layer of fibrin. Normally, there is a layer of decidua interposed between the villi and the myometrium.

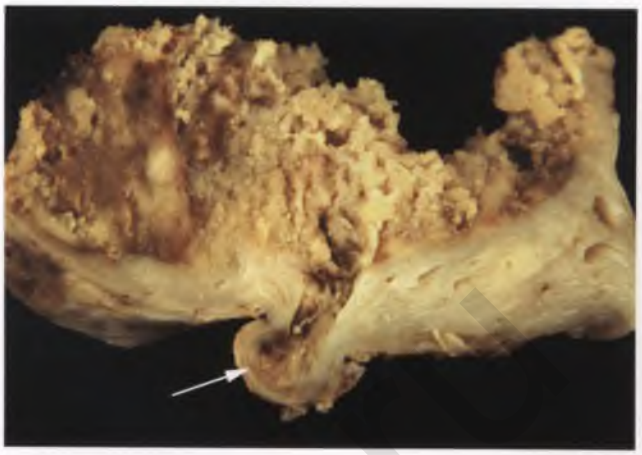

FIGURE 9.9. Placenta increta. This section through a formalin-fixed uterus reveals firmly adherent placental tissue extending into the myometrium. The *arrow* marks a tongue-like protrusion of placental tissue that extends to within 1 mm of the bulging serosal surface. The protrusion is occurring in an area of wall weakness (the patient had a history of three prior cesarean sections).

LAMINAR NECROSIS OF THE FETAL MEMBRANES[7,8]

This lesion is seen in the extraplacental fetal membranes of about 10% of placentas submitted for examination, and is thought to be an indicator of uteroplacental hypoxia. It is diagnosed when at least 10% of the membrane roll exhibits necrosis of this type.

Grossly, laminar necrosis may appear as an area of pale yellow discoloration that may give the false impression of chorioamnionitis (Fig. 9.11A). Histologically, it is characterized by a band of coagulative necrosis involving the decidua and/or trophoblastic cells of the chorion laeve, with sparing of the amnion (Fig. 9.11B).

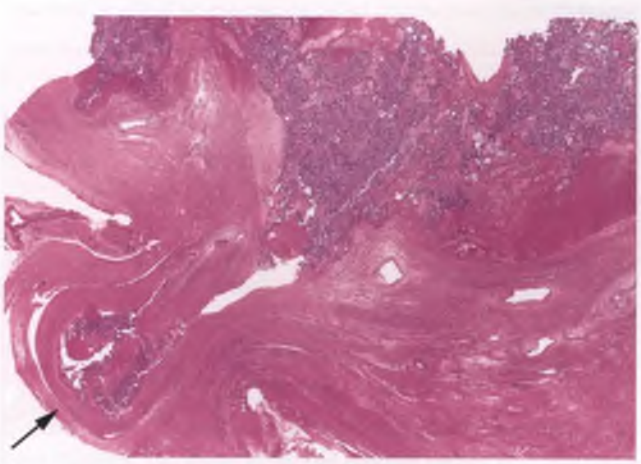

FIGURE 9.10. Placenta increta. This low-magnification view represents the histologic correlate of the specimen in the preceding figure. The area of protrusion of chorionic villi deep into the myometrium is marked by an *arrow*.

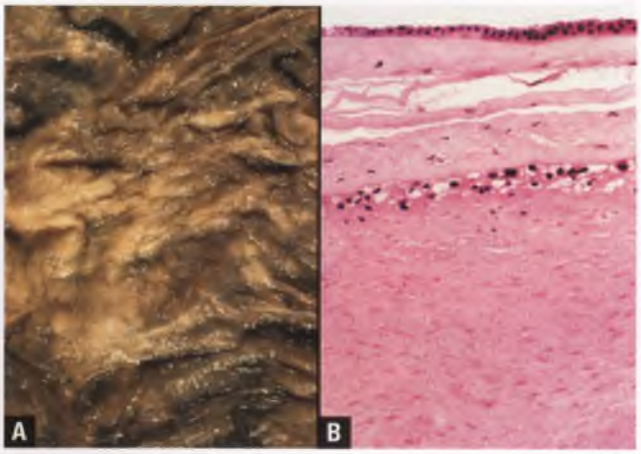

FIGURE 9.11. Laminar necrosis. **A:** The pale yellow areas of the fetal membranes represent a peripheral rim of decidual necrosis. **B:** Note the coagulative necrosis of the decidua beneath the band of trophoblastic cells within the chorion laeve. The nuclei of the necrotic decidual cells are faintly stained and the necrotic tissue contains minute granules of basophilic debris.

MICROSCOPIC CHORIONIC PSEUDOCYSTS OF THE FETAL MEMBRANES[8,9]

Microscopic chorionic pseudocysts are found in about 4% of placentas submitted for examination. Similar to laminar necrosis, this finding is thought to be related to membrane hypoxia. These lesions consist of lakes of colloid-like eosinophilic fluid within the chorion laeve (Fig. 9.12).

SEPTAL AND CHORIONIC CYSTS

Septal cysts are usually <1 cm and occur within the septal pillars that demarcate the cotyledons of the placenta. Although septal cysts are considered to be an incidental finding, they are more prevalent in cases of maternal floor infarction/massive perivillous fibrin deposition. Histologically, septal cysts are filled with proteinaceous material and are lined by intermediate trophoblastic cells (Fig. 9.13).

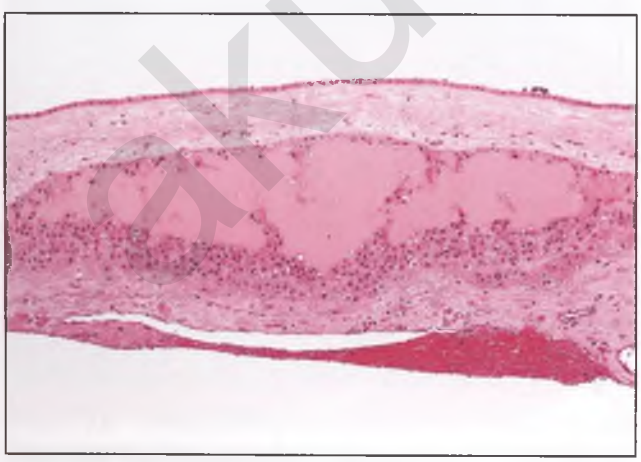

FIGURE 9.12. Microscopic chorionic pseudocyst of the fetal membranes. A lake of eosinophilic fluid is surrounded by intermediate trophoblastic cells of the chorion laeve. (Courtesy of Dr. Jerzy Stanek.)

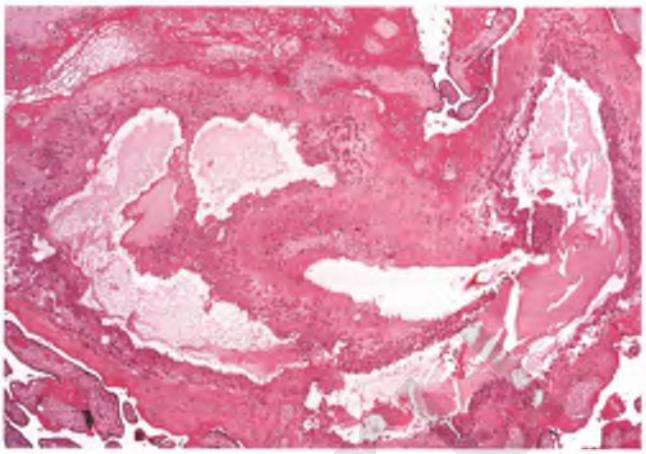

FIGURE 9.13. Septal cyst. The cystic spaces contain proteinaceous fluid and are lined by intermediate trophoblastic cells. The wall of the cyst also contains decidual cells and fibrinoid material. (Courtesy of Dr. Jerzy Stanek.)

Chorionic cysts occur in the chorionic plate and can be of substantial size. Histologically, they resemble septal cysts, except for the absence of decidual cells within their walls. Despite their sometimes impressive gross appearance, these cysts are of no clinical significance.

DIVIDING MEMBRANE IN TWIN GESTATIONS[10,11]

Roughly 70% of twin pregnancies are dizygotic, whereas the remaining 30% are monozygotic. A major part of the evaluation of placentas from twin gestations is the determination of the existence and composition of the dividing membrane, which has implications for the zygosity of the infants. In twin placentas that are monochorionic, the twins are monozygotic (identical). Most dichorionic twin placentas are associated with dizygous (fraternal) twins, but monozygous twins will also have a dichorionic placenta if splitting of the fertilized egg occurs within the first 3 days following fertilization. Separate twin placentas, which account for roughly 35% of cases, are dichorionic–diamniotic by definition, and are examined as if they represented two singleton placentas. A fused placenta with a single sac with no dividing membrane, which accounts for only about 1% of cases, is monochorionic–monoamniotic by definition. This type of placentation is associated with a high rate of fetal morbidity and mortality due to the prevalence of umbilical cord entanglements (Fig. 9.14).

The determination of the type of twin placentation requires more expertise when evaluating a fused twin placenta

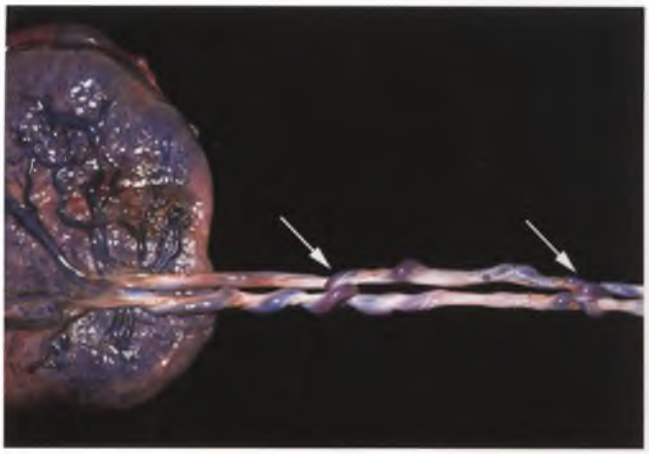

FIGURE 9.14. Monochorionic–monoamniotic twin placenta with umbilical cords. In this rare type of twin placentation, the sharing of a single amniotic cavity by monozygous twins leads to a high incidence of cord complications. In this case, the cords have become entangled and knotted in two separate areas (*arrows*). (Courtesy of Dr. Richard L. Payne.)

FIGURE 9.15. Dichorionic–diamniotic fused twin placenta. **A:** This cross-section at the junction of the two placental beds demonstrates the thick, off-white, opaque nature of the dividing membrane (top portion of image). **B:** This portion of the dividing membrane has been peeled apart, revealing a centrally located, vertical ridge of firm tissue at the point of attachment to the fetal surface that is characteristic of this type of placentation.

with a dividing membrane. In this situation, the incidence of dichorionic–diamniotic placentation accounts for about 35% of the overall number of twin placentas, whereas monochorionic–diamniotic placentation accounts for the remaining 29% in the scenario where the other types of placentation add up to 35% + 35% + 1% = 71%. This distinction can usually be made grossly, since the dividing membrane in dichorionic–diamniotic cases is thick and opaque, difficult to peel apart into its four separate layers, forms a ridge at the point of attachment to the fetal surface, and is not associated with vascular anastomoses between the two placental beds (Fig. 9.15). In contrast, the dividing membrane in monochorionic–diamniotic cases is thin and translucent (unless altered by meconium staining or chorioamnionitis), easily peels apart into two separate layers, has a smooth and continuous point of attachment to the fetal surface, and is often associated with numerous vascular anastomoses between the two placental beds. Note that any peeling maneuvers should be performed on only a portion of the dividing membrane, so that some intact membrane is preserved for histology.

Histologic examination of either a roll of the dividing membrane or a T-shaped section that includes a portion of the dividing membrane attached to the fetal surface is used for confirmation of the type of placentation. The dividing membrane in dichorionic–diamniotic fused twin placentas consists of a central layer of two fused chorionic membranes sandwiched in between the two amniotic membranes (Fig. 9.16). In contrast, the dividing membrane in monochorionic–diamniotic fused twin placentas consists of two fused amniotic membranes without any intervening chorionic tissue (Fig. 9.17). The presence or absence of the central stripe of chorion-derived intermediate trophoblastic tissue is the key distinguishing histologic feature, and the presence of the two fused chorions in the dividing membrane of dichorionic–diamniotic placentas is what makes it thick and opaque rather than thin and translucent.

The fact that there is no chorion in the dividing membrane of the *monochorionic*–diamniotic fused twin placenta can be a source of confusion. The various designations (such as monochorionic–diamniotic) refer to the type of placentation rather than serving as an indicator of the composition of the dividing membrane; the single chorion that is referred to in the monochorionic–diamniotic fused twin placenta forms part of the membrane that envelopes the entire periphery of both

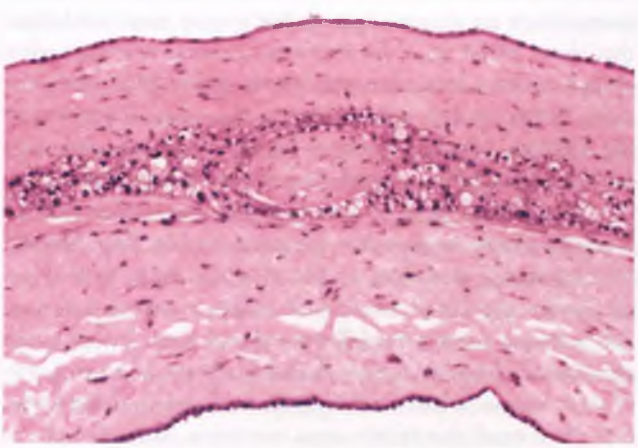

FIGURE 9.16. Dividing membrane of a dichorionic–diamniotic fused twin placenta. The fusion of the two chorions results in a central cellular stripe composed of chorionic-type intermediate trophoblast. The centrally located nodule within the cellular band is a remnant of a chorionic villus that has undergone pressure atrophy. Amniotic epithelium lines both sides of the dividing membrane.

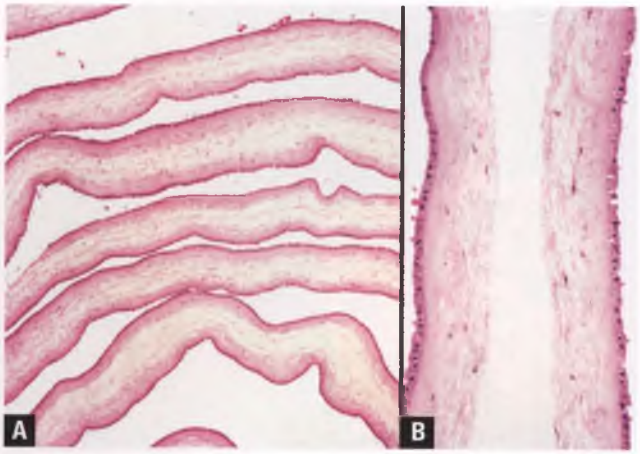

FIGURE 9.17. Dividing membrane of a monochorionic–diamniotic fused twin placenta. **A:** This partial view of a membrane roll demonstrates the presence of two loosely adherent amnions without an interposed layer of chorionic tissue. **B:** Because the two amnions are easily separated from one another, there is often an artifactual space between these two layers.

FIGURE 9.18. Twin–twin transfusion syndrome. In this section through a formalin-fixed placenta from a monochorionic–diamniotic twin placenta at 34 weeks gestational age, the pale and larger placental territory represents that of the donor twin, whereas the smaller, darker, and congested placental territory at right corresponds to that of the recipient twin. The donor twin was smaller, anemic, and died in utero; the recipient twin was larger, polycythemic, and survived. (Courtesy of Dr. Julio A. Lagos.)

twins. Placentas of this type are at risk for twin–twin transfusion syndrome, as discussed in the following section.

TWIN–TWIN TRANSFUSION SYNDROME[10–12]

Twins from monochorionic placentas frequently share portions of their intraplacental vascular circulation. Such twins are at risk for the development of twin–twin transfusion syndrome, which is associated with a high incidence of premature delivery, cerebral palsy, intrauterine fetal demise, and perinatal death. This syndrome develops when significant artery-to-vein communications are present deep within one or more cotyledons that shunt blood from the arteries of a donor twin through a shared capillary network to the venous system of the recipient twin. Artery-to-vein anastomoses in the other direction and the presence of artery-to-artery or vein-to-vein anastomoses may lessen the clinical significance of twin–twin transfusions.

The various types of vascular anastomoses that may be found in monochorionic twin placentas are best demonstrated by cannulating umbilical vessels, flushing them with water to remove the blood from their major placental branches, and injecting them with different colored dyes. Stripping the amnion off of the fetal surface further facilitates the examination of these vessels. When evaluating the fetal vessels of the chorionic plate, recall that arteries cross over veins. Note that tears in the placenta, formalin fixation, and previous in utero treatment of vascular anastomoses with laser coagulation will make it difficult or impossible to demonstrate these interconnections.

In full-blown examples of the twin–twin transfusion syndrome, the result is a donor twin with oligohydramnios related to low urine output that is small, anemic, and pale, and a recipient twin with polyhydramnios related to high urine output that is large, polycythemic, and plethoric. An exception with regard to skin tone occurs when the donor twin dies first and the recipient twin acutely exsanguinates into the low-pressure circulation of the dead donor twin, which paradoxically results in the donor twin having a plethoric appearance and the recipient appearing pale.[13] When performing autopsies on twins where the chronic twin–twin transfusion syndrome is a consideration, it is best confirmed by documenting a discordance in heart size, with the donor heart being smaller and lighter than the recipient heart.

The placental territory corresponding to the donor twin in twin–twin transfusion syndrome is classically pale, whereas that of the recipient twin is dark red (Fig. 9.18). It is not uncommon for there to be unequal sharing of the placental territory, which is true for monochorionic twin placentas in general. Histologically, the donor villi are large, edematous, and relatively immature. The capillaries of the donor terminal villi are depleted of mature red blood cells, but may contain nucleated precursors as a compensatory response to fetal anemia (Fig. 9.19A). In contrast, the recipient villi are more mature and their capillaries are stuffed with mature red blood cells (Fig. 9.19B).

FETUS PAPYRACEUS

A fetus papyraceus is a shrunken dead fetus that has been compressed against the fetal membranes by the growth of a living twin (Fig. 9.20). These flattened and necrotic structures are easily overlooked. Their most recognizable feature is the presence of an eye spot due to persistent retinal pigment.

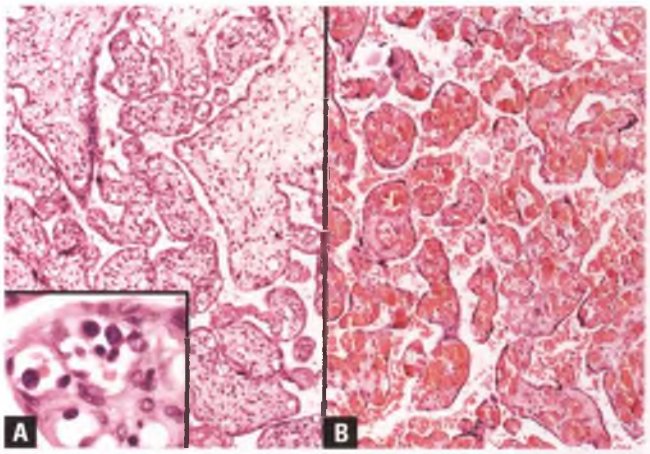

FIGURE 9.19. Twin–twin transfusion syndrome at 34 weeks gestational age. **A:** The donor villi are large, edematous, and noticeably depleted of red blood cells. Nucleated red blood cell precursors are present in some of the villous capillaries, as highlighted in the inset. **B:** The recipient villi are more mature and the villous capillaries are engorged with red blood cells.

CHORIOAMNIONITIS AND FUNISITIS[14,15]

Chorioamnionitis is inflammation of the fetal membranes, whereas funisitis refers to inflammation of the umbilical cord. In most cases, these inflammatory reactions represent a response to an ascending bacterial infection from the cervicovaginal area. Mobilization of maternal neutrophils results in chorioamnionitis, which produces maternal symptoms that include fever, tachycardia, leukocytosis, uterine tenderness, and a malodorous vaginal discharge. However, these findings are neither sensitive nor specific for intrauterine infection. In addition to the maternal component, the fetus can also mount an inflammatory response to an amniotic fluid infection beginning at about 20 weeks of gestation. This response is manifested by acute inflammation of umbilical and chorionic plate vessels, which may spread into neighboring stroma.

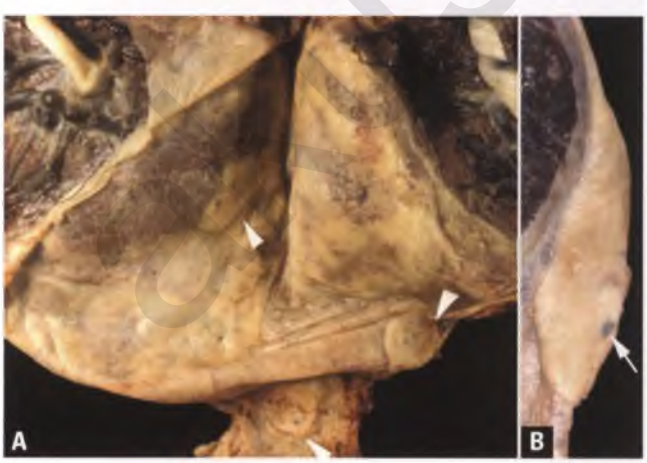

FIGURE 9.20. Fetus papyraceus. **A:** In this specimen from a multigestational pregnancy, note the presence of three separate fetal remnants within the membranes as marked by the white *arrowheads*. **B:** This example features a more prominent eye spot (*arrow*). (Both images courtesy of Dr. Julio A. Lagos.)

FIGURE 9.21. Severe acute chorioamnionitis. The fetal membranes covering the chorionic plate are opaque and pale yellow.

As detailed below, the pathologist should grade and stage chorioamnionitis and funisitis, since their severe and advanced forms are more likely to be associated with complications such as premature delivery, neonatal sepsis, neurologic impairment, and perinatal death.[16] Following these guidelines will provide more clinically relevant and reproducible diagnoses and will assist future efforts in clinicopathologic correlation.

Acute Chorioamnionitis

Subtle examples of acute chorioamnionitis may be grossly inapparent. In well-developed cases, the presence of membranes with an opaque, pale yellow appearance suggests the diagnosis (Fig. 9.21).

The earliest stage of the maternal inflammatory response is referred to as **acute subchorionitis**, during which maternal neutrophils accumulate either in the layer of fibrin that is typically present beneath the chorionic plate or within the decidua of the extraplacental fetal membranes (Fig. 9.22A).* Shortly thereafter, the wave of neutrophils may be found as a localized band within the chorion laeve (Fig. 9.22B). This stage is referred to as **acute chorionitis**, and is also considered to be early in the course of the maternal inflammatory reaction. These early stages are estimated to indicate the presence of an infection that has been ongoing for 6 to 12 hours.

In the typical case of **acute chorioamnionitis**, there is a neutrophilic infiltrate within the fibrous chorion above the

*Whether the presence of neutrophils within the membranous decidua is indicative of a response to an amniotic fluid infection is controversial. Since the lack of an association of this finding with clinical symptoms could be explained equally well by it (a) representing an early, asymptomatic phase of acute chorioamnionitis, or (b) being totally nonspecific, it does not appear that this controversy is easily resolvable.

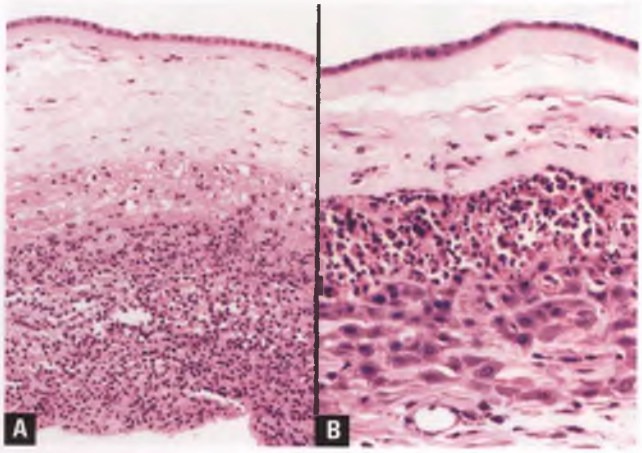

FIGURE 9.22. Early maternal inflammatory response to an infection of the amniotic fluid. **A:** Acute subchorionitis. There is a dense infiltrate of neutrophils in the decidual layer beneath the chorion laeve of the extraplacental fetal membranes, which could descriptively be termed acute membranous deciduitis. **B:** Acute chorionitis. A band of neutrophils has accumulated at the top of the trophoblastic layer of the chorion laeve. The overlying amnion is unremarkable.

chorion laeve and/or the amnion (Fig. 9.23). This reaction represents the intermediate stage of the maternal inflammatory response, and is estimated to develop between 12 and 36 hours after infection of the amniotic fluid. Acute chorioamnionitis is graded as severe when there is a continuous, confluent, and thick band of neutrophils or when subchorionic microabscesses are present. After 36 hours, it is likely that the advanced stage of the maternal inflammatory response will be present. This stage is manifested by **necrotizing chorioamnionitis**, which features karyorrhectic fragments derived from degenerating neutrophils, thickening and hypereosinophilia of the amniotic basement membrane, and degeneration and sloughing of portions of the amniotic epithelium.

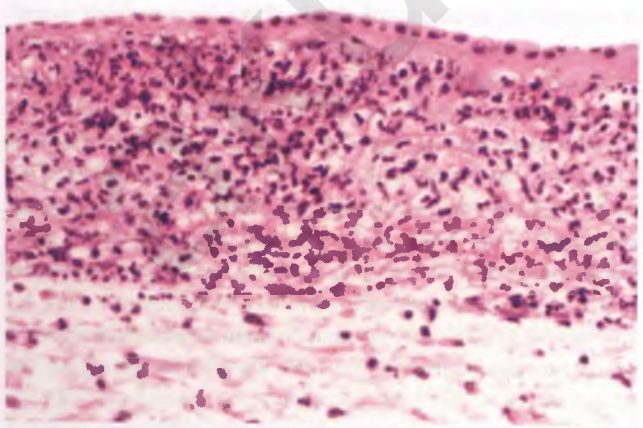

FIGURE 9.23. Severe acute chorioamnionitis. The membrane overlying the chorionic plate contains a dense band of acute inflammatory cells that extends to just beneath the surface layer of amniotic epithelial cells.

Chronic Chorioamnionitis

The definition of this entity has not been standardized, its etiology is unknown, and it is variably described as an unusual variant of chorioamnionitis[17,18] or as being commonly seen in patients with preterm labor and premature rupture of membranes.[19] Most investigators define chronic chorioamnionitis as the presence of a chronic inflammatory infiltrate within the fetal membranes that is dominated by small lymphocytes of T lineage, find an occasional association with acute chorioamnionitis, and note a strong association with villitis of unknown etiology (VUE).[17–19] However, others state that the mononuclear cells that characterize this lesion are predominantly macrophages, which by definition do not include those that are involved in scavenging meconium or hemosiderin, and note that coexistent acute chorioamnionitis should be at least focally present.[14] It seems likely that the former investigators are studying an entity that may often have an immunologic basis related to maternal T cells reacting against fetal tissue. In contrast, the latter authors appear to be studying examples of protracted cases of acute chorioamnionitis that have been smoldering for days or weeks, which should be designated as subacute rather than chronic chorioamnionitis.[20]

Funisitis

The fetal response is manifested by migration of fetal neutrophils from the lumens of umbilical and chorionic plate vessels across their smooth muscle walls and into neighboring stroma. The early stage of the inflammatory response involves neutrophils infiltrating the wall of chorionic plate vessels (chorionic vasculitis) or the umbilical vein (umbilical phlebitis). There is evidence that arterial involvement occurs later and is more likely to be associated with clinically significant adverse events such as neonatal sepsis. For these reasons, involvement of one or both umbilical arteries is considered an intermediate stage of the fetal inflammatory response. Whether veins or arteries are involved, the inflammatory infiltrate is typically oriented toward the source of the infection in the amniotic cavity (Fig. 9.24). Involvement of Wharton's jelly is allowed in either stage, as long as it has not progressed to concentric umbilical perivasculitis or necrotizing funisitis (see below). Given the significance of umbilical arterial versus venous involvement, the unqualified diagnosis of "acute funisitis" is too nonspecific; preferred diagnostic terms include umbilical phlebitis (vein only), umbilical arteritis (one or both arteries only), umbilical vasculitis involving vein and one artery, and umbilical panvasculitis (vein and both arteries).

The advanced stages of the fetal inflammatory response include concentric umbilical perivasculitis and necrotizing funisitis. In the former, dense bands of neutrophils encircle one or more umbilical vessels. Necrotizing funisitis is grossly characterized by a "barber pole" appearance to the unsectioned cord and by perivascular bands or crescents of off-white to pale yellow necrotic tissue when the cord is viewed in cross section.[21,22] Histologically, the necrotic zones within Wharton's

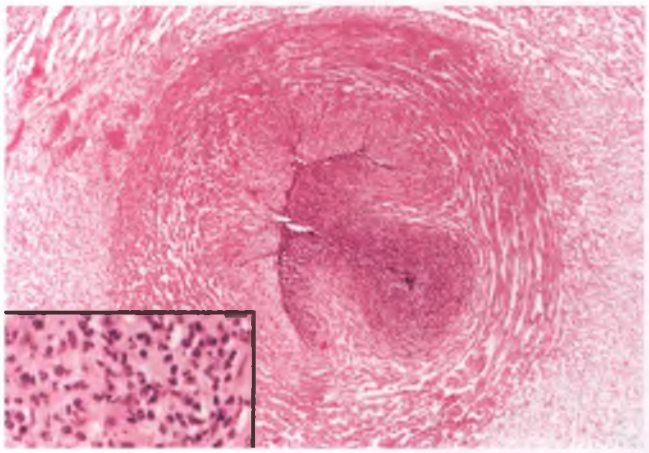

FIGURE 9.24. Acute funisitis with involvement of an umbilical artery. A dense infiltrate of fetal neutrophils is seen migrating through a portion of the wall of an umbilical artery. The inflammation is oriented toward the source of the infection in the amniotic cavity. The inset highlights the neutrophilic nature of the inflammatory infiltrate.

jelly contain areas with abundant amounts of fragmented inflammatory debris and calcified material related to neutrophil karyorrhexis (Fig. 9.25). No exudate is present on the surface of the involved umbilical cord.

Candida Funisitis[23,24]

A distinctive feature of *Candida* chorioamnionitis is the presence of grossly recognizable pale yellow plaques measuring up to 2 mm in diameter that are found on the surface of the umbilical cord. The histologic correlate is a peripheral funisitis

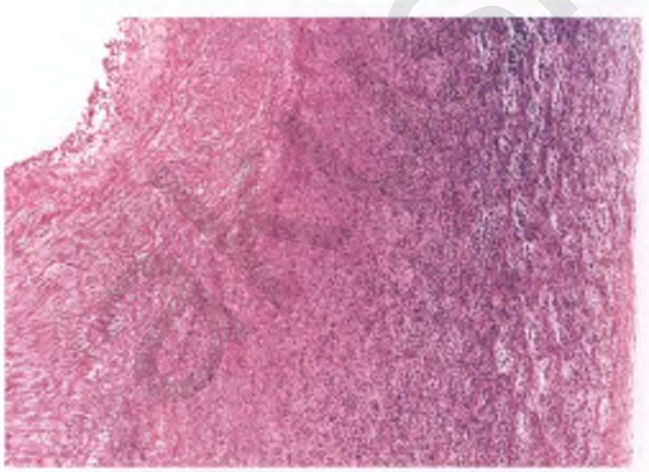

FIGURE 9.25. Necrotizing funisitis. The outer portion of the band of necrosis is darkly stained due to its high content of inflammatory cells and associated basophilic debris. The lumen and smooth muscle wall of the neighboring vessel are in the upper left portion of the image. Note that the normal feathery myxomatous tissue of Wharton's jelly is conspicuously absent. The surface of the umbilical cord at right has lost its amniotic epithelium, but is free of exudative material.

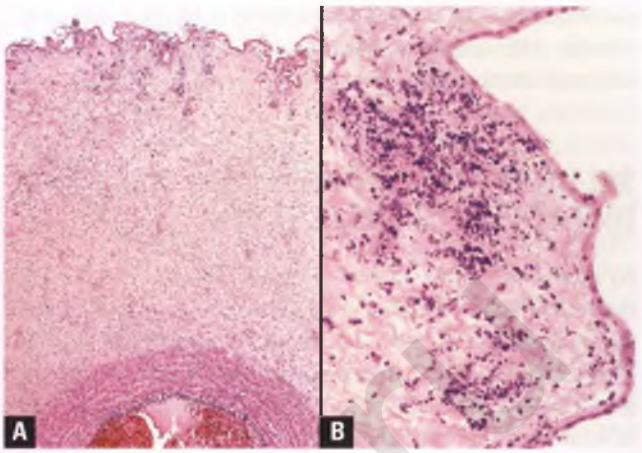

FIGURE 9.26. Peripheral funisitis secondary to infection with *Candida* organisms. **A:** In this low-magnification view, note the presence of a patchy inflammatory infiltrate near the surface of the umbilical cord (top). **B:** At higher magnification, the subamniotic location of the *Candida* microabscesses is apparent. A Gomori methenamine silver stain showed fungal organisms consistent with *Candida* species (not shown). (Glass slide kindly provided by Dr. Cheryl M. Reichert.)

in which inflammatory debris is present at the cord surface and nearby microabscesses are located just beneath the amniotic epithelium (Fig. 9.26). Fungal organisms consistent with *Candida* species are present in the inflamed areas.

CHRONIC DECIDUITIS[15,25]

Chronic deciduitis of the basal plate is characterized by either a diffuse lymphocytic infiltrate or a less impressive chronic inflammatory infiltrate that includes the presence of plasma cells (Fig. 9.27). Some cases may represent preexisting chronic

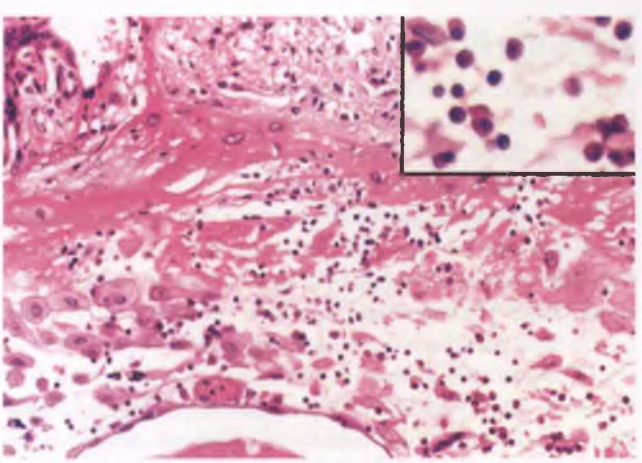

FIGURE 9.27. Chronic deciduitis of the basal plate. Scattered lymphocytes and plasma cells are present, as shown at higher magnification in the inset.

endometritis or an abnormal response to the placental allograft, whereas others may be related to neighboring chronic villitis or maternal arteriopathy.

SELECTED VILLITIS-PRODUCING INFECTIOUS DISEASES OF THE PLACENTA

As mentioned above, the infectious agents that produce chorioamnionitis and funisitis generally ascend from the cervix or vagina to involve the amniotic cavity. In contrast, the so-called TORCH infections[†] have a hematogenous mode of transmission, reach the placenta via the maternal circulation, and result in inflammation of the chorionic villi (villitis).

Cytomegalovirus

Cytomegalovirus (CMV) is the most common recognizable infectious cause of chronic villitis, and may be associated with significant developmental abnormalities or intrauterine fetal demise. Placentas infected by CMV do not have a distinctive gross appearance. Histologically, the villi often appear overly cellular due to an increased number of lymphocytes, plasma cells, histiocytes, and stromal cells. The most characteristic histologic findings of CMV villitis are (a) a lymphoplasmacytic infiltrate associated with remnants of obliterated blood vessels (Fig. 9.28) and (b) large, round to oval, purple intranuclear inclusions surrounded by a clear halo, sometimes accompanied by small cytoplasmic inclusions (Fig. 9.29A). Depending on the case, CMV inclusions may be readily identifiable or vanishingly rare, and may be found within endothelial cells, macrophages, or trophoblastic cells.[26] Immunohistochemical stains using an antibody directed against CMV can facilitate the diagnosis (Fig. 9.29B).[27] Other histologic findings that are seen in some cases of CMV villitis include villous stromal necrosis, hemosiderin deposition, calcification, and fibrosis.

Parvovirus B19[28]

Parvovirus B19 is the etiologic agent of the dermatologic condition known as erythema infectiosum ("fifth disease"), which is a rash-producing illness that is most common in children. Most adults who are infected with parvovirus B19 are either asymptomatic or develop a self-limited arthropathy, but this virus can be transmitted to the fetus and placenta. Parvovirus B19 selectively infects and destroys actively dividing cells, and has a particular affinity for erythroblasts. The consequences to the fetus range from insignificant to fatal, with death occurring in about 10% of cases.

The fetal anemia that may be induced by parvovirus B19 infection typically results in a placenta that is large and pale. Villi are edematous, and features of villitis are conspicuously absent. Careful examination of the villous capillaries reveals erythroblasts with characteristic intranuclear inclusions that are glassy and light purple, which displace the host chromatin to the periphery of the nuclear membrane (Fig. 9.30A). The diagnosis can be further substantiated using immunohistochemistry (Fig. 9.30B). Parvovirus inclusions may also be found in fetal autopsy tissue, particularly within the bone marrow and liver.

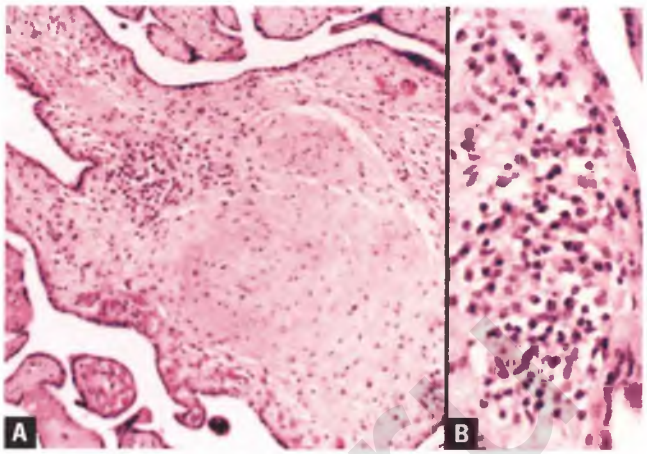

FIGURE 9.28. CMV villitis from a case with intrauterine fetal demise at 28 weeks gestational age. **A:** Note the presence of a focal lymphoplasmacytic villous infiltrate associated with a central nodular aggregate of vessels whose lumens have been obliterated. **B:** This high-magnification view highlights an area with prominent lymphoplasmacytic villitis.

Congenital Syphilis[29–31]

Syphilis is caused by the spirochete *Treponema pallidum*. Pregnant women with this disease can transmit this microorganism to the fetus through the placenta. This is an unusual

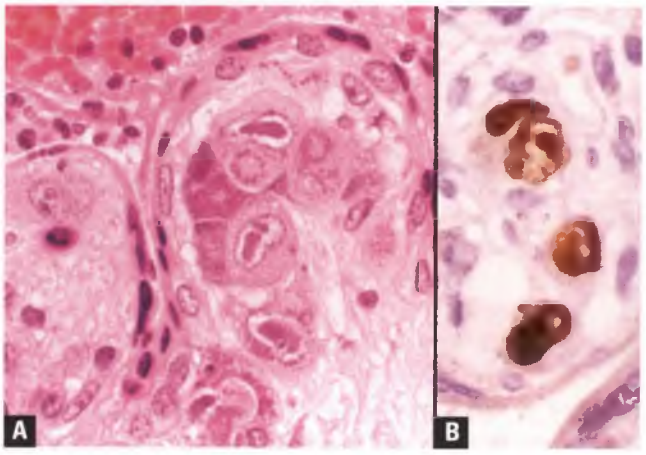

FIGURE 9.29. CMV villitis from a case with intrauterine fetal demise at 17 weeks gestational age. **A:** Characteristic intranuclear inclusions with halos are present, along with granular cytoplasmic inclusions. **B:** This image shows reactivity of the infected cells with a CMV immunohistochemical stain.

[†]TORCH is an acronym for a group of viral, bacterial, and parasitic infections that can infect the placenta, fetus, and neonate. It stands for **T**oxoplasmosis, **O**thers (e.g., syphilis, varicella zoster, parvovirus B19), **R**ubella, **C**ytomegalovirus, and **H**erpes simplex virus.

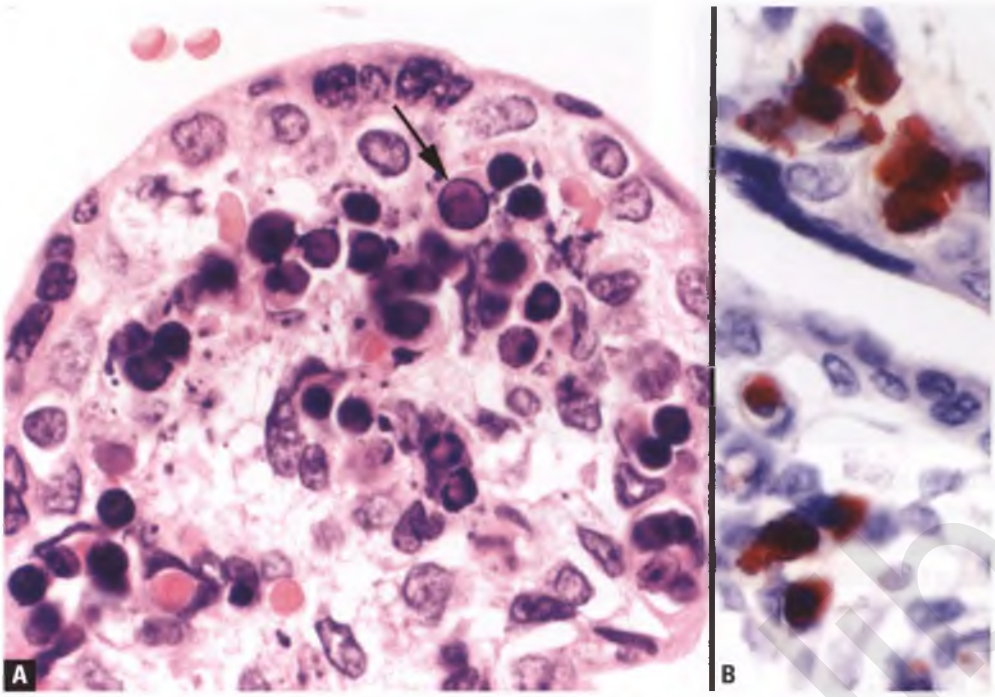

FIGURE 9.30. Chorionic villi with parvovirus B19 infection from a case of intrauterine fetal demise at 23 weeks gestational age. **A:** Several of the erythroblasts within the villous capillaries, such as the one marked by the *arrow*, contain characteristic intranuclear inclusions with peripheral condensation of chromatin. **B:** This image demonstrates the presence of infected erythroblasts using a parvovirus B19 immunohistochemical stain.

occurrence in compliant patients who have access to first trimester screening and effective antibiotic treatment. However, when it occurs, it often leads to abortion and stillbirth.

The placenta in congenital syphilis is usually large and composed of relatively immature villi. These enlarged villi contain an increased number of macrophages, which is the primary reason for their hypercellular appearance (Fig. 9.31). Focal areas of acute or chronic villitis may be present, along with fibrotic vascular changes that may result in villous vessels with luminal narrowing, recanalization, or obliteration. The more subtle vascular changes of congenital syphilis are characterized by a few concentric layers of pericapillary fibrosis, which results in an onion skin pattern (Fig. 9.31). Nucleated red blood cell precursors are commonly seen within the fetal circulation in stillborns with congenital syphilis, which is reflective of fetal anemia and/or hypoxia.[29]

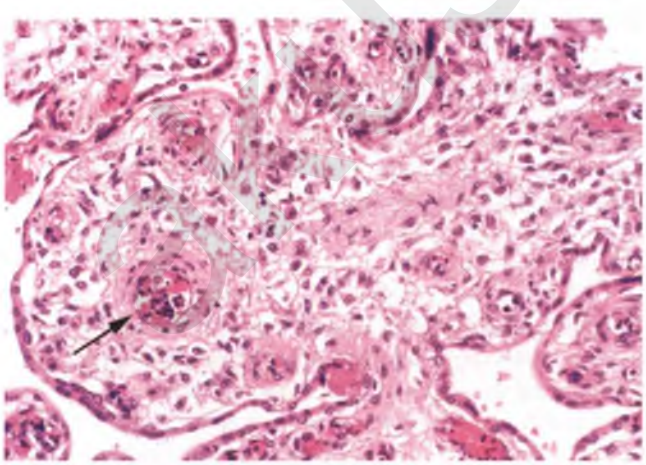

FIGURE 9.31. Placenta from a stillborn fetus with congenital syphilis at 34 weeks gestational age. The enlarged villi are hypercellular and show some concentric pericapillary stromal fibrosis (*arrow*). Several nucleated red blood cell precursors are also present within the villous capillary marked by the *arrow*.

The histologic triad that suggests the diagnosis of congenital syphilis can be summarized as the presence of enlarged hypercellular villi, proliferative fetal vascular changes, and acute or chronic villitis.[30] The identification of spirochetes is required for definitive diagnosis, and may be accomplished by silver stains (Dieterle, Steiner and Steiner, or Warthin-Starry), immunofluorescence, immunohistochemistry, or polymerase chain reaction.[30]

Although one study found a strong association between necrotizing funisitis and congenital syphilis,[21] the bulk of the literature suggests that this severe form of funisitis can be caused by a variety of infectious agents.[22,32,33]

Congenital Listeriosis[31]

Congenital listeriosis is caused by *Listeria monocytogenes*, which is a gram-positive bacterial rod. Infection of the fetus and placenta with this organism may result in premature delivery, neonatal sepsis, meningitis in the first few weeks after birth, or spontaneous abortion.

Listeria villitis is distinctive in that neutrophils rather than chronic inflammatory cells predominate, and only scattered villi are involved (Fig. 9.32). In areas with more extensive involvement, there may be patches of villous necrosis and abscess formation. In some cases, these small abscesses may be grossly visible as punctate pale yellow foci within the substance of the placenta. Chorioamnionitis is also typically present, which may be associated with funisitis.

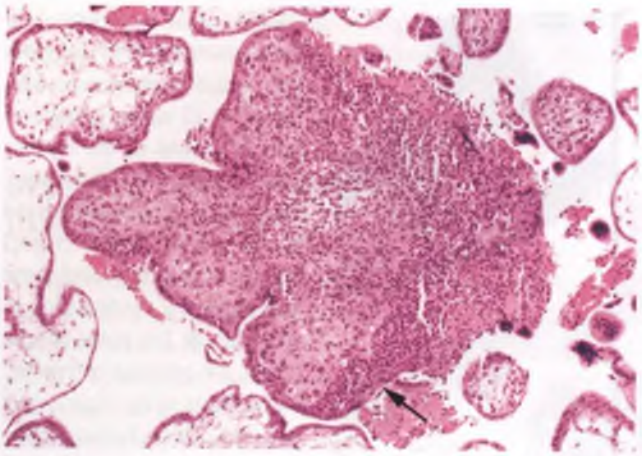

FIGURE 9.32. Congenital listeriosis from a spontaneous abortion at 15 weeks gestational age. The involved villus contains an extensive neutrophilic infiltrate. As is typical, the neutrophils in some areas are sandwiched between the trophoblastic layer and the villous stroma (*arrow*).

VILLITIS OF UNKNOWN ETIOLOGY[31,34,35]

VUE affects approximately 10% of placentas. It is estimated that roughly 95% of cases of chronic villitis fall into this category, with most of the remainder due to TORCH infections. Since VUE is a microscopic finding, adequate sampling of the placenta is necessary to detect it. About 90% of cases can be identified with standard protocols that sample two to three sections of placental parenchyma, although higher detection rates can be obtained with additional sampling.

VUE is characterized by a lymphohistiocytic infiltrate involving villi in a focal and patchy distribution that may preferentially involve distal villi, stem villi, or basal villi (Fig. 9.33). The presence of villous plasma cells should suggest an infectious process such as CMV placentitis. Stem villi involved by VUE may show obliterative loss of vessels, which results in clusters of avascular sclerotic villi in the downstream territory supplied by these vessels. In cases with stromal destruction and trophoblastic necrosis, the involved villi agglutinate in a manner that stands out at low magnification.

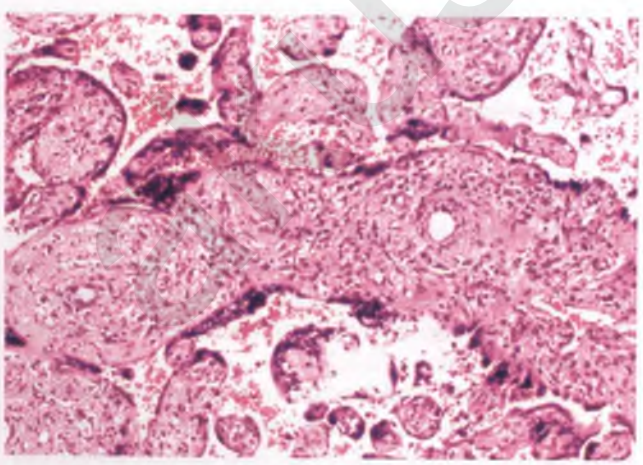

FIGURE 9.33. VUE from a placenta at 40 weeks gestational age with a history of intrauterine growth restriction. The abnormal villi exhibit increased cellularity due to an infiltrate of lymphocytes and histiocytes. Involutional vascular changes are also present.

The finding that most of the intravillous lymphocytes in VUE are T cells of maternal origin suggests that this lesion may represent a host (mother) versus graft (placenta) reaction. However, VUE is a diagnosis of exclusion, and it is not possible in any given case to exclude with complete confidence the presence of an undetected causative infectious agent.

Differential Diagnosis

The differential diagnosis of VUE includes infectious chronic villitis and, in those cases of VUE with obliterative vascular changes, there is also a resemblance to fetal thrombotic vasculopathy (FTV).

- In contrast to villitis related to viral and syphilitic infections, there is no evidence of infection in either the mother or infant with VUE. In addition, VUE tends to occur in placentas from pregnancies that are at or near term, shows patchy villous involvement, and is limited to terminal and stem villi, whereas infectious chronic villitis is usually associated with preterm deliveries, generally involves the entire villous tree, and commonly involves the fetal membranes or umbilical cord as well.
- VUE with stem villous involvement associated with obliterative fetal vasculopathy and FTV can both feature prominent areas of downstream avascular sclerotic villi, but the former lesion is distinguished by the presence of a significant lymphohistiocytic infiltrate within the villous stroma.

Clinicopathologic Correlation

When focal and low grade, as is usually the case, VUE is usually not associated with an adverse pregnancy outcome. However, well-developed examples of VUE are an important cause of intrauterine growth restriction, neurologic impairment, and recurrent pregnancy loss.

VUE has been reported to recur in up to 25% of cases. Recurrent lesions may be of greater severity than their predecessors, which is presumably a reflection of previous antigenic priming and the reactivation of memory T cells.

PLACENTAL INFARCTS[36]

An infarct is a region of coagulative necrosis related to local ischemia that results from obstruction of the blood flow that supplies that area. In placental infarcts, the vessels that are occluded are of maternal origin and are usually branches of the spiral arteries at the

FIGURE 9.34. Acute and subacute infarcts. **A:** This section through fresh placental tissue demonstrates the presence of an acute infarct involving the left half of specimen. **B:** This section through formalin-fixed placental tissue shows extensive involvement by tannish brown infarcts that spare the central aspect. Although these infarcts are older than the red infarct in **(A)**, their colors are not directly comparable because of differences in fixation. The maternal surface is at the bottom of both images.

FIGURE 9.35. Old infarcts. Several old infarcts with a *pale yellow* appearance are present in these cross sections through formalin-fixed placental tissue. Note how the base of the infarcts abuts the maternal surface at the bottom of the slices. (Courtesy of Dr. Julio A. Lagos.)

base of the placenta that normally enter the intervillous space. Placental infarcts are common, especially in women with preeclampsia, essential hypertension, and thrombophilic disorders. When focal, these infarcts represent incidental findings, but multiple or large infarcts or those found during the first two trimesters suggest maternal vascular disease and are more likely to be of clinical significance. Extensive infarction is associated with fetal hypoxia, intrauterine growth restriction, and intrauterine fetal demise.

Acute placental infarcts are red, and are drier and firmer than uninvolved placental tissue (Fig. 9.34A). As the infarcts age, they become brown (Fig. 9.34B) and eventually turn into hard, off-white to pale yellow masses (Fig. 9.35). They classically are wedge shaped, with the base of the wedge abutting the basal plate.

Histologically, early infarcts show collapse of the intervillous space and villous agglutination followed by gradual loss of intensity of basophilic staining of the nuclei of the syncytiotrophoblastic lining (Fig. 9.36). Old infarcts consist of ghost outlines of completely necrotic villi separated by variable amounts of fibrin (Fig. 9.37).

MATERNAL FLOOR INFARCTION/MASSIVE PERIVILLOUS FIBRIN DEPOSITION[37–40]

Maternal floor infarction is an uncommon disorder of unknown etiology that may cause premature delivery, intrauterine growth restriction, neurologic impairment, or fetal death. It may recur in subsequent pregnancies, which is important information to convey to the obstetrician and patient. Most investigators currently think that maternal floor infarction and massive perivillous fibrin deposition are variants of the same entity, with the major difference being the site of the bulk of the fibrinoid deposits. Since intervillous and basal plate fibrin is present to some degree in all placentas, the diagnosis of maternal floor infarction/massive perivillous fibrin deposition can be subjective in borderline cases. It has been suggested that at least a portion of the maternal surface of the placenta have fibrinoid deposits that result in a thickness of ≥3 mm before a diagnosis of maternal floor infarction is rendered.[38]

Maternal floor infarction is somewhat of a misnomer, since the primary abnormality is massive deposition of fibrin in the decidual rim of the basal plate and to varying degrees in the intervillous space, which secondarily leads to villous atrophy, sclerosis, or infarction. Grossly, classic cases of maternal floor infarction exhibit a thickened, firm, pale yellow, corrugated rind over large portions of the basal plate related to deposits of fibrin (Fig. 9.38). The extent to which this fibrinoid material extends into the substance of the placenta is variable from region

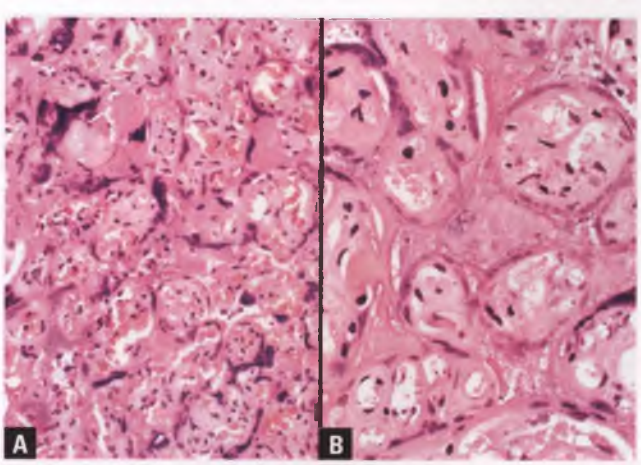

FIGURE 9.36. Acute infarcts. **A:** The terminal villi are crowded together with loss of much of the intervillous space. **B:** In this slightly more advanced example, some of the syncytiotrophoblastic nuclei stain less intensely than normal and have a smudged appearance.

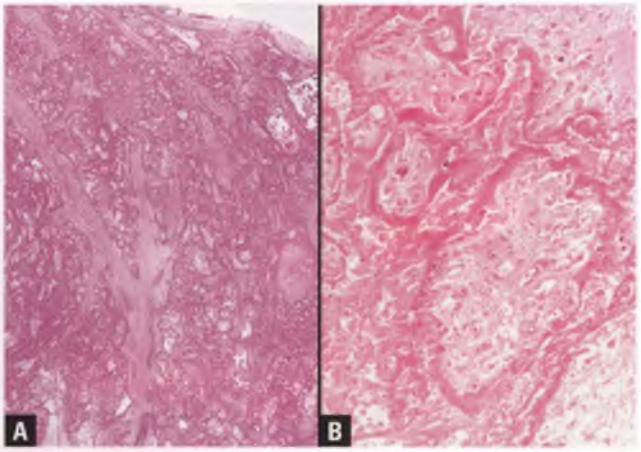

FIGURE 9.37. **A,B:** Old infarcts. Ghost outlines of a confluent mass of necrotic villi are separated by variable amounts of fibrin.

to region and case to case (Fig. 9.39). In some cases, the deposition of this material in a net-like distribution from the basal to chorionic plates imparts a lardaceous or marbled appearance to the sectioned surface, and cystic spaces may be present within the substance of the placenta (Figs. 9.40 and 9.41A). These cystic spaces may represent either residual blood-filled lakes within the intervillous space (Fig. 9.41B) or septal cysts as shown in Figure 9.13.

As mentioned above, chorionic villi in the involved areas show secondary changes related to the effects of encasement and slow strangulation by the fibrinoid deposits (Fig. 9.42). Extravillous intermediate trophoblastic cells have a tendency to migrate into and proliferate within the fibrinoid material (see Figs. 10.38 and 10.39).

In contrast to true infarcts that are caused by an occlusive vascular event, villi entrapped by massive amounts of fibrin do not form a confluent mass. In addition, the villi enmeshed in fibrin maintain their normal spacing, whereas in recent infarcts, the villi are closely approximated due to the collapse of the intervillous space that is caused by a lack of perfusion.

FIGURE 9.38. Maternal floor infarction. The deposition of fibrin over most of the maternal surface has resulted in a pale, corrugated appearance that is sometimes referred to as a "gyriform" pattern. The normal cotyledonoid architecture of the maternal surface is conspicuously absent. (Courtesy of Dr. Julio A. Lagos.)

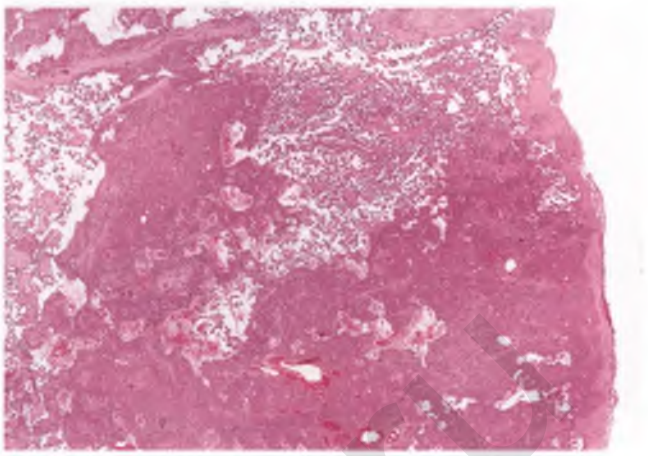

FIGURE 9.39. Maternal floor infarction/massive perivillous fibrin deposition. In this example, excessive fibrinoid material is present in portions of the basal plate at right and throughout most of the placental parenchyma.

SUBCHORIONIC FIBRIN PLAQUES

In term placentas, incidental fibrin plaques that represent thrombosis of maternal blood are commonly found beneath the chorionic plate. These off-white to pale yellow plaques are usually about 2 to 3 cm in diameter and only a few mm thick, and may have a laminated appearance when viewed in cross section (Fig. 9.43). Chorionic villi are not incorporated into these plaques. The most likely explanation for their formation is that they are related to traumatization of the chorionic plate during the course of normal fetal movements.[41]

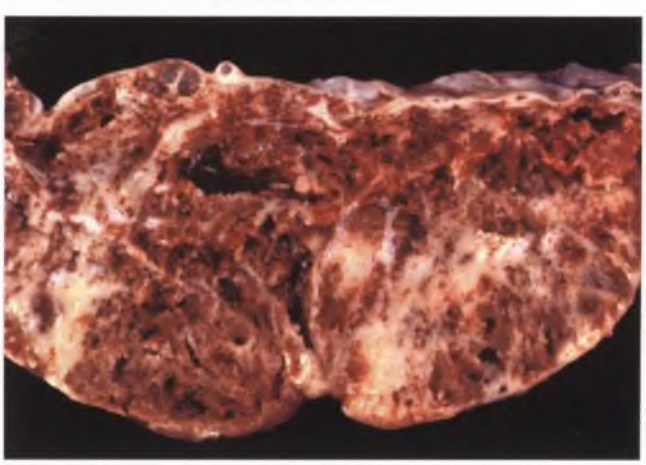

FIGURE 9.40. Maternal floor infarction/massive perivillous fibrin deposition. This cross section reveals placental tissue with massive perivillous fibrin deposition extending from the basal plate (bottom) to the fetal surface (top).

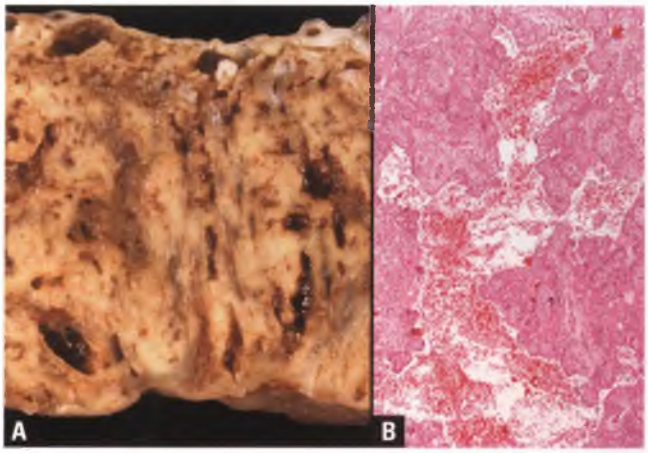

FIGURE 9.41. Maternal floor infarction/massive perivillous fibrin deposition. **A:** This section through a formalin-fixed placenta shows full-thickness lardaceous deposits of fibrin and scattered cysts, some of which are filled with blood. **B:** This histologic section demonstrates an irregularly shaped residual blood lake within the intervillous space. (Gross image courtesy of Dr. Julio A. Lagos.)

INTERVILLOUS THROMBI

Intervillous thrombi are a common finding within the substance of the placenta. They may be single or multiple and typically measure 1 to 2 cm in diameter. When recently formed, they are dark red clots, but over time they evolve into lesions that are laminated and off-white. The section on fetomaternal hemorrhage contains an example of the gross appearance of intervillous thrombi (see Fig. 9.55).

Intervillous thrombi displace villi and are composed of an admixture of fetal and maternal red blood cells and fibrin that are usually at least focally laminated in histologic sections (Fig. 9.44). They are indicative of focal fetal hemorrhage into the maternal blood of the intervillous space that presumably occurs via rupture of a villus at its thinnest and weakest point (the vasculosyncytial membrane). Isolated intervillous thrombi represent an incidental finding, but when multiple these lesions may be an indication of more clinically significant fetomaternal hemorrhage, as discussed later in this chapter.

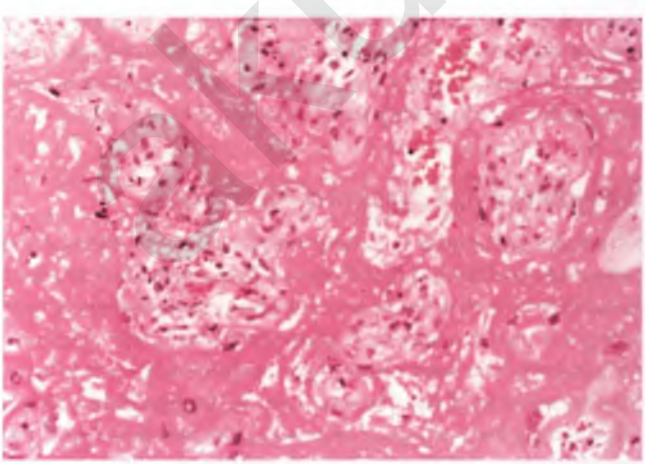

FIGURE 9.42. Maternal floor infarction/massive perivillous fibrin deposition. In this high-magnification view, perivillous fibrinoid material is seen encasing atrophic villi. This histologic pattern differs from that of infarcted placental villi (compare with Figs. 9.36 and 9.37).

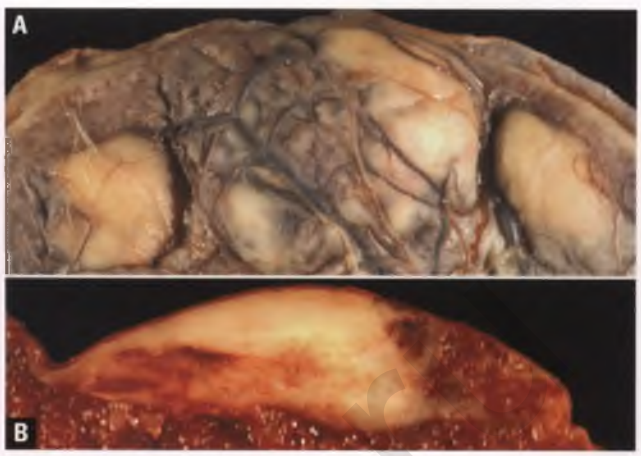

FIGURE 9.43. Subchorionic fibrin plaques. **A:** This portion of the chorionic plate contains several pale yellow plaques. **B:** Cross-sectional view of one of these plaques.

HEMATOMAS

Marginal Hematoma

Marginal hematomas are located at the junction of the peripheral margin of the placental disc and the extraplacental fetal membranes. These crescentic-shaped blood clots may track along the undersurface of the adjacent fetal membranes or extend onto the maternal surface of the placenta (Fig. 9.45).

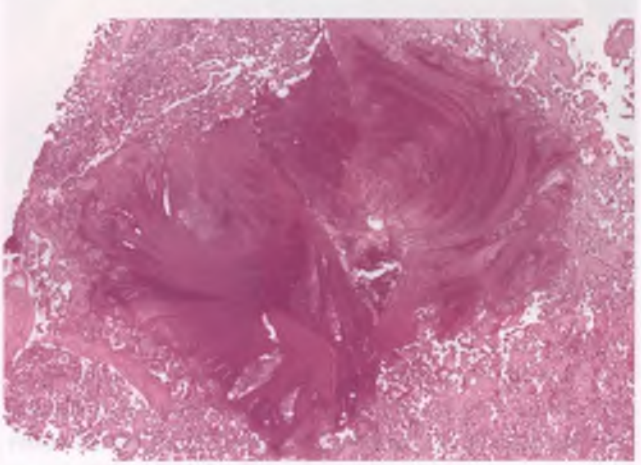

FIGURE 9.44. Intervillous thrombus. Note the laminations, which are most prominent in the upper right portion of the thrombus.

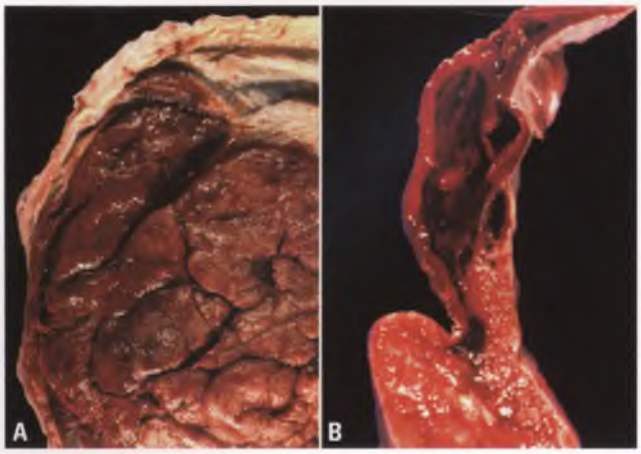

FIGURE 9.45. Marginal hematoma. **A:** In this view of the maternal surface, a crescentic-shaped, dark red blood clot is wedged between the peripheral margin of the placenta and the fetal membranes. **B:** In this section through the marginal hematoma and placenta, the fetal surface is at right and the maternal surface is at left. Note how the hematoma tracks underneath the fetal membranes in the top half of the image.

Retroplacental Hematoma

A large retroplacental hematoma is the type of hematoma that is most often associated with placental abruption, which is discussed at the end of this section. These hematomas are sandwiched in between the basal plate and the superficial aspect of the uterine wall. Indentation and compression of the overlying placental tissue by the hematoma often leads to villous infarction (Fig. 9.46). With time, the hematoma turns brown and may develop string-like strands or degenerative cysts on its path toward resorption.

FIGURE 9.46. Retroplacental hematoma. This section through a formalin-fixed placenta shows a retroplacental hematoma associated with an overlying compressed rim of infarcted tissue. Compare the appearance of the infarcted tissue with that of normal placental parenchyma at right, and note the stringy appearance and cystic degeneration of portions of the peripheral aspect of the hematoma.

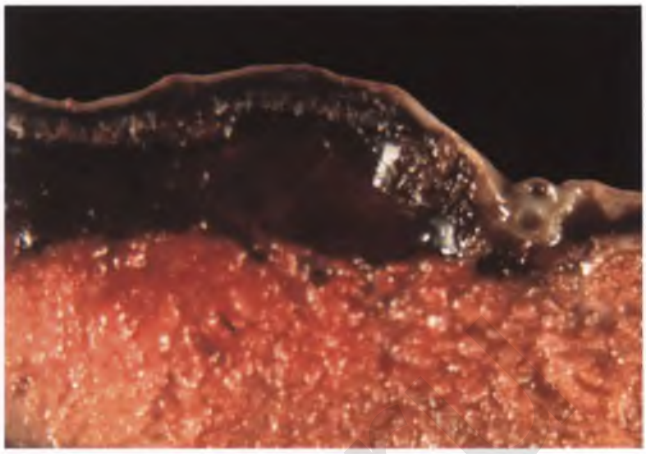

FIGURE 9.47. Subchorial thrombohematoma. Note how the clot is interposed between the chorionic plate and the underlying placental tissue and bulges into the amniotic cavity. The deep margin of the clot is slightly irregular due to focal extensions into the intervillous space.

Massive Subchorial Thrombohematoma[42]

This rare lesion, which is also known as a Breus' mole, represents extravasated blood of maternal origin that dissects and coagulates between the chorionic plate and the underlying villi (Fig. 9.47). These clots bulge into the amniotic cavity, and may extend into the intervillous space. When of sufficient size, these thrombohematomas can be associated with fetal injury or death.

Subamniotic Hematoma[43]

Subamniotic hematomas are secondary to rupture of the fetal vessels that course through the chorionic plate and are separated from the amniotic cavity by only a thin layer of amnion.This type of hematoma rarely occurs in utero and is more often the result of excessive traction on the umbilical cord during delivery. Recent subamniotic hematomas appear as a thin-walled, hemorrhagic cysts protruding into the amniotic cavity. More remote clots of this type are composed of fibrin and brown fluid.

Hematomas and Placental Abruption[44]

When the pathologist encounters a placenta with an attached hematoma or detached blood clot, the major issue that needs to be addressed is whether or not there was a placental abruption (abruptio placentae), which is associated with retroplacental bleeding and clot formation. In this condition, there is premature detachment of the placenta from the uterine implantation site due to a hemorrhagic event at the interface between these two tissue types. If this happens acutely, there will not be sufficient time for clot formation, and the diagnosis will be a clinical rather than pathological one. When extensive and acute, placental abruptions often lead to the death of the fetus and may also result in maternal morbidity or mortality.

The clinical features of abruption include vaginal bleeding coming from the cervical os, pain in the abdominopelvic region, fetal distress, and maternal hypotension. These symptoms may also be seen in other conditions, and are not always present. In cases in which a very recent clot has formed, it may be only loosely attached to the placenta. Such a clot is likely to arrive in the pathology laboratory in separate fragments, which should be measured and weighed (similar clots may form during the normal postpartum period). More established retroplacental hematomas have features as described in the section on these lesions, and their presence should be correlated with the clinical impression of the degree and significance of premature separation from the implantation site.

The varied clinical outcome of placenta-related hemorrhages can best be explained by categorizing them into arterial and venous types.[2] A bleed from a large, centrally located, high-pressure artery is likely to result in the classic acute form of placental abruption and may be associated with a centrally located retroplacental hematoma with compressed and/or infarcted placental tissue. In contrast, hemorrhage from a low-pressure vein is likely to occur in a peripheral, chronically distended vessel and be associated with a marginal hematoma, chronic abruption, and circumvallation. The finding of diffuse chorioamniotic hemosiderosis in this situation can be explained by the passive flow of blood following the path of least resistance, which usually is just beneath the chorion. Hemosiderin may also be deposited within the membranes in cases in which maternal blood has leaked into the amniotic fluid. An example of chorioamniotic hemosiderosis is illustrated in Figure 9.59.

FETAL THROMBOTIC VASCULOPATHY[45–49]

FTV is a chronic disorder that is characterized by thrombi within fetal vessels of the chorionic plate, stem villi, or umbilical cord that result in clustered groups of distal villi with sclerotic and avascular cores and/or stromal-vascular karyorrhexis. Well-developed forms of FTV are associated with intrauterine growth restriction, cerebral palsy, thromboembolic events within the fetus or neonate, and stillbirth. Most commonly, chronic partial or recurrent intermittent obstruction of the umbilical cord is the primary event that leads to the development of FTV via creation of a thrombogenic state (vascular stasis). Arteries and/or veins may be involved. Although fetal arteries of the chorionic plate can be identified using the guideline that arteries cross over veins, differentiation of vessel type is usually not possible in histologic sections.

Grossly, the involved segments of placental parenchyma in florid examples of FTV appear pale and granular, and the occluded fetal vessels can often be identified by (a) their firm, distended appearance, and (b) the presence of discolored thrombotic material within their lumens (Fig. 9.48). In contrast to the agglutinated masses formed by infarcts, the involved placental tissue is not firm, since the abnormal villi remain separated from one another and bathed by the maternal blood in the intervillous space. In those cases in which thrombotic vessels are not grossly identified, they may be found within vessels of stem villi (Fig. 9.49) or their presence may be inferred by the clusters of abnormal villi that demonstrate either avascularity and sclerosis of their cores or stromal-vascular karyorrhexis. These abnormal villi are characteristically found adjacent to or intermingled with functional distal villi that are supplied by a neighboring flowing branch of the fetal vascular system, and are lined by a seemingly unaffected layer of syncytiotrophoblastic cells (Fig. 9.50). Various criteria have been proposed

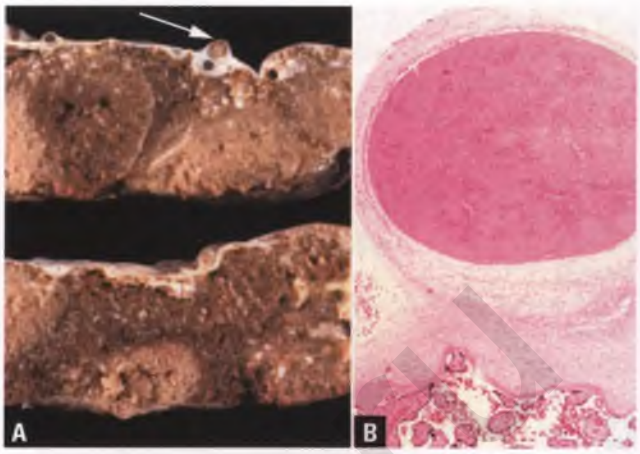

FIGURE 9.48. Fetal thrombotic vasculopathy. **A:** This view of the sectioned surface of two slices of formalin-fixed placental tissue demonstrates the presence of occlusive thrombi within some of the large fetal vessels of the chorionic plate. The largest thrombus (*arrow*) lies within an artery that sits atop a vein that is filled with fresh dark blood. The patches of pale and granular placental tissue correspond to fibrotic avascular villi that are supplied by the occluded arterial vessels. Unlike infarcts, these regions are not firm. **B:** This low-magnification view shows an occlusive thrombus within a large vessel of the chorionic plate. (Gross image courtesy of Dr. Julio A. Lagos.)

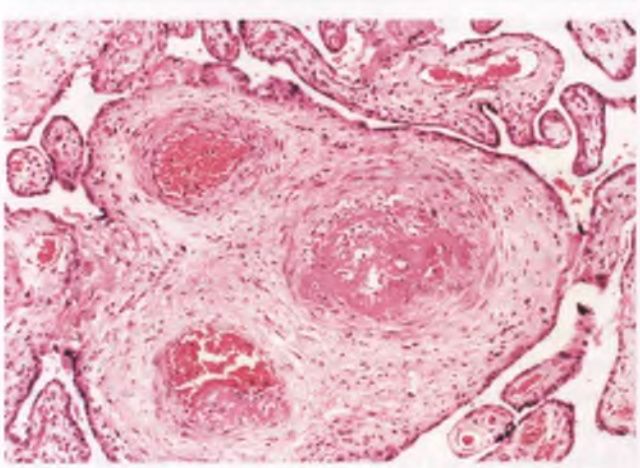

FIGURE 9.49. Fetal thrombotic vasculopathy. In the stem villus that occupies most of this image, recent organizing thrombi are present in two of the three muscularized vessels.

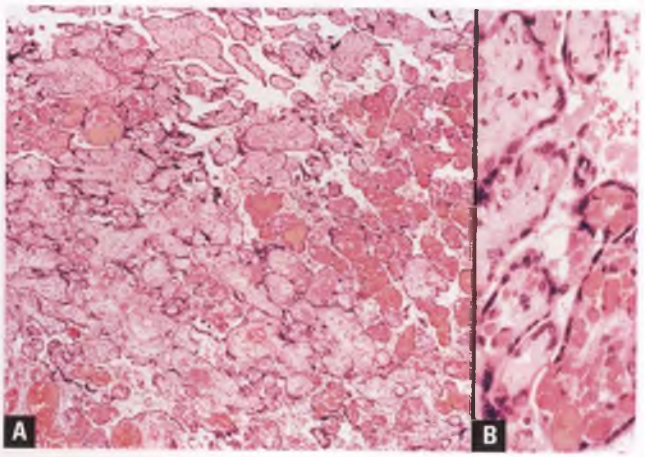

FIGURE 9.50. Fetal thrombotic vasculopathy. **A:** Clusters of fibrotic avascular villi produced by thrombosis of a fetal vessel are intermingled with distal villi whose capillaries are engorged with red blood cells. **B:** Specks of karyorrhectic debris are present within some of the fibrotic villi. Note that the sclerotic villi have a preserved syncytiotrophoblastic lining.

that require these abnormal villi to be of a certain minimum extent in an effort to restrict this diagnosis to lesions of clinical significance. Most recently, an average of >15 affected villi per section of placental parenchyma has been suggested as a minimum diagnostic threshold for FTV.[49]

The lesion that was previously referred to as hemorrhagic endovasculitis is characterized by villous changes that include endothelial and stromal karyorrhexis, organizing thrombi, recanalized vessels, fragmented and extravasated red blood cells, and deposition of hemosiderin,[50] and is now considered to be within the spectrum of FTV. Some examples of this phenomenon may represent an early phase of thrombosis-related villous damage that will gradually progress to the end-stage of avascular sclerotic villi. In other cases, this histologic pattern may be related to venous stasis caused by an upstream venous occlusive thrombus rather than a fetal artery occlusion, with the latter thought by some to be more apt to produce downstream avascular villi without appreciable karyorrhectic changes.

Differential Diagnosis

FTV needs to be distinguished from (a) the normal involutional changes that occur following intrauterine fetal demise and (b) VUE associated with obstructive fetal vasculopathy.

- In contrast to FTV, the vascular and villous changes that are seen following the intrauterine death of the fetus, which are described in the next section, involve the placenta diffusely rather than regionally, and are not associated with microscopic patches of avascular villi or villi with stromal-vascular karyorrhexis adjacent to normal villi.[51]
- The presence of stem villi with a significant lymphohistiocytic infiltrate and obliterative vascular changes in association with downstream avascular villi is most likely related to VUE rather than FTV.[34] This distinction is worth making, since VUE is much more likely to recur in a subsequent pregnancy than FTV.

PLACENTAL CHANGES FOLLOWING FETAL DEATH IN UTERO[51]

Histologic examination of the placenta can be utilized to provide an estimate of the amount of time that has elapsed between fetal death in utero and delivery of the stillborn. The three parameters that are most useful in this regard are (a) intravascular karyorrhexis within small vessels of terminal villi, (b) vascular luminal abnormalities of the stem villi, and (c) extensive fibrosis of terminal villi. Intravascular karyorrhexis is recognized as minute basophilic particles of nuclear debris of capillary endothelial and/or white blood cell origin within the lumens of villous capillaries. The stem villus vascular abnormalities feature muscular vessels with either total luminal obliteration or fibroblastic ingrowth resulting in septation of the lumen into several small blood-filled compartments (Fig. 9.51). These postmortem vascular changes presumably are enabled by the continued oxygenation of the intervillous space of the placenta that is supplied by the maternal circulation. Extensively fibrotic terminal villi have stromal cores that are hyalinized, fibrotic, and completely avascular.

If none of the three findings listed above is present, then fetal death can be presumed to have occurred within 6 hours of delivery. If only intravascular karyorrhexis is found, then the time of fetal death is most likely between 6 hours and 2 days of delivery. If vascular luminal abnormalities of the stem villi have developed without extensive fibrosis of terminal villi, then the time of fetal death can be estimated to be between 2 days and

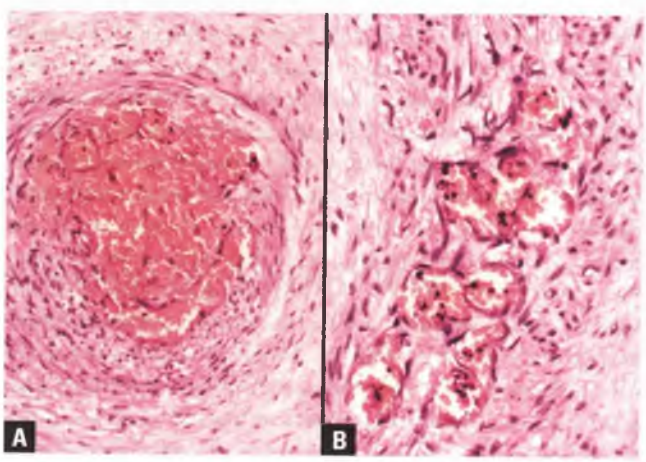

FIGURE 9.51. **A,B:** Postmortem vascular changes in stem villi. The muscular vessels within these stem villi exhibit fibroblastic septation of the vessel lumens, which results in a compartmentalized appearance that somewhat resembles recanalization of a thrombus. The changes in **(A)** are less florid than in **(B).** Clinicopathologic correlation indicated that this stillborn fetus died 4 to 5 days prior to delivery.

2 weeks prior to delivery. If extensive fibrosis of terminal villi is present, then the interval between fetal death and delivery is probably more than 2 weeks. In most cases, the stillborn fetus will also be available for pathologic examination to help establish the time of fetal death.[52,53]

The distinction of the vascular postmortem changes described above from FTV is discussed in the previous section.

ACUTE ATHEROSIS[54,55]

Acute atherosis is characterized by fibrinoid necrosis of the muscularized walls of decidual and superficial myometrial spiral arteries and arterioles coupled with the presence of mural aggregates of lipid-laden macrophages (Fig. 9.52). A perivascular mononuclear cell infiltrate may also be present. Thrombosis of these vessels leads to infarcts of the corresponding villous territory, which may be numerous and extensive. Acute atherosis should not be confused with the fibrinoid necrosis that occurs in spiral arteries as a consequence of invasion by intermediate trophoblastic cells, which represents normal physiologic remodeling of these vessels during pregnancy.

Acute atherosis is most commonly seen in preeclampsia, which is also known as toxemia of pregnancy. Preeclampsia occurs after the 20th week of gestation and affects about 5% of all pregnancies. In addition to the definitional finding of pregnancy-induced hypertension, patients with preeclampsia also have proteinuria and/or generalized edema. Eclampsia refers to the condition in which otherwise unexplained seizures develop in a preeclamptic patient. Following delivery, preeclampsia resolves and the necrotizing arteriopathy regresses.

The identification of acute atherosis in a preeclamptic patient is facilitated by the examination of several sections of the basal plate and the rim of decidua attached to the fetal membranes in order to obtain profiles of a sufficient sample of spiral arteries. Despite these efforts, few or no maternal vessels may be present for evaluation in some cases.

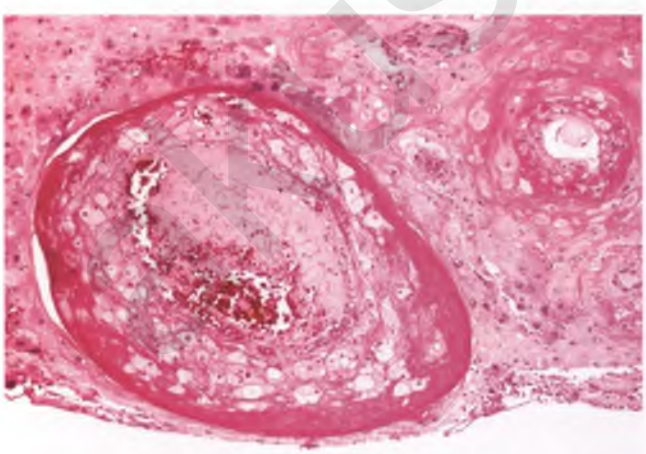

FIGURE 9.52. Preeclampsia-associated acute atherosis of maternal vessels in the placental basal plate. The walls of the spiral arteries have undergone fibrinoid necrosis and contain several lipid-laden macrophages. The larger of the two damaged vessels also contains an organizing thrombus, which was associated with infarction of the neighboring placenta. (Courtesy of Dr. Deborah J. Gersell.)

INCREASED SYNCYTIAL KNOTS (TENNEY-PARKER CHANGE)

Chronic maternal vascular underperfusion of the placenta is associated with several different reaction patterns that may be seen at the level of the chorionic villi, maternal vessels, or umbilical cord.[55] One of these reaction patterns is the presence of patches of villi with an increased number of syncytial knots, which is also known as Tenney-Parker change (Fig. 9.53).[56] Syncytial knots, which represent aggregates of apoptotic syncytiotrophoblastic nuclei, normally become more numerous with increasing gestational age. Thresholds that have been recommended for making the subjective interpretation of increased knots include the presence of knots on more than 30% of the distal villi or simply an impression that the number of knots is excessive for gestational age.

CHORANGIOSIS[57,58]

Chorangiosis refers to the presence of significant numbers of highly vascular terminal villi, and has been quantitatively defined as >10 terminal villi with more than 10 capillary loops per villus occurring in several different regions of the placenta (Fig. 9.54). Chorangiosis is found in about 5% of placentas, and occurs in a variety of settings. In many cases, there is an association with a chronic decrease in oxygen tension within the intervillous space. Chorangiosis is presumably related to elongation and increased coiling of the preexisting capillary network in an attempt to optimize gas exchange.

Congestion of the villous capillary loops may simulate chorangiosis, but simply represents engorgement of the preexisting capillary architecture. The distinction of chorangiosis from chorangiomatosis is discussed in the section on the latter entity.

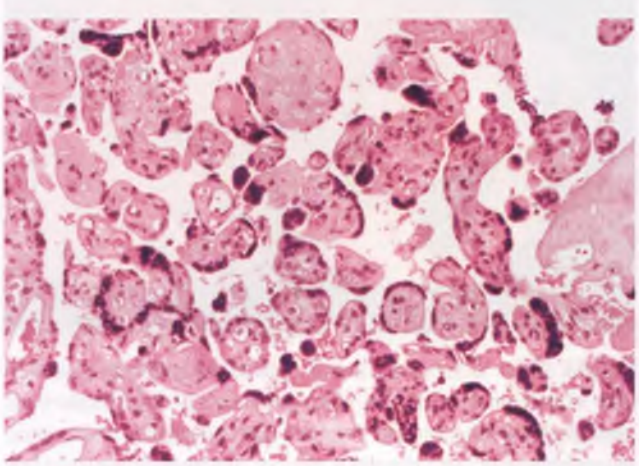

FIGURE 9.53. Increased syncytial knots (Tenney-Parker change).

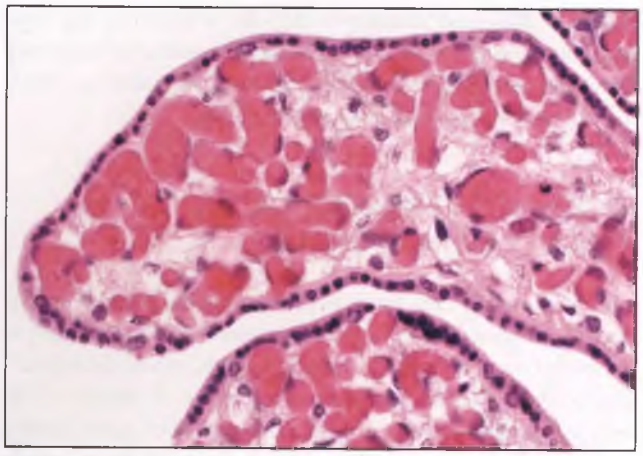

FIGURE 9.54. Chorangiosis. In this high-magnification view from one of several clusters of similar-appearing terminal villi, the number of villous capillary loops is markedly increased from the number that is normally present. (Courtesy of Dr. Deborah J. Gersell.)

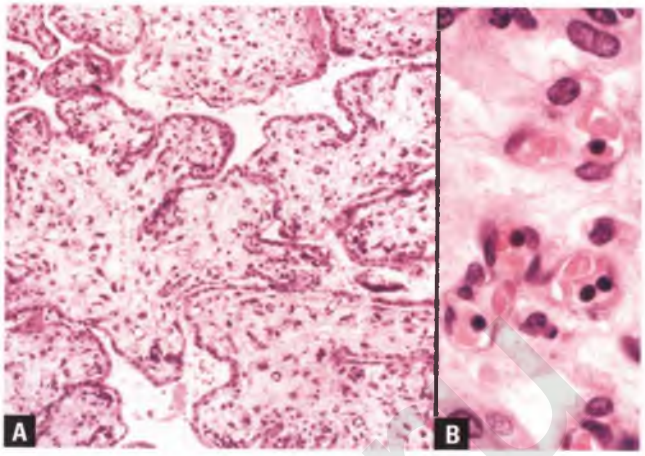

FIGURE 9.56. Severe fetomaternal hemorrhage at 39 weeks gestational age associated with intrauterine fetal demise. **A:** The chorionic villi are edematous and anemic. **B:** Note the presence of nucleated red blood cells within some of the villous capillaries.

FETOMATERNAL HEMORRHAGE[59]

Severe hemorrhage of fetal blood into the maternal circulation is a rare occurrence and may be the cause of fetal anemia or intrauterine fetal demise. In cases of chronic or repeated episodes of fetomaternal hemorrhage, the placenta typically exhibits diffuse villous edema, multiple intervillous thrombi, excessive weight, increased thickness, and nucleated red blood cells within the villous capillaries (Figs. 9.55 and 9.56). The latter finding beyond about 20 weeks of gestation is a reliable indicator that there is some abnormal process stimulating fetal erythropoeisis. When this constellation of features is encountered, the pathologist should recommend that the clinician request a Kleihauer-Betke test on a smear of maternal blood. This test enables the identification of red blood cells that contain fetal hemoglobin and can provide an estimate of the extent of the fetomaternal hemorrhage. Flow cytometric analysis of maternal blood utilizing antibodies directed against fetal hemoglobin can also be used for this purpose.

Possible causes of severe fetomaternal hemorrhage include maternal abdominal trauma, amniocentesis, a placental tumor, and abruption. In most cases, no specific cause is identified.

FIGURE 9.55. Chronic severe fetomaternal hemorrhage associated with intrauterine fetal demise. This section through the formalin-fixed term placenta demonstrates thick and pale (edematous and anemic) parenchyma with two intervillous thrombi. The placenta weighed 900 g, which is almost twice its expected weight.

ERYTHROBLASTOSIS FETALIS[60]

Erythroblastosis fetalis, which is also known as hemolytic disease of the newborn, is largely a preventable disease that is rarely seen in modern obstetrical practice. It is due to the formation of maternal antibodies that develop in response to blood group incompatibility between mother and child (usually differences in the Rh D, A, B, or Kell antigens). Severe forms of this disease are most frequent in the situation with an Rh-negative mother and an Rh-positive child. In order for the mother to develop these antibodies, there must be significant hemorrhage of fetal blood into the maternal circulation, with childbirth serving as the most common opportunity for this occurrence. Given this sequence of events, the risk for erythroblastosis fetalis is much greater in subsequent pregnancies than it is in the first one. Prophylactic use of Rho-gam (immune globulin containing anti-D antibodies) in at-risk mothers markedly reduces the risk of immunization of the mother against the Rh antigen of the fetal red blood cells.

In its full-blown form, the destruction of fetal red blood cells in erythroblastosis fetalis leads to anemia and jaundice. The anemia results in hypoxic injury to the heart and liver that leads to generalized edema and ascites (hydrops fetalis) via cardiac decompensation and decreased plasma oncotic pressure.

The placenta in classic cases of erythroblastosis fetalis is enlarged and pale, may contain one or more intervillous thrombi, and resembles that seen in chronic severe fetomaternal hemorrhage (see Fig. 9.55). Histologically, patches of enlarged and edematous villi are intermingled with normal-appearing terminal villi, the cytotrophoblastic layer is more conspicuous and mitotically active than normal, numerous macrophages are present within the villous stroma, and nucleated fetal red blood cells are found within the villous capillaries. Although typical of erythroblastosis fetalis, many of these findings can also be seen in fetal anemia due to other causes, cardiac failure, hypoproteinemia, and other disorders.

MECONIUM STAINING OF FETAL MEMBRANES[61]

When the near-term fetus is under distress, passage of meconium (fetal intestinal contents) into the amniotic fluid may occur. Meconium is also commonly found within the amniotic fluid of pregnancies that are beyond their due dates. If meconium is aspirated by the fetus, it can induce a chemical pneumonitis that results in respiratory distress (meconium aspiration syndrome).[62]

Grossly, meconium staining is recognized as a green or greenish brown discoloration of the membranes (Fig. 9.57). Meconium induces reactive and degenerative changes within the amniotic epithelium that include pseudostratification, clubbing, and disorganization (Fig. 9.58A). Prolonged exposure of the membranes to the toxic effects of meconium eventually results in epithelial necrosis and sloughing. The presence of golden brown, finely granular, nonrefractile meconium pigment within macrophages of the connective tissue layer of the amnion indicates that the meconium has been present within the amniotic fluid for at least 1 hour (Fig. 9.57B).

Meconium pigment needs to be distinguished from the more coarsely granular, brown refractile deposits of hemosiderin that may be found either extracellularly or within macrophages

FIGURE 9.57. Meconium staining of the fetal membranes of the chorionic plate. The membranes have a *greenish-brown* discoloration.

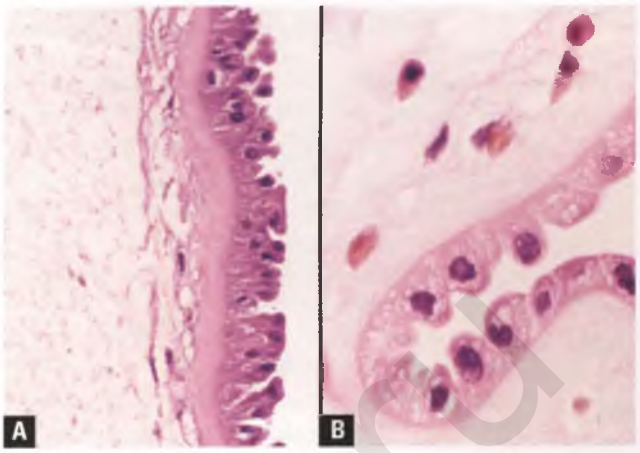

FIGURE 9.58. Meconium staining of the fetal membranes. **A:** Note the reactive changes in the epithelium of the amnion. **B:** This image highlights the presence of amniotic macrophages with golden brown pigment.

of the amnion and chorion (Fig. 9.59A). In contrast to meconium, these granules stain with iron stains such as Prussian blue (Fig. 9.59B). Although diffuse chorioamniotic hemosiderosis has been thought to be an uncommon lesion that is associated with chronic marginal separation of the placenta ("chronic abruption") and circumvallation,[2] this view has recently been challenged.[63]

MECONIUM-ASSOCIATED VASCULAR NECROSIS[64,65]

With prolonged exposure to meconium on the order of ≥16 hours, the cytotoxic effects of its constituent elements may result in a characteristic alteration to umbilical and chorionic

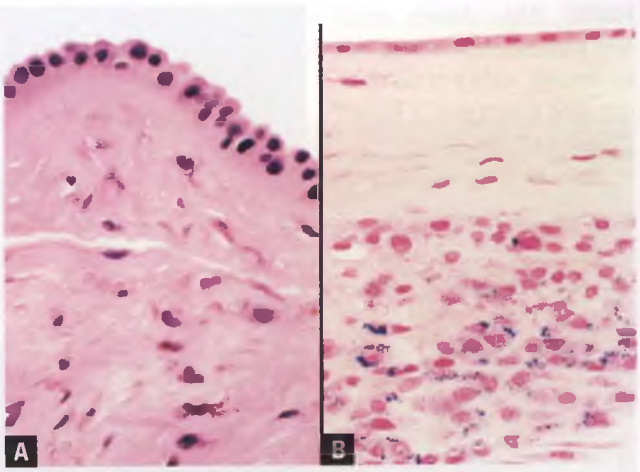

FIGURE 9.59. Fetal membranes with chorioamniotic hemosiderosis from a patient with a history of chronic marginal separation of the placenta and circumvallation. **A:** In the stroma beneath the amniotic epithelium, note the presence of coarsely granular brown pigment within macrophages. **B:** In this portion of the membranes, a Prussian blue stain demonstrates the presence of blue-staining iron particles within the chorion.

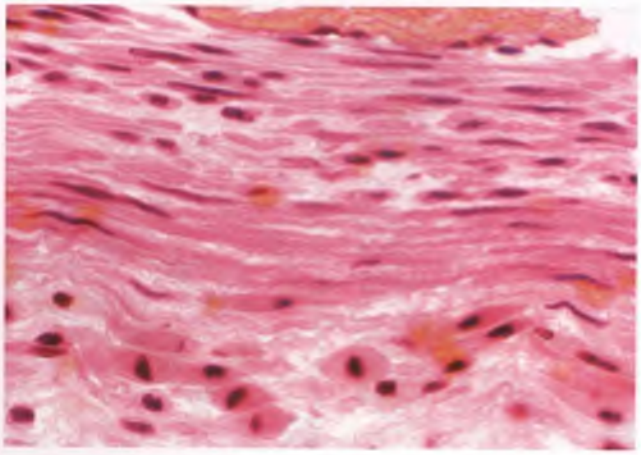

FIGURE 9.60. Meconium-associated vascular myonecrosis of an umbilical vessel. The affected myocytes are at the periphery of the vessel at the bottom of the image. They exhibit eosinophilic to orangeophilic cytoplasmic degeneration with "balling up" and detachment from the vessel wall.

plate vessels. This alteration, termed meconium-associated vascular necrosis, is characterized by apoptosis of smooth muscle cells of the periphery of vessel walls. These apoptotic myocytes form rounded, eosinophilic to orangeophilic bodies that detach from the outer wall of the affected vessels (Fig. 9.60). At scanning magnification, involved vessels are often abnormally dilated, which is a clue to look closely for myonecrosis at the periphery of the vessel walls and to search for pigmented macrophages within Wharton's jelly. The recognition of meconium-associated vascular necrosis may assist in the defense of the obstetrician in medicolegal cases brought forth for an unexpected adverse delivery outcome, since the presence of this rare and easily overlooked lesion is strongly associated with cerebral palsy.

AMNION NODOSUM[66]

Amnion nodosum is a rare lesion that is associated with oligohydramnios, although it also occurs under other circumstances. It is characterized by multiple light gray to yellow-tinged nodules projecting from the amniotic surface, which are most noticeable on the portion of the amnion that covers the chorionic plate (Fig. 9.61). These nodules measure only about 1 to 5 mm in diameter, may coalesce to form small plaques, and are easily removed when gentle pressure is applied.

Histologically, the dominant element within the nodules of amnion nodosum is amorphous eosinophilic material, within which are embedded occasional cell remnants and lanugo hair fragments (Fig. 9.62). These nodules are derived primarily from sloughed fetal skin particles that are a normal constituent of amniotic fluid. In cases that are associated with oligohydramnios, it appears that the reduction of amniotic fluid leads to a condition in which these particles aggregate and deposit on damaged areas of the amniotic surface. The finding of amnion nodosum should prompt the clinician to look for oligohydramnios-associated conditions such as pulmonary hypoplasia and abnormalities of the urinary tract.

Amnion nodosum needs to be distinguished from squamous metaplasia, which is discussed in the following section.

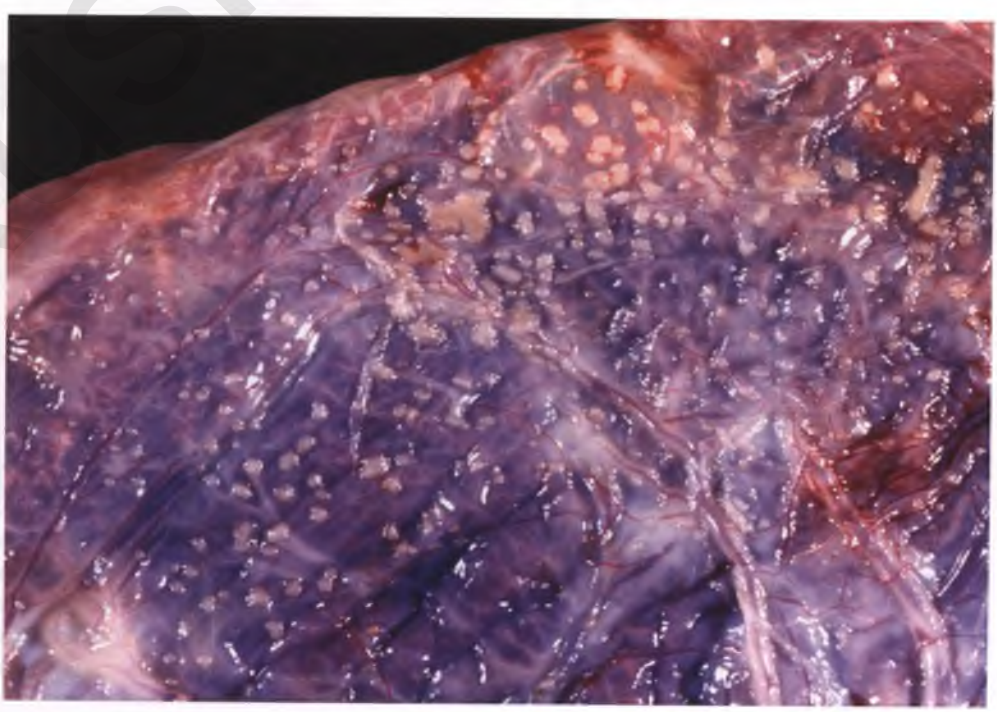

FIGURE 9.61. Amnion nodosum. Multiple small nodules stud the amniotic surface of the chorionic plate. (Courtesy of Dr. Richard L. Payne.)

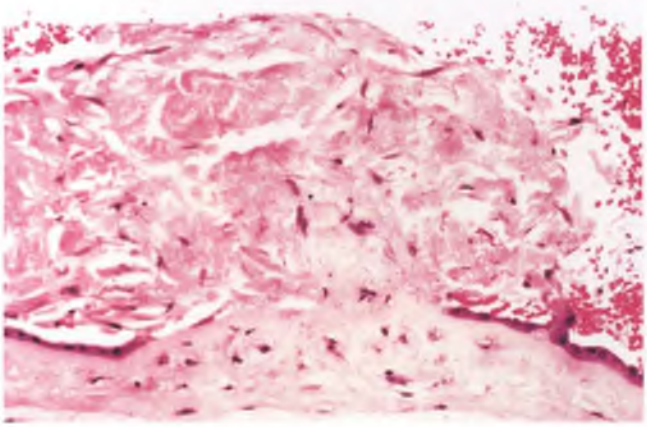

FIGURE 9.62. Amnion nodosum. The lesion consists of a nodule of amorphous eosinophilic material admixed with scattered cellular elements that is loosely attached to the surface of the amnion covering the chorionic plate.

SQUAMOUS METAPLASIA OF THE AMNIOTIC SURFACE

This common abnormality is of no clinical significance and features small pearly-white patches or plaques that have a predilection for the amniotic surface near the insertion site of the umbilical cord. Histologically, this lesion is characterized by the presence of variably keratinized stratified squamous epithelium that is sharply demarcated from the normal epithelium of the amnion (Fig. 9.63).

Squamous metaplasia may be grossly confused with amnion nodosum. However, in contrast to amnion nodosum, the patches and plaques of squamous metaplasia are not easily separated from the amnion. In addition, these two lesions have distinctly different histologic features.

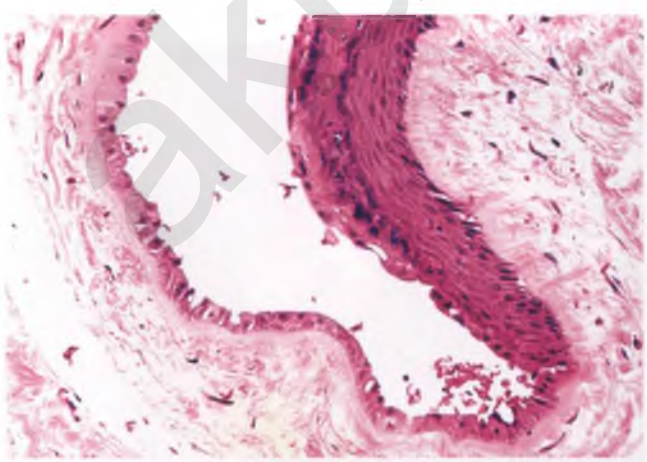

FIGURE 9.63. Squamous metaplasia. There is an abrupt transition between the amniotic epithelium at left and the focus of squamous metaplasia at right.

AMNIOTIC BAND SYNDROME[67]

If the amnion is disrupted and separates from an intact chorion due to trauma or other poorly understood mechanisms, the resulting thin fibrous strands can entangle a wide variety of body parts as a consequence of subsequent fetal movement. These bands can constrict the extremities, digits, neck, umbilical cord, body wall, and craniofacial region, which can result in circular grooves, syndactyly of banded digits, ischemic damage, malformations, and amputations. The fetus may also swallow the free end of one of these strands, leading to its head being drawn toward and held against the placental surface. Each case is unique, the defects are asymmetric, and the risk of recurrence in a future pregnancy is negligible.

Pathologists generally only see cases of this phenomenon that are associated with fetal demise, such as those that occur with strangulation of the umbilical cord or neck or with severe craniofacial involvement. In examining the placenta and fetus, the pathologist should take gross photographs and note the presence, location, and effect of the bands. The residual amnion is typically collapsed around the base of the umbilical cord. Histologically, the bands consist of fibrous tissue that may or may not be lined by amniotic epithelium. Sections of the chorionic plate show an absence of amnion and fibrosis of the chorion, often with superficially adherent proteinaceous debris and fetal squames.

PLACENTAL INSERTION OF THE UMBILICAL CORD

In most placentas, the umbilical cord inserts on the fetal surface in either a central location or with varying degrees of eccentricity. On occasion, the cord inserts at the margin of the placental disc, producing what is also known as a "battledore placenta" (Fig. 9.64). In about 1% of placentas, there

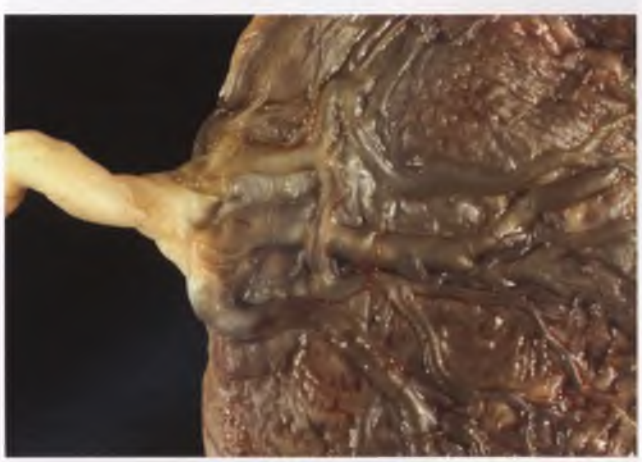

FIGURE 9.64. Marginal cord insertion (Battledore placenta). The chorionic plate has a *greenish-brown* discoloration due to meconium staining.

FIGURE 9.65. Velamentous insertion. The branching vessels of the umbilical cord insert into the fetal membranes instead of into the chorionic plate of the placenta.

FIGURE 9.66. Single umbilical artery. The artery at left can usually be distinguished from the umbilical vein by its thicker wall and lumen that is either collapsed or of smaller diameter. The umbilical vein is typically dilated and filled with fresh blood.

is a velamentous insertion of the cord into the fetal membranes (Fig. 9.65). Velamentous insertions are associated with various fetal anomalies and their exposed and unsupported vessels are susceptible to mechanical injury. The risk of life-threatening injury to the fetus is particularly high when velamentous vessels traverse the internal cervical os, which is a condition known as vasa previa.

SINGLE UMBILICAL ARTERY[68,69]

The normal umbilical cord has two arteries and one vein. Deoxygenated blood within the umbilical arteries travels from the fetus to the chorionic villi, whereas the umbilical vein returns oxygenated blood to the fetus. The only other veins that carry oxygenated rather than deoxygenated blood are the pulmonary veins that empty into the left atrium of the heart.

A single umbilical artery (two-vessel cord) is found in <1% of placentas, and is associated with various congenital anomalies and a low birth weight (Fig. 9.66). Since the umbilical arteries may fuse close to the placenta and give the false impression of a single umbilical artery, cross sections of the umbilical cord that are to be submitted for histologic evaluation should be taken at least 5 cm from the placental insertion site.[70]

TORSION AND STRICTURE OF THE UMBILICAL CORD

The normal umbilical cord is a spiraled structure that resembles an elongated spiral staircase. Umbilical cord torsion is deemed to have taken place when such twisting is focally excessive and associated with a significant decrease in cord diameter. Limiting the definition of torsion in this way facilitates its distinction from cords with a subjective and clinically inconsequential increase in twisting that does not obstruct blood flow. True umbilical torsion is usually located near the fetal end of the cord, but may also occur near the placental end (Fig. 9.67). Umbilical cord torsion may be associated with a stricture, which is characterized by a focal area in which the lumen of the umbilical cord vessels is constricted or obliterated in conjunction with loss of Wharton's jelly. Such lesions are associated with venous congestion, thrombosis, and edema of the cord.

EDEMA OF THE UMBILICAL CORD

Varying degrees of edema of the umbilical cord are found in about 10% of deliveries, and may be associated with respiratory distress of the newborn (Fig. 9.68).[71] When massive and most prominent at the infant's end of the cord, the possibility of retrograde urination into the cord through a patent urachus should be considered.[72]

FIGURE 9.67. Torsion and stricture of the umbilical cord (*arrow*) associated with intrauterine fetal demise.

FIGURE 9.68. Prominent edema of the umbilical cord.

FIGURE 9.70. Nuchal cord. Loops of umbilical cord can be faintly seen through the fetal membranes in the region of the neck of the fetus (*arrow*). The placenta is at left.

TRUE KNOTS OF THE UMBILICAL CORD

Most true knots are loosely tied and are clinically insignificant (Fig. 9.69). If the knot has been tight for a long period of time or has been acutely tightened, it may be responsible for fetal death. True knots need to be distinguished from kinks produced by focal vascular dilatations, vascular loops, and outward projections formed by an overabundance of Wharton's jelly ("false knots").

NUCHAL CORD

In a nuchal cord, the umbilical cord encircles the neck of the fetus one or more times. Nuchal cords can cause fetal demise, usually in mid-pregnancy, through compromise of the umbilical circulation and/or blood flow through the jugular veins (Fig. 9.70). If this situation develops gradually, the neck of the fetus is thin and pale, the head is edematous and congested, and there is thrombosis of the umbilical vessels (Fig. 9.71). Nuchal cords are found fairly frequently in term deliveries, where they are typically not associated with an untoward pregnancy outcome.[73,74]

FIGURE 9.69. True knot of the umbilical cord. Compare the true knot (center) with the false knot located beneath it and to the left.

UMBILICAL CORD HEMATOMA

An umbilical cord hematoma is a rare lesion that forms when bleeding from one of the umbilical vessels is contained by Wharton's jelly. If this barrier is breached, then blood enters the amniotic cavity. Umbilical cord hematomas typically are located near the fetal end of the cord and appear as a reddish purple fusiform enlargement (Fig. 9.72).

The clinical significance of an umbilical cord hematoma varies from inconsequential to being the cause of perinatal

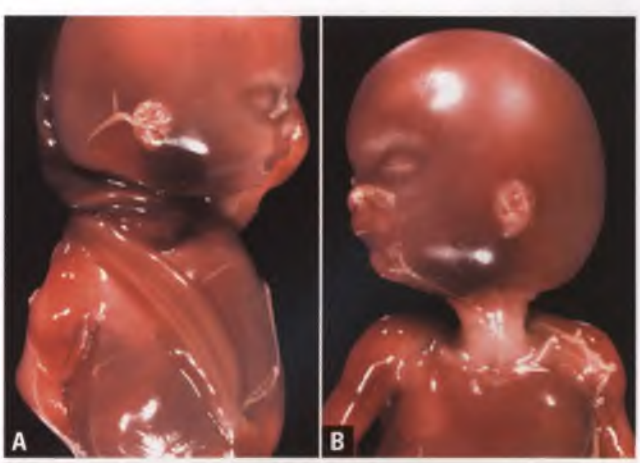

FIGURE 9.71. Nuchal cord (same case as preceding figure). **A:** The umbilical cord is tightly wrapped around the neck of the fetus. Thrombosis of umbilical vessels was also present (not shown). **B:** The neck is thin and pale and the head is spherical, edematous, and congested due to the blockage of venous return to the heart that normally occurs through the jugular veins.

FIGURE 9.72. Umbilical cord hematoma associated with fetal demise. **A:** The reddish-purple hematoma is present at its typical location near the fetus. **B:** Compression of the umbilical vessels by the hematoma has resulted in stasis, dilatation, and thrombosis of the umbilical vein. (Courtesy of Dr. Richard L. Payne.)

mortality. Cases associated with fetal death are related to either significant blood loss or compression of fetal vessels.

PLACENTAL MESENCHYMAL DYSPLASIA

Placental mesenchymal dysplasia is discussed in Chapter 10 as part of the differential diagnosis of partial hydatidiform mole.

CHORANGIOMA[58]

A chorangioma (placental capillary hemangioma) is found in about 0.5% of placentas that are submitted for pathologic examination, making it the most common placental tumor. Most chorangiomas are solitary and measure <0.5 cm, but these tumors may be several cm in diameter. They are usually located in the marginal and/or subchorionic regions of the placenta (Fig. 9.73). These tumors may be composed of one or more nodules, and usually have a tan, brown, red, and/or dark purple sectioned surface (Fig. 9.74). Yellow or white areas within the tumor are typically due to remote infarction.

Histologically, chorangiomas are composed of numerous vascular channels of capillary type with surrounding pericytes (Fig. 9.75A). The supporting stroma varies from inconspicuous to prominent. A characteristic feature of chorangiomas is the presence of a flattened to variably hyperplastic layer of trophoblastic cells that stretch around the periphery of the tumor (Fig. 9.75B). This finding, coupled with the presence of muscle-specific actin-positive pericytes that normally envelope the capillaries of stem rather than terminal villi, supports an origin from stem villi. Degenerative changes, which include myxoid change, hyalinization, necrosis, and calcification, may be present.

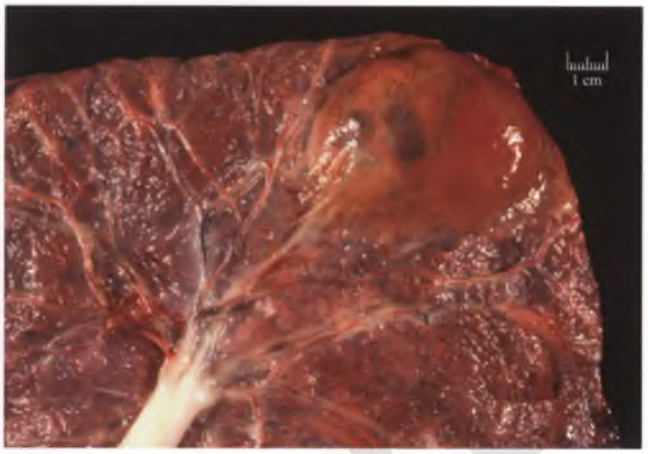

FIGURE 9.73. Chorangioma. The tumor bulges from the fetal surface of the placenta. Note its typical location in the subchorionic region near the placental edge.

Occasional chorangiomas that exhibit increased cellularity, mitotic activity, and nuclear atypia have been referred to as atypical cellular chorangiomas (Fig. 9.76). Despite their worrisome appearance, these tumors behave in a benign fashion. When evaluating a tumor of this type, it is comforting to know that there has yet to be a reported case of primary placental angiosarcoma.

Chorangiomas are generally of no clinical significance, although they may be associated with preeclampsia, multiple gestation, premature delivery, and an increased incidence of fetal hemangiomas. Chorangiomas of intermediate size may be associated with intrauterine growth restriction related to significant amounts of blood being diverted to the chorangioma rather than to functional villi.[75] Those rare chorangiomas that attain a large size (on the order of 10 cm) may function as

FIGURE 9.74. Chorangioma. This view of the sectioned surface demonstrates a solid subchorionic tumor with varying shades of *tan, brown, red,* and *dark purple* that is sharply demarcated from the underlying placental tissue. The yellow area represents a band of necrosis (infarction) with patches of dystrophic calcification.

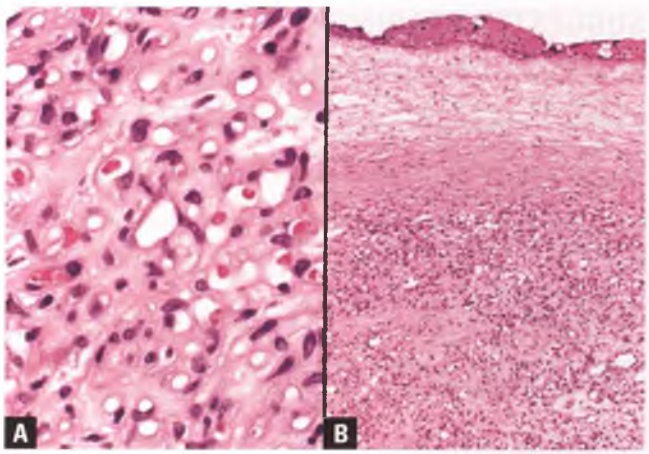

FIGURE 9.75. Chorangioma. **A:** These lesions consist of a proliferation of capillary-like vessels with associated pericytes. **B:** A layer of trophoblastic cells enmeshed in fibrin (top) forms the peripheral rim of the chorangioma (bottom). Interposed between the trophoblastic cells and the vascular proliferation is a band of chorionic connective tissue.

arteriovenous shunts and produce high-output cardiac failure with resultant hydrops fetalis.[76]

CHORANGIOMATOSIS[58]

Chorangiomatosis is similar to chorangioma in its frequency, clinical associations, and histologic features. However, chorangioma is characterized by the formation of an expansile nodular mass, whereas the vascular proliferation in chorangiomatosis is limited to stem villi (Fig. 9.77). Involvement of the placenta may be focal, segmental, or multifocal. Cases that are diffuse and multifocal are more likely to be associated with clinically significant conditions than the more localized

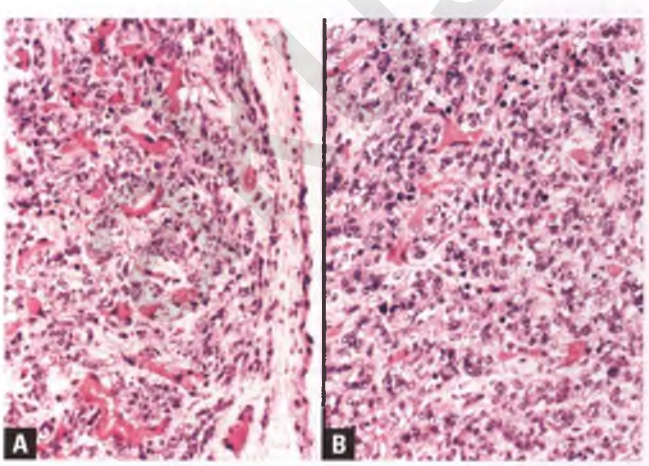

FIGURE 9.76. Atypical cellular chorangioma. **A:** The vascular proliferation is more cellular than usual. Note the presence of a thin rim of trophoblastic cells lining the periphery of the tumor at right. **B:** The vascular nature of the tumor is difficult to appreciate in this area, which is mitotically active.

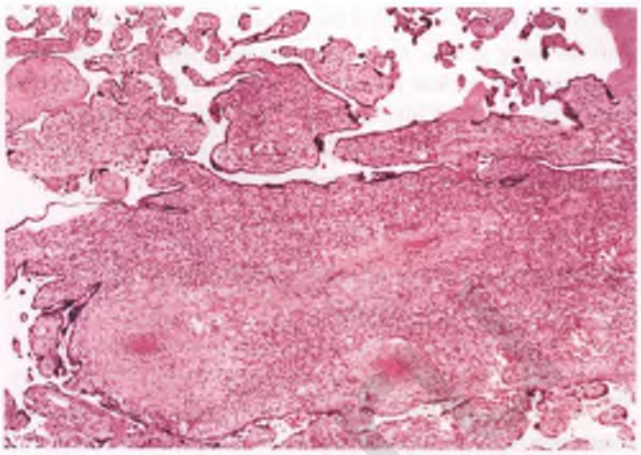

FIGURE 9.77. Chorangiomatosis. The stem villi in this region show histologic features that are similar to that of a chorangioma. The largest stem villus in this image contains thick-walled vessels. The terminal villi are unaffected by this process.

forms of this lesion. Foci of chorangiomatosis may be seen in about 10% of chorangiomas; conversely, about 10% of cases or chorangiomatosis are associated with a chorangioma.

In contrast to chorangiomatosis, chorangiosis features excessive capillarization of *terminal* villi with sparing of stem villi, and lacks the associated muscle-specific actin-positive pericytes that are present in chorangiomatosis and chorangiomas.

LEIOMYOMA INVOLVING THE FETAL MEMBRANES

A few cases of leiomyoma involving the fetal membranes have been reported (Fig. 9.78).[77,78] Although it is possible that these tumors originate from the smooth muscle cells that line the

FIGURE 9.78. Leiomyoma involving the fetal membranes. The bisected leiomyoma, which is intimately associated with the fetal membranes, has a solid, whorled, *pale-tan* sectioned surface. (Courtesy of Dr. Richard L. Payne.)

vessels that nourish the fetal membranes, the only case studied thus far using genetic techniques has been shown to represent a submucosal uterine leiomyoma that had become incorporated into the fetal membranes.[77] Intraplacental leiomyomas are equally rare, and at least one has also been shown by genetic techniques to be of uterine origin.[79]

METASTASES OF MATERNAL CANCER TO THE PLACENTA[80,81]

Metastasis of maternal cancer to the placenta is quite rare. There is often no gross evidence of metastatic disease, with the tumor represented solely by scattered clusters of malignant cells within the maternal blood-containing intervillous space. In such cases, extensive histologic sampling may be required to identify foci of placental involvement. It is important to note if invasion of the chorionic villi and villous vessels is identified, since this is the presumed mechanism by which the maternal cancer cells gain access to the fetal circulation. Actual fetal metastasis of maternal cancer is very uncommon, but may result in a fatal outcome.

Although malignant melanoma represents <10% of the cancers encountered in pregnant women, it is the most common type of cancer found to metastasize to the placenta and/or fetus (Fig. 9.79). The major reason for this overrepresentation appears to be that widespread melanoma at its preterminal and rapidly progressive stage, which is almost always present when the placenta is involved, is more commonly seen in the reproductive age group than other types of aggressive, high-stage tumors that might exhibit a similar behavior.

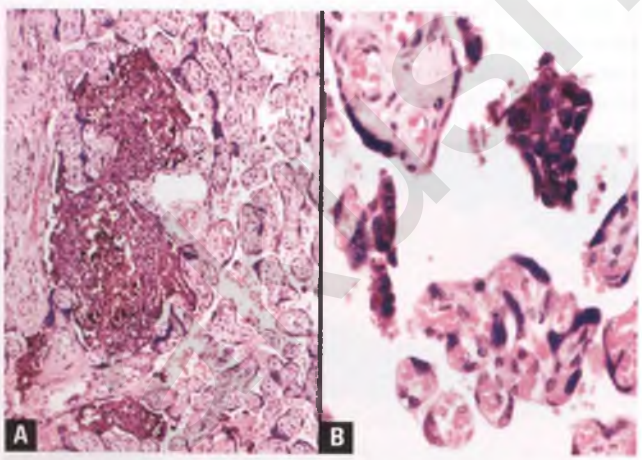

FIGURE 9.79. **A,B:** Maternal malignant melanoma metastatic to the placenta. Pigmented nests of melanoma are present within the intervillous space.

SUGGESTED READINGS

Baergen R. *Manual of Benirschke and Kaufmann's Pathology of the Human Placenta.* New York, NY: Springer; 2005.

Benirschke K, Kaufmann P, Baergen R. *Pathology of the Human Placenta.* 5th ed. New York, NY: Springer; 2006.

Crum CP, Nucci, MR, Lee, K, eds. *Diagnostic Gynecologic and Obstetric Pathology.* 2nd ed. Philadelphia, PA: Elsevier Saunders; 2011.

Fox H, Wells M. *Haines and Taylor Obstetrical and Gynaecological Pathology.* 5th ed. Edinburgh: Churchill Livingstone; 2003.

Kaplan, CG. *Color Atlas of Gross Placental Pathology.* 2nd ed. New York, NY: Springer, 2007.

Kraus FT, Redline W, Gersell DJ, et al. *Placental Pathology (Atlas of Nontumor Pathology).* Washington, DC: American Registry of Pathology; 2004.

Kurman RJ, Ellenson LH, Ronnett BM, eds. *Blaustein's Pathology of the Female Genital Tract.* 6th ed. New York, NY: Springer; 2011.

REFERENCES

1. Huppertz B. The anatomy of the normal placenta. *J Clin Pathol.* 2008;61:1296–1302.
2. Redline RW, Wilson-Costello D. Chronic peripheral separation of placenta. The significance of diffuse chorioamnionic hemosiderosis. *Am J Clin Pathol.* 1999;111:804–810.
3. Suzuki S. Clinical significance of pregnancies with circumvallate placenta. *J Obstet Gynaecol Res.* 2008;34:51–54.
4. Breen JL, Neubecker R, Gregori CA, et al. Placenta accreta, increta, and percreta. A survey of 40 cases. *Obstet Gynecol.* 1977;49:43–47.
5. Khong TY. The pathology of placenta accreta, a worldwide epidemic. *J Clin Pathol.* 2008;61:1243–1246.
6. Jacques SM, Qureshi F, Trent VS, et al. Placenta accreta: mild cases diagnosed by placental examination. *Int J Gynecol Pathol.* 1996;15:28–33.
7. Stanek J, Al-Ahmadie HA. Laminar necrosis of placental membranes: a histologic sign of uteroplacental hypoxia. *Pediatr Dev Pathol.* 2005;8:34–42.
8. Stanek J. Diagnosing placental membrane hypoxic lesions increases the sensitivity of placental examination. *Arch Pathol Lab Med.* 2010;134:989–995.
9. Stanek J, Weng E. Microscopic chorionic pseudocysts in placental membranes: a histologic lesion of in utero hypoxia. *Pediatr Dev Pathol.* 2007;10:192–198.
10. Nikkels PG, Hack KE, van Gemert MJ. Pathology of twin placentas with special attention to monochorionic twin placentas. *J Clin Pathol.* 2008;61:1247–1253.
11. Benirschke K, Masliah E. The placenta in multiple pregnancy: outstanding issues. *Reprod Fertil Dev.* 2001;13:615–622.
12. Sala MA, Matheus M. Placental characteristics in twin transfusion syndrome. *Arch Gynecol Obstet.* 1989;246:51–56.
13. Benirschke K. The contribution of placental anastomoses to prenatal twin damage. *Hum Pathol.* 1992;23:1319–1320.
14. Redline RW, Faye-Petersen O, Heller D, et al. Amniotic infection syndrome: nosology and reproducibility of placental reaction patterns. *Pediatr Dev Pathol.* 2003;6:435–448.
15. Redline RW. Inflammatory responses in the placenta and umbilical cord. *Semin Fetal Neonatal Med.* 2006;11:296–301.
16. Redline RW. Clinically and biologically relevant patterns of placental inflammation. *Pediatr Dev Pathol.* 2002;5:326–328.
17. Gersell DJ, Phillips NJ, Beckerman K. Chronic chorioamnionitis: a clinicopathologic study of 17 cases. *Int J Gynecol Pathol.* 1991;10:217–229.
18. Jacques SM, Qureshi F. Chronic chorioamnionitis: a clinicopathologic and immunohistochemical study. *Hum Pathol.* 1998;29:1457–1461.
19. Kim CJ, Romero R, Kusanovic JP, et al. The frequency, clinical significance, and pathological features of chronic chorioamnionitis: a lesion associated with spontaneous preterm birth. *Mod Pathol.* 2010;23:1000–1011.
20. Ohyama M, Itani Y, Yamanaka M, et al. Re-evaluation of chorioamnionitis and funisitis with a special reference to subacute chorioamnionitis. *Hum Pathol.* 2002;33:183–190.
21. Fojaco RM, Hensley GT, Moskowitz L. Congenital syphilis and necrotizing funisitis. *JAMA.* 1989;261:1788–1790.

22. Jacques SM, Qureshi F. Necrotizing funisitis: a study of 45 cases. *Hum Pathol.* 1992;23:1278–1283.
23. Hood IC, Desa DJ, Whyte RK. The inflammatory response in candidal chorioamnionitis. *Hum Pathol.* 1983;14:984–990.
24. Qureshi F, Jacques SM, Bendon RW, et al. *Candida* funisitis: a clinicopathologic study of 32 cases. *Pediatr Dev Pathol.* 1998;1:118–124.
25. Khong TY, Bendon RW, Qureshi F, et al. Chronic deciduitis in the placental basal plate: definition and interobserver reliability. *Hum Pathol.* 2000;31:292–295.
26. Sinzger C, Muntefering H, Loning T, et al. Cell types infected in human cytomegalovirus placentitis identified by immunohistochemical double staining. *Virchows Arch A.* 1993;423:249–256.
27. Muhlemann K, Miller RK, Metlay L, et al. Cytomegalovirus infection of the human placenta: an immunocytochemical study. *Hum Pathol.* 1992;23:1234–1237.
28. Spruill LS, Batalis N. Parvovirus B19 infection: characteristic placental and autopsy findings in a case of intrauterine fetal demise. *Pathol Case Rev.* 2010;15:50–54.
29. Sheffield JS, Sanchez PJ, Wendel GD Jr, et al. Placental histopathology of congenital syphilis. *Obstet Gynecol.* 2002;100:126–133.
30. Genest DR, Choi-Hong SR, Tate JE, et al. Diagnosis of congenital syphilis from placental examination: comparison of histopathology, Steiner stain, and polymerase chain reaction for *Treponema pallidum* DNA. *Hum Pathol.* 1996;27:366–372.
31. Gersell DJ. Chronic villitis, chronic chorioamnionitis, and maternal floor infarction. *Semin Diagn Pathol.* 1993;10:251–266.
32. Craver RD, Baldwin VJ. Necrotizing funisitis. *Obstet Gynecol.* 1992;79:64–70.
33. Benirschke K. Congenital syphilis and necrotizing funisitis [Letter to Editor]. *JAMA.* 1989;262:904.
34. Redline RW. Villitis of unknown etiology: noninfectious chronic villitis in the placenta. *Hum Pathol.* 2007;38:1439–1446.
35. Redline RW. Placental inflammation. *Semin Neonatol.* 2004;9:265–274.
36. Fox H. The significance of placental infarction in perinatal morbidity and mortality. *Biol Neonat.* 1967;11:87–105.
37. Maloney KF, Baergen RN. Maternal floor infarction. *Pathol Case Rev.* 2010;15:58–61.
38. Katzman PJ, Genest DR. Maternal floor infarction and massive perivillous fibrin deposition: histological definitions, association with intrauterine fetal growth restriction, and risk of recurrence. *Pediatr Dev Pathol.* 2002;5:159–164.
39. Andres RL, Kuyper W, Resnik R, et al. The association of maternal floor infarction of the placenta with adverse perinatal outcome. *Am J Obstet Gynecol.* 1990;163:935–938.
40. Naeye RL. Maternal floor infarction. *Hum Pathol.* 1985;16:823–828.
41. Naeye RL. The clinical significance of absent subchorionic fibrin in the placenta. *Am J Clin Pathol.* 1990;94:196–198.
42. Shanklin DR, Scott JS. Massive subchorial thrombohaematoma (Breus' mole). *Br J Obstet Gynaecol.* 1975;82:476–487.
43. Deans A, Jauniaux E. Prenatal diagnosis and outcome of subamniotic hematomas. *Ultrasound Obstet Gynecol.* 1998;11:319–323.
44. Dimashkieh H, Rumboldt T, Richardson MS, et al. Clinical and pathologic features of placental abruption. *Pathol Case Rev.* 2010;15:45–49.
45. Redline RW, Pappin A. Fetal thrombotic vasculopathy: the clinical significance of extensive avascular villi. *Hum Pathol.* 1995;26:80–85.
46. Kraus FT. Cerebral palsy and thrombi in placental vessels of the fetus: insights from litigation. *Hum Pathol.* 1997;28:246–248.
47. Kraus FT, Acheen VI. Fetal thrombotic vasculopathy in the placenta: cerebral thrombi and infarcts, coagulopathies, and cerebral palsy. *Hum Pathol.* 1999;30:759–769.
48. Redline RW, Ariel I, Baergen RN, et al. Fetal vascular obstructive lesions: nosology and reproducibility of placental reaction patterns. *Pediatr Dev Pathol.* 2004;7:443–452.
49. Redline RW. Fetal thrombotic vasculopathy. *Pathol Case Rev.* 2010;15:37–39.
50. Sander CH. Hemorrhagic endovasculitis and hemorrhagic villitis of the placenta. *Arch Pathol Lab Med.* 1980;104:371–373.
51. Genest DR. Estimating the time of death in stillborn fetuses: II. Histologic evaluation of the placenta; a study of 71 stillborns. *Obstet Gynecol.* 1992;80:585–592.
52. Genest DR, Singer DB. Estimating the time of death in stillborn fetuses: III. External fetal examination; a study of 86 stillborns. *Obstet Gynecol.* 1992;80:593–600.
53. Genest DR, Williams MA, Greene MF. Estimating the time of death in stillborn fetuses: I. Histologic evaluation of fetal organs; an autopsy study of 150 stillborns. *Obstet Gynecol.* 1992;80:575–584.
54. Staff AC, Dechend R, Pijnenborg R. Learning from the placenta: acute atherosis and vascular remodeling in preeclampsia-novel aspects for atherosclerosis and future cardiovascular health. *Hypertension.* 2010;56:1026–1034.
55. Redline RW, Boyd T, Campbell V, et al. Maternal vascular underperfusion: nosology and reproducibility of placental reaction patterns. *Pediatr Dev Pathol.* 2004;7:237–249.
56. Tenney B, Parker F. The placenta in toxemia of pregnancy. *Am J Obstet Gynecol.* 1940;39:1000–1005.
57. Altshuler G. Chorangiosis. An important placental sign of neonatal morbidity and mortality. *Arch Pathol Lab Med.* 1984;108:71–74.
58. Ogino S, Redline RW. Villous capillary lesions of the placenta: distinctions between chorangioma, chorangiomatosis, and chorangiosis. *Hum Pathol.* 2000;31:945–954.
59. Wylie BJ, D'Alton ME. Fetomaternal hemorrhage. *Obstet Gynecol.* 2010;115:1039–1051.
60. Wentworth P. The placenta in cases of hemolytic disease of the newborn. *Am J Obstet Gynecol.* 1967;98:283–289.
61. Miller PW, Coen RW, Benirschke K. Dating the time interval from meconium passage to birth. *Obstet Gynecol.* 1985;66:459–462.
62. Rossi EM, Philipson EH, Williams TG, et al. Meconium aspiration syndrome: intrapartum and neonatal attributes. *Am J Obstet Gynecol.* 1989;161:1106–1110.
63. Khong TY, Toering TJ, Erwich JJ. Haemosiderosis in the placenta does not appear to be related to chronic placental separation or adverse neonatal outcome. *Pathology (Phila).* 2010;42:119–124.
64. Altshuler G, Arizawa M, Molnar-Nadasdy G. Meconium-induced umbilical cord vascular necrosis and ulceration: a potential link between the placenta and poor pregnancy outcome. *Obstet Gynecol.* 1992;79:760–766.
65. Redline RW. Meconium-associated vascular necrosis. *Pathol Case Rev.* 2010;15:55–57.
66. Adeniran AJ, Stanek J. Amnion nodosum revisited: clinicopathologic and placental correlations. *Arch Pathol Lab Med.* 2007;131:1829–1833.
67. Seidman JD, Abbondanzo SL, Watkin WG, et al. Amniotic band syndrome. Report of two cases and review of the literature. *Arch Pathol Lab Med.* 1989;113:891–897.
68. Heifetz SA. Single umbilical artery. A statistical analysis of 237 autopsy cases and review of the literature. *Perspect Pediatr Pathol.* 1984;8:345–378.
69. Leung AK, Robson WL. Single umbilical artery. A report of 159 cases. *Am J Dis Child.* 1989;143:108–111.
70. Fujikura T. Fused umbilical arteries near placental cord insertion. *Am J Obstet Gynecol.* 2003;188:765–767.
71. Coulter JB, Scott JM, Jordan MM. Oedema of the umbilical cord and respiratory distress in the newborn. *Br J Obstet Gynaecol.* 1975;82:453–459.
72. Schaefer IM, Manner J, Faber R, et al. Giant umbilical cord edema caused by retrograde micturition through an open patent urachus. *Pediatr Dev Pathol.* 2010;13:404–407.
73. Mastrobattista JM, Hollier LM, Yeomans ER, et al. Effects of nuchal cord on birthweight and immediate neonatal outcomes. *Am J Perinatol.* 2005;22:83–85.
74. Schaffer L, Burkhardt T, Zimmermann R, et al. Nuchal cords in term and postterm deliveries—do we need to know? *Obstet Gynecol.* 2005;106:23–28.
75. Mucitelli DR, Charles EZ, Kraus FT. Chorioangiomas of intermediate size and intrauterine growth retardation. *Pathol Res Pract.* 1990;186:455–458.
76. Isaacs H Jr. Fetal hydrops associated with tumors. *Am J Perinatol.* 2008;25:43–68.
77. Tarim E, Killicadag E, Kayaselcuk F, et al. Submucosal leiomyoma of the uterus incorporated into the fetal membranes and mimicking a placental neoplasm: a case report. *Placenta.* 2003;24:706–709.
78. Misselevich I, Abramovici D, Reiter A, et al. Leiomyoma of the fetal membranes: report of a case. *Gynecol Oncol.* 1989;33:108–111.
79. Ernst LM, Hui P, Parkash V. Intraplacental smooth muscle tumor: a case report. *Int J Gynecol Pathol.* 2001;20:284–288.
80. Potter JF, Schoeneman M. Metastasis of maternal cancer to the placenta and fetus. *Cancer.* 1970;25:380–388.
81. Baergen RN, Johnson D, Moore T, et al. Maternal melanoma metastatic to the placenta: a case report and review of the literature. *Arch Pathol Lab Med.* 1997;121:508–511.

10

Gestational Trophoblastic Disease

INTRODUCTION

Gestational trophoblastic disease encompasses a spectrum of gestation-related abnormal trophoblastic proliferations ranging from molar pregnancies to trophoblastic neoplasms with varying degrees of aggressiveness. Placental site nodules and the exaggerated placental site are lesions of intermediate trophoblast that are often included in the differential diagnosis of trophoblastic neoplasms. However, since placental site nodules and the exaggerated placental site are nonmolar, nonneoplastic processes that typically present as incidental findings in endometrial curettings, they are discussed in the section on the endometrium and myometrium in pregnancy, abortion, and the postpartum period in Chapter 4.

COMPLETE HYDATIDIFORM MOLE

Classic Complete Mole (13 or More Weeks Gestational Age)

The vast majority of complete moles are diploid or tetraploid,[1] but all genetic material is of paternal origin. This unusual and diagnostically useful genotype is typically the result of fertilization of an egg devoid of functional maternal DNA (a so-called empty egg) by a single sperm that subsequently duplicates its genetic material, but occasionally may also be the result of two separate sperms fertilizing an empty egg.[2] In Europe and the United States, the incidence of complete mole is approximately 1 in every 2,000 clinically recognized pregnancies.[3] If left in utero to run its natural course, a complete mole will typically present with second-trimester vaginal bleeding, a uterus that is large for gestational age, a "snowstorm" pattern on ultrasound, and a markedly elevated serum β-hCG (>100,000 mIU/mL).

Grossly, classic complete moles are voluminous specimens that resemble loosely aggregated grapes, with a mean maximal villous diameter of 0.7 cm (Fig. 10.1).[1] There is generalized villous edema with a range of hydropic swelling, and central villous cavitation (cistern formation) is common. Although some cisterns may rupture and collapse during tissue extraction and processing, those that do not will contain fluid that appears faintly eosinophilic and granular in histologic sections. There is often a thin, well-demarcated, compressed rim of villous stroma surrounding the cisterns. Embryonic tissues are almost always absent, as are recognizable vascular structures within the villous stroma.

In addition to the grape-like villous swelling, the other cardinal feature of the classic complete mole is circumferential villous trophoblastic hyperplasia. This excessive proliferation of trophoblast is easily identified, but its extent and pattern of distribution are haphazard (Figs. 10.2 to 10.5). In the intervillous space, the trophoblastic proliferation may exhibit sheet-like growth and severe cytologic atypia, and may form bridges across villous structures (Fig. 10.6). Intravillous trophoblastic pseudoinclusions may also be present (Fig. 10.7). These pseudoinclusions are typically large and irregularly shaped, and have a different appearance than those that are a regular feature of partial moles (compare with Fig. 10.15).

Classic Complete Mole versus Partial Mole

The main features of a classic complete mole that help to distinguish it from a partial mole are (a) the diffuse and more pronounced nature of the villous edema, which results in a spectrum of villous sizes and more numerous cisterns, (b) the more extensive trophoblastic hyperplasia, (c) the absence of embryonic tissues, (d) the diploid/tetraploid rather than triploid DNA content, and (e) the lack of immunoreactivity for p57 in cytotrophoblast and villous stromal cells (see below). An additional finding that is much more prevalent in complete moles than in partial moles and hydropic abortions is widespread severe nuclear atypia in the intermediate trophoblast of the implantation site (Fig. 10.8).[4]

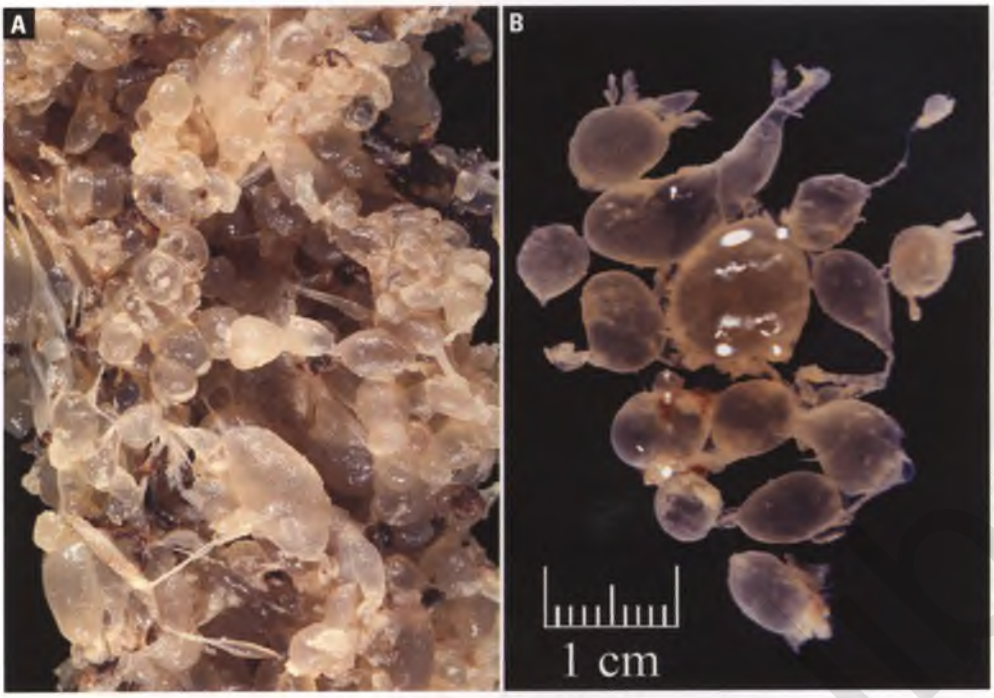

FIGURE 10.1. Complete hydatidiform mole. **A:** The tissue is abundant and composed of loosely aggregated vesicles of variable size. (Courtesy of Dr. Richard L. Payne.) **B:** These vesicles have been suspended in saline for photography.

Clinical Behavior

Complete moles are associated with a 15% to 20% incidence of persistent gestational trophoblastic disease.[5] This complication usually takes the form of persistent or invasive complete mole, although postmolar trophoblastic neoplasms can also occur. The estimated incidence of subsequent choriocarcinoma is 1 in 40 (2.5%).[6]

Early Complete Mole (7–12 Weeks Gestational Age)

With early prenatal care and advances in ultrasound techniques, failed pregnancies are now identified and evacuated with a gestational age as early as 7 weeks.[7] This has had an impact on the ease at which pathologists can recognize complete moles, since moles evacuated at this early stage do not show the pronounced villous edema, cistern formation, and widespread circumferential trophoblastic proliferation that are seen in complete moles several weeks later in gestation. Instead, the low-power clue to the possibility of a very early complete mole (VECM) is the presence of bulbous villi with a myxoid stroma that may be blue tinged (Figs. 10.9 and 10.10). This stroma contains primitive mesenchymal cells with increased cellularity, stromal karyorrhexis, and delicately branching immature vascular networks (Fig. 10.11).[8] The contour of these villi has been variously described as resembling the toes of a foot or that of a cauliflower, phyllodes tumor, knuckle, or club. The primitive capillary-like spaces within these villi are devoid of

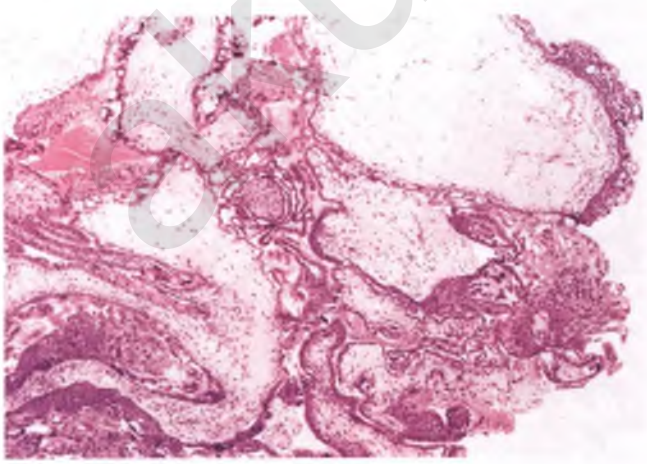

FIGURE 10.2. Complete hydatidiform mole. Note the prominent circumferential trophoblastic hyperplasia and generalized villous edema.

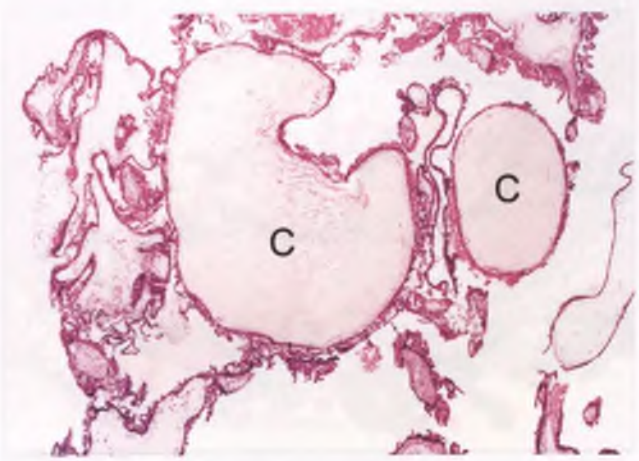

FIGURE 10.3. Complete hydatidiform mole. In this example, cisterns are present (labeled C), and there is less trophoblastic proliferation than in Figure 10.2.

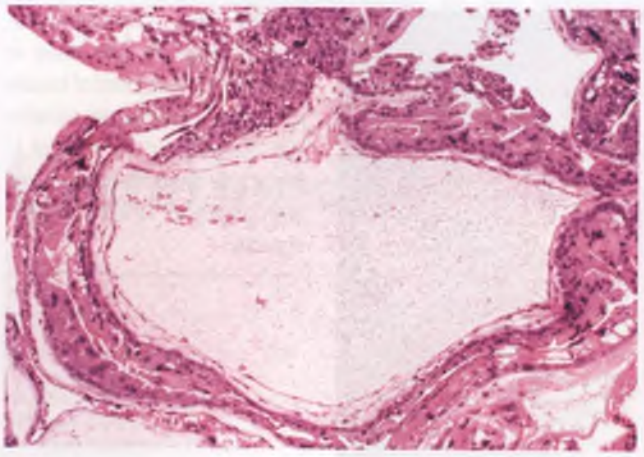

FIGURE 10.4. Complete hydatidiform mole. This molar villus exhibits cistern formation and circumferential trophoblastic hyperplasia. The cistern is surrounded by a compressed rim of villous stroma, and is filled with fluid that contains lightly eosinophilic, granular material.

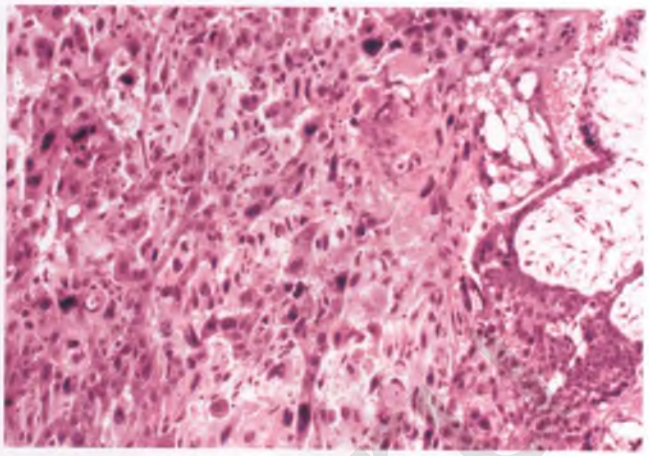

FIGURE 10.6. Complete hydatidiform mole. The molar villus at the far right side of the image merges with an area of sheet-like growth of intervillous trophoblast, which exhibits patches of severe nuclear atypia.

fetal-derived nucleated red blood cells and are destined to degenerate.[9]

The appearance of villi from early complete moles is distinctive and differs from that seen in normal gestation, partial moles, nonmolar gestations with chromosomal abnormalities, and abortions with hydropic degeneration (see below). When villi with low-power features that are suggestive of VECM are encountered, the identification of a subset of villi with circumferential trophoblastic hyperplasia helps to confirm the diagnosis. Although the trophoblastic proliferation is often focal in these cases, those villi that display this feature usually do so in a fairly obvious fashion (Figs. 10.9 and 10.10). Cisterns may be present or in the early stages of development (Fig. 10.12), but are not necessary for a diagnosis of VECM. As in classical complete mole, supportive evidence for a molar pregnancy is the finding of severe nuclear atypia within the intermediate trophoblast of the implantation site.

A recent study has emphasized the importance of villous stromal changes (incomplete vasculogenesis and increased karyorrhexis and apoptosis) over circumferential trophoblastic hyperplasia in the recognition of VECM.[10] When a morphologic diagnosis of VECM cannot be made with confidence, lack of nuclear staining with the p57 antibody in villous stromal cells and cytotrophoblastic cells can help to confirm the presence of a complete mole (see below). Recognition of VECM is of clinical importance, since the incidence of persistent gestational trophoblastic disease with this entity appears to be similar to that of conventional complete moles that are diagnosed later in gestation.[7,9]

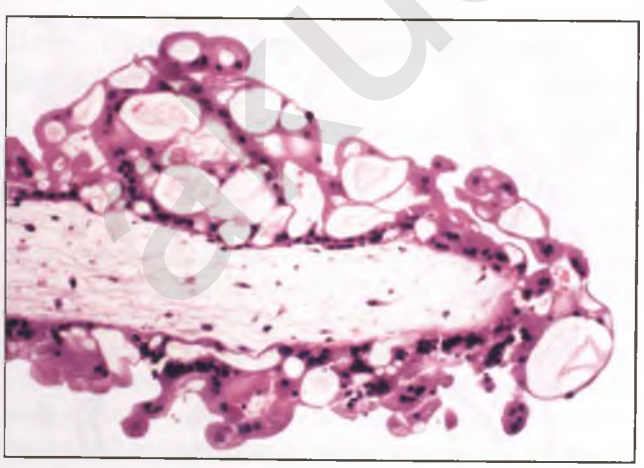

FIGURE 10.5. Complete hydatidiform mole. Prominent vacuolization of the hyperplastic syncytiotrophoblastic cells that surround this molar villus create a lace-like pattern.

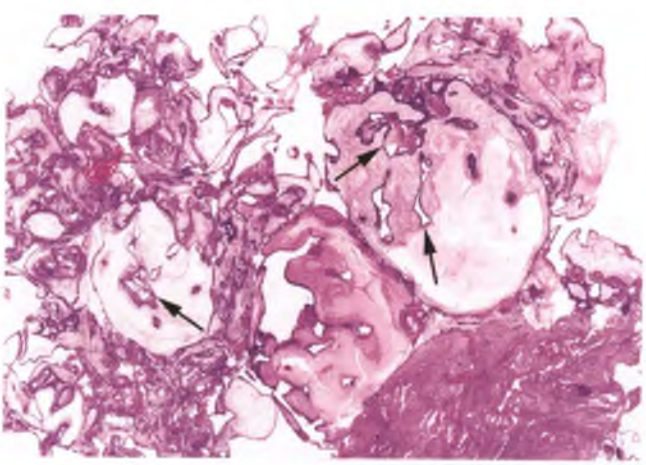

FIGURE 10.7. Complete hydatidiform mole. Molar villi may contain large, irregularly shaped trophoblastic pseudoinclusions, such as those marked by the *arrows*.

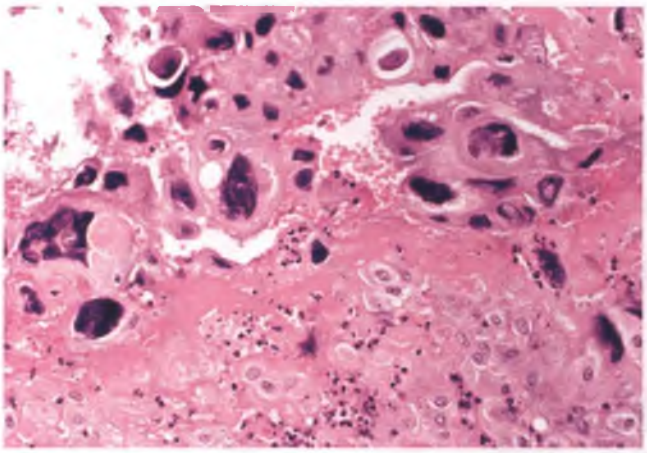

FIGURE 10.8. Complete hydatidiform mole. In this example, the intermediate trophoblast at the implantation site exhibits severe nuclear atypia.

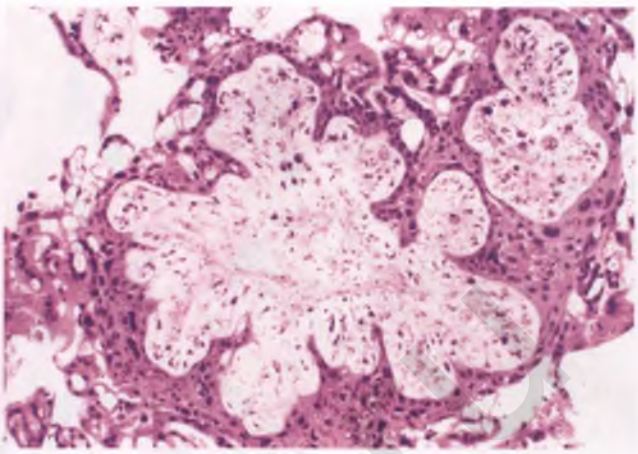

FIGURE 10.9. Very early complete mole. Note the (a) characteristic cauliflower-like villous shape, (b) primitive mesenchymal villous stroma with increased cellularity and necrobiosis, and (c) diffuse, circumferential trophoblastic hyperplasia. The latter finding was present in only a subset of villi.

PARTIAL HYDATIDIFORM MOLE

Partial moles frequently present with late first-trimester vaginal bleeding, a uterus that is of small or normal size for gestational age, a low to normal β-hCG, and the clinical impression of a missed abortion.[11] In a study from Ireland of almost 20,000 pregnancies, the incidence of partial mole was approximately 1 in 700 pregnancies, which presumably reflects the incidence in Europe and the United States as well.[3]

Almost all well-documented partial moles are triploid,[11] with one set of maternal chromosomes and two sets of paternal chromosomes (diandric triploidy) that is the result of fertilization of a normal egg by either two sperms or a single sperm that subsequently duplicates its genetic material. Although most diandric triploid gestations are histologically recognizable as partial moles, a minority of these genetic partial moles show only subtle or no diagnostic features.[12] Nontriploid partial moles should be viewed with a heavy dose of skepticism, since most are reclassified upon critical reexamination.[11] It should also be noted that not all triploid gestations are partial moles, since about one-third have been found to be digynic rather than diandric, and these digynic triploids lack histologic features diagnostic of partial moles.[12]

Gross examination of partial moles may reveal hydropic villi admixed with normal villi, but the hydropic changes are less prominent than in classic complete moles and may not be evident to the naked eye. Histologically, the partial mole can be thought of as a toned-down version of the complete mole when it comes to the extent of hydropic swelling, cistern formation, and trophoblastic proliferation, although it must be kept in mind that these two abnormalities are very different at the cytogenetic level.

Partial moles with classic histology exhibit all of the following features: (a) two distinct populations of villi, with one enlarged and edematous and the other small and often fibrotic (Figs. 10.13 and 10.14); (b) circumferential trophoblastic hyperplasia, usually focal and mild (Figs. 10.13 to 10.15); (c) of the villi that are enlarged and edematous, many exhibit irregular, scalloped outlines (Figs. 10.13 and 10.15); (d) small, round trophoblastic pseudoinclusions, which actually represent cross sections of narrow invaginations of surface trophoblast, are seen within some of the villi with scalloped contours (Figs. 10.15 and 10.16); and (e) within the subset of edematous villi, at least a few exhibit central cavitation (cistern formation) (Figs. 10.14 and 10.16). In contrast to complete moles, evidence of fetal development is usually present,

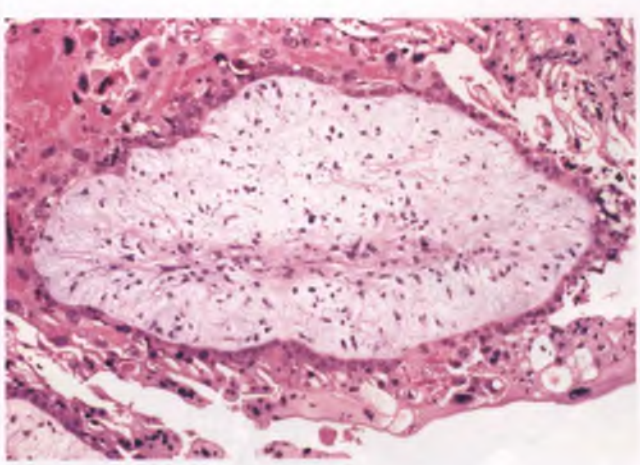

FIGURE 10.10. VECM with circumferential trophoblastic hyperplasia. The villous stroma is myxoid and has a distinctive blue-tinged appearance that bears some resemblance to cartilage or the stroma of a fibroadenoma of the breast.

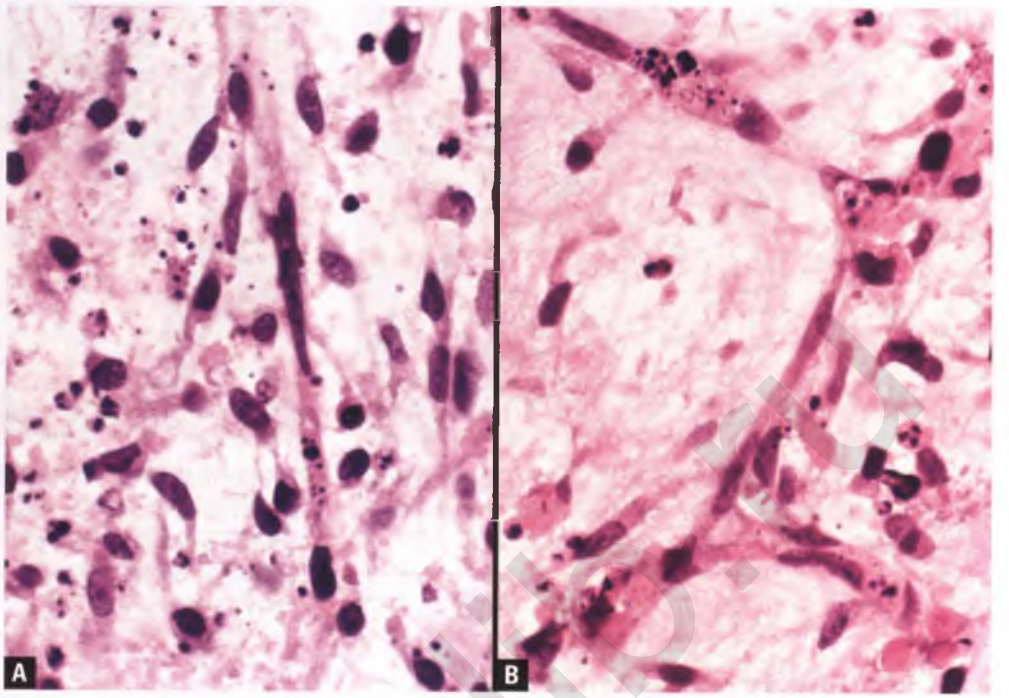

FIGURE 10.11. Villous stroma in VECMs. **A:** Note the stromal hypercellularity and necrobiosis. **B:** Primitive branching capillaries with degenerative changes are present.

often in the form of nucleated red blood cells within villous capillaries (Fig. 10.16 inset).

The histologic features of partial mole can be subtle, and this condition is probably underdiagnosed.[3,11] Some investigators have found that specificity for a diagnosis of partial mole is maintained when three or more of the five features listed above are present,[13] but confirmatory studies such as DNA flow cytometry are suggested when the histologic findings are equivocal. Although circumferential trophoblastic proliferation is one of the diagnostic features of partial mole, it is vaguely defined with no quantitative criteria. Subtle indications of this type of proliferative activity may be manifested by syncytiotrophoblastic micropapillary projections (dubbed syncytiotrophoblastic snouts/sprouts/knuckles/notches or syncytial tags) that when tangentially sectioned may appear to be free-floating adjacent to molar villi (Fig. 10.15), or by a redundant layer of syncytiotrophoblastic cells with a vacuolated, lace-like appearance similar to that illustrated for complete moles (Fig. 10.5).[11] In second-trimester partial moles, another helpful diagnostic clue that is occasionally seen within the villous stroma is the

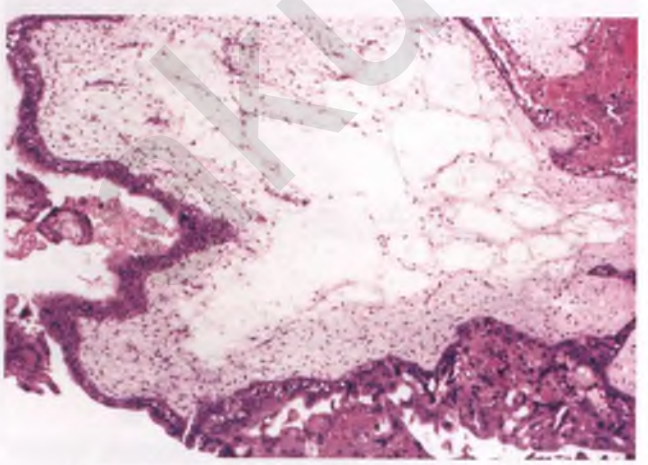

FIGURE 10.12. Very early complete mole. The presence of packets of accumulated fluid within the center of this molar villus is indicative of an early stage of development of a full-fledged cistern.

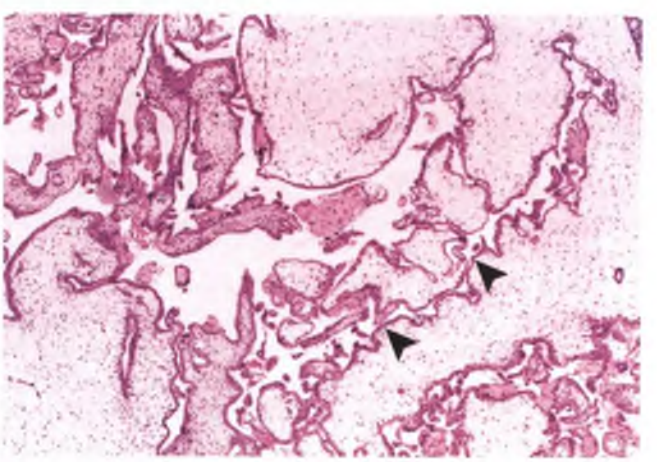

FIGURE 10.13. Partial hydatidiform mole. Large, irregularly shaped, edematous villi are admixed with smaller fibrotic villi, fulfilling the criterion of two distinct villous populations. One of the edematous villi has a scalloped outline (*arrowheads*). Trophoblastic hyperplasia is mild and involves a minority of the villi.

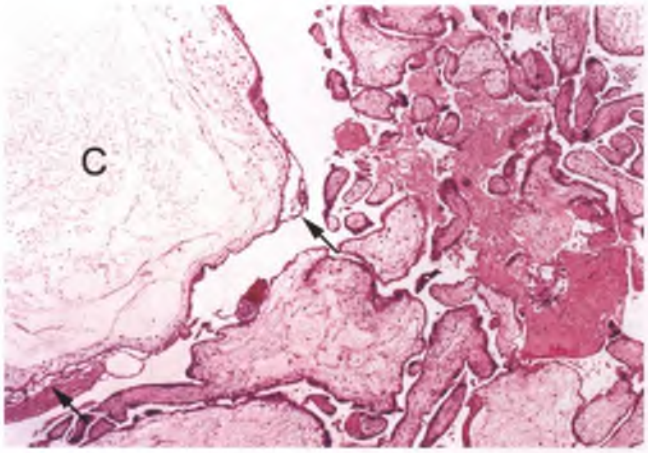

FIGURE 10.14. Partial hydatidiform mole. Two populations of villi are present. The large villus with a central cistern (C) exhibits subtle, lace-like proliferation of syncytiotrophoblast (*arrows*).

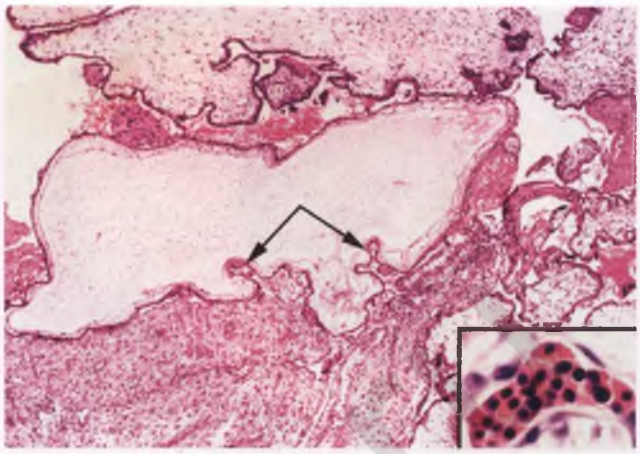

FIGURE 10.16. Partial hydatidiform mole. The central villus with a cistern has been fortuitously sectioned through two trophoblastic invaginations (*arrows*), which are usually seen as "trophoblastic inclusions." The inset shows nucleated red blood cells within a villous capillary of a partial mole, which is indicative of fetal development.

presence of a distinctive maze-like conglomeration of thin-walled, dilated, anastomosing vascular channels (Fig. 10.17).[14]

Clinical Behavior

Although it has been previously estimated that patients with partial moles have a 5% to 10% chance of developing persistent gestational trophoblastic disease, more recent studies have shown this incidence to be <1%.[5,15] Many of the cases reported in years past as partial mole with persistent gestational trophoblastic disease were diploid, and today would be reclassified as either complete mole or complete mole combined with a normal twin gestation.[16] When persistence does occur following a partial mole, it almost always represents retained residual molar tissue or, much less commonly, an invasive mole.[11] Rare, well-documented cases of partial mole with subsequent or concurrent development of choriocarcinoma have been reported, but this incidence appears to be on the order of 1 in 1,000 (0.1%).[15,17] In light of the more recent and credible data documenting the minimal risk of progression of partial moles, it seems reasonable that some investigators are calling

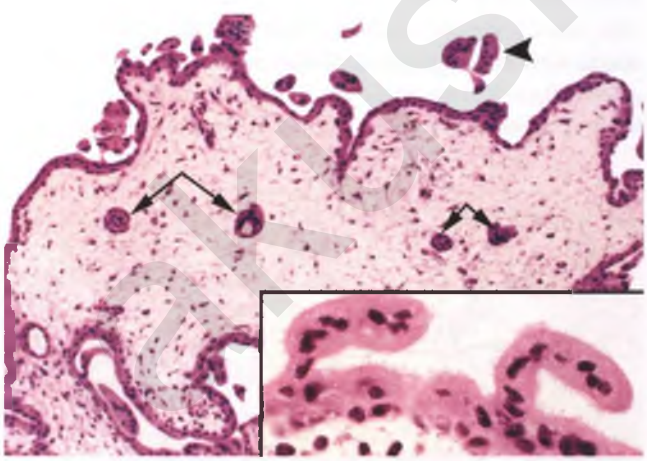

FIGURE 10.15. Partial hydatidiform mole. This image highlights an edematous villus with characteristic scalloped outlines and several trophoblastic pseudoinclusions (*arrows*). Mild trophoblastic proliferation is also present, as manifested by micropapillary projections of syncytiotrophoblast. Most of these trophoblastic sprouts appear to be detached from the perimeter of their associated villus (*arrowhead*). The inset shows micropapillary projections of syncytiotrophoblast attached to and protruding from the surface of another molar villus.

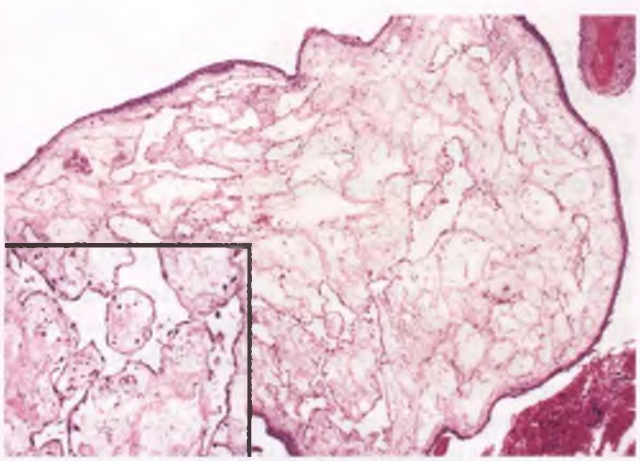

FIGURE 10.17. Partial hydatidiform mole. The stroma of this enlarged villus contains maze-like vascular channels and pockets of edema fluid. The inset highlights a focus of maze-like vessels.

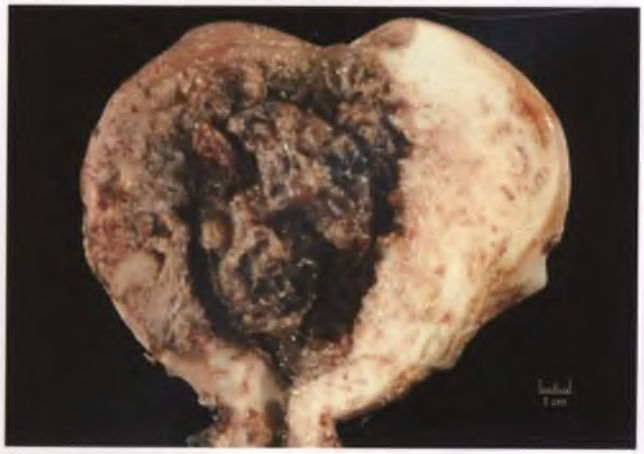

FIGURE 10.18. Invasive hydatidiform mole. In this opened, formalin-fixed uterus, a hemorrhagic, intracavitary mass with scattered vesicles exhibits transmural infiltration of one side of the myometrium. (Courtesy of Dr. Enrique Higa.)

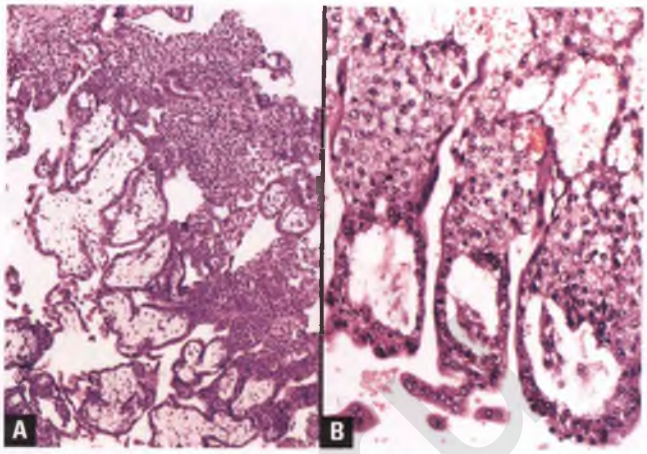

FIGURE 10.19. Normal trophoblastic proliferation in early gestation. **A:** In this abortion specimen, fragments of the trophoblastic shell are seen in association with chorionic villi. **B:** This view of chorionic villi with trophoblastic columns emphasizes the polar nature of the trophoblastic proliferation.

for shortening of the β-hCG surveillance period for those cases that are well documented.[5]

INVASIVE HYDATIDIFORM MOLE

In a small percentage of cases, evacuation of a molar pregnancy is followed by persistent elevation of the serum β-hCG level due to invasion by molar villi into the myometrium or its vascular spaces.[18] When it occurs, this phenomenon usually follows a complete mole, although rare cases of invasive partial mole have also been reported.[19] In the typical example, a ragged, hemorrhagic mass is seen infiltrating the myometrium (Fig. 10.18). Since invasive moles generally respond to chemotherapy, pathologists are unlikely to see such specimens except in hysterectomies from patients treated emergently for uterine perforation.

DIFFERENTIAL DIAGNOSIS OF MOLAR PREGNANCY

Early Gestation with Sampling of Polar Villous Proliferation

It is normal in early gestation for the villous trophoblastic proliferation to extend outward from one tip or edge of the anchoring villi in a polar fashion, forming the trophoblastic columns that contribute to formation of the trophoblastic shell (Fig. 10.19). Abortion specimens obtained during early gestation can contain tissue fragments that contain focally impressive trophoblastic proliferations that can cause confusion with molar pregnancies. This is frequently a problem in ectopic tubal pregnancies, since these are often removed at a time of gestation when the trophoblastic columns and trophoblastic shell are prominent.[20] In contrast to normal early gestations, molar trophoblastic proliferation is circumferential rather than polar. If O. J. Simpson's defense attorney, Johnnie Cochran, had been a pathologist, he might have said "If it grows at one pole, it's not a mole." The presence of chorionic villi with a polar rather than circumferential trophoblastic proliferation, the lack of appreciable villous stromal karyorrhexis, and the limited amount of trophoblastic tissue help to identify cases with these features as simply abortions at an early gestational age.

Hydropic Abortion

Villi from hydropic abortions share the property of villous edema with molar gestations. However, the overall amount of villous tissue is scant, their maximum villous diameter is two to three times smaller than that of villi from molar gestations,[1]

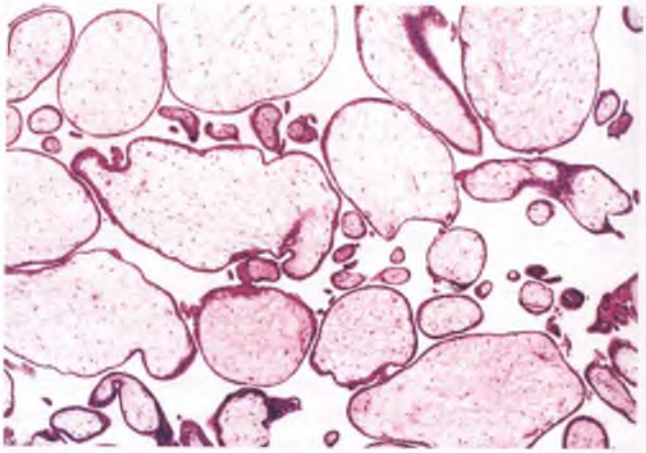

FIGURE 10.20. Hydropic abortus. Edematous villi with a spectrum of sizes are lined by an attenuated rim of trophoblast.

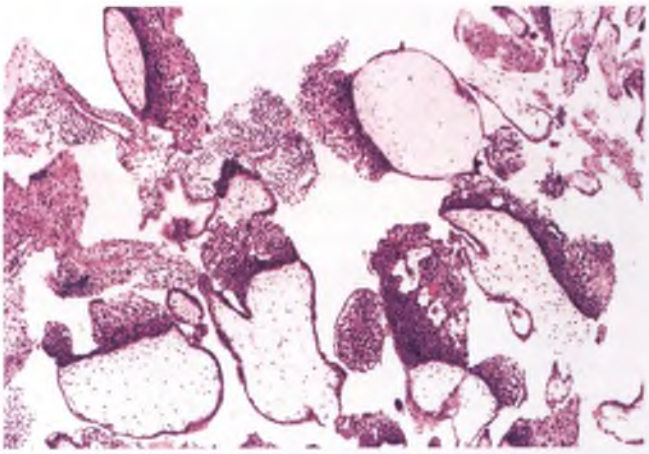

FIGURE 10.21. Hydropic abortus. In this example, many of the edematous villi are capped by a polar trophoblastic proliferation.

cisterns are usually absent, the villi exhibit a spectrum of sizes with a tendency toward round to oval contours, and the overlying trophoblast is usually thin and attenuated rather than hyperplastic (Fig. 10.20). That said, occasional hydropic abortions contain edematous villi that exhibit proliferating trophoblast with the normal polar distribution (Fig. 10.21).

Gestational Sac or Stem Villi with Shearing Artifact

The amnion is easily separated from the chorion, and in suction curettage specimens there is often a clear space between these two layers as a consequence of the shearing forces applied during tissue extraction (Fig. 10.22). This tear-related artifact of the gestational sac, which extends into pseudovillous

FIGURE 10.22. The separation of the amnion from the chorion in this gestational sac mimics the appearance of ruptured hydropic villi with collapsed cisterns.

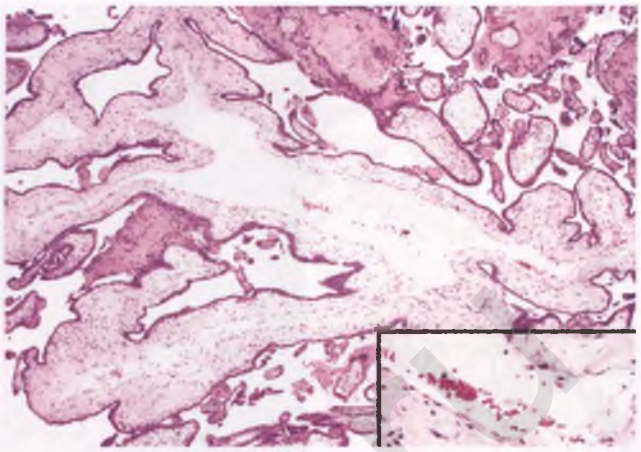

FIGURE 10.23. Stem villus with shearing-related artifact. A slit-like, central clear space is present that follows the normal contour of the villus. The inset highlights the presence of scattered small aggregates of fresh blood within this space, which serves as additional evidence in favor of a traumatic origin.

papillary infoldings of the membrane on the side opposite the chorion laeve, should not be misinterpreted as villi with cistern formation. Cisterns are formed due to hydropic distention of villi, and those that have not ruptured and collapsed prior to tissue processing are typically filled with granular, faintly eosinophilic fluid. It is also not uncommon for large stem villi that have been subjected to shearing forces during tissue extraction or processing to exhibit a similar tear-related artifact that can lead to the false impression of cistern formation (Fig. 10.23).

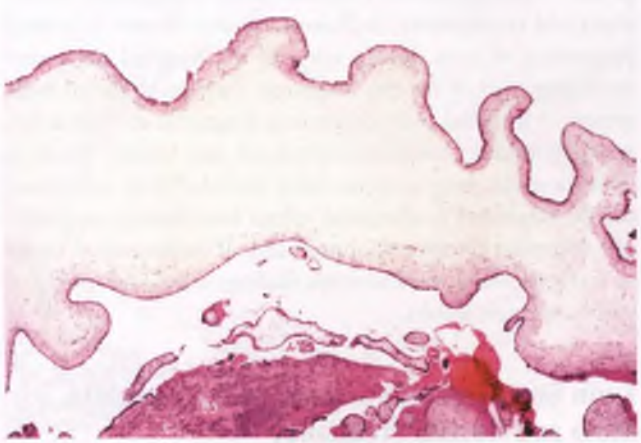

FIGURE 10.24. Portion of an opened early gestational sac composed of amnion that has been turned inside out and folded back upon itself. The formation of a clear pseudocavity, coupled with normal undulations in the amnion, creates the false impression of a cavitated villus with scalloped outlines.

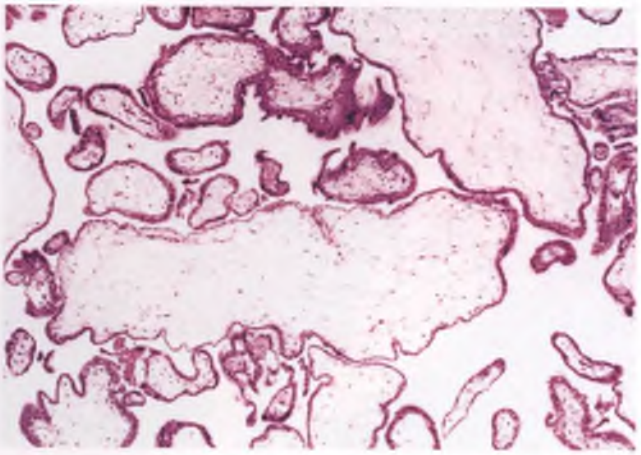

FIGURE 10.25. Abnormal villous morphology in trisomy 21 (Down syndrome). Edematous villi, some with scalloped contours, are present.

Gestational Sac Turned Inside Out

An opened gestational sac folded inside out prior to fusion of the amnion with the chorion, which occurs at about 12 weeks of gestation, can mimic a large hydropic villus (Fig. 10.24).

Abnormal Villous Morphology Due to Nonmolar Chromosomal Abnormalities

Various chromosomal abnormalities, such as trisomy 13, trisomy 18, trisomy 21 (Down syndrome), and 45,XO (Turner's syndrome), are associated with abnormal villous morphology that can cause some resemblance to partial moles (Fig. 10.25).[13] The features most often shared with partial moles are enlarged, edematous villi with scalloped outlines and the presence of what appears to be two discrete populations of villi.[13] Mild degrees of circumferential trophoblastic hyperplasia and trophoblastic inclusions can also be seen in a small proportion of cases, but in none of the reported cases were more than two of the five diagnostic features of partial mole present.[13] If partial mole is a serious diagnostic consideration, ancillary studies should be considered (see below). Cases in which a molar pregnancy has been excluded with confidence can be diagnosed as abnormal villous morphology suggestive of a nonmolar cytogenetic abnormality. If chromosomal analysis was performed, the histologic findings should be correlated with karyotypic results.

Twin Gestation with Simultaneous Complete Mole and Normal Pregnancy

Twin gestations that represent a complete mole occurring in conjunction with a normal twin are quite rare, but have been reported.[21] In this situation, the histologic findings in endometrial curettings will resemble a partial mole, given the admixture of two different populations of villi and evidence of embryonic development. Features favoring a complete mole with simultaneous normal twin gestation over a partial mole are (a) the extensive degree of trophoblastic hyperplasia in those villi with proliferative trophoblast, (b) the lack of scalloped villous contours and small, round trophoblastic pseudoinclusions, (c) severe nuclear atypia of implantation site intermediate trophoblast, (d) p57 negativity in the edematous villi with trophoblastic hyperplasia and p57 positivity in the normal villi, and (e) diploid/tetraploid rather than triploid DNA content. All cases of "diploid partial mole" should be evaluated for this possibility, especially if follow-up discloses the development of choriocarcinoma, which is 25 times more common in complete moles than partial moles.

Placental Mesenchymal Dysplasia

Placental mesenchymal dysplasia is a rare disorder characterized by (a) tortuous chorionic plate vessels with aneurysmal dilatation and thrombosis (Fig. 10.26) and (b) enlarged, edematous villi with a fibromyxoid stroma (Figs. 10.27 and 10.28).[22] The associated fetus may be normal, have growth restriction, undergo intrauterine fetal demise, or have Beckwith-Wiedemann syndrome. The vascular changes develop and progress over time, such that abnormal chorionic plate vessels are not seen before 20 weeks of gestation. The ultrasonographic findings of the placenta in this disorder may resemble a partial mole. However, the presence of a well-formed fetus and the usual presentation in the third trimester help to distinguish this process from a molar gestation.

Histologically, the edematous villi in placental mesenchymal dysplasia may show focal cistern formation, and their admixture with small villi causes further resemblance to partial mole. However, unlike partial moles, the edematous villi in placental mesenchymal dysplasia do not show circumferential trophoblastic proliferation, scalloped outlines, or trophoblastic pseudoinclusions, and are diploid by DNA flow cytometry. The vascular pattern in the edematous villi in placental mesenchymal dysplasia ranges from avascular to normal to chorangiomatous, and there may be an associated chorangioma. Some cases, including many of those associated with Beckwith-Wiedemann syndrome, have peripherally located muscularized vessels within the abnormal villi.[11]

UTILITY OF ANCILLARY STUDIES WHEN EVALUATING DIFFICULT CASES OF SUSPECTED MOLAR PREGNANCY

The most common diagnostic dilemmas in which ancillary studies can prove helpful are partial mole versus complete mole, partial mole versus hydropic abortus, partial mole versus abnormal villous morphology secondary to a nonmolar cytogenetic abnormality, and early complete mole versus hydropic abortus. In exceptional cases, a complete mole associated with a normal twin gestation can also cause diagnostic difficulties, as discussed

FIGURE 10.26. Placental mesenchymal dysplasia. Note the aneurysmal dilatation of the tortuous, thrombosed vessels of the chorionic plate.

above. In difficult cases, one should submit all of the villous tissue for histologic evaluation in the hope of uncovering more readily apparent diagnostic features. If that does not lead to a conclusive diagnosis, special studies should be performed or the slides and representative tissue block should be sent to a consultant. DNA flow cytometry and immunohistochemistry are technologies that can provide useful information in the evaluation of suspected molar pregnancies and are readily available in many pathology laboratories. Digital image analysis and fluorescence in situ hybridization (FISH) are alternative methods to flow cytometry for assessing ploidy, with FISH thought to have the best accuracy of these three technologies.[23] Recently, more sophisticated molecular genetic techniques have become commercially available as kits that allow DNA genotyping to be performed in a practical and cost-effective manner.[24] This powerful genetic test is performed using formalin-fixed,

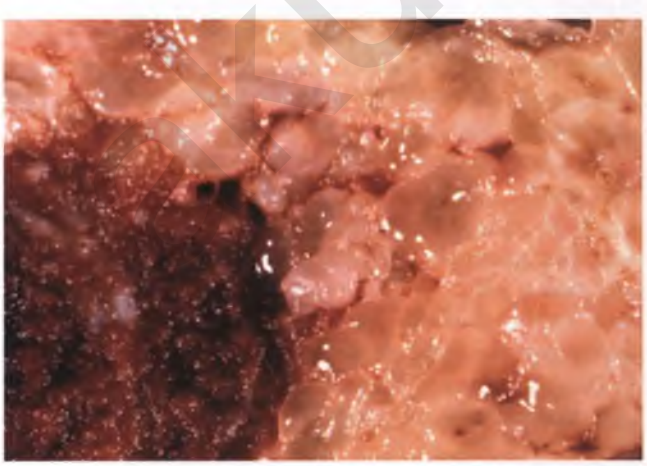

FIGURE 10.27. Placental mesenchymal dysplasia. This sectioned surface demonstrates the presence of enlarged, edematous villi adjacent to normal, reddish-brown placental tissue.

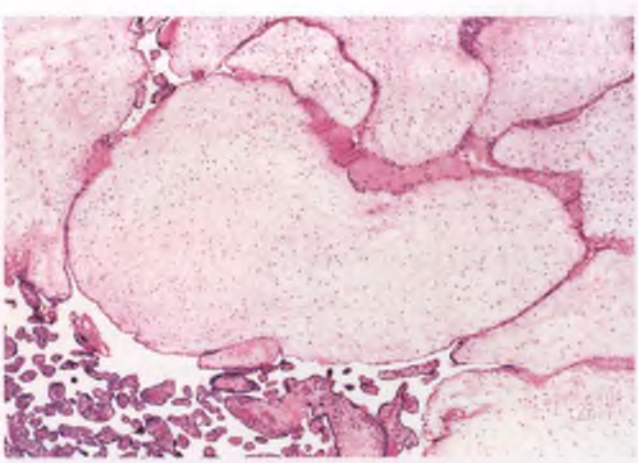

FIGURE 10.28. Placental mesenchymal dysplasia. Enlarged, avascular villi with edematous fibromyxoid stroma are seen adjacent to normal third-trimester villi. The abnormal villi have gradually curved rather than scalloped contours, and lack trophoblastic proliferation and trophoblastic pseudoinclusions.

paraffin-embedded samples of villous and maternal decidual tissue and has the ability to identify the androgenetic diploidy (or androgenetic tetraploidy) of complete mole, the diandric triploidy of partial mole, and the biparental diploidy of nonmolar mimics of molar pregnancy.[24,25] The utility of these various technologies is discussed in more detail in the sections that follow.

DNA Ploidy Analysis

DNA flow cytometry can be performed on either fresh or formalin-fixed, paraffin-embedded tissue, and can help to distinguish a triploid partial mole (69 chromosomes) from a complete mole (46 or 92 chromosomes), a hydropic abortus (46 chromosomes), or a monosomy (45 chromosomes) or trisomy (47 chromosomes) with abnormal villous morphology.[26] The inability of flow cytometry to detect differences in DNA content related to additions or deletions of single chromosomes does not impact its utility in this situation, since the entity to be excluded or confirmed (the partial mole) differs from the other differential diagnostic considerations in DNA content by at least one multiple of 23 chromosomes (±1 chromosome in the case of a monosomy or trisomy). Moreover, since digynic triploids do not produce histologic concerns for partial mole,[12] the finding of triploidy in a specimen that is histologically worrisome for partial mole is strong supportive evidence for that diagnosis.

Although useful in confirming the diagnosis of partial mole, DNA flow cytometry cannot distinguish a complete mole from a normal diploid hydropic abortus (both generally 46 chromosomes). In addition, DNA flow cytometry can be difficult to interpret or give misleading results if most or all of the tissue submitted for evaluation is inadvertently taken from maternal (diploid) endometrium, there is an actively dividing diploid cell population, or there is excessive cellular debris.[23] Although digital image analysis has an advantage over flow cytometry in that it allows for the direct visualization of the cells being analyzed, it is limited by the ability of an actively dividing diploid cell population within a diploid sample to result in histograms that can be misinterpreted as triploid.[23]

p57 Immunohistochemistry

Although technologies that assess ploidy status still have their place in distinguishing partial moles from complete moles, hydropic abortions, and abnormal villous morphology related to nonmolar cytogenetic abnormalities, differentiation of partial versus complete mole can also be accomplished via immunohistochemical detection of the p57 gene product, as can distinction of partial mole from complete mole admixed with normal twin gestation.[27–29] This immunostain is also of great value in distinguishing early complete mole from hydropic abortus, which is a setting where DNA flow cytometry does not provide useful information.

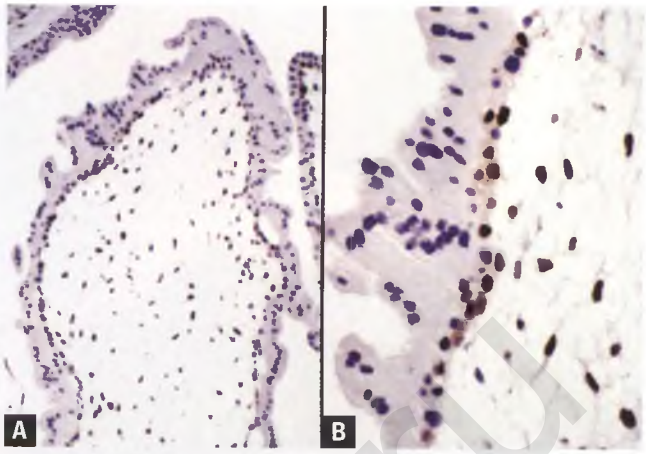

FIGURE 10.29. A,B: p57 immunohistochemistry in partial hydatidiform mole. Several of the cytotrophoblastic and villous stromal cells exhibit nuclear immunoreactivity, but the mildly hyperplastic syncytiotrophoblastic cells are negative. Similar staining patterns are observed in all other types of gestations, with the notable exception of negative staining of cytotrophoblastic and villous stromal cells in complete moles. (p57 immunostain courtesy of Dr. Steve Kargas.)

The p57 gene is located on chromosome 11 and is paternally imprinted, which means that this gene on the paternally derived chromosomes is epigenetically inactivated through a process such as selective DNA methylation. Thus, for tissue types in which the gene has been imprinted, the p57 gene product is entirely derived from the maternal allele, and its detection by nuclear immunoreactivity serves as a marker for the maternal genome. Since complete moles are derived solely from paternal DNA, whereas partial moles, hydropic abortions, and cases with abnormal villous morphology contain maternally derived genetic material, different patterns of expression of the p57 gene product can be used in the differential diagnosis of complete mole versus these other entities. In partial moles, hydropic abortions, and cases with abnormal villous morphology, many of the cytotrophoblastic and villous stromal cells are p57-positive (Fig. 10.29), whereas these cell types are almost always p57-negative in complete moles.[27–29] Decidua and islands of intervillous intermediate trophoblast from all types of gestations serve as internal positive controls (Fig. 10.30).*

Very rarely, aberrant expression of p57 can be seen in numerous cytotrophoblastic and villous stromal cells in complete moles, which is a false-negative test result since it incorrectly argues against the diagnosis of complete mole.[27] This phenomenon has been shown in some instances to be due to the retention of at least a portion of the maternal chromosome 11 that contains the p57 locus.[30,31]

*The positive staining of intervillous trophoblast in complete moles comes as a surprise, and is most likely due to the erasable and tissue-specific nature of genetic imprinting.

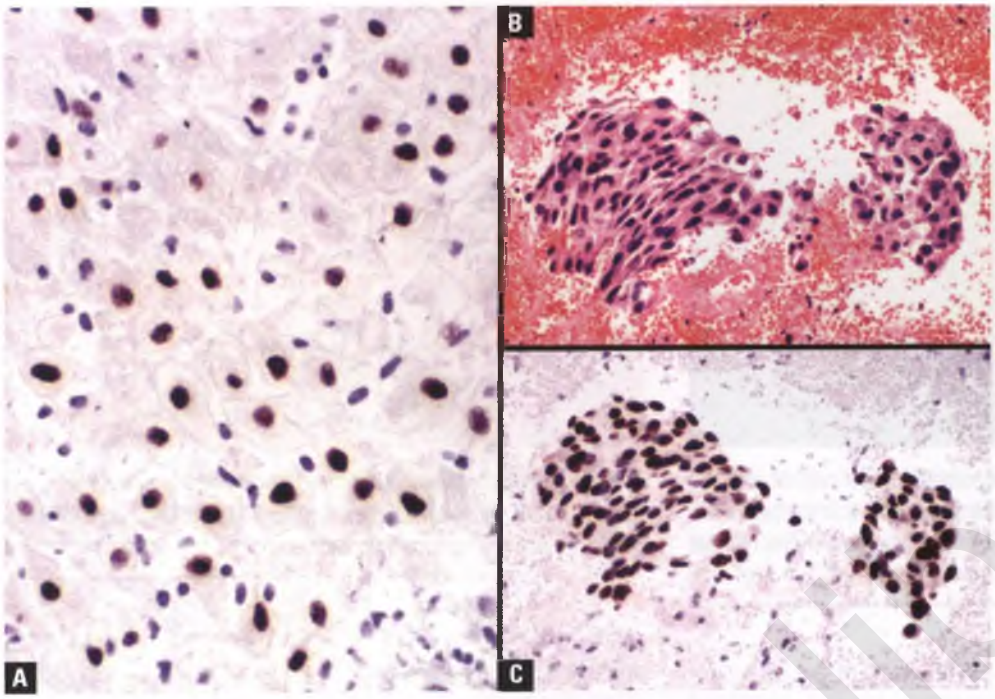

FIGURE 10.30. Internal positive controls used in p57 immunohistochemistry. **A:** Many decidual cell nuclei are p57-positive. **B:** Islands of intervillous intermediate trophoblast. **C:** Serial section of **B** stained with p57, showing strong immunoreactivity. (p57 immunostains courtesy of Dr. Steve Kargas.)

p57 Immunohistochemistry and Molecular Genotyping Move to the Forefront

Recently, it has been proposed that p57 immunohistochemistry be the frontline ancillary test for further evaluation of specimens suggestive of hydatidiform mole by routine histology.[25,32] Cases with negative p57 immunostaining in which complete mole is a leading differential diagnostic consideration can be confidently diagnosed as complete mole, provided that there is appropriate staining of the internal positive control. Other cases suggestive of hydatidiform mole in which the p57 immunostain is positive or equivocal should be subjected to molecular genetic analysis, which will enable identification of partial moles (diandric triploids), nonmolar mimics such as hydropic abortions and abnormal villous morphology related to nonmolar cytogenetic abnormalities (biparental diploids), and the exotic cases of complete mole with aberrant p57 expression (androgenetic diploids with retained genetic material from maternal chromosome 11). Note that ploidy analysis via DNA flow cytometry, digital image analysis, or FISH has been taken out of the loop in this algorithm because of the limitations of some of these techniques as described above and their inability to determine the relative contributions of maternal and paternal chromosomes in a given specimen.

Personally, I do not see the need for p57 immunohistochemistry in routine practice when the histologic differential diagnosis does not include complete mole. For example, when trying to distinguish abnormal villous morphology or hydropic abortus from partial mole, p57 positivity is almost assured and performing this stain only serves to delay the diagnosis and increase the cost of the evaluation. In this situation, I would prefer to proceed directly to genotyping or ploidy analysis. Although genotyping is preferred, the assay chosen may depend upon test availability, the expertise of the pathologists and technologists performing these tests, and cost.

CHORIOCARCINOMA[33]

Choriocarcinoma is the most malignant gestational trophoblastic neoplasm. Approximately 50% of cases are preceded by a hydatidiform mole, with complete moles outnumbering partial moles by a ratio of approximately 25 to 1 in this

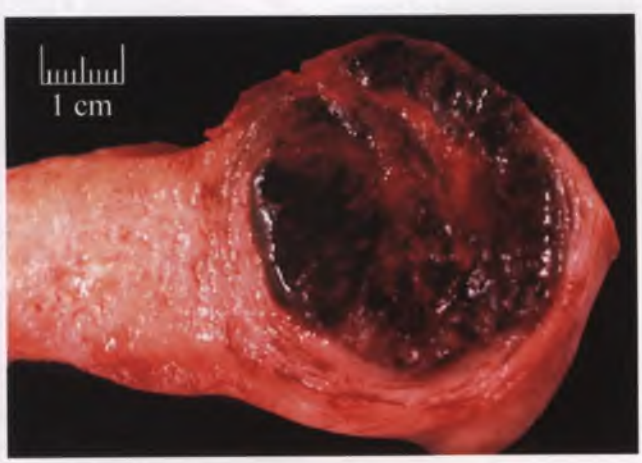

FIGURE 10.31. Choriocarcinoma. The sectioned surface of this uterine choriocarcinoma demonstrates its characteristic gross appearance as a hemorrhagic nodule.

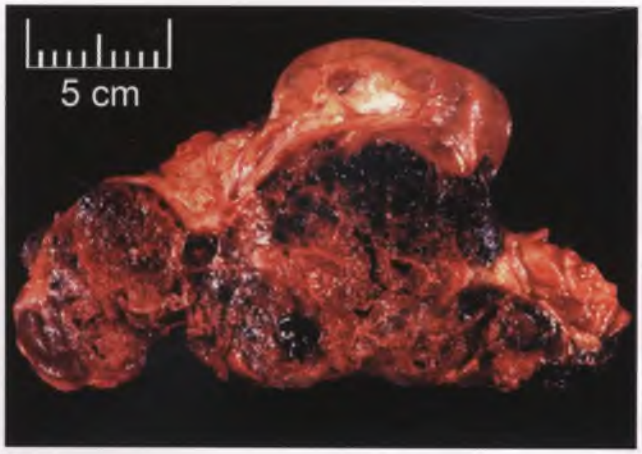

FIGURE 10.32. Choriocarcinoma metastatic to perinephric soft tissues. The sectioned surface of the kidney is located at the top of the image, and is dwarfed by the large hemorrhagic tumor with nodular rather than infiltrative borders.

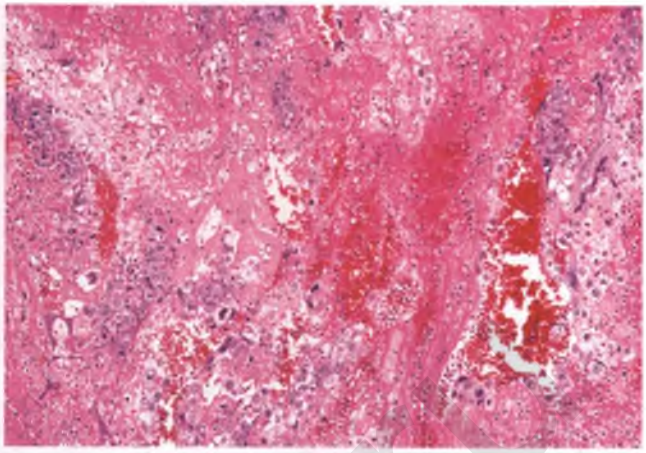

FIGURE 10.33. Choriocarcinoma. As expected from the gross appearance of choriocarcinomas, large portions of the tumor, particularly centrally, are hemorrhagic and necrotic.

circumstance. Choriocarcinoma can also present as a complication of a normal pregnancy, a spontaneous abortion, or an ectopic pregnancy. The estimated frequency of choriocarcinoma is 1:160,000 for normal gestations, 1:16,000 for spontaneous abortions, 1:5,000 for ectopic pregnancies, 1:1,000 for partial moles, and 1:40 for complete moles. Although abnormal uterine bleeding is often present, the first manifestations of the disease may be related to hemorrhagic events from metastatic deposits in such locations as the lung, brain, or liver.

Grossly, choriocarcinomas are circumscribed, hemorrhagic masses at both primary and metastatic sites (Figs. 10.31 and 10.32). Since hemorrhagic necrosis dominates the central regions of these tumors (Fig. 10.33), histologic sections should be taken at the interface with normal tissues, which is where viable tumor is most likely to be found.

Microscopically, choriocarcinoma is composed of nests and sheets of mononucleate trophoblastic cells interlaced with syncytiotrophoblastic cells in a distinctive biphasic pattern (Fig. 10.34). Although traditional descriptions of choriocarcinoma equate the mononucleate trophoblastic component with cytotrophoblast, morphologic evidence and a recent immunohistochemical study indicate that most of

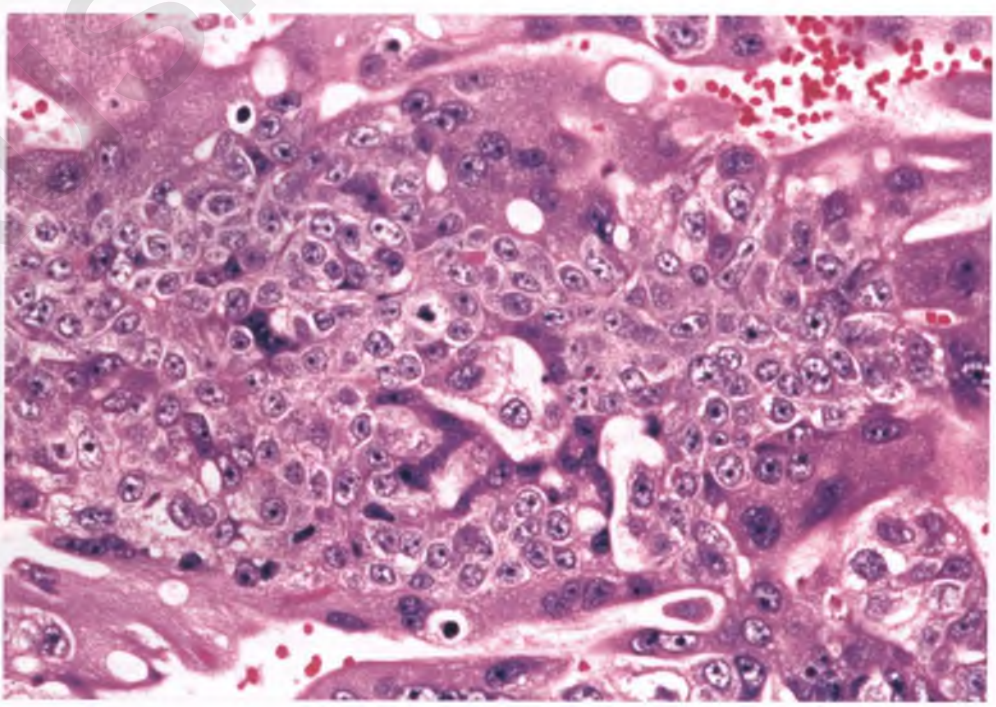

FIGURE 10.34. Choriocarcinoma. Multinucleated, vacuolated syncytiotrophoblastic cells are seen enveloping aggregates of mononucleated trophoblastic cells, which results in a biphasic pattern that is characteristic of this tumor.

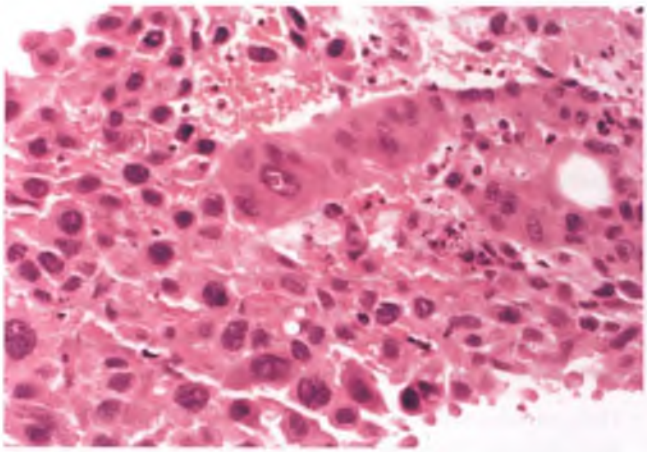

FIGURE 10.35. Choriocarcinoma. Intermediate trophoblastic cells constitute most of the mononucleated cells in this field.

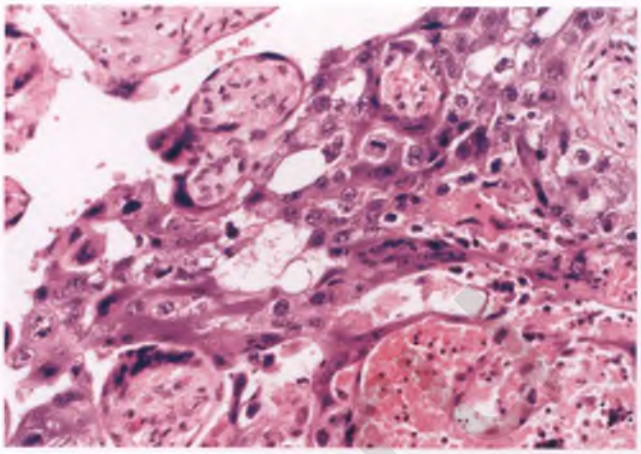

FIGURE 10.37. Intraplacental choriocarcinoma. There is comingling of choriocarcinoma with third-trimester chorionic villi at the edge of the cancerous nodule. (Glass slide kindly provided by Drs. Bruce D. Patterson and Cheryl M. Reichert.)

the mononucleate trophoblastic cells in the majority of choriocarcinomas are actually intermediate trophoblasts.[34] In routine sections, these intermediate trophoblasts (particularly those of implantation type) are distinguished from cytotrophoblastic cells by their larger, more pleomorphic nuclei (Fig. 10.35). The distinction between villous-type intermediate trophoblast and cytotrophoblast within choriocarcinomas may require immunohistochemistry, but this distinction is rarely necessary for diagnostic purposes. Choriocarcinomas lack chorionic villi by definition, with the exception of the intraplacental variant, which is discussed in the following paragraph.

Documented intraplacental choriocarcinomas are extraordinarily rare, and are almost always found in near-term or term gestations (Figs. 10.36 and 10.37).[35,36] Many are of small size, and are easily overlooked on gross examination of the placenta. In general, those that are recognized as a lesion are grossly thought to be an infarct or intervillous thrombus rather than a tumor. Maternal metastatic disease is present at the time of diagnosis of the intraplacental choriocarcinoma in about 60% of cases.[35] These metastases are often asymptomatic at the time of detection, with their identification via radiologic screening prompted by the placental findings. In a small percentage of cases, there are metastases to the infant, which are often fatal. Given that intraplacental choriocarcinoma is often difficult to detect grossly, it is likely that a significant proportion of cases of gestational choriocarcinoma that follow "normal" term gestations represent metastases from small intraplacental choriocarcinomas that were never recognized.

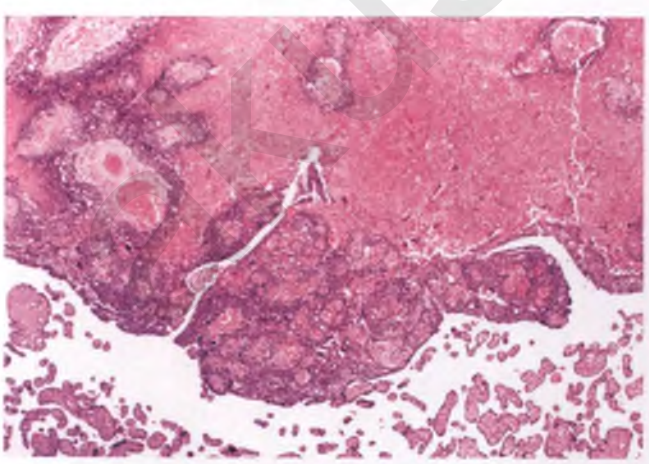

FIGURE 10.36. Intraplacental choriocarcinoma. This low-magnification view demonstrates a portion of a cancerous nodule with extensive hemorrhagic necrosis. Viable tumor is present surrounding vessels and at the tumor interface with third-trimester chorionic villi. (Glass slide kindly provided by Drs. Bruce D. Patterson and Cheryl M. Reichert.)

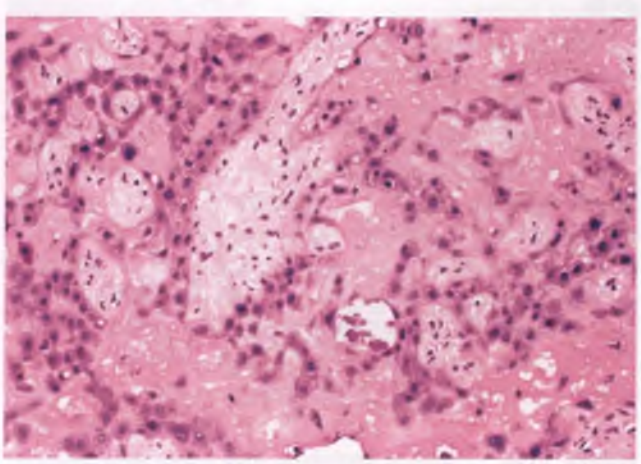

FIGURE 10.38. Aggregates of intermediate trophoblasts embedded within deposits of perivillous fibrin. This is an incidental finding.

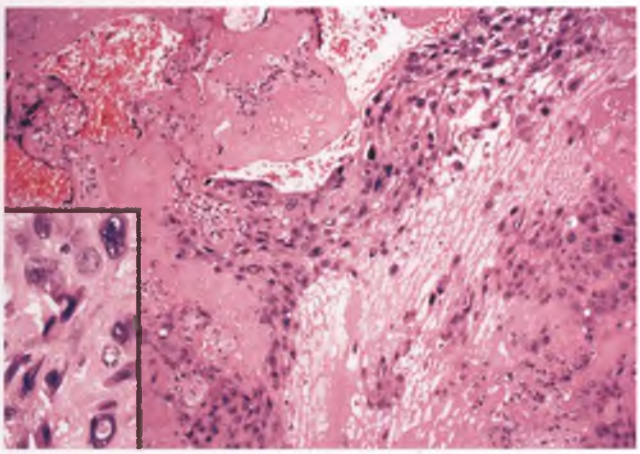

FIGURE 10.39. Aggregates of intermediate trophoblasts embedded within deposits of perivillous fibrin. The inset highlights the presence of incidental degenerative atypia.

Only a few cases of chorangiocarcinoma, which is basically a choriocarcinoma arising in association with a chorangioma, have been reported.[37] Care should be taken not to confuse this entity with the fairly frequent finding of hyperplasia of the trophoblastic elements that are normally seen at the periphery of chorangiomas (see Chapter 9).

Differential Diagnosis

It is important to distinguish early forms of intraplacental choriocarcinoma from the variably cellular aggregates of intermediate trophoblasts that are often incidentally found embedded within perivillous deposits of fibrin (Fig. 10.38). Occasionally, degenerative nuclear atypia can be seen in these trophoblastic elements, resulting in a resemblance to so-called choriocarcinoma in situ (Fig. 10.39). The intimate association of the trophoblastic proliferation with perivillous fibrin, the virtual absence of mitotic activity, and the finding of a pure population of mononucleate intermediate trophoblasts rather than a dimorphic admixture of mononucleate trophoblasts and syncytiotrophoblasts help to distinguish this process from an incipient form of the rare intraplacental choriocarcinoma.

Choriocarcinoma of the usual type can be confused with sampling of previllous trophoblast or the trophoblastic shell from early gestations, complete hydatidiform moles with exuberant trophoblastic proliferations, postmolar trophoblast, anaplastic malignant neoplasms with tumor giant cells, and placental site trophoblastic tumors (PSTTs).

- Only previllous trophoblastic elements may be present in very early abortion specimens, typically admixed with fragments of clotted blood (Fig. 10.40). In slightly more advanced gestations, villi may have formed but they may be overshadowed by fragments of the trophoblastic shell. The dimorphic proliferation of cytotrophoblast and syncytiotrophoblast in these situations creates a microscopic pattern very similar to choriocarcinoma. However, in contrast to choriocarcinoma, the amount of trophoblastic tissue is limited to a few microscopic fragments, and there is not widespread tissue necrosis. Serum β-hCG levels can also be helpful, since they are much lower at this early point in gestation than would be expected for choriocarcinoma. Multiple histologic sections should be examined in an attempt to further exclude choriocarcinoma by finding chorionic villi.
- As discussed above, rare choriocarcinomas have been reported in association with villi from term or near-term placentas. However, the presence of villi in a first- or second-trimester placenta excludes the possibility of choriocarcinoma, even if the trophoblastic proliferation is exuberant and atypical (Fig. 10.41).[38] In an initial curettage, the diagnosis in such situations is either an early gestation or a complete mole. In a

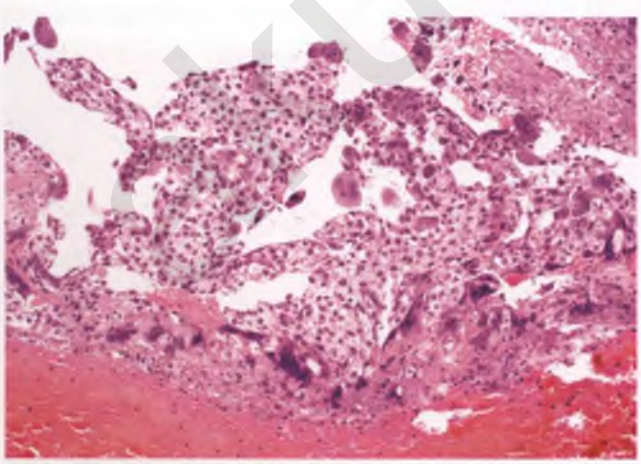

FIGURE 10.40. Previllous trophoblast from a very early gestation. A resemblance to choriocarcinoma is apparent, but this was a focal microscopic finding unassociated with tissue necrosis.

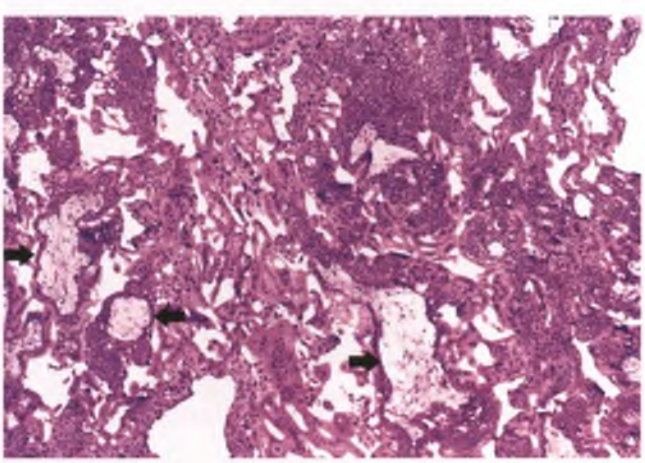

FIGURE 10.41. Exuberant trophoblastic proliferation in an early complete mole. The presence of villi (*arrows*) during this period of gestation excludes the possibility of choriocarcinoma. Follow-up was uneventful.

postmolar curettage, the diagnosis is persistent hydatidiform mole rather than choriocarcinoma as long as any abnormal villi are identified (there may be an underlying invasive mole, but myometrial invasion by molar villi is hardly ever seen in curettage specimens). Even if villi are absent, in the face of a small amount of trophoblastic tissue, the findings are most likely related to sampling issues in a persistent mole rather than to choriocarcinoma. Such cases can be reported as "persistent trophoblast without villi—see comment." However, the presence of abundant sheets of trophoblast in a biphasic pattern with tumor necrosis and/or destructive growth into the myometrium should prompt a diagnosis of choriocarcinoma.

- Metastatic poorly differentiated malignancies should also be considered in the differential diagnosis of choriocarcinoma, and can be differentiated by correlation with clinical history, serum β-hCG levels, and an immunohistochemical panel that includes hCG for the detection of syncytiotrophoblasts. Since neoplasms other than choriocarcinoma can sometimes contain hCG-positive cells, the identification of hCG-positive syncytiotrophoblasts should be reaffirmed by their typical histologic features of multinucleation, violaceous (and often vacuolated) cytoplasm, and biphasic growth pattern before hCG immunoreactivity is taken as evidence of choriocarcinoma. Even then, the possibility of an unusual carcinoma with trophoblastic differentiation needs to be considered. Unlike choriocarcinomas, these tumors will show evidence of transition between their usual and choriocarcinomatous components.
- The distinction of choriocarcinoma from PSTT is discussed in the following section.

PLACENTAL SITE TROPHOBLASTIC TUMOR

PSTT, which in years past has been referred to as atypical chorioepithelioma, syncytioma, and trophoblastic pseudotumor,[39]

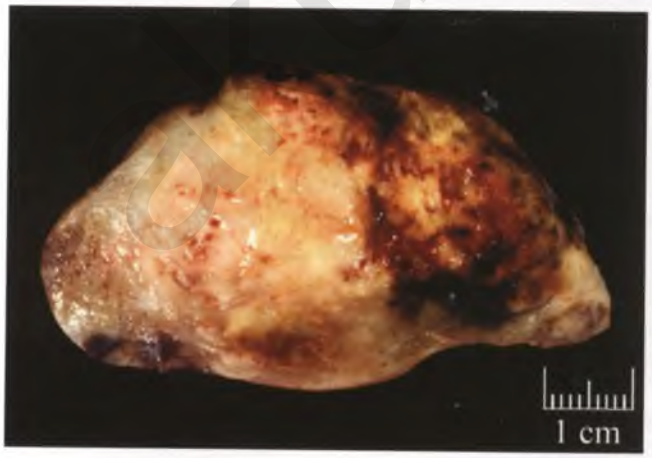

FIGURE 10.42. Placental site trophoblastic tumor. This section through the myometrium demonstrates transmural involvement by the tumor, which is yellow, partially hemorrhagic, and poorly demarcated.

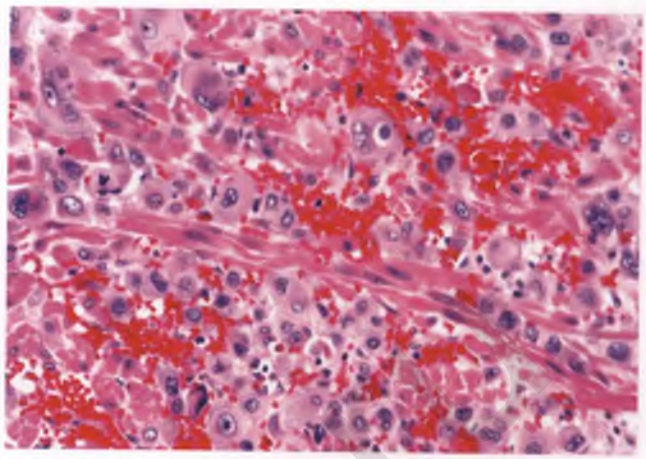

FIGURE 10.43. Placental site trophoblastic tumor. Note the characteristic pattern of myoinvasion, with tumor cells splaying apart and dissecting between muscle fibers, rather than destroying them.

is a rare neoplasm of implantation-type intermediate trophoblast. The most common clinical presentation is amenorrhea or abnormal vaginal bleeding in a 20- to 40-year-old woman with uterine enlargement and slightly elevated levels of serum β-hCG.[40] There is a history of a prior gestational event, typically within the past 2 years, and in 95% of cases this was a normal gestation. In about 5% of cases, there is coexistent nephrotic syndrome due to a distinctive glomerular lesion.[41] Although initial experience with this rare neoplasm suggested that it was benign, subsequent studies have revealed malignant behavior in about 15% of cases.[42] Since PSTT is generally nonresponsive to conventional chemotherapy regimens, hysterectomy is the treatment of choice.

Grossly, PSTT most often forms an ill-defined mass within the myometrium, but it may also appear more well circumscribed or as a polyp projecting into the endometrial cavity. Its sectioned surface is typically soft, tan to yellow, and partially hemorrhagic (Fig. 10.42). Microscopically, the tumor recapitulates the normal growth pattern of implantation-type intermediate trophoblasts infiltrating the myometrium and vessels (Figs. 10.43 and 10.44). The neoplastic counterpart of the deciduoid variant† of the mononucleated, implantation-type intermediate trophoblast typically predominates in PSTTs, with occasional interspersed binucleated and multinucleated cells (Fig. 10.45). Neoplastic cells with features of the hyperchromatic variant of intermediate trophoblast are also present in variable numbers. In addition to the dissecting pattern of myoinvasion, regions of the tumor may exhibit an expansile growth pattern. The mitotic index averages 2 mitotic figures per 10 high-power fields, and the mean Ki-67 proliferation index is 14%.[43] Chorionic villi are almost always absent.

†For descriptive purposes, I have divided implantation-type intermediate trophoblasts into deciduoid and hyperchromatic variants (see Chapter 4).

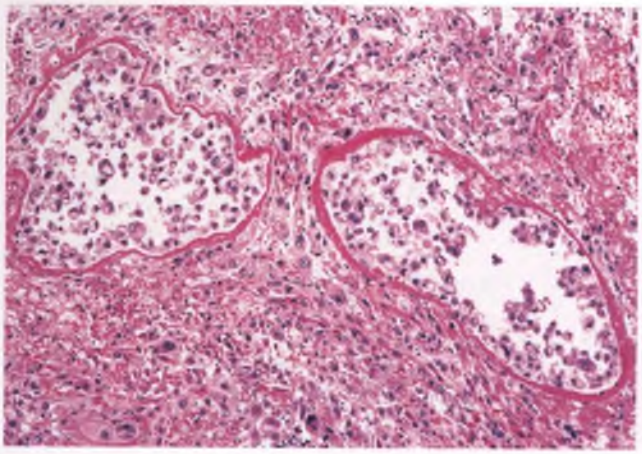

FIGURE 10.44. PSTT with its trademark pattern of vascular invasion recapitulating that seen in the normal implantation site. It is not surprising that hemorrhage is often present in these neoplasms, given the fragile state of the vessels whose walls have been replaced by fibrinoid material.

As discussed below, the most diagnostically useful immunohistochemical features of PSTTs are their diffuse positivity for cytokeratin and human placental lactogen, focal positivity for human chorionic gonadotropin, and negativity for p63 and placental alkaline phosphatase.[42,44,45]

Differential Diagnosis

The differential diagnosis of PSTT includes exaggerated placental site, placental site nodule, choriocarcinoma, epithelioid trophoblastic tumor (ETT), and epithelioid smooth muscle tumor.

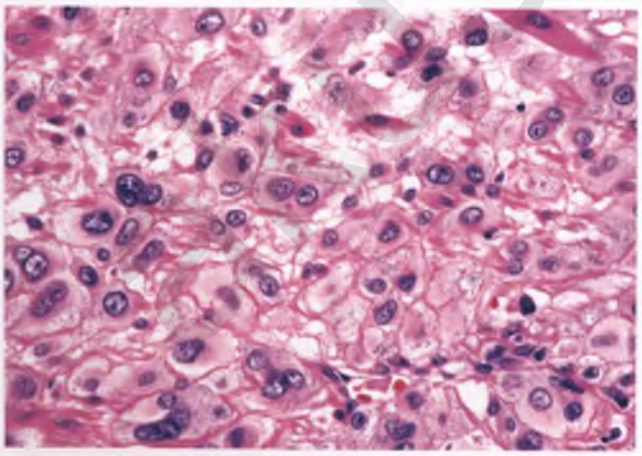

FIGURE 10.45. Placental site trophoblastic tumor. In this area of expansile confluent growth, there are only a few residual wisps of smooth muscle. The tumor is composed predominantly of mononucleated intermediate trophoblastic cells, many of which have a deciduoid appearance.

- Distinguishing between PSTT and an exaggerated placental site can be particularly difficult in a curettage specimen, since both feature myometrium and vessels infiltrated by intermediate trophoblast. Findings that favor an exaggerated placental site include the absence of a clinically detected mass, little or no mitotic activity, the presence of chorionic villi, lack of foci of confluent growth, and a Ki-67 proliferative index of near zero.[43]
- Placental site nodules are distinguished from PSTT by their incidental presentation, small size, circumscribed rather than infiltrative growth pattern, hyalinized stroma, and immunoreactivity for placental alkaline phosphatase[46] and p63.[45]
- PSTTs lack the biphasic growth pattern of choriocarcinoma, the extensive hemorrhagic necrosis, and the diffuse positivity of the syncytiotrophoblastic component of choriocarcinoma for human chorionic gonadotropin. Although isolated syncytiotrophoblasts can be seen in PSTT, most of the multinucleated cells present in this tumor are multinucleated intermediate trophoblasts that have polygonal or round contours with nonvacuolated cytoplasm. This appearance contrasts with the elongated, spider-like, interwoven shapes of vacuolated syncytiotrophoblast typical of choriocarcinoma. Choriocarcinoma also lacks the characteristic pattern of vascular invasion of PSTT.
- Distinction of PSTT from ETT is discussed in the following section.
- PSTTs can be distinguished from epithelioid smooth muscle tumors on the basis of their characteristic pattern of vascular invasion, positivity for human placental lactogen, and negative staining for muscle markers. Diffuse positivity for cytokeratin is also expected in PSTT, but can also be seen in a minority of epithelioid smooth muscle tumors.[47]

EPITHELIOID TROPHOBLASTIC TUMOR

ETT, which was first described in 1998,[48] is a rare trophoblastic tumor thought to be derived from chorionic-type intermediate trophoblast. The typical clinical presentation is abnormal vaginal bleeding in a premenopausal woman with a remote history of a prior gestational event. Serum β-hCG levels are usually elevated at the time of diagnosis, but at relatively low levels (<2,500 mIU/mL). Approximately 25% of tumors will behave in a malignant fashion. Like PSTT, hysterectomy is the usual treatment of choice, since this tumor is not generally successfully treated with chemotherapy.

Grossly, ETTs are solitary, tannish-brown uterine nodules with occasional degenerative cysts and variable amounts of hemorrhage and necrosis. The tumors rarely exceed 4 cm in diameter. In the Shih and Kurman series, half of the tumors presented in the lower uterine segment or endocervical canal.[48]

Microscopically, ETTs are composed of a nodular proliferation of chorionic-type intermediate trophoblastic cells arranged in nests and sheets, which is rimmed by a lymphocytic infiltrate in approximately half of the cases (Fig. 10.46). The tumor has a characteristic hyaline-like matrix that may

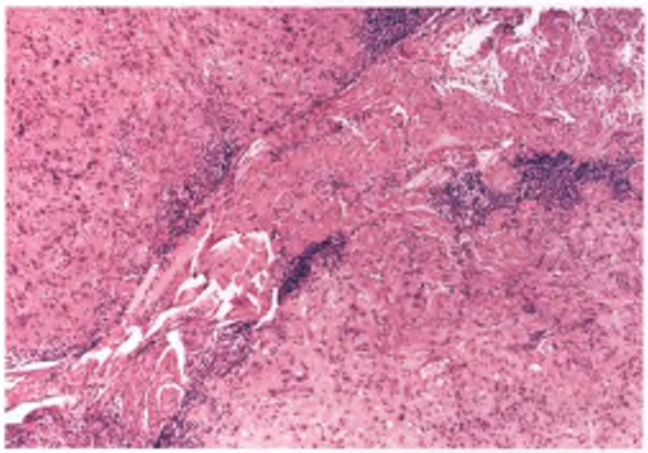

FIGURE 10.46. Epithelioid trophoblastic tumor. This low-magnification view highlights two nodular fragments of tumor from an endometrial curettage. Note the peripheral rim of lymphocytes, which is a helpful diagnostic feature.

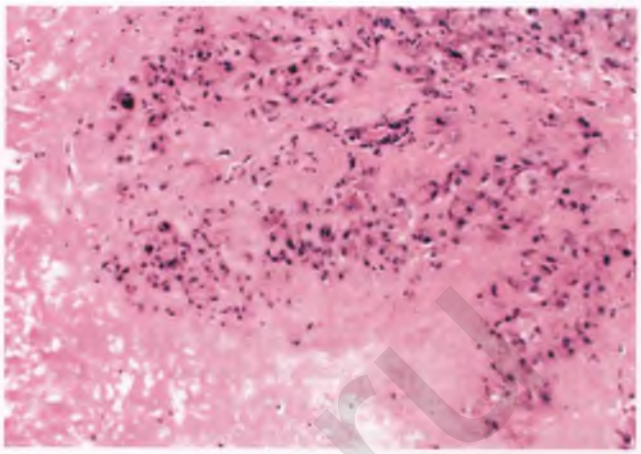

FIGURE 10.48. Epithelioid trophoblastic tumor. A focus of geographic necrosis is present to the left of a serpentine cord of tumor cells.

be seen either surrounding the tumor cells or within the center of tumor cell nests; in the latter situation, the matrix may be punctuated by dots of necrotic debris (Fig. 10.47). Foci of geographic necrosis are usually evident (Fig. 10.48). ETT has an average mitotic index of 2 mitoses per 10 high-power fields, and a mean Ki-67 proliferation index of 18%.[48] Just like their nonneoplastic counterparts in the chorion laeve (Fig. 9.4), the tumor cells can have either eosinophilic or clear (glycogen-rich) cytoplasm (Fig. 10.49). When tumors involve the endocervix, there can be partial replacement of the endocervical epithelium by neoplastic trophoblastic elements in a pattern that can be misinterpreted as endocervical gland involvement by high-grade squamous intraepithelial lesion (pseudo-HSIL).[48]

ETTs are immunoreactive for pancytokeratin, but their most diagnostically useful immunohistochemical features are their immunoreactivity for p63, cyclin E, and HSD3B1, and their lack of strong nuclear staining for p16 (see below).[45,48–50]

It is noteworthy that a handful of primary pulmonary ETTs that mimic non–small cell lung carcinoma have been reported in parous women of reproductive age.[51]

Differential Diagnosis

The main differential diagnostic considerations of ETT are placental site nodule, PSTT, cervical squamous cell carcinoma, and epithelioid smooth muscle tumor.

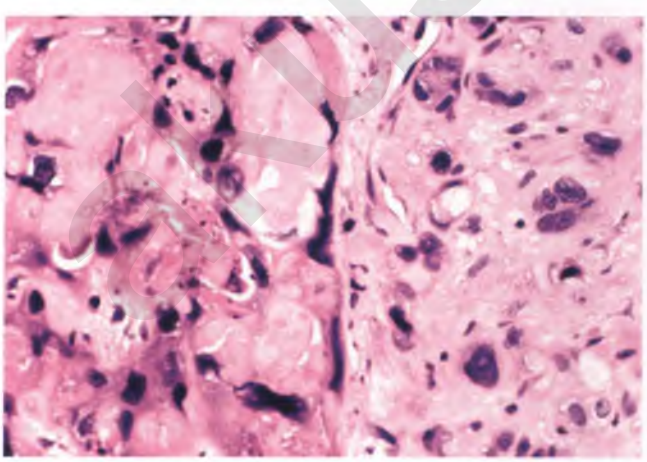

FIGURE 10.47. Epithelioid trophoblastic tumor. Hyaline-like matrix material characteristically surrounds tumor cells (right) and may also be found within the center of tumor cell nests, where it can be mistaken for keratin (left). Some of the aggregates of matrix material contain specks of necrotic debris.

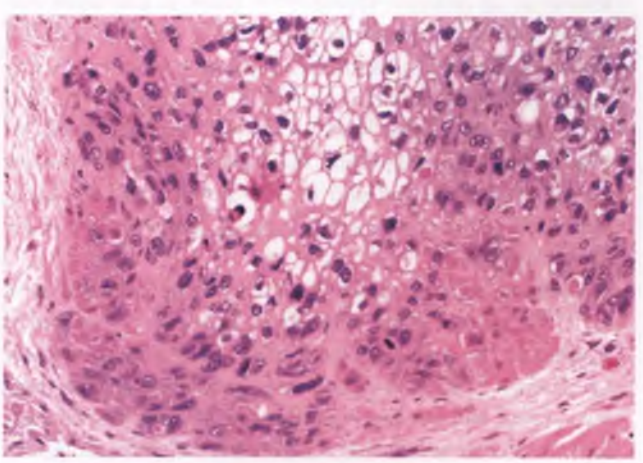

FIGURE 10.49. Epithelioid trophoblastic tumor. This example contains nests of tumor cells with cytoplasm that ranges from clear and glycogen rich to eosinophilic. Note the resemblance to squamous cell carcinoma.

- Placental site nodules are incidental findings of microscopic size rather than mass lesions, lack necrosis, and have a low Ki-67 proliferation index (<10%).[52] Since ETTs are thought to represent the neoplastic counterpart of placental site nodules, it is not surprising that their immunophenotypes are very similar. However, nuclear immunoreactivity for cyclin E is typically diffuse and strong in ETTs and focal and weak in placental site nodules, and this difference can help to distinguish these two processes from one another.[49]
- In contrast to ETTs, PSTTs have an infiltrative rather than nodular growth pattern, lack the characteristic hyalinized stroma of ETT, demonstrate a pattern of vascular invasion that recapitulates that seen in the normal implantation site, and are p63 negative.[45]
- ETTs can be easily misdiagnosed as squamous cell carcinoma, particularly when the tumors are located within the endocervical canal, the pseudo-HSIL lesion is present, and the hyaline-like matrix is misinterpreted as keratin. Clinicopathologic correlation often helps in distinguishing ETT from squamous cell carcinoma, since ETT usually occurs in premenopausal women with a prior gestational event and mildly elevated serum β-hCG, but atypical clinical presentations can occur. Microscopically, a well-circumscribed, or at most focally infiltrative border, particularly when associated with a peripheral rim of lymphocytes, is much more typical of ETT than squamous cell carcinoma. ETTs also lack the intercellular bridges of squamous cell carcinoma. The immunohistochemical markers that are most helpful in making this distinction are p16 and HSD3B1, since ETTs typically exhibit negative to weak cytoplasmic staining for p16 and positive immunoreactivity for HSD3B1, whereas the vast majority of cervical squamous cell carcinomas show diffuse, strong, nuclear and cytoplasmic immunoreactivity for p16 and are HSD3B1 negative (HSD3B1 is an enzyme that holds promise as a sensitive and specific marker for trophoblastic lesions of all different types).[49,50,53] There is also some evidence that CD10 positivity favors ETT and that CK 5/6 positivity favors squamous cell carcinoma, but conflicting results have been reported for CK18, HLA-G, and inhibin when these antibodies have been tested for their ability to help resolve this differential diagnosis.[45,48,53] Immunostains for pancytokeratin and p63 are not useful in this situation, since both of these tumors are typically immunoreactive for these markers.[45]
- Epithelioid smooth muscle tumors may be confused with ETT because of their epithelioid appearance, prominent hyalinized stroma, and occasional immunoreactivity for cytokeratin.[47] When well sampled, epithelioid smooth muscle tumors will usually have transitional foci where more typical smooth muscle differentiation is evident, and immunohistochemical staining with muscle markers will usually document their myogenous phenotype.[54]

SUGGESTED READINGS

Clement PB, Young RH. *Atlas of Gynecologic Surgical Pathology*. 2nd ed. Philadelphia, PA: Elsevier Saunders; 2008.

Crum CP, Nucci MR, Lee K, eds. *Diagnostic Gynecologic and Obstetric Pathology*. 2nd ed. Philadelphia, PA: Elsevier Saunders; 2011.

Kurman RJ, Ellenson LH, Ronnett BM, eds. *Blaustein's Pathology of the Female Genital Tract*. 6th ed. New York, NY: Springer; 2011.

Robboy SJ, Mutter GL, Prat J, et al., eds. *Robboy's Pathology of the Female Reproductive Tract*. 2nd ed. Oxford, UK: Churchill Livingstone; 2009.

Silverberg SG, Kurman RJ. *Tumors of the Uterine Corpus and Gestational Trophoblastic Disease. Atlas of Tumor Pathology*, Third series, Fascicle 3. Washington, DC: Armed Forces Institute of Pathology, 1992:219–285.

REFERENCES

1. Lage JM, Mark SD, Roberts DJ, et al. A flow cytometric study of 137 fresh hydropic placentas: correlation between types of hydatidiform moles and nuclear DNA ploidy. *Obstet Gynecol*. 1992;79:403–410.
2. Kajii T, Ohama K. Androgenetic origin of hydatidiform mole. *Nature*. 1977;268:633–634.
3. Jeffers MD, O'Dwyer P, Curran B, et al. Partial hydatidiform mole: a common but underdiagnosed condition. A 3-year retrospective clinicopathological and DNA flow cytometric analysis. *Int J Gynecol Pathol*. 1993;12:315–323.
4. Montes M, Roberts D, Berkowitz RS, et al. Prevalence and significance of implantation site trophoblastic atypia in hydatidiform moles and spontaneous abortions. *Am J Clin Pathol*. 1996;105:411–416.
5. Niemann I, Petersen LK, Hansen ES, et al. Predictors of low risk of persistent trophoblastic disease in molar pregnancies. *Obstet Gynecol*. 2006;107:1006–1011.
6. Bagshawe KD. Risk and prognostic factors in trophoblastic neoplasia. *Cancer*. 1976;38:1373–1385.
7. Hui P, Martel M, Parkash V. Gestational trophoblastic diseases: recent advances in histopathologic diagnosis and related genetic aspects. *Adv Anat Pathol*. 2005;12:116–125.
8. Keep D, Zaragoza MV, Hassold T, et al. Very early complete hydatidiform mole. *Hum Pathol*. 1996;27:708–713.
9. Kim MJ, Kim KR, Ro JY, et al. Diagnostic and pathogenetic significance of increased stromal apoptosis and incomplete vasculogenesis in complete hydatidiform moles in very early pregnancy periods. *Am J Surg Pathol*. 2006;30:362–369.
10. Kim KR, Park BH, Hong YO, et al. The villous stromal constituents of complete hydatidiform mole differ histologically in very early pregnancy from the normally developing placenta. *Am J Surg Pathol*. 2009;33:176–185.
11. Genest DR. Partial hydatidiform mole: clinicopathological features, differential diagnosis, ploidy and molecular studies, and gold standards for diagnosis. *Int J Gynecol Pathol*. 2001;20:315–322.
12. Redline RW, Hassold T, Zaragoza MV. Prevalence of the partial molar phenotype in triploidy of maternal and paternal origin. *Hum Pathol*. 1998;29:505–511.
13. Chew SH, Perlman EJ, Williams R, et al. Morphology and DNA content analysis in the evaluation of first trimester placentas for partial hydatidiform mole (PHM). *Hum Pathol*. 2000;31:914–924.
14. Szulman AE. Trophoblastic disease: complete and partial hydatidiform moles. In: Perrin E, ed. *Pathology of the Placenta*. New York, NY: Churchill Livingstone; 1984:183–197.
15. Seckl MJ, Fisher RA, Salerno G, et al. Choriocarcinoma and partial hydatidiform moles. *Lancet*. 2000;356:36–39.
16. Niemann I, Hansen ES, Sunde L. The risk of persistent trophoblastic disease after hydatidiform mole classified by morphology and ploidy. *Gynecol Oncol*. 2007;104:411–415.
17. Medeiros F, Callahan MJ, Elvin JA, et al. Intraplacental choriocarcinoma arising in a second trimester placenta with partial hydatidiform mole. *Int J Gynecol Pathol*. 2008;27:247–251.
18. Takeuchi S. Nature of invasive mole and its rational management. *Semin Oncol*. 1982;9:181–186.
19. Gaber LW, Redline RW, Mostoufi-Zadeh M, et al. Invasive partial mole. *Am J Clin Pathol*. 1986;85:722–724.

20. Sebire NJ, Lindsay I, Fisher RA, et al. Overdiagnosis of complete and partial hydatidiform mole in tubal ectopic pregnancies. *Int J Gynecol Pathol.* 2005;24:260–264.
21. Choi-Hong SR, Genest DR, Crum CP, et al. Twin pregnancies with complete hydatidiform mole and coexisting fetus: use of fluorescent in situ hybridization to evaluate placental X- and Y-chromosomal content. *Hum Pathol.* 1995;26:1175–1180.
22. Parveen Z, Tongson-Ignacio JE, Fraser CR, et al. Placental mesenchymal dysplasia. *Arch Pathol Lab Med.* 2007;131:131–137.
23. Kipp BR, Ketterling RP, Oberg TN, et al. Comparison of fluorescence in situ hybridization, p57 immunostaining, flow cytometry, and digital image analysis for diagnosing molar and nonmolar products of conception. *Am J Clin Pathol.* 2010;133:196–204.
24. Bifulco C, Johnson C, Hao L, et al. Genotypic analysis of hydatidiform mole: an accurate and practical method of diagnosis. *Am J Surg Pathol.* 2008;32: 445–451.
25. McConnell TG, Murphy KM, Hafez M, et al. Diagnosis and subclassification of hydatidiform moles using p57 immunohistochemistry and molecular genotyping: validation and prospective analysis in routine and consultation practice settings with development of an algorithmic approach. *Am J Surg Pathol.* 2009;33:805–817.
26. Lage JM, Popek EJ. The role of DNA flow cytometry in evaluation of partial and complete hydatidiform moles and hydropic abortions. *Semin Diagn Pathol.* 1993;10:267–274.
27. Castrillon DH, Sun D, Weremowicz S, et al. Discrimination of complete hydatidiform mole from its mimics by immunohistochemistry of the paternally imprinted gene product p57KIP2. *Am J Surg Pathol.* 2001;25:1225–1230.
28. Merchant SH, Amin MB, Viswanatha DS, et al. p57KIP2 immunohistochemistry in early molar pregnancies: emphasis on its complementary role in the differential diagnosis of hydropic abortuses. *Hum Pathol.* 2005;36:180–186.
29. Hayati AR, Tan GC. Clinicopathologic and immunohistochemical differences in complete and partial hydatidiform moles in a multiracial Malaysian population. *Int J Gynecol Pathol.* 2005;24:277–285.
30. Fisher RA, Nucci MR, Thaker HM, et al. Complete hydatidiform mole retaining a chromosome 11 of maternal origin: molecular genetic analysis of a case. *Mod Pathol.* 2004;17:1155–1160.
31. McConnell TG, Norris-Kirby A, Hagenkord JM, et al. Complete hydatidiform mole with retained maternal chromosomes 6 and 11. *Am J Surg Pathol.* 2009;33:1409–1415.
32. Ronnett BM, DeScipio C, Murphy KM. Hydatidiform moles: ancillary techniques to refine diagnosis. *Int J Gynecol Pathol.* 2011;30:101–116.
33. Silverberg SG, Kurman RJ. *Tumors of the Uterine Corpus and Gestational Trophoblastic Disease. Atlas of Tumor Pathology.* Third series, Fascicle 3. Washington, DC: Armed Forces Institute of Pathology; 1992:219–285.
34. Mao TL, Kurman RJ, Huang CC, et al. Immunohistochemistry of choriocarcinoma: an aid in differential diagnosis and in elucidating pathogenesis. *Am J Surg Pathol.* 2007;31:1726–1732.
35. Sebire NJ, Lindsay I, Fisher RA, et al. Intraplacental choriocarcinoma: experience from a tertiary referral center and relationship with infantile choriocarcinoma. *Fetal Pediatr Pathol.* 2005;24:21–29.
36. Ganapathi KA, Paczos T, George MD, et al. Incidental finding of placental choriocarcinoma after an uncomplicated term pregnancy: a case report with review of the literature. *Int J Gynecol Pathol.* 2010;29:476–478.
37. Ariel I, Boldes R, Weintraub A, et al. Chorangiocarcinoma: a case report and review of the literature. *Int J Gynecol Pathol.* 2009;28:267–271.
38. Elston CW, Bagshawe KD. The diagnosis of trophoblastic tumours from uterine curettings. *J Clin Pathol.* 1972;25:111–118.
39. Kurman RJ, Scully RE, Norris HJ. Trophoblastic pseudotumor of the uterus: an exaggerated form of "syncytial endometritis" simulating a malignant tumor. *Cancer.* 1976;38:1214–1226.
40. Young RH, Scully RE. Placental-site trophoblastic tumor: current status. *Clin Obstet Gynecol.* 1984;27:248–258.
41. Young RH, Scully RE, McCluskey RT. A distinctive glomerular lesion complicating placental site trophoblastic tumor: report of two cases. *Hum Pathol.* 1985;16:35–42.
42. Young RH, Kurman RJ, Scully RE. Proliferations and tumors of intermediate trophoblast of the placental site. *Semin Diagn Pathol.* 1988;5:223–237.
43. Shih IM, Kurman RJ. Ki-67 labeling index in the differential diagnosis of exaggerated placental site, placental site trophoblastic tumor, and choriocarcinoma: a double immunohistochemical staining technique using Ki-67 and Mel-CAM antibodies. *Hum Pathol.* 1998;29:27–33.
44. Kurman RJ, Young RH, Norris HJ, et al. Immunocytochemical localization of placental lactogen and chorionic gonadotropin in the normal placenta and trophoblastic tumors, with emphasis on intermediate trophoblast and the placental site trophoblastic tumor. *Int J Gynecol Pathol.* 1984;3:101–121.
45. Shih IM, Kurman RJ. p63 expression is useful in the distinction of epithelioid trophoblastic and placental site trophoblastic tumors by profiling trophoblastic subpopulations. *Am J Surg Pathol.* 2004;28:1177–1183.
46. Huettner PC, Gersell DJ. Placental site nodule: a clinicopathologic study of 38 cases. *Int J Gynecol Pathol.* 1994;13:191–198.
47. Rizeq MN, van de Rijn M, Hendrickson MR, et al. A comparative immunohistochemical study of uterine smooth muscle neoplasms with emphasis on the epithelioid variant. *Hum Pathol.* 1994;25:671–677.
48. Shih IM, Kurman RJ. Epithelioid trophoblastic tumor: a neoplasm distinct from choriocarcinoma and placental site trophoblastic tumor simulating carcinoma. *Am J Surg Pathol.* 1998;22:1393–1403.
49. Mao TL, Seidman JD, Kurman RJ, et al. Cyclin E and p16 immunoreactivity in epithelioid trophoblastic tumor—an aid in differential diagnosis. *Am J Surg Pathol.* 2006;30:1105–1110.
50. Mao TL, Kurman RJ, Jeng YM, et al. HSD3B1 as a novel trophoblast-associated marker that assists in the differential diagnosis of trophoblastic tumors and tumorlike lesions. *Am J Surg Pathol.* 2008;32:236–242.
51. Lewin SN, Aghajanian C, Moreira AL, et al. Extrauterine epithelioid trophoblastic tumors presenting as primary lung carcinomas: morphologic and immunohistochemical features to resolve a diagnostic dilemma. *Am J Surg Pathol.* 2009;33:1809–1814.
52. Shih IM, Seidman JD, Kurman RJ. Placental site nodule and characterization of distinctive types of intermediate trophoblast. *Hum Pathol.* 1999;30:687–694.
53. Kalhor N, Ramirez PT, Deavers MT, et al. Immunohistochemical studies of trophoblastic tumors. *Am J Surg Pathol.* 2009;33:633–638.
54. de Leval L, Waltregny D, Boniver J, et al. Use of histone deacetylase 8 (HDAC8), a new marker of smooth muscle differentiation, in the classification of mesenchymal tumors of the uterus. *Am J Surg Pathol.* 2006;30:319–327.

General Aspects of Processing and Reporting Surgical Pathology Specimens

Recommendations regarding how to process specific types of gynecologic specimens and suggested wording regarding their reporting are provided in the chapters corresponding to the organ of origin. What follows are guidelines related to the general aspects of processing and reporting all types of surgical pathology specimens for which a histologic interpretation is performed.

PREANALYTICAL HANDLING OF SURGICAL PATHOLOGY SPECIMENS

All specimens must be properly labeled and accompanied by an appropriately completed pathology requisition form. Fresh specimens should be stored in the Gross Room refrigerator until they can be processed. Once specimens from a case have been accessioned and given a surgical pathology number, cassettes are prepared (preferably using an automated cassette labeler). Each cassette should be labeled with unique identifying information. Always double-check to make sure that the cassettes are labeled with the correct case number and alphanumeric designation. Most laboratories find it useful to have color-coded cassettes, with different colors indicating to the histotechnologist the priority of the specimens and the histology protocol.

"GROSSING" THE SPECIMEN

The Gross Description

At the start of every batch of dictations, the prosector (resident, fellow, pathologists' assistant, or pathologist) must identify themselves and indicate the date. For each case, the prosector dictates *both* the patient name and the surgical pathology number at the start of the gross description (two patient identifiers markedly reduce the chance of one case being confused with another). If an intraoperative consultation has been performed, dictate the results of that consultation prior to describing any specimens, and specify the pathologist(s) who performed the consultation.

To begin a gross dictation on an individual specimen, begin with "Received as…" followed by how the specimen is labeled. Some prosectors also prefer to indicate whether the specimen was received in formalin or received fresh, and may also wish to indicate that the specimen is further labeled with the patient's name and surgical pathology number. Describe all organs and tissues in the order received with a clear description of their gross features. Give pertinent data concisely, including the size, shape, color, texture, and relationship of a lesion to adjacent structures. To minimize confusion and typographical errors, it is preferable to give measurements exclusively in centimeters, rather than alternating back and forth between centimeters and millimeters. In general, nongastrointestinal organs that are partially or completely resected should be weighed. If any tissue has been submitted for special procedures, gross photographs have been taken, or the specimen has been decalcified, then that information should be dictated as part of the gross description.

The last part of the dictation of each specimen should be a review of the blocks submitted for histology. Clearly state whether all of the tissue or representative sections have been submitted (e.g., "Submitted entirely in A1" or "Representative sections in A1–A3"). Some prosectors also find it useful to indicate the amount of remaining tissue by using "Jar code" terminology, with "Jar 0" meaning that the entire specimen was submitted and Jar 1 through Jar 4 referring to increasingly larger containers. Use a new paragraph to describe each specimen.

Note: Some prosectors are in the habit of treating the samples that have been submitted for frozen sections as full-fledged, separately submitted specimens. This occurs most often in academic settings in which one pathologist-in-training does the frozen section and another is responsible for dictating the gross description. The result is a needless and confusing discussion about the frozen section sample (e.g., received as "FS1" is a fragment of brown tissue measuring blah, blah, blah). It makes much more sense to readers of the report to describe the specimen as it was received from the operating room. After the submitted tissue has been described, reference to the frozen section can be made as follows: A representative sample is processed for frozen section analysis, and this tissue is now submitted in FS1.

Indications for Inking of Specimens

For cases in which surgical margins are important, the application of India ink to the specimen surface (followed by Bouin's solution as a mordant) is a useful method to identify the margins in histologic sections.* For specimens in which more than one margin is to be evaluated, the use of different colored inks is recommended to identify the different margins. If the margins of resection have been inked, record this information in the gross description. Be careful not to let "ink dribble" from gloves or paper towels come into contact with tissue that does not represent the margin of interest, since this can result in the false impression of a true resection margin when slides are examined microscopically. To help avoid this problem, it is recommended that the prosector change gloves after completing the inking procedure. To evaluate the inked margins, sections may be taken perpendicular to the margin (usually the preferred method) or shaved tangentially from the margin. For specimens that arrive in more than one piece, remember that the edges of these tissue samples are only specimen edges that may or may not represent true surgical margins.

Use of different-colored inks is also an additional safeguard in guarding against transpositions of specimens of the same tissue type either within a case or between patients. Examples include left and right breast core biopsies performed on the same patient on the same day (ink the left cores one color and the right cores another color) or multiple prostate needle biopsies from six different patients received on the same day (color-code by patient, since (a) it is not practical to ink each specimen site a different color, and (b) it is much more important to prevent a transposition between patients than within the same patient in this circumstance).

Submission of Tissue Samples for Histologic Interpretation

Very small specimens that will go through the perforations in the cassettes must be placed between sponges or wrapped in a small piece of lens paper. Small biopsies that are received fresh should be transferred to formalin for a few hours prior to further processing (sandwiching fresh tissue between sponges traumatizes the tissue and creates an artifact with triangular spaces). Small biopsies that are difficult to see may be stained by applying a drop of hematoxylin with a plastic pipette (this will facilitate visualization of the tissue by the histotechnologist). If a tissue sample is large or received late in the day and needs overnight fixation, it may be advantageous to send through a small representative portion ("pilot section") on the day it is received and fix the rest overnight for submission the following day. This protocol may allow for a preliminary diagnosis to be made on the day after the surgical procedure, while still safeguarding against the possibility of inadequate fixation interfering with the ability to make an accurate diagnosis.

Tissue selected or sectioned for histologic evaluation should be ≤3 mm thick and easily fit within the cassette. A cassette should not be packed more than half full with tissue curettings. When handling fresh tissue, consideration should be given to submission of tissue for special procedures (e.g., microbiologic cultures on suspected infectious processes if not obtained by the submitting physician, flow cytometry immunophenotyping for hematolymphoid lesions, cytogenetic analysis on selected products of conception or malignant tumors, storing of frozen tissue for possible special studies or lipid stains, or fixing a sample from an unusual tumor in glutaraldehyde for possible electron microscopy). Large specimens (e.g., uteri, ovarian tumors, or placentas) should be dissected in the fresh state and then fixed in an adequate amount of formalin (~10 times the volume of the tissue) before the tissue blocks are taken. Large specimens must be sliced to achieve adequate fixation. Hollow viscera should be opened and pinned to a corkboard for fixation, unless the prosector elects to inflate the specimen with formalin. In some instances, it may be desirable to preselect 2- to 3-mm-thick sections of tumor for separate fixation (e.g., slices of ovarian lymphoma separately fixed in small jars of formalin and B5). The instruments and cutting board should be cleaned meticulously between specimens to avoid contamination of one specimen with another.

TIDBITS REGARDING MICROSCOPIC EVALUATION AND THE FINAL REPORT

- Before starting the microscopic examination, confirm that the slides match the associated paperwork (transpositions are more likely to occur and less likely to be detected when a batch of specimens from the same tissue site has been delivered). Computer-generated, typed slide labels that list both the case number and the patient's last name in as large a font as feasible reduce the likelihood of such transpositions.
- Review a list of the patient's previous pathology accessions and examine any relevant material.
- After indicating the appropriate patient and pathologist identifying information, the microscopic description is dictated. The degree of detail provided in the microscopic description should be tailored to the reader of the report. Clinicians do not want to have to wade through a tedious description of what the cells look like and what formations they are making in order to get to the relevant diagnostic and prognostic information, and transcription services need to be utilized efficiently. On the other hand, in consultation reports provided at the request of other pathologists, it is appropriate and desirable to go into some detail about the particular microscopic features of a lesion that help to distinguish it from others in the differential diagnosis.
- In cases in which slides are interpreted but no microscopic description is deemed necessary, the pathologist should

*As discussed at the beginning of Chapter 7, I am not a proponent of routinely inking the surface of ovarian tumors.

clearly indicate that a microscopic examination was indeed performed (I prefer the succinct "Microscopic: Performed" over the more loquacious "Microscopic examination substantiates the above-cited diagnosis").

- The report should include the results of all special stains that have been performed and billed. Use of preliminary reports and addenda should be kept to a minimum, particularly when the additional report is describing the results of special stains that will be completed within 24 hours of the initial report. For the clinician and personnel handling the reports, receiving results in a piecemeal fashion is suboptimal, and increases the chances of a miscommunication. Special stains that are clinically relevant and billable should be reported regardless of the result, rather than leaving the clinician hanging by making a statement such as "Special stains for acid-fast bacilli and fungi will be performed and the results will be reported as an addendum if either of these stains is positive." In cases with significant delays, the clinician should be notified of the reason for the delay.
- Pathologists are encouraged to seek consultations with each other on unusual, difficult, subjective, interesting, and high-impact cases. If an intradepartmental consultation is noted in the surgical pathology report, it should specify the pathologist(s) whose opinions are reflected in the report.
- Unexpected pathology results of major clinical importance should be telephoned to the physician, and the conversation should be documented in the pathology report (e.g., no chorionic villi, implantation site, or fetal parts in a specimen submitted as products of conception).
- The diagnosis should be reported as "Organ, specific site, procedure – Diagnosis" (e.g., uterus, cervix, biopsy—no significant abnormality). Pathologists should itemize each specimen in the diagnosis section of the report for the sake of clarity, completeness, and compensation.
- Before signing out the case, confirm that the list of specimens submitted, type of operation, clinical history, and clinical diagnosis have been accurately transcribed by the secretarial staff. Proofread the remainder of the report, correct any typographical errors, approve the charges, and assign an ICD-9 code if this task is not performed by other laboratory or billing personnel.
- Following the procedures of the individual laboratory's quality assurance policy, selected finalized cases should be submitted for review by other pathologists within the group. This review should occur in a timely manner.
- Turnaround time is important. At least 90% of routine surgical pathology cases should be completed within two working days.
- For those cases in which a pathologist initiates slide consultation with a pathologist at another institution, an addendum summarizing the consultant's opinion should be issued once the consultant's report is received. If the consultant is changing the original diagnosis in a significant way, the postsignout report should be in the form of an amendment rather than an addendum. It is recommended that the pathologist telephone the consultant's diagnosis to the treating physician, particularly when the initial report was noncommittal or the consultant's diagnosis is significantly different from the diagnosis that was initially favored.

SUGGESTED READINGS

Rosai J. *Rosai and Ackerman's Surgical Pathology*. 9th ed. St. Louis, MO: Mosby; 2004. Appendices A and B.

Nakhleh RE, Fitzgibbons PL, eds. *Quality Management in Anatomic Pathology*. College of American Pathologists: Northfield, IL: 2005.

Haber S. *Innovations in Pathology: The Best of Thirty Years*. College of American Pathologists: Northfield, IL: 2001.

Billing (CPT and ICD-9 Coding) of Gynecologic and Obstetric Surgical Pathology Specimens in the United States

GENERAL BILLING PRINCIPLES

Basic Billing/Coding Terminology and the Concept of Medical Necessity

Physicians bill for the procedures they perform and services they provide using CPT (Current Procedural Terminology) codes.[1] For surgical pathology, the primary CPT billing codes in increasing order of complexity are 88300, 88302, 88304, 88305, 88307, and 88309, proceeding from specimens that receive a "gross only" examination (88300) to the most complicated surgical resections (88309). ICD-9 codes are used to identify the disease, injury, symptom, or condition of the patient.*

For proper reimbursement, most insurers require proof of medical necessity, which is accomplished by providing the appropriate ICD-9 code for the CPT code that is billed. For many cases in pathology, claims will still be processed and paid using ICD-9 codes that are broad and generic within the correct organ system. For example, using an ICD-9 code of 611.72 (lump or mass in breast) is sufficient to have an 88305 or 88307 CPT code paid, regardless of whether the pathologic diagnosis is fibrocystic change, fibroadenoma, carcinoma, or any other lesion that can produce a mass. However, if the diagnosis is breast carcinoma and immunostains are performed for biomarkers, then the 88342 charges for the immunostains are likely to be denied unless the ICD-9 code for breast cancer (174.9) has been provided with the submitted claim. In other words, the insurance company is only willing to pay for estrogen and progesterone receptor immunostains and an assessment of proliferative activity and HER2 expression if these studies are performed on a breast cancer, which is a situation that is deemed medically necessary. As this example illustrates, accurate ICD-9 coding is most important in situations in which immunostains or other special procedures have been performed.

To minimize the burden of locating the correct ICD-9 code, it is useful to have an "ICD-9 Greatest Hits" list amongst your easily accessible reference materials. ICD-9 codes related to gynecologic surgical pathology that should be on this list

*A government-mandated transition from ICD-9 to ICD-10 codes is currently scheduled for October of 2013. Updating insurance and laboratory software to accommodate this new system and educating physicians and coders on how to use these new codes are tasks that are likely to be quite challenging.

include 622.10 (dysplasia of cervix), 180.9 (cervical cancer), 621.30 (endometrial hyperplasia), 219.1 (benign neoplasm of uterine corpus), 182.0 (malignant neoplasm of uterine corpus), 220 (benign neoplasm of ovary), 183.0 (primary ovarian cancer), 198.6 (metastatic cancer to ovary), and 196.9 (lymph node metastasis).

The Buck Stops with the Pathologist

Although many pathologists delegate the responsibility of CPT and ICD-9 coding to clerical or billing staff, the person ultimately and legally responsible for the accuracy of the bill is the pathologist who signs the pathology report.[2] Pathology groups need to audit their billing codes to ensure that they are accurate and to promote consistent coding within the group. Depending on the size and structure of the pathology group and its degree of billing complexity, it may be desirable to establish a formal compliance program.[2]

If It's Not in the Report, It's Not Billable

For the sake of accuracy and completeness and in order to defend your charges against an insurance audit, justification for any issued charges should be clearly documented in the pathology report. It is grossly inadequate to make a blanket statement such as "Immunohistochemical stains support this diagnosis." Instead, each specific stain performed and its result should be listed (the same applies to other special stains). Make sure that the number and type of primary pathology codes (88300–88309) correspond to the number and type of specimens submitted and reported (with exceptions as outlined in the section on assigning CPT codes). If a specimen requires decalcification, an 88311 charge should be added and the gross description should specify that the specimen was submitted after decalcification. If any intraoperative consultations were performed, appropriate charges should be added and the type and result of each consultation should be listed in a separate section of the pathology report, as outlined in the following example:

Intraoperative Consultation

Ovary, left, oophorectomy (gross consultation)—consistent with dermoid cyst
Ovary, right, oophorectomy (frozen sections 1A and 1B)—endometrioid carcinoma arising within an endometriotic cyst
Lymph nodes, left pelvic, dissection (cytologic evaluation)—negative for malignancy (4/4)

In this example, the charges for the intraoperative consultation would be an 88329-59 for the gross consultation, one 88331 and one 88332 for the two frozen sections on the right ovary, and an 88333 for the cytologic evaluation (see section on billing for intraoperative consultations for further details).

Potential Problems with Billing for Special Stains

In the age of electronic billing and for the sake of efficiency, the hospital may have set up its system to send out its bill shortly after the accession date and to forgo sending any additional bills on what it considers incidental late charges. If the pathologists' billing system keys off of the hospital's system, then charges for special stains that are ordered a few to several days after the accession date will also not be issued by the pathologists' billing service. Although such charges may be considered "incidental" by the hospital, they are of significantly more importance for most pathologists. A similar problem can occur if the charge codes for special stains are not entered into the billing system in a timely manner. For these reasons, it is important to establish a mechanism to ensure that special stains are billed regardless of how many days after the accession date the order was placed.

Mutually Exclusive Edits and the Importance of the "-59" Modifier

Government-sponsored insurance and some insurance companies use edits for combinations of charges that they think are inappropriate, which lead to claim denials. In the battle for proper reimbursement, the "-59" modifier is an important tool that is used to indicate to the insurer that the service performed was medically necessary and distinct from the other services provided on the same day for the same patient. Examples relevant to gynecologic pathology of Medicare's mutually exclusive edits that may result in claim denials without proper use of the "-59" modifier include (a) use of the frozen section code 88331 with intraoperative consultation codes 88329, 88333, or 88334, and (b) consultations on referred material (88321, 88323, or 88325) when special stains (88312, 88313, and/or 88342) are performed or when such a consultation is provided on the same day as a separate in-house surgical pathology or cytopathology service.

Spot-Audit Targeted Cases at High Risk for Billing Errors and Payment Denial

From the previous discussion, it should be obvious that cases with immunostains are ideal candidates for spot-audits. Not only are they at risk for being not being billed, but they are also likely to be rejected for payment if the correct ICD-9 code or modifier has not been applied. Other cases worth auditing are those with multiple CPT codes, high dollar values, intraoperative consultations, and code pairs subject to known mutually exclusive edits. Claims with multiple units of the same CPT code are at risk for being denied for exceeding the limit prescribed by one of Medicare's "Medically Unlikely Edits" (for consultations on referred slides, this applies if there is more than one consultation code). Billing services should be willing and able to set up the group's compliance officer

with remote online access to patient information within the pathologists' account, so that the compliance officer can get immediate and unfiltered feedback for each audit. The billing service should also be able to supply the pathology group with a report listing the claim denials of the major payers so that patterns of denial can be identified and rectified.

Outreach

In some situations, laboratories may try to increase their volume by obtaining business from outreach locations. This may involve discounting the lab charges for specimens derived from these sources. In this scenario, discounted test codes for outreach specimens may be established by using a different prefix letter from those originating from inside the hospital (e.g., R88305 → 88305 charging 80% of the regular rate vs. H88305 → 88305 charging the regular rate).

ASSIGNING CPT CODES FOR GYNECOLOGIC AND OBSTETRIC SURGICAL PATHOLOGY SPECIMENS

Since 1992, the foundation of surgical pathology billing has been based upon the principle that each specimen that has been submitted for individual examination and diagnosis is a separate billable unit of work.[3]

Table A2.1 provides an alphabetized list of selected OB/GYN-related surgical pathology specimens and their corresponding CPT codes.

In general, the number of billable units of work corresponds to the number of specimen containers received for a given case. However, there are exceptions, for which examples are provided below:

1. If both ovaries ± tubes are submitted in a single container without regard for laterality, only one charge can be issued. However, if one of the adnexa is identified in some way (e.g., an attached suture marking the right side or the clinician notes that the right ovary is the one with the 5 cm cyst), then tissue from the left and right sides should be processed separately and two charges are appropriate.
2. For resected ovaries, if one or both fallopian tubes are incidentally removed and are submitted in separate containers, then they are bundled together and included in the ovarian-related charge(s).
3. For resected uteri, if the ovaries and/or fallopian tubes are incidentally removed and are submitted in separate containers, then they are bundled together and included in the single uterine-related charge.
4. If two tissues of obviously different origin are submitted in the same container, such as a uterus along with an appendix, two charges are appropriate.
5. In some situations, tissue from the same surgical specimen is submitted in more than one container. For example, if the amount of tissue obtained from an abortion exceeds the size of the containers that the operating room personnel have on hand, they may submit the specimen in more than one container. In cases of this type, only one charge is appropriate. Other similar examples outside the field of gynecologic pathology include submission of a sample of a brain tumor for frozen section followed by additional brain tumor for permanent sections (charge only one 88307 + an 88331 for the frozen section) and the submission of a breast needle core biopsy that has been separated into two different containers according to whether or not microcalcifications are present (charge only one 88305). When utilizing computer software packages to associate specimens with histology protocols and billing, users may have to get creative in order to avoid the

TABLE A2.1 CPT Codes for Selected OB/GYN-Related Surgical Pathology Specimens

Specimen	CPT Code
Abortion—spontaneous/missed	88305
Abortion—induced	88304
Bartholin gland cyst	88304
Cell block, any source	88305
Cervix, biopsy	88305
Cervix, LEEP or conization	88307
Endocervix, curettage/biopsy	88305
Endometrium, curettage/biopsy	88305
Fallopian tube, biopsy	88305
Fallopian tube, ectopic pregnancy	88305
Fallopian tube, sterilization	88302
Fetus, with dissection	88309
Hydatid cyst of Morgagni	88304
Intrauterine device	88300
Leiomyoma(s), myomectomy	88305
Lymph node, nonsentinel, biopsy	88305
Lymph node, sentinel, biopsy	88307
Lymph nodes, regional resection	88307
Omentum, biopsy	88305
Ovary, w/wo tube, neoplastic	88307
Ovary, w/wo tube, nonneoplastic	88305
Ovary, biopsy/wedge resection	88305
Peritoneum, adhesion	88304
Peritoneum, biopsy	88305
Placenta, other than third trimester	88305
Placenta, third trimester	88307
Polyp, cervical/endometrial	88305
Uterus, w/wo tubes and ovaries, prolapse	88305
Uterus, w/wo tubes and ovaries, high-grade dysplasia/malignancy[a]	88309
Uterus, w/wo tubes and ovaries, other than above	88307
Vagina, biopsy	88305
Vaginal mucosa, incidental	88302
Vulva/labia, biopsy	88305
Vulva, total/subtotal resection	88309

[a]I have substituted the words "High-Grade Dysplasia/Malignancy" for "Neoplastic" to clarify how specimens of this type should be coded (see section on billing gray zones).

computer double-billing in these situations. One solution is to create a specimen type designated "more of same, no charge." This specimen type can be associated with the correct histology protocol, but have a blank billing field so that no charges are issued for the tissue in that particular container. If this approach is utilized, check to make sure that the laboratory information system software does not use this entry field of the specimen type to supersede the listing of specimens as received from the submitting physician, otherwise what was submitted as "right breast core biopsy with microcalcifications" may appear on the report as "more of same, no charge."

BILLING "GRAY ZONES"

For most specimens in gynecologic and obstetric surgical pathology, assignment of a CPT code is a straightforward exercise that involves following the guidelines provided in the previous section. However, there are some "gray zones" in which it is not entirely clear how a specimen should be billed. In these cases, the pathologist should use common sense and see that the amount of work reflects the charge applied. What follows is a brief discussion of some commonly encountered ambiguous billing situations and my approach to them. Depending on the circumstances of an individual case or guidance from a higher authority, deviations from these recommendations may be warranted.

Cervical LEEPs

Although cervical loop electrosurgical excision procedure (LEEP) specimens are generally considered equivalent to cone biopsies and are charged as 88307s, this may not be appropriate when multiple LEEP samples are separately submitted from the same patient. If such samples can be submitted entirely in a single cassette, then an 88305 charge for each of these samples is more appropriate.

Hysterectomies for HSIL/AIS

A hysterectomy that has been performed for a diagnosis of cervical high-grade squamous intraepithelial lesion (HSIL) or adenocarcinoma in situ (AIS) should be coded as an 88309, even if no residual lesion is found.[4] In such cases, the entire transformation zone should be submitted for histologic evaluation to exclude the possibility of occult invasion.

Fibroid Uteri

The CPT coding manual lists "Uterus, with or without Tubes and Ovaries, Neoplastic" as an 88309. Use of the term "Neoplastic" has created some confusion, since some have considered this a license to bill uteri with leiomyomas ("fibroid uteri") as 88309s, when they should be billed as 88307s.[4]

Vaginal Hysterectomies for Prolapse

Probably the most undervalued specimen in all of surgical pathology is the vaginal hysterectomy for uterine prolapse, which is billed as an 88305 (the equivalent of a melanocytic nevus or tubular adenoma submitted in a single cassette). Although no significant pathology is likely to be found, a careful gross examination still needs to be performed and the cervix, endometrium, and myometrium all need to be evaluated histologically. It is appropriate to upgrade these cases to 88307s if abnormalities such as endometrial polyps or leiomyomata are present. Moreover, if vaginal mucosa is also submitted (regardless of whether or not it arrives in the same container), a separate 88302 charge should be issued for its microscopic examination.

Resections of Uteri and Adnexa when the Adnexa Contain Significant Pathology

When the ovaries and/or fallopian tubes are *incidental* specimens that are removed along with the uterus, they do not represent significant additional work and are bundled together with the single CPT code for the uterus, whether or not the adnexa arrive in the laboratory attached to the uterus or in separate containers. However, when the ovary is removed because of a neoplasm and a hysterectomy is also performed, the ovary becomes the primary specimen. The 88307 CPT code for evaluation of an ovarian neoplasm and its associated fallopian tube stands on its own merits, and a separate 88307 or 88309 is warranted for the uterus based upon whether or not it harbors a malignancy.[4] Bilateral ovarian tumors resected with a benign uterus could theoretically be charged as 88307 × 3, but charges should be considered on a case-by-case basis depending upon the amount of work involved.

Twin Placentas

Twin third-trimester placentas should be charged as 88307 × 2 if the placentas can be individually identified by a cord clamp or other means (make sure to diagnose each placenta separately in the pathology report).[4]

Lymph Node Samples

Oncologic procedures in gynecology often generate multiple separate containers of lymph nodes, and it is often unclear whether a given sample should be billed as a biopsy (88305) or a dissection (88307). Billing should correspond to the amount of work necessary to process and interpret the specimen. If it requires minimal dissection to identify the node(s) and all nodal tissue from that specimen is submitted in a single cassette, then an 88305 is most appropriate. If nodes have to be dissected from intimately associated adipose tissue and more than one cassette is needed to process the nodal tissue, then an 88307 charge is indicated.

Sentinel Lymph Nodes

Sentinel lymph nodes are billed as 88307s to reflect the increased amount of work that it takes to process and evaluate these specimens via a protocol that involves histologic sectioning at multiple different levels. However, billing can get out of hand when the surgeon submits two or more "sentinel" lymph nodes

as separately identifiable specimens. If five separately identified sentinel lymph nodes are submitted, five 88307 charges could theoretically be issued. This is excessive, especially since it should not matter to the surgeon which of the five sentinel lymph nodes contains a metastasis, but only the size of each metastasis, the presence or absence of extranodal extension, the number of nodes involved, and the total number of nodes examined. If surgeons realized how the separate submission of sentinel nodes impacted the patient's pathology bill, most would quickly begin submitting their battalion of sentinel nodes as one specimen. Meanwhile, in cases in which multiple sentinel nodes are submitted as separate specimens, the amount of work that it takes to process these nodes can be significantly reduced by color-coding the individual nodes with different inks and submitting as many of them in the same cassette as space constraints allow. With the amount of work to section and examine these nodes reduced, the associated charges can be reduced accordingly.

The Marginal Sample

It is not uncommon for endocervical or endometrial samples to contain scant, nondiagnostic tissue. The reporting of such specimens should describe what little material is present on the slide and the usual CPT code should be billed. It is not any less work for the histotechnologist or pathologist to process a specimen of this type than one that contains an adequate amount of tissue. Moreover, the scant nature of the specimen may provide the gynecologist with relevant clinical information, such as in cases of endometrial atrophy.

The Phantom Sample

On occasion, the laboratory will receive a container labeled with a patient's name with no identifiable specimen. The submitting physician should be notified as soon as possible, and a brief report should be issued that indicates the lack of a specimen. The prosector should not feel obligated to submit a filtered sample of formalin from the container to document the absence of tissue (this will only cause the histotechnologist to panic and suffer eye strain). No charge should be issued in this circumstance.

BILLING FOR INTRAOPERATIVE CONSULTATIONS

An intraoperative consultation may take the form of a gross consultation or microscopic diagnoses that are rendered via analysis of frozen sections and/or cytologic preparations. Billing for gross consultations and frozen sections has remained unchanged for many years. A gross consultation is billed as an 88329, the first frozen section on each individual specimen is billed as an 88331, and each additional frozen section performed on the same specimen is billed as an 88332 ("frozen section" in this context refers to one or more slides generated from a single block of frozen tissue; that is, the frozen tissue block is the unit of service for codes 88331 and 88332). Prior to 2006, intraoperative consultations that utilized cytologic preparations were billed using code 88329 coupled with code 88161. Since 1/1/06, intraoperative cytologic evaluations are billed using CPT code 88333 for the initial site and code 88334 for each additional site.[5]

Billing gets more complicated when frozen sections and cytologic preparations are both utilized to evaluate a specimen. In the usual situation where the frozen section and cytologic evaluations complement one another, Medicare dictates that only the frozen section charge is billable. In occasional cases, such as when one modality is utilized to diagnose carcinoma and the other is performed on a different area of the same specimen to evaluate the resection margin, Medicare allows billing for both the frozen section and the cytologic evaluation. In this situation, the "initial site" code 88331 is used for the frozen section and the "additional site" code 88334 is used for the cytologic prep (append the "-59" modifier to the 88334 code to override the mutually exclusive edit and separately document each result in the intraoperative consultation section of the report).

Note: Cytologic evaluations that are performed outside the context of an intraoperative consultation, at the discretion of the pathologist, and in conjunction with the primary surgical pathology codes, such as smears or touch preps of a fresh lymph node that is suspicious for lymphoma, are not separately billable according to Medicare rules.

BILLING FOR SPECIAL STAINS

CPT codes for special stains used in surgical pathology are provided in Table A2.2.

TABLE A2.2 CPT Codes for Special Stains Used in Surgical Pathology

Stain	Code
Stains for microorganisms (e.g., AFB, GMS, PAS[a])	88312
Most other special stains (e.g., trichrome, retic, iron, PAS for glycogen and/or mucin)	88313
Stains on frozen sections (e.g., oil red O)	88314
Stains to identify chemical components (e.g., copper)	88318
Stains to identify enzyme constituents (e.g., chloroacetate esterase)	88319
Immunostains	88342
Immunofluorescence stains (usually for kidney or skin biopsies)	88346

NOTE: If the pathologist orders a special stain for interest only, or if the pathologist decides not to report the result of a special stain for any reason (e.g., the lesion to be evaluated is focal and no longer present in the specially stained slides), then it is the responsibility of the pathologist to see to it that no charges are issued for the unreported special stains.

[a]When a PAS stain is ordered to detect fungal organisms rather than as a stain for glycogen and/or mucin, it should be ordered as a "PAS fungus" stain. This terminology should alert the histotechnologist to perform a PAS with diastase stain (to remove background "noise" related to glycogen), use a fungus control, and bill the stain as an 88312 rather than an 88313.

Quantity Issues

When the same special stain is performed on more than one block of a particular specimen, or on different levels of the same block, only one special stain charge should be issued.[4] If the same special stain is performed on *different* specimens within the same case, then one special stain charge should be billed for each different specimen. Examples:

There are three blocks of a right ovarian mass with granulomatous inflammation. AFB and GMS stains are performed on all three blocks. Special stain portion of bill = 88312 × 2 (one charge for the AFB and one charge for the GMS).

There are three blocks of a right ovarian mass and two blocks of a left ovarian mass, with granulomatous inflammation in all five blocks. All blocks are stained with AFB and GMS. Special stain portion of bill = 88312 × 4 (AFB right ovary, GMS right ovary, AFB left ovary, GMS left ovary).

Cytokeratin immunostains are performed on three different levels of the same tissue block of a sentinel lymph node. Special stain portion of bill = 88342 × 1.

Medical Necessity Issues

As previously discussed, proper reimbursement for immunostains requires accurate ICD-9 coding to document medical necessity. Insurers may legitimately deny payment for immunostains when they are of questionable medical necessity, such as when endometrial samples are stained with the plasma cell marker CD138 as a screening test for chronic endometritis.

In most situations, the medical necessity of the immunostains is not in question, and it is simply a matter of having the attention to detail to append the appropriate ICD-9 code. One problematic area concerns immunostains that are performed to help establish or refute the presence of a condition when the results suggest that the condition is not present. A common example of this situation is a difficult prostate needle biopsy in which an immunostain highlights a rim of basal cells in the area of interest, thereby supporting a benign process. Ordinarily, Medicare and other insurers will not pay for an immunostain if it is performed on benign prostatic tissue. However, the ICD-9 code V76.44, special screening for malignant neoplasm of the prostate, indicates the medical necessity of the immunostain and should allow for proper reimbursement. In gynecologic pathology, an analogous situation exists when p16, MIB-1, and/or ProExC immunostains are performed on an atypical squamous metaplastic proliferation of the cervix in an effort to identify an HSIL. If the stains support HSIL, then the ICD-9 code for cervical dysplasia can be used, and proper reimbursement should occur. However, if the stains support metaplasia, there is no ICD-9 code that can reliably assure reimbursement. The V code that is analogous to V76.44 is V76.2 (special screening for malignant neoplasm of the cervix). However, this code is specifically for use with a Pap smear, and its use will likely result in denial of the entire claim. Another example of this problem within the field of gynecologic pathology is when a p57 immunostain is performed to address the differential diagnosis of early complete mole versus hydropic abortion in cases in which the immunostain supports the latter diagnosis. Unless and until ICD-9 codes are developed or approved to address situations of this type, the only recourse is to audit these cases and dispute denials on a case-by-case basis, hopefully armed with a pathology report that documents the important role that the immunostain(s) played in arriving at the diagnosis.

BILLING FOR CONSULTATIONS ON REFERRED SLIDES

Most consultations on referred slides will result in an 88321 charge (consultation and report on referred slides prepared elsewhere). If evaluation of this material requires preparation of routine H&E slides from tissue blocks provided by the referral source, then code 88323 is used. In the unusual situation in which the consultation includes comprehensive review of the patient's medical record, code 88325 is appropriate (the number of slides examined or amount of time required to complete the consultation are not factors in making this determination). Note that these codes are not intended to be used for in-house consultations when a pathologist shares a case with a colleague. Although these in-house consultations are in the best interest of patient care and represent an important educational and quality assurance activity, they are not reimbursable.

The consultation code (88321, 88323, or 88325) covers interpretation of all of the preparations included with the case. So even if a case comes with "bug" stains, several immunostains, and photos of electron micrographs, a single consultation code is all that is allowed. However, if special stains are performed in the consultant's laboratory using material received from the referral source, then the consultant can bill for these special stains in addition to the consultation code (remember to append the "-59" modifier to the special stain codes as discussed in the section on mutually exclusive edits). As previously mentioned, consultations on referred slides that are performed on the same day as an in-house surgical pathology or cytopathology service should also be submitted with a "-59" modifier to avoid denial of the claim.

For consultations on referred slides, the unit of work has historically been the number of separate cases submitted for interpretation (usually one). In those situations in which the referring physician has requested an examination of slides from more than one case, such as a primary ovarian cancer from 2008 and a peritoneal recurrence from 2010, then two units of the consultation code (in this example, 88321) could be charged according to historical coding practices.[4] However, despite objections from the College of American Pathologists and many others, Medicare has recently decided to limit the number of outside consultation charges per patient to one per date of service, regardless of the number of cases being examined during the consultation.[6] Pathologists may continue to bill for outside consultations using the historical coding practice for patients not covered by government insurance, and may also attempt to justify more than one unit of service as reasonable and necessary to the government by appending the "-59" modifier, but should brace for a resistance for payment beyond that corresponding to one consultation code.

REFERENCES

1. American Medical Association. *Current Procedural Terminology*. American Medical Association Press: Chicago, IL; 2009.
2. Sidley & Austin law firm. *Compliance Guidelines for Pathologists*. Chicago, IL: College of American Pathologists; 1998.
3. College of American Pathologists. *CPT Coding for Surgical Pathology*. Chicago, IL: College of American Pathologists; 1991.
4. Graziano C. Cracking the code: advice for CPT dilemmas. *CAP Today* July 1999;1+84–90.
5. Hughes J. Proper use of 88333 and 88334 CPT Codes. *CAP Today* Sept. 2006;74,76.
6. Centers for Medicare and Medicaid Services. Medically Unlikely Edits. Available at:http://www.cms.hhs.gov/NationalCorrectCodInitEd/08_MUE.asp#TopOfPage. Accessed 2010.

Page numbers in *italics* designate illustrations; those followed by a "t" indicate tables.